CUMULATIVE INDEX

Volumes 16–20

NUCLEAR SCIENCE ABSTRACTS

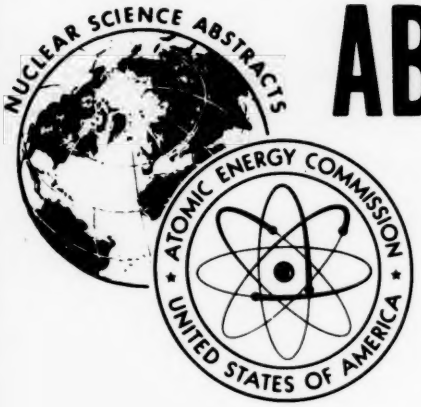

Volumes 16 through 20

1962 – 1966

SUBJECTS (V–Z)

UNITED STATES ATOMIC ENERGY COMMISSION
Division of Technical Information

USAEC DEPOSITORY LIBRARIES

Collections of USAEC reports are maintained in the libraries of the organizations listed below for reference use by the general public. Facilities for making photocopies are available. The USAEC also makes available through these libraries atomic energy reports of countries other than the U. S. that are abstracted in *Nuclear Science Abstracts*.

ALABAMA
Auburn, Auburn University
ALASKA
College, University of Alaska
ARIZONA
Tucson, University of Arizona
ARKANSAS
Fayetteville, University of Arkansas
CALIFORNIA
Berkeley, University of California
Davis, University of California
Los Angeles, University of California
San Diego, Public Library
Stanford, Stanford University
COLORADO
Boulder, University of Colorado
Denver, Public Library
CONNECTICUT
New Haven, Yale University
DELAWARE
Newark, University of Delaware
DISTRICT OF COLUMBIA
Washington, Library of Congress
FLORIDA
Coral Gables, University of Miami
Gainesville, University of Florida
Tallahassee, The Florida State University
GEORGIA
Atlanta, Georgia Institute of Technology
HAWAII
Honolulu, University of Hawaii
IDAHO
Pocatello, Idaho State University
ILLINOIS
Chicago, John Crerar Library
Chicago, University of Chicago
Evanston, Northwestern University
Urbana, University of Illinois
INDIANA
Bloomington, Indiana University
Lafayette, Purdue University
IOWA
Ames, Iowa State University
KANSAS
Manhattan, Kansas State University
KENTUCKY
Lexington, University of Kentucky
Louisville, University of Louisville
LOUISIANA
Baton Rouge, Louisiana State University
New Orleans, Tulane University
MARYLAND
Baltimore, Johns Hopkins University
College Park, University of Maryland
MASSACHUSETTS
Cambridge, Harvard University
Cambridge, Massachusetts Institute of Technology
MICHIGAN
Ann Arbor, University of Michigan
Detroit, Public Library
East Lansing, Michigan State University
MINNESOTA
Minneapolis, University of Minnesota
MISSISSIPPI
State College, Mississippi State University
MISSOURI
Kansas City, Linda Hall Library
Rolla, University of Missouri School of Mines and Metallurgy
St. Louis, Washington University
MONTANA
Bozeman, Montana State College
NEVADA
Las Vegas, Nevada Southern University
Reno, University of Nevada
NEW JERSEY
Princeton, Princeton University
Teaneck, Fairleigh Dickinson University
NEW MEXICO
Albuquerque, University of New Mexico
NEW YORK
Albany, The University of the State of New York
Buffalo, State University of New York at Buffalo
Ithaca, Cornell University
New York, Atomic Industrial Forum, Inc.
New York, Columbia University
New York, New York University
Rochester, University of Rochester
Schenectady, Union College
Syracuse, Syracuse University
Troy, Rensselaer Polytechnic Institute
NORTH CAROLINA
Charlotte, Public Library of Charlotte and Mecklenburg County
Durham, Duke University
Raleigh, North Carolina State College
NORTH DAKOTA
Grand Forks, University of North Dakota
OHIO
Cincinnati, University of Cincinnati
Cleveland, Public Library
Columbus, Ohio State University
Toledo, University of Toledo
Youngstown, Youngstown University
OKLAHOMA
Norman, University of Oklahoma
Stillwater, Oklahoma State University
OREGON
Corvallis, Oregon State University
Portland, Reed College
PENNSYLVANIA
Philadelphia, University of Pennsylvania
Pittsburgh, Carnegie Library
University Park, Pennsylvania State University
PUERTO RICO
Rio Piedras, University of Puerto Rico
RHODE ISLAND
Providence, Brown University
SOUTH CAROLINA
Columbia, University of South Carolina
TENNESSEE
Knoxville, University of Tennessee
Memphis, Public Library
Nashville, Joint University Libraries
Oak Ridge, Oak Ridge Associated Universities
TEXAS
Austin, University of Texas
College Station, Texas A & M University
Dallas, Southern Methodist University
Houston, Rice University
Lubbock, Texas Technological College
San Antonio, Public Library
UTAH
Salt Lake City, University of Utah
VIRGINIA
Blacksburg, Virginia Polytechnic Institute
Charlottesville, University of Virginia
Norfolk, Old Dominion College
WASHINGTON
Pullman, Washington State University
Seattle, University of Washington
WEST VIRGINIA
Morgantown, West Virginia University
WISCONSIN
Madison, University of Wisconsin
Milwaukee, Public Library
WYOMING
Laramie, University of Wyoming

UNITED STATES ATOMIC ENERGY COMMISSION

NUCLEAR SCIENCE ABSTRACTS

Cumulative Index

Volumes 16 through 20

1962 - 1966

SUBJECTS (V-Z)

Division of Technical Information

This eleven-volume set is for sale by the
Superintendent of Documents, U. S. Government Printing Office
Washington, D. C. 20402 Price $36.00

STAFF OF NUCLEAR SCIENCE ABSTRACTS

John W. Norris
Managing Editor

Donald D. Davis
Assistant Managing Editor

David E. Bost
Production Manager

Robert E. Upchurch
Subject Heading Specialist

J. Paul Meredith
Descriptive Cataloging Specialist

Clara L. Fox
Corporate Author Specialist

Mary H. Newman
Reports Evaluator

Brainard L. Patton
Scheduling and Publishing Coordinator

Section Editors

Everett J. Hoffman
Chemistry

Robert C. Kelly
Engineering; Earth Sciences

Lee M. Thompson
General Physics

Charles E. Stuber
High Energy Physics

Hugh E. Voress
Life Sciences

Lawrence T. Whitehead
Nuclear Data

James M. Jacobs
Reactor Technology; Metals and Ceramics

Abstractors

F. S. Armstrong*
Mary M. Brown
Jane G. Buchanan
D. Lamar Cason
Bennie G. Di Bona
Helen G. Donald
James R. Dulaney
Wells L. Green
Bernard O. Griggs
Harry G. Grisham
Mary C. Grissom
Miriam P. Guthrie
Fernando Hamilton
Phyllis C. Hansen
Thomas F. Heagerty
Carolyn D. Houston
Rose V. Jermain
Sidney F. Lanier
Betty L. McDowell
William D. Matheny
John H. Mitchell
Dora H. Moneyhun
Luther Norene
Carol Oen
Jean F. Peckham
Henry D. Raleigh
Mona H. Raridon
Julia S. Redford
Ned W. Rizzardi
Francis L. Sachs
Lila B. Smith
Polly C. Summers
Anne G. Ward
Helen L. Ward
David C. West
Milton O. Whitson
Juanita Wilson

*Atomic Energy of Canada, Ltd.

Acknowledgments

Agreements between the United States Atomic Energy Commission and the following organizations with regard to providing continuing services and specific literature coverage for *Nuclear Science Abstracts* are gratefully acknowledged:

American Institute of Physics; Atomic Energy of Canada Limited; Atomic Energy Research Establishment, United Kingdom; Aktiebolaget Atomenergi, Sweden; European Atomic Energy Community (EURATOM); Gmelin Institute, International Atomic Energy Agency; Japan Atomic Energy Bureau—Japan Atomic Energy Research Institute; Netherlands Patent Office; Reactor Centrum Nederland.

Communication concerning the editorial policy and content of *NSA* should be addressed to the Managing Editor, *Nuclear Science Abstracts*, AEC Division of Technical Information Extension, P. O. Box 62, Oak Ridge, Tennessee 37830.

Use of funds for printing this publication approved by the Director of the Bureau of the Budget, June 28, 1966.

Cumulative Index
Volumes 16-20, Subjects, 1962-1966

NUCLEAR SCIENCE ABSTRACTS

A semimonthly publication of the USAEC Division of Technical Information, Edward J. Brunenkant, Director. Published by the USAEC Division of Technical Information Extension, Robert L. Shannon, Extension Manager.

Nuclear Science Abstracts provides the only comprehensive abstracting and indexing coverage of the international literature on nuclear science and technology. *NSA* covers scientific and technical reports of the U. S. Atomic Energy Commission and its contractors, those of other U. S. Government agencies, and those of other governments, universities, industrial, and research organizations. It also covers patents, books, and journal literature on a worldwide basis. A list of the journals scanned appears in Issues 1 and 13 of each volume. Nearly 400,000 abstracts have appeared in *NSA* through Volume 20. The subject matter covered in *NSA* is described in Issue 1 of each volume and in TID-4552, *Subject Scope of Nuclear Science Abstracts*. The latter is available free from the U. S. Atomic Energy Commission, Division of Technical Information Extension, P. O. Box 62, Oak Ridge, Tennessee 37830.

Abstracts are arranged according to subject categories which are defined in Issue 1 of each volume. If the language of the original item is not English, the language is indicated. Translations are not abstracted if an abstract of the original item has appeared in *NSA*.

AVAILABILITY OF PUBLICATIONS ABSTRACTED

The public availability of all U. S. Atomic Energy Commission reports is indicated in the report number indexes. The availability of other reports, when known, is also indicated. The availability of some unnumbered reports is given in the abstract.

Dissertations abstracted in *Dissertation Abstracts* and included in *NSA* are available from University Microfilms, Inc., 315 N. First Street, Ann Arbor, Michigan 48103.

Information on the availability of the published literature and unpublished conference papers abstracted in *NSA* may be obtained from the Division of Technical Information Extension, P. O. Box 62, Oak Ridge, Tennessee 37830.

HOW TO OBTAIN NUCLEAR SCIENCE ABSTRACTS

NSA is available to the general public on a subscription basis from the Superintendent of Documents, U. S. Government Printing Office, Washington, D. C. 20402, as follows:

For the 24 regular issues, $30.00 domestic, $37.00 foreign. A single issue costs $1.75, plus 25 percent for foreign mailing. Domestic rates apply to the United States, Canada, Mexico, and Central and South American countries except Argentina, Brazil, Guyana, French Guiana, Surinam, and British Honduras. Foreign rates apply to the countries excepted above and to all other countries throughout the world.

For the quarterly, semiannual, and annual indexes, $22.00 domestic, $25.00 foreign.

Multivolume subject and author indexes are available as follows:

Vols. 1-4 (1948-1950). Johnson Reprint Corporation, 111 Fifth Avenue, New York, N. Y. 10003, $30.00.

Vols. 5-10 (1951-1956). Superintendent of Documents, U. S. Government Printing Office, Washington, D. C. 20402, $5.25.

Vols. 11-15, Subjects. Superintendent of Documents, U. S. Government Printing Office, Washington, D. C. 20402, $19.00.

Vols. 11-15, Personal Authors. Superintendent of Documents, U. S. Government Printing Office, Washington, D. C. 20402, $14.25.

Vols. 11-15, Corporate Authors. Superintendent of Documents, U. S. Government Printing Office, Washington, D. C. 20402, $2.50.

Vols. 16-20. (To be issued in 1967.)

Cumulative Report Number Index, Vols. 1—15 Revised, is available from the Superintendent of Documents, U. S. Government Printing Office, Washington, D. C. 20402, $4.00.

Cumulative Report Number Index, Vols. 16—20, is available from the Superintendent of Documents, U. S. Government Printing Office, Washington, D. C. 20402, $4.25.

Annual indexes are available separately from the Superintendent of Documents, U. S. Government Printing Office, Washington, D. C. 20402, as follows:

Vol. 16, Subjects and Authors, $9.75.
Vol. 17, Subjects and Authors, $12.25.
Vol. 18, Subjects and Authors, $12.50.
Vol. 19, Subjects and Authors, $12.50.

Annual indexes for Vol. 20 were not issued since they are a part of the cumulation for Vols. 16–20.

NSA is available on an exchange basis to universities, research institutions, industrial firms, and publishers of scientific information. Inquiries should be directed to the U. S. Atomic Energy Commission, Division of Technical Information Extension, P. O. Box 62, Oak Ridge, Tennessee 37830.

Government agencies may obtain *NSA* free of charge.

INTRODUCTION

Subject entries in this index are generally specific materials, things, and processes. These are followed by modifiers that describe the properties of, and processes applied to, the entries.

The number preceding the colon is the *NSA* volume number, and the number following is the abstract number. The designation (R) following the abstract number indicates that the abstract is of a progress report; (P) indicates a patent; and (T) indicates a translation. Abstracts for reports other than progress reports carry no letter designation. References to report numbers, where appropriate, are included after the abstract number of the citation. Published literature (journal article or book) is identifiable by the absence of a report number.

Special characters are added to modifiers in the field of physics; if the modifier does not establish the experimental or theoretical character of a reference, a symbol (E), (T), or (E/T) is placed immediately after the modifying phrase and before the journal reference number. The value of this identification has been established by the American Institute of Physics.

The user should bear in mind that the ideas presented in the original literature, rather than key words, have been indexed. The indexers have tried to select what seemed the most probable and logical place to look for typical information. Since it is not possible to anticipate where a user would look for information, numerous cross references are included.

Experience in using an index of this type will be the best guide in obtaining the desired information, and a consideration of synonymous or closely related terms as well as recent developments in scientific terminology will prove valuable.

Information must be so indexed as to be of the greatest use to the greatest number of users. This requires that a topic be indexed to headings that most specifically describe it and not ordinarily to the headings that describe its ultimate use, nor to the general class headings that include the specific headings. For example, information on the treatment of thyroid disease with I-131 would be indexed under Thyroid Gland and under Iodine Isotopes I-131, but not necessarily under Radiotherapy. A study of the effects of x radiation on hair would be indexed under both X Radiation and Hair.

The broad, general class headings are used only for general information or for comprehensive reports or articles.

Subject Heading Styles

Generally, the direct form of subject entry is used rather than inverted headings, e.g., Amino Acids rather than Acids, Amino; Helium Isotopes He-4 rather than Helium—isotopes He-4 or Helium—He-4 isotopes. Note, however, that in some cases parenthetic modifying terms or inverted headings of the form Neutrons, Fast are used in preference to a direct entry that would result in the scattering of information. Organic compounds are usually entered in the index in the inverted form so that substituted compounds can be listed near the parent compound; e.g., Benzene, Bromo- rather than Bromobenzene. Subject headings were chosen from TID-5001(5th Rev.) "Subject Headings used by the USAEC Division of Technical Information."

Alphabetization

Subject headings are alphabetized word-by-word. A parenthetic qualifier following a subject heading is disregarded in alphabetizing unless there are two or more headings identical except for the parenthetic qualifier, in which case the qualifier determines the order. Headings involving Greek letters are arranged as if the names of the letters were spelled out.

Examples:

M-Capture
  see Electron Capture
Magnesium
Magnesium Alloys
Manganese Fluorides
Manganese(II) Fluorides
Mesons
Mesons (π)
Mesons (ρ)
3-Pentanol, 2,4-Dimethyl-
2-Pentanol, 2-Methyl-
2-Pentanol, 4-Methyl-

Nomenclature of Inorganic Compounds

Inorganic compounds are indexed in the direct form, listing cations in the order of increasing valence in the case of polycationic salts of varying valence and in alphabetic order for polycationic salts in which all cations have the same valence; e.g., Sodium Aluminum Silicates and Potassium Sodium Sulfates.

Multicomponent Alloys and Other Systems

Multicomponent alloys, except well-known trade names, are indexed under a heading in the form "element alloy" for each element in the alloy. The modifier begins with element symbols for each component arranged alphabetically as if the English name for the element were spelled out.

Example: Copper–Gold Alloy is indexed
  Copper Alloys
    Cu–Au . . .
  Gold Alloys
    Cu–Au . . .

Well-known alloys such as Zircaloy-2 are indexed directly to the trade name; cross references referring from each component of the alloy to the entry for the trade name are included.

Multicomponent systems of nonmetallic elements are indexed in a manner similar to alloys except the main heading used contains the word "Systems" in place of "Alloys."

Example: Silicon–Tungsten Systems are indexed
Silicon Systems
Si–W...
Tungsten Systems
Si–W...

Multicompound systems and mixtures of compounds are indexed under the main heading for each component compound; the modifiers begin with an alphabetical listing of compound formulas.

Example: Lead Titanate–Lead Zirconate is indexed
Lead Titanates
$PbTiO_3$–$PbZrO_3$...
Lead Zirconates
$PbTiO_3$–$PbZrO_3$...

A mixed system of compounds and elements is indexed using a combined form of the above conventions, e.g., a dispersion of copper and alumina would be indexed

Aluminum Oxides
Al_2O_3–Cu...
Copper Systems
Al_2O_3–Cu...

Physical States and Configurations of Materials

Specification of the physical state, if other than normal, or geometric configuration of the material is included in the modifying phrase, i.e., liquid metals would be indexed to the metal with "liquid" in the modifier, and carbon crucibles would be indexed to Carbon with "crucibles" appropriately placed in the modifier and also to Crucibles if appropriate.

Modifying Phrases

The modifiers appearing under a subject heading are written specifically to describe the relation of the item being indexed to that heading. Effort is exerted to begin the modifier with the word judged to be of greatest use to the greatest number of users: this, however, does not obviate the need to consider all modifiers under the main heading(s) of interest.

Modifiers are usually intended to form a meaningful phrase when combined with the main heading. Some are intended to be read following the main heading, e.g., the entry Hydrogen—sorption by charcoal is read "hydrogen sorption by charcoal"; however, as a result of placing the important word first, many modifiers must be arranged for smooth reading, e.g., Formaldehyde—yields in radiolysis of ethyl ether, effects of deuterium on is read "effects of deuterium on formaldehyde yields in radiolysis of ethyl ether" and Uranium—crystal structure of, effect of cooling rate on allotropic transformations in is read "effect of cooling rate on allotropic transformations in crystal structure of uranium." Prepositions are sometimes omitted if no ambiguity results.

SUBJECTS (V-Z)

V

V PARTICLES
see also S Particles
compositeness criteria in Lee model, Salam, 19: 45068
interactions with nucleons, energy eigenvalue functions for, 16: 18355
interactions with mesons ($K\pi_3$) in fermion decay models, 17: 26346
interactions with hyperons (Λ), neutrons, and protons, 18: 7517
interactions with protons, bubble chamber detection efficiency for, 18: 12460 (JINR-P-1489)
interpretation as elementary-particle bound states and resonances in Lee model with form factor, 18: 6030
magnetic moments of, Vigier rotator model for anomalous, 17: 34802
production by meson (π^-)-nucleon interactions, 17: 9360
production by meson (π^-)-proton interactions at 10 Bev/c, 17: 9361
production in cosmic showers, transverse momentum of, 18: 14770
production in meson (π^-)-proton interactions at 6 Bev/c, cross section for, 17: 9427
production in meson (θ)-nucleon interactions, Lee model for, 18: 16778
production in meson (K^-)-proton interactions at 5.5 Bev/c, (Σ), 20: 15416
production in propane by mesons (π^-) at 6.1, 11.6, and 18.1 Bev, 16: 16938 (NP-11592(Vol.I)(p.101-10))
relativistic field theory with, 18: 21039
theory of, nonanalytic cut off function in Lee model for, 18: 32546

VACCINES
against Schistosoma, use of irradiated cercariae as, 19: 8937
against Schistosoma in mice, use of irradiated cercariae for, 19: 43848
against sheep lungworm, preparation from irradiated larvae, 19: 43750
antibody formation against polio, effects of irradiated pantothenic acid on, 19: 29978
effectiveness of irradiated lungworm, in cattle, 18: 528
effectiveness of irradiated *A. caninum*, in dog immunization, 19: 36025
effects of antiplague, on radiosensitivity of mammals, 17: 19865
effects of antituberculosis, during chronic irradiation, 16: 1540
effects of Brucella, in irradiated guinea pigs, 18: 25096 (T) (JPRS-24896)
effects of gangrene-tetanus, on irradiated monkeys, 19: 33945
effects of irradiated trichina larvae as, against trichinosis in swine, 19: 13020
effects of live brucellous serogenic immunization on irradiated guinea pigs, 16: 7467
effects of pertussis, on mouse leukopenia and lymphopenia, 20: 22685
effects of thymectomy on response to, in dogs, 19: 3976
effects on mouse lymph nodes and spleen when used with radiation, 18: 19740
evaluation of irradiated nematodes as, in sheep, 18: 43231 (TID-21203)
gamma-irradiated *Brucella melitensis*, immune reactions of mice to, 19: 22019(R) (UCLA-12-541(p.51-91))
immunity effects in irradiated rabbits, effects of sorption and vaccination time on, 19: 33948
immunogenic activity of, prepared from γ-irradiated *Brucella melitensis*, 20: 18509(R) (UCLA-12-576, pp 61-80)
induction of antileptospiral immunity in irradiated susliks, 16: 1542
preparation by formaldehyde and radiosterilization of, effects on immunity of mice to living bacteria, 17: 17701
preparation by irradiation of live viruses in presence of protective agents, 18: 3583(P)
preparation of *Ancylostoma caninum*, use of irradiated larvae for, 19: 33861
preparation of bacterial and helminthic, use of radiation in, 19: 13829
preparation of *Brucella melitensis* and *Brucella abortus*, using irradiated bacteria, 19: 45868
preparation of *Dictyocaulus filaria*, using γ and x irradiated larvae, 20: 8653
preparation of irradiated, against helminthic parasitic infections, 19: 7175
preparation of *Leptospira icterohemorrhagiae* by gamma irradiation of organisms, 20: 8676
preparation of lungworm, by irradiation, 17: 23100
preparation of *Pasteurella tularensis*, using irradiated bacteria, 19: 25971
preparation of pig-lung-parasite, from irradiated larvae, 20: 23570(P)
preparation of tuberculosis, using gamma-irradiated bacteria, 18: 15824
preparation of virus, inactivation by gamma exposure, 17: 1277
preparation of virus, in irradiated tissue cultures, 18: 27178
preparation of virus, 18: 27181
preparation of virus, 18: 27199
preparation of, feasibility of using zonal centrifuges in, 18: 11515 (ORNL-3502)
protective effects of combined, on immunity in irradiated and normal mice, 17: 19826
protective effects of immunization with live, against radiation sickness in rabbits, 18: 6689
protective effects of sorbed tritoxoid, against gas-gangrene and radiation effects in monkeys, 18: 8191
protective effects of antigen, against radiation sickness in rabbits, 19: 7185
protective effects of typhus against radiation damage to rat liver, 19: 15227
radiation effects on bacteria in smallpox, 17: 30323
radiation effects on gas gangrene, gamma, 18: 3530
radiation effects on lungworm larvae, use for, x, 18: 17392
radiation effects on reproduction of smallpox, in tissue culture, 18: 19687
radiation effects on sensitivity to, in rabbits, 18: 27177
radiation effects on response of guinea pigs to living tularemia, 18: 27193
radiation effects on immune reactions to, in rabbits, 18: 41178
radiation effects on mouse BCG, 19: 2125
radiation effects on response to, in dogs, 19: 3976
radiation effects on tetanus, in monkeys, 19: 19608
radiation effects on response to, in rabbits, 19: 26052
radiation effects on guinea pig and rat immunity to Brucella, x, 19: 28004
radiation effects on antibody synthesis in rabbits injected with leptospirosis, 19: 33953
radiation effects on effectiveness of *Ascaridia galli* larval, in chickens, 19: 35957
radiation effects on distribution of heat-killed *Mycobacterium smegmatis* in 20: 10654
radiation effects on virulence of Brucella, 20: 26700
radiation effects on response of rabbits to typhoid, x, 20: 38641
radiation effects on uptake of heat-killed sulfur-35-labeled mycobacterial, by microsomes and mitochondria in rat spleen, x, 20: 42907
radioprotective effects on mice, evaluation during fractional and prolonged irradiation, 20: 42992
radiosensitivity effects of influenza-virus, in mice treated by bone marrow injections, 18: 23366
radiosensitivity effects of smallpox virus, on chick embryos, x, 20: 14281
radiosensitivity effects of typhoid-paratyphoid, in dogs, x, 20: 42987
response to anthrax, by rabbits, 19: 33836
use of irradiated larvae of *Dictyocaulus viviparus* as, against lungworms in cattle, 18: 38722

VACUUM
bibliography on measurement of, 17: 3099
book: *Leybold Vacuum-Pocketbook*, in German, 18: 18024
book: *Ultrahigh Vacuum and Its Applications*, 18: 22243
contamination of, by residual gases, effects on materials deposited in, 16: 31695 (SCTM-249-61(14))
contamination of refractory metals and alloys by residual gases in high, 18: 39826 (ORNL-3674)
development of ultrahigh, 16: 27161(R) (NYO-9810)
development of ultra-high, 16: 29482(R) (NYO-9811)

dielectric breakdown in, 18: 18461(T) (AEC-tr-6341)
effects of ultra-high, on materials, 20: 45874 (NASA-TM-X-1268)
effects of ultrahigh, on fatigue of refractory alloys at high temperatures, 20: 824(R) (NASA-CR-54458)
effects on electric properties of dielectrics, 18: 10575 (NP-13539(Paper 4))
effects on engineering materials, 18: 2293(R) (FZK-161-1)
effects on engineering materials, 19: 18535(R) (FZK-188-1)
effects on engineering materials, 19: 42902(R) (FZK-243)
effects on engineering materials in combination with cryotemperatures and radiation, 20: 43994(R) (FZK-290)
effects on phase relations in cerium oxide–zirconium dioxide system, 20: 26845
effects on properties of uranium oxide pellets, 18: 32175
effects on properties and structure of tungsten crystallized in, 20: 43937
effects on refractory alloys and stainless steels, 18: 44049(R) (ORNL-3670(p.77-111))
effects on space vehicle materials, 18: 652(R) (FZK-163)
effects on space vehicles, estimates of magnitude and nature of, 20: 2036 (AD-618030)
effects on tensile properties of niobium and zirconium at 1100 to 1300°C, 20: 46198
effects on vaporization of hafnium carbides and tantalum carbides, 20: 35476 (NASA-TN-D-3503)
electric arc cathode emission processes in, 18: 20143
electric breakdown in, field emission in, 17: 36440(R) (NP-13061)
electric breakdown in high, 18: 687(R) (NP-13274)
electric breakdown in, theory of d-c, 18: 20140
electric breakdown in, theory of, 18: 20139
electric breakdown in, mechanisms of, 18: 20142
electric breakdown in ultrahigh, initiation of (E/T), 19: 2899
electric breakdown current in high, 20: 6169
electric discharge in, review of theories for, 20: 11769 (LGI-65/30)
electric discharge in, transverse magnetic field effects on, (E), 20: 11769
electromagnetic fields in, Fresnel's equation of wave normals for polarization in, (T), 19: 33098
gas expansion into, collisionless, 16: 10701
gravitational fields in, uniqueness of central-symmetric, (T), 20: 17582
hydromagnetic wave transmission at plasma boundary with, 18: 13130 (ARA-T-9197-7)
measurement and production of ultrahigh, review, 16: 10693
measurement of high and ultrahigh, 16: 6525
measurement of ultra-high, design of ionization gage for, 16: 31744
measurement of ultra-high, equipment and facilities for, 20: 45874 (NASA-TM-X-1268)
Penning discharge triggering in, effect of nickel-63 on, 20: 45877
photon interactions in, properties of, (T), 19: 47332
photon reactions in, Fresnel's equation for, (T), 19: 33098
physics and technology of, in thermonuclear research, 16: 28298
plasma expansion into, hydrodynamical model for, 19: 23884
plasma recombination processes in, expanding, (T), 20: 26305
plasma wave transformations at boundary of, 18: 32918
procedures in ultra-high, using aluminum foil gaskets, 17: 39222 (UCRL-7393)
production and measurement of ultrahigh, methods for, 17: 36465
production of high and ultrahigh, 16: 6525
production of, low-temperature surface condensation method for, 17: 14425(T) (AERE-Trans-915)
production of ultrahigh, by evaporation of silicon monoxide, 16: 1794
production of ultrahigh, by evaporation of silicon monoxide, 16: 14856(T) (CEA-tr-A-1044)
production of ultrahigh, back-diffusion and backstreaming effects on, 18: 22239
production of ultra-high, 18: 41636
production of ultrahigh, zeolite gettering devices for, 19: 15739
production of, feasibility of economic, 18: 22238
radiation effects on engineering materials in, 18: 20581(R) (FZK-172)
radiosensitivity effects on cinnamic acid and γ-phenyl ethyl acetate, 19: 11226
sorption of argon, helium, and nitrogen in, 20: 45876
technology in atomic industry, review, 16: 10226
technology in industry, 16: 10136
technology of ultrahigh, review of, 20: 11008
use in containment of water-cooled power reactors, 20: 12447
use in preparation and packing of isotopic radiation targets, 20: 25510 (AERE-R-5097, Paper 3)
uses of ultrahigh, 19: 20149

VACUUM FURNACES

book: *Handbook of High Vacuum Engineering*, 18: 14064
characteristics for metal production, 16: 20967
description of flame, for high-temperature studies on beryllium, 18: 25328(R) (SC-DC-64-864)
design, 17: 29344
design and operation of tungsten electrode, for arc melting refractory metals and alloys, 16: 6685 (IS-262)
design and operation of, for refractory alloy creep tests, 18: 44142(R) (NASA-CR-54123)
design and performance of induction coil assembly for uranium remelting, 18: 12599(R) (NLCO-900)
design and performance of sputter-ion-pumped resistance, 19: 24696
design for measuring strength at high temperatures, 18: 37683 (NP-14215)
design for melting and casting uranium, 17: 16579(P)
design for sintering at temperatures up to 2400°C, 16: 11809 (AERE-M-963)
design for use in high-temperature calorimetry, 18: 43440(R) (ANL-6800 (p.305-25))
design of electron bombardment, for annealing refractory metal samples, 17: 6218
design of electronic feedback-controlled, for measuring oxygen solubility in refractory alloys and metals, 20: 25562(R) (EIMAC-TR-66-2)
design of micro-, for high-temperature micrographic analysis, 17: 340(T,R) (EURAEC-342)
design of precision, for Moessbauer measurements, (E), 19: 40858
design, construction, and operation of consumable-electrode arc, for melting molybdenum-niobium-tantalum-tungsten alloys, 18: 44071
induction coil assembly design for uranium melting, 18: 32106 (NLCO-912)
performance, 19: 18401(R) (WANL-PR(Q)-005)
performance of ultrahigh, for annealing of refractory metal alloys, 19: 13955(R) (WANL-PR-(P)-005)

VACUUM FUSION ANALYSIS

equipment and procedures for determination of oxygen in uranium, 17: 14146 (PG-Report-411)
equipment design and operation for determining oxygen in beryllium, 16: 26911
equipment design and operation for determination of oxygen in uranium and plutonium carbides by, 17: 15872 (AERE-R-4216)
pressure monitoring in, use of Statham pressure transducers for continuous, 16: 261(R) (MCW-1465)

VACUUM GAGES

see also Pressure Gages

accuracy of, factors in, 17: 36440(R) (NP-13061)
anomalous residual currents in nude Bayard-Alpert ionization-type, 18: 2004
book: *Handbook of High Vacuum Engineering*, 18: 14064
book: *High Vacuum Engineering*, 18: 22242
book: *Leybold Vacuum-Pocketbook*, in German, 18: 18024
calibration below 100 ptorr, 18: 14190
calibration below 10^{-9} torr, method for, 19: 15845
calibration by orifice method, 16: 7625 (CF-61-5-109(Suppl.3))
calibration in magnetic fields, 16: 9511(R) (ORNL-3239(p.85-95))
calibration of ionization-type for gases other than nitrogen, 17: 27668
calibration of ion, for ultrahigh vacuum system, 17: 36452(R) (TID-19303)
calibration of ion gages at low pressures using leak detectors, 18: 41633
calibration of nude, for pump fluids, 17: 17337(R) (ORNL-3392(p.86-8))
calibration system, 16: 25553 (GCA-TR-61-19-N)
calibration system for, design of, 19: 32415
calibration to 10^{-9} torr, 16: 31750
capabilities and operational principles of, survey of, 17: 16172 (BNL-6796)
characteristics of modulated Bayard-Alpert ion, 19: 32414(R) (WERL-2823-18)
cleanup of inert gases in hot-cathode, 17: 21815
comparison of Bayard-Alpert and magnetron, for measurements below 10^{-10} Torr, 17: 37415
description for controlling and measuring high vacuum processes, 16: 19279
description of radiometric, using tritium source, 17: 32325
description of small ionization manometer with cold cathode, 19: 9453(T) (UCRL-Trans-1169(L))
description of types of, for research uses, 17: 13867
design, 17: 4802(P)
design, 18: 2009
design, 20: 39187
design and construction of alphatron, 16: 29174
design and performance for measuring neutral gas density near magnetically confined plasma, 16: 17202
design and performance of hot-cathode magnetron ionization, for extreme ultra-high vacua, 17: 25574
design and performance of transistorized ionization, with five-decade capability and self-compensating circuit, 18: 1996
design and performance of Penning-type discharge cold cathode, for 10^{-3} to 10^{-14} torr, 18: 12429
design and performance of a-c gas-discharge, 18: 16278 (NP-13717)
design and performance of diamagnetic suspension absolute, 19: 46579
design and performance of hot-filament ionization, 20: 31483
design and theory of ion, 17: 32385
design for density measurements of neutral gas in region of plasma and

strong magnetic field, 18: 27778
design of Bayard-Alpert, effects of lowered x-ray limit, 16: 31745
design of Bayard-Alpert, for pressures down to 100 ptorr, 18: 7011
design of cold-cathode, 20: 35639
design of electrical getter, 16: 1902(P)
design of electrical getter, 16: 1903(P)
design of electric mass filter for use as, 18: 37490(P)
design of electron-single-scatter, for 10^{-5} to 1 torr, 20: 29600
design of hot-cathode ionization type, 16: 31744
design of ion, 18: 37493(P)
design of ion-focusing, 18: 8633
design of ionization, 17: 8575(P)
design of ionization-type, with photocurrent suppression, 17: 27667
design of ionization, with semiconducting electron source, 17: 37418(P)
design of ionization-type, 18: 25757
design of ionization-type, with photocurrent suppression for measurement of very low pressures, 19: 26626 (AD-611007)
design of ionization-type, 20: 29513(P)
design of mass filter partial-pressure, 16: 31753
design of mass filter partial-pressure, 18: 5599(P)
design of modified Bayard-Alpert, with reduced x-ray limit, 17: 32366
design of Pirani-type with automatic control, 17: 342
design of radiometric, 18: 16395
design of, reduction of x-ray limit in, 16: 31746
design of spinning-rotor, for pressures below 10^{-4} torr, 16: 13348
design of two-chamber ionization, 20: 13026 (IPP-2/39)
design of, with high sensitivity and infinite lifetime, 19: 28622
design utilizing ultraviolet light, 16: 31748
design with thermistor sensor, 16: 14919 (SCTM-277-61(14))
development, 18: 12329(R) (ORNL-3564(p.126-9))
development and testing of, 17: 25091(R) (ORNL-3417(p.283-4))
development and uses of, review, 17: 41224
development and uses, 19: 20149
development of friction-type, review, 19: 18234 (EUR-CEA-FC-281)
development of hot-cathode magnetron, 16: 31747
development of ultra-high, 18: 33761
development of, review of, 19: 20142
development of, using electron beam virtual cathode relaxation time, 20: 23434
electric currents in Bayard-Alpert, residual, (E), 19: 15846
emission regulator circuit for ion, 18: 14166 (TID-20301)
extension of high-pressure limit to above 1 μ pressure of commercial, 16: 19130
filament interactions with hydrogen and oxygen in ion, 19: 29812(R) (SRIA-425-4)
filaments for ion, carbon monoxide production by, 19: 11052(R) (SRIA-135)
helium production in, (E), 19: 20146
ion collection in Bayard-Alpert, (T), 20: 16787
ion pumping mechanism for Bayard-Alpert, 18: 22241
mass spectrometer design for use in, 20: 29496
mechanisms of electrical cleanup of gas in the hot cathode ionization type, 16: 29176
operation in magnetic fields, 16: 31749 (MATT-80)
operation of Bayard-Alpert, effects on residual pressures, 18: 41634
operation of, effects of electron-surface interactions on, 18: 33759 (AD-427830)
performance and use of radiometric, 18: 33999
performance below 10^{-10} torr, 20: 5641
performance of, anomalous effects in, 18: 687(R) (NP-13274)
performance of bare and glass-enclosed Bayard-Alpert ionization, 17: 18580
performance of bare and glass-enclosed ionization, at 10^{-10} to 10^{-8} torr in oil-free system, 18: 4054 (MATT-212)
performance of Bayard-Alpert ion gage, 16: 19124
performance of Bayard-Alpert and Redhead, aboard Explorer XVII, 18: 8634
performance of modulated Bayard-Alpert, below 10^{-13} torr, 18: 41632
performance of modulated Bayard-Alpert ion, 19: 32413(R) (WERL-2823-17)
performance of, book on, 20: 31391
performance testing, 18: 22946(R) (ORNL-3591(p.241-8))
Philips Ionization Gage discharge mechanism, 16: 2009
Philips Ionization Gage discharge mechanism, 16: 2010
pressure limits of hot-filament ionization, low-, 19: 20147
properties as gamma detector, 18: 10382 (USAELRDL-TR-2342)
properties of hot cathode magnetron, 20: 29494
properties of inserted and glass-tube Bayard-Alpert, 17: 16184(T) (AERE Trans-920)
review of ultrahigh, 20: 11008
sorption of hydrogen in hot-cathode ionization, effects of, (E), 19: 24694
use in high and ultra-high vacuum systems, 20: 45874 (NASA-TM-X-1268)
use of Bayard-Alpert ion, for low oxygen pressure measurements, 19: 32413(R) (WERL-2823-17)
use of Bayard-Alpert ionization, for cesium partial pressures, 20: 28578
use of cold and hot cathode, for low gas density measurements, 19: 467
use of radiometric, survey on, 20: 20990(T) (AERE-Trans-1048)
use of strain gage as, in vacuum fusion analysis, 18: 29917 (CONF-546-1)
vacuum pump for Orbitron, 19: 4346

VACUUM PUMPS

see also Diffusion Pumps
see also Jet Pumps
argon sorption on surfaces of vac-ion, 19: 39323
book: *Handbook of High Vacuum Engineering*, 18: 14064
book: *High Vacuum Engineering*, 18: 22242
book: *Leybold Vacuum-Pocketbook*, in German, 18: 18024
book: *Ultrahigh Vacuum, An Introduction*, in German, 18: 25683
capabilities and operational principles of, survey of, 17: 16172 (BNL-6796)
characteristics of all-metal-exhaust, for mass spectrometer, 20: 43068(R) (IDO-14679, pp 47-50)
cold trap design for mechanical, using dry ice, 18: 22240
construction and properties of titanium, 16: 29075
control of, equipment for, 19: 18135 (IPP-4/16)
description and performance of titanium-evaporation cryogenic, 19: 9360(T) (ORNL-tr-302)
description of hydrogen-condensation, for pressures near 100 torr, 19: 7691(T) (UCRL-Trans-1166(L))
description of titanium-gettered, 17: 20667
description of types of, for research uses, 17: 13867
description of ultrahigh, 17: 36465
description of 20-ptorr, using magnetic fields, 17: 20668
design, 18: 22238
design, 18: 35645(R) (SC-DC-64-1097)
design and efficiency of diffusion-sorption, 20: 507
design and operation of hydrogen condensation type, 16: 29074
design and operation of getter-ion type, 17: 10944
design and operation of helium-condensation, 17: 21817
design and operation, 19: 40773
design and operation of pump-leak detection system, 20: 39096 (AECD-EP-11)
design and performance of ultrahigh, 18: 8512
design and performance of cryogenic, for production of ultrahigh vacuum, 18: 12333
design and performance of getter-ion, 19: 42633
design and performance for evacuating target space in particle accelerators, 20: 21479
design and performance of cryogenic, with very low coolant consumption, 20: 23275
design for accelerating tubes, 20: 34002(P)
design for cryopumping hydrogen, 16: 31743
design for high pumping speeds, 16: 13196(P)
design for ion gage, 19: 4346
design for isochronous cyclotrons, 20: 46263
design for pressures down to 10^{-9} Torr, 17: 34077
design for ultralow pressures, 17: 1595(P)
design for 10^{-13} torr, 20: 31392
design of cryogenic, 17: 14425(T) (AERE-Trans-915)
design of cyclic cryogenic, for hydrogen removal, 18: 37320(P)
design of electrical getter, 16: 1902(P)
design of electrical getter, 16: 1903(P)
design of evaporative, for ALICE, engineering drawings for, 20: 15922
design of getter-, 17: 12405(P)
design of getter-ion-type, 17: 36425 (NP-13020(p.290-4))
design of high-capacity liquid-nitrogen-cooled, 17: 3158 (TID-16988 (Paper 1))
design of ionic getter, 16: 1899(P)
design of liquid hydrogen cryogenic, 17: 247 (NAA-SR-6490)
design of liquid helium cryo-, for large plasma research machines, 20: 46831 (UCRL-70024)
design of magnetically suspended molecular, 16: 31733
design of multi-beam, gas-discharge, 16: 25511(T,P) (FTD-TT-62-370)
design of Penning-discharge, 18: 29863
design of regenerative cryosorption, 18: 8513
design of rotor-stator, 17: 16215(P)
design of steam–mercury, for pressures of 5×10^{-10} mm Hg, 16: 14857(T) (FTD-TT-62-141)
design of titanium, for betatrons, 17: 31563
design of titanium, for betatrons, (E), 19: 9829
design of titanium nitrate ultra-high, 20: 27141
design of turbo-molecular, for pressures down to 10^{-10} torr, 18: 41637
design of ultra-high mercury diffusion, without internal bakeable seals, 18: 1891
design of ultrahigh, using cryopumping and cryosorption, 19: 15744
design of, for sample furnace for neutron diffraction experiments, 20: 29106
design to remove gases by freezing on sorbent material, 17: 35971(P)
development and performance of, using titanium sublimation, 17: 35952 (BNL-6489)

development and uses, 19: 20149
development for controlled thermonuclear devices, 18: 2985(R) (UCRL-10852)
development for ultrahigh vacuum systems, 20: 9134 (CONF-650512, pp 10-13)
development of cryogenic, 17: 14943(R) (NYO-9812)
development of ion, 18: 41631
development of μ torr, for proton synchrotron, 18: 2499 (PPAD-498E)
development of ultra-high, 18: 33761
development of vapor-jet, 19: 34357 (N64-24831)
ion traps for sputter-ion, use of zeolite for excited, 19: 18248
molecular, for selective pumping of light and heavy gases, 17: 3096
oil vapor contamination from, shielding of proton accelerators against, 20: 31848
operation for pumping gases at low pressures, 16: 19031(P)
operation of triode getter-ion, 19: 13616
performance for Van de Graaff accelerators, 20: 46265
performance of adsorption, 20: 18889 (LNF-65/38)
performance of axial inflow turbomolecular, 20: 35637
performance of cryopumps, review of, 20: 7250
performance of getter-ion, pumping speed measurements for determining, 20: 31645(R) (AD-627094)
performance of, book on, 20: 31391
performance of, contamination effects and limits for, 20: 29396
performance of, survey of, 19: 26526
pressure measurements for, total and partial, 20: 35636
primer for evapor-ion, design of titanium, 18: 35258(P)
review of ultrahigh, 20: 11008
testing "orbitron" ion-sublimation, under plasma-vessel conditions, (E), 19: 32411(R) (LA-3320(p.69-70))
testing turbo-molecular, sorption effects on maximum vacuum and pumped volume, 17: 16184(T) (AERE-Trans-920)
use for production of ultrahigh vacuum, 19: 34358 (UCRL-7925-T)

VACUUM SEALS

see also Seals and Glands
book: *Handbook of High Vacuum Engineering*, 18: 14064
brazing alloys for alumina-to-niobium alloy, 19: 40980 (LA-3302)
description of large rotary, 17: 20132
description of strip-sealed continuous-rotation scattering chamber, (E), 19: 44883
design, 17: 11798(R) (TID-17221)
design, 18: 32893(R) (ORNL-3652)
design and performance of reusable metal ultra-high, 20: 23276
design for aluminum window in helium cryostats, 16: 29072
design for mass spectrometers, 19: 30505(P)
design for mass-spectrometer source-handling systems, (E), 20: 2159
design for photomultiplier tubes, 20: 5787
design of ceramic-to-metal and metal-to-metal, 16: 20566 (IFA/TV/14)
design of electrical pass-through, for mass spectrometer, 16: 29103 (IS-212)
design of flange-aluminum foil gasket for ultra-high vacuum use, 20: 37000 (UCID-4548(Rev.4))
design of, for use with beam windows, 17: 42033(P)
design of glass, 17: 254 (UCRL-6978)
design of liquid metal, for low vacuum pressures, 16: 19033(P)
design of quick, 20: 505 (ORNL-P-1517)
development and testing for high-temperature fission counters and ionization chambers, 18: 21564(R) (GEMP-81)
development and uses, 19: 20149
development for cathode-ray tubes, 17: 30676 (TID-19009)
development of all-metal, 17: 9647(R) (TID-17021)
development of indium, for large bell jars, 19: 6027 (RFP-449)
development of metalizing paint for metal-to-ceramic, 20: 27401(R) (AD-632362)
development of μ torr, for proton synchrotron, 18: 2499 (PPAD-498E)
development of thin film, for uv spectroscopy systems, 18: 29864
flange tests of bakeable aluminum wire, 18: 14061 (ORNL-3509)
methods for optical windows, 20: 9135 (CONF-650512, pp 14-17)
performance of gaskets, factor method for predicting, 19: 44135 (IA-1033)
performance of gold wire, 20: 35638
performance of silicone GE SR-82, in sealing leaks in glass and metal ultrahigh vacuum systems, 18: 8511
review of ultrahigh, 20: 11008
testing metal-to-ceramic, at high temperatures, 18: 39615 (GEMP-298)
use of bellows as, in transmitting motion through vacuum wall, 19: 44234 (MATT-345)

VACUUM SYSTEMS

see also Leak Detectors
see also Vacuum Vessels
analysis for residual gases, design of mass spectrometer for, 16: 31755
analysis for residual gases by mass spectroscopy, 16: 31756
backstreaming in baffled, 18: 1890
baffle design for, circulating liquid-nitrogen-cooled, 16: 31785
bibliography, 17: 28361 (NP-12921)
bibliography on, 17: 3099
book: *Handbook of High Vacuum Engineering*, 18: 14064
book: *High Vacuum Engineering*, 18: 22242
book: *Leybold Vacuum-Pocketbook*, in German, 18: 18024
book: *Ultrahigh Vacuum and Its Applications*, 18: 22243
book: *Ultrahigh Vacuum, An Introduction*, in German, 18: 25683
book: *Vacuum Technology*, 18: 29865
carbon dioxide content in glass, method for lowering, 19: 20148
characteristics for DCX-2, 16: 9505(R) (ORNL-3239(p.10-15))
coating of ultrahigh, with Teflon, 19: 32413(R) (WERL-2823-17)
components of ultrahigh, development of, 20: 9134 (CONF-650512, pp 10-13)
conference on, in Washington, D. C., October 16 to 19, 1961, Vol. I, 16: 31710
conference on, in Washington, D. C., October 16 to 19, 1961, Vol. II, 16: 31761
construction of, problems in, 16: 31715
contamination effects of residual gases in, on refractory metals, 18: 14355 (CONF-373-7)
contamination of ultrahigh, by silicone oil diffusion pump, 17: 20765
cryopumping of, cold-gas-cooling machine for, 19: 22527
cryotrapping in, helium and hydrogen, 18: 8514
degasification of elastomers and plastics from, 17: 35953 (CLM-R-23)
description and operation of portable ultrahigh, 19: 13616
description and testing of ultrahigh, for studies of evaporated films, 17: 36452(R) (TID-19303)
description of alumina sliding-shaft lock, for mass spectrometer, 19: 34424 (BNWL-SA-62)
description of continuous thin film deposition, 20: 19201
description of, for evaporative deposition of films, 17: 6158
description of pyrex ultrahigh, for observation of adhesion between quartz crystal surfaces, 19: 38840
description of strip-sealed continuous-rotation scattering chamber, (E), 19: 44883
description of ultrahigh, for use with polarizing spectrometer in studies of optical properties of surfaces, 18: 18023
description of ultrahigh, 19: 40772 (ORNL-P-1465)
design and construction of portable all-metal high-speed, 16: 31779
design and development for encapsulated electromagnets, 20: 504(R) (ORNL-3836, pp 120-9)
design and operation of, for ZGS injector, 17: 7339 (BNL-6511(p.318-22))
design and operation, 17: 21104 (ANL-6700)
design and operation of cold-cathode gas-discharge getter ion, 17: 40153(R) (AD-290727)
design and operation, 19: 40773
design and operation of, for film preparation by vacuum evaporation, 20: 25512 (AERE-R-5097, Paper 5)
design and performance of PHERMEX hydrogen-purging, 18: 22626 (TID-7691(p.431-41))
design and performance of sputter-ion pump, 19: 36646
design and performance for Ogra-1 magnetic mirror machine, 20: 30701
design and pumping requirements for zero Gradient Synchrotron at Argonne National Laboratory, 16: 31775
design considerations for use of ultrahigh, in metallurgy, 18: 31744 (UCRL-7914)
design for accelerators, 19: 27028 (UCRL-11808)
design for accelerating tubes, 20: 34002(P)
design for boiling liquid metal heat transfer facility, 20: 45874 (NASA-TM-X-1268)
design for Cambridge Synchrotron, 18: 34367 (CEAL-1000)
design for cesium ion thruster testing, 20: 45874 (NASA-TM-X-1268)
design for chalice, 20: 40178(R) (SIT-2582-19)
design for deposition of thin films, 18: 18020 (SC-TM-64-536)
design for electron diffraction studies, 19: 15741
design for fast-wave plasma cyclotron amplifiers, 17: 27650(R) (AD-297382)
design for ion injection and magnetic mirror devices, 16: 29928
design for irradiation or vacuum-coating of specimens, 18: 33763(P)
design for large electromagnetic isotope separator, 16: 31777
design for lunar surface simulation, 19: 36647
design for mass spectrometric analyses above 10^{-4} mm Hg, 18: 37486(T) (NASA-TT-F-141(p.123-31))
design for Ogra-II, 20: 42421(T) (NP-tr-1396)
design for omegatron mass spectrometer, 18: 37483(T) (NASA-TT-F-141(p.96-107))
design for Orsay accelerator, 18: 10716
design for particle accelerators, 20: 13396(P)
design for preparing plasma, 16: 5826
design for preparing plasma, 16: 10682(T) (FTD-TT-61-400)
design for preparing and studying thin metallic films, 18: 24225
design for preparing pure powders of air-sensitive alloys, 18: 30120(T) (ANL-Trans-37)
design for proton synchrotrons, 19: 12036
design for solar absorptivity measurement and ultraviolet irradiation, 18: 39420

design for space environment simulation testing of radiation effects on vehicle materials, 18: 10262
design for Stanford linear accelerator, 19: 37352
design for storage rings for 28-Bev protons, 19: 16324
design for study of friction between single-crystal surfaces, 20: 9500 (UCRL-13190)
design for super-low pressures using sorptive metal coatings, 16: 6523
design for testing mechanical properties of metals, 16: 13564 (AFOSR-2139)
design for 7-Bev proton synchrotron, 17: 902
design incorporating establishment of controlled atmosphere by using mercury vapor pump sets, 16: 31781
design of demountable ultrahigh, 18: 37355(P)
design of greaseless 7-nanotorr, for plasma studies, (E), 19: 32410(R) (LA-3320(p.67-8))
design of high-temperature, for refractory metal research, 20: 21350 (ORNL-TM-1426)
design of liquid-helium and liquid-nitrogen, (E), 19: 41626
design of piston-type expansion system for liquid-hydrogen bubble chamber, 18: 39627 (UCRL-11558)
design of precision cryostat for Moessbauer measurements, (E), 19: 40848
design of sliding-bar vacuum locks, 18: 14178
design of ultra high, for field emission tube, 18: 14063
design of ultra-high, 18: 33764(P)
design of ultrahigh, using evaporated molybdenum, 16: 1895
design of ultrahigh, 17: 2061(R) (TID-16592)
design of ultrahigh, using zeolite getter pumps, 19: 15739
design of ultrahigh, using liquid helium cryopump, 19: 15742
design of ultrahigh, using diffusion pumps, 20: 9133 (CONF-650512, pp 7-9)
design of ultrahigh, for hydrogen ion reactions with surfaces at 30 kev, 20: 31937
design of vacuum evaporator for ultrahigh-vacuum fabrication of multilayer devices, 18: 3973
design of 10^{-13} torr, for space simulation, 19: 15743
design of 10^{-13} torr pumping system and work chamber, 20: 31392
design of, for measuring oxygen solubility in refractory alloys and metals, 20: 25562(R) (EIMAC-TR-66-2)
design of, for use in evaporation of radioactive metals and oxides, 20: 27004
design to get very low pressures by freezing gases on sorbent material, 17: 35970(P)
design to get very low pressures by freezing gases on sorbent material, 17: 35972(P)
desorption in, 17: 21816
desorption spectrometry in ultrahigh, at 77°K to room temperature, 19: 28534
development, 16: 32493(R) (ORNL-3315(p.79-84))
development, 18: 2985(R) (UCRL-10852)
development, 18: 8960(R) (TID-19940(p.1-21))
development, 20: 15882(R) (NP-15868)
development, 18: 12329(R) (ORNL-3564(p.126-9))
development and fabrication for zero Gradient Synchrotron, 16: 31776
development at Hungarian Inst. of Atomic Research, 16: 19020
development at ORNL, 16: 32485(R) (ORNL-3315)
development at ORNL, 17: 17337(R) (ORNL-3392(p.86-8))
development at ORNL, 17: 33159(R) (ORNL-3472(p.107-18))
development for Argonne ZGS, 16: 4882(R) (ANL-6427)
development for Argonne Synchrotron, 19: 28961 (MURA-711)
development for bakeout to 400°C, 18: 20618(R) (NP-13799)
development for bubble chambers, 18: 5607 (BNL-7478)
development for calibration of low-pressure sensors, 18: 7289(R) (GEMP-30A)
development for CEA beam bypass, 20: 11385 (CEAL-TM-157)
development for charge exchange chambers, 19: 16411
development for charge transfer and ionization measurements, 19: 18684(R) (TID-21565)
development for deposition of thin films, 17: 29254 (SCTM-130-63(74))
development for fatigue studies of refractory alloys at high temperatures, 19: 18458(R) (NASA-CR-54286)
development for isotope target preparation, 20: 696(R) (ORNL-3829)
development for linear accelerators, 18: 22625 (TID-7691(p.421-30))
development for microwave plasma components studies, 18: 34977(R) (RADC-TDR-64-94)
development for Sherwood project, 16: 17584(R) (ORNL-3262(p.199-205))
development for Stanford linear accelerator, 17: 29643(R) (SLAC-16)
development for Stanford linear accelerator, 17: 42015(R) (SLAC-18)
development for Stanford linear accelerator, 18: 8958(R) (SLAC-23)
development for Stanford linear accelerator, 18: 22593(R) (SLAC-27)
development for Stanford Linear Accelerator, 20: 13366(R) (SLAC-53)
development for thermonuclear fusion, 19: 23163(R) (ORNL-3650(p.111-86))
development for ultrahigh vacuum systems, 20: 9134 (CONF-650512, pp 10-13)
development for 10^{-13} torr, 18: 41630
development of, 18: 31743(R) (ORNL-3652(p.132-45))
development of condensers for, for testing ion rocket engines, 16: 29060 (NASA-TN-D-1217)
development of fluid-free ultra-high, constructed of stainless steel, 17: 21814
development of, linear accelerator, 17: 17317(R) (SLAC-8)
development of μ torr, for proton synchrotron, 18: 2499 (PPAD-498E)
development of oil diffusion pumps for, 16: 33083 (UCRL-6963-T)
development of single-wall ultrahigh, for thin film deposition, 19: 40774
development of ultrahigh, 16: 15723(R) (UCRL-9969)
development of ultrahigh, 17: 4181(R) (UCRL-10294)
development of ultrahigh, 17: 12230(R) (TID-17638)
development of ultrahigh, 17: 19465(R) (UCRL-10607)
development of ultrahigh, 18: 29861(R) (WERL-9)
development of ultra-high, 18: 33761
development of ultrahigh, using unbaked apparatus with rubber packing, 20: 18890
development of ultrahigh, 20: 39098(R) (WERL-2823-21)
development, use of polyphenyl ethers in, 16: 31734
diffusion pump design optimization for, 16: 31739 (UCRL-6407)
diffusion pump oil deposition in, method for measuring, 19: 20143
diffusion traps for ultrahigh, development of flat, 18: 27692
effects on magnetic fields in proton synchrotrons, 17: 936
electric breakdown in, effects of contamination from thermal decomposition of glass, 17: 4640 (TID-15465)
electron transmission windows for, carbon-coated, 20: 509(P)
flanges for, performance of aluminum foil, 17: 39222 (UCRL-7393)
gage calibration for several gases, 16: 7625 (CF-61-5-109(Suppl.3))
gas desorption and re-emission in, 16: 31714
gas load in ultrahigh, origins and composition of limiting, 16: 31717
gas residuals in ultrahigh, methods for eliminating, 19: 15740
gas sorption and desorption in high, residual, (E), 19: 20144
getter for hydrogen on evaporated titanium films, 16: 5441
getter pumping using vapor-deposited titanium films, 16: 3098 (ORNL-3217)
helium production in ionization gages in, (E), 19: 20146
hydrocarbon formation in ion-pumped, mechanisms for, 18: 41635
hydrogen pressure measurement in ultrahigh, techniques for, 19: 46578
instrumentation development for ultrahigh, 19: 44357
instrumentation for ultrahigh, review, 17: 41224
instrumentation for, design and protection of mechanical, (E), 19: 18136 (UCRL-7830)
ion pumps for, development of, 18: 41631
leak detection in, use of mass spectrometer for, 18: 27777
leak rate of, correlations with phenomena observed in metal to metal contact in gaskets, 16: 31773
leaks and mercury vapor in, light analysis detectors for, 17: 39223 (UCRL-7399-T)
manipulator for, engineering drawings of, 18: 12332
mass spectrometers for, design of omegatron, 18: 29950
mass transport of oil in, 19: 20140(R) (ORNL-3760(p.94-7))
materials for high-temperature, development and testing of, 20: 41440(R) (ALO-3632-4)
measurements of background in, below 10^{-13} torr, 18: 41632
methane decomposition and synthesis in, 19: 31332(R) (ORNL-3789(p.334-40))
modification of, for 1.2-Mev cyclotron, 17: 36724
modifications for increased accuracy and precision in silane irradiation testing, 16: 14770(R) (NYO-9861)
motion transfer in, device for, 20: 41125 (SGAE-PH-41/1966)
oil detection in, methods for, 19: 31332(R) (ORNL-3789(p.334-40))
operation requirements of, with refractory metals at high temperatures, 16: 32038 (ORNL-TM-334)
organic vapor measurements in, polymer film formation for, 19: 38564
oxygen in, effects of molecular, 17: 36440(R) (NP-13061)
partial pressure measurement in, design of r-f mass spectrometers for, 19: 24476
performance determination of, techniques for, 20: 39097(R) (ORNL-3989, pp 128-33)
performance in CERN 25-Gev proton synchrotron, 16: 31778
performance in SNAP-8 ground test facility for, 20: 8451
performance of AGS, 20: 19285(R) (BNL-929, pp 44-57)
performance of, at Canel hot laboratory, 17: 2767
performance of enclosures in, contamination effects and limits for, 20: 29396
performance of mass-spectrometer ultrahigh, under high argon pressures, 20: 31390
performance of MURA accelerator, 18: 42229
performance of Stanford storage ring, 18: 16587 (BNL-7534(p.209-27))
performance of 10-pTorr glass, 19: 43633(R) (NP-15354)
performance of 7-Bev proton synchrotron, 17: 903
performance of, back-diffusion and backstreaming effects on, 18: 22239
performance of, for high-current electron storage rings, (E), 19: 6416 (CEAL-1013)

pressure in ultra-high, processes limiting ultimate, 16: 31711
pressure measurements in, using hot-cathode ionization gages, 20: 16630
pressure stage passages for firing electron or ion beams from, 16: 16813 (UTIA-78)
pressures in, effects of operation modes of ion gages on, 18: 41634
production of pressure difference between interconnected chambers of, apparatus design for, 17: 16215(P)
production of 10^{-11} torr in, with bakeout at 250°C for 15 hr, (E), 19: 4347
pumping system for, cryosorption, 20: 33500
pumping using Penning-type discharges supported on condensible metal vapors, 16: 31740 (UCRL-5598)
pumps for ORNL Van de Graaff accelerator, 19: 42964(R) (ORNL-3782, pp 144-52)
radiation effects on NIMROD proton-synchrotron, dosimetry techniques for measuring, 20: 31832
radioinduced outgassing in aluminum, (E), 19: 28533
research, 20: 10112 (CONF-650512)
research progress at Stanford, 17: 35000(R) (SLAC-10)
residual carbon dioxide in ultrahigh, elimination of, 19: 32413(R) (WERL-2823-17)
residual gas composition, effects of plastics on, 16: 18849 (CLM-R-16)
residual-gas concentrations in, effects of purging, 17: 20771
residual gas effects on ultrahigh, 18: 29861(R) (WERL-9)
residual gases in ultrahigh, analysis of, 19: 26526
residual gases in oil-diffusion-pumped ultrahigh, effects of trapping conditions on, 20: 506
review of ultrahigh, 20: 11008
sorption of residual gases in ultra-high, 16: 31721
symbols for, standards for graphic, 18: 14062 (UCRL-11226)
technology of high, review of, 20: 45874 (NASA-TM-X-1268)
tests of creep unit, for studies of refractory alloys at high temperatures, 18: 30172(R) (NASA-CR-54048)
trap development and testing, 16: 7633(R) (NYO-9807)
traps for diffusion-pump, electric discharges as, 19: 38839 (RFP-572)
traps for Stanford linac, in-line oil, 19: 37358
traps for, use of porous metal isolation, 19: 46573 (UCRL-12393-T)
ultrahigh, preparation and uses, 19: 20149
use in materials evaluation for satellite applications, 16: 31782
use of artificial zeolites in high, review on, 19: 20141
use of ion pump for ultrahigh, 20: 45878
use of plastics in, 20: 43471
uses in chemical engineering, 16: 20315
valves for protection of, design of fast-closing large-aperture, 17: 4650
valves for ultrahigh, modification of Hoke, 19: 20145
windows for ultrahigh, methods for sealing, 20: 9135 (CONF-650512, pp 14-17)

VACUUM TECHNIQUES

at French Pierrelatte gaseous diffusion plant, 18: 25682
bibliography on, 17: 3099
book: *Handbook of High Vacuum Engineering*, 18: 14064
book: *Handbook of Vacuum Physics*, Vol. 3, Parts 1, 2, and 3, 19: 22526
book: *High Vacuum Engineering*, 18: 22242
book: *Leybold Vacuum-Pocketbook*, in German, 18: 18024
book: *Practical Vacuum Techniques*, 20: 508
book: *Ultrahigh Vacuum and Its Applications*, 18: 22243
book: *Vacuum Science and Engineering*, 20: 31391
book: *Vacuum Technology*, 18: 29865
book: *Vacuum Technology*, 18: 33762
conference on, 19: 16296
cryopumping in electric rocket testing vacuum facilities, 16: 31783
degassing of elastomers and plastics, 19: 32417
degassing of metallic surfaces by electron bombardment, 18: 43779(R) (ORNL-3670(p.262-5))
design and performance of cryopumping device for degassing, 16: 13168 (AEDC-TDR-62-57)
development, 16: 12225(R) (NYO-9808)
development, 16: 20315
development, 18: 22946(R) (ORNL-3591(p.241-8))
development and uses, 17: 29388 (EUR-231.d)
development and uses of, 19: 40773
development below 10^{-13} torr, 19: 34357 (N64-24831)
development for Argonne Synchrotron injector linac, 18: 22627 (TID-7691 (p.442-8))
development for deposition of thin films, 17: 29254 (SCTM-130-63(74))
development of, 18: 31743(R) (ORNL-3652(p.132-45))
development of hydrogen-purging, for PHERMEX linacs, 18: 22626 (TID-7691(p.431-41))
development of ultrahigh, 16: 7633(R) (NYO-9807)
development of ultra-high, 16: 29061(R) (NYO-9809)
development of ultrahigh, 17: 14943(R) (NYO-9812)
development of ultrahigh, 17: 16181(R) (TID-18283)
development of ultrahigh, review, 18: 8512
development of ultra-high, 18: 33761
development of, for space simulation and deposition of thin films, 19: 38842
development, review, 17: 20647
developments in ultrahigh, for surface kinetic studies, 18: 33454
for measurement of hydrogen pressure in ultrahigh vacuum systems, 19: 46578
for nonferrous metallurgy, 16: 12046
for production of metals, 16: 20967
gas desorption from stainless steel by flash-filament technique, 16: 31723
gas desorption from metals by photon bombardment, 16: 31722 (NYO-9805)
in metallurgy, conference, 16: 2124
instrumentation developments for ultrahigh, 19: 44357
outgassing data for epoxy resins and rubbers, 16: 31718
outgassing processes and rates, 16: 31713
outgassing rates of contaminated metal surfaces, 16: 31716
performance for electron-bombardment preparation and purification of refractory metals, 16: 32045
production of ultra-high vacuum in nonpreconditioned apparatus, 18: 41636
pumping for ultrahigh vacuum, 19: 34358 (UCRL-7925-T)
research progress on ultrahigh, 18: 29861(R) (WERL-9)
review of metallurgical, 19: 16003 (UCRL-7562)
survey, 17: 16172 (BNL-6796)
use in aluminum outgassing, 17: 23886
use in bubble chamber development, 20: 11141
use in mass spectrometry, 17: 25576
use in metallurgy of nonferrous metals, 17: 23885
use in metallurgy, conference on, 17: 25756
use in research, 17: 13867
use of electron bombardment to desorb gases from surfaces, 19: 9359 (ORNL-P-818)
use of, in organic radiochemical studies, 16: 31636 (ASD-TDR-62-575)
uses of ultrahigh, review of, 20: 11008

Vacuum Tubes
see Electron Tubes

VACUUM VALVES
(Including stopcocks.)
see also Valves

book: *Handbook of High Vacuum Engineering*, 18: 14064
characteristics of bakeable high-conductance, 17: 3097
design and development of magnetically driven gas, 17: 35260(R) (TID-19135)
design and operation of hydraulically actuated ultrahigh, 19: 40776
design and performance for Stanford linac, 19: 37351
design for accelerators, engineering drawings, 17: 21863
design for mass-spectrometer source-handling systems, (E), 20: 2159
design for ultrahigh vacuum systems, 19: 38841
design of all-metal ultrahigh, 18: 16188(P)
design of bakable ultra-high, 17: 12417(P)
design of bakable ultrahigh, 17: 32844(R) (ARF-A218-12)
design of cam-operated fluid pressure, 17: 40969(P)
design of fast-acting electromechanical, for gas bursts, 18: 8510 (63-RL-3441E)
design of fast-closing large-aperture, 17: 4650
design of fast-acting ultrahigh, for gas injection into C stellarator, 18: 15331 (MATT-225)
design of gate, for ALICE magnetic mirror device, engineering drawings of, 20: 6513
design of large-diameter fully openable, 17: 35974(P)
design of pulsed gas, for plasma studies, 20: 5642
design of quick, 20: 505 (ORNL-P-1517)
design of ultra-high, 17: 12421(P)
design of ultrahigh, 16: 16497(P)
design of, with long life, 18: 20199(T)
development and testing of ultrahigh, 19: 40775
development of fast stainless steel, for Stanford linac, 19: 37359
development of, for electron guns, 17: 17317(R) (SLAC-8)
review of ultrahigh, 20: 11008
tests of waveguide, 17: 17317(R) (SLAC-8)

VACUUM VESSELS

beam reactions with circular, electromagnetic fields from, (T), 20: 15169 (SLAC-49, pp 32-5)
book: *Handbook of High Vacuum Engineering*, 18: 14064
book: *Leybold Vacuum-Pocketbook*, in German, 18: 18024
charged-particle beam stability in toroidal, (T), 20: 15170 (SLAC-49, pp 36-48)
contamination in glass, effects on electrical breakdown in, 17: 8974
degasification of, development of flame-sprayed ceramic-metal heating element for acceleration of, 17: 6205 (CERN-62-28)
description of high-temperature, for x-ray diffractometer, 19: 30493(T) (AEC-tr-6559)
description of strip-sealed continuous-rotation scattering chamber, (E), 19: 44883
design and development of reinforced plastic, 16: 8256

design and performance of double-walled, 16: 31780
design and performance of ultrahigh, for simulation testing of SNAP components at 10^{-9} torr and 1000°F, 17: 247 (NAA-SR-6490)
design for electron beam working of large workpieces, 18: 25964(P)
design for evaporation and x-ray diffraction studies of resulting films, 16: 15277 (TID-15255)
design for fatigue tests at high temperature, 19: 34339(R) (NASA-CR-54389)
design for filament preparation for mass spectrometers, engineering drawings for, 19: 34454
design for gamma angular correlation measurements, 18: 2403(R) (PR-P-58)
design for holding radioactive sources, 18: 18334
design for ion rocket testing, 17: 3102(P)
design for radioactive materials, 19: 24379
design for study of heating of metals by ion bombardment, 18: 28109
design for use with scintillation and semiconductor detectors, (E), 20: 7415
design for 15-Mev betatron, 19: 34824
design of charged-particle scattering chamber, (E), 19: 40907
design of double-walled, with variable thermal conductance, 18: 5689(P)
design of scattering chamber, 18: 30822
design of scattering chamber for use with solid-state detectors, 20: 16883
diffusion of gases into, 16: 31712
electric breakdown of electrodes in, by field emission of electrons, 18: 28132
electron transfer in spherical, angular distribution in, (T), 19: 46824
gasket design for, 16: 31773
interlock system for, 17: 16199(P)
joining of sections of accelerator, epoxide-resin glue for, 18: 44333
performance in friction tests on aluminum, 20: 35897 (UCRL-13212)
production and use of ion beams in primary, 18: 28115
radiation effects on electron transfer in, 19: 7825
radiation effects on stainless steel type 205, 20: 9618
radiation effects on saturation properties of spherical, 20: 9308
tungsten ionizer performance in, effects of, 19: 14300
uses in flow rate control in mixers-decanters, 19: 2439 (NP-14343 (p.Id1-4))

VAGINA
cytological analysis of, diagnostic use following radiotherapy, 19: 10961
cytology, in evaluation of effectiveness of radiotherapy of gynecologic cancer, 17: 5864
cytology of, use in evaluation of prognosis and results of radiotherapy of cervical cancers, 20: 10740
effects of radiomimetics on human, 20: 6815
epithelial studies in mouse, autoradiographic method for, 20: 40502(R) (ORNL-3922, pp 115-27)
fistulas of, repair of, 18: 4954
radiation dose to, during cervical carcinoma therapy, 19: 42392
radiation effects on level of nucleic acids and proteins of prepubertal mice submitted to induced hyperplasia, 17: 1262
radiation effects on capacity, 17: 1307
radiation effects on, in rats, 17: 21481
radiation effects on epithelium of, cytology of, 17: 27097
radiation effects on cells of, 18: 33348
radiation effects on epithelium in, protective effects of estrogens against gamma and x, 19: 33959
radiation effects on human, 20: 6815
radiation effects on benign cells of, 20: 10740
radiation effects on cells of, following cervical carcinoma therapy, 20: 18331
radiation effects on cytology of, therapeutic-dose, 20: 29076
radiation injuries of, after radiotherapy, 19: 7062
radiation injuries to, therapy-induced, 19: 22069
radioinduced cornification of cells in rat, x, 20: 40673
radioinduced cytological changes of, radium-therapy, 17: 28707
radioinduced injury to, following therapy of cervical cancer, 20: 38751
radioinduced vesicovaginal fistulas of, repair technique for, 17: 35531
radiosensitivity of, 18: 9906
radiotherapy effects on glucose-6-phosphate dehydrogenase activity in secretions in, cervical, 19: 17735
radiotherapy effects on cell smear from, in patients with cervical cancer, 19: 15254
radiotherapy of cancer, response, 16: 20057
radiotherapy of cancer of, 19: 10932
radiotherapy of carcinomas of, 20: 5457
radiotherapy of cancer of, design and performance of cobalt-60 applicator for, 20: 18511
radiotherapy of cancer of, system for dosimetry of intracavitary radium, 20: 41377
radiotherapy of cancer of, cutaneous eruptions following, 20: 40679
radiotherapy of cancer of, using betatron, 20: 40768
radiotherapy of endometrial carcinoma of, survey on 610 cases of, treated using radium, 18: 15920
radiotherapy of metastases of, radium applicator for, 19: 26197
radiotherapy of pelvic cancer, effects on, therapy for, 18: 21922
radiotherapy of tumors of, design of shielded cobalt-60 applicators for, 20: 6972
radiotherapy of, doses and methods for, 20: 3848
use of linear source in, with 4-Mev x rays for radiotherapy of cervical carcinomas, 20: 33108

VAK REACTOR
(Versuchs-Atomkraftwerk Kahl)
design and development of, review, (E), 19: 43546
electric system of, design review, 20: 1507
fuel elements for radiation testing of, 19: 29676
fuel elements for, radiation testing on boiling-superheat, 19: 29676
heat transfer systems of, description of, 20: 32812
instrumentation for, operation of, 20: 8428
neutron flux distribution in, relaxation method for calculating, 19: 21655
operation of, 18: 6496
operation of Kahl (RWE) Nuclear Power Plant, experience in, 17: 36959
operation of, review, 19: 19400
operation of, review of 3-year, 19: 40201
performance, 18: 23070
radioactivity monitoring of air in Kahl building, 19: 14858
safety features in, review of, 19: 35783
startup and load-change procedures for, 18: 11447 (TID-7672(p.242-6))
testing of 15-Mw boiling, 17: 2597

VALENCY
see also Bonds
effects on chromium-51 uptake by clams, 20: 40575
theory review, 17: 12282

VALERIC ACID
capillary ripple propagation in surfaces of solutions of, 19: 4175 (IS-855)
decomposition of, uranyl sensitized photo-, 17: 10697
effects on radioinduced redox processes in ammonium iron sulfate, 18: 13878
radiolysis of, formation of carbonyls by gamma and ultraviolet, 17: 21748
4-phenyl-, effects on cesium extraction by 4-*sec*-butyl-2-α-methylbenzyl-phenol, 19: 28443(R) (ORNL-3785)

Valeric Acid, α-Amino
see Norvaline

VALERIC ACID, 5-AMINO-
labeling with tritium at α-carbon atom, 19: 46306

Valeric Acid, α-Amino-δ-Guanidino-
see Arginine

Valeric Acid, α,δ-Diamino-
see Ornithine

VALERIC ACID, 3,5-DIHYDROXY-3-METHYL-
preparation of C^{14}-labeled, 16: 13030(T)

VALERIC ACID, 4,4-DINITRO-, ETHYL ESTER
determination in explosives, method for, 20: 14470 (UCRL-7873)

VALERIC ACID, 4,4-DINITRO-, METHYL ESTER
determination in explosives, method for, 20: 14470 (UCRL-7873)

VALERIC ACID, 4,5-DIOXO-
labeling with carbon-14 at 5 position, 20: 7121(T)
synthesis and isolation of, 20: 7121(T)

VALINE
analysis for carbon-14 by continuous scintillation counting, 17: 5709
benzoyl-, substituent effects on hydrogen-tritium exchange in preparation of, 18: 31553
carbon-14 uptake by, in algae proteins during photosynthesis, 19: 24244
complexes with lanthanum, stability of, 19: 36421
determination in mixture with isoleucine and leucine by infrared spectrometry, 19: 46184(T) (ORNL-tr-341)
determination in protein hydrolyzates using carbon-14- or tritium-labeled 1-fluoro-2,4-dinitrobenzene, 16: 16089
determination of, in rabbit urine, design of photometer for, 17: 30214
deuterium exchange of polymers of, with heavy water, sites of, 19: 22276
hydrolysis by hydrochloric acid in tritiated water, hydrogen exchange in free and protein combined, 19: 9243
incorporation in chloroplast proteins, tracer studies of, 19: 25853
incorporation into protein, 18: 33212(R) (NYO-2570-1)
labeling with carbon-14, 20: 26916
labeling with tritium by Wilzbach method, 19: 46311
labeling with tritium following radiolysis of ribonuclease, 20: 18749
preparation of carbon-14-labeled, method for, 18: 258
protective effects against radioinduced hemolysis of erythrocytes, 16: 32725 (HW-SA-2638)
radiation effects on poly-, electron spin resonance spectra of, 17: 23413
radiation effects on ESR spectrum of, temperature effects on, 19: 4229
radiation effects on content of, in nervous system of guinea pigs exposed prenatally, 19: 5673
radiation effects on content of, in kidneys and liver of mice, 19: 7149
radiation effects on uptake of tritium-labeled-, by bean chromosomes, 19: 31851
radiation effects on uptake of tritiated, by *Vicia faba chromosomes*, x, 19: 38417

radio and chemically induced mutants of, in *E. coli*, 19: 15083
radioinduced free radicals in, dose-response relation in yield of, 17: 14353
radioinduced mutations for yeast requirement of, reversion of, 19: 15127
radioinduced radicals in, 16: 30452
radiolysis in presence of nitrogen or oxygen, mechanisms of, 19: 506
radiolysis of oxygenated and oxygen-free solutions, products formed in, 18: 6854
radiosensitivity effects on paramecia, 17: 15737
separation from amines and amino acids by thin-layer chromatography-ionophoresis and ionophoresis, 18: 19854(T) (SC-T-64-49)
synthesis and transformation in uv photolysis of organic compounds in mixtures with ammonium compounds, 18: 23204(T) (JPRS-24164 (p.19-42))
synthesis of tritium-labeled, 18: 10119(T) (NP-tr-1093)
vapor pressure, 18: 15678 (IS-790)

VALINE, *N*-ACETYL-
radiolysis of, electron spin relaxation times at 4.2°K of radicals from, 20: 26997

VALINE, 3-MERCAPTO-
effects on cobalt-60 uptake by rat organs, 19: 5620
effects on immune reactions, 19: 26109(R) (ORINS-49(p.40-62))
effects on radiosensitivity of tumors, 16: 21966
effects on radiosensitivity of *Escherichia coli*, kinetics of, 20: 45477
influence of, on distribution of mercury in rats, 18: 27039
preparation of tritium-labeled, 20: 35571
protective effects against radiation, correlation with instability constant of copper complex formation, 16: 7470
radioinduced free radicals in, 17: 25028
radioinduced free radicals in frozen aqueous solutions of, electron spin resonance studies of, 17: 30590
radiolysis of, electron spin resonance spectra of free radicals produced by, 17: 8165
radiosensitivity effects on Ehrlich tumors, 17: 35479
radiosensitivity effects on Ehrlich carcinomas, 19: 211

VALINOMYCIN
effects on reduction of pyridine nucleotides in rat liver slices, 20: 42759

VALLECITOS BOILING WATER REACTOR
analysis of data for reactivity-flux driving power spectral density function, 18: 9639 (CONF-332-8)
control rod development and testing, 16: 31205 (GEAP-3946)
coolant loss-of-flow in, flow-decay tests for two-pump operation, 18: 40822 (APED-4463)
coolant surface waves in, (E/T), 19: 21684 (GEAP-4061)
corrosion product activation and deposition, 16: 23290
decontamination procedures for, 17: 1119 (GEAP-3372)
experimental facilities for testing superheater fuel elements, uses of E-SADE loop, 20: 5104 (ACNP-65006)
fission product release from uranium-dioxide fuel rods in (E), 19: 1856
fuel analysis for promethium isotopes, fission products, and transuranic isotopes, 19: 24904 (BNWL-45)
fuel assembly testing in, (E), 19: 5474(R) (GEAP-4641)
fuel burnup in, isotopic-composition studies of, 18: 11414 (TID-7672 (p.288-302))
fuel capsule irradiation testing in GeV-2 in, 18: 29000(R) (GEAP-4503)
fuel element burnup, 16: 30093(R) (SRO-71)
fuel element burnup in, 17: 33240(R) (GEAP-4303)
fuel element burnup in, 18: 4762(R) (GEAP-4385)
fuel element cladding corrosion in, 17: 42210
fuel element decay heat in shipping cask, 18: 40808 (GEAP-4704)
fuel element development, 17: 15452(R) (GEAP-3947)
fuel element development and testing, 17: 26858(R) (GEAP-4219)
fuel element development and testing, 17: 40340(R) (GEAP-4309)
fuel element development and testing, 18: 7927(R) (GEAP-4391)
fuel element development and testing, 18: 24885(R) (GEAP-4488)
fuel element development and testing, 18: 29042(R) (GEAP-4609)
fuel element development and testing, 18: 45021(R) (GEAP-4647)
fuel element development, 19: 12780(R) (GEAP-4741)
fuel element fabrication for, by swaging, 17: 18712 (GEAP-3918)
fuel element failure in, operational experience with, 18: 3278
fuel element failure in, operating experience with, 18: 4824
fuel element failure in, location and monitoring system for, 18: 7867
fuel element failures in, review, 19: 3591
fuel element failure in, 20: 7525
fuel element failure in ESADE superheat loop of, radiochemical studies of, 20: 36469 (GEAP-4813)
fuel element irradiation in, 18: 1239(R) (GEAP-4048)
fuel element irradiation in ESADE-VBWR superheat loop in, 19: 42903 (GEAP-4775)
fuel element shipping and chemical reprocessing of, 17: 3761
fuel element shipping casks for, drop testing of, 18: 39528 (APED-4522)
fuel element testing, 17: 35140(R) (GEAP-4215)
fuel element testing in SADE loop in, 17: 40270 (GEAP-4240)
fuel element testing, 17: 40271(R) (GEAP-4301)
fuel element testing in, 18: 1241(R) (GEAP-4332)
fuel element testing, 18: 4761(R) (GEAP-4383)
fuel element testing in, 19: 10541(R) (GEAP-4703)
fuel elements, burnup and operating status, 16: 12750(R) (SRO-65)
fuel elements, development of high-power-density, 17: 13675(R) (GEAP-4001)
fuel elements of, method for processing stainless steel–uranium, 20: 9043 (IDO-14658)
fuel irradiation schedules in, 18: 3134(R) (GEAP-4094)
fuel performance in, effects of cladding on, 18: 29069
fuel rod burnout damage in, 18: 38365 (A/CONF.28/P/469)
fuel rod design for increased thermal output, testing of, 19: 45573 (GEAP-4902)
fuel rod failure in, stainless steel (E), 19: 3686
fuel rod failure in, stainless steel clad, 19: 24123
fuel rod testing in, 18: 21635(R) (GEAP-4481)
fuel testing in, on low-density compacted powder uranium dioxide, 20: 2232
fuel tube fabrication for irradiation in, 20: 2280 (DP-989)
fuels and materials testing for, 18: 24886(R) (GEAP-4565)
fuels and materials testing in, 18: 24884(R) (GEAP-4419)
fuels and materials for, development and testing of, 18: 45020(R) (GEAP-4619)
in-pile loop in, design of E-SADE, 18: 45019 (GEAP-4617)
instrumentation for E-SADE loop in, 17: 21248 (TID-7658(p.123-33))
kinetics of, effects of coolant circulation mode on, 18: 29066
licensing activities for, 18: 1267
neutron distributions in, measurement by wire activation, 17: 38996
neutron flux measurements for local power density using neutron telescope, 16: 8945
neutron resonance activation spectrum, 19: 8617(R) (GEAP-4729)
noise analysis, 18: 40821 (APED-4285)
noise analysis in, (E), 19: 40164
operation, 16: 28542(R) (SRO-68)
operation, 16: 33989(R) (SRO-72)
operation, 17: 1049(R) (SRO-73)
operation, 17: 4305(R) (SRO-74)
operation, Apr.-June 1963, 17: 40271(R) (GEAP-4301)
operation of E-SADE loop in, 17: 21234 (TID-7658(p.58-9))
operation of E-SADE loop in, 17: 36927(R) (GEAP-4075)
operation of E-SADE loop in, 17: 36928(R) (GEAP-4126)
operation of E-SADE loop in, 17: 36929(R) (GEAP-4243)
operation of, experience in, 17: 36959
operation of, fuel element testing in, 17: 21221(R) (GEAP-4159)
operation summary, 16: 17299(R) (SRO-66)
operation, Feb. 1960–Jan. 1961, 18: 40865(R) (NP-14286)
radioactive maintenance experiences, 16: 631
radioactivity deposition from nuclearly superheated steam in, 17: 35096 (GEAP-4141)
safety audit for, 19: 1820 (CONF-446-42)
safety performance of, evaluation of, 19: 38207
spent fuel analysis for fission products and heavy element isotopes, evaluation of chemical, 20: 14435 (BNWL-SA-503)
stability analysis, 18: 23063 (TID-7662(p.91-135))
stability testing of, 17: 22854(R) (GEAP-3935)
stability tests, 18: 1239(R) (GEAP-4048)
stability tests on, 18: 21634 (GEAP-3971)
thermal operating performance, 18: 15434 (TID-7669)
use in fuel cycle developmental program, 16: 3940(R) (GEAP-3781)

VALLECITOS SUPERHEAT REACTOR
construction and operation status, 19: 5487 (SAN-8003(p.1-12))
coolant and moderator chemistry, 20: 12399(R) (GEAP-4941)
coolant chemistry control for, 17: 38469 (TID-7674(p.21-4))
coolant chemistry, 19: 4197 (SAN-8003(p.90-133))
coolant chemistry and fission product release in, 20: 28751(R) (GEAP-5125)
cooling system of, sampling facilities for chemical studies of, 20: 36469 (GEAP-4813)
core physics parameters for startup of ESADA for, 17: 38483 (TID-7674(p.58))
critical experiment facility for, safeguards summary of, 17: 1005 (GEAP-4054)
criticality studies and pre-startup physics calculations, 17: 24678 (GEAP-4213)
criticality studies, 18: 3210
criticality studies, 18: 3211
criticality studies, (E), 19: 5488 (SAN-8003(p.163-89))
description, 16: 31302
design and development, 16: 11271
design and development, Apr.–June 1962, 17: 36927(R) (GEAP-4075)
design and development, July–Sept. 1962, 17: 36928(R) (GEAP-4126)
design and development, Jan.–Mar. 1963, 17: 36929(R) (GEAP-4243)
design and development of, review, (E), 19: 43546
design and development of, 20: 47056
design and operation, 19: 3788

design and operating experience of, 19: 38172 (APED-4784)
design description, 17: 10103
design specification changes, 19: 25636
development, 16: 33990 (TID-7634)
development, 17: 17538(R) (GEAP-4105)
development, 17: 21236 (TID-7658(p.77-8))
development, 17: 21314(R) (GEAP-4146)
development, 18: 33083 (A/CONF.28/P/215)
development and operation of, Sept. to Nov. 1964, 19: 24080(R) (GEAP-4759)
development and operation, Dec. 1964–Feb. 1965, 19: 35757(R) (GEAP-4810)
development of, Dec. 1962–Feb. 1963, 17: 33309(R) (GEAP-4200)
development of, Mar.–May 1963, 17: 33310(R) (GEAP-4277)
development status, 17: 38491 (TID-7674(p.68-9))
fission product release in, xenon-133 and -138, 20: 28750(R) (GEAP-5061)
fuel bundle design for Mark V core, 20: 28751(R) (GEAP-5125)
fuel clusters for, design and fabrication of Mark III, 20: 42627 (GEAP-5051)
fuel development and testing for, summary, 18: 23054(R) (GEAP-4432)
fuel development and testing for, 18: 35145(R) (GEAP-4566)
fuel development and testing for, 19: 19382(R) (GEAP-4714)
fuel development for, 18: 15523(R) (GEAP-4363)
fuel development for, 20: 3472(R) (GEAP-4891)
fuel development for, 20: 28750(R) (GEAP-5061)
fuel development for, 20: 28751(R) (GEAP-5125)
fuel element design and development for, 18: 43028(R) (GEAP-4623)
fuel element design and performance for, Mark III, 20: 45110 (GEAP-4793)
fuel element development and testing for, 18: 1241(R) (GEAP-4332)
fuel element development for, 19: 4597 (SAN-8003(p.13-89))
fuel element development and fabrication for, (E), 19: 10539 (GEAP-4573)
fuel element development and testing for, 19: 10541(R) (GEAP-4703)
fuel element fabrication for E-SADE loop for, 17: 38473 (TID-7674 (p.34-6))
fuel element fabrication and testing for ESADA for, 17: 38475 (TID-7674(p.39-45))
fuel element fabrication, 18: 3251
fuel element fabrication and design for, 20: 36477 (KR-89, pp 197-237)
fuel element failure in, metallurgical evaluation of, 20: 28750(R) (GEAP-5061)
fuel element irradiation testing for, 20: 35024 (GEAP-5135)
fuel element testing in, BONUS, 20: 36460(R) (CEND-244)
fuel elements for, development, (E), 19: 10538 (GEAP-4425)
fuel elements of, mechanical out-of-pile testing of, 18: 35144 (GEAP-4560)
fuel performance evaluation for, DARE code for thermal hydraulic, 19; 29639 (GEAP-4772)
fuel-cladding materials for, 19: 29675
fuels and materials testing for, 18: 24886(R) (GEAP-4565)
fuels and materials testing in, 18: 24884(R) (GEAP-4419)
fuels and materials for, development and testing of, 18: 45020(R) (GEAP-4619)
hazards analysis, 17: 1112 (APED-3958)
instrumentation for, 17: 21248 (TID-7658(p.123-33))
instrumentation for, 17: 38471 (TID-7674(p.28-30))
licensing activities for, 18: 1267
neutron flux in, (kβ/l) pulsed-source technique for, (E), 20: 14162
operation summary for June–Aug. 1965, 20: 12399(R) (GEAP-4941)
performance of, nuclear and thermal, 19: 29667
power distribution analysis of, 20: 3472(R) (GEAP-4891)
power distributions in core of, 20: 28751(R) (GRAP-5125)
power distribution in Mark IV core, 20: 28750(R) (GEAP-5061)
reactivity measurements by pulsed neutron technique, 18: 29041(R) (GEAP-4606)
reactivity of, critical and subcritical, 18: 15581
reactivity of, critical and subcritical, 18: 15582
regulatory review on, 19: 32495
safety audit for, 19: 1820 (CONF-446-42)
safety organization for, 20: 12337
safety performance of, evaluation of, 19: 38207
startup, 18: 43028(R) (GEAP-4623)
transients in, analysis of thermal-hydraulic, (T), 19: 38177 (GEAP-4780)

VALLEY-and-RIDGE PROVINCE (PENN.)
geology and hydrology of Dunning Cove basin for potential use for radioactive waste disposal, 19: 14894 (SAN-413-2)

Valve Packing
see Seals and Glands

VALVES
see also Vacuum Valves
acceleration switching, performance for machine tool control, 19: 48106 (Y-1488)
actuator design for turbopump control, pneumatic linear, 16: 14850 (TIM-612)
availability and specifications for gas-cooled reactors, 18; 15528 (NYO-9788)
cleaning mass spectrometer, 18: 25269(R) (NLCO-905)
control circuit for, testing of, 17: 26765(R) (ORNL-3419)
design, 17: 21332
design, 20: 32762(P)
design and calibration for boiling channel power measurements (E), 19: 3638 (HPR-35(Vol.I)(Sect.6))
design and development of adapter, for refueling machine head, 17: 21310 (AMF-388-TR-3)
design and development for advanced closed-Brayton-cycle space power systems, 17: 36987 (SY-5394-R(Vol.I))
design and operation of multipurpose ball, 17: 23463 (UCRL-10326)
design and testing for reactor primary coolant systems, 17: 32227
design and testing for hydraulic reactor control systems, 18: 24820(R) (GNEC-337)
design criteria for power reactors, 19: 35640
design for accurate timing of electron and x-ray exposures, (E), 19: 41186
design for automatic exit-steam quality control in boiling reactors, 18: 3228
design for burst slug detection systems, 17: 42253(P)
design for coaxial ducting, 16: 7671(P)
design for coaxial ducting, 17: 20145(P)
design for cold traps, 16: 13200(P)
design for coolant control in reactor fuel channel, 19: 8585(P)
design for fluid flow control, 16: 20623(P)
design for fluid flow control, 17: 1623(P)
design for gas control during reactor loading, 19: 10475(P)
design for gas control in particle accelerators, 20: 23843(P)
design for gas-cooled reactor channels, 17: 13752(P)
design for gas injection in plasma studies, 20: 5642
design for gas-cooled reactors, 19: 31485(P)
design for glass blowing on contaminated apparatus, 18: 33718
design for heat exchangers, 16: 5479(P)
design for heat exchanger tubes, 17: 12441(P)
design for Maritime Pressurized Water Reactor containment system, 19: 38250
design for mass spectrometer source, 19: 4448(P)
design for nuclear power plants, 16: 33109(P)
design for passing pebbles into and out of reactor, 19: 5411(P)
design for pressure control in reactor containment vessels, 18: 6429(P)
design for pulsed gas, 20: 40246
design for reactor cooling systems, 20: 22364(P)
design for solids flow, 20: 28853(R) (IDO-14661, pp 45-82)
design for use in ion sources, 18: 28187(R) (ORNL-3578(p.122-6))
design of bakeable, for ALICE, 20: 15923
design of bakeable 12-in., 20: 45848
design of check, for reduction of water hammer, 19: 22471(P)
design of control, 17: 4658(P)
design of control cock for liquefied gases, 17: 21868(P)
design of electromagnetic, for fluid flow control, 18: 12323(P)
design of fast, for injection of gas into vacuum, 17: 6216
design of flow-diverter, for granular solids, 20: 22511 (IDO-14666)
design of flow-regulator, for sodium cooled fast reactors, 20: 16004(P)
design of fluid flow control system for ducts, 16: 25538(P)
design of fluid-flow control, for pressure vessels, 17: 30654(P)
design of fluid-tight, 17: 16208(P)
design of, for gas control, 17: 10032(P)
design of, for high-pressure high-temperature fluorination system, 17: 30615
design of, for use in monitoring operation for reactor coolant, engineering drawings for, 18: 6426
design of gas pressure-relief, for dry boxes, 18: 31709(P)
design of gate type, for controlling separate concentric channels, 16: 13199(P)
design of gate, with obturating member to close off conduit, 20: 5042(P)
design of HBWR coolant-flow calibration, 19: 33604(R) (HPR-57)
design of high-pressure leak-proof needle, 17: 10889 (AD-252467)
design of large sodium, conceptual, 20: 20184 (ACNP-65579)
design of leak, 20: 10498(P)
design of leak, for mass spectrometer ion source, 18: 25652(P)
design of lift and non-rotatable spindle-type flow-control, 20: 14676(P)
design of liquid-sodium flow controller for in-pile uses, (E), 19: 40135
design of magnetically driven, for operation at 400°C, 18: 37315
design of non-return, for concrete containment vessels, 19: 29486(P)
design of palladium, for deuterium generator, 18: 3937
design of piston-controlled stop, 16: 5452(P)
design of pneumatic exhaust, 16: 13171 (DC-57-10-98)
design of pneumatically actuated, 20: 43425 (ORNL-P-2406)
design of pressure-wave actuated control, 18: 31710(P)

design of pulsed gas, 16: 30547(P)
design of purge or bleeder, 17: 25404(P)
design of rotary selector, for variable communication between many conduits for fluids, 17: 35978(P)
design of rotary-selector, for allowing variable communications between assembly of passageways traversed by fluid, 18: 9600(P)
design of safety, for contaminated reactor gases, 16: 21761(P)
design of sampling, for reactor coolant, 16: 26462 (DP-658)
design of sampling, for fuel element rupture detection system, 20: 10315(P)
design of selector, for sampling gas from reactors, 16: 28453(P)
design of stainless steel, for liquid metal loop, 19: 22984(R) (NASA-CR-54167)
design of three-way electropneumatic, for converting electrical signals into pressure pulses, 16: 327 (AD-255794)
design of vapor, for sodium-cooled reactors, 16: 306(P)
design of ventilation, for blast shelters, 20: 39073
design of 12-in. 250-psi ball-type, engineering drawings for, 19: 20104
design of, actuated by heat-sensitive seals, 20: 46128(P)
design to protect reactor containment shells against burst due to excessive pressure, 18: 33000(P)
development and performance of pneumatic solids transfer, in uranium trioxide plant, 18: 35677 (HW-58563)
development and performance of HBWR coolant-flow calibration, 19: 31542(R) (HPR-59)
development and testing for hydraulic reactor control systems, 18: 7859(R) (GNEC-318)
development for circulation systems in gas-cooled high-temperature reactors, 19: 27741
development for flow of powdered or granular solids, 18: 33712 (HW-53440)
development for hydraulic reactor control systems, 18: 1188(R) (GNEC-299)
development for liquid metal cooled reactors, 17: 7606(R) (ORNL-1515)
development for power reactors, 19: 24018
development for space propulsion systems using liquid propellants, 20: 11007(R) (NP-15831)
development for superheaters, 18: 26946
development for use in radiation-resistant pneumatic power systems for space vehicles, 17: 23460(R) (GD/C-63-068)
development for 10000-hr operation with lithium to 1000°F and potassium–sodium alloys to 1200°F, 19: 11682
development of bearings for D-103 by-pass, 16: 23801 (DC-60-1-37)
development of blast-closure, for bomb shelters, 17: 10776 (NP-12454)
development of, for use in pressurized water reactor systems, 16: 31221 (TID-6135)
development of, for use in radiation-resistant pneumatic systems, 17: 10774(R) (GDC-63-001)
development of, for sample scanning in fuel rupture monitoring system, 17: 38492 (TID-19378)
development of frozen-seal type for Molten Salt Reactor Experiment, 16: 10133 (ORNL-TM-128)
development of high-temperature solenoid-operated, 19: 40765(R) (NP-15309)
development of liquid–metal, for Lithium Cooled Reactor Experiment, 18: 27658 (PWAC-401(Pt.II))
development of superconductive, book, 18: 36438
development of, for volatility separation process, 20: 33413(R) (K-1669)
disc motion analysis of, computer programs for, 17: 12426 (WAPD-TM-323)
electromagnetic, for particle accelerators, 17: 21105 (CEA-1936)
engineering drawings for hot air control, for wind tunnels, 18: 39417
evaluation and testing of pneumatic servo type for control of actuators, 16: 7630 (DC-59-10-101)
evaluation of bellows-sealed, 16: 31784 (UCRL-6565-T)
fabrication and testing of 24-in., for reactor cooling systems, 19: 31568
flow testing Tesla static check, for Mercury-Rankine system (E), 19: 2513 (NAA-SR-Memo-10239)
hydraulic characteristics of shield-orifice, 16: 33123 (NAA-SR-Memo-7417)
material and testing requirements for, ASA code for, 16: 31709
operating characteristics of fast electromagnetically operated, 17: 34064 (CONF-78-5)
operation and testing of ART dump, 16: 28646(R) (ORNL-2247(Pts.1-5))
operational characteristics of pilot-actuated water-relief, computer program for, 18: 27644 (WAPD-TM-399)
performance of liquid-metal, 18: 19283
performance of remote bellows-seal air-actuated and solenoid-actuated types flow measurement and sampling, 16: 20631 (CVNA-140)
performance tests of flow controller for sodium service at temperatures up to 1200°F, 18: 5465 (NAA-SR-7534)
plug design for sealing, in pipes, 18: 31708
pressure drop in two-phase flow through gate and globe, 19: 32378 (CONF-640507(p.483-7))
properties of gas injection, for coaxial plasma gun, 20: 46894
radiation effects on NERVA, under dynamic operation conditions, 19: 14867 (FZK-170-Z)
radiation effects on actuator for turbine power control, 19: 14872 (FZK-170-8)
remote operating mechanism for, 19: 11342(P)
remote operation, device for, 19: 2509(P)
seal for, design of corrosion-resistant, 19: 36584(P)
seat materials for HTGR, galling tests of low-cobalt, 19: 11304 (GAMD-3058)
specification guides at HAPO for, 18: 3923 (TID-15246(Vol.I)(Rev.))
specifications for gas-cooled reactor cooling system, 18: 1199
surge pressure from check, prediction of, 17: 8364
surge pressure from check, minimization of, 17: 8365
technology of advanced, review, 19: 20097 (NASA-SP-5019)
testing coolant-loop self-activating relief, for pressurized water reactor, 18: 45011 (DLCS-3070203)
testing for Hanford Production Reactor (N) primary loop, 18: 31016 (HW-79616)
testing manual-controlled reactor coolant loop stop, 16: 30101 (WAPD-PWR-TE-142)
testing of ball and flapper caps, 16: 29059 (HW-69432(Suppl.A))
testing of butterfly, for cavitation in Pathfinder reactor, 17: 22845 (ACNP-62004)
testing of butterfly, in Shippingport reactor hydraulic system, 19: 27777 (DLCS-5680301)
testing of hydraulic system for butterfly, in Shippingport Pressurized Water Reactor, 18: 24880 (DLCS-3570501)
timing circuit for sequence, 20: 23445

VAN ALLEN RADIATION BELTS

see also Cosmic Radiation

anisotropy in, angular, 18: 2722 (AID-Report-P-63-28)
anomalies in radiation intensity as measured by Sputnik II, 18: 18828(T)
artificial, decay time of electrons in, 17: 13310
artificial, energy spectrum and time decay of July 1962, 17: 13303
artificial, fission beta source studies of, 17: 13308
artificial, from nuclear detonation, 17: 13307
artificial, measurements on, 17: 13304
artificial, observations of, 17: 13305
artificial, particle analysis of, 17: 13306
artificial, review of data on, 17: 13309
asymmetry of Jupiter's, 18: 42285
atmosphere in, density of, (T), 19: 37724
atmospheric effects of, D-layer production by electrons from, 16: 29527
auroral effects of, review, 17: 14507
bibliography on, 20: 35985 (NASA-SP-7026)
biological effects of flare-produced and other proton fluxes, 16: 3598 (AD-257272)
boundary during solar maximum, determination from energetic electron trapping, (E), 19: 47462
boundary of, dependence on geographic and geomagnetic coordinates, 17: 19013(T)
boundary of inner, 17: 6934(T)
boundary of outer, 16: 15490
boundary of outer, 17: 6936(T)
boundary of outer, at 1000-km, 18: 21071
bremsstrahlung and electron intensities in, shielding of astronauts from, (T), 20: 28599
bremsstrahlung dosimetry in, 17: 18387 (TID-7652(p.760-72))
Cape Town anomaly in, effect on auroral emission, 17: 6850
characteristics, 16: 10400 (ASD-TR-61-322(p.1-7))
characteristics, 16: 20235
charged-particle densities at 20 to 200 ev at 55000 to 75000 km, 16: 15503
charged particle distribution in outer, 17: 2149
charged particle distribution in, 18: 16731(T) (FTD-TT-64-90(p.110-27))
charged particle distributions in, from high-altitude nuclear tests, (E), 19: 16728 (AD-603599)
charged particle distribution in, solar storm effects on, (T), 19: 21137
charged particle distribution in, 19: 47491
charged particle excitation in, 19: 21154
charged particle flux in inner, 16: 12311
charged particle flux in equatorial regions of, detection of soft, 17: 24257(T)
charged particle flux and trajectories in, 17: 25966
charged particle fluxes in near-earth, (E), 19: 9946 (ASE-546)
charged particle flux in inner, Dec. 19, 1961, (E), 20: 39992
charged particle intensity in, 17: 6935(T)
charged-particle intensities in, geomagnetic storm effects on, 18: 5962
charged particle interactions with transverse waves in, (T), 19: 37722
charged particle intensities in, 17: 19011 (AFCRL-63-242)
charged particle lifetime and time histories in artificial and natural,

18: 28288
charged particle measurements, cadmium sulfide detector for, 16: 6565
charged particle motion in, 17: 26272
charged-particle motion in, adiabatic theory of, 18: 6356
charged particle motion in, at small pitch angles, 18: 7798
charged particle movement in, adelphic-integral method and Stoermer problem for, 18: 26242
charged particle motion in, electromagnetic perturbation effects on, (T), 19: 25433
charged particle measurements in, from Vela Project, 19: 47450 (LA-DC-7365)
charged-particle removal from, time reversal of geocyclotron mechanism for, 18: 7436
charged particles in, magnetic moment nonconservation for, 17: 37920
charged particles in, sources of, 19: 12401(T)
charged-particle acceleration in, post-storm, 19: 35252
charged-particle confinement in, review of, 19: 20902
charged-particle dynamics and origin in outer, 18: 32688
charged-particle distribution in, during geomagnetic storms, 19: 12421
charged-particle diffusion in, 20: 30206(T) (NASA-TT-F-389, pp 426-42)
charged-particle distribution in, review of, 20: 37911
charged-particle energy and flux in, 18: 28458
charged-particle energy spectra and flux in, 20: 15232
charged-particle fluxes in outer, 18: 42519 (SUI-64-1)
charged-particle flux in, determination of, 18: 5955
charged-particle intensity variations in outer, 18: 26444
charged-particle intensity in, 18: 28287
charged-particle intensity distributions in, (E), 20: 24207(R) (AD-625960)
charged-particle intensity in, effects of satellites on, 20: 30223(T) (NASA-TT-F-389, pp 817-21)
charged-particle intensities in, (E), 20: 30235
charged-particle lifetimes in, atmospheric-density effects on, 19: 35235 (N64-25566)
charged-particle motion in, Alfven's theory for, 18: 30648 (AFCRL-64-226)
charged-particle motion during magnetic storms, (T), 19: 21128(T)
charged-particle motion in, 19: 33155
charged-particle motion in outer, trapped, (T), 20: 28133
charged-particle precipitation from, effects on ionospheric v-l-f propagation, 18: 28493
charged-particle streams in, effects of geomagnetic field variations on, 19: 21126
charged-particle transport in, (T), 20: 28099(T)
composition of, 17: 24231
composition of, review of, 20: 39957(T)
composition, properties, and structure of, review, 17: 41669
composition, dynamics, and origin of, 18: 32687
configuration and intensity of, data summary on, 19: 31131 (AD-607814)
contribution to radiation dose in space vehicles, 17: 5646
contribution to radiation dose in space vehicles, 17: 35332 (NP-13060(p.301-38))
current and density of, theory of plasma near magnetic dipole for, 19: 35262
currents in, measurements with Explorer 10, 17: 8984
data from Soviet spaceship measurements, 17: 17777(T) (JPRS-18395 (p.179-202)
decay of artificial electron belt in South American magnetic anomaly, satellite measurements of, 18: 18802
decay of electron flux in artificial, time, (E), 19: 8119
deformation of outer, by ring current, 17: 32878
description of, 17: 22413
description of inner, 18: 948
detection and measurement by satellite-borne detectors, 18: 485
detection and measurement of, instruments for, 18: 2563
detection in South Atlantic magnetic anomaly, 17: 6937(T)
diamagnetism, as source of external geomagnetic field, 16: 24663
distribution, 16: 12317(T)
distribution and properties of electrons and particles in, satellite data on, 17: 41700
distributions and interactions of, theory of, 17: 37895
distributions at 1.2 to 2.3 earth radii, (E), 19: 8118 (NASA-TN-D-2516)
distributions in space, 17: 7676
distributions of electrons and protons in, energy, spatial, and time, (E), 19: 23511
distributions of, in low northern and southern latitudes, 17: 2102(T)
diurnal variations in inner, 18: 11027 (LNF-63/54(p.27))
dosage measurements, 16: 20240
dose measurements in, at 200 to 400 km by satellites and spaceships during 1960–1963, 19: 700
dosimetry in, Sputnik II, 17: 19014(T)
dosimetry of energetic radiation in, data survey on, 16: 24013 (NASA-TN-D-1267)
drag effects on satellites, 16: 14136 (AFOSR-1159)
dynamics of, 17: 12907
dynamics of outer, 17: 12999
effect of Starfish nuclear explosion on, (E), 19: 5072
effects of artificial belt on solar cells, 17: 14426
effects of artificial, on ionospheric D layer, 19: 45166
effects of artificial, on solar-cell power systems, 20: 13131
effects of currents in, on cosmic ray rigidity cutoff, (T), 20: 27774(T)
effects of geomagnetic storms on outer, 17: 12901
effects of high-altitude nuclear explosions on (E), 19: 3147 (D1-82-0372)
effects of hydromagnetic shock waves on, 17: 3596
effects of nuclear explosions in space on, 17: 9009
effects on airglow and aurora excitation, 18: 28470
effects on diodes and transistors, simulation of, 18: 2383
effects on electric components of lunar excursion module, 18: 7015
effects on electronic components, 18: 10358
effects on electronic materials, bibliography on, 19: 1006 (PDL-46195)
effects on gallium arsenide and silicon solar cells, 19: 4543
effects on manned space vehicle and trajectory around, 16: 8082
effects on manned space flight, 18: 12793
effects on manned space flight, computer analyses of, 18: 35048 (AMRL-TDR-64-11)
effects on manned military space vehicles, (T), 20: 2656 (NASA-SP-71, pp 265-86)
effects on metals and plastics, tolerance limits for, 17: 22241
effects on reproduction of *Drosophila melanogaster*, in magnetic fields, (E), 19: 15136
effects on satellites, 16: 34133
effects on satellites, 17: 3908 (RM-3096-PR)
effects on silicon solar cells, 17: 16884
effects on solar cells, 16: 34132
effects on space flights, 20: 30222(T) (NASA-TT-F-389, pp 758-63)
effects on space vehicles, 17: 16876
effects on the F region of the ionosphere, 18: 7595
effects on the geomagnetic field, 17: 4704
electric ring currents in, guiding-center approximation for, 17: 32863
electromagnetic disturbances in, 19: 35281
electromagnetic perturbation effects on particles trapped in, (T), 19: 47485
electromagnetic-wave scattering by relativistic electrons in, 17: 13321
electron acceleration in, 18: 24332
electron and ion distribution in, Coulomb relaxation of, (T), 20: 7981
electron and proton energy spectra and fluxes in inner, review of, 20: 15621
electron and proton intensity in, 20: 17310(T) (AD-623948)
electron and proton energy, spatial, and temporal distribution in, 20: 30204(T) (NASA-TT-F-389, pp 375-86)
electron and proton motion in outer, effects on geomagnetic field variations, 20: 30209(T) (NASA-TT-F-389, pp 464-82)
electron and proton spatial distribution in, analysis of, 20: 30211(T) (NASA-TT-F-389, pp 535-50)
electron and proton distributions in Brazilian magnetic anomaly at 250 to 400 km, spatial and temporal, 20: 30217(T) (NASA-TT-F-389, pp 607-15)
electron and proton energy and spatial distribution in, 20: 30219(T) (NASA-TT-F-389, pp 623-9)
electron and proton energy and intensity in outer, (E), 20: 37905
electron bremsstrahlung in, x-ray flux from, 18: 18823
electron bremsstrahlung from, tissue doses from, 19: 30008
electron capture in outer, equatorial angle distribution between, (T), 19: 47474
electron capture in, from high-altitude explosions, 20: 34353(R) (N-65-34401)
electron content in outer, 20: 30213(T) (NASA-TT-F-389, pp 566-8)
electron currents in, three-electrode traps for measurement of, 18: 497
electron density and temperature in, from exosphere ion-density measurements, 18: 5958
electron density and energy distributions in, 18: 22808
electron density at 200 to 400 km, 19: 21136
electron density distributions in artificial, 19: 45167
electron density diurnal variation in outer, geomagnetic activity correlations with, (E), 20: 19682
electron density distribution in, computer program for mopping, 19: 41954 (NP-15338)
electron density in artificial, computer program for analyzing decay of, 19: 35236 (NASA-TN-D-2874)
electron detection and measurement in, instrumentation for, 20: 15589(R) (ASE-1125)
electron diffusion in, high mirror point, 17: 6294
electron diffusion in, low mirror point, 17: 6925
electron diffusion in, 17: 6930
electron diffusion in, 17: 6941
electron diffusion in outer, inward radial, (E), 19: 41578
electron diffusion in outer, geomagnetic field effects on, (E), 20: 46488

electron directed intensity distribution above 40 kev in inner, (E), 20: 28130
electron distribution in, during July 1962, 17: 13302
electron distribution in, 1600 kev, 17: 41674
electron distribution in outer zone, Explorer XII observations on, 18: 26246
electron distribution in lower regions of outer, (E), 20: 17538 (N-65-17609)
electron distribution in, solar wind effects on, 20: 32260
electron distributions in, spikes in energetic, (E), 20: 37903
electron distribution in outer, effects of solar flares on, (E), 19: 41312
electron distributions in, 19: 16763
electron dosimetry in, 17: 18387 (TID-7652(p.760-72))
electron efflux from, mechanisms for, 17: 15061
electron energy and lifetime in outer, (E), 20: 21815
electron energy distribution in outer, calculation based on modified Fermi heating, 19: 47487
electron energy distributions in, models for, 20: 25989 (NASA-SP-3024(Vol.2))
electron energy distribution and flux in lower edge of inner, (E), 20: 39983
electron energy spectrum in outer, 16: 19662
electron energy spectrum in inner, 17: 3934
electron energy spectrum in, 17: 9172
electron energy spectrum in outer, neutron β-decay calculation of, 17: 15054 (NASA-TN-D-1717)
electron energy spectra at 200 to 355 km, (E), 19: 27342
electron energy spectra in inner, (E), 19: 33144
electron energy spectra in artificial, 20: 9872
electron energy spectra and pitch angle distributions in, from high-altitude explosions, 20: 4732 (UCRL-14368-T(Rev.1))
electron energy spectra in, 20: 32251
electron energy spectra, 18: 2747
electron energy spectra and origin in, 18: 5954
electron energy spectra and angular distributions in, 19: 35303
electron energy-selective distribution in inner, trapped, (E), 20: 34389
electron flux and decay of artificial, following high-altitude nuclear explosion, 17: 32860
electron flux and trajectories in artificial, 17: 34665
electron flux in artificial, correction for altitude dependence in, 20: 34383
electron flux in artificial and outer, 17: 26741 (ORNL-TM-552)
electron flux in outer, 18: 28289
electron flux in outer, 18: 28290
electron flux in outer, temporal variations during geomagnetic storms of, (E), 20: 44454
electron flux in, nuclear-explosion injected, 18: 28491
electron flux in, at 6,600 to 48,800 km, 18: 5963
electron fluxes at latitudes beyond normal boundary of, (E), 19: 37719
electron fluxes in, radial dependence of, 19: 33145
electron fluxes in auroral zone during magnetic storms, outer, (E), 20: 46458(T)
electron fluxes in, 18: 7633
electron fluxes in, from orbiting nuclear reactor, (T), 19: 31589 (AFCRL-64-865)
electron fluxes in, from orbiting reactor, (T), 19: 37733
electron increases in, from high-altitude nuclear explosions, 17: 16875
electron injection by Argus tests, 17: 6839
electron injection into inner, 17: 31262
electron injection by SNAP reactors, 18: 15029
electron injection into artificial, from Starfish explosion, 20: 6209
electron intensities near magnetic equator in outer, local-time dependence of, (E), 19: 45160
electron intensities in outer, 27-day periodicity of, 20: 23910
electron intensities in, distribution of, 17: 18355 (TID-7652(p.1-11))
electron intensities in, 19: 16326 (REIC-37)
electron intensities in Brazilian magnetic anomaly at 200-400 km, 19: 35294
electron intensity measurements in, 16: 8086
electron intensity in outer, 17: 5183
electron intensity in inner zone of, 17: 16920
electron intensity variation at 1000 km, diurnal, 18: 28275
electron intensity distribution in outer, (E), 19: 27340
electron intensity at 180 to 330 km, 19: 29149
electron intensity variations in outer, temporal, (E), 20: 34367
electron intensity and distribution in outer, (E), 20: 46450 (AD-628255)
electron interactions with atmosphere in, 19: 35302
electron leakage from, effects on aurorae, 17: 15063
electron leakage from, correlations with leakage from magnetic mirrors, (E), 20: 21836
electron lifetime in outer, at magnetically quiet times, (T), 20: 21817
electron lifetimes and precipitation from outer, 17: 3942
electron longitudinal drift in, effect of superimposed electric field on, (T), 20: 44434
electron loss and replenishment at middle latitudes and high B values, 19: 45161
electron loss from, due to pitch angle scattering by electromagnetic disturbances, 20: 32288
electron loss rate from outer, 18: 7636
electron losses from outer, into stratosphere, 20: 7982
electron losses in, due to whistlers, 17: 32889
electron losses to atmosphere, 18: 12998 (SSD-TDR-63-204)
electron origin in, trapped, 20: 39957(T)
electron pitch-angle distributions in outer, 16: 15518
electron plasmas in, amplification and generation of whistlers in, 18: 7381
electron precipitation into auroral zones, 17: 3948
electron precipitation from, 17: 12897
electron precipitation from, excitation of aurorae and airglow by, 18: 7632
electron precipitation in inner, flux of energetic quasi-trapped, (E), 20: 34377
electron production and spatial distribution from cosmic-neutron beta decay, 16: 3602
electron source for outer, (T), 19: 33123
electron spatial distribution in outer, 20: 30215(T) (NASA-TT-F-389, pp 576-87)
electron spectra in, following Starfish detonation of July 9, 1962, 18: 30649 (UCRL-7659)
electron spectra in, from Starfish detonation, 20: 4731 (UCRL-7659-T (Rev.1))
electron velocity distributions in, effects of vlf electromagnetic oscillations on, 18: 24519
electron-distribution variations during magnetic storms, correlations with magnetosphere tail, (E), 20: 11831
electrons and protons in inner, model for, 20: 13646 (NASA-SP-3024)
electrons in, source of, 17: 12904
electrons in, formation of slow, 20: 44156
energy transfer to atmosphere from, heating effects of, 18: 6099
exhaustion of, 17: 19012
flux densities and mirror-point distributions, 17: 5182
formation of (T), 19: 3012
formation of, effects of electron and proton drift in magnetosphere on, 20: 30207 (NASA-TT-F-389, pp 442-53)
genetic effects on *Neurospora crassa* in lower, 16: 16191
geographical distribution, 16: 27418 (NP-11961)
geomagnetic field fluctuation effects on, 16: 21245
geomagnetic field deformations in, during magnetic storms, 17: 32864
geomagnetic micropulsations in, 20: 32248
geomagnetic ring-current effects in inner, 17: 37897
hazards to manned space flight, 16: 13848
hydromagnetic wave effects on protons above the proton belt, 16: 10787
hydromagnetic waves in outer, 17: 6926
induced radioactivity in space vehicle materials, 16: 9761(R) (UCRL-9897(p.131-3))
intensities in, following solar chromospheric eruptions, 17: 2150(T)
intensities of artificial belt produced by high-altitude nuclear explosion on July 9, 1962, 16: 32207
intensity and location of outer, at low altitudes, 20: 24213
intensity changes due to reactor power sources in, 17: 5067
intensity in region of Brazilian magnetic anomaly, (E), 19: 23533(T)
intensity in region of Brazilian magnetic anomaly, (E), 19: 33150(T)
intensity in vicinity of Brazilian magnetic anomaly at 300 km, 18: 42543
intensity in vicinity of Brazilian magnetic anomaly at 235 to 345 km, 18: 42544
intensity of inner, time variations of, 17: 5186
intensity time variations in inner, Oct. 1959 to Dec. 1960, 16: 18295
intensity variations with time of inner, Oct. 1959 through Dec. 1960, 16: 29616
intensity variations, 17: 3939
intensity variations at 180–250 km, conjugate points of, 17: 28127(T)
intensity variation with altitude, (E), 19: 32916(T)
intensity variations of outer, during geomagnetic storms, (T), 19: 35240(T)
intensity variations in outer, nocturnal, 20: 30214(T) (NASA-TT-F-389, pp 569-75)
ion density in, low-energy, 19: 35233 (LA-DC-6509)
kinetic instability of outer, (T), 19: 12402(T)
lifetimes of protons at 1 kev to 1 Mev, 16: 919
location and energy spectrum, 16: 32644(R) (UCRL-10211(p.16-42))
magnetic anomaly of 320-km in South Atlantic, 16: 4669
magnetic anomaly of 320-km in South Atlantic, 16: 8080(T) (JPRS-11579)
magnetic disturbances of, 17: 12998
magnetic field of ring-current model, 16: 5845
magnetic field of proton component, quiet-time, 16: 29622
magnetic fields in, 16: 27860(T) (JPRS-13505)

magnetic fields produced by, 17: 3949
measurements and nature, 16: 19660
measurements from Explorer X, 17: 13000
measurements in outer, Aug. 1959, 17: 3941
measurements on, using Explorer VI satellite, 19: 27353
mechanism of mirror point loss in magnetic fields, 17: 12903
motion of outer boundary of, (E/T), 19: 23515
neutron albedo theory of origin of, 17: 12908
neutron intensities in, 17: 19011 (AFCRL-63-242)
neutron spectra in, 19: 47279
nighttime F layer in, recombination coefficient of, 17: 13318
nuclear emulsion experiments, 16: 11340 (UCRL-5967-T)
nuclear explosion effects on, 18: 10817
observation of anomalies in, at 200 to 300 km, 17: 12900
origin, (T), 19: 31163
origin, (T), 20: 15593
origin, (T), 20: 17547(T)
origin and formation of, charged particle drift mechanism for, (T), 20: 37909
origin and properties of, 18: 5956
origin and properties of, review of hypotheses on, 20: 2861
origin and properties of, (E/T), 20: 46456 (NP-16319)
origin of, mechanisms for, 18: 5957
origin of trapped protons in, 20: 39957(T)
particle acceleration in, 17: 8993
particle composition and spectra, measurements by satellites, 16: 9718 (NP-11161)
particle densities in, 17: 12907
particle density in, effect of geomagnetic fluctuations on, 17: 9167 (N62-10690)
particle density in lower, long-term study of time variations in, 17: 9169 (SUI-62-1)
particle density in outer, relation to F-layer critical frequencies, 17: 11453
particle density maxima in, 18: 42339
particle diffusion in, 17: 12905
particle diffusion, acceleration, and losses in, equatorial orbit study of, 20: 37489
particle distribution in, 18: 4412 (ASD-TDR-62-606)
particle dynamics of outer, 17: 12906
particle energies and intensities in, 20: 11840
particle energy spectrum in, August and September 1959, 17: 16937
particle energy, motion, and distribution in, 18: 10817
particle fluxes for vehicle trajectories along, calculation of time-integrated proton and electron, 19: 37491 (N64-29364)
particle intensities at 1000 km, 17: 41709
particle intensity and distribution in, 19: 35300
particle lifetimes in, relations with time, (E/T), 19: 8129
particle losses from, nonadiabaticity effects on, 17: 24249
particle sources and phenomena of, survey of research and theory on, 17: 13297 (NAA-SR-7849)
particle trajectories in, Capetown anomaly and shape, 16: 5843
particle trapping model for outer, 16: 18307
particle trapping in inner, 18: 28278
particles in, review and bibliography on energetic, 17: 36565
photon flux in, determination of, 18: 5955
position of Jupiter's, 20: 27700
production by plasma waves from bow shock wave, 18: 44652
production by Soviet 1962 high-altitude thermonuclear explosions, 18: 26188 (SUI-63-37)
production of artificial, in high-altitude explosions, 19: 31134 (NP-14990)
production of artificial, sources for, 19: 45159 (UCRL-14374)
production of artificial, from high-altitude nuclear explosions, 19: 45166
production of artificial, from Starfish burst, 20: 24210(T) (TG-230-T466)
production of artificial, from high-altitude nuclear explosions, 20: 24226
production of polar aurorae and electrojets by, 16: 29623
profiles and radiation intensity during geomagnetic storms, 18: 5961
propagation of vlf emissions through, 17: 12893
properties, 17: 26276
properties, 17: 28594(T) (FTD-TT-62-202)
properties, 18: 30671
properties, 20: 32274
properties and boundary of, correlation with geomagnetic field variations, (E), 20: 46487
properties and effects on Aurora, 18: 21087
properties, and mathematical analysis of charged particle orbits in geomagnetic fields, 16: 4665 (D1-82-0116)
properties and sources of (E/T), 19: 3004
properties and sources of (E/T), 19: 3168
properties and structure of, review of, 20: 19697
properties of, 19: 35296
properties of, 20: 34359 (N-66-16975)
properties of artificial, produced by Soviet tests on Oct. 22 and 28, 1962, 19: 25414 (NP-14991)
properties of artificial, from satellite data, 20: 7980
properties of outer, at low altitudes, 20: 30216(T) (NASA-TT-F-389, pp 588-606)
properties of, review, 17: 28131
properties of, review of, 17: 29269
properties of the outer, 17: 5184
properties of 320-km height, 16: 8080(T) (JPRS-11579)
properties of, abstracts on, 19: 14420 (ATD-P-64-51)
properties of, research on, 19: 41571(R) (N64-29400)
properties of, review of, 19: 8334
properties of, review of, 19: 14431
properties of, review of, 20: 7990
properties of, review of, 20: 19645 (NASA-SP-97)
properties of, review of, 20: 21837
properties of, review of, 20: 27769
properties of, review of, 20: 30196(T) (NASA-TT-F-389, pp 8-25)
properties of, review of, 20: 37489
properties of, survey (E/T), 19: 3173
properties of, survey on, 20: 30204(T) (NASA-TT-F-389, pp 375-86)
properties, review of, 20: 46492
proton density distribution in, computer program for mapping, 19: 41954 (NP-15338)
proton density in inner, effects of solar cycle variations on, (T), 20: 15590 (NASA-TN-D-3086)
proton density variation with solar cycle, computer program for calculation of, 20: 17539 (N-65-18257)
proton detectors for inner zone of, 18: 7087
proton diffusion in outer, (T), 19: 47461
proton distributions in inner, 18: 44485
proton distributions at 40 to 110 Mev in, 19: 6589
proton distribution and energy in inner, 20: 13647
proton distribution in, altitude and time dependence of 55-Mev, (E), 20: 6200
proton distribution at 0.17 to 3.4 Mev in, 20: 32250
proton distribution in, 19: 16763
proton distribution in outer, effect of solar flare on, (E), 19: 41312
proton energy and intensity in South Atlantic magnetic anomaly, (E), 19: 27336
proton energy and pitch angle variations in outer, 19: 37705 (N64-27247)
proton energy and spatial distributions in inner, 20: 11825
proton energy and spatial distributions in, 20: 39957(T)
proton energy spectra in, 17: 25968
proton energy spectrum of inner, spatial variation of, 17: 31261
proton energy spectra and flux in inner, 18: 7435
proton energy spectra and population in inner, solar-cycle effects on, 19: 37706 (N64-27250)
proton energy spectra and angular distributions in, 19: 35303
proton energy spectra in, 18: 2747
proton energy spectra and origin in, 18: 5954
proton flux and energy measurements, 17: 6920
proton flux and trajectories in artificial, 17: 34665
proton flux at low altitudes in South Atlantic magnetic anomaly, 18: 18801
proton flux distributions in, 19: 1469
proton flux in, 18: 7633
proton flux in, 20: 34363 (N-66-17248)
proton flux in artificial and outer, 17: 26741 (ORNL-TM-552)
proton flux in environment of earth orbiting vehicles, 20: 32244 (N-66-13126)
proton flux in inner, east-west asymmetry in, 17: 16918 (UCRL-10587)
proton flux in lower edge of inner, (E), 20: 39983
proton flux in outer, 18: 28289
proton flux in South Atlantic magnetic anomaly, (E), 19: 27338
proton flux in, at 6600 to 48,800 km, 18: 5963
proton flux in, from decay of solar neutrons, 20: 21495
proton flux in, from orbiting nuclear reactor, (T), 19: 31589 (AFCRL-64-865)
proton flux in, from orbiting reactor, (T), 19: 37733
proton flux in, ring current effects on, 20: 39970
proton flux measurements in inner, 18: 7635
proton fluxes in, 17: 18385 (TID-7652(p.725-38))
proton-induced radioactivity, hazards for space flight, 17: 28686(R) (UCRL-10683(p.1-14))
proton injection into, by cosmic ray and solar proton albedo neutron decay, 20: 21550
proton intensities in outer zone of, 17: 9173
proton intensities in Brazilian magnetic anomaly at 200–400 km, 19: 35294
proton intensities in, distribution of, 17: 18355 (TID-7652(p.1-11))
proton intensity and spectra in South Atlantic magnetic anomaly, (E), 19: 27337

proton intensity at $3.5 \leq L \leq 10$, (E), 20: 17548(T)
proton intensity distribution in, model for, (T), 20: 32292
proton intensity in, 19: 16326 (REIC-37)
proton interactions in, hydromagnetic instabilities, 19: 29151
proton lifetime in, 18: 28291
proton lifetimes in, 16: 4666 (D1-82-0117)
proton longitudinal drift in, effect of superimposed electric field on, (T), 20: 44434
proton motion in, magnetic effects of, 19: 37709 (N64-33627)
proton population in, solar cycle effects on, 18: 42528
proton spatial distribution in, analysis of high-energy, (E/T), 19: 45188
proton spectra in inner, at 30 to 40 Mev, 17: 19019
proton spectra in outer, 19: 35299
proton spectrum, 17: 27596 (NP-12905)
proton spectrum in inner, above 12 Mev, 16: 18296
proton spectrum in inner, spatial variation of, (E), 19: 37725
proton time-integrated flux for low-acceleration vehicle trajectories in, 18: 20816
proton trajectories in, (T), 20: 32261
proton trapping in, solar flare, 17: 12899
proton trapping mechanism, 17: 6921
proton-energy spectra in, 18: 26244
protons from, excitation of low-latitude red aurora by, 17: 12873
protons in inner, origin and losses of trapped, 20: 32243 (AD-634704)
protons in outer, model for origin of, 19: 41577
radiation distributions in, engineering models for, (E), 20: 2654 (NASA-SP-71, pp 47-55)
radiation dose from, minimizing, 20: 39158
radiation doses from inner and outer, 20: 2663
radiation effects on solar cells in, 18: 12753
radiation flux on spacecraft in, computer code for, 17: 35236
radiation hazards, 17: 2815 (AD-275605)
radiation measurement in, Explorer VII high-energy, 19: 44973
radiation types and levels in, 19: 11608
radio wave propagation in, by particle-plasma interactions, 17: 32868
radioactivity induced in sodium iodide by trapped protons of, (E), 19: 23524
relation to ionospheric ionization irregularities, 17: 37893 (AFCRL-62-352)
review, 17: 28055
review, 18: 11093
review, 18: 14755 (AD-401660)
review of satellite studies, 17: 20822
ring currents in, origin, 16: 6888(T) (FTD-TT-61-162)
ring currents in region, origin, 16: 890
shielding manned space vehicles against, (T), 20: 3245 (NASA-SP-71, pp 407-14)
shielding of manned space vehicles from, 17: 16877
shielding space vehicles against, 17: 22769
shielding space vehicles from, use of selective vehicle orientation for, (T), 20: 3249 (NASA-SP-71, pp 473-6)
silicon photoelement lifetime in, 17: 27891 (JINR-P-1247)
solar cell lifetime in, estimation, 16: 18084 (LMSD-703735-1)
solar flare effects on, 16: 27894
solar radiation effects on properties of, 18: 28464
spectra in outer, 16: 29617
spectra of energetic particles in inner, 17: 5195
stability, 16: 23223
stability against interchanges, (T), 19: 37723
stability of outer, kinetic, 20: 39964(T)
stability of, electron and proton critical flux effects on, (T), 20: 37910
stability of, interchange, (T), 20: 11835
structural changes of outer, solar magnetic storm associated, 17: 24246
structure and properties of outer, 16: 8087
structure at 320 km, 18: 28292
structure of, changes in, 18: 5964
structure of inner, correlations with charged-particle motion in magnetosphere, (T), 20: 34393
structure of outer, during main phase of geomagnetic storm, (T), 19: 12420
structure of, effects of ionospheric electrostatic fields on, (T), 19: 41593
structure of, model for, 20: 36109
structure of, review of, 20: 37899
structure variations during geomagnetic storms, (T), 20: 11838
synchrotron radiation calculations for, 17: 31250
trapping mechanism in, 17: 12902

VAN DE GRAAFF ACCELERATORS

acceleration tube for, alternating-gradient, 20: 25667
accelerator tube conditioning for Saclay tandem, 20: 46266
alpha particle acceleration in tandem, 16: 25910(R) (NP-11749)
analysis of data from, DIDJERIDOO program for, (E), 19: 30638 (ANL-6993)
auxiliary equipment for ORNL 5- or 5.5-Mev, engineering drawings for, 17: 33139
beam bunching system for, nanosecond, 19: 16313
beam bunching system at AWRE, klystron, 20: 27670
beam control devices for ORNL, engineering drawings for, 18: 42251
beam current measurement during operation, 18: 24251(T,R) (AEC-tr-6316(p.425-30))
beam deflection system for, using two 45° magnets, 17: 2354
beam energy calibration of, methods for, 18: 739
beam energy calibration by backscattering measurements, 19: 2933
beam energy calibration of Dacca, 20: 19284 (AECD-EP-8)
beam energy fluctuations in, device for reducing, 18: 20709(P)
beam energy of, system for modulating, 19: 20746
beam energy regulation for Princeton Synchrotron, 19: 37299
beam energy resolution at 1.75 Mev in 3-Mev, 16: 29895
beam energy stabilization systems for, design of, 18: 22642
beam focusing and calibration using a magnetic analyzer, 18: 14681 (NP-13617)
beam injection system of, 5.5-Mev ion buncher for, 20: 13379
beam injection system for, design of nanosecond ion pulsed for, 20: 37337
beam ionization stages, spectral method for determining, 20: 19402
beam-pulsing apparatus, design, 16: 13750
beam pulsing in, lens pulser for duoplasmatron, engineering drawings, 17: 22764
beam pulsing system for, design of nanosecond, 18: 26176
beam-pulsing system with rf-type source, 16: 13764
beam stabilization system for 2-Mev, design of fast, 20: 19295 (CERN-66-11)
beam stacking in CERN accumulation and storage ring for, r-f, 19: 28941 (CERN-65-8)
beam transport in, electrostatic lens system for, 19: 29228(R) (AEET/NP/10)
beam-pulsing method on proton, for metastable lifetime measurements, 19: 12512
beams, energy resolution improvement method, 16: 21642 (AD-267612)
beams from, magnet for 90° deflection of, 18: 2505
beams from, properties as atomic emission spectra sources, 17: 29460
calibration of 400-kev, 19: 9727 (ARL-64-151)
characteristics, design, and operation of Trombay, India 5.5-Mev, 17: 15312 (AEET/NP/5)
characteristics of 3-Mev, 18: 24250(T,R) (AEC-tr-6316(p.413-24))
charging characteristics of, 17: 33134
comparison with telecobalt therapy unit, 16: 6284
computer on-line data acquisition for control of, 19: 36927
computer uses on-line with, systems characteristics for, 18: 32019 (LADC-6476)
conference on tandem, 20: 21462 (BNL-948)
construction and performance of tandem, for 2-Mev protons, 17: 22681
control of, development and operation of on-line computer for, 19: 14765(R) (ANL-6977)
control using on-line computer, 20: 19018(R) (ANL-7110, pp 231-310)
corona current in, voltage dependence of, 18: 42623(R) (ANL-6879 (p.21-34))
data analysis for 5-Mev, telemetering equipment for, 18: 36114 (UJV-939/63)
data collection and processing system for, integrated, 17: 38605 (CU(PNPL-227(p.160-2))
data processing system for, computer, 18: 10705
data processing system for tandem, design of, 20: 5939 (LA-DC-7267)
data recording and processing system for Chalk River, automated, 17: 13613 (CREL-883)
data recording system for tandem, automatic, 19: 27033
description and applications of 12-Mev tandem, 17: 33125
description of Dacca 3 Mev, 19: 34817
description of Dacca 3-Mev, 20: 23831
description of double tandem, 20: 21464 (BNL-948, pp 692-703)
description of neutral-beam-injected single-stage tandem, 18: 8966
description of tandem, 16: 33090
description of tandem, 20: 41581(P)
description of 3-Mev electron, at Tokyo, 18: 30353(T,R) (AEC-tr-6231 (p.367-72))
description of 500-kv proton, 18: 6167 (NP-13381)
description of, at installations in India, 20: 5715 (AEET-227
description, design, and operations of 5.5-Mev, (E), 20: 9959(R) (AEET-214)
design, 19: 44890(P)
design, 19: 44891(P)
design, 19: 44892(P)
design and operation of, 17: 24524(R) (NIRL/R/23)
design and operation of 5-Mv, 18: 40091 (NP-14336)
design and operation at Harwell, 19: 48115
design concepts, 18: 20708

design, construction, and operation of, safety measures for, 17: 34171
design for pulsed electrons, 18: 20583 (PAN-473/II)
design of high-intensity nanosecond pulsed, 16: 19823 (TID-15647)
design of pressurized, 18: 36117
design of pressurized ion, 19: 41181
design of tandem, 20: 13401(P)
design of terminal electronic circuits in 2-Mev pulsed, 17: 26656
design of 0.5-Mev, for electrons at University of Guanajuato, Mexico, 16: 7259
design of 12-Mev tandem, engineering drawings for, 17: 35017
design of 12-Mev tandem, 18: 16616
design of 20-Mev, for protons, 17: 22680
design of 3-Mev, 17: 36739
design of 3-Mev, 17: 36740
design of 3-Mev pulsed, for fast neutron time-of-flight experiments, 16: 33252
design of 3-Mev, at Dacca, 20: 13356 (AECD/EP/6)
design of 300-kev, 17: 21123
design of 4.5-Mev pressurized, 16: 7182
design of 6-Mev, 18: 10682 (IKF-7)
design of 600-kv, 18: 34373(T) (JPRS-25692)
design to prevent electron loading, 20: 35980(P)
design with inclined electrodes, 20: 19315
development, 17: 20564(R) (TID-18442)
development, 18: 11195(R) (EANDC(E)-49(L))
development and history of, review of, 18: 4369 (TID-18191)
development and operation, 19: 17179(R) (BNL-841(p.1-17))
development at Karlsruhe Nuclear Research Centre, 19: 17442
development at ORNL, 18: 28187(R) (ORNL-3578(p.122-6))
development for nuclear structure studies, 19: 33704
development in Japan, 19: 36829
development of ion sources and nanosecond pulsers for, 19: 42964(R) (ORNL-3782, pp 144-52)
development of Minnesota Emperor Tandem, 20: 35968(R) (TID-22971, pp 1-40)
development of 2-Mev positive ion, 20: 9608(R) (ANL-7029, pp 13-14)
development of 5-Mv, 20: 41541(R) (ORNL-3875, pp 159-63)
development status of ORNL, 20: 39470(R) (ORNL-3924)
developments at ANL, 17: 41529(R) (ANL-6720(p.29-42))
electrode system for, electrolytic trough measurements for, 20: 46261
electrodes for large, design of high-voltage, 19: 37427(P)
electron beam from, energy spectrum of, 17: 30124
electron beam scanner for, design of wide area, 19: 37295
electron dosimetry in 2-Mev, using cerium sulfate solution, 19: 47177
energy modulation in 3.6-Mev, 17: 7307 (BNL-5792)
energy resolution in 3-Mev, 17: 36669 (WASH-1042)
energy standards for, development of absolute, 19: 28973
equipment for 3- and 5-Mev, engineering drawings of, 18: 5895
helium-3 acceleration in, doubly ionized, 19: 16311
instrumentation, development for 3- and 5-Mv ORNL, 16: 11864(R) (ORNL-3191(p.89-91))
instrumentation development for, 17: 14615(R) (ORNL-3378(p.80-93))
instrumentation development for, 20: 8062(R) (COO-720-058)
instrumentation systems for, development of transistorized, 17: 32347
insulators in, use of sulfur hexafluoride as, 19: 37293
ion beam injector for, design of pulsed, 18: 44326
ion beams from 4-Mev, with high intensity and resolution, 19: 23220
ion beams in, water vapor jet target for charge changing of, 19: 18645
ion pump operation on, 19: 37300
ion source and instrumentation, development, 17: 1175(R) (HW-70050 (p.31-77))
ion source current increase, 16: 14113
ion source design for, 18: 12814
ion source for, gas flow regulator for r-f, 17: 4160
ion source for pressure-type, design of duoplasmatron, (E), 19: 18639
ion source for, design of doubly charged helium, 19: 37291
ion source for, negative, 20: 39500
ion-source leak-control systems design for, 17: 41211
ion source movement by remote control during operation, 16: 13749
ion sources for, engineering drawings of, 17: 35016
ion sources for 3-Mev, design of pulsed, (E), 20: 9977 (TID-22403)
ion sources for, development of duoplasmatron, 19: 11883
ion sources for, divalent helium, 19: 27032
ion sources for, duoplasmatron and r-f, 19: 37289
ion-channel for 2-Mev, development of, 20: 21480
laboratory design for 5.5-Mev, at Padua, 17: 9653
magnetic field regulator development, 17: 15251(R) (CU(PNPL)-220)
measuring equipment for, design of remotely operated, 18: 28195
modification and operation of ANL, 17: 41536(R) (ANL-6767)
neutron experiments at Argonne, 20: 9945
neutron production at 2 to 100 kev in, 16: 14072
operation and testing of tandem, 17: 22264(R) (ANL-6679)
operation and use, 16: 12210(R) (ANL-6488)
operation at Osaka, Japan, experiences in, 18: 30352(T,R) (AEC-tr-6231(p.14-33))
operation of ANL 4.5-Mev, 16: 3529(R) (ANL-6432)
operation of electron, pulsed-beam, 19: 28969
operation of Indian 5.5-Mev, Apr. 1962–Dec. 1963, 18: 42620(R) (AEET/NP/8)
operation of Ohio State, summary for 1961, 16: 12444(R) (TID-15124)
operation of tandem, 17: 2345
operation, ozone generation hazards in, 16: 27296 (HW-SA-2283)
operations of 5-Mev, 18: 10702
performance and use as radiation source, 19: 12020
performance as a neutron source in activation analysis, 20: 36146
performance of inverted cone accelerating tubes, 17: 15335
power fluctuations of, in radiation chemistry studies, 18: 26171(T) (AEC-tr-6372(p.511-20))
power supply regulator for, design of, 17: 2051(R) (CU(PNPL)-219)
properties of positive-ion, for neutron sources, 17: 29568
properties of, for use in food sterilization studies, 20: 39303
pulse generator for 2-Mev, nanosecond, 20: 17217
pulsed beam techniques for, nuclear resonance fluorescence measurements using, 18: 15319
pulsed-beam time-of-flight system of, design of pulse shape discriminator for, 16: 29876 (HW-SA-2637)
pulsing equipment design, 16: 20472(R) (RRL-79)
pulsing modification, 16: 2495(R) (TID-14256)
pumping system for, 20: 46265
radiation damage studies using, solid-state, 18: 32247
radiation dose distribution for electron, inhomogeneity of, 20: 4204
radiation from, medical aspects of exposure to, 17: 22692
radiation levels around 3-Mev Dacca, gamma, 20: 25649 (AECD-HP-4)
radiation monitor system for Los Alamos, 19: 37355
radiation monitor system for large, audio-visual warning, 20: 5733 (LA-DC-6790)
radiation monitoring in vicinity of, at ORNL, 17: 14609(R) (ORNL-3378 (p.22-7))
research at 12-Mev tandem, 20: 4823(R) (ANL-7081, pp 36-69)
research at 4.5-Mev, 20: 4822(R) (ANL-7081, pp 22-35)
research programs for 5.5-Mev, 17: 20564(R) (TID-18442)
research programs using, at Karlsruhe, 18: 24246 (NP-13930(p.137-8))
research progress on tandem, 18: 14592(R) (PR-P-60)
shielding of 12.5-Mev tandem, effectiveness of, 20: 23820 (ANL-7139)
spectrometer for use with, engineering drawings of time-of-flight, 18: 5678
target apparatus for, engineering drawings of, 19: 23231
target cooling system for, 20: 18877
target preparation, carbon and hydrogen, 16: 5388
target preparation and contamination, 17: 10849(R) (HW-73337(p.29-76))
terminal voltage measurements on, using generating voltmeter, 18: 24242 (CONF-22-33)
therapeutic use, beam direction and dosimetry for, 18: 11925
use as fast neutron source in activation analysis, 18: 15955 (NP-13761)
use as high-voltage source in 200-kev accelerator for generating 14-Mev neutrons, 19: 47176
use as neutron source for activation analysis, 17: 32009
use as neutron source in activation analysis, 18: 15956 (NP-13762)
use for generating slow neutrons, 17: 806 (TID-16985)
use for micrometeoroid simulation, 18: 20707
use for research in nuclear physics, 20: 21463 (BNL-948, pp 685-91)
use in biological irradiations, 20: 32902
use in fast neutron time-of-flight systems, 18: 27793
use in industrial radiography, exposure curves of two films for, 18: 26175
use in nuclear physics research program in Pakistan, 19: 25089 (AECD/EP/1)
use in optical atomic spectroscopy, 18: 28254
use in optical spectroscopy, 18: 8969
use in radiation chemistry in Japan, 17: 30044
use in radiation damage studies of metals, 16: 16795
use in soft fruit preservation at Wageningen, 18: 12508
use in space radiation simulation, 18: 29856
use in space radiation simulation, 18: 29857
use of 2-Mev, in radiation chemistry, 20: 43328
use to accelerate micron-size particles up to 14 km/sec, 16: 14123
uses as proton source for irradiation of solids, 20: 25662
voltage calibration of 400-kv, technique for rapid, 20: 37331
voltage stabilization of 400-kv, circuit for, 19: 9727 (ARL-64-151)
voltage stabilizer for, 18: 32247
voltage stabilizer for 500-kev, design of, (E), 20: 7670 (INFN/TC-64/5)

VANADATES

see also Ammonium Vanadates
see also Calcium Vanadates
see also Cerium Vanadates

see also Cesium Vanadates
see also Chromium Vanadates
see also Fluovanadates
see also Gadolinium Vanadates
see also Lanthanum Vanadates
see also Lithium Zinc Vanadates
see also Neodymium Vanadates
see also Plutonium Vanadates
see also Potassium Uranyl Vanadates
see also Potassium Vanadates
see also Rare Earth Vanadates
see also Rubidium Vanadates
see also Scandium Vanadates
see also Sodium Uranyl Vanadates
see also Sodium Vanadates
see also Sodium Vanadyl Vanadates
see also Uranyl Vanadates
see also Yttrium Vanadates
alkyl ortho-, decomposition in ion source of mass spectrometer, 20: 14584(R) (TID-22444)
analytical use as oxidimetric reagent, review, 16: 12984
analytical use with uranium, 19: 9090
determination of, using triphenylarsine oxide, 20: 18607
effects on complexometric titration of zirconium, 18: 41336
hydrolysis of vanadate ions, rate constants for polymeric, 20: 33309
oxidation and reduction of, controlled potential coulometric studies of, 19: 13896(R) (NUMEC-2389-4)

VANADIUM

see also Transition Metals
abundance in 3 Centauri A, 17: 32851
alloying characteristics with rare earths, 18: 41924(R) (IITRI-578P19-13)
alloying effects on properties of niobium, 16: 7897 (WADC-TR-57-344 (Pt.V))
alloying effects on oxidation resistance of aluminum–niobium–titanium–zirconium alloys, 16: 9248(P)
alloying effects on tantalum and tungsten alloys, 16: 13562(R) (AD-259116)
alloying effects on beryllium binary systems, 16: 13593(T) (CEA-tr-X-259)
alloying effects on iron-titanium hardness, 16: 12129
alloying effects on strain-aging in niobium alloys, 16: 21063
alloying effects on oxidation of niobium–zirconium alloys in air and steam, 16: 32078 (AERE-R-4134)
alloying effects on oxidation of $NbAl_3$ at 760°C, 16: 27590(R) (DRI-2043)
alloying effects on corrosion of chromium–molybdenum steel by carbon dioxide, 16: 29344(T) (AEC-tr-5303)
alloying effects on delta-prime phase of plutonium, 17: 3535
alloying effects on aluminum–niobium alloy oxidation, 17: 4902(R) (DRI-2061)
alloying effects on iron–nickel–tungsten alloys, 17: 14826(R) (LAR-14)
alloying effects on iron–nickel–tungsten alloys, 17: 14827(R) (LAR-17)
alloying effects on titanium, 17: 16580(P)
alloying effects of, on oxidation of niobium alloys, 17: 22122
alloying effects on corrosion of zirconium by steam and water, 17: 23889(R) (ARF-B198-39)
alloying effects on mechanical properties of solid-solution-strengthened niobium alloys, 17: 24001
alloying effects on mechanical properties of aluminum alloys, 17: 32608
alloying effects on corrosion resistance of niobium to steam at 540°C, 17: 36221 (BMI-1636)
alloying effects on hardness of chromium, 17: 37548
alloying effects on molybdenum–niobium–uranium–zirconium alloys, 17: 39644
alloying effects on aluminum–zirconium alloys at 800 to 1000°C, 17: 39657
alloying effects on austenitic steel, 17: 41437(T,R) (EURAEC-598)
alloying effects on grain-refinement and beta to alpha transformation in uranium, 17: 41468
alloying effects on corrosion of zirconium by steam, 18: 7134 (AERE-R-4458)
alloying effects on corrosion resistance of zirconium in carbon dioxide, 18: 12576 (GEAP-4089(Vol.I)(Paper 3))
alloying effects on niobium corrosion by lithium, 18: 14409 (ORNL-3551)
alloying effects on oxidation of niobium–zirconium alloy at 500 and 1000°, 18: 14413(T) (FTD-TT-63-1020)
alloying effects on properties of niobium and tantalum for high-temperature use, 18: 14454 (BM-RI-6390)
alpha reactions (α,Li^6) with, 18: 16951(R) (TID-20311)
alpha reactions with, gamma distribution from, 16: 21457
analysis and determination, 20: 14500
analysis for carbon dioxide, carbon monoxide, hydrogen, and nitrogen by hot-vacuum extraction, 17: 14147 (PG-Report-412)
analysis for carbon, 18: 13639 (PG-Report-494)
analysis for chloride, turbidimetric, 17: 17968 (PG-Report-339)
analysis for hafnium or zirconium using catechol violet, colorimetric, 19: 19780
analysis for impurities, chemico-spectrographic, 18: 13708
analysis for nitrogen and oxygen by d-c carbon-arc, gas chromatographic technique, 19: 9069
analysis for oxygen, comparison of inert-gas fusion and vacuum extraction methods for, 16: 28872 (TID-11794)
analysis for oxygen, 17: 27257
analysis for oxygen, activation, 20: 16331 (GA-6568)
analysis for tantalum by anion exchange in hydrofluoric–nitric acid mixtures, 18: 35455
analysis for thorium using *N*-benzoyl-*N*-phenylhydroxylamine, gravimetric, 19: 46194
analysis for titanium, spectrographic, 17: 2907 (WAL-TR-823.5/1)
analysis of, separation of interfering elements prior to activation, 20: 26775
argon ion sputtering, atom ejection patterns in, 16: 2203(R) (TID-14257)
atomic Slater-Condon parameters for, 17: 2426
atomic weight of, from isotopic abundance measurements, 19: 4353 (IS-921)
Auger spectra of, relative intensities of transitions in KLL, 17: 41976
bibliography on, Defense Metals Information Center selected accessions, January 1963, 17: 14739 (NP-12525)
bibliography on, DMIC selected accessions, Sept. 1962, 17: 419 (NP-12170)
bibliography on, DMIC accessions, May 1963, 17: 29246 (AD-407822)
bonding to itself and other refractory metals by solid-state diffusion methods, 19: 16050(P)
bonding to refractory metals, temperature requirements for solid-state diffusion, 17: 25688(R) (GEMP-177A)
bonding to uranium carbide and iron–uranium carbide cermets, 20: 9468
book: *Behavior and Properties of Refractory Metals*, 19: 14066
book: *Critical Review of the Analytical Methods of the Titanium, Vanadium, and Chromium Transition Element Groups*, 18: 3702
book: *Rare Metal Extraction by Chemical Engineering Techniques*, 18: 13952
book: *Vanadium, Niobium, Tantalum. The Metallurgy of the Pure Metals and Their Alloys*, in German, 18: 25906
brazing tubes of, in cryostat and oven fabrication, 19: 16027 (CEA-R-2618)
brittle-ductile transition, 16: 21068
carbon ion reactions in, gamma ray emission from, 16: 29831 (BNL-5922)
carbon-12 reactions, gamma distribution from, 16: 21457
charged particle reactions with, cross sections for, 17: 34886 (UCRL-10783)
chemical properties in lithium chloride-potassium chloride eutectic, 16: 25306 (CEA-2125)
chromium-atom slowdown paths at 20 to 90 ev in, (E), 19: 33512
cladding of, electrolytic, 18: 14439
combustion of, in fluorine, calorimetry of, 16: 28641(R) (ANL-6543)
compatibility of coatings of, with plutonium, thorium, and uranium, 17: 8843
compatibility with bismuth germanium telluride at 500 to 700°C, 17: 23971 (WCAP-1868)
compatibility with sodium at 650°C, 17: 41333(R) (ANL-6677)
compatibility with uranium carbide and uranium carbide–uranium sulfide at 1150°C, 17: 40422(R) (ANL-6784)
compatibility with plutonium carbide–uranium carbide, 18: 8729 (UNC-5074)
compatibility with fissium–plutonium–uranium alloys at 550 to 650°C, 18: 19456(R) (ANL-6840)
compatibility with fissium–plutonium–uranium alloys at 500 and 600°C, 18: 26893(R) (ANL-6868(p.11-108))
compatibility with fissium–plutonium–uranium alloy, 19: 2839
compatibility with uranium carbide and uranium carbide–10 uranium sulfide at 1150°C, 20: 9556
compatibility with plutonium–uranium carbides at 590 and 820°C, 20: 9437
compatibility with plutonium-uranium carbides, 20: 6600(R) (ANL-7105, pp 1-35)
compatibility with plutonium carbides at 1200 to 1400°C, 20: 29820
compressibility at high pressures, 17: 3494 (UCRL-6696-T)
content and distribution patterns of, in natural waters of Umra, Rajasthan, 17: 29098
content in high-purity depleted uranium metal, 19: 24481 (GAT-T-1141)
content in high-velocity A stars, 18: 36135
content in lignites, role of lignin in, 17: 25438
content in organs and tissues of humans outside continental U. S., 19: 21831
content in red giant stars, theory for, 18: 16634

content in red-colored Paleozoic deposits in Northern Tien Shan, 20: 14780(T) (AEC-tr-6579)
content in river waters, 17: 30687
content in sun, deviations from thermodynamic equilibrium in, 18: 30387
corrosion, 16: 27589 (BM-RI-5990)
corrosion by ammonium hydroxide, sodium hydroxide, and sodium hypochlorite at 35 and 60°C, 20: 11230 (BM-RI-6715)
corrosion by cesium at 750°C, 18: 20873
corrosion by chloride solutions at 35, 60, and 100°C, 20: 11230 (BM-RI-6715)
corrosion by formic, hydrochloric, and oxalic acids at 35°C, galvanic, 20: 11230 (BM-RI-6715)
corrosion by impurities in liquid metal coolant in Dounreay Fast Reactor, 16: 26475 (TID-7622(p.35-56))
corrosion by liquid lithium, effects of oxygen on, 18: 14409 (ORNL-3551)
corrosion by lithium, effects of oxygen, 16: 22552
corrosion by lithium at 1500 to 1900°F, 17: 6570 (ORNL-2674)
corrosion by lithium, effects of carbon, nitrogen, or oxygen on, 18: 27914
corrosion by lithium at 1600°F, 19: 36980 (PWAC-355)
corrosion by nitric acid at 35°C, galvanic, 20: 11230 (BM-RI-6715)
corrosion cracking by inorganic and organic acids and inorganic salt solutions, stress-, 20: 2254 (BM-RI-6680)
corrosion in reactors, 19: 20488
corrosion of, book, 18: 22451
corrosion of, by acids and bases, crevice, galvanic, and spray, 20: 11230 (BM-RI-6715)
corrosion resistance to mercury at 900°F, 20: 2264
creep and rupture of, numerical methods for analysis of, 20: 15041 (GEMP-397)
critical fields in films of, (E/T), 20: 21915
crystal lattice calculations for nitrogen impurity in, 19: 1951 (BNL-7906)
crystal lattice calculations for point defects in, 19: 1953 (BNL-8435)
crystal lattice vibrations in, inelastic neutron scattering measurements of, 20: 42573
crystal lattice wave spectrum of, 17: 38033(T) (AEC-tr-5734(p.196-8))
crystal structure, effects of cold-rolling and annealing, 16: 30824
crystal structure of, 17: 41873 (WASH-1044)
crystal structure deformation at 4.2 to 373°K, flow and yield stress measurements of, 18: 44213
crystal structure deformation in, mechanism of thermally activated flow in, 18: 44214
crystal structure at 110 to 400°K, 20: 7614
current fluctuations in superconducting, 18: 26484
deformation by filing at room temperature, x-ray-diffraction study of, 17: 25768 (AD-403526)
deformation, thermally activated, 17: 27879
deposition by electrolytic methods, 20: 35870
deposition from fused salt mixtures, electro-, 20: 11260
deposition from fused fluoride bath, 19: 11711
deposition from molten fluorides, 19: 16034
deposition in organic solvents, electrolytic, 18: 13602 (BM-RI-6303)
deposition of superconducting films, 18: 13014
deposition on other metals by electroplating methods, 19: 42827
determination as cinnamoylphenylhydroxylaminate, photometric, 20: 22942
determination as impurity in and volatilization from tungsten, semi-quantitative spectrographic, 16: 4131 (BM-RI-5903)
determination as trace in standard rocks G-1 and W-1, spectrographic, 16: 20831
determination as trace impurity in uranium, 18: 29591
determination as trace impurity in plutonium–thorium–uranium and thorium–uranium alloys, 19: 17798
determination by activation, substoichiometric, 18: 21997
determination by activation analysis, interference of (n,p), (n,α) to (n,γ) reactions in, (E), 19: 29318
determination by complexometric methods using EDTA, 19: 46219
determination by charged-particle reactions at 2 Mev, 20: 43097
determination by neutron activation, 16: 18827
determination by re-activation, 18: 10007
determination by spectrochemical methods, voltage-fluctuation patterns in, 19: 40416
determination by thermal-neutron activation methods, sensitivity for, 19: 9071
determination in alloys, spectrophotometric, 16: 26943
determination in aluminum, x-ray spectroscopic, 17: 10571
determination in artificial graphite, 18: 9584
determination in aluminum, activation, 18: 43407
determination in aqueous solutions by radio release method using silver-110, 19: 4069
determination in alloys using vacuum cup electrode, spectrographic, 19: 22103 (TIM-904)
determination in aluminum, activation, 19: 28224 (SGAE-CH-13/1964)
determination in automobile lubricants, activation, 20: 14439(R) (GA-5556)
determination in aluminum, activation, 20: 22896
determination in aqueous solutions, design of oxyacetylene burner for measuring sensitivity of spectrophotometric, 20: 29083(R) (UCRL-14767)
determination in biological materials, activation, 16: 23403
determination in beryllium by activation, 19: 24415
determination in biological material by neutron activation methods, 19: 40421
determination in blood using neutron activation analysis with pre-irradiation separation, 20: 1791
determination in biological materials and drinking water, activation, 20: 38565
determination in clay, acetic acid leachates, sand, and silt, spectrochemical, 16: 4379
determination in cerium and erbium, mass spectrographic, 19: 2232
determination in copper, activation, 20: 16332 (GA-6691)
determination in diabase W-1 and granite G-1, spectrographic, 16: 17895
determination in fused lithium chloride–potassium chloride eutectic, controlled potential coulometric, 18: 6748
determination in graphite, activation, 17: 15916
determination in graphite, spectrographic, 18: 3681
determination in ginseng by activation methods, 19: 42446
determination in hydrochloric acid or methanol–nitric acid media, spectrophotometric, 20: 3888 (TID-22402)
determination in high-purity tantalum by spectrography using d-c arc method, 20: 20608
determination in iron, activation, 19: 10980 (EURAEC-1273)
determination in igneous and metamorphic apatites, spectrographic, 20: 26787
determination in Korean Schinseng roots by activation, 17: 30121
determination in lanthanum oxide, spectrographic, 20: 22895
determination in milk powder, activation, 18: 1585
determination in mixture with uranium using potassium dichromate, titrimetric, 18: 33496
determination in mixtures by x-ray fluorescence using promethium-147/aluminum and tritium/zirconium sources, 20: 3883 (ORNL-IIC-5, pp 154-81)
determination in minerals and rocks using paper chromatography, 20: 35389 (CEA-R-2791)
determination in natural water, quantitative spectrographic, 16: 17597
determination in niobium by radioactivation analysis, 16: 23633 (TID-7629(p.239-44))
determination in nuclear-grade graphite, spectrochemical, 17: 40733
determination in nuclear grade graphite, spectrochemical, 19: 43930 (JEN-145-DQ/I-46)
determination in ore concentrates, volumetric, 16: 2965 (PG-Report-264)
determination in organic reactor coolants, spectrographic, 18: 184
determination in ores, activation, 18: 13626(R) (NYO-10174)
determination in oils, activation, 20: 1739(R) (GA-4297)
determination in oil samples in water, activation, 20: 14439(R) (GA-5556)
determination in powdered milk, activation, 18: 10028
determination in petroleum and its products, activation, 18: 15968
determination in presence of cerium and iron using potassium dichromate, potentiometric, 18: 25308
determination in powdered samples by spectrochemical methods, 19: 22120
determination in petroleum, activation, 20: 29139
determination in presence of cerium, amperometric, 20: 35434
determination in plutonium by carrier distillation methods, spectrographic, 20: 40814 (RFP-664)
determination in powder samples by spectrographic methods, semi-quantitative, 20: 43104
determination in rubber, activation, 17: 130
determination in rat liver tissue, activation, 17: 38935
determination in reactor graphites by double arc method, 19: 9084
determination in reactor coolants, polarographic, 19: 11003
determination in stratospheric aerosols, 16: 25609 (AFCRL-62-299)
determination in SAP, x-ray spectrographic, 17: 27226 (EUR-21.f)
determination in surface waters by activation analysis, 18: 37072 (A/CONF.28/P/854)
determination in solids by spark source mass spectrometry, quantitative, 19: 13247
determination in sodium uranate, spectrochemical, 19: 15367
determination in sea water by quantitative solvent extraction and spectrography, 19: 28253
determination in tissue, after neutron activation, 17: 31813 (AERE-R-4309)
determination in tantalum by d-c arc method, spectrographic, 18: 19894
determination in tantalum by anion exchange in hydrofluoric–nitric acid mixtures, 18: 35455
determination in titanium dioxide, activation, 19: 19771(R) (TEES-2671-4(Chap.9))
determination in uranium compounds by reversed-phase partition

chromatography, 16: 23636 (TID-7629(p.276-84))
determination in uranium base alloys, photometric, 16: 26928
determination in uranium tetrafluoride, spectrographic, 17: 1391 (TID-17030)
determination in uranium(IV-VI) oxide by carrier distillation excitation, effects of graphite electrode grade on, 17: 10538 (TID-16295)
determination in uranium-233-labeled uranium dioxide, spectrographic, 18: 9980
determination in uranium, spectrophotometric method using 8-quinolinol, 18: 17754
determination in uranium alloys, photometric, 18: 19845 (JAERI-1053)
determination in uranium and its compounds and alloys, methods for, 19: 19823
determination in uranium compounds, colorimetric, 20: 12802
determination in uranium tetrafluoride, spectrographic, 20: 14473
determination in uranium compounds after separation by solvent extraction using *N*-benzoylphenylhydroxylamine, spectrographic, 20: 24976 (GAT-524)
determination in water, silver-spark spectrographic, 17: 1381 (IDO-14591)
determination in zirconium and zirconium alloys, spectrographic, 17: 2907 (WAL-TR-823.5/1)
determination in zirconium by activation, 19: 24418
determination in Zircaloy-2, spectrographic, 20: 29113
determination in 18/8 steel, thermal neutron activation, 17: 35647
determination of, in residues by iron flux method, spectrographic, 17: 19942 (PG-Report-157)
determination of, in uranium using benzoylphenylhydroxylamine, colorimetric, 17: 23251 (GAT-T-1085)
determination of, in uranium concentrates and ores, spectrographic, 17: 23254 (PG-Report-220)
determination of, in uranium using Xylenol Orange, 17: 38944
determination of trace amounts, catalytic colorimetric method, 17: 1404
determination of traces in marine organisms, activation, 17: 4468
determination of traces in petroleum, activation, 17: 21647
determination of traces of, using oxycellulose, 17: 35656
determination of trace amounts of, in iron, activation, 20: 14471
determination of trace amounts of, in beryllium by spectrography, 20: 16352
determination of trace amounts of, by reactor neutron activation methods, 20: 26760
determination of traces of, in biological materials, activation, 20: 38837
determination of, use of azo dye in spectrophotometric, 17: 35945
determination of, optimum sample position in activation, 18: 19906
determination of, paper chromatographic methods for, 18: 29600
determination of, tracer techniques for, 18: 33483
determination of, properties of formaldoxime for spectrophotometric, 18: 39085
determination of, review on methods for, 19: 22108
determination of, using 5,7-dibromo-8-quinolinol, 19: 36289
determination of, in alloys, cast iron, and steel, differential amperometric, 20: 33246
determination simultaneously with molybdenum or uranium, potentiometric, 17: 38961
determination using aniline, benyidine, or α-naphthylamine qualitative, 16: 25276(T) (AEC-tr-5250)
determination using Xylenol Orange, colorimetric, 18: 43416
determination using plasmochin, colorimetric, 19: 7301
determination using acid alizarin black SN, spectrophotometric, 19: 24408
determination using 5,7-diiodo-8-hydroxyquinoline (diiodoxine), heterometric, 20: 257
determination with titanium(III) salts, amperometric, 16: 11572
deuteron elastic scattering at 27.5 Mev, angular distribution for, (E/T), 20: 3057
deuteron reactions (d,t) at 21.6 Mev, 17: 6780(R) (ANL-6603(p.52-5))
deuteron scattering by carbon and mercury impurities in, cross sections for, 18: 26560
deuteron scattering at 26.5 Mev, total cross sections for, (E), 19: 5164
development and properties of, as braze for joining aluminum oxide and niobium–zirconium alloy, 20: 27445 (LA-DC-7159)
development of coatings of, for thermal protection, 17: 410 (DMIC-175)
diffusion barrier between aluminum and uranium, 20: 855
diffusion coefficient measurements in, for vanadium-48 at 1000 to 1900°C, 18: 4172(R) (ORNL-3470(p.67-74)
diffusion in air at 5000°K, 16: 15312(T)
diffusion in beta titanium, 18: 39906 (NRL-6141)
diffusion in chromium, 18: 39906 (NRL-6141)
diffusion in couples with aluminum, silicon, and uranium, 19: 30731 (EUR-1819.e(p.37-48))
diffusion in molybdenum and tungsten, 16: 2194(R) (NP-11060)
diffusion in molybdenum, niobium, tantalum, and tungsten at 1700 and 1800°C, 17: 1918 (ASD-TDR-62-432)
diffusion in niobium, concentration gradients of, 18: 20512 (ASD-TDR-62-7(Pt.II))
diffusion in titanium, 17: 33859 (ARF-2208-16)
diffusion in, tracer studies of, 19: 11682
diffusion of atoms in bcc, activation energy for interstitial, (T), 19: 40086
diffusion of chromium in, tracer studies of, 18: 16474 (NP-13738)
diffusion of hydrogen in, 19: 16445(R) (ANL-6900(p.304-29))
diffusion of vanadium-48 in, temperature dependence, 18: 27967 (ORNL-3617)
diffusion of vanadium-48 in, 18: 44153 (ORNL-P-425)
diffusion penetration by plutonium–uranium alloys, 16: 28555 (TID-7623 (p.105-21))
diffusion rates of hydrogen through 10-mil-thick, at 500 to 575°C, 18: 2569(R) (ANL-6687(p.188-203))
dislocation on {110} planes in bcc, dissociation of, 20: 33918
dislocation parameters for, 20: 17033
dislocations in primary slip systems of crystals of, dynamical behavior of, 17: 37526
dissociation energy of gaseous and heat of vaporization of solid, correlation of, 17: 6095
dissolution rate in liquid aluminum, 17: 10577 (ANL-FGF-292)
distribution between magnesium chloride and magnesium–zinc alloy at 800°C, 17: 36860(R) (ANL-6648)
distribution coefficient in hydrochloric acid and ion exchange resins, 16: 7503
distribution in tissues and teeth of rats, tracer study of, 18: 38757
ductility of hydrogenated and pure, effects of strain and temperature on, 19: 22980 (IS-T-7)
ductility of, at −269°C, 20: 21416
ductility of, effects of solid-solution hardening at grain boundaries on, 19: 23078
ductility of, effects of nitrogen and oxygen on low-temperature, 20: 4297(R) (IS-1200(Sect.M))
effect on properties of low-alloy steels for reactor pressure vessels, 20: 39444(P)
effects of additions of, on steam corrosion of niobium–tin–zirconium alloys, 20: 2255(R) (EURAEC-1323)
effects of alloy additions of, on mechanical properties of niobium, 20: 11302
effects of alloying additions of, on thermal stability of $TiAl_3$, 20: 11335
effects of, on aluminum-iron alloys, 16: 30820
effects of, on chromium-iron-manganese-nickel alloys, 16: 30822
effects on austenitic grain size and ductility of low-alloy steel, 20: 27481(R) (EURAEC-1419 and App.)
effects on calcium, potassium, and sodium radiation emission spectra in acetylene–air flame, 18: 13701
effects on coatability of niobium, 20: 43827 (GTR-19)
effects on corrosion of chromium–molybdenum steel by carbon dioxide, 16: 22556
effects on corrosion of niobium–tin–zirconium alloys by steam, 18: 18319(T,R) (EURAEC-953)
effects on corrosion of niobium–tin–zirconium alloys by steam, 18: 41938(T,R) (EURAEC-1058)
effects on corrosion resistance of molybdenum–nickel alloys, 18: 41968(P)
effects on corrosion, stability, and strength of niobium, 20: 43905 (ORNL-3212)
effects on crystal field properties of zirconium oxide, 19: 33518 (TID-21946)
effects on crystal field properties of zirconium oxide, 20: 36854
effects on determination of phosphorus in uranium by isotope dilution methods, 20: 8865
effects on ductility of steel, 17: 14862(T) (EURAEC-515)
effects on ductility of iodide chromium, 18: 32189
effects on electric properties of sodium niobates, 16: 22745
effects on fluorescence of uranium in sodium carbonate–sodium fluoride melts, 18: 33506
effects on fracture mechanisms in beryllium single crystals, 20: 23714
effects on hot-cracking susceptibility of Monel, 19: 30751 (WERL-8844-8)
effects on hydrogen embrittlement of steel, 18: 24153(T,R) (EURAEC-1002)
effects on hydrogen distribution in Zircaloy, 20: 11221
effects on mechanical properties of niobium and tungsten, 16: 3443 (ASD-TR-61-3)
effects on mechanical properties of niobium alloys prepared by electron-beam melting, 19: 30768
effects on molybdenum crystallization, 20: 35930
effects on Néel temperature of chromium, (E), 19: 4741 (IS-1033)
effects on oxidation of aluminum–niobium alloys, 16: 10456(R) (TID-14956)
effects on oxidation resistance of refractory metal disilicides, 20: 41424
effects on phase transformations in steel, 18: 24152(T,R) (EURAEC-

1001)
effects on photometric determination of cerium in cast iron and steels, 20: 43143
effects on polarographic determination of uranium, 16: 2982
effects on properties of rare earths, 16: 3474(R) (USBM-U-863)
effects on properties of beryllium–calcium alloys at high temperatures, 18: 35951(P)
effects on properties of tantalum, 19: 41067
effects on properties of boron steel, 20: 39426
effects on properties of beryllium–nickel alloys, 20: 46208
effects on silicide coatings for tantalum-base alloys, 17: 23945(R) (ASD-TDR-63-232)
effects on sintering of zirconium boride, 19: 26794
effects on spectrophotometric determination of aluminum, 19: 13226
effects on spectrophotometric determination of thorium, 19: 24408
effects on spectrofluorimetric determination of scandium, 20: 14476
effects on strength of thorium at high temperatures, 19: 20560 (ORNL-3777)
effects on structure of superconducting Nb_3Al, 18: 34283 (UCRL-11390)
effects on tensile properties of niobium–tungsten alloys, 18: 34197
effects on zirconium alloys for use in reactors, 20: 9560(P)
effects on zirconium alloys for use in nuclear reactors, 20: 9561(P)
elasticity, effects of cerium on, 16: 27660
electric conductivity of, fluctuations in, 17: 666
electric conductivity fluctuations in intermediate state of superconducting, (E), 19: 23578
electric potential fluctuations in mixed state of superconducting, (E), 19: 39709
electric potential of electrodes of, effects of deuterium on, 17: 31989
electrochemical behavior in lithium chloride–potassium chloride eutectic, 17: 30555
electrode potentials, effects of anode polarization on, 17: 25741
electron emission by superconducting films of, on magnesia substrate, 18: 30166(R) (AD-439716)
electron energy loss spectra, 16: 12273
electron energy losses in altered, and mechanisms of, 17: 13165
electron energy loss in films of, 17: 20791
electronegativity, 18: 13797
embrittlement by hydrogen, mechanisms of, 20: 41412(R) (IS-1500 (Sect. M))
energy level fluorescence yields from, K, (E), 20: 15242 (CONF-233 (Vol.3), pp 465-79)
energy level transitions in, Coster-Kronig, (T), 20: 15238 (CONF-233 (Vol.3), pp 398-418)
energy level widths for, K, (T), 20: 15239 (CONF-233(Vol.3), pp 419-39)
explosibility of powders of, 19: 36698 (BM-RI-6516)
extrusion by hydrostatic methods, 19: 18436
extrusion by hydrostatic methods, 19: 44651
extrusion of recrystallized, effects of temperature on, 19: 9604(R) (IS-900(Sect.M))
extrusion of stainless steel-clad, 19: 11711
fabrication and properties as refractory material, 16: 19404
fabrication and properties of, review of, 17: 29253 (NRC-7129)
fabrication and properties for use as superconductors, 18: 34179
fabrication by electroforming, 19: 42827
fabrication of powdered, method for, 18: 34117(P)
fabrication of thin-wall tubes of, methods for, 18: 14423 (CONF-373-9)
fabrication, ore processing, properties, and uses of, 18: 35950
fabrication, oxidation, and properties of, 18: 35986 (ERR-FW-049A)
Fermi surface in vanadium silicides, (E), 19: 23990
fluorescence yields in proportional and scintillation detectors, 18: 3796
forming of, electrolytic process for, 18: 14439
gamma reactions (γ,n) with, neutron angular distribution from, 18: 34935
gamma reactions (γ,n) with, cross sections for, 19: 16961
gamma reactions (γ,α) at 21 and 30 Mev with, spectra and relative yields for, 17: 24481
gamma spectra from 14-Mev neutron activation of, determination by, 19: 26241
gamma spectra of, irradiated by 14.8-Mev neutrons, 17: 2242 (TID-16949)
hardness of cold-reduced, 18: 15426(R) (ANL-6810)
Hartree-Fock potential of neutral atoms of, analytical expressions for, 18: 16656
heat capacity of high-purity, at 0.35 to 25°K, 20: 32684(R) (UCRL-16658, pp 21-38)
helium and hydrogen ion attenuation at 0.1 to 500 Mev, tables for, 20: 41619 (CEA-R-3042)
helium-3 elastic scattering at 20 Mev, differential cross sections for, 18: 21359
helium-3 elastic scattering at 20 Mev, differential cross sections, 18: 26681
hydrolysis in 4-methyl-2-pentanol and acidic sodium perchlorate solutions, distribution of vanadium-48 in, 18: 27415
hydrolysis of pentavalent, scheme for, 19: 46237(R) (ORNL-3832, pp 76-99)
impact testing of, high-velocity, 20: 33490 (CONF-651026, pp 737-68)
interactions in interstitial sites in bcc crystals of, 17: 20460 (UCRL-7184)
ion exchange in concentrated hydrochloric and perchloric acids, distribution coefficients of, 18: 17759
ion exchange paper chromatography of, 18: 17785
iron-57 Mössbauer effect in, localized magnetic moments from, 19: 18511
iron-57 Mössbauer effect at high pressures, 19: 23739
iron-57 Mössbauer spectra in, 20: 30766
machining of, optimum conditions for turning, 19: 30696 (RDB(C)TM-278)
magnetic flux movement through superconducting, energy losses from, (E), 19: 6618
magnetic flux quantization in superconducting cylinders of, 19: 21194
magnetic flux retention in hysteretic superconducting, 20: 44521
magnetic properties of single-crystal, 18: 954 (NP-13274(p.40-6))
magnetic susceptibility, 17: 41333(R) (ANL-6677)
magnetic susceptibilities of, temperature dependence of, 20: 17069
magnetostriction in pure monocrystalline, 19: 39199
mechanical properties of, effects of nitrogen on, 18: 2163(R) (IS-700 (Sect.M))
mechanical properties of electroclad and electroformed, 18: 14439
mechanical properties, 19: 9604(R) (IS-900(Sect.M))
mechanical properties of iodide-refined, effects of nitrogen on strain aging and brittle-ductile transition on, 19: 9658 (IS-994)
mechanical properties of electrorefined, effects of rare earth additions on, 19: 2795 (BM-RI-6553)
melting of, composition of gases evolved during electron beam, 20: 872
melting point of zone-refined, 20: 31721(T) (AD-630971)
melting point of, effects of gas impurities on, 20: 17094
mercury ion sputtering, atom ejection patterns in, 16: 2203(R) (TID-14257)
mesic (μ^-), effect of atomic binding on decay rate of mesons (μ^-) in, 17: 774
meson (μ^-) capture by, K x rays from, (E), 19: 28991 (JINR-P-2039)
meson (μ^-) capture by, probability for, (T), 20: 28456
meson (μ^-) transitions in mesic atoms of, energy of, 20: 4825(R) (ANL-7081, pp 81-93)
meson (μ) capture, Fermi interactions in, 16: 15590
meson (μ^-) capture rate and lifetime in, 17: 775
metabolism in animals, techniques for studying, 20: 32926
metabolism in enamel of teeth, tracer study, 19: 35896
miscibility with other elements, calculation of, 20: 14538
neon ion sputtering, atom ejection patterns in, 16: 2203(R) (TID-14257)
neutron absorption cross section in pitchblende, thermal, 20: 37994
neutron capture by, gamma spectra from thermal, (E), 19: 6695
neutron capture by, gamma spectra from, (E), 19: 19095 (WASH-1053)
neutron capture by, gamma spectra from thermal, (E), 20: 15787
neutron capture cross sections, 16: 26509
neutron capture cross sections, energy dependence of, 18: 15562
neutron capture cross sections at 4 to 220 kev, total, 18: 42650 (TID-21144)
neutron capture gamma spectrum, 16: 28024(R) (ARF-1193-12)
neutron cross sections at 1.44 ev (E), 19: 3288
neutron cross sections at 2.6 to 2.85 Mev, (E), 19: 27400
neutron diffraction at high pressures, 20: 14059(R) (IDO-17104)
neutron diffraction properties of, 20: 26396(R) (IDO-17140)
neutron elastic and inelastic scattering by, cold, 17: 12032
neutron elastic scattering by, spectrum for cold, 17: 38039(T) (AEC-tr-5734(p.227-31))
neutron elastic scattering by, spectra from, (E), 20: 7445(T)
neutron elastic scattering at 3.2 Mev, (E/T), 20: 46644
neutron inelastic scattering cross sections at 0.07 ev, 16: 14064
neutron inelastic scattering in, dispersion curves and phonon spectra from, 16: 32384
neutron inelastic scattering in, phonon scattering spectra from, 16: 32387
neutron inelastic scattering by, 17: 4041
neutron inelastic scattering by, spectrum of, 17: 9064
neutron inelastic scattering by, time-of-flight spectrum for cold, 17: 20972
neutron inelastic scattering by, time-of-flight spectrum for, 17: 20973
neutron inelastic scattering at low energies, 18: 733(R) (TID-19610)
neutron inelastic scattering by, cold, (E), 19: 12076
neutron inelastic scattering by crystals of, properties of cross sections for, (T), 19: 14633
neutron inelastic scattering by, cold, (E/T), 20: 28670
neutron inelastic scattering by polycrystalline, phonon frequency distribution from thermal, 20: 34507
neutron radiative capture cross sections at 30 and 65 kev, 18: 34274(R) (NIRS-2(p.3-15))
neutron reaction rate in foil of, thermal-spectrum, 18: 7026 (AEEW-R-217)

neutron reactions at 3.7 Mev, cross-section measurements, 16: 8224
neutron reactions (n,γ) with, polarization from, (E), 19: 23726
neutron reactions (n,γ) with, spectra of thermal, (E), 19: 35439
neutron reactions (n,γ) at 1 ev to 50 kev, cross sections for, (E), 20: 3032
neutron reactions at 18 to 220 kev, total cross sections for, (E), 20: 40069(R) (EANDC(E)-66(U))
neutron reactions at 21.65 to 152.6 kev, resonance parameters for, (E), 20: 40069(R) (EANDC(E)-66(U))
neutron resonance absorption integrals of, activation measurements of, 17: 26423 (GA-3125)
neutron resonance integrals for dilute solutions of, (T), 19: 29260 (TID-21744)
neutron resonance absorption by, cadmium cutoff energy for, (T), 20: 9951
neutron scattering, phonon frequency distribution in, 16: 7175
neutron scattering angular distribution, 16: 12419 (ANL-5567(Rev.))
neutron scattering, velocity distributions in, 16: 21333 (CRRP-1078)
neutron scattering at 77°K, 16: 31054 (HW-SA-2541)
neutron scattering by, cold, 16: 31873
neutron scattering by, 17: 34560(R) (TID-19195)
neutron scattering by, spectra from inelastic, 18: 24605 (NP-13930(p.59-71))
neutron scattering by, angular distributions in, (E), 19: 8376(R) (GA-5176)
neutron scattering in, multiple, (T), 19: 12577
neutron scattering by, angular distributions of, 19: 31252
neutron scattering at 0.001 to 1 ev, differential cross sections for, (E), 19: 33192(R) (GA-6096)
neutron scattering by, frequency distribution at 20 Mev, (E), 19: 35378(R) (EANDC(E)-57(U))
neutron scattering by, performance of three-axis spectrometer for thermal, 19: 44527
neutron scattering by, spectra for, (T), 20: 26348 (NP-16010, pp 102-39)
neutron scattering by, energy spectra from cold, (E), 20: 31567
neutron spin-orbit interaction in, electronic polarization study of, 17: 15262(R) (TID-18062)
neutron spin-orbit scattering by monocrystalline, polarized, 18: 16894(R) (MIT-3031-1)
neutron spin-orbit interactions in crystals of, 17: 20963
neutron total cross section of, fast, 17: 20982 (HW-SA-2875)
neutron total cross section for, 17: 22568 (WASH-1041)
neutron total cross section at 200 ev to 1 Mev, 17: 36669 (WASH-1042)
neutron total cross section from 3.2 to 5.2 Mev, (E), 19: 14576
neutron total cross sections at 623 to 833 Mev, (E), 19: 35378(R) (EANDC(E)-57(U))
nuclear magnetic resonance and relaxation in superconducting, 18: 7653
nuclear magnetic resonance in superconducting, 18: 15092
nuclear magnetic resonance in superconducting films of, 18: 21117
nuclear magnetic resonance of crystals of, 17: 1926 (D1-82-0194)
nuclear optical potential with i-spin operators for, 18: 9373
nuclear spin relaxation induced by core polarization in, 18: 12787
nuclear spin state amplitudes in, 17: 15262(R) (TID-18062)
occurrence in Cottonwood Wash Mining Area, San Juan Co., Utah, 16: 397 (RME-109(Rev.))
optical properties of small particles of, (T), 20: 5879 (D-910092-6)
oxidation by chromium(VI) ions, 19: 9046(R) (IS-900(Sect.C))
oxidation by water vapor at 1 and 8 torr, 20: 19197
oxidation in hydrochloric, nitric, phosphoric, and sulfuric acids and sodium hydroxide, anodic, 18: 25929
oxidation kinetics and thermochemistry, 16: 4495 (NP-11056(p.3-15))
oxidation kinetics, 20: 29644
oxidation protection of, by ceramic coatings, 20: 7528
oxide films on surface of electrodes of, valency changes in, 17: 25203
oxygen removal from, by contact with gas mixture, 19: 36972(P)
paramagnetic susceptibility of, origin and temperature dependence of, 17: 15262(R) (TID-18062)
particle waves and phonon fission in crystals of, 18: 27874
performance as braze for ceramic-to-metal seals, 18: 44496(R) (MND-2812)
performance as cladding for plutonium–uranium fuel alloys, (E), 20: 14007(R) (ANL-7122, pp 1-41)
performance as coating on fast reactor fuel elements, 18: 26824(R) (ANL-6885)
performance as fuel cladding in fast reactors, 18: 24952(R) (ANL-6880(p.6-48))
performance as fuel cladding for liquid-metal-cooled breeder reactors, (E), 19: 35800
performance as neutron filter, 18: 36080(R) (RPI-328-8)
performance of pelletized, for control of radiant heat transfer in nuclear rockets, (E), 19: 24148 (NASA-CR-210)
phase transformation in, effects of hydrogen content on, 20: 13180(R) (IS-RD-4)
phase transition in alloyed and unalloyed, effects of interstitials on ductile-to-brittle, 16: 25751 (DMIC-Memo-155)
phonon frequency distribution in, 17: 20972
phonon frequency distribution in, low-energy peak in, 17: 20973
phonon frequency distribution function, 19: 20553 (KFK-262)
phonon scattering spectrum of, 17: 38029(T) (AEC-tr-5734(p.167-8))
phonon spectra, 18: 24959 (NP-13910)
phonon spectrum of, by neutron inelastic scattering, 17: 9064
photon reactions with, proton angular distributions and yields at >8 Mev, 17: 28265
physical properties, 16: 15209
plasticity of, effects of hydrogen on, 20: 4297(R) (IS-1200(Sect.M))
polarization in magnetized crystals of, neutron-scattering analysis of electronic and nuclear, 17: 20496
polishing, utilization of "plug" technique in electrolytic, 16: 10440
positron lifetime in, 16: 3626
precipitation using dimethylbenzenearsonic acid, 19: 9136
preparation and properties of single crystals of, 20: 41481
preparation and purification, 20: 4297(R) (IS-1200(Sect.M))
preparation by aluminum reduction of vanadium pentoxide, 20: 2225 (IS-T-40)
preparation by reduction of pentoxide of, using aluminum and carbon, 20: 41412(R) (IS-1500(Sect. M))
preparation, effects of yttrium, 16: 1695
preparation of, by oxide reduction, thermodynamics of, 17: 14269
preparation of crystals of, by electron beam melting, 18: 27871(T)
preparation of, design of apparatus and method for, 17: 20408(P)
preparation of, design of apparatus and method for, 17: 20409(P)
preparation of high-purity, 17: 4447 (IS-500(Sect.M))
preparation of purified, 20: 20365
preparation of, separation of metal from reaction products in, 17: 20410(P)
preparation of single crystals of, 18: 2163(R) (IS-700(Sect.M))
preparation of single crystals of, by arc-zone melting, 18: 18339
preparation of single-crystal, 18: 954 (NP-13274(p.40-6))
preparation of thin films of, use of vacuum-arc process for, 16: 31769
preparation, properties, and purification, 19: 9604(R) (IS-900(Sect.M))
production by proton reactions in iron, 16: 1808(R) (TID-12849)
production in supernova interiors, rapid nuclear processes for, 17: 39835
properties, 16: 3460 (NP-11108)
properties and reactions at elevated temperatures, 16: 4527 (DMIC-160)
properties as cladding for fissium–plutonium–uranium fuel elements, 17: 41333(R) (ANL-6677)
properties as fuel element cladding, 18: 15563
properties as spiked-poison in neutron capture studies of boron, 18: 2798
properties for use as reactor material, 16: 4994
properties for use as canning and structural material for reactors, 17: 35111
properties for use as fuel cladding material, 19: 11679
properties for use as oxidation-resistant coating for uranium, 19: 13925
properties for use as fuel-element cladding, 19: 22884
properties for use as fuel cladding material in reactors, 19: 39206
properties of high-purity, effects of carbon, hydrogen, nitrogen and oxygen, 16: 19337 (BM-RI-5975)
properties of, mechanical and physical, 16: 32134
properties of welded sheaths, sheets, and tubes of, corrosion, mechanical, and physical, 18: 7172
properties of, effects of sodium coolant on, 20: 46995
properties of, for use in furnace for neutron diffraction experiments, 20: 29106
properties of, physicochemical, mechanical, and radiation stability, 19: 26818 (NAA-SR-8617(Vol.III))
properties, mechanical and tensile, 16: 7893 (NP-11196(p.101-4))
proton attenuation at 28.7 Mev in, 17: 37861
proton cross sections at 8.8 Mev, (E), 19: 29276
proton elastic scattering, polarization effects, 16: 4791
proton elastic scattering at 9–22 Mev, optical-model analysis of, 17: 28316
proton inelastic scattering by, effects of E1 resonances on, 16: 33906
proton inelastic scattering at 14.5 Mev, statistical model prediction for yields for, 17: 38206
proton nonelastic scattering cross sections at 10 Mev, 17: 13581
proton reactions (p,n) with, isobaric states from, 18: 14590(R) (NIRL/R/60)
proton reactions (p,n) at 18.5 Mev, angular distributions of quasielastic, 18: 40587
proton reactions (p,Be-7) at 155 Mev with, cross sections for, 19: 1579
proton reactions (p,n) at 30 and 50 Mev, isobaric-state excitation in, (E/T), 20: 6361
proton reactions (p,n) at 30 to 50 Mev, distributions from, 20: 15729(R) (RHEL/R-112, pp 37-66)

proton reactions at 0 to 84 Mev, excitation functions of, 17: 36673
proton reactions at 2.9 Bev, sodium-24 energy spectra from, (E), 19: 8453
proton reactions at 590 Mev and 18.3 Bev, potassium isotope yields in, (E), 20: 17717
proton reactions at 40 Mev to 25 Bev, lithium isotopes from, (E), 20: 31205
proton reactions at 0.05 to 2.9 Bev, induced activity data and cross sections for spallation, (E/T), 20: 32549
proton reactions (p,n) at 3 Mev, gamma and neutron spectra from, 16: 12266
proton reactions (p,n) at 138 Mev, collective excitations in, 17: 38310
proton reactions with, rare gas and tritium production cross sections for, 18: 15189 (CERN-64-12)
proton reactions with, lithium-6 and -7 fragments from, 18: 16977
proton scattering at 45 Mev, polarization in, (E), 20: 22128
purification, 18: 2163(R) (IS-700(Sect.M))
purification by cerium, 19: 22875(T) (JPRS-28849(p.166-78))
purification by electron-beam melting, 17: 34330(R) (USBM-U-1057)
purification by electron-beam melting, 20: 5181(R) (ORNL-3039)
purification by hydrogen reactions, 20: 41412(R) (IS-1500(Sect. M))
purification by zone melting, 18: 8456
purification of, radiochemical method for, 20: 8838 (UCRL-14258)
radiation damage in, cross sections for atomic displacements from 1- to 3-Mev electrons, 19: 39225 (AFCRL-65-286)
radiation effects on fuel rod jackets of, 19: 26876 (ANL-6750)
radioinduced production of helium and hydrogen in, neutron, 19: 26901
reactions of trivalent, with neptunium(V) in perchlorate solutions, 16: 13055
reactions with beryllium, copper, stainless steel, and niobium alloys to 760°C *in vacuo*, 19: 44606 (PWAC-483)
reactions with beryllium in carbon dioxide, 19: 22997 (TRG-Report-842)
reactions with carbon dioxide to 600°C, 19: 22997 (TRG-Report-842)
reactions with crucibles of refractory compounds with boron, carbon, and nitrogen at 400 to 1500°C, 19: 37112
reactions with europium in aqueous perchloric acid solutions, spectrophotometric studies on kinetics of, 20: 43228
reactions with liquid sodium at high temperatures, 20: 38499 (ANL-7120, pp 839-47)
reactions with rare earth metals, 19: 22875(T) (JPRS-28849(p.166-78))
reactions with silver nitrate in nonaqueous solvents, 16: 5311(R) (TID-14361)
reactions with silica, interfacial, 16: 31595
reactions with sodium, high-temperature, 20: 15033(R) (ANL-7152, pp 87-96)
reactions with sodium at high temperatures, 20: 20925(R) (ANL-7055, pp 177-212)
reactions with sodium at 2200°C, 20: 31440(R) (ANL-7175, pp 159-83)
reactions with sulfur dioxide, 20: 33270
reactions with uranium di- and monocarbides and nitride at 1000°C, 16: 30829
reactions with uranium, plutonium–uranium, and fissium–plutonium–uranium alloys at 1100 to 1400°C, 19: 44587(R) (ANL-7000, pp 3-63)
reduction of neptunium by, in perchloric acid, kinetics and thermodynamics of, 18: 23485
reduction of pentaaminecobalt(III) complexes by, kinetics of, 18: 16018
refining powders of, electrolytic, 17: 8270(P)
separation by anion exchange in acetic acid–nitric acid medium, 18: 16131
separation by anion exchange in mixed aqueous and non-aqueous systems, 19: 2243
separation by electrolysis of cryolitic solutions of pentoxide, 16: 10106
separation by reversed-phase column chromatography, 17: 1401
separation by solvent extraction using butyl phosphates, 18: 16157(P)
separation from acid solutions by extraction using amine–ether in hydrocarbon diluent, 20: 12941(P)
separation from aliphatic alcohol-nitric acid solutions by anion exchange, 17: 32194(R) (TID-19068)
separation from alcohol-nitric acid solutions by ion exchange, 17: 35945
separation from aqueous solutions as lead vanadate, 19: 18085(P)
separation from aqueous solutions using lead shot column or bed, 20: 4071(P)
separation from aqueous solutions by extraction using organo-phosphorus solutions, 20: 5605(P)
separation from Beaverlodge ore and tailings by carbonate leaching, 18: 6884(R) (NP-13412)
separation from carbonate leach solutions by precipitation, 16: 11777(P)
separation from carbonate leach solutions by anion exchange, 16: 11778(P)
separation from carrier-free scandium-48 by ion exchange and solvent extraction, 18: 37101
separation from carbonate solutions by precipitation using calcium sulfate, 19: 2460(P)
separation from carbonate leach solutions of uranium ores, 20: 25219(P)
separation from chloride solutions by solvent extraction using amines, 17: 3070(R) (ORNL-TM-265)
separation from coke for production of high-purity artificial graphite, 17: 27741
separation from graphite above 1750°C in inert gases, 19: 38762
separation from hydrochloric acid solutions by solvent extraction using 2-ethylhexanol, 19: 36252
separation from large amounts of uranium, anion-exchange, 19: 7620(R) (TID-21411)
separation from lithium chloride solutions by oxine precipitation-carbon adsorption method, 20: 43092 (Y-1553)
separation from low-grade ores by chlorination, technique for, 18: 3902
separation from low grade ores, reductive chlorination process for, 20: 4072(P)
separation from manganese by ion exchange, 17: 12213
separation from metallic mixture by ion exchange chromatography, 17: 5991
separation from metal ionic mixtures, electrochromatographic, 17: 10753
separation from nitric or sulfuric acid solutions, ion exchange selectivity scales for, 19: 9257
separation from ores, synthesis of extractants for, 16: 5423(P)
separation from ores by carbonate leaching process, 19: 2460(P)
separation from ores by extraction with organophosphates, 19: 44129(P)
separation from other metals by ion exchange, 19: 15692
separation from other inorganic ions by paper chromatography, 20: 12939
separation from rare earths by ion exchange in isopropyl alcohol, 18: 20104
separation from rhenium by anion exchange chromatography, 19: 24433
separation from scandium by ion exchange chromatography, 20: 16574
separation from silver by partition chromatography, 20: 4054
separation from sodium diuranate, 16: 17704(P)
separation from solution by ion exchange using polyamidoximes, 18: 35653(P)
separation from solutions by solvent extraction, review of methods for, 19: 13543
separation from sodium diuranate, 20: 25212
separation from sulfuric acid solutions by solvent extraction using liquid anion exchange resin, 16: 30317
separation from sulfuric acid solutions by solvent extraction using *N*-benzoyl-*N*-phenylhydroxylaminates, 18: 5237
separation from titanium using benzoylphenylhydroxylamine, direct weight gravimetric, 17: 38940
separation from titanium by zone melting, 18: 8456
separation from uranium concentrates, 16: 4208(R) (NLCO-800)
separation from uranium ores, 16: 22259(R) (ACCO-20)
separation from uranium leach solutions (acid) by ion exchange, 16: 23772 (ACCO-37)
separation from uranium by solvent extraction using amyl acetate, 17: 14411
separation from uranium ore concentrates, 18: 5431(P)
separation from uranium ore liquors, ion exchange process for, 19: 4267(P)
separation from uranium by ion exchange, 19: 7641
separation from uranium by ion exchange in hydrofluoric–sulfuric acid solutions, 19: 11297
separation from uranium by cation exchange chromatography, 19: 13245
separation from uranium in fluorine-containing solutions by ion exchange, 19: 15678
separation from zirconium by ion exchange chromatography, 16: 31577
separation from zirconium by solvent extraction using thenoyltrifluoroacetone-xylene, 18: 1808
separation of, from boron, method for, 17: 17999
separation of (IV) and (V) states by paper chromatography, 17: 1402
separation of scandium from, by ion exchange chromatography, 19: 533
separation of uranium from, by ion exchange, 19: 32285
separation of uranium values from waste solutions of, 19: 36567(P)
separation of, from thallium by ion-exchange chromatography, 20: 36935
separation of, from zinc, in hydrochloric acid solutions by ion-exchange chromatography, 20: 45809
shock wave interactions with, thermodynamic parameters from mirror-image approximation for particle velocity and pressure in, 17: 37676
Slater-Condon parameters of, determined from spectral data, 17: 31118
soldering tubes of, in fabrication of cryostats and ovens, 19: 16027 (CEA-R-2618)
solubility in liquid cadmium, 17: 1985
solubility in liquid and solid magnesium, 18: 28002
solubility in liquid zinc, 20: 22966 (ANL-7083)
solubility in molten lithium at 482 to 1010°C, 16: 6718 (NEPA-1465)
solubility in rubidium at 1000 to 2000°F, 17: 16634 (AGN-8063)
solvent extraction using dialkyl methylene diphosphonic acid, 16: 13155
sorption by cellulose ion exchangers from acetone and ethanol mixtures with hydrochloric acid, 18: 16140
sorption from nitric acid by ion exchange paper, 19: 24435

sorption from sulfuric acid by anion exchange resins, 18: 31680
sound-wave attenuation in cylinders of superconducting, energy gap from u-h-f, 17: 41622
spark patterns produced by grinding of, 18: 19493(T) (SC-T-64-47)
specific heat and vibrational spectra of, calculations of, 17: 22190
specific heat at low temperatures, 16: 25806
specific heat of crystals of, 16: 15222
spectra in lithium chloride–potassium chloride, crystal field, 16: 30371 (TID-16693)
spectra of, absorption, 18: 1489(R) (IS-700(Sect.C))
spectra of, arc, 18: 6358
spectra of, atomic absorption, 17: 10549
spectra of, electric discharge, 17: 34642
spectra of, flame, 17: 19990 (IS-517)
spectra of, models for lattice vibrational, 17: 35681 (EUR-366.e)
spectra of oxidation states in lithium chloride–potassium chloride eutectic, 16: 7560
spectra of, in zeta pinch, 19: 25564
spectra of, measurement of K x-ray, 18: 44429
spectra of, muonic K and L x-ray, 18: 42626(R) (ANL-6879(p.69-87))
spectra of, Ohlin structure near limit of continuous x-ray, (E), 19: 44940
spectra of, time evolution of lines in emission, 20: 7062
spectra of, use of fuel-rich premixed oxyacetylene flame for emission, 18: 25278
sputtering at 50 to 600 ev by rare gas ions, 17: 8931(R) (NP-12389)
sputtering by hydrogen ions, yields from, 18: 8926
sputtering by noble-gas ions at 100 to 600 ev, yields from, 16: 22753
sputtering of crystals of, by argon, mercury, neon, and xenon ions at low energies, atom ejection in, 17: 37467
strain aging and transition temperature in, effects of nitrogen on, 20: 5851
structure calculations for, 18: 8920(R) (TID-19940(p.119-39))
structure of electrorefined, effects of rare earth additions on, 19: 2795 (BM-RI-6553)
superconducting critical fields and temperatures for, 17: 41592
superconducting critical current oscillations in, field dependence of, 18: 28512
superconducting energy gap for, ultrasonic measurement of, 18: 4501
superconducting films of, preparation by "protected sputtering", 18: 36535
superconducting films of, preparation and properties of, 18: 36536
superconducting mixed-state structure in, NMR and relaxation studies of, 20: 37963
superconducting point contacts of, macroscopic quantum interference effects in, (E/T), 20: 11911
superconducting properties of, (E), 20: 8014
superconducting single crystals of, ultrasonic attenuation measurements on, 18: 36503
superconducting transition temperatures of films of, 17: 28046
superconducting transition temperature of, pressure dependence of, (E), 20: 19762
superconductivity energy gap of, ultrasonic attenuation measurements of, 17: 25826
superconductivity and uses of, 17: 34451
superconductivity, 17: 36440(R) (NP-13061)
superconductivity, 17: 41604
superconductivity of, 18: 15084
superconductivity of, magnetic field effects on, 18: 15077
superconductivity energy gaps in, electron tunnelling measurements by, 18: 36495
superconductivity of, effects of long-range order on, 18: 42564
superconductivity of, effects of crystal dislocations on, 18: 44688
superconductivity enhancement of, using 3,4,7,8-tetramethyl-1,10-phenanthroline, 19: 40543
superconductivity of, 20: 40047
superconducting properties of, effects of λ transition on, 20: 21875
superconductivity of, Ginzburg-Landau parameter for, 20: 44537
surface tension at melting point, 17: 39612
tensile properties of, effects of interaction of interstitial solute and substructure on, 18: 34204
testing for in-core flux monitoring, 20: 35835(R) (DPST-66-83-5)
testing for use as cladding of fissium–plutonium–uranium alloy fuel, 18: 10572 (CONF-373-2)
thermal capacity at 0.35 to 25°K, measurements of, (E), 19: 33180
thermal capacity of normal and superconducting, 19: 43997(R) (UCRL-11889)
thermal capacity of crystals of, renormalization effects in electronic, 17: 39597
thermal capacity of mixed state in, at 0.5 and 5.4°K, 20: 42116
thermal capacity of normal and superconducting, at 0.5 to 5.4°K, 20: 42115
thermal conductivity of, at 1600 to 1800°K, 16: 31813 (ASD-TR-61-528)
thermal conductivity of superconducting, 17: 567
thermal conductivity of superconducting thermal switches of, at 0.3 to 2°K, (E), 19: 23584
thermal conductivity decrease in superconducting crystals of, in lattice scattering region, 17: 34629
thermal expansion properties at low temperatures, 17: 1967
thermal expansion of, linear, 20: 45106(R) (ANL-7249)
thermal properties at high temperatures, 16: 4551 (WADD-TR-60-904)
thermoelectric power at 4 to 300°K, 17: 22337
toxic properties of, review of, 18: 13423
tracer applications survey, 16: 1359
ultrasonic attenuation in superconducting, 18: 36504
ultrasonic transverse-wave attenuation in superconducting, temperature dependence of, 18: 2760
uptake and distribution in *Ciona intestinalis*, 16: 20119
use as diffusion barrier between aluminum clad and uranium fuel, 18: 13264
use as windows in electric discharge devices, 20: 13052(P)
use for electroless and electrolytic coating of bearings and dies, review of, 19: 4604
uses in nuclear technology, 17: 12679
uses of superconducting, as level gages in liquid helium, 18: 40442
vanadium-51 NMR in, temperature dependence of, 18: 24688
vanadium-52 beta decay in, monocrystalline recoil-atom anisotropic slowdown in, (E/T), 19: 33389
vapor pressure, 20: 331
vaporization by electron bombardment, 19: 34660
vibrational frequency distribution of, neutron inelastic scattering studies of, 17: 39713 (BNL-7240)
voltammetry in phosphoric acid–sulfuric acid or sulfuric acid using pyrolytic graphite electrode, 18: 19967
welding of, argon-arc and electron-beam methods of, 20: 21310
welding sheaths, sheets, and tubes of, techniques for, 18: 7172
welding to niobium sheet, tongue effect in, 16: 2155
welding to type 347 stainless steel, 17: 23864(R) (BMI-1619(Del.))
x-ray absorption at room temperature and −180°C, 17: 39798
x-ray mass absorption at 1.49 to 15.77 kev, (E), 19: 25146(R) (TID-21542)
x-ray spectra from μ-mesic atoms of, nuclear charge distribution from, 19: 27518
yield stress of, correlation of thermal component of, 17: 18793
Young's modulus of, as function of temperature, 18: 39970
zone refining of, method for induction, 18: 14398

VANADIUM ACID SULFATES

chromium-atom slowdown paths at 20 to 90 ev in, (E), 19: 33512

VANADIUM ALLOYS

analysis for tantalum, photometric, 16: 5269 (WAL-TR-823/2)
bonding to themselves or other refractory metal alloys, 19: 16050(P)
book: *Vanadium, Niobium, Tantalum. The Metallurgy of the Pure Metals and Their Alloys*, in German, 18: 25906
coating, development of high-temperature oxidation protective materials, 16: 6706(R) (ARF-2227-3)
coatings for protection against high-temperature oxidation, 16: 12083(R) (ARF-2227-4)
corrosion by inorganic and organic acids at 35, 60, and 100°C, 20: 11230 (BM-RI-6715)
corrosion by liquid sodium, 20: 33822
corrosive effects of sodium on binary, 20: 6601(R) (ANL-7115, pp 1-41)
development as fuel jacket material for fast reactors, 20: 38465 (ANL-7120, pp 289-300)
development for high-temperature uses, 16: 5680 (ARF-2210-6)
development of dispersion-strengthened, 17: 41428(R) (IITRI-B6007-4)
development of dispersion-strengthened, 18: 27858(R) (IITRI-B6007-6)
development of fabricable high-strength, 20: 21333(R) (IITRI-B6042-4)
development with improved creep properties for use at 2200 to 2400°F, 19: 13885(R) (IITRI-B6021-4)
fabrication, 18: 32033 (A/CONF.28/P/255)
fabrication and properties as refractory material, 16: 19404
fabrication and properties of, review of, 17: 29253 (NRC-7129)
fabrication and properties for use as superconductors, 18: 34179
fabrication of, 16: 6707 (ARF-2231-1)
fabrication of, 17: 39562
mechanical properties of, 17: 12656 (AD-277779)
mechanical properties at high temperatures, effects of metal and nonmetal additions on, 17: 25771 (ASD-TDR-62-667)
miscibility with other elements, calculation of, 20: 14538
oxidation above 2000°F, 17: 39562
oxidation at high temperatures, coatings for protection against, 17: 12610(R) (ARF-B6001-2)
oxidation, causes of catastrophic, 16: 4500 (ORNL-TM-51)
oxidation protection of, development of coatings for, 18: 30190
phase studies, 17: 41333(R) (ANL-6677)
production in electric arc furnace, fabrication of consumable electrodes for, 18: 8741(P)

properties, 16: 3460 (NP-11108)
properties above 2000°F, 17: 39562
properties as fuel cladding material, 18: 32033 (A/CONF-28/P/255)
properties at low temperatures, 18: 22493(R) (PB-171809-6)
properties for use as jacket material for fast reactor fuels, 18: 21698(R) (ANL-6860)
properties for use as fuel-element cladding, 19: 22884
properties of, mechanical and physical, 16: 32134
properties of, review, 17: 1826
properties of superconducting, size factor and, 17: 25927
properties of, containing hafnium, niobium, titanium, and zirconium, 18: 7267
strength of, elevated-temperature, 16: 6707 (ARF-2231-1)
superconductivity of, theory for, 17: 18830
tensile properties, 16: 29348 (ARF-2231-5)
thermal capacity at 0.4–4°K, Einstein, 17: 39596
use for electroless and electrolytic coating of bearings and dies, review of, 19: 4604
Al–Co–Fe–Ti–V, properties of aged, 20: 4360(R) (AD-619399)
Al–Co–V, phase studies on intermetallic compounds in, 20: 17075
Al–Cr–Co–Mo–Ni–Ti–V–Zr, surface treatments for IN-100, coating and mechanical, 20: 29706 (NASA-TM-X-53448)
Al–Cr–Cu–Fe–Mo–Sn–Ti–V–Zr, fabrication and properties, 18: 22424(R) (WAL-TR-401/303-2)
Al–Cr–Cu–Fe–Mo–Sn–Ti–V, fabrication and properties, 18: 22424(R) (WAL-TR-401/303-2)
Al–Cr–Cu–Fe–Sn–Ti–V–Zr, fabrication and properties, 18: 22424(R) (WAL-TR-401/303-2)
Al–Cr–Cu–Fe–Sn–Ti–V, fabrication and properties, 18: 22424(R) (WAL-TR-401-303-2)
Al–Cr–Ge–Ti–V, properties of aged, 20: 4360(R) (AD-619399)
Al–Cr–Nb–Ti–V, properties for brazing niobium, 20: 25552(P)
Al–Cr–Ti–V, corrosion by ammoniated water at pH 10 and 600°F, 17: 37482 (KAPL-M-CC-4)
Al–Cr–Ti–V, corrosion by mercury, 18: 10492
Al–Cr–Ti–V, corrosion by sodium chloride, effects of stress on, 20: 33858(R) (AD-634094)
Al–Cr–Ti–V, ductility of, effects of liquid cesium on, 18: 14354(R) (ARF-B215-12)
Al–Cr–Ti–V, fracture modes in surfaces of, 20: 9485 (AD-623567)
Al–Cr–Ti–V, machining characteristics, 17: 14778(R) (ASD-TR-7-532a (IX))
Al–Cr–Ti–V, mechanical and metallurgical properties, 16: 4547 (WADC-TR-59-595(Pt.II))
Al–Cr–Ti–V, properties as brazing alloy for niobium alloy honeycomb structures, 18: 39874
Al–Cr–Ti–V, properties at –400 to 100°F, 19: 26803(R) (AD-611165)
Al–Cr–Ti–V, properties of aged, 20: 4360(R) (AD-619399)
Al–Cr–Ti–V, tensile and creep properties at 1800 to 2300°F, 17: 37506 (BLR-62-26)
Al–Cr–Ti–V, welding characteristics, 16: 4516 (DMIC-Memo-140)
Al–Cr–V, development of refractory, for use in oxygen-contaminated sodium systems, (E), 20: 14007(R) (ANL-7122, pp 1-41)
Al–Cu–Fe–Sn–Ti–V, additive and alloying effects on mechanical properties of, 19: 46985 (AD-613651)
Al–Cu–Fe–Sn–Ti–V–Zr, deformation and heat treatment effects on mechanical properties of, 20: 2309 (AD-615024)
Al–Cu–Fe–Sn–Ti–V–Zr, fabrication and properties of, effects of carbon additions on, 18: 22424(R) (WAL-TR-401/303-2)
Al–Cu–Fe–Sn–Ti–V, fabrication and mechanical properties of forged, effects of carbon, chromium, molybdenum, oxygen, and zirconium additions on, 18: 35944(R) (WAL-TR-401/303-4)
Al–Cu–Fe–Sn–Ti–V, mechanical properties of titanium-base, 20: 33858(R) (AD-634094)
Al–Cu–V, phase studies, 19: 42874
Al–Cu–V, phase studies, 20: 23725
Al–Fe–Mo–Ti–V, properties of aged, 20: 4360(R) (AD-619399)
Al–Fe–Ti–V, properties of aged, 20: 4360(R) (AD-619399)
Al–Mn–Ti–V, properties of aged, 20: 4360(R) (AD-619399)
Al–Mo–Sn–Ti–V–Zr, beta transus temperature of, 19: 20462(R) (NRL-6258)
Al–Mo–Sn–Ti–V, beta transus temperature of, 19: 20462(R) (NRL-6258)
Al–Mo–Sn–Ti–V, corrosion by sodium chloride, effects of stress on, 20: 33858(R) (AD-634094)
Al–Mo–Sn–Ti–V–Zr, corrosion by sodium chloride, effects of stress on, 20: 33858(R) (AD-634094)
Al–Mo–Sn–Ti–V, fracture modes in surfaces of, 20: 9485 (AD-623567)
Al–Mo–Sn–Ti–V, fracture toughness properties of titanium-base, effects of heat treatments on, 20: 11273(R) (NRL-6364)
Al–Mo–Sn–Ti–V, mechanical properties of titanium-base, 20: 33858(R) (AD-634094)
Al–Mo–Ti–V, annealing, 17: 3367 (AD-275092)
Al–Mo–Ti–V, corrosion by mercury, 18: 10492
Al–Mo–Ti–V, corrosion cracking of, mechanisms for stress, 19: 44621 (CONF-651006-1)
Al–Mo–Ti–V, corrosion cracking by salts at 550 to 600°F, stress-, 20: 11227
Al–Mo–Ti–V, corrosion by sodium chloride, effects of annealing on, 20: 33858(R) (AD-634094)
Al–Mo–Ti–V, creep properties of, effects of sheet processing variables on, 16: 21009(R) (AD-264815)
Al–Mo–Ti–V, fabrication characteristics of, 19: 16024 (AD-425058)
Al–Mo–Ti–V, fatigue studies, 19: 30740 (NASA-CR-246)
Al–Mo–Ti–V, fracture modes in surfaces of, 20: 9485 (AD-623567)
Al–Mo–Ti–V, mechanical properties of sheet and welds, 16: 2142(R) (AD-256167)
Al–Mo–Ti–V, mechanical properties, 17: 3468 (ASD-TR-62-7-675)
Al–Mo–Ti–V, mechanical properties of weldments, 17: 14886
Al–Mo–Ti–V, mechanical properties of diffusion-bonded plates of, 19: 20462(R) (NRL-6258)
Al–Mo–Ti–V, mechanical properties of solution-annealed and aged T-19, 19: 20462(R) (NRL-6258)
Al–Mo–Ti–V, mechanical properties of titanium-base, 20: 33858(R) (AD-634094)
Al–Mo–Ti–V, phase studies, 18: 42090
Al–Mo–Ti–V, phase studies, 20: 5851
Al–Mo–Ti–V, properties of rolled sheet, 16: 19294 (AD-267448)
Al–Mo–Ti–V, properties, 17: 3367 (AD-275092)
Al–Mo–Ti–V, properties at –400 to 100°F, 19: 26803(R) (AD-611165)
Al–Mo–Ti–V, radiation effects on, fast-neutron, 19: 6364(R) (NP-14443)
Al–Mo–Ti–V, radiation effects on tensile properties of, irradiated at 30°R, fast-neutron, 20: 27589(R) (NASA-CR-54881)
Al–Mo–Ti–V, rolling, 17: 3367 (AD-275092)
Al–Mo–Ti–V, rolling, 17: 3468 (ASD-TR-62-7-675)
Al–Mo–Ti–V, rolling of, component distribution in, 16: 2143(R) (AD-256168)
Al–Mo–Ti–V, strip processing, 17: 3468 (ASD-TR-62-7-675)
Al–Mo–Ti–V, tensile properties, 17: 3468 (ASD-TR-62-7-675)
Al–Mo–Ti–V, tensile properties at 30 and 540°R, 17: 25776(R) (NP-12812)
Al–Mo–Ti–V, tensile properties, 19: 6364(R) (NP-14443)
Al–Mo–Ti–V, thermal stability of, effects of composition on, 20: 11336
Al–Mo–Ti–V, welding characteristics, 16: 4510 (DMIC-Memo-140)
Al–Nb–Ti–W–V–Zr, properties for use to 1200°F, 20: 4393 (PWAC-472)
Al–Nb–V, corrosion by steam and water, 16: 29346
Al–Nb–V, crystal structure and phase studies of superconducting, 18: 32149(R) (UCRL-11317(p.131-49))
Al–Sn–Ti–U–V–Zr, mechanical properties, 19: 37074
Al–Sn–Ti–V, beta transus temperature of, 19: 20462(R) (NRL-6258)
Al–Sn–Ti–V, corrosion by ammoniated water at pH 10 and 600°F, 17: 37482 (KAPL-M-CC-4)
Al–Sn–Ti–V, corrosion by sodium chloride, effects of stress on, 20: 33858(R) (AD-634094)
Al–Sn–Ti–V–Zr, formability characteristics and mechanical properties of, 20: 2308 (AD-614637)
Al–Sn–Ti–V, fracture toughness properties of titanium-base, plane-strain, 20: 11273(R) (NRL-6364)
Al–Sn–Ti–V–Zr, mechanical properties of, effects of uranium on, 19: 37074
Al–Sn–Ti–V, strength and toughness of titanium-base, effects of aging and annealing on, 20: 33858(R) (AD-634094)
Al–Sn–V–Zr, corrosion by steam at 400°C, 19: 32696(R) (EURAEC-783)
Al–Sn–V–Zr, fabrication and properties, 19: 36965(T,R) (EURAEC-618)
Al–Tc–V, Knight shifts and magnetic susceptibilities in b-c-c region of, 18: 2454
Al–Ti–V, analysis for iron using 4,7-diphenyl-1,10-phenanthroline, spectrophotometric, 16: 2974
Al–Ti–V, bonding of, controlling factors in diffusion, 19: 24964
Al–Ti–V, corrosion by mercury at 700°F, 16: 16683 (TID-7626(Pt.I) (p.107-8))
Al–Ti–V, corrosion by cesium, 17: 30944
Al–Ti–V, corrosion by ammoniated water at pH 10 and 600°F, 17: 37482 (KAPL-M-CC-4)
Al–Ti–V, corrosion of nitrided, by mercury to 538°C, effects of inhibitors on, 17: 41333(R) (ANL-6677)
Al–Ti–V, corrosion by mercury, 18: 10492
Al–Ti–V, corrosion by cesium at 400°C, 20: 4337
Al–Ti–V, corrosion by cesium at 400°C, 20: 11227
Al–Ti–V, corrosion by oxygen-contaminated sodium, 20: 16060(R) (ANL-7152, pp 1-49)
Al–Ti–V, corrosion cracking in titanium-base, stress-, 20: 16967 (AD-628277)
Al–Ti–V, crack initiation in, factors influencing, 19: 36944 (AD-602952
Al–Ti–V, deformation properties of, effects of temperature and deformation velocity on, 17: 20485

Al–Ti–V, ductility of, effects of liquid cesium on, 18: 14354(R) (ARF-B215-12)
Al–Ti–V, embrittlement by hydrogen, 20: 9494 (LA-DC-6833)
Al–Ti–V, extrusion of, high energy rate processes for, 16: 27596(R) (ASD-TR-7-882(VII))
Al–Ti–V, extrusion by Dynapak process, 19: 30686(R) (AD-608945)
Al–Ti–V, fabrication by explosive forming, 16: 2151 (WAL-624.5/1)
Al–Ti–V, fatigue crack propagation in, study of low-cycle, 19: 20462(R) (NRL-6258)
Al–Ti–V, fatigue of, energy criterion for, (T), 20: 27521
Al–Ti–V, fracture modes in surfaces of, 20: 9485 (AD-623567)
Al–Ti–V, fracture toughness of plasmarc welds in titanium-base, 20: 11273(R) (NRL-6364)
Al–Ti–V, fracture toughness properties of titanium-base, plane-strain, 20: 11273(R) (NRL-6364)
Al–Ti–V, fracture toughness properties of titanium-base, 20: 11273(R) (NRL-6364)
Al–Ti–V, friction coefficients with metals and metals with dry lubricants of titanium-base, *in vacuo*, 20: 7571 (NAA-SR-9644)
Al–Ti–V, friction coefficients with alumina, carbon, and other ceramics of titanium-base, *in vacuo*, 20: 7571 (NAA-SR-9644)
Al–Ti–V, hydrogen ion sputtering effects on, 18: 8904
Al–Ti–V, interface friction in hot deformation of, 19: 46981(R) (AD-611821)
Al–Ti–V, machining characteristics, 17: 14778(R) (ASD-TR-7-532a(IX))
Al–Ti–V, mechanical properties, 17: 3468 (ASD-TR-62-7-675)
Al–Ti–V, mechanical properties, 17: 11099(R) (NP-12475)
Al–Ti–V, mechanical properties of diffusion-bonded plates of, 19: 20462(R) (NRL-6258)
Al–Ti–V, mechanical properties of, effects of strain rate on, 20: 11284 (UCRL-14599)
Al–Ti–V, mechanical properties of titanium-base, 20: 33858(R) (AD-634094)
Al–Ti–V, metallurgical bonding to stainless steel by extrusion, 18: 27937
Al–Ti–V, neutron reactions with, activation response of, 20: 28591 (DC-59-3-90)
Al–Ti–V, oxidation by argon–oxygen environment at 1035 and 1685°F, 19: 6240(R) (ASD-8-170(V))
Al–Ti–V, phase transformations kinetics in, 17: 11248
Al–Ti–V, properties at –400 to 100°F, 19: 26803(R) (AD-611165)
Al–Ti–V, properties for NERVA pressure vessel, 19: 38252
Al–Ti–V, radiation effects on, fast-neutron, 19: 6364(R) (NP-14443)
Al–Ti–V, radiation effects on tensile properties at 30°R, fast neutron, 19: 14086(R) (N65-13446)
Al–Ti–V, radiation effects on low-cycle fatigue and tensile properties at cryogenic temperatures, 20: 11345(R) (NASA-CR-54787)
Al–Ti–V, radiation effects on tensile properties of, irradiated at 30°R, fast-neutron, 20: 27589(R) (NASA-CR-54881)
Al–Ti–V, rolling, 17: 3468 (ASD-TR-62-7-675)
Al–Ti–V, self-welding to ceramics, graphite, and metals in SNAP reactor environment at 700 to 1300°F, 20: 7570 (NAA-SR-9643)
Al–Ti–V, stress-corrosion, 17: 6569(R) (NP-12369)
Al–Ti–V, strip processing, 17: 3468 (ASD-TR-62-7-675)
Al–Ti–V, superconducting transition temperature, effects of phase transformation on, 18: 42025(T) (AI-Trans-49)
Al–Ti–V, superconducting properties, 18: 44681
Al–Ti–V, superconductivity and phase transformations, 19: 7965
Al–Ti–V, techniques for cold welding of, 19: 34357 (N64-24831)
Al–Ti–V, tensile properties, 17: 3468 (ASD-TR-62-7-675)
Al–Ti–V, tensile properties at 30 and 540°R, 17: 25776(R) (NP-12812)
Al–Ti–V, tensile properties, 17: 36987 (SY-5394-R(Vol.I))
Al–Ti–V, tensile properties, 19: 6364(R) (NP-14443)
Al–Ti–V, tensile properties of, effects of exposure to cesium at 650°C on, 20: 11227
Al–Ti–V, transformation behavior in, during cooling, 17: 16721
Al–Ti–V, welding by solid-state methods, 19: 22937
Al–Ti–V, welding characteristics, 16: 4510 (DMIC-Memo-140)
Al–Ti–V, welding, explosive techniques for, 16: 3419 (ASD-TR-61-124)
Al–Ti–V–Zr, beta transus temperature of, 19: 20462(R) (NRL-6258)
Al–Ti–V–Zr, corrosion by steam at 400°C, 19: 32696(R) (EURAEC-783)
Al–Ti–V–Zr, fabrication and properties, 19: 36965(T,R) (EURAEC-618)
Al–Ti–V–Zr, welding characteristics, 16: 4510 (DMIC-Memo-140)
Al–Ti–W–V–Zr, properties for use to 1200°F, 20: 4393 (PWAC-472)
Al–U–V, fabrication of reactor fuels of, 19: 44668(P)
Al–V, analysis for iron using 4,7-diphenyl-1,10-phenanthroline, spectrophotometric, 16: 2974
Al–V, crystal structure and phase studies of superconducting, 18: 32149(R) (UCRL-11317(p.131-49))
Al–V, crystallization of intermetallic compounds in, effects of casting temperature on, 20: 27554
Al–V, fabrication and production of stoichiometric, 19: 42831
Al–V, magnetic susceptibility, 17: 41333(R) (ANL-6677)
Al–V, nuclear magnetic resonance, 19: 43986(R) (ANL-7000, pp 201-4)
Al–V, properties of intermetallic compound, 20: 37260
Al–V, solidification and structure of, effects of high cooling rate on, 19: 9673(T) (SC-T-64-2011)
Al–V, superconducting transition in, (E), 20: 9915
Al–V–Zr, corrosion by steam at 400°C, 19: 32696(R) (EURAEC-783)
Al–V–Zr, fabrication and properties, 19: 36965(T,R) (EURAEC-618)
Al–V–Zr, phase studies on intermetallic compounds in, 20: 17075
Al–V–Zr, thermal expansion between 100 and 1100°C, 19: 24982(R) (EURAEC-1270)
Au–Nb–V, phase structure and superconductivity of, 18: 11117
Au–V, structure of, 17: 578
Be–Ca–V, development of corrosion-resistant, 17: 37473(P)
Be–Ti–V, aging characteristics and phase studies, 16: 6746
Be–Ti–V, performance in niobium alloy brazing, 20: 39365
Be–V, crystal structure of intermetallic compound VBe_{12} in, 16: 16717 (DC-58-11-114)
Bi–V, phase studies, 19: 37072
Ce–Mg–V, mechanical properties at 100 to 300°C, 17: 1920 (BM-RI-6078)
Ce–V, analysis of, amperometric, 20: 35434
Ce–V, phase diagram, 16: 18076
Co–Fe–V, electric conductivity and specific heat at 80 to 1150°F, 18: 41928(R) (NASA-CR-54089)
Co–Fe–V, properties of Hiperco 50 and Supermendur for use in space electric power systems, 20: 4379 (NASA-CR-54091)
Co–Fe–V, structural ordering in, 17: 38048(T) (AEC-tr-5734(p.279))
Co–Nb–V, oxidation properties at 2000°F in air, 17: 35997(R) (IITRE-B6001-5)
Co–V, ferromagnetic nuclear resonance and saturation magnetization in, 18: 36032
Co–V, oxidation properties at 2000°F in air, 17: 35997(R) (IITRE-B6001-5)
Co–V, vanadium-48 nuclear orientation in, 20: 24445
Co–V–Zr, atomic arrangements in C14 Laves phase in, 17: 29364
Cr–Fe–Mo–V, erosion by mercury vapor at 640°F of Lapelloy, 20: 11214(R) (NASA-CR-54717)
Cr–Fe–Mo–V, mechanical and thermophysical properties of H-11, at 80 to 1600°F, 18: 41928(R) (NASA-CR-54089)
Cr–Fe–Mo–V, properties of H-11 Steel for use in space electric power systems, 20: 4379 (NASA-CR-54091)
Cr–Mn–V, cryogenic properties, 19: 9767(R) (IS-900(Sect.P))
Cr–Mo–Nb–Ti–V, corrosion by steam at 1000°F, 17: 23890(R) (BMI-X-10040)
Cr–Mo–Nb–Ti–V, corrosion by steam at 540 and 650°C, 18: 8747(R) (BMI-X-10071)
Cr–Mo–Nb–Ti–V, corrosion by steam at 540 and 650°C, 18: 22415(R) (BMI-X-10082)
Cr–Mo–Ni–V, corrosion and oxidation resistance in fused salts, 18: 41968(P)
Cr–Nb–Ti–V, corrosion by steam at 1000°F, 18: 2184
Cr–Nb–Ti–V, corrosion by steam at 540 and 650°C, 18: 8747(R) (BMI-X-10071)
Cr–Nb–Ti–V, corrosion by steam at 540 and 650°C, 18: 22415(R) (BMI-X-10082)
Cr–Nb–Ti–V, corrosion by steam at 540, 565, 650, and 750°C, 18: 32036(R) (BMI-X-10091)
Cr–Nb–Ti–V, corrosion by steam at 540°C, 18: 41933 (TID-11295 (3rd Ed.))
Cr–Nb–Ti–V, corrosion by steam at high temperatures, 19: 2758
Cr–Nb–Ti–V, corrosion by air and superheated steam, 19: 9620 (BMI-1700)
Cr–Nb–Ti–V, fabrication by extrusion and rolling, 18: 22415(R) (BMI-X-10082)
Cr–Nb–Ti–V, mechanical properties of corrosion-resistant, 19: 9620 (BMI-1700)
Cr–Nb–Ti–V, performance in nuclear-superheater environment, 19: 10541(R) (GEAP-4703)
Cr–Nb–Ti–V, properties for use as cladding materials in nuclear superheat applications, 18: 24080 (BMI-X-286)
Cr–Nb–Ti–V, properties as cladding materials, 20: 5846
Cr–Nb–Ti–V, corrosion by steam at 1000°F, 17: 23890(R) (BMI-X-10040)
Cr–Nb–Ti–V, tensile properties at 540, 675, and 815°C, 18: 32036(R) (BMI-X-10091)
Cr–Nb–V, corrosion by steam at 1000°F, 17: 23890(R) (BMI-X-10040)
Cr–Nb–V, corrosion by steam at 540°C, 18: 8747(R) (BMI-X-10071)
Cr–Nb–V, corrosion by steam at 540°C, 18: 22415(R) (BMI-X-10082)
Cr–Nb–V, corrosion of, by steam and water, 16: 29346
Cr–Nb–V, fabrication and mechanical properties of sheet of, 19: 20552(R) (IITRI-B6021-6)
Cr–Nb–V–Zr, development and properties for reactor cladding, 18: 7266
Cr–Ti–V, corrosion by sodium at 650°C, 19: 29468(R) (ANL-7017)
Cr–Ti–V, corrosion by sodium at 650°C, 19: 31462(R) (ANL-7028)
Cr–Ti–V, corrosion by sodium at 650°C, effects of oxygen on, 19: 35604(R) (ANL-7045(p.1-23))

Cr–Ti–V, corrosion by flowing sodium at 650°C, effects of chromium content on, 20: 5851
Cr–Ti–V, corrosion by sodium at 650°C, 20: 36391(R) (ANL-7219, pp 1-27)
Cr–Ti–V, creep measurements on, 20: 46963(R) (ANL-7132)
Cr–Ti–V, creep rate of, 20: 6601(R) (ANL-7115, pp 1-41)
Cr–Ti–V, elastic properties, 20: 6556(R) (ANL-7105, pp 36-58)
Cr–Ti–V, elasticity of, 20: 36392(R) (ANL-7219, pp 28-54)
Cr–Ti–V, fabricability of, effects of composition on, 19: 44587(R) (ANL-7000, pp 3-63)
Cr–Ti–V, fabrication for fuel-coating tests, 19: 14765(R) (ANL-6977)
Cr–Ti–V, fabrication and thermal expansivity of, 20: 24734(R) (ANL-7176, pp 1-44)
Cr–Ti–V, fabrication of, 20: 46963(R) (ANL-7132)
Cr–Ti–V, fatigue burst testing of reactor fuel tubes of, 20: 36391(R) (ANL-7219, pp 1-27)
Cr–Ti–V, magnetization of high-field superconducting type-II, mixed state paramagnetism in, (E), 20: 8018
Cr–Ti–V, mechanical and metallurgical properties, 16: 4547 (WADC-TR-59-595(Pt.II))
Cr–Ti–V, mechanical properties at high temperatures, 19: 40177(R) (ANL-7046(p.1-35))
Cr–Ti–V, mechanical properties at high temperatures, 20: 42579(R) (ANL-7245, pp 29-47)
Cr–Ti–V, phase conversions and properties of, 20: 43970
Cr–Ti–V, properties as fuel cladding, 19: 24064(R) (ANL-6997)
Cr–Ti–V, radiation effects on mechanical properties of, fast neutron, 20: 36391(R) (ANL-7219, pp 1-27)
Cr–Ti–V, radiation effects on mechanical and physical properties of, 20: 45106(R) (ANL-7249)
Cr–Ti–V, thermal expansivity of, 20: 26394(R) (ANL-7193)
Cr–Ti–V, thermal expansion of, linear, · 20: 45106(R) (ANL-7249)
Cr–U–V, phase studies on, 20: 11271 (LFEN-24)
Cr–V, antiferromagnetism of, at 95 to 300°K, 19: 40077 (IS-T-18)
Cr–V, brazing material for joining molybdenum to tungsten for use to 2700°F, 20: 21312
Cr–V, corrosion in sodium at 650°C, 20: 43809 (BNL-50003)
Cr–V, electric conductivity and thermoelectric power of, at 4.2 to 450°K, 19: 40077 (IS-T-18)
Cr–V, electronic specific heat, 17: 16698
Cr–V, Knight shifts and magnetic susceptibilities in, 17: 654
Cr–V, magnetic properties, 19: 23057
Cr–V, nuclear magnetic resonance, 17: 16820
Cr–V, nuclear magnetic resonance in, 18: 2401(R) (IS-700(Sect.P))
Cr–V, nuclear magnetic resonance of, (E), 20: 4476(R) (IS-1200(Sect.P))
Cr–V, paramagnetic susceptibility, 16: 10576
Cr–V, properties of, at high temperatures, 16: 30779 (BMI-1277)
Cr–V, thermal capacity of solid solutions of, at low temperatures, 19: 4703
Cr–V, thermal expansion of, · 20: 43964
Cr–V, thermodynamic properties at 1550°K, 18: 25970(R) (ANL-6868 (p.303-25))
Cr–V–Zr, fabrication of, cracking in, 17: 41427(R) (IITRI-B231-9)
Cr–V–Zr, forgeability and tensile strength, 17: 25771 (ASD-TDR-62-667)
Dy–V, oxidation by air at 500°C and water at 93 and 177°C, 17: 34330(R) (USBM-U-1057)
Dy–V, phase studies, 16: 17967(R) (USBM-U-887)
Dy–V, physical properties, (E), 19: 16188
Er–V, oxidation by air at 400°C and water at 93 and 177°C, 17: 34330(R) (USBM-U-1057)
Er–V, physical properties, (E), 19: 16188
Fe–Mo–Ni–V, effects of ammonium fluoride–formic acid–nitric acid anodic solutions against corrosion of, 18: 35959
Fe–Ti–V, hardness and stability of beta phase in, 16: 12129
Fe–Ti–V, phase studies, 16: 558
Fe–V, analysis of cast, for impurities, 18: 2157(R) (BMI-1644(Del.))
Fe–V, atomic magnetic moments and electron transfer in, 17: 37817
Fe–V, density-of-states effects on magnetic stiffness of, (E/T), 19: 23969
Fe–V, diffusion of iron in, temperature dependence, 19: 968 (UCRL-12029-T)
Fe–V, ferromagnetism and atomic magnetic moments of, effects of solute concentration on, 17: 27801 (TID-17141)
Fe–V, hyperfine structure of iron-57 spectra in, 17: 13236
Fe–V, lattice parameter, 19: 44679(R) (ANL-7000, pp 205-12)
Fe–V, magnetic fields at iron-57 nuclei in, (E), 19: 20578
Fe–V, magnetic properties, 17: 41333(R) (ANL-6677)
Fe–V, Mossbauer effect in, 17: 29627
Fe–V, neutron elastic scattering by, cross sections for, (E/T), 20: 26346 (NP-16010, pp 1-41)
Fe–V, radiation effects on diffusion-controlled reactions in, 17: 31055
Fe–V, solubility of nitrogen in, 19: 41065
Fe–V, thermal capacity of solid solutions of, at low temperatures, 19: 4703
Fe–V, thermodynamic properties at 1400 to 1800°K, 17: 27774 (ANL-6657)
Fe–V, thermodynamic properties, 17: 41333(R) (ANL-6677)
Fe–V, vanadium-48 nuclear orientation in, 20: 24445
Fe–V–Zr, corrosion by steam at 750°F, 17: 6561(R) (ARF-2198-34)
Fe–V–Zr, corrosion by steam, 17: 34347(R) (IITRI-B198-43)
Fe–V–Zr, melting points, 18: 44497(R) (MND-2812-2)
Fe–V–Zr, oxidation by steam at 750°F, hydrogen absorption from, 18: 2162(R) (IITRI-B198-46)
Fe–V–Zr, tensile properties at 70 and 750°F, 18: 2162(R) (IITRI-B198-46)
Ga–V, critical currents of superconducting, 18: 26464
Ga–V, critical field limits at superconducting temperatures, 17: 3635
Ga–V, critical field of superconducting V_3Ga, (T), 20: 37936 (CLM-R-60)
Ga–V, crystal structure of intermetallic compounds in, 20: 871
Ga–V, crystallographic parameters, 17: 18822
Ga–V, effects of processing variables on critical current density and superconductivity of V_3Ga, 18: 4289
Ga–V, effects of orbital field on Fulde-Ferrell state in, 20: 40046
Ga–V, electric conductivity above superconducting transition temperature, 20: 8028
Ga–V, electronic band structure of, 18: 14523
Ga–V, energy state of superconducting V_3Ga, with paramagnetic impurities, 20: 28209
Ga–V, heat-capacity changes during superconducting transition in, (T), 19: 33181
Ga–V, magnetic field effects on superconducting, 18: 15063
Ga–V, magnetic flux distributions in superconductors of, (E), 19: 10194
Ga–V, magnetic properties of superconducting, 16: 15467
Ga–V, magnetic penetration depth in superconducting V_3Ga, 18: 28505
Ga–V, mechanical constraint effects on superconducting transitions of niobium wires coated with, 17: 28098
Ga–V, negative surface energy model of superconductivity of, 17: 9040
Ga–V, nuclear magnetic resonance of gallium-69, -71, and vanadium-51 in, 18: 44229
Ga–V, phase studies, 18: 8845
Ga–V, preparation of superconducting, vapor deposition technique for, 17: 18892 (ASD-TDR-62-1111)
Ga–V, preparation of thin superconducting films of, getter sputtering technique for, 18: 13015
Ga–V, preparation of V_3Ga, 20: 42534
Ga–V, pressure effects on superconductivity of, 18: 15078
Ga–V, properties of superconducting, 18: 6127
Ga–V, properties for use as superconductive wires, 18: 34200
Ga–V, radiation effects on superconducting properties of, fast-neutron, 18: 10583
Ga–V, radiation effects on superconductivity of, neutron, 18: 34683(R) (NP-14136)
Ga–V, spin paramagnetism below critical temperature in superconducting, 18: 4505
Ga–V, strong phonon effects in superconductors of, 18: 40449
Ga–V, superconductivity, 16: 16830
Ga–V, superconductivity of, isotope effects on, 17: 34617
Ga–V, superconductivity, 17: 41604
Ga–V, superconducting properties of, 18: 9262(R) (NP-13492)
Ga–V, superconducting critical currents in transverse fields, 18: 44698
Ga–V, superconducting properties of, current and magnetic field effects on, (E), 19: 19060
Ga–V, superconductivity, 20: 4426
Ga–V, superconductivity of fused, 20: 15123
Ga–V, superconducting critical field of, upper, (E), 20: 34434
Ga–V, superconductivity of V_3Ga in 30-kG fields, 20: 42534
Ga–V, superconducting critical currents in intermetallic compounds of, in high fields, (E), 20: 21922
Ga–V, thermodynamic properties of superconducting, 16: 25804
Ga–V, use of GaV_4 in superconducting magnets, 17: 20438
Gd–Ti–V, properties of, effects of hydrogen on, 16: 12099(R) (LAR-3)
Gd–V, oxidation by air at 450°C and water at 93 and 177°C, 17: 34330(R) (USBM-U-1057)
Gd–V, phase studies, 16: 17967(R) (USBM-U-887)
Gd–V, physical properties, (E), 19: 16188
Ge–Ta–V, phase studies on intermetallic compounds in, 20: 17075
Ge–V, magnetic penetration depth in superconducting V_3Ge, 18: 28505
Ge–V, nuclear magnetic resonance of vanadium-51 in, 18: 44229
Ge–V, preparation of thin superconducting films of, getter sputtering technique for, 18: 13015
Ge–V, preparation and properties of thin films of V_3Ge as hard superconductor, 18: 15055
Ge–V, superconductivity of, isotope effects on, 17: 34617
Hf–Mo–V, forgeability and tensile strength, 17: 25771 (ASD-TDR-62-667)
Hf–Nb–Ta–V, mechanical properties, 17: 14809(R) (ARF-B231-8)
Hf–Nb–Ta–V, oxidation of siliconized, at 2200°F, 17: 23942(R)

(ARF-B6001-3)
Hf–Nb–Ta–V, oxidation life at 2200°F of siliconized, static, 17: 35997(R) (IITRE-B6001-5)
Hf–Nb–V, fabrication and tensile properties of, effects of nitrogen and oxygen on, 16: 16712(R) (ARF-2231-3)
Hf–Nb–V, fabrication and properties of high temperature, 20: 27472 (BM-RI-6777)
Hf–Nb–V, oxidation of siliconized, at 2200°F, 17: 23942(R) (ARF-B6001-3)
Hf–Nb–V, oxidation life at 2200°F of siliconized, static, 17: 35997(R) (IITRE-B6001-5)
Hf–Nb–V, preparation and properties, 16: 22577(R) (ARF-2231-4)
Hf–Nb–V, strength at high temperatures, 20: 2407(P)
Hf–Nb–W–V, oxidation of siliconized, at 2200°F, 17: 23942(R) (ARF-B6001-3)
Hf–Nb–W–V, oxidation life at 2200°F of siliconized, static, 17: 35997(R) (IITRE-B6001-5)
Hf–Ta–W–V, mechanical properties and weldability, 17: 34420(R) (WANL-PR-M-004)
Hf–V, composition and mechanical and physical properties of, 18: 7267
Hf–V, phase diagram, 16: 17967(R) (USBM-U-887)
Hf–V, phase studies, 16: 19374(R) (USBM-U-921)
Hf–V, phase studies, 16: 29319(R) (USBM-U-952)
Hf–V, phase studies at 800 to 1500°C, 16: 6746
Hf–V, phase studies, 17: 3389(R) (USBM-U-978)
Hf–V, phase studies, 17: 17446
Hf–V, phase studies at 900 to 2300°C, 17: 34330(R) (USBM-U-1057)
Hf–V, properties of, effects of hafnium content on, 16: 15169 (BM-RI-5949)
Hf–V, structure of intermetallic compound HfV_2 in, 16: 2253
Hf–V, superconducting transition temperature of, (E), 20: 8021
Ir–V, crystal structure of ordered intermediate phases, 19: 28817
Ir–V, superconductivity in close-packed intermediate phases of, 20: 17624
Mg–V, phase diagrams, 18: 28002
Mn–V, crystal structure and phase studies, 18: 25970(R) (ANL-6868 (p.303-25))
Mo–Nb–Ru–Ti–V, oxidation of siliconized, at 2200°F, 17: 23942(R) (ARF-B6001-3)
Mo–Nb–Ru–Ti–V, oxidation life at 2200°F of siliconized, static, 17: 35997(R) (IITRE-B6001-5)
Mo–Nb–Ti–V, coating for oxidation protection, 19: 20459(R) (IITRI-B6019-6)
Mo–Nb–Ti–V, corrosion by steam at 1000°F, 17: 23890(R) (BMI-X-10040)
Mo–Nb–Ti–V, elastic properties and shear modulus of annealed and quenched, 18: 35999
Mo–Nb–Ti–V, mechanical properties of low-ruthenium content, at 2000°F, 16: 33444(R) (ARF-2231-6)
Mo–Nb–Ti–V, mechanical properties of, at high temperatures, effects of molybdenum, tantalum, and tungsten additions on, 16: 33444(R) (ARF-2231-6)
Mo–Nb–Ti–V, phase studies, 19: 7967
Mo–Nb–Ti–V, preparation and properties, 16: 22577(R) (ARF-2231-4)
Mo–Nb–V, corrosion of, by steam and water, 16: 29346
Mo–Nb–V, corrosion by steam at 1000°F, 17: 493(R) (BMI-X-10003)
Mo–Nb–V, ductility strength, and weldability of, 18: 14448
Mo–Nb–V, fabricability, strength, and weldability of, 20: 29763
Mo–Nb–V, mechanical properties of, effects of composition on, 17: 24001
Mo–Nb–V, preparation and properties, 16: 22577(R) (ARF-2231-4)
Mo–Nb–V, properties, 17: 34419(R) (WADC-TR-57-344(Pt.VII))
Mo–Nb–V–Zr, bend ductility of B-66, effects of argon atmosphere contamination on, 19: 9592(R) (ASD-8-170(IV))
Mo–Nb–V–Zr, bonding of B-66, method for diffusion, 20: 5867
Mo–Nb–V–Zr, casting and testing of B-66 ingots, 18: 571(R) (AD-297246)
Mo–Nb–V–Zr, coating evaluation for B-66, oxidation-resistant, 19: 36945 (AD-610867)
Mo–Nb–V–Zr, coating of B-66, with chromium–silicon–titanium systems and silicides, 18: 14373(R) (NP-13498)
Mo–Nb–V–Zr, coatings for B-66 foils, development of high-temperature oxidation-resistant, 18: 30118(R) (RTD-TDR-63-4006(Pt.I))
Mo–Nb–V–Zr, coatings on B-66, properties of oxidation-resistant, 19: 26801(R) (AD-607530)
Mo–Nb–V–Zr, compatibility of rocket nozzles of, with hydrogen, 20: 19228
Mo–Nb–V–Zr, composition, crystal structure, and phases of precipitates in, 16: 22582 (ASD-TDR-62-7)
Mo–Nb–V–Zr, contamination of B-66 by rolling in argon atmosphere, 19: 9592(R) (ASD-8-170(IV))
Mo–Nb–V–Zr, corrosion protection by silicide coatings, 19: 11682
Mo–Nb–V–Zr, corrosion by cesium and lithium above 2500°F, 19: 28766
Mo–Nb–V–Zr, corrosion of B-66, by lithium, effects of oxygen on, 20: 4301(R) (ORNL-3870, pp 102-35)
Mo–Nb–V–Zr, corrosion by cesium vapor and liquid lithium at 2500 to 3400°F of B-66, 20: 5851
Mo–Nb–V–Zr, corrosion by refluxing potassium at 1800 to 2400°F, 20: 25485 (NASA-TN-D-3429)
Mo–Nb–V–Zr, creep-rupture properties of B-66, temperature dependence, 18: 44049(R) (ORNL-3670(p.77-111))
Mo–Nb–V–Zr, creep-rupture properties of, 20: 2336 (ORNL-P-1634)
Mo–Nb–V–Zr, ductility transition temperature of B-66, effects of protective coatings and welding on, 20: 27466
Mo–Nb–V–Zr, ductility, strength, and weldability of, 18: 14448
Mo–Nb–V–Zr, evaporation tests of B-66 in high vacuum, 18: 44049(R) (ORNL-3670(p.77-111))
Mo–Nb–V–Zr, evaporation losses of B-66, at 1200 to 1500°C in high vacuum, 19: 37043 (ORNL-P-1394)
Mo–Nb–V–Zr, evaporation losses in high vacuum of B-66, 20: 4301(R) (ORNL-3870, pp 102-35)
Mo–Nb–V–Zr, extrusion, 17: 3445(R) (NP-12225)
Mo–Nb–V–Zr, extrusion of tubing from, optimization studies, 17: 11140(R) (AMC-TR-7-775(VII))
Mo–Nb–V–Zr, extrusion of tubes of, 17: 23895(R) (AD-403514)
Mo–Nb–V–Zr, extrusion of, program outline for, 17: 25749(R) (WANL-PR-(N)-001)
Mo–Nb–V–Zr, extrusion by Dynapak process of B-66, 19: 30686(R) (AD-608945)
Mo–Nb–V–Zr, fabrication of rolled sheets of B-66, 18: 12591(R) (AD-409960)
Mo–Nb–V–Zr, fabrication of B-66, by rolling, 18: 12593(R) (AD-411155)
Mo–Nb–V–Zr, fabrication and mechanical properties of B-66, 18: 18292(R) (N63-20341)
Mo–Nb–V–Zr, fabrication of B-66, by extrusion and forging, 18: 20484(R) (AD-418992)
Mo–Nb–V–Zr, fabrication of B-66, by extrusion, 18: 20487(R) (WANL-PR-(N)-002)
Mo–Nb–V–Zr, fabrication and properties of coated B-66, 18: 24068(R) (NP-13955)
Mo–Nb–V–Zr, fabrication of extruded B-66, 18: 24093(R) (AD-424593)
Mo–Nb–V–Zr, fabrication and properties of B-66 tubing, 18: 27924(R) (WANL-PR-(N)-004)
Mo–Nb–V–Zr, fabrication of B-66, by rolling, 18: 30106(R) (AD-430773)
Mo–Nb–V–Zr, fabrication B-66 into sheets, 18: 30146(R) (AD-414497)
Mo–Nb–V–Zr, fabrication of B-66 tubing, 18: 41933 (TID-11295(3rd Ed.))
Mo–Nb–V–Zr, fabrication by forging and by extrusion, 19: 11711
Mo–Nb–V–Zr, fabrication and properties of B-66 sheet, 19: 20499(R) (AD-606291)
Mo–Nb–V–Zr, fabrication and properties of B-66 foil, 19: 24945 (ASD-TDR-63-829(Pt.I))
Mo–Nb–V–Zr, fabrication and properties of B-66 strip and foil, 19: 24946 (ASD-TDR-63-829(Pt.II))
Mo–Nb–V–Zr, fabrication of tubing of B-66, 20: 16998
Mo–Nb–V–Zr, joining of foils of B-66, for honeycomb panel fabrication, 18: 37661 (ASD-TDR-63-799(Pt.I))
Mo–Nb–V–Zr, mechanical properties of Pfaudler silicide and TRW chromium–silicon–titanium-coated B-66, in air at 70 to 2600°F, 18: 20523(R) (NP-13811)
Mo–Nb–V–Zr, mechanical properties of B-66, 19: 13978 (AMRA-TR-64-16)
Mo–Nb–V–Zr, oxidation and mechanical properties of coated B-66, 17: 39525(R) (AD-416459)
Mo–Nb–V–Zr, oxidation protection of B-66 by chromium–silicon–titanium coatings at 2000 to 2700°C, 18: 30127 (ASD-TDR-62-934(Pt.II))
Mo–Nb–V–Zr, properties of B66 sheet, 18: 573(R) (AD-422116)
Mo–Nb–V–Zr, properties as space reactor fuel cladding, 18: 9713 (CONF-375-3)
Mo–Nb–V–Zr, properties of coated B-66, to 2600°F, 18: 14373(R) (NP-13498)
Mo–Nb–V–Zr, properties of B-66, to 2600°F, 18: 14353(R) (AD-408310)
Mo–Nb–V–Zr, properties of B-66 foils at high temperatures, effects of coatings on mechanical and thermophysical, 18: 34128 (RTD-TDR-63-4068)
Mo–Nb–V–Zr, properties of welds in B-66, 19: 40989
Mo–Nb–V–Zr, reactions with cesium at 3400°F, metallographic specimen preparation of B-66, 19: 46954 (NMI-5025(Pt.I), pp 39-58)
Mo–Nb–V–Zr, reactions with uranium carbide, nitride, and dioxide, metallographic specimen preparation of B-66, 19: 46954 (NMI-5025 (Pt.I), pp 39-58)
Mo–Nb–V–Zr, rolling of foils of B-66, 19: 7871(R) (AD-422001)
Mo–Nb–V–Zr, stress-rupture properties of B-66, 19: 40961
Mo–Nb–V–Zr, tensile properties of welded plates of B-66, 20: 4301(R) (ORNL-3870, pp 102-35)
Mo–Nb–V–Zr, tensile properties of B-66, effects of welds on, 20: 29712(R) (WANL-PR-(P)-009)
Mo–Nb–V–Zr, tensile strength of B-66, at 1100 to 1400°C, 17: 30950(R)

(NMI-2117)
Mo–Nb–V–Zr, tests of B-66 tubing, nondestructive, 19: 13950 (ORNL-TM-990)
Mo–Nb–V–Zr, thermal properties, 18: 7201 (ASD-TDR-63-597)
Mo–Nb–V–Zr, thermal properties to melting point, 20: 878
Mo–Nb–V–Zr, weld bend tests of B-66, 19: 13955(R) (WANL-PR-(P)-005)
Mo–Nb–V–Zr, weld stability in B-66, 20: 5866
Mo–Nb–V–Zr, weld structural stability in, 18: 22459(R) (NP-13816)
Mo–Nb–V–Zr, weldability of B-66, 17: 39498 (DMIC-Memo-169)
Mo–Nb–V–Zr, weldability of B-66 sheet, 18: 44049(R) (ORNL-3670 (p.77-111))
Mo–Nb–V–Zr, weldability study of B-66, 19: 24957(R) (WANL-PR(P)-006)
Mo–Nb–V–Zr, weldability studies of B-66, 19: 46966(R) (WANL-PR(P)-007)
Mo–Nb–V–Zr, weldability evaluation of, 20: 39366
Mo–Nb–V–Zr, welding of B66, effects of parameters on T1G welds in, 18: 573(R) (AD-422116)
Mo–Nb–V–Zr, welding of B-66, power force programmed ultrasonic, 18: 12594 (AD-427997)
Mo–Nb–V–Zr, welding of B-66, tungsten-arc, 18: 34058(R) (WANL-PR(P)-003)
Mo–Nb–V–Zr, welding of B-66, equipment and procedures for, 19: 9629(R) (AD-608818)
Mo–Nb–V–Zr, welding parameters for B-66, electron-beam, 20: 5867
Mo–Nb–V–Zr, welding properties of B-66, 20: 27466
Mo–Nb–V–Zr, welds in B-66, thermal stability of, 20: 27467
Mo–Nb–W–V, mechanical properties of, effects of composition on, 17: 24001
Mo–Ta–V, mechanical properties, 17: 31010
Mo–Ta–V, phase diagram, 19: 41036
Mo–Ti–V, aging characteristics and phase studies of, 16: 6746
Mo–Ti–V, corrosion by sodium at 650°C, 19: 31462(R) (ANL-7028)
Mo–Ti–V, corrosion by sodium at 650°C, effects of oxygen on, 19: 35604(R) (ANL-7045(p.1-23))
Mo–Ti–V, creep and tensile properties of, at 1800°F, 16: 6747
Mo–Ti–V, development of refractory, for use in oxygen-contaminated sodium systems, (E), 20: 14007(R) (ANL-7122, pp 1-41)
Mo–Ti–V, elastic properties and shear modulus of annealed and quenched, 18: 35999
Mo–Ti–V, elastic properties, 20: 6556(R) (ANL-7105, pp 36-58)
Mo–Ti–V, fabrication for fuel-coating tests, 19: 14765(R) (ANL-6977)
Mo–Ti–V, properties as fuel cladding, 19: 24064(R) (ANL-6997)
Mo–U–V, properties and structure, 17: 6725
Mo–V, creep and tensile properties of, at 1800°F, 16: 6747
Mo–V, fabrication and properties, 18: 26893(R) (ANL-6868(p.11-108))
Mo–V, properties as brazing material, 19: 24916(R) (GEMP-334A)
Mo–V, thermal expansion of, 20: 43964
Mo–V–Zr, oxidation by steam at 900°F, 18: 2162(R) (IITRI-B198-46)
Nb–Sn–V, superconductivity of fused, 20: 15123
Nb–Sn–V–Zr, corrosion by steam at 400 and 450°C, 19: 30668(R) (EURAEC-1274)
Nb–Ta–Sn–V, superconductivity of, 17: 406 (ASD-TDR-62-269)
Nb–Ta–Sn–V, superconducting properties of (Nb,Ta,V)$_3$Sn, 19: 1504
Nb–Ta–Ti–V, coating by pack siliconization, 18: 37621(R) (IITRI-B6021-3)
Nb–Ta–Ti–V, coating for oxidation protection, 19: 20459(R) (IITRI-B6019-6)
Nb–Ta–Ti–V, creep properties and fabrication, 19: 13885(R) (IITRI-B6021-4)
Nb–Ta–Ti–V, effects of boron, carbon, hafnium, and silicon on fabrication and tensile properties of, 19: 32719(R) (AD-609727)
Nb–Ta–Ti–V, fabrication and properties, 17: 4924(R) (ARF-B231-7)
Nb–Ta–Ti–V, fabrication and properties at high temperatures, 18: 37621(R) (IITRI-B6021-3)
Nb–Ta–Ti–V, fabrication and mechanical properties of sheet of, 19: 20552 (IITRI-B6021-6)
Nb–Ta–Ti–V, mechanical properties of, at 2000°F, 16: 33444(R) (ARF-2231-6)
Nb–Ta–Ti–V, oxidation of siliconized, at 2200°F, 17: 23942(R) (ARF-B6001-3)
Nb–Ta–Ti–V, oxidation life at 2200°F of siliconized, static, 17: 35997(R) (IITRE-B6001-5)
Nb–Ta–Ti–V, preparation and properties, 16: 22577(R) (ARF-2231-4)
Nb–Ta–V, arc melting, 17: 3375(R) (ASD-TR-7-826(II))
Nb–Ta–V, availability, properties, and uses of, 20: 29760
Nb–Ta–V, brazing techniques for, 19: 30690(R) (ML-TDR-64-270)
Nb–Ta–V, coating of, with aluminum–silicon in tin, 16: 24163(R) (NP-11711)
Nb–Ta–V, coating of, with ceramics and metals, 16: 24148(R) (ASD-TR-61-676)
Nb–Ta–V, coating with silicides and silicon for protection against oxidation to 4000°F, 18: 30105(R) (AD-429028)
Nb–Ta–V, coatings for, development of aluminum–tin and silicide, 16: 29341 (NP-11990)
Nb–Ta–V, coatings for, for high-temperature uses, 16: 27687
Nb–Ta–V, development as brazing alloy for refractory metals, 20: 4301(R) (ORNL-3870, pp 102-35)
Nb–Ta–V, development and properties of, 20: 31709(R) (IITRI-B6042-5)
Nb–Ta–V, fabrication of rolled sheet, 17: 6597(R) (DMIC-176)
Nb–Ta–V, fabrication and properties of dispersion-strengthened, 18: 5732(R) (IITRI-B6007-5)
Nb–Ta–V, fabrication and properties of sheet bar of, 18: 10508
Nb–Ta–V, fabrication and mechanical properties of sheet of, 19: 20552(R) (IITRI-B6021-6)
Nb–Ta–V, forging characteristics, 16: 9162 (DMIC-Memo-143)
Nb–Ta–V, mechanical properties and quality of, effects of processing variables on, 16: 19336 (ASD-TR-61-684)
Nb–Ta–V, mechanical properties of, effects of composition on, 17: 24001
Nb–Ta–V, mechanical properties, 17: 31010
Nb–Ta–V, mechanical properties and stability of dispersion-strengthened, 17: 30971(R) (IITRI-B6007-3)
Nb–Ta–V, oxidation of, protective effects of aluminum-tin, beryllide, and silicon-titanium coatings against, 17: 22109(R) (ASD-TDR-63-160)
Nb–Ta–V, phase diagram, 19: 41036
Nb–Ta–V, preparation and properties, 16: 22577(R) (ARF-2231-4)
Nb–Ta–V, properties of, at cryogenic and ultrahigh temperatures, 17: 545
Nb–Ta–V, properties as brazing alloy material, 17: 29320(R) (GEMP-23A)
Nb–Ta–V, properties of, data tabulations of mechanical, metallurgical, and physical, 18: 5774 (DMIC-189)
Nb–Ta–V, tensile properties of vanadium-base, effects of carbon and silicon additions on, 20: 21333(R) (IITRI-B6042-4)
Nb–Ta–V, thermal properties, 18: 7201 (ASD-TDR-63-597)
Nb–Ta–V, thermal properties to melting point, 20: 878
Nb–Ta–V–Zr, strength at high temperatures, 20: 2407(P)
Nb–Ti–V, aging characteristics and phase studies, 16: 6746
Nb–Ti–V, annealing, 17: 35078(R) (ANL-6739)
Nb–Ti–V, coating development for, 16: 2168(R) (ARF-2227-2)
Nb–Ti–V, coating for oxidation protection at high temperatures, 19: 15996(R) (IITRI-B6019-4)
Nb–Ti–V, coating for oxidation protection at 1800 to 2500°F, 19: 20459(R) (IITRI-B6019-6)
Nb–Ti–V, coating of, with nickel by flame spraying, oxidation tests of, 16: 6706(R) (ARF-2227-3)
Nb–Ti–V, coating with silicide, 17: 12610(R) (ARF-B6001-2)
Nb–Ti–V, coating with silicides for high-temperature oxidation protection, 17: 30938(R) (NP-12971)
Nb–Ti–V, coatings of pack-siliconized, effects of processing time at 2000 to 2200°F on thickness of, 17: 35997(R) (IITRE-B6001-5)
Nb–Ti–V, compatibility with sodium at 650°C, 17: 41333(R) (ANL-6677)
Nb–Ti–V, compatibility with sodium at 650°C, 18: 26893(R) (ANL-6868 (p.11-108))
Nb–Ti–V, corrosion of, by steam and water, 16: 29346
Nb–Ti–V, corrosion by steam at 1000°F, 17: 493(R) (BMI-X-10003)
Nb–Ti–V, corrosion by steam at 1000°F, 17: 23890(R) (BMI-X-10040)
Nb–Ti–V, corrosion by sodium at 650°C, 17: 35078(R) (ANL-6739)
Nb–Ti–V, corrosion by sodium at 650°C, 17: 36861(R) (ANL-6764)
Nb–Ti–V, corrosion by flowing sodium at 650°C, 17: 37001(R) (ANL-6780)
Nb–Ti–V, corrosion by sodium at 650°C, 18: 15663(R) (ANL-6808)
Nb–Ti–V, corrosion by sodium at 650°C, 19: 31462(R) (ANL-7028)
Nb–Ti–V, corrosion by sodium at 650°C, effects of oxygen on, 19: 35604(R) (ANL-7045(p.1-23))
Nb–Ti–V, corrosion by acids and bases of vanadium-base, 20: 11230 (BM-RI-6715)
Nb–Ti–V, creep and tensile properties of, at 1800°F, 16: 6747
Nb–Ti–V, creep-rupture testing at 870°C, 18: 4255(R) (ORNL-3470(p.98-125))
Nb–Ti–V, development of, for high-temperature uses, 16: 5680 (ARF-2210-6)
Nb–Ti–V, development and properties of, as brazes for joining aluminum oxide and niobium–zirconium alloy, 20: 27445 (LA-DC-7159)
Nb–Ti–V, development and properties of, 20: 31709(R) (IITRI-B6042-5)
Nb–Ti–V, effect of silicide coatings on ductile-to-brittle transition of, 19: 32592(R) (AD-426040)
Nb–Ti–V, elastic properties and shear modulus of annealed and quenched, 18: 35999
Nb–Ti–V, elastic properties, 20: 6556(R) (ANL-7105, pp 36-58)
Nb–Ti–V, evaluation of properties of, 19: 15995 (IITRI-B231-11)
Nb–Ti–V, evaporation tests of Armour alloy in high vacuum, 18: 44049(R) (ORNL-3670(p.77-111))
Nb–Ti–V, fabrication and high-temperature properties of, effects of nitrogen and oxygen on, 16: 12084(R) (ARF-2231-2)
Nb–Ti–V, fabrication and high-temperature strength, 16: 6707 (ARF-

2231-1)
Nb–Ti–V, fabrication and tensile properties of, effects of nitrogen and oxygen on, 16: 16712(R) (ARF-2231-3)
Nb–Ti–V, fabrication of, evaluation of methods and additives for, 16: 29348 (ARF-2231-5)
Nb–Ti–V, fabrication by rolling, 18: 15663(R) (ANL-6808)
Nb–Ti–V, fabrication and properties at high temperatures, effects of molybdenum, tantalum, and tungsten additions on, 18: 22418(R) (IITRI-B6021-1)
Nb–Ti–V, fabrication and properties, 18: 26893(R) (ANL-6868(p.11-108))
Nb–Ti–V, fabrication for fuel-coating tests, 19: 14765(R) (ANL-6977)
Nb–Ti–V, fabrication and mechanical properties of sheet of, 19: 20552(R) (IITRI-B6021-6)
Nb–Ti–V, forgeability and tensile strength, 17: 25771 (ASD-TDR-62-667)
Nb–Ti–V, hardening by carbide and oxide dispersions, 17: 41428(R) (IITRI-B6007-4)
Nb–Ti–V, hardness of sodium-treated, 17: 35079(R) (ANL-6749)
Nb–Ti–V, mechanical properties of, at 2000°F, effects of interstitials on, 16: 2167(R) (ARF-2210-5)
Nb–Ti–V, mechanical and oxidation properties, 17: 41427(R) (IITRI-B231-9)
Nb–Ti–V, mechanical properties of, effects of pack silicide coatings on, 18: 39819(R) (IITRI-B6019-5)
Nb–Ti–V, melting points, 18: 44497(R) (MND-2812-2)
Nb–Ti–V, microstructure of, effects of annealing temperature on, 19: 44587(R) (ANL-7000, pp 3-63)
Nb–Ti–V, oxidation of aluminum coated, 17: 12656 (AD-277779)
Nb–Ti–V, oxidation of siliconized, at 2200°F, 17: 23942(R) (ARF-B6001-3)
Nb–Ti–V, oxidation life at 2150 to 2200°F of siliconized, effects of preparation method on static, 17: 35997(R) (IITRE-B6001-5)
Nb–Ti–V, oxidation protection by aluminum–tin coatings with chromium and titanium additions, 20: 7580 (TIM-945)
Nb–Ti–V, oxidation by air at 900 to 1200°C, kinetics and mechanisms of, 20: 37191
Nb–Ti–V, preparation and properties, 16: 22577(R) (ARF-2231-4)
Nb–Ti–V, properties as cladding for reactor fuel elements, 18: 6412(R) (GEAP-3888)
Nb–Ti–V, properties as fuel cladding, 19: 24064(R) (ANL-6997)
Nb–Ti–V, protective coatings for, 17: 6562(R) (ARF-B-6001-1)
Nb–Ti–V, radiation effects on mechanical properties up to 750°C, neutron, 20: 41506
Nb–Ti–V, tensile properties of vanadium-base, effects of carbon and silicon additions on, 20: 21333(R) (IITRI-B6042-4)
Nb–Ti–V, use as brazing alloy for fabrication of refractory metals, 18: 44049(R) (ORNL-3670(p.77-111))
Nb–Ti–V–Zr, oxidation of siliconized, at 2200°F, 17: 23942(R) (ARF-B6001-3)
Nb–Ti–V–Zr, oxidation life at 2200°F of siliconized, static, 17: 35997(R) (IITRE-B6001-5)
Nb–Ti–W–V, oxidation of siliconized, at 2200°F, 17: 23942(R) (ARF-B6001-3)
Nb–Ti–V–Zr, phase studies, 18: 549(R) (NP-13241)
Nb–Ti–V–Zr, properties, 19: 26848
Nb–Ti–V–Zr, properties, effects of composition on, 20: 2340 (ORNL-TM-1131)
Nb–Ti–W–V, coating for oxidation protection, 19: 20459(R) (IITRI-B6019-6)
Nb–Ti–W–V, oxidation life at 2200°F of siliconized, static, 17: 35997(R) (IITRE-B6001-5)
Nb–Ti–W–V, preparation and properties, 16: 22577(R) (ARF-2231-4)
Nb–Ti–W–V, properties for elevated-temperature service, 19: 6241 (BM-RI-6558)
Nb–Ti–W–V–Zr, properties for elevated-temperature service, 19: 6241 (BM-RI-6558) (ARF-B6007-2)
Nb–V, coating development for oxidation protection of, at high temperatures, 16: 19334(R) (ARF-2227-5)
Nb–V, coating for oxidation protection, 19: 20459(R) (IITRI-B6019-6)
Nb–V, compatibility with sodium at 650°C, 17: 41333(R) (ANL-6677)
Nb–V, composition and mechanical and physical properties of, 18: 7267
Nb–V, corrosion of, by steam and water, 16: 29346
Nb–V, corrosion resistance, 16: 10464
Nb–V, corrosion by superheated steam, 17: 20417
Nb–V, corrosion by steam at 1000°F, 17: 23890(R) (BMI-X-10040)
Nb–V, corrosion by steam at 1000°F, 18: 2184
Nb–V, corrosion by potassium at 1500 to 1800°F, 18: 5728 (ASD-TDR-63-270(Pt.II))
Nb–V, corrosion by steam at 540 and 650°C, 18: 8747(R) (BMI-X-10071)
Nb–V, corrosion by potassium vapor at 1500 to 1800°F, 18: 18282 (BNL-844)
Nb–V, corrosion by liquid sodium, 18: 21698(R) (ANL-6860)
Nb–V, corrosion by steam at 540 and 650°C, 18: 22415(R) (BMI-X-10082)
Nb–V, corrosion by lithium at 815°C, effects of oxygen on, 20: 2340 (ORNL-TM-1131)
Nb–V, corrosion by acids and bases of vanadium-base, 20: 11230 (BM-RI-6715)
Nb–V, corrosion by hydrochloric, phosphoric, and sulfuric acids, effects of alloy composition on, 20: 14997
Nb–V, corrosion by refluxing potassium at 1800 to 2400°F, 20: 25485 (NASA-TN-D-3429)
Nb–V, creep and tensile properties of, at 1800°F, 16: 6747
Nb–V, creep and tensile properties, 17: 32568 (CONF-53-5)
Nb–V, creep strength and ductility of, effects of mechanical twinning on, 20: 15049(R) (N65-16256)
Nb–V, creep testing of, summary of slow-bend, 18: 4255(R) (ORNL-3470(p.98-125))
Nb–V, deformation twinning in, 18: 42019 (ORNL-3678)
Nb–V, development of, for high-temperature uses, 16: 5680 (ARF-2210-6)
Nb–V, development and properties of, as brazes for joining aluminum oxide and niobium–zirconium alloy, 20: 27445 (LA-DC-7159)
Nb–V, diffusion penetration of, by plutonium–uranium alloys, 16: 28555 (TID-7623(p.105-21))
Nb–V, diffusion in bcc, 19: 23112
Nb–V, diffusion kinetics, 19: 42837 (AD-610234)
Nb–V, dislocation and mechanical twinning in, effects of impurities on, 17: 23961 (ORNL-TM-542)
Nb–V, ductile-to-brittle transitions in, enhancement of, 20: 43893 (KAPL-3119)
Nb–V, ductile-to-brittle transitions in, grain boundary effects on, 20: 43894 (KAPL-3146)
Nb–V, ductility, strength, and weldability of, 18: 14448
Nb–V, effects of additives on dispersion strength of, 17: 23943(R)
Nb–V, evaluation for use in lithium-cooled reactors, 18: 44049(R) (ORNL-3670(p.77-111))
Nb–V, fabrication of, evaluation of methods and additives for, 16: 29348 (ARF-2231-5)
Nb–V, fabrication and properties, 17: 4924(R) (ARF-B231-7)
Nb–V, fabrication, oxidation, and properties for use above 2000°F, 17: 39562
Nb–V, fabrication and properties of dispersion-strengthened, 18: 5732(R) (IITRI-B6007-5)
Nb–V, fabrication and properties, 18: 26893(R) (ANL-6868(p.11-108))
Nb–V, fabrication and properties of, effects of metals and carbon on, 18: 27858(R) (IITRI-B6007-6)
Nb–V, fabrication, properties, testing, and uses of superconducting, 19: 16110
Nb–V, fabrication and mechanical properties of sheet of, 19: 20552(R)
Nb–V, hardness, 20: 15073
Nb–V, hydrogen embrittlement, 16: 2256
Nb–V, interdiffusion in, 19: 47058
Nb–V, lattice defect observations in crystals of, use of electron microscopy for, 18: 4251(R) (ORNL-3470(p.49-52))
Nb–V, machinability, properties, weldability, and workability of, 17: 32581
Nb–V, mechanical properties of, at high temperatures, 16: 19339 (BM-RI-5987)
Nb–V, mechanical properties of, effects of composition on, 17: 24001
Nb–V, mechanical properties and stability of dispersion-strengthened, 17: 30971(R) (IITRI-B6007-3)
Nb–V, melting points, 18: 44497(R) (MND-2812-2)
Nb–V, oxidation protection of, at 2000 to 2400°F, coatings for, 16: 27587 (ARF-2227-6)
Nb–V, oxidation of aluminum coated, 17: 12656 (AD-277779)
Nb–V, oxidation kinetics of, 18: 7156
Nb–V, oxidation of, temperature dependence of, 20: 16982
Nb–V, oxidation rate of, 1100°C, 20: 23614
Nb–V, performance as cladding for plutonium–uranium fuel alloys, (E), 20: 14007(R) (ANL-7122, pp 1-41)
Nb–V, properties of welded, 17: 11242
Nb–V, properties as high-temperature brazing alloys, 17: 25688(R) (GEMP-177A)
Nb–V, properties as brazing alloy material, 17: 29320(R) (GEMP-23A)
Nb–V, properties as fuel element cladding, 18: 15563
Nb–V, properties for high-temperature brazing, 19: 11669(R) (GEMP-41A)
Nb–V, radiation effects on fuel rod jackets of, 19: 26876 (ANL-6750)
Nb–V, radioinduced twinning in, neutron, 20: 39462
Nb–V, structural properties of solid solutions of, 19: 13979 (ASD-TDR-63-567(Pt.II))
Nb–V, tensile and creep properties at 2800 to 3400°F, 17: 37506 (BLR-62-26)
Nb–V, tensile strength of B-33, at 1100 to 1400°C, 17: 30950(R) (NMI-2117)
Nb–V, thermal expansion of, 20: 43964
Nb–V, thermodynamic properties, 16: 13636
Nb–V, twinning in, relation of dislocation substructure to, 20: 4389(R)

(ORNL-3870, pp 61-4)
Nb–V, twinning transition temperature, effects of oxygen and vanadium content on, 19: 30809
Nb–V, twinning transition temperature, effects of cold-rolling reduction and annealing temperature on, 19: 30809
Nb–V–Zircaloy-2, radiation effects on phases in, neutron, 18: 39999 (KAPL-2251)
Nb–V–Zr, corrosion of, by steam and water, 16: 29346
Nb–V–Zr, creep properties of, at 982 and 1204°C, 20: 27545
Nb–V–Zr, creep testing of, summary of slow-bend, 18: 4255(R) (ORNL-3470(p.98-125))
Nb–V–Zr, development and properties of niobium-base Cb-753, 20: 19214 (N-65-22097)
Nb–V–Zr, melting points, 18: 44497(R) (MND-2812-2)
Nb–V–Zr, phase studies, 17: 11108(T,R) (EURAEC-307)
Nb–V–Zr, phase studies, 17: 14749(T,R) (EURAEC-408)
Nb–V–Zr, phase studies, 18: 28036
Nb–V–Zr, preparation and properties, 16: 22577(R) (ARF-2231-4)
Nb–V–Zr, properties of Cb-753, 20: 21411
Nb–V–Zr, radiation effects on phases in, neutron, 18: 39999 (KAPL-2251)
Nb–W–V, mechanical properties of, effects of composition on, 17: 24001
Nb–W–V, oxidation of siliconized, at 2200°F, 17: 23942(R) (ARF-B6001-3)
Nb–W–V, oxidation life at 2200°F of siliconized, static, 17: 35997(R) (IITRE-B6001-5)
Nb–W–V, phase diagram, properties, and structure of vanadium-rich corner of, 19: 9681
Nb–W–V, preparation and properties, 16: 22577(R) (ARF-2231-4)
Nb–W–V, properties for elevated-temperature service, 19: 6241 (BM-RI-6558)
Nb–W–V–Zr, ductility, strength, and weldability of, 18: 14448
Nb–W–V–Zr, mechanical properties of, effects of carbon on, 17: 34419(R) (WADC-TR-57-344(Pt.VII))
Nb–W–V–Zr, properties for elevated-temperature service, 19: 6241 (BM-RI-6558)
Ni–Nb–Ta–Ti–V, corrosion resistance and ductility of, 19: 34735(P)
Ni–Nb–V, corrosion of, by steam and water, 16: 29346
Ni–Nb–V, oxidation of coatings of, 17: 6562(R) (ARF-B-6001-1)
Ni–V, crystal structure of intermetallic compounds in, 19: 987
Ni–V, crystal structure of intermetallic compound VNi_3 in, 19: 9699
Ni–V, crystallographic parameters, 17: 18822
Ni–V, electronic specific heat, 17: 16698
Ni–V, hardness and oxidation properties, 17: 35997(R) (IITRE-B6001-5)
Ni–V, magnetic moment distributions in dilute, 17: 37694
Ni–V, neutron elastic scattering by, cross sections for, (E/T), 20: 26346 (NP-16010, pp 1-41)
Pd–V, crystal structure of intermetallic compounds in, 19: 987
Pd–V, crystal structure of intermetallic compound VPd_3 in, 19: 9699
Pd–V, electric conductivity and Hall constant of, 17: 580
Pd–V, magnetic properties at 90 to 1100°K, 20: 7585(T) (ANL-Trans-251)
Pd–V, thermoelectric powers at 700°C, 18: 25970(R) (ANL-6868 (p.303-25))
Pt–V, crystal structure of intermetallic compounds in, 19: 987
Pt–V, crystal structure of intermetallic compound VPt_3 in, 19: 9699
Pt–V, crystal structure of equiatomic intermetallic compound in, 19: 24994
Pt–V, crystallographic parameters, 17: 18822
Pt–V, magnetic penetration depth in superconducting V_3Pt, 18: 28505
Pu–U–V, corrosion by air, 19: 2753
Pu–U–V, corrosion by air at room temperature, 19: 44587(R) (ANL-7000, pp 3-63)
Pu–U–V, performance as zero-power-reactor fuel, 18: 36751 (ANL-6912)
Pu–V, phase diagram, 17: 16567
Re–V, magnetic susceptibility and specific heat of superconducting binary complex phases of, 18: 37715
Re–V, phase diagram, 17: 8727
Re–V, phase studies at 800 to 1500°C, 16: 6746
Rh–Ti–V, superconductivity, 18: 21112
Ru–V, crystal structure of intermetallic compounds and saturated solid solutions in, 17: 16717
Ru–V, thermal capacity of solid solutions of, at low temperatures, 19: 4703
Sc–V, superconductivity in, (E), 19: 5108
Sm–V, oxidation by air at 500°C, 17: 34330(R) (USBM-U-1057)
Sm–V, physical properties, (E), 19: 16188
Sn–Ti–V–Zr, corrosion by steam at 400°C, 18: 22428(T,R) (EURAEC-838)
Sn–Ti–V–Zr, corrosion by steam at 400°C, 19: 32696(R) (EURAEC-783)
Sn–Ti–V–Zr, fabrication by extrusion, 18: 22428(T,R) (EURAEC-838)
Sn–Ti–V–Zr, fabrication and properties, 19: 36965(T,R) (EURAEC-618)
Sn–V, phase studies at 800 to 1500°C, 16: 6746
Sn–V, preparation and crystal structure of intermetallic compound V_3Sn_3 in, 19: 39189
Sn–V, tin-119 Mössbauer effect in, 18: 5881
Sn–V, use of SnV_3 in superconducting magnets, 17: 20438
Sn–V–Zr, corrosion by steam at 350, 400, and 480°C, 18: 20476(T,R) (EURAEC-916)
Sn–V–Zr, corrosion by steam at 350, 400, and 480°C, 18: 22428(T,R) (EURAEC-838)
Sn–V–Zr, corrosion by steam at 350, 400, and 480°C, hydrogen sorption during, 18: 34060(T,R) (EURAEC-1062)
Sn–V–Zr, corrosion by steam at 400°C, 19: 32696(R) (EURAEC-783)
Sn–V–Zr, corrosion by steam or water, 19: 24982(R) (EURAEC-1270)
Sn–V–Zr, fabrication and tensile properties of extruded, 18: 22428(T,R) (EURAEC-838)
Sn–V–Zr, fabrication and mechanical properties, effects of heat treatments on, 18: 34060(T,R) (EURAEC-1062)
Sn–V–Zr, fabrication and properties, 19: 36965(T,R) (EURAEC-618)
Sn–V–Zr, mechanical properties at 20, 200, 500, and 700°C, 18: 20476(T,R) (EURAEC-916)
Sn–V–Zr, mechanical properties between 20 and 700°C, 19: 24982(R) (EURAEC-1270)
Sn–V–Zr, oxidation of, causes of second transition point in, 16: 7857
Sn–V–Zr, sorptive properties for hydrogen, 19: 24982(R) (EURAEC-1270)
Sn–V–Zr, thermal expansion between 100 and 1100°C, 19: 24982(R) (EURAEC-1270)
stainless steel–V, fabrication of tubular, 18: 15663(R) (ANL-6808)
Ta–Sn–V, superconductivity of, 17: 406 (ASD-TDR-62-269)
Ta–Ti–V, aging characteristics and phase studies, 16: 6746
Ta–Ti–V, compatibility with sodium at 650°C, 17: 41333(R) (ANL-6677)
Ta–Ti–V, compatibility with sodium at 650°C, 18: 26893(R) (ANL-6868 (p.11-108))
Ta–Ti–V, corrosion by sodium at 650°C, 19: 31462(R) (ANL-7028)
Ta–Ti–V, corrosion by sodium at 650°C, effects of oxygen on, 19: 35604(R) (ANL-7045(p.1-23))
Ta–Ti–V, creep and tensile properties of, at 1800°F, 16: 6747
Ta–Ti–V, development as brazing alloy for refractory metals, 20: 4301(R) (ORNL-3870, pp 102-35)
Ta–Ti–V, elastic properties, 20: 6556(R) (ANL-7105, pp 36-58)
Ta–Ti–V, fabrication for fuel-coating tests, 19: 14765(R) (ANL-6977)
Ta–Ti–V, properties as fuel cladding, 19: 24064(R) (ANL-6997)
Ta–Ti–V, use as brazing alloy for fabrication of refractory metals, 18: 44049(R) (ORNL-3670(p.77-111))
Ta–Ti–V–Zr, phase studies, 18: 549(R) (NP-13241)
Ta–V, coating for oxidation protection, 19: 20459(R) (IITRI-B6019-6)
Ta–V, coating with ceramics and metals, 16: 24148(R) (ASD-TR-61-676)
Ta–V, creep and tensile properties of, at 1800°F, 16: 6747
Ta–V, electric conductivity of, effects of magnetic fields on, 19: 27735(R) (NAA-SR-10850)
Ta–V, fabrication and properties at high temperatures, 18: 7178
Ta–V, fabrication and mechanical properties of sheet of, 19: 20552(R) (IITRI-B6021-6)
Ta–V, high-magnetic-field specific heat of superconductors of, 18: 7649
Ta–V, magnetic properties at 77 to 1100°K, 20: 7593
Ta–V, magnetization of, 19: 12865(R) (NAA-SR-10501)
Ta–V, mechanical properties, 17: 31010
Ta–V, phase diagram, existence boundary of σ-phase, 16: 22614
Ta–V, phase studies, 18: 26055
Ta–V, properties as high-temperature brazing alloys, 17: 25688(R) (GEMP-177A)
Ta–V, properties for elevated-temperature service, 19: 6241 (BM-RI-6558)
Ta–V, specific heat at low temperatures, 19: 12865(R) (NAA-SR-10501)
Ta–V, specific heat of superconducting, (T), 19: 19038
Ta–V, thermodynamic properties, 16: 13636
Ta–V, thermodynamic properties of superconducting, 18: 15080
Ta–V, thermodynamic properties of superconducting, 20: 10272(R) (NAA-SR-9339)
Ta–V–Zr, coating for oxidation protection, 19: 20459(R) (IITRI-B6019-6)
Ta–W–V, mechanical properties, 17: 31010
Tc–V, Knight shifts and magnetic susceptibilities in, 17: 654
Tc–V, nuclear magnetic resonance relaxation times, 19: 43986(R) (ANL-7000, pp 201-4)
Tc–V, nuclear spin-lattice relaxation time of technetium-99 and vanadium-51 in, (E), 19: 39403
Tc–V, phase studies on, 17: 11220
Tc–V, superconducting transition temperature, 19: 44678(R) (ANL-7000, pp 186-200)
Tc–V, technetium-99 and vanadium-51 nuclear magnetic resonance in, 16: 22140
Th–V, corrosion by water at 120 to 260°C, 19: 22889 (ANL-7006)
Th–V, phase diagram, 17: 4936
Th–V, phase diagram, 17: 14740 (TID-11295(2nd Ed.))
Th–V, phase studies, 16: 30877

Th–V, phase studies at 800 to 1500°C, 16: 6746
Ti–U, corrosion by sodium at 550 to 750°C, 20: 45106(R) (ANL-7249)
Ti–V, bulk superconductivity in, 18: 24553
Ti–V, compatibility with fissium–plutonium–uranium alloys at 600 and 650°C, 18: 19456(R) (ANL-6840)
Ti–V, compatibility with fissium–plutonium–uranium alloy, 19: 2839
Ti–V, compatibility with plutonium–thorium–uranium alloys, 20: 2230
Ti–V, compatibility with plutonium-uranium carbides, 20: 6600(R) (ANL-7105, pp 1-35)
Ti–V, compatibility with plutonium–thorium–uranium alloy, 20: 31666
Ti–V, composition and mechanical and physical properties of, 18: 7267
Ti–V, corrosion by sodium at 650°C, 18: 15663(R) (ANL-6808)
Ti–V, corrosion by oxygenated sodium at 650°C, 18: 19456(R) (ANL-6840)
Ti–V, corrosion by liquid sodium, 18: 21698(R) (ANL-6860)
Ti–V, corrosion by sodium at 650°C, 18: 26893(R) (ANL-6868(p.11-108))
Ti–V, corrosion by liquid sodium at 650°C, 18: 44925(R) (ANL-6923 (p.14-45))
Ti–V, corrosion by sodium at 650°C, 19: 14765(R) (ANL-6977)
Ti–V, corrosion by sodium at 650°C, 19: 17176(R) (ANL-6965(p.1-41))
Ti–V, corrosion by liquid sodium, 19: 23991(R) (ANL-7003)
Ti–V, corrosion by sodium at 650°C, 19: 29468(R) (ANL-7017)
Ti–V, corrosion by sodium at 650°C, 19: 31462(R) (ANL-7028)
Ti–V, corrosion by sodium at 650°C, effects of oxygen on, 19: 35604(R) (ANL-7045(p.1-23))
Ti–V, corrosion by sodium at 650°C, 19: 40177(R) (ANL-7046(p.1-35))
Ti–V, corrosion by oxygen-contaminated sodium, 19: 44587(R) (ANL-7000, pp 3-63)
Ti–V, corrosion by sodium at high temperatures, 20: 3320(R) (ANL-7082, pp 1-28)
Ti–V, corrosion by oxygenated sodium at 540°C, effects of polarization on, 20: 3321(R) (ANL-7082, pp 29-53)
Ti–V, corrosion cracking by ferric chloride, hydrochloric acid, and nitric acid solutions, stress-, 20: 2254 (BM-RI-6680)
Ti–V, corrosion of TV-20, by sodium at 650°C, 20: 5846
Ti–V, corrosion by acids and bases of vanadium-base, 20: 11230 (BM-RI-6715)
Ti–V, corrosion by sodium at 650°C, 20: 26394(R) (ANL-7193)
Ti–V, corrosion by sodium at 650°C, effects of oxygen content on, 20: 31669
Ti–V, corrosion in sodium at 650°C, 20: 43809 (BNL-50003)
Ti–V, creep and tensile properties of, at 1800°F, 16: 6747
Ti–V, creep at high temperatures, 18: 44925(R) (ANL-6923(p.14-45))
Ti–V, creep rate testing and thermal expansivity of, 20: 30790(R) (ANL-7204, pp 1-31)
Ti–V, critical current density of superconducting, in transverse field of 30 kgauss, 18: 6128
Ti–V, critical current-field relation in superconducting, 17: 41542 (BSD-TDR-63-148)
Ti–V, critical field for superconducting, temperature dependence of lower, (E/T), 19: 19031
Ti–V, critical magnetic field of superconducting, (T), 19: 33181
Ti–V, development for use as cladding on fast reactor fuels, 18: 35060(R) (ANL-6904)
Ti–V, development of refractory, for use in oxygen-contaminated sodium systems, (E), 20: 14007(R) (ANL-7122, pp 1-41)
Ti–V, development for fuel cladding, 20: 20183
Ti–V, diffusion of titanium-44 in, 20: 4385(R) (ORNL-3870, pp 15-19)
Ti–V, elastic moduli of, ultrasonic measurement of, 19: 17177(R) (ANL-6965(p.42-83))
Ti–V, elasticity of, ultrasonic measurements of, as function of temperature, 20: 31708 (ANL-7119)
Ti–V, electric conductivity and magnetization of superconducting, at 4.2°K, (E), 20: 21928
Ti–V, electronic specific heat, 17: 16698
Ti–V, enthalpy, thermal conductivity, and thermal expansion of, 19: 44587(R) (ANL-7000, pp 3-63)
Ti–V, fabricability of TV-20, effects of molybdenum, niobium, and tantalum additions on, 19: 44587(R) (ANL-7000, pp 3-63)
Ti–V, fabrication and properties as reactor fuel cladding material, 18: 19456(R) (ANL-6840)
Ti–V, fabrication and properties, 18: 26893(R) (ANL-6868(p.11-108))
Ti–V, fabrication of tubing of, 19: 2786
Ti–V, fabrication and mechanical properties of, 19: 29468(R) (ANL-7017)
Ti–V, fabrication for fuel jackets, 19: 31462(R) (ANL-7028)
Ti–V, fabrication of TV-20 into bar, rod, sheet, and tubing, 19: 30687 (ANL-6928)
Ti–V, fabrication into tubes by extrusion, 19: 40177(R) (ANL-7046 (p.1-35))
Ti–V, fabrication of TV-20, 19: 44587(R) (ANL-7000, pp 3-63)
Ti–V, fabrication of tubing of, for reactor fuel cladding, 20: 11258
Ti–V, fabrication of TV-20, process development for, 20: 11260
Ti–V, fabrication of, equipment and techniques for, 20: 43846 (ANL-7127)
Ti–V, hardness of cold-reduced, 18: 15426(R) (ANL-6810)
Ti–V, hardness of extruded, 18: 15663(R) (ANL-6808)
Ti–V, hardness of, effects of oxygen and titanium content on, 19: 44587(R) (ANL-7000, pp 3-63)
Ti–V, heat content at −80 to 1150°C, 19: 14765(R) (ANL-6977)
Ti-V, Knight shifts and magnetic susceptibilities in, 17: 654
Ti–V, linear thermal expansion coefficient of, 20: 46963(R) (ANL-7132)
Ti–V, magnetic field effects on superconductivity of, 18: 15077
Ti–V, magnetic induction measurements for superconducting, 17: 37717
Ti–V, magnetization of high-field superconducting type-II, mixed-state paramagnetism in, (E), 20: 8018
Ti–V, mechanical properties for use as fuel cladding, 19: 6827(R) (ANL-6944(p.13-52))
Ti–V, mechanical properties at high temperatures, 19: 40177(R) (ANL-7046(p.1-35))
Ti–V, mechanical properties at high temperatures, 19: 44674(R) (ANL-7000, pp 69-83)
Ti–V, melting points, 18: 44497(R) (MND-2812-2)
Ti–V, neutron reactions in, yields of helium and hydrogen produced by fast, 19: 44746 (NAA-SR-Memo-10626)
Ti–V, nuclear spin-lattice relaxation in type II superconductors of, (E), 19: 41611
Ti–V, paramagnetic susceptibility, 16: 10576
Ti–V, performance as fuel cladding in fast reactors, 18: 24952(R) (ANL-6880(p.6-48))
Ti–V, performance as coating on fast reactor fuel elements, 18: 26824(R) (ANL-6885)
Ti–V, performance as sodium-cooled-reactor fuel cladding, 18: 36751 (ANL-6912)
Ti–V, performance as cladding for plutonium–uranium fuel alloys, (E), 20: 14007(R) (ANL-7122, pp 1-41)
Ti–V, precipitation in β phase, 16: 10600
Ti–V, preparation and properties of thin-film hard superconducting, 18: 28501
Ti–V, preparation for superconductor magnetic field measurements, 19: 40286(R) (NAA-SR-11200)
Ti–V, properties for use as cladding for high-temperature fuels, 18: 44930(R) (ANL-6930(p.17-38))
Ti–V, properties for use as fuel cladding material, 19: 11679
Ti–V, properties as fuel cladding, 19: 17176(R) (ANL-6965(p.1-41))
Ti–V, properties as fuel cladding, 19: 40113(R) (ANL-7071)
Ti–V, radiation effects on mechanical properties of, fast neutron, 20: 36391(R) (ANL-7219, pp 1-27)
Ti–V, radiation effects on mechanical properties up to 750°C, neutron, 20: 41506
Ti–V, radiation effects on mechanical and physical properties of, 20: 45106(R) (ANL-7249)
Ti–V, radioinduced production of helium and hydrogen in, neutron, 19: 26901
Ti–V, reactions with fissium–plutonium–uranium at 600 to 750°C, 19: 40958
Ti–V, reactions with plutonium–thorium–uranium alloys at 650°C, 19: 44674(R) (ANL-7000, pp 69-83)
Ti–V, reactions with fissium–plutonium–uranium alloys at 750°C, 19: 44587(R) (ANL-7000, pp 3-63)
Ti–V, reactions with fissium–plutonium–uranium alloy at 550 to 700°C, 20: 5843
Ti–V, reactions with sodium, high-temperature, 20: 15033(R) (ANL-7152, pp 87-96)
Ti–V, reactions with sodium at 2100°C, 20: 31440(R) (ANL-7175, pp 159-83)
Ti–V, reactions with liquid sodium at high temperatures, 20: 38499 (ANL-7120, pp 839-47)
Ti–V, removal from fuel pins by hydrogen-induced swelling, 19: 40113(R) (ANL-7071)
Ti–V, removal from fuel elements by chlorination, 20: 5594(R) (ANL-6925, pp 21-106)
Ti–V, removal from reactor fuel alloys, chemical methods for, 20: 20802(R) (ANL-7055, pp 21-98)
Ti–V, removal of cladding of, from fuel elements, 19: 14765(R) (ANL-6977)
Ti–V, removal of cladding of, from fuel by chlorination and hydridation, 19: 32279(R) (ANL-7020(p.3-99))
Ti–V, separation from reactor fuel alloys, development of methods for, 19: 6827(R) (ANL-6944(p.13-52))
Ti–V, separation from reactor fuel alloys by flotation in cadmium, 19: 29468(R) (ANL-7017)
Ti–V, specific heat in body-centered-cubic, at low temperatures, 16: 25806
Ti–V, superconductivity of, pulsed-magnetic-field studies of, 17: 18907 (TID-17310)

Ti–V, superconducting transitions in high magnetic fields, 17: 25938
Ti–V, superconductivity, 17: 41604
Ti–V, superconductivity of, 18: 15084
Ti–V, superconducting properties, 18: 44681
Ti–V, superconductivity of, (E), 19: 6613
Ti–V, superconducting transition anomalies in, (E), 19: 10214
Ti–V, superconducting properties and uses, 19: 39750(P)
Ti–V, superconducting critical field of, spin-orbit effects on upper, (E), 20: 32330
Ti–V, superconductivity, 20: 40047
Ti–V, superconducting magnetic field and surface current measurements for, 20: 44535
Ti–V, tensile properties at 20 to 800°C, 18: 25966(R) (ANL-6868 (p.120-32))
Ti–V, thermal conductivity of, 20: 46963(R) (ANL-7132)
Ti–V, thermal expansion of, linear, 20: 45106(R) (ANL-7249)
Ti–V, thermodynamic properties, 16: 13636
Ti–V, transformation characteristics during continuous cooling, 18: 20545
Ti–V, use as brazing alloy, 19: 30690(R) (ML-TDR-64-270)
Ti–V, use as fuel element cladding material in 1000-Mw(e) fast breeder reactor, 20: 38494 (ANL-7120, pp 94-103)
Ti–V–Zr, fabrication and properties, 18: 26893(R) (ANL-6868(p.11-108))
Ti–V–Zr, fabrication and properties, 19: 36965(T,R) (EURAEC-618)
Ti–V–Zr, phase studies, 18: 549(R) (NP-13241)
Ti–V–Zr, tensile properties at room temperature, 18: 18380
Ti–V–Zr, thermal expansion between 100 and 1100°C, 19: 24982(R) (EURAEC-1270)
Ti–V–Zr, use as brazing alloy, 19: 30690(R) (ML-TDR-64-270)
Ti–W–V, aging characteristics and phase studies of, 16: 6746
Ti–W–V, creep and tensile properties of, at 1800°F, 16: 6747
U–V, casting of, testing of products from, 20: 29803
U–V, combustion kinetics of, 20: 43612
U–V, fabrication and properties, 18: 557
U–V, mechanical properties, 20: 29803
U–V, phase studies, 17: 29255 (ZFK-WF-13)
U–V, spectrographic analysis for aluminum, 18: 35451 (PG-Report-390)
U–V, stability of thermal cycled, 17: 39638
V–Y, corrosion by acids and bases of vanadium-base, 20: 11230 (BM-RI-6715)
V–Y, phase studies, 16: 19394
V–Zn, crystal structure and phase studies, 17: 40421(R) (ANL-6766)
V–Zn, phase studies, 17: 1359(R) (ANL-6569)
V–Zn, phase studies, 17: 14116(R) (ANL-6596(p.29-118))
V–Zn, structure of V_4Zn_5, 18: 1483(R) (ANL-6687(p.27-85))
V–Zr, composition and mechanical and physical properties of, 18: 7267
V–Zr, corrosion by steam at 400°C, 18: 24150(T,R) (EURAEC-538)
V–Zr, corrosion by steam, effects of aluminum, tin, or titanium on, 19: 24982(R) (EURAEC-1270)
V–Zr, corrosion by steam, 19: 24982(R) (EURAEC-1270)
V–Zr, crystal structure of, electron microscopic studies of, 18: 20476(T,R) (EURAEC-916)
V–Zr, crystal structure of Brillouin zones in, effects of electron-atom ratios on, 19: 26836
V–Zr, electrochemical potential and hydrogen overvoltage, 17: 34403 (GEAP-4192)
V–Zr, extrusion of, effects on structure, 17: 6654(R) (EURAEC-394)
V–Zr, free energies of formation of Laves phases in, 16: 13636
V–Zr, hardening of, by addition of aluminum, tin, or titanium, 19: 24982(R) (EURAEC-1270)
V–Zr, hardening of, by formation of intermetallic compounds, 19: 24982(R) (EURAEC-1270)
V–Zr, hydrogen overvoltage measurements in, 17: 27728(R) (GEAP-4076)
V–Zr, hydrogen overvoltage at ZrV_2 in sulfuric acid, 18: 12642 (GEAP-4089(Vol.II)(Paper 22))
V–Zr, magnetic induction in hard superconducting, (E), 20: 21893
V–Zr, mechanical properties of, 19: 24982(R) (EURAEC-1270)
V–Zr, oxidation by carbon dioxide up to 600°C, 18: 30192
V–Zr, phase studies, 17: 11204(T,R) (EURAEC-444)
V–Zr, phase studies of, 17: 11213
V–Zr, phase studies and properties of extruded, effects of annealing, quenching, and tempering on, 18: 24150(T,R) (EURAEC-538)
V–Zr, reactions with hydrogen, thermochemical and structural aspects of, 20: 27436
V–Zr, tensile properties, 19: 36965(T,R) (EURAEC-618)
V–Zr, uptake of hydrogen during steam and water corrosion of, 17: 32519
W–V, creep and tensile properties of, at 1800°F, 16: 6747
W–V, magnetic induction measurements for superconducting, 17: 37717
W–V, phase studies of, at 800 to 1500°C, 16: 6746
W–V, properties in bonding tungsten to carbide-coated graphite, 17: 14776(R) (AD-285214)

VANADIUM ARSENIDES
crystal structure, 19: 7945

VANADIUM, BISCYCLOPENTADIENYL-
preparation by reaction of vanadium chloride with magnesium cyclopentadienide, 20: 35493

VANADIUM BORIDES
abrasive properties, 20: 15109
bibliography on preparation and properties of, 17: 10579 (ASD-TDR-62-873)
chemical bonding and electric conductivity of, 20: 16439
electric properties of, effects of non-metallic atoms on, 17: 8854
fabrication and properties of MHD cell electrodes of, 19: 6495
performance as control materials for high-temperature reactors, 18: 22519
preparation by carbon reduction of oxide with boric oxide, 20: 19702
radiation sintering of, 17: 20512 (GEAP-3743(Pt.II))
reactions with carbon, 20: 14555
thermal conductivity, effects of electronic and crystalline structure, 16: 24208

VANADIUM BROMIDES
formation of tetravalent, 17: 23293 (IS-533)
reactions of, with bromine and iodine vapors at 350 to 450°C, 17: 23295 (IS-535)
vapor pressure of, at 590 to 950°K, 17: 23294 (IS-534)
vaporization of, 17: 2956 (UCRL-9840)
vaporization reactions of trivalent, at 644 to 805°K, 17: 23293 (IS-533)
VBr_3–VCl_3, reactions of, with bromine vapor, 17: 23295 (IS-535)

VANADIUM BRONZE
magnetic resonance in lithium, 16: 21123 (AFOSR-1959)

VANADIUM CARBIDES
abrasive properties, 20: 15109
analysis for carbon using electron microprobe, 19: 43966
analysis for oxygen by heat extraction, 16: 7515
bibliography on properties, 17: 27809 (UCRL-7284)
bonding and vacancies in, 18: 16483(T) (AEC-tr-6374)
bonding to tantalum, 16: 15151 (APED-3870)
crystal structure, 18: 25970(R) (ANL-6868(p.303-25))
crystal structure, 19: 37050
deformation properties and hardness of, at high temperatures, 20: 33920
deposition on graphite surfaces, 19: 42836(P)
diffusion of carbon in, at 1700 to 3000°C, 20: 27530
effects on grain growth of uranium carbides, 19: 20515(R) (NCSC-2981-6)
effects on grain growth of uranium carbides, 19: 20516(R) (NCSC-2981-7)
elastic properties of stoichiometric, 20: 39430
electric conductivities and Hall coefficients, 16: 6749
electric properties of, effects of non-metallic atoms on, 17: 8854
emissivity at 800 to 5000°K, relation of structure to, 18: 20566
emissivity of coatings of, to 2000°F, 16: 30801(R) (PWA-1878)
entropy of formation at 298°K, 18: 19974
fabrication by hot-pressing, 20: 31699
figure of merit and atomic characteristics, 19: 2284
formation in vanadium steel, 17: 11209
free energy of formation at 1180 to 1370°K, 18: 19970
friction between surfaces of, at high temperatures in vacuum, argon, helium, and nitrogen atmospheres, 19: 28826
friction between surfaces of, at high-temperatures in vacuum, 19: 28827
hardness of, effects of temperature on, 17: 36316
inflammability of powdered, at 180 to 1100°C, 18: 44211
magnetic susceptibility, 17: 14858(T) (AEC-tr-5651)
melting temperature, evaluation for space technology, 18: 16521
oxidation of, at 1000 to 2000°K, kinetics of, 17: 21665(R) (ASD-TDR-62-203(Pt.II))
phase studies by differential thermal analysis, 20: 9525
physical properties of, band model for determining, 19: 7442
preparation in fluidized beds, 20: 9397
preparation of high-purity, using cobalt or iron-nickel alloy bath, 19: 42828
preparation of high-purity, auxiliary metal bath for, 20: 27452
preparation, properties, and aerospace applications, 19: 37142
pressing of high density, apparatus for hot, 16: 19267
production and properties of, 18: 7262
properties, mechanical and physical, 16: 30853
properties of, effects of temperature on mechanical and physical, 17: 16760
radiation effects on mechanical and physical properties of, 17: 16760
review, 18: 39899 (LA-2942)
screening of metal–metal bonds in, effects on overlapping, 18: 17781(T) (AEC-tr-6388)
spectral emittance at 800 to 5000°F, 16: 18939
superconducting properties, 19: 20572
superconductivity of, negative results, 17: 11391
surface energy of, calculation of approximate, 17: 41475(T)
thermal conductivity, effects of electronic and crystalline structure, 16: 24208
thermal decomposition, 17: 32036 (CONF-40-2)

thermal properties to 5000°F, 16: 18938
thermal properties of, at 500 to 5000°F, 17: 16636 (ASD-TDR-62-765)
thermionic properties at 1400 to 2000°K, 17: 25811
thermodynamic stability of, review of data on, 19: 23064
thermoelectric emission of, on metal substrates, 19: 6351
thermoelectric properties at 1600 to 2130°K, 17: 11436
wetting by liquid cobalt, copper, iron, and nickel, 20: 1837
graphite–VC, fabrication and physical properties of, 20: 39367
MoC–VC, high-field superconductivity of, (E), 19: 25449
NbC–VC, wetting by nickel, 19: 18522(T)
NbN–VC, superconducting properties, 20: 17589 (CONF-650922, pp 541-9)
Nb–VC, wetting by nickel, 18: 7241
SiC–TiC–VC, oxidation tests at 1400 and 1500°C, 19: 9624 (SCNC-270)
SiC–VC, oxidation tests at 1400 and 1500°C, 19: 9624 (SCNC-270)
SiC–VC–ZrC, oxidation tests at 1400°C, 19: 9624 (SCNC-270)
TiC–VC, oxidation tests at 1400°C, 19: 9624 (SCNC-270)
TiC–VC, wetting by liquid copper, 20: 1837
VC–ZrC, oxidation tests at 1400°C, 19: 9624 (SCNC-270)
Vanadium Cesium Sulfates
see Cesium Vanadium Sulfates

VANADIUM CHLORIDES
see also Vanadium Oxychlorides
analytical use in potentiometric determination of bismuth and thallium, 16: 1714
chlorine-35 quadrupole bonding and resonance in solid layer type, 16: 7538
properties of solutions of, in dimethyl sulfoxide, 20: 293 (UCRL-16330)
radiation effects on magnesium reduction of, gamma, 18: 12138 (BNRI-6382)
reactions of, with bromine and iodine vapors at 350 to 450°C, 17: 23295 (IS-535)
separation by reversed-phase partition chromatography using organophosphorus compounds, 18: 25614
spectra of, at liquid helium temperatures, ESR, 20: 31221(R) (UCRL-16658, pp 73-87)
synthesis of anhydrous, 17: 30553
vapor pressure of, at 590 to 950°K, 17: 23294 (IS-534)
vaporization of, 17: 2956 (UCRL-9840)
VBr_3–VCl_3, reactions of, with bromine vapor, 17: 23295 (IS-535)

VANADIUM COMPLEXES
bis(1,3-diphenyl-1,3-propanedione)oxo-, preparation and properties, 18: 39193
catalytic effects on hydrolysis of salicyl phosphate, 16: 28949
chlorophyllin, radiosensitivity effects in mice, gamma, 20: 1692
complexes with 2,4-pentanedione, heat of combustion of, 16: 11609
formation constants and classification of, by spectrophotometric methods, 19: 26365
tris(1,3-diphenyl-1,3-propanedione)-, preparation and properties, 18: 39193
tris(2,4-pentanedionato)-, preparation and properties, 18: 39193
with cyanide in molten lithium chloride–potassium chloride, stability of, 19: 32122(R) (NYO-2747-3)
with cyclopentadiene-cycloheptatriene, structure of, 17: 20018
with EDTA, bonding and structure of, 17: 33896
with ethylenediaminetetraacetic acid, formation and stability of polynuclear, 20: 23035
with gallic acid, absorption spectra of solutions of, 18: 13715 (AFOSR-TN-59-1183)
with *N*-hydroxyethylethylenediaminetriacetic acid, formation and stability of polynuclear, 20: 23035
with porphyrin, separation of, from oil solutions, 18: 5405(P)
with salicylic acid, properties, 16: 18915
with triphenylphosphine, preparation and properties of, 18: 12089
with tropolone, preparation, properties, and structure, 20: 5538
with 1,2-cyclohexanediaminetetraacetic acid, formation and stability of polynuclear, 20: 23035
with 2,4-pentanedione, thermodynamics of solution, 16: 18897
with 2,2′-bipyridine-1,1′-dioxide, preparation and properties of, 20: 25067
with 2,4-pentanedione, chromium-atom slowdown paths at 20 to 90 ev in, (E), 19: 33512
with 2,4-pentanedione, heat of combustion of, 16: 11609
with 2,4-pentanedione, preparation of, 18: 39193
with 3-cyanopentane-2,4-dione, stretching frequency of cyano group in, 16: 20421

VANADIUM COMPOUNDS
analytical uses for determination of cerium in magnesium alloys by potentiometric titration, 20: 274
decomposition of tetraalkoxides in ion source of mass spectrometer, mechanism of, 20: 14584(R) (TID-22444)
preparation of plutonate, with perovskite structure, 18: 23521(P)
use as photosensitizer for polymerization of methyl methacrylate at various pH's, 20: 38934

VANADIUM COUPLES
Al/Si/U/V, multiphase diffusion studies in, 19: 30731 (EUR-1819.e (p.37-48))
Al/U/V, multiphase diffusion studies in, 19: 30731 (EUR-1819.e (p.37-48))
Fe/Nb/stainless steel/V, diffusion in bimetallic tubing of, with iron and vanadium diffusion barriers, inter-, 20: 11215(R) (NASA-CR-54718)
Fe/stainless steel/Ta/V, diffusion in bimetallic tubing of, with iron and vanadium diffusion barriers, inter-, 20: 11215(R) (NASA-CR-54718)
Ta/V, interdiffusion in, 18: 42031

VANADIUM DEPOSITS
mapping of Monument No. 1-Mitten No. 2 Mine, Monument Valley, Navajo County, 16: 4384
mineralogy of deep and intermediate, in Mounana, Gabon Republic, 19: 654

VANADIUM FERROCYANIDES
properties for use as ion exchange material, 20: 12932

VANADIUM FLUORIDES
see also Vanadium Oxyfluorides
heat of sublimation and vapor pressure of, 20: 26874
preparation and properties, 16: 17554(R) (ORNL-3262(p.3-18))
reactions with chlorides, fluorides, and sulfides, 20: 36804
reactions with xenon hexafluoride and xenon tetrafluoride oxide, compound formation in, 20: 45657
separation from uranium hexafluoride, 19: 13553(P)
vanadium-51 NMR in, 19: 13293
vaporization of, 17: 2956 (UCRL-9840)
UF_6–VF_5, Raoult's law deviation in liquid, 18: 39251

VANADIUM HYDRIDES
analysis for hydrogen by combustion method, 19: 22150
chemical bonds in, properties of, 20: 12847
hydrogen vibrations in, (E/T), 19: 5887
neutron inelastic scattering, by localized modes in, cold, (E), 19: 12076
neutron inelastic scattering by, determination of localized modes of hydrogen excess in, (E), 20: 20107 (EUR-2734.e)
neutron inelastic scattering by localized oscillation states in, cold, (E/T), 20: 28670
neutron scattering by, spectra from inelastic, 18: 24605 (NP-13930 (p.59-71))
nuclear magnetic resonance measurements of, 19: 43346
preparation, 20: 26902
structure of, analysis from neutron diffraction patterns of $VD_{0.71}$ at low temperatures, 16: 29484(R) (TID-15143)

VANADIUM IODIDES
phase studies, 20: 3863(R) (IS-1200(Sect. C))
preparation, 18: 2163(R) (IS-700(Sect.M))
preparation, 19: 9604(R) (IS-900(Sect.M))
preparation and phase studies of, 20: 35473 (IS-T-41)
vapor pressure and equilibrium reactions, 20: 40796 (IS-1500(Sect.C))
vaporization of, 17: 2956 (UCRL-9840)

VANADIUM IONS
see also Pervanadyl ions
see also Vanadyl Ions
determination by nuclear magnetic relaxation, 18: 6771
determination of tetravalent, in sulfate solutions using cerium sulfate and ferroin, titrimetric, 20: 43144
effects on cobalt determination in steel, 20: 43145
effects on copper determination, 20: 36726
effects on crystalline electric fields, method for calculating, 20: 5006(R) (ORNL-3870, pp 50-5)
effects on electron spin resonance spectra of irradiated silicate glasses, 20: 42538
effects on oxidation of uranium(IV) by chlorates, 16: 27005
effects on zirconium oxide reflectance, 18: 14722(R) (TID-20233)
electron paramagnetic resonance spectrum of divalent, in calcium oxide single crystals, 18: 2468
electron spin resonance of divalent, in magnesium oxides and sulfides, 18: 2469
electron spin resonance of excited ^2E level of divalent, in magnesium oxides, 20: 46942 (NYO-2150-18)
electron transfer between cobalt(III) and divalent, oxyanions as bridging groups in, 20: 3967
electronic wave functions for nuclear magnetic moment perturbations, tables of, 17: 36374 (BNL-6491)
fluorescence spectra of trivalent, in aluminum oxide single crystals, (E), 20: 10241
oxidation by chromium(VI), 20: 3863(R) (IS-1200(Sect. C))
oxidation by pentammine-organic acid cobalt(III) complexes, 17: 161
oxidation of, in uranium leach liquors by bacteria, 20: 45822(P)
oxidation-reduction reactions of, polarization during, 19: 44002(T) (AEC-tr-6572)
radioinduced in ammonium zinc sulfate, spectra of, 18: 20059

radioinduced in vanadyl-containing ammonium magnesium sulfates, ammonium zinc sulfates, and potassium zinc sulfates, EPR spectra of, 20: 12319
reactions with chromium ions, effects of chloride ions on, 20: 40796(R) (IS-1500(Sect.C))
reactions with graphite at 30 kev, x-ray diffraction studies of products from, 16: 33804
reactions with neptunium(V), kinetics of, 17: 40766 (DP-434)
reactions with uranium(VI), kinetics of, 19: 11106
reactions with uranium(VI) ions in acid perchlorate solutions, kinetics of, 20: 31239
reduction by lead–sodium alloy in acid solution, 19: 17867
separation from titanium using vanillin, 19: 333
separation of tetra- and pentavalent, from 25 metal ions by cation exchange, 16: 25484 (IS-415)
Slater-Condon parameters of, determined from spectral data, 17: 31118
spectra in magnesium oxide, effects of perturbations on optical, 18: 42155 (ML-1190)
spectra in magnesia, effects of perturbations on, 19: 32048(R) (NP-15073)
spectra in rutile, ESR, 18: 25411
spectra of, in sapphire, 17: 22222 (MMPP-NPC-1-3)
stability constants and structure, effects of ligand fields, 17: 28911

VANADIUM ISOTOPES

abundance in terrestrial sources, 19: 4353 (IS-921)
abundance in terrestrial sources, 19: 9046(R) (IS-900(Sect.C))
abundance of, mass spectrographic determination of, 18: 8298
abundances of, determination of absolute, 18: 1489(R) (IS-700(Sect.C))
atomic mass comparisons for, 18: 15228
binding energies and spectra of, from residual two-body interaction theory, 18: 4605
decay scheme, 17: 7138 (PUC-1962-61)
gamma reactions on, cross sections for, 19: 12496
helium-3 elastic scattering by, optical model for, 17: 5364
occurrence in iron meteorites, 17: 3177
proton reactions (p,t) with, analytical uses of, (T), 19: 14498 (ANL-6878(p.425-48))
proton reactions on, chromium-51 yields from, 17: 8153

VANADIUM ISOTOPES V-46

beta decay of, energy level scheme from, 17: 40070
beta decay of, conserved vector current hypothesis and ft values for, (E/T), 19: 39859
beta decay of, CVC theory and ft values for, (T), 19: 21416
beta decay of, f values for, 19: 37795 (NP-15109)
beta decay of, half life for, 18: 21306
beta decay of, phase-space integrals for, (T), 20: 17732
beta decay, energy spectra, and magnetic moment of, $f_{9/2}$ model for, 20: 22131
decay scheme of isomeric, 19: 29258 (NP-15050)
energy levels, inversion of lowest T = 0,1 states in, 16: 13997
energy levels of, excitation in proton reactions (p,n) with titanium-46, 18: 24612 (NP-13930(p.134))
energy levels of, isotope shifts of isobaric-analog, (E), 20: 22095
energy levels of, model for, 20: 22131
half life of isomeric, 17: 9626
isomeric transitions, (E), 20: 46242(R) (TID-23239)
positron decay, 17: 5325 (PUC-1962-62)

VANADIUM ISOTOPES V-47

beta and gamma spectra and energy levels, 16: 17148
beta decay of, log ft values for, (T), 20: 19932
beta decay, energy spectra, and magnetic moment of, $f_{7/2}$ model for, 20: 22131
decay, gamma spectra of titanium-47 spin at 160 kev in, 17: 26480
decay, search for 1.54- and 1.87-Mev gamma rays, 16: 10995
energy level density, 16: 19797
energy level spacings in, 19: 21446
energy levels, 18: 22913
energy levels, (E), 19: 21374
energy levels from chromium-50 (p,α) reactions at 11 and 12 Mev, (E), 20: 10019
energy levels of, model for, 20: 22121
production in nitrogen-14 reactions with chlorine-35, cross section for, 17: 24053(R) (ORNL-3432)
yields in proton spallation of copper at 24 Bev, 16: 24859

VANADIUM ISOTOPES V-48

activity measurements in fragment of Sputnik IV, 17: 28943(R) (TID-18961)
analytical uses, 18: 33483
beta decay of, beta–circularly polarized-gamma correlations in, 16: 33898
beta decay of, circular polarization of gamma radiation following, 18: 21309
beta decay of, Coulomb matrix elements and impurity coefficients in, 18: 28665
beta decay of, matrix elements from β-γ correlations from, (E), 20: 32506
content in Sputnik 4 fragment, 18: 13666
content in Sputnik 4 fragment, 18: 26127
decay of, ratio of electron capture to positron emission in, 18: 2886
decay of, K-capture to positron ratios for, (E), 20: 15711 (CONF-233 (Vol.2), pp 345-58)
decay scheme, 17: 33056
diffusion in titanium at 900 to 1550°C, coefficient for, 18: 4172(R) (ORNL-3470(p.67-74))
diffusion in titanium at 900 to 1550°C, 18: 27865 (ORNL-3616)
diffusion in titanium, temperature dependence of, 18: 44058 (ORNL-P-351)
diffusion in vanadium at 1000 to 1900°C, coefficient for, 18: 4172(R) (ORNL-3470(p.67-74))
diffusion in vanadium, temperature dependence, 18: 27967 (ORNL-3617)
diffusion in vanadium, 18: 44153 (ORNL-P-425)
distribution between 4-methyl-2-pentanol and acidic sodium perchlorate solutions, 18: 27415
energy level at 305 kev, lifetime of, 17: 6958 (UCRL-7091)
energy level density, 16: 19797
energy levels, 18: 22913
energy levels in, low-lying, 16: 15681
energy levels of, lifetimes of, 18: 42624(R) (ANL-6879(p.35-63))
energy levels of, isotope shifts of isobaric-analog, (E), 20: 22095
half life measurements from 440-Mev proton reactions with stone meteorites, 17: 28943(R) (TID-18961)
metabolism in rats, techniques for studying, 20: 32926
neutron reactions (n,2n) at 14.5 Mev, cross section predictions from scandium-45 (α,2n) reactions, (T), 20: 36178 (UCRL-14575)
nuclear orientation in iron and cobalt, 20: 24445
nuclear spin and hyperfine structure, (E), 20: 46242(R) (TID-23239)
positrons from, polarization of, 18: 38190
production by proton reactions in thick iron targets, cross sections for, 18: 26583
production in cyclotrons, yields, 16: 12590
production in proton reactions with iron and nickel at 130 to 400 Mev, cross sections for, 18: 22881
production in proton reactions with iron at 400 Mev, (T), 20: 32560
production in 100-Mev to 1-Bev proton reactions with iron, 17: 28943(R) (TID-18961)
production of carrier-free, in ORNL cyclotron, 19: 22851 (ORNL-TM-1047(p.72-6))
separation from manganese-52, method for, 19: 46210
spin measurement and shell-model calculations, (E/T), 20: 40154
uptake by rats, effects of age and sex on, 18: 43204
yield in alpha and proton reactions with copper, 20: 30531
yields in proton spallation of copper at 24 Bev, 16: 24859

VANADIUM ISOTOPES V-49

activity measurements in fragment of Sputnik IV, 17: 28943(R) (TID-18961)
beta decay of, log ft values for, (T), 20: 19932
energy level density, 16: 19797
energy levels, 18: 22913
energy levels, (E), 19: 27477
energy levels at 89 and 152 kev, lifetimes of, 18: 2871
energy levels from chromium-52 (p,α) reactions at 11 and 12 Mev, (E), 20: 10019
energy levels of, symplectic symmetry in $f_{7/2}$, (T), 19: 6670
yields in proton spallation of copper at 24 Bev, 16: 24859

VANADIUM ISOTOPES V-50

abundance ratio to vanadium-51 in ascidians, 18: 19519 (IS-655)
deuteron reactions (d,α) and (d,p) at 3 to 4.3 Mev, energy levels from, 18: 19046
deuteron reactions (d,α) at 7.5 Mev, levels from, (E), 20: 28336
electron paramagnetic resonance in vanadium oxychlorides and oxyfluorides, hfs of, 18: 17830
energy level density, 16: 19797
energy levels, 18: 22913
energy levels and gamma spectra, (E), 19: 37832(R) (ORNL-3800(p.1-49))
energy levels from vanadium-51 (p,d) reactions at 17.5 Mev, (E), 20: 46596 (PUC-937-211)
energy levels of, symplectic symmetry in $f_{7/2}$, (T), 19: 6670
energy levels of, from proton reactions (p,d) with vanadium-51 at 22 Mev, (E), 20: 4899
energy levels of, isotope shifts of isobaric-analog, (E), 20: 22095
half life, 16: 11002
neutron reactions (n,γ), vanadium-52 energy levels from, (E), 19: 41725
neutron resonance integrals for dilute solutions of, (T), 19: 29260 (TID-21744)
neutron resonance parameters and total cross sections at 3 to 60 kev, (E), 20: 30360 (WASH-1068)
neutron total cross sections at 2.5 to 60 kev, (E), 19: 25475(R) (ORNL-TM-1044)

nuclear electric quadrupole moment, 18: 40601
nuclear magnetic resonance in, compared with vanadium-51, 18: 40601
nuclear moments and spins, 17: 22222 (MMPP-NPC-1-3)
production in meteorite Aroos by cosmic radiation, 16: 918
proton inelastic scattering at 3 to 4.3 Mev, energy levels from, 18: 19046

VANADIUM ISOTOPES V-51

abundance ratio to vanadium-50 in ascidians, 18: 19519 (IS-655)
alpha reactions (α,n) with, manganese-54 production by, (E), 20: 46613
alpha reactions (α,n) at 11 to 20 Mev, spectra from, 16: 23100
alpha reactions (α,p) with, nuclear temperature dependence on incident energies in, 17: 38206
alpha scattering at 50 Mev, level spins and parities from, (E/T), 20: 30460
alpha scattering by, 17: 40436(R) (NYO-10063(p.105-15))
bremsstrahlung reactions (γ,α), (γ,2n), (γ,3n), and(γ,2p), relative yields from, 19: 23209(R) (RPI-328-20)
bremsstrahlung reactions at 25, 29, and 37 Mev, (E), 19: 47596(R) (TID-22141, pp 94-7)
carbon nucleus reactions (C^{13}), copper-61 production, 16: 1064
carbon-12 reactions with, cross sections and excitation functions for, 17: 26426 (NYO-10387)
carbon-12 reactions up to 120 Mev, copper-63 compound nucleus formation in, (E), 20: 38147
carbon-12 reactions (C-12,N-13) with, angular distributions from, (E), 20: 42153 (JINR-E-2824)
carbon-12 reactions (C-12, N-13) with, angular distributions and cross sections for, (E), 20: 46587 (JINR-P-2794)
decay scheme and lifetime of first excited state, 16: 19765
deuteron elastic scattering at 8 to 10.5 Mev, differential cross sections for, 17: 28306
deuteron elastic scattering at 8.0 to 10.5 Mev, analyses of, 18: 34758 (JEN-130-DF/I-41)
deuteron reactions (d,p) at 15 Mev, angular dependence of proton polarization, 16: 21597
deuteron reactions (d,p) at 15 Mev, proton polarization in, 17: 838
deuteron reactions (d,p) with, compound nucleus formation effects in, 17: 38222
deuteron reactions (d,α) and (d,p) at 3 to 3.4 Mev, energy levels from, 18: 19046
deuteron reactions (d,α) with, differential cross sections for, 18: 21157(R) (AFOSR-5284)
deuteron reactions (d,p) at 10.1 Mev, proton spectra from, (E), 19: 31250
deuteron reactions (d,α) with, distorted-wave model in, (E/T), 20: 1238
deuteron reactions (d,p) at 10.1 Mev, (E/T), 20: 1167
deuteron reactions (d,p) with, differential cross sections for, (E), 20: 26104
deuteron reactions (d,p) with, vanadium-52 energy levels from, (T), 20: 42201
deuteron scattering at 8.0 to 10.5 Mev, magnetic spectrograph studies of elastic, 18: 15217
electron elastic scattering from, 18: 14590(R) (NIRL/R/60)
electron energy levels of, g-factors and hyperfine-interaction constants for, (E), 20: 9962(R) (ANL-7029, pp 9-12)
electron inelastic scattering by, at 183 to 600 Mev, 17: 836
electron paramagnetic resonance in vanadium oxychlorides and oxyfluorides, hfs of, 18: 17830
energy level density, 16: 19797
energy level of lifetimes, 17: 41528(R) (ANL-6720(p.16-28))
energy level transitions in, probability for E2, (T), 19: 10311
energy levels, 16: 17075
energy levels, 18: 2841(R) (ORNL-3488(p.1-17))
energy levels, 18: 22913
energy levels, 18: 34855
energy levels from Coulomb excitation by neon-20, 17: 4093
energy levels from chromium-51 decay, 645-kev, (E), 20: 22029
energy levels from chromium-51 decay, (E), 20: 32410
energy levels in, from chromium-51 decay, 17: 40035
energy levels in, nuclear g factor of, 17: 11700
energy levels of, calculated, 17: 24480
energy levels of, gamma-gamma angular correlation for spin of 933-kev, 17: 26436(R) (ORNL-3425(p.30-1))
energy levels of, model for, 17: 29615
energy levels of, reduced widths and strength functions of, (E), 19: 17009
energy levels of, from chromium-51 decay, (E), 19: 47619
energy levels, static moments, and transition rates of, 20: 32513
fluorescence yield from K shell following electron-capture decay of chromium-51, 16: 9441 (TID-14854)
fluorine isotope reactions (F^{19},F^{18}) up to 43 Mev, 16: 21428
gamma absorption cross section, (T), 19: 45366
gamma reactions (γ,π⁻2n) at 150 to 300 Mev, cross sections for, (E), 19: 43352
gamma reactions (γ,n) and (γ,2n), cross sections for, 17: 4097
gamma reactions (γ,α) with, alpha spectra from, 17: 11678
gamma resonance scattering at 325 kev, cross section for, (E), 19: 17021
gamma spectra of, low-energy, 18: 16980
helium ion reactions (He,He⁴He⁴) at 40 Mev, 17: 31516
helium-4 reactions (He⁴,Be⁷) at 40 Mev, 17: 31516
helium-3 elastic scattering at 12 Mev, 18: 38144
helium-3 elastic scattering and reactions (He-3,d) at 22 Mev, (E), 19: 21240 (LA-DC-6232)
helium-3 reactions (He-3,2p) at 12 Mev, Q value for, 20: 16331 (GA-6568)
helium-4 reactions at 6 to 42 Mev, excitation functions for, (E), 20: 34529(R) (UR-3591-2)
hyperfine structure of, analysis by exchange polarization, 19: 27580
ion reactions with, neutron-transfer mechanisms in, (E), 19: 37823(R) (ORNL-3800(p.1-49))
Knight shifts of, in aluminum–technetium–vanadium alloys, 18: 2454
lifetime, magnetic moments, and reduced transition probabilities for, calculated, 17: 24480
lifetime of 320-kev level, 16: 5983
meson (π⁺) reactions at 220 to 320 Mev/c, double charge exchange in, (E), 20: 42316
motion in gases, slowing down in, (E), 19: 17021
neutron capture at 14 Mev, gamma spectra from, (E), 20: 19829 (NIJS-R-455)
neutron capture by, polarization of gamma rays from, (E), 19: 23633 (UJV-1211/64)
neutron capture cross section at 14.7 Mev, (E), 20: 46614
neutron inelastic scattering at 14.1 Mev, evaporation mechanism, (E), 19: 37788 (INR-591/IA/PL)
neutron potential scattering cross sections, 18: 2849
neutron reactions (n,p) at 14 Mev, direct and evaporation mechanisms, 16: 4850
neutron reactions (n,α) at 12 to 20 Mev, cross sections, 16: 5955
neutron reactions (n,He^3) at 14.5 Mev, cross-section upper limits, 16: 8219
neutron reactions (n,nα), cross sections at 12 to 19 Mev, 16: 19818
neutron reactions (n,d), angular distributions from, 16: 21554
neutron reactions (n,γ), activation measurements for, 16: 24787 (NP-11793)
neutron reactions (n,α) at 14.5 Mev, cross sections, 16: 31090
neutron reactions (n,2p) at 14.8 Mev, cross section limit, product half life, and Q value for, 17: 2242 (TID-16949)
neutron reactions (n,p) at 14.8 Mev, cross sections for, 17: 2242 (TID-16949)
neutron reactions (n,helium-3) at 14.8 Mev, cross section limit, product half life, and Q value for, 17: 2242 (TID-16949)
neutron reactions (n,2n) and (n,pn) at 14.8 Mev, cross sections for, 17: 2242 (TID-16949)
neutron reactions (n,p) at 14.8 Mev, separation energies for, 17: 2242 (TID-16949)
neutron reactions [(n,αn) + (n,nα)] at 14.8 Mev, cross section limit, product half life, and Q value for, 17: 2242 (TID-16949)
neutron reactions (n,α) at 14.8 Mev, cross sections for, 17: 2242 (TID-16949)
neutron reactions (n,αγ) and (n,αn) at 14.8 Mev, cross sections for, 17: 2242 (TID-16949)
neutron reactions [(n,αn) + (n,nα)], separation energies for, 17: 2242 (TID-16949)
neutron reactions (n,pγ) at 14.8 Mev, cross sections for, 17: 2242 (TID-16949)
neutron reactions (n,d) at 14.4 Mev, 17: 5385
neutron reactions (n,α) at 14.5 Mev, cross sections for, 17: 11614 (BNL-6044)
neutron reactions (n,p) at 12 to 19 Mev, energy dependence of cross sections for, 17: 26618
neutron reactions (n,nα) with, cross section for, 17: 31797(R) (BNL-782(p.51-9))
neutron reactions (n,d) at 14 Mev, angular distributions and cross sections for ground-state transitions in, 17: 34920
neutron reactions (n,nα) at 14.7 Mev, upper limit for cross section of, 17: 36707
neutron reactions (n,2p) at 14.7 Mev, cross-section limits for, 17: 36707
neutron reactions (n,p) at 14 Mev, 17: 36410 (NP-13020(p.169-73))
neutron reactions (n,nα) at 14.8 Mev, maximum cross-section limits for, 18: 1077
neutron reactions (n,2p) at 14.8 Mev, cross-section limits for, 18: 1077
neutron reactions (n,He^4) at 14.8 Mev, cross-section limits for, 18: 1077
neutron reactions (n,α) at 14 Mev, nuclear shell effects in cross sections for, 18: 18977
neutron reactions (n,n'γ) at 1.0 and 4.0 Mev, cross sections and spectra for, 18: 30736(R) (TID-20658)
neutron reactions (n,2n) at 14 Mev, shell effects in, (T), 19: 12536
neutron reactions (n,p) at 14.8 Mev, cross sections for, (E), 19: 27516

neutron reactions (n,γ) with, energy levels from, (E), 19: 31241(R) (UCRL-12473(p.1-30))
neutron reactions (n,γ), vanadium-52 energy levels from, (E), 19: 41725
neutron reactions (n,p) at 14.8 Mev, cross sections for, (E), 20: 12133
neutron reactions (n,p) with, sensitivity of, for activation analysis, 20: 16332 (GA-6691)
neutron reactions (n,γ) with, vanadium-52 level scheme from thermal, (E), 20: 19899
neutron reactions (n,γ) at to 14 Mev, cross sections for, (T), 20: 30378
neutron reactions (n,p) at 14.8 Mev, cross sections for, (E), 20: 30394
neutron reactions (n,2n) at 14 Mev, cross section for, (E), 20: 34624
neutron reactions (n,γ) with, resonance activation integral cross sections for, (E), 20: 40069(R) (EANDC(E)-66(U))
neutron resonance integrals for dilute solutions of, (T), 19: 29260 (TID-21744)
neutron scattering at 3 to 650 kev, cross sections, phases, and strength functions for, (E), 19: 10319
neutron total cross section at 0.6 to 25 kev, 18: 2943
neutron transmission in, shape elastic cross section for, 17: 38004(T) (AEC-tr-5734(p.27-8))
nitrogen ion reactions at 16.5 and 18.3 Mev, angular distribution of gamma radiation from excited levels from, 16: 33827
nitrogen-14 reactions with, excitation functions for one-neutron-transfer, (E/T), 19: 47586 (ORNL-TM-1218)
nitrogen-14 reactions at 20 to 42 Mev, excitation functions for, (E), 19: 47667
nuclear magnetic moments, 16: 1054
nuclear magnetic resonance in technetium-vanadium alloys, 16: 22140
nuclear magnetic resonance in chromium–vanadium alloys, 17: 16820
nuclear magnetic relaxation in alloys and silicides, 18: 14523
nuclear magnetic resonance in vanadium nitrides, Knight shift and relaxation in, 18: 19980
nuclear magnetic resonance of, temperature dependence of, 18: 24688
nuclear magnetic resonance in, compared with vanadium-50, 18: 40601
nuclear magnetic resonance in intermetallic compounds VB_2, V_3Ge, and V_2Ge, 18: 44229
nuclear magnetic resonance in chromium–vanadium alloys, (E), 19: 4741 (IS-1033)
nuclear magnetic resonance in type II superconductors, (E), 19: 10194
nuclear magnetic resonance in fluoride solutions, measurement of, 19: 13293
nuclear properties of, semiatomic model for, 17: 22629
nuclear quadrupole moment of, (E), 20: 38026
nuclear radius, 17: 36679
nuclear spin-lattice relaxation time in technetium–vanadium alloys, temperature variations of, (E), 19: 39403
nuclear wave functions, (E), 19: 10257(R) (TID-21335(p.33-107))
photon reactions, mechanism and yields of, 18: 38191
proton elastic scattering at 22.2 Mev, angular distributions and cross sections, 16: 9462
proton inelastic scattering at 17.45 Mev, level structure study from, 18: 15280
proton inelastic scattering at 3 to 4.3 Mev, energy levels from, 18: 19046
proton inelastic scattering by, levels from, (T), 19: 14489 (ANL-6878(p.143-73))
proton reactions (p,n) with excitation functions for, 18: 16996
proton reactions (p,d) at 17 to 18.5 Mev, neutron shell configuration studies from, 18: 21291
proton reactions (p,n) at 1.6 to 2.2 Mev, yields from, 18: 24591(R) (LMSC-4-50-62-1)
proton reactions (p,2p) at 150 Mev, 18: 32824
proton reactions (p,n) at 7 to 13 Mev, 18: 34859
proton reactions (p,n) at 155 Mev (E/T), 19: 3313
proton reactions (p,n) with, thresholds for, (E), 19: 6704
proton reactions (p,d) with, distributions from, (E), 19: 10257(R) (TID-21335(p.33-107))
proton reactions (p,α) with, models for, (T), 19: 14496 (ANL-6878(p.335-50))
proton reactions (p,n) with, performance as neutron source, 19: 19137
proton reactions (p,n) at 3.5 to 6.75 Mev, total cross sections for, (E), 19: 23682
proton reactions (p,α) and (p, p) at 6.75, cross sections for, (E), 19: 23682
proton reactions (p,d) with, distributions from, (E), 19: 37823(R) (ORNL-3800(p.1-49))
proton reactions (p,n) at 1.5 to 2.3 Mev, total cross section for, (E), 19: 41676 (ORNL-P-1468)
proton reactions (p,n) at 370 Mev, nuclear-structure effects in, (E/T), 20: 1213
proton reactions (p,d) at 22 Mev, energy levels from, (E), 20: 4899
proton reactions (p,2p) at 460 Mev, (E/T), 20: 11948 (AD-624318)
proton reactions (p,n) with, neutron production for activation analysis in, 20: 16332 (GA-6691)
proton reactions (p,2p) at 140 Mev, energy spectra and angular correlation distributions from, (E), 20: 17741
proton reactions (p,γ) at 0.6 to 2.7 Mev, isobaric analog resonances in chromium-52 from, 20: 19928
proton reactions (p,n) with, cross sections and excitation functions for, (E), 20: 32371 (CEA-R-2832)
proton reactions (p,d) at 17.5 Mev, angular distributions and spectroscopic factors from, (E), 20: 46596 (PUC-937-211)
proton reactions at 660 Mev, lithium-8 emission in, (E), 19: 16887
proton reactions at 660 Mev, lithium-8 production in, (E), 19: 37790 (JINR-P-2093)
proton reactions at 150 to 550 Mev, lithium mass spectra from, (E), 20: 8105
proton reactions (p,n) and (p,γ) at 4.26 Mev, cross sections, 16: 5956
proton reactions (p,α) and (p,p′) at 17.5 Mev, alpha spectra from, 16: 7112
proton reactions (p,n) at 4 to 6.5 Mev, cross sections, 16: 8217
proton reactions (p,n) at 1.67 to 2.05 Mev, resonance in, 16: 8177
proton reactions (p,α) at 18 Mev, seniority wave function effects on angular distributions and cross sections, 16: 21578
proton reactions (p,nγ), cross sections and excitation functions, 16: 21626
proton reactions (p,n) at 14.8 Mev, neutron spectra from, 16: 26326 (UCRL-6733)
proton reactions (p,n) at 17 Mev, effects of excited isobaric states, 16: 26333 (UCRL-6830)
proton reactions (p,n) at 5 to 10.5 Mev, cross sections, 16: 31106
proton reactions (p,n) and (p,p′) at 5 to 11 Mev, statistical theory predictions for, 16: 31107 (UCRL-6686)
proton reactions (p,3p), excitation functions for, 16: 33892
proton reactions (p,n) at 9 to 13 Mev, neutron spectra from, 17: 4063 (UCRL-6530)
proton reactions (p,xp) at 100 to 400 Mev,cross sections for, 17: 5323 (NYO-8921)
proton reactions (p,n), cross section relations with energy, 17: 7144 (TID-17357(Pt.III))
proton reactions (p,n) at 12.1 Mev, residual nucleus excitation in, 17: 13537
proton reactions (p,n) on, spectra from, 17: 17226
proton reactions (p,n) with, analog state neutron angular distribution from, 17: 20994 (UCRL-7233)
proton reactions (p,n) at 6.75 Mev with, cross section for, 17: 22618
proton reactions (p,n) at 40 to 150 Mev, excitation functions of, 17: 24426
proton reactions (p,3p3n) at 30 to 150 Mev, excitation functions for, 17: 29590
proton reactions (p,Be^7) at 33 to 39 Mev, 17: 31516
proton reactions (p,n) at 12.1 Mev, second-term contributions to distorted-wave calculations of isobaric analog excitation in, 17: 38188
proton reactions (p,n) at 12.1 Mev, isospin potential in, 17: 38201
proton reactions (p,n) at 30 and 50 Mev with, excitation of isobaric states in, 17: 41926
proton reactions (p,n) with, use as an absolute neutron source, 18: 1080
proton reactions (p,nγ) with, 18: 2846(R) (TID-19709)
proton reactions (p,d) with, angular distributions for, 18: 9319(R) (TID-19940(p.22-76))
proton reactions (p,t) with, 18: 9319(R) (TID-19940(p.22-76))
proton scattering spectra, 16: 2492(R) (TID-14186)
proton scattering at 9.4–22.2 Mev, local optical potentials for, 17: 38185
proton scattering by, energy levels from, 18: 30867
proton scattering at 50 Mev, differential cross sections for, (E), 20: 15728(R) (RHEL/R-112, pp 23-36)
spin-lattice relaxation in superconducting vanadium silicide at low temperatures, 20: 37964
x-ray fluorescence coefficient of, L-shell, (E), 19: 27492

VANADIUM ISOTOPES V-52
activity of, method for determining gamma, 20: 9196
beta decay in vanadium monocrystals, recoil atom slowdown in, (E/T), 19: 33389
beta decay of, end-point energy in, 17: 40034
beta decay of, energy and half life of, (E), 20: 8157
beta decay of, gamma spectra for, 18: 19048
beta decay of, spectra from, (E), 20: 32564
beta decay of, transitions to vibrational levels in, 18: 36625
beta emission from, hindrance phenomena in, 16: 23073
binding energy, magnetic moment, and spin of ground-state, effective neutron-proton interaction for, 18: 6231
decay, 18: 15209 (UCOL-521)
decay of, weak gamma transitions in, 18: 18948
decay, (E), 19: 5246
energy level structure, (E), 19: 35439

energy levels, (E), 20: 1167
energy levels, (T), 20: 26139
energy levels, 18: 11161 (ANL-6797(p.79-88))
energy levels and gamma spectra of, (E), 19: 31241(R) (UCRL-12473(p.1-30))
energy levels from deuteron reactions (d,p) with vanadium-51 at 10.1 Mev, 19: 31250
energy levels from vanadium (n,γ) reactions, low-lying, (E), 19: 41725
energy levels from vanadium-51 (d,p) reactions, excited, (E), 20: 26104
energy levels of, parity and spin of, (E), 19: 23726
energy-level scheme from thermal neutron reactions (n,γ) with vanadium-51, (E), 20: 19899
energy-level structure of, calculations using shell model with configuration mixing, (T), 20: 42201
gamma dose constants for, 20: 46617
gamma emission by, 18: 8313
gamma emission by, circular polarization in, (E), 19: 23633 (UJV-1211/64)
gamma spectra, 16: 4751 (JAERI-4019)
gamma spectra, 17: 34966
half life, 20: 16331 (GA-6568)
neutron reactions (n,γ) with, gamma spectra from, 18: 11161 (ANL-6797(p.79-88))
neutron reactions (n,α) at 14 Mev, nuclear shell effects in cross sections for, 18: 18977
nuclear structure of, from capture-gamma measurements, 18: 11161 (ANL-6797(p.79-88))
nucleon interactions in, properties from effective, (T), 20: 17735
production in PANACEA, 17: 34195(R) (JLI-2748-0-7)
use in activation determination of vanadium in powdered milk, 18: 10028

VANADIUM ISOTOPES V-53
binding energy, magnetic moment, and spin of ground-state, effective neutron-proton interaction for, 18: 6231
nucleon interactions in, properties from effective, (T), 20: 17735

VANADIUM MINERALS
analysis, handbook of procedures for, 16: 2966 (RMO-3001(Rev.1))
geochemical survey, in San Jose Co., Utah, 16: 27437

VANADIUM MOLYBDATES(VI)
preparation, crystal structure, and magnetic susceptibility of, 20: 26864

VANADIUM NITRIDES
analysis for nitrogen by reaction with chlorine and measurement of nitrogen released, 19: 17800
crystal structure in iron alloys, 19: 22230
electric properties of, effects of non-metallic atoms on, 17: 8854
electron structure of crystals of, 17: 27875
figure of merit and atomic characteristics, 19: 2284
hardness, 16: 7916
hardness of, effects of temperature on, 20: 4297(R) (IS-1200(Sect.M))
physical properties of crystalline, 17: 27875
preparation and properties of, 19: 18472(T) (JPRS-28739)
preparation by decomposition of ammonium fluorovanadate in ammonia, 19: 15541
properties in iron alloys, 19: 22230
review, 18: 39899 (LA-2942)
sintering of, electron density in phase lattices and optimal conditions for, 17: 27767
solubility products in liquid iron at 1550 to 1750°C, 19: 41065
structure, 16: 7916
superconducting properties, 19: 20572
surface energy of, calculation of approximate, 17: 41475(T)
thermal conductivity, effects of electronic and crystalline structure, 16: 24208
vanadium-51 NMR in, Knight shifts and relaxation in, 18: 19980
NbC–NbN–VN, superconducting properties, 20: 17589 (CONF-650922, pp 541-9)
NbN–VN, superconducting properties, 20: 17589 (CONF-650922, pp 541-9)

VANADIUM ORES
analysis for niobium, activation, 18: 13626(R) (NYO-10174)
availability of, review of, 17: 29253 (NRC-7129)
processing by reductive chlorination, 20: 4072(P)
processing with a combined solubilization and extraction solution, 19: 44129(P)

VANADIUM OXIDES
see also Vanadium Bronze
catalytic effects on deuterium-hydrogen exchange, 16: 20433
catalytic effects on hydrocracking of polyphenyls, 17: 28434 (IDO-16858)
catalytic effects on radioinduced isomerization of 2-butene, 18: 23667
catalytic effects on decomposition of tritium-labeled compounds, 19: 7491
catalytic properties of, isotopic exchange studies of, 18: 13739
chromium-atom slowdown paths at 20 to 90 ev in, (E), 19: 33512
corrosive effects on steel, 16: 12059
crystal structure of, vacancy interaction energies in, 17: 35781
effects on densification of thorium oxide–uranium oxide pellets, 16: 7874 (ANL-6375)
effects on density and volume changes of graphite, 17: 36202(R) (SCC-13)
effects on density of sintered uranium dioxide, 18: 44118
effects on neutron-induced contraction in graphite, 20: 31667
effects on physical properties and radiation stability of graphite, 18: 7305 (HW-SA-3020)
effects on radiolysis of water vapor, 20: 9002
effects on sintering behavior of urania powders, 20: 37202
effects on uranium oxide sintering properties, 17: 12637
electric conductivity of, effects of structure on, 19: 42858
electric conductivity of liquid, 19: 9684
electron energy losses in, and mechanisms of, 17: 13165
enthalpy of solution of solid oxides in, at 68°C, 20: 7072
gamma spectra of, irradiated by 14.8-Mev neutrons, 17: 2242 (TID-16949)
heat of fusion of V_2O_4 and V_2O_5, 16: 12192
magnetic properties of, from iron-57 Mössbauer effect in, (E), 20: 3289
magnetic structure of rutile-like crystals of, 19: 8700 (CALT-221-5)
magnetic susceptibility, effects of magnesium and zirconium addition, 16: 15126(R) (NP-11584)
meson (μ^-) capture by, K x rays from, (E), 19: 28991 (JINR-P-2039)
neutron resonance absorption integral of, (E), 20: 14008(R) (ANL-7122, pp 42-69)
oxygen-18 exchange reactions with, kinetics and mechanisms of, 17: 15979
oxygen-18 exchange with sulfur dioxide or trioxide, 19: 7439
phase diagram with potassium phosphate, 16: 121
polarography in lithium and lithium sodium metaphosphates at 750 and 730°C, 18: 1516
properties as growth media for refractory oxide crystals, 18: 4171(R) (ORNL-3470(p.3-5))
properties of, effects of temperature on mechanical and physical, 17: 16760
radiation effects on films of, on glass, 16: 21108
radiation effects on thermo-electromotive force of pentavalent, reactor, 17: 12724
radiation effects on catalytic activity in hydrogen-deuterium exchange, 17: 18125
radiation effects on electrophoresis and specific conductivity of sols of, 18: 10146
radiation effects on catalytic properties of, 19: 26430
radiation effects on mechanical and physical properties of, 17: 16760
reactions with americium oxide, properties of ternary oxides formed in, 19: 28286 (KFK-280)
reactions with ammonium uranyl vanadate in solution, formation of polyvanadate in, 19: 15463(T) (ANL-Trans-33(p.323-5))
reactions with calcium carbonate and oxide in solid phase, 19: 15465(T) (ANL-Trans-33(p.339-49))
reactions with graphite, formation of vanadium carbide coatings by, 19: 42836(P)
reactions with nitrogen dioxide–nitrogen tetroxide, 16: 10018
reactions with oxygen, isotopic exchange, 18: 43496
reactions with protactinium pentoxide, 19: 7603
reactions with tungsten carbide at 1300 to 1400°C, preparation of alloys by, 18: 39833(T)
reactions with uranium oxides, 17: 14244
reactions with uranium oxides, 18: 3784
reactions with uranium dioxide at 900 to 1200°C, formation of UV_2O_6 in, 20: 23674
reduction by aluminum, preparation of vanadium by, 20: 2225 (IS-T-40)
reduction of, thermodynamics of, 17: 14269
reduction of, thermodynamics of, 18: 13763
reduction to metal by reactions with aluminum and carbon, 20: 41412(R) (IS-1500(Sect. M))
screening of metal–metal bonds in, effects on overlapping, 18: 17781(T) (AEC-tr-6388)
spectra, Franck-Condon factor arrays for band, 16: 22129
spectra in low frequency region, infrared, 18: 23549
spectra of, in 300 to 1000 mμ region, reflectance, 17: 15970
spectra of nonstoichiometric, reflectance, 18: 12108
testing for use in shaft seals for potassium space power systems, 20: 2242
thermodynamic properties of gaseous, tables of, 17: 40777(R) (RAD-SR-63-183)
thermoelectric properties of liquid, 19: 9684
vacancy structure, 16: 22573(R) (AD-266459)
valency changes in films of, on electrodes, 17: 25203
Al_2O_3–V_2O_5, deposition on yttrium, 20: 35875(P)
Al–V_2O_5, ignition tests on, in contact with electrically pulsed bridge-wires, 20: 26820(R) (SC-CR-66-2019)

Am_2O_3–V_2O_3, crystal structure, preparation, and properties, 19: 32749
CaO–CoO–V_2O_5–ZnO, analysis by x-ray fluorescence, 18: 25275
CaO–V_2O_5, density and surface ductility of fused, at 1200 to 1650°C, 20: 15076
CoO–V_2O_5, catalytic effects on hydrocracking of polyphenyls, 17: 28434 (IDO-16858)
Cr_2O_3–V_2O_5, density and surface ductility of fused, at 1200 to 1650°C, 20: 15076
Fe_2O_3–V_2O_5, density and surface ductility of fused, at 1200 to 1650°C, 20: 15076
Fe_2O_3–V_2O_5, internal magnetic field in, 16: 13777
Fe_2O_3–V_2O_5, magnetic properties and structure of, 16: 25366
MoO_2–VO_2, phase studies, 19: 42859
Nb_2O_5–V_2O_5, crystal structure of tetragonal phases in, 18: 19942
NbO_2–VO_2, crystal structure of double oxide $NbVO_4$, 20: 16982
Nb_2O_5–V_2O_5, double oxide formation and composition in, after sintering, 18: 12057
Nb_2O_5–V_2O_5, electric conductivity, 17: 1504
Nb_2O_5–V_2O_5, phase studies, 19: 26846
Nb_2O_5–V_2O_5, phase studies, 19: 41049
NbO_2–VO_2, properties of tetragonal rutile phase in, electric and magnetic, 19: 16176
P_2O_5–V_2O_5, electric conductivity of glass systems of, 20: 2316 (COO-1198-220)
P_2O_5–V_2O_5, electric conductivity of glass systems of, 20: 2316 (COO-1198-220)
rare earth oxides–V_2O_5, preparation and magnetic properties, 19: 42463
SiO_2–Ag_2SO_4–V_2O_5, radiation effects on catalytic activity of, in oxidation of sulfur dioxide by air, 20: 29291
SiO_2–V_2O_5, viscosity, 17: 4933 (WADD-TR-60-463(Pt.II))
SiO_2–V_2O_5–ZrO_2, zircon formation in, 18: 42085
Ta_2O_5–V_2O_5, crystal structure of tetragonal phases in, 18: 19942
Ta_2O_5–V_2O_5, double oxide formation and composition in, after sintering, 18: 12057
ThO_2–V_2O_5, phase studies, 19: 11116
ThO_2–V_2O_5, phase studies on, 19: 25034
TiO_2–VO–ZrO_2, phase diagram at 1500°C, 16: 29403
UO_2–V_2O_5, phase studies at 900 to 1200°C, 20: 23674
V_2O_3–V_2O_5, phase studies, 20: 17007(R) (AD-627468)

VANADIUM OXYCHLORIDES
mass spectrometric studies of, 19: 9046(R) (IS-900(Sect.C))
vanadium-50 and -51 EPR in, hft of, 18: 17830

VANADIUM OXYFLUORIDES
equilibrium distribution in complex, 18: 6800
mass spectrometric studies of, 19: 9046(R) (IS-900(Sect.C))
spectra of, appearance potentials and fragmentation of ions in, 20: 8882 (IS-983)
vanadium-50 and -51 EPR in, hft of, 18: 17830

VANADIUM OXYNITRIDES
catalytic effects on hydrolysis of salicyl phosphate, 16: 28949
preparation, 20: 10856

VANADIUM OXYSULFATES
chromium-atom slowdown paths at 20 to 90 ev in, (E), 19: 33512

VANADIUM PHOSPHIDES
crystal structure, 19: 7945

VANADIUM SILICIDES
crystal phase transformations in superconducting, 18: 42568
crystal structure of, phase temperature effects on, 20: 42531
electric conductivity above superconducting transition temperature, 20: 8028
electron spin-pairing in superconducting, (E/T), 20: 30734(R) (TID-22970, pp 1-63)
electron structure of crystals of, 17: 27875
electron-spin pairing in single crystals of superconducting, neutron-diffraction studies of, 20: 20152
electronic band structure of, 18: 14523
electronic instability, temperature effects on, 20: 42531
Fermi surface of, (E), 19: 23990
heats of formation, 16: 20394
magnetic field penetration in superconducting, (E), 20: 8030
magnetic field penetration of superconducting, (E), 20: 21908
magnetic penetration depth in superconducting, 18: 28505
magnetization measurements in, 20: 20109(R) (MIT-3031-3)
magnetization of films of, validity of models for, 17: 9039
microwave surface resistance in superconducting, (E), 20: 21916
phase transformation in superconducting, martensitic, (E), 19: 29161
physical properties of crystalline, 17: 27875
polarization in superconducting, electronic and nuclear, 20: 20109(R) (MIT-3031-3)
preparation and properties of superconducting, 17: 18892 (ASD-TDR-62-1111)
preparation of thin superconducting films of, getter sputtering technique for, 18: 13015
radiation effects on superconducting properties of boron- and uranium-doped, thermal neutron, (E), 20: 30260
solvent properties for aluminum and beryllium, 20: 17043
spin paramagnetism below critical temperature in superconducting, 18: 4505
structural transformation in V_3Si, vanadium-51 Knight shifts and field gradients during, 20: 42118
structure of superconducting, transformation in, (E), 20: 28194
superconducting properties, effects of beryllium, boron, manganese, and molybdenum, 16: 30821
superconducting properties of, current and magnetic field effects on, (E), 19: 19060
superconductive properties of, effects of transition metals on, 19: 39196
superconductivity of crystalline V_3Si, neutron-diffraction analysis of, 18: 16894(R) (MIT-3031-1)
superconductivity of, effects of aluminum, beryllium, germanium, and tin on, 20: 17043
thermionic emissions at 1100 to 1600°K, 17: 25812
vanadium-51 spin-lattice relaxation at low temperatures in superconducting, 20: 37964
$MoSi_2$–WSi_2–VSi_2, phase studies, 20: 27542
U–V_3Si, radiation effects on superconducting current density in, neutron, (E), 19: 14435(R) (NP-14676)

VANADIUM STEEL
carbide formation in, 17: 11209
carbon activity in gamma-phase, 19: 32048(R) (NP-15073)
mechanical properties of, effects of strain rate on, 20: 11284 (UCRL-14599)
B–C–Cr–Mn–Mo–Ni–Nb–V, precipitation of niobium carbide in, 18: 37726
C–Cr–Mn–Mo–Ni–Si–V, strength and toughness of dynamically strain-aged, 20: 7584 (UCRL-16363)
C–Cr–Mo–Ni–V, mechanical properties, effects of composition variations on, 19: 9645 (AD-604867)
C–Cr–Mo–Ni–V, mechanical properties, effects of low-temperature tempering on, 19: 9647 (AD-604876)
Cr–Mn–Mo–V, reactions with carbon dioxide to 400°C, 19: 22997 (TRG-Report-842)
Cr–Mo–Ni–Nb–V, development as HY-180/210 steel, 20: 5851
Cr–Mo–Ni–V, development, 19: 20462(R) (NRL-6258)
Cr–Mo–Ni–V, fatigue crack propagation in, effects of air or salt water environment on, 20: 11273(R) (NRL-6364)
Cr–Mo–Ni–V, mechanical properties, effects of carbon on, 19: 9646 (AD-604872)
Cr–Mo–Ni–V, mechanical properties of, effects of processing on, 20: 33858(R) (AD-634094)
Cr–Mo–V, brittleness in, during time-to-rupture tests, theory of notch-, 20: 25563 (EURAEC-1350)
Cr–Mo–V, creep of, enthalpy and entropy of activation of, 18: 25974 (EURAEC-1037)
Cr–Mo–V, creep-rupture properties of, 17: 3521
Cr–Mo–V, creep-rupture properties, 17: 39531(R) (EURAEC-689)
Cr–Mo–V, effects of cerium on impurities, mechanical properties, and oxidation of, 17: 27859
Cr–Mo–V, friction coefficients with metals and metals with dry lubricants of H-11 Tool, *in vacuo*, 20: 7571 (NAA-SR-9644)
Cr–Mo–V, radiation effects on relaxation of elastic stresses in bent plates of, neutron, 16: 22704
Cr–Mo–V, radiation effects of neutrons on high-temperature creep, 18: 28039(R) (EURAEC-1020)
Cr–Mo–V, rupture mechanisms of, determination by time-to-rupture tests, 20: 41445(R) (EURAEC-1622)
Cr–W–V, erosion by mercury vapor at 640°F of 18-4-1 tool, 20: 11214(R) (NASA-CR-54717)
Mn–Mo–Ni–V, welding procedures for, electro-slag, 20: 2281(R) (EURAEC-1408)
Mn–Mo–V, properties of Ammo, variations in samples of, 20: 41447(R) (EURAEC-1669)
Mn–Mo–V, transformation curves for continuous cooling of, from 1100°C, 20: 46184 (EURAEC-1677)
Mo–Ni–V, fracture toughness, 18: 44138 (KAPL-3031)
Mo–Ni–V, fracture toughness, 19: 24984 (KAPL-3088)
Mo–Ni–V, fracture toughness tests on specimens of, different sizes, 20: 27479 (CONF-660406-1)

VANADIUM SULFATES
see also Cesium Vanadium Sulfates
see also Vanadium Oxysulfates
analytical use in potentiometric determination of bismuth and thallium, 16: 1714
effects on hydrolysis of lactose in oxygen-18-labeled water, catalytic, 19: 30177

VANADIUM SULFIDES
phase studies, 19: 9046(R) (IS-900(Sect.C))

VANADIUM SYSTEMS

miscibility with other elements, calculation of, 20: 14538
Al–C–Cu–H–N–Sn–Ti–V–Zr, mechanical properties of, 19: 46985 (AD-613651)
Al–C–Nb–V, phase studies, 20: 15103
Al–Cr–Si–Ti–V, properties of aged, 20: 4360(R) (AD-619399)
Al–C–Ta–V, phase studies, 20: 15103
Al–C–V, crystal structure and phase studies, 18: 12706
Al–C–V, crystal structure and phase studies of superconducting, 18: 32149(R) (UCRL-11317(p.131-49))
Al–C–V, crystal structure and superconductivity of V_3Al_2C, 18: 32702
Al–C–V, superconductivity of V_2AlC, 20: 6228
Al_2O_3–Nb–V, melting points, 18: 44497(R) (MND-2812-2)
Al–Si–V, crystal structure and phase studies, 18: 12704
Al–Si–V, superconductivity of solid solutions in, 20: 17043
Al–U–V, inter-diffusion in, electron beam analysis of, 18: 39058 (EUR-1643.e(p. 275-300))
B–Co–V, crystal structure, 20: 20685
Be–Si–V, superconductivity of solid solutions in, 20: 17043
B–Fe–V, crystal structure, 20: 14532
B–Ni–V, crystal structure, 20: 20685
B–V, nuclear magnetic resonance of vanadium-51 in, 18: 44229
B–V, preparation, properties, and uses of, review on, 16: 27640(T) (FTD-TT-62-430)
C–Cr–Fe–Mo–Ni–Nb–Ta–W–V, production of corrosion and oxidation resistant, 18: 12618(P)
C–Fe–V, explosibility of powders of, 19: 36698 (BM-RI-6516)
C–Ge–V, crystal structure and phase studies on, 18: 10561
C–Ge–V, crystal structure and phase studies, 18: 12706
C–Hf–Mo–V, fabrication of, cracking in, 17: 41427(R) (IITRI-B231-9)
C–Hf–Nb–V, hardening by annealing, 17: 41428(R) (IITRI-B6007-4)
C–Hf–Nb–V, preparation and properties of dispersion strengthened, 17: 16514(R) (ARF-B6007-1)
C–H–V, formation of ternary compounds in, 18: 39821 (IS-875)
C–Mo–V, phase studies and structure of, 17: 1958(T) (AEC-tr-5459)
C–Mo–V, phase studies, 17: 22195
C–Mo–V, phase studies and thermodynamics of, for use at high temperatures, 20: 29774
C–Mo–V, phase transformations in, thermodynamics of, 17: 22205
C–Mo–V, phase transformations in, thermodynamics of, 18: 44161(T) (AERE-Trans-1009)
C–Mo–V, superconductivity, 19: 43997(R) (UCRL-11889)
C–Nb–Ta–V–Zr, preparation and properties of dispersion strengthened, 17: 16514(R) (ARF-B6007-1)
C–Nb–Ti–V–Zr, evaluation of properties of, 19: 15995 (IITRI-B231-11)
C–Nb–Ti–V–Zr, mechanical properties, 17: 14809(R) (ARF-B231-8)
C–Nb–Ti–V–Zr, mechanical properties, 17: 41427(R) (IITRI-B231-9)
C–Nb–Ti–V–Zr, mechanical properties and oxidation rate, 19: 32754
C–Nb–V–Zr, fabrication, 17: 41427(R) (IITRI-B231-9)
C–Nb–V–Zr, hardening by annealing, 17: 41428(R) (IITRI-B6007-4)
C–Nb–V–Zr, heat treatment of, 20: 14972(P)
C–Nb–V–Zr, mechanical properties, 17: 14809(R) (ARF-B231-8)
C–Nb–V–Zr, preparation and properties of dispersion strengthened, 17: 16514(R) (ARF-B6007-1)
C–O–V, phase studies and thermodynamic analysis, 19: 16148
C–Si–V, crystal structure and phase studies on, 18: 10561
C–Ta–V–Zr, coating for oxidation protection, 19: 20459(R) (IITRI-B6019-6)
C–V, phase studies on, thermal analysis of, (E), 20: 1863
C–V, preparation, properties, and uses of, review on, 16: 27640(T) (FTD-TT-62-430)
C–W–V, phase studies and thermodynamics of, for use at high temperatures, 20: 29774
C–W–V, phase transformations in, thermodynamics of, 17: 22205
C–W–V, phase transformations in, thermodynamics of, 18: 44161(T) (AERE-Trans-1009)
Fe–Si–V, crystal structure of D-phase, (E/T), 20: 30734(R) (TID-22970, pp 1-63)
Fe–Si–V, magnetic hyperfine field and electric quadrupole coupling in, (E), 20: 28657
Ga–N–V, lattice parameters of filled β-manganese structure phases in, 19: 37109
Ga–O–V, crystallographic parameters, 17: 18822
Ge–Si–V, superconductivity of solid solutions in, 20: 17043
graphite–V, deposition of coatings of, at 1500 to 1750°C, 19: 39144(P)
graphite–V, properties of, effects of graphite source material on, 20: 33876(R) (N-66-17087)
HfC–V, solidus at 1790°C, 19: 44612(R) (USBM-RC-1199)
H–V, nuclear magnetic resonance, 19: 43986(R) (ANL-7000, pp 201-4)
H–V, phase relations and magnetic properties, 17: 2130
H–V, phase studies and thermal properties, 18: 13776
H–V, phase studies, 20: 41412(R) (IS-1500(Sect. M))
H–V, phase studies of, by x-ray diffraction, 20: 45688
H–V, preparation of, for transmission electron microscopy, hydrogen concentration in electrothinning procedures for, 20: 31691
H–V, thermodynamic properties of, at 250 to 650°C below 1 atm, 16: 518 (AFOSR-1107)
H–V, thermodynamics of excess partial entropy of hydrogen in, 17: 39609
Mn–O–V, magnetic structures in, 19: 38061
Mo–O–V, reduction by hydrogen at 400 to 800°C, 19: 28823
Mo–Si–V, phase studies and properties, 16: 30849
Nb–N–V–Zr, heat treatment of, 20: 14972(P)
Nb–O–V–Zr, heat treatment of, 20: 14972(P)
Nb–Si–V, phase studies, 18: 42088
N–V, preparation, properties, and uses of, review on, 16: 27640(T) (FTD-TT-62-430)
N–V–Zn, lattice parameters of filled β-manganese structure phases in, 19: 37109
O–Ti–V, aging characteristics and phase studies, 16: 6746
O–V, phase studies on, 20: 13260(R) (NP-15852)
O–V, phase studies, 20: 17007(R) (AD-627468)
O–W–V, phase studies on, 19: 25007
Rh–Si–V, phase study of Cr_3O-type structures in, 19: 44702 (TID-22200)
Si–Sn–V, phase study of Cr_3O-type structures in, 19: 44702 (TID-22200)
Si–Sn–V, superconductivity of solid solutions in, 20: 17043
Si–Ta–Ti–V, phase studies, 18: 549(R) (NP-13241)
Si–Te–V, phase studies on intermetallic compounds in, 20: 17075
Si–Ti–V, aging characteristics and phase studies, 16: 6746
Si–V, barrier effects on diffusion in aluminum–uranium alloys, 19: 42871
Si–V, critical field limits at superconducting temperatures, 17: 3635
Si–V, development of, for tantalum alloy and metal protection, 16: 24148(R) (ASD-TR-61-676)
Si–V, fabrication, properties, testing, and uses of superconducting, 19: 16110
Si–V, magnetic flux distributions in superconductors of, (E), 19: 10194
Si–V, magnetic properties of superconducting, effects of temperature on critical field, 16: 15467
Si–V, magnetic properties of superconducting, 18: 9262(R) (NP-13492)
Si–V, negative surface energy model of superconductivity of, 17: 9040
Si–V, preparation, properties, and uses of, review on, 16: 27640(T) (FTD-TT-62-430)
Si–V, preparation and properties of thin-film hard superconducting, 18: 28501
Si–V, pressure effects on superconductivity of, 18: 15078
Si–V, properties of superconducting, 18: 6127
Si–V, radiation effects on superconducting properties of, fast-neutron, 18: 10583
Si–V, radiation effects on superconductivity of, neutron, 18: 34683(R) (NP-14136)
Si–V, strong phonon effects in superconductors of, 18: 40449
Si–V, superconductivity, 16: 16830
Si–V, superconductivity of, isotope effects on, 17: 34617
Si–V, superconductivity, 17: 41604
Si–V, superconducting transition temperature of V_3Si, effects of stresses on (E), 19: 1496
Si–V, superconductivity of fused, 20: 15123
Te–V–Zr, oxidation by steam at 900°F, 18: 2162(R) (IITRI-B198-46)
TiC–V, analysis of, for titanium using sodium diethyldithiocarbamates, 16: 11571
V–ZrO_2, thermal shock resistance of, 20: 33901
W–UO_2–V, fabrication of cermets of, by isostatic cold pressing, 20: 14962(R) (N65-20803)

Vanadyl Chlorides
see Vanadium Oxychlorides

Vanadyl Fluorides
see Vanadium Oxyfluorides

VANADYL IONS

analytical use as back-titrant in determination of metals in fluoride solutions, 17: 5995
chemical effects on deiodination of thyroxine *in vivo* in mice, 17: 13922 (IA-748)
complex formation by, optimum conditions for, 19: 13374
growth in ammonium zinc sulfate, spectra of, 18: 20059
radiation effects on, in ammonium zinc sulfate, x, 20: 12319
radioprotective effects in mice, 18: 13567
separation from manganese by cation exchange, 19: 13535
sorption by aminodiacetate resin Dowex A-1, 20: 16358
spectra in ammonium zinc sulfate, EPR, 20: 12319
spectra of aqueous solutions of, ESR, 20: 43184 (UCRL-17064)
toxicity of, in mouse, determination by LD_{50} on thirtieth day of, 17: 17719

VANADYL OXALATES

chromium-atom slowdown paths at 20 to 90 ev in, (E), 19: 33512

Vanadyl Sulfates

see Vanadium Oxysulfates

VANDENDRIESSCHEITES
synthesis, 18: 16009

VANILLIC ACID
determination in human urine, equipment for, 20: 45797(R) (ORNL-3945, pp 199-207)
genetic effects on *Drosophila melanogaster*, 17: 1214
synthesis of deuterated derivatives of, 18: 13814

VANURALITES
identification and characteristics, 17: 34121

VAPOR PRESSURE
bibliography on Knudsen effusion method of measuring, 1940 to 1962, 18: 23446 (LA-3006)
determination below 500°C, apparatus for, 17: 30807
determination from beta and gamma ray measurements in isotopic exchange, 16: 1836
determination of, for atomic species by measurement of resonance line absorption, 16: 29483 (R60SD330)
determination of, for binary alloys, 17: 12672(T) (AEC-tr-5626)
equations for, graphical method for determining nonlinear constant in, 17: 10620
isotope effects on, 17: 17944 (BNL-6279)
isotope effects on, relation of molecular structure to, 17: 23332
isotopic effects, 16: 13830
isotopic effects, 16: 25304 (BNL-6050)
measurement at high temperatures, equipment and procedures for, 16: 10407 (ASD-TR-61-322(p.121-39))
measurement at high temperatures, apparatus for, 17: 33856 (AERE-R-3565(Rev.))
measurement at low temperatures, procedures for, 17: 15952 (LADC-5711)
measurement by Knudsen effusion method, problems, 16: 9979(R) (TID-15017)
measurement by Knudsen effusion method, equipment for, 20: 4369 (CEA-R-2871)
measurement for high-boiling and -melting organic compounds, design of isoteniscope for, 20: 23042 (EUR-2170.d)
measurement for metals, isotope methods for, 17: 36100
measurement in Knudsen effusion cell, study of errors due to thermal gradient in, 18: 39568 (LA-DC-6242)
measurement in porous solids by Knudsen effusion method, 17: 27341
measurement in solid materials using a tracer technique, 17: 32050(T) (AEC-tr-5911)
measurement, Knudsen effusion apparatus for, 16: 9142(R) (NP-11264)
measurement of partial, analyzer calibration for, 19: 22984(R) (NASA-CR-54167)
measurement of very low, of organic materials, method and apparatus for, 17: 32391(P)
measurement of, design of torsion-effusion apparatus for, 18: 14165 (TID-18592)
molecular effusion method for measuring, 20: 37307 (LA-3509)
of liquid metals, measurement by carrier gas method, 17: 37519(T) (AEC-tr-5983)
of metal halides, bibliography on, 17: 14202 (BM-IC-8147)
of metals and some refractory metalloids of groups IV, V, VI, VII, and VIII, 20: 331
of reactor fuel materials, equations for, 20: 38433 (ANL-7120, pp 641-53)
of thirty inorganic liquids up to critical point, 18: 41374 (UCRL-7167 (Rev.1))
reduced Frost-Kalkwarf equation for, 17: 14246
tables of, of 32 inorganic liquids at temperatures up to critical point, 18: 3722 (UCRL-7167)

Vapor-Slurry Reactors
see Fluid Fuel Reactors

VAPORIZATION
see also Evaporation
analysis of solid fuel, radiometric, 18: 25874
aspects of high-temperature, Knudsen cell design for study of, 16: 17814 (ANL-6536)
at high temperatures, use in thermodynamic studies, 19: 46234 (COO-1140-123)
equipment for liquid, for gas chromatography, 19: 32115(P)
fission-induced, in uranium dioxide, 17: 3538 (HW-SA-2497)
fundamental aspects, 17: 2060 (TID-14168)
growth of vapor film on rapidly heated plate, 17: 30667
measurement at high temperatures, 17: 16632(R) (AD-274654)
of elements of groups I to VI, bonding in homonuclear molecules in, 19: 36420
of liquid droplets during re-entry ablation, calculation, 19: 27813 (SC-RR-65-138)
of liquid drops on hot surface, 17: 29076(R) (TID-18996)
of metal from cylindrical cells, calculation of rates of, 19: 46943(T) (FTD-TT-65-611)
of metal oxides, measurement, 16: 25403
of metals at melting point, relation of energy and surface tension to, 18: 35530
of molten salts at low pressures, 20: 26821(R) (SRIA-106-38)
of nonstoichiometric compounds, calculation of kinetics of, 19: 6257 (NP-14535)
of nuclear materials at high temperatures, thermodynamics of, 20: 283 (COO-1140-129)
of volatile oxides, methods for studying, 16: 25381
phenomena in, 16: 33126 (UNC-5021)
processes in, fundamental aspects of, 17: 14201 (ANL-6663)
processes, studies, 16: 25389
symposium on, of nuclear materials, 17: 6104
testing equipment design for sodium, 19: 10540(R) (GEAP-4594)
thermodynamics of suboxide, 17: 10645

VARIABLE MODERATOR REACTOR
design, review of, 16: 30119

VASOCONSTRICTOR DRUGS
evaluation in man, tracer method using sodium-22, 19: 26164
radiosensitivity effects, 16: 12940

VBWR
see Vallecitos Boiling Water Reactor

Vector Mesons
see Mesons

Vegetation
see Plants

VEHICLES
see also Space Vehicles
accidents to highway, as potential carriers of radioactive materials, 17: 8431 (NYO-9771)
book: *Nuklearna Propulzija* (Nuclear Propulsion), 18: 4839
collision behavior of, procedure for predicting longitudinal, 20: 7313 (NYO-2539-4)
collision of, analysis of shipping container response to, 19: 40817 (SC-RR-65-98, pp 243-60)
decontamination of, methods for, 20: 27185 (AD-632989)
description of gamma spectrometer mounted, for field measurements, 18: 7086
description of mobile automatic alpha, beta, and gamma counting facility, 18: 29981 (NDL-TM-12)
design for use as field laboratory, 20: 27210(R) (UCRL-14680)
design of carriage for rolling on rails around reactor, 17: 29059(P)
design of mobile manipulator, 17: 2761
design of motor, for protection from fallout, 20: 5679(P)
design of ORNL mobile radiation laboratory, 17: 10877
design of remotely controlled mobile, with manipulators for recovery of aerospace nuclear power devices, 19: 46489 (CONF-640508, pp 327-33)
design of truck for traveling on tracks around reactor, 16: 30528(P)
development at U. S. Army Research Office, 1962 summary, 17: 33413(R) (NP-12967)
engine scale deposits and wear in tractors, neutron activation analysis of, 18: 39756(T) (AEC-tr-6390(p.397-402))
exhaust from automobiles, use of depleted-uranium catalysts for destruction of air pollutants in, 17: 33770 (PB-171980)
exhaust from automobiles, use of uranium oxide in catalyst for oxidation of carbon monoxide and hydrocarbons in, 18: 17715 (BM-RI-6323)
fallout decontamination by remote medical facilities of, 18: 29183
fuel for, methanol synthesis using nuclear power in mobile energy depot system, 20: 12877 (BNL-955)
motor deterioration in tractors, effect of dust on, 16: 13424(T) (AEC-tr-4492(p.53-8))
operation using nuclear energy, survey of energy storage systems for, 19: 2465 (BNL-7447)
power plant for lunar, 20: 45870
propulsion of land, radionuclide heat source for, 20: 46128(P)
propulsion of marine, radionuclide heat source for, 20: 46128(P)
propulsion systems for land, using fuel cells and electric motors, 16: 3983 (DOFL-TR-777)
propulsion using ammonia and liquid hydrogen fuels from energy depot, 19: 15694 (ACNP-64501)
radiation survey by detectors in M60 tank, correction factors for, 18: 25709 (NDL-TR-49)
radiography of railroad rolling stock, gamma, 18: 39731(T) (AEC-tr-6390(p.75-87))
shock waves from hypersonic, propagation in plasma, 17: 5430 (AD-276418)
testing of shielded-cab, for operation in radioactive fields, 17: 25472 (AFSWC-TDR-62-137)
tiedowns for containers for transport of radioactive materials on, 20: 23375 (NYO-2539-2)
trolley for support of scintillation counters, 17: 6213
truck dispatching system, computer simulation, 19: 10674 (K-1623)

weighing system for moving railway, radiometric, 18: 24047(P)
VEIN DEPOSITS (U. S.)
structural controls for, review of, 19: 30433
Veins
see Blood Vessels
VELA PROJECT
see also Antler Operation
see also Cowboy Project
blast effects from Salmon event on residential-type structures, 20: 4189 (VUF-1030)
blast effects from Salmon event on tall industrial and residential structures, 20: 4190 (VUF-1031)
borehole research in, conference on, 19: 20173 (VESIAC-4410-83-X)
cavity behavior in Tatum Salt Dome, Dribble Project, 18: 12337 (TID-20083)
cavity pressure and temperature measurements in Dribble, 20: 4084 (VUF-3017)
cavity stresses in Project Dribble, (T), 20: 12989 (NVO-1312-1(Vol.1))
conference on high-frequency seismic energy, Lakewood, Colorado, October 15 and 16, 1962, 18: 23784 (NP-13956)
containment and ground motion in Salmon Event, predictions and tests for, 20: 7251 (VUF-1026)
data from Satellite program of, 19: 47450 (LA-DC-7365)
data processing for satellite program, modular logic system for, 20: 15597
decoupling in Salmon detonation, seismology of, 20: 14664 (UCRL-14487(Rev.1))
description of Dribble Project, 19: 18174 (TID-21630)
design of satellite and systems for, redundancy, 20: 15598
detection of underground nuclear explosions, airborne spectral reconnaissance system for, 19: 26637 (VESIAC-5436VU)
development of geoelectric techniques for on-site inspection, 18: 33780 (NP-14145)
development of satellite program, 20: 15595
developments in, to July 1961, Congressional hearings on, 16: 20854
developments in, to July 1961, summary of, 16: 20855
developments in VELA-UNIFORM, 17: 34082
earth movement recording using geophones, 19: 9385(R) (NP-14531)
effects of Salmon explosion on nearby oil and gas facilities, 19: 36589 (VUF-1022)
environs monitoring for Salmon Event, 20: 16743 (VUF-1021)
field experiments in Gnome event, Vela-Uniform, 19: 24729 (VESIAC-5218VU)
geologic investigations of Sand Springs Range, Churchill Co., Nevada, 17: 3167 (TID-17224)
geologic maps, photographs, and logs for Sand Springs Range, Churchill Co., Nevada, 17: 3168 (TID-17224(Suppl.))
ground motion from Hardhat event, measurements of close-in, 19: 18177 (VUP-2101)
ground motion from Antler event, surface measurements of close-in, 19: 28556 (VUP-2100)
ground shock spectra from Gnome event, 19: 40713 (VUF-2401)
ground water flow velocities and radioactive decay in Shoal Event, hazards from, 20: 16742 (VUF-1014)
ground-water safety in Salmon Event, evaluation of, 20: 9094 (VUF-1027)
instrumentation, 18: 14586 (AD-416438)
instrumentation development for, 17: 10819(R) (AD-278217)
instrumentation design and performance for Project Dribble, 20: 12990 (NVO-1312(Vol.2))
instrumentation for Salmon Event, 20: 41070 (VUF-3021)
instrumentation in Salmon Event, grout mixtures for, 20: 9138 (VUF-3019)
ocean-bottom seismic data analysis from Pacific, 19: 26551 (AFCRL-64-666)
on-site inspection techniques, syllabus, 19: 24730 (VESIAC-5545VU)
performance of satellite system, computer simulation for, 20: 15599
development of Satellite program, 19: 2471 (SC-DC-64-1591)
pressure spikes from Project Dribble, effects on cavity walls (T), 19: 2473 (UCRL-7916)
progress report on Vela Uniform, 1960 through 1961, 18: 19500
radiation detector electronics for satellite program, 20: 15596
radiation hazards in Salmon event, methods for monitoring, 20: 33561 (VUF-1025)
radiological site survey for Project Shoal underground nuclear explosion, pre- and post-shot, 19: 698 (VUF-1012)
radiological surveillance of Shoal event, off-site, 19: 697 (VUF-1009)
seismic behavior of Gnome event, relation to nuclear test detection, 18: 31045 (AD-428227)
seismic data for CLEARWATER event, long-range, 18: 16189 (AD-427125(Rev.))
seismic data for on-site inspection, 17: 10238(R) (AD-278378)
seismic data for SHOAL event, local, 18: 16190 (NP-13757)
seismic data from BOBAC Event, 17: 3151 (NP-12275)
seismic data from HAYMAKER Event, 17: 3152 (NP-12276)
seismic data from YORK Event, 17: 3153 (NP-12277)
seismic data from WICHITA Event, 17: 3154 (NP-12278)
seismic data from Antler event, analysis of, 18: 10264 (AD-407430)
seismic data from STONES event, 18: 10265 (NP-13586)
seismic data from STONES event, long-range, 18: 16191 (NP-13586(Rev.))
seismic data from SALMON event, long-range, 19: 11403 (NP-14678)
seismic data from Fisher and Gnome events, long-range, 19: 26555 (VESIAC-5197VU)
seismic data from HARDHAT event, 19: 26556 (VESIAC-5439VU)
seismic data from PALANQUIN event, 20: 37010 (AD-631340)
seismic data from RED HOT, long-range, 20: 39124 (AD-632957)
seismic data on AARDVARK, long-range, 17: 34117 (NP-12328(Rev.))
seismic data on SHOAL, comparison with FALLON earthquake, 18: 39476 (NP-14283)
seismic data on, evaluation of, 18: 10211 (AD-402358)
seismic data recording in Vela-Uniform, magnetic tape standards for, 18: 6989 (AD-289031)
seismic discrimination techniques for Vela-Uniform, auditory, 19: 26560(R) (VESIAC-9281VU)
seismic effects of Pre-Dribble detonations in salt and sedimentary deposits, 18: 371 (NP-13279)
seismic measurements of DANNY BOY shot in, 17: 6268 (NP-12419)
seismic measurements of Hyrax event in, 17: 6269 (NP-12420)
seismic measurements from MAD event, 17: 10245 (NP-12524)
seismic measurements of STOAT explosion in, 17: 16262 (AD-297344)
seismic measurements from TENDRAC event, 18: 10263 (AD-404012)
seismic measurements, interpretation of data in long-range, 19: 24731 (VESIAC-7378VU)
seismic measurements on underground explosion in, 20: 20876 (NP-15949)
seismic measurements for CHARCOAL event, 20: 23318 (AD-631043)
seismic measurements from CHASE IV test, 20: 23319 (AD-631052)
seismic measurements on underground explosions in, 20: 41149 (AD-632956)
seismic monitoring of Salmon event in Dribble Project, volunteer team program, 19: 28555 (AD-612711)
seismic research in deep boreholes, 17: 3142 (AD-274106)
seismic source identification using long- and intermediate-period waves, 19: 26550(R) (AD-607946)
seismic velocity determination and distance measurements in salt dome for Salmon Event, 20: 43551 (VUF-3015)
seismic wave propagation from salt-dome environments, 18: 37357 (NP-14227)
seismic wave propagation from explosions, model studies, 19: 26559(R) (VESIAC-8746VU)
seismograms of GNOME event, compilation, 19: 18175 (VESIAC-4260)
seismological data in, for AARDVARK shot, 17: 6267 (NP-12328)
seismological observations on Project SHOAL in granite, 18: 22261 (AD-434785)
seismology, 17: 20196 (NP-12700)
seismology research, bibliography on, 19: 18171 (AD-422423)
shock wave propagation in granite from HARDHAT event (E/T), 19: 648 (SC-4741(RR))
shock wave propagation by nuclear explosion in salt deposit in Salmon event, calculations on, 20: 23323 (UCRL-12326)
site studies for Shoal event, geologic and hydrologic, 19: 26528 (VUF-1001)
status of Vela Uniform, 17: 16906
surface radiation and weather prediction activities for Salmon Event, 20: 5667 (VUF-1020)
use of water wells in Vela Uniform, 18: 43780 (AFCRL-64-177)
vent gas treatment plant for Dribble, analytical systems for, 19: 46471 (UCRL-14123)
vented gases in Dribble project, apparatus for analysis of, 19: 19776 (UCRL-12169)
Velocitrons
see Mass Spectrometers
VELOCITY
see also Acceleration
control and measurement in Mössbauer apparatus, 20: 21081
effects of, combined with γ radiation on Drosophila genetics, 20: 14343
effects of, combined with x radiation on mitosis in mouse marrow, 20: 18439
effects of, in combination with vibrations and x radiation on mouse genetics, 20: 42986
effects of, on earth penetration by projectiles, 20: 45240 (SC-RR-66-376)
effects on mouse genetics, 20: 42986
effects on phage induction and viability of *E. coli* during space flight, 20: 42910
hypervelocity techniques, conference on, 16: 18728
measurement in water, use of neutron activation of oxygen in,

20: 25368(P)
measurement near underground explosions, gage for, 19: 38917 (SC-R-65-904, pp 23-48)
measurement of air, calibration of instruments for, 18: 27755(R) (ORNL-3578(p.78-95))
measurement of reactor-coolant, 18: 35089 (TID-8540(p.177-211))
measurement of ultracentrifuge rotor, by radiotelemetry, 20: 43637(R) (UCRL-16246, pp 168-75)
measurement of, using Mossbauer effect, 17: 36125
measurement of water circulation in boiler-feed water system, design of radioisotope device for, 18: 7101(P)
measurement of, using gamma resonant absorption, 19: 38966(P)
measurements by Mössbauer resonance of gamma rays, 16: 32000 (ARF-1166-22)
of raindrops, equipment for measuring, 20: 31476(R) (BNWL-235-4, pp 21)
transformation of, in special relativity, geometrical demonstration of, 17: 40227

VENEZUELA
fallout monitoring in, 1960 through 1962, 18: 25689
radiation monitoring in, 20: 9143

VENTILATION
see also Exhaust Systems
see also Laboratories
capacity and rate of, in underground shelters, 20: 20920 (AD-621377)
control in beryllium handling, 16: 21878 (ASD-TR-62-7-665)
design and use of systems for, in radioisotope laboratories, 20: 43593(T) (AEC-tr-6642)
design for blast and fall-out shelters, 16: 13393
design for high-alpha facility, 17: 2773
design for laboratory hoods, 19: 18100 (LA-DC-6396)
design for municipal emergency center, 16: 13394
design for nuclear reactor facilities, 16: 13398
design for nuclear facilities, 20: 31453 (STI-PUB-121)
design for radiation hazards control in nuclear power plants, 16: 19190
design of equipment for, in laboratory, 20: 35672
development and operational procedure for GETR, 19: 38261 (APED-4548)
development of air conditioning system for plastic protective suits, 19: 36741
development of lithium hydroxide canisters for carbon dioxide removal, 16: 2054 (NP-10935)
development of systems of, for protective shelters, 20: 39074
effects of overpressures on radon-222 hazards in underground mines, 20: 6694(R) (MIT-952-2)
effects on natural alpha radioactivity level of air-sampling filter, 18: 43879
effects on radon content in living and working environments, 20: 2090
equipment for clean rooms, 16: 25509 (TID-16274)
equipment for, construction and operation of, 16: 33055
equipment for, during beryllium machining, 17: 36260
equipment for, use of plastics in, 19: 18101
evaluation and performance of hood system in plutonium fabrication facility, 16: 2073
evaluation of recyclings and transit times of systems for, use of fumigenes for, 18: 43874
filter design criteria and specifications for, at National Reactor Testing Station, 20: 20933 (IDO-12045)
filter humidity testing for systems of, 18: 14006 (TID-7677(p.572-602))
filter system modification and testing in ALRR, 20: 42681(R) (IS-1500(Sect. R))
filter testing for system of, sodium flame method, 18: 14005 (TID-7677 (p.553-71))
filter testing for cesium-137 and iodine in nuclear plant, efficiency of, 19: 22602 (RISO-94)
for beryllium fabrication facilities, 19: 26584
for clean rooms, system design, 16: 20874 (SC-4673(RR))
for corrosive fumes, use of Quickdraft eductors for, 18: 438 (NLCO-889)
for fallout shelters, 19: 34397 (BNL-9188)
for rock shelters, economics of, 16: 33323
for toxic metal processing plants, 19: 32498
hazards analysis for radiochemical facilities, 16: 29212 (ORNL-TM-346)
in closed underground shelters, techniques and cost analysis of, 18: 12383 (AD-413416)
in operations using radioactive materials, 19: 15820
in uranium mines, 17: 20241 (NP-12692)
measurement of rate of, using radioisotopes, 19: 4564
method for, of fallout shelters by induced draft, 20: 20921 (AD-621998)
monitoring exhaust from laboratory system for, equipment for, 20: 13006 (ORNL-TM-1384)
of crowded shelters cooled by outside air, manual punkah-pump for, 19: 30395 (ORNL-TM-1154)
of hot cells and isotope laboratories at Würenlingen, 19: 9318
of NS *Savannah* reactor compartment, performance of filters in, 19: 27811(R) (ORNL-3775)
of rooms containing gamma sources, 19: 38883
of uranium mines for control of radon and daughters, 18: 20269
particle deposition in ducts from aerosols, 18: 31791 (ORNL-P-4)
protection from fallout contamination in hospitals, 17: 8466
pumps for shelter, durability tests of punkah, 19: 38832 (ORNL-TM-1155)
rate from decay of filter paper air samples of radon or thoron daughters, 16: 10320
removal of radioactive gases and aerosols by, 16: 18709(T) (JPRS-12637)
safety hazards in systems for, 18: 14117 (TID-7677(p.56-72))
specification guides at HAPO for, 18: 3925 (TID-19753)
standards for, radiation industrial buildings, 19: 38884
system design for radiochemical laboratories, 19: 44284 (AWRE-O-24/65)
system design for, in ORNL Transuranium Processing Plant, 18: 14001 (TID-7677(p.86-101))
system design for, in Los Alamos plutonium-processing facility, 20: 27201 (LA-DC-7590)
system evaluation for, use of analog computers in, 18: 13999 (TID-7677 (p.44-55))
system for fallout shelter, 19: 38833(P)
system for fallout shelter, 20: 27127(P)
system for laminar-flow clean rooms, 18: 45182 (SC-R-64-145A)
system for plutonium-processing facility gas purification, 20: 25199(T) (ORNL-tr-1121)
system for reactor maintenance cell, 17: 2753
systems for caves, standardization of, 19: 18103
systems for protective clothing, 19: 36710 (RL-SA-3682)
systems for radioisotope laboratories, 16: 25676
systems for shelters, performance of gravity, 19: 22594 (NP-14976)
systems for use in clean rooms, 19: 21793 (SC-RR-65-47)
systems in fallout shelters, effectiveness in removing fallout particles, 17: 3232(R) (UCRL-7035)
valves for blast shelter systems, 20: 39073

VERA (Versatile Experimental Reactor Assembly)
see Critical Assemblies

VERMICULITES
cesium diffusion in, 16: 2802(R) (ORNL-3189(p.42-9))
diffusion of sodium in, self-, 20: 38858 (BNWL-235-3, pp 23-51)
fixation in glass, 20: 47082 (AEET-250)
fusion and leaching studies for waste fixation, 19: 31618(R) (TID-21882)
ion exchange and fixation properties for cesium, 16: 27021
ion exchange behavior of, for cesium, 18: 19448(R) (ORNL-TM-757)
ion exchange capacity and selectivity, 16: 2809(R) (ORNL-TM-49)
ion exchange in potassium- and sodium-treated, 19: 8673(R) (ORNL-3697(p.3-10))
ion exchange properties for cesium in waste solutions, 16: 12798
ion exchange properties for cesium and strontium, 17: 25315
ion exchange properties under centrifugation, 17: 29865 (AERE-R-4314)
ion exchange properties for strontium in waste solutions, 17: 36999
ion exchange properties for cesium and strontium, 18: 19450(T) (CEA-tr-A-1462)
mitigation of shock wave effects by lightweight concrete containing, 17: 5668 (DASA-1263)
physical characteristics, 16: 2808(R) (ORNL-TM-15)
properties as ion exchange material, effects of heat treatment on, 19: 30342
radiation effects on corrosion of cesium-containing, 20: 18166(R) (TID-22531)
reactions with strontium, tracer studies, 16: 25049 (TID-7628(p.187-97))
sorptive properties for barium, cerium, cesium, cobalt, praseodymium, strontium, and yttrium, 16: 11958(R) (JAERI-5003(p.117-18))
sorptive properties for radionuclides in waste, 17: 19705 (TID-7644 (p.29-45))
sorptive properties for cesium, 17: 37146 (AAEC/TM-205)
sorptive properties for cesium and strontium, 17: 39301(R) (ORNL-3492 (p.62-70))
sorptive properties of potassium-treated, for cesium and strontium, 18: 6537(R) (ORNL-TM-603)
sorptive properties for cesium and strontium, effects of aluminum and iron hydroxides and potassium on, 18: 17344
sorptive properties for cesium, effects of ammonium, cesium, potassium, or rubidium ions on, 18: 27474
sorptive properties for thorium and uranium from solutions, 18: 37050 (A/CONF.28/P/814)
sorptive properties for cesium and strontium from solutions, 19: 4257 (UJV-1106/64)
sorptive properties for cesium from solutions, 19: 36543(R) (TID-21955)
sorptive properties for cesium-137, 20: 20696
sorptive properties for cesium and strontium, 20: 43130
sorptive properties for cesium, 20: 43455

structure determination from cesium sorption, 17: 18296
use in decontaminating waste water, 16: 7337
use in waste processing at AERE, Harwell, 20: 26556
VERMONT
aerial gamma monitoring of, correlation with areal geology, 18: 43798 (CEX-59.4.14)
radiation effects on congenital malformations in infants in, natural background, 19: 33853
radiation exposure in, background, 18: 43838
radioactivity from natural sources, 17: 27629
Versene
see Acetic Acid, (Ethylenediamine)Tetra-, Sodium Salts
Versene Acid
see Acetic Acid, (Ethylenediamine)Tetra-
VERTEBRATES
see also Burros
see also Cats
see also Cattle
see also Dogs
see also Goats
see also Guinea Pigs
see also Hamsters
see also Horses
see also Mice
see also Monkeys
see also Rabbits
see also Rats
Vertex Tubes
see Hilsch Tubes
VESPIDAE
cobalt-58 half life in, following cobalt sulfate feeding, 20: 8574
diapause larvae in Mormoniella, method for producing, 20: 40582(R) (ORNL-3922, pp 65-8)
genetic analysis of induced variability in Habrobracon, 17: 38746(R) (TID-19432)
genetic evolution in populations of, 18: 19506(T) (TID-20401)
genetic variability under prolonged inbreeding in Habrobracon, 18: 8107(R) (NYO-10620)
hatchability of Habrobracon eggs, postirradiation effects of carbon monoxide and nitrogen on, 16: 23452 (BNL-4981)
labeling of, by phosphorus-32 uptake from food or honey, 19: 35913
metabolism and toxic effects of cobalt, copper, magnesium, and zinc in Habrobracon, 19: 10741 (TID-21559)
mud transport by, from White Oak Lake, 19: 21792(R) (ORNL-3650(p.187-219))
mutations in Habrobracon induced by ethyl methanesulfonate and nitrogen mustard treatment of oocytes, 16: 31406
radiation effects on cytoplasm of Habrobracon eggs, 16: 28751(R) (TID-16471)
radiation effects from ingested plutonium-239 on fertility and life span, 17: 13918 (HW-SA-2605)
radiation effects on life span of diploid and haploid *Habrobracon serinopae*, 18: 8129
radiation effects on chromosomes of *Hymenolepis diminuta*, gamma, 18: 19752
radiation effects on mud-dauber wasps from radioactive mud nests, 19: 6931(R) (ORNL-3697(p.65-84))
radiation effects on response to toxic metals in, 19: 10741 (TID-21559)
radiation effects on developing Bracon embryos, photoreactivation of uv, 19: 42368
radiation effects on sperm in, gamma, 19: 43721(R) (ORNL-TM-1217)
radiation effects on unisexual wasp Devorgilla, genetic, 20: 1643
radiation effects on, genetic, 20: 1622 (WT-820)
radiation effects on egg production in, x, 20: 8650
radiation effects on genetic variability in Habrobracon, gamma, 20: 36659
radioactive material transport by, 20: 6711(R) (ORNL-3849, pp 43-100)
radioinduced aging in, effect of ploidy on, 17: 40647
radioinduced dominant lethality in, 18: 43225 (ORNL-P-388)
radioinduced dominant lethals in males of, frequency of x, 20: 20464
radioinduced eye color mutations in Mormoniella, x, 20: 40669
radioinduced mutations, R-locus deleterious, 16: 9871
radioinduced mutations, 16: 30237
radioinduced mutations in Habrobracon oocytes, 17: 21513
radioinduced mutations of Mormoniella, 18: 73
radioinduced mutations of Habrobracon, 18: 13453(R) (TID-20220)
radioinduced mutations of *Dahlbominus fuscipennis*, 20: 3733
simulated flight tests for Habrobracon, 20: 40508(R) (ORNL-3922, pp 196-9)
ultraviolet-induced nontransmissible nuclear damage in, 17: 38787
use in research, 20: 8650
zinc-65 effects on eggs of habrobracon, 16: 26706
VESIR
see Vallecitos Superheat Reactor
VESSELS
(This heading is reserved for containers of various kinds.)
see also Blood Vessels
see also Dissolvers
see also Naval Vessels
see also Pressure Vessels
see also Tanks
see also Vacuum Vessels
analysis of low-level radioactive waste containers in accident environment, 19: 20196 (CONF-650103-6)
book: *The Optimal Design of Chemical Reactors. A Study in Dynamic Programming*, 16: 13507
characteristics of cryogenic, for gas storage in space, 17: 9123
chilldown and boiloff losses of large liquid hydrogen storage dewars, 19: 39686 (LA-DC-7164)
collapse of copper, by external pressure, 16: 5436 (ORNL-TM-102)
concentration changes in Nth vessel of series, nomograph for, 19: 2466 (HW-SA-3261)
connecting device for leak-tight, 19: 34317(P)
containing gas under pressure, method of relieving pressure in, 17: 36911(P)
containment of explosions by, studies, 19: 9283 (LGI-63/23)
convection in cylindrical, 17: 8379
crack failure in cylindrical steel, effects of pressure and temperature on, 18: 18017
criticality control using boron, 17: 27502
criticality of arrays of, for storage of plutonium nitrate solution, 19: 18733 (BNWL-19)
decontamination and dismantling of radioactively contaminated containers, glove box for, 20: 5711(P)
decontamination of fuel storage, 20: 28853(R) (IDO-14661, pp 45-82)
description of transport container for irradiated fuels from power stations in United Kingdom, 19: 40829 (SC-RR-65-98, pp 711-18)
design and evaluation of reactor, (E/T), 19: 8574 (IITRI-578P22-9)
design and properties of, for radio-induced chemical reactions, 20: 16505 (BNL-949)
design for cell preservation by freezing, 17: 35369
design for containment of gaseous fuel reactors, 20: 14054(P)
design for electrolytic melt refining of plutonium and uranium, 19: 4239(P)
design for electron irradiation of gases, 20: 7668(P)
design for fluid-bed denitration, engineering drawings of, 19: 4164
design for fluidized-bed reactions, 19: 24222(P)
design for high pressure infrared spectrometer, portable, 19: 46771
design for liquid hydrogen, 18: 38017 (APCI-541301)
design for petroleum samples for nuclear detonation shock-transition studies, 19: 608 (PNE-112F(Pt.II))
design for production of chemicals by radioinduced reactions, 18: 12139(R) (BNL-823(p.48-56))
design for radiation chemistry studies, 18: 37311 (BNL-874(p.18))
design for radioactive liquid waste disposal, 20: 10445
design for radiochemical reactions, 16: 693
design for reaction of metals with gaseous fluorinating agent for preparation of metal fluorides, 18: 12114(P)
design for safe storage of fissile materials, 18: 44976
design for shipment of radioactive materials, 20: 43492 (ORNL-TM-1312(Vol.2))
design for shipping spent fuel elements, 18: 37422 (A/CONF.28/P/184)
design for shipping of plutonium nitrate, 19: 4402 (RFP-437)
design for shipping plutonium nitrate and oxide, 19: 40825 (SC-RR-65-98, pp 609-19)
design for shipping spent reactor fuels, (E), 19: 40837
design for shipping and storage of radioactive materials, 20: 43476(P)
design for storage and shipping of spent fuel elements, 20: 14679(P)
design for underwater storage of strategic materials, 17: 32229(P)
design for use in measurement of leakage rate, 20: 36978 (NAA-SR-12001)
design of cryogenic, for germanium detectors, 20: 6694(R) (MIT-952-2)
design of insulated, for liquefied gases, 17: 8309
design of reactor, with radiation shield, 17: 28514(P)
design of reusable, for high-temperature reactions, 17: 12607(P)
design of shipping, for uranium hexafluoride, 17: 16126
design of shipping containers for radioactive materials, review, 19: 40823 (SC-RR-65-98, pp 450-72)
design of stainless steel, for recovering radioactive waste, 20: 18160 (CEA-R-2894)
design of vented, for reactor containment, 18: 7947
design of, for collecting radioactive methyl esters in gas–liquid chromatography, 20: 35432
development and tests of accident-resistant shipping, for radioactive materials, 19: 40816 (SC-RR-65-98, pp 141-86)
development of fire-resistant, 18: 26995(P)
development of sample-carrier, for pneumatic tube systems, 17: 35253(R) (IA-775)

development of shipping packages for plutonium dioxide, 19: 30443 (RFP-501)
fabrication and properties of zirconium, for steel casting, 17: 36319
fabrication for liquids to be irradiated, 16: 20574
fill height measurement by radiation absorption in, 18: 5598(P)
fire resistance tests of wood containers for shipping fuel cores, 20: 37024 (NLCO-899)
fire test of finned box, 19: 40827 (SC-RR-65-98, pp 631-50)
fire tests of models of shipping containers, 19: 40815 (SC-RR-65-98, pp 133-40)
fixation of radioactive materials in, calculations of transient temperatures for, 20: 18155 (BNWL-157)
gamma transport, 20: 160
impact tests of birdcage-type, for shipping of fissionable material, 19: 6129 (ORNL-3735)
impact tests of drum-type birdcages for shipping of fissile materials, 19: 15697 (ORNL-P-869)
impact tests of end cap for Containment Capsule Impact Safety Study, 19: 558 (SC-RR-64-530)
impact tests of shipping container for fissionable materials, 19: 26491 (LAMS-2983(Suppl.))
impact tests of steel shells of casks, 18: 6934 (ORNL-TM-680)
insulation compaction in large dewars by thermal cycling, study of perlite, 19: 38779 (LA-DC-7158)
ion exchange on walls of, in monitoring atmospheric radioactivity, 17: 39328
leak testing using radioactive gas, 20: 23249(P)
level indicators for MSRE fuel-processing tanks, (E), 19: 24175(R) (NYO-2910-9)
materials testing for fissile materials storage, 20: 20840(R) (BNWL-193, pp 57-67)
opening of metal, use of lasers for remote, 20: 9105
opening of metal, use of lasers for remote, 20: 5669
packing spheres in cylindrical, computer analysis of, 20: 41063 (BNL-997)
plutonium leakage from, device for measuring, (E), 19: 28329
plutonium penetration through capsules, system for detecting high-temperature, 19: 36750 (LA-DC-6973)
preparation from set oil shale remains and waterproof foil, for waste 19: 5567(P)
pressurization in storage, effects on gas evolution from plutonium residues on, 20: 4364 (AERE-M-1644)
radiation effects on plastic expansion of spherical, 19: 14106
radioactivity in culture, for Paramecium growth studies, 20: 42886
safety characteristics of reactor-containment, (E), 19: 35624
sealing of fission-product-containing, methods of remote welding for, 18: 6536 (HW-79393)
standardization for shipping radioactive materials, 19: 40822 (SC-RR-65-98, pp 442-9)
storage of tritium, in plastic bags, hazards of, 20: 41196 (LA-DC-7996)
stress analysis of plexiglass model of thick-walled, comparison of experimental and numerical, 19: 22503 (GAMD-5503)
survival of waste containers at ocean depths, 16: 11349
tests of Class II container for shipping low-assay uranium compounds, 19: 40819 (SC-RR-65-98, pp 330-56)
tests of container for shipping fissile materials, 18: 6972 (LAMS-2983)
tests of shipping containers for slightly enriched uranium fuel cores, 19: 40820 (SC-RR-65-98, pp 357-76)
tests of shipping containers for plutonium nitrate solutions, 19: 40821 (SC-RR-65-98, pp 423-41)
tests of 10-ton capacity shipping containers for uranium hexafluoride, drop, 19: 40824 (SC-RR-65-98, pp 580-608)
thickness measurement in reactor fuel element processing, ultrasonic facility for, 19: 4342
use of stainless steel, to contain dissolution of stainless steel fuel cladding, 19: 11301(P)

VGL-2 (Russian)
see Magnetic Mirror Machines

Vibrating Conveyers
see Conveyers

VIBRATING REED ELECTROMETERS
design, 18: 41760 (BNL-8378)
design and use with ionization chambers, 17: 18488
sensitivity for beta counting, 17: 18487
use in analysis of organic compounds for carbon-14, 16: 148
use in clinical dosimetry, 19: 46854

VIBRATION TESTING
description of force-controlled, 19: 18132 (SC-TM-65-31)
dynamic data interpretation for weapon systems, 19: 1967 (SCL-DC-64-83)
equipment having low power requirement, 17: 1630(P)
method for measuring elastic constants of small plates, 18: 25679
method for shock testing on shakers, 18: 35700 (NAA-SR-Memo-8162(Rev.))
method for, eddy-current, 20: 2025 (BNWL-SA-349)
methods for determining resonances in SNAP 10, (E), 19: 17342 (NAA-SR-Memo-8339)
of irradiation capsules in vortex flow, 18: 28931 (EUR-1638.e)
of nonlinear systems, methods and data analysis of, 18: 6935 (SC-TM-284-63(72))
of operating machines, preventive maintenance aspects of, 17: 8275 (HW-SA-2149)
of radiator-condenser structure R/C 6, 18: 43740 (NAA-SR-Memo-9963)
of refractory alloys at high temperatures in ultra-high vacuum, 19: 18458(R) (NASA-CR-54286)
of rod and tube bundles in air, 16: 27200(T,R) (EURAEC-106)
of SNAP 2, mockup, 19: 5529 (NAA-SR-Memo-10257)
response of linear lumped spring-mass systems to, graphical methods for, 18: 17360 (TID-18775)
review of random vibration terminology and analysis equipment, 18: 19478 (SCL-R-64-40)

VIBRATIONS
analysis of airborne, system for, 18: 16280 (SC-TM-328-62(72))
analysis of nonlinear, in reactor components, 20: 45061
analysis of vibrating systems, computer program for, 18: 9754 (KAPL-M-EC-33)
biological effects, 17: 37103
damping of, effects of aerospace environments on materials and techniques for, 17: 29262
damping of, shock-absorbing mounts for, 18: 3950(P)
damping of, engineering drawings of mount for, 19: 30359
effects of high-frequency and ultrasonic, on radiophosphorus absorption in dog intestine, 20: 18219
effects of stress induced by, on radiosensitivity of rats and guinea pigs, 19: 40354(T) (FTD-TT-65-48, pp 38–9)
effects of water on natural frequency of beam, 20: 4080 (WAPD-TM-535)
effects of, combined with γ radiation on Drosophila genetics, 20: 14343
effects of, combined with γ radiation on phage production in *E. coli*, 20: 18363
effects of, combined with x radiation on mitosis in mouse marrow, 20: 18439
effects of, combined with proton-irradiation on shielded rats, 20: 18441
effects of, in combination with acceleration and x radiation on mouse genetics, 20: 42986
effects on animal physiology, 19: 45824(T) (NASA-TT-F-354)
effects on bone marrow cells of mice, 19: 17494(T) (FTD-TT-64-1316 (p.205-16))
effects on grain size control in ingots and welds, review of, 17: 30947 (DMIC-Memo-166)
effects on heat transfer from heated tubes to water, 17: 23475(R) (CUA-NE-26)
effects on heat transfer from heated tubes to water, 17: 40974(R) (CUA-NE-27)
effects on heat transfer from heated tubes to water, 18: 396(R) (CUA-NE-28)
effects on hematopoietic organs in mice, 20: 33010
effects on mouse genetics, 20: 42986
effects on oxidation in rat brain, 19: 38358 (AD-612660)
effects on phage induction and viability of *E. coli* during space flight, 20: 42910
effects on phage production in *E. coli*, 20: 18363
effects on radiation sickness, 16: 78
effects on radioinduced changes in bone marrow of mice, 19: 2103
effects on serotonin content in animal blood, 19: 15095
effects on vestibular organs in guinea pigs, synergistic effects of radiation on, 19: 38358 (AD-612660)
experimental techniques in, conference on, 18: 5442
forced, in system with viscous friction and coulomb damping, 16: 4624(T) (SCL-T-389)
frequencies of rod and tube bundles in air, 16: 27200(T,R) (EURAEC-106)
frequency of monatomic chain, effects of anharmonic potential, 16: 17612 (D1-82-0149)
heat transfer effects in aqueous reactor cooling systems, 16: 9624(R) (CUA-NE-17)
measurement during highway transport of SNAP systems, 17: 24744 (NAA-SR-Memo-8074)
measurement in fuel assemblies, eddy-current transducers for, 19: 46716(R) (IDO-17081, pp 77-123)
measurement in reactor fuel assemblies using noise-analysis techniques, 20: 34878
monitoring in PRTR pressure tubes, device for, 19: 14832(R) (HW-81984(p.11.1-14))
of reactor structures, analysis of seismic, 17: 21270
radiosensitivity effects on mice, synergistic, 20: 28968
response of one-degree-of-freedom system to shock pulses, 19: 11308

(NAA-SR-Memo-10591)
statistical analysis of nonstationary, in missiles, 18: 4910 (SC-DC-2049)
theory of nonlinear, 18: 6935 (SC-TM-284-63(72))
uncoupling of modes of, in very large underground structures by suspension, 19: 26481 (AD-608518)
Vidicon Tubes
see Television Equipment
VINCALEUKOBLASTINE
effects of, combined with x radiation on tumors in mice, 20: 38613
sulfate, radioprotective effects, 20: 12719 (NP-15668)
VINYL ACETATE POLYMERS
Vinyl Acetate Polymers
see Acetic Acid, Vinyl Ester Polymers
radioinduced copolymerization with polymethyl methacrylate, 17: 29923
VINYL ALCOHOL POLYMERS
binder effects on grain growth and solarization of sintered uranium dioxide pellets, 18: 34170
diffusion of radium-224 in, 18: 13775
effects as binder on tensile strength of oxides for machining, 20: 11277 (RFP-659)
effects of irradiation followed by heating on gel formation in, 18: 24198(T,R) (AEC-tr-6316(p.118-20))
effects of, on hemopoiesis in irradiated rats, 18: 6696
effects on grain growth in sintered uranium dioxide, 19: 14013
graft-copolymerization with preirradiated vinyl monomers, method for, 20: 23187(P)
heat treatment effects on, effects of boric acid on, 18: 25487(T) (AEC-tr-6372(p.175-84))
mechanical properties of wood impregnated with, 19: 2416
performance in colored films for gamma and neutron dosimetry, 20: 2135
performance in fine-grain nuclear emulsions, 19: 44400 (CERN-65-4 (Vol.II), pp III31-56)
preparation of thermoplastic, with fire-retardant properties, 17: 35623(P)
preparation of tritiated, for luminous paints, 17: 191 (IA-735)
properties of radioinduced methylmethacrylate and styrene grafts polymerized on, 16: 19443
properties of, from gamma-induced polymerization of vinyl acetate, 18: 23593(T,R) (AEC-tr-6316(p.134-6))
radiation effects on electric properties, gamma, 16: 18089
radiation effects on, acetalized with glyoxylic acid, 16: 18951
radiation effects on dyeability of fibers, 16: 22198
radiation effects on aqueous solutions, 16: 22234
radiation effects on properties as electrical insulation, 16: 22666
radiation effects on acetylated and normal, in aqueous solution, 16: 33033
radiation effects on, gamma, 17: 29919
radiation effects on properties of coatings, 17: 36362
radiation effects on viscosity of aqueous solutions of, 18: 17878
radiation effects on gel formation and viscosity of, high-temperature, 18: 24197(T,R) (AEC-tr-6316(p.114-17))
radiation effects on, effects of boric acid on, 18: 25487(T) (AEC-tr-6372(p.175-84))
radiation effects on mechanical properties of acetylated, beta, 18: 25489(T) (AEC-tr-6372(p.193-5))
radiation effects on reactions with chlorine and sulfur dioxide, 18: 25490(T) (AEC-tr-6372(p.197-205))
radiation effects on film in air and vacuum, infrared spectral studies of gamma, 18: 29706(T,R) (AEC-tr-6231(p.125-35))
radiation effects on viscosity of aqueous solutions of, effects of additives on, 18: 29740(T,R) (AEC-tr-6231(p.339-41))
radiation effects on, gamma, 18: 29744(T,R) (AEC-tr-6231(p.418-27))
radiation effects on thermoluminescence, 19: 19983
radiation effects on dye-containing, 19: 32237
radiation effects on dielectric properties of, electron, 20: 1897 (NASA-TN-D-3032)
radiation effects on micro-gel particle size of, gamma, 20: 33343
radiation grafting with monomers, mechanical properties after, 19: 11180
radiation modification of, synthesis of artificial kidney membranes by, 18: 37188 (BNL-874(p.32))
radioinduced chlorination, 16: 22184
radioinduced chlorination, 18: 29724(T,R) (AEC-tr-6231(p.225-9))
radioinduced copolymerization with nylon-6, 17: 29923
radioinduced cross linking of, effects of oxygen and temperature on gel formation in, 16: 31646
radioinduced crosslinking and gelation in aqueous solution of, 16: 33045
radioinduced cross-linking in aqueous solutions, 17: 1545
radioinduced crosslinking of aqueous solutions of, effects of additives on, 17: 27904
radioinduced crosslinking in aqueous solutions of, in absence of air, 17: 30206
radioinduced crosslinking of, effects of allyl acrylate, allyl methacrylate, and diallyl maleate on, 18: 8407 (RAI-329)
radioinduced crosslinking in aqueous solutions, effects of polymerization degree on, 18: 17877
radioinduced crosslinking in fibers and films of, properties of product in beta, 18: 25488(T) (AEC-tr-6372(p.185-92))
radioinduced crosslinking of, 19: 26380(R) (NYO-3329-2)
radioinduced crosslinking with nylon 66 in presence of allyl methacrylate–methanol–water system, 20: 1909
radioinduced crosslinking in, for use as membrane in artificial kidneys, 20: 16505 (BNL-949)
radioinduced free radicals in, singlets in electron spin resonance spectra produced at high doses, 18: 23616(T,R) (AEC-tr-6316(p.306-9))
radioinduced free radicals in, output saturation in electron spin resonance spectra of, 18: 23617(T,R) (AEC-tr-6316(p.310-13))
radioinduced free radicals in, concentration of, 18: 23618(T,R) (AEC-tr-6316(p.314-21))
radioinduced free radicals in, electron spin resonance studies of, 18: 23649(T,R) (AEC-tr-6316(p.538-50))
radioinduced free radicals in, gamma, 18: 23651(T,R) (AEC-tr-6316 (p.573-86))
radioinduced free radicals in, gamma, 18: 23654(T,R) (AEC-tr-6316 (p.609-15))
radioinduced free radicals in, ultraviolet, 18: 23653(T,R) (AEC-tr-6316 (p.598-602))
radioinduced free radicals in, electron spin resonance spectra, 18: 29735(T,R) (AEC-tr-6231(p.292-309))
radioinduced free radicals in, effects of physical state on electron spin resonance spectra of, 18: 29741(T,R) (AEC-tr-6231(p.373-95))
radioinduced free radicals in, reactions with sulfur dioxide, 18: 29747(T,R) (AEC-tr-6231(p.439-50))
radioinduced gas evolution from films of, gamma, 18: 29707(T,R) (AEC-tr-6231(p.136-7))
radioinduced gelation, effects of acids on, 17: 14340
radioinduced gelation at high temperatures, 18: 29703(T,R) (AEC-tr-6231(p.119-20))
radioinduced gelation at 90 to 170°C, 18: 29704(T,R) (AEC-tr-6231 (p.121-2))
radioinduced graft polymerization with methyl methacrylate, 16: 229
radioinduced graft polymerization of methyl methacrylate on films, 16: 22190
radioinduced graft polymerization of styrene on films, 16: 22194
radioinduced graft polymerization of styrene on films, effects of ferrous ions, 16: 22196
radioinduced grafting of, with styrene, 17: 18139
radioinduced graft polymerization on vinyl acetate in aqueous and acetylated solutions, 17: 27444
radioinduced graft polymerization to MMA, gamma, 17: 30049
radioinduced graft polymerization of, on acrylonitrile–butadiene–styrene mixture, 17: 30199
radioinduced graft polymerization to methyl methacrylate, effects of ferrous ions on, 17: 33985
radioinduced graft polymerization to styrene, solvent effects on, 17: 33986
radioinduced grafting of monomer mixtures on, 18: 12226
radioinduced graft polymerization of styrene on, effects of solvents on gamma, 18: 23581(T,R) (AEC-tr-6316(p.66-9))
radioinduced graft polymerization of styrene on, effects of environment on, 18: 23582(T,R) (AEC-tr-6316(p.70-5))
radioinduced graft polymerization of vinyl monomers on, gamma, 18: 23583(T,R) (AEC-tr-6316(p.76-8))
radioinduced graft polymerization of 2-methyl-5-vinyl pyridine and styrene on, 18: 23584(T,R) (AEC-tr-6316(p.79-83))
radioinduced graft polymerization with acrylonitrile, butadiene, and styrene, effects of heat treatment on, 18: 25482(T) (AEC-tr-6372 (p.135-40))
radioinduced graft polymerization on styrene, heat treatment effects on x-ray scattering in, 18: 25483(T) (AEC-tr-6372(p.141-3))
radioinduced graft polymerization on acrylamide, 18: 25485(T) (AEC-tr-6372(p.159-61))
radioinduced graft polymerization of binary mixtures onto, mechanism of, 18: 27547
radioinduced graft polymerization of acrylonitrile–butadiene–styrene onto fibers and powders of, 18: 27548
radioinduced graft polymerization of styrene onto spun fiber of, 18: 27549
radioinduced graft polymerization of styrene onto fibers of, spun from alkali bath, 18: 27550
radioinduced graft polymerization onto polybutadiene, structure of product in, 18: 27551
radioinduced graft polymerization of monomers to, 18: 29698(T,R) (AEC-tr-6231(p.91-101))
radioinduced grafting to styrene in methanol solution above 40°C, 19: 11181
radioinduced graft polymerization of methacrylamide on, 19: 26423
radioinduced graft polymerization of acrylonitrile on, 20: 401

radioinduced main chain scission in, effects of structure on, 19: 18028
radioinduced main-chain scission in, 19: 9179
radioinduced polymerization of methyl methacrylate on film from aqueous solution, 16: 22234
radioinduced production, 18: 3867(P)
radiolysis in various media, 16: 22233
radiolysis of aqueous solutions of, effects of inorganic salts and organic compounds on, 19: 2387
radiolysis of, electron paramagnetic resonance study of radicals from, 17: 33987
radiolysis of, selectivity of scission of various bonds in, 17: 29921
radiolysis of water-swollen films, 16: 22236
radiolysis of, EPR studies of yields of stabilized charges in low-temperature, 20: 40962
radiolysis of, in presence of oxygen, 19: 453
radiolysis of, linear energy transfer effects on yields from, 18: 29779
radiolysis of, mechanisms of gamma, 20: 7141
reactions with acetates, ester interchange and copolymer formation in, 17: 35858
reactions with metals, effects of pH and temperature on, 18: 23542
spectra of, effects of heating and irradiation on infrared, 18: 23590(T,R) (AEC-tr-6316(p.121-8))

Vinyl Bromide
see Ethylene, Bromo-

Vinyl Chloride
see Ethylene, Chloro-

VINYL COMPOUNDS
(See also specific compounds.)
carbon-13 nuclear magnetic resonance spectra, chemical shifts in, 20: 26842
dehydrogenation and isomerization of, radiochromatographical studies of action of catalysts in, 19: 38718
development of radiation-resistant, 17: 3055(P)
effects on radiolysis of ammonia, 18: 29788
esters, radioinduced polymerization of, 20: 23191(P)
graft polymerization onto polymers induced by radiation and ozone, 19: 36450 (AD-610557)
graft-copolymerization of, with cellulose esters, 20: 36906(P)
photopolymerization, rapid, 16: 14806(P)
photopolymerization, catalytic, 16: 30322(P)
polymerization, 17: 3024(R) (NYO-10143)
preparation of oxygen-18-labeled, 18: 10132
properties and radiation effects on polymeric, 20: 21431(R) (WADC-TR-55-58(Pt.9))
radiation effects, 17: 4571 (TID-7643(p.1-16))
radiation effects on, 18: 273 (TID-19535)
radiation effects on emulsion polymerization of, beta, gamma, and x, 18: 1734
radiation effects on, 18: 11512(R) (NARF-63-9p)
radiation polymerization of, in wood, 18: 2117
radioactive contamination of, effects of ratio of radioactive to stable isotopes in contaminating solution on, 19: 9422
radioinduced copolymerization at low temperatures, gamma, 18: 37216(T) (AEC-tr-6398(p.529-37))
radioinduced graft polymerization with cellulose and nylon, 16: 1816(T) (NP-tr-807)
radioinduced grafting on halocarbon polymers, 16: 3057(P)
radioinduced graft copolymerization on polyethylene, 16: 10092(P)
radioinduced graft polymerization on polyethylene, 16: 16449(P)
radioinduced graft polymerization to textile fibers, 17: 4586 (TID-7643 (p.268-99))
radioinduced graft polymerization on polypropylene, 19: 11202
radioinduced grafting to paper, 20: 25178(P)
radioinduced polymerization, 16: 5393(P)
radioinduced polymerization in water for use as waxing dispersion, 16: 16400(P)
radioinduced polymerization in crystalline state, 16: 31365
radioinduced polymerization at high pressures, 17: 1554(P)
radioinduced polymerization of, in solid state, 17: 4578 (TID-7643(p.136-49))
radioinduced polymerization, effects of dose rate, 17: 6175
radioinduced polymerization of, krypton-85, 17: 14575(R) (NYO-10144)
radioinduced polymerization of vinyl carbazole, 17: 14333
radioinduced polymerization, 17: 23587 (BNL-790)
radioinduced polymerization of, studies of variables in, 17: 23398
radioinduced polymerization with fibrous polymers, 17: 39367
radioinduced polymerization, 17: 40867
radioinduced polymerization of N-vinylcaprolactam in liquid and solid states, 18: 12216
radioinduced polymerization of, use for dosimetry of x and gamma radiation, 18: 16077 (NP-13734)
radioinduced polymerization of *N*-vinylcaprolactam and *N*-vinylsuccinimide, 19: 489
radioinduced polymerization with sytrene, 20: 1910
radioinduced polymerization in the presence of zinc chloride, 20: 23192(P)
radioinduced polymerization with cellulose, 20: 23108
radioinduced polymerization of coatings of, on exterior surfaces, 20: 29320(P)
radiopolymerization in solid state, mechanisms for, 17: 34012
use in metal coating, specification for, 17: 22100 (TID-18523)
acrylic monomers–aromatic vinyl monomers–polyisobutylene, radioinduced formation of thermoplastic resin of, 20: 38978(P)

Vinyl Fluoride
see Ethylene, Fluoro-

Vinyl Iodide
see Ethylene, Iodo-

VINYL RADICALS
spectra of carbon-13-labeled, ESR, 20: 38941(R) (RRL-2310-182)

Vinyl Stearate Polymers
see Stearic Acid, Vinyl Ester Polymers

VINYL SULFONE
radioinduced graft polymerization of, on fibrous cotton and nylon, gamma, 20: 35822

Vinylidene Chloride
see Ethylene, Dichloro-

Vinylidene Fluoride
see Ethylene, Difluoro-

Vinylsulfonic Acid Polymers
see Ethenesulfonic Acid Polymers

VIOLURIC ACID, 1,3-DIMETHYL-
analytical use for spectrophotometric titration of alkali and alkaline earths in salt solutions, 16: 12968

VIRGINIA
areal geology and aeroradioactivity surveying of, 20: 20928 (CEX-59.4.17)
cosmic ray measurements, 1956–59, 16: 10803
deuterium content in rainfall in, Nov. 1 and 2, 1963, 19: 47112
fallout patterns in, 18: 31826
gamma aeroradioactivity at 500 ft over, mapping of, 19: 46614
lead isotope ratios in galenas of, 20: 45882
occurrence and properties of niobium–uranium metamict mineral in Powhatan County, 19: 44279
pegmatites in, age estimation of, 20: 43504(R) (COO-689-60, App.A-4)
radioactivity of Norfolk peninsula, aerial measurements, 18: 418 (CEX-6 1.6.4)

Virginium
see Francium

VIRIAL COEFFICIENTS
accuracy of thermodynamic, at low densities, (T), 19: 30848(R) (UCRL-12473(p.31-63))
applications of hypervirial theorems, 16: 16815
calculation and consistency of fifth, for hard-sphere gas, 16: 16847
calculation of fourth, for square-well potentials, 17: 34579
calculation of fourth, from square-well potentials, 18: 34300
calculation of second, for general polyreciprocal potentials, 16: 25875 (AFSWC-TDR-62-21)
calculation of second, for ion-neutral interactions, tables for, 16: 25875 (AFSWC-TDR-62-21)
calculation of second, for one-dimensional Lennard-Jones gas, (T), 19: 28924
calculation of second, for two-dimensional Lennard-Jones gas, (T), 19: 28923
calculations of fourth, fifth, and sixth, for hard disks and spheres, 18: 12832
diagram expressions for, 18: 16548 (AERE-R-4494)
estimation of sixth, for hard-sphere gas, 17: 32778
reformulation for classical fluids, 18: 37847
tables of second, and their derivatives for constituent pairs involving neutral species in high-temperature air, 16: 25875 (AFSWC-TDR-62-21)
use of third, in theory of three-body forces, 18: 153
Wigner distribution function in second, 18: 14986

VIRIAL THEOREM
derivation for many-electron Dirac systems, 16: 3807

VIRUSES
see also Bacteriophages
see also Influenza Virus
see also Rickettsia
action of Riley, 20: 45253
analysis for trace elements in tobacco mosaic, activation, 20: 38846
antibody for neutralizing polio, properties of, 18: 21873
antigen isolation from adeno-, centrifugation for, 20: 7(R) (ORNL-3883)
arginase enzymes induced by, action and structure of, 19: 31678(R) (ORNL-3768(p.137-45))
behavior in hamster tumor cells, 17: 40464
biological differences in variants of *Mengo encephalomyelitis*,

18: 8019(R) (TID-19921)
bonding of tobacco mosaic, to methylmercury and potassium uranyl fluoride, 17: 27043
book: *Problems of Radiation Genetics*, 19: 42348(T)
carcinogenic effects, 18: 9805
carcinogenic effects in mice, 19: 22019(R) (UCLA-12-541(p.51-91))
chemically induced inactivation of, 19: 29916
co-carcinogenic effects in x-irradiated mice, 19: 31678(R) (ORNL-3768 (p.137-45))
control and pathology of diseases caused by, in domestic animals, 20: 42954
control laboratory design, 19: 42617 (TID-22102)
criteria for handling infectious agents in laboratories, 19: 31635 (ORNL-TM-1162)
demonstration in tissues of mice with radioinduced leukemia, 16: 25199
density determination of, in preformed gradient, 17: 35358
desoxyribonucleic acid induction by Polyoma, in x-irradiated mouse and rat embryo cell cultures, 20: 18369
detection, 16: 11380(R) (AD-259234(p.69-87))
deuterium oxide effects on replication, 17: 31837
development, effects of temperature, 16: 1441
development, effects of heavy water and temperature, 16: 1442
development, effects of heavy water and temperature, 16: 1443
digestion of vaccinia, by uranyl acetate solutions, 16: 31414
effect of colamine on reproduction of, in chick embryos, 18: 27055
effects of detergent on biological properties of, 19: 33936
effects of deuterium oxide and x radiation on multiplication of poliomyelitis, 17: 23134
effects of leukemogenic, on tumorigenesis in mouse thymus, 20: 18193
effects of lipo-, on radiosensitivity of human cells, 19: 31875
effects of mutagenic agents in, mechanism of electiveness, 17: 35383
effects of polyoma, on radiosensitivity of hamster cells to transformation, 19: 15197
effects of polyoma, on neoplasm, development in thymectomized mice, 19: 17450
effects of polyoma, on transplant immunity in hamsters, 19: 17593
effects of rabbit antiserum on biological properties of, 19: 33936
effects of Rauscher leukemia, on growth of mouse cells in semisolid agar, 20: 40502(R) (ORNL-3922, pp 115-27)
effects of Riley, on mouse serum levels of enzymes following treatment with substances altering RES, 20: 45252
effects of ultraviolet radiation on physical properties of ribonucleic acid, 16: 20150
effects of water-d_2 on interferon production and titre of Japanese B encephalitis, mechanism of, 19: 29876
effects of water-d_2 on plaque size of western equine encephalitis, 20: 39
effects of 3-methylcholanthrene and nitromin on production of, in chicken sarcomas, 20: 35303
effects of 6-azauracil on growth, nucleic acid synthesis, and uv-induced lysis in *Vibrio cholerae*, 19: 33960
effects of, carcinogenic, 19: 45942
effects of, on DNA synthesis in cells in irradiated tissue cultures, 18: 15835
effects on amino acid metabolism and growth in animal cells, tracer 20: 45320 (LF-29)
effects on aminoacyl-sRNA synthetase systems in host cells, 20: 40632(R) (ORNL-3922, pp 175-91)
effects on etiology of lung cancer, 19: 29910
effects on genetic transduction in rabbits of Shope, 19: 31678(R) (ORNL-3768(p.137-45))
effects on hamster kidney-cell cultures, neoplastic, 20: 18197
effects on human embryos, teratogenic, 20: 3747
effects on luminescence of cells in tissue culture, 18: 27179
effects on lymphoma induction in mice, *in vitro* reactions of lymphocytes in, 20: 35268
effects on morphology of cells in Ehrlich's ascites tumor, 16: 12851
effects on morphology of cells in Ehrlich's ascites tumors, 16: 12852
effects on protein and nucleic acid synthesis, 19: 35894(R) (TID-21973)
effects on rabbits on Shope papilloma, mechanisms for tumorigenic, 20: 40632(R) (ORNL-3922, pp 175-91)
effects on RNA synthesis in cultured cells, 20: 36555(R) (NYO-2643-22)
electrical birefringence of tobacco mosaic, 19: 48104 (UCRL-16278)
encephalomyelitis effects on bone marrow and lymph system in guinea pigs compared with x radiation, 17: 10427
etiology of, in radioinduced leukemia in mice, 19: 27954
function, properties, and structure of, 19: 42212 (NYO-3424-1)
genetic code for spontaneous and chemically induced mutations of, 19: 40296 (TID-21856)
genetic effects in man, 19: 33806
genetic transmittal by DNA in, uv-method for determining mechanism for, 20: 20426
growth in cells in tissue culture, 18: 43181(R) (LA-3132-MS(p.213-17))
growth of x-irradiated Rous sarcoma, on chick embryo chorioallantoic membrane, 20: 103
hamster cells infected with Polyoma, effects of x-irradiated noninfected cells on, 20: 10684
heat and radiation effects on substrains of Newcastle disease, in chicken embryos, 16: 32777
identification in electron microscope by labeled antibodies, 16: 11375(R) (AD-259234(p.9-17))
immune reactions to, in dogs, 19: 31632 (LF-25)
immune reactions to rabbit papilloma, in man, 20: 6700(R) (ORNL-3853, pp 183-207)
immunity in mice to transplanted leukemia, 20: 40502(R) (ORNL-3922, pp 115-27)
inactivation of Newcastle disease, using Acridine Orange and phosphorus-32, 20: 33058
inactivation of, by hydrogen peroxides in buffer solutions, 19: 28027
inclusion of, in leukemic cells of mice, 20: 42882
induction of leukemia in mice, 20: 42893
infection in mice, effects of thorotrast-induced reticuloendothelial blockage on, 18: 17618
infection of human diploid cells in culture by tumor, 20: 20377
infection of irradiated monkeys with pox, 16: 31521
infection of mice with mousepox, effects of deuterium oxide on, 17: 10285
infections with vaccinia, effects of methotrexate and x radiation on recovery from, 16: 32674
infectivity of Gross and Rauscher, in mice injected with tissue extracts of infected mice, 20: 45511(R) (UCLA-12-595, pp 33-66)
injection of sarcoma, effects on phosphorus-32 uptake by nucleic acids in chicken thymus gland, 16: 12867
inoculation of mice with influenza, aerosol, 20: 6700(R) (ORNL-3853, pp 183-207)
interaction with host, physiology of, 20: 40632(R) (ORNL-3922, pp 175-91)
interactions with host, physiology of, 20: 6700(R) (ORNL-3853, pp 183-207)
iron-59 uptake by tobacco mosaic virus, 17: 1229
isolation by zonal centrifugation, 19: 2005(R) (ORNL-3700(p.134-47))
isolation from animal and human tissue, summary of data on, 20: 20360(R) (PRNC-73)
isolation of leukemia, in mice, 20: 16159(R) (ORNL-3900, pp 150-81)
isolation of murine leukemia, 20: 45288(R) (SAN-322-4)
isolation of respiratory syncytial, by B-IX zonal rotors, 20: 40507(R) (ORNL-3922, pp 191-6)
isolation of, from dogs, use of tissue cultures of canine origin for, 20: 4 (LF-26)
labeling with iodine-125, 20: 45288(R) (SAN-322-4)
leukemia induced in mice by, immunological differences in, 20: 3694
leukemia induction by, 20: 45419
leukemia-inducing, in mice, 19: 29847 (ACRH-103(p.48-61))
leukemic cells induced in mice by, long-term cultivation in tissue cultures, 16: 2903
leukemogenesis and, 17: 37038
leukemogenic effects in mice of, deuterium therapy for, 18: 29484
leukemogenic effects of, 18: 38873
lymphoma induction in mice by, 20: 28873
metabolism of magnesium by turnip yellow mosaic, 19: 33782
metabolism of strontium-90 by turnip yellow mosaic, 19: 33782
molecular structures of adeno-, 17: 6792(R) (ISS 62/14)
molecular structure of DNA in phage α of *B. megatherium*, 20: 8508(R) (EUR-2589.e)
molecular weights, determination by radiation target data, 17: 33714
multiplication on human cells, metabolic pattern for, 19: 35931
mutagenic action of radiomimetic agents in, 17: 33717
myeloid leukemia, action and properties in mice and rats, 18: 4928(T) (AEC-tr-6160)
myxo- and rhino-, isolation by continuous-flow centrifugation, 19: 31680(R) (ORNL-3768(p.149-53))
nature of, review, 16: 32643(R) (UCRL-10211(p.9-15))
nucleic acids of tobacco mosaic, analysis for trace elements, neutron activation, 18: 21764 (SGAE-BL-4/1964)
pathological effects on mice, 18: 41073 (COO-1038-4)
photoreactivation of ribonucleic acid in tobacco mosaic, after ultraviolet inactivation, 20: 1659
photoreactivation of plant, effects of morphology on, 20: 18360
photoreactivation of ribonucleic acid of tobacco mosaic, following ultraviolet inactivation, 20: 32957
photosensitivity of, effects of furocoumarins on, 20: 18469
plaquing efficiency of CHAT, effects of water-d_2 at 40°C with limited thermal exposure ratios, 17: 10290
preparation and properties of phosphorus-32-labeled rabbit pox, 16: 26697
propagation of mouse leukemia, in tissue cultures, 19: 2076(R) (ORNL-3700(p.113-26))

purification of radioactive foot-and-mouth disease, 17: 38673
radiation effect on mice infected with, 20: 8677
radiation effects on antigenic hemagglutinating, and infections properties, 16: 1541
radiation effects on course of infection from, 16: 14606
radiation effects on heat-resistant and heat-sensitive hemagglutinating property, 16: 14466(R) (TID-15353)
radiation effects, gamma, heavy ion, and x, 16: 16189
radiation effects on poliovirus yield in cultured kidney cells from rhesus monkey, 16: 20201
radiation effects on infection by and immunity to, 16: 20227
radiation effects on plaque-forming ability of vesicular stomatitis, 16: 14543
radiation effects on measles infection and immunity in monkeys, 17: 4401
radiation effects on spread of tick-borne encephalitis, in lymphatic system in mice, 17: 5786
radiation effects on inactivation of vaccinia Lancy strain, 17: 14006
radiation effects on antigenicity of vaccinia, in rabbits, 17: 17851
radiation effects on growth in cultured monkey kidney cells, 17: 23138
radiation effects on growth of polyoma, in mouse embryo cultures, 17: 24924
radiation effects on toxicity of, to L cells, 17: 28736
radiation effects on tobacco mosaic, 17: 38847
radiation effects on biological properties of, 17: 38745(R) (TID-19427)
radiation effects on electron spin resonance spectrum of, 18: 1432
radiation effects on infectivity of West Nile, ultraviolet, 18: 3548
radiation effects on sensitivity of animal cells to transformation by polyoma, 18: 5060
radiation effects on vaccinia, gamma and uv, 18: 8190
radiation effects on infectivity of vaccinia and encephalomyocarditis, gamma and ultraviolet, 18: 8192
radiation effects on incidence of herpes, 18: 11748
radiation effects on mouse resistance to, x, 18: 13467
radiation effects on cells producing Rous sarcoma, method for detection of, x, 18: 15838
radiation effects on reproduction in guinea pigs and mice of parotitis, x, 18: 19556(T) (JPRS-23956(p.9-17))
radiation effects on immunity to, review, 18: 19747
radiation effects on smallpox, in tissue culture, 18: 19687
radiation effects on vaccinia, Shay leukemia development in rats from uv, 18: 19614
radiation effects on susceptibility of mice to, 18: 23248(T) (JPRS-24696)
radiation effects on infection of mouse spleen by, 18: 25223
radiation effects on reproduction of, in tissue cultures, 18: 27178
radiation effects on reproduction of, in tissue cultures, 18: 27181
radiation effects on reproduction of, in tissue cultures, 18: 27199
radiation effects on immune reactions to, in mice, 18: 29243 (TID-20774)
radiation effects on disease caused by Friend, 18: 31201
radiation effects on response of vaccinated dogs to, 19: 71 (LF-17)
radiation effects on rats infected with, beta and gamma, 19: 3904
radiation effects on genetics of, bibliography on, 19: 3974
radiation effects on infectivity of leukemia-inducing, in mice, 19: 7047
radiation effects on course of encephalitis infections in mice, 19: 15025
radiation effects on susceptibility to Coxsackie B1, in neonatal rat brain and skeletal muscle, 19: 17594
radiation effects on development of, in rat embryo cell cultures, 19: 19563
radiation effects on giant cell formation by, in L-cells, 19: 21879
radiation effects on evolution of encephalitis in mice, 19: 24265
radiation effects on plant infection by tobacco mosaic, temperature and time effects on uv, 19: 26045
radiation effects on plaque-formation in, uv, 19: 27974
radiation effects on growth of, ultraviolet, 19: 29909
radiation effects on tobacco mosaic, ultraviolet, 19: 33936
radiation effects on leukemia induction in mice by, 19: 33793
radiation effects on polyoma, effects of media on gamma, 19: 36081
radiation effects on activation of guanidine- and puromycin-treated infective centers of polio, 19: 46032
radiation effects on production of polio, by monkey-kidney cells, 19: 45955
radiation effects on, and hosts, 19: 45974
radiation effects on survival of Vaccinia, effects of particle aggregation on, ultraviolet, 20: 1651
radiation effects on inflammation induced by herpes zoster, x, 20: 3836
radiation effects on infections of plants caused by, γ, 20: 3768
radiation effects on plant, biological, 20: 5310
radiation effects on bacterial reactions to, target theory for γ and x, 20: 5299(R) (TID-22187)
radiation effects on transforming efficiency of desoxyribonucleic acid extracted from, tracer study of uv, 20: 6760
radiation effects on growth of, in HeLa cells in culture, uv, 20: 6842
radiation effects of inhaled strontium-90 on production of, in feces, nose, and throat of dogs, 20: 8636(R) (LF-28, pp 230-5)
radiation effects on HeLa cells infected with adeno-, uv, 20: 12711
radiation effects on nucleic acids in, uv, 20: 16206
radiation effects on nucleic acids in, uv, 20: 16207
radiation effects on dengue, gamma and x, 20: 20360(R) (PRNC-73)
radiation effects on Puerto Rican animal, 20: 20360(R) (PRNC-73)
radiation effects on reproductive capacity of Rous, 20: 18321
radiation effects on barley stripe mosaic, and its homologous antiserum, uv, 20: 22714
radiation effects on, review of x, 20: 22750
radiation effects on production of, in chicken sarcomas, mechanism of x, 20: 35303
radiation effects on, of foot and mouth tissue cultures, 20: 35319
radiation effects on DNA in, repair mechanisms for uv and x, 20: 36578 (ORNL-P-2240)
radiation effects in inactivation of tobacco mosaic, mechanism for uv, 20: 38584
radiation effects on interactions of Polyoma, with mouse embryo cells, 20: 38702
radiation effects on infectivity of Newcastle disease and Rous sarcoma, uv, 20: 38707
radiation effects on food-borne, review, 20: 41388
radiation effects on, molecular basis for, 20: 45330
radiation effects on infectivity and antigen production by simian virus 40, uv, 20: 45346
radiation injury and recovery mechanisms in, uv, 20: 30139
radiation on immune response to infectious hepatitis, in dogs, 20: 45288(R) (SAN-322-4)
radiation treatment in presence of protective agents for preparation of vaccines, 18: 3583(P)
radiography of models of, 20: 40653
radioinduced inactivation, 16: 26848
radioinduced inactivation of, isotypic interference in, 17: 14025
radioinduced inactivation of, 18: 23246(T) (AERE-Trans-1000)
radioinduced inactivation or airborne, uv, 18: 43836
radioinduced inactivation of foot and mouth disease, 19: 11624
radioinduced inactivation of DNA, 19: 26058
radioinduced inactivation of, in buffer solutions, 19: 28027
radioinduced inactivation of, ultraviolet and x, 19: 29916
radioinduced inactivation of, 19: 32649
radioinduced inactivation of, x, 19: 36046
radioinduced inactivation of reproduction and transformation in polyoma, 19: 36052
radioinduced inactivation of plaque formation and transformation in polyoma, 19: 36053
radioinduced inactivation of tobacco necrosis, ultraviolet, 19: 45962
radioinduced inactivation of Southern bean mosaic, ultraviolet, 20: 126
radioinduced inactivation of Newcastle disease, mechanism for uv, 20: 6884
radioinduced inactivation of, mechanisms for, 20: 14387
radioinduced inactivation of Vaccinia, 20: 20500
radioinduced inactivation of Newcastle, in chickens, uv, 20: 22634
radioinduced inactivation of foot and mouth disease, in tissues of infected animals, gamma, 20: 41392
radioinduced inactivation of, 20: 42954
radioinduced mutations of, ultraviolet, 19: 19549
radioinduced myeloid leukemia in mice as affected by Gross, x, 18: 19578
radiosensitivity of intracellular psittacosis, 17: 21535
radiosensitivity of Friend, in mouse spleen extracts, 17: 37075
radiosensitivity of psittacosis, in tissue culture cells, effect of developmental stage and radioprotective chemicals on, 18: 6636
radiosensitivity of infectious nucleic acid portion and whole tobacco mosaic, to fast electrons, 18: 25159
radiosensitivity of, effects of biological complexity on, 18: 29360
radiosensitivity of vesicular stomatitis, during replication in chick embryo cells, 19: 15185
radiosensitivity of, 19: 22837
radiosensitivity of, in fowls, 19: 28100
radiosensitivity of pathological, 19: 46890
radiosensitivity of, in water, gamma, 20: 1645
radiosensitivity of *Herpes simplex*, effects of bromouracildesoxyriboside and iodouracildesoxyriboside on, 20: 5363
radiosterilization of, for vaccines, 17: 1277
radiosterilization of food contaminated with, 19: 32649
Rauscher leukemia, cytopathologic *in vitro* effects in mice of, 19: 31677(R) (ORNL-3768(p.119-30))
reactivation of polio-, at low temperatures after attenuation by x radiation, 20: 42966
relation of antigenic materials from, to Ehrlich ascites tumor cells, 20: 42712(R) (UCRL-16246, pp 51-7)
reproduction and growth of mouse myeloid leukemia, in tissue culture, 18: 4929(T) (AEC-tr-6161)
reproduction in cells in tissue culture, 19: 35862 (LA-DC-6583)

reproduction on uv-irradiated cultured animal cells, 20: 45475
resistance to infection by, genetic factors, 16: 21951
respiratory syncytial, antigen isolation by zonal centrifugation from, 20: 7(R) (ORNL-3883)
ribonucleic acid conservation, during replication and translations, tracer study, 17: 28749
role in actuation of tumors, 17: 22984
role in leukemia etiology, 19: 45833
role in radioinduced lymphoid leukemia in mice, 19: 28055
role of nucleic acids of, in infective processes, 18: 21742 (SGAE-BL-3/1964)
role of oncogenic, in radioinduced neoplasms, 18: 31189
role in etiology of leukemia, review of, 20: 45250
sarcomas induced by, in monkeys, 19: 21806
sedimentation rates in water at 20°C, 18: 35678(R) (ORNL-3656)
separation and characterization of particles, from natural water, 19: 27897 (ORNL-P-115)
separation by centrifugation, engineering drawings of tubes for, 19: 46515
separation from cancerous cells and tissues, development of zonal centrifuges for, 18: 11514 (ORNL-3415)
separation from cells and tissues, development of zonal centrifuges for, 18: 11515 (ORNL-3502)
separation from culture fluids, plasma, and tissues by fractionation and zonal centrifugation, 18: 35678(R) (ORNL-3656)
separation from other materials using ultracentrifuges, 20: 16159(R) (ORNL-3900, pp 150-81)
separation from tissue culture fluid by continuous-flow centrifugation, 20: 6701(R) (ORNL-3853, pp 207-11)
separation of, engineering drawings of containment system for centrifugal, 20: 16166
separation of, techniques for containment and sterilization in, 19: 45730(R) (ORNL-3752)
size measurements for, use of radioinduced inactivation for, 20: 5310
immune reactions to antisera of, 20: 45288(R) (SAN-322-4)
sorption on glass or silicone surfaces, agglutination and tracer studies of, study, 20: 45288(R) (SAN-322-4)
Soviet studies in, 18: 19508(T) (JPRS-23956)
staining for electron microscopy, use of uranyl formate for, 20: 22533
staining tobacco mosaic, for electron microscopy, 19: 35883
structure from radiosensitivity effects, 16: 7406 (BNL-675(p.1-17))
structure of Newcastle disease, 17: 38745(R) (TID-19427)
sub-cellular particles of, sedimentation coefficients and densities of, 18: 27009(R) (ORNL-3601(p.152-72))
susceptibility of hamsters to infection by, 17: 33451(R) (ANL-6723 (p.50-2))
synthesis of whole TMV, cell-free, 18: 21725(R) (TID-20437)
tracer studies survey, 16: 1409
tumorigenesis effects of SV_{40}, in hamsters immunized by irradiated antigens, 19: 8898
use of sheep spleen extract as protection against Rauscher, 20: 40658
use of uv-inactivated, for production of hybrid heterokaryons from man and mouse cells, 19: 17449

VISCERA

see also Thoracic Viscera

VISCOMETERS

calibration of oscillating bob, at room temperature, 20: 38871(R) (NYO-1769-54)
calibration of, for measurements on alkali metals at high temperatures, 20: 20651(R) (CU-2660-26)
description of capillary, for alkali metal vapors, 19: 24981(R) (CU-2660-16)
design and calibration of oscillating-crucible, 18: 41373(R) (TID-20951)
design and operation for measuring cesium and rubidium coefficients to 2000°F, 19: 578(R) (AGN-8112)
design and operation of, for liquid metals, 20: 41455(R) (NYO-2731-7)
design and performance of interfacial, for studying mass transfer, 16: 11503(R) (ORNL-TM-34)
design for high pressures and temperatures, 18: 33858
design for liquid helium-4 using damping of transverse vibrations of fine wire, 18: 2761
design for measurements on molten salts at high pressure and temperature, 20: 38871(R) (NYO-1769-54)
design of automatic recording multigrade capillary, 19: 22663 (LADC-6436)
design of, for liquid metals, 17: 6671 (NP-12366)
design of, for molten salt measurements, 17: 25062(R) (ORNL-3417(p.41-50))
design of oscillating sphere, for transport studies in molten salts, 20: 38872(R) (NYO-1769-68)
design of radiometric, using cobalt-60, 20: 2200
design of torsional-pendulum, engineering drawings for, 20: 21015
design of vertically oscillating cylinder, for transport studies in molten salts, 20: 38872(R) (NYO-1769-68)
design of vibrating wire, for alkali metal vapors, 20: 22965(R) (AGN-8177)
design of, for use at high pressures and temperatures, 20: 38872(R) (NYO-1769-68)
design of, for use with liquid metals, 20: 41460 (TIM-793)
development for fused salts and liquid metals, 20: 5594(R) (ANL-6925, pp 21-106)
development of fused-salt torsional, 17: 14613(R) (ORNL-3378(p.47-62))
development of, review of, 19: 20142
operating characteristics of oscillating cup, 16: 2926(R) (MLM-1117)
tests of oscillating-cup, 19: 28283(R) (AGN-8143)
use of rotating-spindle, for Molten Salt Reactor Experiment fuel and coolant, 18: 22011(R) (ORNL-3591(p.38-58))

Viscosimeters

see Viscometers

VISCOSITY

calculation for gases, from correlation functions, 19: 1073
calculation of bulk, for Maxwellian particles in a simple gas, 17: 36844
calculation of hard-sphere, 18: 25362
calculations of, for radioinduced branched polymers, 18: 12200
cross sections for screened Coulomb potential, quantum-mechanical values, 16: 3775
effect on leak rate of conical-face seals, 20: 41074 (AECL-2551)
effects in magnetohydrodynamic generators, 17: 9094
equation for determining, of liquid metals, 20: 20656 (UCRL-11930)
measurement method for unstable industrial suspensions, 16: 17881(R) (MITS-47)
measurements, theory of torsional oscillation method for, 16: 16343(T) (NASA-TT-F-88)
of concentrated suspensions of spherical particles, lower bound of, 17: 33868 (CONF-154-1)
of high-temperature ionized mixtures, calculation of, 19: 19941
of liquid metals, design of viscometer for measuring, 17: 6671 (NP-12366)
of liquid metals, relation between activation energy and melting point in, 17: 23988
polyamino acid solutions, effects of gamma rays and pH, 20: 42826
radiation effects on, in solid state polyamino acids, 20: 14588
radiation effects on DNA, uv, 20: 20412
tables for gases at 100 to 5000°K, 16: 13210 (NASA-TR-R-132)
theories of liquid, 17: 3580 (UCRL-6400)
theory for liquid metals, 17: 28828(R) (TID-18951)
theory for quantum systems, 18: 21070
theory of method for determining, of alkali metals, 19: 578(R) (AGN-8112)
theory of, in compressed gases, 19: 25072(T) (LA-tr-65-7)
transport theory, nonlinear effects in, 16: 3560
use in measurement of DNA molecular weight, 17: 30353

Viscous Flow

see Fluid Flow (Laminar)

VISION

see also Eyes
see also Phosphenes

amino acid metabolisms in visual system of rats after unilateral enucleation, tracer study, 18: 31092
analysis of mechanisms of, 18: 28094(R) (TID-20607)
color perception, 17: 35260(R) (TID-19135)
discriminative processes, automatic equipment for measuring, 16: 26681
effects of nuclear weapons on, 17: 35466
effects of nuclear explosions on, 20: 27183(R) (AD-627332)
effects of prenatal radiation exposure in rats, 16: 26681
electronic aids for the blind, review on, 19: 23837
function of rods in, compartment theory for theory of, mathematical representation of compartment, 17: 11028
light sensitivity of, in man, 19: 8806
myopia in children in Hiroshima and Nagasaki, effects of environment, inbreeding, and inheritance on, 16: 33325
optical illusion of three-dimensional objects, 17: 35260(R) (TID-19135)
perception principles for, photograph description model including Gestalt, 18: 2149 (TID-19690)
protection against flash blindness in aviation personnel, 19: 36126
protection from nuclear flashes, design of electrochemical device for, 17: 14529 (MRL-TDR-62-29)
protection from nuclear flashes, design of phototropic ophthalmic device for, 17: 14530 (MRL-TDR-62-46)
radiation detection with, electrons and x, 19: 148
radiation effects, 16: 23500
radiation effects on receptor apparatus of, in man, 17: 5851
radiation effects on animal, x, 17: 35535
radiation effects on rat, from fetal x-irradiation, 17: 35545
radiation effects on, in mammals, 17: 38896
radiation effects on, in cats, 18: 3500 (UCRL-11005)
radiation effects on monkey, psychic blindness from, x, 18: 13503

radiation effects on rabbit, x, 18: 19728
radiation effects on human, 18: 29323
radiation effects on, in man, 18: 33341
radiation effects on, 19: 25903 (AD-608877)
radiation effects on depth perception, in rats, 19: 33878
radiation effects on, of rats, 19: 33879
radiation effects on, in mice, 19: 36017
radiation effects on, of monkeys, 19: 45893
radiation effects on discriminatory, in monkeys, effects of age on x, 20: 3721
radiation effects on Limulus, stimulus-response relationship for x, 20: 8607
radiation effects on rabbit, x, 20: 38689
radiosensitivity of, 19: 13074
recovery time after exposure to high-intensity, short-duration flash, 16: 32657
relation of thalamus to, in monkeys, 19: 31660(R) (ACRH-23(p.40-57))
thermonuclear explosion effects on, 18: 18103
visual receptor processes, mechanisms of, 20: 30963

Vistanex
see Plastics

VISUAL PURPLE
luminescence in, relation of x-ray visibility to, 20: 36587(T)
radiation effects on regeneration of, 17: 35525
radiation effects on, *in vitro* and in eye, 18: 27190
radiation effects on absorption spectrum of, in retina of frogs, 19: 7064

VITAMIN A
see also Carotene
deposition of, in liver of pigs, effects of radiation and copper on, 17: 17729
determination in blood, feces, and tissues by liquid scintillation of tritium, 17: 10552
effects on calcium metabolism in rat bones, 19: 33774
effects on cerium-144 uptake by rat bones, 19: 8749
effects on hemorrhagic syndrome, 16: 6267 (NP-11258)
effects on hemorrhagic syndrome, 16: 6268(R) (NP-11261)
effects on polysaccharide metabolism in blood platelets of rats, 19: 45759(R) (ORO-631, pp 77-82)
effects on radiosensitivity of swine, 16: 32788
effects on skeletal growth in rats, 20: 16148 (NYO-2779-9)
effects on strontium-90 metabolism by rats, 18: 41046 (NP-14333)
effects on strontium-90 uptake by rats, 19: 17486
effects on strontium-90 metabolism in rat bones, 19: 33774
labeling with tritium, 17: 18471
metabolic effects, 17: 16360(R) (NP-12597)
protective effects against radioinduced changes in serum protein in rabbits, 16: 14565
radiation and effects on whale-liver, 18: 35374
radiation effects, in foods, 16: 17948(T) (AERE-Trans-882)
radiation effects on content in foods, gamma, 19: 15043
radiation effects on content in food, 19: 17641
radiolysis of A_1, 19: 2376
radiosensitivity effects on guinea pigs, 17: 33686
radiosensitivity effects on mouse epithelium, x, 18: 43309
radiosensitivity effects on life spans of mice, 19: 10911

VITAMIN B
see also Nicotinic Acid
content in irradiated pork, effects of moisture, 17: 6365
dephosphorylation of, catalytic effects of cerium, lanthanum, manganese, thorium, and zirconium ions on, 20: 20375
determination by inverse isotope dilution using sulfur-35, 20: 7040
effects on erythropoietic index and iron content in patients receiving radiotherapy for uterine cancer, 20: 42908
effects on metabolism of iodine-131, in rats, 19: 38337
effects on radiosensitivity of rats, 16: 21900 (ASD-TR-61-534)
effects on radiosensitivity of nervous system in frogs and lobsters, 18: 11559(R) (TID-19977)
effects on tumor growth and metabolism in irradiated rats, 18: 41133
metabolism in dogs fed irradiated meat, 20: 42793
protective effects against radioinduced changes in serum protein in rabbits, 16: 14565
protective effects against radiation injuries in guinea pigs, 17: 27082
protective effects against radiation in L-ascorbic acid oxidation, 18: 31187
radiation effects on microbiological activity of thiamin hydrochloride, 17: 8141
radiation effects on content in foods, 19: 11632
radiation effects on metabolism of, in mice and rats, 19: 15054
radiation effects on, in presence of calcium carbonate, dibasic calcium phosphate, and sodium chloride, 20: 4018
radiation effects on bacterial metabolism of, y, 20: 5346
radiation effects on metabolism of, in mice, x, 20: 29003
radiation effects on, biological and chemical, y, 20: 38580
radioprotective effects combined with narcotics on nervous tissue, 16: 18775
radiosensitivity effects combined with narcotics on nervous tissues, 16: 26742(T) (FTD-TT-62-831)
radiosensitivity effects on rat leukocytes, beta, 20: 18499
radiosterilization effects on content of, in strawberries, gamma, 20: 13142(R) (UCD-34P80-3, pp 52-4)
reactions with sugar phosphates during photosynthesis, effects of enzymes on, 18: 17403(R) (UCRL-11046(p.15-20))
therapeutic use in radiodermatitis, 18: 38990
transport across intestinal wall, effects of whole-body irradiation, 16: 25180 (TID-16271)

VITAMIN B_1
effects on anaphylaxis in irradiated sensitized guinea pigs, 17: 30405
effects on metabolism porphyrin bodies in tissues, with and without x irradiation, 16: 4083
effects on radiation resistance in rats, dietary, 20: 38721
hydrochloride, irradiation method for stabilization of, 20: 10931(P)
propyl disulfide, protective effects against radiation injuries in dogs, 19: 36116
protective effects against radiation injuries in mice, 16: 1636
protective effects against radiation sickness in monkeys, 16: 26875
protective effects against radiation effects on cholesterol metabolism in guinea pigs, 18: 9928
protective effects against radiation effects on amino acid content in wheat sprouts, 18: 33398
radiation effects, in foods, 16: 17948(T) (AERE-Trans-882)
radiation effects on metabolism, 16: 21922
radiation effects on metabolism in rabbits, 16: 26667(T) (JPRS-13555 (p.7-17))
radiation effects on hydrochloride crystal of, compounded in calcium carbonate powder, gamma, 17: 8904
radiation effects on content of, in brain and liver in rats, 17: 14079
radiation effects on content in foods, gamma, 19: 15043
radiation effects on content of, in eggs and wheat, 19: 17575
radiation effects on content of, in guinea pigs, 19: 17581
radiation effects on activity of, in uterine cervical cancer tissues, 20: 35358
radiation effects on content in oysters, gamma, 20: 45347
radioinduced decomposition of, *in vitro*, 17: 20075
therapeutic effects on radiation sickness of rats, 16: 31529
therapeutic effects of, on radiation sickness in rats, 18: 5139(T) (JPRS-22123)

VITAMIN B_2
chelate formation effects on cobalt-60 distribution in rat, 16: 12873
complexes with hydriodic acid and phenols, spectra of, 20: 10461 (COO-908-7)
complexes with naphthalenediol and phenols, spectra and stability of, 20: 10460 (COO-908-6)
complexes with phenols, properties and spectra of, in solution, 20: 10458 (COO-908-4)
complexes with phenols, electric and magnetic properties of, 20: 10459 (COO-908-4)
dephosphorylation of, catalytic effects of cerium, lanthanum, manganese, thorium, and zirconium ions on, 20: 20375
effects of radioprotective compounds on phosphorescence of, 18: 29400
effects on calcium-45 metabolism in chicken bones, 19: 31746
effects on metabolism porphyrin bodies in tissues, with and without x irradiation, 16: 4083
effects on radiation resistance in rats, dietary, 20: 38721
phosphorescence of riboflavine, effects of oxygen and radioprotective chemicals, 16: 21991
radiation effects, in foods, 16: 17948(T) (AERE-Trans-882)
radiation effects on microbiological activity, 17: 8141
radiation effects on content of, in brain and liver in rats, 17: 14079
radiation effects on, oxygen effect in, 17: 15774
radiation effects on content of, in blood and organs in animals, 17: 17736
radiation effects on urine content of, 17: 31907
radiation effects on metabolism in rats of, x, 17: 37028(T) (JPRS-21171(Del.)(p.24-31))
radiation effects on crystals of, gamma, 18: 3859
radiation effects on content in foods, gamma, 19: 15043
radiation effects on content of, in eggs and wheat, 19: 17575
radiation effects on blood content of, in dogs, x, 20: 5384
radiation effects on aqueous solutions of, review on, 20: 20728 (PB-181506, pp 49-58)
radiation effects on content in oysters, gamma, 20: 45347
radiolysis of, electron and x, 18: 20090
therapeutic effects on radiation sickness of rats, 16: 31529

Vitamin B_4
see Adenine

Vitamin B_6

see Pyridoxine

VITAMIN B_{12}
absorption by gastrointestinal tract, tracer study, 20: 6992
absorption by man, tracer study, 20: 6993
binding by serum proteins of, tracer study, 19: 25835 (BNL-8730)
body retention of hydroxocobalamin and cyanocobalamin in patients with pernicious anemia, 18: 15666 (BNL-6942)
cobalt-58-labeled, absorption by gastrointestinal tract, 18: 15799
complexes with cobalt, cobalt-58 recoil reactions in, 18: 3847
content and retention of cobalt-60 labeled-, in dog liver, 16: 23397 (BNL-4888)
content in sea water, determination using carbon-14 and *Cyclotella nana*, 20: 20368 (CONF-640309-1)
deficiency states, tracer studies, 16: 14408
determination in human blood plasma by saturation technique, 19: 5837
determination in human liver of cobalt-57-labeled, collimator for, 20: 19051
determination in sea water, microbiological, 18: 19486(R) (TID-20433)
diagnostic use of cobalt-58-labeled, 19: 28166
diagnostic uses of labeled, 16: 1419
distribution of cobalt-60-labeled, in tissue and organs, 18: 3450 (BNL-6913)
distribution of cobalt-60-labeled in man, 18: 13390(R) (ORINS-43)
effects of, on nucleic acid content in bone marrow and spleen in irradiated guinea pigs, 17: 14101
effects of, on radiation effects on blood cells in chicks, 17: 31954
effects of, on sulfur-35 uptake by bones in chicks, 17: 19800
effects of, on sulfur-35 uptake and retention by bones and tissues in chicks, 17: 21446
effects on ascites hepatoma in rats, 20: 8679
effects on radiation injuries of hematopoietic system, 17: 35561
effects on radioinduced changes in blood plasma protein levels, 17: 33742
effects on radioinduced alopecia, 20: 5484
half life, biological, 16: 14398
isotope exchange in radiocobalt divalent ion-doped, 20: 29259
labeled with cobalt-57 or cobalt-60, comparative counting efficiency, 16: 21876
measurement of cobalt-58-labeled, count-integrator for, 18: 41780
measurement of cobalt-58-labeled, in urine, 19: 46083
metabolism in irradiated rats, 17: 15836
metabolism in man, tracer studies of, 18: 35279 (TID-7678(p.497-518))
metabolism in man, tracer studies, 20: 6990
metabolism in man, tracer studies, 20: 6991
metabolism in rats, tracer studies, 20: 6990
metabolism of injected in man, effects of cyanocobalamin on, 19: 31624 (BNL-8132)
metabolism of injected in leukemia patients, effects of cyanocobalamin on, 19: 31624 (BNL-8132)
metabolism of radiocobalt-labeled, by man, 20: 27030
metabolism of, tracer studies in man, 19: 15317
metabolism, tracer study, 16: 16159
metabolism, tracer study, 16: 16161
metabolism, tracer study, 16: 16162
metabolism, tracer study using cobalt-57, 20: 28
occurrence in sea water, 16: 4030 (TID-12946(App.I,Vol.II))
preparation of cobalt-60-labeled, by biosynthesis, 16: 18909
preparation of cobalt-60-labeled, 19: 10742(T) (CEA-tr-R-1757)
preparation of cobalt-57- or cobalt-60-labeled, 19: 34056
preparation of radioactive, 17: 21753
preparation of radiocobalt-labeled, method for, 20: 27030
preparation of tritium-labeled, 20: 35571
protective effects against radiation injuries in mice, 16: 25253
protective effects against radiation damage in bone marrow, 18: 11855
protective effects against radiation injuries in mice, 19: 190
radiation effects on biological activity, 16: 7468
radiation effects on level in blood serum, 16: 11479
radiation effects on microbiological activity, 17: 8142
radiation effects on content of, in liver in rats, 17: 14079
radiation effects on content of, in mouse organs, 17: 30445
radiation effects on mouse kidney and liver content of, x, 18: 19743
radiation effects on content of, in rat tissues, 18: 27189
radiation effects on intestinal absorption of, in man, 19: 5639
radiation effects on rat excretion of, x, 19: 3954
radiation effects on intestinal absorption of, 20: 3851
radiation effects on, in meat, effects of lyophilization on γ, 20: 11185
radiation effects on content in oysters, gamma, 20: 45347
radiodecomposition of, external and internal gamma, 17: 10718
radioinduced mutations for Aspergillus, uv, 18: 43287
radioinduced recoil damage in, thermal annealing of neutron, 20: 29259
radiosensitivity effects on ascites hepatoma in rats, x, 20: 8679
radiosensitivity effects on rats, 20: 26704
radiotherapy effects on sorption of, by intestines, 19: 28198
resorption of cobalt-60-labeled, in intestine, whole-body retention test of, 19: 6956
retention in man, comparison with ill patient, 16: 1334(R) (LAMS-2627(p.280-3))
sorption and turnover, 16: 14398
sorption by patients, tracer study, 20: 16303(R) (AD-626384)
sorption of cobalt-58 labeled, 16: 16158
sorption, tracer study using whole-body counting, 17: 5746
structure of, determination of, using x-ray-diffraction analysis, 18: 31067
synthesis and metabolism, tracer study, 17: 23010
therapeutic effects in radiation injuries in rabbits, 16: 9929
tracer study of metabolism in man, 19: 38493
use in acute radiation sickness therapy, 20: 8739
use of cobalt-57-labeled, in radiodiagnosis, 19: 46128
use of cobalt-57-labeled, in differential diagnosis of macrocytic anemias, 20: 45524
use of cobalt-57-labeled, in parathyroid scanning, 19: 5744
uses of cobalt-60 labeled, for radiodiagnosis of chronic myelogenous leukemia, 18: 15914 (TID-7689(p.11-14))

VITAMIN B_C
see also Folic Acid
radiation effects on content in oysters, gamma, 20: 45347

VITAMIN B_1
effects on iodine-131 distribution in tissues of rats and mice, 18: 11562
preparation of carbon-14-labeled, in carboxy and methyl groups, 18: 27478

VITAMIN C
(L-Ascorbic acid)
see also Ascorbic Acid
effect of blood content of, on labeling of erythrocytes with chromium-51, 17: 33495
effects on ascites hepatoma in rats, 20: 8679
effects on erythropoietic index and iron content in patients receiving radiotherapy for uterine cancer, 20: 42908
effects on irradiated rat leukocytes, 20: 42948
effects on metabolism of porphyrin bodies in tissues, with and without x irradiation, 16: 4083
protective effects against radioinduced changes in serum protein in rabbits, 16: 14565
protective effects against radiation injuries in rats, 19: 36119
radiation effects, in foods, 16: 17948(T) (AERE-Trans-882)
radiation effects on content in guinea pigs, 17: 14032
radiation effects on content in potatoes, 17: 30349
radiation effects on oxidation of, protective effects of catalase and nicotinic acid against, 18: 31187
radiation effects on content in foods, gamma, 19: 15043
radiation effects on content in oranges, 19: 44554 (IA-1015)
radiation effects on rat liver microsome synthesis of, x, 19: 10803
radiation effects on papaya content, 20: 18248(R) (UH-235P5-1, pp 52-4)
radiation effects on metabolism of, in guinea pigs and rats, γ and x, 20: 28921
radiation effects on concentration of, in potato tubers, x, 20: 38690
radiosensitivity effects on dog intestinal motor function, x, 18: 17643
radiosensitivity effects on potatoes, gamma, 19: 25932
radiosensitivity effects on ascites hepatoma in rats, x, 20: 8679
radiosensitivity effects of, on growth in peas, fast neutron and gamma, 20: 45387
therapeutic effects of, on radiation sickness in rats, 18: 5139(T) (JPRS-22123)
therapeutic effects on bacterial infections in irradiated rabbits, 19: 33984

VITAMIN D
effects of cholecalciferol on calcium-45 half life in chick, 17: 23058
effects of cholecalciferol on calcium-45 metabolism in chicks, 17: 21450
effects of cholecalciferol on zinc-65 retention by bone and liver in chicks, 17: 21447
effects on absorption of radioisotopes by rachitic chicks, 17: 23024
effects on barium content in rat mitochondria, 20: 8559
effects on calcium metabolism in chicks, tracer study, 17: 19776
effects on calcium absorption from intestine in rachitic chicks, 18: 11618
effects on calcium-45 and strontium-90 removal from rat bones, 18: 31113
effects on calcium-47 levels in rachitics, 19: 6993
effects on calcium-47 absorption in rachitic infants, 19: 7000
effects on calcium metabolism in rachitic infants, 19: 7002
effects on calcium-47 absorption, 19: 7259
effects on calcium-47 metabolism in normal and rachitic children, 20: 3672
effects on calcium metabolism in chickens, 20: 5237(R) (UR-668, pp 55-109)
effects on calcium content in rat mitochondria, 20: 8559
effects on calcium transport across intestinal membrane, tracer study, 20: 14243(R) (TID-22626)

effects on human calcium-47 sorption, 19: 10757
effects on magnesium content in rat mitochondria, 20: 8559
effects on mineral content of bones and teeth in normal and rachitic rats, 18: 33277 (STI/DOC/10/28(p.21-38))
effects on skeletal growth in rats, 20: 16148 (NYO-2779-9)
effects on strontium-90 metabolism by rats, 18: 41046 (NP-14333)
effects on strontium content in rat mitochondria, 20: 8559
effects on urinary excretion of skeletal calcium-45 and phosphorus-32 from intact and parathyroidectomized rats, 16: 7401
effects on zinc content in rat mitochondria, 20: 8559
formation in radiolysis of ergosterol, 17: 27473
physiological effects, 16: 31432
preparation of tritiated, 18: 6843
sorption by rats, intestinal, 18: 21793

VITAMIN D_2

content in irradiated yeast, chromatographic determination, 20: 3690
incorporation of carbon-14 in, method for, 18: 21793
preparation of tritiated, and incorporation in rat tissues, 17: 38710
synthesis, distribution, and metabolism of tritium-labeled, 18: 11614
use with strontium-90 in treatment of rickets in rats, 19: 19680
yields in gamma radiolysis of ergosterol, 16: 22172

VITAMIN D_3

effects of orally administered, on rickets in rats, 17: 35571
effects on calcium metabolism in rats, 19: 38347
effects on rat strontium-90 metabolism, 18: 27057
effects on strontium-90 metabolism in rats, 19: 10760
effects on strontium-90 uptake by rats, 19: 17486
effects on strontium-90 metabolism in rats, 19: 38347
labeling with tritium and purification of product, 19: 22273
labeling with tritium, 19: 30315
preparation of tritiated, and incorporation in rat tissues, 17: 38710
separation from irradiated 7-dehydrocholesterol solution, chromatographic, 20: 22882
synthesis of tritium-labeled, 18: 21793
synthesis, distribution, and metabolism of tritium-labeled, 18: 11614

VITAMIN E

see also Tocopherols
effect on carcinogenicity of methylcholanthrene in mice, 17: 28668(R) (ACRH-19(p.54-6))
effect on radioinduced fatty acid peroxides in rabbit and rat aorta, 20: 42813
effects of, on radiation injuries in mice, 17: 23123
effects on enzyme release from x irradiated lysosomes in rat liver, 20: 38577
effects on reproductive function in hamsters, 18: 43232(R) (TID-21204)
effects on selenium distribution in chick tissues, tracer study, 17: 23064
effects on selenium-75 uptake by sheep blood cells, 18: 3468
metabolism in dogs fed irradiated meat, 20: 42793
radiation effects, in foods, 16: 17948(T) (AERE-Trans-882)
radiation effects on, 19: 32642

Vitamin H

see Biotins

VITAMIN K

effect on protein synthesis in rats, 17: 16359(R) (NP-12596)
effects in irradiated diet on dogs, cats, and rats, 17: 8502
effects of dietary content of, on induction of hemorrhagic syndrome in rats, 17: 40444(R) (NP-13183)
effects of, on hemorrhagic syndrome in rats, 17: 41177(R) (NP-13173)
effects of 2-methyl-1,4-naphthaquinol bis(disodium phosphate) and its tritiated analog on the sulfhydryl content of mouse ascites tumor, 19: 35908
effects on hemorrhagic syndrome, 16: 6267 (NP-11258)
effects on hemorrhagic syndrome, 16: 6268(R) (NP-11261)
effects on hemorrhage in rats, 17: 16364(R) (NP-12602)
effects on hemorrhagic diathesis in rats fed irradiated beef, 18: 33992
effects on hemorrhages induced by irradiated beef in diet of rats, 19: 36881
effects on lipid metabolism in rat liver, 18: 35311(R) (NP-14188)
effects on plasma prothrombin time in rats, 18: 11572(R) (NP-13573)
effects on protein synthesis, 16: 8456(R) (NP-11256)
effects on protein synthesis, 16: 33344(R) (NP-12093)
effects on radiosensitivity of tumors, 19: 10792(T) (JPRS-28345)
effects on radiosensitivity of fruit-spoilage fungi, 20: 13137 (NP-15360)
effects on radiosensitivity of bacteria, spores, and yeasts, 20: 37144
effects on response of tumors to radiotherapy, 17: 104
effects on survival of lung cancer patients treated by radiotherapy, 19: 32010
effects on yeast cultures, 18: 13547
labeling with tritium, 20: 18711
metabolic effects, 17: 16360(R) (NP-12597)
metabolism in dogs fed irradiated meat, 20: 42793
oxidative phosphorylation in, 18: 21775(R) (UCRL-11215(p.13-14))
physiological effects of deficiency of, in baby pigs and in monkeys, 16: 33344(R) (NP-12093)
protective effects against beta radiation damage to liver tissue respiration, 16: 4040
protective effects against reticulo-endothelial function decrease in irradiated mice, 16: 14547
protective effects against radioinduced changes in serum protein in rabbits, 16: 14565
protective effects against radiation lesions in mitochondria in rabbit and rat tissues, 16: 28774
radiation effects on, in beef, 19: 103
radiation effects on, 19: 32642
radiation processing effects on content of, in beef, 18: 11571(R) (NP-13572)
radiosensitivity effects in bacteria, 16: 16220
radiosensitivity effects on bacteria, 19: 44552 (BLG-327)
radiosensitivity effects of K_5 on Salmonellae infections in eggs, 20: 14395
radiosterilized diet effects on deficiency of, in rats, 17: 13939
role in bacterial metabolism, 20: 40571
therapeutic use of tritium-labeled tetrasodium 2-methyl-1:4-naphthaquinol diphosphate, 16: 17393

VITAMIN K_5

effects on gamma sensitivity of spores of food-spoilage fungi and yeasts, 20: 43784

VITAMIN P

see also Hesperidin
see also Rutin
effects on radiation reaction of skin, 16: 8625
protective effects against radiation injury to histo-hematic barrier in, spleen, 18: 1451
radiosensitivity effects on dog intestinal motor function, x, 18: 17643
therapeutic effects of, on radiation sickness in rats, 18: 5139(T) (JPRS-22123)

Vitamin PP

see Nicotinamides

VITAMINS

(For instances of known chemical nature see also as organic compounds.)
content in foods, 19: 30603
content in total diet composites, 17: 33516
determination in biological materials by paper chromatography, 17: 4380(R) (UCRL-10479)
effects on course of radiation sickness in guinea pigs, 20: 33101
effects on excretion and skeletal retention of strontium in mice, 18: 31102
effects on irradiated rat leukocytes, 20: 42948
effects on radiotherapy of cervical cancers, 20: 191
effects on recovery from radiation sickness, 19: 38457
labeling, metabolism and synthesis, tracer studies, 16: 1377
metabolism in dogs fed radiopasteurized meat, 20: 42793
preparation of labeled, by microbial processes, 19: 46409
protective effects against radiation damage, 17: 7912
protective effects of protein complex of, against radiation sickness in rats, 17: 14113
protective effects of pellagra preventive, against radiation effects on cholesterol metabolism in guinea pigs, 18: 9928
radiation effects in complex systems, 16: 9922(T) (JPRS-12310(p.1-14))
radiation effects on fat-soluble, 16: 16623
radiation effects on microbiological activity, 17: 8141
radiation effects on, 17: 25031
radiation effects on intestinal absorption of, 18: 13419(R) (TID-20242)
radiation effects on content of, in clams, 19: 8846
radiation effects on content in foods, 19: 11632
radiation effects on content of, in rye flour, 19: 38423
radiation effects on content of, in oysters, 20: 9316 (CONF-651024, pp 14-17)
radiation effects on content in oysters, γ, 20: 39288(R) (ORO-636)
radiation inactivation of, in fruits and vegetables, 20: 43781
radiation protection by, in dogs, gamma, 17: 30421
radioinduced reactions with HCl, chromatographic method for separating products in, 20: 20738
radioprotective effects in mice, x, 20: 45492
radiosensitivity, 19: 30603
radiosensitivity effects of, 17: 38895
radiosensitivity effects of, 17: 38910
radiosensitivity effects on rat organs, gamma, 18: 41207
radiosterilization effects on content of, in foodstuff, gamma, 18: 17507
radiosterilization effects on contents of, in sweet potatoes, 19: 24895
radiosterilization of, effects on potency, 19: 44559
stability in prepared dog food during storage, 19: 43644(R) (UCD-472-112)
therapeutic effects in radiation injuries, 16: 82
therapeutic effects in radiation sickness, 16: 7468

therapeutic use in radiation sickness, 16: 9923(T) (JPRS-12310(p.15-23))
therapeutic use in radiation injury, 18: 37015

Vitreous Enamels
see Porcelain Enamels

VITREOUS MATERIALS
see also Glass
fabrication of boron-free, for radiation-resistant insulation, 20: 15131(P)
leaching characteristics of, after waste fixation in, 20: 47082 (AEET-250)
radiation effects on properties of, 19: 4195(R) (NYO-10626)
radiation effects on dielectric and tensile properties of crystalline, neutron, 20: 23802
radiation effects on corrosion resistance of, 20: 47082 (AEET-250)
waste fixation in, 20: 47082 (AEET-250)

VMR
see Variable Moderator Reactor

Voids
see Reactor Shield Voids

VOLATILITY SEPARATION PROCESSES
see also Fluoride Volatility Processes
construction materials for fused-salt, corrosion behavior of, 17: 17451
decontamination factor for uranium, 18: 41566(T) (ANL-Trans-74)
description of film-distillation, 18: 37586 (A/CONF.28/P/557)
description of, for short-lived isotopes, review of, 20: 20826
development, 17: 4225(R) (ANL-6635(p.28-50))
development, 17: 10741(R) (ORNL-TM-313)
development, 18: 8455
development, 18: 13975
development, 18: 44931(R) (ANL-6939(p.39-72))
development for carbon-containing fuel elements, 19: 44109 (BLG-331)
development for ceramic fuels and fuel alloys, 20: 20177(R) (BNL-929, pp 83-105)
development for fuel reprocessing, 17: 12057(R) (BNL-742(p.1-85))
development for fuel processing, review, 19: 34284
development for highly enriched and slightly enriched fuels, 20: 25208
development for irradiated molybdenum--uranium alloys, 17: 14379(T) (AEC-tr-5652)
development for processing irradiated fuel, 18: 41583
development for processing spent nuclear fuels, (E), 19: 34286
development for reprocessing fuels, French research program on, 18: 3886(T) (AEC-tr-6177)
development for recovery of plutonium and uranium from fuels, 19: 35605(R) (ANL-7045(p.24-48))
development for recovery of plutonium and uranium, 20: 7192(R) (K-1649)
development for spent fuels, 20: 20183
development of chloride, for nuclear fuels, 18: 39386
development of chloride, for recovery of uranium from spent fuels, 19: 4246(R) (ORNL-3627(p.1-28))
development of chloride-fluoride, for enriched uranium fuels, 19: 14765(R) (ANL-6977)
development of fluid-bed chlorination-fluorination process for uranium alloy fuels, 18: 35060(R) (ANL-6904)
development of fluid-bed, 19: 11293
development of fluidized-bed, for processing irradiated fuel elements, 19: 26468
development of fluid-bed, for irradiated fuels, 20: 33413(R) (K-1669)
development of fluid-bed, for processing irradiated fuels, 20: 36926 (K-L-6091)
development of, for decontamination of irradiated uranium oxide, 16: 31675 (ORNL-3280)
development of, for separation of plutonium from oxide mixtures, 16: 33974(R) (ANL-6610)
development of, for irradiated reactor fuels, 17: 8267
development of halide, for processing irradiated fuels, 18: 16153
development of Nitrofluor, 19: 11293
development of, for spent fuels, 20: 10965
development of, for treatment of irradiated fuels, 20: 36950
development of, *Technical Progress Review*, Spring 1961, 19: 11293
development, removal of chloride from Zircex off-gas, 16: 20537(R) (ORNL-TM-177)
developments in, for irradiated fuels, 19: 22430
economics of, for carbide, metal, and oxide fast-breeder reactor fuels, 20: 43410 (ANL-7137)
fuel element reprocessing by, pilot plant design problems for, 20: 29364
fuel element threading tool for, 18: 20134(R) (ORNL-TM-792)
instrumentation for Volatility Pilot Plant at ORNL, 17: 14612(R) (ORNL-3378(p.44-6))
materials for use in construction of chloride, testing of, 19: 4246(R) (ORNL-3627(p.1-28))
materials of construction for chloride, corrosion testing of, 16: 32883(R) (ORNL-3314(p.1-39))
materials of construction for, corrosion testing of, 20: 7192(R) (K-1649)
operations of hydrogen-distillation plant, 18: 37590 (A/CONF.28/P/754)
performance for ceramic fuels and uranium alloys, 18: 37280 (A/CONF.28/P/771)
performance for fuel reprocessing, 18: 36751 (ANL-6912)
testing of chloride, for plutonium and uranium recovery, 20: 35590 (ORNL-3977)
use in activation analysis, 20: 35457
use of chloride, for processing uranium--zirconium alloys, 18: 41560 (CEA-R-2508)
use of fluidized beds in reprocessing solid reactor fuels, 17: 10730 (BNL-6195)
use of inert fluidized beds for reprocessing fuels, 17: 8233 (BNL-6039)
volatilization of plutonium tetrachloride during chloride volatility processing of fuels, thermodynamic calculations for, 18: 43715 (ORNL-3693)
waste solutions from, economics for management of, 20: 47083(R) (ORNL-3945, pp 79-106)

Volatilization
see Vaporization

VOLCANOES
see also Lava
age estimation of ash from, by carbon-14 method, in New Zealand, 20: 20893
contents of thorium and uranium in lava from Oldoinyo Lengai, Tanganyika, 17: 29105
deposits from Costa Rica, inside and outside of one-story residences, 20: 16659 (AD-629527)
dust deposits in San Jose, decontamination of, 19: 32468
dust particles from ground surface of, method for size analysis of, 20: 4149 (AD-623639)
ion exchange capacity of zeolitic tuffs from Nevada, effects of heating on, 18: 18035
isotopic content of sulfur and uranium in mineralization of Canale Monterano, Italy, 17: 29110
lead isotope contents in magmas from, 20: 43521
lead-206, -207, and -208 ratios in rocks from Japanese, 18: 18029
lead-210 from Mount Vesuvius, specific activity of, 18: 33791
particle clouds from Irazú, fallout patterns of, 20: 33507 (AD-634901)
sulfur isotopic composition and origin in, 19: 18152
sulfur isotopic ratios in, in Wairakei region of New Zealand, 20: 45925

Voltage Breakdown
see Dielectric Breakdown

Voltage Doubler
see Cockcroft-Walton Accelerators

VOLTAGE REGULATORS
see also Power Supplies
design, 17: 12530 (SCTM-134-62(72))
design, 17: 19412 (BNL-6922)
design and construction of three-phase, for 88-in. cyclotron, 20: 15183
design and development of ultra-stable capacitive, 20: 43634 (SLAC-PUB-199)
design for accelerators, 20: 19323(P)
design for cyclotron beam deflector, 20: 7679 (UJV-1386/65)
design for h-f accelerator supplies, 17: 42030
design for power matching in static power conversion systems for space, 17: 34073
design for 500-kev Van de Graaff accelerators, (E), 20: 7670 (INFN/TC-64/5)
design of capacitive divider for pulsed high-voltage measurements, 17: 8552
design of, for image intensifier tubes, 17: 10907 (TID-15860)
design of high-voltage divider, 17: 3299
design of potentiostat, 20: 43512(R) (ANL-7136, pp 315-27)
design of stabilizing circuit for Cockcroft-Walton accelerator, 17: 9657
design of transistorized, 16: 13369(P)
design of transistorized, for photomultiplier tube stabilization, 18: 2002
development and testing for high voltages, 17: 29177(T) (NP-tr-1031)
development and testing of high-temperature, 18: 29928(R) (NP-13979)
development for betatron-magnet excitation, 18: 14687
development of, for digital modules, 17: 2051(R) (CU(PNPL)-219)
development of high-stability solid-state, (E), 19: 36765(R) (TID-21936)
engineering drawing of, for suppressing thermocouple electromotive forces, 19: 749
engineering drawings of, for monitoring instruments, 19: 6173
in x-ray equipment, survey, 17: 30241
properties for electromagnetic isotope separators, 20: 4281 (IAE-926)
testing of automatic, for control of alternator supplying proton synchrotron pulses, 17: 19432
use of cyclotron D, for background reduction in reaction and scattering experiments, 16: 33254
uses of two-state modulation system as, 17: 35260(R) (TID-19135)

Voltameters
see Coulometers

VOLTAMMETRY

boron carbide electrodes for use in, 19: 24409
development for fused salt analyses, 19: 17781(R) (ORNL-3750)
development for liquid fluoride analysis, 19: 23163(R) (ORNL-3650 (p.111-86))
development for use in molten salt studies, 17: 15853(R) (ORNL-3397 (p.24-6))
development of glassy carbon electrode for use in, 19: 13217
developments in controlled-potential, at ORNL, 18: 33452 (ORNL-P-145)
method for x-ray equipment, using photographic film, 20: 16844
methods for solid-electrode, using reversible voltages, 19: 15341 (COO-1148-93)
sensitivity of d-c, effects of various mercury cathodes on, 17: 15851(R) (ORNL-3397(p.1-16))
use of simple quasi reference electrode in, 18: 31427 (ORNL-P-14)

VOLTMETERS
calibration and range conversion of, 17: 23614 (TRG-Report-515)
description of radiometric, for Mv range, 18: 23846
design and performance of peak-reading, 20: 9226 (SC-TM-65-577)
design for Astron accelerator, 20: 10121 (CONF-650512, pp 105-8)
design for photographic film reader, 20: 39258
design for time distribution curves, using beta sources, 16: 15062
design of high-impedance vacuum tube, 20: 41248
design of Kerr-cell, for high-intensity pulses, 18: 29959
design of single-pulse-peak reading, (E), 19: 22653 (BDX-613-67)
design of transistorized micro-, 16: 10176 (DC-60-2-145)
design of wideband, for pulse measurements, 18: 31856
design of, engineering drawings for, 20: 14831
development for measuring high-voltage equipment, 17: 29177(T) (NP-tr-1031)
development of digital, 18: 13628(R) (ORNL-3537(p.1-17))
development using ionization method for measuring contact potential differences, 18: 33863
overload protection for, transistor, 18: 2404(R) (TID-19651)
standardization of, 17: 6395 (HW-SA-2510)
timing systems for readout of digital, 20: 14822(R) (RHEL/R-112, pp 99-128)
use of generating, for measurement of Van de Graaff terminal voltage, 18: 24242 (CONF-22-33)

VOLUMETRIC ANALYSIS
see also Gasometric Analysis
bibliography and review on, for inorganic compounds, 16: 14651
by double precipitation reactions, tracer studies of role of adsorption indicators in, 16: 127 (JEN-77-SI/1-12)
development of biamperometric titrimetry, 17: 35622(R) (TID-19359)
development of micro methods of, 17: 15854(R) (ORNL-3397(p.26-38))
developments in inorganic, review of, 18: 19865
equipment and method for particle, for biological applications, 20: 18186(R) (LA-3432, pp 102-29)
equipment design for determining gas-solid reaction kinetics, 18: 35953 (BM-RI-6359)
use of radioisotopes as indicator in titrations, 16: 22024

Vortex Tubes
see Hilsch Tubes

VSR
see Vallecitos Superheat Reactor

Vulcain Reactor (Belgium)
see Maritime Reactors

W

W-105 Reactors
see Hanford Production Reactors

W-305 Reactor
see Hanford Test Reactor

Wagner Rearrangement
see Molecular Rearrangements

WALES
carbon, potassium, thorium, and uranium content in black shales from coalfield in South, 18: 37416

Walkie-Poppy
see Rate Meters

Walkie-Talkie
see Rate Meters

WALTER REED RESEARCH REACTOR
containment of, secondary and tertiary, 18: 3371
containments during maximum credible accident, secondary and tertiary, 18: 4883

WARFARE
see also Air Warfare
see also Atomic Weapons
see also Biological Warfare
see also Biological Warfare Agents
see also Chemical Warfare
see also Civilian Defense
see also Radiological Defense
see also Radiological Warfare
see also Thermonuclear Weapons
see also Underwater Warfare
book: *Civil Defense Against Atomic, Chemical, and Bacteriological Weapons*, 17: 20274
book: *Nuclear War and Nuclear War Protection*, 16: 24032(T)
casualty rates in nuclear, sensitivity to selected parameters, 20: 23265 (AD-624702)
civilian defense in atomic, 18: 33814
conduct of, effects of science on, 20: 27071
contamination of municipal water supplies during nuclear, 19: 42658 (NP-15328)
effects on contamination of water supplies, 20: 23382(T) (JPRS-34578)
fallout decontamination following thermonuclear, economics and efficiency of, 19: 4393 (AD-450606)
fallout hazards to Canadian hospitals from, 18: 29886
flood problems during post-attack period in nuclear, 19: 11421 (RM-4238-TAB)
food distribution and processing after thermonuclear, 19: 4391(R) (AD-450228)
hospital organization for nuclear, 17: 27623
industrial survival from nuclear, 16: 5616
infectious disease problems in, postattack, 20: 43588 (RM-5090-TAB)
medical personnel in nuclear, 17: 37383
medical problems of nuclear, 17: 39330
military medical services for thermonuclear, 18: 25729
protection of air traffic control system from chemical–biological–radiological warfare agents, equipment for, 19: 9354 (GDC-64-026)
radiation casualties during thermonuclear, 18: 20258
radiation survey by detectors in M60 tank in, correction factors for, 18: 25709 (NDL-TR-49)
radioelectronics for use in, 20: 27073
recovery from thermonuclear, 19: 4392 (AD-450598)
social effects of nuclear, 17: 34174
structural materials development for nuclear, 19: 26753 (AD-610502)
survival rations for use during nuclear, 17: 27621
thermonuclear, casualties from, 17: 37381
thermonuclear, medical consequences of, 18: 14157
use of nuclear craters as obstacles in military defenses, 19: 34300 (UCRL-7966)

WASHINGTON
analysis of water from rivers of, for radioactivity, 18: 37385
bird survey in, 19: 17410 (HW-SA-3359)
cesium-137 content in forests of, effects of climatic zones on, 20: 20879 (BNWL-SA-530)
density-flow regime of Franklin D. Roosevelt Lake, 19: 26527 (BNWL-20)
ecology of Dover sole and sablefish off coast of, 20: 24831(R) (RLO-1731-5)
fallout monitoring, 1963 and 1964, 20: 11011(R) (BNWL-122, pp 181-3)
fallout monitoring, 1961 through 1964, 20: 11012(R) (BNWL-122, pp 184-6)
geochronology of crystalline rocks of northern Cascade Mountains, 18: 14067(R) (NYO-7243)
stratigraphy of late basalt flows, Ellensburg Formation, and lower Ringold Formation in south-central, 19: 38843 (BNWL-SA-135)
stratigraphy of post-basalt sediments in south-central, 19: 38844 (BNWL-SA-140)
strontium-90 deposition in soil from rainfall, Clallam County, 1957–60, 16: 19171
thorium and uranium oxide contents in monazites in, 18: 18060
zinc-65 distribution in plankton from offshore waters of, 20: 43545

Washington (D. C.)
see District of Columbia

WASPALOY
brazing and welding of, criteria for, 17: 11163 (DMIC-181)
corrosion by lithium fluoride, 19: 12150
corrosion by lithium at 1500°F, 19: 36980 (PWAC-355)
corrosion by lithium fluoride in cyclic high-temperature environment, 20: 4326 (TRW-ER-6561)
creep rate, effects of alternating stress, 17: 4965
drilling, 17: 6615
electrochemical machining of, effects of friction, surface finish, and tool erosion on, 17: 34386
joining by brazing, soldering, or welding, 20: 29666 (RSIC-484)
joining by mechanical fastening, 20: 29667 (RSIC-509)
machining properties of, 20: 29665 (RSIC-482)
surface treatments for, coating and mechanical, 20: 29706 (NASA-TM-X-53448)
tensile properties, 17: 36987 (SY-5394-R(Vol.I))

Wasps
see Vespidae

WASTE DISPOSAL

see also Sewage
see also Sewage Systems
see also Stack Disposal
see also Waste Recovery
abstracts on management research, 19: 42194 (NP-15267)
activation, for in-pile conversion of long-lived isotopes to stable or short-lived isotopes, (T), 20: 16132 (BNL-8558)
activities at ORNL for June and July 1961, 16: 2808(R) (ORNL-TM-15)
after incorporation of radioisotopes in glass blocks, 17: 33404
after radiation accidents, 19: 22639
air dispersion, progress in, 16: 29211(R) (NYO-4817)
anaerobic digestion of waste sludge, effects of iodine-131 and phosphorus-32 on, 16: 5103
at AEC facilities, review, 20: 7331
at Argonne and Los Alamos, comparison of operational practices in low- and intermediate-level, 20: 3603 (LA-DC-7249)
at British nuclear power reactors, 16: 23349
at Chalk River, 17: 20256
at Chalk River, procedures and experience in, 18: 36855 (CRIO-1194)
at Hallam Nuclear Power Facility, 20: 5130(R) (TID-22355)
at Hanford Works, effects on radioactivity of Columbia River, 19: 36703 (HW-72229(Rev.))
at Hanford, costs of waste management program, 19: 33677 (RL-SEP-496)
at Hanford, review of, 19: 27832(R) (HW-83609)
at high-level cobalt-60 plant in Ottawa, 19: 30435 (AECL-2233)
at Homestake-New Mexico uranium refinery at Grants, New Mexico, 18: 13350 (TID-19941(p.55-71))
at Homestake-Sapin uranium refinery at Grants, New Mexico, 18: 13351 (TID-19941(p.73-91))
at Idaho Operations Office, 1963, 19: 4398(R) (IDO-12037)
at Japan Atomic Energy Institute, Tokyo, 17: 2661 (JAERI-6011)
at Lawrence Radiation Laboratory, 20: 1552 (UCRL-14320)
at National Reactor Testing Station, data on, 19: 27834 (IDO-12040)
at nuclear installations, sitological studies for, 17: 29870
at nuclear power plants, 19: 31622
at Shippingport Atomic Power Station, 20: 3521
at SL-1 site after reactor excursion, 19: 22639
at Swedish reactor plants, 16: 1193(R) (NP-10915)
at uranium mills, 18: 13346 (TID-19941)
at uranium ore refinery at Edgemont, South Dakota, field study of, 18: 13347 (TID-19941(p.1-18))
at uranium refinery at Gunnison, Colorado, 18: 13348 (TID-19941(p.19-36))
at uranium refinery at Grand Junction, Colorado, 18: 13349 (TID-19941 (p.37-54))
at Windscale, marine environmental monitoring of, 18: 8597
atmospheric, management in a nuclear economy, 16: 5614
bibliography, 16: 20040
bibliography, 16: 23784 (ORNL-2971(Vol.1))
bibliography, 16: 23785 (ORNL-2971(Vol.3))
bibliography, 16: 25476 (ORNL-2971(Vol.4))
bibliography on, 16: 30157 (TID-3555(Suppl.1))
bibliography on, 16: 29038 (ORNL-2971(Vol.7))
bibliography on, 16: 31346 (ORNL-2971(Vol.8))
bibliography on, 17: 3 (ORNL-2971(Vol.6))
bibliography on, 18: 36857 (TID-3311(Suppl.1))
bibliography on, 20: 18153 (AED-C-01-12)
bibliography on, 20: 18154 (AED-C-01-13)
bibliography on biological aspects of, 16: 28730 (TID-3910)
bibliography on biological aspects of, 17: 40515 (TID-3910(Suppl.1))
bibliography on equipment and plants for, 16: 30496 (ORNL-2971 (Vol.5))
bibliography on ultimate, in salt formations, 18: 31041 (KFK-205)
book: *Advances in Water Pollution Research*, Vol. 1, 2, and 3, 20: 20982
book: *Low-Level Radioactive Wastes: Their Handling, Treatment, and Disposal*, 18: 38700
book: *Processing and Disposal of Radioactive Waste from Laboratories*, 19: 27839
book: *Radioactive Waste Materials*, 17: 13874
book: *The Management of Radioactive Wastes Produced by Radioisotope Users*, 20: 40480 (STI-PUB-119)
book: *The Radiochemical Manual*. Second Edition, 20: 36924
book: *Treatment and Disposal of Radioactive Wastes*, 16: 18712
bore hole, method for, 20: 26585(P)
burial and storage, processing for, 20: 12520(T) (CEA-tr-A-1490)
burial at Hanford, 19: 24190 (HW-77274)
burial, development of packaging for, 16: 30682(R) (UCRL-6936)
burial in natural salt formations, 17: 39298(R) (ORNL-3492(p.19-37))
burial in natural salt formations, 19: 8675(R) (ORNL-3697(p.19-31))
burial in Western U. S., possible areas for, 18: 33168 (SRIA-8)
burial of glass-fixed fission products at Chalk River, monitoring of contamination by, 18: 33165 (ERI-6)
burial of liquid wastes from Purex Process, design of routing system and tank farm for, 16: 31343 (HW-72780)
burial of solid wastes at Savannah River Plant, 17: 24733 (DPSPU-63-30-2)
burial, evaluation of bentonite as moisture barrier in, 19: 48076 (DPSPU-62-30-3A)
burial, heat dissipation from, 20: 28853(R) (IDO-14661, pp 45-82)
burial, method for liquid and solid, 19: 43626
burial, method of, at Monticello, Utah, 20: 36535 (RMO-3005(Suppl.))
burial, packaging, and transport for, 20: 43069(R) (IDO-14679, pp 51-9)
burial, temperature distributions in gamma-active ceramic spheres for, 19: 40275
burial, temperature distribution in gamma-active spheres, (T), 19: 42191 (AEET/HP/TH-20)
burning degraded solvents from radiochemical processes, 19: 21748 (DPSPU-64-30-8B)
burning of uranium scrap, facility for, engineering drawings, 17: 22964
by atomic energy industries, effects of, on contamination of biosphere, 17: 37056(T) (FTD-TT-63-664)
by burial, hydraulic press for packaging drums for, 17: 29135(R) (UCRL-7254(p.34-9))
by collection and burial, 16: 23350
by ground storage, 16: 25040 (TID-7628(p.12-16))
by incineration, 17: 10221(T,R) (EURAEC-443)
by incorporation of fission products in concrete, 17: 21378
by industries, 19: 38290
by injection into permeable rocks, 16: 25056 (TID-7628(p.324-46))
by liquid storage in underground fractured rock formations, 17: 29877(P)
by solid storage in phosphate glass, 17: 2461(R) (BNL-731(p.18-46))
by solidification in subterranean formations, 17: 29878(P)
by storage, management of tank farms for, 17: 8268
by uranium ore processing plant, effects of river pollution on radiation exposure of population, 18: 35763 (NP-14161)
calcination, mercury behavior in, 17: 28581(R) (HW-77299)
calcination, pot and spray, 17: 28581(R) (HW-77299)
calcination, procedure for fluorination furnace material, 16: 18702 (CEA-2102)
centralized removal of wastes from sites of accumulation for, 20: 1553
ceramic sponges for, preparation and use of, 16: 32622
compressing and storage at Saclay, 20: 26580
conference on, 17: 19703 (TID-7644)
conference on ground disposal, 16: 25037 (TID-7628)
container design for, 18: 6547(P)
container for, preparation from set oil shale remains and waterproof foil, 19: 5567(P)
containers and procedures for, 17: 1679
containers for low-level, structural integrity of, 19: 20196 (CONF-650103-6)
contamination of area, 16: 9824
contamination of surface waters by, 20: 43598
contamination problems in, survey, 16: 25677
contribution to zinc-65 burdens in marine organisms along Pacific coast of the United States, 20: 27159
control at Paducah Gaseous Diffusion Plant, 19: 35886(R) (KY-484)
control measures for safe, legislation on, 17: 15527
control of, at Marcoule Center, 17: 42424
control of, in Great Britain, 19: 25778
control of, legal aspects of international, 19: 25779
cost and technology study for high-level radioactive liquids in New York state, 17: 15525 (NP-12486)
cost estimates for management of, effects of fission-product removal on, 17: 26188
cost estimates for management of power-reactor, 17: 26187
cost of shipping calcined solids 500, 1000, and 1500 miles for, 16: 32620 (ORNL-3356)
cost studies of interim liquid storage and pot calcination, 16: 25072 (TID-7628(p.532-5))
deep well, geology of 200-m Eurochemic, 16: 34144(T,R) (EURAEC-275)
deep-well injection, survey of geologic basins in U. S., 16: 25057 (TID-7628(p.347-55))
deep well injection, 16: 25058 (TID-7628(p.356-62))
deep well injection, for uranium mill waste water, 17: 2648
deep well, review of Canadian practices, 17: 19706 (TID-7644(p.75-82))
deep well, ion exchange in, 18: 17342
deep well, of radioactive materials for heating minerals *in situ*, 20: 30950(P)
deep well, research on hydrofracturing and permeable formations, 19: 31617(R) (ORNL-TM-1081)
deep-well, methods for, 19: 23996(R) (ORNL-3650(p.1-110))
design and operation of deep injection wells, 16: 25059 (TID-7628(p.363-73))
design of cement containers for sea, 16: 26641 (TID-15431)

design of drum transport equipment, 16: 30158
design of facility for high- and intermediate-level liquid, 16: 18707 (ORNL-TM-211)
development, 17: 1163(R) (ORNL-TM-376)
development in Czechoslovakia, 18: 38686 (A/CONF.28/P/775)
development in, at Pelindaba, South Africa, 20: 20352
development of sites for C.E.N., 16: 30153 (EURAEC-184)
development of technology, summary for July to Sept. 1961, 16: 16020(R) (EURAEC-187)
developments, 17: 28581(R) (HW-77299)
developments in, 16: 2057(R) (ORNL-3189)
developments in, related cooperative projects, 16: 2805(R) (ORNL-3189 (p.77-80))
developments in United States, 17: 2650
developments in, effects on U. S. nuclear power industry, 18: 33161 (A/CONF.28/P/868)
dilution in Clinch River, distribution of radioisotopes in, 16: 2059(R) (ORNL-3189(p.13-27))
dilution in Rhone River in France, 16: 9723 (CEA-2003)
dilution in Rhone River in France, 16: 12796(T) (AEC-tr-5013)
dilution in Rhone from Marcoule plant, tracer study using rhodamine B, 16: 18710
dilution in Rhone River of effluents from Marcoule Center, 17: 29871
dilution in river in Yugoslavia, 17: 41147
dilution in river waters, monitoring radioactivity in, 19: 3800
dilution methods for low-level, from Agesta Reactor, 19: 24193
discharge at nuclear power plants, monitoring of, 18: 8596
dispersion factors for Columbia River at Hanford works, 17: 29119 (HW-SA-3056)
dry wells, injection of grout into shale formation, 16: 2803(R) (ORNL-3189(p.69-72))
dry wells, moisture and radioisotope distribution under test model, 16: 16021 (HW-71573)
dry wells, study of NRTS area for, 17: 19709 (TID-7644(p.151-75))
ecological effects of products from, on freshwater organisms, 16: 22456 (TID-7632(p.360-71))
ecological effects of, bibliography, 19: 24237 (TID-3910(Suppl.3))
ecological survey for Philippine Atomic Research Center, 17: 31791 (PAEC(D)HP-631)
economic aspects of storage, 17: 26933 (ORNL-TM-559)
economic, engineering, and safety evaluations of, 17: 39180(R) (ORNL-3452(p.51-96))
economics, engineering, and hazards, 16: 2804(R) (ORNL-3189(p.72-7))
economics, engineering, and hazards, 17: 2785(R) (ORNL-3347(p.1-46))
economics of, at AEC fuel-processing plants, 20: 45814
economics of, at C.E.N., 19: 24191 (TID-21786)
economics of, for irradiated fuels, 20: 24670 (UJV-1493)
economics of, in tanks, 19: 48080 (ORNL-2873)
economics, engineering, and safety evaluations of, 19: 8676(R) (ORNL-3697(p.54-61))
effects of management on reactor site selection, 17: 19602
effects of radioactive, on Chironomus chromosome aberrations, 20: 40530
effects of radioactive, on hydrobionts, 20: 40527
effects on radioactivity of Columbia River below Hanford, 19: 38874 (BNWL-SA-53)
effects on White Oak Lake bed plants and soils, 17: 4369 (ORO-585)
embedding highly radioactive wastes in concrete, 18: 1315
encapsulation methods for high-level, 18: 19453
engineering geology of, 17: 4373
environmental contamination around reactors, review, 17: 13738
environmental monitoring at nuclear installations, 16: 29271
environs monitoring of radioactivity release at SIC, Jan. to June 1962, 18: 1282 (CENRD/HP/62/2)
equipment and problems in Czechoslovakia, 16: 2812
facilities for aqueous, in Italy, 17: 5649
facilities for, at Japanese Institute of Radiological Sciences, 18: 21925
feasibility studies of, in Black Sea and tributaries, 20: 45227
feasibility studies of, in the Black Sea and tributaries, 20: 43539
fission product containment material for, 20: 35177(P)
fission product incorporation in glass, 17: 5650
fission product movement in chemical waste seepage pits, 19: 6930(R) (ORNL-3697(p.43-8))
fixation and storage on ion exchange beds, dehydration of beds in, 17: 42415 (HW-78893)
fixation in asphalt, hot-cell tests on, 20: 10442 (ORNL-TM-1343)
fixation in basalt, 18: 40962 (UJV-1105/64)
fixation in borate and phosphate glasses, 16: 1649(R) (ORNL-TM-1)
fixation in borosilicate glass, thermal conductivity measurements for, 19: 9650 (AERE-R-4685)
fixation in cement, injection methods for, 18: 17346
fixation in cements, 18: 43093
fixation in cement, injected into shale, 19: 23996(R) (ORNL-3650(p.1-110))
fixation in ceramic material from gas or liquid, 18: 7984(P)
fixation in ceramic-coated clay, method for, 20: 30951(P)
fixation in fired clays, fission product retention in, 17: 40416 (ORNL-2611)
fixation in glass, 18: 43095
fixation in glass, 20: 16141(P)
fixation in glass, transient thermal properties, 19: 17388(R) (HW-84467)
fixation in glass, development of process for, 19: 23355(R) (BNL-867(p.1-117))
fixation in glass, simulation studies on, 20: 18166(R) (TID-22531)
fixation in glass, computer program for glass composition for, 20: 20346 (ORNL-3824)
fixation in glass, simulation studies on, 20: 47082 (AEET-250)
fixation in phosphate glass, method for continuous plant operation for, 16: 34149
fixation in phosphate glass, 20: 3606
fixation in soils by injection, hydrodynamics of, 20: 18163(R) (NP-15859)
fixation in unleachable solids, 18: 3393(P)
fixation in vitreous materials, 16: 16023(R) (NYO-9653)
fixation in vitreous preparations, 18: 38683 (A/CONF.28/P/587)
fixation in vitreous preparations, utilization of heat from, 19: 31620
fixation in vitreous matrices, research program on, 19: 31618(R) (TID-21882)
fixation method for liquid, with useful resultant product, 17: 28587(P)
fixation of americium-241–plutonium-239 raffinate solutions in cement, 19: 21750 (LA-3150)
fixation of cesium on clay minerals by ion exchange, 16: 27021
fixation of fission products on clinoptilolite columns, 16: 23346 (CRCE-1080)
fixation of fission products in ceramic microspheres for, 17: 32327
fixation of niobium chloride by calcium chloride in, 17: 34052(T,R) (EURAEC-634)
fixation of radioactive gases in water-unleachable rocklike products, 20: 3608(P)
fixation on clays, 16: 23351
fixation on peat humic acids, 18: 38688 (A/CONF.28/P/784)
fixation, phosphate glass for, 17: 31795(R) (BNL-782(p.18-43))
flow studies on large shallow pond, (E), 19: 29804
for clinical radioisotope laboratories, 19: 33682
for nuclear industry, 18: 38690 (AEET/HP/RWD/4)
for nuclear ships and submarines, 18: 10320
fresh water, hazards and movement in, 20: 18157 (BNWL-SA-466)
fresh water, safety hazards in, 19: 12858
from isotope laboratories, dilution and storage calculations, 16: 25077
from radiotherapy hospital, 18: 24985
geologic and hydrologic features of Atlantic and Gulf coastal plains, 16: 16024 (TEI-805)
geological evaluations in, 20: 28851 (BNWL-SA-57)
geology and hydrology at Burial Ground 4, Oak Ridge, Tenn., 16: 9725 (ORNL-3182)
ground, analysis of Mol site for, 17: 28579 (EURAEC-295)
ground burial, site selection and operation, 16: 25063 (TID-7628(p.428-36))
ground discharge, 16: 32619 (HW-SA-2707)
ground discharge of NPR decontamination wastes, site evaluation for, 17: 35241 (HW-69426)
ground, laboratory studies of contamination of aquifers by, 17: 39270 (UCRL-13074)
ground, mathematical formulation of steady Darcian transport of fluids in heterogeneous partially saturated media, 16: 34139 (HW-72335(Pt.1))
ground, monitoring of ground waters in Hanford Area, 17: 10822 (HW-SA-2566)
ground, practical application of theory on movement in, 17: 37000
ground, radioisotope migration from single deposit, 16: 18703 (CRER-1077)
ground storage, 16: 25041 (TID-7628(p.67-76))
ground storage, 16: 25043 (TID-7628(p.99-114))
ground storage, 16: 25069 (TID-7628(p.491-505))
ground storage, 16: 25071 (TID-7628(p.513-31))
ground storage, 16: 25073 (TID-7628(p.536-68))
ground storage, 17: 1173(R) (HW-70050)
ground storage area for, 20: 8479(R) (ORNL-3849, pp 1-42)
ground storage at Hanford, monitoring, 17: 1177(R) (HW-70050(p.143-219))
ground storage at Hanford, monitoring results on, 19: 25773 (HW-84577)
ground storage at ORNL, geohydrology evaluation of, 20: 12518 (ORNL-TM-1327)
ground storage, geohydrologic factors, 16: 25042 (TID-7628(p.77-98))
ground storage in U. S., review of, 18: 17337
ground storage method of, 20: 38539(P)
ground storage, safety, 16: 25070 (TID-7628(p.506-12))
ground storage, survey on feasibility, 17: 2785(R) (ORNL-3347(p.1-46))

ground storage, conditions for, 18: 17340
ground storage, evaluation of problems in, 18: 17338
ground storage, hydraulic fracturing method for shale injection in, 20: 8479(R) (ORNL-3849, pp 1-42)
ground storage, international program for, 18: 17339
ground storage, leak development in tanks for, 20: 9420 (DP-990)
ground storage, study of geologic basins for, 19: 14894 (SAN-413-2)
ground water analog test model for Hanford Project, 18: 14066 (HW-80086)
ground, computer program for calculating steady Darcian transport of fluids from, 18: 26975 (HW-72335(Pt.2))
ground, development for EBR-II waste, 19: 40113(R) (ANL-7071)
ground, effects of climate on shallow-depth, 18: 17347
ground, effects of ground water on transport in soil, 20: 8817(R) (BNWL-36, pp 4.1-77)
ground, evaluation and site selection for, 20: 10443 (STI/PUB/103)
ground, geologic and hydrologic studies on, 18: 16207
ground, geologic and hydrologic conditions at National Reactor Testing Station for, 19: 22529(R) (IDO-22046)
ground, ground water transport effects on, 20: 11009 (BNWL-SA-406)
ground, hydrology at National Reactor Testing Station, 19: 40269(R) (IDO-22047-USGS)
ground, in United Arab Republic, 20: 20350
ground, method for analyzing transport by water, 19: 40268 (BNWL-63)
ground, piping intermediate-level liquids to shale beds, equipment for, 19: 21753
ground, use of seismic methods for studying, 20: 14753 (BNWL-47)
guides for, from Plutonium Recycle Test Reactor, 18: 38691
handling at Dresden Power Reactor, liquid, 16: 7333
hazards from radioactive, environmental and human, 19: 1947
hazards from radioactive, in municipal sewage systems, 20: 41217
hazards from radioactive, in Canada, 20: 45942 (AECL-2478)
heat generation in, computer codes for calculation, 16: 20036 (LA-2664)
heat release from buried wastes, 17: 33407
heat release from high-level wastes, 18: 36859
hospital radioactive, hazards from, 18: 22290
hydraulic fracturing methods for injection with cement in shale, 17: 39297(R) (ORNL-3492(p.13-18))
hydraulic fracturing methods for injection with cement and clay in shale wells, 19: 8674(R) (ORNL-3697(p.10-19))
hydraulic fracturing methods for, mechanics of fracture formation and observation and monitoring well design for, 20: 28857
hydrofracturing methods for, 20: 10439(R) (ORNL-3830, pp 285-98)
hydrology and lithology of Savannah River Plant area, 17: 2639 (DPSPU-62-30-21B)
in Antarctic and Arctic glaciers, problems of, 16: 28640
in asphalt, cement, and tar, leach rates from, 18: 43091(R) (ORNL-TM-830)
in basement rock at Savannah River Plant, 18: 29135 (DP-844)
in clay minerals by fixation, 17: 1164
in deep wells and salt formations, summary, 16: 12795(R) (ORNL-TM-133)
in deep wells and natural salt formations, 16: 31347(R) (ORNL-TM-252)
in deep wells and salt formations, 16: 2809(R) (ORNL-TM-49)
in deep wells and natural salt formations, 17: 2785(R) (ORNL-3347(p.1-46))
in deep wells and natural salt formations, 18: 6537(R) (ORNL-TM-603)
in deep wells, by hydraulic fracturing, 17: 17619(R) (ORNL-TM-482)
in deep wells, ion exchange parameters of, 17: 19711 (TID-7644(p.187-99))
in deep wells, mix development and tracer studies of water movement for, 18: 43091(R) (ORNL-TM-830)
in European countries, 19: 19428 (SZS-2)
in fresh water, 17: 24738
in geological formations of Appalachian Basin, survey, 16: 15001 (TEI-791)
in Great Britain, regulations, 16: 19208
in ground at Savannah River Plant, 16: 25044 (TID-7628(p.115-29))
in Irish Sea, radiobiological monitoring, 1959 and 1960, 17: 20191 (AHSB (RP)-R-27)
in Italy, technical and hygienic aspects of, 20: 3604 (RT/PROT(65)-12)
in natural salt formation, 17: 17619(R) (ORNL-TM-482)
in natural salt formations, development of methods for, 18: 43091(R) (ORNL-TM-830)
in ocean by Marcoule establishment, 17: 15526
in radioisotope hospital wards, 20: 38790
in rivers, hydrological problems in, 20: 2082 (CEA-Bib.-59)
in salt mines, for calcined materials, 17: 17453
in sea of radioisotopes fixed on ion-exchange resins, re-distribution after, 20: 47089
in seepage pits, percolation of plutonium species in soil, 16: 25054 (TID-7628(p.248-81))
in sewer, behavior of radioisotopes in, 17: 36061
in soil, studies of fission product migration rates for, 17: 1159 (HW-SA-2744)
in Solway Firth, measurements of water and silt movement for studies of, 19: 10662 (PG-Report-605)
in streams, monitoring of, 20: 38742
in streams, operations research on liquid, 20: 22513 (NYO-10447)
in subterranean rock formation, 18: 4894(P)
in Tennessee River System, effects on radioactivity at various sites downstream from ORNL, 17: 37055 (ORNL-3409)
in tidal estuaries, dispersion factors in, 19: 25780
in underground mined caverns, 16: 25061 (TID-7628(p.380-95))
in vaults in crystalline rock, 19: 33681
in water streams used for irrigation, safety hazards from, 19: 10666
in White Oak Creek, Tenn., effects of geology and soils on, 19: 27835 (ORNL-TM-1108)
incineration at Chalk River, 19: 31616 (AECL-2248)
incineration of uranium-containing oil solutions, 18: 1313 (NLCO-894)
incineration, factors affecting combustion in, 20: 26558
incineration, plant for, 20: 26566
incineration, purification of off-gases from, 18: 39563
incineration, review of U. S. experience with, 20: 26577
incinerator for plutonium, engineering drawings for, 19: 12861
incinerators for low-activity, operation of Chalk River, 20: 10448
incinerators for, review on, 20: 22508 (AEET-220)
incorporation in asphalt, 19: 31617(R) (ORNL-TM-1081)
incorporation in asphalt, 20: 12524
incorporation in asphalt, feasibility of, 20: 18020(R) (ORNL-3900, pp 2-81)
incorporation in basalt, efficiency of, 20: 26552
incorporation of radioisotopes in glass, 17: 33405
injection into deep sandstone formations, 16: 25055 (TID-7628(p.303-23))
injection of gases into lithosphere, appraisal at National Reactor Testing Station, 19: 48077 (IDO-12024)
inventory control and regulation of, computer program for, 19: 45687 (DP-966)
iodine-129 content in reactor, limits for, 20: 32884
iodine-131 release and monitoring during, 18: 37443 (ORNL-NSIC-3)
ion exchange, properties of clay minerals for, 17: 21385
ion exchange, use of natural earth materials, 16: 20535(R) (IDO-14583)
Irish Sea, of low-activity radioactive effluent from Windscale, 20: 45229
land burial, 16: 25062 (TID-7628(p.396-427))
land burial, 16: 25064 (TID-7628(p.437-59))
land burial, effects of bentonite on permeability of soil by moisture, 16: 25066 (TID-7628(p.462-8))
land burial methods of, technical progress review on, 18: 17350
land burial of solid packaged wastes in U. S. for, evaluation of, 16: 34146
land burial, site survey in northeastern U. S., 16: 25065 (TID-7628 (p.460-1))
land burial, withdrawal of AEC from commercial program of, 18: 8453
laws, West Germany, 16: 21864
legal aspects and licensing for, in sea water, 16: 11348
limits for release of effluents from the Plutonium Recycle Test Reactor, 16: 30046 (HW-SA-2475)
liquid injection in permeable formations, 17: 39296(R) (ORNL-3492 (p.3-12))
liquid injection into deep permeable formations, 19: 8673(R) (ORNL-3697(p.3-10))
liquid, portable facility design, 16: 18705 (NP-11496)
liquid release and storage at BNL, summary for 1965, 20: 25120(R) (BNL-954, pp 114-21)
liquid storage development, 16: 18706 (ORNL-TM-210)
liquid storage, heat problems in, 16: 1282(T) (CEA-tr-X-402)
liquid storage, heat generation problems in deep geological formations, 16: 11346
liquid storage in abnormal-pressure underground reservoirs, 16: 16028
liquid storage in underground tanks, activity in seepage from, 19: 21752
liquid storage, migration of radioactive liquid in sands, 17: 26941
liquid storage, mineral cycling in drained lake bed after, 18: 10 (TID-19618(p.5-37))
liquid storage, movement of radioisotopes through ecosystem from, 18: 9 (TID-19618)
liquid storage of uranium mill effluent underground, 16: 5594
liquid storage of processed Purex and Thorex wastes in tanks, economic evaluation of, 17: 2655
liquid storage, tank design for, 18: 4893
liquid storage, use of asphalt composition in, 20: 2248(P)
low activity, discharge rate from Windscale Works to Irish Sea, 18: 25723
low-level radioactive, volume reduction for, 18: 24986
management of high-level, future possibilities of, 16: 30160
management of, economics of, 20: 14208 (ORNL-P-1926)
management, survey of administrative and technical aspects, 16: 7267
marine, 16: 29261

marine, design of containers for, 17: 17453
marine, ecological effects, 17: 29151
marine, effects on radioactivity of marine organisms, 18: 1341(R) (TID-19608)
marine, effects on zinc-65 content in ocean waters, 18: 4952
marine, evaluation of containers for, 17: 29874
marine, factors in selecting sites for, 16: 32623
marine, health hazards, 16: 18711
marine, health hazards, 16: 19210
marine, monitoring, 16: 10348
marine, of Windscale effluent in Irish Sea, beta activities of sea materials following, 17: 24737
marine, problems in, 17: 29873
marine, purification of water after, 17: 29875
marine, standards for radiopollution from, 17: 29876
marine, strength tests of prototype containers for, 16: 11344 (TID-13942)
marine, survey of Solway Firth, as site for, 18: 4890 (PG-Report-500)
marine, survival of waste containers at ocean depths, 16: 11349
marine, testing of containers for, 16: 3981 (TID-13226)
marine, U. S. Pacific Coast site survey, 16: 1280 (TID-13665)
marine, control and evaluation of, 18: 36860
marine, effects of high levels of zinc-65 on ecology of trophic level crustaceans, 20: 42731(R) (RLO-1751-2)
marine, effects on radioactivity of marine organisms, 18: 33230
marine, effects on radioactivity of organisms and water, 18: 33779
marine, effects on environment, 19: 24748(R) (PG-Report-647)
marine, effects on radioactivity of sea foods, 20: 11054
marine, from nuclear-powered ships, safety in, 18: 15657 (NP-13685)
marine, in coastal sea water, 18: 40955 (AEET/HP/RWD/3)
marine, in inert bituminous encasements, 18: 31042
marine, near Japan, 19: 27837
marine, physicochemical properties of cesium-137, cobalt-60, strontium-89, and strontium-90 in, 20: 38537
marine, problems in, 18: 11503
marine, radioisotope diffusion from, 19: 27838
marine, review of, 19: 8677
marine, site survey and monitoring program for, 19: 24767
method and device for inclusion of solutions in alumina cement, 18: 23120(P)
method for liquid, 18: 4892
method for radioactive, hydraulic-fracturing, 20: 28856
method for, at Institute for Radiochemistry and Research Reactor FRM at Munich, Germany, for low- and intermediate-level liquid, 20: 26582
methods, 17: 14574
methods and facilities in France, 18: 38679 (A/CONF.28/P/86)
methods and operations, review, 16: 16464
methods and problems of, in Japan, 20: 30945
methods and safety aspects for, 18: 45157
methods at Hanford Radiometallurgy Facility, 16: 678
methods at HNPF, 19: 33609(R) (TID-21861)
methods at National Institute of Radiological Science in Chiba, Japan, 20: 5672
methods at Saxton Reactor, 20: 1508
methods at Sioux Falls Power Reactor, 19: 45593(R) (TID-22168)
methods at South African National Nuclear Research Center, Pelindaba, 20: 26553
methods development, review, 16: 18996
methods development for, *Technical Progress Review*, Spring 1964, 19: 12859
methods development at BNL, 20: 20177(R) (BNL-929, pp 83-105)
methods development for solidification and storage of high-activity wastes, 20: 35174
methods evaluation for ultimate, of liquids and solids, 17: 28583 (ORNL-3357)
methods for, 18: 20246
methods for, 20: 5207
methods for, at Harwell, 17: 10222
methods for Eurochemic, 20: 4048(R) (NP-15406)
methods for, from nuclear medicine buildings, 17: 7704
methods for fuel, management, 20: 8482
methods for gas-, organic-, sodium-, and water-cooled power reactors, 16: 28638
methods for gaseous, 19: 38902
methods for gases, 20: 12522
methods for glass melter condensates containing sulfuric acid, 20: 18159 (BNWL-SA-514)
methods for hospitals and medical research establishments, 19: 28603
methods for hospitals and research laboratories, ICRP recommendations for, 20: 45989
methods for Humboldt Bay Power Reactor, 20: 12435
methods for LCBWR, 20: 5105 (ACNP-65544(Vol.I))
methods for liquid, at SM-1 power plant, 19: 29620 (AP-Note-442)
methods for, of solutions, 17: 28586(P)
methods for permanent low-activity, in Czechoslovakia, 16: 34147
methods for radioactive and toxic metallurgical wastes, 17: 25717
methods for radioactive, 19: 1947
methods for radioactive, in Switzerland, 19: 12860
methods for radioactive, 20: 23383(T) (JPRS-34927)
methods for radioactive solid, from reactors, 20: 30947
methods for radiochemical laboratories, 18: 38692
methods for radiochemical laboratories, 18: 38693
methods for separating long-lived isotopes from high-level wastes, (E), 19: 42197
methods for SNAP reactors, 19: 42140 (NAA-SR-11353)
methods for solid, for Philippine Atomic Research Center, 17: 29868 (PAEC(D) HP-622)
methods for uranium mills and mines, 19: 32495
methods for wastes from SM-1 shield tank water, 16: 18663 (OSB-13)
methods for, at Atomic Energy Establishment Trombay, 18: 38689 (A/CONF.28/P/794)
methods for, at Shippingport Atomic Power Station, 20: 40481 (WAPD-T-1851)
methods for, developments in studies on, 20: 30943(R) (ORNL-TM-1465)
methods for, in Great Britain, 20: 36536
methods for, in Hungary, 18: 29142
methods for, research at European Nuclear Energy Agency on, 20: 26587(R) (NP-15919)
methods for, review on, 19: 24198
methods for, review of, 20: 12519 (TID-8541, pp 149-248)
methods for, review of Saclay, 20: 26581
methods for, review of IAEA research on, 20: 32883
methods for, survey of, 20: 45222
methods in Hanford waste management program, 18: 33166 (HW-81481)
methods of, at uranium mills, 17: 21384
methods of, evaluation of, 18: 9744
methods of, for small amounts and low activities, 17: 10223
methods of gases, liquids, and solids, 19: 1987
methods of, review, 17: 21800
methods of safe, from industrial uranium ore processing plants, 19: 43627
methods of safe, research summary on, 19: 13671(R) (WASH-1052)
methods of survey, 16: 17332(R) (EURAEC-25)
methods of, control of radioisotope release to water in, 19: 2536
methods of, following processing of irradiated fuel elements, 19: 46435
methods of, for gaseous, liquid, and solid wastes from uranium mines and mills, 20: 30948
methods of, for intermediate and high-level wastes, review of development of, 20: 47087
methods of, for radioactive gases from nuclear reactors, 20: 30949
methods of, injection in shale wells, hydraulic fracturing, 20: 35175
methods of, possibility of total containment in, 18: 26979
methods of, review of research and development activities on, 19: 48083
methods of, review of safety precautions in, 20: 16577
methods of, review of, 20: 16582
methods of, technical progress review of, 20: 38538
methods, review, 17: 15528
methods survey, 16: 16026(T) (CEA-tr-A-1106)
methods, technical progress review, 16: 28448
methods used at Hanford plant, (E), 19: 42196
methods used by AEC installations, 19: 31621
methods using tanks and retention basins for radioactive liquids from 300 Area at Hanford, 16: 26637 (HW-64292)
monitoring at Brookhaven, 1963, 19: 46640 (BNL-915)
monitoring at ORNL, 19: 32469(R) (ORNL-3820)
monitoring for wastes from beryllium production plants, 20: 43629
monitoring in Clinch and Mohawk Rivers, 19: 46646(R) (PHS-999-RH-13)
monitoring of ground water for radioactivity, 17: 8457
monitoring of, in Clinch River, 17: 2810 (ORNL-3370)
monitoring of radioactive, at Savannah River Plant, January to June 1966, 20: 43577(R) (DPST-66-30-2)
monitoring sea water after, procedures for, 16: 9726
nuclear safety research and development program, 18: 32962 (A/CONF.28/P/282)
nuclear underground explosions in, 20: 43463 (UCRL-14756)
nuclear-explosion produced rubble chimneys for, 20: 35176
Oak Ridge National Lab., effects on radioactivity in Clinch River, 20: 22514 (ORNL-P-2021)
ocean contamination by, review on, 20: 23312
of aqueous radioactive waste from civil nuclear power stations in Great Britian, site evaluation for, 20: 47090
of area 300 effluent in Columbia River, dispersion, 17: 26928 (HW-73672)
of Hanford NPR decontamination wastes, 17: 35242 (HW-71929)
of Hanford NPR reactor decontamination wastes, 16: 30154 (HW-73482)
of high-activity liquids from nuclear power plants, 17: 13873
of high-level wastes, 17: 33398

of highly-radioactive wastes, 17: 10227
of highly radioactive solutions, 17: 33401
of low- and intermediate-level radioactive wastes, 18: 21694
of low- and medium-level liquid wastes at Savannah River Plant, 20: 1548 (DPSPU-65-30-30)
of low-level wastes produced by radioisotope users, code of practice on, 19: 27840
of radioactive liquid wastes from industrial and medical uses, 19: 3799
of radioactive materials, review, 18: 18106
of radioactive wastes, effects on the environment, 17: 33544
of solid wastes, 17: 10230
of solutions into ground, 17: 10220(T, R) (EURAEC-367)
of solutions into sand, 17: 10221(T, R) (EURAEC-443)
of solutions into ground, 18: 24979(T,R) (EURAEC-202)
of solutions into ground, 18: 24980(T,R) (EURAEC-300)
of solutions into ground, 19: 10659(R) (EURAEC-703)
of unenriched uranium chips by burning, 16: 7772 (TID-14647)
on nuclear-powered ship Walter F. Perry, system for, 19: 12825
open pit, vadose flow in layered and nonlayered materials, 17: 1656
operation of phosphate glass and rotary calcination processes for, 18: 3671(R) (BNL-799(p.26-54))
operational management of KAPL, 16: 31348 (TID-6767)
operations at BNL, July 1962 to July 1963, 18: 7988(R) (BNL-806 (p.125-47))
operations, summary, 17: 26932(R) (ORNL-TM-516)
operations, summary, 17: 30582(R) (IDO-14611)
packaging in hot cells, 19: 40270 (JUL-249-RW)
packaging of long-lived fission products, engineering of demonstration facilities for, 18: 21691 (HW-77163)
permissible levels for, 20: 26559
piping system for, at Argonne National Lab., 17: 19737
plant design for, at Saxon, 17: 2644
pond storage at National Reactor Test Station, 17: 1655
possibilities at Ispra, Italy, 16: 25074 (TID-7628(p.569-82))
practices in Great Britain, 16: 25075 (TID-7628(p.583-9))
practices used in disposal of radioisotopes in hospitals in Russia, 20: 42796
principles governing radioactive contaminants, 17: 27613
principles of, legal and nuclear, in Germany, 20: 42686
problems for radiochemical processing plants, 16: 15024 (ORNL-TM-164)
problems in liquid, at Institute of Atomic Energy, Brazil, 20: 16134 (IEA-102)
problems in ocean, effects on human and marine life, 16: 17921
problems in sludge, at Harwell, 17: 19715
problems of field, 18: 6539
problems of ocean, 16: 11347
problems of sewerage or water basin, 18: 7983
problems, review, 16: 34145
procedures for, review, 17: 15518 (AHSB(RP)-R-29)
procedures for various activity levels, 16: 9311
procedures for, at radiochemical laboratories, 20: 31469
processing of, review of, 17: 34063
public health aspects, 17: 8440
public health hazards of pond storage of calcined highly active wastes, 20: 40482
radiation effects on vitreous materials used in, 19: 30242
radiation hazards to environmental health from, 19: 15812
radiation hazards of marine, 19: 24809
radiation hazards in, environmental, 19: 38289
radiation hazards from, in sewer systems and purification plants, 20: 36533 (BMWF-FBK-66-04)
radiation hygiene in, review, 20: 43602
radiation monitoring at Center for Nuclear Energy, Mol, 19: 46631 (A/AC.82/G/L.986)
radiation protection practices in German, 16: 5618
radiation protection standards for, 17: 14573
radiation protection standards for, 18: 6712 (DPSPU-63-30-42)
radiation protection in, 20: 13017
radioactive and industrial, literature review, 1961, 18: 9743
radioactive contamination of marine environments by, 19: 36702 (EUR-2407.f)
radioactive, ocean and river contamination by, 18: 14145
radioactive, ocean contamination by, 20: 29405 (NP-14694)
radioactivity control in, methods for, 18: 12393
radioactivity from, in Tennessee River System, 20: 45216 (ORNL-3721)
radioactivity in sewage disposal systems from, 18: 18090
radioactivity monitoring in, 18: 40961 (UJV-1104/64)
radioactivity, methods for dust and gaseous, 19: 31685
radiobiological monitoring, 17: 33566
radiological monitoring of Clinch and Tennessee Rivers below Oak Ridge, 16: 29272
reactor coolant, radioisotope behavior in sea water after, 19: 33668
recommendations for, 17: 26930 (ISS-63/23)
regulations in Germany, 17: 7654
removal of radioactive gases and aerosols from the atmosphere, 16: 18709(T) (JPRS-12637)
requirements and problems related to high-activity at Eurochemic Reprocessing Plant, 20: 45232
research programs at Norwegian Institute on ecological aspects, 16: 14233(R) (KR-16)
research programs, summary for AEC in 1961, 16: 12827
research programs of the International Atomic Energy Agency, 16: 25076 (TID-7628(p.590-601))
research programs on, 16: 32882(R) (ORNL-3314)
research programs on, in Japan, 17: 17624(R) (JAERI-5006)
research programs on, AEC, 17: 19747 (TID-18468(p.353-63))
research programs on, in Federal Republic of Germany, 19: 48112
research progress on, 18: 23139(R) (NP-13876)
review, 16: 287
review, 17: 17449
review, 17: 28792
review, 19: 35857
review of methods used at ORNL, 16: 28636 (ORNL-TM-282)
review of methods, 17: 21379
review of methods for gases, liquids, and solids, 18: 45149 (HW-SA-3575)
safety aspects, 16: 15041
safety aspects of, in USSR, 17: 4752
safety aspects of, review, 18: 45158
safety in tunnel or cavern, 20: 42686
safety in, review of 1964 Geneva papers on, 19: 24779
safety in, to atmosphere and water, 19: 40277
safety of tank storage of high-level liquid wastes, environmental aspects of, 18: 6537(R) (ORNL-TM-603)
safety precautions, 16: 8443
safety precautions in, 19: 13678
salt deposit, problems in, 19: 40272
salt mine, concept and field test of, 19: 3802
salt mine, concept and field test of high-level, 20: 8483
salt mine, demonstration of, 20: 10439(R) (ORNL-3830, pp 285-98)
salt mine, field demonstration of, 20: 18020(R) (ORNL-3900, pp 2-81)
salt mine, field experiment for demonstration of high-level, 19: 21751 (ORNL-P-1064)
salt mine, field experiment for demonstration of high-level, 20: 18169
salt mine, influence of stress, temperature, and radiation on flow and stability of, 20: 45217 (ORNL-P-2126)
salt mine, instrumentation for, 19: 42689(R) (ORNL-3782, pp 84-90)
salt-formation, development of methods for, 19: 17781(R) (ORNL-3750)
sea, biological consequences of, 20: 26549(R) (NP-15915)
sea, of radioactive residual water from The Hague Center, 20: 45228
seafood contamination by, 19: 24759
sealing in refractory vessels, method for, 20: 5209(P)
self-formation, method for, 19: 23996(R) (ORNL-3650(p.1-110))
settling pond, effects of algal grout on effectiveness of, 20: 24815
site evaluation methods for liquid, 17: 21373 (IDO-12027)
soil adsorption of, studies in France on, 17: 2536
soil contamination by, 19: 24760
solid conditioning and storage, techniques for, 17: 26937
solid storage, cement processing for, 18: 6537(R) (ORNL-TM-603)
solid storage, economic evaluation of interim, 17: 42416 (ORNL-3355)
solid storage in solidified glass, monitoring of activity from, 16: 25039 (TID-7628(p.9-12))
solid storage, welding procedure for, 17: 15522 (HW-73933)
solidification of sludge by inglobation in concrete, 17: 31792
solidification of waste solutions, 17: 33406
solidification, development of calcining and glass-forming systems for, 19: 31617(R) (ORNL-TM-1081)
solidification, heat generation by calcine from, 20: 28853(R) (IDO-14661, pp 45-82)
solidification, leachability of calcine and glass from, 20: 28853(R) (IDO-14661, pp 45-82)
solidification, processes for high-level materials, 20: 18020(R) (ORNL-3900, pp 2-81)
solvent extraction for recovery and removal of fission products from Purex 1WW, 17: 28581(R) (HW-77299)
sorption and release of cesium on clinoptilolite, 17: 15523 (HW-74927)
sorption by alumino-silicates for, 17: 19712 (TID-7644(p.201-10))
sorption on ion exchangers, 17: 28581(R) (HW-77299)
sorptive properties of soil in, 16: 8(T) (AEC-tr-4142(p.33-42))
sorptive properties of peat for fission products, (E), 19: 33680
standards in U.S. and U.S.S.R., comparison of, 20: 12521
storage at Arco waste calcining facility, new facilities for, 19: 24610(R) (IDO-14638)
storage at Oxford University, design of central store for, 18: 13353
storage building for, Federal Institute of Reactor Research, Würenlingen, Switzerland, 18: 13344 (EIR-56)
storage, concrete tanks for, 17: 30071

storage containers for, remote welding closure of stainless steel, 18: 14424 (HW-79522)
storage in buried tanks, heat dissipation from, 18: 35234(R) (HW-81862)
storage in buried tanks, heat dissipation from, 18: 45148(R) (HW-83320)
storage in concrete vaults, granite, and salt formations, comparison of costs of, 17: 42417 (ORNL-TM-664)
storage in mined-out salt mines, 16: 25067 (TID-7628(p.469-76))
storage in mined-out salt mines, 16: 25068 (TID-7628(p.477-90))
storage in reservoirs, 16: 14371
storage in salt caverns, dimensioning for maximum credible accidents in, (T), 20: 16722 (BMwF-FBK-65-03)
storage in salt formations in Europe, 18: 38687 (A/CONF.28/P/783)
storage in salt formations, 19: 31617(R) (ORNL-TM-1081)
storage in salt formations, equipment for, 20: 18165 (ORNL-P-1987)
storage in salt mines, heat generation by, 20: 3605
storage in salt mines, 20: 8479(R) (ORNL-3849, pp 1-42)
storage in salt mines, design and operation of Project Salt Vault for, 20: 20347 (ORNL-P-2058)
storage in salt mines, demonstration of, 20: 45571(R) (ORNL-3945, pp 248-55)
storage in stainless steel leak-tight containers, design of packaging facilities for, 20: 20348 (RL-SA-60)
storage in tanks, calculation of maximum temperature for, 19: 25777(R) (HW-84603(p.37-49))
storage in tanks, cost of form for, 19: 31617(R) (ORNL-TM-1081)
storage in tanks, heat generation rate for, 20: 8477(R) (BNWL-139)
storage in tanks, calculation of maximum temperature for, 20: 8477(R) (BNWL-139)
storage in tanks, effects of leaks on soil and tank temperatures in, 20: 35172 (BNWL-181)
storage in tanks, economics and safety of, 20: 47083(R) (ORNL-3945, pp 79-106)
storage in underground tanks, sampling of sludge by rotary core drilling, 18: 15654 (HW-74040)
storage in West Germany, study of possible underground, 19: 31619(T) (AEC-tr-6549)
storage of high-level solids in salt mine, demonstration of, 18: 7982 (ORNL-TM-734)
storage of high-level wastes, review, 18: 43098
storage of high-level solids in salt mine, demonstration experiment on, 19: 42195 (ORNL-P-1479)
storage of high-level solids in salt mine, demonstration of, 19: 45689 (ORNL-P-1568)
storage of irradiated uranium, relation of fission product management to economics of, 20: 22517
storage of liquid wastes in soils, seepage rates for, 17: 36993(R) (TID-19164)
storage of liquid wastes in soils, seepage rates for, 17: 36994(R) (TID-19186)
storage of liquid wastes in soils, seepage rates for, 17: 36995(R) (TID-19187)
storage of liquid wastes in soils, seepage rates for, 17: 36996(R) (TID-19188)
storage of liquid wastes in soils, seepage rates for, 17: 36997(R) (TID-19189)
storage of plugs and experimental devices from reactors, 16: 17331 (CEA-2084)
storage of Purex and Thorex wastes in salt formations, evaluation of, 17: 2654
storage of, concrete block design for, 20: 27210(R) (UCRL-14680)
storage practices, review of current, 16: 30159 (HW-SA-2478)
storage principles and techniques for fissionable materials, 20: 35698
storage tank development, 17: 28581(R) (HW-77299)
storage, calculation of temperature rises in high-level, 18: 33167 (LADC-5940)
storage, design of concrete cells for, 19: 10663
storage, design of facility for Hanford, 20: 16135 (RL-SA-62)
storage, economic aspects of, 18: 19448(R) (ORNL-TM-757)
storage, economy and safety in long-term, 20: 8478(R) (KFK-357)
storage, engineering drawings, tanks for, 19: 6881
storage, environs monitoring program at Czechoslovakian facility for, 20: 23408
storage, evaluation of salt cavern and sea, 20: 8478(R) (KFK-357)
storage, pressure in calcined waste pots for, 20: 12517(R) (BNWL-170)
storage, suitability of German salt mine cavities for, 19: 19429(T) (AEC-tr-6544)
subsurface, geology of Williston Basin, Montana and North and South Dakota for, 16: 27419 (TEI-809)
summary at ORNL, May–Oct. 1963, 18: 19448(R) (ORNL-TM-757)
surface water, migration and retention in lithosphere from, 18: 17349
survey for clinical and biological applications, 16: 20904
survey, of Bogue Sound area, North Carolina, 17: 31817(R) (TID-19122)
survey of management of high-level wastes by AEC contractors, 18: 7980 (HW-SA-3279)
survey of methods, 16: 11342(R) (EURAEC-83)
survey of methods, 16: 26636(R) (EURAEC-84)
survey of methods, 17: 33399
survey of U. S. operational experience in waste management, 18: 33162 (A/CONF.28/P/869)
survey of U. S. practices for liquid wastes, 1963, 18: 11502
system development for large closed-cycle pressurized-water reactors, 19: 48001(R) (WCAP-3743)
system for Shippingport Pressurized Water Reactor, performance, 16: 7332
system for Sodium Reactor Experiment, operation, 16: 7334
systems for, at Selni power plant, 18: 7950
systems for, materials for nuclear power plant, 20: 30815
tank storage for separation plant wastes, limitations in, 16: 2798 (HW-59919)
tank storage methods of, thermal effects of leaks, 18: 26976 (HW-80848)
tank storage methods of, 20: 26551
tank storage of acid and alkaline solutions, economics of, 20: 14208 (ORNL-P-1926)
tank storage, economic and safety evaluations of, 20: 10438(R) (ORNL-3830, pp 96-139)
tank-storage of purex solutions, 19: 17388(R) (HW-84467)
tank-storage, engineering aspects of, 19: 38285(R) (BNWL-76)
tank-storage, liquid-level telemetering systems for, 18: 27755(R) (ORNL-3578(p.78-95))
through boreholes to sub-surface areas, 16: 25060 (TID-7628(p.374-9))
to concrete vaults, granite formations, and salt mines, economics of, 19: 5558(R) (ORNL-3627(p.73-114))
to deep wells and salt formations, development of techniques for, 17: 7653(R) (ORNL-TM-396)
to dry wells, study of Jackass Flats area for, 17: 4370 (TEI-829)
to fresh-water streams, evaluation of effects of, at Hanford, 17: 2641 (HW-SA-2748)
to ground and water tables, economics, and hazards of liquid, 20: 28852 (IDO-12052)
to ground, facilities at Chalk River plant, 16: 25038 (TID-7628(p.3-9))
to ground in Canada, 19: 12857
to ground, migration of cations in, 17: 29869(T) (EURAEC-417)
to ground, purification process based on mineral exchanges in, 17: 29872
to ground, review of methods for, 17: 8268
to ground, suitability of Powder River Basin (Wyo.) for, 17: 3155 (TEI-823)
to ground-water aquifers, effects of density and viscosity of liquid contaminants on dispersion, 16: 3979 (HW-69627)
to ground water aquifers, 17: 2785(R) (ORNL-3347(p.1-46))
to ground, measurement of soil parameters for partially saturated flow in, 19: 1945(R) (HW-81746(p.4.39-42))
to ground, migration and deposition of gross gamma emitters in, 19: 1944(R) (HW-81746(p.4.32-6))
to rivers and lakes at North American atomic energy sites, experience, 18: 33160 (A/CONF.28/P/287)
to sea, from nuclear-powered ships, 16: 8421
treatment of Purex stored waste sludge, 17: 28581(R) (HW-77299)
tritium movement from Chalk River liquid disposal area, 17: 29866 (CRER-1146)
underground tanks, model study of flow in, 17: 17615(R) (HW-76262)
uses of radioisotopes, review, 17: 12521
vessel for radioactive liquid, design of, 20: 10445
waste gas handling system for Army Reactor (PL-3), 16: 16018 (APAE-Memo-313)
waste movement through ground water and soil, 16: 28634 (CRER-1089)
water dilution, economic evaluation of model for, 17: 40537 (TID-7664 (p.353-89))
water dilution methods at Marcoule Center, 17: 42423
zinc-65 in Pacific Ocean plankton from Hanford Reactor, 20: 43545

WASTE PROCESSING

see also Waste Disposal
see also Waste Recovery
abstracts on management research, 19: 42194 (NP-15267)
activated sludge methods, 20: 29353
activated sludge, evaluation, 19: 24196
activated sludge, evaluation, 19: 24197
active mud, efficiency of, 18: 36858
activity release in, review of consequences, 16: 3303
aerobic, pilot plant study of, 18: 43099
aluminum nitrate recovery from Redox acid waste, computer study of process for, 18: 45147 (HW-82771(Pt.1))
at Argonne and Los Alamos, comparison of operational practices in low- and intermediate-level, 20: 3603 (LA-DC-7249)
at British nuclear power reactors, 16: 23349
at Chalk River, procedures and experience in, 18: 36855 (CRIO-1194)
at Enrico Fermi Nuclear Research Center, Milan, 18: 29140(T)

(ORNL-tr-143)
at Eurochemic reprocessing plant, 19: 24192
at Eurochemic, proposals for, 18: 40957 (NP-8519)
at Hanford, management aspects of high-level, 16: 32617 (HW-SA-2515)
at Hanford, review of, 19: 27832(R) (HW-83609)
at Ispra, design and operation of plant for, 17: 21377
at Kjeller, operation of plant for, 19: 29808(R) (KR-94)
at Lawrence Radiation Laboratory, 20: 1552 (UCRL-14320)
at Marcoule, procedure and results in, 17: 40419
at nuclear power plants, 19: 31622
at Shippingport Pressurized Water Reactor, system performance, 17: 4372 (WAPD-T-1280)
at Windscale fuel reprocessing plants, 18: 38681 (A/CONF.28/P/187)
baling and compacting in, process units for, 20: 26569
bibliography of UKAEA publications available to public, 16: 17339 (NP-11504)
bibliography on, 16: 30157 (TID-3555(Suppl.1))
bibliography on, 16: 31346 (ORNL-2971(Vol.8))
bibliography on, 18: 9743
bibliography on, 18: 36857 (TID-3311(Suppl.1))
bibliography on decontamination of radioactive water, 17: 12043 (NP-12482)
book: *Low-Level Radioactive Wastes: Their Handling, Treatment, and Disposal*, 18: 38700
book: *Management of Radioactive Wastes*, 19: 31623
book: *Processing and Disposal of Radioactive Waste from Laboratories*, 19: 27839
book: *Radioactive Waste Materials*, 17: 13874
book: *The Management of Radioactive Wastes Produced by Radioisotope Users*, 20: 40480 (STI-PUB-119)
buildings and facilities for, in India, 20: 36539(R) (NP-16171)
burning spent solvent from radiochemical separations processes, 19: 21747 (DP-942)
by adsorption and ion exchange, 17: 8268
by anion exchange, for plutonium in Recuplex Process, 17: 8236 (HW-59983)
by calcination and radiant-heat spray solidification at Hanford, design of equipment for, 17: 21380
by calcination and formation of phosphate glass, 17: 19723 (BNL-759 (p.14-38))
by calcination and ion exchange, methods for, 19: 5562
by calcination, development, 16: 20534(R) (IDO-14574)
by calcination, development of processes for high-level materials, 17: 7653(R) (ORNL-TM-396)
by calcination, development, 17: 10741(R) (ORNL-TM-313)
by calcination, development of radiant-heat spray process for, 17: 19700 (HW-SA-2722)
by calcination in fluidized beds, 16: 20535(R) (IDO-14583)
by calcination, radiant-heat spray process for, 17: 28585
by calcination, review of processes for, 17: 40418
by coagulation and ion exchange, 16: 21863
by coagulation, efficiency for Hanford Production Reactor coolant effluent decontamination, 17: 12041 (HW-SA-2192)
by denitration using sugar, 17: 35243 (HW-77080)
by electrodialysis, 16: 28637(T) (AEC-tr-5079)
by evaporation, apparatus development for, 17: 24736
by fixation in glass, pilot plant design and operation for, 18: 43097
by fixation of fission products on clinoptilolite columns, 16: 23346 (CRCE-1080)
by fixation of fission products in glass, 17: 10232
by flocculation of solutions, 16: 21862
by flotation, decontamination factors in, 17: 35240 (EUR-262.e)
by incineration, development of apparatus for, 16: 20035 (GEAP-3542)
by incineration, design and performance of incinerator and gas cleaning equipment for, 17: 29867 (NDL-TM-8)
by incineration, leaching, and solidification, 16: 26636(R) (EURAEC-84)
by ion exchange, 16: 21865
by ion exchange, 17: 19705 (TID-7644(p.29-45))
by ion exchange for cerium removal, 17: 33396 (HW-SA-2920)
by ion exchange of alkaline intermediate-level solutions, 17: 31790 (ORO-604)
by mineral reactions, 17: 19708 (TID-7644(p.115-50))
by mixing with gamma-absorbing materials, 16: 2813(P)
by precipitation, procedure at ANDUJAR uranium mill, 17: 13871 (JEN-108-DMa/1-15)
by radioisotope sorption on coal columns, 18: 38697
by solidification in subterranean formations, 17: 29878(P)
by solvent extraction, 16: 26639(R) (HW-73412)
by solvent extraction, 17: 31788 (CONF-49-1)
by solvent extraction for recovery of cesium, strontium, and rare earths, 17: 35244 (HW-SA-2982)
by sorption on ion exchange materials, 16: 26639(R) (HW-73412)
by vitrification of concentrated fission product solutions, 16: 26634 (CEA-2130)
calcination, 16: 26639(R) (HW-73412)
calcination, 16: 26640 (ORNL-TM-259)
calcination, 16: 27744 (NYO-9701)
calcination, 16: 27124(R) (ORNL-TM-257)
calcination, 16: 30155(R) (HW-74375)
calcination, 17: 33403
calcination, 18: 12256(R) (IDO-14621)
calcination and evaporation, off-gas scrubber development, 16: 29247 (TID-7627(p.557-80))
calcination and evaporation methods of, review, 18: 43098
calcination and evaporation of Purex FTW-65 wastes, effects of sodium sulfate additions on, 18: 41303(R) (ORNL-TM-642)
calcination and fixation by mineral reactions, developments in, 16: 2799(R) (HW-70517)
calcination and fixation, development of processes for, 16: 32885(R) (ORNL-3314(p.58-95))
calcination and fixation in solids, conference on, Washington, D. C., February 1 and 2, 1962, 17: 12044 (TID-7646)
calcination and fixation of Purex FTW-65, heating tests of susceptor-pot system for, 19: 18052(R) (ORNL-TM-1027)
calcination and fixation, methods development for, 19: 22405(R) (HW-83298(p.4.1-25))
calcination and sorption processes, 16: 5100(R) (HW-71374)
calcination and solidification methods development, 18: 17332(R) (HW-80526)
calcination and solidification of high-level Purex and Redox wastes, development of equipment and techniques for, 18: 24975(R) (HW-81829)
calcination and solidification of high-level Purex and Redox wastes, development of equipment and techniques for, 18: 35234(R) (HW-81862)
calcination and solidification of high-level Purex and Redox products, 18: 45148(R) (HW-83320)
calcination and solidification in glass, methods for, 19: 17388(R) (HW-84467)
calcination and solidification studies, 19: 25775(R) (HW-84603(p.8-31))
calcination and solidification studies for, 20: 8477(R) (BNWL-139)
calcination and solidification of Purex solutions, pilot plant studies on, 20: 24809(R) (BNWL-213)
calcination and solidification of Purex solutions, pilot plant studies on, 20: 40476(R) (BNWL-267)
calcination at Arco, off-gas cyclone performance in, 18: 43090 (IDO-14633)
calcination by fluidized-bed techniques, engineering drawings of filter blowback system for, 17: 35249
calcination, calculation of particle surface areas and volumes for fluidized-bed, 18: 3389 (IDO-14617)
calcination, cost factors for Purex and Thorex wastes, 17: 10218 (IDO-14595)
calcination, design of pilot plant for, 16: 30497(R) (ORNL-TM-157)
calcination, design of pilot plant for demonstration of, 17: 17616 (IDO-14596)
calcination, development of process for, 16: 1286(P)
calcination, development of fluidized bed techniques, 16: 1855(R) (IDO-14560)
calcination, developments in, 16: 7615(R) (ORNL-TM-35)
calcination, development of techniques in, 16: 8666(R) (IDO-14567)
calcination, developments in, 16: 1854(R) (IDO-14553)
calcination, development of fluidized-bed calciner for, 17: 1160 (IDO-14586)
calcination, development of fluidized bed equipment and techniques for aluminum nitrate waste, 17: 2652
calcination, development of fluidized-bed equipment for, 17: 4368 (IDO-16794)
calcination, development of pot process of, 17: 21374 (ORNL-TM-549)
calcination, development of gravity-feed operation for, 17: 21777(R) (ORNL-TM-441)
calcination, development of equipment and methods for pot, 17: 38579 (ORNL-3277)
calcination, development of pot and spray methods of, 18: 8445(R) (HW-78388(p.4.1-15))
calcination, effects of magnesium and sugar on ruthenium volatility in, 17: 17615(R) (HW-76262)
calcination, evaporation, and incineration, air cleaning in, 16: 29211(R) (NYO-4817)
calcination, extraction, in-tank solidification, and sorption studies, 16: 12793(R) (HW-72324)
calcination facility at Arco, development and operation of fluidized-bed, 18: 45152 (TID-7699(p.1-23))
calcination facility operation at Arco Plant, April-June 1964, 19: 20042(R) (IDO-14646)
calcination facility at Arco, operation, 19: 24610(R) (IDO-14638)
calcination facility, analytical services for, 19: 32059(R) (IDO-14655)

calcination facility operation for, Dec. 1963 to 1966, 20: 47086
calcination, filling rates for pot, 16: 14617(R) (ORNL-TM-136)
calcination-fixation test of Purex FTW-65 waste, 17: 35257(R) (ORNL-TM-628)
calcination, fluid-bed studies using high-level materials, 17: 19699 (HW-66384RD)
calcination, hot-cell calciner equipment for radiant-heat spray, 16: 31344 (HW-SA-2513)
calcination, hot-cell studies on Purex solutions, 17: 19701 (HW-SA-2877)
calcination in, development and performance of fluidized beds for, 17: 12045 (TID-7646(p.3-19))
calcination in fluidized beds, development of potassium–sodium alloy heating system for, 18: 39453
calcination in molten sulfur, 17: 19697 (DP-713)
calcination in molten sulfur, 17: 33402
calcination, melt formation in, 17: 4366 (HW-69780)
calcination methods for, development of, 17: 21594(R) (ORNL-TM-355)
calcination methods of, economic, engineering, and safety evaluations of, 17: 39302(R) (ORNL-3492(p.70-6))
calcination methods of, use of calcium nitrate to reduce sulfate volatility in, 17: 40931(R) (ORNL-TM-613)
calcination methods of, technical progress review on, 18: 17350
calcination methods of, safety analysis of ICPP facility for, 18: 26977 (IDO-14620)
calcination methods of, development and evaluation of pot, 18: 26978 (ORNL-TM-857)
calcination methods of, design of stainless steel pot for, 18: 29139 (ORNL-TM-839)
calcination methods of, review of pot and spray, 19: 43625
calcination methods of, fluid-bed, 20: 26551
calcination methods of, fluid-bed, 20: 38538
calcination of aluminum-type and zirconium-bearing, 16: 16023(R) (NYO-9653)
calcination of aluminum nitrate wastes, factors affecting alumina intra-particle porosity in, 17: 1161 (IDO-14587)
calcination of aluminum nitrate wastes in fluidized bed, 18: 17333 (IDO-14618)
calcination of aluminum nitrate wastes in fluidized bed, process studies on, 18: 36856 (IDO-14627)
calcination of aluminum nitrate wastes in Arco facility, fluidized-bed, 19: 33675 (IDO-14608)
calcination of aqueous wastes in molten sulfur, 17: 12046 (TID-7646(p.20-36))
calcination of aqueous wastes, development of pot method for, 17: 12049 (TID-7646(p.52-68))
calcination of aqueous wastes, development of radiant spray method for, 17: 12051 (TID-7646(p.83-93))
calcination of Darex, Purex, and TBP-25 wastes, calciner-evaporator component and control material balances for, 16: 33070(R) (ORNL-TM-297)
calcination of Darex, Purex, and TBP-25 wastes, engineering studies of pot, 17: 40417 (ORNL-TM-619)
calcination of, equipment feasibility studies for, 17: 17619(R) (ORNL-TM-482)
calcination of full-level Purex and Redox waste, pilot plant tests of pot and spray, 19: 25772 (HW-83896)
calcination of high-level Purex wastes, 16: 2809(R) (ORNL-TM-49)
calcination of high-level Purex wastes, batch, 17: 26929 (HW-74043)
calcination of high-level liquid wastes, uses of hot cells in, 18: 1316
calcination of high-level wastes using rotary ball kiln, studies of continuous, 18: 33163 (BNL-832)
calcination of high-level aluminum nitrate wastes, 18: 31658(R) (IDO-14635)
calcination of high-activity-level liquids, 18: 43091(R) (ORNL-TM-830)
calcination of high-level wastes in pots, 19: 23996(R) (ORNL-3650 (p.1-110))
calcination of Purex and TBP-25 wastes, 16: 14690(R) (ORNL-TM-121)
calcination of Purex and Thorex wastes, economic evaluation of pot, 17: 2655
calcination of Purex-65 wastes, 17: 26931(R) (ORNL-TM-453)
calcination of Purex wastes, development of pot and spray methods for, 17: 38578(R) (HW-78188)
calcination of Purex wastes, development of pot and spray methods for, 18: 4886(R) (HW-79140)
calcination of Purex wastes, development of phosphate glass process for, 18: 4886(R) (HW-79140)
calcination of Purex FTW-65 wastes, 18: 6537(R) (ORNL-TM-603)
calcination of Purex FTW-65 waste, evaporator-calciner tests for, 18: 7981 (ORNL-TM-715)
calcination of Purex FTW-65 wastes in glass, 18: 35644(R) (ORNL-TM-836)
calcination of Purex FTW-65 wastes, filling rates for pot, 19: 11264(R) (ORNL-TM-937)
calcination of simulated Purex-65 waste, 17: 33768(R) (ORNL-TM-541)
calcination of TBP-25, performance of evaporator-calciner close-coupled system, 16: 11503(R) (ORNL-TM-34)
calcination of wastes, development of pot process for, 17: 12050 (TID-7646(p.69-82))
calcination of zirconium fluoride wastes, 19: 20042(R) (IDO-14646)
calcination of zirconium fluoride wastes, pilot plant study of fluid-bed, 19: 43623 (IDO-14653)
calcination on fluidized beds, analog calculation of elutriated fines in, 18: 19447 (IDO-14626)
calcination, operation of facility for 1050 hr, 17: 1564(R) (IDO-14593)
calcination, operation of gravity feed in pot systems, 17: 20100(R) (ORNL-TM-412)
calcination, operation of Demonstrational Waste Calcining Facility for, 18: 5415(R) (IDO-14599)
calcination, optimum fill volumes in pot, 16: 2810 (ORNL-TM-59)
calcination, pilot plant design and operation for hot pot, 17: 2651
calcination, pilot plant studies with simulated ICPP wastes, 17: 19698 (HW-65838 RD)
calcination processes for, 17: 8268
calcination process developments, summary, 17: 30582(R) (IDO-14611)
calcination process operation for liquids, 20: 35173 (IDO-14662)
calcination, programing of calciner wall temperature in pot, 17: 38580 (ORNL-TM-600)
calcination run on Purex FTW-65 waste, 17: 40684(R) (ORNL-TM-608)
calcination, shielding calculations for pot, 17: 33397 (ORNL-TM-595)
calcination studies in small-diameter columns, 16: 2923(R) (ANL-6379)
calcination studies of, spray and pot, 17: 37003(R) (HW-78118)
calcination, study, 16: 14817(R) (ORNL-TM-112)
calcination, techniques for, 18: 6538
calcination test run on high-level Purex waste, 17: 40930(R) (ORNL-TM-581)
calcination test run, melting of hole in pot during, 19: 2205(R) (ORNL-TM-936)
calcination, testing of mercury trap in, 17: 10219(R) (ORNL-TM-343)
calcination using close-coupled evaporator and calciner system, 16: 1858(R) (ORNL-TM-32)
calcination using rotary ball kiln, 17: 2653
calcination, volume reduction in, 16: 28639
calcination, analog computer simulation of low-temperature-evaporation method of pot, 18: 19444 (HW-75223)
calcination, biological availability of radionuclides after, 19: 32467 (IDO-12042)
calcination, comparison of four processes for, 18: 29137 (IDO-14622)
calcination, design and development of facility for, 18: 17930(R) (IDO-14625)
calcination, design of furnace for, 19: 4256(R) (ORNL-TM-886)
calcination, development of pot and spray methods of, 18: 27278(R) (HW-79280(p.4.1-28))
calcination, development of air distributor caps for fluidized-bed, 18: 29138 (IDO-14629)
calcination, development of control system and equipment for, 18: 40963
calcination, development of pot and spray methods of, 19: 12859
calcination, effluent decontamination during, 19: 25781(P)
calcination, engineering drawings of pot for liquid-waste, 19: 5565
calcination, facility and methods for, 20: 28853(R) (IDO-14661, pp 45-82)
calcination, fission product volatilization from alumina product of, 19: 24610(R) (IDO-14638)
calcination, flowsheet for Purex 1WW-phosphoric acid, 19: 38285(R) (BNWL-76)
calcination, level detection in canisters for product of, 19: 25771 (HW-77979)
calcination, operation of facility for, 18: 17929(R) (IDO-14616)
calcination, pilot plant studies on pot and spray, 20: 20345 (BNWL-SA-569)
calcination, process tests of pneumatic atomizing nozzles in fluidized-bed, 18: 45150 (IDO-14631)
calcination, product analysis in, 19: 7274(R) (IDO-14636)
calcination, public health aspects, 20: 40482
calcination, removal of particulates from Waste Calcining Facility off-gas, 18: 15658 (TID-7677(p.280-96))
calcination, rising level glass run on Purex waste, 19: 28444(R) (ORNL-TM-1094)
calcination, ruthenium-106 release in, 19: 44773 (BNL-914, pp 57-64)
calcination, segregation of fission products in, 19: 13524(R) (HW-81984(p.4.1-20))
calcine powder melter development for spray kilns, 18: 27278(R) (HW-79280(p.4.1-28))
calcining facility for, removal of particles from off-gas of, 18: 39412 (IDO-14607)
ceramics preparation from irradiated fuel swarf, 20: 1554
cerium sulfate precipitation from Purex waste, 19: 5986 (HW-71589)

cesium and strontium separation by absorption on vermiculite, leaching studies for, 20: 43130
cesium recovery in Purex process, 16: 31342 (HW-70874)
cesium separation by adsorption on ammonium-12-molybdophosphate, 16: 14813 (AERE-R-3884)
cesium separation by solvent extraction using dipicrylamine, 17: 28580 (HW-76222)
cesium separation by solvent extraction using 4-sec-butyl-2-methylbenzylphenol, pilot plant studies, 18: 19446 (HW-80686)
cesium separation from Hanford Alkaline Supernate by solvent extraction using 4-*sec*-butyl-2-methylbenzylphenol, 19: 2432 (HW-80876)
cesium separation from Purex 1WW by phosphotungstate precipitation, 19: 8672 (HW-81092)
cesium separation from alkaline supernatant waste by ion exchange, breakthrough study of, 19: 10661 (HW-83461)
cesium-137 separation, 17: 38581
chemical methods for, 18: 1314
classification, production, and treatment of sludge at Harwell, 17: 19715
coagulation and precipitation, effect of surface active agents on, 16: 2795 (AAEC/E-74)
coagulation and precipitation, 16: 2796 (AAEC/E-75)
coagulation of radioisotopes from reactor effluent, 17: 19717
coagulation precipitation methods of, effects of synthetic detergent on, 19: 48084
coating sludges with bitumen, 18: 4885(CEA-2331)
combustion of high boilers from organic-moderated reactors, 16: 2684 (NAA-SR-5410)
combustion of plutonium wastes, tests of incinerator-scrubber for, 18: 3386 (HW-68788)
combustion, at Risö, Denmark, 20: 26562
concentration and storage, 17: 10228
concentration and purification methods of, design of plant for, 18: 26992
concentration methods for sludges, 17: 30072
concentration of liquids and solids, design of Berlin collecting station for, 17: 42422
concentrator for, dewatering property of, 18: 24984
conference on, 18: 21693
conference on Air Cleaning, BNL, Upton, New York, October 10 to 12, 1961, 16: 29214 (TID-7627)
conference on fixation of high-level wastes, 18: 45151 (TID-7699)
consolidation in alloys, 19: 17176(R) (ANL-6965(p.1-41))
conversion to glasses, 20: 26551
conversion to glasses, 20: 38538
conversion to solids, for highly active materials, 17: 17453
criteria for, of low and intermediate level wastes, 20: 30944
deactivation by electrodialysis, 16: 12797(T) (NP-tr-863)
decontamination of aluminum nitrate wastes by freeze-melt technique, 18: 31658(R) (IDO-14635)
decontamination of polluted air and waste water, review, 19: 8678
dehydration after mixing with sulfur and solidification of aqueous waste solutions, 18: 45159(P)
dehydration of radioactive slimes, effects of polymers on, 20: 45218(T) (KFK-tr-201)
denitration of Purex 1WW waste using sugar, 17: 38578(R) (HW-78188)
denitration of Purex 1WW waste using sugar, 18: 4886(R) (HW-79140)
denitration of Purex Process acid wastes using formaldehyde, 18: 15655 (HW-79622)
design of remote-controlled purification plant at Wurenlingen, 18: 6541
design of spray calciner, 17: 33411(P)
design of system at Wurenlingen, 18: 6540
development, 17: 1163(R) (ORNL-TM-376)
development at Eurochemic, 18: 13962
development in Czechoslovakia, 18: 38686 (A/CONF.28/P/775)
development in, at Pelindaba, South Africa, 20: 20352
development of, 16: 30495(R) (IDO-14589)
development of calciner-evaporator using Purex-type feed, 16: 4227(R) (ORNL-TM-33)
development of, for high- and low-level materials, 16: 31347(R) (ORNL-TM-252)
development of methods for low-level, 16: 2800(R) (ORNL-3189(p.1-6))
development of methods for cesium-137 removal from sodium ion-containing wastes, 18: 34006(R) (ORNL-TM-889)
development of methods for low-level, 19: 5558(R) (ORNL-3627(p.73-114))
development of methods for, (E), 19: 34286
development review, 16: 6515
development summary for Hanford laboratories, 1958–1964, 19: 27833(R) (HW-83610)
developments in, 16: 2057(R) (ORNL-3189)
developments in, 17: 31795(R) (BNL-782(p.18-43))
developments in, at ORNL, 17: 39201(R) (ORNL-3452(p.240-51))
developments in EURATOM-U. S. project for, 16: 34144(T,R) (EURAEC-275)
developments in, related cooperative projects, 16: 2805(R) (ORNL-3189 (p.77-80))
developments in, summary, 17: 31681(R) (HW-76559)
developments in United States, 17: 2650
developments in, at Eurochemic radiochemical processing plant, 18: 27618(R) (ORNL-TM-833)
developments in, effects on U. S. nuclear power industry, 18: 33161 (A/CONF.28/P/868)
developments, summary, 17: 36860(R) (ANL-6648)
economic and engineering problems, 16: 7331
economic aspects of Purex and Thorex, 17: 26933 (ORNL-TM-559)
economic, engineering, and safety evaluations of, 17: 39180(R) (ORNL-3452(p.51-96))
economics, engineering, and hazards, 16: 2804(R) (ORNL-3189(p.72-7))
economics of, at Mol, Belgium, plant, 20: 8480 (TID-22427)
economics of, by fluidized-bed fluoride volatility, 20: 24810 (ORNL-TM-1441)
effectiveness of organic cation exchange resins, 16: 11350
effects on radium-226 and strontium-90, 18: 18050
effluent treatment at Windscale, 16: 11351
electrodeionization, of intermediate-level materials, 19: 22405(R) (HW-83298(p.4.1-25))
engineering equipment for, catalog of, 16: 30515 (TID-4100(1st Rev. Index 2))
environmental effects of, at National Reactor Testing Station, 20. 45219
equipment and methods for liquid from hot laboratory, Würenlingen, Switzerland, 16: 26635 (EIR-24)
equipment and methods development for, 17: 39180(R) (ORNL-3452 (p.51-96))
equipment and methods for improved, at ORNL, 20: 10439(R) (ORNL-3830, pp 285-98)
equipment and methods for, at Eurochemic fuel reprocessing plant, 20: 18167
equipment and methods for, of solids, 20: 27039 (NP-15946)
equipment and method for, at Tokai Power Station in Japan, 20: 42688
equipment and procedures for, at Mol, Belgium, 18: 38698
equipment design and operation for, at Cadarache Center, 20: 36537
equipment for, at Saclay, 20: 24813
equipment for, use of plastics in, 19: 18101
equipment used in France for, 18: 38680 (A/CONF.28/P/88)
evaporation and calcination of solutions, 16: 8444(P)
evaporation and chlorination, furnace apparatus for, 16: 10119(P)
evaporation and denitration of Purex solutions, performance of equipment for, 20: 20344 (BNL-10047)
evaporation and fixation in bitumens, Karlsruhe, 1963 to 1965, 20: 18171
evaporation, decontamination factor in, 17: 10224
evaporation, design and performance of perforated plate column demister, 16: 3982
evaporation, design and characteristics of installations for, 17: 12053
evaporation, design of installation at Wurenlingen for, 18: 6542
evaporation, design of falling-film evaporator for, 18: 6543
evaporation, evaluation of two evaporator systems for, 17: 2642 (KT-530)
evaporation methods of, apparatus development for, 19: 12854 (UJV-1110/64)
evaporation methods of, comparison of economics and performance of installations for, 20: 22516
evaporation of aqueous wastes, heat transfer coefficients of vertical tube evaporator for, 19: 43624 (RFF-534)
evaporation of Eurochemic hot waste, tests of evaporator for, 18: 4888 (NP-13289)
evaporation of low-level and decayed high-level solutions, engineering drawings of apparatus for, 17: 19719
evaporation of radioactive liquids in fluidized bed, 20: 30946
evaporation of, heat transfer properties of fluidized-bed spray-type evaporator for, 19: 48079(R) (NP-15371)
evaporation, concentrator with disposable vessel for, 18: 11498 (AD-404279)
evaporation, efficiency and cost of, 18: 21695
evaporation, filters for, 18: 40960 (UJV-1103/64)
evaporation, installation for, 18: 45156 (UJV-1109/64)
evaporation, plant for solar, 20: 26554
evaporation, plant at Risö, Denmark, for, 20: 26561
extraction of long-lived nuclides in, 17: 2461(R) (BNL-731(p.18-46))
facilities and equipment for, at Shippingport Atomic Power Station, 20: 40481 (WAPD-T-1851)
facilities and methods for, design and engineering aspects of, 20: 5207
facilities at AERE, Harwell, for, filtration and ion-exchange, 20: 26555
facilities at Marcoule, chimney baffle model studies, 16: 4367 (CEA-2004)
facilities for low-level, at Reactor Centrum Nederland, 20: 26578
facilities for, engineering drawings of WAFRAX, 20: 16139
facility at Karlsruhe Nuclear Research Center for, 20: 26560
film evaporation methods of, design of plant for, 19: 48086

filtration and freeze-drying method for, 20: 47088(P)
filtration and vacuum freeze drying, 19: 33683(P)
filtration and vacuum freeze drying, apparatus for, 20: 3607(P)
filtration of sludges, two processes for, 20: 14210
filtration through soil, factors affecting, 17: 41088
fission product incorporation in glasses in, 17: 42420
fission product recovery in Purex waste, 16: 30492 (HW-SA-1939)
fission product release in, effects of volatilization on, 20: 18156 (BNWL-SA-453)
fission product separation by sorption by pyroclastic rocks in, 17: 35940 (UJV-951/63)
fission product separation from acidic effluents by inorganic ion exchangers, 18: 37281 (A/CONF.28/P/772)
fixation in annular containers, correlation for maximum transient temperature in, 19: 25775(R) (HW-84603(p.8-31))
fixation in asphalt for intermediate materials, 20: 10438(R) (ORNL-3830, pp 96-139)
fixation in basalt, extraction of cesium and strontium following, 20: 24814
fixation in borosilicate glass of highly radioactive wastes from Risö, Roskilde, Denmark, 20: 45230
fixation in cement block, 19: 3798 (UJV-1111/64)
fixation in cement, 20: 26557
fixation in ceramic sponges, description of pilot plant operation for, 19: 5563
fixation in glass-type material, 16: 20037
fixation in glass, 17: 17619(R) (ORNL-TM-482)
fixation in glass of concentrated fission product solutions from Marcoule, France, 20: 45231
fixation in glass of concentrated solutions of fission products, process at Fontenay-aux-Roses, France for, 20: 45233
fixation in glass, United Kingdom work on, 18: 38682 (A/CONF.28/P/188)
fixation in glass, evaluation of, 19: 10665
fixation in glass, development of cell for, 19: 13524(R) (HW-81984 (p.4.1-20))
fixation in glass, process for, 19: 21754(P)
fixation in glass, studies, 19: 25775(R) (HW-84603(p.8-31))
fixation in glass, rising level test, 19: 26219(R) (ORNL-TM-1069)
fixation in glass, development of, 19: 34302(R) (HW-84384(p.4.1-9))
fixation in glass, factors affecting products of, 19: 38285(R) (BNWL-76)
fixation in glass, testing rising-level method for, 20: 12928(R) (ORNL-3868)
fixation in glass, Fingal's cave for, 20: 24812
fixation in glass, properties of input melts for, 20: 40476(R) (BNWL-267)
fixation in glasses by calcination, efficiency of, 20: 38998(R) (ORNL-3958)
fixation in glassy solids, development and evaluation of methods for, 18: 26978 (ORNL-TM-857)
fixation in phosphate glass, laboratory studies, 18: 35236 (ORNL-3612)
fixation in phosphate glass, pilot plant operation for, 18: 45153 (TID-7699(p.24-35))
fixation in phosphate glass, methods for, 19: 15331(R) (BNL-841(p.18-42))
fixation in phosphate glass, flowsheet development for, 19: 36216(R) (BNL-900(p.29-72))
fixation in phosphate glass, methods for, 19: 36535(R) (HW-84609 (p.4.1-7))
fixation in phosphate glass, 20: 3606
fixation in phosphate glass, Brookhaven process for continuous, 20: 22509 (BNL-10109)
fixation in phosphate glass, process for, 20: 36534 (BNWL-200)
fixation in solids, transient thermal behavior of, 18: 45148(R) (HW-83320)
fixation method of, effects of adding lithium and sodium to glass-forming mixture in, 20: 42690(P)
fixation of calcined alumina in phosphate glass, 19: 24610(R) (IDO-14638)
fixation of cesium and strontium on ion exchange beds in storage containers, 18: 9742 (HW-SA-3233)
fixation of fission products in glass, pilot plant study, 17: 10235
fixation of fission products in glass, pilot plant study, 17: 10236
fixation of fission products in glass, treatment of off-gas, 17: 10237
fixation of fission products in melted silicates, 17: 10226
fixation of fission products in titanates and titanium oxides by co-precipitation, 17: 10234
fixation of fission products in glass, 17: 13872
fixation of high-level wastes in inert solid materials, 18: 24976 (LADC-6398)
fixation of high-level wastes in glass, development of continuous melting system for, 18: 43091(R) (ORNL-TM-830)
fixation of molybdenum and fission products in phosphate glass, 19: 5566(P)
fixation of Purex and TBP-25 wastes in glass, 17: 10246(R) (ORNL-TM-403)
fixation of Purex waste solutions in glass, development, 19: 33676 (ORNL-3640)
fixation of Purex wastes in phosphate glass, study of composition range in, 19: 42192 (BNWL-80)
fixation of Purex solutions in phosphate glass, evaluation of, 20: 22510 (BNWL-SA-564)
fixation of radioactive muds on bitumen, 18: 26980(P)
fixation of radioactive in polysilicates, thermite process for, 20: 45226
fixation of ruthenium in solids, 17: 17618 (ORNL-TM-263)
fixation of ruthenium in solids, 18: 11504(P)
fixation of TBP-25 wastes in glass, 18: 35641(R) (ORNL-TM-785)
fixation of TBP-25 wastes in glass, 18: 35642(R) (ORNL-TM-798)
fixation of TBP-25 wastes in glass, 18: 35643(R) (ORNL-TM-823)
fixation of wastes in phosphate glass, 17: 12048 (TID-7646(p.43-51))
fixation of wastes in ceramic sponges, 17: 12052 (TID-7646(p.94-101))
fixation of water-unleachable solids, 17: 40420(P)
fixation on clays, 17: 2647
fixation, effects of additives on purex solution, 19: 17388(R) (HW-84467)
fixation, methods for, 19: 38080(R) (HW-84609)
fixation, research program on, 19: 25774(R) (HW-84603)
flocculation of low-level-waste waters by aluminum phosphate, 16: 14368(T) (AEC-tr-5045)
flocculation, effects of pH on reactor effluent, 20: 8980(R) (BNWL-36, pp 3.1-122)
flocculation, for separation of radioactive ruthenium, 18: 24983
flocculation, of low-level liquid wastes from regeneration of ion-exchange units from high-flux reactors, 20: 26584
flocculation, use of humic acid as coagulation agent in, 18: 24982
floculation and ion exchange, for low-level effluents, 18: 19450(T) (CEA-tr-A-1462)
flotation method for, 20: 10447
fluorination of solid wastes for plutonium removal, 19: 32280(R) (ANL-7020(p.100-49))
foam countercurrent extraction methods for, 19: 18055
foam separation and ion exchange, review of, 17: 17453
foam separation and scavenging-precipitation-ion exchange processes for low-level wastes, 18: 6537(R) (ORNL-TM-603)
foam separation column system for, description, 16: 11503(R) (ORNL-TM-34)
foam separation column for, performance of, 17: 40684(R) (ORNL-TM-608)
foam separation in, centrifugal foam breaker for, 17: 33768(R) (ORNL-TM-541)
foam separation methods for, 16: 29039(R) (RAI-101)
foam separation methods for, 17: 26931(R) (ORNL-TM-453)
foam separation methods for low-activity wastes, 17: 28584(R) (RAI-113)
foam separation methods for waste water, 17: 39180(R) (ORNL-3452 (p.51-96))
foam separation methods, 18: 16129(R) (RAI-116)
foam separation methods of, technical progress review on, 18: 17350
foam separation methods of, engineering drawings of column for, 18: 31682
foam separation methods of, 18: 43091(R) (ORNL-TM-830)
foam separation methods for low-activity wastes, condensation techniques in, 18: 41303(R) (ORNL-TM-642)
foam separation methods for intermediate- and low-level wastes, 19: 31617(R) (ORNL-TM-1081)
foam separation of cesium and strontium from low-level, 16: 7328(R) (TID-14472)
foam separation of low-level solutions, use with scavenging-precipitation methods, 19: 5558(R) (ORNL-3627(p.73-114))
foam separation of strontium from low-level waste, 19: 30322 (ORNL-3527)
foam separation treatment of low-activity wastes at ORNL, 19: 40271(R) (RAI-350)
for nuclear industry, 18: 38690 (AEET/HP/RWD/4)
for plutonium recovery, 20: 5595(R) (ANL-6925, pp 107-64)
for protection of water supplies, 16: 9046
for separation and recovery of strontium-90 and cesium-137 from fission product mixtures, 16: 8(T) (AEC-tr-4142(p.33-42))
fractionization and packaging technology in, development of, 17: 33395 (HW-SA-2786)
freezing and ion-exchange separation methods for, 18: 38684 (A/CONF.28/P/609)
ground storage, insolubilization using petroleum tar, 16: 25050 (TID-7628(p.198-210))
heating to form compact bodies insoluble in water, use of alumino-thermics in, 18: 33171(P)
hydrogen burner testing for, catalytic, 17: 15520 (DLCS-3670101)
in European countries, 19: 19428 (SZS-2)
in Purex Process by preparation of phosphate glass, flowsheets for, 16: 23352(R) (BNL-705)
incineration, 16: 11342(R) (EURAEC-83)

incineration, 16: 17332(R) (EURAEC-25)
incineration, design and operation of incinerators and gas cleaning equipment, 16: 29239 (TID-7627(p.416-60))
incineration of carbon-14-containing wastes, incinerator design, 16: 5440
incineration of solid wastes, design and operation of equipment for, 17: 42419(T,R) (EURAEC-697)
incineration, design and operation of Marcoule equipment for, 19: 27836
incineration, design and operation of plants for, 20: 45214 (AEET-243)
incineration, fixation of ash from, in glass, 20: 18166(R) (TID-22531)
incineration, gas cleaning at facility for, 18: 15659 (TID-7677(p.331-47))
incineration, gas-cleaning techniques in, 20: 26570
incinerator for, 20: 14212(P)
incinerators for low-activity, operation of Chalk River, 20: 10448
incinerators for volume reduction, commercial, 18: 23116
incinerators for, design and economics of, 20: 28854 (RFP-735)
incorporation in asphalt, effects of radioactivity levels on, 20: 12517(R) (BNWL-170)
incorporation in asphalt for, 20: 38538
incorporation in silicate glasses, 18: 15661
incorporation of ashes and semi-dry sludges in asphalt, 17: 28579 (EURAEC-295)
incorporation of fission products into glass, 17: 10231
incorporation of radioisotopes in glass blocks, 17: 33404
incorporation of radioisotopes in glass, 17: 33405
incorporation of wastes in vitreous materials, 20: 1556
insolubilization in asphalt, pilot studies, 18: 38685 (A/CONF.28/P/774)
insolubilization of concentrates by asphalt coating, 17: 42418(T,R) (EURAEC-695)
installation at Mol, 16: 7329(T) (AEC-tr-4954)
installations for, in Euratom countries, 19: 29470 (EUR-2271.f)
instrumentation for pilot plant for low-level, engineering drawings for, 20: 1557
ion exchange and evaporation of low-level process water containing bicarbonate ions, 17: 31789 (ORO-603)
ion exchange and freeze drying methods of, 20: 26551
ion exchange and solvent extraction methods for Purex wastes, 18: 35234(R) (HW-81862)
ion exchange, cell design for continuous measurement of radioactive eluates, 16: 17712
ion exchange decontamination of high-level Savannah River waste supernate, 18: 26974 (BNL-853)
ion exchange, development of, for low level materials, 16: 32885(R) (ORNL-3314(p.58-95))
ion exchange, Harwell experiments, 16: 20034 (AERE-R-3496)
ion exchange methods for low-level waste water, 17: 39180(R) (ORNL-3452(p.51-96))
ion exchange methods of, use of resins of locally available soil material in, 18: 5415(R) (IDO-14599)
ion exchange methods of, technical progress review on, 18: 17350
ion exchange methods of, 20: 14643
ion exchange methods of, for mine waters, 20: 26575
ion exchange methods for, 18: 1314
ion exchange of low-level solutions, use with scavenging-precipitation methods, 19: 5558(R) (ORNL-3627(p.73-114))
ion exchange on vermiculite platelets, effects of particle diffusion, 16: 2802(R) (ORNL-3189(p.42-9))
ion exchange process at Shippingport Pressurized Water Reactor, modification proposals for, 16: 1281 (WAPD-BT-23(p.75-81))
ion exchange processing of low-level wastes, 16: 2809(R) (ORNL-TM-49)
ion exchange procedures for, 18: 38699
ion exchange separation of Sr^{90} and Cs^{137}, 17: 33408
ion exchange separation of cesium-137, 18: 23118
ion exchange separation of chromium-51 and cobalt-60 from citrate and permanganate solutions, 18: 35235 (IDO-12036)
ion exchange, suitability of peat, 16: 7335
ion exchange treatment of process condensate wastes, 18: 7979 (HW-79174)
ion exchange use in holding tanks for, 17: 30073
ion exchange using peat, 16: 14370
ion exchange, utilization of silicate clays, 16: 5102
ion exchange-scavenging, development of procedures for, 19: 38285(R) (BNWL-76)
ion exchange, development for low-level solutions, 18: 17929(R) (IDO-14616)
ion exchange, development for low-level aqueous wastes, 19: 31617(R) (ORNL-TM-1081)
ion exchange, evaluation of natural earth materials for, 18: 12256(R) (IDO-14621)
ion exchange, evaluation of resins for, 19: 3806(R) (KR-79)
ion exchange, for removal of strontium-90 from biologic waste, 19: 45692 (UCD-472-112, pp 141-7))
ion exchange, sorptive properties of zeolites for, 18: 15656 (HW-SA-3333)
ion exchange, use of peat-clay exchange for, 18: 19449 (ZFK-RCH-2)
ion exchange, use of earth materials for, 18: 33164 (CONF-179-5)
ion exchange, use of mobile unit for, 18: 40966
ion exchange, use of natural organic materials for, 18: 40967
ion exchange, use of peat and bentonite clay for, 18: 40968
ion exchange, use of earth materials for, 19: 23996(R) (ORNL-3650(p.1-110))
ion separation methods in, 18: 35648
ion-exchange methods of, properties of zeolite taff for, 19: 44123
ion-exchange methods of, for low- and intermediate-level-activity wastes, 20: 38538
ion-exchange, uses of natural cation exchangers in, (E), 19: 40130 (ZFK-RN-17(p.165-78))
leaching, 16: 17332(R) (EURAEC-25)
leaching of cement-vermiculite-water mixtures in sea water, 19: 14767(R) (KR-86)
liquid storage, cycling of fission products in natural vegetation, 16: 34143 (ORO-580)
low-level decontamination by foam column surfaceactants, 17: 20100(R) (ORNL-TM-412)
management at Studsvik, economics and operations associated with, 20: 26548 (AE-225)
management of, economics and engineering studies of, 18: 19448(R) (ORNL-TM-757)
materials by ion exchange scavenging, low-level, 17: 7653(R) (ORNL-TM-396)
method for liquid, 18: 4892
method for low- and intermediate-level liquid and solid, at Kjeller, Norway, 20: 26583
method for low-level, liquid-foam, 20: 12526
method for medium-level liquid, at Pelindaba, South Africa, 20: 47084 (PEL-102)
method for PW-1 and PW-2, effects of melter products on, 20: 12517(R) (BNWL-170)
method for strontium-90-containing biologic, 17: 38643(R) (UCD-108 (p.123-42))
method for, at Hahn-Meitner Institute, Berlin, 20: 26576
method for, using complexing and electrodialysis or molecular filtration, 19: 28459(P)
method of thermal, for volatilization of cesium-137 and ruthenium-106, 20: 26573
method of, for low-level radionuclide separation, 20: 40483
method of, using sulfuric acid dissolution, 20: 5208(P)
method review, 16: 247
methods, 16: 28636 (ORNL-TM-282)
methods, 17: 14574
methods allowing reuse of acid leach solution within mill, 16: 21859 (BM-RI-6011)
methods and facilities in France, 18: 38679 (A/CONF.28/P/86)
methods at Bois-Noirs mine-plant complex, 17: 42427
methods at center for radioactive waste and sewage, 18: 38695
methods at Grenoble Nuclear Research Center, France, 17: 26939
methods at Karlsruhe Atomic Research Center, 20: 32881
methods at Karlsruhe Atomic Research Center, 20: 32882
methods at radiometallurgy facility at Hanford, 16: 3148
methods at South African National Nuclear Research Center, Pelindaba, 20: 26553
methods development, 16: 7475(R) (ORNL-TM-81)
methods development at ORNL, 16: 23348(R) (ORNL-TM-169)
methods development and evaluation, 17: 17619(R) (ORNL-TM-482)
methods development for disposal of high- and low-level waste solutions, 17: 35618(R) (ORNL-TM-545)
methods development for, *Technical Progress Review*, Spring 1964, 19: 12859
methods development for, in Czechoslovakia, 19: 17389
methods development, 20: 1352(T,R) (JPRS-31526)
methods for, 18: 11375
methods for, 18: 40961 (UJV-1104/64)
methods for, comparison of calcination, 18: 3392
methods for, development of calcination, foam-separation, and ion-exchange, 18: 9744
methods for disposal, management, and storage, (E), 19: 35858
methods for, effects of processing-site location on, 17: 41087
methods for fuel, management, 20: 8482
methods for gaseous effluents, 16: 12704
methods for gaseous, liquid, and solid wastes, 16: 9727
methods for glass melter condensates containing sulfuric acid, 20: 18159 (BNWL-SA-514)
methods for high- and low-activity, (E), 19: 35858
methods for high-, intermediate-, and low-level solutions, 20: 47083(R) (ORNL-3945, pp 79-106)
methods for intermediate- and low-level, economics and evaluation of, 20: 10441 (ORNL-TM-1289)

methods for liquids at Argonne National Lab., 16: 8441
methods for liquid, at Casaccia, 20: 45220
methods for organic, 17: 38582
methods for polonium process wastes, 18: 15689(R) (MLM-1155)
methods for radioactive waste water, review, 17: 5652
methods for, research progress in Belgium, 17: 17620(T,R) (EURAEC-518)
methods for, review of, 17: 10225
methods for separating long-lived isotopes from high-level wastes, (E), 19: 42197
methods for, at Institute of Atomic Energy, Brazil, 20: 16134 (IEA-102)
methods for, at Marcoule, Mol, and Windscale, 20: 12520(T) (CEA-tr-A-1490)
methods for, burial and storage, 20: 12520(T) (CEA-tr-A-1490)
methods for, construction and management of research center for studying, 18: 38696
methods for, developments in studies on, 20: 30943(R) (ORNL-TM-1465)
methods for, in Hungary, 18: 29142
methods for, in uranium ore processing plants, 19: 43627
methods for, research progress in Belgium on, 18: 24979(T,R) (EURAEC-202)
methods for, research progress in Belgium on, 18: 24980(T,R) (EURAEC-300)
methods for, review of, 18: 43096
methods for, review of, 20: 12519 (TID-8541, pp 149-248)
methods for, survey of, 20: 45222
methods in Denmark, 20: 3646
methods in low-level, 18: 36861
methods in Norway, 19: 48114
methods of, at National Reactor Testing Station, 18: 3390 (IDO-16925 (p.119-29))
methods of, comparison of European and Japanese, 17: 22961
methods of, development at Marcoule Center, 17: 42425
methods of, for liquids, 17: 21800
methods of, for Purex Tank Farm condensate, 17: 24734 (HW-SA-2968)
methods of, for solid wastes, 17: 17614 (CEA-2195)
methods of, in Czechoslovakia, 17: 19716
methods of low-level, review of, 17: 42421
methods of, review, 17: 12054
methods of safe, research summary on, 19: 13671(R) (WASH-1052)
methods of, used at various installations, review of, 17: 22963
methods of, at Chinon Reactor Installation, 20: 9029
methods of, at Gundremmingen Nuclear Power Plant, 20: 8416
methods of, for radioisotope separation at Hanford, 19: 13848
methods of, for recovery of highly enriched uranium from aluminum–uranium alloy scrap, 19: 13538
methods of, for sewage from radiological hospitals, 19: 38288
methods of, in reactor fuel reprocessing facilities, 20: 16582
methods of, possibility of total containment in, 18: 26979
methods of, recovery of fission products as energy and radiation sources in, 20: 42689
methods of, review of, 19: 40276
methods of, review of research and development activities on, 19: 48083
methods of, technical progress review of, 20: 38538
methods, review, 16: 19208
methods, review, 16: 20314
methods, review, 17: 15528
methods survey, 16: 16026(T) (CEA-tr-A-1106)
methods used at AERE, Harwell, chemical, 20: 26556
methods used at Hanford plant, (E), 19: 42196
methods used at Karlsruhe Atomic Research Center, 16: 32621 (KFK-36)
methods used in United States, survey of, 17: 24763
mineral exchange, Canadian developments in, 17: 19706 (TID-7644 (p.75-82))
neutralization by concentration or dilution, review, 16: 20037
neutralization of Purex-type wastes, 16: 11343 (ORNL-TM-127)
of ferrous metal scrap containing radium, 16: 5615
of high- and low-level materials, 16: 20537(R) (ORNL-TM-177)
of high-level wastes, 17: 33398
of laboratory radioactive waste waters by contact precipitation, 19: 5564
of laboratory wastes, 18: 38694
of liquid and solid laboratory wastes, 18: 38693
of long-lived nuclides, by neutron-absorption conversion, 16: 31341 (BNL-5010)
of low-level effluents at Risö decontamination plant, 17: 22962
of low level effluents, methods and problems of, 17: 26940
of low-level solid material at Marcoule Center, France, 17: 26938
of low-level waters, 16: 8440 (UCRL-6641)
of low- and intermediate-level radioactive wastes, 18: 21694
of low- and medium-level liquid wastes at Savannah River Plant, 20: 1548 (DPSPU-65-30-30)
of low-level wastes produced by radioisotope users, code of practice on, 19: 27840
of medium-activity liquid wastes by lyophilic processing, 17: 10229
of nitric acid solutions, 17: 33400
of plutonium-containing wastes, radiation hazards from explosion during oxidation in, 18: 43843
of Purex wastes for neptunium removal, 17: 40923 (DP-453)
of radioactive liquid wastes from industrial and medical uses, 19: 3799
of solid radioactive materials at Saclay, 18: 43094
of solid wastes, 17: 10230
of zirconium oxide sludge by electrolytic dissolution, 17: 4295(R) (DP-740)
operations at Shippingport, nuclide identification during, 16: 9724 (DLCS-2180101)
operations, summary, 17: 37292(R) (ORNL-TM-586)
oxidation of radioactive sewage, 18: 19454
packaging in concrete, costs and techniques of, 20: 26565
particle growth kinetics in fluidized calciner, 16: 13025
performance of plant design at ORNL for low-level, 17: 36998
phosphate glass formation methods of, review of, 19: 43625
pilot plant and techniques for solids, 16: 25034 (CEA-2147)
pilot plant for, at Wurlingen, 17: 2649
pilot plant for, at Junta de Energia Nuclear, Spain, 20: 26567
plant at Japan Atomic Energy Research Institute, test operation and cost estimation of, 18: 11500 (JAERI-1048)
plant at Rocky Flats for, operation of aqueous, 20: 1940 (RFP-638)
plant design and operation for radioactive, at Rey, Czechoslovakia, 17: 17621
plant design at Japan Atomic Energy Research Institute, 16: 17334 (JAERI-1021)
plant design for low-level, at Latina, Italy, 16: 31349
plant for low-level, at Karlsruhe Nuclear Research Center, 20: 26574
plant for, description of, at The Hague, 19: 40273
plant management and accounting procedure at Mol, Belgium, 20: 8481 (TID-22428)
plant-scale recovery of promethium-147 at Hanford, 20: 1551 (RL-SA-53)
pot calcination, 16: 32618 (HW-SA-2592)
pot calcination of Darex, Purex, and TBP wastes, 17: 39180(R) (ORNL-3452(p.51-96))
pot calcination of Darex, Purex, and TBP wastes, 19: 5558(R) (ORNL-3627(p.73-114))
precipitation in, for decontamination of radioactive waste water, 17: 2646
precipitation methods for low-level aqueous solutions, design of plant using, 19: 45693
precipitation methods for, 18: 1314
precipitation of calcium and magnesium prior to foam separation, 16: 25036 (ORNL-TM-260)
precipitation of strontium from IWW Purex waste, 17: 10246(R) (ORNL-TM-403)
precipitation of uranium acid leach residues, 17: 8228
precipitation–phenolic ion exchange techniques for, 16: 1649(R) (ORNL-TM-1)
precipitation using radiochemical compounds, 16: 2811
precipitation-ion exchange, economics of plant using, 20: 20349
precipitation, improvement of Wirbos method for, 18: 40969
problems and methods, 16: 14369
problems in, 17: 26934
problems in liquid, at Fontenay and Saclay, 17: 26936
problems in Paris region, 17: 26935
radiation monitoring system for, effluent, 20: 41272(R) (ORNL-3875, pp 53-74)
radiation use in, 18: 17612
radioactive and industrial, literature review, 1961, 18: 9743
radioactivity monitoring equipment for, 19: 18065
recovery of plutonium from incinerator ash, 18: 40959 (RFP-396)
remote-control equipment for use in, 18: 41610(P)
removal of strontium by calcite-phosphate column, 16: 25051 (TID-7628 (p.211-13))
research facilities for, Casaccia, Italy, 20: 36540
research programs, summary for AEC in 1961, 16: 12827
research programs of the International Atomic Energy Agency, 16: 25076 (TID-7628(p.590-601))
research programs on calcination, extraction, and sorption techniques for, 17: 7652(R) (HW-75290)
research programs on, AEC, 17: 19747 (TID-18468(p.353-63))
research programs on, review of Euratom, 19: 14931
research progress at Argonne National Lab., October to December 1961, 16: 20296(R) (ANL-6477)
research progress on, *Technical Progress Reviews*, Spring 1964, 19: 11290
research, review, 16: 8806 (IDO-14555)
review, 16: 287
review, 17: 28792
review, 18: 35239

review, 19: 35857
review of methods and cost factors, 17: 21379
review of methods for gases, liquids, and solids, 18: 45149 (HW-SA-3575)
ruthenium separation by periodate precipitation, 20: 26572
safety in, review of 1964 Geneva papers on, 19: 24779
scavenging by ion exchange materials, 16: 25053 (TID-7628(p.237-47))
scavenging-ion exchange process for, 16: 2808(R) (ORNL-TM-15)
scavenging, metallic ion removal by foaming agents and suspensions, 17: 12366(R) (RAI-104)
scavenging of NPR decontamination solutions, 17: 7651 (HW-74507)
scavenging-precipitation ion-exchange method for low-level, pilot plant demonstration of, 17: 24735 (ORNL-3349(Pt.II))
separation of cesium and strontium from low-level solutions by foam columns, 16: 22269(R) (TID-15919)
separation of cesium by solvent extraction using phenols, 17: 17949(R) (ORNL-TM-449)
separation of cesium, ruthenium, and strontium by ion exchange, 18: 6548(P)
separation of cesium by ion exchange, 18: 20097 (CONF-179-1)
separation of cesium-137 and strontium-90 by ion exchange, 19: 12856
separation of chromium, iron, and nickel from stainless steel solutions by electrolysis over mercury cathode, 16: 12794 (IDO-14570)
separation of fission products by solvent extraction, 18: 4889 (ORNL-3518)
separation of iodine-131 from sewage by use of trickling filters, 16: 11345 (TID-14867)
separation of mercury prior to calcination or fixation, 17: 21375 (ORNL-TM-568)
separation of mercury in, by amalgamation, 18: 24977 (ORNL-TM-827)
separation of radium from uranium mill effluents by adsorption, 17: 17949(R) (ORNL-TM-449)
separation of radioactive materials from solutions using aluminum or iron hydroxides and flotation agent, 18: 19452
separation of radioisotopes for use as heat sources, 18: 33983 (HW-SA-3080(Rev.))
separation of strontium from aqueous sodium-salt solutions by ion exchange, properties of zeolites for, 17: 8240 (HW-SA-2364)
separation of strontium and rare earths from Purex 1WW by solvent extraction using di(2-ethylhexyl)phosphoric acid, 17: 17949(R) (ORNL-TM-449)
separation of strontium from fission product solutions, 18: 11499 (AERE-R-4493)
separation of uranium values as uranium tetrafluoride, 19: 36567(P)
sludge filtration in, use of filter aids for, 20: 10446
soil sorption and retention, 16: 25052 (TID-7628(p.214-36))
solidification by absorption into hydraulic binders, 18: 6546(P)
solidification by mixing with hydraulic binding agent and granulated material, 18: 33170(P)
solidification by rising-liquid-level (RL-Potglass) process, 18: 35237 (ORNL-3629)
solidification by pot calcination to glass, 18: 40958 (ORNL-TM-882)
solidification by evaporation, operating experience on in-tank, 19: 45691 (RL-SA-41)
solidification by phosphate glass process, properties of platinum crucible for use in, 20: 23644 (BNL-10132)
solidification condensate treatment, 20: 12517(R) (BNWL-170)
solidification, effects of concentration and temperature on, 17: 2640 (HW-74371)
solidification in tank by submerged combustion, 16: 8438 (HW-71752)
solidification in storage tanks by hot air injection, 17: 19702 (HW-SA-2958)
solidification in storage tank, information manual on, 19: 10660 (HW-83218)
solidification in storage tanks, heat transfer from, 19: 38285(R) (BNWL-76)
solidification in underground tanks, tests of immersion heaters for, 19: 42193 (BNWL-101)
solidification in ceramics, 20: 26568
solidification methods for, 20: 16142(P)
solidification of fission products into glasses and mica, 16: 16027(T) (NP-tr-874)
solidification of fuel processing wastes by incorporation in glass, 17: 19714
solidification of waste solutions, 17: 33406
solidification of intermediate-level solutions by mixing with asphalt and concrete, 19: 5558(R) (ORNL-3627(p.73-114))
solidification of high-activity wastes, methods development for, 20: 35174
solidification using bitumens, 18: 36862(P)
solidification using bitumen, 20: 26564
solidification with asphalt, 16: 11342(R) (EURAEC-83)
solidification with asphalt, 16: 17332(R) (EURAEC-25)
solidification, calcination and glass formation for high-level materials, 20: 10438(R) (ORNL-3830, pp 96-139)
solidification, costs of Hanford program for, 19: 33677 (RL-SEP-496)
solidification, development of processes for, 18: 45154 (TID-7699 (p.73-95))
solidification, development for high-level materials, 19: 22405(R) (HW-83298(p.4.1-25))
solidification, development of engineering prototypes for demonstration of, 19: 25776(R) (HW-84603(p.32-6))
solidification, development of pilot plant for, 19: 38286 (HW-SA-3604)
solidification, design of engineering prototypes for, 20: 12517(R) (BNWL-170)
solidification, design verification tests on prototype equipment for, 20: 12517(R) (BNWL-170)
solidification, equipment prototype development for, 19: 38285(R) (BNWL-76)
solidification, equipment and methods for, 20: 40477 (HW-80056)
solidification, flow diagram for engineering prototypes for, 20: 12517(R) (BNWL-170)
solidification, hazards evaluation of installation unit for in-tank, 19: 19427 (RL-SEP-65)
solidification, methods for high-level materials, 20: 12524
solidification, methods for, 20: 24971(R) (BNL-954, pp 50-83)
solidification, objectives and plans for engineering prototypes for, 20: 18158 (BNWL-SA-467)
solidification, tests on in-tank, 20: 12517(R) (BNWL-170)
solidification, transient behavior in, 20: 24809(R) (BNWL-213)
solidification, using materials that shield against radiation, 18: 15660(T,P) (CEA-tr-A-1413)
solidification, use of computers for evaluation of engineering prototype for, 20: 12517(R) (BNWL-170)
solvent extraction for recovery of strontium and rare earths from Purex 1WW, 16: 8439 (ORNL-3204)
solvent extraction processes for recovering fission products from solutions, 18: 6883 (HW-SA-3211)
solvent extraction of strontium in, 18: 11505(P)
solvent extraction of strontium and rare earths from Purex acid waste, 18: 29136 (HW-79762(Pt.2))
solvent extraction of strontium and rare earths from Purex waste, 18: 31655 (HW-79762(Pt.1))
solvent extraction, for separation of cerium and rare earths, 18: 39365 (HW-78987(Rev.))
solvent extraction, demonstration of CSREX process for, 19: 5557 (HW-81091)
solvent extraction of molybdenum from wastes using alkyl phosphoric acids, 19: 8679
sorption by natural minerals, 16: 30155(R) (HW-74375)
sorption method using peat, 16: 25078
sorption methods for, use of flocculants in, 20: 16138
sorption of calcium and strontium by hydrous ferric oxide and limonite, 17: 36993(R) (TID-19164)
sorption of cesium and strontium on Victorian brown coal, 16: 25033 (AAEC/TM138)
sorption of cesium-137 on zeolite, effects of gamma leakage on thermal conditions for, 17: 12040 (HW-74712)
sorption of cesium and strontium in, 17: 36995(R) (TID-19187)
sorption of cesium and strontium in, 17: 36997(R) (TID-19189)
sorption of cesium and strontium by countercurrent contact with coagulated slurries of natural adsorbents, 18: 43092 (UJV-973/63)
sorption of fission products by electrocoagulated aluminosilicates, 19: 48082 (UJV-1296/65)
sorption of radioactive contamination from reactor effluent water on aluminum beds, 16: 23347 (HW-72215)
sorption of radioisotopes on minerals, 16: 2801(R) (ORNL-3189(p.27-42))
sorption of radioisotopes from reactor effluent on minerals, 16: 25035 (HW-69225)
sorption of radioisotopes from solution, evaluation of natural earth materials from Eastern Idaho for, 18: 13345 (IDO-14624)
sorption of strontium by minerals, 16: 25049 (TID-7628(p.187-97))
sorption on cellulose material, 16: 9728(P)
sorption on clay, 19: 21755(P)
sorption on clays and sands, 17: 29982
sorption on hydrated oxides precipitated by anodic dissolution of aluminum and iron, 19: 5560 (UJV-1112/64)
sorption on ion exchangers, 16: 34138 (HW-69263)
sorption, use of bitumen in, 16: 1279 (CEA-1992)
sorption, use of bitumen in, 16: 5101(T) (AEC-tr-4900)
sorption, development of inorganic materials for, 18: 45155(R) (TID-20980)
sorption, properties of Italian clays for fixation of cesium-137 and strontium-89, 20: 14209 (RT/PHOT(65)29)
sorption, using ferric hydroxide, 18: 20102 (UJV-850/63)
sorptive properties of clay minerals for strontium-90 for, 18: 21696
strontium recovery by solvent extraction followed by ion exchange,

18: 45160(P)
strontium recovery from Purex wastes by sulfate precipitation, 19: 5987 (HW-74036)
strontium-90 separation in, 16: 30505
strontium-89 effects on microflora of sewer water biofilters, 18: 19451(T) (JPRS-23903)
summary at ORNL, May–Oct. 1963, 18: 19448(R) (ORNL-TM-757)
summary of high- and low-level, 16: 12795(R) (ORNL-TM-133)
survey of management of high-level wastes by AEC contractors, 18: 7980 (HW-SA-3279)
survey of methods, 17: 33399
system design for, at Rospo and Ispra-2 Reactors, 20: 45220
system development for organic reactors, 17: 1123 (NAA-SR-5675)
systems for boiling reactor gases, 18: 35181
techniques for liquid and solid, in India, 20: 20351
temperature rises resulting from storage of high-level wastes, analytical evaluation of, 17: 17617 (LADC-5366)
testing of KRB reactor facility for, 20: 42638(R) (TID-23299)
treatment and packaging of solid wastes, 17: 33410
treatment of effluents at Latina station, 16: 8442
uranium recovery in, 16: 23637 (TID-7629(p.285-94))
use of centrifuged beds of vermiculite for, 17: 29865 (AERE-R-4314)
use of chemical heat in liquid, 20: 28855
use of nuclear energy for, economics of, 20: 45631(R) (ORNL-3945, pp 259-69)
vitrification of concentrated solutions of fission products, 17: 10233
vitrification of pulps, continuous process for, 18: 38683 (A/CONF.28/P/587)
vitrification, pilot-plant studies of, 18: 4891
volume reduction for disposing low-level radioactive wastes, 18: 24986
volume reduction of sludges by freezing and thawing, plant for, 18: 6544

WASTE RECOVERY
from sea water, using radioisotope uptake by marine algae, 16: 26677
of protactinium and uranium from ethereal sludge, 17: 4632
separation of plutonium from dross in, 17: 1555 (CEA-2161)

Waste Slurries
see Hanford Waste Slurries

WASTE SOLUTIONS
analyses of stored sludge at Hanford, 18: 40956 (HW-77380)
analysis for barium, calcium, and strontium in strontium-90, methods for, 16: 23601 (HW-69677)
analysis for beta activity, methods for, 20: 14450(R) (NLCO-970, pp 8.1-4)
analysis for fission products, methods for, 20: 22862 (CEA-R-2553)
analysis for fluoride, volumetric, 17: 33795 (PG-Report-449)
analysis for gross beta activity, 20: 43072(R) (IDO-14679, pp 193-229)
analysis for iodine-131, 16: 22006 (PG-Report-334)
analysis for iodine-131, phosphorus-32, and thallium-204 in solid fractions of, method for, 18: 41338
analysis for lead-210 by precipitation and beta counting, 16: 2961 (AERE-R-3795)
analysis for lead-210, radiochemical, 20: 5505
analysis for low-level beta activity, 20: 43072(R) (IDO-14679, pp 193-229)
analysis for neptunium-237, 17: 40693 (DP-748)
analysis for plutonium using zinc sulfide scintillator, 16: 26909 (CEA-2090)
analysis for plutonium, methods for, 20: 20976
analysis for polonium-210 by ion exchange and gamma counting, 20: 3879(R) (MLM-1266)
analysis for radioisotopes, development of methane flow counter for, 17: 32019
analysis for radioisotopes in polonium waste disposal process, 18: 13357(R) (MLM-1148)
analysis for radioisotopes in, 19: 8724 (NLCO-933)
analysis for radiocerium by precipitation and beta counting, 19: 9260
analysis for samarium-151 by isotope dilution mass spectrometry, 20: 43068(R) (IDO-14679, pp 47-50)
analysis for scandium-46, phosphorus-32, and chemical forms of radioactive ions in Hanford, 17: 1176(R) (HW-70050(p.78-142))
analysis for strontium-90 in presence of strontium-89, 19: 46196
analysis for sulfur in solid, by combustion and colorimetry, 20: 38795 (BNWL-265)
analysis for trace amounts of uranium by controlled-potential polarography, 20: 16389
analysis for traces of uranium, 20: 25015
analysis for trace amounts of uranium, fluorescence, 20: 29128
analysis for tritium, 16: 2980
analysis for uranium, polarographic, 19: 7290
analysis for uranium for nuclear materials management, review of methods for, 20: 18619
analysis for volatile products, gas-chromatographic, 16: 22033
analysis for zinc-65, 16: 28863 (AERE-R-3945)
analysis of decontaminated, for radionuclides, gamma spectrometric, 18: 43385 (ORNL-P-447)
analysis of dilute, for radionuclides by computer resolution of gamma spectra, 19: 9063 (ORNL-3744)
analysis of Harwell effluent for cesium-137, radiometric, 17: 25112 (AERE-R-4318)
analysis of Harwell effluent for radium-228, 18: 6741 (AERE-R-4460)
analysis of polonium-process, 18: 13358(R) (MLM-1151)
analysis of uranium remelt, for radium, 19: 8724 (NLCO-933)
calcination of aluminum nitrate and zirconium fluoride, 16: 1854(R) (IDO-14553)
calcination of aluminum nitrate, development of fluidized bed waste process for, 17: 21382
calcination of high-level, operation and performance of fluidized bed for, 18: 23119
calcination of Purex FT-65, R-73 test conditions and results for, 17: 37292(R) (ORNL-TM-586)
calcination to solids for use in saline water conversion, 17: 30787
calcined, biological availability of radionuclides in, 19: 32467 (IDO-12042)
cesium recovery from Purex Alkaline Supernate by solvent extraction using 4-*sec*-butyl-2(α-methylbenzyl)phenol, 19: 48075 (BNWL-68)
cesium-137 separation from, 18: 1314
cesium-137 diffusion from simulated phosphate ceramic, 20: 24809(R) (BNWL-213)
characteristics of, in uranium milling industry, 17: 21383
characterization of Purex FTW-65, 18: 19448(R) (ORNL-TM-757)
clarification, effects of carbonate and phosphates on hardness of effluent, 17: 10246(R) (ORNL-TM-403)
clarification of development of methods for, 18: 43091(R) (ORNL-TM-830)
coagulation and precipitation, effect of surface active agents on, 16: 2795 (AAEC/E-74)
composition of simulated Purex 1WW and FTW solutions, 17: 31681(R) (HW-76559)
concentration at river mouths, 20: 45225
concentration by evaporation, equipment for, 16: 1285(P)
concentration by freezing and thawing, plant for, 18: 6544
concentration by solar evaporation, 20: 26554
concentration in tanks, studies, 19: 25777(R) (HW-84603(p.37-49))
concentration of contaminated potassium tetraborate, by evaporation, 19: 38287 (NDL-TM-20)
concentration of intermediate-level, using finned circulator-evaporator, 20: 40477 (HW-80056)
concentration of low-level, operation and performance of facility for, 20: 22507 (AD-622372)
concentration of radioactivity by electrodialytic cell using ion exchange sheet, 17: 1176(R) (HW-70050(p.78-142))
concentration of radioactive, effects of polymer addition on, 17: 35247
concentrator for radioactive, design of, 17: 35248
consolidation and encapsulation of fission products from fuel wastes, 16: 27743 (NYO-9700)
consolidation of, methods development for, 17: 28586(P)
contamination of plants by, 19: 30006 (CEA-Bib-53)
contamination of rivers by, problems in, 18: 6539
contamination of surface waters by, review of conference on, 19: 20234
conversion to solid, processing, and storage, review on problems in, 19: 5561
conversion to solid, process for, 20: 35173 (IDO-14662)
corrosive effects of Purex, on stainless steel and titanium, 16: 30735 (HW-73378)
corrosive effects on calciner construction materials, 17: 8266
corrosive effects of Purex, on stainless steel, 17: 10246(R) (ORNL-TM-403)
corrosive effects of high-level, on stainless steel, 17: 14767 (IDO-14600)
corrosive effects of acidic nitrate, on stainless steel, 17: 39490 (ORNL-3474)
corrosive effects of refluxing FTW-65, on metals, 18: 19448(R) (ORNL-TM-757)
corrosive effects of Purex–colemanite, on construction materials at 900°C, 19: 25775(R) (HW-84603(p.8-31))
corrosive effects of Purex, on calciner materials, 19: 31617(R) (ORNL-TM-1081)
corrosive effects on Inconel and stainless steel spray calciners, 19: 38285(R) (BNWL-76)
cost estimates for management of, effects of fission-product removal on, 17: 26188
cost estimates for management of high-level power-reactor, 17: 26187
crib disposal of decontamination wastes, 16: 30154 (HW-73482)
criticality accidents in solutions of fissile material, estimation of neutron and gamma dose from, 18: 27723 (NP-13724)
decontamination, 17: 10851(R) (HW-73337(p.158-237))
decontamination by coagulation and precipitation, 16: 2796 (AAEC/E-75)
decontamination by electrodialysis, 16: 28637(T) (AEC-tr-5079)

decontamination by precipitation of calcium and ferric phosphates, 17: 26942
decontamination by ferric hydroxide flocculation, 17: 35246
decontamination by ion exchange using clinoptilolite and Linde AW 400, 18: 3806(R) (BNL-799(p.55-63))
decontamination by ferric hydroxide flocculation, 18: 24981
decontamination by ion exchange, 18: 38699
decontamination by cation exchange, 18: 40964
decontamination by sorption of radioisotopes on blast-furnace slags, 18: 40965
decontamination by distillation, economics and safety of evaporators for, 19: 4286
decontamination by cation exchange using humic acid, 19: 33678
decontamination by recycle scavenging–precipitation ion exchange process, 20: 10440 (ORNL-3863)
decontamination by contact precipitation and ion exchange, 20: 20349
decontamination from radioisotopes by sorption on aluminum, 16: 14373(P)
decontamination of hospital wastes, 16: 33096
decontamination of, design of concentrator for, 16: 34148
decontamination of aqueous radioactive, by ferric hydroxide flocculation, 17: 42426
decontamination of, methods for, 18: 7983
decontamination of polonium process, 18: 16376(R) (MLM-1157)
decontamination of polonium-process, 18: 19468(R) (MLM-1176)
decontamination of, sorptive properties of pyroclastic rocks for, 19: 24444
decontamination of low-level, by scavenging-precipitation and foam separation, 20: 1549 (ORNL-3811)
decontamination of Harwell, by filtration, 20: 7295 (AERE-R-3880)
decontamination of, filter aids for, 20: 10446
decontamination of, effects of acidity and chemicals on, 20: 8979(R) (BNWL-36)
decontamination of, using Yazoo and Zilpha clays, 20: 45221
decontamination of low-level, for reuse, 20: 47083(R) (ORNL-3945, pp 79-106)
decontamination using bentonites and vermiculites, 16: 7337
decontamination using activated sludge, 19: 24196
decontamination using activated sludge, 19: 24197
decontamination using clay minerals, 20: 12527(P)
decontamination using caustic-carbonate precipitants in sludge-blanket column, 20: 18168
denitration of, additive effects of sugar on, 17: 36991 (HW-75565)
denitration of Purex, by reactions with sugar, 17: 35243 (HW-77080)
determination of, by aerobic treatment, 20: 40483
diffusion of cesium-137 from simulated, during fixing and melting, 20: 8477(R) (BNWL-139)
dilution and dispersal in Clinch River, 20: 40479 (ORNL-P-2328)
dilution in slow-moving recipients following high-velocity jet release, 19: 24193
dilution in Winnipeg River, use of rhodamine B in tracer study on, 20: 7293 (AECL-2295)
dilution of, in Ottawa River, use of rhodamine B for study of NPD, 17: 22960 (CRER-1128)
dilution, dispersion, and sedimentation in British estuaries, 20: 45224
discharge into Clinch River from ORNL, 20: 45223
discharge into Escaut River in Belgium, proposed sewer for, 20: 22515(T) (ORNL-tr-965)
dispersion in Clinch River, effects of river flow and temperature on, 19: 1946 (ORNL-P-605)
dispersion in northeast Pacific by Columbia River effluent, · 20: 31448 (RLO-1725-15)
dispersion in northeast Pacific by Columbia River effluent, · 20: 31449 (RLO-1725-16)
dispersion in northeast Pacific by Columbia River effluent, · 20: 31450 (RLO-1725-17)
dispersion in northeast Pacific by Columbia River effluent, · 20: 31451 (RLO-1725-18)
dispersion in northeast Pacific by Columbia River effluent, · 20: 31452 (RLO-1725-19)
disposal and handling of, 17: 15531
disposal in clays and sands, 18: 24980(T,R) (EURAEC-300)
disposal in Durango-type uranium milling process, 16: 2797 (BM-RI-5874)
disposal in ocean, relation to marine ecology, 16: 9835
disposal in shale wells by hydraulic fracturing, 19: 8674(R) (ORNL-3697(p.10-19))
disposal in underground waters, flow measurement using tracer techniques, 18: 24979(T,R) (EURAEC-202)
disposal in underground waters, flow measurement using tracer techniques, 18: 24980(T,R) (EURAEC-300)
disposal in underground waters, flow measurement using tracer techniques, 19: 10659(R) (EURAEC-703)
disposal of, in Italy, 17: 5649
disposal of, in uranium milling, 17: 7650 (BM-RI-6114)
disposal of low-activity, into Irish Sea, review of, 20: 45229
disposal of residual radioactive, from The Hague Center into sea, 20: 45228
disposal of, to ground or water table, economics and hazards of, 20: 28852 (IDO-12052)
distribution in rivers, use of iodine-131 determination for studying, 20: 29099
distribution of tritium in, 16: 30156 (HW-74536)
effects of Hanford reactor, on growth of salmon, 20: 10538(R) (BNWL-122, pp 198-201)
effects of nitrate, on carbon steel, 20: 35848 (DP-1023)
effects on swimming ability of salmon, 18: 41016(R) (HW-80500(p.205-8))
electrodialysis in, 18: 27278(R) (HW-79280(p.4 1-28))
elution of, in bitumen, 17: 10220(T,R) (EURAEC-367)
elution of, in bitumen, 17: 10221(T,R) (EURAEC-443)
elution of, in bitumen, 18: 24979(T,R) (EURAEC-202)
elution of, in bitumen, 18: 24980(T,R) (EURAEC-300)
evaporation and calcination to solids, 16: 2808(R) (ORNL-TM-15)
evaporation and calcination in fluidized oxide bed, 16: 8444(P)
evaporation and storage of high-level, Hanford program for, 17: 21381
evaporation by solar energy, design of equipment for, 20: 18164(R) (NP-15874)
evaporation by solar energy, 20: 32883
evaporation, design of system for, 16: 14372
evaporation, design of system for, 16: 21861
evaporation of radioactive, in fluidized bed, 20: 30946
evaporation of, separation of radioactive droplets by plate column during, 17: 40945
evaporation of, calculations and equipment for solar, 20: 10437(R) (NP-15662)
evaporation of, design and operation of equipment for, 19: 12854 (UJV-1110/64)
evaporation of, operational characteristics of fluidized-bed spray evaporator for, 19: 45688(R) (NP-15367)
evaporator for, design and operation of, 17: 24732 (CR-IO-1144)
extraction and recovery of, at uranium mills, 17: 21384
fission product diffusion from simulated solid, 20: 12517(R) (BNWL-170)
fission product leaching from, diffusion and sorption in cement mortars, 18: 1315
fission product recovery from reactor fuel reprocessing wastes, 16: 27121 (HW-SA-2569)
fixation of intermediate-level, in asphalt, 20: 47083(R) (ORNL-3945, pp 79-106)
fixation of low-level, in glass, 20: 47082
flocculation of ammoniacal filtrates from uranium dioxide–plutonium oxide preparation, 18: 25895(R) (NUMEC-2389-3)
flow in soils, 20: 8821(R) (BNWL-36, pp 4.1-77)
flow in soils, tracer studies of, 20: 42687
flow-diverter valve for, design of, 20: 22511 (IDO-14666)
handling and storage of demineralizer-resin slurries, 20: 40481 (WAPD-T-1851)
handling of, safety in, 18: 29142
hazards of radioactive aqueous, assessment of, 20: 12525
hazards of, from medical use of unsealed radioactive sources, 20: 36678
hazards, origin, and treatment, 17: 12054
inventory at BNL, 19: 36452(R) (BNL-900(p.105-20))
management of tritium-bearing, problems in, 19: 24198
monitoring, 16: 28635 (DLCS-2180102)
monitoring, 16: 28636 (ORNL-TM-282)
monitoring and treatment of, review of conference on, 19: 20234
monitoring at ORNL, detector calibration for, 18: 12461 (ORNL-TM-786)
monitoring at ORNL, 1963, 18: 37442(R) (ORNL-3665)
monitoring equipment and methods, direct continuous, 16: 16613
monitoring equipment and methods for, 18: 12391
monitoring equipment and methods for, 18: 40961 (UJV-1104/64)
monitoring for beryllium, 18: 29876 (CEA-TP-472)
monitoring for radioactivity in, equipment and methods for, 18: 35858
monitoring for strontium-90 content, 16: 1283
monitoring heavy water reactor, for tritium, · 20: 23357 (CONF-640413, pp 34-9)
monitoring of, beta counter for, 17: 30089
monitoring of radioactive, 18: 2022(R) (HW-77609(Sect.5))
monitoring using salmon, 16: 25143(R) (HW-72500(p.144-7))
nature, volume, and activity of, from uranium mills, 17: 40913
nitrate content reduction, 19: 3803(P)
origin of radioactive aqueous, in nuclear industry, 20: 12525
physical properties of simulated decontaminant, 16: 18704 (HW-72531)
precipitation of calcium and magnesium from low-level, 17: 10246(R) (ORNL-TM-403)
processing at AERE, Harwell, 20: 26556
processing by anionic coprecipitation using periodate, 20: 26572
processing by flocculation, 20: 26584
processing by foam and ion exchange methods, 19: 12859

processing by ion exchange, 19: 24198
processing by solvent extraction, 17: 4625 (HW-SA-2767)
processing chromium-51-containing, precipitation method for, 20: 10444(T) (ORNL-tr-916)
processing developments, summary, 17: 36860(R) (ANL-6648)
processing fission-product, by vitrification, 18: 4891
processing for americium and curium recovery, 16: 24343
processing for arsenic-76 and phosphorus-32 separation from, 16: 30325 (HW-73972)
processing for cesium-137 removal, ion exchange, 18: 22179
processing for cesium and strontium recovery, 19: 6879 (UJV-1108/64)
processing for cesium separation by ion exchange, 19: 19426 (HW-84105)
processing for chromium-51 separation, precipitation method for, 19: 12855
processing for conversion to form for handling and storage, 19: 33683(P)
processing for neptunium recovery by solvent extraction, 20: 27036(R) (IDO-14661, pp 1-44)
processing for plutonium separation, solvent extraction, 16: 32927
processing for promethium recovery by ion exchange, 19: 18050 (HW-83299)
processing for ruthenium separation by cellulose derivative-bentonite flocculation, 19: 33679
processing for strontium recovery by lead sulfate carrier precipitation, 19: 24198
processing for technetium-99 separation by ion exchange, 16: 31345 (HW-SA-2581)
processing, furnace apparatus, 16: 10119(P)
processing low- and intermediate-level, at NRTS, 20: 26571
processing low- and intermediate-level, at Institute for Radiochemistry and Research Reactor FRM at Munich, Germany, 20: 26582
processing low-activity, by co-precipitation at Saclay, 20: 26581
processing low-level, at Kernforschungszentrum, Karlsruhe during 1961 and 1962, 18: 21692
processing low-level, 18: 36861
processing low-level, methods for, 20: 10438(R) (ORNL-3830, pp 96-139)
processing methods, 16: 13409
processing methods for, from cobalt-60 and iodine-131 production, 20: 14211
processing monazite, production of rare earth oxides by, 20: 23220
processing of high- and low-level, for disposal, 17: 35618(R) (ORNL-TM-545)
processing of high-level, by direct conversion to phosphate glass, 20: 36534 (BNWL-200)
processing of low-level, flowsheet for water-recycle, 19: 31617(R) (ORNL-TM-1081)
processing of low-level, at Reactor Centrum Nederland, 20: 26578
processing of low- and intermediate-level, at Kjeller, Norway, 20: 26583
processing of Purex IWW, by ion exchange methods, 17: 35618(R) (ORNL-TM-545)
processing of, effects of strontium-89 on nitrifying bacteria in biological, 18: 27732
processing of, using chemical heat, 20: 28855
processing organic reactor, 18: 29141
processing radioactive, from hospitals, 19: 38288
processing radioactive, using manganese dioxide, 20: 5206
processing sulfate-containing, for strontium recovery, 20: 5210(P)
processing systems for, at Rospo and Ispra-2 Reactors, 20: 45220
production in large closed-cycle pressurized-water reactors, 19: 48001(R) (WCAP-3743)
production, control, and release at Studsvik, Sweden, 19: 27831 (AE-182)
properties of calcined, effects of additives and blending on, 20: 28853(R) (IDO-14661, pp 45-82)
properties of phosphoric acid-treated radioactive, 19: 17388(R) (HW-84467)
properties of simulated solid, effects of temperature and time on, 20: 24809(R) (BNWL-213)
properties of sulfate-bearing versus sulfate-free samples of, 20: 12517(R) (BNWL-170)
properties of, effects of composition on, 19: 22405(R) (HW-83298(p.4.1-25))
purification by contact precipitation, method for, 18: 33169
purification by electrodialysis using ion-exchange membranes, 20: 26563
purification by ion exchange, properties of Albanian clays for, 17: 2647
purification of laboratory radioactive, by contact precipitation, 19: 5564
purification with Radgendorf clay, 16: 23351
radiation monitoring of aqueous, methods for, 18: 6545
radioactive, effects of marine disposal on contaminstion of fish, 18: 33248
radioactive, effects on biological conditions in rivers, 18: 35238 (STI/DOC/10/28(p.9-20))
radioactivity in, monitoring of low-level beta, 17: 380
radioactivity measurement in, review methods for, 19: 19749 (EUR-2118.f)
radioactivity of, apparatus and methods for measuring, 17: 5651
radioactivity of aqueous reduction by precipitating aluminum and bismuth hydroxides in hydrolysis cell, 18: 15688(R) (MLM-1152)
radioactivity of, sampling techniques for monitoring, 18: 465
radioactivity of, monitoring before discharge and in receiving waters, 19: 3800
radioisotope concentrations in, 17: 30071
radiological monitoring, 18: 35762 (NAVDOCKS-MO-218)
radionuclides in reactor, effect of SiO_2 on, 20: 45215 (BNWL-282)
recovery of, design of equipment for, 20: 18160 (CEA-R-2894)
reduction of radioisotopes in, effects of chemical additives and coating materials on, 18: 1487(R) (HW-77609(Sect.3))
reuse, in uranium ore processing plants, 16: 31340 (BM-RI-6045)
ruthenium removal from intermediate-level, by electrodialysis, 19: 30317 (BNWL-72)
ruthenium separation from, by cellulose–bentonite flocculation, 20: 36929
sampling and monitoring of, instrumentation and techniques for, 20: 16137
sampling flowing, for radioactivity monitoring, 16: 3295
sampling in underground storage tanks by rotary core drilling, 18: 15654 (HW-74040)
separation and purification of americium-241 from, by chromatographic ion exchange, 19: 20041 (HW-84352)
separation of actinium-227 from, by ion exchange, 20: 3879(R) (MLM-1266)
separation of actinides and lanthanides from, extractants for, 20: 27069(P)
separation of aluminum nitrate nonahydrate from Redox acid, by crystallization techniques, 20: 36925 (HW-82771(Pt.3))
separation of americium, curium, and rare earths from, anion exchange method for, 18: 3391
separation of americium oxides from, by acid leaching and calcination, 19: 22407 (RFP-442)
separation of americium from plutonium aqueous, by solvent extraction using dibutyl butylphosphonate, 20: 436 (RL-SEP-518)
separation of barium-137, cesium-137, cobalt-60, and strontium-89 from, using coal humic acid column, 20: 36930
separation of bismuth from, by electrolytic deposition, 19: 20047 (MLM-734)
separation of cerium, cesium, and strontium from acid, solvent extraction process for, 19: 5988 (HW-75537)
separation of cesium from, by adsorption, 16: 1854(R) (IDO-14553)
separation of cesium from, by vermiculites, 16: 12798
separation of cesium and strontium from condensate, containing ammonia, 16: 26638 (HW-71627)
separation of cesium from, by solvent extraction using dipicrylamine, 17: 28580 (HW-76222)
separation of cesium-137 and strontium-90 from, using clay, lime, phosphate, and soda ash, 17: 36998
separation of cesium from alkaline, ion-exchange, 18: 3387 (HW-76449)
separation of cesium from, by ion exchange, 18: 23700 (DP-876)
separation of cesium from, by ion exchange using iron cyanide–molybdenum oxide, 18: 31400
separation of cesium and strontium from acid, by ion exchange, 19: 7613 (BLG-267)
separation of cesium-137 and strontium-89 from, by Korean acid clay, 19: 24194
separation of cesium from Purex IWW, by solvent extraction using mixer-settler, 19: 28444(R) (ORNL-TM-1094)
separation of cesium-137 from fission-product, for transport, 19: 29803 (ORNL-3765)
separation of cesium from, by ion exchange, 19: 30349(P)
separation of cesium-137 and strontium-90 from, by sorption on ion exchange materials, 20: 14434 (BNWL-180)
separation of cesium-137, strontium-90, and yttrium-90 from, using multiclone dust, 20: 18170
separation of cesium from high-level, by ion exchange, 20: 16570
separation of cesium from fission-product, by ion exchange on ammonium molybdophosphate, 20: 20818
separation of chromium, iron, nickel, radioisotopes, and zirconium from, 16: 1855(R) (IDO-14560)
separation of fission products from, by solvent extraction, 17: 31788 (CONF-49-1)
separation of fission products from, by foam extraction, 18: 1797 (NYO-10038)
separation of fission products from, 18: 9744
separation of fission products from, by sorption on bentonites, 18: 37296 (NP-14178)
separation of fission products from, use of electrodialysis in, 19: 13523 (EUR-2199.e)

separation of fission products from, review, 19: 35857
separation of fission products from, at Hanford, 19: 45690 (RL-SA-40)
separation of fission products from, 20: 26551
separation of fission products from, methods for, 20: 27039 (NP-15946)
separation of fission products from, by sorption using clay minerals, 20: 29332 (ORNL-P-1811)
separation of fission products from, by solvent extraction, 20: 45796(R) (ORNL-3945, pp 195-8)
separation of manganese and rare earths from, solvent extraction methods for, 20: 16329 (BNWL-187)
separation of mercury from, by amalgamation with aluminum or copper, 18: 24977 (ORNL-TM-827)
separation of neptunium from Purex, by anion exchange, 17: 40923 (DP-453)
separation of neptunium-237 and plutonium-238 from, design of ion exchange column for, 18: 41571
separation of neptunium-237 from, method for, 20: 20561 (JAERI-1099)
separation of phosphorus from, by activated sludge methods, 20: 29353
separation of plutonium from, by steam stripping, 16: 1854(R) (IDO-14553)
separation of plutonium from analytical laboratory, 20: 435 (RFP-551)
separation of promethium-147 from, plant-scale demonstration of processes for, 20: 1551 (RL-SA-53)
separation of protactinium-231 from uranium-processing, efficiency of ion exchange and solvent extraction for, 18: 20105
separation of radium from uranium, foam, 17: 19718
separation of radium-226 from, by precipitation, 17: 42427
separation of radioisotopes from, by ion exchange, 18: 17332(R) (HW-80526)
separation of radioactive materials from, by sorption on peat, 19: 3801
separation of radium from, in uranium mills by ion exchange, 19: 34273
separation of radium from, by sorption on manganese dioxide, 19: 34269
separation of radioactive isotopes by coagulation and ion exchange, 19: 36549
separation of radioisotopes from, by precipitation, filtration, lime and soda treatment, and ion exchange, 19: 40276
separation of radioisotopes from, sorptive properties of peat for, 20: 7002 (INR-609/XIX/D)
separation of rare earths and strontium from Purex, by ion exchange, 18: 25606 (ORNL-3585)
separation of rare earths from complexed, by solvent extraction using bis(2-ethylhexyl)phosphate, 19: 46432 (ORNL-P-1603)
separation of rare earth fission products from, by solvent extraction using TBP, 20: 14635 (CONF-660305-5)
separation of rhodium and ruthenium from aqueous, 18: 3907(P)
separation of rhodium from aqueous, 18: 3908(P)
separation of ruthenium from Purex, by ion exchange, 18: 8445(R) (HW-78388(p.4.1-15))
separation of ruthenium-103 and -106 from, 18: 9990
separation of ruthenium from, by cellulose derivative-bentonite flocculation, 18: 24983
separation of ruthenium from alkaline, ion-exchange, 18: 27278(R) (HW-79280(p.4.1-28))
separation of ruthenium from, processes of, 20: 25033 (CEA-R-2842)
separation of solid suspensions from uranium, methods for, 16: 23385 (TID-7616(p.223-34))
separation of strontium from, by ion exchange on alumina or vermiculite, 17: 36999
separation of strontium-90 from organic, by ion exchange, 18: 35240
separation of strontium from, by solvent extraction followed by ion exchange, 18: 45160(P)
separation of strontium from stored Purex, by lead sulfate carrier precipitation, 19: 20035 (BNWL-4)
separation of strontium-90 from, by sorption by aluminum oxide, 20: 16330 (CEA-R-2851)
separation of technetium from, by ion exchange, 20: 1963
separation of uranium by precipitation with ferrocyanide, 16: 12799
shipping solidified, hazards of, 20: 24809(R) (BNWL-213)
solidification and storage of medium-level, 20: 47084 (PEL-102)
solidification of high-level, 20: 47083(R) (ORNL-3945, pp 79-106)
solidification of, in-tank, 19: 22405(R) (HW-83298(p.4.1-25))
solidification of, performance of engineering prototypes for, 20: 8477(R) (BNWL-139)
solidification of, performance of in-tank, 20: 18161 (ISO-SA-1)
solubility and drip temperature of, effects of temperature and time on, 20: 12517(R) (BNWL-170)
solubility and temperature of phosphate, containing fission product and process oxides, 20: 12517(R) (BNWL-170)
sorption of iodine-131 from, by charcoal, 16: 1284
sorption of radioisotopes from, by rhyodacite tuff, 19: 48085
sources of, industrial and non-industrial, 20: 12520(T) (CEA-tr-A-1490)
storage at Oxford University, design of central store for, 18: 13353
storage in underground tanks, activity in seepage from, 19: 21752
storage in vaults in crystalline rock, 19: 33681
strontium-90 uptake by, 18: 3459
strontium-90 recovery, 16: 25651 (HW-71574)
sulfate precipitation from, 19: 25777(R) (HW-84603(p.37-49))
sulfate precipitation from, 20: 8477(R) (BNWL-139)
temperatures in storage tanks for, effects of leaks on, 20: 35172 (BNWL-181)
thermal properties of solidified, 20: 12517(R) (BNWL-170)
toxic effects of reactor, on fish, 17: 35323(R) (HW-76000(p.211-14))
toxic effects of reactor, on fish, 17: 35325(R) (HW-76000(p.219-22))
toxic effects of uranium mill, on river fauna, 17: 33586
transport by ground water, sequence for predicting, 20: 11009 (BNWL-SA-406)
transport of solidified, hazards in, 20: 12517(R) (BNWL-170)
transportation of solidified, hazards in, 20: 8477(R) (BNWL-139)
transportation of, analysis of aircraft capabilities for, (T), 19: 24065 (AFWL-TDR-64-81)
treatment, 20: 5207
treatment and disposal, summary, 17: 26932(R) (ORNL-TM-516)
treatment and release, 18: 13352
treatment and storage of small amounts of, survey of, 17: 26943
treatment at Juelich research center, 19: 48078 (JUL-261-DE)
treatment of high- and low-level, summary, 18: 19448(R) (ORNL-TM-757)
treatment of intermediate-level, 19: 25777(R) (HW-84603(p.37-49))
treatment of low-level aqueous, methods for, 16: 31349
treatment of low-level, development of scavenging-precipitation ion-exchange process for, 17: 28582 (ORNL-3322)
treatment of low-level, summary, 17: 30582(R) (IDO-14611)
treatment of radioactive design of falling-film evaporator for, 18: 6543
treatment of, economics and problems in, 19: 40274
uptake by marine organisms, 19: 10732
uranium sorption from, using sawdust, 20: 26579
use in generating electricity, method of, 20: 9360(P)
use in generation of electric current, 20: 33757(P)
use of sugar beet pulp base as cation exchanger for, 16: 20039

WATER

see also Body Water
see also Ground Waters
see also Ice
see also Natural Waters
see also Radioactive Waters
see also Rain Water
see also Sea Water
see also Steam
see also Surface Waters

acidities in, substituent effects on, 18: 43488
acidity and conductivity of distilled, in Czechoslovak nuclear reactor, 18: 1309
activation of, in secondary and auxiliary circulating systems of a reactor, 17: 42204
activation of, by X-agent, 18: 26146
aerosol particle washout with, 18: 35260(R) (AERE-PR/HPM-5)
alpha activity in flowing, monitor for, 20: 21038 (K-1656)
alpha monitoring in, apparatus for, 18: 23828(R) (UCRL-7637)
alpha reactions with, neutron yields from, 17: 9527
alpha reactions with molecules of, 17: 39308(R) (ORNL-3492(p.134-43))
analyses for uranium, spectrophotometric, 19: 11029
analyses of reactor coolant, 19: 42084(R) (CVNA-239)
analysis for alkali and alkaline earth metals in mineral, flame photometric, 20: 38798 (NIJS-R-465)
analysis for alpha and beta sources, radiochemical methods for, 20: 16337 (RMO-3001(Rev.1)(Suppl.))
analysis for aluminum, chromium, copper, iron, manganese, molybdenum, and nickel by extraction photometry, 19: 15388
analysis for aluminum, iron, and silicon, 19: 26229 (INR-590/VIII)
analysis for americium, evaluation of radiochemical method for, 20: 8980(R) (BNWL-36, pp 3.1-122)
analysis for ammonia traces, 18: 11964 (HW-79296)
analysis for beta sources, 17: 1412
analysis for beta-emitting radioisotopes, 18: 1525
analysis for beta activity, cesium-137, sodium-24, strontium-90, and tritium, radiochemical procedures for, 18: 13642 (SC-4783(RR))
analysis for beta-emitting radioisotopes, 18: 15982
analysis for boric acid, neutron absorptiometric, 16: 2962 (ANL-6439)
analysis for boric acid, automated colorimetric, 19: 40404 (BNWL-SA-167)
analysis for boron traces, spectrophotometric, 18: 11972 (PG-Report-532)
analysis for boron and strontium, spectrochemical, 19: 39265(R) (IA-1021)
analysis for boron and strontium, spectrochemical, 20: 256
analysis for bromine-82 and iodine-131, 17: 30155
analysis for cadmium traces, atomic spectrophotometric, 18: 31366

(CRDC-1193)
analysis for calcium by isotope dilution, 19: 11028
analysis for carbon-14, sampling techniques for, 19: 36681
analysis for cations, silver-spark spectrographic, 17: 1381 (IDO-14591)
analysis for cerium, lanthanum, phosphorus, and strontium by counting after adsorption on phosphate gel, 16: 12953 (PAN-268/X)
analysis for cesium-137, iodine-131, and strontium-89 and -90, methods for, 18: 35471
analysis for cesium-137, iodine-131, strontium-89, and strontium-90, 19: 13232
analysis for cesium-137, rapid method for, 19: 19805
analysis for cesium-137, chromium-51, and potassium-40, source of error in gamma spectroscopic, 19: 32596
analysis for cesium-137 by ion exchange and gamma spectroscopy, 20: 16342
analysis for cesium-137, iodine-131, and strontium-89 and -90, gamma spectrometric, 20: 31180
analysis for chlorine, magnesium, and sodium, thermal neutron activation, 18: 5220
analysis for chloride ions, colorimetric, 18: 6762
analysis for chlorine and copper, activation, 20: 12768 (IEA-97)
analysis for chlorine, radiochemical method for, 20: 43063 (EUR-2990.f)
analysis for chromates, absorptiometric, 16: 11520 (PG-Report-310)
analysis for chromium-51 by precipitation with iron hydroxide and gamma spectroscopy, 20: 20603
analysis for cobalt-60, spectrophotometric, 19: 15384
analysis for coliform bacteria using carbon-14, 18: 39534
analysis for copper, spectrophotometric, 17: 17972 (PG-Report-434)
analysis for corrosion products, method for, 20: 33201
analysis for corrosives and solids in swimming pool reactor coolant, activation and chemical, 20: 38800 (PAEC(C)RE-652)
analysis for deuterium at 0.003 to 0.02%, absorptiometric, 16: 14662(T)
analysis for deuterium, mass spectrometric, 16: 20333
analysis for deuterium and tritium, design of infrared monitor for, 16: 32918 (CRRP-1099)
analysis for deuterium, infrared analyzer for, 17: 1415(P)
analysis for deuterium using thermal conductivity cell, 17: 2731
analysis for deuterium, falling-drop, 17: 10566
analysis for deuterium by thermal conductivity, 17: 33807
analysis for deuterium, hydrogen, and oxygen, 18: 7853(R) (KR-58)
analysis for deuterium, methods for, 19: 319
analysis for deuterium, infrared method for, 19: 2209 (CRDC-1141)
analysis for deuterium by density measurements after normalizing oxygen-18 content, 19: 13210
analysis for deuterium and oxygen-18 by differential pycnometric method, 19: 13211
analysis for deuterium, 20: 1801(P)
analysis for deuterium, infrared spectroscopic, 20: 7030
analysis for deuterium by photodissociation methods, 20: 22893
analysis for deuterium by infrared spectroscopy, 20: 31640(R) (NYO-755-1, pp 130-72)
analysis for deuterium by decomposition and gas chromatography, 20: 35441
analysis for dissolved hydrogen, design of automatic instrument for, 16: 348 (WAPD-BT-23(p.27-30))
analysis for dissolved oxygen, radiochemical method, 16: 11514 (ORO-483)
analysis for dissolved oxygen, 16: 23610 (PG-Report-335)
analysis for dissolved oxygen, radiometric, 16: 25282
analysis for dissolved oxygen, review of methods for, 18: 8266 (CEA-Bib-36)
analysis for dissolved gases, 18: 27290 (TID-19180)
analysis for dissolved oxygen, radiometric, 19: 17782 (ORO-592)
analysis for dysprosium-165m, selenium-77, and tellurium-131, activation, 19: 10983(R) (TEES-2671-3)
analysis for ethanol using beta-excited x-ray sources, absorptiometric, 20: 3882 (ORNL-IIC-5, pp 51-71)
analysis for fallout, activity losses by evaporation during, 17: 19802
analysis for fallout nuclides, 20: 7021
analysis for fission products, apparatus, 16: 27172(P)
analysis for fission products and uranium, 18: 6471 (NP-13445)
analysis for fission products, design of monitor for, 20: 3909
analysis for fluorine, 17: 27589 (CNI-111)
analysis for fluorides by radiometry using tantalum-182, 19: 39265(R) (IA-1021)
analysis for heavy water by infrared absorption, 16: 18847
analysis for heavy water in Concepción Region, Chile, 16: 25621
analysis for heavy water at 25°C, 16: 28883
analysis for heavy water, infrared, 17: 32006
analysis for heavy water by electrochemistry of cadmium in water-heavy water systems, 19: 40427
analysis for heavy water by nuclear magnetic resonance spectra, 20: 239
analysis for heavy water, leak detector for, 20: 2099 (AECL-2291)
analysis for heavy water by infrared spectroscopy, 20: 16377
analysis for hydrazine, absorptiometric, 16: 22007 (PG-Report-336)
analysis for hydrogen peroxide, ultraviolet spectrophotometric, 18: 15948 (CEA-2391)
analysis for hydrogen peroxides in irradiated, polarographic, 20: 16327 (AAEC/TM-301)
analysis for impurities, in nuclear reactor for marine propulsion, methods for, 17: 33789 (EUR-224.i)
analysis for impurities, survey of methods for, 18: 1505 (ORNL-TM-724)
analysis for impurities, spectrographic method using gallium oxide, 19: 19774 (UCRL-7962)
analysis for iodine-131 by liquid ion exchange and activity counting, 20: 26807
analysis for isotopes, book, 16: 23661
analysis for isotopic impurities, infrared analyzer for, 18: 25312(P)
analysis for isotopic content, infrared absorptiometric, 19: 2207 (CEA-R-2441)
analysis for isotopic impurities, apparatus for radiation absorption, 19: 34134(P)
analysis for low levels of uranium, 18: 43397
analysis for low-level alpha and beta radioactivity, method for, 18: 10017
analysis for metallic impurities by atomic absorption spectrometry, 18: 33461 (DP-879)
analysis for metal traces, polarographic, 19: 11030
analysis for metallic impurities, atomic absorption spectroscopy for, 19: 46166 (DP-980)
analysis for oxygen-18 by conversion of oxygen to carbon dioxide, 16: 2971
analysis for oxygen, radiometric, 16: 24577
analysis for oxygen-17 and oxygen-18, 17: 5956 (KR-30)
analysis for oxygen, activation, 18: 1523
analysis for oxygen-18 by neutron activation, 18: 23426
analysis for oxygen-18 by infrared spectrometry, 18: 35459
analysis for oxygen, activation, 18: 37092
analysis for oxygen-18, activation, 19: 7341
analysis for oxygen-18, by activation methods, 19: 40419
analysis for oxygen-18, activation, 19: 45679(R) (NYO-1859-11)
analysis for oxygen-18, mass spectrometric, 20: 8852
analysis for oxygen-18, vapor pressure osmometer for, 20: 9368
analysis for oxygen-18, mass spectrometric, 20: 12800
analysis for oxygen, radiochemical method for, 20: 43064 (EUR-2991.f)
analysis for peroxide in reactor coolant, titrimetric, 20: 43071 (IDO-14679, pp 75-191)
analysis for phosphate traces, radiometric, 16: 15076
analysis for phosphorus and sulfur simultaneously, activation, 18: 11989
analysis for phosphorus-32, 19: 15383
analysis for plutonium by solvent extraction using cupferron, 16: 17604
analysis for plutonium, radiochemical method for, 19: 44296 (NYO-4700(Rev.)(Suppl.II))
analysis for polonium-210 by coprecipitation with tellurium by stannous chloride and alpha counting, 20: 26762
analysis for radioisotopes, compilation of procedures for, 16: 4192
analysis for radioisotopes in Russia, 16: 10312(T) (JPRS-12166)
analysis for radioactivity, 16: 16325
analysis for radioactive materials, methods used at Czechoslovakian water-work laboratories for, 17: 7979
analysis for radioisotopes by gamma spectrometry, 17: 40702 (TID-7655 (p.107-18))
analysis for radioisotopes in treatment plants for, 18: 19448(R) (ORNL-TM-757)
analysis for radioisotopes in swimming pool reactor, 18: 31037
analysis for radioisotope traces, gamma spectrometric, 18: 33485
analysis for radionuclides, training course manual on, 18: 39531 (NP-14255)
analysis for radioactive niobium and ruthenium, 18: 41357
analysis for radioactive materials, methods for, 19: 324
analysis for radioactivity, method for, 19: 43974
analysis for radioisotopes, 20: 40819(T) (CEA-tr-A-1883)
analysis for radium by sorbe-mulsion method, 17: 32013
analysis for radium isotopes, methods for, 18: 35486
analysis for radium-226 and radon-222, assay methods for, 18: 35487
analysis for radium, use of activated carbon for, 19: 13236
analysis for radium-226, radiochemical method for, 19: 44296 (NYO-4700(Rev.)(Supp.II))
analysis for radium-226, 20: 40809 (NP-16235)
analysis for radon, radiochemical, 17: 7974
analysis for radon, method for scintillation, 18: 21967
analysis for radon, radiometric, 18: 31401
analysis for radon-222, 19: 2208 (CLOR-28)
analysis for radon, radiometric method using a liquid scintillator for, 19: 5790

analysis for Rhodamine B, spectrophotometric, 16: 16320
analysis for strontium-90 by ion exchange, 16: 8684(T) (AERE-Trans-881)
analysis for strontium isotopes, 16: 18818 (TID-15415)
analysis for strontium-90, radiometric, 16: 22031
analysis for strontium by x-ray fluorescence, 17: 38962
analysis for strontium-90 by chelate extraction and counting, 18: 166 (NP-13232)
analysis for strontium, flame photometric, 18: 11983
analysis for strontium-90 by ion exchange and counting, 18: 13687
analysis for strontium-90 by using carrier technique, triple precipitation, and counting, 18: 25267 (K-1521)
analysis for strontium-90, radiochemical, 18: 39509
analysis for strontium, flame spectrophotometric, 19: 5766 (AE-163)
analysis for strontium-90, method for rapid control, 19: 24445
analysis for strontium-90, 20: 1754
analysis for thorium, spectrophotometric, 16: 26927
analysis for thorium and uranium in solutions of, by beta absorption, 17: 32014
analysis for total beta activity by ion exchange and counting, 18: 13687
analysis for trace elements, spectrographic, 17: 2929
analysis for traces of dissolved oxygen, 18: 31367 (HW-79194(Rev.1))
analysis for trace elements by activation, use of paper chromatography and computers in, 19: 7338
analysis for trace amounts of barium, cesium, copper, nickel, rubidium, and uranium, activation, 20: 24990
analysis for trace elements, neutron activation, 20: 33248
analysis for tritium, development of continuous monitoring technique for, 16: 694
analysis for tritium, photographic, 16: 1707
analysis for tritium, radiometric, 16: 25592
analysis for tritium using liquid scintillator, 18: 41340
analysis for tritium, radiochemical, 19: 7266 (AERE-M-1219)
analysis for tritium, review on methods for, 20: 1728 (AD-618562)
analysis for tritium, method for, 20: 5517
analysis for tritium, survey of concentration and counting methods for, 20: 5521
analysis for tritium, efficiency of flow counter for, 20: 29098
analysis for tritium by distillation, electrolysis, and scintillation counting, 20: 31398(T) (NSJ-tr-49)
analysis for tritium, method for, 20: 40826
analysis for uranium, spectrophotometric, 16: 17592(T) (CEA-tr-R-1569)
analysis for uranium by alpha counting, 17: 1374 (AERE-AM-85)
analysis for uranium using sodium diethyldithiocarbamate, photometric, 17: 35648
analysis for uranium, method for, 19: 30132
analysis for uranium, activation, 20: 14461(R) (ORNL-3889, pp 48-70)
analysis for uranium, methods for, 20: 16337 (RMO-3001(Rev.1)(Suppl.))
analysis for water-d_1 by infrared spectroscopy, 16: 26903(T) (AEC-tr-5270)
analysis for water-d_1 by drops falling in *o*-fluorotoluene, automatic timer design for, 16: 14659
analysis for water-d_2 by falling-drop method using inclined tube, 19: 6149 (SGAE-CH-6/1964)
analysis for water-d_2 by specific weight measurement, 19: 43983(P)
analysis for zirconium, automated fluorescence, 19: 40403 (BNWL-SA-166)
analysis in primary reactor cooling systems, chromatographic method for, 20: 26777
analysis loops, for oxygen, volumetric, 16: 9942 (CRDC-732)
analysis, methods and standards for radiochemical, 16: 28888
analysis of boiling, for gases, instrument for automatic, 17: 40705 (TID-7655(p.147-175))
analysis of borehole, for beta activity, 17: 17970 (PG-Report-357)
analysis of effluent for actinium-227, radiochemical, 19: 10979 (AERE-R-4747)
analysis of, for deuterium by measurement of variation of vanadium electrode potential, 17: 31989
analysis of, for lithium, flame photometric, 17: 23250 (AE-105)
analysis of, for sulfur, activation, 17: 19958
analysis of, for tritium, radiometric, 16: 31544 (IA-739)
analysis of pressurized, for gases, 18: 41310 (CEA-R-2509)
analysis of pure and tap for trace elements, by reactor neutron activation methods, 20: 26760
analysis of reactor effluent for radionuclides, 18: 43372 (HW-SA-3680)
analysis of reactor coolant, 19: 11003
analysis of reactor-coolant, for chlorides by neutron activation, 20: 41418(R) (GEAP-5150)
analysis of void fractions in boiling, by neutron attenuation, (E), 19: 18109 (CONF-654-53)
analysis of, for cesium-137 and strontium-90 by beta-counting after chemical separation, 20: 43532
analysis of, for deuterium oxide, by infrared spectrophotometry, 20: 35410
analysis of, for oxygen-18, preparation of carbon dioxide for mass spectroscopic, 20: 26790
analysis of, for oxygen-16 and oxygen-18 by mass spectrometry, 20: 45598
analysis of, for radium, evaluation of methods for, 20: 31191
analysis of, for various elements, by neutron activation methods using freezing, 20: 45602
analysis of, infrared absorption equipment for isotopic, 20: 18620(P)
analysis of, methods for, 20: 16337 (RMO-3001(Rev.1(Suppl.))
analysis of, review on methods for, 19: 22110
analysis of, use of interferometer for isotopic, 19: 13212
analysis, operation of rotating filter infrared spectrometer for isotopic, 17: 333 (IM-48)
analytical chemistry of, review on, 17: 19949
anharmonicity constants of isotopically substituted, 17: 4546(T)
antenna performance in fresh, cylindrical and spherical, 20: 3632 (SC-DR-65-459)
argon thermodynamic properties in, 19: 13318
atomic frequency spectra of moderators of, integral parameters for, 20: 36404 (AE-228)
beta absorption and backscattering by, calculation of elemental stopping powers from, 19: 30127
beta activity measurement in, reliability of techniques for, 18: 15979
beta measurement sensitivities in, 16: 17834
beta particle detection in, using Cherenkov effect, 20: 31506 (CEA-R-2915)
beta radioactivity in Hawaii during 1962 Pacific nuclear tests, 19: 13629 (NP-14778(Pt.III))
bibliography on pollution and purification of, 16: 31999 (SB-498)
bibliography on saline conversion, 16: 2815 (TID-3567)
boiling, analysis of liquid superheat for nucleate, 19: 13576 (ANL-6980)
boiling burnout and natural circulation stability in seven-rod bundle at high pressures, 19: 7678 (EURAEC-1163)
boiling burnout and flow instability at 500 to 1500 psia in heated parallel tubes, 19: 7685 (TID-21403)
boiling burnout at 1000 psia in swirl-flow tube heater, 18: 43760 (TID-21101)
boiling burnout at atmospheric pressure, saturation pool, 20: 25258
boiling burnout conditions for, flowing in vertical ducts, 18: 1880
boiling burnout conditions for flow in vertical 3- and 7-rod clusters, (E/T), 20: 11000
boiling burnout data for clusters of reactor fuel rods cooled by, 20: 35615 (AEEW-R-468)
boiling burnout detection method for, 20: 14694
boiling burnout heat flux, 19: 24673 (NP-14953)
boiling burnout heat flux in internally cooled tubes, effects of inlet flow conditions on, 20: 4101(R) (EURAEC-1354)
boiling burnout in flow through vertical annuli, 17: 10789 (AE-100)
boiling burnout in, investigation of critical, 17: 10807(T,R) (EURAEC-449)
boiling burnout in ducts, survey of experimental data on, 18: 35162 (TID-8540(p.131-76))
boiling burnout in flow of, over vertical rod clusters, 18: 39424 (AE-153)
boiling burnout in vertical tubes, compilation of world data on, 19: 2511 (AEEW-R-356)
boiling burnout in heated tubes, 19: 11349(R) (EURAEC-1224)
boiling burnout in flow in ducts, annuli, and rod clusters, tables of data on, 19: 26498 (AE-177)
boiling burnout in vertical round ducts, development of correlation for, 19: 30367 (AE-178)
boiling burnout in, comparisons of analyses of, (T), 19: 38814
boiling burnout in pressurized loops in natural circulation conditions, 19: 46536 (RT/ING(65)1)
boiling burnout in annular flows at 1000 psi, (E), 20: 4105 (TID-22321)
boiling burnout in, in internally cooled tubes, 20: 14686(R) (EURAEC-1448)
boiling burnout of subcooled, in forced flow through tubes, 19: 32383 (EUR-2432.d)
boiling burnout of, flowing through nonuniformly heated tubes, (E), 20: 9113(R) (BAW-3238-10)
boiling burnout studies, 18: 33737 (ORNL-P-18)
boiling burnout, effects of electric fields on, 19: 38807(R) (NYO-2404-70)
boiling critical heat flux in internally cooled channels at 70 and 100 atm, effects of length/diameter ratio on, 19: 44184(R) (EURAEC-1281)
boiling detection in, tests of acoustic instrument for, 20: 2014 (ORNL-P-1678)
boiling, effect of channel diameter on critical thermal load, 17: 20179
boiling, effects of size range of active nucleation cavities and surface conditions on nucleate, 16: 27212
boiling, equipment and techniques for measuring burnout heat flux in, 17: 276(T,R) (EURAEC-303)
boiling, equipment and techniques for measuring burnout heat flux in, 17: 278(T,R) (EURAEC-404)
boiling flow in parallel rod array, pressure profiles of, 20: 25256

boiling flow in tubes at low pressures, nucleate subcooled, 19: 11350 (NASA-TN-D-2626)
boiling flow of, momentum transfer and void fraction in, 20: 33468
boiling flow over heated rod, visual observations of high-pressure transitional, 19: 4306 (GEAP-4636)
boiling flow over heated rods, photography of high-pressure transitional, 20: 25242 (GEAP-5094)
boiling flow regimes at 500 psia, 19: 26500(R) (NYO-3304-4)
boiling flow regimes in high-pressure, research program on, 19: 44193(R) (NYO-3304-5)
boiling heat flux in, effects of induced whorls on critical, 18: 16183(T) (EURAEC-639)
boiling heat transfer at low heat flux, 17: 37336(R) (TID-19371)
boiling heat transfer from rod bundles in forced flow of, at 1000 psia, 18: 3952 (DP-857)
boiling heat transfer in forced convection in, at 600 to 1400 psia, 18: 29837 (GEAP-4492)
boiling heat transfer from platinum, effects of reduced gravity on, 18: 35685(R) (APL-TDR-64-19)
boiling heat transfer in, effects of electric fields on, 18: 35690(R) (NYO-2404-4)
boiling heat transfer by, 19: 18126
boiling heat transfer from outside surfaces of tubes to saturated, at 535 to 1550 psia, 19: 28503 (SROO-260-6)
boiling heat transfer from two-rod geometry to, in forced convection at 1000 psia, 19: 30371 (GEAP-4721)
boiling heat transfer, effects of applied voltage on, 19: 32365 (CONF-640507(p.217-52))
boiling heat transfer scaling laws in tubes of, forced-convection, 19: 32345 (AEEW-R-363)
boiling heat transfer at 300 psi, effects of electric fields on, 19: 40735(R) (NYO-2404-5)
boiling, hydrodynamic model for nucleate pool, 16: 20605
boiling in annular channels with heating from two sides, critical heat flux, 19: 30383(T) (WAPD-Trans-17)
boiling in forced flow of, calculation of critical heat flux in, 18: 10233(T) (AEC-tr-6290)
boiling in heated tubes, burnout in, 19: 46541
boiling in Inconel tubes under forced convection, subcooled nucleate, 16: 27220
boiling in natural circulation loop, oscillations in, 20: 14684 (ANL-7073)
boiling in rod bundles, critical, (T), 20: 36992
boiling in stainless steel tubes, heat transfer burnout in, 17: 1613
boiling in tubes, critical heat loads during, 17: 1614
boiling in tubes, forced convection, 16: 17812
boiling in tubes, local heat flux and pressure drop in forced-convection, 18: 43761 (UCRL-13062)
boiling instability in forced-convection flows through small tubes, subcooled, 19: 46534 (NP-15437)
boiling kinetics of, nucleate, 18: 6933
boiling, mechanism of saturated nucleate pool, 18: 25671
boiling of, acoustic noise production in nucleate, 17: 32251 (TRG-Report-549)
boiling of subcooled, burnout heat flux limits in annulus, 17: 11979(R) (DP-805)
boiling of subcooled, void volume in nucleate pool, 18: 12322
boiling of, surface temperature fluctuations during bubble formation in nucleate, 18: 20162 (EUR-1622.f)
boiling of, transition from discrete-bubble to merging-bubble regime in nucleate, 18: 39459
boiling of, void fraction-measuring instruments for, 18: 35809(R) (NYO-10559)
boiling of, void fraction-measuring instruments for, 18: 35810(R) (NYO-10610)
boiling on horizontal plate, film, 16: 16508
boiling on horizontal surfaces, analysis of nucleate pool, 18: 1881
boiling on mercury and metal surfaces, nucleate, 16: 20618
boiling on mercury surface, nucleate, 16: 20617
boiling on metal ribbons at atmospheric pressure, transient pool-type, 16: 13232
boiling on vertical surface of submerged metallic ribbon with step in Joule heating, transient, 16: 27213
boiling peak heat flux for, flowing normal to cylinders, 17: 12434
boiling phenomena in high-pressure, photographic studies of, 17: 16235 (WAPD-T-1566)
boiling point and vapor pressure of, 20: 38921
boiling point, effects of magnetic field on, 19: 7358 (MATT-235)
boiling, velocity of rising steam in, 16: 24510
boiling void distribution along cylindrical reactor channels, 20: 33469
bonding in alumina, beryllia, and silica during dehydration at 150 to 1100°C, 20: 16413 (CEA-R-2703)
bonding to clays, NMR study of, 18: 16031
book: *Radioactive Materials and Water. A Review*, in German, 16: 8443
book: *The Radiation Chemistry of Water and Aqueous Solutions*, 16: 249
book: *Water Circuit in Thermal Power Stations*, 19: 35633
bremsstrahlung and electron transport in, (T), 20: 3246 (NASA-SP-71, pp 437-48)
bubble entrainment in flow of, 19: 32387 (NP-15051)
bubble formation in initially subcooled, 18: 6920 (AD-424629)
bubble growth and collapse times in, 16: 14854 (WAPD-TH-453)
bubble growth rate in, at atmospheric pressure, 16: 13219
bubble motion in, 16: 6535
burnout conditions for flow of boiling, in vertical round ducts, 17: 7528 (AE-87)
burnout conditions for single rod in annular flow path at 600 to 1400 psia, 18: 5464 (GEAP-3899)
burnout heat flux in boiling, effects of ultrasonic vibrations, 16: 19042 (ATL-A-123)
burnout heat flux of forced convection in channels, 16: 19056
burnout in flow through tubes, effects of axial heat-flux distribution on, 17: 12433
burnout in pool boiling, effects of pressure transients on, 17: 12436
calcium uptake from, by trout, tracer study, 20: 10555
cation hydration in, (T), 20: 8895
cavitation bubble collapse in flow of, in venturi, 19: 32386 (NP-15023)
cavitation damage to materials in, 19: 9623 (NP-14632)
cavitation damage on aluminum and gold foils, 19: 13915 (NP-14771)
cavitation damage on coated impellers, studies, 19: 44197 (TIM-895)
cavitation damage to materials in, (E), 20: 16974 (NP-15889)
cavitation effects on materials in venturi, 18: 3955 (NP-13319)
cavitation number measurements in, effects of air on, 19: 9330 (NP-14605)
cerium compound absorption spectra in, 20: 36831
cesium-137 maximum permissible concentration, 16: 1320(R) (LAMS-2627(p.175-82))
cesium-137 content in Amsterdam, 1960 to 1963, 20: 20949
cesium-137 content in, Bombay, 1964 to 1965, 20: 43532
chemical and radioactive wastes in, effects on fish ecologies, 17: 14528 (HW-SA-2862)
chemical binding in, 18: 15675 (IS-530)
chemical properties, determination by quantum theory, 16: 15364
chemical properties of ruthenium nitrate in, 20: 25033 (CEA-R-2842)
chemical reactions in reactors, 18: 22012(R) (ORNL-3591(p.67-9))
chemistry in boiling reactors, 18: 3059
chemistry in Hanford Production Reactors (N), automatic system for monitoring, 19: 24144
chemistry of, in water-cooled reactors, 17: 4907
chemistry of, in water-cooled power reactors, 17: 31740
chemistry of pressurized-reactor, in-pile loop studies of, 19: 23996(R) (ORNL-3650(p.1-110))
chemistry of reactor, 18: 24886(R) (GEAP-4565)
chemistry of reactor coolant, 18: 24898 (NP-13900(Sect.3))
chemistry of reactor, 18: 24884(R) (GEAP-4419)
chemistry of, in Bulgarian IRT-1000 reactor, (E), 19: 19421
chloride ion transfer to heavy water, calculation of free energy of, 18: 25338
circulation in boiler-feed water system, design of device for measurement of velocity of, 18: 7101(P)
coalescence of drops of, with solids, rate measurements, 19: 28471(R) (TID-21855)
collection of atmospheric, for tritium sampling, 19: 22125
collision of molecular beam of, with water vapor, cross sections, 17: 624
condensation tests in zero gravity, 19: 583 (NP-14431)
conservation of resource, use of nuclear explosions in, 18: 1843 (UCRL-6588)
contact angle hysteresis studies, 16: 17881(R) (MITS-47)
contamination by fall-out, maximum permissible, 16: 28733
contamination by uranium and its isotopes, maximum permissible concentrations for, 19: 13674
contamination of, origin, 17: 13874
content and reactions in upper atmosphere, 19: 14120
content in barium–hydrogen loaded resins, determination of, 18: 36896 (TID-19539)
content in blood plasma and urine of rats, 20: 40561
content in building materials, neutron scattering for determination of, 17: 34206
content in cereals, determination of, using neutron thermalization, 20: 37154
content in concretes, gamma and neutron shielding parameter variations with, 20: 3253
content in concretes, effect on shielding properties of, 20: 10227
content in concretes, thermal neutron scattering determination of, 20: 18610
content in concretes, neutron transmission method for determining, 20: 25355
content in crude ores, use of fast neutron elastic scattering for measuring,

18: 35910
content in Earth's surface, book on, 20: 7254
content in Leda clay, calibration of neutron meter for measuring, 18: 33897
content in living tree trunks, radiometric device for measuring, 18: 39576
content in materials, statistical correlation of neutron scattering for determination of, 17: 34204
content in materials, neutron transmission method for determining, 20: 25355
content in nickelveyite uranium mineral, 19: 40799
content in organic soils, measurement of, using neutron method, 20: 14756
content in rat liver after gamma irradiation, effects of dietary casein level, 20: 42864
content in rat organs, effects of diet and radiation on, 17: 30244
content in rhyolitic lava, 18: 33788
content in seeds, effects on reactions to x radiation, 19: 21946
content in snow at Lysa Hora, performance of radiometric snow gage for measuring, 18: 18151
content in snow deposits, gamma spectroscopic determination of, 20: 549
content in soil, determined by gamma ray absorption method, 17: 8508
content in soil of Neotoma Valley, Ohio, ecological effects in forest environment, 19: 6900 (TID-21354)
content in soil, gamma attenuation measurement of, 19: 17837
content in soil, neutron probe measurement of, 20: 20915
content in soil, radiometric methods for determining, 20: 29505
content in soil, theory of neutronic method for determining, 19: 26234 (RISO-97)
content in soil, use of neutron meters in measuring, 20: 39131
content in soils, neutron scattering method for measuring, 19: 11405
content in soils, volume of influence of neutron probe for determining, 19: 36678
content in soils, effects of bulk density and hydrogen form on calibration of meter for measuring, 19: 38948
content in soils, determination by neutron thermalization, 20: 544
content in soils, cost comparison of neutron-moderation and gravimetric methods for determination of, 20: 43094
content in soils, measurement by neutron attenuation and scattering, 20: 43558
content in thalenites from Japan, 20: 29399
content in trees, tracer study, 20: 45267
content in upper atmosphere, 18: 7616
content in upper atmosphere, from rocket soundings, 18: 37794(T) (NASA-TT-F-141(p.1-21))
content in zircon from Kyoto Prefecture, Japan, 19: 36296
content measurement by neutron attenuation, 17: 30729
content of, in building materials, thermal neutron diffusion method for determination of, 17: 15902
content of soil, device for measurement of, 17: 41011
contents in meteorites, 18: 34398
convection transients from flat vertical surfaces, natural, 17: 16246
cooling capacities of, as reactor coolant, 18: 6424
corrosion effects of oxygenated, on chromium–nickel steel, 20: 2262 (WCAP-2056(Pt.6))
corrosive effects on Zircaloy-2 at 680°F, 16: 7889 (NP-11196(p.16-20))
corrosive effects of ammoniated and lithiated, on Zircaloy under nucleate boiling conditions, 16: 19287 (KAPL-2203)
corrosive effects on aluminum and aluminum alloys, 16: 22548
corrosive effects on aluminum alloys at high temperatures, 16: 22550
corrosive effects on zirconium alloys at high temperatures and pressures, effects of anions, 16: 22557
corrosive effects on steels at critical parameters, electrochemistry, 16: 22562
corrosive effects on uranium, uranium–zirconium alloys, and zirconium, effects of cathodic polarization, 16: 22154
corrosive effects in pressurized-water-cooled reactors, 16: 30738
corrosive effects on Zircaloy-2 and -4 at high temperatures, 16: 33433 (WAPD-TM-307)
corrosive effects on steels at 546°F, 16: 33439
corrosive effects on aluminum in reactor environment, 16: 33442
corrosive effects on reactor metals and alloys, review, 17: 3431
corrosive effects on Zircaloy-2 at 360°C, 17: 11097(R) (NMI-7257)
corrosive effects on annealed Zircaloy-2 at 550°F, 17: 11132 (KAPL-M-AA-4)
corrosive effects on nickel-plated steel, 17: 13878(R) (KR-36)
corrosive effects on iron, 17: 16600
corrosive effects on aluminum, 17: 18698 (JAERI-1035)
corrosive effects on aluminum alloys, groove pitting in, 17: 27747 (HW-74359(Rev.))
corrosive effects on Zircaloy-2 at high temperatures, effects of radiation and cold work on, 17: 27729 (HW-76636)
corrosive effects on reactor materials, 17: 37001(R) (ANL-6780)
corrosive effects on Zircaloy-2, effects of carbon content on, 17: 37465 (WAPD-T-1508)
corrosive effects of simulated N-reactor secondary system, on materials, 17: 37480 (HW-76358)
corrosive effects on beryllium at 325°C, 18: 4192 (AERE-R-4422)
corrosive effects on aluminum and aluminum alloys, bibliography on, 18: 7150 (VDIT-81)
corrosive effects on zirconium alloys at high temperatures, effects of fluorides on, 18: 10469 (CONF-187-52)
corrosive effects on mild steel equipment in HWCTR, 18: 13331 (DP-801)
corrosive effects on niobium–tin–zirconium alloy, 18: 12574 (APED-4364)
corrosive effects on niobium–tin–zirconium alloy, 18: 14358(R) (EURAEC-135)
corrosive effects on niobium–tin–zirconium alloy, 18: 14360(R) (EURAEC-199)
corrosive effects on Zircaloy-2, additive effects of nitrogen, oxygen, and silicon on, 18: 16440 (WAPD-283)
corrosive effects on Zircaloy-2 at 680°F, 18: 27884 (KAPL-2000-21(p. VI.1-4))
corrosive effects on uranium nitrides at 100°C, 18: 30108(R) (BMI-X-10083)
corrosive effects on niobium–tin–zirconium alloy at 350°C, 18: 30110 (EUR-86.d)
corrosive effects on uranium, effects of oxygen on, 18: 34072 (AWRE-O-40/64)
corrosive effects on construction materials under Advanced Test Reactor conditions, 18: 34074 (IDO-24460)
corrosive effects on reactor materials, 18: 36817
corrosive effects on scratched Zircaloy-2 cladding of NPR fuel element, 18: 37640 (HW-75359)
corrosive effects on zirconium alloys at high temperatures, 18: 37668 (A/CONF.28/P/158)
corrosive effects on zirconium alloys, 18: 37633 (A/CONF.28/P/342)
corrosive effects on reactor materials, 18: 37635 (A/CONF.28/P/445)
corrosive effects on niobium–tin–zirconium alloy at 600 and 680°F, 18: 41957 (KAPL-3018)
corrosive effects on materials, galvanic, 18: 41959 (WCAP-1844)
corrosive effects on Zircaloy-2, effects of oxide films on, 18: 44037(R) (HW-82651(p.5.1-33))
corrosive effects on uranium nitride, 19: 885 (BMI-1692)
corrosive effects on aluminum and its alloys at high temperatures in reactors, survey, 19: 922 (HW-69876)
corrosive effects on consolidated Zircaloy-2 powder at 680°F, effects of nitrogen and oxygen on, 19: 927 (KAPL-3060)
corrosive effects on mild steel, 19: 3806(R) (KR-79)
corrosive effects on Zircaloy-4 tubing at 360°C, 19: 4587 (GEAP-4739)
corrosive effects on steels at high temperatures, 19: 7865(R) (EURAEC-1237)
corrosive effects on aluminum, 19: 7855(R) (RISO-90)
corrosive effects on zirconium alloys, microprobe studies of, 19: 9621 (DP-906)
corrosive effects on Zircaloy, effects of environmental factors on hydrogen pickup in, 19: 9625 (WAPD-TM-411)
corrosive effects on sintered aluminum–iron–nickel compacts at 350°C, 19: 4607(P)
corrosive effects on Zircaloy-2 at 275°C, 19: 13883(R) (HW-81984 (p.9.1-6))
corrosive effects on nuclear structural materials, review, 19: 16013 (CEA-R-2600)
corrosive effects on rare-earth-rich alloys, (E), 19: 16188
corrosive effects on cadmium-indium-silver alloys, effects of added metals on, 19: 18402 (WCAP-3269-29)
corrosive effects of high-temperature, on Zircaloy-2 and Zircaloy-4, 19: 22870(R) (HW-83601)
corrosive effects on Zircaloy-2 at 280°C, 19: 22895(R) (HW-83298(p.9.1-3))
corrosive effects on Zircaloy-2 and -4 at 300 and 320°C, (E), 19: 24941
corrosive effects on steels at high temperatures, 19: 24936(R) (EURAEC-1308)
corrosive effects on ceria–urania and urania–zirconia, 19: 25044(R) (CEND-2936-222)
corrosive effects on HFIR materials, 19: 28756 (ORNL-TM-1029)
corrosive effects on steel at high temperatures, studies, 19: 29808(R) (KR-94)
corrosive effects of ammoniated and deionized, on sintered ceramic fuel wafers, 19: 31556(R) (WAPD-MRP-112)
corrosive effects on aluminum and carbon steel, tests of inhibitors for, 19: 30666 (BNWL-29)
corrosive effects on zirconium alloys at 360°C, 19: 30681
corrosive effects on gadolinium–stainless steel alloys at 354°C, 19: 32675 (BM-RI-6636)
corrosive effects on aluminum–beryllium alloys at 232°C, 19: 32679(R) (IDO-17037)

corrosive effects on aluminum–beryllium alloys at 232°C and 350 psig, 19: 32680(R) (IDO-17052)
corrosive effects on reactor materials, (E), 19: 33628
corrosive effects on zirconium alloys during irradiation, 19: 32693 (AECL-2257)
corrosive effects on Zircaloy at 280°C, 19: 37167(R) (HW-84609(p.8.1-7))
corrosive effects on chromium–iron–nickel alloys, 19: 40967(R) (COO-1319-27)
corrosive effects on A288 and X8001 aluminum alloys, 19: 44616(R) (ANL-7000, pp 122-37)
corrosive effects on aluminum, effects of polarizing current on, 19: 44617(R) (ANL-7000, pp 213-26)
corrosive effects of boiling, on carbon steel, 19: 44627
corrosive effects on nickel-plated aluminum at 330°C, 19: 46945 (BNWL-98)
corrosive effects on superalloys at high temperatures, 19: 46946 (BNWL-100)
corrosive effects on high-silicon aluminum alloys, 20: 763 (BNWL-125)
corrosive effects on type 304 stainless steel, effects of surface finish on, 20: 765(R) (EURAEC-1387)
corrosive effects on Creusot 1.2 MD 07 boilerplate steel, effects of flow rate on, 20: 765(R) (EURAEC-1387)
corrosive effects on type 410 stainless steel, effects of surface finish on, 20: 766(R) (EURAEC-1445)
corrosive effects on type 304 stainless steel, effects of flow rate on, 20: 766(R) (EURAEC-1445)
corrosive effects on Zircaloy-4 under heat-transfer conditions, 20: 4331
corrosive effects on carbon- and nitrogen-stabilized plutonium–uranium monoxide at 550°F, 20: 4327(R) (UNC-5138)
corrosive effects on europium molybdate at 100 and 250°C, 20: 4305(R) (ORNL-3870, pp 187-90)
corrosive effects on aluminum–yttrium alloys, effects of yttrium content on, 20: 4320(R) (ORNL-3870, pp 70-4)
corrosive effects on beryllium, 20: 6666(R) (ANL-7115, pp 68-77)
corrosive effects on beryllium at 100 and 120°C, 20: 5844
corrosive effects on type 1100 aluminum alloy, methods of inhibiting, 20: 5846
corrosive effects on low-alloy and stainless steels, effects of surface treatments on, 20: 5846
corrosive effects on Zircaloy-2 powders at 680°F, effects of nitrogen and oxygen additions on, 20: 5851
corrosive effects on stainless steel claddings in Saxton and Yankee Power Reactors, 20: 8429
corrosive effects on uranium carbides, 20: 9433
corrosive effects on uranium monocarbide and uranium monocarbide–10 iron at 80°C, 20: 9434
corrosive effects on aluminum, kinetics of, 20: 11227
corrosive effects on nickel plating on plutonium–aluminum fuel elements, 20: 11227
corrosive effects on carbon and stainless steels, effects of flow rate and surface treatments on, 20: 14978 (EURAEC-1546)
corrosive effects on aluminum–beryllium alloys at 163°C, 20: 19178(R) (IDO-17154)
corrosive effects on welded joints of niobium–zirconium alloys, 20: 19195
corrosive effects on zirconium alloys, effects of fast neutrons on, 20: 23767 (BNWL-88)
corrosive effects on europia–titania and europia–stainless steel 304L–titania cermets at high temperatures, 20: 31678 (HIT-3583-24)
corrosive effects on carbon steels, stainless steels, and Zircaloy-2 at high pressures and temperatures, 20: 33815(R) (EURAEC-1625)
corrosive effects on uranium, in-pile, 20: 35837 (KR-89, pp 63-81)
corrosive effects on stainless steel, gamma radiation effects on, 20: 37182
corrosive effects on zirconium single crystals at 680°F, 20: 41423
corrosive effects on aluminum coupled to copper and nickel, 20: 43824 (ANL-6236)
corrosive effects at pH 5 and 100°C of flowing, on potential HFIR materials, 20: 43833 (ORNL-TM-1030)
corrosive effects on steel in evaporator environments, review, 20: 43834 (ORNL-TM-1612)
cosmic meson (μ) spectra at great depths in, (E), 19: 41293
cosmic meson (μ) reactions with, energy losses from relativistic, (T), 20: 37707
critical heat flux for high-pressure bulk-boiling water flow, 17: 8347
critical heat fluxes in high-pressure boiling water flows, 17: 8348
critical heat flux for subcooled, flowing normal to cylinder, 17: 8352
critical heat flux for nearly saturated, flowing normal to cylinder, 17: 8353
critical heat fluxes for flow of subcooled, in circular channels at 100 to 180 atm, 18: 22224(T) (AEC-tr-6393)
critical heat flux of, effects of test section geometry on, 18: 39460
critical heat flux and flow regimes in boiling, (E), 20: 2012(R) (NYO-3304-6)
critical heat load in tubes, effects of tube diameter on, 18: 8489(T) (AEC-tr-6287)
critical heat loads for low-velocity flow of subcooled, around a tube in a square channel, 18: 8490(T) (AEC-tr-6291)
critical solution temperatures of phenols in, 20: 18720
critical specific volume, 18: 39440(T)
critical state of, studies, 19: 17863(T) (AI-Trans-76)
criticality effects on enriched uranium cylinders, 16: 32261 (LAMS-2744)
criticality studies on water-reflected spheres of aqueous homogeneous plutonium-nitrate systems, (E/T), 19: 37511(R) (HW-84608(p.5-29))
decomposition and recombination, radiation effects, 16: 11703(R) (TID-15123)
decomposition by electron beams of deuterium-labeled, isotope effects in, 18: 35518
decomposition by electron impact, kinetic energy distribution in, 19: 28912(R) (ANL-6819)
decomposition by electric-arc heating of vaporous, plasma radiation from, (E/T), 20: 17936
decomposition by fission recoils in thoria–urania slurries, 17: 25305
decompression in reactors, analysis of, (E), 20: 3324(R) (IITRI-578P21-13)
decompression into air, one-dimensional analysis of shock waves from, 20: 16023(R) (IITRI-578P21-16)
decompression of, in reactors, 17: 7532(R) (ARF-K6018-3)
decontamination, 17: 25434
decontamination and demineralization by electrodialysis, 16: 16603 (ERDL-1671-TR)
decontamination by flocculation, 16: 32631
decontamination by magnetite filter unit, 17: 25064(R) (ORNL-3417(p.61-3))
decontamination by chemical precipitation, 18: 20266
decontamination by ion exchange, 18: 38699
decontamination by sorption of radioisotopes by ion exchange materials, 19: 539
decontamination by sorption of radioisotopes on bentonites, gypsum, and superphosphate, 20: 22924
decontamination by radioactive ion sorption on heated alkali-treated clays, 20: 23040(P)
decontamination effects of distilled, with ultrasonics on rat skin contaminated with ^{131}I, ^{32}P, or ^{90}Sr, 20: 42811
decontamination, electrodialytic, 17: 15867(P)
decontamination, equipment and methods, 16: 13409
decontamination from radioactive substances, review of methods for, 16: 11993
decontamination from radioisotopes by sorption on aluminum, 16: 14373(P)
decontamination in nuclear war, 16: 16591 (AD-264822)
decontamination in Krupp installation, 16: 32632
decontamination of waste, using sugar beet pulp base as cation exchanger, 16: 20039
decontamination of radioactive, bibliography on, 17: 12043 (NP-12482)
decontamination of radioactive waste, by ferric hydroxide flocculation, 17: 42426
decontamination of, barium sulfate sorption of strontium in, 18: 29883 (UJV-936/63)
decontamination of cistern, for drinking, in Switzerland, 19: 2188
decontamination of, review, 19: 8678
decontamination of, fast-filtration and ion-exchange methods for, 20: 4068
decontamination of, for human consumption, 20: 23383(T) (JPRS-34927)
decontamination of, by precipitation of radioisotopes, 20: 31318 (BMwF-FBK-65-04)
decontamination of, by sorption of iodine-131 on hydrated ferric oxide containing silver, 20: 36800
decontamination of, procedures for, 20: 45831
decontamination studies, 18: 37428 (A/CONF.28/P/849)
decontamination using water organisms, bibliographic review, 17: 1669
decontamination using clay minerals, 20: 12527(P)
demineralization of boiling-reactor cooling, 20: 3539 (ACNP-65558 (Rev.1))
density of oxygen-18-labeled, 17: 18069
deoxygenation of, performance of amine–copper and sulfite-type resins for, 18: 27476
desalination by nuclear plant in southern Tunisia, study, 19: 14861
desalination of, use of radioisotope heat source in, 18: 27818(R) (PB-181469)
desalination program, fuel element development and testing for, 18: 4765(R) (ORNL-3470(p.232-4))
desalination research, 19: 16819(R) (ORNL-3714(Vol.I))
desalination, using nuclear energy, cost factors, 17: 31675 (CONF-14-6)
desalination using conventional and nuclear energy, review, 18: 19499
desalination, conference on, 19: 17332 (ORNL-3783)

desalination, possible improvements in nuclear, 18: 32968 (ORNL-P-20)
detection and identification of, method for underground, 17: 29115(P)
detection and separation from sodium loops, in-line devices for, 19: 44162(R) (APDA-174, pp 33-55)
detection of, neutron gage for, 17: 29886
detection of, neutron gage for, 17: 29887
detection of, radiometric density gage for, 17: 29888
detection of surfaces of boiling, ultrasonic instruments for, 18: 33830(R) (NYO-10556)
detection of surfaces of boiling, ultrasonic instruments for, 18: 33831(R) (NYO-10558)
detection of surfaces and voids in boiling, ultrasonic instruments for, 18: 33832(R) (NYO-10560)
detection of thin layer of, radiometric apparatus for, 20: 25369(P)
detection of thin film of, on surfaces, radiometric device for, 20: 25372(P)
determination as adsorbed phase in tantalum oxide films by infrared spectroscopy, 19: 15490
determination by neutron scattering, method for finding sensitivity and precision of, 19: 7766 (IFA-MR-21)
determination by neutron scattering, 19: 26728
determination in anhydrous hydrofluoric acid, conductometric, 16: 17589 (PG-Report-292)
determination in argon and helium, instruments for, 18: 25264 (CNLM-4016)
determination in asbestos and plywood slabs by neutron scattering, 19: 5791
determination in beryllium carbide, methods for, 16: 6366 (NEPA-940)
determination in building materials by gamma absorption, 16: 24048
determination in brown coal by elastic back-scattering of fast neutrons, 16: 25296
determination in building materials, radiometric, 19: 11612
determination in building materials by neutron absorption, gage for, 20: 5819
determination in beryllium oxide, evaluation of methods for, 20: 26772
determination in benzene from 10 to 60°C, isotopic dilution method for, 20: 43113
determination in boreholes using NMR method, 20: 45931(P)
determination in barium chloride, silica gel, and silicate iron ore by isotope dilution analysis, 20: 45595
determination in coal by neutron moderation, 16: 25682(R) (TID-16013)
determination in coal, radiometric, 16: 28651(R) (TID-16338)
determination in coal storage piles, development of neutron-moderation method for, 17: 14576(R) (TID-17973)
determination in cotton leaves, beta ray gaging technique for, 18: 12021
determination in coal and soil using neutron moderation, 18: 39565 (COO-712-73)
determination in concretes and soils by neutron scattering, 18: 41600
determination in crude and fertilizer lime by neutron moderation, 19: 26247
determination in coffee beans by neutron scattering, 19: 34131
determination in cattle, tracer technique for whole-body, 19: 43694
determination in concretes, reliability of neutron-absorption, 20: 8848
determination in coke by neutron absorption, 20: 16922
determination in coke, concretes, and sand using neutron probes, 20: 16926
determination in catalyst and silastic resin, by titration, handling methods for, 20: 29083(R) (UCRL-14767)
determination in compacted soils, radiometric methods for, 20: 29581 (AD-633785)
determination in drugs by beta absorption, 16: 6368 (TID-14330)
determination in fused uranium dioxide by electrochemical and manometric methods, 17: 1380 (DP-766)
determination in friable materials, neutron meter for, 18: 33466(T) (AEC-tr-6399(p.43-50))
determination in friable bodies by neutron slow-down, 18: 33470(T) (AEC-tr-6399(p.83-91))
determination in fine-grained concrete sand, activation, 18: 39105
determination in forest products, using radiation, 19: 13841
determination in gas streams containing hydrogen fluoride, equipment for continuous, 20: 20581
determination in hydrated diamagnetic salts by oxygen-17 nuclear resonance techniques, 17: 35263(R) (UCRL-10706(p.1-110))
determination in halogenated solvents, infrared, 19: 5775 (RFP-419)
determination in highway construction materials using nuclear gages, 19: 9446 (NP-14604)
determination in helium coolant in Dragon Reactor, evaluation of methods for, 19: 22155
determination in iron during sintering by neutron scattering, 17: 27282
determination in iron ores by neutron slowing down, 19: 7336
determination in irradiated terphenyl by gas chromatography, 20: 26924(R) (MIT-334-48)
determination in kerosene--TBP and TBP, 19: 29808(R) (KR-94)
determination in lime, sand, silicates and wood, development of cadmium probe for, 16: 22504
determination in living plants, radiometric, 16: 26905(T) (CEA-tr-A-1127)
determination in lactose by neutron thermalization, 18: 39097
determination in liquids of low water solubility, using impregnated silica gel, 19: 21783(P)
determination in lignites by gamma absorption, 20: 41154
determination in materials, sensitivity of neutron moisture probe for, 16: 698
determination in methanol using krypton-85, 17: 27639(R) (TID-18881)
determination in materials by neutron reactions, development of scintillation probes for, 17: 30867
determination in materials, activation, 17: 32017
determination in materials by neutron scattering, effects of density on, 18: 13672
determination in materials, radiometric, 19: 7767 (IFA-MR-24)
determination in methanol using kryptonated calcium carbide, 19: 36267
determination in oxide fuels, coulometric, 18: 2161(R) (HW-76302)
determination in organic solvents using krypton-85, 18: 37566(R) (NYO-2757-3)
determination in organic reactor coolant, 19: 15342 (DCI-52)
determination in ores by radiometric methods, 19: 22836
determination in organic liquids using kryptonates, sensitivity of, 20: 18570(R) (NYO-2757-5)
determination in peat by neutron stopping, 17: 10559
determination in porous rock in boreholes by gamma scattering methods, 18: 31774
determination in plutonium and uranium dioxides, electrolytic, 18: 31368 (HW-82487)
determination in polyphenyls by Karl Fischer method, 19: 292 (NAA-SR-9734)
determination in polyphenyls by Karl Fischer method, 19: 301 (RT/CHI(64)-10)
determination in plywood green veneer by radiation readout, 19: 2584
determination in plutonium and uranium oxides, 19: 9603(R) (HW-81601(p.2.1-35))
determination in plutonium and uranium oxides, electrolytic, 19: 22869(R) (HW-83298(p.5.1-38))
determination in roadbed, radiometric, 18: 22390
determination in rats by scintillation counting of tritium water, 19: 26236
determination in rock strata using well logging, 20: 14777
determination in soils, calibration of neutron probes, 16: 5545
determination in solids, microwave apparatus, 16: 8704
determination in soils using fast-neutron sondes, 16: 13411 (NP-11381)
determination in soils, neutron-thermalization, 16: 11998 (NP-11380)
determination in soil by nuclear methods, bibliography, 16: 23982 (AERE-Bib-140)
determination in snow using gamma-radiation, 17: 347
determination in soils by neutron scattering, 17: 1414
determination in sand by neutron absorption, 17: 32018
determination in soils, calibration of neutron probe for, 17: 35400
determination in soil, use of radioisotopes for, 17: 35401
determination in soil by neutron scattering, 17: 35402
determination in soils using radiation probes, comparison of methods for, 18: 425
determination in soils, neutron probe for, 18: 5541(P)
determination in solids by neutron reflection, 18: 6758
determination in solids by neutron moderation, 18: 8303
determination in soil, variance in neutron-scattering, 18: 10004
determination in soil, neutron radiometric, 18: 12424
determination in soils and building materials, neutron moderation method for, 18: 19905
determination in soils using radioisotopes, 18: 25699(T) (OTS-63-11008 (p.15-21))
determination in soils by using neutron sources, 18: 27821
determination in soils using neutron probe, 18: 29929 (NP-13993)
determination in sand and building materials by neutron attenuation method, 18: 31384
determination in soils, neutron monitor for, 18: 35808 (HW-82009)
determination in soil by gamma scattering measurements, effects of soil density on, 18: 39106
determination in solid propellants, techniques for, 19: 5590 (UCRL-13136)
determination in soils, neutron radiometric, 19: 7720
determination in soils using nuclear gages, 19: 9447 (NP-14610)
determination in soils, design of radiometric devices for, 19: 13656
determination in soils by neutron scattering, cadmium standards for, 19: 38869
determination in sand, by neutron thermalization, 20: 3913(P)
determination in soils, neutron meter for, 20: 14771
determination in samples by neutron absorption, gage for, 20: 16924
determination in soils by neutron energy losses, 20: 19118
determination in solvents, chromatographic, 20: 31641(R) (NYO-755-1,

pp 173-208)
determination in soils by neutron probing, 20: 31435
determination in solids by neutron recoil methods, 20: 31627
determination in soils, gamma and neutron well logging equipment for, 20: 33537
determination in soils by neutron scattering, 20: 41115(P)
determination in SAP, methods for, 20: 45574 (EUR-3064.f)
determination in snow by gamma counting, Fichtelberg, Germany, 20: 550
determination in tributyl phosphate by Karl Fischer methods, 16: 18816 (PG-Report-255)
determination in thorium nitrate–tributyl phosphate solutions, 16: 22265 (AERE-CE/M-190)
determination in TBP, infrared absorption spectrographic, 17: 27239 (PG-Report-467)
determination in terphenyls, using Karl Fischer titration method, 19: 7270 (EUR-2159.e)
determination in uranium dioxide and tetrafluoride, 16: 11516 (PG-Report-247)
determination in uranium tetrafluoride, methods for, 19: 19785
determination in uranium tetrafluoride by gas volumetric methods using calcium hydride, 20: 20609
determination in vented gases from underground nuclear explosion, apparatus for, 19: 19776 (UCRL-12169)
determination in water-d_2 mixture, quantitative spectrophotometric, 18: 9986
determination in water-d_2, photometric, 20: 3970(P)
determination of, in powders of metals and metal compounds by vacuum distillation, 17: 5963 (PG-Report-350)
determination of moisture in soil, neutron scattering method, 17: 25136
determination of moisture content in top soil layer, prediction method for, 18: 16206 (USNRDL-TR-662)
determination of moisture in cellulose, use of oxygen-18 exchange reaction with carbon dioxide in, 18: 23397(T,R) (AEC-tr-6316 (p.274-82))
determination of soil levels using neutron probe, 16: 9424
determination of soil, on lysimeters and small watersheds, 17: 35403
determination of traces of, in organic liquids, using kryptonates, 18: 33450(R) (NYO-2757-4)
determination of, using neutrons, 18: 8319(P)
determination of, on remote surfaces, combination neutron technique for, 20: 31211
determination of, use of krypton-85 hydroquinone clathrate in, 20: 35422
determination of, in soils by neutron scattering, 20: 39141
determination on surfaces, deuterium exchange with water-d_2, spectrometric, 17: 40759
determination, review of physical methods, 17: 4465
deuterium content of crystallization, of saline minerals, 19: 44240
deuterium content in, in petroleum deposits, 20: 7261
deuterium content, 17: 22570(T) (NP-tr-993)
deuterium enrichment of, process for, 17: 14226(T,P) (CEA-tr-A-1227)
deuterium enrichment in, method for, 18: 12530(P)
deuterium exchange with hydrogen sulfide, 16: 465(P)
deuterium exchange with hypophosphorous acid, kinetics, 17: 15988
deuterium exchange with p-xylene, geometric factor in catalytic, 17: 15863
deuterium exchange between solvated protons and, equilibrium constant of, 17: 23328
deuterium exchange with hydrogen ions, equilibrium constant, 17: 27380
deuterium exchange between propyne and, 18: 2133(R) (TID-19592(Sect.V))
deuterium exchange with hydrogen, catalyst recycling in, 18: 4152(P)
deuterium exchange with hydrogen in, poisoning of platinum–carbon catalyst during, 18: 33527 (IFA-28-IS)
deuterium exchange between acetylene and, equilibrium in, 19: 7509
deuterium exchange with dissolved hydrogen using diethylamine as catalyst, rate of, 19: 17856 (MIT-2249-1)
deuterium exchange with anion exchange resin, 19: 19865
deuterium exchange with salts of trioctylamine or benzyldilaurylamine, 19: 19864
deuterium exchange between dissolved hydrogen and, 19: 26739(R) (MIT-2249-2)
deuterium exchange between, and deuterium-labeled hydrogen sulfide, 19: 32665
deuterium exchange between propyne and, equilibrium constant for, (E/T), 19: 42497
deuterium exchange with hydrogen between ammonia and, in hot-and-cold plant, 19: 44574
deuterium exchange with isobutyraldehyde, effects of acids, amines, and oxygen bases on, 20: 5565
deuterium exchange with, catalytic effects of ruthenium chloride on, 20: 16423
deuterium exchange between acetylene and, factors affecting, 20: 31640(R) (NYO-755-1, pp 130-72)
deuterium exchange with aromatic compounds, 16: 17380
deuterium–hydrogen exchange in, mechanism of, 18: 8349
deuterium-hydrogen exchange between heavy water and silk fibroin and, 18: 23470
deuterium–hydrogen exchange in, effect of poisons on catalytic, 20: 7106
dibutyl ester dibutyl phosphinic acid–UO_2SO_4–H_2O, phase equilibria in, 18: 37122
dibutyl ester dibutyl phosphinic acid–H_2SO_4–H_2O, phase equilibria in, 18: 37122
dielectric constant at 0 to 40°C, 18: 206 (NYO-10695)
dielectric constant at 0 to 800°C, calculations of, 19: 30151(R) (ORNL-3789(p.139-63))
dielectric constant at 0 to 40°C, 19: 40527
dielectric relaxation time and volume fraction of free volume for, 19: 13303
differentiation from petroleum by fast neutron scattering, 19: 4082
diffusion at 23°C, effects of ions on self-, 19: 32159
diffusion in alkaline earth chlorides and water at 25°C, coefficients of, 20: 1865
diffusion in geological cores and silica-sphere lattices, self-, 17: 33943
diffusion in silica glass, tritium tracer technique for study of, 18: 10085
diffusion into polymers, 18: 25022(T) (ANL-Trans-15)
diffusion, neutron scattering studies of, 16: 24271 (AERE-R-4043)
diffusion of iodine-131 from carbon dioxide bubbles through, 18: 6528(T) (AEC-tr-6144)
diffusion of oxygen-18-labeled, in concentrated aqueous solutions of cesium and lithium chlorides at 25°C, 18: 1621
diffusion of water-t in, at 25°C, 17: 28881
diffusion through lipid membranes, 20: 42725
discharge from long cylindrical container at high enthalpy, 16: 7660 (NEI-156)
discharge of high-enthalpy, from broken pipe, 19: 10461 (TDVI-33)
disposal in shale wells by hydraulic fracturing, 19: 8674(R) (ORNL-3697(p.10-19))
disposal of radioactive, 19: 31685
dissociation constants of carboxylic acids and dinitrophenols in, 17: 39092
dissociation in dioxane mixtures with water or water-d_2, deuterium solvent isotope effects in, 18: 39240
dissociation of, isotopic effects on, 18: 1634
dissolution of irradiated sodium chloride in, quenching effects of oxygen on luminescence from, 17: 10612
distillation at low pressure for heavy water production, 19: 11651
distillation of, isotopic fractionation during, 17: 23333
dose distribution in, from electron beam irradiation, three dimensional, 20: 21470 (PB-181506, pp 116-29)
drop coalescence at planar interface with anisole, hydrodynamic mechanism for, 16: 25956 (UCRL-10097)
droplet behavior on hot surface, 18: 16177(R) (TID-20133)
droplet growth in vapor of, in expanding cloud chambers, (T), 20: 43674
droplet interchange with vapor, 18: 35260(R) (AERE-PR/HPM-5)
economic aspects as energy source, 18: 40216
effect of, on electron paramagnetic resonance spectrum in wheat flour after irradiation, 17: 8497
effect of, on rubidium-86 uptake by soil, 17: 36015
effect on radioinduced ionic polymerization of styrene, 17: 23410
effectiveness in removal of radioisotopes from leafy vegetables, 18: 5555
effects in radiation biology, electron spin resonance studies, 20: 40597
effects of adsorbed, on transfer of uv-induced excitations in solid proteins, 20: 32938
effects of borated and lithiated, on wear of cylinders and pistons, 19: 45601(R) (WCAP-3750)
effects of bound and free, on radiopreservation of fish, 20: 7475
effects of bound, on radiosensitivity of *Escherichia coli*, 19: 21894
effects of content in pea seeds of, on radiosensitivity, 18: 17577
effects of content of, on radiosensitivity of oat seeds, 18: 25181
effects of depth of, on integral radiation dosage measurement in water phantom, 17: 28617
effects of flooding, on reactivity of gas- and steam-cooled fast reactors, 20: 38439 (ANL-7120, pp 826-36)
effects of hot, on cold work recovery of Zircaloy-2, 19: 6294 (HW-80309)
effects of irradiated, on spore *A. aureofaciens*, 18: 17514
effects of irradiated, on nylon at pH 10.5 and 40 to 45°C, 20: 31280
effects of movement of, on ion movement into tomato root xylem, 18: 21723 (TID-18877)
effects of oxygen-17-enriched, on ESR spectra of oxygen-17-labeled benzoquinone, 20: 43224
effects of stress of, on γ-irradiated pine seedlings, 20: 12674
effects of, on acidity change in gamma-irradiated potato and corn starch, 20: 33367
effects on active transport of arabinose, glucose, and sodium in hamster intestine, 20: 18212

effects on aluminum, stainless steel, uranium, and zirconium in reactor environment, 20: 14996
effects on analysis of alkali metals in glove box atmosphere, 20: 7015 (ORNL-TM-1357)
effects on association of cadmium ions with bromide ions in molten nitrate, 19: 34142(R) (NYO-2873-7)
effects on atomic hydrogen yields from low-pressure hydrogen discharge, 20: 18663
effects on carbon steel in operating pressure boilers, 20: 31681 (NAA-SR-Memo-11707)
effects on cesium-137 excretion by rats, 18: 43174(R) (LA-3132-MS(p.37-41))
effects on chemisorption of ethylene by yttrium oxide, 20: 29186
effects on chlorination of uranium(IV) oxide, 20: 43443
effects on chlorosulfonated polyethylene, 18: 17916
effects on chromatographic and electrophoretic behavior of metal ions in lithium chloride–potassium chloride eutectic, 18: 43479
effects on corrosion of iron by terphenyl, 20: 777
effects on corrosion of rhenium at 25 and 100°C, 20: 21275
effects on corrosive properties of biphenyl, 20: 25491(T) (AECL-2330, pp 179-95)
effects on crystal structure of oxide films on zirconium, 20: 778
effects on decay of free radicals radioinduced in egg albumin, 18: 8410
effects on decontamination of equipment, land targets, and vehicles, 20: 27185 (AD-632989)
effects on desorption of radioiodine from clays and sediments, 20: 600 (ORNL-P-1581)
effects on electric conductivity of molten lithium chlorides, 18: 26019
effects on electrochemistry of molten alkali halides, 18: 39156 (EUR-1643.e(p.327-45))
effects on electrochemical reduction of aliphatic nitro compounds, 20: 18636(R) (TID-22725)
effects on emission of X-agent, 18: 720
effects on energy transfer in proteins, 20: 5270
effects on energy transfer in sulfur dioxide vibrations, 16: 3026
effects on EPR spectra of manganese ions in maple leaves and pine needles, 19: 25892
effects on fluorescence of uranyl ions, 19: 19863
effects on formation of corrosion-resistant films on titanium and zirconium oxides, 18: 20481
effects on free radical formation in irradiated mustard seed, 18: 31165
effects on free radicals in irradiated brine shrimp eggs, 19: 25892
effects on friction and wear of materials, 19: 22449 (EDI-123)
effects on gamma radiation effects on potato starch, 20: 36599
effects on graphite and pyrolytic carbon under high heat flux conditions, 19: 20463 (ORNL-TM-431)
effects on heat transfer from surfaces in organic-cooled reactors, 19: 31463 (CRCE-1189)
effects on iodine exchange reactions with 1-phenyl-2,3-dimethyl-4-iodopyrazolone, 20: 35515
effects on ion exchange of uranium and other elements in system with organic acids, 18: 25305
effects on irradiation behavior of Inconel, 16: 9260 (KAPL-M-EEB-17)
effects on molecular weight distribution in radioinduced polymerization of α-methylstyrene, 17: 11285
effects on natural frequency of beam vibration, 20: 4080 (WAPD-TM-535)
effects on neon in spark chambers, 18: 14210 (JINR-P-1498)
effects on neutron multiplication in heavy-water-moderated reactor, 17: 17432
effects on oxygen effect in irradiated barley seed, 20: 18389
effects on oxygen-18 exchange between water and copper and iron sulfates, 20: 29153
effects on polymerization in irradiated hydrocyanic acid, 16: 17744
effects on post-shot thermal effects and secondary explosions in cavities in tuff, 20: 20939 (NVO-1163-70)
effects on procaine activity in mice, 17: 33519
effects on properties of quartz, 19: 22279
effects on pulse radiolysis of organic solutes, 20: 1920
effects on radiation effects on wheat seeds, 19: 38412
effects on radioinduced graft polymerization, 17: 16041(R) (NCSC-2477-10)
effects on radioinduced polymerization of styrene, 18: 5361 (CONF-117-31)
effects on radioinduced graft polymerization of styrene on polyvinyl alcohol, 18: 23582(T,R) (AEC-tr-6316(p.70-5))
effects on radioinduced post polymerization of trioxane, 18: 27532
effects on radioinduced graft polymerization, 18: 31611
effects on radioinduced grafting of styrene to cotton fabric, 18: 31626
effects on radioinduced grafting of vinyl monomers to wool, 20: 7154
effects on radioinduced luminescence and photoconductivity in zinc oxide, 20: 7128(R) (NYO-2206-1)
effects on radioinduced paramagnetic centers in sodium selenite, (E), 20: 15972
effects on radioinduced fluorescence in terbium chelate systems in, 20: 18683
effects on radioinduced polymerization of styrene at 25°C, 20: 23140
effects on radioinduced decomposition of pectins, 20: 36879
effects on radioinduced polymerization of allyl alcohol, 20: 36880
effects of radioinduced polymerization of styrene, 20: 43338
effects on radioinduced polymerization of acrylonitrile on cellulose, 17: 8131 (PAN-310/XVII)
effects on radioinduced grafting of vinyl monomers on cellulose, 18: 12163
effects on radioisotope movement through soils, 19: 36661
effects on radiolytic formation of hydrogen from silane, 16: 20478
effects on radiolysis of ketones, 18: 33621 (UJV-977/64)
effects on radiolysis of methanol, 19: 13425(R) (NYO-2383-12)
effects on radiolysis of 2-propanol, 19: 13423 (KFK-243)
effects on radiolysis of hydrocarbons and crude oils, 19: 22335
effects on radiolysis of dichlorobutanes and dichloropropanes, 20: 9020
effects on radiolysis of potato starch, 20: 20737
effects on radiolysis of butyl chloride, 18: 25598
effects on radiomimetic effects of nitrosoamides on herb seeds, 19: 43870
effects on radiosensitivity of molecules in biological systems, 18: 1433
effects on radiosensitivity of barley seeds, 19: 15089
effects on radiosensitivity of barley seeds, correlation of temperature effects with, 19: 24316
effects on radiosensitivity of artemia eggs, 20: 18342
effects on radiosensitivity of bromouracil-substituted coliphages, 20: 45471
effects on radiosensitivity of barley and ionions treated with 2-amino-purine and 5-bromouracil, 20: 45400
effects on reaction of carbonate hydrolase, 18: 27056
effects on reactivity of metal ions with hydrated electrons, 19: 17913
effects on reactor building materials, 20: 31682 (NP-16003)
effects on saturation in radioinduced polymerization of 3,3-bis-chloromethyloxacyclobutane, 18: 12206
effects on sintered density of urania powders, 19: 44595(R) (EURAEC-1338)
effects on soil volume weight determination by gamma scattering, 19: 26566
effects on solvolysis of diethyl dicarbonate and ethyl chloroformate at 25°C, 20: 23065
effects on sorption of carbon monoxide on zinc oxide, 19: 40578
effects on sound dispersion in ethylene, 16: 3025
effects on spectra of neodymium complexes, 20: 14560
effects on stress corrosion cracking of titanium and zirconium in alcohol–acid solutions, 20: 14988
effects on stress corrosion cracking of chromium–iron–nickel alloy, 20: 31676(R) (COO-1319-39)
effects on thermal neutron flux trapping by water-d_2, 16: 33785
effects on thermal denaturation of DNA, 19: 12919(T)
effects on yield in radioinduced reactions between 1-bromobutane and tin, 20: 7125 (BMI-1745, Sect. H)
effects on yield of radioinduced reactions between 1-bromobutane and tin, 20: 7488(R) (BMI-1742(Del.))
effects on yields of atomic hydrogen from electric discharge in low-pressure hydrogen, 19: 38590 (UCRL-16050)
effects on yields of hydrogen peroxide from radiolysis of methanol, 20: 5581
effects on yields from gamma radiolysis of acetone, 20: 18737
effects on Zircaloy-2 at 300°C, 20: 25499
ejection from pressurized column on depressurization, 20: 22350
electric conductivity and pH monitoring in Czech research reactors, 16: 26924
electric conductivity in thoria capillary, 18: 22015(R) (ORNL-3591 (p.102-12))
electric conductivity of very pure, 19: 17852 (CEA-R-2633)
electric conductivity of ions in, at 25°C, 20: 14540
electric discharge in vapor of, stimulated infrared emission in, (E), 19: 9792
electric discharges in, temperature of, 20: 7970
electric discharge in, channel expansion rate, energy balance, and particle density for pulsed, (T), 20: 28086
electric power production from jets of ionized vapor in energy conversion device, 16: 19623
electrolysis for in-field synthesis of ammonia fuel, conceptual study, 19: 1968 (TID-20441(Vol.I))
electrolysis in electrochemonuclear systems, for production of hydrogen and oxygen, 19: 12770 (BNL-8754)
electrolysis of, description of cells for, 17: 29234(T) (CEA-tr-A-1331)
electrolysis of, economics of ammonia and hydrogen production using nuclear power for, 20: 45631(R) (ORNL-3945, pp 259-69)
electrolysis, survey of technology of, 18: 27360 (TID-19978(Vol.II))

electrolytic properties of, with reactor-irradiated platinum electrodes, 18: 27952(R) (EURAEC-926)
electron absorption, 16: 16555
electron absorption and backscattering by, 18: 32773
electron attenuation at 24 Mev, gamma emission in, 18: 44921
electron beam collisions with, emission spectra from, 18: 16700
electron beam reactions, proton production in, 17: 18110 (UCRL-6967)
electron binding in solutions of, model for, 18: 25577
electron capture by, mechanism of, 19: 9229
electron capture by, (E/T), 20: 18557 (ORNL-TM-1409)
electron depth-dose distribution in, calculation of, 19: 5600
electron elastic scattering at 295°K, cross sections, 16: 33844
electron energy at various bond angles, 17: 2058(R) (NP-12207)
electron energy deposition in, at 20-Bev, 18: 7841(R) (ORNL-3499 (Vol.II)(p.9-11))
electron energy levels, configuration interaction study, 16: 12219(R) (NP-11304)
electron excitation of jets of, radicals from, 17: 34009
electron, gamma, and x-ray reactions with, computer analysis of secondary electron emission from, 17: 41525 (AFSWC-TDR-63-50)
electron inelastic scattering from oxygen nuclei, 16: 5941
electron polarization in molecules of, effects of temperature on, 20: 29230
electron reactions at 6.5 Mev to 50 Bev, 16: 3887(R) (ORNL-3193 (p.329-39))
electron reactions at 30 ev, spectra from, 17: 25266
electron reactions with, dose distributions from, 17: 34558 (RISÖ-53)
electron reactions at 10 to 16 ev, ionization potentials from, 18: 31538
electron reactions at 66 Mev, photoneutron yields from, (E), 19: 16867
electron reactions with, excitation of long-lived states in, (E), 19: 23320
electron reactions in phantoms of, angular distribution of bremsstrahlung from, 19: 28996
electron reactions at 24 Mev, photon energy spectra from showers from, (T), 20: 23940
electron reactions with, isotope effect in Cherenkov radiation from, 20: 35435
electron scattering intensities of, calculation of, 18: 777
electron scattering by, inelastic 390 v, 18: 14836
electron scattering by, 18: 32781
electron scattering by, Rydberg transitions in spectra from, 19: 32142
electron scattering by, cross sections for, (T), 20: 973
electron slowing-down spectra in, 17: 32826
electron spectra produced by cobalt-60 gamma rays in, 16: 17853
electron spin resonance in, hyperfine structure in, 20: 33287
electronic energy, 16: 16357
elimination from deuterated acetates and alcohols, mass spectrographic investigation of, 18: 27480
energy absorption in, in cylindrical shield voids, (T), 19: 8567
enthalpy data at 2850 to 4300 psia and 360 to 400°C, 16: 7958 (ANL-6505)
enthalpy, measurements of excess in, 16: 14755
equation of state for, in critical region, 17: 39078
equilibria and reactions with metal fluorides at 565 to 970°C, 19: 30067(R) (ORNL-3789(p.56-98))
equilibrium with heavy water, evaluation of constant for, 19: 19891
erosive effects on rotating metal disks, 19: 44625 (TIM-894)
erosive effects on metals and alloys at 70°F, cavitation, 20: 29640 (NP-16048)
europium ion spectra in, absorption and fluorescence, 18: 13759
evaporation from artificial rough surfaces, 19: 44245 (BNL-914, pp 125-32)
evaporation of, deuterium and oxygen-18 exchange effects in, 17: 37190
evaporation of drops of, computer program for, 19: 41110 (BNWL-74)
evaporator for treatment of contaminated, automatic control of, 20: 16594
exchange between aquorhodium and oxygen-18-labeled solvent water, 18: 17793
exchange in linear transfer system, interfusion effect in, 19: 2324
exchange in fish, tracer study of, 17: 2715
exchange of deuterium between hydrogen and, apparatus for, 20: 264
exchange of deuterium oxide with, in plants, 20: 8556
exchange of molecules in aqueous ferric solutions, nuclear magnetic resonance studies, 16: 5371 (UCRL-9846)
exchange of oxygen-17-enriched, with first coordination sphere cations, 16: 3017
exchange on metal ions, NMR studies of, 20: 31218(R) (UCRL-16658, pp 1-9)
exchange reaction with hydroxyl ions, equilibrium constant for, 17: 37202
exchange reactions with complex ions, oxygen-17 nuclear magnetic resonance studies of, 18: 31431(R) (UCRL-11317(p.1-14))
exchange reactions with heavy water, thermodynamic functions of, 18: 33567
exchange with chromous and cupric ions, nuclear magnetic resonance study using oxygen-17, 19: 9099 (UCRL-11704)
exchange with deuterium on nickel wire catalyst in alkaline solution, 18: 227
exchange with ferric and gadolinium ions in solution, nuclear magnetic resonance study, 19: 43997(R) (UCRL-11889)
explosions in, pressure produced by contained, 20: 38459 (ANL-7120, pp 720-33)
expulsion from heated channels, pressures and temperatures in, 19: 14765(R) (ANL-6977)
extraction from rocks, feasibility of nuclear versus solar power for, 19: 34360 (AD-608225)
fall-out monitoring, 16: 441
fallout contamination, 18: 13396
fallout contamination in Austria, 18: 18046
fallout contamination at Argonne, New York, and New Zealand, 20: 521(R) (HASL-164)
fallout content of, factors affecting, 18: 43865
fallout in, data on, 18: 22257
fallout monitoring in, design of gamma detection unit for, 16: 27403(R)
fallout monitoring, radiological health data, July 1962, 16: 28739
fallout monitoring, 1961 and 1962, 17: 21955
fallout monitoring in, Germany, 1958 and 1959, 18: 14086
fallout monitoring in, Canada, March 1966, 20: 33556 (NP-16124)
fallout uptake by, in England, 18: 20208 (AERE-R-4415)
fallout-contamination of, 18: 27743
film flow on heated rod, burnout and nucleation of climbing, 19: 28510
films of, measurement of thickness of, 17: 25860(R) (PR-P-56(p.43-67))
fissile-material critical mass in, distribution effects on, (T), 20: 18062
fission product content in drinking, in England, 16: 20126
fission products in, permissible concentrations of, 18: 1967
flow characteristics in expansion through converging-diversion nozzle, 16: 10151 (UCRL-6665-T)
flow distribution in annular fuel elements for TSR-II, 20: 4299(R) (ORNL-2711)
flow from nuclear-explosion-produced rubble chimneys, 20: 35176
flow in annular channel with roughened heated inner wall, heat transfer in, 20: 25255
flow in cavitating venturi, pressure distribution, velocity, and void fraction in choked two-phase, 20: 25245 (NP-16038)
flow in cylindrical tubes, effects of flow rate and pressure on burnout heat fluxes in, 18: 14043
flow in cylindrical cavitating venturi, void fraction distribution and axial pressure profile for two-phase, 20: 33473
flow in ducts with and without heat transfer, friction factors for turbulent, 18: 8500
flow in heating channels, with forced convection, 16: 4271 (CEA-1825)
flow in irregular annular gaps, turbulent, 16: 8879(T) (AEC-tr-4960)
flow in parallel tubes, stability of boiling, 19: 33601(R) (DP-965)
flow in partially saturated soil, equations for relating parameters in, 19: 603(R) (HW-81746(p.4.42-7))
flow in porous materials, use of gamma attenuation for measuring, 17: 34131
flow in pressurized loop, effects of physical properties on two-phase adiabatic, 18: 397 (EURAEC-152)
flow in rectangular channels, burnout, friction, and heat transfer in forced turbulent, 18: 10237
flow in rectangular channels, boiling burnout heat flux in low-pressure, 18: 10238
flow in round tubes, power distribution effects on burnout and hydrodynamic instability in forced, 20: 2009 (EUR-2490.e)
flow in soils, application of diffuse theory to, 17: 39280
flow in tubes, critical heat load and wall temperature dependence on mass flow-rate, subcooling, and water pressure, 18: 27659(T) (AEC-tr-6401)
flow in vertical tubes, flooding velocities for countercurrent annular, 16: 16498 (AEEW-R-123)
flow in vertical tubes, heat transfer effects on laminar, (T), 20: 27115
flow in vertical, rectangular conduit, two-phase, 20: 31340 (ANL-7093)
flow measurement in steam generators, isotopic speedmeters for, 16: 30628
flow of boiling, in vertical round ducts, burnout conditions for, 17: 29079
flow of boiling, burnout conditions for vertical-duct, (T), 19: 11357
flow of boiling, critical heat flux in long tubes for, 20: 14695
flow of boiling, effects of gravity on, 18: 38558 (A/CONF.28/P/801)
flow of boiling, in heated tubes, 20: 31346
flow of, bubble motion in turbulent, 17: 32250 (TID-19224)
flow of, in single-tube branch and multi-tube branch systems, 17: 20173 (PWAC-213)
flow of open currents, tracer measurement of, 17: 3089
flow of saturated, through tubes, 18: 39450
flow of saturated, through apertures, (E), 19: 44196(R) (TID-22145)
flow of, burnout heat fluxes for, 18: 37330 (A/CONF.28/P/327a)
flow of, critical parameters in two-phase, 18: 20170 (TID-7694(p.11-17))

flow of, dynamics of vortex, 19: 40236 (LA-3229, pp 237-50)
flow of, heat transfer in two-phase, 18: 20171 (TID-7694(p.18-23))
flow of, pressure drop in two-phase, 18: 20172 (TID-7694(p.24-34))
flow patterns for peripherally injected, in vortex tubes, 20: 6653 (D-910091-7)
flow rate measurements in pipes, tracer methods, 16: 30697 (DPR/INF/268)
flow rates of, radiometric measurement of, 20: 43662
flow through heat exchangers, total-sample method for measuring rate of, 18: 33750
flow through packed beds, parameters for glass-bead, Raschig-ring, and soil packings, 18: 45155(R) (TID-20980)
flow through pipes, burnout heat flux for vertical boiling, 17: 29075(R) (TID-18978)
flow through porous media, tracer studies of, 19: 13830
flow through tube apertures at high pressures, analyses of, 20: 36990
flow through turbines, tracer studies of, 19: 13830
flow through two eccentrically positioned orifices in series, pressure drop characteristics, 19: 38810 (RL-SA-31)
flow, tracer techniques for discharge rate in porous media, 16: 5629
flow transients and heat-driven pressure in supercritical thermodynamic region of, 19: 13595
flow velocity through channels of finite bundles of hollow rods, turbulent, 20: 31350
flows in curved copper tubes, friction factors for, 18: 32893(R) (ORNL-3652)
flows through components of TSR-II, measurement of, 18: 28937(R) (ORNL-3578(p.100-21))
fluoridated, effects on calcium-45 and strontium-85 uptake by bones in rats, 17: 27044
force constants and infrared spectrum of, calculation of, 18: 5277
force constants of deuterated from normal, method for adjusting vibrational, 19: 7396
formation in dehydration and dehydrogenation of 2-propanol, kinetics, 18: 1719
formation of, in radiolysis of *p*-benzhydroquinone and phenol, 20: 4332
free energy of formation at 1100°F, 17: 32571(R) (MSAR-63-105)
fuel element storage in, criticality studies for enriched uranium, (E), 19: 35752 (BNWL-52)
fuel element weighing in, equipment for error elimination in irradiated, 20: 16780 (TID-22689)
gamma absorption, buildup factors for, 16: 710
gamma absorption by, 19: 10454 (P-157(RAND))
gamma absorption by, (E), 20: 27348
gamma absorption coefficients, polynomial approximation of linear, 16: 11114 (DC-57-8-158)
gamma absorption coefficients, 16: 12454
gamma absorption coefficient, 16: 11453(R) (ANL-6464(p.133-42))
gamma absorption coefficients at 0.14 to 2.76 Mev, 16: 21695
gamma absorption coefficients of, equations for, 18: 30938(T,R) (AEC-tr-6231(p.56-60))
gamma absorption doses for, 16: 16004
gamma absorption in, calculation of, 19: 38023
gamma absorption in hemispheres of, from central point source, (T), 19: 41959
gamma activity of, effects of energy and measuring volume on measurements of, 18: 29587
gamma and neutron reflection and scattering by, 20: 7315(R) (ORNL-3849, pp 151-82)
gamma angular and energy distributions in, cobalt-60, (E), 19: 41953 (NP-15131)
gamma angular distributions and energy spectra in, calculation using Monte Carlo method, 20: 5181(R) (ORNL-3029)
gamma attenuation from point sources, 16: 11122 (DC-59-12-229)
gamma attenuation, point source, 16: 14200 (DC-61-1-101)
gamma attenuation by, effects of spherical voids in, 17: 17404(R) (BNL-164)
gamma attenuation in, build-up factors for, 19: 35566 (RT/FI(65)-7)
gamma attenuation coefficients at 0.03 to 10 Mev, 19: 35569
gamma attenuation coefficients at 0.01 to 100 Mev, 20: 36350
gamma attenuation in, tables of equivalent thickness of, 20: 44989
gamma attenuation, 16: 3838(R) (ORNL-3193(p.4-9))
gamma attenuation by, calculation methods for, 16: 17161
gamma attenuation coefficients, 16: 23246
gamma backscattering from spherical surfaces of, at 0.7 and 1.25 Mev, (E), 20: 6525
gamma buildup factors for, 0.5- to 10-Mev, 18: 26814(T) (ORNL-tr-80)
gamma buildup factors and sorption, 20: 10225
gamma buildup factors for, calculation of, (T), 20: 12261 (AFRRI-TM-65-2)
gamma buildup factors and energy spectra in, Monte Carlo calculation of, 16: 2620 (NASA-TN-D-850)
gamma distribution from cobalt-60 source in, 16: 18331
gamma distributions in, collimated-source, 19: 31435
gamma dose albedos for, (T), 20: 3274
gamma dose buildup factors for, 20: 10228
gamma dose buildup factors in plane parallel barriers of, (E/T), 20: 26338
gamma dose rates in, from point isotropic fission sources, (T), 19: 45464 (ORNL-TM-1167)
gamma heating in slabs of, 20: 4999(R) (ORNL-2599)
gamma heating in, calculations for, (E/T), 20: 6517 (CONF-651101-41)
gamma measurement sensitivity in, 16: 17834
gamma radiation penetration, 17: 3976
gamma reactions (γ,n) at 5 to 10 Mev with nuclei in, yields from, (E), 19: 34392(T)
gamma reactions (γ,n) at 2.25 to 15 Mev with nuclei in, yields from, (T), 19: 34393(T)
gamma reactions (γ,n) with deuterium in reactor shielding of, flux distribution for, (T), 20: 24801
gamma reactions, buildup factor studies, 16: 10668 (DC 60-2-215)
gamma reactions, ratio of Compton scattering and total attenuation coefficients, 16: 11113 (DC-57-8-83)
gamma reactions with, energy deposition from, 18: 44751
gamma scattering at 0.66 Mev, energy distributions from, 16: 24693 (NP-11538)
gamma scattering at 1 Mev, total field for multiple, (T), 20: 1321
gamma scattering at 4.0 Mev in barriers of, intensity angular distribution of, (T), 20: 6526
gamma scattering by, build-up factors for, 16: 31031
gamma scattering by, discrepancies in calculations of energy distributions from, 18: 42393
gamma scattering by duct in, streaming in, (T), 20: 6530
gamma scattering by semi-infinite slabs of, 20: 26336
gamma scattering fluxes in, 17: 31635 (ORNL-3466)
gamma scattering from point isotropic source of cesium-137 by, energy distributions from, 18: 42661
gamma scattering in, pulse height spectra, 17: 15109
gamma scattering in, 0.662-Mev, 19: 31436
gamma shielding buildup factors for, 17: 22767
gamma shielding by, nomograms for determining thicknesses for, 19: 21598
gamma shielding by, thickness calculations for, 20: 17964(T) (ORNL-tr-1061)
gamma shielding properties of, 17: 29973
gamma shielding properties of, factors for, 18: 3029 (RISO-62)
gamma shielding properties of slabs of, Monte Carlo analysis of, 18: 4684 (NRL-5981)
gamma spectra from reactor moderator of, 19: 25749 (NP-15022(Vol.I))
gamma spectra in, at 0.2 to 6 Mev, 20: 30722 (KAPL-M-6497)
gamma spectrometry of methods for, 18: 39111
gamma transmission through slabs of, 18: 35051
gamma transmission through slabs of, Monte Carlo calculations of, (T), 19: 14733 (WAPD-BT-31(p.43-9))
gamma transmission through slabs of, Monte Carlo calculations of, 19: 14732(R) (TO-B-63-83)
gamma transport in, solutions using Tschebyscheff polynomial expansions and method of moments, 18: 13181
hazards from contamination of drinking, evaluation, 20: 41217
heat exchange during bubble boiling, 16: 4279(T) (FTD-TT-61-153)
heat exchanger for use with sodium and, 19: 36628(P)
heat flux in surface and volume boiling of, critical, (E/T), 20: 25267
heat fluxes during burnout, (E), 20: 14694
heat of adsorption of, 18: 31743(R) (ORNL-3652(p.132-45))
heat of adsorption on thorium oxide, 20: 16456
heat of dilution and solution of rare earth chlorides in, 20: 3956
heat of formation, 17: 27322 (UCRL-7301-T)
heat of immersion of thorium dioxide in, 19: 349 (ORNL-P-542)
heat of mixing with methanol, deuterium isotope effects on, 17: 28876
heat transfer above critical heat flux at high subcritical pressures, forced-convection, 19: 13583 (WCAP-2056(Pt.V))
heat transfer and pressure gradients in forced-flow bulk-boiling, round tube data, 16: 13211 (TID-14632)
heat transfer and pressure drop in eccentric annuli, 16: 25526 (NYO-9649)
heat transfer and pressure drop in tubes containing bluff-body promoters, 16: 27229
heat transfer and fluid dynamics in boiling, survey of, 18: 1879
heat transfer and laminar flow of, in circular cavity, 19: 13596
heat transfer burnout measurements in boiling, design test loop for, 18: 20180 (TID-7694(p.87-8))
heat transfer burnout in pressurized, in cosine-heated tubes, 18: 39436 (TID-21031)
heat transfer burnout and stability of natural circulation, in seven-rod bundle, 19: 20120
heat transfer by, 18: 17322(R) (TID-19971)

heat transfer by bubble boiling of, effects of pressure on, 19: 24682
heat transfer by boiling, burnout heat flux in, 20: 2023
heat transfer by plates in flowing, 16: 7669
heat transfer by supercritical, 20: 3485(R) (WCAP-2120)
heat transfer by, critical forced-flow, 18: 31723 (NP-14072)
heat transfer characteristics in two-phase flow, 20: 16605 (NYO-3304-8)
heat transfer coefficients, 16: 27214
heat transfer coefficients for film boiling beyond burnout in annular flow, 17: 8346
heat transfer coefficient, 17: 20178
heat transfer coefficients, nucleate boiling, 19: 7688
heat transfer from plate to supercritical, by free convection, 17: 8341
heat transfer from cylinder rotating in, convective, 17: 27533 (AE-107)
heat transfer from fluidized particles to, correlations of, 18: 12317 (NYO-10702)
heat transfer from plate to near-critical, by turbulent free convection, 18: 39426 (COO-1177-16)
heat transfer from tubes to supercritical, forced-convection, 19: 36614 (WCAP-5449)
heat transfer in annular flows of subcooled, 18: 24882(R) (DP-905)
heat transfer in boiling, effects of induced vortices on burnout flux, 16: 20598(T) (EURAEC-146)
heat transfer in boiling, electroconvection effects on, 16: 25533
heat transfer in boiling, in vertical tube, 17: 3120
heat transfer in bulk boiling, nonuniform axial, 20: 4104 (NP-15622)
heat transfer in forced flow of, 17: 4662(T) (AEC-tr-5538)
heat transfer in flows through pipes, 18: 24910(R) (SRO-101)
heat transfer in forced-flow transition boiling in two-rod test sections at high pressures, 19: 13594
heat transfer in flow in tubes at near-critical temperatures and supercritical pressures, forces-convection, 19: 24677 (WCAP-2056(Pt.IV))
heat transfer in open lattices of rods, boiling burnout, (E), 19: 13584 (WCAP-3736(Vol.I))
heat transfer in open lattices of rods, boiling burnout, (E), 19: 13585 (WCAP-3736(Vol.II))
heat transfer in pressurized, review of research on, 19: 35620
heat transfer in, review of effects of additives on boiling and critical heat flux, 16: 13209 (NAA-SR-Memo-6946)
heat transfer in small-diameter high-pressure tubes, 17: 10806(T) (AEC-tr-5602)
heat transfer in sub- and supercritical, 20: 18862 (COO-1177-19)
heat transfer in supercritical, model for, (T), 20: 25241 (GEAP-5093)
heat transfer in two-phase swirl flows of, in boiling reactors, (E), 19: 28497 (EURAEC-1114)
heat transfer in uniformly heated tubular test sections, 19: 36621
heat transfer in, voltage effects on boiling, 19: 9345
heat transfer of boiling, forced- and natural-circulation, 18: 20160(R) (AD-423679)
heat transfer of boiling, forced- and natural-circulation, 18: 20166(R) (NP-13810)
heat transfer of, effect of pressure transients on pool boiling burnout, 16: 27232
heat transfer properties in 50- to 60-kgauss magnets, 16: 15439
heat transfer to boiling, review of, 17: 285
heat transfer to boiling, on nickel and platinum wires, 17: 35995
heat transfer to, in small tube at 200 psia, 17: 35983 (ANL-6715)
heat transfer to liquid hydrogen from, in heat exchangers, 19: 44186 (LA-DC-7148)
heat transfer to near-critical, in vertical tubes, (E), 20: 18861 (COO-1177-18)
heat transfer to supercritical, free convective, 16: 5464 (ANL-6486)
heat transfer to subcooled, effects of upstream compressibility on, 19: 46546
heat transfer to, in electrically heated vertical tube in turbulent flow, single- and two-phase, 18: 18002 (TID-20407)
heat transfer to, in one- and two-phase flows through annuli, 18: 23766(R) (GEAP-4431)
heat transfer to, mechanism of, 18: 39429 (NDA-10-51)
heat transfer to, at high pressures after critical heat flux, 19: 46554
heat transfer to, at coexistence of nucleate and film boiling, 20: 31345 (T) (NSJ-tr-471)
heat transfer to, from high temperature fuel particles, 20: 42580(R) (ANL-7245, pp 60-73)
heating by energy released by nuclear explosion, 18: 5446(P)
heating, effects of temperature difference on turbulent forced-convection, 16: 27215
hydrated electron reactions with, rate constants for, 18: 23691
hydration equilibria of aliphatic aldehydes in, 18: 6842
hydrogen atom and proton reactions with vaporous, emission spectra from, 17: 41641(T)
hydrogen bond elongation in, isotopic substitution effects on, 18: 25417(T)
hydrogen bonding in, infrared spectral study of, 20: 5552
hydrogen exchange with thiols, 17: 1461
hydrogen exchange between chlorophyll and pheophytin and, 17: 7950(T)
hydrogen exchange with hydrogen sulfide, heavy water production by, 18: 18257 (NP-13766(p.7-26))
hydrogen ion dissociation in, hydrogen ion production in, 17: 33155(R) (ORNL-3472(p.56-69))
hydrogen ion reactions with, anion production in, 17: 39756
hydrogen ion reactions at 10 to 50 kev, equilibrium fractions in, (E), 19: 14243
hydrogen ion reactions with molecular, at 1 to 55 kev, particle production cross sections for, 20: 29919 (UCRL-14214)
hydrogen isotope disproportionation in, 20: 33283
hydrogen isotope exchange with, homogeneous catalysis of, 17: 23816
hydrogen isotope exchange with oxonium ions, 17: 40428(R) (NYO-10063(p.7-22))
hydrogen isotope fractionation in perchloric acid solutions of, 18: 19968
hydrogen isotopic fractionation between equilibrium vapor phase and hydroxide solutions in, 18: 35550
hydrogen-tritium exchange reactions between lactones and, effects of triethylamine catalyst on, 20: 41017
hydrolysis of procaine in, stability in, 19: 11102
hydroxyl radical split from, statistical model for angular momentum conservation for abnormal rotation of, 18: 16024
hypersonic and ultrasonic velocities in, effects of relaxation on, 20: 4479(R) (TID-22179, pp 1-83)
impact shock for blunt-nosed missile on, 18: 45188 (SC-TM-64-987)
incorporation of radium in, for clinical baineological uses, 20: 8780
ingestion of radon-enriched, radiation dose to man from, 16: 30688
injection of boiling, into terphenyl, heat transfer during, (E/T), 20: 33464
interaction between nonpolar groups in, role in protein structure, 19: 13290
interface with oil in rocks, determination of, 20: 43553
intermolecular reactions in, infrared spectroscopic studies of, 19: 26361
iodine transfer with dry steam, 18: 39178
iodine-131 deposition from, in thyroid gland, 17: 31849
iodine-131 maximum permissible concentration, 16: 1325(R) (LAMS-2627(p.204-12))
ion attenuation by, energy-range curves for heavy, 17: 25968
ion species in oxygenated, transient, 19: 26452
ionic, structure and stability of hydrated, 18: 5396
ionization and proton transfer in, effects of tritium on, 20: 16424
ionization by alpha particles and electrons, cross sections and mass spectra for, (E), 20: 44122
ionization by x rays at high energies, spectra of, 18: 41506(R) (ML-TDR-64-169)
ionization distribution in, from fast electrons, 17: 24101
ionization efficiency curves, effects of instrumental factors on, 16: 15296
ionization of, in mass spectrometry, formation of H_3O^+ in, 20: 45681
ionization potentials of, 17: 19935
isotope effects on α-chymotrypsin-catalyzed hydrolysis, 16: 26999
isotope effects on, review on, 19: 28432
isotope exchange between nitric oxide and nitric acid in, oxygen-18 concentration in, 17: 18656
isotopic analysis, 17: 27313(R) (ASD-TDR-62-843)
isotopic analysis of, equipment for falling-drop method of, 20: 26795
isotopic exchange of oxygen-18-labeled, with plutonyl oxygen, 17: 14252
isotopic exchange between oxygen-16-enriched, and vitreous or crystallized silicates, 17: 23836
isotopic exchange of hydrogen between hydrogen and, 18: 9752 (IA-900)
isotopic exchange of deuterated toluene, 19: 38693
isotopic molecular weight, determination of, 16: 2997(T) (NP-tr-808)
labeling with dysprosium by activation, 16: 6446
labeling, with oxygen-18, 19: 32222
leakage from concrete reactor housings, 20: 10272(R) (NAA-SR-9339)
leakage from pipes, detection by sodium-24 tracer, 19: 39265(R) (IA-1021)
leakage in pressure vessels, mechanism and rate, 20: 30810
liberation by thermal treated silical gel, deuterium exchange method for determination of internal and surface, 18: 1674
light absorption in, visible-region, 17: 30543
light scattering by, Cabannes factor and Rayleigh ratio for, 20: 3941
loss of, effect on uranium and thorium in metamorphism, 20: 45935
mass difference with water-*d*, (E), 19: 28336
mass spectra of ionized, in strong electrical fields, 20: 1829
measurement on surfaces, design of neutron device for, 17: 10925
meson (μ) absorption at 10^{10} to 10^{13} ev, energy transfer in cosmic, (T), 20: 23953
meson (μ) energy loss in, (E/T), 19: 41345
meson (μ) collision losses in, 16: 16919
meson (μ^+) repolarization in, as a function of external field, 17: 9237
meson (π^-) capture by hydrogen in, 17: 7083 (JINR-P-1081)
metabolism and turnover in dogs, tracer study using deuterium, 18: 19530

metabolism by irradiated rats, 18: 6655
metabolism of tritium-labeled, climatic effects on animals, 19: 2017
mixing in narrow bubble column, 18: 27642(T) (ORNL-tr-118)
mixing with air, tracer study of, 20: 36989 (WAPD-TM-492)
mixing with heavy water, thermodynamic functions of, 19: 865(R) (ORNL-3679(p.23-38))
mixtures with air, design and construction of equipment for preparation and separation, 16: 17794 (EURAEC-49)
moderating properties, for use in flux-trap reactors, 16: 31059
molecular diffusive motion in, (T), 19: 7474
molecular motion in beryl, neutron scattering studies of, 19: 12069
molecular motion in, neutron scattering studies of, 20: 36821
molecular spectra, 16: 15365
molecular structure and solvent properties, 16: 25327(T) (AEC-tr-5126)
molecular structure in actinides and rare earth hydration, 17: 25260
molecular structure of, atomic displacements from anharmonic vibrations, 17: 31117
molecular structure, 18: 27396
molecular structure of, electron-diffraction studies of, 19: 11091
molecular structure of, x-ray scattering determination of, 19: 46161(R) (ORNL-3832, pp 116-50)
molecular structure model of, 20: 2520(R) (IA-920)
molecular structure of ground-state and excited, angular correlation diagrams for, 18: 27384
molecular wave functions of isoelectronic sequence of, 18: 24296(R) (AD-417517)
molecule scattering by, cross sections for inelastic, 19: 14265
monitoring at Ispra, 20: 45979
monitoring for alpha activity, 16: 364
monitoring for arsenic-76 content, automatic system for, 18: 24821 (HW-75374)
monitoring for radioactivity in U. S., Nov. 1961, 16: 2089
monitoring for radioactivity, 1961, 16: 27510
monitoring for radioactivity near uranium mines and processing plants, 17: 41154
monitoring for radioactivity in, equipment and methods for, 18: 35858
monitoring for tritium, 20: 23363 (CONF-640413, pp 83-6)
monitoring low-level radioactivity in, review of methods for, 17: 1668
monitoring of low-level waste, for strontium-90, 16: 1283
monitoring of tap, sampling device for, 20: 39218
monitoring of, for tritium, design of portable device for, 20: 33635
monitoring of, gas-flow counter for large-area, (E), 19: 18287
monitoring purity of reactor, system for, 18: 24932 (HW-SA-3018)
monitoring Savannah River Plant, Jan. to June 1965, 19: 44288(R) (DPST-65-30-2)
motion and heat transfer of organic droplets in, 19: 15719 (TID-21531)
movement, 17: 19746 (TID-18468(p.311-52))
movement in bodies of, isotopic current analyzer for, 20: 23527 (CONF-651206)
movement of, in ice-covered lake, tracer study of, 18: 10270
neutron absorption by, from polonium-beryllium source, 18: 21136
neutron absorption by gold foils in, effects of flux anisotropies on, 19: 826
neutron absorption in, fast, (E), 20: 9265
neutron absorption, dosages from, 16: 16004
neutron age, 16: 1007
neutron age and higher moments in, 19: 10675(R) (NAA-SR-9999)
neutron age, fission, 16: 15264(R) (HW-71747)
neutron age from uranium-233 fission, 16: 3867(R) (ORNL-3193(p.203))
neutron age in, 16: 3611 (NASA-TN-D-1102)
neutron age in, from uranium-235 fission, 16: 13969
neutron age in, moments calculations of, 16: 22977
neutron age in, Monte Carlo calculation of, 18: 42592 (TID-7050(p.125-37))
neutron age measurements in, fission, (T), 20: 9379(R) (NAA-SR-11650, Sect.4)
neutron age to indium resonance in, fission, 18: 2800
neutron age-to-indium resonance in, fission, 18: 4514 (NAA-SR-8621)
neutron age to indium resonance in (E), 19: 1532
neutron age to indium resonance in, computer analysis, (E), 19: 6620 (NAA-SR-Memo-8662)
neutron age-to-indium resonance in, RBU Monte Carlo calculations of, 18: 38054 (NAA-SR-Memo-9500)
neutron ages in, 18: 9296
neutron albedos on, hydrogen content dependence of, 18: 19257 (BRL-1224)
neutron attenuation, 16: 6076 (XDC-57-1-32)
neutron attenuation, 16: 15612 (GA-2544)
neutron attenuation, 16: 17237 (NASA-TN-D-1184)
neutron attenuation by boron-containing and pure, fast, 16: 14076
neutron attenuation by boron-containing, 16: 24366
neutron attenuation by, thermal, 17: 3817
neutron attenuation by, fast, 17: 28221 (EUR-107.f)
neutron attenuation by, with polymer-chip additives, 17: 41375(P)
neutron attenuation by, nomograms for calculations in, 17: 42157
neutron attenuation in, fast, 18: 986(T) (AEC-tr-6113)
neutron attenuation by, fast, 18: 2826
neutron attenuation by, diffusion approximation for fast, 18: 38283 (A/CONF.28/P/721)
neutron attenuation and thermalization in, fast, (E/T), 19: 29202
neutron attenuation in, analysis using S_n method, 20: 10224 (ORNL-TM-1196)
neutron attenuation and thermalization in, fast, (E/T), 20: 30340
neutron attenuation in, 16: 3838(R) (ORNL-3193(p.4-9))
neutron attenuation, calculation methods for, 16: 17161
neutron background in, 20: 43547
neutron backscattering by plane and spherical layers of, 18: 16896 (NP-13720)
neutron capture with charged-particle emission in, determination for source calibration, (E), 19: 45232
neutron collisions in, critical removal angles for, (E), 19: 38020
neutron cross sections, thermal, 18: 38038 (A/CONF.28/P/651)
neutron cross sections at 1.44 ev (E), 19: 3288
neutron decay constants in, spectral correction analysis of pulsed- (T), 19: 3205
neutron decay constants in, pulsed, (T), 20: 9938 (BNL-9770)
neutron diffusion length measurements in, 16: 737
neutron diffusion length measurements in, 16: 738
neutron diffusion and thermalization at 0.5 to 286°C, 16: 7166
neutron diffusion, thermal, 16: 9419
neutron diffusion length at 16 to 89°C, thermal, 16: 9421
neutron diffusion parameters at 26.7°C, 16: 12407
neutron diffusion, thermal, 16: 12416
neutron diffusion parameter determination by pulsed method, 16: 14255
neutron diffusion lengths in, calculational model for, 16: 24373
neutron diffusion and thermalization at 0.5 to 286°C, 16: 24765(T) (AEC-tr-5143)
neutron diffusion in, extrapolation distances for, 16: 26208
neutron diffusion length in, thermal, 17: 2209
neutron diffusion at ~0°C, 17: 2211
neutron diffusion parameters in, temperature dependence of, 17: 4028
neutron diffusion parameters of, 17: 5308
neutron diffusion parameters in, thermal, 17: 15204 (BNL-719 (Vol.IV)(p.1186-1210))
neutron diffusion parameters and buckling in, 17: 15210 (BNL-719 (Vol.IV)(p.1331-59))
neutron diffusion parameters in, 17: 15220 (TID-18007)
neutron diffusion in, 17: 15191 (BNL-719(Vol.III)(p.799-804))
neutron diffusion in, measurement by pulsed and poisoning methods, 17: 15197 (BNL-719(Vol.III)(p.946-65))
neutron diffusion length at 20 to 50°C, thermal, 17: 19210
neutron diffusion lengths in, thermal, 17: 20956 (GEAP-4018)
neutron diffusion parameters for, 17: 22666(R) (TID-18561)
neutron diffusion parameters of, research on, 17: 24369(R) (GA-3542)
neutron diffusion parameters for, 17: 26066
neutron diffusion parameters in, 17: 26398 (PAN-403/IX)
neutron diffusion lengths in, thermal, 17: 28437 (KAPL-2000-20)
neutron diffusion in, for various scattering laws, 17: 32972 (CONF-11-7)
neutron diffusion in, as function of temperature, 17: 32976
neutron diffusion in, for cube, slab, and sphere geometry, 17: 34560(R) (TID-19195)
neutron diffusion in, 17: 34847
neutron diffusion in, 17: 38052(T) (AEC-tr-5734(p.286-7))
neutron diffusion in, at 0 and 20°C, 17: 38053(T) (AEC-tr-5734(p.288-92))
neutron diffusion in, around a point source of uranium-235, ratio of flux to source strength for, 17: 39959
neutron diffusion in, parameters for thermal, 18: 992
neutron diffusion parameters for, measurement using pulsed neutron method, 18: 9301
neutron diffusion in, 18: 15169
neutron diffusion length and pulse parameters for, 18: 26516
neutron diffusion parameters of, measurement using pulsed-source method, 18: 26828
neutron diffusion lengths in, thermal, 18: 30691
neutron diffusion length in, experiment for thermal, 18: 30949 (NYO-9077)
neutron diffusion and thermalization in spheres of, 18: 34752(R) (CU(PNPL)-234)
neutron diffusion constant measurements in, 18: 37113 (A/CONF.28/P/763)
neutron diffusion parameters, 18: 38043 (A/CONF.28/P/678)
neutron diffusion constants of, scattering measurements on, 18: 40475 (JÜL-160-NP)
neutron diffusion parameters in, review of, 18: 40490
neutron diffusion hardening in, re-analysis of data on, 18: 44709 (WAPD-T-1634)

neutron diffusion parameters for, thermal (E/T), 19: 1520 (CRRP-1203)
neutron diffusion cooling coefficient and asymptotic spectrum temperature in (E/T), 19: 3206
neutron diffusion parameters in, computer analysis of thermal, (T), 19: 6843 (WAPD-TM-373)
neutron diffusion cooling and heating in, thermal, (E), 19: 12465
neutron diffusion in, design of pulse generator for measuring, 19: 14479
neutron diffusion measurements in, using pulsed source, (E), 19: 27392 (INR-573/IXA)
neutron diffusion in, capture effects on, (T), 19: 27399
neutron diffusion in, pulsed-source measurements of fast, (E), 19: 29207
neutron diffusion in iron and lead in, spectra of, (E), 19: 31205
neutron diffusion parameters in, pulsed, (T), 19: 33216
neutron diffusion in, thermal parameters of, (E), 19: 35378(R) (EANDC(E)-57(U))
neutron diffusion in, P_3 calculations of pulsed, (T), 19: 37767 (WAPD-T-1788)
neutron diffusion in, using oscillating source, 19: 41641(R) (MIT-2344-3, pp 137-54)
neutron diffusion length in, from time-decaying fields, (E), 19: 47560
neutron diffusion in, pulsed thermal, 20: 2944
neutron diffusion parameters in, sample geometry effects on, (E), 20: 2952
neutron diffusion parameters for, pulsed, (E), 20: 13729
neutron diffusion in spherical containers of, parameters for, (E), 20: 15686
neutron diffusion length at 18 to 255°C, thermal, (E), 20: 15679
neutron diffusion in cylindrical geometries of, 20: 26533(R) (BNL-954, pp 16-49)
neutron diffusion parameters in, temperature dependence of thermal, (E), 20: 28240
neutron diffusion length and temperature in boron-poisoned, 20: 34469 (DP-MS-66-30)
neutron diffusion length and temperature in boron-bearing, thermal, (E), 20: 34503
neutron diffusion parameters of, measurement using pulsed-neutron techniques, 20: 34508
neutron diffusion in, parameters for thermal, (E), 20: 36141 (IEA-107)
neutron diffusion lengths in poison-bearing, calculations using diffusion theory and transport theory, 20: 40053
neutron diffusion parameters in, measurement and calculation of, (E/T), 20: 40055
neutron diffusion in, extrapolation length measurements for, 20: 46966(R) (NAA-SR-12010)
neutron diffusion parameters in, poisoned with boron or cadmium, 17: 32975
neutron distributions in, 17: 13472
neutron distributions at 1.5 to 12 Mev in, from swimming-pool reactors, (E), 19: 21735 (ORNL-P-1092)
neutron distributions in, first- and last-flight expectation values in Monte Carlo calculations of fast, (T), 19: 27395 (ORNL-RSIC-3)
neutron distributions in, fission, 19: 31435
neutron distributions in multilayered media containing, in well logging, 19: 34390(T)
neutron distribution along cylindrical ducts in, fission, (E), 20: 38351
neutron dose and radiative capturerates in, (T), 19: 14743
neutron dose rates behind slabs of, fast, 17: 36628 (ORNL-TM-646)
neutron dose rates in, from point isotropic fission sources, (T), 19: 45464 (ORNL-TM-1167)
neutron effective cross sections of, thermal, 17: 40219(T) (AEC-tr-6058)
neutron elastic scattering by, slow, (T), 20: 28252
neutron energy deposition in, fast, 18: 10372 (CONF-187-55)
neutron energy distributions in, at 20 to 90 cm from 15-Mev source, 17: 26401
neutron energy distributions at boundary with graphite, 17: 34895
neutron energy distribution in plane geometry of, effects of diffusion cooling on, 19: 3194
neutron energy distribution in, performance of threshold detector for measuring, 19: 15047
neutron energy-exchange kernels and spectra in, 18: 2814
neutron energy spectra behind shielding of, method of counting efficiencies for studying, 19: 31440
neutron energy spectra in, (T), 19: 47964
neutron extrapolation length in, thermal, 18: 2810
neutron extrapolation lengths in slabs of (E), 19: 1533
neutron extrapolation length in, (T), 20: 46562(R) (RPI-328-68, pp 84-144)
neutron flux distributions in spherical containers of, thermal, 17: 3331
neutron flux distributions in, multigroup approximation calculation of, 17: 29566 (WAPD-T-1563)
neutron flux distributions in, from point source in spherical cavity, 18: 34731 (NASA-CR-54110)
neutron flux distributions from point isotropic fission source in, transfusion-method computer calculation of, 18: 36555 (ORNL-3487)
neutron flux distributions in shields of, thermal, 19: 3221
neutron flux distributions in, expectation values for (T), 19: 3222
neutron flux distribution in bent air duct immersed in, 19: 27701 (EIR-78)
neutron flux distribution in, asymptotic spectra of, (E), 19: 29177 (RPI-328-29)
neutron flux distribution in, 19: 32787(R) (NIRS-3(1-17))
neutron flux distribution in EBWR shielding of, 19: 35760 (IEA-85)
neutron flux distributions in, extrapolation distances from pulsed, (E), 20: 13726
neutron flux in moderators of, multi-velocity corrections in activation measurements of, 20: 29539
neutron flux in, pulsed-source measurements of thermal, (E), 19: 29209
neutron flux measurements in voids in, 17: 3799
neutron flux measurements in, using gold activation, thermal, 20: 5181(R) (ORNL-3029)
neutron flux perturbation by aluminum–dysprosium foils in, thermal, 20: 15669 (NASA-TN-D-3237)
neutron flux perturbation by re-entrant holes, thermal, 20: 34501
neutron fluxes and spectra in reactor shielding of, fast, (E/T), 20: 1318
neutron inelastic scattering, 16: 1021 (IDO-16699)
neutron inelastic scattering cross sections at 0.07 ev, 16: 14064
neutron inelastic scattering by, 16: 32364 (TID-16691)
neutron inelastic scattering by, cold, 17: 4042
neutron inelastic scattering at 25°C, 17: 22308
neutron inelastic scattering at 25 and 75°C, energy distributions for, 17: 37806
neutron inelastic scattering by, cold, 18: 7403 (BNL-7414)
neutron inelastic scattering at 90°C, thermal, 18: 24625 (WASH-1046)
neutron inelastic scattering by, down-scattering effects in, 18: 36080(R) (RPI-328-8)
neutron inelastic scattering on, 18: 38610 (A/CONF.28/P/615)
neutron inelastic scattering at low energy, chopper study of (E), 19: 3191(R) (RPI-328-16)
neutron inelastic scattering at fixed angles, time-dependent pair correlation function from thermal, (T), 19: 10225
neutron inelastic scattering by, differential cross sections for, (E), 19: 23599(R) (RPI-328-20(p.24-34))
neutron inelastic scattering by, epithermal, (E/T), 19: 47549(R) (TID-22141, pp 34-49)
neutron inelastic scattering by, cross sections for, (E), 20: 4807(R) (RPI-328-40, pp 56-66)
neutron inelastic scattering at 0.83 to 1.8 ev, differential cross sections for, (E), 20: 30334
neutron inelastic scattering by, dynamic processes in slow, 20: 40338
neutron lifetime measurements in, thermal, 17: 15195 (BNL-719 (Vol.III)(p.932-4))
neutron mean free paths in, containing cylindrical voids, (T), 19: 23608
neutron moderating properties for use as cold-neutron source, 16: 7170
neutron moderation in, 18: 24888 (HW-SA-3507)
neutron moderation in, properties for, 18: 38044 (A/CONF.28/P/680)
neutron moderation in, pulsed measurement of, 18: 42589 (PAN-503/IX-A)
neutron moderation by, at 20, 77, and 300°K, (E), 20: 11944
neutron multigroup calculations for, 18: 32950 (WAPD-TM-448)
neutron partial differential scattering cross sections for, reduced slow, 16: 28026 (IDO-16699(Rev.))
neutron penetration, calculations, 16: 3880(R) (ORNL-3193(p.299-304))
neutron penetration through, fast, 18: 16891(R) (GA-4881)
neutron penetration in cylindrical air ducts in, 18: 38046 (A/CONF.28/P/688)
neutron photoemission in contact with oil, use in prospecting, 19: 22572
neutron propagation in, from thermal columns of pulsed reactors, 17: 34871
neutron propagation in, from monoenergetic sources, (E), 19: 14462 (EUR-2161.f)
neutron pulse decay constants in, (T), 19: 10230
neutron pulse parameters in, temperature dependence of, 18: 15155
neutron pulses in systems with plutonium-239 and uranium-235, approach to equilibrium of, (T), 19: 27403
neutron quasi-elastic scattering at 22°C, 16: 31055 (HW-SA-2542)
neutron quasi-elastic scattering by, cold, 17: 36630 (TID-17871)
neutron quasi-elastic scattering by, spectrum for cold, 17: 38039(T) (AEC-tr-5734(p.227-31))
neutron range in, for polonium–beryllium sources, 16: 3658 (NP-11106)
neutron reactions in, cross sections and spatial distributions, 16: 17059
neutron reactions in, cross section and spatial distribution for, 16: 22971(T) (JPRS-13609)
neutron reactions (n,γ) with, dose distributions from, 18: 16962
neutron reactions with, distributions from, 18: 37741 (A/CONF.28/P/167)

neutron reactions with, energy deposition from, 18: 44751
neutron reactions (n,p) with oxygen-16 in, nitrogen-16 specific activity from, (T), 19: 14847 (WAPD-BT-31(p.37-42))
neutron reactions with, fluorine-17, fluorine-18, and nitrogen-13 production in, (E), 20: 45728
neutron reflection at 0.5 to 8 Mev, 16: 3878(R) (ORNL-3193(p.288-94))
neutron reflection by surfaces of, absorbed dose in air from, (T), 20: 6528
neutron reflector savings in polystyrene-plutonium(IV) oxide arrays, 18: 22850(R) (HW-80020(p.31-7))
neutron rethermalization in, 17: 7055 (HW-SA-2415)
neutron scattering at 0.03, 0.06, and 0.12 ev, space time correlation function for, 16: 7161
neutron scattering at 0.18×10^{-3} to 2.8×10^{-3} ev, 16: 7162
neutron scattering, spectral studies of water structural dynamics from, 16: 7163
neutron scattering, angular and energy distributions, 16: 7164
neutron scattering, inelastic and quasi-elastic, 16: 7165
neutron scattering, production of cold neutrons in, 16: 7169
neutron scattering, cross sections and spectra, 16: 7178
neutron scattering, studies using spinning sample method, 16: 7158
neutron scattering, thermal, 16: 9653 (KAPL-2000-16)
neutron scattering, 16: 18447
neutron scattering law, 16: 21331 (AERE-R-4019)
neutron scattering, velocity distributions in, 16: 21333 (CRRP-1078)
neutron scattering cross section, constants for approximation functions, 16: 21342
neutron scattering at low energies, calculation of angular distribution, 16: 21343
neutron scattering displacement cross sections, fast, 16: 22964 (CEA-2142)
neutron scattering at 0.15 to 0.40 ev and 22°C, 16: 31054 (HW-SA-2541)
neutron scattering in, total cross sections for thermal, 16: 32368
neutron scattering in, diffusive atomic and vibratory motions from cold, 16: 32373
neutron scattering at 22 and 150°C, 16: 32382
neutron scattering, thermal, 16: 12409
neutron scattering, thermal, 16: 13925 (AERE-R-3931)
neutron scattering, diceway curves for, 17: 2341(R) (TID-17186)
neutron scattering at 0.10, 0.15, and 0.25 ev at 22°C, quasi-elastic, 17: 5297 (HW-75147)
neutron scattering by, comparison of Nelkin and Radkowsky kernels for, 17: 9482 (WAPD-T-1481)
neutron scattering by, thermal, 17: 11589 (HW-75526)
neutron scattering in, comparison of Nelkin's kernel with experiment, 17: 11303(R) (HW-75228)
neutron scattering, comparison of differential cross section values with Nelkins kernel, 17: 13678(R) (HW-75914)
neutron scattering by, space-time correlation function representation of cross section for, 17: 15219 (PAN-355/I-B)
neutron scattering by, thermal, 17: 15161 (BNL-719(Vol.I)(p.26-53))
neutron scattering by, experimental and theoretical values, 17: 15162 (BNL-719(Vol.I)(p.54-65))
neutron scattering by, calculations of, from models allowing for chemical binding, 17: 15185 (BNL-719(Vol.II)(p.614-55))
neutron scattering cross sections, thermal, 17: 15189 (BNL-719 (Vol.II)(p.706-97))
neutron scattering by, cross sections, 17: 19379
neutron scattering cross sections at 0.035809 ev, 17: 22537 (TID-18481)
neutron scattering by rotating molecules of, cross sections for thermal, 17: 22545
neutron scattering by, thermal, 17: 22539 (TID-18587)
neutron scattering by, alteration of Nelkin's model for, 17: 24369(R) (GA-3542)
neutron scattering law for, 17: 26392(R) (GA-3853)
neutron scattering law for, research on, 17: 31079(R) (HW-77311(p.4-11))
neutron scattering in, computer program for Nelkin calculations on, 17: 31384 (HW-78288)
neutron scattering at low energies, small-energy rotational transitions in, 17: 36634
neutron scattering by molecules of, thermal, 18: 2815
neutron scattering by, thermal, 18: 2805
neutron scattering, calculated moments for thermal, 17: 38418 (KAPL-M-FDF-3)
neutron scattering by, 17: 38026(T) (AEC-tr-5734(p.119-39))
neutron scattering by, total cross section for, 17: 38037(T) (AEC-tr-5734(p.219-21))
neutron scattering law for, 17: 39943(R) (GA-4176)
neutron scattering at 95°C, law for slow, 18: 8912(R) (HW-78388 (p.10.1-25))
neutron scattering law for, 18: 11147(R) (HW-79054(p.12-20))
neutron scattering by, cold, 18: 15128 (AE-133)
neutron scattering at 22 and 150°C, 18: 15129 (AERE-R-4484)
neutron scattering law for, research on, 18: 28088(R) (HW-80284 (p.10.1-28))
neutron scattering and thermalization by, calculations of, 18: 33010 (A/CONF.28/P/258)
neutron scattering by, kernel including anisotropic molecular motion for, 18: 34739
neutron scattering cross sections at 0.001 to 10 ev, 18: 36551 (GA-5373)
neutron scattering by, cross sections for slow, 18: 40474 (IDO-16977 (p.23-43))
neutron scattering cross sections for, thermal, 18: 42599 (TID-7050 (p.289-330))
neutron scattering cross sections for, computer program for slow, 18: 44703 (IDO-16984)
neutron scattering model for (T), 19: 3510 (CEA-R-2473)
neutron scattering by, angular- and position-dependent spectrum of (E), 19: 3201
neutron scattering by, angular distributions in, (E), 19: 8376(R) (GA-5176)
neutron scattering by liquid and solid, cold, 19: 12457 (JINR-P-1903)
neutron scattering kernel for, (E/T), 19: 16817(R) (GA-5554)
neutron scattering at 0.15 to 1.81 ev, cross sections for, (E), 19: 19095 (WASH-1053)
neutron scattering by, cold, (E), 19: 19077
neutron scattering by vaporized, at 0.018 to 0.080 ev, (E), 19: 21200 (KFK-264)
neutron scattering by, effects on kinetics of pulsed fast reactors, (T), 19: 24029 (EUR-2285.e)
neutron scattering by, differential cross section of thermal, (E/T), 19: 27389 (GA-6295)
neutron scattering by, cross sections and kernels for thermal, (T), 19: 29169 (GA-6281)
neutron scattering by, differential cross sections for thermal, (E/T), 19: 29216
neutron scattering by model for slow, 19: 32680(R) (IDO-17052)
neutron scattering at 0.001 to 1 ev, differential cross sections for, (E), 19: 33192(R) (GA-6096)
neutron scattering cross sections in, slow, (T), 19: 45228 (NP-15469)
neutron scattering by liquid, dynamics of, (E), 19: 45235
neutron scattering by, van Hove function for, (E), 19: 45236
neutron scattering kernels and laws for, thermal, 20: 3412
neutron scattering by, differential cross sections for thermal, (E/T), 20: 4801(R) (GA-6634)
neutron scattering by, angular distributions and diffusion constants from thermal, (E), 20: 6270
neutron scattering near melting point, differential cross sections for slow, (T), 20: 9946
neutron scattering by, thermal, (T), 20: 19781 (JAERI-1095)
neutron scattering by, differential cross sections and corrections for thermal, (E), 20: 21939(R) (GA-6930)
neutron scattering by, theory of, 20: 26396(R) (IDO-17140)
neutron scattering by, Monte Carlo solutions for multiple, 20: 26062 (CEA-R-2971)
neutron scattering model for, sensitivity to thermal reactor parameters, 20: 28714 (BNWL-SA-616)
neutron scattering by, angular distributions for, (E), 20: 28597
neutron scattering at 3.3 and 8.0 Mev, energy and dose-rate distributions in, 20: 28598
neutron scattering by, model for thermal, (E/T), 20: 30330
neutron scattering at 0.15 to 1.8 ev, differential cross sections for 302°K, (E/T), 20: 32350 (KAPL-M-6536)
neutron scattering by, energy spectra from cold, (E), 20: 31567
neutron scattering at 0.304 ev, width of 0.200-ev vibration level from, (E), 20: 34480
neutron scattering cross sections for, thermal, (T), 20: 36139 (GA-7055)
neutron scattering in, double differential cross sections for thermal, 20: 36140(R) (GA-7091)
neutron scattering by, hindered-translator model for one-particle motions in slow, 20: 37999
neutron scattering kernels at 423 and 550°K, thermal, (T), 20: 42138 (IN-1019)
neutron scattering laws for, 20: 44587 (NP-16291)
neutron scattering by, quasi-elastic cold, 17: 15246
neutron scattering studies of crystalline-bound, 19: 9095 (JINR-P-1904)
neutron shielding efficiency of, measurement of, 19: 35572
neutron slowdown at 1.46 ev in, time distribution and spatial dependence of, (E), 20: 26067
neutron slowing-down spectra in, 16: 9411 (AAEC/E-78)
neutron slowing-down in, 17: 15198 (BNL-719(Vol.III)(p.966-76))
neutron slowing down and thermalization in, 18: 7656 (AE-125)
neutron slowing down in, below 2.1 Mev, (E/T), 19: 29201
neutron slowing down in, (E/T), 19: 29203
neutron slowing down distributions in fresh and saline, 19: 35370(T)
neutron slowing down in, without polarization loss, (T), 20: 1134

(ORNL-P-1604)
neutron slowing down in, spin polarization effects on fission, (T), 20: 2969
neutron slowing down in, space- and time-dependent density for, (E), 20: 11927 (AE-208)
neutron slowing down in, effects of spin polarization on age of fission, 20: 30329
neutron slowing down times in, 17: 34829 (CONF-39-63)
neutron slowing-down time to cadmium edge in, 18: 21148
neutron slowing-down in, from radium–beryllium sources, 18: 44710
neutron slowing-down and thermalization in, (E), 19: 35353
neutron slowing-down time in, spatial dependence of, (E/T), 20: 34487
neutron slowing-down time in, spatial dependence of, (E), 20: 34488
neutron spatial distribution at indium resonance energy, 16: 1009
neutron spatial distribution, foil activation analysis of, 16: 1010
neutron spatial distribution of fission source in, 17: 3784
neutron spectra at 0.5 to 15 Mev, (E), 19: 27386 (GA-5750)
neutron spectra at absorption discontinuities in, thermal, (E/T), 19: 33231
neutron spectra in, methods for measurement of, 17: 15173 (BNL-719(Vol.II)(p.318-36))
neutron spectra in, 18: 733(R) (TID-19610)
neutron spectra in, with dispersed resonance absorbers, 18: 15157
neutron spectra in slab geometry in, thermal, 18: 15158
neutron spectra in, with absorbers, 18: 34733
neutron spectra in, kernel calculations of thermal, 18: 42600 (TID-7050 (p.330-49))
neutron spectra in poisoned, (E), 19: 5114(R) (GA-5486)
neutron spectra in borated, (E), 19: 8376(R) (GA-5176)
neutron spectra in critical solutions in, (E), 19: 18734 (CEA-R-2455)
neutron spectra in, comparison with scattering model, (E/T), 19: 27388 (GA-6291)
neutron spectra in, spatially dependent asymptotic, (E), 19: 33215
neutron spectra in poisoned, (E), 19: 41646
neutron spectra in, spatially dependent asymptotic, (T), 19: 47548(R) (TID-22141, pp 3-33)
neutron spectra in cooled, thermal, (E), 20: 2945
neutron spectra in, containing erbium and gadolinium, temperature-dependent, (E/T), 20: 2966
neutron spectra in, temperature dependent, 20: 19778(R) (GA-6824)
neutron spectra in, (E/T), 20: 24312
neutron spectra in, time-dependent thermal, (T), 20: 28232 (AE-226)
neutron spectra in, (T), 20: 30326
neutron spectra in, thermal, 20: 36140(R) (GA-7091)
neutron spectra in, 20: 36428 (GA-7072)
neutron spectra near temperature discontinuity in, thermal, (E/T), 20: 30331
neutron spectrum in, energy exchange kernel calculations of, 17: 32970 (CONF-11-5)
neutron spectrum measurements in, extraction hole effects on thermal, 16: 26199 (NP-11932)
neutron temperature distribution effects in reactor core, 17: 29835 (PAN-405/IX)
neutron temperature across interface with boron-poisoned water, (E/T), 19: 21207
neutron thermalization, 16: 18449
neutron thermalization and transport effects in, analytical expressions for, 17: 2505
neutron thermalization in, 17: 37993(R) (GA-4426)
neutron thermalization in, 18: 22848(R) (GA-4659)
neutron thermalization in, 18: 24566 (NP-13912)
neutron thermalization in, parameters for, 18: 26871
neutron thermalization in, 18: 38011 (A/CONF.28/P/366)
neutron thermalization, 18: 38031 (A/CONF.28/P/360)
neutron thermalization in, scattering-law parameters for (T), 19: 1518 (AE-154)
neutron thermalization in, chemical binding effects in, (T), 19: 19071
neutron thermalization in, time dependence of, (E), 19: 33226
neutron thermalization in, time-dependent, (T), 19: 33227
neutron thermalization in, integral, 19: 41640(R) (GA-6323)
neutron thermalization in, (E/T), 20: 8035 (GA-5798)
neutron thermalization in, (E/T), 20: 9944 (RPI-328-44)
neutron thermalization in, pulsed-source measurements of, (E), 20: 13739
neutron thermalization in, integral, (E/T), 20: 19778(R) (GA-6824)
neutron time-decay constants in, upper bounds for pulsed, (T), 19: 47553
neutron total cross section of, 17: 26392(R) (GA-3853)
neutron total scattering cross sections for, 16: 28019
neutron transmission at low energies, angular distribution, 16: 3877(R) (ORNL-3193(p.278-87))
neutron transmission in, at 0.5 to 14 Mev, 17: 9478 (BRL-1174)
neutron transmission by, flux and reflection in thermal, 17: 34828 (BRL-1204)
neutron transmission by finite slabs of, 20: 4999(R) (ORNL-2599)
neutron transmission through energy spectra after fast, (E), 20: 12268
neutron transport cross section, temperature dependence, 16: 2494 (TID-14223)
neutron transport in, measurement of extrapolation lengths for, 17: 11600 (WAPD-T-1490)
neutron transport in, Monte Carlo calculations of fast, 17: 34843
neutron transport in slabs of, leakage spectra for fast, 18: 6143 (R) (ORNL-3499(Vol.I)(p.108-15))
neutron transport in, eigenfunction analysis of, 18: 36080(R) (RPI-328-8)
neutron transport in, fast, 18: 40735 (EUR-1643.e(p.87-108))
neutron transport in, fast (E/T), 19: 3223
neutron transport equations for, eigenvalues of Boltzmann, (T), 19: 33217
neutron transport in, fast, (E), 20: 8035 (GA-5798)
neutron transport in, analysis of, (E/T), 20: 35001 (BNWL-222)
neutron transport in, Monte Carlo calculations of buildup factors and energy spectra, 16: 2620 (NASA-TN-D-850)
neutron utilization in reactor moderators of, thermal, (T), 19: 10493
neutrons age from fission in, comparisons of calculations and measurements, 18: 15153
nitrogen bubble kinetics in, 19: 38244 (N64-24160)
nitrogen-17 production in reactor, by (n,p) and (n,d) reactions in oxygen-17 and oxygen-18, 17: 20983 (IA-755)
nitrogen-16 distribution between steam and, in boiling reactors, 20: 6638
nuclear magnetic resonance relaxation in silica gel sorbed, temperature dependence of, 17: 32134
nuclear magnetic resonance of sorbed, on thorium oxide, temperature dependence of, 18: 20632 (TID-18689)
nuclear magnetic resonance of adsorbed, on thorium oxide, 18: 27426
nuclear magnetic resonance in flow-type generator, theory of, 18: 31526
nuclear magnetic resonance in, thermal relaxation time in, (E), 19: 15511
nuclear spin coupling constants in, molecular orbital theory for, 18: 44773
nuclear spin-lattice relaxation in, 18: 784
nuclear spin states, measurements, 16: 2354
nuclear spin states in molecular crystals, detection by neutron scattering, 16: 10735
nuclear spin-lattice relaxation in, (T), 19: 7474
nuclear spin-lattice relaxation in, (T), 19: 23186
nucleate pool boiling of, equation for statistical analysis of heat flux in, 16: 30564
orientation of molecular, in field of alkali ions, 18: 5285
origin of brines in oil wells, 20: 41161
oxidation by perxenate, intermediates in, 19: 34162
oxidation of tungsten by, effects of hydrogen on, 20: 2261(R) (UCRI-326)
oxidation of tungsten by, mass spectrometric study of, 20: 2261(R) (UCRI-326)
oxidizing effects on graphite at 775 to 975°C, 19: 30672(R) (ORNL-3789(p.202-7))
oxygen exchange with plutonyl ions in solution, 17: 12267
oxygen exchange with magnesia at 50 and 100°C, 17: 27313(R) (ASD-TDR-62-843)
oxygen ion reactions at 15 to 50 kev in, equilibrium fractions for, (E), 19: 18687
oxygen isotope exchange in, 16: 29295(R) (NYO-8771)
oxygen removal from HWCTR cooling, by sulfite, 19: 11668(R) (DP-945)
oxygen removal from, using resin columns, 16: 28415 (WAPD-BT-25)
oxygen-18 coupling constants with protons in, 16: 7976
oxygen-18 exchange, equilibrium constants and partition function ratios for, 16: 18876
oxygen-18 exchange between molecular sieve adsorbent and, 17: 23837
oxygen-18 exchange with uranium(VI) oxide and peroxide, 17: 23353
oxygen-18 exchange between carbon dioxide and, effects of catalysts on, 18: 2134(R) (TID-19592(Sect.VI))
oxygen-18 exchange between neptunyl ions and, rates of, 18: 5281
oxygen-17 NMR absorption in, effects of electrolytes on, 19: 39265(R) (IA-1021)
oxygen-17 NMR in, effects of chromium(II) and perchlorate ions on, 17: 32134
oxygen-17 spectra in enriched, effects of temperature on NMR, 20: 43171 (LA-DC-7394(Rev.))
oxygen-18 enrichment of, by fractional distillation, 19: 32659
oxygen-18 exchange with phosphorous acid, mechanism and rate of, 18: 19965
oxygen-18 exchange with carbon dioxide in moisture determination in cellulose, 18: 23397(T,R) (AEC-tr-6316(p.274-82))
oxygen-18 exchange with benzoates, 19: 28346(R) (TID-21662)
oxygen-18 exchange with orthotungstate or 12-tungstocobaltate at 25°C, 20: 14525
oxygen-18 exchange reactions between *p*-substituted benzoate anions and, mechanism of, 20: 16542(R) (TID-22646)
oxygen-18 exchange reactions between *p*-substituted benzophenones and, 20: 16542(R) (TID-22646)

oxygen-18 exchange with cupric, ferric, and ferrous sulfates, 20: 29153
oxygen-18 exchange between, and phenols and quinone in acidic media, mechanisms of, 20: 43276
oxygen-18/-16 ratio in saline, in oil wells, 20: 41161
particle transport on ideal surface at 0.08 slope, 16: 20594 (USNRDL-TR-436)
particle transport on surfaces by films of, effects of slope on, 19: 30444 (USNRDL-TR-834)
partition between aqueous and tributyl phosphate–hexane phase, 16: 24646
penetration into plastically deformed potassium bromide and sodium chloride crystals, 18: 4919 (TID-19729)
performance as moderator for critical experiments, (E), 19: 35706 (LA-3219)
performance as power-reactor coolant, 20: 30910
performance as reactor shielding, (E/T), 19: 14753
performance as reactor shielding, (E/T), 19: 14755
performance as reactor shielding, 19: 17156(R) (EUR-2197.d)
performance as shielding for neutron detectors, (E), 19: 13723 (HW-84329)
performance as shielding for FRG-2 research reactor, (E), 19: 17156(R) (EUR-2197.d)
performance as space-vehicle propellant, 17: 10201
performance as thermal columns in heavy-water reactors, (E), 19: 17358 (ANL-6915)
performance in EHD cells as charge carrier, (E), 19: 14287 (AD-603681)
performance of ionized vapors of, in direct-energy conversion devices, 18: 36249
performance of particle-seeded, as rocket-reactor coolant, (E), 19: 24149 (NASA-CR-212)
permissible levels of radioactivity in, 19: 4379
phase analysis of boiling, for determination of height and liquid content of foam, 17: 14601 (NYO-10011)
phase equilibrium in uranium and vanadium systems, 16: 17888
photolysis at 1470 Å, primary processes in, 20: 10881
photolysis by green algae in light, mechanisms of oxygen evolution, 17: 1187
photolysis in photosynthetic organisms, tracer study, 17: 7770
photolysis of, and aqueous solutions, 16: 30471
physical properties of oxygen-18 containing, 17: 2700
physical properties of, at 32 to 690°F and high pressures, 20: 43173 (NAA-SR-Memo-12006)
physiochemical properties of oxygen-16 and -18 labeled, 17: 10657
placental transfer in rabbits and swine, tracer study, 19: 38344
polarographic behavior in molten potassium nitrate–sodium nitrate at 350°C, 19: 17859 (TID-21511)
positron and positronium decay in, 19: 4899 (NRS-21)
positron annihilation in, 16: 18882
positron annihilation in, 15-kgauss magnetic field effects on, 16: 21175
positron lifetimes in, 16: 32354
positronium decay in, magnetic quenching of, 18: 26221
positronium decay in, (E), 19: 15867 (NP-14701)
positronium production in, (E/T), 19: 39509
potential energy functions for, determination from spectral data, 20: 31949
potentials of nickel electrode in, 16: 25322 (TID-16292)
preparation of very pure, 19: 17852 (CEA-R-2633)
pressure pulse production in fixed volume of, by pulse heating, 20: 3338
pressure-drop flow characteristics of subcooled, at atmospheric pressure in narrow heated channels, 20: 39047 (AERE-M-1739)
processing aboard space vehicles, using electric-power plants, (E/T), 20: 5820 (NASA-CR-316)
processing and use at Chinon nuclear power plant, 18: 12666
processing for Marcoule nuclear center, 18: 12296
processing in space vehicles, use of radioisotopes for, 20: 21174 (SAN-575-12)
production and methods of collection of, in combustion of samples for scintillation counting, 20: 43139
production by desalination, economic comparison of two evaporators for, 19: 40699 (ORNL-TM-826)
production by distillation of sea water, survey of large-scale processes for, 19: 11302 (AERE-M-1504)
production from labeled glucose in obese patients, 19: 21758 (BNL-8864)
production from saline water, economic aspects of nuclear power for, 17: 19633(R) (PB-161062)
production from saline water by heat from radioactive wastes, Project Artesia, 17: 30787
production from saline water, design of small nuclear reactor for use in plant for, 19: 17334
production from wastes in shelters, evaluation of processes for, 18: 16228 (NP-13740)
production in ion exchange resin irradiation in heavy water, 18: 17777 (NP-13766(p.119-33))
production of fresh, using dual-purpose reactors, 20: 45187
production of potable, by flash distillation of sea water, (E), 19: 29649 (PB-181694)
production of thin flowing sheets for radiation target use, 20: 11409
properties as catalyst for vibrational energy transfer, 17: 3644
properties as fast-neutron shield, experiment for, 18: 30949 (NYO-9077)
properties as heavy water-moderated power reactor coolant, 18: 43024 (DPW-64-135)
properties as moderator in research reactors, 18: 4857
properties as neutron reflector in fast-breeder reactors, 18: 4700
properties as reactor moderator, 16: 18050
properties as reactor coolant, 16: 23830 (BNL-5377)
properties as reactor coolants, 16: 28545 (TID-7623(p.2-8))
properties as reactor reflector, 17: 42224
properties as reactor coolant, 18: 11373
properties as reactor material, 18: 12665
properties as reflector in fast reactor, 18: 4746
properties as working fluid in Rankine power cycle, 20: 41398
properties for cooling lead radiation shield, 16: 18593 (TIM-80)
properties for polarographic reduction of organic compounds, 20: 18636(R) (TID-22725)
properties for use as shielding for ship reactor, 19: 3770
properties for use as reactor coolant and moderator, review of, 19: 22885
properties for uses in reactors, 19: 45678 (JEN-149-DQ/I-50)
properties for use as DCX-2 coolant, 20: 10128 (CONF-650512, pp 177-81)
properties in damped oscillating manometer, time-dependent, 17: 27654 (LADC-5535)
properties of, effects of isotopic substitutions on physical and thermodynamic, 16: 25307 (CEA-Bib-15)
proton absorption by, depth-dose measurements in, 18: 27790(R) (ORNL-3578(p.46-59))
proton attenuation, 17: 18909 (TID-18436)
proton attenuation by, energy-range curves for, 17: 25968
proton depth-dose distribution in spherical phantom filled with, 17: 27059 (ORNL-3457)
proton motion in, from cold neutron scattering measurements, 18: 43499
proton motions in, fluctuation of, 18: 27440
proton reactions (p,γ) at 160 Mev, gamma spectra from, 18: 16315
proton reactions at 160 Mev, secondary-nucleon production in, 18: 7693(R) (ORNL-3499(Vol.II)(p.73-84))
proton reactions at 160 Mev, neutron and proton spectra for, 18: 7694(R) (ORNL-3499(Vol.II)(p.89-93))
proton reactions at 160 Mev, 0.6- to 11-Mev gamma rays from, (E), 19: 21243 (ORNL-3506)
proton reactions at 160 Mev, proton production in, (E), 20: 44649 (ORNL-3887)
proton reactions with, energy deposition from, 18: 44751
proton reactions with nuclei in, cross sections at 160 Mev, (E), 19: 14536 (ORNL-P-848)
proton self-diffusion coefficient in, nuclear resonance measurements on, 19: 8115
proton transfer by, Grotthuss mechanism in, 20: 340
proton transfer reactions in, product and rate isotope effects in, 19: 389
purification, 16: 11522(R) (TID-15082)
purification, 18: 41304(R) (ORNL-TM-775)
purification by ion exchange, 18: 33713
purification by ion exchange, design of fallout treatment kit for, 20: 12942(P)
purification for Dragon Reactor, 19: 48042
purification for reactor coolant uses, 18: 152 (HW-68716)
purification for reactors, 19: 42130 (HW-68387)
purification for use in Hanford Production Reactors, 18: 23443 (HW-77710)
purification in Bulgarian IRT-1000, 19: 19419
purification in Parr Shoals Power Reactor, properties of zirconium oxide and phosphate ion exchangers for, 16: 14612 (CVNA-135)
purification of, at Hanford Atomic Facility, 17: 14205 (HW-76389)
purification of, automatic system for adding clarifying chemicals at treatment plant, 17: 8487(P)
purification of, emergency measures of, 17: 39336
purification of radioactive, by ion exchange, 17: 10710
purification of radioactive, effects of radiostability of exchange resins on, (E), 19: 40129 (ZFK-RN-17(p.114-26))
purification of reactor coolant and moderator, 17: 14235
purification of reactor-coolant, 18: 40915
purification of reactor primary-coolant, ion-resin methods for, 19: 40123 (IAE-787)
purification of reactor coolant, ion exchange materials for, 19: 38759 (ZFK-RN-17(p.95-117))
purification of reactor coolant, electrophoretic filter for, 20: 6568

purification of reactor coolant, evaporator design for, 20: 26406
purification of, use of cellulose filters for, 18: 39554
purification with cobalt-60, 16: 24054
purity monitoring in reactor primary coolant loops, standardization of, 19: 40124 (IAE-789)
radiation attenuation in, effects of thickness on, 17: 36347(R) (NARF-62-18P)
radiation chemistry, 15: 238
radiation chemistry, in sulfuric acid, 16: 7593
radiation chemistry, precursors of molecular hydrogen formed in, 16: 20505
radiation chemistry of, in relation to biological systems, 17: 25012
radiation chemistry of, effects of initial linear energy transfer of protons in, 17: 25338
radiation chemistry of, effects on radiosensitivity of biological systems, 18: 1433
radiation chemistry of, isotope effects in, 19: 36475
radiation chemistry of, 19: 42335
radiation chemistry of, under alpha bombardment at 30 Mev, 20: 18809
radiation chemistry of liquid and frozen, 20: 18190(R) (UCRL-16613)
radiation chemistry of, structural model of hydrated electron in, 20: 43322
radiation chemistry of glasses of, at 77 to 150°K, ESR studies of gamma and ultraviolet, 20: 45730
radiation dose calculations for, x-ray, 19: 10960
radiation dosimetry in, use of Cherenkov detector for measuring cosmic, 19: 8124
radiation effects on reactions with aluminum, stainless steel, uranium, and Zircaloy-2, 16: 11575 (ANL-6250)
radiation effects at 1 Mev, secondary electron energies, 16: 14199 (DC-57-4-67)
radiation effects on extracellular, in rabbits, 17: 14102
radiation effects on, fluorescence and thermoluminescence spectra of gamma, 17: 40871
radiation effects on gastrointestinal absorption of, in rats and dogs, 18: 11654 (USNRDL-TR-693)
radiation effects on rat consumption of, age effects on protons, 18: 15815 (USNRDL-TR-712)
radiation effects on balance of, in rat gastrointestinal tract, 18: 17541
radiation effects on, comparison with free radical reactions, 18: 27501
radiation effects on diffusion through polyethylene, gamma, 18: 37770(T) (AEC-tr-6398(p.521-8))
radiation effects on platinum-catalyzed deuterium exchange between, and benzene in, 18: 43648
radiation effects on electric conductivity of, gamma, 19: 437(T) (JPRS-26808(p.132-9))
radiation effects on reactions with uranium monocarbide, in-pile, 19: 7948
radiation effects on beef as affected by pre-irradiation soaking in, 19: 15964
radiation effects on, review on theory of, 19: 15231
radiation effects on reactions with uranium, 19: 23991(R) (ANL-7003)
radiation effects on cavitation threshold of degassed, neutron, 19: 28383
radiation effects on, 19: 32642
radiation effects on exchange of, in rat liver, 19: 33919
radiation effects on ammoniated and oxygenated solutions, 19: 40548 (BNWL-82)
radiation effects on, behavior of ion spurs and tracks in alpha and gamma, (T), 20: 370
radiation effects on, mechanism and rate of, 20: 390
radiation effects on content of, in forest soils, 20: 3653 (BNL-8466)
radiation effects on content in muscle, γ and x, 20: 18293 (NP-14898)
radiation effects on, electron, 20: 38947
radiation effects on gastrointestinal absorption of, in rats, tracer study of x, 20: 42971
radiation effects on content in oysters, gamma, 20: 45347
radiation heating deposition rates in, cross sections for, 17: 36347(R) (NARF-62-18P)
radiation measurements in phantoms of, 18: 31073
radiation monitoring, 17: 13874
radiation monitoring of, methods for, 18: 6545
radiation monitoring in, instruments and methods for, 18: 6981
radiation monitoring of, sample preparation for, 19: 26588
radiation monitoring at Paducah Plant, 19: 35886(R) (KY-484)
radiation monitoring of process, detector calibration for, 19: 42715(R) (ORNL-3782, pp 35-51)
radiation monitoring in German, 1965, 20: 4164
radiation monitoring of Swiss, 1963, 20: 7273
radiation penetration in, half-value thickness equivalents for, 19: 7229
radiation scattering from, measurement of bremsstrahlung and gamma, 18: 44920
radiation scattering in, radiation doses from, gamma and x, 19: 31444
radiative processes in solutions of, formation of compounds of bound nitrogen by, 20: 25160
radioactive contamination, deactivation and protection against, 16: 2066(T) (NP-tr-793)
radioactive contamination, hazards to man, 16: 10340
radioactive contamination of, methods of measuring and controlling, 17: 41073
radioactive contamination of, detection by beta counting, 18: 11969 (PAN-452/XIX)
radioactive contamination of, hygienic aspects of, 18: 18106
radioactive contamination of, Federal Republic of Germany, 1955 to 1962, 19: 24788
radioactive waste disposal in, safety precautions for, 19: 40277
radioactive waste solutions of, assessment of industrial hazards from, 20: 12525
radioactivity, 19: 28597
radioactivity at off-site stations during Operation DOMINIC in Pacific, 19: 15752 (NP-14778(Pt.I))
radioactivity at off-site stations during Operation DOMINIC in Pacific, 19: 15753 (NP-14778(Pt.II))
radioactivity buildup in coolant, 16: 29994 (AEET/HP/3(Rev.))
radioactivity content in Mexican, 1962, 20: 9155
radioactivity content of, from fallout in West Germany, 20: 40570
radioactivity content of, from fallout in West Germany, 20: 43626
radioactivity, evaluation of methods for counting gross, 16: 5509
radioactivity in Antarctic, 18: 35749
radioactivity in German, 1965, 20: 23412
radioactivity in German, 1965, 20: 23413
radioactivity in, monitoring of low-level beta, 17: 380
radioactivity in, methods for determination of low-level, 17: 37168
radioactivity in, measurement techniques for, 18: 1976
radioactivity in, performance of vibrating condenser electrometers for determination of, 17: 12566
radioactivity in potable and rain, ORNL summary for 1965, 20: 33557(R) (ORNL-3969)
radioactivity in Spain, 18: 35754
radioactivity in West Germany, 16: 30677 (NP-12019)
radioactivity in, wet ashing ion exchange method for determination of, 17: 37169
radioactivity in, maximum permissible concentrations of uranium-235 fission products in, 19: 38872 (AEET/HP/TH-15)
radioactivity in, importance of measuring, 20: 20961
radioactivity in, performance of scintillation materials for detecting, 20: 31499 (AD-633752)
radioactivity in, methods for measuring, 20: 40819(T) (CEA-tr-A-1883)
radioactivity measurement devices, 16: 23868
radioactivity measurement under unsaturation conditions, 16: 30605
radioactivity measurement in waste, apparatus and methods for, 17: 5651
radioactivity measurement in, continuous, 17: 4815
radioactivity measurement in, discontinuous, 17: 4816
radioactivity measurement in, direct, 17: 30082
radioactivity measurements in New Zealand, 20: 40521(R) (NP-16270)
radioactivity monitoring, design of spray evaporation, 16: 13329
radioactivity monitoring in, instrument for, 17: 29222(P)
radioactivity monitoring in continuously contaminated, 18: 10429(P)
radioactivity monitoring in, design of equipment for continuous, 18: 14252
radioactivity monitoring in, using scintillation ion exchange resins, 19: 2640
radioactivity monitoring in Savannah River Plant area, 19: 7725(R) (DPSPU-64-30-1)
radioactivity of drinking, removal of, 17: 36078
radioactivity of, evaporation unit with Geiger-Mueller tube for measuring, 17: 40765(P)
radioactivity of, in Czechoslovakia, measurement methods of, 17: 15616(T) (JPRS-18391)
radioactivity of mineral, in Italy, natural, 20: 9151
radioactivity of reactor coolant, effects of low-cobalt stainless steel on cobalt-60, 19: 45495 (WAPD-T-1653)
radioactivity of, design of equipment for measuring, 18: 14087
radioactivity of, regulations on control of, in Germany, 18: 22287
radioactivity of, methods for monitoring, 19: 13672
radioactivity of, system for monitoring, 19: 13713
radioactivity of, hazards to human organs from, 20: 7324(T) (CEA-tr-R-1350)
radioactivity of, equipment for measuring total beta, 20: 22912
radioactivity releases in, studies using bromine-82, 18: 37500 (A/CONF.28/P/610)
radioinduced Cherenkov radiation from, intensity of, at 3000 to 10,000 A, 16: 33690 (PAN-329/ZVII)
radioinduced decomposition of, effects of osmium tetroxide on, 19: 13450
radioinduced defects in, fast-neutron, 19: 991 (CEA-R-2510)
radioinduced formation in ion exchange resins immersed in water-d_2, 17: 35868 (EIR-50)
radioinduced free radicals, biochemical effects, 16: 14487
radioinduced free radicals in, diffusion kinetics of, 18: 3827

radioinduced heating rates in AARR thermal column, 19: 35606(R) (ANL-7045(p.49-59))
radioinduced ice formation in supercooled, gamma, 20: 9288
radioinduced in baked glass bulbs, gamma, 20: 44011
radioinduced ionization in, (T), 19: 46401
radioinduced ionization of, diffusion-controlled radical reactions in particle tracks during, 20: 31294
radioinduced nucleation of bubbles in, theory, 17: 28032
radioinduced reactions in, studies using fluorescence of aromatic compounds, 16: 5787
radioinduced reactions in acidified, isotope effects on, 17: 35873
radioinduced reactions with carbon monoxide, gamma, 18: 29044(R) (HW-79280(p.6.1-16))
radioinduced reactive species in, 19: 468
radioinduced synthesis of, energy transfer from carbon dioxide in alpha, 18: 22138
radioinduced synthesis of, energy transfer from carbon dioxide in, 19: 429(R) (ORNL-3679(p.39-48))
radioinduced thermoluminescence of, 19: 26418
radioinduced yields of positive oxygen ions in, electron, 19: 40581
radioisotope behavior in, 19: 31685
radioisotope concentrations in, maximum permissible, 18: 25733
radioisotope content of Hanford reactor effluent, effects of filter flow rate on, 19: 683(R) (HW-81746(p.3.29-30))
radioisotope content of, in Ispra environs, Italy, 1965, 20: 33553 (EUR-2965.e)
radioisotope distribution in, in closed vessels, 20: 36711
radioisotope levels in tap, 17: 5751(R) (HASL-132)
radiological decontamination of drinking, by ion exchange, 17: 12496 (NP-12463)
radiological monitoring near Nevada Test Site, 16: 9030 (TID-14776)
radiological monitoring after Shoal nuclear explosion, 19: 697 (VUF-1009)
radiolysis, 16: 1811(T) (AEC-tr-4564)
radiolysis, 17: 24974
radiolysis, 19: 22385
radiolysis, (T), 19: 46401
radiolysis, 18: 10139(R) (AD-403358)
radiolysis by fission fragments, 17: 3901
radiolysis by fission fragment recoil energy in aqueous slurry of uranium-thorium oxides, 17: 21770
radiolysis by proton beam at 1 to 2 Mev, yields of hydrogen peroxide in, 18: 23578 (LFEN-15)
radiolysis by 1.57-Mev proton pulses, 19: 44058 (LFEN-23)
radiolysis, effects of reducing radical on hydrogen ion, hydrogen peroxide, and oxygen yields in, 16: 10071
radiolysis, electron spin resonance of free radicals produced in gamma, 16: 7600
radiolysis, electron paramagnetic resonance of free radicals produced by beta and gamma, 16: 11711
radiolysis, formation of two kinds of H atoms in, 16: 6457
radiolysis, free radicals produced in, 16: 8783
radiolysis G values, 16: 20514
radiolysis, gamma and neutron, 16: 27047
radiolysis in acid, basic, and neutral solutions, review of free radical yields in, 18: 20037 (BNL-6978)
radiolysis in boiling water reactors, hermetic sealing and recombiner problems from, 18: 21672 (NAA-SR-Memo-9507)
radiolysis in flow irradiator, calculated product accumulation in, 19: 44061(T) (AEC-tr-6567)
radiolysis in Halden Reactor, effects of power, pressure, subcooling, and additions of deuterium and nitrogen on, 18: 19368(R) (HPR-33)
radiolysis in High Flux Isotope Reactor, 18: 22013(R) (ORNL-3591 (p.70-6))
radiolysis in PM-3A spent core storage tank, hydrogen evolution in, 19: 40188 (NYO-3420-2)
radiolysis in power reactors, 17: 14114 (ANL-6562)
radiolysis in presence of azide, 16: 29004
radiolysis in presence of hydrogen, kinetics of, 19: 9170 (TID-21232)
radiolysis in reactors, rate of, 19: 38698 (ZFK-RN-17(p.199-207))
radiolysis in solutions with fumaric acid, gamma, 20: 10875
radiolysis in water-cooled power reactors, 17: 28538
radiolysis, kinetic behavior of products, 16: 1837
radiolysis kinetics, analysis, 16: 20521
radiolysis mechanism, 16: 6442(T) (CEA-tr-R-1448)
radiolysis mechanism, 16: 25462
radiolysis mechanism in, 17: 1327
radiolysis mechanism, 17: 10509(R) (ORNL-3320(p.30-46))
radiolysis mechanism of, 19: 429(R) (ORNL-3679(p.39-48))
radiolysis, nature of reducing radical formed in, 16: 13107
radiolysis, nature of hydroxyl radical and hydrogen atom, 16: 30469
radiolysis, nature of excited water molecules formed in, 18: 9752 (IA-900)
radiolysis of acid solutions of, yields of products of, 20: 18745
radiolysis of adsorbed, hydrogen yields in, 20: 45714(R) (ORNL-3945, pp 218-20)
radiolysis of basic solutions of, yields from gamma, 18: 23674
radiolysis of, concentration and temperature dependence of hydrogen molecule and hydroxyl radical production in, 17: 34020
radiolysis of, determination of quantity of free radicals formed in, 18: 1733
radiolysis of, effects of pH on radical yields in, 17: 4614
radiolysis of, effects of pH on hydrogen peroxide formation in, 17: 16058(R) (AEC-tr-5687)
radiolysis of, effects of hydroxyl radical on hydrogen yield in, 17: 37265
radiolysis of, effects of solutes on reactivity of H_3O^-, 18: 5375
radiolysis of electron slowing down spectrum of, 19: 11428
radiolysis of, evidence for, reactions of ions in spurs in, 17: 40882
radiolysis of frozen potassium hydroxide solutions in, EPR of radicals from, 19: 7549
radiolysis of hydrogen peroxide in, gamma, 19: 2393
radiolysis of, in relation to use in nuclear reactors, 17: 25296
radiolysis of, lectures on effects in EBWR, 17: 17403 (ANL-6640)
radiolysis of, mechanism and yields in, 16: 31665
radiolysis of, mechanism of hydrogen peroxide formation in, 17: 10686
radiolysis of, mechanisms of, 17: 18109 (TID-18305)
radiolysis of, mechanism of gas formation process in electron, 18: 327
radiolysis of oxygenated, transient species in, 20: 14614
radiolysis of, prediction of order of magnitude or number of molecules originally decomposed in, 18: 1771
radiolysis of, primary species formed in, 17: 25020
radiolysis of, reaction constants of the hydrated electron in, 17: 23399
radiolysis of, reaction mechanisms and polaron production during, 17: 34024
radiolysis of, reactions of hydrated electrons from, 17: 40865
radiolysis of, review of, 17: 25332
radiolysis of, role of primary processes in pH effect on, 16: 22219
radiolysis of, role of oxygen in the primary formation of H and H_3O^- in, 17: 8187
radiolysis of shielding, for high-power gamma facility, 20: 5670
radiolysis of silica-sorbed, G values for, 20: 8982(R) (ORNL-3830, pp 233-5)
radiolysis of sodium formate solutions, deuterium isotope effects, 16: 33030
radiolysis of, solute kinetics in, 17: 25021
radiolysis of, acid-base dissociation constants for intermediates from, 19: 46343
radiolysis of, at pH of 9.5 to 14, gamma, 20: 26958
radiolysis of, catalytic recombination of products from, 19: 4197 (SAN-8003(p.90-133))
radiolysis of, chemical reactions of products from gamma, 19: 439
radiolysis of, chemical yields from neutron and gamma, 20: 43377
radiolysis of, detection of hydrated electrons in, 19: 5959
radiolysis of, deuterium effects on molecular hydrogen formation in, 19: 13459
radiolysis of, diffusion kinetics for alpha and gamma, (E/T), 20: 43288(R) (CALT-532-1)
radiolysis of, effects of oxygen on free radicals formed in, 18: 29789
radiolysis of, effects of acidity, deuterium, and solute additions on pulse, 18: 43663
radiolysis of, effects of alkaline media on, 19: 505
radiolysis of, effects of water-soluble stable free radicals on, 19: 509
radiolysis of, effects of linear energy transfer on isotope effects in hydrogen formation in, 19: 18029
radiolysis of, effects of inert salts on yields from neutron, 19: 26397
radiolysis of, effects of copper ions, hydrogen peroxide, and oxygen on electron, 19: 42542
radiolysis of, effects of salts on, 20: 8981 (CEA-R-2794)
radiolysis of, effects of hydrogen and oxygen on yields of hydrogen peroxide from, 20: 16520
radiolysis of, effects of iodine and methyl iodide on, 20: 25167
radiolysis of, effects of deuterium on gamma, 20: 43352
radiolysis of, energy releases in reactions following, 20: 9008
radiolysis of, formation and detection of intermediates in, 18: 25576
radiolysis of, formation of hydroxyl radicals in pulsed-electron, 20: 10924
radiolysis of, formation of molecular hydrogen peroxide in gamma, 20: 25142
radiolysis of, free radical formation by, 18: 16080
radiolysis of, free radical model for, 20: 38959
radiolysis of, hydrated electron absorption spectrum and reaction constants in, 18: 23691
radiolysis of, hydroxyl ions in mass spectrum from electron, 18: 43656
radiolysis of, hydrated electrons in, 19: 469
radiolysis of, in sodium acid phosphite–sodium nitrate solutions, effects of pH on, 20: 14601
radiolysis of, intermediate-product interactions with added acceptors in,

18: 37210(T) (AEC-tr-6398(p.451-61))
radiolysis of, isotope effects on hydrogen production by, 20: 2520(R) (IA-920)
radiolysis of, isotope effects on vapor-phase gamma, 20: 25138
radiolysis of, kinetics of pulsed electron beam, 18: 25578
radiolysis of, linear energy transfer in gamma and neutron, 18: 27497 (WAPD-BT-30(p.53-64))
radiolysis of, linear energy transfer effects on yields from, 18: 29779
radiolysis of, mechanisms of formation of molecular products in electron and gamma, 18: 20050
radiolysis of, mechanism of acidity and solute concentration effects on yields in, 18: 23681
radiolysis of, method for estimating ratio of rate constants in, 19: 444
radiolysis of, model for, 18: 29695 (UJV-734/62)
radiolysis of, nature of free radicals induced by, 19: 19968
radiolysis of, nitrous oxide as scavenger in, 19: 38720
radiolysis of, precursor of molecular hydrogen in, 19: 4206
radiolysis of, primary processes in, 18: 35636
radiolysis of, processes in in-pile, 18: 38243 (A/CONF.28/P/20)
radiolysis of, properties of reducing component produced in, 18: 39311
radiolysis of, production and properties of excited molecules in, 19: 26917(R) (IA-984)
radiolysis of, production of H_3O precursor to molecular hydrogen in, 19: 46332(R) (ORNL-3832, pp 50-65)
radiolysis of, properties of excited molecules from, 20: 2520(R) (IA-920)
radiolysis of, rates of reaction of hydroxyl radical from, 19: 26444
radiolysis of, reactions of tetranitromethane with hydrated electrons produced in gamma, 18: 37219
radiolysis of, reactions of hydrated electrons and hydrogen atoms from, 19: 22292
radiolysis of, reactions of hydrated electron, hydrogen atom, and hydroxyl radical in, 20: 7132
radiolysis of, reactions of alanine with reducing species formed in gamma, 20: 7152
radiolysis of, reaction rates and yields in, (T), 20: 16509 (TID-22666)
radiolysis of, reactions of hydroxyl radicals from, 20: 26928
radiolysis of, reactions of hydrated electrons in, 20: 33373
radiolysis of, reducing radical yields in gamma, 19: 46332(R) (ORNL-3832, pp 50-65)
radiolysis of, review on, 19: 13462
radiolysis of, scavenging of atomic hydrogen formed in, 19: 22339
radiolysis of, solute scavenging effects in regions of high radical concentration from gamma, 19: 26446
radiolysis of, solute concentration effects of, on hydrogen yields from gamma, 20: 7151
radiolysis of, spectra of electron scattering in, 19: 9213
radiolysis of, standard electrode potential of hydroxide ions formed in, 19: 22327
radiolysis of, tracer studies of kinetics of electron, 20: 29315
radiolysis of, yields from, 19: 30255
radiolysis, rate constants of radical processes in, 16: 10070
radiolysis, separation of effects of fast neutrons and gamma radiations, 16: 10053
radiolysis, temperature effect, 16: 17739
radiolytic hydrogen yield in loop, 17: 40266(R) (EURAEC-728)
radionuclide contents in, 19: 9365(R) (HASL-155)
radioprotective effects of sulfurated mineral, 20: 38709
radiosensitivity effects in barley, 16: 1619
radiosensitivity effects on pine seeds, 16: 17470
radiosensitivity effects on shrimp eggs, 16: 17504
radiosensitivity effects in barley and maize seeds, 17: 15799
radiosensitivity effects on *Staphylococcus aureus*, 17: 23187
radiosensitivity effects on seeds, 17: 31869
radiosensitivity effects on plants, 17: 31951
radiosensitivity effects on Lupinus seed, 17: 35481
radiosensitivity effects on pea seeds, mechanism of, 17: 38880
radiosensitivity effects of, on *Bacillus megaterium* spores, 17: 40614
radiosensitivity effects on *Bacillus megaterium* spores, gamma, 18: 13505
radiosensitivity effects on wheat grain, gamma, 18: 13529
radiosensitivity effects on biological systems, 18: 21871
radiosensitivity effects on tomato seed and pollen, 18: 35377
radiosensitivity effects on seeds and spores, 19: 29886(R) (ANL-6971 (p.29-46))
radiosensitivity effects on Artemia eggs, 19: 43814
radiosensitivity effects on peas, 19: 45863
radiosensitivity effects on Lupinus, x, 19: 45847
radiosensitivity effects on mutagenesis in Arabidopsis, x, 20: 5357
radiosensitivity effects on germination in *Phleum pratense*, γ and x, 20: 14349
radiosensitivity effects on *Rauwolfia serpentina* seed, γ, 20: 16249
radiosensitivity effects on *Vicia sativa*, x, 20: 16276
radiosensitivity effects on pea flour, 20: 16297(R) (EUR-2548.f)
radiosensitivity effects on grass seeds, 20: 18382
radiosensitivity effects on mutation frequency in tomato pollen, γ, 20: 18393
radiosensitivity effects on Pisum meal, 20: 18429
radiosensitivity effects on pine seeds, x, 20: 22744
radiosensitivity effects of sulfurated mineral, in mice, 20: 22775
radiosensitivity effects on barley seeds, 20: 38736
radiosensitivity effects of content of, in peas treated with vitamin C, fast neutron and gamma, 20: 45387
radiosensitivity effects of content of, in sunflower seed, gamma, 20: 45416
radiosterilization of, gamma, 19: 6224
radium-226 content of drinking, maximum permissible limits for, 18: 33820
rationing in postattack recovery period, 20: 45940 (AD-639710)
reactions in system with butyl phosphates, hydrochloric acid, and uranyl chlorides, hydrolytic and photolytic, 16: 1828
reactions of hydrated electron with, in pulse radiolysis, 20: 10894
reactions of ions of, with gases, mass spectrometry of dissociation in, 18: 220
reactions of jets of, with liquid aluminum, pressure-wave generation by, 20: 18050(R) (STL-372-22)
reactions of, with zirconium at high temperatures, 16: 30718 (ANL-6548)
reactions of, with uranium, kinetics, products, and mechanism of, 20: 45682
reactions with aluminum and magnesium alloys (liquid), 16: 31614
reactions with aluminum–nickel–uranium alloy plates during TREAT transients, 18: 1486(R) (ANL-6687(p.167-87))
reactions with aluminum and its alloys, 18: 35060(R) (ANL-6904)
reactions with aluminum, magnesium, and reactor fuels, 18: 44922(R) (ANL-6800(p.326-402))
reactions with aluminum, laser-induced, 19: 17174(R) (ANL-6900(p.232-303))
reactions with aluminum, induced by laser heating, 19: 32447(R) (ANL-7020(p.175-97))
reactions with aluminum, laser-induced, 20: 20925(R) (ANL-7055, pp 177-212)
reactions with ammonia, production of deuterium and water-d_3 by isotopic exchange in, 18: 44014
reactions with ATJ graphite in flowing helium at 775 to 925°C, 20: 23607
reactions with barium oxides, 17: 41534(R) (ANL-6720(p.77-89))
reactions with barium oxide, 18: 42295(R) (ANL-6879(p.114-29))
reactions with benzyl chlorides, chlorine isotope effects in, 16: 25344
reactions with bidentate phosphine oxides and trioctylphosphine oxide to form complexes, 19: 24621
reactions with bismuth chloride, effects of unknown agent on bismuth oxychloride precipitation in, 17: 29015
reactions with carbon dioxide, effects of pressure and temperature on isotopic fractionation in, 17: 4511
reactions with carbon dioxide and zinc, preparation of methane for tritium counting by, 18: 16075
reactions with ceramics and metals, 19: 17178(R) (ANL-6965(p.91-8))
reactions with cesium in ethylenediamine, kinetics of, 18: 260
reactions with chromium oxalate ions, 17: 25166(R) (TID-18769)
reactions with deuterated water, (E), 19: 24522
reactions with dicarboxylic acids, kinetics of proton abstraction in, 20: 350
reactions with fission products, effects of chemical agents on, 20: 4185(R) (ORNL-3843, pp 169-234)
reactions with fluoride complexes, thermodynamic functions of, 17: 40798
reactions with graphite, magnesium, and uranium in reactor environment, 18: 1258 (NP-13223)
reactions with graphite up to 3000°K (E/T), 19: 2354
reactions with graphite at high temperatures, 19: 25052(R) (ORNL-3731 (p.154-206))
reactions with graphite, rate measurements on, (E), 19: 35622
reactions with graphite under in-pile conditions, 19: 36962(R) (ORNL-3807, pp 145-76)
reactions with heavy water, mass spectrometric determination of equilibrium constant for disproportionation, 20: 38875 (UCRL-14703-T)
reactions with hydrogen ions to form hydronium ions in alcohols and formates, tracer studies of, 18: 5368
reactions with hydrated electrons in aqueous solutions, rate constants, 18: 27488
reactions with hydrated electrons, review on, 20: 5525 (IA-1041)
reactions with lanthanum germanides, 20: 46214
reactions with liquid reactor fuels and claddings, 18: 19309(R) (ANL-6725(p.201-23))
reactions with liquid sodium in Sodium Reactor Experiment pipe gallery, hazards analysis of, 18: 24894 (NAA-SR-Memo-7743)
reactions with metals, 16: 2923(R) (ANL-6379)
reactions with metals, 16: 12843
reactions with metals, exploding wire study, 17: 9107

reactions with metals under reactor transient conditions, 17: 13729
reactions with metals used in fuel elements, energy release in, 18: 245
reactions with methyl iodide, calculated carbon-13 and deuterium isotope effects in, 18: 33612 (BNL-8066)
reactions with metals in reactor environment, TREAT studies of, 19: 25765
reactions with metals in reactors, (E), 19: 35624
reactions with metals at high temperatures during core meltdown, (E/T), 19: 47960(T) (ORNL-TR-694)
reactions with metals, analysis in LOFT meltdown, (T), 20: 26518(R) (IDO-17145)
reactions with metals during reactor meltdown, hydrogen combustion in, 20: 28685(R) (BMI-X-10163)
reactions with molten beryllium fluoride–beryllium oxide–lithium fluoride at 500 to 700°C, 19: 30155 (ORNL-TM-1129)
reactions with molybdenum at 1100 to 1700°C, 20: 5846
reactions with molten urania, 20: 27406(R) (BNWL-198, pp 4.1-42)
reactions with molten aluminum, pressure generation and effects in, 20: 33808
reactions with neodymium oxide, infrared spectra of products of, 20: 14568
reactions with oxygen and uranium, kinetics and products of, 20: 45683
reactions with potassium–sodium alloys, 17: 2939 (HW-67717)
reactions with potassium chloride, heat of, 17: 27323 (UCRL-7325-T)
reactions with pure metals, theory of, 18: 27432
reactions with radioisotope-containment materials in launch pad abort environments, 20: 19192 (SC-DC-65-1918)
reactions with rare earth dicarbides, formation of gaseous products in, 20: 17048
reactions with silica gel, radioinduced, 16: 13664
reactions with sodium, thermodynamics of, 18: 33528 (NP-14080)
reactions with sodium owing to small leaks in steam generators, 18: 35663(R) (TID-20936)
reactions with sodium in boiler, engineering analysis, 19: 7676(R) (BAW-1280-20)
reactions with sodium, thermodynamic calculations of, 19: 9107
reactions with sodium, analysis of, 19: 13577(R) (BAW-1280-21)
reactions with sodium in steam generators, studies of problems produced by, 19: 20107(R) (BAW-1280-22)
reactions with sodium, literature review on, 19: 28284 (APDA-167)
reactions with sodium, effects on design of superheaters, 19: 31474 (BAW-1280-23)
reactions with sodium, effects on design of superheaters, 19: 31475 (BAW-1280-24)
reactions with sodium in reactors, testing of, 19: 35608(R) (APDA-170)
reactions with sodium in steam generators, 19: 38803(R) (BAW-1280-26)
reactions with sodium, test loop for, 19: 44161(R) (APDA-174, pp 25-32)
reactions with sodium in prototype boiler, analysis, 19: 46529 (APDA-175)
reactions with sodium in boiler, engineering analysis, 19: 46531(R) (BAW-1280-28)
reactions with sodium in loops, separation of products of, 20: 1960
reactions with sodium, effects on design of steam generators, 20: 4100 (BW-67-2(a))
reactions with sodium, loop for testing small leak, 20: 10285(R) (APDA-178, pp 18-29)
reactions with sodium in pipes, 20: 9417 (CONF-650620, pp 156-65)
reactions with sodium, research program on, 20: 9419 (CONF-650620, pp 232-43)
reactions with sodium, test facility for studying, 20: 10290 (CONF-650620, pp 244-54)
reactions with sodium in steam generator, 20: 12386 (APDA-176)
reactions with sodium in sodium-heated steam generators, 20: 12391 (BAW-1280-28(Vol.3))
reactions with sodium, loop development for analyzing, 20: 14024(R) (APDA-182)
reactions with sodium in steam generators, 20: 14149(T,R) (ORNL-tr-900)
reactions with sodium, 20: 28691(R) (APDA-185)
reactions with stainless steel 302 under simulated nuclear incident conditions, 18: 1486(R) (ANL-6687(p.167-87))
reactions with stainless steel and zirconium during reactor accidents, 20: 16019(R) (BMI-X-10154)
reactions with steel at high temperatures, survey of mechanism, 17: 16601
reactions with tetracyanoethylene and polyacrylonitrile under high pressure, addition, 19: 36457 (NYO-3185-1)
reactions with thorium ions in pores of silica gel, 18: 5279
reactions with thorium dioxide particles, 18: 22015(R) (ORNL-3591 (p.102-12))
reactions with thorium carbides, products of, 20: 9044(R) (ORNL-3830, pp, 30-68)
reactions with tungsten and uranium sulfides, thermodynamic properties of, 17: 38428 (ANL-6656)
reactions with type 316 stainless steel at 315°C and 1500 psi, 17: 36860(R) (ANL-6648)
reactions with uranium monocarbide, 16: 1649(R) (ORNL-TM-1)
reactions with uranium carbide, 17: 10246(R) (ORNL-TM-403)
reactions with uranium at 35 to 100°C, 18: 10467 (AWRE-O-94/63)
reactions with uranium carbides, mechanism of, 18: 41364 (CEA-R-2350)
reactions with uranium carbide and uranium sulfide at high temperatures, 19: 14765(R) (ANL-6977)
reactions with uranium in TREAT meltdown excursion, 19: 29570
reactions with uranium carbide at 30 to 86°C, kinetics, 19: 38581 (NAA-SR-11401)
reactions with uranium carbides at high temperatures, 20: 18824(R) (EURAEC-1536)
reactions with uranium nitride and uranium carbide oxides at 80 to 300°C, 20: 29645
reactions with uranium, reactor excursion initiation, 20: 30802
reactions with uranium, condenser discharge method for nonisothermal, 20: 29189
reactions with uranium, effects of temperature on, 20: 31666
reactions with uranium monocarbide, 20: 31666
reactions with uranium hydride, kinetics and products from, 20: 45682
reactions with water, 18: 3038(R) (ANL-6801)
reactions with water-d_2 at 25°C, equilibrium constant value for, 18: 39218
reactions with water, analysis of, 19: 46530(R) (BAW-1280-27)
reactions with xenon di- and hexafluorides, 20: 1881
reactions with yttrium oxides, infrared spectroscopy studies of, 20: 26917
reactions with zirconium at high temperatures, 17: 17447
reactions with zirconium using laser-beam heating, 18: 15426(R) (ANL-6810)
reactions with zirconium using laser-beam heating, 18: 19456(R) (ANL-6840)
reactions with Zircaloy-2 in reactor core meltdown, 19: 35607(R) (ANL-7045(p.60-9))
reactions with zirconium in reactors, analysis of, 19: 35619
reactions with zirconium at high temperatures, 19: 40195(R) (WCAP-3269-5)
reactions with Zircaloy-2 at 900 to 1200°C, kinetics of oxidation, 20: 762(R) (BNWL-120, pp 5.1-18)
reactions with Zircaloy-2 during meltdown experiments, 20: 5843
reactions with Zircaloy-2 and Zircaloy-4 at 630 and 650°F, 20: 33827
reactions with Zircaloy-4 in LOFT experiment, 20: 45112 (IDO-17168)
reactions with 4-chlorobutanol to form tetrahydrofuran, deuterium isotope effects in, 19: 22268
reactivity effects on aqueous plutonium-239–240 slabs, 18: 18612 (ORNL-TM-821)
reactivity effects in NERVA reactor, 20: 35121 (LA-3428)
reactivity worth of, measurement of, (E), 20: 30347(R) (IDO-17147, pp 13-28)
reactor criticality effects on hydride cores, 17: 26057
reactor criticality effects on hydride cores, 17: 26058
reactor criticality effects in heavy water reactors, 18: 3116
reactor criticality effects, 18: 23011 (GAMD-2871)
reactor criticality effects in JRR-2, 18: 44978
reactor criticality effects of (E), 19: 3573
reactor criticality effects in Kiwi ocean-drop test, 19: 38238 (LA-DC-6447)
reactor criticality effects of, in moderator of heavy water reactor, (T), 20: 10331 (UJV-1412/65)
reactor impact on, cavity generation by SNAP 10A, 18: 15591 (NAA-SR-Memo-9105)
recovery and storage of, use of underground explosions in, 20: 43463 (UCRL-14756)
relationship between tumor incidence and radium, uranium and radon content in, 20: 38739
removal of, from melting rods, 20: 33884(R) (SC-CR-66-2029)
resources of, uses of radioisotopes in investigations of, 19: 13830
rotation of molecule of, in solid argon, infrared spectroscopic evidence for, 17: 8042
sampling of tap, evaporator collector for continuous, 20: 1757
sampling river, engineering drawings of equipment for, 20: 39185
self-diffusion in, at 25°C, effects of electrolytes and heavy water on, 17: 10613
separation by solvent extraction using tributyl phosphate–n-hexane, 17: 4634
separation from air and steam by gravity, carry-under studies, 17: 16240
separation from air and steam, development of centrifugal separators for, 17: 23457(R) (ACNP-63013)
separation from air and steam, development of centrifugal separators for, 17: 32206(R) (ACNP-63021)
separation from air and steam, development of centrifugal separators for, 17: 38477 (TID-7674(p.48))

separation from air and steam using full circle radial vane separator, 17: 38476 (TID-7674(p.46-8))
separation from air and steam, development of centrifugal separators for, 17: 40954(R) (ACNP-63028)
separation from air and steam, development of centrifugal separators for, 18: 10205(R) (ACNP-63035)
separation from air and steam, development of centrifugal separators for, 18: 33693(R) (ACNP-64026)
separation from air and steam, development of centrifugal separators for, 19: 555(R) (ACNP-64028)
separation from air and steam, development of radial vane separator for, 19: 6026(R) (GEAP-4728)
separation from air by precipitation-type cyclone separator, 19: 11328 (NP-14547)
separation from anisole, methods for, 20: 19135(R) (K-C-718)
separation from ethanol by ion exchange, 20: 2520(R) (IA-920)
separation from fats and oils, tritium used for measurement of, 18: 22383
separation from graphite by helium purging at 700°C, 18: 1659
separation from helium, 16: 12833
separation from helium, 18: 1608 (JAERI-4025)
separation from heavy water, U. S. facilities for, 18: 31996 (A/CONF.28/P/290)
separation from heavy water, technology of, 18: 36809(R) (SRO-105)
separation from heavy water, film-distillation, 18: 37586 (A/CONF.28/P/557)
separation from helium by sorption, 19: 4256(R) (ORNL-TM-886)
separation from lunar rocks using nuclear explosives, 18: 10213 (UCRL-7515)
separation from mixed potassium and sodium nitrates by nitrogen dioxide bubbling, 20: 10272(R) (NAA-SR-9339)
separation from MSRE graphite, 18: 22011(R) (ORNL-3591(p.38-58))
separation from radioactive materials, development of process for, 16: 2811
separation from saturated steam mixtures, separator design, 16: 11814 (GEAP-3787)
separation from sodium chloride by hyperfiltration through cellulose acetate and ion exchange filters, 18: 1615(R) (ORNL-3488(p.123-8))
separation from steam in boiling reactors, centrifugal, 16: 14874 (EURAEC-148)
separation from steam, design of baffle separators for, 17: 13785
separation from steam, loop for testing equipment for, 17: 21249 (TID-7658(p.134-8))
separation from steam in reactor, development of radial vane separator for, 17: 21250 (TID-7658(p.139-45))
separation from steam in boiling water reactor, methods for, 18: 11463
separation from steam, development of radial vane separator for, 19: 26490(R) (GEAP-4847)
separation from steam in boiling reactors, separator for, 19: 27795
separation from steam in high pressure loop, void fraction, 19: 28490 (ACNP-65002)
separation from steam, methods development for, 19: 32344(R) (ACNP-65001)
separation from steam, development of devices for, 19: 38801(R) (ACNP-65004)
separation from steam, development of separators for, 19: 44131 (ACNP-65003)
separation from steam, design of device for, 20: 2024(P)
separation from steam, performance of radial-vane separator for, 20: 18864 (GEAP-4935)
separation from steam, radial vane separator development for, 20: 28696(R) (GEAP-5084)
separation from water-d, physical and thermodynamic aspects, 16: 16628
separation from water-d_2 by vaporization, separation factor for, 17: 28879
separation from water-d_2 by freezing, 19: 4571(T) (MLM-1206(Tr))
separation of air from, development of separators for, 16: 17778(R) (EURAEC-99)
separation of air and steam from, development of centrifugal separators for, 18: 20128(R) (ACNP-64021)
separation of cesium-137 from, 16: 2075
separation of cesium and strontium from, using Victorian brown coal, 16: 25033 (AAEC/TM138)
separation of cesium from, by precipitation with Prussian blue, 18: 5420
separation of cesium-137 and strontium-90 from fuel storage basin effluent, by ion exchange, 19: 40651 (IDO-14657)
separation of cobalt-60 from, by adsorption by peat soils, 19: 22412
separation of cobalt-60 from, by adsorption by peat, 20: 26550
separation of fission products from, by precipitation, 16: 2958(P)
separation of fission products from, by foaming, 20: 36934
separation of oxygen-18- and tritium-enriched, by column extraction, effects of pressure and reflux rate on, 20: 45775
separation of polonium, radium, thorium, and uranium from waste, 20: 26575
separation of radioactive compounds from, by zone melting, 18: 29803
separation of radioisotopes from, by sorption by bentonites and diatomaceous earth, 20: 16138
separation of radon from, by aeration, 20: 23296
separation of strontium-90 from calcium in, method for, 17: 19788 (CRER-1134)
separation of strontium-90 from, by solvent extraction using TTA, 18: 13930
separation of strontium from, method for, 18: 33484
separation of strontium-90 and yttrium-90 from, by ion exchange using bentonites and gypsum, 20: 29348
shape calculation, 17: 2901
shear transmission, 16: 20557 (AD-269396)
shielding attenuation factors for, radioisotope and fission-product, 18: 22984 (NYO-10721)
shielding calculations for, for cylindrical gamma sources, 20: 32678
shielding properties of, 17: 33256
shielding properties in fuel element storage ponds, 18: 40812 (NP-10375)
shielding properties of, fast-neutron, (E), 19: 17157(R) (ORNL-3714 (Vol.I)(p.43-67))
shielding properties at 0.5 to 10.0 Mev, point isotropic source, 19: 31432
shock wave propagation in, following sudden decompression, 18: 36759 (IITRI-578P21-6)
sodium compound dissolution in, heats of, 20: 1825
softening of, regeneration using ion exchange in, 19: 15693
soil content of, performance of neutron-scattering probes for measurement of, 18: 27774
solubility in aromatic hydrocarbons and halides, 17: 25100
solubility in bis(2-chloroethyl) ether at 25°C in various electrolytes, 16: 8737
solubility in *o*-terphenyl at 225, 300, and 375°C, 18: 13233(R) (BNL-823 (p.1-19))
solubility in organic diluents, 19: 20039 (EUR-2246.e)
solubility in polyphenyl mixture, 19: 292 (NAA-SR-9734)
solubility in TBP at 0 to 100°C, 19: 11072
solubility in terphenyls, 18: 11366 (BNL-7650)
solubility in tributyl phosphate, 17: 1453
solubility in tributyl phosphate at 25°C, 18: 23712
solvation and transference of potassium chloride in, 16: 1786
solvation effects on radioinduced gaseous ammonium ions, 19: 30262
solvent effects on keto-enol interconversion of 2-acetylcyclohexanone, kinetics, 16: 11614
solvent effects on stability constants of copper acetylacetonates, 16: 13015(R) (TID-15227(p.65-79))
solvent effects on molecular weight determinations of organophosphorus acids in volatile solvents, 16: 13052
solvent effects on gamma-irradiated methyl vinyl ether polymers, 16: 18772
solvent effects on radioinduced graft polymerization of cotton cellulose and rayon on polystyrene, 17: 31808
solvent effects on alkaline earth metals, theory of, 18: 27432
solvent properties for molybdic oxide and its hydrates, 16: 168
solvent properties for rare gases, 16: 163
solvent properties for cadmium and copper dioxalato complexes, 16: 10024
solvent properties for methyl halides, initial state and transition state isotope effects in, 16: 11617
solvent properties for krypton and oxygen, 16: 18878
solvent properties for hydrogen sulfides, 16: 18879
solvent properties for silver halides and strontium thiocyanate, 16: 23706
solvent properties for strontium sulfate, effects of particle size, 16: 23592
solvent properties for oxygen with and without platinum catalyst, 16: 25324 (TID-16392)
solvent properties for helium at 200 to 280°C, 17: 3378(R) (BMI-1583(Del.))
solvent properties for mercury at 25 to 90°C, activation study, 17: 4451
solvent properties for lithium hydroxide at high temperatures, 17: 4520
solvent properties for silver bromate, 17: 28882
solvent properties for copper(II) iodate, 17: 28883
solvent properties for silver bromate, electrolyte effects on, 17: 28884
solvent properties for hydrobromic acid, 17: 30619(R) (NYO-6552)
solvent properties for scandium nitrates, 17: 32115
solvent properties for aluminum hydroxide, 17: 40789
solvent properties for hydrocarbons, at 50 to 220°C, 18: 3777
solvent properties for uranium tetrafluoride at 0, 25, and 50°C, 18: 8340
solvent properties for cesium borosilicate and cesium-enriched kaolins, 19: 13843(R) (SAN-366-1)
solvent properties for alkyl halides, role of initial state structure in kinetic isotope effects in, 19: 13294

solvent properties for magnetite at 164 to 260°C, 19: 30150(R) (ORNL-3789(p.113-21))
solvent properties for alkaline earth sulfates, 19: 30156 (ORNL-tr-649)
solvent properties for lithium bromate, 19: 44003(T) (BNL-tr-6)
solvent properties for actinium oxalate, 20: 1846
solvent properties for rare earth acetates, temperature effects on, 20: 1869
solvent properties for erbium and yttrium phosphates, 20: 1873
solvent properties of actinium hydroxide, aging effects on, 20: 1847
solvent properties for cerium(IV) nitrates, 20: 3954
solvent properties for cerium, cobalt, and promethium sorbed on charcoal powders, 20: 5675
solvent properties for iodine at 5 to 50°C, 20: 5539
solvent properties for magnetite at high temperatures, 20: 17158(R) (ORNL-3900, pp 82-149)
solvent properties for benzenesulfonic acid, isotope effects on, 20: 18643
solvent properties of carbon dioxide-charged, for rare earth carbonates, 20: 45636
solvent properties of boiling, for cobalt compounds, at 185 atm, 20: 45680
sorption and desorption of residual, in high vacuum, (E), 19: 20144
sorption and flow of, tracer studies of, 17: 25533
sorption by beryllium oxide, infrared study of, 20: 25604
sorption by colloidal thoria, 20: 38926
sorption by ferric oxide at 25 and 35°C, 17: 35617(R) (NYO-10329)
sorption by graphite, tracer study using tritium, 18: 628
sorption by graphite oxides, 18: 41432
sorption by intestine and stomach in dogs, effects of centimeter band radio waves on, 17: 10315
sorption by poly-glutamic acid, 17: 28789
sorption by powdered uranium(IV) oxides, oxidation inhibition by, 19: 34200(P)
sorption by quartz under benzene, effects of hysteresis angles on, 17: 11091(R) (MITS-49)
sorption by synthetic zeolites, mechanism of, 19: 13330
sorption by thorium dioxide, 18: 41469
sorption by thorium oxide at 25°C, mechanisms of, 20: 26869
sorption by thorium oxides, 20: 36843
sorption from atmospheric gases by nuclear graphite, 20: 23039
sorption from electrolytes using illites and montmorillonites, 18: 17820
sorption from helium streams by fixed beds of type 5A Linde molecular sieves, kinetics of, 18: 35643(R) (ORNL-TM-823)
sorption from helium streams by fixed beds of type 5A Linde molecular sieves, kinetics of, 18: 35642(R) (ORNL-TM-798)
sorption from intestine to lymph and blood, tracer study, 16: 25130(R) (HW-72500(p.84-7))
sorption from passive films on stainless steel, tracer studies of, 19: 34183
sorption from plutonium and uranium oxide fuels, 18: 30113(R) (HW-76304(p.2.1-43))
sorption from rat colon, effects of serotonin on, tracer study of, 20: 32912
sorption in rat ileum, factors affecting, 20: 22568
sorption on beryllium oxide, 18: 20014
specific heat data at 14.22 to 4300 psia and 680 to 800°F, review, 16: 3167 (ANL-6436)
spectra and optical transmission in irradiated, absorption, 17: 12346
spectra and structure of water-d in, Raman, (E), 19: 42483
spectra at −20 to 250°C, near-infrared, 19: 13279 (ORNL-P-925)
spectra at zero scattering angle, electron-impact, 19: 7399
spectra at 1220 to 1240 Å, absorption, 17: 12241
spectra at 20°C, Raman, 16: 9295(T) (CEA-tr-R-1408)
spectra at 500 to 600 cm^{-1}, effects on centrifugal distortion on infrared, 17: 4771 (NP-12236)
spectra, cation and isotope effects on Raman, 19: 34196
spectra, effects of lithium and potassium halides on Raman, 16: 30401
spectra in crystals, low frequency motions in neutron, 18: 22045
spectra in near-infrared at -20 to 250°C, absorption, 19: 46237(R) (ORNL-3832, pp 76-99)
spectra in tributyl phosphate, effects of dissolved salts on, infrared, 16: 10015
spectra of distilled, visible absorption, 18: 3791
spectra of hydrated electron in, effects of carbon dioxide and water on, 17: 1436
spectra of neodymium ions in alcohol solutions, 16: 30397
spectra of, in vacuum ultraviolet region, vibrational analysis of, 19: 26331
spectra of, infrared absorption, 18: 13748
spectra of, infrared and Raman, 18: 27396
spectra of, intensities of stretching vibrations in infrared, 19: 26361
spectra of, intensity measurements of absorption bands in, 20: 43178 (NRL-6394)
spectra of, molar extinction coefficients for infrared-absorption, 20: 25092
spectra of, uv absorption, 20: 10823
spectra of, vibrational, 18: 12100(T)
spectral distribution of scattered radiation in phantom of, irradiated by gamma beam or x rays, 16: 32795
spectral distribution of scattered radiation in phantom of, irradiated by cesium-137 gamma source, 16: 32796
spectral effects on free radicals radioinduced in DNA and RNA, ESR, 18: 12232
spectrum, effects of dissolved alkali halides on Raman, 16: 6415
spectrum of ammonia in, effect of hydrated electrons on transient, 17: 12345
steam void determination in, method for, 19: 20294
steam void measurements in stainless steel channels at high pressure by x-ray absorption, 16: 318 (TID-14156)
sterilization by chlorination and gamma radiation, combined method for, 18: 5697(T) (JPRS-21975(Del.)(p.10-12))
strontium uptake from, by trout, tracer study, 20: 10555
strontium-90 concentration in, of Palermo in November and December 1961, 17: 13958
strontium-90 distribution in, data tabulation, 16: 14448 (NYO-9934)
strontium-90 removal from, by hydrophytes and organic wastes, 18: 3459
strontium-89 extraction by marine organisms, 16: 30686(T) (JPRS-14974(p.16-19))
strontium-90 contamination in drinking, factors affecting uptake by man, 20: 41142
strontium-90 content in London, 19: 14991
strontium-90 contents in, 19: 34365(R) (HASL-161)
strontium-90 content in tap, in Belo Horizonte, Brazil, 20: 42999 (NP-15934)
strontium-90 content of, in Bombay, 1964 to 1965, 20: 43532
structure in biological systems, oxygen-17 magnetic resonance studies of, 20: 22560
structure in ionic solutions, near-infrared spectra of, 17: 40803
structure of, diffraction determination of, 17: 37225
structure of hydrogen-bonded molecules of, in hydrated crystals, 16: 18888
structure of liquid, model using strong hydrogen bonds, 18: 6788 (IA-875)
structure of pure, near-infrared spectra of, 17: 40802
structure of, spectral study of, 18: 25368
structure of, spectral study of, 18: 25369
sulfurated, protective effects on x-irradiated mice, 20: 45490
surface tension measurement from photographed menisci, 19: 34681 (LA-DC-6514)
systems for de-ionized, for cleaning stations, 20: 16590 (SC-TM-66-49)
temperature distribution in superheated layer above nucleate pool boiling of, 19: 13598
temperature distribution along heat conducting wall under transient boiling, 20: 9115(T) (ANL-Trans-236)
temperature fields in flowing, 16: 10155(T) (FTD-TT-62-57)
temperature measurements in wells, design of instruments for, 16: 29101 (HW-73994)
thermal capacity at constant volume near critical point, 17: 40794
thermal capacity at constant volume near critical point, 20: 7069
thermal capacity during phase transition in supercritical region, 16: 15291
thermal capacity of, in supercritical state, 18: 12055
thermal conductivity in pool boiling, 16: 13229
thermal conductivity in supercritical region, 16: 13250
thermal conductivity in supercritical region, 16: 13271
thermal conductivity of 5000-psi supercritical, at high flow rates through round tubes, 16: 13249
thermal conductivity of gaseous, at 380 to 525°K, 18: 16020
thermal conductivity, 20: 4310(R) (ORNL-P-1699)
thermal conductivity of, device for measuring, 20: 43270 (AEET-245)
thermal expansion of oxygen-18-enriched, 18: 23546
thermal expansion below 260°C, 18: 29653
thermal expansion of oxygen-18-labeled, 17: 18069
thermodynamic and transport properties of, significant-structure theory for, 20: 12858
thermodynamic functions for, at −10 to 1000°C and 1 to 250,000 bars, 17: 6055 (UCRL-7118)
thermodynamic properties at 1200 kg/cm^2 pressure at 300°C, 16: 1738(T) (CEA-tr-R-1411)
thermodynamic properties, 18: 591(R) (AD-293487)
thermodynamic properties at 5000 psi, 19: 4309 (NDA-10-56(Rev.))
thermodynamic properties of, (E), 20: 30182
thermodynamic similarity with water-d_2, 17: 6059(T) (CEA-tr-R-1541)
tracer study of balance of, with saline in human body, 20: 42782
transfer to water-d_2 by hydrated solutions of electrolytes, 17: 6096
transference and solvation phenomena of sodium chloride in, 16: 2944
transport properties, 16: 3553
transport properties, 16: 18933

treatment at Hanford, 19: 1955 (HW-83801)
treatment in Tsing-Hua research reactor, review on, 19: 12848
treatment of primary coolant of VVR-M reactor, 18: 38666
treatment problems in water-cooled power reactors, lectures on, 18: 5744 (KR-53)
tritium concentration in, review on methods for, 20: 1728 (AD-618562)
tritium content, 17: 22570(T) (NP-tr-993)
tritium content in stratospheric, origin of, 16: 7763
tritium content in, maximum permissible, 20: 23370 (CONF-640413, pp 117-23)
tritium exchange with succinate, 16: 23390
tritium exchange with iron and nickel hydroxides, 16: 31367
tritium exchange with alkylbenzenes, 20: 347(R) (TID-22251)
tritium exchange with methane, 20: 469(R) (ORNL-TM-1275)
tritium exchange with aromatic compounds, 16: 17380
tritium origin in hydrothermal, 20: 39132
tungsten sputtering in vapor of, model for chemical, 17: 37178
uptake by roots of sunflowers, tracer study, 19: 33777
uptake by soil, tracer technique for measuring, 18: 24045
uptake by trees, use of tritium in tracer study on, 19: 8736
uptake by wheat, effects of thermal treatment on, 20: 18323
uranyl ion dielectric properties and luminescence in, 19: 11065
uranyl nitrate hexahydrate dissociation and electric conductivity in, 16: 2945
use for decontamination of fabrics for protective clothing, 20: 9203
use for reactor thermal column, experiment for, 18: 30949 (NYO-9077)
use in decontaminating protective clothing, 20: 39161
use in multilayer enclosure shields in real fallout field, 20: 41201 (RRA-T55 and Summary)
use in shielding, cobalt-60 well irradiator, 20: 43613
use of, as moderator in rocket reactors, 16: 32580 (NASA-TN-D-1407)
use of fluoridated, in hemodialysis, 20: 5237(R) (UR-668, pp 55-109)
use of vapor jet targets of, for charge changing of fast ion beams, 19: 18645
Van Hove self-correlation functions for protons, 17: 8919 (CRNP-1121)
vapor pressure at 0 to 374°C, tables of, 17: 39079
vapor pressure equations for, 17: 39814
vapor pressure of, isotope effects on, 17: 2701
vapor pressure of, measurement of, 18: 25436
vapor pressure of, hydrogen isotope effects on, 18: 31425 (LADC-5905)
vapor pressure over uranyl nitrate solutions in nitric acid, 19: 32158
vaporization and wave propagation in shock tubes, 16: 13735
vaporization by decompression, 18: 9578(R) (IITRI-A6042-3)
vaporization phenomena, 16: 33126 (UNC-5021)
vaporization rate of, deuterium isotope effects on, 19: 32132
vibrational frequencies of perturbed and substituted, exact isotope rule for, 18: 12073
vibrational potential function of bent molecules of, third-order, 20: 14559
vibrational properties and spectra, 16: 14740
vibrational spectra in salt hydrates, 16: 6424
vibrations of trapped, in molecular sieves, 20: 41651
vibratory motions in, cold neutron scattering study of, 17: 15245
void fraction determination in boiling, method for, 19: 3577
void measurements in cold, impedance instruments for, (E), 19: 22655 (CONF-640607(Vol.II)(Paper D-1))
void measurements in, instruments for transient, (E), 19: 22656 (CONF-640607(Vol.II)(Paper D-2))
volatilities of oxygen-16, -17, and -18 labeled, relative, 16: 23667 (IA-728)
volatility of oxygen-17-labeled, relative, 16: 28961
volatility of oxygen-17-labeled-to-oxygen-16-labeled, determination of relative, 17: 35253(R) (IA-775)
volatility of tritium-labeled water in, 19: 15471
volatilization of boron from, effects of mannitol on, 16: 2972
water-d_2 content in, determination using osmometer, 19: 15392
weightless, dynamic behavior of surface of, 18: 5855
X agent effects on transmittance of, 18: 18484
X-agent scattering by, 18: 2682
x-ray-diffraction analysis of, radial distribution functions from, 18: 1491(R) (ORNL-3488(p.102-22))
x-ray dose distribution in, isodose plotter for, 17: 34212
x-ray scattering at 50 to 250 kev by slabs of, spectra, 16: 24293
x-ray scattering intensities of, calculation of, 18: 777
x-ray attenuation coefficients, 16: 23246
x-ray dose distribution in, 19: 29443
x-ray scattering at 4 to 200°C, diffraction studies on, 20: 43180 (ORNL-3997)
x-ray scattering cross sections, 18: 20035
x-ray scattering in phantoms of, angular distributions in, 19: 28996
x-ray spectral distributions in, 20: 41322
yields from gamma radiolysis of ethanol, 20: 20746
yields from x radiolysis of carbon monoxide–oxygen–water system, 20: 23169
yields in gamma radiolysis of carbon dioxide–hydrogen mixture, 20: 26922 (BNWL-SA-591)
yields in radioinduced oxidation of isobutane using hydrobromic acid catalyst, 20: 12883 (ORO-634)
acetic acid–TBP–H_2O, effect of hydrogen bonding on uranium distribution in, 20: 18845
acetic acid–2-pentanone, 4-methyl-–water, electric conductivity, 16: 20534(R) (IDO-14574)
acetic acid–4-methyl-2-pentanone–H_2O, flow properties of, in stacked-clone contactor, 20: 45798(R) (ORNL-3945, pp 230-2)
acetone–H_2O, critical heat flux, 18: 39460
acetone–H_2O, effects of deuterium on rate of solvolysis of substituted bromo- and chlorohydrocarbons in, 20: 336
acetone–H_2O, equivalent conductivity of hydrochloric acid in, 20: 336
acetone–H_2O, rate laws for uranium(IV)–uranium(VI) exchange in, 18: 1638
acetone–water, tritium recoil reactions with, 16: 27068
acetonitrile–H_2O, effects on ESR spectra of oxygen-17-labeled benzoquinone, 20: 43224
adipic acid–TBP–H_2O, effect of hydrogen bonding on uranium distribution in, 20: 18845
$AgClO_4$–H_2O, radioinduced free silver atoms in solid solutions of, EPR of x, (E), 20: 15975(T)
AgF–H_2O, radioinduced free silver atoms in solid solutions of, EPR of x, (E), 20: 15975(T)
$AgNO_3$–H_2O, radioinduced free silver atoms in solid solution of, EPR of x, (E), 20: 15975(T)
Ag_2SO_4–H_2O, radioinduced free silver atoms in solid solutions of, EPR of x, (E), 20: 15975(T)
air–H_2O, boiling flow in parallel rod array, pressure profiles of, 20: 25256
air–H_2O, density disturbances in flow of, 20: 29375(R) (ANL-7190, pp 193-200)
air–H_2O, droplet entrainment in annular flow of, 18: 8485(R) (NYO-10488)
air–H_2O, flow in tubes, load losses and vacuum fractions in, 18: 14024(R) (EURAEC-53)
air–H_2O, flow in vertical tubes, effects of fluid properties and tube size on void fraction in upwards, 19: 6073(R) (NYO-3114-3)
air–H_2O, flow in vertical tubes, pressure drop and void fractions for, 20: 18869(R) (NYO-3114-10)
air–H_2O, flow measurements in horizontal, converging-diverging nozzles, analysis of two-phase, 17: 35984 (ANL-6754)
air–H_2O, flow of circulating and non-circulating, slip ratios in, 19: 36622
air–H_2O, flow stability analyses in, annular, 18: 1867(R) (NYO-10487)
air–H_2O, flow theory for, 18: 14030(R) (NYO-10489)
air–H_2O, heat transfer in flows through parallel-rod arrays, 17: 10812
air–H_2O, heat transfer in nine-rod assemblies, 19: 22483(R) (GEAP-4798)
air–H_2O, heat transfer in, bibliography on, 20: 35617 (AERE-Bib-150)
air–H_2O, heat transfer in multirod geometries, 20: 35621(R) (GEAP-5161)
air–H_2O, momentum flux measurement by impulse method for flow of, 20: 5624 (MIT-3496-1)
air–H_2O, propagation of density disturbances in flow of, 20: 9112 (ANL-7053)
air–H_2O, swirl flows in tubes, (E/T), 20: 12960 (EURAEC-1515)
air–H_2O, void wave propagation in, electric probe for determining, 19: 23991(R) (ANL-7003)
air–water, bubbly flow upward in tubes, hydrodynamic characteristics of, 20: 36988 (TID-23261)
air–water, density disturbances in flow of, 20: 29375(R) (ANL-7190, pp 193-200)
air–water, flow through tubes, 17: 16233(R) (TID-18141)
air–water, heat transfer in, mechanisms of two-phase, 18: 35684 (ANL-6862)
air–water, heat transfer in BWR, 19: 42623 (EURAEC-1363)
air–water, theory of two-phase annular flows of, 18: 25657(R) (NYO-3114-1)
air–water, two-phase flows on four-rod assembly, effects of twist strips on, 18: 16182(T) (EURAEC-638)
air–water, two-phase flow pressure drops in annular test section, 19: 40733(R) (GEAP-4863)
air–water, voidage measurements in upward two-phase flow through tube, 20: 39045 (AEEW-M-650)
Al–B_4C–H_2O, neutron propagation through, 17: 26071
alcohol–$Fe(NH_4)_3(SO_4)_3$–O–H_2SO_4–H_2O, effects of alcohol structure on radioinduced redox processes in, 18: 13877
Al–H_2O, fission neutron age measurements in, (T), 20: 9379(R) (NAA-SR-11650, Sect.4)
Al–H_2O, fission neutron lifetime to 1.46-ev indium resonance in, (E), 20: 46568

Al–H_2O, fission-neutron age to indium resonance in, (E), 20: 2970
Al–H_2O, gamma heating in, calculations for, (E/T), 20: 6517 (CONF-651101-41)
Al–H_2O, neutron age in, moments calculations of, 16: 22977
Al–H_2O, neutron age measurements for mixtures of, 20: 8316(R) (NAA-SR-11450, Sect.7)
Al–H_2O, neutron angular and energy distribution at interface of, (E), 19: 8382
Al–H_2O, neutron diffusion in laminar arrays of, (T), 19: 19355 (BNL-8950)
Al–H_2O, neutron diffusion in plutonium-fueled lattices of, thermal, (E), 20: 12396(R) (EURAEC-1505)
Al–H_2O, neutron slowing-down moments in, Monte Carlo code for, (T), 20: 8040 (NAA-SR-Memo-11239)
Al–H_2O, performance as reflector for MTR fueled with high-exposure (Hx) plutonium, (T), 19: 31605 (HW-84575)
Al–H_2O, reaction thermodynamics, 16: 12843
Al–H_2O, stabilization using bentonite strengtheners and phosphate salt stabilizers, 18: 18294(R) (NP-13758)
allyl methacrylate–methanol–H_2O, effects on radioinduced crosslinking of nylon 66 and poly (vinyl alcohol), 20: 1909
$Al(NO_3)_3$–HNO_3–H_2O, distribution coefficients for plutonium between anion exchange resin and, calculation, 19: 20046 (LA-3188)
$Al(NO_3)_3$–HNO_3–$UO_2(NO_3)_2$–H_2O, phase diagrams, 17: 10616
Al_2O_3–H_2O, flow in circular pipe, analysis of laminar, 20: 2020
Al–Pu–H_2O, criticality measurements on, 18: 11397(R) (HW-79054(p.43-6))
Al–Pu–H_2O, neutron spectra in, 18: 11436(R) (HW-79054(p.31-42))
Al–Th–H_2O, neutron age, 16: 1007
Al–U–H_2O, criticality studies, 18: 3104
amyl alcohol–H_2O, critical heat flux, 18: 39460
Ar–ethanol–H_2O, hydrodynamic characteristics in circular tubes, 19: 1875(R) (EURAEC-1011)
Ar–H_2O, density measurements of two-phase mixtures in, 18: 398 (EURAEC-205)
Ar–H_2O, heat transfer properties, 18: 17999(R) (EURAEC-923)
Ar–H_2O, hydrodynamic characteristics in circular tubes, 19: 1875(R) (EURAEC-1011)
Ar–H_2O, performance in ionization chambers, 18: 20393
Ar–H_2O, phase and velocity distribution in two-phase adiabatic dispersed flow, 19: 22477 (CISE-98)
Ar–H_2O, spectroscopic properties of induction-coupled plasmas of, (E), 20: 7005 (IS-T-51)
Ar–H_2O, two-phase flow of adiabatic, liquid volume fraction in, (E), 20: 9116
$BaCl_2$–HCl–H_2O, activity coefficients of, determination by ultracentrifugation, 19: 347(R) (ORNL-3679(p.60-83))
$BaCl_2$–NaCl–H_2O, activity coefficient determination by ultracentrifugation, 19: 46237(R) (ORNL-3832, pp 76-99)
bentonites–H_2O, relation between sodium ion activity and diffusion in, 20: 33260(R) (ORO-648, pp 103-22)
benzene–trioctylamine–water, distribution of nitric acid in, 18: 27421
benzene–water, drop coalescence at planar interfaces in, hydrodynamic mechanism for, 16: 25956 (UCRL-10097)
benzene–water, interfacial tension by falling-drop method, 16: 2926(R) (MLM-1117)
benzene–water, performance as gamma dosimeter, 16: 6656
benzene–N_2O–H_2O, production of biphenyl–terphenyl mixtures in radiolysis of, 20: 10930(P)
benzene–water, radiation effects on chemical reactions in, neutron and gamma, 16: 8758 (NP-11262)
benzene–H_2O, radiation effects on coalescence rates in liquid, 20: 5571 (ORNL-TM-1283)
benzenethiol–H_2O, radioinduced oxidation of, gamma and x, 20: 45735
benzene–water, radiolysis products, identification of liquid and solid, 16: 218
benzene–HNO_3–H_2O, radiolysis of, 17: 20061
benzene–H_2SO_4–trioctylamine–H_2O, solvent properties for uranyl sulfate, mass action and non-ideality in, 20: 43423 (ORNL-P-2354)
benzene–didecylamine–H_2SO_4–H_2O, solvent properties for uranyl sulfate, mass action and non-ideality in, 20: 43423 (ORNL-P-2354)
benzene-didecylamine–Na_2SO_4–H_2SO_4–H_2O, solvent properties for uranyl sulfate, interface and transferring species in, 20: 43424 (ORNL-P-2359)
benzene–water, use in calibration of teletherapy machines, 19: 7328
benzene–ethanol–H_2O, use in paper chromatography of compounds labeled with iodine-125 and iodine-131, 20: 5515
benzene–water, use of saturated solutions, as gamma dosimeters, 16: 8758 (NP-11262)
benzilic acid–uranyl acetate–water, coordination compounds in, 17: 32085
benzoic acid–TBP–H_2O, effect of hydrogen bonding on uranium distribution in, 20: 18845
$Be(OH)_2$–BeO–H_2O, thermodynamic properties, 19: 17851 (CEA-R-2611)
B–H_2O, corrosive effects on control rod and fuel cladding, 20: 12418(R) (WCAP-3739)
B–H_2O, neutron infinite-medium spectra in, (T), 19: 33192(R) (GA-6096)
B–H_2O, neutron spectra in, 17: 37993(R) (GA-4426)
B–H_2O, neutron spectra in, tabulation, (E/T), 19: 16814 (AERE-R-4776)
B–H_2O, neutron spectra in, thermal, 19: 42037(R) (BNWL-95, pp 4-17)
B–H_2O, neutron spectra in, (E), 20: 15731(R) (RPI-328-49)
B–H_2O, neutron spectra in, thermal, (E), 20: 28237(R) (TID-22844, pp 1-35)
B–H_2O, temperature-dependent neutron spectra in, 17: 39943(R) (GA-4176)
B–H_2O, thermal neutron spectra in, 18: 2818
biphenyl–water, drop coalescence at planar interfaces in, hydrodynamic mechanism for, 16: 25956 (UCRL-10097)
boric acid–H_2O, corrosive effects on aluminum, 20: 1467(R) (IDO-28649)
boric acid–H_2O, heat transfer to boiling, in open lattices of rods, (E), 19: 13584 (WCAP-3736(Vol.I))
boric acid–H_2O, heat transfer to boiling, in open lattices of rods, (E), 19: 13585 (WCAP-3736(Vol.II))
boric acid–H_2O, neutron diffusion length at 18 to 255°C, thermal, (E), 20: 15679
boric acid–water, neutron spectra for, in slab geometry, 17: 24369(R) (GA-3542)
boric acid–H_2O, neutron spectra hardening in, thermal, 19: 45226 (KFK-294)
boric acid–H_2O, thermal neutron spectra in, determination using integral activation techniques, (E), 20: 2965
B–$UO_2(NO_3)_2$–H_2O, critical mass of, 20: 3379 (ORNL-TM-1207)
butanol–H_2O, nucleate boiling kinetics of, 18: 6933
butyl dibutylphosphinate–CCl_4–HNO_3–$UO_2(NO_3)_2$–H_2O, phase separation in, 18: 10187
butyl phosphate–H_2O, drop coalescence at planar interfaces in, hydrodynamic mechanism for, 16: 25956 (UCRL-10097)
butyl phosphate–kerosene–water, radiolysis of, separation of dibutyl hydrogen and monobutyl dihydrogen phosphate from yields in, 16: 25420(R) (SRIA-62)
$CaCl_2$–H_2O–$ZrOCl_2$, solubility in hydrochloric acid at 25°C, 18: 1682
$Ca(NO_3)_2$–H_2O, phase diagram of, 20: 38994(R) (AE-232)
$Ca(NO_3)_2$–$UO_2(NO_3)_2$–H_2O, activity coefficients of, at 25°C, 20: 29196
catechol–H_2O–$ZrOCl_2$, chelate formation in, adiabatic compressibility and ultrasonic studies of, 20: 45666
catechol–$Th(NO_3)_4$–H_2O, chelate formation in, adiabatic compressibility, and ultrasonic studies of, 20: 45666
CCl_4–TBP–H_2O, azeotropic distillation of, 20: 36731
CCl_4–TBP–H_2O, phase studies, 18: 41439
CCl_4–TBP–$UO_2(NO_3)_2$–H_2O, phase equilibria in, 18: 22183
CCl_4–TBP–$UO_2(NO_3)_2$–H_2O, solvent partition studies on, 18: 1830
$CdCl_2$–H_2O–$ZnCl_2$, thermodynamic properties, 16: 14378(R) (NYO-2302)
Cd–H_2O, neutron capture and thermalization in, 18: 15133 (JEN-127-DF/I-39)
Cd–H_2O, neutron capture and diffusion in, 18: 38043 (A/CONF.28/P/678)
Cd–H_2O, neutron scattering in, reaction rate curves for, (E/T), 20: 19776 (AE-223)
Cd–H_2O, neutron spectra in, 18: 22848(R) (GA-4659)
Cd–H_2O, neutron spectra in, tabulation, (E/T), 19: 16814 (AERE-R-4776)
CdI_2–catechol–H_2O, chelate formation in, adiabatic compressibility and ultrasonic studies of, 20: 45666
$CdSO_4$–H_2O, neutron diffusion length at 18 to 255°C, thermal, (E), 20: 15679
$CeCl_3$–KCl–H_2O, chemical and physical properties, 20: 8945
$CeCl_3$–NaCl–H_2O, chemical and physical properties, 20: 8945
$Ce_2(CO_3)_3$–$Ce_2(SO_4)_3$–H_2O, phase studies, 17: 35829
cellulose–H_2O, NMR relaxation times in, 19: 15511
$Ce(NO_3)_3$–$Ce(NO_3)_4$–HNO_3–TBP–H_2O, oxidizing potentials of cerium in, 19: 407
$Ce(NO_3)_4$–HNO_3–TBP–H_2O, method for presenting data on phase diagrams and separations in, 19: 2286
$Ce(NO_3)_3$–K_2CO_3–H_2O, composition of, effects of reactant concentration on, 20: 20664
$Ce(NO_3)_3$–$LiNO_3$–H_2O, solubility ratios in, at 10, 20, and 30°C, 19: 40519
$Ce(NO_3)_4$–TBP–$UO_2(NO_3)_2$–H_2O, method for presenting data on phase diagrams and separations in, 19: 2286
$Ce(NO_3)_4$–TBP–$UO_2(NO_3)_2$–H_2O, phase diagram, 20: 10952
$Ce(NO_3)_4$–$Th(NO_3)_4$–TBP–H_2O, method for presenting data on phase diagrams and separations in, 19: 2286
$Ce(NO_3)_3$–$UO_2(NO_3)_2$–H_2O, compound formation in, 20: 20682
cesium oxalates–H_2O–YCl_3, phase studies, 20: 33304
$CHCl_3$–H_2O, dissociation of 2,4-hexanedione and 6-methyl-2,4-

heptanedione in, 19: 40423
chlorobiphenyl–H_2O, settling mechanism in separation of, 18: 23452 (UCRL-10625)
chloroform–Gd–1-phenyl-1,3-butanedione–H_2O, complex formation and stability in, 17: 35813
chloroform–trioctylamine–water, distribution of nitric acid in, 18: 27421
chloroform–H_2O, separation of neodymium from, by solvent extraction using selenoylacetone and selenoyltrifluoroacetone, 20: 26813
$(C_2H_5)_3N$–H_2O–D_2O, isotope separation and solubility in, 17: 1793
C–H_2O, neutron propagation through, 17: 26071
clay–H_2O, cation movement in, 19: 46239(R) (ORO-631, pp 132-41)
Cl–O–H_2O, corrosive effects on 304 and 347 stainless steels, 18: 24125(R) (CEND-3256-209)
CO_2–H_2O, oxygen-18 exchange in, 16: 12839
CO_2–H_2O, oxygen-17 and oxygen-18 distribution equilibrium in, 19: 44007
CO_2–H_2O, reactions of, with beryllium at 700°C, 16: 12060
CO–H_2O, radiolysis of vapors of, yields in gamma, 20: 25122 (HW-SA-3440)
Co–O–H_2O, radiolysis of, yields from x, 20: 23169
CO_2–H_2O, oxygen-18 equilibrium distribution in, 20: 26790
CO_2–U–H_2O, electrochemical equilibrium diagrams for, at 25°C, 20: 26877
$CsNO_3$–$UO_2(NO_3)_2$–H_2O, chemical potential of water in, at 25°C, 18: 3776
$CsNO_3$–$UO_2(NO_3)_2$–H_2O, thermodynamic properties of compound formation in, at 25°C, 20: 18696
$CuFeS_2$–UO_2SO_4–H_2O, phase studies at 200 to 360°C, 19: 17868
Cu–H_2O, neutron diffusion in, 17: 31385 (JEN-114-DF/I-33)
CuO–NiO–SO_3–UO_3–H_2O, phase studies, 19: 23163(R) (ORNL-3650 (p.111-86))
$CuSO_4$–D_2SO_4–UO_2SO_4–H_2O–D_2O, spectrophotometry of reactor fuel solutions of, 20: 20600
$CuSO_4$–H_2O, pressure effects on temperature of liquid-liquid immiscibility in, 17: 33923
dioxane–H_2O, cerium compound absorption spectra in, 20: 36831
dioxane–H_2O, dielectric properties of, 18: 19957
dioxane–H_2O, dissociation constants for acetylacetone and metal acetylacetonates in, 19: 26295 (TID-21811)
dioxane–H_2O, effects on equilibrium in keto-enol tautomerism of 2,4-pentanedione, 20: 16416(R) (NYO-906-68)
dioxane–H_2O, effects on isotopic exchange between elementary iodine and 1-phenyl-2,3-dimethyl-4-iodopyrazolone, 20: 16502
dioxane–H_2O, solvent effects of, on stability constants of copper acetylacetonates, 16: 13015(R) (TID-15227(p.65-79))
dioxane–water, electric conductivity of cesium chloride at 25°C in, 17: 37151
dioxane–H_2O, electric conductivity of lithium-7-labeled lithium chloride in, 18: 19976
dioxane–H_2O, electrochemical properties of rare-earth compounds in, 18: 6829
dioxane–H_2O, isotope effects on dissociation of acetic acid and water in, 18: 39240
dioxane–water, nuclear magnetic resonance spectra of electrolytes in, 17: 40800
dioxane–H_2O, solvent effects of, on acetylacetone equilibrium constants with copper perchlorate, 16: 13013(R) (TID-15227(p.3-32))
dioxane–H_2O, spectra of, frequency shifts in infrared, 18: 3434(T) (UCRL-Trans-994(L))
dioxane–H_2O, tautomeric equilibria, 19: 36343(R) (TID-21847)
dioxane–H_2O, thermodynamic properties of acetylacetone in, 16: 13014(R) (TID-15227(p.33-64))
dioxane–water, use of, in hydrolysis of cyclic acetals, 20: 45703
dodecane–dodecylammonium chloride–quartz–H_2O, contact angle hysteresis, 18: 13604(R) (MITS-51)
dodecane–HNO_3–TBP–$UO_2(NO_3)_2$–H_2O, equilibrium relations for, for nitric acid-uranyl nitrate extraction, 20: 18844
dodecane–quartz–H_2O, sorption in dodecylammonium chloride-modified, 19: 9362(R) (MITS-52)
dodecyldimethylbenzylammonium nitrate–kerosene–octanol–$Pu(NO_3)_4$–H_2O, plutonium(IV) distribution in, effect of acid concentration on, 18: 13959
D_2O–H_2O, analysis of, 17: 2729
D_2O–H_2O, neutron diffusion in, 17: 3792
D_2O–H_2O, properties as reactor moderator, 18: 28921(R) (TID-20649)
ethanol–H_2O, bubble motion in, 16: 6535
ethanol–H_2O, dissociation constants for acetylacetone and metal acetylacetonates in, 19: 26295 (TID-21811)
ethanol–H_2O, effects of deuterium on rate of solvolysis of substituted bromo- and chlorohydrocarbons in, 20: 336
ethanol–H_2O, effects on isotopic exchange between elementary iodine and 1-phenyl-2,3-dimethyl-4-iodopyrazolone, 20: 16502
ethanol–H_2O, electric conductivities of cesium and potassium chlorides in, 18: 206 (NYO-10695)
ethanol–H_2O, electrochemical properties of uranium(IV) in, 19: 46292
ethanol–H_2O, equivalent conductivity of hydrochloric acid in, 20: 336
ethanol–H_2O, flow in pressurized loop effects of physical properties on two-phase adiabatic, 18: 397 (EURAEC-152)
ethanol–H_2O, nucleate boiling kinetics of, 18: 6933
ethanol–H_2O, pressure drop in, effects of test-section geometry on, 16: 17291(R) (EURAEC-222)
ethanol–$FeSO_4$–O–H_2SO_4–H_2O, radioinduced oxidation of iron in, mechanism of electron and gamma, 19: 13426 (PAN-547/XVII)
ethanol–NO–H_2O, radiolysis of, nitrous oxide yields from, 20: 23168
ethanol–H_2O, rate laws for uranium(IV)–uranium(VI) exchange in, 18: 1638
ethanol–H_2O, solvation and transference of potassium chloride in, 16: 1786
ethanol–H_2O, solvation and transference of sodium chloride in, 16: 2944
ethanol–H_2O, solvent effects of, on stability constants of copper acetylacetonates, 16: 13015(R) (TID-15227(p.65-79))
ethanol–H_2O, solvent properties for beryllium in sulfated ores, 19: 24631(P)
ethanol–H_2O, uranium(IV) polarography in, 19: 22135
ethylene glycol–H_2O, nucleate boiling kinetics of, 18: 6933
ethylene glycol–H_2O, rate laws for uranium(IV)–uranium(VI) exchange in, 18: 1638
ethyl ether–$FeCl_3$–HCl–H_2O, method for presenting data on phase diagrams and separations in, 19: 2286
Fe–H_2O, fission neutron age-to-indium resonance energy in (E), 19: 3532
Fe–H_2O, gamma heating in, calculations for, (E/T), 20: 6517 (CONF-651101-41)
Fe–H_2O, gamma scattering by, build-up factors for, 16: 31031
Fe–H_2O, neutron age in, moments calculations of, 16: 22977
Fe–H_2O, neutron age to indium resonance in, calculation of, 19: 12865(R) (NAA-SR-10501)
Fe–H_2O, neutron age to indium resonance in, (E/T), 19: 31193 (NAA-SR-Memo-10918)
Fe–H_2O, neutron age measurements for mixtures of, 20: 8316(R) (NAA-SR-11450, Sect.7)
Fe–H_2O, neutron age to indium resonance energy in, fission, (E), 20: 17659
Fe–H_2O, neutron angular and energy distributions at interface of, (E), 19: 8382
Fe–H_2O, neutron attenuation in, 16: 26192 (AEEW-R-125)
Fe–H_2O, neutron attenuation, 18: 40739
Fe–H_2O, neutron attenuation in, few- and multigroup P3 analyses of, (T), 20: 2939 (WAPD-T-1710)
Fe–H_2O, neutron attenuation in, 20: 42517
Fe–H_2O, neutron flux distributions in, 16: 24597
Fe–H_2O, neutron fluxes in, diffusion-theory method for calculating, 16: 8290 (GNEC-187)
Fe–H_2O, neutron flux distributions in, 19: 17163
Fe–H_2O, neutron flux distributions and spectra in shielding of, (E/T), 20: 40287
Fe–H_2O, neutron multigroup calculations for laminated shields, 18: 32950 (WAPD-TM-448)
Fe–H_2O, neutron scattering and slowing down in lattices of, 19: 27735(R) (NAA-SR-10850)
Fe–H_2O, neutron slowing down density distributions in, Monte Carlo code for, 20: 17660
Fe–H_2O, neutron transport in, (E/T), 20: 4998 (JINR-P-2359)
Fe–H_2O, neutron transmission through mixtures of, 20: 34784
Fe–H_2O, performance of layers of, as gamma and neutron shielding, (E), 19: 14752
Fe–H_2O, properties as laminated reactor shield, (E), 19: 5521 (EUR-1888.d)
Fe–H_2O, proton reactions at 170 to 660 Mev, neutron production in, (T), 20: 4998 (JINR-P-2359)
Fe–H_2O, thermal neutron flux distributions in shields of, 19: 3221
$Fe(NH_4)_2(SO_4)_2$–$CuCl_2$–H_2SO_4–H_2O, properties as gamma dosimeter, 19: 44372 (AFCRL-65-470)
$Fe(NH_4)_2(SO_4)_2$–isobutyl alcohol–O–H_2SO_4–H_2O, radioinduced oxidation and reduction of iron in, 18: 13876
Fe–2-methyl-1-propanol–O–H_2SO_4–H_2O, radioinduced oxidation and reduction reactions of iron ions in, 20: 388
Gd–H_2O, neutron scattering in, reaction rate curves for, (E/T), 20: 19776 (AE-223)
Gd–H_2O, neutron spectra in, thermal, 19: 42037 (BNWL-95, pp 4-17)
$Gd(NO_3)_3$–HNO_3–H_2O–$Y(NO_3)_3$, phase studies, 18: 25434
gelatin–H_2O, NMR relaxation times in, 19: 15511
glycerol–H_2O, fluorescein fluorescence polarization in, 17: 12815
glycerol–H_2O, radiosensitivity effects on *Staphylococcus aureus*, surface adsorption in, 16: 31397(R) (ANL-6535(p.104-11))
glycerol–H_2O, uranyl ion dielectric properties and luminescence in, 19: 11065

graphite–U–H_2O, critical dimensions of cylinders, slabs, and spheres, 18: 807 (LAMS-2955)
graphite–H_2O, neutron angular and energy distribution at interface of, (E), 19: 8382
graphite–H_2O, neutron moderation length in, 19: 25461
graphite–H_2O, neutron thermalization in, 18: 38011 (A/CONF.28/P/366)
graphite–H_2O, neutron thermalization in, at large temperature gradients, (E), 20: 13740
graphite–MoS_2–Na_2SiO_3–H_2O, radiation effects on properties as solid-film lubricants, 17: 36347(R) (NARF-62-18P)
H_3BO_3–H_2O, neutron attenuation in, 16: 15612 (GA-2544)
H_3BO_3–H_2O, neutron transmission at low energies in, angular distribution from, 16: 3877(R) (ORNL-3193(p.278-87))
HBr–methanol–H_2O, effects on ion exchange of metals, 19: 30085(R) (TID-21853)
HCl–H_2O, dual temperature exchange of deuterium in, 17: 22075
HCl–H_2O, effects on operation of mass spectrometer, 19: 36751 (NASA-TM-X-1111)
HCl–H_2O, flow in circular tube, magnetic field effects on, (E), 20: 28064
HCl–$NdCl_3$–$PrCl_3$–TBP–H_2O, separation factors for neodymium and praseodymium in, 20: 40904
HCl–$NdCl_3$–$PrCl_3$–TBP–H_2O, solvent distribution of neodymium and praseodymium in, 20: 7004 (IS-T-42)
HCl–$NdCl_3$–$SmCl_3$–TBP–H_2O, solvent distribution of neodymium and samarium in, 20: 7004 (IS-T-42)
$HClO_4$–H_2O, rotation of hydronium groups in, neutron studies, 19: 26283 (INP-360)
HCl–UCl_4–H_2O, phase studies at −107 to 40°C, 20: 25049
HCl–2-propanol–H_2O, effects on ion exchange of metals, 19: 30085(R) (TID-21853)
He–H_2O, corrosive effects on nickel-base alloys at 1700, 1900, and 2100°F, 20: 5846
He–H_2O, effects of, on subcooled boiling burnout heat flux for internally heated annulus, 16: 27193(R) (TID-15969)
hematite–isovalerone–water, sorption in, 17: 35617(R) (NYO-10329)
heptane–water, radiolysis yields from, 18: 10161
HfF_4–H_2O, compound formation in, 18: 27412
HF–H_2O, proton magnetic resonance, relations of concentration with proton chemical shifts, 17: 15963 (TID-18200)
HF–H_2O, thermal neutron scattering by, 18: 11195(R) (EANDC(E)-49(L))
HF–K_2NbF_7–K_2TaF_7–H_2O, solubilities at 25°, 17: 39029(T) (AEC-tr-6069)
HF–ThF_4–H_2O, phase studies, 19: 28333
Hf–U–H_2O, neutron transport in enriched critical assemblies of, resonance interference in, (E/T), 19: 21643 (WAPD-T-1728)
H–H_2O, hydrogen isotope exchange in, 19: 24910(P)
H–H_2O, isotopic equilibrium constants in, at 250 to 900°K, 16: 8712 (IFA-DF-13)
H–H_2O, reactions with uranium hexafluoride, kinetics of, 20: 35479 (ORNL-TM-1454)
H–H_2O, tritium exchange in, 17: 2664 (ORNL-3334)
H–H_2O, uses for purification of molybdenum and molybdenum–rhenium alloys, 20: 7499(R) (GEMP-53A)
HNO_3–H_2O, distillation for hydrogen isotope separation, 17: 2681
HNO_3–H_2O, isotope separation factors in distillation of, 17: 2682
HNO_3–$Nd(NO_3)_3$–H_2O, phase studies at 25°C, 19: 26305
HNO_3–$Pr(NO_3)_3$–H_2O, phase studies at 25°C, 19: 26305
HNO_3–$Pr(NO_3)_3$–$RbNO_3$–H_2O, solubility isotherm at 25°C, 17: 35842
HNO_3–TBP–H_2O, calculation of cascade stagewise conditions for rare earth separation, 18: 20098 (IS-780)
HNO_3–TBP–H_2O, molecular interactions in, 17: 4446 (IS-500(Sect.E))
HNO_3–TBP–H_2O, nitric acid concentration in mixer-settler extractor as function of time, 20: 1953 (IS-T-34)
HNO_3–TBP–H_2O, phase studies, specific gravity, and viscosity of, 17: 7944
HNO_3–TBP–$UO_2(NO_3)_2$–H_2O, method for presenting data on phase diagrams and separations in, 19: 2286
HNO_3–$Th(NO_3)_4$–TBP–H_2O, method for presenting data on phase diagrams and separations in, 19: 2286
HNO_3–$Th(NO_3)_4$–TBP–$UO_2(NO_3)_2$–H_2O, phase equilibrium in, 19: 26476
HNO_3–$Th(NO_3)_4$–TBP–H_2O, phase studies, 18: 5268
HNO_3–$UO_2(NO_3)_2$–H_2O, nitric acid–water partial pressures over, 20: 9052(R) (ORNL-3830, pp 248-51)
HNO_3–$UO_2(NO_3)_2$–H_2O, phase diagrams, 16: 11580 (TID-15080)
HNO_3–$UO_2(NO_3)_2$–H_2O, phase diagram, 20: 38994(R) (AE-232)
HNO_3–$UO_2(NO_3)_2$–H_2O, phase equilibrium in, 17: 10615
HNO_3–$UO_2(NO_3)_2$–H_2O, refractive index measurements on, 20: 40804 (KR-108)
HNO_3–$UO_2(NO_3)_2$–H_2O, separation of uranyl nitrate from, using TBP, 19: 4253(R) (ORNL-3627(p.231-2))
HNO_3–$UO_2(NO_3)_2$–H_2O, vapor pressures of nitric acid and water over, 19: 32158
HNO_3–2-propanol–H_2O, ion exchange of rare earths from, 18: 25395
HNO_3–2-propanol–H_2O, lead complexing in, 18: 25384
H_2O–D_2O, acid-base equilibria in, 19: 34143(R) (NYO-3041-1)
H_2O–D_2O, analysis for deuterium and hydrogen, 17: 10240(R) (NP-12208)
H_2O–D_2O, analysis, infrared interference method for isotopic, 18: 33460 (CEA-R-2440)
H_2O–D_2O, boiling temperature and vapor pressure of, 20: 38921
H_2O–D_2O, effects on reactor fuel burnup, 18: 30972 (BLG-222)
H_2O–D_2O, ionic product, 17: 27379
H_2O–D_2O, ionization of ammonium ion, chloroacetic acid, and hydrazoic acid in, 18: 12091
H_2O–D_2O, neutron diffusion parameters in, (E), 19: 35351 (TID-21851)
H_2O–D_2O, neutron diffusion parameters for cylinders of, 20: 2951
H_2O–D_2O, neutron diffusion parameters in, thermal, (E), 20: 40061
H_2O–D_2O, neutron spectra in, (E/T), 20: 24312
H_2O–D_2O, properties as reactor moderator, 18: 28921(R) (TID-20649)
H_2O–D_2O, proton magnetic resonance shifts in, 17: 11342
H_2O–D_2O, radiation effects on, origin of isotope effects on, 19: 22333
H_2O–D_2O, radiolysis of, yields from, 19: 30255
H_2O–D_2O, radiolysis of, isotope effects in hydrogen production in gamma, 20: 38938 (IA-1074)
H_2O–D_2O, solvent isotope effects in, 18: 39239
H_2O–D_2O, solvent properties for argon, 20: 40897
H_2O–D_2O, spectra of solutions in, effects of solute on near-infrared, 20: 45643
H_2O–D_2O, thermal conductivity at 380 to 525°K, 18: 16020
H_2O–D_2O, thermal conductivity, 19: 7410
H_2O–D_2O, use as research reactor moderator, 19: 24189(P)
H_2O–D_2O, use as research reactor moderator, 20: 24805(P)
H_2O–D_2O, use of field ion-mass spectra for determining hydrogen/deuterium ratio in, 19: 30135
H_2O–D_2O, vapor pressure equilibria in, 18: 15974
H_2O–D_2O, vapor pressure of saturated salt solutions of, 20: 38994(R) (AE-232)
H_2O–HDO, diffusion in, 17: 21706
H_2O–HDO–D_2O, molecular motion in, proton spin-lattice relaxation study of, (E), 20: 34097
H_2O–HDO–D_2O, spectra of, infrared absorption, 18: 13748
H–O–H_2O, detonation properties, 16: 18874
H_2O_2–H_2O, electron spin resonance in, of free radicals produced by irradiation at 90°K, 16: 5260
H_2O_2–H_2O, radical concentration and recombination in irradiated, 18: 10163
H_2O_2–H_2O, solvent properties for cesium and rubidium nitrates, effects of cation size on, 16: 13059
H_2O_2–K_2CO_3–$UO_4(NO_3)_2$–H_2O, complex formation in, 18: 13770
H_2O–Xe, electron density decay rate in afterglow vapors of, 18: 32439
H_2O–Zircaloy, neutron ages and fluxes to indium resonance in, (T), 19: 31192 (KAPL-3080)
H_2O–Zr, fission neutron ages to indium resonance in, 18: 28555
H_2O–Zr, fission-neutron age-to-indium resonance in, 18: 44708 (NAA-SR-Memo-9965)
H_2O–Zr, gamma heating in, calculations for, (E/T), 20: 6517 (CONF-651101-41)
H_2O–Zr, neutron age in, moments calculations of, 16: 22977
H_2O–Zr, neutron age-to-indium resonance in, fission, 18: 40476 (NAA-SR-9503)
H_2O–Zr, neutron age and higher moments in, 19: 10675(R) (NAA-SR-9999)
H_2O–Zr, neutron ages in, 20: 10272(R) (NAA-SR-9339)
H_2O–Zr, reaction thermodynamics, 16: 12843
H_2O–Zr, reactivity calculations for uranium-235-containing, 16: 28421 (WAPD-BT-25(p.87-94))
H_3PO_4–pyridine–SO_2–H_2O, sulfur-34 exchange in, thermal phase reversal in, 20: 33298
H_2S–H_2O, temperature profiles of, in countercurrent exchange columns, 16: 14826
H_2SO_4–H_2O, pressure effects on temperature of liquid-liquid immiscibility in, 17: 33923
H_2SO_4–H_2O, radiolysis of oxygenated solutions of, 20: 14614
H_2SO_4–trioctylamine–H_2O, activity coefficient for equilibria in, 20: 45795(R) (ORNL-3945, pp 176-88)
ice–water, positronium decay in, 18: 7418
ice–water, reactions between foreign particles and organic matrix materials in, 18: 15722 (TID-20332)
KCl–H_2O–YCl_3, phase studies, 17: 35841
KCl–$SmCl_3$–H_2O, phase studies, 17: 35841
K_2CO_3–H_2O, phase diagram of, 20: 38994(R) (AE-232)
kerosene–octanol–$Pu(NO_3)_4$–tridodecylammonium nitrate–H_2O, plutonium(IV) distribution in, effect of acid concentration on, 18: 13959
kerosene–TBP–H_2O, solvent properties for nitric acid, 18: 17948
KOH–H_2O, radiolysis of oxygenated solutions of, 20: 14614

lactic acid–uranyl acetate–water, complexes in, 17: 1519
$La(NO_3)_3$–HNO_3–TBP–H_2O, method for presenting data on phase diagrams and separations in, 19: 2286
$La(NO_3)_3$–HNO_3–H_2O–$Y(NO_3)_3$, phase studies, 18: 25434
$La(NO_3)_3$–K_2CO_3–H_2O, composition of, effects of reactant concentration on, 20: 20664
lauric acid–TBP–H_2O, effect of hydrogen bonding on uranium distribution in, 20: 18845
$LiNO_3$–H_2O, phase diagram of, 20: 38994(R) (AE-232)
Li_2SO_4–H_2SO_4–water, critical phenomena and solubilities of, 17: 25067(R) (ORNL-3417(p.77-98))
Li_2SO_4–water, critical phenomena and solubilities of, 17: 25067(R) (ORNL-3417(p.77-98))
mandelic acid–uranyl acetate–water, complexes in, 17: 1518
methane–H_2O, tritium exchange in, 20: 41067(R) (ORNL-TM-1582)
methanol–H_2O, activity coefficients of salts in, rule for calculation of, 16: 16375
methanol–H_2O, diffusion of potassium chloride in, 18: 15712(R) (TID-20260)
methanol–H_2O, dissociation constants for acetylacetone and metal acetylacetonates in, 19: 26295 (TID-21811)
methanol–$HClO_4$–H_2O, electron exchange reactions between thallium and uranium in, 18: 27418
methanol–H_2O, equilibrium and standard free energy constants for alkali metals in, 18: 8362
methanol–H_2O, radiolysis of, yields of hydrogen from gamma, 20: 18736
methanol–NO–H_2O, radiolysis of, nitrous oxide yields from, 20: 23168
methanol–H_2O, solvent effects of, on acetylacetone equilibrium constants with copper perchlorate, 16: 13013(R) (TID-15227(p.3-32))
methanol–H_2O, solvent effects of, on stability constants of copper acetylacetonates, 16: 13015(R) (TID-15227(p.65-79))
methanol–H_2O, solvent effects of, on gamma-irradiated polyvinyl acetate, 16: 18950
methanol–H_2O, thermodynamic properties of acetylacetone in, 16: 13014(R) (TID-15227(p.33-64))
methanol–H_2O, use in paper chromatography of compounds labeled with iodine-125 and iodine-131, 20: 5515
$Mg(NO_3)_2$–$UO_2(NO_3)_2$–H_2O, activity coefficients of, at 25°C, 20: 29196
$Mg(NO_3)_2$–$UO_2(NO_3)_2$–H_2O, chemical potential of water in, at 25°C, 18: 3776
$MoSi_2$–H_2O, zeta potential, 18: 18294(R) (NP-13758)
MoS_2–UO_2SO_4–H_2O, phase studies at 200 to 360°C, 19: 17868
Na_2CO_3–H_2O, phase diagram of, 20: 38994(R) (AE-232)
Na_2CO_3–H_2O, radiolysis of oxygenated solutions of, 20: 14614
Na–H_2O, reaction thermodynamics, 16: 12843
NaOH–H_2O, radiolysis of oxygenated systems of, 20: 14614
Nb_2O_5–SO_3–H_2O, preparation and solubility constants, 17: 28915
$Nd(NO_3)_3$–HNO_3–H_2O, phase studies at 25°C, 18: 17794
$Nd(NO_3)_3$–HNO_3–$Pr(NO_3)_3$–TBP–H_2O, separation factors for neodymium and praseodymium in, 20: 40904
$Nd(NO_3)_3$–HNO_3–$RbNO_3$–H_2O, solubility isotherm at 25°C, 17: 35842
$Nd(NO_3)_3$–HNO_3–$Pr(NO_3)_3$–TBP–H_2O, solvent distribution of neodymium and praseodymium in, 20: 7004 (IS-T-42)
$Nd(NO_3)_3$–TBP–H_2O, complex formation in, 18: 25393
Ne–H_2O, performance in spark chambers, 19: 22750
NH_4F–BeF_2–H_2O, phase studies at 0°C, 19: 2277(T) (ANL-Trans-116)
NH_4F–UF_4–H_2O, crystallographic properties, solubility, and spectra of solid phases in, 18: 13749
NH_3–methane–H_2O, formation of cyanamide and dicyanamide in radiolysis of, 19: 9217
NH_4NO_3–$Gd(NO_3)_3$–HNO_3–H_2O, phase studies, 19: 28334
NH_4NO_3–$La(NO_3)_3$–TBP–H_2O, phase studies and solvent properties of, 19: 24423
N–H_2O, hydrodynamic characteristics in circular tubes, 19: 1875(R) (EURAEC-1011)
N–H_2O, oxidative effects on uranium, mechanism of, 20: 16986
N–H_2O, radiation effects on oxidation of reactor graphite, 19: 1008(T) (JPRS-26808(p.157-68))
N–H_2O, radiation effects on production of ammonia in, effects of acidity on γ and uv, 20: 31289
NaCl–H_2O, spectra of, molar extinction coefficients for infrared-absorption, 20: 25092
NH_3–H_2O, radiolysis of, hydrogen yields from gamma, 20: 29295
N–H_2O, yields from d-c discharges in, 18: 20013
NH_4OH–H_2O, corrosive effects on ceramic fuels, 19: 24093(R) (WAPD-MRP-111)
NH_3–O–H_2O, radiolysis of, hydrogen yields from gamma, 20: 29295
NH_4F–UO_3–H_2O, properties of solid phases in, chemical and physical, 20: 29200
NH_4SCN–methanol–H_2O, distribution coefficients of metals in, 19: 40447
NH_3–UO_3–H_2O, structure and x-ray diagrams of compounds in, 17: 33921
NH_3–$UO_2(NO_3)_2$–$CO(NH_2)_2$–H_2O, precipitation of compounds from, 17: 167
Ni–H_2O, gamma heating in, calculations for, (E/T), 20: 6517 (CONF-651101-41)
Ni–H_2O, neutron angular and energy distributions at interface of, (E), 19: 8382
NiO–N_2O_5–UO_3–H_2O, formation of NiO · $3UO_3$ at 300°C in, 18: 12084
NiO–SO_3–UO_3–H_2O, formation of NiO · $3UO_3$ at 300°C in, 18: 12084
nitric acid–U–H_2O, criticality data for, 20: 1410 (AHSB(S)HANDBOOK-1(1st.Rev.))
nitric acid–Pu–H_2O, criticality data for, 20: 1410 (AHSB(S)HANDBOOK-1(1st.Rev.))
N–O–H_2O, oxidative effects on uranium, mechanism of, 20: 16986
N_2O–H_2O, radioinduced hydroxyl radicals in, 20: 10924
NO–SO_3–UO_3–H_2O, uranyl sulfate liquid–liquid immiscibility in, above 300°C, 16: 10022
NO–2-propanol–H_2O, radiolysis of, nitrous oxide yields from, 20: 23168
O_2–H_2O, atomic processes in atmospheric, (T), 19: 23508(R) (AD-603532)
O–H_2O, atomic processes in atmospheric, (T), 19: 23508(R) (AD-603532)
O–H_2O, oxidative effects on uranium, mechanism of, 20: 16986
O–H_2O, reactions of, with hafnium and zirconium borides and carbides at 3000°K, kinetics and thermodynamics of, 16: 25747 (ASD-TDR-62-204(Pt.I))
oleic acid–TBP–H_2O, effect of hydrogen bonding on uranium distribution in, 20: 18845
O–NaOH–Na_2SO_3–H_2O, radiolysis of, hydrogen yield in, 16: 23716 (PAN-290/ChR)
oxalic acid–TBP–H_2O, effect of hydrogen bonding on uranium distribution in, 20: 18845
Pb–H_2O, calculation of gamma transmission by stratified slabs of, 18: 19263
Pb–H_2O, gamma heating in, calculations for, (E/T), 20: 6517 (CONF-651101-41)
Pb–H_2O, gamma scattering by, build-up factors for, 16: 31031
Pb–H_2O, gamma transmission through, as function of thickness, (T), 19: 45466
Pb–H_2O, neutron angular and energy distributions at interface of, (E), 19: 8382
Pb–H_2O, performance as reactor shielding, (E/T), 19: 14753
Pb–H_2O, shielding efficiency for gamma rays and neutrons, (T), 20: 32676
PbS–UO_2SO_4–H_2O, phase studies at 200 to 360°C, 19: 17868
phenol–H_2O, compound formation in, 18: 34131 (TID-20849)
plutonium oxalate–H_2O, criticality data, 20: 1410 (AHSB(S)HANDBOOK-1(1st.Rev.))
propanol-H_2O, critical heat flux, 18: 39460
propionic acid–TBP–H_2O, effect of hydrogen bonding on uranium distribution in, 20: 18845
Pu–H_2O, criticality studies, 16: 7792
Pu–H_2O, criticality studies, 16: 12700
Pu–H_2O, criticality studies on, (E), 19: 16437 (HW-83603)
Pu–H_2O, criticality studies of, (E), 19: 18735 (HW-79572)
Pu–H_2O, criticality data for, 20: 1410 (AHSB(S)HANDBOOK-1(1st.Rev.))
Pu–H_2O, criticality studies on, 20: 3368 (BNWL-SA-214)
Pu–H_2O, criticality of, effects of plutonium-240 concentrations on, 20: 3368 (BNWL-SA-214)
Pu–H_2O, neutron buckling and cross sections for homogeneous, calculation of critical dimensions from, 16: 26463 (DP-701)
Pu–H_2O, neutron flux distributions in, 18: 23012(R) (HW-80020(p.8-13))
Pu–H_2O, neutron multiplication factor for, (T), 19: 18735 (HW-79572)
Pu–H_2O, neutron spectra in, tabulation, (E/T), 19: 16814 (AERE-R-4776)
PuO_2–H_2O, criticality data for, 20: 1410 (AHSB(S)HANDBOOK-1(1st.Rev.))
PuO_2–H_2O, criticality parameters for plutonium-240 enriched, (T), 20: 16031
PuO_2–UO_3–H_2O, critical masses and neutron buckling in lattices of (E/T), 19: 3531
PuO_2–UO_2–H_2O, criticality data for, 20: 1410 (AHSB(S)HANDBOOK-1(1st.Rev.))
PuO_2–UO_2–H_2O, criticality studies using pulsed sources, (E), 20: 14078
PuO_2–UO_2–H_2O, criticality parameters for, containing enriched and natural uranium, (T), 20: 16032
PuO_2–UO_2–H_2O, criticality studies in lattices of, 20: 47006(R) (EURAEC-1666)
PuO_2–UO_2–H_2O, neutron decay constants in lattices of, (E), 20: 12397(R) (EURAEC-1506)
Pu–U–H_2O, neutron cross sections and thermal spectra in, 20: 12370
Pu–UO_3–H_2O, criticality studies, 17: 41732(R) (HW-77871(p.58-61))
Pu–UO_2–H_2O, criticality studies, 20: 6607(R) (GEAP-4965)
pyridine–H_2O, radiolysis of, yields of hydrogen from gamma, 20: 18736
pyridine–SO_3–H_2O, sulfur-34 enrichment in, 19: 18371
pyrocatechol–uranyl acetate–H_2O, complex formation in, 18: 17808
quartz–water, oxygen isotope fractionation in, 18: 35576

$RbNO_3$–$UO_2(NO_3)_2$–H_2O, formation and nature of complexes in, 18: 41443
rubidium oxalates–H_2O–YCl_3, phase studies, 20: 33304
Sm–H_2O, neutron spectra in, thermal, 19: 42037 (BNWL-95, pp 4-17)
SO_4–UO_2–H_2O, distribution of copper and nickel oxides between liquid phases in labeled and unlabeled, 16: 18896
SO_4–UO_2–H_2O, equilibrium compositions of heavy- and light-liquid phases in labeled and unlabeled, 16: 18895
SO_4–UO_2–H_2O, liquid immiscibility and critical phenomena at 298 to 380°C, 17: 8067
SO_4–UO_2–H_2O, pressure effects on liquid phase formation in, 17: 33923
SO_4–UO_2–water, fluid equilibria in, pressure effects on, 17: 25067(R) (ORNL-3417(p.77-98))
$Sr(NO_3)_2$–$UO_2(NO_3)_2$–H_2O, activity coefficients of, at 25°C, 20: 29196
steam–H_2O, boiling burnout in vertical tubes, empirical correlation for, 20: 12968
steam–H_2O, bubble- and slug-flow effects on volume fraction of, 20: 23257
steam–H_2O, burnout in flows with axially nonuniform heat flux, (E), 20: 14696
steam–H_2O, BWR power-to-void transfer functions for, (E/T), 20: 8344 (ANL-7041)
steam–H_2O, calculation of steam volume fractions in boiling, 17: 14466
steam–H_2O, corrosive effects on Zircaloy-2, 20: 6566(R) (EURAEC-1382)
steam–H_2O, critical flow, (T), 20: 488
steam–H_2O, critical flow tests for, 17: 1148 (HW-69488)
steam–H_2O, critical heat flux in forced flow, 18: 31723 (NP-14072)
steam–H_2O, density in boilers, radiometry of, 20: 9348
steam–H_2O, flow in radial-vane separators, 20: 39019(R) (GEAP-5149)
steam–H_2O, flow in vertical tubes, 20: 18869(R) (NYO-3114-10)
steam–H_2O, flow through apertures, 17: 35990(R) (TID-19326)
steam–H_2O, flow void fractions in, 17: 3111 (NASA-TN-D-1440)
steam–H_2O, heat flux dryout in internally heated annuli, (E), 20: 4099 (AECL-2332)
steam–H_2O, heat transfer in mixture of, 20: 27108(R) (GEAP-5146)
steam–H_2O, heat transfer in, bibliography on, 20: 35617 (AERE-Bib-150)
steam–H_2O, heat transfer in circular pipes, 20: 43477 (CONF-661102-1)
steam–H_2O, heat transfer and pressure drop data for flow in round vertical tubes, 20: 5623 (EURAEC-1325)
steam–H_2O, heat transfer and hydrodynamics in, 20: 6566(R) (EURAEC-1382)
steam–H_2O, mixing methods for, development of, 17: 1115(R) (EURAEC-48)
steam–H_2O, momentum flux measurement by impulse method for flow of, 20: 5624 (MIT-3496-1)
steam–H_2O, phase and velocity distribution in vertical upflow in round tubes, (E), 20: 7227 (EURAEC-1283)
steam–H_2O, phase velocity distribution for flowing, 20: 18874
steam–H_2O, pressure drop in natural-circulation single-component flow at low pressures, 20: 2021
steam–H_2O, research program on mixing and separation, 17: 15389(R) (EURAEC-46)
steam–H_2O, research programs on separation of, 17: 14414(R) (ACNP-62033)
steam–H_2O, separator testing for, 20: 35033
steam–H_2O, separator development for, radial-vane, 20: 10291(R) (GEAP-4967)
steam–H_2O, sound propagation in, speed of, 20: 35614 (AEEW-M-452)
steam–H_2O, void fraction measurement using acoustic methods, 20: 20187 (EURAEC-1361)
steam–H_2O, separator design for, 17: 42389(P)
steam–water, analysis of boiling convection channel flows of, (E), 19: 46538(R) (TID-22148)
steam–water, analytical model for critical flow of, (T), 19: 36620
steam–water, behavior of, in low-pressure critical discharge from constant area pipes, 16: 8870 (HW-68934(Rev.))
steam–water, behavior of, under fog flow conditions, droplet diffusion model for predicting, 16: 19991(R) (NDA-2169-2)
steam–water, boiling burnout, review, 19: 2518
steam–water, boiling heat transfer in upward flow in tubes, CAN-2-experimental data on, 19: 6069 (EURAEC-1084)
steam–water, boiling in coiled tubes, departure from nucleate, 18: 37348 (TID-20983)
steam–water, burnout and pressure drops in flow of, in round tubes, 16: 23816 (EURAEC-42)
steam–water, burnout heat flux and flow dynamics in, 16: 13237
steam–water, burnout heat flux in annulus, 18: 33730 (AERE-R-4352)
steam–water, burnout heat fluxes in forced flow of, 18: 37330 (A/CONF.28/P/327a)
steam–water, burnout in annular flow, effects of test section geometry on, 19: 9323 (AERE-R-3961)
steam–water, corrosive effects of, on stainless steel and Zircaloy-2 at 245 to 287°C at flows of 266 to 553 g/cm²/sec, 16: 7853 (EURAEC-151)
steam–water, corrosive effects on Zircaloy-2, 18: 8476(R) (EURAEC-830)
steam–water, corrosive effects on Zircaloy-2 tubes, 18: 37636 (A/CONF.28/P/574)
steam–water, corrosive effects on stainless steel and Zircaloy-2 claddings at 2000°F, 19: 7862 (APED-4413)
steam–water, corrosive effects on high-purity and industrial 18-10 stainless steels, 19: 11690(R) (EURAEC-1213)
steam–water, corrosive effects on stainless steel, 19: 24997
steam–water, corrosive effects on chromium-nickel and stainless steels, 19: 34644
steam–water, critical discharge from pipe elbows and tees, 19: 22475 (BNWL-34)
steam–water, critical flow through short tubes, 17: 37332 (HW-77594)
steam–water, critical flow from pipe at high upstream pressures, 18: 29838 (HW-80535)
steam–water, critical flow through short pipes, choking in, 19: 32377 (CONF-640507(p.479-81))
steam–water, critical flow in blowdown of tanks, analysis, 19: 38083 (WAPD-T-1791)
steam–water, critical heat load in tubes, effects of tube diameter on, 18: 8489(T) (AEC-tr-6287)
steam–water, critical heat fluxes for flow of, in circular channels at 100 to 180 atm, 18: 22224(T) (AEC-tr-6393)
steam–water, critical heat flux in forced-convective high-quality flow in tubes and roughened annuli, 19: 13574 (AECL-2109)
steam–water, critical heat flux and film thickness in, 19: 30369 (APPE-24)
steam–water, critical mass velocity in, comparison of results with homogeneous- and separated-flow models, 16: 31792 (HW-65739)
steam–water, density of, use of neutron source for measurement of, 16: 13273 (AERE-EL/M-97)
steam–water, design of separator device for, 16: 11814 (GEAP-3787)
steam–water, development for use as reactor coolant, 17: 40267(R) (EURAEC-750)
steam–water, discharge of critical, from pipes, 16: 835
steam–water, effect of pipe and entrance properties on flow rates of, 20: 41107
steam–water, effects of geometrical factors on dryout of flowing, 17: 32260
steam–water, effects of flow rate and pressure on burnout heat fluxes in cylindrical tubes, 18: 14043
steam–water, expansion of very low quality steam through nozzles, 16: 14882 (UCRL-6152)
steam–water, expansion process through de Laval nozzle, models for, 16: 14883 (UCRL-6230)
steam–water, film boiling in heated tubes, 18: 6928(T) (AEC-tr-6252)
steam–water, flow and heat transfer properties, 19: 588 (TID-21221 (p.7-86))
steam–water, flow and heat transfer in experimental loops, 19: 11348(R) (EURAEC-1219)
steam–water, flow during metastable conditions, critical, 18: 1849(R) (TID-19493(Sect.3))
steam–water, flow in BWR, (T), 19: 42624
steam–water, flow in forced-circulation boiler tubes, review, 19: 26507
steam–water, flow in riser channel, true steam content in natural, 18: 27660(T) (AEC-tr-6402)
steam–water, flow in vertical tubes, pressure drops in, 18: 20164 (EURAEC-1004)
steam–water, flow of, adiabatic two-phase, 16: 17804
steam–water, flow of, holdup vapor fractions in two-phase countercurrent, 18: 8482 (KAPL-2295)
steam–water, flow of, in elbows, pressure drop in, 16: 19046 (HW-SA-2564)
steam–water, flow of, in overexpanded nozzles, shock effects in, 16: 7663 (UCRL-6676)
steam–water, flow of, in pipes, analyses of, 16: 4277(T) (AEC-tr-4496)
steam–water, flow of, slip ratios at high void fractions, 18: 1848(R) (TID-19493(Sect.2))
steam–water, flow of, through aperture, 16: 20615
steam–water, flow of, analysis using turbine flowmeters, (E/T), 19: 22478 (CONF-640607(Vol.II)(Paper D-6))
steam–water, flow parameter correlation in annular flow of, 19: 15718(R) (NYO-3114-5)
steam–water, flow past fuel cylinders, vibrations in axial, 19: 18106 (AECL-2225)
steam–water, flow patterns of, two-phase, 17: 7613(R) (UNC-5042)
steam–water, flow pressure drop across thick plate restrictions in, 18: 25665
steam–water, flow through apertures, 17: 35990(R) (TID-19326)
steam–water, flow with liquid entrainment in circular pipes, (T), 20: 28056

steam–water, fluid flow and heat transfer in high-pressure, 16: 18624
steam–water, fluid flow in simulated, 16: 8869 (EURAEC-150)
steam–water, fluid flow and heat transfer properties in circular tubes, 19: 1875(R) (EURAEC-1011)
steam–water, heat transfer by, 16: 14327
steam–water, heat transfer by, design of facility for studies on, 16: 8867 (EURAEC-41)
steam–water, heat transfer by, in round tubes, 16: 25530(T) (EURAEC-42)
steam–water, heat transfer properties, 16: 2690(T) (TT-985)
steam–water, heat transfer properties, 16: 26603(T,R) (EURAEC-36)
steam–water, heat transfer properties, 16: 26640(T,R) (EURAEC-38)
steam–water, heat transfer properties, 16: 34082(T,R) (EURAEC-40)
steam–water, heat transfer by, 17: 21872 (CISE-R-62)
steam–water, heat transfer of, in round vertical tubes, 17: 32244 (EURAEC-637)
steam–water, heat transfer to, flowing in round vertical tubes with non-uniform axial power distribution, 17: 32245 (EURAEC-671)
steam–water, heat transfer by, 17: 34092(R) (EURAEC-299)
steam–water, heat transfer, 18: 8476(R) (EURAEC-830)
steam–water, heat transfer experiments on, equipment for, 18: 8478 (EURAEC-862)
steam–water, heat transfer and pressure drop in sprays of, 18: 14025 (EURAEC-153)
steam–water, heat transfer to, flowing in heated tube, 18: 16171 (EURAEC-929)
steam–water, heat transfer in flows through pipes, 18: 24910(R) (SRO-101)
steam–water, heat transfer properties in circular tubes, 18: 28932(R) (EURAEC-1013)
steam–water, heat transfer crisis in, 18: 29853
steam–water, heat transfer from fuel assembly to, 18: 37324 (A/CONF.28/P/16)
steam–water, heat transfer parameters of channel flows of, 19: 590
steam–water, heat transfer crisis in forced convection, review of experimental studies of, 19: 15715 (EURAEC-1085)
steam–water, heat transfer crisis in, 19: 18123
steam–water, heat transfer, from rod cluster type fuel elements to, 19: 22473 (AERE-R-3960)
steam–water, instabilities in two-phase flow of, 17: 34088 (AERE-M-1105)
steam–water, interfaces of, detection using ultrasonic instruments, (E), 19: 24013 (CONF-640607(Vol.I)(Paper A-14))
steam–water, kinetics of mixing and separation, 16: 17799(R) (EURAEC-209)
steam–water, liquid film breakdown in annular two-phase flow, 19: 28509
steam–water, moisture separation in, 16: 1921
steam–water, performance in reactor spray cooling, 18: 17999(R) (EURAEC-923)
steam–water, phase composition in heated pipes, 18: 12320
steam–water, pressure drop in vertical heated and unheated annuli for forced convective flow, 16: 25519 (AERE-R-3808)
steam–water, pressure drop in forced boiling flow, 18: 33745
steam–water, pressure drop in two-phase flow of, 19: 32376 (CONF-640507(p.459-78))
steam–water, pressure drop in two-phase flow through piping components, 19: 32378 (CONF-640507(p.483-7))
steam–water, pressure gradients in critical flow of, theory for predicting, 17: 39247
steam–water, pressure pulsations in heat transfer by, 20: 43478(R) (EURAEC-1620)
steam–water, properties of, for use as reactor coolant, 16: 33980(R) (EURAEC-332)
steam–water, properties as reactor coolant, 19: 25672(P)
steam–water, separation of water entrainment from, efficiency of screens for, 16: 26470 (KAPL-2000-18)
steam–water, separator development for, (E), 19: 4330 (SAN-8003 (p.190-9))
steam–water, slip ratio of, at 212°F, 20: 43482 (ORNL-TM-1519)
steam–water, slug-annular flow regime, transition at high pressures, 18: 17997 (ANL-6796)
steam–water, sound velocity in two-phase flows of, (E), 19: 13586(T) (WAPD-Trans-15)
steam–water, specific gravity in boilers, 17: 6378
steam–water, steam volume fractions in flowing and static (E), 19: 3579
steam–water, theoretical model for predicting maximum flow rate of, 18: 41623
steam–water, thermal conductivity of, during evaporation in horizontal tubes, 16: 13227
steam–water, thermal conductivity characteristics of, flowing in annulus, 16: 13238
steam–water, two-phase critical flow in annuli, 17: 16239
steam–water, two-phase critical flow model, use in calculations for liquid metal systems, 18: 6921 (ANL-6779)
steam–water, two-phase critical flow rates, comparison of calculated and observed, 18: 8480 (GEAP-4395)
steam–water, two-phase expansion through convergent-divergent nozzle, 18: 25662
steam–water, two-phase flow through apertures, 18: 27652 (COO-926-31)
steam–water, two-phase pressure drop in piping components, 18: 35689 HW-80970(Rev.1))
steam–water, two-phase flow at 600 to 1400 psia in pipes and channels, pressure drop, 18: 41614 (GEAP-4616)
steam–water, two-phase pressure drop across contractions and expansions, 18: 41615 (GEAP-4622)
steam–water, two-phase flow of, heat transfer and hydrodynamic studies, 19: 32358 (CONF-640507(p.79-87))
steam–water, two-phase vessel blowdown from pipes, theory, 19: 38802 (APED-4827)
steam–water, two-phase flow at 1200 psig, orifice and venturi measurements of, 19: 46526 (AECL-2273)
steam–water, vapor volume fractions in vertical flow in duct, 19: 11344(R) (ACNP-64029)
steam–water, vaporization of, during flow, growing-bubble model for, 16: 16504(R) (TID-15429)
steam–water, velocity of rising steam in, 16: 24510
steam–water, void fraction measurements in, by gamma attenuation techniques, 17: 32241(R) (ACNP-63020)
steam–water, void fractions in, instruments for measuring, (E), 19: 24071 (CONF-640607(Vol.II)(Paper D-8))
steam–water, void fraction measurement by x-ray attenuation in two-phase flow of, 19: 40745
stearic acid–TBP–H_2O, effect of hydrogen bonding on uranium distribution in, 20: 18845
TBP–H_2O, cerium compound absorption spectra in, 20: 36831
TBP–H_2O, chemical activity coefficients of, 20: 9049(R) (ORNL-3830, pp 193-221)
TBP–H_2O ,dielectric constants for, 20: 9049(R) (ORNL-3830, pp 193-221)
TBP–H_2O, phase studies, specific gravity, and viscosity of, 17: 7944
TBP–UO_2–H_2O, solvent partition at 0 to 100°C, 19: 11072
TBP–$UO_2(NO_3)_2$–H_2O, phase equilibria in, 18: 22183
Th–H_2O, neutron age in, 16: 1007
Th–H_2O, neutron resonance escape probability in lattices of, (E), 20: 34985
$Th(NO_3)_4$–TBP–$UO_2(NO_3)_2$–H_2O, method for presenting data on phase diagrams and separations in, 19: 2286
ThO_2–UO_2–H_2O, neutron parameters in lattices of uranium-233-enriched (E/T), 19: 3529
$TlNO_3$–$UO_2(NO_3)_2$–H_2O, chemical potential of water in, at 25°C, 18: 3776
tributyl phosphate–H_2O, dielectric constants, 19: 7424
trimethylamine–H_2O–D_2O, deuterium isotope effects in, 18: 8391
UC–H_2O, criticality parameters for, 19: 44112 (CONF-651103-4)
U–H_2O, asymptotic thermal neutron spectra in, 18: 2821
U–H_2O, buckling measurements in, design of exponential facility for, 17: 35253(R) (IA-775)
U–H_2O, conversion ratios, 16: 725
U–H_2O, critical and safe limits of slightly enriched, 19: 47955 (CONF-651103-6)
U–H_2O, critical parameters for slightly enriched, 16: 933 (HW-69273)
U–H_2O, criticality studies, 16: 12699
U–H_2O, criticality studies in critical and subcritical assemblies, 16: 24354
U–H_2O, criticality studies of over-moderated, 16: 761
U–H_2O, criticality studies of superheated, 16: 760
U–H_2O, criticality studies on enriched, 16: 7792
U–H_2O, criticality studies, 18: 33024
U–H_2O, criticality of slightly enriched, 18: 35113 (TID-8540(p.529-609))
U–H_2O, criticality studies, (E), 19: 10496
U–H_2O, criticality parameters for, 19: 44112 (CONF-651103-4)
U–H_2O, criticality calculations on, 19: 47959 (WCAP-3269-52)
U–H_2O, criticality data for, 20: 1410 (AHSB(S)HANDBOOK-1(1st.Rev.))
U–H_2O, criticality parameters for, (T), 20: 16031
U–H_2O, criticality studies, (E), 20: 22375(R) (BNWL-193, pp 45-56)
U–H_2O, kinetics of enriched lattices, 16: 23352(R) (BNL-705)
U–H_2O, neutron buckling and disadvantage factor for slab lattices of, 17: 26060
U–H_2O, neutron bucklings and flux distributions in, 18: 38315 (A/CONF.28/P/667)
U–H_2O, neutron buckling in 3% enriched, Monte Carlo calculations of, 19: 47954 (BNWL-127)
U–H_2O, neutron decay and modal analysis of enriched assemblies, 17: 37993(R) (GA-4426)
U–H_2O, neutron distribution in, 19: 12753
U–H_2O, neutron disadvantage factor for, 20: 30855

U–H_2O, neutron epi- and sub-cadmium absorption in, 17: 26062
U–H_2O, neutron flux distribution in subcritical, 16: 15528
U–H_2O, neutron flux distributions in, 18: 23012(R) (HW-80020(p.8-13))
U–H_2O, neutron flux distribution in, 18: 33025
U–H_2O, neutron infinite multiplication factor in lattices of, (E/T), 19: 10495
U–H_2O, neutron multiplication factor for, (T), 19: 18735 (HW-79572)
U–H_2O, neutron physics measurements, 18: 21594 (BNL-6975)
U–H_2O, neutron physics parameters of, 18: 37862 (A/CONF.28/P/358)
U–H_2O, neutron resonance capture integrals, high-energy, 16: 24396
U–H_2O, neutron resonance integrals for slab lattices of, 19: 29337
U–H_2O, neutron spectra temperature distribution in, 16: 1002 (PAN-233/IX)
U–H_2O, neutron spectra for, 17: 26392(R) (GA-3853)
U–H_2O, neutron spectra in, measured and theoretical, 19: 33192(R) (GA-6096)
U–H_2O, neutron spectra in, method for measuring, 19: 38136
U–H_2O, optimization of spacing in subcritical assemblies, 16: 11172
U–H_2O, reaction thermodynamics, 16: 12843
U–H_2O, reactivity calculations for systems with zirconium, 16: 28421 (WAPD-BT-25(p.87-94))
U–H_2O, reactivity, 18: 15471 (GA-4838)
U–H_2O, resonance escape, calculation of, by QUERY program, 16: 4676(R) (CEND-104)
U–H_2O, shielding properties of, gamma and neutron, 20: 36352
U–H_2O, spatial and spectral distribution of thermal neutrons in, 16: 32362 (MITNE-17)
U–H_2O, subcritical material buckling in, 18: 42916 (CEA-R-2490)
U–H_2O, thermal neutron distributions in, 17: 38493 (WAPD-T-1594)
U–H_2O, thermal neutron flux distribution in rectangular lattice of, 18: 38327 (A/CONF.28/P/826)
U–H_2O, thermal neutron activation ratios in lattices of, 19: 29569
U–H_2O, thermal neutron spectra in cylindrical lattices of, (T), 20: 9954
U–H_2O–Zr, critical bucklings and extrapolation distance for uranium-235, (T), 19: 40159 (WAPD-T-1774)
U–H_2O–Zr, criticality of water-reflected uranium-235, (E/T), 19: 29524
U^{235}–H_2O–Zr, reactivity of, effects of water gaps and uranium-238 on, 17: 41734 (WAPD-T-1483(Rev.))
U–H_2O–Zr, reactivity effect of water-gap spacing and uranium-238 on enriched, 20: 26434
UO_2F_2–H_2O, critical thickness of, calculation of, 17: 21266
UO_2F_2–H_2O, neutron dosage and leakage spectra calculations for highly enriched, 16: 3612
UO_2F_2–H_2O, neutron flux perturbation by aluminum–dysprosium foils in, thermal, 20: 15669 (NASA-TN-D-3237)
UO_2F_2–H_2O, pressure effects on temperature of liquid-liquid immiscibility in, 17: 33923
UO_2–H_2O, analysis of bucklings in assemblies, 17: 40262 (BNL-7293)
UO_2–H_2O, critical and safe limits of slightly enriched, 19: 47955 (CONF-651103-6)
UO_2–H_2O, criticality studies on multiregion low-enrichment systems of, 16: 12669 (WCAP-1933)
UO_2–H_2O, criticality, minimum uranium-235 enrichment requirements for, 16: 13857 (HW-70310)
UO_2–H_2O, criticality, minimum uranium-235 enrichment requirements for, 16: 13857 (HW-70310)
UO_2–H_2O, criticality calculations on, 19: 47959 (WCAP-3269-52)
UO_2–H_2O, criticality data for homogeneous, 20: 1410 (AHSB(S)HANDBOOK-1(1st.Rev.))
UO_2–H_2O, criticality parameters for, (T), 20: 16031
UO_2–H_2O, criticality studies of mixtures of, 20: 33597
UO_2–H_2O, Dancoff effect on temperature coefficients of resonance integrals in, 19: 30780
UO_2–H_2O, effects of plutonium-240 on criticality of homogeneous, 18: 16736 (HW-79413)
UO_2–H_2O, fission recoil separation effects in, 16: 12709
UO_2–H_2O, kinetic characteristics, 16: 9652(R) (IDO-16726)
UO_2–H_2O, multiplication factors for slightly enriched, 16: 13857 (HW-70310)
UO_2–H_2O, neutron capture-to-fission ratio in lattices of, (E), 20: 26435
UO_2–H_2O, neutron disadvantage and thermal utilization factors in square cells of, (E), 20: 10333
UO_2–H_2O, neutron flux variations and multiplication in, 16: 12707
UO_2–H_2O, neutron migration in slightly-enriched, 17: 26063
UO_2–H_2O, neutron migration in, 17: 35119
UO_2–H_2O, neutron migration, multiplication factor, and reflector savings for, 19: 42053
UO_2–H_2O, neutron multiplication in, comparison of analytical and cadmium-ratio, 16: 24426
UO_2–H_2O, neutron multiplication factors for, infinite-medium, 20: 46997
UO_2–H_2O, neutron parameters in lattices of (E/T), 19: 3530
UO_2–H_2O, neutron resonance integrals for slab lattices of, 19: 29337
UO_2–H_2O, neutron spectra, 18: 40783 (KR-87)
UO_2–H_2O, neutron thermal utilization in, 18: 3115
UO_2–H_2O, neutron thermal disadvantage factors for, 20: 5073
UO_2–H_2O, reactivity of reflected critical assemblies of, (E), 19: 12778(R) (GEAP-4644)
UO_2–H_2O, reactivity of variable-pitch lattices of, kinetic and steady-state measurements of, (E/T), 20: 14079
UO_2–H_2O, reactivity temperature coefficient for, reflector effects on, (E), 20: 5067
UO_2–H_2O, resonance escape, calculation by QUERY program, 16: 4676(R) (CEND-104)
UO_2–H_2O, separation of, from fission products, 16: 11259
UO_2–H_2O, solvent properties of, for copper oxide, nickel oxide, and sulfur trioxide at 300°C, 16: 11636
UO_2–H_2O, stability of, 17: 22784(R) (ARF-3124-1)
UO_2–H_2O, volume ratio effects on reactor fuel cycle cost, 20: 5176 (EUR-2468.e)
UO_3–H_2O, water bonding in, types of, 17: 14292
UO_3–H_2O–D_2O, criticality and reactivity of, 18: 3169 (BAW-1274)
UO_3–H_2O–D_2O, nuclear properties of, 17: 29706(R) (BAW-1271)
UO_2–H_2O–Zircaloy-2, chemical reactions of, 20: 23765(R) (ANL-7176, pp 86-93)
UO_2–H_2O–Zr, neutron parameters for lattice of, 18: 9580 (WAPD-T-1632)
$UO_2(NO_3)_2$–H_2O, criticality studies, 16: 3859(R) (ORNL-3193(p.159-67))
$UO_2(NO_3)_2$–H_2O, criticality studies at 93 wt.% uranium-235 enrichments, 16: 3856(R) (ORNL-3193(p.131-2))
$UO_2(NO_3)_2$–H_2O, criticality studies of mixtures of, 20: 33597
$UO_2(NO_3)_2$–H_2O, criticality studies on effectiveness of control elements, 20: 35692
$UO_2(NO_3)_2$–H_2O, nuclear parameters in cylindrical and spherical vessels, 16: 12326
$UO_2(NO_3)_2$–H_2O–$Zn(NO_3)_2$, activity coefficients of, at 25°C, 20: 29196
$UO_2(NO_3)_2$–$Zn(NO_3)_2$–H_2O, chemical potential of water in, at 25°C, 18: 3776
UO_2SO_4–H_2O, corrosive effects on stainless steel, 16: 17563(R) (ORNL-3262(p.90-8))
UO_2SO_4–H_2O, phase equilibria, 16: 31311
UO_2SO_4–H_2O, phase studies, 16: 11168
UO_2SO_4–H_2O, phase studies, 16: 18634
UO_2SO_4–H_2O, pressure effects on liquid-liquid immiscibility at 290 to 430°C, 17: 33923
UO_2SO_4–H_2O–ZnS, phase studies at 200 to 360°C, 19: 17868
UO_2SO_4–water, liquid-liquid immiscibility and phase studies of, 17: 25067(R) (ORNL-3417(p.77-98))
UO_3–$UO_2(NO_3)_2$–H_2O, phase studies, 20: 10841
U^{235}–UO_2–H_2O, physics of undermoderated cores of, 18: 13234 (CONF-187-35)
U-235–H_2O–Zr, critical bucklings and extrapolation distance for, (T), 19: 40159 (WAPD-T-1774)
1-propanol–H_2O, dissociation constants for acetylacetone and metal acetylacetonates in, 19: 26295 (TID-21811)
2-butanone–H_2O, bubble growth rate in, at atmospheric pressure, 16: 13219
2-butanone–H_2O, critical heat flux, 18: 39460
2-butanone–H_2O, effects of hexane on solvent distribution of iodine-131 and technetium-99 in, 19: 22099 (ORNL-TM-1058)
2-ethoxyethanol–H_2O, condensation of gaseous, mass transfer effects in, 19: 22484(R) (NYO-2765-1)
2-methyl-1-propanol–H_2O, ferric thiocyanate distribution in, effects of fluoride on, 20: 16335(R) (NBS-TN-276)
2-propanol–H_2O, dissociation constants for acetylacetone and metal acetylacetonates in, 19: 26295 (TID-21811)
2-propanol–H_2O, effects on photoreduction of benzophenone, 20: 7129(R) (NYO-2499-17)
2-propanol–H_2O, thermodynamics of reactions between nickel(II) and 2,4-pentanedione in, 20: 16416(R) (NYO-906-68)

WATER-*d*

analysis for isotopic impurities, apparatus for radiation absorption, 19: 34134(P)
content in Martian atmosphere, infrared spectral evidence for, 19: 8061
determination in water, infrared method for, 19: 2209 (CRDC-1141)
deuterium exchange between hydrogen and, kinetics of catalytic, 17: 21680
deuteron two-quantum transitions in, 17: 32765
dissociation of, isotopic effects on, 18: 1634
effects on growth of Agrostemma hypocotyl and Avena coleoptile cylinders, 19: 45763(T) (AD-468388)
effects on Napier relaxation frequency of oxygen, 19: 40483
electron excitation of jets of, radicals from, 17: 34009
enthalpy, measurements of excess in, 16: 14755
exchange with water in plants, 20: 8556
hyperfine structure of, microwave, 18: 12060
ion products of, 19: 38608

light absorption in, visible-region, 17: 30543
mass difference with water, (E), 19: 28336
neutron thermalization in, (E/T), 20: 9944 (RPI-328-44)
potential energy functions for, determination from spectral data, 20: 31949
properties review, physical and thermodynamic, 16: 25307 (CEA-Bib-15)
radioinduced yields of positive oxygen ions in, electron, 19: 40581
rotation of molecule of, in solid argon, infrared spectroscopic evidence for, 17: 8042
separation from water, physical and thermodynamic aspects, 16: 16628
spectra and structure in liquid water, Raman, (E), 19: 42483
spectra, effects of lithium and potassium halides on Raman, 16: 30401
spectra in water-d_2 solutions, near-infrared, 20: 45643
spectra of valence bands in liquid and solid, temperature dependence of infrared, 19: 9093 (CEA-R-2463)
spectra of, absolute intensities of infrared, 19: 26361
spectra of, infrared absorption, 18: 13748
spectra of, molar extinction coefficients for infrared-absorption, 20: 25092
spectra of, vibrational, 18: 12100(T)
spectrum, hyperfine structure of rotational, 16: 16355
spectrum, proton magnetic resonance, 16: 29519
structure of, spectral study of, 18: 25369
uptake and distribution in intestinal tissues of dog, *in vitro*, compartmental analysis of, 20: 42748
vapor pressure of, at −40 to 0°C, 20: 29149
H_2O–HDO, diffusion in, 17: 21706
H_2O–HDO–D_2O, molecular motion in, proton spin-lattice relaxation study of, (E), 20: 34097
H_2O–HDO–D_2O, spectra of, infrared absorption, 18: 13748

WATER-d_2
acidities in, substituent effects on, 18: 43488
activation and fission product concentrations in, sequential analysis of, 18: 27287 (DP-886)
algae growth in, 16: 1341
alkali halide activity and osmotic coefficients in, at 25°C, 20: 16488
analyses of reactor coolant-moderator, 19: 42084(R) (CVNA-239)
analysis and purification for RA Reactor, Yugoslavia, 16: 26918
analysis for deuterium by deuteron reaction (d,n) with oxygen-16 induced by reactor neutrons, 16: 4134 (IA-692)
analysis for deuterium, methods for quantitative, 18: 8296
analysis for deuterium, gas-chromatographic, 20: 265
analysis for deuterium in low concentration by drop method, 20: 22903
analysis for deuterium in low concentration by drop method, 20: 22904
analysis for hydrogen, spectrometric, 18: 33539
analysis for hydrogen by thermal neutron transmission, 20: 36740
analysis for impurities, review of problems in, 20: 7020
analysis for isotopic purity, apparatus for continuous, 16: 23623 (TID-7629(p.91-109))
analysis for isotopic impurities, infrared analyzer for, 18: 25312(P)
analysis for isotopic content, infrared absorptiometric, 19: 2207 (CEA-R-2441)
analysis for isotopic impurities, apparatus for radiation absorption, 19: 34134(P)
analysis for light water, infrared analyzer for, 17: 1415(P)
analysis for light water, photometric, 20: 3970(P)
analysis for metallic impurities, atomic absorption spectroscopy for, 19: 46166 (DP-980)
analysis for radioisotopes and trace constituents in PRTR, 16: 23333 (HW-69924)
analysis for trace impurities, automated, 19: 40406 (CONF-650919-2)
analysis for water by infrared spectroscopy, 16: 26903(T) (AEC-tr-5270)
analysis of CVTR, 19: 40179(R) (CVNA-236)
analysis of low-enrichment, using infrared radiation, 19: 7274(R) (IDO-14636)
analysis of, method for, 17: 35197
analysis of reactor, 17: 1150 (JAERI-1024)
analysis of, for deuterium ion concentration, 20: 35407
analysis of, for hydrogen by neutron activation methods, 20: 45728
analysis of, methods for, 18: 17726 (NP-13766(p.135-54))
analytical methods for, review, 19: 5806
analytical use in isotope dilution analysis of barium chloride, silica gel, and silicate iron ore for hydrogen ion and water, 20: 45595
analytical uses in determination of manganese, 19: 19806
argon thermodynamic properties in, 19: 13318
atomic frequency spectra of moderators of, integral parameters for, 20: 36404 (AE-228)
basicity of amino acids in, 16: 1790
beta scattering by, measurement of saturated backscattering from, 18: 35057
boiling flow in vertical round duct, void fractions in, 18: 1859 (AE-106(2nd rev. ed))
boiling point and vapor pressure of, 20: 38921
cation hydration in, (T), 20: 8895
chloride ion transfer to, from water, calculation of free energy of, 18: 25338
circulation as moderator in power reactors, 16: 5014 (DP-628)
concentration during electrolysis of water, 16: 5632(T)(P) (CEA-tr-X-283)
concentration, equipment and method for electrolytic, 16: 17965
concentration in hot-cold columns, method for, 18: 12530(P)
concentration in light water using surface-active agents, 17: 1806(P)
concentration in salt water liquor by precipitation of salts and removal of crystallization water, 19: 866(T) (ORNL-tr-335)
concentration using magnetohydrodynamic effect, 19: 44578(P)
conference on, 18: 17716 (NP-13766)
conference on heavy water reactor lattices, 18: 6413
content in aqueous solutions, determination of, using absorption spectrum displacement, 20: 35526
content in crystallization water of saline minerals, 19: 44240
content in Martian atmosphere, infrared spectral evidence for, 19: 8061
content in natural waters of Concepción Region, Chile, 16: 25621
content in water, determination using osmometer, 19: 15392
corrosive effects on beryllium at high temperatures, 16: 17563(R) (ORNL-3262(p.90-8))
corrosive effects on Type 304 stainless steel, 17: 32516 (DPSPU-62-30-26)
corrosive effects on zirconium alloys at 400°C, 17: 37003(R) (HW-78118)
corrosive effects on Zircaloy-2 and Zircaloy-4, 18: 7142(R) (HW-77954 (p.5.16-17))
corrosive effects on Zircaloy-2 and Zircaloy-4, 18: 7148(R) (HW-78962 (p.5.13-23))
corrosive effects on SS 304 (E), 19: 3643 (HPR-35(Vol.II)(Sect.10))
corrosive effects on materials, in HWCTR, 19: 11668(R) (DP-945)
corrosive effects on Zircaloy-2 at 275°C, 19: 13883(R) (HW-81984 (p.9.1-6))
corrosive effects on mild steel components in reactor cooling system, 19: 16014 (CONF-446-81)
corrosive effects on mild steel, 19: 43603
corrosive effects on steel in Savannah River Components Test Reactor, 20: 29654
corrosive effects on types 304, 316, and 17-4 PH stainless steel at 315°C, 20: 31669
critical solution temperatures of phenols in, 20: 18720
critical specific volume, 18: 39440(T)
criticality studies of two-region uranyl sulfate systems with, (E/T), 19: 31510
decomposition in HBWR moderator, effects of deuterated ammonia, nitrogen, and oxygen on, 19: 33604(R) (HPR-57)
decomposition of, effects of air ammonia, deuterium, nitrogen, and oxygen, 20: 40409(R) (NP-16230)
decontamination from colloidal and particulate suspensions by electrophoresis, 17: 33766 (HW-77950)
demand and supply for heavy water reactors, forcast to 1985, 20: 42516 (66-CNA-301)
density at 250 to 372°C, 16: 26966(T) (AECL-1560)
density at 275 to 425°C, 16: 31631
density of oxygen-18-labeled, 17: 18069
density of, temperature dependence of, 20: 28049
detection in water, leak detector for, 20: 2099 (AECL-2291)
determination by float method, 17: 1410
determination by falling drop method, 19: 7297
determination by falling-drop method, 19: 13215
determination by infrared spectroscopy, 16: 7511
determination in air by infrared absorption, 16: 17864(P)
determination in air and liquids, design of infrared monitor for, 16: 32918 (CRRP-1099)
determination in blood plasma, micromethods for, 19: 15390
determination in liquids below 25°C, float method for densimetric, 18: 17727 (NP-13766(p.155-68))
determination in light water by electrochemistry of cadmium in water–heavy water systems, 19: 40427
determination in light water by nuclear magnetic resonance spectra, 20: 239
determination in light water, 20: 8813
determination in natural water at 25°C, 16: 28883
determination in water by infrared absorption, 16: 18847
determination in water, by drops falling in *o*-fluorotoluene, automatic timer design for, 16: 14659
determination in water by recording hydrometer, 17: 329 (CEA-2184)
determination in water, falling-drop, 17: 10566
determination in water, infrared, 17: 32006
determination in water mixture, quantitative spectrophotometric, 18: 9986
determination in water, infrared method for, 19: 2209 (CRDC-1141)
determination in water by falling-drop method using inclined tube, 19: 6149 (SGAE-CH-6/1964)

determination in water mixture, system for, 19: 13713
determination in water by specific weight measurement, 19: 43983(P)
determination in water by infrared spectroscopy, 20: 16377
determination in 1 to 99% concentration range, infrared spectrophotometric methods for, 16: 11510 (CRDC-1051)
determination of purity by infrared absorption, 16: 8674 (IDO-14576)
determination of small concentrations, falling-drop method, 16: 7514
determination of, methods for, 18: 37585 (A/CONF.28/P/496)
determination of, in water by infrared spectrophotometry, 20: 35410
determination of, at 0 to 10.5 mol %, by falling-drop method using n-butyl benzoate, 17: 12211
deuteration of Euglena grown in, 19: 2057
deuterium exchange with benzene, radiation effects on catalytic, 19: 11170(R) (TID-21443)
deuterium exchange with nylon-6, structure studies by, 19: 11147
deuterium exchange with nylon and proteins, 19: 11154
deuterium exchange with hydroxyl groups of silica aerosols or gels, 19: 13372
deuterium exchange with poly-L-leucine and poly-L-valine, 19: 22276
deuterium exchange with cobalt ethylenediamine complexes, NMR studies of, 19: 26349
deuterium exchange with α-hydrogen of 2-phenylethyldimethylsulfonium or 2-phenylethyltrimethylammonium ions, 19: 26368
deuterium exchange between, and amide groups, 19: 32195
deuterium exchange between, and aromatic compounds, effects of π-complex absorption on transition metals on, 19: 32199
deuterium exchange with organics, group VIII metal catalysis of, 19: 38597
deuterium exchange between, and hydridoplatinum complex, 19: 38627
deuterium exchange between, and *trans*-hydridochlorobis(triethylphosphine)platinum(II), 20: 20701
deuterium exchange between, and amino acids or peptides, 20: 20714
deuterium exchange with 3-heptanone, 20: 23061
deuterium exchange with methylenecyclopropanecarboxylic acids, 20: 25113
deuterium exchange with hydrocarbons or hydrogen sulfide, 20: 29611(P)
deuterium exchange with active methyl hydrogens of pyrylium and tropylium compounds, 20: 31260
deuterium exchange between, and aniline, effects of temperature and catalytic activity of cobalt, nickel, and platinum on, 20: 43275
deuterium NMR in, quadrupole effects in, 18: 11242
deuterium-hydrogen exchange between chlorophyll and, location of, 18: 16042(T)
deuterium-hydrogen exchange between light water and silk fibroin and, 18: 23470
deuterium-oxygen bonds in, length of, 18: 25417(T)
deuteron quadrupole relaxation in liquid, measurement of, 18: 19962
deuteron quadrupole in, constants for, (T), 20: 12287
deuteron two-quantum transitions in, 17: 32765
dielectric constant at 0 to 40°C, 18: 206 (NYO-10695)
dielectric constant at 0 to 40°C, 19: 40527
dielectric properties in dioxane, 16: 27022
dielectric relaxation time of, effects of free volume and temperature on, 19: 13303
diffusion in clay systems, relation between exchangeable ion conductance and activation energies for, 16: 13075
diffusion of dioxane in electrolytic solutions of, coefficients of self-, 17: 40800
diffusion of thermal neutrons in, at 20 to 220°C, 17: 7058 (TID-15165)
diffusion through sulfonated polystyrene cation membrane, 17: 33890
diffusion through lipid membranes, 20: 42725
dilution by ion exchange resin treatment and irradiation, 18: 17777 (NP-13766(p.119-33))
dissociation constants of carboxylic acids and dinitrophenols in, 17: 39092
dissociation of deuteriophosphoric acid in, at 5 to 50°C, 19: 7427
dissociation of, isotopic effects on, 18: 1634
effect in mice, enhancement with anticancer drugs, 16: 11447(R) (ANL-6464(p.93-6))
effect in mice, enhancement with anticancer drugs, 16: 11447(R) (ANL-6464(p.93-6))
effect of lipid content of animal cells in tissue culture, 17: 23062
effect on nonenzymatic transamination of glutamic acid, 19: 25975
effect on sound dispersion in ethylene, 16: 3025
effects in sea urchin eggs, effects of hydrostatic pressure on antimitotic, 19: 35996
effects of incorporated, on development of roots, 19: 12961(R) (TID-21604)
effects of ingested, on sterility of mice, 20: 10550
effects of ingested, on normal and pregnant mice and rats, 20: 30975
effects of ingested, on gonads, 16: 12865
effects of, on circulating antibody levels in mice, 20: 28988
effects on acid ionization constants, 17: 16022
effects on action current of striated muscle, 19: 2012
effects on active transport of arabinose, glucose, and sodium in hamster intestine, 20: 18212
effects on algae, metabolic, 16: 23364
effects on animal cells, 16: 32780
effects on ascites tumor cells, metabolic, 18: 38763
effects on bacteria, 16: 23388
effects on bacteria, 16: 23404
effects on bacteria, mutagenic, 16: 26675
effects on beef heart aconitase and pancreatic lipase, 20: 42738(R) (ANL-7136, pp 255-65)
effects on biochemical and physiological reactions, 20: 45302
effects on carbon-14 uptake by proteins in Arbacia eggs, 18: 38764
effects on cells, review, 20: 3651
effects on cellular and protein resistance to heat and hydrostatic pressure, 20: 18218(T)
effects on citric acid and pyruvate carboxylase formation in *Aspergillus niger*, 20: 35205
effects on crystallinity of Cellulose II film at 170 to 220°C, 17: 37217
effects on desoxyribonucleic acid in bacteriophage, 18: 38743
effects on development of fish eggs and fingerlings, 19: 29898 (HW-SA-3627)
effects on differentiation and proliferation of mononuclear leukocytes to fibroblasts, 18: 1337
effects of dissociation constants of nitrophenols and salicylic acid, 20: 7088
effects on dissociation constant of acetic acid at 5 to 50°C, 20: 35514
effects on DNA and proteins, chemical, 18: 3441
effects on Drosophila, mutagenic and physiological, 19: 2015(T)
effects on Drosophila, genetic, 18: 17522
effects on *E. coli*, mutagenic, 19: 42234
effects on energy transfer in sulfur dioxide vibrations, 16: 3026
effects on enolization of oxalacetic acid, 16: 23532
effects on enzymatic activity of phosphopyruvic kinase in presence of alkaline ions, 17: 23049
effects on fluorescence yield of rare earth ions, 18: 3752
effects on fluorescence and absorption spectra of europium chloride solutions, 19: 38636
effects on fluorescence of dysprosium, neodymium, and samarium chlorides, 20: 25102
effects on fluorescence of trivalent europium ions, 20: 35505
effects on fluorine-19, chemical shift, 17: 25261
effects on glucose, phosphate, and potassium uptake in yeast, 19: 3878
effects on growth of *Azotobacter*, 16: 18751
effects on growth and respiration of yeast, 16: 25137(R) (HW-72500 (p.113-18))
effects on growth and metabolism in cichlid fish embryos and larvae, 17: 35319(R) (HW-76000(p.187-97))
effects on growth of mint plants, 18: 15861
effects on growth of peppermint plants, *Mentha piperita*, 18: 38759
effects on growth of algae, bacteria, molds, and yeasts, 18: 38763
effects on growth of yeast, 18: 41086(R) (HW-80500(p.153-6))
effects on growth and development of *Atropa belladonna*, 19: 25866
effects on growth in cell cultures and microorganisms, review, 20: 3651
effects on growth of yeasts as function of inoculum age, 20: 1601
effects on growth of Lemna, 20: 22553
effects on helical stability of DNA in salmon sperm, 20: 35204
effects on hydrolysis of 4-methyl-1,3-dioxane and 1,3-dioxane, 19: 44011
effects on hypochromicity of synthetic polynucleotides, 20: 35204
effects on incorporation of phosphorus-32 into rat liver desoxyribonucleic acid, 17: 1224
effects on interferon production and titre of Japanese B encephalitis virus, mechanism of, 19: 29876
effects on isometric contraction of muscle, 16: 32754
effects on lipase activity, 20: 30995
effects on lipid composition of tissue culture cells, 18: 123
effects on luminescence of rare earth ions in aqueous solutions, 20: 26849
effects on macromolecule synthesis in developing sea urchin eggs, 19: 43709
effects on meiosis and mitosis in *Tetrahymena pyriformis*, 20: 8532
effects on meiosis in oocytes of starfish, effects of hydrostatic pressure on, 20: 30986
effects on metabolism in yeast, 17: 35319(R) (HW-76000(p.187-97))
effects on mice, morphological, 18: 15800
effects on mitosis in onion roots, 19: 21924
effects on mitosis in dividing sea urchin eggs, effects of pressure and temperature on, 20: 32917
effects on muscle relaxation in rabbits, 20: 18228
effects on Napier relaxation frequency of oxygen, 19: 40483
effects on neutral red uptake by frog sartorius muscle, 20: 5317
effects on oxidation of cholesterol and sodium octanoate by rat liver mitochondria, 20: 18217

effects on palladium–deuterium electrode potential, 19: 38608
effects on phage-resistant mutations in *E. coli*, 20: 31033(R) (NASA-CR-59196)
effects on plants, photochemical, 16: 14429
effects on plaque size of western equine encephalitis virus, 20: 39
effects on plaquing efficiency of polio virus at 40°C with limited thermal exposure ratios, 17: 10290
effects on poliovirus multiplication, 17: 23134
effects on potential and resistance of isolated frog skin, 18: 31107
effects on procaine activity in mice, 17: 33519
effects on products in hydrolysis of aluminum, thorium, and uranium carbides, 20: 40905
effects on properties of cytoplasm and gelatin, 18: 38764
effects on proton relaxation times of aqueous solutions of manganese ions, 19: 2350
effects on radio and thermal sensitivity of myosin, 16: 14509
effects on radioinduced fluorescence in terbium chelate systems in, 20: 18683
effects on rat brain, infrared spectra of, 19: 6978
effects on rate of hydrolysis of 2,2,2-trifluoro-*N*-methylacetanilide, 20: 43280
effects on rats, 18: 33250
effects on reactivity of large steam-cooled fast power reactors, 20: 38438 (ANL-7120, pp 815-25)
effects on replication of virus, 17: 31837
effects on reproduction of rats, 19: 22287(R) (UCRL-11948)
effects on sea urchin eggs, morphological, 17: 26975
effects on solvolysis of diethyl dicarbonate and ethyl chloroformate at 25°C, 20: 23065
effects on spectra of neodymium complexes, 20: 14560
effects on starving *Aerobacter aerogenes*, 18: 36939
effects on sterility of male mice, 18: 1325(R) (UCRL-10934)
effects on structure of polypeptides, 19: 33817
effects on thermal denaturation of desoxyribonucleic acid, 17: 4389
effects on thermal denaturation of algal chromoprotein phycocyanin, 18: 3445
effects on thermal stability of phycocyanin, 18: 38763
effects on thermal denaturation of DNA, 19: 12919(T)
effects on thermal stability of proteins, 19: 46318
effects on thermal fractionation of *E. coli* DNA-DNA hybrids, 20: 32896
effects on unfertilized sea urchin eggs, parthenogenic, 16: 28707
effects on wound healing in rats, 19: 19484
effects on yeast growth, 16: 7398
effects on yeast, metabolic, 17: 13917 (HW-SA-2570)
effects with growth regulators on peppermint, 19: 35920
electric conductivity of tetraalkylammonium halides in, at 25°C, 20: 7085
electric conductivity of ions in, at 25°C, 20: 14540
electric discharge in vapor of, stimulated infrared emission in, (E), 19: 9792
electron absorption and backscattering by, 18: 32773
electron capture by, swarm measurements of cross sections for dissociative, 18: 29768
electron capture in, 17: 39308(R) (ORNL-3492(p.134-43))
electron excitation of jets of, radicals from, 17: 34009
electron polarization in molecules of, effects of temperature on, 20: 29230
electron reactions with, neutron yield from, 18: 11934
enrichment, adaptability of packed columns for industrial, 16: 13499
enrichment by high-pressure exchange, effects of additives on, 16: 32017 (KFK-92)
enrichment, electrochemical process for, 17: 16493
enrichment using liquid ion exchangers, 18: 22404(P)
enrichment using zirconium phosphate ion exchangers, 18: 22405(P)
enthalpy at 350 to 460°C and 250 to 500 kg/cm², (E), 19: 22187(T)
enthalpy, measurements of excess in, 16: 14755
equation of state and maximum density, 16: 11673
equilibrium with light water, evaluation of constant for, 19: 19891
exchange reaction with *p*-xylene, catalytic effects of alumina–nickel, rhodium, and silver on, 18: 13822
exchange reactions with hetero- and polycyclic hydrocarbons, platinum-catalyzed, 16: 16344
exchange reactions with hydrocarbons, labeling in, 18: 13802
exchange reactions of deuterium with propene in, 18: 27369
exchange reactions with water, thermodynamic functions of, 18: 33567
exchange reactions with hydrogen in alkylaromatic hydrocarbons and toluic acid derivatives, nickel-catalyzed, 19: 38688
exponential void coefficient measurements for natural uranium tubes in, 16: 2399 (DP-643)
feasibility as moderator in light-water-cooled reactors, 18: 24882(R) (DP-905)
flow monitoring alarm and trip system for, 18: 36847 (AECL-1974)
flow of boiling, void fractions for, 17: 27532 (AE-106)
flow of, sieve tray testing in, 18: 13292(R) (SRO-98)
fluid flow of, design of loop to study two-phase, 20: 45854 (AE-238)
force constants and infrared spectrum of, calculation of, 18: 5277
gamma absorption doses in, 16: 16004
gamma reactions (γ,n) at 2.25 to 15 Mev, yields from, (T), 19: 34393(T)
gamma reactions (γ,n), with yields from, (E), 20: 26096 (TID-22889)
gamma reactions (γ,n), photoneutron production in, 16: 29823
handling and storage, 20: 7020
handling at SPERT II facility, 18: 40945 (IDO-16997)
hazards of tritium from, to skin of laboratory personnel, 20: 41185 (AECL-2594)
heat conductivity, 17: 23366
heat conductivity of gaseous, at 100 to 500°C, 17: 32076
heat of vaporization of, calculations of, 19: 28295
heat transfer by, in NPD reactor, fabrication and testing of system for, 19: 5485 (R63CAP-71)
hydration equilibria of aliphatic aldehydes in, 18: 6842
hydrogen bonding in, infrared spectral study of, 20: 5552
hydrogen exchange with indene, kinetics of triethylamine-catalyzed, 18: 13736
hydrogen isotope exchange with benzene and its derivatives, effects of nickel on, 17: 27384
hydrolysis in, metal ion catalyzed, 18: 13753
hydrolysis of procaine in, stability in, 19: 11102
infrared absorption by, temperature dependence, 18: 3731
ionization constant of, self-, 19: 34143(R) (NYO-3041-1)
ionization of, in mass spectrometry, formation of D_3O^+ in, 20: 45681
iron(III) molar extinction coefficients, 16: 16387
isotope effects in irradiated, 17: 35873
isotope effects on α-chymotrypsin-catalyzed hydrolysis, 16: 26999
isotope effects on physical properties of wheat gluten due to hydrogen bonding, 18: 23477
isotope effects on, review on, 19: 28432
isotope exchange reactions with benzene, π-complex substitution mechanisms in transition metal-catalyzed, 19: 4186
isotope exchange with aliphatic amines or dimethylhydrazine, 16: 6412
isotope exchange with anisole and xylene, effects of catalysts on, 17: 27387
isotope exchange with propene, effects of nickel on, 17: 27390
isotope exchange with cellulose and cellulose derivatives, 18: 27441
isotopic analysis, temperature-float method, 16: 8698
isotopic analysis by nuclear resonance, 16: 31548(T) (AEC-tr-5328)
isotopic analysis of, by infrared spectrometry, 20: 18590
isotopic exchange reactions with *p*-xylene, 17: 18067
isotopic exchange with active hydrogens in organic compounds, 19: 15368
isotopic exchange with fluorimide, 19: 40537
isotopic exchange with substituted benzenes, steric effect in platinum-catalyzed, 20: 45641
laser action in d-c discharge vapors of, continuous-wave submillimeter, (E), 20: 28047
leakage from mechanical pumps, 16: 20564 (DP-666)
light scattering by, Cabannes factor and Rayleigh ratio for, 20: 3941
loss during operation of HWCTR, 18: 15520(R) (DP-895)
loss from HBWR, Oct. 1964–Mar. 1965, 20: 5123(R) (HPR-61)
losses in Plutonium Recycle Test Reactor, 16: 26616 (HW-73735)
magnetic resonance of photolyzed single-crystal, 19: 46161(R) (ORNL-3832, pp 116-50)
management of, accounting systems at AECL for, 19: 47906 (AECL-2282)
mass spectra of ionized, in strong electrical fields, 20: 1829
measurement and status in HBWR, 20: 1466(R) (HPR-63)
micelle formation and hydrophobic bonding of sodium decyl and sodium dodecyl sulfates in, 20: 18687
mixing with normal water, thermodynamic functions of, 19: 865(R) (ORNL-3679(p.23-38))
molecular structure of, atomic displacements from anharmonic vibrations, 17: 31117
molecular structure, 18: 27396
molecular structure of, electron-diffraction studies of, 19: 11091
neutron absorption, dosages from, 16: 16004
neutron age in, moments calculations of, 16: 22977
neutron attenuation by boron-containing, 16: 24366
neutron capture gamma spectrum of, thermal, 17: 41873 (WASH-1044)
neutron coherent scattering at 0.04 to 0.1 ev, (E), 19: 33192(R) (GA-6096)
neutron cross sections at 1.44 ev (E), 19: 3288
neutron decay constants in, effects of temperature on thermal, 20: 8337
neutron decay constants in, pulsed, (T), 20: 9938 (BNL-9770)
neutron die-away, mean emission time, and spectra in borated, 17: 24369(R) (GA-3542)
neutron diffusion in, measurements by pulsed source method, 16: 739
neutron diffusion in, 16: 9641(R) (DP-685)
neutron diffusion coefficients in, at 20 to 220°C, 16: 24374
neutron diffusion length in, 16: 28018

neutron diffusion coefficients at 20 to 220°C, thermal, 17: 2212
neutron diffusion parameters, 17: 2219
neutron diffusion parameters in, thermal, 17: 15204 (BNL-719 (Vol.IV)(p.1186-1210))
neutron diffusion in, 17: 15193 (BNL-719(Vol.III)(p.879-99))
neutron diffusion parameters for, 17: 26067
neutron diffusion coefficients in, at 20 to 220°C, 17: 26415
neutron diffusion coefficient measurements in, corrections for, 17: 26416
neutron diffusion in, analysis by pulsed-source method, 17: 34870
neutron diffusion in, parameters for thermal, 18: 992
neutron diffusion in, at 10 to 50°C, parameters for, 18: 993
neutron diffusion parameters in, thermal, 18: 4519
neutron diffusion constant measurements in, 18: 37113 (A/CONF.28/P/763)
neutron diffusion constants of, scattering measurements on, 18: 40475 (JÜL-160-NP)
neutron diffusion parameters in, review of, 18: 40490
neutron diffusion parameters for, thermal (E/T), 19: 1520 (CRRP-1203)
neutron diffusion cooling coefficient and asymptotic spectrum temperature in (E/T), 19: 3206
neutron diffusion parameters of, thermal (E), 19: 3207
neutron diffusion in, time-dependent spectra for, 19: 23605
neutron diffusion parameters in, pulsed, (T), 19: 33216
neutron diffusion parameters at 25 to 250°C, (E), 19: 33224
neutron diffusion in, thermal parameters of, (E), 19: 35378(R) (EANDC(E)-57(U))
neutron diffusion parameters in, pulsed thermal, (E), 19: 42045(R) (MIT-2344-3, pp 55-108)
neutron diffusion parameters in, measurement using pulsed neutron techniques, 20: 2954
neutron diffusion coefficient in, containing voids, thermal, (E), 20: 2957
neutron diffusion in, thermal, (E/T), 20: 11931 (CONF-651101-53)
neutron diffusion constant of, pulsed-source technique for measuring, (E), 20: 14076
neutron diffusion length and temperature in boron-poisoned, 20: 34469 (DP-MS-66-30)
neutron diffusion length and temperature in boron-bearing, thermal, (E), 20: 34503
neutron energy spectra in, (T), 19: 47964
neutron flux distribution and leakage through perforated iron plates in, 19: 37774
neutron flux distributions around single uranium fuel rod in, (E/T), 19: 42047 (MIT-2344-3, pp 115-24)
neutron flux in laminates with iron, (E/T), 19: 21210
neutron flux trapping by, effects of water on thermal, 16: 33785
neutron incoherent scattering, model for thermal, 16: 24379
neutron inelastic scattering, 16: 1021 (IDO-16699)
neutron inelastic scattering by, temperature dependence of inelastic, 18: 38042 (A/CONF.28/P/673)
neutron inelastic scattering by, dynamic processes in slow, 20: 40338
neutron intermolecular scattering by, thermal, 17: 20965
neutron intramolecular scattering by, thermal, 17: 20964
neutron lifetimes in thermal system of, 18: 44715
neutron moderating properties in split-core pool reactors, 18: 4848 (EANDC(OR)-26U)
neutron moderating properties, in flux-trap reactors, 16: 31059
neutron moderation in, properties for, 18: 38044 (A/CONF.28/P/680)
neutron moderation by, at 77 and 300°K, (E), 20: 11944
neutron partial differential scattering cross sections for, reduced slow, 16: 28026 (IDO-16699(Rev.))
neutron penetration, calculations, 16: 3880(R) (ORNL-3193(p.299-304))
neutron reaction rates in, in ZEEP loop, 18: 7885 (AEEW-M-363)
neutron reactions with, neutron yield in, 18: 24625 (WASH-1046)
neutron reactions with, fluorine-17, fluorine-18, and nitrogen-13 production in, (E), 20: 45728
neutron resonance capture by uranium-238 in, 19: 29502 (CEA-R-2475)
neutron scattering at 0.03, 0.06, and 0.12 ev, space time correlation function for, 16: 7161
neutron scattering, spectral studies of water structural dynamics from, 16: 7163
neutron scattering, angular and energy distributions, 16: 7164
neutron scattering law, 16: 21331 (AERE-R-4019)
neutron scattering displacement cross sections, fast, 16: 22964 (CEA-2142)
neutron scattering at 0.0026 to 10.4 kev, spectra from, 16: 25586
neutron scattering in, diffusive atomic and vibratory motions from cold, 16: 32373
neutron scattering in, analysis, 16: 32374
neutron scattering at 22°C, 16: 32382
neutron scattering, thermal, 16: 12409
neutron scattering, thermal, 16: 13925 (AERE-R-3931)
neutron scattering by, thermal, 17: 15161 (BNL-719(Vol.I)(p.26-53))
neutron scattering law for, at 22 and 150°C, 18: 28528 (AERE-R-4582)
neutron scattering and thermalization by, calculations of, 18: 33010 (A/CONF.28/P/258)
neutron scattering model for (T), 19: 3510 (CEA-R-2473)
neutron scattering by poisoned, spectra of thermal (E), 19: 3202
neutron scattering model for, (E), 19: 5114(R) (GA-5486)
neutron scattering by, cold, (E), 19: 19077
neutron scattering by, molecular conglomerates in, 19: 21221
neutron scattering by, differential cross section of thermal, (E/T), 19: 27389 (GA-6295)
neutron scattering by, cross sections and kernels for thermal, (T), 19: 29169 (GA-6281)
neutron scattering by, differential cross sections for thermal, (E/T), 20: 4801(R) (GA-6634)
neutron scattering by, angular distributions and diffusion constants from thermal, (E), 20: 6271
neutron scattering at 0.06 to 10 ev, differential cross section for, 20: 2963
neutron scattering by, thermal, (T), 20: 19781 (JAERI-1095)
neutron scattering by, cross sections for slow, (E/T), 20: 19778(R) (GA-6824)
neutron scattering by, differential cross sections and corrections for thermal, (E), 20: 21939(R) (GA-6930)
neutron scattering model for, sensitivity to thermal reactor parameters, 20: 28714 (BNWL-SA-616)
neutron scattering by, model for calculating thermal, (T), 20: 42139 (IN-1020)
neutron scattering laws for, 20: 44587 (NP-16291)
neutron slowdown and thermalization in, time dependence of, (E), 20: 26068
neutron slowing-down spectra in, 16: 9411 (AAEC/E-78)
neutron slowing down in, Greuling-Goertzel approximation, 16: 19726 (TID-15645)
neutron slowing down process in, effect of chemical bonding on, 17: 15226
neutron slowing down times in, 17: 34829 (CONF-39-63)
neutron slowing down and thermalization in, time dependence of, (E/T), 20: 21936 (AE-216)
neutron spectra in, measurement of time dependence of, 18: 24571(R) (RPI-328-6)
neutron spectra in, time-dependent (E/T), 19: 3191(R) (RPI-328-16)
neutron spectra in poisoned, (E), 19: 5114(R) (GA-5486)
neutron spectra in borated, (E), 19: 8376(R) (GA-5176)
neutron spectra in, 19: 23209(R) (RPI-328-20)
neutron spectra in, comparison with scattering model, (E/T), 19: 27388 (GA-6291)
neutron spectra in, time-dependent, (E), 19: 29208
neutron spectra in boron- and cadmium-poisoned, thermal, (E/T), 19: 33231
neutron spectra in, analysis of time-dependent, 19: 37766 (RPI-328-23)
neutron spectra in poisoned, (E), 19: 41646
neutron spectra in, time-dependent, (T), 19: 47548(R) (TID-22141, pp 3-33)
neutron spectra in, pulsed-source measurement of time-dependent, (E/T), 20: 13736
neutron spectra in, (E/T), 20: 24312
neutron spectra in, time-dependent thermal, (T), 20: 28232 (AE-226)
neutron spectra in, time-dependent, (E/T), 20: 30324(R) (RPI-328-56, pp 52-93)
neutron spectra in, 20: 36428 (GA-7072)
neutron streaming in, in pipes, 17: 3803
neutron streaming in pipes, 17: 11588 (AE-98)
neutron streaming in ducts filled with, (E/T), 19: 14755
neutron thermalization, 16: 18449
neutron thermalization in, 18: 22848(R) (GA-4659)
neutron thermalization in, scattering-law parameters for (T), 19: 1518 (AE-154)
neutron thermalization spectra in, time-dependent, (E/T), 19: 31196(R) (RPI-328-35(p.1-34))
neutron thermalization in, time dependence of, (E), 19: 33226
neutron thermalization in, time-dependent, (T), 19: 33227
neutron thermalization in, integral, 19: 41640(R) (GA-6323)
neutron thermalization in, interference scattering effects on, (T), 19: 47559
neutron thermalization in, (E/T), 20: 8035 (GA-5798)
neutron thermalization in, integral, (E/T), 20: 19778(R) (GA-6824)
neutron thermalization in, (T), 20: 46562(R) (RPI-328-68, pp 84-144)
neutron time-dependent spectra in, 18: 36080(R) (RPI-328-8)
neutron transport length in, thermal, 18: 24625 (WASH-1046)
neutron transport in, fast-pulse measurement of, 18: 44972 (MIT-2344-1)
neutron transport in enriched lattices, thermal, (E/T), 19: 5433 (MITNE-33)
oxygen-17 spectra in enriched, effects of temperature on NMR, 20: 43171

(LA-DC-7394(Rev.))
oxygen-17 to oxygen-18 ratios in, neutron activation methods for measuring, 20: 45728
performance as moderator for critical experiments, (E), 19: 35706 (LA-3219)
performance as thermal columns in heavy-water reactors, (E), 19: 17358 (ANL-6915)
performance of particle-seeded, as rocket-reactor coolant, (E), 19: 24149 (NASA-CR-212)
photoneutron production in, by delayed gammas following uranium-235 irradiation, 16: 24495
piezo-optic coefficients, 20: 4484
potential energy functions for, determination from spectral data, 20: 31949
preparation, 16: 7816(T,P) (CEA-tr-X-282)
preparation, 19: 32665
preparation by GS process, economic aspects of, 18: 12261
preparation by isotopic exchange, 17: 11058
preparation by isotopic monothermic ammonia-hydrogen exchange process, 19: 18376(P)
preparation from ammonia by isotope exchange with hydrogen, economic aspects for coal fields from, 18: 32003
preparation of, evaluation of catalysts for isotope-exchange, 17: 27388
preparation of, sieve tests in plants for, 17: 17546(R) (SRO-80)
preparation of, testing of sieve trays used in, 18: 23137(R) (DPST-64-83-3)
preparation, summary of methods for, 19: 2699
processing by ion exchange, dilution on, 18: 17777 (NP-13766(p.119-33))
processing of moderator, 18: 38384 (A/CONF.28/P/29)
processing of, distillation column for, 18: 17775 (NP-13766(p.85-93))
processing of, for nuclear power plants, 20: 8421
processing reactor, review on, 18: 17776 (NP-13766(p.95-118))
production, 16: 10397(T) (JPRS-12674)
production, 20: 8813
production, 18: 37585 (A/CONF.28/P/496)
production and market status, 16: 20936
production and market status, 16: 27552(T) (AEC-tr-5200)
production and properties for reactors, 18: 15452
production and treatment for reactors, 17: 1150 (JAERI-1024)
production at different degrees of purity, process and apparatus, 16: 3371(T,P) (CEA-tr-X-396)
production at natural gas fertilizer factory, methods for, 20: 25464 (AECD/CH-8)
production at Savannah GS plants, sieve tray capacity for, 18: 28916(R) (DPST-64-83-4)
production at Savannah River, 19: 22845 (ORNL-TM-1047(p.30-1))
production by ammonia-hydrogen exchange, 17: 1805(P)
production by ammonia–hydrogen deuterium exchange, factors affecting, 19: 11645
production by cascade system, optimum, 16: 2105
production by cascade electrolysis, 17: 11056(T) (CEA-tr-A-1159)
production by catalytic hydrogenation of carbon monoxide, 16: 17957(T)
production by catalytic isotope exchange with hydrogen, 16: 20927(P)
production by catalytic isotope exchange between hydrogen and water, 17: 25675(P)
production by catalytic exchange between steam and hydrogen in the presence of fissionable material, 20: 1884(P)
production by distillation at low pressure, 19: 11651
production by dual temperature process, determination of variables, 16: 453(T) (CEA-tr-X-410)
production by dual-temperature exchange, control of, 17: 4873
production by dual temperature process, development of materials for plants, 17: 8717
production by dual-temperature exchange reactions, 19: 24910(P)
production by electrolysis of water, 17: 29241(P)
production by exchange reaction and electrolysis, 16: 454(T) (CEA-tr-X-411)
production by exchange between ammonia and hydrogen, 18: 37577 (A/CONF.28/P/91)
production by exchange between ammonia and hydrogen, 19: 32049
production by high pressure exchange, construction and operation of pilot plant for, 16: 32016 (KFK-90)
production by hydrogen sulfide exchange, economics, 16: 452 (TID-13964)
production by hydrogenation of carbon monoxide, process for, 17: 30898(P)
production by hydrogen distillation, method for, 17: 34312
production by hydrogen distillation at low temperature, 18: 41569
production by isotope exchange, 16: 12839
production by isotope exchange with hydrogen sulfide, heat exchange in, 17: 1802(P)
production by isotopic exchange of electrolytic hydrogen gas scrubbing in, 18: 18259 (NP-13766(p.37-52))
production by isotopic exchange between ammonia and water, 18: 44014
production by isotopic exchange between hydrogen sulfide and water, gas cooling in, 19: 36897(P)
production by isotopic exchange between ammonia and hydrogen, 19: 40942(P)
production by nitric acid–water countercurrent distillation, 18: 16405(P)
production by platinum-catalyzed isotopic exchange, Spanish Sabinanigo plant for, 19: 26740
production by rectification, theoretical considerations in, 18: 32004
production by the electrolytic method, 16: 20926
production, combination of fractional distillation and electrolysis methods, 16: 3369(T,P) (CEA-tr-X-281)
production economics, 17: 2601
production, electrolytic concentration method and cell for, 16: 19230
production, flow diagrams for large conceptual plant, 16: 22510 (TID-15733)
production for reactors, analysis of demands and review of methods, 16: 12005
production from concentrated saline solutions, 18: 22406(P)
production in ammonia synthesis, 16: 13500(P)
production in Argentina, design and cost analysis for H_2S–H_2O exchange process for, 18: 4143 (NP-13340)
production in GS plant, evaluation of sieve tray capacity in, 18: 17998(R) (DPST-64-83-2)
production in GS plant, evaluation of sieve tray capacity in, 18: 40751(R) (DPST-64-83-7)
production in India, economics of, 18: 37589 (A/CONF.28/P/753)
production methods, survey, 16: 16036
production methods and uses of, review of, 17: 23806
production methods in Japan, 18: 18262
production of, by dual-temperature process involving hydrogen and water, 17: 14707(T) (CEA-tr-A-1164)
production of, economics and performance of processes for, 17: 32136
production of, electrochemical method for, 17: 1804(P)
production of, procedure and apparatus for continuous, 17: 25667(T) (CEA-tr-A-1231)
production of, abstracts of patents on, 20: 1951 (AECL-2279)
production of, analytical control of installations for, 20: 9367
production of, by GS process, performance testing of sieve trays for, 20: 37160 (DP-1025)
production of, design of rectification plants for, 19: 26744
production of, distillation column for, 18: 18261 (NP-13766(p.77-83))
production of, evaluation of methods for, 18: 10440
production of, for Czechoslovakian power reactors, economics of, 20: 33761
production of, improvements in, 18: 18257 (NP-13766(p.7-26))
production of, methods for, 18: 39398
production of, optimization of electrolyzer-isotope exchanger system for, 18: 18260 (NP-13766(p.53-76))
production of, pilot plant for electrolytic, 19: 44576
production of, process for, 20: 29611(P)
production of, sieve tray testing for, 18: 21633(R) (DPST-64-83-1)
production of, Spanish Sabinanigo plant for, 18: 18258 (NP-13766 (p.27-36))
production, operation of water rectification tower for, 16: 27539
production processes, review, 16: 17956
production, survey of industrial methods and plants, 16: 15094
production technology of, review, 18: 22396
production, bibliography on, 18: 34008 (TID-3091(Suppl.1))
properties as catalyst for vibrational energy transfer, 17: 3644
properties as heavy water-moderated power reactor coolant, 18: 43024 (DPW-64-135)
properties as moderator in research reactors, 18: 4857
properties as moderator in subcritical assemblies, 18: 28984
properties as moderator in mixed-fuel lattices, 18: 28986
properties as moderator in externally heated critical lattices, 18: 28987
properties as reactor moderator, 16: 18050
properties as reactor coolant, 16: 23830 (BNL-5377)
properties as reactor material, 18: 12665
properties as reactor moderator, 18: 15577
properties review, physical and thermodynamic, 16: 25307 (CEA-Bib-15)
protective effects against mousepox in mice, 17: 10285
proton attenuation at 18 to 550 kev, (T), 19: 27704 (PAN-556/IA)
proton exchange with ribonuclease, nuclear magnetic resonance spectra of, 17: 6073
proton motions in, fluctuation of, 18: 27440
proton reactions (p,n) at 6 Bev, 18: 21698(R) (ANL-6860)
proton reactions at 160 Mev, secondary-nucleon production in, 18: 7693(R) (ORNL-3499(Vol.II)(p.73-84))
proton reactions at 160 Mev, neutron and proton spectra for, 18: 7694(R) (ORNL-3499(Vol.II)(p.89-93))
proton reactions at 450 Mev with, neutrons from, 18: 18933
proton reactions at 450 Mev and 6 Bev, neutron yields in, (E),

19: 31215(R) (ANL-7010(p.1-19))
proton reactions with nuclei in, cross sections at 160 Mev, (E), 19: 14536 (ORNL-P-848)
proton transfer reactions in, product and rate isotope effects in, 19: 389
purification by ion exchange, efficiency of, 19: 11287
purification by ion exchange, efficiency of, 20: 35025 (NP-16014)
purification for reactors, 18: 37263 (A/CONF.28/P/433)
purification in Polish EVA reactor, system for, 16: 34120
purification in production reactors by ion exchange, 16: 16335(R) (DP-678)
purification of, by miniature ion exchange columns, 17: 19556(R) (DP-806)
purification of oil-contaminated, by passage through column of activated charcoal, 19: 42603
purification of reactor coolant and moderator, 17: 14235
purity control by conductivity measurements, 16: 6392(T) (CEA-tr-X-405)
radiation effects on deuterium exchange with benzene, cyclohexane, and *n*-hexane, gamma, 20: 36866
radioactivity, in NRX reactor, 17: 10126 (CRDC-1126)
radioinduced thermoluminescence of, 19: 26418
radioinduced yields of positive oxygen ions in, electron, 19: 40581
radiolysis, electron spin resonance of free radicals produced in gamma, 16: 7600
radiolysis, electron paramagnetic resonance of free radicals produced by beta and gamma, 16: 11711
radiolysis, free radicals produced in, 16: 8783
radiolysis G values, 16: 20514
radiolysis in boiling reactors, effects of ammonia and deuterium on, 20: 6638
radiolysis in Halden Boiling Reactor, 18: 38479 (A/CONF.28/P/595)
radiolysis in presence of aluminum oxide–platinum catalyst, rate and yields of, 19: 17977
radiolysis of frozen potassium hydroxide solutions in, EPR of radicals from, 19: 7549
radiolysis of, mechanism of alpha and beta, 16: 31665
radiolysis of sodium formate solutions, deuterium isotope effects, 16: 33030
radiolysis of, acidity effects on yields in gamma, 19: 38710
radiolysis of, isotope effects in, 20: 8981 (CEA-R-2794)
radiolysis of, processes in in-pile, 18: 38243 (A/CONF.28/P/20)
radiolysis of, yields from, 19: 30255
radiosensitivity effects on *E. coli*, 16: 69
reactions of deuterium atoms from, in radiolysis of organic solutes, 16: 17740
reactions with acetylene, equilibrium in exchange, 18: 39209
reactions with diborane, isotopic effects in, 20: 306
reactions with dicarboxylic acids, kinetics of proton abstraction in, 20: 350
reactions with nitriles, 16: 11594
reactions with water at 25°C, equilibrium constant value for, 18: 39218
reactions with water, mass spectrometric determination of equilibrium constant for disproportionation, 20: 38875 (UCRL-14703-T)
reactor criticality effects in JRR-2, 18: 44978
reconcentration of downgraded, performance criterion for process unit, 16: 27533 (DP-652)
removal of, from heavy water reactors, 17: 7588(P)
research on uranium lattices moderated by, experimental and theoretical, 17: 17419(R) (MITNE-26)
rotation of molecule of, in solid argon, infrared spectroscopic evidence for, 17: 8042
self-diffusion effects of, on water at 25°C, 17: 10613
separation from air at reactor installations, 19: 38907
separation from fission products in slurry type reactor by distillation, 16: 25496(P)
separation from light water by distillation, efficiency of Stedman stainless steel packings for, 19: 20068
separation from reactor degradation products, design and operation of plants for, 19: 8573
separation from sea water, MHD method for, 18: 22192(P)
separation from water, electrolytic, 16: 3376(P)
separation from water, U. S. facilities for, 18: 31996 (A/CONF.28/P/290)
separation from water, technology of, 18: 36809(R) (SRO-105)
separation from water, film-distillation, 18: 37586 (A/CONF.28/P/557)
separation from water by freezing, 19: 4571(T) (MLM-1206(Tr))
separation of cobalt-60 from, from RA reactor, 20: 23389
shielding effects of, in reactors, 18: 28939
sodium compound dissolution in, heats of, 20: 1825
solvent effects on keto-enol interconversion of 2-acetylcyclohexanone, kinetics, 16: 11614
solvent effects on uv absorption spectra of anions, 18: 43500
solvent properties for cadmium and copper dioxalato complexes, 16: 10024
solvent properties for methyl halides, initial state and transition state isotope effects in, 16: 11617
solvent properties for helium at high pressures and 50 to 280°C, 16: 25303 (BMI-1587)
solvent properties for helium at 50 to 280°C, 17: 3378(R) (BMI-1583(Del.))
solvent properties in chemical reactions, isotope effects on, 17: 5063
solvent properties for silver bromate, 17: 28882
solvent properties for copper(II) iodate, 17: 28883
solvent properties for silver bromate, electrolyte effects on, 17: 28884
solvent properties for silver sulfate, 18: 1614(R) (ORNL-3488(p.65-90))
solvent properties for hydrocarbons, at 50 to 220°C, 18: 3777
solvent properties for alkyl halides, role of initial state structure in kinetic isotope effects in, 19: 13294
solvent properties for alcohols, amino acids and hydrocarbons, 19: 46318
solvent properties for iodine at 5 to 50°C, 20: 5539
solvent properties for benzenesulfonic acid, isotope effects on, 20: 18643
solvent properties for azo dyes, isotope effects on role of intramolecular hydrogen bonds in, 20: 43287
solvolysis of cobalt(III) complexes in, 19: 17892
sonolysis of, hydrogen isotope effects in, 18: 12067
sorption by synthetic zeolites, mechanism of, 19: 13330
sorption from intestine of rat, effects of serotonin on, 19: 5608
sorption in rat ileum, factors affecting, 20: 22568
sorption of vapor by lysozyme at 17 to 57°C, exchange effects in, 16: 460
specific volume at 250 to 500°C to 100 to 500 kg/cm², 16: 26967(T) (CEA-tr-R-1579)
specific volume measurements at 275 to 425°C and 50 to 34 kg/cm², 17: 32060
spectra at −20 to 250°C, near-infrared, 19: 13279 (ORNL-P-925)
spectra at 1220 to 1240 Å, absorption, 17: 12241
spectra at 20°C, Raman, 16: 9295(T) (CEA-tr-R-1408)
spectra, effects of lithium and potassium halides on Raman, 16: 30401
spectra, hyperfine structure of microwave rotational, 16: 27780
spectra in near-infrared at -20 to 250°C, absorption, 19: 46237(R) (ORNL-3832, pp 76-99)
spectra of adenosine triphosphate complexes in, effects of pD on infrared, 19: 5936
spectra of helix-coil transitions of DNA in, infrared, 20: 35193
spectra of, visible absorption, 18: 3791
spectra of, for infrared, 20: 1877
spectra of, in vacuum ultraviolet region, vibrational analysis of, 19: 26331
spectra of, infrared absorption, 18: 13748
spectra of, intensities of stretching vibrations in infrared, 19: 26361
spectra of, intensity measurements of absorption bands in, 20: 43178 (NRL-6394)
spectra of, molar extinction coefficients for infrared-absorption, 20: 25092
spectra of, uv absorption, 20: 10823
spectra of, vibrational, 18: 12100(T)
sporulation effects on *Aspergillus niger* fungi heated in, alteration of, 16: 17369
structure from 4 to 100°C, two-state theory of, 20: 44032
structure of, spectral study of, 18: 25369
thermal capacity at constant volume near critical point, 20: 7069
thermal capacity in supercritical region, 17: 25172
thermal capacity of supercritical, 17: 23365
thermal capacity of, liquid and vapor, 17: 33935
thermal conductivity at 10 to 80°C, 16: 28931(T) (AECL-1581)
thermal conductivity at 10 to 60°C, 16: 28932(T) (AECL-1582)
thermal conductivity of gaseous, at 380 to 525°K, 18: 16020
thermal conductivity of, at 40°C to critical temperature, 19: 42469
thermal expansion of oxygen-18-labeled, 17: 18069
thermodynamic and transport properties, of compressed and saturated, 16: 7520 (CVNA-54(Rev.1))
thermodynamic and transport properties of, significant-structure theory for, 20: 12858
thermodynamic properties, 17: 1434
thermodynamic properties of, tables of, 17: 12224 (AECL-1673)
thermodynamic properties of, computer program for calculating, 17: 32038 (CVNA-129)
thermodynamic properties of, 19: 44008
thermodynamic properties of electrolytes in, 20: 10847
thermodynamic properties of, (E), 20: 30182
thermodynamic similarity with light water, 17: 6059(T) (CEA-tr-R-1541)
transfer rate across isolated pericardium, 16: 31456
transfer to light water by hydrated solutions of electrolytes, 17: 6096
transport across dog intestinal mucosa membranes, tracer study of, 18: 31091

tritium content build-up with time in PRTR, 16: 33983 (HW-61151)
ultrasonic attenuation and relaxation time in vapor, 20: 29172
uranyl citrate complexes in, NMR spectra of, 19: 38623
use as reflector for Polish high-flux research reactor, 20: 47071
use in Plutonium Recycle Critical Facility, operating experience from, 18: 45023 (HW-81473)
use in preparation of deutero-hydrocarbons, 20: 43409(P)
use in radial reflector of Polish high-flux research reactor, 20: 32871
use in reactors, physico-chemical problems of, 19: 24020
use in reactors, problems in, 20: 5143
use in tumor therapy, potential of, 18: 23209
uses in studies of free radical formation from potassium nitroform, 19: 7524
vapor pressure of, measurement of, 18: 25436
vapor pressure of, hydrogen isotope effects on, 18: 31425 (LADC-5905)
vapor pressure of, saturated, 18: 35570
vapor pressure of, at −40 to 0°C, 20: 29149
vaporization phenomena, 16: 33126 (UNC-5021)
vaporization rate, 19: 32132
vibrational potential function of bent molecules of, third-order, 20: 14559
vibrational properties and spectra, 16: 14740
vibrational spectra in salt hydrates, 16: 6424
vibratory motions in, cold neutron scattering study of, 17: 15245
viscosity of, temperature dependence of, 18: 37124
void volume fraction in boiling, measurement by (γ,n) reaction, 17: 264 (AE-83)
x ray scattering by, structure analysis from, (E/T), 20: 35395 (ORNL-3960)
x-ray scattering at 4 to 200°C, diffraction studies on, 20: 43180 (ORNL-3997)
yields in gamma radiolysis of gaseous deuterium–oxygen mixtures, 20: 12881 (AD-626609)
$AgClO_4$–D_2O, radioinduced free silver atoms in solid solutions of, EPR of x, (E), 20: 15975(T)
AgF–D_2O, radioinduced free silver atoms in solid solutions of, EPR of x, (E), 20: 15975(T)
$AgNO_3$–D_2O, radioinduced free silver atoms in solid solutions of, EPR of x, (E), 20: 15975(T)
Ag_2SO_4–D_2O, radioinduced free silver atoms in solid solutions of, EPR of x, (E), 20: 15975(T)
air–Al–D_2O, neutron diffusion in air-filled aluminum-tube lattices in heavy water, (E/T), 20: 13705(R) (MIT-2344-4, pp 135-44)
alcohol–O_2O, NMR spectra of, 19: 22265
B–D_2O, neutron spectra in, 17: 39943(R) (GA-4176)
B–D_2O, neutron spectra in, tabulation, (E/T), 19: 16814 (AERE-R-4776)
$Ca(NO_3)_2$–D_2O, phase diagram of, 20: 38994(R) (AE-232)
$(C_2H_5)_3N$–H_2O–D_2O, isotope separation and solubility in, 17: 1793
CO_2–D_2O, oxygen-17 and oxygen-18 equilibrium distribution in, 19: 44007
CO_2–D_2O, oxygen-18 equilibrium distribution in, 20: 26790
CuO–NiO–SO_3–UO_3–D_2O, critical phenomena and liquid-liquid immiscibility at 260 to 410°C, 17: 33922
CuO–NiO–SO_3–UO_3–water-d_2, liquid-liquid immiscibility and phase studies of, 17: 25067(R) (ORNL-3417(p.77-98))
CuO–SO_3–D_2O, liquid immiscibility and critical phenomena at 320 to 430°C, 17: 8067
CuO–SO_3–UO_3–D_2O, critical phenomena and liquid-liquid immiscibility at 260 to 410°C, 17: 33922
CuO–SO_3–UO_3–water-d_2, liquid-liquid immiscibility and phase studies of, 17: 25067(R) (ORNL-3417(p.77-98))
$CuSO_4$–D_2SO_4–UO_2SO_4–H_2O–D_2O, spectrophotometry of reactor fuel solutions of, 20: 20600
dioxane–D_2O, dielectric properties of, 18: 19957
dioxane–D_2O, isotope effects on dissociation of acetic acid and water in, 18: 39240
D–O–D_2O, detonation properties, 16: 18874
D_2O–H_2O, analysis of, 17: 2729
D_2O–H_2O, neutron diffusion in, 17: 3792
D_2O–U, neutron multiplication in, 17: 3790
D_2O–U, neutron spectra in, calculation by Wilkins' theory, 17: 790
ethanol–water-d_2, deuterium exchange with hydrogen in phenylphosphonous acid in, 17: 40839
Fe–D_2O, fast neutron slowing-down in laminar, (E), 19: 29457
Fe–D_2O, neutron energy spectra in laminated, variations in, (E/T), 19: 47561
Fe–D_2O, neutron flux determinations in laminations of, 18: 28908
Fe–D_2O, neutron flux distributions in, 18: 42874
Fe–D_2O, neutron fluxes and leakage through perforated laminates of, (E/T), 20: 4800 (AE-198)
Fe–D_2O, neutron spectra in laminated, fast, (E/T), 20: 1304 (AE-196)
Fe–D_2O, neutron transmission through ducts in laminar, (T), 19: 12723 (AE-166)
Fe–D_2O, performance as reactor shielding, (E/T), 19: 14755
H_2O–D_2O, acid-base equilibria in, 19: 34143(R) (NYO-3041-1)
H_2O–D_2O, analysis for deuterium and hydrogen, 17: 10240(R) (NP-12208)
H_2O–D_2O, analysis, infrared interference method for isotopic, 18: 33460 (CEA-R-2440)
H_2O–D_2O, boiling temperature and vapor pressure of, 20: 38921
H_2O–D_2O, dissociation constants of nitrophenol, dinitrophenol, and imidazole in, 19: 34143(R) (NYO-3041-1)
H_2O–D_2O, effects on reactor fuel burnup, 18: 30972 (BLG-222)
H_2O–D_2O, ionic product, 17: 27379
H_2O–D_2O, ionization of ammonium ion, chloroacetic acid, and hydrazoic acid in, 18: 12091
H_2O–D_2O, neutron diffusion parameter in, (E), 19: 35351 (TID-21851)
H_2O–D_2O, neutron diffusion parameters for cylinders of, 20: 2951
H_2O–D_2O, neutron diffusion parameters in, thermal, (E), 20: 40061
H_2O–D_2O, neutron spectra in, (E/T), 20: 24312
H_2O–D_2O, properties as reactor moderator, 18: 28921(R) (TID-20649)
H_2O–D_2O, proton magnetic resonance shifts in, 17: 11342
H_2O–D_2O, radiation effects on, origin of isotope effects on, 19: 22333
H_2O–D_2O, radiolysis of, yields from, 19: 30255
H_2O–D_2O, radiolysis of, isotope effects in hydrogen production in gamma, 20: 38938 (IA-1074)
H_2O–D_2O, solvent isotope effects in, 18: 39239
H_2O–D_2O, solvent properties for argon, 20: 40897
H_2O–D_2O, spectra of solutions in, effects of solute on near-infrared, 20: 45643
H_2O–D_2O, thermal conductivity at 380 to 525°K, 18: 16020
H_2O–D_2O, thermal conductivity, 19: 7410
H_2O–D_2O, use as research reactor moderator, 19: 24189(P)
H_2O–D_2O, use as research reactor moderator, 20: 24805(P)
H_2O–D_2O, use of field ion-mass spectra for determining hydrogen/deuterium ratio in, 19: 30135
H_2O–D_2O, vapor pressure equilibria in, 18: 15974
H_2O–D_2O, vapor pressure of saturated salt solutions of, 20: 38994(R) (AE-232)
H_2O–HDO–D_2O, molecular motion in, proton spin-lattice relaxation study of, (E), 20: 34097
H_2O–HDO–D_2O, spectra of, infrared absorption, 18: 13748
K_2CO_3–D_2O, phase diagram of, 20: 38994(R) (AE-232)
$LiNO_3$–D_2O, phase diagram of, 20: 38994(R) (AE-232)
Li_2O–SO_3–UO_3–D_2O, critical phenomena and liquid-liquid immiscibility at 300 to 410°C in, 18: 12085
Li_2O–SO_3–UO_3–D_2O, critical phenomena and liquid-liquid immiscibility in, 18: 22014(R) (ORNL-3591(p.84-101))
Li_2SO_4–H_2SO_4–water-d_2, critical phenomena and solubilities of, 17: 25067(R) (ORNL-3417(p.77-98))
Li_2SO_4–SO_3–D_2O, critical phenomena, 17: 25207
Li_2SO_4–water-d_2, critical phenomena and solubilities of, 17: 25067(R) (ORNL-3417(p.77-98))
Na_2CO_3–D_2O, phase diagram of, 20: 38994(R) (AE-232)
NiO–SO_3–UO_3–D_2O, critical phenomena and liquid-liquid immiscibility at 260 to 410°C, 17: 33922
NiO–SO_3–UO_3–water-d_2, liquid-liquid immiscibility and phase studies of, 17: 25067(R) (ORNL-3417(p.77-98))
phenol-d–water-d_2, vapor pressure, 18: 16066 (NP-13736)
propane–D_2O, radiolysis of, neutralization of hydronium ions in gamma, 20: 33363
SO_3–UO_3–D_2O, liquid immiscibility and critical phenomena at 280 to 410°C, 17: 8067
steam–water-d_2, electric conductivity of, impedance void meter for (E), 19: 3641 (HPR-35(Vol.I)(Sect.9))
ThO_2–water-d_2, exponential experiments, 16: 13859
ThO_2–water-d_2, neutron age in, 16: 734
ThO_2–water-d_2, neutron age in, 16: 1232(R) (BAW-1221)
ThO_2–water-d_2, neutron age in, 16: 6096 (BAW-1234)
trimethylamine–H_2O–D_2O, deuterium isotope effects in, 18: 8391
U–D_2O, buckling for natural uranium rods in heavy water, comparison with exponential piles, 16: 758
U–D_2O, buckling in natural uranium rod lattices, 16: 12683
U–D_2O, buckling in natural uranium rod lattices, 16: 12684
U–D_2O, buckling in subcritical two-zone, 16: 1207
U–D_2O, calculation of fast fission factor for, 20: 30859
U–D_2O, critical experiments on Ispra-1, 16: 9693 (CNEN-100)
U–D_2O, critical level in, pulsed-neutron determination of, 18: 21595 (CEA-R-2376)
U–D_2O, criticality studies, 16: 24355
U–D_2O, criticality studies of 3-wt.% uranium-235-enriched, 16: 8093 (DP-644)
U–D_2O, fast fission effects in subcritical, 16: 15526 (NYO-9661)
U–D_2O, gamma measurements in lattices of, 19: 29475
U–D_2O, neutron absorption in, pulsed-neutron measurement of, 18: 42950
U–D_2O, neutron age and slowing-down flux at indium resonance, from line

uranium source, 16: 12415
U–D_2O, neutron buckling measurements in, 16: 4678 (DP-640)
U–D_2O, neutron buckling in, 17: 35086 (DP-832)
U–D_2O, neutron buckling in, 18: 3117
U–D_2O, neutron buckling in lattices of, 18: 13236 (EIR-57)
U–D_2O, neutron buckling and flux distributions in lattices of, (E), 19: 42049(R) (MIT-2344-3, pp 155-64)
U–D_2O, neutron capture and fast fission, 16: 24429
U–D_2O, neutron cadmium-ratio for, 17: 26035
U–D_2O, neutron decay constants in enriched lattices of, pulsed, 19: 42045(R) (MIT-2344-3, pp 55-108)
U–D_2O, neutron fast-fission factor for, 17: 26017
U–D_2O, neutron fission of uranium-235 and -238 in, ratio of fast, (E), 20: 1147 (CRRP-1220)
U–D_2O, neutron flux distributions in, 16: 24430
U–D_2O, neutron flux distribution in, 18: 33025
U–D_2O, neutron lattice parameters in two-region assemblies of, (E), 19: 42048 (MIT-2344-3, pp 125-36)
U–D_2O, neutron migration anisotropy in void-containing, 17: 26059
U–D_2O, neutron multiplication in, effects of reflectors and voids on, 16: 24415
U–D_2O, neutron multiplication in poisoned lattices of, 19: 42046(R) (MIT-2344-3, pp 109-14)
U–D_2O, neutron parameters of slightly enriched lattices of, 18: 44972 (MIT-2344-1)
U–D_2O, neutron physics of, 17: 35087 (DP-833)
U–D_2O, neutron spectra in lattice cells of, 18: 3092 (AE-123)
U–D_2O, nuclear parameters of rod lattices of, 18: 7893 (DP-777)
U–D_2O, optimization of spacing in critical assemblies, 16: 11172
U–D_2O, parameters for natural uranium rod lattices in heavy water, 16: 757
U–D_2O, physics calculations for organic cooled lattices of, 18: 21596 (EUR-597.e)
U–D_2O, physics of partially enriched lattices of, 18: 42923(R) (MITNE-46)
U–D_2O, space-dependent neutron spectra in lattices of, 19: 29568
UO_2–D_2O, buckling measurements on 19-rod clusters, 16: 15766 (AE-66)
UO_2–D_2O, exponential experiments, 16: 13859
UO_2–D_2O, neutron buckling and void effects in, 16: 24414
UO_2–D_2O, neutron buckling in, 19: 9641(R) (DP-685)
UO_2–D_2O, neutron buckling in, 16: 34008
UO_2–D_2O, neutron buckling in, 18: 3118
UO_2–D_2O, neutron buckling in lattices of, 18: 36777 (DP-873)
UO_2–D_2O, neutron buckling and diffusion coefficients in lattices of, 20: 46993 (DP-1054)
UO_2–D_2O, neutron multiplication factor for, 16: 24427
UO_2–D_2O, neutron spectra, 18: 40783 (KR-87)
UO_2–D_2O, reactivity, 16: 32556
UO_2–H_2O, criticality studies, 18: 3093 (APED-4236)
UO_2–H_2O–D_2O, criticality and reactivity of, 18: 3169 (BAW-1274)
UO_2–H_2O–D_2O, nuclear properties of, 17: 29706(R) (BAW-1271)
$UO_2(NO_3)_2$–D_2O, properties as reactor fuel, 17: 5605(P)
UO_2SO_4–D_2O, critical experiments on enriched, 17: 15431
UO_2SO_4–D_2O, criticality studies of enriched, 18: 38344 (A/CONF.28/P/845)
UO_2SO_4–D_2O, properties as reactor fuel, 16: 18634
1-butanol–D_2O, nuclear magnetic resonance spectra, 20: 26824
2-butanol–D_2O, nuclear magnetic resonance spectra, 20: 26824
2-methyl-1-propanol–D_2O, nuclear magnetic resonance spectra, 20: 26824
2-methyl-2-propanol–D_2O, nuclear magnetic resonance spectra, 20: 26824

WATER-*d₂*
spectra of, vibrational, 18: 12100(T)
uptake and transport by onion roots, 18: 11607

WATER-*t*
analysis for tritium, development of liquid scintillation detector for, 16: 16093
analysis for tritium, correction for, 18: 25309
analysis for tritium, design of internal gas counter for, 18: 37088
analysis for tritium using internal gas counter, method for, 18: 37089
content in atmosphere, 20: 37028
content in southern hemisphere precipitation from thermonuclear explosions, 20: 27164
conversion into tritiated butane, 16: 8787
counting standards for, recalibration of NBS, 18: 30070
determination by scintillation, estimation of total water content in rats by, 19: 26236
determination in blood plasma, radiometric, 18: 9999
determination in soils, liquid scintillation counting method for, 18: 23419
determination in urine by scintillation counting, 16: 23642 (UCLA-504)
determination of, in urine, rapid radiochemical method for, 17: 35338(R) (UCLA-515(p.33-46))
diffusion in soils, method for measurement of, 17: 39281
diffusion in water at 25°C, 17: 28881
diffusion through dry-box rubber gloves, 18: 5546 (LAMS-2962)
distribution and expiration of injected, 16: 9823
distribution in plants, 19: 31740
distribution in plants, 19: 31741
effects on chromosome aberrations in root-tip meristems of *Allium cepa*, 19: 12946
effects on growth of bacteriophage on *Escherichia coli*, 19: 29973
effects on HeLa cells, 18: 25156
effects on *Hemophilus influenzae*, 16: 1307(R) (LAMS-2627(p.82-93))
effects on postnatal development of rat progeny, 19: 17579
effects on protein synthesis by HeLa cells in culture, 19: 25952
measurement in air, method for, 20: 25411
metabolism in man, 19: 7206(R) (ORNL-3697(p.173-7))
production in heavy water reactors, hazards from, 20: 23357 (CONF-640413, pp 34-9)
properties review, physical and thermodynamic, 16: 25307 (CEA-Bib-15)
radioinduced tritium exchange with benzene and toluene, 20: 36868
reaction with hydrocarbons to produce radioactive hydrocarbons, 20: 5593(P)
reactions with n-butylmagnesium bromide, production of tritiobutane by, 17: 8176
sorption by burned and normal skin, 20: 14255
sorption from rat colon, effects of serotonin on, tracer study of, 20: 32912
specific activity of, use of heated ionization chamber for measurement of, 19: 523
spectra of, vibrational, 18: 12100(T)
toxic effects of, in rabbits, 19: 40337
toxic effects of, pathology and treatment in rabbits, 19: 40340
tritiation effects on benzene and pyridine derivatives in ammonium chloride, 17: 32142
use as tracer for water flow measurements in oil fields, 16: 16074
uses in tracing ground waters, 19: 22581
vapor pressure of, measurement of, 18: 25436
vaporous exchange with rain water, calculation of, 17: 34140
volatility in light water solutions, 19: 15471
yields in oxidation of tritiated aldoses by iodine, isotope effects in, 18: 5359
methane–HTO, tritium exchange with hydrogen in, 20: 23236(R) (ORNL-TM-1496)

WATER-t_2
content in atmosphere, 20: 37028
density at 5 to 54°C, 18: 8366
deposition at Chalk River in snow, 16: 20858 (AECL-1518)
determination in reactor coolant gas, 17: 33797 (PG-Report-469)
determination in reactor coolant gas, 19: 24404 (PG-Report-469(Rev.))
diffusion through plastic films, measurement of, 17: 20345 (DP-792)
distribution in embryonate eggs, 16: 1467(R) (TID-14093)
effects of environmental, on guppies, 19: 33(R) (NYO-3039-1)
effects of, on growth of HeLa tissue cultures, 17: 14082
effects of perfused, on cholesterol and fatty acid metabolism in rat liver, 20: 38559
effects on anaerobic rumen bacteria, 16: 17392
effects on cell mitosis in chick embryo skeletal muscle tissue, 16: 31480
effects on chromosome aberrations in hamster cells, comparison with radiation and tritiated thymidine, 19: 15179
effects on chromosome aberrations in apical root-tip cells of *Vicia faba*, 19: 42269
effects on growth of Rickettsiae and influenza virus in eggs, 16: 17390
effects on metabolism in algae, 16: 14521
effects on mice and rats of injected, pathological, 20: 38568
effects on peas, mutagenic, 19: 35962
effects on root growth of corn and pea seedlings, 20: 16227(R) (NYO-3561-2)
hazards and time limits of accidental exposure in regenerated or stable atmospheres, 18: 43876
hazards of, produced in heavy water reactors, 20: 927
light emission from aqueous solution of, 20: 18813
metabolism in *Zea mays* roots, 19: 43702
monitoring of vapors of, scintillation detector for, 20: 4235 (AECL-2283)
packaging for shipping, design of, 17: 40998
properties review, physical and thermodynamic, 16: 25307 (CEA-Bib-15)
radiation effects on positron-annihilation lifetime spectra in, gamma, 20: 29268
radiation hazards of gaseous, in air, 16: 23717 (USNRDL-TR-565)
radioactivity measurements of National Bureau of Standards 1954 standards, 19: 7306
radioactivity of, use of proportional counter for absolute determination of, 18: 39102
reactions with methane, effects of tritium on products from, 20: 14455(R) (ORNL-3889, pp 25-32)

separation from water by vaporization, separation factor for, 17: 28879
sorption of vapor of, by foamed poly(vinyl chloride), 18: 20458 (USNRDL-TR-717)
spectra of, vibrational, 18: 12100(T)
toxic effects on mice, rabbits, and rats, 19: 25881
tracer use in studies on flow in Timavo River, Italy, 20: 35656
tritium beta decay in, atomic structure studies of organic compounds by, 20: 29326
tritium counting in, equipment and method for, 18: 15978
tritium exchange between, and amino acids or peptides, 20: 20714
tritium exchange with animal tissues, 16: 17382
tritium exchange with *tert*-butyl alcohol, effects of perchloric acid on, 20: 36849
uptake of, by rabbit eye lens in culture, 20: 5256
use as tracer in measurements of lean body and total fat content of man, 16: 16151
use for leak detection in heat exchangers in petroleum refinery, 18: 16389 (TID-7688(p.80-3))
use in determining body water, 20: 10557
use in skin water-uptake analysis, 19: 14966
use in testing autoradiographic images, 20: 22834
uses for labeling menaquinone and phylloquinone, 20: 18711
vapor pressure of, measurement of, 18: 25436
vapor pressure of, hydrogen isotope effects on, 18: 31425 (LADC-5905)

Water Boiler
see Los Alamos Water Boiler

WATER BOILER NEUTRON SOURCES
abnormal incidents in AE-6, review, 17: 13741
fission gas release from AE-6 on March 25, 1959, analysis, 16: 5071 (NAA-SR-Memo-3757)
gas evolution delay in FRF, effects on dynamic behavior, 16: 22471
neutron flux monitoring system using argon activation for L-77, 16: 17850
power transient of Dec. 20, 1958, analysis, 16: 5070 (NAA-SR-Memo-3756)

WATER COOLED REACTORS
see also Advanced Test Reactor
see also Argonne Low Power Research Reactor
see also Babcock and Wilcox Test Reactor
see also Beznau Power Reactor
see also Boiling Reactors
see also Japanese Materials Testing Reactor
see also Oskarshamn Power Reactor
see also Pressurized Water Reactors
see also San Onfre Power Reactor
see also Swimming Pool Reactors
see also VAK Reactor
accidents in, iodine deposition on surfaces following, 20: 45045(R) (BMI-X-10173)
accidents in, metal-water reaction data for predicting, 20: 14996
analysis of fog cooling, 18: 7936
auxiliary systems development for 395-Mwe, (E), 19: 45597 (WCAP-3269-31)
boiler design for, 19: 26512(P)
boiler design for, 20: 14041(P)
boiler design for, vertical-tube, 20: 10411(P)
boiling burnout in, conditions for, 19: 35759(R) (HW-84384(p.10.1-13))
boiling burnout of 19-rod fuel bundles in, (E), 19: 8569 (HW-83443 (Rev.1))
boiling effects on power and reactivity in, 17: 7574 (WAPD-T-1225)
boiling in, departure from nucleate, 17: 21892
boiling indicator for, design of film, 20: 22367(P)
book: *Chemical Aspects of Nuclear Reactors. Vol. II. Water-Cooled Reactors*, 18: 11373
burnout and pressure drop in steam-water systems for, 16: 25530(T) (EURAEC-42)
burnout heat flux in, 17: 9864(T,R) (EURAEC-401)
burnout heat transfer studies in, 18: 15520(R) (DP-895)
burnout of fog-cooled fuel-rod clusters in, (E), 19: 31551(R) (SRO-115)
containment building for, design of filter system of, 17: 14415 (DP-812)
containment in lined outer casing, 19: 35642(P)
containment of, dry, 20: 12447
containment systems for, review, 17: 41091
containment system for, vapor suppression, 20: 28710(P)
contamination and decontamination of piping in, 17: 31676 (DP-793)
contamination from cooling system of, method and apparatus for removal of, 19: 40119(P)
contamination of aluminum and stainless steel in, 18: 19267 (DP-829)
control by variation of water-d_2 concentration, 17: 17527(P)
control equipment for, 19: 42019(T) (ORNL-tr-669)
control method for overmoderated, 17: 10011(P)
control method for, 20: 30822(P)
control of boiling, utilizing evolved steam circulated through core, 19: 21661(P)
control of heavy water moderated, (T), 20: 10330 (RT/ING(65)13)
control of, use of soluble poisons for, 18: 38267 (A/CONF.28/P/70)
control of, use of soluble poison and xenon-135 for, 20: 14099(P)
control rod actuator for large, design of hydraulically operated, 17: 26794 (TID-18727)
control rod positioning actuator design for, 18: 3082
control rod requirements for power, review of, 20: 35049
control rods for closed-cycle, feasibility of boron automatic, 20: 12418(R) (WCAP-3739)
control rods for power, performance of boron-bearing, 20: 35050
control system design for, 17: 9986(P)
control systems for, description of hydraulic-ball, (E), 19: 17206
control using boric acid shim, 18: 11401 (WCAP-3729)
coolant analysis and sampling system for Hanford 100-N, 20: 26744 (HW-SA-3099)
coolant analysis for chemical and radioactive contamination, 20: 12509
coolant analysis in water moderated EWA, 19: 17365 (PAN-581/XIV)
coolant and moderator purification in, 17: 14235
coolant boiling detection in, evaluation of acoustic and reactor-power spectra methods for, 16: 30142 (ORNL-TM-274)
coolant boiling in, detection and quenching by period meters, 18: 3076
coolant burnout data for, interpretation of, 19: 4338
coolant characteristics in Hungarian research, (E), 19: 40264 (ZFK-RN-17(p.54-67))
coolant chemistry, 18: 32964 (GEAP-4291)
coolant chemistry and corrosion studies for, 19: 30066(R) (ORNL-3789)
coolant circulation in water-moderated, dynamics of, 18: 38451 (A/CONF.28/P/382)
coolant conductivity and pH measurements in Czech research-type, 16: 26924
coolant development for steam–water spray-cooled CAN-2, 17: 35092(R) (EURAEC-612)
coolant development for steam–water spray-cooled CAN-3, 17: 35093(R) (EURAEC-622)
coolant flow density distribution through core of, (T), 20: 10270 (EUR-2547.e)
coolant flow in boiling maritime, two-phase, 18: 38558 (A/CONF.28/P/801)
coolant flow in channel of water-moderated, computer program for analysis of, 18: 40833 (GN-37)
coolant flow in, hydrodynamic instability of, 17: 1027 (IDO-16791 (p.189-208))
coolant flow monitoring, design of radiation-resistant rotameter for, 16: 27393(P)
coolant kinetics of heterogeneous, research on, 20: 20178(R) (STL-372-27)
coolant loss accidents in, computer program for analysis of, 17: 18664 (WCAP-2059)
coolant loss accidents in, model for tank blowdown in, 19: 29572
coolant loss accidents in closed-cycle power, flow analysis of, (T), 20: 12418(R) (WCAP-3739)
coolant loss accidents in, metal–water reactions in, 20: 45112 (IDO-17168)
coolant loss in, post-incident cooling system analysis for, 18: 38454 (A/CONF.28/P/436)
coolant loss in, research facilities for studying, 16: 28526(R) (ARF-4226-1)
coolant loss-of-flow in Canada-India, primary, 18: 38624 (A/CONF.28/P/793)
coolant maintenance, 18: 38290
coolant mixing device for, steam–water, 20: 16011(P)
coolant monitoring for fission products, evaluation of Cherenkov detectors for, 17: 23764
coolant monitoring by polarography, 19: 11003
coolant monitoring system for homogeneous, radioisotope identification, 20: 36408 (NP-16006)
coolant pump wear in, effects of chemical shim environments on, 19: 21606 (WCAP-3269-9)
coolant purification in, ion-resin methods for primary, 19: 40123 (IAE-787)
coolant purification for, electrophoretic filter for, 20: 6568
coolant purity monitoring in primary loops of, standardization of, 19: 40124 (IAE-789)
coolant radioactivity from contamination by dissolved radionuclides, 16: 21717 (DP-682)
coolant radioactivity in, effect of oxygen-16 (n,p) reactions on, 16: 28417 (WAPD-BT-25(p.27-35))
coolant reactions with zirconium in, analysis of, 19: 35619
coolant supply for, 18: 40915
coolant systems for, design of, 18: 24930(P)
coolant temperature, computation method, 16: 1192 (NARF-61-35T)
coolant temperature monitor for, design of, 20: 20186 (DP-834)

coolant void coefficients for steam-cooled fast, extrapolation from critical assembly measurements, 20: 38425 (ANL-7120, pp 585-97)
coolant void effects in plutonium fueled, 18: 3223
coolant void formation in, in-pile capsule measurements of transient, (E), 20: 20179(R) (STL-372-27, pp 3-12)
coolant void fraction determination using simulated boiling in exponential piles, (E), 20: 20216
coolant-loss accidents in water-moderated, fission product release in, 19: 28574(R) (BMI-X-10119)
coolant-loss accidents in, metal–water reaction calculations for, 20: 20925(R) (ANL-7055, pp 177-212)
coolant-loss accidents in, analysis of simulated, 20: 31440(R) (ANL-7175, pp 159-83)
coolants for, evaluation of performance of fog as, (E), 19: 42020
cooling by fog flow, 16: 807
cooling by fog or superheated steam, 17: 289
cooling by steam–water spray, 17: 40266(R) (EURAEC-728)
cooling by steam–water spray, 17: 40267(R) (EURAEC-850)
cooling channels, burnout analysis, 16: 17226 (AEEW-R-117)
cooling circuit design for, 17: 9989(P)
cooling circuit design for, 17: 10000(P)
cooling of, research on steam-water spray, 17: 34092(R) (EURAEC-299)
cooling pipe fracture modes, review, 19: 953 (GEAP-4446)
cooling pipe rupture in, survey of parameters for study of, 19: 38175 (GEAP-4445)
cooling purification by ion exchange, (E/T), 19: 14857
cooling system design for heavy-water-moderated, 16: 34038(P)
cooling system development for closed-cycle, with chemical-shim control, (E), 19: 19346 (WCAP-3269-32)
cooling system for heavy water moderated, spray evaporation method for core, 16: 18624
cooling system for, development of steam–water spray, 20: 6566(R) (EURAEC-1382)
cooling system joints of vapor-cooled, support for, 19: 38121(P)
cooling systems, mechanism for film formation in, 16: 4491 (AECL-1265(Paper 9))
core components for chemically shimmed, design of, 19: 40198(R) (WCAP-3721)
core configuration of VVR-M, optimization of, 20: 18140
core lattice design for, 17: 9974(P)
core lattice for water-moderated, design of, 18: 23033(P)
core meltdown in, metal–water reactions in, (E/T), 19: 47960(T) (ORNL-tr-694)
corrosion and erosion problems in pressurized, 16: 30738
corrosion and oxygen production in, effects of ammonia on suppression of, 20: 26920 (AECL-2562)
corrosion and water treatment problems in power, lectures on, 18: 5744 (KR-53)
corrosion loop operation in, 17: 9864(T,R) (EURAEC-401)
corrosion of aluminum in low-temperature, 18: 41966
corrosion of aluminum and its alloys at high temperatures in, survey, 19: 922 (HW-69876)
corrosion of materials in high-temperature, 17: 6567 (HW-SA-2745)
corrosion problems, 16: 10460
corrosion problems survey, 16: 16036
corrosion problems in, 16: 32083(T) (CEA-tr-A-1148)
corrosion problems, 17: 12614
corrosion problems in, 18: 16445
corrosion resistance in, process for improving, 19: 36989(P)
criticality parameters of, 20: 6582 (EUR-2461.f)
criticality studies of, with plutonium recycling, 18: 35168
criticality studies of heterogeneous, 19: 38133(R) (STL-372-13)
decontamination process evaluation, 16: 15780(R) (HW-71259)
description, 19: 6862
description and performance of pressure-tube, 17: 5612
description and prospects of pressurized, 17: 5611
description of graphite-reflected Ispra-2 swimming-pool, 16: 28609 (RT/ING(62) 3)
description of McMaster University swimming pool, 16: 28615
description of SILOE, 17: 10147
description of, at Kyoto Univ., 18: 33155
design, 20: 1425(P)
design analysis of thorium-fueled, 17: 28456 (TID-7650(p.172-93))
design and construction of graphite-moderated Polish, 16: 34119
design and construction of Manchester/Liverpool Universities, 18: 23113
design and development of 100-Mw(e) steam-generating heavy-water-moderated, 18: 38412 (A/CONF.28/P/129)
design and development of Hermes fast breeder steam-cooled, 18: 38458 (A/CONF.28/P/516)
design and development of 100-Mw(e) steam-generating heavy-water-moderated, 18: 38418 (A/CONF.28/P/143)
design and development of large closed-cycle, (E/T), 19: 5490(R) (WCAP-3269-2)
design and development of large, 19: 29651(R) (WCAP-3269-3)
design and economic studies, 16: 3942 (NDA-2132-6)
design and economic aspects of 300-, 500-, and 1000-Mw(e) heavy water-moderated, 17: 38550 (SL-2008)
design and operation for steam generation in core, 19: 33651(P)
design and technology of, chemical and metallurgical problems in, 17: 4907
design characteristics of Steam Cooled Breeder Reactor, 19: 29580
design development of Mixed Spectrum Superheater, 16: 1243 (GEAP-3590(Rev.1))
design development for CIRENE, 20: 1489
design feasibility of heavy-water-moderated, up to 8300 Mw(th), 18: 35143(R) (DP-915)
design for inherent safety and natural circulation cooling, 18: 13244(P)
design for superheat production, 17: 9998(P)
design for superheating, 17: 10003(P)
design for superheating steam, 19: 38223(P)
design for underwater service, 19: 38215
design for water desalinization, 17: 28499
design of Beloyarsk graphite-moderated steam-superheating, (E), 19: 43547
design of boiling superheating, 19: 21659(P)
design of boiling, heavy-water-moderated, 19: 19369(P)
design of boiling, with increased boiling surface, 20: 42602(P)
design of Candu-type boiling, conceptual, 19: 31529 (AECL-2211)
design of double-cycle, for power production, 19: 10594
design of fast supercritical, 18: 23032 (HW-78953)
design of fog-cooled, water-moderated, 16: 18618(R) (NDA-2132-2)
design of fog-cooled, light water-moderated, 17: 9862(R) (UNC-5008-II)
design of fog-cooled, with subcooled water inlet, 18: 38353(P)
design of graphite-moderated, 16: 15851(P)
design of graphite-moderated steam-generating and superheating, 20: 30919(P)
design of, having crossed layers of pressure tubes, 17: 10080
design of heavy water-moderated steam-cooled pressure tube, 16: 21757(P)
design of heavy water moderated steam-cooled, 17: 9973(P)
design of heavy-water-moderated, 17: 29775(P)
design of heavy water-moderated steam-cooled, 18: 24928(P)
design of heterogeneous steam-moderated power, 20: 30918(P)
design of liquid-moderated steam-cooled, 17: 21353(P)
design of marine steam-cooled light-water-moderated, 17: 12006
design of maritime, 18: 38565
design of multi-pass vapor moderated, for power production, 20: 30916(P)
design of multipass superheated-steam-cooled, 17: 29815(P)
design of portable 10-Mw(t), using thermoelectric generator, 18: 2566 (WCAP-1818(Vol.I)(Del.))
design of portable thermal circulation reactor using thermoelectric elements, 18: 2574 (WCAP-1818(Vol.II)(Del.))
design of pressurized H_2O–D_2O, 20: 34991(P)
design of self-stabilized, 17: 2568(P)
design of Soviet research, 18: 13329 (AID-P-63-60)
design of spherical, 17: 3846
design of spiked-core, 16: 12731 (CEND-150(Pt.V))
design of steam-cooled, 17: 21355(P)
design of steam moderated power reactors, 20: 30915(P)
design of steam system, 17: 9963(P)
design of steam-cooled water-moderated power, 18: 21662(P)
design of steam-cooled power reactor, 19: 1921(P)
design of steam-cooled, as superheater, 19: 38224(P)
design of steam-generating heavy-water-moderated prototypic 100-Mwe, 18: 30983 (DPR/INF/274)
design of superheating, for power production, 17: 42391(P)
design of superheated-steam-cooled multi-zone, 18: 23079(P)
design of superheating steam-cooled, 19: 21662(P)
design of thermionic package-power, 18: 3236
design of three-pass water-moderated maritime, 16: 28593(P)
design of variably controlled and moderated power, using hydrogen-isotope-bearing moderator vapor, 20: 30917(P)
design of water-moderated, parameter optimization in, 18: 38433 (A/CONF.28/P/304)
design of water-moderated steam-generating, 19: 8648(P)
design of water-moderated, 20: 30869(P)
design of water-moderated, for power production, 20: 30912(P)
design of water-moderated thermal, boiler- and turbine-less, 20: 40435(P)
design of 300-Mwe, 17: 5579 (NDA-2132-5)
design of 40- and 300-Mwe fast breeder, 16: 15912 (NDA-2148-5)
design of 500-Mw(e) thorium power breeder, (E), 19: 14849 (WAPD-LPR-181)
design of 500-Mw(e) thorium power breeder, (E), 19: 14850 (WAPD-LPR-256)

design of, fast supercritical, 20: 1515
design of, optimum parameters for, 18: 36828
design of, with integral steam generation apparatus, 18: 43057(P)
design of, with provision for dissipation of decay heat from fission products, 20: 26445(P)
design studies of fog concept, 18: 13743
design study of advanced indirect cycle for maritime uses, 16: 24971 (CEND-150(Pt.I))
design using fixed-bed fuel elements, 18: 9612(P)
design using mixed heavy and light water as moderator-coolant, 20: 30868(P)
design using water as primary and secondary coolants, 18: 43072(P)
design with local boiling, 16: 18644(P)
design, development program, and economics of breeder-type, 18: 15576
development, 16: 2669(R) (ANL-6454)
development, 19: 35790
development, 20: 10276(R) (NP-15580)
development and economic evaluations of Canadian, 17: 24673 (AECL-1730)
development and principles of graphite-moderated pressure-tube, 20: 1493
development and research program for large closed-cycle, 20: 30884(R) (WCAP-3269-16)
development for use in power stations, 17: 36956
development of, design and testing of equipment for studies in, 17: 17407(R) (EURAEC-537)
development of direct-cycle steam-superheating, 20: 5113 (CONF-650602-59)
development of Euratom CAN-1, 16: 8868(R) (EURAEC-97)
development of Euratom CAN-1, 16: 26603(T,R) (EURAEC-36)
development of Euratom CAN-1, 16: 26604(T,R) (EURAEC-38)
development of EURATOM CAN-1, 16: 28571(T,R) (EURAEC-37)
development of EURATOM CAN-1, 16: 28572(T,R) (EURAEC-39)
development of Euratom CAN-1, 16: 34082(T,R) (EURAEC-40)
development of heavy water moderated, 16: 9615 (AECL-1318 (Paper 10))
development of heavy-water-moderated, for desalination plants and power production, 17: 28526(R) (DP-845)
development of heavy-water-moderated power, 17: 42335 (AECL-1807 (p.59-67))
development of Hermes steam-cooled fast power breeder, (E/T), 19: 35808
development of large closed-cycle, 19: 40195(R) (WCAP-3269-5)
development of large closed-cycle power, 20: 12417(R) (WCAP-3269-15)
development of large closed-cycle power, 20: 12418(R) (WCAP-3739)
development of plutonia–urania-fueled fast, 19: 38264(R) (GEAP-4781)
development of pressurized, heavy-water moderated, power, 17: 10099
development of, review of present and future, 17: 28536
development of steam-water-spray-cooled, 18: 9575(R) (EURAEC-831)
development of steam-water spray-cooled, 19: 1875(R) (EURAEC-1011)
development of steam-cooled heavy-water-moderated, in Canada, 19: 33613
development of, with in-pile thermionic cells, 18: 6490 (MND-2903 (Vol.II))
dynamics of fog cooling in, 17: 10044 (CRARE-1108)
economic analysis of desalination-plant, 18: 36833 (TID-20039)
economic and potential aspects of, comparison with heavy water reactors, 18: 15558
economic and technical aspects of, for power production, 19: 10579
economic aspects of, for power production and sea water desalination, 19: 45620
economic assessment of large dual-purpose, for desalination, 18: 36834
economic evaluation of light, long-term, 18: 17306
economics and thermal efficiency of water-moderated power, 19: 27805
economics of dual-purpose, for desalination, 18: 45036(T) (JPRS-26497)
economics of low-temperature, water moderated, for desalination, 19: 42097 (ORNL-TM-1152)
experimental facilities for tank-type, hydraulic sample changer for, 18: 26973(P)
experimental facilities for VVR-M, beam holes and thermal column, 20: 18139
feasibility of heavy-water-moderated, 18: 24882(R) (DP-905)
feasibility of mixed-spectrum steam-superheat power reactors, (T), 20: 3471(R) (GEAP-4861)
fuel and fuel cycle parameters of, 20: 6582 (EUR-2461.f)
fuel bundle burnout heat flux testing in, effects of rod spacing on, 18: 33060(R) (DPST-64-83-5)
fuel bundle burnout heat flux testing in, effects of rod spacing on, 19: 14804(R) (DPST-64-83-11)
fuel burnout in rod-type geometry in, 16: 27219
fuel burnup in, computer analysis of, 18: 30972 (BLG-222)
fuel burnup monitors for VVR-S, description of flux-wire, (E), 19: 30524 (NP-14972)
fuel burnup processes in, methods of calculating, 18: 11399 (TID-7672(p.347-66))
fuel cartridge failure detection in, 16: 31271 (NP-11754(Vol.II)(Sect.II))
fuel channel design for, 17: 35127(P)
fuel channel vibration in, hydro-flutter theory of self-excited, 20: 6564
fuel channels of, sealing plug for, 19: 38113(P)
fuel cladding for, zirconium and stainless-steel, 18: 37610 (A/CONF.28/P/419)
fuel cladding material for, properties of aluminum, 20: 35838 (KR-89, pp 97-111)
fuel cladding material for, properties of stainless steel, 20: 35839 (KR-89, pp 112-30)
fuel cycle costs, 17: 36876 (ORNL-TM-678)
fuel cycles and loading programming for, 16: 26620 (ORNL-TM-277)
fuel cycles for power, 18: 7908
fuel dispersal in, heat conduction criteria for preventing molten, (T), 20: 20180(R) (STL-372-27, pp 22-35)
fuel element assembly for, design of, 19: 35821(P)
fuel element burnout testing in, effects of rod spacing on, 17: 28423(R) (DPST-63-69-6)
fuel element cans for, development of "nuclear vapotron," (E), 20: 5088(R) (EURAEC-1337)
fuel element cladding performance in, stainless steel, 18: 38279 (A/CONF.28/P/593)
fuel element claddings for breeder, mechanical and physical properties of, 20: 33861 (BAW-237)
fuel element cladding materials for, properties of zirconium-base, 20: 35849 (KR-89, pp 82-86)
fuel element cladding for, development of, 20: 39356(R) (GEAP-5134)
fuel element cooling in VVR-S, asymmetry effects in, 18: 23110
fuel element design for generation of superheated steam, 18: 11423(P)
fuel element design for, 18: 43017(P)
fuel element design for heterogeneous, 19: 12765(P)
fuel element development, 18: 16422(R) (CEND-204)
fuel element dryout heat flux in, 20: 38409 (AECL-2586)
fuel element failure in, detection units for, 19: 17280 (NP-14703)
fuel element failure in, detection system for, 19: 42715(R) (ORNL-3782, pp 35-51)
fuel element preparation for, cost analysis of, 17: 42239
fuel element testing for, 18: 7202(R) (CEND-199)
fuel element welding development for, 20: 12377(R) (CEND-2863-236)
fuel elements, development of uranium dioxide, 16: 20951(R) (CEND-149)
fuel elements for, preparation of ceramic, 17: 42319(P)
fuel elements for, testing uranium-dioxide, 18: 24854(R) (CEND-2863-211)
fuel elements for, testing of uranium dioxide, 18: 45001(R) (CEND-2863-217)
fuel elements for, development of, 18: 44073
fuel elements for, development of "nuclear vapotron" finned, (E), 19: 10518(T) (EURAEC-1005)
fuel elements for, properties of metallic uranium, 20: 36448 (KR-89, pp 174-80)
fuel elements, heat transfer in cylindrical, 16: 21712 (AEEW-R-96)
fuel for, properties of metallic uranium, 20: 35837 (KR-89, pp 63-81)
fuel performance in fog-cooled, 18: 37324 (A/CONF.28/P/16)
fuel rod development and testing, 17: 23897(R) (CEND-178)
fuel rod spacing effects on heat transfer burnout in heavy-water moderated, 18: 28916(R) (DPST-64-83-4)
fuels for Belgian, use of plutonium, 20: 28797
gamma dose rates from primary water loop of Avogadro RS-1, 17: 36865 (EUR.304.e)
hazards evaluation in STEP project, 18: 24956(R) (IDO-16961)
heat energy production in, method of utilizing, 16: 28512(P)
heat exchangers of, radioactive contamination of, 18: 28950
heat flow in, effects of fuel and cladding on, 18: 7899 (AEEW-R-196)
heat flux in, critical, 18: 32956 (A/CONF.28/P/224)
heat fluxes in, effects of subcooled water flow velocity on burnout, 18: 39441
heat removal from, steady-state, 18: 38258
heat transfer, 17: 19611(R) (DP-825)
heat transfer and hydraulics in maritime, 20: 8449
heat transfer burnout in, 17: 38540(R) (DP-855)
heat transfer burnout in, 19: 18108(R) (BAW-3238-6)
heat transfer burnout in heavy water-moderated, effect of rod spacing on, (E), 19: 22479(R) (DPST-65-83-2(p.3-7))
heat transfer by steam–water mixtures in, 18: 20182 (TID-7694 (p.108-49))
heat transfer in, 17: 24652
heat transfer in, during power increase, 18: 9572
heat transfer in fog-cooled, 18: 45031(R) (SRO-106)
heat transfer in fog-cooled, 18: 45032(R) (SRO-107)
heat transfer in fog-cooled, 19: 10571(R) (SRO-111)
heat transfer in fuel-rod bundles in superheated-steam-cooled, (E), 20: 3471(R) (GEAP-4861)
heat transfer in heterogeneous, transient, 18: 23776

heat transfer in, dynamic studies, 19: 44194 (SGAE-RE-2/1965)
heat transfer kinetics in heterogeneous, 17: 42215
heat transfer limitations on fuel elements, 20: 38484
heat transfer properties of, improvements for, 18: 4797 (GEAP-4203)
heat transfer under fog flow conditions in, 16: 23272(R) (NDA-2169-3)
heat transfer, analysis for, 19: 35623
hydrodynamic and thermal characteristics of VVR-S, 18: 7973
hydrodynamics of high pressure argon loop in, 17: 9864(T,R) (EURAEC-401)
instrumentation, conference, 16: 11225 (HPR-16)
instrumentation of, 16: 31265 (NP-11754(Vol.I))
instrumentation of, 16: 31270 (NP-11754(Vol.II))
kinetics of heavy water moderated, (T), 20: 10330 (RT/ING(65)13)
kinetics of heavy-water–water cooled-and-moderated, 18: 38245 (A/CONF.28/P/176)
kinetics of heterogeneous, 20: 18050(R) (STL-372-22)
kinetics of mixed-spectrum steam-superheat, (E/T), 20: 3471(R) (GEAP-4861)
kinetics of Philippine Research Reactor PRR-1, 18: 1307
kinetics of supercritical, natural circulation, 16: 28436
kinetics of, analysis by boron-poisoning method, (T), 19: 10478 (CEA-R-2489)
kinetics of, survey, (E/T), 19: 17246
loading closed-cycle power, using automatic boron control, 20: 12418(R) (WCAP-3739)
materials for, properties of niobium–zirconium alloys as, 20: 41422
materials for, review of, 19: 22885
materials for, survey of zirconium alloys as, 18: 10566
materials selection for, 17: 4230 (DL-51)
materials specification for, ASTM, 16: 32595
materials testing for, corrosion loop for, 20: 21266
mechanical equipment problems in, survey, 17: 42375
neutron absorber efficiency in homogeneous uranium, heterogeneous, (E/T), 19: 45536
neutron buckling and void effects in heavy water moderated, 17: 26061
neutron buckling and void effects in heavy-water-moderated, with uranium dioxide rod clusters, 17: 28483 (TID-18895)
neutron buckling in heavy water-moderated, 18: 36777 (DP-873)
neutron leakage escape probability for, 19: 10491
neutron reactions with coolant in, nitrogen-16 specific activity from, (T), 19: 14847 (WAPD-BT-31(p.37-42))
neutron shielding calculations for, 19: 14745
neutron spectrometer design for water-moderated, 18: 8686
neutron spectrum in thermal column of Triga Mark II, (E), 19: 42184
operation manual for research, (E), 19: 25767
operation of Canada-India, 18: 24949 (AEET/ROD/7)
operation of Hungarian WWRS, 18: 38598 (A/CONF.28/P/451)
operation of steam-generating, in fog-flow conditions, 17: 13692
operation of WWR-C, at Rossendorf, Germany, (E), 19: 40261 (ZFK-RN-17(p.179-98))
operations of MSSCEF, 20: 3471(R) (GEAP-4861)
optimization of power, 18: 35179
performance as saline water distillation power source, economic aspects 17: 19633(R) (PB-161062)
performance evaluation, review of, 16: 30119
performance of Canada-India, 18: 24948 (AEET/ROD/6)
performance of steam–water spray, 18: 17999(R) (EURAEC-923)
performance of steam-cooled power breeders, evaluation, (T), 19: 35806
performance of steam-cooled fast power breeder, at 1200 psi, 20: 38496 (ANL-7120, pp 136-40)
performance of urania elements in, 20: 11222
physics methods development for large, 20: 5134(R) (WCAP-3269-12)
physics of, 17: 5585
physics parameter study of large steam-cooled fast power, 20: 38438 (ANL-7120, pp 815-25)
plutonium burnup and production in, calculation methods for, 20: 3535
power excursion tests in highly enriched plate-type, 18: 44970 (IDO-17000)
power excursions in experiments for measuring pressure transients and transient steam void formation, 17: 21259(R) (TID-17005)
power excursions in, steam void formation during, 18: 28924
power level determination from nitrogen-16 activity in coolant, 20: 14019
power level increases in water-moderated, by fuel element replacement, 18: 11489
power measurement using Cherenkov detectors, 17: 23765
power modulation of, high-pressure loop for measuring boiling void response to, 20: 18872(R) (STL-372-27, pp 13-21)
power monitoring, Cherenkov detector, 16: 25597(P)
pressure peaks following burst of pressure vessel in, means of flattening, 18: 33049(P)
pressure transients in vessel of, following loss-of-coolant accidents, (T), 20: 24674
pressure tube design for, 19: 25682(P)
process instrumentation for, review, 17: 10996
production of superheated steam in, 17: 10117(P)
properties of, computer program for hydrodynamic, nuclear, and thermal, 20: 36389 (AEEW-R-441)
properties of, summary of reports on, (E/T), 19: 17181 (WCAP-3728)
pumps for, shaft-seal systems for, 19: 17316
reactivity changes in, kinetic response prediction for, 20: 38449
reactivity control of, subcritical, (E), 19: 14796
reactivity coolant loss accidents in, calculational model for dynamics of, (T), 19: 38134 (WAPD-T-1792)
reactivity during loss of coolant accident, (T), 19: 29571
reactivity excursion simulation in, 20: 16029
reactivity excursions in, pressure pulses and voids from, 18: 35068(R) (STL-6312)
reactivity feedback in ceramic-fueled fast, 18: 38496 (A/CONF.28/P/687)
reactivity fluctuations in boiling, mean-square minimization of, 17: 12008
reactivity modulator for, design for parameter measurements, 19: 40197(R) (WCAP-3718)
reactivity modulator for, design for parameter measurements, 19: 40198(R) (WCAP-3721)
reactivity of heterogeneous, effects of epithermal processes on, 19: 1843
reactivity of water-moderated, 18: 38446 (A/CONF.28/P/359)
reactivity of, effects of stainless steel- and zirconium-clad fuel loading on, 20: 30884(R) (WCAP-3269-16)
reactivity transients in urania-fueled SPERT-I, feedback effects in, (E/T), 19: 38269 (IDO-17054)
review and survey of commercial power, 18: 35160 (TID-8540(p.1-69))
safety hazards analysis for Pegase, (E), 19: 10638 (CEA-R-2518)
safety hazards analysis for UCLA Training Reactor, (E/T), 19: 19418 (UCLA-NEL-2)
safety hazards and precautions at Pegase installation, 19: 42151 (CEA-R-2518(Vol.II))
safety hazards in, evaluation of metal-water reactions as, 18: 33678(R) (ANL-6875)
safety in progressive development of, 18: 43051
safety of steam-cooled fast, during flooding, 20: 38439 (ANL-7120, pp 826-36)
safety of water-moderated, 17: 10134
shielding of, heat release by iron-water thermal, 18: 13199
shielding performance in Westinghouse Test Reactor, 18: 4851 (ORNL-TM-332)
shutdown margin in, measurement of, 18: 9690
shutdown of steam-generating, heat removal during, 19: 38225(P)
shutdown system for, 20: 42597(P)
stability of boiling, models for dynamic, 18: 3134(R) (GEAP-4094)
stability of, hydrodynamic aspects, 17: 2524
stability of steam-cooled fast ceramic, models for, (T), 19: 8597 (EIR-71)
startup and adjustment of water-moderated, procedures for, 18: 38434 (A/CONF.28/P/305)
steam generator designs for, tubulous, 16: 34101(P)
steam generator design for, 17: 31746(P)
steam generator design for, 17: 31747(P)
steam systems of, technology of, 20: 26497
steam-water mixtures in, 16: 2690(T) (TT-985)
steam–water mixer for, 18: 42961(P)
structural materials for, review of, 16: 20013
superheating in boiling, 17: 9961(P)
temperature monitor for large, design of, 20: 24676 (DP-836)
thermal efficiency and condenser output of, 20: 22420
thermal models for dioxide-fueled, (T), 19: 29522
thermal transient analysis for, with exponential power increase, 17: 28496
thermodynamic cycles of power plants with, (T), 20: 24765(T)
transients in, fuel–steam reactions during, 18: 36751 (ANL-6912)
water characteristics in primary circuits of research, (E), 19: 40260 (ZFK-RN-17(p.68-74))
water chemistry in, 17: 31740
water chemistry measurements in Czech WWR-S, (E), 19: 40263 (ZFK-RN-17(p.32-43))
water chemistry problems in, 17: 28538
water level in, measurement of, 16: 31272 (NP-11754(Vol.II)(Sect.III))
water pH in, problems in measurement of, (E), 19: 40127 (ZFK-RN-17 (p.9-23))
water problems in, conference, (E/T), 19: 40117 (ZFK-RN-17)
water purification in, performance of resins for, (E), 19: 40128 (ZFK-RN-17(p.75-94))
water purification equipment for, performance of ion-exchange, (E), 19: 40130 (ZFK-RN-17(p.165-78))
water radiolysis in, 17: 25296
zirconium alloy uses in, evaluation, 16: 11274

WATER MODERATED REACTORS

see also Air Force Engineering Test Reactor
see also Aircraft Shield Test Reactor
see also ANP Reactor (SCW)
see also Arbor Reactor
see also Argonaut Reactor
see also Armour Research Reactor
see also Army Reactors (SM-1)
see also Belgian Reactor-3
see also Beznau Power Reactor
see also Boiling Reactor Experiments
see also Brookhaven Medical Reactor
see also Brookhaven Neutron Source Reactor
see also Bulk Shielding Facility
see also Carrier Vessel Reactor
see also Dresden Power Reactor
see also Elk River Power Reactor
see also Engineering Test Reactor
see also Experimental Boiling Water Reactor
see also Fontenay-aux-Roses Reactors (Triton)
see also General Electric Test Reactor
see also Grenoble Reactors (Melusine)
see also Homogeneous Reactor Experiment
see also Indian Point Power Reactor
see also Japanese Materials Testing Reactor
see also LIDO
see also Los Alamos Omega West Reactor
see also Los Alamos Power Reactor Experiments
see also Los Alamos Water Boiler
see also Low Power Research Reactor
see also Lynchburg Test Reactor
see also Materials Testing Reactor
see also Materials Testing Reactor Mockup
see also Michigan Research Reactor
see also NASA Research Reactor
see also North Carolina Research Reactor
see also NRL Research Reactor
see also Nuclear Test Reactor
see also Obrigheim Power Reactor
see also ORNL High Flux Isotope Reactor
see also ORNL Research Reactor
see also Oskarshamn Power Reactor
see also Pennsylvania Research Reactor
see also Radiation Effects Reactor
see also Saclay Reactors (Proserpine)
see also San Onfre Power Reactor
see also Shippingport Pressurized Water Reactor
see also Sioux Falls Power Reactor
see also Spanish Reactors (JEN-1)
see also Submarine Advanced Reactor
see also Submarine Reactors
see also Swedish Reactors (R-2)
see also TRX Reactor
see also VAK Reactor
see also Vallecitos Superheat Reactor
see also Water Boiler Neutron Sources
see also Yankee Power Reactor
acidity and conductivity of distilled water in Czechoslovak, method for continuous measurement of, 18: 1309
analysis and feasibility of thermoelectric direct-conversion, 16: 21791 (AD-267442)
analysis by Deutsch method, (T), 19: 14798
analysis of water-reflected zirconium hydride moderated, 17: 36898
boiling effects on power and reactivity in, 17: 7574 (WAPD-T-1225)
boiling void distribution along cylindrical channels in, 20: 33469
breeding coefficient in uranium–thorium intermediate-energy, (T), 20: 32831
bubble formation delay time after large insertion of reactivity in, 19: 21653
calandria arrangement for, design of, 20: 3354(P)
characteristics of plutonium fueled, survey of, 20: 35003 (BNWL-232)
Cherenkov production in, 18: 3355
Cherenkov production in, 18: 37956
conference on, Gatlinburg, Tenn., June 11 to 14, 1962, 18: 3322 (TID-7663)
construction and design of 50-Mwe Netherlands SEP, 18: 30984(R) (EUR-1811.n)
containment building for, design of filter system of, 17: 14415 (DP-812)
containment in lined outer casing, 19: 35642(P)
containment systems for, review, 17: 41091
control by moderator variations, 17: 9970(P)
control by moderator temperature variation, 19: 42031(P)
control of accidents in power-producing, by spray systems, 18: 19372 (JAERI-1054)
control of suspension-fueled, by moderator flow rate, 18: 24842(P)
control of, use of soluble poisons for, 18: 38267 (A/CONF.28/P/70)
control of, use of soluble poison and xenon-135 for, 20: 14099(P)
control rod design for, 17: 26834(P)
control rod design for, to reduce flux peaking, 20: 42588(P)
control rod drive systems, feasibility studies, 16: 8313 (GNEC-155)
control rod economics, 16: 24485
control rod effects in H_2O–D_2O, 18: 3114
control rod reactivity worths for uranium oxide fueled, cadmium–indium–silver, 20: 20210 (WCAP-3269-39)
control rod requirements for, with chemical shim, 18: 13197 (WCAP-3727)
control rod theory and worth calculations for, 16: 33981 (GEAP-3937)
control rod worth, 18: 19375 (NP-13714)
control rods for, homogenization of cruciform, 20: 22357 (RT-FI-(65)50)
control rods for, performance of neutron-absorber-filled tubes as, (E/T), 20: 40381
control using boric acid shim, 18: 11401 (WCAP-3729)
controls by moderater temperature and composition variation, 19: 42030(P)
coolant analysis in water cooled EWA, 19: 17365 (PAN-581/XIV)
coolant and moderator purification in, 17: 14235
coolant boiling detection in, methods for, 20: 46973
coolant characteristics in Hungarian research, (E), 19: 40264 (ZFK-RN-17(p.54-67))
coolant circulation in, effects of stoppage of, 17: 1088
coolant circulation in water-cooled, dynamics of, 18: 38451 (A/CONF.28/P/382)
coolant conductivity and pH measurements in Czech research-type, 16: 26924
coolant density profile in, computer program for, 20: 38450
coolant flow in water-cooled, computer program for analysis of, 18: 40833 (GN-37)
coolant-loss accidents in water-cooled, fission product release in, 19: 28574(R) (BMI-X-10119)
cooling by steam–water spray, research program, 16: 7290(R) (EURAEC-173)
cooling system joints of vapor-cooled, support for, 19: 38121(P)
core configuration of VVR-M, optimization of, 20: 18140
core design for, 20: 42595(P)
core lattice for water-cooled, design of, 18: 23033(P)
core parameters for Cornell Univ. zero-power, 19: 10658
corrosion problems in, review of, 19: 20488
costs of single and dual spectral-shift control pressurized-water-reactor power plants, (T), 19: 31550 (NYO-3289-1)
critical experiments in, analysis of problems of, 17: 18994
critical experiments on dioxide-fueled, 18: 36779(R) (HW-81659(p.4-9))
critical experiments for, reliability of data from, 18: 36781(R) (HW-81659(p.26-32))
critical experiments for plutonium-fueled, 18: 36782(R) (HW-81659 (p.33-44))
critical size and flux distribution in highly enriched, 18: 3104
criticality and lattice-parameter calculations for, (T), 19: 8603 (WCAP-3269-25)
criticality calculations for mixtures of light and heavy water, computer code for, 16: 17286 (BAW-1230(Pt.II))
criticality calculations for, computer program for, 18: 13232 (BAW-207)
criticality calculations for uniform, (T), 19: 42054
criticality effects of beryllium oxide reflector elements in, 16: 12711
criticality of glass-clad uranium-fueled, 20: 22415 (RPI-321-4)
criticality of low enrichment homogeneous, hydrogen–uranium ratios, 16: 18316
criticality of multi-region uranium oxide-fueled, 17: 18997
criticality of, parametric study of minimum dimensions for, (E/T), 19: 31504 (LA-3221)
criticality of, pulse techniques for measuring, 18: 38328 (A/CONF.28/P/846)
criticality parameters of, 20: 6582 (EUR-2461.f)
criticality parameters for epithermal, (E/T), 20: 18053
criticality studies, 16: 7287 (DC-51-9-5)
criticality studies of spectral shift controlled, 17: 26767 (PAN-106/IX)
criticality studies of Japan's Tank Type Critical Assembly, 17: 36971 (JAERI-Memo-1122)
criticality studies of, with plutonium recycling, 18: 35168
criticality studies of plutonium enriched, 19: 10484(R) (GEAP-4730)
criticality studies on homogeneous, (E), 19: 10487 (LA-3166-MS)
criticality studies on, (E), 19: 35706 (LA-3219)
criticality studies of heterogeneous, 19: 38133(R) (STL-372-13)
criticality studies in, review, (E), 19: 40163
criticality studies on spectral-shift, review, (E), 19: 40163
decontamination, chemicals and procedures for, 16: 20984
description, 19: 6862
description and performance of pressure-tube, 17: 5612
description and prospects of pressurized, 17: 5611

description of graphite-reflected Ispra-2 swimming-pool, 16: 28609 (RT/ING(62)3)
description of McMaster University swimming pool, 16: 28615
description of SILOE, 17: 10147
description of, at Kyoto Univ., 18: 33155
design, 20: 5086(P)
design and characteristics of closed-cycle boiling, 16: 21786(P)
design and construction of Manchester/Liverpool Universities, 18: 23113
design and criticality studies of AC-100A, 16: 7283(APEX-229)
design and performance characteristics of 19-cell 630, 17: 35141 (GEMP-232)
design and technology of, chemical and metallurgical problems in, 17: 4907
design directory of experimental, research, and test types, 16: 14343
design for inherent safety and natural circulation cooling, 18: 13244(P)
design, nuclear calculation methods review, 16: 468 (AEEW-R-64)
design of air-cycle type with folded-metal-screen fuel elements, 16: 17288 (DC-52-4-37)
design of boiling, with steam recirculating system to control reactivity, 17: 29741(P)
design of compact plutonium-fueled power, 18: 29091
design of emergency cooling systems for, 20: 12434
design of experimental heterogeneous, 19: 48074(P)
design of fog-cooled, 16: 18618(R) (NDA-2132-2)
design of gas-cooled, 16: 6149(P)
design of heavy water-moderated steam-cooled, 18: 24928(P)
design of heterogeneous steam-cooled power, 20: 30918(P)
design of marine steam-cooled, 17: 12006
design of maritime, 18: 38565
design of moderator-controlled thermal breeder, 19: 27759(P)
design of multi-pass steam cooled, for power production, 20: 30916(P)
design of organic-cooled, 18: 11429 (CEND-175(Vol.I))
design of pressurized H_2O–D_2O, 20: 34991(P)
design of self-stabilized, 17: 2568(P)
design of Soviet research, 18: 13329 (AID-P-63-60)
design of spiked-core, 16: 12731 (CEND-150(Pt.V))
design of steam cooled power reactors, 20: 30915(P)
design of steam-cooled power, 18: 21662(P)
design of steam-cooled, as superheater, 19: 38224(P)
design of steam-cooled power, 20: 30917(P)
design of three-pass water-cooled maritime, 16: 28593(P)
design of water-cooled, parameter optimization in, 18: 38433 (A/CONF.28/P/304)
design of water-cooled steam-generating, 19: 8648(P)
design of water-cooled, 20: 30869(P)
design of water-cooled, for power production, 20: 30912(P)
design of water-cooled thermal, boiler- and turbine-less, 20: 40435(P)
design of, with reactivity automatically controlled by rate of supply of water, 17: 31709(P)
design of WWR-M, 18: 38610 (A/CONF.28/P/615)
design of 500-Mw(e) thorium power breeder, (E), 19: 14849 (WAPD-LPR-181)
design of 500-Mw(e) thorium power breeder, (E), 19: 14850 (WAPD-LPR-256)
design of, optimum parameters for, 18: 36828
design of, with arrangement for rapid lowering of liquid level, 18: 44992(P)
design of, with hold-down arrangement for fuel elements, 20: 1431(P)
design study of advanced indirect cycle for maritime uses, 16: 24971 (CEND-150(Pt.I))
design using combined graphite moderation, 20: 6592(P)
design using mixed heavy and light water as moderator-coolant, 20: 30868(P)
design with easily replaceable core, 17: 36912(P)
design with removable solid-moderator elements, 17: 38521(P)
design with superheating system, 19: 45628(P)
design with superheating system for power plants, 20: 24774(P)
development, 17: 17404(R) (BNL-164)
development, 20: 10276(R) (NP-15580)
development and economic aspects, 18: 38514 (A/CONF.28/P/779)
development for power production, 17: 28526(R) (DP-845)
development of, joint US-EURATOM progress on, April 1 to June 30, 1961, 17: 24662
development of large closed-cycle, 20: 10382(R) (WCAP-3269-13)
development of large closed-cycle power, 20: 12417(R) (WCAP-3269-15)
development of large closed-cycle power, 20: 12418(R) (WCAP-3739)
development of plutonium recycle fuels for use in, 17: 14732(R) (GEAP-4051)
development of plutonium recycle for, 17: 28431(R) (GEAP-4216)
development of plutonia–urania-fueled fast, 19: 38264(R) (GEAP-4781)
development of superheated, 18: 9674
economic assessment of large dual-purpose, for desalination, 18: 36834
economics and thermal efficiency of water-cooled power, 19: 27805
economics as nuclear process heaters, 18: 15585
economics of dual-purpose, for desalination, 18: 45036(T) (JPRS-26497)
economics of low-temperature, water cooled, for desalination, 19: 42097 (ORNL-TM-1152)
economics of spectral-shift controlled, 17: 40378
economics of spectral-shift pressurized-water thorium power breeders, (E), 19: 42109
experimental facilities for VVR-M, beam holes and thermal column, 20: 18139
feasibility for water desalination, 19: 31572
feasibility of, fueled with natural uranium pins and highly enriched stainless steel-uranium plates, (E), 19: 33575 (AP-Note-444)
fission rates in slightly enriched, 17: 24657
fuel and fuel cycle parameters of, 20: 6582 (EUR-2461.f)
fuel balances for, 19: 19394
fuel burnup calculations for, computer code for, 19: 24032
fuel burnup in plutonium-fueled (E/T), 19: 3589 (HW-82043)
fuel burnup in, computer analysis of, 18: 30972 (BLG-222)
fuel burnup in, plutonium centered natural uranium, (T), 20: 14102 (BNWL-183, Sect.II)
fuel burnup in, plutonium, 20: 35003 (BNWL-232)
fuel burnup monitors for VVR-S, description of flux-wire, (E), 19: 30524 (NP-14972)
fuel can damage in, detection limits of, 17: 5007
fuel consumption in slightly enriched, effects of water-to-uranium ratio, 16: 753
fuel cost relation to reactor size, 16: 5056
fuel costs of SSCR, uranium-233 and -236 recycle, (T), 19: 29595
fuel cycle costs, 17: 36876 (ORNL-TM-678)
fuel cycle development for plutonium-enriched, 19: 8617(R) (GEAP-4729)
fuel cycle evaluation for power-producing, 18: 23075
fuel cycles for power, 18: 7908
fuel development for, plutonium recycle, 18: 15429(R) (GEAP-4482)
fuel development for, plutonium-recycle, 18: 32965(R) (GEAP-4603)
fuel element assembly with burnable poison for, 19: 42072(P)
fuel element burnup in, evaluation of plutonium recycle in, 17: 33240(R) (GEAP-4303)
fuel element burnup in, evaluation of plutonium recycle in, 18: 4762(R) (GEAP-4385)
fuel element cooling in VVR-S, asymmetry effects in, 18: 23110
fuel element development for large closed-cycle, stress analysis of, (E), 20: 10382(R) (WCAP-3269-13)
fuel element guarantees for, problems in, 17: 29810
fuel lattice for, with optimum K(eff) and negative temperature coefficient, 18: 38253 (A/CONF.28/P/695)
fuel management optimization programs for, 19: 24099
fuel plate temperature in Spert I destructive power excursions, 18: 38287 (IDO-16884)
fuel processing for, economics of, 18: 13978
fuel recycling in plutonium–uranium fueled, 18: 35128(R) (GEAP-4642)
fuel rod development and testing, 17: 23897(R) (CEND-178)
fuel-element guide tube design for, 19: 45517(P)
gamma flux distribution in VVR, 16: 28605
gamma spectra from stainless steel core of, 17: 12764(R) (ORNL-3360 (p.3-11))
hazards evaluation in STEP project, 18: 24956(R) (IDO-16961)
heat transfer in, transient, 18: 4751
heat transfer kinetics in heterogeneous, 17: 42215
inspection, 16: 15937
kinetic behavior during rapid power surge, theoretical interpretation of, 18: 11405
kinetic characteristics, 16: 9652(R) (IDO-16726)
kinetic characteristics, effects of fuel subcooling and temperature, 16: 9652(R) (IDO-16726)
kinetics equation for, coefficients and roots of, 18: 7894 (IDO-16904)
kinetics of heavy-water–water cooled-and-moderated, 18: 38245 (A/CONF.28/P/176)
kinetics of Philippine Research Reactor PRR-1, 18: 1307
kinetics of plutonium-fueled thermal, 18: 38299 (A/CONF.28/P/165)
kinetics of, theoretical aspects, 17: 18996
kinetics of, survey, (E/T), 19: 17246
lattice studies in, review of, 18: 33012 (A/CONF.28/P/264)
lattice theory on enriched-uranium fueled, 17: 18990
moderator design with variable concentrations of water and lead or magnesium, 18: 13211(P)
moderator flow circuit for, introduction of gas bubbles to reduce moderator density in, 18: 19301(P)
moderator flow-control device for, 17: 33293(P)
moderator mixing, heavy and light, 19: 24189(P)
moderator reactivity worths in, oscillating-level technique for, 18: 33031
neutron buckling and reaction rates in, 18: 21591 (AEEW-M-425)
neutron buckling and flux distribution in, 18: 38315 (A/CONF.28/P/667)

neutron constants of, calculations of thermal, 18: 40795
neutron cross sections and thermal spectra in plutonium-uranium-fueled, 20: 12370
neutron diffusion and spectra in pulsed, 17: 22538 (TID-18565)
neutron flux calibrations, 17: 19684
neutron flux density distributions in, activation detectors for measuring, 19: 35711
neutron flux distribution in, internal thermal columns for amplifying, 16: 24955
neutron flux distributions in, effects of energy on, 18: 21608
neutron flux distributions in IRR-1 swimming-pool, 18: 38612 (A/CONF.28/P/666)
neutron flux distribution and coolant density profile of, method for calculating, 20: 3500
neutron flux distribution in, computer program for, 20: 38450
neutron flux distribution in VVR, 16: 28605
neutron kinetics in, analysis of, 20: 36424 (CEA-R-2883)
neutron leakage escape probability for, 19: 10491
neutron migration areas in uranium dioxide-fueled, 17: 35119
neutron multiplication in, comparison of analytical and cadmium-ratio, 16: 24426
neutron multiplication factor of, fueled with uranium dioxide, 17: 24656
neutron reactions with moderator in, nitrogen-16 specific activity from, (T), 19: 14847 (WAPD-BT-31(p.37-42))
neutron shielding calculations for, 19: 14745
neutron spectra and fast-fission effect in, fast, 20: 22506
neutron spectra from split-core swimming-pool, 18: 4848 (EANDC(OR)-26U)
neutron spectra in heterogeneous, transport equation for calculating, 18: 23030
neutron spectra in heavy and light, 18: 40783 (KR-87)
neutron spectra in uranium-235-fueled subcritical, (E), 19: 35723
neutron spectra in, calculation of thermal, 19: 47968
neutron spectrometer design for water-cooled, 18: 8686
neutron spectrum in thermal column of Triga Mark II, (E), 19: 42184
neutron temperature in Rossendorf, 16: 1264 (ZFK-RN-5)
neutron temperature in Rossendorf, 16: 1265 (ZFK-RN-13)
neutron thermal utilization in, 16: 24425
neutron thermal utilization in, calculational models for, 19: 38229 (WCAP-5492)
neutron thermalization in, parameters for, 18: 26871
neutron thermalization in, computer program for, 20: 10323 (KR-101)
neutron thermalization in, computer program for calculating, 20: 10329 (RT/FI(65)24)
neutron transport in, few-group calculations for, 18: 42596 (TID-7050 (p.197-229))
neutron transport in cylindrical, enriched-uranium, 18: 44714
neutron-density disadvantage factors in enriched lattices of, temperature dependence of thermal (T), 19: 3528
operation manual for research, (E), 19: 25767
operation of Hungarian WWRS, 18: 38598 (A/CONF.28/P/451)
operation of WWR-C, at Rossendorf, Germany, (E), 19: 40261 (ZFK-RN-17(p.179-98))
operation of WWR-M, 18: 38595 (A/CONF.28/P/325)
operation with uranium–plutonium fuel cycles, feasibility studies of, 17: 31695
performance, 18: 4859
performance as saline water distillation power source, economic aspects of, 17: 19633(R) (PB-161062)
performance of low-enrichment thermal, methods for analysis of, 18: 33087 (A/CONF.28/P/266)
physics calculations for plutonium-fueled, methods for, 19: 14788(R) (HW-81984(p.10.1-15))
physics of, 17: 5585
physics of, facility for studying, 17: 15422
physics parameters of gas-cooled, computer program for calculating, 20: 3381 (UJV-1309b/65)
plutonium burnup in, model for, 17: 16738(R) (GEAP-4081)
plutonium distribution in fuel rods for, optimization, 20: 3457
plutonium recycle economics for, (T), 20: 1436 (GEAP-4907)
power excursion tests of low-enrichment uranium dioxide core in SPERT-I, 16: 15782 (IDO-16751)
power excursion tests in highly enriched plate-type, 18: 44970 (IDO-17000)
power excursions in, self-limiting behavior of, 17: 19668 (IDO-16819)
power excursions in low-power, equations for analysis of, 17: 24713 (HW-SA-2997)
power excursions in highly enriched, self-shutdown effects in, (T), 19: 5434 (NP-14501)
power level increases in water-cooled, by fuel element replacement, 18: 11489
power levels of, use of Cherenkov radiation in measuring, 18: 6467(P)
power measurement using Cherenkov radiation, 16: 1975
power of, use of Cherenkov-radiation intensity for determining, (E), 19: 25738
power sensitivity to neutron cross section uncertainties below 100 ev, 20: 26422 (BNL-10058)
pressure vessel design with moderator-level regulator, 18: 17268(P)
proton flux in, fluorine-18 and nitrogen-13 production by recoil, 18: 30763
reactivity calculations and experimental correlations, 17: 42234
reactivity change for bubbling void in JRR-2, 18: 43087
reactivity changes in, kinetic response prediction for, 20: 38449
reactivity control, 16: 17269(P)
reactivity control in, by changing ratio of light to heavy water in, 18: 42897(P)
reactivity control of, subcritical, (E), 19: 14796
reactivity Doppler feedback in oxide fueled, analysis of, 18: 26868
reactivity effects of moderator expulsion from enriched, 16: 28438
reactivity excursion simulation in, 20: 16029
reactivity excursion termination by steam formation, 16: 14301 (MND-C-2487(p.223-31))
reactivity in highly enriched uranium, 16: 15795
reactivity measurements using kinetic techniques, subcritical, 17: 2470 (EIR-28)
reactivity measurements in enriched, 18: 38314 (A/CONF.28/P/650)
reactivity measurement for, analog system for, 18: 42917 (CEA-R-2513)
reactivity of aluminum–plutonium fueled, 20: 12494 (BNWL-160)
reactivity of, effects of long-term fuel burnup on, 17: 19557(R) (GEAP-4161)
reactivity of enriched water-cooled, 18: 38446 (A/CONF.28/P/359)
reactivity of heavy water–light water moderated, 18: 28921(R) (TID-20649)
reactivity of heterogeneous, effects of epithermal processes on, 19: 1843
reactivity of homogeneous, 20: 5062
reactivity of, effects of cross section sensitivity on, 20: 24707 (CONF-660303-6)
reactivity parameters of heavy-water–water moderated, 18: 38255(R) (KR-72)
reactivity transients in urania-fueled SPERT-I, feedback effects in, (E/T), 19: 38269 (IDO-17054)
reactivity transients in, computer program for calculation of, 19: 40160 (WAPD-TM-479)
reactivity, void coefficients in Pool Critical Assembly, 16: 3837(R) (ORNL-3193(p.3-4))
reactivity void coefficient, 16: 18629
reactivity worths of poison strips in, 18: 28943
safety aspects of, 17: 1087
safety hazards analysis for Pegase, (E), 19: 10638 (CEA-R-2518)
safety hazards and precautions at Pegase installation, 19: 42151 (CEA-R-2518(Vol.II))
safety of low-enrichment uranium dioxide-fueled, analysis of maximum credible accidents in, 18: 19319
safety of water-cooled, 17: 10134
safety of, effects of neutron cross section uncertainties on, 20: 45068 (CONF-660303, pp 430-53)
shielding of, heat release by iron-water thermal, 18: 13199
shielding performance in Westinghouse Test Reactor, 18: 4851 (ORNL-TM-332)
startup and adjustment of water-cooled, procedures for, 18: 38434 (A/CONF.28/P/305)
survey of U.S., for power production, 17: 29812
thermal models for dioxide-fueled, (T), 19: 29522
transient behavior of, preestimation of, 18: 4877
uranium–plutonium fuel cycle in, 17: 36886
water chemistry measurements in Czech WWR-S, (E), 19: 40263 (ZFK-RN-17(p.32-43))
water level in, measurement of, 16: 31272 (NP-11754(Vol.II)(Sect.III))
water pH in, problems in measurement of, (E), 19: 40127 (ZFK-RN-17 (p.9-23))
water problems in, conference, (E/T), 19: 40117 (ZFK-RN-17)
water radiolysis in, 17: 25296
water treatment for convertible light water-heavy water-type, 17: 24767

Water Pipes
see Pipes

WATER PURIFICATION EQUIPMENT
decontamination factor of Warsaw plant for Vistula River water, 18: 20229 (CLOR-23)
decontamination properties of Krupp, 16: 32632
description of Marcoule Reactor (G-1), 18: 12667
description of VVR-M research reactor unit, 18: 38667
design and operation of Hungarian reactor, 20: 24678 (NP-15892)
design and performance of mobile, 18: 25726(T)
design and performance of mobile unit for demineralization of reactor water, 19: 28470 (INR-582/XIV,XI)

design and performance of electrophoretic, for reactor coolants, 20: 6568
design for fast-breeder reactors, 20: 40413 (TID-23257(Vol.1))
design for operation on high-purity coolant of hermetically sealed boiling reactors, 20: 18089 (NAA-SR-Memo-10178)
design for PRTR, 19: 11472 (HW-83447)
design for reactor feed water purification, 18: 33713
design for Shippingport Pressurized Water Reactor, engineering drawings for, 17: 29049
design of CANDU-type reactor for desalination, 19: 38216
effectiveness of polyelectrolyte coagulants for removal of fission products, 16: 3980 (NP-11105)
efficiency for radioisotopes in water, 19: 36717
efficiency in low-level waste treatment, 20: 40483
efficiency of rapid-filter, for decontamination of surface waters, 17: 18410
efficiency of, use of sodium-24 for determination of, 19: 2671
evaluation, 17: 10850(R) (HW-73337(p.77-157))
evaluation, for removal of radioactive contamination, 16: 9061
feasibility of filtration unit for, 20: 2072 (AD-616006)
for removal of radioactive contamination, 16: 9044
for removal of radioactive contamination, 16: 9046
modification of, for fallout removal, 17: 39293(R) (NP-13151)
operation of, in primary coolant system of Polish EVA reactor, 16: 34120
performance for reactor coolants and moderators, 17: 14235
performance of condensate polishing equipment, 16: 2769
performance of ion-exchange, for reactors, (E), 19: 40128 (ZFK-RN-17 (p.75-94))
performance of ion-exchange, using natural cations, (E), 19: 40130 (ZFK-RN-17(p.165-78))
performance of soil and sand filters for removal of fallout fission products, 19: 15754 (NP-14781)
performance of synthetic-resin, in radioactive circuits, (E), 19: 40129 (ZFK-RN-17(p.114-26))
radium-226 removal by, 18: 18050
silver adsorption on surfaces in silver-based disinfecting systems, 18: 45176 (NYO-10544(Rev.))
strontium-90 removal by, 18: 18050
study of Redox plant demineralizer, 19: 2431 (HW-77023)
testing of filter conditioner for alum-filter conditioner treatment of raw water, 17: 35955 (HW-75299)
testing of sieve tray capacity in heavy water plant, 18: 40751(R) (DPST-64-83-7)
use in treatment of Clinch River water at Oak Ridge Gaseous Diffusion Plant, 20: 592 (K-C-785)
use of chemonuclear reactors for ozone production, 20: 5568 (BNL-9664)
use of chemonuclear reactors for ozone production, 20: 46971
use of radiation sources in, 19: 17541
use of radioisotopes in, 17: 30184

WATER SUPPLIES

(Including plants, sources, distribution, storage, etc.)
see also Water Purification Equipment

alpha activity due to radium and decay products, measurement of, using nuclear emulsions, 20: 11044
analysis for alpha activity, spectroscopic, 16: 17433
analysis for barium-140, radium-226, and strontium-90 by ion exchange, 18: 23421
analysis for beta activity, method for radium-226, and strontium-90, 18: 10018
analysis for cesium-137 and strontium-90, 19: 26543
analysis for fall-out radioactivity, 1962, 16: 30693
analysis for fallout radioactivity, radiochemical, 18: 8281 (NYO-4700 (Rev.))
analysis for fallout fission products in, 19: 9367 (IAEA-R-1)
analysis for radioactivity, 16: 30694
analysis for radioactivity, spectrometric, 17: 5733
analysis from radioactivity in France, 18: 16204(R) (SCPRI(RM)-XII-1963)
analysis for radioisotopes, methods for, 20: 16369
analysis for radioactive contaminants, methods for, 20: 18615
analysis for radium, radiochemical, 18: 1574
analysis for strontium x-ray fluorescence spectrometric, 17: 10553
analysis for strontium-90, samples collected in 1962, 17: 27592(R) (HASL-138)
analysis for strontium-90 and yttrium-90, design of equipment for, 18: 6763
analysis for strontium-89 and -90, chromatographic, 18: 39131
analysis for strontium-90, method for, 20: 3867 (CEA-R-2844)
analysis for strontium-89 and -90, method for, 20: 24980 (SZS-2(1966))
analysis for uranium and radium, spring water from Cotes-du-Nord region, France, 16: 27455
analysis for vanadium in Swedish, activation, 20: 38565
at Argonne National Lab., 17: 19737
beta activity of, in Italy, 1962, 18: 18040 (BIO/03/63)
carbon-14 content of, 19: 32437
cesium-137 content in, Japan, 1964, 19: 42639 (NP-15278)
cesium-137 content in, in Japan, 1960 and 1961, 20: 43518(T) (NSJ-tr-54)
cesium-137 content of Japanese, 16: 5550 (A/AC.82/G/L.690)
cesium-137 content of, in UK, 1961, 16: 24033
cesium-137 content in, in Great Britain, 1961, 17: 14549
cesium-137 content in, in Great Britain, 1962, 17: 36028 (NP-13035)
cesium-137 removal in reservoirs, effects of hydrodynamic factors on, 18: 36928(T) (JPRS-26056(p.1-8))
civilian defense measures to protect, 18: 27727
construction of water conveyance system in California, feasibility of nuclear excavation in, 18: 35675 (TID-7695(p.363-70))
consumption and inspection of, in event of nuclear conflict, 19: 38882
contamination by fall-out after nuclear attack, radiation hazards from, 16: 24014 (NP-11715)
contamination by fall-out from nuclear weapons, problems in, 16: 29263
contamination by fallout, vulnerability of U. S., 18: 8535 (AD-426044)
contamination control for, 19: 38290
contamination of, by fallout, problems of radiation hazards in, 17: 15527
contamination of, during radiological warfare, 17: 39293(R) (NP-13151)
contamination of municipal, by nuclear attacks, 18: 20233 (NP-13806)
contamination, protection, and purification of, in event of mass attack, 20: 23382(T) (JPRS-34578)
costs of treatment programs for, possible reduction of, 19: 20087 (GAT-P-33)
decontamination after nuclear attack, 16: 9062
decontamination, by filtration through sand and soil, 17: 30765
decontamination for drinking, development of ion exchange unit for small-scale, 18: 441 (NP-13260)
decontamination from radioisotopes using natural sorbents, efficiency of, 19: 24424
decontamination in bacteriological, chemical, and radiological warfare, 20: 4192(T) (JPRS-32686)
decontamination of, methods for, 16: 29263
decontamination of radioactive, emergency procedure for individuals or families, 17: 1659(T) (AEC-tr-5455)
decontamination of fallout strontium-90 in reservoirs by accumulation by hydrophytes and detritus, 17: 28644(T) (JPRS-19937(p.29-37))
decontamination of, review on methods for, 17: 36047
decontamination of Warsaw, by filtration, 19: 13684
decontamination of household, 19: 15754 (NP-14781)
decontamination of, 19: 20240
decontamination of, feasibility of filtration unit for, 20: 2072 (AD-616006)
decontamination of, using sanitary water-treatment process, 20: 22512 (K-1651)
decontamination of, sorptive properties of peat for, 20: 7002 (INR-609/XIX/D)
decontamination using sanitary treatment process, 20: 592 (K-C-785)
desalination for Northeast U. S., potential, 20: 45186 (NP-16148)
determination in milk samples collected during 1961, 17: 1677
development and management of, use of nuclear explosions in, 19: 38791 (TEI-857)
development and management of, use of atomic explosion in, 20: 41073
effects of high-altitude explosions on, evaluation on, 18: 33811
effects of nuclear attack on, recovery from, 19: 9418
effects on radiation dose to gastrointestinal tract, system for continuous monitoring of, 20: 27191 (BNWL-SA-212)
emergency measures for protection during nuclear disaster, 16: 22468
fall-out contamination, 16: 22453 (TID-7632(p.306-11))
fall-out content from Project Chariot explosions, 16: 17918 (TEI-810)
fallout contamination of, during nuclear warfare, 18: 18071
fallout contamination of, effects of redistribution of fission products on, 18: 37368 (HNS-1229-46)
fallout contamination of, pathological effects, 19: 21895
fallout contamination of, manual on control of, 19: 30441 (NP-15066)
fallout contamination of, radiation dose to man from, 19: 46633 (AD-276187)
fallout monitoring in samples collected in 1962, 17: 21954
fallout monitoring in, 1963, 18: 18041(R) (HASL-144)
fallout monitoring in U. S., 1964, 19: 637
fallout monitoring in Japan, 1963, 19: 9369 (NP-14502)
fallout radioactivity in samples collected from 1960 through 1962, 17: 18454
fallout radioactivity in samples collected in 1962, 17: 18455
filtration at increased rates at Hanford, 19: 7653 (RL-REA-1)
fission product removal, effectiveness of polyelectrolyte coagulants, 16: 3980 (NP-11105)
for fallout shelters, procurement, storage, preparation, and service of, 18: 12379 (AD-403714)
iodine-131 content in, from fallout, 19: 26596
manganese-54 content in German, from fallout, 19: 15792

maximum permissible limits for beryllium in, 20: 42755
monitoring equipment and methods for, 18: 12391
monitoring for beta activity and strontium-90 content in, in Poland, 1961, 17: 25474 (CLOR-13)
monitoring for beta activity in Austria, 1962, 19: 15804
monitoring for fall-out radioactivity, 16: 6645(R) (HASL-117)
monitoring for fallout radioactivity, 1963, 17: 18322(R) (HASL-135)
monitoring for radioactivity, 16: 20889
monitoring for radioactivity, 16: 20901
monitoring for radioactivity, in Great Britain, 19: 4379
monitoring for radioactivity in German Federal Republic, Jan.-March 1961, 19: 18227
monitoring of bacterial contamination in, 18: 11565
monitoring of, contaminated by fallout in Connecticut, 17: 18426
monitoring of, design of apparatus for, 17: 381
monitoring of, for radioactivity in New England and Middle Atlantic States, 17: 18424
monitoring of, after explosion of nuclear weapon, 18: 12385 (NP-13568)
monitoring of, at Juelich research center, 19: 48078 (JUL-261-DE)
monitoring of, system for continuous, 18: 10430(P)
monitoring, 1961, 16: 20906
monitoring, 1961, 16: 20905
monitoring, 1961 and 1962, 16: 20907
pollution of, review of, 18: 9743
pollution prevention at ORNL, reduced pressure principle backflow preventer for, 19: 36719
postattack recovery procedures for, 20: 45940 (AD-639710)
protection and decontamination of, against radiological, chemical, and bacteriological warfare agents, 18: 31802(T) (JPRS-25214)
protection from fallout contamination in hospitals, 17: 8466
radiation control of *Entamoeba histolytica* in, 20: 5366
radiation disinfection of, gamma, 20: 1645
radiation dose to population from, in regions with uranium ores, 20: 4193
radiation monitoring of, sample preparation for, 19: 26588
radioactive contamination measurement, in Prague, 16: 7778
radioactive contamination, 16: 9046
radioactive contamination, public health aspects, 17: 8440
radioactive contamination of, control of, 17: 21950
radioactive contamination of, 18: 29911
radioactive contamination of, review, 19: 4379
radioactive contamination of, transfer to man, 19: 24758
radioactive contamination of, review, 19: 24790
radioactive contamination removal, 16: 9061
radioactive decontamination, 19: 24771
radioactivity and hardness of, relation of cancer mortality rates to, 17: 20255
radioactivity content in, in Italy Jan.–June 1962, 17: 36024 (BIO/26/62)
radioactivity due to fallout, 1964, 18: 31784(R) (HASL-146)
radioactivity due to fallout in, 1964 and 1965, 19: 20154(R) (HASL-158)
radioactivity due to fallout, 1965, 20: 20882(R) (HASL-171)
radioactivity from cesium-137 and strontium-90 in Faeroe Islands, 1964, 20: 7320 (RISO-108)
radioactivity from cesium-137 and strontium-90 in Greenland, 1964, 20: 7321 (RISO-109)
radioactivity from cesium-137 and strontium-90 in, in Japan, 1964, 20: 16731 (NP-15883)
radioactivity from fallout in, 1965 and 1966, 20: 41131(R) (HASL-172)
radioactivity in British, 17: 6337
radioactivity in, device for detection and measurement of, 17: 12565
radioactivity, in Prague, 16: 20878(T) (AECL-1498)
radioactivity in U. S., 1964, 20: 33589
radioactivity in West German Republic, 19: 38904
radioactivity in, 1961 and 1962, 16: 14447(R) (HASL-122)
radioactivity in, Great Britain, 1963, 19: 24703 (NP-15013)
radioactivity in, of Great Britain, 20: 5409
radioactivity in, method for determining alpha, beta, and gamma, 20: 16407
radioactivity in, Jan. to July, 1965, 20: 18972
radioactivity, maximum permissible concentrations, 17: 23546 (HW-77690)
radioactivity monitoring in West German Republic, July–Sept. 1964, 19: 15816
radioactivity monitoring in Italy, 19: 42637 (BIO/32/63)
radioactivity of Canadian, June 1965, 19: 44251 (NP-15519, pp 23-51)
radioactivity of Hanford area, 1964, 19: 38874 (BNWL-SA-53)
radioactivity of, in Brazil, naturally occurring, 17: 30774
radioactivity of Maine and New Hampshire, 20: 37006
radioactivity of samples collected in U. S., 1964, 18: 41644(R) (HASL-149)
radioactivity of, in Brazil, 18: 41649 (TID-20955)
radioactivity of, in Lima, Peru, 19: 15795
radioactivity of, in Alaska, 19: 18164
radioactivity of, in Austria, 1963, 19: 38860
radioactivity of, in Australia, United Kingdom, and United States, 19: 40805 (NRS-30)
radioactivity of, in India, Nov. 1963, 20: 7294 (AEET/HP/Environ/4)
radioactivity of, in Hanford area, Wash., Jan. to June 1965, 20: 7297 (BNWL-165)
radioactivity of, in Savannah River Plant area, July through Dec. 1965, 20: 27195(R) (DPST-66-30-1)
radioactivity of, permissible levels, 16: 9311
radioactivity, maximum permissible, 16: 9044
radioisotope contamination of, following nuclear warfare, 19: 42658 (NP-15328)
radioisotope decontamination using U. S. Army equipment, 19: 36717
radiological monitoring in November 1962 in France, 17: 14537 (SCPRI(M)62-11)
radiological monitoring in Dec. 1962 in France, 17: 14538 (SCPRI(RM)-62-12)
radiological monitoring, 18: 35762 (NAVDOCKS-MO-218)
radiological monitoring, 18: 41648 (NP-14254)
radiological monitoring in West Germany, 19: 15819
radiosterilization of, 19: 17541
radium content in, analysis of deciduous teeth for monitoring, 20: 4160
radium content of Savannah River Area, South Carolina, 17: 20239 (DPSPU 63-30-10)
radium-226 intake from, in Great Britian, 16: 27482
recharge of ground water as, economics of artificial, 19: 45717 (UCRL-7850(Rev.1))
requirements of nuclear center, 18: 12295
research on underground, using gamma and neutron scattering, 20: 37135
restoration of metropolitan water works following nuclear attack, 17: 27595 (NP-12902)
saline contamination of coastal, tracer study of, 19: 32419
separation of cerium-144, cesium-137, and strontium-90 from, by ion exchange chromatography, 20: 20627
separation of cesium-137 from, by solvent extraction using nitrobenzene, 17: 8455
separation of radon from, by aeration, design of pilot plant for, 20: 14649
shortages in, desalination of sea water for meeting, 19: 34293 (BNWL-SA-134)
size distribution and storage characteristics of potable, in U. S., 18: 37356 (NAA-SR-Memo-9311)
standards of radioactive pollution, 17: 27613
strontium-90 deposition in, effects on dietary intake through water-living organisms, 16: 5135(T) (CEA-tr-R-1416)
strontium-90 accumulation by plants growing in reservoirs, 18: 35282(T) (AEC-tr-6447)
strontium-90 content in U. S., 1963, 18: 12401
strontium-90 content in Don River basin, Russia, 18: 35776(T) (AEC-tr-6458)
strontium-90 content in, radiochemical measurement of, 18: 39509
strontium-90 content in, Weser River, 18: 39536
strontium-90 contents in Poland in 1962, 19: 24701 (CLOR-32)
strontium-90 content in German, 19: 38876 (NP-14927)
strontium-90 content in, Japan, 1964, 19: 42639 (NP-15278)
strontium-90 content in U. S., 1965, 20: 16662(R) (HASL-165)
strontium-90 content in, in Japan, 1960 and 1961, 20: 43518(T) (NSJ-tr-54)
strontium-90 content in Japanese, 16: 5550 (A/AC.82/G/L.690)
strontium-90 content of, in United Kingdom, 1961, 16: 24033
strontium-90 content in, in Great Britian, 1961, 17: 14549
strontium-90 content in, in Great Britian, 1962, 17: 36028 (NP-13035)
strontium-90 hydrologic transport to, from atmosphere, 20: 41141
tritium content in, in Japan in 1961 and 1962, 17: 30083
turbidity monitoring system for treatment plant of PRTR, 19: 11472 (HW-83447)
uranium contamination of, 19: 36743
uranium content in, effects on content in man, 19: 19490
use of tritium in measuring subterranean, in South Africa, 20: 41167
uses of radioisotopes, review, 17: 12521
utility planning for nuclear attack, 18: 1971
vulnerability of U. S., to nuclear attack, 19: 22588 (AD-602677)
water treatment system for, automatic, 17: 8487(P)
water-hammer in complex piping system for, comparison of theory and experiment for, 19: 4270 (HW-SA-3512)

WATER VAPOR

see also Steam

analysis for tritium by gas counting, 16: 18814 (ORO-484)
analysis of ionized, mass spectrometric, 17: 4457 (GA-3358)
bubble growth and transition characteristics in nucleate boiling, dynamics of, 18: 10235
collision with ammonia and water molecular beams, cross sections, 17: 624
compatibility with pyrolytic-carbon-coated carbide fuel particles at 1000°C, 20: 11224
condensation of, irreversible, 18: 34323

content in atmosphere above 100 km, 18: 7617
content in lunar atmosphere, effects of solar wind on, 18: 18546
content in middle stratosphere over southern England, 1956 to 1960, 16: 13384
convection in atmosphere, 20: 4153(R) (UCRL-14360, pp 73-85)
corrosive effects on beryllium above 500°C, 16: 25725
corrosive effects on iron, 17: 8742(R) (EURAEC-448)
corrosive effects on uranium, 18: 8757 (SC-DC-64-204)
corrosive effects on uranium, effects of hydrogen, nitrogen, and oxygen on, 18: 10483
corrosive effects on uranium at 100°C in absence of oxygen, effects of pressure on, 18: 25921 (AWRE-O-25/64)
corrosive effects on beryllia tubes at 1800 to 2600°F, 18: 27880 (APEX-760)
corrosive effects on graphite at 725 to 840°C, 18: 29048(R) (HW-80284(p.6.1-10))
corrosive effects on plutonium, thorium, uranium, and their carbides, bibliography on, 18: 32090 (UCRL-7836)
corrosive effects on beryllia tubes, 19: 2748 (UCRL-7663)
corrosive effects on Hastelloy X and Haynes 25 Alloy at 1200°C, 19: 13883(R) (HW-81984(p.9.1-6))
corrosive effects on tungsten, 19: 18410
corrosive effects on Zircaloy-2 and zirconium at 600 to 850°C, 19: 22870(R) (HW-83601)
corrosive effects on chromium–iron alloys, 19: 22863(R) (AD-606809)
corrosive effects on high-temperature structural alloys in helium at 1700°F, 19: 30820 (BNWL-23)
corrosive effects on iron–plutonium–uranium alloys, 19: 30665 (AWRE-O-18/65)
corrosive effects on uranium at 25 and 40°C, effects of oxygen on, 19: 44618 (AWRE-O-42/65)
corrosive effects on uranium arsenides and sulfides at 25 and 40°C, 19: 44618 (AWRE-O-42/65)
corrosive effects on uranium carbide metallographic specimens, 19: 46953 (NMI-4997, pp 62-75)
corrosive effects on uranium, 20: 1805 (AWRE-O-69/65)
corrosive effects on Inconel 600, 625, 702, and 718 at 815, 930, and 1038°C, 20: 9409 (BNWL-155)
corrosive effects on Hastelloy C, N, R-235, and X-280 at 815, 930, and 1038°C, 20: 9409 (BNWL-155)
corrosive effects on Haynes Alloy 25 and Incoloy 800 at 815, 930, and 1038°C, 20: 9409 (BNWL-155)
corrosive effects on uranium, mechanism of, 20: 33310
corrosive effects on graphite, effects of metal additions on, 20: 31667
decomposition of, using fission fragment recoil energy, 20: 29317
deposition from air to snow surfaces, tracer studies, 19: 1031 (CRL-86)
determination in argon in gas chromatography, electron drift velocity detector for, 18: 33476
determination in air system of underground counting facility, 20: 22853(R) (ANL-7060)
determination in gases, design of electrolylic device for, 17: 23613 (TID-18574)
determination in gases using carbon-14-labeled calcium carbide, 18: 19848 (ORO-591)
determination in gases by hydrolysis of organic chloride and activation of formed hydrochloric acid, 18: 31365 (CEA-R-2357)
determination in klystrons during operation and life-testing, 16: 31757
determination in lunar atmosphere, 16: 26049
determination in stratosphere, alpha radiation hygrometer for, 19: 32501 (AD-608498)
determination in wood chips by slowing down of fast neutrons, 19: 17846
determination, neutron moderation method, 16: 25271(R) (TID-16156)
determination of traces in gases, 16: 8705(P)
determination of traces of, in gases, chromatographic, 19: 28228(T) (NP-tr-1231)
deuterium exchange with hydrogen at high temperatures and pressures, catalyst for, 17: 27719(P)
deuterium exchange with hydrogen, properties of chromium trioxide–nickel catalyst for, 20: 5534
deuterium-hydrogen exchange in, kinetics of, 16: 20923 (NP-11789)
distribution in atmosphere over Hyderabad, India, 17: 39269 (TID-19483)
distribution in stratosphere and troposphere, review on, 20: 23279
effect on external surface adsorption capacity of charcoal for methyl iodide, 20: 41202 (UCRL-14990)
effect on hydridation of Zircaloy-2, 19: 34639(R) (BNWL-79(p.5.1-11))
effects as impurity on performance of carbon dioxide-filled proportional detectors, 18: 7068
effects in irradiated uranium dioxide fuel elements, 20: 2468
effects of absorbed, on pyrophoric properties of uranium dioxide, 18: 1666
effects on argon ion-platinum reactions at 22 kev, 17: 25989
effects on atmospheric absorption at 1.35 cm wavelength, 20: 4479(R) (TID-22179, pp 1-83)
effects on beryllium corrosion by carbon dioxide, 18: 14416
effects on decomposition of magnesium hydroxide, 17: 18070
effects on densification during sintering of beryllium oxide, 19: 24963
effects on efficiency of electron multiplier, 19: 32413(R) (WERL-2823-17)
effects on electron spin resonance of irradiated silicon oxides, 19: 28384
effects on fatigue of molybdenum, 19: 44730
effects on fluorine–trifluoroacetic acid reaction, 20: 1881
effects on gamma radioinduced recombination rate of hydrogen and oxygen, 20: 20749
effects on gas plating rate for nickel carbonyl, 17: 2942 (K-1533)
effects on graphite oxidation by oxygen at 510 to 650°C, 20: 21285
effects on ignition of magnesium alloys in carbon dioxide, 19: 7849 (CEA-R-2494)
effects on initial sintering of calcia, 20: 43813(R) (COO-1122-3)
effects on iodine-131 sorption by activated charcoal, 20: 278 (CONF-650407, pp 814-29)
effects on kinetics of graphite oxidation by nitrogen–oxygen mixtures, 20: 23608
effects on Magnox alloy corrosion by carbon dioxide, 20: 7524
effects on methyl iodide retention in charcoals, 20: 279 (CONF-650407, pp 852-68)
effects on Napier relaxation frequency of oxygen, 19: 40483
effects on oxidation of cerium–magnesium alloys by nitrogen at 475 to 600°C, 19: 20485
effects on oxidation of graphite at 620°C, 19: 30677
effects on plutonium corrosion by air at 30 to 100°C, 20: 21280
effects on preparation of sulfur- and xenon-containing fluorine compounds, 20: 1881
effects on radioinduced reactions between carbon dioxide and graphite, 19: 11159 (AERE-R-4332)
effects on radioinduced reactions of carbon dioxide with graphite, 19: 19954 (AERE-R-4839)
effects on radioinduced recombination of hydrogen with oxygen, 19: 40549 (COO-1032-1)
effects on radioinduced recombination of hydrogen and oxygen, 20: 36910
effects on removal of iodine vapor and methyl iodide from air by activated charcoals, 20: 280 (CONF-650407, pp 869-84)
effects on solubility of beryllium oxide in molten alkali metal hydroxides, 20: 8897
effects on transition metals at 1 and 8 torr, 20: 19197
effects on volatilization of molybdenum, 19: 32161
effects on Zircaloy-2 hydridation at 320°C, 20: 7497(R) (BNWL-150, pp 3.1-30)
effects on zirconium and zirconium alloys at 375 and 575°C, 20: 25498
electron attachment coefficients and drift velocities in mixtures with other gases, 17: 29441
electron collisions with, on tungsten surface, 17: 12761(R) (NYO-9813)
electron drift velocity in, slow, 16: 19470 (NP-11617)
electron drift velocity in, at 77 to 443°K, 16: 27742 (NP-11983)
electron quasi-trapping in, low-energy, 16: 25973
electron reactions at 0.1 to 20 kev, ionization cross sections for, (E), 20: 29928
enthalpy data at 2850 to 4300 psia and 360 to 400°C, 16: 7958 (ANL-6505)
equation of state for critical region, 16: 9292 (ANL-6508)
equation of state for, in critical region, 17: 39078
exchange of tritiated, between air and snow, 19: 32785 (AECL-2232)
exchange reactions with gaseous tritium, 20: 23356 (CONF-640413, pp 17-26)
flow of atmospheric, determination of, 18: 22547(T) (ANL-Trans-12)
heat of adsorption on graphite, 16: 27654
heat transfer by, 18: 37324 (A/CONF.28/P/16)
heat transfer by, 18: 17322(R) (TID-19971)
heat transfer in laminar flow, 17: 21879 (TID-18556)
heat transfer properties, 17: 289
heat transfer properties, 16: 31801
hydrogen ion growth in supersaturated, 17: 39018 (AWRE-O-55/63)
ionization effects in nitrogen-filled chambers, 17: 11047
ionization in reactor by fission products, conversion to electric energy, 18: 18630
isotopic exchange of hydrogen between molecular hydrogen and, 17: 27326
isotopic exchange of hydrogen and tritium in beta decay-induced, 19: 4214
laser action in d-c discharge, continuous-wave submillimeter, (E), 20: 28047
measurement in atmosphere and clouds using microwave radiometers, 20: 4479(R) (TID-22179, pp 1-83)
measurement of very low humidity, performance of electrolytic hygrometer for, 20: 45944 (AERE-PR-HPM-9, pp 1-6)
monitoring of tritiated, scintillation detector for, 20: 4235 (AECL-2283)

neutron scattering at 0.18×10^{-3} to 2.8×10^{-3} ev, 16: 7162
neutron scattering at low energy, (T), 19: 33212
neutron scattering cross sections at 18 and 32 Mev, frequencies of, (E), 19: 35378(R) (EANDC(E)-57(U))
oxidation of graphite by, in presence of hydrogen, rate of, 20: 29626
oxidation of niobium, mechanism and rate of, 17: 1441
particle capture mechanisms for airborne, 16: 30664 (TID-16578 (Pts.1&2))
particle formation in supersaturated, kinetic analysis of, 17: 14224(T) (AEC-tr-5683)
performance as reactor coolant, 18: 36809(R) (SRO-105)
photoionization and absorption cross sections, 18: 16718
poisoning effects on thermionic emission from thoriated tungsten cathodes, 16: 17845
production for humidity calibrations, generator for, 18: 9762 (SC-TM-102-63(24))
properties as atmospheric tracer, 18: 10617
properties in cloud chambers at −75 to 0°C, 16: 8006
protective effects of, against radiation injury of brine shrimp eggs, 17: 40622
radiation chemistry of, isotope effects in, 19: 36475
radiation effects on production of ions from, alpha, 20: 31270
radioinduced reactions with carbon monoxide, production of carbon dioxide and hydrogen in, 17: 8214
radiolysis of deuterated and normal, molecular and radical yields in gamma, 18: 12189
radiolysis of, effects of cyclohexane, ethanol, ether, and methane on gamma, 17: 39148
radiolysis of, hydrogen yields in alpha, 17: 39140
radiolysis of, effects of nitrous oxide on electron and hydrogen yields from, 19: 22376
radiolysis of, effects of presence of vanadium oxide and zinc oxide semiconductors on, 20: 9002
radiolysis of, effects of temperature and cyclohexane scavenger on yields of hydrogen from gamma, 20: 16536
radiolysis of, formation of molecular hydrogen in gamma, 18: 16105
radiolysis of, hydrogen yields from gamma, 20: 29295
radiolysis of, ion yields in alpha, 20: 1936
reactions with barium oxide at 1485 to 1785°K, 18: 9780 (TID-20017)
reactions with barium oxide, formation of vapor species in, 19: 17436 (UCRL-12225-T)
reactions with beryllia, 17: 40778 (TID-6036)
reactions with beryllium oxide at 1065 to 1380°C, 18: 20016
reactions with beryllium, kinetics, 19: 11051(R) (SC-DC-64-1432)
reactions with beryllium in simulated launch pad abort environments at 800 to 1500°C, 20: 2341 (SC-DC-65-1637)
reactions with calcium, magnesium, molybdenum, tantalum, and zirconium, combustion, 20: 29641(R) (SC-DC-65-1691)
reactions with carbon-coated fuel particles at 1000°C, 19: 36960(R) (ORNL-3807, pp 80-142)
reactions with cerium tetrafluoride, 19: 39182
reactions with fission fragment tracks in crystals, etching in, 18: 18437
reactions with graphite at high temperatures, 17: 469
reactions with graphite at high temperatures, 18: 39157 (HW-75072)
reactions with graphite at 750 to 900°C, mechanism of, 19: 13421(R) (HW-81984(p.6.1-14))
reactions with graphite at 750 to 900°C, kinetics, 19: 17855 (HW-SA-3439)
reactions with graphite in carbon dioxide–helium mixtures at high temperatures, 19: 23996(R) (ORNL-3650(p.1-110))
reactions with lead azide, 18: 6557 (SC-DC-3440)
reactions with lithium at 20 to 45°C, 17: 10622
reactions with magnetite cylinders, mechanism 19: 12882 (TID-21573)
reactions with magnesium fluoride at high temperatures, kinetics of, 19: 15418 (UCRL-9821(Rev.))
reactions with magnesium fluoride at high temperatures, mechanism of, 19: 15419 (UCRL-11103(Rev.1))
reactions with mercury isotopes, photochemical, 19: 20429 (MLM-1214)
reactions with neodymium oxides, 19: 374
reactions with niobium pentachloride, kinetics of, 18: 5263
reactions with niobium and tantalum during annealing and melting, 19: 40490
reactions with niobium, embrittling effects of, 19: 46296
reactions with potassium hydroxide and superoxide, kinetics, 19: 40462 (SC-TM-65-183)
reactions with pyrolytic-carbon-coated uranium dicarbide at 700 to 1100°C, 18: 18316 (ORNL-3598)
reactions with pyrolytic-carbon-coated uranium carbide particles at temperatures up to 1100°C, 19: 20463 (ORNL-TM-431)
reactions with pyrolytic carbon fuel particle coatings at 1000°C, 19: 39129(R) (ORNL-TM-1116)
reactions with pyrolytic-carbon-coated fuel particles at 1000°C, 20: 13261(R) (ORNL-3885, pp 87-149)
reactions with sintered uranium dioxide, 17: 41367(T) (EURAEC-711)
reactions with uranium(IV) oxide at 1400 to 1708°C, 16: 4450(R) (BMI-1546(Del.))
reactions with uranium nitride, 16: 8707 (AERE-R-3710)
reactions with uranium carbides, 16: 14815(R) (EURAEC-23)
reactions with uranium in flowing moist gases, mechanism of, 18: 8756 (SC-DC-64-203)
reactions with uranium at 35 to 100°C, 18: 10467 (AWRE-O-94/63)
reactions with uranium oxides, kinetics and phases of, 18: 41377 (UJV-940/63)
reactions with uranium at 160 to 410°C, kinetics of, 19: 26281 (CEA-R-2596)
reactions with uranium, growth of oxide films in, 19: 44619 (AWRE-O-66/65)
reactions with uranium at 30 to 80°C, kinetics, 20: 1804 (AWRE-O-68/65)
reactions with uranium carbide, factors affecting, 20: 12925(R) (EURAEC-1446)
reactions with uranium carbide, effects of hydrogen on, 20: 40870 (NAA-SR-Memo-7310)
reactions with vapor-deposited uranium films, kinetics of, 17: 25180
reactions with Zircaloy-2 and zirconium at 300 to 360°C, kinetics of, 20: 24995
removal from argon, 18: 27862 (NASA-SP-41(p.313-16))
separation from barium, cadmium, molybdenum, and yttrium oxides for neutron transmission measurements, 20: 3914 (AERE-M-1654)
separation from gas-cooled reactor helium coolants, 16: 29240 (TID-7627 (p.461-74))
solubility in alkali nitrates, thermodynamics of, 20: 1812 (EUR-2495.e)
solvent properties for aluminum hydroxide, 17: 40789
sorption by iron oxide, analysis of isotherms in, 16: 17881(R) (MITS-47)
sorption by lysozyme at 17 to 57°C, exchange effects in, 16: 460
sorption by molecular sieves, 19: 27879 (SC-RR-65-160)
sorption by thoria gel, 17: 35705 (TID-19276)
sorption by uranium tetrafluoride, uranyl fluoride, and their mixtures, thermodynamics of, 20: 45625 (MCW-1448)
sorption by vapor-deposited titanium films, probability factors for, 18: 4329(R) (ORNL-3470(p.237-9))
sorption by vapor-deposited titanium films, 18: 14591 (ORNL-3481)
sorption in nuclear power plant components, 18: 7934
sorption in ultrahigh vacuum systems, 19: 28534
sorption of, tracer studies on pulmonary, 18: 35414 (TID-7678(p.213-36))
sorption on cleaved surfaces of LiF, 17: 4545
sorptive and retention properties for chondroitin sulfates and heparin, 17: 40841
sources and control of, in fallout shelters, 18: 37433 (AD-600423)
sources and control of, in fallout shelters, 18: 37434 (AD-600437)
specific heat data at 14.22 to 4300 psia and 680 to 800°F, review, 16: 3167 (ANL-6436)
sticking factors for, on titanium film, 17: 17337(R) (ORNL-3392 3392(p.86-8))
thermal capacity at 500 to 600°C and 200 to 500 atm, 16: 5467(T) (CEA-tr-R-1410)
thermal conductivity at 320 to 560°C, 16: 6532(T) (CEA-tr-R-1436)
tritium content in atmospheric, method for measuring, 20: 37028
tritium exchange with tritium gas, beta-decay-induced, 18: 3862
ultrasonic attenuation and relaxation times in, 20: 29172
yields in gamma radiation decomposition of potassium sodium tartrates, mass spectra of, 19: 15599
ethylene–water vapor, electron diffusion in, 17: 39308(R) (ORNL-3492(p.134-43))
ethylene–H_2O, electron diffusion coefficient and drift velocity in, (E), 20: 33289
H–H_2O, effects on volatilization of tungsten, 18: 31493
H–H_2O, isotopic exchange kinetics in, 19: 26742
H–water vapor, dissociations in, at 600 to 1700°C, 17: 33858 (ANL-6747)
methane–water vapor, rate of tritium exchange reactions with hydrogen in, 20: 14662(R) (ORNL-TM-1394)

WATER WAVES

buoy dynamics from, submerged, (T), 20: 6686(R) (NVO-98-12)
detection and measurement of Tsunami-like, 19: 42210(R) (NVO-98-8)
detection of tsunami, operational and support requirements plan for, 20: 543(R) (NVO-98-9)
detection of tsunami, system design and development for, 20: 2058(R) (NVO-98-10)
energy flux for spectrum of ocean, evaluation of, 17: 20184
energy transfer in spectrum of gravity, equations for, 17: 20183
formation, motion, and ship behavior in, 16: 8417
interactions of, Feynman diagrams and rules for, 20: 18936
measurement of deep ocean tsunami, design and operation of taut-line buoy system for, 19: 17414(R) (NVO-98-3)
measurement of deep ocean tsunami, testing of taut-line buoy system for, 19: 17415(R) (NVO-98-4)

measurement of deep Tsunami-like, instrumentation for, 19: 40288(R) (NVO-98-5)
measurement of deep water tsunami, equipment and methods for, 19: 13619(R) (NVO-98-1)
measurement of tsunami, pressure sensors for, 20: 2059(R) (NVO-98-11)
motion of solitary breaking and shoaling, (T), 20: 12551 (UCRL-12186)
production by nuclear explosion in unconfined aquifer, model study, 19: 26484 (UCRL-13119)
production in atomic explosions, characteristics, 16: 2841
propagation from atomic explosions, simulation using explosions, 20: 14660 (AD-620468)
propagation from underwater nuclear explosions, simulation of, 20: 37306 (AD-636408)
properties of small, 16: 4370 (ONR-9(Vol.3))
run-up effects of dispersive, feasibility of modeling, (T), 20: 4142 (AD-619053)
velocity potential of surface, on sloping beach, (T), 19: 10708 (UCRL-12185)

Wave Mechanics
see Quantum Mechanics

Waveguides
see Microwave Equipment

WAXES
see also Greases
see also Oils
see also Paraffin
analysis of natural, chromatographic, 16: 28670(R) (UCLA-507)
composition of coelacanth fish, 19: 43681(R) (UCLA-12-565, pp 17-31)
composition of, from fish, 18: 11574(R) (UCLA-520(p.15-25))
composition of, from fish, 19: 21819(R) (UCLA-12-541(p.15-24))
dosimetric properties of beeswax and carnauba, 16: 9052
effects on buoyancy of fish, 20: 18210(R) (UCLA-12-576, pp 16-25)
plant metabolism, tracer study, 17: 13986(R) (UCLA-510)
preparation of improved waxing dispersions by irradiation, 16: 16400(P)
properties as dip-coat packaging, 16: 4589(R) (NP-11146)
radiation effects on electric conductivity and structure of synthetic ceresin, 16: 15257
radiation effects on gloss stability of coating compositions, 17: 25841(P)
radioinduced electret production in, 17: 29382
selenium incorporation in leaf, tracer study, 17: 17657
separation of natural, chromatographic, 17: 35337(R) (UCLA-515 (p.15-31))
use of, as laps on vibratory polishers, 17: 6516 (IS-439)

WBNS
see Water Boiler Neutron Sources

WEAPONS
see also Atomic Weapons
see also Biological Warfare Agents
see also Chemical Warfare Agents
see also Radiological Warfare Agents
see also Radiological Weapons
see also Thermonuclear Weapons
cessation of testing of, effects on strontium-90 contamination in East Germany, 20: 43538
development, 20: 27071
testing of, correlation with appearance of debris in New Zealand, 20: 43530

WEAR
see also Abrasion
analysis of engine, iron-55, 18: 2113
behavior of non-metallic materials, 16: 30518
determination in drawing die, tracer techniques, 16: 12078
evaluation of, by tracer techniques, 17: 1587
factors affecting frictional, 20: 43788
measurement between bearing materials, survey of, 17: 32208(R) (GDC-63-140)
measurement for automobile tires using thallium-204 beta source, 18: 39728(T) (AEC-tr-6390(p.51-6))
measurement for machine parts by activation analysis, 18: 16165 (TID-7689(p.137-42))
measurement in cylinders and piston rings, tracer techniques for, 17: 32226
measurement in gasoline engines by neutron activation, 19: 2472
measurement in lathe tools using radioactive tracers, 17: 8511
measurement in pressurized water environment to 500°F, test rig for, 19: 22462 (WAPD-288)
measurement in refractory materials by radiological means, safety aspects, 16: 16066
measurement in shearing dies and punches, radiological, 16: 16067
measurement of, engineering drawings of system using tracer techniques for, 17: 32380
measurement of gear pitting, tracer technique for, 17: 30190
measurement of, on chromed piston rings and cylinder liners by gamma spectrometry, 17: 12520
measurement of tool, radiometric method for, 18: 20426
measurement of, use of radioisotopes for, 17: 16377
measurement of, for pipes, radiometric, 19: 24898
measurement of, for refractories in blast furnaces, using radiometric methods, 20: 715
measurement of, use of radioisotopes in, 18: 14318
measurement of, use of kryptonate beta sources in, 20: 43765
measurement on engine parts, use of gamma sources for, 17: 30188
measurement on piston ring in diesel engine, tracer technique for, 17: 30189
measurement on piston rings, tracer techniques for, 18: 2108 (TID-16050)
measurement on piston rings, use of radioisotopes in, 18: 39735(T) (AEC-tr-6390(p.108-13))
measurement on piston rings, activation method for, 19: 30611
measurement using krypton-85, 17: 35261(R) (TID-19318)
measurement using krypton-85, 18: 37566(R) (NYO-2757-3)
measurement using radioisotopes, 20: 46115
measurement without system radioactive contamination, activation method for, 18: 22196(P)
measurements in steel, use of gold diffusion as tracer in, 19: 32753
measurements on ball bearings using radioisotopes, 19: 7829
measurements on cylinder bushings of engines, radioisotope uses in, 19: 9557
mechanism of wire-drawing dies, 16: 8982
of plated coatings for use in rotary switches, 19: 42216 (SC-DR-65-269)
of tool for punching sheet metal, 16: 24068
pitting of metals by, tracer studies, 17: 41371
processes in small-scale uses, study by tracer methods, 16: 16063
radiation effects on, 17: 36366
radiation effects on, of solid-film lubricants in reactor environment, 18: 40000 (NARF-63-11T)
radiation effects on, of polyethylene, gamma, 20: 7640
radiadtion effects on, of refractory materials at high temperatures, 16: 10604 (APEX-671)
studies using phosphorus-32-labeled tricresyl phosphate, effects of labeled impurities on, 19: 13840
study in large diesel engines by tracer methods, 16: 16062
study in turbo-assembly suspension bearings, by tracer methods, 16: 16065
testing cylinder and piston, in reactor shim solutions, 19: 45601(R) (WCAP-3750)
testing SAP reactor pressure tubes, 19: 8634 (EUR-1816.e)
tracer methods for, 20: 43788
tracer study in turbo-assembly suspension bearings by tracer methods, 16: 24037(T) (AEC-tr-5189)

Weighing
see Balances

WELDED JOINTS
see also Welds
aging behavior in niobium–zirconium alloy, 17: 8769
analysis for carbon and oxygen, activation, 20: 16331 (GA-6568)
analysis of steel, chemical, 17: 39509(T,R) (EURAEC-615)
analysis of steel, chemical, 18: 10501(T,R) (EURAEC-787)
brittle failure in steel, effects of symmetry on, 20: 9441(R) (EURAEC-1352)
brittle fracture of steel plates, 17: 39469(T) (EURAEC-602)
corrosion of hafnium-Zircaloy-2, 17: 10074 (WAPD-TM-337)
corrosion of Incaloy-to-Zircaloy, by steam under reactor conditions, 19: 45572(R) (GEAP-4755)
corrosion of niobium–zirconium, effects of heat treatments on lithium, 19: 36980 (PWAC-355)
corrosion of niobium–zirconium, by water and steam, 20: 19195
corrosion of stainless steel-to-Zircaloy, by steam under reactor conditions, 19: 45572(R) (GEAP-4755)
cracking in steel, effects of deposited-metal phase transformation temperatures on, 18: 39858(R) (EURAEC-1117)
design for explosive welding, 19: 40989
design for Zircaloy-4 tubes, end closure, 20: 5865 (WCAP-3269-37)
design of swaged, in aluminum-clad target rods, 20: 5175(R) (ORNL-3870, pp 230-7)
ductility of high-tensile steel, parameters affecting, 17: 12636(T,R) (EURAEC-501)
ductility of high-tensile steel, parameters affecting, 17: 39506(T,R) (EURAEC-539)
ductility of, on high-strength steels, 17: 11113(T,R) (EURAEC-430)
ductility of steel, effects of weld composition and fabrication techniques on, 18: 39856(R) (EURAEC-1021)
ductility of steel, effects of hot work-hardening on, 18: 39863(T,R) (EURAEC-1118)
embrittlement of steel, effect of time at high temperatures on, 20: 21393
evaluation for chromium–molybdenum steel and stainless steel,

18: 43062(R) (NASA-CR-54111)
fabrication and properties of reactor steel, 19: 9634(R) (EURAEC-1166)
fabrication of niobium loop for liquid metals, 20: 43879
fatigue effects in, 17: 38552(R) (SWRI-5-1348-7-1)
fatigue properties of, between dissimilar metals, 19: 34658(R) (SWRI-1228-64)
hardness of heat-affected zones of, effects of welding technique on, 19: 44686(R) (EURAEC-1362)
heat treatment, 16: 10443
in very thick steel plates, research program on, 19: 42820(R) (EURAEC-1252)
inspection of steel, methods for, 20: 29389
leakage rate in pressure vessel gas and liquid, 20: 30810
mechanical properties of, effects of gas confinement and thickness of, 17: 12634(T,R) (EURAEC-378)
mechanical properties, 17: 39509(T,R) (EURAEC-615)
mechanical properties of high-tensile steel, effects of additives and processing on, 18: 2237(T,R) (EURAEC-729)
mechanical properties, 18: 10501(T,R) (EURAEC-787)
mechanical properties, 18: 10503(T,R) (EURAEC-813)
mechanical properties, 18: 16458(T,R) (EURAEC-811)
mechanical properties, 18: 34089(T,R) (EURAEC-915)
mechanical properties, 19: 9633(R) (EURAEC-1106)
mechanical properties of Incoloy and Inconel, effects of temperature on, 19: 24081(R) (GNEC-361)
mechanical properties of steel, 19: 22863(R) (AD-606809)
mechanical properties, 19: 32703(R) (EURAEC-1297)
mechanical properties of Hastelloy and Haynes 25, effects of aging on, 20: 43888 (BNWL-290(Pt.1))
mechanical shock resistance in thick, 17: 11171(T,R) (EURAEC-330)
performance of fuel element end seals, determination of, 20: 14196
performance of, effects of multiple repairs and 400°F interpass temperature on, 19: 34655 (NP-15134)
procedures and properties of joining boron-10 stainless steel by resistance foil-seam welding process, 16: 3423 (KAPL-M-SAT-7)
properties and structure of seam welds in reactor pressure vessel, 17: 17440
properties of manually fabricated thick, 17: 14750(T,R) (EURAEC-459)
properties of seams, effects of rare earth additions on, 19: 22930(T) (JPRS-28849(p.244-9))
properties of, in thick plates of 1.2 MD07 steel, 20: 11239(R) (EURAEC-1468)
radiation effects on, neutron, 17: 38552(R) (SWRI-5-1348-7-1)
radiation effects on Inconel and stainless steel, in-reactor, 20: 44027
radiography of steel plate, for flaws, 16: 24058
shrinkage of, in reactor assemblies, testing of, 16: 28647(R) (ORNL-2340(Pts.1-5))
stress distributions in, from vertical ascending method, 18: 35973(T,R) (EURAEC-1023)
stress distributions in, from ascending vertical method, 19: 13939(R) (EURAEC-1097)
stress relief of, between Conoseal flange and component piping, 20: 11214(R) (NASA-CR-54717)
study of tube-to-tube sheet design, 19: 7873 (APED-4612)
tensile properties of, normalized vs. quenched and tempered, 18: 4279
tensile properties of steel, containing defects, 20: 9441(R) (EURAEC-1352)
testing equipment for, 18: 18019
testing in pipelines, radioisotope carrier for, 16: 7736(P)
testing of, development of nondestructive methods for, 17: 1901(T,R) (EURAEC-375)
testing of niobium–zirconium, nondestructive, 20: 13320
testing of steel tube, regulations for radiation protection in x-ray, 17: 32307
testing of Zircaloy-to-stainless steel, 19: 5405(R) (WCAP-3374-2)
testing pressure-vessel, nondestructive methods for, 20: 14709
testing, survey of test specimens used in, 16: 11828 (DMIC-165)
thermal cycle measurement of submerged-arc, method for, 19: 24947(R) (EURAEC-1280)
thermal cycling calculations for, 18: 8776(T,R) (EURAEC-433)

WELDING

see also Brazing
see also Soldering
arc-initiation circuit for remote fuel rod, 19: 44587(R) (ANL-7000, pp 3-63)
argon-arc method of, uses of carbon dioxide in, 19: 20534
automatic, evaluation of power source for, 18: 27916 (KAPL-2000-21 (p.VIII.1-7))
bibliography of Soviet literature on electroslag, 1956–1962, 17: 18720(T,R) (EURAEC-470)
bibliography on electron beam, 1957 to 1961, 16: 22566 (NP-11777)
bibliography on fusion, of aluminum, 18: 12600 (NP-13628)
bibliography on hot pressure, 18: 5748 (AD-423723)
bibliography on methods of, 20: 15005 (NASA-SP-5024)
bibliography on pressure, 1944 to 1961, 16: 20995 (NP-11776)
bibliography on vacuum-cold, 17: 22129 (NP-12731)
bibliography on, 1957–1962, 17: 18728
book: *Metals Reference Book.*, Vol. I and II, 3rd edition, 18: 32080
book: *Welding and Brazing Techniques for Nuclear Reactor Components*, 18: 34100
characteristics and developments in electron beam, 18: 34112
collet for zirconium fuel element, 18: 17977(R) (ORNL-TM-793)
conference, 17: 23907 (TID-7620(Pt.I))
conference, AWS and ASME, Cleveland, Ohio, April 9 to 13, 1962, 16: 25741
conference on, Chicago, Oct. 1959, 17: 18717 (TID-7624)
defect frequency in acetylene or arc, mathematical model for estimations of, 18: 22457 (HW-76573)
defects, effects on fatigue of pressure vessels, 17: 14792(R) (TID-17930)
description of projection, 17: 4915
development and uses of electro-key method, 16: 18004(R) (EURAEC-219)
development for metal working, 18: 25955
development for reactor materials, 17: 7606(R) (ORNL-1515)
development for reactor materials, review of, 17: 11123
development for refractory metals, 18: 579(R) (NP-13267)
development of apparatus and methods of electric-arc, for aligned tubes, 17: 41404(P)
development of arc, for molybdenum and niobium alloys, 17: 509 (CW-R&DL-29)
development of automatic assembly device for fuel, 16: 28372(R) (ORNL-3302(p.46-56))
development of automated processes for, 17: 12634(T,R) (EURAEC-378)
development of electron-beam, 19: 4743(R) (NP-14444)
development of electron-beam, 19: 40765(R) (NP-15309)
development of explosive, 16: 3419 (ASD-TR-61-124)
development of explosive, 20: 11260
development of filler materials and procedures for, high-strength low-alloy steels, 20: 5867
development of, for reactor fuel element fabrication, 16: 30168(R) (ORNL-3313(p.65-132))
development of, for reactor steels, 17: 1902(T,R) (EURAEC-397)
development of gas shielded-arc, 16: 25740
development of inspection techniques for, 16: 29358(T,R) (EURAEC-244)
development of magnetic force resistance, 19: 22870(R) (HW-83601)
development of methods for joining very thick steel pieces, 18: 39862(T,R) (EURAEC-1007)
development of parameters for clad fuel element end-plug, 18: 4795(R) (GEAP-3924)
development of projection, for stainless steel and Zircaloy, 18: 45001(R) (CEND-2863-217)
development of processes for, 19: 4634(R) (EURAEC-1098)
development of procedures for EVESR fuel elements, 19: 24080(R) (GEAP-4759)
development of projection, for fuel element spacing, 20: 12377(R) (CEND-2863-236)
development of resistance techniques for thermocouple attachment to fuel elements, 16: 10472 (DC-55-5-16))
development of techniques for Zircaloy fuel assembly, 16: 494 (CVNA-93)
development of tungsten-arc techniques, 16: 6693 (NAA-SR-Memo-5887)
development of ultrasonic techniques for, 16: 2145 (CEND-80)
development of ultrasonic, for refractory metals, 16: 19295 (ASD-TR-7-888(1))
development of ultrasonic system for, 17: 12627(R) (ASD-TR-7-888 (Vol.III))
development of ultrasonic, for fabrication of flat-plate fuel elements, 17: 14789 (NYO-10456)
developments at ORNL, 17: 23915 (TID-7620(Pt.I)(p.144-54))
developments in industry, 16: 506
edge, using an electron beam for, 17: 4921(P)
effects of electron-beam, on properties of molybdenum, 20: 23623
effects of melting methods on argon-arc and electron-beam, 18: 22465
effects of TIG, on properties of niobium–zirconium alloy, 20: 23731
effects on brittle fracture of thick steel plates, bend test for measurement of, 20: 11240(R) (EURAEC-1520)
effects on properties of metals, 20: 29623(R) (TID-22970, pp 121-256)
effects on recrystallization in molybdenum, niobium, tantalum, and tungsten, 20: 13267(T) (AD-624909)
electric butt-welding by flashing, 18: 2195 (CEA-2295)
electrogas, stresses generated in, 17: 22133(T,R) (EURAEC-532)
electron beam and TIG, comparison of, 18: 4220
electron beam and TIG, of niobium, stainless steel, and Zircaloy-2 reactor components, 18: 14447

electron-beam, equipment and methods, 16: 2153
electron beam equipment and techniques at 100 to 150 kv, 16: 19272
electron beam equipment and techniques, 16: 19271
electron-beam, equipment and materials for, 17: 34378
electron beam guns and method for, 16: 19283
electron beam methods for, 16: 19284
electron beam method for, of sintered aluminum, 17: 25743 (EUR-39.e)
electron-beam, of reactive and refractory metals, 17: 30955
electron-beam, of refractory metals in ionizer fabrication, 17: 32557
electron beam, principles and apparatus design, 16: 21000
electron-beam, review of industrial uses of, 17: 29296 (PB-181458)
electron beam techniques, 16: 19273
electron-beam, use for fabricating reactor fuel cladding configurations, 18: 4210 (HW-79143)
electron-beam, use for ceramics, graphite, metals, and steel, 18: 4220
electron-beam and vacuum arc, 18: 24108
electron-beam and TIG, equipment and techniques for, 18: 34058(R) (WANL-PR(P)-003)
electron-beam engineering drawing of equipment for, 19: 4293
electron-beam methods of, 18: 20491
electron-beam methods of, control of distortion in, 19: 42833
electron-beam, of tube to tubesheet joints, 20: 2283 (KAPL-3110)
electron-beam, plutonium bearing fabrication of particulate fuel elements by, 18: 20492
electron-beam, vacuum chamber for large workpieces, 18: 25964(P)
electroslag, equipment and techniques for, 19: 9634(R) (EURAEC-1166)
engineering drawings of portable welder, 18: 44121
engineering drawing of remotely operated heliarc equipment for capsules in hot cells, 19: 4290
equipment and methods for ultrasonic, of refractory metals, 17: 22126(R) (AD-402406)
equipment and procedure for electron-beam vacuum sealing of capsules, 17: 23913 (TID-7620(Pt.I)(p.120-5))
equipment and procedures for heat exchanger, 17: 23919 (TID-7620 (Pt.I)(p.193-205))
equipment and procedures for cylinders, design of automatic, 18: 35971 (NP-14177)
equipment and procedures for refractory metals and alloys, 19: 9629(R) (AD-608818)
equipment and process for tube-to-tube-sheet, for heat exchanger, 20: 13219 (RL-SEP-710)
equipment and techniques for resistance seam-, of stainless steel sheaths, 17: 32549
equipment and techniques for friction, 17: 41333(R) (ANL-6677)
equipment and techniques for consumable-electrode inert-gas arc, of refractory metals, 18: 573(R) (AD-422116)
equipment and techniques for TIG, of reactor tubing, 18: 14438
equipment and techniques for electroslag, reactor steels, 19: 13940(R) (EURAEC-1242)
equipment, chamber with means for rapid filling with inert gas, 17: 18254(P)
equipment, design and operation of ultrasonic, 16: 15157 (HW-69461)
equipment design for welding fuel element end caps, 16: 9177
equipment design for bench or remote operation, 17: 2764
equipment, development of power supply for electron beam welder, 16: 27252 (DP-731)
equipment for arc, using magnetic fields, 19: 34307(P)
equipment for automatic, of thin-wall tubes, 17: 41384 (HW-79182)
equipment for automatic, 18: 17977(R) (ORNL-TM-793)
equipment for, development of electron-beam, 17: 30921 (SC-4920(M) (p.73-6))
equipment for electron-beam, 16: 30544(P)
equipment for electron-beam, 17: 16631(P)
equipment for fabrication of pressure vessel for Czechoslovakian nuclear power plant, 19: 13958(T) (ORNL-tr-408)
equipment for heating the work adjacent a weld, 16: 30532(P)
equipment for high-temperature burning, plasma-jet, 17: 22103(T) (AERE-Trans-931)
equipment for inert-gas welding of end cap to sheathed fuel elements, 18: 25959(P)
equipment for joining end cap to reactor fuel tube by U-shaped weld, 17: 42280(P)
equipment for, of reactive metals under controlled atmosphere, 17: 23900 (KR-38)
equipment for plasma-jet, 18: 14451
equipment for pressure tube seal welding and cutting at CVTR, 18: 33100 (CVNA-99)
equipment for recording current, voltage, and position during vertical, 19: 42822(R) (EURAEC-1401)
equipment for refractory metals, 17: 27768
equipment for remote heliarc cutting, 17: 8764
equipment for remote rewelding of process tube joints in sodium–graphite reactors, 19: 40125 (NAA-SR-9821)
equipment for sealing tubes to tube sheets, 18: 25961(P)
equipment for thermocouple fabrication, 17: 34377 (TID-19268)
equipment for thin-walled tube, 19: 33709(P)
equipment for TIG-MIG, with visual inspection device, 20: 15019
equipment for tubular elements, 20: 2304(P)
equipment for welding ribs on thin-walled tubing, electron-beam, 20: 23620 (DP-996)
equipment for Zircaloy-clad plutonium-containing fuel elements, 19: 2765 (HW-SA-3486)
equipment for, design and operation of ultrasonic, 19: 22920 (HW-70938(Del.))
equipment for, development of automatic, 18: 20134(R) (ORNL-TM-792)
equipment for, engineering drawings of, 19: 28483
equipment using electron beams for, 17: 511 (DMIC-174)
equipment using pulsed electron beam, 16: 18012(P)
evaluation of electron-beam, 16: 31763
explosive, of incompatible metals, 18: 4222
facilities at Sandia, 17: 23916 (TID-7620(Pt.I)(p.155-8))
facility for refractory metals, construction of CANEL, 19: 24652 (CNLM-5537)
facility for refractory metal, controlled atmosphere, 19: 36997 (CNLM-5245)
filler products for, performance of molybdenum and nickel alloys for, 17: 11171(T,R) (EURAEC-330)
filler products, properties of, 17: 14750(T,R) (EURAEC-459)
friction, of similar and dissimilar metals, 17: 1908
fusion, of end caps in beryllium tubes, 17: 8767
grain growth of austenitic steel during, effects of temperature and time on, 17: 39514(T,R) (EURAEC-699)
improvement in inert-arc, 17: 8789(P)
inert-arc process for high vacuums, development, 17: 23915 (TID-7620(Pt.I)(p.144-54))
instrumentation and control systems for automatic, 20: 41230(R) (ORNL-3875, pp 24-34)
joining of boron steel, 17: 8766
materials and processes for refractory metals, development of, 18: 572(R) (AD-421974)
materials and procedures for high-tensile-strength steels, 19: 26797
materials for high-tensile-strength steels, 19: 26796
materials for steel, 18: 15565
method for cold, 19: 34357 (N64-24831)
method for fabricating rod bundle fuel elements for fluid flow and heat transfer studies, 20: 7501(R) (TID-22426)
method for fuel rod end caps, 19: 24967(P)
method for fuel-element-end-cap, 19: 24972(P)
method for reactor fuel elements and end enclosures, 20: 5868(P)
method for remote, fission product containers, 17: 15522 (HW-73933)
method for remote, development, 19: 17308
method for tube-to-plate, 17: 12652(P)
methods development for closure fabrication of autoclave liners, 18: 4171(R) (ORNL-3470(p.3-5))
methods development for reactor materials, 18: 14446
methods development for reactor materials, 18: 32119
methods development for reactor materials, 18: 41987
methods for aluminum-plutonium, 17: 23914 (TID-7620(Pt.I)(p.126-43))
methods for aluminum, gas-torch and WIG-, 18: 20490
methods for APM alloys, evaluation of cold pressure, 17: 36248 (NAA-SR-Memo-7748)
methods for austenitic stainless steel-boron-alloy steel, 17: 23914 (TID-7620(Pt.I)(p.126-43))
methods for automatic, 17: 23909 (TID-7620(Pt.I)(p.35-40))
methods for capsule, 20: 11263(P)
methods for fuel element end closures, development of magnetic force, 20: 27406(R) (BNWL-198, pp 4.1-42)
methods for fuel element cladding and end caps, 20: 37208
methods for high-strength and -temperature alloys, 16: 4510 (DMIC-Memo-140)
methods for Inconel, 17: 23911 (TID-7620(Pt.I)(p.70-92))
methods for magnetic-force resistance, for SAP materials, 18: 10509
methods for pressure tubes, explosive, 20: 37168(R) (BMI-1771)
methods for pressure tubes, explosive, 20: 37169(R) (BMI-1774)
methods for reactor tube, remote gas tungsten-arc, 19: 46973
methods for refractory materials, 16: 19397
methods for refractory metals, 20: 43848(R) (BNWL-269, pp 5.1-36)
methods for remote application, 16: 28359(R) (BAW-1107)
methods for Sean reactor pressure vessel, 20: 40417
methods for thick steel plates, development of, 20: 7534(R) (EURAEC-1208)
methods for thick steel plates, development of, 20: 9442(R) (EURAEC-1518)
methods for thick steel plates, development of, 20: 9443(R) (EURAEC-1473)
methods for titanium–Zircaloy-2, 17: 23914 (TID-7620(Pt.I)(p.126-43))

methods for type-410 stainless steel, 17: 23912 (TID-7620(Pt.I) (p.95-116))
methods for zirconium, electron beam, 19: 24973(P)
methods for, of 0.75-in. thick 6061 aluminum alloy, 20: 3609 (ACF-11)
methods of, for high-temperature gas loop, 18: 7162(R) (HW-77954(p.6.5-11))
methods of, for thick steel, 17: 22137(T,R) (EURAEC-586)
methods of, for beryllium, 19: 11680
methods of, for fabrication of space-age hardware, 19: 6286
methods of, for high-temperature fuel elements, 20: 20183
methods of, for use in reactor construction, 19: 22885
methods using glove boxes for HFIR targets, 18: 14426 (ORNL-3558 (p.61-83))
of capsules containing radioactive materials, design of mechanism for bench or remote operation, 17: 3713
of fuel element end seals, control of fusion, 19: 6281
of fuel rods to wire spacers in fabrication of clusters, 18: 5750(R) (CEND-157)
of low-alloy steels on site, 17: 524(P)
of metals for use in aircraft and missile components, review, 16: 10424 (ASD-TR-61-322(p.661-76))
of metals in nuclear plants, requirements for quality control in, 19: 22922 (HW-SA-3510)
of metals, review of, 17: 11166 (HW-SA-2527)
of plutonium-bearing fuel elements, facility for, 19: 2789
of plutonium-containing fuel elements, 19: 6274 (HW-82825)
of reactive and refractory metals by solid-state methods, 19: 22937
of reactor fuel elements and cores, 18: 32114(T) (AI-Trans-48)
of reactor pressure vessels, effects of manganese and silicon content of weld metal on, 19: 14051
of reactor steels, effects of flux and rod compositions on, 16: 29359(T,R) (EURAEC-251)
of reactor steels, research on electroslag techniques for, 17: 22136(T,R) (EURAEC-585)
of reactor steels, research program on electroslag, 17: 39511(T,R) (EURAEC-659)
of reactor steels by electroslag techniques, 17: 41389(T,R) (EURAEC-763)
of reactor steels by electroslag techniques, 18: 10504(T,R) (EURAEC-849)
of reactor steels by electroslag techniques, 18: 20488(T,R) (EURAEC-970)
of refractory metals, review of, 17: 29301
of refractory metals, survey of state-of-the-art of, 17: 34368 (NP-13045)
of refractory metal alloys, 18: 5752(R) (WANL-PR(P)-001)
of refractory metals, effects of InFab atmosphere on, 18: 16450(R) (AD-431672)
of refractory metals, electron beam, 18: 34092
of refractory metal alloys, 19: 13954(R) (WANL-PR(P)-004)
of refractory metal alloys, 19: 13955(R) (WANL-PR-(P)-005)
of refractory metals, method for flash, 19: 34662
of stainless steel-clad carbon steel, for fabrication of piping, 20: 788 (SWRI-1228-73)
of thick steel plates, specimen testing for, 20: 41450(R) (EURAEC-1684)
of titanium alloys and reactive metals, problems, 16: 10488(T) (FTD-TT-61-251)
of tubes to tube sheet in boiler, technique for internal, 19: 24951 (NAA-SR-8541)
operator qualification standards for, 20: 43821
plasma jet uses in, 20: 1277 (TID-22136)
problems in nuclear installations, 16: 10497
problems of, in Japanese nuclear power plants, 19: 12798
procedures for boiler tubesheets, 19: 31474 (BAW-1280-23)
procedures for boiler tubesheets, 19: 31475 (BAW-1280-24)
procedures for nickel, 20: 33413(R) (K-1669)
procedures for reactor steel, 19: 22948
procedures for reactor steels, process development for electro-slag, 20: 2281(R) (EURAEC-1408)
procedures for tube-to-tube-sheets in boilers, 20: 11214(R) (NASA-CR-54717)
procedures for tube-to-tube-sheet, in boilers, 20: 11215(R) (NASA-CR-54718)
procedures for, in inert gas chambers, 20: 35110 (CNLM-5584(Vol.3))
procedures, specifications, and qualification test records for, Hanford guide for, 18: 24102 (TID-20625(Vol.I))
procedures, specifications, and qualification test records for, Hanford guide to, 18: 24103 (TID-20625(Vol.II))
procedures, specifications, and qualification test records for, Hanford guide to, 18: 24104 (TID-20625(Vol.III))
procedures, specifications, and qualification test records for use at Hanford, 19: 20521 (TID-20625(Vol.I(Rev.I))
procedures, specifications, and qualification test records for use at Hanford, 19: 20522 (TID-20625(Vol.II)(Rev.I))
procedures, specifications, and qualification test records for use at Hanford, 19: 20523 (TID-20625(Vol.III)(Rev.I))
procedures, specifications, and qualification test records for use at Hanford, 19: 20524 (TID-20625(VolIV)(Rev.I))
process development for very thick steel plates, 20: 23621(R) (EURAEC-1548)
process development for explosive, of dissimilar metals, 20: 14957(R) (BMI-1754)
process for fuel element end closures, 17: 36922 (ACNP-63023)
processes for nuclear power stations, 16: 507
processes for Zircaloy fuel element spacers, 19: 33601(R) (DP-965)
processes of, summary of Hanford, 16: 30749 (HW-SA-2112)
refractory metals, facility for, 20: 5867
refractory metals, parameters for electron-beam, 20: 5867
residual stresses produced by upward vertical, 18: 8779(T,R) (EURAEC-820)
resistance, prevention of contamination from electrodes in, 16: 19326(P)
review of joining of exotic materials, 17: 34360 (CONF-94-5)
safety requirements for, stainless steel for nuclear reactor plants, 20: 11259
seam-testing by non-destructive methods, 16: 29352(R) (EURAEC-304)
specification guides at HAPO for, 18: 3924 (TID-15246(Vol.II)(Rev.))
specification guides at HAPO for, 18: 4215 (TID-15247(Rev.))
specifications for, of stainless steel for structural quality welds for mildly corrosive nonradioactive service, 17: 32540 (TID-19161)
specifications for stainless steel heat exchangers, 17: 34371 (TID-19155)
specifications for stainless steel, 17: 34372 (TID-19156)
specifications for fusion, of stainless steel, 17: 34373 (TID-19157)
specifications for stainless steel, 17: 34374 (TID-19158)
specifications for fusion, of stainless steel, 17: 34376 (TID-19160)
specifications for dissimilar welding in iron- and nickel-base alloys, 19: 4592(R) (MSAR-61-114)
stainless steel tapes to heavy-gage steels, process development for, 19: 36998(R) (EURAEC-1296)
stress analysis of deposits in single-pass, 17: 1900(T,R) (EURAEC-331)
stress distributions from vertical ascending method of, 18: 35973(T,R) (EURAEC-1023)
stress distributions from vertical-ascending, 19: 13939(R) (EURAEC-1097)
stress from vertical-ascending, 18: 30156(T,R) (EURAEC-914)
stresses from rising vertical process of, analysis of residual, 17: 11172(T,R) (EURAEC-391)
stresses from rising vertical electroslag, analysis of residual, 17: 39510(T,R) (EURAEC-617)
stresses from rising vertical electroslag, analysis of residual, 18: 10500(T,R) (EURAEC-739)
stresses in rising vertical processes of, residual stressed from, 17: 11173(T,R) (EURAEC-446)
stresses produced by electrogas and electroslag, measurement of, 20; 25524 (EURAEC-1562)
sulfur distributions in mild steels used for, 17: 29892
techniques for aluminum, stainless steel, and steel tubes, 18: 7173
techniques for Bradwell heat exchanger shells, 16: 19314
techniques for, development of, 17: 11130
techniques for fabrication of thermionic cells, 19: 47282(R) (NYO-3429-4)
techniques for nuclear structures, 18: 7172
techniques for, of reactor steels, 17: 16616
techniques for reactor pressure vessels, 16: 19313
techniques for reactor steels, electro-slag, 16: 33460(T,R) (EURAEC-315)
techniques for stand pipe pressure vessel, 16: 19315
techniques for steel pressure vessels, submerged-arc, 17: 39513(T,R) (EURAEC-672)
techniques for steel pressure vessels, submerged-arc, 18: 10505(T,R) (EURAEC-853)
techniques for steel pressure vessels, submerged-arc, 18: 16459(T,R) (EURAEC-962)
techniques for thick carbon steel pressure vessels, 16: 19312
techniques for thick steels, 17: 39509(T,R) (EURAEC-615)
techniques for thick steels, 18: 10501(T,R) (EURAEC-787)
techniques for thick steels, 18: 10503(T,R) (EURAEC-813)
techniques for thick steels, 18: 16458(T,R) (EURAEC-811)
techniques for thick steels, 18: 34089(T,R) (EURAEC-915)
techniques for thick steels, 19: 9633(R) (EURAEC-1106)
techniques for thick steels, submerged-arc, 19: 11691(R) (EURAEC-1221)
techniques for tube-to-tubesheet, 17: 29293 (APAE-123)
techniques of, in USSR, 17: 32541(T) (FTD-TT-62-1677)
testing equipment for simulating, 17: 39507(T,R) (EURAEC-601)
thermal cycle measurement during submerged-arc, method for, 19: 24947(R) (EURAEC-1280)
thermal cycling calculations for, 18: 8776(T,R) (EURAEC-433)
thick steel plates, cracking and hardness changes from, 20: 15000 (EURAEC-1517)

thick steel plates, process development for, 20: 25523(R) (EURAEC-1277)
trip report of American Welding Society delegation to Soviet Union, July 3 to 17, 1962, 17: 14800
ultrasonic, fundamentals of, 16: 4515 (NP-11054)
ultrasonic, improvements in equipment for non-destructive, 17: 22132(T,R) (EURAEC-525)
ultrasonic methods for heat exchanger components, 16: 19308 (PWAC-165)
ultrasonic, of refractory metals and alloys, 17: 20430 (AD-299397)
ultrasonic, of refractory metals, 17: 36240(R) (AD-290604)
ultrasonic, bibliography on, 20: 13210 (AWRE/LIB/BIB/13)
ultrasonic, methods and equipment for, 18: 45203(P)
ultrasonic, of aluminum alloys, 19: 30689 (HW-51911)
ultrasonic, of refractory metals, 18: 12592(R) (AD-410514)
ultrasonic, power-force programming for refractory metals and alloys, 18: 12594 (AD-427997)
use of electronic, for sealing plastic bags containing alpha sources, 20: 45953 (ISO-SA-23)
use of electroslag, for large dimensional construction, 19: 11703(T) (ORNL-tr-407)
use of plasma jets for, 20: 16593
uses in reactor materials fabrication, 18: 18338
uses of lasers for, 20: 11260
wire development with rare earth additions for open-arc, 19: 22930(T) (JPRS-28849(p.244-9))
wires to thin metal films, method for ultrasonic, 20: 23632

WELDING RODS

cooling resistance-, method for, 20: 5867
development for high-strength steels, 17: 23932
development for thick steel plates, 20: 9443(R) (EURAEC-1473)
development of cerium-niobium, for reducing interstitial content in niobium, 18: 29617
development of filler properties for automatic and manual processes, 17: 12634(T,R) (EURAEC-378)
evaluation for stainless steel, 16: 3428 (NYO-9725)
for ferritic steel-austenitic steel welds, 17: 23921 (TID-7620 (Pt.I)(p.209-16))
performance of, effects of composition on, 16: 29359(T,R) (EURAEC-251)
performance of steel, effects of additives on, 17: 11171(T,R) (EURAEC-330)
properties of Hastelloy X, for joining Hastelloy X-280 to stainless steel or Haynes 25 Alloy, 19: 34627(R) (BNWL-79(p.6.1-20))
properties of Hastelloy W, for joining Hastelloy X-280 to stainless steel or Haynes 25 Alloy, 19: 34627(R) (BNWL-79(p.6.1-20))
properties of steel, 17: 39509(T,R) (EURAEC-615)
properties of steel, 18: 10501(T,R) (EURAEC-787)
properties of steel, 18: 10503(T,R) (EURAEC-813)
properties of steel, 18: 10504(T,R) (EURAEC-849)
properties of steel, 18: 16458(T,R) (EURAEC-811)
properties of steel, 18: 34089(T,R) (EURAEC-915)
properties of steel, 19: 9633(R) (EURAEC-1106)
properties of steel, 19: 9634(R) (EURAEC-1166)
radiation effects, 17: 6735 (AE-90)
radiation effects on properties of A302B steels, neutron, comparison of U. S. and Japanese, 20: 46236
stress-rupture properties of high-nitrogen, 17: 6723

WELDS

analysis and control by gammascopy, 16: 13489(T) (AEC-tr-4492(p.390-2))
bibliography on effects of weld-pool agitation on properties and characteristics of, 17: 32533 (AD-409795)
bonding in, ultrasonic method for testing, 19: 38546(R) (RFP-552)
brittle fractures in steel, review of, 17: 37520(T) (TRG-Inf-Ser-88)
built-joint, in sandwiched materials, 17: 23913 (TID-7620(Pt.I) (p.120-5))
corrosion of nickel, by gas environments in fluid-bed fluoride volatility process, tests, 19: 26764 (ANL-6979)
crack effects on fatigue strength of carbon steel pipe, 20: 759
crack testing of, in steel, (E), 19: 22974(R) (EURAEC-1275)
cracking in steel plates, 17: 39508(T,R) (EURAEC-614)
cracking in steel plates, 18: 8781(T,R) (EURAEC-881)
cracking in steel, effects of phase transformation temperatures on, 18: 39858(R) (EURAEC-1117)
cracking of, ultrasonic detector design for, 16: 29121(T) (FTD-TT-62-368)
cracking of, in steel, review of theories, effects, causes, and control of, 18: 25941 (DMIC-197)
creep properties in filler, 17: 39509(T,R) (EURAEC-615)
cutting machine for, for PWR Core 2, instruction manual, 20: 42649 (WAPD-PWR-2230)
cutting machine for, for PWR Core 2, instruction manual, 20: 42650 (WAPD-PWR-2232)
defects in, radiographic inspection for, 17: 14470 (IA-750)
defects in, effects of, 18: 35208
deposition and properties of beads on steel, 18: 14435(T,R) (EURAEC-907)
deposition and properties of beads on manganese–molybdenum steel, 18: 32115(T,R) (EURAEC-1018)
deposition and properties of beads on manganese–molybdenum steel, 19: 11691(R) (EURAEC-1221)
deposition of beads on manganese–molybdenum steel for bending tests, 17: 41390(T,R) (EURAEC-768)
detection of flaws by gamma spectroscopy, 16: 3291(T) (JPRS-9706 (p.79-80))
distortion of, electron-beam methods of controlling, 19: 42833
ductility of steel, effects of composition and fabrication techniques on, 18: 39856(R) (EURAEC-1021)
ductility of steel, effects of hot work-hardening on, 18: 39863(T,R) (EURAEC-1118)
effects of defects in, on fatigue strength of steel, 20: 45862(R) (SWRI-1228P1-28)
effects on corrosion of stainless steel waste tanks, 20: 27036(R) (IDO-14661, pp 1-44)
effects on fatigue strength of steel, 19: 45503(R) (SWRI-1228-69)
effects on reactor accident containment, limiting, 20: 5034 (NOLTR-63-140)
electrodes for dissimilar-metal, in thermal-cycling situations, 17: 23921 (TID-7620(Pt.I)(p.209-16))
embrittlement of nickel-alloy, effects of aging and temperature on, 19: 30737(R) (HW-84573(p.6.1-11))
embrittlement of steel, by high temperatures, 19: 23090
etching of, procedures and reagents for, 20: 43821
failure in pressure vessels, mechanisms of, 19: 13999(R) (SWRI-1228-43)
fatigue notch sensitivity of Zircaloy, 19: 2846
fatigue strength of omega seals in chromium–iron–nickel Alloy 600, 18: 27860 (KAPL-2000-21(p.I.1-11))
fatigue strength of carbon steel-to-stainless steel, 20: 39404 (SWRI-1228-4-20)
flaw detection in, using gamma sources, 18: 14306
flaw detection in, portable isotope pencil for, 19: 32335(P)
flaw detection in, using iridium-192 gamma sources, 19: 42628
flaw detection in, methods development for x-ray, 20: 13177(R) (EURAEC-1504)
flaw detection using gamma sources for, 18: 4139
flaws in fuel element cladding, detection of, 20: 23261
gamma photographs, 16: 13451(T) (AEC-tr-4492(p.214-16))
grain size control in, effects of sonic vibrations on, review of, 17: 30947 (DMIC-Memo-166)
hardness and microstructure of L-605 to molybdenum–titanium alloy, 17: 29070(R) (NP-12934)
impact properties of, effect of heat-treatment on Charpy keyhole, 17: 23923 (TID-7620(Pt.I)(p.225-42))
inspection in pipes at New Zealand geothermal steam power station using gamma radiography, 19: 597
inspection in tubes, ultrasonic apparatus for, 16: 2018(P)
inspection methods for, 19: 32394(R) (EURAEC-1341)
inspection of pressure vessel nozzle, ultrasonic, 16: 7746
inspection of pressure vessel, methods of, 19: 13999(R) (SWRI-1228-43)
inspection of submarine cable butt, equipment and method for gammagraphic, 19: 36631
inspection of, betatron detector with scintillation counters for, 20: 19233
inspection of, design of lead muff on gamma source for, 18: 43775
inspection of, efficiency of ultrasonics for, 19: 28518(R) (EURAEC-1342)
inspection of, methods for radiographic and ultrasonic, 20: 12973(R) (EURAEC-1519)
inspection of, procedures for, 20: 35110 (CNLM-5584(Vol.3))
inspection of, radiographic methods of, 19: 46564
inspection of, radiographic methods for, 20: 45865
inspection of, uses of x-ray radiography for, 20: 20864
inspection using bremsstrahlung, 20: 23259(T) (AEC-tr-6466/1, pp 131-4)
inspection using 8-Mev linear accelerator, 16: 10271
integrity of thermionic converter component, 19: 23347(R) (NYO-3429-2)
internal defects in high-strength steel, causes and effects of, 17: 519 (WAL-TR-642.4/1)
mechanical properties of, for high-strength steels, 17: 23932
mechanical properties of dissimilar, in stainless steel and superalloys, 17: 39501 (HW-78574)
mechanical properties in manganese–molybdenum steel plate, 17: 39512(T) (EURAEC-667)
mechanical properties of electroslag, in manganese–molybdenum steel, effects of oxidation on, 18: 8731(T) (EURAEC-510)

mechanical properties of filler, 18: 16458(T,R) (EURAEC-811)
mechanical properties of Incoloy and Inconel tube, effects of temperature on, 19: 24081(R) (GNEC-361)
mechanical properties of high-tensile steels, preparations for research on, 20: 41448(R) (EURAEC-1670)
mechanical properties of heavy-gage steel, preparations for research on, 20: 41410(R) (EURAEC-1612)
nondestructive testing of, 20: 25268 (ORNL-P-2107)
porosity in heat-resisting alloys, causes and effects of, 20: 13264(R) (WANL-PR(P)-008)
post heating by electron beam in steel and titanium alloys, 17: 25764
production methods for, in Incoloy 800 and Inconel 600 and 625, (E), 20: 6624 (TID-22425)
properties of electroslag, in thick reactor steels, 19: 9634(R) (EURAEC-1166)
properties of filler, 18: 10503(T,R) (EURAEC-813)
properties of filler, 19: 32703(R) (EURAEC-1297)
properties of steel filler, 18: 10501(T,R) (EURAEC-787)
properties of steel filler, 18: 34089(T,R) (EURAEC-915)
properties of steel filler, 19: 9633(R) (EURAEC-1106)
properties of, effects of weld parameters on mechanical and physical, 18: 573(R) (AD-422116)
properties of, on very thick steel pieces, 18: 39862(T,R) (EURAEC-1007)
properties testing for use in Elk River Reactor pressure vessel, 20: 42636(R) (SWRI-1228-4-22)
quality control for resistance, in aluminum alloys, 17: 20429 (AD-294774)
quality control in ferrous metallurgy by irradiation method, 16: 13485(T) (AEC-tr-4492(p.369-73))
quality control in thin-walled cylinders, use of radioisotopes in, 16: 13492(T) (AEC-tr-4492(p.403-5))
radiation effects on notch ductility of, 17: 23918 (TID-7620(Pt.I) (p.168-90))
radiographic inspection of, equipment for, 17: 25427(P)
radiographic techniques for, betatron, 16: 19151
radiography in shipbuilding, use of radioisotopes, 16: 13491(T) (AEC-tr-4492(p.399-402))
radiography of butt joints of pipes, 16: 13486(T) (AEC-tr-4492(p.374-8))
radiography of small-diameter tube, x-ray generator for, 20: 7242 (LA-DC-6977)
radiography of steel pipe, x-ray, 17: 292 (HW-74643)
radiography of, surface finish standard for, 17: 13686 (WAPD-BT-27(p.53-7))
radiography of, in circulation pipes, gamma, 18: 39732(T) (AEC-tr-6390(p.88-90))
radiography of, method for neutron, 20: 11005(P)
sonic inspection using twin-angle beam technique, 17: 27761 (TID-18871)
stability in niobium alloys, 18: 22459(R) (NP-13816)
stress-corrosion cracking by boiler water at 500°F and sea water at 550°F, 17: 27749 (KAPL-M-CC-3)
stress corrosion in Hallam reactor sodium system, 20: 10378 (NAA-SR-Memo-11607)
stress elimination in fuel element, 18: 4774(P)
stress-relieving, 17: 23922 (TID-7620(Pt.I)(p.218-24))
stresses in heavy steel, measurement of residual, 19: 42819 (DF65SL-205)
tensile properties of, in steel pipes, effects of cycle loading on, 17: 18746 (HW-75484)
tensile properties for joining wrought depleted uranium, design allowables for, 20: 2342 (SC-DR-58-61)
testing in steel, development of radiographic and ultrasonic, 18: 12563(T) (EURAEC-192)
testing in steel, nondestructive, 17: 8821(T,R) (EURAEC-450)
testing of bridgewire, nondestructive, 18: 9761 (SC-DR-251-63)
testing of electric resistance and flash butt, 20: 16618
testing of, for determination of surface stresses, 18: 8779(T,R) (EURAEC-820)
testing of pressure vessel, fatigue, 19: 24090(R) (SWRI-1228-56)
testing of pressure-vessel, 20: 43851(R) (EURAEC-1671)
testing of, specifications for radiographic, 17: 34375 (TID-19159)
testing of steel, radiographic, 19: 595(R) (EURAEC-1151)
testing of steel, ultrasonic, 19: 596(R) (EURAEC-1152)
testing of steel, evaluation of variables in radiographic, 19: 40753(R) (EURAEC-1378)
testing of thick steel, ultrasonic, 18: 43771(R) (EURAEC-882)
testing of, validity of requirements for nondestructive, 17: 11168 (TID-15756)
testing of, in NPR pipe, design of hydrostatic and vibratory-fatigue machines for, 18: 22234 (HW-77831)
testing of, radiographic and ultrasonic, 18: 39463(R) (EURAEC-663)
testing of, radiographic and ultrasonic, 18: 39464(R) (EURAEC-762)
testing of, radiographic and ultrasonic, 19: 34338(R) (EURAEC-1393)
testing of, radiographic and ultrasonic methods of, 19: 42024
testing steel pressure vessel, ultrasonic methods of, 19: 42025
testing type-410 stainless steel, 17: 23912 (TID-7620(Pt.I)(p.95-116))
thermal cycling effects on stainless steel wire-to-tube, 18: 16422(R) (CEND-204)
ultrasonic inspection of, in thick wall steel pipe, 17: 6243 (HW-74597)
ultrasonic inspection of spot, 19: 8685 (BDX-613-14)

WELL LOGGING

activation analysis, systems for automatic, 19: 19773 (TID-20467)
activation, radiation source-detector apparatus for, 17: 8573(P)
age and paleotemperature analyses of deep-sea cores by, 16: 29201
analysis of iron-bearing ores and rocks in boreholes, activation, 20: 37019
analysis of rocks in boreholes, activation, 20: 37018
anomalies in gamma borehole measurements, quantitative measurements of, 17: 37357
book: *Radioactive Investigations of Oil and Gas Wells*, 19: 36687(T)
borehole and formation parameters in, computer code for, 20: 14775
borehole size determination in, radiometric method for, 19: 24741(P)
coal layer determination and identification by gamma-log correlations, 18: 5503
coal seam thickness determination by gamma-gamma, 16: 3363
computer analysis of gamma-ray, 17: 25439
curves for radiometric, effects of logging speed and time constant of integration circuit on, 19: 24737
density determination for borehole fluids, radiometric apparatus for, 18: 12377(P)
density logging of earth formations, gamma-gamma, 18: 5502
design for cyclic activation, 17: 8677(P)
design of gamma-gamma diffusion device for, for detecting materials of high atomic number, 17: 1739(P)
design of radiometric, 17: 8574(P)
determination and correlation of, glauconite sandstones with phosphorites, natural gamma, 18: 5504
determination of chemical composition of natural ore deposits, methods for, 18: 5497
development, 20: 14770
development of radiometric, 17: 10243 (NP-12381)
development of radiometric techniques for, 18: 5535
device with one source and two detectors for detecting oil, 19: 2550(P)
effects of tool position, borehole fluid, and source-detector spacing on pulsed-neutron, 18: 5509
efficiency of gamma-gamma, effects of caverns, 16: 3364
equipment and methods for study of waste-disposal hydrology, 16: 25043 (TID-7628(p.99-114))
equipment and method for chlorine detection in boreholes, 18: 5537(P)
equipment and method for neutron–gamma, for detection of hydrocarbons, 20: 4170(P)
equipment and method for neutron–gamma, 20: 25314(P)
equipment and methods for, in Hungary, review on, 20: 33538
equipment and method for neutron-gamma, 20: 39137(P)
equipment and techniques for neutron and γ, 17: 305
equipment and techniques for gamma and neutron, 17: 36016
equipment and techniques for neutron-gamma, 18: 5540(P)
equipment calibration and errors, 20: 39131
equipment calibration for, 20: 45930(P)
equipment design, 20: 39138(P)
equipment design and performance, pulsed high-energy neutron-induced spectral, 16: 419
equipment design and performance for gamma, 17: 298 (AERE-R-3197)
equipment design and method for radioactive, for exact identification of substrate formations, 17: 29113(P)
equipment design and method for determination of carbon and hydrocarbons in earth formations, 18: 6963(P)
equipment design and method for determination of oxygen in earth formations, 19: 38871(P)
equipment design and method for, 20: 9162(P)
equipment design and method for, 20: 9163(P)
equipment design for lunar probes, 16: 20659
equipment design for, neutron source, 16: 30670
equipment design for simultaneous gamma and neutron logging, 17: 8579(P)
equipment design for simultaneous density and natural gamma-ray logging, 17: 16408(P)
equipment design for obtaining samples from bore holes, 17: 36018(P)
equipment design for high-pressure, 18: 5539(P)
equipment design for dispersing liquid isotopes into bore holes, 19: 11408
equipment, design of heat-insulated radiation counter, 16: 20697(P)
equipment development for, 18: 1317(R) (NP-13210)
equipment for, 19: 32443(P)
equipment for chlorine detection in a non-ferrous environment, neutron-gamma, 20: 29446(P)

equipment for density and moisture measurements in gamma and neutron, 20: 33537
equipment for, design of multiplex system for, 17: 30747(P)
equipment for, design of neutron source as, 18: 8639(P)
equipment for determining injectivity profiles of fluid injection wells, 16: 16590(P)
equipment for flow measurement in boreholes, 19: 15852(P)
equipment for flow measurements in boreholes, 20: 41170(P)
equipment for gamma-neutron, 16: 16571(P)
equipment for, gamma-neutron and pulsed, 17: 12485
equipment for gamma or neutron-gamma, using multiple detectors, 20: 21145(P)
equipment for gamma-gamma, 20: 33542
equipment for gamma, 20: 39139(P)
equipment for gamma-gamma, during drilling, 20: 41171(P)
equipment for gamma, electrode calibration for, 20: 41165
equipment for hydrogen-independent chlorine, neutron–gamma, 20: 27179(P)
equipment for injecting tracer into borehole, 18: 6965(P)
equipment for measuring temperature and vertical currents, 17: 10851(R) (HW-73337(p.158-237))
equipment for neutron-neutron and neutron-gamma, 18: 35825(P)
equipment for neutron-gamma, modernization of, 19: 40794(T) (AEC-tr-6577)
equipment for neutron-neutron, 19: 46622(P)
equipment for neutron–gamma, calibration of, 20: 4171(P)
equipment for neutron–gamma, for determination of salt water, oil, or gas, 20: 25315(P)
equipment for neutron-gamma, scintillation-type detector for, 20: 29445(P)
equipment for neutron-gamma, for chlorine, temperature compensation circuit for, 20: 39136(P)
equipment for NMR method for, 20: 45931(P)
equipment for nuclear, using pair spectrometer, 18: 6964(P)
equipment for nuclear, using a scintillation counter, 18: 7049 (NP-13416)
equipment for productivity logging using gamma radiation, 19: 2590(P)
equipment for radiometric, design of cobalt-60 gamma-gamma, 18: 27717
equipment for radiometric, using semiconductor detector, 19: 13658(P)
equipment for radiometric, 19: 46624(P)
equipment for radiometric, design of neutron–gamma, 20: 33723(P)
equipment for radiometric, pulsed-neutron, 20: 43163(P)
equipment for simultaneous natural-gamma and neutron-source logs, 16: 14983(P)
equipment for soil moisture measurements, 20: 20915
equipment for, calibration of, 20: 9161(P)
equipment for, control system for artificial radioactivity sources for, 19: 36688(P)
equipment for, cooling system for, 20: 39140(P)
equipment for, design of accelerator tube for neutron source for, 19: 34395(P)
equipment for, development of electronic and mechanical, 19: 28420(R) (NP-14825)
equipment for, in reservoirs using fast neutrons, 20: 35657
equipment for, NMR, 20: 9159(P)
equipment for, scintillation, 20: 5658(P)
equipment, power supply for ionization devices, 16: 30643(P)
equipment shielding for neutron–gamma for chlorine determination, 20: 29443(P)
equipment, techniques, and uses, review, 16: 422
equipment with coincident pulse suppression for simultaneous neutron and gamma logging, 18: 35826(P)
fission product transport through soil, 17: 10820 (BNL-6554)
fluid invasion in borehole in neutron, effects of, 19: 34382
gamma caliper instrument for measuring borehole size, 18: 27783(P)
gamma, design of coincidence Compton spectrometer, 17: 1783(P)
gamma detection in, semiconductor detector for, 19: 34585(P)
gamma distribution in, 17: 18300
gamma/gamma, equipment and method for locating coal, 16: 25637
gamma instrument for measuring density of formations, 16: 20698(P)
gamma intensity calculations for drill holes, 16: 7766
gamma radiation detection, survey of natural, 18: 35733
gamma radiation measurement, 17: 4865(P)
gamma scattering device for locating borehole cement, 18: 2017(P)
gamma scintillation methods of, for studies of dispersion of gamma emitters from waste disposal sites, 19: 1944(R) (HW-81746(p.4.32-6))
gamma spectral logs for, curves for quantitative interpretation of, 20: 27173
gamma spectrometer apparatus design for, 17: 23734(P)
gamma spectrometer design for, 17: 29225(P)
gamma, factors affecting in, 19: 30416
gamma, method for locating ore deposits, 18: 33782
health physics problems in, 20: 41216
humidity determinations, using fast-neutron sondes, 16: 13411 (NP-11381)
instrumentation and techniques development for, 16: 423
instruments and techniques for, radiometric, 20: 37060
instruments for radiometric, description of Russian, 19: 34380(T) (AEC-tr-6578)
instruments in, equipment for insulating and refrigerating, 18: 5689(P)
interpretation of gamma logs from, 17: 300
interpretation of nuetron-gamma logs for Zechstein carbonates in German Democratic Republic, 18: 5496
log analysis for uranium ores, computer program for gamma, 19: 34379 (RME-143)
method for barren log interpretation in radioactive, information theory in, 19: 34394(T)
method for carbon and oxygen determination by nuclear resonance fluorescence, 19: 32444(P)
method for chlorine, using neutron-capture gamma rays, 20: 25316(P)
method for detecting and identifying hydrocarbons and water, 17: 29115(P)
method for determining gas-oil boundaries in hydrocarbon mixtures using neutron-gamma indicators, 19: 28559
method for determining uranium-deposit rock density using computer program and system, 20: 14778
method for gamma, 19: 38867
method for gamma, 20: 25309
method for gamma radiometric, 19: 46892(P)
method for locating cement in boreholes, 17: 16414(P)
method for locating water-producing zones, 18: 18054(P)
method for locating fluid-entry regions in, 19: 24741(P)
method for mapping formation permeability, 17: 29114(P)
method for oil prospecting using fast neutrons, 18: 12374(P)
method for radiometric, using gamma detection at several levels, 19: 15772
method for radiometric, elimination of interference of iron casing effect in, 20: 29442(P)
method for simultaneous tracer and natural gamma logging, 18: 25703(P)
method for strata shrinkage measurement using cobalt-60, 20: 11024
method of, by bombardment with nuclear particles, 17: 12489(P)
method of, for measuring ground sinkage at Niigata City, Japan, 17: 30180
method of gamma-gamma, for heavy element concentration in rocks, 20: 12993
method of ground water flow investigations by, 19: 28566
method of radiometric, 17: 3199(P)
method of radiometric, 18: 8532
method of strata content determination using oxygen and silicon activation by neutrons, 18: 12373(P)
method of, using delayed neutrons, 20: 41157
method using computer learning program, 20: 14777
methods and uses of, review of, 20: 35655
methods for, book on, 18: 5536
methods for oil wells using radioactive fluid tracers, 18: 16192 (TID-7689(p.38-45))
methods for potassium-salts prospecting and potassium determination, 16: 16044
methods for, using (γ,n) reactions, 19: 34391(T)
methods in neutron, 18: 4009
methods in radiometric, 17: 8423
methods of oil and gas borehole investigations in USSR, 18: 5493
methods of prospecting for potassium and sodium salts, 18: 5525
methods of radiometric, 18: 20225
methods of, gamma-gamma and neutron-gamma, 20: 18182
methods of, using fast neutrons and scintillation detector, 19: 7722(P)
methods using magnetic resonance of free radicals produced by radiation, 18: 3708(P)
methods using radiation, 16: 8986 (CEA-NOTE-352)
Monte Carlo calculations for gamma, 20: 27174
Monte Carlo fast convergence method in, 20: 4168
neutron activation, 16: 31971
neutron-activation analysis of bauxites and coals, 18: 5507
neutron activation methods of, for location of copper sulfide ores, 18: 43825
neutron activation methods of, for location of copper in drill holes, 18: 43826
neutron activation method of, for bauxite prospecting, 20: 43554
neutron age equations for, fast, 17: 10833
neutron apparatus with spectral selectivity, 17: 16412(P)
neutron apparatus for, calibration method for, 18: 12375(P)
neutron asymptotic time distribution in pulsed, 19: 34384(T)
neutron boundary effects in, 19: 13654
neutron calculations in, Monte Carlo method for, 20: 12994
neutron-capture gamma ray logging system, 16: 22394(P)
neutron-capture gamma ray logging system, 16: 22395(P)
neutron density in, group method for determining, 19: 34388(T)

neutron diffusion in, 18: 26506
neutron diffusion theory for, 20: 14774
neutron distribution in borehole after source cutoff, 19: 34385(T)
neutron distribution in media with cylindrical interfaces, 19: 34387(T)
neutron distributions in soils and oil-bearing limestone in, 19: 34389(T)
neutron distribution in multilayered media in, 19: 34389(T)
neutron, effects of instrument sensitivity and transport on, 17: 1640
neutron-epithermal neutron apparatus for measuring porosity, 17: 16410(P)
neutron-gamma apparatus with sodium iodide crystal at liquid nitrogen temperature, 16: 27409(P)
neutron-gamma apparatus, 17: 16395(P)
neutron-gamma apparatus for identifying elements by delayed coincidence, 17: 16413(P)
neutron-gamma device for activation and detection of non-radioactive tracers, 16: 17861(P)
neutron-gamma logging instrument with control of neutron output, 16: 17874(P)
neutron-gamma spectrometry in boreholes, chemical composition of rocks from, 18: 5522
neutron-gamma system for logging aluminum and silicon, 16: 17906(P)
neutron-gamma system with calibration means, 16: 20699(P)
neutron generator for, 17: 3200(P)
neutron generator for, 17: 18585(P)
neutron generator for, design of, 18: 5508
neutron generator for, 18: 40497(P)
neutron generator for, pulse transformer design for, 18: 39604(P)
neutron lifetime in borehole model, thermal, (E/T), 19: 18184
neutron method for determining points of entry of different liquids, 16: 20919(P)
neutron methods for soil moisture measurements, model study of, 18: 5524
neutron–neutron, coal seam thickness determination by, 17: 34123
neutron-neutron device for petroleum prospecting, 16: 17858(P)
neutron-neutron pulse, methods for oil and gas boreholes, 18: 5495
neutron one-energy-group diffusion theory in borehole geometry, problems in, 18: 5494
neutron, porous-strata models for, 18: 4008
neutron probe calibration curve for soil moisture measurements, effect of borehole diameter on, 18: 5523
neutron, proportional detector for, 16: 27387(P)
neutron, scintillation detector for, 17: 25662(P)
neutron slowdown, distributions for depth of rock in pulsed, 19: 34386(T)
neutron slowing down and absorption method and apparatus for, 18: 23868(P)
neutron soil moisture probe, 18: 35808 (HW-82009)
neutron source design for petroleum detection, 17: 8314(P)
neutron source design for, 17: 16415(P)
neutron source design for, self-contained, 18: 1934(P)
neutron source design for, 18: 5542(P)
neutron source design for, 20: 9160(P)
neutron source design for, linear accelerator, 19: 2934(P)
neutron source for, design of, 20: 29444(P)
neutron source for pulsed neutron-neutron, in gas and oil wells, 20: 37017
neutron source output stabilization, 16: 18282(P)
neutron sources for, 16: 8986 (CEA-NOTE-352)
neutron sources for petrolium prospecting, 17: 20224
neutron sources for, 18: 5498
neutron-gamma apparatus for detecting oil or salt water in earth formations, 18: 12367(P)
neutron-gamma apparatus with shielded detector for, 18: 18055(P)
neutron-gamma instrument for distinguishing between hydrocarbon oil and gas in earth formations, 19: 2592(P)
neutron, boundary value problem in theory of pulsed, 19: 34383(T)
neutron, temperature effects in, 18: 10292
nitrogen content determination using neutrons, 18: 13713(P)
nuclear, equipment and methods for, 17: 41013(P)
nuclear magnetic, for liquid content of earth formations, 16: 27398(P)
nuclear magnetic resonance apparatus, 16: 23961(P)
nuclear magnetic resonance, determining of magnetic properties of drilling mud, 16: 27407(P)
performance in ore composition analysis, 20: 2063
probe design for, 20: 14773
probe design for gamma and neutron, 17: 10836
pulsed neutron-neutron methods in, Monte Carlo calculations in, 20: 35658
radiation caliper apparatus, 19: 2591(P)
radiation detection instrument for, 19: 34586(P)
radiation die-away in pulsed neutron, 19: 42649
radiation protection in, 17: 6342
radioactive metallo-organic compounds for use in, 18: 5538(P)
radioactive resin use in, 17: 8674(P)
radioactive, improvement of efficiency of data transmission in, 18: 33853(T) (AEC-tr-6399(p.207-20))
radioisotope injection for tracer surveys, 17: 3090
radioisotope uses in, for exploitation of natural gas and petroleum reservoirs, 20: 27142
radiometric control of flooding of oil deposits, 18: 5520
radiometric equipment for, 18: 5519
radiometric equipment design for reducing well-fluid effects, 19: 24740(P)
radiometric equipment for, circuitry for, 19: 46623(P)
radiometric, for uranium deposits, 18: 1910 (CEA-2330)
radiometric methods of, development of neutron source for use in, 19: 18189(P)
radiometric methods of, using gamma scattering, 19: 22830
radiometric methods of, for petroleum exploration, 19: 30419
radiometric methods of, review, 19: 36679
radiometric methods of, for measuring petroleum contents, 20: 23564
radiometric, equipment and techniques for neutron, for boron deposits, 19: 13261
radiometric, survey of methods for, 18: 22263
radiometric, uses for determining water resources, 19: 22573
radiotracer determination of permeable zones in water injection wells, 18: 5531
radium content variation in borehole water, 18: 5533
reactor for use in, design of, 19: 33652(P)
rock density evaluation from natural-gamma logs, method for, 18: 5499
scintillation counter design for, 17: 4863(P)
soil bulk-density determination using gamma sources, devices for, 18: 5506
soil density and moisture measurements using gamma and neutron scattering, 20: 37135
soil moisture determination by a neutron method, 18: 5505
soil-moisture measurements by neutron, 20: 31435
sources for, 17: 20225
spectrometer design for, 17: 22023
techniques in, 17: 10842
techniques in gas and oil prospecting, gamma and neutron, 17: 12487
telemetering systems for, design of, 20: 35765(T) (AD-630996)
theory development and calculations for neutron, 19: 46619
theory for epithermal-neutron, 20: 18932
theory of neutron, 18: 5501
tracer method for locating and identifying subterranean fluids, 18: 22264(P)
tracer technique for detecting leaks and studying porosity of layers, 19: 2551(P)
tracer techniques for determining fractures in oil-bearing layers, 18: 5527
use of neutron thermalization for water determination in soils, 16: 11998 (NP-11380)
use of nuclear geophysical methods for testing natural gas reservoirs, 19: 28562
use of open radio-sources in oil boreholes, 18: 5534
use of radioactive tracers to measure fluid productivity in wells, 18: 12376(P)
using neutron sources, 17: 8678(P)
using neutron sources, 17: 8679(P)
using neutron sources, apparatus for, 17: 9496(P)
waste disposal monitoring using gamma, 19: 25773 (HW-84577)

WELLS

analysis of borehole water for beta activity, 17: 17970 (PG-Report-357)
book: *Radioactive Investigations of Oil and Gas Wells*, 19: 36687(T)
construction materials corrosion in domestic, near Savannah River Plant, 17: 29283 (TID-17257)
core mineralogy of Joy No. 1, 17: 26932(R) (ORNL-TM-516)
deep injection waste disposal, site survey, 16: 25057 (TID-7628(p.347-55))
design and operation of deep injection waste disposal, 16: 25059 (TID-7628(p.363-73))
drilling of, control of well fluid circulation by radioactivation of fluid during, 18: 6962(P)
effects of Salmon explosion on nearby oil and gas facilities, 19: 36589 (VUF-1022)
fluid productivity profile log of, use of tracers for studying, 18: 12376(P)
heating of underground formations, reactor for, 18: 19404(P)
isotopic composition of brines in oil, 20: 41161
logs for wells and test holes drilled in Nevada Test Site prior to 1960, 16: 8992 (TEI-804)
neutron diffusion in timbered-layer-intersected, attenuation decrement and mean lifetime for nonstationary, (E), 20: 27175
operation of deep injection waste disposal, 16: 25058 (TID-7628(p.356-62))
pressure cementing of, to prevent contamination at National Reactor Testing Station, 17: 30752 (IDO-12030)
pressure rise in dry, 18: 3429(R) (TID-19733)
productivity of natural gas, improvement by underground nuclear explo-

sions, 20: 36961 (UCRL-12229)
resources of water, at Nevada test site, 17: 1633 (TEI-788)
seismic signals in cased and open deep, 19: 7716(R) (AFCRL-62-878)
tool orienting in, radially collimating window for instruments for, 20: 29517(P)
use in earthquake and explosion detection, 18: 43780 (AFCRL-64-177)
use of water level and pressure fluctuations in, to detect seismic signals, 19: 26557(R) (VESIAC-7724VU)
waste disposal by hydraulic fracturing, 16: 2808(R) (ORNL-TM-15)
waste disposal in deep, mechanisms for, 17: 26932(R) (ORNL-TM-516)
waste disposal in deep, 18: 6537(R) (ORNL-TM-603)
waste disposal in deep, operations summary of, 18: 19448(R) (ORNL-TM-757)
waste disposal in shale, by hydraulic fracturing, 19: 8674(R) (ORNL-3697(p.10-19))
waste disposal into, 17: 4373
water level in, radioisotopes uses in measuring, 19: 42647
water temperature logging system for, 16: 29101 (HW-73994)

WEST INDIES

fall-out monitoring, 1960 to 1961, 16: 394 (AERE-R-3766)
iodine-127 and iodine-131 metabolism in Jamaica, 19: 3869
radioactivity of Jamaican bauxite and terra rossa, 20: 33547
uptake by normal subjects in Jamaica, thyroidal, 19: 3869

WEST VIRGINIA

areal geology and aeroradioactivity surveying of, 20: 20928 (CEX-59.4.17)
gamma aeroradioactivity at 500 ft over, mapping of, 19: 46614

Westinghouse Test Reactor (WTR)
see Research Reactors

WETTING

detection in liquid sodium, apparatus for, 18: 33827 (EUR-1823.d)
of heat transfer surfaces during boiling, effects of applied voltage on, 17: 8366
radiation effects on surface, gamma, 16: 12201

Wetting Agents
see Surface-Active Agents

WHALES

radioisotope content in, 20: 38560

WHEAT

activation analysis of, methods for, 20: 23527 (CONF-651206)
adenosine triphosphatase synthesis in roots of, effects of calcium and strontium on, 20: 30992
alpha radioactivity, 18: 35382
analysis for cesium-137 in, from 1962 crop, 18: 6944(R) (HASL-142)
analysis for mercury, activation, 19: 19771(R) (TEES-2671-4(Chap.9))
analysis for mercury, activation, 20: 1738(R) (GA-4041)
analysis for mercury contamination, activation, 20: 1739(R) (GA-4297)
analysis for mercury by neutron activation, 20: 1755
analysis for protein fractions in irradiated flour of, electrophoretic, 17: 4766
analysis for strontium-90 content, 1961 and 1962, 16: 1447(R) (HASL-122)
analysis for strontium-90 in United States, 1959-60, 16: 17928
analysis for strontium, atomic-absorption spectrophotometric, 16: 26913
beta radioactivity and potassium content in, 16: 25644 (CLOR-9)
breeding 56-chromosomal Triticum × Agropyron from gamma-irradiated seed for fertility increase, 20: 35194
calcium content in Canadian, 20: 41198 (NP-16192)
calcium content of U. S., 1958-62, 18: 14147
calcium uptake and distribution in, relation to strontium-90, 20: 42766
carbohydrate metabolism in plants of, from irradiated seeds, 18: 17590
cation metabolism in seedlings of, 20: 38548(R) (ORO-2410-1)
cerium-144 content in, from U. S., 1962, 18: 25265 (HASL-143)
cerium-144 content of U. S., 18: 33818
cerium-144 uptake by, effects of lime and humus on, 16: 14451
cesium-134 and -137 content, relation to content in man, 19: 20225
cesium-137 content in, effects of calcium, potassium, sodium, and soil acidity on, 19: 14982
cesium-137 content in German, effects of precipitation on, 20: 11017
cesium-137 content in flour from French, 1960 to 1962, 20: 45892
cesium-137 content of U. S., 18: 33818
cesium-137 content of Canadian, 16: 5148 (CRER-1000)
cesium-137 uptake by roots of, effects of di- and mono-saccharides on, 19: 50
cesium-137 uptake by, effects of alkali metal and ammonium cations on, 19: 51
cesium-137 uptake by seedlings of, cultured with ammonia, 19: 29878
cesium-137 uptake by, effects of potassium content in soil on, 19: 35898
cesium-137 uptake by, effects of respiration inhibitors on, 18: 9752 (IA-900)
cesium-137 uptake from contaminated soil, 18: 15761
cesium-137 uptake by Canadian, 18: 39537
chromosome aberrations in winter, frequency of chemical induced, 19: 31836
chromosomes of, space flight effects on, 18: 1327(T) (FTD-TT-63-968(p.332-41))
cobalt-60 uptake by, effects of respiration inhibitors on, 18: 9752 (IA-900)
content of cesium-137, iodine-131, strontium-89, and strontium-90 in U. S., 1965, 20: 38743
cytology and physiology of T. *durum* and T. *monococcum*, effects of alkylating compounds on, 19: 43653
development of parenchyma in, effects of auxins on, 20: 40631(R) (ORNL-3922, pp 161-6)
effects of alkylating chemicals on *Lakota durum*, 20: 33064
effects of free lipid fraction from irradiated seedling bean leaves on seed of, toxic, 20: 36598
effects of irradiated, on reproduction by rats, 19: 7079
effects of irradiated, on growth and survival of rats, 19: 7080
effects of space flight on seeds of, 20: 31058
effects of space flight on chromosome aberrations in roots of, 20: 42909
effects of transplantation of non-irradiated embryo on γ-irradiated endosperm, seedling-growth, 20: 45452
effects on development and growth of irradiated bean lipid, 20: 5265(T)
ethylenimine-induced mutations of, 20: 1655
fallout monitoring in, Canada, March 1966, 20: 33556 (NP-16124)
fission products transfer to, from contaminated soil, 17: 38725
gamma attenuation coefficients for, (E/T), 20: 716
genetic control of strontium-89 and calcium-45 accumulation, 20: 40532(R) (COO-1097-17)
genetic studies of, 20: 26655(R) (NP-15975)
genetic variability in *durum*, effects of ethylmethanesulfonate on, 19: 42267
germination and growth of seedlings of, 19: 2009(R) (ORNL-3700(p.176-9))
gluten in, effects of heavy water on physical properties of, 18: 23477
growth, effects of irradiated seeds on, 16: 1598
growth of seedlings of, effects of radiation and weightlessness on, 19: 43717 (NASA-CR-303)
growth of, effects of blood serum and gastric juices from irradiated animals on, 18: 41125
growth of, effects of supragravitation on, 18: 11801
growth, effects of chemical mutagens on, 16: 25194 (CNEN-124)
manganese-54 content of, 20: 23300
metabolism in seed of, effects of cysteine and quinone on, 20: 31002
mutagenesis in, effects of ethylenimine and x radiation on, 20: 42919
mutations in, chemically induced, 20: 22658
mutations in, chemically induced, 17: 15731
mutations in, chemically induced, 19: 3888 (EUR-1829.f)
mutations in, chemically induced, 19: 2161
mutations in, effects of chemicals on, 16: 28762 (CNEN-124)
mutations in, frequency of chemical, 17: 38689
mutations of, induced by gamma radiation or ethyleneimine, 18: 17594
nitrogen incorporation in grain and stalk of ripening, tracer study of, 17: 2717
phosphorus-32 uptake by seeds of, effects on metabolism of, 18: 23205(T) (JPRS-24290(p.36-42))
properties of nuclei in seeds of, microspectrophotometric study of, 20: 40631(R) (ORNL-3922, pp 161-6)
protection of grain and grain products from contamination by radioactive, chemical, or bacteriological substances, 18: 31803(T) (JPRS-25250)
quality and yield of, effects of fission products on, 19: 35963
radiation and supragravitational effects on growth of, 18: 11801
radiation effects in seeds of, effects of dose rate on, 19: 43781
radiation effects in vinyl pyrrolidon monomer treated, electron paramagnetic resonance spectra for, 17: 30347
radiation effects on morphophysiological characteristics of seed, 16: 1609
radiation effects on seedling growth in, 16: 1612
radiation effects on cross-fertilization, 16: 4052
radiation effects on diploid, comparison of beta and gamma, 16: 12932
radiation effects on, flour, 16: 19218(T) (CEA-tr-R-1424)
radiation effects on flour, 16: 24041
radiation effects, genetic, 16: 28762 (CNEN-124)
radiation effects on *durum* and *vulgare* varieties of, chronic gamma, 16: 28767 (RT/BIO(62)43)
radiation effects, genetic, 16: 28790
radiation effects on light-scattering properties of gliadin portion of gluten, 16: 14489
radiation effects on flour from Italian, gamma, 17: 3544(T) (NP-tr-926)
radiation effects on chemical and physical properties of flour protein of, 17: 4766
radiation effects on flour and baking products from, electron paramagnetic resonance spectra of, 17: 8497
radiation effects on flour flavor and odor, germination, respiration, and surface molds, cathode, 17: 10374
radiation effects on species with different ploidy, x, 17: 10381
radiation effects on growth and survival of, comparison with effects of

mutagenic agents, 17: 10388
radiation effects on embryonic-endosperm ratio in, gamma, thermal neutron, and x, 17: 10386
radiation effects on cell growth in leaves, 17: 15651
radiation effects on, seed and seedling neutron exposure, 17: 15748
radiation effects on flour proteins, 17: 21961(T) (AEC-tr-5775)
radiation effects on proteins of flour of, 17: 23039(T) (AEC-tr-5794)
radiation effects on gluten proteins in flour of, 17: 23040(T) (AEC-tr-5798)
radiation effects on properties of gluten from, 17: 23096(T) (AEC-tr-5795)
radiation effects on properties of gluten from, 17: 23097(T) (AEC-tr-5797)
radiation effects, genetic, 17: 23144
radiation effects, genetic, 17: 28713
radiation effects on seedlings of einkorn, acute and chronic, 17: 30224
radiation effects on, gamma, thermal neutron, x, 17: 30055
radiation effects on frequency and types of chromosome aberrations and mutations in seeds of, 17: 40588
radiation effects on growth, development, and survival of, 17: 40541
radiation effects on growing of, 18: 2120
radiation effects on rheology of, x, 18: 3539
radiation effects on variability of spring, during conversion to winter habit, 18: 3562
radiation effects on fatty acid peroxide derivatives from, gamma, 18: 5116
radiation effects on seeds of, plant sensitivity from gamma, 18: 9850
radiation effects on, during vegetation, 18: 11692
radiation effects on leaves of, gamma, neutron, and x, 18: 13494
radiation effects on, review of gamma, 18: 13528
radiation effects on, effects of moisture content on gamma, 18: 13529
radiation effects on seed germination in, gamma, neutron, and x, 18: 13494
radiation effects on chromosomes of, gamma, neutron, and x, 18: 13494
radiation effects on seedling height in, gamma, neutron, and x, 18: 13494
radiation effects on mitotic inhibition in, gamma, 18: 17488
radiation effects on mutation rate and polyploidy of *Triticum*, x, 18: 19748
radiation effects on grain yield and bread yield of eleven varieties of, from irradiated seeds, 18: 21833(T) (OTS-63-11453/2(p.87-98))
radiation effects on straw of, for use by rumen microorganisms, 18: 21849
radiation effects on meristematic cells of seeds of, 18: 27125
radiation effects on amino acids in grains of, 18: 29275(T)
radiation effects on seed of, effects of oxygen tension and storage temperature on neutron, 18: 31221
radiation effects on amino acid content in sprouts of, protective effects of magnesium sulfate, niacin, and thiamin against, 18: 33398
radiation effects on Einkorn, RBE of fast-neutron and gamma, 18: 41227
radiation effects on seeds of, gas-plasma, 19: 185
radiation effects on fertility of, chronic gamma, 19: 7058
radiation effects on gluten of, 19: 7126
radiation effects on grain yield, growth, and quality of *Triticum aestivum*, 19: 10887
radiation effects on genetic mutability increase in, 19: 15113
radiation effects on durum and bread, gamma, 19: 15161
radiation effects on growth of, factors affecting, 19: 15167
radiation effects on growth inhibitors in, x, 19: 15171
radiation effects on seeds of, gamma and x, 19: 15173
radiation effects on genetic variance in hexaploid and tetraploid, 19: 15079
radiation effects on content of B-complex vitamins in, 19: 17575
radiation effects on development and growth of, photoperiod and temperature effects on uv, 19: 19545
radiation effects in, biological, 19: 21917
radiation effects on gluten in, 19: 24318
radiation effects on germination and seedlings of, small-dose, 19: 25931
radiation effects on germination of, x, 19: 25935
radiation effects on, effects of dose on x, 19: 25935
radiation effects on, effects of gibberellic acid on gamma, 19: 31795(R) (ORNL-3768(p.181-6))
radiation effects on, gamma, 19: 32651
radiation effects on epidermal hairs of, chronic gamma, 19: 33891
radiation effects on yields of, seed-irradiation, 19: 36008
radiation effects on mutations by seed exposure, fast neutron and gamma, 19: 36061
radiation effects on development and growth of, gamma, 19: 36076
radiation effects on seeds of, effects of water content on, 19: 38412
radiation effects on genetic variability in *durum*, fast neutron and x-ray, 19: 42267
radiation effects on content and quality of spring, gamma, 19: 42328
radiation effects on nutritive value in animals, gamma, 20: 50
radiation effects on lipids in, effects of dose on gamma, 20: 1637
radiation effects on development of embryos of, 20: 1666
radiation effects on seeds of, x, 20: 5403
radiation effects on microorganisms in stored, γ and neutron, 20: 7472
radiation effects on quality of flour from, effects of moisture content on γ, 20: 7473
radiation effects on, gamma, 20: 6876
radiation effects on cell division in seedlings of, γ, 20: 6787(R) (ORNL-3853, pp 177-81)
radiation effects on genetic variability in, 20: 10603(R) (IAEA-2466-11)
radiation effects on genetic variability in, 20: 12641 (TID-22582)
radiation effects on, effects of pre- and post-irradiation thermal treatment on, 20: 18323
radiation effects on, mutagenic, 20: 18409
radiation effects on, following seed soaking in phosphorus-32 solutions, 20: 18442
radiation effects on water content of leaves of, γ, 20: 31110
radiation effects on development of, γ, 20: 31113
radiation effects on metabolism in seeds of, γ, 20: 31002
radiation effects on seeds of, and plants grown from them, 20: 31058
radiation effects on growth and mutations in Triticum, fast and fission neutron and gamma, 20: 31080
radiation effects on growth and yield of, effects of age of seed on, 20: 32978
radiation effects on *Lakota durum*, x, 20: 33064
radiation effects on dry matter and water content in varieties of, dosage effects on gamma, 20: 33013
radiation effects from phosphorus-32 on, effects of feed solution additives on, 20: 35226
radiation effects on seeds of summer, γ, thermal neutron, uv, and x, 20: 35317
radiation effects on mutations in embryos of, gamma, 20: 36650
radiation effects on constituents of flour of, gamma, 20: 40599
radiation effects on seeds of pure and hybrid, gamma, 20: 42897
radiation effects combined with ethylenimine on mutagenesis in durum, 20: 42919
radiation effects on diploid and polyploid species of, recurrent-exposure x, 20: 45395
radiation effects on genetics of, thermal neutron, 20: 45392
radiation effects on *durum* and bread, first generation, 16: 1599
radiation effects on growth of, 18: 11801
radiation effects on growth of, 16: 25194
radiation effects, biological, 19: 21913
radiation injuries to cells of, protective effects of acrylamide and propionamide against, 18: 3586
radiation process of flours, cereals, and baked products, 17: 21960(T) (AEC-tr-5773)
radiation processing of, and wheat products for control of insect infestation, 18: 13446 (NP-13640)
radiation processing of, effects on quality, 19: 15946 (CONF-641002 (p.4-7))
radiation processing for disinfestation of insect pests, 19: 36883
radiation processing for sprout inhibition, 19: 36883
radiation studies on, use of low-power research reactor for, 17: 38685
radioactivity due to fallout in Canadian, Nov. 1965, 20: 20883 (NP-15914)
radioactivity due to fallout in Canadian, Dec. 1965, 20: 20938 (NP-15921)
radioactivity of Canadian, June 1965, 19: 44251 (NP-15519, pp 23-51)
radioinduced and chemically induced mutations in *Triticum durum*, 18: 23320
radioinduced chlorophyll mutations, 16: 26811
radioinduced chromosomic aberrations in "Cappelli", 17: 10389
radioinduced chromosome aberrations in embryos of, by incorporated tritium, 18: 1424
radioinduced chromosomal aberrations in, gamma, 18: 17607
radioinduced chromosomal aberrations and mutation in, effects of boron on gamma and thermal neutron, 19: 2153
radioinduced chromosomal aberrations in radicals of, 19: 7096
radioinduced chromosome aberrations in winter, frequency of, 19: 31836
radioinduced free radicals in moist seeds of, 19: 5668
radioinduced growth acceleration, after low-dose irradiation of seed, 16: 6336
radioinduced micro-mutations in, 18: 43218(R) (EUR-1882.e(p.7-26))
radioinduced multiple carpel mutation in H 167, 18: 6634
radioinduced mutants, 16: 25195 (CNEN-126)
radioinduced mutations, 16: 6315(T) (JPRS-11322(p.429-46))
radioinduced mutations, economic significance and genetic basis, 16: 8542(R) (TID-14829)
radioinduced mutations, 16: 25196 (CNEN-120)
radioinduced mutations, 16: 31515
radioinduced mutations, 16: 32735(R) (TID-16979)
radioinduced mutations, 17: 2834(R) (TID-17287)
radioinduced mutations in "Cappelli" durum, 17: 10390
radioinduced mutations, 17: 15731
radioinduced mutations, 17: 24894(R) (TID-18673)

radioinduced mutations, 17: 28714
radioinduced mutations, 17: 28715
radioinduced mutations in, evaluation of use in breeding of macro- and micro-, 17: 38688
radioinduced mutations for rust resistance in, neutrons and x, 17: 39362
radioinduced mutations in bread, frequency and spectrum of beta, neutron, and x, 18: 9853
radioinduced mutations of, 18: 11649 (TID-20031)
radioinduced mutations of, 18: 13453(R) (TID-20220)
radioinduced mutations in, 18: 13484
radioinduced mutations in Triticum by gamma irradiation of seed, 18: 17484(T) (OTS-62-11755/4(p.17-28))
radioinduced mutations for disease resistance in, gamma, 18: 31224
radioinduced mutations of, yield from, 18: 33279(R) (TID-20823)
radioinduced mutations in, fast neutrons, 18: 33374
radioinduced mutations of, 18: 38777(R) (TID-21068)
radioinduced mutations of, 18: 41115
radioinduced mutations in, x, 19: 2154
radioinduced mutations in, neutron and x, 19: 2161
radioinduced mutations in, gamma, 19: 3888 (EUR-1829.f)
radioinduced mutations in, for breeding, 19: 7147
radioinduced mutations in winter, 19: 17621
radioinduced mutations in, 19: 21861(R) (NP-14937(p.116-25))
radioinduced mutations of *Triticum durum* and *T. monoccum*, 19: 24261(R) (TID-21649)
radioinduced mutations in different varieties of, phylogenetics of, 19: 26047
radioinduced mutations of, gamma, 19: 25994
radioinduced mutations in, 19: 36077
radioinduced mutations of, applications in plant breeding programs, 19: 42260 (TID-22115)
radioinduced mutations of, γ and fast neutron, 20: 1655
radioinduced mutations of *Triticum monococcum*, 20: 3762
radioinduced mutations in winter, γ, 20: 6795(T) (JPRS-33170, pp 226-32)
radioinduced mutations in, effects of ploidy on, 20: 6897
radioinduced mutations in, classification of, 20: 12632(R) (EUR-2546.f)
radioinduced mutations in, γ and x, 20: 16285
radioinduced mutations in, 20: 16286
radioinduced mutation in, use in breeding program, 20: 18322
radioinduced mutations for quantitative traits in Durum, x, 20: 20501
radioinduced mutations in seeds of, effects on dose rate on beta, gamma, and fast-neutron, 20: 22743
radioinduced mutations in, effects of post-irradiation soaking and temperature changes on gamma, 20: 22779
radioinduced mutations in, fast-neutron and gamma, 20: 22658
radioinduced mutations in buck-, gamma, 20: 22665
radioinduced mutations in, effects on gluten content and quality, 20: 22672
radioinduced mutations of, γ and neutron, 20: 28960
radioinduced mutations in, fast neutron and gamma, 20: 36620
radioinduced mutations in, x, 20: 42846 (IAEA-2466-13)
radioinduced mutations in, frequency of, 17: 38689
radioinduced smut resistance in, gamma, 18: 31245
radioinduced sterility in pollen of, γ, 19: 43767
radioinduced striping in Einkorn, beta, gamma, and neutron, 19: 2152
radioinduced variegation mutations in, Einkorn, beta, fast neutron, gamma, and thermal neutron, 20: 20497
radiosensitivity, 20: 28864(R) (NP-15976)
radiosensitivity and cytological characteristics, effects of variety, 16: 9848(T) (JPRS-11485(p.158-63))
radiosensitivity and cytological changes in, effects of variety on, 17: 5903
radiosensitivity, effects of polyploidy on thermal neutron and x, 16: 12933
radiosensitivity of, effects of variety on, 18: 5027
radiosensitivity of growth of germinating seeds of, 18: 27013(R) (ORNL-3601(p.210-15))
radiosensitivity of varieties of bread, gamma, 19: 2155
radiosensitivity of embryos from seeds of, effects of carbohydrate metabolism on, 19: 33888
radiosensitivity of, effects of elements on gamma, 19: 42369
radiosensitivity of German winter wheat varieties, x, 20: 35321
radiosensitivity of, effects of polyploidy on gamma, 20: 36648
radiosterilization, safety and wholesomeness of, 19: 32651
radiosterilization of, status, 20: 16918 (AECL-PAK/RB-7)
radiosterilization effects on wholesomeness of bread and cake, 20: 27372
ruthenium-106 uptake by, effects of lime and humus on, 16: 14451
sodium-22 content in, relation to content in man, 19: 20225
strontium accumulation in grain of, effects of genotype and calcium content on, 18: 21789
strontium-85 uptake by plants, plant parts, and seed of, 19: 33753
strontium-89 accumulation in grain, stems, and leaves, genetic factors in, 17: 27055
strontium-89 uptake by, effects of genotype on, 17: 13896
strontium-89 and -90 content in German, effects of precipitation on, 20: 11017
strontium-89 uptake by, heritability in, 19: 14975
strontium-89 uptake by, effects of lime and humus on, 16: 14451
strontium-90 activity in 1959 harvest, 16: 15037
strontium-90 content in Canadian, 1962, 17: 41026 (NP-13193)
strontium-90 content in Idaho and Montana, effects of spring precipitation on, 18: 10286
strontium-90 content of Canadian, 1962, 18: 14148
strontium-90 content in U. S., 1963, 18: 18041(R) (HASL-144)
strontium-90 content of, from 1963 harvest, 18: 23804
strontium-90 content of, for U. S. 1963 crop, 18: 35787
strontium-90 content in plant parts and milling fractions, 18: 35788
strontium-90 content in Canadian, 1958 to 1963, 19: 9379
strontium-90 content of flour from British, 19: 36733
strontium-90 content of U. S., 1958 to 1964, 19: 46662
strontium-90 content in Canadian, 1963, 20: 7304 (NP-15641, pp 3-8)
strontium-90 content in Canadian, 1964, 20: 14736 (NP-15853, pp 3-7)
strontium-90 content in, in Japan, 1964, 20: 16731 (NP-15883)
strontium-90 content in, effects of washing with decontaminating solutions on, 20: 29473
strontium-90 content in Canadian, 1963, 20: 33588
strontium-90 content in Canadian, 1966, 20: 41198 (NP-16192)
strontium-90 content in domestic and imported, in Finland, 1963 and 1964, 20: 43006
strontium-90 content in Japanese, 20: 45887 (NP-16290)
strontium-90 content in flour from French, 1960 to 1962, 20: 45892
strontium-90 content of U. S., 1958 through 1962, 18: 14147
strontium-90 contents in Canadian, 16: 5148 (CRER-1000)
strontium-90 effects on, 18: 31171
strontium-90 levels in United States, 1959, 16: 13405
strontium-90 levels in, 17: 5751(R) (HASL-132)
strontium-90 uptake by, 18: 3619
strontium-90 uptake by, environment effects on, 18: 13403 (HW-SA-2977)
strontium-90 uptake by, grown in open and under tents, 19: 25842
strontium-90 uptake by, effects of liming and soil types on, 20: 6745
strontium-90 uptake by, effects of variety on, 20: 18970
strontium-90 uptake and distribution in, relation to calcium, 20: 42766
strontium-90 uptake from contaminated soil, 18: 15761
strontium-90 uptake by Canadian, 18: 39537

WHEATSTONE BRIDGE
design of pulse-size, for calibration of scintillation spectrometers, 17: 37421
performance in temperature distribution measurements, 20: 9115(T) (ANL-Trans-236)

WHEELS
design of shock-absorbing, 19: 33707(P)

WHISTLERS
analysis of proton, for density determination in ionosphere, (T), 20: 37885
cutoff theory for, evaluation of upper, 17: 41666 (D1-82-0245)
cyclotron damping of proton, ionospheric temperature from, 20: 39972
detection and measurement at Durban, 18: 40425
detection of helium, Alouette II Satellite, 20: 25993
diagnostic use for magnetospheric plasma density, (T), 19: 41596
dispersion of, protonosphere electron temperature effects on, (T), 19: 21140
distribution, production, and structure of, review on, 19: 16755
electron trajectories in presence of magnetospheric waves from, (T), 19: 21099
excitation by electromagnetic pulses from nuclear explosions, 17: 41678
excitation by gyrating electron streams in plasma, 18: 11333
frequency of proton, from vlf data, (E), 20: 11821
frequency of vlf proton, hydrogen ion ionospheric content from crossover, 20: 11822
interactions with electrons, v-l-f emissions from, 17: 41684
interactions with ionized stream, 18: 22976
interactions with ionized stream, 19: 25550 (AD-607091)
interactions with ionospheric charged particles, gyroresonance, 19: 29134 (SU-SEL-64-063)
interactions with electrons and protons in magnetosphere, gyroresonance radiation from, (T), 20: 4747
measurements on proton, hydrogen ion/electron content ratio from, (T), 20: 2847 (AD-614716)
modes for, equations for exact nonlinear electromagnetic, 20: 29899
power of magnetospheric electron velocity spectra from cyclotron absorption of, (E), 19: 47463
power spectra of, electron velocity distributions from, (T), 20: 17558
production by helical electron beams in ionosphere, 18: 36422
production by streams of gyrating electrons, 20: 7659(R) (ORNL-3849,

pp 101-50)
production of proton ion-cyclotron, in ionosphere, (E/T), 19: 23517
production of proton ion-cyclotron, in ionosphere, (E/T), 19: 47445 (AD-611828)
propagation along magnetized plasma slab, effect of collisions on, (T), 20: 40196
propagation during geomagnetic storms, (E), 19: 5076
propagation in electron stream, 18: 11064
propagation in hot plasma, anomalous damping of, (T), 19: 31363
propagation in ionosphere, echoes in, 19: 25429
propagation in magnetosphere, theory for group, 20: 44469
propagation in plasma in magnetic field, negative ion effects on, (T), 19: 10413
propagation in plasma, ion effects on, (E/T), 19: 10437
propagation in plasma with electron beams, (T), 19: 29423
propagation in plasma, thermal cutoff to, 17: 33143 (D1-82-0229)
propagation of echoes of, in low latitudes, (E), 19: 39674
propagation of long-wave-emitted signals, optical path variation, (E), 20: 44429
propagation of micropulsation, in atmosphere, 18: 44659
propagation of, theory for, 18: 2745
propagation of, interpretation of, (T), 20: 6207
properties, 18: 30671
theory for, magnetoionic, (T), 19: 47464
theory of hydromagnetic, 20: 19666
theory of multiple discrete well-defined components in, 18: 11064
use for determining helium and hydrogen ion distribution in magnetosphere, (E), 20: 6198
use for electron density, hydrogen ion concentration, and proton gyrofrequency determination, (E), 20: 19669
use in magnetospheric electron density measurements, 18: 38015
use in magnetospheric ionization density structure determination, (E), 20: 19667
use in magnetospheric electron content and density determinations, (E), 20: 19668

WHITE OAK CREEK
cesium-137 content of sedge plants from drained waste disposal area fed by, 17: 33549
cesium-137 content in sediments of, 20: 10449
cesium-137 distribution and fixation in sediments of lacustrine origin in, 19: 46681
chromosomal aberrations in *Chironomus tentans* population of, exposed to chronic low-level radiation, 18: 8108 (ORNL-3531)
contamination and hydrology of, 16: 31347(R) (ORNL-TM-252)
contamination, determination of sources of, 16: 2808(R) (ORNL-TM-15)
diffusion of ground water in basin of, tracer studies of, 18: 43091(R) (ORNL-TM-830)
dispersion of radioactive waste from, in Clinch River, effects of river flow and temperature on, 19: 1946 (ORNL-P-605)
ecological survey, 1950 to 1953, Oak Ridge National Laboratory area, 17: 18332 (ORO-587(Vol.I))
ecological survey of vertebrate fauna, 1954, 17: 21932 (ORO-587(Vol. III))
ecology and fission product uptake in plants and animals, 17: 2786(R) (ORNL-3347(p.47-72))
ecology and radioisotope accumulation of smallmouth buffalo fish in, 18: 8061 (ORNL-3530)
ecology of drained lake, 16: 17374
ecology of mammal populations, 17: 33581
ecology of plants, 19: 38331
ecology studies in watershed area of, 19: 6931(R) (ORNL-3697(p.65-84))
fission product distribution and movement in drainage basin of, analysis, 18: 19448(R) (ORNL-TM-757)
fission product movement in, 19: 21792(R) (ORNL-3650(p.187-219))
flow studies of, use of analog computer in, 18: 20134(R) (ORNL-TM-792)
geology and soils of basin of, 19: 27835 (ORNL-TM-1108)
health physics studies of, 17: 39303(R) (ORNL-3492(p.76-8))
hydrology studies of drainage basin of, 18: 19448(R) (ORNL-TM-757)
mapping and radioactivity of watershed of, 19: 6932(R) (ORNL-3697(p.85-94))
mineral cycling in natural vegetation on drained lake bed, 16: 34143 (ORO-580)
monitoring, 16: 2058(R) (ORNL-3189(p.6-13))
monitoring for cesium-137, cobalt-60, ruthenium-106, and strontium-90 in, methods for, 18: 14092
monitoring of, for radionuclides, 17: 7653(R) (ORNL-TM-396)
plant taxa of drained bed of lake fed by, 1956 to 1960, 18: 12 (TID-19618(App.A))
radiation monitoring operations, summary, 17: 26932(R) (ORNL-TM-516)
radioactive waste dispersion in drained lake bed fed by, 18: 10 (TID-19618(p.5-37))
radioactive waste disposal in White Oak Lake and, effects on Chironomus cytogenetics, 20: 40530
radioactivity, from waste Burial Ground 4, 16: 9725 (ORNL-3182)
radioactivity in, 19: 7734(R) (ORNL-3697(p.32-42))
radioactivity in bottom sediments in, 18: 6537(R) (ORNL-TM-603)
radioactivity in drainage basin and sediments in, 19: 6930(R) (ORNL-3697(p.43-8))
radioactivity in plants and soils of former drainage basin of, 17: 39304(R) (ORNL-3492(p.81-95))
radioactivity in sediments in, from waste disposal, 19: 26591
radioactivity in, 1963, 18: 37442(R) (ORNL-3665)
radioactivity of, Aug. to Oct. 1962, 17: 17619(R) (ORNL-TM-482)
radiobiological monitoring of effluent, use of strontium-90 in clam shells, 16: 21889
radioinduced chromosome aberrations in *Chironomus tentans* larvae from, as result of waste contamination, 18: 25212
radioisotope content of drainage basin of, 17: 39300(R) (ORNL-3492 (p.51-62))
radioisotope content in, 17: 39306(R) (ORNL-3492(p.107-15))
radionuclide content in sediments of, 20: 45223
ruthenium flow in, 18: 17348
ruthenium movement in, 17: 39275
strontium distribution, 16: 12795(R) (ORNL-TM-133)
strontium-90 and cesium-137 content in insects inhabiting the area, 17: 33550
waste disposal area, bioaccumulation of radioactive isotopes by herbivorous mammals of area, 16: 9824
waste disposal area, fate of radioisotopes, 17: 2785(R) (ORNL-3347 (p.1-46))
waste disposal in, effects on lake bed plants and soils, 17: 4369 (ORO-585)
waste disposal in, effects on radioactivity of, 1961 and 1962, 17: 37055 (ORNL-3409)
waste disposal in, radioactivity from, 1962 to 1963, 20: 45216 (ORNL-3721)

White Sands Fast Burst Reactor
see Fast Burst Reactor Facility

WHITESHELL REACTOR NO. 1
commissioning program, 20: 42668 (AECL-2552)
construction of, 20: 42667 (66-CNA-309)
coolant behavior in, 20: 42669 (AECL-2553)
coolant tube material testing for, 18: 38265 (A/CONF.28/P/23)
description, 17: 22876
design and development, 18: 13339
design and development, Sept. 1964, 19: 12769(R) (AECL-2082)
design and development, 19: 38282
design of, review of, 20: 8471
design parameters for, (E), 19: 40218
development, 20: 45183
development, 19: 38168 (AECL-2220)
development, 20: 45234 (AECL-2460)
environs monitoring, 20: 14738 (NP-15853, pp 21-33)
environs monitoring, January 1966, 20: 29053 (NP-15951)
environs monitoring of, March 1966, 20: 33556 (NP-16124)
fuel behavior in, 20: 42669 (AECL-2553)
fuel sheathing development and testing for, 18: 38265 (A/CONF.28/P/23)
materials behavior in, 20: 42669 (AECL-2553)
radioactive contamination of milk near, 20: 14738 (NP-15853, pp 21-33)
research programs on, at AECL, 19: 45694(R) (AECL-2251)
shielding for, design of primary, 20: 20308 (AECL-2544)
shielding for, design of secondary, 20: 20309 (AECL-2545)

Whole-Body Counters
see particular sensing (detector) components used in whole-body techniques

WIGNER EFFECT
neutron fluxes for, calculation of, 17: 435
survey on, 20: 39455 (EUR-3056.e)

WIGWAM OPERATION
radiation monitoring at, aerial, 20: 23381 (USNRDL-TR-981)

WILBERFORCE AREA (ONTARIO)
ages of uranium minerals, 16: 29197

WILLISTON BASIN (MONT., N. DAK., S. DAK.)
geology of, for subsurface waste disposal in, 16: 27419 (TEI-809)
uranium occurrence in southwestern, 19: 30434

WIND
agitation of surface water by, wave patterns from, 19: 1030 (AECL-2051)
analysis of, using digital computers, 19: 17427 (SC-TM-8-62(51))
covariance, directional component means, and variances of, for 5 years, tabulation by season for 9 locations, 17: 6251 (CDRP-182-109)
device for analyzing, 20: 9167(R) (BNWL-36, pp 5.1-102)
direction measurement for diffusion parameter determinations, method for, 20: 514 (CONF-650407, pp 429-38)
direction of enhanced solar, and sudden commencement hydromagnetic waves, 16: 19649

distributions and profiles of prevailing, as function of altitude, 17: 3144 (AFSWC-TDR-62-35)
distributions at 100,000 to 300,000 ft, 16: 10277 (SC-4482(RR))
distributions in stratosphere, 16: 4374 (TID-13093)
distributions of, three-dimensional studies of, 18: 14574(R) (ANL-6769 (p.181-96))
effects of local, on fallout deposition, 18: 37365(R) (AD-600447)
effects of northerly and southerly, on gamma activity in air, 18: 2393
effects of shear and speed on accuracy of fall-out predictions, 16: 22440 (TID-7632(p.122-35))
effects on cloud formation from chemical explosives, 20: 4152 (TID-22266)
effects on diffusion of radioactive gases from nuclear power plants, 19: 18555
effects on dye tracer in ocean water, 19: 31630 (CU-2663-22)
effects on fallout deposition, 17: 3143 (AD-276185)
effects on fallout transport and deposition, 20: 4154(R) (AD-620003)
effects on fallout level, near New Delhi, 20: 16680
effects on ground deposition of microspheres released from 50 km, 20: 11033 (SC-TM-65-398)
effects on iodine-131 levels near Brookhaven Reactor, 20: 43608
effects on ionospheric F region, auroral-generated atmospheric, (E), 20: 44437
effects on missile launching, 18: 40984 (NAA-SR-Memo-9560)
effects on non-tidal drift at Cape Canaveral, 18: 15715 (TID-20322)
effects on particulate matter in atomic clouds, 20: 16160 (UCRL-14739 (Pt.2))
effects on sound wave propagation in atmosphere, (T), 19: 16258 (SC-RR-64-1756)
equations for inrush, development of, 20: 36995 (AD-636794)
fallout dose reduction effects of, 18: 20237 (USNRDL-TR-700)
fallout perturbations by local sea breezes, 20: 16661(R) (ECOM-00392-F)
fluctuations of, structure of, 18: 45161 (BNL-7328)
height and velocity variations of, equations for, 20: 18988(R) (ORNL-929, pp 58-66)
hydrodynamic effects on gravity waves from large explosions, 16: 27769
ionospheric, measurement by gun-launched projectiles, 20: 44447
measurement of, constant-temperature-difference meter for, 20: 516 (TID-22278)
measurement of, design of remote-recording weather vane for, 17: 25470(P)
measurements in atmosphere, similarity with temperature, 19: 47110 (RISO-100)
measurements in mesodecline over Nevada Test Site, 17: 4701
measurements in mesodecline over Tonopah test range, Nevada, 17: 8305
meteorological measurements at Risoe on, 1962 through 1964, 20: 27145 (RISO-121)
motion in conducting atmosphere, MHD equations for, 20: 11808(T)
prediction of activities of, for Salmon Event, 20: 5667 (VUF-1020)
predictions of, at National Reactor Testing Station, 20: 41129
profile in lowest 400 feet of atmosphere, 16: 14995(R) (BNL-697)
profile in lowest 400 feet of the atmosphere, 16: 25611 (BNL-718)
profile laws for, evaluation of, 18: 14575(R) (ANL-6769(p.197-219))
profiles at Lucas Heights in Australia, Sutton's turbulence index from, 18: 40038 (AAEC/TM-243)
profiles for 41 weather bureau stations in U. S., 17: 320
profiles in upper atmosphere determined from sodium cloud drifts at twilight, 16: 30663(R) (TID-16336)
profiles of, review, 19: 44794 (BNL-914, pp 158-60)
properties of stratospheric, during IGY, 20: 4151 (MIT-2241-14)
radioactivity transport across trade wind inversion in Hawaii by, 20: 45900
scattering in atmosphere by, role in atmospheric turbulent diffusion, 18: 10611(T) (AEC-tr-6128(p.231-47))
structure of, in micrometeorology, 19: 44798 (BNL-914, pp 175-7)
topographic effects on surface, at Lucas Heights, 18: 40039 (AAEC/TM-244)
turbulence at Douglas Point, Ontario, (E), 19: 18170
turbulence in boundary layer of atmosphere, analog simulation for, 19: 40282 (BNWL-SA-171)
turbulence in, analog-computer analysis of, (E), 19: 13859 (HW-84448-10)
turbulence in, low-level, 19: 44793 (BNL-914, pp 156-7)
turbulence measurements in, Theta–N instrumentation system for, 18: 14582 (TID-7677(p.384-91))
turbulence of components of, vertical structure of, 19: 44799 (BNL-8516)
turbulence of, formulas for anemometer dissipation of, 19: 20654(R) (ANL-6938(p.242-51))
velocity at 90 to 160 km, (E), 19: 43224
velocity fluctuations at Risö, Denmark, micrometeorological measurements of, 17: 12454 (RISO-45)
velocity in troposphere, factors affecting, 16: 27418 (NP-11961)
velocity measurement method for, 19: 29819(P)
velocity of, device for measuring and recording two-dimensional patterns of, 18: 45200(P)
velocity profiles of, method for measuring, 20: 25280

WIND RIVER FORMATION (WYO.)
uranium isotopic fractionation in granite and sandstone deposits in, 18: 39525

WIND TUNNELS
applications in the study of wind profiles, 16: 25611 (BNL-718)
calibration of ion velocities in, (E), 19: 15847
design and performance of hypersonic, 18: 20119 (ARL-64-5)
design for calibration of wind-measuring devices, 19: 20655(R) (ANL-6938(p.252-6))
design of ARGMA 8000-kw plasma, for reentry simulation, 16: 25499 (ARGMA-TN-2H5N)
design of hypersonic, engineering drawings of, 18: 12299
design study of arc-jet simulated hypersonic, 16: 24885 (ASD-TR-61-283)
development, 16: 12789(R) (NP-11384)
development of plasma, experiments for, 20: 17904
developments, 16: 6244 (NP-11177)
flow of hydrogen at 13,000°K and 1000 atm in, equilibrium in, 19: 20124
force and dynamic tests of re-entry vehicle in, 19: 8710 (SC-TM-64-1288)
force tests of tangent ogive shape at Mach 2.0 in, 19: 8709 (SC-TM-64-1281)
gas heating by rotating electric arc for (T), 19: 1699 (ARC-CP-743)
heat transfer to models in, at super- and hypersonic speeds, 16: 17791 (AFOSR-1591)
hypersonic flow in, production using electrostatic acceleration of frozen air particles, 20: 24176(R) (AD-624563)
hypersonic force tests of RFD-2 configuration in 48-in., 18: 33187 (SC-DC-64-1016)
hypersonic, measurement of low densities in gas flow in, 17: 30672
hypervelocity production by traveling-wave plasma acceleration, 18: 1108 (ARL-63-151(p.203-25))
hypervelocity techniques, conference on, 16: 18728
model tests on flow from radiochemical building ventilation stack in, 18: 22545 (AEEW-R-227)
performance of hyperthermal (E/T), 19: 2741
plasma flow in low-density hypersonic, gasdynamics of, 18: 17136
plasma flow in supersonic, microwave measurements, 16: 2589 (USCEC-83-208)
plasma flow production in low-density, system for, 19: 6805
plasma jet production in, arc heaters for, 19: 38796
pressure control system for, 16: 33081 (TID-16698)
properties and uses of, (E/T), 19: 9795
rocket test model static stability in Mach 7.6, correlation to flight data, 18: 45179 (SC-DC-64-1450)
temperature variation in hypersonic, reduction of stagnation, 18: 13365 (SC-4976(RR))
tests of Terrier-Tomahawk rocket system, 19: 1966 (SC-TM-64-984)
use in reactor-site gas diffusion studies, 20: 39105
use in scale model smoke diffusion experiments, 19: 44764 (BNL-914, pp 14-17)
use in scale-model smoke plume-rise tests, 19: 20656(R) (ANL-6938 (p.257-73))
valves for, engineering drawings for hot air control, 18: 39417
vehicle testing in Mach-5 and -7.5, STRYPI-II, 18: 45187 (SC-TM-64-981)
wind velocity measurements in, calibration of instruments for, 16: 30186 (ANL-6474(p.73-81))

WINDOWS
blast effects of atomic explosions on, 18: 1888 (WT-7)
brazing of thin beryllium, to supports, 17: 6605
cleaning of clouded oil-filled shielding, 17: 3707
design for fallout shelters, 19: 44218(P)
design for high-activity cells, 19: 36601(P)
design for hot cell use, 16: 3884(R) (ORNL-3193(p.318-19))
design for hot cells with means for autoregeneration, 18: 3947(P)
design for hot cells with means for autoregeneration, 18: 3948(P)
design for hot-cell use to prevent opacification of lead glass, 18: 6918(P)
design for hot cells, 18: 31742
design for hot cells, 19: 7671
design for hot cells, 19: 36600(P)
design for pressure vessel inspection, 20: 45062
design for shielded enclosures, 17: 32235(P)
design of double glazed prismatic type for radiation chambers, 16: 27171(P)
design of hermetically sealed, for radiation beams, 17: 42033(P)
design of irradiation, for electron accelerators, 20: 41574(P)
design of liquid-filled, for biological shielding, 19: 35580(P)
design of radially collimating, for well-tool orienting instruments, 20: 29517(P)

design of radiation shielding, 16: 27182(P)
design of shielded, for hot cells, 18: 39413 (ORNL-TM-932)
design of vanadium-foil, for electric discharge devices, 20: 13052(P)
design of zinc bromide type for gamma and neutron shielding, 16: 3154
design of zinc bromide-filled shielding, 17: 7498 (USNRDL-TR-594)
design of zinc bromide-filled shielding, with argon atmosphere and mild steel container, 18: 11363
design using reflection mirrors for nuclear reaction chambers, 19: 1831(P)
fabrication of soft phosphate glass, for shielding, 16: 27618(P)
failure of beryllium, of CEA hydrogen bubble chamber, 20: 19038 (NYO-10742)
for electron accelerators, design of metal gaskets for, 20: 46270(P)
haziness in hot-cell viewing, determination and elimination of, 18: 27811(R) (ORNL-TM-198)
installation techniques and sealing of kilocurie gamma shielding type, 16: 3156
ion beam transmission in aluminum oxide, 18: 37821
neutron shielding calculations, comparison with concrete, 16: 3153
opacification of hot cell, preventive design for, 18: 3944(P)
preparation for G-M tubes, 20: 35801
production of beryllium-coated plastic, 19: 938 (MLM-1194)
properties of bubble chamber, mechanical and optical, 17: 39423
radiation effects on optical transmission properties of, in space environment, 19: 39059
radiation effects on glass hot-cell, gamma, 19: 47102
radiation effects on materials for spacecraft, electromagnetic and proton, 20: 25617(R) (N-65-33370)
radiation effects on shielding, charge accumulation from gamma, 20: 30727
radioinduced clouding of oil in shielding-type, 16: 3155
radioinduced heating of, in EBR-II fuel cycle facility, 20: 31313 (ANL-6853)
radioinduced opacification in hot cells, method for preventing, 16: 27176(P)
seal for aluminum, in helium cryostats, 16: 29072
sealing structure for glove-box, 19: 34310(P)
shielding, fracture of irradiated by electric discharge, 18: 675
shielding, procedure for cleaning clouded oil-filled, 17: 2758
specification and testing of bubble-chamber, 17: 39426
standards for hot cell, 18: 8468
thickness of mica, in end-window counters, use of alpha particles for measuring, 20: 14826
use of beryllium, for gamma rays in cryostat, 17: 8300

WINDSCALE ADVANCED GAS COOLED REACTOR
civil engineering and plant layout, 17: 21330
commissioning measurements, 17: 33346
containment and safety systems, review, 16: 1250(R) (NDA-2159-2)
containment building for, 17: 21331
containment building fabrication, 17: 24702
control and instrumentation, 17: 21336
control of power, safety of, 20: 24750
control rod calibration in, (E), 19: 17322
control rod system of HERO, 17: 31741
coolant circulator design for, 17: 21333
coolant flow control system and equipment, 17: 31742
coolant-moderator reactions in, 17: 21347
coolant pressure circuit design, 17: 21332
core design, 17: 21334
core performance, (T), 20: 1498
core physics and kinetic studies, 17: 21343
cost factors, 16: 26606
description, 17: 22861
design, 17: 21328
design, 17: 21329
design, 18: 43049
design and characteristics, 16: 8375
design and operation, 20: 16092
design and performance of, 18: 11455
design and performance, 18: 38408 (A/CONF.28/P/125)
design concept, 16: 8374
design for use in power plants for export, 20: 28781
development, 19: 35789
development, 20: 26479
development, 20: 30798(R) (NP-16043)
development and operation, 16: 28668
development and research program, 17: 21339
development of, review of experimental and theoretical work for, 17: 42219
development of, fuel design and irradiation and physics of, 19: 27796
electric system of, design review, 20: 1507
evaluation, 17: 22885
experimental facilities, 17: 21340
experimental physics on, review, 17: 21344
fuel and can metallurgy, 17: 21341
fuel can oxidation tests, 18: 37631 (A/CONF.28/P/157)
fuel cans for, development of, 18: 26946
fuel cans for, fabrication of stainless steel, 19: 39134
fuel clusters for, conversion and fast fission ratios in, 20: 40399 (AEEW-M-654)
fuel costs, effects of coolant selection, 17: 5616
fuel cycle costs for, 18: 38420 (A/CONF.28/P/159a)
fuel cycle for, analysis of, 20: 45180
fuel economics for, 20: 16087 (TRG-Report-1115)
fuel element burnup distributions in, analysis of, (E), 19: 44463 (TRG-Report-1005)
fuel element design, 17: 21335
fuel element failure, fission product release in, 19: 44303 (TRG-Report-888)
fuel element heat transfer, 17: 21345
fuel elements for, development of dispersion, 18: 21659
fuel elements for, development of standardized, 18: 38360 (A/CONF.28/P/149)
fuel fabrication and processing facilities for, (E), 19: 45612
fuel for, plutonium uses in, 19: 19398
fuel for, pyrolytic carbon-coated uranium carbide dispersed in silicon carbide as, 20: 36494 (TRG-Report-1210)
fuel handling, 17: 21334
fuel pin bowing analysis, 18: 9621 (TRG-Report-587)
fuels for, development of dispersion, 18: 29079
kinetics and safety of, (E/T), 19: 17247
material compatibility, 18: 11460
materials aspects of, review of, 17: 30924
materials used in, compatibility of, 17: 21342
moderator for, properties of graphite, 20: 1497
moderator radiation effects, 17: 21346
moderator radiation absorption rate in, calorimeter for determining, 19: 48031
moderator weight loss in, (T), 20: 26485
operating experience, 20: 5164
operation and performance of, (E), 19: 45613
operation and safety control of, 19: 27797
performance, 18: 11460
reactivity, 17: 26073
reactivity, temperature coefficients at 300 to 450°K, 16: 18608 (AERE-M-911)
research and development program, 17: 24703
safety characteristics of, 18: 38430 (A/CONF.28/P/183)
safety review, 16: 31278 (UNC-5029)
startup and performance, 17: 21337
startup and performance of, 18: 11454
startup reactivity behavior, 17: 21338
steam drum for, steady state and transient measurements, 20: 40398 (AEEW-M-631)
uses of, two-year plan for, 17: 21338
waste disposal from fuel processing for, into Irish Sea, 20: 45229
waste processing, 16: 11351

WINDSCALE PRODUCTION REACTORS
accident at, tritium release to atmosphere in, 20: 20889
environs monitoring of, marine, 18: 8597
fuel burnup, long-term reactivity changes, 16: 9251 (AERE-R-3787)
waste discharge from, to Irish Sea, 18: 25723
waste disposal in Irish Sea, radiobiological monitoring 1959 and 1960, 17: 20191 (AHSB(RP)-R-27)

Wineglass
see Pinch Devices

WINES
beta activity in Rumanian, 20: 45982
potassium-40 content in Rumanian, 20: 45982
preparation, use of radiation and radioisotopes in, 16: 27516
radiation effects on, gamma, 18: 523
radiation effects on, gamma, 18: 12514
radioactivity of, from vineyards of Cotnari region of Rumania, 1960, 17: 30282
radioactivity of, in Husi vineyards, Rumania, 20: 25293
radiopreservation of, effects of dose on organoleptic qualities in, 20: 2197
strontium-89 and -90 content in, in France, 1958-59, 16: 19194
ultrasound effects on, in presence of air, carbon dioxide, hydrogen, nitrogen, and oxygen, 18: 12514

WINGS
see also Aircraft
hypersonic flow over delta, 19: 28493 (ARL-65-18)

WINNIPEG RIVER
dilution of waste solutions in, use of rhodamine B in tracer study on, 20: 7293 (AECL-2295)

monitoring for radioactivity, August 1965, 20: 7311 (NP-15642, pp 33-45)
radiation monitoring, 20: 14738 (NP-15853, pp 21-33)
Wire Recorders
see Magnetic Recording Systems
Wire Spark Chambers
see Spark Chambers
WIRES
(See also specific metals from which wires are fabricated.)
see also Exploding Wire Phenomena
see also Reactor Fuel Wires
activity measurement, automatic recording device for, 18: 37533
availability and properties of irradiated polymer, 17: 30144
coating of, development of electrolytic techniques for, 18: 20134(R) (ORNL-TM-792)
coating of, methods for continuous electrolytic, 19: 26750(R) (NYO-1480-16)
coating with cross-linked polyvinylidene fluoride polymers using radiation, 20: 12909(P)
critical currents in superconducting, 17: 24062 (UCRL-10402)
crystal structure of nitrided type 304 stainless steel, dilatometric studies of, 20: 41449(R) (EURAEC-1676)
cutting tool for, in instrumented reactor fuel elements, 20: 21018(P)
development of alkali metal-resistant insulated conductors, 18: 37304 (APL-TDR-64-42)
development of high-temperature alkali-metal-resistant insulated, 18: 10466(R) (AD-404273)
development of very high strength beryllium, 19: 13934(R) (AD-608190)
diameter measurements by eddy-current techniques, 16: 15184 (KAPL-2000-17)
distortion of helical wrappings of, on reactor fuel rods, 17: 6743 (HW-SA-2445)
drawing and mechanical properties of ultrafine beryllium, 17: 41382(R) (AD-419008)
electromagnetic wave propagation along four-wire transmission lines, 19: 6890 (SC-R-64-174)
energy absorption from tension, by cylindrical shell, analysis, 19: 36580 (UCRL-13160(Pt.2))
explosion of, destructive effects of plasma from, 17: 7495
fabrication and properties of drawn and swaged nickel and niobium, 18: 35933(R) (ML-TDR-64-56)
fabrication and properties of chromium-iron-nickel alloys, 19: 9596(R) (COO-1319-18)
fabrication and properties of superconducting, 19: 24958
fabrication developments for superconducting, 17: 41333(R) (ANL-6677)
fabrication from beryllium, 18: 16451(R) (AD-432273)
fabrication of beryllium, 17: 30951(R) (NP-12964)
fabrication of fine, high-strength beryllium, 18: 25938(R) (AD-439498)
fabrication of fine high-strength beryllium, 18: 35972(R) (NP-14193)
fabrication of high-strength beryllium fine, 19: 16026 (BBC-TR-382-243)
fabrication of, bremsstrahlung measurement of cross-section variations for, (E/T), 20: 14838
installation of, for reactor in-core instruments, 16: 31268 (NP-11754 (Vol.I)(Sect.III))
magnetic fields of straight, 18: 32275(R) (ORNL-3652(p.105-31))
magnetization of iron, by step-increased magnetic fields, (T), 19: 25625(T) (AI-Trans-84)
neutron activation in, automatic apparatus for flux determination by, 17: 37437
neutron activation of, scanner with decay correction system for determining, 18: 4111
neutron resonance absorption by gold, self-shielding effects in, 18: 28720
performance of superconducting, for signal transmission, 20: 9889 (EGG-1183-1192)
properties of column packing, in isotope separation, 19: 9570
properties of gauzes of, flow friction, geometric, and heat transfer, 20: 35624(R) (TUBIK-1, pp 34-72)
radiation effects on, 18: 8873 (NP-13505)
radiation effects on polyethylene-coated, 18: 14570
radiation effects on performance of, neutron, 18: 30240 (WANL-TME-109)
radiation effects on performance of, in telemetry electronics, 18: 33839 (RTD-TDR-63-4287(Vol.II))
radiation effects on mechanical properties of polyester enameled, 19: 14108
radiation effects on insulated magnet and lead, 19: 25049 (NP-15022 (Vol.II))
radiation effects on, gamma, 20: 27605
radiation effects on, for use as sensors, 20: 29486(R) (NASA-CR-54964)
radiation effects on film-insulated magnet, gamma, 20: 41503
radiation processing of, facility design for, 20: 9108(P)
scanner for reactor-flux, design of automatic, 20: 26396(R) (IDO-17140)
soldering of noble-metal, 19: 1964 (SC-DR-64-645)
superconducting critical field intensity of, pulse methods for measuring, 20: 9899
superconductive, properties of materials for, 18: 34200
superconductivity of niobium–oxygen–titanium, effects of crystal structure on, 20: 37267
superconductivity of tantalum–titanium, effects of crystal structure on, 20: 37268
tensile properties of high-purity zone-refined beryllium, 18: 7199 (AD-414490)
tensile properties of as-drawn chemical-milled beryllium ultrafine, 18: 25975 (NAEC-AML-1909)
tensile properties of tungsten, at 1200 to 2500°F, 20: 37251
testing for residual strain and working at high temperatures, device for, 19: 44213
tests of Novathene-insulated low-temperature, for SNAP-10A, 19: 2468 (NAA-SR-Memo-10175)
transition propagation in superconducting, 19: 25439
use in reactor neutron flux measurements, 19: 28646
use of magnetostrictive, for spark chamber delay line, 19: 787 (UCRL-11620)
use of tension, for support of sphere, analysis, 19: 36579 (UCRL-13160(Pt.1))
use of tension, for support of sphere in cylindrical shell, model studies, 19: 36581 (UCRL-13160(Pt.3))
use of tungsten, for reinforcement of tungsten-matrix rocket motor components, 20: 46176
vortex lines near, in liquid helium II, 18: 18845
WISCONSIN
lead isotope ratios in galenas of, 20: 45882
mineral content of native plants of, 18: 43134 (TID-21006)
radiation monitoring of lakes in, 20: 7265
tritium-hydrologic research in, 18: 12372
WITWATERSRAND GOLD FIELDS (UNION OF SOUTH AFRICA)
ore analysis, radiochemical examination of errors in, 16: 25635
uranium deposits in, book on, 17: 29112
WITWATERSRAND REEFS (UNION OF SOUTH AFRICA)
age estimation of galenas, monazites, and uraninites in Dominion Reef conglomerates, 16: 13377
lead isotope compositions of galenas, 16: 13378
Wolfram
see Tungsten
Wolframates
see Tungstates
WOLLASTONITES
crystal structure and symmetry of strontium germanate as model for α-, 16: 20441
WOLSENDORFITES
synthesis, 18: 16009
WOOD
see also Lignin
see also Plywood
analysis for moisture, development of cadmium probe for, 16: 22504
analysis for moisture by fast neutron slowing down, 19: 17846
analysis in crime detection, activation, 20: 1738(R) (GA-4041)
analysis in criminal cases, activation, 20: 14439(R) (GA-5556)
carbon-14 content in 18th- and 19th-century, correlation of sunspot activity with, 19: 36675
carbon-14 natural content in Taiwan, 18: 31759
combustion of, produced by high-altitude nuclear explosions, (T), 19: 43221 (USNRDL-TR-866)
criticality studies of containers, 16: 12841
defects in logs, poles, and trees, use of gamma radiation backscatter and transmission for evaluation of, 16: 32008 (ORO-487)
density determination across growth rings by beta absorption, 16: 17954
density determination for radioactive containers, 16: 20861 (AHSB(S)R-36)
density measurements on, before and after solvent extraction of rosin, by beta absorption methods, 20: 23561
density of, design of device using beta particles for measurement of, 17: 18464
density of pressed, tracer techniques for determining bulk, 17: 324(T) (OTS-60-51035)
density of, gamma radiation measurement of, 19: 9467(P)
electron beam dose distributions in, three-dimensional, 20: 21470 (PB-181506, pp 116-29)
equation of state of balsa, for use in reactor blast shield, (E), 19: 38092 (IITRI-578P21-9)
gamma attenuation by, air-scattered, 19: 29439 (CEX-63.3)
gamma attenuation by pine, 20: 1313
gamma scattering by, analysis of back-scattered radiation in, 17: 31435
gamma shielding by, in basement fallout shelters, (E), 20: 7298 (CEX-59.7B(Pt.3))
Hausbock larvae and resulting damage observations by use of roentgen

rays, 16: 13496
heat generation in, due to decay of plutonium dioxide, 19: 9406 (RFP-418)
impregnation of, by methyl methacrylate, methods for, 20: 33335 (ORO-2945-4)
impregnation with polymers, use of radiation in, 18: 2117
ion exchange capacity, 16: 14706
ion-exchange properties of products of, 18: 35238 (STI/DOC/10/28 (p.9-20))
measurement of density of, using gamma radiation, 19: 36798(P)
neutron absorption in, fast, (E), 20: 9265
neutron effective cross sections of, thermal, 17: 40219(T) (AEC-tr-6058)
neutron isolation characteristics, 19: 38013 (LA-DC-7139)
neutron transmission at 4.5 and 14.5 Mev by, asymptotic, 19: 1812(R) (HW-81746(p.2.36-8))
penetration of sodium pentachlorophenolate in, radioactivation analysis of, 20: 29161
plastic alloys of, economics and properties for commercial uses of, 18: 37062 (BNL-874(p.14-15))
preparation and properties of plastic-impregnated, 17: 18461(R) (ORO-600)
preparation of kryptonated, by diffusion, 20: 18570(R) (NYO-2757-5)
preservation of marine piling, development of uranium-containing creosote, 16: 11383(R) (NP-11409)
processing of, radioisotopes in, 20: 706
processing of, uses of radioisotopes in, 20: 710
processing of, uses of radioisotopes in, 20: 711
production and properties of plastic-impregnated, using radiopolymerization, 19: 2416
production of radioinduced polymer-impregnated, commercial aspects of, 20: 33743 (TID-22774)
production, review of uses of radiation in, 19: 2686
properties as neutron reflector, 20: 3390
properties as neutron reflector, 20: 3391
pulp flow through mills, tracer technique for studying, 20: 16921 (TID-22627)
radiation absorption by, compton effect, pair production, and photoelectric effect in gamma, 19: 24555
radiation effects on properties of impregnated, 16: 10642
radiation effects, chemical, 16: 9083
radiation effects, 17: 16108
radiation effects, 17: 18461(R) (ORO-600)
radiation effects on plastic-containing, 17: 23587 (BNL-790)
radiation effects on chemistry of, gamma, 19: 30259
radiation effects on morphology of beechwood, gamma, 19: 29931
radiation effects, 19: 36451(R) (BNL-900(p.73-104))
radiation effects on compressibility, sorptive properties, and tensile strength of beech, pine, and spruce, gamma, 20: 26976
radiation effects, gamma, 18: 37771(T) (AEC-tr-6398(p.538-46))
radiation scattering from, measurement of bremsstrahlung and gamma, 18: 44920
radioinduced combination of, with plastic, economic aspects of, 20: 31624 (BNWL-261)
radioinduced combination of, with plastic, economic aspects of, 20: 31625 (NYO-3569-1)
radioinduced graft polymerization with polymers, 17: 27896 (TID-18907)
radioinduced graft polymerization of polystyrene to cellulose in red pine sapwood, 17: 31807
radioinduced polymerization of monomer-impregnated, 17: 3687
radioinduced polymerization of monomers impregnated in, 17: 4589 (TID-7643(p.335-44))
radioinduced polymerization of monomers impregnated in, 18: 13906
radioinduced polymerization of methyl methacrylate, styrene, and vinyl acetate in, to produce wood-plastic combinations, 18: 17889
radioinduced polymerization with plastics, properties of products of, 18: 37190 (BNL-874(p.37-8))
radioinduced polymerization of monomers in, commercial utility of wood-plastic composites produced by, 19: 11617 (TID-21434)
radioinduced polymerization of styrene with cellulose in, 19: 24586
radioinduced polymerization of monomers in, gamma, 19: 30234 (ORO-628)
radioinduced polymerization of monomers in, to produce wood–polymer composites, 19: 36458 (NYO-3334-1)
radioinduced polymerization of monomer-impregnated, to produce wood–plastic combination, 20: 5818
radioinduced polymerization of methyl methacrylate in, effects on dimensional stability of, 20: 23110
radioinduced polymerization in plastic-impregnated, method for, 20: 33750
radioinduced sugar depolymerization in, gamma, 18: 30248
radioisotope shipping container made of, fire effects on, 18: 22271 (COO-277)
shielding properties of, 17: 33256
shock impingement testing, 18: 36759 (IITRI-578P21-6)
shock impingement analysis of redwood, 19: 25640(R) (IITRI-578P21-12)
shock wave effects on sugar-pine, (E), 20: 5023(R) (IITRI-578P21-15)
shock wave impingement analysis for balsa, 18: 3040(R) (IITRI-A6042-2)
shock-wave impingement analysis for balsa, 18: 9578(R) (IITRI-A6042-3)
shock-wave impingement analysis for balsa, 18: 23001(R) (IITRI-T6042-4)
shock-wave impingement analysis for balsa, 18: 28935(R) (IITRI-T6042-5)
shock-wave impingement analysis for balsa, 19: 6832(R) (IITRI-578P21-8)
shock-wave impingement analysis for balsa, 19: 6833(R) (IITRI-T6042-7)
stress analysis of, 17: 7532(R) (ARF-K6018-3)
stress analysis of balsa, 17: 11937(R) (ARF-4132-16)
technologies in forest products industry, possible applications of nuclear radiation in, 19: 2685
thermal radiation effects on balsa, maple, and willow, 16: 28654 (WT-1339)
use as ion exchange for decontamination of radioactive wastes, 18: 40967
use in shipping container for radioactive materials, 19: 40816 (SC-RR-65-98, pp 141-86)
use of densified laminates of, as neutron shielding, 20: 33777
methyl methacrylate–wood, radioinduced polymerization of, economics and properties of products from, 20: 39287 (KLX-1876)
plastic–wood, AEC program on materials of, 20: 21178 (ORNL-IIC-7, pp 1-5)
plastic–wood, commercial development and uses of, 20: 21182 (ORNL-IIC-7, pp 49-58)
plastic–wood, commercial possibilities of irradiated, in Pacific Northwest, 20: 21185 (ORNL-IIC-7, pp 76-80)
plastic–wood, commercial potential of irradiated combinations of, 20: 21186 (ORNL-IIC-7, pp 81-8)
plastic–wood, commercial production of irradiated combinations of, 20: 21187 (ORNL-IIC-7, pp 89-94)
plastic–wood, commercial use of irradiated combinations of, 20: 21189 (ORNL-IIC-7, pp 99-105)
plastic–wood, conceptual design and feasibility study of combinations of, 20: 21181 (ORNL-IIC-7, pp 32-48)
plastic–wood, development, properties, and commercial future of, 20: 21183 (ORNL-IIC-7, pp 59-63)
plastic–wood, development-production program for Lockwood, 20: 21188 (ORNL-IIC-7, pp 95-8)
plastic–wood, mechanical properties of radioinduced, 19: 30234 (ORO-628)
plastic–wood, mechanical and physical properties of irradiated combinations of, 20: 21348 (ORNL-IIC-7, pp 22-5)
plastics–wood, radiation processing of materials of, 20: 16505 (BNL-949)
plastic–wood, radiation processing of, 20: 21177 (ORNL-IIC-7)
plastic–wood, radiation processing and testing of, method for, 20: 21179 (ORNL-IIC-7, pp 6-14)
plastic–wood, radiation processing of, commercialization aspects of, 20: 21184 (ORNL-IIC-7, pp 64-75)
plastic–wood, radiation processing of, program for evaluation of, for commercial use, 20: 21349 (ORNL-IIC-7, pp 26-31)
plastic–wood, radiation processing of, economic aspects of, 20: 27376
plastics–wood, radiation processing of, review of technical aspects of, 20: 27375
plastic–wood, radioinduced polymerization reactions in, 20: 21180 (ORNL-IIC-7, pp 15-21)
plastics–wood, radioinduced graft polymerization of, properties of products formed by, 20: 27384
plastic–wood, radioinduced polymerization, 20: 37145
plastic–wood, use of irradiated combinations of, in sporting-goods industry, 20: 21190 (ORNL-IIC-7, pp 106-11)
polymer–wood, physical properties of radiation-produced, 18: 8694 (ORO-612)
polymer–wood, properties of radiation-processed composites of, 19: 36458 (NYO-3334-1)

WOOL

see also Glass Wool

analysis by activation for animal nutrition studies, 19: 22818(R) (ORNL-3650(p.221-38))
analysis for molybdenum, activation, 19: 46192
analysis for trace elements by activation, 19: 17781(R) (ORNL-3750)
analysis of biosynthetically labeled, direct liquid scintillation method, 17: 14185
evaluation for protective clothing against radioactive materials, 16: 3285(T) (JPRS-9706(p.40-9))
gamma attenuation by, 18: 39736(T) (AEC-tr-6390(p.114-16))
identification of Australian, activation analysis and gamma spectra, 18: 35907(R) (NCSC-2477-2)
ignition by nuclear explosions, effects of burst heights and atmospheric

conditions, 17: 27945 (NP-12936)
labeling of fibers with iodine-131, 17: 27216
radiation effects on mechanical properties, 16: 24257
radiation effects on fibers, 17: 27899
radiation effects on yellowing of, tracer studies of role of amino acid decomposition in uv, 20: 18281
radioactivity in, 16: 5122
radioactivity, natural and fission-product, 17: 23025
radioinduced graft polymerization of acrylonitrile, methyl methacrylate, and styrene on, 17: 27900
radioinduced graft polymerization of monomers on fibrous, parameters affecting, 19: 7537(R) (NCSC-2477-11)
radioinduced grafting of vinyl monomers to, effects of methanol and water on, 20: 7154
sorptive properties for ruthenium, 20: 27517
strontium-90 decontamination using detergents and EDTA, 18: 43864
uranium nitrate decontamination using detergents and EDTA on, 18: 43863

WORMS

bioluminescence of *Balanoglossus biminiensis*, 18: 15703 (TID-18659)
cesium-137 distribution in tree-foliage-feeding, 20: 6711(R) (ORNL-3849, pp 43-100)
chromium distribution in polychaete, 20: 36552
deuterium uptake in nereid polychaete, 18: 21787
disaggregation of planarians, 18: 1325(R) (UCRL-10934)
ecology of *Nephtys caecoides* in Yaquina Bay, Oregon, 20: 45263(R) (RLO-1750-8(Vol.3), (Paper 1))
effects of irradiated cercariae of *Schistosoma mansoni* on humoral immunity of mice, 19: 7121
electrophoretic behavior of trypanosomes, effects of uranyl ions on, 19: 31718
immunogenic efficiency of double vaccination with x-irradiated *Ancylostoma caninum* in dogs, effects of age on, 20: 31043
labeling with tantalum-182, effects of, 18: 1335
organic-compound uptake by planarians, tracer studies of, 18: 1325(R) (UCRL-10934)
preparation of irradiated vaccines against parasitic Helminths, 19: 7175
radiation effects on cysticercoids of *Hymenolepis diminuta*, genetic, 17: 40548 (TID-17729)
radiation effects on rat intestine population of *N. brasiliensis*, x, 18: 70
radiation effects on *Fasciola hepatica*, 18: 25128
radiation effects on development of Ascaris eggs, 18: 27138
radiation effects on development of Ascaris eggs, 18: 27139
radiation effects on enzyme systems in marine, 18: 27062(R) (NYO-1680-1)
radiation effects on development of Ascaris eggs, 18: 27163
radiation effects on growth and production of *Hymenolepis diminuta* in rats, 18: 27206
radiation effects on mutation frequency in silk-, fractionated vs. single x, 18: 31143
radiation effects on eggs and larvae of *Ascaridia galli*, 18: 38793
radiation effects on virulence of Schistosoma, in monkeys, x, 19: 15201
radiation effects on suppression of reproductive potential of potato tuber-, gamma, 19: 17573
radiation effects on activity of neurosecretion cells in earth-, light, 19: 24281
radiation effects on growth and mortality of *Ophryotrocha puerilis*, 19: 26046
radiation effects on sensitivity of nerves in, gamma, 19: 26086
radiation effects on spermatocyte chromosomes in silkworm, microbeam uv, 19: 31670(R) (NIRS-3(p.19-56))
radiation effects on silkworm spermatogonia, x, 19: 31670(R) (NIRS-3(p.19-56))
radiation effects on reproduction of potato tuberworm, 19: 33803
radiation effects on eggs of helminth parasites, 19: 35988
radiation effects on larvae of *Dictyocaulus filaria*, γ and x, 19: 42275
radiation effects on egg viability in Hoemonchus, γ, 19: 42281
radiation effects on, beta, 20: 6711(R) (ORNL-3849, pp 43-100)
radiation effects on virulence of *Schistosoma japonicum* cercariae in mice, x, 20: 12545(R) (PAEC(A)AR651)
radiation effects on development of external genital organs in embryos of *Anguis fragilis*, 20: 24880
radiation effects on embryos of blindworm, x, 20: 36615
radiation effects on African giant and red wiggler, gamma, 20: 40637(R) (ORO-2754-7)
radiation effects on RNA content in regenerating *Polycelis nigra*, x, 20: 42933
radioinduced giant and neoplastic cells in, 19: 15072
radioinduced sterility in male *Prodenia litura* by carbon-14, 18: 1412
radioisotope uptake by, in Clinch River, 17: 40529 (TID-7664(p.193-207))
radiosensitivity of evergreen bag, 20: 6711(R) (ORNL-3849, pp 43-100)
radiosterilization of navel orangeworm *Paramyelois transitella*, effectiveness of, 18: 3573
strontium-89 retention by apple maggot, 19: 25863
vaccine for lungworm, effectiveness of radiation-produced, 18: 528
vaccine for sheep lungworms, preparation from irradiated larvae, 19: 43750
zinc uptake by tubificid, from silts, 18: 45176 (NYO-10544(Rev.))

WOUNDS

see also Trauma
analysis for plutonium-239, 19: 26162(R) (ORINS-49(p.98-110))
analysis for plutonium-239, development of miniature counters for, 19: 38546(R) (RFP-552)
contamination by plutonium, method for treatment of, 20: 20943 (RFP-453)
decontamination of, resulting from radiation accident, 19: 22637
detection and measurement of plutonium-239 in, design of instrument for, 17: 1741 (AERE-M-595)
deuterium oxide effects on rat, 18: 33250
effect of tendency to report minor, on accident statistics, 18: 15691 (ORNL-3563)
effects of open skin, with radiation on mortality of mice, 19: 17645
effects of skin, on septicemia in irradiated mice, 20: 12704
effects of whole-body irradiation on healing, in rats, 16: 20289
effects with radiation on excretion of taurine and urea in rabbit urine, 20: 35248
fallout absorption through open, 18: 29232
healing effects of serum from irradiated animals on, of rats, 18: 43248
healing of, effects of immune reactions on, in mice, 18: 8119 (USNRDL-TR-683)
healing of radioinduced microlesions on mouse skin, 17: 23154
healing of rat, effects of ascorbic acid and water-d_2 on, 19: 19484
monitoring for plutonium, instrument for, 20: 39267
of potato tubers, effects on resistance to fungi, 18: 13466(T) (OTS-63-11011(p.76-9))
plutonium-contaminated puncture, treatment, monitorings, and decontamination, 17: 31962 (DPSPU-63-30-5)
plutonium contamination of, 18: 29211
plutonium deposition and removal in, 20: 31030 (BNWL-SA-39)
plutonium-239 contamination of, equipment for monitoring, 20: 9262
plutonium-239 content in, errors in measurement of, 20: 20951
radiation effects on healing of infected, repeated, 16: 16211
radiation effects on healing of, in rats, 18: 11900(R) (AD-412857L)
radiation effects on healing of, in mice, effect of homologous bone marrow and lymph node cells transplantation on, 18: 23273
radiation effects on healing of, in rats, 18: 31131(R) (RRA-T42)
radiation effects on healing of, 19: 15019(R) (RRA-N318)
radiation effects on maxillo-facial, review on course and therapeutic measures for, 19: 17636
radiation effects on tetanus vaccination in monkey, 19: 19608
radiation effects on collagen content and cystine and methionine metabolism in healing, in rats, 19: 33900
radiation effects on healing of mouse, effects of radioprotective compounds on x, 20: 6878
radiation effects on healing time of mouse, x, 20: 12684
radiation effects on healing of, after radical neck dissection, x, 20: 14303
radiation effects on healing of rat skin, effects of hormones on γ, 20: 31061
radiation sickness effects on deferred treatment of firearm, in rabbits, 18: 25202
radioactive contamination of, action levels in medical treatment of, 19: 46008
radioactivity in, detection and measurement of, 19: 44538
radioinduced in rabbits, protective effects of proteic blood substitute against, 17: 38899
radioinduced on skin, blood vessel regeneration during healing of, 18: 11752
radioisotope absorption by, 18: 35779
radioisotope effects on vascularization of healing, 16: 1436
radioisotope sorption in rat, 20: 14253
radiotherapy induced, effects of hydrogen perioxide on healing of, 19: 22023
repair mechanism in skin, 17: 28601
sodium-22 absorption in, 18: 29218
synergistic effects with radiation sickness, in mandible, 16: 14393(T) (JPRS-12169(p.39-46))
synergistic effects with gunshot fractures, 16: 14394(T) (JPRS-12169 (p.47-50))
therapy of plutonium-contaminated, 19: 2552 (HW-SA-3676)
therapy of radioactively contaminated, 17: 28640
treatment of plutonium-contaminated, use of tetrasodium EDTA in, 16: 4393 (HW-66309)
treatment of skull and brain, during radiation sickness, 18: 9914(T) (FTD-TT-63-581)
treatment of, plutonium-contaminated, by incision, 19: 2183 (HW-SA-

3730)
with radioactive material imbedded, design of treatment facility, 19: 11325 (HW-82153(Rev.1))
WR-1
see Whiteshell Reactor No. 1
Wriggle Instability
see Pinch Effect
WRRR
see Walter Reed Research Reactor
Wylfa Reactors
see Calder Hall Reactors
WYOMING
(See also headings of the form Wyoming (Carbon Co.))
carbon isotope abundances in carbonates of Gas Hills Uranium District, 17: 20235
carbon-13 content of calcite in epigenetic pyrite deposits, Gas Hills Area, 20: 16675
carbon, oxygen, and sulfur isotope ratios in uranium deposits in Gas Hills district, 20: 16670
environmental radiation measurements in, 20: 38735(R) (NYO-1704-13)
fallout monitoring, 1963, 20: 5649(R) (COO-1340-2, pp 54-83)
geology of Powder River Basin, 17: 3155 (TEI-823)
mapping and geochemical analysis of Shirley Basin uranium district in, 18: 41671
radioactivity levels in fossil fuels from, 20: 152(R) (NYO-3086-1 Pt.VIII)
uranium isotopic fractionation in sandstone of Powder River Basin, 19: 20187
uranium occurrence in, survey of, 19: 46629
uranium sandstone deposits in Gas Hills area, stable isotopic geology and origin of, 19: 22587
zoning of mineral deposits in, hydrothermal, 17: 34116 (CONF-123-1)
WYOMING (CARBON CO.)
protactinium-231 and thorium-230 contents in sandstone deposits of Shirley Basin, 18: 31778
uranium isotope fractionation in Shirley Basin, 18: 31777
WYOMING (FREMONT CO.)
uranium isotopic fractionation in granite and sandstone deposits in Wind River Basin in, 18: 39525
WYOMING (NATRONA CO.)
uranium isotope and daughter product fractionation in sandstone deposits in, 20: 2057
uranium occurrence in Shirley Basin Area, paleotopographic control of mineral belt, 16: 5584
WYOMING (SWEETWATER CO.)
uranium-bearing coal deposits, 16: 13385
uranium occurrence in Green River Formation in, 19: 40799
WYOMING (YELLOWSTONE NATIONAL PARK CO.)
rare gas content and nature in thermal springs in, 19: 26252

X

X-10 Reactor
see ORNL Graphite Reactor
X AGENT
activation of water by, 18: 26146
directional properties, 20: 14622
effects of, on alkaline dye solutions, 20: 45757
effects on aqueous kaolin solutions, 18: 12227
effects on bacterial growth, time fluctuations in, 18: 17613
effects on cloudiness of bismuth oxychloride suspensions in cardboard, lead, and tin boxes, 18: 10968
effects on cloudiness of collidal bismuth oxychloride solutions, 19: 28410
effects on erythrocytes, 17: 38681
effects on erythrocyte optical density, relative to space and time, 18: 17608
effects on erythrocytes, 18: 26144
effects on glass vessel transmittance, photoelectric cells, and water, 18: 18484
effects on growth of *P. vulgaris*, 17: 38666
effects on growth of *P. vulgaris*, influence of various materials on, 17: 38667
effects on growth of seeds, 17: 38668
effects on kaolin colloids, 20: 5587
effects on neutral red precipitation or crystallization, 18: 33671
effects on neutral red precipitation or crystallization, 18: 33672
effects on neutral red precipitation or crystallization, 18: 33673
effects on neutral red sedimentation, effects of color on, 19: 11230
effects on neutral red sedimentation, effects of aluminum-foil shielding on, 19: 11231
effects on neutral red sedimentation, 19: 11232
effects on neutral red sedimentation, effects of environment on, 19: 26448
effects on neutral red solutions, 19: 26449
effects on protein solutions, 17: 38669
effects on proteins, time fluctuations in, 18: 17614
effects on sensitivity of photoelectric cells, 20: 21163
effects on transmittance of frosted glass, 18: 12247
effects on turbidity of proteins, 17: 38670
emission of, effects of water or lead on, 18: 720
flux of, annual and diurnal fluctuations in, 20: 30955
frosted glass effects on light transmittance, 18: 12749
influence of, on sedimentation rate of erythrocytes, 17: 35395
interference of thermal radiation by, 18: 26144
mirror-imaging effects of, 18: 26145
patterns of, effects of light on, 20: 11536
presence in sunlight, 19: 11232
production by cosmic radiation, 17: 35395
production by light conversion, 19: 28411
properties of, annual and diurnal variations of, 18: 22577
scattering by water, 18: 2682
studies on, summary of, 20: 30956
X Particles
see Mesons (X)
X RADIATION
see also Bremsstrahlung
see also Gamma Radiation
see also Photons
absorption and emission by elements, wavelength tables, (E), 19: 8065 (NYO-10586)
absorption and emission by elements, energies for, 19: 33704
absorption by argon and neon, coefficients for, 17: 39731
absorption by argon, fine structure of K edge of, 18: 7425
absorption by argon and xenon, cross sections for, (T), 19: 8099
absorption by argon, one-electron model for spectra of K, 19: 39411
absorption by atoms, near K absorption edge, 17: 9217
absorption by atoms, energy levels from, (T), 20: 960 (AROD-2810.18)
absorption by bone and muscle, 17: 28676(R) (NYO-10050)
absorption by bone, 19: 30016
absorption by concretes, lead, and steel, 16: 24223
absorption by copper at 1.5 to 1.8 kev, coefficients for, 17: 29396 (TID-18947)
absorption by copper at 1.49 to 17 kev, mass coefficients for, 17: 34658
absorption by crystals, phonon excitation effects on coefficients for, (T), 19: 25632
absorption by crystals, corrections for, (T), 20: 12308
absorption by elements, coefficients for, 16: 23966 (ANL-6515(p.53-80))
absorption by fluoroscopic screens, 19: 46150
absorption by gallium single crystals, fine structure of extended K edge of, (E), 19: 9913
absorption by gallium single crystals, extended fine structure of K-edge, (T), 20: 32707
absorption by krypton and xenon, photoionization cross sections for, (T), 19: 47216 (AD-613675)
absorption by man of, during diagnostic radiography, 20: 3816
absorption by matter, J-phenomena in, 18: 44435
absorption by metals at 7 to 17 Å, coefficients for, (E), 19: 6394
absorption by metal films at low energies, (E), 19: 25146(R) (TID-21542)
absorption by mouse and rat bone marrow, relative biological effectiveness, 16: 17517
absorption by personnel during fluoroscopy and radiography, protection against, 18: 8242
absorption by pituitary gland, 16: 6273
absorption by plutonium particles, self-, 20: 20951
absorption by powdered materials, measurement of particle size distribution by, 19: 4602
absorption by samarium hexaboride, edge structure in, 19: 22185
absorption by shielding, 19: 33704
absorption by silicon, (E), 19: 28674
absorption by tissues, man vs. phantom, 19: 13188
absorption by 14 elements of $1 \leq Z \leq 30$, 20: 923
absorption curve for aluminum, optical constants from infrared to x-ray frequencies from, 18: 18565
absorption curves for, radiographic data from, 18: 31991
absorption in crystals, extended fine structure of edges for, 18: 7431
absorption in crystals, photoelectric, (T), 20: 20147
absorption in dose-equated materials, 20: 23373(R) (N-65-29998)
absorption in electron beam apparatus, provision for, 20: 11418(P)
absorption in gallium single crystals, spectra for, (E), 19: 16129
absorption in interfaces, 20: 25331
absorption in K shell of silicon in gaseous silicon chlorides, spectra of, (E), 20: 19389
absorption in L shell of germanium in gaseous germanium chlorides, spectra of, (E), 20: 19389
absorption in man and phantoms, measurements of, 20: 4207
absorption in materials, coefficients for, 18: 42300
absorption in metallic foils and organic films, thickness measurements

from, 17: 41222
absorption in silicon, cross sections for, 18: 32779
absorption measurements of monochromatic, in contrast media, 18: 2414
absorption measurements for evaluating settling rates of suspensions, equipment for, 20: 22914
absorption of cosmic, by interstellar and intergalactic matter, 20: 37485
absorption of, effects of temperature on K-edge, 17: 39798
absorption of, fabrication of strontium filters for, 20: 5692
absorption of, use in determining fuel distribution in fuel plates, 19: 11598
absorption spectra of L shell of lutetium, forbidden lines in, (E), 20: 39613
absorption, temperature effects on extended fine structure, 16: 21126 (D1-82-0164)
absorption, use for measurement of steam voids in water at high pressure, 16: 318 (TID-14156)
alopecia induced by therapeutic doses to head, effects of vitamin B_{12} on, 20: 5484
angular correlations with gamma radiation, relaxation effects in, 19: 39849
atmospheric ionization by, from high-altitude explosions, 17: 16292
atmospheric spectral intensities of solar, 16: 19654 (GCA-61-37-A(Chap.2))
attenuation and sorption coefficients for beryllium oxide and enriched lithium deuterides and hydrides, 20: 27210(R) (UCRL-14680)
attenuation by aluminum, iron, and lead, 19: 17169
attenuation by elastically deformed germanium crystals, (E), 19: 14052
attenuation by Z = 6 to 18 elements, coefficients for, 17: 22433 (NP-12661)
attenuation coefficients for low Z elements at 6 to 14 kev, 16: 9291 (TID-14860)
attenuation in aluminum, copper, lead, and tin, half-value thickness, 16: 4628
attenuation in lead, sand, and water, 16: 23246
attenuation in reactor materials, measurement of, 20: 29707 (ORNL-TM-1457)
attenuation of, in argon and carbon dioxide, 16: 31013 (TID-16419)
attenuation of, survey of application of, 17: 30242
attenuation of 320 kv, secondary electron spectrum from, 18: 40134
attenuation of, equipment for automatic display of curves of, 18: 12489(P)
attenuation through light-sensitive emulsions in color radiography, 17: 3139(P)
auroral zone, conjugate balloon observations, 20: 37914
avoidance by mice, effects of dose rate, 16: 32793
avoidance by rats, peripheral neural paths mediating, 16: 26747
avoidance by rats, conditioned, 17: 5837
avoidance by rats, physiological receptor mechanisms of, 17: 5857
avoidance conditioning of rats by exposure to nonlethal doses of, 18: 1425
biochemical studies in barley mutants induced by, 20: 45335
biological action of sieve exposure, 16: 9793
biological and morphological effects, utilization of incisor as test organ in rats, 16: 4107
biological and pathological effects, thresholds for, 16: 6334
biological dosimetry, based on percentage of chromosomal aberrations, 17: 31897
biological effectiveness of deep and superficial at 200 kev, 16: 11481
biological effectiveness of 200-kv, on yeast cultures, 16: 14488
biological effectiveness in tissue-equivalent phantom, relative, 16: 23448
biological effects, effects of partial-body shielding, 16: 12903
biological effects on mice, protective effects of AET and MEA against, 16: 76
biological effects of mammalian erythrocytes, 16: 1570
biological effects, genetic and somatic, 16: 4009(R) (UCSF-21)
biological effects on developing male germ cells of flour beetle, *Tribolium confusum*, 16: 4048
biological effects in mice, 16: 4060
biological effects, assessment using cystine, 16: 4089
biological effects on closure of hole in gastric wall with homotransplant, 16: 4114(T) (JPRS-10882)
biological effects in protozoa, 16: 7423(R) (TID-14567)
biological effects on tissue-culture cells, survival kinetics, 16: 7447
biological effects of sieve, 16: 9782
biological effects of sieve, comparison with full field, 16: 9787
biological effects, histamine hypothesis, 16: 9806
biological effects on longevity of *Drosophila melanogaster*, 16: 11459(R) (TID-14970)
biological effects on pathogenicity of *Fasciola hepatica* in mice, 16: 12929
biological effects in rats and guinea pigs, 16: 12907
biological effects of lethal doses on digestive organs of rats, protective effects of desoxyribonucleic acid, 16: 12925
biological effects of lethal doses on kidney enzyme activity, 16: 12926
biological effects on tumor cells, effects on growth of rats, 16: 12927
biological effects on desoxyribonucleic acid, 16: 14797
biological effects on eyes in rabbits, 16: 14484(T) (JPRS-13499 (p.10-21))
biological effects of 20-Mev and 200-kv, 16: 14519
biological effects on Pseudomonas colonies and enzyme synthesis, 16: 14544
biological effects on erythrocytes in mice, 16: 14545
biological effects on toxicity of cholinergic phosphorothioate in rats, 16: 14458(R) (NP-11359(p.28-34))
biological effects on children, small doses, 16: 14579
biological effects on behavior development in fetuses, 16: 16272
biological effects on Purkinje fibers of calf and sheep hearts, 16: 16279
biological effects in *Escherichia coli*, chemical protection, 16: 16297
biological effects on electric properties of frog muscles, 16: 16181(T) (JPRS-13154(p.8-15))
biological effects on electric properties of cerebral cortex, 16: 16183(T) (JPRS-13154(p.21-34))
biological effects on bacteria, DNA, eggs, enzymes, mammalian cells, virus, and yeast, 16: 16189
biological effects on eyes of rabbits, 16: 16175 (ASD-TR-61-415)
biological effects in chick embryos, 16: 17521
biological effects, 16: 17522
biological effects on kidney, 16: 17403
biological effects on mice thymus, 16: 17404
biological effects in nerve cells, 16: 17440(T) (JPRS-12921(p.12-33))
biological effects on tumors, 16: 17463(T)
biological effects on development of thiophosphate-oxidizing enzyme in liver of rats, 16: 18765(R) (NP-11660(p.76-84))
biological effects on skin, mechanism of radioprotective substances, 16: 18801
biological effects on leukocytes in patients, protective effects of dexamethasone against, 16: 20269
biological effects on mice infected with lymphocytic choriomeningitis, 16: 20271
biological effects on mice infected with lymphocytic choriomeningitis, 16: 20272
biological effects on spleen cells in mice, 16: 20274
biological effects on antibody formation in rabbits, 16: 20275
biological effects on skin graft take and immune response in rabbits, 16: 20276
biological effects on blood platelets in mice, 16: 20277
biological effects on body temperature in rabbits, 16: 20279
biological effects of lethal irradiation on bone marrow and spleen, protective effects of desoxyribonucleic acid, 16: 20283
biological effects on ultraviolet-thrombopoietic factor in mice, 16: 20290
biological effects on erythrocyte transmission across mouse placenta, radiation effects, 16: 20066
biological effects on transmission of maternal serum albumin to fetus in mice, 16: 20067
biological effects on *Trichinella spiralis*, 16: 20135
biological effects on immunogenicity of *Trichinella spiralis* larvae, 16: 20137
biological effects on ovary grafts in eyes of mice, 16: 20139
biological effects on adrenergic transmission and nictitating membrane in cats, 16: 20143
biological effects on resorption time of cutaneous wheals, 16: 20145
biological effects on hair, protective effects of erotonin against, 16: 20162
biological effects on leg buds of chick embryos, 16: 20164
biological effects on metabolism of Yoshida ascites hepatoma cells, 16: 20194
biological effects on *Schistosoma masoni* cercariae, 16: 20202
biological effects on tritium incorporation in brain and liver of mice, 16: 20221
biological effects on rat testes, comparison of single and fractionated doses, 16: 20225
biological effects on anaphylaxis in guinea pig, 16: 20252
biological effects on mice, protective effects of spleen cells against, 16: 20263
biological effects of radiotherapeutic doses on blood, 16: 20264
biological effects of diagnostic doses on reproductive function of women, 16: 20265
biological effects on immune responses of mice, 16: 20267
biological effects on tumor metastasis in mice, 16: 20268
biological effects on immunity of mice to *Trichinella spiralis*, 16: 21935
biological effects on survival of isografted fetal mouse hearts, 16: 21936
biological effects of, on gonads in male mice, protective effects of unsaturated fatty acid esters against, 16: 20285
biological effects of, on rat liver, effects of adrenal hormones on, 16: 20247

biological effects on intestine, protective effects of ileum shielding against, 16: 26748
biological effects on *E. coli* in combination with ultraviolet radiation, cross-induction transfer, 16: 26772
biological effects on healing of rat liver, 16: 26793
biological effects on regenerative capacity of extremities of salamanders, 16: 26794
biological effects on function of oocytes in ovulation and on ovogenesis in fish, 16: 26795
biological effects on HeLa cells, production of giant cells, 16: 26817 (UCRL-9226)
biological effects on bones in mice, effects of energy absorbed, 16: 28743(R) (NYO-10152)
biological effects on development of embryonic gonads, 16: 28758
biological effects on embryonic gonads, 16: 28760
biological effects on mouse cerebellum, 16: 28768
biological effects on heart of chicken embryo during 80 to 88th hour of incubation, 16: 28779
biological effects on muscles, protection by transplanted pulverized tissue, 16: 30230
biological effects in dry bacterial spores, reaction mechanisms, 16: 30268
biological effects on reticulocytes in rats, 16: 30287
biological effects on blood and spermatozoa of rabbits, 16: 30291
biological effects on cholesterol content of blood serum of dogs and rabbits, 16: 30294
biological effects on metabolism by dogs, 16: 30296
biological effects on adrenal glands and hormones, 16: 30297
biological effects on mice, protection by dextran, 16: 30306
biological effects on abdominal region, effects of bile on diarrhea in, 16: 31524 (HW-SA-2646)
biological effects on beetles at different stages in life cycle, 16: 31525
biological effects on blood serum density in rats, 16: 31493
biological effects on electrophoretic mobility of tumor cells in mice, 16: 31496
biological effects on liver cells, 16: 31418
biological effects of 200-kv, compared with 730-Mev proton particles, 16: 32645(R) (UCRL-10211(p.43-9))
biological effects on virus-induced tumor cells, 16: 32673
biological effects on recovery of guinea pigs from vaccinia virus infections, 16: 32674
biological effects on micromotility of small intestine, 16: 32753
biological effects on esterase activity in rat testes, 16: 32757
biological effects on β-glucuronidase activity in rat testes, 16: 32758
biological effects of therapeutic doses on brain, 16: 32767
biological effects on growth of rabbit cartilage, 16: 32769
biological effects on hands, from x-ray machines, 16: 32771
biological effects of small daily doses on skin of guinea pigs, 16: 32775
biological effects on hands from fluoroscopy, 16: 32818
biological effects on elevation of thymidylate synthetase during liver regeneration, 16: 32846
biological effects on myelopoietic cells in bone marrow, recovery from, 16: 32847
biological effects on intestine, 16: 32850
biological effects on reactions of animals to burns by fire, 16: 32858
biological effects on maxillary systems, role of humoral factors in, 16: 32861
biological effects on antimicrobial and antitoxic immunity of animals, 16: 32862
biological effects of repeated doses, 16: 32864
biological effects on infantile larynx of rabbits, 16: 32870
biological effects on hematopoiesis of prenatal whole-body, 16: 32872
biological effects on response of leukocytes to electrical skin shock, 16: 32856
biological effects as function of dose rate and time, 17: 25019
biological effects compared with 660-Mev protons, 17: 17779(T) (JPRS-18395(p.363-8))
biological effects, effects of dose on recovery rate, 17: 5909 (TID-14019)
biological effects of whole-body, on metabolic function of rat liver, 17: 17867
biological effects of whole-body doses on blood count in rats, 17: 25056
biological effects of whole-body doses on mice, protective effects of diethyl stilbestrol propionate against, 17: 30457
biological effects of whole-body doses on albumins and globulins of blood plasma, 17: 30452
biological effects of whole-body doses on histochemistry of lymph and spleen in mice, 17: 30383
biological effects of whole-body doses on mitotic activity of shielded cornea, indirect, 17: 30392
biological effects of whole-body doses on electrophoretic mobility of hemoglobin in dogs, 17: 30410
biological effects of whole-body doses on electrophoretic pattern of liver and serum proteins in dogs, 17: 30411
biological effects of whole-body doses on protein fractions of rabbit brain, 17: 30412
biological effects of whole-body doses on guinea pigs, 17: 30414
biological effects of whole-body doses on rabbit brain activity induced by sulfur injections, 17: 30442
biological effects of whole-body doses on leukocytes in mice, 17: 30443
biological effects of whole-body doses on glycogen content of leukocytes in mice, 17: 30444
biological effects of whole-body doses on vitamin B_{12} contents of mouse organs, 17: 30445
biological effects of whole-body doses on antibody formation in rabbits, 17: 30446
biological effects of 200-kv, 17: 28759
biological effects of 22-Mevp and 200-kvcp, compared with effects of gamma radiation, 17: 40549 (TID-18210)
biological effects of 50 kvp and 250 kvp in dogs, 17: 17767 (USNRDL-TR-616)
biological effects of clover seed irradiation on hybrid generation, 17: 30332
biological effects of divided doses in large and small mammals, 17: 15804 (USNRDL-TR-606)
biological effects of, effects of intensity on, 17: 27105
biological effects of fractionated doses on skin of rat tails, 17: 24999
biological effects of heavy, on survival and mitosis of cells in tissue culture, 17: 40551(R) (TID-19515)
biological effects of localized exposure to, on mammals, 17: 31883
biological effects of, minimal dose rates for delayed, 17: 25485
biological effects of, relative, 17: 1328
biological effects of, time-dose relations compared with fast electrons and gamma, 17: 37133
biological effects on attenuation of tubercle bacilli, 17: 51
biological effects on amino acid levels in plasma and urine of cancer patients, 17: 15784
biological effects on appearance of metastases of transplantable mammary epithelioma of rats, 17: 17824
biological effects on action current curve of frog nerve, 17: 25000
biological effects on antibody formation, mechanism of stimulation in, 17: 27121
biological effects on autolysis of rat blood, 17: 30384
biological effects on antitoxin formation in guinea pigs and rabbits, 17: 30402
biological effects on anaphylaxis in sensitized guinea pigs, 17: 30405
biological effects on blood vessels of mice and rats in conjunction with high-fat diets, 17: 13974(R) (NP-12484(p.63-93))
biological effects on blood, 17: 27160
biological effects on bactericidal properties of rabbit blood platelet serum, 17: 27125
biological effects on chickens, comparison with gamma rays, 17: 10471
biological effects on catalase and peroxidase activities of rabbit blood, 17: 30430
biological effects on cardiac muscle of white rats, 17: 40580
biological effects on diploid and hexaploid species of *Avena*, 17: 10457
biological effects on DNA, 17: 15792
biological effects on Drosophila embryos at 200 kv and 14 Mv, 17: 17892
biological effects on dogs and rabbits in combination with acute blood losses, treatment, 17: 30448
biological effects on encephalomyelitis in guinea pig, 17: 81
biological effects on electron paramagnetic resonance spectra of desoxyribonucleic acid, 17: 50
biological effects on embryonal development of mice, 17: 5897
biological effects on *Escherichia coli*, 17: 21494
biological effects on female genital glands and fetuses in mice, 17: 30394
biological effects on genital systems of female mice and rabbits, 17: 30447
biological effects on graft-host immune reactions in mice, 17: 27122
biological effects on hamsters, protective effects of diethyl stilbestrol against, 17: 30458
biological effects on immune response of rabbit skin, 17: 28744
biological effects on kidneys and submaxillary glands of rats in presence of cortisone, 17: 10470
biological effects on longevity and total body weight of mice, 17: 17920
biological effects on lysine content in guinea pigs, 17: 33711
biological effects on lung cells, tracer studies using tritiated thymidine, 17: 38821
biological effects on mice, comparison with neutrons, 17: 2886
biological effects on myocardium, electrocardiogram studies of, 17: 17939
biological effects on mammalian cells, 17: 23171
biological effects on mammalian tissue cells, wavelength-dependent effects on, 17: 27057 (MMPP-196-2)
biological effects on metabolism in sprouting plant seeds, 17: 30330
biological effects on monocellular organisms, 17: 31890

biological effects on neurological disturbances in tortoises, 17: 30382
biological effects on nervous systems of dog embryos, 17: 30401
biological effects on nucleic acid, effects of target size on, 17: 35457(R) (TID-19345)
biological effects on ovary development in chicken and chick embryos, 17: 30328
biological effects on oxygen consumption, blood sugar, and leukocyte glycogen in rats, 17: 30451
biological effects on oocytes in rats, 17: 31913
biological effects on planaria, 17: 28679 (TID-18949)
biological effects on rats, effects of praseodymium nitrate on, 17: 13973(R) (NP-12484(p.54-62))
biological effects on rats, effects of hypothermia on, 17: 30449
biological effects on reticulo-endothelial system, tracer studies of, 17: 40595
biological effects on swimming times of rats, 17: 5934
biological effects on skin, 17: 5813
biological effects on skin, 17: 15757
biological effects on spleen lymphoid centers in mice, effects of thymus on, 17: 15752
biological effects on sperm acting as fertilizer or activator in planaria, 17: 17810
biological effects on spermatogenesis in mice, 17: 30329
biological effects on sprouting seeds of root crops, 17: 30331
biological effects on skin, protective effects of Delial against, 17: 30393
biological effects on transaminase activity in organs of infantile rats, 17: 24918
biological effects, synergistic effects of microwaves in dogs, 17: 2823 (RADC-TDR-62-102)
biological effects on grasshopper embryos, 17: 24896 (TID-18723)
biological effects on mice, 17: 5671(R) (LAMS-2780(p.85-129))
biological effects on mice and hamsters, 17: 5779(R) (UCSF-22)
biological effects on mice, effects of age at exposure, 17: 23174
biological effects on mice, effects of linear energy transfer on early response, 17: 10358 (BNL-6575)
biological effects of, compared with lethal effects of 440- and 730-Mev protons on mice, 18: 43 (CONF-250-3)
biological effects on properties of compound lipids in rabbits, 18: 53
biological effects on blood pressure in rabbits, relation of dose and time to, 18: 87
biological effects of, effects of energy level and dose rate on, 18: 97
biological effects and therapeutic efficiency of, compared with effects of gamma radiation and electron beams, 18: 1479
biological effects of, review, 18: 3603
biological effects in mice, effects of caging on, 18: 5003(R) (NP-13281 (p.104-14))
biological effects in hamsters, 18: 6621(R) (UCSF-23)
biological effects in progeny of mice receiving gonad exposure, 18: 6621(R) (UCSF-23)
biological effects of, tissue factors for measuring, 18: 8262
biological effects of sublethal doses on tolerance to red-cell auto-antigens in mice, 18: 8171
biological effects on spleen, production of antimitotic factor in, 18: 8172
biological effects on estrus cycle of white mice, 18: 8185
biological effects in Paramecium, 18: 9831(R) (AD-403109)
biological effects in Tribolium populations, 18: 9864
biological effects in rats and dogs, 18: 11654 (USNRDL-TR-693)
biological effects on permeability of cells in *Allium cepa* L., 18: 11675
biological effects on HeLa cells in fractionated doses, recovery from, 18: 11754
biological effects on intracellular formation of phages by *Escherichia coli*, 18: 11805
biological effects on oxidation processes in tissues, 18: 11807
biological effects on nervous system of frogs, 18: 13474
biological effects on brain development in rat embryos, comparison with nitrogen mustard, 18: 15834
biological effects on blood serum and enzymatic system of rabbits, 18: 15879
biological effects on spore *A. aureofaciens* with and without water, 18: 17514
biological effects on bone tissue regeneration in tibia of rats, 18: 17515
biological effects of, compared to gamma rays and fast neutrons in mice, 18: 17559
biological effects in mice and rats, effects of fractional doses on, 18: 17624
biological effects of, relative, 18: 19685
biological effects on cartilages of growing larynx in rabbits, 18: 19700
biological effects on phosphonucleoside contents of organs of rats, 18: 19702
biological effects on mice, effects of hypoxia on, 18: 21892
biological effects of, relative to gamma radiation, 18: 21894
biological effects on eye lens in frogs, 18: 23268
biological effects on mice, protection against, using chlorotrianise, 18: 23371
biological effects of massive localized doses of, in treatment of lung carcinoma, 18: 25252
biological effects of, effect of dose fractionation on, 18: 25192
biological effects in mammalian cells, calculation of survival curves based on multi-target or multi-hit model, 18: 25171
biological effects on mice, protection against, by olive oil, 18: 27226
biological effects on barley and lily seed at 150 kev, 18: 27083
biological effects on corticoid content and weight of adrenal gland of rats, 18: 27089
biological effects of, compared with effects of protons, 18: 27067(R) (ORNL-3601(p.110-15))
biological effects on mice, protective effects of ethyl palmitate and plant oils against, 18: 27214
biological effects on mice, protective effects of callicrein and callicrein-inactivator against, 18: 27234
biological effects on animals and plants at doses to 12 Mr, 18: 29366
biological effects on protein fractions of goats after repeated irradiations, 18: 29367
biological effects of, in yeast, 18: 29339
biological effects on mice after injections of Endoxan, 18: 29350
biological effects in dogs, cats, rats, mice, and rabbits, 18: 29256
biological effects in sheep, 18: 31228
biological effects of high-voltage, units of measurement for, 18: 31184
biological effects on proliferative capacity of cancer cells *in vivo*, 18: 31138
biological effects on sprout growth and material changes in potatoes, 18: 31149
biological effects in mice, rats, and dogs, 18: 33286(T) (UCRL-Trans-1068)
biological effects in rat and mouse embryos, effects of dose fractionation and protraction on, 18: 33423
biological effects on the pocket mouse, 18: 35362
biological effects on respiratory control and adenosinetriphosphatase activity of liver mitochondria, 18: 36958(T) (JPRS-25741(p.87-94))
biological effects on hamster cells in culture, 18: 38778(R) (TID-21082)
biological effects on animal cells in tissue culture, 18: 41181
biological effects of, oxidation mechanism in, 18: 41149
biological effects on *Micrococcus radiodurans*, effects of p-hydroxymercuribenzoate on, 18: 41089(R) (NYO-3319-3)
biological effects on Saccharomyces after pretreatment with actinomycin, 18: 41150
biological effects in rats, synergistic effects of copper toxicity on, 18: 43219 (HW-SA-3716)
biological effects, 18: 43230(R) (ORNL-TM-924)
biological effects on hamsters, 18: 43232(R) (TID-21204)
biological effects, 18: 43270
biological effects on adrenal activity and corticoid content in rats, 18: 43296
biological effects, 19: 21902
biological effects in yeast, effects of incubation time on, 19: 38422
biological response to, nonvisual, 18: 47(R) (TID-19617)
bleeding effects on bone marrow cell proliferation in mice following, 20: 40722
book: *Dose Distribution and Dose Determination in Pendulum Irradiation (200 kv to 17 Mev)*, 19: 38534
book: *Effects of Nuclear Radiation on Solids*, 19: 30841
book: *Fundamentals of X-Ray and Radium Physics*, 20: 25641
book: *Physical Foundations of Radiology*, 17: 4431
book: *The Collected Papers of Lord Rutherford*. L., 16: 15351
book: *The Encyclopedia of X Rays and Gamma Rays*, 18: 8043
book: *The Fundamentals of X-Ray and Radium Physics*, 16: 9329
book: *Tissue Grafting and Radiation*, 20: 31120
book: *X-Ray and Nuclear Physics for Medicine and Biophysics*, 20: 6985
burden and exposure time of, at 60 to 200 kv, effect of various screen combinations on, 17: 15676
bursts of solar, short intensity increases of heavy cosmic nuclei accompanying, 20: 29965
cancerogenic effects on lymph system in mice, 17: 10406
carcinogenetic effects of, on animals and man, 17: 27187
carcinogenetic effects on rats, partial and whole-body, 17: 27094
carcinogenic effects, skin tumor induced by, 16: 5201(T)
carcinogenic effects on mouse kidneys undergoing compensatory hyperplasia, 16: 11465 (USNRDL-TR-532(Rev.))
carcinogenic effects in rats, whole-body exposure, 16: 21871
carcinogenic effects on bones in mice, 16: 31389(R) (ANL-6535(p.33-5))
carcinogenic effects on mammary gland in rats, hormonal factors, 16: 32791
carcinogenic effects on tubercular lupus, 17: 10441
carcinogenic effects of soft, on mice, 17: 15823
carcinogenic effects in rats, 17: 17659

carcinogenic effects of, combined with N-nitrosodiethylamine in Wistar rats, 17: 27155
carcinogenic effects on human skin, 17: 33674
carcinogenic effects on human skin, histopathology, 17: 35513
carcinogenic effects, review of, 17: 35582
carcinogenic effects on mouse skin, 17: 40638
carcinogenic effects on rats, effect of age and strain on, 18: 1427
carcinogenic effects on thyroid gland in rats, 18: 8161
carcinogenic effects on thyroid gland in adults and children, 18: 8163
carcinogenic effects on mouse tails of fractionated, comparison of electrons to, 18: 13553
carcinogenic effects in mice, comparison with effects of fast neutrons, 18: 21828 (USNRDL-TR-713)
carcinogenic effects of castration by, 18: 29547
carcinogenic effects of, 18: 29488
carcinogenic effects in rat kidneys, factors affecting, 18: 29506
carcinogenic effects following cervical cancer therapy with, 18: 29463
carcinogenic effects on skin, treatment of, 18: 38980
carcinoma induced by, 19: 22020
carcinoma induction in rat intestine, 17: 23155
carcinoma therapy using supervoltage, effects on nervous system of, 18: 29541
case in therapy, absorbed dose calculations for, 18: 3667
cataract development in frogs and mice caused by wounds after, 16: 20200
cataract induction in sympathectomized eyes in rabbits by, developmental course of, 17: 21486
cataract induction in mice, 18: 8105(R) (NYO-2740-1(p.81-154))
cataract induction by embryonic and fetal exposure of mice to, 18: 29344
cataract induction by, in rats, 18: 35370
cataract induction in rabbits by, effects of lens glutathione content on, 18: 38874
cataract induction in rats by, effectiveness relative to gamma radiation, 19: 19612
cataractogenic effects of, effect of dose fractionation on, 18: 25200
cataracts induced in rabbits, 16: 1547
cataracts induced in mice by, effects of age on lamellar, 17: 14080
cataracts induced in rabbits by, effects of removal of cervical sympathetic ganglion on, 17: 21490
cataracts induced by, in rabbit eyes, 18: 31209
chemical effects on polyvinyl acetate, dependence on linear energy transfer, 16: 20501
chemical effects on ionosphere in high-altitude nuclear explosions, 16: 28648 (RM-3204-PR)
chemical effects on oxidation of formic acid at platinum electrode, 16: 28996
chemical effects on nucleic acids, 17: 212
chemical effects on nucleic acids and nucleoproteins, 17: 15771
chemical effects on glucose oxidase and riboflavin, 17: 15774
chemical effects on 3-indoleacetic acid, 17: 15776
chemical effects on DNA, 17: 15792
chemical effects on cattle serum globulin isoelectric points, 17: 17872
chemical effects on nucleic acids *in vitro* and *in vivo*, 17: 40558
chemical effects on adenine, diphosphopyridine nucleotide, and nicotinamide, 18: 6852
chemical effects on gelatin, 18: 6861
chemical effects on mercuric chloride, 18: 8424
chemical effects on behavior of platinum electrodes in irradiated solutions, 18: 8438
chemical effects on aqueous solutions of chloral hydrate, hydrochloric acid formation in, 18: 12234
chemical effects on colloidal systems, 18: 12148(R) (TID-20067)
chemical effects on potassium hydrogen maleate, free radical produced in, 18: 13833 (CONF-403-1)
chemical effects on reactions of isobutane and olefins, effects of electrophilic additives on, 18: 13836(R) (NYO-10025)
chemical effects on tetrafluoroethylene oxidation, 18: 13872
chemical effects on alkali nitrate solutions, 18: 20080
chemical effects on vitamin B_{12}, 18: 20090
chemical effects on normal and secondary butyl chlorides, 18: 25598
chemical effects on hexane, 18: 25555
chemical effects on cyclopentanone, 18: 27496 (TID-20713)
chemical effects on proteins, 18: 27502
chemical effects of, comparison with action of free radicals, 18: 27501
chemical effects on catalase, protective effects of glycerol against, 18: 27218
chemical effects on desoxyribonucleic acid, 18: 31564 (EUR-1646.f)
chemical effects on potassium azide, 18: 33647
chemical effects on ESR spectra of N-alkylureas, 18: 41528
chemical effects on luminescence decay times in scintillator solutions, 18: 41529
chemical effects on paramagnetic absorption spectrum of L-cystine, 18: 41531
chemical effects on diphenyl phosphine oxide, mechanism and spectra of, 18: 41534
chemical effects on electric conductivity of polyamide copolymers, effects of benzophenone and hydroquinone on, 18: 41535
chemical effects on reactivity of ammonium perchlorate, 18: 43603
chemical effects on urea crystal mixtures with adipic, fumaric, and succinic acids, ESR spectra of radicals produced by, 18: 43625
chimera induction in rats, effects of bone marrow, lymph node, and thymus cell injections on, 17: 24948
chimeras, effects of lymphoid cells on skin homograft tolerance in long-lived, 16: 2901
chimeras of mice, effects of bone marrow and spleen cells on colony-forming units in, 19: 17679
chimeras of mice, mortality from secondary disease in, 19: 45910
chromatid aberrations induced in Vicia by, effect of DNA on, 18: 8158
chromosomal aberration gradients induced in *Tradescantia* anthers by, yields in, 17: 10454
chromosomal aberrations induced by, mechanisms for, 18: 17598
chromosome aberrations induced by, effects of oxygen, 16: 12904
chromosome aberration induction in MN, 16: 14583
chromosome aberrations induced by, 16: 12911
chromosome aberrations induced by, 16: 12912
chromosome aberration induction in Ehrlich ascites tumors, effects of oxygen tensions on, 16: 17490
chromosome aberrations induced in *Vicia faba* root tips by, effects of cupferron and 2,4-dinitrophenol on, 16: 30248
chromosome aberrations induced in Tradescantia by, metabolic repair of, 16: 30252
chromosome aberrations induced by, effects of post-irradiation temperature, 17: 1303
chromosome aberrations induced by, effect of fractionated dose, 17: 28709
chromosome aberrations induced in bean roots by, in combination with 5-fluorodeoxyuridine, 17: 28723
chromosome aberrations induced by, in normal and tumorous cells, effects on cell viability, 17: 31897
chromosome aberrations induced by, in human cells, 17: 33652
chromosome aberrations induced by, in root tip cells, 18: 46 (TID-19578)
chromosome aberration induction in human leukocytes, 18: 1394
chromosome aberration induction in bean roots, relation of DNA synthesis and structure to, 18: 8164
chromosome aberrations induced in *Trillium komtschaticum* by, effects of mitomycin-c on frequency of, 18: 8198
chromosome aberrations in human leukocytes *in vivo* and *in vitro* induced by, 18: 29354
chromosome aberrations induced in *Vicia faba* by, effects of time of cell cycle on, 18: 29293
chromosome aberrations induced by, in mouse liver cells, 18: 35372
chromosome aberrations induced by, in human cells, 18: 35302(R) (AD-438540)
chromosome aberrations induced by, in human cells, 18: 35303(R) (AD-438541)
chromosome aberrations induced by, in rat liver, 18: 36973
chromosome aberrations induced by, in Tradescantia, 18: 36991
chromosome aberrations induced by, in Tradescantia, 18: 36992
chromosome aberrations induced by, in Tradescantia, 18: 36993
chromosome aberrations induced by, in *Limotettix striola*, 19: 27985
chromosome aberrations induced by, in man, 19: 28054
chromosome breakage and reunion induction, 16: 1591
chromosome breakage induced by, in salamander oocytes, 18: 27005(R) (ORNL-3601(p.60-8))
chromosome damage, growth reduction, and mitotic inhibition by, in *Vicia faba* roots, 16: 30251
chromosome healing following, in mice, 17: 31958
chromosome rearrangement induced by, in translocated heterozygotes of *Tipula oleracea*, 17: 10402
clinical practices and problems of sieve irradiation, 16: 9784
clinical results of sieve irradiation, 16: 9783
color centers in cesium bromides induced by, optical and thermal properties of, 20: 45036
color centers induced by, in potassium chlorides, 20: 45041(T)
comparison of conventional and supervoltage, in radiotherapy, 20: 35375
conditioned stimulation by, in rats following surgical ablation of olfactory bulbs, 20: 45412
conditioning exposure of mice to, effects on recovery from lethal injury, 18: 35365
de-excitation effect of, 17: 11289(T)
depth dose and intensity of, effects of focus-skin distance on, 20: 33127
detection and absolute measurement below 12 kev, proportional counter for, 16: 27301
detection and analysis of cosmic, research programs on, (E),

20: 41667(R) (MIT-2098-251, pp 1-13)
detection and distribution of galactic sources of, (E), 20: 9637
detection and measurement, 16: 4009(R) (UCSF-21)
detection and measurement, photographic density laws, 16: 8919(T) (NP-tr-845)
detection and measurement in bone marrow, 16: 10222
detection and measurement instruments calibration, 16: 11881
detection and measurement of solar, 16: 15505
detection and measurement in auroral zone on Sept. 27 and Oct. 1 and 2, 1960, 16: 15519
detection and measurement, performance of semiconductor detectors in radiodiagnosis, 16: 16556
detection and measurement of diffracted, using thallium-activated sodium iodide crystal, 16: 19503
detection and measurement of scattered, during dental radiography, 16: 20884
detection and measurement, sensitivity of Geiger-Mueller counter for, 16: 20656
detection and measurement of beta-excited, by proportional counter, 16: 22352
detection and measurement using selenium photocell combined with phosphors, 17: 8658
detection and measurement by free-air ionization chambers, 17: 16423 (ISS-62/9)
detection and measurement by use of air ionization chambers, 17: 16424 (ISS-62/10)
detection and measurement of pulsed, 17: 22044
detection and measurement of, calibration of Victoreen cavity chamber for, 17: 23739 (HASL-133)
detection and measurement at 100 km, space-time association with auroral glow, 17: 24239
detection and measurement by proportional detectors, 17: 25632
detection and measurement of, development of proportional detectors for, 17: 25633
detection and measurement of, efficiency of proportional detectors for, 17: 25634
detection and measurement of soft, sensitivity of counter for, 17: 25659
detection and measurement to 10,000 r, photographic film development techniques for, 17: 27594 (NBS-TN-161)
detection and measurement of soft, time resolution of proportional counters for, 17: 27709
detection and measurement of, efficiency of manganese-activated calcium sulfate for, 17: 28820 (AE-109)
detection and measurement of, use of ionometric methods in, 17: 30759
detection and measurement of, using insulating materials, 17: 30095
detection and measurement of, problems in, 17: 30846 (CEA-2281)
detection and measurement of, design of high-performance fluoroglass dosimeter for, 17: 34241(T) (UCRL-Trans-984)
detection and measurement of, energy dependence characteristics of ionization chambers for, 17: 36166
detection and measurement of, scintillation method for, 17: 41269
detection and measurement of, sensitivity of photomultiplier tubes for, 17: 41273
detection and measurement of, evaluation of 6 types of instruments for, 18: 5675
detection and measurement of solar, August 19 and 20, 1960, 18: 7398
detection and measurement of solar, below 10 A by Russian geophysical rockets and sputniks, 18: 7450
detection and measurement of, from high-voltage electronic equipment, 18: 8599
detection and measurement up to 1 Mev, use of G-M tubes for, 18: 8690
detection and measurement of low-level, 18: 11940
detection and measurement of, during diagnostic radiography, 18: 11941
detection and measurement of low-level, during diagnostic radiography, 18: 11946
detection and measurement of soft to hard, design of apparatus for, 18: 12480(P)
detection and measurement of, spherical proportional counter for, 18: 12487(P)
detection and measurement of pulsed, from radar, 18: 12442(R) (AD-412461)
detection and measurement around electronic equipment, 18: 12465 (RADC-TDR-63-29)
detection and measurement of, self-powered dosimeter for, 18: 14256
detection and measurement of monoenergetic, design of calorimeter for, 18: 13445 (MMPP-196)
detection and measurement of solar, thermoluminescent properties of manganese-activated calcium sulfates for, 18: 18229(T)
detection and measurement using proportional counters, electronic reduction of background for, 18: 23974
detection and measurement of, design of proportional counter for, 18: 25834
detection and measurement of scattered, 18: 25838
detection and measurement of 1- to 10-kev, plastic scintillator for, 18: 25845
detection and measurement of, design of photovoltaic cell exposure rate meter for, 18: 25867
detection and measurement of, proportional counter for, 18: 27790(R) (ORNL-3578(p.46-59))
detection and measurement of pulsed, low-inertia silicon n-p and n-i-p detectors for, 18: 31925
detection and measurement of, ionization chambers for, 18: 31961
detection and measurement of 17-kev, instrument for, 18: 31981(P)
detection and measurement of small-wavelength cosmic, total-reflection telescope for, 18: 33970
detection and measurement of, portable ionization chamber for, 18: 37524
detection and measurement of, performance of photographic film detectors for, 18: 39678
detection and measurement of, performance of photographic film detectors for, 18: 39681
detection and measurement of, sensitivity of Geiger-Mueller tubes and scintillation detectors for, 18: 39684
detection and measurement using colored methacrylate polymer, 18: 39610 (AERE-R-3360)
detection and measurement of, development of integrating multipoint remote-area safety monitor for, 18: 41792
detection and measurement of, devices for, 19: 2191 (ORNL-P-658)
detection and measurement of, design of Geiger-Mueller tube for, 19: 2657(P)
detection and measurement of, arrangement for discrimination of various hardnesses in, 19: 2658(P)
detection and measurement of dose absorbed by specimens, 19: 2661(P)
detection and measurement of interstellar, (E), 19: 5569(R) (MIT-2098-64)
detection and measurement of, design and performance of silicon n-p junction cells for, 19: 7794
detection and measurement of, design and performance of ionization chambers for, 19: 9479 (HW-SA-3773)
detection and measurements of soft, ionization chamber for, 19: 9483 (NP-14419)
detection and measurement of, performance of photographic film detectors for, 19: 9526
detection and measurement of, design of instruments for medical applications, 19: 9535
detection and measurement of, design of instruments for medical applications, 19: 9536
detection and measurement of, cadmium sulfide response for, 19: 11596
detection and measurement using photographic method, 19: 13785
detection and measurement of astronomical, (E), 19: 14199 (MIT-2098-99)
detection and measurement, long-life monitor for, 19: 13736 (SC-TM-64-1674)
detection and measurement of absorbed dose in tissue, 19: 15015(R) (N64-29573)
detection and measurement of, sensitivity of silver bromide emulsions for, 19: 18291
detection and measurement of scattered, during diagnostic radiographic procedures, 19: 22052
detection and measurement of, development of fluoroglass dosimeters for, 19: 22723
detection and measurement, design of calorimeter for, 19: 22767
detection and measurement by dosimetric films, effects of energy on optical density in, 19: 30518 (CLOR/GUM-35)
detection and measurement of solar, use of photographic emulsions for, 19: 30549
detection and measurement of complete spectrum of, apparatus for, 19: 32609
detection and measurement of solar, photographic emulsions for, 19: 32864
detection and measurement of soft, design of gridded proportional counter for, 19: 39046(P)
detection and measurement using matched pairs of cadmium sulfide crystals, (E), 19: 40598
detection and measurement from pulsed sources, plastic scintillators for, 19: 43415 (MATT-347)
detection and measurement of, design of portable survey meter for, 19: 42730
detection and measurement of solar, using rockets and satellites, (E), 19: 43020
detection and measurement of, energy dependence of alanine dosimeter for, 20: 394
detection and measurement of pulsed or steady, monitor design for, 20: 2121 (AD-614832)
detection and measurement of ultra-soft, gas counters for, 20: 7433
detection and measurement at 1 to 10 kev, proportional counter for, 20: 7434

detection and measurement of, from iron-55, 20: 8580
detection and measurement of, instruments for, (E), 20: 13092
detection and measurement of low-energy, performance of proportional counter for, 20: 14879
detection and measurement of absorbed dose, performance of ionization chambers for, 20: 14894
detection and measurement of low-energy, solid-state detection for, 20: 14910(P)
detection and measurement of, design of narrow-band apparatus for, 20: 16823 (NYO-3160-1)
detection and measurement of, design of extrapolation chamber for, 20: 16852
detection and measurement of cosmic, using gas proportional counters, 20: 16901
detection and measurement of solar, instruments for, 20: 16904
detection and measurement of cosmic, counter telescope for, 20: 19030 (N-65-17266)
detection and measurement in stratosphere, radiosonde for, 20: 23479
detection and measurement of, using silicon *p-n* junction detectors operated as photodiodes, 20: 29540
detection and measurement of, photographic film detector with intensifier screen for, 20: 29573(P)
detection and measurement of, from deposited plutonium-239 in dogs, 20: 30968 (BNWL-SA-11)
detection and measurement of soft solar, fabrication and operation of ionization chamber for, 20: 31511 (N-66-16936)
detection and measurement of, using image intensifiers with gas-filled detectors, 20: 33687
detection and measurement of, evaluation of instruments for, 20: 35767
detection and measurement of, ion chamber detector for, 20: 39249(P)
detection by ionization and scintillation methods, review of, 19: 18261 (NP-14685)
detection from source in cylindrical proportional counter, efficiency of, (T), 19: 34501
detection of beta-excited, 16: 22507
detection of biological effects of, method for immediate, 18: 25134
detection of, counting-loss and pulse pile-up in, 18: 4120
detection of, development of system for Ranger, 17: 2662(R) (MLM-1135)
detection of galactic, rocket-borne instrumentation for, 20: 39229
detection of K and L, using sodium iodide crystals, 17: 8643
detection of low-energy, design of scintillation camera for, 20: 19089
detection of low-energy, using scintillation detectors and semiconductor detectors, 20: 21107
detection of lunar, theories on, 20: 2666
detection of narrow band, apparatus for, 19: 39047(P)
detection of short bursts of, gas scintillators for, 18: 30049
detection of soft, 16: 12633
detection of soft stellar, rocket, 19: 39332
detection of soft, windowless resistance strip detector for, 19: 22721
detection of soft, ionization chamber saturation in, 19: 28645
detection of 0.1 to 1.5 Mev, design and performance of miniature pocket dosimeter for, 19: 22726
detection of, calorimeter design and performance for, 20: 14908
detection of, design and performance of gas-filled image intensifier spark chamber for, 20: 41299
detection of, design of 1–12 Å range scintillation detector for, 20: 43726
detection of, dosimeter for, 20: 25430
detection of, performance of liquid argon-filled chambers for, 20: 15259
detection of, photomultipliers for, 18: 33904
detection of, pulse height shifts in gas proportional detectors for, 20: 41331
detection of, scintillation counter efficiency for, 20: 16836
detection of, scintillation response of sodium iodide crystals for, 20: 25373 (AD-631709)
detection of, sensitive monitor for, 20: 25420
detection of, survey of devices for, 20: 21023 (AD-624231)
detection using antimony sulfide single crystals, (E), 19: 18008
detection using cadmium sulfide cells, increased sensitivity in, 19: 30617
detection using chromosome aberrations, 18: 19643
detection using europium-activated single crystals of calcium fluorides, 20: 21135
detection using internally amplifying gallium-diffused junctions, 20: 21100
detection using lithium-drifted p-i-n semiconductor device, 20: 25433(P)
detection using plastic scintillator, energy dependence of efficiency of, 20: 19066
detection using scintillators, pulse-height asymmetry in, 17: 1778
detection using semiconductor detectors, sensitivity of, 19: 6205
detection using semiconductor detectors, 19: 26680
detection with gamma spectrometer, 19: 13803
determination of absorbed dose in tissue, 17: 23173
determination of personnel exposure dose by film badge, 18: 5149
diagnostic dose reduction, methods for, 18: 18104
diagnostic, effects of prenatal exposure on childhood cancer, 16: 18779
diagnostic exposure, effects on induction of neoplasms in offspring, 17: 27185
diagnostic use for aortic calcification, 18: 37045
diagnostic use for plasma density measurements, 18: 38232
diagnostic use for plasma, 19: 33402(R) (AFCRL-65-315)
diagnostic use of, protective measures for, 18: 39017
diffraction and transmission by single crystals, intensity distributions in, (T), 19: 32789
diffraction at Bragg angle, propagation of wave field from, 19: 23366
diffraction by alpha-irradiated silicon crystals, 20: 12281
diffraction by copper crystals, anomalous transmission in, (E), 19: 16117
diffraction by crystals, Pendelloesung fringes in, (E/T), 19: 39287
diffraction by crystal dislocations, theory and uses of, 20: 5003 (CEA-R-2875)
diffraction by curved crystals, (E/T), 19: 4828 (TID-7705(p.194-213))
diffraction by germanium single crystals, effects of alpha irradiation on intensities of, 19: 26880 (EUR-2188.e)
diffraction by germanium and silicon, effects of fast neutrons and impurities on, (E), 20: 24612
diffraction by liquids, planetary-electron effects on, (T), 19: 14254
diffraction by molybdenum, radioinduced line-width changes in, 20: 15136 (RL-REA-2595, pp 51-62)
diffraction by natural quartz, defect structure from, 20: 32695
diffraction by radiation-damaged molybdenum, 16: 2265 (HW-SA-47)
diffraction from deformed cerium containing extrinsic stacking faults, 19: 42811
diffraction from infinitely thick ideal crystal, kinetic theory for, 20: 34863
diffraction in mosaic crystals, secondary extinction in, (T), 19: 32810
diffraction line broadening in calcium fluorides, 18: 22039
diffraction of, line breadths and peak height for α_1 α_2 doubling effects in, 17: 15873 (AERE-R-4218)
diffraction of, dynamical theory of, 18: 34354
diffusion in crystals by thermal agitation, 19: 38032
distribution of absorbed, in atmosphere, 17: 14947 (SC-4759(RR))
distribution of high-energy scattered, in water phantoms irradiated by electron beams or x radiation, 20: 23808(R) (NIRS-4, pp 3-12)
distribution of stray, from industrial radiography, 18: 8505
dosage absorbed in radiology, line integral method for calculating, 18: 9946
dosage absorbed in Grenz-ray region by phantom materials, determination of, 19: 24784
dosage determinations, use of film badges for, 16: 4039(T) (NP-tr-824)
dosage determination for fluoroscopic procedures, 16: 8473
dosage determination, units and measurements, 16: 15042
dosage determinations during diagnostic uses, 16: 17527
dosage determinations by detector using radioinduced polymerization, 16: 20857(R) (AD-265757)
dosage determinations received by radiographers, 16: 27480
dosage determinations near interfaces between hard and soft tissue, 16: 26676
dosage determination of absorbed megavoltage, in tissue-equivalent phantoms, 17: 1311
dosage determinations in megavolt therapy, 17: 1312
dosage determinations for occupational exposure of personnel in medical x-ray departments, 17: 8447
dosage determinations, methods for, 17: 13977(R) (NP-12484(p.134-58))
dosage determinations for, in esophagus, 18: 148
dosage determinations of, calculation of integral whole-body dose for 200 Kv, 18: 17702
dosage determinations for sheep, lethal, 20: 20487
dosage measurements, from unshielded klystron radar tube, 16: 8646
dosage measurements in medical radiological examinations, effects of image intensifiers, 17: 21935(T) (NP-tr-996)
dosage measurements for diagnostic procedures, 17: 23091 (TID-18031)
dosage measurement in water phantom, effects of water depth on integral, 17: 28617
dosage of, for lethality in dormant Guar seed, 19: 40376
dosage received by patients from diagnostic radiography, 17: 20251
dosage received by patients from diagnostic radiography, 17: 20252
dosage to bones, measurement by calorimetry, 17: 32305
dosage to man during fluoroscopy, factors contributing to, 20: 33133
dosage to patient in fluoroscopy, performance of nomogram for measurement, 17: 35564
dosage to radiographer and roentgenologist in fluoroscopic examination of the digestive tract, 16: 2070
dosage to roentgenologist and assisting staff in fluoroscopic examinations of heart and lung, 16: 2069
dose absorbed by man of, during diagnostic radiography, 20: 5440
dose and dose loss, phantom study of, 18: 1966

dose and dose rate measurement of, equipment for, 20: 46067
dose calculation for therapeutic, backscatter factors for, 19: 22062
dose calculations of, for radiotherapy of carcinoma of uterus, 19: 31940
dose calculations of, for radiotherapy of Peyronie's disease, 19: 31976
dose calculations for rotational therapy, computer program for IBM-709, 19: 36145
dose calculations for radiotherapy, design of isodose plotter for, 19: 36146
dose calculations for use in radiotherapy, 20: 38750
dose concept, 17: 40592
dose definition and measurement, method for, 18: 29322
dose delivered to mediastinum during preoperative irradiation of lung tumors, comparison at 9 centers, 18: 25253
dose depth for therapy using, tables of, 19: 17710
dose determination using Compton effect, 18: 12494(P)
dose determination, dosimetric fundamentals in volume, 16: 17941
dose distribution measurements for high intensity microsecond pulses, 16: 21895(R) (AD-266956)
dose distribution in dogs, phantom measurement accuracy of, 18: 15753
dose distribution measurements from discoloration of triphenyltetrazolium chloride in agar-agar, 18: 22350
dose distribution of, in tumors, computer analysis of data on, 18: 33434
dose distribution of, during therapy of uterine carcinomas, 19: 263
dose distribution of, in tangential mammary irradiation, 19: 9027
dose distribution in tumors, 19: 19672
dose distribution in nonuniform phantoms, isodose curves of, 19: 28585
dose distribution of 6-Mv, in water, 19: 29443
dose distribution in man, computer analysis, 19: 34098
dose distribution in laryngeal carcinoma therapy, methods for, 19: 42391
dose distribution in head irradiation, effects of stainless steel mesh skull prosthesis on, 20: 8762
dose distribution in therapy, 20: 24960
dose distribution measurements, 20: 29073
dose distribution in dogs, effects of partial-body shielding on, 20: 35276
dose distribution in tissue, effects of bone dimensions on, 20: 38791
dose distribution of pelvic, using modified Marburg method, 20: 43047
dose distribution, depth, 17: 28672 (BNL-6348)
dose distributions for rectangular fields, calculation of, 18: 27246
dose distributions from, in fallout, (T), 20: 2048 (USNRDL-TR-888)
dose distributions in radiotherapy, atlas of single-field, 20: 8749 (STI/PUB/96(Vol. 1))
dose distributions for uterine carcinoma, 20: 40769
dose effects on cataract induction, 20: 40771
dose effects on chromosome aberrations in human blood cells, 20: 40665
dose effects on erythropoiesis in rats, 20: 42957
dose effects on recurrent mouse mammary carcinoma, 20: 43035
dose effects on thyroid metabolism in rats, x, 20: 43029
dose estimates of, used for therapy of benign diseases, 20: 8785
dose estimation to hand from old unit, 1920 to 1934, 18: 31317
dose estimation to personnel using, 18: 31817
dose estimations for, current intensity and flux in, 20: 37091
dose for $LD_{50/30}$ in jackrabbits, 20: 40494(R) (COO-1329-3)
dose for mice, determination of lethal, 19: 45990
dose fractionation of, therapeutic advantages of, 18: 6726
dose fractionation of, effects on carcinolytic action, 19: 10940
dose fractionation effects on cataracts of rats, 20: 40690
dose from, effects of phantom materials on depth, 17: 38675
dose in soft-tissue cavities of bone, calculation of absorbed, 19: 13685
dose measurement for therapeutic use, 19: 10930(T) (JPRS-27527)
dose measurement of, film scanner for, 19: 18239
dose measurement of, using photostimulated polarization transients in zinc sulfide, (E), 20: 40333
dose measurements in gonad region of infant phantom under superficial radiation conditions, 16: 6661
dose measurements, 17: 16350
dose measurements of, simultaneously with gamma dose measurements, performance of luminescent detectors for, 18: 510
dose measurements at surface and various depth in water phantoms, 18: 3553
dose measurements by discoloration of glass or plastics, 18: 5651
dose measurements at quantum limit, 18: 9809
dose measurements in vicinity of interface between two media of different atomic compositions exposed to, of 11 to 20 Mv, 18: 23388
dose measurements of, during diagnostic radiographic procedures, 18: 38997
dose measurements of, during diagnostic cineradiography, 18: 41298
dose measurements of, for treatment of thyroid carcinomas, 19: 253
dose measurements in medical radiography and radiotherapy, 19: 9044
dose measurements of, during diagnostic radiography of chest, 19: 10971
dose measurements of, in pregnant women and fetuses, 19: 12968
dose measurements of, in bone, 19: 13056
dose measurements of, in gel brain phantom, 19: 24307
dose measurements for therapeutic use of, 19: 30052
dose measurements of, design of tissue-equivalent phantom for, 19: 32019
dose measurements for fractionated exposures, 19: 36162
dose measurements for eyes of, during diagnostic radiography of head and neck region, 19: 43885
dose measurements of, for gonads of children during diagnostic radiography, 20: 3854
dose measurements of, from diagnostic radiography during pregnancy, 20: 3823
dose measurements in medical radiography, 20: 35364
dose measurements, problems in, 19: 15143
dose measurements, depth, 17: 19822
dose modification by grids, 17: 12085
dose of, during diagnostic applications, 19: 5738
dose of, from repeated diagnostic radiography, 20: 3834
dose of, received by patients from conventional radiography, multisection radiography, tomography, and radiographic subtraction procedures, 18: 11942
dose rate determination in vinyl chloride, absorbed, 19: 39016
dose rate effects and significance in survival time curves, 16: 4405 (UCLA-455)
dose rate measurements of low-level, modification of Geiger-Mueller counter for, 20: 29553
dose rates and energy spectra from stray, 17: 21953
dose rates from radioisotope and fission-product sources, 18: 22984 (NYO-10721)
dose rates from unfiltered beams, 20: 45951 (HASL-179)
dose rates of, in irradiations through grids, 20: 29056
dose received by gonads during diagnostic radiography, 19: 10925
dose received by population from medical use of sources of, 19: 46112
dose received by urologist, from retrograde pyelogram examinations, 20: 5459
dose reduction during diagnostic radiography, 19: 10924
dose reduction in diagnostic, use of, 19: 46146
dose response of mammalian and bacterial cells in culture to, parameters for multi-target and multi-hit survival curves in, 18: 25170
dose standards, national intercomparison, 17: 21937
dose-survival curves for human kidney cells in tissue cultures, 16: 12930
dose tables and isodose charts for medium energy, depth, 17: 27633
dose to abdominal tissues from cervical cancer therapy, 19: 42392
dose to bone marrow during diagnostic radiography, 17: 20253
dose to bone marrow in fluoroscopic examination of gastrointestinal tract, 18: 455
dose to children of, from radiographic diagnosis of congenital heart disease, 20: 5455
dose to dentists during radiography, 20: 5430
dose to fetus during radiographic localization of placenta, 20: 6973
dose to fetus in radiography, 20: 31146
dose to gonads during fluoroscopic chest examination, 16: 33333
dose to gonads during diagnostic radiography, 20: 1703
dose to gonads during dental radiography, 20: 4206
dose to gonads during therapy of hemangiomas in children, 20: 31156
dose to gonads from dental radiography in Japan, 20: 4196
dose to gonads of, from therapy of dermatological diseases in man, 20: 5445
dose to head in diagnostic dental radiography, measurement of, 19: 19676
dose to Japanese people from fluoroscopy, 20: 31466
dose to patient during urography, effects of contrast media dose in reducing, 20: 3857
dose to patient from diagnostic, hazards of, 20: 6921
dose to skin during diagnostic radiography, 20: 1704
dose-absorbed estimation from dosimeter readings, 19: 18220
dose-rate measurements of high-energy, in water phantoms, 18: 39631
dose-time relations for, for therapy of laryngeal carcinomas, 18: 25250
doses from diagnostic gonadal, 19: 28157
doses from prenatal, fetal, 19: 15262
doses to human gonads from diagnostic, calculation procedure for, 20: 43026
dosimeter for measuring, photochemical, 18: 29986
dosimeter for, design of multi-element, 19: 28693
dosimetric control of, 18: 456
dosimetry, 16: 26835
dosimetry, (E), 19: 13801
dosimetry, advantages and basic principles of film, 16: 24028
dosimetry along central axis of beam of, from tissue-air ratios, 18: 29530
dosimetry at interfaces, 20: 18952
dosimetry at 10 kev to 2 Mev, review of film, 19: 26658 (SZS-6)
dosimetry at 200 Kvcp and 22 Mevp, calibration of ionization chamber for, 16: 17513
dosimetry by ionization chambers, energy dependence of dose sensitivity of, 18: 35856
dosimetry by ionization and scintillation method, review of, 19: 18261 (NP-14685)

dosimetry during fluoroscopy, parameters affecting, 20: 43050
dosimetry during intravenous pyelogram examinations, 20: 22824
dosimetry during mouth radiography, 20: 40795
dosimetry during pregnancy, phantom for, 19: 30539
dosimetry for bone marrow during chest radiography, 20: 180
dosimetry for dental procedures, 20: 14419
dosimetry for therapy of head and neck neoplasms, 20: 41210
dosimetry in biological studies, equipment and methods for, 20: 35349
dosimetry in bladder tumor therapy, 18: 41291
dosimetry in bone and lungs using lithium fluoride thermoluminescent dosimeters, 20: 43747
dosimetry in bones, review of experimental and theoretical methods for, 20: 18954
dosimetry in cephalometric radiography, 20: 20543
dosimetry in cervical cancer therapy, 19: 42381
dosimetry in chickens, lethal, 20: 38676
dosimetry in cylindrical cavities in bones, method for measuring, 17: 21498
dosimetry in diagnostic radiology, filtration and kilovoltage effects on depth, 19: 46144
dosimetry in dog tissues, method for, 20: 604
dosimetry in dogs and phantoms, 20: 20432 (AD-630332)
dosimetry in pharyngeal phantom, 20: 43020
dosimetry in pituitary tumors, 20: 38761
dosimetry in radiotherapy, 17: 25001
dosimetry in rat tissues, effects of age on, 20: 25336
dosimetry in sheep phantoms, 19: 36823 (USNRDL-TR-842)
dosimetry in sheep, 20: 38625
dosimetry in therapy of Hodgkin's disease, 20: 31151
dosimetry in thin phantoms, 20: 18977
dosimetry in tissues, 19: 38499
dosimetry in Tradescantia, performance of lithium fluoride thermoluminescent detector for, 20: 46030(R) (AERE-PR-HPM-9, pp 6-17)
dosimetry near interface of soft tissue and bone, 17: 4850
dosimetry of, 19: 13175
dosimetry of, 19: 32588
dosimetry of betatron, 18: 42241
dosimetry of, calorimetric method for, 18: 4106
dosimetry of criticality accident, 19: 36699 (BNWL-SA-5)
dosimetry of, description of direct-reading meters for, 17: 29993
dosimetry of diagnostic, during pregnancy, 19: 26186
dosimetry of diagnostic, collimation effects on, 19: 46145
dosimetry of diagnostic, ionization chambers for, 19: 46857
dosimetry of diagnostic, scintillator-photomultiplier combination for, 19: 46858
dosimetry of diagnostic, in Japan, 20: 14799
dosimetry of diagnostic, in Japan, 1960, 16: 28800
dosimetry of, evaluation of dosimeters for, 17: 39409(R) (AD-296591)
dosimetry of exit dose for lungs, during radiotherapy, 20: 1699
dosimetry of fractionated, nomogram for, 20: 16749
dosimetry of high voltage pulsed r-f tube, 20: 21022 (AD-624230)
dosimetry of high-energy, 19: 2193
dosimetry of high-energy, radiation quantities and units for, 19: 9479 (HW-SA-3773)
dosimetry of high-energy, 19: 32787(R) (NIRS-3(1-17))
dosimetry of intensive soft, applicability of instruments to, 19: 26696
dosimetry of low levels of, latensification of film sensitivity for, 19: 30550
dosimetry of low-level, fluorescence apparatus for, 18: 25855(P)
dosimetry of low-level, 20: 12999 (CEA-R-2746)
dosimetry of medical, 20: 16843
dosimetry of medical, survey using film packs, 20: 41213
dosimetry of megavoltage, 17: 1776
dosimetry of Mv, calibration of ionization chambers for, 18: 31960
dosimetry of radiographic, 17: 34159
dosimetry of radiological, in Britain, 17: 34183
dosimetry of radiographic, tables for, 20: 16751
dosimetry of scattered, 16: 6663
dosimetry of scattered, during diagnostic radiography, 19: 43917
dosimetry of scattered, from therapeutic electron beam, 20: 43012 (BMwF-FBK-66-03)
dosimetry of shell irradiation, phantom studies, 19: 46127
dosimetry of soft, 16: 29258
dosimetry of soft, using ionization chambers, 19: 22727
dosimetry of soft, using G-M counters, 20: 13085
dosimetry of supervoltage, numerical method for determination of moving field isodose curves, 18: 21932
dosimetry of surface, during rotational irradiation, 18: 3663
dosimetry of therapeutic, 18: 37058
dosimetry of therapeutic doses of, 19: 30016
dosimetry of therapeutic doses, use of phantoms for, 20: 5481
dosimetry of therapeutic, 20: 33122
dosimetry of, use of film badge for personnel, 17: 20375
dosimetry of, use of calcium fluoride (manganese) and lithium fluoride thermoluminescence, 17: 22031
dosimetry of, using cerium sulfate solutions, 17: 41255
dosimetry of 15.5-Mev betatron, effects of field size on, 17: 5899
dosimetry of 15-Mev, in cervical cancer therapy, 20: 12747
dosimetry of, automatic system for, 20: 29070
dosimetry of, calibration of ionization chambers for, 18: 31959
dosimetry of, calorimetric method for, 20: 15858
dosimetry of, chemical method for, 18: 12475
dosimetry of, chemical, 19: 2621
dosimetry of, circuit arrangement for, 20: 13124(P)
dosimetry of, design of thermoluminescent detector for, 19: 36862(P)
dosimetry of, design and performance of luminescent dosimeters for, 20: 9291
dosimetry of, design of integrating dose-rate meter using ionization chamber for, 20: 21078
dosimetry of, detector for, 19: 32603(P)
dosimetry of, development of chromium, cobalt, and lead glasses for, 19: 840
dosimetry of, during diagnostic radiographic examinations, 18: 27266
dosimetry of, during diagnostic radiographic examinations, 18: 27267
dosimetry of, during diagnostic radiographic examinations, 18: 27268
dosimetry of, during diagnostic radiographic examinations, 18: 27269
dosimetry of, during diagnostic radiography, 19: 43889
dosimetry of, during benign tumor therapy, 20: 13013
dosimetry of, during diagnostic radiography, 20: 22845
dosimetry of, during extraoral radiography of jaws and skull, 20: 23391
dosimetry of, effects of selective absorption on, 19: 270
dosimetry of, effects of bone geometry on soft-tissue, 20: 18978
dosimetry of, equipment for, 19: 13802
dosimetry of, equipment for, 20: 21062
dosimetry of, evaluation of methods for, 20: 27269(T) (CEA-tr-A-1871)
dosimetry of, extrapolation ionization chamber for, 18: 43987
dosimetry of, filter analysis for film, 20: 7328
dosimetry of, Finnish and Swedish standard chambers for, 20: 37078
dosimetry of, for post-operative treatment of breast cancer with opposed tangential fields, 18: 43346
dosimetry of, for treatment of carcinoma of uterus, 19: 31995
dosimetry of, for diagnostic use, 19: 43901
dosimetry of, for cancer therapy, 20: 5439
dosimetry of, for therapeutic use, 20: 5478
dosimetry of, for therapy of lymphosarcomas, 20: 5485
dosimetry of, for therapy of skin carcinomas, 20: 6928
dosimetry of, for tumor radiotherapy, 20: 18521
dosimetry of, for mammary carcinoma therapy, 20: 18545
dosimetry of, from internally administered radionuclides, 19: 15314
dosimetry of, from magnetrons in radar installations, 19: 46673
dosimetry of, from chaoul-type tubes, 20: 3838
dosimetry of, in bone marrow, 19: 13044
dosimetry of, in gonads during thoracic radiography, 20: 6934
dosimetry of, ionization chamber standardization for, 18: 31958
dosimetry of, ionization chamber for, 19: 22792
dosimetry of, liquid photographic emulsions for, 20: 16845
dosimetry of, methods for determining errors in, 20: 23394
dosimetry of, oxygen enhancement ratio for, 20: 16750
dosimetry of, performance of semiconductor detectors for, 19: 34066
dosimetry of, performance of scintillation detectors for, 20: 2157
dosimetry of, performance of ionization chambers for, 20: 13113
dosimetry of, phantom studies for tumor therapy, 20: 6977
dosimetry of, phantom for, 20: 43053(P)
dosimetry of, phosphate glass element for, 20: 4258(P)
dosimetry of, photographic, 19: 26710
dosimetry of, photographic, 19: 46853
dosimetry of, portable microcalorimeter for, 20: 21024 (AD-630693)
dosimetry of, silicon junctions for, 18: 23967
dosimetry of, theory of electronic equilibrium and transition stages in, 19: 25174
dosimetry of, thermoluminescent powders for, 18: 31957
dosimetry of, thermoluminescence detectors for, 19: 39044(P)
dosimetry of, training manual on, 20: 23416
dosimetry of, units for, 20: 18951
dosimetry of, using erythrocyte enzyme activity in rats, 18: 9832(R) (AD-403354L)
dosimetry of, using cyanides of triphenylmethane dyes, 20: 16521
dosimetry of, using Compton effect detectors, 20: 25415
dosimetry of, using thermoluminescence, 20: 33719
dosimetry on plutonium and plutonium oxide–uranium dioxide surfaces, effects of isotopic composition on, (E/T), 20: 27188 (BNWL-SA-22)
dosimetry, performance of photographic film detectors, 17: 3240
dosimetry, scintillation detector for, 16: 10338
dosimetry system for terminating pre-set exposure to, 19: 2627
dosimetry, theory of film, 16: 9045
dosimetry using chromosomal abberations, 18: 19643

dosimetry using ferroelectric transducer elements, 18: 31914 (SC-R-64-197)
dosimetry using ferrous sulfate, 18: 31954
dosimetry using films, equivalent dose relation in, combined with gamma rays, 17: 36052
dosimetry using film badges, 19: 4417
dosimetry using film detectors, effectiveness of, 19: 18201
dosimetry using fluoroglass, 20: 31538
dosimetry using free-air ionization chamber, 19: 4459 (ISS-64/30)
dosimetry using human leukocytes, 20: 22633
dosimetry using ionization chambers, 18: 41777
dosimetry using ionization chambers, 19: 28645
dosimetry using lithium fluoride, (E), 19: 4484 (UCRL-11613)
dosimetry using photocell, 18: 22376(P)
dosimetry using plastic scintillators, 19: 46105
dosimetry using scintillation detectors, 19: 30557
dosimetry using scintillating phantoms, 19: 38893
dosimetry using thermoluminescent phosphor, (E), 19: 4455 (HW-84398)
dosimetry using volume expansion, 19: 32555
dosimetry with cavity chambers, stopping power ratios for, 16: 7786
dosimetry with silver-activated phosphate glass, 16: 9051
dosimetry within tissue using glass microdosimeter, 18: 39628 (UR-651)
dosimetry, problems in personnel, 18: 16364
dosimetry, using photographic film and scintillators, 19: 28676
effect on anthocyanin production in detached flower petals of *Impatiens balsamina*, 18: 25064
effect on blood platelet production and survival in rats, 20: 6785(R) (ORNL-3853, pp 128-40)
effect on bone marrow cells in mice, 20: 31071
effect on homozygous yeast, 16: 20226
effect on leukocyte phagocytic activity, effects of tumor growth, 16: 6351
effect on lifespans of erythrocytes labeled with chromium-51 or iron-59, 19: 42297
effect on luminescence of alkali-halide phosphors pre-exposed to electric field, 19: 40571
effect on lymphoid repopulation in mouse graft-versus-host reaction, 20: 8717
effect on production of fatty acid peroxides in rabbit and rat aorta, 20: 42813
effect on synthesis of desoxyribonucleic acid, 16: 21974
effectiveness in treatment of allergic dermatitis, 17: 1244
effectiveness in treatment of tumors, 17: 5779(R) (UCSF-22)
effectiveness in tumor treatment, 17: 17835
effectiveness of, in treatment of acne vulgaris, 18: 25235
effects after head therapy, tumorigenic, 20: 16245
effects as stress factor in pathogenesis of myocardial necroses in rats, 19: 24320
effects combined with prednisolone on mitosis in MTK sarcomas, 16: 8603
effects combined with maleic acid on mitosis in MTK sarcomas in mice, 16: 8604
effects combined with igrocin on chromosomes and mitosis in rat sarcomas, 16: 14556
effects combined with citric acid on mitosis in rat sarcoma, 16: 14557
effects combined with the sodium salt of arsphenamine on mitosis in MTK sarcomas, 16: 8594
effects combined with chemotherapy on ovary and tumor cells in hamsters, 17: 28613
effects combined with actinomycin D on skin and tumors on man and mice, 17: 28741
effects combined with tetanus toxoid on mice, protective effects of bone marrow cells against, 17: 38802
effects combined with immunization on serum glycoprotein content in rabbits, 17: 40576
effects combined with methylated purines on mutational synergism in *E. coli*, 18: 9863
effects combined with *N,N'*-bis(2-chloroethyl) methylbenzylamine on ATP content in rats, 19: 3977
effects combined with chemicals on growth and mutation frequency of rice seeds, 19: 8854
effects combined with cholesterol-fat feeding on coronary arteries in rabbits, 19: 13010
effects combined with electric shock as warning stimulus in pigeons, 19: 13087
effects combined with starvation on carbon dioxide production in yeast cells, 19: 25968
effects combined with spleen cells and thymus grafts on graft tolerance in mice, 19: 29983
effects combined with bone marrow and thymectomy on skin grafting in mice, 19: 29984
effects combined with novoembichine on amino acid accumulation in *Mycobacterium cyaneum* 416, 20: 31005
effects combined with aging on rat exercise performance, 20: 40604 (AD-635251)
effects combined with urethan on tumor-resistant mice, 20: 42873
effects combined with ethylenimine mutagenesis in durum wheat, 20: 42919
effects during pregnancy, 20: 14380
effects for calcifying epithelioma, therapeutic, 19: 38494
effects in animals, microorganisms, and plants, genetic, 19: 21922
effects in *Arabidopsis thaliana*, genetic, 17: 33502
effects in *Arabidopsis thaliana*, genetic, 19: 19548
effects in *Ascabolus immersus*, mutagenic, 19: 111
effects in bacterial spores, protective effects of glycerol against, 18: 31279
effects in barley seed, genetic, 20: 97
effects in cats, biological, 20: 43
effects in controlling immune responses following human kidney transplants, 20: 43032
effects in diploid yeast, genetic, 19: 21920
effects in Drosophila, genetic, 17: 15681
effects in Drosophila, genetic, 19: 10790(R) (TID-21601)
effects in Drosophila, genetic, 19: 10791(R) (TID-21608)
effects in Drosophila, genetic, 19: 10840
effects in Drosophila, genetic, 19: 10841
effects in Drosophila, genetic, 19: 10842
effects in Drosophila, genetic, 19: 10843
effects in Drosophila, genetic, 19: 12999
effects in Drosophila sperm, effects of nitrogen on, 19: 25981
effects in Drosophila males, genetic, 19: 28103
effects in Drosophila, genetic, 19: 31888
effects in Drosophila populations, genetic, 19: 35948(R) (TID-22031)
effects in Drosophila, lethal, 19: 43787
effects in Drosophila, genetic, 19: 43787
effects in Drosophila, genetic, 19: 45949
effects in Drosophila populations, genetic, 19: 36003
effects in Drosophila, genetic, 20: 18332
effects in *Escherichia coli*, genetic, 19: 5672
effects in *Escherichia coli*, genetic, 19: 10789(R) (TID-21591)
effects in *Escherichia coli*, biological, 19: 31787(R) (NYO-2740-2)
effects in *Escherichia coli*, biological, 19: 33798
effects in *Escherichia coli*, lethal, 19: 43794
effects in *Escherichia coli*, genetic, 19: 43794
effects in *Escherichia coli*, 19: 43795
effects in grasshoppers, genetic, 18: 9831(R) (AD-403109)
effects in guinea pigs and rats, effects of stress induced by vibration, physiological, 19: 40354(T) (FTD-TT-65-48, pp 38-9)
effects in hamster cells, biological, 19: 33798
effects in insects, pathologic, 19: 10719 (AECL-2107)
effects in living cells, biochemical, 16: 30270
effects in *Macaca mulatta*, whole-body, 19: 28072
effects in mammals, delayed pathological, 20: 1716
effects in man following brain therapy, leukemogenic, 20: 22760
effects in man, genetic, 19: 45967
effects in man, leukemogenic, 20: 94
effects in man, leukemogenic, 20: 6958
effects in man, pathological, 19: 22071
effects in mice and rats, dose-rate dependence of early, 17: 4421
effects in mice, protective effects of cysteamine and reserpine against, 17: 35470
effects in mice, protective effects of ethyl palmitate against, 17: 35471
effects in mice, carcinogenic, 19: 19594
effects in mice, effects of fetal thymus cell transplantation on, 18: 19766
effects in mice, effects of strain on, 19: 33881
effects in mice, fractionated doses, 19: 43792
effects in mice, genetic, 19: 28076
effects in mice, genetic, 19: 28062
effects in mice, hematological, 19: 27955
effects in mice, immunological, 19: 45806 (AD-621543)
effects in mice, lethal, effects of microwave exposure on, 19: 10785 (RADC-TDR-63-352)
effects in mice, late somatic, 19: 10814
effects in mice, leukemogenic, 19: 24274
effects in mice, leukemogenic, 19: 24275
effects in mice, lethal, 19: 25938
effects in mice, leukemogenic, 19: 38372
effects in mice, lethal, 19: 45982
effects in mice, leukemogenic, 19: 45911
effects in mice, mechanism for leukemogenic, 20: 3696
effects in mice, pathological, 19: 38450 (USNRDL-TR-851)
effects in mice, pathological, 19: 43771
effects in mice, pathological, 19: 45808(R) (NYO-901-36)
effects in mouse oöcytes, genetic, 19: 43788
effects in mouse oöcytes, genetic, 19: 43789
effects in mouse spermatogonia, genetic, 19: 43788

effects in mouse spermatogonia, genetic, 19: 43789
effects in mouse spermatogonia, effects of dose, dose rate, and radiation quality on pathological, 19: 43788
effects in *Mycobacterium bovis*, biological, 19: 31807
effects in nervous system of man, pathological, 19: 40349 (BNL-9345)
effects in Neurospora, mutagenic, 19: 2111
effects in Neurospora, biological, 19: 21893
effects in plants, genetic and morphological, 19: 12961(R) (TID-21604)
effects in plants, genetic, 19: 21861(R) (NP-14937(p.116-25))
effects in polycythemia patients, 20: 22849
effects in potassium and sodium chloride crystals, F center formation, 18: 36067
effects in producing giant polynucleate cells in virus-transformed hamster cells, 20: 35255
effects in producing lymphomatoses of thymic origin in mice, 20: 36613
effects in rabbits, whole-body, neurological, 19: 40355(T) (FTD-TT-65-48, pp 111-12)
effects in rabbits, biological, 20: 43
effects in rat brain, metabolic, 19: 43810
effects in rat liver, pathological, 19: 43735
effects in rats, protective effects of 2-methylpiperazine dithioformate against, 17: 37134
effects in rats, protective effects of hypothermia against, 17: 40609
effects in rats, biological, 20: 43
effects in rats, carcinogenic, 19: 19606
effects in rats, carcinogenetic, 19: 25973
effects in rats, carcinogenic, 19: 33942
effects in rats, effects of early biological stress on, 19: 42278
effects in rats, effects of cortisone on, metabolic, 19: 43837
effects in rats, genetic, 19: 10719 (AECL-2107)
effects in rats, genetic, 19: 45808(R) (NYO-901-36)
effects in rats, pathological, 19: 5718
effects in rats, pathological, 19: 33810
effects in rats, physiological, 19: 40360(T) (FTD-TT-65-48, pp 666)
effects in rats, physiological, 19: 43808
effects in rice seeds, effects of dose rate on biological, 19: 43781
effects in rice, genetic, 19: 21917
effects in *Schistosoma japonicum* cercariae, biological, 19: 43848
effects in silkworms, genetic, 19: 21916
effects in silkworms, genetic, 19: 43784
effects in silkworms, genetic, 19: 43787
effects in silkworms, lethal, 19: 43787
effects in sodium chloride crystals, 18: 12773
effects in Tetrahymena, genetic, 19: 10788(R) (TID-21584)
effects in thyroid gland, physiological, 19: 40374
effects in Tradescantia and Vicia, genetic, 19: 36014
effects in Tradescantia, genetic, 19: 38360 (TID-21695)
effects in tritium plant cells, genetic, 20: 71
effects in *Vicia faba*, morphology of mutagenic, 19: 3928
effects in *Vicia faba* roots, synergistic effects of sulfonamides on, 19: 21950
effects in *Vicia faba*, genetic, 19: 36094
effects in wheat seed, genetic, 19: 42260 (TID-22115)
effects in wheat seeds, effects of dose rate on biological, 19: 43781
effects in wheat, mutagenic, 19: 2154
effects in wheat, mutagenic, 19: 2161
effects in yeast, genetic, 19: 10789(R) (TID-21591)
effects of acute, whole-body exposure on metabolism, 16: 6308(T) (JPRS-11322(p.316-36))
effects of acute, on adrenal gland function, 18: 13540
effects of behavior of rats, 18: 23238 (FSU-2690-15(Paper 4))
effects of bipolar gain of transistors, Q-factor technique for, 19: 32613(R) (AD-608960)
effects of brain exposure on life span of rats, 16: 2892 (TID-14294)
effects of brain irradiation on respiration, 18: 1396
effects of chronic exposure for several generations, on longevity and reproductive performance in mice, 17: 28682(R) (TID-18992)
effects of, combined with infrared radiation on plant physiology, 17: 7795(R) (TID-17446)
effects of, combined with antigen on plasma cell reactions in spleen of rabbits, 17: 17860
effects of, combined with dehydroascorbic acid on Yoshida sarcoma in rats, 17: 17905
effects of, combined with lipoxidase on mortality of mice, 17: 17921
effects of combined ultraviolet radiation and, on chromosome breakage in pollen, 17: 25013
effects of combined, and microwaves on hematologic response of dogs, 20: 40650
effects of consecutive exposures on skin radiosensitivity, 16: 18773
effects of cranial, on fixated behavior and maze performance in rats, 17: 10430
effects of cranial exposure to, on psychological processes in rats, 18: 11651 (TID-20121)
effects of daily sub-total doses on hematopoietic tissues and blood cells, 16: 12889
effects of deoxynucleoproteins in *E. coli*, 19: 19576
effects of diagnostic, during delivery, 17: 35365
effects of dietary copper and molybdenum on response to stress of exposure to, in rats, 17: 35317(R) (HW-76000(p.178-82))
effects of dose levels on relative biological effectiveness and elimination of chromosomal aberrations, 16: 1603
effects of dose on induction of foreign spleen reaction, 16: 26838
effects of dose rate, on filament formation in *Escherichia coli*, 16: 6320
effects of *E. coli* B, protective effects of oxygen against lethal, 19: 28047
effects of embryonic exposure on life span of rats, 19: 42259(R) (TID-22005)
effects of embryonic exposure to, on aging of chickens, 20: 1611(R) (COO-1119-4)
effects of exposure of seed, on seedling growth, 16: 1525
effects of exposure of central nervous system on liver nucleic acids, 16: 2895
effects of exposure of central nervous system on pancreas, 16: 2896
effects of exposure during puberty, on reproduction of female dogs, 16: 5204
effects of exposure of leaves, on plant metabolism, 16: 6317(T) (JPRS-11322(p.458-62))
effects of exposure of male chickens on sex ratio, 16: 12891
effects of exposure of rat gonads to various doses for several generations, on learning ability of offspring, 16: 32789
effects of exposure of jaw on buccal epithelium in rabbits, protective effects of cysteamine, 17: 1345
effects of exposure of testes to, on weight of offspring in swine, 17: 10414
effects of exposure of humoral factors on reflexes of intestinal chemoreceptors, 17: 30338
effects of exposure of mice to, on aging of progeny, 18: 15808(R) (LAMS-3034(p.116-23))
effects of exposure for 15 generations to, on breeding characteristics of mice, 18: 15809(R) (LAMS-3034(p.124-8))
effects of exposure of seeds to low-dose, on plant growth and development, 18: 23253(T) (OTS-61-11326)
effects of exposure of cerebrospinal axis to, combined with chemotherapy for treatment of mouse leukemia, 18: 29476
effects of exposure of tubal ova to, on embryonic development of hamsters, 18: 29308
effects of exposure of ovarian ova to, on embryonic development of hamsters, 18: 29309
effects of exposure of buffer solutions to, on subsequent inactivation of virus in, 19: 28027
effects of exposure to, *in utero* in rats, physiological, 19: 38361(R) (TID-21951)
effects of exposure to, *in utero* in rats, psychological, 19: 38361(R) (TID-21951)
effects of exposure of adrenal glands to, on recovery from cardiac decompensation, 19: 43919
effects of exposure of rat adrenal glands on pulmonary histaminase activity, 20: 24885
effects of exposures to, with and without precise focusing, 18: 27270
effects of extracorporeal exposure of blood to, on lymphocyte content in calves, 18: 35335
effects of fetal exposure on subsequent behavior and learning ability, 16: 16221
effects of fetal irradiation on behavior of 100-day-old male rats, 17: 15655
effects of focal-head exposure on behavior of monkeys, 16: 26808
effects of fractionated doses in Drosophila ova, biological, 19: 24308
effects of frequent exposure of chest on incidence of leukemia, 17: 5816
effects of fungi cultures *in vitro* at 29 kv, 19: 17663
effects of grid and sieve, on phosphorus-32 transport velocity from skin of guinea pig, 16: 1568
effects of high-level whole-body exposure in man, 16: 8657
effects of high-level, on heart of dogs, 17: 23094 (UR-625)
effects of high-altitude explosion, on ionospheric electron and ion dissociative recombination, 18: 11086
effects of high-energy, from linear accelerator for cancer therapy, 18: 17684
effects of human cells, oxygen effects on, 19: 26151
effects of lesion induction in brain on behavior in pigeon, 19: 26108
effects of lethal dose on metabolism in mice, 17: 21528
effects of lethal dose in mice given bone marrow protection, effects of stimulation of reticular-endothelial system on, 19: 36056
effects of lethal doses on rats treated with bone marrow transplantations, 20: 42956
effects of liver exposure on metabolic activities in rabbits, effects of

dose on, 20: 6879
effects of local applications on growth capacity of kidney, 16: 9888
effects of local abdominal exposure on response to nephrotoxic serum, 16: 16195
effects of local exposure of head on histochemical properties of skin, oral mucosa, and bone marrow, 17: 1248
effects of local irradiation of heads of rats on spermatogenesis, 20: 42961
effects of localized, on bone marrow, destruction and restoration phases in, 18: 23265
effects of low-intensity, motor responses of moths to, 17: 19808 (USNRDL-TR-622)
effects of low-level exposure on blood picture, 16: 4101
effects of low-level exposure on developing brain in embryos, 17: 7883
effects of low-level exposure on developing brain in embryos, 17: 7852
effects of low level exposure on developing brain and nervous system, 17: 7857
effects of low-dose diagnostic, on development of fetuses and babies, 20: 18536
effects of low-energy, on mammalian tissue cells, wavelength, wavelength dependence of, 18: 19757
effects of low-level, on skin, 19: 28145
effects of low-level, and high-frequency electromagnetic waves in man, 17: 37366(T) (JPRS-20872)
effects of massive and acute doses of, on conditioned behavior of monkeys, 18: 35310 (NP-14043)
effects of medium exposure to, on chick embryo cells, 20: 38707
effects of multiple radiation sickness on induction of lesions in dog gastrointestinal tract, 20: 40645
effects of multiple and single doses of, on blood coagulation in rabbits, 20: 45326
effects of, on adrenocortical steroid synthesis in rats, whole-body, 17: 15808
effects of, on adrenal gland in rats, 17: 23104
effects of, on alkaline phosphatase activity of sebaceous gland in guinea pigs, 17: 17853
effects of, on antibody responses to influenza virus in mice, 17: 14043
effects of, on antibody cell response to antigens in radiochimeras in mice, 17: 17871
effects of, on antibody formation in rabbits immunized with bacteriophage ϕX 174, 17: 21518
effects of, on antibody formation, 17: 30399
effects of, on arterial blood pressure in cats and dogs, effects of drugs on, 17: 23216
effects of, on autolysis of DNA and RNA in bone marrow in rabbits, 17: 12139(T)
effects of, on blood serum density in rats, 17: 17909
effects of, on blood cells in chicks, effects of folic acid, tetracycline, and vitamin B_{12} on, 17: 31954
effects of, on bone marrow regeneration in parabiotic rats, 17: 17861
effects of, on bone marrow and gonads in mice and monkeys, protective effects of cysteamine against, 17: 19913
effects of, on Bromsulfalein conjugation with glutathione in rat bile, 17: 17859
effects of, on buccal cells in rabbits, sensitizing effects of testosterone on, 17: 15666
effects of, on calcium metabolism in rabbits, 17: 19790 (TID-18422)
effects of, on capillaries in tongue in frogs, 17: 23194
effects of, on carbohydrate, protein, and RNA metabolism in rat lens, 17: 17726
effects of, on carbon-14-labeled orotic acid uptake by Ehrlich ascites cells, 17: 17817
effects of, on cardiovascular malformations by destruction of regions behind heart rudiments in chick embryos, 17: 17850
effects of, on catabolism of hexobarbital in mice, 17: 17716
effects of, on cell elements in bone marrow and spleen in mice, 17: 23131
effects of, on central nervous system in rats, 17: 14045
effects of, on central nervous system of rabbits and rats, effects of rate on, 17: 21551
effects of, on chick embryos and mouse ascites tumors and testis, relative, 17: 12143
effects of on children exposed *in utero*, 17: 10875
effects of, on chromium-51 uptake by mice, protective effects of serotonin against, 17: 14021
effects of, on cleft palate development in mouse embryos, 17: 21482
effects of, on conditioned and non-conditioned reflex reactions in leukocytes, 17: 12149
effects of, on coronary arteries of hypercholesteremic rabbits, 17: 21476
effects of, on course of *Trypanosoma lewisi* infection in rats, 17: 15573
effects of, on cytoplasm of distal tubule cells of kidneys in mice, 17: 15713
effects of, on degeneration and regeneration of peripheral nerves in rabbits, 17: 12160
effects of, on denerved and normal legs of rabbits, 17: 19824
effects of, on density of blood serum in rats, whole-body, 17: 21548
effects of, on differentiation and induction of spermatogenesis in grasshoppers, 17: 14040
effects of, on digestive rudiments in chick embryos, 17: 17849
effects of, on distribution of potassium in rat tissues, 17: 15687
effects of, on DNA content in fibroblasts and HeLa cells in rabbits, 17: 14013
effects of, on DNA synthesis and mitosis in rat lens epithelium, 17: 21485
effects of, on DNA synthesis by *E. coli*, effects of chloramphenicol on, 17: 23127
effects of, on dogs, protective effects of bone marrow infusions or lead shielding against lethal, 17: 21581
effects of, on double helix in DNA, 17: 19827
effects of, on *E. coli*, oxygen enhancement ratio for, 17: 12144
effects of, on *E. coli*, protective effects of bacterial fermentation compounds against, 17: 17802
effects of, on elimination of dextran from blood plasma in rabbits, 17: 17731
effects of, on enzyme activity and mortality of rats, protective effects of chemicals against, 17: 19875
effects of, on epilation in mice, protective effects of chemicals against, 17: 17818
effects of, on erythropoiesis in rats, reactivation effects of cobalt on, 17: 15810
effects of, on erythrocytes, protection against, using nonreducing agents, 17: 17942
effects of, on erythropoiesis depression in rabbits, protective effects of splenectomy against, 17: 21559
effects of, on estrous, ovaries, and vagina in rats, 17: 21481
effects of, on fertility of male mice, effects of olive oil on, 17: 12154
effects of, on glomerulus and proximal tubule of kidneys, in mice, 17: 15712
effects of, on glutathione content in lens of eye in cattle and pigs, 17: 17864
effects of, on glycogen and reducing compounds in yeasts, 17: 12162
effects of, on glycogen metabolism in skin of dogs, 17: 17852
effects of, on guinea pig skin, protective effects of serotonin and related compounds against, 17: 21504
effects of, on heart in therapy of chest tumors in man, 17: 17786
effects of, on hematopoietic cells in mice and salamanders, microcinematography method for determination of, 17: 21542
effects of, on immune reactions to injected bone marrow in mice, 17: 35315(R) (HW-76000(p.167-73))
effects of, on incidence and latent period of leukemia in mice, 17: 15724
effects of, on incidence of mammary and ovarian tumors in mice, 17: 17819
effects of, on intestines and skin of rats, relative biological, 17: 12145
effects of, on intercapillary glomerulosclerosis in young mice, 17: 17862
effects of, on leukemia and secondary syndrome in mice, effects of bone marrow transfusions on, 17: 14011
effects of, on leukemic mice, protective effects of bone marrow and chemical agents against, 17: 14019
effects of, on leukocytes in peripheral blood in rats, effects of ribonucleic acid on, 17: 15692
effects of, on leukemia in rats induced by extracts from human leukemic tissue, 17: 17681
effects of, on Leydig cells in rats, 17: 15693
effects of, on lipid metabolism in liver in dogs, 17: 17904
effects of, on liver in mice, protective effects of 2-methylpiperazine dithioformate against, 17: 15809
effects of, on loss of soluble materials from lymphocytes in rat thymus, 17: 23110
effects of, on lungworm larvae vaccines in cattle, 17: 21423
effects of, on lymphocyte polysaccharides and serum glycoproteins in guinea pigs, whole-body, 17: 14008
effects of, on meiosis of *L. esculentum* and *L. peruvianum*, 17: 19833
effects of, on metabolism of nucleic acids in liver and spleen in rats, effects of injected DNA on, 17: 13929
effects of, on methemoglobin formation in hemolysates and erythrocytes with different catalase concentration, 17: 17840
effects of, on mice, protective effects of spleen cell injection or splenectomy on, 17: 15811
effects of, on mice, effects of lipoxidase and olive oil on, 17: 15813
effects of, on mice and rats, mechanism of protective effects of cysteamine against, 17: 19876
effects of, on mitosis in crystalline lens in rabbits, 17: 15818(T)
effects of, on mitosis of kidney cells cultured *in vivo*, 17: 21501
effects of, on mutations in *Neurospora crassa*, 17: 15652
effects of, on nervous systems, 17: 17887
effects of, on nervous system of rats exposed *in utero*, 17: 21508

effects of, on nicotinic acid metabolism in rats, 17: 14050
effects of, on oocyte maturation in ovaries in mice, 17: 15816(T)
effects of, on organs and skin of guinea pigs, effects of radar waves on, 17: 21545
effects of, on ovaries in mice, local and whole-body, 17: 12169
effects of, on oxidative phosphorylation in mitochondria, effects of dinitrophenol on, 17: 12137
effects of, on oxidative phosphorylation in kidney and liver in rats treated with homogenates, 17: 17890
effects of, on oxygen consumption in chickens, rabbits, and rats, whole-body, 17: 14071
effects of, on parasite multiplication and tissue culture mitosis, 17: 21495
effects of, on peripheral blood in guinea pigs after acute bleeding, 17: 7808
effects of, on pericardium, in treatment for pulmonary carcinoma, 17: 19818
effects of, on peroxide formation in barley and bean seedlings, 17: 23129
effects of, on phenotypic expression of isoantigens of H-2 system in embryonic and newborn mice, 17: 21519
effects of, on protein-bound mercapto groups in testis in rats, 17: 17788
effects of, on reactivity of cerebral cortex in monkeys, 17: 17908
effects of, on repopulation of bone marrow and spleen cells during serial transfer in mice, 17: 23130
effects of, on serum aldolase activity in rabbits, variation with open field and with grate of, 17: 17875
effects of, on serum lactic dehydrogenase activity in rats, 17: 17789
effects of, on skin of pigs, fractionated and single, 17: 12146
effects of, on skin and tumors, reduced oxygen enhancement effect in, 17: 12147
effects of, on skin epithelium in young axolotls, 17: 14000
effects of, on skin, follow-up studies of occupational, 17: 17916
effects of, on somatic segregation from heterozygous diploids of *Penicillium chrysogenum*, 17: 17886
effects of, on staphylococci injections on rabbit skin, 17: 21520
effects of, on sterility in mice, cause of, 17: 19910
effects of, on sulfur-35 uptake and distribution by rat tissues, 17: 21437
effects of, on survival of rats receiving heterotransplants of Ehrlich ascites tumor, 17: 17868
effects of, on synthesis of serum proteins in mouse/rat chimeras, 17: 19843
effects of, on testes in mice, fractionated and single dose, 17: 19911
effects of, on thermal denaturation of DNA in mice, 17: 21539
effects of, on thymidine uptake by spleen in rats, effects of erythropoietin on, 17: 19853
effects of, on transduction by *Salmonella typhimurium* phage P22, 17: 23203
effects of, on *Trichinella spiralis*, immunity in mice, 17: 15654
effects of, on tumors in rats, oxygen effect in, 17: 12142
effects of, on tympanal mesenchyme cycle in ear of rats, 17: 21487
effects of, on urinary formaldehydogenic steroid levels in rats, protective effects of ACTH against, 17: 23099
effects of, on 5-hydroxytryptamine in small intestine in guinea pigs, mice, rabbits, and rats, 17: 15705
effects of oxygen on recovery of tumor cells from damage by, 20: 45409
effects of parasitism and, on Tribolium populations, 19: 21987
effects of parental exposure to, on life spans and reproduction in non-irradiated mouse progeny, 20: 45394
effects of partial cell exposure to, morphological and biochemical, 19: 17565
effects of penicillin-resistant *E. coli*, 18: 3531
effects of pituitary gland exposure to, on adrenal gland and excretory system, 18: 95
effects of pituitary exposure on excretory systems in rats, 18: 96
effects of porphyrin on sensitivity of mouse sarcoma to, 20: 40657
effects of post-surgical, on bronchial carcinomas, 20: 24958
effects of pre- and postnatal, on locomotor behavior and neuromorphologic anomalies in rats, 20: 40688
effects of prenatal exposure to, on subsequent gonadal hormone secretion by rats, 20: 22595
effects of prenatal exposure on audiogenic seizures in rats, 17: 1288
effects of protracted low-level ancestral exposure of mice to, on sensitivity to gamma radiation, 17: 5777 (TID-15181)
effects of pulsed on turn-off characteristics of silicon-controlled rectifiers, 18: 648 (D2-9878-3(Sect.F))
effects of pulsed, on peroxidation of *p*-xylene, 20: 43369
effects of pulsed, on amplitude distribution of boron trifluoride counters, 20: 43756
effects of pulses of, on electronic properties of silver chloride surface layers, 19: 35867 (NYO-2471-2)
effects of repeated sublethal doses of, on radioresistance and radio-excitability in rats, 18: 25127
effects of seed exposure, on characteristics and kernel composition of soybeans, 17: 27071(T) (OTS-62-11755/2(p.99-100))
effects of sieve exposure of rabbit testis to, 19: 15290
effects of sieve-controlled, on rabbit ears, 20: 18357
effects of single and repeated exposure on gonads of mice and rats, 18: 17623
effects of single dose at 7500 r on the oxygen consumption of chicken embryo intestine, 18: 25124
effects of single and fractionated doses on tumor induction in mouse thymus, 20: 42892
effects of single or fractionated dose of, on testicular development in mouse embryos, 17: 37066(T) (JPRS-20960)
effects of single and fractionated doses of, on hematopoietic system in mice, 17: 40628
effects of small dosages on blood picture, 16: 4063
effects of small doses on leukocyte chromosomes in man, 18: 25163
effects of soft, on homogeneous tissue, 18: 11786
effects of soft, on excitation threshold of frog nerves, mechanisms for, 20: 42868
effects of solar nonflare, in ionospheric D region, 18: 42537
effects of spermatogenic line of mice, protective effect of 2-(2-aminoethyl)-2-thio-pseudourea, 17: 28726
effects of spleen exposure on peripheral blood picture, 16: 8577
effects of spleen exposure on response of chronic lymphatic leukemia patients to phytohemagglutinin, 20: 6843
effects of synthesis of histone and DNA in cell nuclei, 18: 8151
effects of therapeutic doses on induction of radiation sickness, 16: 8652
effects of therapeutic doses of, on morphology of bone marrow, 18: 3656
effects of therapeutic doses of, on human skin, 18: 21945
effects of therapeutic doses of, on morphology of bone marrow cells, 18: 33399
effects of therapeutic doses of, carcinogenic, 20: 3841
effects of therapeutic doses of, on oral mucosa, 20: 3744
effects of therapeutic doses of, on enzyme activity of tumors, 20: 3763
effects of therapeutic doses of, on intestine, pathological, 20: 3820
effects of therapeutic doses on cytology of normal and neoplastic oral cells, 20: 8750
effects of therapeutic doses of, delayed carcinogenic, 20: 16242
effects of therapeutic, on spinal cord, pathological, 20: 20545
effects of therapeutic use on excretion of β-glucuronidase, 20: 43025
effects of therapeutic exposure on thyroid function, tracer study, 17: 14033
effects of two successive exposures on tissue development of crown-gall, 16: 26782
effects of ultrahard, combined with radium on uterine carcinomas, 20: 24965
effects of various doses on rat leukocyte counts, whole-body, 20: 40697
effects of wheat gluten, rheological, 18: 3539
effects of whole-body exposure on pattern and threshold of electroshock seizures, 16: 75
effects of whole-body exposure, on activation of folic acid in liver, spleen, and bone marrow, 16: 1552
effects of whole-body exposure on kidney weight, effects of high-protein diet, 16: 5211
effects of whole-body exposure on intestinal epithelium, 16: 6309(T) (JPRS-11322(p.337-52))
effects of whole-body or head exposure on neuromotor ability, 16: 7347(R) (TID-14692)
effects of whole-body exposure on metabolic processes, 16: 7347(R) (TID-14692)
effects of whole-body exposure on enzyme activity in intestinal mucosa, 16: 7422 (ORO-503)
effects of whole-body exposure on enzyme systems of liver and spleen, in rats, 16: 7423(R) (TID-14567)
effects of whole-body exposure, on retention of cesium-137, 16: 8537 (AMRL-504)
effects of whole-body exposure, on vital staining characteristics of tissues, 16: 9847(T) (JPRS-11485(p.122-30))
effects of whole-body exposure, on liver magnesium levels, 16: 9860(T)
effects of whole-body or partial-body exposure on urinary excretion of corticosteroid and glucose, 16: 20209
effects of whole-body exposure, on carcinogenic effects of urethan, in mice, 17: 28699 (USNRDL-TR-641)
effects of whole-body repeated exposure to, on blood picture of rats, 17: 29879(R) (IA-822)
effects of whole-body, on bone marrow function, 17: 30078
effects of whole-body exposure to, on oxygen consumption by rats, 17: 38904
effects of whole-body exposure to, on leukemia incidence in mice, 17: 40630
effects of whole-body, on ascorbic acid and glutathione content in rat brain, 20: 38679
effects of whole-body exposure to, on mice protected by various agents post-irradiation, 20: 45492

effects of wide-field to trunk, pathological, 19: 32017
effects of 10-kev, on mice, 20: 20475
effects of 15-Mev, on mice, RBE for, 20: 31072
effects of 180-kev, on Chlorella, RBE for, 20: 45353 (CEA-R-2984)
effects of 200-kv, on *Escherichia coli*, relative biological efficiency in, 20: 31107
effects of, alone or in combination with 2-aminopurine and 5-bromouracil on mitosis and yield of chromosome aberrations in barley and onion roots, 20: 45400
effects of, combined with actinomycin on mouse testes, 20: 6865
effects of, combined with stilbestrol and surgery on prostate carcinomas, 20: 8765
effects of, combined with 6-purinethiol on skin graft survival in rats, 20: 10506
effects of, combined with radium therapy and surgery on cervical carcinomas, complications from, 20: 14377
effects of, combined with diethyl sulfate on barley seeds, 20: 14384
effects of, combined with radium therapy and surgery on cervical carcinomas, 20: 14409
effects of, combined with trauma on function of rabbit kidney, 20: 14325
effects of, combined with cold on cesium-137 retention in rats, 20: 16180
effects of, combined with cytostatic drugs on polycythemia, complications from, 20: 16233
effects of, combined with cyclophosphamide and hyperbaric oxygen in leukemic mice, 20: 16262
effects of, combined with magnetic fields on barley seeds, 20: 18387
effects of, combined with magnetic field on plant germination and seedling development, 20: 18388
effects of, combined with acceleration or vibrations on mitosis in mouse marrow, 20: 18439
effects of, combined with radium on cervical cancer, 20: 18309
effects of, combined with radium on cervical cancer, 20: 18550
effects of, combined with procarbazine on tumors, 20: 20504
effects of, combined with surgery on cervical carcinomas, 20: 20526
effects of, combined with gamma radiation and surgery on mammary carcinomas, 20: 22839
effects of, combined with fast neutrons on Drosophila chromosomes exchange yield, 20: 24914
effects of, combined with thermal burns on early mortality in rats, 20: 24931
effects of, combined with cyclophosphamide on rats, therapeutic, 20: 33120
effects of, combined with gamma radiation on phagocytic index in cervical cancer patients, 20: 45459
effects of, effects of BUDR on, 18: 38985
effects of, in combination with acceleration and vibrations on mouse genetics, 20: 42986
effects of, in mice, leukemogenic, 19: 2092
effects of, on developing embryos and fetuses, 19: 19699
effects of, on lymphocytes in guinea pig lymph nodes, 20: 28976
effects of, on photosensitivity of molybdenum trioxide single crystals, 20: 46235
effects of, on yield and food value of corn irradiated prior to sowing, 20: 45455
effects of, review of biological, 20: 12999 (CEA-R-2746)
effects of, review of LET and RBE in, 20: 18362
effects of, used with antibiotics on scale homograft survival in fish, 18: 19726
effects of, with vincaleucoblastine on mouse tumors, synergetic, 20: 38613
effects on abdomen and head of rabbits, irritating, 17: 27070(T) (JPRS-19806)
effects on aberration frequencies in bean root meristem cells, 16: 1587
effects on aberrations of Trillium chromosomes, 19: 3930
effects on ability of blood to induce immunological tolerance in chickens, 16: 28783
effects on ability of hookworm larvae to produce infection in dogs, 17: 33492
effects on abnormal chromosomes in leukemic patients, 18: 21878
effects on abortion, infant death, and sterility in off-spring of workers, 16: 25214
effects on absorbing capacity of reticulo-endothelial system in rabbits, effects of bleeding on, 20: 33054
effects on absorption and retention of strontium-90 by rats, whole-body, 16: 31474 (UR-617)
effects on absorption spectra of magnesium fluoride, 18: 17898
effects on absorption spectra, electron emission, and luminescence of lithium fluoride crystals, 18: 33632
effects on absorption spectra of sodium fluoride, 18: 41542
effects on absorption spectra of peritoneal dialysate from rats, 18: 41081(R) (HW-80500(p.132-3))
effects on absorption and luminescence spectra of activated alkali halide phosphors, 19: 47884(T) (IS-Trans-18)
effects on absorption spectra of activated sodium chlorides, 20: 7172
effects on absorption spectra of alkali halide crystals, 20: 21424 (N-65-23332)
effects on absorption spectra of silver, 20: 34092
effects on absorption of labeled sodium iodide by rat skin, 17: 31957
effects on absorption of fatty acids by small intestines, 17: 40505
effects on abundance of lymphocytes in blood when externally shunted blood is chronically irradiated, 20: 35308
effects on acanthosis in guinea pig skin, quality effects on, 19: 24285
effects on acceptance of transplanted fin by goldfish, *Carassius auratus*, 19: 2099
effects on acceptance of autogenous bone grafts in dogs, 19: 43835
effects on acetylene, methylacetylene, and ethylacetylene, 19: 46334 (TID-22231)
effects on acid and alkaline phosphatase activity in guinea pig skin, 19: 130
effects on acid and alkaline phosphatase and esterase activity in guinea pig skeletal muscle, 19: 19574
effects on acid and alkaline phosphastases in mouse tibiae, 20: 32943
effects on acid deoxyribonuclease activity in spleen and thymus in mice, 19: 10895
effects on acid deoxyribonuclease activity in mouse spleen and thymus, whole-body, 19: 24345
effects on acid phosphatase in Yoshida ascites sarcoma, 16: 8607
effects on ACTH and cortisone effects on phosphatide content and metabolism in rat testes, 18: 33256
effects on ACTH, magnetic, 20: 18479
effects on actinomycetes, 16: 1488(T) (JPRS-10170(p.335-60))
effects on action of cercariae in immunization against *Schistosoma japonicum* in rhesus monkeys, 19: 36045
effects on activation of amino acids from rat thymus nuclei, 18: 1385
effects on activation of green gram 3′-nucleotidase, protective effects of 2-amino-2-hydroxymethyl-1,3-propanediol against, 17: 40587
effects on active and trace conditioned reflexes in rats, effects of staphylococcal toxin on, 17: 7898(T)
effects on activity of 5-hydroxytryptophan decarboxylase in mouse liver, 18: 5068
effects on activity of catalases and peroxidases in solution, 18: 13445 (MMPP-196)
effects on activity, learning, mortality, and seizure susceptibility of rats exposed *in utero*, 19: 19618
effects on activity of ATPase in mitochondria in rat heart, liver, and spleen, 19: 21869
effects on activity of mouse phagocytes, 19: 31676(R) (ORNL-3768 (p.112-18))
effects on activity of nickel hydrogenation catalysts, 19: 36521(P)
effects on activity of N-demethylase, in rat liver, 19: 43720(R) (NP-15310, pp 26-35)
effects on activity of carboxypeptidase A, 20: 46 (PRNC-40)
effects on activity of alkaline phosphatase in human leukocytes, 20: 5269
effects on activity of alanine–2-oxoglutarate and aspartate–2-oxoglutarate-aminotransferase in rat CNS and muscles, 20: 10593
effects on activity of lenticular epithelial enzymes in rabbits, 20: 10630
effects on activity of lipolytic enzymes, 20: 14279
effects on activity and synthesis of red-cell carbonic anhydrase *in vivo*, 20: 28922
effects on activity of acetyl- and butyrylcholinesterase in developing rat brain, 20: 35242
effects on activities of desoxyribonuclease and phosphatase in liver of rats, whole-body exposure, 17: 1317
effects on activity of central nervous system in rats, effects of diphtheria toxin on, 17: 7899(T)
effects on activity of bacteriophages, protective effects of sulfhydryl compounds against, 17: 23186
effects on activity of nickel carbonate catalase model, 17: 33982
effects on activity of proteolytic enzymes in mouse spleen, 17: 33631
effects on acute coronary insufficiency in rabbits by heart and whole-body exposure, 18: 6688
effects on adaptation for secondary antibody response in rabbits, 17: 7865
effects on adaptive response of rats, 20: 5319
effects on adenine nucleotide content in rat blood and liver, 20: 14270
effects on adenosinephosphoric acid levels in rat tissues, 18: 3521
effects on adenosine triphosphate synthesis in rat thymus nuclei, 17: 38796
effects on adensonine triphosphatase activity in rat liver mitochondria, 20: 40695
effects on adrenalin-forming function of sympathetic nervous system, whole-body exposure, 16: 17462(T)
effects on adrenal morphology and function in mice, 18: 17627

effects on adrenal transplant vascularization in rats, 18: 21838
effects on adrenal activity in man, 18: 25104
effects on adrenalin and serotonin secretion in rats, 18: 33277 (STI/DOC/10/28(p. 21-38))
effects on adrenal function in monkeys, 18: 43281
effects on adrenal glands used as transplants in rats, 19: 107
effects on adrenal cortex mitoses in mice, comparison of detoxified snake venom effects with, 19: 8814
effects on adrenal cortex in rats, 19: 31670(R) (NIRS-3(p.19-56))
effects on adrenal lipids in rats, 20: 6768
effects on adrenal cortex in rats, histochemical, 20: 10576
effects on adrenal cortex in dogs, 20: 14280
effects on adrenaline content in blood of dogs, 20: 28941
effects on adrenaline content in rats, 20: 28964
effects on adrenal function in rats, whole-body, 20: 38638
effects on adrenal function in hypophysectomized rats with pituitary transplants, whole-body exposure, 17: 1258
effects on adrenocortical-hypophyseo function, 17: 4406
effects on adrenocorticotropic hormone activity and ascorbic acid content in rats, 17: 23179
effects on *Aedes aegypti* cytogenetics, 18: 23262
effects on Aedes populations, 20: 12668
effects on aerobic glycolysis of thymocytes in rats, 17: 40577
effects on aerosol formation and concentration decay, 16: 33523(R) (TID-16694)
effects on afferent nerve activity in cats and rats, low-level, 19: 26107
effects on age specific mortality rate in female mice, effects of estrogen on, 17: 1301
effects on agglutination in animal, 16: 5194
effects on aging in invertebrates, mutagenic mechanism for, 18: 27119
effects on aging in rats, immobilization of proteins in, 19: 7097
effects on aging in mice, 17: 4418
effects on aging of onion seeds, 16: 17482
effects on aging of chicken embryos, 20: 36605(R) (COO-1119-5)
effects on aging simulation of adrenal cortex in hamsters, 19: 17597
effects on agricultural plants, effects of genotype and species, 20: 45393
effects on albumin synthesis in liver and blood serum albumin content in chicks, 18: 6664
effects on albumin–sulfathiazole, 18: 13847
effects on aldolase and transaminase activity in rats, 19: 15077
effects on algae, 20: 25124(R) (NYO-3383-3)
effects on algae, biological, 20: 1681
effects on alkali halide crystals containing divalent impurities, 18: 25585(T)
effects on alkali halides, mechanism of defect formation and recombination in, 18: 34280(R) (NYO-2680-1)
effects on alkali halide crystals, M′ and R′ centers from, 20: 34854
effects on alkaline-phosphatase in rats, 18: 1384
effects on alkaline phosphatase production in mouse bones, 19: 45729(R) (NYO-910-23, pp 1-111)
effects on alkaline phosphatase activity in blood, 20: 20415
effects on allergic reactions in cancer patients, 19: 21969
effects on *Allium cepa* root tips, relation of dose and two-hit aberrations, 16: 8545 (TID-14857)
effects on Allium root tip, relation to potential difference change, 18: 3532
effects on Allium permeability, 18: 11783
effects on Allium nuclei, quantitative study, 18: 41197
effects on allometry of radiosulfate metabolism and weight changes in mouse embryos, 20: 42765
effects on alloxan monohydrate single crystals, ESR spectral studies on, 20: 35530
effects on α-aminoisobutyric acid crystals at 77°K, ESR spectral studies on free radicals in, 20: 18750
effects on α-phage infected *Bacterium megaterium*, 19: 36082
effects on alterations in deoxyribonucleic acid from regenerating rat liver, *in vivo*, 16: 20199
effects on aluminate solutions, 19: 38738
effects on aluminum-doped silicon oxide, bleaching of, 18: 12742
effects on ameboid migration of human leukocytes, 16: 32800
effects on amination in rat liver and kidney following whole-body exposure, 20: 45456
effects on amino acid incorporation into normal and regenerating liver in rat, 16: 70
effects on amino acid content of developing meal worm embryos, 18: 3495(R) (TID-19463)
effects on amino acid content in blood of C_3H mouse, 18: 11718
effects on amino acid transport by lymphatic tissues, 18: 11781
effects on amino acid content in blood serum, 18: 23319
effects on amino acid metabolism in rabbits, 18: 25198
effects on amino acid metabolism in mice, protective effects of splenectomy against, 18: 27233
effects on amino acid content of wheat grains, 18: 29275(T)
effects on amino acid decarboxylase activity in liver and spleen of mice, 18: 31195
effects on amino acid content of meal worm embryos, 19: 73 (NYO-2814-1)
effects on amino acid content in nervous system of guinea pigs, prenatal, 19: 5673
effects on amino acids in blood serum of rabbits, 19: 27953
effects on amino acid synthesis in rat liver, 20: 20410
effects on amino acids, electron spin relaxation time measurements of, 20: 26997
effects on amino acids, endothermic decay of free radicals induced by, 20: 40504(R) (ORNL-3922, pp 146-60)
effects on amino acid incorporation into mouse cell nuclei of, 17: 31887
effects on aminoacyl-cRNA synthetase activity in azotobacter, 20: 22588
effects on ammonia and hydrazine, 16: 10619 (NASA-TN-D-1193)
effects on ammonium perchlorate propellants, 18: 29756
effects on ammonium fluorophosphate, ESR studies of, 20: 38949
effects on amniotic fluid content in mouse embryos, 19: 17592
effects on amoeba, recovery from supralethal, 19: 15101
effects on amphibian gastrulas, 18: 19649
effects on amyloidosis development in mice injected with casein, 17: 25046
effects on Anacystis pigments, mutagenic, 20: 28958
effects on anaerobic glycolysis in mouse spleens, 19: 13070
effects on anal fin rays in *Oryzias latipes*, 19: 102
effects on anaphylactic sensitivity, whole-body exposure, 16: 26744
effects on anaphylactic shock in guinea pigs, 18: 5055
effects on anaphylactic reactions in guinea pigs, whole-body exposure, 17: 5783
effects on anatomy and function of kidney from pelvic exposure, 17: 14075
effects on Ancylostoma infectivity in dogs, 20: 22689
effects on anemia development in mice and rats, protective effects of erythropoietin against, 19: 26110
effects on anemia development in splenectomized mice injected with spleen cells, 19: 25986
effects on anesthetized mice, 18: 3545
effects on anesthetized animals, 18: 19612(T)
effects on angiomas, effects of age on, 20: 12745
effects on animal growth, protective effects of mercamine against, 19: 2175
effects on animal immunogenesis, protective effects of chemical agents against, 19: 2177
effects on animal reactivity in space, (E), 19: 3898(T) (FTD-TT-64-1077(p.234-46))
effects on animal cell cultures, protective effects of 5-bromodeoxyuridine against, 19: 7188
effects on animal cells, review on recovery from, 19: 17697
effects on animal cells, recovery from, 19: 26068
effects on animal cells in culture, genetic, 19: 25941
effects on animal cells in tissue culture, mitotic, 19: 45867
effects on animal cells in tissue culture, protective effects of cysteine and MEA against, 20: 5418
effects on animal cells in tissue culture, protective effects of aminoethylisothiuronium against, 20: 5419
effects on animal cells, biological, 20: 10650
effects on animal cells, morphological, 20: 12635(R) (NYO-2786-1)
effects on animal cells, antibodies, and viruses, review, 20: 22750
effects on animal cells in culture, effects of oxygen on biological, 20: 31123
effects on animal cells, direct and indirect, 17: 15769
effects on animal vision, 17: 35535
effects on animals, protective effects of Synkavite against, 18: 17687
effects on animals, alteration of initial, 19: 7202
effects on animals, biophysics of threshold dose for, 19: 8810
effects on animals and plants, small-dose, 19: 19516
effects on animals and man, 20: 5301(R) (UR-668, pp 1-54)
effects on animals, lethal, 20: 42934
effects on animals treated with apilac, 20: 43009
effects on annealed polyethylene crystals, mechanism of, 19: 9241
effects on anomalies in interkinetic nuclei, 16: 20215
effects on anoxic tumor cells, fractionated-dose, 18: 41142
effects on anterior hypophysis of frogs, local and whole-body, 17: 30341
effects on anthracene crystals, 20: 12893
effects on antibiotic formation by Streptomyces, 18: 38804
effects on antibody response to antigen in rats, whole-body exposure, 16: 26857
effects on antibody synthesis in spleen cells, 16: 28784
effects on antibody level and *Rickettsia prowazekii* retention in guinea pigs, 18: 17619
effects on antibody formation in animals administered antigen, 19: 12988

effects on antibody formation in diphtheria immunized rabbits, 19: 17630
effects on antibody production in rabbits, 19: 24282
effects on antibody formation in mice, 19: 24301
effects on antibody production in rabbits, 19: 26052
effects on antibody production in rabbits, 19: 33821
effects on antibody production by transferred spleen cells in mice, 19: 45986
effects on antibody formation in mice, injected with sheep erythrocytes, 20: 1661
effects on antibody response of rabbits to antigens, 20: 1680
effects on antibody formation by spleen cells of mice, 20: 6780(R) (ORNL-3853, pp 93-7)
effects on antibody production in dog kidneys, 20: 8630(R) (LF-28, pp 103-7)
effects on antibody formation in rabbits, 20: 32958
effects on antibody titers in rabbits, 20: 35254
effects on antibody production in mice, 20: 40626(R) (ORNL-3922, pp 80-3)
effects on antibody synthesis in rats, 20: 42835(R) (ANL-7136, pp 63-80)
effects on antibody production in guinea pigs, 20: 42887
effects on antibody formation to ovine luteinizing hormone in rats, 20: 45334
effects on antibody formation, bone marrow, and spleen in rats, after doses of Endoxan or Trenimon, 18: 29365
effects on antibody formation in mice, tracer study, 17: 10255(R) (TID-17648)
effects on antibody dissociation from transferred cells to serum albumin in cattle, 17: 13898
effects on antibody response to antigen, 17: 27178
effects on antibody formation in rabbits, 17: 33676
effects on antibody response in rabbits, 17: 38803
effects on antigenicity of mouse donor cells, 18: 38853
effects on antigenic properties and chemical structure of ovalbumin, 19: 8803
effects on antigenic characteristics of virus-induced mouse leukemia, 20: 3694
effects on antigenic properties of Schistosoma cercaria in monkeys and rats, 20: 24917
effects on antigen localization in rats, 20: 42835(R) (ANL-7136, pp 63-80)
effects on antigenicity of mouse liver on lymphoid cells incubated with phytohemagglutinin, 20: 40588
effects on antioxidant activity in ascites tumors, 19: 8945
effects on antithrombin activity in dog blood plasma, 19: 17521
effects on antithromboplastin and antithrombin activity in rabbits, 17: 35485
effects on antitoxin localization in rabbits, 19: 42306
effects on aortic sclerosis incidence in rabbits, 18: 17548
effects on apomixis in *Poa pratensis*, 16: 1611
effects on aqueous solutions of aniline, 19: 11211
effects on aqueous solutions of C_{18}-fatty acids, mechanism of oxidation in, 19: 13477
effects on aqueous sodium chlorite solutions, 19: 13482
effects on aqueous solutions of DNA, 19: 45729(R) (NYO-910-23, pp 1-111)
effects on aqueous solutions of ADP, 19: 45729(R) (NYO-910-23, pp 1-111)
effects on Arabidopsis, mutagenic, 19: 28010
effects on *Arabidopsis thaliana*, genetic, 20: 40710
effects on Arbacia eggs, effects of AET on, 20: 40619(R) (NYO-2740-3, pp 216-57)
effects on aromatics in boric acid glass, spectra of free radicals in, 18: 10157
effects on arousing stimulus in rats, role of olfactory system in, 19: 15140
effects on Artemia oocytes, effects of ploidy on recovery from, 20: 22618 (RT-BIO-(65)31)
effects on arterial prostheses in dogs, 20: 14344
effects on arterial prostheses in dogs, 20: 14345
effects on Ascites tumor cells, effects of light and thionine on, 18: 17413
effects on ascites hepatoma in rats, effects of diet on, 20: 8679
effects on ascites tumor antioxidant activity, 20: 40642
effects on ascites tumors, metabolic, 18: 27079
effects on ascorbic acid metabolism in organism, 16: 11480
effects on ascorbic acid content in adrenal glands in hypophysectomized rats, 18: 9855
effects on ascorbic acid content of guinea pigs and mice, 17: 37096
effects on aspartate transcarbamylase activity in *Escherichia coli*, 20: 22585
effects on Aspergillus, 20: 45338
effects on astroglial cells and blood vessels in rat brain, glycogen accumulation from, 20: 38674
effects on asynaptic rice plant cytogenetics, 18: 13543
effects on atherosclerosis development in pigeons, 18: 25087(R) (TID-20641)
effects on atherosclerosis development and lipid metabolism in pigeons, 20: 110
effects on atherosclerosis in rabbits and man, 18: 33277 (STI/DOC/10/28(p.21-38))
effects on ATP content in rat organs and tissues, 19: 17626
effects on ATP content in Tradescantia anthers, 20: 20418
effects on ATP-ase and potassium retention in rat liver erythrocytes, 19: 10849
effects on ATP, DNA, RNA, and oxidative phosphorylation in rats, protective effects of cystamine and cysteamine against, 19: 33976
effects on auricles of rabbits, 20: 20451
effects on autolysis in rat liver, protective effects of acrylamide and vinylpyrrolidine against, 19: 42370
effects on autonomic functions of vagus nerve in cats, dogs, and rabbits, 18: 41176
effects on autonomic regulatory functions of cerebellum in cats, 18: 41177
effects on autotransplants of mouse mammary adenocarcinoma, 19: 7041
effects on Avena chromosome number, 18: 38822
effects on avoidance conditioning in rats, role of autonomic nervous system in, 19: 26103
effects on avoidance behavior of rats, 20: 18339
effects on B^3 chromosomes in maize, use of A-B translocations in mutation studies on, 18: 19513
effects on *B. breslau* virulence in mice, 19: 33950
effects on *Bacillus subtilis*, effects of purine and pyrimidine on, 19: 2172
effects on *Bacillus cereus*, biochemical, 20: 14263
effects on *Bacillus cereus* endospores, 18: 38840
effects on bacteremia in mice, 20: 8721
effects on bacteriophages, effects of cysteamine and cysteine on, 16: 20293
effects on bactericidal activity of phagocytin, whole-body exposure, 16: 23462
effects on bacteriophage formation in *Escherichia coli*, 16: 30266
effects on bactericidal activity of fixed phagocytes in liver and spleen of mice, 18: 109
effects on bacteria and yeast, synergistic action of nitrogen mustard in, 18: 1416
effects on bacteriophage, 18: 11693
effects on bacteria, protective effects of nitric oxide against, 18: 15901
effects on bacteriophage T1, effects of freeze-drying, low temperature, and sulfhydril compounds on, 18: 19634
effects on *Bacterium paratyphosum* agglutinin production in rabbits, 18: 19738
effects on bacterial DNA synthesis, 18: 21889
effects on bacterial agglutination by rabbit liver polypeptides, 18: 25110
effects on bacteriophage reproduction in *Escherichia coli*, 18: 27180
effects on bacteria, protective effects of hydrogen sulfide against, 18: 29414
effects on bactericidal activity of guinea pig serum, 18: 38851
effects on bacterial spores, mechanisms for, 19: 181
effects on bacterial luciferase, mechanism of, 19: 13088
effects on bacteriophage nuclei acid, 19: 21864(R) (TID-21679)
effects on bacteria, protective effects of magnesium ions and sulfones against, 19: 26123
effects on bacteriophage, genetic, 19: 28098
effects on bacteriophage, genetic, 19: 28099
effects on bacteriophage, biological, 19: 33840
effects on bacteriophages, 19: 35944(R) (NP-14902)
effects on bacteriophage, mechanisms of inactivation, 19: 36054
effects on bacteriophages, ESR spectra of, 20: 1623
effects on bacteria, biological, effects of p-hydroxymercuribenzoate on, 20: 1618 (NYO-3319-6)
effects on bacterial reactions to phages and viruses, target theory for, 20: 5299(R) (TID-22187)
effects on bacteriophage, inactivating, 20: 14260 (NP-15856)
effects on bacteria, effects of iodoacetamide on, 20: 18446
effects on bacteria, 20: 18481
effects on bacteriophage, genetic, 20: 22765
effects on bacteriophage, genetic, 20: 22766
effects on bacteriophage, genetic, 20: 22767
effects on bacteriophage, genetic, 20: 28948
effects on bacteriophage, inactivating, 20: 38628
effects on bacteriophage, inactivating, 20: 38712
effects on bacteriophage, inactivation, 18: 29304
effects on bacteriophage in *E. coli*, induction, 17: 12170
effects on bacteria, iodoacetamide sensitization of, 17: 12163
effects on bacteriophage properties, 17: 15790

effects on bacterial infection in dogs, 17: 27204
effects on barbiturate response in rats, effects of methysergide, 5-hydroxytryptamine, and cysteamine on, 17: 10418
effects on barium nitrate crystals, nitrate ion ESR from, 19: 38730
effects on barley seed, wave length effects, 16: 1619
effects on barley embryo roots cultured in exposed potato mash, 16: 17505
effects on barley seeds, protective effects of tyramine and tryptamine against x, 18: 3589
effects on barley seedlings, protective effects of radioresistant plant extracts on, 18: 31308
effects on barley and wheat seeds, sensitivity, 19: 15173
effects on barley seeds, genetic, 19: 36122
effects on barley seeds, genetic, 19: 45819(R) (TID-22176)
effects on barley seedlings, 20: 10619
effects on barley seeds, effects of magnetic fields on, 20: 18387
effects on barley seedlings and seeds, 20: 18411
effects on barley seeds, genetic, 20: 18418
effects on barley seeds, protective effects of carbonates and phosphates against, 20: 18435
effects on barley roots, biological, 20: 31052
effects on barley seeds, genetic, 20: 45464
effects on barley, relation of embryo structure, node position, planting depth and tillering to, 17: 10453
effects on barley, rice, and wheat, 17: 30055
effects on barley seeds, effects of temperature on, 17: 40610
effects on barley, genetic, 20: 12714
effects on barley, effects of zygosity on, 20: 40701
effects on barley, genetic, 20: 40711
effects on barley, genetic, 20: 40712
effects on barley, genetic, 20: 40717
effects on barley, induction of resistance to, 20: 18411
effects on base composition and cells of DNA, ESR spectral studies on, 20: 31014
effects on beagle reproduction as affected by aging, 18: 23341
effects on beagles, effects of thickness of central beam dose received on, 20: 113
effects on bean sprouts, oxygen pressure effects on, 19: 7094
effects on beans, genetic, (E), 19: 10824
effects on behavior, 16: 23513
effects on behavior and learning capacity of rats, 16: 32733(R) (TID-16849)
effects on behavior aging in monkeys, 18: 81
effects on behavior of aging dogs, 18: 25091(R) (UCD-472-109(p.49-52))
effects on behavior and brain electrical activity in rabbits, effects of adrenalectomy and tranquilizers on, 19: 15230
effects on behavior of reduced glutathione in rat erythrocytes, heart muscle, liver, and spleen, 19: 17650
effects on behavior and EEG in hippocampal system in cat brain, 19: 26100
effects on behavior of rats, fetal exposure, 19: 45894
effects on behavioral changes in rats, prenatal, 19: 26102
effects on behavior of parabiotic rat partners, 20: 3706 (AD-623365)
effects on behavior traits in swine, genetic analysis of, 20: 3784
effects on behavior of larvae of *D. melanogaster*, 20: 5295 (NP-15559)
effects on behavior of monkeys, 20: 8695
effects on behavior of rats, prenatal exposure, 20: 8623 (CONF-631008, pp 92-110)
effects on behavior of rats, prenatal exposure, 20: 8625 (CONF-631008, pp 118-26)
effects on behavior in monkeys, 20: 14286 (AD-625837)
effects on behavior of primates, 20: 18283 (AD-611869, pp 375-89)
effects on behavior of rats, 16: 5212
effects on behavior of rats after prenatal irradiation, 17: 17808
effects on behavior of rats, 18: 23236 (FSU-2790-15(Paper 2))
effects on behavior of rats, 18: 23237 (FSU-2690-15(Paper 3))
effects on behavior of rats, 18: 23239 (FSU-2690-15(Paper 5))
effects on behavior of rats, 18: 23240 (FSU-2690-15(Paper 7))
effects on behavior of rats, 19: 5664
effects on behavior and neural activation in rats, 17: 19809 (USNRDL-TR-624)
effects on behavior, in dogs, 17: 31863(R) (UCD-107(p.74-85))
effects on benign tumors in children, dose to attendant and patient from, 20: 13013
effects on beryl crystals, EPR and hfs from, 20: 15982(T)
effects on beryllium oxide crystals and powders, (E), 19: 26357
effects on β-glucuronidase activity and glucuronide synthesis in duodenal mucous membrane in rats, 16: 8554
effects on β-carotene in oleic acid, 18: 37011
effects on bile acids and taurine metabolism in rat liver, 20: 32944
effects on bile salt absorption in rat intestine, 19: 31716
effects on bilirubin concentration in the rat, 18: 5034
effects on bilirubin conjugation and excretion in rat liver, 18: 19632
effects on binary mixtures of benzene and alcohols at 77°K, ESR and tracer studies of, 20: 12890
effects on binding of chromium-51 by liver nucleic acids and proteins, 17: 27084
effects on biochemical events in regenerating liver, 16: 25132(R) (HW-72500(p.92-6))
effects on biochemical and physicochemical properties of hemoglobin in dogs, 16: 26796
effects on biochemical activity in thymus in mice, whole-body exposure, 16: 30241
effects on biochemical processes, small-dose, 18: 29380
effects on biochemical activity and physiological functions in dogs, 20: 20435 (CONF-650560-15)
effects on biochemicals, ESR studies of role of molecular structure in, 20: 25132
effects on biochemicals, ESR and thermoluminescence studies of, 20: 29249
effects on bioelectric activity of nerves, 16: 23503
effects on bioelectric activity in isolated rat stomachs, 19: 2141
effects on bioelectric activity in rat stomach, factors affecting x, 19: 2140
effects on biogenesis of karyokinesis, 16: 9889
effects on biological properties of globulins, 18: 6667
effects on biological half life of iodine-131 labeled *L*-thyroxine and 3,5,3'-triiodo-*L*-thyronine in rats, 18: 13479
effects on biological activity of blood serum in rats, 18: 27150
effects on biological activity of snake venom, of *Ancistrodon piscivorus*, 18: 33385
effects on biologically active amines, 19: 35950(R) (TID-22047)
effects on biological systems, effects of dose fractionation, 20: 6827
effects on biological materials, parameters of, 20: 40504(R) (ORNL-3922, pp 146-60)
effects on biological systems, standards for, 20: 43602
effects on biological and structural properties of hemic cells *in vitro*, 17: 5862
effects on biological life of injected fibrinogen, whole-body exposure, 17: 31916
effects on biometric traits in offspring of mice, 19: 42347
effects on biosynthesis and biotransformation of corticosteroids, 18: 23348
effects on biosynthesis in HeLa cells, 17: 40585
effects on bird populations, 19: 29894(R) (ANL-6971(p.215-23))
effects on birefringence induced by light in potassium chloride crystals, 18: 798
effects on bis(2-guanidoethyl) disulfide and 2-mercaptoethylguanidine distribution and metabolism in mice, 18: 19772
effects on bladder of, following therapy, 18: 38802
effects on bladder tumors, therapeutic, 19: 30020
effects on bladder cancer, therapeutic, 19: 34036
effects on bladder, 19: 36212
effects on blast cell development in lymphocytes in culture, effects of phytohemagglutinin on, 20: 6877
effects on blood and lymph circulation in dogs, 20: 33018
effects on blood-brain barrier, local exposure, 17: 30298
effects on blood cells and hematopoietic organs, 16: 60
effects on blood cells *in vitro*, 16: 26821
effects on blood circulation in eye of rabbits, 18: 8138(T)
effects on blood coagulation in rats, 18: 8140(T)
effects on blood circulation in hypothalamic region of cat brain, 18: 41174
effects on blood components of antibiotic-treated rabbits, 19: 3971
effects on blood cell count and malignant tumors in man, mice, and rats, small dose, 19: 7042
effects on blood circulation in dogs, 19: 10795
effects on blood coagulation in dogs, 19: 15024(T) (OTS-64-11410/4 (p.524-33))
effects on blood coagulation, in cancer patients, 19: 21963
effects on blood coagulation *in vitro*, 19: 28058
effects on blood circulation between parabiotic rats, 19: 45838
effects on blood coagulation in rabbits, 20: 5325
effects on blood coagulation and blood plasma, 20: 5365
effects on blood coagulation time in dogs and rats, 20: 6867
effects on blood cells, globulins, and proteins in mice, fractionated-dose, 20: 16224 (CEA-R-2848)
effects on blood coagulation in dogs and rats, 20: 20490
effects on blood coagulation in dogs, 20: 20491
effects on blood coagulation time of chronically exposed medical personnel, 20: 22749
effects on blood coagulation, reaction mechanisms of, 20: 26637 (CEA-R-2949)
effects on blood coagulation, 20: 28985
effects on blood circulation in rabbits, 20: 29010
effects on blood coagulation, 20: 31032 (CEA-R-2953)

effects on blood coagulation in rats, 20: 45376
effects on blood count and protein in animals at 3270 to 5400 r, 18: 19703
effects on blood coagulation in man, occupational, 17: 10446
effects on blood cells in silkworm larvae, 17: 30221
effects on blood cells, bone-therapy, 17: 33695
effects on blood coagulability, 17: 35474
effects on blood coagulation in rats, 17: 35583
effects on blood enzyme activity in rats following whole-body exposure, 20: 42955
effects on blood flow in human skin, telangiectasis development as repair sign in, 19: 10827
effects on blood glucose content, 19: 13037
effects on blood glycogen content, 17: 17783(T) (JPRS-18479)
effects on blood lipid levels, whole-body exposure, 16: 21975
effects on blood levels in rabbits, prolonged repeated exposure, 18: 3541
effects on blood levels of ascorbic acid, 17: 23212(R) (AD-285937)
effects on blood of medical personnel, data on, 17: 27620
effects on blood picture and gonads in cockerels, whole-body, 16: 9872
effects on blood picture in dogs and rabbits, 16: 9898
effects on blood pressure in rat, 16: 18769 (USNRDL-TR-562)
effects on blood picture and phagocytic ability of leukocytes, partial-body exposure, 16: 21952
effects on blood plasma protein in man, 16: 23412 (CEA-2132)
effects on blood pressure in rats, whole-body, 16: 25222
effects on blood platelet-endothelial adhesion in pituitary gland of rats, 16: 32724 (BNL-6229)
effects on blood picture in starch-injected and normal parabiotic rabbits, 18: 25150
effects on blood picture and body weight of rabbits, whole-body, 18: 27105
effects on blood plasma iron clearance time in sheep, whole-body, 18: 31179
effects on blood picture and constituents in dogs, 18: 35317 (RTD-TDR-63-3012)
effects on blood picture in rats, 18: 38966
effects on blood picture in guinea pigs, 18: 38854
effects on blood picture in rabbits, 18: 38963
effects on blood picture in rats, 18: 38964
effects on blood picture in rabbits, effects of diphacil on, 18: 39020
effects on blood picture in rats, effects of cell-free thymus extracts on, 19: 4003
effects on blood picture in ischemic rabbits, 19: 10916
effects on blood picture in rats, 19: 13036
effects on blood picture of hospital personnel, 19: 19525
effects on blood picture of conventional and germfree mice, whole-body, 19: 19619
effects on blood plasma creatine and creatinine content in rats, 19: 21970
effects on blood picture in radiology technicians, 19: 24317
effects on blood platelet size in dogs, 19: 31800 (UR-663)
effects on blood pressure and breathing of dogs, protective effects of drugs against, 19: 36116
effects on blood platelets, biochemical, 19: 43714 (EUR-2438.f)
effects on blood platelets, morphological, 19: 43714 (EUR-2438.f)
effects on blood protein content in rabbits, 20: 3709 (CEA-R-2865)
effects on blood picture in rabbits, 20: 5325
effects on blood picture in rabbits, 20: 3709 (CEA-R-2865)
effects on blood picture and survival in monkeys, 20: 14302
effects on blood picture of chickens, 20: 26695
effects on blood plasma proteins in Hiroshima bomb survivors, cancer patients, and personnel, 20: 36581
effects on blood picture and weight organs in mice, fractionated-dose, 17: 7819
effects on blood picture in guinea pigs, whole and partial-body exposure, 17: 21474
effects on blood picture in dog and monkey, 17: 33452(R) (ANL-6723 (p.61-2))
effects on blood plasma and skin heparin content in rats, 17: 37076
effects on blood retraction, 16: 20205
effects on blood, reinjection study on, 17: 14001
effects on blood serum protein fractions, whole-body exposure, 16: 21964
effects on blood serum proteins in rats, whole-body exposure, 16: 30235
effects on blood supply and protein synthesis in cartilage and bone, 18: 6620(R) (TID-19929)
effects on blood serum, protective effects of chemical agents against, 18: 11850
effects on blood serum protein content in rabbits, effect of infection on, 18: 23174
effects on blood serum protein content in rats, 18: 25140
effects on blood serum proteins in mice, 18: 27158
effects on blood serum proteins in guinea pigs infected with brucellosis, 18: 27025
effects on blood serum proteins in mice, 18: 29276(T)
effects on blood serum absorption and protein content in rats, 18: 33335
effects on blood serum proteins in mice, 19: 8908
effects on blood system and skin grafts in rabbits, protective effects of lysozyme against, 19: 17671
effects on blood serum complement titer in rats, 20: 6767
effects on blood serum, measurement of, by consumption of complement of a Paramecium culture, 20: 32932
effects on blood serum proteins, chemical, 20: 36579
effects on blood serum proteins in gestating hamsters, 20: 38598(R) (TID-22955)
effects on blood serum proteins of patients with cervical carcinoma, therapeutic dose of, 20: 45531
effects on blood serum protein levels, whole-body exposure, 17: 1354
effects on blood serum proteins, effects of age, 17: 27171
effects on blood typing sera, 20: 20425
effects on blood urea level in nephrectomized rats, protective effects of carbohydrates against, 18: 27219
effects on blood vessels in internal organs in rabbit, fractional whole-body, 16: 8592
effects on blood vessel control, whole-body exposure, 16: 23438
effects on blood vessels in mammals, 18: 27062(R) (NYO-1680-1)
effects on blood vessel permeability, tracer study in dogs, 18: 41192
effects on blood vessel circulation in rat mesentery, effects of topical agents on whole-body, 19: 17501
effects on blood vessels in mice, pathological, 19: 36023
effects on blood vessels around joints, 20: 31163
effects on blood vessels in neck of rabbits, 20: 45373
effects on blood volume, whole body exposure, 17: 21566
effects on blood-brain barriers in rabbits, 19: 45970
effects on blood-serum and hepatic proteins, biochemical, 17: 15770
effects on blood, extracorporeal-exposure, 20: 28927 (BNL-9647)
effects on blue-green algae sensitivity to isoniazid and streptomycin, 19: 35966
effects on body and renal weight in nephrectomized mice, 20: 16282
effects on body fluids in rats, physiological, 19: 40369
effects on body growth and incisor development in rats following head-only exposure, 20: 45350 (AD-640158)
effects on body temperature of mice, 18: 38817(T)
effects on body water content in rabbits, 19: 12973
effects on body weight and tumor incidence in mice irradiated embryonically or fetally, 20: 22724
effects on bone composition in mice, 18: 33276(R) (NYO-910-7)
effects on bone growth in rats, 16: 8615
effects on bone growth in rats, 18: 77
effects on bone growth in children and dogs, therapeutic dose, 18: 8218
effects on bone growth in rabbits, 18: 36957(R) (UCRL-11387(p.140-51))
effects on bone growth in rats, 20: 3707 (AD-623641)
effects on bone growth in rats, protective effects of MEG against, 20: 12729
effects on bone growth in rats, 20: 20486
effects on bone growth in rats, 20: 24875
effects on bone growth in parabiotic rats, 20: 26652 (AD-632540)
effects on bone growth, 17: 7789 (BNL-6595)
effects on bone growth and calcium uptake, tracer study, 17: 30308
effects on bone marrow cells in rats, 16: 4097
effects on bone marrow synthesis of desoxyribonucleic acid in rat, 16: 14558
effects on bone marrow myelopoietic precursors, 16: 14562
effects on bone marrow and phosphorus-32 uptake in rabbit, 16: 14569
effects on bone marrow and iron-59 uptake by red blood cells in rats, relative biological, 16: 17516
effects on bone marrow transplantations in dogs, effects of 6-mercaptopurine and urethan on, 16: 26869 (USNRDL-TR-571)
effects on bone marrow repopulation in rabbit chimeras, 18: 13526
effects on bone marrow functions in rats, 18: 17558
effects on bone marrow repopulation in man and mouse, 18: 19592
effects on bone marrow and leukocyte chromosomes, 18: 27075
effects on bone marrow transplants in mice, 18: 31207
effects on bone marrow in mice, 18: 43282
effects on bone marrow of mice in combination with low-frequency vibration, cytological, 19: 2103
effects on bone marrow in rats, quantitative distant and indirect, 19: 7036
effects on bone marrow cells of mice, 19: 17494(T) (FTD-TT-64-1316 (p.205-16))
effects on bone marrow cells in culture, 19: 31784 (EUR-2415.e)
effects on bone marrow cells in mice, 19: 33911
effects on bone marrow in mice, pathological, 20: 5320
effects on bone marrow of leukemia patients, fibrotic, 20: 10746
effects on bone marrow in man, 20: 18381
effects on bone marrow, effects of lysozyme on, 20: 18494
effects on bone marrow stem cells, pathological, 20: 22703

effects on bone marrow megakaryocytes and thrombocytes in rats, 20: 22625
effects on bone marrow cells in rats, effects of splenectomy on, 20: 24881
effects on bone marrow in rabbits, hematological, 20: 38633
effects on bone marrow and peripheral blood cells in chickens, 20: 45324
effects on bone marrow allografts in dogs, 18: 8209
effects on bone marrow cells in atomic bomb survivors, 17: 5785
effects on bone marrow and lymph system in guinea pigs compared with encephalomyelitis virus, 17: 10427
effects on bone marrow, tracer study, 17: 23019
effects on bone marrow lipid levels, whole-body exposure, 17: 24970
effects on bone metabolism in rats, 20: 42785
effects on bone, effects of dose fractionation on tumor induction by, 17: 40641
effects on bone, tumor induced by, 17: 40590
effects on bones in young rabbits, 16: 31506
effects on bones in rats, effects of pituitary growth hormone on, 17: 33663
effects on bones of therapeutic doses, pathological, 20: 3856
effects on bones, blastomogenic, 19: 36183
effects on bones, mechanism for osteomyelitic, 20: 20371
effects on bovine serum albumin denatured by heat and urea, 19: 27977
effects on brain and nervous system of monkeys, 18: 8102 (BNL-7620)
effects on brain and skeleton malformations in mice exposed *in utero*, 19: 17646
effects on brain and central regulation of electrocardiogram, 20: 42925
effects on brain cells, biochemical, 19: 10786(R) (TID-21440)
effects on brain content of 5-hydroxytryptamine in rats and mice, 17: 27110
effects on brain, damage sequence in mice, 16: 23481
effects on brain development in mouse embryos, 19: 10794
effects on brain excitability, whole-body exposure, 16: 1555
effects on brain electrical activity of rabbits, 19: 25987
effects on brain electrical activity in rabbits, 20: 33056
effects on brain function, whole-body exposure, 17: 5886
effects on brain function, whole-body exposure, 17: 5888
effects on brain function and serotonin levels, 17: 21524
effects on brain growth, 16: 23477
effects on brain in rats, physiopathological, 17: 10459
effects on brain lipid metabolism, whole-body exposure, 17: 5882
effects on brain of fetal rats, 16: 23473
effects on brain of rabbits, 19: 31818
effects on brain of external head exposure to, in a child, 19: 33866
effects on brain of guinea pig, histochemical, 20: 10638
effects on brain of rabbits, pathological, 20: 29011
effects on brain of rabbits receiving skin doses via slit-shaped field, 17: 38757
effects on brain of rats, prenatal-irradiation, 17: 38813
effects on brain serotonin in rats, relation of barbiturate hypnosis to, 20: 31007
effects on brain tumor cultures, 18: 29283
effects on brain tumors, therapeutic, 19: 34031
effects on brain tissues of therapeutic doses of, delayed, 20: 1713
effects on brain wave activity during conditioned activity of cats, 20: 38602(R) (UCLA-34P60-1)
effects on brain 5-hydroxytryptamine levels, whole-body exposure, 16: 17478
effects on breakdown of desoxyribonucleic acid in *E. coli*, 16: 8561
effects on breast development, 16: 20170
effects on breast tumors and myeloma in mice, potentiation effects of 5-iododeoxyuridine on, 19: 10921
effects on breast tumors prior to radical surgery, 20: 3861
effects on breeding in two-rowed barley, 19: 8915
effects on breeding characteristics of mice, 10-generation exposure of sires, 17: 27101
effects on bromine-82 and chlorine-36 exchange between ethylenediamine cobalt or rhodium complexes and hydrobromic or hydrochloric acids, 20: 38960
effects on bronchial, esophageal, and lung carcinomas, moving-beam, 20: 16317
effects on "brown spot" character in Drosophila, 17: 10379
effects on budding of yeast cells, 18: 27154
effects on bull semen of testicular, 18: 23337
effects on cable properties and functional changes in central nervous system of rats, 19: 26095
effects on cadmium- and nickel-activated sodium metaphosphate glass, spectra of ion formation in, 19: 25060
effects on cadmium sulfide single crystals, photochemical, 16: 22249
effects on cadmium sulfide single crystals, 18: 34286(T) (AEC-tr-6399 (p.186-95))
effects on calcification of cartilage in rats, 19: 2096
effects on calcium metabolism in rats, whole-body, 18: 6606
effects on calcium metabolism by bones and teeth, role of denervation in, 18: 37003
effects on calcium metabolism in rabbits, 18: 43269
effects on calcium-doped sodium chloride crystals, polarized absorption characteristics of color centers induced by, 19: 17409 (COO-1197-10)
effects on calcium metabolism in skeleton of mice, influence of age, 19: 21975
effects on calcium-45 uptake by *Nitella flexilis*, 19: 43818
effects on calcium fluoride single crystals, temperature dependence of thermoluminescence from, 20: 30767
effects on calcium–sodium chloride–silver crystals, color centers from, 20: 38396
effects on calcium fluoride crystal absorption, fluorescence, and bleaching, 20: 45006
effects on calcium-45 storage by bones in mice, 17: 4425
effects on calf thymus deoxyribonucleoprotein, chemical, 19: 13083
effects on calf-thymus DNA, protective effects of disulfides against, 20: 36665
effects on cancer of thoracic wall, 18: 27169
effects on cancer development in children exposed prenatally, 19: 7029
effects on cancer cells, 19: 10932
effects on cancer metastases in lymph nodes, 19: 26181
effects on Candida albican infection in mice, 16: 17483
effects on capacity of *Escherichia coli* to reproduce bacteriophage, 19: 70 (IAEA-R-18)
effects on capillary hematocrit findings, whole-body exposure, 16: 11434(R) (ANL-6464(p.19-21))
effects on capillary circulation, 18: 43257
effects on capillaries in frogs and guinea pigs, 17: 37123
effects on Carassius lifespans, effects of adrenalectomy and hypophysectomy on, 19: 31670(R) (NIRS-3(p.19-56))
effects on carbohydrate metabolism in liver, 16: 14500
effects on carbohydrate and fat metabolism in mice, 19: 28013
effects on carbon dioxide and oxygen balance in blood, 16: 9899
effects on carbon dioxide production in starved yeasts, effects of glucose supplementation on, 20: 1653
effects on carbon uptake by Hassall's corpuscles in guinea pig thymus, 20: 6847
effects on carbon dioxide in exchange reactions between labeled carbon dioxide and oxygen, 20: 12882 (IA-1065)
effects on carbon monoxide–oxygen–water systems, yields from x, 20: 23169
effects on carbon tetrachloride, dioxane, and hexane, ion mobilities and yields from, 20: 25141
effects on carbon dioxide, mechanism of, 20: 40996
effects on carbon dioxide production and ripening of apples, 17: 21962(T) (NP-tr-995)
effects on carbon-14-labeled L-tyrosine uptake and melanin production in tadpoles, 18: 27205
effects on carbon-14-labeled leucine uptake by cell nuclei in regenerating rat liver, 19: 15138
effects on carbon-14-labeled orotic acid incorporation into rat RNA, 20: 18263
effects on carbonic anhydrase content of rat erythrocytes, 19: 21820(R) (UCLA-12-541(p.25-44))
effects on carboxylation of n-pentane, 20: 43333
effects on carcinogenic activity of azo dyes, 18: 9937
effects on carcinogenic action of benzopyrene, 19: 13114
effects on carcinoma development in beagle thyroid, whole-body, 19: 15038
effects on carcinoma incidence in women, 19: 28036
effects on carcinomas in larynx and pharynx, 19: 42393
effects on carcinoma cell cultures, 19: 43802
effects on carcinomas of skin, concentrated serial exposure, 20: 1718
effects on carcinomas of bronchi, protracted exposure, 20: 1720
effects on carcinomas of cervix, late pathological effects of therapeutic doses of, 20: 6929
effects on carcinomas of lungs, therapeutic, 20: 8769
effects on carcinomas of cervix, evaluation of, 20: 8775
effects on carcinoma of penis, therapeutic, 20: 8766
effects on carcinomas of cervix, therapeutic, 20: 10727
effects on carcinoma of bladder, effects of dose fractionation on therapeutic, 20: 10743
effects on carcinoma of cervix during pregnancy, 20: 10751
effects on carcinostatic properties of gastric cancer extracts, 20: 12625
effects on carcinogenesis following childhood radiotherapy, 20: 18412
effects on carcinogenic effects of implanted plastic in rats, effects of exposure time on, 20: 42840(R) (ANL-7136, pp 164-90)
effects on carcinogenicity of retrorsine in rats, 17: 35488
effects on cardiac function, 20: 18328
effects on cardiovascular system in rabbits, 19: 8924
effects on cardiovascular and hematopoietic system of rats, 19: 38441
effects on cardiovascular function, therapeutic doses in cancer

patients, 17: 19860
effects on carotenoids and phthalocyanines, chemical, 19: 2376
effects on carried lifetimes in silicon, transient, 18: 36038(R) (AD-433623)
effects on carrier mobility and trap density in anthracene and polystyrene, 20: 40952 (SC-DC-66-1823)
effects on carrot tissues and tomato stems, photoreactivation of, 20: 120
effects on cartilage of developing larynx in rabbits, 19: 2082(T) (ANL-Trans-121)
effects on cartilage of rats, biological, 20: 14291(R) (TID-22494)
effects on cat brain, relation to craniocerebral injury, 18: 15818(T) (JPRS-23544)
effects on catalase activity in mouse liver, 18: 9890
effects on catalase activity in *Mycobacterium tuberculosis* strains, 18: 19607
effects on catalase activity in rats, effects of electric stimulation on, 18: 27200
effects on catalase activity of cells in tissue culture, 19: 5708
effects on catalase content in progeny of exposed mice, 19: 7014(R) (ANL-6906(p.75-7))
effects on catalase, protective effects of metal ions against, 19: 11218
effects on catalase, protective effects of dimethyl sulfoxide against, 19: 33970
effects on catalase inactivation, 18: 29244 (TID-20780)
effects on catalase accumulation in conidia of *Aspergillus niger*, 17: 10397
effects on catalytic activity of magnesium and sodium sulfates, comparison with sulfur-35 additions, 16: 227
effects on catalytic activity in silica gel, 19: 13455
effects on cataract development in rabbit eyes, pathology of, 20: 32973
effects on cataract induction, comparison of RBE of x rays with, 20: 40618(R) (NYO-2740-3, pp 166-215)
effects on catecholamine content in nervous system of rats, (E), 19: 31829
effects on catecholamine content in ground squirrels, 20: 18291 (N-65-17058)
effects on catecholamines content of rat adrenal glands and heart, 20: 28964
effects on catecholamine content in tissues in squirrels during hibernation, 17: 35504
effects on cattle and horses, general clinical, 19: 5719
effects on cattle serum, protection against, 17: 17943
effects on caudal regeneration in *Syllis amica*, 17: 5808
effects on cell aging and swelling in rat liver, 19: 7102
effects on cell biochemistry and morphology in rabbit tissue cultures, 18: 25117
effects on cell culture survival in man, pulsed-source, 19: 10876
effects on cell cycle of rat tooth germ cells, 20: 45384
effects on cell division in Ehrlich's ascites tumors, whole-body, 16: 25209
effects on cell division in corneal epithelium in mice, 18: 8142(T)
effects on cell division and morphology of algae, partial-cell exposure, 18: 13441 (BL-85)
effects on cell distribution changes in mouse bone marrow, electronic particle counting, 19: 21940
effects on cell division of the ciliate *Spathidium spathula*, 20: 40623(R) (ORNL-3922, pp 32-49)
effects on cell division in pea seedlings, 17: 10359 (HW-SA-2606)
effects on cell division and growth, 17: 27136
effects on cell growth in mouse testicles, 18: 27106
effects on cell growth and viability of carcinoma in mice, 17: 58
effects on cell homogeneity in regenerating rat livers, 19: 29926
effects on cell membranes in Nitella, light effects on, 19: 26085
effects on cell membranes, traumatic, 20: 1636
effects on cell mitosis, 16: 26760
effects on cell morphology and weight of spleen in mice, 18: 3493 (TID-18352)
effects on cell nuclei in bone marrow, synergistic effects of vibration, whole-body, 19: 38358 (AD-612660)
effects on cell nuclei, biological, 19: 45992
effects on cell permeability of onion skins, 18: 9899
effects on cell permeability in onions, effects of storage on, 19: 7076
effects on cell population kinetics and growth of *Tradescantia paludosa* roots, 19: 36028
effects on cell reorganization and repopulation in meristems in bean roots, mechanisms, 16: 7432
effects on cell structure resultant from subcellular functional changes, 18: 17610
effects on cell survival, 19: 26063
effects on cell survival in mouse sarcomas, effects of oxygen inhalation on, 20: 12725
effects on cells, 19: 17566
effects on cells at base of rat's incisor teeth at various energies, morphological, 19: 161
effects on cells from clinical and occupational exposures, 19: 42353
effects on cells in hamsters, protective effects of actinomycin D against, 18: 17665
effects on cells in flagellate *Astasia longa*, 20: 31085
effects on cells in tissue culture, metabolic, 16: 26764
effects on cells in developing beetle wing, 17: 33730
effects on cells of Ehrlich's ascitic carcinoma, radioautographic studies in mice, 18: 13482
effects on cells of bone sarcoma, morphological, 19: 245
effects on cells of transplanted mouse tumors, 20: 3750
effects on cells, tumor-growth, 17: 5824
effects on cells, mechanism for, 19: 26064
effects on cells, role of genetic damage in lethal, 20: 31042
effects on cellular differentiation, 16: 26758
effects on cellular proliferation changes in staminal hairs of *Tradescantia occidentalis*, 18: 1405
effects on cellular permeability of *Allium cepa* L. bulbs, effects of storage on, 18: 11713
effects on cellular components of rat lungs, 20: 6899
effects on cellular infiltrates of mouse liver tissues, 20: 22639
effects on cellular permeability in onions, effects of dose on, 20: 28900
effects on cellular components of rabbit liver and gastric mucosa, 20: 33060
effects on cellular composition of tissues from therapeutic doses of, 20: 38769
effects on cellular proliferation, 17: 28601
effects on cellular and nuclear growth in *Paramecium aurelia*, 17: 10408
effects on cellular permeability in coats of *Allium cepa* L., 17: 24926
effects on cellulose-decomposition activity of rumen bacteria, 16: 20206
effects on central nervous system in hamsters, brain exposure, 16: 17506
effects on central nervous system, 16: 23480
effects on central nervous system response to analgesics and other drugs, 18: 47(R) (TID-19617)
effects on central nervous system in mice, rabbits, and rats, protective effects of drugs against, 18: 5014
effects on central nervous system in dogs and monkeys, 18: 29382
effects on central nervous system of dogs and guinea pigs, microdose, 19: 3947
effects on central nervous system and endocrine stimulation in rats, protective effects of ACTH and phenobarbital against, 19: 8972
effects on central nervous system in rat embryos, *in utero*, 19: 26083
effects on central nervous system reactions in rats, 19: 31839
effects on central nervous system tissues in embryos, morphological, 20: 8620 (CONF-631008, pp 33-47)
effects on central nervous system in fetuses, morphological, 20: 8621 (CONF-631008, pp 48-81)
effects on central nervous system in embryos, morphological, 20: 8621 (CONF-631008, pp 48-81)
effects on central nervous system in cats and rats, 20: 18292(R) (N-65-17068)
effects on central nervous system in normal and parabiont rats, 20: 22720
effects on central nervous system, review of research on, 20: 22687
effects on central nervous system in rats, whole-body, 20: 26671
effects on central regulation of automatic functions in rabbits, 20: 38654
effects on central nervous system, fine-structure study, 16: 9810
effects on central nervous system in rats, histopathological, 17: 7902(T)
effects on central nervous system, exposure of head, 17: 5887
effects on central nervous system in monkeys, whole-body, 17: 12176
effects on central nervous system of rat embryo, 17: 15745
effects on cercaria, production of immunization against Schistosoma in rhesus monkey, 16: 14402
effects on cerebellar defects in mice, 18: 11740
effects on cerebellum development in mice, 18: 23284
effects on cerebellar granule in rats, 17: 7871
effects on cerebral cortex and subcortex of prenatally exposed rabbits, 16: 25247
effects on cerebral cortex in rats, 16: 31398(R) (ANL-6535(p.113-20))
effects on cerebral cortex bioelectric activity, 18: 23308
effects on cerebral cortex in mice, 19: 170
effects on cerebral cortex function development in rats exposed *in utero*, 19: 17618
effects on cerebral cortex in fetal rats, effects of fractionated and single exposure on, 20: 24920
effects on cerebral cortex of monkeys, 20: 36656
effects on cerebral cortex of rats exposed as fetuses, 17: 19899
effects on cerebral content of adenosinephosphoric acids in rats, 17: 35563
effects on cervical nerves, whole-body exposure, 16: 23442
effects on cervical and bladder cancer, mega- and supervoltage *vs.* kilovoltage, 20: 5451
effects on cervical carcinomas, therapeutic, 20: 8773

effects on cervical carcinomas, cytological, 20: 12659
effects on cervical carcinomas, 20: 14409
effects on cervical cancer, 17: 33751
effects on cesium bromide crystals, thermoluminescence from, 18: 39340
effects on cesium bromide color centers at low temperature, 19: 40098
effects on cesium monoiodide crystals, emf from, 20: 40335(T)
effects on chain scission and hydrogen bond breakage in DNA, 19: 34236
effects on Chang liver cells, 18: 21835
effects on changes in domain structures of Rochelle salt crystals, 19: 44031(T)
effects on changes in different types of nervous systems in rats, 17: 7895(T)
effects on charge transfer between ions in crystals, 19: 40575
effects on charge distributions in silicon oxides, 20: 37285
effects on chemical composition of brain tissues, 16: 26829
effects on chemical composition of brain tissues, 16: 26831
effects on chemical conversion in uranium salt solutions, 16: 3321(T) (AEC-tr-4497(p.145-59))
effects on chemical properties of fatty acids, 18: 17557
effects on chemical and physical properties of rat blood, 19: 38440
effects on chemical reactions between 3,4-benzopyrene and DNA, 20: 18788
effects on chemiluminescence induction in organic compounds in presence of oxygen, 19: 46344
effects on chick embryo development, 18: 37005
effects on chick embryos, protective effects of compounds against, 19: 10920
effects on chick embryos from eggs exposed to, 20: 5306
effects on chick embryos, pathological, 20: 6895
effects on chick embryos, pathological, 20: 12706
effects on chick embryos, effects of inoculation with smallpox virus vaccine on, 20: 14281
effects on chick embryos, pathological, 20: 29012
effects on chicken lifetime and size, 18: 31252
effects on chicken embryos, direct and indirect, 19: 91
effects on chicken heart myoblasts, 20: 24936
effects on chicken embryos and post-hatching growth of survivors, 20: 29015
effects on chickens, biological, effects of breed on, whole-body, 20: 38677
effects on chickens, pathological, 20: 42833(R) (ANL-7136, pp 16-46)
effects on chicken body weight, genetic transmission to progeny, 20: 45427
effects on chicks, comparison with gamma rays, 18: 29539
effects on children, epilating dose, 19: 2124
effects on children, pathological, 19: 10883
effects on children, carcinogenic, 20: 8767
effects on children in Israel, leukemogenic, 20: 22678
effects on chinchillas, biological, 20: 6900
effects on Chinese hamster cells recovery from acute vs chronic, 18: 35354
effects on Chinese hamster cells, recovery from, 19: 26073
effects on Chinese hamster cells, protective effects of serum in media against, 20: 14400
effects on $CHI_3 \cdot 3S_8$, protective effects of sulfur, 17: 19923
effects on chloral hydrate, 18: 1737
effects on chlorates, electron paramagnetic resonance study of defects induced in, 19: 24568(T)
effects on Chlorella, genetic, 20: 3716(T) (JPRS-31514, pp 65-76)
effects on Chlorella pigmentation, mutagenic, 20: 22674
effects on chloride ion excretion in rats, 19: 3967
effects on chlorine-substituted ethylenes, 16: 8762 (TID-14851)
effects on chlorine exchange between chlorine gas and sodium chlorides, 19: 2344
effects on chlorine-35 NQR in sodium chlorates, 20: 20118
effects on chlorine-36 exchange between rhodium complexes and chlorides, 20: 20706
effects on chlorophyll synthesis in leaves, 16: 26818
effects on chlorophyll mutation rates in barley, 20: 3782
effects on cholesterol metabolism in rats, 19: 19511(T) (JPRS-29364(p.1-4))
effects on cholesterol metabolism in rat muscle and spleen, 19: 26017
effects on cholesterol and fatty acid synthesis in rats, effects of adrenalectomy on, 19: 29921(T)
effects on cholesterol metabolism in rat testes, 19: 33863
effects on cholesterol content in rat blood, 20: 28992
effects on cholesterol content in rat tissues, 20: 28995
effects on cholesterol-blood complexes in dogs, 20: 28998
effects on cholesterol and fatty acid synthesis in liver in rats, 17: 5792
effects on cholesterol content in adrenal gland, in rats, 17: 40646
effects on cholic acid excretion by liver in rats, tracer study, 20: 78
effects on cholinesterase activity in blood serum and liver, 16: 4076
effects on chorioallantoic membrane in chick embryo, 16: 1546
effects on chromatid aberration induction in Tradescantia, 19: 5657
effects on chromatin structure and histone components of rat thymocyte nuclei, 19: 7077
effects on chromatin anomalies in HeLa cells, protective effects of organophosphorus derivatives against, 20: 20515
effects on chromium oxidation state in acetone, 19: 7571
effects on chromium, manganese, and nickel contents in dog blood, liver, and spleen, 19: 17537
effects on chromium divalent and tetravalent ion content in rubies, 20: 12305
effects on chromium metabolism in mice, tracer study, 17: 30312
effects on chromosomes of rat liver, 16: 7433
effects on chromosome structure and stability, 16: 9891
effects on chromosomes and mitosis in carcinoma and onion root cells, effects of synkavite on, 16: 14555
effects on chromosomes in mice tumor cells with chloramphenicol post treatment, 16: 17540
effects on chromosomes and nucleoli in rat liver, 18: 11772
effects on chromosomes, protective effects of thymidine against, 18: 11773
effects on chromosomes in man and mouse, 18: 19583
effects on chromosomes, biological, 19: 2062 (BNL-8462)
effects on chromosome abnormalities and pollen grain sterility in jute, 19: 5680
effects on chromosome transfer during conjugation in *E. coli* strain, 19: 7054
effects on chromosome rearrangement in *Chrysanthemum carinatum*, 19: 7074
effects on chromosome aberrations in Trillium, 19: 8866
effects on chromosome aberrations in Trillium, 19: 8867
effects on chromosomes in giant cells induced in Chinese hamsters *in vitro*, 19: 10850
effects on chromosomes in human cells in culture, 19: 12964
effects on chromosomes of *Sorghum vulgare* seeds, 19: 13085
effects on chromosomal breakage in Vicia, hydroxylamine effects on, 19: 15129
effects on chromosome aberrations in barley, effects of 2,4-dinitrophenol on frequency of, 19: 15093
effects on chromosome rearrangements in *Crepis capillaris* seedlings, reproduction and structure of, 19: 17610
effects on chromosome breakage in *Crepis capillaris*, 19: 17614
effects on chromosome aberration induction in male *Drosophila*, effects of AET, glutathione, and MEA on, 19: 17557
effects on chromosome damage in man, effects of time in culture on *in vivo*, 19: 17559
effects on chromosome aberrations in human leukocytes, 19: 19596
effects on chromosomes of human thyroid tumor, 19: 21903
effects on chromosomes, aberrant, 19: 26063
effects on chromosomes in insects, 19: 28070
effects on chromosomes in human leukocytes, aberrant, 19: 31792(R) (ORNL-3768(p.94-8))
effects on chromosome breakage in hamster cells, 19: 31864
effects on chromosome number in HeLa cells, continuous, 19: 31850
effects on chromosomes in plant cells, protective effects of nutrients, 19: 33874
effects on chromosomal DNA in human cells as related to mutagenicity, 19: 33829
effects on chromosomes in rat embryos, 19: 35989
effects on chromosomes in Tradescantia, genetic, 19: 36016
effects on chromosome aberrations in barley and *Vicia faba*, modifying effects of acridine orange and methylene blue on, 19: 38462
effects on chromosomes in Tradescantia, synergism with infrared radiation on aberrant, 19: 38416
effects on chromosome break induction in barley, interaction in, 19: 38399
effects on chromosomes, dose-response equations for aberrant, 19: 42290
effects on chromosome aberrations in apical root-tip cells of *Vicia faba*, 19: 42269
effects on chromosome replication in *E. coli*, 19: 43741
effects on chromosome aberrations in leukocytes, 19: 45915
effects on chromosomes of lymphocytes in man, morphological, 19: 45916
effects on chromosomes of lymphocytes in man, morphological, 19: 45917
effects on chromosomes of leukocytes in tissue culture, 20: 88
effects on chromosomes in mouse fibroblasts, effects of culture density on aberrant x, 20: 3691
effects on chromosomes in man, 20: 3705(R) (AD-617601)
effects on chromosomes in leukocytes in humans, monkeys, and rabbits, 20: 5304(T) (JPRS-32985, pp 45-50)
effects on chromosomes in fish embryos, pathological, 20: 6819
effects on chromosomes of cells in culture, 20: 8666
effects on chromosomes of Vicia, x, 20: 8667
effects on chromosomes of barley seeds, 20: 8702
effects on chromosomes in human blood, pathological conditions affecting,

20: 8707
effects on chromosomes of Vicia roots, genetic, 20: 8720
effects on chromosomes in Vicia roots, effects of N-ethylmaleimide on, 20: 10624
effects on chromosomes in hypothermic mice, mutagenic, 20: 12693
effects on chromosomes in Vicia root-meristem, dose-response parameters for aberrant, 20: 18350
effects on chromosomes in Ehrlich ascites tumor cells, oxygen enhancement ratio for, 20: 18352
effects on chromosomes in Tradescantia pollen grains, morphological, 20: 20438 (EUR-2518.f)
effects on chromosomes in radiographic personnel and their families, 20: 20447
effects on chromosomes of bone marrow cells, 20: 22582
effects on chromosomes in cultured leukocytes, 20: 22614(R) (NIRS-4, pp 28-34)
effects on chromosomes in mouse bone marrow, 20: 22649
effects on chromosomes in human leukocytes, 20: 26672
effects on chromosomal bridges at anaphase in barley seeds and Tradescantia, 20: 29031
effects on chromosomes in Vicia, genetic, 20: 31124
effects on chromosome aberrations in mouse embryo fibroblasts exposed at different phases of mitotic cycle, 20: 35271
effects on chromosomes in cultured blood leukocytes from Down's-syndrome and normal patients, 20: 35273
effects on chromosomes of human lymphocytes, 20: 38615
effects on chromosomes in Chinese hamster cells and human leukocytes, 20: 40628(R) (ORNL-3922, pp 89-93)
effects on chromosomes, repair mechanisms for, 20: 40609 (CONF-660418-1)
effects on chromosomes in Drosophila oocytes, frequency of crossover-suppressing aberrant, 20: 40625(R) (ORNL-3922, pp 59-64)
effects on chromosome aberration frequency in cultured kidney cells, 20: 42837(R) (ANL-7136, pp 124-40)
effects on chromosomes in *Crepis capillaris* sprouts, 20: 42936
effects on chromosomes in *Vicia faba* roots, genetic, 20: 45386
effects on chromosomes in *Vicia faba*, 18: 33318
effects on chromosomes, RBE for aberrant, 18: 41228
effects on chromosomal patterns in normal and leukemic mice, 17: 23118
effects on chromosomes in root tips of *Avena sterilis*, 17: 27087
effects on chromosome fragmentation, 17: 31935
effects on chromosome aberrations in regenerating rat liver, effects of hypothermia on, 17: 38748 (USNRDL-TR-666)
effects on chronic inflammation in rabbits, long-term, 19: 10862
effects on chrysanthemum, mutagenic, 19: 5646
effects on chrysanthemums, mutagenic, 19: 5653
effects on chrysanthemum, (E), 19: 15141
effects on Chrysanthemum chromosomes, aberrant, 20: 22645
effects on chymotrypsin kinetics, 18: 19666
effects on circulating stem cells in mice partial body, 19: 10853
effects on *Cl. perfringens*, genetic, 19: 38445
effects on coagulation factors in rat blood, 19: 28095
effects on coaxial cables and electric condensers, method for reduction of, 20: 5805(R) (AD-617782)
effects on coenzyme I content in chick embryo heart, 19: 3922
effects on coenzyme A in bone marrow of rats, 18: 21859
effects on coenzyme A content in mice, protective effects of chemicals against, 17: 38837
effects on coercive magnetic field of Rochelle salt, 20: 3995
effects on collagen and luciferase-luciferin at –20 to 30°C, 19: 15196
effects on collagen metabolism and urinary excretion of pyrrole-2-carboxylic acid in rats with polyethylene sponge implants, 19: 17553
effects on collagen in skin of hamsters, 20: 5330
effects on collagen gel, 20: 14593
effects on collagen, determination by magnetic resonance spectroscopy, 20: 36585
effects on collagen levels in muscle, local exposure, 17: 1265
effects on collagen maturation in urinary bladder, local exposure, 17: 1266
effects on collagen fraction in rat skin, 17: 1329
effects on collagen fraction in atrophic muscle, 17: 10465
effects on colloidal systems and suspensions, 20: 4015
effects on colony formation in tissue cultures of animal cells, 19: 35997
effects on colony formation by green algae, 20: 8701
effects on colony development in animal cells, cytological analysis of, 17: 24927
effects on colony-forming cells among spleen colonies in mice, 19: 120
effects on color and phosphorescence of borate glass, 20: 31283
effects on color and x-ray luminescence of calcium fluorides as function of temperature, 20: 42556
effects on color centers in potassium bromides and chlorides at low temperatures, prolonged, 18: 20668
effects on color center formation in potassium chloride crystals, 19: 22362
effects on color center formation in sodium chloride crystals, 19: 34239
effects on color center formation in ionic crystals, 19: 34241
effects on color center formation and emission spectra of alkali halide crystals, 19: 34242
effects on color center formation in ionic crystals, 19: 34250
effects on color centers and luminescence of silver-activated alkali halides, 19: 34251
effects on color center formation in potassium chlorides, 19: 34253
effects on color centers and luminescence of silver-activated alkali halide crystals, 19: 34254
effects on color center induction in sodium silicate glass, effects of cerium on kinetics of, 19: 42912
effects on color center distribution in potassium chloride crystals, 19: 46371
effects on color center formation in sodium fluoride crystals, 20: 1908
effects on color centers in potassium and sodium chlorate single crystals, 20: 7143
effects on color center formation in quartz, uv re-excitation of, 20: 10233
effects on color center development in sodium fluoride at 80 and 200°K, 20: 20106 (COO-1044-23)
effects on color center formation in potassium chloride crystals, 20: 26979
effects on color centers in alkali-halide crystals, 20: 32691
effects on color center formation in lithium fluorides, 20: 34847
effects on color centers, crystal structure, and optical properties of potassium chloride crystals, 20: 43306
effects on color center formation in lithium fluoride, 20: 46940 (AD-640317)
effects on color centers in quartz, 19: 32048(R) (NP-15073)
effects on color of quartz crystals, 19: 18551
effects on color of bile pigments, 19: 5638
effects on color-center destruction and recombination luminescence in silver-doped sodium chlorides, 20: 32693
effects on color-center, destruction and recombination luminescence in calcium–silver activated sodium chlorides, 20: 32694
effects on coloration and thermoluminescence of borate glasses, relation between, 19: 39244
effects on coloration and d-c conductivity of pure and doped sodium chloride crystals, 20: 38373
effects on coloring and luminescence of ionic crystals, (E), 19: 27717
effects on colorless and pigmented bacteria, lethal, 20: 18361
effects on compensatory hypertrophy of rat kidney, 16: 8586
effects on compensatory hypertrophy of rat kidney, abscopal, 19: 26000
effects on compensatory mechanisms of nervous system in labyrinthectomized rabbits, 20: 26643
effects on competence of gastrula ectoderm in batrachia, 17: 5807
effects on complementary components of blood in guinea pigs, 16: 1508
effects on complement content of blood serum of rats, 19: 27973
effects on complement content of blood serum of rats, 19: 27983
effects on complement content of blood serum of rats, 19: 27984
effects on composition and thermal resistance of rabbit blood serum, 18: 31283
effects on concentration of oxidized and reduced TPN in rat organs, 20: 18343
effects on conditioned behavior in fish, 16: 18792
effects on conditioned reflexes in normal and bromide-treated dogs, 18: 33319
effects on conditioned emotional responses in rats, x, 19: 10853
effects on conditioned saccharin aversion in rats, 19: 17598
effects on conditional behavior in rats, low dose, 19: 26104
effects on conditioned response to rats, 19: 26105
effects on conditioned-reflex activity of dogs exposed *in utero*, 20: 1627(T)
effects on conditioned behavior in parabiont rats, x, 20: 16284
effects on conditioned reflexes in rats exposed *in utero*, 20: 20492
effects on conditioned aversion to saccharin in rats, 17: 23162
effects on conditioned avoidance behavior of rats, effects of prior saccharin habituation on, 17: 23182
effects on conductivity of cadmium sulfide single crystals, 18: 37767(T) (AEC-tr-6398(p.192-8))
effects on conductivity of halogen derivatives of benzene and methane in diethyl ether, 19: 30278
effects on conductivity of cadmium sulfide and cadmium selenide, electron-hole pair separation energy and quantum yield from, 20: 24627(T)
effects on congenital deformities in mice, 17: 17764(R) (TID-18338)
effects on conjugation of steroids by liver and kidney, whole-body exposure, 17: 24888(R) (COO-227(p.151-69))
effects on connective tissue, whole-body exposure, 16: 14592
effects on connective tissue cells, metabolic, 19: 45895
effects on connective tissue of rabbits, effects of vasoconstricting drugs on, 20: 38640
effects on content of phosphorus compounds in rabbit brain, 18: 3528

effects on content of free amino acids in rat brain, whole-body, 18: 11629 (NADC-MA-6315)
effects on content and molecular structure of glycogen in rat liver, 18: 29353
effects on content of 5-hydroxyindolyl compounds in rat brain, 19: 7100
effects on content of 17-ketosteroids in blood plasma, 19: 7144
effects on content of chromium, magnesium, and nickel in dog tissues, 19: 19540
effects on content of diphtheria and tetanus antibodies in guinea pigs, 19: 24283
effects on content of trypsin inhibitor in dogs, 19: 33828
effects on content of glutamic-pyruvic transaminase and glutamic-oxalacetic transaminase in blood serum of mice, 19: 36012
effects on content of monoamine oxidase in rat brain, 19: 35950(R) (TID-22047)
effects on content of glycoprotein in blood serum of rats, 20: 14378
effects on content of nucleic acids in *Escherichia coli*, 20: 31023
effects on content of 5-hydroxyindoleacetic acid and 5-hydroxytryptamine in rat urine, 20: 32946
effects on content and metabolism of phosphoproteins in denerved and intact muscles in rabbits, 20: 36602
effects on content of various lipids in rat tissues following lethal dose of, 20: 38701
effects on content of lymphocytes and morphology of thymus of infant mice, 20: 42880
effects on contractive ability of mitochondria, 20: 10678
effects on conventional and germ-free mice, 19: 25908 (ORNL-P-81)
effects on copper and zinc content and enzyme activity in blood of mammals, 20: 16222 (AFWL-TR-65-112)
effects on copper and iron contents of rat serum, 20: 24855
effects on copper-64 metabolism in rats, 18: 41082(R) (HW-80500(p.138-9))
effects on corrosolum-induced brain seizures in rats, 17: 30340
effects on cork layer formation on wounded cortex of sweet potatoes, 17: 36097
effects on corn seeds, metabolic, 16: 1492(T) (JPRS-10170(p.405-17))
effects on cornea of young axolotls, 18: 1418
effects on cornea and lens of eyes in newborn mice, pathogenesis of *in utero*, 19: 13032
effects on cornea of salamanders, pathological, 20: 82
effects on corneal mitosis in mice, partial and whole-body exposure, 18: 17629
effects on corneal graft reaction in rabbits, 19: 36080
effects on corneal graft material, 20: 3719
effects on coronary occlusion leading to heart damage in rabbits, 19: 17552
effects on corrosion properties of metals and alloys, 18: 8900
effects on corrosion of quartz by hydrofluoric acid, 18: 42132
effects on cortical response of rats, 19: 33879
effects on corticosterone levels in rats, 18: 35266(R) (UCLA-12-529 (p.41-7))
effects on corticosterone levels in rat adrenals and plasma, 19: 5703
effects on *Cosmos bipinnatus*, mutagenic, 19: 21912
effects on course of candidiasis (moniliasis) of lungs, 16: 5173(T) (JPRS-11242(p.115-19))
effects on course of skin infection in rabbits, 18: 23315
effects on course of viral diseases in mice, 18: 29243 (TID-20774)
effects on course of lead poisoning in rats, 19: 31835
effects on course of anthrax infections in rabbits, 19: 33836
effects on course of intercapillary glomerulosclerosis in mice, 19: 38409
effects on course of leukemia in man and mice, whole-body, 20: 1700
effects on course of leukemia in man and mice, whole-body, 20: 1701
effects on course of bacteremia in mice, 20: 12704
effects on course of homologous disease in mice, whole-body exposure, 17: 17889
effects on cranial bones, 18: 33338
effects on creatine and creatinine electron spin resonance of free radicals in, 18: 12194
effects on creatine excretion in thyroparathyroidectomized rats, 18: 15876
effects on creatine metabolism in rats, 19: 5705
effects on creatine metabolism in man, 20: 32931
effects on creatinuria incidence in rats, 16: 31499
effects on creatinuria incidence in adrenalectomized rats, 17: 40616
effects on *Crepis capillaris* chromosomes, aberrant, 20: 22671
effects on crop plants, protective effects of chemicals against seed, 19: 43877
effects on crown-gall regeneration in Scorsonere, protective effects of RNA growth factor against, 19: 31914
effects on crypt cell survival in mice, 18: 1389
effects on crystal structure of germanium-activated quartz, 18: 20587
effects on crystalline acrylonitrile, chemical, 19: 485
effects on crystal structure of alkali metal halides, 19: 14091(R) (TID-21625)
effects on crystallographic parameters of potassium iodate and triglycine sulfate, 19: 13501
effects on crystalline sugars, 20: 4020
effects on crystals of alkali metal halides, (E), 20: 13973(R) (NYO-3033-1)
effects on crystals of deuterated glycine, controlled-temperature ESR spectral studies on, 20: 16525
effects on crystal orientation in ethylene and propene polymers, 20: 40949(R) (NYO-3003-29)
effects on crystal structure of barium, calcium, and strontium molybdates, EPR studies of, 20: 45759
effects on cultural mammalian tumor cells, potentiation effects of hadacidin on, 19: 15155
effects on culture media, 16: 20204
effects on cultured human cells, modification of, 18: 11880
effects on cultured KB cells, 20: 16258
effects on cultured hamster and HeLa cells, lethal effects of colchicine on, 20: 40618(R) (NYO-2740-3, pp 166-215)
effects on cultured neoplastic mast cells, 20: 42834(R) (ANL-7136, pp 46-63)
effects on cultured hamster cells, biological, 20: 42841(R) (ANL-7136, pp 266-89)
effects on cyanidine pigment in *Maranta leuconeura* leaves, (E), 19: 40362
effects on *Cyathodium tuberosum*, mutagenic, 19: 45901
effects on cyclonucleotide formation in adenosine monophosphate, 20: 32950
effects on cysts in guinea pigs, 18: 21857
effects on cytochrome c in eyes, 20: 18261(T)
effects on cytochrome c oxidase and glucose-6-phosphatase activity in rat liver, whole-body exposure, 20: 20417
effects on cytochrome c content in mitochondria, 20: 22586
effects on cytochromoxidase and succinic dehydrogenase activity in liver, nervous system, and skeleton in rabbits, fractionated, 17: 31979
effects on cytology and structure of bone marrow in rats, whole-body, 16: 23429 (BNL-5032)
effects on cytology HeLa tumor cells, 18: 9898
effects on cytolytic and transforming abilities of Polyoma virus, 20: 38702
effects on cytoplasm of wasp Habrobracon eggs, 16: 28751(R) (TID-16471)
effects on cytoplasmic movement, 18: 23274
effects on cytoplasmic streaming in plant cells, 19: 8900
effects on cytoplasmic budding in human lymphocytes, 19: 8821
effects on cytoplasmic organelles, 19: 26154
effects on cytoplasmic streaming in Nitella, 19: 25958
effects on cytoplasm in chick embryo muscle, effects of dose on, 20: 14321
effects on cytoplasmic streaming in *Nitella flexilis* Ag., 17: 24919
effects on cytoplasmic streaming in cell adjacent to irradiated one, 17: 24921
effects on cytoplasmic organelles in rat liver cells, 17: 40582
effects on cytotoxins of *in vitro* KB cells, 17: 38818
effects on D-glucose absorption by intestines in active and hibernating ground squirrels, 19: 45841
effects on dacron prostheses, 20: 14345
effects on daily rhythm of mitosis in root tips of *Vicia faba*, 19: 8878
effects on *Datura stramonium*, 18: 13522
effects on death process and longevity in grain weevils, 20: 45466
effects on decarboxylase activity and protein content of mouse livers, 20: 12782
effects on deesterification and light scattering properties of orange pectin nitrate, 17: 33983
effects on defect induction in sodium azide, ESR spectral studies on, 20: 15942 (NYO-2150-11)
effects on defects in potassium chlorate monocrystals, 20: 20117
effects on deficiency and translocation induction in *Drosophila melanogaster*, effects on crossing over, 19: 15090
effects on deformed potassium chloride crystals, color centers induced by, 19: 11721 (CONF-543-20)
effects on degradation process in DNA, repeated, 18: 19656
effects on degradation of DNA in *E. coli*, 20: 31015
effects on dehydrogenase, diaphorase, and phosphatase activities in kidney, abdominal exposure, 16: 55
effects on dehydro-ascorbic acid metabolism in rabbit, 16: 14582
effects on dehydrogenase activity in rat tissues, 16: 26661(R) (NP-11966 (p.65-78))
effects on dehydrogenases and transaminases in sporulating *B. subtilis*, 18: 15845
effects on dehydrogenase activity in liver of rats, 18: 38811
effects on dehydrogenase activity in rat liver and spleen, 18: 43286
effects on dehydrogenase activity in rats, 17: 37097
effects on dehydrogenase activity in rats, protective effects of shielding on, 17: 38761

effects on delayed hypersensitivity in guinea pigs and rabbits, 20: 36655
effects on delocalization in normal and substituted cytosine and guanine, 19: 30269
effects on δ-aminolevulinic acid synthetase in chicken erythrocytes, 19: 24276
effects on denaturation of desoxyribonucleic acid extracted from *Escherichia coli*, 17: 5855
effects on density and oxidation properties of plutonium nitrides, 19: 11679
effects on density changes and F-center concentration in potassium chlorides, 20: 20163
effects on dental caries, 16: 4121
effects on dental caries, 16: 12885(T) (FTD-TT-62-183)
effects on dental lesions in rats whole-body exposure, 17: 19807 (USNRDL-TR-620)
effects on dentinogenesis in rats, fractionated, 19: 28023
effects on deoxynucleoproteins in *Bacterium coli*, 19: 19576
effects on deoxyribonuclease activity in liver, mitochondria, and spleen, 18: 43289
effects on deoxyribopolynucleoproteins in animal tissues, 19: 29933
effects on deoxyribonucleoproteins in rabbit cornea, 20: 32961
effects on depolymerization of bacterial desoxyribonucleic acid, 19: 36083
effects on depolymerization of rat-liver DNA, prevention of, 17: 30364
effects on deposition of injected fibrinogen in rats, tracer study, 20: 18294(R) (TID-22766)
effects on depression and enhancement of hemolysin response in rabbits, effects of antigens on, 19: 7099
effects on depth perception in rats, 19: 33878
effects on descendants of irradiated male rats, 19: 26054
effects on desoxyribonucleic acid synthesis, 16: 6292(T) (JPRS-11322(p.1-21))
effects on desoxyribonucleic acid in thymus, 16: 8621
effects on desoxyribonucleic acid synthesis, 16: 8560
effects on desoxyribonucleic acid, 16: 1807 (NP-10955)
effects on desoxyribonuclease activity of liver and spleen in rats, 18: 8124(T) (JPRS-22613(Del.)(p.12-28))
effects on desoxyribonucleic acid content of bone marrow in guinea pigs and rats, 18: 13541
effects on desoxyribonucleic acid content and morphology of lymph nodes in guinea pigs, whole-body, 18: 25102
effects on desoxyribonucleic acid synthesis in bone marrow and tumor cells in rats and mice, 18: 25166
effects on desoxyribonucleic acid synthesis in bone marrow and tumor cells in rats and mice, 18: 25173
effects on desoxyribonucleic acids of rat spleen, whole-body, 18: 25084 (NYO-2568-1)
effects on desoxyribonucleic acid synthesis in mouse spleen *in vitro*, 18: 25186
effects on desoxyribonucleic acid in RNA polymerase system, tracer study of, 18: 41103
effects on desoxyribonucleic acid from bacteriophage, 19: 70 (IAEA-R-18)
effects on desoxyribonuclease content of rat thymus and spleen, 19: 5659
effects on desoxyribonuclease content of liver and spleen in mice, 19: 13059
effects on desoxyribonucleic acid metabolism in rat liver and intestinal cells, 19: 19506 (TID-21703)
effects on desoxyribonucleic acid in bacteriophages, 19: 35944(R) (NP-14902)
effects on desoxyribonucleic acid synthesis in carcinoma cells, 19: 35982
effects on desoxyribonucleic acid, EPR studies of, 19: 42539
effects on desoxyribonucleic acid content of cells of corneal epithelium of rats, 20: 1633
effects on desoxyribonucleic acid synthesis in *Escherichia coli*, 20: 1639
effects on desoxyribonuclease activity in rat spleen, 20: 10622
effects on desoxyribonucleotide content of mouse and rat bone marrow, spleen, and thymus, single and repeated exposure, 20: 10633
effects on desoxyribonucleic acid content in rat thymus, 20: 14311
effects on desoxyribonucleoproteins at molecular and supermolecular levels, 20: 28908
effects on desoxyribonucleic acid synthesis and mitosis in epidermis of mice, tracer study, 17: 59
effects on desoxyribonucleic acid synthesis in rat cells, whole-body, 17: 30342
effects on desoxyribonucleic acid in *Escherichia freundii*, reaction mechanisms, 17: 31899
effects on desoxyribonucleic acid, 17: 31922
effects on desoxyribonucleic acid synthesis in bean roots, 17: 38794
effects on destruction of endotoxins by tissues in rats, 17: 33709
effects on deuterated and normal methane in presence of argon, krypton, and xenon, 20: 379
effects on development of Ephestia larvae, 16: 25134(R) (HW-72500 (p.102-3))
effects on development, growth, and sensitivity of Yoshida ascites sarcomas, 16: 25221
effects on developing brain and nervous system, 16: 28830
effects on development of Morgan's toxinfection in monkeys, 16: 30244
effects on developing germ cells in male Drosophila, fast and fractionated-dose, 18: 8157
effects on development of limb skeleton in chick embryos, 18: 9834 (TID-20063)
effects on developing hematopoietic system in mouse embryos, 18: 17625
effects on development of leukemia in mice protected by cells from high-leukemia-incidence strain, 18: 21912
effects on development of transplanted tumors in rats, 18: 25197
effects on developing chick embryos, 18: 27107
effects on developing fetuses, 18: 27144
effects on developing nervous system in rat embryos and fetuses, 18: 31251
effects on development of snail eggs, 18: 38835
effects on development of snails exposed as eggs, 18: 38836
effects on development of rat oocytes, 19: 3913(T)
effects on development of fish eggs, 19: 5662
effects on developing skeleton, 19: 7109
effects on developing ear of salamanders, 19: 8864
effects on development of sarcomas in guinea pigs, chronic, 19: 8891
effects on development of continuous variation in *Drosophila melanogaster*, 19: 10888
effects on development and course of osteonecrosis of cranial vault in man, long-term, 19: 12995
effects on development of phosphorothioate-oxidizing enzyme in liver of young rats, 19: 13089
effects on development of runt disease in mouse intestine, 19: 15108
effects on development of mammary gland in pregnant mice, 19: 17617
effects on developing embryos, 19: 19466
effects on developing hematopoietic tissues in chick embryos, 19: 21959
effects on development of maize seeds, 19: 21870
effects on developing fetus, 19: 27964
effects on development of neuroblast cells of salamanders, 19: 28026
effects on development of fetuses, in rats, 19: 28042
effects on developing connective tissue, 19: 29888(R) (ANL-6971(p.59-82))
effects on development of embryos of the cockroach, *Blaberus craniifer*, 19: 29903(R) (TID-21877)
effects on developing embryos, 19: 29987
effects on development of amphibian embryos, 19: 33809
effects on development of grasshopper embryos, 19: 33813
effects on developing fetuses, of mice and monkeys, 19: 31787(R) (NYO-2740-2)
effects on developing gonads in male rats, 19: 35972
effects on development of oocytes in insects, head exposure, 19: 36060
effects on development of algae, morphological, 19: 36067
effects on development of algae, morphological, 19: 36068
effects on developing nerves, in insect larvae, morphological, 19: 43849
effects on developing fetuses and ovaries, 20: 214
effects on development of wheat embryos, 20: 1666
effects on development of myelitis, 20: 3771
effects on development of bones in children, pathological, 20: 3808
effects on development of teeth, in monkeys, 20: 3743
effects on developing fetuses, pathological, 20: 5476
effects on development of axial skeleton and spinal cord in salamanders, 20: 5312
effects on development of chick embryos, 20: 6881
effects on development of mouse embryos, 20: 6785(R) (ORNL-3853, pp 128-40)
effects on developing central nervous system in fetuses, biological, morphological, and physiological, 20: 8622 (CONF-631008, pp 82-91)
effects on development of central nervous system in fetuses, 20: 8619 (CONF-631008, pp 2-36)
effects on development of central nervous systems in fetuses, 20: 8620 (CONF-631008, pp 37-47)
effects on development and growth of maize following seed exposure, 20: 10613(T) (NP-tr-1344)
effects on developing mouse fetuses, effects of dose on, 20: 12683
effects on developing mouse embryos, pathological, 20: 12650
effects on developing mouse fetuses, pathological, 20: 12650
effects on development of *Oryzias latipes* females, effects of steroids on, 20: 16263
effects on developing rat brain, pathological, 20: 16275
effects on development of mouse embryos, 20: 22614(R) (NIRS-4, pp 28-34)

effects on developing nerve cells, 20: 22620(R) (TID-22823)
effects on development of ulcer and epithelioma following radiotherapy for lymphoma, 20: 35377
effects on development of barley seeds, 20: 38736
effects on development of mice exposed *in utero*, 20: 40619(R) (NYO-2740-3, pp 216-57)
effects on development of monkeys exposed *in utero*, 20: 40619(R) (NYO-2740-3, pp 216-57)
effects on development of *Heterakis gallinarum* embryos, 20: 40667
effects on development of experimental allergic encephalomyelitis in rats, 20: 40728
effects on development of rats exposed *in utero*, pathological, 20: 42879
effects on development of autoimmunity following radiotherapy, 20: 43027
effects on development and growth of chicken embryos, 20: 45414
effects on development of thiophosphate-oxidizing enzyme system in livers of rats, 17: 13969(R) (NP-12484(p.15-25))
effects on development of transplanted tumors in rats, whole-body, 17: 5860
effects on development of planaria, 17: 5789
effects on development of larvae of *Ephestia kuehniella*, 17: 7790 (HW-SA-2281)
effects on development of *Bombyx mori* eggs, 17: 7829
effects on development of eye pigmentation in young mice, 17: 7847
effects on developing eye in embryos, 17: 7848
effects on development of enzyme system in rat liver, 17: 23080(R) (NP-12760(p.1-12))
effects on development of glomerulosclerosis in mice, 17: 23163
effects on development of liver metastasis after tumor cell injection, 17: 26974
effects on development of transplanted mouse eggs, 17: 27117
effects on development of hyperostosis interna and ovarian tumors in mice, 17: 28747
effects on development and activity of enzyme systems in liver of rats, 17: 33482(R) (NP-13010(p.11-22))
effects on developing brain in rats, 17: 35565
effects on developing rat embryos, pathological, 17: 35569
effects on development of awn characteristics and fatuoids in oats, 17: 38843
effects on development of segmentary heterochromia of eyes of children exposed *in utero*, 17: 40648
effects on dichloroacetamide, ESR studies of coupling in, 20: 43297
effects on *Dictyocaulus filaria* larvae, immunologic, 19: 42275
effects on dielectric loss factor of polytetrafluoroethylene, 18: 8888
effects on dielectric properties of cordierites and beryls, 18: 40022
effects on dielectric permittivity of triglycine sulfate single crystals, (E), 19: 18541
effects on dielectric and optical properties of potassium sodium tartrates, 19: 23139
effects on dielectrics and lattice constants of lithium fluoride, effects of dose on, 20: 43307
effects on dietary patterns, whole-body exposure, 16: 18780
effects on different Drosophila strains, 20: 32994
effects on diffusion in guinea pig skin, effects of induced hiberation on, 17: 24908
effects on digestive processes and excretion in dogs operated by Pavlov or Heidenhain methods, 20: 45402
effects on digestive function of intestinal epithelium in rats, 20: 45332
effects on digestive tracts of rats on different diets, 17: 37027(T) (JPRS-21171(Del.)(p.14-23))
effects on dilute aqueous solutions, 17: 10717
effects on dimethylglyoxime, ESR spectra of radical pairs induced by, 19: 4207
effects on diphosphorpyridine nucleotide content in organs and tumors of rats, 18: 27148
effects on diphosphopyridine nucleotide metabolism in liver and Ehrlich ascites tumor cells in mice, whole-body exposure, 17: 68
effects on dipicolinic acid content in *Bacillus cereus* spores, 20: 35240
effects on diploid mutation induction in *Oenothera berteriana*, trisomic mutants in descendents of, 19: 33943
effects on diploid and haploid Saccharomyces, biological, 20: 18405
effects on diploid and polyploid species of wheat, genetic, 20: 45395
effects on dislocation motion in alkali halide crystals, acoustic attenuation study of, 18: 34276 (NP-14129)
effects on distant chromosomes in mouse bone marrow, 20: 18356
effects on distribution and specific activity of enzymes in rat spleen fractions, whole-body, 16: 17491
effects on distribution of phosphorus-32-labeled staphylococcus, 19: 2127
effects on distribution of colloidal gold-198 in lymph nodes in guinea pigs, 19: 27961
effects on distribution of heat-killed *Mycobacterium smegmatis* in mice, 20: 10655
effects on distribution of transplantation antigens in mice, effects on skin graft survival, 20: 24930
effects on distribution of strontium-90 and yttrium-90 in tissues in mice, 17: 19848
effects on division cycle of algae, 19: 7075
effects on division and growth rate of *Paramecium aurelia*, 19: 15137
effects on DNA, 18: 37002
effects on DNA, 19: 10910
effects on DNA, 20: 14283
effects on DNA, 20: 38542(T) (UCRL-Trans-10029)
effects on DNA activity in rat liver and spleen, effects of cysteine on whole-body, 20: 35249
effects on DNA activity on catalase extracted from rat liver, 20: 45343
effects on DNA and RNA content in chick embryo, 16: 25207
effects on DNA and RNA in liver and spleen, 16: 25208
effects on DNA and RNA in HeLa cells, tracer studies of, 18: 31139
effects on DNA and RNA in rabbit bone marrow, autolytic, 19: 10809(T)
effects on DNA and nucleoprotein synthesis in rat testes, 19: 38370
effects on DNA and RNA metabolism in rat spleen, 20: 18341
effects on DNA and RNA contents in liver and spleen of rats, 20: 35326
effects on DNA bases, protective effects of amino acids against, 18: 27216
effects on DNA binding capacity of hemoglobin, 19: 5704
effects on DNA catabolism in rats, 20: 5382
effects on DNA content in rat liver, effects of ploidy on, 20: 18260
effects on DNA content and weight of mouse kidneys, 20: 22726
effects on DNA content and mitotic activity in rat kidneys, 20: 24909
effects on DNA content of *E. coli*, 20: 45323
effects on DNA degradation in *E. coli*, 18: 19641
effects on DNA, direct and indirect, 16: 28804
effects on DNA from rat kidney, spleen, and thymus, 20: 6762
effects on DNA in vitular thymus, latent, 18: 3552
effects on DNA in *Escherichia coli*, 19: 2077(R) (ORNL-3700(p.180-6))
effects on DNA in bacteria, 20: 45(R) (EUR-2471.1)
effects on DNA in *E. coli*, 20: 14265
effects on DNA in *Micrococcus radiodurans*, 20: 18269
effects on DNA in *Escherichia freundii* in culture, effects of chemical content of medium, 17: 27113
effects on DNA, local, 17: 30353
effects on DNA metabolism in rats, 20: 26690
effects on DNA mitosis and synthesis on onion root tips, 18: 29399
effects on DNA molecule, site and mechanism of action, 20: 42821
effects on DNA, nucleoproteins, and RNA content in organs and tissues in chickens, 17: 31955
effects on DNA phosphorus-32 uptake in tumor cells, 18: 5049
effects on DNA polymerase activity, 18: 13507
effects on DNA priming ability in RNase system, 19: 45849
effects on DNA replication in *E. coli*, effects of amino acid deprivation and chloramphenicol on, tracer study, 20: 6836
effects on DNA solutions from calf thymus, 18: 17566
effects on DNA susceptibility to DNase and uptake in Ehrlich ascites carcinoma cells, 18: 5062
effects on DNA synthesis, 18: 1398
effects on DNA synthesis and mitosis in Ehrlich ascites tumor cells, 18: 8182
effects on DNA synthesis, inhibitory effects of guanine and thymidine on, 18: 11761
effects on DNA synthesis in viral-infected tissue cultures, 18: 15835
effects on DNA synthesis in rat liver, whole-body, 18: 17583
effects on DNA synthesis and mitosis in antigen-injected mice, 18: 36986
effects on DNA synthesis in regenerating rat liver, 19: 15184
effects on DNA synthesis in rats with partial hepatectomy, dose rate relation in, 19: 21947
effects on DNA synthesis and DPN content in ascites tumor cells, 19: 28041
effects on DNA synthesis in guinea pigs and rats, 19: 29934
effects on DNA synthesis, review on, 19: 31892
effects on DNA synthesis in rat liver as function of time, 20: 12638 (TID-21474)
effects on DNA synthesis in mammalian cells, 20: 16230(R) (TID-22644)
effects on DNA synthesis in human cell cultures, 20: 18264
effects on DNA synthesis in embryonic mouse cells, 20: 18265
effects on DNA synthesis in HeLa cells, effects of DNA replication on, 20: 18267
effects on DNA synthesis and DPN content in Ehrlich ascites carcinoma cells, tracer study, 20: 18270
effects on DNA synthesis in normal and tumorous tissue, 20: 18271
effects on DNA synthesis in mouse ascites tumor cells, 20: 18266
effects on DNA synthesis in hamster organs, 20: 22630
effects on DNA synthesis in rat liver, 20: 22576 (TID-21907)
effects on DNA synthesis in intestine and liver of rats, x, 20: 22577 (TID-21908)
effects on DNA synthesis in regenerating rat liver, 20: 22578 (TID-21914)

effects on DNA synthesis in uterine epithelium of mice, 20: 31088
effects on DNA synthesis in rat body and kidneys, systemic factor in recovery from, 20: 32952
effects on DNA synthesis in intestines and liver of rats, effects of dose rate on, 20: 32942
effects on DNA synthesis in regenerating rat liver, mechanism of, 20: 36593
effects on DNA synthesis in rat tissues, 20: 38576 (TID-22103)
effects on DNA synthesis in chick fibroblasts and myoblasts, 20: 40587
effects on DNA synthesis in peripheral blood cells in rabbits, 17: 10291
effects on DNA synthesis and DPN content in tumor cells, 17: 33639
effects on DNA transforming activity, rescue of, 19: 3909
effects on DNA transforming activity, 20: 22613(R) (NIRS-4, pp 21-8)
effects on DNA transforming activity, 20: 45321(R) (SAN-632-1)
effects on DNA uptake of carbon-14-labeled adenine in bacteria, 19: 27952(T) (OTS-63-11455/3-4(p.111-16))
effects on DNA-ase activity in mouse urine, 19: 28005
effects on DNA-ase and RNA-ase activity in Ehrlich ascites cells, 20: 38578
effects on DNA-strand scission in *E. coli*, effects of 5-bromodeoxyuridine on, 20: 35245
effects on DNA, effects of purine deprivation on, 20: 18256
effects on DNA, phosphatase, and RNA in cerebral nerve cells in rats, 20: 31010
effects on DNA, quantum biological analysis of, 19: 31670(R) (NIRS-3(p.19-56))
effects on DNA, repair mechanisms for, 20: 36578 (ORNL-P-2240)
effects on DNAse activity in rat thymus, 20: 14311
effects on dodecahydrotriphenylene inclusion compounds, 20: 9011
effects on dog arteries, auto- and homovenous repair of, 20: 20478
effects on dog behavior, 19: 5702
effects on dog blood count, 18: 17597
effects on dog gall bladder, 18: 38819
effects on dog glucose tolerance, 18: 11778
effects on dog heart, pathological, 19: 45835
effects on dog hemopoiesis when used with decortication, 18: 19733
effects on dog immunity to anthrax, 18: 15858
effects on dog intestinal motor function, chemical prophylaxis for, 18: 17643
effects on dog kidneys, mechanism of, 18: 13440(R) (AD-401681)
effects on dog kidneys under high oxygen tension, 18: 15880
effects on dog leukocytes, 50- *vs.* 250-kvp, 18: 19585
effects on dog lungs, pathophysiology of, 19: 43799
effects on dog lymphocytes, protective effects of bone marrow against, 18: 17636
effects on dog nervous system of head, 18: 31142
effects on dog pancreas, 17: 37061 (BNL-6608)
effects on dog sperm production, 18: 15892
effects on dog thyroid gland, 19: 10804
effects on dogs and mice, protective effects of thiophosphates against, 18: 31306
effects on dogs and sheep, 18: 41222
effects on dogs and rats, protective effects of hypothermia against, 19: 2174
effects on dogs and rats, synergistic effects of anesthesia and trauma, 19: 8781(R) (AD-422394)
effects on dogs and rats, protective effects of chemical compounds against, 20: 10699(T) (NASA-TT-F-353, pp 210-38)
effects on dogs and rats, RBE of, 20: 10611(T) (NASA-TT-F-353, pp 185-93)
effects on dogs and rats, RBE of, 20: 10612(T) (NASA-TT-F-353, pp 194-209)
effects on dogs and rabbits, pathological, 20: 38688
effects on dogs, partial and whole-body, 16: 23419 (UR-609)
effects on dogs, protective effects of dimercaptosuccinic acid against, 17: 35413
effects on dogs, blood transfusion therapy of, 19: 7203
effects on dogs, biological, 19: 8783 (BNL-8571)
effects on dogs, combined effects of trauma, 20: 5302(R) (UR-668, pp 161-6)
effects on dogs, effects of polyglucine on, 20: 12723(T) (JPRS-33766, pp 3-7)
effects on dogs, graft-vs-host specificity of lymph cells transformed from marrow allografts on, 20: 24921
effects on dogs, long-term pathological, 19: 27950(R) (UCD-472-111)
effects on dogs, mechanism for protective effects of bone marrow against, 20: 8730
effects on dogs, protective effects of 2-(2-aminoethyl)-2-thiopseudourea and *p*-aminopropiophenone against, 18: 19794
effects on dogs, protective effects of 2-(2-aminoethyl)-2-thiopseudourea and *p*-aminopropiophenone against, 18: 19795
effects on dogs, protective effects of bone marrow against, 18: 21915
effects on dogs, protective effects of pyridoxal phosphate against, 19: 8964
effects on dogs, pathological, 20: 12645
effects on dogs, pathological, 20: 40638(R) (UCD-472-113, pp 1-16)
effects on dogs, protective effects of typhoid-paratyphoid vaccine against, 20: 42987
effects on dogs, rats, and rabbits, protective effects of selachyl alcohol, 20: 38731
effects on dogs, recovery rate from, 20: 45431
effects on dogs, synergistic effects of microwaves on, 19: 8857
effects on dogs, use of hyperbasophilic cells as index of proliferation of marrow transplants in, 19: 17691
effects on dominant lethal mutations in mature sperm and gonad damage in animals, RBE of, 19: 17607
effects on dominant lethal mutation induction in mouse spermatogonia, 19: 38394
effects on dominant lethal induction in rats, 20: 10609(T) (NASA-TT-F-353, pp 151-6)
effects on dominant and recessive genotypes of desynaptic barley mutants, 20: 42923
effects on dominant lethality in Drosophila oocytes, factors affecting, 18: 19622
effects on dominance-submission patterns, in female dogs, 17: 31864(R) (UCD-107(p.86-97))
effects on donor bone marrow cells exposed *in vivo*, 18: 25201
effects on dormant seeds, protective effects of cysteine and sodium hydrosulfite against, 18: 21923
effects on dorsal ganglion root cells in rats, protective effects of AET against, 19: 15224
effects on doubling-time and mitotic delay in Chinese hamster and L-cells, 19: 25961
effects on DPN content in sarcoma cells, 20: 14370
effects on DPN distribution in sarcoma cells, 18: 29378
effects on DPN metabolism in Ehrlich ascites and Yoshida sarcoma cells, 20: 35259
effects on DPNH binding and titratable sulfhydryl group loss in glutamate and lactate dehydrogenase solutions, 19: 25848
effects on Drosophila, gametic genotype effects on, 18: 3567
effects on Drosophila, genetic, 18: 5117
effects on *Drosophila melanogaster*, 18: 9851
effects on *Drosophila melanogaster*, anoxia effects on, 18: 11831
effects on Drosophila genetics, 18: 13491
effects on Drosophila sperm, effects of temperature on, 18: 23279
effects on Drosophila spermatogonia, 18: 27112
effects on Drosophila, 18: 35379
effects on Drosophila, nondisjunction, 18: 43253
effects on Drosophila, genetic, 19: 2069(R) (ORNL-3700(p.58-62))
effects on Drosophila genetic variation, 19: 5650
effects on Drosophila, mutagenic, 19: 8848
effects on Drosophila chromosomes, lethal, 19: 8850
effects on Drosophila genetic variation, phenocopy method for detecting, 19: 8852
effects on Drosophila, genetic, 19: 10822
effects on Drosophila genetics, 19: 15067
effects on Drosophila brood-patterns, mutagenic, 19: 15130
effects on Drosophila progeny, relation between paternal age and sex ratio in, 19: 15088
effects on Drosophila, genetic, 19: 21973
effects on drosophila progeny, relation between paternal age and sex ratio in, 19: 15088
effects in Drosophila, genetic, 19: 28062
effects on Drosophila sperm, protective effects of nitrogen against, 19: 29960
effects on Drosophila, mutagenic, 19: 31670(R) (NIRS-3(p.19-56))
effects on Drosophila population, genetic, 20: 1642
effects on Drosophila males, genetic, 20: 1644
effects on Drosophila, genetic, 20: 1619(R) (TID-22293)
effects on Drosophila, genetic, 20: 3713(T) (JPRS-31514, pp 29-43)
effects on Drosophila, genetic, 20: 3714(T) (JPRS-31514, pp 44-58)
effects on Drosophila, genetic, 20: 3715(T) (JPRS-31514, pp 59-64)
effects on Drosophila, genetic, 20: 5338
effects on Drosophila, genetic, 20: 5358
effects on Drosophila, effects of argon and oxygen on genetic, 20: 6898
effects on Drosophila, genetic, 20: 6778(R) (ORNL-3853, pp 62-5)
effects on Drosophila genetics, effects of dose on, 20: 18324
effects on Drosophila, genetic, 20: 18333
effects on Drosophila sperm, mutagenis, 20: 18336
effects on Drosophila, genetic, 20: 18415
effects on Drosophila spermatogenesis, 20: 18310
effects on Drosophila, genetic, 20: 22761
effects on Drosophila, genetic, 20: 22616(R) (NIRS-4, pp 58-69)
effects on Drosophila, genetic, 20: 22653
effects on Drosophila spermatogenesis, effects of temperature on, 20: 22662

effects on Drosophila chromosomes, mechanisms for, 20: 24892
effects on Drosophila sperm and spermatogonia, effects of dose on mutagenic, 20: 24893
effects on Drosophila and silkworms, genetic, 20: 26655(R) (NP-15975)
effects on Drosophila, genetic, 20: 26681
effects on Drosophila, genetic, 20: 26683
effects on Drosophila, genetic, 20: 28956
effects on Drosophila, effects of ATP on genetic, 20: 29046
effects on Drosophila, genetic, 20: 31036(R) (SAN-529-3)
effects on Drosophila, genetic, 20: 31047
effects on Drosophila, genetic, 20: 31049
effects on Drosophila males, effects of AET and N_2 treatment on genetic, 20: 33073
effects on Drosophila, genetic, 20: 38596(R) (SAN-590-1)
effects on Drosophila, genetic, 20: 38650
effects on Drosophila, x, 20: 38646
effects on Drosophila, comparison of RBE of fast neutrons with, 20: 38645
effects on Drosophila populations, genetic, 20: 40622(R) (NYO-3096-8)
effects on Drosophila, genetic, 20: 40706
effects on Drosophila, genetic, 20: 40707
effects on Drosophila mosaics, 18: 19618
effects on drug toxicity in animals, 18: 11882
effects on drug-injected rabbits, 18: 11884
effects on dry mass distribution changes in mouse bone marrow, 19: 15055
effects on dry mass of Ehrlich ascites tumors, 20: 42817
effects on dry seeds of *Arabidopsis thaliana*, 18: 63
effects on dual-nucleated transplants of Acetabularia, 16: 16240
effects on Dunning leukemia in rats, protective effects of bone marrow and MEG against, 19: 31913
effects on duodenal crypts in mice, ultrastructural, 20: 33007
effects on duration of mitosis in corneal epithelium of mice, 18: 41165
effects on durum and bread wheats, first generation, 16: 1599
effects on dynamics of lymphoid and myeloid hemopoiesis in rats, dose effects on, 19: 8830(T)
effects on dysplastic changes in growing hair, 16: 21981
effects on *E. coli*, recovery from, 18: 1397
effects on *E. coli*, protective effects of oxygen against, 17: 33682
effects on *E. coli* genetic recombination after female irradiation, 18: 19620
effects on *E. coli* culture medium, carcinoma growth-inhibition, 18: 21890
effects on *E. coli*, effects of oxygen on reparation of, 18: 25229
effects on *E. coli* hexoses and pentoses contents, 18: 27116
effects on *E. coli* growth, mitosis, and nucleic acid metabolism, 18: 29252
effects on *E. coli* pyridoxal phosphate content, 18: 31147
effects on *E. coli*, protective effects of compressed nitrogen gas against, 18: 31293
effects on *E. coli* and *S. cerevisiae* survival, 18: 41231
effects on *E. coli* growth, 19: 84
effects on *E. coli*, effects of nucleic acid content on, 19: 2083(T) (JPRS-27239)
effects on *E. coli* DNA, degradation, 19: 8823
effects on *E. coli*, mechanisms for chemical protection against, 19: 10917
effects on *E. coli*, effects of temperature on mutagenic, 19: 15125
effects on *E. coli*, radiation chemistry of, 19: 26059
effects on *E. coli* B capacity for phage T3, sensitization effects of iodoacetamide on, 19: 38455
effects on *E. coli*, protective effects of ribonuclease against, 19: 38465
effects on *E. coli* phage ϕX174, mutagenic, 19: 42289
effects on *E. coli* B/r, effects of organic nitroxide-free radicals on sensitization of, 19: 43875
effects on *E. coli* mutants, protective effects of phenylbenzamidine against, 19: 46012
effects on *E. coli*, effects of bromouracil content in DNA on, 20: 22651
effects on *E. coli* and yeasts, initial sites of action of, 20: 33062
effects on *E. coli*, repair mechanisms for, 20: 35288
effects on *E. coli*, genetic, effects of genetic factors on, 20: 38621
effects on *E. coli*, lethal, 20: 38630
effects on *E. coli*, effects of protein synthesis on, 20: 40629(R) (ORNL-3922, pp 94-8)
effects on *E. coli* RNA, 20: 42814
effects on early stages of spermatogenesis of adult *D. melanogaster* males, 20: 12637 (TID-21466)
effects on ears in young rats, 19: 26082
effects on ears of Amblystoma embryos, protective effects of parabiosis against, 18: 25148
effects on EDTA complexes of cobalt, copper, nickel, and zinc, 19: 30250
effects on egg production in Habrobracon, 20: 8650
effects on egg production by chickens, 20: 10626
effects on egg-to-adult viability in *D. melanogaster*, 20: 36618
effects on eggs and larvae of *Ascaridia galli*, 18: 38793
effects on Ehrlich ascites tumor cells, 18: 29543
effects on Ehrlich ascites tumor cells, sensitivity effects of potassium cyanides on, 19: 5721
effects on Ehrlich ascites tumor cells, ploidy effects on, 19: 29932
effects on Ehrlich ascites tumors at various times following inoculation into mice, 19: 38402
effects on Ehrlich ascites cells in mice, 20: 118
effects on Ehrlich's adenocarcinoma, qualitative and quantitative, 20: 18396
effects on Ehrlich's carcinoma, mitotic, 16: 28821
effects on elasticity of skin, 16: 21921
effects on elastic fibers in rabbit ear, 17: 27133
effects on electrical and mechanical activity of muscle, whole-body exposure, 16: 14510
effects on electrical activity and membrane permeability of isolated nerves, 18: 47(R) (TID-19617)
effects on electric activity and content of γ-aminobutyric and glutamic acids in brain of rats, 18: 6663
effects on electric properties of dielectrics, 18: 10575 (NP-13539(Paper 4))
effects on electric conductivity of alkali halides, effects of impurities on, 18: 20588
effects on electric conductivity and ion mobility in silicone oils, 18: 27498
effects on electric activity in brain of rabbits, 18: 27191
effects on electric conductivity of lead-doped and strontium-doped potassium chloride crystals, 18: 31584
effects on electric properties of high-pressure polyethylene, 18: 44265
effects on electric activity of nerves in cats and rabbits, 19: 3915(T)
effects on electrical activity of brain, 19: 17490 (CEA-Bib-20)
effects on electrical response of compound eyes in cockroach *Blaberus*, 19: 17603
effects on electric conductivity of doped ionic crystals, 19: 18552
effects on electric conductivity of polyethylene, 19: 20017
effects on electric conductivity of alkali halides doped with divalent cations, (E), 19: 26386
effects on electrical activity of chicken embryo heart, 19: 27968
effects on electric conductivity of tetramethylammonium polyiodides, 19: 30247
effects on electric conductivity induction in polyethylene at high dosage, 19: 36465
effects on electric insulators, 19: 37156(R) (AD-425904)
effects on electric conductivity of gallium selenides, 20: 2439 pp 34-58)
effects on electrical activity of brain of rabbit embryos, effects of developmental stage on, 20: 31037(T) (JPRS-35315, pp 65-75)
effects on electric and magnetic properties of calcium fluoride crystals, (E), 20: 42555
effects on electric properties and unit cell volume of lithium fluoride crystals, 20: 42564(T)
effects on electric conductivity of mercury sulfide films, (E), 20: 46961
effects on electric potentials in algae, 18: 27092
effects on electric activity of brain in rabbits, 18: 27093
effects on electric properties of muscles and nerves in rats, 17: 24961
effects on electrical activity of central nervous system, 17: 33627
effects on electrical activity in eye of cockroaches, 17: 33716
effects on electric and electrochemical properties of muscles, 17: 40542 (AD-296342)
effects on electron spin resonance spectra of keratins, 16: 8589
effects on electrophoretic mobility of Ehrlich ascites tumor cells, 16: 8585
effects on electroencephotographs of brain tumors, 16: 16260
effects on electrolyte permeability in skin, local high-level exposure, 16: 16301
effects on electrophysiological parameters of skeletal and heart muscle, 16: 17473
effects on electroencephalographic pattern and adrenaline sensitivity in rabbits, prenatal exposure, 16: 25244
effects on electrophoretic behavior of proteins and colloidal lability in cancerous tissues, 16: 26834
effects on electroshock seizure responses in rats, dose-dependent, 18: 8180
effects on electroshock seizures in rats, 18: 9885
effects on electrophoretic pattern of mouse serum, 18: 29328
effects on electron traps in potassium chloride, 18: 32250
effects on electrophoretic distribution of proteins in blood serum exposed *in vitro*, 18: 33353
effects on electrolyte shift in rats, 18: 38866
effects on electron spin resonance of bovine serum albumin, 18: 41141
effects on electrolyte balance in rats, 19: 3902

effects on electron spin resonance centers in alanine, 19: 7542
effects on electron nuclear double resonance spectra of adipic acid crystals, 19: 9786
effects on electron paramagnetic resonance of dl-α-alanine, 19: 9232
effects on electron paramagnetic resonance of sodium thiosulfate, 19: 9233
effects on electron spin resonance of sodium polyphosphate, 19: 9181
effects on electronic resonance of glycine, 19: 9235
effects on electrolyte transport in mouse spleen, 19: 13070
effects on electron spin resonance absorption of succinic acid and deuterated succinic acid, 19: 13445
effects on electrokinetic potential of sarcoma cells, 19: 15144
effects on electrolyte and water balance in rats, 19: 15031
effects on electroshock seizures in rats, cysteine and dose effects on, 19: 19514
effects on electrophoretic mobility in nuclear membranes in rabbit kidney and L cells, 19: 24297
effects on electrocorticography in rats, bilateral and unilateral cranial, 19: 24342
effects on electrophoretic properties of serum proteins, in cancer patients, 19: 26029
effects on electrophoretic properties of serum proteins in normal and tumor-bearing rats, 19: 26030
effects on electrophysiological properties of plants, 19: 25933
effects on electroretinographic response to partial retinal stimulation in man, 19: 25915
effects on electrophysiology of central nervous system in dogs, low-level, 19: 26098
effects on electrophysiology of neural activity in rat brain, 19: 26106
effects on electrophoretic properties of proteins, 19: 28088
effects on electrophoretic properties of proteins, 19: 28089
effects on electroencephalographic activity in rat brain, 19: 36018
effects on electroluminescence of activated alkali halides, 19: 41981
effects on electroluminescence of alkali halides, 19: 40572
effects on electroluminescent screens, (E), 19: 46341(T) (FTD-TT-65-24)
effects on electrophysical properties of germanium, 20: 4465
effects on electrical activity of rabbit brain, 20: 22615(R) (NIRS-4,
effects on electron postemission of calcium sulfate, 20: 20769
effects on electrophysiological parameters in Planorbis nerve cells, 20: 22591
effects on electrophoretic mobility of animal cells in suspensions, 20: 28905
effects on electron-induced color centers in alkali halides, (E), 20: 30776
effects on electrolyte transport in ascites tumor cells, 20: 45445
effects on electroluminescent screens, 16: 22248
effects on electroretinal response in frogs, 16: 21976
effects on electrolyte balance of heart and skeletal muscles, whole body exposure, 17: 21566
effects on electrocortical activity in prenatal and neonatal rats, 17: 35502
effects on elimination of solid particles from lungs in rats, 19: 24322
effects on embryo of *Balberus cranilfer*, 16: 9839(R) (TID-14662)
effects on embryo of mice, dose dependence of, 20: 33027
effects on embryo-endosperm ratios in seeds, 17: 10386
effects on embryogenesis, analysis of injuries and reparation, 16: 5221
effects on embryonic hematopoietic tissues, 16: 26790
effects on embryonic organs, 18: 5033
effects on embryonic human fibroblasts, chromosomal aberrations from, 18: 8149
effects on embryonic development of goldfish by exposure of mother, 19: 169
effects on embryonic development in planarians, 19: 31826
effects on embryonic mice exposed *in utero*, seasonal effects on low dose whole-body, 19: 42298
effects on embryonic lethality of mice by paternal spermatozoa exposure, 19: 42303
effects on embryonic cells of mice and rats, effects on DNA induction by Polyoma virus, 20: 18369
effects on embryonic mortality and sex-chromosome loss during cleavage in mice, 20: 33008
effects on embryonic heart of chicken, early reversible, 17: 1283
effects on embryonic development of mice, 17: 33672
effects on embryos and fetuses in mice, 16: 9855
effects on embryos and fetuses of mice, 19: 31964
effects on embryos of mice, delayed pathological, 20: 14315
effects on embryos of blindworm, 20: 36615
effects on embryos of mice, RBE of neutrons, 20: 40618(R) (NYO-2740-3, pp 166-215)
effects on embryos of mice, whole-body preimplantation, 17: 17911
effects on emergence of house flies from pupae, 20: 14306
effects on emotional display of aged female beagles, early adult, 19: 7139
effects on endocrine reactions in dogs, 20: 26686
effects on endocrine function in rabbits, 20: 45254
effects on endogenous respiration in mouse spleens, 19: 13070
effects on endogenous respiration and histone synthesis in Ehrlich ascites tumor cells, 20: 10691
effects on endosperm-embryo relations in Triticum seeds, 18: 43218(R) (EUR-1882.e(p.7-26))
effects on energy metabolism in mouse Ehrlich ascites tumor cells, 18: 29332
effects on enzymatic activity of regenerating rat liver, 17: 15785
effects on enzyme activity in MTK sarcoma III tumor cells, 16: 4100
effects on enzyme formation, 16: 7458
effects on enzyme activity in Tetrahymena, 16: 9862
effects on enzyme activity in skin, 16: 12918
effects on enzyme activity in spleen and liver, whole-body exposure, 16: 14573
effects on enzyme activity in atrophic thymus, whole-body exposure, 16: 14576
effects on enzyme synthesis of S-adenosylmethionine in yeasts, 16: 17738
effects on enzyme activity in regenerating liver, whole-body exposure, 16: 17523
effects on enzyme synthesis during liver regeneration in rats, 16: 17464
effects on enzyme activities in rat tissues, protective effects of chemicals against, 16: 26659(R) (NP-11966(p.43-54))
effects on enzyme activity in heart mitochondria, 16: 28750(R) (TID-16446)
effects on enzyme activity in heart mitochondria, 16: 28749(R) (TID-16447)
effects on enzyme activity in protozoa, 16: 28772
effects on enzyme activity of leukocytes in guinea pigs, 18: 1435
effects on enzyme activity in heart, liver, and kidney of mice, whole-body, 18: 3555
effects on enzyme activity in rat liver, 18: 9870
effects on enzyme system in rat liver, whole-body, 18: 11630(R) (NP-13555(p.1-14))
effects on enzyme activity in brain of rats, effects of various drugs on, 18: 11631(R) (NP-13555(p.15-33))
effects on enzyme activity in extracts of tissue cultures, 18: 15831
effects on enzyme activity and phosphate metabolism in mitochondria of rat spleen, 18: 17467(R) (ANL-6790(p.145-9))
effects on enzyme activity in DNA–ribonuclease complex, 18: 17573
effects on enzyme activity in rat liver, 18: 23241(R) (NP-13918(p.13-27))
effects on enzyme activity in stomach of rats, 18: 25086(R) (TID-20636)
effects on enzyme systems in marine organisms, 18: 27062(R) (NYO-1680-1)
effects on enzyme activity in tissues, effects of chloroprene on, 18: 27201
effects on enzyme activity of guinea pig heart muscle, 18: 29267
effects on enzyme activity and metabolism in intestinal mucosa of guinea pigs, 18: 31162
effects on enzyme activity in rats, 18: 35327(T) (JPRS-25630)
effects on enzyme development in rat liver, 18: 35363
effects on enzyme activity in rat tissues, 18: 43242
effects on enzyme activity in mice, 19: 2075(R) (ORNL-3700(p.101-11))
effects on enzyme activity in muscles of mice and rabbits, 19: 7146
effects on enzyme activity in skin of guinea pigs, 19: 8882
effects on enzyme activity in rat liver, 19: 8787(R) (NP-14448(p.1-12))
effects on enzyme activity in rat liver, 19: 8788(R) (NP-14448(p.13-20))
effects on enzyme activity in rat liver, 19: 8789(R) (NP-14448(p.21-35))
effects on enzyme release by mitochondria and ribosomes, 19: 8818
effects on enzyme activity in liver and kidney of guinea pigs, 19: 10793
effects on enzyme activity in mouse liver, 19: 21858(R) (NP-14779 (p.1-14))
effects on enzyme activity in rat liver, 19: 21859(R) (NP-14779(p.15-28))
effects on enzyme activity in rats, whole-body, 19: 21976
effects on enzyme activity in rat liver, 19: 27978
effects on enzyme activity in rat liver, 19: 31785(R) (NP-15072(p.17-28))
effects on enzyme activity and cell growth in mouse thymus, 19: 31801 (USNRDL-TR-840)
effects on enzyme activity in erythrocytes and liver of rats, 19: 33841
effects on enzyme activity in sarcoma tissue homogenates, 19: 36013
effects on enzyme activity in Tetrahymena, 19: 43856
effects on enzyme content in rat intestine, 19: 45927
effects on enzyme levels in monkey blood, 20: 3692
effects on enzyme activity in excised bovine lens, 20: 8594
effects on enzyme activity of mitochondria from rat liver, spleen, and thymus, 20: 14376
effects on enzyme activity in rat tissue homogenates, 20: 16289
effects on enzyme synthesis in rat liver, 20: 20429(R) (AD-629311, pp 15-25)

effects on enzyme activity in chick embryos, 20: 20440(R) (EUR-2643-f)
effects on enzyme activity in rat testes, 20: 22613(R) (NIRS-4, pp 21-8)
effects on enzyme activity in rat testes, head-exposure, 20: 22615(R) (NIRS-4, pp 34-58)
effects on enzyme activity, effects of moisture on, 20: 28902
effects on enzyme locational specificity in Neurospora, 20: 31012
effects on enzyme release from rat liver lysosomes, 20: 38577
effects on enzyme inactivation, 19: 19517
effects on enzyme activity of cells of cervix carcinoma and surrounding cells, 18: 19701
effects on enzyme activity of seeds of *Pisum sativum* L., 17: 7828
effects on enzyme systems in rat liver, 17: 10479(R) (NP-12251(p.12-21))
effects on enzyme systems in rat liver, 17: 10478(R) (NP-12251 (p.1-11))
effects on enzyme activity in kidneys, whole-body exposure, 17: 27066 (USNRDL-TR-640)
effects on enzyme activity, physiological, 16: 1553
effects on enzyme systems in thymus mitochondria, 17: 27086
effects on enzyme activity in rats, 17: 38762
effects on enzymes in guinea pig lungs, 18: 19675
effects on enzymes in monkey kidney tissue cultures, 18: 21861
effects on enzymes, 18: 29321
effects on enzymes in rat liver, 18: 35314(R) (NP-14210(p.1-13))
effects on enzymes, effects of estrogens on, 19: 15275
effects on enzymes in hypertensive rats, 19: 15040
effects on enzymes in guinea pig adrenal glands, local and whole-body, 19: 17595
effects on enzymes in beef heart muscle, 20: 63(R) (STI/DOC/10/42, pp 45-55)
effects on enzymes in *E. coli*, 17: 31960
effects on enzymes, protective effects of disulfides against, 17: 37127
effects on enzymes in thymus nuclei of rats and mice, whole-body, 17: 40573
effects on eosinophilia in healthy and tumorous rats, 16: 8578
effects on Ephestia, effects of developmental stage on spectra of mutagenic, 20: 42970
effects on epididymal spermatozoa in bovine testes, 20: 29013
effects on epilation in guinea pigs, protective effects of bufotenine, isoserotonin, and serotonin against, 18: 31274
effects on epilation of mouse skin, protective effects of blood serum against, 20: 33081
effects on epilation of guinea pigs, 17: 17896
effects on epinephrine and nor-epinephrine secretion in guinea pigs, histochemical determination, 20: 24862
effects on epithelium of bladder and abdomen in rats, single acute exposure, 18: 8122(T) (JPRS-22556(p.14-26))
effects on epithelial tumors of lacrimal glands, 20: 14410
effects on EPR of potassium chlorate, 20: 12888
effects on EPR spectra of stretched polypropylene, 18: 23679
effects on EPR spectra of quartz with aluminum impurity, 20: 16539(T)
effects on equilibrium in electrolytic solutions, 18: 12165
effects on Eranthis embryos, recovery from, 19: 15145
effects on erythrocyte metabolism in man, whole-body, 18: 1419
effects on erythrocytes, anemia induction in rabbits by, 18: 27113
effects on erythropoiesis and survival of rabbits, post-, 18: 27140
effects on erythrocyte carbonic anhydrase activity in rabbits, 18: 31145
effects on erythrocytes, 18: 33334
effects on erythropoietin production by dog kidneys, 18: 38783
effects on erythropoietic activity in mice, protective effects of fresh and frozen bone marrow against, 19: 192
effects on erythropoiesis in rabbit spleen, 19: 10868
effects on erythropoiesis in rats, 19: 12982
effects on erythropoiesis in anemic rabbits, 19: 17629
effects on erythrocyte volume and hemoglobin content in rats, 19: 21872
effects on erythrocytes in blood and saline suspensions, 19: 24350
effects on erythropoiesis in mouse marrow, effects of postirradiation temperature on, 19: 31905(R) (ORNL-3768(p.99-108))
effects on erythrocyte fragility, 19: 31743
effects on erythroid clone formation in polycythemic animals, bone marrow effects on, 19: 36079
effects on erythropoiesis in cross-circulated dogs, 19: 38382
effects on erythrocytes in salamanders, morphological, 19: 43730
effects on erythropoiesis in rat embryos, 19: 45826
effects on erythrocytes, hemolytic, 20: 14275
effects on erythrocyte morphology in man, chronic-exposure, 20: 16250
effects on erythrocyte membranes, 20: 18454
effects on erythropoiesis in rats, chronic low-level exposure, 20: 22706
effects on erythrocyte mass and plasma volume following cancer therapy, 20: 22737
effects on erythrocyte membranes, protective effects of chemical agents against, 20: 24943
effects on erythropoiesis in rats, effects of endocrine gland removal and hormones on, 20: 29043
effects on erythropoiesis in dogs, 20: 45349 (AD-639299)
effects on erythrocyte creatine content, 17: 5856
effects on erythropoietin, calculation of molecular characteristics from, 17: 12158
effects on erythrocytes, effects of monoiodoacetic acid on, 17: 15786
effects on erythropoiesis in rats, tracer study, 17: 23018
effects on erythrocytes in man, rabbits, and roosters, 17: 27166
effects on *Escherichia coli* capacity for bacteriophage, effects of cysteine and glycerol on, 18: 41111
effects on *Escherichia coli* in presence of substituted nitroxides, 19: 7194
effects on *Escherichia coli*, effects of oxygen on lethal, 19: 21923
effects on *Escherichia coli*, biological, 19: 21894
effects on *Escherichia coli*, physiological, 19: 21871
effects on *Escherichia coli*, biochemical, 19: 33864
effects on *Escherichia freundii*, protective effects of fluoroacetate against x, 19: 46015
effects on *Escherichia coli* mutants, 19: 45948
effects on *Escherichia coli*, genetic, 20: 26678
effects on *Escherichia coli*, effects of nutrients on biological, 20: 40618(R) (NYO-2740-3, pp 166-215)
effects on *Escherichia coli*, effects of cysteine, MEA, and penicillamine on, 20: 45477
effects on *Escherichia coli* and yeast, reaction mechanisms for, 20: 46121
effects on *Escherichia coli* in glucose, sensitivity, 17: 30336
effects on ESR in ammonium fluophosphate and magnesium hypophosphite, 20: 414
effects on ESR of rare earth-doped calcium fluoride at 50 kv, 18: 2470
effects on ESR spectra of hexamethylenediammonium adipate single crystal, 18: 20075
effects on ESR spectra of methionine, 18: 22149
effects on ESR spectra of cystine, glycine, glycylglycine, and valine, temperature effects on, 19: 4229
effects on ESR spectra in single crystals of dimethylglyoxime-d_2, glyoxime, and methylglyoxime at 77°K, 20: 14598
effects on ESR spectra of albumin and methionine, 20: 18791
effects on ESR spectra of potassium sulfate at 77 and 300°K, 20: 18734
effects on esterase activity of rat brain and blood serum, 18: 5064
effects on esterase and β-glucuronidase activities and state of cells in rat gonads, 19: 31845
effects on esterase content in rat blood, 20: 38682
effects on esterase activity in rats, 20: 42824
effects on estrogen production in female rats, 17: 37073
effects on estrone in acetic acid, chemical, 20: 5274
effects on estrus cycle in mice, 20: 18403
effects on etching of quartz, 18: 16535
effects on ethanol and sodium formate in heavy and light water, hydrogen yields in, 19: 5960
effects on ethanol or methanol mixtures with naphthalene, spectra of hydrogen atom reactions in, 20: 16524
effects on ethyl isocyanide binding reaction in hemoglobin, 16: 8581
effects on ethyl mercaptan, ESR studies on, 20: 43320
effects on ethyl- and propylmalonic acids, 20: 33375
effects on ethylene vapors, effects of xenon on chemical, 19: 5949 (TID-21389)
effects on Euglena survival, effects of culture conditions on, 19: 24267
effects on European corn borer fertility and mortality, 18: 5052
effects on exchange between nitrogen-14 and -15 in gaseous nitrogen, 18: 23680
effects on excretion of 5-hydroxyindoleacetic acid by rats, 18: 41122
effects on excretion of iodides in thyroidectomized rats, 17: 40668
effects on expansion of melanophore pigment in hypophysectomized frogs, 18: 33277 (STI/DOC/10/28(p.21-38))
effects on experimental bladder calculus formation in rats, 20: 20467
effects on experimental allergic encephalomyelitis in guinea pigs, 17: 5801
effects on exteriorized intestine and spleen of rabbits, 20: 3775
effects on exteriorized rat kidneys, 20: 6894
effects on exteriorized intestine and spleen of rats, 20: 3775
effects on extracellular structures in animals, 20: 33063
effects on extracts and fragments of chloroplasts, 17: 10458
effects on extremities and life span of salamanders, protective effects of DNA and RNA against, 19: 26118
effects on eye lens regeneration in salamanders, 19: 2070(R) (ORNL-3700(p.69-76))
effects on eye lenses of mice, 20: 18185(R) (BNL-929, pp 126-47)
effects on eye lens in mice, 17: 33453(R) (ANL-6723(p.63-4))
effects on eyes, 19: 7133
effects on eyes, 20: 22772
effects on eyes, delayed, 17: 31861(R) (UCD-107(p.44-9))
effects on eyes following therapy of canthus and eyelid carcinomas,

20: 40689
effects on eyes in mice embryos after whole-body exposure to mother, 16: 14549
effects on eyes in developing mouse embryos, 16: 25215
effects on eyes of dogs, 18: 25090(R) (UCD-472-109(p.45-8))
effects on eyes of rabbits, 19: 31806
effects on eyes of rabbits, 19: 33794
effects on eyes of mice, pathological, 19: 34098
effects on eyes of dogs exposed during fetal stages, 20: 10675
effects on F center spectra in alkali halide crystals, 19: 11214(T)
effects on F centers in pure and activated potassium chloride crystals of, 19: 24567(T)
effects on F centers and photostimulated emission in sodium chlorides, (E), 19: 41980
effects on F-bands in sodium bromide–sodium chloride mixed crystals, 20: 14605
effects on F-center formation in sodium chloride monocrystals, 19: 34252
effects on F-center formation in potassium chloride crystals, (E), 20: 14000
effects on F-center absorption in sodium fluoride, 20: 12892
effects on F-center formation in ionic crystals, temperature dependence of, 20: 32724(T)
effects on F-center formation in doped potassium chlorides, 20: 42557
effects on *Fasciola hepatica* in liver in mice, 18: 1411
effects on fasting rats of, pathological, 20: 3766
effects on fatty acid uptake by sarcoma cells in rats, 19: 12937
effects on fatty acids in rabbit liver, 19: 17526
effects on fatty acids and phosphatides in rat liver, whole-body, 19: 26034
effects on fatty acids in mice, 19: 29963
effects on fatty acid content of blood plasma of pregnant rats and fetuses, 19: 33790
effects on fatty acid synthesis in rat liver slices, 19: 36011
effects on fatty acid synthesis in liver, 20: 63(R) (STI/DOC/10/42, pp 45-55)
effects on fatty acid absorption in rats, 20: 3754
effects on fatty acid metabolism in rats, 20: 14379
effects on fatty acid content in free lipid fraction beam leaves, 20: 36598
effects on fatty acids, biochemical, 18: 52
effects on fatty acid composition of skin lipids, 17: 5825
effects on fatty acid content of testes of rats, 17: 35450 (TID-17882)
effects on fatty infiltration of mouse liver, protective effects of lipotropic substances on, 17: 40586
effects on feathers, electron spin resonance studies of free radicals produced in, 18: 27085
effects on feeder layers in mouse tissue cultures, 20: 12654
effects on female germ cells of Drosophila, 18: 23281
effects on female rat gametes at antenatal and postnatal periods, 18: 38832
effects on female Drosophila longevity, 19: 122
effects on female mice, cytogenesis of bone marrow cell grafts in, 19: 26142
effects on female genital organs, whole-body exposure, 17: 5795
effects on femoral neck following therapy for gynecological cancer, 20: 18407
effects on ferrochelatase activity in rabbit organs, 19: 5641
effects on ferroelectric Rochelle salt, 18: 5397
effects on fertilization phenomena and gametic lethality in *Drosophila melanogaster*, 16: 9845(R) (TID-15021)
effects on fertility of male mealy bug, *Planococcus citri*, 16: 30236
effects on fertility of male mice, pre- and post-natal, 18: 11665
effects on fertilized eggs of roundworms treated with 5-bromodeoxyuridine, 18: 11717
effects on fertility of rats exposed 8 or 17 days after birth, 18: 13480
effects on fertility, growth, and sexual maturity of rats, protective effects of cysteine against, 18: 13544
effects on fertility and mortality of *Drosophila melanogaster*, 18: 19750
effects on fertility of guinea pigs, 18: 25230
effects on fertility of male guinea pig, 18: 25191
effects on fertility of male guinea pigs, 19: 10875
effects on fertility of female mice exposed during infancy, 17: 23178
effects on fertilized eggs and developing embryos in hamsters, 17: 27119
effects on fetus after male exposure, protective effects of S-β-aminoethylisothiuronium against, 16: 25211
effects on fetus of cervical carcinoma therapy, 19: 34034
effects on fetuses in hamsters, 18: 33322
effects on fetuses, heterochromia resulting from, 18: 29445
effects on fibrinogen and fibrolytic activity in dog blood, 19: 42312
effects on fibrinolysis in rabbits, whole-body, 20: 5325
effects on fibrinogen and fibrinolytic activity in blood, 20: 6867
effects on fibrinoid lesions in rabbits, effects of toxin on, 17: 2848
effects on fibroblast-DNA synthesis and mitotis, 18: 11723
effects on fibrous proteins, electron spin resonance study of, 17: 4429
effects on fin transplantability in Carassius, 19: 31670(R) (NIRS-3 (p.19-56))
effects on fine structure of liver and spleen in mice, 19: 7170
effects on fine structure in frog nerve cells, 19: 42285
effects on fine structure in fetal rat cells, 20: 14262
effects on fine structure of guinea pig retina, 20: 31118
effects on fine structure of Paneth cells in mice, 20: 31083
effects on fish adrenal cortex, histological, 18: 33272(R) (NIRS-2(p.31-42))
effects on fish intestinal epithelium histological, 18: 33272(R) (NIRS-2 (p.31-42))
effects on fish pituitary control of melanization, 18: 33272(R) (NIRS-2 (p.31-42))
effects on fish, protective effects of reserpine against, 18: 33272(R) (NIRS-2(p.31-42))
effects on fitness of mouse populations, 18: 35345
effects on fitness of mouse populations, 18: 35348
effects on fitness factors of Drosophila populations, 17: 10384
effects on flexibility of denatured and native DNA, 19: 33903
effects on flour beetles, effects of pathogenic bacteria on, 19: 45908
effects on flower primordia formation in Xanthium, 20: 42842(R) (ANL-7136, pp 290-301)
effects on flowering of Xanthium, 18: 17471(R) (ANL-6790(p.228-9))
effects on fluid and sodium balance in rats, protective effects of mercaptamine against, 19: 33792
effects on fluorescence of lithium fluoride crystals, 18: 797
effects on fluoride systems, 19: 2402
effects on fluorine-19-activated beryllium oxide, ESR spectra of, 18: 33657
effects on fluorobenzene in aqueous and organic solutions, 19: 11209
effects on folic acid, 20: 10904
effects on food intake by rats, effects of chlorpromazine on, 20: 18367
effects on formation of 5-deoxycytidylic acid deaminase in regenerating liver, whole-body exposure, 16: 17449
effects on formation of oxidation products in lipids in organs in rats, 18: 3522
effects on formation of lipid oxidation products in liver mitochondria in rats, 18: 9892
effects on formation of radiomimetic substance in rabbit liver, 18: 13460(T) (JPRS-23507)
effects on formation of lipid oxidation products in rat intestine, kidneys, and liver homogenate, 18: 33305
effects on formation of bladder calculi in rats, 20: 8604
effects on formation of leukocyte-regulating factor in rabbits, 20: 16265
effects on formation of mononucleated giant erythropoietic cells, 20: 18325
effects on formation of organic peroxides in mice, 20: 38660
effects on Forssman-antigen synthesis in hamster and mouse cells, 18: 33317
effects on free lipid fraction in bean sprouts, biochemical, 20: 5265(T)
effects on free radical formation in a biological system, factors controlling, 16: 5257
effects on free radical formation in amino acids, 18: 27014(R) (ORNL-3601(p.216-21))
effects on free radicals in solid DNA, 19: 440
effects on free radical density in polymethylmethacrylate, 19: 38706
effects on free radical yield in DNA, effects of DNA molecular weight on, 20: 420
effects on free radical induction in solid DNA, EPR spectral studies on, 20: 32934
effects on free radical production in biological substances, 17: 15767
effects on frequency and properties of genetic recombinations in *E. coli*, 19: 19537
effects on frequency of chromosome breaks at different stages of spermatogenesis in *D. melanogaster*, 20: 32995
effects on frequency of chromatid and chromosome aberrations in dry seeds of *Vicia faba*, 20: 42920
effects on frequency and types of chromosome aberrations and mutations in wheat seeds, 17: 40588
effects on freshly sutured bronchial stumps and esophageal anastomoses in dogs, 17: 27127
effects on Friend virus disease, 18: 31201
effects on Friend virus, 17: 37075
effects on frog electroretinogram, 18: 84
effects on frog heart, physiological, 19: 12953 (NP-14664)
effects on frog heart, physiological, 19: 12955(R) (NP-14666)
effects on frog muscle cells, 18: 43234
effects on frog retina, 18: 33343
effects on frog retinas, 19: 28087
effects on frogs and mice, protective effects of low temperature against, 18: 29387
effects on frogs, repair of, 18: 19781(T)
effects on frozen iron sulfate solutions, 20: 36867

effects on fruit development in orchids, 20: 38597(R) (TID-23057)
effects on fruits, ESR spectral studies on, 20: 35247
effects on fumarase activity in *Tetrahymena pyriformis GL* during cell division, 17: 10409
effects on *Funaria hygrometrica* plants, genetic, 20: 3781
effects on function of hematopoietic system, 16: 23445
effects on function and growth of regenerated or transplanted adrenocortical tissue in rat, 16: 23417(R) (TID-16122)
effects on function of adrenal glands, tracer study, 16: 28688
effects on function of endocrine glands, 18: 29240(R) (COO-119-229 (p.80-92))
effects on functional mechanisms in rats, 18: 43243
effects on function of rabbit intestines, 19: 17585
effects on function of reticulo-endothelial system in rabbits by liver exposure, 19: 25982
effects on function of rat hematopoietic system, 19: 45984
effects on function and morphology of endocrine glands, 20: 1671
effects on function and histology of rabbit kidneys, 20: 16234
effects on function of nucleic acids in HeLa cells, 20: 26647
effects on function and structure of dog pancreas, 20: 26662
effects on function and morphology of dog kidneys, 20: 29025
effects on function and ultrastructure of isolated rat sympathetic ganglion, 20: 31055
effects on function and structure of bull testicle, single whole-body or fractionated dose, 20: 40610(R) (COO-895-9)
effects on function of vestibular apparatus in dogs and rabbits, 20: 45413
effects on function and structure of villus epithelial cells in mice, 17: 4420
effects on fungal spores, 19: 19558
effects on fungal spores, 19: 19559
effects on fungi, physiological, 20: 10620
effects on fused chloride and fluoride salts, 18: 34050(R) (ORNL-3626 (p.59-164))
effects on fusion of body segments of planaria, 18: 31232
effects on gadolinium-doped calcium fluoride, preferential emission in afterglow of, (E), 20: 6550
effects on *Gallus domesticus*, whole-body, 18: 11702
effects on gamete mutation frequency, maximum permissible dose from, 20: 107
effects on gamma globulin content in mice, effects of thymectomy followed by isologous restoration on, 19: 24280
effects on γM antibody response in mice, 20: 6863
effects on gamma-globulins in benign diseases, 19: 24355
effects on gamma-irradiated sodium chloride, coloration from, 19: 40105
effects on γ-mutated *E. coli*, 20: 45454
effects on ganglionic cells in chicken embryos, 19: 36071
effects on ganglioside content in rat brain, 20: 45329
effects on gas metabolism in rats, protective effects of methandrostenolone against, 19: 13115
effects on gaseous tetramethylsilicone, chemical, 19: 17956(R) (NYO-2007-8)
effects on gaseous butadiene, 19: 46336 (TID-22236)
effects on gaseous propene, 19: 46337 (TID-22244)
effects on gaseous 1-butene and *cis*-2-butene, 19: 46335 (TID-22232)
effects on gastric retention, whole-body exposure, 16: 12898
effects on gastric secretion in stomach of dogs, effects of histamine on, 18: 5105
effects on gastric secretion in dogs after feeding, whole-body, 18: 5106
effects on gastric passage time in rats, 18: 25172
effects on gastric retention in rats, 18: 33277 (STI/DOC/10/28(p.21-38))
effects on gastric acid secretion in ulcer patients, 19: 27958
effects on gastric juice secretion and enzyme activity in dogs, 20: 5384
effects on gastric motility in dogs, 20: 6789(T) (AD-620967)
effects on gastric emptying in rats, part-body, 20: 36628
effects on gastrointestinal tract in mice, whole-body, 16: 14504
effects on gastrointestinal tract in mice, head exposure, 16: 14505
effects on gastrointestinal tract in mice, abdomen exposure, 16: 14506
effects on gastrointestinal tract in guinea pig, relative potency of 250 kvp, 16: 31475 (USNRDL-TR-576)
effects on gastrointestinal tract, lymphatic system, and respiratory system of rabbits, 19: 7163
effects on gastrointestinal tract function in rabbits, 20: 38659
effects on gastrointestinal absorption of water in rats, 20: 42971
effects on gastrointestinal tract in conventional and germfree mice, 20: 45359 (ORNL-P-2407)
effects on gastrointestinal motility and glucose absorption in guinea pigs, 17: 37139 (TID-19388)
effects on gelation of triethylene glycol dimethacrylate at 14 Mev, 20: 20720 (AD-630891)
effects on gemmation in *Saccharomyces cerevisiae*, 17: 40593
effects on gene function in bacteriophage T4, 20: 33066
effects on genetic marker in transforming desoxyribonucleic acid, 18: 5024
effects on genetics of barley seeds, post-treatment modification of, 18: 11842
effects on genetics and population size in Drosophila, 18: 13493
effects on genetic response of Drosophila spermatozoa, 18: 19647
effects on genetic recombination in microorganisms, 19: 3945
effects on genetic loads in Drosophila, 19: 8849
effects on genetic variability in *Nicotiana tabacum*, R_1 evaluation of, 19: 10885
effects on genetic mutability increase in Drosophila population and plants, 19: 15113
effects on genetic variance in hexaploid and tetraploid wheat, 19: 15079
effects on genetics of panicle formation in rice, 19: 24287
effects on genetic variability in *durum* wheat, 19: 42267
effects on genetic loads and inbreeding in *D. melanogaster*, 19: 45952
effects on genetic variability in maize and wheat, 20: 10603(R) (IAEA-2466-11)
effects on genetic variability in maize and wheat, 20: 12641 (TID-22582)
effects on genetic transcription in Rhodopseudomonas, 20: 31033(R) (NASA-CR-59196)
effects on genetic structure of plants, 17: 27100
effects on genic duplication frequency in Drosophila, 18: 11728
effects on genital development in worms, 20: 24880
effects on germ cells in rabbits, 20: 29019
effects on germ-free mice, 19: 2135
effects on germ-free mice, lethal, 20: 3778
effects on germ-free mice, biological, 20: 6907(R) (EUR-2511.e)
effects on germ-free mice, effects of diet and strain on lethal, 20: 22730
effects on German winter wheat varieties, 20: 35321
effects on germanium diodes, 18: 40016
effects on germinating power of water-sensitive barley seeds, 18: 5038
effects on germination of jute seeds, 19: 5716
effects on germination and survival of *Arabidopsis thaliana*, 19: 15157
effects on germinal line and gonad regeneration in *Asterina gibbosa*, 19: 17532
effects on germination of seeds and spores, 19: 29886(R) (ANL-6971 (p.29-46))
effects on giant cells in mouse bone marrow, dose relation to, 19: 5676
effects on giant cell formation in RCP cell strain, 20: 5323
effects on gill formation and regeneration in *Branchiura sowerbyi*, 18: 25135
effects on gladiolus hybrids, seeds, and tubers, 20: 35290
effects on glass, stabilization of coloring, 19: 32607(P)
effects on glasses, ESR studies of, 20: 5019
effects on glasses, bibliography on, 20: 15134 (N65-15819)
effects on glioma growth in mice, 18: 17690
effects on globular-plasmatic transfer of potassium ion, 18: 11719
effects on glomerulosclerosis development in mice, effects of AET, age, exposure, and shielding on, 19: 42368
effects on glomerular lesions in kidneys in mice, pathogenesis of whole-body, 17: 10433
effects on glucose metabolism in yeast, 16: 2899
effects on glucose metabolism by heart muscle, 16: 4096
effects on glucose-6-phosphate dehydrogenase content in erythrocytes, 18: 6659
effects on glucose-6-phosphate phosphatase activity in liver of fasting rats, 18: 27128
effects on glucose metabolism in rats, tracer study, 20: 3678
effects on glucose absorption in rat intestine, 20: 16274
effects on glucose metabolism in rats, tracer study, 20: 42856 (TID-23213)
effects on glucose and fatty acid metabolism in mice, 17: 35512
effects on glucose-6-phosphatase activity in liver in rats, 17: 35524
effects on glucose absorption by guinea pig intestine, 17: 38771
effects on glucose metabolism in monkeys, whole-body, 17: 38885 (SAM-TDR-63-40)
effects on glucuronidase activity in mouse thymocytes, 20: 24867
effects on glutamic dehydrogenase within and without intact mitochondria, 16: 23456
effects on glutaminase activity in mouse brain and liver, whole body exposure, 17: 7862
effects on glutathione content in organs in rabbits with and without implanted sarcoma, 17: 7877
effects on glycine metabolism in rats, 19: 35993
effects on glycine peptides of, chemical, 20: 5273
effects on glycine, ESR spectra of radicals in, 20: 29281
effects on glycogen content of nerve cells in rabbit brain, whole body, 18: 1383(T) (OTS-62-11069(No.3)(p.797-808))
effects on glycogen content in rat brain, 18: 6624
effects on glycogen content of dog and rabbit eyes, 18: 15837(T)
effects on glycogen content of mouse spleen leukocytes, when used with

antigens, 18: 19741
effects on glycogen content of leukocytes, 18: 27195
effects on glycogen metabolism in rat liver, 19: 2087
effects on glycogen content of rat liver, 19: 8879
effects on glycogen and mucopolysaccharides in guinea pig skin, 19: 10835
effects on glycogen metabolism in rat brain and liver, age effects on, 19: 36063
effects on glycogenolysis in rat liver slices, mechanism for, 20: 6761
effects on glycogen content in nervous system in frogs, 17: 37069(T) (JPRS-21170(Del.))
effects on glycolysis in chicken normal and tumorigenic tissues, 18: 29335
effects on glycolysis and respiration in guinea pig and rat retina, 20: 36630
effects on glycolysis hindrance in ascites tumor cells, 17: 5900
effects on glycolysis, oxygen uptake, and protein synthesis in hepatoma cells in mice, 17: 23151
effects on glycoprotein content in rat serum, 20: 18258
effects on glycoprotein and hexose content in blood serum in rats with hyperthyroidism, 20: 42805
effects on glyoxime single crystals, ESR spectra of free radicals in, 19: 36498
effects on gold-198 uptake by lymph nodes in dogs, 20: 18306
effects on goldfish survival and susceptibility to *Aeromonas salmonicida* and *Gyrodactylus* species infections, 16: 17498
effects on goldfish intestine, effects of temperature on histopathological, 19: 31670(R) (NIRS-3(p.19-56))
effects on goldfish lifespans, effects of temperature on, 19: 31670(R) (NIRS-3(p.19-56))
effects on goldfish, effects of water temperature on lethal, 20: 16236
effects on gonad development in fish, effects of season and temperature on, 20: 14307
effects on gonad development in fruit flies, 20: 42847(R) (NP-16176)
effects on gonadal and gonadotropic hormones in man, 20: 31034(R) (RLO-1780-7)
effects on gonadotropic hormone response of rat testes, 18: 17532
effects on gonads, protective effects of casein against, 16: 25233
effects on gonads of female mice progeny, 19: 7032
effects on gonads in women, 19: 28036
effects on gonads of male insects, 19: 36098
effects on gonads and liver in rabbits, biochemical, 19: 40375
effects on gonads of viviparous lizard embryos, biological, 20: 5324
effects on gonads of monkeys, pathological, 20: 31117
effects on gonads of mice, histological, 17: 31891
effects on gonads of immature female rats, 17: 5838
effects on gonads and developing embryos in mice, 17: 38905
effects on gonads, ovaries, thymus, and thyroid of animals, review on, 19: 17635
effects on gonocytes in testes of rats, 19: 38369
effects on graft-versus-host reaction in mice, 20: 24887
effects on grain beetle *Tribolium castaneum*, genetic, 19: 7021 (TID-20082)
effects on grain weevils, protective effects of hypoxia against, 18: 31296
effects on grain weevils, effects of oxygen concentration and temperature, 20: 5385
effects on grain yield and bread yield from wheat plants from irradiated seeds, 18: 21833(T) (OTS-63-11453/2(p.87-98))
effects on granulocyte release from bone marrow, 19: 29945
effects on granulocytic alkaline phosphatase activity in rats, 20: 6763
effects on granulocyte blood picture in man, 20: 18381
effects on granulocyte distribution in blood, bone marrow, and other organs in rats, whole-body, 20: 32930
effects on grass seeds, effects of moisture content on, 20: 18382
effects on grasshopper neuroblast cells, cytological, 20: 6844
effects on ground squirrels, effects of hibernation and temperature on, 20: 42835(R) (ANL-7136, pp 63-80)
effects on growing bone, 16: 8612
effects on growing bones, 17: 17879
effects on growth of wheat seedlings of different ploidy, 16: 1612
effects on growth of wheat, seed exposure, 16: 1598
effects on growth and viability of sweet clover after seed exposure, compared with thermal neutron, 16: 1600
effects on growth of transplanted tumor, 16: 4053
effects on growth in *Sinapis alba*, 16: 8558
effects on growth in *Sinapis alba*, 16: 11467(T) (AEC-tr-5016)
effects on growth and morphology of Ehrlich's ascites carcinoma cells, 16: 17481
effects on growth of rats, whole-body exposure, 16: 18780
effects on growth of cells in tissue culture, 16: 26750
effects on growth and spread of malignant tumor cells, 16: 30213(R) (ORO-566)
effects on growth of yeast, 18: 8126(T) (UCRL-Trans-1025)
effects on growth of *Escherichia coli*, 18: 8146
effects on growth of rat fangs, 18: 11688
effects on growth of rabbit skeleton, 18: 21837
effects on growth of malignant melanomas, 18: 27166
effects on growth of *Escherichia coli*, 18: 29247 (TID-20785)
effects on growth of mice compared to fast neutrons, 18: 31198
effects on growth of barley seeds, effects of chlorides of sodium, calcium, and magnesium on, 18: 33409
effects on growth and reactivity of anthrax culture in meat-peptone bouillon media, 18: 38925
effects on growth of tumor cells in culture, effects of corticosterone and mercaptopurine on, 18: 41093(R) (TID-21126)
effects on growth of bone marrow cells, 18: 43349
effects on growth of parental bone marrow transplants in hybrid mice, 18: 43224 (ORNL-P-346)
effects on growth of mammalian cells in culture, synergistic effects of nitrogen mustard on, 18: 43277
effects on growth of transplanted sarcoma in mice, 19: 124
effects on growth of transplanted fetal liver cells in mice, 19: 125
effects on growth of melanomalignomas, 19: 147
effects on growth of tumor cells in mice disseminated at surgery, preoperative, 19: 243
effects on growth of transplanted tumor cells in mice, 19: 5660
effects on growth of mammalian cells in culture, effects of ultraviolet light on, 19: 5667
effects on growth of transplanted tumor cells in rats, 19: 7081
effects on growth of *Streptococcus bovis*, 19: 7169
effects on growth of *Pisum sativum* L., 19: 7104
effects on growth of cells in tissue culture, 19: 8876
effects on growth of nerves in chicken embryos, 19: 10802
effects on growth of transplanted tumors in rats, 19: 10855
effects on growth of transplanted rat tumors, 19: 10939
effects on growth of transplanted tumors in mice, 19: 12975
effects on growth of fibroblast cells in tissue culture, 19: 12977
effects on growth inhibitors in wheat endosperm, 19: 15171
effects on growth and senescence of primary antibody forming potential in mouse spleen, 19: 15104
effects on growth of rat incisors, 19: 17529
effects on growth of polyoma virus induced tumors in hamsters, 19: 17593
effects on growth and regression of bone marrow grafts in hybrid mice, 19: 17655
effects on growth of roots, 19: 21906
effects on growth of transplanted tumors in mice, 19: 21957
effects on growth and mortality of *Ophryotrocha puerilis* and its eggs, 19: 26046
effects on growth of jaws and teeth of cats, 19: 27966
effects on growth of animal cells in tissue culture, 19: 28071
effects on growth of aluminum oxide crystals, 19: 28874(T) (AD-610971)
effects on growth and survival of chickens, 19: 29889(R) (ANL-6971 (p.90-116))
effects on growth and metabolism in seeds, 19: 29893(R) (ANL-6971 (p.166-205))
effects on growth of transplanted carcinoma cells in mice, 19: 31960
effects on growth and division of *Escherichia coli*, 19: 33852
effects on growth of tumor cells, effects of oxygen tension on, 19: 36095
effects on growth of *Escherichia coli*, influence of amino acids in growth media, 19: 36123
effects on growth of tumor transplants in mice, 19: 38387
effects on growth of progeny of male rats exposed in infantile period, 19: 40365
effects on growth hormone levels in acromegalics, 19: 42287
effects on growth of transplanted sarcoma in rats, 19: 43772
effects on growth of wheat seedlings, 19: 43717 (NASA-CR-303)
effects on growth of *Vicia faba* roots, of continuous low dose-rate exposure, 20: 87
effects on growth of jaws in kittens, 20: 91
effects on growth of transplanted sarcomas in mice, protective effects of sodium cysteinethiosulfonate against, 20: 131
effects on growth of bone marrow transplants in mice, effects of arabinofuranosylcytosine on, 20: 1687
effects on growth of lymphoid cells, on monolayers of mouse embryo cells in culture, 20: 1658
effects on growth of transplanted tumors in rats, 20: 3695
effects on growth of tumor transplants in mice, 20: 3751
effects on growth of thymus transplants in mouse kidney, 20: 5376
effects on growth of *Escherichia coli*, 20: 6779(R) (ORNL-3853, pp 88-92)
effects on growth on bone marrow cells in spleen of mice, biological, 20: 8710
effects on growth of tissue cells of Topinambour, 20: 10621
effects on growth of tumor transplants in rats, 20: 10665
effects on growth in newborn mice, effects of dose and strain on,

20: 10673
effects on growth inhibition by rat serum, protective effects of cysteine against, 20: 16208
effects on growth of wheat, effects of thermal treatment on, 20: 18323
effects on growth of cellular transplants in mice, 20: 18304
effects on growth of transplanted mouse tumors, 20: 18460
effects on growth of carcinoma and embryonal tissues in culture, effects of actinomycin on, 20: 18461
effects on growth of hamster melanomas, 20: 18463
effects on growth of uv-irradiated ascites tumor cells, 20: 20483
effects on growth of carcinoma transplants in mice, effects of inhaled carbon dioxide on, 20: 22802
effects on growth of transplanted mouse tumors, effects of temperature on, 20: 22746
effects on growth kinetics of leukemia cells, 20: 28962
effects on growth of Kalanchoe, effects of air, carbon dioxide, and nitrogen atmospheres on, 20: 31076
effects on growth and yield of wheat, effects of age of seed on, 20: 32978
effects on growth of lymphoma cells by exposure of culture medium, 20: 36633
effects on growth of transplanted hematopoietic cells in mice, 20: 38592 (ORNL-P-2158)
effects on growth of transplanted lymphoma cells in mice, effects of anoxia on, 20: 38699
effects on growth of mouse tumors, sensitizing effects of uracil on, 20: 40668
effects on growth of cells from mouse experimental fibrosarcoma, 20: 42888
effects on growth of Yoshida ascites sarcoma in rats, 20: 42962
effects on growth of cells of Jerusalem artichoke rhizomes in cultures, 20: 45437
effects on growth patterns of paramecium, mathematical model for estimation of, 20: 45472
effects on growth of human hair, 17: 38791
effects on growth and metabolism of sunflower seeds, relation between, 19: 33894
effects on growth of ovarian grafts in eye in mice, 17: 1255
effects on growth of injected peritoneal cells in mice, 17: 7805 (USNRDL-TR-597)
effects on growth and survival of durum wheat, comparison with effects of mutagenic agents, 17: 10388
effects on growth of *Serratia marcescens*, 17: 24968
effects on growth of gastrointestinal tract epithelium, local-exposure, 17: 27103
effects on growth of radioinduced bone sarcomas in rats, 17: 30367
effects on growth of fungi in media, 17: 34197
effects on growth of internodal cells in *Chara vulgaris*, 17: 33722
effects on growth of plants, 17: 35448 (TID-17490)
effects on growth and development of maize, repeated and single, 17: 38844
effects on growth of cells of Ehrlich ascites tumors in tissue cultures, 17: 40549 (TID-18210)
effects on growth-stimulating properties of injected, in mice, 19: 21897
effects on growth, iodine-131 uptake, and morphology of transplanted thyroid in rats, 20: 24907
effects on guinea vaccinal process following BCG immunization, 16: 62
effects on guinea pig skin melanocytes, 18: 5053
effects on guinea pig skin, protective effects of cysteamine against, 18: 11861
effects on guinea pig muscle enzymes, 18: 17494
effects on guinea pigs, protective effects of calf serum and human γ-globulin against, 18: 17669
effects on guinea pig histamine sensitivity, 18: 21841
effects on guinea pigs, protective effects of serotonin against, 18: 29391
effects on guinea pig heart muscle cells, 18: 29336
effects on guinea pig and rat intestinal tryptophan content, 18: 29278
effects on guinea pigs, effects of autoinfection on hemorrhagic syndrome, 19: 3997
effects on guinea pigs, synergistic effects of radar on, 19: 7108
effects on guinea pig brain, 19: 15078
effects on guinea pigs and rats, protective effects of spleen transplants against, 19: 24372
effects on guinea pigs and rats, protective effects of anaphylatoxin against, 19: 26147
effects on guinea pigs, effects of pre-irradiation on lethal, 20: 5356
effects on guinea pigs, carcinogenic, 20: 6814
effects on guinea pig skin, biological, 20: 22793
effects on guinea pigs, protective effects of gibberellic acid against, 20: 24944
effects on guinea pig kidneys, effects of fractionated and single exposure on, 20: 24933
effects on guinea pig kidneys, fractionated or whole-body exposure, 20: 45434
effects on guinea pigs, fractionated-dose epilatory, 17: 1281
effects on guinea pigs, fractionated-doses epilatory, 17: 1282
effects on guinea pig intestine, cytological and cytochemical, 17: 33642
effects on guinea pigs, protective effects of meso-dithiosuccinic acid against, 17: 35486
effects on guinea pigs, protective effects of DL-dithiosuccinic acid against, 17: 35487
effects on guinea pigs and rabbits, protective effects of chemical agents against, 17: 38804
effects on hair, 18: 38857
effects on hair dysplasia in mice, effects of cysteamine on, 17: 27174
effects on hair follicles and skin on mice, elongate microbeam, 17: 23154
effects on hair growth, 19: 33868
effects on hair of mice, 19: 5658
effects on hair of mice, local and whole-body, 19: 43833
effects on halite subjected to pressure, 19: 5972
effects on halogenated alkenes, chemical, 19: 5948 (TID-21388)
effects on hamsters, protective effects of bone marrow against, 18: 11877
effects on hamster melanomas, 18: 11907
effects on hamster lung cells, 18: 19670
effects on hamster cells, effects of oxygen on, 19: 26153
effects on hamster cells in culture, 19: 29886(R) (ANL-6971(p.29-46))
effects on hamster mouth, pathologic, 19: 36092
effects on hamster cells in tissue culture, fractionated doses, 19: 43791
effects on hamster and HeLa cells after plating and trypsinization, dose response in, 20: 36664
effects on hamster cells *in vitro*, carcinogenic, 20: 42927
effects on hamster melanoma, effects of cold, cytostatics, and immunology on, 18: 27108
effects on hands, pathological, 19: 19524
effects on hands, surgical treatment of, 17: 21475
effects on haploidy in *Petunia hybrida*, 19: 7173
effects on hardening of silver-doped potassium chlorides at low temperatures, (E), 20: 22321
effects on hardness of crystals of potassium chloride and lithium fluoride, 20: 43304
effects on hatchability of *Artemia salina* oocytes, effects of low temperature on, 20: 18447
effects on hatching of chicken eggs, 18: 31255
effects on hatching of chick embryos, 17: 38840
effects on head of rats, 18: 27161
effects on heading time in mutant strains of rice plants, 19: 7093
effects on healing of infected wounds in rabbits, repeated, 16: 16211
effects on healing of closed fractures of bones in rabbits, 19: 7164
effects on healing of bone fractures in rabbits, 19: 10817
effects on healing of skin wounds of mice, effects of radioprotective compounds on, 20: 6878
effects on health and fertility of dentists exposed occupationally, 20: 59(R) (NYO-901-37, pp 31-2)
effects on heart, acute local exposure, 17: 23140
effects on heart function, 20: 213
effects on heart in rabbits, 16: 26669(T) (JPRS-14767(p.1-13))
effects on heart muscle fiber in dogs, 16: 4080
effects on heartbeat of frog, 16: 25216
effects on HeLa and L cell survival, effects of ploidy on, 20: 24854
effects on HeLa cell size, protective effects of AET and thymidine analogues against, 18: 11873
effects on HeLa cell fine structure, 18: 19723
effects on HeLa cells and water phantoms, quality and RBE, 19: 24339
effects on HeLa cells, sensitivity effects of trypsinization on, 19: 25960
effects on HeLa cells in tissue culture, fractionated doses, 19: 43790
effects on HeLa cells in culture, effects of anoxia and *N*-ethylmaleinimide on, 20: 31130
effects on HeLa cells in culture, biological, 20: 31056
effects on HeLa cells, protective effects of AET and sodium tripolyphosphate against, 19: 17678
effects on HeLa cells, 17: 35484
effects on HeLa S3 mitosis, 18: 29306
effects on HeLa S3 cells *in vitro*, kinetics of, 20: 33065
effects on hemangiomas in children, 20: 12750
effects on hemato-encephalic barrier permeability in rats, 20: 14312
effects on hematoencephalic barrier and cerebral blood vessels, 16: 23493
effects on hematology and pathology in monkeys, effects of bone marrow transplants on whole-body, 20: 33071
effects on hematopoietic and thrombopoietic systems in rabbits, whole-body, 16: 4059
effects on hematopoietic system in weanling rats, 16: 4093
effects on hematopoietic system in weanling mice, 16: 8597
effects on hematopoiesis in mice, rats, and guinea pigs, 18: 107

effects on hematopoietic system of mice, effects of toxin on recovery from, 18: 43315
effects on hematopoietic system in goldfish, 19: 2101
effects on hematopoietic system of mice injected with foreign bone marrow, 19: 5722
effects on hematopoietic system of rats, 19: 10867
effects on hematopoietic system in rabbits and rats, 19: 19499(R) (NP-14899)
effects on hematopoiesis and survival of mice, 19: 21889
effects on hematopoietic system in man, whole-body, 19: 21874
effects on hematopoiesis in rats, effects of tumor growth on, 19: 28049
effects on hematopoiesis in mouse spleens, effects of biological materials on, 19: 29935
effects on hematopoietic colonies in mouse spleen, 19: 31852
effects on hematopoietic system in Carassius, effects of temperature on, 19: 31670(R) (NIRS-3(p.19-56))
effects on hematopoietic system in mice, pathological, 19: 36100(R) (NP-15170)
effects on hematopoietic system, 19: 36192
effects on hematopoietic system, leukemogenic, 20: 3730
effects on hematopoietic system of rabbits, fractionated exposures, 20: 5364
effects on hematopoietic activity of bone marrow cells in culture, 20: 6784(R) (ORNL-3853, pp 118-27)
effects on hematopoiesis in mice, protective effects of intestinal shielding against, 20: 18432
effects on hematopoiesis in mice and rabbits, effects of mucopolysaccarides on, 20: 20510
effects on hematopoietic stem cells in mice, 20: 22640
effects on hematopoiesis, effects of fractionated exposure on, 20: 28984
effects on hematopoietic systems of dogs, lower-body, upper-body, and whole-body, 20: 29029
effects on hematopoietic system in mammals, 20: 42844 (BNL-10385)
effects on hematopoietic system in guinea pigs, mice, and rats, single whole-body, 17: 4398
effects on hematopoietic system in rabbits, 17: 4428
effects on hematopoietic system in mammals, 17: 17757 (TID-16572)
effects on hematopoiesis in rats, 17: 40627
effects on heme synthesis in rabbits, 18: 33400
effects on heme synthesis in rabbit bone marrow cells, 19: 33873
effects on heme synthesis in rabbit bone marrow cells, effects of hormones on, 20: 28912
effects on hemoglobin recombination, 18: 38909
effects on hemoglobin synthesis in chick marrow cells in culture, 19: 24300
effects on hemoglobin synthesis in chickens, 20: 76
effects on hemoglobin synthesis in rabbits, whole-body exposure, 17: 61
effects on hemoglobin in rabbits from abdominal skin exposure, 17: 4426
effects on hemolysis and membrane permeability of erythrocytes, 20: 18468
effects on hemolysin synthesis in rabbits, 20: 42835(R) (ANL-7136, pp 63-80)
effects on hemopoiesis in sheep, 19: 19600
effects on hemopoietic system in guinea pigs, chronic low-dose, 20: 28945
effects on hemopoiesis in monkeys, tracer study after whole-body exposure, 17: 54
effects on hepatic regeneration in rats, 19: 8843
effects on hepatic enzymes induced by phenobarbital or phenaglycodol, 17: 33691
effects on hepatic regeneration, whole- and partial-body exposure, 17: 5854
effects on heredity, 19: 36088
effects on heritable histocompatibility changes in mice, hypothesis on, 20: 35309
effects on heterozygous female Drosophila, mutagenic, 20: 22655
effects on hexacyanoferrates in acid, alkaline, and neutral solution, 20: 23179
effects on hexane, determination of ion mobilities and yields from, 20: 25140
effects on hexobarbital inhibition of respiratory centers in rat fetuses, 19: 15075
effects on hibernating ground squirrels, lethal, 20: 42834(R) (ANL-7136, pp 46-63)
effects on higher nervous system in rats, repeated, 17: 7897(T)
effects on higher nervous activity in rats, 17: 30362
effects on Hill activity and phosphorylation of chloroplasts, 20: 20428
effects on hippocampal spike activity in rat brain, 19: 26099
effects on hippuric acid synthesis in rat liver, effects of glycine on, 18: 19631
effects on histamine and histaminase content of rat tissues, 18: 27186
effects on histamine content in blood and tissues of rabbits, effects of antibiotic therapy on, 18: 35325(T) (JPRS-25464(p.8-13))
effects on histamine content of tissues, 19: 15023(T) (FTD-TT-64-644)
effects on histamine content of tissues of rabbits and rats, 20: 26677
effects on histidine decarboxylase activity in rat stomach, 19: 17604
effects on histidine decarboxylase in rat stomach, 19: 35950(R) (TID-22047)
effects on histidine decarboxylase content of stomach, 17: 30228(R) (TID-19086)
effects on histochemical and histological changes in rat central nervous system, 19: 26090
effects on histology and nucleic acid content of cerebellum in guinea pig, 16: 32824
effects on histology and cytology of thymus gland, in mice, whole-body, 18: 3557
effects on histology and saline-soluble DNA content in mouse spleen, 18: 23257
effects on histology and tumor development in rat bones, 19: 21886
effects on histology of axolotl extremities, cell regenerative effects of RNA in, 19: 26137
effects on histology of rat spleen during immune response, local, 20: 36637
effects on histologic structure of hair follicles of the skin in castrated mice, 17: 1249
effects on histology and function of kidneys in rabbits, 17: 5904
effects on histone localization and structure in rat thymocytes, 19: 7078
effects on histone synthesis in mouse tumors by inhibition of DNA replication, 19: 15052
effects on histones in rat thymocytes, staining technique for studying x, 20: 22709
effects on homocysteinethiolactone, ESR spectra of, 20: 386
effects on homograft reactions in mice, 16: 11487
effects on homograft reactions to bladder transplants in dogs, 20: 22718
effects on homograft tolerance in mice with and without urethan, 17: 24993
effects on homologous bone marrow transfusions, 18: 3544
effects on homologous skin grafts in rats, 18: 25114
effects on hormone synthesis in rat adrenal gland, 19: 33905
effects on hormone synthesis in adrenal cortex, whole-body exposure, 17: 1259
effects on horse bean plantules, effects of oxygen pressure on, 18: 23299
effects on host response to tapeworms, 20: 36607(R) (TID-23114)
effects on human amnion cells, 19: 31788(R) (ORNL-3768(p.33-57))
effects on human brain from scalp epilation, 18: 136
effects on human blood, 18: 13486
effects on human blood platelets in plasma suspension, 19: 133
effects on human blood coagulation, therapeutic, 19: 15117
effects on human breasts, carcinogenic, 19: 27979
effects on human cells at various oxygen concentrations, equations for, 18: 31144
effects on human chromosomes, 18: 33334
effects on human cells in tissue culture, genetic, 19: 43844
effects on human chromosomes, aberrant, 20: 5351
effects on human cells in culture, biological, 20: 40623(R) (ORNL-3922, pp 32-49)
effects on human chromosomes, 18: 21856
effects on human cell nuclei, 17: 30358
effects on human chromosomes, spinal-irradiation, 17: 38792
effects on human cells, protective effects of nucleosides against, 17: 40613
effects on human embryos and fetuses, injurious, 19: 25965
effects on human electrocardiographs, 20: 20474
effects on human erythrocyte diameter and volume from occupational exposure to, 20: 40678
effects on human genetics by infant exposure, 19: 19568
effects on human gonads, 20: 31034(R) (RLO-1780-7)
effects on human kidney cells, methods for modification of, 18: 19760
effects on human kidney cultures, protective effects of iododeoxyuridine and heavy ions against, 19: 26125
effects on human kidney cells, factors affecting RBE, 20: 40725
effects on human leukocyte chromosomes, 18: 15840
effects on human lymph vessels, 18: 19604
effects on human leukocyte chromosomes, 18: 21879
effects on human lymphocyte chromatics, aberrant, 19: 2130
effects on human lymphocytes, toxic, 18: 23294
effects on human nervous system, electroencephalographic study, 18: 29302
effects on human pituitary, tumorigenic, 19: 24294
effects on human populations, low-dose, 20: 14331
effects on human recovered amnion cells, 19: 21986
effects on human stomach, 19: 5715
effects on human skin following breast radiotherapy, 19: 8901
effects on human skin, ultracellular, 19: 8902
effects on human skeleton following skin hemangioma therapy,

20: 22636
effects on human skin, late, 20: 35381
effects on human spermatogonia, 20: 40627(R) (ORNL-3922, pp 84-8)
effects on human thyroid, 20: 42857(R) (TID-23228)
effects on hyaline cartilage regeneration in rabbits, 18: 38785
effects on hyaluronidase activity and release in guinea pig and rat spermatozoa, x, 18: 17506
effects on hyaluronidase-hyaluronic acid system in rats and rabbits, 18: 27194
effects on hyaluronidase activity, 18: 43257
effects on hyaluronidase activity and tissue permeability in animals, 19: 17580
effects on hybrid mice grafted with skin from parents, 20: 40651
effects on hybridization between species and varieties of fruit trees, 19: 5717
effects on hydrogen bond rupture in DNA in spleen and thymus in rats, 19: 8916
effects on hydrolysis of salicyl phosphate, 20: 20744
effects on *Hymenolepis microstoma*, 20: 36662
effects on hypertaurinuria induction in rats, effects of cysteine on, 19: 26134
effects on hypertensive damage in blood vessels, 17: 5844
effects on hyperthyroidism, therapeutic, 19: 15288
effects on hypertrophied breast tissue after estrogen therapy for prostate cancer, 20: 22825
effects on hypophysectomized and normal rats treated with sex hormones, 16: 20185
effects on hypophysis during hibernation, 16: 26833
effects on hypothermic mice, protective effects of MEA against, 19: 3994
effects on hypoxanthine production by microorganisms, 18: 10177(P)
effects on immature bones in young mice, 16: 4092
effects on immune response, effects of intestinal shielding, 16: 6340
effects on immune reactions to skin grafts in mice, 16: 17549
effects on immune reactions in bone marrow chimeras, 16: 21918 (USNRDL-TR-560)
effects on immune reactions, 16: 28785
effects on immune reactions to skin grafts, 18: 115
effects on immune reactions in guinea pigs, 18: 15825
effects on immune reactions in rabbits, 18: 15881
effects on immune reactions in guinea pigs, 18: 27193
effects on immune reactions to tumor transplants in mice, 18: 29318
effects on immune reactions in rats, 18: 33387
effects on immune reactions in tumor cells in mice, 18: 35326(T) (JPRS-25464(p.22-30))
effects on immune response in rats, 18: 35302(R) (AD-438540)
effects on immune response in mice, 18: 35303(R) (AD-438541)
effects on immune reactions in rats, 18: 36980
effects on immune reactions in rabbits, 18: 41178
effects on immune reactions in xenogenic mouse chimeras, 18: 41079(R) (HW-80500(p.124-6))
effects on immune reactions in mice, 18: 43324
effects on immune reactions in dogs, 19: 71 (LF-17)
effects on immune reactions in mice, 19: 2075(R) (ORNL-3700(p.101-11))
effects on immune reactions in mice, 19: 3905
effects on immune reactions in dogs, 19: 3976
effects on immune reactions in mice, 19: 5642
effects on immune reactions in hibernating ground squirrels, 19: 7013(R) (ANL-6906(p.23-6))
effects on immune reactions in rats, 19: 8863
effects on immune reactions in thymectomized rats, 19: 8872
effects on immune response in thymectomized mice, protective effects of thymus grafts against, 19: 8978
effects on immune reactions in mice, 19: 8838
effects on immune reactions in mice, 19: 10797
effects on immune reactions in chickens, 19: 10854
effects on immune response in rabbits, 19: 13001
effects on immune reactions in mice, 19: 13012
effects on immune reactions in mice, 19: 13014
effects on immune responses of spleen cells in thymectomized mice, 19: 15217
effects on immune reactions in rabbits, 19: 15022 (USNRDL-TR-799)
effects on immune globulin sequence in rabbits following immunization, 19: 15105
effects on immune response to transplanted tumors in mice, 19: 17503
effects on immune reactions in mouse chimeras, 19: 17504
effects on immune reactions in mouse chimeras, 19: 17505
effects on immune reactions in mouse chimeras, 19: 17506
effects on immune reactions to transplanted kidney in dogs, 19: 19519
effects on immune reactions to kidney transplants, 19: 19520
effects on immune reactions to spleen transplants in dogs, 19: 19521
effects on immune reactions to spleen transplants, 19: 19522
effects on immune reactions to lung transplants, 19: 19523
effects on immune reactions in rats, 19: 22003
effects on immune reactions in mice, 19: 21896
effects on immune reactions to skin grafts of burn wounds in rabbits, 19: 21905
effects on immune reactions in mouse chimeras, 19: 21943
effects on immune reactions to bone marrow transplants in mice, 19: 21961
effects on immune reactions to bone marrow grafts in mice, 19: 25909 (ORNL-P-1211)
effects on immune reactions in tumor-bearing rats, 19: 26040
effects on immune reactions in rats, 19: 28091
effects on immune reactions to skin grafts in mice, 19: 28093
effects on immune reactions to kidney grafts in dogs, 19: 28094
effects on immune reactions to kidney transplants in man, whole-body, 19: 27987
effects on immune reactions to renal homografts, 19: 27995
effects on immune reactions in rabbits, 19: 29892(R) (ANL-6971(p.143-58))
effects on immune reactions of embryonic chick spleen, 19: 29837
effects on immune reactions in mice, 19: 29896 (EUR-2201.f)
effects on immune reactions in germ-free mice, 19: 29939
effects on immune reactions to skin grafts, in rabbits and rats, 19: 29942
effects on immune reactions in man and rabbits, 19: 29981
effects on immune reactions to kidney transplants, whole-body, 19: 31956
effects on immune reactions to kidney transplants in dogs, 19: 33820
effects on immune reactions to kidney transplants, 19: 33828
effects on immune reactions in mice, 19: 33855
effects on immune reactions in mice, 19: 33859
effects on immune reactions to spleen cell transplants in mice, 19: 36029
effects on immune reactions to tuberculosis infection in guinea pigs, 19: 38375
effects on immune reactions in mice, 19: 42338
effects on immune reactions to injected spleen cells in rats, 19: 42339
effects on immune reactions in mice, 19: 45827
effects on immune response to transplanted kidneys in man, 19: 45888
effects on immune reactions to parental spleen cell grafts in rats, 20: 86
effects on immune reactions to transplanted kidneys, 20: 125
effects on immune reactions in mice to injected allogenic and syngenic bone marrow, 20: 1660
effects on immune reactions in mice and rats, 20: 1632
effects on immune reactions to sheep erythrocytes in rabbits, 20: 3689
effects on immune reactions in rabbits, 20: 3738
effects on immune reactions in injected thymocytes and lymph node cells in mice, 20: 3777
effects on immune reactions in rabbits, 20: 3746
effects on immune reactions in thymectomized mice, 20: 5408 (USNRDL-TR-920)
effects on immune reactions in mice, 20: 5413
effects on immune reactions to marrow transplants in mice, methods for assaying, 20: 5372
effects on immune reaction to baboon kidney transplants in man, 20: 6813
effects on immune reactions to bone marrow transplants in mice, effects of previous transfusions on, 20: 6886
effects on immune reactions in mice and rats, 20: 6893
effects on immune reactions in guinea pigs, 20: 6833
effects on immune reactions to injected bone marrow, in leukemic man and mouse, 20: 8793
effects on immune reactions in rabbits, 20: 8669
effects on immune reactions in thymectomized rabbits, 20: 8669
effects on immune reactions in thymectomized-appendectomized rabbits, 20: 8669
effects on immune reactions of mice to rat tissue transplants, 20: 10505(R) (BNWL-122, pp 146-9)
effects on immune properties of sarcoma cells in suspension, 20: 10634
effects on immune reactions to allogenic skin grafts in mice, 20: 12656
effects on immune reactions to injected bone marrow and lymph cells in mice, 20: 20472
effects on immune reactions in mice, 20: 22615(R) (NIRS-4, pp 34-58)
effects on immune reactions in mice, 20: 24918
effects on immune response of thymectomized chickens, 20: 29014
effects on immune reactions in blood cells of dogs, 20: 33015
effects on immune response of rats, 20: 35280
effects on immune response in rabbits, 20: 35301
effects on immune reactions in rabbit eyes, 20: 38608
effects on immune reactions in adrenal cortex of rabbits, 20: 38697
effects on immune system and lymphatic tissues in estradiol-injected mice, effects of marrow transplants on, 20: 40577
effects on immune reactions to tissue transplants, 20: 43013(R) (ORO-2459-1)
effects on immune reactions in rabbits, 20: 42855(R) (TID-23203)
effects on immune reactions in rabbits, 20: 42830 (AD-635598)
effects on immune reactions to bone marrow grafts in dogs and mice,

20: 45484
effects on immune response, 17: 7698
effects on immune reactions in mice, 17: 7850
effects on immune reactions in mice, 17: 7851
effects on immune reactions to injected bone marrow cells in mice, 17: 19812 (USNRDL-TR-630)
effects on immune response in mice, 17: 22981
effects on immune response, 17: 31914
effects on immune reactions to transplanted tumors, 17: 31915
effects on immune responsiveness in rabbits, 17: 38793
effects on immune responses in rabbits, 17: 38808
effects on immunity to gas-gangrene and tetanus in guinea pigs, 16: 7459(T)
effects on immunity and leukocytic response in rabbits, 16: 9876
effects on immunity to transplanted tumors in mice, 18: 11799
effects on immunity transfer to sarcoma I homografts in newborn mice, 19: 17574
effects on immunity to Brucella vaccine in guinea pigs and rats, 19: 28004
effects on immunity in rabbits, role of humoral factors in, 19: 35953
effects on immunity against tumor tissue, 19: 42292
effects on immunity and lymphopoiesis of mouse thymus, 18: 17498
effects on immunity to *Trichinella spiralis* infection in mice, 17: 10424
effects on immunity to *Schistosoma mansoni cercariae* in mice, 17: 24992
effects on immunity to intestinal infections in monkeys, 17: 24953
effects on immunogenic uveitis development in rabbits, 18: 38847
effects on immunogenicity of tendon grafts, 19: 45964
effects on immunogenicity of tendon grafts, 19: 45965
effects on immunogenicity of *Dictyocaulus filaria* larvae, 20: 8653
effects on immunogenic efficiency of double vaccination with *Ancylostoma caninum*, 20: 31043
effects on immunological reactions, 16: 8627
effects on immunological reactions in rabbits, 16: 8639(T)
effects on immunological factors, 16: 12909
effects on immunological restoration by thymus in rats, 18: 15869
effects on immunological response to diphtheria antitoxin in rabbits, 19: 28078
effects on immunological reconstruction in guinea pigs, 19: 33947
effects on immunological paralysis in mice, 20: 8716
effects on immunologically competent cells in graft-versus-host reaction in mice before and after antigenic contact, 20: 33083
effects on immunological tolerance to skin homografts in mice, 17: 96
effects on immunological recovery in mice, role of thymus in, 17: 10412
effects on immunologic tolerance in rats, 17: 15761
effects on implantation frequency of rat ova, 18: 11661
effects on implanted ascites hepatoma in mice, therapeutic, 20: 45516
effects on *in vitro* or *in vivo* mouse oocyte survival, 19: 8861
effects on *in vitro* hamster cells, 17: 33673
effects on *in vitro* guinea pig cells, 17: 35475
effects on inactivation of pathogenic bacteria, use as biological dosimeter, 19: 13075
effects on inactivation of bacterial spores, heat effects on, 19: 17539
effects on inactivation of *E. coli* T5, protective effects of cystamine, cysteamine, and hydrogen sulfide against, 19: 26146
effects on inactivation of replicative factor-DNA, 19: 42295
effects on inactivation of papain coupled with poly-p-aminophenylalanine, 19: 45976
effects on inactivation of bacteriophage T1, protective effects of cystamine and cysteamine against, 20: 33094
effects on inactivation of lambda phage in bacteriophage, protective effects of chemicals against, 20: 33078
effects on inactivation and mutability in Saccharomyces, 20: 45469
effects on incidence of *Streptococcus equi* infections in burros, 20: 14288 (AD-627986)
effects on incidence and latency of lymphosarcomas in mice, 20: 18317
effects on incidence of bacteremia and hemorrhage in guinea pigs, 20: 38656
effects on incidence of plasmocytoma, 17: 91
effects on incidence of tumors and life span of mice injected with Ehrlich ascites tumor cells, 17: 40640
effects on inclusions in chicken heart and liver mitochondria, 18: 36974
effects on inclusion compounds between urea and ethers, ESR studies of, 19: 22323
effects on incompatibility in *Oenothera organensis*, 20: 14382
effects on incorporation of amino acids into proteins, 18: 23259
effects on incorporation of DNA precursors in mammalian cells *in vivo*, 17: 12164
effects on incretory and secretory function in dog pancreas, dietary effects on, 19: 21938
effects on induction of hereditary cataracts in young rats, 19: 15139
effects on induction of giant and neoplastic cells in earthworms, 19: 15072
effects on induction of isoleucine- and valine-requiring mutants of *E. coli*, biochemistry and genetics of, 19: 15083
effects on induction of immunologic disorders in man and mice, hypothesis on, 19: 17507
effects on induction of streptomycin resistant mutations in *Cholera vibrio*, hard and soft, 19: 17547
effects on induction of electronic energy levels in n-type germanium, 19: 20612 (AFCRL-64-839)
effects on induction of viral leukemia in mice, 19: 33793
effects on induction of chromosome aberrations, 19: 36096
effects on induction of neoplasms in rat thyroid, by exposure of single lobe, 19: 38367
effects on induction of mutations in male mice, superlethal, 19: 38393
effects on induction of leukopenia in rabbits, 20: 5315
effects on induction of allergic encephalomyelitis in rats, whole-body exposure, 17: 27124
effects on induction of mammary tumors, in dogs, 17: 31860(R) (UCD-107(p,30-43))
effects on industrial radiographers, 19: 42667
effects on infants, leukemogenic, 19: 3946
effects on infective capacity of *Schistosoma mansoni* cercariae in mice, 19: 126
effects on infectivity of viruses in mice, 19: 7047
effects on infection latency in guinea pigs and mice, 19: 24269
effects on infectious processes in mice, 19: 33950
effects on infectivity of larvae of *Ancylostoma caninum* in dogs, 19: 33861
effects on infectivity of viruses, 19: 36046
effects on inflammation associated with Mikulicz's disease, 20: 3826
effects on inflammation of herpes zoster, 20: 3836
effects on inheritable metabolic deficiencies in animal cells in culture, 18: 41072 (CONF-534-3)
effects on inhibition of nucleoside phosphorylase in rat erythrocytes, 18: 8174
effects on inhibition of antitumoral immunity in mice, protective effects of cystamine against, 19: 8961
effects on inhibition of homogenate of regeneration blastemas in salamanders, 19: 15076
effects on inhibition of glycolysis of Ehrlich ascites carcinoma, labile phase of, 17: 31959
effects on initiation of DNA replication in *E. coli*, 19: 26070
effects on inoculation tumors in rats, histological, 18: 3558
effects on insect spermatocytes, 18: 29338
effects on insects, bibliography on, 19: 5628 (TID-3579)
effects on insemination and sperm retention in *Drosophila melanogaster*, 18: 9859
effects on inseminated and virgin Drosophila females, mutagenic, 20: 12663
effects on insulation resistances in polyethylene and Teflon, 18: 43621
effects on insulated gate field effect MOS transistors, 20: 39273(R) (AD-635198)
effects on insulators, bulk photovoltaic, 18: 18442
effects on insulin distribution in rats, tracer study of, 20: 42932
effects on interaction of induced chromosome breaks in barley seed, 19: 42343
effects on interconversion of cystine and cysteine, 19: 34228
effects on internal and middle ear in rabbit, 16: 1501
effects on interstitial mucopolysaccharides in hibernating animals, 16: 11484
effects on intestinal vascular permeability, 16: 1503
effects on intestinal glucose absorption, 16: 5178
effects on intestinal permeability by macromolecules, whole-body exposure, 16: 14517
effects on intestinal function in rats, whole-body, 18: 3492 (TID-18282)
effects on intestinal absorption of vitamins, 18: 13419(R) (TID-20242)
effects on intestinal stenosis following therapy for gynecologic carcinoma, 18: 13488
effects on intestines in rats, protective effects of MEA and mesenteric vessel clamping against, 18: 27204
effects on intestinal permeability to polyvinylpyrrolidone in rats, 18: 41080(R) (HW-80500(p.127-8))
effects on intestinal mucosa of mice, 19: 10832
effects on intestines in rats, use of polyvinylpyrrolidone leakage for measurement of, 19: 10891
effects on intestinal epithelium of goldfish, effects of temperature on, 19: 10880
effects on intestinal mucosa of germfree mice, whole-body, 19: 25997
effects on intestinal absorption of sugars in rats, 19: 33842
effects on intestinal motor function in dogs, 19: 35956
effects on intestine in chick embryos, protective effects of cysteamine against, 19: 42357
effects on intestinal cells of hedgehog, effects of hibernation on histologic, 20: 5377
effects on intestinal flora following cervical tumor therapy, 20: 6866

effects on intestinal sorption following abdominal cancer therapy, 20: 8713
effects on intestinal absorption of bile salts in rats, 20: 10599(R) (BNWL-122, pp 128-30)
effects on intestinal mucosa after abdominal therapy, 20: 14339
effects on intestinal epithelium in mice, lethal whole-body exposure, 20: 16223 (BNL-8952)
effects on intestine following radiotherapy, 20: 24966
effects on intestinal secretory functions in dogs, effects of dietary fatty acids on, 20: 28993
effects on intestinal mucosa in mice, 20: 31082
effects on intestinal absorption of iron in rats, iron-59 tracer study of, 20: 33003
effects on intestinal cells of rats and amphibians, 20: 40607 (BNL-10518)
effects on intestine, cytological, 16: 14575
effects on intestine, protective effects of β-mercaptoethylamine and blood vessel clamping on, 17: 27112
effects on intestinal absorption and elimination of N^1-methylnicotinamide in rats, whole-body, 17: 40661 (TID-18205)
effects on intra- and extra-cellular potassium content in mice, use of EKG to study, 20: 45444
effects on intracellular organelles in mice, 20: 20413
effects on intracellular enzyme oxidation-reduction state in mouse and rat organs, 20: 22708
effects on intracellular virus, 17: 21535
effects on intracutaneous and intramuscular resorption of gold-198 and iodine-131 in man, 19: 8918
effects on intraocular tumors, therapeutic, 20: 12740
effects on intrasplenic ovarian transplants in rats, 19: 33925
effects on inulin space in rats, 18: 8128
effects on inverse mutation induction in *E. coli*, 19: 15188
effects on iodide ions in acetone solutions, 19: 13464
effects on iodine-131 uptake and thyroid hormone synthesis in chick embryo, 16: 31473 (UR-616)
effects on iodine metabolism and thyroid function in mice, 19: 13081
effects on iodine-131 metabolism in rat thyroid, 18: 9881
effects on iodine-131-labeled triolein absorption in man, 19: 15111
effects on iodine-131-labeled triolein absorption by rat intestine, 19: 17498
effects on ion mobilities in carbon tetrachloride, dioxane, ethyl ether, and hexane, 20: 18724 (BNL-10012)
effects on ion mobility in liquid dodecane, hexadecane, and tetrodecane, 20: 20734
effects on ionic crystals, mechanisms of coloration from, 18: 39332
effects on ionic conductivity of potassium bromide crystals, (E), 19: 23150
effects on ionic permeability of rat and rooster erythrocytes, 19: 19577
effects on ionization of germanium and silicon as function of temperature, 20: 46959(T)
effects on iridindiphosphate glucose content in rat liver, 20: 10590
effects on iron catalase, resonance in, 18: 12145 (PRNC-14)
effects on iron content of erythrocytes, in rats, 19: 33940
effects on iron incorporation in erythrocytes, protective effects of AET, cysteine, and serotonin against, 19: 212
effects on iron metabolism in rat, whole-body single exposure, 16: 4091
effects on iron metabolism in bone marrow and erythrocytes, time-factor, 16: 14554
effects on iron metabolism in blood, whole-body exposure, 16: 23430
effects on iron metabolism in liver, tracer study, 16: 28755(T) (JPRS-13953(p.39-47))
effects on iron metabolism in dogs, whole-body, 16: 30221(T) (AEC-tr-5354)
effects on iron metabolism in bone marrow cells in tissue culture, 19: 10866
effects on iron metabolism in rat blood, effects of erythropoietin on, 19: 21948
effects on iron storage in rat liver, 19: 5713
effects on iron-59 uptake by rat bone marrow megakaryocytes *in vivo*, 16: 4073
effects on iron-59 incorporation into rat liver cells, effects of preliminary cysteamine injection, 17: 14061
effects on iron-59 uptake by organs in mice, 17: 30386
effects on iron-59 uptake by erythrocytes in mouse bone marrow, 17: 33624
effects on iron-59 uptake by rat mucosa, protective effects of MEA against, 18: 19787
effects on iron-59 uptake by bone marrow, erythrocytes, liver, and spleen in rabbits, dynamics of, 18: 27141
effects on iron-59 uptake by intestines in rats, 18: 27204
effects on iron-59 metabolism, 18: 35353
effects on iron-59 uptake by mice, sex differences in, 19: 17652
effects on iron-59 uptake by bone marrow and spleen in intact and splenectomized mice, 20: 22610 (AD-632049)
effects on iron-59 metabolism in rat blood, 20: 40561
effects on islet-cell tumors in pancreas in rats, 17: 10432
effects on isograft resistance to Rous sarcomas in mice, 20: 6825
effects on isolated tissues of cockroach, 19: 10800
effects on isolated ascites tumor cells, metabolic, 18: 27087
effects on isolated adrenal gland, 17: 72
effects on isolated tobacco leaves transmitted to shielded parts of plant, 17: 38847
effects on isomerization of stilbene, 20: 33334 (NYO-3242-13)
effects on jaw bone and teeth in rats, 17: 24952
effects on jaws and teeth of weanling rabbits, x, 20: 45354(R) (COO-119-234, pp 227-50)
effects on jaws and teeth in rats, 17: 5867
effects on jute leaves, aberrant, 18: 43292
effects on jute plants, genetic, 20: 18385
effects on jute, cytogenetic study of mutagenic, 20: 22686
effects on karyokinetic activity in embryonal cells, 19: 7184
effects on KB tumor cells, 17: 38817
effects on keratins, radical state, 16: 27086
effects on keratinization in squamous cell carcinomas following radio-therapy, 20: 18255
effects on ketone–urea inclusion compounds, ESR studies of, 19: 22323
effects on kidney function and hypertrophy in nephrectomized rats fed high protein diet, 16: 8555
effects on kidney transplant immunity in dogs, 18: 17495
effects on kidney transplant survival in, 19: 12969
effects on kidney homografts in dogs by local graft exposure, 19: 38425
effects on kidney function in dogs, 20: 14342
effects on kidney tissue cultures after foot-and-mouth disease infection, 20: 35319
effects on kidney tissues and renal clearance of mice, 20: 36608
effects on kidney function in man, early, 17: 27077
effects on kidney morphology and function, single, local exposure, 17: 30291 (UR-626)
effects on kidneys in dogs, 18: 21834
effects on kidneys of mice exposed at birth, pathological, 20: 22733
effects on kidneys and survival of rats, effects of suprarenal shielding on whole-body, 20: 34334
effects on kidneys, effects of nephrectomy on neoplastic, 16: 18778
effects on kidneys in rabbits, 17: 24910
effects on kinetics and optics of pancreatic ribonuclease, 19: 11219
effects on kinetics of DPN-enzyme coupled reactions, 17: 33625
effects on Kurloff bodies in guinea pig lymphocytes, 20: 22690
effects on L cells, effects of age on, 19: 26074
effects on L cells, recovery from fractionated-dose, 19: 26074
effects on L-ascorbic acid synthesis in rat liver microsomes, 19: 10803
effects on L-cells, restoration of viability following, using isologous subcellular fractions, 18: 19783
effects on L-cells, protective effects of depolymerized DNA and DNA-nucleotides against, 20: 8733
effects on L-leucine crystallization by exposure to human blood serum, 19: 15094
effects on labeled bone marrow cells appearance in peripheral blood in rat, 16: 14559
effects on labeled phosphate uptake by rat liver, 18: 17422
effects on labeled orotic acid uptake by RNA and DNA polymerase and thymidylic kinase activities in rats, 19: 21877
effects on lachrymal system of rabbits, 20: 35304
effects on lactate dehydrogenases, protective effects of glycerol against, 18: 21914
effects on lactate dehydrogenase enzyme in rat brain, 19: 15106
effects on lactate metabolism in animal cells in tissue culture, 19: 21909
effects on lactate dehydrogenase activity, 20: 18451
effects on lactic acid dehydrogenase of guinea pig and mucosa, 18: 17652
effects on lactic acid and pyruvic acid content of bovine and rabbit lenses, 18: 29268
effects on lactic dehydrogenase activity in mouse blood plasma, 19: 45844
effects on lactic dehydrogenase content in blood and muscles, whole-body exposure, 17: 28760
effects on lactic- and malic-acid dehydrogenases in extracts of rat liver and spleen, 20: 10583
effects on lactic-acid bacteria, metabolic, 17: 1235 (NP-12155)
effects on *Lactobacillus delbruckii*, protective effects of EDTA against, 20: 33095
effects on lamb testes, 18: 23338
effects on lamella in detergents, 20: 33364
effects on lameness in horses, 20: 22822
effects on lampbrush chromosome breakage in salamander oocytes, 19: 29961
effects on large intestine after cervical carcinoma therapy, 18: 17611
effects on larvae of sheep lungworm, lethal, 19: 43750
effects on laryngeal carcinomas, 19: 7230

effects on laryngeal mucosa, pathological, 20: 166(T) (N64-20943, pp 1–8)
effects on lead silicate glass, electric polarization from, 20: 410
effects on lead-doped potassium chloride, bleaching of, 18: 20038 (COO-1044-13)
effects on leakage of cellular constituents from yeast, 18: 41085(R) (HW-80500(p.150-2))
effects on leakage of protein into small intestine, 18: 13517
effects on learning behavior, *in utero* exposure, 16: 23507
effects on learning ability of rats, 19: 7086
effects on lens epithelium, radioautographic study of, 18: 11662
effects on lens epithelium of rats, 19: 8826
effects on lens epithelium in rabbits, *in vitro* and *in vivo*, 19: 10847
effects on lens epithelium in rabbit eyes, 19: 15183
effects on lens epithelium in rats, 17: 35497
effects on lens of rat eye, 19: 5629 (TID-21392)
effects on lens proteins, lens rigidity, and spectral transmission in eyes of rabbits, 18: 6619 (TID-19920)
effects on lens regeneration in salamanders, 18: 27006(R) (ORNL-3601(p.69-82))
effects on lenticular epithelial enzymes in rabbit epithelial cells and mitochondria, 19: 15216
effects on lesion formation on heart of chicken embryo, ultrastructural, 19: 17531
effects on lethal anaphylactic shock suppression in mice, whole-body, 19: 26050
effects on lethal mutations in heterochromatinic region of *D. melanogaster*, effects of development temperature on, 20: 35272
effects on lethality of *Fasciola hepatica* in mice, 18: 5037
effects on lethality in flour beetles, dose ratio to fast neutrons, 19: 10852
effects on lethality in mice, protective effects of cyclobutane derivatives against, 19: 10922
effects on lethality in mice, modifying effects of microwaves on, 19: 24375
effects on lethality in mice, protective effects of sodium nitrate against, 19: 24376
effects on lethality in mice, fractionated, 19: 33895
effects on lethality in dogs, dose and exposure effects on, 19: 43832
effects on lettuce seed germination at 26°C, 16: 1584
effects on leukemic lymphocytes, protective effects of phytohemagglutinin against, 18: 11868
effects on leukemia development in children, relation of fetal, 19: 7030
effects on leukemia incidence in polycythemia patients, 19: 7106
effects on leukemia incidence in radiological workers, 19: 8897
effects on leukemia incidence in patients exposed therapeutically, 19: 8897
effects on leukemia incidence in germ-free mice, 19: 10871
effects on leukemia development in mice, effects of croton oil on, 19: 15092
effects on leukemia induction in mice, protective effects of ACTH against, 19: 17692
effects on leukemia induction in man, 19: 24277
effects on leukemia transplants in mice, 19: 33876
effects on leukemia incidence of exposure to, 19: 33854
effects on leukemic cells, dosimetry for, 19: 34032
effects on leukemia genesis, 19: 42277
effects on leukemia, extracorporeal, 19: 42388
effects on leukemia induction, 19: 45915
effects on leukemic cells in mice, 20: 5368
effects on leukemia in germfree mice, 20: 18371
effects on leukemia cells in mouse lymph nodes, 20: 22642
effects on leukemia induction in mice, potentiation of, with urethane, 20: 33005
effects on leukemia induction in mice, effects of thymectomy and thymus implantation on, 20: 35327
effects on leukemia induction in mice, 20: 42867
effects on leukergic reaction in rabbits, 17: 14072
effects on leukergic reaction in rabbits caused by bacteria, 17: 14073
effects on leukocyte count, variations with dose, 16: 23446
effects on leukocyte reactions to transfusions in rats, 18: 6668
effects on leukocytes, 18: 13496
effects on leukocyte peroxidase in children, 18: 13516
effects on leukocyte number and kind in rat peripheral blood, 18: 21831(T) (JPRS-24301(Del.)(p.9-16))
effects on leukocyte phagocytic activity in rabbits, 18: 27176
effects on leukocyte chromosomes in man, 18: 35320 (TID-19531)
effects on leukocyte cytoplasm, 19: 166
effects on leukocytes, 19: 2137
effects on leukocytosis in rabbits, 19: 7105
effects on leukocytes in rabbits, protective effects of lysozyme against, 19: 17670
effects on leukocyte chromosomes in human infants, 19: 33875
effects on leukocyte blood picture in guinea pigs, effects of dose and time on, 20: 1670
effects on leukocytic reaction to adrenaline in dogs, 20: 10594
effects on leukocytic chromosomes after abdominal or pelvic therapy, aberrant and ploidy, 20: 12658
effects on leukocytic chromosomes following radiodiagnosis, 20: 22624
effects on leukocyte count in radiotherapy patients, 20: 24940
effects on leukocytes in culture, morphological, 20: 28920
effects on leukocyte counts in rats administered endoxan, 20: 42965
effects on leukocyte counts and mucosa of bladder and rectum, following use for therapy of uterine cancer, 20: 45540
effects on leukocyte isoantigenic factors, 20: 45319 (AD-640261)
effects on leukocyte alkaline phosphatase in cancer patients, 17: 23098
effects on leukocytes in rat thymus, effects of sodium chloride fixation, 17: 35506
effects on leukopenia development in rabbits, protective effects of marinamycin against, 19: 15222
effects on leukopenia production in mice, dose duration effects in local, 19: 24343
effects on level of anti-heart antibodies, 16: 8593
effects on levels of cholinesterase, mercapto groups, and peroxides in mouse tissues, 19: 35952(T) (JPRS-29641(p.44-52))
effects on levels of nucleic acids and proteins of uterus and vagina of prepubertal mice submitted to induced hyperplasia, 17: 1262
effects on liberation of amines in frogs, whole-body exposure, 16: 12916
effects on liberation of 5-hydroxytryptamine in brain stem of adrenalectomized rats, 20: 31069
effects on life span of descendants of irradiated mice, 16: 1310(R) (LAMS-2627(p.103-9))
effects on life span of mice, 16: 1313(R) (LAMS-2627(p.121-3))
effects on life span of mice, five-generation exposure, 16: 17503
effects on life span of mice, whole-body, 16: 31382(R) (ANL-6535(p.5-12))
effects on life span of, in mice, with and without rare earth nitrates, 16: 4003(R) (NP-11020(p.96-104))
effects on life span of diploid and haploid *Habrobracon serinopae*, 18: 8129
effects on life span of mice, fractionated, 18: 11666
effects on life span of Drosophila, 18: 19554 (TID-20550)
effects on life span of dogs, statistical analysis of, 18: 25094(R) (UCD-472-109(p.173-7))
effects on life span, radiosensitivity, and productivity of mice, chronic long-term, 18: 31128 (LADC-6472)
effects on life span of mice, 18: 41094(R) (TID-21156)
effects on life span of mice, 19: 13005
effects on life span of *Drosophila melanogaster*, 19: 17648
effects on life span of *Sarcophaga peregrina*, 19: 25990
effects on life span of mice, 19: 28076
effects on life span of house fly, after exposure of pupae, 19: 33858
effects on life spans of mouse progeny, protective effects of cysteamine against, 19: 42366
effects on life span of mice, effects of genotype on, 20: 3711(R) (NYO-3314-2)
effects on life span of hamsters, 20: 5330
effects on life span of house fly, *Musca domestica*, 20: 5331
effects on life span of mice, computer program for evaluation of, 20: 5300 (UCLA-12-573)
effects on life span and reproduction of *Sarcophaga peregrina*, 20: 16291
effects on life span of mice, 20: 26684
effects on life spans in mice, effects of age at exposure on, 20: 40633 (ORNL-P-2287)
effects on life span of rats, effects of single or divided exposure, 17: 7796 (TID-17451)
effects on life span of mice, protective effects of pantothenic acid against, 17: 28740
effects on life spans of mice, 17: 33754
effects on life spans in Drosophila, 17: 35501
effects on life span of mice, 17: 40649
effects on life span in mice, 17: 40651
effects on life span of mice, 17: 40654
effects on life span of offspring of exposed mice, 17: 23090(R) (NP-12760(p.166-80))
effects on life-span of x-ray technicians, 20: 3760
effects on life-span of germ-free mice, effects of diet and mouse strain on, 20: 6785(R) (ORNL-3853, pp 128-40)
effects on lifespans of mice, 20: 45443
effects on lifetime of $^5D_4$ level in terbium chlorides, (E), 20: 42539
effects on light emission by amino acid and trypsin powders, effects of temperature on, 19: 42530
effects on light response in rabbits, prenatal, 19: 25944
effects on light-scattering properties of gliadin portion of wheat gluten, 16: 14489

effects on light-sensitivity of film, 20: 36895
effects on Lilium after seed irradiation, 18: 31215
effects on limb development in mouse embryos, 19: 28003(T)
effects on limb regeneration in salamanders, role of normal epidermis in recovery from, 20: 20465
effects on limb tissue grafts in urodeles, 18: 13499
effects on *Limulus ommatidia*, stimulus-response relationship for, 20: 8607
effects on lipid and iodine content of rabbit blood, 20: 38652
effects on lipid composition of tissue culture cells, 18: 123
effects on lipid composition of testes of guinea pigs and rats, 19: 8949
effects on lipid content of rabbit blood, 20: 77
effects on lipid content of brain of guinea pigs, 20: 10636
effects on lipid content in fetal rat cells, 20: 14262
effects on lipid content in mouse liver, 20: 14268
effects on lipid composition of liver mitochondria in rats, 17: 5772 (TID-13322)
effects on lipid levels in liver mitochondria, 17: 12125 (TID-15755)
effects on lipid metabolism in rats and monkeys, whole-body, 18: 13419(R) (TID-20242)
effects on lipid metabolism in dogs, 18: 27196
effects on lipid metabolism in rat liver, 19: 17524
effects on lipid metabolism in rabbits, 19: 17492(R) (TID-21493)
effects on lipid metabolism in rabbits and rats, 19: 17493(R) (TID-21496)
effects on lipid metabolism in rabbits and rats, 20: 18375
effects on lipid metabolism in rats, effects of phosphatides on, 20: 28992
effects on lipid metabolism in rats, effects of diet on, 20: 45381
effects on lipid metabolism in leukocytes, 17: 10365(R) (TID-17692)
effects on lipid metabolism in leukocytes, 17: 13980 (TID-17747)
effects on lipid metabolism in leukocytes and blood platelets, 17: 21537
effects on lipid peroxide levels in rat liver, whole-body exposure, 17: 19868
effects on lipid synthesis in rat brain and liver, effects of cysteamine and Synkayvite on, 19: 26092
effects on lipids in rat tissue, 19: 25959
effects on lipids in liver mitochondria in rats, 17: 38744(R) (TID-19410)
effects on lipids, protein, and glycogen in liver of guinea pig, 18: 15813 (NP-13733)
effects on lipoprotein content of liver and phosphatides in rabbit sera, protective effects of vitamin B_6 against, 17: 30350
effects on liquid tetramethylsilane, mechanism and yields from, 20: 18729(R) (NYO-2007-9)
effects on lithium and sodium fluorides containing nickel ion, 19: 457
effects on lithium fluoride, F-center luminescence from, (E), 20: 22331
effects on lithium fluoride crystals, 17: 18142
effects on litter size of swine, 19: 7082
effects on liver after uterine carcinoma therapy, effects of halothane on, 18: 25119
effects on liver cells, latent lesion, 16: 11482
effects on liver cell glycogen content in rats, after central nervous system exposure, 18: 3512
effects on liver carcinogenesis, 18: 36959
effects on liver cell populations in rats, 19: 29925
effects on liver cells of pregnant rats, pathological, 20: 14294
effects on liver cells of fetal rats, pathological, 20: 14294
effects on liver enzyme development in rats, 18: 5000(R) (NP-13281(p.1-24))
effects on liver enzyme development in rats, 18: 5001(R) (NP-13281 (p.25-33))
effects on liver enzymes after carcinoma therapy, 19: 15191
effects on liver enzyme activity, 17: 23082(R) (NP-12760(p.22-8))
effects on liver glycogen synthetase in fasting rats, 19: 3939
effects on liver glycogen phosphorylase activity in rats, whole-body, 19: 13021
effects on liver glycogen metabolism, head exposure, 17: 4393
effects on liver in animals, 18: 9889
effects on liver lipid metabolism, whole-body exposure, 16: 25178(R) (TID-16131)
effects on liver levels of adenine nucleotides, water, and lipids, local exposure, 17: 34
effects on liver mitochondria in mice, whole-body, 16: 8602
effects, on liver mitochondria, whole-body exposure, 16: 11450(R) (ANL-6464(p.114-15))
effects on liver mitochondria in rats, electron microscopy of, 18: 9895
effects on liver mitochondria in rats, 19: 26033
effects on liver metabolism in rats, whole-body exposure, 17: 15570
effects on liver of awake and hibernating porcupine, 18: 13472
effects on liver proteins in rabbits and rats, 19: 24360
effects on liver proteins, immunochemical analysis of, 17: 30344
effects on liver regeneration after partial hepatectomy, 19: 19512
effects on liver transplantation in dogs, 17: 25047
effects on liver, pathogenesis of, 19: 2136
effects on liverworts, effects of apical cell number on, 20: 31065
effects on lizard populations, gonadal-exposure, 20: 12585
effects on localizing response to antigen of different tissues in immunity, 16: 11460(R) (TID-15042)
effects on logarithmic damping decrements of quartz oscillators, 20: 21155
effects on long-term aging of skin on mice, 18: 3574
effects on loss of pregnancy in rats, 18: 27131
effects on loss of regeneration capacity in extremities of salamanders, 19: 19544
effects on luciferase and luciferin solutions at various temperatures, protective effects of cysteine against, 18: 27212
effects on luciferin and luciferase, 17: 38759
effects on luminescence of lithium fluoride crystals, 18: 17892
effects on luminescence of cells in tissue culture, 18: 27179
effects on luminescence of phosphors, 18: 40015
effects on luminescence of alkali halide crystals, 19: 2388
effects on luminescence of thallium-activated alkali halide crystals, 19: 11204
effects on luminescence of quartz, 19: 13468
effects on luminescence of gases, 19: 13480
effects on luminescence of alkali halides, 19: 15514(T)
effects on luminescence of alkali halide phosphors in presence of F-band illumination, 19: 15626(T)
effects on luminescence of copper-doped potassium and sodium chloride crystals, 19: 19964
effects on luminescence of cadmium zinc sulfide phosphors in presence of infrared radiation, 19: 19965
effects on luminescence of thallium-activated alkali halides, 19: 19966
effects on luminescence of alkali halide phosphors, 19: 22313
effects on luminescence of nickel-activated sodium chloride phosphor, (E), 19: 27719
effects on luminescence of pure alkali halide crystals, (E), 19: 27723
effects on luminescence and scintillation behavior of thallium-activated sodium iodides, (E), 19: 27725
effects on luminescence of calcium fluoride and sodium chloride single crystals, 19: 30274(T)
effects on luminescence of thallium- and indium-activated alkali halide crystals, 19: 34244
effects on luminescence of thallium-activated alkali metal halide crystals, 19: 34238
effects on luminescence centers of silver-activated alkali halide phosphors, 19: 41977
effects on luminescence of europium-activated potassium- and sodium-chloride phosphors, 19: 40567
effects on luminescence spectra of thallium-activated sodium iodide crystal phosphors, 19: 40568
effects on luminescence of thallium-activated potassium iodides, in electric field, 19: 40573
effects on luminescence of doped alkali metal halides at 90 and 295°K, 19: 45488
effects on luminescence of lymphocytes, 20: 5383
effects on luminescence of thallium-activated cesium iodide and sodium iodide phosphors, (E), 20: 6537
effects on luminescence of acridine-orange-stained Tetrahymena, 20: 5267
effects on luminescence and photoconductivity in zinc oxide, effects of oxygen and water on, 20: 7128(R) (NYO-2206-1)
effects on luminescence and photoconductivity of zinc oxide, 20: 7128(R) (NYO-2206-1)
effects on luminescence of potassium iodide, 20: 12891
effects on luminescence of thallium-activated cesium iodide and sodium iodide crystals, 20: 14611(T)
effects on luminescence of thallium-activated sodium-iodide crystals, excitation mechanism of, 20: 17991(T)
effects on luminescence of Z_3 center in magnesium-doped lithium fluoride, 20: 28634
effects on luminescence in alkali halide crystals, 17: 5112
effects on lung cancer, 20: 14420
effects on lung carcinomas, effects of actinomycin D and 5-fluorouracil on, 20: 18539
effects on lung cancers, effects of actinomycin on, 20: 18541
effects on lung parenchyma in rabbits, effects of dose on morphologic, 19: 42264
effects on lung reflexes in cats, effects on cardiovascular system of, 20: 14371
effects on lung resistance to tumorigenic action of urethan, 17: 28721
effects on lung tissue, pathological, 20: 33043
effects on lungs following therapeutic, injurious, 19: 31861
effects on lungs in silicotic rabbits, 16: 14550
effects on lungs in radiotherapy of bronchial carcinomas, 18: 1402
effects on lungs of rabbits and rats, 20: 1675
effects on lungs of hamsters and rats, morphologic, 20: 3785

effects on lungs of rabbits, pathological, 20: 8684
effects on lungs, pathology of pulmonary lesions, 16: 4074
effects on lungs, x, 20: 45542
effects on lungworm larvae, used for vaccination, 18: 17392
effects on lungworm larvae, cattle immunity induced by, 18: 31077
effects on Lupinus, protective effects of moisture against mutagenic, 19: 45847
effects on Lupinus seeds, protective effects of moisture content against, 17: 35481
effects on lutein cells of rat ovary, 20: 40672
effects on Luzula, seed-irradiation, 19: 3929
effects on lymph cells in culture, immunological, 20: 32980
effects on lymph nodes in mice, whole-body, 16: 14531
effects on lymph node plasmacytic reaction in mice and rats, 18: 19557(T) (JPRS-23956(p.18-26))
effects on lymph nodes and vessels in rats, 20: 3718
effects on lymph node cells in mice, 17: 33728
effects on lymph of the lung, 17: 37137
effects on lymph system in mammary gland, 16: 32749(T) (JPRS-15018 (p.135-43))
effects on lymph system, whole-body exposure, 16: 32750(T) (JPRS-15018(p.144-50))
effects on lymph system of neck, 19: 27965
effects on lymph system in rats, 19: 28056
effects on lymph system of therapeutic doses of, 20: 3852
effects on lymph vessels in rats, morphological, 20: 26674
effects on lymphatic tissue, biological, 20: 38612
effects on lymphatic dynamics, lymph nodes, and lymph vessels following cancer therapy, 20: 42976
effects on lymphocyte segment index in guinea pigs, 18: 25203
effects on lymphocyte ultrastructure in rat spleen, 18: 31210
effects on lymphocytes in rabbit appendix, 19: 10873
effects on lymphocytes in mice, 19: 21883
effects on lymphocytes in rat thymus, protective effects of cysteamine against, 19: 26131
effects on lymphocyturia in dogs with renal homografts, 19: 26039
effects on lymphocyte nuclei, morphological, 20: 1612 (EUR-2505.e)
effects on lymphocyte distribution in rat spleen and thymus, effects of cell size on, 20: 14318
effects on lymphocytes in blood and peritoneal cavity of mice, 20: 26651 (AD-632282)
effects on lymphocyte blood picture, effects of adrenaline on, 20: 38678
effects on lymphocyte-neutrophil index in guinea pigs, 20: 45458
effects on lymphocytosis and whole-body immunity by hypophysis exposure, 17: 4407
effects on lymphoid and myeloid leukemia incidence in mice, 20: 6788 (ORNL-P-1703)
effects on lymphoid cells in blood and bone marrow in dogs, 20: 31086
effects on lymphoid leukemia induction in mice, lactic dehydrogenase activity and characteristics in, 20: 33051
effects on lymphoma cells, effects of 5-bromouracil on, 20: 18445
effects on lymphoma induction in mice, *in vitro* reactions of lymphocytes in, 20: 35268
effects on lymphosarcomas, effects of bone marrow transplants on, 20: 6971
effects on lyophilized mouse liver, effects of cysteine and oxygen on radicals from, (E), 20: 8688
effects on lysine, 18: 1736
effects on lysogenicity in *Staphylococcus alba*, 20: 22771
effects on lysomal hydrolases of beef heart tissue, 18: 13449 (TID-20139)
effects on lysosomes of heart tissue, 19: 10874
effects on lysosomes in rat liver and thymus, 19: 29849(R) (ANL-6971 (p.1-28))
effects on lysozyme, protective effects of hydrogen sulfide against, 18: 29414
effects on lysozyme activity in organs of mice, 19: 2113
effects on lysozyme activity in rat intestine, whole-body, 19: 45933
effects on lysozyme aqueous solutions, inactivating, 20: 20423
effects on M-center formation in potassium chlorides, 20: 34859
effects on *Macaca mulatta* embryo cell cultures, protective effects of serotonin and thiourea against, 20: 31121
effects on magnesium fluoride crystals, 19: 20618 (NBS-8614)
effects on magnesium oxide, ESR studies of, 19: 34231
effects on magnesium-doped single crystals of lithium fluoride, color centers from, (E), 20: 10258
effects on magnetic properties of lithium fluoride, 19: 9743
effects on magnetic properties of lithium fluorides, 19: 9744
effects on magnetic properties of desoxyribonucleic acid, 19: 43723(R) (TID-22128)
effects on maize, genetic, 17: 28765
effects on maize root meristems, 18: 5016
effects on maize root morphogenesis, 18: 11780
effects on maize seeds, genetic, 20: 31092
effects on maize seed, biological RBE of, 20: 42843 (BNL-10358)
effects on maize seeds, mutagenic, 20: 45361 (TID-22622)
effects on maize, mutagenic, 19: 43712 (BNL-9383)
effects on maize, genetic, 20: 12678
effects on maize, genetic, 20: 18334
effects on maize, genetic, 20: 38617
effects on maize, genetic, 20: 40708
effects on male breast, 17: 1251
effects on male germ cells of *D. melanogaster*, effects of age on mutagenic, 20: 12636 (TID-21459)
effects on malignant tumor induction, hypothesis on somatic mutation origin of, 19: 17555
effects on malignant lymphoma in dogs, 19: 28207
effects on malignant melanomas, pre-operative, 20: 38764
effects on malonic and substituted malonic acids, ESR studies of, 20: 45755
effects on mammalian embryos, low-level exposure, 16: 16212
effects on mammalian retina, 16: 23501
effects on mammalian cells, recovery during inhibition of synthesis of DNA, 19: 7120
effects on mammalian cells, model for recovery from, 19: 26072
effects on mammalian chromosomes in embryonic fibroblast, 20: 22668
effects on mammalian bone marrow cells in different phases of cycle, 20: 32997
effects on mammalian chromosomes *in vitro*, 19: 178
effects on mammalian nervous system, 18: 48 (USNRDL-TR-670)
effects on mammals, 20: 40694
effects on mammary gland activity, physiological, 19: 40353(T) (FTD-TT-65-48, pp 16-17)
effects on man after cervical carcinoma therapy, review of indirect, 20: 10670
effects on man of therapeutic doses of, pathological, 20: 1717
effects on man, effects of polyvinylpyrrolidone on, 20: 14396
effects on man, effects of pyridine diphosphate nucleotides on therapeutic, 20: 18535
effects on man, leukemogenic, 20: 10647
effects on man, low doses, biological, 20: 3779
effects on man, pathological, 20: 6841
effects on man, pathological, 20: 26668
effects on man, permanent epilatory, 18: 29394
effects on man, protective effects of bone marrow grafts against, 20: 5420
effects on manganese content of tissues in dogs, guinea pigs, and rabbits, 18: 38872
effects on manifestation of candida infection in mice, 16: 14532
effects on marrow production in chickens by exposure of spinal cord graft to chorioallantoid, 19: 43761
effects on mast cells in rat skin, 16: 25206
effects on mating activity of male Drosophila, 20: 10644
effects on maze-learning in rats, 17: 38801
effects on mean viability of Drosophila autosomes, 20: 12661
effects on mechanical-structural properties of gelatin, 19: 1024
effects on mechanical resistance of human erythrocytes, 19: 19595
effects on mechanism of sodium and potassium exchange through erythrocyte cell membrane, 17: 1264
effects on *Medicago polymorpha*, 20: 18312
effects on medullar vessels in rabbits, 18: 17563
effects on medullary cells of the rat in combination with Endoxane, 16: 28778
effects on medullary hemopoiesis in guinea pigs, 17: 37099
effects on meiosis in *Luzula purpurea*, 18: 75
effects on meiosis in progeny of x-irradiated *Luzula purpurea*, 18: 76
effects on meiosis in mouse oocytes, 18: 8154
effects on meiosis in Trillium, 19: 7124
effects on meiosis induction in asynaptic and male-sterile mutants of peas, 19: 17658
effects on meiotic irregularities in plants, 16: 1585
effects on meiotic and mitotic stages in Habrobracon eggs, 18: 3568
effects on meiotic stages in Artemia oocytes, 20: 5359
effects on melanin synthesis in chicken feathers, 18: 5018
effects on melanization in goldfish skin, effects of adrenocorticotropic hormone on, 17: 12167
effects on melanomas, sensitizing effects of cesium eosinate on, 18: 3635
effects on melanophores in fish skin, physiological, 20: 22614(R) (NIRS-4, pp 28-34)
effects on membrane penetrability and enzyme reactions in artificial system, 18: 17570
effects on membranes of animal cells, 19: 35964
effects on membrane permeability in monkey erythrocytes, 20: 6765
effects on meprobamate metabolism in rats, 17: 35480
effects on mercapto groups in guinea pig blood, 19: 3953

effects on mercuric chloride reduction, 19: 15585
effects on meristematic cells in rye and wheat seeds, 18: 27125
effects on mesenteric mast cells in normal and adrenalectomized rats, 20: 10686
effects on mesothelial tissues in rabbits, 18: 38967
effects on metabolism of zinc-65, 16: 42
effects on metabolism, sprouting, and weight loss of potato tubers, 16: 1614
effects on metabolism of trichloroacetic acid in yeast, 16: 4095
effects on metabolism of zinc-65, 16: 5209
effects on metabolism in leaves, 16: 6314(T) (JPRS-11322(p.422-8))
effects on metabolism in tumors, 16: 12902
effects on metabolism, whole-body dose, 16: 14499
effects on metabolism of adenine and phenylalanine in thymus cell nuclei, 16: 14518
effects on metabolism of ribonucleic acid, whole-body exposure, 16: 12901
effects on metabolism of vitamin B_{12}, 16: 21922
effects on metabolism of vitamin B_6 in rabbits, 16: 26667(T) (JPRS-13555 (p.7-17))
effects on metabolism in cell nuclei and entire cells, biochemical, 16: 30273
effects on metabolism in heart, in guinea pigs, local and whole-body, 18: 3554
effects on metabolism in liver of mice, chronic exposure, 18: 5002(R) (NP-13281(p.92-103))
effects on metabolism in rat skin, 18: 11741
effects on metabolic and phagocytic activities of polymorphonuclear leukocytes, 18: 23242(R) (TID-20379)
effects on metabolism in mouse ascites tumor cells, 18: 29515
effects on metabolism in isolated erythrocytes, 18: 31244
effects on metabolism of iodine-131-labeled insulin, 18: 38885
effects on metabolism in lungs of rabbits, 18: 38968
effects on metabolism in reticulocytes *in vitro*, 19: 101
effects on metabolism in rats, 19: 3895(R) (ORO-625(p.103-8))
effects on metabolism in mice, 19: 5665
effects on metabolism of adenosinephosphoric acids in rats, 19: 8933
effects on metabolism of folic and folinic acids in dogs, 19: 13049
effects on metabolism in seeds and seedlings, 19: 12959 (TID-21460)
effects on metabolism in liver of rats, 19: 13054
effects on metabolism in regenerating liver cells, 19: 21983
effects on metabolism of cholesterol and lipids in rat liver, 19: 24361
effects on metabolism of desoxyribonucleic acid in rabbit eye, 19: 25905 (NYO-2456-1)
effects on metabolism in frog skin, 19: 29901(R) (RLO-1754-1)
effects on metabolism of phospholipids in rats, 19: 35946(R) (NYO-1864-21)
effects on metabolism in rat embryos, 19: 42259(R) (TID-22005)
effects on metabolism in man and rats, use in exposure diagnosis, 19: 43852
effects on metabolism in rat kidney tissue sections, 20: 5352
effects on metabolism of calcium and sulfur, tracer study in rat bones, 20: 5370
effects on metabolism in animal lenses, effects of age on, 20: 5333
effects on metabolism in dog brain, effects of arsenic compounds on, 20: 6817
effects on metabolism in cultured chick embryo tissues, 20: 8649
effects on metabolism of rats, delayed, 20: 14368
effects on metabolic activity in rat spleen and stomach, 20: 20433 (AD-630390)
effects on metabolism of methylnaphthalene in rats, 20: 20439 (EUR-2628.f)
effects on metabolism of nuclear acids and proteins, 20: 22794 (EUR-2769.f)
effects on metabolism in mouse spleen, effects of injected bone marrow on, 20: 22797
effects on metabolic changes accompanying phagocytosis in guinea pigs, 20: 24922
effects on metabolism of vitamin C in guinea pigs and rats, 20: 28921
effects on metabolism in erythrocytes, 20: 28924
effects on metabolism of carbon-14-labeled glycine and acetate in rat liver sections, 20: 35253
effects on metabolism in Ascites tumor cells, 20: 38599 (TID-22968)
effects on metabolism in bone marrow and peripheral blood of whole-body irradiated rats, 20: 42788
effects on metabolism of injected liver desoxyribonucleic acid in rats, 17: 21530
effects on metabolism of proteins in lymph tissue, tracer study of, 17: 31932
effects on metal halides, 16: 6790 (TID-14395)
effects on metal ions with varying valency dissolved in acetone, chemical, 19: 480
effects on metal-oxide transistors, (E), 19: 28701
effects on metaphase/prophase ratio in man and mice, 17: 10411
effects on metastatic rate in rats injected with Guerin epithelioma, 18: 23264
effects on metastases following therapy for breast cancer, 20: 40793
effects on metastasis frequency of whole-body, 17: 15831
effects on methane, evaluation of ionic reactions in, 19: 7556
effects on methane and propane, effects of temperature on hydrogen yields in, 20: 381
effects on methemoglobin formation in human red blood cells, 16: 18777
effects on methyl iodide, coulombic "explosion" from inner shell vacancies, 19: 430 (ORNL-P-591)
effects on methyl methacrylate polymers, protective effects of organic additives against, 20: 4036
effects on methylation of guanidinacetic acid in rat liver, 20: 36603
effects on methylene blue solutions, 19: 30249
effects on mice, 18: 38859
effects on mice, 19: 21890
effects on mice, 19: 45990
effects on mice, 18: 21827(R) (UCRL-11184(p.128-35))
effects on mice after exposure of 35 generations, 20: 18289(R) (LA-3432, pp 56-101)
effects on mice and rats, protective effects of cystamine and mercamine against, 18: 8206
effects on mice and rats, effects of S-phosphorylated thiols on, 18: 11851
effects on mice and rabbits, effects of sodium pentobarbital on, 19: 205
effects on mice and rats, physiological, 19: 2132
effects on mice and rabbits, protective effects of plasma properdin against, 19: 42355
effects on mice and rats at 250 kev, pathological, 20: 1614 (NASA-SP-71, pp 97-103)
effects on mice and rats, protective effects of sulfur compounds against, 20: 16297(R) (EUR-2548.f)
effects on mice and rats, hematological, 20: 22705
effects on mice and rats, protective effects of sodium gallate on pathological, 20: 38728
effects on mice and rats, protective effects of sulfur and thiol compounds against, 20: 42998(R) (EUR-2992.f)
effects on mice and rats, protective effects of sodium cyanide against, 17: 28677 (TID-17148)
effects on mice, application of probit method to study, 16: 6329
effects on mice, cyclic variation in, 17: 40621
effects on mice, effects of age, 16: 1311(R) (LAMS-2627(p.110-16))
effects on mice, effects of natural and purified diets on, 17: 23181
effects on mice exposed *in utero*, stunting, 19: 10796
effects on mice, factors in spleen cell therapy of, 17: 14106
effects on mice, hematological factors, 16: 23(R) (TID-13432)
effects on mice injected with fetal liver, bone marrow, or isogenic spleen, 18: 5035
effects on mice in air and impure oxygen, protective effects of cysteine against, 17: 40583
effects on mice, protective effects of aminoethylisothiourea against, 16: 23517
effects on mice, protective effects of antimitotic chemicals and bone marrow graft against, 16: 26872
effects on mice, protective effects of catalase against, 18: 5026
effects on mice, protective effects of human blood serum on, 17: 28742
effects on mice, protective effects of chemicals against, 17: 37067(T) (JPRS-20964)
effects on mice under mild hypothermia, whole-body exposure, 16: 1544
effects on mice with transplantation immunity antigens, 16: 21917 (USNRDL-TR-556)
effects on mice, amyloidosis in chimeras and relation to lymphoid hypoplasia in whole-body, 19: 19650
effects on mice, biological, 19: 2072(R) (ORNL-3700(p.83-8))
effects on mice, biological, 19: 25911 (TID-21727)
effects on mice, biological, 20: 18454
effects on mice, biological, 20: 18467
effects on mice, biological, 20: 20430(R) (AD-629311, pp 26-32)
effects on mice, biological, 20: 22615(R) (NIRS-4, pp 34-58)
effects on mice, biological, 20: 33055
effects on mice, biological, 20: 38648
effects on mice, carcinogenic, 19: 29887(R) (ANL-6971(p.47-58))
effects on mice, circadian rhythmicity of, 20: 5336
effects on mice, carcinogenic, 20: 14373
effects on mice, carcinogenic, 20: 18286 (EUR-2462.1)
effects on mice, carcinogenic, 20: 22697
effects on mice, delayed somatic, 17: 24971
effects on mice, effects of bone marrow injections and influenza virus on, 18: 9917
effects on mice, effects of gonadectomy, sex, and strain on, 18: 23347
effects on mice, effects of bleeding on, 18: 25116
effects on mice, effects of splenectomy on whole-body, 19: 8906

effects on mice, effects of sex on protective effects of AET against, 19: 8957
effects on mice, effects of benzopyrene on carcinogenic, 19: 13114
effects on mice, effects of blood transfusions on subsequent marrow transplants, 19: 19653
effects on mice, effects of phytohemagglutinin on lymphoid noduli formation in, 19: 25984
effects on mice, effects of injections of bone marrow and spleen cells in, 19: 31918
effects on mice, effects of hyperbaric oxygen on, 19: 31903(R) (NP-15072(p.88-102))
effects on mice, effects of age, dose, and sex on leukemogenic, 20: 5367
effects on mice, effects of estradiol and estriols on, 20: 6864
effects on mice, effects of age and dose fractionation on, 20: 8691
effects on mice, effects of hereditary anemia on, 20: 14290(R) (NYO-1800-12)
effects on mice, etiology of tumorigenic, 20: 18359
effects on mice, effects of adrenal hormones on, 20: 18437
effects on mice, effects of bacterial endotoxin on, 20: 18496
effects on mice, effects of tissue transplants on, 20: 22784
effects on mice, effects of spleen cell transplants on, 20: 22789
effects on mice, effects of mixture of radioprotective compounds on genetic, 20: 24882
effects on mice, effects of time of day on lethal, 20: 28938
effects on mice, effects of injected parental bone marrow or spleen cells on leukemogenic, 20: 31127
effects on mice, effects of acridine orange on leukemogenic, 20: 33080
effects on mice, effects of AET and hypoxia on recovery from, 20: 42988
effects on mice, effects of age and strain, whole-body exposure on neoplastic, 17: 1276
effects on mice, fractionated-dose lethal, 19: 2081 (USNRDL-TR-784)
effects on mice, factors affecting survival of protective bone marrow transplants against, 19: 31905(R) (ORNL-3768(p.99-108))
effects on mice, genetic, 19: 5681
effects on mice, genetic, 19: 7090
effects on mice, genetic, 19: 7130
effects on mice, genetic, 19: 45809(R) (NYO-1979-12)
effects on mice, genetic, 20: 3711(R) (NYO-3314-2)
effects on mice, genetic and leukemogenic, 20: 3765
effects on mice, genetic, 20: 6781(R) (ORNL-3853, pp 98-101)
effects on mice, genetic, 20: 28957
effects on mice, genetic, 20: 31048
effects on mice, high dose-rate, 20: 24923
effects on mice, hematological fractionated-dose, 20: 42831 (AD-635600)
effects on mice, *in vitro* studies of lymphoid recovery following, 20: 42984
effects on mice, leukemogenic, 19: 12997
effects on mice, leukemogenic, 20: 6901
effects on mice, lethal, 20: 12685
effects on mice, late somatic, 20: 20441 (ORNL-P-1173)
effects on mice, leukemogenic, 20: 22646
effects on mice, leukemogenic, 20: 33016
effects on mice, leukemogenic, 20: 38715
effects on mice, mutagenic, 20: 6828
effects on mice, mechanisms for leukemogenic, 20: 18317
effects on mice, mechanisms in aminothiol and anoxia protection against, 20: 18431
effects on mice, mechanism for protective effects of lymphoid and myeloid cell transplants against, 20: 40727
effects on mice, number and type of cells required for protection against, 19: 26135
effects on mice, protective effects of cysteamine against, 18: 11852
effects on mice, protective effects of trithiocarbonates of guanidine derivatives against, 18: 11866
effects on mice, protective effects of human platelets against, 18: 17649
effects on mice, protective effects of ozone against, 18: 17654
effects on mice, protective effects of bone marrow against, 18: 19770
effects on mice, protective effects of cysteamine against, 18: 19775
effects on mice, protective effects of 2-(2-aminoethyl)-2-thiopseudourea and bone marrow against, 18: 19796
effects on mice, protective effects of frozen and stored bone marrow against, 18: 19805
effects on mice, protective effects of 3-alkyl-1,3-thiazane derivatives against, 18: 23370
effects on mice, protective effects of ethyl palmitate against, 18: 25216
effects on mice, protective effects of chemical agents against, 18: 31273
effects on mice, protection against, 18: 33406
effects on mice, protective effects of histamine against, 18: 33414
effects on mice, protective effects of bone marrow transplants and estradiol against, 18: 35390
effects on mice, protective effects of drugs against, 18: 36966
effects on mice, protective effects of bone marrow and chemicals against, 18: 37024
effects on mice, protective effects of gallates against, 18: 38978
effects on mice, protective effects of cysteamine and histamine against, 18: 41247
effects on mice, protective effects of castration against, 18: 41248
effects on mice, protective effects of chemicals against, 18: 41253
effects on mice, protective effects of AET, glutathione, and serotonin against whole-body, 19: 199
effects on mice, peroxide induction in, 19: 5666
effects on mice, protective effects of cloned bone marrow and spleen cells against, 19: 8979
effects on mice, protective effects of heterocyclic nitrogen compounds against lethal, 19: 13092 (CEA-R-2582)
effects on mice, protective effects of bone marrow and spleen cell transplantation against midlethal, 19: 17675
effects on mice, protective effects of allogenic marrow inoculation against, 19: 19648
effects on mice, protection from killing effect of spleen cells in, 19: 19651
effects on mice, protective effects of Pyrexal against, 19: 28115
effects on mice, protective effects of D- and L-cysteine against, 19: 31906(R) (ORNL-3768(p.179-80))
effects on mice, protective effects of hematopoietic transplants against, gamma and x, 19: 33979
effects on mice, protective effects of cobalt–chlorophyll and glucuronic acid against whole-body, 19: 38456
effects on mice, protective effects of orotic acid against, 19: 38458
effects on mice, protective effects of hematoporphyrin against, 19: 42354
effects on mice, protective effects of nitrogenous heterocyclics against, 19: 43863
effects on mice, protective effects of *p*-aminopropiophenone and MEA against, 19: 43873
effects on mice, protective effects of hematoporphyrin against, 19: 43862
effects on mice, protective effects of AET, glutathione, and serotonin against, 19: 46016
effects on mice, pathological, 20: 60(R) (NYO-901-37, pp 33-68)
effects on mice, protective effects of bone marrow grafts against lethal, 20: 138
effects on mice, protective effects of mercaptoethylamine, 20: 5407(R) (AD-623599, pp 37-44)
effects on mice, pathological, 20: 6919
effects on mice, pathological, 20: 6784(R) (ORNL-3853, pp 118-27)
effects on mice, protective effects of bone marrow cells against, 20: 6908(R) (NYO-2862-1)
effects on mice, protective effects of bone marrow therapy against, 20: 12720(R) (TID-22466)
effects on mice, protective effects of sodium hyposulfite against, 20: 14393
effects on mice, protective effects of 1,3,4-oxadiazolium salts and *s*-triazole derivatives against, 20: 16490(R) (TID-22681)
effects on mice, protective effects of endogenous sulfhydryl compounds against, 20: 18433
effects on mice, protective effects on 5-BUdR combined with MEA against, 20: 18498
effects on mice, protective effects of 5-BUdR against, 20: 18498
effects on mice, protective effects of MEA against, 20: 18498
effects on mice, protective effects of psychotropic drugs against, 20: 18501
effects on mice, protective effects of antioxidant inhibitors against, 20: 20506
effects on mice, protective effects of drugs against, 20: 20513
effects on mice, pathological, 20: 33085
effects on mice, protective effects of *Bacillus subtilis* preparations against, 20: 36673
effects on mice, protective effects of drinking sulfurated mineral water, 20: 38709
effects on mice, protective effects of glycine on, 20: 38714
effects on mice, protective effects of bone marrow against, 20: 40718(R) (ORNL-3922, pp 99-105)
effects on mice, protective effects of transplants of parental tissue against, 20: 40718(R) (ORNL-3922, pp 99-105)
effects on mice, protective effects of nibufin against, 20: 40724
effects on mice, pathological, 20: 42833(R) (ANL-7136, pp 16-46)
effects on mice, protective effects of cysteine and MEA given intravenously or in water or gum arabic solution on, 20: 42997(R) (ANL-7136, pp 191-204)
effects on mice, protective effects of vaccines, thiophosphates, and AET against, 20: 42992
effects on mice, protective effects of sulfurated water against, 20: 45490
effects on mice, protection against epilatory, by macromolecules, 17: 35472
effects on mice, therapeutic effects of stimulants against, 18: 43313
effects on mice, tumorigenic, 19: 31817

effects on mice, use of nicotinic acid derivative in treatment for, 18: 23365
effects on mice, use of testis weight for evaluation of, 20: 42841(R) (ANL-7136, pp 266-89)
effects on microcirculation in kidneys, 16: 20214
effects on microcirculation of rat mesentery, later response to serotonin, 20: 42978
effects on microcolony formation in *Salmonella typhimurium*, 18: 13556
effects on *Micrococcus radiodurans*, relation of guanine cytosine content to, 18: 43274
effects on *Micrococcus radiodurans*, 19: 24324
effects on microhardness and dislocation mobility of sodium chloride crystals, (E), 20: 45005
effects on micromutation production in barley, 20: 35320
effects on microörganisms, lethal, 19: 76(R) (UCRL-11387(Suppl.) (p.19-51))
effects on microorganisms, use in size estimations, 20: 18314
effects on microorganisms and metazoa, repair mechanisms for, 20: 31040
effects on microorganisms, genetic control of, 20: 31041
effects on microorganisms, effects of light on, 20: 45363(R) (TID-23347)
effects on microörganisms, 17: 24937
effects on microscopic structures of intestinal mucosa in man, 17: 24990
effects on microsporogenesis in sugar beet plants, 20: 12676
effects on microstructures in regenerating liver cells, 16: 21920
effects on microstructure of duodenum cells, early, 18: 23266
effects on midbrain-posterior lobe system of rats in whole-body irradiation, 19: 162
effects on midbrain hypophyseal system in rats, protective effects of AET against, 20: 35335
effects on Mikulicz's disease, therapeutic, 20: 16316
effects on milk production by cattle and goats after mammary gland exposure, 20: 22594
effects on Mimosa responses, 18: 19574
effects on mineral content of blood in rabbits, 19: 8927
effects on mineral metabolism in mouse bones, 19: 45729(R) (NYO-910-23, pp 1-111)
effects on mineral metabolism in rat skeleton, localized-exposure, 20: 10587
effects on mitochondria in rat cells, 19: 35951 (UR-666)
effects on mitochondria function and structure in mouse liver, 19: 38424
effects on mitoses in cornea of *Axolotl* and *Triton punctatus*, 19: 15044
effects on mitosis in leaves, reaction mechanisms, 16: 30279
effects on mitosis in sea urchin eggs, 18: 9835 (UCRL-10979)
effects on mitosis and DNA synthesis in Ehrlich ascites tumor cells, 18: 11800
effects on mitosis in HeLa cells, 18: 17599
effects on mitosis in rats, 18: 25101
effects on mitosis and regeneration in rat liver, whole-body, 19: 82
effects on mitosis in soybeans, 19: 96
effects on mitosis duration in corneal epithelium in fasting rats, 19: 8832(T)
effects on mitosis in *Helianthus annuus* and *Vicia faba* root tips, 19: 8839
effects on mitosis rate of cells in tissue culture, 19: 13073
effects on mitosis in mouse bone marrow, 19: 29936
effects on mitosis in Tradescantia, synergism with infrared radiation, 19: 38416
effects on mitosis in Planaria, dose effects on regenerating capacity in, 19: 40366
effects on mitosis in brain of rat embryos, 19: 43768
effects on mitosis in plant cells, 20: 3764
effects on mitosis in animal cells, 20: 3764
effects on mitosis in mouse cornea, 20: 5421
effects on mitosis in RCP cell strain, 20: 5323
effects on mitosis in sea urchin eggs, mechanisms for, 20: 6861
effects on mitosis in cells of Phalaris, 20: 8697
effects on mitosis in HeLa cells in culture, 20: 14375
effects on mitosis in Saccharomyces, 20: 16255
effects on mitosis in rat lens epithelium, 20: 16256
effects on mitosis in rat bone marrow cells, protective effects of sodium against, 20: 18326
effects on mitosis in regenerating rat liver, 20: 18457
effects on mitosis of *Vicia faba* root meristem, comparison of, with effects of DNA, 20: 32976
effects on mitosis in *E. coli*, factors affecting, 20: 40630(R) (ORNL-3922, pp 106-8)
effects on mitosis, comparison with Endoxan, 16: 28777
effects on mitosis in bone marrow cells in tissue cultures, 17: 1290
effects on mitosis-stimulating activity in hepatectomized rat serum, 17: 24922
effects on mitosis in male mice, 17: 30335
effects on mitosis in mammalian cells in tissue cultures, 17: 37079
effects on mitotic index and succinic dehydrogenase activity in hepatomas, 16: 14560
effects on mitotic delay in dog erythroblasts, 18: 15874
effects on mitotic index in pea roots, 18: 31222
effects on mitotic activity in mouse corneal epithelium, 19: 10813
effects on mitotic activity in regenerating rat liver cells, 19: 19510(T) (JPRS-29250(p.27-32))
effects on mitotic activity in regenerating rat liver, 19: 21892
effects on mitotic activity of corneal epithelium of mice, 19: 33825(T)
effects on mitotic mechanism in *E. coli*, repair of, 20: 16200
effects on mitotic delay in spermatogenesis of *Drosophila melanogaster*, 20: 18354
effects on mitotic frequency of Haplopappus embryos, 20: 26666
effects on mitotic recombination in heterozygous Saccharomyces, mechanism of, 20: 33053
effects on mitotic response of thymus-derived cells to sheep erythrocytes and skin grafts in mice, 20: 35339
effects on mitotic stages in Tradescantia microspores, 17: 31937
effects on mitotic inhibition in liver, recovery from, 17: 2874
effects on moisture content of rat tissues, 19: 45896
effects on mold cells and pectic enzymes, 20: 63(R) (STI/DOC/10/42, pp 45-55)
effects on molecular weight of egg albumin, 19: 29924
effects on molecular reactions in DNA, mechanisms of, 19: 31893
effects on molecular changes in DNA, 16: 26836
effects on mongolism occurrence, maternal exposure, 17: 10436
effects on monkey kidney cells in tissue culture, 18: 8150
effects on monkey behavior, 18: 13501
effects on monkey social behavior, evidence of psychic blindness from, 18: 13503
effects on monkey and rat responses, 18: 19586
effects on monkey jaw bones, effects of dose fractionation on necrotic, 20: 3742
effects on monkey testes, cytological, 18: 38898
effects on monkey heart cell nuclei size, 17: 38833
effects on monkeys, protective effects of bone marrow transplants against, 19: 31915
effects on monkeys, protective effects of cysteine–AET against, 20: 140
effects on monkeys, pathological, 20: 31101
effects on monkeys, pathological, 20: 31103
effects on monomers, kinetics of chemical, 19: 490
effects on Mormoniella, mutagenic, 19: 31674(R) (ORNL-3768(p.64-9))
effects on Mormoniella males, mutagenic, 20: 20464
effects on morphogenesis of embryonic chick tibiotarsus, 18: 19657
effects on morphology of tumor cells, electron microscope examination, 16: 1566
effects on morphology of adrenal and pituitary glands, ovaries, and thymus, in rats, 16: 4051
effects on morphology and metabolism of *Paramecium caudatum*, 16: 4109
effects on morphology and metabolism of cartilage, localized, 16: 14533
effects on morphology of desoxyribonucleic acid, 16: 17451(T)
effects on morphology of deoxyribonucleic acid, 16: 21919(T) (JPRS-14140)
effects on morphology of fertilized ova and embryo development in hamster, ova exposure, 16: 23416 (TID-16121)
effects on morphology and metabolite transport of intestinal wall, whole-body exposure, 16: 25179 (TID-16270)
effects on morphology and metabolite transport of intestinal wall, whole-body exposure, 16: 25180 (TID-16271)
effects on morphology and biochemical properties of thymus, 16: 26803 (UAC-5718)
effects on morphology of mammalian cells in tissue culture, large doses, 16: 32728 (TID-16732)
effects on morphology of bacilli Sal., 16: 14568
effects on morphology and hatching percent of chick embryos, 18: 108
effects on morphology of rat intestine, whole-body, 18: 3492 (TID-18282)
effects on morphology of lymphocytes, 18: 6626
effects on morphology and physiology of rat spleen, 18: 15822
effects on morphology and genetic factors in *Chlorella vulgaris*, 18: 17581
effects on morphology of erythrocytes in rabbits, 18: 27162
effects on morphology of mammalian cells in cultures, 18: 29377
effects on morphology of lymph node cells in rats, 19: 5706
effects on morphology of liver cells in rats, 19: 5709
effects on morphology of spore-forming bacteria, 19: 7165
effects on morphology of carcinomas, 19: 21972
effects on morphology and physiology of immature cerebral cortex in cat brain, 19: 26094
effects on morphology of peritoneal leukocytes in mice, 19: 31802 (USNRDL-TR-841)
effects on morphology of cells of peritoneal cavity of mice, 20: 18285 (AD-630103)

effects on morphology of mouse intestinal crypt cells, 20: 31128
effects on morphology of jute, comparison of ethylenimine with, 20: 33048
effects on morphology of thymus gland of animals, 20: 38685
effects on morphology of granulocytes, whole-body exposure, 17: 5797
effects on morphology of granulocytes, whole-body exposure, 17: 5798
effects on morphology of central nervous system in rats, 17: 7901(T)
effects on morphology of leukocytes in monkeys, 17: 19820
effects on morphology and blood picture of thymus in mice, 17: 35467
effects on morphology of seedlings of *Vicia sativa* and *Vicia villosa* exposed as seeds, 17: 38692
effects on mortality rate in mice, protective effects of organic compounds against, 16: 4000(R) (NP-11020(p.65-77))
effects on mortality in female mice, backscatter and beam direction, 16: 17495
effects on mortality in rats, protective effects of Zymosan-stimulated Properdin against, 19: 7182
effects on mortality in goldfish, effects of adrenalectomy and hypophysectomy on, 19: 10869
effects on mortality of grain beetles, oxygen effects on, 19: 17622
effects on mortality from *Pseudomonas aeruginosa* in mice, protective effects of antibiotics against, 19: 36121
effects on mortality of mice, rabbits, and rats, mechanism of, 20: 38666
effects on mortality of gastropods exposed at various stages of life cycle 20: 40700
effects on mortality in monkeys treated with antibiotics, blood platelets, and bone marrow, 20: 42980
effects on mortality of dentists, 20: 45502 (PHS-999-RH-18)
effects on mortality and nodulation in alfalfa treated with β-indolylacetic acid, 20: 45391
effects on mortality of mice infected with *Trichinella spiralis*, 17: 10431
effects on MOS field-effect transistors, transient, 20: 16913
effects on MOS semiconductors, 20: 31615
effects on MOS transistor capacitance-voltage characteristics, (E), 20: 19113
effects on MOS transistors, positive charge distributions in dielectric layer from, (E), 20: 37130
effects on motility and contraction in nerve-muscle preparations from worms, 16: 30283
effects on motivation in rats, humoral factor in, 20: 5303 (USNRDL-TR-925)
effects on motor defense reflexes elaborated with visual stimuli in rabbits, 17: 7894(T)
effects on motor performance in rats, 17: 35518
effects on mouse and rabbit retinas, 18: 17540
effects on mouse and rat serum protein metabolism, 18: 19590
effects on mouse aging and kidney function, 18: 23291
effects on mouse and rabbit ear, skin recovery processes in, 19: 45987
effects on mouse body temperature, 18: 17550
effects on mouse bone marrow and spleen, protective effects of homologous cell against, 18: 19767
effects on mouse blood cell and hematopoietic system metabolism, 18: 19730
effects on mouse bone marrow, effects of incubation temperature on x, 19: 31905(R) (ORNL-3768(p.99-108))
effects on mouse bone marrow proliferative activity, 20: 20452
effects on mouse bone marrow, immuno-electrophoretic technique for determining, 20: 24913
effects on mouse bone marrow cells, effects of vibrations on, 18: 41182
effects on mouse blood formation, 17: 31941
effects on mouse cerebellum, single high-level exposure, 18: 15830
effects on mouse chromosomes and sterility, 18: 15893
effects on mouse carbohydrate metabolism, relation to phagocytosis in hematopoietic system, 18: 19734
effects on mouse collagen, factors affecting, 18: 27118
effects on mouse chromosomes, protective effects of streptomycin against whole-body, 19: 196
effects on mouse chromosomes, aberrant, 19: 10879
effects on mouse chromosomes, effects of age on aberrant, 19: 43729(T) (BNL-tr-12)
effects on mouse chromosomes during leukemia induction, 19: 45911
effects on mouse chromosomes, aberrant, 20: 65(R) (TID-22174)
effects on mouse disease immunity, 18: 13467
effects on mouse embryos, 18: 11672
effects on mouse embryos and fetuses, 18: 11753
effects on mouse embryos, 18: 15891
effects on mouse embryonic development, 18: 41203
effects on mouse eyes, prenatal, 18: 41203
effects on mouse epithelium, protective effects of vitamin A against, 18: 43309
effects on mouse embryos, pathological, 19: 45852
effects on mouse embryos, cataractogenetic, 20: 40619(R) (NYO-2740-3, pp 216-57)
effects on mouse embryos, 20: 40649
effects on mouse epithelium, cytological, 20: 42834(R) (ANL-7136, pp 46-63)
effects on mouse embryos, cytokinetic, 18: 35329
effects on mouse fetus limbs, 18: 11739
effects on mouse fibroblasts, chemical protection against, 18: 11875
effects on mouse fibroblasts, protective effects of cysteamine against, 18: 17639
effects on mouse fertility, 18: 23325
effects on mouse fetuses, protective effects of splenectomy against x, 20: 18436
effects on mouse gonads, pathological, 20: 14404
effects on mouse genetics, 20: 42986
effects on mouse hind limb circulatory system, 18: 19640
effects on mouse hematopoietic tissue transplants, 18: 37009
effects on mouse heart and resultant electrocardiograms, 20: 40648
effects on mouse immunological tolerance, 18: 25157
effects on mouse immunity to Ehrlich tumors, 18: 31155
effects on mouse immunity to skin carcinomas, 18: 35357
effects on mouse influenza, 18: 38805
effects on mouse immunity to syngeneic bone marrow transplants, 20: 6824
effects on mouse immunity to uv-irradiated transplants of ascites tumor cells, 20: 20484
effects on mouse immunity to sarcoma J, 20: 42890
effects on mouse kidneys, neoplastic, 16: 4033 (USNRDL-TR-532)
effects on mouse liver mitochondria, 18: 1429
effects on mouse liver catalase activity, 18: 17600
effects on mouse lymphoid regeneration, effects of thymus on, 18: 19546
effects on mouse lymph nodes and spleen when used with vaccination, 18: 19740
effects on mouse lymphocytic choriomeningitis, 18: 29462
effects on mouse leukocytes, 18: 41206
effects on mouse lungs, co-carcinogenic effects of chemicals and viruses on tumorigenic, 19: 31678(R) (ORNL-3768(p.137-45))
effects on mouse L cell cultures, protective effects of halogenated pyrimidines against, 19: 38459
effects on mouse life spans, effects of genetic damage on, 19: 45969
effects on mouse lungs, carcinogenic, 20: 1606 (AD-623079)
effects on mouse lymph nodes, effects of serum injection on recovery from, 20: 6809
effects on mouse leukocytes, effects of pertussis vaccine on, 20: 22685
effects on mouse leukemia cells, effects of biochemical changes on, 20: 22710
effects on mouse liver and spleen, whole-body, 20: 45434
effects on mouse mortality, effects of age on spleen cell transfusions for, 18: 19727
effects on mouse mammary glands, comparison of effects of carcinogens and, 20: 20502
effects on mouse marrow cells, factors affecting recovery from, 20: 40634 (ORNL-P-2312)
effects on mouse ovaries, 18: 21876
effects on mouse population productivity, 18: 29300
effects on mouse production of bacteriophage-neutralizing antibody, 18: 29301
effects on mouse progeny survival, protective effects of chemical agents against, 19: 2179
effects on mouse pituary system, protective effects of chemicals against, 19: 26124
effects on mouse plasma lipids and serum lipoproteins, 20: 3704
effects on mouse populations, biological, 20: 38590(R) (NYO-1979-13)
effects on mouse RES, Riley virus effects on plasma enzyme levels following, 20: 45252
effects on mouse spermatogonia, 16: 31487
effects on mouse splenic uptake of iron-59, 18: 19594
effects on mouse survival, protective effects of cysteamine against, 18: 19788
effects on mouse spleen proteolysis, 18: 19744
effects on mouse spleen cell transplants, 18: 27120
effects on mouse spleen, Friend's disease development from, 18: 29284
effects on mouse skin grafts, effects of prior newborn liver injection on, 18: 31237
effects on mouse spleen after foreign cell infection modification of, 18: 38863
effects on mouse spermatozoa mutagenesis, protective effects of AET against, 18: 38987
effects on mouse spermatogenesis, protective effects of AET against, 19: 206
effects on mouse survival, protective effects of chemicals against, 19: 2181
effects on mouse spermatogonia, mutagenic, 19: 5651
effects on mouse spermatogonial genes, lethal, 19: 5652
effects on mouse sarcomas, effects of nicotinic acid on, 19: 13113

effects on mouse spermatogonia, mutagenic, 19: 15132
effects on mouse stem cells, 19: 28066
effects on mouse spleens, hybrid resistance to protective grafts against, 19: 31677(R) (ORNL-3768(p.119-30))
effects on mouse spleen cells, cytological, 20: 12681
effects on mouse survival, electrolytic balance as predictor of, 20: 14266
effects on mouse spermatozoa, effects of dose on lethal mutagenic, 20: 18351
effects on mouse survival, protective effects of organophosphorus derivatives against, 20: 20515
effects on mouse spleen, cytological, 20: 22614(R) (NIRS-4, pp 28-34)
effects on mouse skin, protective effects of heparinized rabbit serum against epilation, 20: 24915
effects on mouse spermatogenesis, 20: 24934
effects on mouse skin epithelial cells, dose-response relations for, 20: 28990
effects on mouse spleen and thymus, synergistic effects of Mitomycin C and Endoxan in, 20: 31131
effects on mouse spermatogonia, biological, 20: 22632
effects on mouse skin, biological, 20: 38627
effects on mouse spermatogonia, effects of dose on frequency of mutagenic, 20: 40627(R) (ORNL-3922, pp 84-8)
effects on mouse sex chromosomes, aberrant, 20: 40627(R) (ORNL-3922, pp 84-8)
effects on mouse spermatogenic epithelium, pathological, 20: 42942
effects on mouse skin carcinogenesis in combination with dimethylbenzanthracene, 20: 42969
effects on mouse skin, comparison with effects of electrons and neutrons, 20: 45426
effects on mouse thrombocyte count, protective effects of ultraviolet against, 18: 3537
effects on mouse tumor grafts, x, 18: 5012
effects on mouse thrombocytes, 18: 11745
effects on mouse thrombocyte count, protective effects of ultraviolet radiation against, 18: 17648
effects on mouse transplantation antigens, 18: 19589
effects on mouse tolerance to skin grafts, 18: 43293
effects on mouse tumors, protective effects of AET against, 19: 7179
effects on mouse testes, RBE of, 19: 10860
effects on mouse tumor cells, evaluation of radioprotectant by, 17: 35575
effects on mouse vestibular apparatus, 19: 3969
effects on mouth following facial therapy, 20: 14324
effects on MPA metabolism in mice, 18: 33373
effects on mucin production by glands in rats and mice, high-level local exposure, 17: 23103
effects on mucopolysaccharides in rat connective tissue, 18: 33277 (STI/DOC/10/28(p.21-38))
effects on mucopolysaccharides in aortic wall in animals and man, 17: 24904
effects on mucoprotein excretion in rats following whole-body exposure, 20: 42960
effects on mucosa of exteriorized rat intestine, pathological, 20: 14364
effects on mucosa weight and enzyme activity in intestine, 20: 45351 (BNL-10534)
effects on mucous membranes in rats, 20: 6858
effects on mucus synthesis in rat intestine, 20: 10600 (BNWL-122, pp 131-4)
effects on multipolar mitosis in KB human cell line, 19: 15074
effects on muramidase activity in mouse lymph cells, 19: 31906(R) (ORNL-3768(p.179-80))
effects on murine leukemia cells *in vitro*, survival curves for, 20: 5361
effects on murine Ehrlich ascites tumor cells *in vitro* and *in vivo*, 20: 22713
effects on muscle membrane, depolarization, 17: 17761 (TID-18220)
effects on muscle morphology and metabolism, 17: 15641 (TID-18221)
effects on muscles in mice, protective effects of cysteamine against, 17: 31967
effects on mutability of female and male *Drosophila melanogaster* mature sperm, 19: 15085
effects on mutagenesis in rye grass seed, 19: 17527
effects on mutagenic properties of tissue extracts, 20: 28959
effects on mutation rates in first and later formed sprouts in barley seeds, 16: 1578
effects on mutation rate and polyploidy of *Triticum*, 18: 19748
effects on mutation frequency patterns in Drosophila, 19: 109
effects on mutational mosaicism in rice, 19: 7140
effects on mutation frequency in dormant rice seed, 19: 8855
effects on mutation breeding of six-rowed barley in X_1 and X_2 generations, 19: 10826
effects on mutation induction in A3-3 region of *Neurospora crassa*, kinetics of, 19: 15153
effects on mutation induction in *Neurospora crassa*, physiological and structural relations within TD locus in, 19: 17517
effects on mutation induction in cultivated rice, 19: 17533
effects on mutation induction in *Chrysanthemum carinatum*, 19: 17534
effects on mutation induction in *Act. antibioticus*, comparison of chemicals with, 19: 26023
effects on mutation induction in *Schizosaccharomyces pombe*, comparison of nitrite induced mutations with, 19: 26035
effects on mutation induction in different wheat varieties, phylogenetics of, 19: 26047
effects on mutations in Chlorella, 19: 28080
effects on mutations in *E. coli*, mechanism of, 19: 33912
effects on mutation induction in peas, segregation in, 19: 35961
effects on mutation induction in peas, 19: 35960
effects on mutation induction in male Drosophila, effects of sperm maturity on frequency of, 19: 38390
effects on mutation induction in Dahlbominum oogonia, 19: 38392
effects on mutation induction in fodder peas, 19: 42268
effects on mutation induction in potato plants, 19: 42318
effects on mutation induction in region of X chromosome in *D. melanogaster* DNA, 19: 45879
effects on mutations in bacteriophage, 20: 80
effects on mutation rate in murine cell line resistant to purine analogs, 20: 1678
effects on mutation induction in *Pisum sativum*, effects of mutant gene penetrance on, 20: 6773 (EUR-2510.d)
effects on mutation rate in *Drosophila melanogaster* in presence of serotonin, 20: 14398
effects on mutation rates in ad-3 regions of *Neurospora*, 20: 16159(R) (ORNL-3900, pp 150-81)
effects on mutation rates in Drosophila, 20: 31108
effects on mutations of economically important plants, 20: 31109
effects on mutation induction in barley and rice seeds, 20: 31050
effects on mutations in Sippe 50 of *Antirrhinum majus*, 20: 33052
effects on mutation frequency in hydrated wild-type tomato pollen, 20: 35299
effects on mutation and selection in *Trifolium subterraneum*, second cycle, 20: 35300
effects on mutation induction in Schizosaccharomyces, environmental effects on, 20: 36653
effects on mutation frequency in *Drosophila* sperm, effects of cyanide and dose rate on, 17: 24901
effects on mutations in X_1 and X_2 *Vicia faba* L., 17: 28648
effects on mutation rate in Drosophila sperm, 17: 31895
effects on mutation rates in Drosophila, 17: 35567
effects on myocardium of rabbits, pathological, 20: 8668
effects on myoglobin single crystals, 16: 30260
effects on myosin ATPase activity, 18: 23258
effects on myotactic reflexes in rabbits, 17: 2869
effects on *n*-heptane and 2,2,4-trimethylpentane, mechanism of dialkylperoxide formation in, 19: 24552
effects on *N,N*-diethyl-*p*-phenylenediamine, 19: 2414
effects on nail tissues of rats, 19: 21956
effects on natural populations of mice and toads of periodic exposure of males to, 18: 8113 (TID-19982)
effects on natural population of lizards, whole-body, 20: 20444(R) (TID-22820)
effects on natural populations of vertebrates, 17: 30398
effects on necrosis of myocardium in rabbits, 20: 33017
effects on negative ion vacancy formation in alkali halides, 20: 36356 (CEA-S-3)
effects on neoblast transplants in planarians, tracer study, 19: 35987
effects on neonatal and prenatal mortalities in mice after fetal or maternal exposure, 19: 43760
effects on neoplasm cytology, 18: 38883
effects on nerve action potentials in cold-blooded animals, 20: 29021
effects on nerve cells in rabbit brain, pathological whole-body, 18: 1381(T) (OTS-62-11069(No.3)(p.768-80))
effects on nerve cells of the sympathetic ganglia in rabbits, 19: 5637
effects on nerve fiber action-potential, effects of sodium azide on, 18: 23277
effects on nerve-muscle preparation from Annelids, 17: 33626
effects on nerve regeneration, 20: 1635
effects on nerve structures in dog and rabbit liver, 18: 23309
effects on nerve sensitivity in rabbits, 18: 35380
effects on nerves at low doses, mechanism, 16: 6319
effects on nerves, 19: 7145
effects on nerves of gastrointestinal tract in rabbits, 19: 21910
effects on nerves, physiological, 20: 40606 (BMwF-FBK-66-02)
effects on nervous system of monkeys and rats, demyelination, malacic myelopathy, and myodegeneration, 16: 23483
effects on nervous system, survey of Russian work, 16: 23487
effects on nervous system of rat progenies, antenatal exposure,

16: 25240
effects on nervous system in dogs, whole-body, 18: 9838
effects on nervous system, effects of phenothiazine on, 18: 17711
effects on nervous activity of antenatally irradiated dogs, 18: 19608(T)
effects on nervous system of rabbits exposed *in utero*, 18: 25121
effects on nervous system in cats and rats, 18: 33278 (ST1/DOC/10/28 (p.39-66))
effects on nervous system development in rabbit embryos, 18: 41105(T)
effects on nervous system, electroencephalographic study of occupational, 19: 8859
effects on nervous activity of rats, prenatal, 19: 17619
effects on nervous activity of dogs, antenatal, 19: 19536
effects on nervous system development in rat embryos, 20: 60(R) (NYO-901-37, pp 33-68)
effects on nervous system of dogs, effects of fluoroacetate on, 20: 6817
effects on nervous system in animals, clinical and experimental studies on low-dose, 20: 33037
effects on nervous response of rabbits, 20: 33057
effects on nervous system, cytochemical, 16: 1477(T) (JPRS-10170 (p.128-34))
effects on nervous system in rats, 18: 6622 (USNRDL-TR-682)
effects on nervous system function, acute, chronic, and fractionated exposure, 17: 17778(T) (JPRS-18395(p.311-20))
effects on nervous system, local and whole-body exposure, 17: 27069(T) (JPRS-19284)
effects on neural tube of chick embryo, 16: 23476
effects on neuro-endocrine system in dogs and rabbits, 18: 23377
effects on neurons in supraoptic cytoplasm and nucleus in rats, 17: 7868
effects on neurosecretion release in rat, whole-body, 18: 13506
effects on neurosecretion in pituitary gland, protection against, by 5-hydroxytryptamine, 18: 27224
effects on Neurospora, biochemistry and genetics of mutagenic, 19: 15082
effects on Neurospora, functional inactivation of mutagenic, 19: 31788(R) (ORNL-3768(p.33-57))
effects on Neurospora, protective effects of anoxia against mutagenic and lethal, 19: 42363
effects on Neurospora, protective effects of MEA against, 19: 42364
effects on Neurospora conidia, protective effects of endogenous anoxia and MEA against, 19: 42365
effects on Neurospora, mutagenic, 19: 15081
effects on Neurospora conidia, biological, 20: 3780
effects on Neurospora, genetic, 20: 6777(R) (ORNL-3853, pp 54-61)
effects on Neurospora, photoprotection against, 20: 14358
effects on Neurospora, utilization of mutagenic, 20: 18347
effects on Neurospora chromosomes, nonallelic complementation studies, 20: 42926
effects on Neurospora conidia germination, protective effects of calcium gluconate against, 17: 40612
effects on newborn, head exposure, 16: 23475
effects on nicotinamide-adenine-N^1-oxide-dinucleotide formation in nicotinamide adenine dinucleotide decomposition, 19: 44062
effects on nicotinamide adenine dinucleotides content in rat thymocytes, 20: 36590
effects on nictitating membrane in eye in cat, 17: 24906
effects on *Nippostrongylus brasiliensis* larvae on immunity level in rats, 19: 24363
effects on Nitella cyclosis, recovery from, 20: 3698
effects on *Nitella flexilis*, biological, 20: 42998(R) (EUR-2992.f)
effects on nitrogen fixation in rumen lining, 18: 21893
effects on nitrogen content in mice, effects of bone marrow injections on, 19: 138
effects on nitrogen metabolism in frog liver, 19: 31882
effects on nitrogen distribution in mice treated with bone marrow, 20: 20407 (ORNL-P-1118)
effects on nitrogen metabolism in rat brain, 20: 26696
effects on nitrogen balance in mouse chimeras, 20: 38636
effects on nitrogen metabolism in yeast, 17: 5881
effects on nitrogen excretion by spleen, protective effects of histamine and cysteamine, 17: 23159
effects on non-specific antibody production and reticulo-endothelial system after liver exposure, 16: 14540
effects on non-infected hamster cells, effects on contacted Polyoma-infected cells, 20: 10684
effects on nonallelic mutations in Neurospora, 20: 40624(R) (ORNL-3922, pp 52-8)
effects on normal and rachitic rats, metabolic, 19: 40351(R) (NYO-1913-1)
effects on nuclear membrane of spermatocytes of *Lebistes reticulatus* R., 18: 1392
effects on nuclear diameters of cells of Walker carcinomas, 18: 19699
effects on nuclear division in Paramecium, 18: 35303(R) (AD-438541)
effects on nuclear ATP synthesis in mice and rats, 19: 26062
effects on nuclear inactivation in Neurospora, protective effects of anoxia against, 19: 31788(R) (ORNL-3768(p.33-57))
effects on nuclear structure of rat thymocytes, 20: 18455
effects on nuclear emulsions, 20: 27616
effects on nuclear reorganization in paramecia, 20: 29007
effects on nuclear processes in *Paramecium putrinum*, 20: 33047
effects on nuclear proteins in *Vicia faba*, cytophotometric measurements on, 20: 36588
effects on nuclear spin in nucleic acids and bases, 17: 39152
effects on nuclei of mouse liver cells, 18: 33350
effects on nuclei in Triton erythroblasts, 19: 45925
effects on nuclei acid and phosphate metabolism in carrot tissues and tomato stems, effects of dose-rate on, 20: 120
effects on nucleic acid, phosphate, and phospholipid contents in liver and spleen in rat, 16: 14552
effects on nucleic acid metabolism in mice, 16: 25212
effects on nucleic acid metabolism in *Azotobacter agile*, 16: 30226(T) (JPRS-15220)
effects on nucleic acid metabolism in nerve cells of rabbit brain, whole-body, 18: 1382(T) (OTS-62-11069(No.3)(p.781-96))
effects on nucleic acids in fish embryos, 18: 11722
effects on nucleic acid synthesis in rabbit thymus, whole-body, 18: 17473 (NYO-2565-1)
effects on nucleic acid metabolism during embryonic development in barley seed, 18: 25175
effects on nucleic acids in *Escherichia coli*, 18: 27153
effects on nucleic acid synthesis in liver of partial-hepatectomized rats, whole-body, 18: 33294
effects on nucleic acid metabolism in HeLa cells in culture, 18: 43240
effects on nucleic acid synthesis in mammalian cells, 18: 43276
effects on nucleic acids, free radicals formed in, 19: 5957
effects on nucleic acid composition of rabbit tissues, 19: 8923
effects on nucleic acid metabolism in brain of rats, 19: 8929
effects on nucleic acid content of Yoshida sarcoma cells, 19: 13031
effects on nucleic acid contents in extremities of larval salamanders, 19: 25942
effects on nucleic acid content in guinea pig brain, 19: 28097
effects on nucleic acid content of *Escherichia coli*, 19: 29923
effects on nucleic acid metabolism in rat liver, 19: 33815
effects on nucleic acid content in liver of rat embryos, 19: 45826
effects on nucleic acid synthesis in ϕX174-infected *E. coli*, tracer study, 19: 45851
effects on nucleic acid metabolism in rat lens, tracer study, 20: 89
effects on nucleic acid synthesis in rats, 20: 18495
effects on nucleic acid and protein content in *E. coli*, effects on survival, 20: 22651
effects on nucleic acid synthesis in rat thymus cells, 20: 28953
effects on nucleic acid in rats and guinea pigs, metabolic, 18: 49(T) (JPRS-21472(Del.))
effects on nucleic acid content in regenerating liver, 17: 1289
effects on nucleic acid distribution and metabolism in *Zea mays* seedlings, 17: 1322
effects on nucleic acid and protein metabolism in barley seedlings, 17: 10456
effects on nucleic acid metabolism in rats, whole-body exposure, 17: 15684
effects on nucleic acid metabolism in rats, whole-body exposure, 17: 15685
effects on nucleic acids, 17: 19845
effects on nucleic acid content in organs of rats, effects of sodium gallate, 17: 24900(T) (JPRS-19355)
effects on nucleic acid metabolism in thymus and liver, tracer study of, 17: 33736
effects on nucleic acid metabolism in central nervous system in rats, 17: 40602
effects on nucleic acid synthesis in thymus, whole-body, 17: 33737
effects on nucleic acid synthesis in thymus, whole-body, 17: 33738
effects on nuclein metabolism by skeletal muscles in rats, 17: 37068(T) (JPRS-20997)
effects on nucleohistone, 20: 14592
effects on nucleolar structures of *Cannabis sativa* seedlings, morphological, 19: 45940
effects on nucleoli in Chang liver cells, 17: 27063 (TID-18846)
effects on nucleoproteins in Tetrahymena, 20: 5267
effects on nucleoprotein density, 20: 8595
effects on nucleoproteins in cells, 16: 30269
effects on nucleoprotein loss in cell nuclei in liver, thymus, and spleen in first four hours after irradiation, 17: 27157
effects on nucleosides, free radicals formed in, 19: 5955
effects on nucleotide metabolism, 16: 9859(T)
effects on nucleotides, free radicals formed in, 19: 5956
effects on nucleotide oxidation in suspensions of cattle heart mitochondria,

20: 20496
effects on nucleus of Habrobracon eggs, 16: 1621
effects on nucleus size of ascites tumor cells, 18: 13554
effects on number and growth rate of lateral roots in Vicia, 20: 24910
effects on oat chromosome number, 18: 31159
effects on oat seeds, genetic, 20: 45369
effects on oats and wheat, 18: 13494
effects on oats cultured in phosphorus-deficient solutions, 17: 37091
effects on oats, genetic, 20: 10645
effects on occurrence frequency of mutations in Drosophila, 17: 31936
effects on octacosane and polyethylene films, spectral studies on hydrogen liberation and *trans*-vinylene development in, 20: 26919 (AD-632666)
effects on *Oenothera hookeri*, mutagenic, 20: 22763
effects on *Oenothera berteriana*, genetic, 20: 22764
effects on *Oenothera berteriana*, genetic, 20: 22770
effects on *Oenothera berteriana*, genetic, 20: 22762
effects on offspring from dysgerminoma therapy, 18: 13521
effects on offspring and reproductive cycle in dogs, 17: 24954
effects on olfactory epithelium of salamanders, pathological, 19: 35965
effects on olfactory receptors in rats, 20: 8708
effects on olfactory bulb neurons in rats, effects of gases in nasal cavities on, 20: 16215 (AD-628443)
effects on omentectomized and splenectomized mice and rats, time dependence of, 18: 41205
effects on onion cell permeability, 17: 38832
effects on onions, radioprotective effects of chloral and hexachlorocyclohexane against cytological, 19: 8967
effects on onset of sarcoma in rats, 19: 13042
effects on oöcyte maturation in mice, 16: 23520
effects on oocyte maturation in mice, 16: 30225(T) (FTD-TT-62-501 (p.24-30))
effects on oocytes and oogonia in fetal rats, short-term, 19: 15154
effects on oocytes in cattle and swine, 19: 36026
effects on optical absorption in sodium bromate crystals, 18: 10154
effects on optical masers, 18: 20625 (N63-21469)
effects on optical absorption in magnesium oxide single crystals, 18: 37220
effects on optical absorption in F centers of potassium chloride crystals, 19: 18017(T)
effects on optical absorption bands in lithium fluorides, 19: 20817
effects on optical properties of lithium fluorides, impurity effects in, 19: 19998
effects on optical absorption of copper centers in potassium halides, (E), 19: 40107
effects on oral cancers, therapeutic, 20: 175
effects on oral tissues in hamsters, whole-body exposure, 17: 1308
effects on orange juice, 18: 10435
effects on orchitis development and *Treponema pallidum* content in antigens in rabbits, 20: 31119
effects on organic liquids, excimer emission from, 20: 23132
effects on organic peroxide production in mice, whole-body exposure, 17: 67
effects on organs and tissues in rat, with and without europium nitrate and nitric acid, 16: 4004(R) (NP-11020(p.105-16))
effects on organs and tissues in man, relation of dose to, 20: 8808
effects on oriented calf thymus DNA, ESR spectra from, (E), 20: 8606
effects on *Oryzias latipes*, effects of temperature on biological, 20: 22731
effects on osmoregulation in fish, 20: 42885
effects on osmosis in Allium bulbs, effects of electrolytes on, 19: 42270
effects on osmotic processes in Begonia leaves, 18: 11691
effects on osmotic resistance of red blood cells in rabbits, whole-body, 19: 12972
effects on osmotic resistance of rat leukocytes, 20: 10614
effects on osmotic resistance of rat leukocytes, 20: 12705
effects on osmotic resistance of rat leukocytes, 20: 45377
effects on osmotic resistance of leukocytes, 17: 35584
effects on osteogenesis of long bones of mouse embryos, 19: 45872
effects on osteogenic sarcomas, therapeutic, 20: 6941
effects on ova distribution in rat uterus, 18: 17492
effects on ovarian estrogen level and tumor development in rats, 19: 8831(T)
effects on ovarian function in rats, 17: 1297
effects on ovaries in mammals, 18: 35322(R) (TID-20941)
effects on ovaries in mice, direct, partial, and whole-body, 19: 15029
effects on ovaries of rabbits, pathological, 19: 35999
effects on ovaries after irradiation of salivary glands, 16: 20217
effects on ovary development in young female rats, whole-body, 19: 13066
effects on ovary growth in Oryzias during sexually active seasons, 19: 31670(R) (NIRS-3(p.19-56))
effects on ovary in chick embryos, 19: 3933
effects on ovulary time in orchids, 19: 24331
effects on ovulation in rats, 19: 21933
effects on ovulation cycle of women following ovarian and pituitary exposure, 20: 45546
effects on oxalic acid content in urine of mice, 16: 21962
effects on oxidase activity in rat liver, 19: 8795 (SAM-TDR-64-29)
effects on oxidation reactions in liver, 16: 1496(T) (JPRS-10170 (p.454-7))
effects on oxidative-reduction processes in plants, 16: 8565(T)
effects on oxidation in bacteria, protective effects of cysteine against, 16: 25223
effects on oxidative phosphorylation uncoupling in rabbits and rats, whole-body, 16: 28774
effects on oxidation of gluconic and pyruvic acids in *Bacterium cadaveris*, 16: 32787
effects on oxidative phosphorylation in spleen of rats, 18: 8200(T)
effects on oxidative phosphorylation in rat liver mitochondria, 18: 23233(R) (ANL-6823(p.157-60))
effects on oxidative phosphorylation in ascitic fluid from tumor-bearing mice, 19: 3899
effects on oxidative phosphorylation in mitochondria of rat liver cells, 19: 7016(R) (ANL-6906(p.110-12))
effects on oxidation kinetics of tetrafluoroethylene, 19: 7577
effects on oxidative phosphorylation in rat liver mitochondria, effects of insulin and other compounds on, 19: 17669
effects on oxidative phosphorylation processes in rat liver mitochondria, whole-body, 19: 17627
effects on oxidation of cumene, effects of impurities on hydrogen peroxide accumulation in, 19: 30271
effects on oxidation of iron ions in sulfuric acid solutions, 19: 30287
effects on oxidation of sulfuric acid by oxygen, dose rate effects on, 20: 412
effects on oxidation and reduction properties of zinc oxide, 20: 7128(R) (NYO-2206-1)
effects on oxidation of unsaturated fatty acids, device for chemiluminescence studies on, 20: 25165
effects on oxidative enzymes in mouse epididymis and testis, 20: 31090
effects on oxidative phosphorylation in chicken embryos, 20: 33042
effects on oxidation of benzenethiol, 20: 45735
effects on oxidation of bilirubin in aqueous solution, 17: 1184
effects of oxidation of bilirubin in aqueous solution, 17: 1186
effects on oxidative phosphorylation of isolated liver mitochondria in rats, 17: 5784
effects on oxidative phosphorylation and optical density in rat liver, whole-body, 17: 30354
effects on oxygen supply in bean root meristems, 16: 1529
effects on oxygen consumption in bone marrow in guinea pigs, 16: 25204
effects on oxygen consumption in the rat, effects of thyroxine and triiodothyronine on, 18: 5036
effects on oxygen consumption by rats, effects of insulin on, 18: 19806
effects on oxygen uptake by human skin, 18: 29269
effects on oxygen uptake by planaria, 18: 31248
effects on oxygen attachment in rabbit hemoglobin, equation for calculating, 19: 19529(T)
effects on oxygen consumption in mice, protective effects of bone marrow against, 19: 31905(R) (ORNL-3768(p.99-108))
effects on oxygen concentrations in Neurospora conidia, 19: 42365
effects on oxygen uptake by *Tenebrio molitor*, 20: 5314
effects on oxygen uptake in rat brain tissues, 20: 20436 (CONF-650560-17)
effects on oxygen consumption in mice, 17: 1291
effects on oxygen consumption, 17: 14031
effects on oxygen consumption by muscle *in vitro*, 17: 17762 (TID-18222)
effects on oxygen-carrying capacity of blood in rabbits, 17: 30420
effects on oxygen uptake by yeast cells, Cartesian diver respirator for measurement of, 17: 33647
effects on oxytocin content of rat pituitary, 18: 23275
effects on oxytoxin-induced contractility of rat uterus, 18: 13519
effects on ozone in man, mouse, rats, and rabbits, 18: 19538
effects on *p*-aminobenzoic acid solutions, 18: 16110
effects on *p*-aminobenzoic acid conjugates, 20: 10904
effects on *p*-chlorobenzaldoxime, free radical ESR spectra from, 20: 23119
effects on p-i-n junction detectors, pulsed and steady-state, 20: 11173 (D2-84071-1)
effects on palatine arch and tonsilar carcinomas, 20: 14416
effects on pancreatic secretion in dogs, effects of hydrochloric acid on, 18: 5107
effects on pancreatic morphology and physiology in dogs, 20: 31089
effects on parabiosis intoxication in inbred rat pairs, 18: 117
effects on parabiosis intoxication in rats, sublethal, 18: 1421
effects on paraffin base system for use as dosimeter, 19: 36501

effects on paramagnetic resonance spectra of cysteine, 18: 12193
effects on paramagnetic defect centers in ammonium bromides and chlorides, 20: 28636
effects on paramecium mitochondria, 16: 4104
effects on Paramecium nucleus, 18: 35302(R) (AD-438540)
effects on Paramecium, mutagenic, 19: 31788(R) (ORNL-3768(p.33-57))
effects on Paramecia, aging, 19: 31788(R) (ORNL-3768(p.33-57))
effects on Paramecia, protective effects of age against, 19: 31788(R) (ORNL-3768(p.33-57))
effects on *Paramecium aurelia*, time course of recovery from lethal, 19: 45978
effects on *Paramecium aurelia*, effects of streptomycin on recovery from mutagenic, 20: 5417
effects on *Paramecium aurelia*, equation for survival from, 20: 16273
effects on Paramecium, temperature-sensitive mutagenic, 20: 18348
effects on Paramecium, conditions affecting yield of temperature-sensitive mutagenic, 20: 18349
effects on Paramecium, genetic, 20: 40623(R) (ORNL-3922, pp 32-49)
effects on parotid gland excretion of sodium and potassium, local exposure, 17: 1293
effects on parotitis virus in guinea pigs and mice, 18: 19556(T) (JPRS-23956(p.9-17))
effects on pathogenicity of Pseudomonas strains in mice, 19: 31905(R) (ORNL-3768(p.99-108))
effects on pathology of monkey fetuses exposed *in utero*, 19: 8811
effects on pathology of atherosclerosis in rats, 20: 28996
effects on pathology of rat brain, 20: 33025
effects on pea seeds, genetic, 20: 81
effects on pea sprouts and seeds, physiological, 17: 1285
effects on peanut plants, genetic, 19: 15020 (TID-20442)
effects on peanuts, genetic, 20: 16247
effects on peas, effects of seed size on, 20: 22676
effects on peas, genetic, 19: 43734
effects on peas, genetic, 20: 5238
effects on peas, mutagenic, 19: 35962
effects on peas, role of DNA synthesis in determining aberrant, 20: 22660
effects on penetration of blood-brain barrier by anticonvulsant drug in rats, 18: 43283
effects on penicillin-resistant *E. coli*, 18: 1401
effects on penicillin production by *Penicillium nigricans*, 19: 19556
effects on peptides and amino acids, free radicals formed in, 19: 5958
effects on percutaneous absorption, 18: 29282
effects on performance capacity of mice and rats, 19: 45823(T) (JPRS-31933, pp 1-5)
effects on performance of tests requiring visual discrimination by monkeys, 19: 45893
effects on performance of learned response by rats, effects of nembutal on, 20: 3772
effects on performance of neutron threshold detectors, 20: 41333
effects on periodontal tissues of rats, 17: 38755
effects on peripheral blood in rats, effects of serotonin on, 18: 23376
effects on peripheral nerves in rats, regeneration following, 20: 35263
effects on peritrichs, 20: 16295
effects on permeability of mitochondria, 16: 1556
effects on permeability of cattle and rat skin, 18: 17646
effects on permeability of blood-brain barrier in rats after head exposure, 18: 29248 (TID-20786)
effects on permeability of membranes of plant cells, 18: 29289
effects on permeability of intestinal membrane in mice, 18: 38789
effects on permeability of frog heart, tracer study, 19: 12954(R) (NP-14665)
effects on permeability of membranes of connective tissue in rats, 19: 36019
effects on permeability of isolated frog heart, 20: 3794
effects on permeability of blood-brain barrier in rats, 20: 38609
effects on permeability of tumor cells, whole-body exposure, 17: 62
effects on permeability of muscle membranes, 17: 17760 (TID-18219)
effects on permeability of yeast cells, 17: 21466 (HW-SA-2280)
effects on permeability of aorta wall in rats, 17: 24947
effects on permeability of the blood brain barrier in rats, 17: 28746
effects on peroxidase activity in Mycobacteria, 18: 25111
effects on peroxide decay in rat spleen DNA, 19: 19541
effects on peroxide formation in mice, 16: 1482(T) (JPRS-10170(p.213-19))
effects on peroxide formation in mice, 16: 1483(T) (JPRS-10170(p.220-33))
effects on peroxidase activity of granulocytes, 17: 5811
effects on persistence of leukemia in mice, 19: 21985
effects on petite yeast strains, 18: 35358
effects on phage induction in *E. coli*, 18: 19739
effects on phage induction in *E. coli*, protective effects of AET and MEA against, 20: 29045
effects on phage production in lysogenic bacteria, protective effects of cystamine, 2-mercaptopropylamine, and urethan against, 19: 7214
effects on phage proteins, protective effects of thiourea against, 19: 42289
effects on phage, recovery from, 20: 12617(R) (NP-15863)
effects on phagocytic ability in leukocytes, 16: 14526
effects on phagocytic response of leukocytes in rabbits, effects of hemorrhage on, 18: 27174
effects on phagocytic activity of reticulo-endothelial system, 18: 27183
effects on phagocytic activity of neutrophils in rabbits, 18: 33277 (ST1/DOC/10/28(p.21-38))
effects on phagocytosis by leukocytes, 19: 19507(R) (TID-21712)
effects on phagocytic activity of reticulo-endothelial cells in rat thymus, 19: 21907
effects on phagocytic activity of, rat reticuloendothelial cells in tissue culture, 20: 85
effects on phagocytic activity of leukocytes in preserved blood, 20: 12698
effects on phagocytosis and immunity mechanism in mice, 20: 33011
effects on phagocytic mechanisms of antibacterial defense in mice, 17: 35520
effects on phase transition in diglycine nitrate and triglycine sulfate, (E), 20: 33355
effects on *Phleum pratense*, 20: 14349
effects on phosphatase activity in tumor cells, 16: 21984
effects on phosphate-transfer reactions in cell nuclei, 16: 30227
effects on phosphate esterification and hydrolysis in mitochondria from spleen in rats, 18: 8176
effects on phosphatase activity in mouse tissues, 19: 31870
effects on phosphate glass, (E/T), 19: 39256
effects on phosphatase content of granulocytes, of man, 19: 43829
effects on phosphatase content in rat tissues, physiological, 19: 43739
effects on phosphate metabolism in Phycomyces, 20: 14264
effects on phosphatide content in rats, 20: 36606(R) (NYO-1864-23)
effects on phosphate metabolism in liver, local exposure, 17: 34
effects on phosphatase activity in liver and spleen, effects of hematopoietic tissue injection on, 17: 27111
effects on phosphorus-32 uptake into deoxyribonucleic acid of thymus, spleen, and intestine of rats, 16: 4068
effects on phosphorus metabolism by rat organs, 16: 14530
effects on phosphorus content in microsomal lipoproteins in rats, 16: 23450
effects on phosphorus-32 excretion in rat urine, 18: 1413
effects on phosphorus-32 RNA-labeling, 18: 3533
effects on phosphorus-32 distribution in organs of rats, 18: 6690
effects on phosphorescence decay of thallium-activated potassium chloride, 18: 13882
effects on phosphorus-32 uptake by rat bone marrow, 18: 17603
effects on phosphorus-32 incorporation by DNA, 19: 141
effects on phosphorus-32 uptake by rat brains, 19: 3950
effects on phosphorus-32 metabolism by rat nucleic acids, 19: 3970
effects on phosphorescence in rocks, 19: 13650
effects on phosphorus-32 uptake by rat femur, local, 19: 25974
effects on phosphoprotein metabolism in guinea pig livers, effects of ATP on, 19: 28112(T) (FTD-TT-64-1163)
effects on phosphorus metabolism in tissue cultures of glioma, 19: 33882
effects on phosphorescence of alkali halide phosphors, influence of F-band illumination on, 19: 40570
effects on phospholipid content in rat-liver particulate fractions, 19: 42262
effects on phosphorus-32 pulse labeling of RNA in *Salmonella typhimurium*, 19: 43743
effects on phospholipase activity of intestinal mucosa of rats, 19: 45820(R) (TID-22227)
effects on phosphors, dose dependence of, 20: 669
effects on phosphorylation in nuclei of tumor cells, 20: 1626
effects on phosphorus metabolism in glioma cultures, 20: 5255
effects on phosphorescence induction in plastics containing dibenzanthracene, effects of heat on, 20: 7128(R) (NYO-2206-1)
effects on phosphorus-32 uptake by rat kidney and liver, 20: 18379
effects on phosphorus metabolism in isolated nuclei from rat bone marrow, 20: 22580
effects on phosphorus-32 metabolism in rats, 20: 22605
effects on phosphorylative capacity of mitochondria from rat liver, 20: 45430
effects on phosphorus-32 incorporation into phosphoethanolamine of rat thymus cells, 18: 29288
effects on phosphorus-32 uptake by *E. coli* fractions, 17: 12141
effects on phosphorus incorporation in organs of rats, 17: 14052
effects on phosphorus-32 uptake by leukocytes in dogs, 17: 17733
effects on phosphorus-32 uptake by erythrocytes in dogs, 17: 17734
effects on phosphorus-32 uptake by DNA in mammary adenocarcinoma in

mice, 17: 23183
effects on phosphorus-32 uptake by DNA in mammary adenocarcinoma in mice, local and whole-body, 17: 23184
effects on phospholipid content of liver mitochondria, whole-body exposure, 17: 28681(R) (TID-18980)
effects on phospholipids in liver mitochondria in rats, 17: 28705
effects on phosphorus-32 uptake in rat gonads, 17: 30008
effects on photoconductivity in anthracene crystals, (E), 19: 22381
effects on photoconductivity of zinc oxide, effects of bromophenol, erythrosin, and pinakrytol green on, 20: 7128(R) (NYO-2206-1)
effects on photoconductivity of cadmium sulfide, 20: 17123(R) (N-65-17505)
effects on photoconductivity of anthracene, 20: 36873
effects on photodynamic inactivation of DNA, 19: 31670(R) (NIRS-3 (p.19-56))
effects on photoelectric sensitivity of antimony–cesium and cesium–silver phototubes, 18: 28055
effects on photographic emulsions, 19: 24558
effects on photoluminescence of silver-activated sodium chlorides, 19: 40569
effects on photomultiplier tubes, 18: 35813 (USNRDL-TR-763)
effects on photophosphorylation and Hill reaction, effect of concentration of isolated chloroplast on, 16: 26814
effects on photostimulated emission from potassium chloride and sodium chloride crystals, 19: 34243
effects on photosynthesis in isolated chloroplasts, 19: 10877
effects on photosynthetic reactions in isolated chloroplasts, 20: 5402
effects on phthalocyanines, 20: 36886
effects on physical properties of polymethyl methacrylate, 19: 39231 (COO-1224-8)
effects on physiology of mouse testis, divided-dose, 18: 17588
effects on physiology of mineral contents in developing guinea pig brain, 19: 19534
effects on physiological properties of cystamine-treated mouse ascitic cell and normal tissue homogenates, 20: 5412
effects on physiology of reticulum cells in rat thymus, 20: 16293
effects on physiology of muscles, 20: 18293 (NP-14898)
effects on physiology of chicken germ cells, 20: 20440(R) (EUR-2643.f)
effects on physiology and respiration in chick embryos, 20: 20440(R) (EUR-2643.f)
effects on physiology of rat thyroid gland, 20: 22643
effects on physiology and weight of adrenal gland, 17: 28702(T) (JPRS-20037)
effects on phytohemagglutinin-treated leukocytes, 18: 1407
effects on phytoncidal activity of white mustard seeds, 17: 30373
effects on pig skin, fractionated, 19: 21888
effects on pig skin, biological, 19: 32001
effects on pig skin, effects of dose fractionation on, 20: 3735
effects on pigments in mouse hair, effects of melanogenetic substrates on, 20: 18502
effects on pigment mosaics in human skin, cellular survival curve test for, 20: 32981
effects on pigmentation of skin of guinea pigs, 17: 1280
effects on piperidine and pyridine, 18: 31635
effects on *Pisum sativum* root meristem mitosis, 18: 13531
effects on *Pisum sativum*, genetic, 19: 5686
effects on *Pisum sativum*, genetic, 19: 25992
effects on *Pisum sativum*, genetic, 19: 25993
effects on *Pisum sativum* seeds, genetic, 20: 8660
effects on pituitary gland in parabiosed rats, 16: 30214 (TID-6875)
effects on pituitary tumors compared with gamma, 19: 30037
effects on pituitary tumors, therapeutic, 20: 1708
effects on pituitary gland function in female rats, effects of gonadectomization on, 20: 6818
effects on pituitary tumors, 20: 8794
effects on pituitary function following nasopharyngeal carcinoma therapy, 20: 40660
effects on pivalic acid, ESR spectra of *t*-butyl radical formation in, 19: 7557
effects on planarian survival of chronic, 18: 31249
effects on plant cells, genetic, 19: 2073(R) (ORNL-3700(p.95-7))
effects on plant embryos, biological, 20: 38588(R) (COO-1400-10)
effects on plant germination and seedling development, 20: 18388
effects on plant growth, 19: 2065 (BNL-8491)
effects on plant metabolism, 16: 25135(R) (HW-72500(p.104-8))
effects on plant reproduction, 20: 8647
effects on plant seedlings, metabolic, 20: 31115
effects on plants, 19: 33956
effects on plants, genetic, 20: 8647
effects on plants, genetic, 20: 18420
effects on plants, genetic, 20: 26644
effects on plants, genetic, 20: 29018
effects on plants, leaves and leaf extracts premature aging and autumnal events, 20: 36609
effects on plants, genetic, effects of exogenous factors on, 20: 40709
effects on plants, genetic, 20: 40714
effects on plants, electrophysiological, 18: 27091
effects on plaque forming ability of vesicular stomatitis virus, 16: 14543
effects on plasma lipids in mice, 16: 9755(R) (UCRL-9897(p.84-90))
effects on plasma volume and vascular permeability in rabbit skin, 19: 2142
effects on plasma iron clearance in dogs, 19: 38388
effects on plasma globulin levels in rabbits, whole-body exposure, 17: 97
effects on plasma protein levels, whole-body exposure, 17: 1355
effects on plasma lactic dehydrogenase activity in mice and rabbits, 17: 33632
effects on plasma lipase clearing factor activity in rats, whole-body, 17: 40679
effects on plasmocytomas, therapeutic, 20: 18551
effects on plasmologen content in brain in rats, 17: 24995
effects on pleural inflammation induced by Croton oil in guinea pigs, 18: 15877
effects on ploidy of mouse spermatocytes, 18: 11663
effects on ploidy in Chinese hamster cell cultures, 18: 33383
effects on ploidy in human leukocyte cultures treated with colchicine, 19: 25953
effects on ploidy in Drosophila gametes, 20: 24892
effects on pneumococcal infection in mice, time factors in, 17: 4413
effects on pneumonia development in mice inoculated with influenza virus, sparing, 19: 8899
effects on *Poa pratensis*, mutagenic, 19: 43778
effects on point defects in plastically deformed lithium fluoride at low temperature, 20: 38368
effects on point-contact germanium diodes, (E), 19: 4548
effects on polarization of paraffin-sulfur mixtures, 18: 33622
effects on poliovirus yield in cultured kidney cells from rhesus monkey, 16: 20201
effects on poliovirus production by monkey kidney cells, 19: 45955
effects on poliovirus multiplication, 17: 23134
effects on pollen, 16: 12931
effects on pollen of maize, genetic, 20: 1656
effects on pollen germination and growth in thirteen plant species, 20: 8699
effects on polycythemia, therapeutic, 20: 5483
effects on polycythemia, 20: 6954
effects on polycythemia, therapeutic, 20: 6958
effects on polycythemia, therapeutic, 20: 8806
effects on polyethylenes, hydrogen yields in chemical, 19: 15574 (WL-TR-64-150)
effects on polymerization of chloroethylene, structure of polymer formed by, 19: 7591
effects on polymerization of solid acrylonitrile in presence of electric field, 19: 40582
effects on polymerization of mixtures of vinyl chloride and argon, krypton, or xenon, 19: 40584
effects on polymerization of methyl methacrylate with isobutylene and ethylene–propylene rubbers, 20: 367
effects on polymerization of diphenylvinylphosphine oxide in presence of oxide powders, 20: 408
effects on polymerization of vinylidene chloride on polyethylene film, 20: 1902
effects on polymerization of hexamethylcyclotrisiloxane in solid phase, 20: 1903
effects on polymerization of methyl methacrylate and styrene in presence of zinc oxide, 20: 7128(R) (NYO-2206-1)
effects on polymerization of styrene to polyethylene, 20: 9014
effects on polymerization of chloroethylene, dosage and rate effects on, 20: 23160
effects on polymerization of dichloroethylene at −35 to 25°C, 20: 25151
effects on polymerization of diallylsilanes, 20: 25163
effects on polymer formation in pyridine at 25°C, 20: 26960
effects on polymerase–DNA in *E. coli*, 17: 31832
effects on polynucleotides in solid phase, 20: 10877
effects on polypropylene, ESR spectra of, 18: 16097
effects on polysaccharide metabolism, whole-body exposure, 17: 5828
effects on polysaccharide metabolism in bones and cartilage, whole-body exposure, 17: 13983(R) (TID-17911)
effects on poplar root growth, protective effects of indoleacetic acid against, 19: 15158
effects on populations, genetic, 19: 10925
effects on population dynamics of human kidney cells, tracer study, 19: 28001
effects on population dynamics of mosquitoes, 20: 10692
effects on population dynamics in Drosophila heterozygous or homozygous for irradiated chromosomes, 20: 42922

effects on porphyrin bodies in tissues, with oxidation-reduction agents, 16: 4083
effects on postnatal mouse mortality following prenatal exposure, 20: 6860
effects on postnatal activity and excretion by mice, neonatal whole-body, 20: 33036
effects on potassium excretion in adrenalectomized rats, whole-body, 18: 6632
effects on potassium bromide and cyanide crystals, color center formation in, 18: 20040 (COO-1044-15)
effects on potassium iodides, temperature dependence of F-band production rate in, 18: 20656
effects on potassium transfer by erythrocytes, 18: 21855
effects on potassium levels in regenerating rat liver, 18: 33301
effects on potassium bromide and chloride, multiple ionization in, (E), 19: 5894
effects on potassium bromide, recombination of interstitials and vacancies in, 19: 9745
effects on potassium efflux in *Micrococcus radiodurans* and *Sarcina lutea*, 19: 24344
effects on potassium bromide crystals with copper impurities, luminescence in, 19: 30275
effects on potassium chloride and sodium chloride phosphors, de-excitation of light sums from, 19: 46379(T)
effects on potassium bromide crystals at room temperature, F centers produced in, 20: 46 (PRNC-40)
effects on potassium chloride crystals, F center accumulation kinetics in, (E), 20: 15980(T)
effects on potassium chloride external surface energy, 20: 17137
effects on potassium and sodium content in animal cell nuclei, 20: 20422
effects on potassium iodides, color center formation from, (E), 20: 30748
effects on potassium chlorate crystals at room temperature, absorption bands from, 20: 32686
effects on potassium dihydrogen arsenate, ESR studies of, 20: 36884
effects on potassium content in blood of rabbits, 20: 38697
effects on potato chimeras, 19: 15159
effects on potato germination and metabolism, 19: 25934
effects on potato chemical composition and yield, after tuber exposure, 20: 38690
effects on potatoes, 18: 31170
effects on potatoes, genetic, 19: 45853
effects on potatoes following tuber exposure, 20: 24898
effects on potential and electrochemical processes at platinum electrode, 19: 504
effects on pregnancy and sexual cycle in mice, 16: 8591
effects on pregnant animals, peripheral blood change in the progeny, 16: 18774
effects on prepyriform electrical activity in rats, whole-body, 17: 10373
effects on preservation of apple juice, 20: 31629
effects on presoaked Arabidopsis seeds, mutagenic, 20: 5357
effects on primary thrombus formation in pituitary gland of rats, 18: 13442 (BNL-6935)
effects on priming activity of DNA, 18: 9879
effects on primordial germ cells in female rats, 20: 24906
effects on process of recovery from cerebral injury in rats, 19: 17637
effects on productivity of mice, 18: 11734
effects on production of chromosomal aberrations in *Vicia faba* seeds, role of free radicals in, 19: 8877
effects on production of dihaploid plants in *Solanum tuberosum*, 19: 17657
effects on production of pituitary hormones and gonad weight in rats, 17: 23170
effects on production in coffee plants, 17: 34201
effects on productivity of female wasps, 17: 33684
effects on progress of mouse cells through division cycle *in vitro*, 18: 3575
effects on proliferative capacity and immunologic activity of spleen cells in mice, whole-body, 18: 114
effects on proliferation of stem-cells developed from human lymphocytes, 19: 8890
effects on proliferative capacity of mouse ascites tumors, 19: 31798(R) (UCRL-11833(p.80-94))
effects on proliferative capacity of isolated carrot root cells, 20: 18395
effects on proliferation of human leukocytes in culture, 20: 31067
effects on proliferation of bone marrow cells in mice, 20: 35289
effects on proliferation of stem cells from cultured human lymphocytes, 20: 42872
effects on propagation of cleavage cracks in sodium chloride single crystals, 20: 16513
effects on propane, decompositon yields from, 20: 29266
effects on properdin systems in dogs, 20: 31013
effects on properties of tobacco crown-gall, 18: 5032
effects on properties of hemoglobins from rats and pigeons, 18: 17567
effects on properties of blood proteins in rabbits, 18: 29255
effects on properties of carbohydrates, 19: 4195(R) (NYO-10626)
effects on properties of desoxyribonucleic acid in bone marrow, 19: 29918(T)
effects on properties of ruby for use as laser, 20: 20110 (NASA-TN-D-3379)
effects on properties of serum proteins in animals, 20: 26650
effects on properties of pyridoxine derivatives, 20: 28901
effects on properties of DNA in rat tissues, whole-body, 20: 36591
effects on properties of fractionated desoxyribonucleic acid from mouse tumor cells, whole-body exposure, 17: 1240 (TID-17010)
effects on properties of fatty acids in rat liver, 17: 30327
effects on protein concentration in serum albumins, 16: 1567
effects on protein synthesis and viability in *Rhodopseudomonas spheroides*, 16: 8562
effects on protein metabolism in connective tissue, whole-body exposure, 16: 17476
effects on protein metabolism in connective tissue, whole-body exposure, 16: 17477
effects on protein electrophoretic patterns of rat blood plasma, whole-body, 18: 1423
effects on proteins and amino acids, effects of environment on, 18: 1434
effects on protein catabolism, protective effects of dianabol against, 18: 3595
effects on protein in dog, 18: 23306
effects on protein content and sulfur-35-labeled methionine uptake in rat blood serum, 18: 27172
effects on protein metabolism in blood serum of mice, 18: 29328
effects on protein structure of enzymes, 19: 160
effects on protein activity, effects of disulfide links on, 19: 180
effects on protein metabolism in rat liver, 19: 5661
effects on proteinic nitrogen and potassium content in muscle tissues of rats, 19: 7157
effects on protein fractions in animal testes, 19: 15016 (NP-14408)
effects on protein metabolism in kidney and liver of mice, 19: 17662
effects on protein metabolism in rats, 19: 29849(R) (ANL-6971(p.1-28))
effects on protein metabolism in *E. coli*, 19: 31890
effects on protein metabolism in mice and rats, 19: 31891
effects on protein metabolism in rat brain, 19: 35983
effects on protein synthesis in rat brains, 19: 43682(R) (UCLA-12-565, pp 33-57)
effects on proteins, inactivating, 19: 45839
effects on protein solutions in presence of inorganic ions, 20: 49
effects on protein synthesis in stem of rat brain, 20: 18295(R) (UCLA-12-576, pp 27-56)
effects on protein metabolism in mice, 20: 22607
effects on proteins in blood serum of rats, 20: 26687
effects on protein synthesis in Ehrlich mouse ascites tumor cells, 20: 28923
effects on protein metabolism in rats, tracer study, 20: 28997
effects on protein loss into gastrointestinal tract in mice, dose effects on, 20: 32933
effects on proteins in rats, effects of serum lyophilization and tumors on whole-body, 20: 36582
effects on protein synthesis in rat tissues, 20: 38595(R) (ORO-3295-2)
effects on protein fractions in serum of rabbits injected with bone marrow and trace elements, 20: 42870
effects on protein metabolism in dogs, partial-body exposure, 20: 42939
effects on protein metabolism in rabbit ovaries, x, 20: 42941
effects on proteins in rat liver mitochondria, 20: 45339
effects on protein-free solutions of hemin, 17: 7910
effects on protein metabolism by liver cells, 17: 15750
effects on protein metabolism in central nervous system and liver, 17: 15781
effects on protein synthesis in intestine, tracer study, 17: 17754 (BNL-6274)
effects on proteins in dry state, 17: 23160
effects on proteins in dry state, 17: 23161
effects on protein nitrogen and DNA decomposition in isolated liver cell nuclei, 17: 24958
effects on protein synthesis in *Bacterium cadaveris*, 17: 27109
effects on protein synthesis, 17: 30302
effects on *Proteus vulgaris*, reduction of triphenyltetrazolium chloride, 18: 31235
effects on Proteus bacteremia in mice, 18: 9867
effects on protoporphyrin III affinity in central nervous system, 16: 14539
effects on pseudochiasmata in onion root tips, with and without infrared treatment, 16: 1594
effects on Pseudomonas enzyme synthesis, 18: 15871
effects on *Pseudomonas aeruginosa*, protective effects of acriflavin and diet against, 19: 46014
effects on Pseudomonas susceptibility in mouse chimeras, 20: 10669
effects on Pseudomonas susceptibility in mice, 20: 10669

effects on Pseudomonas, mechanism of protective effects of freezing against, 20: 14394
effects on Pseudomonas bacteremia in mice, 18: 9868
effects on pseudouridine excretion, 20: 14269
effects on psittacosis virus in tissue cultures, 18: 6636
effects on pulmonary thromboemboli in rats, thoracic, 19: 24338
effects on pulmonary tissues, inflammatory, 20: 18543
effects on pupae of *Tribolium confusum*, effects of age on pathological, 20: 32975
effects on pupal mortality and reproductive capacity in mosquitoes, 20: 24904
effects on pupal weight and reproductive fitness of Tribolium, 20: 40671
effects on purine-starved *E. coli*, 18: 11874
effects on Purkinje cells in animals, 17: 10460
effects on pyridine nucleotides in rat liver, 19: 29919
effects on pyridine nucleotidase activity of rat liver and spleen, 20: 14362
effects on pyridine nucleotides of thymocytes, 17: 27085
effects on pyridoxal phosphate in *E. coli*, 18: 25103
effects on pyrimidine mutation induction in *Salmonella typhimurium*, genetic analysis of, 19: 45878
effects on pyrophosphatase activity in mouse liver and brain, 17: 40596
effects on quantity of porphyrin bodies in tissues in guinea pigs, 16: 4082
effects on quantitative characters in heterozygous Drosophila populations, genetic, 19: 31670(R) (NIRS-3(p.19-56))
effects on quartz, microwave phonon reactions with paramagnetic centers formed in, 20: 30768
effects on quinone content of tissues, 17: 5880
effects on rabbit proteins, effects of horse gamma globulin on, 18: 11879
effects on rabbit lenses, cataract induction from, 18: 13545
effects on rabbit lipids, 18: 19561
effects on rabbit metabolism of carbon-14-labeled palmitic acid, 18: 19665
effects on rabbit visual analyzers, 18: 19728
effects on rabbit leukocyte phagocytosis, 18: 19736
effects on rabbit immune reactions to smallpox, 18: 19737
effects on rabbit blood picture, 18: 21865
effects on rabbit skin, protective effects of esculin against, 18: 23372
effects on rabbit serum iron, 18: 25164
effects on rabbit skin, 18: 27078
effects on rabbit blood-labyrinth barrier to fluorescein, 18: 29376
effects on rabbit epidermis, 18: 29470
effects on rabbit granulopoietic reserve, 18: 29334
effects on rabbit lymph nodes, comparison with gamma rays, 18: 29539
effects on rabbit embryos, 18: 29262
effects on rabbit melanocytes, 18: 29315
effects on rabbit blood serum electric conductivity, 18: 31230
effects on rabbit rectum unconditioned interoceptive exchange reflexes, 18: 31253
effects on rabbit cortex electric activity and brain formations, 18: 31257
effects on rabbit cortex electric activity and reticular formations, 18: 31254
effects on rabbit typhoid immunity, 18: 33369
effects on rabbit skin zinc content, 18: 38908
effects on rabbit eyes, 18: 41196
effects on rabbit reaction to blood loss, 19: 3959
effects on rabbit reaction to physiological solutions, 19: 3959
effects on rabbit ova and uteri, 19: 8942
effects on rabbit erythrocytes, effects of blood catalase levels on, 19: 15112
effects on rabbit liver cells, ultrastructural, 19: 26013
effects on rabbit blood circulation, effects of orthostatic disturbance on, 19: 27951(T) (FTD-TT-65-53)
effects on rabbit ears, effects of Scarlet Red on metaphasia of sebaceous glands in, 19: 28085
effects on rabbit serum conductivity, 19: 31855
effects on rabbit skin, 19: 31816
effects on rabbit eyes, pathological, 19: 31821
effects on rabbit kidneys, renograms of, 19: 38379
effects on rabbit lungs, histological, 19: 43846
effects on rabbit tibia, time factors for, 19: 45989
effects on rabbit muscle tissues, ESR of free radicals produced in, 19: 45947
effects on rabbit immunity to snake venom, 19: 45970
effects on rabbit hearts, effects of sodium thiosulfate on, 20: 18456
effects on rabbit leukocytes, biochemical and morphological, 20: 38681
effects on rabbit liver, cytological, whole-body, 20: 38716
effects on rabbit brain, pathological, 20: 42862
effects on rabbit erythrocytes, effects of iodoacetic acid, sodium iodide, and *Salmonella typhi* endotoxin on, 20: 45371
effects on rabbit lung morphology, 17: 37125
effects on rabbits, restoration effects of immune donor nucleoproteins on, 18: 19765
effects on rabbits receiving cortisone treatment, 18: 23267
effects on rabbits, protective effects of polysaccharides against, 18: 25218
effects on rabbits, protective effects of lysozyme against, 18: 27213
effects on rabbits, protective effects of properdin against, 18: 29384
effects on rabbits, protective effects of calf-thymus polypeptide against fractionated and whole-body, 19: 26115
effects on rabbits, protective effects of hemopoietic tissue transplants against, 19: 33978
effects on rabbits and rats, biological, 20: 22622(T) (AD-625779)
effects on rabbits, pathological, 20: 29051
effects on rabbits, effects of adrenaline on, 20: 38686
effects on radiation-resistant electronic equipment, 18: 33869
effects on radiologists, carcinogenic and genetic, 17: 87
effects on radioluminescence of alkali halide crystals, 19: 27714
effects on radioresistance of sarcoma cells in suspension, 20: 10634
effects on radiosensitivity of *Bacillus subtilis* spores, 19: 33851
effects on rare earth ions in calcium fluorides, (E), 20: 40341
effects on rat adrenal functions, 18: 17538
effects on rat adrenal cortex function, 18: 33272(R) (NIRS-2(p.31-42))
effects on rat adrenal glands, 18: 41154
effects on rat and rabbit immune reactions, 18: 19722
effects on rat at 200 Kvcp and 22 Mevp, relative biological, 16: 17515
effects on rat behavior, threshold for, 19: 13079
effects on rat blood cell levels, protective effects of *N*-phenylthiophenecarboxamidine against, 18: 1457
effects on rat blood and tissue cholinesterase levels, 18: 17517
effects on rat blood proteolysis, 18: 33362
effects on rat blood serum proteins, immunoelectrophoretic measurement of, 20: 35243
effects on rat blood and bone marrow, whole-body lethal, 20: 42955
effects on rat body weight, heritable, 19: 45880
effects on rat bone growth, 18: 19555 (USNRDL-TR-721)
effects on rat bones, 19: 2094
effects on rat bones, 19: 2095
effects on rat bone marrow and thymus cells in cultures, effects of calcium and phosphate contents on, 20: 6906 (EUR-2485.e)
effects on rat bone marrow, cytological, 20: 18534
effects on rat bone marrow, kinetics of hemopoietic regeneration following, 20: 42871
effects on rat brain, acute, 18: 13520
effects on rat brains, fractionated vs single dose, 18: 21888
effects on rat brain, 19: 8874
effects on rat brain, pathological, 19: 13019
effects on rat brain, electrophysiology and pharmacology of, 19: 26093
effects on rat brain, 19: 31841
effects on rat cartilage, 18: 38784
effects on rat carcinomas, effects of cytotoxic and antimetabolite drugs on, 20: 18377
effects on rat central nervous system, 18: 15836(T)
effects on rat chromosomes, 17: 38773
effects on rat chromosomes, 17: 38816
effects on rat chromosomes, 17: 38855
effects on rat conditioning behavior, x, 18: 11782
effects on rat conditioning behavior, 17: 40617
effects on rat DNA polymerase, 18: 82
effects on rat ears, 18: 19562
effects on rat electroshock seizure, protective effects of chlorpromazine and reserpine against, 18: 29412
effects on rat electroshock convulsions, 18: 31216
effects on rat embryos during mesoderm formation, 16: 8588
effects on rat embryos, maternal role in, 18: 15894
effects on rat embryos, parental-exposure, 18: 37012
effects on rat embryos, pathological, 20: 60(R) (NYO-901-37, pp 33-68)
effects on rat embryos *in utero*, protective effects of uterine vascular clamping of mother against, 17: 23153
effects on rat embryos and fetuses exposed *in utero*, 17: 24944
effects on rat eosinophilic response, effects of injected sterilized trichinella larvae on, 18: 17516
effects on rat erythropoiesis, protective effects of alcohols against, 18: 5146
effects on rat excretion of vitamin B_{12}, 19: 3954
effects on rat fetuses, pathological, 20: 10616
effects on rat gastrointestinal tract, 18: 17541
effects on rat gas metabolism, 19: 150
effects on rat gastrointestinal tract, protective effects of MEG against, 19: 31913
effects on rat gastrointestinal tract, effects of bile on, 20: 6910
effects on rat hair, protective effects of cystamine and cysteamine against, 18: 19784
effects on rat hair, 18: 38844

effects on rat hair, protective effects of cysteamine against, 19: 24369
effects on rat hearts, protective effects of nibuphin against, 19: 15119
effects on rat hematology, 18: 23296
effects on rat hematopoiesis, protective effects of splenic homogenates against, 20: 22782
effects on rat intestine population of *N. brasiliensis*, 18: 70
effects on rat intestinal pyridoxine absorption, x, 18: 11779
effects on rat intestine, protective effects of cysteine and shielding against, 19: 5697
effects on rat intestine, effects of adrenal factors on, 20: 10697
effects on rat intestine, physiological, 20: 38604
effects on rat kidneys, pathological, 20: 18284 (AD-629512)
effects on rat kidneys, pathological, local exposure, 20: 45382
effects on rat lens epithelium, 18: 38814
effects on rat leukemic lymphocytes, 18: 17493
effects on rat liver glycogen levels, 18: 13470
effects on rat liver blood bed, 18: 17601
effects on rat liver mitochondria, 18: 17602
effects on rat liver, effects of irradiated bone marrow on, 18: 19790
effects on rat liver, 18: 33380
effects on rat liver, effects of spleen cell injection and splenectomy on, 18: 38981
effects on rat liver, method for determining, 19: 13071
effects on rat liver mitochondria *in vitro*, 19: 15193
effects on rat liver, protective effects of typhus vaccine against, 19: 15227
effects on rat liver mitochondria, 19: 15098
effects on rat liver, 19: 31872
effects on rat liver, whole-body, 19: 33844
effects on rat liver enzyme systems, head or whole-body exposure, 20: 22734
effects on rat liver mitochondria, morphological, 20: 26675
effects on rat liver mitochondria, biochemical and morphological, 20: 38639
effects on rat liver DNA and ploidy, 19: 29925
effects on rat liver cells, 17: 38775
effects on rat lungs, effects of dose fractionation on histological, 20: 3700
effects on rat lungs, pathological, 20: 6804
effects on rat lungs, pathological, 20: 20434 (AD-630870)
effects on rat mammary epithelium, relation to DNA synthesis, 20: 42840(R) (ANL-7136, pp 164-90)
effects on rat mating behavior, 18: 37000
effects on rat metabolism, 19: 28043
effects on rat mouth bones and tissues, 18: 17537
effects on rat nerve cells, cytochemical, 17: 33638
effects on rat neurosecretory system, 18: 3529
effects on rat neurohypophysis, 18: 9875
effects on rat neural system, 18: 19729
effects on rat nucleus habenulae and pineal glands, 18: 27074
effects on rat offspring, 20: 36643
effects on rat oocytes, 20: 36632
effects on rat operant behavior, 18: 17531
effects on rat phosphatase systems, effects of injected glycine on, 20: 20517 (NP-15925)
effects on rat polysaccharide phosphorylase activity, 18: 25115
effects on rat pregnancy from pre-fertilization exposure, 18: 17539
effects on rat respiratory enzymes, 19: 28043
effects on rat sarcomas transplanted into chicks, 19: 5647
effects on rat sarcoma cells, effects of anoxia on, 20: 22776
effects on rat serum proteins, 18: 19754
effects on rat serum globulins, protective effects of fatty acids against, 18: 29401
effects on rat serum protein levels, 17: 38814
effects on rat serum proteins, x, 17: 38815
effects on rat skin, pathological, 19: 45957
effects on rat skin, recovery from necrotic, 20: 22638
effects on rat spinal cord, neurological changes from, 18: 17528
effects on rat spinal cord, 19: 3920
effects on rat spinal cords, 20: 6826
effects on rat spinal cord, 17: 38811
effects on rat spleen, single and divided dose, 18: 3556
effects on rat spleen, 18: 15863
effects on rat spleen lysosomes, 18: 17633(R) (ANL-6790(p.150-5))
effects on rat spleen, hematologic, 19: 31820
effects on rat spleen, effects of fractionated doses on regeneration of, 20: 40702
effects on rat stress accommodation, 18: 25100
effects on rat sulfur metabolism, tracer study of, 18: 13420
effects on rat suprarenals, 18: 19676
effects on rat suprarenal corticosteroids, 19: 3924
effects on rat testes, protective effects of MEA against, 20: 20509
effects on rat thymocyte nucleoproteins, 18: 17505
effects on rat thymus after head irradiation, 18: 21850
effects on rat thyroid growth function, method for measurement of, 18: 23260
effects on rat thymocytes, use of chromium-51 as criterion of regeneration of whole-body, 19: 8837
effects on rat thymocyte nuclei, 19: 12993
effects on rat thymocyte and thymus cells, immediate, 19: 15134
effects on rat thymocyte pycnosis, inhibitory, 19: 28000
effects on rat thymocytes, 19: 31670(R) (NIRS-3(p.19-56))
effects on rat thyroid, latent, 19: 42286
effects on rat thymocytes, lethal, 20: 22615(R) (NIRS-4, pp 34-58)
effects on rat thymus, regeneration processes following whole-body, 20: 35262
effects on rat thymus, mitotic, 20: 38720
effects on rat tumors, protective effects of bone marrow transplantation against, 19: 7183
effects on rat tumors, effects of hyperoxia on, 17: 37128
effects on rat vision, fetal-irradiation, 17: 35545
effects on rat zona fasciculata, 17: 38774
effects on rate of thermal decomposition of silver nitrite, 20: 41000
effects on rate of vegetative fission in Paramecium, 17: 5778 (TID-15521)
effects on rate of cholesterol synthesis in hypophysectomized rats of, 17: 33641(T)
effects on rats, 20: 33059
effects on rats after abdominal exposure, 18: 19587
effects on rats after administration of radioisotopes, whole-body, 17: 12148
effects on rats, correlation with bremsstrahlung, 16: 28808
effects on rats combined with chilling, 17: 35577
effects on rats deprived of food, 18: 80
effects on rats, effects of physical burden and mandibular injury on, 18: 3527
effects on rats given carbon monoxide therapy, 17: 37145
effects on rats, head exposure, 16: 23474
effects on rats in state of hyperthermia, 20: 42959
effects on rats, protective effects of hypo- and hyperthermia against, 18: 3588
effects on rats, biological, 19: 7017 (BNL-7727)
effects on rats, biochemical, 20: 5341
effects on rats, biological, 20: 16287
effects on rats, biological, 20: 16288
effects on rats, biological, 20: 22732
effects on rats, biological, 20: 22786
effects on rats, biological, 20: 26704
effects on rats, biological, 20: 36654
effects on rats, chemical protection against, 18: 19779
effects on rats, dietary effects of B group vitamins, folic acid, and phosphatide on, 20: 38721
effects on rats, effects of 19-norandrostenolone on acute, 19: 19624
effects on rats, effects of strain differences on leukemogenic, 19: 42272
effects on rats, effects of plastic polypropylene implants on carcinogenic, 20: 6806
effects on rats, effects of dose fractionation time on, 20: 8715
effects on rats, effects of pre-irradiation on, 20: 12701
effects on rats, effects of stress on, 20: 12703
effects on rats, effects of parabiosis on tumorigenic, 20: 18318
effects on rats, effects of hypoxia on, 20: 18272
effects on rats, effects of calf tissue extract on, 20: 18497
effects on rats, effects of anoxia on lethal, 20: 22792
effects on rats, effects of uneven exposure and irradiated bone marrow autografts on, 20: 31133
effects on rats, effects of thymectomy on immune response in whole-body, 20: 33077
effects on rats, effects of hypoxia on hemapoiesis regeneration in whole-body, 20: 33092
effects on rats, effects of escin and rutin on, 20: 35343
effects on rats, efficacy of sulfonamide therapy of, 20: 45491
effects on rats, genetic, 19: 7084
effects on rats, hematological, 20: 38619
effects on rats, hematological, 20: 40603 (AD-635086)
effects on rats, leukopenic, 20: 18504
effects on rats, morphological, 20: 5341
effects on rats, metabolic, 20: 38600(R) (TID-23034)
effects on rats, metabolic, 20: 42835(R) (ANL-7136, pp 63-80)
effects on rats, narcotic effects of amobarbital and barbital on, 18: 9922
effects on rats, protective effects of bone marrow and lymph cells against, 18: 11867
effects on rats, protective effects of antibiotics against, 18: 17644
effects on rats, protective effects of bone marrow and plasma against, 18: 17659
effects on rats, protective effects of propylthiouracil against, 18: 19780

effects on rats, protective effects of cysteamine and cysteamine against, 19: 8963
effects on rats, protective effects of 8-methoxypsoralen against, 19: 15225
effects on rats, protective effects of bulbocapnine against, 19: 24377
effects on rats, pathological, 20: 3795
effects on rats, pathological, 20: 5411
effects on rats, pathological, 20: 10598(R) (BNWL-122, pp 107-9)
effects on rats, protective effects of methylandrostenolone against, 20: 14392
effects on rats, physiological, 20: 18458
effects on rats, protective effects of cysteine against, 20: 40729
effects on rats, synergism with thermal burns, 20: 18184(R) (BNL-929, pp 115-25)
effects on rats, testing of lysozyme as possible protective substance against, 20: 42993
effects on reaction of liver ribonucleic acid with formaldehyde, 16: 26780
effects on reactions of organic compounds, 19: 22346
effects on reactions between graphite and humid helium, mass transfer rate in, 19: 30833
effects on reactions of rat nervous system to burns, 19: 33921
effects on reactions of hydrocarbons with carbon dioxide, 19: 38727(T)
effects on reaction to injected dyes in rabbits, whole-body exposure, 17: 31924
effects on reactivity to chloropromazine in rats, 17: 7909
effects on reactor fuel processing materials, 19: 15571(R) (TID-21385)
effects on rearrangement of chromosomes in corneal cells in mice following adrenalectomy, 18: 1395
effects on receptor apparatus of cutaneous and visual analyzers in man, 17: 5851
effects on recombination of linked characters in tomatoes, 16: 26786
effects on recombination in barley, genetic, 19: 8948
effects on recombination luminescence of activated potassium chlorides, (E), 19: 27720
effects on recombination luminescence of silver-activated sodium chlorides, (E/T), 19: 27722
effects on recovery from burns in rats, 18: 38971
effects on recovery of erythropoietin-responsive erythrocytes in plethoric or spleen-shielded mice, 20: 45479
effects on rectal mucosa of rats, whole-body, 19: 45918
effects on rectal mucous membrane of mice, effects of cysteamine on, 20: 42983
effects on rectum and sigmoid colon, injurious, 19: 28008
effects on rectum following bladder therapy, 20: 3734
effects on red cell catalase *in vitro*, 20: 28911
effects on red cell volumes and plasma volumes in Rhesus monkeys, whole-body exposure, 17: 55
effects on red cell volumes in monkeys, 17: 56
effects on red cell membranes, 17: 15787
effects on red clover, morphological and mutagenic, 20: 5491
effects on redox conversion of copper chlorides in acetone solutions, 17: 35898
effects on reductase activity of livers of mice and rats, 17: 13968(R) (NP-12484(p.1-14))
effects on reductase activity in liver of rats, 17: 33483(R) (NP-13010 (p.23-9))
effects on reflex activity of spinal cords in rabbits, 16: 1480(T) (JPRS-10170(p.178-97))
effects on regeneration after trauma, 16: 32743(T) (JPRS-15018(p.73-82))
effects on regeneration of intestinal membranes after trauma, 16: 32744(T) (JPRS-15018(p.83-97))
effects on regeneration of thermal burns in rats, whole-body, 18: 8121(T) (JPRS-22556(p.1-13))
effects on regeneration of tissues in salamanders and mice, 18: 19553(R) (TID-20513)
effects on regeneration in planaria, 18: 29263
effects on regeneration of rat muscles from trauma, 18: 38972
effects on regeneration of skeletal muscle in rats, fractionated, 19: 8925
effects on regeneration of hemopoietic elements in rat bone marrow, 19: 10892
effects on regeneration of extremities in salamanders, 19: 19546
effects on regenerating rat liver, mechanism for x, 19: 29926
effects on regeneration in planarians, 19: 31826
effects on regeneration process in rat sciatic nerve, 19: 33909
effects on regenerative growth in salamanders, 20: 6837
effects on regeneration in Axolotl, 20: 18337
effects on regenerative capacity of axolotl limbs, effects of RNA on recovery from, 20: 29038
effects on regeneration of marrow stem cells in mice, 20: 45348 (AD-637782)
effects on regeneration of *Cordylophora* (Coelenterata), comparison of ectoderm and endoderm, 20: 45383
effects on regeneration and nucleic acid content of extremities in salamanders, 17: 7834
effects on regenerative capacity of extremities of axolotls, factors affecting restoration, 17: 33665
effects on regenerative power of liver in white rats, 17: 33670
effects on regeneration of rhodopsin, 17: 35525
effects on renal damage secondary to ischemia, 19: 28064
effects on renal hemodynamics and function in dogs, whole-body, 19: 33899
effects on renal hemodynamic functions of dogs, 20: 29026
effects on renal homotransplantation in dogs, 17: 33690
effects on renal tumors, morphological, 19: 13137
effects on renal transplantation in sheep, sublethal whole-body, 17: 30380
effects on replacement and viability of X chromosomes, 17: 40601
effects on replication of *E. coli* chromosomes, tracer technique for determining, 19: 15099
effects on replication microorganisms, 19: 21856 (COO-878-15)
effects on replication in *Brachiomonas submarina*, 19: 24340
effects on reproductive rhythm of birds, whole-body exposure, 16: 12913
effects on reproduction in rats, 16: 32748(T) (JPRS-15018(p.128-34))
effects on reproductive capacity of male minks, 18: 83
effects on reproductive rate in mice, 18: 9831(R) (AD-403109)
effects on reproduction of smallpox virus in tissue culture, 18: 19687
effects on reproductive capacity, 18: 23324
effects on reproduction in beagles, 18: 23345
effects on reproduction in female hamsters, 18: 23344
effects on reproductive capacity of female dogs, 18: 25092(R) (UCD-472-109(p.53-61))
effects on reproductive fitness of mouse populations, 18: 35346
effects on reproduction and growth of mice, 18: 35303(R) (AD-438541)
effects on reproductive performance of flour beetles (*Tribolium castaneum* and *T. confusum*), effects of age, temperature, and coexistence on, 18: 41083(R) (HW-80500(p.144-6))
effects on reproductive function of female hamsters, 18: 43232(R) (TID-21204)
effects on reproductive capacity of HeLa and L cells, 18: 43306
effects on reproduction in mice, 19: 5701
effects on reproduction of mice, 19: 7083
effects on reproduction in mice, 19: 7085
effects on reproduction of chickens, 19: 7087
effects on reproduction in mice, 19: 7092
effects on reproduction genetics in female mice, spermatogonial, 19: 7117
effects on reproduction of *Ophiostoma multiannulatum*, 19: 7135
effects on reproduction of yeast cells, 19: 7174
effects on reproduction of monkey kidney cells, 19: 8841
effects on reproductive capacity of rats, 19: 21959
effects on reproduction of yeast, 19: 24357
effects on reproductive capabilities of women, 19: 27986
effects on reproductive capabilities of women, 19: 28036
effects on reproductive capacity of *Tribolium castaneum*, 19: 28070
effects on reproduction in adult ticks, 19: 36039
effects on reproduction and transformation of polyoma virus, 19: 36052
effects on reproduction in Tribolium, effects of dose and temperature on, 19: 43715 (HW-SA-3747)
effects on reproductive performance in Tribolium, effects of genetics and temperature on, 19: 43716 (HW-SA-3748)
effects on reproduction, Drosophila, 20: 5296(R) (NP-15585)
effects on reproductive ability of female mice, small fractionated doses, 20: 6880
effects on reproduction of cells in culture, 20: 8666
effects on reproduction of mallow moth, *Pectinophora malevella*, 20: 9349(T)
effects on reproduction of cereal leaf beetle, 20: 9347
effects on reproduction of Tribolium, effects of sulfoxide compounds on, 20: 10504(R) (BNWL-122, pp 142)
effects on reproduction of *Tribolium castaneum*, 20: 11184(R) (BNWL-122, pp 137-9)
effects on reproduction of mice, 20: 22611 (CEA-R-2874)
effects on reproductive ability and survival of rats, effects of fractionated doses on, 20: 26665
effects on reproductive power of male alfalfa weevils, 20: 35279
effects on reproductive system of queen honeybee, 20: 38631
effects on reproduction in *Tribolium castaneum* Herbst, 17: 4417
effects on reproduction, in dogs, 17: 31865(R) (UCD-107(p.98-111))
effects on reproduction, mutations, and life span of flour beetles, 17: 35320(R) (HW-76000(p.198-201))
effects on reproduction and survival of *Brachiomonas submarina*, 17: 35451 (TID-17981)
effects on reproductive system of infant female rats, 17: 40656
effects on RES system in rats as related to tumor growth, 19: 13052
effects on resistance to infection, in mice, 16: 74

effects on resistance to focal staphylococcal infection in rats, time interval effects on, 18: 38923
effects on resistance of mice to Ehrlich ascites tumor cells, 20: 29017
effects on resistance to fungus infections in mice, 17: 38809
effects on respiration in normal and tumor cells, 16: 1507
effects on respiration of buckwheat after soaking seeds in boron-containing water, 18: 9849
effects on respiratory activity in normal and tumor tissues, 18: 25168
effects on respiration of liver mitochondria in rats, 18: 38858
effects on respiration in tumor cells, 18: 38892
effects on respiratory mechanisms in yeast, 19: 21881
effects on respiratory gas exchange in aorta, cerebral cortex, and hypothalamus in rats, whole-body, 19: 26091
effects on respiratory metabolism in rats, 19: 29937
effects on respiration in chick embryos, 19: 33800
effects on respiration in rat thymocytes in culture, 20: 5340
effects on respiratory center of man, 20: 12702
effects on respiration in Bombyx eggs, 20: 18301
effects on respiratory tract function in rabbits, 20: 38659
effects on respiration and phosphorylation in isolated mitochondria from radiosensitive organs, 17: 1246
effects on respiration in rat tissue, formula for analysis of dose dependence in, 17: 23177
effects on response of thyroid gland to radioprotective compounds, 16: 1640
effects on response to anti-tumor sera in tumor-bearing mice, 16: 17460(T)
effects on response of cholinergic and enteric nerve endings to drugs in guinea pig, 16: 28752 (UCLA-461)
effects on response to homografts, effects of thymus gland on, 18: 113
effects on response to hematopoietic tissue infusions in dogs, 18: 116
effects on response to blood transfusions in rats, 18: 8141(T)
effects on response of peripheral blood vessels to nervous stimulation and adrenalin in rabbit ears, 18: 21832(T) (JPRS-24301(Del.)(p.17-22))
effects on response of spleen to virus infection, in mice, 18: 25223
effects on response of guinea pigs to Brucella vaccine, 18: 25096(T) (JPRS-24896)
effects on response to alloxan in rabbits, 18: 27173
effects on responses to muscular activity in dogs, 18: 36952(R) (TID-20979(Add.))
effects on response of man to conditioned reflex, 18: 37016
effects on response to drug-induced convulsions in rats, 18: 41175
effects on response of dogs to induced muscular contraction, 18: 41217
effects on response of Habrobracon to toxic metals, 19: 10741 (TID-21559)
effects on response of limbs of adult urodeles to tissue grafts, 19: 13013
effects on response of muscular contraction in dogs *in vivo*, 19: 17600
effects on response to muscle relaxant drugs in rabbits, physiological, 19: 43871
effects on response of animal cells to virus infections, 19: 45974
effects on response of salamanders to tissue grafts, 19: 45897
effects on response to barbiturates by rats, 20: 1662
effects on response of olfactory neurons, 20: 20431 (AD-630323)
effects on response of animals to space flight conditions, 20: 22623(T) (UCRL-Trans-1232)
effects on response of dogs to hemorrhagic stress, 20: 38703
effects on response to bacterial antigens of rabbits, 20: 38641
effects on response of mice to sodium fluoroacetates and radiation, 17: 1261
effects on response of rats to barbiturates, whole-body exposure, 17: 5788
effects on response of rats to plutonium, 17: 10318
effects on response to electrical excitation in isolated nerves, 17: 10417
effects on response to heterohemotransfusion reactions, whole-body exposure, 17: 13992(T) (JPRS-17819(p.32-6))
effects on response to skin grafts in mice, 17: 15760
effects on response to skin grafts in mice, 17: 21468 (USNRDL-TR-628)
effects on response to toxins in mice, 17: 23116
effects on response to electro-shock, whole-body exposure, 17: 30299
effects on responsiveness of stem cells to erythropoietin, 17: 33733
effects on response to skin grafts, in mice, 17: 33749
effects on rest potential of striated muscle tissue in frog legs, effects of external media on, 19: 25954
effects on resting potentials of frog muscles, 19: 24362
effects on resting cells in liver in rats after partial hepatectomy, 17: 24943
effects on reticulo-endothelial system in mice, single whole-body, 16: 14546
effects on reticulo-endothelial system in mice after administration of protective agents, 16: 14547
effects on reticulo-endothelial system in mice, fractional, 16: 14548
effects on reticulocytes in peripheral blood of patients with dermatologic diseases, 18: 19712
effects on reticulo-endothelial function in rabbits, 18: 27182
effects on reticulo-endothelial function, 18: 27184
effects on reticular cell transformation in guinea pigs, inhibitory, 19: 33947
effects on reticulo-endothelial function in mice, 20: 14374
effects on reticulum cell sarcoma of skin, alone and combined with laser radiation, therapeutic, 20: 45568
effects on retina of rabbit eyes, 18: 27132
effects on retina in newborn mice, 20: 117
effects on retina of frogs, 17: 23167
effects on retina of rabbits eyes, pathological, 20: 38689
effects on retinal pigments and visual receptor units in crabs, 19: 15182
effects on retinal development in embryos, 20: 3724
effects on retinal response, compared to that of light, 17: 35507
effects on reversed metacentric compound X chromosome in Drosophila, 18: 31158
effects on reversion of transition mutations in *E. coli*, 19: 7052
effects on reversible depression of *Photobacterium fischeri* luminescence, 19: 17602
effects on reversion of white-ivory mutants in Drosophila, 20: 10693
effects on rhizogenesis of hypocotyls of lupine, 19: 5644
effect on rhizogenesis in tissue of Jerusalem artichoke cultivated *in vitro*, 17: 35495
effects on rhodopsin, *in vitro* and in eye, 18: 27190
effects on riboflavin content in blood of dogs, 20: 5384
effects on riboflavin metabolism in rabbits, 17: 37028(T) (JPRS-21171 (Del.)(p.24-31))
effects on ribonucleic acid metabolism in seedlings of corn, seed-exposure, 16: 17452
effects on ribonucleic acid in eye lens, 18: 35370
effects on ribonucleic acid in rat livers, 17: 1306
effects on ribonuclease activity in *Zea mays* seedlings, 17: 1323
effects on ribonucleic acid metabolism in nervous system, 17: 10356 (BNL-6546)
effects on ribonucleic acid metabolism in rat liver, 17: 15798
effects on ribosomes in *Escherichia coli*, 20: 45463
effects on ribosomes in *E. coli*, 17: 35483
effects on rice, 16: 32762
effects on rice early heading, mutagenic, 19: 10825
effects on rice embryos, 18: 21906
effects on rice plants, genetic, 20: 18416
effects on rice seeds, 16: 1608
effects on rice seeds, biological, 20: 1669
effects on rice seeds, genetic, 20: 5393
effects on rice seed, genetic, 20: 18414
effects on rice seed, chlorophyll mutations from, 20: 40641
effects on rice seeds, cytological and genetic, 16: 32763
effects on rice yields, 16: 1607
effects on rice, mutagenic, 20: 8652
effects on rice, wheat, and other plants, genetic, 20: 26655(R) (NP-15975)
effects on Rickettsia eggs, 16: 1536
effects on RNA content in regenerating *Polycelis nigra*, 20: 42933
effects on RNA in lymphatic cells in rabbit appendix, 18: 9872
effects on RNA metabolism in Ehrlich ascites cell and thymocyte nuclei, 19: 15063
effects on RNA metabolism and synthesis in HeLa tumor cells, 19: 19602
effects on RNA of regenerating rat liver, 19: 8817
effects on RNA of rat thymus, 19: 8819
effects on RNA synthesis and tyrosine-α-ketoglutarate activity in rat liver, 19: 24358
effects on RNA synthesis in derivatives of *E. coli*, 19: 38381
effects on role of radiotoxins in sunflower, 18: 35343
effects on root cells, 19: 5632(T) (ANL-Trans-114)
effects on root development in *Zea mays*, 17: 35444 (BNL-6548)
effects on root formation in cultured Jerusalem artichoke tubers, 20: 45438
effects on root growth of Chenopodiaceae, Cruciferae, and Umbelliferae, 17: 27068(T) (CEA-tr-R-1678)
effects on root meristem quiescent centers, 18: 21806 (BNL-805(p.46-58))
effects on root tips of *Scilla obtusifolia*, summary, 16: 57
effects on root tips of exposed jute seed, cytologic, 19: 5679
effects on root-knot nematode propagation in sweet potatoes, 20: 28942
effects on roots of *Vicia faba* in gaseous medium, 20: 26669
effects on roots of *Zea mays* seedlings, 17: 1321
effects on Sabin poliovirus, following, 20: 42966
effects on saccharin response in rats, 18: 19667
effects on saccharin avoidance in rats, 18: 29311
effects on Saccharomyces, protective effects of RNA against, 18: 33410
effects on *Saccharomyces cerevisiae*, 19: 7171
effects on Saccharomyces, genetic, 20: 3717(T) (JPRS-31514, pp 77-91)
effects on Saccharomyces radiosensitivity, mutagenic, 20: 5360

effects on *Saccharomyces cerevisiae*, effects of ploidy on, 20: 28961
effects on *Saccharomyces cerevisiae* cells, protective effects of cystamine against, 20: 33088
effects on salamander eyes, 19: 21866(T) (JPRS-28782(p.36-41))
effects on salamanders, 19: 21899
effects on salamander reproduction, 20: 26663
effects on saline-extractable polydeoxyribonucleotides in rat lymphoid tissue, physico-chemical studies, 20: 22570 (AD-631144)
effects on salivary gland excretion, effects of cysteamine, 19: 13053
effects on salivary gland function in rabbits, 19: 15110
effects on salivary glands and lymph nodes of rats, histochemical, 19: 21932
effects on salivary excretion of rubidium-86 in rats, 17: 37143
effects on salmon sperm, protective effects of cysteamine against, 17: 23233
effects on *Salmonella typhi*, biological, 19: 7046
effects on *Salmonella typhimurium* LT2, protective effects of alcohols against, 19: 7192
effects on *Salmonella typhi*, morphological, 20: 6854
effects on *Salmonella typhi*, biochemical, 20: 6854
effects on Salmonella antibody formation by allogeneic and syngeneic bone marrow chimeras in mice, 20: 22573 (ORNL-P-1316)
effects on sarcoma sensitivity of irradiated autograft transplant, 18: 21877
effects on sarcoma growth in mice after injection of sarcoma-fluid, 18: 41073 (COO-1038-4)
effects on sarcoma induction in man, 19: 12986
effects on sarcoma development in mouth of monkey, 19: 17599
effects on sarcoma induction in man, 19: 28038
effects on sarcoma, therapeutic, 20: 16312
effects on sarcoma, immunological method for increasing, 18: 29483
effects on sarcomatous mice, protective effects of testosterone against, 17: 38823
effects on sarcosomes of housefly flight muscle, 19: 42345
effects on Schistosoma cercariae, 18: 5113
effects on *Schistosoma mansoni* infestation in mice, 19: 7063
effects on Schistosoma cercariae infectivity in mice, 20: 42947
effects on Schizosaccharomyces germinating spores, 18: 17510
effects on Schizosaccharomyces germinating spores, 18: 17511
effects on sebaceous glands in hamsters, 20: 5322
effects on second chromosome in Drosophila, heterozygosity, 20: 22669
effects on secondary structure of meta hemoglobin, device for measurement of, 18: 3542
effects on secondary antibody response in rabbit, 18: 29317
effects on secondary disease in mouse chimeras, protective effects of thymectomy against, 18: 38988
effects on secondary gill formation and tail regeneration in *Branchiura sowerbyi*, 19: 21951
effects on secondary antibody-forming potential of mouse spleen cells, recovery from, 19: 31676(R) (ORNL-3768(p.112-18))
effects on secondary syndrome in rats following rabbit marrow and spleen transplantation, 20: 22637
effects on secondary response to tetanus toxoid, 17: 35530
effects on sedimentation coefficients of DNA from *E. coli*, 16: 25218
effects on sedimentation of DNA from *E. coli*, 17: 33636
effects on seed, 16: 12884(T) (AEC-tr-5052)
effects on seed maturation in *Brassica juncea*, 17: 23199
effects on seed potato production, 18: 33376
effects on seedling development in Vicia spp. for fodder, 17: 38691
effects on seedling roots of *Vicia faba*, 17: 40607
effects on seeds in storage, effects of moisture content, 19: 21946
effects on seeds of jute, genetic, 19: 116
effects on seeds of jute, genetic, 19: 165
effects on seeds of *Arabidopsis thaliana*, genetic, 19: 27971
effects on seeds of *Pisum sativum*, genetic, 19: 29897 (EUR-2218.e)
effects on seeds of red clover, Ultuna, genetic, 19: 45882
effects on seeds of *Trifolium subterraneum*, genetic, 20: 8704
effects on seeds of *Vigna sinensis*, biological, 20: 14341
effects on seeds of Vicia, genetic, 20: 16276
effects on seeds of barley, genetic, 20: 22679
effects on seeds of *Lakota durum*, biological and mutagenic, 20: 33064
effects on seeds of sweet clover and barley, importance of experimental conditions on, 20: 36658
effects on seeds, with and without embryo transplantation, 16: 1573
effects on seeds, free radicals formed in, 19: 5687
effects on seeds, free radicals formed in, 19: 5688
effects on seeds, genetic, 20: 3759
effects on seeds, genetic, 20: 6776(R) (ORNL-3853, pp 50-3)
effects on seeds, effects of infrared radiation on genetic, 20: 16278
effects on selected chemical constituents of blood serum in rats, 17: 43
effects on self-friction of potassium chloride, 19: 20011
effects on semen and testicles of cattle, 19: 17572
effects on seminiferous epithelium in rats and mice, whole-body exposure, 17: 1269
effects on sensitivity of animal cells to transformation by polyoma virus, 18: 5060
effects on sensitivity to vaccines in rabbits, 18: 27177
effects on sensitization of *Pneumococcus* cells and DNA, effects of 5-bromodeoxyuridine on, 19: 7056
effects on sensitivity to toxins, of mice, 17: 31921
effects on sensitometric characteristics of Kodak film, 18: 40026
effects on serological specificity of human serum gamma globulin, 16: 18757 (AMRL-532)
effects on serological properties of proteins, 18: 36968
effects on serotonin concentration in spleen, in rat, 16: 73
effects on serotonin content in blood and tissues of rabbits, effects of antibotic therapy on, 18: 35325(T) (JPRS-25464(p.8-13))
effects on serotonin content of rabbit blood, 19: 12989
effects on serotonin content in animal blood, 19: 15095
effects on serotonin levels in rabbit blood, 20: 18257
effects on serotonin content in rabbit blood, 20: 22615(R) (NIRS-4, pp 34-58)
effects on serotonin content in blood of mice, 20: 24884
effects on *Serratia marcescens*, effects of humidity and inositol on, 18: 17551
effects on *Serratia marcescens*, protective effects of chemicals against, 18: 19785
effects on *Serratia marcescens* and phage kappa, host-cell reactivation of, 19: 29986
effects on *Serratia marcescens*, protective effects of calcium, 19: 36114
effects on serum albumin synthesis in rat liver, effects of food ingestion on, 19: 19603
effects on serum complement of blood of cancer patients, comparison with betatron effects, 16: 11409
effects on serum creatine phosphokinase activity in rabbits, whole-body, 19: 7112
effects on serum complement in man and rabbits, 17: 37126
effects on serum dextran clearance in dogs, 17: 38772
effects on serum glycoproteins, 18: 38901
effects on serum glutamic-oxalacetic transaminase in rats, 17: 40611
effects on serum levels of lysozyme in rats and rabbits, 20: 42944
effects on serum lipoproteins, 17: 38830
effects on serum protein fractions in rabbits, 16: 4087
effects on serum protein fractions in rabbits, 16: 14565
effects on serum protein fractions and Wassermann antibody in rabbits having induced syphilis, 16: 4049
effects on serum proteins of rat, whole-body, 18: 3525
effects on serum proteins in pulmonary diseases, 18: 29542
effects on serum protein fractions, 18: 43257
effects on serum proteins in mice following transplants of rat-to-mouse chimeras, 19: 38404
effects on serum protein content in rats, 19: 43766
effects on serum proteins in mice, 20: 28899
effects on serum proteins in mice, 20: 35316
effects on serum proteins in hamsters, whole-body, 17: 1318
effects on serum protein fractions in rabbits, whole-body exposure, 17: 1336
effects on serum transaminase activity in mice, 20: 12545(R) (PAEC(A)AR651)
effects on serum-resistant syphilis, 18: 23391
effects on severity of contact dermatitis, 17: 2843
effects on sex ratio shifts, 18: 15823
effects on sex ratio of offspring of women exposed during diagnostic radiography, 20: 10657
effects on SH content of *Serratia marcescens*, 20: 18448
effects on SH-groups in liver and spleen of rats, effects of cysteine on, 18: 6706
effects on SH-groups in rat tissues, effects of cysteine and cysteamine on, 18: 6707
effects on shape of dielectric hysteresis loop in triglycine sulfate, 18: 34242
effects on sheep lymph nodes and lymphocyte production, 18: 35352
effects on sheep reproductive potential, 18: 23342
effects on sheep, swine, and dogs, recovery from injuries from, 20: 42996
effects on shielded lymphatic tissue after irradiation of transplanted adrenal cortex, 16: 18768 (TID-15697)
effects on shoot development in potatoes, 19: 15159
effects on shrinkage and swelling properties of housefly sarcosomes, effects of ATP on, 19: 42300
effects on sialic acid content in blood of whole-body irradiated rabbit, 17: 33739
effects on silicon transistor gain, 19: 22814
effects on silicon carbide conductivity and n-p effect, (E), 20: 15967
effects on silicon detectors, noise from, (E), 20: 14923
effects on silkworm spermatogonia, cytological, 19: 31670(R) (NIRS-3(p.19-56))

effects on silkworms, biological, 20: 22614(R) (NIRS-4, pp 28-34)
effects on silver fixation by Kupffer liver cells, 19: 17638
effects on silver nitrate at 77°K, electron spin resonance studies of, 19: 34225
effects on silver nitrate at 77°K, ESR studies of, 20: 29310
effects on silver chlorides, defect formation from, 20: 32731
effects on silver-activated potassium and sodium nitrates, optical properties of fragments produced by, 19: 2384
effects on silver-doped sodium chlorides at 40 kv, de-excitation curves from, 20: 42561
effects on single crystals of dimethylglyoxime at 77°K, 19: 15622
effects on sister chromatid exchange in chromosomes of hamster cells in culture, 18: 33329
effects on Sitophilus pupae, 18: 11737
effects on size and volume of rat embryos, 17: 37129
effects on skeletal development in fetal mice, 19: 21927
effects on skeletal development in fetal mice, 19: 21928
effects on skeletal development in fish embryos, 19: 31670(R) (NIRS-3(p.19-56))
effects on skeletal development of mouse embryos, 20: 5395
effects on skeletal development in mouse embryos, 20: 5316
effects on skeletal development of mouse embryos, 20: 5326
effects on skeletal development in mouse embryos, 20: 5327
effects on skeletal development in mouse embryos, 20: 5337
effects on skeletal development in mouse embryos, 20: 6891
effects on skeletal muscles, 17: 14056
effects on skeleton of therapeutic doses of, 20: 38767
effects on skeleton in chick embryos, 17: 19850
effects on skin, 19: 8905
effects on skin, 19: 21939
effects on skin capillary permeability, 19: 24286
effects on skin, enzymatic study, 16: 4106
effects on skin, enzymatic and histological study, 16: 8625
effects on skin epitheliomas, late carcinogenic, 20: 3811
effects on skin graft survival in neonatal rabbits, 16: 14403
effects on skin grafting in mice, 18: 8119 (USNRDL-TR-683)
effects on skin graft acceptance in mice, effects of immune reactions on, 18: 33388
effects on skin graft acceptance in rabbits, effects of post-irradiation time on, 18: 33386
effects on skin graft immune reactions in mice, 20: 22741
effects on skin grafting in rabbits, role of antibodies in, 17: 10425
effects on skin in accidental exposure, 18: 19706
effects on skin in treatment of skin carcinomas, 18: 19714
effects on skin of guinea pigs, chronic, 19: 8891
effects on skin of guinea pigs, multiple exposures, 19: 35990
effects on skin of guinea pigs, pathological, 19: 45869
effects on skin of guinea pigs, protective effects of chloroquine against, 19: 46019
effects on skin of swine, pathological, 20: 1609 (BNL-9477)
effects on skin of, post-operative therapeutic doses used for breast carcinoma, 20: 3847
effects on skin of guinea pigs and rabbits, mechanism for, 20: 12623
effects on skin of urethan-treated mice, 20: 20476
effects on skin of mice and rats, role of adipose tissue in repair of, 20: 28946
effects on skin of pigs, effects of dose fractionation, 17: 15662
effects on skin of man, energy dependence of, 17: 37109
effects on skin pigmentation, synergistic effects of dimethylchlortetracycline on, 19: 12971
effects on skin wheal resorption, 19: 28146
effects on skin, effects of dose fractionation on, 20: 22745
effects on skin, pathological, 19: 25940
effects on skin, pathological, 19: 33993
effects on skin, role of enzymes in depletion and restoration of, 19: 21941
effects on skin, treatment of, 18: 35340
effects on sleeping time in mice, effects of anesthetics and narcotics, 17: 1342
effects on small intestine after cervical cancer therapy, 20: 10654
effects on small intestine following radiotherapy, 20: 22677
effects on smallpox immunity in rabbits, 20: 18408
effects on *Snagamus trachea*, 19: 70
effects on snail population kinetics, effects of age on, 19: 2138
effects on snail population kinetics, 19: 2139
effects on sodium chloride susceptibility in rats, whole-body, 16: 17494
effects on sodium ion flux in human erythrocytes, 18: 15873
effects on sodium fluoride crystals, temperature dependence of color center growth in, 18: 20039 (COO-1044-14)
effects on sodium chloride coloration and volume, 18: 20598
effects on sodium thiocyanate space, 18: 23285
effects on sodium transport in erythrocytes, 18: 29342
effects on sodium chloride, relations between dislocations and point defects in, 18: 37779
effects on sodium and rubidium metabolism in salivary glands of rats, 18: 43247
effects on sodium excretion by fish, 18: 43280
effects on sodium chloride, F-center, 19: 22379(T)
effects on sodium silicate glass, color centers produced by, 19: 7985
effects on sodium thiosulfate, ESR spectra of free radicals induced by, 19: 34222
effects on sodium chloride crystal plastic flow, 19: 40594
effects on sodium thiosulfate single crystals, ESR spectra of free radicals in, 20: 374
effects on sodium chlorate crystals, color center paramagnetism from, (E), 20: 15961
effects on sodium nitrate crystals, nitrate ion ESR and hfs from, (E), 20: 15965
effects on sodium sulfate metabolism in rat liver, 20: 20410
effects on sodium chloride single crystals, Schottky disorder and lattice relaxation from, (E), 20: 32712
effects on sodium fluorides, N-band formation in, (E), 20: 34838
effects on sodium azide, ESR studies of, 20: 40966
effects on sodium transport across cell membranes in erythrocytes, 17: 4412
effects on sodium content of saliva, whole-body exposure, 17: 15719
effects on sodium-22 efflux in isolated rat nerves, 19: 26087
effects on solid solutions of silver salts, EPR of free atoms in, (E), 20: 15975(T)
effects on solid-state polymerization of *N*-vinylsuccinimide with succinimide, 20: 18776
effects on solubilization of cholinesterase from plaice muscle by bacteria, 20: 28933
effects on soluble albumin in rabbit spleen, 19: 3968
effects on solute radical formation in frozen solutions of alanine, DNA, and gelatins, ESR spectra of, 19: 34237
effects on somatic genetics in Drosophila, 18: 5114
effects on somatic recombination in Drosophila, 18: 43255
effects on somatic mutation frequency induction in oats, 20: 31078
effects on somatic crossing over in *D. melanogaster*, effects of age on location of, 20: 36619
effects on sorghum species, 18: 13534
effects on sorption of carbon monoxide and oxygen by aluminum oxide, 20: 8998
effects on sorption of carbon dioxide by aluminum oxide at 20 to 350°C, 20: 19264
effects on sorptive properties of rabbit serum proteins, 20: 32959
effects on sound-induced seizures in rats, 18: 69
effects on Southern Pine seed, effects of moisture content and stratification on, 20: 22744
effects on soybeans, 18: 38848
effects on soybean seeds, genetic, 20: 45388
effects on space flight sensitized cultures of *Escherichia coli*, 20: 42912
effects on spatial avoidance behavior of rats, 20: 14366
effects on specific activity of DNA and RNA, 20: 8613
effects on specific-pathogen-free mice, 17: 35380
effects on spectral characteristics of oxyhemoglobin, 18: 6661
effects on spectra of lithium fluorides, 18: 22543
effects on spectra of somatic mutations in butterflies, effects of temperature on, 17: 23206
effects on spectrum of colored lithium fluoride crystals, 18: 32249
effects on spermatogenesis, 16: 21939
effects on spermatogenesis in Drosophila, 18: 35302(R) (AD-438540)
effects on spermatogenesis in monkeys, 18: 36999
effects on spermatogenesis in *Drosophila melanogaster*, 19: 31889
effects on spermatogenesis in mice, effects on fertility of, 20: 65(R) (TID-22174)
effects on spermatogenesis in *Drosophila melanogaster*, 20: 38607
effects on spermatogenesis in rats following exposure at birth, 20: 40682
effects on sperms in Drosophila males, effects of nitric oxide, oxygen, and temperature on, 17: 7885
effects on spin transfer in crystalline solid solutions, (E), 20: 43317
effects on spin-lattice relaxation time of praseodymium ions in lanthanum chloride, 20: 40350
effects on spin, protective effect of serotonin against, 17: 2879
effects on spinal cords of neonatal rats, 16: 26788
effects on spinal cord, diagnosis of, 18: 38830
effects on spinal cord, 18: 41161
effects on spinal cord convulsions in aging and newborn rats, whole-body, 19: 26089
effects on spinal cord of developing rat embryos, 19: 33834
effects on spinal cord, pathological, 20: 16251
effects on spinal cord, late pathological, 20: 18406
effects on spinal cord in rodents, pathological manifestations of, 20: 24908
effects on spinal cord after tumor therapy, 17: 95

effects on spinal cord in rabbits and dogs, 17: 33628
effects on spinal cord of neonatal rats, 17: 35521
effects on spinal cord histology in neonatal rats, 17: 35522
effects on spleen response to injected bone marrow, whole-body exposure, 16: 11435(R) (ANL-6464(p.22-3))
effects on spleen proliferation by transplanted marrow cells in mice, 18: 25189
effects on spleen and thymus of rats after head exposure, 19: 10851
effects on spleen cell effects on immune response in mice, 19: 17538
effects on spleen of rats, 19: 36010
effects on spleen and thymus, 19: 39265(R) (IA-1021)
effects on spleen of mice, nodule formation from, 19: 43682(R) (UCLA-12-565, pp 33-57)
effects on spleen cells of *Molge vulgaris* in tissue culture, morphological, 19: 43826
effects on spleen weight in mice, genetic factors, 19: 45956
effects on spleen colonization by transplanted bone marrow cells in mice, 20: 22707
effects on spleen desoxyribonucleic acid, whole-body exposure, 17: 15636(R) (TID-18061)
effects on spleen enzyme content, whole-body exposure, 17: 24966
effects on spleen and testes in rats pre-exposed to low doses, 17: 27137
effects on spleen, therapeutic value for splenic enlargement and leukemia, 17: 38660
effects on spleen, in rats, 19: 29905(T) (JPRS-29112(p.19-25))
effects on splenectomized mice, protective effects of splenic tissue homogenates on, 18: 31285
effects on splenic and thymic weight in mice, 19: 31670(R) (NIRS-3 (p.19-56))
effects on spore germination and stability of virulence in *Ustilago avenae*, 20: 38672
effects on spores of *Bacillus cereus*, 20: 18344
effects on spores of *Bacillus megaterium*, protective effects of water against, 17: 40614
effects on spread of tick-borne encephalitis in lymphatic system in mice, 17: 5786
effects on spreading effect in skin, India ink study, 16: 14578
effects on sprouting and yield of potatoes, 20: 28966
effects on stainability of rat skin cells, 18: 41135
effects on staphylococcus pneumonia in rabbits, 16: 8632(T) (JPRS-11848(p.13-24))
effects on *Staphylococcus aureus*, 19: 29886(R) (ANL-6971(p.29-46))
effects on stem cell pool in transplanted mouse marrow, 19: 3942
effects on stem cells in mouse marrow, 19: 31677(R) (ORNL-3768 (p.119-30))
effects on Stenobothrus germ cell cytochemistry, 18: 19615
effects on sterility of premature female mice, 19: 8816
effects on sterility in female *Phaseolus mungo*, 20: 14347
effects on sterility in *Rhodnius prolixus*, 18: 3519
effects on sternal-marrow regeneration in man, dosage, 19: 7141
effects on steroid synthesis by testes, 19: 10783(R) (COO-119-231(p.76-84))
effects on steroid content of urine, in guinea pigs, 19: 29854(R) (TID-21859)
effects on steroid content in guinea pigs, 20: 28975
effects on stilbene, effects of naphthalene, phenanthrene, and triphenylene on isomerization by, 20: 18735
effects on stimulating properties of chicken and frog liver extracts in frogs, 19: 8917
effects on stimulation of solar plexus nerve ganglions, 20: 38687
effects on stored energy in sodium chloride, calorimetric measurements, 16: 13644 (TID-15043)
effects on stored ascites-tumor cells, effects of ATP and glucose on, 19: 10838
effects on sotred energy of lithium fluoride crystals, 19: 22309
effects on stored onion seedlings, 19: 42781
effects on stored onion seedlings, 19: 42782
effects on stored maize kernels, 17: 28716
effects on strength of chromatography paper, 19: 20630
effects on striated rabbit muscles, 20: 24883
effects on strontium-90 uptake in rat teeth, 18: 19655
effects on strontium-85 and yttrium-91 sorption by rat intestine, effects of dose on, 20: 22600
effects on strontium chloride single crystals, V_k centers from, 20: 40319
effects on structure and function of ovaries, 16: 6325
effects on structure of fibrin clots, 16: 21961
effects on structure and viscosity of desoxyribonucleic acid, 18: 6660
effects on structure of DNA, 18: 8144(T)
effects on structure of cadmium sulfides, 18: 16125
effects on structure of pentaerythritol, 18: 26083
effects on structure of nucleic acids, 18: 33277 (STI/DOC/10/28(p.21-38))
effects on structure of collagen fibrils, 18: 38893
effects on structure of pentaerythritol, 18: 40032
effects on structure of fibers and nerve endings of hair follicles, 19: 7142
effects on structure of DNA molecules in solution, 19: 12994
effects on structure of Y chromosomes in *Drosophila hydei* spermatocytes, 19: 24298
effects on structure of RNA extracted from mouse brain, 20: 45345
effects on structure of cerebral cortex in rat, 17: 14076
effects on structure of interauricular septum in frogs by, 17: 30368
effects on subcellular responses in liver cells in culture, 18: 15864
effects on subcutaneous tissue in rabbits, effects of medicinal agents on, 16: 14600
effects on subcutaneous resorption of thyroxine, 3,5,3'-triiodo-*L*-thyronine, and sodium iodide in rats, 17: 40665
effects on submicroscopic structures of liver cells of mice, early, 20: 33041
effects on subsequent pharyngo-laryngectomy, 20: 5463
effects on successive generations of mouse populations, 19: 7116
effects on succinamide single crystals, ESR and tracer studies of, 20: 18757
effects on sugars in aqueous solutions, 20: 20748
effects on sulfate metabolism in rat brain, 18: 29327
effects on sulfhydryl content of blood, 20: 20415
effects on sulfhydryl groups in thymus nuclei in rats, protective effects of oxidized glutathione against, 18: 129
effects on sulfhydryl content of nucleoproteins in rat liver, 17: 33640(T)
effects on sulfomucopolysaccharide metabolism in rat aorta, 20: 8590
effects on sulfonamide-induced and normal volutin in bacteria, 19: 43759
effects on sulfoxidation of hexane, chemical, 19: 473
effects on sulfur-35-labeled methionine uptake by rat blood serum, 18: 23247 (JPRS-24164(p.1-8))
effects on sulfur-35 uptake by mouse knee joints, 19: 2090
effects on sulfur-35 uptake by rat aorta, 19: 15028
effects on sulfur-35 uptake by soft tissues in mouse hind limb, 19: 21887
effects on sulfuric acid, electron-nuclear double resonance of hydrogen trapped in, 18: 41437
effects on sulfurous acid, 19: 5967
effects on sulfurous acid, 19: 5968
effects on sulhydryl groups in tissue, 18: 41204
effects on summer wheat seeds, mutagenic, 20: 35317
effects on suppressor genes in Drosophila, egg-irradiation, 19: 45968
effects on surface conductivity of polyvinyl chloride, 18: 2299
effects on surface phenomena of polyacrylic acid molecules, 18: 23690
effects on surface-area and -energy of calcia irradiated during calcination, 20: 19271
effects on surface area of calcium oxide, 20: 36904
effects on survival of homologous skin grafts in rats, whole-body, 16: 32820
effects on survival of cells in tissue cultures, 18: 8100 (BNL-7542)
effects on survival of rats, protective effects of abdomen, chest, and head screening against, 18: 25225
effects on survival in fish, dose-dependence of, 18: 33272(R) (NIRS-2 (p.31-42))
effects on survival of HeLa tumor cells, growth medium effects on dose-response curves for, 19: 7060
effects on survival of mice, effects of methyl cellulose on whole-body, 19: 8920
effects on survival of skin grafts in mice, effects of 6-mercaptopurine and 5-bromodeoxyuridine on, 19: 8909
effects on survival and repair of L-cells in culture, 19: 13002
effects on survival time of conventional and germ-free mice, 19: 17587
effects on survival of Chinese hamster cells, effects of age on, 19: 26073
effects on survival of human cell cultures, theoretical curves of, 19: 26075
effects on survival of skin grafts in rabbits, 19: 29944
effects on survival of *Macrobiotes areolatus* in active and dormant states, 19: 38373
effects on survival and recovery of rat growth cartilage, 19: 38407
effects on survival of animal cells in tissue culture, dose effects on, 20: 1617(R) (NP-15149)
effects on survival of transplanted tumors in mice, 20: 3751
effects on survival in mice with carcinoma transplants, 20: 6852
effects on survival in virus-infected mice, 20: 8677
effects on survival of mice after tissue transplants, 20: 8718
effects on survival of rabbit allografts, effect of 6-purinethiol on, 20: 8719
effects on survival of tumor cells in culture, effects of anoxia and antimetabolite drug on, 20: 10664
effects on survival of 5-bromo-deoxycytidine-treated bone marrow cells, 20: 14333

effects on survival in Chlorella, mathematical analysis of, 20: 16246
effects on survival of *Paramecium aurelia* and *Tetrahymena pyriformis*, 20: 36661
effects on survival of mice, effects of 19-nor-testosterone phenylpropionate on, 20: 38610
effects on survival of mammalian cells, effects of metabolic inhibitors on, 20: 38710
effects on survival in mice, protective effects of AET or glutathione combined with bone marrow treatments against, 20: 40719(R) (ORNL-3922, pp 136)
effects on survival time in mice protected by iproniazid or serotonin, 20: 42991
effects on survival of HeLa cells at 250 kvp, 17: 1325
effects on survival of Drosophila, periodic and chronic exposure, 17: 7791 (TID-14624)
effects on survival of partially synchronized hamster cells, effects of division on, 17: 38820
effects on susceptibility of mice to leukemia transmission by cell-free extracts, 18: 8147
effects on susceptibility to Coxsackie B1 virus in neonatal rat brain and skeletal muscle, 19: 17594
effects on susceptibility of mice exposed *in utero* to congenital anomalies, 20: 31066
effects on susceptibility of mice to leprosy bacillus, combined with thymectomy, 20: 45408
effects on suspended uterine horn, effects of pretreatment with tryptophan, 17: 112
effects on sweet cherry trees, genetic, 20: 16244
effects on swine, 19: 5635
effects on swine, biological, 20: 10618
effects on swine, effects of conditioning exposure on pathological, 20: 40605 (AD-635735)
effects on synaptic activities in cat spinal cord, 19: 26088
effects on synaptic mechanisms in cats, whole-body, 20: 26657(R) (SRIA-115P53-1)
effects on synaptic activity of spinal cord, acute exposure, 17: 23172
effects on synchronized HeLa S3 cultures, 19: 26069
effects on synchronized Chinese hamster cells, sensitivity, 19: 31788(R) (ORNL-3768(p.33-57))
effects on syncyte formation in rice plants, 19: 36005
effects on syngenetic preference in mice, 20: 42889
effects on synthesis of desoxyribonucleic acid by tumor cells, 16: 5180
effects on synthesis of glycogen by skin, 16: 6345
effects on synthesis of creatine by liver, whole-body exposure, 16: 23463
effects on synthesis of desoxyribonucleic acid in mammalian cells in tissue culture, 18: 11756
effects on synthesis of ATP by human erythrocytes, 18: 13481
effects on synthesis of ribonucleic acid in *Escherichia coli*, 18: 29305
effects on synthesis of rat liver enzymes, 18: 35315(R) (NP-14210 (p.14-24))
effects on synthesis of ribonucleic acid in rat liver, 18: 41112
effects on synthesis of desoxyribonucleic acid in mouse spleen and intestine after repeated exposure, 18: 41169
effects on synthesis of polylysine and polyphenylalanine *in vitro*, 18: 43236
effects on synthesis of DNA-like RNA in yeast cells, 19: 33830
effects on synthesis of hepatic microsomal enzymes in rats, 20: 5282(R) (AD-623599, pp 1-15)
effects on synthesis of hepatic microsomal enzymes in rats, 20: 5283(R) (AD-623599, pp 16-27)
effects on synthesis of induced β-D-galactosidase in *E. coli*, 20: 31004
effects on synthesis of corticosteroids in rats, 20: 31011
effects on synthesis of desoxyribonucleic acid in liver cell nuclei, tracer study, 17: 75
effects on synthesis of ascorbic acid in rat liver, whole-body exposure, 17: 15656
effects on synthesis of desoxyribonucleic acid in liver, 17: 24956
effects on tadpole tissues, effects of starvation during irradiation on, 20: 10676
effects on tadpoles in aqueous solutions of carbon-14-labeled acrylamide, autoradiographic studies of, 20: 32986
effects on take of autologous skin transplants, local-exposure, 16: 17454
effects on take of allogenic skin grafts in mice, effects of mercaptopurine and bromodeoxyuridine on, 19: 26027
effects on take of skin homografts in rats, 20: 5335
effects on take of kidney homotransplants treated with immunosuppressive drugs, 20: 6936
effects on take of skin grafts in mice, effects of antisera, 17: 19810 (USNRDL-TR-625)
effects on tartronic acid, ESR spectra of, 19: 26438
effects on taste response in rats, 20: 18294(R) (TID-22766)
effects on taste sensitivity in man, 20: 8789
effects on taurine excretion in rats, 18: 27145
effects on taurine excretion in mice, effects of AET and cysteine on, whole-body, 20: 38717
effects on taurine levels in urine, whole-body exposure, 17: 60
effects on teeth in newborn rats, head and whole-body exposure, 20: 14322
effects on teeth of rats, pathological, 19: 45845
effects on teeth, pathological, 19: 33831
effects on tensile strength of rat vibrissae, 20: 42834(R) (ANL-7136, pp 46-63)
effects on testes of prenatally irradiated rats, protective effects of 2-(2-aminoethyl)-2-thiopseudourea against, 18: 21913
effects on testes of infant rats, protective effects of AET against, 19: 93
effects on testes development in young rats, whole-body, 19: 13067
effects on testes of newborn rat, fractionated, 19: 17563
effects on testes of lizards, pathological, 19: 36015
effects on testes of hamsters, mice, and rats, 20: 33069
effects on testes of rats, histological, 18: 19709
effects on testicles of bulls, 18: 25185
effects on testicles after irradiation of salivary glands, 16: 20216
effects on testicular development and spermatogenesis in mice, effects of age at irradiation on, 20: 20499
effects on testicular function in man, pathological, 20: 22617(R) (RLO-1780-1)
effects on testis in cock, relation between dose and grade of degeneration, 16: 14566
effects on texture of beef and pork, 18: 36983
effects on the brown-spots character of *Drosophila melanogaster*, 20: 42945
effects on the decrease in hatching of eggs of *Artemia salina*, 20: 35291
effects on the development of *Ascaridia galli*, 20: 42968
effects on the ichneumonid wasp, Devorgilla, genetic, 20: 1643
effects on the insect *Rhodnius prolixus*, effects of mitotic state on pathological, 19: 94
effects on thermal conductivity of skin, 18: 3561
effects on thermal decomposition of calcium azide, 19: 22358
effects on thermal de-excitation processes in potassium and sodium chloride phosphors, 19: 41101(T)
effects on thermal sensitivity of fungi and yeast, 20: 1640
effects on thermal hemolysis of rat erythrocytes, 20: 12697
effects on thermal decomposition of mercury oxalate, 20: 36898
effects on thermoluminescence of potassium chloride crystals, 18: 16083
effects on thermoluminescence afterglow of proteins and synthetic polymers, 19: 19983
effects on thermoluminescent reduction of chromium ions in magnesium oxide crystals, 19: 40631
effects on thermoluminescence fading in dosimetric lithium fluoride, storage effects on, 19: 44076
effects on thermoluminescence and trapping centers of thallium-activated sodium iodides, 20: 7160(T)
effects on thermoluminescence of lithium fluoride phosphors, 20: 14887
effects on thermoluminescence of rare earth ions in calcium fluoride, 20: 29318
effects on thermoluminescence of inorganic and organic materials, 20: 34828
effects on thermoluminescence of alkali metal halide phosphors, 20: 45739
effects on thermoluminescence in biological materials, measurement of, 18: 37523
effects on thermoregulation in mice, 18: 1428
effects on thermostability of collagen in rats, 18: 5045
effects on thermostable inhibitors in rabbit blood serum, 20: 35306
effects on thermostable inhibitor effects on staphylococcus toxin in rabbit blood serum, 20: 35306
effects on thiamine metabolism in mice and rats, mechanism of, 19: 15054
effects on thiamine metabolism in mice, 20: 29003
effects on *Thiobacillus thiooxidans*, effects of anoxia, chemicals, and pH on, 20: 31139
effects on thiocyanate solutions, oxidation-reduction, 18: 37206(T) (AEC-tr-6398(p.408-11))
effects on thiol content of rat thymus cell nuclei, 18: 3517
effects on thiol content of hamster cheek pouches, 19: 3906
effects on thiol content of Ehrlich ascites carcinoma cells and thymocytes, 19: 7065
effects on thiol content in rat liver and spleen, whole-body, 20: 108
effects on thrombocytes, effects of suspension media on, 20: 5365
effects on thymectomized and sham-thymectomized mice, 19: 7193
effects on thymectomized mice, 20: 18193
effects on thymic hypertrophy, delayed, 16: 28819
effects on thymic amino acid incorporation, 18: 41143
effects on thymic lymphoid tissue in chicks, restoration after local and whole-body exposure, 20: 42935

effects on thymidine, 19: 2377
effects on thymidine uptake by DNA in mice, four-factor model for analysis of, 19: 24337
effects on thymidine metabolism in intestinal epithelium of goldfish, effects of temperature on, 20: 5374
effects on thymidine index in nephrectomized rats, tracer study, 20: 14258 (AD-627569)
effects on thymidine catabolism in rats, 20: 42806
effects on thymidine metabolism in intestine, effects of AET treatment, 17: 10486 (TID-15931)
effects on thymine metabolism in rats, 18: 41139
effects on thymocytes in rats, protective effects of nicotinamide against, 19: 7187
effects on thymocyte survival in rats, dose effects on, 19: 31670(R) (NIRS-3(p.19-56))
effects on thymocyte survival in rats, effects of temperature on, 19: 31670(R) (NIRS-3(p.19-56))
effects on thymocyte nuclei, effects of phosphate metabolism and respiration on x, 20: 42928
effects on thymocytes in tissue culture, effects of media salinity on, 18: 41109
effects on thymus, organ weight and histological modifications, 16: 8620
effects on thymus cortex of rats, 19: 13006
effects on thymus tumors in mice, absence of synergistic effects of local and whole-body, 19: 17556
effects on thymus weight in mice, genetic factors, 19: 45956
effects on thymus gland in mice, cytological, 19: 45871
effects on thymus cytology in mice, 20: 22697
effects on thymus in mice, metabolic, 20: 38606
effects on thymus of children, therapeutic doses of, 20: 45433
effects on thyroid function in rats, 16: 23431
effects on thyroid gland, histochemical and histological, 16: 32802
effects on thyroid function in rats, 18: 8161
effects on thyroid gland in sheep, 18: 8162
effects on thyroid function in pigs, 18: 36975
effects on thyroid gland of rats, pathological, 19: 8892(T)
effects on thyroid following laryngeal cancer therapy, 19: 42286
effects on thyroid function, 19: 43890
effects on thyroid glands of therapeutic doses of, carcinogenic, 20: 3739
effects on thyroid gland in rats, 20: 29047
effects on thyroid glands of adult male rats, post-traumatic changes in muscle tissue from, 17: 30339
effects on tibia in living mice, 16: 26740(R) (TID-16395)
effects on time of mitosis of Yoshida sarcoma cells, 16: 4078
effects on tissue serotonin levels, whole-body exposure, 16: 28845
effects on tissue respiration in rats, effects of chloroprene intoxication on, 18: 38780(T) (JPRS-26278(p.17-23))
effects on tissue culture cells, 18: 38915
effects on tissue eosinophil counts in rats, 20: 6799
effects on tissue proteinases, 17: 30355
effects on tissue response to surgery, 17: 38767
effects on tissue-graft acceptance by newt limbs, 18: 29314
effects on tissues, mechanism of, 20: 45256
effects on toad embryos, protective effects of dinitrophenol against, 18: 33272(R) (NIRS-2(p.31-42))
effects on tobacco resistance to blue mold disease, mutagenic, 20: 40613 (N-66-18147)
effects on tolerance of amoebae to transplanted cytoplasm, 16: 21956
effects on tolerance of mice to explosive decompression, effects of oxygen on, 18: 11624 (AD-407916)
effects on tolerance to bovine serum albumin in rabbits, 19: 45902
effects on tomato seeds, genetic, 20: 40713
effects on tomatoes, seed-irradiation, 18: 13533
effects on tomatoes, mutagenic, 20: 22663
effects on tongue epitheliomas, 20: 22809
effects on tooth socket healing in rats, 18: 3507
effects on topazes, electron spin resonance studies of, 19: 42562
effects on total microsomal and soluble ribonucleic acid of rat liver, 16: 26781
effects on total-body nitrogen in mice, protective effects of bone marrow against, 19: 31905(R) (ORNL-3768(p.99-108))
effects on toxemia in dogs, perfusion method for, 17: 30337
effects on toxic effects of cysteamine, in mice, 17: 31898
effects on toxic response of mice to dietary 2-mercaptoethylamine or *p*-aminopropiophenone, 18: 23358(R) (NP-13918(p.116-28))
effects on toxicity of amphetamine in mice, 20: 18380
effects on toxicity of various drugs in mice, 20: 45448
effects on toxicity of rat blood serum, 20: 45465
effects on toxicity of praseodymium nitrate in rats, 17: 10484(R) (NP-12251(p.90-8))
effects on toxoplasmosis in rats, mechanism for, 18: 21840
effects on TPN photoreduction in isolated chloroplasts, 16: 21987
effects on trace conditioned reflex systems in rats, 17: 7896(T)
effects on trace element content in spleen in rats, 17: 40547(R) (NYO-10569)
effects on Tradescantia meristematic cells, 18: 3478 (BNL-6898)
effects on Tradescantia, effects of light on genetic, 19: 2068(R) (ORNL-3700(p.34-57))
effects on Tradescantia chromosomes, aberrant, 19: 24328
effects on Tradescantia, effects of ATP, histidine, and proline on recovery from, 20: 12728
effects on Tradescantia, effects of cupferron on frequency of chromosome aberrations in, 20: 29028
effects on Tradescantia chromosomes, cytological studies, 20: 42706(R) (NYO-2373-1)
effects on transfer and maintenance of adoptive immunologic tolerance to Shigella antigens in mice, 19: 36078
effects on transference mechanism in parabiont rats, 20: 16284
effects on transfer capacity of rat small intestine, whole-body, 20: 31081
effects on transformation of injected bone marrow cells in dogs, 18: 33337
effects on transformation of hidden spotted to spectacled in potatoes, role of gene M in, 19: 17542
effects on transforming DNA, inactivating, 20: 12620
effects on transformation of blood lymphocytes to blast cells in man, 20: 42903
effects on transistors in single circuits, 19: 22815
effects on transistors, 19: 36870
effects on translocation induction in mouse spermatogonia, 19: 38396
effects on translocations in Drosophila, linear dose dependence of, 18: 23282
effects on translocation of nucleic acids and proteins in germinating barley, 17: 15775
effects on transplantation of malignant tumor cells, hard and soft, 16: 14580
effects on transplantability of ascites tumor cells, 18: 19651
effects on transplantability of mouse tumors, 18: 29522
effects on transplanted tumors in mice, 20: 8662
effects on transplantable brain tumors in mice, protective effects of AET and iododeoxyuridine against, 20: 33090
effects on transplanted tumors in mice, immune response to subsequently transplanted tumors, 20: 40643
effects on traumatic behavior of rabbit brain, 19: 15118
effects on treatment of chronic homologous disease in mice, 19: 9042
effects on *Tribolium castaneum*, genetic, 20: 11184(R) (BNWL-122, pp 137-9)
effects on Tribolium, factors affecting, 20: 18302
effects on Tribolium, 20: 24874
effects on *Tribolium castaneum*, effects of dimethylsulfoxide on, 20: 35260
effects on Trillium, genetic, 19: 8868
effects on Trillium, genetic, 19: 8869
effects on Trillium, genetic, 19: 8870
effects on Trillium chromosomes, aberrant, 19: 42291
effects on tritiated cytidine uptake by HeLa cell RNA, 18: 19599
effects on tritiated-thymidine uptake by neuroblasts in grasshoppers, 19: 15073
effects on tritiated thymidine uptake by Physarum DNA, 19: 15100
effects on tritiated-thymidine uptake by slime mold, 19: 17554
effects on tritiated phenylalanine uptake by serum proteins in perfused rat liver, 19: 26006
effects on tritiated valine uptake by *Vicia faba* chromosomes, 19: 38417
effects on tritiated thymidine uptake by mouse brain, 20: 22688
effects on tritiated thymidine incorporation into DNA, 17: 33729
effects on tritium content in organs and skin of mice, 17: 27181
effects on trypsin digestion of desoxyribonucleoproteins, 18: 17574
effects on trypsin, 18: 37222
effects on trypsin solutions, thermal after-effects in, 19: 18023
effects on trypsin solutions, thermal after-effects of, 19: 24572
effects on trypsin solutions, effects of agar on, 20: 31017
effects on tryptamine content in rat brain tissues, 20: 20437 (CONF-650560-18)
effects on tryptophan metabolism in mice after adrenal and testicle exposure, 16: 14570
effects on tryptophan metabolism in rabbit, 16: 14584
effects on tuberculosis in guinea pigs, 18: 19715
effects on tularemia bacteria and infection in vaccinated guinea pigs and mice, 20: 26701
effects on tulip plants, genetic, 19: 3931
effects on tulip plants, genetic, 19: 3932
effects on tumor beds in mice, 20: 31073
effects on tumor cell reproductive capacity under anoxic and oxygenated conditions, dose-response relation in, 16: 17496
effects on tumor cell reproductive capacity, modification by pharmacological agents, 16: 17497
effects on tumor cells, mechanism for, 18: 29548

effects on tumor cell populations, model for, 18: 31242
effects on tumor cells in culture, metabolic, 19: 24364
effects on tumor cells, 20: 6882
effects on tumor cells, biological, 20: 10650
effects on tumor cells, biological, 20: 10651
effects on tumor cells, mechanism of, 17: 27035
effects on tumor development in monkeys, 19: 7033
effects on tumor development in mice, 19: 15027
effects on tumor development in cerebral cortex in rats, histopathology of, 19: 17589
effects on tumor development in rat liver, 19: 17634
effects on tumor development in *D. melanogaster* eggs and larvae, 19: 27982
effects on tumor grafts, 16: 1513
effects on tumor growth and regression, whole-body and tumor-directed exposure, 16: 20131 (UR-575)
effects on tumor growth and development of metastases in mice, 18: 25162
effects on tumor growth in mice, direct and indirect, 18: 29535
effects on tumor growth and metabolism in rats, effects of thiamine on, 18: 41133
effects on tumor growth in rats, role of reticulo-endothelial system in, 19: 13051
effects on tumor growth in rats, 19: 28057
effects on tumor growth in rat lungs and lymph node metastasis, 19: 28052
effects on tumor growth in mice, synergistic effects of ultrasound on, 19: 29972
effects on tumor growth in F_1 hybrid mice, dose dependence of, 19: 38403
effects on tumor growth in mice, synergistic effects of cruzine on, 19: 38428
effects on tumor growth in rabbits, effects of regional oxygenation on, 19: 38374
effects on tumor growth in mice, 17: 22981
effects on tumor incidence in mice, effects of injected cholesterol on, 19: 29915
effects on tumor implants in mice, effects of oxygen on, 19: 46003
effects on tumor induction in mouse lung, effects of urethane on, 20: 33022
effects on tumor induction in pharynx, following therapy of thyrotoxicosis, 20: 3806
effects on tumor incidence lymph system in hamsters, 17: 14012
effects on tumor of head, therapeutic, 20: 5484
effects on tumor recurrence in rats and mice, 17: 23113
effects on tumorigenesis in Drosophila, 19: 8829
effects on tumors of, 19: 28170
effects on tumors in mice as affected by diurnal variations of exposure, 20: 43048
effects on tumors, radiosensitivity effects of sodium cyclohexyl-succinate on, 18: 13599
effects on tumors, synergistic, 19: 4019
effects on tumors, pre-surgical, 19: 15258
effects on tumors, effects of sensitizing exposure on, 19: 26190
effects on tumors, biological, 20: 22719
effects on two varieties of peanuts, 20: 22683
effects on T1 phages, effects of cysteamine and glycerine on, 16: 20294
effects on T2-bacteriophages, protective effects of cysteamine–oxygen, 16: 9865
effects on T2 bacteriophages, effects of cysteamine on, 16: 20292
effects on T5 receptor, factors affecting inactivation, 20: 3787
effects on ulceration of healing rat epidermis, 19: 26007
effects on ultramicroscopic structure of retina of rabbits, 20: 42958
effects on ultrasonic vibration propagation in dog blood, 18: 38837
effects on ultrasound resistance of blood platelets and erythrocytes, 19: 17721
effects on ultrastructure of duodenal crypts in mice, 19: 33896
effects on ultrastructure of gastric fundus glands in mice, whole-body, 20: 111
effects on ultrastructure of male germ cells in rats following exposure at birth, 20: 40683
effects on ultrastructure of guinea pig brains, 20: 45442
effects on ultrastructure of neurons of Gasser ganglion in rats, 17: 10461
effects on ultraviolet fluorescence of bone marrow and blood cells, whole-body exposure, 16: 31485(T)
effects on ultraviolet fluorescence of nuclei and mitochondria, 17: 37093
effects on uncoupling of oxidation and phosphorylation in mitochondria of green plants, 20: 28947(T)
effects on unirradiated graft of mouse tumor bed, 18: 19695
effects on unsaturation variations in serum lipids in rabbits, 16: 25229
effects on uptake of carbon-14-labeled methionine by rat tissue, 18: 23293
effects on uptake of heat-killed sulfur-35-labeled mycobacterial vaccines by microsomes and mitochondria in rat spleen, 20: 42907
effects on urethan induced leukemia and lung tumor incidence in mice, fractionated and regional, 19: 7069
effects on urethan-induced tumors in mice, effects of dose on inhibitory, 20: 10671
effects on uridine diphosphate glucose pyrophosphorylase activity in rat liver, 19: 43747
effects on urinary excretion of 5-hydroxyindoleacetic acid, 16: 12908
effects on urinary excretion of desoxycytidine in animals, 16: 16293
effects on urinary excretion of noradrenaline or adrenaline by rats, 16: 20173
effects on urinary excretion of 5-hydroxyindoleacetic acid in rats, 18: 19626
effects on urinary excretion of 5-hydroxyindoleacetic acid by rats, effects of cystamine on, 18: 19639
effects on urinary excretion of creatine and 2-methyl-β-alanine in rats, 18: 23234 (EUR-591.d)
effects on urinary excretion in rats, whole-body, 18: 38886
effects on urinary excretion of amines by rats, 19: 28102
effects on urinary excretion of thymidine by rats, 20: 5382
effects on urinary tract following cervical carcinoma therapy, 20: 6802
effects on urinary electrolyte excretion in mice, fractionated doses, 20: 6889
effects on urinary excretion of injected phosphorus-32 in rats, effects of dinitrophenol on, 20: 10666
effects on urinary excretion of ammonia and phosphates in rats, 20: 14270
effects on urinary glucuronide excretion by rats, 20: 18287 (EUR-2638.1)
effects on urinary excretion of glucuronic acid and glucuronides by rats, 20: 22575 (PRNC-80)
effects on urinary excretion and production of cortisols in guinea pigs, 20: 38547(R) (NYO-918-15)
effects on urinary excretion of sodium and potassium in rats, 17: 10463
effects on urinary excretion of phosphorus and desoxyribose in rats, 17: 27037
effects on urine quotients, 16: 4077
effects on uterine leakage of histamine, 18: 3587
effects on uterine sarcomas, therapeutic, 20: 14301
effects on uv emission from alkali halides, 18: 39278 (EUR-1643.e(p.265-74))
effects on uv-induced thrombopoietic serum, 18: 11744
effects on V center formation in alkali halides at 200°K, 20: 14604
effects on vacancy center formation in potassium bromides at low temperature, (E), 20: 13999
effects on vaginal epithelium, restorative effects of estrogen on, 19: 33959
effects on vagus nerve center, protective effects of histamine and serotonin against, 18: 37023
effects on vanadium pentoxide electrokinetics, 18: 10146
effects on vanadyl ions in ammonium zinc sulfate, 20: 12319
effects on various abdominal segments of queen honey bees, 18: 13456 (TID-20299)
effects on vascular permeability of chicks, 19: 29889(R) (ANL-6971 (p.90-116))
effects on vascular changes in rat intestines, role of catecholamines in, 17: 33688
effects on vegetative development and sexual maturity in Lactuca, Spinacia, Pisum, and Vicia, 18: 1378(T) (CEA-tr-X-490)
effects on verrucous carcinoma of oral cavity, anaplastic, 20: 18547
effects on vertebral malformations in mouse embryos, *in utero*, 19: 42279
effects on vertebrates, gynogenetic, 18: 23335
effects on vestibular analyzers in persons exposed occupationally, 19: 36042
effects on vestibular apparatus in dogs and rabbits, 20: 10610(T) (NASA-TT-F-353, pp 157-84)
effects on viability of skin grafts, 18: 25113
effects on viability of Drosophila populations, 18: 29295
effects on viability of Schistosoma cercariae, 19: 8937
effects on viability of *Fasciola hepatica* metacercariae, 19: 21962
effects on viability of skin autografts, 19: 28105
effects on viability of planaria sperm, 19: 35971
effects on viability of Ehrlich ascites tumor cells, use of dyes for assaying, 20: 36631
effects on viability of tumor cells circulating in blood, 17: 2876
effects on viability of cancer cells circulating in blood, 17: 17690
effects on viability, in Drosophila, 17: 28748
effects on Vicia chromosomes, aberrant, 19: 15128
effects on Vicia chromosomes, repair of aberrant, 19: 31788(R) (ORNL-3768(p.33-57))
effects on *Vicia faba* seeds, 16: 1595
effects on *Vicia faba*, protective effects of gaseous vs nongaseous narcotics against, 18: 35386(T) (JPRS-25703(p.1-10))
effects on *Vicia faba*, factors affecting protective effects of nitrogen

against, 18: 35387(T) (JPRS-25703(p.11-18))
effects on *Vicia faba* roots, protective effects of chemical against, 18: 43301
effects on *Vicia faba* root penetrability, 19: 118
effects on *Vicia faba* cells, 19: 24336
effects on *Vicia faba* chromosomes, sensitivity, 19: 31788(R) (ORNL-3768(p.33-57))
effects on *Vicia faba* seedlings, oxygen effects on, 19: 42326
effects on *Vicia faba* cells, biological, 20: 22793
effects on *Vicia faba* chromsomes, protective effects of actinomycin D against aberrant, 20: 40581(R) (ORNL-3922, pp 50-1)
effects on *Vicia faba* meiosis, 20: 42921
effects on *Vicia faba*, protective effects of alcohols and inert gases against, 20: 43007
effects on viral-transformed hamster cells, 20: 10684
effects on virulence Schistosoma cercariae in monkeys, 19: 15201
effects on virulence of tumor grafted in successive generations of mice, 19: 43762
effects on virulence of *Schistosoma japonicum* cercariae in mice, 20: 12545(R) (PAEC(A)AR651)
effects on virus infection in conventional and germfree mice, 20: 8677
effects on virus-infected cultured monkey kidney cells, 17: 23138
effects on virus leukemogenesis potentiation in mice, 18: 36988
effects on virus production in chicken sarcomas, mechanism of, 20: 35303
effects on virus reproduction in tissue cultures, 18: 27178
effects on virus reproduction in tissue cultures, 18: 27181
effects on virus reproduction in tissue cultures, 18: 27199
effects on virus-producing sarcoma cells in chick embryos, 18: 15838
effects on viruses of, lethal, 19: 29916
effects on viruses, 19: 45974
effects on viscosity of bacteriophage desoxyribonucleic acid, 19: 3908(T)
effects on viscosity of hyaluronic acid solutions, post-, 19: 9177
effects on vision in man, 18: 33341
effects on visual cells of mouse retina, 19: 36017
effects on visual discrimination in monkeys, effects of ageing on, 20: 3721
effects on visual cells of retina in tissue culture, 17: 78
effects on vitamin B_{12} in mice, 18: 19743
effects on vitamin B_{12} content of rat tissues, 18: 27189
effects on vitamin C content in papayas, 20: 18248(R) (UH-235P5-1, pp 52-4)
effects on volume expansion and color centers of sodium chlorides, 18: 16106
effects on volume expansion and coloration of LiF, 18: 16107
effects on volume resistivity of organic electrical insulators, 18: 42125
effects on water circulation in gastrointestinal tract in rats, 18: 25155
effects on water exchange between blood and gastric cavity during glucose absorption, 16: 1523
effects on water in presence of water-soluble free radicals, chemical, 19: 509
effects on weight of mouse organs, 18: 31199
effects on weight and desoxyribonucleic acid content of rat kidney, 19: 8796 (USNRDL-TR-783)
effects on weight gain of swine progeny, 20: 1677
effects on weight of rat embryos, 17: 24923
effects on wheal resorption time, mechanism for, 19: 33812
effects on wheat seeds, genetic, 19: 24261(R) (TID-21649)
effects on wheat seeds, genetic, 20: 5403
effects on wheat seed, genetic, 20: 16285
effects on wheat seeds, genetic, 20: 16286
effects on wheat seeds, mutagenic, 20: 20501
effects on wheat species of different ploidy, 17: 10381
effects on wheat, genetic, 20: 42846 (IAEA-2466-13)
effects on wild-type and mutant *Bacillus cereus*, 17: 40550(R) (TID-19486)
effects on wing scales of Ephestia moth, comparison of 5-bromodeoxyuridine with, 19: 24291
effects on work capacity and life span of dogs, 16: 25183(R) (UCD-105)
effects on work capacity and life span of dogs, delayed, 17: 31857(R) (UCD-107)
effects on wound healing, local exposure, 16: 16198
effects on wound healing in mice, effect of injections of homologous bone marrow and lymph node cells on, 18: 23273
effects on wound healing time in mice, 20: 12684
effects on wound healing after surgical resection for tumors, 20: 12646
effects on wound healing after radical neck dissection, 20: 14303
effects on X and Y chromosomes in Drosophila, 19: 15080
effects on X and Y chromosomes at four-strand stage in Drosophila spermatocytes, 17: 28737
effects on X chromosomes in Drosophila oocytes, effects of dose on, 19: 10837
effects on X chromosome translocations in Drosophila, 19: 31789(R) (ORNL-3768(p.58-63))
effects on X chromosome in Drosophila females, 20: 12689
effects on X chromosomes in female Drosophila, 20: 12690
effects on X chromosome of Chinese hamster cells, 20: 22790
effects on X chromosomes in heterozygous and homozygous Drosophila females, 20: 40625(R) (ORNL-3922, pp 59-64)
effects on *Xiphosure polyphemus*, effect of nucleic acid content, 19: 21900
effects on XXX No. 18 trisomy syndrome development in baby, etiologic, 19: 43811
effects on yeast cells along with starvation, 18: 8179
effects on yeast cells, protective effects of pyridoxine on, 18: 9916
effects on yeast cells, genetic, 19: 25912 (UCRL-8268)
effects on yeast cells, kinetics of recovery from sublethal, 19: 26002
effects on yeast cytochrome systems, 20: 38680
effects on yeast cells, protective effects of tetrahydrooxyquinone and neighboring compounds against, 17: 5919
effects on yeast cells, chemical modification of, 17: 30423
effects on yeast genetics, 18: 5054
effects on yeast genes, recovery from mutagenic, 20: 22654
effects on yeast reactivation, 18: 15819(T) (UCRL-Trans-1029)
effects on yeast reproduction, 20: 26698
effects on yeast sterols, 20: 45415
effects on yeast, effects of catalase activity on, 18: 38989
effects on yeast, biological, 19: 29904 (UCRL-16030)
effects on yeast, biological, 19: 29990
effects on yeast, biological, 20: 1663
effects on yeast, metabolic, 20: 16240
effects on yeast, genetic, 20: 18190(R) (UCRL-16613)
effects on yeast, genetic, 20: 26661(T) (ORNL-tr-1234)
effects on yeast, biological, 20: 45355(R) (COO-1249-4)
effects on yeast, genetic, 20: 45364 (UCRL-16851)
effects on yeasts, effects of plating time on recovery from, 18: 8183
effects on yeasts, protective effects of phosphorus-32 against, 17: 37072
effects on yeasts, dark recovery from, 19: 5698
effects on yeasts, effects of storage in dark on recovery from, 20: 8724 (UCRL-16545)
effects on yeasts, effects of dark recovery and glycerol on, 20: 16231 (UCRL-16377)
effects on Yoshida ascites sarcoma cells as affected by hypothermia, 18: 29500
effects on Yoshida ascites tumor cells in rats, recovery mechanism in, 20: 31070
effects on young mouse embryos, 19: 36007
effects on young mice, effects of anoxia on epilatory, 18: 33408
effects on young oocytes in mice, 17: 5835
effects on yttrium-doped calcium fluoride crystals, EPR of color centers from, 20: 40321
effects on *Zea mays*, RBE for cytogenetic, 19: 5696
effects on zeolites in presence of oxygen, ESR spectra of, 20: 375
effects on zinc content in urine, 20: 3693
effects on zinc content of pancreas, 20: 42917
effects on zinc in aqueous carbonic anhydrase, 20: 3693
effects on zinc-65 uptake of mouse testes, 17: 33725
effects on zinc-65 metabolism by mouse liver, 18: 19531
effects on zinc-65 uptake by mouse testes, 18: 33270(R) (NIRS-2(p.23-6))
effects on zinc-65 metabolism in rat erythrocytes, 18: 35265(R) (UCLA-12-529(p.23-40))
effects on Zollinger-Ellison syndrome, 20: 3821
effects on zone-refined potassium bromide and chloride, 19: 5895
effects on 17-ketosteroid urinary excretion, 17: 35586
effects on 17-ketosteroid content in dog blood, whole-body, 20: 38684
effects on 2-methyl-1,4-naphthoquinone, 20: 33082
effects on 2md chromosomes in Drosophila, mutagenic, 19: 45876
effects on 3,1,6,1-aryl-sulfate sulfohydrolase activity in guinea pig brain and liver, *in utero*, 19: 19573
effects on 4-aminobutyric acid content in brain of guinea pigs, 19: 45979
effects on 4-aminobutyric acid content of brain in dogs, 19: 45979
effects on 5-bromodeoxyuridine-labeled chromosomes, 20: 46 (PRNC-40)
effects on 5-hydroxytryptamine content of blood serum of dogs, 19: 8968
effects on 5-hydroxytryptamine in rat brain, 20: 8603
effects on 7-day chick embryo, relative biological, 16: 14551
effects on 9,10-dimethyl-1,2-benzanthracene tumorigenesis, 16: 17492
effects with actinomycin D on cell growth in tissue cultures, 16: 25232
effects with and without beta particles on mutation induction in summer barley, 19: 17582
effects with and without iodoacetic acid on phosphorus-32 and tritium uptake by rat thymus, 19: 17633
effects with and without chemotherapy on function and morphology of rat blood, bone marrow, and spleen, 19: 17644
effects with and without thermal trauma on intestinal mucosa in rats, 20: 12630 (BNL-8383)

effects with chemical mutagens, on tobacco seeds, 16: 25193 (CNEN-118)
effects with chemical carcinogens on morphology of rat tumor cells, 18: 35303(R) (AD-438541)
effects with chemical carcinogens on morphology of rat tumor cells, 18: 35303(R) (AD-438541)
effects with heat on tumors implanted on feet of mice, 17: 17821
effects with myleran on mouse thymus, leukemogenic, 16: 6272
effects with praseodymium in rats, 17: 23089(R) (NP-12760(p.155-65))
effects with streptomycin on mutation frequency in Chlorella, 20: 32993
effects with supranormal gravity on growth of wheat seedlings and chick-embryo muscle tissue, 18: 11801
effects with thymectomy on immunity and intoxication in parabiotic mice, 19: 28006
effects with trauma in production of shock in rabbits, 18: 3503(T) (JPRS-22001)
effects with 5-fluorouracil in treatment of malignant tumors, 18: 5200
effects, biological, 19: 33922
emission by bulk lithium metal, spectra, (T), 19: 18678 (BNL-7965)
emission by cadmium, Ly_α, 18: 34411
emission by californium-252 fission fragments, (E), 19: 21229 (BNL-8841)
emission by californium-252 fission fragments, (E), 20: 38095
emission by Crab Nebula, 18: 42294
emission by Crab Nebula, measurement of, 19: 36220(R) (MIT-2098-142)
emission by fission fragments from spontaneous fission of californium-252, (E), 19: 21265(R) (UCRL-11828(p.95-7))
emission by fission fragments from plutonium-239 and uranium-235, 20: 40158
emission by heavy elements, yields of L_{II} and L_{III} shells, 18: 5928
emission by highly ionized helium and hydrogen plasma, 17: 13642
emission by magnetically compressed plasma, 18: 28878
emission by moon and night sky, research program on, 19: 43017 (AD-501274)
emission by neutron stars, 18: 20711
emission by neutron stars, 18: 42257
emission by pinch plasma column, 18: 19137 (SIT-121)
emission by plasma, 17: 33153(R) (ORNL-3472(p.24-49))
emission by plasma, 17: 36810
emission by praseodymium, silver, and xenon, yields of, 18: 28253
emission by Scorpius, 18: 18534 (CONF-455-1)
emission by solar flares, 16: 894
emission by solar flares, 16: 895
emission by stars, spectra of, 18: 10741
emission by sun, 17: 37916
emission by sun, (T), 19: 14218(T)
emission by sun, correlation to radio wave production, 18: 4395
emission by sun during flare and non-flare sunspot maximum conditions, 18: 5910
emission by sun, mechanisms for, 18: 5908
emission by sun, spectral anomalies of, 18: 28218
emission by supernova shells, 18: 42258
emission by supernovae, effects of early radiation field and high-energy electrons on, 20: 21499
emission by thulium-169, isomeric shift in $K\alpha_{1,2}$, 17: 31429
emission during solar subflare activity, spectra of, 18: 28217
emission during solar flares, by inverse Compton effect, (E/T), 19: 4807
emission during solar flares, mechanisms for, 20: 23852
emission from (K^-) mesic atoms of helium-4, (E), 19: 35494
emission from (K^-) mesic atoms of helium, effects of $\bar{K}$-N interactions on, 20: 29938
emission from aluminum (liquid), spectra of soft L, 17: 27865
emission from auroral atmosphere, spatial asymmetry and time variation in microburst, (E), 19: 47470
emission from betatrons, system for extending, 18: 2506
emission from beta reactions with matter, 19: 47223
emission from cement, problems in use of pulse-height analyzer for analysis of, 19: 6200
emission from cobalt-iron alloys, spectra of soft M_{23}, 17: 29470
emission from compressed plasma, (E), 20: 28582
emission from copper-target tubes, ratio of $K\alpha$ to white, 18: 2544
emission from cosmic sources, observation and theory of, 20: 17248
emission from Crab Nebula, lunar occultation of, (E), 19: 4819
emission from decay of iodine-125, 19: 22021
emission from deuterium Z-pinched plasma, spectroscopy of, (E), 19: 5277(T) (AEC-tr-6518(p.20-7))
emission from elastic discharge in T.A. 2000 device betatron effect for, 20: 24521
emission from electron-irradiated nuclei at 80 to 180Å, 16: 8129
emission from electron microscopes, hazards of, 18: 13578
emission from electron reactions with compounds, intensity corrections for, 20: 14431 (ANL-7078)
emission from explosive solar flares, 18: 44395
emission from fission products, (E), 20: 4849(R) (UCRL-14360, pp 1-50)
emission from fission fragments, design and performance of nanosecond scintillation detectors for determining half life from, 20: 41325
emission from flares behind solar disk, (T), 19: 44894(T) (AD-424481)
emission from galactic sources, free-free emission model for discrete, 20: 29881
emission from gas discharges, energy and time distribution of, 16: 27855
emission from heavy elements, K series E1 transition intensities from, (T), 20: 9663(T)
emission from hollow exploding aluminum wire, mechanisms of, 18: 16566
emission from hot fully ionized hydrogen plasma, (T), 20: 29881
emission from Japanese television equipment, 20: 13014
emission from laser spark of soft, determination of electron temperatures by, (E), 20: 42475
emission from liquid and solid aluminum, (E), 19: 23964
emission from lunar surface following electron bombardment, 20: 17246
emission from mesic atoms (μ) $12 \leq Z \leq 50$, nuclear radii from, 17: 26578
emission from mesic (μ) atoms, energies for (2p-1s), 18: 34435
emission from mesic atoms, energy spectra of, (E), 20: 21534
emission from meson (μ) cascades in metals, 16: 15692
emission from mu-mesic atoms, computer analysis of, 20: 11440(R) (COO-614-34, Sect. IID)
emission from μ-mesic atoms, isotope effects on spectra of, (T), 20: 27736
emission from neutron stars, 18: 18547
emission from neutron stars with magnetosphere, (T), 19: 18664
emission from neutron stars, (T), 20: 17240
emission from planetary auroral zones, magnetic moment from, (T), 19: 12409(T)
emission from plasma, mechanisms of (T), 19: 1703 (MATT-239)
emission from plasma, diagnostics from, 19: 19251 (NP-14689)
emission from proton-emitting solar flares, (E/T), 19: 25135(T)
emission from proton reactions with beryllium at 1.6 Mev from electron acceleration and bremsstrahlung, (E/T), 20: 11501
emission from radars, 20: 9188
emission from solar flares, relation to radio bursts, 17: 41695
emission from solar flares, correlation to type III radiobursts, 18: 7397
emission from solar flares, theory of inverse Compton effect as cause of, 18: 22661
emission from solar flares, 18: 44388
emission from solar flares, 18: 44389
emission from solar flares, 18: 44390
emission from solar flares, theory of, 18: 44405
emission from solar flares, 18: 44407
emission from solar flares, (T), 19: 20890
emission from solar flares, 19: 32856
emission from solar corona, soft, 19: 41209(T) (N64-22932)
emission from solar flares, models for, 19: 44931
emission from solar flares, correlation with radio and visible emission, 20: 2582
emission from solar flares, correlation with microwave bursts, 20: 44101
emission from solid electron targets, angular intensity distributions at surface, 18: 16685
emission from spark-triggered discharge, (E), 19: 39305
emission from stars, optical focusing systems for, 19: 14224
emission from sun, variability of spectra of, 18: 28216
emission from sun, during quiet period, 19: 18663
emission from sun, production and spectra of, 19: 41213
emission from sun, review on, 20: 9647
emission from sun, processes involved in, (E), 20: 34073
emission from supernova remnants, mechanism for, (T), 19: 4801
emission from thin aluminum films, determination of surface density from proton-induced, 20: 17051
emission from TM-2 device, 18: 6305 (NP-13335)
emission from tungsten at 300 to 1100°K, interference maxima of, 18: 16687
emission from tungsten exploding wires, 20: 25636
emission from 4.0- to 6.3-Bev electrons, (E), 20: 39473
emission in bremsstrahlung excitation of $14 \leq Z \leq 50$ elements, detection efficiency for, (E), 20: 15258
emission in a toroidal pinched discharge, mechanisms, 16: 15730
emission in auroral zones, west-east motion, 16: 7978
emission in auroral zone, correlation with ionospheric radio-wave absorption and geomagnetic disturbances, 18: 949
emission in auroral zone, correlation with geomagnetic bays and micropulsations, 18: 951
emission in auroral storms, (E), 19: 27343
emission in double electron transitions in sodium, 18: 18579
emission in electron reactions with glasses, proportional counter for detecting small-angle, 17: 37438
emission in electron reactions with gold at 1 to 2 Mev, 18: 14719 (LFEN-7)
emission in electron reactions with copper at 20 to 50 kev, intensity of

Kα, 18: 26205
emission in electron capture, measurement of, 19: 20384
emission in electric multipole transitions, effects of nuclear finite size on, (T), 19: 23798
emission in electron reactions with single crystals of copper, orientation effects on, (E), 20: 1331
emission in fission-product collisions with atoms, 18: 10764 (ANL-6797(p.464-8))
emission in flash x-ray discharges, (E), 20: 15573
emission in mesic atom (K^-) decay, 17: 26522
emission in meson (μ) interactions, 17: 41531(R) (ANL-6720(p.48-58))
emission in meson (μ^-) transitions in carbon, 18: 34947
emission in meson (μ^-) transitions in calcium isotopes, spectra of, 18: 42732
emission in polonium-210 alpha decay, 17: 11616 (BNL-6166)
emission in powerful pulse discharges, (T), 19: 5311
emission in proton impact on aluminum, 18: 20734(T) (UCRL-Trans-1050(L)
emission in proton reactions with atoms at 25 to 100 kev, characteristic, 18: 28259
emission in solar flare, 17: 5091
emission in solar flares, 17: 13291(T)
emission in solar flares, radio astronomy study of, 18: 32337(T) (AD-428086)
emission in solar flares, 18: 44387
emission in solar flares, (T), 19: 47197
emission in solar flares, relation to radio bursts, 16: 5848
emission in the auroral zone by electrons, energy spectrum variations of, 17: 37898
emission in theta pinch, (E), 19: 19234 (IPP-1/20)
emission in tin-119 internal conversion, coefficients for, 18: 26642
emission line widths, K, 17: 18925
emission mechanisms in galactic centers, external galaxies, and intergalactic media, 18: 7373
emission of burst of, during solar flares, (T), 20: 27704
emission of cosmic, from electron belts of magnetic neutron stars, (T), 19: 42980
emission of galactic, due to suprathermal particles, 18: 28226
emission of high-energy, from Crab nebula, (E), 20: 34044
emission of K, analysis of compound nucleus lifetimes in alpha reactions (α,p) by, 17: 38220
emission of K, from proton reactions with aluminum, copper, and magnesium at 60 to 500 kev, 18: 7775
emission of K, during uranium-235 thermal fission, (E), 19: 45294
emission of K, from electron reactions with thick targets, (T), 19: 16371
emission of K, from continuous fission of uranium-235, (E/T), 20: 24351(R) (MIT-905-52, pp 1-41)
emission of K, in californium-252 fission, (E), 19: 29259 (PPAD-2137-536)
emission of K, in meson (μ^-) capture by chromium and vanadium metals and oxides, (E), 19: 28991 (JINR-P-2039)
emission of K, in fission, (E/T), 20: 20365
emission of Kα, theory of absolute intensity of, 17: 25973
emission of monoenergetic, from alpha-emitting isotopes, (E/T), 20: 4268 (ORNL-IIC-5, pp 353-73)
emission of strong, during solar flare, 19: 28979
emission of thermal, by quiet sun, (T), 20: 27703
emission of, under electron, proton, and x-ray excitation, 18: 36093
emission of, use for film thickness measurements, 20: 493
emission of, 2θ values for first-order, 18: 14718 (JEN-128-DQ/I-38)
emission spectra from sun, isothermal quiet-corona model for line intensities in soft, 20: 19338
energy and intensity of solar, (E), 19: 32857
energy from, determination of total, 19: 38878 (ORNL-P-1405)
energy of, from 2p-1s meson(μ) transitions, 17: 15147
energy spectra and flux of primary cosmic, at 20 to 50 kev, (E), 20: 37580
energy spectra from Scorpius (SCO-XR-1) and sun, (E), 20: 2585
energy spectra in auroral zone atmosphere, (E), 19: 47471
energy spectra of solar, (E), 19: 39333
energy spectra of galactic, interpretation of, 20: 37488
energy spectra of isotropic galactic, (E), 20: 37500
energy spectrum at 20 to 150 kev of auroral, diurnal variations of, (E), 20: 34366
evaluation of 70-Mev, for treatment of tumors, 18: 6621(R) (UCSF-23)
excitation in coatings for thickness measurements, 18: 24046 (PAN-485/1-A)
excitation in light elements by radioisotopes, 17: 30114
excitation of nitrogen by, spectra of first negative and second positive band, (E), 20: 6181 (AD-619288)
excitation of photoelectron emission by soft, effective depth of, 18: 5875(T)
exposure control in cineradiography, device for, 18: 19829
exposure dose measurements in air, magnetic induction field for, 19: 40838
exposure frequency during pregnancy, survey of, 20: 18506
exposure of dentist to, effects of, 17: 10872
exposure of gonads during 31-Mev therapy, 20: 38746 (NYO-3364-19)
exposure to compact bone and lucite slabs, electron energy distributions in, 19: 15057
exposure to high-energy, maximum permissible, 18: 31829
exposure to, activation of infections by whole-body, 16: 14572
exposure to, during diagnostic and dental radiography, survey of, 18: 16248
exposure to, measurement units for, 20: 18951
exposure to, survey of U. S., 18: 27738
field boundary and scatter at 200 kv, 16: 24026
filters for, properties of, 16: 20086
filtration of, for production of monoenergetic, 16: 29100 (HASL-129)
fluorescence excitation in transition elements, 17: 11368
fluorescence in microprobe analysis, tables of corrections for, 19: 295 (NLCO-917)
fluoroscopic, television equipment for monitoring, 20: 40781
flux and spectra in auroral zone (E), 19: 3042
flux at balloon altitudes in South American anomaly, 18: 18823
flux at balloon altitudes, omnidirectional, (E), 19: 35260
flux in atmosphere at 40 to 190 kev, albedo, (E), 20: 4752
flux in auroral-zone atmosphere, 18: 5953
flux measurements in ionosphere, description and performance of monitor for, 16: 14959
flux measurements in northern and southern auroral zones, electron precipitation in, 17: 24240
flux of auroral-zone, periodicity in, (E), 20: 4751
flux of solar, (E), 19: 41231
flux of solar, from 2 to 18 Å, (E), 19: 30927
flux of solar, variations in, 18: 28219
focus localization during moving field radiotherapy, 18: 3665
focusing of, production of short-focal-length lenses for, 20: 7347
free radical induction in alkyl ester-urea inclusion compounds by, ESR spectra and molecular motion of, 18: 33641
free radical induction in polyethylene by, ESR studies of, 20: 7179
free radicals induced in lettuce seeds by, formation and decay, 16: 1574
free radicals induced by, in liver and spleen lipids in rats, 17: 31927
free radicals induced by, in bone grafts, electron spin resonance studies of, 18: 29347
genetic effects on *Drosophila melanogaster*, unequal crossing-over in Bar region, 16: 17471
genetic effectiveness of, compared with protons, 17: 30365
genetic effects, aberrations induced in tomato chromosomes by, 16: 4018
genetic effects, chromosome aberrations in root tips, 16: 14514
genetic effects, chromosomal aberrations induced in mammalian cells in tissue culture, 16: 32729 (TID-16735)
genetic effects, chromosome aberrations induced by, in leukocytes in culture, 17: 7826
genetic effects, chromosome aberrations induced in Chinese hamster by, 17: 35548
genetic effects, effects of dose rate, 16: 58
genetic effects, effects of AET, 16: 4094
genetic effects, effect of dose rate, in mice, 17: 28700 (USNRDL-TR-644)
genetic effects, effects of meiotic stage and species, 17: 19874
genetic effects in *Escherichia coli*, 16: 2894
genetic effects in mice, 16: 5207
genetic effects in Drosophila spermatogonia and spermatozoa, 16: 1527
genetic effects in *Escherichia coli*, chromosome breakage, 16: 7446
genetic effects in paramecium, 16: 7451
genetic effects in Mexican toad, 16: 7466
genetic effects in chrysanthemum plants, 16: 9851(T) (NP-tr-848)
genetic effects in barley seeds, 16: 14491
genetic effects in Drosophila, 16: 16202
genetic effects in plants, 16: 18786
genetic effects in Drosophila, 16: 20175
genetic effects in Drosophila, 16: 20176
genetic effects in wheat seeds, 16: 23454
genetic effects in Drosophila, 16: 28680
genetic effects in Drosophila, 16: 28746(R) (TID-16428)
genetic effects in leeches, 16: 28764
genetic effects in Drosophila, 16: 28789
genetic effects in maize, 16: 28828
genetic effects in Habrobracon, 16: 30237
genetic effects in *Escherichia coli*, 16: 30274
genetic effects in seeds, acute exposure of successive generations, 16: 31516
genetic effects in male swine, whole-body exposure, 16: 31490
genetic effects in Neurospora, 16: 31491
genetic effects in Drosophila, 16: 7455

genetic effects in algae, 17: 33719
genetic effects in *Chondrococcus columnaris*, 17: 5769 (HW-SA-2540)
genetic effects in Drosophila, 17: 74
genetic effects in Drosophila, 17: 10415
genetic effects in Drosophila, 17: 19838
genetic effects in *Drosophila melanogaster*, protective effects of cysteine against, 17: 35526
genetic effects in Drosophila, 17: 24983
genetic effects in Drosophila, 17: 27099
genetic effects in Drosophila, effect of maternal nutrition, 17: 27102
genetic effects in Drosophila, 17: 28599(R) (TID-18979)
genetic effects in fungi, effects of chemical treatments, 17: 1191
genetic effects in Habrobracon oocytes, 17: 21513
genetic effects in maize seedlings after seed exposure to, 17: 38694
genetic effects, in maize, 17: 28711
genetic effects in mice, fractionated dose, 17: 1314
genetic effects in mice, 17: 15629 (LADC-5278)
genetic effects in mice, 17: 15637(R) (TID-18135)
genetic effects in mice, long-term exposure, 17: 27101
genetic effects in moths, 17: 7858
genetic effects in paramecium, effects of dose fractionation, 17: 21515
genetic effects in *Paspalum dilatatum*, 17: 7831
genetic effects in *Paspalum dilatatum*, 17: 7832
genetic effects in plants, effects of far-red pretreatment, 17: 13982(R) (TID-17890)
genetic effects in rats, 17: 35569
genetic effects in root meristems, acute exposure, 17: 23146
genetic effects in seeds of wheat, maize, and tobacco, 17: 24894(R) (TID-18673)
genetic effects in spinach seed, 17: 15682
genetic effects in the moth Ephestia, 17: 31856(R) (TID-19166)
genetic effects in wheat seeds, 17: 28714
genetic effects in wheat seeds, 17: 28715
genetic effects in yeast, 17: 5809
genetic effects in plants, 18: 64
genetic effects in mealy bug, 18: 67
genetic effects in mealy bug, 18: 68
genetic effects in Mormoniella, 18: 73
genetic effects in maize, 18: 1374 (BNL-7367)
genetic effects in Tradescantia, 18: 1376(R) (TID-19516)
genetic effects in Delphinium, 18: 1391
genetic effects in yeast, 18: 1438
genetic effects in hybrid corn, 18: 1440
genetic effects in plants, 18: 3496(R) (TID-19724)
genetic effects in wheat, 18: 5027
genetic effects in Drosophila, 18: 5046
genetic effects in Drosophila, 18: 5047
genetic effects in mosquitoes, 18: 5067
genetic effects in Drosophila, silkworms, Salmonella, wheat, and rice, 18: 8046(R) (NP-13507)
genetic effects in plants, 18: 8107(R) (NYO-10620)
genetic effects in barley, 18: 8112(R) (TID-19964)
genetic effects in maize, wheat, and tomatoes, 18: 11649 (TID-20031)
genetic effects in agricultural plants, 18: 13452(R) (TID-20220)
genetic effects in mice, long-term, 18: 15812(R) (LAMS-3034(p.303-6))
genetic effects in hamster lung cells in tissue culture, 18: 17468(R) (ANL-6790(p.156-60))
genetic effects in hamster cells in tissue culture, 18: 17469(R) (ANL-6790(p.161-70))
genetic effects in yeast, 18: 17479 (UCRL-11191)
genetic effects in rodents, 18: 17622
genetic effects in male Drosophila, 18: 25108
genetic effects in peanuts, 18: 25132
genetic effects in plants, 18: 25133
genetic effects in onion seeds, 18: 25179
genetic effects in oats, 18: 25184
genetic effects in Drosophila, 18: 27135
genetic effects in Drosophila, 18: 27136
genetic effects in *Tribolium castaneum*, 18: 27061 (COO-965-21)
genetic effects in Vicia, 18: 27066(R) (ORNL-3601(p.105-9))
genetic effects in barley, 18: 27003(R) (ORNL-3601(p.27-46))
genetic effects in mice, 18: 27007(R) (ORNL-3601(p.83-91))
genetic effects in Drosophila, 18: 29242(R) (TID-20728)
genetic effects in Drosophila, 18: 29295
genetic effects in Drosophila, 18: 29296
genetic effects in Drosophila, 18: 29297
genetic effects in Neurospora, 18: 29292
genetic effects in yeast, 18: 29294
genetic effects in agricultural crop plants, 18: 33213 (STI/DOC/10/28 (p.79-103))
genetic effects in bacteriophage, 18: 33278 (STI/DOC/10/28(p.39-66))
genetic effects in mouse populations, 18: 33281(R) (TID-20844)
genetic effects induced in R_2 generation of *Nicotiana tabacum* by, 17: 38693
genetic effects, mutability of polygenes, 16: 4032(R) (TID-13959)
genetic effects, mutation induction in cabbage seeds, 17: 35527
genetic effects, mutations in Drosophila, 16: 21945
genetic effects, mutations induced in maize seeds by, frequency of, 17: 38690
genetic effects, mutations of Arabidopsis, 16: 21943
genetic effects, mutations of Collinsia induced by, 16: 21944
genetic effects of exposure for 20 consecutive generations, in mice, 17: 31853 (LADC-5618)
genetic effects of, followed by heat, 17: 38876
genetic effects of, in barley, synergistic effects of ethylmethanesulfonate on, 17: 5861
genetic effects of, in Drosophila, 17: 38788
genetic effects of, on nuclear structures of cells in microörganisms, 17: 19916
genetic effects of 10 generations exposure in mice, 17: 19840
genetic effects of low-level exposure in Drosophila, 16: 11427 (A/AC.82/G/L.734)
genetic effects of low levels of, in Tradescantia, 18: 11758
genetic effects of fractionated doses on embryonic development of mice, 18: 19719
genetic effects of, in castorbean seeds, 18: 25180
genetic effects of, in barley seeds, 18: 25182
genetic effects of diagnostic use of, in females, 18: 27073
genetic effects of, in Drosophila, 18: 27004(R) (ORNL-3601(p.47-59))
genetic effects of, in seedlings of *Haplopappus gracilis*, 18: 29246 (TID-20784)
genetic effects of hydration and, on tomato seed and pollen, 18: 35377
genetic effects of, in mouse populations, 18: 43220(R) (LA-3132-MS (p.109-41))
genetic effects on adult male mosquitoes, 17: 10385
genetic effects on Arabidopsis, 17: 35590
genetic effects on cells, 17: 40553
genetic effects on chromosomes in polymorphic *Drosophila pseudoobscura*, 17: 7887
genetic effects on corn, 17: 27091
genetic effects on crossingover process in Drosophila, 17: 38877
genetic effects on disjunction of chromosomes, 17: 38878
genetic effects on *Drosophila melanogaster*, 17: 24808
genetic effects on *Drosophila melanogaster*, 17: 27064(R) (TID-18855)
genetic effects on *Drosophila melanogaster* wing spread, effects of oxygen on, 17: 30307
genetic effects on *E. coli* mutant, effects of native wild DNA on reversions in, 17: 24917
genetic effects on maize under different physiological conditions, 17: 10380
genetic effects on mice, 17: 53
genetic effects on *Nicotiana tabacum*, polygenic mutability, 17: 10387
genetic effects on plants, use of probability theory in calculating, 17: 23205
genetic effects on prolan stimulation of ovaries, 17: 5817
genetic effects on seeds of Delphinium, 17: 19763
genetic effects on seed, environmental factors in, 17: 31869
genetic effects on sex-linked recessive lethals in Drosophila, 17: 10392
genetic effects on spring wheat, comparison with gamma rays and thermal neutrons, 17: 12155
genetic effects on testes of rats, 17: 38780
genetic effects on tomato seeds and pollen, 17: 17765(R) (TID-18414)
genetic effects on tree seeds, 17: 33661
genetic effects on *Vicia sativa* L, 17: 10395
genetic effects on barley seedlings, 16: 1572
genetic effects on mammals, 16: 1486(T) (JPRS-10170(p.279-312))
genetic effects on *Vicia faba* roots, mechanism, 16: 1623
genetic effects on mature sperm and primordial cells, relative resistance, 16: 8618
genetic effects on sweet potatoes, 16: 9873
genetic effects on mutation of *Drosophila melanogaster*, 16: 12883(R) (TID-15001)
genetic effects on sterility mutations in chromosomes of *Drosophila melanogaster*, 16: 12847(T) (AEC-tr-5051)
genetic effects on box elder, 16: 14522
genetic effects on chromosomes and genes in tissue cultures of normal human cells, 16: 14468(R) (TID-15410)
genetic effects on seeds, 16: 17526
genetic effects on jute plants, 16: 17480
genetic effects on somatic mutations in meal moth, at low doses, 16: 20281
genetic effects on rice, 16: 20179
genetic effects on spermatogonia and spermatozoa of *Drosophila melanogaster*, 16: 20197
genetic effects on fertility, deformities, postnatal and infant mortality, and sex ratio in mice, 16: 20220

genetic effects on populations by dermatological therapy using, 16: 20223
genetic effects on *Sciara coprophilia*, sex-linked recessive lethal mutations, 16: 20138
genetic effects on nuclear differentiation in *Tetrahymena pyriformis*, 16: 21938
genetic effects on chromosomes in root meristems, 16: 25217
genetic effects on *E. coli*, analysis of mutations, 16: 28788
genetic effects on *Marchantia polymorpha* liverwort, nutritionally deficient mutations in, 16: 31497
genetic effects on rice, 16: 32761
genetic effects on rabbits, relation of nucleic exchange to sex of progeny, 16: 32849
genetic effects on guinea pigs, 16: 32867
genetic effects on chromosome rings of Tradescantia, 16: 9880
genetic effects on fungi, 18: 71
genetic effects on populations of *Drosophila pseudoobscura*, 18: 72
genetic effects on wheat, 18: 1390
genetic effects on hair cells of *Tradescantia occidentalis* by 250-kvp, RBE of, 18: 1409
genetic effects on maize, 18: 3499 (TID-19787)
genetic effects on colony formation ability of *E. coli*, search for smallest biologically effective dose in, 18: 6627
genetic effects on growth rates in populations of *Drosophila pseudoobscura*, 18: 6633
genetic effects on multiple carpel mutation in bread wheat, 18: 6634
genetic effects on male Drosophila, 18: 8155
genetic effects on *Oenothera berteriana*, 18: 11676
genetic effects on Drosophila, effects of sperm storage techniques on, 18: 13490
genetic effects on Drosophila, X-Y nondisjunction and exchange, 18: 13492
genetic effects on chloroplasts in *Chara vulgaris* algae, 18: 23287
genetic effects on chromosomes of reproductive cells in mice, protective effects of streptomycin against, 18: 23359(T) (JPRS-24593(p.120-5))
genetic effects on xanthine dehydrogenase in Drosophila, 18: 25208
genetic effects on male rats, 18: 25215(T) (AEC-tr-6227/1(p.25-44))
genetic effects on recessive lethal mutations in saccharomyces, 18: 27095
genetic effects on *Drosophila melanogaster*, 18: 27097
genetic effects on *Escherichia coli*, 18: 27098
genetic effects on first-generation Wistar rats after whole-body irradiation at 9th day of pregnancy, 18: 27167
genetic effects on mice, protective effects of AET and cysteine against, 18: 27217
genetic effects on *Drosophila melanogaster* in presence of ultraviolet radiation, 18: 29272
genetic effects on maize and wheat, 18: 33279(R) (TID-20823)
genetic effects on Drosophila sperm, 18: 35344
genetic effects on maize pollen, 18: 36967
genetic effects on cotton, 18: 41116
genetic effects on cosmos plants, 18: 41117
genetic effects on *Crotalaria intermedia*, 18: 36994
genetic effects on rice, 18: 36995
genetic effects on mice, 18: 41094(R) (TID-21156)
genetic effects on plants, 18: 38774(R) (EUR-1881.e)
genetic effects on wheat seeds, 18: 41115
genetic effects on human somatic cells, 18: 43227 (ORNL-P-419)
genetic effects on gonads of man, 18: 43271
genetic effects on male mice following whole body and gonad exposure, 18: 43295
genetic effects on chlorophyll mutation in *Pisum sativum*, 19: 3948
genetic effects on seeds, 19: 3982
genetic effects on wheat and maize, 18: 38777(R) (TID-21068)
genetic effects to chromosome system of pre-spermatocytic cells, 16: 11461(R) (TID-15047)
genetic hazards from diagnostic use, 17: 23210
gonadal doses from diagnosis, 18: 29525
gonadal doses from dental examinations, method for reduction of, 18: 31333
gonadal doses from diagnostic, 18: 33419
hazards combined with electromagnetic waves to personnel in electron tube fabrication, 19: 8982
hazards evaluation of, during industrial radiography, 20: 45994
hazards from, 17: 39329
hazards from dental, 20: 20519
hazards from diagnostic, 18: 31809
hazards from, at radar stations, 20: 27221
hazards, nature, and production of, review on, 17: 16335
hazards of diagnostic, 18: 5154
hazards of medical, 18: 8232
hazards of, from radiodiagnosis, 18: 14152
hazards of, in small-animal clinics, 19: 8981
hazards to children, 18: 20263
hematological effects in rabbits, modification by formaldehyde and 8-quinolinol, 17: 33662
hemorrhage induction in dogs, effects of soybean phosphatides on, 16: 14593
herpes zoster induction by, 18: 17685
hyaluronic acid depolymerization by, 20: 40591
images of sun, soft, 19: 27054
immune response to, in man and animals, 19: 8800(T) (NP-tr-1204)
inactivation effects on neurospore conidia, 16: 4105
inactivation induced in purified 3-hydroxyanthranilic acid oxidase by, 17: 35514
inactivation of aldolase induced by, 17: 31961
inactivation of bacteria and bacteriophage by, effects of oxygen on, 16: 6343
inactivation of bacteriophage by, 17: 35549
inactivation of bacteriophage by, 18: 45191(R) (TID-21152)
inactivation of crystal liver alcohol dehydrogenase, 16: 6327
inactivation of papain by, 17: 24965
inactivation of papain and CoA in solutions by, protective effects of cysteamine against, 18: 6680
inactivation of Rous virus by, isotypic interference after, 17: 14025
induced by Sept. 28, 1961 solar flare, high altitude distribution, 16: 21238 (NP-11658)
induction in metals, use of, for measuring metallic corrosion, 20: 19196
induction of anti-infection mechanisms in mice, protective effects of cysteine against, 16: 25258
induction of antibiotic-resistant mutations in rhizobium by exposure, 16: 7427
induction of atherosclerosis by whole-body exposure, 17: 7866
induction of atomic hydrogen in human teeth by, electron magnetic resonance spectra of, 18: 3648
induction of breast tumors in rats by, 17: 5839
induction of burns on rabbits by, effects of auto- and homografts on, 17: 17865
induction of cauliflower-head and single-leaf mutation in alfalfa by, morphology of, 17: 21499
induction of chromosomal aberrations in rice plants, 17: 37089
induction of chromosome aberration in leukocytes cultured from human blood, rates and types, 16: 14571
induction of chromosomal aberrations in human skin cultures by, 18: 19563
induction of congenital deformities in mice by, effects of anoxia and fasting on, 18: 8117(R) (TID-20029)
induction of diploid gynogenesis in fish by, 17: 37100
induction of double kernels in rice seed by, 17: 35579
induction of electroretinogram in frogs, 17: 35581
induction of erythroblastic malignancy by, in dogs, 17: 30319
induction of giant cells of HeLa strain, protective effects of cysteamine against, 17: 35541
induction of goldfish melanophores, responses of, 19: 189
induction of hypothyroidism in dogs and resulting effects on metabolism, 20: 40698
induction of intramedullary tumor metastases, diagnosis of, 18: 38830
induction of jute aberrant growth by, 18: 19725
induction of killing effect in jute by, 17: 35580
induction of latent lesions in Topinambour rhizomes by, 17: 14026
induction of leukemia following whole-body, in mice, 16: 25199
induction of leukopenia, effects of orotic acid on, 16: 4086
induction of leukopenia by, 19: 10902
induction of lung carcinoma in rats by total-body, 20: 40614 (NYO-901-39)
induction of lymphatic leukemia in mice, 20: 42893
induction of mutagenic substance in plants by, 16: 6318(T) (JPRS-11322(p.463-7))
induction of rabbit cataracts by, 18: 25195
induction of radiodermatitis by low-level exposure to, 18: 27151
induction of skin lesions in rabbits by, 17: 35477
induction of skin ulcers by, treatment of, 19: 195
induction of sterilization in female and male chick embryos, 17: 10375
induction of uterine cancer by, 18: 147
inhibitory effects on thymidine incorporation into DNA by mammalian cells *in vitro*, 20: 42777
injuries from, compared with gamma and neutron, 18: 41233
injuries in mice from fractionated or split dose of, kinetics of, 18: 8215
intensity distributions from large-surface anode, volumetric, 16: 19084
intensity distribution in presence of structure pseudosymmetry, statistical, 19: 40067
intensity during auroral storms, (E), 20: 11855
intensity from sun, satellite measurements, 17: 15065(T)
intensity in auroral zone event, 17: 8994
intensity in auroral zone, (E), 20: 28118

intensity in auroral zones, balloon observations of, 20: 39990
intensity in ionosphere, sunspot activity correlations with, 20: 19647
intensity measurements of, by non-dispersive spectrometry, 17: 38948
intensity measurements of high-energy, absolute, 16: 1967
intensity measurement of, instrumentation for calorimetric, 20: 16856
intensity of bursts in auroral zone, 17: 12897
intensity of, from meson (π) magnetic deceleration, 17: 37925
intensity of, accuracy in measurement of, 20: 18017
intensity pulsations of auroral-zone, spatial and time, (E), 20: 11826
intensity variations of solar, 20: 29874(T) (NASA-TT-F-389, pp 714-31)
interaction with matter, summary, 17: 30240
interactions in detectors, 17: 4820
interactions of, in the D-layer, 16: 32250 (RAD-SR-62-19)
intensity of auroral, correlations with cosmic neutrons, (E), 19: 25196
intensity of auroral, correlation with auroral luminosity, (E), 19: 39672
intensity of solar, (E), 19: 23246
intensity of solar, (T), 19: 47210
intensity variations in geomagnetically conjugate auroral zones, (E), 19: 33131
intensity variations in geomagnetically conjugate auroral zones, (E), 19: 33132
interactions with electrons in crystals, recoil resonance in, 18: 35242 (CALT-221-2)
interactions with deuterons at 230 Mev, meson (π^-) and (π^+) production in, (E), 19: 43039 (COO-1195-34)
interference structure in specularly reflected, thin film thickness from, 18: 704
ion pair formation at 100 to 300 kv, mean energy, 16: 246
ionization of gases by, electron conductivity in, 17: 5072
ionization of gases by high-energy, spectra of, 18: 41506(R) (ML-TDR-64-169)
ionization of krypton by, K- and L-shell, 18: 20730 (CONF-481-7)
isolation of components of $K\alpha$, reflection-type quartz monochromator for, 18: 8627
isotope shift in uranium $K\alpha$, 19: 9767(R) (IS-900(Sect.P))
isotope shift of K_{α}, in uranium, 20: 17285
lethal dosage determinations for Ehrlich ascites tumor cells, 16: 12906
lethal dosage determinations for fish, 16: 18792
lethal dosage determinations of, for germfree and conventional mice, 18: 1426
lethal dosage determinations of, for mice, 18: 25165
lethal dosage measurements for two species of flour beetle, *Tribolium confusum* and *Tribolium castaneum*, 16: 25146(R) (HW-72500(p.156-8))
lethal dosage measurements for dogs, 16: 32736 (UR-615)
lethal dosage measurements for hamsters, 16: 32794
lethal dosage measurements of, for pocket mouse, 18: 35362
lethal dosage measurements for rats, effects of age on, 18: 43285
lethal dosages of, for swine, 19: 7044
lethal dose determinations of, for green and colorless *Euglena gracilis*, 18: 41187
lethal dose measurements of, for chick embryos, 18: 29341
lethal dose measurements of, in mice, computer calculations of, 20: 6909(R) (ORNL-3853, pp 116-17)
lethal doses of for Lumbricus, 17: 35532
lethal doses of, mammalian syndrome from, acute, 18: 29319
lethal effect on first generation hybrid mice, 16: 26785
lethal effects, effects of previously administered radioisotopes, 16: 23443
lethal effects, effects of previously administered radioisotopes on, 16: 30223(T) (FTD-TT-62-501(p.9-16))
lethal effects in chemically protected monkeys, 16: 1624 (AF-SAM-61-102)
lethal effects in yeasts, protective effects of sulfhydryl compounds, 16: 1635
lethal effects in mice, protective effects of iodothyronines, 16: 14493
lethal effects in Chlamydomonas, 16: 21980
lethal effects in mice, effects of dose rate, 17: 80
lethal effects in mice receiving homologous bone marrow, 17: 25050
lethal effects in rats, effects of population density and sex on, 17: 38888 (UR-631)
lethal effects in young chickens, protective effects of AET against, 17: 40676
lethal effects in mammalian species, 18: 8101 (BNL-7603)
lethal effects in mice, 18: 11847(R) (NP-13555(p.118-30))
lethal effects in mice of protracted, split, and fractionated exposure, model for, 18: 17463(R) (ANL-6790(p.21-5))
lethal effects in rats, effects of partial and whole-body exposure on, 18: 27069 (RTD-TDR-63-3011)
lethal effects, modification by ultraviolet radiation, 16: 9866
lethal effects of, effects of spleen on whole-body, 17: 90
lethal effects of massive doses, on muscle cells in culture, 17: 17825
lethal effects of, on guinea pig, radioprotective effect of *meso*-2,3-dimercaptosuccinic acid against, 17: 17839
lethal effects of, protective effects of serotonin on, 17: 27154
lethal effects of whole-body exposure to, protective effects of ethyl stearate in mice, 17: 27156
lethal effects of, effects of botulinum toxin in mice on, 17: 31901
lethal effects of, in mice, protection effects of β-mercaptoethylamine or *p*-aminopropiophenone against, 17: 33490(R) (NP-13010(p.107-26))
lethal effects of, in mice, effect of dose rate on, 17: 38886 (UCRL-11014)
lethal effects of soft and medium energy, on *Chlorella pyrenoidosa* Chick, 18: 1393
lethal effects of whole-body, on rats aged 8 or 17 days, 18: 3524
lethal effects of high-energy, in mice, effects of dose rate on, 18: 5004(R) (UCRL-11033(p.12-18))
lethal effects of, in normal and neoplastic cells, 18: 5043
lethal effects of 800-r doses on mice, protective effects of *N*-methyl-aminoethylthiosulfuric acid against, 18: 33418(P)
lethal effects of, inefficiency of butyl alcohol in protection against, in mice, 18: 13569
lethal effects of, protective effects of thiogel against, 18: 13577
lethal effects on chicken embryos, effects of cysteamine, cystamine, 5-hydroxytryptamine, and diethyldithiocarbamate, 16: 14494
lethal effects on mice, protective effects of chemicals, 16: 14459(R) (NP-11359(p.35-75))
lethal effects on mice, protective effects of sodium nitrite, 16: 14460(R) (NP-11359(p.76-80))
lethal effects on gastrointestinal tract, protective effects of 2-aminoethanethiol and serotonin, 16: 14461(R) (NP-11359(p.81-5))
lethal effects on mice, effects of diet, 16: 14464(R) (NP-11359(p.106-23))
lethal effects on *Rhodopseudomonas spheroides*, 16: 17525
lethal effects on 4-day chick embryo, relative biological, 16: 17518
lethal effects on rats, effects of oxygen consumption during irradiation, 16: 20280
lethal effects on *Escherichia freundii*, protective effects of fluoroacetate against, 16: 20144
lethal effects on *Shigella sonnei*, effects of nitric oxide and N-ethylmaleimide, 16: 21959
lethal effects on grasshopper embryos, 16: 23413 (TID-15962)
lethal effects on cells in tissue culture, 16: 26764
lethal effects on *E. coli*, effects of temperature and growth rate, 16: 28799
lethal effects on radicular apices cells, protective effects of cysteamine, 16: 28820
lethal effects on mice, protective effects of complex amine oxides against, 16: 31519
lethal effects on mice, protective effects of phencyclidine against, 16: 31522
lethal effects on HeLa cells, effects of freezing, 16: 31494
lethal effects on rats exposed to hypothermia, 16: 32778
lethal effects on chick embryo after egg exposure, 16: 14581
lethal effects on mice, effects of dose output, 16: 9805
lethal effects on bacilli Sal., 16: 14567
lethal effects on rats at body temperatures lower than 10°C, 17: 1305
lethal effects on yeast cells, protective effects of tetrahydroxyquinone against, 17: 2841
lethal effects on white mice, protective effects of pantothenic acid against, 17: 7914
lethal effects on rats, morning and night exposure, 17: 10467
lethal effects on thymocytes, effects of cystamine on, 17: 10487
lethal effects on rats at various intervals after injection of cysteamine, 17: 10488
lethal effects on guinea pig cells cultivated *in vitro*, 17: 10383
lethal effects on rats, partial and whole-body exposure with fractionated doses, 17: 14002
lethal effects on mice, protective effects of allogenic bone marrow grafts against, 17: 14027
lethal effects on chicken embryos at 13-somite stage, 17: 14062
lethal effects on mice fed isologous fetal liver, effects of thymus gland removal on lymphatic regeneration in, 17: 23114
lethal effects on *P. aurelia* during interdivision growth cycle, 17: 23125
lethal effects on mice, protective effects of ozone against, 17: 28772
lethal effects on mice, protective effects of antibiotics and chlorinated drinking water against, 17: 28773
lethal effects on fungi, 17: 28708
lethal effects on Ehrlich ascites tumor cells, effects of nonprotein sulfhydryl level on, 17: 28745
lethal effects on mice, effects of dose rate and fractionation on, 17: 30459
lethal effects on birds, 17: 30416
lethal effects on rats, protective effects of oxycaine against, 17: 30450
lethal effects on golden carp, 17: 33655
lethal effects on cancer cells, mechanisms of, 17: 40623
lethal effects on rats, effects of diurnal variation on, 18: 3550
lethal effects on human and tumor cells, effects of 6-aminonicotinamide on, 18: 8210

lethal effects on mice, comparison with gamma rays and fast neutrons, 18: 17560
lethal effects on metacercaria of *Fasciola hepatica*, 18: 25128
lethal effects on mice, protective effects of gallates against, 18: 31133(T) (JPRS-25274)
lethal effects on cancer cells, protective effects of AET against, 18: 33407
lethal effects on mice, effects of splenectomy on, 18: 41198
lethal effects on mice, 18: 43233 (UR-649)
lethal effects, protective effects of mercazole, in mice, 16: 9178
lethal effects, protective effects of olive oil, 17: 5859
lethal effects, protective effects of vegetable oils, 17: 14111
lethal effects, reaction mechanisms, 16: 14590
lethal mutations induced by, protective effects of β-aminoethylisothiourea on, 17: 40667
leukemia induced by, clinical course of, 16: 6338
leukemia induced by, transfer in cell-free extract in mice, 17: 77
leukemia induced by, in mice, 18: 6653
leukemia induced by, in mice, 19: 7122
leukemia induced by, in mice, 19: 10856
leukemia induced in rats by methylcholanthrene and, transmission of, 17: 10258
leukemia induced in mice by, effects of injected leukemic tissue on, 19: 33824
leukemia induction by health examination, 17: 35493
leukemia induction in mice by, cell-free transmission of, 17: 40599
leukemia induction in mice, 18: 11795
leukemia induction in mice by, plasma lactic dehydrogenase activity in, 18: 23256
leukemia induction in mice by, protection against, using sheep spleen homogenates, 18: 27222
leukemic cells induced in mice by, long-term cultivation in tissue cultures, 16: 2903
leukemic effects on mice, 16: 1514
leukemogenesis by, synergistic effects of urethan, 16: 5213
leukemogenetic effects, effects of urethan and bone marrow injections, 16: 6332
leukemogenic effects in urethan-treated mice, protective effects of bone marrow against, 18: 15899
leukemogenic effects in mice, 18: 17561
leukemogenic effects in mice, protective effects of estrogens and tissue transplant against, 18: 17658
leukemogenic effects in mice, physical factors affecting, 18: 19577
leukemogenic effects in mice, virus effects on, 18: 19578
18: 19512
leukemogenic effects in mice, effects of ACTH on, 18: 21921
leukemogenic effects during pregnancy, 18: 25152
leukemogenic effects on mice, 18: 33311
leukemogenic effects in germ-free mice, 18: 36962
leukemogenic effects on man, 18: 38865
leukemogenic effects on cancer patients, 18: 39029
leukemogenic effects in germfree mice, 18: 41158
leukogenic effects on mice treated with cortisone, 17: 4396
leukoplakia induction by, 18: 19624
lymphosarcoma induced in mice by, lymphoma induction by extracts from, 20: 18359
measurement in auroral zone, 19: 27359
measurement in coincidence with gamma radiation, corrections for, 19: 42737
measurement in coincidence with gamma radiation, corrections for, 19: 42738
measurement in dogs using silver-activated glass rods, 20: 5745(R) (UR-668, pp 117-23)
measurement in therapy range, r-unit absolute, 18: 19826
measurement in water phantoms, 18: 31073
measurement of electron-plasma produced, 19: 17080(R) (TID-21380 (p.63-84))
measurement of extra-terrestrial, review on, 19: 27127
measurement of scattered, from phantom exposed to 100 to 300 kvp x rays, 17: 24913
measurement of soft, using secondary electron multiplier, 17: 25658
measurement of soft, resolution of thallium-activated sodium iodide scintillation detector for, 19: 36849
measurement of, at eye position of fluoroscopic screen assemblies, 18: 25249
measurement of, efficiency of counters for, 18: 33896
measurement of, from non-point sources, 18: 27800
measurement of, from plutonium-239 deposited in lungs, 20: 18186(R) (LA-3432, pp 102-29)
measurement of, performance of hollow ionization chamber for, 19: 24850
measurement of, standards for, 19: 2558
measurement with silver-activated metaphosphate dosimeter, 18: 4103
measurements on solar, survey of, 18: 10726 (NP-13522)
mesic atom (μ) yields of, deficiency in carbon, nitrogen, and oxygen, 17: 26567
meson (π^+) production by polarized, at 227–373 Mev, 17: 26336
metabolic effects, protective effects of cysteamine, 17: 5858
monitoring, 18: 23901
monitoring in personnel in Prague, use of film dosimeters for, 20: 37035
monitoring low doses of, by blood film technique, 17: 28717
monitoring of, bell-alarm personnel meters for, 17: 29994
monitoring of scattered, in exposure facilities, 20: 14812
monochromatization by filtration, voltage diagrams for, 16: 11871(T) (NP-tr-833)
monochromatizing methods, 18: 24224
morphological effects on liver cells, fine structure, 16: 9884
morphological effects on cells in tissue culture, 16: 26751
morphological effects on cells in tissue culture, 16: 26756
morphological effects in amoeba, 17: 7803 (TID-17695)
morphological effects on mouse kidney during early post-natal life, whole-body, 18: 55
morphological effects on ultrastructure of leucocytes and lymphocytes of rabbits, 18: 13536
morphological effects on ultrastructure of rat hepatic cells, 18: 13537
morphology of bursts in auroral zones, 16: 10706
mutagenic effects, induction of R-locus deleterious in Mormoniella, 16: 9871
mutagenic effects in rice, 16: 1618
mutagenic effects on endosperm and seedlings of maize, 16: 1602
mutagenic effects on *Tetrahymena pyriformis* induced by exposure, 16: 7353
mutagenic effects on barley, 16: 17469
mutagenic effects on leaf color, 16: 20207
mutagenic effects on plants, 16: 20208
mutagenic effects on *Artemia salina*, 16: 26771
mutagenic effects in Drosophila, 16: 26789
mutagenic effects on maize seedlings, effects of temperature on somatic, 16: 28765 (RT/BIO(62)44)
mutagenic effects on Drosophila spermatogenesis, 16: 2911
mutagenic effects on Drosophila, modification with 2,4-dinitrophenol, 16: 6360
mutagenic effects on "Cappelli" durum wheat, 17: 10390
mutagenic effects on tomato seeds, comparison with spontaneous mutability, 17: 10391
mutagenic effects on Drosophila, 17: 10393
mutagenic effects on maize seedlings, effect of temperature on, 17: 10394
mutagenic effects in spermatogenesis of Drosophila, 17: 31892
mutagenic effects on phage kappa, 17: 35383
mutagenic effects in lead plastids of *Arabidopsis thaliana*, 17: 35589
mutagenic effects in wheat, 17: 39362
mutagenic effects in Drosophila, 17: 38766
mutagenic effects in Triticum, 18: 3520
mutagenic effects in Drosophila, protective effects of 2,4-dinitrophenol against, 18: 3594
mutagenic effects in Drosophila, review, 18: 11733
mutagenic effects on yeasts during meiosis and mitosis, rates of, 18: 11832
mutagenic effects on mouse germ cells, effects of dose rate and fractionation on, 18: 11837
mutagenic effects on bees, 18: 13447(R) (NYO-2315-1)
mutagenic effects on crops in Japan, 18: 13484
mutagenic effects on Streptomyces, 18: 17486
mutagenic effects in jute, x, 18: 17519
mutagenic effects in Drosophila, 18: 17520
mutagenic effects in *Pisum sativum*, 18: 17617
mutagenic effects in *E. coli*, gene locus of, 18: 21839
mutagenic effects in groundnut, 18: 21868
mutagenic effects in *Phaseolus mungo*, 18: 23263
mutagenic effects in silkworms, fractionated vs. single dose, 18: 31143
mutagenic effects in *Vicia faba*, 18: 33303
mutagenic effects in *Phaseolus mungo*, 18: 33324
mutagenic effects in *E. coli*, 18: 35355
mutagenic effects in Drosophila, protective effects of sulfhydryls against, 18: 36987
mutagenic effects on bacterial chromosomes, 18: 38855
mutagenic effects on Pisum, 18: 38914
mutagenic effects on moth wing scales, 18: 41090 (TID-21097)
mutagenic effects on Pisum chlorophyll genes, 18: 41155
mutagenic effects, 18: 43218(R) (EUR-1882.e(p.7-26))
mutagenic effects on Drosophila chromosomes, 18: 43251
mutagenic effects of, in *Vicia sativa*, 20: 45476
mutant characterization in potatoes by exposure to, 17: 33721
mutation induced in tomatoes by exposure by seeds, 16: 25197 (CNEN-119)
mutation induced in *Medicago sativa L.*, cytogenetics of single-leaf,

17: 10398
mutation induced in *Medicago sativa L.*, morphology of single-leaf, 17: 10399
mutation induction in barley by, comparison of methanesulfonates and, 18: 3543
mutation induction in *Saccharomyces cerevisiae* by, allelic mapping of, 18: 11794
mutation induction in *Drosophila melanogaster*, effects of chloramphenicol, penicillin, and streptomycin on, 18: 11886
mutation induction in Datura, 18: 13523
mutation induction in *Paramecium aurelia*, distribution of chromosomal strands to, 19: 7114
mutation induction in *Neurospora crassa* by, spectra of allelic complementation and leakiness in, 19: 8862
mutation induction effects on mouse skeleton, frequency of, 19: 24290
mutation induction effects on *D. pseudoobscura*, 19: 24292
mutations in wheat induced by, 16: 25196 (CNEN-120)
mutations induced in rice by, 16: 32764
mutations induced in rice by, analysis of reciprocal translocations in, 16: 32765
mutations induced in Drosophila by, effects of gases on, lethal, 17: 7886
mutations induced by, effects of environment on, on yeast growth, 17: 17842
mutations induced in Drosophila by, effects of oxygen and metabolic state, 17: 28710
mutations induced in wheat seeds by, frequency of chlorophyll, 17: 38689
mutations induced in Saccharomyces by, rates of lethal allele, 18: 5063
mutations induced in *Hymenolepis diminuta*, review on behavior and structure of, 18: 9841
mutations induced in bread wheat by, frequency and spectrum of, 18: 9853
mutations induced in Drosophila spermatogonia, dose-frequency response of, 18: 9860
mutations induced in Drosophila by, effects of chloramphenicol, dinitrophenol, nitrogen, oxygen, and ribonuclease on, 18: 11887
mutations induced in homozygote and isogenic Saccharomyces yeast strains by, ploidy effects on, 18: 33394
mutations of *Marchantia polymorpha* induced by, nutritionally deficient, 18: 9847
neurological effects on frog nerve-muscle preparation response to electric stimuli, 16: 16257
neurological effects on presynaptic failure of neuromuscular transmission, 16: 16258
neurological effects on electroretinal response of frog eyes, 16: 16259
neurological effects on ventral root potentials in spinal cords of cats, 16: 16261
neurological effects on neuronal activity in spinal cord of cats, 16: 16262
neurological effects on brain electrical activity in cats and rabbits, 16: 16264
neurological effects on brain activity in cats and rats, 16: 16268
neurological effects on developing embryos, 16: 16270
neurological effects of pre-natal irradiation on behavior of rats, 16: 16271
neurological effects on neurosecretory activity of neurons of supra-optic and paraventricular nuclei in rats, 16: 16278
neurological effects on central nervous system in rats, 16: 16282
neurological effects, comparison of response variability and degree of higher activity of nervous system, 16: 16283
neurological effects of spinal-cord irradiation in white mice, 16: 16285
neurological effects on brains of pigeons and rabbits, comparison of sensitivity of various parts, 16: 16281
neurological effects on 3-(2-aminoethyl)-5-indolol content of brain in rats, 16: 16273
neurological effects on nervous system of animals under interoceptive stimulation, 16: 17444(T) (JPRS-13342(p.4-11))
neurological effects on nervous system of rats, 16: 23420 (USNRDL-TR-561)
neurological effects on brains of pigeons and rabbits, comparison of sensitivity of various parts, 16: 23421(T) (AEC-tr-5141)
neurological effects on spinal reflexes in rabbits, 16: 30299
neurological effects on ganglia of peripheral nervous system of guinea pigs, 16: 30304
neurological effects in rats and monkeys, delayed, 16: 7416 (BNL-675(p.200-3))
neurological effects on electroencephalographic changes in brain, 17: 5902
neurological effects on nervus ischiadicus of frogs, method of measuring effects of dose rate on, 17: 7816
origin of cosmic, (T), 19: 39425
origin of cosmic, (T), 19: 44971
origin of cosmic isotropic, (T), 20: 29958
oxidation of fatty acids, 18: 25570
pathogenic effects in rabbits and rats, 18: 29410
pathologic effects on kidneys, 18: 33288
pathological characteristics of leukemic reticulosarcomatosis induced by, 20: 42729
pathological effects on gonads, hazards from diagnostic procedures, 16: 1561
pathological effects on embryos, 16: 5184
pathological effects, effects of gut shielding and eventration, 16: 5225
pathological effects, comparison with electron and gamma radiation, 16: 5155 (CNB-20)
pathological effects of head exposure, on nervous response, 16: 6304(T) (JPRS-11322(p.248-73))
pathological effects in mice, effects on antibiotic therapy, 16: 9887
pathological effects on hematopoietic system, 16: 9896
pathological effects on hemopoietic tissues, 16: 12924
pathological effects on bones, therapeutic doses, 16: 14492
pathological effects on liver cytoplasm, whole-body exposure, 16: 16235
pathological effects in bone and cartilage, 16: 17448
pathological effects on thymus gland, 16: 21930(T)
pathological effects on head and mouth, 16: 21973
pathological effects on skin of rats, curative effect of serum therapy on, 16: 26873
pathological effects in developing fetus, 16: 26807
pathological effects of therapeutic doses on thyroid gland in children, 16: 30210 (NP-12021)
pathological effects on nerves in red bone marrow, 16: 32742(T) (JPRS-15018(p.64-72))
pathological effects on eye, 17: 5794
pathological effects of fractionated exposure in mice, 17: 7804 (USNRDL-TR-595)
pathological effects and dosage determination of pulsed, high-energy, in man, 17: 8449
pathological effects of chronic, low-level exposure in rats, 17: 15805(T) (JPRS-18153)
pathological effects on mouse embryos, 17: 17870
pathological effects in man, 17: 20254
pathological effects in mice, protective effects of aminoethylisothiuronium, 17: 19817
pathological effects of therapeutic doses in children, delayed, 17: 21478
pathological effects of local exposure of lungs, 17: 23215 (TID-16982)
pathological effects in brain, low-level exposure, 17: 23126
pathological effects on testis, effects of dose fractionation, 17: 24967
pathological effects in developing mouse fetuses, 17: 27169
pathological effects in offspring of exposed females, 17: 30311
pathological effects on ovaries, delayed, 17: 31866(R) (UCD-107 (p.112-28))
pathological effects in dogs, delayed, 17: 31867(R) (UCD-107(p.129-274))
pathological effects on arterial wall of hypercholesterolaemic rabbits, 17: 31900
pathological effects, long-term in dogs, 17: 31859(R) (UCD-107(p.13-29))
pathological effects in mice, protection against, using β-mercaptoethylamine, 17: 33489(R) (NP-13010(p.81-106))
pathological effects on eye lens of mice, 18: 1375 (BNL-7371)
pathological effects on embryos and fetuses of laboratory animals, 18: 8106(R) (NYO-2740-1(p.155-98))
pathological effects of, in dogs, 18: 25093(R) (UCD-472-109(p.62-172))
pathological effects on skin, 18: 25214 (AHSB(RP)R-39(p.87-93))
pathological effects in monkeys, effects of treatment with antibiotics and vaccine on, 18: 27223
pathological effects in rats, effects of electrical stimulation on, 18: 27238
pathological effects in dog kidneys, 18: 27171
pathological effects on intestine in rats and mice, 18: 29421
pathological effects of embryonic exposure to, in rats and mice, 18: 33280(R) (TID-20831)
pathological effects in mice, effects of liver shielding on, 18: 35316(R) (NP-14210(p.81-9))
pathological effects on developing human embryos, 18: 38910
pathological effects on salamanders, 18: 38969
pathological effects on rats, 18: 39021
pathological effects on mice, 18: 41073 (COO-1038-4)
pathological effects on bones during tumor radiotherapy, 19: 3980
pathomorphological effects on vascular system of dogs, 16: 8631(T) (JPRS-11848(p.1-12))
pathomorphological effects on parotid glands in rats, 16: 8633(T) (JPRS-11848(p.25-33))
performance for detection of shallow buried objects, 18: 23782 (NP-13943(p.117-27))
performance in radiological flaw-detection systems, 17: 8384
peroxidase inactivation by, reaction mechanisms for, 18: 29249 (TID-20815)
peroxides induced by, in mice, effects of MEA on, 18: 6709
personnel monitoring by test films in industrial radiography in Poland, 20: 41212

photographic film detector with multi-element filters, design of energy-independent, 20: 658
pneumonitis induction by, histopathological study of, 18: 29409
polarization of, from electron bombardment of mercury vapor, 20: 7739
pre-operative exposure of tumors to, 18: 29489
preoperative treatment of cervical cancer with, 17: 35560
prevention of leukemia induced by, using sheep spleen extract, 20: 40658
production and properties of non-solar, in interstellar space, 19: 44969
production and spectrum in outer space, (T), 19: 18673
production and use of, from tritium, 17: 35862 (AERE-R-3086)
production by beta particle bombardment, 16: 9975
production by californium-252 fission, timing of, (E), 20: 6298(R) (PPAD-2137-566)
production by exploding wires, 17: 13208
production by gamma excitation of target materials, 19: 7828
production by magnetrons in radar installations, 19: 46673
production by proton bombardment, (E), 19: 23326
production by proton bombardment, use of, in determining film surface density, 20: 11281 (UCRL-12107)
production by runaway electrons in hydrogen toroidal pinch discharge, intensity of, 17: 42103
production by stars, 17: 36550
production efficiency of pure thick targets, 16: 8137
production from capacitor discharges, 20: 9607
production from discharges in spark chambers, 20: 43714
production from electron precipitation in auroral-zone ionosphere, (E), 20: 19671
production from electron oscillations in betatrons, maximum, 20: 41560
production in aluminum and magnesium by proton bombardment at 25 to 100 kev, 19: 30946 (UCRL-7700)
production in auroral zone from electron precipitation in atmosphere, 20: 19665
production in auroral-zone D region, energetic electron-precipitation determination from, (E), 20: 19672
production in betatrons, method for increasing yield of, 20: 25665
production in carbon by proton bombardment at 15 to 110 kev, 19: 28993 (UCRL-7826)
production in electron reactions in atmosphere, 20: 30218(T) (NASA-TT-F-389, pp 616-23)
production in electron beam probing of solids, 20: 36359(R) (TID-22992)
production in galaxy, processes for, 18: 28232
production in galactic sources, bremsstrahlung and synchrotron-emission, (T), 19: 20765
production in interplanetary space, (T), 19: 34855
production in linear stabilized pinch devices, 16: 2605(T) (NP-tr-814)
production in linear accelerators, parameters for, 16: 14116
production in magnetosphere by electron bunches, 17: 3924
production in meson(μ) capture by nuclei, nuclear structure research with, 17: 36646 (CERN-63-28(p.143-71))
production in neutron stars, effects of nuclear forces on, 19: 32866
production in nitrogen ion reactions with gold and lutetium, spectra of, (E), 20: 24359(R) (UCRL-16580, pp 95-106)
production in proton reactions with ytterbium at 30 to 100 kev, 18: 40575
production in proton inelastic scattering by copper at 25 to 1700 kev, L shell, (E), 20: 42169(R) (UCRL-14744, pp 1-18)
production in space, (T), 19: 27057
production in theta pinch discharges, 17: 7478
production mechanisms in supernova remnants, 18: 30377 (CONF-320-5)
production of beta-induced, 20: 12545(R) (PAEC(A)AR651)
production of copper L-shell, by proton bombardment, 18: 16663
production of cosmic, by solar flares, (E), 19: 43019 (NASA-TN-D-2798, pp 163-8)
production of high-energy, by linear accelerators, 18: 17684
production of high-energy, in electron beam reactions with plasma, (T), 19: 43429
production of high-energy, in electron beam reactions with plasma, (T), 19: 43428
production of, in fission of uranium-235, 17: 17250
production of inactivation and protective substances by, in agar, 17: 17910
production of K, by electron bombardment of solids, 17: 37871
production of line, effective depth of, 18: 700
production of mixture of electrons and, for irradiation, 20: 23250(P)
production of monochromatic soft beams at 5 to 40 kev, 16: 12182(R) (TID-15122)
production of pulsed, facility design for, 20: 20838 (AD-624019)
production of selected wavelength, method for, 19: 41163(P)
production of soft, design of apparatus for, 17: 18237
production of soft, by proton bombardment, 19: 12324
production of ultrasoft, with potentials of about 200 v, 18: 2413
production of, flash tubes for, 18: 20308
production of, using Josephson-type superconducting tunnel junctions, 20: 28212
production outside solar system, 17: 9176
production yields from 1.5-Mev proton bombardment of thick targets, 18: 14664
propagation modes of wave field of, for single diffraction, 19: 23366
properties of very soft, for skin therapy, 17: 35364
protection against lethal effects, by inorganic condensed phosphates, 16: 4069
protection against, review, 16: 24034
protection against, development of system for, 17: 4748
protection against effects of, using polyanions, 17: 30428
protection against, effects of MEG in mice, 18: 17656
protection against, effects of cysteine in mice, 18: 17657
protection against, effects of cytochrome c on carbon monoxide, 18: 23383
protection against, using bone marrow, in man, 18: 29407
protection against, by sulfhydryl compounds, 18: 29416
protection against, development of compounds for, 19: 43883(R) (UCLA-12-565, pp 65-85)
protection against, manual for, 20: 31445 (N-65-12416)
protection from, in laboratories, 17: 6319 (TID-15445)
protection from, during occupational use, 17: 8448
protection of tissue cultures from, by anoxia and/or cysteamine, 16: 14598
protective effect of imidazole derivatives as a function of dose, 17: 30429
protective effects of cystamine against, in spleen DNA in rat, whole-body exposure, 16: 56
protective effects of bone marrow injections against, in guinea pigs, 16: 1628
protective effects of cysteamine on survival of fetal germ cells, 16: 1632
protective effects of cystamine and cysteamine against, in tissue culture cells, 16: 12887
protective effects of cysteine and 2-(2-aminoethyl)-2-thiopseudourea against lethal, in rhesus monkeys, 16: 17539
protective effects against arrhythmia induced by adrenaline and noradrenaline in anesthesized dogs, 16: 20218
protective effects of monoamine oxidase inhibitors against whole-body, in mice, 16: 25252 (TID-16160)
protective effects of imidazole and its derivatives against, 16: 26783
protective effects of, against acanthosis induced on guinea pig skin, 17: 21502
protective effects of hypoxia against, in mice, 17: 30346
protective effects of post-irradiation oxygen starvation against injuries from, in rat thymocyte nuclei, 20: 42989
psychological effects, 16: 2892 (TID-14294)
pulsations of auroral bremsstrahlung, analysis of, (E), 19: 12416
radiation distribution from, in water phantoms, 20: 23808(R) (NIRS-4, pp 3-12)
radiation effects on metabolism of desoxyribonucleic acid in epithelial cells of rats, 20: 1634
radioactivity in foods induced by, 18: 23815 (AERE-R-4601)
radioinduced emission from pure elements, efficiency of electron, 18: 9006
radioinduced injuries from use of, in therapy of cervical cancer, 20: 38751
radioinduced injuries following use for uterine cancer, 20: 38754
radioinduced mutations in rice, 20: 40640
radioinduced sex-linked recessive lethal, in Drosophila by, 17: 21516
radioinduction of eye color mutations in Mormoniella, 20: 40669
radiology training programs in Germany, 19: 5728
radiosensitivity effects of chronic doses of, on tumor cells, 19: 158
radiosensitivity of rat central nervous system, behavioral responses indicating perception of, 20: 35267
radiotherapy of tumors using, 18: 29471
radiovaccination effect, combined with injection of dinitrophenol, methylene blue, and aminothiazole, 16: 18737
RBE for human body, 20: 42865
reactions in air and hexane, energy dependence of ionization currents from, 18: 10142
reactions in alkali halide crystals, production and destruction of F and M centers in, 18: 10600
reactions in alkali halide crystals, F center production in, 18: 10601
reactions in emulsions, beta multiple production in, 16: 13916
reactions in ionosphere, ionization rate for, 18: 18829
reactions in ionospheric D region, ionization from, (E/T), 19: 12385 (AFCRL-63-747)
reactions in low- and medium-Z absorbers at 852 ev to 40 kev, photoelectric cross sections for, (E), 20: 21523
reactions in lysine monohydrochloride dihydrate, electron spin resonance of radicals formed in, 18: 3853
reactions in paraffin oils, mobility of ions produced in, 18: 10582
reactions in platinum at 5 to 90 Mev, electron pair production in, 18: 28669
reactions in potassium chloride crystals, color center production in,

18: 13889
reactions of soft, electron energy distribution from, 18: 18590(T)
reactions with alkali halide crystals at 4 to 80°K, luminescence spectra from, 18: 33648
reactions with alkali azides, EPR study of nitrogen free radicals from, 20: 13970 (AD-611432, pp 135-47)
reactions with antimony–indium alloys, induced defects in, 19: 16236
reactions with argon, readjustment to vacancies in K and L shells in, (E), 19: 16392
reactions with atoms, model for ionization, 20: 15270
reactions with beryllium, oxidation effects on ionization absorption cross sections for, 18: 26215(T)
reactions with cadmium sulfides, quantum yield of conductivity in, (E/T), 19: 36510
reactions with cadmium sulfide crystals, infrared conductivity quenching in, 20: 8312
reactions with calcium fluorides, EPR studies of V_F centers in, 19: 20003
reactions with calcium fluophosphates, paramagnetic color centers in, 19: 26436
reactions with copper, electron emission in, 19: 28994
reactions with copper, gold, and dielectrics, number of electrons emitted in, 17: 22380
reactions with deuterated and normal hydriodic acid and methyl iodide, recoil-energy spectra and relative abundances of ions produced in, 20: 33354
reactions with disodium hydrogen arsenates, ESR of radicals formed in, 18: 22148
reactions with emulsion nuclei at 5 to 90 Mev, pair and triplet production in, 16: 11029
reactions with frozen hydrochloric and hydrofluoric acids, EPR of hydrogen atoms formed in, 20: 32719(T)
reactions with gases, ion pair production in, 17: 16086
reactions with helium-4, meson (π^-) production in, 19: 23809
reactions with holmium-165, proton production from, 20: 27310
reactions with light nuclei at 600 kev, computer analysis of secondary electron emission from, 17: 41525 (AFSWC-TDR-63-50)
reactions with liquid argon, measurement of ionization in, 20: 15259
reactions with lithium-doped sodium fluorides, color centers in, 19: 33524
reactions with massive cathodes, photoeffect mechanisms in, 16: 24328
reactions with mercury vapor, electricity production in, (E), 19: 47283(T) (BNL-tr-8)
reactions with monofluoroacetamide, ESR spectra of radicals trapped in, 18: 22146
reactions with n-hexane at low stresses, induced conduction from, 20: 7133
reactions with neon, ionization readjustment processes in K-shell, 18: 5929
reactions with neon at 167 to 913 ev, double Auger electron emission in, (E), 19: 20844
reactions with nitrogen, excitation of first negative and second positive bands by, 20: 21834
reactions with nuclei at 15 to 30 Mev, total cross sections for, (E), 19: 12573
reactions with nuclei, gamma energies and half lives from excitation in, 19: 29227 (AEET/ANAL/32)
reactions with nuclei at low energies, excitation in, 20: 13782 (ORNL-P-1927)
reactions with organic substances, luminescence duration from, 18: 8427(T)
reactions with phosphor NE-102, fluorescence yield from, 18: 10156
reactions with potassium bromide crystals, thermoluminescence from plastic deformation of charged traps and color centers from, 18: 27584
reactions with potassium chloride crystals, M centers in, 19: 26450
reactions with potassium iodide crystals, V_K centers in, (E), 19: 40103
reactions with potassium bromide and chloride, color centers in, 19: 22365
reactions with potassium bromide crystals, α and F centers induced in, 20: 1919
reactions with quartz containing aluminum, induced thermoluminescence in, 18: 27585
reactions with quartz crystals, coloration and elastic strain in, 19: 18030
reactions with quartz crystals, induced optical absorption in, 19: 34232
reactions with rare gases in electric fields, luminescence from, 17: 28011
reactions with silica, volume changes in, 18: 5834
reactions with sodium chloride, F-coloration level from, 19: 42550
reactions with thallium-activated alkali metal iodide crystals, scintillation response in, 19: 9209
reactions with xenon, ionization of 4d electrons in, (E), 19: 8098
reflection by crystal lattices, 17: 24278 (UCRL-Trans-926(L))
reflection by crystals, computer analysis of distributions from, (E), 19: 8002 (IS-954)
reflection from crystals, 18: 44315
reflection from thick ideal calcite crystals, coefficient for, (T), 20: 34863
reflection intensities of, statistical distribution of (T), 19: 2964
reflection of, anomalous surface, 18: 42162(R) (TID-20963)
relation between integral dose and image contrast in diagnostic radiography, 18: 39026
relation of dose-fractionation and spacing in time to skin damage, 20: 40764
relation of solar, to radio bursts, 17: 12923
relative biological effectiveness, compared with gamma ray, 16: 1565
relative biological effectiveness, 19: 5631(T) (ANL-Trans-111)
relative biological efficiency of, comparison with gamma radiation and high energy electrons, 20: 40665
repair of chromosome aberrations induced by, in Tradescantia microspores, 20: 42977(R) (ORO-2669-2)
reparative effects of DNA on rat sperm following total body, 20: 40723
response of film badges containing multi-element filters to, 18: 22336 (LA-3001)
response of x-ray workers to cystine and Widal test, 16: 4090
response of 67 leukemia patients to different application methods for, 18: 3655
response to photographic, 16: 360
review of effects, 20: 23418
scattering as particles, 16: 3619
scattering at small angles from cylinders, intensities, 16: 12349
scattering at small angles by neutron-irradiated metals, 20: 27569(R) (BNWL-207, pp 3.7-13)
scattering, bibliography on small-angle, 17: 714 (SRB-62-4)
scattering by acridine III, 17: 6062
scattering by aluminum, K_α fluorescence from, 17: 42017
scattering by ammonia and water, calculation of intensities of, 18: 777
scattering by amorphous matter, elimination of Compton components from, 19: 9476 (CONF-640702-3)
scattering by aqueous sodium caprylate, intensity of, (E), 20: 4483
scattering by atoms, dispersion corrections for, 17: 5045 (TID-14794)
scattering by atoms, parameters for, 18: 20809
scattering by atoms, anomalous dispersion terms for, (T), 19: 9899
scattering by atoms and ions, calculation of factors from Dirac-Slater wave functions for, (T), 19: 9900
scattering by atoms, Hartree-Fock calculations of incoherent, 19: 20824
scattering by atoms, Compton line displacement in, (T), 19: 29005
scattering by beryllium, boron, lithium, lithium fluoride, and lithium oxide, 17: 3979
scattering by beryllium, graphite, and polystyrene, spectral analysis for Smekal-Raman absorption in, 18: 27323
scattering by beryllium and boron, Raman lines in spectra from Compton, (E), 20: 34104
scattering by bound electrons, broadened Compton line in, 17: 39706(R) (AD-296764)
scattering by carbon and organic materials, coherent and incoherent Compton, (E/T), 19: 6393
scattering by chromium oxide crystals, electron momentum from spectra of, 18: 14714(R) (AD-411482)
scattering by conducting spheres, amplitude, 16: 943
scattering by crystals, effects of anharmonicity, 16: 12294
scattering by crystals with dislocations, 17: 13444
scattering by crystals, thermal factor for, 18: 8852(T)
scattering by crystals, defect observation by, 18: 30270
scattering by crystals, theory for, 18: 34452
scattering by crystalline beryllium powder, 19: 1055 (SC-RR-64-1207)
scattering by crystals, (T), 19: 12090
scattering by crystals, effect of anharmonic vibration on Debye-Waller factor for diffuse, (T), 19: 25630
scattering by cylinders, intensity relation for small-angle, (T), 19: 17166
scattering by diamond crystal defects, small-angle, 19: 39230 (BNL-9332)
scattering by disordered crystals, 17: 20049
scattering by electron plasma, Coulomb correlation effects in, 19: 1766
scattering by electron plasma, (T), 19: 37969
scattering by fast-neutron irradiated copper crystals, anomalous, 19: 999(R) (ORNL-3676(p.27-31))
scattering by filament molecules, effects of electron density distribution on, 19: 14269
scattering by finely pulverized graphite at small angles, use in investigation of disperse structure, 19: 42860
scattering by fluid composed of nonspherical molecules, (T), 19: 16382
scattering by fog, use in estimating steam quality in pipes, 16: 25551 (CRRP-1086)
scattering by grains in interstellar space, small-angle, 19: 30919
scattering by ground state helium, factor for, 17: 20748

scattering by heavy atoms, anomalous L-shell dispersion in, 18: 9002(T) (AEC-tr-6269)
scattering by heavy atoms in K- and L-region, dispersion theory for, 18: 10770(T) (AEC-tr-6317)
scattering by heavy water, structure analysis from, (E/T), 20: 35395 (ORNL-3960)
scattering by helium and hydrogen, coherent and incoherent, 16: 4858
scattering by helical filament molecules, 19: 14270
scattering by ionic single crystals, effects of charged defects on, 16: 22919
scattering by irradiated beryllium oxide, intensity distribution of, 18: 20607
scattering by isotactic and syndiotactic polymethylmethacrylate in solution, small-angle, (T), 19: 6391
scattering by K shells, atom factors, 16: 4626(T) (UCRL-Trans-749(L))
scattering by lead, Kohn anomaly measurement by, 17: 5146
scattering by lead, energy spectra of electron emission from, 17: 19062
scattering by lead, secondary electron emission from, 18: 34274(R) (NIRS-2(p.3-15))
scattering by liquid-like binary, description of, 17: 28137 (BNL-6364)
scattering by liquids, radial distribution curve determination by, 17: 37225
scattering by liquid metals and alloys, computer program for analysis of, 18: 609 (TID-19548)
scattering by liquids and solutions, cross sections for, 18: 20035
scattering by liquid xenon, calculation of radial-distribution functions from, 19: 30950
scattering by lithium hydride crystals, coherent, 17: 2078
scattering by lithium deuterides, energy-gap determination from small-angle Compton, (E), 19: 46286
scattering by melt-crystallized polyethylene, 20: 5022
scattering by metal surfaces, anomalous, (E), 19: 18591
scattering by molecular crystals, theory of diffuse, 18: 31507
scattering by molybdenum, elimination of Compton component in, (E), 19: 9929
scattering by neutron-irradiated graphite, 20: 17130
scattering by neutron-irradiated diamond crystals, (E/T), 20: 19273(R) (BNL-929, pp 3-43)
scattering by nitrogen, theory, 17: 27953
scattering by nitrogen, oxygen, and their mixtures, diffraction of, 18: 4615
scattering by nuclei, formation of characteristic modified lines in, 16: 22854 (TID-15828)
scattering by nuclei, resonance elastic, 16: 23109
scattering by nuclei $1 \leq Z \leq 6$ at 1 to 150 kev, cross sections for, (T), 20: 21516 (UCRL-14403)
scattering by potassium permanganate single crystals, 18: 37238
scattering by pyrolytic, small-angle, 18: 2259
scattering by rare-gas atoms, abundances of ionic species from, (E), 19: 37456(R) (ORNL-3778(p.9-12))
scattering by RNA molecules in solution, low-angle, (T), 20: 36586(T)
scattering by silicon crystals, anti-Stokes and Stokes modified lines in, 18: 35242 (CALT-221-2)
scattering by single crystals of lithium fluoride, use of Mössbauer effect to measure elastic, 18: 8935
scattering by single crystals, broad diffuse bands from electron-lattice resonance in, 18: 16551 (TID-20364)
scattering by single-crystal silicon, small-angle, 18: 20555
scattering by solid hydrocarbons, carbon determination from ratio of incoherent to coherent, 19: 10990
scattering by solid solutions, intensity relation to metastable miscibility gap in, 19: 38028 (ORNL-P-1396)
scattering by solids, thickness measurements by, 19: 16230
scattering by thin films, angular distribution of specular, (E), 19: 23298
scattering by thin copper films, interference fringes from, (E/T), 20: 17163
scattering by titanium, effects of crystal distortions on, 19: 2803 (NYO-2994-2)
scattering by two-electron systems and atoms, 19: 37464
scattering by water slabs at 50 to 250 kev, spectra, 16: 24293
scattering by water, angular distribution of, 19: 28996
scattering by xenon, relativistic wave functions for form factors for, 20: 27745
scattering by xenon, form factors for, (T), 20: 29949
scattering effects of, on dimensioning of shielding, 17: 15379
scattering factors for, analytical expressions for Thomas-Fermi-Dirac atomic, 18: 773
scattering factors for, analytical expressions for, 18: 16656
scattering factors of, corrections for incoherent, 19: 39379
scattering from a cuboid shaped tissue-equivalent phantom, factors affecting angular variation of, 20: 41211
scattering from cavities in galvanic copper, small-angle, 17: 24359
scattering from crushed coal, determination of ash content by back-, 20: 37153
scattering from lattice structures, relative intensity in, (E), 20: 5010
scattering in air and water, radiation doses from, 19: 31444
scattering in amorphous materials, theory of multiple, 20: 30734(R) (TID-22970, pp 1-63)
scattering in dilute solutions, review on small-angle, 18: 29186
scattering in heat-treated, graft-polymerized PVA, 18: 25483(T) (AEC-tr-6372(p.141-3))
scattering in matter, bibliography, 16: 19882 (TID-15419)
scattering in matter, measurement and theory of, 19: 38524
scattering in triaxial ellipsoids, small-angle, (T), 19: 12063
scattering intensities of, structure factor calculation from, 17: 37951
scattering of celestial, by interstellar grains, 18: 36124 (MIT-2098-60)
scattering of, effects of surface layers on back-, 17: 29972
scattering of 60- to 80-kev, dose measurements in water phantom, 18: 25255
scattering of, analysis of J-phenomenon in, 19: 41357
scattering of, analysis of J-discontinuity in, (T), 20: 8277
scattering of, asymptotic expansion for integrals in, 18: 34022
scattering of, design of total-reflection monochromator for studying small-angle, 18: 41732
scattering of, LET for electrons from, 17: 34180
scattering of, Raman lines in, (E), 20: 18559 (CALT-221-14)
scattering of, singularities in coherent diffuse, (T), 20: 39586
scattering on atomic gases, factors for, 17: 39772
scattering on copper-65 and tin-116 at 1.114 and 1.29 Mev, source effects on resonance, 17: 41981
scattering on drift rings, theory of small-angle, 17: 36591
scattering width of small-angle, 16: 29708
scintillator quenching by, 18: 20352
secondary, contribution of grid radiation to total dose, 16: 4017
single dose effects on mandibular growth, 20: 40652
single-hit effects by, on Drosophila, water snails, and RNase, 20: 40515
site location of sieve fields, 16: 9792
skin cancer induced by, 20 years after exposure, 17: 40589
skin wounds induced by, blood vessel regeneration during healing process of, 18: 11752
sorption of, by soft tissue near bone, 17: 15702
sorption of soft, by psoriatic parakeratotic stratum corneum, 17: 5689
sources of cosmic, outside solar system, 19: 25187
sources of cosmic, neutron-star and supernova, (T), 19: 44923(T)
sources of cosmic, stellar, 20: 29900
sources of 20- to 58-kev, stellar, (E), 20: 37376
spectra and location of stellar sources of, (E), 20: 15220
spectra from electron-bombarded silver-foil, 18: 26224
spectra from reactions with naphthalene and pyrene, (E), 20: 7659(R) (ORNL-3849, pp 101-50)
spectra from solar flares, 20: 37360
spectra from uranium-235 fission products, (E), 20: 42170 (UCRL-70045)
spectra in beta decay at 0 to 20 kev, 18: 24408
spectra in cosmic cascade showers at high altitudes, (E/T), 19: 41299
spectra in therapy beam, in 200 to 300 kvp range, 20: 41322
spectra of Crab nebula, (E), 20: 9664
spectra of Cyg XR-1, Tau XR-1, and Sco XR-1, 20: 29901
spectra of electron cyclotron resonance discharge-induced, (E/T), 20: 28497(R) (TID-22956, pp 55-147)
spectra of elements, screening doublets in, (E/T), 19: 37478
spectra of lithium, (T), 19: 37479
spectra of μ-mesic, analysis of, 19: 13863(R) (TID-21413)
spectra of primary and secondary, 16: 2465
spectra of prompt, from californium-252 fission fragments, (E), 19: 19093 (UCRL-11902)
spectra of, solar, 17: 24227
spectra of solar, 18: 10731
spectra of solar, at 8 to 20 Å, 17: 26259
spectra of solar, review on, 19: 27059
spectra of solar, measurement using stabilized rockets, (E), 19: 28983
spectra of, emitted from anode in Penning discharge, 18: 21502
spectra of, from flash discharges, (E), 20: 40233
spectrum in solar radiation, review of, 19: 20785
spectrum measurements from a plastic window tube, 16: 7644
spectrum of solar, 17: 26257
spectrum of solar, 19: 32855
spectrum of solar, (E), 19: 4814
standard for, wavelength, (E), 19: 9920
standard units for ionizing, definition, 16: 18127(T) (DC-58-9-84 (p.1-13))
standardized technique of radiotherapy for breast cancer, 20: 40773
standards for, design of laboratory for Swedish, 17: 39320
supervoltage, in cancer therapy in gynecology, 20: 40768
therapeutic applications of, computer patient simulation for, 18: 33435
therapeutic dosages, subsequent development of leukemia, 16: 17455

therapeutic effects of small daily doses on carcinomas, 16: 32775
therapeutic effects of Mev-range, on cancers, 17: 27000
therapeutic effects of, in pituitary adenomas, 18: 27258
therapeutic effects on skin diseases, 18: 29469
therapeutic effects on cancer using 200-kv, 18: 29539
therapeutic effects on bronchogenic carcinoma, combined AB-132 and, 18: 31330
therapeutic effects on cervical carcinoma, 20: 40772
therapeutic results of sieve irradiation, 16: 9785
therapeutic results with and without a grid exposure comparative results, 16: 9786
therapeutic results of high-energy, 18: 21946
therapeutic use, 19: 38499
therapeutic use, 19: 46078
therapeutic use during lung cancer surgery, 18: 35428
therapeutic use for cervical carcinoma, leukemia as possible complication in, 16: 18770(T) (AEC-tr-4956)
therapeutic use for pituitary-endocrine activity, 18: 11920
therapeutic use for leukemia, 18: 13590
therapeutic use for lung carcinoma, 18: 41098
therapeutic use for bronchial carcinomas, efficiency of sieve, 19: 13187
therapeutic use for cancer in children of, 19: 28143
therapeutic use for lung cancers, 19: 31950
therapeutic use for joint diseases, 19: 32022
therapeutic use for carcinomas, late pathological effects, 19: 32037
therapeutic use for cancer, 19: 31947
therapeutic use for prostate carcinomas, efficiency of supervoltage, 19: 34074
therapeutic use for arthrotic bone diseases, radiation dose to gonads during, 19: 36155
therapeutic use for carcinomas of breast, post-mastectomy, 19: 36199
therapeutic use for lymphosarcoma, 19: 36200
therapeutic use for cancer, 19: 38487
therapeutic use for cancer of larynx, effects on thyroid function, 19: 38484
therapeutic use in herpes keratitis, 19: 26165
therapeutic use in man, nephritis induced by, 18: 38791
therapeutic use of ultrahard, 17: 38677
therapeutic use of, dosimetry in, 18: 41163
therapeutic use of grid, for bladder tumors, 19: 7241
therapeutic use of, in palpebral carcinoma, 19: 22068
therapeutic use of, 19: 34023
therapeutic use of, depth-dose tables for, 19: 34077
therapeutic use of, computer calculation of dose distribution for, 19: 34088
therapeutic use of, in carotid sinus syncope, 19: 34093
therapeutic use of, for tumor therapy, 19: 43900
therapeutic use of, for carcinomas of esophagus, 19: 46051
therapeutic use of, for basal cell carcinoma, 19: 46059
therapeutic use of, for Hodgkin's disease, 19: 46067
therapeutic use on malignant tumors, advantages of conventional vs ultra-hard, 19: 34020
therapeutic use, beam direction and dosimetry for, 18: 11925
therapeutic use, evaluation of, 18: 41226
therapeutic uses, complications from, 19: 13173
therapy for childhood hemangiomata, effects on growth, 18: 17500
therapy for chronic myeloid leukemia, 19: 22043
therapy for retinoblastomas, 18: 27248
therapy for uterine carcinomas, pelvic injuries from, 18: 17489
therapy of breast carcinomas using, effects on bones, 18: 19673
therapy of cervical carcinoma using, followed by pregnancy, 18: 19565
therapy of cervical carcinomas using, complications after, 18: 25167
therapy of gynecological tumors using, isodose modulation during, 18: 149
therapy of mammary tumors, effects on vanillylmandelic acid excretion, 18: 21898
therapy of thymus, thyroid carcinomas from, 18: 17497
therapy of thyroid carcinoma using, 18: 13597
tolerance limits of skin to convergent pendulum, 19: 140
tolerance to, acquired by transfer of tolerant state in mice, 17: 19769
transmission by bone, measurement of mineral content by, 20: 3886 (ORNL-IIC-5, pp 290-4)
transmission by imperfect silicon crystals, 17: 6064
transmission by perfect silicon crystals, abnormal, 17: 6063
transmission factors for rectangular shapes, exact calculation of, 18: 5874
transmission in copper crystals, anomalous, 17: 18922
transmission in copper crystals, anomalous, 17: 34546(R) (ORNL-3480(p.17-28))
transmission in doped germanium single crystals, γ-radiation effects on, 19: 44756
transmission in germanium single crystals, Borrmann effect in, (E/T), 19: 18698
transmission through germanium single crystals, anomalous, 17: 16861(T)
transmission through germanium, temperature dependence of, 18: 22569
transmission through zinc crystals, thermal vibration effects on anomalous, (E), 19: 18693
transmission through air, calculations for, (T), 19: 27164 (SC-RR-65-141)
transmission through crystals, effects of crystal perfection on, 20: 20365
transmission through silicon, fast-neutron effects on, (E), 20: 42567(T)
transport in atmosphere from nuclear explosions, 18: 27596
tumor induction by fractionated and protracted whole-body exposure, 16: 21982
tumor induction by, in rats exposed *in utero*, 17: 17811
tumor induction by, in golden hamsters, 17: 28722
tumor induction by, in mice and rats, 17: 40637
tumor induction by, in children treated for thymic enlargement, 18: 6637
tumor induction by, in children treated for thymic enlargement, 18: 6638
tumor induction by, in children treated for thymic enlargement, 18: 6639
tumor induction in mice ovaries, effects of age and racial stock, 17: 17823
tumor induction in tobacco seedlings by exposure, 17: 23147
tumor induction in parabiont rats, osteogenic, 18: 8169
tumor induction in strains of *Drosophila melanogaster*, genetics of, 18: 9857
tumorigenic effects in mice, 18: 23231(R) (ANL-6823(p.20-43))
tumorigenic effects on rat islets, 18: 23286
tumorigenic effects in rat testes, 18: 38880
tumors induced by exposure, in Drosophila embryos, 17: 1273
tumors induced in kidneys in rats by, 17: 35464
tumors of salivary gland induced by, 16: 26826
urease inactivation by, effects of amino acids, buffer salts, and proteins on, 16: 1530
use as warning stimulus for rats, 20: 42852(R) (ORO-2903-28)
use for cancer therapy, comparison with other radiotherapeutic methods and triiodothyronine therapy, 20: 45558
use for diagnosis of gastrointestinal diseases, 17: 26986
use for post-operative therapy of brain tumors, 20: 20530
use for propulsion of interstellar vehicles, (T), 20: 36997
use for quartz crystal alignment for acoustic wave propagation at low temperatures, 20: 38366
use for radiotherapy of brain tumors, 20: 45560
use for therapy of skin tumors, 20: 171
use for therapy of cancers of uterus, effects of vitamin therapy on, 20: 191
use for therapy of benign skin lesions, 20: 3812
use for therapy of tumors of head and neck, 20: 5441
use for therapy of bladder cancers, 20: 5454
use for therapy of cervical carcinomas, effects of estradiol, 20: 5472
use for therapy of ear cancers, 20: 5474
use for therapy of carcinomas of larynx, 20: 5486
use for therapy of skin carcinomas, 20: 6928
use for therapy of eye tumors, 20: 6952
use for therapy of thyroid cancers, 20: 16307
use for therapy of scalp carcinoma, 20: 16308
use for therapy of stomach carcinomas, use of lead grating with, 20: 38763
use for therapy of facial tumors, absorbed dose in brain from, 20: 38765
use for therapy of uterine carcinomas, high voltage, 20: 38786
use for therapy of lymphomas, 20: 43014(R) (RLO-581-10, pp 33-6)
use for therapy of primary lung cancers, 20: 43041
use for therapy of pharyngeal cancers, 20: 43042
use for therapy of pharyngeal cancers, technique and dose distribution for, 20: 43020
use for therapy of skin metastases, 20: 43039
use for therapy of mouse leukemia, effects of allogeneic lymphoid cell transplants on, 20: 45552
use for therapy of tumors of head and neck regions, 20: 45556
use for therapy of ocular tumors in children, 20: 45375
use for therapy, RBE of electron beams and γ rays compared with, 20: 45543
use in angiography, 18: 31321
use in association with urethane to induce pulmonary adenomas, 20: 42891
use in astronomy, 19: 47207
use in astronomy, 20: 17244
use in cancer therapy combined with surgery, 20: 35363
use in cervical cancer therapy, intestinal injuries from, 18: 17535
use in commercial radiopreservation of food, costs of, 20: 31635
use in dentistry, exposure from, 18: 20261
use in detecting calcium microquantities, 18: 17431
use in determination of core position in reactor fuel elements, 19: 20135(P)
use in development of radioresistant line of Ehrlich ascites tumor, 18: 3559
use in diagnosis of placenta previa, 18: 29512

use in high-energy radiography, developments in, 18: 12327
use in inspecting solid rocket fuels and motors, 16: 5465 (USNRDL-TR-534)
use in lung therapy, pneumonitis induced in, 18: 27152
use in lymphosarcoma therapy, pneumonitis induction after, 18: 19566
use in materials testing, conference on, 20: 4116
use in medical diagnosis and therapy, review, 20: 5434
use in medicine, genetic burden of Hamburg, Germany from, 16: 4421
use in medicine, protective measures for, 19: 28128
use in menopause induction, complications from, 18: 29474
use in menopause induction, 18: 29427
use in moving-beam therapy, protective device for, 18: 17698
use in nondestructive testing of materials, 19: 598
use in pituitary ablation, brain necrosis induced by, 18: 38790
use in plant breeding programs, 20: 42846 (IAEA-2466-13)
use in production of transmission pictures of virus models, 20: 40653
use in radiodiagnostic ionography, 20: 43028
use in radiography of shipbuilding materials, 16: 24067
use in radiography, comparison with neutrons, 18: 39471
use in radiography, preparation of exposure charts for, 19: 46561
use in radiosterilization of pears, 16: 10370(T) (NP-tr-846)
use in radiotherapy, biophysical aspects of, 18: 17708
use in radiotherapy of cancers, 19: 32001
use in radiotherapy of laryngeal cancer, 20: 38782
use in radiotherapy, role in etiology of leukemia, review of, 20: 45250
use in respiratory function studies, 20: 20546
use in salmonellae control in meat, economic feasibility of, 19: 44557 (NYO-3426-1)
use in space communication systems, effects of cosmic noise, 16: 4667 (RADC-TN-61-87)
use in space communication, 16: 18698 (RADC-TR-61-219)
use in sterilization of ophthalmological pharmaceutical preparations, 18: 525
use in therapy, 19: 46077
use in therapy of eyelid carcinomas, 19: 46052
use in therapy of metastatic tumors, dose factors, 19: 46101
use in therapy of lymphosarcomas, 20: 5485
use in therapy of inflammations, 20: 16314
use in therapy of face, neck, and oral cancers, 20: 22818
use in therapy of mediastinal teratomas, 20: 33086
use in therapy of hemophilic pseudotumors of foot bones, 20: 33115
use in therapy of cervical carcinoma during pregnancy, technique to safeguard fetus, 20: 38759
use in therapy of sarcoma of limbs, tourniquet application to produce anoxia prior to, 20: 45517
use in therapy of hemorrhagic diathesis resulting from thrombocytopenia, development of acute leukemia following, 20: 45539
use in therapy of cerebral tumors in, sarcoma induction, 16: 20171
use in treatment of postoperative parotitis, 20: 45535
use in treatment of Hodgkin's disease, time-dose relations for, 18: 25251
use in treatment of leukemia, whole-body exposure followed by marrow infusion in, 16: 7469
use of beta-excited, analytical, 16: 22507
use of fluorescent beta-excited, for analysis, 16: 22508
use of fractionated-dose whole-body, for therapy, 20: 29069
use of high-energy, medical, 18: 11921
use of, in inspection for flaws, 16: 31954 (D2-9518)
use of, in medicine, status of, 17: 17698
use of iodine-125-produced, in thyroid autoradiography, 20: 45526
use of low-dose, for therapy in children, 20: 36707
use of orthovoltage, combined with cobalt-60 radiotherapy, economics and effectiveness of, 20: 38792
use of scattered, in radiography, 18: 11914
use of ultrahard, in therapy of gynecological carcinomas, 18: 41279
use of 4-Mev, with linear vaginal source for radiotherapy of cervical carcinomas, 20: 33108
use of, recommendations of Joint Committee on Chest X-ray, American College of Radiology and American College of Chest Physicians concerning safety of routine diagnostic, 20: 35359
use of, with open surgery for carcinoma of the bladder, 20: 35366
used for placenta previa diagnosis, evaluation of, 18: 29549
used with cortisone, effects on rabbit skin homografts, 18: 19613(T)
uses for radiation preservation of food, 20: 14938
uses in Commonwealth X-Ray and Radium Laboratory, 16: 2056 (NP-10982)
uses in diagnosis and therapy of diseases of endocrine system, 18: 29550
uses in diagnosis and therapy, effects of filter material on, 19: 268
uses in Finland, survey, 18: 9957
uses in measurement of porosities and saturations in porous media, 20: 29595
uses in medicine, control and hazards of, 19: 19657(R) (ANL-6938 (p.97-119))
uses in radioscopy for quality control, 18: 39752(T) (AEC-tr-6390 (p.342-6))
uses in textile industry to eliminate static electricity, 19: 30613
visibility of, relation of rhodopsin luminescence to, 20: 36587(T)
wavelength conversion factor for, (E), 19: 8197
wavelength variation effects on diffractometer accuracies, 16: 7711
wavelengths of, errors in measurement of, 20: 11069
wavelengths of, silicon-crystal determination of absolute scale of, 18: 34340
yields from atomic L_2 and L_3 shells, approximation formulas for, (T), 19: 41245
yields from light elements, K-, 17: 32789
yields from nuclei ($40 \leq Z \leq 51$), L-shell, 18: 40573
yields from proton inelastic scattering by nuclei at 15 to 1900 kev, (E), 19: 39881
yields from thermal fission of uranium-235 and plutonium-239, (E), 20: 26182
yields from 2p–1s meson (μ^-) transfer to neon, 17: 9586

X-RAY-ABSORPTION ANALYSIS

book: *Advances in X-Ray Analysis.* Vol. 5. Proceedings of the Tenth Annual Conference on Application of X-Ray Analysis, Denver, Colorado, August 7 to 9, 1961, 16: 25298
book: *Advances In X-Ray Analysis*, Vol. 6, 17: 34424
book: *Advances in X-Ray Analysis* Vol. 8, 19: 46185
book: *The Encyclopedia of X Rays and Gamma Rays*, 18: 8043
book: *X-Ray Optics and X-Ray Microanalysis*, 20: 7045
coefficient determination using scintillation counters, 16: 19078 (TID-15696)
coefficients of, for 87 elements, 17: 22266 (BM-IC-8166)
design of system for determination of elements, 18: 7023(P)
development of, for elements 23 to 46, and 58 to 94, 16: 31545 (LADC-5198)
developments in, review of, 18: 19862
differential method for photons of varying energy, 16: 14780
equipment, 17: 21401(R) (TID-18585)
equipment and method for comparative, 18: 5249(P)
equipment and methods for fluorescence, 18: 12016
equipment and methods development for, 19: 17781(R) (ORNL-3750)
equipment and methods for, 20: 17158(R) (ORNL-3900, pp 82-149)
equipment and method for, of process streams, 20: 39191(P)
equipment for, design of high-pressure, 17: 4848
equipment for monochromatic, of mixed samples, 20: 14505(P)
equipment for sulfur determination in liquid oil products, 18: 33472(T) (AEC-tr-6399(p.98-114))
gamma-emitter activity in, method for calculating, 20: 14498
industrial uses, 19: 9348(T) (FTD-MT-63-261)
method for silver determination in x-ray film, 19: 32078
methods and uses, 16: 28866 (HW-SA-1972)
methods and uses in nuclear chemistry, 17: 33790 (EUR-270.e)
methods development for, 18: 13633(R) (ORNL-3537(p.60-4))
methods for elemental analysis, 17: 40761
methods using alpha or beta particles for exciting x-ray spectra, 18: 6778(P)
of powdered minerals and ores, instrument for automatic continuous, 20: 37152
parameters for defectoscopy, 16: 29180
performance for alloys and coatings, 17: 29957
performance of, using beta-excited sources, 20: 23527 (CONF-651206)
quantitative, with beta-excited x rays, 16: 691
quantometer for, design of 10-channel single-crystal focusing, 17: 40751
sensitivity of absorption, formulas for, 19: 28251
source for, design of gamma-excited, 19: 36876
sources for, use of beta-excited copper, iron, and molybdenum, 20: 3882 (ORNL-IIC-5, pp 51-71)
survey of theory and operation, 17: 10947
use for analyses of carbonaceous fuels, 17: 29890
use for determination of cobalt in complex mixtures, 17: 4462
use for gas composition and density measurements, 17: 29889
use for sediment determination in surface waters, (E), 19: 29133(R) (NYO-10221)
use for testing dispersion fuel plates for fuel inhomogeneity, 19: 12761 (ORNL-3737)
use for thin film measurements, 18: 5573 (CONF-229-2)
use of beta-excited x-ray sources in, 20: 22877(R) (TID-22846)
use of iron-55 in analysis of petroleum products, 19: 28230
uses for inspection of reactor fuel plates, 18: 27846(R) (ORNL-3578 (p.60-6))
x-ray sources in, beta-excited, 20: 33235

X-RAY ABSORPTION CROSS SECTIONS

mass absorption coefficients near K absorption edge, 17: 9217

X-RAY BEAMS

attenuation by body compositions, 20: 3885 (ORNL-IIC-5, pp 277-89)

bibliography on, 17: 38647 (WP/22/6)
biological effects of high-intensity microsecond pulsed, 16: 21895(R) (AD-266956)
bremsstrahlung determination in, using scintillation spectrometry, 16: 19677 (TID-15698)
characteristics of, in 15-Mev betatron for nondestructive testing, 17: 36001
collimation of, design of adjustable-aperture devices for, (E), 20: 2162
delineation of diagnostic, circular and elliptic, 17: 10273
development of, for use in therapy, 18: 6725
direction of, in treatment of bladder tumors, 19: 9031
dosage determinations for sterilization of graft materials, 16: 26810
dose correction factors for, exit-surface skin, 18: 11930
dose distribution in water, isodose plotter for, 17: 34212
dosimetry at edge of, effects of ionization chamber size on, 17: 6445
dosimetry of, 20: 8712
dosimetry of radar, 20: 9188
dosimetry of single or multiple fields of linear accelerator, computer calculation of, 19: 2194
dosimetry of therapeutic, 20: 22844
dosimetry of wide, in finite phantom thickness, 19: 40881 (UR-667)
dosimetry of 6 Mev, entrance and exit, 18: 11929
dosimetry of, contribution of scattered radiation to, 18: 25838
dosimetry of, from accelerator, 20: 1721
effectiveness in therapy of gynecologic tumors, 17: 2846
effects on leaching rate of bauxite and hydrargillite in alkaline aluminate solutions, 19: 36516
effects on tissues, biological, 20: 8712
effects on tissues, biological, 20: 18548
electrons from betatron, secondary scattered, 17: 39342
energy distribution of, from 250-kv constant-potential machine, 19: 20256 (HASL-151)
energy distribution of unfiltered, from 250-kv constant potential machine, 20: 45951 (HASL-179)
energy flux in 6-Mv, calorimetric measurements of, 19: 28677
energy of, determination of total, 18: 34274(R) (NIRS-2(p.3-15))
energy transported by, measurement of total, 16: 33186
exposure to, shutter design for accurate timing of, (E), 19: 41186
focusing of, tube design with elimination of off-focus rays for, 18: 14181
geometry of, for radiotherapy, 19: 4036
intensity at 20 to 90 Mev, design and performance of ionization chamber and quantometer for measuring, 19: 7795
intensity measurement of, design of apparatus for, 17: 10975
intensity measurements using thermoluminescent dosimeters, 17: 32402(R) (TID-19112)
intensity regulation in polychromatic, device for, 16: 29130
measurement of intensity of, with silver-activated glass block dosimeters, 19: 34558
measurement of quality of, using solid-state detectors, 18: 22364
positioning method for small-diameter, for back-reflection analysis, 16: 19134
production by electron linear accelerators, parameters for, 17: 33135
production in linear accelerators, 16: 23976 (ANL-6515(p.218-47))
production of filtered pulsating, for calibration of ionization chambers, 17: 23739 (HASL-133)
production of modulated, 20: 29516(P)
production of monoenergetic 63-, 105-, 150-, and 180-kev, 16: 29100 (HASL-129)
production of pulsed, equipment for, 19: 34461(P)
production of very narrow, 18: 43919
profile measurements on, automatic scanner for, 17: 39399
properties for use in therapy, comparison of cobalt-60 radiation with, 19: 28159
protective effects of hardening, during radiography, 20: 3815
proton energy range in 45- to 105-kvp diagnostic, 20: 26726
quality of, effects on dose to patient during fluoroscopy, 20: 43050
quality of, factors affecting, 18: 39039
radiation dose from 200-kv, during therapeutic radiography, 18: 17702
radiation dose measurements for betatron, 19: 22729
reduction of, in dental radiography, 17: 36062
scattering by matter, method for absolute intensity measurement of small-angle, (E), 20: 24633
scattering by matter, perturbation reduction in small-angle, 20: 24634
scattering by polished surfaces, anomalous, (E), 19: 6408
skin surface ionization reactions, 17: 31871
spectral measurements on high and supervoltage therapy, 19: 10096
therapeutic use of high-energy, 19: 28174
therapeutic use of accelerator supervoltage, 19: 34015
therapeutic use of betatron, radioactivity induced in patients by, 19: 40392 (NYO-3364-6)
use for diagnostics of cold cathode glow discharge gas densities, 18: 19188
use for gas density measurements, 18: 12415 (GNE/Phys/63-14)
use of betatron, in treatment of brain tumors, 17: 37024(T) (JPRS-21086)
use of high-LET, for therapy, 20: 18507 (BNL-10009)
use of narrow, for reduction of patient dose during diagnostic radiography, 20: 1698

X-RAY CAMERAS

applications in studies of lung parenchyma, 19: 10935
calibration and performance of Guinier for interplanar lattice parameters, 16: 19060 (AE-67)
collimator and shutter coupling for, 20: 5693
description and performance of rocket-borne, for measuring solar x-ray flux, 16: 14959
description of microbeam, for determining orientation of small metallurgical samples, 17: 18572
design, 19: 9462
design, 19: 17756
design and operation of vacuum high-temperature, 16: 14904 (CEA-2076)
design and operation of microbeam, 18: 13441 (BL-85)
design and performance of microbeam, 19: 32514
design for metallography at high temperatures, 17: 29353
design for study of single crystals, 17: 8531 (PAN-333/I-B)
design modification for Debye-Scherrer diffraction, for powder patterns of alpha emitters, 20: 11075
design of pinhole, for use in dentistry, 17: 5688
design of precession, for crystal structure studies, 18: 29830
design of precision back-reflection Laue, 20: 14820 (RFP-636)
design of symmetrical back reflection focusing, with microfocus tube, 20: 46012 (INR-697/XIV/PS)
design of 12-ton high-pressure, engineering drawings of, 19: 40865
development for micrographs, 18: 29831
development of high-temperature, for use in diffraction of uranium powder, 18: 27947 (CEA-R-2426)
development of Lang, 17: 5037(R) (ORNL-3364(p.27-56))
development of low-temperature, for use in x-ray spectrography, 17: 27670
film holder for, modification of Polaroid, 18: 1491(R) (ORNL-3488 (p.102-22))
filters for, fabrication of strontium, 20: 5692
industrial uses, 19: 9348(T) (FTD-MT-63-261)
modifications of, 17: 33436
performance for stellar sources, 19: 14224
photographs from, short-exposure-time, 19: 46729(T) (LA-tr-65-21)
temperature errors in high-temperature powder diffraction, 16: 26899 (AERE-R-3818(p.69-78))
use of Berg-Barrett, for studying grains in alpha plutonium, 18: 16482 (UCRL-7651)

X-RAY-DIFFRACTION ANALYSIS

area weight calculations for uranium planes, 19: 946 (DP-904(p.7-21))
beam smearing and desmearing in small-angle, 20: 33187(T) (ORNL-tr-1113)
beam transmission in anomalous absorption in, 17: 37540(T)
book: *Advances in Structure Research by Diffraction Methods*, 18: 41477
book: *Advances In X-Ray Analysis*, Vol. 6, 17: 34424
book: *Advances in X-Ray Analysis*, 18: 41728
book: *Advances in X-Ray Analysis* Vol. 8, 19: 46185
book: *Advances in X-Ray Analysis, Vol. 9*, 20: 43267
book: *Apparatuses for X-Ray Diffraction Analysis*, 16: 155
book: *Single Crystal Diffractometry*, 20: 46962
book: *The Encyclopedia of X Rays and Gamma Rays*, 18: 8043
book: *The Theory of Crystal Structure Analysis*, 16: 4654(T)
book: *X-Ray Studies of Materials*, 18: 5810
book: *X-Ray Diffraction Analysis of Raw Materials*, 20: 36386
book: *X-Ray Optics and X-Ray Microanalysis*, 20: 7045
Bragg angles in powder, computer program for, 17: 25842 (AAEC/TM-190)
calculation of grain orientation distribution function and thermal expansion coefficients in, 17: 29393 (TID-17080)
calculation of unit cell parameters from powder patterns, 16: 5311(R) (TID-14361)
centroid wavelength determination for powder profiles for Kα satellite group, 18: 14611
comparison with neutron-diffraction analysis, 16: 27697(T) (AEC-tr-5170)
computer program for Fourier analysis of data from, 17: 12582 (RFP-297)
computer program for indexing powder patterns, 18: 4905 (IS-683)
computer program for lattice type and cell constants from x-ray powder diffraction data, 18: 26108 (IS-839)
computer program for indexing powder patterns of, for cubic case, 19: 19834 (HW-74393)
computer program for indexing powder patterns of, for orthorhombic case, 19: 19835 (HW-89062)
computer program for indexing powder patterns, 19: 30729 (BNWL-22)
conference on, 16: 26890 (AERE-R-3818)

conference on, West Concord, Mass., Dec. 7 and 8, 1961, 17: 30975 (NMI-4992)
crystal lattice parameters for, fundamental and modulated reciprocal, 20: 34802 (ANL-7147)
crystal structure determination by, table for dispersion corrections in, 20: 29722
data from, computer program for handling, 18: 9971 (ORNL-TM-750)
data handling for crystallographic, computer programs for, 18: 41905 (AROD-3083.14)
data handling for crystallographic, computer program for, 19: 23955 (LA-3198)
design of high-pressure cell for powder patterns up to 500 kilobars, 18: 8621
determination of structure of Vitamin B_{12} using, 18: 31067
development for thoria and urania crystallite size determination, 20: 15044(R) (MCW-1493, pp 15-25)
development of computerized, 20: 23527 (CONF-651206)
development of, for indexing powder patterns, 16: 33465 (ANL-FGF-360)
development of high-temperature, 19: 6142 (ARL-64-82)
developments in, review of, 18: 19866
diffraction peaks in, crystallite size distribution from broadening of, 20: 34858
diffuse scattering due to static atomic displacement and thermal motion in method for correcting for, 20: 4391(R) (ORNL-3870, pp 75-82)
dispersion corrections for cobalt and silver, 17: 41575
dispersion corrections for Z = 10 to 98 elements, anomalous (T), 19: 2961 (LADC-6146)
electron correlation in, 18: 40124
end point detection in, 19: 9067
equations for minimum receiving aperture widths in single-crystal, 19: 10703 (UCRL-7680)
equipment and techniques for, 18: 25971(R) (ANL-6868(p.331-7))
equipment design for narrow-beam small-angle, 18: 43919
equipment design for, 17: 10894 (HW-SA-2616)
equipment for alpha-active powder, design modification for, 20: 11075
equipment for cooling crystals in, 18: 1853
equipment for crystallized gas, cryostat, 19: 38946
equipment for electron probe, 17: 41233(P)
equipment, vacuum chamber for films, 16: 15277 (TID-15255)
extinction correction in crystals, 16: 2310
goniometer design for orientation of single crystals, 19: 30484 (INR-587/II)
goniostat design for use in, 17: 12571
industrial uses, 19: 9348(T) (FTD-MT-63-261)
instrumentation for precision, 18: 43937 (NP-14265)
intensity corrections for weakly absorbing polycrystals, 18: 26104 (BM-RI-6455)
intensity measurements in, physical factors affecting total, 16: 26892 (AERE-R-3818(p.5-18))
intensity measurements in, goniostat for three-dimensional, 19: 24827
intensity measurements in, conference on accuracy of, 20: 18017
intensity measurements of irradiated samples during, automatic device for, 20: 43646
interference in, kinetic theory for, 20: 34863
lattice constant measurement with recording goniometers at high temperatures, errors in, 19: 42855(T) (AERE-Trans-1027)
line breadths and peak height for α_1 α_2 doubling effects, correction tables for, 17: 15873 (AERE-R-4218)
line profile correction in, Mercury computer program for, 16: 26898 (AERE-R-3818(p.61-8))
line profile evaluations in, review of methods for, 16: 26897 (AERE-R-3818(p.54-60))
line profile in, physical factors affecting, 16: 26891 (AERE-R-3818 (p.1-4))
measurement errors in, for determination of d spacings, 17: 34428
measuring strain in ceramic bodies, biaxial and triaxial, 16: 1998
method for determination of background intensities for preferred orientation measurements, 18: 22563
methods and experimental considerations in small-angle, 18: 36077 (AD-602781)
methods for biological material, 18: 10655
methods of, in crystal lattice dynamics, 18: 10656
methods of, uses of chloral hydrate in, 19: 30251
modified Polaroid film holder for, 18: 5591
of liquid-like binaries, radial density functions for, 17: 37524
of liquid metals, high-temperature furnace for, 19: 22882
of liquid metals, review, 19: 26812 (CEA-Bib-54)
of liquids, beryllium sample cell design for, 16: 16560
of metals at high temperatures, method for, 17: 39265
of mosaic crystals, secondary extinction coefficient for, 17: 32829
of new alloys and compounds, 18: 44048(R) (ORNL-3670(p.56-63))
of phases in type 316 stainless steel subjected to high temperatures, 20: 41419(R) (GMAD-3643-5)
of powders, computer program written in FORTRAN for calculating diffraction patterns in, 17: 25677 (UCRL-7196)
of radiation damage in perfect crystals, 18: 39992 (EUR-1643.e(p.231-45))
of structural change phenomena, effects of time on, 19: 38826
of thermal motions in crystals, 16: 13697 (NP-11338)
of thermal stresses near welds in steel pipes, 17: 292 (HW-74643)
pattern indexing for tetragonal, hexagonal, and orthorhombic crystals, charts for, 19: 40080 (NP-15182)
pattern line breadth in, computer program for correcting, 20: 9505 (WAPD-TM-521)
performance of, using beta-excited sources, 20: 23527 (CONF-651206)
point-by-point study of crystal surfaces by Berg-Barrett methods, 18: 25035(T) (UCRL-Trans-1055(L))
pole figures for aluminum, preparation of accurate, 18: 29150 (SC-DC-64-765)
positioning method for small-diameter x-ray beams, 16: 19134
powder pattern generation and structure factor calculations for, computer program for, 19: 47877 (LA-3335)
pseudo-Kossel patterns of uranium single crystals, 19: 16066 (CONF-650210-2)
radiation hazards in, 17: 20247
reflections from crystal monochromators, relative intensities of higher order, 19: 26627 (CALT-221-7)
reflections from dislocations in crystals, model calculations, 18: 44293(T) (AERE-Trans-1010)
research progress on, 18: 15711(R) (TID-20256)
resolution in holography, method for improving, 19: 20297
silicon-crystal measurement of absolute scale of x-ray wavelengths, 18: 34340
singularities in coherent diffuse scattering, 20: 39586
standards for, site measurements on tungsten samples, 19: 721 (DP-904 (p.29-33))
statistical fluctuations in intensity, use in substructure measurements, 19: 46993 (CONF-650810-3)
summary of, 16: 30170(R) (ORNL-3313(p.179-208))
survey of theory and operation, 17: 10947
tables for radioactive-mineral, d spacing and intensity, 18: 33794 (NP-14176)
technique development for biological studies, 20: 232(R) (NYO-901-37, pp 80-4)
techniques for atomic local arrangements and displacements in solid solutions, 19: 31447 (ORNL-P-1240)
techniques for liquid metals, 18: 10542(R) (TID-20065)
techniques of high-temperature, using metal ribbon furnaces, 17: 19978
temperature errors in, 16: 26899 (AERE-R-3818(p.69-78))
theory for short-range-order studies, 17: 36289 (ASD-TDR-63-567(Pt.1))
thermal expansion measurements from lattice parameters of Debye-Scherrer specimens, 18: 26109 (LA-2687)
use for crystal defect structure studies, 20: 9379(R) (NAA-SR-11650, Sect.4)
use for detecting second-order stresses and measuring crystal block sizes, 17: 30989(T) (TRG-Inf.-Ser.-310)
use for monitoring plant streams, 18: 37495(P)
use in continuous study of structural changes in materials, 17: 25429(P)
use in crystallite size analysis, 16: 30806 (TID-16573)
use in mineralogic and petrographic studies of Tyrrhenian Sea sediments, 20: 22536(R) (TID-22837)
use in studies of lattice defects, 17: 35795
use of high-temperature, in metallurgy, 17: 16667
use of Polaroid film in, 16: 8962
use of proportional detectors in, 16: 17844
use to measure preferred grain orientation in uranium, conference on, 19: 888 (DP-904)
uses, 17: 27242 (TID-18925)
uses at ANL, 20: 31167(R) (ANL-7175, pp 217-25)
uses in metallography, conference on, 20: 15943 (RL-REA-2595)
x-ray collimators for, development of, 19: 7312
x-ray sources for, iron-55, 20: 24992

X-RAY DIFFRACTOMETERS

adaptation of, for x-ray reflection studies of thin films, 18: 8624
book: *Single Crystal Diffractometry*, 20: 46962
comparison with neutron diffractometers, 16: 27697(T) (AEC-tr-5170)
construction of theta-theta, 17: 37464(R) (TID-19394)
data collection from, automatic counting and recording system for, 18: 27786 (CEA-2335)
description for wavelengths above 10 Å, 18: 2097
description of commercial counter, adapted for high-temperature operation, 17: 39372 (BNL-6728)
design, 20: 15064(T) (AD-625748)
design and development for examining irradiated uranium carbide, 17: 41364(T,R) (EURAEC-562)
design and performance of germanium bent-crystal, 17: 23624

design and performance of, for liquid structure analysis, 20: 35395 (ORNL-3960)
design for high-temperature operation, 16: 23837 (ARL- 62-315)
design for scanning fluorescent x-ray spectra, 17: 8578(P)
design modifications for examination of gamma emitters, engineering drawings for, 20: 3910
design modification of, with continuous averaging technique for avoiding drift effects in scattering measurements, 20: 41327
design of automatic, for pole-figure analysis of polymer orientation, 19: 36767 (TID-21952)
design of computer-controlled, 19: 280(R) (ORNL-3679(p.94-116))
design of double bent-crystal, 18: 7058 (TID-19849)
design of, for medium-level radioactive samples, 17: 40703 (TID-7655 (p.119-34))
design of, in combination with electron probe microanalyzer, 17: 33855(P)
design of modulated, for radioactive materials, 18: 10347(T) (JPRS-22697(p.146-62))
design of punched tape-controlled, 17: 25578
design of small-angle, with linear collimation, 16: 13763
design of theta-theta, with stationary sample holder, 17: 37400 (TID-19393)
development and testing of automated, 16: 33476 (HW-74429(p.67-79))
development for stellar x rays, 19: 14224
development of, for use at 2000 to 2400°C, 16: 31830 (UCRL-6835-T)
Dewar vessels for, design of double, 17: 39400
furnace design for high-temperature, 19: 44340 (AERE-M-1361)
geometry for three-dimensional studies of single crystals at high and low temperatures, 19: 15822 (AERE-M-1515)
goniometer scanning of, design of program controller for, 20: 41222 (DP-900)
goniometer with single-crystal orienter and grinder, 19: 44694(R) (NP-15432)
imperfections in, errors in measurements resulting from, 17: 34428
measurement accuracies, relation to wavelength variations, 16: 7711
operation of, safety in, 20: 16782
operation of, systematic absences in, 19: 4457 (ISS-64/20)
performance for residual-stress analysis in uranium, 20: 15945 (RL-REA-2595, pp 43-50)
performance of double-diffracting and standard, comparison, 20: 14823 (RL-SA-2595, pp 73-9)
performance of, effects of scintillation-counter window width on, 18: 41783
radiation hazards during use, 16: 8556
radiation intensity distributions in, effects of Soller slits on, 20: 2161
sample cask for shielded, 19: 32059(R) (IDO-14655)
sample heating in, furnace for, 19: 38941
sample temperature measurement in, calibration procedure for, 20: 7337 (AERE-R-4556)
shield design for, 17: 6220
slit mount for, design of radiation proof, 20: 43661
specimen table design for, 17: 20341(P)
spinner for, averaging principles and uses of flat-specimen, 17: 39379 (NAA-SR-Memo-8902)
survey, 17: 18571
use for analysis of deliquescent and pyrophoric samples, 20: 43068(R) (IDO-14679, pp 47-50)
use for lattice parameter determination on single crystals, 17: 39016 (AAEC/TM-211)
use of Geiger-counter, in determination of lattice constants, 19: 44722
vacuum chamber for high temperatures up to 2500°C, 19: 30493(T) (AEC-tr-6559)

X-RAY EQUIPMENT

(See also specific items of equipment.)
see also Radiography
see also X Radiation
see also X-Ray-Diffraction Analysis
adjustment of, to reduce patient dose during diagnostic radiography, 18: 11938
beam intensity regulation in, device for, 16: 29130
beryllium window for, development of mechanical, demountable seal for, 19: 15703
betatron for nondestructive, materials testing, portable, 18: 25677
book: *Advances in X-Ray Analysis, Vol. 9*, 20: 43267
book: *Apparatuses for X-Ray Diffraction Analysis*, 16: 155
book: *The Encyclopedia of X Rays and Gamma Rays*, 18: 8043
book: *X-Ray Optics and X-Ray Microanalysis*, 20: 7045
bremsstrahlung from 600-kvp unit, 16: 22330 (TID-16041)
bremsstrahlung production in 1.5 Mv electrostatic generator, spectra of, (E), 19: 11869
calibration of diagnostic machines, 17: 1271
calibration of pulsed, 20: 9166(R) (BNWL-36, pp 2.1-58)
calibration procedures for, for clinical radiology, 18: 31356
coincidence losses in, nonlinearity correction equation for, 16: 8959
collimator and detector system design for scattering analyses, 18: 43937 (NP-14265)
collimator design, high-resolution, 19: 15828
control of physical standards for, 18: 25248
control of voltage and voltage variation in, 17: 30241
control of, in California, 19: 34413
conversion efficiencies of conventional image amplifiers, 19: 46151
dental and medical, Alaska program for control of, 20: 37042
dental, design for dose reduction, 17: 36062
dental, design of collimator for reduced gonadal exposure in, 17: 20267
dental device to reduce patient dose and improve film quality, 17: 34175
dental, methods for reduction of exposure from, 17: 20261
dental, safety measures in, 17: 16349
dental, survey of hazards and safety practices in use of, 17: 20272
dental, survey of operation of naval, 17: 20268
description of fine focus medium energy tube for radiobiology and crystallography, 19: 20291
description of innovations in, 17: 20326
description of 250-kv facility for calibrating radiation detectors, 19: 20256 (HASL-151)
design alterations of materials testing unit for use in animal irradiation, 18: 29370
design and performance for analysis of metal specimens, 16: 26894 (AERE-R-3818(p.22-37))
design and performance in detecting beryllium impurities, 17: 15890 (Y-1403)
design and performance of IBM 300 kev flash, 18: 14348(R) (RTD-TDR-63-3051)
design and performance of low-inductance flash system, 20: 23433
design and performance of dilatometer, for measuring strain in crystals, 20: 35716
design and performance of specimen-testing, with temperature control using gas streams, 20: 37047
design and use of autofluoroscope, 20: 43051
design developments, 19: 10955
design for autofluorography, 19: 17760
design for chest radiography using ytterbium-169, 20: 3804 (ORNL-IIC-5, pp 309-28)
design for kinescopic recording of fluoroscopic information, 18: 11948
design for measuring paper web density, 18: 12437(P)
design for radiation chemistry, 16: 1829
design for radiography of circumferential welds in small-diameter tubes, 20: 7242 (LA-DC-6977)
design for radiotherapy, 20: 4517
design for reduction of gonadal dose during radiodiagnosis, 18: 3653
design for use in x-ray microprobes and spectrographs, 19: 309
design for use in urethrographic examinations, 20: 5459
design modifications for obsolete, to improve radiation protection, 19: 43909
design modification of portable, to reduce radiation dose, 20: 8796
design of apparatus for determining cardiac chamber volume from cinefluorographic films, 17: 19755
design of cone, 17: 4800(P)
design of digital integrating dose meter for use in therapy, 17: 27164
design of emission analyzer, 18: 16292(P)
design of film holder and filter for dental, 17: 18433
design of fluorescence, for spectral analysis of rare earths and yttrium, 18: 39135
design of fluoroscope using gamma source instead of x-ray tube, 18: 25234 (SGAE-IB/IA-2/1964)
design of, for generation of soft x rays, 17: 18237
design of, for high-energy inspection, radiological aspects of, 17: 10192 (AD-275297(p. 173-91))
design of furnace for intensity measurements on powders, 19: 47009 (NP-15514(Vol.2))
design of high-pressure, 17: 4848
design of high-pressure cell for powder patterns up to 500 kilobars, 18: 8621
design of image intensifier tubes for fluoroscopy, 18: 43958
design of image intensifier, 19: 7775
design of instrument for rapid measurement of field flatness, 17: 30310
design of low-voltage generator, 17: 24892(R) (NYO-10451)
design of miniature, using iodine-125, 20: 14677(P)
design of orienting device for metal single crystals, 17: 12543
design of port structure for rectangular beams, 18: 26994(P)
design of portable low dose, 18: 13598
design of portable fluorescent, using radioisotope sources, 18: 25275
design of reflectometer for thin film studies, 18: 8624
design of serialograph with movable cassettes, 19: 38955(P)
design of shutter apparatus, 16: 27186(P)
design of soft tube for radiotherapy of hemangiomas, 17: 26991
design of tube with reentrant cavity for material to be irradiated,

16: 21895(R) (AD-266956)
design of tube with secondary target for producing K lines, 17: 20766
design of tube with anode-specimen contact, 17: 41221
design of tube with off-focus x-ray eliminator, 18: 14181
design of ultrasoft tube, 18: 27636(P)
design of vacuum reflectometer, for determination of radiation deflection on films, 17: 12704
design of variable-aperture collimators, (E), 20: 2162
design of very-thin-window tube, 18: 8647(R) (NYO-2740-1(p.75-90))
design of x-ray tubes with mercury-vapor targets, 19: 746
design of, for dental radiography, 19: 22066
design of, for fluoroscopic image intensification during diagnostic radiography, 18: 11946
design of, for fluoroscopic image intensification during diagnostic radiography, 18: 11944
design of, for microanalysis of low atomic number elements, 19: 4094
design of, for reduction of patient dose during diagnostic radiological examinations, 18: 11937
design of, for x-ray spectroscopic analysis using promethium-147 beta source, 20: 36765
design of, to reduce radiation dose to patients and physicians during radiography, 18: 25241
design using iodine-125 for measuring mineral changes in bones, 20: 3803 (ORNL-IIC-5, pp 257-76)
design, for radiation dose reduction during diagnostic chest radiography, 19: 13177
development and use of, for fluoroscopic fuze evaluation, 17: 10190 (AD-275297(p. 116-20))
development at Grenoble Nuclear Center, 19: 46512
development for determining minute inhomogeneities in solids, 19: 22514
development for low-dose diagnostic fluororadiography, 18: 15936
development for use in diagnostic radiography, 19: 31931(T) (NP-tr-1237)
development in Japan, 19: 33644
development of diagnostic, to reduce radiation exposure of patients, 19: 34070
development of flash tubes and pulsers, 16: 6551 (UCRL-13025)
development of flash, for analysis of radiolysis of condensed systems, 16: 10050(R) (TID-14969)
development of fluorescent screens for use in diagnostic radiography, 18: 11954
development of, for photographing high-speed phenomena, 17: 10194 (AD-275297(p. 302-4))
development of, for analysis of various metals and welds, 17: 15857(R) (ORNL-3397(p.57-70))
development of, for use in calibration of radiac equipment, 17: 23736(R) (AD-285660)
development of grids for image intensifier fluoroscopy and cineradiography, 18: 11953
development of image intensifier tubes for use in, for fluoroscopic examinations, 18: 11945
development of image intensifier tubes for use in, for fluoroscopic examinations, 18: 12427
development of optic glass fibers for fluoroscopy, 17: 31822
development of portable fluorescent, using promethium-147/aluminum source, 19: 13221
development of portable fluorescent, using promethium-147/aluminum source, 20: 3883 (ORNL-IIC-5, pp 154-81)
development of 2-Mv radiographic flash, 19: 9451(R) (UCRL-13134)
development of, for image intensification, 19: 26172
development of, for reduction of radiation hazards, 20: 12757
development of, for fluorescence analysis of ore slurries, 20: 18593
development of, in dental offices in Jefferson County, Alabama, 18: 16247
development of, to reduce patient dose during diagnostic radiography, 18: 11939
developments in analytical, review on, 20: 22885
developments in, review, 18: 3647
device for exposure control in cineradiography, 18: 19829
device for genetic protection in chest radiology, 17: 39319
dosage to man during fluoroscopy, factors contributing to, 20: 33133
dose distribution using, 18: 15943
dose-limiting factors for diagnostic, 17: 39339
dose measurements in vicinity of dental x-ray unit, 17: 32308
dosimetry and radioprotection near Pulsed High Energy Radiographic Machine Emitting X-rays (PHERMEX), 17: 1657 (LADC-5501)
effects of high-speed systems on image quality using, 18: 11951
effects on radiation dose during diagnostic fluoroscopy, 19: 28138
efficiency of radiographic intensifying screens in, 18: 11955
electron diffusion in x-ray microanalyzer specimens, (E/T), 19: 26937
electron impact on tube targets, backscatter from, 18: 8635
energy spectrum of pulsed tubes, hard-component, 19: 6061
evaluation in Mississippi, 18: 22303
evaluation of efficiency of diagnostic, 19: 13797
evaluation of possible hazards from dental, used in U. S., 20: 45975
filters for diagnostic, aluminum and iron, 19: 13152
filters for, aluminum wedge, 18: 31325
flash tubes for roentgen-ray generation, 18: 20308
for diagnostic chest examinations, evaluation of, 19: 10971
for diagnostic radiography, survey of, 18: 13579(T) (JPRS-23317)
grid evaluation for diagnostic, 19: 46147
hazards in industrial use, 16: 11981
hazards of, in medicine, 17: 20265
hazards of, review on external, 17: 16335
hoist for, design with automatic securing means, 19: 32341(P)
hygiene in dental, 17: 10871
image quality and speed of film-screen combinations in diagnostic, 19: 46149
image-retaining panel for, evaluation of dental use of, 18: 33443
inspection program for, evaluation of, 18: 41264
inspection to assure accurate dosage of therapeutic, 16: 17942
installation and testing of, radiation hazards of, 18: 3601
leakage detection in tubes, development of apparatus for, 17: 11018
limitations of optical image intensification, technical, 19: 46744
mercury vapor target tubes, 18: 20653
modification of films for chest examination, diagnostic value and economics of, 17: 27610
nomenclature and properties of, 20: 4228
operation of, 20: 23418
operation of, design of protective nozzle for use in, 18: 3670(P)
operation of, to reduce patient dose during diagnostic radiography, 19: 10924
output and tube current characteristics of, 19: 241
output of, effects on dose to patient during fluoroscopy, 20: 43050
parasitic radiations in tubes, 17: 18573
pendulum-type arrangement of, for mammary cancer radiotherapy, 20: 35365
performance for detection of shallow buried objects, 18: 23782 (NP-13943(p.117-27))
performance for fluidized-bed reactor analysis, 19: 40224 (LA-3229, pp 63-82)
performance in radiography, effect of tube-voltage and -current waveforms and kvp on, 19: 24656
performance of a stereoscopic televised fluoroscopy system, 18: 11949
performance of flash, 19: 46735
phosphors for diagnostic, efficiency of, 19: 46148
power supply for, design of automatically adjustable, 19: 32343(P)
properties and uses, review, 16: 9329
properties as radiation source, 16: 5628
properties of dental, photographic film for determining, 20: 16844
properties of grids to reduce scattered radiation in medical radiography, 18: 27254
protective device for, design of, 18: 17698
quantum statistics of x-ray-image-intensifying systems for, for fluoroscopy, 18: 11947
radiation dosage reduction in fluoroscopy, methods for, 17: 20248
radiation dose during fluoroscopic procedures, 16: 8473
radiation dose to personnel from, in past, 18: 31817
radiation dose to hand from old, estimation of, 18: 31317
radiation dose to personnel working near, 20: 45998
radiation doses received in cardiac, chest, and gastrointestinal fluoroscopy, 17: 20258
radiation exposure reduction in dental units in Alabama, program, 19: 28129
radiation exposure reduction during fluoroscopy, 20: 8747
radiation from IBM 300 kev flash, 18: 14348(R) (RTD-TDR-63-3051)
radiation hazards from dental, 17: 14572
radiation hazards from dental, 17: 25482 (TID-18708)
radiation hazards from mobile image intensifier, 18: 39001
radiation hazards to operators from, 20: 45968
radiation injuries to right hand from handling of, 18: 19706
radiation protection during, 18: 8242
radiation protection of operators of fluoroscopic equipment, 18: 25249
radiation protection during industrial uses of, 18: 41696
radiation protection during operation of industrial, 20: 38737
radiation protection for, 20: 45518
radiographic effects of tube voltage and current in, 18: 40063
radiography specifications for, 18: 15930
regulations for Polish, 18: 43330
reliability of timers and output on various types of dental x-ray units, 20: 35372
safety measures for, 18: 5154
safety of, 19: 3981
safety of dental, 19: 7753
safety of dental, survey in Australia, 20: 9187
safety of, in physician's offices, Baltimore, 1963, 18: 35793
safety survey of diagnostic, 19: 11456
scattering reduction in therapeutic machines, 16: 20569

screens for, contrast transfer functions for, 18: 21929(T) (NP-tr-1135)
sensitivity of dental x-ray films, survey of, 20: 45969
sensitivity of films for evaluation of, 18: 15938
shielding of dental, 17: 6344
shielding of diagnostic, 16: 17920
shutter design for accurate exposure timing, (E), 19: 41186
spectra from 250-kv constant potential, 20: 45951 (HASL-179)
standards for x-ray amplifier foils and light screens, 19: 42693
survey for radiation dose to skin and gonads during diagnostic use, 18: 38997
survey of dental, 18: 5157
survey of dental, in Idaho, 17: 16340
survey of dental, in Utah, 19: 7754
survey of medical, in Los Angeles, Calif., 17: 21955
surveys of, personnel for, 18: 22301
television in, 17: 34157
therapeutic use of supervoltage, 19: 28212
tubes for beam concentration in irradiation of breast cancers using, 17: 35393
use as source of mixed radiation, 20: 25236
use for food preservation, 19: 26725
use in nondestructive testing of radioactive materials, 20: 4122
use in pipeline weld inspection, 20: 45865
use in therapy, method for correction of timing errors during, 20: 35361
use of fluoroscope to study two-phase flow patterns, 19: 13575 (ANL-6958)
use of iron filters to prolong x-ray tube life, 20: 35376
use of x-ray fluorescence in determination of lead, bismuth, mercury, and strontium separated by paper electrophoresis, 17: 1406
use of x-ray tube for void fraction measurement in two-phase flow, 19: 40745
voltage measurements in, 20: 21087
x-ray emission in copper-target tubes in, ratio of Kα to white, 18: 2544
x-ray dosimetry of 1.5 Mv electrostatic generator, (E), 19: 11868
x-ray production in tubes, voltage wave form effects on, (T), 20: 4091

X-RAY FLUORESCENCE ANALYSIS
bibliography on, 20: 35385 (AERE-Bib-136(Pt.1))
bibliography on, 20: 43058 (AERE-Bib-136(Pt.2))
book: *Advances in X-Ray Analysis* Vol. 8, 19: 46185
book: *X-Ray Optics and X-Ray Microanalysis*, 20: 7045
data for, of crystals, 20: 43057 (AAEC-TM-321)
detector design for, narrow-band, 20: 16823 (NYO-3160-1)
development of instruments and radiation sources for, 20: 37150
dosimetry of medical, survey using film packs, 20: 41213
efficiency and techniques of, review of, 20: 45583
efficiency of in energy range from 1 to 5 kev, 19: 22154
efficiency of, effects of particle size on, 20: 26773
efficiency of, for determining major constituents in multi-element matrices by coherent to incoherent scattering ratios, 20: 20644
efficiency of, survey of, 19: 22152
equipment and techniques for, 20: 23560
filter systems for, differential, 20: 14487
interelement effects in, correction for, 20: 22957
measuring line background in, determination of, 19: 15398
method for measuring salt deposits on electric insulators, 20: 29103
methods and uses of, 20: 8839
of aqueous suspensions of minerals and ores, instrument for automatic continuous, 20: 37152
of light elements, using radioisotopes, 19: 19741 (CEA-R-2539)
performance of, using isotopic sources, 20: 23527 (CONF-651206)
radioisotope uses as radiation sources in, 19: 46201
sensitivity in analysis of gases, 19: 15360
sensitivity of isotopic, 19: 34108 (ORO-627)
sensitivity of, for solution analysis, 20: 33148 (EUR-2951.f)
sensitivity of, increase by filters in primary beam, 19: 30069 (AAEC/TM-289)
sensitivity of, matrix effects on, 19: 15373
use for automation of mail sorting, 20: 9354
use for measuring uranium contamination on reaction fuel elements, 20: 27120 (BNWL-SA-646)
use for nondestructive determination of burnup in nuclear fuel, 20: 11004
use for thickness measurements on metal coatings, 20: 37151
use for three-component samples, nomographic interpretation method in (E), 19: 332
use in continuous analysis of gas mixtures, 20: 36766
use in detecting iron, magnesium, and silicon on Mars, 20: 46106
use in zinc determination in geochemical standards, 19: 36276
use of alpha-particle, for beneficiation products and ores, 20: 33184(T) (AEC-tr-6639, pp 118-21)
use of slit probe in spectrometer for, 19: 11493
use of, for determination of trace amounts of metals, 20: 8846
use of, for light elements, Weibull function for pulse-height distributions from, 20: 29124
use of, in industry and geophysics, review on, 20: 39291
use with radioactive sources for cement-mixing control, 19: 42784
use with radioactive sources for ore analysis, 20: 18593
uses for heavy element determination by gamma excitation, 19: 24477
uses in cement industry, 19: 30252
x-ray emission in electron microprobe, dependence on accelerating voltage, 19: 11042

X-RAY MICROSCOPY
alpha source preparation and handling for electron-microprobe analyzer for, 20: 16554
applications in studies of lung parenchyma, 19: 10935
development of projection technique for coated fuel particles, 18: 17291
equipment, design of emission microscope, 16: 19126
method for calcium determination in blood vessel sections, 18: 36929
use of projection, in examination of coated fuel particles, 19: 30645
19: 30645 (EUR-1819.e(p.105-44))

X-RAY MONOCHROMATORS
description, 18: 24224
design and construction of, 18: 16287
design and performance of curved-crystal, 30- to 250-kev, 16: 21443
design of double curved-crystal, 18: 7058 (TID-19849)
design of total-reflection, for studies of small-angle scattering, 18: 41732
efficiency, spectral analysis, 16: 11871(T) (NP-tr-833)
parameters of, wavelength distributions, 17: 4779
reflections of crystal, relative intensities of higher order, 19: 26627 (CALT-221-7)
theory of, 17: 4778
use of balanced Ross filter chopper as, description and characteristics, 16: 17832
use of bent-crystal, for isolation of α_1 or α_2 components of K x rays, 18: 8627

X-RAY PHOTOMETERS
development of, for *in vivo* use, 18: 7001

X-RAY PHOTOMETRY
development of, for determination of plutonium in castings, 17: 120 (HW-26499(Del.))
film sensitivity in, evaluation, 16: 1953(T) (NP-tr-813)
x-ray polarization in, 17: 8138(R) (TID-17674)

X-RAY SHIELDING
calculation for maximum radiation protection, 20: 45518
design equations for, 19: 32787(R) (NIRS-3(1-17))
design of, for gonads during radiodiagnosis, 18: 3653
device for genetic protection in chest radiology, 17: 39319
evaluation of, for diagnostic radiography, 20: 5677
fabrication of gloves and aprons, 16: 27183(P)
fluxes and spectra behind water slabs, for photons at 50 to 250 kev, 16: 24293
for industrial radiography, 19: 17167
materials for, 20: 1314
performance of lead and lead alloys for, 16: 28314
requirements of, in reference to electron-beam therapy, 17: 31824

X-RAY SOURCES
(For x-ray tubes see also X-Ray Equipment.)
see also Gamma Sources
see also X-Ray Equipment
book: *Safety Standard for Non-Medical X-Ray and Sealed Gamma-Ray Sources*. Part I. *General*, 19: 15818
calibration and dosimetry of 17-kev, 16: 15028(R) (UCRL-6658(Rev.))
calibration of chaoul-type tubes for therapeutic use, 20: 3838
calibration of, efficiency of 4π scintillation detectors for, 18: 39654
characteristics of low-energy radioisotopic, 19: 26718 (ORNL-3802)
characterization of high-intensity monochromatic, for resonance radiation studies, 18: 12145 (PRNC-14)
description of multi-mC, using iodine-125, 17: 7693
description of soft, using proton bombardment, 19: 12324
design and operation of soft micro-beam, 18: 13441 (BL-85)
design and performance of beta-excited, 16: 15051
design and use of radioisotopic, 17: 3675
design and uses of beta-excited, (E), 19: 15849
design and uses of gamma-excited, 19: 36876
design and uses of beta-excited, 20: 36915 (N-66-17678)
design for small-field irradiation of dogs, with holding and field-limiting units, 16: 8845
design for soft fluorescent x rays, 16: 13358
design for use in x-ray microprobes and spectrographs, 19: 309
design of barium–strontium-90, 18: 3657
design of beta-excited, 16: 15052
design of beta-excited portable, 16: 27185(P)
design of cadmium-109, for sediment gage, 20: 43561
design of demountable high-power, for low-energy region, 20: 27243

design of, for analysis of biological samples, 17: 12220
design of iodine-125, 17: 39365
design of low-voltage, 19: 31787(R) (NYO-2740-2)
design of PHERMEX linear accelerator, 19: 8046
design of twin-tube 50 kvp beryllium-window, for microradiobiology, 19: 15187
design of x-ray tubes with mercury-vapor targets, 19: 746
design of, for use in ionization studies, 18: 41506(R) (ML-TDR-64-169)
design of, safety features in, 20: 9205
design of, using iodine-125, 20: 26738(P)
design with adjustable electron beam cross section, 19: 38964(P)
detection and distribution in galaxy, (E), 20: 9637
detection and location of cosmic, (E), 19: 12126
detection and resolution at low-galactic longitudes, 20: 44091
detection of galactic, 18: 28227
detection of, in direction of north galactic pole, 20: 44095
development and fabrication of iodine-125 and promethium-147, 18: 27814(R) (ORNL-TM-434)
development of alpha-excited, 20: 23527 (CONF-651206)
development of gamma-excited, 19: 7828
development of gamma-excited, 19: 28707
development of high-intensity field-emission, 20: 46 (PRNC-40)
development of isotopic, 16: 1876 (ARF-1122-27)
development of light-weight 160-kv portable, 20: 20867
development of medical, using mercury-197, 19: 46141
development of multiple element soft, 19: 18249
development of pulsed, 17: 16044 (TID-18144)
development of radioisotope, for x-ray fluorescence analysis, 20: 37150
development of strontium-90–yttrium-90-base, 18: 33989(T) (AEC-tr-6399(p.243-57))
development using beta-particle energy as power, 16: 1887 (TID-13170)
developments and uses of low-energy, conference on, 20: 4111 (ORNL-IIC-5)
diagnostic, protective housing for, 20: 33132
dose distribution for food irradiation facility, homogeneous, 16: 16624
dose rate and spectra measurements from pulsed, (E), 20: 13057 (AD-627567)
dosimetry of flash, development of system for, 19: 13721 (AD-603608)
dosimetry of large-surface anodes, 16: 19084
efficiency of tritium–zirconium, for excitation in x-ray spectroscopy, 20: 2136
energy spectra from, theoretical calculation of, 19: 45729(R) (NYO-910-23, pp 1-111)
evaluation of radiographic tubes, 19: 13797
for radiobiological irradiations, 16: 28679
galactic, evidence for, 18: 8987
intensity yields of beta-excited, for use in industrial radiography, 16: 22506
iodine-125 as, for diagnostic radiography, 19: 42377 (NYO-3481-1)
mechanisms of localized astronomical (E/T), 19: 2935 (MIT-2098-96)
observations and theory of celestial, 18: 26200
performance for radiation effects studies on electronics, 20: 27365 (SC-DC-3127A)
performance of iron-55, for diffraction analysis, 20: 24992
performance of machine and radioisotope, 20: 23527 (CONF-651206)
performance of radioisotope and machine, in aerospace applications, 20: 35812 (ORO-647)
performance of tritium–zirconium, 18: 28252
performance of, effects of krypton-85-loaded charcoal on, 19: 6216
performances in analytical procedures, 17: 35642
power and radiation field of high-power, evaluation of, 17: 37406
preparation and uses of, 19: 26696
preparation and uses, 20: 27369
preparation of beta-excited, 19: 47223
preparation of iodine-125 2-curie, 17: 29156 (ORNL-TM-562)
preparation of iron-55, 20: 43384
preparation of low-energy, methods for, 20: 10932 (ORNL-P-1928)
preparation of soft, by electroplating of cadmium-109 on copper wires, 19: 44139 (ORNL-TM-1174)
production and uses of, 20: 9353
production of low-energy, developments in, 19: 42775
properties of beta-excited, for nondestructive testing devices, 18: 518 (IITRI-1209-9)
radiation characteristics of flash, 18: 10374 (D2-9878-4)
sizing targets for, 17: 11353
spectra from K-fluorescent, 19: 40834(R) (UCRL-14151)
spectra of tritium–zirconium, 19: 34261
use for altitude measurement and terrain identification, 20: 31493
use for radiography in Japan, 20: 7469
use in industrial absorption and fluorescence analysis, 18: 21981
use in radiography, 20: 41116(P)
use in thickness gaging, 18: 31862(P)
use in thickness measurement, 16: 29117(T) (AEC-tr-5097)
use of beta-excited, for absorptiometry, 20: 3882 (ORNL-IIC-5, pp 51-71)
use of beta-excited, in absorptiometry, 20: 22877(R) (TID-22846)
use of beta-excited, in absorption and diffraction studies, 20: 23527 (CONF-651206)
use of beta-excited, in absorption analysis, 20: 33235
use of beta-excited, in helicopter signaling system, 20: 41221(R) (COO-1471-1)
use of cadmium-109 as, 18: 39709 (ORNL-TM-805)
use of gamma-excited, for alloy analysis and coating weight determination, 19: 15376
use of high-energy, for radiotherapy, 19: 26216
use of isotopic, in fluorescence analysis, 19: 34108 (ORO-627)
use of machine and radioisotope, for aerospace applications, 20: 31339
use of soft, for determining response characteristics of plastic phosphors, 18: 22162
use of standard crystallographic 90-kv x-ray generators for, 18: 7002
uses in control of cement mixing, 20: 23568
x-ray emission from spark-triggered discharge, (E), 19: 39305
x-ray purity from gamma-excited, K, 19: 46407 (AAEC/TM-226(Suppl.1))

X-RAY SPECTRA

analysis and compilation of beta-stimulated, 19: 47223
analysis of, method for, pulse-height, 18: 3706(P)
analysis of quality specifications and derivation of approximate distributions of, 17: 22306
analytical uses of, promethium-147 beta source for, 17: 27280
angular distributions at surface of electron target, 18: 16685
characteristics of, 19: 9348(T) (FTD-MT-63-261)
chemical shifts in, 17: 40429(R) (NYO-10063(p.23-51))
chemical shifts in, (E), 19: 5569(R) (MIT-2098-64)
compilation of beta-excited, 20: 23527 (CONF-651206)
conversion of experimental scattering intensities to absolute scale, 17: 22383
data on scattered, secondary, and leakage, 17: 21953
distortion of, corrections for asymmetric and symmetric, 17: 9015(T)
distortion of, correction of instrumental, 19: 34187(T)
distribution of scattered radiation in water phantom, 16: 32795
effects of alloying on, (E/T), 19: 16205
effects of chemical bonding on soft, 19: 44944
effects of chemical bonding on, 20: 16160 (UCRL-14739(Pt.2))
emission of characteristic atomic, following low-energy proton bombardment, 16: 33633
field theoretical effects in (E/T), 19: 1181
fine structure of, effects of nuclear size on, 18: 779
fission product, (E), 19: 36220(R) (MIT-2098-142)
fluorescence lines of barium stearate crystals, tables, 18: 41378 (Y-1470-1)
identification, use of transparent overlay for spectrographic charts in, 16: 26973 (SCR-495)
intensity distributions of low-energy continuous, effects of target electrons, 16: 23032
intensity of L, of light elements, 19: 27070
intensity of satellites in, (T), 20: 2645
isotope shifts in, formula for, 18: 17064(T)
limit of continuous, high-frequency, 18: 20653
measurement of muonic, performance of germanium detectors for, 20: 29525 (CONF-660209-9)
measurement of solar, by soft-x-ray spectrometer on Orbiting Solar Observatory, 18: 7396
measurement of, using tritium–zirconium excitation source, 18: 28252
measurement using scintillation detector and collimator, 20: 46030(R) (AERE-PR-HPM-9, pp 6-17)
modification by filtration of, 19: 43901
of orbital electrons in Frascati synchrotron, 17: 36723
plasmon satellites of soft, 17: 13424
production, 17: 27242 (TID-18925)
production by Bragg reflection from concave crystals, 17: 20313(T) (AEC-tr-5764)
satellites and nondiagram lines in emission, relations between, 17: 32777

X-RAY SPECTROMETERS

beam emission in, characteristics of, 19: 19747 (CONF-650214-1)
coincidence circuits for, design and performance of, 20: 37093
coincidence losses in, nonlinearity correction equation for, 16: 8959
crystal alignment and preparation for precision, 20: 2126 (CONF-650657-1)
crystal cutting, mounting, and performance of thin sodium iodide crystals for use in 15 to 100 kev, 16: 3224
description for wavelengths above 10 Å, 18: 2097
design, 18: 25852
design and performance for measurement of capture gamma radiation, 16: 23012(T) (UCRL-Trans-792(L))
design and performance of roller, 16: 23948

design and performance of scintillation-type, for soft x rays, 17: 1760
design and performance of nondispersive fluorescence, 17: 39369 (AERE-R-3667)
design and performance of scanning single-crystal multichannel, 18: 2073
design and performance of noncrystal, with proportional counter, 18: 37549
design and performance of semiconductor detector, for *n*-mesic atom spectra, 20: 42311
design and testing of URS-1I, for spectral fine structure, 20: 31581
design and use for study of hot plasma, 16: 1986
design for fluorescence analysis, 17: 4799(P)
design for measuring short-wavelength solar x-ray spectrum from rocket or satellite, 16: 33180
design for Orbiting Solar Observatory for solar-flare spectra, 18: 7396
design for parallel solar x rays, 17: 16486(P)
design for satellite observations of solar x-ray spectra, 18: 7088
design for studying x-ray spectra of deuterium plasma in Scylla, 16: 29908 (TID-12518)
design for use in determination of light elements in solid samples, 20: 43161
design of absorption, 19: 42762
design of analyzer using beta radiation, 18: 25768(P)
design of double-diffracting, engineering drawings for, 17: 39444
design of high-resolution, for fluorescence analysis of materials, 19: 2589(P)
design of high-resolution, 20: 27321
design of nondispersive, for lunar and planetary geochemical analysis, 20: 21128
design of parallel analyzing channel attachment, for analysis of double layers, 19: 8687 (BDX-613-34)
design of portable, 20: 20365
design of proportional-counter, 18: 487 (AFCRL-62-1105)
design of pulse-operated, containing electronic gray wedge, 17: 8609
design of scanning mechanism for satellite-borne, 17: 4808 (NASA-TN-D-1097)
design of sequential, for automatic measurements, 17: 16485(P)
design of solar, for satellite uses, 17: 13320
design of three-crystal, 19: 18332
design of time-constant control system for, 20: 640(P)
design of total-absorption scintillation, 17: 4854
design of two-crystal scintillation pair-coincidence, 18: 7075
design of ultrahigh vacuum grating, with grazing incidence, 20: 41350
design of vertically rotating double-crystal, 18: 41729
design of x-ray sources for, 19: 309
design using concave crystals, 17: 20313(T) (AEC-tr-5764)
design using curved-surface crystal, 18: 5601(P)
design using lithium-drifted germanium crystals, 19: 34524
development, 17: 10948
development and performance of, for microanalysis, 17: 25564
development for dual-channel microanalyzer, 17: 25565
development for line-width measurements in tenths of seconds, 17: 34546(R) (ORNL-3480(p.17-28))
development for simultaneous analysis of several elements, 18: 37537
development for soft x rays, 19: 34476 (IPP-1/32)
development of, for *in vivo* use, 18: 7001
development of microprobe, for uranium analysis, 18: 43380(R) (NLCO-920(p.13-17))
development of, using iodine-125 as radiation source, 20: 6955
diffraction gratings for, thickness of stearate, 19: 9534
efficiencies of bent-crystal, 17: 40429(R) (NYO-10063(p.23-51))
medical uses of, 18: 21998
modification of commercial, for analysis of light elements, 19: 19801
operation and control of system of, computer for, 20: 16869
operation principles and resolution of Bragg, 16: 12182(R) (TID-15122)
performance, 20: 11069
performance in conjunction with pulse-height discriminators, 18: 18196
performance of p-n junctions as, 17: 6458
performance of proportional counter, 19: 34561
performance of proportional counter, 20: 31544
performance of proportional counter, 20: 31545
performance of, corrections for nondispersion-like distortions in, 19: 34187(T)
performance using promethium-147 beta source for K x-ray spectra, 20: 11133
performance with radioisotope source for fluorescence analysis of traces, 16: 15053
power supplies for, design of, 19: 42685(R) (ORNL-3782, pp 24-8)
properties of, analytical, 17: 27242 (TID-18925)
pulse analyzers for, performance of, 19: 28636 (NP-14874)
pulse-height selection for scanning, device for, 17: 18582
resolution of scintillation-type, at low energies, 18: 41872
rubidium-strontium measurements by, matrix effects in, 18: 3995(R) (NYO-10517(p.121-2))
sensitivity improvement using polarization analysis, 17: 37160
shielding effectiveness in microprobe examination of specimens, 20: 40460(R) (IDO-17191)
standardizing continuous readout on-line, apparatus and procedure for, 19: 44545(P)
use in chemical analysis with electron microprobes, 20: 3912
use in mesic atom studies, 19: 4480 (TID-7705(p.240-54))
use in rubidium/strontium determination, 18: 3678(R) (NYO-10517 (p.135-41))
use of pyrolytic graphite as crystal in, 19: 6414

X-RAY SPECTROSCOPY

absorption correction tables for microprobe analysis, 19: 26231 (NLCO-944)
alignment procedures and spurious spectral effects in two-crystal, 16: 25545 (AFOSR-2418)
analysis of adjacent elements by, using radioisotopes, 17: 30484
analysis of minerals, multielement calibration in, 17: 15893
analysis of reactor materials by, review, 19: 5813
beta source uses in, 20: 22961
bibliography and review on absorption and emission, 16: 14650
book: *Developments in Applied Spectroscopy*, Vol. 3, 19: 11041
book: *Instrument and Chemical Analysis Aspects of Electron Microanalysis and Macroanalysis*, 20: 29119
book: *The Encyclopedia of X Rays and Gamma Rays*, 18: 8043
book: *X-Ray Studies of Materials*, 18: 5810
broadening of Fermi edge in, convolution, (T), 19: 12088
computational methods in electron-probe x-ray microanalysis, 17: 40741
correction factors for electron penetration in microanalysis, 19: 19746 (CEA-R-2728)
correction formulas for quantitative microprobe analysis, 19: 9058 (EUR-2156.e)
crystal structure studies by, development of low-temperature camera for use in, 17: 27670
data recording system for low-level, incremental, 19: 36805 (BNWL-SA-121)
development and use as analytical tool, 20: 3911
development for determining trace metals in solutions, 17: 497(R) (KAPL-2000-19(p.I.1-I.28))
development for use in rockets, 18: 32359
development using radioisotopes as radiation sources, 16: 19118
development using radioisotopes as radiation sources, review of, 17: 23260(T) (AERE-Trans-933)
developments for use in chemical analysis, review on, 20: 22885
developments in high-resolution, 17: 2930
developments in, review of, 18: 19862
device for electron microscope, 17: 20342(P)
diffraction line broadening in curved-crystal, correction for, (E/T), 19: 4478 (TID-7705(p.175-93))
diffraction line broadening by stacking faults in bcc crystals, (E/T), 19: 4827 (TID-7705(p.163-74))
electron beam production for, 18: 12795(P)
equipment for, proportional gas-flow, 18: 4123
equipment for, using promethium-147 beta source, 18: 31403
errors in fluorescence analysis, 18: 9963 (AERE-R-4483)
evaluation of, in analysis of blood, 16: 32646(R) (UCRL-10211(p.62-8))
fluorescence lines of gypsum crystal, tables, 18: 28096 (Y-1470-E)
fluorescence lines of mica-48 crystals, tables, 18: 27361 (Y-1470-F)
fluorescence lines of crystals, calculation, 18: 31437 (Y-1470-A)
fluorescence lines of potassium acid phthalate crystal, tables, 18: 31438 (Y-1470-H)
fluorescent, use for chemical analysis, 17: 10949
in highly ionized helium and hydrogen plasma, 17: 13642
in Scylla magnetic mirror machine, 17: 13639
method of absolute intensity by fluorescent, for quantitative analysis, 17: 24786
method of, for iodine determination in blood serum, 18: 4972
methods of, for analysis of solutions, 17: 40762
noise rejection in low-energy scintillation, 18: 32281(R) (UCRL-11213 (p.139-53))
performance in electron-probe microanalyzers, 18: 17760
performance in electron-probe microanalysis of low-Z elements, 18: 17744
performance of proportional detectors in, 16: 6615
physical basis of electron-probe x-ray microanalysis, 17: 40740
precision redetermination of standard reference wavelengths, 18: 34341
promethium-147 as beta source for use in, 17: 30113
sample preparation by isoformation, 17: 10950
semiconductor detectors for use in, 20: 16887
sensitivity improvements for determining traces of elements using direct electron excitation, 19: 38571
sensitivity of, effects of instrumental errors on, 20: 8857
silicon-crystal measurement of absolute scale of x-ray wavelengths, 18: 34340

source for, efficiency of tritium–zirconium, 20: 2136
spectrometer angles as function of x-ray energies and wavelengths for gypsum and lithium fluoride diffraction crystals, 19: 25146(R) (TID-21542)
survey of theory and methods for chemical analysis, 17: 10947
technique for electron-microprobe, for studying oxidation of chromium–iron–nickel alloys in steam, 19: 17774 (GEAP-4490)
use for determination of elements, 18: 7023(P)
use for determining composition of niobium stannides (E), 19: 335
use for materials analysis, design of equipment for, 17: 41233(P)
use for measurement of spectrum of theta-pinch plasma at 15 to 25 A, 17: 35050
use for plasma diagnostics, 17: 13641
use for plasma thermometry in 10^8 °K range, 17: 31617
use for plasma thermometry, 18: 26708(T) (AEC-tr-5589(p.861-8))
use for thin film measurements, 18: 5573 (CONF-229-2)
use in analysis of geochemical samples, 16: 32922(T) (CEA-tr-A-1032)
use in analysis of blood serum for 66 chemical elements, 18: 9975
use in analysis of human blood serum for 29 chemical elements, 18: 15728 (UCRL-10873)
use in analytical work at A.E.R.E., 17: 14135 (AERE-R-4210)
use in crystallographic and nuclear studies, 18: 43151 (ISS-63/50)
use in determination of crystal lattice constants, 16: 32950 (HW-SA-2639)
use in plasma diagnostics, (T), 20: 8260
use of cathodoluminescence as ancillary technique to microprobe analysis, 18: 43379(R) (NLCO-920(p.7-12))
use of electron microprobe to study phase equilibria, 19: 15348 (MLM-1163(p.K-1-10))
use of electron microprobe to chemical analysis, 19: 13199 (LA-3157)
use of, for determination of elements, 16: 29122(T) (SCL-T-430)
use of micro-, in determination of light elements, 17: 30483
use of nondispersive, in elementary chemical analysis, 18: 12011
use of radioisotope fluorescence, for analysis of copper and zinc ores, 18: 39056 (AERE-R-4474)
use of semiconductor detectors in, 20: 22859(R) (UCRL-16580, pp 149-205)
use of windowless tubes for increased intensities from light elements, 17: 25993
use to determine protein-bound iodine in human serum, 16: 20331
use with electron-beam excitation for determination of light elements, 17: 15908
uses at ANL, 20: 31167(R) (ANL-7175, pp 217-25)
utilization in space research, 17: 27669
wavelength conversion factor determination using calcite-crystal, 19: 8197

XANTHATES

carbon isotope exchange with carbon disulfide, 16: 15097(P)
contact angle hysteresis in gas-aqueous solution-solid system, 17: 35617(R) (NYO-10329)
contact angle of potassium ethyl xanthate with galena in nitrogen atmosphere, hysteresis in, 18: 13604(R) (MITS-51)
preparation of sulfur-35-labeled potassium ethyl xanthate, 18: 25460
preparation of sulfur-35-labeled ethyl and *n*-butyl, 18: 3829
radiation effects on flotation properties of, for pure minerals and commercial ores, gamma, 20: 36893
reactions of potassium ethyl xanthate with galena, 19: 9362(R) (MITS-52)
solvent properties for technetium and rhenium, 20: 40856
sulfur isotope exchange with carbon disulfide, 16: 15097(P)
use of potassium ethyl xanthate for synthesis of 2-amino-2-deoxy-1-thio-D-glucose derivatives, 17: 39086
CS_2–xanthate, isotope effects in, 17: 2702
CS_2–xanthogenate, carbon-13 enrichment and exchange in, 18: 24057(P)

XANTHENONES

analytical use for photometric determination of niobium, 18: 5222
analytical use of 1-hydroxy-3-methoxyxanthone in determination of cerium, 16: 22034
analytical use of phenylfluorone for determination of tantalum traces, 19: 40414 (UCRL-7967)
complexes with beryllium, rare earths, thorium, and uranium, preparation and stability of colored, 18: 27366
trioxy-, analytical use of, in photometry of multivalent metals, 17: 18084
1-hydroxy-, analytical use of, for gravimetric determination of thorium and uranium, 16: 9966

XANTHIC ACID

enrichment of compounds of, in carbon and sulfur by isotope exchange with carbon disulfide, 19: 18045(P)

Xanthine, 2-Aminohypo-
see Guanine

Xanthine, 1,3,7-Trimethyl-
see Caffeine

XANTHINES

determination in human urine, equipment for, 20: 45797(R) (ORNL-3945, pp 199-207)
effects with uv and x radiation on mutational synergism in *E. coli*, 18: 9863
reactions with hydroxyl radicals, ESR spectral studies on, 20: 36806

XANTHYDROL

analytical use of labeled, in urea determination, 17: 6032(P)
preparation of carbon-14 labeled, 17: 6032(P)

XENIC ACID

Raman spectra, 18: 27394
reduction to xenon at dropping-mercury electrode, 18: 16053

XENON

see also Rare Gases

absorption and emission at electron cyclotron frequency of plasma of, 18: 15711(R) (TID-20256)
absorption coefficient from 3.6 to 10×10^3 Å, (T), 19: 20833
absorption cross sections, (E/T), 20: 44642 (JINR-P-2808)
acoustic-wave production in low-pressure, r-f breakdown for, 18: 28846
alkali-atom electron-spin-resonance spectra in, at 4.2°K, 16: 23702
alkali metal scattering by, cross sections and rainbow effect in, (E/T), 20: 2636
alkali-atom optical absorption spectra in matrices of, (E/T), 19: 7477
alkali-metal negative-ion dissociation in, cross sections for, (T), 20: 22947
alpha energy loss and ionization in, 16: 6931
alpha reactions with liquid and solid, emission spectra from, (E), 19: 12101
alpha scattering at 40 Mev, effect of nuclear surface density on, (E/T), 19: 29295
alpha scattering by, excitation and ionization effects in, 18: 23972
alpha-particle trajectory in, distribution of photons and ions along, 18: 26121
analysis for krypton-85, 17: 7660(R) (MLM-1137)
analysis for krypton-85 by gamma, Geiger, or proportional counting, 18: 35464
analysis for krypton-85 by scintillation counting, 19: 13201(R) (MLM-1217)
analysis for krypton-85 by counting, 19: 28717(R) (MLM-1221)
analysis for krypton-85 by internal gas phase proportional counting, 19: 32061 (MLM-1247)
analysis for krypton-85 by scintillation counting, 19: 36889(R) (MLM-1250)
analysis for krypton-85 by scintillation counting, 20: 20553(R) (MLM-1142)
analysis for krypton-85 by liquid scintillation counting, 20: 20582
argon ion reactions with, cross sections for, 20: 25747
atomic potential functions for, 18: 42313
atomic transitions of, negative tensor susceptibility for, 17: 17374
behavior in Homogeneous Reactor test, 16: 830
behavior of fission-product, in urania and uranium fuels, 18: 28014
binding theory for, 18: 5343
binding to halogens, alkali metals, and to itself, 17: 16007
bond lengths and polarities and electronegativity of, 19: 24512
bonding interactions and thermodynamic properties of, 17: 22268 (IS-409)
bremsstrahlung emission from plasma of, in thermodynamic non-equilibrium, 17: 42111
bremsstrahlung spectra, 19: 9445 (LA-3130)
bubble release and swelling in solids, model for, 18: 26080
buildup and decay in shutdown reactor, 17: 26812
buildup effects on power-reactor kinetics, 16: 1260
buildup in ALRR, reactivity change from, 20: 42681(R) (IS-1500(Sect. R))
buildup in high-flux reactors, design of circuits to simulate, 17: 10993
buildup in reactors, control of time-to-poison in, 18: 21687
buildup in reactors, optimal feedback control of spatial oscillations in (T), 19: 3534
buildup in reactors, control-induced oscillations in (T), 19: 3535
buildup in reactor shutdown, control of, 20: 3410
buildup in reactors after shutdown, 20: 5074
buildup in reactors, time optimal shutdown problem in, 20: 5075
buildup in reactors, simulator for studying, 20: 12498(R) (IDO-17112, pp 1-51)
buildup in reactors, absorbing foil determination of, 20: 30843
buildup in thermal reactors, optimal flux shutdown programs for, 19: 21639 (IA-988)
cesium beam scattering by, effects of apparatus resolution on cross sections for, 20: 34114
cesium spin relaxation in, (E), 19: 41278
charge exchange in, atom-ion resonance, (T), 19: 19931
charge-exchange with xenon ions, cross sections for, 16: 6868
charge transfer with protons, cross sections for Lyman alpha emission from, 18: 26235
chemistry, 19: 2281
chemistry of, predicted, 17: 33894

chemistry of, in aqueous solution, 18: 25358
chemistry of, review of, 19: 17873
collisions of atoms of, with alkali metal atoms, ionization produced in, (E), 20: 2639
collisions of atoms of, with singly charged krypton ions, profound stripping and scattering in, (E), 20: 2644
content and nature of, in thermal springs in California and Wyoming, 19: 26252
content in atmosphere and meteorites, 17: 25466
content in Bruderheim meteorite, 20: 7716
content in Bruderheim meteorite, 20: 11430
content in lunar atmosphere, effects of solar wind on, 18: 18546
content in meteorites, use in chronometry, 16: 33660
content in natural gases, 19: 44239
content in nuclear reactor, equations and phase-plane for determining, 16: 21741
content in ocean water, 19: 2530
content in periodically operating reactor, time variation of, (T), 19: 12755
content in samarskites, 19: 46598
content in silicates from Estherville Mesosiderite meteorites, 20: 31859
content in upper atmosphere, from rocket soundings, 18: 37794(T) (NASA-TT-F-141(p.1-21))
corresponding states theory, 16: 16374
corresponding states theory, 16: 19480 (UCRL-10029)
costs and uses, review of future and present, 17: 31681(R) (HW-76559)
critical and inversion temperatures, 17: 30460
crystal stability of, three-body interactions in, 18: 34706
cyclotron emission from plasma of, in thermodynamic non-equilibrium, 17: 42111
determination and separation from krypton, gas chromatographic, 16: 145
determination in air, analytical facility for, 19: 17775 (HNS-1229-57)
determination in HRT off-gas stream for poisoning measurements, 16: 19915 (ORNL-TM-228)
determination in irradiated urania pellets using electron microprobe analysis, 20: 11365
determination in irradiated uranium carbide and uranium dioxide fuel elements by isotope dilution and mass spectrometry, 20: 26757
determination in off-gas from burnup capsules, gas chromatographic, 19: 36217(R) (IDO-14656)
determination in pure helium, chromatograph for, 19: 28220 (BNWL-12)
determination in reactor test capsules, chromatographic, 17: 15855(R) (ORNL-3397(p.38-54))
determination in sea water, mass spectrometric, 19: 2247
determination of trace amounts of, by reactor neutron activation methods, 20: 26760
determination using omegatron, 20: 3908
deuteron reactions at 19.6 Mev, optical model parameters for, 18: 1051
deuteron reactions at 0.5 to 25 kev, Lyman alpha emission cross sections for, 18: 32446
diffusion and precipitation in metals, 16: 30852
diffusion and precipitation in aluminum–lithium alloys, 20: 23803
diffusion and release from uranium and uranium monocarbide, 16: 30814(T,R) (EURAEC-360)
diffusion and sorption in high-density graphite at 750 and 1000°C, 16: 23700
diffusion from calcium fluoride–uranium monocrystals, 20: 1324(R) (EURAEC-1428)
diffusion from coated and uncoated ceramic fuel particles, 18: 25983 (SGAE-ME-1/1964)
diffusion from dispersion-type fuels, 17: 35115
diffusion from graphite–thorium carbide–uranium carbide systems, 16: 24628
diffusion from irradiated uranium, effects of burnup and irradiation level on, 16: 25841 (HW-72321)
diffusion from irradiated uranium dioxide, kinetics of, 17: 27886 (AERE-M-969)
diffusion from irradiated uranium carbide at 150 to 975°C, 18: 36003
diffusion from irradiated uranium dioxide pellets and rods, 18: 36063
diffusion from single-crystal uranium carbide, 17: 27784 (GA-4267)
diffusion from sodium at high temperatures, factors affecting, 20: 40357 (NAA-SR-11766)
diffusion from uranium carbide and uranium dioxide single crystals, 18: 16486(T,R) (EURAEC-969)
diffusion from urania in reactor coolant-loss accidents, 19: 28574(R) (BMI-X-10119)
diffusion from uranium carbide monocrystals, 20: 1324(R) (EURAEC-1428)
diffusion from uranium nitride, tracer study of, 20: 43981
diffusion from zirconium carbide, temperature effects on, 19: 36949(R) (BNL-900(p.121-97))
diffusion in alumina, effects of fission recoil damage, 16: 24619
diffusion in aluminum and stainless steel coatings and aluminum–nickel couples, 16: 29368 (BNL-5113)
diffusion in copper, 20: 35841(R) (NAA-SR-11900)
diffusion in gases, coefficients of, 16: 33613
diffusion in graphite, 18: 18361(T) (CEA-tr-X-531)
diffusion in helium, effects of temperature on, 20: 35828(R) (MLM-1300)
diffusion in irradiated uranium fuel elements, 18: 26903
diffusion in irradiated uranium dioxide, 19: 22975(R) (EURAEC-1314)
diffusion in irradiated uranium dioxide, effects of radiation dose on, 19: 26902
diffusion in irradiated uranium, coefficient of, 20: 2358(T) (AERE-Trans-1034)
diffusion in metals, 16: 5736
diffusion in metals and oxides, 19: 16088
diffusion in niobium, 16: 5711 (CNLM-2154)
diffusion in pyrolytic carbon, 18: 37676 (A/CONF.28/P/573)
diffusion in single-crystal uranium carbide, 17: 31019 (GA-4267)
diffusion in sintered uranium dioxide, activation energy of, 18: 34214 (EURAEC-1126)
diffusion in spherical uranium dicarbide particles, coefficient for, 20: 5848
diffusion in tantalum at 820 to 2400°C, 19: 23115
diffusion in thorium dioxide, uranium carbide, and uranium dioxide, 16: 21049(T,R) (EURAEC-121)
diffusion in thorium and uranium dioxides and uranium carbide, 17: 4927(R) (EURAEC-312)
diffusion in thorium and uranium dioxides, 17: 22170(T,R) (EURAEC-526)
diffusion in uranium carbide and oxide, 16: 18150(R) (EURAEC-65)
diffusion in uranium carbide and dioxide at 1000 to 2500°C, 16: 18038(R) (NYO-9046)
diffusion in uranium carbides and oxides, 16: 21047(T,R) (EURAEC-17)
diffusion in uranium dioxide, kinetics, 16: 27686 (WAPD-T-1155)
diffusion in uranium carbide and uranium oxide, 17: 1962(T,R) (EURAEC-385)
diffusion in uranium dioxide, 17: 39549(T,R) (EURAEC-646)
diffusion in uranium dioxide, mechanisms of, 18: 14512
diffusion in uranium, 18: 18304
diffusion in uranium dioxide single crystals, 18: 27972(T,R) (EURAEC-1043)
diffusion in uranium carbide at 2040°C, 18: 32061(R) (UCRL-11317 (p.198-203))
diffusion in uranium oxides, 18: 37617 (A/CONF.28/P/857)
diffusion in uranium carbide and uranium dioxide crystals, 18: 39915(T,R) (EURAEC-1105)
diffusion in uranium carbide, 19: 7946
diffusion in uranium dioxide matrix containing trapping sites, 19: 28845
diffusion in uranium dioxide, impurity effects on, 19: 28846
diffusion in uranium dioxide monocrystals, literature review, 20: 1324(R) (EURAEC-1428)
diffusion in uranium carbide monocrystals, 20: 2317 (EURAEC-1380)
diffusion in urania single crystals at 1000 to 1800°C, activation energy for, 20: 5843
diffusion in uranium, effects of heating on coefficient of, 20: 5848
diffusion in uranium dioxide, 20: 9507
diffusion in uranium at 950 and 1000°C, coefficient for, 20: 15090
diffusion in uranium dioxide single crystals and particles at 600 to 2400°C, 20: 17103
diffusion in uranium-doped calcium fluoride single crystals at 900 to 1200°C, 20: 21332(R) (EURAEC-1573)
diffusion in uranium, effects of beta-to-gamma transition on, 20: 23803
diffusion in uranium at 700 to 1060°C, effects of phase transformation on, 20: 27518
diffusion in uranium dioxide, effects of additions of, lanthanum, niobium, or yttrium oxides on, 20: 31666
diffusion in urania at 1330 to 1800°C, effects of radiation dose on, 20: 31666
diffusion in uranium dioxide, effects of oxide impurities on, 20: 37256
diffusion in urania, effects of trapping sites on, 20: 37293
diffusion in zirconium carbide powder, 19: 23355(R) (BNL-867(p.1-117))
diffusion in zirconium carbides, 20: 20177(R) (BNL-929, pp 83-105)
diffusion of charge carriers in rarefied ionized, study by diffusion-wave method, 17: 9775
diffusion of fission-produced, in uranium dioxide, 18: 18386
diffusion of fission-recoil, in ionic crystals and sinters, 20: 3944
diffusion of hydrogen in, 18: 16054
diffusion of, in thorium oxide, 16: 32124(T,R) (EURAEC-250)
diffusion of, in thorium dioxide, 17: 8822(T,R) (EURAEC-457)
diffusion of, in uranium carbide and oxides, 16: 32124(T,R) (EURAEC-250)
diffusion of, in uranium dioxide crystals, 17: 8822(T,R) (EURAEC-457)
diffusion of, in uranium carbide, 17: 8822(T,R) (EURAEC-457)
diffusion of, in uranium monocarbide crystals at 1000 to 2000°C, 17: 21670 (UCRL-10462)
diffusion of irradiated sintered compacts of urania, 19: 44595(R)

(EURAEC-1338)
diffusion of xenon in liquid and solid, 17: 2136
diffusion rates in irradiated uranium dioxide, dependence on radiation dose, 18: 7321
distillation at low temperatures, 17: 2662(R) (MLM-1135)
distributions in finite reactors, oscillatory behavior of, 17: 31699
distributions in reactors, 18: 4853 (UCRL-7353)
distributions in reactors, calculation using centers and limit cycles, (T), 19: 21634 (BNL-9010)
distributions in reactors, spatial oscillations of, 20: 3326 (WAPD-T-1732)
dysprosium ion stopping in (E/T), 19: 2984
effects as buffer on spin relaxation of optically pumped cesium, 18: 30403 (NP-14066)
effects as inert moderator in recoil tritium reaction with ethane, 20: 45746
effects on cesium vapor diodes, apparatus for determining, 18: 20856
effects on cesium thermionic converter short-circuit currents, 20: 21580
effects on decomposition of nitrous oxide, 19: 26404
effects on density shifts of sodium-23 hyperfine frequency, 19: 30951
effects on growth rates in Neurospora, 20: 20378
effects on hydrogen formation in gamma radiolysis of gaseous, liquid, and solid ethylene, 16: 7591
effects on labeling reactions of methane with tritium, 19: 28363 (UCRL-16009)
effects on lifetime of metastable helium atoms, 18: 26238
effects on molecular spectra, 17: 178
effects on noncylindrical Z-pinch in deuterium, (E), 20: 8185(T) (LA-tr-65-26)
effects on oxygen-18 exchange in carbon dioxide-nitrogen oxide photolysis, 18: 12192
effects on products from radiolysis of methane, 19: 479
effects on propane radiolysis, 20: 29266
effects on radioinduced exchange of hydrogen isotopes, 18: 12142(R) (NYO-7988)
effects on radioinduced isotopic exchange in nitrogen, 19: 36482
effects on radioinduced polymerization of solid methane, 20: 29314
effects on radioinduced exchange between deuterium and methane, 18: 12190
effects on radioinduced crosslinking of polyethylene, 18: 13861
effects on radiolysis of carbon monoxide, 18: 20087
effects on radiolysis of ethylene vapors, 19: 5949 (TID-21389)
effects on radiolysis of acetylene, 19: 17991
effects on radiolysis of ethane, 19: 22293
effects on radiolysis of deuterated and normal methane, 20: 379
effects on radiolysis of ethylene, 20: 5582
effects on radiolysis of deuterated hydrocarbons in presence of hydrogen, proton-transfer, 20: 18742
effects on radiolysis of liquid propane, 20: 43368
effects on reactor neutron dynamics, 18: 33016 (A/CONF.28/P/271)
effects on reactor kinetics, adiabatic analysis of, (T), 19: 33564 (GA-6283)
effects on reactor stability, analog simulation of, 20: 34909 (WAPD-T-1781)
effects on safety of HFBR, 20: 42672 (BNL-10388)
effects on sporulation in Neurospora, 20: 20378
effects on stability of Brookhaven Beam Research Reactor, 20: 35170
effects on temperature drop in clad-fuel clearance in reactor fuel elements, 18: 11410 (EUR-521.e)
effects on x radiolysis of acetylene, methylacetylene, and ethylacetylene, 19: 46334 (TID-22231)
electric breakdown potential of, measurement of a-c, 20: 3160 (AD-618503)
electric conductivity of plasma of, (E), 19: 17099
electric discharges in, transport theory, 16: 4936
electric discharge, radiation temperature in, 16: 19578
electric discharge, striations in toroidal excited by traveling magnetic fields, 16: 19601
electric discharge, emission luminosity in cold low-pressure arcs, 16: 19636
electric discharge in, channel brightness, 16: 24289(T) (NP-tr-898)
electric discharge in, negative radiation temperature, 17: 5461
electric discharge in, characteristics at high and low filling pressures, 17: 15370
electric discharge stabilization in, in magnetic field, 17: 29406
electric discharge in, laser action from, 18: 18624
electric discharge in, plasma constriction in, 18: 21463
electric discharge in low-pressure, instabilities in, 18: 21479
electric discharge in, microwave resonance emission spectra of, 18: 24772
electric discharge in, electron density decay rate in afterglow of, 18: 32439
electric discharge in, traveling density variations in glow, (E/T), 19: 14141 (RLE-TR-424)
electric discharges in, plasmoid production by h-f, 19: 23853
electric discharge in hot cathode, plasma frequencies from, (E), 19: 25555 (RADC-TDR-64-244)
electric discharges in, stable plasmoids from h-f, (E), 20: 10188
electric discharge in, converging-cylinder shock-wave model for Z-pinch, (E), 20: 24565
electric discharges in, high-pressure electrodeless, (E), 20: 42509
electromagnetic radiation from, measurement of anomalous cyclotron, 18: 28094(R) (TID-20607)
electromagnetic-wave propagation in partially ionized, helicon, (E), 19: 21552
electron and ion densities and temperatures in high-pressure plasma of, 20: 6480
electron and photon reactions with, electron cascade curves for, (T), 20: 21514 (INR-598/VI/PH)
electron beam interactions with plasma of, microwave amplification in, (E), 20: 46923
electron binding energies of, K- and L-shell, 20: 46603 (UCRL-16798)
electron capture by, excitation by, 18: 16709
electron collision frequency and density in plasma of, impedance method for measuring, (E/T), 19: 14694
electron density and temperature in high-pressure plasma of, (E), 19: 6807
electron density and temperature in arc plasma of, current density dependence of, (E), 20: 28587
electron density, magnetic susceptibility, and polarizability of atomic, statistical model for, 17: 41625
electron diffusion in plasmas of, in magnetic fields, 17: 27650(R) (AD-297382)
electron distribution in, solution of Thomas-Fermi-Dirac equation for, 20: 19366
electron drag by traveling magnetic wave in plasma of, (E/T), 19: 27680
electron drift velocity in, slow, 16: 19470 (NP-11617)
electron drift velocity in, at 77 to 443°K, 16: 27742 (NP-11983)
electron drift velocity and mean energy in, determination of, 19: 47124(T) (SLAC-Trans-19)
electron elastic scattering by, resonances in, 18: 44447
electron elastic scattering by, momentum-transfer cross sections for slow, (T), 19: 39397
electron emission by solid, secondary, 18: 26156
electron energy levels of neutral, at 380 to 600 Å, existence of auto-ionizing, 18: 10784
electron energy levels of, optically forbidden transitions in, 18: 10785
electron energy loss on thin films, at 20°K, 16: 5789
electron energy loss, penetration, and range at 5 to 100 Mev, 19: 9445 (LA-3130)
electron inelastic scattering at 500 to 1000 ev, oscillator strengths for, 18: 32401
electron mobility in, 17: 40153(R) (AD-290727)
electron momentum-transfer cross sections in, slow (E/T), 19: 2985
electron multiple scattering at 40 to 130 kev, linear displacement distributions in, 18: 21316
electron-photon shower fluctuations in, 4-Bev total energy, 17: 37883
electron reactions with, appearance potentials for ions produced in, 18: 28134
electron reactions at 0.36 to 1.9 ev, threshold laws for ionization in, 18: 32427
electron reactions at 12 to 14 ev, ionization efficiency curves for, 18: 32428
electron reactions with, excitation and ionization in, 18: 36167
electron reactions with, ionization cross sections in, (E/T), 19: 23261
electron reactions with, ionization probabilities in, 19: 23273
electron reactions with, excitation of long-lived states in, (E), 19: 23320
electron reactions at 0.1 to 20 kev, ionization cross sections for, (E), 19: 43016
electron reactions with, ionization cross sections for, (E/T), 20: 5989
electron reactions with, excitation total cross sections for, (T), 20: 9661
electron reactions with atomic, metastable excitation in, (E), 20: 11455 (UCRL-14450)
electron reactions at 0.001 to 20 ev, cross sections for elastic, 20: 25723 (RT-FI-(65)-60)
electron reactions at 0.5 to 18 kev, multivalent ion production mechanisms for, (E), 20: 27753
electron scattering by, cross sections extrapolated to zero energy for, 17: 18963
electron scattering at 25 kev, cross sections for and optical transitions in, 18: 20764
electron scattering at 50 kev, luminescence from, 18: 44428
electron scattering at 100 kev, Lenz theory for small-angle, (E/T), 19: 8106
electron scattering by, at 25 kev, 17: 22274 (NP-12721)
electron scattering by, Lenz and Thomas-Fermi-Dirac models for small-

angle, (T), 19: 8107
electron scattering by, elastic resonances in, (E), 19: 18702
electron scattering by, screening angles for multiple, (T), 19: 23293
electron scattering on, electron-photon cascades from, (T), 20: 28350
electron spin resonance spectra of cesium, lithium, potassium, sodium and rubidium atoms in matrices of, at liquid helium temperatures, 16: 5246
electron thermalization in, calculation of, (T), 20: 28042 (RT-FI-(65)-61)
electron transfer collisions near adiabatic conditions with bromine ions, carbon atoms and ions, hydrogen ions, lithium ions, and oxygen atoms, 16: 16868
electron velocity distributions in mixtures of mercury and, 18: 22815
electron-ion recombination coefficient of plasma of, (E), 20: 36333
electronic partition functions at high temperatures, (T), 19: 6406
energy level widths for, K, (T), 20: 15239 (CONF-233(Vol.3), pp 419-39)
energy levels in solid argon–xenon films, 17: 34620
energy levels of solid, Hartree calculation of ground-state, 17: 642
energy levels of, correspondence with argon energy levels, (E), 19: 14143 (UCRL-7907(Rev.I))
energy of crystalline, temperature dependence of anharmonic free, 18: 6113
energy transfer to, in iodine fluorescence, 19: 2382
enthalpy-entropy diagram, 16: 10713
enthalpy–entropy diagram for, at 0 to 150°C, 16: 23701
equation of state for solid, experimental, 18: 10086
equation of state for, high-pressure, 20: 20365
equilibrium distribution and uptake in organs and tissues in dog, 16: 7389
exciton spectra in liquid and solid, (E), 19: 47893
fission fragment energy-losses in, (E), 20: 44685
fission product, separation of krypton-85 and xenon-136 from, 19: 34607(R) (MLM-1239)
fixation in p-fluorophenol and quinol clathrate crystals, 16: 163
fluorescence of, alpha-excited, 17: 29212
fluorination of, radiation-catalyzed, 17: 31795(R) (BNL-782(p.18-43))
formation and loss in ATR, analog simulation and calculation of, 18: 31034 (IDO-24456)
formation by xenic acid reduction at dropping mercury electrode, 18: 16053
gamma–gamma angular correlations from nuclear transitions in, (E/T), 19: 5191
glow discharges in, energy balance of steady-state, 20: 44961
heat of absorption by molecular sieves, 20: 20806(R) (MLM-1274)
heat of fusion and heat of vaporization of, calculation from rigid-sphere 18: 224
heat transfer in ionized, stagnation-point, (T), 19: 11360
heat transfer to cylinder in plasma of, (E/T), 19: 6793
heats of absorption on molecular sieves, 19: 36889(R) (MLM-1250)
helium elastic scattering by, total cross section for, (E), 19: 44957
helium ion charge exchange in, cross sections for, 18: 14738
helium ion reactions at very low energy, optical radiation from, (E), 20: 7730
helium scattering on, velocity dependence of total cross sections for, (E), 20: 2614
hydrogen halides infrared spectra in liquid, absolute intensities and band structures of, 20: 311
hydrogen ion reactions at 10 to 50 kev, equilibrium fractions in, (E), 19: 14243
hydrogen negative-ion dissociation in, cross sections for, (T), 20: 29947
interactions of, with mesons (π^-) at 8.4 Bev, 16: 33688 (PAN-327/VI)
interactions with metastable helium atoms, de-excitation cross sections, 16: 30972
interactions with metastable helium atoms, calculation of de-excitation cross sections, 16: 30973
interactions with graphite, constants for (6-exp) potential in, 17: 29442
interactions with argon atoms, dipole-quadrupole effects on cross sections for elastic, 18: 20733 (WIS-TCI-41)
ion decay rate in pulsed discharge ionization of, in thermionic converter, 17: 40153(R) (AD-290727)
ion mobilities and recombination coefficients in plasma of, positive, 18: 28827
ion reactions at 1 to 30 kev, charge exchange cross sections for alkali metal, (E), 20: 34112
ionic reactions of, mass-spectrometric studies of, 17: 38988
ionization by alpha particles, impurity and temperature effects on energy of, 18: 18467
ionization by electrons at 150 to 550 Mev, 16: 21288
ionization by electron impact, instrumentation and relative transition probabilities for, 16: 22120
ionization by electron impact at energies up to 100 ev, cross sections for, 17: 31126
ionization by electrons, cross sections for, 18: 20768
ionization by electrons, cross section for, (E), 19: 15886
ionization by electrons at 0.6 to 20 kev, (E/T), 19: 20850
ionization by electron impact, autoionization in, (E), 19: 20963
ionization by electron and proton impact at high energies, cross sections for, (T), 19: 47246
ionization by fission fragments in nuclear thermionic cells, 17: 27985
ionization by fission products, 18: 16740(R) (AD-425231)
ionization by fission fragments, 18: 30487 (TID-7687(p.45-50))
ionization by fission fragments, plasma production in, (E/T), 20: 13939
ionization by in-pile fission fragments, (E/T), 19: 16366(R) (AD-609177 (Sect.A))
ionization by light, multi-photon, (T), 19: 16398
ionization by metastable helium atoms, cross sections, 16: 24296
ionization by metastable helium ions, relative cross sections for, 19: 6479
ionization by shock waves, continuum radiation from, 17: 969
ionization by shock waves, impurity effects on, 18: 34361
ionization cross section for, electron-impact, 19: 38630
ionization efficiency curves, effects of instrumental factors on, 16: 15296
ionization in mass spectrometer, formation of multiply charged ions in, 20: 14584(R) (TID-22444)
ionization in shock tubes, magnetically induced, 18: 7423
ionization induced by magnetic field in shock tube MHD generator, 19: 31321(R) (AD-609273)
ionization lifetime, effects of electric field, 17: 10197 (NASA-TN-D-1563)
ionization of, kinetics of thermal, 17: 29425
ionization of, by electrons at 0.6 to 20 kev, cross sections for, (E/T), 20: 31906
ionization of, cross sections for ruby-laser-multiphonon, (T), 20: 15276
ionization of, cross sections for shock-produced, 20: 40896
ionization of, magnetically induced, (E), 19: 9801
ionization of, modes of magnetically induced, 18: 42785(R) (AD-600531)
ionization potentials, multiple, 16: 17708(R) (TID-14812)
ionization potentials of multiply charged, 18: 22117(R) (RRL-133)
ionization processes in MHD generator, (E), 20: 41786
ionization rates in shock-heated, 17: 36539
isotopic composition of, from calcium-poor achondrites, (E), 20: 39984
isotopic thermal diffusion factor of, at 245 to 543°K, (E), 19: 42480
lamp for producing retinal burns, 18: 23254
laser beam interactions with atomic, ionization from, (E/T), 20: 27721(T) (NP-tr-1380)
laser oscillations in, 5d-6p transitions from pulsed, (E), 19: 39394
light emission from pinched plasma of, 18: 42153 (AROD-3323:4)
lithium halide infrared spectra in matrix of, 18: 27405
lithium reactions at 80 kev, energy losses in, (E), 19: 6443
lithium scattering on, interaction potentials from cross sections for, 17: 25933
lithium-7 scattering at 700 to 3800 m/sec, 17: 823
lithium-6 reactions with, Massey-Mohr total elastic cross sections for, (E/T), 20: 19872
lithium-7 scattering at 7 to 60 kev, angular distributions from, 18: 21318
magnetic field shift at xenon-129 nuclei in liquid and solid, local, (E), 20: 44142
magnetic field shift in solid, local, (T), 20: 44143
magnetic properties of, Hartree-Fock-Slater wavefunction calculations of, 19: 27086
maser collision processes in, optical, 18: 32484
mass spectra, 18: 5316
mass spectra and yields from thermal-neutron irradiation of uranium dioxide, 19: 26912
melting temperature of, equations for calculating, 18: 25990
meson (μ^-) capture rates from hydrogen, (E), 19: 35384 (JINR-P-2153)
meson (π^-) interactions with nucleons in, at 9 Bev/c, (E), 19: 8446
meson (π^-) interactions at 9 Bev/c, hyperon (Λ) and meson (K^0) production in, (E), 20: 15841
meson (π^-) reactions with, hyperon (Σ^0) production in, 18: 18641 (JINR-P-1529)
meson (π^-) reactions at 9 Bev/c, meson (π^0) production in, 18: 34949
meson (π^-) reactions at 9 Bev/c, meson (π^0) production in, 18: 36305
meson (π^-) reactions at 9 Bev/c, cross sections for meson (π^0) production in, (E), 19: 5250
meson (π^-) reactions at 9 Bev/c, mean-free-path of, (E), 19: 35380 (IFA-CR-51)
meson (π^-) reactions at 9 Bev/c, cross sections for hyperons (Λ) and (K^0) from, 19: 39472 (JINR-P-2178)
meson (π^-) reactions at 2.8 Bev/c, meson (π^0) multiple production in, 19: 43279 (NP-15383)
meson (π^-) reactions at 9 Bev/c, cross section for, (E), 19: 47689
meson (π^-) reactions at 9 Bev/c, neutron emission in high four-momentum transfer, (E), 19: 47698
meson (π^-) reactions at 9 Bev, secondary angular distributions from, (E),

20: 34519 (INR-683/VI/PH)
meson (π^-) reactions at 5 and 9 Bev/c, angular, energy, and multiplicity distributions of mesons (π^0) produced in, 20: 39755 (JINR-P-2736)
meson (π^-) reactions at 2.8 Bev, angular distribution and cross sections for, 16: 24695 (NP-11757)
meson (π^-) reactions at 2.8 Bev, K^0 and Λ^0 production in, 16: 26189
meson (π^-) reactions at 1.0 to 1.1 Bev, cross sections, 16: 27925
meson (π^-) reactions at 2.8 Bev/c, K^0–Λ^0 resonances from, 16: 27987
meson (π^-) reactions in liquid, meson (K^0) pair production in, 17: 7039
meson (π^-) reactions with, cross sections for, 17: 9347
meson (π^-) reactions at 8.4 Bev/c, meson (π^0) production in, 17: 11673
meson (π^-) reactions, meson (π^0) production in, 17: 20932
meson (π^-) reactions with, mass spectra for, 17: 26425 (NP-12886)
meson (π^-) reactions at 2.8 Bev/c, meson (π^0) angular distributions from, 17: 41980
meson(π^-) reactions at 9 Bev/c, 18: 40549
meson(π^-) reactions at 9 Bev, meson and photon production from, 18: 40550
microwave absorption in weakly ionized plasma of, in magnetic fields, (E), 20: 3204
microwave emission at cyclotron resonance in plasma of, in magnetic field, 18: 9488
microwave penetration through plasma of, polarization modifications in, (E), 20: 1292
microwave radiation in, negative radiation temperature in cyclotron-resonance, 18: 28874
mobility of positive ions in liquid, 17: 163
molecules of, binding energy for triatomic, (T), 19: 9917
neon ion ionization cross sections, 16: 6880
neon ion reactions with, cross sections for, 20: 25747
neutron absorption and scattering at (3 to 25) $\times 10^{-3}$ ev, cross sections for, 17: 29588
neutron absorption by, in slabs, 18: 28537
neutron activation of, transport system for in-pile, 19: 19416 (IS-1012)
neutron capture by, gamma radiation intensity from, 16: 32176(R) (PR-P-53)
neutron scattering by, effective potential for electron-neutron interactions from, (E), 19: 45098
neutron scattering by, cross sections and electron-neutron interaction from thermal, (E), 20: 40129
neutron-proton ratio on periphery of nucleus of, from meson (π^-) reactions with xenon at 9 Bev/c, (E), 19: 35381 (JINR-P-2097)
nitrogen ion reactions with, cross sections for, (E), 20: 25747
nitrogen metastable molecule reactions in discharges and afterglows, 18: 32494
noise resonance in afterglow plasma of, narrow-band, 18: 28872
nuclear magnetic resonance of liquid, 17: 25271
nuclear relaxation of xenon-129 and -131 in gaseous, 16: 26975
optical gains at 3.5 μ in plasma of, high, 17: 31583
origin of atmospheric, 17: 11445 (NASA-TN-D-1685)
oscillations with flow feedback in reactors, natural modes of, (T), 20: 36439
oxygen ion elastic scattering at 153 Mev, 16: 25990
oxygen ion reactions at 15 to 50 kev in, equilibrium fractions for, (E), 19: 18687
performance as working gas in nuclear-thermionic plasma diodes, (E/T), 19: 16440(R) (AD-609177)
performance in magnetic wave plasma engine, 19: 13608 (NASA-TN-D-2676)
performance in mm-wave beam-plasma amplifiers, (E), 19: 13705 (RADC-TDR-64-207)
performance in scintillation detectors for alpha particles and electrons, 19: 20361
performance in scintillation dE/dx counter, 19: 42724
performance of alkali-seeded, as carrier gas in MHD generator, (T), 19: 34999 (NASA-TN-D-2873)
photoabsorption calculations for, using model for atomic excited states, 20: 15270
photoemission spectra of plasma of, transition probabilities for, (T), 19: 33486
photoionization cross sections for, calculation from model wave functions, (T), 19: 47216 (AD-613675)
photoionization efficiency curves of, fine structure and measurement of ionization potentials from, 17: 37752
photoionization of 4d electrons in, cross sections for, (E), 19: 8098
photon absorption by, cross sections for, 18: 16717
photon reactions at .01 to 10 Bev, electron pair production cross sections for, (T), 20: 27720 (JINR-P-2636)
photon scattering on, electron-photon cascades from, (T), 20: 28350
pinch effect in, spectroscopic studies of, 18: 21422
plasma, containment by alternating magnetic fields in Mc range, 16: 23217
plasma in magnetic field, anomalous microwave radiation from, 17: 22718 (IPPJ-6)
plasma interactions with medium microwave power, shock-produced, 17: 21164
plasma interactions with high microwave power, shock-produced, 17: 21165
plasma of, microwave reflection by shock-produced, 18: 1130 (R63SD77)
plasma of, light emission from, (E/T), 20: 46849
plasma of, microwave diagnostics of high-density, 18: 28767 (RADC-TDR-63-477)
plasma of, microwave amplification in magnetic field, (E), 19: 31370
poisoning of high-flux reactors by, calculation, 17: 4261
poisoning of reactors by, effects on stability, 18: 44982
polarizabilities of metastable, measurement of, 18: 22696
polarizability of liquid, corrections for zero-field many-body, 17: 4526
polarization of excited, tensor measurements of, 19: 32048(R) (NP-15073)
positron lifetime spectra in, (E), 19: 18872
positron mean life in, 18: 707
potassium atomic beam scattering by, 18: 17121(R) (TID-20362)
potassium beam attenuation in, cross section for, 17: 13628(R) (TID-17888)
potassium beam scattering by, at three temperatures, 17: 36376 (CONF-186-1)
potassium ion scattering at 350 to 1550 m/sec, 17: 823
potassium ion scattering by, total cross sections for (E), 19: 2980
potassium scattering on, velocity dependence of total cross section for, (E/T), 19: 34876
potential energy integrals at 0°K of solid, (T), 20: 42123
pressure-volume characteristics at low temperatures, 17: 14936 (IS-623)
production and acceleration of plasma of, in betatrons, (E), 19: 12008
production in operation of power reactor, methods of calculation, 17: 15478
production in proton-induced fission of uranium, cross sections for, 17: 34893
production in reactors during shutdown, minimization of, 18: 28962
production in reactors, steady-state concentrations from, 18: 28963
production of xenon-124-enriched, by thermal diffusion, design and performance of equipment for, 20: 46133
properties as bubble chamber liquid, 16: 31900
properties as working fluid in Brayton power cycle, 20: 41398
properties in aqueous solutions, 18: 25357
properties in scintillation detectors, 17: 29209
properties of, 19: 13384
properties of, as contrast medium for, 17: 35352
properties of, thermodynamic and transport, 18: 1112 (ARL-63-151 (p.294-321))
proton reactions at 1 to 25 kev, Lyman alpha emission cross sections for, 18: 32446
proton reactions at 1 to 23 kev, metastable 2S hydrogen atom production in, (E), 20: 982
proton reactions at 10 to 40 kev, excitation cross sections for hydrogen-atom formation in, (E), 20: 25748
proton reactions (p,xn), production of cesium-129 and -132 by, 17: 30164
proton reactions with, cross sections for Lyman alpha production in, 17: 25953
purification and separation, 16: 32881(R) (MLM-1126)
purification method for, 17: 15855(R) (ORNL-3397(p.38-54))
purification of, by low-temperature distillation, 17: 4374(R) (MLM-1129)
purification plant for, 19: 30325 (RT/FI(65)-6)
radiation absorption in plasma of, optical, (E/T), 19: 25588
radiation attenuation by, critical energies and units for, 17: 38420
radiation effects on diffusion in solids, 18: 36050(T,R) (EURAEC-1006)
radiation effects on electric properties of plasma of, in thermionic diodes, 19: 18743
radiation effects on fluorescence spectra of, 19: 30264
radiation stopping power of, shell corrections to, (T), 19: 4401 (ORNL-P-659)
radiation temperature in positive-column plasma at $\lambda = 4$ and 8 mm, 16: 19594
radio wave emission from plasma of, negative-absorption effects on anomalous bremsstrahlung and cyclotron, (E), 20: 17921
radioinduced ionization in thermionic cells, fission fragment, 18: 20860
radioinduced ionization of, electron dosimetry by, 18: 29764
radioinduced luminescence in uniform electric fields, (E/T), 19: 26379 (NP-14813)
radioinduced luminescence of, electric field effects on decline of alpha, (E), 20: 21521
radioinduced polymerization of, with vinyl chloride, 19: 40584
radioinduced reaction with fluorine, compound formation in, 17: 39119
radioinduced reactions with fluorine, 18: 22132
radioinduced reactions with fluorine, 19: 15331(R) (BNL-841(p.18-42))
radioinduced reactions with fluorine, proton, 20: 23109
radioinduced scintillations in, 18: 32282
radiolysis effects on methane and propane mixture, 16: 7597

radiolysis effects on labeled and unlabeled propane, 17: 4601
radiolysis effects on yields in labeled gaseous isobutane, 17: 12338
radiolysis of mixtures with acetylene, ionic complexes produced in, 16: 11722
radiosensitivity effects on mice, 18: 11878
radiosensitization of deuterium exchange with hydrogen in methane, 17: 8161
range in tungsten single crystals, 18: 18577
rare-gas-ion scattering at 80 kev by, energy losses from, 18: 34416
reactions with acetylene, deuterium, ethylene, and nitrous oxide, cross sections for, 19: 13324
reactions with antimony fluoride and fluorine, formation of xenon hexafluoroantimonate by, 18: 17822
reactions with carbon monoxide and nitrogen at high pressure, spectra of, 17: 4527
reactions with carbon black surfaces, 17: 20050
reactions with cesium, excitation transfer in, (E), 20: 15253
reactions with charged particles, stopping powers and straggling in, (T), 20: 39611
reactions with deuterated and undeuterated propane, dissociative charge-exchange, 18: 3743
reactions with dioxygen difluoride, 19: 26303
reactions with fluorine fluorosulfate, oxygen difluoride, peroxydisulfuryl difluoride, and trifluoromethyl hyperfluorite, 17: 33946
reactions with fluorine, design of circulations loop for studies on, 18: 5315
reactions with fluorine and silicon fluoride, formation of xenon hexafluorosilicate by, 18: 17822
reactions with fluorine, catalysis of, 19: 4144
reactions with fluorine at 350 to 450°C, 19: 28343(P)
reactions with fluorine, production of xenon difluoride in photochemical, 20: 35496
reactions with graphitized carbon black at 2700°C, third order gas-surface, 17: 4534
reactions with helium, ionization cross sections, 16: 26238
reactions with hydrogen mesic atoms, meson (μ) exchange in, (E), 20: 7734
reactions with hydrogen negative ions at 0.2 to 7 kev, electron detachment in, (E), 20: 7735
reactions with inert-gas atoms, van der Waals forces for, 18: 34345
reactions with iodine, energy transfer processes in, 19: 25157
reactions with mercury, cross sections for line broadening from, (E), 20: 2637
reactions with mercury-199 and -201, hyperfine-level excitation in, (E), 20: 4544
reactions with methane, mass-spectrometric studies of, 17: 38988
reactions with oxygen difluoride or fluorine in presence of light, 19: 42477
reactions with p-cresol, heat of formation of clathrate compounds formed in, 20: 20688
reactions with platinum and rhodium hexafluorides, composition of compounds formed in, 18: 5313
reactions with revolving surfaces, 18: 40154
reactions with sodium, spin relaxation cross sections for, 18: 30418
reactions with xenon ions (divalent), total-charge-transfer cross sections for, 16: 22800
reactions with xenon, potential energy curve for, 17: 21690
reactivity effects in HTRE-1, analysis of predictions of various methods, 16: 19984 (DC-60-4-118)
reactor criticality effects after shutdown, 16: 15803
reactor criticality effects, calculations of effective steady state, 16: 15798
reactor criticality effects, spatial oscillations, 16: 18630
reactor criticality effects, time behavior in German Geesthacht research-type, 16: 23336
reactor criticality effects, effect of modal interaction on, 16: 28443
reactor criticality effects of oscillations of, 18: 23028 (TID-7662 (p.548-81))
reactor criticality effects in PRTR at power, 18: 40834 (HW-80253)
reactor criticality effects, 18: 40781 (KAPL-3061)
reactor criticality effects, control of, 19: 29651(R) (WCAP-3269-3)
reactor criticality effects in HBWR, (E/T), 19: 29714 (HPR-58)
reactor criticality effects of, nonconvergence calculations for, 19: 35709 (WAPD-T-1673)
reactor criticality effects in slab matrices, 19: 45539
reactor criticality effects of, calculations of, 17: 24661
reactor criticality effects on heavy-water-moderated natural-uranium thermal reactor, 17: 26762 (IA-741)
reactor criticality effects of, calculation for equilibrium conditions, 17: 28425 (EUR-102.f)
reactor criticality effects of, under different operating conditions, 17: 29726 (RT/ING(63)6)
reactor criticality effects in PWR, (E/T), 20: 3383 (WCAP-3269-48)
reactor criticality effects in VVR-S, (T), 20: 24803
reactor poisoning effects on control rod speeds, 16: 15773 (CEA-2081)
reactor poisoning, effects on shutdown behavior, 16: 21738
reactor poisoning with, optimization of (T), 19: 3522
reactor poisoning by, (T), 19: 42010
reactor stability effects of, feedback control of spatial, 19: 3654 (TID-21273)
recovery from irradiated reactor fuels during dissolution, 20: 15133(R) (GEAP-4893)
release from enriched fuels, analytical method for determining, 19: 15394
release from graphite, effects of fission fragment damage, 17: 3547
release from irradiated thorium carbide-uranium carbide systems in graphite matrix at 900 to 2000°C, 16: 25752 (GA-3211)
release from irradiated fuel elements, 17: 30927
release from irradiated molten fluoride reactor fuel, 17: 34481 (CONF-126-8)
release from irradiated uranium dioxide containing niobium and titanium oxides, 17: 41490 (CRFD-1012)
release from irradiated EGCR fuel elements, 18: 14538(R) (ORNL-3523 (p.69-100))
release from irradiated uranium metal by heating, 19: 2721 (JAERI-4030)
release from irradiated polycrystalline uranium monocarbide, 19: 14082 (EUR-1752.e)
release from niobium and niobium, silicon, and titanium oxides at 50 to 800°C, 16: 4167
release from thorium oxide, uranium carbide, and uranium dioxide crystals, 17: 34333(T,R) (EURAEC-655)
release from thorium dioxide, uranium carbide, and uranium dioxide, 18: 8736(T,R) (EURAEC-859)
release from thorium dioxide, uranium carbide, and uranium dioxide crystals, 18: 10457(T,R) (EURAEC-875)
release from uranium dioxide fuels, 19: 28896
release of fission-product, from melting urania fuel rods, 18: 28069
release rate from pools of water, 20: 39103(R) (BNWL-235-3, pp 51-69)
rubidium-vapor spin relaxation in, (E), 19: 39400
scattering by molecules at thermal energies, total cross sections for, 18: 34407 (UCRL-11071)
scattering of atomic beams of, by argon at thermal energies, cross sections for, 16: 18264
scattering of molecular beams of, by silver single crystals, (E), 20: 44121
scattering on beryllium–copper alloys and nickel at 5 to 25 kev, secondary electrons from, 20: 41620 (NIJS-R-471)
scintillations produced in, by α particles, effect of electric field on, 18: 3824
separation by gas chromatography, 16: 27767
separation from argon, krypton, nitrogen, and oxygen by gas chromatography, 16: 4228 (USNRDL-TR-535)
separation from fission gases and krypton, gas-chromatographic, 18: 39147
separation from flowing helium stream by fixed-bed adsorption, 16: 26489 (TID-7622(p.218-35))
separation from gas mixtures, 19: 40695(P)
separation from helium, 18: 1608 (JAERI-4025)
separation from helium by adsorption on charcoal at low temperatures, 19: 22432
separation from krypton, 16: 16455 (CEA-2111)
separation from krypton-85 by low-temperature distillation, 17: 7659(R) (MLM-1136)
separation from krypton by chromatography, 18: 19467(R) (MLM-1175)
separation from krypton by gas chromatography, 18: 21707(R) (MLM-1177)
separation from krypton, methods testing for, 18: 27810(R) (MLM-1183)
separation from krypton, effects of carrier gas on chromatographic, 18: 29146(R) (MLM-1192)
separation from krypton by chromatography, 18: 45173(R) (MLM-1203)
separation from krypton-85 by chromatography, 18: 45174(R) (MLM-1204)
separation from krypton-85 by chromatography, 18: 45175(R) (MLM-1209)
separation from krypton, chromatographic, 19: 7274(R) (IDO-14636)
separation from krypton-85 by chromatography, 19: 14911(R) (MLM-1216)
separation from krypton-85 by chromatography, 19: 24611(R) (MLM-1227)
separation from krypton-85 by gas chromatography, 19: 28717(R) (MLM-1221)
separation from krypton by chromatography, 19: 30629(R) (MLM-1238)
separation from krypton by gas chromatography, 20: 18825 (KFK-365)
separation from krypton, gas chromatography method for, 20: 25022
separation from krypton by chromatography, 20: 35828(R) (MLM-1300)
separation from neon, thermal diffusion factors for, 20: 39321(R) (MLM-1312)
separation from nitrogen, oxygen, and rare gases by sorption on zeolite, gas chromatographic, 18: 41328
separation from power reactor fuels, economics of, 19: 20036 (BNWL-25)
separation from products of fission-fragment-induced radiolysis, 20: 40951

(RPI-321-6)
separation methods evaluation for, chromatographic, 18: 16376(R) (MLM-1157)
separation of, 19: 13384
separation of krypton from, comparison of helium and nitrogen as carrier gas in chromatographic, 18: 35246(R) (MLM-1196)
separation of krypton-85 from, by chromatography, 20: 39321(R) (MLM-1312)
separation of, from uranium fission products by solvent extraction using carbon tetrachloride, 20: 35594
shock propagation in, properties of, 19: 41128 (UCRL-12466)
shock waves in, density-pressure curves for, (T), 19: 14709
solubility in molten fluoride systems, 16: 18877
solubility of, in fused salts, 16: 28646(R) (ORNL-2247(Pts.1-5))
sorption by activated charcoal, 16: 14814 (BNL-689)
sorption by activated charcoal and various inorganic absorbers, 16: 3068 (ORNL-3228)
sorption by activated carbon, 18: 14361(R) (EURAEC-254)
sorption by activated carbon, 18: 38392 (A/CONF.28/P/44)
sorption by boron nitrides, 20: 43067(R) (IDO-14679, pp 6-46)
sorption by carbon black, many-body effects in, 17: 26251
sorption by carbon, 19: 13901(R) (TID-21415)
sorption by carbon, 20: 9381(R) (TID-22507)
sorption by charcoal and graphite at high temperatures, 16: 29216 (TID-7627(p.24-42))
sorption by charcoal, 17: 40344(R) (NP-13123)
sorption by evaporated molybdenum films, 19: 40463(R) (SRIA-425-5)
sorption by evaporated metallic films, 20: 21387
sorption by glass and molybdenum film at low temperatures, mechanism of chemi-, 19: 26822 (TID-20853)
sorption by glass and molybdenum film, 20: 916(R) (SRIA-425-6)
sorption by graphite at 750 and 1000°C, 16: 13067
sorption by graphitized carbon black, isotherms for, 16: 31536
sorption by molecular sieves, heat of, 20: 35827(R) (MLM-1299, pp 22-33)
sorption by molybdenum films and glass supports, 18: 18021(R) (TID-20411)
sorption by molybdenum films at −195 and −185°C, 19: 11052(R) (SRIA-135)
sorption by molybdenum films and Pyrex glass in ultrahigh vacuum, kinetics of, 20: 21351(R) (SRIA-425-8)
sorption by pyrex glass, physical, 19: 29812(R) (SRIA-425-4)
sorption by surfaces of glass and uranium dioxide, 18: 14387(T,R) (EURAEC-860)
sorption by synthetic zeolite for gas chromatography, effects of lithium, potassium, and sodium on, 18: 41328
sorption by synthetic zeolite, 20: 14444(R) (MLM-1268)
sorption in reactor dehydrator unit, tracer technique for measuring dynamic and static, 20: 18626 (GA-6865)
sorption on activated charcoals and molecular sieves at −78 to 25°C and 10^{-3} mm Hg to 1 atm, 19: 17910
sorption on activated charcoal and boron nitride, 19: 32059(R) (IDO-14655)
sorption on charcoal and silica gel, heat of, 19: 30630(R) (MLM-1245)
sorption on evaporated metal films, relation of surface area determination to, 17: 39589
sorption on glass and molybdenum films, 20: 31242
sound propagation in plasma of, damping in, (E), 19: 17087
sound velocity in plasma of, 18: 13138(R) (ORNL-3564(p.44-62))
spectra at 160 to 190 Å, absorption, 19: 2282
spectra, excited by alpha and electron impacts in pure, 16: 21147
spectra in neon–xenon mixtures, detection of laser lines in (E), 19: 1173
spectra of deuterated and normal methane in, rotation-vibration, 17: 33951
spectra of, effects of added carbon monoxide on emission, 17: 40855(R) (TID-19512)
spectra of highly ionized, in plasma, 18: 40706
spectra of hydrobromic, hydrochloric, and hydriodic acids in, deuterium effects on, 20: 12857
spectra of mercury and sulfur isolated in, at high temperatures, 20: 1818 (UCRL-11976)
spectra of molecules trapped in solid, 20: 18016
spectra of normal and deuterated hydrochloric acid in solid, infrared, 20: 25069
spectra of sulfur molecules in solid, u-v absorption, (E), 19: 45480 (UCRL-10771)
spectra of, accelerator methods for obtaining optical atomic, 18: 28254
spectra of, L absorption, (E), 19: 16389
spectra with hydrocarbon solids at 4.2 and 20.4°K, transition of C_2 molecule, 16: 5258
spin-exchange collisions between singly-ionized ground state and metastable state of neutral, (E), 20: 41650
stability in absorbing-layer slab reactor, absorber effects on, 20: 32771
stability in reactors, two-group analysis of, 17: 28416 (AE-108)
structure of hydrated, in biological systems, 20: 22560
thermal accommodation during adsorption of potassium and cesium on tungsten, 17: 16027
thermal capacity of liquid, at boiling point, 18: 19929 (CONF-417-20)
thermionic properties in diodes, 18: 20831 (APL-TDR-64-28)
thermodynamic and transport properties of liquid, 16: 18932
thermodynamic critical point exponents of, quantum theory of corresponding states for, (E/T), 19: 32806
thermodynamic properties at extremely high pressures, corresponding states rule from, 19: 30846 (UCRL-7907)
thermodynamic properties in molten fluoride systems, 16: 18877
transition probabilities of forbidden lines of, 18: 14736
transport coefficients at high temperatures, 16: 25880 (ARL-62-328)
transport properties in pure gaseous and liquid, 16: 18933
triton energy losses in, 16: 2491 (TID-14145)
triton ranges and stopping cross sections in, 17: 17212
triton scattering and slowing-down by, at 2.7 Mev, 16: 27782
ultraviolet refractive indices of gaseous, Rayleigh scattering method for vacuum, 17: 28029
uses in industry, 19: 13384
vapor pressure of liquid, up to critical point, 18: 3722 (UCRL-7167)
vapor pressure up to critical point, 18: 41374 (UCRL-7167(Rev.I))
wavefunctions for, calculation of approximate analytical, 19: 23277
x-ray absorption, 17: 22044
x-ray scattering by atomic, factors for, 17: 39772
x-ray absorption cross sections of, model for maxima in, (T), 19: 8099
x-ray emission by, yields of L-shell, 18: 28253
x-ray scattering by liquid, calculation of radial-distribution functions from, 19: 30950
x-ray scattering by, relativistic wave functions for form factors for, 20: 27745
x-ray scattering form factors, (T), 20: 29949
xenon-atom reactions at 0.3 to 3 kev on, electron spectra from, 16: 33635
xenon ion inelastic reactions at 20 to 60 ev, electron capture in, 18: 32463
xenon ion reactions with, charge-exchange cross sections for, (E/T), 19: 34877
xenon-129 chemical shift and relaxation in gaseous, 17: 25220
xenon-129 nuclear magnetic resonance in gaseous, 17: 25219
xenon-129 nuclear magnetic resonance in liquid and solid, density-dependent shifts in, 17: 26583
xenon-129 NMR in, chemical shift of (T), 19: 385
xenon-129 NMR shift in, density dependence of, 18: 34919
xenon-131 NMR in gaseous, quadrupolar relaxation in, (T), 19: 19200
xenon-131 NMR in liquid and solid, at 4.2 to 250°K, (E), 20: 38404
xenon-131 NMR shift in, at 4.2 to 250°K, 19: 23813
xenon-131 quadrupole relaxation time in liquid and solid, temperature dependence of, (T), 20: 38392
yields from thermal-neutron fission of uranium, 17: 27416 (HW-73394)
yields from uranium fission, 18: 13636(R) (ORNL-3537(p.71-105))
yields in neutron fission of plutonium and uranium, 18: 18869 (HW-60431)
yields in uranium-235 fission, 19: 36217(R) (IDO-14656)
Ar–Xe, ionization of, at 5000 to 9000°K, shock-induced atom-atom, 20: 41632
hexane–Xe, radiolysis of, charge transfer in, 20: 29314
naphthalene–Xe, radiolysis of, spectra of naphthalene triplet state in pulse, 18: 43627

XENON CHLORIDES
ionization potential of, method of calculating, 19: 22208
ionization potentials, calculated, 19: 46161(R) (ORNL-3832, pp 116-50)
structure of, Mössbauer effect evidence for, 18: 33559

XENON COMPOUNDS
chemistry and preparation of, 19: 2281
electron structure of, models for, 18: 37153
Mössbauer effect in, 17: 41531(R) (ANL-6720(p.48-58))
Mössbauer effect in, 18: 42626(R) (ANL-6879(p.69-87))
preparation and composition of xenon hexafluoroantimonate and silicate, 18: 17822
preparation and properties of, review on, 18: 16050
preparation and properties of, review of, 19: 17873
preparation and properties, 19: 26364
preparation and properties of, review on, 20: 18623 (CEA-Bib-58)
preparation of xenon-133-labeled, by neutron irradiation of lithium fluoride–uranium dioxide powder, 19: 36500
preparation of, review on, 18: 35440
preparation, structure, and chemistry of, 18: 12058
production by iodine-129 beta decay in iodine compounds, 19: 13519
radioinduced formation and retention of radioxenon in, Szilard-Chalmers effects in neutron, 20: 43373
spectra and structure of perxenates, 17: 35680 (CONF-126-18)
spectra of, infrared, 18: 43447 (TID-19201)

structure of, Mössbauer effect studies of, 18: 10034 (CONF-303-15)
synthesis of, developments in, 18: 27374
uses of clathrates, 19: 34607(R) (MLM-1239)
with platinum fluorides, structure and magnetic properties of, 20: 40882

XENON FLUORIDE OXIDES

hydrolysis of, in hydrofluoric acid solutions, Raman spectra of products of, 20: 40906

XENON FLUORIDES

analysis by mass spectrometry, 17: 14243
binding energy of divalent, theory of, 17: 28852
binding in divalent, theory of, 17: 28854
binding theory for di, 18: 5343
bond length in, theory, 17: 25192
bond lengths and molecular shapes of, theory for prediction of, 18: 5345
bond vibration modes of, Bradley-Urey force constants for, (T), 20: 1845
bonding and heats of sublimation of di- and tetra-, 17: 18038
bonding in, d-hybrid and ionic, 18: 5346
bonding in, high-resolution magnetic spectrum of fluorine-19, 17: 17963
bonding in, theories on, 18: 25372
bonding of, 18: 39208
bonding of, from infrared spectra, 17: 19993 (TID-18460)
bonding wavefunctions in, 17: 33898
chemical bonds in, 17: 28839
chemical properties of tetra-, 18: 5320
chemical shifts in, calculation of, 18: 19960
chemical structure, 17: 27744
complexes with arsenic and boron fluorides, properties of, 18: 19999
complexes with cesium and rubidium fluorides, preparation and properties of, 19: 388
crystal and molecular structure of, neutron diffraction studies of, 17: 12249
crystal and molecular structure of, x-ray diffraction studies of, 17: 12250
crystal and molecular structure of, neutron and x-ray diffraction analysis of, 18: 1491(R) (ORNL-3488(p.102-22))
crystal structure, 17: 12247
crystal structure of XeF_6, 17: 25060(R) (ORNL-3417(p.3-16))
crystal structure of tetravalent, x-ray study of, 17: 35676 (BNL-6828)
crystal structure of tetravalent, 17: 35709 (UCRL-10804)
crystal structure of addition compound XeF_2–XeF_4, 17: 37205
crystal structure of di- and tetra-, 18: 5332
crystal structure, 18: 22010(R) (ORNL-3591(p.3-15))
crystal structure from neutron diffraction, 18: 37143
crystal structure, 19: 23163(R) (ORNL-3650(p.111-86))
crystal structure, 20: 12844
electric conductivity and solubility of di-, hexa-, and tetra-, in hydrous hydrofluoric acid, 18: 5339
electron structure of di-, hexa-, and tetra-, programmed semi-empirical LCAO molecular-orbital theory of, 18: 5347
electron structure of di- and tetra-, experimental and theoretical, 18: 5349
electron structure of hexa-, semi-empirical molecular-orbital treatment of, 18: 5348
electron structure and spectrum of tetra-, 18: 8358
electron structure of, 18: 17810
electron transitions in, forbidden, 18: 9046
energy levels of, determination of semi-empirical molecular orbital, 20: 43237
enthalpy of formation and lattice energies of, Madelung constants for, 20: 26352
fluorine exchange with, rate of, 18: 5319
fluorine NMR in, 17: 14242
fluorine-19 NMR and spin-lattice relaxation in, 20: 40892
fluorine-19 spin-lattice relaxation in, 18: 15711(R) (TID-20256)
fluorine-19 spin-lattice relaxation in crystalline tetravalent, 18: 18474
force constants of, calculation of molecular, 19: 46899(R) (ORNL-3832, pp 33-49)
formation and role in xenon-photosensitized reactions of perfluoroalkanes, 19: 22217
formation from beta decay of iodine-131 in iodine pentafluoride, 20: 27014
handling of, safety precautions for, 18: 5327
heat capacity and thermodynamic properties of tetra-, 18: 5328
heat of formation, 17: 17962
heat of formation of tetra-, 17: 27321 (UCRL-7298-T)
hydrolysis in aqueous solutions, products formed in, 18: 5330
hydrolysis of aqueous solutions of, preparation of sodium perxenates by, 18: 25357
hydrolysis of di-, hexa-, octa-, and tetra-, in acid and alkaline solutions, 18: 5329
hydrolysis of divalent, in aqueous solution, 18: 25358
hydrolysis of, preparation of oxyfluoride by, 17: 25234
identification of difluoride and oxyfluoride, mass spectrometric evidence for, 17: 28880
identification of XeF_2, 17: 33948
ionization potential of, method of calculating, 19: 22208
ionization potentials, calculated, 19: 46161(R) (ORNL-3832, pp 116-50)
magnetic properties of tetravalent, 17: 31107
magnetic resonance of fluorine-19 in, 17: 20721
magnetic resonance spectra of, in hydrofluoric acid, 18: 27403
magnetic susceptibility of tetra-, theoretical, 18: 8355
mass spectra of di-, hexa-, and tetra-, 18: 5316
molecular constants and thermodynamic functions of, (T), 20: 29921
molecular structure of, symmetry in, 17: 12248
molecular structure of tetravalent, spectral studies of, 17: 28846
molecular structure of, (T), 19: 11117
molecular structure of, bond lengths in, 19: 13375
molecular structure of hexa- and tetra-, electron-diffraction analysis of, 19: 24531
molecular structure of gaseous, 20: 12860
molecular structure of XeF_6, electron-diffraction studies of, 20: 35475 20: 35475 (IS-T-93)
molecular vibrations of, bond-bond interaction constants for, 20: 10829
Mössbauer effect in, 17: 32089
Mössbauer effect in xenon-129 in di- and tetra-, 18: 5340
Mössbauer effect in, 18: 42626(R) (ANL-6879(p.69-87))
nuclear magnetic resonance of, chemical shifts in, 17: 35752
nuclear magnetic resonance spectra, 18: 2127(R) (ORNL-3488(p.21-41))
nuclear magnetic resonance in, calculation of chemical shifts in, 18: 41470
phase studies and structure, 18: 7129(R) (ORNL-3529(p.71-143))
preparation, 17: 18024
preparation, 18: 41435
preparation, 20: 24971(R) (BNL-954, pp 50-83)
preparation, 20: 2520(R) (IA-920)
preparation and magnetic susceptibility, 17: 14241
preparation and melting point of pure hexavalent, 18: 33593
preparation and properties, 17: 162
preparation and properties of hexavalent, 17: 12244
preparation and properties of hexavalent, 17: 12245
preparation and properties of divalent, 17: 12256
preparation and properties of di-, hexa-, and tetra-, 17: 27327
preparation and properties of, review of, 17: 33863 (CONF-126-1)
preparation and properties of XeF_4 and XeF_6 by electric discharge method, 17: 33947
preparation and properties of hexa- and tetra-, 18: 5321
preparation and properties, 18: 8380
preparation and properties, 19: 9105
preparation and properties, 19: 26364
preparation and properties, 19: 28343(P)
preparation and properties of, review on, 20: 3915 (CEA-Bib-61)
preparation and properties, 20: 8923
preparation and properties of XeF_2, 20: 20678
preparation and properties of, 20: 20659
preparation and reactions of, review on, 20: 35486
preparation and structure of, review on, 18: 25401
preparation and thermal properties of XeF_6, 20: 20665
preparation at room temperature and high pressures, 18: 23476
preparation by fission recoil in neutron-irradiated uranium dioxide–lithium fluoride mixtures, 20: 12898
preparation by heating fluorine and xenon gases at 200 to 400°C, 19: 30213(P)
preparation by reaction of xenon with dioxygen difluoride, 19: 26303
preparation of, design of circulating loop for, 18: 5315
preparation of di-, by high-voltage discharge in xenon–carbon tetrafluoride mixtures, 17: 18042
preparation of di-, hexa-, and tetra-, spectra of penta- in, 18: 5317
preparation of di-, by electric discharge method, 18: 5323
preparation of divalent, photochemical, 17: 8162
preparation of divalent, 18: 17787
preparation of hexavalent, pressure-temperature effects on, 17: 14265
preparation of hexa- and tetra-, by electric discharge method, 18: 5321
preparation of octavalent, 17: 30524
preparation of tetra-, by electric discharge, 17: 12253
preparation of tetra-, 18: 5314
preparation of XeF_4, 17: 25061(R) (ORNL-3417(p.17-40))
preparation of XeF_2, by exposure of fluorine–xenon mixtures to light, 20: 22977
preparation of, by reactions of xenon and oxygen difluoride or fluorine in presence of light, 19: 42477
preparation of, review of, 19: 28323
preparation, properties, and reactions of, review on, 18: 16050
preparation, properties, and structure of, review on, 20: 33299
production by photochemical reactions between fluorine and xenon, 20: 35496
production from fluorine and xenon, catalytic effects in, 19: 4144
properties, 17: 1456
purity of, design of circulating loop for studies on, 18: 5315

radiation effects on tetra-, electron spin resonance spectra of XeF radical, 18: 5336
radioinduced formation of, 17: 39119
radioinduced formation of di-, photochemistry of, 18: 5322
radioinduced formation in mixtures of fluorine and xenon, 18: 22132
radioinduced formation, 19: 36216(R) (BNL-900(p.29-72))
radioinduced formation of, proton, 20: 23109
radioinduced preparation of, 17: 31795(R) (BNL-782(p.18-43))
radioinduced radicals in tetra-, electron spin resonance spectra of, 17: 21758
radioinduced synthesis of, electron and gamma, 17: 25286 (BNL-6948)
radiolysis, 20: 20678
radiolysis and radiosynthesis, 18: 3671(R) (BNL-799(p.26-54))
reactions in aqueous solutions, 18: 1604 (CONF-126-19)
reactions of tetra-, with water, 18: 31361(R) (UCRL-11213(p.87-138))
reactions of, with water, formation of xenon hydroxide in, 17: 12284
reactions with ammonia, antimony fluoride, hydrochloric acid, and perfluorocyclopentene, 19: 5857
reactions with antimony fluoride, octafluorocyclopentene, and water, 20: 1881
reactions with fluorine, design of circulations loop for studies on, 18: 5315
reactions with nitrogen oxides at 300 to 350°K and 0.1 to 30 mm, kinetics of, 18: 29642
reactions with olefins, 19: 4133
reactions with vanadium fluoride, compound formation in, 20: 45657
reactions with water, 17: 16020
reduction in acidic solutions at dropping mercury electrode, 18: 43505
shielding anisotropies in, sign in, 18: 33558
spectra of circulating loop for measurement of infrared, 17: 41196
spectra of coupling and shielding in di, hexa-, and tetra-, nuclear magnetic resonance, 18: 5337
spectra of di-, far ultraviolet, 17: 18037
spectra of di-, hexa-, and tetra-, magnetic resonance, 18: 5338
spectra of di, hexa-, and tetra, infrared and Raman, 18: 5342
spectra of di-, infrared, 17: 18042
spectra of, infrared, 17: 18008 (TID-18276)
spectra of, infrared and Raman, 17: 33865 (CONF-126-9)
spectra of, infrared and Raman, 18: 2127(R) (ORNL-3488(p.21-41))
spectra of tetra-, anisotropy of fluorine chemical shift tensor in, 17: 40804
spectra of tetra-, far ultraviolet, 17: 18039
spectra of tetravalent, infrared and Raman, 17: 28846
spectra of XeF in irradiated XeF_4, electron spin resonance, 17: 33996
spectra of, appearance potentials and fragmentation of ions in, 20: 8882 (IS-983)
spectra of, effects of temperature on near ultraviolet absorption, 20: 31221(R) (UCRL-16658, pp 73-87)
spectra of, ultraviolet emission, 19: 22182
spectrum of, explanation of uv, 18: 23469
spectrum of, interpretation of uv, 18: 23468
structure of di-, 17: 14286
structure of divalent and tetravalent, 17: 12246
structure of gaseous, 18: 5335
structure of gaseous hexavalent, (E), 19: 42494
structure of second crystalline phase of tetra-, 17: 12273
structure of tetra-, neutron diffraction study, 17: 16023
structure of tetra-, crystal and molecular, 18: 5333
structure of, x-ray-diffraction study of, 19: 280(R) (ORNL-3679 (p.94-116))
synthesis of hexa- and octa-, conditions for, 18: 5318
Szilard-Chalmers effect in, 18: 31580
Szilard-Chalmers effect in solid tetravalent, 18: 33666
thermochemical properties of, 17: 33864 (CONF-126-7)
thermochemical properties of di- and tetra-, 18: 1658
thermodynamic functions and mean amplitudes of vibration of tetravalent, 18: 43452
XeF_2–XeF_4, crystal structure of, 18: 5334

XENON HYDROXIDES

preparation and properties of, review on, 20: 3915 (CEA-Bib-61)
preparation of, by reaction of water with xenon tetrafluoride, hazards in, 17: 12284

XENON IONS

beams of, analysis of duoplasmatron, 19: 47267
charge exchange in collisions in argon, 16: 18278
charge exchange in air, cross sections for, 18: 34409
charge-exchange with xenon, cross sections for, 16: 6868
charge transfer with atoms, cross sections for, 17: 8979
charge-transfer cross section in xenon, single, 18: 28246
detection using photographic emulsions, 18: 37521
diffusion in aluminum at high bombardment energies, 19: 47080 (EUR-2478.e)
effects on gain of electron multiplier tubes, (E), 20: 43659
effects on germanium, 19: 11682
effects on glass surfaces up to 30 kev, 20: 45017
effects on gold films at 15 to 250 ev, 17: 20708
effects on structure of amorphous germanium, 19: 6373
electron energy levels of, long-lived excited, 18: 36166
electron-capture cross sections at 0.4 to 3.6 kev, 18: 26229
emission of glass-surface sorbed, rare-gas ion bombardment for, 18: 29862
energy in Zeta pinch discharge in deuterium plasma, 17: 42089
ionization by electrons, cross sections for, 17: 41653
ionization of monovalent, by electrons, cross sections for, 18: 20768
mobility determinations for, based on current-voltage relations for mobility-controlled sheaths, 18: 5860
mobility in helium, 17: 35019 (AD-411955)
penetration in aluminum single crystals, channeling in, 18: 28098
performance in ion propulsion systems, 18: 1838
production by high-temperature hollow cathode ion source, 20: 19002
properties of beams of, in electromagnetic separator, 17: 41320
radiation effects of, on gold at 42.5 kev, 16: 33555
range distribution in tungsten, effects of crystal orientation on, 18: 18576
range in monocrystalline silicon, 18: 28097
ranges in aluminum and gold, 17: 24139
ranges in silicon crystals at 20 to 80 kev, 18: 20812
ranges in solids at 50 to 500 kev, 16: 18247
ranges in tungsten and tungsten oxide at 40 and 125 kev, 19: 23263
reactions and valences in aqueous sodium perxenate solutions, 17: 35679 (CONF-126-11)
reactions on krypton and xenon at 0.3 to 3 kev, electron spectra from, 16: 33635
reactions on metals, secondary electrons from, 17: 16836
reactions with aluminum foils, defect cluster formation in, 17: 31030
reactions with beryllium–copper alloys at 3 to 90 kev, secondary electron emission from, (E), 20: 21538
reactions with carbon films, optical atomic spectra from, 18: 28254
reactions with ceramics and ionic crystals at 40 kev, lattice disorders from, (E), 20: 27597
reactions with copper, gold, and graphite at 100 to 30,000 ev, yields of secondary ions from, 17: 7268
reactions with gases and solids below 1 Mev, range determinations, 16: 10954 (EFINS-61-68)
reactions with germanium, displacement spike crystallization in, 17: 41503 (TID-19534)
reactions with gold, sputtered spectrum from, 17: 439
reactions with metals, secondary emission and sputtering in, 17: 39709 (ARL-63-125)
reactions with methane at 2 to 200 ev, 19: 22319
reactions with metal foils, sticking factors for, (E), 19: 34610
reactions with metal single crystals at 1 to 10 kev, secondary-electron emission in, (E), 19: 39404
reactions with metal surfaces, secondary emission factors for, 20: 31926
reactions with molecules at 15 to 200 ev, charge exchange in, 18: 20742
reactions with neon atoms, ionization cross sections for, 16: 6880
reactions with nickel surfaces, isotopic effect in secondary electron emission in, (E), 19: 41249
reactions with nuclear emulsions, effects of energy and mass on grain darkening in, 18: 23916
reactions with organic compounds, fragmentation and ionization in, 19: 17874
reactions with pentaborane-9, mass spectrometric studies of, 19: 13315
reactions with rare gases, cross sections for charge exchange in, (E/T), 19: 34877
reactions with tungsten at 4 kev, oxygen adsorption in, 19: 42904 (IPP-2/40)
reactions with tungsten at 200 ev to 4 kev, diffusion of trapped gas following, 20: 20128
reactions with xenon, total-charge-transfer cross sections for divalent, 16: 22800
reactions with xenon gas at 20 to 60 ev, electron capture in, 18: 32463
recombination coefficient of molecular, 18: 786
reflection by copper crystals at 50 kev, 18: 4341
Slater-Condon parameters of, determined from spectral data, 17: 31118
sorption and desorption on platinum at 30 to 1290°C, 16: 19568
sorption by tungsten at 40 ev to 5 kev, thermal desorption energies for, 18: 14604
spectra of multi-ionized, in plasma at high temperatures, 16: 8007
sputtering of bcc metal single crystals by, at up to 800 ev, atom ejection in, 17: 37467
sputtering of copper and gold crystals by, high-energy, 16: 19562
sputtering of copper by, energy distributions from, 18: 7404(R) (NP-13430)
sputtering of germanium at 100 to 800 ev by, target temperature depend-

ence at 0 to 350°C, 18: 2526
sputtering of gold at 0 to 1 kev, 16: 9280 (ERR-AN-072)
sputtering of gold at 43 kev, effects of thermal spikes, 16: 23158
sputtering of gold by, spike effects in spectra from, 17: 12730
sputtering of gold by, velocity distribution of particle emission in, 19: 33527
sputtering of metals by, at 0.1 to 2 kev, 16: 19566
sputtering of silicon carbides by, at 10 to 600 ev yields from, 16: 19564
sputtering of silver at 3 to 7 kev by, tracer study of, 18: 751
sputtering of solids at 100 to 600 ev, yields from, 16: 22753
sputtering on copper, molybdenum, and tungsten at 1.5 to 30 kev, (E), 20: 4546
sputtering on copper at 75 to 1 Mev, yield from, (E), 20: 25744
sputtering on copper at 100 kev to 1 Mev, 20: 37468
sputtering on gold at 40 to 100 ev, yields from, (E/T), 20: 13420
sputtering on metals at 25 to 60 kev, energy dependence of, 18: 20785
sputtering on metals at 20 to 1000 ev, mass dependence of, 18: 20786
sputtering on metals at 45 kev, thermal spikes in, (E), 19: 20838
sputtering on silver at 3 to 7 kev, 18: 37853
sputtering ratio for metals at 45 to 65 kev, 16: 9115
sputtering reactions on oriented gold foils at 50 kev, (E), 20: 19372
van der Waals radii of, relation of hydration energy to, 18: 16016
yields from duoplasmatron ion source, pressure dependence of, (E), 19: 45385 (D1-82-0437)

XENON ISOTOPES
abundance in Achilles, LaLande, and Peace River chondrites, 20: 16672
abundance in meteorites and natural gas, anomalies in, 18: 34399
abundance in meteorites, anomaly patterns in, 19: 47213
abundance in meteorites, fission, neutron capture, and spallation anomalies in, 20: 31875
abundance ratios in meteorites, 19: 37450
abundance ratios in Earth's atmosphere and meteorites, 20: 25715
abundances in chondrite pantar, 16: 19167
abundances in monazites from pegmatites, 17: 29101
content in air and water of swimming pool reactor, 18: 24947 (AEET/AM/38)
content in meteorites, histories from, 17: 23528
content in meteorites, 18: 18033
content in Pasamonte meteorite, anomalies from, 20: 17239
content in Renazzo chondrite, 18: 34390
contents in chondritic meteorites, general anomalies in, 16: 17892
decay characteristics of, 19: 17775 (HNS-1229-57)
detection of radioactive, in stack exhausts, 18: 27789(R) (ORNL-3578 (p.37-45))
detection of, from underground nuclear explosions, 19: 22702 (UCRL-12272)
determination in atmosphere, application in calculation of age of earth, 16: 22447 (TID-7632(p.223-41))
determination in meteorites as indication of fission, neutron capture, and spallation anomalies, (E/T), 20: 11424 (NP-15629)
determination in tellurium ores, 19: 33351
determination of fission-product, new method for, 18: 9993
determination of radioactive, method for, 18: 41541
diffusion from irradiated uranium dioxide, 16: 24219
diffusion from irradiated uranium dioxide fuels, 17: 2005 (NP-12193)
distribution in the Bruderheim chondrite, 16: 415
distribution variations in terrestrial samples, 17: 23536
energy levels, interactions, nuclear moments, and transitions in, 17: 24381 (AD-403411)
excited states in even, first, 16: 12518
gamma reactions on, cross sections for, 19: 12496
half life, 17: 7194
half lives of, from uranium fission, (E), 19: 29371
helium-3 elastic scattering by, optical model for, 17: 5364
isomeric transitions, M_4-type, 16: 22985 (NP-11747)
isomeric transitions of E_3 type, 16: 31066 (NP-11746)
isotopic mixing constants of, volume, (T), 20: 19970
mass ratio determinations, 16: 22389
masses and neutron separation energies of even-A, 17: 38102
masses of stable, 19: 10358
meson (π^-) reactions at 8.4 Bev/c on, mesons (π^0) from, 17: 9551
meson (π^-) reactions on, strange particles from, 17: 28339
production and properties of radioactive and stable, 18: 29796
production in spontaneous fission of plutonium-244, 20: 25715
production in thermal-neutron fission of uranium-235, (E), 19: 45260(R) (IDO-14660)
radioinduced formation and retention in solid xenon compounds, neutron, 20: 43373
reactor criticality effects of fission-product, in large pressurized-water power reactors, (T), 20: 8401 (WAPD-T-1732(Rev.))
retention of radioactive, in neutron-irradiated xenon tetrafluoride, 18: 31580
separation and purification, 16: 11502(R) (MLM-1119)
separation by thermodiffusion concentration distribution in tubes for, 17: 11059
separation by thermal diffusion, 18: 21707(R) (MLM-1177)
separation by thermal diffusion, 18: 24050(R) (ORNL-3607)
separation by thermal diffusion, 18: 35246(R) (MLM-1196)
separation by thermal diffusion, 18: 45174(R) (MLM-1204)
separation by thermal diffusion, 18: 45175(R) (MLM-1209)
separation by thermal diffusion, 19: 14911(R) (MLM-1216)
separation by thermal diffusion, equilibration for, 19: 13201(R) (MLM-1217)
separation by thermal diffusion, 19: 22846 (ORNL-TM-1047(p.32-9))
separation by thermal diffusion, 19: 30632(R) (ORNL-3815)
separation by thermal diffusion, 20: 14444(R) (MLM-1268)
separation by thermal diffusion, 20: 39321(R) (MLM-1312)
separation from other fission products, large-scale, 18: 31649 (A/CONF.28/P/252)
separation of, effectiveness of thermal diffusion columns for, 17: 11051 (TID-15343)
separation of radioactive, from water containing oxygen, 17: 8271(P)
separation of xenon-124 from, by thermal diffusion, 20: 39320 (MLM-1311)
separation of, possibility of photochemical, 19: 34607(R) (MLM-1239)
separation of, review of methods for, 19: 11642
separation of, thermodynamic effects in, (E/T), 19: 9568 (NP-14359)
separation on-line from californium-252 spontaneous fission, 20: 19888
thermal diffusion factor for, temperature dependence in, 20: 39326
use of stable, in fuel burnup determination, 19: 28222 (IDO-14642)
vapor pressures, 16: 30704
yields from thermal-neutron fission of thorium-229, 20: 28303
yields from uranium proton fission at 0.6 and 24 Bev, 19: 35511
yields in helium-4 and thermal neutron fission of uranium-235, 17: 22567 (UCRL-10673)
yields in proton reactions with uranium, (E), 19: 29374
yields in thorium-232 helium-ion fission, 17: 22567 (UCRL-10673)
yields in uranium-233 thermal fission, (E), 20: 3010(R) (IDO-14663)

XENON ISOTOPES Xe-118
decay properties, (E), 19: 10262

XENON ISOTOPES Xe-119
decay properties, (E), 19: 10262

XENON ISOTOPES Xe-120
decay properties, (E), 19: 10262
energy levels, (E/T), 19: 45285 (UCRL-16040)
half life of, produced by iodine spallation at 340 Mev, 19: 27495

XENON ISOTOPES Xe-121
decay of, half life and gamma and positron energies in, 19: 27495
decay properties, (E), 19: 10262

XENON ISOTOPES Xe-122
decay properties, (E), 19: 10262
energy levels, (E/T), 19: 45285 (UCRL-16040)
energy levels of, parity and spin of collective, (E), 19: 21316

XENON ISOTOPES Xe-123
decay properties, (E), 19: 10262
energy levels from cesium-123 decay, (E), 20: 30403

XENON ISOTOPES Xe-124
abundance in Bruderheim meteorite, 17: 8990
concentration by thermal diffusion, 18: 37576 (A/CONF.28/P/90)
concentration in gaseous xenon by thermal diffusion, 20: 20807(R) (MLM-1287)
content in Bruderheim meteorite, 20: 11430
content in terrestrial samples, 17: 25461
energy levels of, parity and spin of collective, (E), 19: 21316
enrichment, methods development for, 18: 27812(R) (ORNL-TM-415)
enrichment, methods development for, 18: 27813(R) (ORNL-TM-428)
enrichment, operation of thermal diffusion column for, 18: 27811(R) (ORNL-TM-198)
mass yield spectrum from cosmic-ray spallation reactions, (E), 20: 44079
neutron capture cross sections and resonance integrals, 18: 11237
neutron reactions with, electron-capture iodine-125, 18: 18263
neutron reactions (n,γ), production of carrier-free iodine-125 by, 19: 24598
production in meteorites by cosmic rays, 20: 7694
production in stars, 16: 12308
production of xenon enriched with, by thermal diffusion, design and performance of equipment for, 20: 46133
separation by thermal diffusion, relations with mass difference and pressure, 18: 2128(R) (ORNL-TM-658)
separation by thermal diffusion, cascades for, 18: 7103 (K-OA-1008)
separation by thermal diffusion, 18: 7104 (K-OA-1178)
separation by thermal diffusion, development of systems for, 18: 10438(R) (ORNL-TM-736)
separation from natural xenon by thermal diffusion, 20: 20806(R) (MLM-1274)
separation from other xenon isotopes by thermal diffusion, 20: 35828(R)

(MLM-1300)
separation from xenon isotopes by thermal diffusion, 20: 39320(R) (MLM-1311)

XENON ISOTOPES Xe-125
attenuation by tungsten single crystals at 0.25 to 160 kev, 18: 44457
beta decay of, iodine-125 energy-level transitions from, (E), 20: 46640
concentration on metal foils, sticking factors for, 19: 34610
decay, 16: 7955(R) (PR-P-51)
decay, 18: 14592(R) (PR-P-60)
decay of, 17: 25858(R) (PR-P-56(p.19-33))
decay of, conversion electron spectra from K-capture, (E), 20: 15701 (CONF-233(Vol.2), pp 128-41)
decay properties, (E), 19: 10262
energy level lifetime, 16: 7955(R) (PR-P-51)
energy levels in, five-particle isomeric, (T), 20: 15837
gamma dose constants for, 20: 46617
gamma spectra and half life of isomeric, (E), 19: 41802(T)
hyperfine structure (E/T), 19: 1568(R) (TID-21113)
production of isomeric, (E), 19: 41802(T)
range distribution in tungsten, effects of crystal orientation on, 18: 18576
range distributions in amorphous oxides at 0.5 to 160 kev, 18: 36588
range in tungsten single crystals, 18: 18577
ranges in silicon crystals at 20 to 80 kev, 18: 20812
ranges in tantalum oxide, 20: 20136
reactions with metal foils, method of depth determination of embedded atoms from, 17: 41181
reactions with monocrystalline tungsten at 0.1 to 1.5 Mev, range distributions from, (E), 20: 20135
use in studies of anodic oxidation of metal foils, 17: 32532

XENON ISOTOPES Xe-126
abundance in Bruderheim meteorite, 17: 8990
content in Bruderheim meteorite, 20: 11430
content in terrestrial samples, 17: 25461
energy level structure, (E), 20: 1173
energy level transitions in, M1-M2 mixing ratios as test of purity of vibrational, (T), 19: 25503
energy levels, 16: 17081
energy levels, 16: 23073
energy levels, (E), 20: 15845
energy levels in, structure of low-lying 2^+, 17: 11698
energy levels of, half life of first-excited, 18: 2942
energy levels of, measurement of lifetime of first excited, 18: 34772 (NP-14184)
energy levels of, doublet of two-phonon, 18: 40561
energy levels of, parity and spin of collective, (E), 19: 21316
energy levels of, structure of first and second excited, 20: 10092
energy-level transitions from iodine-127 (p,2ny) reactions, anisotropy of conversion electrons from, 20: 46684
mass yield spectrum from cosmic-ray spallation reactions, (E), 20: 44079
neutron capture cross sections, thermal, (E), 19: 35412
neutron reactions (n,y), cross sections for, (E), 19: 43313
production in meteorites by cosmic rays, 20: 7694
production in stars, 16: 12308
separation from other xenon isotopes by thermal diffusion, 20: 35828(R) (MLM-1300)
surface oscillations of, 18: 13114

XENON ISOTOPES Xe-127
beta decay of, half life and M/L ratio in electron-capture, (E), 19: 43313
beta decay of, iodine-127 energy level lifetime from, 20: 34636
beta decay of, iodine-127 energy-level transitions from, (E), 20: 46640
beta decay scheme for, (E), 19: 6688
decay of, conversion electron spectra from K-capture, (E), 20: 15701 (CONF-233(Vol.2), pp 128-41)
decay of, gamma angular correlations in, (E), 20: 6384
electron capture ratios, M/L, 20: 40153
electron-capture decay of, L/K capture ratios in, 18: 36630
gamma angular correlations from, (E), 20: 9978(R) (TID-22462)
gamma dose constants for, 20: 46617
hyperfine structure (E/T), 19: 1568(R) (TID-21113)
occurrence in recovered satellites, 17: 4708

XENON ISOTOPES Xe-128
content in Bruderheim meteorite, 20: 11430
content in terrestrial samples, 17: 25461
content in thucholites, 19: 15745
content of fissiogenic, in Pasamonte meteorite, 19: 16344
energy level transitions in, M1-M2 mixing ratios as test of purity of vibrational, (T), 19: 25503
energy levels, 16: 17081
energy levels, 16: 23073
energy levels of, parity and spin of collective, (E), 19: 21316
energy-level quantum numbers and transitions from decay of iodine-128, (E), 20: 42147
mass yield spectrum from cosmic-ray spallation reactions, (E), 20: 44079
neutron cross sections at 0.414 ev to 10 Mev, 16: 9427 (GA-2451 (Vol.III))
preparation by neutron irradiation of aluminum iodide, 20: 18731
production in meteorites by cosmic rays, 20: 7694
production in reactors, method for, 18: 3851
production of, techniques for, 18: 41892 (BNL-864)
properties and uses of, produced at Brookhaven, 19: 22853 (ORNL-TM-1047(p.113-16))
proton reactions (p,y) in stars, 16: 12308
surface oscillations of, 18: 13114

XENON ISOTOPES Xe-129
abundance in atmosphere, 17: 5172
abundance in Bruderheim meteorite, 17: 8990
abundance in the atmosphere, 17: 5171
chemical shift and relaxation of, in xenon gas, 17: 25220
content in basic rocks, 20: 7267
content in Bruderheim meteorite, 20: 11430
content in chondrites, 19: 25141
content in meteorites, origin of, 20: 29891
content in minerals from Indarch meteorite, (E), 19: 9863
content in terrestrial samples, 17: 25461
content in thucholites, 19: 15745
content of fissiogenic, in Pasamonte meteorite, 19: 16344
coupling with fluorine-19 in hydrofluoric acid, 18: 5337
coupling with fluorine-19 in xenon fluorides and oxyfluoride, 18: 5338
distribution in stone meteorites, origin of excess, 16: 418
energy level lifetime, 16: 7955(R) (PR-P-51)
energy level transitions in, probabilities for M1, 18: 28598
energy level transitions in, probabilities of E2 and M1, (E), 19: 23717
energy level transitions in, conversion coefficients for, (E), 20: 36245
energy levels, 17: 4117
energy levels, 18: 42626(R) (ANL-6879(p.69-87))
energy levels from cesium-129 decay, (E), 20: 1200
energy levels of, asymmetric rotator model with intermediate coupling for properties of low-lying, 17: 26531
energy levels of, E2 moment of first-excited, 18: 36654
energy levels of, lifetime of first excited, (E), 19: 8450
energy levels of, structure from isomeric transition in, (T), 20: 19970
energy levels of, half life of 40-kev, (E/T), 20: 19273(R) (BNL-929, pp 3-43)
energy-level spins and transitions from beta decay of cesium-129, (E), 20: 46681
gamma dose constants for metastable, 20: 46617
gamma transitions in, conversion coefficients for, (E), 20: 3038
magnetic field shift at nuclei of, in liquid and solid xenon, (E), 20: 44142
magnetic moments, 17: 38104
Mössbauer effect in compounds of, 17: 32089
Mössbauer effect in, 17: 41531(R) (ANL-6720(p.48-58))
Mössbauer effect in, in fluorides, hydroquinone clathrate, and sodium perxenates, 18: 5340
nuclear magnetic resonance of, in gaseous xenon, 17: 25219
nuclear magnetic resonance in xenon (liquid and solid), density-dependent shifts in, 17: 26583
nuclear magnetic resonance shift in xenon, density dependence of, 18: 34919
nuclear magnetic resonance in xenon gas, chemical shift of (T), 19: 385
nuclear quadrupole moment, 18: 42626(R) (ANL-6879(p.69-87))
nuclear relaxation in gaseous xenon, 16: 26975
nuclear spin coupling with oxygen-17 in xenon oxyfluoride, 19: 30168
production and uses of, 20: 31642 (ORNL-P-2190)
production in meteorites by iodine-129 decay, 18: 20726
production in meteorites, mechanisms for, 20: 5978
production of isomeric, by secondary neutron capture in iodine-127, (E), 19: 28720
production of isomeric, by neutron reactions (n,y) with iodine-127, 20: 26089 (ORNL-3839)
spin relaxation in gases and liquids, momentum-dependent, 18: 12053
spin-spin relaxation time in liquid and solid natural xenon, 17: 2136
transitions in, conversion line intensity ratios for M4, 17: 4072
transport in meteorites, mechanism of, 20: 18901
uses in Mössbauer spectroscopic studies of chemical bonding, 19: 22369

XENON ISOTOPES Xe-130
content in Bruderheim meteorite, 20: 11430
content in terrestrial samples, 17: 25461
content in thucholites, 19: 15745
content of fissiogenic, in Pasamonte meteorite, 19: 16344
determination in tellurium ores, 20: 32385
energy levels from cesium-130 decay, 20: 34635
energy levels in, beta transition to first excited, (E), 20: 34679
energy levels of, parity and spin of collective, (E), 19: 21316
internal-conversion electron spectra of, from tellurium-128 (α,2n) reactions, (E), 19: 43381

mass yield spectrum from cosmic-ray spallation reactions, (E), 20: 44079
neutron cross sections at 0.414 ev to 10 Mev, 16: 9427 (GA-2451 (Vol.III))
proton reactions (p,γ) in stars, 16: 12308
rotation states of deformed axial symmetry in, 17: 19282
separation by rectification, 16: 30704
vapor pressure of, saturated, 17: 2998

XENON ISOTOPES Xe-131
abundance of fission-produced, in Pasamonte meteorite, 20: 29892
concentration by thermal diffusion, 20: 3879(R) (MLM-1266)
concentration in gaseous xenon by thermal diffusion, 20: 20806(R) (MLM-1274)
content in Bruderheim meteorite, 20: 11430
content in terrestrial samples, 17: 25461
content in thucholites, 19: 15745
content of fissiogenic, in Pasamonte meteorite, 19: 16344
decay properties, (E), 19: 10262
determination by liquid-scintillation counting, 18: 39075
determination in uranium-233 and -235 fission products, (E), 20: 11960(R) (IDO-14667)
determination of, by beta counting, ionization chamber for, 20: 43106
energy level at 364 kev, half life of, (E), 20: 38031
energy level lifetime, 638 kev, 16: 6027
energy level spins in, 17: 12802(R) (PR-P-55)
energy level transitions in, probabilities for M1, 18: 28598
energy level transitions in, retardations in l-allowed M1, (T), 19: 21323
energy levels, 17: 13520
energy levels, 19: 10983(R) (TEES-2671-3)
energy levels from iodine-131 decay, parities and spins for, (E), 20: 28366
energy levels of, lifetimes of, 17: 5335
energy levels of, E2 moment of ground-state, 18: 36654
energy levels of, internal conversion coefficient of 164-kev, 19: 26922(R) (PR-P-64)
energy levels of, structure from isomeric transition in, (T), 20: 19970
energy levels of, energy ratios and spins of, (E/T), 20: 38022
formation of metastable, by beta decay of iodine-131 in compounds, 20: 40851
gamma activity in air, effects of northerly and southerly winds on, 18: 2393
gamma dose constants for metastable, 20: 46617
gamma spectrum of, low-energy, 17: 7142 (TID-15548)
gamma transitions in, search for low-energy, 17: 19239
gamma transitions in, independent particle model for M4, 19: 17051
internal conversion, charge spectra, 16: 6475
magnetic moments, 17: 38104
mass yield spectrum from cosmic-ray spallation reactions, (E), 20: 44079
meson (π^-) reactions, cross sections of particle production in, 18: 24587 (JINR-P-1584)
neutron cross sections at 0.414 ev to 10 Mev, 16: 9427 (GA-2451 (Vol.III))
nuclear magnetic resonance in xenon gas, quadrupolar relaxation in, (T), 19: 19200
nuclear magnetic resonance shift in xenon at 4.2 to 250°K, 19: 23813
nuclear magnetic resonance in liquid and solid xenon at 4.2 to 250°K, (E), 20: 38404
nuclear quadrupole moment, 18: 42626(R) (ANL-6879(p.69-87))
nuclear quadrupole relaxation time in liquid and solid xenon, temperature dependence of, 20: 38392
nuclear relaxation in gaseous xenon, 16: 26975
production and uses of, 20: 31642 (ORNL-P-2190)
production of isomeric, by secondary neutron capture in iodine-129, (E), 19: 28720
production of isomeric, by neutron reactions (n,γ) with iodine-129, 20: 26089 (ORNL-3839)
production of metastable, 19: 26718 (ORNL-3802)
ranges in metals at 5 to 30 kev, 18: 20672
separation by thermal diffusion, 19: 24611(R) (MLM-1227)
separation from xenon-136 using thermal diffusion columns, method for, 17: 32469
separation from xenon-136 in thermal diffusion column, 18: 13358(R) (MLM-1151)
separation from xenon-132 by thermal diffusion, 19: 24611(R) (MLM-1227)
separation from xenon-136 by thermal diffusion, 19: 28717(R) (MLM-1221)
separation from xenon-136 by thermal diffusion, 19: 34607(R) (MLM-1239)
separation from xenon isotopes by thermal diffusion, 20: 39321(R) (MLM-1312)
sorption by activated charcoal, collector design measuring, 20: 18994 (SGAE-PH-31/1965)
spin lattice relaxation time in solid xenon, (E/T), 20: 38404
transitions in, conversion line intensity ratios for M4, 17: 4072
use of isomeric, in study of inert gas-cleanup in Penning discharge, 18: 12771
uses in tracer studies of pumping mechanism of getter ion pump, 18: 31701
yields from uranium-235 thermal fission, 19: 29313
yields in plutonium-241 thermal fission, (E), 19: 8495
yields in thermal neutron fission of uranium-233 and -235, 20: 43067(R) (IDO-14679, pp 6-46)

XENON ISOTOPES Xe-132
abundance in Bruderheim meteorite, 17: 8990
abundance of fission-produced, in Pasamonte meteorite, 20: 29892
content in Bruderheim meteorite, 20: 11430
content in carbonaceous chondrite and earth, 16: 17892
content in chondrites, 18: 20726
content in chondrites, 19: 25141
content in minerals from Indarch meteorite, (E), 19: 9863
content in natural gases, from uranium-238 spontaneous fission, 19: 630 (TID-21206)
content in thucholites, 19: 15745
content of fissiogenic, in Pasamonte meteorite, 19: 16344
decay scheme for, beta and electron-capture, 17: 19291
determination in uranium-233 and -235 fission products, (E), 20: 11960(R) (IDO-14667)
energy level lifetime, 673 kev, 16: 6026
energy level schemes for cesium-132 and iodine-132 decay-produced, (E), 19: 47584(R) (ORNL-3832, pp 1-28)
energy level transitions in, internal conversion coefficients for, (E), 20: 13883
energy level transitions in, conversion coefficients for E2, (E), 20: 15704 (CONF-233(Vol.2), pp 164-76)
energy levels, 16: 10957 (JINR-P-826)
energy levels, 16: 22989(R) (ORNL-3268(p.19-23))
energy levels, 17: 4117
energy levels, 17: 11685
energy levels, (E), 19: 23743
energy levels and gamma spectra of, 17: 5371
energy levels and transitions of, 18: 42769
energy levels from iodine-132 beta decay, 16: 6012
energy levels from decay of iodine-132 and cesium-132, (E), 19: 41745
energy levels of, parity and spin of collective, (E), 19: 21316
gallium-69 inelastic scattering by, dynamic deformation in, (T), 19: 35382 (JINR-P-2103)
gamma emission, directional correlations of, 16: 26246
mass yield spectrum from cosmic-ray spallation reactions, (E), 20: 44079
neutron cross sections at 0.414 ev to 10 Mev, 16: 9427 (GA-2451 (Vol.III))
nucleon binding energies, 16: 11007
proton reactions (p,γ) in stars, 16: 12308
reactions with gallium-69, dynamic deformation in inelastic, (T), 20: 13794
rotation states of deformed axial symmetry in, 17: 19282
separation from xenon-131 by thermal diffusion, 19: 24611(R) (MLM-1227)
separation from xenon isotopes by thermal diffusion, 20: 39321(R) (MLM-1312)
yields from uranium-235 thermal fission, 19: 29313
yields in plutonium-241 thermal fission, (E), 19: 8495
yields in thermal neutron fission of uranium-233 and -235, 20: 43067(R) (IDO-14679, pp 6-46)

XENON ISOTOPES Xe-133
activity in reactor coolant following diffusion from hole in fuel can, (T), 20: 34995
attenuation by tungsten single crystals at 0.25 to 160 kev, 18: 44457
beta decay of, β-γ circular polarization correlation in, (E), 20: 30553
beta decay of, spin dependence of Rayleigh scattering from, (E), 20: 3082
beta decay scheme, 16: 3678
beta emission, charge spectra, 16: 6476
clearance from lung of, 18: 29176
concentration on metal foils, sticking factors for, 19: 34610
content in equal volumes of air and blood, partition coefficients for, 20: 1599
content in troposphere, source and variation of, 17: 30701
conversion-electron emission from, in monocrystalline tantalum, 20: 20129
decay of 5.27-day fission-product, 16: 30930(R) (NYO-2669)
detection in brain, design of depth-focusing collimator for, 18: 35436
determination in lungs using collimated scintillation counters, 19: 42727
determination in magnox reactor coolant, method for, 19: 21616
determination of, by beta counting, ionization chamber for, 20: 43106
determination simultaneously with xenon-135, equations for, 20: 43069(R) (IDO-14679, pp 51-9)
diffusion coefficients in uranium dioxide at 1000 to 1650°C, 17: 22216 (BMI-1623)
diffusion during temperature changes in reactor, 16: 23255 (AERE-R-3093)
diffusion from alkali metal chloride crystals during thermal annealing,

17: 10638
diffusion from beryllia-coated beryllia-based thoria–urania–yttria fuels, 19: 44599(R) (GEMP-50A)
diffusion from bulk uranium monocarbide at 950 to 1900°C, 16: 30816(T,R) (EURAEC-362)
diffusion from carbide fuels, 16: 30854
diffusion from chromium–iron alloy at 1000 to 1200°C, 17: 14815(R) (BMI-X-10031)
diffusion from fuels during low-dose, low-temperature irradiation, (E), 20: 4471
diffusion from graphite, 17: 16690
diffusion from irradiated uranium dioxide powders and spheroids, 17: 32563 (AERE-R-4347)
diffusion from irradiated urania–zirconia plates at 700 to 1250°C, 17: 39678 (WAPD-TM-313)
diffusion from irradiated uranium carbides, 18: 24072(R,T) (EURAEC-934)
diffusion from irradiated uranium dioxide, 18: 30157(T,R) (EURAEC-933)
diffusion from irradiated uranium carbides at high temperatures, 19: 13874(R) (EURAEC-1179)
diffusion from irradiated uranium carbonitride, 19: 39089 (AERE-M-1389)
diffusion from irradiated thoria and urania, effects of titania additions on, 20: 39381 (AECL-2585)
diffusion from neutron-irradiated uranium oxide compacts, 16: 24144 (AERE-R-4062)
diffusion from neutron-irradiated iron foils, 20: 33922
diffusion from pyrolytic carbon, 17: 29372 (BMI-1634)
diffusion from thorium oxide–yttrium oxide and uranium oxide–yttrium oxide systems, 19: 11679
diffusion from uranium(IV) oxides, activation energy, 16: 6757
diffusion from uranium(IV) oxides, activation energy, 16: 27636(T) (AEC-tr-5256)
diffusion from uranium monocarbide powders, 16: 30815(T,R) (EURAEC-361)
diffusion from uranium dioxide compacts, 17: 4889(T,R) (EURAEC-322)
diffusion from uranium dioxide, in-pile, 17: 4896
diffusion from uranium carbides, 17: 10148
diffusion from uranium carbide, 18: 4160(R) (BNL-799(p.74-100))
diffusion from urania at 800 to 1600°C, coefficients for, 20: 11224
diffusion in alumina at 703 to 1101°C, 16: 4450(R) (BMI-1546(Del.))
diffusion in aluminum and magnesium oxides, 17: 3378(R) (BMI-1583 (Del.))
diffusion in aluminum oxide and beryllium oxide, 18: 20570
diffusion in calcium oxide and uranium-activated calcium fluoride single crystals, activation energies for, 20: 7561(R) (EURAEC-1489)
diffusion in ceramic oxides, thermal release study of, 18: 18373
diffusion in chromium, 17: 3471(R) (BMI-X-10017)
diffusion in coated uranium dioxide particles, 18: 2241
diffusion in graphite, mechanisms for, 17: 16744(R) (TID-18112)
diffusion in graphites and uranium dicarbides at high temperatures, 19: 13875(R) (GA-4022(Pt.1))
diffusion in graphite–uranium dicarbide dispersions and pyrolytic-carbon-coated uranium dicarbide fuels at 1400 to 1700°C, 19: 13877(R) (GA-5016(Pt.1))
diffusion in graphite, 19: 13901(R) (TID-21415)
diffusion in irradiated uranium monocarbide, 17: 26150
diffusion in irradiated uranium dioxides, 18: 14387(T,R) (EURAEC-860)
diffusion in molybdenum-uranium alloy and uranium, 18: 37733 (A/CONF.28/P/62)
diffusion in pyrolytic carbon, 17: 23864(R) (BMI-1619(Del.))
diffusion in single-crystal alpha-alumina, 16: 26491 (TID-7622(p.245-53))
diffusion in sintered uranium carbides at 1000 to 1400°C, 19: 16114
diffusion in thorium and uranium oxides and uranium carbide, 16: 24183(T) (AEC-tr-5206)
diffusion in thorium dioxide, 16: 23674(T) (AEC-tr-5178)
diffusion in thorium dioxide, uranium carbides, and uranium dioxide, 18: 611(T,R) (EURAEC-183)
diffusion in thorium(IV) oxide–uranium(IV) oxide dispersions in beryllium oxides, 18: 20572
diffusion in uranium carbide, 16: 5548
diffusion in uranium carbide, 16: 24184(T) (AEC-tr-5213)
diffusion in uranium monocarbide powder at 1000 to 1400°C, 17: 3394
diffusion in uranium, 17: 34407 (NAA-SR-6761)
diffusion in uranium monocarbide at 1000 to 2000°C, 17: 35265(R) (UCRL-10706(p.204-19))
diffusion in uranium dioxide, 17: 39471(T,R) (EURAEC-648)
diffusion in uranium carbide at 950 to 1830°C, 20: 4450
diffusion in xenon mixtures with argon, helium, krypton, and neon, 19: 13295
diffusion of, apparatus for post-irradiation annealing studies on, 17: 37459 (NAA-SR-Memo-8481)
diffusion of, from iron–chromium alloys, postirradiation heating effects on, 17: 16638 (BMI-1611)
diffusion of, from uranium carbide and graphite at 800 to 1600°C, 17: 16665(T,R) (EURAEC-363)
diffusion of, from irradiated uranium carbide–zirconium carbide, 17: 33272
diffusion of, from impregnated graphite shells of fuel elements, 17: 33273
diffusion of gaseous, from lightly irradiated uranium dioxide at 1000 to 2200°C, 17: 35076 (AERE-R-4342)
diffusion of gaseous, in graphite, 18: 7131(R) (TID-19896)
dispensing and handling of, in diagnostic tracer studies, 19: 30027
dispersion in ocean water after simulated nuclear explosion, 19: 24718
electron emission in monocrystalline tungsten, angular dependence of conversion, (E), 19: 21339
energy level lifetime, 16: 7955(R) (PR-P-51)
energy level scheme from iodine-133 beta decay, (E), 20: 30473
energy level transitions in, conversion coefficients for, (E), 20: 36245
formation in xenon compounds by neutron irradiation of lithium fluoride–uranium dioxide powder, 19: 36500
gamma dose constants for, 20: 46617
gamma emission, charge spectra, 16: 6475
gamma spectra, 20: 35594
impregnation of cast graphite by, method for, 18: 44108
injection in monocrystalline copper at 40 kev, thermal release following, 20: 20145
partition between human blood and brain tissues at 37°C, measurements on, 19: 38353
preparation of pure, for adsorption measurements, 18: 8733(T,R) (EURAEC-734)
production and uses, 18: 29796
production and use for lung function studies, 20: 26735
production and uses of, 20: 31642 (ORNL-P-2190)
production of, process improvement for, 19: 26718 (ORNL-3802)
production process improvement, 20: 16914(R) (ORNL-3900, pp 182-93)
properties of, affecting use as biological tracer, 18: 35413 (TID-7678 (p.189-212))
properties of, for use in radiodiagnosis of spinal cord tumors, 19: 7242
radiation dose to tissues from, during diagnostic use, 18: 37051
radiation hazards from, following nuclear incidents, 20: 20962
range and retention in metals at 1–150 kev, energy and flux dependence of, 17: 28002
range in tungsten at kev energies, 17: 32747
ranges in aluminum at 0.5–2.40 Mev, 17: 28001
ranges in gold, 20: 20136
ranges in uranium dioxide, 20: 20136
reactions with gold crystals at 40 kev, channeling in, (E), 19: 10308
reactions with monocrystalline tungsten at 0.1 to 1.5 Mev, range distributions from, (E), 20: 20135
recovery from fuel materials, method development for, 18: 27812(R) (ORNL-TM-415)
release at IRL research reactor, 18: 4880
release from chromium–iron alloy, gold foils, and iron–nickel alloy at 400 to 1400°C, 17: 23946(R) (BMI-X-10039)
release from chromium-iron alloy at 600 to 1200°C, 17: 30964(R) (BMI-X-10050)
release from chromium–iron alloy at 600 to 1200°C, 18: 10522(R) (BMI-X-10072)
release from chromium–iron alloy at 800, 1025, and 1190°C, 18: 22477(R) (BMI-X-10081)
release from chromium–iron alloy at 900 and 1000°C, 18: 32136(R) (BMI-X-10093)
release from coated uranium carbide and dioxide fuel particles, 17: 23864(R) (BMI-1619(Del.))
release from coated-particle fuels during irradiation, 17: 35251(R) (BMI-1632(Del.))
release from coated fuel spheres at 1500 and 1700°F, 18: 4764(R) (ORNL-3470(p.129-56))
release from enriched fuels, analytical method for determining, 19: 15394
release from EVESR fuel elements, 20: 28750(R) (GEAP-5061)
release from EVESR fuel elements, 20: 28751(R) (GEAP-5125)
release from Fissium-uranium alloy, 16: 826
release from fuel-impregnated graphite at 1070 ± 15°C, 16: 4450(R) (BMI-1546(Del.))
release from fueled-graphite-matrix specimens, 16: 17966(R) (BMI-1541 (Del.))
release from Hastelloy-X-clad beryllium oxide–uranium(IV) oxide systems, 16: 4450(R) (BMI-1546(Del.))
release from irradiated pyrolytic-carbon-coated uranium carbide particles, 16: 17966(R) (BMI-1541(Del.))
release from irradiated fuel on heating, 17: 2022
release from irradiated alumina crystals at 1000°C, 17: 13876(R) (BMI-1603(Del.))

release from irradiated uranium dioxide, 17: 14740 (TID-11295(2nd Ed.))
release from irradiated uranium carbide and dioxide fuel specimens, 17: 25685(R) (BMI-1624(Del.))
release from irradiated carbon–uranium systems at 550 to 1540°C, 17: 35251(R) (BMI-1632(Del.))
release from irradiated uranium dioxide pellets at 1330 to 1565°C, 17: 39665(R) (EURAEC-774)
release from irradiated uranium oxide, measurement using gamma spectrometry, 17: 41488 (CEA-2284)
release from irradiated uranium sesquicarbide at 1000 to 1300°C, 17: 40424(R) (BMI-1642(Del.))
release from irradiated thorium dioxide–uranium dioxide and uranium dioxide, effects of stress on, 18: 8727 (ORNL-TM-740)
release from irradiated uranium carbide, 18: 10456(T,R) (EURAEC-733)
release from irradiated uranium carbide particles, mechanisms of, 18: 15491(R) (ORNL-3523(p.103-26))
release from irradiated uranium dioxide fuel element, 18: 15493(R) (ORNL-3523(p.193-226))
release from irradiated uranium carbides and nitrides at 450 to 1700°C, 18: 15664(R) (BMI-1655(Del.))
release from irradiated coated fuel particles, 18: 15664(R) (BMI-1655(Del.))
release from irradiated uranium dioxide pellets, 18: 16524(R) (EURAEC-979)
release from irradiated uranium carbides at 1000 to 1600°C, 18: 24988(R) (BMI-1665(Del.))
release from irradiated coated fuel particles, 18: 24988(R) (BMI-1665(Del.))
release from irradiated graphite-matrix uranium carbide fuel, 18: 30232 (EURAEC-854)
release from irradiated beryllia-matrix fuel dispersions, 18: 35963 (BMI-1675)
release from irradiated uranium carbonitride, 19: 2715 (AERE-R-4700)
release from irradiated UHTREX extruded elements and beads, 19: 9734 (LA-DC-6713)
release from irradiated coated fuel particles, 19: 13871(R) (BMI-1691 (Del.))
release from irradiated uranium dioxide pellets, 19: 20633
release from irradiated uranium dioxide, apparent diffusion coefficient, 20: 38464 (AERE-M-1607)
release from metal-clad uranium dioxide, 17: 6645 (BMI-1604)
release from neutron-irradiated uranium-dioxide pellets, 18: 28042 (EURAEC-1048)
release from oxide ceramics, 18: 8712 (BMI-1651)
release from pyrolytic carbon-coated fuel particles, 19: 39228 (BMI-1734)
release from reactor fuel spheres, 17: 33321(R) (ORNL-3445(p.111-37))
release from thoria–yttria and urania–yttria solid solutions at 800 to 1600°C, 18: 14453 (AERE-M-1251)
release from uranium carbide and uranium(IV) oxide, effects of postirradiation heat treatments at 815 to 1320°F on, 16: 4450 (BMI-1546(Del.))
release from uranium dioxide pellets at 1000 to 2000°C, 16: 27722
release from uranium dioxide crystals, 17: 33320(R) (ORNL-3445(p.63-108))
release from uranium dioxide pellets, 17: 34484(R) (EURAEC-656)
release from uranium dicarbide particles at 1000 to 1800°C, 17: 41337(R) (GA-4260)
release from uranium carbide powder at 1600°C, 18: 27951 (EURAEC-806)
release from uranium carbide and nitride, in-pile, 18: 41933 (TID-11295 (3rd Ed.))
release from uranium carbide and dioxide, effects of evaporation on, 19: 11725(R) (EURAEC-1245)
release from uranium dioxide irradiated at 800 to 1600°C, 19: 18532 (AERE-R-4714)
release in aircraft fuel pin meltdown, 17: 35117
release of, from irradiated alpha alumina, at 500 to 1500°C, 16: 32138 (BMI-1592)
release of, from uranium dioxide, 17: 9841(R) (EURAEC-492)
release of recoiled, from zirconium hydride, 19: 25047 (NAA-SR-Memo-10509)
separation from iodine-133 by solvent extraction using carbon tetrachloride, 19: 13544
separation from irradiated bismuth–uranium alloys at 1050°F, 17: 14377 (NSEC(T)-15)
separation from irradiated uranium-235 fuels, 18: 31997 (ORNL-TM-804)
separation from other short-lived uranium fission products, 18: 39393
separation from other fission products, 19: 46414
separation from uranium-235 fission products by sorption on charcoal or molecular sieve, 20: 12772 (ORNL-3840)
separation from uranium fission products, method for, 20: 41034 (JEN-160-DQ/I-54)
separation method for, 20: 46102(R) (ORNL-4013)
solubility in blood, 20: 14415
sorption by activated carbon, 17: 34333(T,R) (EURAEC-655)
sorption by activated carbon, 18: 14361(R) (EURAEC-254)
sorption on activated carbon, from air, argon, carbon dioxide, and helium, 20: 1969
sorption on surfaces, uses for surface measurement, 18: 30157(T,R) (EURAEC-933)
tracer use for diagnosis of circulatory shunts, 19: 43904
tracer use for measurement of blood circulation in lungs, 19: 46070
tracer use for measuring sorption isotherms for coolant in HTGR, 20: 18626 (GA-6865)
tracer use for studies of, arterial clearance in man, 19: 36160
tracer use in atmospheric studies, 20: 8980(R) (BNWL-36, pp 3.1-122)
tracer use in atmospheric diffusion studies, 20: 45884
tracer use in pulmonary function of bronchial asthma, 17: 33497
tracer use in studies of renal blood flow, 19: 10974
tracer use in studies of blood circulation, 19: 31689
tracer use of, for cerebral blood flow measurements, 20: 1711
tracer use of, in measurements of brain blood flow, 19: 28181
tracer uses in blood circulation studies, 19: 10751
tracer uses in lung ventilation and perfusion, 18: 35415 (TID-7678 (p.237-47))
tracer uses in pulmonary function, 16: 12855
tracer uses in studies of blood circulation in muscles, 18: 38755
transfer between human blood and brain measurement of partition coefficient for, 19: 24253
use in hematology and radiodiagnosis, 18: 17695
use in measurement of myometrial blood flow during pregnancy, 20: 38747
use in scintiphotography studies of lungs, 20: 40749
use in surface area measurements by B.E.T. adsorption method, 19: 36410
use in surface measurement for uranium dioxide, 19: 4585 (EURAEC-1177)
use in thoracography, 16: 7380
use in tracer measurement of process gas flow rates, 18: 16387 (TID-7688(p.76-8))
use of, as tracer for determination of residual volume in the lungs, 17: 38662
use of, in studying function of various regions of lung, 16: 20065
use with nuclear image amplifier for blood flow and respiration measurements, 20: 3802 (ORNL-IIC-5, pp 239-42)
uses of, survey of, 19: 46414
yields from fission reactions, 16: 24351
yields from fission of thorium-232, and uranium-233, -235, and -238, 20: 30533
yields from thermal neutron fission of uranium-235, 16: 32388 (BNL-1652)
yields in neutron fission of uranium at 14.7 Mev, 18: 44835
yields in plutonium-241 thermal fission, (E), 19: 8495

XENON ISOTOPES Xe-134

abundance of fission-produced, in Pasamonte meteorite, 20: 29892
content in basic rocks, 20: 7267
content in Bruderheim meteorite, 20: 11430
content in natural gases, from uranium-238 spontaneous fission, 19: 630 (TID-21206)
content in natural gases, 19: 44239
content in terrestrial samples, 17: 25461
content in thucholites, 19: 15745
content of fissiogenic, in Pasamonte meteorite, 19: 16344
determination in uranium-233 and -235 fission products, (E), 20: 11960(R) (IDO-14667)
diffusion from BeO–UO_2 and UO_2 fuel elements during reactor operation, 20: 37303
energy levels, 16: 10957 (JINR-P-826)
energy levels, 17: 11685
neutron activation cross section, 17: 32398 (CEA-2215)
neutron cross sections at 0.414 ev to 10 Mev, 16: 9427 (GA-2451 (Vol.III))
proton reactions (p,γ) in stars, 16: 12308
separation by gaseous diffusion, economics and rate of, 19: 22855 (ORNL-TM-1047(p.127-36))
separation from xenon isotopes by thermal diffusion, 20: 39321(R) (MLM-1312)
yields from uranium-235 thermal fission, 19: 29313
yields in plutonium-241 thermal fission, (E), 19: 8495
yields in thermal neutron fission of uranium-233 and -235, 20: 43067(R) (IDO-14679, pp 6-46)

XENON ISOTOPES Xe-135

activity in reactor coolant following diffusion from hole in fuel can, (T), 20: 34995
buildup and decay in homogeneous reactor regions, computer program for, 16: 14229 (DC-59-8-130)
buildup and decay in natural-uranium fueled gas-cooled graphite-moderated reactors, reactivity controlled by, 18: 1271
buildup in reactor, reactivity control by, 20: 14099(P)

content in reactors, reactivity effects of oscillations in, (T), 20: 6590
decay of 9.20-hr fission-product, 16: 30930(R) (NYO-2669)
decay properties, (E), 19: 10262
determination in magnox reactor coolant, method for, 19: 21616
determination simultaneously with xenon-133m, equations for, 20: 43069(R) (IDO-14679, pp 51-9)
diffusion coefficients in uranium dioxide at 1000 to 1650°C, 17: 22216 (BMI-1623)
diffusion during temperature changes in reactor, 16: 23255 (AERE-R-3093)
diffusion from beryllia-coated beryllia-based thoria–urania–yttria fuels, 19: 44599(R) (GEMP-50A)
diffusion from irradiated uranium dioxide, 18: 30157(T,R) (EURAEC-933)
diffusion from neutron-irradiated uranium oxide compacts, 16: 24144 (AERE-R-4062)
diffusion from uranium dioxide, in-pile, 17: 4896
diffusion from urania at 800 to 1600°C, coefficients for, 20: 11224
diffusion in graphite at 400, 800, and 1200°C, 16: 11766
diffusion in irradiated uranium dioxides, 18: 14387(T,R) (EURAEC-860)
diffusion in pyrolytic-carbon-coated uranium dicarbide fuels at 1700°C, 19: 13877(R) (GA-5016(Pt.1))
diffusion in uranium carbide, 16: 5548
diffusion in uranium carbide, 16: 24184(T) (AEC-tr-5213)
diffusion of, from irradiated uranium carbide–zirconium carbide, 17: 33272
diffusion of, from impregnated graphite shells of fuel elements, 17: 33273
effects on neutron flux stability in reactors, kinetic equations for, 19: 14800
effects on power reactor kinetics, stochastic model for, (T), 19: 33611 (WAPD-T-1684)
energy levels, (E), 20: 38099
energy levels from xenon-136 (d,t) reactions, (E), 20: 44842
energy levels of, structure from isomeric transition in, (T), 20: 19970
gamma dose constants for, 20: 46617
gamma spectra, 20: 35594
gamma transitions in, effects of radial matrix elements on probabilities of M4, 18: 2861
half life, 18: 13075
neutron absorption in, temperature dependence of cross sections for, 18: 23064 (TID-7662(p.299-316))
neutron absorption in reactors, optimum power decrease for minimizing, (T), 20: 8358
neutron cross sections at 0.414 ev to 10 Mev, 16: 9427 (GA-2451 (Vol.III))
neutron cross sections, 16: 33781 (AEEW-R-116)
neutron reactions (n,α) at 14 Mev, nuclear shell effects in cross sections for, 18: 18977
neutron resonance cross sections, correction to Doppler broadening in, 17: 28307
production by neutron reactions (n,α) with barium-138, cross sections for, (E/T), 20: 17809
production in neutron reactions (n,α) with barium-138 at 14 Mev, isomer-pair cross-section ratios, 16: 7054
production in reactors, calculation as function of time after power change, 16: 15899 (FXM-1471)
production in shutdown reactors, minimization of, (T), 19: 17222 (UCRL-12261)
production in thermal-neutron fission, cumulative and direct yields in, (E), 20: 11990
radiation hazards from, following nuclear incidents, 20: 20962
radioactivity, 19: 17368
ratio to uranium-235 in reactors, curves for reactivity calculations, 16: 11193 (DC-55-8-109)
reactivity effects in thermal reactors, effects of time-varying shutdown, 16: 781
reactivity effects in steady-state reactors, 18: 38301 (A/CONF.28/P/169)
reactivity effects in Advanced Test Reactor, 18: 40753 (IDO-16977(p.1-20))
reactor criticality effects of, tables for calculating transients from, 20: 12352 (DP-958)
reactor criticality effects of, compensation for oscillations in, 20: 36503(P)
reactor poisoning by, method of compensating, 20: 3359(P)
reactor stability effects of, (T), 19: 5431 (IDO-16985)
release at IRL research reactor, 18: 4880
release from chromium–iron alloy at 900 and 1000°C, 18: 32136(R) (BMI-X-10093)
release from coated uranium carbide and dioxide fuel particles, 17: 23864(R) (BMI-1619(Del.))
release from coated-particle fuels during irradiation, 17: 35251(R) (BMI-1632(Del.))
release from coated fuel spheres at 1500 and 1700°F, 18: 4764(R) (ORNL-3470(p.129-56))
release from enriched fuels, analytical method for determining, 19: 15394
release from fuel-impregnated graphite at 1070 ± 15°C, 16: 4450(R) (BMI-1546(Del.))
release from irradiated uranium carbide and dioxide fuel specimens, 17: 25685(R) (BMI-1624(Del.))
release from irradiated carbon–uranium systems at 550 to 1540°C, 17: 35251(R) (BMI-1632(Del.))
release from irradiated uranium sesquicarbide at 1000 to 1300°C, 17: 40424(R) (BMI-1642(Del.))
release from irradiated uranium dioxide fuel element, 18: 15493(R) (ORNL-3523(p.193-226))
release from irradiated uranium carbides and nitrides at 450 to 1700°C, 18: 15664(R) (BMI-1655(Del.))
release from irradiated coated fuel particles, 18: 15664(R) (BMI-1655(Del.))
release from irradiated uranium carbides at 1000 to 1600°C, 18: 24988(R) (BMI-1665(Del.))
release from irradiated coated fuel particles, 18: 24988(R) (BMI-1665(Del.))
release from irradiated reactor fuels after shut-down, method of compensating for immediate restartup, 18: 33002(P)
release from irradiated coated fuel particles, 19: 13871(R) (BMI-1691 (Del.))
release from metal-clad uranium dioxide, 17: 6645 (BMI-1604)
release from uranium dioxide crystals, 17: 33320(R) (ORNL-3445(p.63-108))
release from uranium dioxide irradiated at 800 to 1600°C, 19: 18532 (AERE-R-4714)
separation from homogeneous reactor fuel, 17: 9892
separation from homogeneous suspension reactor fuels, method for, 19: 46426 (NP-15362)
separation from iodine-135 by solvent extraction using carbon tetrachloride, 19: 13544
separation from MSRE fuel by stripping, 19: 30067(R) (ORNL-3789(p.56-98))
separation from uranium fission products, method for, 20: 41034 (JEN-160-DQ/I-54)
spatial instabilities in reactors, analog study, 16: 3906
yields from fission reactions, 16: 24351
yields from fission of excited uranium-236, 17: 24750(R) (UCRL-10624)
yields from fission of thorium-232 and uranium-233, -235, and -238, 20: 30533
yields from thermal neutron fission of uranium-235, 16: 32388 (BNL-1652)
yields in fission of plutonium-239 and -241 and uranium-233 and -235, direct, 19: 29314
yields in fission of uranium-233 and -235, 19: 32680(R) (IDO-17052)
yields in neutron fission of uranium-233 and -235, 18: 32725 (A/CONF. 28/P/269)
yields in neutron fission of uranium at 14.7 Mev, 18: 44835
yields in plutonium-241 thermal fission, (E), 19: 8495

XENON ISOTOPES Xe-136

abundance in atmosphere, 17: 5172
abundance of fission-produced, in Pasamonte meteorite, 20: 29892
content in basic rocks, 20: 7267
content in Bruderheim meteorite, 20: 11430
content in natural gases, from uranium-238 spontaneous fission, 19: 630 (TID-21206)
content in natural gases, 19: 44239
content in terrestrial samples, 17: 25461
content in thucholites, 19: 15745
content of fissiogenic, in Pasamonte meteorite, 19: 16344
decay of, quasi-particle, 18: 32745(R) (UCRL-11213(p.1-48))
deuteron reactions (d,p) and (d,t) at 15 Mev, xenon-135 and xenon-137 energy levels from, (E), 20: 38099
deuteron reactions (d,p) and (d,t), xenon-135 and, 20: 44842
deuteron reactions (d,2n) with, cesium-136 nuclear properties from, (E), 20: 46605 (UCRL-16998)
energy levels, 17: 40040
energy levels of, second-vibrational, (T), 20: 13793
neutron capture cross sections, thermal, (E), 19: 35412
neutron cross sections at 0.414 ev to 10 Mev, 16: 9427 (GA-2451 (Vol.III))
proton reactions (p,n) with, cesium-136 nuclear properties from, (E), 20: 46605 (UCRL-16998)
proton reactions (p,γ) in stars, 16: 12308
separation by gaseous diffusion, economics and rate of, 19: 22855 (ORNL-TM-1047(p.127-36))
separation by rectification, 16: 30704
separation by thermal diffusion, 18: 45173(R) (MLM-1203)
separation by thermal diffusion, 19: 30629(R) (MLM-1238)

separation by thermal diffusion, 19: 30630(R) (MLM-1245)
separation from fission xenon by thermal diffusion, 19: 34607(R) (MLM-1239)
separation from xenon-131 using thermal diffusion columns, method for, 17: 32469
separation from xenon-131 in thermal diffusion column, 18: 13358(R) (MLM-1151)
separation from xenon-131 by thermal diffusion, 19: 28717(R) (MLM-1221)
separation from xenon isotopes by thermal diffusion, 20: 39321(R) (MLM-1312)
vapor pressure of, saturated, 17: 2998
yields in plutonium-241 thermal fission, (E), 19: 8495

XENON ISOTOPES Xe-137
beta decay, 18: 21361
core isomerism in, (T), 19: 17051
decay, 17: 41932
decay, gamma spectra, 16: 2554
decay scheme, 19: 14646
decay scheme, 19: 45679(R) (NYO-1859-11)
determination in fission gases, spectrometric, 16: 25295
energy levels, (E), 20: 38099
energy levels from, (E), 20: 44842
energy levels from xenon-136 (d,t) reactions, (E), 20: 44842
gamma spectra, 16: 27767
gamma spectra, (E), 19: 12616
gamma spectra, 20: 35594
half life, (E), 19: 29371
half life measurement, 20: 38017
half life of, determination of, 19: 45276 (NP-15304)
preparation and separation from krypton-87, 16: 2554
release from enriched fuels, analytical method for determining, 19: 15394
release from fuel impregnated graphite at 1070 ± 15°C, 16: 4450(R) (BMI-1546(Del.))
release from fuel-impregnated graphite at 1070 ± 15°C, 16: 4450(R) (BMI-1546(Del.))
release from irradiated pyrolytic-carbon-coated uranium carbide particles, 16: 17966(R) (BMI-1541(Del.))
separation in fission of uranyl stearate using on-line isotope separator, 20: 19887
yield from californium-252 fission, (E), 20: 6298(R) (PPAD-2137-566)
yields from plutonium-239 and uranium-233 thermal fission, (E), 19: 12597

XENON ISOTOPES Xe-138
decay properties, (E), 19: 10262
decay scheme, 19: 35615(R) (NP-15037)
determination in fission gases, spectrometric, 16: 25295
diffusion from pyrolytic carbon deposits, 20: 5089(R) (GA-6181)
diffusion in uranium dicarbide at high temperatures, 19: 13875(R) (GA-4022(Pt.1))
diffusion in uranium dicarbide at 1400 to 1600°C, 19: 13877(R) (GA-5016(Pt.1))
gamma spectra, 16: 27767
gamma spectra, (E), 19: 12616
gamma spectra, 20: 35594
half life, 18: 13075
half life, (E), 19: 29371
half life measurement, 20: 38017
half life of, determination of, 19: 45276 (NP-15304)
production and escape from irradiated uranium dioxide, 16: 4963 (EXP-NRX-6304)
release from chromium–iron alloy at 900°C, 18: 32136(R) (BMI-X-10093)
release from enriched fuels, analytical method for determining, 19: 15394
release from EVESR fuel elements, 20: 28750(R) (GEAP-5061)
release from EVESR fuel elements, 20: 28751(R) (GEAP-5125)
release from irradiated uranium dioxide in pressurized water systems, 16: 3893 (RLI-4(Rev.))
release from uranium dicarbide particles at 1000 to 1800°C, 17: 41337(R) (GA-4260)
yield from californium-252 fission, (E), 20: 6298(R) (PPAD-2137-566)
yields from plutonium-239 and uranium-233 thermal fission, (E), 19: 12597
yields from uranium-235 and -238 fission at 14 Mev, (E), 19: 12597
yields in plutonium-241 thermal fission, (E), 19: 8495
yields of, in fission of uranium, 17: 15306

XENON ISOTOPES Xe-139
determination in fission gases, spectrometric, 16: 25295
diffusion from pyrolytic carbon deposits, 20: 5089(R) (GA-6181)
diffusion in uranium dicarbide at high temperatures, 19: 13875(R) (GA-4022(Pt.1))
diffusion in uranium dicarbide at 1400 to 1600°C, 19: 13877(R) (GA-5016(Pt.1))
gamma decay radiations, 17: 19265
gamma spectra, 16: 27767
half life, (E), 19: 29371
half life measurement, 20: 38017
half life of, determination of, 19: 45276 (NP-15304)
release from chromium–iron alloy at 900°C, 18: 32136(R) (BMI-X-10093)
separation in fission of uranyl stearate using on-line isotope separator, 20: 19887
yield from californium-252 fission, (E), 20: 6298(R) (PPAD-2137-566)
yield in uranium fission by 14-Mev neutrons, 17: 21076
yields from plutonium-239 and uranium-233 thermal fission, (E), 19: 12597
yields from uranium-235 and -238 fission at 14 Mev, (E), 19: 12597
yields from uranium-238 fission at 14 Mev, (E), 20: 36171 (NP-16155)

XENON ISOTOPES Xe-140
book: *Isobaric Nuclei with Mass Number A = 140*, 18: 2961
decay scheme and energy level, 16: 31125
determination in fission gases, spectrometric, 16: 25295
diffusion of, from impregnated graphite shells of fuel elements, 17: 33273
gamma spectra, 16: 27767
half life, (E), 19: 29371
half life measurement, 20: 38017
half life of, determination of, 19: 45276 (NP-15304)
release from fuel-impregnated graphite at 1070 ± 15°C, 16: 4450(R) (BMI-1546(Del.))
release from irradiated pyrolytic-carbon-coated uranium carbide particles, 16: 17966(R) (BMI-1541(Del.))
separation in fission of uranyl stearate using on-line isotope separator, 20: 19887
yield from californium-252 fission, (E), 20: 6298(R) (PPAD-2137-566)
yields from plutonium-239 and uranium-233 thermal fission, (E), 19: 12597
yields from uranium-235 and -238 fission at 14 Mev, (E), 19: 12597
yields from uranium-238 fission at 14 Mev, (E), 20: 36171 (NP-16155)

XENON ISOTOPES Xe-141
determination in fission gases, spectrometric, 16: 25295
diffusion of, from impregnated graphite shells of fuel elements, 17: 33273
half life, (E), 19: 29371
half life of, determination of, 19: 45276 (NP-15304)
yield from californium-252 fission, (E), 20: 6298(R) (PPAD-2137-566)
yields from plutonium-239 and uranium-233 thermal fission, (E), 19: 12597
yields from uranium-235 and -238 fission at 14 Mev, (E), 19: 12597
yields from uranium-238 fission at 14 Mev, (E), 20: 36171 (NP-16155)

XENON ISOTOPES Xe-142
half life, (E), 19: 29371
half life of, determination of, 19: 45276 (NP-15304)
yield from californium-252 fission, (E), 20: 6298(R) (PPAD-2137-566)
yields from plutonium-239 and uranium-233 thermal fission, (E), 19: 12597
yields from uranium-238 fission at 14 Mev, (E), 20: 36171 (NP-16155)

XENON ISOTOPES Xe-143
half life, (E), 19: 29371
half life of, determination of, 19: 45276 (NP-15304)
yield from californium-252 fission, (E), 20: 6298(R) (PPAD-2137-566)
yields from plutonium-239 and uranium-233 thermal fission, (E), 19: 12597

XENON ISOTOPES Xe-144
half life of, determination of, 19: 45276 (NP-15304)
half-life of, method for measuring, 20: 44706
yields from plutonium-239 and uranium-233 thermal fission, (E), 19: 12597

XENON NITRIDES
spectra between 4920 and 4750 Å, 17: 28866

XENON OXIDES
bond lengths and molecular shapes of, theory for prediction of, 18: 5345
bonding of, from infrared spectra, 17: 19993 (TID-18460)
chemistry of tri-, formed by hydrolysis of xenon tetrafluoride, 18: 5330
chemistry of tri-, in aqueous solutions, 18: 31361(R) (UCRL-11213(p.87-138))
crystal structure of XeO_3, 17: 25060(R) (ORNL-3417(p.3-16))
crystal structure of hexavalent, 17: 35708 (UCRL-10803)
crystal structure of tri-, 18: 31361(R) (UCRL-11213(p.87-138))
formation by beta decay of iodine-133 in potassium iodide, 20: 27015
formation from beta decay of iodine-131 in potassium iodate, 19: 46411
handling of tri-, safety precautions for, 18: 5327
heat of formation of hexavalent, 17: 35707 (UCRL-7343-T)
heat of formation, 19: 28308
mass spectrum of tetravalent, 18: 13778
molecular structure of, (T), 19: 11117
molecular structure of, semiempirical, (T), 20: 18641
molecular vibration of, mean amplitudes of, 18: 43461

oxidative effects on bromine and iodine ions, kinetics of, 18: 5331
preparation and properties of tri-, 17: 18040
preparation and properties of tetravalent, 18: 16052
preparation and properties of, review on, 18: 16050
preparation and properties, 19: 9105
preparation and properties of, review on, 20: 3915 (CEA-Bib-61)
preparation and properties of, 20: 20659
preparation of, review of, 19: 28323
preparation, properties, and structure of, review on, 20: 33299
properties of, formed by beta decay of iodine-131 in alkali metal iodates, 20: 38984
reactions of tri-, with bromide and iodide ions in aqueous solution, kinetics, 18: 31361(R) (UCRL-11213(p.87-138))
reactions of tri-, with potassium hydroxide in solution, 19: 19847(R) (UCRL-11828(p.182-3))
reactions with potassium hydroxide, formation of $K_4XeO_6 \cdot 2XeO_3$ in, 20: 33280
reactions with trivalent plutonium ions, kinetics of, 19: 22199
separation from iodic acid using zirconium phosphate, 20: 41054
separation from iodate and periodate solutions by ion exchange chromatography, 20: 40851
spectra and potential of, analysis of vibrational, 20: 12842
spectra of, infrared, 17: 18008 (TID-18276)
stability in basic solutions, effects of hydroxyl ion concentration and temperature on, 19: 7384
structure of tri-, 17: 18041
thermodynamic functions at 100 to 2000°K, 18: 43461
uses in titrimetric determination of primary and secondary alcohols, 20: 20579
uses in titrimetric determination of organic acids, 20: 31196

XENON OXYFLUORIDES

bond lengths and molecular shapes of, theory for prediction of, 18: 5345
chemical shifts in, calculation of, 18: 19960
density and refractive index, 20: 14528
handling of, safety precautions for, 18: 5327
heat of formation, 19: 28308
mass spectra, 18: 5316
molecular structure of, from microwave spectra, 18: 27408
nuclear magnetic resonance spectra, 18: 2127(R) (ORNL-3488(p.21-41))
oxygen-17 nuclear magnetic resonance spectra in, 19: 30168
preparation, 18: 5321
preparation and properties of, 17: 25234
preparation and properties of, by electric discharge method, 17: 33947
preparation and properties of tetra-, 18: 5325
preparation and properties of, review on, 20: 3915 (CEA-Bib-61)
preparation and properties of, 20: 20659
preparation by electric discharge method, 18: 5321
preparation of, design of circulating loop for, 18: 5315
preparation of, review of, 19: 28323
properties of, chemical and physical, 20: 14523
reactions with alkali metal, antimony, and arsenic fluorides, 20: 14523
reactions with vanadium fluoride, compound formation in, 20: 45657
spectra and valence force constants of, 19: 15488
spectra of coupling and shielding in, nuclear magnetic resonance, 18: 5337
spectra of, high-resolution fluorine-19 and xenon-129 magnetic double resonance, 17: 33902
spectra of, infrared and Raman, 17: 33865 (CONF-126-9)
spectra of, infrared and Raman, 18: 2127(R) (ORNL-3488(p.21-41))
spectra of, infrared and Raman, 18: 5342
spectra of, magnetic resonance, 18: 5338
spectra of, Raman, 19: 865(R) (ORNL-3679(p.23-38))
structure model of, 19: 865(R) (ORNL-3679(p.23-38))
Urey-Bradley force constants, 20: 12841

XENON SYSTEMS

diffusion of krypton-58 in multicomponent, 19: 2343
Ar–Xe, alpha ionization of, 17: 24052 (ORNL-3422)
Ar–Xe, diffusion coefficients at 0 to 120°C, 19: 7393
Ar–Xe, diffusion of xenon-133 in, 19: 13295
Ar–Xe, electron reactions at 50 kev, luminescence from, (E), 19: 41246
Ar–Xe, thermal diffusion at 0 to 120°C, 19: 30153(R) (ORNL-3789(p.183-201))
Ar–Xe, xenon impurity states in solid, 17: 34620
Cs–Xe, performance in thermionic cells, 18: 36234
Cs–Xe, performance as working gas in Brayton-cycle MHD cells, (T), 19: 16447 (NASA-TN-D-2651)
Cs–Xe, potential curves and spectra for collisions in, 18: 32486
Cs–Xe, thermal diffusion in, 20: 21567 (FEI-15)
F–Xe, identification of XeF, in, 17: 33948
F–Xe, preparation of xenon fluoride from, by exposure to daylight at room temperature, 20: 22977
hexafluoroethane–Xe, energy transfer in gamma radiolysis of, 20: 10884
hexane–Xe, radiolysis of, electron and energy transfer in, at −78°C, 19: 32217
He–Xe, atomic and ionic processes in plasma of, 17: 35019 (AD-411955)
He–Xe, characteristics of electric discharge in, 17: 11431
He–Xe, diffusion coefficients at 0 to 120°C, 19: 7393
He–Xe, diffusion of xenon-133 in, 19: 13295
He–Xe, electric discharge in, atomic temperature and Doppler broadening in, 17: 31606
He–Xe, energy levels of ionized, pressure effects on, 20: 42491
He–Xe, ionization of, by electrons at 150 to 550 Mev, 16: 21288
He–Xe, noise resonance in afterglow plasma of, 18: 28872
He–Xe, performance in scintillation detectors, 19: 20361
He–Xe, properties for use in closed Brayton cycle space power plants, 19: 44205
He–Xe, thermal diffusion at 0 to 120°C, 19: 30153(R) (ORNL-3789(p.183-201))
He–Xe, xenon atomic transitions in, 17: 17374
H_2O–Xe, electron density decay rate in afterglow vapors of, 18: 32439
H–Xe, characteristics of electric discharge in, 17: 11431
H–Xe, dissociation rates of hydrogen in, 16: 7975
H–Xe, electric discharges in multi-cathode, 20: 6168
H–Xe, use of Platt electrostatic model for calculation of properties of diatomic ions of, 18: 12074
Kr–Xe, adsorption of PL-2-generated, evaluation of adsorption device for, 16: 30090 (NYO-4815)
Kr–Xe, diffusion of xenon-133 in, 19: 13295
Kr–Xe, electron reactions at 50 kev, luminescence from, (E), 19: 41246
Kr–Xe, thermal diffusion in, 16: 3561
methane–Xe, counting plateau characteristics, 18: 13357(R) (MLM-1148)
methane–Xe, radiolysis of gaseous, hydrocarbon and hydrogen yields from charge and energy transfer in electron, 20: 23167
Na–Xe, excitation transfer in first excited states of sodium, cross sections for collision-induced, (E), 20: 11499
Ne–Xe, diffusion of xenon-133 in, 19: 13295
Ne–Xe, spectra of xenon in, detection of laser lines in (E), 19: 1173
NO–Xe, mutual charge neutralization of ions in, pressure dependence at 10 to 600 torr, 18: 7407 (UCRL-10904)
N–Xe, electric discharge in, constriction, volt-ampere characteristics, and volume recombination of the positive column of, 16: 21179
N–Xe, electron reactions at 50 kev, luminescence from, (E), 19: 41246
O–Xe, electron transfer collisions near adiabatic conditions in, 16: 16868
O–Xe, radiolysis of, ozone formation in, 18: 20095

XENOTIMES

analysis for rare earths and thorium, 18: 19885
analysis for yttrium, x-ray-fluorescence, 18: 37080
analysis for yttrium, fluorometric, 20: 29094

Xerography
see Electrophotography

Xeroradiography
see Radiography

XMA-1
see Initial Engine Test

XYLENE

analysis for hydrogen by thermal neutron bombardment, 20: 33204
analysis for oxygen by activation, 18: 21953 (AERE-R-4576)
association constants of, with chloranil, deuterium isotope effects in, 17: 15991
behavior of pyrene in *p*, effects of concentration on, 17: 5938
density and viscosity, 20: 14648
determination in humidrier liquors by gas chromatography, 20: 26749 (PG-Report-695)
deuterium exchange with water, geometric factor in catalytic, 17: 15863
deuterium exchange between, and heavy water, effects of π-complex absorption on transition metals on, 19: 32199
deuterium-hydrogen exchange reactions in, effects of nickel on, 19: 28347
diffusion in CGB graphite, 20: 4308(R) (ORNL-3870, pp 243-60)
effects on activity of leukocyte alkaline phosphatase, toxicity, 20: 5269
effects on inflammatory edema in rabbit ears, role of adrenals and central nervous system in, 20: 35342
effects on radiolysis of monoimine of phenanthrene-9,10-quinone, 20: 397
effects on solvent properties of diisopentyl methylphosphonate for thorium in nitric acid solutions, 20: 36942
electron capture in, 19: 7539(R) (ORNL-3697(p.131-43)
electron reactions in ethylene mixture, cross sections for momentum transfer and drift velocities in, 20: 5985 (ORNL-TM-1262)
electronic energy transfer to *p*-terphenyl, 18: 10620 (AFCRL-63-610)
electronic spectra of, tables, 19: 9156 (IS-450)
energy transfer of 1,6-diphenylhexatriene and *p*-terphenyl in, 18: 6850(R) (TID-19902)
exchange reactions with deuterium oxide, catalytic effects of alumina–nickel, rhodium, and silver on, 18: 13822

fluorescence quenching in cyclohexane solution of, by oxygen, 17: 4566
hydrogen abstraction from, by methyl radicals, 19: 21760 (NYO-2728-4)
hydrogen isotope exchange with deuterium oxide, effects of nickel on, 17: 27384
ionization potentials, 16: 7985
isotope effects and spin-spin coupling in partially deuterated, paramagnetic resonance spectra of, 18: 12126
isotope exchange with deuterium oxide, catalytic activity of nickel, palladium, and platinum in, 16: 22080
isotope exchange with deuterium oxide, effects of catalysts on, 17: 27387
isotopic exchange reactions with heavy water, 17: 18067
luminescence of, alpha/beta ratio in, 18: 300
luminescence quenching in benzene solution, effects of aromatic halides on, 17: 4563
luminescence spectra and quantum yields of pure and cyclohexane solutions of, 19: 21771 (TID-21684)
melting point of powdered, alpha absorption determination of, 19: 32169
neutron cross sections, thermal, 18: 38038 (A/CONF.28/P/651)
neutron diffusion parameters for, pulsed, (E), 20: 13729
neutron scattering cross section spectra, 16: 29522 (BNL-5979)
neutron scattering by bound protons in, cold, 18: 11195(R) (EANDC(E)-49(L))
photoionization of, energy spectra of electrons from, 18: 281
positron annihilation in, 17: 9300
properties as diluent in amine solvent-extraction systems, 18: 37275 (A/CONF.28/P/755)
properties as working fluid in Rankine power cycle, 20: 41398
protective effects against radiation damage in polymethyl methacrylate, 19: 15646
proton exchange with hydrogen fluoride, 18: 29679
proton frequency spectra in *meta-*, *ortho-*, and *para-*, from cold neutron scattering, 18: 37151
radiation effects on liquid-phase oxidation by oxygen, 16: 214(T) (NP-tr-794)
radiation effects on scintillation efficiency of 2,5-diphenyloxazole in, 17: 3557
radiation effects on electric conductivity, 17: 22218(R) (GA-4164)
radiation effects on solubility of polyallyl amine and polyethylene in, 18: 22127(T) (JPRS-24289(Del.)(p.89-99))
radiation effects on, ESR spectra of, 18: 25520(T) (AEC-tr-6372(p.481-90))
radiation effects on oxidation of, 19: 476
radiation effects on oxidation of, effects of temperature on kinetics of, 20: 41002
radioinduced oxidation on alumina, alumina–silica system, and silica, 18: 1725(R) (ORNL-3488(p.42-54))
radioinduced oxidation of, effects of bromohydrocarbons and hydrogen bromide on, 19: 479
radioinduced oxidation of, adsorbed on alumina, aluminosilicate, and silica gel, 19: 4215
radioinduced oxidation of, radiation effects on catalysts for, 19: 26430
radioinduced oxidation of para-, effects of organic bromine compounds on, 19: 32225
radioinduced peroxidation of, pulsed-x, 20: 43369
radioinduced thermoluminescence of liquid, effects of *p*-terphenyl on electron, 18: 27543
radiolysis of, electron spin resonance of free radicals produced by, 17: 8168
radiolysis of, hydrocarbon and hydrogen yields from, 17: 31796(R) (BNL-782(p.44-50))
radiolysis of isomeric, products of, 17: 19724 (BNL-759(p.39-46))
radiolysis of isomers of, product yields in, 17: 35865 (BNL-6423)
radiolysis of sulfur in, yields in, 18: 27505
radiolysis of, radical captor properties of dinaphthofuranoxyl and DPPH in, 18: 43607
radiolytic oxidation of *p-*, 17: 6143
reactions with organic matrix materials in ice-water system, 18: 15722 (TID-20332)
solvent effects in tertiary amine extraction of iron in hydrochloric acid, 16: 25481 (PAN-303/V)
solvent effects on gamma-irradiated polyvinyl acetate in methanol, 16: 18950
solvent properties for Santowax R, 16: 14613(R) (IDO-16734)
solvent properties in mixtures with butyl, dichlorodiethyl, and ethyl ethers for uranyl nitrates, 19: 20072
spectra of neptunium, plutonium, and uranium hexa- and tetravalent nitrates in tri-n-octylamine solutions, absorption, 16: 2947
surface stresses in TBP mixtures in equilibrium with aqueous lanthanum nitrate solutions, 19: 22232
tritium exchange with tritiated ethyl malonate, effects of catalysts on, 20: 16492
uses as medium for drifting lithium into germanium, (E), 20: 5702
uses in preparation of radiation-resistant lubricants, 18: 41503(P)
x-ray scattering cross sections, 18: 20035
CCl_4–xylene, solvent properties for uranium, 18: 13937
dibutyl butylphosphonate–xylene, solvent properties for americium from nitrate solutions, 19: 38750 (HW-81166)
dodecylamine–xylene, stability of plutonium-containing, 20: 33188(T,R) (ORNL-tr-1238)
HNO_3–xylene, solvent properties for various elements, 20: 27037 (JAERI-1106)
octylamine–xylene, solvent properties for tetra- and pentavalent protactinium, 17: 29030
TBP–xylene, density and viscosity of, 20: 14648
thenoyltrifluoroacetone–xylene, solvent properties for zirconium, 18: 1808
tributyl phosphate–xylene, solvent properties for uranium, 19: 18074
tridodecylamine–xylene, distribution of bismuth and polonium between, and, hydrobromic or hydrochloric acids, 18: 35535
triisooctylamine–xylene, activation energies and coefficients of plutonium and uranium diffusion in, 18: 10192
triisooctylamine–xylene, mass transfer of nitric acid, plutonium, and uranium from aqueous solutions to, 18: 31663(T) (UCRL-Trans-1078)
triisooctylamine–xylene, solvent properties for plutonium, ruthenium, uranium, and zirconium from aqueous nitric acid solutions, 18: 31663(T) (UCRL-Trans-1078)
trioctylamine–xylene, solvent properties for ruthenium, 20: 14650
TTA–xylene, solvent properties for zirconium, 20: 25004

o-XYLENE, 4-BROMO-
radiation effects on, thermal annealing of neutron, 19: 40576

XYLENOL
tritium rate effect in tyrosinase-catalyzed hydroxylation of, 16: 31450

2,4-XYLENOL
preparation of deuterated, from 2,4,6-tri-d_3-methylpyrylium perchlorate, 20: 16501

XYLENOL ORANGE
analytical use for spectrophotometric determination of indium, 17: 2922
analytical use for spectrophotometric determination of cerium, lanthanum, neodymium, and yttrium, 17: 12199
analytical use for differential spectrophotometric determination of hafnium in presence of zirconium, 17: 12221
analytical use for spectrophotometric determination of rare earths, 17: 25126
analytical use for determination of rare earths, 17: 25147
analytical use for spectrophotometric determination of scandium, 17: 33805
analytical use for spectrophotometric determination of zirconium, 18: 17750
analytical use for spectrophotometric determination of rare earths, 18: 25285
analytical use for complexometric determination of thorium, titanium, and zirconium in solution, 18: 39125
analytical use for colorimetric determination of vanadium, 18: 43416
analytical use for colorimetric determination of scandium, 19: 7296
analytical use for colorimetric determination of lanthanum, scandium, thorium, and uranium on paper chromatograms, 20: 22910
analytical use for complexometric determination of cerium and magnesium in iron and rare earth alloys, 20: 25008
analytical use in determination of thorium in ores, 16: 7510
analytical use in photometric determination of niobium, 17: 12215
analytical use in photometric determination of rare earths, 18: 27341
analytical use of, for spectrophotometric determination of thorium, 17: 15910
analytical use of, for photometric determination of niobium, 17: 30496
analytical uses for spectrophotometric determination of niobium, 18: 1543
analytical uses for determination of scandium and thorium, 18: 5221
analytical uses for spectrophotometric determination of rare earths, 18: 19883
analytical uses in spectrophotometric determination of rare earths, 18: 43394
analytical uses in determination of thorium, 19: 22121
analytical uses in determination of fluorides by titration using uranium, 20: 5520
analytical uses in determination of fluorides by titration using thorium nitrate, 20: 7032
complex with hafnium and zirconium, 17: 19960
complexes with aluminum and molybdenum, association constants and composition of, 17: 40757
complexes with cerium, lanthanum, and yttrium, formation and spectra of, 18: 27341
complexes with iron and uranyl ions, spectrophotometric study of, 17: 137
complexes with lanthanum, lutetium, scandium, and yttrium, composition and chemical properties of, 20: 38924
complexes with scandium, spectra of, 18: 13703

reactions with niobium, 16: 9992
reactions with thorium, 18: 10104
reactions with zirconium, 16: 18918
separation of components of, by complex formation with zirconium, 16: 32978
use in the determination of lanthanum, 20: 40860
uses for determination of rare earths in selenides, sulfides, and tellurides, 20: 16395
uses for spectrophotometric determination of lanthanum, 20: 16394
uses in complexonometric determination of thorium in uranium in presence of tributyl phosphate, 20: 22953
uses in determination of rare earths, 20: 22949
uses in photometric determination of neptunium, 20: 16408
uses in spectrophotometric determination of tetravalent plutonium in presence of hexavalent uranium, 20: 22951

XYLOSE
analysis for oxygen-18, spectrographic, 16: 17711
effects on cesium-137 uptake by wheat roots, 19: 50
intestinal sorption of, measurement of, 20: 28871(R) (EUR-2636.f,i)
labeling with tritium in C-5 position, 19: 22274
oxidation by bromine, tritium isotope effects in, 18: 20031
oxidation by iodine, isotope effects and water-t yield in, 18: 5359
oxidation by sodium chlorite, tritium kinetic isotope effects in, 18: 25459
radiation effects on cyanohydrin reaction, background, 17: 33981
radiation effects on reactions of, with hydroxylamine, background, 19: 4201
radioinduced free radicals, 16: 13113
radioinduced free radicals in, gamma, 18: 23651(T,R) (AEC-tr-6316 (p.573-86))
radiotherapy effects on sorption by intestine, abdomen-pelvic, 19: 17725
separation of protium and deuterium forms of, by gas chromatography, 19: 36546
spectra of trimethylsilylation products of, 17: 4561(R) (UCRL-10350)
yield in gamma radiolysis of oxygenated solutions of D-sorbitol, 16: 219
yield in gamma radiolysis of deaerated solutions of D-sorbitol, 16: 220

Y

Y Particles
see Hyperons
Yankee Atomic Electric Co. Reactor
see Yankee Power Reactor

YANKEE POWER REACTOR
accident analysis using probabilistic methodology, 20: 1461 (CONF-650407, pp 1035-56)
bibliography on, 17: 31734 (TID-3556(Rev.2))
control and instrumentation system installation and operating history, 16: 31308
control and instrumentation of, bibliography on, 20: 47044
control of, boric-acid shim, 18: 21652
control rod and fuel element corrosion testing, 17: 1131 (YAEC-182(Pt.I))
control rod characteristics of cadmium-indium-silver alloys in, 16: 25796
control rod configuration in, analysis of critical, 18: 3217
control rod drive analysis, 16: 32534 (DANATOM-06-61)
control rod evaluation for, 18: 35165(R) (WCAP-6063)
control rod worth, 16: 24469
control rod worth, 16: 24404
control rods for, radiation effects on nickel-plated cadmium–indium–silver, 20: 39461 (WCAP-6074)
coolant sampling in, analysis of, 20: 12418(R) (WCAP-3739)
coolant, transient boiling behavior following flow loss, 16: 14323 (YAEC-132)
core and fuel element evaluation, Apr.–June 1963, 17: 38553(R) (WCAP-6055)
core and fuel element evaluations for, 17: 42363(R) (WCAP-6056)
core design for, (E), 19: 17241
core evaluation for, 17: 15475(R) (WCAP-6053)
core evaluation for, 20: 20272(R) (WCAP-6079)
core evaluation in, (E), 19: 17283(R) (WCAP-6070)
core evaluation program, 17: 33361
core evaluation program, 19: 3655(R) (WCAP-6064)
core-I instrumentation, 16: 24470
core-I reactivity, 16: 24471
core-I reactivity, 16: 24472
core performance analysis for, (E), 20: 16091(R) (WCAP-6078)
critical experiments for, reliability of data from, 18: 36781(R) (HW-81659(p.26-32))
criticality calculations for, 19: 47959 (WCAP-3269-52)
criticality studies, 20: 12418(R) (WCAP-3739)
description, 17: 5611
design and operation data, 19: 33704
development, 20: 36458 (BNL-10309)
development of, core evaluation program in, 17: 2588(R) (WCAP-6052)
development of, program plans for, 19: 24095(R) (YAEC-124)
development program for, summary for Jan. to June 1960, 19: 24096(R) (YAEC-143)
development, Jan.-March 1966, 20: 36496(R) (WCAP-6080)
fuel analyses of Core I, spent, 20: 26467 (WCAP-6068)
fuel analysis for promethium isotopes, fission products, and transuranic isotopes, 19: 24904 (BNWL-45)
fuel assemblies for, remote underwater devices for post-irradiation examination of, 20: 5136 (WCAP-5564)
fuel assemblies from, evaluation of irradiated (E), 19: 3658
fuel assemblies from, remote-control equipment for underwater inspection of irradiated, 20: 2117
fuel assembly shipping from, experience in irradiated, 19: 19392 (WCAP-6062)
fuel burnup and neutron flux distribution in Core I of, 17: 13783 (WCAP-6051)
fuel burnup and power distributions in Core I, 20: 35054
fuel burnup distributions in, 18: 35165(R) (WCAP-6063)
fuel burnup distributions in, evaluation of gamma scanning for, 19: 29663
fuel burnup distributions in, (E/T), 19: 29598
fuel burnup distributions in, gamma scanning for, 19: 38191 (WCAP-5490)
fuel burnup in, 20: 3504
fuel burnup in Core I and II from gamma activity measurements, 19: 35782 (WCAP-6067)
fuel burnup in core I, composition analysis for, 19: 38194 (WCAP-6071)
fuel burnup in lattice cells of, (T), 19: 43519 (WCAP-6069)
fuel burnup in, economics of, 20: 22446
fuel burnup in, model for, 19: 38192 (WCAP-5494)
fuel cladding performance at high burnup, stainless steel (E), 19: 3687
fuel cycle analysis, computer code for, 16: 5653
fuel cycle development, 16: 24468
fuel element and core evaluation program for, 17: 26872(R) (WCAP-6054)
fuel element burnup calculations for, 20: 36496(R) (WCAP-6080)
fuel element cladding corrosion in, analysis of products from, 20: 8429
fuel element cladding corrosion in, analysis of products from, 20: 45126 (WCAP-6072)
fuel element gamma scanning for, 20: 36496(R) (WCAP-6080)
fuel element irradiation testing and radiochemical analysis of, 20: 36496(R) (WCAP-6080)
fuel element testing, 17: 20516 (YAEC-182(Pt.II))
fuel element testing, core-1, 18: 3261
fuel element testing in cores I and II, 20: 7642
fuel elements for, statistical analysis of alpha-25 from spent, 18: 4803 (WCAP-6057)
fuel elements of, fission gas release from, 20: 36496(R) (WCAP-6080)
fuel pellet temperature for Doppler broadening of uranium-238 resonance, 20: 5135 (WCAP-3269-40)
fuel pelletization procedures for, 16: 13552 (YAEC-159)
fuel performance evaluation in, summary, 18: 23067(R) (WCAP-6061)
fuel reprocessing costs, 16: 8817
fuel-pellet temperature for Doppler broadening of uranium-238 resonance, 19: 29659
hazards summary, 17: 38547 (NP-13088)
instrumentation operation and maintenance, 18: 31015
licensing activities for, 18: 1267
loading and operation problems, 19: 43568
loading experience at, 19: 8646
materials burnup and radiation damage in, (E/T), 19: 31560(R) (WCAP-6075)
materials for, properties of concrete, 16: 25781
materials selection on, review of, 17: 30928
neutron flux measurements by automatic activated-wire mapping system, 16: 8942
operating and refueling experience through February 1963, 17: 33355
operating experience through October 1961, 16: 635
operating experience of, 17: 2537
operating experience, 18: 3285
operation, 16: 31293
operation, 16: 31295
operation and performance of, evaluation of, 18: 35175
operation and safeguards of, regulatory actions relative to, 19: 12795
operation data availability, 16: 21816 (NYO-2482)
operation during 1962, 17: 36953
operation experience, 18: 33070 (A/CONF.28/P/202)
operation experience, 18: 33071 (A/CONF.28/P/203)
operation experience with cores 1, 2, and 3, 19: 35791
operation experience 1960–1965, 20: 22457
operation of, nuclear performance of, Core I in, 18: 11441 (TID-7672 (p.1-32))
operation of, review of experience in, 18: 15554
operation of, review, 19: 19395

operational experience, 16: 24466
operational experience with, 18: 9677
performance, 16: 24467
performance, 20: 22444
performance of Core I, 17: 2598
performance of, reliability of, 20: 45181
power disturbances in, local, (E/T), 20: 5134(R) (WCAP-3269-12)
pressure vessel surveillance, evaluation of irradiated specimens in, 19: 11780 (NRL-6179)
pressure vessel, radiation damage surveillance, 19: 11781(R) (NRL-Memo-1556)
radiation and thermal damage in pressure vessel in, 20: 17126 (NRL-6349)
radioisotope production in, economic and technical feasibility of, 19: 28723
radiological safety at, personnel organization and rules for, 16: 31313
reactivity and reactivity coefficients in Core I, fuel burnup effects on, 20: 8402 (WCAP-6076)
reactivity coefficients in, burnup effects on, 19: 45602 (WCAP-5493)
reactivity of Core I data, 17: 13782 (WCAP-6050)
reactivity of, effects of fuel cladding corrosion products on, 20: 45126 (WCAP-6072)
reactivity transients in, spectra of, 18: 15583
safeguards inspection of, international, 19: 17317
safeguards, inspection procedures for, 20: 45108 (BNWL-119)
safety analysis of, probabilistic methodology for, 20: 30883 (SAN-570-2)
safety features in, review of, 19: 35783
safety review, 16: 31278 (UNC-5029)
shielding and radiation levels, 17: 33281
spent fuel analysis for fission products and heavy element isotopes, evaluation of chemical, 20: 14435 (BNWL-SA-503)
startup and operating experience, 16: 23325
startup data, fits with reactor physics models, 17: 2593
startup, primary system and reactor characteristics, 16: 12759 (YAEC-184)
thermal operating performance, 18: 15434 (TID-7669)
vapor container systems of, leakage monitoring in, (E), 20: 6631 (YAEC-1005)

YEASTS

alkali metal ion transport in, mechanisms of, 20: 5251(R) (UR-668, pp 123-49)
autolysate, effects on infections in irradiated rats, 16: 14574
catalase activity in, effects of mercury and uranyl ions on, 19: 10764
cell division and respiration, effects of irradiated methyl linolenate on, 16: 11471
cerium metabolism in, tracer study, 19: 25840(R) (ORINS-49(p.63-71))
cerium-144 uptake by *Saccharomyces cerevisiae*, mechanism of, 20: 40560
cesium-137 content in, used for brewing, 20: 45957 (NYO-3364-23)
chemically induced mutations for radioresistance in, β, uv, and x, 20: 5360
complementation map of *S. cerevisiae*, 20: 26661(T) (ORNL-tr-1234)
content of potassium and sodium in growing, 20: 5251(R) (UR-668, pp 123-49)
cytochrome C metabolism in, 20: 5251(R) (UR-668, pp 123-49)
cytology of Saccharomyces and Candida, 19: 29849(R) (ANL-6971 (p.1-28))
deuterium effects on growth and metabolism in *Saccharomyces cerevisiae*, 17: 23060
deuterium–hydrogen exchange in dehydrogenase from, 17: 40501
dominant lethality in, LET studies with HILAC, 16: 9764(R) (UCRL-9897(p.147-50))
effect of photoreactivation on ultraviolet-induced segregation, 16: 7465
effects of chemical mutagens on Schizosaccharomyces, 20: 38589(R) (EUR-2761.f)
effects of deuterium oxide on growth and respirstion, 16: 25137(R) (HW-72500(p.113-18))
effects of deuterium oxide on metabolism, 17: 13917 (HW-SA-2570)
effects of deuterium oxide, on growth of, 18: 41086(R) (HW-80500 (p.153-6))
effects of dimethyl sulfoxide on, inhibitory, 20: 18206(R) (N-65-16815)
effects of endogenous, on spoilage of radiation processed fish, 20: 9315 (CONF-651024, pp 10-13)
effects of freezing and thawing of isolated cells on morphology and viability, 18: 45177 (ORNL-P-445)
effects of heat on Saccharomyces, 18: 33393
effects of heat treatments combined with γ radiation on *Saccharomyces cerevisiae*, 20: 41387
effects of incorporated carbon-14 on DNA and protein structures in adenine-dependent, mutagenic, 20: 32998
effects of incorporated phosphorus-32 on adenine-dependent diploid, mutagenic, 20: 32999
effects of incorporated carbon-14, phosphorus-32, and sulfur-35 on adenine-dependent, mutagenic, 20: 33000
effects of mitomycin C on, genetic, 20: 8663
effects of nitrogen mustard on, effects of plating time on recovery from, 18: 8183
effects of nitrogen mustard on, lethal, 19: 76(R) (UCRL-11387(Suppl.) (p.19-51))
effects of oxidizing radicals on irradiated and normal, chemiluminescence from, 20: 32916
effects of oxygen on role of oleic acid oxidation products in, 18: 33390
effects of starvation on cells of, 18: 8179
effects of tritiated water on *Rhodotorula gracilis*, effects of cystamine on, 17: 5719
effects of ultraviolet radiation on leakage of amino acids and on amino acid pools, 16: 6330
effects of water-d_2 on growth of, as function of inoculum age, 20: 1601
effects of 5-fluorodeoxyuridine on, genetic, 20: 8663
effects on survival time of irradiated erythrocytes, 16: 9809
enzyme purification and methionine biosynthesis in Saccharomyces, 18: 23193(R) (ANL-6823(p.128-40))
enzymes from, purification of photoreactivating, 18: 27003(R) (ORNL-3601(p.27-46))
extracts, protective effects against radiation injuries in rat spleen, 19: 43860(R) (NP-15310, pp 14-25)
fatty acid metabolism in, enzyme reactions for, 18: 35298
fatty acid metabolism in, 19: 21819(R) (UCLA-12-541(p.15-24))
formate metabolism in *Saccharomyces cerevisiae*, tracer study, 19: 35933
free nucleotide concentration in acid extracts, 16: 12869
function of cytoplasmic granules during sporulation of, 20: 42702(R) (ANL-7136, pp 243-55)
galactose transport system in *Saccharomyces chevalieri*, tracer study, 19: 35936
genetic analysis of *Saccharomyces cerevisiae*, 20: 18194
genetic analysis of Saccharomyces, 20: 18195
genetic transfer in, 20: 45355(R) (COO-1249-4)
growth and metabolism of, effects of rare earths and yttrium on, 20: 16191
growth cycle of *Schizosaccharomyces pombe*, 19: 45820(R) (TID-22227)
growth in heavy water, rate of, 18: 38763
growth in irradiated sole, effects of sodium benzoate on, 19: 22831
growth in water-d_2, nutritional requirements, 16: 7398
invertase production in, mechanisms, 20: 5251(R) (UR-668, pp 123-49)
malic acid metabolism in *Saccharomyces cerevisiae*, radio-gas chromatography apparatus for study of, 20: 45580
metabolism and reproduction in, effects of radiomimetic compounds on, 20: 16240
metabolism in, effects of deuterium oxide and radiation on, 17: 35319(R) (HW-76000(p.187-97))
metabolism in *Saccharomyces carlsbergensis*, 19: 17526
metabolism in, effects of fatty acid from irradiated rabbit liver, 19: 17526
metabolism in, effects of cystamine on, 20: 18372
metabolism in, tracer studies, 19: 29849(R) (ANL-6971(p.1-28))
metabolism of amino acids by, tracer studies of, 17: 7760
metabolism of irradiated, role of trichloroacetic acid, 16: 4095
metabolism of thymidine during cell division, tracer study, 16: 25136(R) (HW-72500(p.109-12))
Mössbauer resonance spectra of ironized, 19: 24585
mutants of, cytochrome c-deficient, 18: 8051
mutation rates in, 18: 27005(R) (ORNL-3601(p.60-8))
mutations, extrachromosomal induced by ultraviolet radiation, 16: 16222
mutations for the isoleucine locus in, suppressor, 17: 31821
mutations in growing, effects of 5-aminoacridine on, 20: 16159(R) (ORNL-3900, pp 150-81)
mutations in Saccharomyces, super-suppressors as addition-deletion, 20: 40582(R) (ORNL-3922, pp 65-8)
mutations in Schizaraccharomyces, chemical-induced, 19: 26035
mutations in, effects of subcritical temperatures on, 17: 37088
mutations induced in *Schizosaccharomyces pombe* by *N*-nitroso-*N*-methyl-*N'*-nitroguanidine, *N*-nitroso-*N*-methyl-urethan, nitrous acid, and uv light, 19: 42266
mutations of Saccharomyces, reversion in, during growth, 20: 6696(R) (ORNL-3853, pp 66-77)
mutations of *Schizosaccharomyces pombe*, genetic analysis of chemically induced, 20: 1654
mutations of, chemically induced, 19: 2002(R) (ORNL-3700(p.63-8))
phosphate metabolism in *Saccharomyces cerevisiae*, effects of 2,4-dinitrophenol and antimycin A on, tracer study, 19: 35934
phosphate metabolism by, tracer studies of, 20: 31108
phosphate release and reproduction of irradiated, effects of radioprotective compounds on, 20: 18503 (AD-611869, pp 169-83)
phosphorus-32 transmutation in, biological effects of, 17: 15793
phosphorus-32 transmutation efficiency in Saccharomyces, 18: 15870
photo-reactivation of ultraviolet radiation damage in DNA, kinetics of, 17: 1299
photo-reactivation of ultraviolet damage in DNA, formation of enzyme-

substrate complex in, 17: 1300
photoreactivating enzymes of, preparation, 19: 31788(R) (ORNL-3768 (p.33-57))
physiology of Saccharomyces and Candida, 19: 29849(R) (ANL-6971 (p.1-28))
potassium retention and survival, effects of high oxygen pressure on, 16: 8546 (TID-14866)
preparation of photoactivating enzyme from, 20: 6775(R) (ORNL-3853, pp 36-49)
protective effects of polysaccharide prepared from, against x-radiation injuries of mice, 20: 10703
radiation affects on, genetic, uv, 20: 8663
radiation damage in cells of, effects of membranes on, 20: 5251(R) (UR-668, pp 123-49)
radiation damage, protective effects of sulfhydryl compounds, 16: 1635
radiation effects on glucose metabolism, 16: 2899
radiation effects on protein synthesis, 16: 7422 (ORO-503)
radiation effects, gamma, heavy ion, and x, 16: 16189
radiation effects on enzyme synthesis of S-adenosylmethionine in, 16: 17738
radiation effects on genetics of saccharomyces, 16: 28745(R) (TID-16401)
radiation effects on phosphate efflux from cells, 16: 30217(R) (TID-16507)
radiation effects on biochemical mutations in *Torulopsis utilis*, 16: 30256
radiation effects from ion beams, 16: 30281
radiation effects on, protection by treatment with vinylpyrrolidone, 16: 32807
radiation effects, relative gamma- and 200-kv x-, 16: 14488
radiation effects on growth and protein synthesis, 17: 2833 (TID-17225)
radiation effects on, protective effects of tetrahydroxyquinone against, 17: 2841
radiation effects on nitrogen metabolism, 17: 5881
radiation effects on, protective effect of tetrahydrooxyquinone and neighboring compounds against, 17: 5919
radiation effects on glycogen and reducing compounds in, 17: 12162
radiation effects on diploid, recovery from, 17: 15740
radiation effects on diploid and haploid, effects of post-irradiation nutrient and temperature on, 17: 15739
radiation effects on, lethal curves for beta and ultraviolet, 17: 15793
radiation effects on permeability, 17: 21466 (HW-SA-2280)
radiation effects on death and degeneration of cells in, 17: 21541
radiation effects of ultraviolet light on mutation rates of *Saccharomyces*, 17: 23204
radiation effects of space flight on diploid and haploid cells of, 17: 24942
radiation effects on diploid and haploid, effects of oleic acid on cosmic, 17: 27199
radiation effects on, model of viability recovery in, 17: 30360
radiation effects on uptake of oxygen by, Cartesian diver respirator for measurement of, 17: 33647
radiation effects on trace element content in nucleic acids in, 17: 35540
radiation effects on, protective effects of phosphorus-32 against, 17: 37072
radiation effects on restoration of viability in, alpha, 17: 37098
radiation effects on reactions between cysteine and peroxides in, gamma, 17: 37094
radiation effects on gemmation in, ultraviolet and x-ray, 17: 40593
radiation effects on diploid and haploid, synergistic action of nitrogen mustard in uv and x, 18: 1416
radiation effects on loss of inorganic phosphates from, ultraviolet, 18: 3551
radiation effects on genetics of, x, 18: 5054
radiation effects on growth of, 18: 8126(T) (UCRL-Trans-1025)
radiation effects on, effects of plating time on recovery from, 18: 8183
radiation effects on *Saccharomyces carlsbergensis* 4228, protective effects of pyridoxine in x, 18: 9916
radiation effects on *Sacch. cerevisiae* under aerobic and anaerobic conditions, recovery from, 18: 11721
radiation effects on mutation reversals as function of ploidy, 18: 13483
radiation effects on catalase activity in, uv, 18: 13525
radiation effects on vitamin-K_1-treated, 18: 13547
radiation effects on reactivation in, x, 18: 15819(T) (UCRL-Trans-1029)
radiation effects on germinating spores in Schizosaccharomyces, x, 18: 17510
radiation effects on germinating spores in Schizosaccharomyces, x, 18: 17511
radiation effects on growth of, ultraviolet, 18: 17579
radiation effects on survival of, effects of dose on ultraviolet, 18: 17580
radiation effects on nucleic acids in, 18: 17867 (SGAE-BL-1/1964)
radiation effects on diploid and polyploid cells of, 18: 19678
radiation effects on enzyme activity in Rhodotorula, protective effects of cystamine against, beta, 18: 19786
radiation effects on, protective effects of antibiotics against, 18: 23380
radiation effects on budding of, 18: 27154
radiation effects on mutants of Saccharomyces, x, 18: 29294
radiation effects on nucleotides and amino acid content in, ultraviolet, 18: 29310
radiation effects on, lysis effects on recovery from, 18: 31220
radiation effects on desoxyribonucleic acid in, 18: 31564 (EUR-1646.f)
radiation effects on role of oleic acid oxidation products in, 18: 33390
radiation effects on, protective effects of RNA against x, 18: 33410
radiation effects in *Saccharomyces cerevisiae*, ultraviolet, 18: 35347
radiation effects from heavy ion beams in, effects of environment on, 18: 36954(R) (UCRL-11387(p.25-34))
radiation effects of heavy ion beams in *Saccharomyces cerevisiae*, 18: 36955(R) (UCRL-11387(p.35-53))
radiation effects on Saccharomyces and Rhodoturula, 18: 38869
radiation effects on, protective effects of catalase activity against x, 18: 38989
radiation effects on leakage of cellular constituents from, 18: 41085(R) (HW-80500(p.150-2))
radiation effects on, after pretreatment with actinomycin, 18: 41150
radiation effects on survival of, fast-neutron and x, 18: 41231
radiation effects on metabolism in, 18: 43279
radiation effects, 19: 11624
radiation effects combined with starvation on carbon dioxide production in cells of, 19: 25968
radiation effects in diploid *Saccharomyces cerevisiae*, genetic, 19: 21920
radiation effects on, lethal, 19: 76(R) (UCRL-11387(Suppl.)(p.19-51))
radiation effects on gene multiplicity in, uv, 19: 2116
radiation effects on, factors affecting recovery from, 19: 5669
radiation effects on, mechanism of recovery from, 19: 5669
radiation effects on, dark recovery from uv, 19: 5698
radiation effects on, external and internal alpha and gamma, 19: 7127
radiation effects on *Saccharomyces cerevisiae*, gamma and x-ray, 19: 7171
radiation effects on reproduction of, 19: 7174
radiation effects on survival of, effects of ploidy and temperature on gamma, 19: 8884
radiation effects on growth and metabolism of, 19: 11616 (SGAE-BL-9/1964)
radiation effects on metabolism in, 19: 12958 (SGAE-BL-12/1964)
radiation effects on colony-forming ability in, effects of heat treatments on gamma, 19: 13108
radiation effects on mutation reversion in, uv, 19: 15127
radiation effects on lifespans of, uv, 19: 15169
radiation effects on survival of, temperature effects on uv, 19: 19626
radiation effects on, ultraviolet, 19: 21921
radiation effects on respiration in, 19: 21881
radiation effects on reproduction of, 19: 24357
radiation effects on, kinetics of recovery from sublethal, 19: 26002
radiation effects on cellular ultrastructure in, electron, 19: 26065
radiation effects on, recovery mechanisms for, 19: 29904 (UCRL-16030)
radiation effects on technological characteristics of working, gamma, 19: 33814
radiation effects on synthesis of DNA-like RNA in cells of, 19: 33830
radiation effects on haploid, RBE of 30 Mev electron, 19: 35978
radiation effects on survival of, effects of incubation on, 19: 38422
radiation effects on incorporation of carbon-14-labeled adenine, orotic acid, and uracil in RNA in diploid, 19: 40367
radiation effects on glycolysis rate in, uv, 19: 43765
radiation effects on *Schizosaccharomyces pombe*, morphological, 19: 45820(R) (TID-22227)
radiation effects on growth of, regeneration ability in, 20: 79
radiation effects on carbon dioxide production in starved, effects of glucose on, 20: 1653
radiation effects on, biological, 20: 1663
radiation effects on wine, effects of dose on, 20: 2197
radiation effects on Saccharomyces, x, 20: 3717(T) (JPRS-31514, pp 77-91)
radiation effects on Saccharomyces, uv, 20: 3717(T) (JPRS-31514, pp 77-91)
radiation effects on survival in, heavy-ion, 20: 6859
radiation effects on, effects of storage in dark on recovery from, 20: 8724 (UCRL-16545)
radiation effects on, effects of oxygen on recovery from, 20: 14399
radiation effects on, protective effects of dark recovery and glycerol against α and x, 20: 16231 (UCRL-16377)
radiation effects on metabolism and reproduction of, x, 20: 16240
radiation effects on mitosis in, uv and x, 20: 16255
radiation effects on, mechanisms of lethal, 20: 18405
radiation effects on, charged particle-beam, 20: 18190(R) (UCRL-16613)
radiation effects on transfer RNA in, uv, 20: 18249
radiation effects on phosphate release by *Saccharomyces cerevisiae*, 20: 18503 (AD-611869, pp 169-83)

radiation effects on *S. cerevisiae*, uv and x, 20: 26661(T) (ORNL-tr-1234)
radiation effects on, lethal γ, 20: 26697
radiation effects on reproduction of, x, 20: 26698
radiation effects on reproduction of, uv, 20: 26699
radiation effects on reproduction of, 20: 28950
radiation effects on *Saccharomyces cerevisiae*, effects of depth in irradiated medium on electron-beam, 20: 28963
radiation effects on, analysis of dose survival dependence of gamma, 20: 33001
radiation effects on chromosomes in, kinetics of gamma, 20: 33002
radiation effects on, initial sites of action of uv and x, 20: 33062
radiation effects on *Saccharomyces cerevisiae*, protective effects of cystamine against x, 20: 33088
radiation effects on, protective effects of glycerol against, 20: 33093
radiation effects on *Saccharomyces vini*, kinetics of cell restoration in alpha and gamma, 20: 35261
radiation effects on lethality in, genetic control in, 20: 35264
radiation effects on, kinetics of viability recovery from gamma, 20: 35275
radiation effects on fermentation and respiration in, effects of glucose on, 20: 35312
radiation effects on *Saccharomyces vini*, protective effects of propyl gallate and vinylpyrrolidone against gamma, 20: 35336
radiation effects on, in fruit juices, 20: 37156
radiation effects on, kinetic regularities in regeneration of, 20: 36642
radiation effects on cytochrome systems in, x, 20: 38680
radiation effects on alcohol dehydrogenase of, alpha and gamma, 20: 42816
radiation effects on, causing spoilage of fruit juices, 20: 43787
radiation effects on assays of, on fish fillets following refrigerated storage, gamma, 20: 43793
radiation effects on, biological, x, 20: 46121
radiation effects on sterols in Saccharomyces, x, 20: 45415
radiation effects on cells of, 18: 8179
radiation effects on *Saccharomyces cerevisiae* strains of, 18: 33393
radiation effects, ultraviolet, 19: 21919
radiation injuries to, protective effects of antibiotics against, 17: 28731
radiation injuries to cells of, protective effects of acrylamide and propionamide against, 18: 3586
radiation injuries of, protective effects of *p*-chloromercuribenzoate against, 18: 25224
radiation injuries and recovery of, 18: 38947
radiation injuries of, effects of cytoplasmic structures on recovery from, 18: 38950
radiation injuries in, effects of propyl gallate and vinyl pyrrolidine on, 19: 221(T) (JPRS-26757(p.11-14))
radiation injuries in, effects of ploidy on recovery from x, 20: 28961
radiation injury restoration in, 19: 17496(T) (JPRS-28405(p.1-32))
radiation injury to, effects of dose on regeneration mechanism from, 17: 33669
radiation resistance, 16: 24043
radioinduced adenine-1 mutants of, mutagen specificity among reversions of uv, 20: 6830
radioinduced antibody production in, uv, 20: 10695
radioinduced fatility of, mechanism of, 18: 13546
radioinduced formation of giant cells in *Candida tropicalis*, 18: 29331
radioinduced free radicals in, 19: 221(T) (JPRS-26757(p.11-14))
radioinduced genetic effects in, ultraviolet, 18: 5048
radioinduced growth mutations in, effects of environment on, 17: 17842
radioinduced inactivation, effects of oxygen, anoxia, ultraviolet light, and dye, 17: 1315
radioinduced inactivation of *Saccharomyces*, effects of degree of ploidy and genotype on, 17: 40566
radioinduced inactivation of *Saccharomyces cerevisiae*, 18: 29339
radioinduced inactivation of transfer ribonucleic acid in *Torulopsis utilis*, ultraviolet, 19: 28019
radioinduced inactivation and mutability in Saccharomyces, uv and x, 20: 45469
radioinduced lethal allele mutations in Saccharomyces, rates of, 18: 5063
radioinduced mitotic reversion in *Saccharomyces cerevisiae*, allelic mapping of, 18: 11794
radioinduced mitotic recombination in heterozygous Saccharomyces, mechanism of uv and x, 20: 33053
radioinduced mutant, 17: 5809
radioinduced mutants in Schizosaccharomyces, uv, 19: 110
radioinduced mutants in, gene control of pigmentation in specific lysine requirement in, 19: 8729
radioinduced mutants in, complementation of, uv, 19: 8847
radioinduced mutation effects on cell division, effects of genetic background on direction and frequency, 16: 7435
radioinduced mutations in saccharomyces, 17: 19839
radioinduced mutations in *Saccharomyces pombe*, 17: 40569
radioinduced mutations of, effects of dose rate and mitotic state on, 18: 1438
radioinduced mutations during meiosis and mitosis in, rates of uv and x-ray, 18: 11832
radioinduced mutations, 18: 17479 (UCRL-11191)
radioinduced mutations in saccharomyces, effects of dose rate and ploidy on uv, 18: 27096
radioinduced mutations in Saccharomyces, effects on protein synthesis of, uv, 18: 29286
radioinduced mutations of Saccharomyces, ultraviolet, 18: 29294
radioinduced mutations for ethionine-resistant, uv, 18: 31071
radioinduced mutations in homozygote and isogenic Saccharomyces strains of, ploidy effects on, 18: 33394
radioinduced mutations of Saccharomyces, enzyme reactions in carbohydrate metabolism in, 18: 41138
radioinduced mutations in, gamma and neutrons, 19: 2091
radioinduced mutations in, 19: 10789(R) (TID-21591)
radioinduced mutation of glutamate auxotroph, 19: 19593
radioinduced mutations of *Saccharomyces cerevisiae*, 19: 25912 (UCRL-8268)
radioinduced mutations of, 19: 36002
radioinduced mutations of *Schizosaccharomyces pombe*, ultraviolet, 20: 1654
radioinduced mutations for radioresistance in, β, uv, and x, 20: 5360
radioinduced mutations in, heavy-ion, 20: 6859
radioinduced mutations of extrachromosomal factor in, uv, 20: 8628 (COO-1249-3)
radioinduced mutations of *Schizosaccharomyces pombe*, recombination among uv, 20: 14327
radioinduced mutations at melezitose locus in Saccharomyces, uv, 20: 12655
radioinduced mutations of *Saccharomyces cerevisiae*, genetic analysis of uv and x, 20: 45364 (UCRL-16851)
radioinduced mutations in *Schizosaccharomyces pombe*, 19: 26035
radioinduced mutations in, uv, 17: 37088
radioinduced premutational damage in, recovery from uv and x, 20: 22654
radioinduced prototrophic mutations in, effects of ploidy on gamma and uv, 19: 3963
radioinduced recessive lethal mutations in saccharomyces, uv and x, 18: 27095
radioinduced reciprocal recombination, gene conversion, and mutation to phototrophy in, photoreactivation of uv, 20: 22783
radiomimetic action of oxidized oleic acid on, effects of oxygen, 16: 25200
radiophotosynthesis in, isolation of labeled free and 2′,3′-ribonucleotide in, 17: 7758
radioprotective activity of imidazole derivatives in, 20: 42979
radioprotective effects of lysates, on mice, 20: 42992
radioresistance of *Saccharomyces cerevisiae* during mitosis, 17: 33653
radiosensitivity, 18: 23311
radiosensitivity as function of germination process and state of exhaustion, 16: 32809
radiosensitivity and production of petite strains, 18: 35358
radiosensitivity, effects of different carbohydrates and osmotic ratios, 16: 6354
radiosensitivity, effects of strain, 16: 16223
radiosensitivity, effect of mutated alleles, 16: 20226
radiosensitivity, effects of oxygen, 16: 30285
radiosensitivity effects of, 17: 38910
radiosensitivity effects of phenoxazine on, 18: 23378
radiosensitivity effects of extracts of, on rats, 20: 20503(R) (AD-629311, pp 1-14)
radiosensitivity effects on streptomycin-sensitive strains of *Proteus mirabilis*, uv, 20: 22758
radiosensitivity of phosphorus-32-labeled, 16: 4043
radiosensitivity of oxidation-reduction reactions, 16: 6299(T) (JPRS-11322(p.142-61))
radiosensitivity of cells, review, 16: 7410 (BNL-675(p.62-75))
radiosensitivity of haploid, effects of anoxia and glycerol on, 16: 21916 (UCRL-10181)
radiosensitivity of, effects of acrylamide, acrylonitrile, and vinyl pyrrolidone on, 17: 2864
radiosensitivity of aα strain of *Saccharomyces*, 17: 17907
radiosensitivity of, isolated from codfish, effects of age and temperature on, 17: 24909
radiosensitivity of diploid and haploid, effects of cysteine and potassium iodide on, 17: 30220
radiosensitivity of, effects of chemical compounds on, 17: 30423
radiosensitivity of soluble ribonucleic acid molecular weight in, 18: 35361
radiosensitivity of ribonucleic acid of, ultraviolet, 18: 41101
radiosensitivity of, 19: 29990
radiosensitivity of, effects of reactivation ability on uv, 19: 17623
radiosensitivity of *Saccharomyces cerevisiae*, effects of catalase forma-

tion on, 19: 24327
radiosensitivity of *Saccharomyces cerevisiae*, effects of metabolic factors on, 19: 27960
radiosensitivity of mitosis in, 20: 1664
radiosensitivity of meiosis in, 20: 1664
radiosensitivity of, effects of uv and x radiations on thermal, 20: 1640
radiosensitivity of, effects of amino acids in culture on, 20: 10695
radiosensitivity of, effects of cystamine on β, 20: 18372
radiosensitivity of, genetic control of, 20: 22699
radiosensitivity of mitotic recombination in, 20: 22616(R) (NIRS-4, pp 58-69)
radiosensitivity of *Saccharomyces cerevisiae*, effects of cystamine on, 20: 29023
radiosensitivity of, genetic control of, 20: 31041
radiosensitivity of, uv and x, 20: 33062
radiosensitivity of, effects of chemicals on, 20: 37144
radiosensitivity of food-spoilage, effects of chemical radiosensitizers on γ, 20: 43784
radiosensitivity of, 20: 43787
radiosensitivity of intact, uv and x, 20: 45355(R) (COO-1249-4)
radiosensitivity of, effects of light on x, 20: 45363(R) (TID-23347)
radiosensitization by iodoacetamide, 20: 42901
radiosterilization effects on, in pork, 18: 22391
radiosterilization in Dover sole, 20: 9346 (TID-22289)
reactions of, with manganese, mercury, and uranyl ions in membrane ligands of, 17: 13931
reactivation of irradiated, significance of fat reserves in, 16: 14495
ribonucleic acid labeling with carbon-14 and phosphorus-32 in, by biosynthesis, 18: 43570
ribosomes, effects of nutrition, 16: 20103
selenium-75 metabolism in *Saccharomyces cerevisiae*, 20: 3661 (NP-15594)
sorbose transport in, use of uranyl ion in studies on, 18: 9823
survial of frozen and thawed, 20: 6756(R) (ORNL-3853, pp 111-15)
survival of centrifugally frozen, effects of warming rate on, 19: 45730(R) (ORNL-3752)
survival of, effects of time-temperature variations on, 19: 31794(R) (ORNL-3768(p.131-6))
synthesis of carbon-14-labeled compounds by, 18: 38746
tissue cultures of, for use in Gulliver program, 19: 33739 (N64-22793)
toxic effects of *Candida albicans* in irradiated mice, 17: 23116
toxic effects of intermediate oxidation products of oleic acid, similarity to gamma ray effects, 16: 20063
tritium content of nucleobases of, radiometric determination of, 18: 1511
tryptophan synthetase activity in, 19: 31674(R) (ORNL-3768(p.64-9))
tryptophan synthetase assay in, using carbon-14 tracer techniques, 20: 40582(R) (ORNL-3922, pp 65-8)
uptake by 3,4-benzopyrene, 19: 31678(R) (ORNL-3768(p.137-45))
uptake of alkali metal cations and hydrogen by, effects of acidity on, 19: 8762
uptake of arsenate and phosphate by fermenting, 17: 13931
uptake of glucose, phosphate, and potassium, effects of deuterium on, 19: 3878
use of compacted, to simulate human tissue, 19: 15015(R) (N64-29573)
vitamin D_2 content in irradiated, chromatographic determination, 20: 3690
3,4-benzopyrene metabolism in, 19: 31678(R) (ORNL-3768(p.137-45))

Yolks
see Egg Yolks

YTTERBIUM
abundance in meteorites and terrestrial matter, 18: 10753
abundance in meteoritic, terrestrial, and solar matter, review on, 19: 13620
abundance in solar atmosphere, 16: 29599 (AFOSR-3024)
alloying characteristics with transition metals, 18: 41924(R) (IITRI-578P19-13)
alloying effects on oxidation of chromium at 2300°F, 16: 18079(P)
alpha reactions (α,xnγ) at 27 to 52 Mev, gamma spectra from, (E), 20: 6348
analysis for calcium and sodium, atomic absorption spectrophotometric, 17: 40727
analysis for lutetium using DEHPA, activation, 19: 32084
analysis for oxygen by neutron activation, 20: 3863(R) (IS-1200(Sect. C))
analysis of neutron-irradiated, for gadolinium and samarium by gamma spectral methods, 16: 132(T) (AEC-tr-4686)
analysis of target foils of, methods for, 20: 8855
analysis of, for trace amounts of lutetium by activation methods, 20: 29082 (SGAE-CH-27/1966)
atomic scattering factors for, 16: 12125
Auger electron spectra and energy level widths, (E), 19: 25495
binding by sodium amalgam, 16: 14756
cohesive energy and ionization of, relation between, (T), 19: 47062
compressibility at room temperature, 18: 20553
content and relative abundances in terrestrial materials, 18: 20202
content in Gulf of Mexico surface water, 20: 43087(R) (TID-23295, Sect.4)
content in sea water and sediments, 17: 30719
content in standard diabase W-1 and standard granite G-1, 19: 26529
content of, in marine organisms, 17: 15604
crystal structure and phase studies, 17: 35263(R) (UCRL-10706 (p.1-110))
crystal structure of, pressure-induced polymorphic transitions in, 18: 14613
deposition on platinum anode, electrolytic, 17: 18204
determination by complexometric titrations using acetic acid compounds, 18: 43417
determination by complexometric photometric titration, 19: 15375
determination by potentiometric titration using arsenazo III, 19: 7299
determination by radioactivation on chromatographic paper, 18: 39120
determination by spectrochemical methods, voltage-fluctuation patterns in, 19: 40416
determination by spectrometry using 4,5-dihydroxy-3-[(*p*-sulfophenyl)azo]-2,7-naphthalenedisulfonic acid, 20: 12806
determination by thermal-neutron activation methods, sensitivity for, 19: 9071
determination in aluminum as trace impurity, activation, 17: 10546
determination in aqueous solutions and thulium oxide powders, activation, 18: 8314
determination in americium by emission spectrography, 20: 8835 (RFP-414)
determination in cerium and erbium, mass spectrographic, 19: 2232
determination in carbonatites by ion exchange chromatography and oxalate precipitation, 20: 16346
determination in diabase and granite by spark source mass spectrography, 19: 11406
determination in europium oxide, spectrographic, 17: 2931
determination in EDTA complexes, spectrophotometric, 17: 6010
determination in hydrochloric acid or methanol–nitric acid media, spectrophotometric, 20: 3888 (TID-22402)
determination in hydrochloric acid solutions, spectrographic carrier-distillation, 20: 36729
determination in holmium oxides by neutron activation, 20: 40796(R) (IS-1500(Sect.C))
determination in iron–yttrium garnet powders, spectrographic, 17: 34431
determination in lithium chloride and lithium iodide, polarographic, 20: 249
determination in mixture with europium, lanthanum, and yttrium flame photometric, 16: 28876(T) (AEC-tr-5291)
determination in minerals and rocks, spectrographic, 17: 6008
determination in minerals by neutron activation, 19: 30424
determination in monazite sand by cathode-ray polarography, 20: 22913
determination in minerals and rocks, activation, 20: 22950
determination in minerals and ores, spectrometric, 20: 29134
determination in niobium by radioactivation analysis, 16: 23633 (TID-7629(p.239-44))
determination in oxalate precipitates, complexometric titration methods for, 18: 1584
determination in presence of other rare earths, spectrophotometric, 17: 32002
determination in potassium chloride medium, polarographic, 20: 1795
determination in rare earth oxides, 17: 6019
determination in rare earth mixtures, polarographic, 20: 26792
determination in rocks, chemical spectrographic method for, 20: 29083(R) (UCRL-14767)
determination in rare earths using acetonitrile, controlled-potential coulometric, 20: 38812
determination in standard igneous rocks G-1, W-1, and G-B by x-ray fluorescence, 20: 29101
determination in silicon carbide by neutron activation, 20: 33167(T) (AEC-tr-6639, pp 42-5)
determination in solutions, spark method for spectrographic, 20: 38832
determination in thorium using xylenol orange, spectrophotometric, 18: 19883
determination in thorium and uranium, spectrographic, 20: 26746 (ISO-SA-13)
determination in TBP extracts, spectrophotometric, 20: 29125
determination in thorium dioxide by isotope dilution methods, 20: 33203
determination in uranium compounds, spectrographic, 20: 29129
determination of, in residues by iron flux method, spectrographic, 17: 19942 (PG-Report-157)
determination of, in rice plant and soil by activation and focusing chromatography, 17: 30219
determination of, review on x-ray spectrographic, 17: 23252 (IS-550)
determination of traces of, by electrochemical stripping, 19: 7331
determination of trace amounts of, by reactor neutron activation methods, 20: 26760
determination of, in rare-earth mixtures, photometric, 20: 252

determination of, use of organic acids for, 20: 14490
determination of, using Pyrocatechol Violet, Arsenazo I, or Methylthymol Blue, spectrophotometric, 20: 45581
determination using arsenazo III, absorptiometric, 16: 14653
determination using Xylenol Orange, spectrophotometric, 18: 25285
determination using 4-(2-pyridylazo)resorcinol, 18: 35461
determination using 2-(*p*-sulfophenylazo)-1,8-dihydroxynaphthalene-3,6-disulfonic acid, spectrophotometric, 18: 41341
determination using xylenol orange, spectrophotometric, 18: 43394
determination using thenoyltrifluoroacetone, photometric, 20: 8859
determination using Chromotrope 2B, photometric, 20: 1772
determination using *N*-methylanabasine-α′-azo-β-naphthol, photometric, 20: 26801
determination using neutron activation analysis, 20: 33231
deuteron elastic scattering at 15 Mev, strong absorption model analysis of, 18: 42708
diffusion in germanium, (E), 19: 11755(T)
diffusion of nitrogen and oxygen in, internal friction in interstitial, 18: 26050
effects of subcutaneous implantations of, in mice, 19: 38334 (COO-1170-1)
effects on grain growth and recrystallization of tantalum, 20: 4424
effects on x-ray fluorescent spectrometric determination of yttrium, 20: 18611
electric and galvanomagnetic properties of, effects of temperature on, 20: 7620
electric conductivity of, effects of pressure on, at various temperatures, 17: 18832
electric conductivity of, effects of pressure on, 17: 25817
electric conductivity of, effects of pressure on, 17: 35263(R) (UCRL-10706(p.1-110))
electric conductivity of, pressure effects on, 18: 18358 (UCRL-11220)
electric conductivity and Hall coefficient, effects of magnetic ordering and temperature on, 18: 27993
electric conductivity of, effects of pressure on, 18: 42069
electric resistance at 25 to 250 mg/cm², 16: 2213(T) (JPRS-10499)
electrochemical characteristics of, in phosphoric acid, 17: 25165 (TID-18697)
electron band structure of, from absolute reflectance measurements, (E), 19: 35594
electron band structure of, x-ray isochromats for, (E), 20: 28681
electron bound state model of, 17: 3607
electron energy levels in, self-consistent wave functions for, 17: 11394
electron interactions in, s-f, 18: 1667
electron structure of, 17: 31075 (CONF-20-4)
electron structure of, measurement from positron annihilation, 18: 20552
energy level widths for, K, (T), 20: 15239 (CONF-233(Vol.3), pp 419-39)
energy levels of, ionization energies from, (T), 20: 37439
energy levels of, lifetimes of $6s6p\,^1P_1$ and $6s6p\,^3P_1$, 20: 39597
enthalpy and related thermodynamic properties at 0 to 1100°C, 17: 4929 (IS-327)
fluorescence of, preparation of targets for studies of L-shell, 17: 36664 (UCRL-6989)
gamma spectra from neutron capture by, 16: 8162(R) (ARF-1193-6)
heat of solution in liquid tin at 726°K, 18: 30164(R) (AD-429007)
heat of solution in liquid tin at 770°K, 20: 11304
heat of sublimation and surface energy of, calculation of, 18: 626
helium-3 elastic scattering at 20 Mev, differential cross sections for, 18: 21359
helium-3 elastic scattering at 20 Mev, differential cross sections, 18: 26681
ion exchange and solubility in potassium carbonate solutions, 18: 31453
ion exchange behavior in hydrochloric acid–organic solvent media, 18: 39124
ion exchange in concentrated hydrochloric and perchloric acids, distribution coefficients for, 18: 17759
ionization at single-crystal tungsten surfaces, 19: 20871
ionization on tungsten surface, (E/T), 19: 8097
ionization potentials of, electron-impact method for measuring, 20: 43235
Knight shift of, determination of, 18: 7774
liquid, solubility of tantalum and tungsten in, at high temperatures, 20: 41412(R) (IS-1500(Sect. M))
magnetic moment stability of, model for high-pressure, (T), 20: 10265
magnetic properties, 19: 38054
magnetic properties at 2 to 300°K, 20: 43939
magnetostrictive strain in, 19: 38051
melting at high pressures, phase transitions in, 18: 34184
metallurgical properties, 18: 18307
neutron absorption properties of, burnup effects on, (E), 19: 40163
neutron absorption resonance integrals, 20: 14059(R) (IDO-17104)
neutron absorption cross section in pitchblende, thermal, 20: 37994
neutron capture by, gamma spectra from thermal, 17: 19329
neutron capture cross sections, 16: 26509
neutron capture gamma spectra, 16: 19745(R) (ARF-1193-9)
neutron capture, gamma spectra following, 16: 29750 (ANL-6589)
neutron cross sections at 0.015 to 0.3 ev, 17: 7078 (IEA-51)
neutron elastic scattering at 0.3 to 1.5 Mev, differential cross sections for (E), 19: 3381
neutron elastic scattering at 0.3 to 2.2 Mev, angular distributions from, (E), 19: 19095 (WASH-1053)
neutron inelastic scattering by, fast, (E/T), 20: 19805(R) (ANL-7110, pp 1-28)
neutron radiative capture cross sections, 16: 14059
neutron radiative capture cross sections, 17: 4037
neutron radiative capture cross sections at 30 and 65 kev, 18: 34274(R) (NIRS-2(p.3-15))
neutron reactions with, effects of burn-up on thermal absorption cross sections for, 17: 15214 (GEAP-4017)
neutron reactions at 0.0005 to 1 ev, total cross sections for, 19: 39779 (IEA-86)
neutron reactions (n,α) with, cross sections for thermal, (E), 19: 41809(T)
neutron resonance absorption integrals for, reactivity measurements for, 19: 29338
neutron resonance absorption integrals, (E), 19: 47576(R) (IDO-17081, (pp 49-76))
neutron resonances in, spectra of, 19: 41661 (JINR-P-2158)
neutron scattering by, cross sections for, 17: 41873 (WASH-1044)
neutron total cross sections at 0.015 to 0.3 ev, (E), 19: 16841 (IEA-75)
nuclear magnetic moments, spin-orbit coupling, and hyperfine fields, 16: 16831
oxidation at high temperatures, 17: 14773(R) (TID-18063)
oxidation in dry and moist air at 100 to 800°C, rate of, 20: 21265 (RPI-2714-8)
oxidation kinetics of, effects of moisture and temperature on, 20: 35854
oxidation of, kinetics of high-temperature, 20: 5859
paramagnetic resonance spectra of tetravalent, in calcium fluoride crystal, 16: 2331
partition coefficients and reciprocal ionic radii, 17: 27562 (INSJ-54)
performance of cathodes of, in diode ion pumps, 20: 10976 (IS-T-46)
phase transformations at 6 to 65 kbar, solid-liquid and solid-solid, 19: 40095
phase transition at 41 kilobars, 17: 16662 (UCRL-10332)
phase transitions induced by high pressure in, 17: 25791
phase transitions in, to 46 kbars, 19: 34713
phase transitions in, 17: 39553
photonuclear reactions, production of short-lived isomers, 16: 12530
polarographic behavior in tetraethylammonium bromide at dropping mercury electrode, 18: 23463
polarographic behavior in dimethylformamide and dimethylsulfoxide, 19: 40681
polarography in acetonitrile, 18: 41354
polarography in anhydrous ethylenediamine, 18: 1517
polarography of, in acetone solution, 17: 14253
precipitation by benzenephosphinic and benzenephosphonic acids, 18: 27308
preparation and purification, 19: 40948 (IS-1195)
preparation of isotopic foils from oxides of, 19: 36307
preparation of isotopic bulk materials and foils of, from oxide, 20: 13216 (ORNL-P-1899)
preparation of thin films of, by electrodeposition, 20: 7538 (ORINS-48)
properties, physical and thermodynamic, 19: 40948 (IS-1195)
proton elastic scattering at 55 Mev, effects of nuclear deformation on, 18: 24665
proton elastic scattering at 55 Mev, 19: 29312
proton reactions at 0.1 to 0.5 Mev, characteristic x-ray yields from, 16: 33633
proton reactions at 30 to 100 kev, x-ray production in, 18: 40575
proton reactions at 660 Mev, cross section of fragment production in, (E), 20: 28470
purification techniques, 19: 30338
radioinduced production of helium and hydrogen in, neutron, 19: 26901
reactions with cerimolybdic acid and its salt in chloride and nitrate solutions, precipitations in, 19: 2287
reactions with dichalcogenides and powdered graphite, preparation of intercalation compounds by, 20: 20648 (AD-621029)
reactions with rare earth sulfides, formation of ytterbium(II) rare earth sulfides by, 19: 2297
reduction and deposition potentials, 19: 7362(T) (UCRL-Trans-1153(L))
reduction in acetonitrile solutions, color production in controlled-potential coulometric, 20: 38813
relaxation processes in, resonance coupling in, 18: 22056
semiconducting properties, 17: 25817
semiconductive transitions in, 17: 39353
separation by anion exchange in acetic acid–nitric acid medium,

18: 16131
separation by anion exchange in EDTA, effects of temperature on, 18: 20110
separation by anion exchange in acid-organic solvent media, 18: 23707(R) (TID-20609)
separation by electrophoresis on zirconium phosphate paper, 17: 4467
separation by partition chromatography using di-(2-ethylhexyl)-orthophosphoric acid as column material, 18: 3889
separation by reversed-phase partition chromatography using organophosphorus compounds, 18: 25614
separation by solvent extraction using amines, 17: 14375 (BM-RI-6205)
separation from actinides and other lanthanides by solvent extraction, 18: 39382
separation from aqueous chloride solutions by solvent extraction using di-n-octyl phosphinic acid, tracer studies of, 19: 46443
separation from europium by ion exchange, 16: 17696
separation from europium and samarium using organic acids, 20: 14490
separation from gadolinium and samarium by zone crystallization in nitrate medium and by precipitation using ammonium oxalate, 18: 16137
separation from lithium chloride solutions by ion exchange, 19: 32318
separation from lutetium and thorium by ion exchange, 16: 8818
separation from lutetium and thulium by cation exchange, 17: 20104
separation from lutetium by ion exchange at 90°C, 20: 10760 (IS-1305)
separation from methanol-nitric acid systems using anion exchange resins, 16: 25280 (TID-15598)
separation from metal ions by ion exchange in isopropyl alcohol, 18: 20104
separation from nitric acid solutions by solvent extraction using TBP, 17: 14393
separation from nitric or sulfuric acid solutions, ion exchange selectivity scales for, 19: 9257
separation from other rare earths, 18: 5434(P)
separation from other rare earths by paper chromatography, 19: 15675
separation from other rare earths by thin-layer chromatography, 20: 7202
separation from other elements by solvent extraction using TBP, 20: 10952
separation from other inorganic ions by paper chromatography, 20: 12939
separation from other rare earths by paper chromatography, 20: 27049
separation from perchloric acid solutions by ion exchange materials, 20: 20823
separation from rare earth mixtures by chromatography using di-(2-ethylhexyl) phosphoric acid on Kel-F, 17: 34060
separation from rare earths, thorium, and uranium by reverse-phase paper chromatography, 19: 7302
separation from rare earths by cation exchange using ammonium α-hydroxyisobutyrate and lactate, 19: 24432
separation from rare earths by reversed phase partition chromatography using 2-ethylhexyl phenylphosphonate, 19: 24431
separation from rare earths, thorium, and uranium by reversed-phase chromatography using methylenebis(di-n-hexylphosphine oxide), 20: 18599
separation from scandium and thorium by solvent extraction using thiocyanate-tributyl phosphate, 18: 1807
separation from scandium by cation exchange chromatography, 18: 25613
separation from scandium sulfate by solvent extraction using sulfuric acid, 19: 30196
separation from scandium and thorium by reversed-phase chromatography, 19: 44125
separation from sulfuric acid by diisobutylphosphoric acid, 18: 1829
separation from thulium, chromatographic, 16: 31567
separation from thiocyanate solutions by solvent extraction using tributyl phosphate, 17: 12371
separation from thulium by solvent extraction using tertiary amines and diethylenetriaminopentaacetic acid or EDTA, 20: 38995 (BM-RI-6809)
separation from transplutonium elements by ion exchange using EDTA, 20: 35596
separation from uranium by anion exchange, 19: 2451
separation from uranium by combined ion exchange-solvent extraction using nitric acid–tetrahydrofuran solutions, 20: 20811
separation from yttrium group, 17: 6019
separation of, from rare earth concentrates by solvent extraction using amalgams, 17: 16157
separation of, from yttrium by solvent extraction using amines, selectivity in, 17: 23430 (BM-RI-6242)
separation of microgram amounts, high-efficiency electromagnetic, 16: 9118
separation using iminodiacetic acid chelating resin, binding ratios in, 17: 18202
solubility and ion-exchange properties in potassium carbonate solution, 19: 13536
solubility in bismuth, 17: 31798(R) (BNL-782(p.60-91))
solubility in cadmium(liquid), 16: 16464
solubility in liquid cadmium at 325 to 550°C, 16: 32059
solvent distribution in perchloric acid–TBP systems, 18: 25381
solvent properties for tantalum, 20: 13180(R) (IS-RD-4)
sorption by ion exchange resins from nitric acid–2-propanol–water solutions, 18: 25395
sorption from lithium nitrate solutions by ion exchange resin, effects of nitric acid on, 18: 35551
sorption from nitric acid by ion exchange paper, 19: 24435
specific heat at 0.4 to 4°K, 16: 32121 (TID-16704)
spectra, flame, 16: 30400
spectra in barium, calcium, and strontium fluorides, absorption and luminescence, 17: 4547(T)
spectra in borides and oxides, fine structure of L_{III} absorption, 18: 39195
spectra in calcium fluoride crystal, absorption, 17: 8915 (AFCRL-62-628)
spectra in lithium nitrate–potassium nitrate system at 0.35 to 2.6 microns, absorption, 16: 17598
spectra in thorium oxide at 100°K, nephelauxetic effects on reflection, 18: 25423
spectra in yttrium-aluminum and yttrium-gallium garnets, paramagnetic resonance, 16: 517 (AFCRL-775)
spectra of doubly and triply ionized, emission, 19: 32155
spectra of, emission and x-ray fluorescence, 18: 183
spectra of, isotope shift in λ 5556Å, 17: 10625
spectra of spin-lattice relaxation of, in cadmium fluorides, 17: 37230(T)
spectra of, analytical applications of flame, 18: 11982
spectra of, atomic absorption, 18: 31513
spectra of, determination of K_α x-ray, 18: 22693
spectra of, electron-transfer, 20: 23033
spectra of, ESR, 18: 28269
spectra of, in liquid ammonia, electronic, 20: 14526
spectra of, in solution, effects of intra-f^n electronic transitions on absorption, 19: 26314
spectra of, intensities, wavelengths, and Zeeman patterns for, 20: 27732
spectra of, isotopic shift of, 19: 30178(T)
spectra of, isotope shifts in, (E), 20: 24438(T)
spectra of, isotope shifts of resonance lines in, 20: 44133(T)
spectra of, use of fuel-rich premixed oxyacetylene flame for emission, 18: 25278
spectra, Zeeman effect of arc and spark type, 16: 24270 (AERE-R-4029)
spectral properties in rare earth oxide matrices, 18: 13869
spectrum in potassium chloride, sodium chloride, and potassium bromide crystals, 19: 11010
spectrum in ytterbium ferrite and yttrium aluminate, 18: 10619 (AFCRL-63-103)
stacking-fault energy, 18: 20550
thermal capacity at 0.4 to 4°K, 17: 16015
thermal capacity at 15 to 350°K, 18: 1489(R) (IS-700(Sect.C))
thermal capacity at 3 to 25°K, 20: 17080
thermal conductivity at 2 to 100°K, (E), 20: 11329
thermal expansion coefficient at low temperature, 17: 18829
thermal expansion at 1.3 to 300°K, coefficient of, 18: 1489(R) (IS-700(Sect.C))
thermal expansion at 1.5 to 12°K, 18: 37716
titration of, comparison of methods for complexometric, 18: 1583
toxicity in laboratory animals, 20: 30970 (COO-1170-5)
vapor pressure of solutions of, in liquid ammonia at −75.9°C, 20: 18689
vapor pressure of, saturated, 19: 34728

YTTERBIUM ACETATES

dissociation constants of, electrolytic, 20: 36830
polarography of, in anhydrous ethylenediamine, 17: 4486
preparation by oxide solubility in alcohols containing ammonia, 20: 20686
preparation of anhydrous, by desolvation, 16: 23697
preparation of anhydrous, by desolvation, 17: 6082
spectra of, infrared absorption, 18: 41446

YTTERBIUM ALCOHOLATES

preparation and properties of, 20: 18652
preparation of, and thermal decomposition to oxide coatings and powders, 20: 36851

YTTERBIUM ALLOYS

properties, 18: 1489(R) (IS-700(Sect.C))
Al–Yb, crystal structure, 19: 7950
Al–Yb, Knight shift from ytterbium-171 nuclear magnetic resonance in, 18: 7774
Al–Yb, magnetic properties of intermetallic compounds of, 20: 39433
Al–Yb, nuclear magnetic resonance of aluminum-27 in, 18: 44229
Al–Yb, properties of intermetallic compounds in, tabulation of, 20: 43972
Au–Yb, magnetic susceptibilities at 2 to 300°K, 20: 27494(R) (NYO-3454-6)
Au–Yb, oxidation of, kinetics of high-temperature, 20: 5859
Au–Yb, phase studies of solid solutions in, 19: 41062
Au–Yb, phase studies, 20: 17016 (IS-1175)

Be–Yb, crystal structure, 17: 36330
Be–Yb, crystal structure, 18: 18399(T)
Be–Yb, structure of $YbBe_{13}$, 19: 23009 (JPRS-28849(p.195-6))
Bi–Yb, crystal structure and magnetic susceptibility, 19: 13289
Bi–Yb, phase studies, 19: 37072
Ca–Yb, crystal structure and electric conductivity of, 20: 41412(R) (IS-1500(Sect. M))
Ca–Yb, phase diagrams, 20: 4297(R) (IS-1200(Sect.M))
Ca–Yb, phase studies, 19: 9604(R) (IS-900(Sect.M))
Ca–Yb, phase studies on, by differential thermal analysis, 20: 13254 (IS-T-70)
Cd–Yb, crystal structure of intermetallic compound $YbCd_4$, 19: 16162
Cd–Yb, eutectic temperature in YbCd–Yb region, 19: 32279(R) (ANL-7020(p.3-99))
Co–Yb, crystal structure of Laves phases in, 19: 47052
Co–Yb, preparation and structure of $MgCu_2$-type, 20: 2385(T)
Cu–Yb, analysis for AlB_2 and $CeCu_2$ type intermetallic compounds, 17: 29335
Fe–Yb, anisotropy of exchange in garnets of, 20: 1802 (AD-618038)
Fe–Yb, preparation and structure, 20: 15110
Ga–Yb, phase studies, 19: 16173
Ga–Yb, preparation and properties of MX_3-type compounds in, 18: 37723
Ge–Yb, crystal structure of intermetallic compounds in, 19: 11762
Ge–Yb, crystal structure of Yb_3Ge_5, 19: 28819
Ge–Yb, crystal structure, 20: 7591
Ge–Yb, crystal structure of, at or near equiatomic proportions, 20: 19225
Ge–Yb, crystal structure of intermetallic compound YbGe in, 20: 33886 (UCRL-14152)
Ge–Yb, structure of germanide, 19: 23006(T) (JPRS-28849(p.184-7))
Hg–Yb, crystal structure of $YbHg_3$, 20: 17060
In–Yb, crystal structure of intermetallic compound $YbIn_3$ in, 18: 39964(T)
In–Yb, crystal structure of $YbIn_3$, 20: 17060
In–Yb, preparation and properties of MX_3-type compounds in, 18: 37723
La–Yb, superconducting transition temperature of, pressure dependence of, (E/T), 20: 37965
Mg–Yb, hexagonal crystal structure in $YbMg_2$, 18: 44181
Mg–Yb, phase studies, 19: 25016
Mg–Yb, phase studies, 20: 4297(R) (IS-1200(Sect.M))
Mg–Yb, structure of intermetallic compounds in, 19: 23008(T) (JPRS-28849(p.191-4))
Ni–Yb, atomic radii and interatomic distances in intermetallic compounds in, 18: 28029
Ni–Yb, magnetic properties of, antiferromagnetic effects on, 16: 22624
Pb–Yb, crystal structure of intermetallic compound type RPb_3 in, 19: 4677
Pb–Yb, crystal structure of $YbPb_3$, 20: 17060
Pb–Yb, phase diagrams, 20: 4297(R) (IS-1200(Sect.M))
Pb–Yb, phase diagrams, 20: 41412(R) (IS-1500(Sect. M))
Pb–Yb, phase studies, 20: 13180(R) (IS-RD-4)
Pb–Yb–Zn, component distribution is recrystallized, 20: 39435
Pd–Yb, phase studies, 19: 47051
Pd–Yb, preparation and properties, 19: 16068 (EUR-1894.i)
Po–Yb, preparation and properties of, 20: 35909
Ru–Yb, process for improving workability of, 19: 40999(P)
Sb–Yb, crystal structure and magnetic susceptibility, 19: 13289
Sb–Yb, crystal structure of $YbSb_2$ in, 20: 37238
Sb–Yb, phase studies of compounds in, 18: 37115 (ANL-6856)
Sb–Yb, phase studies, 20: 21401
stainless steel–Y, corrosion by steam at 650°C, 19: 44616(R) (ANL-7000, pp 122-37)
Th–Yb, phase studies, 16: 13614
Tl–Yb, preparation and properties of MX_3-type compounds in, 18: 37723
Yb–Zn, crystal structure of intermetallic compound $YbZn_2$ in, 19: 47030
Yb–Zn, crystal structure of intermetallic compounds in, 20: 9515
Yb–Zn, crystal structure of intermetallic compounds Yb_2Zn_{17} and $YbZn_{13}$ in, 20: 39417
Yb–Zn, crystallography and transformations in AB_2-type compounds in, 20: 24589(R) (NYO-3560-3)
Yb–Zn, intermetallic compound with $CeCu_2$-type structure in, 20: 21352 (TID-21745)
Yb–Zn, lattice parameters of intermetallic compounds in, 19: 24989(R) (TID-21673)
Yb–Zn, melting point and transformation temperature of intermetallic compounds in, 19: 24989(R) (TID-21673)
Yb–Zn, melting point of $YbZn_2$, 20: 31743

YTTERBIUM ALUMINATES
physical properties, 20: 45639

YTTERBIUM ARSENIDES
crystal structure and magnetic susceptibility, 19: 13289

YTTERBIUM AZIDES
preparation and spectra of, 19: 13389
thermal decomposition of, differential thermal analysis of, 18: 25446

YTTERBIUM BORATES
crystal structure, 17: 27837
crystal structure of vaterite-type, polymorphism in, 20: 12837
polymorphism, x-ray analysis, 16: 162
preparation and properties, 19: 7498
spectra of, infrared, 20: 35519
$LaBO_3$–$YbBO_3$, structural polymorphism of, 17: 32124

YTTERBIUM BORIDES
boron-11 NMR in hexa-, Knight shifts in, 17: 32083
electric conductivity of hexa-, 17: 16726
electric resistance, 19: 6356
electron structure and physical properties of crystals of, 17: 27875
physical properties of hexa-, 16: 12154
preparation and structure of dodeca-, 17: 39020 (BNL-6741)
preparation, properties, and uses, 17: 2959(T) (AEC-tr-5264)
preparation, properties, and structure of hecto-, 18: 35540
spectra of, valence state determination from x-ray absorption, 19: 30194
thermal conductivity, 17: 28843
x-ray absorption by, edge structure in, 19: 22185
ytterbium absorption spectra in, fine structure of L_{III}, 18: 39195

YTTERBIUM BROMIDES
electric conductivity of methanol solutions of anhydrous, at 20 and 45°C, 20: 22991
spectra of, electron-transfer, 20: 25104
thermal decomposition of hydrates of, mechanisms of, 19: 46271

YTTERBIUM CARBIDES
crystal and electronic structure, 17: 3488 (TID-14175)
crystal and electron structure of, correlation between interatomic distances and carbide valency in, 17: 37813
lattice parameters and phase transformation temperatures in, 19: 41014 (LA-DC-6819)
microhardness, 19: 41014 (LA-DC-6819)
neutron diffraction study, 16: 10563

YTTERBIUM CARBONATES
complexes of, composition in solution of, 20: 10824
preparation and thermal decomposition, 18: 17774 (LADC-6082)
preparation by heating water solution of rare earth chloride and ammoniumtrichloroacetate, 19: 36399
preparation from acetates and propionates, 20: 26911
preparation, properties, and structure, 17: 15950 (LADC-5566)
spectra of solid, electron transfer, 20: 35506
spectra of, electron-transfer, 20: 25104

YTTERBIUM CHLORIDES
chemical properties of aqueous solutions of, 20: 40796(R) (IS-1500 (Sect.C))
complexes with phenanthroline, preparation and properties, 19: 40514
crystal field of hydrated, 20: 10860
cyclopentadienyl-, complex with tris-(tetrahydrofuranates), magnetic susceptibility of, 18: 1712(R) (TID-19613)
cyclopentadienyl-, complexing with acetate, benzoate, methoxide, and phenoxide, 18: 1712(R) (TID-19613)
cyclopentadienyl-, magnetic susceptibility, 18: 1712(R) (TID-19613)
cyclopentadienyl-, synthesis, 18: 1712(R) (TID-19613)
entropy of formation and vapor pressure over, 18: 25426
formation and stability, 17: 35834
heat of dilution of aqueous, at 25°C, 20: 3956
heat of dilution of aqueous solutions of, 20: 38870 (IS-1356)
heat of dilution of aqueous, at 25°C, 20: 38903
heat of vaporization and vapor pressure of, above melting point, 17: 37185
pharmacological and toxic effects, 16: 26686 (TID-16385)
preparation and vapor pressure at 1200 to 1400°C, 18: 8382
preparation of, method for, 18: 6832
properties of aqueous solutions of, thermodynamic and transport, 20: 22968 (IS-1344)
properties of di- and trivalent, review on, 19: 22229
reactions with gaseous alkali and alkaline earth metals and hydrogen, thermodynamics of, 20: 43222
specific gravity and apparent molal volume of aqueous solutions of, at 25°C, 20: 38905
spectra in molten chloride eutectic, near-infrared, 19: 17870
spectra of hydrated, absorption, 16: 31609 (UCRL-6564-T)
spectra of, diffuse reflectance, 18: 13689
spectra of, electron-transfer, 20: 25104
spectrum of $YbCl_3 \cdot 6H_2O$, absorption, 16: 10696
stability, 17: 8004 (TID-14716)
thermal capacity of aqueous solutions of, at 25°C, 20: 12818 (IS-T-52)
thermal capacity of aqueous solutions of, at 25°C, 20: 29144 (IS-1355)
thermal capacity of aqueous solutions of, at 25°C, 20: 38906
thermodynamic properties, 18: 10108
vapor pressure, 17: 32118
vapor pressure, 18: 31525
ytterbium-171 nuclear magnetic resonance in, magnetic moment from, 18: 7774
alkyl aluminum–$YbCl_3$, catalytic effects of, on directional polymerization

of 1,3-butadiene in nitrogen, 19: 2318
$KCl-YbCl_3$, phase diagrams, 18: 17844
$KCl-YbCl_2$, phase diagrams, 18: 17844
$KCl-YbCl_2$, vapor pressure, 18: 25435

YTTERBIUM CHROMATES
preparation and structure, 17: 37238

YTTERBIUM CHROMITES
spectra of, infrared, 20: 36807

YTTERBIUM COMPLEXES
absorption spectra of carbonate, 16: 5338
molecular structure of carbonate, cryoscopic measurements of, 19: 15477
preparation and properties of cyclohexylisonitrilocyclopentadienyl, 19: 28293
properties of, as laser material, 17: 25843(R) (AD-282296)
spectra and stability constants, 19: 5873
spectra of trivalent ytterbium in, crystal-field splitting in emission and optical, 19: 7400
stability of cationic nitrate, 17: 14393
with [(2-hydroxyethyl)imino]diacetic acid, dissociation constant of, 19: 38671
with acetic acid chelates, preparation of mixed, 17: 14259
with acetonitrile, pyridinium salts, and triphenylphosphonium, preparation and properties of, 20: 43231
with acetylacetone, magnetic properties of, at low temperatures, 16: 3016
with α-hydroxygluconate, isobutyrate, and lactate, formation constants, 16: 11635
with α-hydroxyisobutyric acid, ion exchange determination of stability constants of, 18: 35521
with α-methylmandelic acid, stability of, 20: 40902
with α-picolinic acid and α-picolinic acid *N*-oxide, stability constants, 19: 13307
with arsenazo, composition of, 18: 19948
with beta-diketones, preparation, 19: 5866
with butyl phosphates, formation and stability of, 20: 26883
with dibenzoylmethide, preparation and thermal stability of, 18: 12088
with dibutyl phosphate, solubility in dialkyl phosphoric acids in benzene at 25°, 17: 32148
with dibutylphosphoric acid, properties, 16: 17686
with dicyclopentadienyl acetate, amide, benzoate, formate, methoxide, and phenoxide, synthesis, 16: 25321(R) (TID-16224)
with diethylenetriaminepentaacetic acid, formation and stability constants of, 17: 16001
with diglycolic acid, stability constant for, 18: 8338
with diglycolic and dipicolinic acids, thermodynamic properties of, 18: 13733
with dilactic, mandelic, and quinic acids, formation and stability constants of, 20: 12817 (IS-1311)
with EDTA, entropy and thermal effects of formation of, 19: 30198
with Eriochrome Violet B, dropping mercury electrode and polarographic behavior, 16: 14707
with gluconic acid in aqueous solution, 16: 9993
with gluconic acid, stability constants for, 16: 27012
with gluconic acid, stability of, 18: 1697
with gluconic acids, stability constants, 19: 40508
with glycine, stability constants for, 19: 22227
with glycolic and lactic acids, thermodynamic properties of, 20: 43215
with glyoxylic acid, formation constant of, 18: 22101
with HEDTA, stability constants of, 16: 32045 (IS-304)
with hydroxycitrate, structure, 18: 43525
with isobutyrate and α-hydroxy- and α,β,β′-trihydroxyisobutyrate ligands, stability constants of, 18: 10124
with malic acid, formation and properties of, 17: 18082
with methoxyacetic, propionic, and thioglycolic acids, formation constants of, 18: 17859
with methylethyl and methylpropyl glycolates, stability of, 18: 22095
with *N*-(hydroxyethyl)ethylenediaminetriacetic acid, electrophoresis of hydrolysis products of, 17: 14264
with nicotinic acid, formation and stability, 17: 35832
with nitric acid, formation and stability, 16: 31627
with nitrilotriacetic acid, enthalpy and entropy of formation, 16: 11601
with nitrilotriacetic acid, properties and structure of hydrated, 18: 17838
with octyl phosphate, solubility in dialkyl phosphoric acids in benzene at 25°, 17: 32148
with organic reagents, preparation and stability of colored, 18: 27366
with Pyrocatechol violet, Arsenazo I, or Methylthymol Blue, preparation of, 20: 45581
with S-ethylthioglycolate and mercaptopropionate ions, stability constants of, 17: 25102
with saccharic acid, preparation of, 20: 33216
with serine, stability and composition, 19: 19874
with serine, stability of, 20: 26896
with tartaric acid and trihydroxyglutaric acid, stability constants for, 20: 36838
with triphenylphosphine oxide, properties and spectra of, 19: 42466
with triphosphate, stability constants, 17: 2963
with trisacetylacetone, trisbenzoylacetone, and benzil, crystal field splitting in, (E/T), 20: 7109
with trisbenzoylacetonate and trisbenzoylmethide, luminescence, 16: 14739
with 1-hydroxycyclopentanecarboxylic acid, stability of, 20: 26910
with 1-hydroxycyclopentanecarboxylic acid, preparation, properties, and structure of, 20: 26837
with 1,10-phenanthroline, preparation and composition of, 19: 30197
with 1,10-phenanthroline, magnetic properties and structure of acetate and nitrate, 19: 36405
with 2,2,6,6-tetramethyl-3,5-heptanedione, preparation and volatility of, 20: 7074
with 2,4-pentanedione, preparation, properties, and solvates, 16: 10016
with 2,4-pentanedione, solubilities of, in solvents, 17: 23446
with 2,4-pentanedione, complexity constants for, 18: 25385
with 8-quinolinol, composition and thermal stability of, 18: 17784

YTTERBIUM COMPOUNDS
cyclopentadienyl, preparation and composition of, 20: 26856
hexaammoniate, preparation and properties of, 20: 18689
preparation and properties of dicyclopentadienyl-, 19: 36408
preparation of dicyclopentadienyl and methylcyclopentadienyl chlorides, 16: 9980(R) (TID-15018)
preparation of organic, 17: 3014(R) (TID-17309)
spectra of isopropoxides and 2-pentoxides, infrared, 19: 15552
synthesis and properties of dicyclopentadienyl, 16: 1651(R) (TID-14260)

YTTERBIUM ETHYL SULFATES
spectra at 0.9 to 1.1 microns, 19: 11046(R) (AROD-2099:22)
spectra of, absorption, 18: 3753
spin-lattice relaxation in, 18: 23528
thermal decomposition, effects of atmosphere, particle size, and upheat rate on, 16: 13048

YTTERBIUM FERRATES
exchange field splitting in, 16: 30958
iron-57 magnetic resonance in, 16: 18481
magnetic properties of yttrium-substituted, 16: 28933(T) (FTD-TT-61-114)
nuclear magnetic resonance spectra of iron-57 in, 16: 6847
spectrum of ytterbium in, 18: 10619 (AFCRL-63-103)
$SrNb_2O_6-YbFeO_3$, ferroelectric properties of, 17: 22199(T)
$Yb_3Fe_5O_{12}-Yb_3Ga_5O_{12}$, growth and properties of, 20: 36380

YTTERBIUM FERRATES(III)
anisotropy of exchange in garnet, 20: 1802 (AD-618038)
crystal structure, 19: 46256
crystal structure, 20: 25038
damping mechanisms in, 19: 32048(R) (NP-15073)
magnetic properties of, Curie point pressure dependence for, (E), 20: 24597

YTTERBIUM FLUORIDES
effects on freezing point depression in sodium fluoride, 18: 5284
preparation and magnetic moments, 20: 7089
preparation, properties, and structure, 17: 15950 (LADC-5566)
$LiF-YbF_3$, phase studies, 19: 30149(R) (ORNL-3789(p.3-35))
$NaF-YbF_3$, phase diagrams at 300 to 1300°C, 20: 33278
$NaF-YbF_3$, phase studies, 19: 30149(R) (ORNL-3789(p.3-35))
NH_4F-YbF_3, chemical properties and crystal structure, 18: 16013

YTTERBIUM GALLATES
growth and properties of garnet, 20: 36380
magnetic susceptibility of, orbit-lattice interaction effects on static, 18: 710
structural properties of $Yb_3Ga_2(GaO_4)_3$, 17: 14210 (NBS-MON-25(Sect.1))
$Yb_3Fe_5O_{12}-Yb_3Ga_5O_{12}$, growth and properties of, 20: 36380

YTTERBIUM GERMANATES
crystal structure of, ir spectral studies on, 20: 43218

YTTERBIUM HYDRIDES
crystal structure, 18: 39192
dissociation and properties, 16: 5307 (NP-11180)
electronic structure, 17: 11329 (TID-15934)
magnetic properties, 17: 2130
magnetic properties, 17: 25708(R) (TID-18766)
properties, 16: 23686
properties and structure, 20: 16453
spectra of normal and deuterated, 20: 25043
structure of high-pressure forms, 16: 32070
$LiH-YbH_2$, phase studies, 19: 19881
LiH–YbH, preparation and structure, 18: 39192
$Yb-YbH_2$, equilibrium hydrogen dissociation pressure in, 20: 12829 (TID-22502)

YTTERBIUM HYDROXIDE OXIDES
preparation and crystal structure, 20: 8892
preparation and crystal structure of, 20: 36791

YTTERBIUM HYDROXIDES

decomposition of, products of thermal, 20: 16441
preparation and properties of oxy-, 19: 34152(T) (ORNL-tr-660)
preparation and structure of, 19: 42865
reactions with formic acid, properties of formate formed by, 19: 38669
reactions with hafnium hydroxides at 100 to 1000°C, 19: 22191
thermal decomposition of, thermographic and x-ray studies on, 20: 25061

YTTERBIUM HYPOPHOSPHITES
spectra of, infrared and Raman, 18: 35533

YTTERBIUM IODIDES
preparation and structure of tri-, 18: 29602 (LADC-6087)
preparation of hydrates of, 18: 39227

YTTERBIUM IODATES
solubility of, in water, 20: 45656

YTTERBIUM IONS
covalency in octahedrally coordinated trivalent, (T), 20: 28674
crystal field potential in calcium fluorides, 18: 27435
crystal-field interactions of, linear and nonlinear shielding of, (E/T), 19: 40101
crystalline electric field for, origin of, (T), 19: 15545
effects on fluorescence of praseodymium-doped lanthanum fluorides, 19: 28309
effects on spectrophotometric determination of erbium, holmium, and neodymium, 20: 43100
electron energy levels and Stark splitting of, in calcium fluoride crystals, 19: 4142
electron paramagnetic resonance of trivalent, in strontium titanate, 18: 2466
electron paramagnetic resonance in calcium tungstates, 18: 23525
electron paramagnetic resonance in calcium fluorides, relaxation in, 18: 23526
electron paramagnetic resonance in calcium fluorides, spin-lattice relaxation in, 18: 23527
electron paramagnetic resonance of, in single-crystal lead molybdate, 19: 44017
electron paramagnetic resonances in cesium oxide single crystals at 10 Bc, (E), 20: 38391
electron spin resonance of trivalent in hexa-antipyrene iodides, 16: 13074
electron spin resonance measurements in calcium fluoride crystals, 17: 35253(R) (IA-775)
electron spin resonance spectra of, in calcium oxide crystals, evidence for covalent bonding from, 17: 36495
electron spin resonance of trivalent, hyperfine structure constants from, 17: 37785
electron spin resonance spectrum of trivalent, in irradiated and thermally treated calcium fluoride, 18: 2471
electron spin resonance spectrum of trivalent, in cadmium fluoride single crystals, 18: 2473
electron spin resonance of trivalent, in thorium oxide, (E), 19: 5893
electron spin resonance in cerium oxide, spectra for, (E), 20: 10242
energy exchange from neodymium ions in calibo glass, (E), 19: 29463
energy matrix elements and eigenvalues in cubic potentials and exchange field, 19: 7486
energy transfer from neodymium ions to, luminescence in silicate glass by, 19: 25172(T)
energy transfer to trivalent erbium ions in silicate glass, (E), 19: 14240
exchange interactions with thulium aluminates and gallates, paramagnetic g-value shifts in, 18: 709
Faraday rotation of trivalent, in garnets, (E), 20: 8293
hydrolysis in aqueous solutions of sodium perchlorate at 25°C, constants for, 20: 43221
hyperfine interactions in tetravalent and trivalent, constants for, 17: 37686
infrared emission of, in silicate glass, 17: 34572
interactions in semiconducting europium chalcogenides, magnetic exchange, 18: 32697
interactions with iron(III) ions in crystalline lattices, exchange splittings of L–S multiplets by, 18: 2481
laser oscillations in barium crown glass containing neodymium and uranyl ions, 20: 8291
light emission in triply activated glass systems, stimulated, (E), 19: 14241
luminescence energy transfer to, from cerium ions in silicate glass, 19: 11060
magnetic moment in crystalline state and in solution, 18: 25350
magnetic resonance in lutetium aluminate and gallate, 16: 15261 (AFCRL-987)
magnetic resonance in calcium tungstate, 20: 2520(R) (IA-920)
paramagnetic resonance in calcium fluoride crystals, 16: 12801(R) (IA-685)
paramagnetic resonance spectra of, in calcium fluoride crystal field, 17: 2935 (AD-274000)
paramagnetic resonance in calcium tungstate, 18: 31505
polarographic reduction at mercury electrode, reversible and irreversible processes in, 16: 32962
polarography at mercury electrode, derivative, 16: 32963
positron mean life in divalent, 17: 25944
preparation of cerium oxide single crystals containing, (E), 20: 43818
radiolysis of aqueous solutions of, pulse, 19: 38728
reactions with Arsenazo III, 18: 6755
relaxation time in calcium fluoride, spin-lattice, (T), 19: 41982
resonance spectrum in yttrium oxides, paramagnetic, 17: 23313
spectra in alkaline earth fluorides, EPR, 19: 26917(R) (IA-984)
spectra in barium, calcium, and strontium fluorides, absorption and luminescence, 19: 19854
spectra in cadmium fluoride crystals, absorption and electron paramagnetic resonance, 16: 24334
spectra in calcium fluoride crystals, absorption, 16: 28951
spectra in lutetium and yttrium chlorides, magnetic properties in paramagnetic resonance, 18: 39212
spectra in rubidium chlorides, pseudolocalized vibrational frequencies in, 19: 28319
spectra in silicate glass, fluorescence, 19: 47886(T) (N64-21857, pp 1-6)
spectra in synthetic lead molybdate single crystals, EPR, (E), 19: 41986(T)
spectra in ytterbium complexes, crystal-field splitting in emission and optical, 19: 7400
spectra of divalent and trivalent, 19: 30941 (AD-609419)
spectra of, near-infrared transitions in, 17: 35759
spectra of trivalent, in hydrated chloride lattices, 20: 10860
spectra of, effects of chemical bonding and transitions on, 20: 36845
spin-lattice relaxation times in strong exchange fields, computation methods for, 16: 22115
spin-lattice relaxation of trivalent, in cadmium fluoride single crystals, 18: 2473
spin-lattice relaxation rate in garnets, 19: 14121 (AD-608278)
spin-lattice relaxation time in calcium fluoride lattice, (T), 19: 41995(T)
spin-lattice relaxation of, in lanthanum fluorides, 20: 42540

YTTERBIUM ISOTOPES
alpha decay of, with N = 84 and 85 (E), 19: 3356
decay of isomeric, energy and half life for, (E), 19: 10329
deuteron reactions at 15 Mev, isomeric states from, (E), 20: 15856
energy levels of, multiple Coulomb excitation of rotational, 17: 31396 (CONF-46-28)
energy levels of odd-A, calculations using single-particle potential with pairing interaction, (T), 20: 46635
energy levels of, rotational, (T), 20: 44843
gamma reactions on, cross sections for, 19: 12496
isomeric transitions of E_3 type, 16: 31066 (NP-11746)
masses of, mass-spectrographic measurements of, 17: 815
nuclear compressibility, 16: 18531
nuclear gyromagnetic ratios and quadrupole moments, 16: 21446
oxygen-16 reactions (O-16,xn) with, alpha-active platinum isotopes from, (E), 20: 32458
preparation of bulk materials and foils of, from oxide, 20: 13216 (ORNL-P-1899)
preparation of foils of, from ytterbium oxides, 19: 36307
preparation of self-supporting foils of, 20: 31696
production and separation of stable, at Seibersdorf Reactor Center, Germany, 20: 23572 (SGAE-PH-32/1965)
production by neutron reactions (n,γ) at 15 Mev, 17: 30159
separation, contamination in electromagnetic, 16: 9101
separation, electromagnetic, 16: 9107
separation in calutrons, 18: 34007(R) (ORNL-TM-890)
spectra of, shifts in x-ray, 18: 17064(T)
yields of, in proton spallation of tantalum at 660 Mev, 18: 4576 (NP-13165(Vol.2)(p.87-100))

YTTERBIUM ISOTOPES Yb-154
alpha decay of, energies and rates for, 18: 26640

YTTERBIUM ISOTOPES Yb-162
decay scheme of, conversion electron and positron spectra and half life for, 17: 34947

YTTERBIUM ISOTOPES Yb-164
beta-gamma transitions in, 18: 21174 (JINR-P-1479(p.3-25))
conversion electron spectra of, (E), 20: 32415
decay scheme and electron conversion spectra, 16: 15624 (JINR-P-475 (Pt.II))
electron conversion at 150 to 900 kev, 18: 4552 (NP-13165(Vol.1) (p.101-5))
energy levels of, gamma cascade from rotational, 18: 44738 (UCRL-11402)
energy levels of, large-spin rotational, (T), 19: 5224
energy levels of, rotational, (T), 19: 45285 (UCRL-16040)
energy levels of, high-spin rotational, (E/T), 20: 19953
energy states of, large-spin rotational, (E/T), 20: 3008 (COO-1420-104)

half life, 18: 32760
YTTERBIUM ISOTOPES Yb-165
beta decay of, gamma spectra from, (E), 20: 19862
decay scheme and electron conversion spectra, 16: 15624 (JINR-P-475 (Pt.II))
half life, 18: 32760
YTTERBIUM ISOTOPES Yb-166
decay scheme and electron conversion spectra, 16: 15624 (JINR-P-475) (Pt.II))
decay to erbium-166, comparison with Bohr-Mottelson collective theory of nucleus, 16: 4828
electron-capture decay scheme for, 17: 19296
electron conversion in, 18: 4550 (NP-13165(Vol.1)(p.83-94))
energy levels, 18: 32745(R) (UCRL-11213(p.1-48))
energy levels in, properties of high-spin rotational, 18: 15288
energy levels of, gamma cascade from rotational, 18: 44738 (UCRL-11402)
energy levels of, large-spin rotational, (T), 19: 5224
energy levels of, rotational, (T), 19: 45285 (UCRL-16040)
energy levels of, rotational, (E), 20: 6348
energy levels of, high-spin rotational, (E/T), 20: 19953
energy states of, large-spin rotational, (E/T), 20: 3008 (COO-1420-104)
gamma decay, 17: 34904
gamma decay, 18: 4549 (NP-13165(Vol.1)(p.65-82))
nucleon pairing correlations in, coupling effects of nuclear rotation on, 20: 36199
YTTERBIUM ISOTOPES Yb-167
beta and electron-capture decay of, thulium-167 energy levels from, (E), 20: 46621
beta decay, 18: 1014 (JINR-P-1361)
beta decay (E), 19: 3325
decay of, conversion electron spectra in, (E), 19: 33357
decay scheme and electron conversion spectra, 16: 15624 (JINR-P-475 (Pt.II))
energy levels of, single quasiparticle, (T), 19: 17052
YTTERBIUM ISOTOPES Yb-168
abundance in meteorites and terrestrial matter, 18: 10753
axial asymmetry in, 16: 11001
decay scheme and electron conversion spectra, 16: 15624 (JINR-P-475 (Pt.II))
deformation parameter, energy level transition probabilities, and nuclear quadrupole moment, (E/T), 20: 24438(T)
energy level from lutetium-168 decay, (E), 20: 28344
energy level of, excitation energy and transition probability for first rotational, 17: 31449
energy level transitions from thulium-169 (p,2n) reactions, ground state rotational, 20: 38008(R) (AECL-2595)
energy levels, 17: 880
energy levels, (T), 19: 16890
energy levels, (E), 20: 6366
energy levels of, properties of octupole, 18: 21172 (JINR-E-1561)
energy levels of, in superfluid model, 18: 28568 (JINR-E-1621)
energy levels of, quadrupole, 18: 36684
energy levels of, corrections in Bohr-Mottelson model for rotational, 19: 17048
energy levels of, rotational, (E), 20: 6348
energy levels of, vibrational, (E/T), 20: 46604 (UCRL-16986)
nuclear octupole deformation, 16: 3745
production in stars, 16: 12308
YTTERBIUM ISOTOPES Yb-169
behavior towards blood serum proteins, 16: 5138
decay of, isomeric shift in $K\alpha_1$ x ray from electron-capture, 17: 31429
decay of, thulium-169 energy level properties from electron-capture, 17: 34923
decay of, energy levels from, 18: 16982
decay of, thulium-169 properties from (E), 19: 3309
decay of, thulium-169 level half lives from, (E), 20: 28380
decay scheme and electron conversion spectra, 16: 15624 (JINR-P-475 (Pt.II))
decay scheme for, 17: 2260
decay scheme of, conversion electron spectrum of, 17: 40069
distribution in mice, 18: 31087
electron capture by, gamma spectra from, (T), 19: 8392 (IS-993)
energy level transitions in, E1, (T), 19: 12620
energy levels, 17: 880
energy levels and gamma spectra, 16: 26254
energy levels of, single quasiparticle, (T), 19: 17052
gamma angular correlations from, in lutetium iron garnet, (E), 20: 17994
gamma dose constants for, 20: 46617
gamma emission, 16: 24583
gamma spectra at 40 to 280 kev, 17: 19329
half life, 18: 4578 (NP-13165(Vol.2)(p.112-16))
production by Osaka Radiation Center linear accelerator, 17: 35006
properties for use in radiography of teeth, evaluation of, 19: 13176
properties in portable devices for chest radiography, 20: 3804 (ORNL-IIC-5, pp 309-28)
separation of, electrolytic, 17: 14357
uptake and distribution in rats, 18: 21783
use in radiography, 16: 24584
use in radiography of aluminum and steel, 18: 20425
use of portable sources of, for diagnostic radiography, 18: 3634
YTTERBIUM ISOTOPES Yb-170
alpha scattering at 2.5 to 4.0 Mev, K-shell conversion coefficients from, 18: 37836
axial asymmetry in, 16: 11001
energy level at 84 kev, structure splitting, 16: 17135
energy level at 84-kev, life time of, 16: 28169
energy level lifetime, (E), 20: 7449
energy level lifetimes of, excited, (E), 20: 9960(R) (AEET-228)
energy level transitions in, conversion coefficients and directional correlations in, 18: 42772
energy level transitions in, E2 conversion coefficients of rotational, (T), 19: 21308
energy level transitions in, 84.2-kev E2, (E), 19: 31271
energy level transitions in, conversion coefficients for E2, (E), 20: 15700 (CONF-233(Vol.2), pp 120-7)
energy level transitions in, conversion coefficients for E2, (E), 20: 15706 (CONF-233(Vol.2), pp 191-7)
energy level transitions in, L-subshell ratios of E2 rotational, 20: 32516
energy level transitions from thulium-170 decay, conversion coefficients for, (E), 20: 32443
energy level transitions of, ratio of internal conversion coefficients of L and M subshells of 84.3-kev E2, 20: 36195
energy level transitions of, K-conversion coefficient for 84-kev, (E), 20: 36233
energy level transitions of, anomalies in E2 conversion coefficients for, (E), 20: 36234
energy level transitions of, K and L particle parameters from 84.2-kev E2, (E), 20: 36256
energy level transitions in, L subshell ratios for E2, (E), 20: 36260
energy level transitions in, L subshell measurements of E2, (E), 20: 36262
energy level transitions in, conversion coefficients for, (E), 20: 42523(R) (IS-1500(Sect.P))
energy levels, 17: 880
energy levels from lutetium-170 decay, (T), 20: 17742
energy levels, lifetimes, 16: 21440
energy levels of, properties of first-excited 2^+, 17: 15289
energy levels of, rotational excitation of first-excited, 17: 33015
energy levels of, vibrations in low-lying, 18: 18970
energy levels of, properties of octupole, 18: 21172 (JINR-E-1561)
energy levels of, vibration-rotation interactions in, 18: 34846
energy levels of, quadrupole, 18: 36684
energy levels of, measurement of lifetimes of, 18: 38070 (NP-14171)
energy levels of, gamma vibrational, (T), 19: 14597
energy levels of, corrections in Bohr-Mottelson model for rotational, 19: 17048
energy levels of, gyromagnetic ratio of 84-kev, (E), 19: 21377
energy levels of, half life of 84-kev, (E), 19: 27502
energy levels of, gyromagnetic ratio of 84-kev, (E), 19: 33305
energy levels of, lifetime of, (E), 20: 1175
energy levels of, half life of first excited, (E), 20: 4877
energy levels of, rotational, (E), 20: 6348
energy levels of, gyromagnetic ratio and mean life of first excited rotational, 20: 19945
energy levels on, lifetime of 84.2-kev, (E), 20: 12082
energy-level transitions in deformed, E2, (E), 20: 44701
energy-level transitions in, L conversion intensity ratios in E2, (E), 20: 46673
gamma decay of, internal conversion coefficients in, (E), 19: 31218 (IS-1032)
gamma radiation from, measurement of internal conversion coefficients of, (E), 19: 30522 (IS-1159)
gamma reactions (γ,n) in stars, 16: 12308
gamma spectra, E2 emission parameters, 16: 21444
gamma spectra, internal conversion of E2 $2^+ \rightarrow 0^+$, 17: 15304
gamma spectra of, hyperfine structure of Mössbauer, 17: 13244
gamma transition in, conversion coefficient of 84-kev, 20: 3155
gyromagnetic ratio of, (E), 20: 8062(R) (COO-720-058)
half life of, (E), 20: 8062(R) (COO-720-058)
internal conversion coefficients, 16: 11032
internal conversion coefficient of, K, 17: 2294
internal conversion coefficient of, 17: 31389(R) (ARF-A6027-2)
internal conversion coefficients, 17: 31402(R) (IITRI-A6027-3)
internal conversion (K) coefficients for E2 transitions in, 18: 18995
internal conversion coefficients for E2 transitions in, nuclear structure

effects on, (T), 19: 47620
internal conversion coefficients of $2^+ \rightarrow 0^+$ transitions in, E2, (E), 20: 15745
Mössbauer effects in, bibliography on, 18: 14650
Mossbauer spectra in oxides, 17: 2309
neutron strength functions for, target spin dependence of, 19: 41656 (BNL-9245)
nuclear octupole deformation, 16: 3745
nuclear rotations, 16: 11042
nuclear shape parameters for, 18: 11221
nucleon pairing correlations in, coupling effects of nuclear rotation on, 20: 36199
nucleon vibrational-rotational interactions in, 18: 34950
oxygen-16 reactions (O-16,xn), alpha spectra and excitation functions, (E), 19: 21248(R) (UCRL-11828(p.21-5))
oxygen-16 reactions (O-16,O-16γ) at 42 Mev, intrinsic quadrupole moment from, (E), 20: 22072
oxygen-16 reactions (O-16,O-16γ) at 42 Mev, intrinsic quadrupole moment from, (E), 20: 22072
properties of, effects of pairing forces on, (T), 19: 21434

YTTERBIUM ISOTOPES Yb-171

energy level scheme for, (E), 20: 17158(R) (ORNL-3900, pp 82-149)
energy level transitions in, E1, (T), 19: 12620
energy level transitions from thulium-171 decay, conversion coefficients for, (E), 20: 32443
energy levels, 17: 880
energy levels, 18: 2949
energy levels, 18: 32277(R) (PR-P-61)
energy levels of, single quasiparticle, (T), 19: 17052
energy levels of, M1 transitions of rotational, (E), 20: 40072 (LA-DC-8061)
energy levels of, g-factor and transition multipolarity for 66.7-kev, (E), 20: 44752
energy levels of, magnetic properties of $K = \frac{1}{2}$ rotational band, (E), 20: 44753
gamma decay of, internal conversion coefficients in, (E), 19: 31218 (IS-1032)
gamma reactions (γ,n) in stars, 16: 12308
gamma spectra, E2 emission parameters, 16: 21444
gyromagnetic ratios, (E/T), 20: 44791
hyperfine structure and nuclear magnetic moment, 18: 21235
hyperfine structure in cesium oxide single crystals at 10 Bc, EPR determination of, (E), 20: 38391
internal conversion coefficients, 16: 4805
moment of inertia of excited, (T), 20: 9988
Mössbauer effect in, properties of, (E), 19: 14521 (CONF-640606-18)
multipolarity of 19.3 kev transition, 16: 19814
neutron resonances in, spectra of, 19: 41661 (JINR-P-2158)
neutron resonances at 0 to 150 ev, (E), 20: 15839
neutron strength functions for, target spin dependence of, 19: 41656 (BNL-9245)
nitrogen-14 inelastic scattering by, Coulomb excitation in, (E), 20: 19959
nuclear magnetic moment, 18: 7774
nuclear magnetic moments, (E), 20: 40073 (LA-DC-8065)
transition spectra in, Alaga's rules for electromagnetic, 18: 26628

YTTERBIUM ISOTOPES Yb-172

decay, lutetium-172 rotational-band shifts from, 16: 15688
electron conversion, 18: 18911
energy level de-excitation characters for, experimental 1^-, 17: 17201
energy level transitions in, E2 conversion coefficients of rotational, (T), 19: 21308
energy level transitions in, M1-M3 mixing in gamma angular correlations of 3-2-0, (T), 20: 8116
energy levels, 17: 880
energy levels, 17: 22625
energy levels, 18: 18956
energy levels, 18: 32277(R) (PR-P-61)
energy levels in, gyromagnetic ratio of first-excited rotational, (E), 20: 12064
energy levels, lifetime of first-excited rotational, 16: 18514
energy levels of, half lives of 78.7- and 1174-kev, 17: 17178
energy levels of, vibrations in low-lying, 18: 18970
energy levels of, properties of octupole, 18: 21172 (JINR-E-1561)
energy levels of, rotational bands from two-particle, 18: 28612
energy levels of, g -factor of rotational, 18: 28671
energy levels of, vibration-rotation interactions in, 18: 34846
energy levels of, quadrupole, 18: 36684
energy levels of, decay properties of isomeric, 19: 1595
energy levels of, gamma vibrational, (T), 19: 14597
energy levels of, corrections in Bohr-Mottelson model for rotational, 19: 17048
energy levels of, rotational, (E), 20: 6348
energy levels of, gyromagnetic ratio and mean life of first excited rotational, 20: 19945
energy levels of, vibrational, (E/T), 20: 44797
energy levels of, octupole vibrational, (T), 20: 44825
gamma reactions (γ,n) in stars, 16: 12308
gamma transitions from $K = 3^+$ to rotational bands of ground state in, 17: 26503
gyromagnetic ratio, 18: 17095
gyromagnetic ratio of, (E), 20: 8062(R) (COO-720-058)
half life of, (E), 20: 8062(R) (COO-720-058)
inertia moment of, 17: 24390 (JINR-P-1216)
moment of inertia of excited, (T), 20: 9988
neutron resonances in, spectra of, 19: 41661 (JINR-P-2158)
neutron resonances at 0 to 150 ev, (E), 20: 15839
neutron strength functions for, target spin dependence of, 19: 41656 (BNL-9245)
nuclear electric quadrupole moments, 18: 18904
nuclear rotations, 16: 11042
oxygen-16 inelastic scattering at 43.5 Mev, vibrational-state excitation in, (E), 19: 45321
oxygen-16 reactions (O-16,xn), excitation functions, (E), 19: 21248(R) (UCRL-11828(p.21-5))
properties of, effects of pairing forces on, (T), 19: 21434
rotation states of deformed axial symmetry in, 17: 19282
spin of excited, inertial moment of, (T), 19: 19126
spin of, Coriolis anti-pairing and blocking effects on, 18: 34775 (TID-20875)

YTTERBIUM ISOTOPES Yb-173

Coulomb excitation at levels to 1.8 Mev, 18: 9335
decay, probability of single-particle transitions, 16: 4835
energy level at 351 kev, E1 transition probability and lifetime, 16: 12535
energy level transitions of, reduction factors from pairing correlations for E1, 18: 30741(T) (UCRL-Trans-1081)
energy level transitions in, analysis of E1, 18: 44769
energy level transitions in, effects of pairing correlations on E1 (T), 19: 3321
energy level transitions in, reduced probabilities for E1, (T), 19: 5210
energy level transitions in, E1, (T), 19: 12620
energy level transitions in, K-shell particle parameter in 272-kev E1, (E), 19: 21320
energy level transitions in, E2/M1 mixing ratios and K conversion coefficients in rotational, (E), 20: 6386
energy level transition probabilities in, pairing correlations in E1, (T), 20: 15766
energy level transitions in, delayed E-1, (T), 20: 15765
energy level transitions of, K conversion coefficients of mixed E2-M1 rotational, (E), 20: 36237
energy level transitions in, particle parameters for K-conversion coefficients from pure E1, (E), 20: 36254
energy levels, 17: 880
energy levels, 18: 1026 (ZFK-PHA-9)
energy levels from beta decay of thulium-173, (E), 20: 28344
energy levels in strongly deformed, relative E1 transition probabilities for, 17: 13563
energy levels of, electron capture by ground, 18: 4544 (NP-13165 (Vol.1)(p.7-22))
energy levels of, parity and spin of, 18: 6226
energy levels of, single quasiparticle, (T), 19: 17052
energy levels of, equilibrium deformations of excited, (T), 20: 28417
energy levels of, M1 transitions of rotational, (E), 20: 40072 (LA-DC-8061)
gamma emission from second-excited state of, 16: 33901
gamma reactions (γ,n) in stars, 16: 12308
gamma spectra, E2 emission parameters, 16: 21444
gamma spectra from lutetium-173 decay, (E), 19: 47661
gamma spectra of, probabilities for E1, 17: 13507
gamma transitions and internal conversion in, probabilities of, (E/T), 19: 21284
gyromagnetic ratio, 16: 1087
gyromagnetic ratio, 18: 17095
gyromagnetic ratios, (E/T), 20: 44791
hyperfine structure and nuclear magnetic moment, 18: 21235
hyperfine structure in cesium oxide single crystals at 10 Bc, EPR determination of, (E), 20: 38391
magnetic moments of, spin-polarization effect on, (T), 19: 29238 (INP-361)
magnetic octupole moments, 16: 8226
moment of inertia of excited, (T), 20: 9988
neutron capture resonances in, 18: 42622(R) (ANL-6879(p.2-20))
neutron resonances in, degrees of freedom of partial radiation widths for, 18: 1055
neutron resonances in, spectra of, 19: 41661 (JINR-P-2158)
neutron resonances at 0 to 150 ev, (E), 20: 15839

neutron strength functions for, target spin dependence of, 19: 41656 (BNL-9245)
nuclear magnetic moments, 16: 16831
nuclear magnetic moment, 18: 7774
nuclear quadrupole moment of, 17: 844
separation of lutetium-172 from, by cation exchange chromatography, 20: 43067(R) (IDO-14679, pp 6-46)
transition probabilities in, gamma, (E/T), 19: 14553
transition spectra in, Alaga's rules for electromagnetic, 18: 26628
transitions in, shell effects on E1, (T), 19: 12498

YTTERBIUM ISOTOPES Yb-174

abundance in meteorites and terrestrial matter, 18: 10753
carbon-12 fission at 109 and 125 Mev, energy-mass distributions in, 18: 26558 (UCRL-11377)
carbon-12 fission of, fragment energy and mass distributions in, (E), 19: 43399
carbon-12 fission, excitation energy, (E/T), 19: 21259(R) (UCRL-11828(p.77-80))
carbon-12 reactions, 18: 15210 (UCRL-11193)
decay scheme, 18: 11195(R) (EANDC(E)-49(E))
energy level transitions in, E2 conversion coefficients of rotational, (T), 19: 21308
energy levels, 17: 880
energy levels, 18: 1026 (ZFK-PHA-9)
energy levels, (T), 19: 16890
energy levels, (E), 19: 21272
energy levels, (E), 19: 23634
energy levels from lutetium-174i electron-capture decay (E/T), 19: 3294
energy levels from lutetium-174 decay, collective and two-particle, (E), 19: 47661
energy levels from thulium-174 decay, parity and spin of, (E), 20: 19944
energy levels in, gyromagnetic ratio of first-excited rotational, (E), 20: 12064
energy levels in, lifetime of 76.5-kev, (E), 20: 12082
energy levels, lifetime of first-excited rotational, 16: 18514
energy levels of, properties of octupole, 18: 21172 (JINR-E-1561)
energy levels of, in superfluid model, 18: 28568 (JINR-E-1621)
energy levels of, measurement of half life (850 μsec) of isomeric, 18: 34896
energy levels of, gamma vibrational, (T), 19: 14597
energy levels of, corrections in Bohr-Mottelson model for rotational, 19: 17048
energy levels of, gyromagnetic ratio and mean life of first excited rotational, 20: 19945
energy levels of, vibrational, (E/T), 20: 44797
energy levels, properties of 1315-kev, 16: 8201
gamma reactions (γ,n) in stars, 16: 12308
gyromagnetic ratio, 18: 17095
gyromagnetic ratio of, (E), 20: 8062(R) (COO-720-058)
half life of, (E), 20: 8062(R) (COO-720-058)
Mössbauer effect in, following Coulomb excitation, 20: 34844
neutron capture by, total cross section for thermal, 17: 38024(T) (AEC-tr-5734(p.109-12))
neutron reactions (n,γ) with, activation cross sections for short-lived isomers in, 18: 15219
neutron reactions (n,γ), activation cross sections for thermal, (E), 19: 31244 (ZfK-RN-23)
neutron resonances in, spectra of, 19: 41661 (JINR-P-2158)
neutron resonances at 0 to 150 ev, (E), 20: 15839
nuclear rotations, 16: 11042
oxygen-16 inelastic scattering at 43.5 Mev, vibrational-state excitation in, (E), 19: 45321
oxygen-16 reactions with, fission excitation functions for, 18: 32839
properties of, effects of pairing forces on, (T), 19: 21434

YTTERBIUM ISOTOPES Yb-175

beta decay of, lutetium-175 half lives of levels from, (E), 20: 28380
beta decay scheme, 16: 24808
beta transitions of, Kotani parameters for first-forbidden, 20: 24408
decay half life, from (n,γ) reaction, (E), 19: 31244 (ZfK-RN-23)
decay scheme, 16: 8194
distribution in benzene–thenoyltrifluoroacetone systems, effects of TBP on, 18: 41586
energy levels and gamma spectra, 16: 26254
energy levels from thulium-175 decay, parity and spin of, (E), 20: 19944
energy levels of, neutron activation cross sections for isomeric, 17: 38024(T) (AEC-tr-5734(p.109-12))
energy levels of, single quasiparticle, (T), 19: 17052
gamma dose constants for, 20: 46617
gamma spectra, 17: 34966
gamma spectra at 40 to 280 kev, 17: 19329
gamma-gamma angular correlations of, perturbed, (E), 19: 10290
production by Osaka Radiation Center linear accelerator, 17: 35006
production of short-lived isomer of, by thermal neutron reactions (n,γ), cross sections for, 18: 15219

YTTERBIUM ISOTOPES Yb-176

deuteron reactions (d,p) at 12 Mev, angular distributions and cross sections for, 18: 1065
energy level transitions in, E2 conversion coefficients of rotational, (T), 19: 21308
energy levels, (T), 19: 16890
energy levels in, gyromagnetic ratio of first-excited rotational, (E), 20: 12064
energy levels, lifetime of first-excited rotational, 16: 18514
energy levels of, vibrations in low-lying, 18: 18970
energy levels of, properties of octupole, 18: 21172 (JINR-E-1561)
energy levels of, spin values for three-particle isomeric, 18: 28614
energy levels of, in superfluid model, 18: 28568 (JINR-E-1621)
energy levels of, quadrupole, 18: 36684
energy levels of, gamma vibrational, (T), 19: 14597
energy levels of, corrections in Bohr-Mottelson model for rotational, 19: 17048
energy levels of, isomeric, (E), 19: 45357
energy levels of, gyromagnetic ratio and mean life of first excited rotational, 20: 19945
gamma reactions (γ,n) in stars, 16: 12308
gamma spectra, E2 emission parameters, 16: 21444
gyromagnetic ratio of, (E), 20: 8062(R) (COO-720-058)
half life of, (E), 20: 8062(R) (COO-720-058)
internal conversion coefficients, 16: 11032
isomeric state of, 17: 11690
neutron capture cross sections, 16: 20302(R) (ANL-6477(p.217-23))
neutron capture cross section measurements, 20: 46963(R) (ANL-7132)
neutron reactions (n,2n) at 14.8 Mev, cross sections for, 16: 7072
neutron reactions (n,2n) at 14.8 Mev, cross section for, 18: 19036
neutron reactions (n,2n) at 14 Mev, shell effects in, (T), 19: 12536
neutron reactions (n,2n) at 14.8 Mev, cross section for, (E), 19: 14614
neutron reactions (n,γ) at 10 kev to 3 Mev, cross sections for, (E), 20: 32370(R) (ANL-7175, pp 212-16)
neutron reactions (n,γ) with, energy-level transitions in isomeric ytterbium-177 from, (E), 20: 44709
neutron resonances in, spectra of, 19: 41661 (JINR-P-2158)
neutron resonances at 0 to 150 ev, (E), 20: 15839
nuclear rotations, 16: 11042
oxygen ion reactions with, double Coulomb excitation in, 17: 801 (TID-16963)
oxygen-16 inelastic scattering at 43.5 Mev, vibrational-state excitation in, (E), 19: 45321

YTTERBIUM ISOTOPES Yb-177

beta and conversion-electron emission, 18: 2403(R) (PR-P-58)
decay, 17: 32724(R) (PR-P-57(p.21-36))
decay scheme, 18: 8918(R) (PR-P-59(p.21-36))
energy level transitions in, delayed E-1, (T), 20: 15765
energy levels, 18: 1065
energy levels and gamma spectra, 16: 26254
energy levels in deformed E1 transition probabilities in, 18: 40501 (AE-152)
energy levels of, single quasiparticle, (T), 19: 17052
energy-level transitions in isomeric, from ytterbium-176 (n,γ) reactions, (E), 20: 44709
gamma dose constants for, 20: 46617
gamma magnetic transitions in, orbit-flip effects on, 17: 5350
gamma spectra, 18: 18214
gamma spectra, (E), 19: 8415
gamma spectra of metastable, 17: 9549
half life of isomeric, (E), 20: 15688 (AD-620384)
half lives of excited states of, (E), 19: 5197

YTTERBIUM ISOTOPES Yb-178

gamma spectra, 18: 40474 (IDO-16977(p.23-43))

YTTERBIUM MANGANATES

Curie point determination of, 19: 41059(T)
magnetic properties and manganese ion moment configurations of, 18: 24128 (CONF-405-34)
preparation, crystal structure, and optical properties of, 17: 40785
properties of, electric and magnetic, 18: 30431(T)

YTTERBIUM MOLYBDATES

preparation and crystal structure of, 20: 31740

YTTERBIUM NIOBATES

distribution in strontium molybdate single crystals, coefficients of, 20: 29746
effects on phase stability of zirconia, 20: 46153(P)
preparation and structure of perovskite type, 20: 844
preparation and thermal properties, 19: 38617
transition temperature of, relation of ionic radii to, 18: 12113
$CaMoO_4$–$YbNbO_4$, preparation and spectra of, 18: 26017
$CaWO_4$–$YbNbO_4$, preparation, luminescent properties, and structure of, 18: 26017

YTTERBIUM NITRATES
analysis of, for gadolinium, 17: 21661
complex formation with dipyridine, 18: 1686
properties of aqueous solutions of, thermodynamic and transport, 20: 22968 (IS-1344)
separation from aqueous solutions by solvent extraction using TBP-nitric acid system, 17: 37307
solubility in di- and tributyl phosphate, 16: 5342
specific gravity and apparent molal volume of aqueous solutions of, at 25°C, 20: 38905
spectra of solid, electron transfer, 20: 35506
stability, 17: 8004 (TID-14716)
toxicity in mice and rats, 18: 17458

YTTERBIUM NITRIDES
magnetic properties at 2 to 300°K, 20: 43939
properties of, electric and magnetic, 17: 32081

YTTERBIUM OXALATES
carbon-14 exchange between, and alkali metal oxalates, 20: 45634
dynamic decomposition of, effects of air, carbon dioxide, and nitrogen on, 18: 23507
solubility in EDTA at 25 and 40°C, 19: 9149
spectra of hydrate of, infrared, 20: 8898
spectra of solid, electron transfer, 20: 35506
spectra of, electron-transfer, 20: 25104
thermal decomposition of hydrated, 18: 8378
thermal decomposition of, mechanism of, 18: 31484
thermal decomposition of hydrates of, differential thermal analysis of products of, 20: 40900
thermal dissociation of hydrates of, 20: 35509

YTTERBIUM OXIDES
see also Sodium Ytterbium Oxides
atomic charge and permittivity of, (E/T), 19: 47901(T)
catalytic effects on dehydrogenation of cyclohexane at 515 to 590°C, 19: 30222
catalytic properties, 17: 2991
content in mckelveyite uranium mineral, 19: 40799
crystal structure at pressures of 25 to 40 kbars and 900 to 1020°C, 19: 4155
crystal structure of, effects of pressure on polymorphism in, 19: 17885
crystal structure and petrography of, 20: 24590 (ORNL-P-1158)
crystalline parameters and transformations of, stable above 2000°C, 20: 23679
determination in thorium oxide by emission spectroscopy, 20: 16393
determination of hydrated, from ytterbium hydroxide thermal decomposition, 20: 16441
effects on hydrogen oxidation, catalytic, 19: 26343
effects on optical properties of silicate glasses, 19: 44030
electric properties, 19: 28825
electronegativity and ion radii of, prediction of phases in binary systems with other oxides from, 19: 23061
enthalpy and entropy at high temperatures, 17: 12661 (BM-RI-6175)
enthalpy and thermal capacity at 298.1 to 1600°K, 19: 22240
magnetic susceptibility at 4.2 to 300°K, 18: 23513
magnetic susceptibility at 4 to 300°K, 20: 3318
magnetic susceptibility at 1.1 to 4.2°K, (E), 20: 24606
magnetic susceptibility of Yb_2O_3 at 1.3 to 4.2°K, (E), 20: 36378
oxygen-18 exchange between molecular oxygen and, 19: 46266
phase studies at 400 to 2200°C, 20: 25048
phase transformations in, at 50 to 1500°C, 20: 5536
phase transformations in, at high pressure and 550 to 1450°C, 20: 26833
polymorphism, 16: 3014
precipitation from calcium oxide crystalline solutions, kinetics of, 20: 7110
preparation of lower, 20: 38867(R) (COO-1109-22, Paper 6)
properties of, chemical and physical, 19: 11120
reactions with barium carbonates, ternary oxide formation in, 19: 46242(R) (TID-22207, Paper B)
reactions with calcium fluoride, 16: 32050
reactions with sodium oxide in presence of nitric acid, 19: 42514
reduction for preparation of isotopic foils, 19: 36307
reduction of, kinetics of aluminothermal, 19: 7371
refraction of, calculation of molar and specific, 19: 13395
separation of, from silicon oxides in liquid state, 17: 14287
solubility in ethyl, isopropyl, methyl, and propyl alcohols in presence of ammonia, 20: 20686
spectra from 50 to 700 cm^{-1}, infrared lattice, 20: 28629
spectra in low frequency region, infrared, 18: 23549
spectra of, infrared absorption, 17: 27840
spectra of, x-ray absorption, 19: 30194
spectral properties of rare earth-activated, 18: 13869
thermal expansion below room temperature, 20: 20168
thermodynamic properties, 16: 96 (TID-14101)
thermodynamic properties at 10 to 350°K, 16: 26963 (TID-16400)
toxicity in mice and rats, 18: 17458
x-ray absorption by, edge structure in, 19: 22185
ytterbium absorption spectra in, fine structure of L_m, 18: 39195
ytterbium-170 Mossbauer spectra in, 17: 2309
ytterbium-170 Mössbauer spectra in, hyperfine structure of, 17: 13244
actinide oxides–Yb_2O_3, preparation of sols of, 20: 39341(P)
Al_2O_3–Yb_2O_3, phase studies, 20: 45639
BaO–Yb_2O_3, optical properties of compounds formed in, 20: 13278
BaO–Yb_2O_3, phase studies, 20: 302
BaO–Yb_2O_3, preparation and properties of, $BaYb_2O_4$, 20: 45687
B_2O_3–Yb_2O_3, liquid immiscibility in, 20: 40910
CaO–Yb_2O_3, grain boundary precipitation in, 20: 31738
CaO–Yb_2O_3, phase diagrams, 20: 10822
CaO–Yb_2O_3, phase studies and solid state reactions in, 20: 7110
CaO–Yb_2O_3, phase studies, 20: 17087
CeO_2–Yb_2O_3, equilibrium phase studies on, 18: 23509
CuO–Yb_2O_3, crystal structure of sintered, 19: 42876
HfO_2–Yb_2O_3, crystallization of, from reactions of hafnium and ytterbium hydroxides, 19: 22191
IrO_2–Yb_2O_3, phase studies in air, 19: 32751
La_2O_3–SiO_2–Yb_2O_3, phase studies, 16: 18871
ReO_2–Yb_2O_3, analysis for platinum and rhodium using electron microprobe, 20: 26340(R) (AD-631987)
ReO_2–Yb_2O_3, crystal structure of Yb_2ReO_5 in, 20: 26340(R) (AD-631987)
ReO_2–Yb_2O_3, magnetic properties and structure of compounds formed in, 20: 36784(R) (AD-636054)
ReO_2–Yb_2O_3, phase studies at 1130 and 1300°C, 20: 17007(R) (AD-627468)
SiO_2–Yb_2O_3, crystal structure of compound formed in, 19: 36375
SiO_2–Yb_2O_3, phase diagram, 16: 6736
SiO_2–YbO, preparation and crystal structure, 19: 38621
SiO_2–YbO, spectra and crystal structure of, infrared, 19: 38622
SrO–Yb_2O_3, optical properties of compounds formed in, 20: 13278
SrO–Yb_2O_3, phase studies, 20: 302
SrO–Yb_2O_3, properties of compounds formed by interactions in, 20: 17044
ThO_2–Yb_2O_3, phase studies at 1200 to 1800°C, 16: 13584 (TID-14808)
ThO_2–Yb_2O_3, phase studies of temperature effects on solid solubility, 18: 8856
Yb_2O_3–TiO_2, phase studies, 19: 42464
Yb_2O_3–ZrO_2, crystal structure, differential thermal analysis, and thermal expansion of, 18: 23503
Yb_2O_3–ZrO_2, electric conductivity, 19: 37094
Yb_2O_3–ZrO_2, phase studies, 19: 42464
Yb_2O_3–ZrO_2, phase transformations in, fluorite, 19: 358(T) (ORNL-tr-201)
Y_2O_3–ZrO_2, crystal structure, evolution, 16: 2224

YTTERBIUM OXYBROMIDES
preparation and structure of, 20: 869

YTTERBIUM PERCHLORATES
reactions of, with *N,N*-dimethylacetamide, adduct formation in, 19: 36397
stability constants of, thermal, 19: 40509

YTTERBIUM PERRHENATES
preparation and properties of, 20: 43217

YTTERBIUM PHOSPHATES
crystal structure of, infrared spectral studies on, 20: 43219
preparation and properties of, conductometric and potentiometric studies on, 20: 38883
preparation and single crystal growth of ortho-, 18: 25356
spectra of solid, electron transfer, 20: 35506
spectra of, electron-transfer, 20: 25104

YTTERBIUM PHOSPHIDES
crystal structure and magnetic susceptibility, 19: 13289

YTTERBIUM SELENIDES
crystal structure, 17: 32125
crystal structure, 18: 1628
crystal structure and magnetic susceptibility, 19: 13289
crystal structure and stability, 19: 36365
crystal structure, 19: 44010
electric conduction in, 18: 37115 (ANL-6856)
electric conductivity and properties of, 18: 42068
phase studies at 600 to 1300°C, 20: 25579
preparation, semiconducting properties, and structure of, 19: 22965 (AL-TDR-64-239)
properties, 16: 32068
structure and electric properties, 16: 15260(R) (AD-262215)
thermoelectric properties of sesqui-, 17: 11292 (AD-277043)
thermoelectric properties, 17: 11296 (AD-278352)
CaSe–Yb_2Se_3, crystal structure, 19: 42467
CaSe–Yb_2Se_3, phase studies, 20: 10857
NdSe–YbSe, electric conductivity and properties of, 18: 42068
NdSe–YbSe, thermoelectric properties, 17: 11296 (AD-278352)

YTTERBIUM SILICATES
preparation of $Yb_2O(SiO_4)$ and $Yb_2Si_2O_7$ monocrystals, 20: 40919

YTTERBIUM SILICIDES
crystal structure, 19: 11125
crystal structure, 19: 42864
structure, 19: 23006(T) (JPRS-28849(p.184-7))

YTTERBIUM SULFATES
crystal structure and magnetic properties at 100 to 300°K, 16: 24304
crystal structure and bond types of octahydrates, 19: 19915
crystal structure of, infrared spectral studies on, 20: 43219
dissociation constants of, electrolytic, 20: 36830
heat of dehydration, 16: 1783
preparation, properties, and structure, 17: 15950 (LADC-5566)
spectra of solid, electron transfer, 20: 35506
spectra of, electron-transfer, 20: 25104
thermal decomposition, 16: 26993

YTTERBIUM SULFIDES
crystal structure, 18: 1628
crystal structure and magnetic susceptibility, 19: 13289
electron structure of mono-, electric conductivity and magnetic susceptibility from, 17: 32082
preparation of mono-, by fused salt electrolysis, 16: 10007
properties of crystals of, chemical and physical, 17: 8080
properties of, electric and magnetic, 17: 32081
reactions with ytterbium, formation of ytterbium(II) ytterbium(III) sulfide by, 19: 2297
spectra of, nephalauxetic effect in reflection, 19: 36390
ytterbium-171 nuclear magnetic resonance in, magnetic moment from, 18: 7774
Ce_2S_3–YbS, compound formation in, 20: 16431
Cu_2S–Yb_2S_3, phase studies, 20: 18644
Dy_2S_3–YbS, compound formation in, 20: 16431
Gd_2S_3–YbS, compound formation in, 20: 16431
Ho_2S_3–YbS, compound formation in, 20: 16431
La_2S_3–YbS, compound formation in, 20: 16431
Nd_2S_3–YbS, compound formation in, 20: 16431
Pr_2S_3–YbS, compound formation in, 20: 16431
Sm_2S_3–YbS, compound formation in, 20: 16431
Tb_2S_3–YbS, compound formation in, 20: 16431
YbS–Y_2S_3, compound formation in, 20: 16431

YTTERBIUM SYSTEMS
B–C–Yb, phase studies, 18: 25319 (COO-1140-103)
graphite–Yb, preparation and magnetic susceptibility of, 20: 21413
graphite–Yb, preparation and properties of intercalation compounds in, (E), 20: 44999
Yb–YbH_2, equilibrium hydrogen dissociation pressure in, 20: 12829 (TID-22502)

YTTERBIUM TANTALATES
preparation and structure of perovskite type, 20: 844

YTTERBIUM TELLURIDES
crystal structure, 17: 32125
crystal structure, 18: 1628
crystal structure and magnetic susceptibility, 19: 13289
electric conductivity and properties of, 18: 42068
preparation, semiconducting properties, and structure of, 19: 22965 (AL-TDR-64-239)
properties, 16: 32068
structure and electric properties, 16: 15260(R) (AD-262215)
thermoelectric properties, 17: 11296 (AD-278352)

YTTERBIUM TUNGSTATES
preparation and crystal structure of, 20: 31740

Yttria
see Yttrium Oxides

YTTRIUM
abundance in meteorites and terrestrial matter, 18: 10753
abundance in meteoritic, terrestrial, and solar matter, review on, 19: 13620
abundance in solar atmosphere, 16: 29599 (AFOSR-3024)
abundance in solar system, (T), 19: 6433
abundance in sun, (E), 20: 17237
alloying characteristics with transition metals, 18: 41924(R) (IITRI-578P19-13)
alloying effects on properties of niobium, 16: 7897 (WADC-TR-57-344 (Pt.V))
alloying effects on structure and magnetic properties of Heusler alloys, 16: 9185 (AD-261209)
alloying effects on lattice constant of cerium, 16: 32056
alloying effects on hcp-bcc phase transition in zirconium, 16: 33499
alloying effects on oxidation of molybdenum at 1000 to 1540°C, 17: 8739 (AD-277355)
alloying effects of, on oxidation resistance of molybdenum, 17: 20411 (AD-282638)
alloying effects on mechanical properties of aluminum alloys, 17: 32608
alloying effects on mechanical properties and oxidation resistance of chromium alloys, 17: 36288(R) (ASD-TDR-63-493)
alloying effects on heat of transport of hydrogen in Zircaloy-2, 18: 5800
alloying effects on corrosion resistance of zirconium in carbon dioxide, 18: 12576 (GEAP-4089(Vol.I)(Paper 3))
alloying effects on corrosion properties of types 405 and 406 stainless steel, 18: 26894(R) (ANL-6868(p.109-16))
alloying effects on corrosion properties of tantalum, 18: 30975(R) (LAMS-3096)
alpha reactions (α,n) at 12 to 18 Mev, (E/T), 19: 3362
analysis for impurities by chemical-spectral method, 19: 30137
analysis for impurities, spectral, (T), 19: 32296
analysis for lanthanum, extraction-photometric, 20: 35449
analysis for nitrogen and oxygen by d-c carbon-arc, gas chromatographic technique, 19: 9069
analysis for oxygen, 20: 20572
analysis for rare earths, activation, 16: 2963 (IS-376)
analysis for scandium after solvent extraction using diantipyrilmethane, 18: 13702
analysis for tantalum traces, activation, 19: 17777 (IS-1117)
analysis of neutron-irradiated, for gadolinium and samarium by gamma spectroscopic, 16: 132(T) (AEC-tr-4686)
analysis of, methods for, 20: 4299(R) (ORNL-2711)
analytical chemistry review, 16: 32945
anion-exchange behavior in ethanol-containing dilute sulfuric acid, 16: 4148
availability, costs, and purity of, (E), 19: 31532 (BMI-X-151)
bibliography, 16: 12116 (WADD-TR-60-864)
binding to blood serum proteins and nucleic acids, tracer study, 17: 10307 (TID-17522)
binding with bone and organic compounds, tracer study, 17: 15567
bonding of tube to end plug, 18: 8770 (NAA-SR-Memo-8528)
book: *The Technology of Scandium, Yttrium, and the Rare Earth Metals*, 18: 4189
bremsstrahlung reactions (y,n) at 55 Mev, angular distributions from, 16: 13988
bremsstrahlung reactions with, isomer production in, (E), 20: 46733
chelates of, urinary excretion of, 20: 14256
chemical properties, 20: 7093
coating of, method for alumina–vanadium oxide, 20: 35875(P)
coatings for, development of protective, 18: 1834(R) (IS-700(Sect.E))
coatings for, oxidation-resistant, 17: 41377(P)
coatings for, development of protective, 19: 9281(R) (IS-900(Sect.E))
combustion with fluorine, products and yields from, 20: 5523(R) (ANL-6925, pp 175-85)
concentration using cation exchange with alkali metal- and alkyl ammonium phosphomolybdates, 16: 18898
content and distribution in acid igneous rocks of Africa, 18: 37358
content and relative abundances in terrestrial materials, 18: 20202
content in alkali igneous rocks, 16: 31970
content in eclogites from Nowa Wies in Snieznik Klodzki, Poland, 20: 18900
content in granitoids of Susamyr Batholite in central Tian-Shan, 18: 6966
content in Gulf of Mexico surface water, 20: 43087(R) (TID-23295, Sect.4)
content in meteorites and terrestrial specimens, 17: 30690
content in meteorites and basaltic, granitic, and sedimentary rocks, 19: 36648
content in minerals and rocks of batholith of Southern California, (E), 19: 38848
content in red-colored Paleozoic deposits in Northern Tien Shan, 20: 14780(T) (AEC-tr-6579)
content in soils of Tomsk region, 20: 2065
content in standard diabase W-1 and standard granite G-1, 19: 26529
content of, in marine organisms, 17: 15604
contents in meteoritic and terrestrial matter, 19: 37428(R) (N64-32896)
coordination chemistry of, review on, 19: 22179
corrosion by acids, air, bases, salts, and distilled water at 25 and 30°C, 16: 5671(R) (TID-14467)
corrosion by aluminum, lead, tin, and zinc at 800 to 1100°C, 19: 40961
corrosion by aqueous chloride and nitrate solutions, rate of, 20: 23618
corrosion by atmosphere at high temperatures, 16: 5315 (WADD-TR-61-123)
corrosion by chromium–uranium and manganese–uranium eutectics, 20: 41064(R) (IS-1500(Sect.E))
corrosion by hydrofluoric and oxalic acid mixtures, 19: 9281(R) (IS-900 (Sect.E))
corrosion by hydrofluoric acid at high temperatures, 20: 4077(R) (IS-1200(Sect. E))
corrosion by liquid metals and their alloys with thorium and uranium, 19: 4617 (IS-888)
corrosion by liquid chromium–uranium and manganese–uranium alloys, 20: 4077(R) (IS-1200(Sect. E))
corrosion by manganese–plutonium–uranium alloys at 900°C,

18: 30975(R) (LAMS-3096)
corrosion by molten uranium alloys at 850°C, 16: 22549
corrosion protection by hydrofluoric acid, 19: 44628
crystallization with thionalid, tracer study of, 16: 12961 (USNRDL-TR-551)
crystallography, interplanar angles, 17: 2095
deformation and microhardness, 16: 12155
deformation mechanisms of, 20: 4299(R) (ORNL-2711)
deformation of polycrystalline, effects of second phases on, 20: 41412(R) (IS-1500(Sect. M))
deposition in and elimination from tissues, 16: 28847
deposition in bone, reaction mechanisms, 17: 10332
deposition on platinum anode, electrolytic, 17: 18204
determination as molybdate, conductometric, 20: 35433
determination as trace in standard rocks G-1 and W-1, spectrographic, 16: 20831
determination by activation using 14-Mev neutrons, 18: 9966 (CEA-2358)
determination by arsenate-iodometric method, 19: 38551
determination by carrier distillation, spectrographic, 18: 9985
determination by consecutive chelatometric titration, 18: 43413
determination by complexometric photometric titration, 19: 15375
determination by complex formation with methyl thymol blue photometric, 19: 17840
determination by charged-particle reactions at 2 Mev, 20: 43097
determination by flame-photometric method, emission sensitivity for, 16: 22028
determination by neutron activation and gamma spectrometry, 19: 5787
determination by neutron activation methods, 19: 32072
determination by neutron-activation methods, 20: 25011
determination by precipitation as diliturate, gravimetric, 18: 31447
determination by potentiometric titration using arsenazo III, 19: 7299
determination by radioactivation on chromatographic paper, 18: 39120
determination by solvent extraction and spectrophotometry using 1-(2-pyridylazo)-2-naphthol, 16: 139
determination by spectrochemical methods, voltage-fluctuations patterns in, 19: 40416
determination by thermal-neutron activation methods, sensitivity for, 19: 9071
determination by x-ray absorption, 16: 31545 (LADC-5198)
determination in Al–Cr–Fe and Cr–Ni alloys, spectrophotometric, 18: 8300
determination in aqueous solutions and minerals in presence of dysprosium by neutron activation, 18: 29581
determination in americium by emission spectrography, 20: 8835 (RFP-414)
determination in aqueous solutions by x-ray fluorescent spectrometry, 20: 18611
determination in aqueous solutions, design of oxyacetylene burner for measuring sensitivity of spectrophotometric, 20: 29083(R) (UCRL-14767)
determination in beryllium–copper alloys, spectrographic, 18: 8299
determination in cast steels, spectrophotometric, 16: 17602
determination in chondrites and sediments, activation, 16: 20841
determination in cerium, erbium, and lutetium, mass spectrographic, 19: 2232
determination in copper–yttrium and chromium–nickel alloys using Arsenazo-III, spectrophotometric, 20: 10773
determination in diabase W-1 and granite G-1, spectrographic, 16: 17895
determination in diabase and granite by spark source mass spectrography, 19: 11406
determination in dysprosium oxide, spectrographic, 19: 22089 (AEET/Spec/14)
determination in dysprosium and terbium using bis(2-ethylhexyl) phosphate, chromatographic, 20: 16385
determination in europium oxide, spectrographic, 17: 2931
determination in fergusonites and xenotimes, fluorometric, 20: 29094
determination in geological samples, activation, 19: 36243(R) (X64-17610)
determination in glass, emission spectrographic, 20: 12810
determination in hydrochloric acid or methanol–nitric acid media, spectrophotometric, 20: 3888 (TID-22402)
determination in hydrochloric acid solutions, spectrographic carrier-distillation, 20: 36729
determination in iron and nickel base alloys, spectrographic, 16: 11539
determination in igneous and metamorphic apatites, spectrographic, 20: 26787
determination in lithium fluoride–magnesium fluoride–yttrium fluoride, 20: 4999(R) (ORNL-2599)
determination in mixture with europium, lanthanum, and ytterbium, flame photometric, 16: 28876(T) (AEC-tr-5291)
determination in minerals and rocks, spectrographic, 17: 6008
determination in mixture with zirconium oxide, x-ray fluorescence, 18: 39135
determination in minerals using Alizarin Red S, photometric, 19: 13258
determination in mixtures of actinides and fission products by paper chromatography, 20: 5509
determination in minerals and ores, spectrometric, 20: 29134
determination in magnesium alloys by successive potentiometric titration, 20: 38830
determination in natural waters, tracer studies of ion adsorption on glass and plastic surfaces in, 19: 30097
determination in ores by x-ray fluorescence, 16: 9967
determination in oxide mixtures with lanthanum and scandium, photometric, 16: 28899
determination in oxalate precipitates, complexometric titration methods for, 18: 1584
determination in presence of dysprosium, activation, 18: 3705
determination in presence of niobium and zirconium by x-ray spectrum method, 18: 5226
determination in presence of aluminum, arsenate method for iodometric, 20: 5506
determination in presence of lanthanum by infrared spectra of oxinate, 20: 8851
determination in rare earth mixtures, spectrographic, 17: 127
determination in rare earth oxides, spectrographic, 17: 17993
determination in rare earth groups, flame photometric, 18: 1548
determination in rare earth oxide mixtures and xenotime ores, x-ray-fluorescence, 18: 37080
determination in rare earth mixture by x-ray fluorescent spectrometry, 20: 18611
determination in rocks, chemical spectrographic method for, 20: 29083(R) (UCRL-14767)
determination in solutions of fission products, development of radio-electrochromatographic method for, 16: 3347(T) (AEC-tr-4497(p.382-8))
determination in silicate rocks, combined cation exchange-spectrochemical, 16: 25287
determination in soil and rocks, 17: 6019
determination in standard silicate rocks, activation, 18: 39128
determination in steel by solution spectrographic method, 20: 266
determination in silicate ores, activation, 20: 2056
determination in silicates, activation, 20: 26782
determination in standard igneous rocks G-1, W-1, and G-B by x-ray fluorescence, 20: 29101
determination in solutions, spark method for spectrographic, 20: 38832
determination in tantalum–yttrium alloys, spectrophotometric, 19: 288 (LA-3123)
determination in tantalum and tantalum–tungsten alloys, spectrographic, 19: 21690(R) (LA-3244)
determination in thorium and uranium dioxides, x-ray spectrographic, 20: 18558 (AECL-2526)
determination in uranium thermal neutron fission products by ion exchange, 16: 12965
determination in uranium-233-labeled uranium dioxide, spectrographic, 18: 9980
determination in yttrium and samarium oxides, activation, 16: 25292
determination in zircons, x-ray fluorescence, 20: 35666
determination, micro-coulometric, 16: 25285
determination of, design of quantometer for x-ray, 17: 40751
determination of, in residues by iron flux method, spectrographic, 17: 19942 (PG-Report-157)
determination of, in hydrochloric acid by powder sifting method, spectrographic, 17: 19972
determination of, in presence of cesium and lanthanum, photometric, 17: 21656
determination of micro amounts of, in rare earth oxides by x-ray fluorescence, 19: 40440
determination of, review on x-ray spectrographic, 17: 23252 (IS-550)
determination of radioactive, by electrophoresis, use of EDTA in, 20: 10792
determination of traces of, in tantalum, spectrophotometric, 19: 5773 (LA-3133)
determination of trace amounts of, by reactor neutron activation methods, 20: 26760
determination of, gravimetric, 19: 11016
determination of, using flame photometer, 19: 36311
determination of, in rare-earth mixtures, photometric, 20: 252
determination of, complexometric, 20: 10779
determination of, evaluation of titrimetric EDTA method with visual indicator end points for, 20: 43067(R) (IDO-14679, pp 6-46)
determination of, in solution using Chrome Azurol S, spectrophotometric, 20: 43110
determination of, in mixture of rare earths, fluorimetric, 20: 43150
determination of, as chromate by conductometric titration, 20: 45600
determination, spectrophotometric, 17: 19987
determination, using arsenazo III, absorptiometric, 16: 14653
determination using diammonium-5,5'-indigo disulfonate, 17: 10568

determination using xylenol orange, spectrophotometric, 17: 12199
determination using wall-stabilized arc discharge, 17: 25124
determination using methylthymol blue, 18: 3688
determination using 4-(2-pyridylazo)resorcinol, spectrophotometric, 18: 19895
determination using cyclohexanediaminetetraacetic acid, potentiometric, 18: 33507
determination using 4-(2-pyridylazo)resorcinol, spectrophotometric, 18: 35461
determination using 2-(*p*-sulfophenylazo)-1,8-dihydroxynaphthalene-3,6-disulfonic acid, spectrophotometric, 18: 41341
determination using xylenol orange, spectrophotometric, 18: 43394
determination using thoron, photometric, 19: 327
determination using chromotrope 2B, photometric, 19: 328
determination using *p*-(2-azo-pyridine)-resorcinol, spectrophotometric, 19: 2236
determination using *N,N'*-bis(2-hydroxy-5-sulfophenyl)-*C*-cyanoformazan, photometric, 19: 7324
determination using mercury-suspension electrodes, polarographic, 19: 36268
determination using methylthymol blue, spectrophotometric, 20: 8860
determination using Chromotrope 2B, photometric, 20: 1772
determination using *N*-methylanabasine-α'-azo-β-naphthol, photometric, 20: 26801
determination using neutron activation analysis, 20: 33231
determination with thorium in monazites, thorium phosphates, and xenotimes, 18: 19885
determination, x-ray spectrometric, 16: 11568
determination, use of pulsed neutrons in activation, 19: 36323
deuteron elastic scattering at 15 Mev, strong absorption model analysis of, 18: 42708
deuteron elastic scattering by, angular distributions from, 20: 46580(R) (BNwF-FBK-66-05)
deuteron reactions (d,n) with, cross sections and mechanism of, (E), 20: 38159
deuteron scattering at 52 Mev, 20: 46580(R) (BNwF-FBK-66-05)
development for use as reactor material, 17: 14740 (TID-11295(2nd Ed.))
diffusion in yttrium oxide, 17: 23292 (IS-518)
diffusion of carbon, nitrogen, and oxygen in, at 1235 to 1460°C in electric field, 20: 5599
diffusion of carbon, nitrogen, and oxygen in, at 1235 to 1460°C, 20: 21254
diffusion of hydrogen in, (E), 20: 23755
diffusion penetration by plutonium-uranium alloys, 16: 28555 (TID-7623 (p.105-21))
discovery and development of, review on, 17: 10618
dissociation energy of gaseous and heat of vaporization of solid, correlation of, 17: 6095
dissociation energies at high temperatures, 18: 3795
dissociation energy of gaseous molecule Y_2, 18: 7218 (WADD-TR-60-782(Pt.XIX))
dissociation energy and free energy functions of, calculation of, 18: 8357
dissociation pressure, 18: 31417 (AWRE-O-22/64)
dissolution and ion exchange in ammonium and potassium carbonate solutions, 17: 12240
dissolution and ion exchange behavior in ammonium carbonate solutions, 17: 39035
distribution between lead and zinc at 500°C, 18: 42089
distribution between magnesium chloride–potassium chloride–sodium chloride and aluminum–magnesium alloy at 550 and 600°C, 19: 32279(R) (ANL-7020(p.3-99))
distribution coefficients in Dowex-1 and lithium nitrate solutions, 16: 11637
distribution coefficient in aluminum, mathematical determination of, 20: 21369
distribution, elimination, and uptake in guinea pigs after inhalation, 17: 37052
distribution in accessory minerals and earth's crust, 17: 8424
distribution in blood, liver, and skeleton, of tracer, 16: 1385
distribution in tissues of mice of ionic and chelated form, tracer study, 17: 10308 (TID-17542)
distribution of, between nitric acid and ion-exchange resin, synergistic effects of thorium on, 17: 15948 (LA-2836)
effects of subcutaneous implantations of, in mice, 19: 38334 (COO-1170-1)
effects on chromium–iron alloys oxidation by carbon dioxide, 20: 2263
effects on corrosion resistance of tantalum to liquid iron–plutonium alloy, 18: 32085 (LADC-6026)
effects on corrosion properties of tantalum, 18: 45002(R) (LA-3163-MS)
effects on corrosion properties of tantalum, 19: 13886(R) (LA-3208-MS)
effects on crystallization of molybdenum, 20: 35905
effects on crystal structure of cobalt, iron, and nickel intermetallic compounds, 20: 37243
effects on determination of europium and terbium in potassium carbonate solutions, 20: 33217
effects on dog and rabbit membranes of contact with, 20: 25(R) (TID-22294)
effects on ductility of iodide chromium, 18: 32189
effects on ductility of chromium, 19: 26860
effects on ductility of fissium–uranium–zirconium alloys, 19: 47004 (NMI-4997, pp 45-54)
effects on ductility of austenitic stainless steel, 20: 31669
effects on grain size of tungsten, 20: 39400 (NASA-TN-D-3531)
effects on grain structure of tantalum and tantalum alloys, 20: 46219(P)
effects on growth and metabolism of bacteria, fungi, molds, and yeasts, 20: 16191
effects on high-temperature properties of eutectic alloys, 20: 17108
effects on hot hardness of zirconium oxides, 20: 5846
effects on hydrogen distribution in Zircaloy, 20: 11221
effects on mechanical properties and microstructure of cobalt and nickel alloys, 20: 27550
effects on microstructure of cast iron, 19: 22999(T) (JPRS-28849(p.31-46))
effects on niobium, additive, 20: 4299(R) (ORNL-2711)
effects on nitrogen and oxygen content in niobium-based alloys, 19: 40953 (PWAC-441)
effects on oxidation resistance of chromium, 18: 16423(R) (GEMP-197)
effects on oxidation of zirconia, 20: 11227
effects on oxidation resistance of chromium–nickel–niobium steel in carbon dioxide at high temperature, 20: 35914
effects on phase transformation of cerium, 16: 1694
effects on plasticity of zirconia, 18: 27882 (GEAP-4473)
effects on plutonium(IV) sorption on platinum in nitric acid, 17: 20082
effects on properties and structure of molybdenum, 17: 8811 (NP-12481)
effects on properties of electrorefined vanadium, 19: 2795 (BM-RI-6553)
effects on properties of cast austenite chromium–nickel steel, 19: 22879(T) (JPRS-28849(p.319-25))
effects on rabbit skin, effects of various solvents on toxic, 20: 25(R) (TID-22294)
effects on radioinduced color center formation in calcium and strontium fluorides, 17: 18146
effects on rats, tumorigenic, 20: 8654
effects on spectrophotometric determination of uranium, 20: 7031
effects on spectrofluorimetric determination of scandium, 20: 14476
elastic properties at 4 to 900°K, 18: 25968(R) (ANL-6868(p.267-86))
electric conductivity of, from electron-phonon scattering in, 17: 11221
electric conductivity of, effects of temperature on, 19: 9281(R) (IS-900 (Sect.E))
electric conductivity and magnetic susceptibility below 300°K, (E), 19: 30797
electric conductivity at 2 to 20°K, 19: 37084
electrochemical characteristics of, in phosphoric acid, 17: 25165 (TID-18697)
electrochemical properties in phosphoric acid, 17: 32034 (CONF-20-22)
electron binding energies of, measurements for, 17: 18924
electron slowing down by, spectra from, (E/T), 20: 7659(R) (ORNL-3849, pp 101-50)
electron structure of, analysis using positron annihilation, (E), 20: 11323
electronic structure of, (T), 20: 4476(R) (IS-1200(Sect.P))
electrophoresis in hydrochloric acid, mobility and spot area in paper, 19: 19810
elimination of deposited, from man, effect of therapy on, 19: 13097
energy level transitions in, Coster-Kronig, (T), 20: 15238 (CONF-233 (Vol.3), pp 398-418)
enthalpy and related thermodynamic properties at 0 to 1675°C, 17: 4929 (IS-327)
exchange in sulfonated polystyrenes, velocity of self-, 18: 43503
extrusion of clad and unclad, into rods and tubing, 19: 44636 (IS-1031)
extrusion of, high-velocity, 18: 2163(R) (IS-700(Sect.M))
extrusion of, high-energy-rate, 20: 783 (IS-1227)
extrusion of, methods for, 20: 41412(R) (IS-1500(Sect. M))
fabrication by extrusion and rolling, 19: 9604(R) (IS-900(Sect.M))
fabrication by rolling, swaging, and drawing, 18: 2163(R) (IS-700 (Sect.M))
fabrication process development, 16: 498 (NMI-1247)
fabrication techniques and properties, 16: 32058
fabrication, ore processing, properties, and uses of, 18: 35950
Fermi surface, (T), 20: 22338
friction and wear properties of, in vacuum, effects of crystal structure on, 20: 21365
friction characteristics in vacuum, 19: 6255 (NASA-TN-D-2513)
gamma attenuation by, effects of hydridation on, 16: 6074 (DC-57-7-51)
gamma reactions (γ,n) with, neutron angular distribution from, 18: 34935
gamma spectra from 14-Mev neutron activation of, determination by, 19: 26241

geochemistry and mineralogy of, in Cherry Mountains (Urals), USSR, book, 19: 20190
growth and nucleation on tungsten, field emission from epitaxial, 19: 25018
growth of single crystals of, method for, 17: 41372
hardening of, effects of dispersion additives on, 20: 4297(R) (IS-1200 (Sect.M))
helium and hydrogen ion attenuation at 0.1 to 500 Mev, tables for, 20: 41619 (CEA-R-3042)
ion exchange and solubility in potassium carbonate solutions, 18: 31453
ion exchange in concentrated hydrochloric and perchloric acids, distribution coefficients for, 18: 17759
ion exchange on ammonium phosphomolybdate and phosphotungstate, mechanism, 19: 11055 (UJV-1139/64)
ion exchange on zirconium-base and clay-mineral ion exchangers, 17: 25364
ion exchange with hydrogen, elution dynamics of, 18: 27459
liquid, solubility of tantalum and tungsten in, at high temperatures, 20: 41412(R) (IS-1500(Sect. M))
magnetic properties of, effects of crystalline field and structure on, 18: 24186
magnetic properties at 2 to 300°K, 20: 43939
mechanical properties, 16: 1693
mechanical properties, 16: 5315 (WADD-TR-61-123)
mechanical properties, 17: 14740 (TID-11295(2nd Ed.))
meson (μ^-) capture by, probability for, (T), 20: 28456
metabolism by marine organisms, tracer study of, 17: 30281(R) (TID-19104)
metabolism in feces, tissues, and urine, 20: 25(R) (TID-22294)
Mössbauer effect of gold-197 in, relation between chemical shift and electronegativity in, 20: 7055 (UCRL-16436)
neutron absorption cross section in pitchblende, thermal, 20: 37994
neutron activation at 14.3 Mev, (E), 20: 19809 (CEA-R-2900)
neutron attenuation in hydrided, 16: 6076 (XDC-57-1-32)
neutron attenuation by, effects of hydridation on, 16: 6074 (DC-57-7-51)
neutron capture cross sections, 16: 26509
neutron capture gamma spectra, high-energy, 19: 25468(R) (ARF-1193-17)
neutron cross sections, 16: 7012 (DC-59-7-171)
neutron cross sections for, nine and sixteen group, 17: 22789 (GEMP-173)
neutron elastic scattering anisotropy in, 18: 15199 (NAA-SR-Memo-9022)
neutron elastic scattering at 3.3 Mev, asymmetry in polarized, (E/T), 19: 10343
neutron elastic scattering at 3.2 Mev, (E/T), 20: 46644
neutron inelastic scattering at 6 Mev, compound-nucleus and direct reactions in, 17: 38207
neutron intermediate resonances and total cross sections at 3 to 650 kev, (E), 19: 35462
neutron radiative capture cross sections at 30 and 65 kev, 18: 34274(R) (NIRS-2(p.3-15))
neutron reactions at 3.7 Mev, cross-section measurements, 16: 8224
neutron reactions, yttrium-90-isomer production in fast, 16: 3705
neutron reactions (n,γ) at 0.025 ev, spectra from, 19: 40896
neutron resonance parameters for, 18: 11195(R) (EANDC(E)-49(L))
neutron scattering by, measurement of polarization in, 17: 2243(R) (TID-17083)
neutron scattering by, amplitude of thermal, 17: 26615(T)
neutron scattering length of, 19: 47888
neutron total cross section of, fast, 17: 20982 (HW-SA-2875)
neutron total cross sections at high energies, fluctuations in, 20: 38173
nuclear magnetic fields in iron, (E), 20: 44824
nuclear magnetic resonance in, 19: 9767(R) (IS-900(Sect.P))
nuclear magnetic resonance of, Knight shifts and relaxation times in, (E), 19: 9141
nuclear magnetic resonance in, (E), 20: 4476(R) (IS-1200(Sect.P))
oxidation, 18: 2163(R) (IS-700(Sect.M))
oxidation, alloying effects of impurities, 17: 14740 (TID-11295(2nd Ed.))
oxidation by air at 500 to 1400°C, 19: 2750
oxidation by air at 500 to 1400°C, 19: 9604(R) (IS-900(Sect.M))
oxidation by air, impurity effects and mechanisms of, 20: 4297(R) (IS-1200(Sect.M))
oxidation by moist air, kinetics of, 20: 31686
oxidation in air at 900 and 1400°C, 18: 25930
oxidation in air at 1100°C, scale formation in, 20: 4334
oxidation in dry and moist air at 100 to 800°C, rate of, 20: 21265 (RPI-2714-8)
oxidation kinetics at 200 to 650°C, 19: 36988
oxidation kinetics of, effects of moisture and temperature on, 20: 35854
oxidation of, in air at 500 to 1400°C, 17: 4447 (IS-500(Sect.M))
oxidation of, kinetics of, 18: 35952 (AWRE-O-45/64)
oxidation of, kinetics of high-temperature, 20: 5859
oxidation protection of, coatings for, 20: 4077(R) (IS-1200(Sect. E))
partition between magnesium alloys and magnesium chloride–potassium chloride–sodium chloride mixture, 20: 3865 (ANL-7064)
partition coefficients and reciprocal ionic radii, 17: 27562 (INSJ-54)
performance of cathodes of, in diode ion pumps, 20: 10976 (IS-T-46)
pharmacology of, 16: 5127(R) (ORO-480)
phase transformation temperature, 16: 5315 (WADD-TR-61-123)
phase transformations in, relation of c/a ratio and elastic moduli temperature dependence with, 19: 44676(R) (ANL-7000, pp 176-82)
plasticity of, effects of temperature on, 20: 4297(R) (IS-1200(Sect.M))
polarographic properties of, on fused potassium acid sulfate electrolyte, 20: 29210
positron annihilation in, effects of local structure on angular correlation of gamma rays from, 18: 18485
positron annihilation in, effects of local structure on angular correlation of gamma rays from, 18: 18485
positron annihilation in, photon angular distributions from, (T), 20: 22338
positron mean life in, 17: 25944
precipitation by benzenephosphinic and benzenephosphonic acids, 18: 27308
precipitation using dimethylbenzenearsonic acid, 19: 9136
precipitation using trichlorobenzenearsonic acid, 19: 9137
precipitation with cerium–cadmium intermetallic compounds from liquid cadmium, 18: 34192
precipitation with ferric hydroxide, tracer studies of, 18: 39172(T) (AEC-tr-6390(p.460-5))
precipitation with aluminum tris-(8-hydroxyquinolate), 18: 39255
precipitation with calcium oxalate, tracer studies of, 19: 9108
preparation and properties of distilled, 17: 23948 (IS-521)
preparation and properties of crystals of, 17: 36211
preparation and properties, 20: 4297(R) (IS-1200(Sect.M))
preparation and purification, 19: 40948 (IS-1195)
preparation and purification of, process development for, 20: 13180(R) (IS-RD-4)
preparation as radiation target substrate for tritium, 18: 27815(R) (ORNL-TM-718)
preparation by metallothermic reduction of halides, 17: 29247 (BM-RI-6259)
preparation by reduction of yttrium chloride by magnesium, 19: 18437
preparation of crystals of, by zone refining and vacuum distillation, 17: 41395
preparation of high-purity, 17: 4447 (IS-500(Sect.M))
preparation of high-purity, methods for, 20: 41412(R) (IS-1500(Sect. M))
preparation of monocrystals of, by zone melting in vacuum, 20: 9388
preparation of self-supporting radiation targets of, 20: 17218
preparation of single crystals of, 18: 2163(R) (IS-700(Sect.M))
preparation of single crystals of, by arc-zone melting, 18: 18339
preparation of single crystals of, by arc-zone melting, 18: 18339
production, 18: 3798(P)
production, 20: 4299(R) (ORNL-2711)
production from yttrium fluoride, 20: 4999(R) (ORNL-2599)
production of pure microspheres of, 17: 27789(R) (MLM-1156)
properties and uses, 19: 23005(T) (JPRS-28849(p.158-65))
properties as fuel element cladding, 18: 15563
properties as nitrogen and oxygen scavenger in molybdenum and tungsten, 16: 25696(R) (DRI-2010)
properties for use as fuel-element cladding, 19: 22884
properties of, chemical and physical, 17: 18071
properties of, chemical and physical, 17: 32648
properties of, review on mechanical, metallurgical, and physical, 18: 14507
properties, physical and thermodynamic, 19: 40948 (IS-1195)
properties, structure, and uses review, 16: 24201 (IS-222)
proton reactions (p,n) at 18.5 Mev, angular distributions of quasielastic, 18: 40587
proton reactions at 100 Mev, isomeric state from, 17: 17141
proton reactions (p,pn) at 20 to 150 Mev, excitation functions for, 16: 28042
proton reactions with, cross section ratios of isobars from, 20: 30531
purification, 18: 2163(R) (IS-700(Sect.M))
purification, 19: 22999(T) (JPRS-28849(p.31-46))
purification by electron-beam melting, 17: 34330(R) (USBM-U-1057)
purification by electron-beam melting, 19: 44588 (BM-RI-6661)
purification by electron-beam melting, 20: 4999(R) (ORNL-2599)
purification by electrotransport, 20: 41412(R) (IS-1500(Sect. M))
purification by fused zone technique, 19: 42429
purification by vacuum distillation, 16: 5315 (WADD-TR-61-123)
purification by zone refining with vacuum envelopes, 16: 2127
purification by zone refining, 20: 4299(R) (ORNL-2711)
purification of commercial-grade, 19: 9604(R) (IS-900(Sect.M))
purification of, in vacuum, (E), 19: 32296
purification of, radiochemical method for, 20: 8838 (UCRL-14258)
purification techniques, 19: 30338
purification using magnesium chloride, 18: 43732(P)
purification using condensation column with temperature gradient, vacuum-

distillation, 19: 42814
purification, chemical process for, 19: 6252 (IS-984)
quantum defect for ^3S state, 17: 20736
radiosensitivity effects on plants, 19: 42369
reactions of, with uranium dioxide, 16: 32034(R) (GEMP-15A)
reactions with cerimolybdic acid and its salt in chloride and nitrate solutions, precipitations in, 19: 2287
reactions with chlorine at 300 to 1700°K, mass spectrometry of surface, 18: 43476
reactions with elements of periodic table, review on, 18: 14507
reactions with hexamethylenediaminetetraacetic acid, 16: 17622(T) (AEC-tr-4456(p.15365))
reactions with hydrogen in liquid magnesium and zinc solvents, 18: 35548
reactions with hydrogen, 19: 15466(T) (LA-tr-65-2)
reactions with manganese–plutonium–uranium alloys, 17: 22855(R) (LAMS-2875)
reactions with physiological ligands, 19: 5624
reactions with physiological ligands, 20: 5237(R) (UR-668, pp 55-109)
reactions with plutonium and uranium at high temperatures, 17: 10239(R) (MLM-1140)
reactions with potassium phosphate, 20: 1873
reduction and deposition potentials, 19: 7362(T) (UCRL-Trans-1153(L))
refining by electrotransport, 20: 21254
scavenging effects on carbon, nitrogen, and oxygen in chromium, 18: 12692
sedimentation and sorption of carrier-free solutions of, effects of surface treatment on, 18: 39247
separation by anion exchange in acetic acid–nitric acid medium, 18: 16131
separation by anion exchange in EDTA, effects of temperature on, 18: 20110
separation by anion exchange in potassium sulfate, 19: 11283
separation by ion exchange and elution with alpha-hydroxy acids, 16: 23571
separation by ion exchange using phosphonic and iminodiacetic acid resins, 18: 37295 (BM-RI-6510)
separation by paper chromatography, effects of ester composition in alcohol and ketone mixtures on, 17: 40947
separation by reversed-phase partition chromatography using organophosphorus compounds, 18: 25614
separation by solvent extraction, 16: 14824
separation by solvent extraction using hydrogen 2-ethylhexyl phenacyl phosphonate, steric effects in, 16: 16366
separation by sorption on calcium oxalate, 18: 23714
separation from actinides and other lanthanides by solvent extraction, 18: 39382
separation from alkaline earths by reversed-phase chromatography, 18: 39096
separation from americium and curium by electrophoresis in EDTA and α-hydroxyisobutyric acid solutions, 20: 18562(R) (EUR-2640.e)
separation from aqueous solutions into organic solvents containing thenoyltrifluoroacetone, 17: 34053
separation from aqueous solutions of organic acids by solvent extraction using high-molecular-weight amines, 19: 40657
separation from aqueous chloride solutions by solvent extraction using di-*n*-octylphosphinic acid, tracer studies of, 19: 46443
separation from aqueous solutions by solvent extraction using naphthenates, 20: 4051
separation from bone ash solutions by solvent extraction using di-(2-ethylhexyl) phosphoric acid, 19: 17801
separation from cadmium by coprecipitation with cadmium–cerium alloy, 16: 16464
separation from calcium and magnesium by reversed-phase partition chromatography, 18: 39078
separation from californium–magnesium–zinc alloys by solvent extraction using lithium chloride–magnesium chloride, 19: 17176(R) (ANL-6965 (p.1-41))
separation from cerium by anion exchange, 16: 126 (HW-69737)
separation from cesium by sorption on ammonium phosphotungstate, 16: 13049
separation from cerium, cesium, and strontium by paper chromatography using iron(III) hydroxide, 17: 21782
separation from cerium and lanthanum by solvent extraction, 19: 11267
separation from cerium and lanthanum as chloromandelate, 19: 11016
separation from chloride solutions by solvent extraction using mono-2-ethylhexyl phosphoric acid, synergistic effects in, 17: 6188 (TID-15271)
separation from chloride solutions by solvent extraction using amines, 18: 1799(R) (ORNL-3496)
separation from dysprosium by countercurrent electrolytic methods, mass effect in, 18: 20112
separation from europium and promethium by ion exchange, effects of aqueous organic media on, 19: 40663
separation from europium by ion exchange, effects of alcohols on, 19: 40666
separation from europium by ion exchange using ammonium acetate eluant, 19: 40680
separation from fission products by solvent extraction using TBP and TOPO, 17: 243
separation from fission products by solvent extraction using D2EHPA, 18: 16147
separation from fission products by sorption on ferric hydroxide, 18: 20102 (UJV-850/63)
separation from fission products in air samples by paper chromatography, 19: 317
separation from fission products by solvent extraction, 19: 7274(R) (IDO-14636)
separation from fission products by solvent extraction and ion exchange, 20: 7203
separation from fused-salts baths by electrowinning, 16: 478 (BM-RI-5868)
separation from hydrochloric acid solutions by solvent extraction using alkyl esters of phosphoric acid, 19: 7631
separation from hydrochloric acid solutions by solvent extraction using 2-ethylhexanol, 19: 36252
separation from hydrochloric acid solutions by solvent extraction using dialkyl alkylphosphonates, 20: 36941
separation from Idaho euxenite concentrate, 19: 9247 (BM-RI-6577)
separation from lanthanides and other metals, chromatographic, 16: 27140
separation from lanthanum and neodymium, effects of solvent mixture on chromatographic, 17: 6009
separation from lanthanum and uranium using ammonium nitrate–trioctylamine, chromatographic, 19: 2234
separation from magnesium–thorium alloy by transfer to liquid scrub alloy in fused salt, 19: 20066
separation from methanol-nitric acid systems using anion exchange resins, 16: 25280 (TID-15598)
separation from metal ions by ion exchange in isopropyl alcohol, 18: 20104
separation from milk by solvent extraction using TBP, 17: 17977(T) (JPRS-18632)
separation from molten magnesium–zinc alloys by fused chloride extraction, 20: 5594(R) (ANL-6925, pp 21-106)
separation from neodymium by ion exchange, 18: 1817
separation from neodymium and praseodymium by solvent extraction, 19: 11268
separation from niobium and rubidium by carrier precipitation, 17: 2242 (TID-16949)
separation from nitric or sulfuric acid solutions, ion exchange selectivity scales for, 19: 9257
separation from nitrate solutions by solvent extraction using tricapryl-methylammonium nitrate, 20: 20812
separation from nitrate solutions by solvent extraction using long-chain tertiary amines, 20: 27063
separation from other fission products by paper electrochromatography, 18: 41575
separation from other rare earths by paper chromatography, 19: 15675
separation from other rare earths by ion exchange, 19: 15682
separation from other fission products by solvent extraction, 19: 18075
separation from other rare earths by ion exchange, 19: 18057
separation from other rare earths by paper electromigration and focusing chromatography, 19: 30327
separation from other metals by reversed-phase chromatography, 19: 30331
separation from other metals by partition chromatography of chloride solutions, tracer studies of, 19: 32288
separation from other fission products by solvent extraction using benzene–oxine solutions, 19: 46440
separation from other rare earths by thin-layer chromatography, 20: 7202
separation from other elements by precipitation with bismuth phosphate carrier, 20: 7204
separation from other elements by electrophoresis and chromatography, 20: 9070
separation from other elements by solvent extraction using TBP, 20: 10952
separation from other inorganic ions by paper chromatography, 20: 12939
separation from other metals by extraction chromatography using TOPO, tracer studies of, 20: 27054
separation from other rare earths by cation exchange in ammonium lactate solutions, 20: 26800
separation from other fission products by ion exchange, 20: 35587 (IEA-101)
separation from other fission products and uranium by chromatography using ion-exchange paper, 20: 35440
separation from other elements by ion exchange using triisooctylamine,

20: 43439
separation from oxygen, 17: 23876(R) (USBM-U-1031)
separation from oxalic acid solution by solvent extraction using triisooctylamine, 19: 22409
separation from perchloric acid solutions by ion exchange materials, 20: 20823
separation from promethium by pulsed solvent extraction, 17: 10746 (TID-15792)
separation from praseodymium by fused salt extraction, 20: 20802(R) (ANL-7055, pp 21-98)
separation from products of fission-fragment-induced radiolysis, 20: 40951 (RPI-321-6)
separation from promethium in fission product solutions, eluting agents for ion-exchange, 20: 43411 (BNWL-SA-677)
separation from rare earths after extraction from euxenite by solvent extraction, 16: 8802 (BM-RI-5910)
separation from rare earths by solvent extraction using amines, 16: 8803 (BM-RI-5923)
separation from rare earths by cation exchange, 16: 20554(P)
separation from rare earths by chromate precipitation, 17: 16168(P)
separation from rare earths by solvent extraction, 17: 40951(P)
separation from rare earths by ion exchange centrifuge chromatography, 18: 17940
separation from rare earths by ion exchange centrifuge chromatography, 18: 17940
separation from rare earths, thorium, and uranium by reverse-phase paper chromatography, 19: 7302
separation from rare earths by reverse-phase paper chromatography, 19: 7298
separation from rare earths by cation exchange using ammonium α-hydroxyisobutyrate and lactate, 19: 24432
separation from rare earths, fast ion exchange method for, 19: 30326 (USNRDL-TR-836)
separation from rare earth mixture by ion exchange, 19: 30348(P)
separation from thorium by ion exchange in ammonium thiocyanate–methanol–water systems, 19: 40447
separation from rare earths by solubility of carbonates in water, 20: 7019(T) (LA-tr-65-24)
separation from rare earths, thorium, and uranium by reversed-phase chromatography using methylenebis(di-*n*-hexylphosphine oxide), 20: 18599
separation from rare earths by thin-layer chromatography, 20: 45597
separation from rhenium by anion exchange chromatography, 19: 24433
separation from rubidium, cesium, and strontium by chromatography, 18: 31669
separation from salts by solvent extraction using 8-mercaptoquinoline in chloroform, 20: 10759 (INP-427/C)
separation from scandium by solvent extraction, 17: 27369
separation from scandium by cation exchange chromatography, 18: 25613
separation from scandium by solvent extraction of diantipyrinylmethane complex, 19: 20080
separation from scandium sulfate by solvent extraction using sulfuric acid, 19: 30196
separation from scandium and thorium by reversed-phase chromatography, 19: 44125
separation from scandium by ion exchange chromatography, 20: 20821
separation from sewage water by sorption on multiclone dust from gasification of coke, 20: 18170
separation from siliceous thorite ore by solvent extraction, 18: 27612 (BM-RI-6457)
separation from soil, radiochemical methods for, 18: 22185
separation from strontium by thin-layer chromatography, 18: 17949
separation from strontium by thin-layer chromatography, 18: 17949
separation from strontium by sorption on gelatin foam, 18: 23735
separation from strontium-89 and strontium-90 by paper electrophoresis, 19: 36285
separation from strontium by ion exchange, 19: 38774
separation from strontium, chromatographic, 19: 44120
separation from strontium by ion exchange, 19: 46196
separation from strontium by chromatographic methods, 19: 46436
separation from strontium by paper electrophoresis, 20: 29336
separation from strontium by paper chromatography, effects of calcium on, 20: 29349
separation from strontium by rapid solvent extraction using bis(2-ethylhexyl) phosphate, 20: 33191
separation from strontium by ion exchange, 20: 43430
separation from sulfuric acid by diisobutylphosphoric acid, 18: 1829
separation from tantalum by passing through tungsten filter, 16: 292(P)
separation from thorium by solvent extraction using 2,4-pentanedione, 18: 20106
separation from thorium and uranium by paper chromatography, 18: 33505
separation from thulium by ion exchange, prediction of efficiency of, 18: 39065
separation from thorium and other rare earths by ion exchange in ammonium thiocyanate–organic solvent–water systems, 20: 1959
separation from titanium by cation exchange chromatography, 17: 32054
separation from transuranic elements by solvent extraction, 18: 352
separation from uranium by oxidation-reduction in fused salts, 16: 10100 (IS-286)
separation from uranium leach waste liquors, 17: 4637(P)
separation from urine by solvent extraction using mono-2-ethylhexyl phosphoric acid, 17: 37297
separation from uranium by anion exchange using carbonate solutions, 18: 361
separation from uranium-free acid solutions by ion exchange, 19: 11299(P)
separation from uranium by cation exchange chromatography, 19: 13245
separation from uranium by reversed-phase partition chromatography, 20: 10784
separation from uranium by combined ion exchange-solvent extraction using nitric acid–tetrahydrofuran solutions, 20: 20811
separation from waste water, methods for, 19: 40276
separation from water by ion exchange using bentonite and gypsum, 20: 29348
separation from water by precipitation, kinetics of, 20: 31318 (BMwF-FBK-65-04)
separation from water, effect of cation-anion resin ratio on slurry, 20: 35595
separation from water by foaming, 20: 36934
separation from zirconium by ion exchange on pyrocatechol-*O*,*O*-diacetic acid, 18: 33508
separation of, by solvent extraction using thenoyltrifluoroacetone, 17: 23253 (IS-561)
separation of fission product, radiochemical, 16: 24564
separation of, from rare earths by solvent extraction using amines, selectivity in, 17: 23430 (BM-RI-6242)
separation of interstitial impurities from by electrotransport, 20: 5599
separation of scandium from, by ion exchange chromatography, 19: 533
separation of trace elements from, by precipitation ion exchange, 20: 1958
separation of zirconium-89 from irradiated carrier-free, by solvent extraction using cupferron, 20: 20626
separation of, from rubidium and strontium by precipitation with iron hydroxide, 20: 33422
separation of, from zinc, in hydrochloric acid solutions by ion-exchange chromatography, 20: 45809
separation of, from other elements by precipitation using ammonium cinnamate, 20: 45611
solubility and ion exchange properties in potassium carbonate solution, 19: 13536
solubility in acids, 19: 44628
solubility in aluminum–magnesium alloy at 550 and 600°C, 19: 32279(R) (ANL-7020(p.3-99))
solubility in beryllium, 17: 20474
solubility in beryllium, 18: 18305
solubility in bismuth at 300 to 700°C, 16: 24216
solubility in liquid zinc, 20: 22996 (ANL-7083)
solubility in yttrium chloride, 18: 1489(R) (IS-700(Sect. C))
solvent distribution in ammonium thiocyanate–methanol–water systems, distribution coefficients for, 19: 40447
solvent extraction by mono(2-ethylhexyl)phosphoric acid, synergistic effects, 17: 8066
solvent extraction by synergic mixtures of phosphonates and thenoyltrifluoroacetone, steric effects, 17: 14382
solvent extraction from perchlorate solutions by phosphoric acid esters, 19: 28441 (NIJS-R-440)
solvent partition in tetrahydrated ammonium cerium sulfate, 18: 10194
solvent properties in D2EHPA–hydrochloric acid, 18: 16147
solvent properties for nitrogen, 20: 13180(R) (IS-RD-4)
solvent properties for tantalum, 20: 13180(R) (IS-RD-4)
sorption by ammonium phosphomolybdates, mechanism of, 18: 25378
sorption by bismuth iodates, 20: 43448
sorption by cation exchange resin Mykion MK, kinetics, 17: 8019
sorption by glass and polyethylene, 20: 23211
sorption by hydroxyapatite systems, tracer study of reaction mechanisms for, 19: 27940
sorption by peat, 19: 11261 (NP-14668)
sorption by platinum, 17: 7662(R) (MLM-1139)
sorption by soil, effects of acidity and concentration on, 20: 40914
sorption by strongly acidic cation exchanger, effects of aqueous solutions of alcohols on, 19: 40664
sorption by turfy-meadow soil, effects of iron on, 20: 28881
sorption by Type X zeolite in presence of sodium, equilibrium in, 19: 22416
sorption by zirconium phosphate gel, 19: 9256
sorption from hydrochloric acid solutions by zirconium phosphates,

16: 16390
sorption from hydrochloric acid solutions by zirconium phosphates, 16: 32958(T) (KFK-tr-112)
sorption from nitric acid by ion exchange paper, 19: 24435
sorption of trace amounts on manganese hydroxide, 16: 27059
sorption on ion exchanger, effects of glycols on, 19: 40662
sorption on ion exchanger, tracer studies of effects of alcohol solutions on, 19: 50665
sorptive properties for tritium, 20: 22976
specific heat at low temperatures, 16: 1797
spectra, flame, 16: 2976
spectra, flame, 16: 30400
spectra in reaction zone of acetylene air flame, excitation of atomic, 17: 27371(T)
spectra of, absorption, 18: 1489(R) (IS-700(Sect.C))
spectra of, atomic absorption, 17: 10549
spectra of, analytical applications of flame, 18: 11982
spectra of, automatic data handling and analysis of, 19: 5885
spectra of, excited by hydrogen–oxygen flame, 18: 17767
spectra of, use of fuel-rich premixed oxyacetylene flame for emission, 18: 25278
sputtering at 50 to 600 ev by rare gas ions, 17: 8931(R) (NP-12389)
superconductivity of, transition temperature for, 18: 36487
superconductivity of, 20: 40047
synthesis in halo red giant star HD 122563, spectral analysis of, 19: 28982
tensile properties, 18: 2163(R) (IS-700(Sect.M))
thermal conductivity at 715 to 1615°F, 19: 6306(R) (TID-6728)
thermal conductivity at 2 to 20°K, 19: 37084
thermal expansion of crystals of, at 4.2 to 273.2°K, anisotropic, 16: 9233
thermodynamic properties at high temperatures, 17: 10580 (BM-RI-6155)
titration of, comparison of methods for complexometric, 18: 1583
toxicity in laboratory animals, 20: 30970 (COO-1170-5)
toxicology of, 16: 5127(R) (ORO-480)
uptake by body organs and skeleton, effects of sodium phosphates on, 16: 32706
uptake by *Cladophora fracta*, concentration effects on dynamics of, 19: 25858
use of deuterium-impregnated, in neutron source, 19: 10376(P)
use to improve properties of iron, nickel, and cobalt, 19: 23021(T) (JPRS-28849(p.303-9))
uses in ceramics, cermets, and metallurgy, 16: 1695
uses of granular or powdered, in fuel element end cap cavity to reduce pressure, 18: 42988(P)
vapor pressure, 16: 10003
vapor pressure, 17: 4515
vapor pressure at 1360 to 1760°K, 16: 25405
vapor pressure of solid, at 1100 to 1480°C, 18: 24177
welding of, methods for, 16: 33453 (NAA-SR-Memo-7283)
with 2,4-pentanedione, preparation, properties, and solvates, 16: 10016
yields from helium ion-induced fission of lead-207 at 41.1 to 26.3 Mev, 20: 37996
yttrium-89 NMR in, Knight shift anisotropy in, (E), 19: 16976

YTTRIUM ACETATES

preparation and crystal structure of ammoniated, 19: 40507
preparation by oxide solubility in alcohols containing ammonia, 20: 20686
preparation of anhydrous, by desolvation, 16: 23697
preparation of anhydrous, by desolvation, 17: 6082
spectra of, infrared absorption, 18: 41446

YTTRIUM ALCOHOLATES

preparation and properties of, 20: 18652
preparation of, and thermal decomposition to oxide coatings and powders, 20: 36851
spectra of isopropoxides, infrared, 18: 1720

YTTRIUM ALLOYS

crystallographic angles in hcp, computer program for calculation of, 20: 22315 (IS-1337)
development for low-weight high-temperature uses, 16: 10419 (ASD-TR-61-322(p.563-86))
mechanical properties and oxidation resistance of, 19: 6334
phase diagrams, handbook, 16: 10512 (DC-59-5-210)
properties of, chemical and physical, 17: 32648
Ag–Tb–Y, crystallography, 20: 4391(R) (ORNL-3870, pp 75-82)
Ag–Y, crystal structure studies, 19: 44678(R) (ANL-7000, pp 186-200)
Ag–Y, crystal structure of intermetallic compound YAg_2 in, 20: 15102
Ag–Y, electric conductivity, 20: 25583
Ag–Y, phase diagrams, 19: 7941
Al–Cr–Fe–Y, corrosion by steam at 3000 psi, 17: 13678(R) (HW-75914)
Al–Cr–Fe–Y, corrosion by oxygenated steam at 500°C and 3000 psi, 17: 38466 (TID-7674(p.16))
Al–Cr–Fe–Y, corrosion by superheated steam at 550°C, 18: 32139(R) (HW-81269(p.5.1-23))
Al–Cr–Fe–Y, corrosion by steam, 18: 41933 (TID-11295(3rd Ed.))
Al–Cr–Fe–Y, corrosion by steam in superheat environment, 19: 4197 (SAN-8003(p.90-133))
Al–Cr–Fe–Y, corrosion by air and steam at high temperatures, 19: 18390(R) (GEMP-43A)
Al–Cr–Fe–Y, corrosion under reactor conditions, 19: 24916(R) (GEMP-334A)
Al–Cr–Fe–Y, corrosion by steam at 500 to 1300°C, 19: 40961
Al–Cr–Fe–Y, corrosion by steam at 550°C of 1041, effects of preoxidation and strain on, 19: 44598(R) (GEMP-49A)
Al–Cr–Fe–Y, corrosion by steam at 730°C, 19: 44598(R) (GEMP-49A)
Al–Cr–Fe–Y, corrosion by steam at 550°C, effects of pre-oxidation and strain on, 20: 2223(R) (GEMP-51A)
Al–Cr–Fe–Y, corrosion by carbon dioxide, helium, nitrogen, and steam, 20: 9408 (BNWL-154)
Al–Cr–Fe–Y, corrosion cracking by magnesium chloride at 154°C, stress-, 20: 9408 (BNWL-154)
Al–Cr–Fe–Y, corrosion by air or steam, effects of chromium content on, 20: 27411(R) (GEMP-400A, pp 135-63)
Al–Cr–Fe–Y, corrosion, fabrication, and preparation of, 19: 11669(R) (GEMP-41A)
Al–Cr–Fe–Y, descaling by sodium carbonate–sodium hydroxide solutions, 18: 22441 (HW-79048)
Al–Cr–Fe–Y, development of compacts with europium oxides for high temperatures, 16: 2175(R) (GEMP-3A)
Al–Cr–Fe–Y, development of fuel-bearing, for high-temperature use, 16: 15178(R) (GEMP-9A)
Al–Cr–Fe–Y, development for fuel cladding, 19: 24916(R) (GEMP-334A)
Al–Cr–Fe–Y, diffusion of uranium into fuel cladding of, 19: 36952(R) (GEMP-47A, pp 13-26)
Al–Cr–Fe–Y, diffusion of uranium through cladding of, 20: 2223(R) (GEMP-51A)
Al–Cr–Fe–Y, diffusion of uranium through fuel cladding of, at 950°C, 20: 7499(R) (GEMP-53A)
Al–Cr–Fe–Y, diffusion of uranium through cladding of, 20: 13179(R) (GEMP-55A, pp 13-28)
Al–Cr–Fe–Y, ductility and strength of, effects of powder preparation by atomization on, 20: 27411(R) (GEMP-400A, pp 135-63)
Al–Cr–Fe–Y, elastic constants at 30 to 1200°C of 2541, dynamic, 19: 44598(R) (GEMP-49A)
Al–Cr–Fe–Y, fabrication and oxidation, 16: 2175(R) (GEMP-3A)
Al–Cr–Fe–Y, fission gas diffusion from iron–uranium fuels clad with, 20: 7499(R) (GEMP-53A)
Al–Cr–Fe–Y, grain structure and mechanical properties of, effects of composition on, 20: 33816 (GEMP-414)
Al–Cr–Fe–Y, impact properties of, 19: 40961
Al–Cr–Fe–Y, impact properties of powder-metallurgy, effects of atomized powders on, 20: 13179(R) (GEMP-55A, pp 13-28)
Al–Cr–Fe–Y, oxidation above 1200°C, 16: 2175(R) (GEMP-3A)
Al–Cr–Fe–Y, oxidation by air at 1200 to 1425°C, 16: 15179 (GEMP-106A)
Al–Cr–Fe–Y, oxidation mechanism, 19: 20470 (GE-TM-63-7-3)
Al–Cr–Fe–Y, oxidation in air and steam to 1100°C, 19: 36952(R) (GEMP-47A, pp 13-26)
Al–Cr–Fe–Y, oxidation by air at 900 and 1100°C, effects of composition on, 19: 44598(R) (GEMP-49A)
Al–Cr–Fe–Y, oxidation by air at 900 and 1100°C, 20: 2223(R) (GEMP-51A)
Al–Cr–Fe–Y, oxidation resistance in air at 450 to 1100°C, effects of alloy composition on, 20: 7499(R) (GEMP-53A)
Al–Cr–Fe–Y, oxidation of, effects of composition on, 20: 33816 (GEMP-414)
Al–Cr–Fe–Y, performance in nuclear-superheater environment, 19: 10541(R) (GEAP-4703)
Al–Cr–Fe–Y, properties for cladding high-temperature fueled cermets, 19: 11669(R) (GEMP-41A)
Al–Cr–Fe–Y, properties of oxidation-resistant, 19: 20470 (GE-TM-63-7-3)
Al–Cr–Fe–Y, properties as high-temperature cladding material to 2500°F, 19: 36947 (APEX-681)
Al–Cr–Fe–Y, radiation effects on, in nuclear superheater environments, 18: 45020(R) (GEAP-4619)
Al–Cr–Fe–Y, radiation effects on mechanical properties of, 19: 18390(R) (GEMP-43A)
Al–Cr–Fe–Y, radiation effects on mechanical properties of, neutron, 19: 36952(R) (GEMP-47A, pp 13-26)
Al–Cr–Fe–Y, radiation effects on mechanical properties of, 20: 2409(R) (AD-617319)
Al–Cr–Fe–Y, radiation effects on ductility of, fast-neutron, 20: 7499(R) (GEMP-53A)
Al–Cr–Fe–Y, radiation effects on tensile properties of, fast-neutron, 20: 9378(R) (GEMP-54A)
Al–Cr–Fe–Y, radiation effects on tensile properties of, fast-neutron, 20: 13179(R) (GEMP-55A, pp 13-28)

Al–Cr–Fe–Y, radiation effects on ductility of, effects of annealing at 350°C on fast-neutron, 20: 27411(R) (GEMP-400A, pp 135-63)
Al–Cr–Fe–Y, reactions with uranium oxides and sulfides, 17: 3381(R) (GEMP-17A)
Al–Cr–Fe–Y, reactions with iron–urania at 950 and 1100°C in air, 19: 44598(R) (GEMP-49A)
Al–Cr–Fe–Y, testing of, as cermet fuel cladding at 750 to 1100°C, 20: 33770(R) (GEMP-59A)
Al–Cr–Fe–Y, transition temperature of, effects of yttrium on ductile-to-brittle, 19: 36952(R) (GEMP-47A, pp 13-26)
Al–Cr–Re–Y, properties, development for high-temperature applications, 16: 13565 (APEX-680)
Al–Cr–Y, crystal structure of intermetallic compounds in, 20: 39414
Al–Cr–Y, fission-product permeability at 2200 to 3200°F, 17: 6645 (BMI-1604)
Al–Cu–Y, crystal structure of intermetallic compounds in, 20: 39414
Al–Er–Y, crystal structure of intermetallic compound $(Y_xEr_{1-x})Al_3$ in, 20: 11305
Al–Fe–Y, crystal structure of intermetallic compounds in, 20: 39414
Al–Li–Mg–Y, preparation and properties at high temperatures, 19: 37154(P)
Al–Mn–Y, crystal structure of intermetallic compounds in, 20: 39414
Al–Mo–Y, magnetic susceptibility at 4 to 300°K, 19: 30743(R) (NYO-3454-1)
Al–Y, corrosion by water at 200°C, effects of yttrium content on, 20: 4320(R) (ORNL-3870, pp 70-4)
Al–Y, crystal structure, 19: 7950
Al–Y, crystal structure of intermetallic compound Y_3Al_2 in, 19: 14020
Al–Y, crystal structure of beta-phase, 20: 4297(R) (IS-1200(Sect.M))
Al–Y, crystal structure of intermetallic compound YAl_3 in, 20: 11305
Al–Y, crystal structure and stability of intermetallic compounds in, 20: 21415
Al–Y, crystal structure of intermetallic compound YAl_3 in, 20: 29721
Al–Y, crystal structure of intermetallic-compound polymorphs of, 20: 41412(R) (IS-1500(Sect. M))
Al–Y, evaluation of, as coating for vanadium alloys, 16: 2168(R) (ARF-2227-2)
Al–Y, phase diagrams and properties, 17: 39581
Al–Y, phase diagram, 19: 23005(T) (JPRS-28849(p.158-65))
Al–Y, phase diagram of, mathematical determination of, 20: 21369
Al–Y, phase equilibria in, 16: 25814
Al–Y, phase studies and crystal structure determination for intermetallic compounds, 19: 14057
Al–Y, properties of intermetallic compounds in, tabulation of, 20: 43972
Al–Y, structure of YAl and Y_3Al_2, 17: 22172
Al–Y, structure of intermetallic compounds in, 18: 7243
Au–Y, crystal structure, 17: 16658 (TID-18197)
Au–Y, crystal structure studies, 19: 44678(R) (ANL-7000, pp 186-200)
Au–Y, crystal structure of intermetallic compound YAu_2 in, 20: 15102
Au–Y, electron transfer in dilute, 17: 37189
Au–Y, oxidation of, kinetics of high-temperature, 20: 5859
Au–Y, phase studies of solid solutions in, 19: 41062
Be–Y, crystal structure and properties of type ABe_{13} intermetallic compounds in, 18: 7247(T)
Be–Y, crystal structure and phase studies, 19: 6306(R) (TID-6728)
Be–Y, dissociation at high temperatures, 18: 34154
Be–Y, dissociation of YBe_{13} at 1040 to 1290°C, 20: 7603
Be–Y, properties to 2750°F, 17: 532 (GEMP-105)
Be–Y, structure of YBe_{13}, 19: 23009 (JPRS-28849(p.195-6))
Be–Y, thermal etch figures in crystalline, 19: 9714(T)
Be–Y, vaporization rates of components at 1080 to 1270°C, 18: 39932
Be–Y, vaporization of YBe_{13}, 19: 40959
Bi–Y, crystal structure and magnetic susceptibility, 19: 13289
Bi–Y, structure of YBi, 17: 20498(T)
Cd–Y, crystal structure, 18: 12708
Cl–Y, crystal structure of intermetallic compound YCd_6, 19: 16162
Cd–Y, phase studies, 19: 32048(R) (NP-15073)
Ce–Y, electric conductivity of, 18: 30196
Ce–Y, electric conductivity at low temperatures, 20: 5888 (NP-15592)
Ce–Y, electric conductivity of dilute, at low temperatures, (E), 20: 15098
Ce–Y, magnetic properties, 17: 25824
Ce–Y, magnetic properties and phase transformations in, 20: 21414
Ce–Y, magnetic susceptibility of delta-phase, temperature dependence of, 18: 20519 (IS-551)
Ce–Y, phase studies, 17: 11186 (DRI-2080)
Ce–Y, phase studies, 19: 6306(R) (TID-6728)
Ce–Y, phase transformations and magnetic ordering in, pressure-induced, 20: 40326
Ce–Y, properties and structure of, 18: 34160
Co–Fe–Y, magnetic susceptibilities of YFe_2–YCo_2 in, at 4.2 to 300°K, 20: 27494(R) (NYO-3454-6)
Co–Gd–Y, magnetic properties of intermetallic compounds of, (E/T), 20: 20141
Co–Gd–Y, magnetic properties of, 20: 30756
Co–Y, cobalt ion EPR in intermetallic compounds of, 20: 15963
Co–Y, crystal structure, 19: 9604(R) (IS-900(Sect.M))
Co–Y, crystal structure of intermetallic compound Y_2Co_{17}, 19: 18481
Co–Y, crystal structure of intermetallic compounds YCo_3 and Y_2Co_{17} in, 19: 37057
Co–Y, crystal structure, 20: 4297(R) (IS-1200(Sect.M))
Co–Y, crystal structure of intermetallic compound YCo_3 in, 20: 7586
Co–Y, crystal structure of intermetallic compound YCo_3 in, 20: 11308
Co–Y, crystal structure of intermetallic compound in, 20: 33896
Co–Y, crystal structure of intermetallic compounds in, 20: 37243
Co–Y, ferrimagnetism of intermetallic compounds of, (E), 20: 24656
Co–Y, magnetic properties of, antiferromagnetic effects on, 16: 22624
Co–Y, magnetic properties of intermetallic compounds in, 20: 9511
Co–Y, magnetic properties of intermetallic compound of, (E), 20: 34823
Co–Y, magnetic structure of, 17: 6706
Co–Y, magnetic structure of YCo_5, 17: 37702
Co–Y, magneto-optic properties of intermetallic compound YCo_5 in, 19: 41084
Co–Y, mechanical properties, 16: 5315 (WADD-TR-61-123)
Co–Y, phase diagram, 19: 47053
Co–Y, phase studies and atmospheric corrosion of, 16: 5315 (WADD-TR-61-123)
Co–Y, phase studies, 20: 21402
Co–Y, preparation of oriented single-crystal spheres of YCo_5, 19: 15989 (AFML-TR-64-362)
Co–Y, preparation of intermetallic compound YCo_5 by zone melting, 19: 16168
Co–Y, thermomagnetic properties of, down to liquid helium temperatures, 16: 16742
Cr–Fe–Y, corrosion by carbon dioxide, helium, nitrogen, and steam, 20: 9408 (BNWL-154)
Cr–Fe–Y, corrosion cracking by magnesium chloride at 154°C, stress-, 20: 9408 (BNWL-154)
Cr–Fe–Y, development of compacts of, with europium oxides for high temperatures, 16: 2175(R) (GEMP-3A)
Cr–Fe–Y, fabrication and oxidation of, 16: 2175(R) (GEMP-3A)
Cr–Fe–Y, fabrication of, by melting and extrusion, 16: 22563 (DC-61-6-29)
Cr–Fe–Y, fission-product permeability at 2200 to 3200°F, 17: 6645 (BMI-1604)
Cr–Fe–Y, oxidation of, internal, 16: 10467
Cr–Y, properties of, development of, for high-temperature applications, 16: 13565 (APEX-680)
Cr–Y, crystal structure and phase studies, 18: 12623 (ASD-TDR-63-204)
Cr–Y, ductility, 19: 26860
Cr–Y, fabrication for internal friction studies, 19: 46913(R) (BMI-1733 (Del.))
Cr–Y, internal friction studies on recrystallized wires of, 20: 7493(R) (BMI-1748(Del.))
Cr–Y, internal friction in recrystallized, effects of nitrogen concentration on, 20: 7490(R) (BMI-1745, Sect.A)
Cr–Y, oxidation by air at 500 to 1400°C, 19: 2750
Cr–Y, phase diagram, 19: 23005(T) (JPRS-28849(p.158-65))
Cr–Y, phase studies and structure, 17: 39581
Cr–Y, phase studies, 18: 1489(R) (IS-700(Sect.C))
Cr–Y, phase studies of solid solution formation in, 19: 41050
Cr–Y, preparation by arc-melting, comparison with powder metallurgy techniques, 17: 14779 (BMI-X-203)
Cr–Y, properties of, at high temperatures, 16: 30779 (BMI-1277)
Cr–Y, properties of, as cladding for reactor fuel elements, 17: 8820 (XDCL-60-8-40)
Cr–Y, properties of chromium-base, effects of interstitial nitrogen and oxygen on, 20: 37168(R) (BMI-1771)
Cr–Y, radiation effects on thermal stability of hydrided, 18: 4306 (TID-19501)
Cr–Y, solubility of nitrogen in chromium-base, 20: 37169(R) (BMI-1774)
Cu–Y, analysis for AlB_2 and $CeCu_2$ type intermetallic compounds, 17: 29335
Cu–Y, analysis for yttrium using Arsenazo-III, spectrophotometric, 20: 10773
Cu–Y, crystal structure of YCu_2, 17: 34423
Cu–Y, crystal structure of AB_2-type compound in, 20: 24589(R) (NYO-3560-3)
Cu–Y, intermetallic compound with $CeCu_2$-type structure in, 20: 21352 (TID-21745)
Cu–Y, magnetic properties and crystal structure of intermetallic compounds in, 19: 9695
Cu–Y, phase diagram, 16: 2248
Cu–Y, phase studies, 20: 41412(R) (IS-1500(Sect. M))
Dy–Y, electric conductivity at low temperatures, 20: 5888 (NP-15592)
Dy–Y, electric conductivity of dilute, at low temperatures, 20: 15098

Dy–Y, magnetic and structural properties, 17: 25708(R) (TID-18766)
Dy–Y, magnetic cooling of, study of properties for, 18: 36545
Dy–Y, magnetic properties and structure of, 17: 37712
Dy–Y, magnetic properties of solid solutions of, 18: 8860
Dy–Y, magnetic properties of, 18: 25981(R) (ORNL-3582(p.11-16))
Dy–Y, magnetic properties, 19: 27732
Dy–Y, magnetic structure, 19: 18462 (ORNL-TM-1063)
Dy–Y, magnetic transition properties of, 17: 26455(R) (ORNL-3425 (p.118-19))
Dy–Y, preparation, and magnetic and structural properties of, 16: 18039 (TID-14769)
Er–Y, electric conductivity at low temperatures, 17: 34443
Er–Y, electric conductivity at low temperatures, 20: 5888 (NP-15592)
Er–Y, electric conductivity of dilute, at low temperatures, 20: 15098
Er–Y, magnetic properties of, 18: 25981(R) (ORNL-3582(p.11-16))
Er–Y, magnetic properties, 19: 27732
Er–Y, magnetic susceptibility at 1.5 to 20°K, 17: 34444
Er–Y, magnetic structure, 19: 18462 (ORNL-TM-1063)
Er–Y, mechanical properties, 16: 5315 (WADD-TR-61-123)
Er–Y, phase studies and atmospheric corrosion of, 16: 5315 (WADD-TR-61-123)
Er–Y, phase studies and structure, 18: 42092
Er–Y, temperature dependence of magnetic properties of, (E), 19: 26828
Fe–Ti–Y, magnetic and structural properties of Laves phases in, 19: 30743(R) (NYO-3454-1)
Fe–Ti–Y, magnetic properties and structure of Laves phases in, 20: 27494(R) (NYO-3454-6)
Fe–Y, analysis for rare earths in powders of, spectrographic, 17: 34431
Fe–Y, crystal structure of intermetallic compound Y_2Fe_{17}, 19: 18481
Fe–Y, crystal structure of intermetallic compound YFe_3 in, 20: 11308
Fe–Y, crystal structure of Y_6Fe_{23} in, 20: 17096(T)
Fe–Y, crystal structure of intermetallic compounds in, 20: 37243
Fe–Y, isomer shift of iron in YFe_2 at 300 and 800°K, 19: 44678(R) (ANL-7000, pp 186-200)
Fe–Y, magnetic properties of, antiferromagnetic effects on, 16: 22624
Fe–Y, Mössbauer effect of iron-57 in Laves phases in, 16: 10565
Fe–Y, Mössbauer effect measurements of hyperfine interactions in Laves phase in, 19: 4683
Fe–Y, oxidation by air at 500 to 1400°C, 19: 2750
Fe–Y, phase diagram, 16: 2248
Fe–Y, preparation of oriented single-crystal spheres of YFe_2, 19: 15989 (AFML-TR-64-362)
Fe–Y, preparation of intermetallic compound YFe_2 by zone melting, 19: 16168
Fe–Y, preparation and structure, 20: 15110
Fe–Y–Zr, magnetic and structural properties of Laves phases in, 19: 30743(R) (NYO-3454-1)
Fe–Y–Zr, magnetic properties and structure of Laves phases in, 20: 27494(R) (NYO-3454-6)
Fe–Y–Zr, thermal capacity of YFe_2–$ZrFe_2$ Laves phases in, 20: 27494(R) (NYO-3454-6)
fissium–U–Y, fabrication of reactor fuel, 17: 41418(P)
Ga–Y, crystal structure of AB type compound in, 19: 37063
Ga–Y, crystallization of Y_5Ga_3 with $D8_8$ structure, 18: 42027
Ga–Y, phase studies, 19: 16173
Ga–Y, structure of intermetallic compounds in, 18: 7243
Ga–Y, structure of intermetallic compounds of, 19: 32755
Gd–Os–Y, magnetic and superconducting ordering in, 20: 13694
Gd–Os–Y, thermal capacity at 0.25 to 20°K, 20: 13694
Gd–Os–Y, thermal capacity of intermetallic compounds of, at 0.25 to 20.0°K, 20: 15061 (UCRL-11580)
Gd–Pu–Y, phase studies, 19: 42849 (MLM-1262)
Gd–Y, disorder resistivity in, 18: 38022
Gd–Y, electric conductivity at low temperatures, 17: 34443
Gd–Y, electric conductivity of, 18: 38021
Gd–Y, electric conductivity of, 19: 983
Gd–Y, electric conductivity at low temperatures, 20: 5888 (NP-15592)
Gd–Y, electric conductivity of dilute, at low temperatures, 20: 15098
Gd–Y, gadolinium ion ESR in, g-factors from, (E), 19: 20698
Gd–Y, magnetic ordering in, gadolinium-content effects on g factor for, 20: 32716
Gd–Y, magnetic properties, 19: 23000(T) (JPRS-28849(p.64-70))
Gd–Y, magnetic properties of, effects of composition and temperature on, 20: 11341
Gd–Y, magnetic susceptibility at 1.5 to 20°K, 17: 34444
Gd–Y, magnetic susceptibility at 300 to 1500°K, 18: 18368
Gd–Y, microwave resonance absorption in magnetic states of, gyromagnetic ratios from, 17: 37707
Gd–Y, paramagnetic resonance absorption in, at 20 to 200°C, 19: 20581
Gd–Y, phase studies, 17: 4981
Gd–Y, phase transformations and magnetic ordering in, pressure-induced, 20: 40326
Ge–Y, crystal structure of AB type compound in, 19: 37063
Ge–Y, crystal structure of intermetallic compound Y_5Ge_4 in, 20: 33910
Ge–Y, preparation and crystal structure of intermetallic compounds in, 19: 28835
Ge–Y, structure of germanide, 19: 23006(T) (JPRS-28849(p.184-7))
Ge–Y, structure of intermetallic compounds of, 19: 32755
Hf–Nb–W–Y, development and evaluation of C-129Y, 19: 11667 (D2-20282-1)
Hf–Nb–W–Y, development and evaluation of C-129Y, 20: 11227
Hf–Nb–W–Y, evaporation tests of C-129Y in high vacuum, 18: 44049(R) (ORNL-3670(p.77-111))
Hf–Nb–W–Y, evaporation losses of C-129Y, at 1200 to 1500°C in high vacuum, 19: 37043 (ORNL-P-1394)
Hf–Nb–W–Y, evaporation losses in high vacuum of C-129Y, 20: 4301(R) (ORNL-3870, pp 102-35)
Hf–Nb–W–Y, fabricability, strength, and weldability of, 20: 29763
Hf–Nb–W–Y, properties of welds in C-129Y, 19: 40989
Hf–Nb–W–Y, properties for use in aerospace vehicles, 20: 15119
Hf–Nb–W–Y, properties for high-temperature service, 20: 39445(P)
Hf–Nb–W–Y, tensile properties of C-129Y, effects of welds on, 20: 29712(R) (WANL-PR-(P)-009)
Hf–Nb–W–Y, weld bend tests of C-129Y, 19: 13955(R) (WANL-PR-(P)-005)
Hf–Nb–W–Y, weldability evaluation of C-129Y, 18: 41979 (ORNL-TM-929)
Hf–Nb–W–Y, weldability of C-129Y sheets, 18: 44049(R) (ORNL-3670 (p.77-111))
Hf–Nb–W–Y, weldability study of C-129Y, 19: 24957(R) (WANL-PR(P)-006)
Hf–Nb–W–Y, weldability studies of C-129Y, 19: 46966(R) (WANL-PR(P)-007)
Hf–Nb–W–Y, weldability evaluation of, 20: 39366
Hf–Nb–W–Y, welding of C-129Y, electron-beam and tungsten-arc, 18: 22426(R) (WANL-PR(P)-002)
Hf–Nb–W–Y, welding of C-129Y, tungsten-arc, 18: 34058(R) (WANL-PR(P)-003)
Hf–Nb–W–Y, welding parameters for C-129Y, electron-beam, 20: 5867
Hf–Y, oxidation at high temperatures, 17: 30937(R) (NP-12968)
Hf–Y, oxidation at high temperatures, surface, 18: 5729 (ASD-TDR-63-744)
Hf–Y, phase studies, 16: 13634
Hg–Y, crystal structure of HgY and Hg_2Y, 18: 12708
Hg–Y, preparation and structure of intermetallic compounds of, (E), 19: 4666
Hg–Y, thermodynamic properties and vapor pressure measurements, 20: 21384
Hg–Y–Zn, phase studies, 20: 11317
Ho–Fe–Y, Mössbauer effect of iron-57 in Laves phases in, 16: 10565
Ho–Y, electric conductivity at low temperatures, 20: 5888 (NP-15592)
Ho–Y, electric conductivity of dilute, at low temperatures, 20: 15098
Ho–Y, magnetic properties, 17: 36313
Ho–Y, magnetic properties of solid solutions of, 18: 8860
Ho–Y, magnetic properties of, 18: 25981(R) (ORNL-3582(p.11-16))
Ho–Y, magnetic properties, 19: 27732
Ho–Y, magnetic structure, 19: 18462 (ORNL-TM-1063)
Ho–Y, preparation, and magnetic and structural properties of, 16: 18039 (TID-14769)
In–Y, crystal structure of intermetallic compound YIn_3 in, 18: 39964(T)
In–Y, structure of intermetallic compounds in, 18: 7243
Ir–Pt–Y, crystal structure studies, 19: 44678(R) (ANL-7000, pp 186-200)
Ir–Y, superconductivity of, 18: 15087
La–Y, dissociation energies at high temperatures, 18: 3795
La–Y, dissociation energy of gaseous molecule YLa, 18: 7218 (WADD-TR-60-782(Pt.XIX))
La–Y, dissociation energy and free energy functions of YLa in, 18: 8357
La–Y, electric conductivity at low temperatures, 20: 5888 (NP-15592)
La–Y, electric conductivity of dilute, at low temperatures, (E), 20: 15098
La–Y, magnetic properties and phase transformations in, 20: 21414
La–Y, phase studies, 17: 4981
La–Y, phase studies, 17: 11186 (DRI-2080)
La–Y, phase transformations and magnetic ordering in, pressure-induced, 20: 40326
La–Y, properties and structure of, 18: 34160
La–Y, superconductivity of, 18: 36487
Li–Mg–Th–Y, preparation and properties at high temperatures, 19: 37154
Li–Mg–Y, preparation and properties at high temperatures, 19: 37154(P)
Lu–Y, electric conductivity, 17: 11190 (IS-477)
Lu–Y, electric conductivity at low temperatures, 20: 5888 (NP-15592)
Lu–Y, electric conductivity of dilute, at low temperatures, 20: 15098
Mg–Y, aging behavior and mechanical properties of, 20: 23669
Mg–Y, atomic number effects correction in electron probe microanalysis of, 17: 27268

Mg–Y, crystal structure of Y_5Mg_{24} in, 17: 20469
Mg–Y, crystal structure, 19: 9604(R) (IS-900(Sect.M))
Mg–Y, enthalpies of formation and vapor pressures of, 20: 4297(R) (IS-1200(Sect.M))
Mg–Y, enthalpy of formation, 19: 9604(R) (IS-900(Sect.M))
Mg–Y, hexagonal crystal structure in YMg_3, 18: 44181
Mg–Y, magnetic susceptibility and specific heat of superconducting binary complex phases of, 18: 37715
Mg–Y, phase diagram, 19: 23005(T) (JPRS-28849(p.158-65))
Mg–Y, phase diagrams, 20: 4297(R) (IS-1200(Sect.M))
Mg–Y, phase studies and properties, 17: 39581
Mg–Y, phase studies, 18: 2163(R) (IS-700(Sect.M))
Mg–Y, preparation by reduction of yttrium chloride by magnesium in fused salt bath, 19: 18437
Mg–Y, preparation by magnesium salt reduction of halides, 19: 40955
Mg–Y, structure of intermetallic compounds in, 19: 23008(T) (JPRS-28849(p.191-4))
Mg–Y, thermodynamics of compound formation in, determination of, from vapor pressure measurements, 16: 19353 (IS-440)
Mg–Y, thermodynamics of formation of intermediate phases in, 19: 37069
Mn–Hg–Y, preparation, 18: 34026 (AD-428771)
Mn–Hg–Y, preparation, 18: 34027 (AD-428772)
Mn–Y, analysis by x-ray fluorescence, 18: 27340
Mn–Y, atomic radii and interatomic distances in intermetallic compounds in, 18: 28029
Mn–Y, crystal structure of intermetallic compound Y_6Mn_{23} in, size-factor limitation in, 19: 23079
Mn–Y, crystal structure of Y_6Mn_{23} in, 20: 17096(T)
Mn–Y, crystal structure and magnetic properties of intermetallic compounds of, 20: 21403
Mn–Y, existence of Y_6Mn_{23} compound in, 19: 14074
Mn–Y, magnetic properties of intermetallic compound YMn_5 in, at 80 to 1400°K, 20: 7610
Mn–Y, phase diagram, 17: 14740 (TID-11295(2nd Ed.))
Mn–Y, phase studies, 16: 13633
Mn–Y, phase studies of, at 75 to 90 at.% manganese, 16: 16744
Mn–Y, phase studies by differential thermal, thermomagnetic, and x-ray analysis of, 19: 46989 (AD-614466)
Mn–Y, preparation, phase studies, and properties of, 19: 46987 (AD-614462)
Mn–Y, preparation and structure, 20: 15110
Mn–Y, structure of YMn_2 and YMn_4, 18: 34026 (AD-428771)
Mn–Y, structure of Laves phase YMn_2, 18: 34027 (AD-428772)
Mo–Y, mechanical properties and preparation, 17: 14818 (DRI-2039)
Mo–Y, oxidation at high temperatures, effects of yttrium content on, 20: 41421
Mo–Y, phase studies, 18: 12623 (ASD-TDR-63-204)
Mo–Y, phase studies of solid solution formation in, 19: 41050
Nb–Ta–Y–Zr, grain size and hardness of, effects of yttrium additions on, 19: 40953 (PWAC-441)
Nb–W–Y–Zr, corrosion by refluxing potassium at 1800 to 2400°F, 20: 25485 (NASA-TN-D-3429)
Nb–Y, corrosion by lithium at high temperatures, 20: 4299(R) (ORNL-2711)
Nb–Y, crystal structure and phase studies, 18: 12623 (ASD-TDR-63-204)
Nb–Y, phase diagram, 19: 23005(T) (JPRS-28849(p.158-65))
Nb–Y, phase studies, 16: 19394
Nb–Y, phase studies and atmospheric corrosion, 16: 5315 (WADD-TR-61-123)
Nb–Y, phase studies of solid solution formation in, 19: 41050
Nb–Y–Zr, corrosion by steam at 400-500°C, 20: 2276(P)
Nb–Y–Zr, grain size and hardness of, effects of yttrium additions on, 19: 40953 (PWAC-441)
Nb–Y–Zr, preparation for use in nuclear reactors, 20: 9561(P)
Nd–Pu–Y, phase studies, 19: 42849 (MLM-1262)
Nd–Y, electric conductivity at low temperatures, 17: 34443
Nd–Y, electric conductivity at low temperatures, 20: 5888 (NP-15592)
Nd–Y, electric conductivity of dilute, at low temperatures, (E), 20: 15098
Nd–Y, magnetic properties, 17: 25824
Nd–Y, magnetic properties and phase transformations in, 20: 21414
Nd–Y, magnetic susceptibility at 1.5 to 20°K, 17: 34444
Nd–Y, magnetic susceptibility of delta-phase, temperature dependence of, 18: 20519 (IS-551)
Nd–Y, phase diagram, 18: 20520 (IS-841)
Nd–Y, phase studies and atmospheric corrosion, 16: 5315 (WADD-TR-61-123)
Nd–Y, phase studies, 17: 11186 (DRI-2080)
Nd–Y, phase studies, 18: 1489(R) (IS-700(Sect.C))
Nd–Y, phase studies, 16: 32057
Nd–Y, phase transformations and magnetic ordering in, pressure-induced, 20: 40326
Ni–Y, crystal structure, 19: 9604(R) (IS-900(Sect.M))
Ni–Y, crystal structure of YNi, 19: 9677
Ni–Y, crystal structure of equiatomic intermetallic compound in, 19: 24994
Ni–Y, crystal structure, 20: 4297(R) (IS-1200(Sect.M))
Ni–Y, crystal structure of intermetallic compound YNi_3 in, 20: 7586
Ni–Y, crystal structure of intermetallic compound YNi_3 in, 20: 11308
Ni–Y, crystal structure of intermetallic compounds in, 20: 37243
Ni–Y, evaluation of, as coating for vanadium alloys, 16: 2168(R) (ARF-2227-2)
Ni–Y, gadolinium EPR in, 18: 33587
Ni–Y, magnetic and structural characteristics of intermetallic compound of type LaNi in, 18: 37697
Ni–Y, magnetic properties of, antiferromagnetic effects on, 16: 22624
Ni–Y, magnetic properties of YNi_5 at 4–300°K, 17: 37713
Ni–Y, magnetic properties of intermetallic compounds in, 20: 9511
Ni–Y, oxidation by air at 500 to 1400°C, 19: 2750
Ni–Y, oxidation of nickel-rich, effects of yttrium content on high-temperature, 20: 33812 (BM-RI-6800)
Ni–Y, phase diagram, 16: 2248
Ni–Y, phase studies and atmospheric corrosion, 16: 5315 (WADD-TR-61-123)
Ni–Y, production of splatcooled, 19: 41021(R) (NMI-8002.1)
Pb–Y, crystal structure of intermetallic compound type RPb_3 in, 19: 4677
Pb–Y, phase diagrams, 20: 4297(R) (IS-1200(Sect.M))
Pb–Y, phase diagrams, 20: 41412(R) (IS-1500(Sect. M))
Pb–Y, phase studies, 20: 13180(R) (IS-RD-4)
Pb–Y, structure of intermetallic compounds in, 18: 7243
Pb–Y, structure of Y_5Pb_3 in, 19: 37066
Pb–Y–Zn, component distribution in recrystallized, 20: 39435
Pd–Y, preparation and properties, 19: 16068 (EUR-1894.i)
Po–Y, preparation and properties of, 20: 35909
Pr–Y, electric conductivity at low temperatures, 20: 5888 (NP-15592)
Pr–Y, electric conductivity of dilute, at low temperatures, (E), 20: 15098
Pr–Y, magnetic properties and phase transformations in, 20: 21414
Pr–Y, magnetic susceptibilities at 2 to 300°K, 20: 27494(R) (NYO-3454-6)
Pr–Y, phase transformations and magnetic ordering in, pressure-induced, 20: 40326
Pt–Y, crystal structure of equatomic intermetallic compound in, 19: 24994
Pu–Y, phase studies, 17: 41350(R) (MLM-1162)
Pu–Y, phase studies, 18: 4166(R) (MLM-1171)
Pu–Y, phase studies, 18: 7125(R) (LAMS-3021)
Pu–Y, phase studies, 18: 24815(R) (MLM-1184)
Pu–Y, phase studies, 19: 11679
Pu–Y, phase studies, use of metallography in, 19: 16073 (MLM-1163 (p.L-1-14))
Pu–Y, solubility studies, 17: 22855(R) (LAMS-2875)
rare earth–Y, solid solutions of, electronic states of, 20: 21398
Re–Y, crystal structure and phase studies, 19: 6306(R) (TID-6728)
Rh–Ti–Y, superconductivity, 18: 21112
Rh–Y, crystal structure of equiatomic intermetallic compound in, 19: 24994
Rh–Y, superconductivity of, 18: 15087
Ru–Y, process for improving workability of, 19: 40999(P)
Sb–Y, crystal structure and magnetic susceptibility, 19: 13289
Sb–Y, structure of YSb, 17: 20498(T)
Sc–Y, nuclear magnetic resonance in, 18: 2401(R) (IS-700(Sect.P))
Sc–Y, phase studies, 17: 27785 (IS-569)
Sc–Y, phase studies, 18: 18307
Sc–Y, phase studies and structure, 18: 42092
Sc–Y, scandium-45 hyperfine interactions in, 20: 9658 (IS-T-38)
Sn–Y, evaluation of, as coating for vanadium alloys, 16: 2168(R) (ARF-2227-2)
Sn–Y, phase diagram, 19: 23005(T) (JPRS-28849(p.158-65))
Sn–Y, phase studies and structure, 17: 39581
Sn–Y, phase studies, 18: 2280
Sn–Y, phase studies and crystal structure determination of intermetallic compound Y_5Sn_3, 19: 16086
Sn–Y, structure of intermetallic compounds in, 18: 7243
Sn–Y, structure of Y_5Sn_3 in, 19: 37066
Ta–W–Y, carburization for fuel capsules, methods for, 20: 1534(R) (LA-3370)
Ta–W–Y, corrosion by iron–plutonium at 700°C, effects of yttrium content on, 20: 5846
Ta–W–Y, corrosion by cerium–cobalt–plutonium alloy fuels, effects of carbon on, 20: 31679(R) (LA-3524)
Ta–W–Y, corrosion by molten plutonium alloys, carbon effects on, 20: 43829(R) (LA-3582)
Ta–W–Y, welds of, fusion zone hardness of, 19: 35613(R) (LA-3316)
Ta–Y, analysis for yttrium, spectrophotometric, 19: 288 (LA-3123)

Ta–Y, annealing of, effects on grain size of, 20: 8390(R) (LA-3431)
Ta–Y, oxidation by air at 500 to 1400°C, 19: 2750
Ta–Y, phase studies, 16: 19394
Ta–Y, phase studies and atmospheric corrosion, 16: 5315 (WADD-TR-61-123)
Ta–Y, phase studies, 18: 12623 (ASD-TDR-63-204)
Ta–Y, phase studies of solid solution formation in, 19: 41050
Tb–Y, electric conductivity at low temperatures, 17: 34443
Tb–Y, electric conductivity at low temperatures, 20: 5888 (NP-15592)
Tb–Y, electric conductivity of dilute, at low temperatures, 20: 15098
Tb–Y, magnetic properties, 17: 36313
Tb–Y, magnetic properties of solid solutions of, 18: 8860
Tb–Y, magnetic properties of, 18: 25981(R) (ORNL-3582(p.11-16))
Tb–Y, magnetic properties, 19: 27732
Tb–Y, magnetic properties of, pressure dependence of Curie and Néel temperatures for, (E), 20: 24661
Tb–Y, magnetic susceptibility at 1.5 to 20°K, 17: 34444
Tb–Y, magnetic structure properties of, 17: 37703
Tb–Y, magnetic structure, 19: 18462 (ORNL-TM-1063)
Tb–Y, preparation, and magnetic and structural properties, 16: 18039 (TID-14769)
Th–U–Y, mechanical properties and phase studies at high temperatures, 17: 12660 (ATL-A-128)
Th–Y, corrosion by water at 120 to 260°C, 19: 22889 (ANL-7006)
Ti–Y, oxidation by air at 500 to 1400°C, 19: 2750
Ti–Y, phase diagram, 16: 29409
Ti–Y, phase diagram, 19: 23005(T) (JPRS-28849(p.158-65))
Ti–Y, phase studies, 16: 13634
Tm–Y, magnetic properties of, 18: 25981(R) (ORNL-3582(p.11-16))
Tm–Y, magnetic properties, 19: 27732
Tm–Y, magnetic structure, 19: 18462 (ORNL-TM-1063)
U–Y, metallographic tests on arc melted, 20: 29775
V–Y, corrosion by acids and bases of vanadium-base, 20: 11230 (BM-RI-6715)
V–Y, phase studies, 16: 19394
W–Y, phase studies, 18: 12623 (ASD-TDR-63-204)
W–Y, phase studies, 19: 6306(R) (TID-6728)
W–Y, phase studies of solid solution formation in, 19: 41050
Y–Zn, crystal structure, 18: 5791
Y–Zn, crystal structure of intermetallic compounds in, 20: 7623
Y–Zn, crystal structure of intermetallic compounds in, 20: 9515
Y–Zn, crystal structure of intermetallic compound YZn_{12} in, 20: 15102
Y–Zn, crystal structure of AB_2-type compound in, 20: 24589(R) (NYO-3560-3)
Y–Zn, intermetallic compound with $CeCu_2$-type structure in, 20: 21352 (TID-21745)
Y–Zn, lattice parameters of intermetallic compounds in, 19: 24989(R) (TID-21673)
Y–Zn, magnetic susceptibility from parallel pumping in planar Zn_3Y, 17: 37700
Y–Zn, melting point and transformation temperature of intermetallic compounds in, 19: 24989(R) (TID-21673)
Y–Zn, phase diagram and thermodynamic properties of, 17: 23950 (IS-538)
Y–Zn, phase studies, 17: 4447 (IS-500(Sect.M))
Y–Zn, phase studies, 18: 1483(R) (ANL-6687(p.27-85))
Y–Zn, structure of YZn, 17: 36304 (TID-19337)
Y–Zn, structures of YZn_3, YZn_5, YZn_4, and Y_3Zn_{11} intermetallic compounds, 19: 7892 (CONF-640702-2)
Y–Zn, vapor pressure of, tracer dew-point method for measuring, 17: 25825
Y–Zr, diffusion and solubility of hydrogen in, 19: 13349
Y–Zr, mechanical properties, 16: 5315 (WADD-TR-61-123)
Y–Zr, metallurgical properties and phase studies on, 20: 5891(R) (NYO-2159-1)
Y–Zr, oxidation at high temperatures, 17: 30937(R) (NP-12968)
Y–Zr, oxidation at high temperatures, surface, 18: 5729 (ASD-TDR-63-744)
Y–Zr, oxidation in dry air at 1200 and 1600°C, 19: 47034
Y–Zr, phase studies, 16: 13634
Y–Zr, phase studies, 20: 35924
Y–Zr, preparation and properties, 16: 2128
Y–Zr, surface tension of liquid, 17: 4943

YTTRIUM ALUMINATES
gadolinium paramagnetic resonance in ortho-, 18: 39234
iron paramagnetic resonance in ortho-, 18: 39234
magnetic structure of ortho-, 18: 10619 (AFCRL-63-103)
physical properties, 20: 45639
praseodymium ion energy levels in, covalency effects on, 19: 11046(R) (AROD-2099:22)
preparation and paramagnetic resonance spectra, 16: 517 (AFCRL-775)
preparation of single crystals, 16: 22114
spectra of praseodymium-doped, absorption and fluorescence, 17: 33915

YTTRIUM ARSENIDES
crystal structure and magnetic susceptibility, 19: 13289

YTTRIUM AZIDES
preparation and spectra of, 19: 13389
thermal decomposition of, differential thermal analysis of, 18: 25446

YTTRIUM BORATES
crystal structure, 17: 27837
polymorphism, x-ray analysis, 16: 162
preparation and properties, 19: 7498
spectra of, infrared, 17: 18048
spectra of, infrared, 20: 35519
structure of vaterite-type, 16: 32075
$LaBO_3$–YBO_3, structural polymorphism of, 17: 32124

YTTRIUM BORIDES
boron-11 NMR, in hexavalent, 17: 676
boron-11 NMR, in hexa-, Knight shifts in, 17: 32083
crystal structure, 20: 25096
crystal structure and thermionic properties of, (E), 20: 38359
effects on thermoelectric properties of MCC 50, 19: 12129(R) (ASD-TDR-62-896(Pt.II))
electric properties, 17: 11306 (IS-473)
electrical properties, Hall effect, 17: 2131
mechanical properties of, (E), 20: 38359
melting of, induction heating in floating zone, 17: 8719
performance as control materials for high-temperature reactors, 18: 22519
physical properties of hexa-, 16: 12154
porosity and mechanical properties of vacuum-sintered, 20: 29738
preparation, properties, and uses, 17: 2959(T) (AEC-tr-5264)
properties as thermionic cathodes, 17: 27966
radiation sintering of, 17: 20512 (GEAP-3743(Pt.II))
testing for use as reactor absorber material, 16: 32072
thermal conductivity, 17: 28843
thermionic properties of hexa-, 17: 14819(R) (GEST-2009)
thermophysical properties at high temperatures, 18: 14469 (TID-7676 (p.101-4))
CeB_6–YB_6, properties, 17: 2959(T) (AEC-tr-5264)
LaB_6–YB_6, properties, 17: 2959(T) (AEC-tr-5264)

YTTRIUM BROMATES
thermal decomposition of, search for perbromate in, 19: 36402

YTTRIUM BROMIDES
preparation of high-purity, 17: 29247 (BM-RI-6259)
thermal decomposition of hydrates of, mechanisms of, 19: 46271

YTTRIUM CARBIDES
binding energy, 20: 5540
crystal lattice parameters, 19: 41014 (LA-DC-6819)
eutectic temperature between carbon and dicarbide, 19: 41014 (LA-DC-6819)
hydrolysis of, gaseous products from, 20: 29220
microhardness, 19: 41014 (LA-DC-6819)
neutron diffraction study, 16: 10563
phase studies, 20: 4297(R) (IS-1200(Sect.M))
phase transformation temperatures in, 19: 41014 (LA-DC-6819)
physical properties of, band model for determining, 19: 7442
preparation and hydrolysis in mineral acids and water, 18: 39221
preparation and properties, 16: 9217(T) (AEC-tr-4997)
preparation and properties, 16: 30408
preparation and properties, 19: 356(T) (JPRS-26877(p.1-24))
preparation and properties, 19: 2346
preparation and properties of, 19: 18472(T) (JPRS-28739)
preparation of high-purity, 17: 29247 (BM-RI-6259)
properties at 20 to 1300°C, 20: 36811
properties of, chemical and physical, 20: 17048
reactions with hydrogen, effects on carbide structure, 19: 9670(T) (AI-Trans-69)
reactions with water, formation of gaseous products in, 20: 17048
structure of dicarbide, 19: 5860
structure of, correlation between interatomic distances and carbide valency in crystal and electron, 17: 37813
structure, crystal and electronic, 17: 3488 (TID-14175)
thermodynamic properties, 20: 5540

YTTRIUM CARBONATES
complexes of, composition in solution of, 20: 10824
complexing in ion exchange studies, 19: 36293
decomposition at 25 to 1500°C, formation of compounds in, 16: 26954 (BM-RI-6029)
decomposition of, mechanism of thermal, 17: 4553
preparation and thermal decomposition, 18: 17774 (LADC-6082)
preparation from acetates and propionates, 20: 26911
solubility in complexone III, 20: 23026
solubility of, in water charged with carbon dioxide, 20: 45636
thermal decomposition at 155 to 700°C, 20: 29223

YTTRIUM CHLORIDE HYDROXIDES
chemical properties and crystal structure of $Y(OH)_2Cl$, 19: 42516

crystal structure, 20: 7066

YTTRIUM CHLORIDES
crystal lattice energy of, relation of self energy of gaseous ions to, 18: 16017
heat of vaporization and vapor pressure of, above melting point, 17: 37185
mass spectra of vapor-phase, 19: 15489
melting points and vapor pressure, 18: 8386
osmotic and activity coefficients of aqueous solutions of, 18: 13722 (IS-770)
preparation, 19: 9604(R) (IS-900(Sect.M))
preparation by reactions of carbonyl chloride with yttria, 20: 41412(R) (IS-1500(Sect. M))
preparation of high-purity, 17: 29247 (BM-RI-6259)
properties of di- and trivalent, review on, 19: 22229
radiation dose to gastrointestinal tract from ingested yttrium-90-labeled, 20: 43043
rare earth ion paramagnetic resonance in, 18: 39212
rare-earth-ion fluorescent lifetimes in crystals of, 20: 12317
reaction with sodium phosphates, 19: 38619
reactions with ammonium or sodium hydroxides, preparation of yttrium hydroxides by, 20: 26873
reactions with chlorides of other metals, 19: 7502
reactions with gaseous alkali and alkaline earth metals and hydrogen, thermodynamics of, 20: 43222
reactions with isopropylamine, thermogravimetric study of, 20: 36853
reactions with potassium chlorides at 25°C, 19: 38620
reactions with sodium fluosilicates, precipitation in, 20: 1870
reduction by magnesium in fused salt bath for preparation of magnesium–yttrium alloys and yttrium, 19: 18437
reduction for preparation of metal, methods for, 20: 41412(R) (IS-1500 (Sect. M))
separation by reversed-phase partition chromatography using organophosphorus compounds, 18: 25614
separation from salts by extraction chromatography using organic phosphorus compounds, 20: 10759 (INP-427/C)
solvent properties for yttrium, 18: 1489(R) (IS-700(Sect.C))
spectra and energy levels of trivalent erbium in, 19: 11082
spectra of chlorine-35- and -37 containing, visible, 20: 14569
spectra of, in gadolinium chlorides, ultraviolet-absorption, 17: 20047
thermodynamic properties, 18: 10108
tricyclopentadiene, preparation and properties of, 17: 33964
vapor pressure and heat of sublimation, 17: 18086
alkyl aluminum–YCl_3, catalytic effects of, on directional polymerization of 1,3-butadiene in nitrogen, 19: 2318
cesium oxalates–H_2O–YCl_3, phase studies, 20: 33304
CsCl–YCl_3, phase studies, 19: 22248
KCl–H_2O–YCl_3, phase studies, 17: 35841
KCl–NaCl–YCl_3, phase studies on, 20: 1872
KCl–YCl_3, phase diagrams, 18: 13792
$LaCl_3$–YCl_3, phase studies, 20: 8938
NaCl–YCl_3, phase diagrams, 18: 13792
rubidium oxalates–H_2O–YCl_3, phase studies, 20: 33304
UO_2Cl–YCl_3, fluorescence spectra of, 19: 15548
Y–YCl_3, phase studies and properties of, 18: 6832
Y–YCl_3, phase studies and reduction reactions of, 20: 26834

YTTRIUM CHROMATES
preparation and properties, 17: 32105
preparation and solubility of, 17: 35828

YTTRIUM CHROMITES
phase studies, 20: 36812
spectra of, infrared, 20: 36807
CeO_2–$YCrO_3$, ceramic properties, 17: 14801(R) (AD-278452)
TiO_2–$YCrO_3$, ceramic properties, 17: 14801(R) (AD-278452)
$YCrO_3$–ZrO_2, ceramic properties, 17: 14801(R) (AD-278452)

YTTRIUM CITRATES
solubility in perchloric acid solutions, 19: 22244

YTTRIUM COMPLEXES
equilibrium quotients and stability of bromide and chloride, 16: 25356
formation of, 18: 6711
formation of, of physiological interest, 20: 5237(R) (UR-668, pp 55-109)
stability constants of, determination of, by metal distribution between aqueous phase and ion exchanger, 20: 16481
stability of, equations for, 20: 8934
with [(2-hydroxyethyl)imino]diacetic acid, dissociation constant of, 19: 38671
with acetic acid chelates, preparation of mixed, 17: 14259
with acetyl-, benzoyl-, and propionylacetonates, stability of, 18: 25389
with acid phosphates, ion exchange studies on composition and stability of, 20: 38878(T) (ORNL-tr-1257)
with Alizarin Red S, composition, nature, and stability of, 18: 16039
with alizarin S and ammonia, formation and structure of, 18: 31518
with α-hydroxygluconate, isobutyrate, and lactate, formation constants, 16: 11635
with α-hydroxyisobutyric acid, ion exchange determination of stability constants of, 18: 35521
with α-hydroxycarboxylic acids, stability constants, 19: 24483 (IS-1122)
with Aluminon, composition and stability of, spectrophotometric studies of, 20: 29180
with antipyrine-salicylates, benzene solvent extraction studies on, 20: 43256
with arsenazo III, formation mechanism of, 17: 6007
with ascorbic acid, absorption spectra of, 18: 31527
with benzoylacetone, dibenzoylmethane, and TTA, preparation and properties of, 20: 26830
with carboxylic acids, stability constants of, 20: 29232
with chromotrope 2B, composition and stability of, 18: 35542
with citric acid, preparation and properties, 17: 14324
with citric acid, preparation and properties of, 18: 41460
with complexones, stability, 16: 11791(T) (AWRE/TRANS/27)
with dibutylphosphoric acid, properties, 16: 17686
with dicarboxymethylethylenediaminobismethylphosphinic acid, stability and dissociation constants, 19: 22237
with dicyclopentadiene, preparation and properties of, 17: 33964
with diethylenediaminepentaacetic and ethylenediaminetetraacetic acids, 16: 10037
with diethylenetriaminepentaacetic acid, formation and stability constants of, 17: 16001
with diglycolic acid, stability constant for, 18: 8338
with diglycolic and dipicolinic acids, thermodynamic properties of, 18: 13733
with dilactic, mandelic, and quinic acids, formation and stability constants of, 20: 12817 (IS-1311)
with dimethyl formamide, preparation and properties of, 20: 35491
with dimethyl formamide, preparation and properties of, 20: 35510
with dimethyl sulfoxide, preparation and composition of, 20: 25051
with DTPA, EDTA, HEDTA, and iminodiacetic acid, preparation and infrared, pH titration, and x-ray diffraction studies of, 20: 26872
with EDTA, formation and stability, 18: 1692
with EDTA, entropy and thermal effects of formation of, 19: 30198
with ethylenediaminetetraacetic acid, 17: 21730
with gluconic acid in aqueous solution, 16: 9993
with gluconic acid, stability of, 18: 1697
with gluconic acids, stability constants, 19: 40508
with glycine, stability constants for, 19: 22227
with glycolic, α-hydroxyisobutyric, and lactic acid, formation of negative chelate, 16: 1784
with glycolic and lactic acids, thermodynamic properties of, 20: 43215
with glyoxylic acid, formation constant of, 18: 22101
with halides, stability constants of, 17: 23351
with HEDTA, stability constants of, 16: 32045 (IS-304)
with humic acid, formation constants and stability, 16: 28973
with hydroxycitrate, structure, 18: 43525
with isobutyrate and α-hydroxy- and α,β,β′-trihydroxyisobutyrate ligands, stability constants of, 18: 10124
with kojic acid and 2,4-pentanedione, stability constants of, 19: 2294
with lactic acid, formation, 16: 1740(T) (UCRL-Trans-535(L))
with methoxyacetic, propionic, and thioglycolic acids, formation constants of, 18: 17859
with methyl thymol blue, stability and optical properties, 19: 17840
with nicotinic acid and hexathiocyanatochromium in aqueous solutions, formation and stability of, 17: 18080
with nicotinic acid, formation and stability, 17: 35832
with nitrilotriacetic acid, enthalpy and entropy of formation, 16: 11601
with nitrilotriacetate, stability constants and thermodynamic properties of, 16: 32977
with nitrilotriacetic acid, properties and structure of hydrated, 18: 17838
with organic acids, composition and stability constants, 16: 18916
with organic reagents, preparation and stability of colored, 18: 27366
with organophosphorus esters and TTA, proton magnetic resonance spectra of, 18: 12132
with oxybis(ethylenenitrilo)tetraacetic acid and carboxymethylaminobis-(ethylenenitrilo)tetraacetic acid, stability of, 16: 30416
with phenanthroline, infrared spectra of, 20: 16437
with phenols, association constants for, 20: 33276
with polyaminocarboxylic acids, preparation and properties, 18: 27445
with S-ethylthioglycolate and mercaptopropionate ions, stability constants of, 17: 25102
with salicylaldehydes, association constants for, 20: 33276
with serine, stability and composition, 19: 19874
with serine, stability of, 20: 26896
with solochrome violet RS, polarography of, 20: 16406
with sulfosalicyclic acid, effect of, on absorption spectra of erbium and neodymium complexes, 20: 40926

with tartaric acid, stability constants of, 17: 39037
with tartaric acid, spectra and thermal decomposition of, 20: 40909
with thoron, composition and stability of, 19: 327
with triphenylphosphine oxide, properties and spectra of, 19: 42466
with triphosphate, stability constants, 17: 2963
with tropolone, preparation, properties, and structure, 20: 5538
with Xylenol Orange, formation and spectra of, 18: 27341
with Xylenol Orange, composition and chemical properties of, 20: 38924
with 1-hydroxycyclopentanecarboxylic acid, stability of, 20: 26910
with 1-hydroxycyclopentanecarboxylic acid, preparation, properties, and structure of, 20: 26837
with 1,10-phenanthroline–thenoyltrifluoroacetone, preparation and composition of, 20: 29221
with 2,2′-bipyridyl, infrared spectra of, 20: 16437
with 2,2′-dipyridyls, preparation and properties of, 20: 43258
with 2,2,6,6-tetramethyl-3,5-heptanedione, preparation and volatility of, 20: 7074
with 2,4-hexanedione, formation of, 18: 35546
with 2,4-pentanedione, preparation and crystal structure of, 20: 20700
with 2,4-pentanedione and bipyridine or 1,10-phenanthroline, spectra and structure of, 20: 26887
with 2,4-pentanedione, solubilities of, 17: 23446
with 2,4-pentanedione, effects of ionic size on stability of, 18: 25389

YTTRIUM COMPOUNDS
alcoholysis of alkenoxide, mechanism, 19: 15552
solubility in water and thermolysis of diliturate, 18: 31447
spectra of alkoxides, infrared, 19: 15552
spectra of isopropoxide, infrared, 19: 7359(R) (ML-TDR-64-124)

YTTRIUM DEUTERIDES
dissociation pressure and entropy, 18: 31417 (AWRE-O-22/64)
thermodynamic properties, 16: 25395
thermodynamic properties, 17: 10597 (TID-15795)

YTTRIUM ETHYL SULFATES
absorption spectra, electron levels, and Zeeman effect of trivalent erbium ions in, 17: 153(T) (AEC-tr-5396)
crystal field splitting in, thermal analysis of, 17: 8058
erbium-167 hyperfine spin lattice relaxation in erbium-doped, (E), 20: 28644
holmium spin-lattice relaxation in, 20: 5020
ion spin lattice relaxation at 1.2 to 5°K, (E), 20: 28644
proton polarization in ytterbium-doped crystals of, (E), 20: 15964
proton spin polarization in crystals of, (E), 19: 7479
rare-earth ion spin-lattice relaxation in, (E), 20: 12300

YTTRIUM FERRATES
see also Neodymium Yttrium Ferrates
analysis for gallium, method of, 17: 37159
ferromagnetic resonance of, effects of rare earths on anisotropy and relaxation in, 18: 27391
gallium-69 and -71 NMR in substituted, 18: 25413
hardness of crystalline, 16: 10728
iron-57 gamma absorption in ferrimagnetic and paramagnetic, internal fields from Zeeman splitting in spectra of, 17: 37778
iron-57 magnetic resonance in, 16: 18481
iron-57 nuclear resonance in, effects of dipolar field, 16: 18190
iron-57 nuclear relaxation in, 16: 13726
iron-57 nuclear relaxation in, mechanism, 16: 13727
magnetic hysteresis of, critical fields for, 20: 28637
magnetic interactions and spin arrangements in garnets, 16: 25882 (ASD-TR-61-630)
magnetic properties of ytterbium-substituted, 16: 28933(T) (FTD-TT-61-114)
magnetic resonance in pure and substituted, 16: 9996
magnetic structure of polycrystalline, 17: 25819(T)
magnetic structure of ortho-, 18: 10619 (AFCRL-63-103)
Mössbauer effect in, measurement, 16: 14697(T) (AEC-tr-5068)
neutron diffraction pattern of polycrystalline, 17: 37417(T)
nuclear magnetic resonance spectra of iron-57 in, 16: 6847
nuclear magnetic resonance of, calculations for, 18: 30303 (CEA-R-2336)
performance in magnetometers for point field measurements, 20: 2104 (MATT-362)
preparation and properties of garnet, 17: 3369 (AD-276084)
preparation of monocrystals, conditions for, 16: 11665
radiation effects on magnetic properties of, neutron, 17: 2042
structure of lanthanum-, neodymium-, and praseodymium-substituted, 16: 5320
structure of monocrystals of, in magnetic field, 17: 1459(T)
structure of $3Y_2O_3 \cdot 3Fe_2O_3 \cdot 2Ga_2O_3$, 18: 13113(T)
thermal conductivity, 16: 31616
tin-114 Mössbauer effect in, 19: 35423(T)

YTTRIUM FERRATES(III)
crystal structure, 19: 46256
ion interactions in, iron–yttrium, 20: 22313 (AD-624719)
magnetic properties of, Curie point pressure dependence for, (E), 20: 24597
magnetic properties of, exchange field formalism of, 20: 26904
neutron inelastic scattering by spin waves in, polarization dependence of, 20: 24647

YTTRIUM FLUORIDES
see also Sodium Yttrium Fluorides
analysis for oxygen, 18: 19907
chemical properties of, effects of temperature on, 18: 16013
crystal structure of, effects of temperature on, 18: 16013
density from melting point to 2500°K, 16: 8740
distribution of colloidal solutions of, in animal tissues, 17: 10443
effects on freezing point depressions in sodium fluorides, 18: 5284
enthalpy of formation, 19: 36411
enthalpy of formation of YF_3, 20: 20650(R) (ANL-7055, pp 167-76)
equilibrium distribution in complex, 18: 6800
heat of formation, 19: 32118(R) (ANL-7020(p.165-74))
heat of sublimation and vapor pressure of, 20: 26874
heat of sublimation and sublimation pressure of, mass spectrometric studies of, 20: 29183
melting point, 16: 6411
precipitation with calcium fluoride, effects of gases on, 18: 13766
production, 20: 4299(R) (ORNL-2711)
production by fluorination of yttrium oxide, 20: 4999(R) (ORNL-2599)
reactions with sodium carbonate at 550 to 700°C, 20: 29223
reduction, evaluation of metals for use in, 16: 2992 (IS-374)
rotational states, 18: 43502
solubility in molten fluoride mixtures, 16: 23595
spectrum of mono-, electronic band, 18: 26163
thermal decomposition at 450 to 800°C, 20: 29223
thermodynamic functions of interactions with water, 17: 40798
thermodynamic properties, 20: 36950
BaF_2–YF_3, phase studies, 19: 38615
CaF_2–NaF–YF_3, crystal structure and solubility, 18: 3774
CaF_2–YF_3, defect character in crystalline solutions of, 17: 37212
CaF_2–YF_3, formation and structure, 18: 23533
CaF_2–YF_3, mixed crystal formation, 18: 5253 (NP-13337)
CaF_2–YF_3, phase studies, 19: 38615
KF–YF_3, density and molar volume of, 20: 43165 (BM-RI-6836)
LiF–MgF_2–YF_3, analysis for magnesium and yttrium, 20: 4999(R) (ORNL-2599)
LiF–MgF_2–YF_3, analysis for oxygen, 20: 4299(R) (ORNL-2711)
LiF–YF_3, density and molar volume of, 20: 43165 (BM-RI-6836)
LiF–YF_2, phase diagram, 20: 4999(R) (ORNL-2599)
LiF–YF_3, phase diagram, 20: 4999(R) (ORNL-2599)
LiF–YF_3, solvent properties for uranium dioxide at 1150°C, 19: 11050 (MCW-1490)
NaF–YF_3, density and molar volume of, 20: 43165 (BM-RI-6836)
NaF–YF_3, phase diagrams at 300 to 1300°C, 20: 33278
NaF–YF_3, phase equilibria in, 17: 39045
NaF–YF_3, phase studies, 16: 17554(R) (ORNL-3262(p.3-18))
NaF–YF_3, phase studies, 17: 25060(R) (ORNL-3417(p.3-16))
NaF–YF_3, phase studies of order-disorder effects and solid solutions, 17: 30506 (CONF-20-21)
SrF_2–YF_3, phase studies, 19: 38615
YF_3–Y_2O_3, phase studies, 18: 1489(R) (IS-700(Sect.C))

YTTRIUM GALLATES
magnetic properties of, exchange field formalism of, 20: 26904
preparation and paramagnetic resonance spectra, 16: 517 (AFCRL-775)
spectra of erbium-doped, absorption, 17: 23375
structural properties of $Y_3Ga_5(GaO_4)_3$, 17: 14210 (NBS-MON-25(Sect.1))

Yttrium Gallium Sulfides
see Gallium Yttrium Sulfides

YTTRIUM GERMANATES
crystal structure of, ir spectral studies on, 20: 43218

YTTRIUM HALIDES
reduction in magnesium salt bath, 19: 40955

YTTRIUM HYDRIDES
cladding for use at high temperatures, 16: 9196(R) (GEMP-103A)
crystal structure, 16: 7567
development as reactor moderator material, 17: 17445
development as shielding for space reactors, 18: 32955
dissociation pressure, 18: 31417 (AWRE-O-22/64)
dissociation pressure, 20: 5844
ductility, 19: 6306(R) (TID-6728)
fabrication, 16: 10487 (XDCL-58-7-23)
fabrication for use at high temperatures, 16: 9196(R) (GEMP-103A)
fabrication of, 17: 20403 (NAA-SR-Memo-6836)
hydrogen vibration frequencies in labeled and unlabeled, 16: 11623
molecular binding of deuterium and hydrogen in, (E/T), 19: 16817(R) (GA-5554)
neutron moderating properties of, 18: 28558
physical properties, (E), 19: 31532 (BMI-X-151)
preparation and properties of, 19: 15466(T) (LA-tr-65-2)

preparation by direct action, 16: 22100
production, 20: 4299(R) (ORNL-2711)
properties as reactor moderator, review of, 18: 32032 (A/CONF.28/P/254)
properties for use as reactor material, 19: 7470
properties for use as space shielding material, 19: 37104
properties of, 17: 20403 (NAA-SR-Memo-6836)
radiation effects on thermal stability of, in-pile, 18: 4306 (TID-19501)
radiation effects at high temperatures, 20: 4299(R) (ORNL-2711)
spectra of deuterated and normal, infrared absorption, 17: 30537
thermal capacity, 17: 7655(R) (ANL-6600)
thermal expansion at 80 to 1650°F, 19: 6306(R) (TID-6728)
thermal stability, 17: 3906
thermodynamic functions of labeled and unlabeled, 16: 11623
thermodynamic properties, 16: 25395
thermodynamic properties, 17: 10597 (TID-15795)
thermodynamic properties of deuterated and normal, at 15 to 350°K, 17: 30537
thermodynamic properties, 19: 40959
thermodynamics of nonsubstitutional solid solutions of, statistical model for, 18: 25421
use of, 17: 20403 (NAA-SR-Memo-6836)
yttrium NMR in, Knight shifts and relaxation times in, (E), 19: 9141

YTTRIUM HYDROXIDE OXIDES
crystal structure, 20: 8893

YTTRIUM HYDROXIDES
crystal structure, 19: 22250
dehydration, 20: 26873
heats of formation and solution, 19: 34152(T) (ORNL-tr-660)
precipitation from aqueous solutions for strontium-90 determination, 19: 2244
preparation and properties of, 19: 34153(T) (ORNL-tr-661)
preparation by reactions of yttrium chlorides with ammonium or sodium hydroxides, 20: 26873
properties as carrier for actinium-228, 20: 43442
reaction with germanium oxides, 16: 30418
reactions with hafnium hydroxides at 100 to 1000°C, 19: 22191
solubility in sodium hydroxides, 16: 123
thermal decomposition of, thermographic and x-ray studies on, 20: 25061

YTTRIUM HYPOPHOSPHITES
preparation and properties of, 20: 16426

YTTRIUM IODATES
solubility of, in water, 20: 45656

YTTRIUM IODIDES
crystal lattice energy of, relation of self energy of gaseous ions to, 18: 16017
crystal structure, 17: 33877
preparation and structure of tri-, 18: 29602 (LADC-6087)
preparation of high-purity, 17: 29247 (BM-RI-6259)
preparation of hydrates of, 18: 39227
stability and thermodynamic properties, 18: 1675
$Y-YI_3$, phase diagram, 17: 22210
$Y-YI_3$, phase studies on, 20: 26834

YTTRIUM IONS
diffusion in bentonite clay-water pastes, self-, 16: 20425
effects on alkaline earth fluoride color centers, 17: 22251
effects on reduction of rare earth ions in calcium fluoride, (E), 19: 38595
effects on spectrophotometric determination of erbium, holmium, and neodymium, 20: 43100
electron spin of trivalent, in hexa-antipyrene iodides, 16: 13074
entropy and heat of formation in aqueous solution, equation for calculation of, 18: 22066
exchange on natural and synthetic exchangers, 16: 20356 (JÜL-32-RC)
exchange with hydrogen ions, theory of sorption dynamics of, 18: 27463
hydrolysis equilibria of perchlorate solutions of, 18: 39177
hydrolysis in aqueous solutions of sodium perchlorate at 25°C, constants for, 20: 43221
interactions with iron ions in garnets, 20: 22313 (AD-624719)
polymerization by hydroxyl bridge formation in aqueous solutions, 20: 7093
radiolysis of aqueous solutions of, pulse, 19: 38728
radioprotective effects in mice, 18: 13567
reactions with derivatives of Arsenazo III, spectrophotometric studies of, 19: 40426
relaxation of, in ferrimagnetic resonance of erbium yttrium ferrates, 17: 37698
separation by thin-layer ionophoresis, 18: 10185
separation of, from aqueous acidic chloride solutions by solvent extraction using mono-octylphosphinic acids, 20: 45806
Slater-Condon parameters of, determined from spectral data, 17: 31118
sorption from aqueous solutions by peat, 20: 7002 (INR-609/XIX/D)
sorption from perchloric acid solutions by cellulose and resin sulfonic acid exchangers, 18: 35473
sorption of trivalent, by phosphorus-containing ion exchangers, from acetic acid–sodium acetate solution, 20: 35593
spectra of, optical, (T), 19: 22218
spectra of, with *o*-semiquinones, electron spin resonance, 18: 39190
toxicity of, in mouse, determination by LD_{50} on thirtieth day of, 17: 17719
van der Waals radii of, relation of hydration energy to, 18: 16016

YTTRIUM ISOTOPES
determination in mixed fission products, radiochemical, 17: 10850(R) (HW-73337(p.77-157))
determination in reactor effluents using gamma spectrometers, 20: 8980(R) (BNWL-36, pp 3.1-122)
energy levels, interactions, nuclear moments, and transitions in, 17: 24381 (AD-403411)
gamma reactions on, cross sections for, 19: 12496
isomeric transitions, M_4-type, 16: 22985 (NP-11747)
nuclear masses and binding energies, 16: 1066
nucleon interactions in, effective, (T), 20: 6337
production in fission of uranium-235, yields, 16: 6438(R) (TID-14466)
removal of internally deposited, effectiveness of chelates of diethylenetriaminepentaacetic acid for, in rats, 19: 5612
separation from biological and dust samples, 19: 10999

YTTRIUM ISOTOPES Y-82
half life, 17: 26507
half life, 17: 28247(R) (TID-18788)
half life, 19: 27496
half life of, determination of, 17: 9516 (UCRL-9995)

YTTRIUM ISOTOPES Y-83
half life, 17: 26507
half life, 17: 28247(R) (TID-18788)
half life, 18: 13082
half life of, determination of, 17: 9516 (UCRL-9995)
half life of isomeric and natural, 19: 27496
photon scattering at 4 to 24 Mev, cross sections for inelastic, 16: 21641
production in strontium-84 (p,2n) reactions, 18: 13082

YTTRIUM ISOTOPES Y-84
half life, 17: 26507
half life of, determination of, 17: 9516 (UCRL-9995)
positron decay scheme, 16: 31184

YTTRIUM ISOTOPES Y-85
beta decay of isomeric, half life for, (E), 20: 17670 (AD-629576)
decay of isomers of, strontium-85 levels from, (E), 20: 26186
decay scheme, (E), 19: 23355(R) (BNL-867(p.1-117))
decay scheme, 18: 13048 (JINR-P-1510)
decay schemes of isomeric, 18: 2927
electron conversion spectra of, 18: 13048 (JINR-P-1510)
energy levels of, parity and spin of, (E), 20: 17670 (AD-629576)
half life, 17: 26507
half life, 17: 28247(R) (TID-18788)
half life of isomeric and natural, 19: 27496
positron decay scheme, 16: 32425

YTTRIUM ISOTOPES Y-86
decay of, K-conversion coefficients and gamma intensities and multipolarities from, (E), 20: 36229
decay of, level scheme for strontium-86 from, (E), 19: 47584(R) (ORNL-3832, pp 1-28)
decay scheme, 16: 12488
decay scheme, (E), 19: 6659
energy level assignments from zirconium-86 decay, (E), 20: 13856
energy levels, 18: 30761
gamma spectra, (E), 19: 16840(R) (IDO-17050)
gamma spectra of, conversion coefficients from, (E/T), 20: 3019 (ORNL-P-1657)
production and properties of metastable, 16: 17115
production at ORNL, 19: 26718 (ORNL-3802)

YTTRIUM ISOTOPES Y-87
beta decay branching ratios for, (E), 19: 14530 (NP-14606)
decay scheme and gamma spectra of ground- and isomeric-state, 18: 18971
decay scheme of isomeric, 17: 19226 (TID-16648)
electron conversion spectra of, 18: 13048 (JINR-P-1510)
energy level transitions in isomeric, 381-kev M4, (E), 20: 24358(R) (UCRL-16580, pp 1-93)
energy levels of, (E/T), 20: 30353(R) (ORNL-3940, pp 1-61)
energy levels of, structure from isomeric transition in, (T), 20: 19970
formation by nuclear de-excitation with neutron emission, charged-particle emission in, (T), 20: 29436
internal conversion coefficient, 16: 7066
photoproduction of isomeric, yield ratios for, (E/T), 20: 1246
photoproduction of isomeric, (E), 20: 46733
production, 19: 30306
production at ORNL, 19: 26718 (ORNL-3802)
production by alpha reactions with rubidium at 35 Mev, 20: 12917

production in (He-3,t) reactions at 27.5 Mev, ratio of ground- and isomeric-state, 18: 18971
production in (^{3}He,t) reactions at 27.5 Mev, ratio of ground- and isomeric-state (E/T), 18: 18971
production in alpha reactions with rubidium, 17: 31797(R) (BNL-782 (p.51-9))
production of strontium-87 from, 19: 10951
separation of metastable strontium-87 from, 18: 3672(R) (BNL-799 (p.64-73))

YTTRIUM ISOTOPES Y-88

beta decay, (E), 19: 17060
beta decay of, gamma spectra from, 20: 24358(R) (UCRL-16580, pp 1-93)
beta transitions in, strontium-88 levels from, (E), 20: 32453
calibration of, by sum peak method using sodium iodide crystal, 19: 32276
content in air samples collected at Richland, Wash., 1962, 1963, and 1964, 19: 2541
content in atmosphere, 1962 through mid-1964, 20: 8980(R) (BNWL-36, pp 3.1-122)
content in rainwater at Ispra during 1963 and 1964, 19: 34373
content in stratospheric and tropospheric samples in Project Star Dust, 1963, 20: 16727(R) (HASL-168)
content in stratospheric and tropospheric samples in Project Star Dust, 1964, 20: 16728(R) (HASL-169)
content on air filters at Hanford, methods of gamma spectrometry for monitoring, 19: 620(R) (HW-81746(p.3.51-5))
contents in air in Hanford Works Area, 19: 13626 (HW-SA-3742)
decay of isomers of, 17: 7294
decay of, K conversion coefficients from, (E/T), 20: 8080 (ORNL-P-1700)
decay rate of, 19: 11584
decay scheme, 18: 2962
decay scheme, 20: 3982(R) (AGN-8156)
decay scheme of isomeric, 19: 29258 (NP-15050)
decay scheme of, removal of fictitious cascades from, 18: 21251
determination in simulated high-altitude radionuclide samples, radiometric, 19: 13203(R) (NYO-3276-8)
determination of, on zirconium-95 fallout particles on grass, spectrometric, 17: 17998
electron pair production cross section near threshold, (E), 19: 21252(R) (UCRL-11828(p.35-8))
electron-capture decay, 18: 36600
energy levels, (E), 19: 37823(R) (ORNL-3800(p.1-49))
energy levels from proton reactions on Sr-88, 16: 4741(R) (TID-14157)
energy levels in, low-lying, 16: 15681
gamma spectra, 16: 11883
gamma spectra, 16: 18467
gamma spectra, 16: 20628 (ANL-6499)
gamma spectra, 19: 31696
gamma spectra, 20: 26396(R) (IDO-17140)
gamma spectra, 20: 44634(R) (IDO-17188)
gamma spectra and half lives of millisecond isomeric, (E), 20: 28431
gamma spectra of, effects of nonlinear response of NaI(Tl) on single-crystal summing, 17: 25891
gamma spectrum from, 18: 7054(R) (ORNL-3499(Vol.II)(p.120-4))
gamma spectrum of, 17: 22008 (LADC-5609)
gamma transitions at 898.2 and 1836.2 kev, (E), 20: 3043
half life, 16: 2541
half life, 20: 8076 (NP-15663)
nucleon interaction potentials in, shell model calculation of, 17: 40031
positron decay, 17: 7254
production and separation of, method for, 17: 10676 (NP-12231)
production at ORNL, 19: 26718 (ORNL-3802)
production by gamma reactions (γ,n) at 20 Mev, 17: 30161
production in 20-Mev linear electron accelerator, purity and yield in, 19: 32836
production of carrier-free, in ORNL cyclotron, 19: 22851 (ORNL-TM-1047(p.72-6))
production of isomeric, in neutron activation of yttrium at 14.3 Mev, (E), 20: 19809 (CEA-R-2900)
production using ORNL 86-in. cyclotron, 20: 2212
soil content and motion, 19: 36661
solvent distribution between bis(2-chloroethyl) ether and hydrochloric acid, coefficient of, 20: 18571 (ORNL-TM-1420)
spectra of, design of 4π scintillation positron spectrometer for, 18: 4125
strontium-88 mass difference, 16: 7078

YTTRIUM ISOTOPES Y-89

abundance in meteorites and terrestrial matter, 18: 10753
alpha inelastic scattering at 42 Mev, level structure from, (E), 20: 22138
alpha scattering at 42 Mev, 18: 16951(R) (TID-20311)
core deformability and electric quadrupole moments, 16: 7026
deuteron elastic scattering at 15 Mev, optical model for, 19: 14604
deuteron inelastic scattering by, distributions from, 17: 9546
deuteron reactions (d,α) at 15 Mev, mechanisms for, 16: 32422
deuteron reactions (d,p) at 15 Mev, neutron-proton residual interactions in, 17: 24491
deuteron reactions (d,p) with, cross section and isomer ratio for, 18: 7697(R) (TID-19931)
deuteron reactions (d,p) at 5 to 12 Mev, cross sections and isomer ratios for production of yttrium-90g and -90m in, 18: 21279
deuteron reactions (d,p) at 12 Mev, 18: 34834
deuteron reactions (d,He-3) with, 18: 42625(R) (ANL-6879(p.65-8))
deuteron reactions (d,t) at 11.8 Mev, angular distributions from, (E), 19: 21326
deuteron reactions (d,p) at 15 Mev, yttrium-90 energy levels from, (E), 19: 23705
deuteron reactions (d,He-3) with, (E), 19: 27446
deuteron reactions (d,n) at 11.8 Mev, total cross sections for, (E), 19: 35438
deuteron reactions (d,p) with, isomeric cross section ratios for, (E), 19: 41820
deuteron reactions (d,p) at 11.95 Mev, yttrium-90 levels from, (E), 20: 15799
deuteron reactions (d,He-3) at 21 Mev, angular distributions from, (E), 20: 34530(T) (CONF-660107-46)
deuteron reactions at 11.8 Mev, energy spectra from, 20: 40065(R) (BMwF-FB-K-66-01)
effect of configuration mixing on M4 transitions of (T), 19: 1643
energy levels, 17: 2243(R) (TID-17083)
energy levels, 18: 2846(R) (TID-19709)
energy levels, 18: 18985
energy levels, excitation energies and spins for, 16: 26287 (IS-408)
energy levels in, search for 1.5-Mev $^9/_2$ +, 16: 33856
energy levels in, excitation of isobaric analog, 18: 15287
energy levels of, (E), 20: 34530(T) (CONF-660107-46)
energy levels of, detection of isomeric, 17: 29953
energy levels of, shell model, 18: 30795
energy levels of, isobaric analogue, 19: 14640
energy levels of, effects of collective vibrational motion on anomalous coupling, (T), 20: 28420
energy-level density and transitions, (E), 20: 42331
Fermi gas coefficient and nuclear temperature, 18: 998 (AD-299005)
gamma dose constants for metastable, 20: 46617
gamma emission by, 18: 8313
gamma spectra, 17: 34966
gamma spectra of metastable, 17: 9549
gamma transitions in, independent particle model for M4, 19: 17051
half life of isomeric, from neutron reactions (n,n'), (E), 20: 16336(R) (NYO-10175)
half life of metastable state of, 17: 19262
helium-3 reactions (He-3,d) with, distorted-wave analysis of, 18: 21204 (LADC-6302)
helium-3 reactions (He-3,d) at 22 Mev, zirconium-90 energy levels from, 18: 24663
isomer yield from deuteron reactions, 17: 11634(R) (TID-17696)
neutron activation cross sections for, (E), 20: 30360 (WASH-1068)
neutron capture by, gamma radiation from thermal, (E), 19: 37805(R) (ORNL-3778(p.44-53))
neutron capture by, isomer ratios from fast, (T), 20: 19920
neutron capture by, cross sections for production of isomeric yttrium-90 in fast, (E), 20: 42326
neutron capture cross sections at 10^3 to 10^8 ev, 16: 26518
neutron capture cross sections of, energy dependence of, 17: 26521
neutron capture cross sections at 4 kev to 3 Mev, (E), 20: 26394(R) (ANL-7193)
neutron capture cross section at 14.7 Mev, (E), 20: 46614
neutron capture gamma spectra from, thermal, (E), 19: 25475(R) (ORNL-TM-1044)
neutron elastic scattering at 1.509 Mev, polarization in, 17: 31410 (TID-19051)
neutron inelastic scattering on, optical model for cross sections of, 17: 33048
neutron inelastic scattering by, levels and spins from, (T), 20: 28343
neutron inelastic scattering at 5.0 Mev, Q values for, (E), 20: 30360 (WASH-1068)
neutron inelastic scattering at 5 Mev, cross sections for, (E), 20: 39470(R) (ORNL-3924)
neutron potential scattering cross sections, 18: 2849
neutron reactions (n,n'γ), angular distributions for, 16: 4741(R) (TID-14157)
neutron reactions at 14.6 Mev, mechanisms and shell effects, 16: 12487
neutron reactions (n,α) and (n,p) at 7.0 to 19.8 Mev, cross sections for, 16: 19782
neutron reactions (n,2p) at 14.8 Mev, cross section limit, product half life, and Q value for, 17: 2242 (TID-16949)
neutron reactions (n,α) at 14.8 Mev, cross sections for, 17: 2242 (TID-

16949)
neutron reactions (n,p) at 14.8 Mev, separation energies for, 17: 2242 (TID-16949)
neutron reactions (n,αγ), (n,αn), (n,2n), (n,pγ), and (n,pn) at 14.8 Mev, cross sections for, 17: 2242 (TID-16949)
neutron reactions (n,γ) at 14.8 Mev, cross sections, product half life, and Q value for, 17: 2242 (TID-16949)
neutron reactions on, widths of resonances in, 17: 13557
neutron reactions at 2–10 kev, inelastic scattering and radiative capture cross sections for, 17: 29631
neutron reactions (n,2p) at 14.7 Mev, cross-section limits for, 17: 36707
neutron reactions (n,γ) at 14.7 Mev, cross sections for, 17: 36707
neutron reactions (n,2p) at 14.8 Mev, cross-section limits for, 18: 1077
neutron reactions (n,γ) at 14.8 Mev, cross section of, 18: 1077
neutron reactions (n,2n) with, 18: 11195(R) (EANDC(E)-49(L))
neutron reactions with, scattering widths for resonance, 18: 17034
neutron reactions with, gamma radiation from, 18: 30735(R) (TID-20657)
neutron reactions (n,n′γ) at 1.0 and 4.0 Mev, cross sections and spectra for, 18: 30736(R) (TID-20658)
neutron reactions (n,xγ) at 14.8 Mev, cross section and gamma spectrum for, 18: 30736(R) (TID-20658)
neutron reactions at 15 kev, level parameters from, (E), 19: 5172
neutron reactions (n,2n) at 14 Mev, shell effects in, (T), 19: 12536
neutron reactions (n,γ) at 225 to 925 kev, cross section for, (E), 19: 19095 (WASH-1053)
neutron reactions (n,2n) with, fission-averaged cross sections, 19: 29319
neutron reactions (n,n′γ) at 14 Mev, cross sections for, (E), 19: 41781
neutron reactions (n,γ) at 0.145 to 1.225 Mev, cross sections and isomer ratios for, (E), 19: 45376
neutron reactions (n,n′), activation cross section for, (E), 20: 16336(R) (NYO-10175)
neutron reactions (n,γ) at 10 kev to 3 Mev, cross sections for, (E), 20: 32370(R) (ANL-7175, pp 212-16)
neutron reactions (n,n′γ) near 4 Mev, gamma production cross sections for, (E/T), 20: 34515 (CONF-660303-34)
neutron reactions (n,p) at 14.7 Mev, cross section for, (E), 20: 46614
neutron reactions (n,2n) at 3 Mev above threshold, cross section for, (E), 20: 46614
neutron scattering by, gamma decay of excited levels following, 17: 2243(R) (TID-17083)
neutron scattering at 6 Mev, angular distributions for, (E), 19: 5171
neutron scattering at 3 to 650 kev, cross sections, phase shifts, and strength functions for, (E), 19: 10319
neutron scattering at 0.00064 to 8.0 ev, cross sections for, (E/T), 20: 22010(R) (NYO-72-28)
neutron strength functions for, 18: 8919(R) (PR-P-59(p.65-78))
nuclear magnetic resonance in yttrium, Knight shift anisotropy in, (E), 19: 16976
nuclear properties of isomeric, 18: 13626(R) (NYO-10174)
nuclear radius, 17: 36679
nucleon scattering at 20 Mev, energy levels from, (T), 19: 14603
photoactivation of isomeric, cross sections for, 18: 7705
photon reactions at 300-Mev peak, isomer production in, (E/T), 20: 1246
photon reactions (γ,n) on, threshold of, 17: 17158
production of isomeric states in yttrium-89 (n,n′γ) reactions at 14 Mev, cross sections for, (E), 19: 41781
production of isomeric, in neutron reactions with zirconium-90 at 14 Mev, (E), 19: 47566 (AERE-R-5009)
proton reactions (p,n) and (p,p) at 4 to 5.5 Mev, compound resonances from, 18: 15287
proton reactions (p,γ) at 5.5 to 8.5 Mev, isobaric analog states from, 18: 36642
proton reactions (p,γ) with, isobaric spin analog state for (E/T), 19: 1568(R) (TID-21113)
proton reactions (p,n) with, gamma spectra and resonances for (E/T), 19: 1568(R) (TID-21113)
proton reactions (p,n) with, thresholds for, (E), 19: 6704
proton reactions (p,n), spectra from, (E), 19: 19095 (WASH-1053)
proton reactions (p,n) at 4.6 to 5.6 Mev, angular distributions in, (E), 19: 21356
proton reactions (p,n) at 4.65 to 5.05 Mev, isobaric analog states in, (E), 19: 25511
proton reactions (p,n), cross sections near isobaric analog resonances for, (E), 19: 25475(R) (ORNL-TM-1044)
proton reactions (p,n) at 3.6 to 5.1 Mev, cross sections, (E), 19: 37813(R) (ORNL-3778(p.97-100)
proton reactions (p,d) with, distributions from, (E), 19: 37823(R) (ORNL-3800(p.1-49))
proton reactions (p,xn) at 400 Mev, cross sections for, 19: 37835(R) (TID-22024)
proton reactions (p,α) at 20.2 Mev, distributions from, (E), 19: 37823(R) (ORNL-3800(p.1-49))
proton reactions (p,n), (p,2n), and (p,pn) at 120 to 670 Mev, cross sections for, 19: 43272 (JINR-P-2218)
proton reactions (p,α) at 20.2 to 22.5 Mev, alpha angular distributions and spectra from, (E/T), 19: 47670
proton reactions (p,α) at 6 to 14 Mev, zirconium-90 level widths from, (E), 20: 8135
proton reactions (p,n) at 14.2 Mev, angular distributions, Q values, and spectra from, (E), 20: 13345(R) (NP-15772)
proton reactions (p,n) at 4.5 to 5.5 Mev, cross sections for, (E), 20: 22010(R) (NYO-72-28)
proton reactions (p,xn) and (p,pxn) at 5 to 85 Mev, excitation functions for, (E), 20: 22133
proton reactions (p,n), (p,2n), and (p,pn) at 120 to 670 Mev, cross sections for, (E), 20: 24405
proton reactions (p,n) at 4.6 to 5.3 Mev, excitation functions and angular distributions for, (E), 20: 26094 (ORNL-P-2117)
proton reactions (p,γ$_0$) at 2.2 to 6.3 Mev, excitation function and spin-flip giant resonance from, (E), 20: 28398
proton reactions (p,α) with, zirconium-90 level widths from, (E/T), 20: 30360 (WASH-1068)
proton reactions (p,d) at 36 Mev, deuteron spectra from, (E/T), 20: 30353(R) (ORNL-3940, pp 1-61)
proton reactions (p,α) at 20.2 Mev, alpha spectra from, (E/T), 20: 30353(R) (ORNL-3940, pp 1-61)
proton reactions (p,n) at 14.2 Mev, Q-values and differential cross sections for, (E/T), 20: 34520 (INS)-97)
proton reactions (p,n) at 8 to 14 Mev, neutron spectra from, (E), 20: 44739
proton reactions (p,pn), excitation functions, 16: 5963
proton reactions (p,γ) in stars, 16: 12308
proton reactions (p,pn) at 20 to 155 Mev, excitation functions for, 16: 21484
proton reactions (p,n) at 14.8 Mev, neutron spectra from, 16: 26326 (UCRL-6733)
proton reactions (p,pn) at 19.2 Mev, isomeric states from, 16: 32441
proton reactions (p,n) at 11.2 Mev, cross sections for, 17: 29586
proton reactions (p,n) on, cross sections for, 17: 33072
proton reactions (p,d) at 22 Mev, excited energy levels in, 17: 38234
proton reactions (p,d) and (p,n) at 11.2 Mev, cross sections for, 17: 40056
proton reactions (p,n) at 1.5 to 6.0 Mev, threshold measurements on, 18: 6200
proton reactions with, through analog states, 18: 38154
proton scattering at 14.71 Mev, angular distribution from elastic and inelastic, 20: 28408
proton spallation, bromine-80 yield cross sections, 16: 3696
solvent extraction from biological materials by bis(2-ethylhexyl) phosphate, 20: 8507(R) (COO-119-233, pp 88-93)

YTTRIUM ISOTOPES Y-90

activity measurements, absolute, 16: 6604
activity of mixtures with strontium-90 and, external emission from, (E), 19: 22400
administration to fish, force-feeding method for, 17: 40465
analysis of, for contaminant in radioapplicator of, 17: 15911
beta activity of aqueous solutions of, measurement using Cherenkov radiation, 19: 13508
beta activity of, design of 4π beta plastic scintillator for measurement of, 17: 6459
beta activity of, method for measuring relative, 19: 15648 (NP-14698)
beta activity of, method for measuring relative, 19: 15649 (NP-14700)
beta and conversion-electron spectra, 20: 5768
beta counting of strontium-90–yttrium-90, corrections for foil absorption in 4π, (E), 19: 26654 (EUR-2248.e)
beta decay of, Coulomb corrections to internal bremsstrahlung in, 17: 26619
beta decay of isomeric, 18: 36668
beta decay of, scintillation performance for, 18: 5398
beta decay of, bremsstrahlung from, (T), 19: 8558 (HW-83784)
beta decay of, bremsstrahlung spectra in, (E), 20: 13761 (CONF-233 (Vol.4), pp 656-68)
beta decay of, direct-interaction ionization probability for, (T), 20: 19934
beta decay of, double internal bremsstrahlung in, (E/T), 20: 10030
beta decay of, end-point energy in, 18: 15236
beta decay of, inner bremsstrahlung from, 18: 22917
beta decay of, internal bremsstrahlung from, 18: 34837
beta decay of, internal bremsstrahlung spectra from, 19: 21302
beta decay of, internal bremsstrahlung in, 19: 33273
beta decay of, internal bremsstrahlung spectra in, (T), 20: 36209
beta decay of, performance of proportional counters for low activity, 19: 30541
beta decay of, polarization of Cherenkov radiation produced in cellulose acetate by, 20: 25797
beta depth-dose measurement in lucite, 17: 4851
beta dose determination, 16: 2077

beta emission by, bremsstrahlung circular polarization from attenuation of, 17: 20954
beta emission by, scintillation counter for measuring, 20: 14874
beta emission from, determination of end-point energy of, 17: 28183
beta emission from, 18: 8253(T) (NP-tr-1087)
beta emission of, backscattering from aluminum in 2π geometry, (E), 20: 30369
beta particles from, polarization of, 18: 34877
beta particles from, bremsstrahlung production by, (E), 19: 45284 (TID-22169)
beta polarization from, (E), 20: 28395
beta radiation dose distribution around sources of, suitable for pituitary implantation, 17: 19780
beta reactions with, x-ray emission in, (E), 19: 15849
beta sorption from, as function of atomic number, 17: 28184
beta sorption from, by toad skin, 19: 12915
beta spectra from, silicon counters for measuring, 20: 29520 (CLOR-45/D)
beta spectra of, (E), 19: 45283 (SGAE-PH-23/1965)
beta spectra of, allowed and first-forbidden (E), 19: 3330
beta spectra of, effect of secondary electron emission on, 19: 23312
beta spectra of, form factors for, 18: 44767
beta spectra of, shape measurements for, 18: 32832
beta transition in, circular polarization of internal bremsstrahlung in first-forbidden, 17: 29582
bibliography on properties and separation processes, 16: 5080 (MND-P-2581-III(Pt. I))
bremsstrahlung energy loss in, 17: 21015
bremsstrahlung excitation by, in thin absorbers, 20: 5000 (ORNL-IIC-5, pp 91-8)
bremsstrahlung spectra from, internal, 16: 17107
colloids, use in treatment of malignant effusions, 19: 15323
contamination of pig skin by, 18: 4953
contamination of rabbit skin by, 18: 12392
content in Balkan Mountains from fallout, 19: 15800
content in bones of humans, 17: 8463
content in contaminating solutions, effects on degree of surface contamination, 19: 9422
content in lake waters, equilibrium with strontium-90, 17: 21940
content in Pacific Ocean fish livers, 18: 29208
content in sea water, effects on development of fish spawn, 20: 20445(T) (TRG-Inf. Ser.-166)
content in seawater, 20: 43688
content in Tyrrhenian Sea plankton, 19: 30411
decay in solutions, 18: 8647(R) (NYO-2740-1(p.75-90))
decay of, correction factors for, 17: 24384 (AERE-R-4237)
decay of, calibration of ionization chamber for particles from, 19: 6194
decay of, contribution to total beta activity of coastal sediments of Ligurian Sea from, 20: 526
decay scheme, 17: 24891(R) (COO-227(p.204-14))
decay scheme and energy levels, 17: 34887 (UCRL-10865)
deposition of, use of molecular plating for quantitative, 20: 41011 (SGAE-CH-34/1966)
deposition on surfaces for preparation of large-dimension beta sources, 18: 28064
detection and measurement in solutions, sensitivity of scintillation counters for, 18: 29967 (AERE-R-4638)
detection and measurement on clothing, design of monitor for, 19: 26648 (AECL-2245)
detection and measurement of, using scintillation ion exchange resin, 19: 32098
detection and measurement of, *in vivo*, 20: 7316(R) (ORNL-3849, pp 215-29)
detection in clothing, instrument for, 19: 32544 (AECL-2245)
determination by autoradiography using ring-oven method, temperature effects on fading effect in, 20: 251
determination, by β-spectrum analysis, 16: 9958
determination in air by beta measurement, efficiency of counter for, 19: 20169
determination in aerosols, methods and equipment for, 19: 34258 (NP-15102)
determination in aqueous solutions by Cherenkov counting, 19: 42581
determination in aqueous solutions by detection of Cherenkov radiation, 19: 46215
determination in animals and plants in presence of calcium-45 and strontium-89 and -90, 20: 26623
determination in drinking water, design of equipment for, 18: 6763
determination in French air and rain water, 18: 4036
determination in fallout-contaminated waters by solvent extraction and counting, 19: 11017
determination in human urine and waste solutions, 16: 2980
determination in man and phantoms, whole-body counting, 16: 16140
determination in milk, 17: 38920 (IEA-60)
determination in milk, ion exchange, 18: 41343
determination in mixture with strontium-89 and -90 using semiconductor detector, spectrometric, 19: 32111
determination in milk, 19: 38856
determination in milk as an indirect measure of strontium-90 content, slide-rule method for, 20: 35352
determination in natural waters, 16: 28886
determination in Pacific Ocean, 18: 39109
determination in presence of strontium-90 by liquid scintillation spectrometry, 20: 1766
determination in presence of strontium-90, beta counting technique for, 20: 31188
determination in radioisotope mixtures, microcalorimetric, 20: 3866 (CEA-R-2630)
determination in solution using scintillation detector, 17: 6446
determination in urine, using Cherenkov effect, 19: 28278
determination in urine using Cherenkov effect, 19: 46198
determination in urine by anion exchange and beta counting, 20: 20583
determination in waste water, 17: 380
determination in water, 20: 40819(T) (CEA-tr-A-1883)
determination of physicochemical state of, in liquid media by paper electrophoresis and radioactivity recording, 18: 33590
determination of, efficiency of beta scintillation sandwich counting method for, 20: 5783
distribution and retention in trout, 16: 25117(R) (HW-72500(p.26-9))
distribution in benzene–thenoyltrifluoroacetone systems, effects of TBP on, 18: 41586
distribution in organs of mice after intratumoral injections, 17: 30213
distribution in tissues of molting crayfish, 20: 10515(R) (BNWL-122, pp 46-8)
distribution of injected, in rhesus monkey, 17: 38729
dose rates from, measurement of surface, 18: 31786 (LADC-4467)
dosimetry of beta particles from cylinders of, implanted in pituitary hypophysis, 18: 29519
dosimetry of granules of, method for measuring, 17: 11029
dosimetry of oxide rods containing, 19: 22037
dosimetry of sources suitable for pituitary implantation, 17: 19781
effects from intracellular implantation of, on pituitary function, 19: 30029
effects ingested in fish, 17: 5701 (HW-SA-2255)
effects of colloidal, on leukemia and advanced tumors, 16: 17421
effects of combined strontium-90 and, on tumorigenesis in rats, 20: 8654
effects of DTPA-incorporated, on hemorrhagic diathesis in dogs, 18: 19600
effects of implants of, on meningeal and nerve centers in cats, dogs, and rabbits, regeneration following, 20: 35265
effects of ingested, on rat intestine, 17: 38765
effects of ingested, pathological, 16: 25131(R) (HW-72500(p.88-91))
effects on blood picture, 16: 18794
effects on cancer, 20: 24950 (TID-22862)
effects on chick embryos, 18: 38775(R) (ORO-624)
effects on Cushing's disease, therapeutic, 20: 8753
effects on cutaneous angiomas, 20: 18528
effects on harvest and grain quality of field crops, 19: 19508(T) (JPRS-28977)
effects on human intestine, 19: 137
effects on human pituitary, surgical, 19: 26207
effects on lungs, carcinogenic, 18: 31349
effects on lymphatic dynamics, lymph nodes, and lymph vessels following cancer therapy, 20: 42976
effects on mice, carcinogenic, 19: 29887(R) (ANL-6971(p.47-58))
effects on mice, tumorigenic, 18: 23231(R) (ANL-6823(p.20-43))
effects on pancreatic and liver cancer, 20: 12738
effects on pituitary in diabetic children, 20: 8755
effects on pituitary, dosimetry for ablative, 20: 8751
effects on pituitary gland, effects on mammary carcinoma of, 20: 10752
effects on pituitary gland, 20: 18532
effects on pituitary gland, histological, 17: 10451
effects on quality and yield of grain crops, 19: 35963
effects on rats, tumorigenic, 20: 8654
effects on specific lymphopenia induction in dogs, 20: 42902
effects on treatment of transplanted lung tumors in rats, 19: 28150
effects with phosphorus-32 on tissue homografts in dogs by lymphatic ablation, 20: 36641
electron conversion spectra of, 18: 13048 (JINR-P-1510)
electron polarization in, method for measuring longitudinal, 18: 21339
energy level parameters, (E), 19: 5172
energy levels, 16: 5985
energy levels, 16: 21352 (NP-11667)
energy levels, 18: 34834
energy levels, (E), 19: 23705
energy levels from deuteron reactions (d,p) with yttrium-89 at 11.95 Mev, (E), 20: 15799
energy levels from deuteron reactions (d,α) with zirconium-92 at 12.0 Mev,

(E), 20: 15799
energy levels of, 17: 13557
energy levels of, low-energy, 17: 31518
energy levels of, shell model of, 19: 23363(R) (NP-14954)
energy levels of, central and tensor potentials in shell model calculations of, 20: 28360
energy levels of, shell-model potential parameters for low-lying, (T), 20: 38145
energy levels, configuration mixing, and proton-neutron interaction in, (T), 19: 23678
excretion of deposited, effects of EDTA on, in dogs, 20: 5248(R) (COO-119-232, pp 200-2)
half lives of ground and metastable states of, 17: 19262
hyperfine-structure, moments, and spin, 16: 8216
implantation for pituitary ablation, 20: 12753
iridium-192 contamination of, 18: 13593
isomeric states of, characteristics of, 17: 28327
isomers, detection and properties, 16: 3710
localization of injection of, in organs in dogs and rabbits, 17: 21405
metabolism and toxic effects of, in avian embryos, 20: 32909(R) (ORO-648, pp 91-102)
metabolism by Chlorella, 18: 41064
metabolism by marine plankton, 19: 24242(R) (NP-14901)
metabolism by plankton, 18: 35238 (STI/DOC/10/28(p.9-20))
metabolism by plants, 19: 45804
metabolism in man, 17: 7750 (TID-17547)
metabolism in rats after oral administration of mixed uranium fission products, 19: 40322
mobility of, on paper electrochromatograms, 18: 10159
movement in soils, 20: 30943(R) (ORNL-TM-1465)
movement in soils, method for study of, 18: 16216
neutron reactions (n,α) at 14 Mev, nuclear shell effects in cross sections for, 18: 18977
neutron reactions (n,γ) at 0.14 to 1.22 and 14.5 Mev, cross sections for, (E), 20: 9981 (WASH-1064)
neutron-proton residual interaction in, 18: 34870
nuclear magnetic fields in iron, (E), 20: 44824
nucleon coupling in, 19: 14644
nucleon interaction potentials in, shell model calculation of, 17: 40031
preparation and isolation of carrier-free, 18: 33665
preparation and purification of carrier-free, by elution of strontium-90-charged cation exchanger, 17: 29033
preparation and standardization as beta source, 18: 39605 (AAEC/TM-239)
preparation for therapeutic use, 18: 13875
preparation of carrier-free, 16: 5372(T) (CEA-tr-R-1339)
preparation of carrier-free, method for, 20: 10759 (INP-427/C)
preparation of carrier-free, 20: 27054
preparation of, for radioecological studies, 20: 28879
production by rubidium-87(α,n), strontium-88(He-3,p), and yttrium-89(d,p) reactions, isomeric cross section ratios for, (E), 19: 41820
production from strontium-90, 17: 3021 (BNL-5454)
production in neon-22 and oxygen-18 reactions with thorium-232, 18: 24690
production in reactors, 17: 3022 (BNL-6407)
production of ground and metastable states of, in rubidium-87 (α,n) and yttrium-89 (d,p) reactions, cross sections and isomer ratios in, 18: 21279
production of high-purity from strontium-90, 17: 18396 (UCRL-10215)
production of isomer pairs of, from helium-3 reactions (He-3,p) with strontium-88 at 14 to 19 Mev, (E), 20: 32430
production of metastable, by fast neutron reactions with yttrium and zirconium, 16: 3705
production of, techniques for, 18: 41892 (BNL-864)
properties and useful range in thickness measurements, 16: 2097
properties and uses of, produced at Brookhaven, 19: 22853 (ORNL-TM-1047(p.113-16))
properties of colloidal, for biomedical studies, 20: 26635
properties of radioapplicators of strontium-90 and, 20: 18522
properties of, chemical, physical, radiological, and toxicological, 19: 11422 (RSG-A-1)
radiation dose to mouse gonads from injected, 18: 23185(R) (ANL-6823(p.76-80))
radiation dose to gastrointestinal tract from ingested, calculation of, 20: 43043
radiation effects of ingested, on rats, 16: 30208 (HW-SA-2660)
radiation effects on tissue distribution in mice, 17: 19848
radiation effects of implanted, on pituitary in cancer patient, 17: 27191
radiation effects of implanted, on cat brain tissue, 17: 28729
radiation effects on dog lymph system, from labeled DTPA, 18: 19601
radiation hazard from atmospheric, in mixture with strontium-90, 20: 31528
radiobiology of, 18: 41278
removal from leafy vegetables, effectiveness of detergents and water for, 18: 5555
removal from surface by chemicals, 19: 4419
removal from textiles used for radioprotective clothing, 19: 17834
separation by ion exchange (E), 19: 868
separation from aqueous solutions of strontium-90, 16: 2102(T) (CEA-tr-X-403)
separation from cerium-144 by ion exchange, 17: 240
separation from cesium-137 and strontium-90 by ion exchange on allyl phosphate, 19: 11024
separation from cesium-137 and strontium-90, chromatographic, 19: 26235(T) (CEA-tr-A-1801)
separation from fission products by amalgam exchange, radiochemical, 18: 16148
separation from fission products in foods by solvent extraction using di-(2-ethylhexyl) phosphoric acid, 19: 15386
separation from fission products by thin layer chromatography, 19: 24467
separation from rare earth fission products, 16: 7497
separation from radioisotopes in aqueous solutions by foam chromatography using colloidal manganese dioxide, 20: 20628
separation from rain water, 20: 37029
separation from sea water, 20: 31249
separation from strontium-90 in carbonate solution by ion exchange, 16: 3077
separation from strontium-90 using anion exchange resins, 16: 3038(T) (CEA-tr-X-353)
separation from strontium-90 by ion exchange papers, 16: 11536
separation from strontium-90 in carrier-free state, electrochromatographic, 16: 13103
separation from strontium-90, chromatographic, 16: 27078
separation from strontium-90 by adsorption on various materials, 17: 2662(R) (MLM-1135)
separation from strontium-90 by selective sorption on platinum, 17: 7660(R) (MLM-1137)
separation from strontium-90 by selective adsorption on materials, 17: 7659(R) (MLM-1136)
separation from strontium-90 by sorption, 17: 25295
separation from strontium in carrier-free state using diaryl phosphates, 17: 25324
separation from strontium-90, use of pyridine in precipitation with ferric hydroxide, 17: 27447
separation from strontium-90, 17: 35893
separation from strontium-90 by solvent extraction using benzene and TTA, 18: 1803(T) (CEA-tr-X-175)
separation from strontium-90 by ion exchange on tin phosphate, 18: 13922
separation from strontium-90 by coprecipitation with ferric hydroxide, 18: 22182
separation from strontium-90, by ion exchange, 18: 23717
separation from steel surfaces by electrolysis, 18: 35946
separation from strontium-90 by anion exchange, 18: 41568
separation from strontium-90 by ion exchange and residue adsorption, 18: 45175(R) (MLM-1209)
separation from strontium-90, system for, 19: 2706(P)
separation from strontium-90 using thin-layer chromatography, carrier-free, 19: 5982
separation from strontium by ion exchange, 19: 7626
separation from strontium-90 by ion exchange, 19: 36293
separation from strontium-90 by elution process, 20: 2211
separation from strontium-90 using organic bases as precipitants, 20: 23202
separation from strontium-90 by ion exchange in DTPA and HEDTA, 20: 25197 (ORNL-3903)
separation from uranium fission products using ring oven method, 19: 11021
separation from waste solutions by ion exchange, 17: 31790 (ORO-604)
separation from water by solvent extraction using thenoyltrifluoroacetone, 19: 11017
separation from waste solutions using manganese dioxide, 20: 5206
separation from water using bentonites, gypsum, and superphosphate, 20: 22924
separation in insoluble barium and strontium sulfate columns, 17: 192 (JEN-105-DQ/I-32)
separation of carrier-free, by solvent extraction using TBP, 17: 8211
separation of strontium from, by amalgam exchange technique, 17: 34038
separation using chromatographic paper treated with tri-*n*-octyl phosphate, 17: 35943
shielding of, bremsstrahlung attenuation factors for, 20: 3254
shielding requirements for, 17: 8156
sorption by ion exchange collectors, 18: 12258 (PAN-453/XIX)
sorption by ion ion exchange materials from water, 19: 539
sorption by iron and zirconium hydroxides from acid solutions, 19: 376
sorption by rat skin, 20: 14253

sorption on vermiculite from acidic and neutral solutions, 16: 11958(R) (JAERI-5003(p.117-18))
sorption through burns and wounds in rats, 18: 29232
standards of, for diagnostic and therapeutic use, 17: 21744
therapeutic effects on diabetic angiopathy, 19: 15245
therapeutic effects for pituitary ablation, 19: 19667
therapeutic effects on breast cancer, 19: 28178
therapeutic use for polycythemia vera in humans, 16: 7391
therapeutic use for, 17: 38680
therapeutic use in large animals, method for, 18: 3638
therapeutic use of DTPA chelates of, maintenance of curie quantities in, 18: 8257
therapeutic use of, 18: 41278
therapeutic use of, dosimetry in intra-sellar implantation, 19: 4031
therapeutic use of, tumor to total body radiation dose ratio in, 19: 15289
therapeutic use of ceramic spheres containing, 19: 22045
therapeutic use of applicators of, 19: 43906
therapeutic use on skin tumors, 19: 34005
therapeutic use, applicator needle for, 18: 15912(R) (ACRH-20(p.25-36))
therapeutic uses, 18: 35431
therapeutic uses of suspended, by intratumoral deposition, 16: 8551(T) (JPRS-11903)
therapeutic uses of colloidal injected, in tumor-bearing rats, 16: 14438
therapeutic uses of, arterial-injection methods in, 17: 7742
therapeutic uses of suspended, by intra-arterial deposition in animals and man, 17: 38783
therapeutic uses of, review on, 19: 274
therapy for spinal pain, 18: 17691
transport in mouse serum, 16: 31464
uptake and distribution in developing roe of Black Sea fish, 19: 25879
uptake and excretion in rats, effects of zirconium citrate on, 18: 3460
uptake by carp, 18: 5148(T) (JPRS-21989(p.5-10))
uptake by eggs and tissues of chickens following intramuscular and oral administration, 18: 38775(R) (ORO-624)
uptake by fish roe, 16: 28723
uptake by human body, 19: 7735(R) (ORNL-3697(p.222-6))
uptake by human liver, profile counting studies on, 19: 19492
uptake by *in vitro* produced melanin, 18: 3451(R) (COO-228(p.133-9))
uptake by legume and grain plants from soil, 20: 26627
uptake by lymph nodes, carcinoma therapy using, 18: 21939
uptake by *Melanogrammus aeglefinus* developing spawn, 19: 17483
uptake by salmon and trout eggs from contaminated water, 16: 12878 (PG-Report-288)
uptake, distribution and excretion by animals, 17: 28637
use as beta source in irradiation of brain tumors, 16: 16245
use as beta source for hypophysectomy, 18: 6723(T) (NP-tr-1080)
use as beta source of, for pituitary ablation, 20: 3809
use as beta source for therapy of hemangiomas in children, 20: 5443
use as β source for ablation of pituitary gland, 20: 5468
use as beta source for pituitary ablation, 20: 6938
use as beta source for pituitary ablation, 20: 6939
use as beta source for therapy of eye tumors, 20: 6952
use as beta source, for pituitary ablation, 20: 8764
use as beta source for pituitary ablation, 20: 8783
use as beta source for therapy of skin lesions, 20: 8791
use as beta source for therapy, 20: 8798
use as radioapplicator for pituitary gland ablation in man, 19: 28063
use for bremsstrahlung production in metals, 19: 2672
use for destruction of pituitary gland, method of, 19: 19660
use for destruction of pituitary gland, therapeutic effects of, 19: 19664
use for hypophysiolysis in treatment of breast cancer, comparison with adrenal surgery, 19: 42380
use for pituitary ablation, 20: 24964
use for radiotherapy of metastasized mammary carcinomas, 20: 31153
use for studying oyster self-decontamination, 18: 17441
use for therapy of skin tumors, 20: 16325
use for therapy of skin metastases, 20: 43039
use in beta applicators, 20: 40766
use in clinical diagnosis using ORINS linear scanner, 16: 7704
use in control of vascularization in corneal grafts, 17: 38778
use in dog prostate embolization, 18: 11743
use in evaluation of scrubbing tests on textiles, 19: 24887
use in hemangioma therapy, 20: 10745
use in hypophysectomy, 18: 19824
use in hypophysectomy, nursing care of patients following, 20: 33105
use in internal therapy, survey of techniques for, 20: 14406
use in interstitial, radiotherapy, 17: 5695
use in microspheres for therapy of malignant tumors in animals and man, 19: 10938
use in pituitary gland ablation, 20: 12748
use in pituitary surgery, 18: 13582
use in radiotherapy, dose calculations for hypophysial implantation of cylindrical sources for, 17: 40466
use in radiotherapy of epilepsy, 20: 38779
use in radiotherapy of cancer, 18: 29485
use in therapy by intra-arterial injection, method for, 19: 19661
use in therapy for advanced breast cancer, clinical evaluation of, 19: 17716
use in trans-sphenoidal hypophysectomy, results compared with use of gold-198, 20: 38758
use in treatment of hemangioma, 19: 7249
use in x-ray source, 18: 3657
use of bead of, for pituitary cancer radiotherapy, 20: 38744 (DP-1066(Vol.1), pp IV.47-66)
use of bremsstrahlung radiation from, for activation determination of beryllium and deuterium, 18: 37081
use of colloidal, in treatment of malignant effusions, energy levels for, 19: 38515
use of colloidal, calculation of absorbed dose and dose distribution for therapeutic, 17: 40454
use of, in microspheres for cancer therapy in animals and man, 17: 10288
use of injected, in treatment of multiple myeloma, 16: 20070
use of injections of, in dogs and man for preparation of bone marrow transplants, 17: 21480
use of internally deposited particles of, for cancer therapy, 20: 29059 (TID-22860)
use of pellets of, as beta source for ablation of pituitary hypophysis, 18: 31318(T) (OTS-63-11409/6(p.949-58))
use with strontium-90 as beta source for radiation chemistry studies, 16: 7585
use with strontium-90 as divided beta source in irradiation facility, 20: 23102
used with strontium-90, bremmsstrahlung efficiency in bone of, 18: 23173
uses of colloidal, medical, 17: 30010
yield in alpha fission of thorium-232 at 20 to 40 Mev, (E), 19: 41779
yield in neutron fission of uranium-235 at 14.9 Mev, (E), 19: 41779
yields from fission of plutonium-239, uranium-235, and uranium-238, 18: 19516

YTTRIUM ISOTOPES Y-91

accumulation coefficients of, in marine organisms, 18: 21780(T) (JPRS-24227)
accumulation in sea algae, 16: 4023
activity measurements, absolute, 16: 6604
behavior towards blood serum proteins, 16: 5138
beta decay of, angular correlations in, 17: 19325
beta decay of, internal bremsstrahlung from, 18: 34837
beta decay of, internal bremsstrahlung spectra from, 19: 21302
beta decay of, internal bremsstrahlung in, 19: 33273
beta decay of, internal bremsstrahlung spectra in, (T), 20: 36209
beta emission from, determination of end-point energy of, 17: 28183
beta sorption from, as function of atomic number, 17: 28184
beta spectra, 18: 30019
beta spectra, 18: 30768
beta spectra of, shape measurements for, 18: 32832
binding of, in bone, 18: 6610
characteristic state of, in blood serum, 18: 6608
chemical behavior in trace quantities, 17: 2960(T) (UCRL-Trans-599(L))
clearance of inhaled, effects of DTPA on, 18: 35296
complexes of, with EDTA and other chelating agents in blood, formation of, 18: 6609
content in fallout, 1964, 20: 11018
content in fallout and precipitation near Leningrad, 20: 16704
content in ground-level air along 80th meridian (west) during 1961, 17: 14477 (NRL-5869)
content in plants and soil, methods for decreasing, 19: 18209
content in stratosphere, 19: 20657(R) (DASA-1309)
content in stratospheric and tropospheric samples in Project Star Dust, 1963, 20: 16727(R) (HASL-168)
content in stratospheric and tropospheric samples in Project Star Dust, 1963, 20: 16728(R) (HASL-169)
decay of, correction factors for, 17: 24384 (AERE-R-4237)
deposition in body, effectiveness of chelating agents in reducing, 16: 31453(T)
determination in air samples, 16: 6639 (DASA-1300(Vol.1))
determination in air by beta measurement, efficiency of counter for, 19: 20169
determination in drinking and rain water, 20: 7021
determination in reactor effluents, methods for, 17: 35627(R) (AFSWC-TDR-62-146)
determination in simulated high-altitude radionuclide samples, radiometric, 19: 13203(R) (NYO-3276-8)
determination in sea water, methods for, 20: 1749 (USNRDL-TR-912)
determination of, radiochemical, 18: 8281 (NYO-4700(Rev.))
determination of, gamma spectrometric, 19: 32545 (CEA-R-2461)

diffusion in irradiated artificial graphite, 18: 632
diffusion in irradiated Zircaloy-4 at 800°C, 20: 21232 (BMI-1763)
diffusion in uranium(IV) oxides, 16: 10602
diffusion in uranium (IV) oxides, 16: 21046(T) (AEC-tr-5171)
distribution and excretion of inhaled, in guinea pigs, 17: 38727
distribution and volatility in air-burst debris, 20: 9184 (USNRDL-TR-933)
distribution from nuclear excavation in basalt, 20: 613
distribution in mouse tissues, whole-body autoradiographic study of, 20: 22550
distribution in rats and dogs from inhalation, 17: 40510
effects on blood and hematopoietic system, 20: 28982
effects on blood picture, 16: 18794
effects on dogs after intravenous injection, pathological, 19: 40377
elimination of, effects of chelating agents on, in rats, 18: 6611
energy levels in shell model, three-particle low-lying, (T), 20: 24448
energy levels of, effects of collective vibrational motion on anomalous coupling, (T), 20: 28420
energy loss as beta source, spectra of linear, 19: 36062
excretion by goats, 18: 31118
excretion by man, 18: 13433
excretion by rats, effects of deferoxamine and DTPA on, 20: 6746
excretion from mice using TTHA chelate promoter, 20: 10556
excretion in rats, effects of diethylenetriaminepentaacetic acid, 19: 35924
excretion of, from efficacy of EDTA, DTPA, and TTHA for promoting, 20: 18438
gamma transitions in, independent particle model for M4, 19: 17051
half life, 16: 2541
half life, 17: 38111
incorporation in tetrahydrated ammonium cerium sulfates, mixed crystal formation in, 20: 43252
ion exchange on ammonium phosphomolybdates, 18: 13801
metabolism by aquatic insect larvae in spiked water, 19: 42247(T)
metabolism by mice after inhalation in liquid aerosol, 18: 19544
metabolism by mice, effects of hexametaphosphate aerosols on, 19: 3865
metabolism in man, 17: 7750 (TID-17547)
metabolism in rats after inhalation, 19: 40314
mobilization in rats, effects of esterified polyaminopolycarboxylic acids on, 16: 28705(T) (NP-tr-907)
motion in soil, effects of chelating agents on, 19: 38329 (TID-20471)
nuclear properties, 17: 863
proton reactions (p,d) at 22 Mev, angular distributions and cross sections for, 17: 26566
radioactivity, 19: 17368
release in aircraft fuel pin meltdown, 17: 35117
release to atmosphere in SPERT I destruct, (E), 19: 24172 (IDO-12039)
removal of, from rat skin using ultrasonic energy, 16: 3994 (HW-51938)
retention in mammals, effect of chelating agents on, 16: 29327 (KFK-76)
retention of inhaled, in guinea pigs, 18: 29534
separation from animal tissues using complexing agents, 19: 12945
separation from aqueous solution by sorption on diatomaceous earth, 20: 12938
separation from fission products by solvent extraction using TBP, (E), 19: 22417
separation from promethium-147 by solvent extraction in pulse column, 17: 18199
separation from rare earth fission products, 16: 7497
separation from radioisotopes in aqueous solutions by foam chromatography using colloidal manganese dioxide, 20: 20628
separation from uranium fission products using ring oven method, 19: 11021
separation from water by chemical precipitation, 18: 20266
separation of, electrolytic, 17: 14357
sorption by calcium phosphate, 16: 28639
sorption by river silts, 18: 35238 (STI/DOC/10/28(p.9-20))
sorption by soils, effects of disodium salt of EDTA on, 20: 35227
sorption from aqueous solutions by manganese dioxide, 16: 16389
sorption of, by marine silts, 17: 37021(T) (JPRS-20795(p.1-6))
sorption of trace amounts of, on aluminum, chrome steel, or paint films, 19: 17920
tracer use in intestinal absorption studies, 18: 13433
transfer from contaminated soil to plants, 17: 38725
transfer from mother to progeny in rats, 18: 13432
transport in mouse serum, 16: 31464
uptake and distribution in rats, 18: 21783
uptake and distribution in developing roe of Black Sea fish, 19: 25879
uptake and elimination by guinea pig, effects of diethylenetriamine-pentaacetic acid on, 19: 3864
uptake by algae, effects of EDTA on, 20: 38570
uptake by aquatic insects, coefficient of accumulation for, 19: 25857
uptake by barley, bean, and tomato roots, effects of oxygen on, 19: 15003
uptake by bean plants, effects of chelating agents on, 16: 26685 (TID-16380)
uptake by embryos, placental, 16: 6288
uptake by food plants under field conditions, 17: 40541
uptake by *Gammarus lacustris*, 17: 15623
uptake by larvae of aquatic insects, 19: 8774
uptake by marine organisms, correlation with buildup factor, 20: 18215
uptake by rat organs, effects of calcium, cobalt, and zinc complexes with DTPA on, 19: 26256
uptake by soft tissues, effect of fluoroacetate, 17: 17732
uptake by white mice, 17: 21460
uptake, distribution, and excretion by animals, 17: 28637
uptake from soil by crop plants, 18: 19515 (NP-13796)
uptake of injected, in bones, kidney, and teeth in pocket mouse, 16: 44
uptake, distribution and excretion by kidneys, liver, and spleen in rats, 19: 17471
use for studying oyster self-decontamination, 18: 17441
use in study of movement of liquid and solid in small intestine in rats, 17: 10281
yields from neutron fission of thorium-232, 18: 9311 (IS-558)
yields in thermal neutron fission of plutonium-239, 19: 16873

YTTRIUM ISOTOPES Y-92
decay scheme, 16: 29828 (LADC-5293)
energy levels of, structure from isomeric transition in, (T), 20: 19970
production in neon-22 and oxygen-18 reactions with thorium-232, 18: 24690
release to atmosphere in SPERT I destruct, (E), 19: 24172 (IDO-12039)
yields from uranium-235 fission, 18: 42778
yields from uranium 235 thermal fission, (E), 20: 30476

YTTRIUM ISOTOPES Y-93
beta decay, mass discrepancies from, 16: 26287 (IS-408)
energy levels, (E), 19: 17056
energy levels and gamma spectra, 16: 31089
energy levels and gamma spectra of, 19: 1594
production in neon-22 and oxygen-18 reactions with thorium-232, 18: 24690
radioactivity, 19: 17368
sorption by humic acids and peat, 16: 11591
spectra of, gamma, 19: 29228(R) (AEET/NP/10)
yields from uranium-235 fission, 18: 42778
yields from uranium 235 thermal fission, (E), 20: 30476
yields in neutron fission of uranium at 14.7 Mev, 18: 44835
yields in neutron fission of natural thorium at 14.7 Mev, 18: 44836

YTTRIUM ISOTOPES Y-94
beta decay of, gamma transitions in, 20: 28315
decay of, determination methods for, 19: 35615(R) (NP-15037)
radioactivity, 19: 17368
yields from uranium-235 fission, 18: 42778
yields from uranium 235 thermal fission, (E), 20: 30476

YTTRIUM ISOTOPES Y-95
beta decay, mass discrepancies from, 16: 26287 (IS-408)
beta decay of, gamma transitions in, 20: 28315
beta decay of, zirconium-95 energy levels from, (E), 20: 44722
decay of, determination methods for, 19: 35615(R) (NP-15037)
yields from uranium-235 fission, 18: 42778
yields from uranium 235 thermal fission, (E), 20: 30476

YTTRIUM ISOTOPES Y-96
half life and chemical separation, 16: 12468

YTTRIUM ISOTOPES Y-97
half life, (E), 20: 13783 (ORNL-TM-1333)

YTTRIUM MANGANATES
Curie point determination of, 19: 41059(T)
magnetic properties and manganese ion moment configurations of, 18: 24128 (CONF-405-34)
magnetic properties of monocrystals of $YMnO_3$, at 4.2 to 300°K, 20: 28620
magnetic properties and structure, 18: 3772
magnetic structure, 17: 28891
preparation, crystal structure, and optical properties of, 17: 40785
properties of, electric and magnetic, 18: 30431(T)

YTTRIUM MINERALS
see also Thalenite
analysis for yttrium by neutron activation, 18: 29581
composition and structure of datolite group, 18: 12342(T)

YTTRIUM MOLYBDATES
physical properties at 600 to 1325°C, 16: 13003(R) (NP-11299)
preparation and crystal structure of, 20: 31740
preparation and structure, 19: 4119

Yttrium Neodymium Ferrates
see Neodymium Yttrium Ferrates

YTTRIUM NIOBATES
distribution in strontium molybdate single crystals, coefficients of, 20: 29746
fluorescence of trivalent neodymium ions in, 19: 36419

fluorescence spectra, 18: 26017
preparation and structure of, 18: 12673
preparation and structure of perovskite type, 20: 844
transition temperature of, relation of ionic radii to, 18: 12113
$CaWO_4$–$YNbO_4$, preparation, luminescent properties, and structure of, 18: 26017

YTTRIUM NITRATES
binding energies in, infrared spectral studies of ammoniated, 20: 40886
complex formation with dipyridine, 18: 1686
decomposition at 25 to 1500°C, formation of compounds in, 16: 26954 (BM-RI-6029)
reactions with ammonium nitrates in nitric acid solutions, 16: 30438
separation by reversed-phase partition chromatography using organophosphorus compounds, 18: 25614
solubility in TBP, 18: 13927
solubility in tributyl phosphate, 16: 5342
$Ca(NO_3)_2$–$Y(NO_3)_3$, sorption by antimony and arsenic sulfide sols, 19: 11073
$Gd(NO_3)_3$–HNO_3–H_2O–$Y(NO_3)_3$, phase studies, 18: 25434
$La(NO_3)_3$–HNO_3–H_2O–$Y(NO_3)_3$, phase studies, 18: 25434

YTTRIUM NITRIDES
formation in scaling of high-purity yttrium metal, 20: 4334
magnetic properties at 2 ro 300°K, 20: 43939
phase studies, 20: 4297(R) (IS-1200(Sect.M))
preparation and properties, 17: 21678
preparation by reactive arc melting, 20: 21244
properties of electric and optical, 17: 32652
properties, electric and optical, 18: 18472
superconducting properties, 19: 20572

YTTRIUM OXALATES
carbon-14 exchange between, and alkali metal oxalates, 20: 45634
decomposition at 25 to 1500°C, formation of compounds in, 16: 26954 (BM-RI-6029)
decomposition of, mechanism of thermal, 17: 4553
dynamic decomposition of, effects of air, carbon dioxide, and nitrogen on, 18: 23507
radioactivity measurements, production of uniform layers by means of centrifugal force for, 16: 16427
solubility in EDTA at 25 and 40°C, 19: 9149
thermal decomposition, 17: 1494
thermal decomposition, 17: 37193
thermal decomposition of hydrated, 18: 8378
thermal decomposition of hydrates of, differential thermal analysis of products of, 20: 40900
thermal dissociation of hydrates of, 20: 35509

YTTRIUM OXIDES
analysis for dysprosium and scandium, activation and spectrometric, 16: 2975
analysis for dysprosium by activation analysis, 19: 22122
analysis for dysprosium, activation, 19: 28273
analysis for dysprosium, activation, 20: 38833
analysis for impurities, chemico-spectrographic, 19: 5795
analysis for impurities by chemical-spectral method, 19: 30137
analysis for oxygen, 18: 19907
analysis for traces of other rare earths, x-ray fluorescence, 20: 7029
analysis, neutron activation, 16: 25292
atomic charge and permittivity of, (E/T), 19: 47901(T)
bonding to refractory metals, 20: 2292
compatibility with molybdenum and tungsten in cesium vapor, 18: 12857(R) (GESR-2017)
compatibility with tungsten at 1600°C in cesium, 18: 15489(R) (GESR-2007)
compatibility with refractory metals at high temperatures, 19: 7851 (CNLM-5942)
content in mckelveyite uranium mineral, 19: 40799
content in thalenites from Japan, 20: 29399
content in zircon from Kyoto Prefecture, Japan, 19: 36296
corrosion by manganese–plutonium–uranium alloy at 900°C, 16: 22549
crystal structure at pressures of 25 to 40 kbars and 900 to 1020°C, 19: 4155
crystal structure powder diffraction patterns, 19: 17795
crystal structure of, effects of pressure on polymorphism in, 19: 17885
crystal structure of, single-crystal x-ray diffraction studies of, 19: 47027
crystal structure, 16: 25350
crystal structure of nonstoichiometric, 19: 46273
crystalline parameters and transformations of, stable above 2000°C, 20: 23679
deformation by press-forging, mechanism of, 20: 23690
deformation characteristics, 20: 4297(R) (IS-1200(Sect.M))
dehydration to 600°C for neutron transmission measurements, 20: 3914 (AERE-M-1654)
deposition coatings of, on graphite by wash-coating or flame-spraying, 16: 495 (NAA-SR-5833)
deposition of coatings of, on graphite crucibles for thorium and uranium casting, 17: 12599
deposition on actinide oxides, 19: 22958(P)
determination in thorium oxide by emission spectroscopy, 20: 16393
dielectric constants and losses, 18: 7214 (NP-13431)
diffusion in, coefficient of, 17: 23292 (IS-518)
dissociation energies at high temperatures, 18: 3795
dissociation energy of, mass spectrographic study of, 19: 30171
effects of dispersions of, on hardness of niobium–titanium–vanadium alloys, 17: 41428(R) (IITRI-B6007-4)
effects of inhaled, on blood and lungs of dogs, 20: 14257
effects of, on magnetic properties of manganese ferrites, 17: 14880
effects of, on magnetic properties of magnesium manganese ferrates, 17: 16019
effects on creep properties of uranium dioxide, 19: 14022
effects on crystal structure of beryllium oxide, 16: 5689 (ORNL-TM-94)
effects on dehydrogenation of cyclohexane at 515 to 590°C, 19: 30222
effects on diffusion in uranium dioxide, mechanism of, 20: 37256
effects on dispersion strengthening of zirconium, 18: 4260 (TID-18430)
effects on dispersion strength of niobium–vanadium alloys, 17: 2394(R) (ARF-B6007-2)
effects on elastic properties of zirconia, 20: 39438
effects on electric conductivity of hafnia, 19: 18394 (ML-TDR-64-294)
effects on hardness of zirconia to 725°C, 17: 32484(R) (GEAP-4284)
effects on hydrofluorination kinetics of urania, 20: 23612
effects on irradiation performance of urania, 20: 39447 (AECL-2581)
effects on linear thermal expansion of hafnia, 19: 18394 (ML-TDR-64-294)
effects on mechanical properties of sintered and extruded tungsten, 20: 21374
effects on plasticity of uranium oxides at 940°C, 16: 12133
effects on polymorphism of zirconium oxide, 20: 3953
effects on properties of Zircaloy-2, 19: 7930
effects on sintered density of plutonia powders, 19: 40981 (NUMEC-2389-6)
effects on sintering of plutonium dioxide, 18: 27863(R) (NUMEC-2389-1)
effects on strength of zirconium, 19: 44676(R) (ANL-7000, pp 176-82)
effects on thermal conducting of thorium and uranium dioxides, 19: 18448 (AECL-2169)
effects on thermal conductivity of uranium dioxide, 17: 27814(T) (EURAEC-103)
effects on xenon diffusion in urania, 20: 31666
elastic properties, 20: 4077(R) (IS-1200(Sect. E))
elastic properties of, 20: 41064(R) (IS-1500(Sect.E))
elasticity of, 19: 9281(R) (IS-900(Sect.E))
elasticity of polycrystalline, from room temperature to 1658°C, 19: 30770
electric conductivity, 19: 24916(R) (GEMP-334A)
electric conductivity and defect structure of, 19: 42898
electron emission in presence of thermal emission current, secondary, 17: 37546(T)
electron paramagnetic resonance spectra of trivalent erbium ions in single crystals of, 20: 29192
electron spectra of, 20: 31219(R) (UCRL-16658, pp 11-20)
electron transport number in zirconium oxide, 18: 18377
electronegativity and ion radii of, prediction of phases in binary systems with other oxides from, 19: 23061
electronic spectra of mono-, 19: 36345 (UCRL-11927)
electronic symmetry determination in, by electric deflection, (E), 19: 42493
energy transfer effects in europium doped, nonradiative resonant, 18: 25564
entropy and heat content at high temperatures, 16: 30356 (BM-RI-6033)
erbium ion absorption and fluorescence spectra in single crystal, 18: 34305
europium ion spectra in, energy levels for absorption and fluorescence, 19: 2305
evaluation of coatings of, for high-temperature protection of vanadium alloys, 16: 2168(R) (ARF-2227-2)
fabrication of, 19: 894(R) (GEMP-39A)
fabrication of crucibles of, by pressure-sintering, 19: 34657(R) (RFP-518)
fabrication of crucibles of, method for, 20: 41412(R) (IS-1500(Sect. M))
fluorescence and stimulated emission of trivalent europium at 6113 Å in, 18: 2426
fluorescent properties of europium-activated, effects of cathode rays on, 19: 9186
formation in scaling of high-purity yttrium metal, 20: 4334
formation of, free energy of, 18: 14401 (BNL-7553)
internal friction of polycrystalline, from room temperature to 1658°C, 19: 30770
luminescence of Y_2O_3:Eu, emission and excitation spectra studies of, 20: 40315
melting point, 17: 39717 (GEST-2021)

melting point, effects of oxygen content, 17: 4447 (IS-500(Sect.M))
melting temperature, evaluation for space technology, 18: 16521
neodymium ion energy levels and crystal-field splittings in, 20: 30744
optical absorption and fluorescence intensities in single crystals of, at room temperature, (E), 20: 28645
optical absorption and fluorescence intensities in rare earth-doped single crystals of, at room temperature, (E), 20: 28645
performance as crucible for carbon reduction of uranis, 20: 13180(R) (IS-RD-4)
phase studies, 16: 25350
phase studies at 1700 to 2400°C, 20: 3939
phase studies of, bibliography on, 16: 33480 (UCRL-6262(Pt.2))
phase transformations in, at 50 to 1500°C, 20: 5536
phase transformations in, at high pressure and 550 to 1450°C, 20: 26833
photoluminescence of europium-activated, 19: 28312
physical properties at 600 to 1325°C, 16: 13003(R) (NP-11299)
physical properties of, bibliography on, 20: 43911 (UCRL-6262(Pt.1))
preparation, 19: 37142
preparation by calcination of yttrium oxalate in air, 20: 41064(R) (IS-1500(Sect.E))
preparation of high purity, from rare earths by ion exchange, 16: 6512
preparation of nonstoichiometric, 19: 46273
preparation of single crystal, 20: 41064(R) (IS-1500(Sect.E))
properties as nuclear thermionic device material, 18: 24367 (GEST-2022)
properties as temperature sensor materials, 17: 29712(R) (GEMP-77)
properties for carbon reduction crucibles, 20: 41411 (IS-1379)
properties for high-temperature insulation of thermocouples, 20: 41461(R) (UCRL-7361(Pt.3))
properties for use as uranium dioxide sintering additives, 17: 546(T,R) (EURAEC-5)
properties in in-pile thermionic cells, 19: 44685 (CONF-650908-5)
properties of, 19: 37142
properties of coatings of, on electron tube cathodes, 17: 25810
properties of nonstoichiometric, magnetic and paramagnetic, 20: 880
properties of press-forged, mechanical and optical, 20: 23690
properties of, bibliography on, 16: 33480 (UCRL-6262(Pt.2))
properties of, for use as insulator in thermionic converters, 20: 27531
properties, x-ray diffraction studies of heat treatment effects, 16: 15171 (DC-61-3-71)
protective effects of coatings of, on graphite, against thorium alloys, 17: 40393
purification for electronics application, 18: 36037
radiation damage, neutron, 19: 26883 (LA-3285)
radiation effects on dimensions and electric resistivity of, fast- and thermal-neutron, 20: 27588 (LA-DC-6822)
radioinduced luminescence of thin films of, containing rare-earth oxides, (E), 19: 13427
rare-earth-ion fluorescent lifetimes in crystals of, 20: 12317
reactions with alcohols and products of alcohol decomposition, infrared spectroscopy studies of, 20: 26917
reactions with barium carbonates, ternary oxide formation in, 19: 46242(R) (TID-22207, Paper B)
reactions with barium, potassium, and sodium chlorides, 20: 26816 (HW-72369)
reactions with calcium fluoride, 16: 32050
reactions with carbonyl chloride for production of yttrium chloride, 20: 41412(R) (IS-1500(Sect. M))
reactions with ferric oxide at 700 to 1400°C, 19: 40515
reactions with lanthanum and neodymium oxides in solid state, 20: 36840
reactions with niobium, 20: 27531
reactions with rhodium oxides, 17: 39044
reactions with tungsten in metallization of ceramics, 19: 899 (LA-DC-6468)
refraction of, calculation of molar and specific, 19: 13395
separation of, from silicon oxides in liquid state, 17: 14287
separation of zirconium-89 from irradiated, by ion exchange, 20: 16353
sintering and grain-growth mechanisms of, 18: 1834(R) (IS-700(Sect.E))
sintering mechanisms of, 20: 4077(R) (IS-1200(Sect. E))
sintering mechanisms of, 20: 41064(R) (IS-1500(Sect.E))
sintering of, 19: 9281(R) (IS-900(Sect.E))
sintering of, mechanism of first stage in, 18: 4217(T) (AEC-tr-6159)
sintering of, resonant frequency determinations in, 20: 7535 (IS-T-48)
sintering rates of, at 1210 to 1643°C, 20: 33838 (IS-T-90)
solubility in complexone III, 20: 23026
solubility in ethyl, isopropyl, methyl, and propyl alcohols in presence of ammonia, 20: 20686
sorptive properties for ethylene, effects of water on, 20: 29186
sorptive properties for ethylene and hydrogen, infrared spectroscopic studies of, 20: 35521
spectra at 200 to 1600°C, emission, 17: 30510 (IS-578)
spectra from 50 to 700 cm^{-1}, infrared lattice, 20: 28629
spectra in low frequency region, infrared, 18: 23549
spectra of europium-activated, absorption, excitation, and fluorescence, 18: 6820
spectra of gaseous, ground state and hyperfine-structure separation in optical, (E), 19: 42495
spectra of, in 300 to 1000 mμ region, reflectance, 17: 15970
spectra of, infrared absorption, 17: 27840
spectra of neodymium-activated single crystals of, at 77°K, 18: 5854
spectra of, parameters for emission, 17: 1433
spectra of, Ohlin structure near limit of continuous x-ray, (E), 19: 44940
spectral properties of rare earth-activated, 18: 13868
stabilization effects on thermal expansion of zirconium oxide at 200 to 2200°C, 18: 16500
thermal conductivity and expansion, 16: 22585 (DC-61-6-4)
thermal conductivity at high temperatures, 18: 39895 (GEMP-296)
thermal conductivity at 1000 to 2200°C, 20: 820 (GE-TM-64-10-4)
thermal conductivity in helium and hydrogen at 1600 to 2500°K, 19: 894(R) (GEMP-39A)
thermal expansion coefficients at 25 to 1000°C, 16: 16715(R) (CAL-PI-1273-M-10)
thermal expansion at 25 to 1000°C, 17: 14813 (BM-RI-6180)
thermal expansion to above 2000°C, 18: 25355
thermodynamic properties, 16: 25386
thermodynamic properties at 300 to 2000°K, 17: 14203 (BM-RI-6198)
thermodynamic properties of gaseous mono-, 18: 12075
use as temperature sensor, 16: 33982(R) (GEMP-74)
use of intravascular injections of, in cancer radiotherapy, 20: 24950 (TID-22862)
uses for dispersion strengthening of Zircaloy-2, 20: 5851
uses in aerospace, 19: 37142
vaporization of, species produced by, 20: 43901(R) (NBS-D-154)
ytterbium ion paramagnetic resonance spectrum in, 17: 23313
actinide oxides–Y_2O_3, preparation of sols of, 20: 39341(P)
Ag–Y–Y_2O_3, preparation and semiconducting properties of, 19: 22965 (AL-TDR-64-239)
Al_2O_3–SiO_2–Y_2O_3, phase studies and structure of, 18: 43466
Al_2O_3–UO_2–Y_2O_3, phase studies of, after heating in air at 1400 to 1800°C, 20: 43900(R) (NBS-D-150)
Al_2O_3–Y_2O_3, bonding to niobium using tungsten interlayer, 17: 34365 (LADC-5598)
Al_2O_3–Y_2O_3, bonding to niobium–1 zirconium, brazing alloy for, 19: 40980 (LA-3302)
Al_2O_3–Y_2O_3, corrosion by manganese–plutonium–uranium alloy at 900°C, 16: 22549
Al_2O_3–Y_2O_3, crystal structure, 16: 27644
Al_2O_3–Y_2O_3, phase studies and structure, 18: 43465
Al_2O_3–Y_2O_3, radiation damage, neutron, 19: 26883 (LA-3285)
Al_2O_3–Y_2O_3, radiation effects on dimensions and electric resistivity of, fast- and thermal-neutron, 20: 27588 (LA-DC-6822)
BaO–Y_2O_3, optical properties of compounds formed in, 20: 13278
BaO–Y_2O_3, preparation and properties of BaY_2O_4, 20: 45687
BeO–ThO_2–UO_2–Y_2O_3, creep and fuel retention of, effects of high temperatures on, 18: 39815(R) (GEMP-38A)
BeO–ThO_2–UO_2–Y_2O_3, fuel loss at 1200 to 1400°C, effects of coating on, 19: 30646(R) (GEMP-46A)
BeO–ThO_2–UO_2–Y_2O_3, fuel retention at high temperatures, 18: 34040(R) (GEMP-36A)
BeO–ThO_2–UO_2–Y_2O_3, fuel retention in, effects of air temperature on, 19: 13879(R) (GEMP-42A)
BeO–ThO_2–UO_2–Y_2O_3, irradiation testing of tubular fuel elements of, 20: 2467
BeO–ThO_2–UO_2–Y_2O_3, mechanical and thermal properties of, 18: 34040(R) (GEMP-36A)
BeO–ThO_2–UO_2–Y_2O_3, preparation and properties as internal conversion ceramic fuel material, 18: 2159(R) (GEMP-28A)
BeO–ThO_2–UO_2–Y_2O_3, properties as reactor fuel, 19: 24916(R) (GEMP-334A)
BeO–ThO_2–UO_2–Y_2O_3, radiation effects, 19: 24916(R) (GEMP-334A)
BeO–ThO_2–UO_2–Y_2O_3, radiation effects at 1000 to 1550°C, 19: 30646(R) (GEMP-46A)
BeO–UO_2–Y_2O_3, preparation procedures, ceramographic, 19: 46937 (NMI-5025(Pt.I), pp 1-25)
BeO–Y_2O_3, crystal structure and phase studies, 16: 20381
BeO–Y_2O_3, structure of, 17: 12663 (DC-61-7-10)
B_2O_3–Y_2O_3, liquid immiscibility in, 20: 40910
CaO–Fe_2O_3–SnO_2–Y_2O_3, superexchange inducing of magnetic fields on nuclei of diamagnetic tin atoms in iron garnets, 19: 23961
CaO–UO_2–Y_2O_3–ZrO_2, phase studies of, after heating in air at 1400 to 1800°C, 20: 43900(R) (NBS-D-150)
CaO–Y_2O_3–ZrO_2, ionic conductivity of cubic solid solutions in, 18: 16014
CeO_2–ThO_2–Y_2O_3, phase studies on, 18: 23516
CeO_2–Y_2O_3, equilibrium phase studies on, 18: 23509

$CuO-Y_2O_3$, crystal structure of sintered, 19: 42876
$Er_2O_3-SiO_2-Y_2O_3$, phase studies, 16: 22113
Fe–$SrTiO_3-Y_2O_3$–ZrH, electric and thermal properties, 17: 29854(R) (MND-2584-4)
$Gd_2O_3-Fe_2O_3-Y_2O_3$, phase diagrams, 16: 29402
$Gd_2O_3-La_2O_3-Y_2O_3$, luminescence of europium in, 19: 14015
$HfO_2-Y_2O_3$, crystallization of, from reactions of hafnium and yttrium hydroxides, 19: 22191
$HfO_2-Y_2O_3$, electric conductivity at 900 to 1600°C, effects of composition on, 20: 21370
$HfO_2-Y_2O_3$, mechanical and thermal properties of plasma-sprayed, 20: 16943(R) (IITRI-B237-45)
$HfO_2-Y_2O_3-ZrO_2$, thermal expansion to 4000°F, 18: 30105(R) (AD-429028)
$IrO_2-Y_2O_3$, phase studies in air, 19: 32751
$La_2O_3-Y_2O_3$, analysis of, for lanthanum and yttrium, photometric, 16: 28899
$La_2O_3-Y_2O_3$, phase diagrams, 16: 13598
$MgO-Y_2O_3$, phase studies, 18: 7239
$MgO-Y_2O_3$, phase studies, 18: 18396
$MgO-Y_2O_3$, thermal expansion to above 2000°C, 18: 25355
$MgO-Y_2O_3-ZrO_2$, phase studies of, on annealing and cooling, 20: 3953
$Mo-Y_2O_3$, phase studies, 17: 39717 (GEST-2021)
$Mo-Y_2O_3$, stability and strength at 1650 to 2210°C, 19: 26853
$Nb_2O_5-Y_2O_3$, properties and structure of compounds formed in, 18: 34199
$PuO_2-Y_2O_3$, preparation of sols of, 20: 39341(P)
$ReO_2-Y_2O_3$, magnetic properties and structure of compounds formed in, 20: 36784(R) (AD-636054)
$ReO_2-Y_2O_3$, preparation and ferromagnetic properties of phases in, 20: 13260(R) (NP-15852)
$Re-Y_2O_3$, phase studies, 17: 39717 (GEST-2021)
$Ru_2O_4 \cdot Y_2O_3$, magnetic susceptibility, 17: 630
$Sc_2O_3-Y_2O_3$, analysis of, for scandium and yttrium, photometric, 16: 28899
$Sc_2O_3-Y_2O_3$, phase diagram, 20: 840
$SiO_2-Y_2O_3$, preparation and properties of $Y_2O(SiO_4)$ in, 16: 17689
$SrO-Y_2O_3$, optical properties of compounds formed in, 20: 13278
$SrO-Y_2O_3$, properties of compounds formed by interactions in, 20: 17044
$Ta_2O_5-Y_2O_3$, properties and structure of compounds formed in, 18: 34199
$Ta-Y_2O_3$, measurement of insulation heat loss of, 20: 43798(R) (ALO-3634-2)
$Ta-Y_2O_3$, phase studies, 17: 39717 (GEST-2021)
$ThO_{1.5}-YO_{1.5}$, crystal structure and composition of, 19: 11743
$ThO_2-UO_2-Y_2O_3$, fission gas release from beryllia coated, 19: 44599(R) (GEMP-50A)
$ThO_2-UO_2-Y_2O_3$, fission product release kinetics in beryllia-based fuel elements containing, 19: 32678(R) (GEMP-48A)
$ThO_2-UO_2-Y_2O_3$, fuel retention capability of beryllia-based fuel elements containing, 19: 32678(R) (GEMP-48A)
$ThO_2-UO_2-Y_2O_3$, lattice parameters of face centered cubic structures in, high-temperature effects on, 18: 39815(R) (GEMP-38A)
$ThO_2-UO_2-Y_2O_3$, phase studies, 18: 34040(R) (GEMP-36A)
$ThO_2-UO_2-Y_2O_3$, phase studies, 19: 2800(R) (GEMP-40A)
$ThO_2-UO_2-Y_2O_3$, phase studies, 19: 24916(R) (GEMP-334A)
$ThO_2-UO_2-Y_2O_3$, preparation and properties as internal conversion fuel material, 18: 24065(R) (GEMP-34A)
$ThO_2-UO_2-Y_2O_3$, properties and reactions of internal conversion fuel compositions of, 18: 16424(R) (GEMP-270A)
$ThO_2-UO_2-Y_2O_3$, uranium loss from beryllia-dispersions at high temperatures, effects of sintering on, 19: 2800(R) (GEMP-40A)
$ThO_2-UO_2-Y_2O_3$, vapor pressure of uranium trioxide over, 19: 24916(R) (GEMP-334A)
$ThO_2-Y_2O_3$, defect structure and electrical properties of, 19: 42896
$ThO_2-Y_2O_3$, defect structure and electric conductivity of, 20: 843
$ThO_2-Y_2O_3$, diffusion of xenon-133 from, 19: 11679
$ThO_2-Y_2O_3$, electric and ionic conductivities, 19: 34194
$ThO_2-Y_2O_3$, electric conductivity of solutions of, electronic and ionic components of, 20: 29216
$ThO_2-Y_2O_3$, ionic conductivity and phase studies, 17: 30978(R) (NP-12969(Paper I))
$ThO_2-Y_2O_3$, phase relations and solid solubility in, 20: 843
$ThO_2-Y_2O_3$, preparation and fabrication, 17: 30978(R) (NP-12969 (Paper I))
$ThO_2-Y_2O_3$, Seebeck coefficient, 19: 36338(R) (NP–15160)
$ThO_2-Y_2O_3$, use as solid electrolyte in high-temperature cell, 19: 38586 (UCRL-11957)
$ThO_2-Y_2O_3$, xenon-133 release from irradiated solid solutions of, at 800 to 1600°C, 18: 14453 (AERE-M-1251)
$TiO_2-Y_2O_3$, phase studies, 20: 17032
$UO_x-Y_2O_3$, vaporization mechanisms of, 20: 43900(R) (NBS-D-150)
$UO_2-UO_3-Y_2O_3$, crystal structure of $UO_3 \cdot 3Y_2O_3$ phase in, 18: 6836
$UO_2-UO_3-Y_2O_3$, phase studies on, 18: 6836
$UO_2-UO_3-Y_2O_3$, phase studies, 18: 18370
$UO_2-UO_3-Y_2O_3-ZrO_2$, phase equilibria in air at high temperatures, 20: 43901(R) (NBS-D-154)
$UO_3-Y_2O_3$, crystal structure, 20: 26909
$UO_3-Y_2O_3$, diffusion of xenon-133 from, 19: 11679
$UO_3-Y_2O_3$, formation of $UO_{3.90} \cdot 6YO_{1.5}$, kinetics and mechanism of, 16: 25350
$UO_x-Y_2O_3$, O/U ratios in, after heating in air at 1400 to 1800°C, 20: 43900(R) (NBS-D-150)
$UO_2-Y_2O_3$, oxidation of solid solutions of, kinetics of, 20: 31685
$UO_2-Y_2O_3$, phase equilibria in air at high temperatures, 20: 43901(R) (NBS-D-154)
$UO_2-Y_2O_3$, preparation and properties as internal conversion fuel material, 18: 24065(R) (GEMP-34A)
$UO_2-Y_2O_3$, radiation effects on, effects of density, fissioning rate, and temperature on thermal-neutron, 20: 23778 (WAPD-TM-455)
$UO_3-Y_2O_3$, stability of, in oxidizing environment at high temperatures, 16: 10011
$UO_2-Y_2O_3$, thermal conductivity at high temperatures, 18: 39895 (GEMP-296)
$UO_2-Y_2O_3$, thermal conductivity up to 2000°C, 20: 820 (GE-TM-64-10-4)
$UO_2-Y_2O_3$, thermodynamic properties of solid solutions in, 20: 23713
$UO_{3+x}-Y_2O_3$, vapor pressure of oxygen over, 17: 29324 (KR-48)
$UO_x-Y_2O_3$, vaporization of, species produced by, 20: 43901(R) (NBS-D-154)
$UO_2-Y_2O_3$, xenon-133 release from irradiated solid solutions of, at 800 to 1600°C, 18: 14453 (AERE-M-1251)
$UO_2-Y_2O_3-ZrO_2$, phase studies of, after heating in air at 1400 to 1800°C, 20: 43900(R) (NBS-D-150)
$UO_2-Y_2O_3-ZrO_2$, preparation and properties as internal conversion fuel material, 18: 24065(R) (GEMP-34A)
$UO_2-Y_2O_3-ZrO_2$, preparation of solid solution powders of, for use as reactor fuel, 19: 39094 (CONF-117(p.11-19))
$UO_2-Y_2O_3-ZrO_2$, preparation procedures, ceramographic, 19: 46937 (NMI-5025(Pt.I), pp 1-25)
$WO_3-Y_2O_3$, phase diagram and properties of, 17: 14873
$W-Y_2O_3$, extrusion of, elongation and microstructure from, 20: 27510
$W-Y_2O_3$, phase diagrams, 20: 39437
$W-Y_2O_3$, phase studies, 17: 39717 (GEST-2021)
$YF_3-Y_2O_3$, phase studies, 18: 1489(R) (IS-700(Sect.C))
$Y_2O_3-TiO_2$, phase studies, 19: 42464
YO_1-ZrO_2, analysis for zirconium by precipitation using cupferron, 18: 25277
$Y_2O_3-ZrO_2$, crystal structure and properties at 1700 to 1750°C, 18: 556
$Y_2O_3-ZrO_2$, electric and ionic conductivities, 19: 34194
$Y_2O_3-ZrO_2$, electric conductivity at 1000 to 2400°K, 19: 25005
$Y_2O_3-ZrO_2$, electric conductivity, 19: 37094
$Y_2O_3-ZrO_2$, electric conductivity at 850 to 1300°C, 19: 42470
$Y_2O_3-ZrO_2$, electric current passage through, at 1300°C, zirconium nitride production in, 19: 42470
$Y_2O_3-ZrO_2$, formation and properties of solid solutions of, 17: 34453
$Y_2O_3-ZrO_2$, phase equilibria in air at high temperatures, 20: 43901(R) (NBS-D-154)
$Y_2O_3-ZrO_2$, phase studies, 17: 25792
$Y_2O_3-ZrO_2$, phase studies, 17: 32653
$Y_2O_3-ZrO_2$, phase studies and structure, 16: 28945
$Y_2O_3-ZrO_2$, phase studies of, after heating in air at 1400 to 1800°C, 20: 43900(R) (NBS-D-150)
$Y_2O_3-ZrO_2$, phase transformations in, fluorite, 19: 358(T) (ORNL-tr-201)
$Y_2O_3-ZrO_2$, preparation and properties of, 18: 6822
$Y_2O_3-ZrO_2$, preparation of dense and homogeneous samples by melting techniques, 20: 798
$Y_2O_3-ZrO_2$, preparation of sols of, 20: 8958(P)
$Y_2O_3-ZrO_2$, properties of, x-ray diffraction studies of heat treatment effects on, 16: 15171 (DC-61-3-71)
$Y_2O_3-ZrO_2$, vacancies in stabilized cubic, Mössbauer study, 19: 36338(R) (NP–15160)
$Y_2O_3-ZrO_2$, x-ray fluorescence analysis for yttrium, 18: 39135
Y–Y_2O_3, phase diagram, 17: 14740 (TID-11295(2nd Ed.))

YTTRIUM OXYBROMIDES
preparation and crystal structure, 20: 1834

YTTRIUM OXYCHLORIDES
structural properties, 17: 14210 (NBS-MON-25(Sect.1))

YTTRIUM OXYFLUORIDES
preparation and properties, 18: 17839

YTTRIUM OXYSELENIDES
preparation and properties of, hydrogen bonding in, 18: 19981

YTTRIUM OXYSULFIDES
preparation and properties of, hydrogen bonding in, 18: 19981

YTTRIUM PERCHLORATES
reactions of, with *N,N*-dimethylacetamide, adduct formation in, 19: 36397
separation by reversed-phase partition chromatography using organophosphorus compounds, 18: 25614

YTTRIUM PERRHENATES

preparation and properties of hydrates, 19: 22234
preparation and properties of, 20: 43217
YTTRIUM PHOSPHATES
crystal structure of, infrared spectral studies on, 20: 43219
distribution of colloidal solutions of, in animal tissues, 17: 10443
preparation and properties, 19: 38619
preparation of hydrated, 19: 38620
solubility in salt solutions, sulfuric acid, and water, 20: 1873
YTTRIUM PHOSPHIDES
crystal structure and magnetic susceptibility, 19: 13289
preparation and crystal structure of, 17: 12673
YTTRIUM PYROPHOSPHATES
preparation and properties, 18: 41454
YTTRIUM RUTHENATES
magnetic susceptibility at 2 to 1300°K, 16: 16837
YTTRIUM SELENIDES
crystal structure, 18: 1628
crystal structure and magnetic susceptibility, 19: 13289
crystal structure and stability, 19: 36365
crystal structure, 19: 44010
thermoelectric properties of sesqui-, 17: 11292 (AD-277043)
CaSe–Y_2Se_3, crystal structure, 19: 42467
CaSe–Y_2Se_3, phase studies, 20: 10857
YTTRIUM SILICATES
see also Thalenite
distribution of colloidal solutions of, in animal tissues, 17: 10443
preparation of colloidal, for use as beta emitter, 17: 5656(R) (KR-29)
preparation of radioactive, 19: 7610
preparation of $Y_2O(SiO_4)$ monocrystals, 20: 40919
reactions with strontium silicates, products from, 17: 1471
structure of, polymorphic, 20: 14537
Ca_2SiO_4–$Y_4(SiO_4)_3$, phase studies and structure, 17: 4548
YTTRIUM SILICIDES
crystal structure, 19: 11125
crystal structure and microhardness, 19: 42862
crystal structure, 20: 33910
preparation and properties, 19: 357(T) (JPRS-26877(p.25-47))
preparation and properties, 19: 42513
preparation and structure, 16: 16377
preparation of, method for, 20: 37176
preparation using arc smelting, 20: 46168
properties of, physicochemical, 20: 17047
structural characteristics, 16: 7913
structural studies, 16: 1697
structure, 19: 23006(T) (JPRS-28849(p.184-7))
thermal capacity of superconducting, anomalous, (E), 20: 21883
YTTRIUM SULFATES
see also Ammonium Yttrium Sulfates
crystal structure and bond types of octahydrates, 19: 19915
decomposition at 25 to 1500°C, formation of compounds in, 16: 26954 (BM-RI-6029)
gadolinium ion paramagnetic resonance in octohydrate, zero-field, 16: 16384
heat of dehydration, 16: 1783
reduction of anhydrous, by carbon monoxide, 18: 25427
thermal decomposition, 16: 26993
YTTRIUM SULFIDES
see also Gallium Yttrium Sulfides
crystal structure, 18: 1628
crystal structure and magnetic susceptibility, 19: 13289
homogeneity regions in, 20: 3938
preparation and crystal structure of, 20: 22975
preparation and structure of poly-, 18: 10063
reactions with chromium and iron sulfides, 16: 18863
reactions with sulfides of divalent metals, 16: 18864
reactions with ytterbium, formation of ytterbium(II) yttrium sulfide by, 19: 2297
thermoelectric properties of sesqui-, 17: 11292 (AD-277043)
Cu_2S–Y_2S_3, phase studies, 20: 18644
YbS–Y_2S_3, compound formation in, 20: 16431
YTTRIUM SYSTEMS
Ag–Y–Y_2O_3, preparation and semiconducting properties of, 19: 22965 (AL-TDR-64-239)
Al–C–Y, phase diagram at 950°C, 19: 34723
Al–C–Y, phase studies of, atomic size effects in, 19: 23111
B–Co–Y, crystal structure, 20: 14532
B–Ni–Y, crystal structure, 20: 14532
calcium oxalate–Y, precipitation reactions in, distribution coefficients of, 20: 36794
C–Cr–Co–Mo–W–Y, oxidation resistance of, at high temperatures, 19: 37155(P)
C–Cr–Co–Nb–W–Y, oxidation resistance of, at high temperatures, 19: 37155(P)
C–Cr–Co–Ta–W–Y, oxidation resistance of, at high temperatures, 19: 37155(P)
C–Hf–Nb–O–W–Y, design for improved fabricability and strength at high temperatures, 20: 25610(P)
C–H–Y, formation of ternary compounds in, 18: 39821 (IS-875)
C–Mo–W–Y, corrosion by hydrochloric, phosphoric, and sulfuric acids at high temperatures, 20: 46158
C–Nb–O–W–Y–Zr, design for improved fabricability and strength at high temperatures, 20: 25610(P)
C–Nb–W–Y–Zr, corrosion by potassium at 2000 to 2200°F, 18: 24091
C–Nb–W–Y–Zr, corrosion by potassium at 2000°F of AS-55, 20: 768(R) (NASA-CR-54226)
C–Nb–W–Y–Zr, microstructure of AS-55 sheet, 19: 13955(R) (WANL-PR-(P)-005)
C–Nb–W–Y–Zr, properties of AS-55 for containment of alkali metals, 17: 41339 (GE-62FPD365)
C–Nb–W–Y–Zr, tensile properties of D-43Y, effects of welds on, 20: 29712(R) (WANL-PR-(P)-009)
C–Nb–W–Y–Zr, weldability study of AS-55, 19: 24957(R) (WANL-PR(P)-006)
C–Nb–W–Y–Zr, weldability of D-43Y, 20: 13264(R) (WANL-PR(P)-008)
C–U–Y, phase diagram, 18: 41933 (TID-11295(3rd Ed.))
C–U–Y, phase diagram, 20: 9552
C–U–Y, phase studies, 18: 39892 (BMI-1685)
C–Y, oxidation in air at 500 to 1400°C, 19: 2750
C–Y, phase diagram, 20: 9552
C–Y, phase studies, 18: 39892 (BMI-1685)
C–Y, phase studies, 20: 13180(R) (IS-RD-4)
C–Y, phase studies, 20: 41412(R) (IS-1500(Sect. M))
D–Y, deuterium desorption from targets of, 19: 28953 (EUR-1815.e (Rev.)(p.263-70))
Gd–H–Y, crystal structure, 20: 14546
H–Sc–Y, phase studies, 20: 5909
H–Y, crystal structure and phase studies, 19: 6306(R) (TID-6728)
H–Y, oxidation in air at 500 to 1400°C, 19: 2750
H–Y, phase relations, 16: 9979(R) (TID-15017)
H–Y, phase relationships in, at 900 to 1350°C, 16: 28958
H–Y, phase studies and thermal properties, 18: 13776
H–Y, statistical model for thermodynamics of nonsubstitutional solid solutions of, 18: 25421
H–Y, thermodynamic properties at 250 to 350 and 650 to 950°C, 19: 38642
Mn–O–Y, magnetic structure, 19: 38057
Nb–O–Ti–Y, crystal structure of $YTiNbO_6$ in, 20: 26863
N–Y, oxidation in air at 500 to 1400°C, 19: 2750
N–Y, phase studies, 20: 41412(R) (IS-1500(Sect. M))
O–Ta–Ti–Y, crystal structure of $YTiTaO_6$ in, 20: 26863
O–Ti–W–Y, crystal structure of $YTi_{1.5}W_{0.5}O_6$ in, 20: 26863
O–Ti–Y, reactions in gases, properties of compounds formed by, 20: 45640
O–W–Y, phase studies of, 17: 14873
O–Y, phase diagram, 18: 35499 (IS-812)
O–Y, phase diagram, 18: 39897 (IS-848)
O–Y, phase studies and atmospheric corrosion of, 16: 5315 (WADD-TR-61-123)
O–Y, phase studies, 18: 2163(R) (IS-700(Sect.M))
O–Y, phase studies, 19: 9604(R) (IS-900(Sect.M))
Sb–O–Ti–Y, crystal structure of $YTiSbO_6$ in, 20: 26863
Si–Y, crystal structure, 18: 13795
T–Y, fabrication as radiation target, 18: 27813(R) (ORNL-TM-428)
T–Y, neutron yield of targets of, 19: 28953 (EUR-1815.e(Rev.) (p.263-70))
Y–YCl_3, phase studies and properties of, 18: 6832
Y–YCl_3, phase studies and reduction reactions of, 20: 26834
Y–YI_3, phase diagram, 17: 22210
Y–YI_3, phase studies on, 20: 26834
Y–Y_2O_3, phase diagram, 17: 14740 (TID-11295(2nd Ed.))
YTTRIUM TANTALATES
fluorescence of trivalent neodymium ions in, 19: 36419
fluorescence spectra, 18: 26017
preparation and structure of, 18: 12673
preparation and structure of perovskite type, 20: 844
YTTRIUM TELLURIDES
crystal structure, 18: 1628
crystal structure and magnetic susceptibility, 19: 13289
crystal structure and stability, 19: 36365
crystal structure, 19: 44010
thermoelectric properties of sesqui-, 17: 11292 (AD-277043)
YTTRIUM TITANATES
preparation and properties, 19: 2319
YTTRIUM TUNGSTATES
hydration, 20: 307
preparation and crystal structure of, 20: 31740
preparation and properties, 18: 39183

rare-earth-ion fluorescent lifetimes in crystals of, 20: 12317
YTTRIUM URANATES
crystal structure, 20: 26832
YTTRIUM VANADATES
europium-ion uv fluorescence in polycrystalline matrices of, 20: 20119
fluorescence of europium-activated, 19: 28330
photoluminescence of europium-activated, 19: 28312
preparation and properties, 19: 22245
properties of europium-activated, for color television tubes, 18: 37217
properties of rare earth-activated, as phosphor, 19: 36392
properties of single crystals of YVO_3, electric, magnetic, and semiconducting, (E), 20: 24664
structure of, x-ray diffraction analysis of, 17: 10663
YTTRIUM ZIRCONATES
grain growth and sintering at 1600 to 2000°C, atmospheric effects on, 18: 34212
YUCCA FLAT QUADRANGLE (NEV.)
geologic map of, 17: 4727
YUCCA LAKE QUADRANGLE (NEV.)
geologic map of, 17: 4733
YUGOSLAVIA
age estimation of uraninites using lead isotopes, 17: 4709
atomic energy developments in, legislation and publications on, 16: 32633
carbon-14-labeled compounds preparation in, 19: 42589
cesium-137 content in atmosphere in, from weapons testing in 1962 and 1963, 20: 16682
cesium-137 content in hops and malt from, 20: 45957 (NYO-3364-23)
fission product content in Balkan Mountains in, from fallout, 19: 15800
industrial aspects of ionization radiation in Croatia, 17: 25520(T) (JPRS-19545)
monitoring atmospheric radioactivity at Sljeme and Zagreb, Feb. to May 1962, 17: 27569
monitoring for radon in uranium mine in, 19: 4414
nuclear power development in, 19: 38211
potassium-40 activity in precipitation and waters in Vinca, 19: 46590(T) (JPRS-31469)
production of radioisotopes in, 16: 28986(T) (JPRS-14524)
radiation and radioisotope production and uses in, 20: 23565
radiation chemistry activities and development at Boris Kidric Nuclear Science Institute, Vinca, 18: 20082
radiation exposure of population of, 19: 34416
radiation protection standards, 19: 46654(T) (JPRS-31993)
radioisotope and labeled compound production in, review of, 19: 42586
radioisotope and labeled compound production at Boris Kidric Institute of Nuclear Sciences in, 19: 42587
radioisotope production at Vinca, 18: 10439(T) (JPRS-23279)
radioisotope production development at Boris Kidric Institute, 19: 36890(T) (JPRS-30769)
radioisotope production and uses in, 19: 36891(T) (JPRS-30771)
radioisotope production and uses in, 20: 37137
radioisotope uses in metallurgy in, survey of, 17: 36093(T) (JPRS-20805)
radioisotope uses in, economics of industrial, 20: 27377
uranium beds in, geochemical studies, 19: 36691(T) (JPRS-30963)
uranium content in urine of uranium miners in, 18: 20271
uranium deposits in tertiary volcanites of northeastern Macedonia, 18: 37403 (A/CONF.28/P/415)

Z

Zamboni Piles
see Dry Batteries
ZEBRA
control rod worths in, measurement of, (E), 19: 17200
description, (E), 19: 35855
design description, 16: 31331
neutron buckling measurements in, 18: 6454
neutron Doppler measurements in core 5, 20: 20310 (AEEW-R-465)
reactivity Doppler coefficients for, (T), 20: 32869
reactivity Doppler coefficient in core 5, 20: 32840
ZEEP
(Canadian zero energy exponential pile.)
critical experiments with, 17: 42384
design data, 16: 14347
heat flux distribution in annular pellet rod mockup in, 19: 31602 (AECL-2247)
hot-channel capture and fission measurements in, 17: 17402 (AECL-1684)
lattice parameters, 18: 38294 (A/CONF.28/P/25)
neutron leakage from closely packed lattices in, 18: 33018 (CRRP-627)
neutron reaction rates in deuterium oxide loop of, calculations on, 18: 7885 (AEEW-M-363)
neutron reaction rates in, multi-group calculations on, 18: 7888 (AEEW-R-186)
neutron slowing-down spectra in, (E/T), 19: 19070
neutron spectra in cylinder of hot heavy and light water mixtures, 16: 17233 (CRRP-985-D)
reaction rate measurements of, iterative five-group analysis of, 18: 27841 (AEEW-M-424)
Zenith
see High Temperature Gas Cooled Reactor Experiment
Zeolites
see Ion Exchange Materials
ZEPHYR
(Zero energy fast reactor at Harwell, England, using Pu cylindrical fuel rods and a U reflector.)
design, 16: 21732
neutron fission cross-section ratios for, 16: 15996 (AEEW-M-184)
Zero Energy Tank Reactor (ZETR)
see Critical Assemblies
Zero Gradient Synchrotron (ZGS)
see Argonne Synchrotron
ZERO POWER REACTOR (MARK II)
criticality studies in, 20: 6587 (NASA-TN-D-3097)
criticality studies in, 20: 38532 (NASA-TN-D-3555)
hazards summary, 17: 26894 (NP-12892)
Zero-Power Reactors
see Critical Assemblies
Zeta
see Thermonuclear Reactors
ZEUS
(Zero Energy Uranium System)
design, 16: 21732
Zeus (Radiation Instrument)
see Radiation Detection Instruments (Ion Current Type)
Zeuto
see Radiation Detection Instruments (Ion Current Type)
ZINC
see also Transition Metals
abrasion of, friction, wear, and work-hardening during, 18: 18363
abundance in solar atmosphere, 16: 29599 (AFOSR-3024)
abundance in 3 Centauri A, upper limit, 16: 4659
alloying effects on properties of magnesium–thorium alloys, 16: 9246
alloying effects on magnesium corrosion and mechanical properties, 16: 17990
alloying effects on nuclear spin-lattice relaxation of aluminum at 0.37 to 1.2°K, 16: 21184
alloying effects on aluminum corrosion, 17: 1881
alloying effects on negative thermal expansion of delta plutonium, 17: 29340
alloying effects on ignition temperature of plutonium in air and oxygen, 17: 36860(R) (ANL-6648)
alloying effects on corrosion of aluminum–nickel–silicon systems, 17: 37005(R) (KR-49)
alloying effects on radiation effects on aluminum at low temperatures, 17: 37614
alloying effects on critical temperature of manganese, 18: 2287
alloying effects on magnesium, 18: 4267
alloying effects on Magnox alloys for use as canning material, 18: 27999
alloying effects on composition and mechanical properties of magnesium–neodymium alloys, 18: 28000
alpha reactions (α,Li^8) with, 18: 16951(R) (TID-20311)
alpha reactions (α,n), 19: 33252(T) (ORNL-tr-627)
alpha reactions (α,p), proton spectra from, 16: 2538
alpha scattering at 43 Mev, excitation of collective levels by inelastic, 16: 21514
analysis and determination, 20: 14500
analysis for arsenic using Gutzeit method, 17: 10563
analysis for cadmium by x-ray fluorescence, use of gamma-excited x-ray sources for, 19: 15376
analysis for copper and iron by x-ray fluorescent spectroscopy, 17: 2913
analysis for copper, effects of threshold reactions on activation, 19: 4085
analysis for copper and silver by isotopic dilution and activation methods, 19: 28231
analysis for europium by chemical stripping, 18: 19851(R) (TID-20548)
analysis for fluorine in electrorefining solutions of, feasibility of activation, 20: 16339(R) (TID-22662)
analysis for impurities, methods of spectrochemical, 16: 22038
analysis for rare earths, 20: 20607
analysis for trace amounts of gold by activation methods, 19: 15402
analysis for trace amounts of copper by activation methods, 19: 43973
analysis for zinc-65 by radiometric titration, 16: 26926
analysis for zinc-65 and -69, calculation method for, 18: 20069
analysis of, derivative activation, 19: 28256
argon ion reactions with surface of, 18: 747(T) (NP-tr-1068)

atomic structure, random-phase approximations for calculation of, 17: 8954 (UCRL-10510)
atomic volume and thermal expansion of liquid, gamma absorption measurements of, 20: 27559
behavior in fused lithium chloride–potassium chloride eutectic, chromatographic and electrophoretic, 18: 43479
beta absorption and backscattering by, 19: 30127
beta scattering by, measurement of saturation backscattering from, 18: 35057
bonding to aluminum, hot-press, 19: 40949 (ISC-640)
boron deposition on, properties of boride layers formed by, 18: 6824
bremsstrahlung reactions (γ,p) at 24 Mev, direct photoeffect and evaporation contributions in, 17: 38209
charged particle reactions with, cross sections for, 17: 34886 (UCRL-10783)
coatings of, beta-backscattering gage for measuring thickness of, 20: 14839
combustion in fluorine, calorimetry of, 17: 14118(R) (ANL-6596 (p.164-74))
combustion in fluorine, 18: 1485(R) (ANL-6687(p.153-66))
compressibility at high pressures, 17: 3494 (UCRL-6696-T)
concentration by marine organisms, 17: 12112
content and distribution in beef heart, 19: 45753 (AE-191)
content in blood and skin in rabbits with radiodermatitis, 19: 33910
content in blood and skin of man and rabbits suffering from radiodermatitis, 20: 45309
content in bone, effects of age and diet on, 16: 11400 (TID-15045)
content in brain in Huntington's chorea, 18: 4976
content in high-purity depleted uranium metal, 19: 24481 (GAT-T-1141)
content in human brain, 17: 35419
content in human diet, effects of zinc content in sea foods and water supplies on, 19: 42669
content in human erythrocytes and serum, 17: 10148
content in human heart, neutron activation determination of, 18: 33457 (AE-146)
content in human organs, variability, 17: 13935
content in human serum and muscles, 16: 20098
content in mammalian cells, effects of cell cycle stage on, 20: 18204(R) (LA-3432, pp 130-77)
content in marine organisms, 19: 31696
content in marine organisms, 20: 16725(R) (EUR-2543.e)
content in normal and leukemic leukocytes, activation analysis of, 18: 33517
content in organs and tissues of humans outside continental U. S., 19: 21831
content in oysters in Fishers Island Sound and Thames River, Conn., 16: 1432(R) (TID-13509)
content in oysters and marine algae, 16: 32690(R) (TID-16635)
content in pulmonary tissue relative to beryllium, 17: 28647
content in rat kidney mitochondria, effects of vitamin D on, 20: 8559
content in red-colored Paleozoic deposits in Northern Tien Shan, 20: 14780(T) (AEC-tr-6579)
content in river waters, 17: 30687
content in rocks, effects of clay content on, 20: 29417
content in schlieren granite segregations, 19: 24699
content in teeth after use in dental restorations, 20: 27
content in tissues of young and aged dogs, 20: 40540(R) (UCD-472-113, pp 17-56)
content in total diet in Japan, 19: 13681
content of, in sediments of Bay of Roquebrune, 20: 36553
corrosion, 17: 6572 (OTS-61-31480)
corrosion by aluminum–silicon and water of coatings of, on uranium, 19: 40949 (ISC-640)
corrosion, by humid air containing 0 to 0.5% sulfur dioxide, 16: 9157(T) (AEC-tr-5008)
corrosion by impure Santowax, 17: 23891 (NAA-SR-7755)
corrosion by oxygen, and by sodium chloride, nitrate, and sulfate solutions, tracer studies on, 18: 25927
corrosion by water, electrochemical, 16: 12055
corrosion of, by ammonium and sodium chlorides and sulfates, 17: 22123
corrosion of, book, 18: 22451
corrosion of, review, 19: 7868
corrosion processes under adsorbed films of moisture, electrochemical kinetics, 16: 10458(T) (AEC-tr-5003)
corrosion resistance to mercury at 900°F, 20: 2264
corrosive effects of, vapors on series 300 and 400 stainless steel at 900°C, 17: 36860(R) (ANL-6648)
corrosive effects on container metals, 19: 4617 (IS-888)
corrosive effects on Inconel, niobium, and yttrium at 800 to 1100°C, 19: 40961
corrosive effects on refractory metals in presence of molten chlorides, 20: 2266
crystal dislocations in, anisotropy effects on, 16: 33604
crystal dynamics of, neutron diffraction analysis of, 19: 36817 (RT/FI(64)-20)
crystal lattice dynamics, Debye-Waller factors, and heat capacity of, model for, 19: 23056
crystal lattice vibrational spectra, 18: 24168
crystal structure of, neutron diffraction analysis of, 18: 7213 (JINR-P-1440)
crystal structure from neutron diffraction, 18: 37674 (A/CONF.28/P/488)
crystal structure at 4.2, 77, and 300°K, 19: 9766(R) (COO-623-105)
crystallization in lanthanide-lead melts, mechanisms of, 20: 39435
crystallization with thionalid, tracer study of co-, 16: 12961 (USNRDL-TR-551)
cycle in lakes and streams, tracer study, 17: 33601
de Haas-Van Alphen effect in, exhibiting a resistance minimum, 17: 13155
deformation and flow of polycrystalline, effects of pressure on, 19: 37048 (WVT-6431)
deformation of single crystals of, at high strain rates, 19: 43997(R) (UCRL-11889)
deposition of coatings of, on niobium, 16: 499 (NRL-5643)
deposition on beryllium, 20: 27454
deposition on uranium by electrolysis, porosity test method for, 17: 36264
deposition on uranium, electrolytic, 19: 28786
deposition on uranium, hot-dip, 19: 40949 (ISC-640)
determination, activation, 16: 18821
determination as impurity in and volatilization from tungsten, semiquantitative spectrographic, 16: 4131 (BM-RI-5903)
determination as impurity in bismuth, spectrographic, 17: 27309
determination as impurity in natural fluorites by activation methods, 19: 17835
determination as trace impurity in uranium, 18: 29591
determination as trace impurity in plutonium–thorium–uranium and thorium–uranium alloys, 19: 17798
determination by activation and isotope dilution, substoichiometric, 18: 21997
determination by bremsstrahlung-activation gamma spectra, 20: 22960
determination by back-titration with EDTA using silver-110m-labeled silver iodate as indicator, 20: 26769
determination by charged-particle reactions at 2 Mev, 20: 43097
determination by flame spectrophotometry, emission sensitivity for, 16: 22028
determination by isotope dilution, substoichiometric, 18: 21997
determination by neutron activation, 20: 35390 (CEA-R-2965)
determination by plasma spectroscopy, limits for, 17: 40427(R) (NYO-10063(p.1-6))
determination by potentiometric titration of acid liberated by complex formation, 19: 46205
determination by potentiometric titration using EDTA, equipment for, 20: 5502
determination by radiometric titration, 20: 16386
determination by spectroscopy using high-frequency plasma flames, 18: 10020
determination by substoichiometric isotope dilution, tracer studies of effects of equilibrium time, interfering ions, and pH on, 20: 26766
determination by thermal-neutron activation methods, sensitivity for, 19: 9071
determination by titration, suitability of tetraethylenepentaminehepta-acetic acid for, 19: 19813
determination in aluminum as trace impurity, activation, 17: 10546
determination in aluminum, x-ray spectroscopic, 17: 10571
determination in aluminum, hydrochloric acid, and zirconium, oscillopolarographic, 18: 6759
determination in air, chemical procedures for, 18: 13642 (SC-4783(RR))
determination in aluminum, activation, 18: 21993
determination in ammonium diuranate, uranium, and uranium compounds, absorptiometric, 18: 35454 (PG-Report-579)
determination in aluminum and iron, activation, 18: 37071 (A/CONF.28/P/829)
determination in aluminum by solvent extraction and activation methods, 19: 9082
determination in aluminum and copper–nickel alloys by x-ray fluorescence methods, 19: 15373
determination in aluminum, activation, 19: 28224 (SGAE-CH-13/1964)
determination in aluminum ingots, x-ray fluorescence, 20: 8828 (K-1638)
determination in airborne dusts, spectrochemical, 20: 14475(R) (ORNL-3889, pp 36-39)
determination in automobile lubricants, activation, 20: 14439(R) (GA-5556)
determination in automobile tire rubber, activation, 20: 14439(R) (GA-5556)
determination in automobile paint, activation, 20: 14439(R) (GA-5556)
determination in asbestos using ion exchange, activation, 20: 16336(R)

(NYO-10175)
determination in aluminum, activation, 20: 22896
determination in aluminum by x-ray spectrography using direct electron excitation, 20: 26755
determination in antimony, activation, 20: 26814
determination in aluminum by neutron activation, 20: 33164(T) (AEC-tr-6639, pp 28-31)
determination in americium and plutonium by spark-source mass spectrography, 20: 40816 (RFP-699)
determination in biological tissue ash by x-ray fluorescence, 16: 11521 (TID-15046)
determination in biological materials, 16: 18823
determination in biological materials, activation, 16: 23403
determination in beryllium, activation, 17: 25123
determination in blood and tissues, activation, 17: 39012
determination in biological materials by ion exchange and gamma spectrometry, 18: 13660
determination in beryllium by activation, 19: 24415
determination in biological materials, x-ray fluorescence spectrometric, 19: 43939(R) (UCD-472-112, pp 59-72)
determination in biological tissues, activation, 19: 15333 (AE-168)
determination in biological materials by neutron activation analysis, 20: 7046
determination in brass by x-ray fluorescence methods, 20: 20642
determination in blood serum by neutron activation, 20: 33224
determination in blood and hair of man, activation, 20: 36728
determination in blood in arthritic and healthy patients, activation, 20: 38845
determination in blood serum, activation, 20: 38851
determination in bone, 16: 11400 (TID-15045)
determination in cadmium, cobalt, and nickel, 16: 3334(T) (AEC-tr-4497(p.243-50))
determination in clay, acetic acid leachates, sand, and silt, spectrochemical, 16: 4379
determination in chicken by neutron activation, 16: 20337
determination in *Crassostrea virginica*, colorimetric, 17: 7783
determination in carbonatites, spectrographic, 17: 27228 (EUR-32.f)
determination in chromium and thorium nitrates, spectrophotometric, 18: 10011
determination in concentrates and ores, x-ray fluorescence, 18: 21981
determination in corn leaves, method for, 18: 39067
determination in cerium and erbium, mass spectrographic, 19: 2232
determination in cobalt, activation, 19: 5829
determination in copper by activation, 19: 40422
determination in commercial plastics, activation, 20: 14439(R) (GA-5556)
determination in conductive tissue of beef heart, activation, 20: 31176
determination in dioxides of titanium, zirconium, and thorium by x-ray fluorescence, 17: 144
determination in drugs, activation, 19: 24400 (KR-91)
determination in europium oxide, spectrographic, 17: 2931
determination in enamel of teeth, neutron activation, 19: 38562
determination in erythrocytes and plasma in human blood, activation, 20: 38852
determination in fluid inclusions from fluorite and quartz, activation, 17: 25134
determination in gallium, isotopic dilution, 16: 9957
determination in gallium arsenide, activation, 17: 32004
determination in G-1 and W-1 geochemical standards by neutron activation and x-ray fluorescence, 19: 36276
determination in grease samples, activation, 20: 1738(R) (GA-4041)
determination in germanium by neutron activation methods, 20: 46759
determination in human teeth, gamma spectrometric, 16: 8671 (AE-61)
determination in human mandibular articular disc by gamma spectrometry and neutron activation, 17: 28811
determination in human whole blood, activation, 17: 40739
determination in hydrochloric and nitric acids, activation, 18: 25286
determination in hydrochloric and nitric acids and hydrogen peroxide, activation, 18: 31390
determination in hair by activation methods for identification of individuals, 19: 17824
determination in human lung tissue by neutron activation methods, 19: 40452
determination in human blood serum, activation, 20: 1586
determination in high-purity germanium dioxide by isotope dilution, 20: 26766
determination in high-purity bismuth by neutron activation, 20: 26767
determination in human heart tissue, activation, 20: 31175
determination in indium by amalgam polarography, 17: 25145
determination in iron meteorites, activation, 18: 39098
determination in indium–tin–zinc alloys, volumetric, 19: 8690 (BDX-613-37)
determination in iron, activation, 19: 10980 (EURAEC-1273)
determination in iron–niobium alloys, chromatographic, 20: 14455(R) (ORNL-3889, pp 25-32)
determination in lithium chloride–potassium chloride eutectic, controlled potential coulometric, 16: 16310
determination in lactose, method for, 18: 179
determination in lubricants, computer routine for activation, 18: 19918
determination in lubricating oils by neutron activation methods, 18: 39074
determination in lung tissue, activation, 20: 16335(R) (NBS-TN-276)
determination in magnesium–zinc alloys, x-ray fluorescence, 16: 5283
determination in Magnox alloys, spectrochemical, 17: 40734
determination in Magnox alloys, spectrographic, 18: 3682
determination in magnesium, spectrochemical, 18: 11967(R) (MCW-1482 (p.37-46))
determination in molybdenum and its compounds, spectrographic, 18: 17766
determination in mill products and ores by activation, 18: 27298
determination in minerals and rocks by neutron activation methods, 19: 7283
determination in minerals by neutron activation, 19: 30424
determination in Magnox alloys, spectrochemical, 19: 42414 (JEN-146-DQ/I-47)
determination in meteorites, activation, 19: 42451
determination in marine organisms, polarographic, 20: 16175(R) (RT/BIO(65)-1)
determination in minerals and rocks using paper chromatography, 20: 35389 (CEA-R-2791)
determination in mosaic virus and nucleic acids in tobacco plants, activation, 20: 38846
determination in natural water, quantitative spectrographic, 16: 17597
determination in niobium and zirconium by radioactivation analysis, 16: 23633 (TID-7629(p.239-44))
determination in nucleic acids, activation, 18: 19892
determination in nickel, activation, 19: 2237
determination in nickel plating solutions, spectrographic, 19: 13265
determination in niobium by activation, 19: 24416
determination in ointments and pastes by beta backscattering, 16: 24065
determination in ores by radioisotope x-ray fluorescence, 18: 39056 (AERE-R-4474)
determination in ores by radiometric fluorescence analysis, 19: 43971
determination in organic coating pigments, activation, 20: 38853
determination in polyphenyls by activation analysis, 17: 38945
determination in pharmaceutical preparations by beta backscattering, 18: 182
determination in petroleum and its products, activation, 18: 15968
determination in polyphenyls, x-ray-spectrographic, 18: 19844 (ISPRA-455)
determination in plants, activation, 20: 3901
determination in paint in criminal cases, activation, 20: 8827(R) (GA-6152)
determination in plutonium by carrier distillation methods, spectrographic, 20: 40814 (RFP-664)
determination in plant materials, activation, 20: 43060 (CEA-R-2967)
determination in powder samples by spectrographic methods, semi-quantitative, 20: 43104
determination in quartz crystals from Providencia area, Zacatecas, Mexico, activation, 20: 18631 (NYO-2266-1)
determination in rare earths at 1 to 1000 ppm level, 17: 1377 (BM-RI-6097)
determination in ores and rocks, method for gamma activation, 19: 28277
determination in pharmaceuticals by measuring reflected beta particles, 19: 10994
determination in paint by activation, age estimation of white lead by, 19: 11035
determination in ppm range by d-c arc excitation, spectrochemical, 19: 19827
determination in powdered samples by spectrochemical methods, 19: 22120
determination in pure indium, activation, 19: 28273.
determination in reactor coolants, polarographic, 19: 11003
determination in rocks, gamma-gamma logging method for, 20: 12993
determination in sea water in Chesapeake Bay area, 16: 14998(R) (NYO-8100)
determination in stratospheric aerosols, 16: 25609 (AFCRL-62-299)
determination in sea water, activation, 17: 4469
determination in silicon dioxide by activation and ion exchange chromatography, 17: 19979
determination in SAP, x-ray spectrographic, 17: 27226 (EUR-21.f)
determination in silicon carbide, activation, 17: 38964
determination in selenium, activation, 18: 21988
determination in soil, activation, 18: 21994
determination in superconductor materials, activation, 18: 31389
determination in silicon, activation, 18: 33502
determination in surface waters by activation analysis, 18: 37072

(A/CONF.28/P/854)
determination in silicon, activation, 19: 2240
determination in solids by spark source mass spectrometry, quantitative, 19: 13247
determination in spleen tissue and RNA, neutron activation, 19: 13206 (SGAE-BL-13/1964)
determination in SAP powders by different laboratories, statistics on, 19: 19750 (EUR-2286.f)
determination in sea water by neutron activation methods, 19: 22574
determination in sea water by quantitative solvent extraction and spectrography, 19: 28253
determination in snake venom by activation, 19: 28274
determination in sea water and silts, spectroscopic, 19: 36315
determination in snake venom, activation, 20: 2520(R) (IA-920)
determination in sea water, activation, 20: 18576(R) (TID-22660)
determination in silicon dioxide, activation, 20: 20634
determination in sulfide ores by neutron activation methods, 20: 26759
determination in silicates, activation, 20: 26782
determination in seawater, activation, 20: 40834
determination in seawater, activation, 20: 43085(R) (TID-23295, Sect.2)
determination in SAP, methods for, 20: 45574 (EUR-3064.f)
determination in terphenyls, activation, 17: 28813
determination in tissue, after neutron activation, 17: 31813 (AERE-R-4309)
determination in tissues, activation method, 18: 29571
determination in trace amounts in aluminum by x-ray spectrography, 19: 38571
determination in thorium, photometric and polarographic, 20: 20601
determination in tissue samples, activation, 20: 26754
determination in uranium leach solutions, 16: 14668
determination in uranium compounds by reversed-phase partition chromatography, 16: 23636 (TID-7629(p.276-84))
determination in uranium, spectrophotometric, 17: 6001
determination in uranium(IV-VI) oxide by carrier distillation excitation, effects of graphite electrode grade on, 17: 10538 (TID-16295)
determination in uranium using dithizone, spectrophotometric, 18: 1532
determination in uranium using dithizone, spectrophotometric, 18: 1533
determination in uranium-233-labeled uranium dioxide, spectrographic, 18: 9980
determination in uranium concentrates, oxides, and metal, activation, 20: 16399
determination in water, silver-spark spectrographic, 17: 1381 (IDO-14591)
determination in white lead for age determination of paintings, activation, 19: 5820
determination in zirconium, polarographic, 16: 18820
determination in zirconium alloys, 17: 6020
determination in zinc ores, activation, 18: 39121
determination in zinc ores by x-ray fluorescence using tritium/zirconium source, 19: 5819
determination in zirconium by activation, 19: 24418
determination, micro-coulometric, 16: 25285
determination of, in uranium fission products, 17: 15892
determination of, in residues by iron flux method, spectrographic, 17: 19942 (PG-Report-157)
determination of, ionization methods for mass-spectrometric, 17: 38975
determination of, in erythrocytes and blood serum, radiometric, 17: 40477
determination of, method for, 17: 28801 (IDO-14316(Suppl.4))
determination of radioactive, in marine organisms, 20: 33215
determination of traces in germanium dioxide, activation, 17: 27297
determination of traces of, using oxycellulose, 17: 35656
determination of traces of, in polyphenyls, 19: 302 (RT/CHI(64)-11)
determination of trace amounts of, using 1-(2-thiazolylazo)-2-naphthol, spectrophotometric, 19: 19814
determination of trace, in aluminum and lead, activation, 19: 36288
determination of trace amounts of, in iron, activation, 20: 14471
determination of trace amounts of, by reactor neutron activation methods, 20: 26760
determination of trace amounts of, by derivative neutron activation, 20: 29136
determination of traces of, in crude oils, by nondestructive activation analysis, 20: 33196
determination of trace amounts of, in tungsten and molybdenum by atomic absorption spectrophotometry, 20: 43154
determination of, radiometric titration, 18: 27311
determination of, paper chromatographic methods for, 18: 29600
determination of, use of azo dyes in spectrophotometric, 20: 22925
determination of, by neutron activation methods, 20: 29078(R) (AD-633252)
determination of, in presence of cobalt by radiometric titration using EDTA, 20: 38806
determination of, in blood by radioisotopic dilution, 20: 40844
determination of, evaluation of titrimetric EDTA method with visual indicator end points for, 20: 43067(R) (IDO-14679, pp 6-46)
determination of, in carbazole by neutron activation methods, 20: 43116
determination of, in thallium by neutron activation methods, 20: 45596
determination using cyclohexanediaminetetraacetic acid, potentiometric, 18: 33507
determination using sulfatoceric acid, titrimetric, 18: 41355
determination using mercury cyanate and EDTA, 19: 19779
deuteron elastic scattering at 11.8 Mev, angular distributions, 16: 3637
deuteron elastic scattering at 11.8 Mev, optical model analysis of, 17: 38192
deuteron elastic scattering at 26 Mev, angular distributions from, 18: 28634
deuteron elastic scattering at 15 Mev, strong absorption model analysis of, 18: 42708
deuteron elastic scattering at 26 Mev, optical model analysis of, (E/T), 20: 3053
deuteron inelastic scattering at 13.6 Mev, angular distributions from, 18: 40633
deuteron reactions (d,α) at 15 Mev, cross sections and energy distributions for, 16: 11020
deuteron reactions (d, helium-3) at 21.6 Mev, determination of configurations of states by, 16: 21562
deuteron reactions (d,p) at 13.6 Mev, proton spectra from, 16: 26356
deuteron reactions at 11.8 Mev, optical model parameters for, 18: 1051
deuteron reactions (d,p) with, angular distributions from, (T), 19: 12596
deuteron scattering at 12 Mev, angular distributions, 16: 13953 (JÜL-30-KP)
deuteron scattering at 26.5 Mev, total cross sections for, (E), 19: 5164
development of coatings of, for tantalum alloy and metal protection, 16: 24148(R) (ASD-TR-61-676)
diffusion coefficients in hydrochloric and perchloric acids, 19: 348(R) (ORNL-3679(p.117-26))
diffusion in air at 5000°K, 16: 15312(T)
diffusion in cadmium, 18: 40994(R) (TID-21052)
diffusion in copper-zinc crystals, enhancement by 30-kev neon ion bombardment, 16: 2282
diffusion in gallium arsenides, 19: 23164(R) (SU-SEL-64-103)
diffusion in gallium arsenide, effects of partial pressures on, (E), 19: 39269(R) (SU-SEL-64-133)
diffusion in liquid solutions, coefficient determination for, 19: 11109
diffusion in pure and zinc-doped sodium chloride monocrystals, 18: 25969(R) (ANL-6868(p.287-302))
diffusion in silver–zinc alloy, 18: 9773 (TID-19979)
diffusion of cadmium and gold in, 16: 29318(R) (TID-16386)
diffusion of cadmium-115m and gold-198 in crystals of, anisotropic coefficients for, 17: 25804
diffusion of cobalt-57 in, mechanism for, (E), 20: 28662
diffusion of copper, gallium, and iron in, 18: 40994(R) (TID-21052)
diffusion of indium-114 and silver-110 tracers in crystals of, anisotropic, 16: 6753
diffusion of iron and mercury into, 19: 42459(R) (RPI-1044-7)
diffusion of uranium in liquid, 17: 1359(R) (ANL-6569)
diffusion of uranium in liquid, 17: 40421(R) (ANL-6766)
diffusion of uranium in liquid, at 600 to 800°C, 20: 2368
dislocation mobility in pure single crystals of, basal, 19: 48089 (CALT-473-4)
dislocation structure in, use of ion bombardment for study of, 17: 37544(T)
dissociation energy of gaseous and heat of vaporization of solid, correlation of, 17: 6095
dissolution and ion exchange behavior in ammonium carbonate solutions, 17: 39035
dissolution in sulfuric acid, valency of ions formed during, 16: 3401
dissolution in zinc chloride, thermodynamic studies of, 20: 24971(R) (BNL-954, pp 50-83)
distribution and turnover in rats, tracer study, 17: 10275
distribution between anion exchange resin and aqueous chloride solutions, 17: 10588 (IA-764)
distribution between γ-alumina and molten chlorides, 20: 3959
distribution coefficient between fused bismuth and fused salt eutectic, 17: 21683
distribution in nature, 17: 33615
distribution in tissues, effects of hepatic damage, tracer study, 16: 14440
distribution in tissues in rats, tracer study, 16: 28670(R) (UCLA-507)
distribution of, between nitric acid and ion-exchange resin, synergistic effects of thorium on, 17: 15948 (LA-2836)
distributions in electric arc discharges, image-spectrogram studies of, 19: 30108
effect on determination of copper in bismuth by neutron activation methods, 19: 43941
effects of carrier, on metabolism of zinc-65 in rats, 19: 35906
effects of decontaminating and descaling solution on metal loss on, 20: 21238 (NP-15928)

effects of diet content of, on metabolism of injected zinc-65 in chickens and embryos, 20: 35228
effects of dietary, on zinc-65 uptake by rat tissues, 19: 35915
effects of dietary, zinc-65 sorption in humans and rats, 16: 17417
effects of nitrogen mustard on content of, in spleen in rats, 17: 40547(R) (NYO-10569)
effects of, on potentiometric-acidimetric determination of zirconium, 17: 23288
effects of, on shielding properties of lead, 17: 33256
effects of vapor-phase, on stainless steels at 900°C, corrosive, 19: 26778
effects on complexonometric determination of holmium and lanthanum, masking of, 19: 17822
effects on copper or silver infiltrants in graphite, 20: 29764
effects on corrosion resistance of beryllium, 19: 22913(P)
effects on decomposition of tritium-labeled compounds, 19: 7491
effects of dietary, on zinc-65 retention by bone and liver in chicks, 17: 21447
effects on diffusion of niobium, 17: 23876(R) (USBM-U-1031)
effects on discontinuous precipitation in beryllium–copper alloys, 20: 37253
effects on fluorescence of salicylate, 17: 33879
effects on fluorescence of uranium in sodium carbonate–sodium fluoride melts, 18: 33506
effects on fusion welding of beryllium, 16: 5692 (WADD-TR-60-917)
effects on gastrointestinal absorption of copper-64 in rats, 20: 16182
effects on growth in γ-irradiated barley seeds, 20: 45328
effects on heterometric determination of vanadium, 19: 36289
effects on heterometric determination of vanadium using 5,7-diiodo-8-hydroxyquinoline, 20: 257
effects on hydrochloric acid cleavage of organotin compounds in methanol–water, 20: 6687(R) (NYO-3453-1)
effects on magnetic moment saturation of mixed ferrites at 0°K, 17: 8001 (PAN-335/IX)
effects on manganese sorption by barley roots, 20: 16174(R) (RLO-1547-3)
effects on nuclear electric quadrupole resonance in copper, 17: 18825
effects on oxygen overvoltage and proton diffusion in nickel oxide, 18: 27457
effects on physiology of male reproductive organs of rats, 20: 12601 (TID-22526)
effects on properties of magnesium-base alloys for fuel-element cladding, 20: 39443(P)
effects on reconstitution of blastocyst formation in rabbits, 19: 25864
effects on selenium-75 uptake by sheep blood cells, 18: 3468
effects on separation of magnesium, plutonium, and uranium from halide salt baths, 17: 36860(R) (ANL-6648)
effects on spectra of nitrogen-15 in ATP, 20: 29083(R) (UCRL-14767)
effects on spectrophotometric determination of aluminum, 19: 13226
effects on spectrophotometric determination of thorium, 19: 24408
effects on spectrophotometric determination of cerium, 19: 32075
effects on stability of delta-phase plutonium–gallium alloys, 20: 11224
effects on steel corrosion by water, 19: 29808(R) (KR-94)
electric conductivity, effects of magnetic fields up to 400 kgauss, 16: 15451
electric conductivity of, effects of lattice vacancies on, 17: 11231
electric conductivity and Hall constant of liquid, in pseudopotential, 18: 22494 (TID-19959(Rev.))
electric conductivity of liquid, 20: 41476
electric discharge in, ion concentration and spectral broadening in, 17: 9060
electric properties of contacts with hard superconductors, 17: 36453 (TID-19310)
electrolysis of irradiated, for copper-64 separation, 17: 8213
electrolysis of solid lithium sulfate on electrodes of, cathode reactions and isotope effects in, 18: 33596
electron backscattering at 1 to 3.5 Mev, 16: 12344
electron elastic scattering by, cross sections for, 18: 32381
electron emission from, after high-energy molecular bombardment, 18: 18564
electron energy levels of, lifetime of $^1P_1$, 18: 22695
electron plasma resonances in, analysis using photon scattering, (T), 20: 1326 (ORNL-P-1600)
electron reactions with, K x-ray emission in, (E), 19: 16377
electron reactions with, optical spectra from, (E), 20: 7659(R) (ORNL-3849, pp 101-50)
electron scattering at 0.8 and 1.5 Mev, energy-loss spectra, 16: 8136
electron scattering by Coulomb field of, phase shift approximation for, 17: 31417
electron scattering by, 18: 40167
electron scattering at 600 to 1200 kev by, coefficient of, 19: 27069
electron transport phenomena in, at liquid helium temperatures, 17: 11378
energy level lifetimes, $^1P_1$ and $^3P_1$, 18: 15267
energy level lifetimes, $^3P_1$, 18: 15266
energy level transitions in, Coster-Kronig, (T), 20: 15238 (CONF-233 (Vol.3), pp 398-418)
energy level widths for, K, (T), 20: 15239 (CONF-233(Vol.3), pp 419-39)
equilibrium in cadmium–cadmium iodide systems, 16: 15223
erosion of electrodes of neutron-activated, in spark discharge, 19: 47134
exchange in chelating ion resin, self-, 18: 19972
explosibility of powders of, 19: 36698 (BM-RI-6516)
films of, tunneling in superconducting bismuth–indium films superimposed on, (E), 20: 42109
fluorescence yields in proportional and scintillation detectors, 18: 3796
gallium atom ranges at low energies in, 18: 34441
gamma attenuation of liquid, 16: 9226
gamma attenuation at 0.1 to 10 Mev, coefficients for, 18: 35058
gamma attenuation coefficient of, temperature dependence of cobalt-60, (E), 19: 5391
gamma backscattering at 662 kev, (E), 19: 13789
gamma backscattering at low energy, spectral angular distribution for, (E), 20: 34783
gamma quanta in single crystal, angular correlation of annihilation, 16: 5934
gamma reactions (γ,α) at 31 Mev, alpha spectra from, (E), 20: 38037
gamma scattering by electrons of, at 662 kev, (E), 20: 41625
gamma spectra from 14-Mev neutron activation of, determination by, 19: 26241
grain boundaries, structure and properties, 16: 19429
Hall constant for liquid, 18: 9000 (TID-19959)
Hartree-Fock wave functions, 16: 18162 (MRL-103)
Hartree-Fock potential of neutral atoms of, analytical expressions for, 18: 16656
heat of fusion, 20: 4297(R) (IS-1200(Sect. M))
heat of fusion, 20: 41412(R) (IS-1500(Sect. M))
hyperfine structure, 16: 21129(R) (NP-11640)
influence of, content of soils on wheat and barley growth variations, 20: 40532(R) (COO-1097-17)
internal friction in crystals of, at 4.2 to 300°K and 4 to 40 kc, 16: 2199 (TID-14140)
ion exchange behavior in hydrochloric acid–organic solvent media, 18: 39124
ion exchange in concentrated hydrochloric and perchloric acids, distribution coefficients for, 18: 17759
ion exchange paper chromatography of, 18: 17785
ion exchange properties for neodymium and praseodymium separations, 18: 10200
ion exchange with aluminum, copper, and zinc on Dowex 50W resin, rate of, 17: 32053
ionization by electron bombardment from 0 to 500 v, multiple, 17: 29409
ionization cross section measurements using mass spectrometry, 16: 5782(T) (AD-257713)
ionization of, by thermal methods after complex formation, 17: 38975
ionization of, Auger effect in, 18: 16698
iron-57 displacement in lattice of polycrystalline, Mössbauer-effect measurements of, 19: 40097
iron-57 Mössbauer effect in, mean-square nuclear displacement from, (E), 19: 23740
iron-57 Mössbauer effect in, Debye-Waller factor for, (E), 20: 28662
iron-57 Mössbauer spectra in, 20: 30766
laser beam reactions on surfaces of, momentum transfer by giant-pulsed, (E), 20: 31810
laser beam reactions with, uv spectra from plasma produced from, (E), 20: 38300
light emission by foils of, electron-induced, (E), 19: 16278
magnetic flux penetration and tunneling in superimposed layers of indium–bismuth alloys and, in magnetic fields, (E), 19: 39699
magnetic resonance in, 17: 8093
magnetic susceptibility, low field de Haas–Van Alphen effect, 16: 13563 (AFOSR-1757)
magnetoacoustic absorption in crystalline, low-temperature Landau level oscillations in, (E), 19: 8117
magnetoplasma resonance in, 17: 16841
mass spectrum of secondary ions from, 17: 32389
melting temperature of, equations for calculating, 18: 25990
mesic atom (μ^-) decay in, anomaly in, 17: 6888
mesic atoms of, meson (μ^-) decay in, 16: 24278 (JINR-P-971)
mesic (μ^-), effect of atomic binding on decay rate of mesons (μ^-) in, 17: 774
meson (μ^-) capture by, x rays from, 18: 19044
meson (μ^-) capture by, probability for, (T), 20: 28456
meson (μ) capture and decay in, 16: 15690
meson (μ) capture, Fermi interactions in, 16: 15590
meson (μ) cascades in, x-ray emission from, 16: 15692
meson (μ) decay in, 16: 24819

meson (μ) scattering, x-ray emission in, 16: 19705
meson (μ) x-ray transition energies for, 16: 25909 (NEVIS-105)
meson (μ^-) capture rate and lifetime in, 17: 775
meson (μ^-) capture by, x-ray spectra from, 17: 26578
mesons (μ) bound in, decay, 16: 22870
metabolism and pathway in mouse, 16: 8489
metabolism and toxic effects in Habrobracon, 19: 10741 (TID-21559)
metabolism by aquatic organisms, tracer study, 17: 33601
metabolism by benthic marine algae, tracer study, 17: 24864
metabolism by marine organisms, tracer study of, 17: 30281(R) (TID-19104)
metabolism by plants, effect of soil zinc content on, 17: 40498(R) (TID-19389(App.C))
metabolism by snails, tracer study, 17: 24865
metabolism, effects of whole-body irradiation, 16: 18750
metabolism in chickens, tracer study, 19: 21820(R) (UCLA-12-541(p.25-44))
metabolism in cirrhotic and normal liver of man, tracer study, 20: 18222
metabolism in domestic animals, tracer study, 17: 31816(R) (ORO-605)
metabolism in gastrointestinal tract of cattle, 19: 31752
metabolism in mammals, tracer study, 17: 7762
metabolism in mice, tracer study of, 19: 6947 (BNL-7745)
metabolism in plants, tracer study, 16: 32715
metabolism in rabbits, tracer study of, 19: 8772
metabolism in rats, effects of cadmium on, 18: 43188(R) (TID-21200)
metabolism in rats and sheep, effects of cadmium on, 19: 5604 (HW-SA-3729)
metabolism in rats, tracer study, 19: 33767
metabolism in sheep, effects of cadmium on, 18: 41039(R) (HW-80500 (p.140-3))
metabolism in sheep, tracer study, 19: 8739 (HW-SA-3746)
metabolism of, by mollusks and plankton, 17: 35407(R) (TID-19332)
metabolism of, in marine organisms, 18: 6598(R) (TID-19922)
metabolism, physiological effects, and biological specificity of, in man, 17: 38704 (BNL-7252)
metabolism, tracer studies, 16: 1393
metabolism, tracer study, 16: 18750
microwave properties of superconducting, in energy-gap frequency region, (E), 20: 28204
Mössbauer effect of gold-197 in, relation between chemical shift and electronegativity in, 20: 7055 (UCRL-16436)
movement in peppermint plant, 16: 23389
neutron absorption cross sections at 24 kev, (E), 19: 45230
neutron capture by, average level widths of compound nucleus from, (E), 20: 32424
neutron capture cross sections, 16: 26509
neutron capture cross sections at 0.2 to 105 kev, total, 18: 42650 (TID-21144)
neutron cross sections of, shell effects on thermal, (E), 19: 47618
neutron diffraction patterns of crystals of, 16: 6538 (IFA-FN-21)
neutron diffraction by, scattering length for, (E), 20: 17667
neutron elastic scattering at 14 Mev, cross sections for small-angle, 16: 28044
neutron elastic scattering cross sections at 0.3 to 1.5 Mev, 17: 36861(R) (ANL-6764)
neutron elastic scattering cross sections at 0.3 to 1.5 Mev, 18: 15426(R) (ANL-6810)
neutron elastic scattering at 0.65 Mev, angular distributions for, 18: 17089
neutron elastic scattering at 0.3 Mev, angular distributions for, 18: 17090
neutron elastic scattering at 0.5 to 0.8 Mev, cross sections for, 18: 26568
neutron elastic scattering at 400 kev, cross section for, 18: 38074(T) (AEC-tr-6398(p.64-9))
neutron elastic scattering at 0.3 to 1.5 Mev, differential cross sections for (E), 19: 3381
neutron elastic scattering at 3.3 Mev, asymmetry in polarized, (E/T), 19: 10343
neutron elastic scattering at 3.5 to 4.8 Mev, differential cross sections for, (E/T), 19: 14564
neutron elastic scattering at 0.3 to 1.5 Mev, angular distributions from, (E), 19: 19095 (WASH-1053)
neutron elastic scattering at 0.2 to 2.0 Mev, compound, (T), 19: 19190
neutron elastic scattering at 0.8 Mev, angular distributions from, (T), 19: 37884
neutron elastic scattering at 1 Mev, differential cross sections for, (E/T), 20: 9981 (WASH-1064)
neutron elastic scattering at 0.8 Mev, cross sections for, (T), 20: 15770
neutron elastic scattering at 0.68 to 1.25 Mev, (E/T), 20: 19805(R) (ANL-7110, pp 1-28)
neutron elastic scattering at 3.2 Mev, (E/T), 20: 46644
neutron inelastic scattering by, collective nuclear energy levels from fast, 17: 848
neutron inelastic scattering cross sections at 1.0 to 1.5 Mev, 18: 15426(R) (ANL-6810)
neutron inelastic scattering at 14 Mev, collective-state excitation by, (E/T), 19: 23697
neutron inelastic scattering by crystals of, at low energies, phonon dispersion relations from, 16: 27674
neutron inelastic scattering in single crystals of, phonon dispersion relations from thermal, 16: 32370
neutron inelastic scattering by crystals of, lattice dynamics from, 17: 39601
neutron inelastic scattering by liquid, structure factor from, 20: 27535
neutron radiative capture cross sections at 30 and 65 kev, 18: 34274(R) (NIRS-2(p.3-15))
neutron reactions (n,n'γ), cascade gamma energies for, 16: 4741(R) (TID-14157)
neutron reactions at 3.7 Mev, cross-section measurements, 16: 8224
neutron reactions at 0.1 to 100 Mev, total cross sections for, 16: 11021
neutron reactions (n,p) at 14 Mev, angular distributions and spectra from, 16: 11028
neutron reactions at 3 to 15 Mev, removal cross sections, 16: 29739
neutron reactions at high energies, table of radioisotopes produced in, 17: 794 (CERN-62-22)
neutron reactions at 4 to 5 Mev, compound-nucleus level widths from, 18: 36645
neutron reactions (n,2n) with, fission-averaged cross sections, 19: 29319
neutron reactions (n,n'γ) at 0.3 to 2.6 Mev, excitation cross sections for, (E/T), 19: 31284
neutron reactions (n,n'γ) with, cross section for, 19: 45263 (JAERI-1078)
neutron resonance parameters for, 18: 11195(R) (EANDC(E)-49(L))
neutron resonance absorption integral of, (E), 20: 14008(R) (ANL-7122, pp 42-69)
neutron scattering at 0.4 to 24 Mev, optical model for, 16: 3872(R) (ORNL-3193(p.237-50))
neutron scattering at 1 Mev, 16: 3662
neutron scattering, polarization effects, 16: 4792
neutron scattering angular distribution, 16: 12419 (ANL-5567(Rev.))
neutron scattering at 3.4 to 4.6 Mev, angular distributions, 16: 26507
neutron scattering by, measurement of polarization in, 17: 2243(R) (TID-17083)
neutron scattering by, in beta brass, 17: 6705
neutron scattering by, cross sections for, 17: 41873 (WASH-1044)
neutron scattering at 0.4 to 1.2 Mev, cross sections for, 18: 9331
neutron scattering by, 18: 24625 (WASH-1046)
neutron scattering at 0.3 to 1.5 Mev, optical model analyses of, 18: 28695
neutron scattering at 3 to 650 kev, cross sections, phase shifts, and strength functions for, (E), 19: 10319
neutron scattering at 2.2 Mev, (E), 19: 26674
neutron scattering by, angular distribution in, 19: 31252
neutron scattering by crystals of, near 1 Å, 16: 22356
neutron total cross sections at 28.4 Mev, 16: 5969
neutron total cross section, 17: 15272
neutron total cross section of, fast, 17: 20982 (HW-SA-2875)
neutron total cross section at 200 ev to 1 Mev, 17: 36669 (WASH-1042)
neutron total cross sections at 28 Mev, 18: 44711
neutron total cross sections at high energies, fluctuations in, 20: 38173
nucleon scattering at 2.8 and 6.8 Mev, angular distributions from, 18: 38080(T) (AEC-tr-6398(p.120-5))
nutritional needs of, in man, 19: 21990
optical properties of films of, in vacuum ultraviolet region, 19: 42213 (ORNL-TM-1164)
orientation of crystals of, in vapor-deposited layers, 16: 32908(T) (AEC-tr-5392)
particle size measurement for crystals of, microbeam x-ray width methods for, 17: 18780(T) (TRG-Inf-Ser-107)
particle-density radial distribution in arc plasma of, (E), 20: 8241
phase transformations in, relation of c/a ratio and elastic moduli temperature dependence with, 19: 44676(R) (ANL-7000, pp 176-82)
phonon dispersion curves in, (T), 19: 42892
photon elastic scattering at particle threshold energy, cross sections for, 17: 17153
photon reactions up to 80 Mev, neutron emission in, 18: 38152
photon reactions with, proton angular distributions and yields at >8 Mev, 17: 28265
physical properties of liquid, 19: 28821
plastic deformation of polycrystalline, 17: 20446 (AD-284284)
plastic deformation, 18: 39835
polarographic behavior in ammonium solutions, effects of separan suppressor on, 17: 14139 (IEA-56)
polarographic behavior in lithium chloride–potassium chloride eutectic, 18: 8381
porosity of coatings of, electrodeposited on uranium, 17: 34353
positron annihilation in, temperature effects on, 18: 44169
positron annihilation in, angular correlations from, (E), 19: 41285

positron lifetime in, 16: 3626
positron mean lifetime in, 17: 24260 (AD-286667)
precipitation from homogeneous solution by 8-hydroxyquinaldine, 18: 9777 (TID-20010)
precipitation using trichlorobenzenearsonic acid, 19: 9137
precipitation using dimethylbenzenearsonic acid, 19: 9136
preparation of crystals of, by Bridgman method, 16: 91 (PAN-244/I-B)
preparation of kryptonated, by ion bombardment, 20: 18570(R) (NYO-2757-5)
preparation of single crystals of, 18: 1834(R) (IS-700(Sect.E))
preparation of single crystals of, 20: 41064(R) (IS-1500(Sect.E))
preparation of single-crystal, 17: 32575(R) (TID-19181)
preparation of, use of vacuum techniques in, 17: 23885
production of bicrystal and single-crystal, equipment for, 20: 43910(R) (TID-23269)
properties evaluation for coating niobium, 16: 21031 (DC-60-8-25)
properties of liquid, 16: 19370 (TIM-65)
properties of liquid, as reactor coolant, 16: 23830 (BNL-5377)
properties of, for use in electric discharge machining of SAP, 20: 33851
properties, theory of infrared and optical, 16: 25758 (NP-11675)
protective effects against nucleic acid decomposition by nuclease, 18: 25085 (SGAE-BL-5/1964)
protective effects of coatings of, against oxidation of niobium–vanadium alloys at 2000 to 2400°F, 16: 27587 (ARF-2227-6)
proton cross sections at 8.8 Mev, (E), 19: 29276
proton elastic and inelastic scattering at 6.8 Mev, 17: 24414
proton elastic scattering at 6.8 Mev, 16: 7120
proton elastic scattering at 9–22 Mev, optical-model analysis of, 17: 28316
proton elastic scattering at 17.8 Mev, polarization of, (E), 20: 32439
proton inelastic scattering by, effects of E1 resonances on, 16: 33906
proton inelastic scattering at 14.5 Mev, statistical model prediction for yields in, 17: 38206
proton nonelastic scattering cross sections at 10 Mev, 17: 13581
proton reactions at 160 Mev, proton production cross sections, 16: 14019
proton reactions at high energies, table of radioisotopes produced in, 17: 794 (CERN-62-22)
proton reactions at 590 Mev and 18.3 Bev, potassium isotope yields in, (E), 20: 17717
proton reactions at 0.05 to 2.9 Bev, induced activity data and cross sections for spallation, (E/T), 20: 32549
proton reactions (p,n) at 14.8 Mev, neutron spectra from, 16: 26326 (UCRL-6733)
proton reactions (p,2n), 16: 29880(R) (ORNL-1345)
proton reactions with, proton spectra from, 17: 18376 (TID-7652(p.409-32))
proton scattering by, optical models for, 17: 19342
proton total cross sections at 8.5 to 11 Mev, (E), 19: 43323
proton total cross section at 17 Mev, (E), 20: 44662 (USC-136-111)
purification of, by redistillation in New Jersey type columns, 17: 8251 (PAN-345/XVI)
purification of, radiochemical method for, 20: 8838 (UCRL-14258)
radiation effects on availability in soils, 16: 16176 (NP-11578)
radiation effects on diffusion in brass, 16: 22656
radiation effects on electric conductivity of, neutron, 16: 31267 (NP-11754(Vol.I)(Sect.II))
radiation effects on electric resistance of, 17: 6732 (62-GC-207)
radiation effects on, 17: 6733 (62-GC-209)
radiation effects, 17: 8877 (AFCRL-62-316)
radiation effects on K absorption spectrum, neutron, 17: 14319
radiation effects on yield strength of coated, 17: 31022
radiation effects on microhardness, 17: 31024
radiation effects on plastic deformation of, 17: 32684
radiation effects on properties of, neutron, 17: 32694
radiation effects on content of, in yeast nucleic acids, 17: 35540
radiation effects on content of, in spleen of rats, 17: 40547(R) (NYO-10569)
radiation effects on mechanical properties of, 18: 2364
radiation effects on electric conductivity at 77°K, recovery from neutron, 18: 4322
radiation effects on mechanical properties of mercury-coated crystals of, 18: 10590
radiation effects on properties and mercury diffusion in, 18: 12740
radiation effects on deformation of single crystals of, 18: 26090
radiation effects on rabbit skin content of, 18: 38908
radiation effects on mechanical properties of, neutron and proton, 18: 44262
radiation effects on electron work function of oxidized surfaces of, 19: 4737
radiation effects on mechanical properties of crystalline, in presence of surface-active mercury, 19: 23131
radiation effects on deformation of single crystals of, electron and proton, 19: 32780
radiation effects on metabolism of, in rats, 19: 43852
radiation effects on internal friction in crystals of, 16: 575(T) (AEC-tr-4693)
radiation effects on plasticity of crystals of, 17: 2015
radiation effects on deformation of mercury-coated crystals of, 17: 16676
radiation effects on mechanical properties of crystals of, in presence of mercury films, 17: 16749
radiation effects on mechanical properties of crystals of, in presence of mercury, 17: 29381
radiation effects on plastic behavior of, beta, gamma, and neutron, 17: 37576
radiation effects on, in aqueous solutions of carbonic anhydrase, x, 20: 3693
radiation effects on content in human urine of, x, 20: 3693
radiation effects on expansion of, under cyclic torsion stress, 20: 9584
radiation effects on content in blood serum of mammals, 20: 16222 (AFWL-TR-65-112)
radiation effects on metabolism of, in horses and swine, neutron, 20: 32907(R) (ORO-648, pp 62-70)
radiation effects on electrodes of, gamma, 20: 33944(R) (N-65-34010)
radiation effects on, at 11 to 7°K, electron, 20: 41499
radiation effects on pancreas content, x, 20: 42917
radiation scattering from, measurement of bremsstrahlung and gamma, 18: 44920
radiodermatitis effects on content of, in skin and blood, 18: 33285(T) (JPRS-25502)
radioinduced growth of, 17: 470
radioinduced ionization of, cross sections for electron, 20: 10885
radioinduced lattice defects in, electron microscopic observations of, 19: 11812
radioinduced production of helium and hydrogen in, neutron, 19: 26901
radioinduced sputtering deposit patterns in, collision processes in ionic, 17: 37600
radiolysis of aqueous solutions of, spectra of abnormal valency states in, 17: 35909
reactions of gaseous, with rare earth chlorides, thermodynamics of, 20: 43222
reactions of hydrogen with calcium, cerium, lanthanum, thorium, and yttrium in liquid, 18: 35548
reactions with allyl compounds in solvents, 19: 5932 (TID-21381)
reactions with benzenearsonic acid and its derivatives in acid media, precipitation, 17: 12198
reactions with carbon dioxide and water, preparation of methane for tritium counting by, 18: 16075
reactions with crucibles of refractory compounds with boron, carbon, and nitrogen at 400 to 1500°C, 19: 37112
reactions with fast neutrons, helium and hydrogen production in type 347 stainless steel in, 20: 7490(R) (BMI-1745, Sect.A)
reactions with hydrogen at –195°C, 16: 112
reactions with magnesium to 340°C, 19: 22997 (TRG-Report-842)
reactions with Magnox alloy to 300°C in argon, 19: 22997 (TRG-Report-842)
reactions with niobium, kinetics of vapor, 18: 7271
reactions with organic matrix materials in ice-water system, 18: 15722 (TID-20332)
reactions with silver nitrate in nonaqueous solvents, 16: 5311(R) (TID-14361)
reactions with sodium in liquid ammonia, intermetallic phase production in, 18: 23149(T) (ANL-Trans-8)
reactions with the halides of molybdenum, niobium, tantalum and tungsten to yield pure metals, 20: 9405(P)
reactions with uranium chlorides in molten alkali chlorides, 18: 3730
reactions with uranium chloride for precipitation of uranium from chloride melt, 18: 41379(T) (KFK-tr-158)
reactions with uranium and uranium carbide at 540 to 800°C, 19: 24482 (IS-1061)
reactions with uranium monocarbide at 540 to 800°C, phase formations in, 20: 2404
reactions with uranium monocarbide at 500 to 800°C, 20: 14991
recrystallization of, by thermal cycling, 17: 6698(T) (NP-tr-929)
reduction of niobium by, 17: 25150
retention by clays, 19: 36300
scanning for zinc-65, slit effects on counting rates in, (E/T), 19: 32592
separation as ferrocyanide on filter paper by precipitation chromatography, 17: 40932
separation by anion exchange in acetic acid–nitric acid medium, 18: 16131
separation by anion exchange in acid-organic solvent media, 18: 23707(R) (TID-20609)
separation by anion exchange in mixed aqueous and non-aqueous systems, 19: 2243

separation by continuous electrolysis in flowing solution, 19: 7647
separation by electrophoresis on zirconium phosphate paper, 17: 4467
separation by ion exchange using triisooctylamine, effects of diluent on, 20: 43439
separation by solvent extraction using dibenzoylmethane as chelating agent, 17: 19974
separation by solvent extraction of the dibenzoylmethane complex, 17: 21790
separation from actinide transition elements by ion exchange, 19: 24449
separation from aqueous solutions by solvent extraction using 8-hydroxyquinoline-N-oxide, tracer studies of, 17: 21783
separation from aqueous solutions by solvent extraction using diphenylarsinic acid, 17: 21787
separation from aqueous solution by dithizone–cellulose acetate column, 19: 40642 (AERE-R-4969)
separation from aqueous solutions by solvent extraction using dinonylnaphthalenesulfonic acid or sodium dinonylnaphthalenesulfonate, effects of neutral donors on, 20: 27050
separation from bismuth, cadmium, copper, lead, and silver by anion exchange, 16: 16463
separation from bismuth by ion exchange, 17: 32195(T) (KFK-tr-130)
separation from buffered solutions by solvent extraction using TTA with TBP or TBPO, tracer studies of, 19: 32289
separation from calcium by cation exchange, 16: 2978
separation from cadmium and mercury, chromatographic method using ion exchange resin, 19: 2450(T) (ORNL-tr-300)
separation from cadmium cobalt, manganese, and nickel by cation exchange, 19: 13535
separation from cadmium, activation-electrochemical, 19: 17772 (EUR-2165.i)
separation from cadmium by ion exchange, 19: 30334
separation from chloride solutions by solvent extraction using amines, 17: 17949(R) (ORNL-TM-449)
separation from chromium, cobalt, iron, manganese, and silver in aqueous solution by solvent extraction using dithizone–chloroform, 19: 26471
separation from cobalt, copper, iron, and manganese by anion exchange using tartaric acid, 17: 40917 (AD-288767)
separation from copper, iron, mercury, and uranyl ions by paper precipitation chromatography, 18: 1565
separation from dilute solutions of zinc, 18: 31566 (TID-18567(p.2-6))
separation from ethanolic hydrochloric acids by ion exchange, 19: 39265(R) (IA-1021)
separation from fission products, thorium, and uranium, 17: 29630
separation from gallium, indium, and thallium by volatilization, 17: 12296
separation from gallium by thin-layer chromatography, 18: 17949
separation from gallium, indium, and transition elements by ion exchange chromatography, 20: 20634
separation from germanium and nickel by carrier precipitation, 17: 2242 (TID-16949)
separation from hydrochloric acid solutions by solvent extraction using acetylacetone, 18: 31389
separation from hydrochloric acid solutions by solvent extraction using 2-ethylhexanol, 19: 36252
separation from iron by reversed-phase chromatography, 16: 11734
separation from iron by extraction-chromatography using tetrabutyl hypophosphate–tetrabutyl pyrophosphate mixture, 19: 42439
separation from lead by solvent extraction of thiocyanates, 19: 30094
separation from lithium chloride in ethanol by ion exchange, 19: 26917(R) (IA-984)
separation from lithium chloride solutions by oxine precipitation-carbon adsorption method, 20: 43092 (Y-1553)
separation from metal ionic mixtures, electrochromatographic, 17: 10753
separation from metal mixtures by thin layer chromatography, 20: 36753
separation from neutron-irradiated biological materials by ion exchange, 20: 36762
separation from nitric or sulfuric acid solutions, ion exchange selectivity scales for, 19: 9257
separation from other metals by ion exchange chromatography in tartrate medium, tracer studies of, 19: 7627
separation from other metals by ion exchange, 19: 9046(R) (IS-900 (Sect.C))
separation from other metal ions on silica columns treated with dinonyl naphthalenesulfonic acid, 19: 15691
separation from other metals by ion exchange, 19: 15692
separation from other metals by ion exchange in hydrobromic acid–organic solvent, 19: 30085(R) (TID-21853)
separation from other metals by partition chromatography of chloride solutions, tracer studies of, 19: 32288
separation from other inorganic ions by paper chromatography, 20: 12939
separation from other metals by extraction chromatography using TOPO, tracer studies of, 20: 27054
separation from perchloric acid solutions by ion exchange materials, 20: 20823
separation from perchlorate solutions by solvent extraction using bis-(2-ethylhexyl) phosphate, 20: 45795(R) (ORNL-3945, pp 176-88)
separation from plutonium by anion exchange, 17: 4629
separation from plutonium by ion exchange, 20: 35585 (EURAEC-1639)
separation from pure metals using thionalide, 16: 18835
separation from rare earths by ion exchange in isopropyl alcohol, 18: 20104
separation from rare earths by ion exchange chromatography, 20: 18827
separation from rhenium by anion exchange chromatography, 19: 24433
separation from salts by extraction chromatography using organic phosphorus compounds, 20: 10759 (INP-427/C)
separation from salts by solvent extraction using Schiff bases in chloroform, 20: 10759 (INP-427/C)
separation from scandium by precipitation using cinnamic acid, 18: 43426
separation from scandium by ion exchange chromatography, 20: 16574
separation from scandium by ion exchange chromatography, 20: 20821
separation from silver by solvent extraction using tri-n-octylphosphine sulfide, 19: 19753 (IS-T-3)
separation from solutions by solvent extraction, review of methods for, 19: 13543
separation from sulfate solution by ion exchange, relative effectiveness of mineral cation exchangers, 16: 30389
separation from thorium, titanium, and zirconium using ammonium cinnamate, 16: 28900
separation from thorium by ion exchange, 16: 30435
separation from thorium by ion exchange in nitric acid solution, 20: 20624
separation from titanium by cation exchange chromatography, 17: 32054
separation from titanium using benzoylphenylhydroxylamine, direct weight gravimetric, 17: 38940
separation from tin by reversed-phase chromatography, 20: 40796(R) (IS-1500(Sect.C))
separation from uranium by ion exchange and elution with ascorbic acid, 18: 25611(T) (AEC-tr-6227/1(p.1-8))
separation from uranyl ions by solvent extraction using dithizone, 18: 29582
separation from uranium by cation exchange chromatography, 19: 13245
separation from uranium by ion exchange, 19: 32285
separation from uranium by chromatography on cellulose columns, tracer studies of, 19: 40687
separation from uranium by ion exchange, 19: 44119
separation from uranium by extraction chromatography, 20: 433 (INP-412/C)
separation from uranium by combined ion exchange-solvent extraction using nitric acid–tetrahydrofuran solutions, 20: 20811
separation from uranium by extraction chromatography using trioctylamine, 20: 27055
separation from zirconium by ion exchange chromatography, 16: 31577
separation of, from indium and gallium using cinnamic acid, 17: 15924
separation of magnesium fro , by complex formation and solvent extraction, 19: 19833 (CEA-R-2628)
separation of rare earths from, by precipitation using ammonium cinnamate, 20: 45611
separation of scandium from, by ion exchange chromatography, 19: 533
separation of scandium from, by precipitation using ammonium cinnamate, 20: 25012
separation of silver from, by cation exchange chromatography, 20: 40847
separation of trace amounts of, from alkali metals, alkaline earths, and rare earths, 20: 1958
separation of, from thallium by ion-exchange chromatography, 20: 36935
separation of, from germanium and germanium dioxide, by precipitation using 8-hydroxyquinoline, 20: 46759
separation using aromatic Schiff bases, 20: 45802
shock wave interactions with, thermodynamic parameters from mirror-image approximation for particle velocity and pressure in, 17: 37676
Slater-Condon parameters of, determined from spectral data, 17: 31118
slip in, effects of aluminum on basal, 20: 1560 (CALT-473-5)
slip mechanisms in, 20: 31714(R) (UCRL-16658, pp 99-103)
soaps of, preparation and properties of, 20: 35931
solubility in indium arsenide, determination by Hall coefficient, 19: 39269(R) (SU-SEL-64-133)
solvent distribution in ammonium thiocyanate–methanol–water systems, distribution coefficients for, 19: 40447
solvent extraction by tris(2-butoxyethyl) phosphate, 17: 12189
solvent partition in aqueous bromide–TBP systems, 18: 25382
solvent partition in tributyl phosphate–hydrochloric acid or –nitric acid systems, 18: 33685
solvent properties of liquid, for uranium, 16: 16464
solvent properties for palladium, rhodium, ruthenium, uranium, and zirconium, 16: 28555 (TID-7623(p.105-21))
solvent properties of liquid, for molybdenum, niobium, palladium, thorium, and zirconium, 16: 544

solvent properties of liquid, for uranium–zirconium fissium alloys, 16: 11796
solvent properties of liquid, for cerium, ruthenium, uranium, and zirconium, 17: 1359(R) (ANL-6569)
solvent properties for strontium at 428 to 727°C, 17: 14116(R) (ANL-6596 (p.29-118))
solvent properties of liquid, for manganese, plutonium, rhenium, and technetium, 17: 35078(R) (ANL-6739)
solvent properties for technetium at 428 to 758°C, 17: 36860(R) (ANL-6648)
solvent properties for barium, cerium, lanthanum, neodymium, praseodymium at 550°C, 17: 40421(R) (ANL-6766)
solvent properties of liquid, for barium and neodymium, 18: 1483(R) (ANL-6687(p.27-85))
solvent properties of liquid, for plutonium, 18: 17769(R) (ANL-6725(p.99-111))
solvent properties for metals, 20: 22966 (ANL-7083)
sorption by ammonium molybdo-, tin, titanium, and zirconium phosphates, comparison of, 20: 45795(R) (ORNL-3945, pp 176-88)
sorption by cellulose ion exchangers from acetone and ethanol mixtures with hydrochloric acid, 18: 16140
sorption by Dowex-1 anion exchange resin from hydrobromic acid solution, 16: 28936
sorption by peat, 19: 11261 (NP-14668)
sorption by river silts, 18: 38711 (NYO-10544)
sorption from hydrochloric acid by cellulose and resin paper ion exchangers, 18: 16139
sorption from nitric acid by ion exchange paper, 19: 24435
sorption in rats, effect of dietary level of cadmium on gastrointestinal, 17: 35318(R) (HW-76000(p.183-6))
sorption on anion exchange papers in hydrobromic and hydrochloric acids and lithium chloride, 18: 25374
sorptive properties for hydrogen and hydroxyl ions, 17: 25853 (PAN-372/V)
sorptive properties for fission-product iodine from various environments, 20: 574 (CONF-650407, pp 730-46)
sorptive properties for ionic radioisotopes in aqueous solutions, effects of acidity on, 20: 7003 (INR-634/V/C)
spectra in reaction zone of acetylene air flame, excitation of atomic, 17: 27371(T)
spectra in spark discharges, electron-ion recombination in, 18: 27319
spectra, lifetime of first excited resonance state, 16: 29481(R) (NP-11989)
spectra of, correlation of dissociation energies and excitation potentials in flame, 17: 14234
spectra of, fine structure of excitation, 18: 762
spectra of, from electron excitation, 18: 759
spectra of, low energy neutron-capture gamma, 17: 15943(R) (ARF-1193-20)
spectra of, spin-orbit coupling in band structure, 17: 16845
spectra of, in cooling spark discharges, (E), 19: 27103
spectra of, measurement of K x-ray, 18: 44429
spectra of, muonic K and L x-ray, 18: 42626(R) (ANL-6879(p.69-87))
sputtering by argon ions at 30 kev, 17: 36523
sputtering by argon ions, yields and ejection patterns from, 19: 1169(R) (ORNL-3676(p.74-8))
sputtering by argon ions at 1 to 50 kev, 20: 34815 (IBK-435)
sputtering by ions at 45 kev, thermal spikes in, (E), 19: 20838
sputtering by xenon at 25 to 60 kev, energy dependence of, 18: 20785
sputtering of, by argon ions, 17: 5038(R) (ORNL-3364(p.57-84))
strain-rate testing of crystals of, 17: 32575(R) (TID-19181)
structural properties of, effects of thermal cycling on, 18: 22510
structure of powdered, neutron diffraction method for determining, 18: 32174
superconducting critical fields and temperatures for, 17: 41592
superconducting energy gap in polycrystalline, 18: 20627(R) (NP-13815)
superconducting energy gap anisotropy in (E), 19: 3181
superconducting transition temperature in, 16: 15334
superconducting transition temperature in, pressure dependence of, (E), 20: 34451
superconducting transition temperature of, isotope effects on, (E), 20: 37959
superconductivity of, energy gap and critical field in, 17: 6877
superconductivity in, criteria for, (T), 19: 12448
superconductivity of, 20: 40047
surface tension, 16: 1772
surface tension of liquid, relation to critical temperature and surface energy, 16: 25351
temperature of plasma of, spectroscopic determination of, 20: 26275
temperature of transient discharge plasma of, determination using Stark broadening, (T), 20: 34736
thermal conductivity of superconducting thermal switches of, at 0.3 to 2°K, (E), 19: 23584
thermal expansion coefficients, 17: 18818
thermal expansion down to 1.5°K, 18: 18837
thermal expansion of crystals of, at 4.2 to 273.2°K, anisotropic, 16: 9233
thermodynamic properties at high pressures and temperatures, 19: 40459 (NP-15324)
thickness as coating on copper and iron, beta-x-ray fluorescence analysis of, 18: 27322
toxic effects of, in snails, 18: 19489(R) (TID-20469)
toxic effects on man, 19: 21990
ultrasonic attenuation in superconducting, 18: 36504
ultrasonic attenuation in, spin-splitting of De Haas-Van Alphen oscillations in, (E), 19: 33522
ultraviolet emission from electron-bombarded foils of, 20: 14004
uptake by *Cladophora fracta*, concentration effects on dynamics of, 19: 25858
uptake by corn plants, effects of soil fertility on, 20: 40735 (NYO-2744-37)
uptake by phytoplankton, 16: 4030 (TID-12946(App.I,Vol.II))
uptake by woody plants, regularities in, 19: 6964
uptake from silts by soft clams and tubificid worms, 18: 45176 (NYO-10544(Rev.))
use as threshold detector for fast neutrons, (E), 19: 39007
use as tracer, survey, 16: 1359
use in bonding aluminum and aluminum alloys, 17: 41402(P)
use in fast-neutron activation dosimetry, 17: 34288
use in radiation protection pastes for skin in radiotherapy, 18: 19832
use in reduction of yttrium fluorides, 16: 2992 (IS-374)
use in the ion exchange separation of the cerium-group rare earths, 16: 1672
use of kryptonated, as indicator in fluoride determination by titration, 19: 36266
vapor pressure at 660 to 826°C, 18: 4166(R) (MLM-1171)
vapor pressure of liquid, effects of temperature on, 19: 39163(R) (MLM-1244)
vapor pressure over liquid and solid calcium–zinc alloys, 20: 4297(R) (IS-1200(Sect.M))
vapor pressures of liquid, at 7 to 200 torr and 847 to 1062°K, 18: 41927(R) (MLM-1199)
vaporization from probe surface in electric arcs, (E), 20: 32593
viscosity of liquid, 18: 16153
viscosity of liquid, 19: 16074 (MLM-1163(p.M-1-17))
viscosity of liquid, based on atomic parameters, 20: 20656 (UCRL-11930)
viscosity of, relation of atomic mobility to, 17: 4945
viscosity to 1000°C, 17: 29365
wettability with mercury, effects of microrelief on, 17: 3503
x-radiation production efficiency, 16: 8137
x-ray absorption at room temperature and −180°C, 17: 39798
x-ray emission lines of, widths of K, 17: 18925
x-ray spectra of, using promethium-147 beta source, 17: 27280
x-ray spectrum from mesic (μ), 17: 22264(R) (ANL-6679)
x-ray mass absorption at 1.49 to 16.61 kev, (E), 19: 25146(R) (TID-21542)
x-ray spectra from μ-mesic atoms of, nuclear charge distribution from, 19: 27518
x-ray transmission in crystals of, thermal vibration effects on anomalous, (E), 19: 18693
yields from radiolysis of zinc phthalocyanine, 20: 36886

ZINC ACETATES
effects on platinum catalysts in hydrogenation reactions, 16: 13006 (SRO-44)
formation constants, 16: 22104
magnetic resonance of irradiated, 19: 9207

ZINC ALLOYS
analysis for iron and magnesium using butylamine and chloroform, photometric, 18: 13645(T) (AEC-tr-6346)
analysis for molybdenum and tin using 8-quinolinol, 16: 16314
analysis of surface for nitrogen, 17: 7971
corrosion of, review, 19: 7868
reactions with uranium for separation from spent fuels, 17: 6184 (NBS-7582)
soldering to beryllium, 18: 10511
superconducting, transition temperature of, model for, 18: 40455
vapor pressure of zinc over binary, 18: 2163(R) (IS-700(Sect.M))
Ag–Zn, crystal structure studies, 19: 44678(R) (ANL-7000, pp 186-200)
Ag–Zn, diffusion in, activation energies for, 17: 35264(R) (UCRL-10706(p.111-203))
Ag–Zn, diffusion activation energies in dilute solid solutions of, relation with Zener relaxation activation energy, 18: 9773 (TID-19979)
Ag–Zn, heat of formation and phase studies, 16: 10502 (AROD-2287.15)
Ag–Zn, phase studies, 16: 551
Ag–Zn, properties and structure, 16: 15198(R) (TID-15390)
Ag–Zn, radiation effects on diffusion-controlled reactions in, 17: 31055
Ag–Zn, relaxation studies of vacancy annealing in solid solutions of, 18: 15723(R) (TID-20334)

Ag–Zn, relaxation studies of vacancy annealing in solid solutions of, 19: 22988(R) (NYO-2811-23)
Ag–Zn, solute distribution and thermal curves of solidification of, 17: 20500
Ag–Zn, Zener relaxation distribution parameter, 16: 12230 (TID-15085)
Al–Cu–Mg–Zn, corrosion resistance of, effects of age hardening, chromium, and silver on stress, 18: 25946(T) (RSIC-177)
Al–Cu–Mg–Zn, mechanical and structural properties of type 7075, effects of zirconium additions on, 16: 9222
Al–Cu–Mg–Zn, mechanical properties, review, 16: 13617
Al–Cu–Mg–Zn, tensile properties of welded, 16: 6697 (NP-11227)
Al–Cu–Zn, oxidation of, kinetics, mechanism, and microstructure of internal, 20: 23619
Al–Hf–Zn, phase studies, 19: 14059
Al–Mg–Mn–Zn, corrosion, 19: 6271(T) (JPRS-27451)
Al–Mg–Mn–Zn, plastic anisotropy of AZ31B sheet, 19: 39149 (AD-425880)
Al–Mg–Zn, aging sequences in, 17: 1976
Al–Mg–Zn, bonding of AZ31, surface preparation and epoxy adhesive for, 19: 36995 (BDX-613-68)
Al–Mg–Zn, deformation stacking after cold-working, 16: 10594
Al–Mg–Zn, dispersion hardening of, effect of pre-aging on, 16: 10598
Al–Mg–Zn, effects of polarization on stress corrosion of, 17: 32530
Al–Mg–Zn, fatigue at low endurance, during strain and stress, 16: 13615
Al–Mg–Zn, mechanical properties, review, 16: 13617
Al–Mg–Zn, precipitation in vicinity of grain boundaries, 16: 19420
Al–Mg–Zn, stress corrosion under constant tensile and bend stress, 16: 10468
Al–Mg–Zn, stress-corrosion cracking of, effect of corrosion conditions on, 17: 22124
Al–Mg–Zn, temperature dependence in stress corrosion, 17: 11139
Al–Mg–Zn, tensile properties of welded, 16: 6697 (NP-11227)
Al–Ti–Zn, phase studies, 19: 14059
Al–Zn, age-hardening, effects of magnesium on resistivity changes during, 19: 9612(T) (AI-Trans-68)
Al–Zn, annealing neutron-irradiated, 17: 39693
Al–Zn, beta scattering from, 18: 35057
Al–Zn, clustered vacancy annihilation and precipitation in, 18: 7244
Al–Zn, corrosion by aluminum–silicon and water of coatings of, on uranium, 19: 40949 (ISC-640)
Al–Zn, deformation stacking after cold working, 16: 10594
Al–Zn, deposition on uranium, hot dip, 19: 40949 (ISC-640)
Al–Zn, dislocations in slightly rolled, long rectilinear, 16: 27651
Al–Zn, effect of cold working on phase segregation in, 17: 11246
Al–Zn, effects of clustering on superconductivity properties of, 17: 39615
Al–Zn, electric conductivity and phase diagram, 16: 15213
Al–Zn, evaluation of, as coating for vanadium alloys, 16: 2168(R) (ARF-2227-2)
Al–Zn, gamma attenuation in, 16: 9226
Al–Zn, grain boundary diffusion in, 16: 19427
Al–Zn, high-ductile state in, 17: 11247
Al–Zn, intergranular fragility in, effect of elimination of point faults on, 16: 19419
Al–Zn, phase studies and thermodynamic properties, 16: 4559
Al–Zn, phase studies, effects of interlamellar spacing on eutectic solidification rate, 16: 15195 (TID-15338)
Al–Zn, pre-precipitation of zinc in neutron-irradiated, (T), 19: 4732
Al–Zn, precipitation of Guinier-Preston zones in, heat tone, 19: 39173(T) (ORNL-tr-634)
Al–Zn, properties evaluation of, for coating niobium, 16: 21031 (DC-60-8-25)
Al–Zn, radiation effects on electric conductivity of, recovery from electron, 17: 25836
Al–Zn, radiation effects on diffusion-controlled reactions in, 17: 31055
Al–Zn, radiation effects on Guinier-Preston zone formation in, deuteron, 17: 41333(R) (ANL-6677)
Al–Zn, radiation effects on formation of Guinier-Preston zones in, deuteron, 18: 7283 (CONF-339-4)
Al–Zn, radiation effects on pre-precipitation rate in, neutron, 18: 24206
Al–Zn, radiation effects on zone formation in crystalline, 18: 26069(R) (ANL-6868(p.373-417))
Al–Zn, radiation effects on electric conductivity of, stage I and II recovery from electron, 20: 5918
Al–Zn, radiation effects on crystal structure of, at −196°C, neutron, 20: 19260
Al–Zn, sorptive properties for iodide, phosphate, and sulfate ions, 19: 9253 (UJV-1115/64)
Al–Zn, structure evolution through annealing, 16: 19386
Al–Zn, superconducting properties of, 20: 8003(R) (MIT-3226-8)
Al–Zn, thermal cycling effects on structural properties of, 18: 22510
Al–Zn, transformation of beta to zeta phase in single crystals of, 20: 8484 (COO-1198-234)
Al–Zn, vacancy concentration in, measurement of, 19: 24980(R) (COO-987-4)
Al–Zn, vapor pressure of, tracer dew-point method for measuring, 17: 25825
Al–Zn, zone formation in, factors affecting, 16: 16766
Al–Zn–Zr, phase studies, 19: 14059
Au–Ag–Zn disorder and reflectivity of beta phase, 17: 23965(R) (TID-18632)
Au–Zn, electron transfer in dilute, 17: 37189
Au–Zn, heat of formation and phase studies, 16: 10502 (AROD-2287.15)
Au–Zn, heat of formation of AuZn, 19: 39168(R) (TID-22015)
Au–Zn, solute distribution and thermal curves of solidification of, 17: 20500
Be–Mg–Zn, diffusion of beryllium to surface of, on heating at 300 to 500°C, 19: 47071
Be–Mg–Zn, effects of heat on beryllium distribution in, 19: 30769
Be–Zn, corrosion resistance, 19: 22913(P)
Be–Zn, structure, effects of ultra-rapid quenching on, 17: 14812(R) (ASD-TDR-62-181)
Bi–Zn, superconductivity, 20: 44554
Ca–Pu–U–Zn, phase studies, 17: 35079(R) (ANL-6749)
Ca–Zn, crystal structure of AB_2-type compound in, 20: 24589(R) (NYO-3560-3)
Ca–Zn, heat of fusion of intermetallic compound, 20: 41412(R) (IS-1500(Sect. M))
Ca–Zn, intermetallic compound with $CeCu_2$-type structure in, 20: 21352 (TID-21745)
Ca–Zn, phase studies, 17: 27800 (TID-17136)
Ca–Zn, phase studies, 17: 36860(R) (ANL-6648)
Ca–Zn, phase studies, 17: 40421(R) (ANL-6766)
Ca–Zn, solvent properties for plutonium and uranium at 400 to 850°C, 17: 35079(R) (ANL-6749)
Ca–Zn, solvent properties for uranium at 700, 750, and 800°C, 17: 40421(R) (ANL-6766)
Ca–Zn, solvent properties for uranium at 700 to 800°C, 18: 1483(R) (ANL-6687(p.27-85))
Ca–Zn, solvent properties for plutonium and uranium, 18: 16153
Ca–Zn, solvent properties of liquid, for plutonium and uranium, 18: 43359(R) (ANL-6800(p.43-196))
Ca–Zn, thermodynamic properties, 20: 13180(R) (IS-RD-4)
Ca–Zn, thermodynamic properties, 20: 21335 (IS-T-76)
Ca–Zn, thermodynamic properties of, 20: 41412(R) (IS-1500(Sect. M))
Ca–Zn, zinc vapor pressure over liquid and solid, 20: 4297(R) (IS-1200 (Sect.M))
Cd–Ag–Zn, phase studies, 16: 22634
Cd–Mg–Pu–Zn, stability in mild steel and stainless steel containers at 600°C, 20: 5594(R) (ANL-6925, pp 21-106)
Cd–Mg–U–Zn, corrosive effects on ferrous alloys in presence of chloride flux, at 600 and 650°C, 19: 32279(R) (ANL-7020(p.3-99))
Cd–Mg–U–Zn, corrosive effects with chloride flux on carbon steel, Croloy, and stainless steel at 600 to 650°C, 20: 5594(R) (ANL-6925, pp 21-106)
Cd–Mg–U–Zn, corrosive effects in fused chloride mixtures, on stainless steel, 20: 20802(R) (ANL-7055, pp 21-98)
Cd–Mg–U–Zn, phase studies, 20: 5594(R) (ANL-6925, pp 21-106)
Cd–Mg–U–Zn, precipitation of U_2Zn_{17} from, cadmium and magnesium substitution in, 19: 32279(R) (ANL-7020(p.3-99))
Cd–Mg–Zn, corrosive effects on carbon steel, stainless steel, and tantalum at 500, 750, and 850°C, 20: 2265
Cd–Mg–Zn, creep properties, 17: 11179 (AERE-M-1149)
Cd–Mg–Zn, distribution of praseodymium between magnesium chloride–potassium chloride–sodium chloride and, at 600°C, 19: 32279(R) (ANL-7020(p.3-99))
Cd–Mg–Zn, solubility of praseodymium and uranium in, 18: 33678(R) (ANL-6875)
Cd–Mg–Zn, solvent properties for uranium, 17: 37001(R) (ANL-6780)
Cd–Mg–Zn, solvent properties for uranium at 600°C, 17: 40422(R) (ANL-6784)
Cd–Mg–Zn, solvent properties for uranium at 600 and 700°C, 18: 15426(R) (ANL-6810)
Cd–Mg–Zn, solvent properties for uranium at 600 and 650°C, 18: 15663(R) (ANL-6808)
Cd–Mg–Zn, solvent properties for praseodymium, 18: 24952(R) (ANL-6880(p.6-48))
Cd–Mg–Zn, solvent properties of liquid, for uranium, 18: 43359(R) (ANL-6800(p.43-196))
Cd–Mg–Zn, solvent properties of liquid, for plutonium and uranium, 19: 15662(R) (ANL-6900(p.45-142))
Cd–Mg–Zn, solvent properties for fissium–plutonium–uranium fuel pins, 19: 23991(R) (ANL-7003)
Cd–Mg–Zn, solvent properties for plutonium at 350 to 700°C, 19: 32279(R) (ANL-7020(p.3-99))
Cd–Mg–Zn, solvent properties of melts of, for plutonium and uranium,

20: 447
Cd–Pb–Zn, phase studies, 19: 9604(R) (IS-900(Sect.M))
Cd–Zn, analysis by beta reflection, 18: 13690
Cd–Zn, eutectic solidification reactions in, 18: 44144 (NYO-2558-1)
Cd–Zn, eutectic solidification in, atom redistribution in, 19: 42853 (TID-21229)
Cd–Zn, radiation effects on elasticity and microhardness of, 16: 18088
Cd–Zn, radiation effects on contact melting of, 18: 16538
Ce–Mg–Zn–Zr, ultrasonic wave attenuation and delay in, 19: 32761
Ce–Zn, compound formation and electromotive behavior of, 17: 14859(T) (AEC-tr-5674)
Ce–Zn, crystal structure of intermetallic compounds in, 20: 29719
Ce–Zn, heat of fusion of intermetallic compound, 20: 41412(R) (IS-1500(Sect. M))
Ce–Zn, heats of formation and fusion of CeZn in, 19: 19838 (IS-1070)
Ce–Zn, lattice parameters of intermetallic compounds in, 19: 24989(R) (TID-21673)
Ce–Zn, melting point and transformation temperature of intermetallic compounds in, 19: 24989(R) (TID-21673)
Ce–Zn, melting point of $CeZn_2$, 20: 31743
Ce–Zn, phase diagram, 19: 23083
Ce–Zn, phase studies, 16: 6748
Ce–Zn, phase studies, 17: 14860(T) (AEC-tr-5678)
Ce–Zn, phase studies, 17: 36860(R) (ANL-6648)
Ce–Zn, phase studies, 17: 40421(R) (ANL-6766)
Ce–Zn, phase studies, 19: 9604(R) (IS-900(Sect.M))
Ce–Zn, preparation and properties, 17: 14747(T) (AEC-tr-5677)
Ce–Zn, thermodynamic properties, 19: 23083
Ce–Zr, phase studies, 18: 2163(R) (Sect.M))
Co–Zn, critical temperature of superconducting, transition metal impurity effects on depression of, (E), 20: 37955
Cr–Zn, superconducting critical temperature of, transition metal impurity effects on depression of, (E), 20: 37955
Cu–Au–Zn, disorder and reflectivity of beta phase, 17: 23965(R) (TID-18632)
Cu–Au–Zn, electron diffraction diagrams of antiphases with non-integral periods, 17: 22179
Cu–Fe–Zn, deformation and flow of polycrystalline, effects of pressure on, 19: 37048 (WVT-6431)
Cu–Gd–Zn, magnetic properties of intermetallic compounds of, conduction-electron concentration effects on, (E), 20: 24657
Cu–Mg–Zn, liquid miscibility of, at high temperatures, 20: 31314(R) (ANL-7175, pp 1-41)
Cu–Mg–Zn, thermal capacity, 20: 27494(R) (NYO-3454-6)
Cu–Mn–Zn, diffusion in solid, mechanisms of, 19: 42843(R) (COO-359-10)
Cu–Mn–Zn, effects on properties of magnesium and magnesium–zirconium alloy for use as fuel element can, 19: 20610(P)
Cu–Mn–Zn, paramagnetism and valency in, 17: 32561 (AE-111)
Cu–Ni–Zn, analysis of, for cobalt by isotope dilution, 16: 5276
Cu–Ni–Zn, crystal structure of, neutron diffraction study of, 19: 32762
Cu–Ni–Zn, neutron diffraction study of long-range order in single-crystal, 19: 25026
Cu–Pb–Zn, radiation effects on wear resistance of lead bronze, fast-neutron, 20: 15140
Cu–Tb–Zn, crystallography, 20: 4391(R) (ORNL-3870, pp 75-82)
Cu–Zn, analysis by x-ray fluorescence using radioisotopes, 17: 17976(T) (AEC-tr-5696)
Cu–Zn, analysis of, using fluorescent beta-excited x rays, 16: 22508
Cu–Zn, analysis of, x-ray-fluorescence, 17: 29957
Cu–Zn, angular correlation of positron annihilation radiation in, 17: 24260 (AD-286667)
Cu–Zn, cavitation damage in water, 20: 16974 (NP-15889)
Cu–Zn, crystal properties of, thermal effects on, 16: 4550 (WADD-TR-60-893)
Cu–Zn, crystal structure and phase studies, 16: 22050 (NP-11764)
Cu–Zn, crystal structure of stoichiometric, 19: 32048(R) (NP-15073)
Cu– Zn, de Haas-van Alphen effect in β, 19: 11774
Cu–Zn, deformation of, stored-energy measurements during, 18: 4249(R) (ORNL-3470(p.33-9))
Cu–Zn, diffusion in single, enhancement of, by 30-kev neon ion bombardment, 16: 2282
Cu–Zn, diffusion of nickel in, 18: 7994(R) (GTR-21)
Cu–Zn, effects of short-range order on dislocations and stacking fault energy in, 18: 8815
Cu–Zn, elastic constants of, relation to cohesion and stability of intermetallic phases, 18: 44228
Cu–Zn, elastic properties of, improvement of, by abnormal hardening, 16: 12161
Cu–Zn, erosion by water at 70°F, effects of annealing on cavitation, 20: 29640 (NP-16048)
Cu–Zn, formation and growth of intermetallic phases in, 20: 25564 (INR-643/XIV/PB)
Cu–Zn, heat capacity at 1.4 to 4.2°K of gamma-phase, 18: 964
Cu–Zn, heat of formation and phase studies, 16: 10502 (AROD-2287.15)
Cu–Zn, heat of formation of alpha, at 573°K, 18: 32153(R) (UCRL-11317(p.176-97))
Cu–Zn, isotopic exchange of zinc(II) ions between, and zinc sulfate solutions, 16: 22050 (NP-11764)
Cu–Zn, lattice dynamics and structure of, 18: 14592(R) (PR-P-60)
Cu–Zn, lattice vibrations in beta-phase, 18: 9317(R) (PR-P-59(p.37-45))
Cu–Zn, neutron diffraction of short-range order in beta, 17: 22193
Cu–Zn, ordering in beta CuZn, effects of long-range interactions on, 18: 32264 (BNL-7452)
Cu–Zn, radiation effects on diffusion-controlled reactions in, 16: 33567
Cu–Zn, radiation effects on diffusion-controlled reactions in, 17: 31055
Cu–Zn, radiation effects on defect-diffusion in, neutron, 18: 39993 (EUR-1643.e(p.246-53))
Cu–Zn, small-angle cold neutron scattering by, 17: 38034(T) (AEC-tr-5734(p.199-202))
Cu–Zn, thermal cycling effects on structural properties of, 18: 22510
Cu–Zn, thermal vibrations in beta-phase, (E/T), 19: 11767
Cu–Zn, x-ray scattering in, effects of long-range order on, 16: 24212
Cu–Zn, x-ray spectra for content ratio in, 17: 27280
Cu–Zr, copper-63 nuclear spin echoes in, r-f excitation of, (E/T), 19: 41988
Dy–Zn, crystal structure, 18: 5791
Dy–Zn, crystal structure of intermetallic compounds in, 20: 9515
Dy–Zn, crystal structure of intermetallic compounds Dy_6Zn_{23} in, 20: 39417
Dy–Zn, lattice parameters of intermetallic compounds in, 19: 24989(R) (TID-21673)
Dy–Zn, melting point and transformation temperature of intermetallic compounds in, 19: 24989(R) (TID-21673)
Dy–Zn, melting point of $DyZn_2$, 20: 31743
Dy–Zn, structure of DyZn, 17: 36304 (TID-19337)
Er–Zn, crystal structure, 18: 5791
Er–Zn, crystal structure of int rmetallic compounds in, 20: 9515
Er–Zn, crystal structure of intermetallic compound Er_2Zn_{17} in, 20: 39417
Er–Zn, melting point and transformation temperature of intermetallic compounds in, 19: 24989(R) (TID-21673)
Er–Zn, melting point of $ErZn_2$, 20: 31743
Er–Zn, structure of ErZn, 17: 36304 (TID-19337)
Eu–Zn, crystal structure of intermetallic compounds in, 20: 9515
Eu–Zn, crystal structure of intermetallic compound $EuZn_{13}$ in, 20: 39417
Eu–Zn, melting point of $EuZn_2$, 20: 31743
Eu–Zn, properties of intermetallic compounds in, 19: 37081
Fe–Mn–Zn, spin wave dispersion in, 17: 38031(T) (AEC-tr-5734(p.188-92))
Fe–Zn, anodic oxidation products at ambient temperature, 17: 14869
Fe–Zn, critical temperature of superconducting, transition metal impurity effects on depression of, (E), 20: 37955
Fe–Zn, crystal structure of nitrogen-containing, 16: 2259
Fe–Zn, phase studies of nitrogen-containing, 16: 16768
Ga–Hf–Zn, phase studies, 19: 14059
Ga–Pu–Zn, properties of delta-stabilized, 19: 24987 (RFP-506)
Ga–Pu–Zn, tensile properties and thermal expansion of delta-stabilized plutonium-base, 20: 11224
Ga–Ti–Zn, phase studies, 19: 14059
Ga–Zn, isotopic exchange of zinc-65 between aqueous solution and, 19: 46209
Gd–Ag–Zn, magnetic properties of intermetallic compounds of, conduction-electron concentration effects on, (E), 20: 24657
Gd–In–Zn, magnetic properties of intermetallic compounds of, conduction-electron concentration effects on, (E), 20: 24657
Gd–Zn, crystal structure, 18: 5791
Gd–Zn, crystal structure of intermetallic compounds in, 20: 9515
Gd–Zn, crystal structure of intermetallic compounds Gd_6Zn_{23} and $GdZn_{12}$ in, 20: 39417
Gd–Zn, melting point and transformation temperature of intermetallic compounds in, 19: 24989(R) (TID-21673)
Gd–Zn, melting point of $GdZn_2$, 20: 31743
Gd–Zn, structure of GdZn, 17: 36304 (TID-19337)
Ge–Zn–Zr, phase studies, 19: 14059
Hf–Zn, crystal structure of intermetallic compounds in, 20: 11328
Hf–Zn, crystallographic parameters, 17: 18822
Hg–Y–Zn, phase studies, 20: 11317
Hg–Zn, electro- and radiochemical studies of electrode reactions of, 17: 27398
Hg–Zn, reaction with protactinium, 20: 45694
Ho–Zn, crystal structure, 18: 5791
Ho–Zn, crystal structure of intermetallic compounds in, 20: 9515
Ho–Zn, crystal structure of intermetallic compound $HoZn_{12}$ in, 20: 39417

Ho–Zn, crystallography and transformations in AB_2-type compounds in, 20: 24589(R) (NYO-3560-3)
Ho–Zn, lattice parameters of intermetallic compounds in, 19: 24989(R) (TID-21673)
Ho–Zn, magnetic susceptibility of AB_2-type compound in, 20: 24589(R) (NYO-3560-3)
Ho–Zn, melting point and transformation temperature of intermetallic compounds in, 19: 24989(R) (TID-21673)
Ho–Zn, melting point of $HoZn_2$, 20: 31743
Ho–Zn, structure of HoZn, 17: 36304 (TID-19337)
In–Mg–Zn, corrosion, 19: 6271(T) (JPRS-27451)
In–Sn–Zn, analysis, volumetric, 19: 8690 (BDX-613-37)
In–Zn, diffusion coefficient measurements on liquid, during molecular distillation, 20: 21334 (IS-1325)
In–Zn, diffusion coefficients of liquid, 20: 41064(R) (IS-1500(Sect.E))
In–Zn, distillation of, surface effects in, (E), 19: 28328
In–Zn, distillation of liquid, surface concentration changes in, 20: 29346
In–Zn, radiation effects on contact melting of, 18: 16538
La–Zn, crystal structure of AB_2-type compound in, 20: 24589(R) (NYO-3560-3)
La–Zn, crystal structure of intermetallic compound $LaZn_{13}$ in, 20: 39417
La–Zn, intermetallic compound with $CeCu_2$-type structure in, 20: 21352 (TID-21745)
La–Zn, lattice parameters of intermetallic compounds in, 19: 24989(R) (TID-21673)
La–Zn, melting point of $LaZn_2$, 20: 31743
La–Zn, phase studies, 17: 14860(T) (AEC-tr-5678)
La–Zn, phase studies, 17: 14116(R) (ANL-6596(p.29-118))
La–Zn, phase studies, 17: 36860(R) (ANL-6648)
La–Zn, phase studies, 17: 40421(R) (ANL-6766)
Li–Mg–Th–Zn, preparation and properties at high temperatures, 19: 37153(P)
Li–Mg–Zn, phase transitions and tensile properties, 16: 24164 (NP-11778)
Li–Zn, performance in fuel cells, 18: 24355 (ANL-6802(p.53-63))
Lu–Zn, crystal structure of intermetallic compounds Lu_6Zn_{23}, Lu_2Zn_{17}, and $LuZn_{12}$ in, 20: 39417
Lu–Zn, melting point of $LuZn_2$, 20: 31743
Mg–misch metal–Zn, plastic anisotropy of ZE10A sheet, 19: 39149 (AD-425880)
Mg–Pu–U–Zn, corrosive effects on type 405 stainless steel, 20: 20802(R) (ANL-7055, pp 21-98)
Mg–Pu–Zn, liquid miscibility of, at high temperatures, 20: 31314(R) (ANL-7175, pp 1-41)
Mg–rare earths–Zn–Zr, crystal structure, 20: 2399
Mg–rare earth–Zn, preparation and properties, 19: 4709(P)
Mg–Th–Zn–Zr, corrosion, 19: 6271(T) (JPRS-27451)
Mg–Th–Zn–Zr, mechanical properties of, at high temperatures, 16: 27688(P)
Mg–U–Zn, corrosive effects on refractory metals in presence of molten chlorides, 20: 2266
Mg–U–Zn, corrosive effects with fused chlorides, on carbon and zirconium boride, 20: 20802(R) (ANL-7055, pp 21-98)
Mg–U–Zn, stability of, effects of impurities on, 18: 17921(R) (ANL-6725(p.31-88))
Mg–Zn, alloying effects of uranium on, 16: 5719 (NP-11169)
Mg–Zn, analysis for ruthenium using 1-nitroso-2-naphthol, spectrophotometric, 20: 12788
Mg–Zn, analysis of, for zinc, x-ray fluorescence, 16: 5283
Mg–Zn, corrosion of, effects of indium on, 18: 20482
Mg–Zn, crystal structure, 20: 2399
Mg–Zn, diffusion of beryllium to surface of, on heating at 300 to 500°C, 19: 47071
Mg–Zn, direct reduction of thorium dioxide by, 17: 3872
Mg–Zn, distillation, 17: 36860(R) (ANL-6648)
Mg–Zn, distillation of, apparatus for, 18: 43359(R) (ANL-6800(p.43-196))
Mg–Zn, distribution of elements between molten magnesium chloride and, 17: 40421(R) (ANL-6766)
Mg–Zn, distribution of praseodymium between magnesium chloride–potassium chloride–sodium chloride and, at 600°C, 19: 32279(R) (ANL-7020(p.3-99))
Mg–Zn, effects on throium dioxide reduction in liquid halide salts, 19: 9618(P)
Mg–Zn, elastic constants of, relation to cohesion and stability of intermetallic phases, 18: 44228
Mg–Zn, enthalpy of formation of intermetallic compounds MgZn, $MgZn_2$, and Mg_2Zn_{11} in, 16: 4581
Mg–Zn, evaluation of, as coating for vanadium alloys, 16: 2168(R) (ARF-2227-2)
Mg–Zn, exchange of plutonium in liquid systems with chlorides, thermodynamics of, 20: 43819
Mg–Zn, heat of fusion of intermetallic compound, 20: 41412(R) (IS-1500(Sect. M))
Mg–Zn, heats of formation and fusion of intermetallic compound $MgZn_2$ in, 19: 19838 (IS-1070)
Mg–Zn, phase separation in, x-ray studies of, 17: 8861
Mg–Zn, phase separation of, supernatant solutions from uranium, 17: 36860(R) (ANL-6648)
Mg–Zn, phase studies by neutron diffraction, 20: 12545(R) (PAEC(A)AR651)
Mg–Zn, precipitation and recrystallization of, 17: 34446
Mg–Zn, reactions with uranium oxides, 18: 17922(R) (ANL-6725 (p.88-99))
Mg–Zn, reactions with thorium dioxide, 20: 742 (ANL-7058)
Mg–Zn, reactions with plutonium dioxide, 20: 2220 (ANL-7059)
Mg–Zn, reactions with uranium oxide, 20: 741 (ANL-7057)
Mg–Zn, reduction of plutonium, thorium, and uranium oxides using, 16: 828
Mg–Zn, separation of uranium from liquid, by hydridation, 19: 17176(R) (ANL-6965(p.1-41))
Mg–Zn, separation of plutonium from, by fused chloride extraction, 20: 5594(R) (ANL-6925, pp 21-106)
Mg–Zn, separation of californium and yttrium from, by fused chloride extraction, 20: 5594(R) (ANL-6925, pp 21-106)
Mg–Zn, solvent properties for plutonium and uranium, 17: 1359(R) (ANL-6569)
Mg–Zn, solvent properties of liquid, for zirconium, 17: 1359(R) (ANL-6569)
Mg–Zn, solvent properties for zirconium at 482 to 758°C, 17: 14116(R) (ANL-6596(p.29-118))
Mg–Zn, solvent properties for thorium at 750 to 850°C, 17: 36860(R) (ANL-6648)
Mg–Zn, solvent properties for uranium at 500 to 900°C, 17: 36860(R) (ANL-6648)
Mg–Zn, solvent properties for thorium, 17: 40421(R) (ANL-6766)
Mg–Zn, solvent properties of liquid, for transuranic elements, 19: 36553
Mg–Zn, solvent properties for rare earth elements in molten chloride salts, 20: 3865 (ANL-7064)
Mg–Zn, solvent properties of, for chromium, iron, niobium, and zirconium, 20: 31314(R) (ANL-7175, pp 1-41)
Mg–Zn, sorption of impurities in magnesium–thorium alloy by liquid, in fused salt, 19: 20066
Mg–Zn, sorptive properties for curium in presence of americium, 18: 43733(P)
Mg–Zn, thermal stability at 150 to 300°C, 17: 34461
Mg–Zn, thermodynamic properties, 18: 2163(R) (IS-700(Sect.M))
Mg–Zn, thermodynamic properties, 19: 9604(R) (IS-900(Sect.M))
Mg–Zn, vapor pressure, 17: 12672(T) (AEC-tr-5626)
Mg–Zn–Zr, bonding of ZK60, surface preparation and epoxy adhesive for, 19: 36995 (BDX-613-68)
Mg–Zn–Zr, casting, 18: 14452(P)
Mg–Zn–Zr, corrosion resistance of, to carbon dioxide and air at 500°C, alloying effects of beryllium and manganese on, 16: 30892(P)
Mg–Zn–Zr, corrosion, 19: 6271(T) (JPRS-27451)
Mg–Zn–Zr, creep properties of, for use as fuel element can, 16: 15236(P)
Mg–Zn–Zr, hot brittleness of, 19: 37092
Mg–Zn–Zr, oxidation by carbon dioxide–carbon monoxide mixtures at 500 to 700°C, 17: 25739
Mg–Zn–Zr, preparation for casting, 18: 22469(P)
Mg–Zn–Zr, structure, 18: 2258
Mg–Zn–Zr, thermal stress in Z.W. 1, 16: 20811(P)
Mg–Zn–Zr, ultrasonic wave attenuation and delay in, 19: 32761
Mn–Zn, analysis for beryllium, spectrophotometric, 19: 5789
Mn–Zn, crystal and magnetic structure of, 19: 9704
Mn–Zn, crystal structure of nitrogen-containing, 16: 2259
Mn–Zn, crystal structure, 18: 2403(R) (PR-P-58)
Mn–Zn, de Haas-van Alphen effect in, exhibiting a resistance minimum, 17: 13155
Mn–Zn, magnetic structure of, 18: 9317(R) (PR-P-59(p.37-45))
Mn–Zn, phase studies of nitrogen-containing, 16: 16768
Mn–Zn, spin scattering in superconducting, (E), 20: 34464
Mn–Zn, superconductivity in, effects of s-d exchange interactions in, 18: 24555
Mn–Zn, superconducting critical temperature of, transition metal impurity effects on depression of, (E), 20: 37955
Nb–Zn, crystal structure of intermetallic compounds in, 20: 11328
Nb–Zn, oxidation resistance of intermetallic compounds, 18: 7271
Nb–Zn, phase diagram, 16: 499 (NRL-5643)
Nb–Zn, phase diagram, 16: 6543 (ONR-9(Vol.I)(p.104-27))
Nb–Zn, phase diagram, 20: 31669
Nb–Zn, phase studies, 19: 23077
Nb–Zn, properties of, as protective coating for niobium, 16: 6543 (ONR-9(Vol.I)(p.104-27))
Nb–Zn, properties as high-temperature coating, 20: 29650

Nb–Zn, structure of intermetallic compound $NbZn_3$ in, 16: 5731
Nb–Zn, superconductivity of, critical persistent currents in, 17: 6875
Nb–Zn, vapor pressures of compounds in, 16: 499 (NRL-5643)
Nb–Zn–Zr, mechanical properties, 18: 7292(R) (HW-77954(p.4.1-12))
Nd–Zn, crystal structure, 18: 5791
Nd–Zn, crystal structure of intermetallic compounds in, 20: 9515
Nd–Zn, crystal structure of intermetallic compound Nd_2Zn_{17} in, 20: 39417
Nd–Zn, lattice parameters of intermetallic compounds in, 19: 24989(R) (TID-21673)
Nd–Zn, melting point of $NdZn_2$, 20: 31743
Nd–Zn, phase studies, 17: 36860(R) (ANL-6648)
Nd–Zn, phase studies, 17: 40421(R) (ANL-6766)
Nd–Zn, structure of NdZn, 17: 36304 (TID-19337)
Ni–Zn, critical temperature of superconducting, transition metal impurity effects on depression of, (E), 20: 37955
Ni–Zn, crystal structure of nitrogen-containing, 16: 2259
Ni–Zn, diffusion of copper in, 18: 7994(R) (GTR-21)
Ni–Zn, phase studies of nitrogen-containing, 16: 16768
Pb–rare earths–Zn, component distribution in recrystallized, 20: 39435
Pb–Zn, atomic volume, density, and thermal expansion of liquid, gamma absorption measurements of, 20: 27559
Pb–Zn, distribution of rare earths in, at 500°C, 18: 42089
Pb–Zn, distribution of cerium in liquid, 18: 42089
Pb–Zn, phase studies of, at 650 to 800°C, 16: 28641(R) (ANL-6543)
Pb–Zn, phase studies at 648 to 795°C, 17: 40421(R) (ANL-6766)
Pb–Zn, self-diffusion of zinc in, at 400 to 550°C, 16: 10543(R) (TID-14773)
Pb–Zn, solute distribution and thermal curves of solidification of, 17: 20500
Pb–Zn, solvent properties of liquid, for cerium and palladium, 16: 16464
Pb–Zn, solvent properties for cerium, palladium, plutonium, strontium, and uranium, 18: 31495
Pr–Zn, crystal structure studies, 19: 44678(R) (ANL-7000, pp 186-200)
Pr–Zn, crystal structure of intermetallic compound Pr_2Zn_{17} in, 20: 39417
Pr–Zn, lattice parameters of intermetallic compounds in, 19: 24989(R) (TID-21673)
Pr–Zn, melting point of $PrZn_2$, 20: 31743
Pr–Zn, phase studies, 17: 36860(R) (ANL-6648)
Pr–Zn, phase studies, 17: 40421(R) (ANL-6766)
Pr–Zn, thermodynamic properties, 19: 24064(R) (ANL-6997)
Pu–Zn, electric conductivity of, at 0 to 300°K, 16: 29424
Pu–Zn, enthalpy, entropy, and free energy of $PuZn_{13}$, 19: 7926
Pu–Zn, phase diagram, 17: 4984
Pu–Zn, phase studies and properties of intermetallic compounds in, 18: 42048
Pu–Zn, phase transformation of delta-stabilized, 17: 8733(P)
Pu–Zn, preparation of stabilized, by application of high pressure, 19: 5930(P)
Pu–Zn, structure of intermetallic compounds in, 17: 3536
Pu–Zn, thermal expansion of delta phase, 16: 4464
Pu–Zn, thermal expansion of delta, 17: 23953 (LADC-5466)
Pu–Zn, thermodynamic functions, 18: 1483(R) (ANL-6687(p.27-85))
Pu–Zn, thermodynamic properties, 18: 17769(R) (ANL-6725(p.99-111))
Pu–Zn, thermodynamic properties of, 18: 44224
Pu–Zn, thermodynamic properties, 19: 7926
rare earths–Zn, crystal structure of intermetallic compounds in, 19: 41040
rare earth–Zn, crystal structure of, CsCl-type intermediate phases in, 20: 31737
rare earths–Zn, crystallography and transformations in AB_2-type compounds in, 20: 24589(R) (NYO-3560-3)
rare earths–Zn, melting points, 20: 24589(R) (NYO-3560-3)
rare earth–Zn, phase studies and structure of intermetallic compounds in, 19: 24989(R) (TID-21673)
Ru–Zn, process for improving workability of, 19: 40999(P)
Sb–Bi–Sn–Zn, thermoelectric properties, 16: 15283(T,P) (FTD-TT-61-264)
Sb–Zn, development and properties as thermoelectric material, 17: 23861(R) (AD-282505)
Sb–Zn, electronic and solidification characteristics of, for use in thermoelectric cells, 16: 9187 (AFCRL-830)
Sb–Zn, radiation effects on thermoelectric properties at 50 to 200°C, 16: 27696 (WCAP-1680)
Sb–Zn, thermoelectric properties of intermetallic compound in, 20: 29709(R) (TID-22970, pp 65-119)
Sc–Zn, preparation and structure of, 17: 39587
Sm–Zn, crystal structure, 18: 5791
Sm–Zn, crystal structure of intermetallic compounds in, 20: 9515
Sm–Zn, crystal structure of intermetallic compound $SmZn_{12}$ in, 20: 39417
Sm–Zn, crystallographic and thermodynamic data on intermetallic compound, 20: 41412(R) (IS-1500(Sect. M))
Sm–Zn, magnetic susceptibility of AB_2-type compound in, 20: 24589(R) (NYO-3560-3)
Sm–Zn, melting point of $SmZn_2$, 20: 31743
Sm–Zn, phase diagrams, 20: 4297(R) (IS-1200(Sect.M))
Sm–Zn, structure of SmZn, 17: 36304 (TID-19337)
Sn–Zn, beta scattering from, 18: 35057
Sn–Zn, distillation of, surface effects in, (E), 19: 28328
Sn–Zn, distillation of liquid, surface concentration changes in, 20: 29346
Sn–Zn, entropy of liquid, electronic contribution in mixing to, 17: 6044 (NP-12311)
Sn–Zn, eutectic solidification reactions in, 18: 44144 (NYO-2558-1)
Sn–Zn, evaluation of, as coating for vanadium alloys, 16: 2168(R) (ARF-2227-2)
Sn–Zn, radiation effects on microhardness, 17: 31024
Sn–Zn, solute distribution and thermal curves of solidification of, 17: 20500
Sn–Zn, superconducting transitions at 3.0 to 3.7°K, (E), 20: 28190
Sr–Zn, crystal structure of $SrZn_2$ in, 18: 8814 3560-3)
Sr–Zn, crystal structure of AB_2-type compound in, 20: 24589(R) (NYO-
Sr–Zn, intermetallic compound with $CeCu_2$-type structure in, 20: 21352 (TID-21745)
Ta–Zn, crystal structure of intermetallic compounds in, 20: 11328
Ta–Zn, thermal analysis, 17: 36860(R) (ANL-6648)
Tb–Zn, crystal structure, 18: 5791
Tb–Zn, crystal structure of intermetallic compounds in, 20: 9515
Tb–Zn, magnetic structure, 18: 39954
Tb–Zn, magnetic susceptibility of AB_2-type compound in, 20: 24589(R) (NYO-3560-3)
Tb–Zn, melting point of $TbZn_2$, 20: 31743
Tb–Zn, structure of TbZn, 17: 36304 (TID-19337)
Tc–Zn, chemical properties, 18: 3038(R) (ANL-6801)
Tc–Zn, decomposition pressure of intermetallic compound $TcZn_6$ in, at 470 to 570°C, 18: 23488
Tc–Zn, decomposition pressure of intermetallic compounds in, 18: 43359(R) (ANL-6800(p.43-196))
Tc–Zn, formation of Tc_4Zn_{11} in, 17: 37001(R) (ANL-6780)
Tc–Zn, phase studies and thermodynamic properties, 18: 33678(R) (ANL-6875)
Tc–Zn, phase studies on technetium-99-labeled, 18: 36013
Tc–Zn, phase studies, 18: 43359(R) (ANL-6800(p.43-196))
Tc–Zn, phase studies, 17: 40421(R) (ANL-6766)
Th–Zn, crystal structure of $ThZn_4$, 17: 18772(R) (TID-18412)
Th–Zn, melting point and transformation temperature of intermetallic compounds in, 19: 24989(R) (TID-21673)
Th–Zn, production of solid, by electrolysis in fused salt above 1100°C, 19: 16083(T) (NP-tr-1221)
Th–Zn, reactions of Th_2Zn_{17} with thorium tetrachloride in fused lithium chloride–potassium chloride eutectic, 19: 24484 (IS-T-11)
Th–Zn, separation of thorium from, by precipitation using lithium, 19: 6004(P)
Th–Zn, separation from fluoride systems by electrolysis at 1100°C, 17: 39209
Th–Zn, thermodynamic properties of, 18: 44224
Th–Zn, thermodynamic properties, 19: 7926
Th–Zn, vapor pressure of, tracer dew-point method for measuring, 17: 25825
Ti–Zn, crystal structure of intermetallic compounds in, 20: 11328
Ti–Zn, crystallographic parameters, 17: 18822
Tl–Zn, solute distribution and thermal curves of solidification of, 17: 20500
Tm–Zn, crystal structure, 18: 5791
Tm–Zn, crystal structure of intermetallic compounds in, 20: 9515
Tm–Zn, crystal structure of intermetallic compounds, Tm_6Zn_{23} and $TmZn_{12}$ in, 20: 39417
Tm–Zn, crystallography and transformations in AB_2-type compounds in, 20: 24589(R) (NYO-3560-3)
Tm–Zn, melting point of $TmZn_2$, 20: 31743
Tm–Zn, structure of TmZn, 17: 36304 (TID-19337)
U–Zn, phase studies, 16: 6748
U–Zn, phase studies, 17: 1359(R) (ANL-6569)
U–Zn, phase studies, 17: 14116(R) (ANL-6596(p.29-118))
U–Zn, phases in $UZn_{8.5}$–Zn region of, 19: 32055(R) (ANL-7020 (p.231-7))
U–Zn, precipitation of U_2Zn_{17} from cadmium–magnesium–zinc solution, cadmium and magnesium substitution in, 19: 32279(R) (ANL-7020 (p.3-99))
U–Zn, preparation of intermetallic, 19: 32769(P)
U–Zn, separation of uranium from, by precipitation using lithium, 19: 6004(P)
U–Zn, structures in $UZn_{8.5}$–UZn_{12} region of, 19: 32055(R) (ANL-7020

(p.231-7))
U–Zn, thermodynamic properties of, at 450°C, 16: 25397
U–Zn, thermodynamic properties of, 18: 44224
U–Zn, thermodynamic properties, 19: 7926
V–Zn, crystal structure and phase studies, 17: 40421(R) (ANL-6766)
V–Zn, phase studies, 17: 1359(R) (ANL-6569)
V–Zn, phase studies, 17: 14116(R) (ANL-6596(p.29-118))
V–Zn, structure of V_2Zn_{11}, 18: 1483(R) (ANL-6687(p.27-85))
Yb–Zn, crystal structure of intermetallic compound $YbZn_2$, 19: 47030
Yb–Zn, crystal structure of intermetallic compounds in, 20: 9515
Yb–Zn, crystal structure of intermetallic compounds Yb_2Zn_{17} and $YbZn_{13}$ in, 20: 39417
Yb–Zn, crystallography and transformations in AB_2-type compounds in, 20: 24589(R) (NYO-3560-3)
Yb–Zn, intermetallic compound with $CeCu_2$-type structure in, 20: 21352 (TID-21745)
Yb–Zn, lattice parameters of intermetallic compounds in, 19: 24989(R) (TID-21673)
Yb–Zn, melting point and transformation temperature of intermetallic compounds in, 19: 24989(R) (TID-21673)
Yb–Zn, melting point of $YbZn_2$, 20: 31743
Y–Zn, crystal structure, 18: 5791
Y–Zn, crystal structure of intermetallic compounds in, 20: 7623
Y–Zn, crystal structure of intermetallic compounds in, 20: 9515
Y–Zn, crystal structure of intermetallic compound YZn_{12} in, 20: 15102
Y–Zn, crystal structure of AB_2-type compound in, 20: 24589(R) (NYO-3560-3)
Y–Zn, intermetallic compound with $CeCu_2$-type structure in, 20: 21352 (TID-21745)
Y–Zn, lattice parameters of intermetallic compounds in, 19: 24989(R) (TID-21673)
Y–Zn, magnetic susceptibility from parallel pumping in planar Zn_xY, 17: 37700
Y–Zn, melting point and transformation temperature of intermetallic compounds in, 19: 24989(R) (TID-21673)
Y–Zn, phase diagram and thermodynamic properties of, 17: 23950 (IS-538)
Y–Zn, phase studies, 18: 1483(R) (ANL-6687(p.27-85))
Y–Zn, phase studies, 17: 4447 (IS-500(Sect.M))
Y–Zn, structure of YZn_7, 17: 36304 (TID-19337)
Y–Zn, structures of YZn_2, YZn_3, YZn_4, and Y_3Zn_{11} intermetallic compounds, 19: 7892 (CONF-640702-2)
Y–Zn, vapor pressure of, tracer dew-point method for measuring, 17: 25825
Zn–Zr, crystal structure of intermetallic compounds in, 20: 11328
Zn–Zr, ferromagnetic resonance in intermetallic compounds of, (E), 20: 15960
Zn–Zr, itinerant electron ferromagnetism in, 18: 20556
Zn–Zr, structure of intermetallic compound $ZrZn_{22}$ in, 16: 5730

ZINC ALUMINATES
preparation of single crystals, 16: 22114

ZINC BORATES
luminescence of antimony-, arsenic-, bismuth-, and manganese-activated, 16: 6877
luminescence of rare earth ions in, 19: 46269
preparation, 16: 13008(R) (TID-15006)
spectra of, infrared, 17: 18048

ZINC BROMATES
Szilard-Chalmers reaction in, bromine isotope effects in, 17: 40891
thermal decomposition of, search for perbromate in, 19: 36402

ZINC BROMIDES
electron energy losses in, and mechanisms of, 17: 13165
reactions in fused salts, formation constants of complex ions, 16: 4128
thermodynamic properties of solid, liquid, and gaseous, 18: 15700 (SRIA-109)
use as biological shields in radiology, 19: 15301
use in shielding windows with argon atmosphere and mild steel container, 18: 11363
use in shielding windows, 17: 7498 (USNRDL-TR-594)
use in windows for gamma and neutron shielding, 16: 3154
vaporization of, 17: 2956 (UCRL-9840)
zinc ion diffusion in liquid, 16: 22149
$CdBr_2$–$ZnBr_2$, phase diagrams, 20: 36787 (YALE-2723(Vol.1))

Zinc Cadmium Sulfides
see Cadmium Zinc Sulfides

ZINC CARBONATES
sorptive properties for organic compounds, 18: 25032(T) (SC-T-64-618)
sorptive properties of basic, for plutonium and uranium from alkaline solutions, 19: 5985 (AERE-R-4516)
sorptive properties of basic, for uranium in sea water, 19: 24634(P)
thermoluminescence properties of, for use as radiation dosimeter, 20: 36913

ZINC CERIUM NITRATES
cobalt-57 intermediate state reorientation in, 17: 28819 (AD-405844)
cobalt-60 orientation in, spin-spin interaction effects on gamma angular distributions from, (T), 20: 36371
iron-57 paramagnetic resonance in, at 4.2, 77, and 193°K, 19: 34170
spectra of, infrared, 18: 235

Zinc Cesium Ferrocyanides
see Cesium Zinc Ferrocyanides

ZINC CHLORIDES
complexes of, polarization in benzene and dioxane solutions, 18: 31487
corrosive effects on stainless steels under stress, mechanism of, 16: 30733 (ARF-2181-12)
diffusion in molten, effects of temperature on self-, 19: 26338
displacement by cadmium chloride on anion exchangers, frontal analysis and development, 16: 23673(T) (AEC-tr-5098)
effects as calcergen, relation to histamine liberators in rats, 20: 36557
effects on oxidation of plutonium, uranium, and zirconium in halide salt–metal systems, 17: 36860(R) (ANL-6648)
effects on platinum catalysts in hydrogenation reactions, 16: 13006 (SRO-44)
effects on self-diffusion of water at 23°C, 19: 32159
effects on spectra of niobium complexes with thiocyanate, 18: 31392
electric conductivity of melts, temperature coefficients for, 18: 23456(T) (AI-Trans-46)
electron energy losses in, and mechanisms of, 17: 13165
fixation on anion exchange resin, quantitative, 16: 17640(T) (AEC-tr-5027)
gamma absorption by aqueous solutions of, for shielded windows, (E), 20: 10226
ion mobilities in liquid, 16: 157 (IS-344)
paramagnetic ion ESR in, temperature effects, 16: 13018 (UCRL-9944)
polarographic behavior in pyridine, 16: 13016 (TID-15229)
polarography in mixture of lithium and potassium chlorides, 16: 2953
polarography in mixture of potassium and sodium chlorides, 16: 2954
properties of complexes with, 16: 22082
properties of solutions of, in dimethyl sulfoxide, 20: 293 (UCRL-16330)
radiation effects on fused, gamma, 19: 39265(R) (IA-1021)
reactions in dioxane–water solutions, nuclear magnetic resonance spectra of, 17: 40800
reactions in fused salts, formation constants of complex ions, 16: 4128
reactions with methanol, methoxide complex formation equilibrium in, 19: 11075
separation by reversed phase partition chromatography using organophosphorus compounds, 18: 25614
separation from salts by extraction chromatographic using organic phosphorus compounds, 20: 10759 (INP-427/C)
solubility in sodium chloride, 19: 44677(R) (ANL-7000, pp 183-5)
solvent properties for zinc, 20: 24971(R) (BNL-954, pp 50-83)
sorption in guinea pigs, percutaneous tracer study, 19: 12927
spectra in argon, krypton, and xenon matrices, infrared, 17: 4497 (UCRL-10451)
spectra in tri-*n*-octylamine nitrate solutions, infrared, 18: 10075
spectra of liquid, Raman, 20: 38871(R) (NYO-1769-54)
spectra of uranium(IV) chloride in, 17: 14261
thermodynamic properties of solid, liquid, and gaseous, 18: 15700 (SRIA-109)
use as catalyst in radioinduced polymerization of vinyl esters, 20: 23192(P)
uses as catalyst in preparation of radiation-resistant lubricant, 18: 41503(P)
uses as catalyst in preparation of radiation-resistant lubricant, 18: 41504(P)
vaporization of, 17: 2956 (UCRL-9840)
volatility of, effects of ammonia on, 20: 26821(R) (SRIA-106-38)
$BaCl_2$–$ZnCl_2$, phase diagrams, 20: 36787 (YALE-2723(Vol.1))
Bi–NaCl–$ZnCl_2$, spectra of reaction products of, absorption, 20: 3921(R) (ORNL-3870, pp 56-60)
$CaCl_2$–$ZnCl_2$, phase diagrams, 20: 36787 (YALE-2723(Vol.1))
$CdCl_2$–H_2O–$ZnCl_2$, thermodynamic properties, 16: 14378(R) (NYO-2302)
$CdCl_2$–$ZnCl_2$, phase diagrams, 20: 36787 (YALE-2723(Vol.1))
CuCl–$ZnCl_2$, phase diagrams, 20: 36788 (YALE-2723(Vol.2))
$GaCl_3$–$ZnCl_2$, phase diagram, 19: 5846(T) (ANL-Trans-105)
$HgCl_2$–$ZnCl_2$, phase diagrams, 20: 36788 (YALE-2723(Vol.2))
$InCl_3$–$ZnCl_2$, phase diagram, 16: 2931(T) (AEC-tr-4870)
$InCl_3$–$ZnCl_2$, phase diagrams, 20: 36788 (YALE-2723(Vol.2))
KCl–$ZnCl_2$, phase diagrams, 20: 36788 (YALE-2723(Vol.2))
KCl–$ZnCl_2$, properties of fused, as simulated reactor fuels, 17: 27797 (PAN-414/V)
KCl–$ZnCl_2$, spectra of fused, infrared, 17: 37175 (URS-74)
LiCl–KCl–$ZnCl_2$, oxidizing effects of liquid, on thorium, 20: 4297(R) (IS-1200(Sect.M))
LiCl–KCl–Zn–$ZnCl_2$, reactions with uranium monocarbide at 580 to 802°C, 19: 24482 (IS-1061)
LiCl–KCl–Zn–$ZnCl_2$, reactions of uranium monocarbide at 540 to 802°C

in, 20: 2404
LiCl–KCl–$ZnCl_2$, reactions with uranium carbide at 540 to 800°C, 20: 4297(R) (IS-1200(Sect.M))
LiCl–KCl–$ZnCl_2$, reactions with uranium monocarbide–zinc at 500 to 800°C, 20: 14991
LiCl–KCl–$ZnCl_2$, spectra of liquid, effects of composition on Raman, 20: 35481(R) (ORO-2073-11)
LiCl–$MgCl_2$–MgF_2–Zn–$ZnCl_2$, corrosive effects on tungsten alloys at 800°C, 17: 36860(R) (ANL-6648)
LiCl–Mg–$MgCl_2$–MgF_2–Zn–$ZnCl_2$, corrosive effects on anodized beryllium at 800°C, 17: 36860(R) (ANL-6648)
LiCl–$ZnCl_2$, spectra of fused, infrared, 17: 37175 (URS-74)
$MgCl_2$–$ZnCl_2$, phase diagrams, 20: 36788 (YALE-2723(Vol.2))
NaCl–$ZnCl_2$, diffusion and ionic conductivity in, 19: 44677(R) (ANL-7000, pp 183-5)
$PbCl_2$–$ZnCl_2$, phase diagrams, 20: 36788 (YALE-2723(Vol.2))
RbCl–$ZnCl_2$, phase diagrams, 20: 36788 (YALE-2723(Vol.2))
$SnCl_2$–$ZnCl_2$, phase diagrams, 20: 36788 (YALE-2723(Vol.2))
$SrCl_2$–$ZnCl_2$, phase diagrams, 20: 36788 (YALE-2723(Vol.2))
TlCl–$ZnCl_2$, phase diagrams, 20: 36788 (YALE-2723(Vol.2))
Zn–$ZnCl_2$, analysis of, spectrophotometric, 18: 3671(R) (BNL-799 (p.26-54))
Zn–$ZnCl_2$, electromotive force studies of species in liquid, 18: 11511 (NAA-SR-8881)
Zn–$ZnCl_2$, electromotive force measurements on, 17: 40815
Zn–$ZnCl_2$, free energy of solution of, 19: 11103
Zn–$ZnCl_2$, zinc-65 exchange mechanism and rate in, at 433 to 681°C, 16: 6420

ZINC CHROMATES
effects of decontaminating and descaling solution on coating of, 20: 21238 (NP-15928)
effects on radiation behavior of polymers, 18: 24199(T,R) (AEC-tr-6316 (p.359-67))

ZINC COMPLEXES
bis-(dipivaloylmethanido)-, crystal and molecular structure, 17: 32040 (NYO-10552)
chlorophyllin, radiosensitivity effects in mice, gamma, 20: 1692
effects on radiation sickness in mice, 18: 9931
formation of, thermodynamics and kinetics of, 18: 17717(R) (TID-20438)
reactions with 8-hydroxy-5-quinolinesulfonic acid, 19: 15571(R) (TID-21385)
tetrachloro-, bonding and pseudo-lattice energies in tetrahedral, 17: 17947 (NYO-9873)
with adenosine triphosphate, infrared spectra of, in heavy water, 19: 5936
with adenosine triphosphate, stability constants of, 16: 7556
with adenosinephosphoric acids, stability constants of, 16: 28948
with $\alpha,\beta,\gamma,\delta$-tetraphenylporphine, Szilard-Chalmers recoil reactions in, 19: 15647
with α, β, γ, δ-tetraphenylporphines, retentions in Szilard-Chalmers (α,γ) recoil reactions in, 19: 40612
with aminoacetone-*N*,*N*-diacetic acid, dissociation and stability constants of, 18: 19946
with arsenazo III, formation mechanism of, 17: 6007
with ascorbic acid, absorption spectra of, 18: 31527
with azo dyes, composition of, radiometric and spectrophotometric studies of, 20: 22925
with carbamic acid, synthesis, 16: 6425
with cupferron, thermal dissociation, 19: 7366
with diacetamide, properties and spectra of, 20: 8494 (TID-22449)
with dialkyl phosphoric acids, preparation and properties, 18: 25429
with dialkyl phosphorodithioic acids, formation, 17: 15858(R) (ORNL-3397(p.71-112))
with diethyldithiophosphate, solvent extraction from mineral acids using carbon tetrachloride, 16: 28926(T) (AEC-tr-5202)
with DPTA and EDTA, effects on zinc-65 retention in rats, 20: 42789
with DTPA, effectiveness in removing cerium-144 and yttrium-91 from rat organs, 19: 26256
with EDTA, bonding and structure of, 17: 33896
with EDTA, destruction by oxidation, 19: 32047 (KFK-287)
with EDTA, effects on growth of rough lemon and trifoliate orange seedlings, 19: 29813 (TID-20741)
with EDTA, radiation effects on stability, 19: 30250
with EDTA, substitution reactions in, 19: 28357
with ethylenediaminetetraacetic acid, radioprotective effects of, in mice, 18: 13567
with hexamethylphosphoramide, NMR contact shifts in, 20: 12828 (TID-21587)
with MEG, preparation and structure of, 19: 17911
with MEG, protective effects against radiation damage in mice, 19: 17911
with mercaptohydroquinone and 4-mercaptoresorcinol, stability of, 19: 26237
with mercaptosuccinic acid and 2,3-dimercaptosuccinic acid, formation and properties of, 18: 8394 (TID-20013)
with *N*-(2-pyridylmethyl)iminodiacetic acid, stability of, 17: 15993
with naphthazarin, composition and thermal stability, 16: 18893
with phosphoorganic compounds in TTA and 2,4-pentanediones, synergism in, 20: 261
with pyridine, separation from aqueous solutions by solvent extraction, effects of ion charge magnitude on, 19: 546
with rare earths and complexone(III), solubility in water and thermal stability, 19: 22239
with salicylaldehydes, association constants for, 20: 33276
with solochrome violet RS, polarography of, 20: 16406
with substituted 2-(pyridyl)- and 2-(quinolyl)-1,3-indanediones, acid dissociation and formation constants of, 18: 25457
with sydnones, formation and properties, 18: 11528 (TID-20062)
with tetraphenylporphine in dioxane, gamma radiolysis of, 20: 36889
with thenoyltrifluoroacetone and trioctylphosphine oxide, preparation and properties, 19: 15680
with thiocyanate, solvent extraction in three-phase system using diantipyrilmethane, 18: 13950
with thiodibenzoylmethane, stability of, 20: 20693
with thiols, radiosensitivity effects in mice, 20: 18450
with 1-(2-pyridylazo)-2-naphthol, formation constants and distribution equilibria of, 17: 14381
with 1,3-bis(2'-pyridyl)-1,2-diazaprop-2-ene, spectra, 17: 33816
with 1-substituted tetrazoles, 19: 15417 (TID-19078)
with 1,10-phenanthroline, formation constants, 19: 42456 (IS-T-20)
with 2-methyl-4,6-heptanedione, stability constants of, 19: 11056(T) (AEC-tr-6227/3(p.183-92))
with 3-cyanopentane-2,4-dione, stretching frequency of cyano group in, 16: 20421
with 4-methylpyridine–thenoyltrifluoroacetone, preparation, 19: 3811 (TID-20074)
with 8-quinolinol derivatives, electronic absorption spectra, 19: 43989 (MIT-905-20)
with 8-quinolinols, luminescence yields of, 20: 10456 (COO-773-3)

ZINC COMPOUNDS
effects on radioinduced vulcanization of rubber, 19: 495
effects on radiolysis of water, 20: 8981 (CEA-R-2794)
neutron total cross sections of, temperature effects of magnetic order on, 18: 36034
preparation and properties of bis-(β-diketone) polymers, 17: 12188
with manganese nitrides, ferromagnetic properties of, 20: 4402(T) (ANL-Trans-230)

ZINC CYANIDES
distribution coefficients in lithium chloride ion exchange systems, 18: 25297
properties for precipitation of cesium from sea water, 17: 30726
spectra of complexes, infrared, 16: 2937
spectra of, infrared absorption, 16: 2937

ZINC, DIMETHYL-
decomposition in ion source of mass spectrometer, mechanism of, 20: 14584(R) (TID-22444)
spectra of hydrogen and lithium-7 in ether solutions of methyllithium complexes with, NMR, 20: 43393

ZINC FERRATES (III)
see also Manganese Zinc Ferrates

ZINC FERROCYANIDES
see also Cesium Zinc Ferrocyanides
ion exchange properties for cesium, 18: 27331
ion exchange properties for separation of alkali metals, tracer studies of, 18: 43721
properties for use as ion exchange material, 20: 7198

ZINC FLUORIDES
cobalt-57 electron capture decay in, lifetime of iron ions from, 19: 26393
decomposition voltage at 1100°C in calcium fluoride–thorium fluoride melts, 16: 20966
effects on freezing point depressions in sodium fluoride, 17: 37213
effects on homomolecular isotopic exchange of carbon monoxide, catalytic, 19: 26328
electrolytic effects in molten fluorides, 16: 13131 (PAN-280/IV)
growth of highly perfect single crystals of, for use in lasers, 17: 37744
hardness of crystalline divalent, 16: 10728
heat of formation, 18: 1485(R) (ANL-6687(p.153-66))
heat of formation, 17: 40421(R) (ANL-6766)
vaporization of, 17: 2956 (UCRL-9840)
AgF–ZnF_2, phase diagrams, 20: 36787 (YALE-2723(Vol.1))
CaF_2–ThF_4–ZnF_2, electric and ionic conductivity of, at 1100°C, 16: 23672 (PAN-287/IV)
KF–ZnF_2, phase diagrams, 20: 36788 (YALE-2723(Vol.2))
LiF–K_3AlF_6–ZnF_2, phase diagram of, 18: 35503 (ORNL-3594)
LiF–ZnF_2, phase diagrams, 20: 36788 (YALE-2723(Vol.2))
NaF–ZnF_2, phase diagrams, 20: 36788 (YALE-2723(Vol.2))

$RbF–ZnF_2$, phase diagrams, 20: 36788 (YALE-2723(Vol.2))
$ThF_4–ZnF_2$, analysis for thorium–zinc alloys by electrolysis at 1100°C, 17: 39209

ZINC GERMANATES
preparation of kryptonates of, by diffusion, 20: 18570(R) (NYO-2757-5)

ZINC HALIDES
spectra of molecular, electronic, 19: 34148 (UCRL-11979)

ZINC HYDRIDES
properties of diatomic ions of, use of Platt electrostatic model for calculation of, 18: 12074
spectra of normal and labeled, ultraviolet, 17: 3637

ZINC HYDROXIDES
dehydration, emanation during, 16: 31661

ZINC IODIDES
electron energy losses in, and mechanisms of, 17: 13165
equilibrium in cadmium–cadmium iodide–zinc systems, 16: 15223
iodine exchange with alkyl iodides, 19: 46294
vaporization of, 17: 2956 (UCRL-9840)
$KI–ZnI_2$, spectra of liquid equimolar mixtures of, Raman, 20: 35481(R) (ORO-2073-11)

ZINC IONS
diffusion in zinc bromide (liquid), 16: 22149
effects on contraction regulation by action potential duration in frog muscles, 19: 45736
effects on copper determination, 20: 36726
effects on foils of copper, 20: 15146
effects on hydrogen yields from radiolysis of water, 19: 26397
effects on hydrolysis of α-D-glucose 1-phosphate, 20: 16421
effects on radiation damage in ribonuclease and trypsin, 20: 32939
effects on radiobiological behavior in rats, 17: 35253(R) (IA-775)
effects on spectrophotometric determination of erbium, holmium, and neodymium, 20: 43100
effects on structure of ribonucleic acid, 19: 9157(R) (NYO-2567-1)
hydration numbers, 17: 30544
isotopic exchange of trivalent, between copper–zinc alloys and zinc sulfate solutions, 16: 22050 (NP-11764)
polarography in nitrate melt, oscillographic, 19: 2271 (EUR-1908.e)
precipitation with calcite from aqueous solutions, 20: 18631 (NYO-2266-1)
production of, source for, 19: 9457
production using laser light, 18: 34297
radioinduced reduction of divalent, gamma, 18: 17905
radiolysis of aqueous solutions of, pulse, 19: 38728
radioprotective effects in mice, 18: 13567
reactions in copper at 150 kev, thermal annealing of damage from, 20: 38378
reactions in EDTA complexes, 19: 28357
reactions with hydrated electrons, pulse radiolysis studies of, 19: 17913
salting out effects in thorium nitrate–TBP systems, 18: 13944
separation by thin-layer ionophoresis, 18: 10185
separation from metal ions by extraction using 8-quinolinethiol, 17: 10768
separation from titanium using vanillin, 19: 333
Slater-Condon parameters of, determined from spectral data, 17: 31118
solvent extraction from molten nitrate by liquid silicone–TBP at 150°C, 19: 19833 (CEA-R-2628)
sorption by aminodiacetate resin Dowex A-1, 20: 16358
sorption by cotton cloth, acidity effects on, 18: 35515
sorption from aqueous solutions by peat, 20: 7002 (INR-609/XIX/D)
sorption from perchloric acid solutions by cellulose and acid resin sulfonic acid exchangers, 18: 35473
sorption from water by peat, 20: 218(R) (STI/DOC/10/42, pp 1-22)
sorption of divalent, by phosphorus-containing ion exchangers, from acetic acid–sodium acetate solutions, 20: 35593
sorption on zirconium phosphates, tracer studies of, 19: 32293
spectra of, with o-semiquinones, electron spin resonance, 18: 39190
sputtering ratio for polycrystalline copper, 16: 9114
stability constants and structure, effects of ligand fields, 17: 28911
toxicity of, in mouse, determination by LD_{50} on thirtieth day of, 17: 17719

ZINC ISOTOPES
alpha elastic scattering by, angular distribution of, 19: 21459
alpha inelastic scattering at 44 Mev, 18: 36700
alpha inelastic scattering by even-even, 18: 40608
atomic mass comparisons for, 18: 15228
distribution and natural carriers of, in sea water, 20: 31422
energy levels, interactions, nuclear moments, and transitions in, 17: 24381 (AD-403411)
gamma emission by, radiative widths for, (E), 19: 23626 (JINR-P-1995)
gamma reactions on, cross sections for, 19: 12496
isomeric transitions, M_4-type, 16: 22985 (NP-11747)
neutron reactions (n,p) at 14.5 Mev, pairing-energy effects on, 16: 23103
nuclear moments of, theoretical configuration mixing model calculations of, 17: 14926(R) (AD-296893)
preparation, determination, and properties of radioactive, 16: 1349
preparation of foil targets of, 20: 19297 (IAE-973)
production in meson (π^-) reactions, cross sections and yields for, 17: 11650 (UCRL-10531)
proton elastic scattering at 14.5 Mev, cross sections for, 19: 47705
proton elastic scattering at 14.5 Mev, cross sections for, (E/T), 20: 34638
proton reactions (p,t) with, analytical uses of, (T), 19: 14498 (ANL-6878(p.425-48))
proton reactions at 30 Mev, 18: 42655
proton reactions at 14.5 Mev, total cross sections for, (E), 20: 42162 (LA-DC-8075)
proton reactions (p,n) at 17 Mev on even, effects of excited isobaric states, 16: 26333 (UCRL-6830)
proton reactions (p,α) at 20.5 Mev on, cross sections, 17: 33070
radiation effects on incorporation of, by blood cells, x, 20: 28922
separation from aqueous solutions, ion exchange, 17: 1176(R) (HW-70050(p.78-142))
separation of, performance of separator for, 20: 16928(R) (INSJ-92)

ZINC ISOTOPES Zn-60
energy levels of, Hartree-Fock calculations for, 20: 34564
mass, (E), 19: 31320
properties of, Hartree-Fock calculations of, (T), 20: 24323 (AD-624314)

ZINC ISOTOPES Zn-61
decay scheme for isomeric, (E), 20: 32373(R) (COO-1530-1)

ZINC ISOTOPES Zn-62
decay properties, 17: 26533
gamma spectra, 16: 11883
positron emission, half life, and production of, 18: 5179 (TID-7673(p.371-87))
production in copper-63(p,2n) reactions, 18: 1021 (ORNL-TM-663)
separation of neutron-deficient, from copper-63, 20: 43067(R) (IDO-14679, pp 6-46)
yields in proton spallation of copper at 24 Bev, 16: 24859

ZINC ISOTOPES Zn-63
decay properties, 17: 26533
energy levels, 16: 28091 (UCRL-6756)
energy levels from proton reactions (p,n) with copper-63 at 4 to 9 Mev, (E), 20: 30406
gamma spectra, (E), 19: 16840(R) (IDO-17050)
half life, (E), 19: 35441
production in gamma reactions (γ,n) at 20.5 Mev, 16: 18512
production in proton reaction with copper at 9.3 Mev, 17: 4103
separation from copper, rapid carrier-free method for, 16: 8785

ZINC ISOTOPES Zn-64
alpha inelastic scattering at 43 Mev, 16: 5957
alpha inelastic scattering, excitation by, 16: 24777 (CEA-2146)
alpha inelastic scattering at 44 Mev, 18: 16925 (ANL-6848(p.137-42))
alpha inelastic scattering at 43 Mev, collective excitations by, 17: 22627
alpha inelastic scattering at 43 Mev, collective states excited in, 17: 38266
alpha reactions (α,n) and (α,pn) at 10 to 24 Mev, cross sections and excitation functions for, (E), 19: 43316
alpha reactions at 3 to 10 Mev, gamma yields from, 16: 23065
alpha reactions with, excitation functions for, (T), 20: 32373(R) (COO-1530-1)
alpha scattering at 43 Mev, distributions from, 17: 5358
alpha scattering at 42 Mev, magnetic analysis, 16: 16542
alpha scattering at 22 Mev, angular distributions for, (E/T), 19: 10333
bremsstrahlung reactions (γ,n) and (γ,2n) at 24 Mev, direct photoeffect and evaporation contributions in, 17: 38209
determination in ratio with zinc-68 in minerals and rocks, activation, 18: 27299
deuteron elastic scattering by, cross sections for, 17: 33071
deuteron elastic scattering at 6.5 Mev, angular distributions from, (E), 19: 5251
deuteron inelastic scattering at 13.6 Mev, differential cross sections for, 17: 38259
deuteron inelastic scattering at 13.6 Mev, differential cross sections for, 17: 40016
deuteron inelastic scattering at 15 Mev, energy levels from, (E), 19: 47642
deuteron reactions (d,αn), excitation functions and thick-target yields for, 17: 17235
deuteron reactions (d,2p), excitation functions and thick yields for, 17: 17235
deuteron reactions (d,p) and (d,t) at 15 Mev, nuclear structure studies from, 18: 2932
deuteron reactions (d,n) at 11.7 Mev, neutron spectra from, (E), 19: 33365
deuteron reactions (d,p), proton polarization from, (E), 20: 6422
energy level structure of, 17: 22568 (WASH-1041)
energy levels, 16: 28071

energy levels, 18: 40608
energy levels of, determination of, from 43-Mev alpha scattering reactions, 16: 32400 (TID-16665)
fabrication as radiation target, 18: 27813(R) (ORNL-TM-428)
formation and decay in compound-nucleus reactions, 20: 38152
gamma reactions, (γ,p) with, cross sections, (E/T), 19: 14528 (LAL-1120)
gamma reactions at 20.1 to 21.2 Mev, activation cross sections, 16: 4755 (TID-13492)
gamma reactions (γ,n) at 20.5 Mev, cross sections, 16: 18512
gamma spectra from Coulomb excitation of, (E), 19: 37817(R) (ORNL-3778(p.116-19))
gamma transition at 991.7 kev following Coulomb excitation, (E), 20: 3043
helium-3 elastic scattering at 12 Mev, 18: 38144
neutron reactions (n,p) at 12 to 18 Mev, cross sections for, 17: 853
neutron reactions (n,np) and (n,pγ) at 14 Mev, cross sections for, 17: 2242 (TID-16949)
neutron reactions (n,t) at 14 Mev, cross sections and Q values for, 17: 2242 (TID-16949)
neutron reactions (n,p), separation energies for, 17: 2242 (TID-16949)
neutron reactions (n,2n) and (n,p) at 14.8 Mev, cross sections for, 17: 2242 (TID-16949)
neutron reactions (n,2n) at 14.1 Mev, cross sections for, 17: 15299
neutron reactions (n,2n) at 12 to 19.6 Mev, cross sections, 17: 19344
neutron reactions (n,p) with, product half life for, 17: 25857(R) (PR-P-56(p.4-18))
neutron reactions (n,2n) and (n,p) at 12 to 19 Mev, energy dependence of cross sections for, 17: 26618
neutron reactions (n,α) and (n,nα) at 14.8 Mev, differential cross sections, energy spectra, and level density parameters for, 17: 26606
neutron reactions (n,p) with, cross sections for fast, 17: 31056
neutron reactions (n,p), production of copper-64 by, 17: 30165
neutron reactions (n,2n) at 12–20 Mev, cross sections for, 17: 38213
neutron reactions (n,p) at 14 Mev, cross section ratio to zinc-66 and 67, 16: 6019
neutron reactions (n,2n) at 14.8 Mev, cross sections for, 16: 7072
neutron reactions (n,2n), excitation functions for, 16: 21352 (NP-11667)
neutron reactions (n,p) at 1.8 to 4.8 Mev, excitation functions, 16: 31082
neutron reactions (n,p), production of copper-64 by, 19: 2701
neutron reactions (n,p), production of copper-64 by, 19: 11253
neutron reactions (n,2n) at 14 Mev, shell effects in, (T), 19: 12536
neutron reactions (n,p), production of carrier-free copper-64 by, 19: 30267
neutron reactions (n,2n) at 12.6 to 19.6 Mev, cross sections for, (E), 19: 35378(R) (EANDC(E)-57(U))
neutron reactions (n,2n) at 12.6 to 19.6 Mev, excitation functions of, (E), 19: 35441
neutron reactions (n,2n) at 12.6 to 19.6 Mev, excitation function for, (E/T), 19: 47571 (EUR-2456.e)
neutron reactions (n,d) at 14 Mev, energy levels from, (E), 20: 4896
neutron reactions (n,2n) at 10 to 20 Mev, cross sections for, 20: 19810 (EUR-119.e(Vol.2))
neutron reactions (n,p) at 0 to 20 Mev, cross sections for, 20: 19810 (EUR-119.e(Vol.2))
neutron reactions (n,np) and (n,p) at 14 Mev, cross section, energy spectra, and angular distributions from, (E), 20: 22048
neutron reactions (n,p) at 14.8 Mev, cross sections for, (E), 20: 28447
neutron reactions (n,d) with, angular distributions from, (E), 20: 40069(R) (EANDC(E)-66(U))
neutron reactions (n,2n) at 3 Mev above threshold, cross section for, (E), 20: 46614
neutron reactions (n,2n) at 14.6 Mev, cross section for, (E), 20: 46614
neutron reactions (n,2n) and (n,p) at 13.8 to 14.8 Mev, cross sections and isomeric ratios for, 16: 21385
neutron resonance activation integrals for, 18: 1038
neutron resonance integrals for dilute solutions of, (E), 19: 29260 (TID-21744)
neutron resonance at 288 ev, radiation width of, (E), 20: 3133
neutron threshold reactions with, cross sections for, 17: 36653 (EUR-119.e)
nuclear moment of inertia, determination of, 17: 38206
production in compound-nucleus reactions, analysis of, (E), 19: 19090 (UCRL-11862)
properties as neutron threshold detector, 17: 35260(R) (TID-19135)
proton elastic and inelastic scattering at 6.8 Mev, 17: 24414
proton elastic scattering, isotopic, isotonic, and shell closure effects on polarized, 17: 19360
proton elastic scattering at 9.5 to 22.2 Mev, angular distributions and cross sections, 16: 9462
proton inelastic scattering, gamma angular distribution from, 17: 17205
proton inelastic scattering at 14.65 Mev, 16: 28071
proton inelastic scattering at 10 Mev, differential cross sections for, 18: 7763
proton inelastic scattering by, angular correlations for, 18: 7780
proton inelastic scattering by, energy level structure from, 19: 17043
proton reactions (p,p′γ) at 5.8 Mev, angular correlations for, 18: 30727 (NP-14053)
proton reactions (p,α) at 1.75 Mev, angular distributions from, (E/T), 20: 8083 (PUC-937-171A)
proton reactions (p,xpyn) at 370 Mev, cross sections for, (E), 20: 8120
proton reactions (p,p′) with, cross sections for, (T), 20: 17692 (ORNL-TM-1414)
proton reactions at 12 Mev, energy levels from, 20: 6296(R) (ORNL-3858 (Vol.1), pp 1-12)
proton reactions (p,p′γ) on, excited states from, 17: 36712
proton reactions (p,p′γ) at 5.0 Mev, second 2+ level properties, 16: 3714
proton scattering at 9.6 and 11.7 Mev by, differential cross sections for, 17: 11643 (UCRL-6930)
proton scattering at 6.9 Mev, 17: 11656
proton scattering at 9.6 and 11.7 Mev, excitation levels determined by, 17: 17239
proton scattering at 9.4–22.2 Mev, local optical potentials for, 17: 38185
proton scattering at 5.8 Mev by, gamma-proton angular correlations in inelastic, 18: 26582
proton scattering at 50 Mev, angular distributions and differential cross sections for, (E), 19: 28962(R) (NIRL/R/81)
proton scattering by, excited states from, (T), 19: 37803(R) (ORNL-3778 (p.37))
proton scattering at 12 Mev, cross sections for, 19: 47585 (ORNL-3851)
proton scattering by, isobaric analog states from, (E), 20: 44761
spectra of II, shift in ultraviolet lines of, 17: 33011
transition mixing ratios (E2/M1) for, measurement of $2^{+\prime} \rightarrow 2^{+}$, 17: 17205

ZINC ISOTOPES Zn-65

analysis of, for carrier by isotopic dilution, 20: 38814
beta decay of, intensity of 1.114-Mev gamma transition in, (E), 20: 40093
body burden in Alaska, 18: 20231 (HW-SA-3048)
chemical behavior in trace quantities, 17: 2960(T) (UCRL-Trans-599(L))
content in animals of California coast, 19: 38895
content in animals, birds, fish, and plants in region of Cape Thompson, Alaska, 1959 to 1962, 20: 7319 (PNE-480)
content in Columbia River invertebrates, 1964 and 1965, 20: 20382 (BNWL-SA-623)
content in Columbia River whitefish, 20: 20382 (BNWL-SA-623)
content in *Crassostrea virginica* in Fishers Island Sound, Conn., 17: 7783
content in deep bottom ocean feeders, sinking rates for, 18: 8526
content in fish in Barents Sea, 19: 24724
content in fish in Northeast Pacific Ocean, 20: 40523(R) (RLO-1750-8 (Vol.1))
content in fish, milk and water supplies in Hanford, Washington, Jan. to June 1965, 20: 7297 (BNWL-165)
content in Hanford personnel, 18: 36920 (HW-82409)
content in Hanford reactor effluent, 19: 685(R) (HW-81746(p.3.33-6))
content in invertebrates in Columbia River estuary, 20: 40523(R) (RLO-1750-8(Vol.1))
content in Japanese people, 19: 13681
content in marine organisms near Columbia River mouth, interspecies differences in, 17: 24866
content in marine organisms off southern California coast, 18: 32
content in marine organisms in northeast Pacific Ocean, 20: 18903 (RLO-1750-3)
content in marine organisms along Pacific coast of the United States, 20: 27159
content in nekton and macroplankton in Pacific Ocean off Oregon coast, 18: 1341(R) (TID-19608)
content in Nevada cattle in 1959, 16: 1329(R) (LAMS-2627(p.226-33))
content in ocean fish, effects of content in sea water on, 20: 11054
content in oysters in Fishers Island Sound and Thames River, Conn., 16: 1432(R) (TID-13509)
content in oysters and marine algae, 16: 32690(R) (TID-16635)
content in oysters in Thames River, Conn., 1964, 19: 631(R) (TID-21241)
content in Pacific Ocean fish livers, 18: 29208
content in particles suspended in Columbia River, 19: 622(R) (HW-81746 (p.3.84-6))
content in personnel at Hanford, summary of whole-body counter results for 1960, 18: 35760 (HW-67245(Rev.))
content in polonium process waste stream, 18: 13358(R) (MLM-1151)
content in reactor effluent water, effects of sodium silicate addition on, 18: 36752 (HW-75782)
content in reactor effluent, effect of SiO_2 on, 20: 45215 (BNWL-282)
content in reservoir water in Umatilla, Oregon, 20: 8980(R) (BNWL-36, pp 3.1-122)
content in salmon in northeast Pacific Ocean, 20: 45961(R) (RLO-1750-8(Vol.3), (Paper 2))
content in salmon, reared in Hanford reactor effluent, 20: 10538(R) (BNWL-122, pp 198-201)

content in Savannah River water, July through Dec. 1965, 20: 27195(R) (DPST-66-30-1)
content in sediments in Columbia River estuary, 20: 40523(R) (RLO-1750-8(Vol.1))
content in silts in Columbia River estuary, 20: 45890(R) (RLO-1750-8 (Vol.2)(Paper 2))
content in tissues of fin whale captured off Oregon coast, 19: 6936
content in vegetation in Northern Alaska from fallout, 17: 27053 (HW-SA-3050)
content in whales, 20: 38560
content of, in mollusks and plankton of Thames River, Conn., 17: 35407(R) (TID-19332)
content of, in marine organisms, 19: 10732
content of, in tuna from Western Pacific, 1962, 18: 27703 (UWFL-90)
contents in animals and plants from Chariot site environment, 19: 25796 (PNE-445)
contents in animals, plants, rain water, and soils from Chariot site environment, 19: 25797 (PNE-446)
contents in animals and plants from Chariot site environment, 19: 25799(R) (PNE-448)
decay in irradiated zinc sulfide crystals, copper center formation from, 19: 34230
decay of, branching ratios in, 17: 12802(R) (PR-P-55)
decay of, ratio of electron capture to positron emission in, 18: 2886
decay of, branching ratios for electron-capture, (E), 20: 19831 (NP-15912)
decay of, K conversion coefficients from, (E/T), 20: 8080 (ORNL-P-1700)
decay of, K/L ratio for electron-capture, (E/T), 20: 15713 (CONF-233 (Vol.2), pp 365-8)
decay of, peak-to-total ratios for, 18: 18884 (TID-20390)
decay of, x-ray emission rates for electron-capture, (E), 20: 15242 (CONF-233(Vol.3), pp 465-79)
decay properties, 17: 26533
deposition on aluminum, copper, and tin, 16: 7872
deposition on copper, glass, and tin, 16: 6421
deposition on platinum electrodes, procedure for electrolytic, 18: 16104
detection and measurement of, performance of whole-body plastic scintillation detector for, 19: 20377
detection in gastrointestinal tract from drinking water, continuous monitoring system for, 20: 27191 (BNWL-SA-212)
determination as impurity in phosphorus-32 by sorption in humus column, 17: 27284
determination in Alaskan vegetation, gamma spectrometric, 19: 9366 (HW-SA-3316)
determination in crushed oil shales, activation, 20: 23236(R) (ORNL-TM-1496)
determination in Columbia River plume at sea, techniques for, 20: 25282 (RLO-1750-4)
determination in IRL Reactor pool by gamma spectrometry, 17: 40702 (TID-7655(p.107-18))
determination in irradiated polyphenyls, 16: 7496
determination in irradiated stainless steel by group separation and gamma spectrometry, 18: 41325
determination in irradiated materials by extraction and precipitation, gamma spectrometric, 20: 16336(R) (NYO-10175)
determination in man, whole-body gamma spectrographic, 18: 17721 (BNL-7885)
determination in man, whole-body, 19: 2707 (BNL-8432)
determination in man, whole-body, 19: 13637
determination in mixture with cerium-144, method for, 19: 43962
determination in nuclear industrial workers by whole-body counting, quantitative, 16: 17927
determination in oysters, from Thames River, Conn., 1960 and 1961, 17: 33558
determination in Pacific Ocean, 18: 39109
determination in presence of phosphorus-32 in plant material, method for, 19: 42444
determination in reactor effluent water, monitor for, 18: 13619 (HW-66689)
determination in sediments near mouth of Columbia River, 17: 15530
determination in sewage plants, spectrometric, 17: 36063
determination in silts, use of *in situ* probe for, 19: 26267
determination in shellfish by radiochemical techniques, 19: 46218
determination in urine, gamma spectrometric, 19: 32 (HW-SA-3641)
determination in waste solutions, 16: 28863 (AERE-R-3945)
determination in zinc, radiometric, 16: 26926
determination of, in Connecticut oysters and limpets, 1961 to 1963, 18: 6598(R) (TID-19922)
determination of, in Columbia River effluent, 18: 12338 (TID-20200)
diffusion in pure and zinc-doped sodium chloride monocrystals, 18: 25969(R) (ANL-6868(p.287-302))
distribution in closed and flowing aqueous systems, 20: 6715
distribution in Columbia River effluent, 19: 46680
distribution in fish tissue, 17: 12114
distribution in mollusks of Columbia River estuary, 20: 40523(R) (RLO-1750-8(Vol.1))
distribution in pancreas of rats, 18: 31116
distribution in plankton from offshore waters of Oregon and Washington, 20: 43545
distribution in protein fractions of guinea pig serum, 20: 42791
distribution in shallow fresh-water ponds, 17: 40521 (TID-7664(p.43-60))
distribution in tissues in man, 16: 7386
distribution in tissues, tracer study, 16: 25133(R) (HW-72500(p.97-101))
distribution in water and silt of British estuaries, 20: 45224
distribution of Hanford-produced, in marine organisms, sediments, and water from coastal and offshore waters, 19: 27910 (UWFL-86)
distribution of, in *Phaseolus vulgaris* L. during seed germination and young plant development, 17: 15551
distribution of ingested, in tissues in trout, 17: 35306(R) (HW-76000 (p.111-14))
effects of chronic ingestion of, in trout, 20: 10528(R) (BNWL-122, pp 101-6)
effects of ingested, on reproduction of Habrobracon, 19: 10741 (TID-21559)
effects on antigen structure, protein fractions, and tissues in rabbits, 20: 35315
effects on erythropoietic index and iron content in man, 20: 42908
effects on habrobracon wasp and its eggs, 16: 26706
effects on immune reactions in rabbits, 20: 31112
effects on rabbits, pathological, 20: 31112
effects on yeast cells, internal, 19: 7127
electron capture decay, K-shell fractions, 16: 26336
electron capture decay of, L/K ratio, 16: 31101
electron capture ratios, M/L, 20: 40153
electron (K) capture fractions, 16: 7732
electron (K) fluorescence yields, 16: 7732
elimination by mice and rats, effects of DTPA, pectin, and zirconium phosphate on, 20: 38733
elimination of chloride-incorporated, chelation and isotope exchange methods for, 20: 18216
elution during isolation of rat liver nuclei, 18: 41051
energy levels and gamma spectra of, 19: 1589
energy levels of, isobaric-spin splitting of single-particle and single-hole, 17: 9572
exchange mechanism and rate in zinc–zinc chloride systems at 433 to 681°C, 16: 6420
excretion by man, effects of chelating agents on, 20: 1691
excretion by man, effects of chelates on, 20: 20397
excretion by rats, 17: 24869
excretion by rats, effects of deferoxamine and DTPA on, 20: 6746
formation and detection in stainless steel loop coolant, 16: 11957(R) (JAERI-5003(p.112-14))
gamma dose constants for, 20: 46617
gamma emission at 92 kev, Mössbauer spectra, 16: 23143
gamma emission from, measurement of, 18: 179
gamma specific emission coefficient, 17: 6431 (CEA-2036)
gamma spectra, 17: 16438
gamma spectra, 17: 34966
gamma spectra, 17: 34967
gamma spectra of, dependence of shape on measuring conditions of scintillation, 18: 18232
gamma spectra of, least-squares analysis of, 18: 33926
gamma spectrum, (E), 19: 20342
gamma spectrum, 18: 18174 (BRL-1230)
gamma transition at 1115.6 kev, (E), 20: 3043
half life, 20: 8076 (NP-15663)
half life of, biological, 19: 13681
half life, spectrophotometric determination, 16: 10973
hyperfine interaction constants of, 18: 5847(R) (NP-13401)
hyperfine structure, optical detection of level crossings in, 17: 8928(R) (NP-12325)
hyperfine structure of $(4s4p)^3P_1$ state of, 18: 15266
hyperfine structure and Landé g factor for, 18: 15267
ingestion by man of, in oysters, 20: 553 (BNWL-SA-293)
metabolism by algae and fish, 17: 23033 (DPSPU-63-30-3)
metabolism by animals and plants in flowing ecosystem, 20: 26607 (TID-22873)
metabolism by dairy cattle, 19: 3836(R) (ORO-625(p.70-85))
metabolism by marine organisms, 19: 43669(R) (NP-15159)
metabolism by marine fish and invertebrates, 20: 26549(R) (NP-15915)
metabolism by rat erythrocytes, effects of x radiation and plasma concentration on, 18: 35265(R) (UCLA-12-529(p.23-40))
metabolism by rats, scintillation-counter measurements of whole-body retention in, 18: 43175(R) (LA-3132-MS(p.42-8))
metabolism by swine, 19: 3835(R) (ORO-625(p.64-9))
metabolism by trophic level crustaceans of Northeast Pacific Ocean,

20: 42731(R) (RLO-1751-2)
metabolism in aquatic organisms, 20: 16160 (UCRL-14739(Pt.2))
metabolism in blood cells of swine, effects of dietary calcium, zinc, and fats on, 19: 45759(R) (ORO-631, pp 77-82)
metabolism in domestic animals, 18: 11645(R) (ORO-614)
metabolism in dragonflies, effects of body size and temperature on, 19: 45789
metabolism in fish, 20: 32914
metabolism in leukemia patient, 16: 1332(R) (LAMS-2627(p.263-9))
metabolism in mammals, effects of environment on, 19: 35904
metabolism in man, 17: 5670(R) (LAMS-2780(p.17-84))
metabolism in man, 19: 17480
metabolism in man, effects of dietary calcium on, 19: 45787
metabolism in mice, effects of irradiation, 16: 42
metabolism in mice, effects of irradiation, 16: 5209
metabolism in rabbits, 18: 43190
metabolism in rabbits, 19: 39265(R) (IA-1021)
metabolism in rat prostate, effects of hormones on, 19: 35914
metabolism in rats, effects of ethylenediaminetetraacetic acid and carrier zinc on, 19: 35906
metabolism in rats, 20: 38556
metabolism in rats, effects of calcium- and zinc-chelates of EDTA and DPTA on, 20: 42789
metabolism in salt marsh ecosystems, 20: 40573
metabolism in tropical marine organisms, 16: 5132 (TID-14420)
metabolism in trout, 18: 41036(R) (HW-80500(p.109-12))
metabolism of, in small vertebrates under natural environments, 18: 6591(R) (TID-19895)
metabolism of, in rats, effects of dietary levels of copper and molybdenum on, 18: 15794
metabolism of, in rats, effects of dexamethasone and prednisolone on, 20: 40563
methods for measuring content of, in silt, 20: 25282 (RLO-1750-4)
monitoring in human farm population near Hanford, 19: 22617
motion in soil, effects of chelating agents on, 19: 38329 (TID-20471)
nuclear magnetic and quadrupole moments, 18: 15266
nuclear spin, 18: 15266
nuclear spin and magnetic and quadrupole moments, 17: 8928(R) (NP-12325)
occurrence in marine organisms and particulate material, 17: 30255
positron spectra, 17: 32424
positron spectrum measurement, 17: 8634
precipitation from waste water, 17: 2646
preparation of high-purity, method for separating 19 impurities during, 20: 45809
preparation of reference samples for detector calibration, 18: 30073
production by neutron reactions (n,γ), 18: 37592
production in copper-65(p,n) reactions, 18: 1021 (ORNL-TM-663)
production in deuteron reactions (d,2n) with copper-65, cross sections for, 20: 16508(R) (NYO-2771-13)
production in nuclear reactions, 17: 33615
production in proton reaction with copper at 9.3 Mev, 17: 4103
production in proton reactions on copper, yields from, 17: 8153
production of, by 16-Mev cyclotron in Yugoslavia, 17: 17321
production of high-specific-activity, by Szilard-Chalmers reaction, 16: 13080 (CEA-2072)
production using Rossendorf Reactor in East Germany, 19: 20436
radiation effects on uptake in mouse testes, x, 17: 33725
radiation effects on mouse liver metabolism of, x, 18: 19531
radiation effects on mouse testicular uptake of, x, 18: 33270(R) (NIRS-2(p.23-6))
radioactivity of, absolute measurement of, 20: 15690 (CEA-R-2813)
scanning in zinc crystals, slit effects on counting rates in, (E/T), 19: 32592
scintillation spectra, relation to source thickness, 16: 4630
secretion by pig pancreas, hormonal effects on, 18: 38775(R) (ORO-624)
secretion of, in milk of sheep, 20: 10527(R) (BNWL-122, pp 94-8)
separation by isotopic exchange between aqueous solution and gallium-zinc alloy, 19: 46209
separation by solvent extraction using phosphoörganic compounds in 2,4-pentanediones and TTA, synergism in, 20: 261
separation from copper-64 and manganese-54 in sea water, method for, 20: 18576(R) (TID-22660)
separation from fission products by amalgam exchange, radiochemical, 18: 16148
separation from manganese-52, method for, 19: 46210
separation from neutron-irradiated biological materials, use of Szilard-Chalmers effect in, 20: 18583
separation from water by adsorption on minerals, 16: 25035 (HW-69225)
separation from water by precipitation on aluminum hydroxide, 18: 15688(R) (MLM-1152)
separation from water using U. S. Army equipment, 19: 36717
separation from yttrium-90 in food by solvent extraction using di-(2-ethylhexyl) phosphoric acid, 19: 15386
sorption and distribution in chicks, effects of vitamin D, 17: 23024
sorption by calcium phosphate, 16: 28639
sorption by Columbia River particulate material, 18: 35761 (HW-79279)
sorption by glass, plastic, and rubber materials, 19: 5920
sorption by guinea pig skin, disappearance measurements of, 20: 32910
sorption by mammalian erythrocytes, effect of plasma on, 18: 6597 (TID-19847)
sorption by PA-2 aluminum alloys and stainless steel, effects of pH on, 20: 25073
sorption from aqueous solutions by manganese dioxide, 16: 16389
sorption from reactor effluent by particles in Columbia River, 19: 215(R) (HW-81746(p.3.81))
sorption from sea water by montmorillonite clay, 20: 18576(R) (TID-22660)
sorption in rat gastrointestinal tract, effects of segmental ligation on, 19: 33768
sorption of, by lithium halide cation exchange resins, 17: 15992
sorption of ionic, by metal surfaces, 20: 7003 (INR-634/V/C)
sorption of orally administered, effects of dietary zinc on humans and rats, 16: 17417
sorption on Columbia River silts, 20: 45261(R) (RLO-1750-8(Vol.2), (Paper 1))
sorption on sediments in Columbia River, 19: 15784(R) (HW-83614)
spectra of, design of 4π scintillation positron spectrometer for, 18: 4125
transfer from mother to progeny in rats, 18: 13432
transfer in rats, placental, 18: 15794
transfer in rats, prenatal and postnatal, 18: 1365
transfer of, in rodent progeny, pre- and post-natal, 17: 40491 (TID-18075)
transport across intestinal membranes, 18: 43188(R) (TID-21200)
transport in aqueous environment, 20: 26608 (TID-22876)
transport in Columbia River, 20: 25290
transport in Columbia River, 19: 20(R) (HW-81746(p.3.86-94))
uptake and accumulation by plankton, seasonal variations, 20: 10536(R) (BNWL-122, pp 187-9)
uptake and distribution in sheep, dosimetry of, 16: 28712 (HW-SA-2338)
uptake and distribution by body, eggs, and excreta of hens, dietary effects on, 19: 14962
uptake and distribution in normal and tumor tissue in man, 19: 43699
uptake and distribution in clays, plants, sediments, and suspensions in aqueous environment, 20: 26608 (TID-22876)
uptake and distribution in dogs and monkeys, 20: 35214
uptake and retention of, by bone and liver in chicks, effects of breed and diet on, 17: 21447
uptake and retention by aortic tissue, hair, and organs of rats, 18: 36933
uptake and retention by marine algae, mechanisms of, 20: 8582
uptake and retention by man from Columbia River fish, 20: 30969 (BNWL-SA-45)
uptake and translocation by rough lemon and trifoliate orange rootstock, 19: 25877
uptake by algae in sea water, 19: 17469
uptake by aquatic insects, 17: 5702 (HW-SA-2848)
uptake by aquatic insects, coefficient of accumulation for, 19: 25857
uptake by aquatic foodstuffs from radioactive wastes in fresh water, 20: 18157 (BNWL-SA-466)
uptake by barley roots, mechanism for, 20: 5258
uptake by biological organisms in fresh-water pond, 18: 25079
uptake by brain tumors, 18: 1471
uptake by Columbia River algae, factors affecting, 20: 20382 (BNWL-SA-623)
uptake by Columbia River plankton, 20: 20382 (BNWL-SA-623)
uptake by crustacea, mollusks, and plankton in Bay of Venice, 20: 20386(R) (NP-15916)
uptake by Ehrlich ascites cancer cells *in vitro*, 20: 42775
uptake by euphausiids off Oregon coast, relation to Columbia River of, 18: 23182
uptake by human hair, 19: 3873
uptake by marine mollusks, 20: 40528
uptake by microscopic marine algae, 16: 26677
uptake by oysters, 19: 43663
uptake by Pacific Ocean fish, 18: 29892
uptake by plants, effects of neutrons on, 20: 6711(R) (ORNL-3849, pp 43-100)
uptake by rat hair, 20: 1695
uptake by rats, effects of age and sex on, 18: 43204
uptake by rats, effects of DTPA and unitiol on excretion of, 19: 17482
uptake by swine blood cells in vitro, effects of dietary calcium, zinc, and corn oil on, 20: 40556
uptake by tissues in rats, effects of dietary copper, molybdenum, and zinc on, 19: 35915
uptake by tissues of laying hens and chicken embryos, effects of dietary zinc and calcium on, 20: 35228

uptake by tree branches, leaves, needles, roots, and stems from soil, 19: 45773
uptake by tumor cells in mice, effects of antimony and complexes on, 19: 33783
uptake from infected intestine of chickens, 20: 36566
uptake of amino acid chelates containing, by pancreas, scintillation scanning of, 16: 7392
uptake of, by prostate gland in dogs, 17: 17730
use as gamma source in well logging, 20: 41165
use as tracer for external localization of brain tumors by positron scanning, 19: 10929(R) (NYO-1242-1)
use as tracer for DTPA excretion in rats, 20: 38556
use as tracer in biological studies, 17: 33615
use as tracer to study extraction of metal ions, 20: 45802
use in control of blast furnace lining wear, 18: 6914 (NP-13436)
use in determining metal ion adsorption on platinum catalysts, 16: 13006 (SRO-44)
use in labeling fish, 17: 7703
use in measurement of energy flow at population level, 17: 33588
use in placental permeability studies, review of, 18: 1345
use in radiation source, 17: 30785(T) (JPRS-20129)
use in scintiscanning of the prostate gland, 20: 35214
uses for determining transition temperatures of crystal systems, 20: 18677
uses of, review of diagnostic and therapeutic, 18: 17693
yields from deuteron reactions in zinc, 17: 17235
yields in copper-65 (d,2n) reactions at 20 Mev, (E), 19: 19109
yields in proton spallation of copper at 24 Bev, 16: 24859

ZINC ISOTOPES Zn-66

alpha inelastic scattering at 43 Mev, collective excitations by, 17: 22627
alpha inelastic scattering at 43 Mev, collective states excited in, 17: 38266
alpha inelastic scattering at 43 Mev, 16: 5957
alpha inelastic scattering, excitation by, 16: 24777 (CEA-2146)
alpha inelastic scattering at 44 Mev, 18: 16925 (ANL-6848(p.137-42))
alpha reactions (α,n), (α,pn), and (α,3p) at 10 to 24 Mev, cross sections and excitation functions for, (E), 19: 43316
alpha reactions at 3 to 10 Mev, gamma yields from, 16: 23065
alpha reactions with, comparison to gallium-69 proton reactions, 17: 26533
alpha scattering at 22 Mev, angular distributions for, (E/T), 19: 10333
bremsstrahlung reactions (γ,np) at 50 to 300 Mev, (E), 19: 37860
deuteron elastic scattering at 6.5 Mev, angular distributions from, (E), 19: 5251
deuteron inelastic scattering at 15 Mev, energy levels from, (E), 19: 47642
deuteron reactions (d,α), excitation functions and thick-target yields for, 17: 17235
deuteron reactions (d,p) and (d,2n) at 3 to 11.6 Mev, absolute cross sections and excitation functions for, 17: 31520
deuteron reactions (d,p) and (d,t) at 15 Mev, nuclear structure studies from, 18: 2932
deuteron reactions (d,n) at 11.7 Mev, neutron spectra from, (E), 19: 33365
deuteron reactions (d,p), proton polarization from, (E), 20: 6422
energy level transition in, M1-M2 mixing ratios as test of purity of vibrational, (T), 19: 25503
energy levels, 16: 23073
energy levels, 18: 40608
energy levels of, determination of, from 43-Mev alpha scattering reactions, 16: 32400 (TID-16665)
energy levels of, in alpha-particle model, 19: 1619
gamma spectra from Coulomb excitation of, (E), 19: 37817(R) (ORNL-3778(p.116-19))
gamma transition at 1039.2 kev following Coulomb excitation, (E), 20: 3043
neutron compound inelastic scattering at 3 Mev, angular correlation functions for, 18: 9402
neutron reactions (n,np) and (n,pγ) at 14 Mev, cross sections for, 17: 2242 (TID-16949)
neutron reactions (n,2n) at 14 Mev, cross sections for, 17: 26551
neutron reactions (n,2n) with, cross sections for fast, 17: 31056
neutron reactions (n,p) at 14 Mev, cross section ratio to zinc-64, 16: 6019
neutron reactions (n,p) with, cross section for, 18: 11195(R) (EANDC(E)-49(L))
neutron reactions (n,p) at 12.6 to 19.6 Mev, excitation functions for, (E), 19: 6669
neutron reactions (n,2n) at 14 Mev, shell effects in, (T), 19: 12536
neutron resonance at 328 ev, radiation width of, (E), 20: 3133
proton elastic scattering, isotopic, isotonic, and shell closure effects on polarized, 17: 19360
proton inelastic scattering, gamma angular distribution from, 17: 17205
proton inelastic scattering by, angular correlations for, 18: 7780
proton reactions (p,p' γ) at 5.8 Mev, angular correlations for, 18: 30727 (NP-14053)
proton reactions (p,$\gamma\gamma$) with, triple correlations in, (E), 19: 23628 (NRL-6186)
proton reactions (p,α) at 1.75 Mev, angular distributions from, (E/T), 20: 8083 (PUC-937-171A)
proton reactions (p,α) at 17.5 and 28 Mev, J-dependence of angular distributions from, 20: 32489
proton reactions (p,α) and (p,p') at 9.5 to 10.5 Mev, energy spectra from, (E), 20: 36176(R) (TID-22971, pp 41-140)
proton reactions (p,pn) at 2.9 Bev with, cross section for, 17: 22621
proton reactions (p,p'γ) on, excited states from, 17: 36712
proton reactions (p,p'γ) at 5.0 Mev, second 2+ level properties, 16: 3714
proton reactions (p,t) with, 18: 9319(R) (TID-19940(p.22-76))
proton reactions with, distributions from, (E), 19: 10257(R) (TID-21335 (p.33-107))
proton scattering at 5.8 Mev by, gamma-proton angular correlations in inelastic, 18: 26582
proton scattering by, isobaric analog states from, (E), 20: 44761
separation from zinc-67 by amalgam exchange, 19: 46899(R) (ORNL-3832, pp 33-49)
spectra of II, shift in ultraviolet lines of, 17: 33011
transition mixing ratios (E2/M1) for, measurement of $2^{+\prime} \rightarrow 2^{+}$, 17: 17205

ZINC ISOTOPES Zn-67

alpha reactions (α,2n) and (α,p2n) at 10 to 24 Mev, cross sections and excitation functions for, (E), 19: 43316
Coulomb excitation by nitrogen ions, (E), 19: 16895
Coulomb excitation of, gamma angular distribution from, (E), 19: 16896
deuteron elastic scattering at 6.5 Mev, angular distributions from, (E), 19: 5251
deuteron inelastic scattering at 15 Mev, energy levels from, (E), 19: 47642
deuteron reactions (d,αn), excitation functions and thick-target yields for, 17: 17235
deuteron reactions (d,p) and (d,t) at 15 Mev, nuclear structure studies from, 18: 2932
deuteron reactions (d,p), proton polarization from, (E), 20: 6422
energy level crossings, optical detection, 16: 13177(R) (NP-11413)
energy levels, 17: 2242 (TID-16949)
energy levels from Coulomb excitation by neon-20, 17: 4093
energy levels, hyperfine structure of metastable ^{3}P, 16: 24849
energy levels of, isobaric-spin splitting of single-particle and single-hole, 17: 9572
energy levels of, structure from isomeric transition in, (T), 20: 19970
fabrication as radiation target, 18: 27813(R) (ORNL-TM-428)
gamma decay, Mössbauer effect on 92-kev transition, 16: 13946 (JINR-P-845)
hyperfine interaction constants of, 18: 5847(R) (NP-13401)
hyperfine structure of, 17: 36442(R) (NP-13084)
hyperfine structure of $(4s4p)^3P_1$ state of, 18: 15266
hyperfine structure and Landé g factor for, 18: 15267
internal conversion coefficients for, calculations using relativistic Hartree-Fock model, (T), 20: 46699
Mössbauer effect in, bibliography on, 18: 14650
Mössbauer effect on 92-kev transition, 16: 21362(T) (AEC-tr-5115)
neutron reactions (n,p), separation energies for, 17: 2242 (TID-16949)
neutron reactions (n,p) with, copper-67 yields from, 17: 39980 (ORNL-TM-666)
neutron reactions (n,p) at 14 Mev, cross section ratio to zinc-64, 16: 6019
neutron reactions (n,p) with, copper-67 production by, 18: 41532
neutron reactions (n,p), production of copper-67 by, 19: 2701
neutron resonance at 226 ev, radiation width of, (E), 20: 3133
neutron resonance at 456 ev, radiation width of, (E), 20: 3133
neutron resonant scattering by, 20: 7430
nuclear orientation by optical pumping, 18: 13078
photon reactions (γ,p) at 5 to 30 Mev, shell effects in cross sections of, (E), 20: 34554(T)
proton reactions (p,n) with, thresholds for, (E), 19: 6704
proton reactions (p,n) at 1.5 to 5 Mev, gallium-67 levels from, (E), 20: 22053
separation from zinc-66 by amalgam exchange, 19: 46899(R) (ORNL-3832, pp 33-49)

ZINC ISOTOPES Zn-68

alpha inelastic scattering at 43 Mev, collective excitations by, 17: 22627
alpha inelastic scattering at 43 Mev, collective states excited in, 17: 38266
alpha inelastic scattering at 43 Mev, 16: 5957
alpha inelastic scattering, excitation by, 16: 24777 (CEA-2146)
alpha inelastic scattering at 44 Mev, 18: 16925 (ANL-6848(p.137-42))
alpha reactions (α,αp) at 10 to 24 Mev, cross sections and excitation functions for, (E), 19: 43316
alpha reactions at 3 to 10 Mev, gamma yields from, 16: 23065

alpha scattering at 43 Mev, distributions from, 17: 5358
alpha scattering at 22 Mev, angular distributions for, (E/T), 19: 10333
determination in ratio with zinc-64 in minerals and rocks, activation, 18: 27299
deuteron elastic scattering by, cross sections for, 17: 33071
deuteron elastic scattering at 6.5 Mev, angular distributions from, (E), 19: 5251
deuteron inelastic scattering at 13.6 Mev, differential cross sections for, 17: 38259
deuteron inelastic scattering at 13.6 Mev, differential cross sections for, 17: 40016
deuteron inelastic scattering at 15 Mev, energy levels from, (E), 19: 47642
deuteron reactions (d,He^3), excitation functions for, 17: 17234
deuteron reactions (d,p) and (d,2n) at 3 to 11.6 Mev, absolute cross sections and excitation functions for, 17: 31520
deuteron reactions (d,He^3), 16: 14378(R) (NYO-2302)
deuteron reactions (d,p) and (d,t) at 15 Mev, nuclear structure studies from, 18: 2932
deuteron reactions (d,He-3) with, analysis of, 18: 21204 (LADC-6302)
deuteron reactions (d,n) at 11.7 Mev, neutron spectra from, (E), 19: 33365
deuteron reactions (d,p), proton polarization from, (E), 20: 6422
deuteron reactions (d,p) at 15 Mev, isomeric yield ratios for, 20: 16508(R) (NYO-2771-13)
energy level transitions in, M1-M2 mixing ratios as test of purity of vibrational, (T), 19: 25503
energy levels, 16: 23073
energy levels, 18: 40608
energy levels, (E), 19: 27477
energy levels from gallium-68 decay, 16: 28066
energy levels of, determination of, from 43-Mev alpha scattering reactions, 16: 32400 (TID-16665)
energy levels of, from decay of copper-68, 18: 19057
energy levels of, 0^+, 18: 36620
excited state with energy 232 kev, 17: 17142
gamma spectra from Coulomb excitation of, (E), 19: 37817(R) (ORNL-3778(p.116-19))
gamma transition at 1077.6 kev following Coulomb excitation, (E), 20: 3043
mass difference between, and copper-68, 18: 19057
neutron activation cross section at 24 kev, (E), 20: 12135
neutron reactions (n,α) at 14.8 Mev, cross sections for, 17: 2242 (TID-16949)
neutron reactions (n,γ), cross sections for, 17: 7100 (NP-12330(p.95-6))
neutron reactions (n,γ) at thermal energies, cross sections for, 16: 29812
neutron reactions (n,p) at 14 Mev, copper-68 decay studies from, 18: 19057
neutron reactions (n,γ), activation cross section for, (E), 20: 16336(R) (NYO-10175)
neutron resonance activation integrals for, 18: 1038
neutron resonance integrals for dilute solutions of, (E), 19: 29260 (TID-21744)
neutron resonance at 530 ev, radiation width of, (E), 20: 3133
neutron total cross section, 17: 36669 (WASH-1042)
neutron total cross section, 17: 41873 (WASH-1044)
nitrogen-14 reactions (N-14, N-13), isomeric ratios in, 19: 22282(R) (NYO-1930-40)
nitrogen-14 reactions (N-14, N-13) at 40 to 150 Mev, isomeric pair production ratios in, 19: 41674 (NYO-1930-44)
preparation as radiation target material, 18: 27811(R) (ORNL-TM-198)
proton elastic and inelastic scattering at 6.8 Mev, 17: 24414
proton elastic and inelastic scattering at 11 Mev, distorted waves approximation in, 17: 38182
proton elastic scattering, isotopic, isotonic, and shell closure effects on polarized, 17: 19360
proton elastic scattering at 40 Mev, cross sections for, (E/T), 20: 30353(R) (ORNL-3940, pp 1-61)
proton inelastic scattering by, angular correlations for, 18: 7780
proton reactions (p,2p) at 80 to 430 Mev, recoil ranges in, 18: 13106
proton reactions (p,p' γ) at 5.8 Mev, angular correlations for, 18: 30727 (NP-14053)
proton reactions (p,n) with, thresholds for, (E), 19: 6704
proton reactions (p,α) at 1.75 Mev, angular distributions from, (E/T), 20: 8083 (PUC-937-171A)
proton reactions (p,n) and (p,p) with, isobaric analog states of gallium-69 from, (E), 20: 12079
proton reactions (p,n) at 1.5 to 5 Mev, gallium-68 levels from, (E), 20: 22053
proton reactions (p,α) at 17.5 Mev, J-dependence of angular distributions from, (E), 20: 32489
proton reactions (p,xp) at 100 to 400 Mev, cross sections for, 17: 5323 (NYO-8921)
proton reactions (p,2p) at 400 Mev to 6.2 Bev, cross sections and excitation functions for, 17: 11650 (UCRL-10531)
proton reactions (p,p' γ) at 4.7 Mev, second 2+ level properties, 16: 3714
proton reactions (p,2p), excitation functions for, 16: 33892
proton scattering at 6.9 Mev, 17: 11656
proton scattering at 5.8 Mev by, gamma-proton angular correlations in inelastic, 18: 26582
proton scattering by, isobaric analog states from, (E), 20: 44761
spectra of II, shift in ultraviolet lines of, 17: 33011

ZINC ISOTOPES Zn-69

beta spectra, 16: 7128
decay properties, 17: 26533
decay properties of isomeric, 17: 26533
decay scheme, 18: 18939
decay scheme (E), 18: 18939
energy levels and gamma spectra of, 19: 1589
energy levels of, structure from isomeric transition in, (T), 20: 19970
energy-level transitions from beta decay of copper-69, (E), 20: 46735
gamma dose constants for metastable, 20: 46617
gamma spectra, 17: 34966
gamma spectra, 16: 4751 (JAERI-4019)
gamma transitions in, independent particle model for M4, 19: 17051
half life of isomeric, from neutron reactions (n,γ), (E), 20: 16336(R) (NYO-10175)
isomeric-pair production by neutron activation, yield ratios of, 17: 7248
isomeric ratio, 17: 31520
production by neutron reactions (n,γ), 18: 37592
production by neutron irradiation of zinc-68, 20: 18818(P)
production of isomeric, in deuteron reactions (d,p) at 15 Mev, 20: 16508(R) (NYO-2771-13)
separation from neutron-irradiated aluminum, chromatographic, 20: 33164(T) (AEC-tr-6639, pp 28-31)
separation of isomeric, 17: 14361

ZINC ISOTOPES Zn-70

alpha reactions at 3 to 10 Mev, gamma yields from, 16: 23065
deuteron elastic scattering by, cross sections for, 17: 33071
deuteron elastic scattering at 6.5 Mev, angular distributions from, (E), 19: 5251
deuteron inelastic scattering at 13.6 Mev, differential cross sections for, 17: 38259
deuteron inelastic scattering at 13.6 Mev, differential cross sections for, 17: 40016
deuteron reactions (d,p), proton polarization from, (E), 20: 6422
gamma spectra from Coulomb excitation of, (E), 19: 37817(R) (ORNL-3778(p.116-19))
gamma transition at 883.7 kev following Coulomb excitation, (E), 20: 3043
neutron reactions (n,2n), (n,pγ) and (n,pn) at 14.8 Mev, cross sections for, 17: 2242 (TID-16949)
neutron reactions [(n,αn) + (n,nα)] at 14.8 Mev, cross sections, product half life, and Q value for, 17: 2242 (TID-16949)
neutron reactions (n,$\alpha\gamma$) and (n,αn) at 14.8 Mev, cross sections for, 17: 2242 (TID-16949)
neutron reactions [(n,αn) + (n,nα)], separation energies for, 17: 2242 (TID-16949)
neutron reactions (n,nα) at 14.7 Mev, cross section for, 17: 36707
neutron reactions (n,γ) at thermal energies, cross sections for, 16: 29812
neutron reactions (n,nα) at 14.8 Mev, cross section for, 18: 1077
neutron reactions at 14 to 15 Mev, nickel-67 production in, (E), 19: 27564
neutron reactions (n,γ), activation cross section for, (E), 20: 16336(R) (NYO-10175)
neutron reactions (n,2n) at 3 Mev above threshold, cross section for, (E), 20: 46614
proton elastic and inelastic scattering at 6.8 Mev, 17: 24414
proton reactions (p,n) with, thresholds for, (E), 19: 6704
proton reactions (p,α) at 1.75 Mev, angular distributions from, (E/T), 20: 8083 (PUC-937-171A)
proton reactions (p,n) at 1.5 to 5 Mev, gallium-70 levels from, (E), 20: 22053
proton reactions (p,γ) in stars, 16: 12308
proton scattering at 6.9 Mev, 17: 11656

ZINC ISOTOPES Zn-71

beta decay of, coincidence measurements for, 18: 30775
decay of, triple cascade in, 17: 20564(R) (TID-18442)
decay of, gamma cascades in (E/T), 19: 1570 (TID-21201)
decay scheme, 17: 29879(R) (IA-822)
decay schemes for isomers, 16: 7094
gamma dose constants for, 20: 46617
gamma emission by, 18: 8313
gamma spectra, 17: 35253(R) (IA-775)
gamma spectra, 16: 4751 (JAERI-4019)
gamma spectra, 18: 1050
gamma spectra, 18: 24657

gamma spectra and half life, 17: 29879(R) (IA-822)
half life of isomeric, from neutron reactions (n,γ), (E), 20: 16336(R) (NYO-10175)
half life of, from neutron reactions (n,γ), (E), 20: 16336(R) (NYO-10175)
neutron reactions (n,α) at 14 Mev, nuclear shell effects in cross sections for, 18: 18977
yields from helium ion-induced fission of lead-207 at 41.1 to 26.3 Mev, 20: 37996

ZINC ISOTOPES Zn-72
decay of, beta and gamma spectra from, 17: 28281
decay scheme, 17: 11723
decay scheme and half life, 17: 38119
gamma decay, 17: 29630
production in 80-Mev proton fission of terbium-159, absolute cross section for, 17: 16052(R) (TID-18261(p.44-8))
proton reactions at 2.9 Bev, isobaric yields from, 16: 23126
yield from neutron fission of uranium-235, 16: 21347 (AWRE-0-58/61)
yield in proton fission of uranium-238 at 150 Mev, kinetic energy and range of, 19: 27498
yields from helium ion-induced fission of lead-207 at 41.1 to 26.3 Mev, 20: 37996
yields from thermal and epi-cadmium neutron fission of plutonium-239, 20: 28448
yields in lead-206 helium-ion-induced fission, 18: 2844 (TID-19654)
yields in proton fission of uranium-238 at 150 Mev, excitation energy and momentum transfer of, 19: 27499

ZINC LANTHANUM NITRATES
cobalt-59 nuclear relaxation in, 17: 16014
iron-57 paramagnetic resonance in, at 4.2, 77, and 193°K, 19: 34170

Zinc Manganese Ferrates
see Manganese Zinc Ferrates

ZINC MINERALS
analysis of, use of radioisotope methods for, 20: 3884 (ORNL-IIC-5, pp 206-21)

Zinc Nickel Ferrites
see Nickel Zinc Ferrites

ZINC NIOBATES
luminescence of, self-activated, 18: 20060

ZINC NITRATES
see also Zinc Lanthanum Nitrates
analytical use for ion exchange separation of americium, curium, and rare earths, 20: 18562(R) (EUR-2640.e)
salting-out properties in uranyl nitrate extraction from aqueous solutions, 17: 10770
separation by reversed-phase partition chromatography using organophosphorus compounds, 18: 25614
solubility in aqueous solutions of uranyl nitrate, 16: 18994
spectra in tri-*n*-octylphosphine oxide solutions, infrared, 18: 10075
spectra in tributyl phosphate, infrared, 16: 31610 (AERE-R-3031)
$Th(NO_3)_4$–$Zn(NO_3)_2$, crystal structure of octahydrates, 19: 19852
$UO_2(NO_3)_2$–H_2O–$Zn(NO_3)_2$, activity coefficients of, at 25°C, 20: 29196
$UO_2(NO_3)_2$–$Zn(NO_3)_2$–H_2O, chemical potential of water in, at 25°C, 18: 3776

ZINC ORES
analysis for iron and zinc by x-ray fluorescence using tritium/zirconium source, 19: 5819
analysis for lead by absorption, 18: 13683
analysis for zinc by radioisotope x-ray fluorescence, 18: 39056 (AERE-R-4474)
analysis for zinc, activation, 18: 39121
analysis of, nomographic interpretation method in x-ray fluorescence (E), 19: 332

ZINC OXALATES
pyrolysis of anhydrous, carbon-13 isotope effects in, 18: 27424

ZINC OXIDES
analysis by x-ray fluorescence using promethium-147/aluminum source, 20: 3883 (ORNL-IIC-5, pp 154-81)
analysis, thermal, 16: 28878
catalytic effects on dehydrogenation of isopropanol, 17: 18011 (TID-18423)
catalytic effects on radioinduced polymerization of isobutene, 18: 12220
catalytic effects on radioinduced isomerization of 2-butene, 18: 23667
catalytic properties, effects of gallium and lithium on, 17: 35798
catalytic properties of, isotopic exchange studies of, 18: 13739
chemical effects on reduction of uranium(VI) oxides by decomposition products of ammonia, 18: 12056
chemical effects on radioinduced polymerization of isobutene, 19: 487
cleavage of wurtzite structure in, 18: 13729 (UCRL-7288)
composition, electrochemical method for determining deviations from stoichiometry in, 16: 32960(T) (UCRL-Trans-834(L))
crystal structure of, neutron diffraction analysis of, 18: 7213 (JINR-P-1440)
crystal structure from neutron diffraction, 18: 37674 (A/CONF.28/P/488)
dielectric losses in, frequency dependence of, 19: 19851(T) (ORNL-tr-491)
diffusion of radon-224 recoil atoms in, 17: 14275
effects of powdered, on radioinduced polymerization of isobutene and styrene, 19: 2380
effects of, as filler on tensile strength of irradiated butadiene–styrene elastomers, 18: 27594
effects on absorption of irradiated sodium silicate glass, 18: 32202
effects on densification during sintering of beryllium oxide, 19: 24963
effects on densification of thorium oxide–uranium oxide pellets, 16: 7874 (ANL-6375)
effects on density and volume changes of graphite, 17: 36202(R) (SCC-13)
effects on fritting of beryllium oxide, 18: 22500(T) (UCRL-Trans-1042(L))
effects on gamma radiolysis of aqueous solutions of benzene, 19: 44051 (AE-192)
effects on gamma-induced polymerization of isobutene, 19: 18021
effects on photolysis of nitromethane, 20: 8988
effects on physical properties and radiation stability of graphite, 18: 7305 (HW-SA-3020)
effects on radiation behavior of polymers, 18: 24199(T,R) (AEC-tr-6316 (p.359-67))
effects on radioinduced polymerization of acrylonitrile, 18: 12171
effects on radioinduced polymerization of butadiene with isobutene, 19: 7594
effects on radioinduced copolymerization, 19: 18000
effects on radioinduced polymerization of isobutylene with vinylidene chloride, 20: 403
effects on radioinduced polymerization of diphenylvinylphosphine oxide, 20: 408
effects of radioinduced polymerization of styrene, 20: 43338
effects on radioinduced polymerization of cyclohexane, isoprene, methyl methacrylate, and styrenes, 18: 10167
effects on radiolysis of water vapor, 20: 9002
effects on radiolysis of benzene in aqueous solutions, 20: 20768
effects on rate of polymerization of allyl alcohol, 20: 36880
effects on reduction of uranium trioxides by ammonia, 17: 10726
effects on spectrochemical analysis of niobium–tantalum mixtures, 17: 15899
electric conductivity, 17: 18772(R) (TID-18412)
electric conductivity of, effects of oxygen adsorption on, 17: 14370
electric properties of, effects of lattice energy and temperature on, 19: 21601(T) (ORNL-tr-490)
evaporation of, Knudsen-Langmuir studies of, 18: 39168 (UCRL-7521)
hardness of crystals of, 16: 10728
hardness of, microcrystals of, 17: 27343
incorporation into uranium dioxide lattice, 17: 27487
luminescence in, effects of traps on, 18: 10174
luminescence of, electric-field-induced, 17: 27342
luminescence yield of, effects of adsorbed oxygen on, 17: 14370
meson (μ^-) capture in, (E), 19: 37896
neutron resonance absorption integral of, (E), 20: 14008(R) (ANL-7122, pp 42-69)
oxygen exchange in, effects of additives and temperature on, 18: 10080
oxygen-18 exchange with carbon dioxide and oxygen, 20: 8899
photoconducting properties of dye-sensitized films, 18: 41302 (NP-14281 (p.219-37))
polarographic behavior in molten borax, 16: 17770
positron annihilation in, angular correlations from, 18: 33605
positronium lifetime in, (E), 20: 37819
preparation of kryptonated, by diffusion, 20: 18570(R) (NYO-2757-5)
properties for use as radiation dosimeter, 20: 7128(R) (NYO-2206-1)
radiation effects on magnetic properties, 17: 12737
radiation effects on catalytic activity in hydrogenation and isotope-exchange reactions, 17: 18125
radiation effects on catalytic activity for ethanol dissociation, 16: 20509
radiation effects on reactions with methanol, 16: 20516
radiation effects on electric conductivity, kinetics of, 16: 27707
radiation effects on sorptive properties for oxygen, review, 16: 31664
radiation effects on electric properties of, effects of radiolytic absorbent materials on, 18: 36053
radiation effects on electrodes in aqueous solutions, 18: 37769(T) (AEC-tr-6398(p.495-504))
radiation effects on catalytic reactions of, in formic acid decomposition, 19: 4196(R) (ORNL-3627(p.220-3))
radiation effects on adsorptive and catalytic properties of, for heterogeneous oxidation of carbon monoxide, 19: 17952 (CEA-R-2604)
radiation effects on, mechanisms in, 19: 20019
radiation effects on catalytic activity in conversion of cyclohexane, 19: 26417
radiation effects on catalytic properties of, 19: 26430

radiation effects on catalytic oxidation of carbon monoxide on, at 270°C, 19: 40577
radiation effects on sorption of carbon monoxide on, gamma, 19: 40578
radiation effects on catalytic effects of, on gaseous reactions, 19: 46329 (EUR-2455.e)
radiation effects on films of, on glass, 16: 21108
radiation effects on films of, on glass, 17: 5020
radiation effects on adsorbed layers of hydrogen, isobutene, and oxygen on powders of, gamma, 16: 13666
radiation effects on oxidation and reduction properties of, 20: 7128(R) (NYO-2206-1)
radiation effects on polymerization of organic compounds by, 20: 7128(R) (NYO-2206-1)
radiation effects on crystal structure of, neutron, 20: 11359
radiation effects on chemical activity of solid catalysts of, reactor, 20: 25121(R) (CU-2791-5)
radiation effects on, electron and neutron, 20: 37281
radiation effects on catalytic activity of, in decomposition of hydrogen peroxide, 20: 43364
radioinduced grafting of methyl methacrylate to surface of powders of, 18: 320
radioinduced luminescence and photoconductivity of, uv and x-ray, 20: 7128(R) (NYO-2206-1)
radioinduced luminescence and photoconductivity in, effects of oxygen and water pressure on, 20: 7128(R) (NYO-2206-1)
radioinduced photoconductivity in, effects of bromophenol, erythrosin, and pinakrytol green on sensitization of, 20: 7128(R) (NYO-2206-1)
radiolysis of azoethane adsorbed on, 18: 39316
radiolysis of azoethane adsorbed on, energy transfer in gamma, 20: 23116
reactions with aluminum oxides and lanthanum or neodymium oxides at 1400 to 1500°C, 20: 16482
reactions with uranium(IV-VI) oxide at high pressure and temperature, 16: 17966(R) (BMI-1541(Del.))
reactions with uranium oxides at high pressure and 900 to 1200°C, 16: 25302 (BMI-1585)
reactions with uranium(IV-VI) oxide, formation of uranate in, 19: 15450(T) (ANL-Trans-33(p.220-3))
reduction by carbon monoxide in absence and presence of strontium oxide, kinetics of, 16: 28943
sintering of, effects of oxygen on, 17: 1838
sintering of, mechanism of first stage in, 18: 4217(T) (AEC-tr-6159)
solubility in vanadium oxide at 685°C, enthalpy for, 20: 7072
sorptive properties for hydrogen, infrared spectral studies, 16: 31599
spectra in low frequency region, infrared, 18: 23549
spectra, infrared absorption at 2 to 22μ, 16: 18859(T) (UCRL-Trans-795(L))
spectra of suspensions of, in thin polyethylene films, infrared transmission, 19: 19917
structure of, electron microscopic studies of, 18: 8041(T) (UCRL-Trans-982(L))
structure of powdered, neutron diffraction method for determining, 18: 32174
thermal conductivity at 400, 600, and 800°C, 17: 29331(T) (AEC-tr-5872)
thermoluminescence of, mechanisms of, 17: 22275 (NP-12725)
Al_2O_3–ZnO, reactions with zirconium titanates at high temperatures, 16: 5352
Al_2O_3–ZnO, sorptive properties for phosphorus-32 and sulfur-35 in aqueous solutions, 19: 36274
CaO–CoO–V_2O_5–ZnO, analysis by x-ray fluorescence, 18: 25275
Cr_2O_3–ZnO, electric conductivity, 17: 18772(R) (TID-18412)
Fe_2O_3–MnO–ZnO, neutron magnetic inelastic cross section of, 17: 36669 (WASH-1042)
Fe_2O_3–MnO–ZnO, neutron radiation effects on magnetic properties of, 17: 2042
Fe_2O_3–NiO–ZnO, neutron radiation effects on magnetic properties of, 17: 2042
Nb_2O_5–ZnO, formation of spinel in, 17: 12597
Nb_2O_5–ZnO, phase studies, 16: 4563
Nb_2O_5–ZnO, phase studies, 19: 26846
PbO–ZnO, analysis by beta backscattering, 18: 41350
rare earth oxides–ZnO, preparation and magnetic properties of, 19: 42463
Sc_2O_3–ZnO, phase studies, 20: 29168
SiO_2–Na_2O–ZnO, absorption in gamma-irradiated, 18: 32202
2-methylpropene–ZnO, radioinduced polymerization of, effects of *n*-hexane on, 20: 23161

ZINC PERCHLORATES

reactions with dioxane, structure of addition compound formed in, 17: 4452
separation by reversed-phase partition chromatography using organophosphorus compounds, 18: 25614

ZINC PHOSPHATES

performance with radioisotopes in thermometers based on luminosity, 17: 29965
radiation effects on catalytic effects of, on gaseous reactions, 19: 46329 (EUR-2455.e)
$Sr_3(PO_4)_2$–$Zn_3(PO_4)_2$, phase equilibria and tin-activated luminescence, 16: 3009

ZINC SELENIDES

chromium-53 EPR in, parameters for, 18: 20019
displacement of selenium in, by electron bombardment, 17: 11320 (NP-12360)
dissolution kinetics, 20: 29623(R) (TID-22970, pp 121-256)
electron band structure of, high-pressure determination of, 20: 14221 (COO-1198-230)
fluorescence of rare-earth-doped, (E), 19: 17936
imperfection ionization energies and photoelectronic properties, 16: 21222
radiation damage at low temperatures in, thresholds and annealing of electron, 19: 26877 (ARL-65-60)
radiation effects on, electron, 17: 16757
radiation effects on electric conductivity of crystals of, gamma, 17: 5005
radiation effects on, ESR studies of, 20: 2492
radiation effects on double acceptor defects in n-type, 20: 2499
radioinduced defects in crystals of, correlation with thermally produced defects, 17: 37851
radioinduced defects in, fluorescence studies of, 20: 2498
radioinduced defects and fluorescence bands in, annealing of electron, 20: 28659
ZnSe–ZnS, concentration-dependent ESR in, 18: 27439

ZINC SILICATES

luminescence efficiency of, effects of excitation by alpha, beta, and ultraviolet radiation and structure and preparation on, 18: 18203
performance with radioisotopes in thermometers based on luminosity, 17: 29965
preparation of kryptonated, by diffusion, 20: 18570(R) (NYO-2757-5)
pressure effects on spectral characteristics of manganese-activated crystals of, at 1 to 7000 atm, 16: 29491(T) (AEC-tr-5293)
proton radiation effects at 30 kev on, luminescence emission, 20: 44035
radioinduced luminescence of manganese-doped, energy variation of ion, 20: 5573
sorptive properties for cesium, 17: 36995(R) (TID-19187)
sorptive properties for cesium, 18: 45155(R) (TID-20980)

ZINC SULFATES

see also Ammonium Zinc Sulfates

activity and osmotic coefficients in heavy water at 25°C, 20: 16488
analysis for bromine by activation analysis, 18: 8304
analysis for cobalt, iron, and manganese using ion exchange chromatography and activation methods, 20: 36757
analysis for copper and nickel using ion exchange and activation methods, 20: 36756
analysis for metals, interfering reactions in activation, 20: 36755
determination of, fluorescein, 18: 1487(R) (HW-77609(Sect.3))
effects of, on radiation inactivation of trypsin, 17: 33731
effects on acrylonitrile polymerization in aqueous solution, 16: 30455
effects on barley and Vicia chromosomes after ethyl methanesulfonate treatment, 18: 13568
effects on gamma-induced polymerization of acrylonitrile in aqueous solution, 18: 29716(T,R) (AEC-tr-6231(p.175-85))
incorporation in plastic neutron detection, 20: 46093
isotopic exchange of zinc(II) ions between, and copper-zinc alloys, 16: 22050 (NP-11764)
radiation effects on electric conductivity of solutions of, gamma, 20: 36912
radiolysis of hydrated, yields in, 19: 40610
radiolysis of hydrated, gamma, 20: 36903
transfer between heavy and light water, ionic hydration in, 17: 6096
transition temperature in iron or magnesium sulfates, tracer studies of, 20: 18677

ZINC SULFIDES

see also Cadmium Zinc Sulfides

activation of crystals of, by strange atoms, penetration mechanism for, 16: 13725
analysis for cobalt and nickel, spectrometric, 16: 11569
analysis for cobalt, iron, and manganese using ion exchange chromatography and activation methods, 20: 36757
analysis for copper by neutron activation, 17: 19985
analysis for metals, interfering reactions in activation, 20: 36755
band emission in copper-activated crystals of, with indium as coactivator, 16: 6876
beta backscattering, 16: 9409
bombardment conductivity pulse variation in non-uniform electric field distribution in crystals of, 16: 18185
carrier distribution in crystals of, in strongly inhomogeneous excitation, 17: 12819

charge drift velocity in crystalline, field dependence of, 19: 32048(R) (NP-15073)
chromium-53 EPR in, parameters for, 18: 20019
cleavage of wurtzite structure in, 18: 13729 (UCRL-7288)
composition of vaporous, equilibrium, 17: 33905
compressibility of, volume, (E), 19: 41984
content in atmosphere, apparatus for recording, 20: 9165(R) (BNWL-36, pp 1.1-84)
crystal structure powder diffraction patterns, 19: 17795
deposition from atmosphere on vegetation, 19: 44248 (BNL-914, pp 141-3)
deposition from flowing gas in vertical conduit, 17: 29039 (HW-73404)
deposition of, in thin layers, for alpha detection by scintillation, 17: 4847
determination after deposition on membrane filter, development of detector for, 16: 332 (HW-55917)
determination of pigment in air, recording instrument for, 19: 14906 (HW-SA-3317)
determination of trace amounts on air filters by counting phosphorescence emission, 17: 1176(R) (HW-70050(p.78-142))
determination of trace amounts of, on air filters by counting phosphorescence emission, 16: 9944 (HW-63261)
diffusion of cadmium-115 in crystals of, 19: 13977 (AD-609726)
dispersion in clean room, measurement of contamination from particulate, 19: 24747 (ORNL-TM-1049)
dissociation energy of, 17: 33906
dissociation pressure at 800 to 1100°C, 17: 28837(T) (UCRL-Trans-958)
dissolution in acid media, 16: 30790(R) (MITS-48)
dissolution kinetics, 20: 29623(R) (TID-22970, pp 121-256)
dissolution of, by aqueous sulfuric acid, kinetics of, 16: 28921(R) (TID-15718)
efficiency of copper-activated crystals of, for detection of high-energy electrons, 20: 2164
electric conductivity and luminescence of copper-activated crystals of, 16: 25413(R) (NP-11882)
electroluminescence in powdered, carrier injection, 17: 3564 (AFCRL-62-142)
electroluminescence in castor wax and tricresyl phosphate matrices, effects of polarization, 16: 20470(R) (NP-11604)
electroluminescence of crystals of, determination of frequency factor and trap depth from temperature dependence of, 17: 37881
electroluminescence of single crystals of, 16: 19540
electroluminescence of copper–manganese-activated crystals of, 16: 6557
electroluminescence of crystals of, presence of delayed recombinations in, 17: 12279
electroluminescence of unactivated and copper- and manganese-activated crystals of, 17: 12807
electroluminescence centers in crystals of, trap filling by field excitation, 17: 37882
electroluminescence of aged copper-doped, voltage dependence of, 20: 26387
electroluminescent spectra of crystals of, time-dependence of, 17: 12806
electron band structure of, high-pressure determination of, 20: 14221 (COO-1198-230)
electron bombardment of crystals of, space charge effects in ambipolar diffusion of carriers induced by, 16: 2349
electron emission mechanisms in crystals of, induced photo and thermal, 16: 860
electron paramagnetic resonance of copper- and silver-activated, 16: 30928 (NP-11996)
electron penetration depths in, at 1 to 30 kev, 18: 44476
electrophotoluminescence in d-c field, 16: 7938(R) (NP-11277)
emission characteristics of tritium-excited, 18: 23693
excitation of trivalent erbium ions in copper-containing, by a-c field, 18: 2458
fluorescence of rare-earth-doped, (E), 19: 17936
fluorescence properties of crystals of, 17: 6092
fluorescent emission spectrum of copper-activated crystals of, 16: 19489
hardness of crystals of, 16: 10728
hardness of microcrystals of, 17: 27343
imperfection ionization energies and photoelectronic properties, 16: 21222
ion penetration depths at 1 to 30 kev, 18: 44476
ion range-energy relations for, (T), 19: 30967
iron-57 luminescence and nuclear resonance absorption spectra in, 19: 19855
light centers in crystals of, nature of, 16: 6878
light emission and photoconductivity in, 16: 7938(R) (NP-11277)
luminescence band model for crystals of, 16: 10746
luminescence buildup and decay of copper-activated crystals of, 16: 21150
luminescence build-up and decay of copper-activated crystals of, 17: 8958
luminescence by beta excitation, light yields from, 17: 41565(T) (AEC-tr-6081)
luminescence centers in activated phosphors of, 18: 743 (CONF-254-1)
luminescence centers of copper-activated crystals of, reversible transformation of, 17: 31236
luminescence characteristics of copper- and silver-activated crystals of, 16: 1806(R) (NP-10912)
luminescence efficiency of, effects of excitation by alpha, beta, and ultraviolet radiation and structure and preparation on, 18: 18203
luminescence excitation of crystals of, by electrons, positive temperature coefficients and saturation of, 17: 32833
luminescence in crystals of, optical flash and quenching in, 17: 35917
luminescence intensity in crystals of, as function of electron beam density and temperature, 16: 6873
luminescence mechanisms in crystals of, 16: 33655
luminescence of chlorine-, copper-, and manganese-activated crystals of, effects of electric field on gamma, 17: 11229(T)
luminescence of copper-activated, effects of coactivators on, 17: 11228(T)
luminescence of copper and silver activated, effects of temperature on, 18: 41521
luminescence of copper-doped, quenching effects on, 19: 7480
luminescence of copper-activated crystals of, beta, 16: 2320
luminescence of copper-activated crystals of, effects of preparation method on, 16: 6874
luminescence of copper- and silver-activated crystals of, effects of lithium and titanium on, 16: 13743
luminescence of copper-activated crystals of, de-excitation effect of x ray in, 17: 11289(T)
luminescence of crystals of, model for electric-field quenching of, 17: 11362
luminescence of electric field enhancement and quenching of, 18: 13884
luminescence of thallium-activated crystals of, 16: 13742
luminescence of, effect of iron ions on, 18: 20003
luminescence of, energy and mass dependence of ion-excited, 18: 20011
luminescence of, effects of copper on photo- and x-ray-induced, 19: 17929(T)
luminescence response of silver-activated, to electrons, (E), 19: 44520
luminescent properties for determining fuel element surface contamination, 18: 12459 (HW-78268)
luminescent properties of crystals of, prepared at room temperature, 17: 12280
meson (μ^-) capture in, (E), 19: 37896
neutron absorption by boron in crystals of, efficiency of, as for slow-neutron detection, 17: 3332
particle sampling in air stream, errors in subisokinetic, 20: 20927 (BNWL-217)
performance as phosphor in radioisotope lamps, 17: 29963
performance in neutron scintillation detectors, 19: 18296
performance of crystals of, in radioisotopic self-luminous systems, 17: 29964
performance with radioisotopes in thermometers based on luminosity, 17: 29965
photoconductivity induced in films, by electron bombardment, 16: 29547
photoconductivity of crystals of, induced by electron bombardment, 16: 29547
photoelectroluminescence of single crystals of, 17: 12808
photoluminescence of dysprosium-, neodymium-, terbium-, and thulium-activated, 19: 34171
photovoltaic effect in crystals of, model for anomalous, 17: 24048 (NP-12795)
physical properties of activated crystals of, 17: 22029
preparation of crystals of, factors affecting size, form, and properties in, 17: 12237
preparation of crystals of, 16: 25878 (ARL-62-319)
preparation of scintillation screens of, method for, 20: 7441
preparation of silver-doped, for phosphor-screen alpha detectors, 20: 9260
preparation of thallium-activated crystals of, 16: 13742
preparation, properties, and performance of silver-activated, 18: 23963
properties and uses of radiation-activated luminescent phosphors of, 17: 25605(T) (AEC-tr-5700)
properties of boron-10 containing, as neutron detector, 16: 14079
properties of crystals of, as neutron detectors, 16: 31874
properties of crystals of, electrical and optical, 16: 25878 (ARL-62-319)
properties of rare earth-doped, as optical masers, 19: 23164(R) (SU-SEL-64-103)
properties of rare earth doped, electric and optical, 20: 20122
properties of silver-activated, for scintillation counting of carbon-14 and tritium in chromatographic flow cells, 19: 22118
properties of silver-activated, in radiation dosimetry, 19: 30557
radiation effects on luminescence and quenching centers of activated, 17: 28995

radiation effects on luminescence, 16: 13296 (PAN-248/XIII)
radiation effects on electric conductivity and luminescence of, electron, 18: 17910
radiation effects on excitation spectra of copper-activated and pure, fast neutron, 18: 24575
radiation effects on luminescence, 19: 19967
radiation effects on absorption spectra of, neutron, 19: 32209
radiation effects on ESR in, asymmetry and annealing of neutron, 19: 32210
radiation effects on, thermal neutron, 19: 34230
radiation effects on luminescence of, electron, 19: 40587
radiation effects on luminescence of, electron, gamma, and uv, 19: 44757
radiation effects on spectra of copper-activated crystals of, neutron, 17: 1539
radiation effects on crystals of, 17: 5039(R) (ORNL-3364(p.85-124))
radiation effects on electric conductivity of crystals of, gamma, 17: 5005
radiation effects on electron spin resonance and luminescence in crystals of, neutron, 17: 30127
radiation effects on luminescence of copper- or silver-activated crystals of, neutron, 17: 34493
radiation effects on thermoluminescence of crystals of, neutron, 17: 34494
radiation effects on electron spin resonance of copper- or silver-activated crystals of, neutron, 17: 34495
radiation effects on optical transmission spectra of single crystals of, fast-neutron, 20: 31272
radiation effects on electric conductivity and Hall effect in monocrystals of, fast-neutron, 20: 36865
radiation effects on scintillation properties of silver-activated, 20: 41342
radioinduced damage in single crystals of, thermoluminescent trapping states from electron, (E), 20: 13990
radioinduced phase transitions in, fast neutron, 18: 23665
radioinduced scintillation in silver-doped single crystals of, temperature quenching of alpha, electron, and proton, 20: 23505
radioinduced thermoluminescence of, electron, gamma, and uv, 19: 32231
radioluminescence output-function of silver-doped, correlation with scintillation-spike duration from alpha, 20: 24637
reactions with yttrium sulfide, 16: 18864
sampling of particles of, in isokinetic and subisokinetic air streams, 20: 39103(R) (BNWL-235-3, pp 51-69)
scavenging from aerosols by rain, effects of drop size on, 19: 4397(R) (HW-83602)
solubility in sulfuric acid, 16: 17881(R) (MITS-47)
sorptive properties for copper, mercury, and silver, 18: 1614(R) (ORNL-3488(p.65-90))
spectra of copper–indium-activated crystals of, 17: 12810
spectra of crystals of, effects of electric fields on absorption-edge, 17: 12809
spectra of dysprosium-doped crystalline, emission, (E), 19: 39269(R) (SU-SEL-64-133)
spectra of neutron-irradiated, optical quenching of ESR, 18: 23664
spectra of terbium-doped crystalline, emission, (E), 19: 39269(R) (SU-SEL-64-133)
structure of crystals of, 16: 16804 (AFOSR-2300)
surface structure of unactivated and copper-activated crystals of, effects of darkening in moist air on, 16: 20477
trap properties of electroluminescent phosphors of crystals of, 17: 32834
use as intensifying screen for reducing radiation doses in radiography, 20: 33130
use in dual atmospheric tracer technique, 19: 44800 (BNWL-103)
use of photostimulated crystals of, in radiation dosimetry, 20: 40333
use of silver-activated, for preparation of neutron scintillation detector, 16: 1005(T) (UCRL-Trans-689)
use of silver-activated, as intensifier in alpha autoradiography, 20: 12563
use of silver-activated, in solid angle alpha counter, 20: 46056(T) (NP-tr-1428)
use with fluorescein to study atmospheric dispersion and transport, 17: 20193 (HW-70892)
x-ray intensities of one-dimensional disordered Wurtzite crystals, 18: 6575(T) (AI-Trans-20)
x-ray absorption by, energy dependence of, 19: 46150
Al–Cu–ZnS, electroluminescence of, temperature dependence of (E), 19: 383
CdS–ZnS, luminescence of, electric-field effects on alpha-induced, 19: 448
CdS–ZnS, performance of crystals of, in radioisotopic self-luminous systems, 17: 29964
CdS–ZnS, radioluminescence of copper-doped, from beta emission from promethium-147, 20: 33645
Cl–ZnS, electroluminescence in magnetic field of thin film of, 18: 1126(R) (NBS-7973)
Cu–ZnS, electroluminescence of thin film of, in magnetic fields, 18: 1126(R) (NBS-7973)
FeS_2–PbS–SiO_2–ZnS, analysis for lead, x-ray fluorescence, 19: 5825
FeS_2–PbS–SiO_2–ZnS, analysis for lead by gamma-excited x-ray fluorescence, 19: 24477
fluorescein–ZnS, performance as atmospheric tracer, 20: 9165(R) (BNWL-36, pp 1.1-84)
Mn–ZnS, electroluminescence in magnetic field of thin film of, 18: 1126(R) (NBS-7973)
plastic–ZnS, design of phosphor using, 18: 31646(P)
UO_2SO_4–H_2O–ZnS, phase studies at 200 to 360°C, 19: 17868
ZnSe–ZnS, concentration-dependent ESR in, 18: 27439

ZINC SYSTEMS
Al–C–Nb–Zn, phase studies, 20: 15103
Al–C–Ta–Zn, phase studies, 20: 15103
As–Cu–Sn–Zn, corrosion of arsenical Admiralty metal by simulated N-reactor secondary water, 17: 37480 (HW-76358)
As–Sn–Zn, radiation effects on thermal conductivity of superconducting, 20: 2488
$CaCl_2$–CaF_2–Mg–$MgCl_2$–Zn, corrosive effects on silicon carbide at high temperatures, 19: 17176(R) (ANL-6965(p.1-41))
$CaCl_2$–Mg–$MgCl_2$–MgF_2–U–Zn, reactions with alumina crucibles at 800°C, 17: 36860(R) (ANL-6648)
C–Co–Zn, phase studies of, atomic size effects in, 19: 23111
Cd–Cu–S–Zn, radiation and temperature effects on luminescence of, 17: 37642(R) (ARF-1214-TR-3)
Cd–I–Zn, equilibrium pressure of iodine in, at 831°K, 16: 15223
Cd–LiCl–Mg–$MgCl_2$–NaCl–U–Zn, corrosive effects on reactor materials, 18: 36751 (ANL-6912)
Cd–Mg–UCl_4–Zn, corrosive effects of, on stainless steel at 650°C, 20: 31314(R) (ANL-7175, pp 1-41)
C–Fe–Zn, phase studies of, atomic size effects in, 19: 23111
C–Hf–Zn, structure of filled Ti_2Ni type compounds in, 19: 37107
C–Mn–Zn, magnetic properties of Mn_3ZnC in, 20: 22312(R) (AD-622796)
C–Mn–Zn, phase studies of, atomic size effects in, 19: 23111
C–Nb–Zn, structure of filled Ti_2Ni type compounds in, 19: 37107
C–Ni–Zn, phase studies of, atomic size effects in, 19: 23111
Co–N–Zn, crystal structure, 16: 2259
Co–N–Zn, phase studies, 16: 16768
C–Ti–Zn, structure of filled Ti_2Ni type compounds in, 19: 37107
C–Zn–Zr, structure of filled Ti_2Ni type compounds in, 19: 37107
Hf–N–Zn, structure of filled Ti_2Ni type compounds in, 19: 37107
Hg–Zn, optical maser collision processes in, 18: 32484
LiCl–KCl–Zn, properties for use in countercurrent extraction of thorium and uranium, 19: 34272
LiCl–KCl–Zn–$ZnCl_2$, reactions with uranium monocarbide at 580 to 802°C, 19: 24482 (IS-1061)
LiCl–KCl–Zn–$ZnCl_2$, reactions of uranium monocarbide at 540 to 802°C in, 20: 2404
LiCl–$MgCl_2$–MgF_2–Zn–$ZnCl_2$, corrosive effects on tungsten alloys at 800°C, 17: 36860(R) (ANL-6648)
LiCl–Mg–$MgCl_2$–MgF_2–Zn–$ZnCl_2$, corrosive effects on anodized beryllium at 800°C, 17: 36860(R) (ANL-6648)
LiCl–Mg–$MgCl_2$–NaCl–Zn, corrosive effects on reactor materials, 18: 36751 (ANL-6912)
Mg–$MgCl_2$–Zn, distribution studies in, 17: 3871
Mn–Zn–Fe_3O_4, neutron magnetic inelastic cross section of, 17: 36669 (WASH-1042)
Nb–N–Zn, phase studies, 19: 42872
Nb–N–Zn, structure of filled Ti_2Ni type compounds in, 19: 37107
Nb–O–Zn, phase studies, 19: 42872
N–Ti–Zn, structure of filled Ti_2Ni type compounds in, 19: 37107
N–V–Zn, lattice parameters of filled β-manganese structure phases in, 19: 37109
N–Zn–Zr, structure of filled type Ti_2Ni compounds in, 19: 37107
UC–Zn, reactions with potassium chloride–lithium chloride–zinc chloride at 500 to 800°C, 20: 14991
Zn–$ZnCl_2$, analysis of, spectrophotometric, 18: 3671(R) (BNL-799 (p.26-54))
Zn–$ZnCl_2$, electromotive force measurements on, 17: 40815
Zn–$ZnCl_2$, electromotive force studies of species in liquid, 18: 11511 (NAA-SR-8881)
Zn–$ZnCl_2$, free energy of solution of, 19: 11103
Zn–$ZnCl_2$, zinc-65 exchange mechanism and rate in, at 433 to 681°C, 16: 6420

ZINC TANTALATES
luminescence of, self-activated, 18: 20060

ZINC TELLURIDES
chromium-53 EPR in, parameters for, 18: 20019
electron band structure of, high-pressure determination of, 20: 14221 (COO-1198-230)
imperfection ionization energies and photoelectronic properties, 16: 21222

optical rectification in, with laser beams, (E/T), 19: 31647 (TID-21807)
radiation effects on electric conductivity of, gamma, 17: 5005
tellurium-125 Mössbauer effect in, (E), 20: 20148
ZINC TETRATHIOCYANATOMERCURATE(II)
precipitation with microquantities of cerium-144, cesium-137, and strontium-89, 20: 20619
ZINC TITANATES
radiation effects on electric conductivity, slow-neutron, 16: 24266
ZINC TUNGSTATES
luminescence decay after excitation with uv light and electrons, 16: 19539
ZINC URANATES
formation and structure of, from reactions of zinc oxide with uranium oxide, 19: 15450(T) (ANL-Trans-33(p.220-3))
preparation and properties, 18: 20012
Zinn Fast Reactor
see Experimental Breeder Reactor
Zippers
see Fasteners
ZIRCALOY-2
alloy element distribution in bulk metal and oxide film on, 20: 5851
analysis for boron by direct absorptiometric method, 17: 5965 (PG-Report-362)
analysis for boron, spectrophotometric, 17: 21641
analysis for distribution of alloying elements in, using electron microprobe, 17: 27746(R) (DPST-63-71-1)
analysis for hydride contamination, eddy-current, 18: 27750(R) (HW-79280(p.7.1-22))
analysis for hydrogen, chromatographic, 17: 2909(T,R) (EURAEC-383)
analysis for hydrogen by micrograph studies, 19: 11680
analysis for hydrogen by isotopic equilibration, 19: 19831
analysis for hydrogen, method for, 20: 766(R) (EURAEC-1445)
analysis for impurities, spectrographic, 20: 29113
analysis for oxygen, activation, 17: 497(R) (KAPL-2000-19(p.I.1-I.28))
analysis for oxygen by argon carrier fusion method, 18: 21969
analysis for oxygen by isotope dilution, comparison with vacuum fusion method, 19: 26245
analysis for oxygen, activation, 20: 3907
analysis of, by electron microprobe and x-ray fluorescence spectrometer, 17: 24687(R) (SRO-82)
analysis of, for tungsten by solvent extraction using 8-quinolinol, 17: 19952
analysis of moderator cladding, for hydrogen and oxygen, 19: 12865(R) (NAA-SR-10501)
analysis of surface layers of water-d_2-oxidized, for deuterium, activation, 19: 7351
anisotropy in, strain and yield, 20: 4304(R) (ORNL-3870, pp 171-83)
bibliography on properties of, 19: 39097 (GEMP-346)
bonding of aluminum to oxidized, effects of flow pattern on extrusion, 19: 26783 (AECL-2244)
bonding to aluminum and stainless steel, explosive, 19: 26780 (AECL-2209)
bonding to aluminum, extrusion, 19: 26782 (AECL-2243)
bonding to aluminum, diffusionless, 19: 28774 (CRE-1139)
bonding to aluminum, extrusion process for, 19: 28775 (CRE-1195)
bonding to aluminum, method for diffusionless, 20: 46179(P)
bonding to graphite, process using copper, 18: 37663 (NAA-SR-9604)
bonding to Inconel 600, explosive, 18: 29043 (GNEC-345)
bonding to Inconel-800 and stainless steel, 19: 10541(R) (GEAP-4703)
bonding to Inconel, methods for, 19: 19380(R) (CEND-513)
bonding to steel, hot-swaging method for diffusion, 20: 27456
bonding to thorium, effects of fabrication on, 19: 14806(R) (HW-81984 (p.5.1-55))
bonding to type 304 stainless steel, diffusion, 20: 13222
bonding to uranium–zirconium fuels, mechanisms of, 20: 39361 (WAPD-305)
bonding to Zircaloy, methods of cleaning for, 18: 4216 (WAPD-TM-375))
bonding to Zircaloy, gas pressure, 18: 29058 (WAPD-BT-30(p.65-79))
brazing to stainless steel, 17: 4889(T,R) (EURAEC-322)
brazing to stainless steel, 18: 14361(R) (EURAEC-254)
brazing to thorium fuels, evaluation, 17: 31681(R) (HW-76559)
brittleness of, effects of hydrogen on, 19: 18498
brittleness of, effects of hydrogen on, 20: 11227
burst strength of, effects of temperature on, 18: 8866(R) (HW-78388 (p.8.1-7))
burst strength of, effects of temperature on, 18: 7297(R) (HW-77954 (p.6.3-4))
burst test of irradiated pressure tube of, 17: 39667 (HW-77855)
bursting of cladding tubes of, in loss-of-coolant accident in boiling and pressurized water reactors, 17: 32620
cadmium contamination of reactor surfaces exposed to heavy water (E), 19: 3618 (CEA-R-2504)
cesium ion deposition on, under oxidizing conditions, 18: 5747
chloride ion deposition on, under oxidizing conditions, 18: 5747
cladding thickness testers for, 17: 6391 (DP-663)
coating of, with uranium dioxide by spraying, 16: 3814(R) (ATL-A-121)
coating with aluminum for hydrogen barrier, 17: 36298 (NAA-SR-Memo-8060(Rev.))
coating with copper, 18: 39846
coating with copper, method for electrolytic, 18: 44109
coating with copper to prevent hydrogen absorption, electrolytic, 20: 5867
compatibility with lead telluride at 600 to 700°C, 17: 23927 (WCAP-1703)
compatibility with bismuth germanium telluride and lead telluride at 500 to 700°C, 17: 23971 (WCAP-1868)
compatibility with fissionable materials, 17: 29255 (ZFK-WF-13)
compatibility with uranium nitrides at high temperatures, 18: 542(R) (BMI-X-10061)
compatibility with plutonium carbide–uranium carbide, 18: 8729 (UNC-5074)
compatibility with plutonium carbide–uranium carbide systems at 1100 and 1500°F, 18: 16426(R) (UNC-5068)
compatibility with aluminum–plutonium alloy at 600°C, 18: 26893(R) (ANL-6868(p.11-108))
compatibility with uranium nitrides at 700 to 900°C, 18: 32035(R) (BMI-X-10073)
compatibility with uranium nitrides at 600 to 900°C, 18: 32037(R) (BMI-X-10092)
compatibility with uranium nitride at 900°C, 18: 34035(R) (BMI-X-20053)
compatibility with uranium nitride, 19: 2717(R) (BMI-X-10100)
compatibility with plutonium carbide–uranium carbide, 19: 24923(R) (UNC-5081)
compatibility with Incoloy and Zircaloy-2 at 475 to 1200°C, 20: 5914(R) (GEAP-3771-17)
compatibility with aluminum, copper, and nickel, 20: 23613
compatibility with cadmium sulfate, 20: 38447 (WCAP-2867)
corrosion, 18: 5753
corrosion and hydrogen absorption by electron-beam-welded nickel-free, 20: 25489 (WAPD-TM-533)
corrosion and hydrogen absorption by nickel-free and normal, effects of silicon on, 20: 25490 (WAPD-TM-544)
corrosion and oxidation of annealed and etched, by air and water, 20: 4319 (EURAEC-1457)
corrosion at RT by deionized water, 17: 31681(R) (HW-76559)
corrosion behavior of, effects of alloying elements on, 17: 19611(R) (DP-825)
corrosion by acid lithium chloride at 55°C, 19: 28214(R) (ORNL-3739)
corrosion by ammonium hydroxide, lithium hydroxide, steam, and water at high temperatures, hydrogen sorption from, 18: 21643(R) (WAPD-MRP-107)
corrosion by ammonium and lithium hydroxides, 18: 22442 (KAPL-M-6102)
corrosion by ammonium hydroxide, lithium hydroxide, steam, and water at high temperatures, hydrogen sorption from, 18: 29060(R) (WAPD-MRP-108)
corrosion by ammonium hydroxide, lithium hydroxide, steam, and water at high temperatures, hydrogen sorption from, 18: 45034(R) (WAPD-MRP-109)
corrosion by ammonium hydroxide, lithium hydroxide, steam, and water at high temperatures, hydrogen sorption from, 19: 12785(R) (WAPD-MRP-110)
corrosion by aqueous solutions, electrochemistry of, 17: 25066(R) (ORNL-3417(p.69-76))
corrosion by aqueous homogeneous reactor solutions, 18: 2190
corrosion by aqueous solutions, review, 18: 32081 (A/CONF.28/P/243)
corrosion by aqueous solutions, galvanic, 18: 41959 (WCAP-1844)
corrosion by boiling water, 18: 3134(R) (GEAP-4094)
corrosion by boiling hydrochloric acid, effects of oxygen on, 18: 27280(R) (ORNL-3597)
corrosion by boiling lithiated water in crevices of simulated PRTR fuel elements, 19: 40965 (BNWL-83)
corrosion by borated water at 600°F, 20: 5846
corrosion by boric acid at 600°F, 19: 42816 (WCAP-3725)
corrosion by carbon dioxide at 450°C, 17: 27730(R) (HW-77052)
corrosion by carbon monoxide at 600°C, 18: 7141(R) (HW-77954(p.5.14-15))
corrosion by carbon dioxide and carbon monoxide, 18: 7147(R) (HW-78962 (p.5.1-12))
corrosion by carbon dioxide at 800 to 1300°F, 18: 12576 (GEAP-4089 (Vol.I)(Paper 3))
corrosion by chemical cleaning, evaluation of, 19: 36984
corrosion by coolant in HWCTR, 19: 46917(R) (DP-975)
corrosion by deuterated lithium hydroxide, 18: 27856(R) (HW-79280 (p.9.1-4))
corrosion by deuterated and undeuterated lithium hydroxide solutions at 275°C, 18: 1440(R) (HW-79766(p.5.1-16))
corrosion by flowing water at 300 and 320°C, (E), 19: 24941

corrosion by fuel storage-basin water, electrochemical, 20: 28853(R) (IDO-14661, pp 45-82)
corrosion by fused potassium nitrate–sodium nitrate–sodium nitrite mixture at 400 to 600°C, 20: 25506
corrosion by fused potassium nitrate–sodium nitrate–sodium nitrite mixture at 400 to 600°C, 20: 25506
corrosion by heavy-water steam at 400°C, 17: 27730(R) (HW-77052)
corrosion by heavy water at 275°C, 18: 7142(R) (HW-77954(p.5.16-17))
corrosion by heavy water, 18: 7148(R) (HW-78962(p.5.13-23))
corrosion by heavy water in HWCTR, 19: 11668(R) (DP-945)
corrosion by high-pressure flowing steam at 300, 400, and 500°C, 17: 34346(R) (GEAP-4211)
corrosion by high-temperature aqueous solutions, effects of copper sulfate on, 18: 22446(R) (ORNL-3591(p.77-83))
corrosion by high-temperature water, fretting, 19: 40961
corrosion by hydrochloric–nitric acid solutions, 17: 25090(R) (ORNL-3417(p.280-2))
corrosion by hydrochloric and nitric acids, 18: 14410 (ORNL-3558(p.104-12))
corrosion by hydrochloric and nitric acids, 18: 22173(R) (ORNL-3591 (p.201-4))
corrosion by hydrochloric acid, effects of additives and oxygen on, 19: 7263(R) (ORNL-3651)
corrosion by hydrochloric–nitric acids, 19: 28214(R) (ORNL-3739)
corrosion by hydrochloric acid–organic mixtures, 19: 28214(R) (ORNL-3739)
corrosion by hydrochloric acid, hydrogen pickup in, 19: 30671(R) (ORNL-3789(p.122-5))
corrosion by hydrogen–water vapor in crevices in mechanical structures of, mechanism for, 20: 7497(R) (BNWL-150, pp 3.1-30)
corrosion by hydrochloric acid, 20: 23602(R) (ORNL-3913, pp 53-73)
corrosion by hydrochloric acid at 35 to 105°C, 20: 41039(R) (ORNL-3880)
corrosion by hydrogen, carbon monoxide, and water, effects of oxide films on, 18: 44037(R) (HW-82651(p.5.1-33))
corrosion by iodine vapor, mechanisms of, 20: 25505
corrosion by irradiated water, 18: 14407(R) (HW-79766(p.5.1-16))
corrosion by irradiated water, 18: 27857(R) (HW-80284(p.9.1-3))
corrosion by lithiated water at 550°F, effects of annealing on, 17: 11132 (KAPL-M-AA-4)
corrosion by lithium hydroxide solutions at 300°C, 18: 5743 (HW-78819)
corrosion by lithium hydroxide, steam, and water at high temperatures, hydrogen sorption from, 18: 7932(R) (WAPD-MRP-106)
corrosion by moist hydrogen at 100 to 200°C, 19: 16217(R) (HW-84281 (p.5.31-5))
corrosion by molten fluoride salts, cathodic protection in, 20: 35853
corrosion by nitrate–nitrite fused salt mixture at 400 to 600°C, 17: 25724 (TID-18773)
corrosion by oxygen and water vapor at high temperatures, kinetics of, 17: 495 (HW-73511)
corrosion by oxygen and steam at 500°C, 17: 32520
corrosion by oxygenated sodium at 650°C, 18: 19456(R) (ANL-6840)
corrosion by potassium hydroxide and potassium sulfate at 50 to 90°C, effects of electrode potential on, 20: 16979
corrosion by reactor solutions, radiation effects on, 17: 25066(R) (ORNL-3417(p.69-76))
corrosion by reactor environments, effects of preoxidation on nickel-free, 20: 5851
corrosion by Santowax OM coolant at 320 to 400°C, out-of-pile and in-pile, 19: 13911 (AECL-2118)
corrosion by sodium, temperature dependence of, 18: 25937
corrosion by steam and water, 17: 6581
corrosion by steam at 280 to 500°C and 15 to 800 lb/in.², 17: 12619
corrosion by steam at 400°C and water at 360°C, effects of nitrogen, oxygen, and silicon on, 17: 27751 (WAPD-T-1567)
corrosion by steam at 300, 400, and 500°C, 17: 32484(R) (GEAP-4284)
corrosion by steam–water spray, 17: 35093(R) (EURAEC-622)
corrosion by steam–water system, 17: 34092(R) (EURAEC-299)
corrosion by steam and water, alloying effects on, 17: 37495(T) (TRG-Inf-Ser-100)
corrosion by steam at 500°C, 17: 39468(T,R) (EURAEC-520)
corrosion by steam at 300, 400, and 500°C, 18: 545(R) (GEAP-4368)
corrosion by steam at 750°F and 1,500 psi, effects of new heat treatment procedure on, 18: 570
corrosion by steam–water mixtures, 18: 8476(R) (EURAEC-830)
corrosion by steam at 750°F and 1500 psi, 18: 10452 (TID-20058)
corrosion by steam at 400°C, hydrogen pickup in, 18: 10471 (HW-67437)
corrosion by steam at 750°F, 18: 12558 (ORNL-TM-739)
corrosion by steam at 300, 400, and 500°C, 18: 12542(R) (GEAP-4484)
corrosion by steam at 400°C hydrogen pickup in, 18: 14545(T,R) (EURAEC-863)
corrosion by steam and water, effects of nitrogen, oxygen, and silicon on, 18: 16440 (WAPD-283)
corrosion by steam–water sprays, 18: 17999(R) (EURAEC-923)
corrosion by steam–water mixtures, 18: 20182 (TID-7694(p.108-49))
corrosion by steam at 350, 400, and 480°C, 18: 20476(T,R) (EURAEC-916)
corrosion by steam at 350 and 480°C, 18: 22428(T,R) (EURAEC-838)
corrosion by steam at 400°C, hydrogen sorption during, 18: 34060(T,R) (EURAEC-1062)
corrosion by steam and water in reactor environment, 18: 34076 (TID-8540(p.213-330))
corrosion by steam-water flows, 18: 37636 (A/CONF.28/P/574)
corrosion by steam and water, 18: 37612 (A/CONF.28/P/477)
corrosion by steam and water, 18: 37635 (A/CONF.28/P/445)
corrosion by steam at high pressure and temperature, effects of flexing on, 18: 44037(R) (HW-82651(p.5.1-33))
corrosion by steam, impedance measurements on film formation in, 18: 44089
corrosion by steam–water sprays, 19: 1875(R) (EURAEC-1011)
corrosion by steam at 400°C, effects of dispersed yttrium oxide on, 19: 7930
corrosion by steam and water at high temperatures, 19: 22870(R) (HW-83601)
corrosion by steam, effect of selected fabrication variables on, 19: 26767(R) (GEAP-4821)
corrosion by steam, influence of the structure on, 19: 30682
corrosion by steam under nuclear superheat reactor conditions, 19: 45572(R) (GEAP-4755)
corrosion by steam–water sprays, 20: 6566(R) (EURAEC-1382)
corrosion by steam, effects of heat treatments on, 20: 5846
corrosion by steam at 750°F or water at 680°F, effects of nitrogen and oxygen additions on, 20: 5851
corrosion by steam at 2000°F, 20: 5851
corrosion by steam, 20: 9427 (WAPD-TM-546)
corrosion by steam at 1200 to 1600°C, 20: 9378(R) (GEMP-54A)
corrosion by steam and water, effects of nitrogen and oxygen interstitial impurities on, 20: 25499
corrosion by steam at 1200 and 1400°C, 20: 27430(R) (GEMP-400A, pp 203-20)
corrosion by steam and water at high pressures and temperatures, 20: 33815(R) (EURAEC-1625)
corrosion by steam at high temperatures, 20: 41422
corrosion by stream and water, 18: 30134(T,R) (EURAEC-955)
corrosion by steam and water, effects on tensile properties, 19: 4616(R) (EURAEC-1161)
corrosion by steam, 18: 39847
corrosion by superheated steam at 500°C, hydrogen sorption during, 17: 39470(T,R) (EURAEC-619)
corrosion by superheated steam at 400°C, 18: 8735(T,R) (EURAEC-782)
corrosion by superheated steam at 500°C and water at 350°C, hydrogen uptake from, 18: 14386(T,R) (EURAEC-822)
corrosion by terphenyl, 19: 2759
corrosion by Tramex Process solutions, 17: 12183(R) (ORNL-3375)
corrosion by uranyl sulfate solution at 280°C, in-pile, 17: 27750 (ORNL-3099)
corrosion by water at 600°F, radiation effects on, 17: 1131 (YAEC-182 (Pt.I))
corrosion by water at 680°F and by steam at 750°F, 17: 6561(R) (ARF-2198-34)
corrosion by water at 360°C, effects of heat treatment in salt, 17: 11097(R) (NMI-7257)
corrosion by water at 680°F, 17: 30905(R) (ARF-B198-42)
corrosion by water at 320°C, effects of welding on, 17: 36236
corrosion by water, 18: 2188
corrosion by water at 540°F, 18: 7138(R) (HW-77954(p.5.1-4))
corrosion by water, effects of beryllium and uranium on, 18: 7148(R) (HW-78962(p.5.13-23))
corrosion by water, in-pile, 18: 14407(R) (HW-79766(p.5.1-16))
corrosion by water at 260 and 280°C, 18: 22450
corrosion by water, oxide film tenacity and release of retained film radioactivity in, 18: 24082 (HW-79811)
corrosion by water and steam, additive effects of nitrogen and oxygen on, 18: 27884 (KAPL-2000-21(p.VI.1-4))
corrosion by water at high temperatures, composition effects on, 18: 37644
corrosion by water, 18: 37633 (A/CONF.28/P/342)
corrosion by water and steam, in-pile, 18: 41933 (TID-11295(3rd Ed.))
corrosion by water vapor at 300 to 500°C, 19: 2760
corrosion by water or water vapor in radiation environment, 19: 7870
corrosion by water and steam at 500 to 950°F, 19: 11682
corrosion by water at 280°C, impact and fretting studies of, 19: 11682
corrosion by water and heavy water at 275°C, 19: 13883(R) (HW-81984(p.9.1-6))
corrosion by water at 280°C, 19: 22895(R) (HW-83298(p.9.1-3))
corrosion by water in ETR G-7 loop, 19: 30669(R) (HW-84573(p.5.1-22))
corrosion by water during neutron irradiation, 19: 32693 (AECL-2257)

corrosion by water at 518°F, fretting, 19: 35759(R) (HW-84384 (p.10.1-13))
corrosion by water at 280°C, 19: 37167(R) (HW-84609(p.8.1-7))
corrosion by water at high temperatures, 19: 39234 (GEAP-4597)
corrosion by water at high temperatures, effects of cold work and radiation on, 17: 27729 (HW-76636)
corrosion by wet steam, 18: 6913 (NP-13409)
corrosion cracking by iodine at 350°C, stress-, 20: 5914(R) (GEAP-3771-17)
corrosion during a-c heating in stainless steel loops, 17: 3424 (KAPL-M-WKA-16)
corrosion films on, composition and properties of, 17: 501(R) (KAPL-2000-19(p.V.1-V.31))
corrosion films on, composition of, 18: 12580 (GEAP-4089(Vol.II) (Paper 19))
corrosion films on, microprobe studies of, 19: 9621 (DP-906)
corrosion in aqueous homogeneous reactor solutions, in-pile, 19: 13932
corrosion in boiling-water reactor environment, 18: 12723 (GEAP-4089 (Vol.II)(Paper 17))
corrosion in decontamination of pressurized-water reactors, 19: 2746 (HW-SA-2333(Rev.))
corrosion in PRTR pressure tubes, 18: 44037(R) (HW-82651(p.5.1-33))
corrosion in PRTR pressure tubes, causes and minimization of, 20: 1367
corrosion in PRTR, wear and crevice, 20: 764 (BNWL-SA-313)
corrosion in reactor, ETR test of, 20: 27425(R) (BNWL-207, pp 5.1-12)
corrosion in water-cooled reactors, problems of, 18: 16445
corrosion in 8 *M* hydrochloric acid solution at 35 to 105°C, hydrogen pickup in, 19: 46428(R) (ORNL-3847)
corrosion mechanisms of, electron microprobe determination of, 17: 18697(R) (DPST-62-71-4)
corrosion mechanisms, electron microprobe analyses of, 17: 36223(R) (DPST-63-71-2)
corrosion mechanisms of, electron microprobe analysis of, 18: 562(R) (DPST-63-70-8)
corrosion mechanism, 18: 3190(R) (SRO-95)
corrosion mechanisms of, electron microprobe analyses of, 18: 21633(R) (DPST-64-83-1)
corrosion of, 17: 39472(T,R) (EURAEC-668)
corrosion of, and hydrogen sorption by, in reactors, 17: 16598
corrosion of annealed peroxidized, by steam and water, 18: 563 (KAPL-2285)
corrosion of, by ammoniated water at 680°F, 17: 499(R) (KAPL-2000-19(p.III.1-III.9))
corrosion of, by lithium hydroxide and related solutions at high temperatures, 16: 33433 (WAPD-TM-307)
corrosion of, by polyphenyls at 330 to 400°C, 16: 22547
corrosion of, by steam at 500°C and 1 atm. pressure, 17: 8715(T,R) (EURAEC-451)
corrosion of, by steam–water spray, 17: 11941(R) (EURAEC-475)
corrosion of, by steam-water spray, 17: 17406(R) (EURAEC-519)
corrosion of, by steam, sorption of hydrogen during, 16: 5674
corrosion of, by steam and hot water, 16: 24128 (WAPD-T-1281)
corrosion of, by steam and water up to 400°C, effects of stresses on, 16: 20985
corrosion of, by steam at 500°C, hydrogen uptake in, 16: 485 (AERE-R-3768)
corrosion of, by steam at 800 to 1200°F, 16: 17980 (KAPL-M-AA-1)
corrosion of, by terphenyls, 16: 22551
corrosion of, by uranyl sulfate solutions, 16: 11168
corrosion of, by uranyl sulfate solutions, 16: 18634
corrosion of, by water, fretting, 16: 9151 (HW-68613)
corrosion of, by water at 580°F and pH 10, 16: 27592 (HW-SA-2454)
corrosion of, by water in pressurized water reactors, resistance to, 16: 7855
corrosion of, by wet steam, 16: 22554
corrosion of cladding of, irradiation effects on pressurized-water, 18: 39990 (CRFD-1178)
corrosion of consolidated-powder, effects of nitrogen and oxygen on, 18: 24081 (CONF-509-1)
corrosion of consolidated powder of, effects of nitrogen and oxygen on aqueous, 19: 927 (KAPL-3060)
corrosion of, during long exposures, 16: 17291(R) (EURAEC-222)
corrosion of, effects of metallurgical properties on, 17: 38551(R) (SRO-93)
corrosion of, effects of surface contamination with hydrofluoric acid–nitric acid etchant on, 16: 27593 (WAPD-T-1095)
corrosion of, fretting, 17: 16588 (HW-75626)
corrosion of fuel rods coated with, in chemical-shim environment, 19: 28765
corrosion of hydrided, 18: 27856(R) (HW-79280(p.9.1-4))
corrosion of Inconel bonds of, by ammoniated water at 600°F, 17: 499(R) (KAPL-2000-19(p.III.1-III.9))
corrosion of irradiated, by steam, 18: 7147(R) (HW-78962(p.5.1-12))
corrosion of pressure tubes of, in PRTR, 18: 19426 (HW-80158)
corrosion of pressure tubes of, in Plutonium Recycle Test Reactor, 18: 45083 (HW-80021)
corrosion of PRTR pressure tube, detection in coolant, 18: 29045(R) (HW-79280(p.11.1-10))
corrosion of PRTR pressure tubes of, 17: 14766
corrosion of scratches on cladding of, by water and steam, 18: 37640 (HW-75359)
corrosion of stainless steel bonds of, by ammoniated water at 600°F, 17: 499(R) (KAPL-2000-19(p.III.1-III.9))
corrosion of, studies by electron microprobes, 17: 19634(R) (SRO-81)
corrosion of, studies by electron microprobes, 17: 28533(R) (SRO-83)
corrosion of, studies by electron microprobes, 17: 42352(R) (SRO-94)
corrosion of tubes of, by steam–water at 2000°F, 19: 7862 (APED-4413)
corrosion of tubing of, by steam, 19: 4587 (GEAP-4739)
corrosion of weld joints to hafnium, 17: 10074 (WAPD-TM-337)
corrosion of, effects of high heat flux on, 18: 34082
corrosion of, effects of environmental factors on hydrogen pickup during aqueous, 19: 9625 (WAPD-TM-411)
corrosion of, effects of heat flux on, 19: 40961
corrosion of, effects of heat treatment on, 19: 22870(R) (HW-83601)
corrosion of, research programs on aqueous, 19: 4627
corrosion of, review of oxidation and hydriding kinetics and radiation effects in, 19: 16011 (AERE-R-4820)
corrosion product release and deposition rates, in boric acid solutions at high temperatures, 19: 13918 (WCAP-5368)
corrosion properties of, high-temperature, 17: 14744 (WAPD-T-1549)
corrosion resistance of, review on, 16: 12836
corrosion resistance of, effects of fabrication variables on, 16: 25726
corrosion resistance of preoxidized, effects of stress-relief annealing on, 18: 24081 (CONF-509-1)
corrosion resistance of, effects of nitrogen and oxygen on aqueous, 19: 11682
crack propagation in pressure tubes of, detection and mechanisms of, 20: 37172
creep and fatigue properties, 18: 14359(R) (EURAEC-136)
creep and stress-rupture properties at 300°C, 20: 11227
creep at 450 to 650°F, 17: 15532(R) (BMI-1607(Del.))
creep at 450 to 750°F, 17: 22966(R) (BMI-1614(Del.))
creep at 550 to 750°F, 17: 6511(R) (BMI-1593(Del.))
creep in, estimates of grain boundary diffusion, 20: 23709
creep of, activation energies for stresses between 20,000 and 30,000 psi and at 50 to 500°C, 16: 21033 (HW-70151)
creep of annealed and cold-worked, 18: 40970(R) (BMI-1674(Del.))
creep of cold-worked, activation energies for in-pile, 17: 31681(R) (HW-76559)
creep of cold-worked pressure tubes of, equation for, 20: 19203 (AECL-2528)
creep of, in-reactor measurements of, 18: 7293(R) (HW-77954(p.4.13-18))
creep of pressure tubes of, in transverse direction, 16: 12088 (CRGM-1040)
creep of, activation energies for, 19: 14029
creep of, activation energy for, 20: 31669
creep of, in-pile, 18: 41933 (TID-11295(3rd Ed.))
creep of, microdisplacement readout systems for measuring in-pile, 18: 31837 (HW-80271)
creep properties, 17: 3378(R) (BMI-1583(Del.))
creep properties, 17: 3379(R) (BMI-1596(Del.))
creep properties, 17: 8807 (HW-75267)
creep properties, 18: 13354(R) (BMI-1657(Del.))
creep properties at 550 to 750°F, 18: 20450(R) (BMI-1661(Del.))
creep properties at 1200 and 1300°F, 19: 32733 (NAA-SR-11047)
creep properties at 450 to 750°F, effects of cycling stress and temperature on, 20: 5851
creep properties at high temperatures, 20: 31669
creep properties, effects of in-pile irradiation, 17: 12602
creep properties of annealed and 15% cold-worked, 17: 1937 (HW-SA-2803)
creep properties of annealed and cold-worked, at 450 to 750°F, 17: 23864(R) (BMI-1619(Del.))
creep properties of annealed and cold-worked, at 450 to 750°F, 17: 25685(R) (BMI-1624(Del.))
creep properties of pressure tubes of, 17: 27822
creep properties of, in-reactor measurements of, 17: 27730(R) (HW-77052)
creep properties of sheet of, at 550 to 750°F, 17: 40423(R) (BMI-1639(Del.))
creep properties of annealed, effects of hydrogen on, 18: 600 (CRGM-1169)
creep properties of sheet, long-term, 18: 7985(R) (BMI-1650(Del.))
creep properties of, in-reactor, 18: 14537(R) (HW-79766(p.4.1-76))
creep properties of cold-worked, in-reactor, 18: 32222 (HW-SA-3477)
creep properties, radiation effects, 17: 14740 (TID-11295(2nd Ed.))

creep rate in fast neutron field, 17: 32697
creep rupture at 450 to 750°F of annealed and cold-worked, long-term, 19: 16061 (BMI-X-10113)
creep-rupture properties of annealed and 15% cold-worked, at 450 to 750°F, 17: 29314(R) (BMI-X-238)
creep-rupture properties of, research program on long-term, 17: 37507(R) (BMI-X-257)
creep-rupture properties of sheet, long-term testing results on, 18: 2157(R) (BMI-1644(Del.))
creep-rupture properties at 450 to 750°F at 19000 to 53000 hr, 18: 5772(R) (BMI-X-266)
creep testing in NRX reactor, in-pile facility for, 18: 9730 (NP-12385)
creep testing of annealed and cold-worked, at 550 to 750°F, 17: 35251(R) (BMI-1632(Del.))
creep testing, use of centrifugal machine for, 17: 20400 (AGN-8062)
creep tests, 18: 18307
creep tests at 550 to 750°F, 17: 41424(R) (BMI-1642(Del.))
creep tests at 550 to 750°F, 18: 34032(R) (BMI-1668(Del.))
creep tests at 550 to 750°F, 18: 34033(R) (BMI-1669(Del.))
creep tests at 550 to 750°F, 18: 34034(R) (BMI-1672(Del.))
creep tests of sheet, 17: 26944(R) (BMI-1630(Del.))
creep, theory of in-reactor, 17: 13678(R) (HW-75914)
creep-rupture properties of annealed and cold-worked sheet of, at 550 to 750°F, 18: 15664(R) (BMI-1655(Del.))
creep-rupture properties of annealed and cold-worked, at 550, 650, and 750°F, 18: 16467(R) (BMI-X-277)
creep-rupture properties of annealed and cold-worked sheet of, at 550, 650, and 750°F, 18: 24988(R) (BMI-1665(Del.))
creep-rupture properties of annealed and cold-worked, at 550, 650, and 750°F, 18: 32135(R) (BMI-X-296)
creep-rupture testing, 18: 17351(R) (BMI-1659(Del.))
creep, hardness, and tensile properties of, effects of dispersed yttrium oxide on, 19: 7930
crystal structure of thin-walled tubes of, effects of fabrication on, 20: 37237
crystallization of, after cold rolling and annealing, 19: 41034
crystallographic orientations in tubing of, effects of fabrication method on preferred, 20: 11251
crystallographic pole figures from microhardness measurements, 18: 44052(R) (ORNL-3670(p.147-59))
decontamination of, using acid oxalate–peroxide solutions, 19: 4046(R) (ORNL-3627(p.247-8))
decontamination research, 19: 9047 (ORNL-P-718)
defects at room temperature, origin and development of cup and cone, 18: 27933
defects in tubes of, 18: 12547(R) (HW-76303(p.3.1-37))
defects in tubular, sonic inspection of, 20: 43812(R) (BNWL-269, pp 4.1-9)
deformation of PRTR pressure tubes, 17: 14766 (HW-73697)
deformation properties of, effects of oriented hydride precipitates on, 20: 27421
deposition of copper coatings on, method of, 19: 40989
deuterium absorption from heavy water at 275°C, 18: 27857(R) (HW-80284(p.9.1-3))
deuterium absorption in deuterated lithium hydroxide, 18: 27856(R) (HW-79280(p.9.1-4))
development, 17: 14744 (WAPD-T-1549)
development for use as fuel cladding, 18: 45022(R) (GNEC-327)
development of thin-walled tubes of, with internal spiralled ribs, 18: 8773 (TID-19987)
diffusion of cesium-137 in, 19: 8615(R) (GEAP-3771-14)
diffusion of hydrogen in, mathematics of thermal, 16: 10507 (CRT-1049)
diffusion of hydrogen in oxide films on, polarographic measurements of, 18: 12641 (GEAP-4089(Vol.II)(Paper 21))
diffusion of hydrogen in, effects of thermal cycling on, 20: 16981
diffusion penetration of, by plutonium–uranium alloys, 16: 28555 (TID-7623(p.105-21))
dimensional changes during annealing in, temperature gradient effects on, 18: 26028
disintegration of, in nitric acid, electrolytic, 16: 1854(R) (IDO-14553)
dislocation arrangements in cold-rolled, 18: 12718 (AE-130)
dissolution by ammonium fluoride, 18: 13969
dissolution by Citriflex process, chemistry of, 20: 11272 (NP-15661)
dissolution by hydrofluoric acid, 18: 16152
dissolution by hydrofluoric acid in fluoride melt at 650°C, 18: 30128 (BMI-X-288)
dissolution in Citriflex Process, 18: 27618(R) (ORNL-TM-833)
dissolution in fused salt-hydrofluoric acid systems, 17: 20100(R) (ORNL-TM-412)
dissolution in hydrofluoric acid-nitrosyl chloride and -nitrosyl fluoride solutions, 18: 3671(R) (BNL-799(p.26-54))
dissolution in molten fluoride mixture, 17: 40424(R) (BMI-1642(Del.))
dissolution in nitric acid, electrolytic, 17: 4295(R) (DP-740)
dissolution in nitric acid, electrolytic, 17: 20097(R) (DP-824)
dissolution in nitric acid solutions, electrolytic, 17: 32192(R) (DP-839)
dissolution in Zirflex process, 17: 23434 (ORNL-3404)
dissolution of cladding of, on aluminum–plutonium fuel elements, flowsheet for, 20: 10948 (HW-76472)
dissolution of fuel cladding of, methods for, 19: 13524(R) (HW-81984 (p.4.1-20))
dissolution of, development of Citriflex Process for, 18: 13970
dissolution rate in molten fluoride mixture in hydrofluorinator at 500°C, 17: 36222 (BMI-X-253)
dissolution using hydrofluoric acid, 18: 13962
dissolution using hydrochloric acid, 19: 29468(R) (ANL-7017)
dissolver solutions for, corrosive effects of, on pre- and de-filmed titanium, 17: 35618(R) (ORNL-TM-545)
distribution of alloying elements in, effects of thermal treatment on, 20: 11287 (WAPD-T-1809)
distribution of hydrogen in, during hydrogenation and oxidation, 20: 5851
ductility at −33 to 300°C, 20: 746(R) (BNWL-120, pp 6.1-11)
ductility of thin-walled tubular, effects of hydride orientation on, 18: 40751(R) (DPST-64-83-7)
ductility of tubular, effects of hydride platelet orientations on, 19: 10571(R) (SRO-111)
ductility of, effects of liquid cesium on, 18: 14354(R) (ARF-B215-12)
ductility of, effects of hydrogen on, 19: 18486
ductility of, effects of zirconium hydride platelets on, 20: 31669
ductility of, effects of high temperatures on, 20: 41422
ductility transition temperature of, effects of hydrogen on nil, 20: 9489(R) (BNWL-166, pp 6.9-14)
effects on reactions of bromine pentafluoride with uranium, 20: 20803(R) (ANL-7055, pp 99-162)
engineering properties of tubes of, produced by vacuum powder metallurgy, 17: 32623
etching by cathodic arc, 17: 11089 (HW-SA-2559)
evaluation for fuel clad in Connecticut Yankee reactor, 19: 27784 (UNC-5095)
extrusion by hydrostatic methods, 19: 18436
extrusion by hydrostatic methods, 19: 44651
extrusion of thin-walled tubes of, with internal straight ribs, 18: 10499 (TID-20048)
extrusion of tubes, 17: 17546(R) (SRO-80)
extrusion of tubes of, feasibility of cold, 16: 19298(R) (ATL-A-119)
extrusion of tubes of, feasibility of cold, 16: 19299(R) (ATL-A-120)
extrusion of, clad thorium–uranium fuel tubes, 20: 782 (DP-943)
fabrication and properties, 17: 32484(R) (GEAP-4284)
fabrication and properties, 18: 545(R) (GEAP-4368)
fabrication and properties, 18: 12542(R) (GEAP-4484)
fabrication and properties of resistance-gathered projections on sheets of, 18: 15664(R) (BMI-1655(Del.))
fabrication and testing of irradiated cladding tensile specimens of, in-cell, 17: 3714
fabrication effects on mechanical properties of, 20: 37232
fabrication for uniformly high corrosion resistance, 17: 20441(P)
fabrication into cladding for thorium–uranium fuel tubes, 18: 30152 (HW-79843)
fabrication into pressure tubes for EL4 Reactor, by extrusion and drawing, 19: 9631 (CEA-R-2580)
fabrication methods for, 20: 43425 (ORNL-P-2406)
fabrication of, by extrusion and drawing, 16: 27614
fabrication of crack-free small tubing, 17: 1906
fabrication of fuel elements, collapse-clad, 18: 29043 (GNEC-345)
fabrication of fuel element cladding of, 20: 29658 (ANL-6283)
fabrication of high-pressure capsules from tubes of, 20: 43989(R) (BNWL-269, pp 3.1-30)
fabrication of irradiated fuel element cladding tensile-test specimens of, in-cell, 17: 2765
fabrication of process tubes of, by vendors for N-Reactor, 18: 32102 (HW-80566)
fabrication of projections on sheet of, 19: 28773 (BMI-X-10096)
fabrication of reactor components of, by electron beam and TIG welding, 18: 14447
fabrication of rhombic rods, 17: 3444 (KAPL-M-RXH-1)
fabrication of tubes of, 17: 11979(R) (DP-805)
fabrication of tubes of, for fuel elements, 17: 34390
fabrication of tubes of, by cold extrusion, 17: 39497(R) (ATL-A-138)
fabrication of tubular, by drawing and extrusion, 17: 41333(R) (ANL-6677)
fabrication of tubular, by cold extrusion, economics and feasibility of, 18: 4209(R) (ATL-423)
fabrication of tubular, 18: 25939(R) (ANL-6868(p.201-18))
fabrication of tubular, by explosive sizing, 19: 30642(R) (BMI-1707(Del.))
fabrication of tubing of, stress-orientation developed during, 19: 44634(R) (DPST-65-83-7)
fabrication of tubing of, texture control during, 20: 4304(R) (ORNL-

3870, pp 171-83)
fabrication of tubes of, by hot drawing, 20: 41432
fabrication of tubular, for fuel jackets and thermocouples, 20: 46162 (ANL-6621)
fabrication of, into fuel element brackets and cladding, 20: 46143(R) (HW-66081)
failure in reactors, effects of stainless steel cladding lining on, 18: 22456 (GEAP-4555)
failure of fuel rod cladding of, in BWR at critical heat flux, 19: 24057
fatigue notch sensitivity of welds of, 19: 2846
fatigue of, effects of hydrogen and stress on, 17: 526(R) (ARF-2230-12)
fatigue of, effects of hydrogenation on susceptibility to delayed-static, 18: 18406
fatigue properties, 18: 14360(R) (EURAEC-199)
fatigue strength of, studies of, by alternating torsion at room temperature, 16: 21065
flaw examination in PRTR pressure tubes, 19: 19387 (HW-84440)
forging bars of, 16: 15162
fracture analysis diagram for pressurized tubing of, 20: 9489(R) (BNWL-166, pp 6.9-14)
fracture and yielding characteristics of, effect of combined stress on, 16: 5735
fracture of, effects of corrosion and hydrogen pickup on brittle, 18: 1255 (NP-13220)
fracture of irradiated, 19: 14084(R) (HW-81984(p.8.1-3))
fracture of, effects of hydride precipitates on mode of, 19: 4669
fracture of, effects of hydrogen content and temperature on, 19: 26839
fracture of, effect of hydrogen on angle of bend to, 19: 32733 (NAA-SR-11047)
fracture of, effects of hydride precipitates on mode of, 20: 5849
fracture properties of, variables in, 18: 39896 (HW-82631)
fracture properties of, effects of hydrogen and temperature on, 20: 31669
fracture toughness of, data summary, 20: 46186 (GEAP-5014)
fracture transition temperatures of, review of effects of hydrogen and grain size on, 20: 37187
grain growth in cones at 1000°C, effects of time and wall thickness on, 19: 25024
grain growth in high-temperature phase, 18: 34139
grain structure and hydride orientation in, effects of processing variables on, 20: 35911
growth of large single crystals of, using electron-beam furnace, 18: 44052(R) (ORNL-3670(p.147-59))
growth of single crystals of, by electron-beam techniques, 18: 4252(R) (ORNL-3470(p.55-62))
growth of single crystals of, using electron-beam heating, 19: 39137
hardness, 18: 35938(R) (NMI-2129)
hardness anisotropy measurements in, 18: 4252(R) (ORNL-3470(p.55-62))
heat of transport of hydrogen in, alloying effects of yttrium on, 18: 5800
heat transfer between uranium dioxide and, coefficient of, 16: 25523 (CRFD-1075)
heat transfer from uranium dioxide to, effects of pressure on contact, 19: 2521
heat transfer to sheaths of, from uranium dioxide cores, 19: 2522
heat treatment effects on texture of, 20: 37198
hydridation, 18: 41945
hydridation, 20: 11225
hydridation, 18: 551(T,R) (EURAEC-224)
hydridation at 320°C, effects of water vapor on, 20: 7497(R) (BNWL-150, pp 3.1-30)
hydridation at 400 and 500°C, 18: 545(R) (GEAP-4368)
hydridation at 400 and 500°C, 18: 12542(R) (GEAP-4484)
hydridation at 400 to 423°C, 18: 32139(R) (HW-81269(p.5.1-23))
hydridation at 425°C, 19: 10512(R) (HW-81601(p.3.1-27))
hydridation, effects of supercharging with hydrogen on, 17: 13678(R) (HW-75914)
hydridation, effects of water vapor on, 17: 36225 (HW-76562(Rev.))
hydridation in crevice regions in fuel rod end caps, effects of closure type on, 20: 7497(R) (BNWL-150, pp 3.1-30)
hydridation in steam, 18: 560 (AERE-R-4348)
hydridation in steam and water, 18: 30134(T,R) (EURAEC-955)
hydridation in steam and water, effects on tensile properties, 19: 4616(R) (EURAEC-1161)
hydridation of cold-worked and heat-treated, at 280 to 500°C, 20: 9439 (AECL-2511)
hydridation of, effects of excess hydrogen on, 17: 1873 (HW-73382)
hydridation of, effects of stress on, 17: 15958 (TID-16476)
hydridation of, effects on properties, 17: 32484(R) (GEAP-4284)
hydridation of, effects of thick films on, 18: 7146(R) (HW-77954(p.5.33-5))
hydridation of, factors affecting, 18: 2192
hydridation of, in reactors, 17: 11157 (CEND-153(Vol.II)(p.77-99))
hydridation of, metallographical studies of, 17: 39470(T,R) (EURAEC-619)
hydridation of, nondestructive eddy-current methods for measuring, 18: 8606(R) (HW-78388(p.7.1-10))
hydridation of, bibliography on, 18: 18285 (DP-803(Del.))
hydridation of, effects of stress on orientation of, 19: 17337(R) (HW-84281(p.6.11-13))
hydridation of, effects on mechanical properties, 20: 30902
hydridation of, effects of heat treatments on, 19: 22870(R) (HW-83601)
hydridation of, in water, 20: 11221
hydridation of, in steam, effects of initial oxide layer formation on, 20: 25500
hydridation of, nondestructive eddy-current apparatus for detecting, 19: 30394
hydridation of, orientation of zirconium hydride platelets in, 18: 23137(R) (DPST-64-83-3)
hydridation of, water vapor inhibition of, 19: 34639(R) (BNWL-79 (p.5.1-11))
hydridation studies on, 18: 24910(R) (SRO-101)
hydride detection in, nondestructive, 17: 14740 (TID-11295(2nd Ed.))
hydride detection in surface of, by critical-angle ultrasonic tests, 18: 18014 (HW-79928)
hydride embrittlement of fuel supports of, prevention of, 19: 3710 (HW-80117)
hydride nucleation and growth in, 20: 2253 (AECL-2297)
hydride orientations and mechanical properties of thin-walled tubes of, 18: 2218(R) (DPST-63-74-9)
hydride orientation and mechanical properties of thin-walled tubes of, 18: 28916(R) (DPST-64-83-4)
hydride orientation on, dependence on crystallographic texture, 20: 33828
hydride orientation in tubular, effects of fabrication on, 20: 35835(R) (DPST-66-83-5)
hydride phase estimation in process tubes of, metallographic, 18: 20518 (HW-74949)
hydride platelet orientations in tubing of, effects of stresses and fabrication on, 17: 36292(R) (DPST-63-74-7)
hydride platelet orientations in tubing of, effects of fabrication and stresses on, 18: 21633(R) (DPST-64-83-1)
hydride platelet orientation in thin-walled tubing of, effects of fabrication and stresses on, 18: 35061(R) (DPST-64-83-6)
hydride platelet orientation in thin-walled tubing of, effects of fabrication and stresses on, 19: 14804(R) (DPST-64-83-11)
hydride platelet stress orientation in thin-walled tubing of, 18: 8791(R) (DPST-63-74-10)
hydride plates pole figure in, method for determining, 20: 4304(R) (ORNL-3870, pp 171-83)
hydride pole figure determination by quantitative metallography, 18: 44052(R) (ORNL-3670(p.147-59))
hydride pole figures in, rapid metallographic technique for determination of, 19: 34687 (ORNL-P-1266)
hydride precipitation in, effects of strain on directional, 18: 44052(R) (ORNL-3670(p.147-59))
hydride precipitation in, effects of elastic stresses on orientation of, 19: 44697 (ORNL-TM-1239)
hydride precipitation in, effects of preferred orientation and stress on, 20: 4304(R) (ORNL-3870, pp 171-83)
hydride precipitate orientation in, effects of stress on, 20: 15120
hydride precipitation in, effects of preferred orientation and stresses on, 20: 33843 (NLCO-946, pp 79-102)
hydriding by gas mixtures containing hydrogen, effects of oxidation rate on, 18: 4203
hydriding in hydrogen, carbon monoxide, and water, effects of oxide films on, 18: 44037(R) (HW-82651(p.5.1-33))
hydriding of, effects of heat flux on rate of, 19: 40961
hydrogen absorption in deuterated and undeuterated lithium hydroxide solutions at 275°C, 18: 14407(R) (HW-79766(p.5.1-16))
hydrogen absorption in steam, 18: 39847
hydrogen diffusion in, effects of thermal cycling on, 19: 13883(R) (HW-81984(p.9.1-6))
hydrogen distribution in oxidized, tritium autoradiographic studies of, 19: 13910 (AECL-2085)
hydrogen embrittlement of, 17: 8715(T,R) (EURAEC-451)
hydrogen embrittlement in steam at 750°F and 1,500 psi, effects of new heat treatment procedure on, 18: 570
hydrogen embrittlement of inner supports of, effects of annealing on, 19: 2720 (HW-80178)
hydrogen pickup by peroxidized, in water, 18: 563 (KAPL-2285)
hydrogen pickup by, in 680°F water and 750°F steam, 18: 24081 (CONF-509-1)
hydrogen pickup by irradiated, from in-pile loop water, 18: 44037(R) (HW-82651(p.5.1-33))
hydrogen pickup by, effects of oxygen on, 19: 22870(R) (HW-83601)
hydrogen pickup in steam and water, effects of nitrogen, oxygen, and silicon on, 18: 16440 (WAPD-283)
hydrogen pickup in steam and water at high temperatures, 20: 33815(R)

(EURAEC-1625)
hydrogen pickup in water at high temperatures, effects of radiation and cold work on, 17: 27729 (HW-76636)
hydrogen solubility in, effects of temperature on, 20: 39379 (AECL-2453)
hydrogen uptake by, 20: 7520
ignition properties of wastes from machining operations on, 20: 15001 (HW-66930)
inspection of tubes of, eddy current technique for, 17: 4689
inspection of tubular, sonic, 19: 17177(R) (ANL-6965(p.42-83))
joining of, to stainless steel by hard-soldering, 16: 16649(R) (EURAEC-194(App.6))
joining of tubes of Inconel and, by explosive welding, 19: 18422 (BMI-1715)
joining of tubular, to stainless steel sheet, by rolling techniques, 17: 510 (CWAED-54)
joining to carbon steel, 18: 31016 (HW-79616)
joining to Incoloy-800 and Type 304L stainless steel in tubular joints by hot tandem extrusion, 19: 24948 (GEAP-4756)
joining to Inconel by explosive methods, 19: 24081(R) (GNEC-361)
joining to stainless steel, explosive, 18: 2208
joining to stainless steel, 18: 11432(R) (DP-875)
joining to stainless steel by diffusion, 19: 16028 (CEA-R-2634)
joining tubing of, to iron–nickel alloy, 16: 5021 (GNEC-176(Del.))
joint with carbon steel, evaluation of expanded, 17: 8806 (HW-75135)
joint with carbon steel in coextruded process tube, strain measurements in, 18: 12549 (HW-78788)
length variations induced by thermal cycling in tubes of, 18: 14359(R) (EURAEC-136)
measurements on preferred orientation in, microhardness and x-ray diffraction, 19: 22991 (ORNL-P-1165)
mechanical properties of, effects of hydridation on, 17: 412 (KAPL-2221)
mechanical properties of, at 25 to 850°C, effects of niobium addition and oxygen on, 17: 1947 (TID-17174)
mechanical properties of, hydrogen effects on, 17: 6696(T) (EURAEC-353)
mechanical properties of, effects of hydrogen content on, 17: 39470(T,R) (EURAEC-619)
mechanical properties of, effects of hydrogen content on, 17: 39468(T,R) (EURAEC-520)
mechanical properties of, effects of hydrogen content on, 17: 41368(T,R) (EURAEC-784)
mechanical properties of extruded tubing of, 16: 5021 (GNEC-176(Del.))
mechanical properties of, effects of hydrogen on, 16: 7875(R) (ARF-2230-3)
mechanical properties of, effects of cold work on, 16: 12089 (CRGM-1046)
mechanical properties of, effects of grain size on, 16: 15184 (KAPL-2000-17)
mechanical properties of, effects of heat treatment under vacuum on, 18: 7167
mechanical properties at room temperature, 18: 12558 (ORNL-TM-739)
mechanical properties of extruded, at 580°F, 18: 14465 (KAPL-2296)
mechanical properties of NPR pressure tubes, effects of hydriding on, 18: 14367(R) (HW-79766(p.6.1-21))
mechanical properties, 18: 25894(R) (NMI-2128)
mechanical properties of welded, 18: 37680 (A/CONF.28/P/757)
mechanical properties of cold-worked, effects of hydrogen and neutrons on, 18: 42108 (AECL-1986)
mechanical properties of tubing of, effects of oriented hydrides on, 18: 44129 (AECL-1989)
mechanical properties of consolidated powder of, effects of nitrogen and oxygen on, 19: 6295 (KAPL-3032)
mechanical properties, 19: 22870(R) (HW-83601)
mechanical properties of thin-walled tubing of, effects of hydride orientation on, 19: 22970(R) (DPST-65-83-2(p.8-12))
mechanical properties of, effects of nitrogen and oxygen content on, 19: 30784
mechanical properties of, summary of, 19: 39097 (GEMP-346)
mechanical properties of, effects of hydrogen on, 20: 11221
mechanical properties of, effects of hydrogen on, (E), 20: 21386
mechanical properties, microstructure, and texture of thin-walled tubes of, 20: 25609
mechanical properties, 20: 32796(R) (AI-CE-3)
mechanical properties of alpha-phase, effects of preferred orientation on, 20: 37226
mechanical properties of, effects of preferred orientation on, 20: 37232
mechanical properties of, 17: 39472(T,R) (EURAEC-668)
mechanical properties of, effects of temperature on, 18: 44036(R) (HW-82651(p.4.1-49))
mechanical testing of, effects of embrittling factors in, 20: 11227
metallographic studies of oxide layers on, preparation of samples for, 16: 22546
metallography and stress analyses of, 20: 18020(R) (ORNL-3900, pp 2-81)
micrographic appearance of, effects of heat treatment under vacuum on, 18: 7167
microstructure of, method for determining preferred orientation in, 20: 23750
microstructure of, in failed PRTR tube of, 20: 27577(R) (BNWL-207, pp 6.1-6)
morphology of, effects of carbonium and oxygen diffusion on, 18: 44182
movement of zirconium hydride in, electrothermal effects on, 19: 30737(R) (HW-84573(p.6.1-11))
neutron reactions in, yields of helium and hydrogen produced by fast, 19: 44746 (NAA-SR-Memo-10626)
optical properties of oxide films on, 18: 4252(R) (ORNL-3470(p.55-62))
oxidation and mechanical properties, 17: 32621
oxidation and rupture of uranium fuel rods clad by, by water at 200 to 300°C, 20: 7515 (HW-61799)
oxidation and sorption of deuterium in heavy water by, 18: 8752(R) (HW-78388(p.9.1-4))
oxidation by carbon dioxide at 450 and 550°C, 17: 37003(R) (HW-78118)
oxidation by carbon monoxide at 600°C, 18: 8752(R) (HW-78388(p.9.1-4))
oxidation by carbon dioxide at 350 and 450°C and steam at 425°C, 18: 32139(R) (HW-81269(p.5.1-23))
oxidation by dry air at 20 to 270°C, 18: 37639(R) (EURAEC-1130)
oxidation by hydrogen fluoride–oxygen, 19: 31462(R) (ANL-7028)
oxidation by lithium hydroxide solutions at 275°C, 18: 32139(R) (HW-81269(p.5.1-23))
oxidation by oxygen and steam, effects of pressure on, 17: 36234
oxidation by oxygen and water vapor at 600 to 800°C, properties of, 18: 10489
oxidation by oxygen or water vapor at 300 to 360°C, kinetics of, 20: 24995
oxidation by steam, effects of dissolved oxygen on, 18: 567
oxidation by steam at 750°F and water at 680°F, hydrogen absorption from, 18: 2162(R) (IITRI-B198-46)
oxidation by steam, oxide films from, 19: 2763 (AECL-1999)
oxidation by steam at 500°C and 1000 psi, inhibiting effects of boric acid on, 19: 20492
oxidation by triple carbonate salt, 17: 23957(R) (NMI-7247)
oxidation by water vapor at 425°C, effects of thermal cycling on, 19: 16018(R) (HW-84281(p.5.26-30))
oxidation by water at 900 to 1200°C, kinetics of, 20: 762(R) (BNWL-120, pp 5.1-18)
oxidation by water vapor at 375 and 575°C, kinetics of, 20: 25498
oxidation films on, effects of environment and surface preparation on structure of, 20: 19188(R) (GEAP-5001)
oxidation in heavy water, 18: 8752(R) (HW-78388(p.9.1-4))
oxidation in oxygen and water vapor at 600 to 850°C, 19: 22870(R) (HW-83601)
oxidation in reactor, electric conductivity study of, 19: 7846 (AECL-2066)
oxidation in steam, 18: 560 (AERE-R-4348)
oxidation in Thermox process for irradiated fuel elements, 17: 40918 (AE-120)
oxidation in water vapor at 400°C, 17: 36225 (HW-76562(Rev.))
oxidation kinetics and oxide film breakaway at 600 to 850°C, 20: 25497
oxidation of, 17: 32621
oxidation of, causes of second transition point in, 16: 7857
oxidation of cladding of, by steam in TREAT transient experiments, 19: 38132 (ORNL-P-1287)
oxidation of cold-worked and heat-treated, by steam at 280°C, 18: 32139(R) (HW-81269(p.5.1-23))
oxidation of, electron microprobe analysis of chromium and iron in oxide film, 18: 6493(R) (SRO-96)
oxidation of, factors affecting, 18: 2192
oxidation of prefilmed, effects of vacuum annealing on, 20: 9412(R) (BNWL-166, pp 5.7-10)
oxidation of process tubes of, in PRTR, 20: 27427(R) (BNWL-207, pp 5.16-18)
oxidation of, distribution of tin in oxide film in, 20: 25504
oxidation of, effects of thermal cycling on, 18: 44037(R) (HW-82651 (p.5.1-33))
oxidation of, electrochemical studies of kinetics of film formation in, 19: 28758
oxidation of, mechanism of breakaway, 20: 25496
oxidation of, structure of oxide films from, 19: 973
oxidation rates in water-d_2 at 400°C, 17: 37003(R) (HW-78118)
oxide film formation on, hot hardness tests of plasticity of, 19: 25009
penetration by aluminum–plutonium alloy at 500 to 650°C, 17: 37001(R) (ANL-6780)
performance as boiling-reactor fuel cladding, 18: 29069
performance as ceramic fuel element capsules, 20: 36470 (GEAP-4870)
performance as cladding on uranium dioxide fuel tubes, 18: 11432(R) (DP-875)

performance as cladding for uranium dioxide powder for pressurized-water reactors, 18: 42965 (EXP-NRX-20605)
performance as cladding in borated water at high pressures and temperatures, 20: 33791
performance as fuel element cladding, 19: 14883(R) (HW-81602 (p.5.1-16))
performance as fuel cladding in superheater environment, 19: 24081(R) (GNEC-361)
performance as fuel coatings in PWR, 19: 34632
performance as fuel element ribs and spacers, (E), 20: 8371 (DP-1002)
performance as fuel cladding under coolant-loss conditions, 20: 20221
performance as PRTR pressure tubes, 19: 22870(R) (HW-83601)
performance as reactor pressure tube material, 17: 7552(R) (HW-74761 (p.8.1-15))
performance as Saxton fuel rod cladding, (E), 20: 10382(R) (WCAP-3269-13)
performance as SRE moderator and reflector cladding, 20: 12404 (NAA-SR-11160)
performance in nuclear-superheater environment, 19: 10541(R) (GEAP-4703)
performance in reactor components, design criteria for, 18: 28023
performance of pressure tubes of, in PRTR, 18: 9727 (HW-SA-3008)
performance on urania fuel elements in thermal cycling tests, 20: 43989(R) (BNWL-269, pp 3.1-30)
phase composition in, determination of second, 17: 6719
phase transformations in, during hot working, 16: 12141
phase transformation studies, 19: 30682
phase transformation in temperature cycles at 500 to 1100°C, beta-alpha, 17: 39605
physical properties and uses of, review on, 17: 32503
physical properties of, effects of hydride orientation and grain structure on, 20: 35911
pickling of, in hydrofluoric acid–nitric acid bath, formation and thermal decomposition of zirconium fluoride during, 17: 35700 (TID-17478)
plastic deformation of, kink bands in, 17: 23966(R) (TID-18637)
plastic deformation of, twinning in, 16: 2201(R) (TID-14185)
plastic flow of, determination by hardness, 20: 37230
polishing of, development of methods for mechanical, 17: 16656 (TID-16475)
preferred orientation of, effects of fabrication on, 17: 14843 (ORNL-TM-460)
preferred orientation in rolled, 17: 31681(R) (HW-76559)
preferred orientation in, x-ray method for measuring, 20: 9504 (WAPD-TM-472)
preparation of hydrided, for microscopic examination, 19: 24926
preparation of powders of, 20: 2222 (EURAEC-1390)
pressure-deflection and rupture of plates of, 18: 44064 (WAPD-282)
processing claddings of, on spent uranium fuel elements, 19: 28452
procurement and evaluation for fuel element fabrication, 19: 896 (HW-82400(p.2.1-13))
production in single-melt electric arc furnace, fabrication of electrodes for, 18: 8741(P)
production of reactor-grade ingots of, from scrap, 17: 15184 (KAPL-2000-17)
properties, 19: 28870(R) (BMI-X-10121)
properties and uses of thin-wall tubing of, 17: 35154(R) (SRO-92)
properties as cladding and structural materials in reactors, 18: 32072
properties as cladding and structural material in reactors, 18: 41947
properties as fuel element cladding, 18: 15563
properties as fuel cladding, 18: 30973(R) (HW-76304(p.3.1-19))
properties as pressure tubes in power reactors, 19: 17328
properties, effects of carbon content on corrosion and tensile, 17: 37465 (WAPD-T-1508)
properties for Bonus reactor fuel element cladding, 19: 19380(R) (CEND-513)
properties for fuel element canning, 18: 42034
properties for fuel cladding for water-cooled reactors, 20: 35849 (KR-89, pp 82-96)
properties for use in pressure tube in PRTR, surveillance program on, 18: 15525 (HW-78456)
properties for use in water-cooled reactors, 18: 37668 (A/CONF.28/P/158)
properties for use as fuel cladding for water-cooled power reactors, 18: 37692
properties of bonded joints with stainless steel, 17: 13672(R) (DP-815)
properties of, data manual on, 16: 27632 (TRG-Report-108)
properties of extruded and forged, for use in reactors, 17: 34435
properties of splatcooled, effects of beryllium on, 18: 14372(R) (NMI-2124)
properties of, as core structure for N.S. *Savannah* reactor, (E), 19: 40218
properties of, effects of annealing and heat treatments on, 18: 39928
properties of, effects of temperature on mechanical and physical, 17: 16760
properties of, mechanical and physical, 20: 4400 (WCAP-3269-41)
properties of, review on mechanical and physical, 16: 626
properties of, summary of corrosion, hydridation, and oxidation, 19: 39097 (GEMP-346)
properties, effects of impurities on, 18: 44031 (BM-RI-6536)
radiation effect on mechanical properties at 70 to 600°F, 18: 34233
radiation effects on corrosion by water, 17: 2018
radiation effects on mechanical properties of, in-cell testing of, 17: 2765
radiation effects on tensile properties, 17: 3537 (HW-75052)
radiation effects, 17: 4230 (DL-51)
radiation effects on creep, 17: 7553(R) (HW-74761(p.9.1-37))
radiation effects, 17: 6735 (AE-90)
radiation effects on properties of PRTR pressure tubes, 17: 8706 (HW-73698(Rev.))
radiation effects on mechanical properties, 17: 11129
radiation effects on mechanical properties, 17: 12717 (HW-62422)
radiation effects on mechanical properties and structure of, 17: 12718 (HW-67949(Rev.))
radiation effects on creep properties, 17: 12602
radiation effects on oxidation of, 17: 12621
radiation effects on mechanical properties of, 17: 13678(R) (HW-75914)
radiation effects on corrosion of, in-reactor, 17: 13678(R) (HW-75914)
radiation effects on creep properties, 17: 14740 (TID-11295(2nd Ed.))
radiation effects, 17: 17447
radiation effects on, 17: 22221 (HW-67072)
radiation effects on chemical and mechanical properties of, program for studying, 17: 22229(T-R) (EURAEC-560)
radiation effects on, 17: 27730(R) (HW-77052)
radiation effects on mechanical properties of, 17: 27730(R) (HW-77052)
radiation effects on corrosion of, by water at 280°C, 17: 27730(R) (HW-77052)
radiation effects on tensile properties of, neutron, 17: 29375 (HW-SA-3012)
radiation effects on rupture-stress properties of, neutron, 17: 31068
radiation effects on embrittlement and hardening of, neutron, 17: 31063
radiation effects on tensile properties of, fast neutron, 17: 32665 (HW-74955)
radiation effects on stress-rupture properties of, 17: 34557(R) (ORNL-3480(p.117-42))
radiation effects on, in-reactor measurements of, 16: 30907 (HW-SA-2673)
radiation effects on creep properties of cold-worked, 16: 14989 (CRGM-1047)
radiation effects on hydridation of purposely defected, 16: 12177 (HW-65465)
radiation effects on mechanical properties of, 16: 24239 (HW-SA-2547)
radiation effects on mechanical properties of, neutron, 16: 22701
radiation effects on stress relaxation in, 16: 5757 (DP-623)
radiation effects on mechanical properties of, 17: 37003(R) (HW-78118)
radiation effects on corrosion by water at 280°C, 17: 37003(R) (HW-78118)
radiation effects on corrosion and hydridation of, neutron, 18: 2343
radiation effects on tubes of, 18: 2355
radiation effects on tensile properties at 343°C, 18: 4761(R) (GEAP-4383)
radiation effects on corrosion rate of, by water at 540°F, 18: 7138(R) (HW-77954(p.5.1-4))
radiation effects on corrosion of, 18: 7147(R) (HW-78962(p.5.1-12))
radiation effects on tandem-extruded joints between stainless steel and, neutron, 18: 7284 (DP-859)
radiation effects on creep, 18: 7293(R) (HW-77954(p.4.13-18))
radiation effects on mechanical properties of, 18: 7294(R) (HW-77954 (p.4.19-77))
radiation effects on creep of, 18: 7301(R) (HW-78962(p.4.45-9))
radiation effects on mechanical properties of, 18: 7302(R) (HW-78962 (p.4.50-126))
radiation effects on burst strength of, 18: 7929(R) (HW-78962(p.6.11-19))
radiation effects on mechanical properties, 18: 8866(R) (HW-78388 (p.8.1-7))
radiation effects on mechanical properties of, neutron, 18: 8868 (HW-SA-3268)
radiation effects on corrosion, 18: 8752(R) (HW-78388(p.9.1-4))
radiation effects on corrosion of, by boiling water, 18: 12723 (GEAP-4089(Vol.II)(Paper 17))
radiation effects on electrochemical properties of, 18: 14406(R) (EURAEC-852)
radiation effects on corrosion by water, 18: 14407(R) (HW-79766(p.5.1-16))
radiation effects on creep properties of, neutron, 18: 14537(R) (HW-79766(p.4.1-76))
radiation effects on tensile properties of, neutron, 18: 14537(R) (HW-79766(p.4.1-76))
radiation effects on corrosion and mechanical properties of, neutron,

18: 18418(T,R) (EURAEC-971)
radiation effects on tensile properties of, 18: 18307
radiation effects on corrosion in steam–oxygen mixtures, 18: 22446(R) (ORNL-3591(p.77-83))
radiation effects on deformation and fracture of cold-worked, 18: 24191 (HW-SA-3194)
radiation effects on tensile properties of, neutron, 18: 26096
radiation effects on mechanical properties, neutron, 18: 28043(R) (HW-79280(p.8.1-6))
radiation effects on creep of, 18: 28043(R) (HW-79280(p.8.1-6))
radiation effects on, in-pile, 18: 27952(R) (EURAEC-926)
radiation effects on corrosion in water, neutron, 18: 27856(R) (HW-79280(p.9.1-4))
radiation effects on corrosion of, in-pile, 18: 28932(R) (EURAEC-1013)
radiation effects on mechanical properties of sheaths of, fast neutron, 18: 30231 (DP-888)
radiation effects on mechanical properties of, fast-neutron, 18: 30263
radiation effects on engineering properties of, review, 18: 32216 (A/CONF.28/P/242)
radiation effects on creep of cold-worked, neutron, 18: 32222 (HW-SA-3477)
radiation effects on corrosion and mechanical properties of, neutron, 18: 32235(T,R) (EURAEC-1068)
radiation effects on mechanical properties of annealed and cold-worked, 18: 32043(R) (HW-81269(p.4.1-64))
radiation effects on flow and fracture behavior of annealed and cold-worked, fast-neutron, 18: 36047 (HW-82102)
radiation effects on oxidation of, by dry argon–nitrogen–oxygen, argon–oxygen, and oxygen systems at 20°C, 18: 37639(R) (EURAEC-1130)
radiation effects on, in-pile neutron, 18: 37732 (A/CONF.28/P/21)
radiation effects on corrosion by fog, neutron, 18: 37324 (A/CONF.28/P/16)
radiation effects on pressurized-water corrosion of cladding of, 18: 39990 (CRFD-1178)
radiation effects on mechanical properties of hydrided cold-worked, 18: 42108 (AECL-1986)
radiation effects on corrosion and properties of, 18: 41933 (TID-11295 (3rd Ed.))
radiation effects on mechanical properties of pressure tubes of, fast-neutron, 19: 6362 (HW-83164)
radiation effects on tensile properties of, 19: 8615(R) (GEAP-3771-14)
radiation effects on creep of, 19: 11777(R) (EURAEC-1243)
radiation effects on mechanical properties of tubular, 19: 13883(R) (HW-81984(p.9.1-6))
radiation effects on tensile properties of, neutron, 19: 14110
radiation effects on oxidation by low-oxygen water, neutron, 19: 16016(R) (HW-84281(p.5.1-5))
radiation effects on oxidation of tubular, 19: 16018(R) (HW-84281 (p.5.26-30))
radiation effects on corrosion and mechanical properties of, neutron, 19: 16208(R) (EURAEC-1249)
radiation effects on mechanical properties of, at high temperatures, 19: 16214(R) (HW-84281(p.4.14-15))
radiation effects on PRTR pressure tubes, 19: 21686 (HW-84540)
radiation effects on electric conductivity of corrosion films on, gamma, (E), 19: 20621
radiation effects on PRTR pressure tubes of, evaluation of fast neutron post-, 19: 23120 (BNWL-5)
radiation effects on crystal structure of, 19: 23124(R) (HW-83298(p.8.1-4))
radiation effects on fuel rod cladding of, in-pile, 19: 24123
radiation effects on hydrogen pickup by, neutron, 19: 25046(R) (HW-83615)
radiation effects on type 304, fission-fragment, 19: 28870(R) (BMI-X-10121)
radiation effects on pressure tubes of, neutron, 19: 30821 (BNWL-42)
radiation effects on mechanical properties of tubular, 19: 30649(R) (HW-84573(p.4.1-31))
radiation effects on corrosion by steam, fast neutron, 19: 30650(R) (ORNL-3789(p.126-38))
radiation effects on tubular, fast neutron, 19: 30737(R) (HW-84573 (p.6.1-11))
radiation effects on tensile properties of transition joint between Inconel 600 and, fast neutron, 19: 34742(R) (BNWL-79(p.4.1-30))
radiation effects on ductile-to-brittle transition temperature in, fast neutron, 19: 34627(R) (BNWL-79(p.6.1-20))
radiation effects on mechanical properties of, neutron, 19: 37162 (BNWL-SA-236)
radiation effects on, neutron, 19: 37167(R) (HW-84609(p.8.1-7))
radiation effects on, neutron, 19: 40286(R) (NAA-SR-11200)
radiation effects on properties of, summary of, 19: 39097 (GEMP-346)
radiation effects on mechanical properties of, fission-fragment and neutron, 19: 39229(R) (BMI-X-10134)
radiation effects on mechanical properties of, 19: 39234 (GEAP-4597)
radiation effects on corrosion and tensile properties of welded joints of hafnium-to-, fast neutron, 19: 41092 (WAPD-TM-457)
radiation effects on tensile properties of, neutron, 19: 40961
radiation effects on corrosion of oxide films on, gamma and neutron, 19: 47099
radiation effects on stress-rupture of, fast neutron, 20: 746(R) (BNWL-120, pp 6.1-11)
radiation effects on ductility of, fast neutron, 20: 2420(R) (DPST-65-83-8)
radiation effects on in-pile corrosion of, by aqueous solutions, 20: 5852(R) (EURAEC-1522)
radiation effects on tensile properties of, effects of hydrogen content on neutron, 20: 5851
radiation effects on mechanical properties of, fast-neutron and fission-fragment, 20: 7628(R) (BMI-X-10146)
radiation effects on creep at 315°C of annealed, in-reactor, 20: 9568(R) (BNWL-166, pp 4.1-7)
radiation effects on tensile properties and tube burst pressure of, fast-neutron, 20: 9569(R) (BNWL-166, pp 6.1-3)
radiation effects on collapsible sheaths of, 20: 2415 (AECL-2276)
radiation effects on corrosion and mechanical properties of, neutron, 20: 11354
radiation effects on fuel cladding of, reactor, 20: 17120 (GEAP-4916)
radiation effects on tensile properties of, fast-neutron, 20: 23585(R) (GEAP-3771-18)
radiation effects on iodine reactions with, neutron, 20: 23585(R) (GEAP-3771-18)
radiation effects on corrosion of, by water, effects of fabrication history on fast-neutron, 20: 23767 (BNWL-88)
radiation effects on transition joints between Inconel 600 and, fast-neutron, 20: 23768 (BNWL-190)
radiation effects on fuel claddings of, 20: 28733(R) (GEAP-4919)
radiation effects from fission fragments on mechanical properties and strain of, 20: 27567 (BMI-1766)
radiation effects on mechanical properties of, 20: 27574(R) (BNWL-207, pp 4.32-4)
radiation effects on transition joints between Inconel 600 and, neutron, 20: 27574(R) (BNWL-207, pp 4.32-4)
radiation effects on tensile properties of PRTR tubes of, 20: 27577(R) (BNWL-207, pp 6.1-6)
radiation effects on fracture toughness of, neutron, 20: 27576(R) (BNWL-207, pp 4.44-55)
radiation effects on sorptive properties of, for hydrogen and oxygen, fast-neutron and gamma, 20: 27599
radiation effects on hydrogen sorption and mechanical properties of, fast-neutron, 20: 27601
radiation effects on impact properties of hydrided, fast-neutron, 20: 27602
radiation effects on creep of, at 300°C, fast-neutron, 20: 27603
radiation effects on deformation of hydrided, fast-neutron, 20: 27421
radiation effects on tensile properties at room and 650°F temperatures, 20: 30884(R) (WCAP-3269-16)
radiation effects on impact properties of, effects of hydrogen on fast-neutron, 20: 31669
radiation effects on fuel element cladding of, in-pile, 20: 33867 (GEAP-4849)
radiation effects on, neutron, 20: 33964
radiation effects on mechanical properties of, fast neutron, 20: 39457 (GEAP-5100-9)
radiation effects on, as fuel cladding, 20: 46144(R) (HW-67765)
radiation effects on mechanical and physical properties of, 17: 16760
radiation effects on burst strength of, 18: 7297(R) (HW-77954(p.6.3-4))
radiation effects on mechanical properties of, 18: 44036(R) (HW-82651 (p.4.1-49))
radioinduced corrosion by oxygen, 20: 23602(R) (ORNL-3913, pp 53-73)
radioinduced production of helium and hydrogen in, neutron, 19: 26901
radioinduced swelling of, clad thorium–uranium fuel tubes, reactor, 20: 782 (DP-943)
reactions of clad of, with steam at 1500°C and 15 psig, 19: 32447(R) (ANL-7020(p.175-97))
reactions of oxidized, with aluminum at 400 to 500°C, 20: 39380 (AECL-2570)
reactions with copper during extrusion, prevention of, 19: 27781 (NMI-7263)
reactions with iodine at 250 to 700°C, 18: 35127(R) (GEAP-3771-13)
reactions with iodine at 350°C, 19: 8615(R) (GEAP-3771-14)
reactions with iodine at 350°C and 150 PSIG, 19: 22868(R) (HW-81603 (p.4.1-12))
reactions with iodine, 19: 31519(R) (GEAP-3771-15)
reactions with iodine at 350 to 455°C, 19: 42804(R) (GEAP-3771-16)
reactions with iodine in helium–steam mixtures, 20: 20940(R) (ORNL-

3915)
reactions with iodine, effects of oxide films on, 20: 23585(R) (GEAP-3771-18)
reactions with organic reactor coolants, 20: 33832
reactions with plutonium–uranium carbides at 820°C, 20: 9437
reactions with plutonium uranium carbide and uranium monocarbide at 820°C, 20: 27416(R) (UNC-5134(Vol.1))
reactions with steam during reactor transients, 18: 36751 (ANL-6912)
reactions with steam in simulated reactor loss-of-coolant accident, 19: 45496 (WCAP-3269-30)
reactions with steam and water at high temperatures, 20: 4183(R) (ORNL-3843, pp 2-70)
reactions with steam at 900 to 1500°C, 20: 31669
reactions with steam at high temperature, 20: 33806
reactions with steam at high temperatures, 20: 43828 (HW-66911)
reactions with steam, 19: 28771
reactions with uranium monocarbide at 1000 to 2400°C, 18: 8795 (HW-72031)
reactions with uranium dioxide at 950 to 1575°K, interfacial, 19: 44597 (GEAP-4679)
reactions with uranium nitride at 600 to 900°C, 20: 19187 (BMI-1760)
reactions with water in core meltdown, 19: 35607(R) (ANL-7045(p.60-9))
reactions with water during meltdown experiments, 20: 5843
reactions with water at 630 and 650°F, 20: 33827
reactor fuel element end caps of, 17: 4237 (HW-74287)
recovery and recrystallization of, effects of annealing on, 17: 20433 (HW-69680)
removal from uranium dioxide, fluid-bed fluoride volatility process for, 20: 12923 (ANL-6898)
sealing to glass, development of methods for, 18: 20134(R) (ORNL-TM-792)
segregations in, electronic probe microanalyzer study of, 18: 543 (CEA-2291)
shearing fuel tubes of, developments in, 19: 22429
shearing of, fire hazard from, 18: 35643(R) (ORNL-TM-823)
solubility in hydrofluoric acid at low temperatures, 19: 22429
sorption of hydrogen beyond terminal solubility by, 18: 8752(R) (HW-78388(p.9.1-4))
sorptive properties of, for hydrogen, 16: 24128 (WAPD-T-1281)
sorptive properties for hydrogen, 17: 3472 (CRGM-1081)
sorptive properties for hydrogen beyond terminal solubility, 17: 7552(R) (HW-74761(p.8.1-15))
sorptive properties of, for hydrogen in steam at 500°C and 1 atm. pressure, 17: 8715(T,R) (EURAEC-451)
sorptive properties for hydrogen, 17: 27751 (WAPD-T-1567)
sorptive properties for hydrogen from steam at 500°C, 17: 39468(T,R) (EURAEC-520)
sorptive properties for deuterium from heavy water at 275°C, 18: 7142(R) (HW-99754(p.5.16-17))
sorptive properties for hydrogen, 18: 7148(R) (HW-78962(p.5.13-23))
sorptive properties for deuterium, 18: 7148(R) (HW-78962(p.5.13-23))
sorptive properties for hydrogen in charging beyond terminal solubility, 18: 7209(R) (HW-77954(p.5.18-19))
sorptive properties for hydrogen from water, effects of applied electric potential on, 20: 9411(R) (BNWL-166, pp 5.4-6)
sorptive properties for hydrogen during aqueous corrosion, effects of environment on, 20: 11227
sorptive properties for hydrogen from hydrochloric acid, 20: 11227
sorptive properties for hydrogen to 400°C, effects of stresses on, 16: 20985
specific heat at 0 to 1050°C, 18: 2157(R) (BMI-1644(Del.))
strain anisotropy in tubing of, apparatus for studying, 20: 4304(R) (ORNL-3870, pp 171-83)
strain behavior of round and sheet tensile specimens of, 19: 47012 (ORNL-TM-1226)
strengthening with yttria dispersions, 20: 5851
stress-corrosion cracking by boiler water at 500°F and sea water at 550°F, 17: 27749 (KAPL-M-CC-3)
stress orientation of hydride platelets in tubing of, 18: 17998(R) (DPST-64-83-2)
stress relaxation in, by annealing, 18: 37622 (KAPL-M-6155)
stress-rupture in-pile testing, 17: 5040(R) (ORNL-3364(p.125-50))
stress-rupture properties of annealed, effects of hydrogen on, 18: 600 (CRGM-1169)
stress rupture tests on pressure tubes of, 19: 22966 (BNWL-8)
stress testing of tubing, 17: 14740 (TID-11295(2nd Ed.))
stresses in cladding of, during fuel powder loading by vibratory compaction, 20: 21289 (BNWL-194)
stresses in, effects of hydrogen embrittlement on, 17: 7555(R) (HW-74761(p.11.1-14))
stresses on tubular, during fuel compaction, 19: 39125(R) (BNWL-91)
structural analysis of fuel element containers for NS *Savannah*, 17: 34411 (ORNL-TM-483)
structure, 19: 28870(R) (BMI-X-10121)
structure of alpha-, effects of preferred orientation on creep, deformation, and fracture in, 20: 2339 (ORNL-P-1753)
structure of, influence of heat treatments on, 19: 30682
temperature distributions in, as fuel element end cap, 19: 30790
temperature effects, 17: 4230 (DL-51)
17: 14814 (BMI-1616)
tensile properties at 68 and 680°F, 17: 30905(R) (ARF-B198-42)
tensile properties of, effects of cold work and radiation on, 17: 32665 (HW-74955)
tensile properties at 300 to 1600°F, 17: 35104 (NAA-SR-Memo-3034)
tensile properties of, at 600°F, 16: 15231
tensile properties of pressure tubes of, 16: 18034 (HW-73398)
tensile properties of, impact and slow notch-bend testing of, 17: 1931 (HW-74339)
tensile properties of, prediction of, 17: 6691 (WAPD-T-1335)
tensile properties of, effects of high temperature and strain aging on,
tensile properties of, effects of hydrogen on, 18: 2276
tensile properties at 70 and 680°F, 18: 2162(R) (IITRI-B198-46)
tensile properties, 18: 7860(R) (HW-77954(p.6.20-6))
tensile properties, 18: 7294(R) (HW-77954(p.4.19-77))
tensile properties, 18: 7302(R) (HW-78962(p.4.50-126))
tensile properties, 18: 10452 (TID-20058)
tensile properties of, effects of hydride morphology and hydrogen on, 18: 14480 (WAPD-275)
tensile properties of irradiated and unirradiated, 18: 14537(R) (HW-79766(p.4.1-76))
tensile properties, notch, 18: 20843(R) (HW-79280(p.8.1-6))
tensile properties, effects of hot-water treatments on cold work recovery, 19: 6294 (HW-80309)
tensile properties of hydrided, 19: 4690
tensile properties, 19: 11682
tensile properties of, effects of cold work on, 19: 14110
tensile properties of, effects of specimen geometry on, 19: 26805 (AECL-2207)
tensile properties of, effect of texture on, 19: 30805
tensile properties, 20: 5846
tensile properties of hydrided, restoration of, at 100 to 200°C, 20: 5849
testing for in-core flux monitoring, 20: 35835(R) (DPST-66-83-5)
testing for SCE fuel cladding, 19: 45601(R) (WCAP-3750)
testing fuel cladding of, loss-of-coolant, 18: 38363 (A/CONF.28/P/438)
testing of, development of equipment for, 17: 7555(R) (HW-74761 (p.11.1-14))
testing of fuel claddings of, economics of nondestructive, 20: 14032
testing of fuel cladding of, eddy current, 20: 14033
testing of, nondestructive, 18: 9636 (ANL-6632)
testing of pressure tubes of, 17: 10128 (HW-74731)
testing of pressure tubes of, 18: 32044(R) (HW-81269(p.6.1-7))
testing of reactor pressure tubing of normal and hydrided, crack-propagation, 18: 27955 (HW-80567)
testing of reactor tube, 18: 44038(R) (HW-82651(p.6.1-8))
testing of reactor pressure tubes of, crack propagation, (E), 20: 10287 (BNWL-SA-179)
testing of sheath tubing of, 16: 3237 (HW-64452)
testing of thin-wall tubing of, ultrasonic, 18: 35699 (HW-81956)
testing of tubes of, ultrasonic, 16: 31955 (HW-72802)
testing of tubes of, for hydride by eddy-current testing, 17: 37003(R) (HW-78118)
testing of tubes of, for Hanford K Reactor, 18: 44039 (HW-82774)
testing of tubes of, ultrasonic equipment and method for nondestructive, 20: 14714
testing of tubing of, for EBWR fuel elements, 18: 2161(R) (HW-76302)
testing of, ultrasonic, 17: 4305(R) (SRO-74)
testing PRTR pressure-tube, 19: 17361(R) (HW-84281(p.6.1-10))
testing reactor tubes of, nondestructive method for, 20: 14711
testing tubes of, for JPDR, 19: 27793
testing tubular, 19: 22895(R) (HW-83298(p.9.1-3))
tests of pressure tubes of, 17: 40341(R) (GNEC-141(Del.))
thermal capacity at 50 to 700°C, 20: 13310
thermal cycling, effects on crystal structure and dimensional stability, 17: 14729 (CRGM-1106)
thermal cycling of, changes in length by, 16: 19380(T,R) (EURAEC-201)
thermal expansion in, analysis of slip lamellae in, 17: 39605
thermal expansion of, x-ray method for measuring, 20: 9504 (WAPD-TM-472)
thermal expansion of, effects of hydride phase on, 20: 31745
thermal stress fatigue behavior, 17: 14740 (TID-11295(2nd Ed.))
thermal stress fatigue tests, 19: 13980(R) (ATL-A-144)
thermal stress fatigue, 20: 11227
thermal stresses in, fatigue behavior in, 16: 33467 (ATL-A-127)
thickness measurement of claddings and tubes of, eddy current tester for, engineering drawings, 17: 21897
thickness measurement, autoradiographic technique for, 19: 46964 (NMI-4996, pp 149-63)

use as cladding for plasma-spray-coated ceramic fuel plates, 17: 20431(R) (ATL-A-126)
uses in nuclear reactors, 19: 39108
welding, 18: 5753
welding, 18: 8715(R) (CEND-186)
welding by electron beams, effects on properties, 17: 30955
welding for corrosion-resistant joints, 17: 6630
welding fuel element end closures of, process development for magnetic force, 20: 27406(R) (BNWL-198, pp 4.1-42)
welding of, at 100 to 150 kv, electron beam equipment and techniques for, 16: 19272
welding of, development of thermocouples for measurements in, 17: 11105 (TID-17734)
welding of, electron-beam, 17: 28526(R) (DP-845)
welding of fuel element spacer to, projection, 20: 12377(R) (CEND-2863-236)
welding of Inconel 600 to, joint design for explosive, 19: 40989
welding of, inspection and procedures for resistance, 17: 34381
welding of plates of Inconel and, experiments on explosive, 19: 11697 (BMI-X-328)
welding of tubes of, to stainless steel tube sheets, 20: 15019
welding of, argon shielded metal-arc, 19: 37015
welding of, to assemble or seal plutonium-containing fuel elements, 18: 24100 (HW-SA-3146)
welding ribs on thin-walled tubing of, apparatus for electron-beam, 20: 23620 (DP-996)
welding to Inconel, explosive, 18: 34033(R) (BMI-1669(Del.))
welding to Inconel, explosive, 18: 34034(R) (BMI-1672(Del.))
welding to Inconel flat plates, 18: 40970(R) (BMI-1674(Del.))
welding to Inconel using explosive methods, 19: 2716(R) (BMI-1681 (Del.))
welding to Inconel, explosive, 19: 13871(R) (BMI-1691(Del.))
welding to stainless steel, 17: 11084(R) (EURAEC-388)
welding to stainless steel type 410, explosive, 18: 4222
welding to titanium, 17: 23914 (TID-7620(Pt.I)(p.126-43))
welding with Inconel 600 to flat and contoured surfaces, explosive, 19: 39156(R) (CEND-532)
x-ray absorption coefficients at 40 to 130 kev, 17: 12600
x-ray attenuation coefficients, 17: 14740 (TID-11295(2nd Ed.))
x-ray attenuation in, measurement of, 20: 29707 (ORNL-TM-1457)
zirconium hydride precipitation in, effects of strain on directional, 17: 20453 (CRGM-1135)
zirconium self-diffusion in beta phase of, 17: 18820
Al–Zircaloy-2–ZrO_2, phase studies, 20: 39380 (AECL-2570)
BC–Zircaloy-2 dispersion, remote preparation of irradiated metallographic specimens of, 17: 6526 (TID-7625(p.20-9))
B_4C–Zircaloy-2, burnup of boron-10 in, at 400 to 650°F, 17: 23864(R) (BMI-1619(Del.))
B_4C–Zircaloy-2, corrosion by water at 600°F, 17: 23864(R) (BMI-1619(Del.))
B_4C–Zircaloy-2, radiation effects on, at high boron burnups at 400 to 500°F, 17: 24004 (BMI-1627)
B_4C–Zircaloy-2, radiation effects, 17: 26862(R) (MND-MD-2560-7)
B_4C–Zircaloy-2, release of helium from irradiated, effects of heat treatment on, 17: 23864(R) (BMI-1619(Del.))
Be–Th–Zircaloy-2, corrosion, 18: 29001(R) (HW-79280(p.5.1-25))
Be–Zircaloy-2, corrosion of, effects of thorium on, 18: 8721(R) (HW-78388(p.5.1-22))
Be–Zircaloy-2, corrosion by water at 300°C, effects of thorium contamination on, 19: 14806(R) (HW-81984(p.5.1-55))
Be–Zircaloy-2, fabrication of SLIS, 18: 5735(R) (NMI-2122)
Be–Zircaloy-2, fabrication and properties of splatcooled SLIS, 18: 35938(R) (NMI-2129)
Be–Zircaloy-2, fabrication and properties of splatcooled SLIS, 19: 34654(R) (NMI-1263)
Be–Zircaloy-2, hardness, 18: 25894(R) (NMI-2128)
Be–Zircaloy-2, microstructure of cast, effects of aging on, 18: 8726(R) (NMI-2123(p.47-51))
Be–Zircaloy-2, preparation and properties, 18: 18293(R) (NMI-2125)
Be–Zircaloy-2, preparation and properties of braze, 19: 26819 (NMI-4787)
Cr–Zircaloy-2, corrosion cracking by iodine at 350°C, stress-, 20: 5914(R) (GEAP-3771-17)
H_2O–Zircaloy, neutron ages and fluxes to indium resonance in, (T), 19: 31192 (KAPL-3080)
Nb–O–Zircaloy-2, phase studies and hardness measurements, 17: 30972 (KAPL-2286)
Nb–V–Zircaloy-2, radiation effects on phases in, neutron, 18: 39999 (KAPL-2251)
Nb–Zircaloy-2, radiation effects on phases in, neutron, 18: 39999 (KAPL-2251)
UO_2–H_2O–Zircaloy-2, chemical reactions of, 20: 23765(R) (ANL-7176, pp 86-93)
UO_2–Zircaloy-2, radiation effects on burnup at increased heat rating, 20: 2421 (EXP-NRX-22902)
U–Zircaloy-2, dissolution by hydrofluoric acid process, 17: 1564(R) (IDO-14593)
U–Zircaloy-2, dissolution in hydrofluoric acid, rates of, 20: 33411 (IDO-14674)
U–Zircaloy-2, fluid-bed fluoride volatility process for uranium separation from, 20: 12924 (ANL-6973)
U–Zircaloy-2, processing by fluoride volatility for uranium recovery, 19: 24064(R) (ANL-6997)
U–Zircaloy-2, processing for uranium recovery by fluoride volatility, 20: 5595(R) (ANL-6925, pp 107-64)
U–Zircaloy-2, processing for uranium recovery by fluoride volatility, 20: 20803(R) (ANL-7055, pp 99-162)
U–Zircaloy-2, separation by chlorination-fluorination reactions, 17: 36861(R) (ANL-6764)
U–Zircaloy-2, separation by chlorination and fluorination reactions, 18: 15663(R) (ANL-6808)
U–Zircaloy-2, separation of uranium from, fluid-bed fluoride volatility process for, 19: 18046 (ANL-6829)
U–Zircaloy-2, separation of uranium from, by precipitation and extraction, 20: 43438
Zircaloy-2–ZrB_2, burnup of boron-10 in, at 400 to 650°F, 17: 23864(R) (BMI-1619(Del.))
Zircaloy-2–ZrB_2, corrosion by water at 600°F, 17: 23864(R) (BMI-1619(Del.))
Zircaloy-2–ZrB_2, radiation effects on, at high boron burnups at 400 to 500°F, 17: 24004 (BMI-1627)

ZIRCALOY-3

corrosion by steam at 280 to 500°C and 15 to 800 lb/in.², 17: 12619
corrosion by steam and water, alloying effects on, 17: 37495(T) (TRG-Inf-Ser-100)
corrosion by steam at 750°F and 1500 psi, 18: 10452 (TID-20058)
corrosion by water at 280°C, 19: 37167(R) (HW-84609(p.8.1-7))
corrosion of, by steam and water, effects of impurities on, 16: 486 (BM-RI-5865)
corrosion of, by water at 360°C, effects of annealing atmosphere, cold-work, temperature, and time on, 16: 4492 (HW-69681)
corrosion resistance of, review on, 16: 12836
development, 17: 14744 (WAPD-T-1549)
hydridation of, effects on mechanical properties, 20: 30902
hydride orientation on, dependence on crystallographic texture, 20: 33828
mass transfer by sodium, 18: 15568
performance in reactor components, design criteria for, 18: 28023
phase composition in, determination of second, 17: 6719
radiation effect on mechanical properties at 70 to 600°F, 18: 34233
radiation effects, 17: 17447
reactions with steam at high temperature, 20: 33806
recovery and recrystallization of, effects of annealing on, 17: 20433 (HW-69680)
tensile properties, 18: 10452 (TID-20058)

ZIRCALOY-4

abrasion between cylinders and flats of, in water at 550°F, 20: 7488(R) (BMI-1742(Del.))
abrasion between cylinders and flats of, in water at 550°F, 20: 7490(R) (BMI-1745, Sect.A)
bibliography on properties of, 19: 39097 (GEMP-346)
burst testing of pressure tubes of, 17: 9837 (CVNA-144)
composition of commercial, 19: 39152(R) (BMI-X-10132)
corrosion and hydriding of, under heat-transfer conditions, computer program for prediction of, 20: 4331
corrosion and hydrogen absorption by electron-beam-welded, 20: 25489 (WAPD-TM-533)
corrosion and hydrogen absorption characteristics of, effects of silicon on, 20: 25490 (WAPD-TM-544)
corrosion by ammonium hydroxide, lithium hydroxide, steam, and water at high temperatures, hydrogen sorption from, 18: 21643(R) (WAPD-MRP-107)
corrosion by ammonium hydroxide, lithium hydroxide, steam, and water at high temperatures, hydrogen sorption from, 18: 29060(R) (WAPD-MRP-108)
corrosion by ammonium hydroxide, lithium hydroxide, steam, and water at high temperatures, hydrogen sorption from, 18: 45034(R) (WAPD-MRP-109)
corrosion by ammonium hydroxide, lithium hydroxide, steam, and water at high temperatures, hydrogen sorption from, 19: 12785(R) (WAPD-MRP-110)
corrosion by aqueous solutions, review, 18: 32081 (A/CONF.28/P/243)
corrosion by aqueous chlorides, 19: 29651(R) (WCAP-3269-3)
corrosion by aqueous chemical shim solutions at 600°F, 19: 40198(R) (WCAP-3721)
corrosion by boiling water, 18: 3134(R) (GEAP-4094)

corrosion by boric acid–potassium hydroxide solutions, 18: 30133 (WCAP-3737)
corrosion by boric acid, (E), 19: 5490(R) (WCAP-3269-2)
corrosion by deuterated lithium hydroxide, 18: 27856(R) (HW-79280 (p.9.1-4))
corrosion by deuterated and undeuterated lithium hydroxide solutions at 275°C, 18: 14407(R) (HW-79766(p.5.1-16))
corrosion by flowing water at 300 and 320°C, (E), 19: 24941
corrosion by fuel storage-basin water, electrochemical, 20: 28853(R) (IDO-14661, pp 45-82)
corrosion by halide solutions at 680°F, 17: 30941
corrosion by heavy water, 18: 7148(R) (HW-78962(p.5.13-23))
corrosion by heavy water at 275°C, 18: 7142(R) (HW-77954(p.5.16-17))
corrosion by heavy water in HWCTR, 19: 11668(R) (DP-945)
corrosion by hydrochloric and nitric acids, 18: 14410 (ORNL-3558(p.104-12))
corrosion by hydrochloric and nitric acids, 18: 22173(R) (ORNL-3591 (p.201-4))
corrosion by lithium hydroxide, steam, and water at high temperatures, hydrogen sorption from, 18: 7932(R) (WAPD-MRP-106)
corrosion by pressurized water, 19: 40195(R) (WCAP-3269-5)
corrosion by Santowax OM coolant at 320 to 400°C, out-of-pile and in-pile, 19: 13911 (AECL-2118)
corrosion by steam at 400°C, hydrogen pickup in, 18: 10471 (HW-67437)
corrosion by steam and water in reactor environment, 18: 34076 (TID-8540(p.213-330))
corrosion by steam and water, 19: 22870(R) (HW-83601)
corrosion by steam, effects of air introduction on, 20: 2257(R) (GEMP-52A, pp 47-52)
corrosion by steam at 1200 to 1600°C, 20: 9378(R) (GEMP-54A)
corrosion by steam at 1200 and 1400°C, 20: 27430(R) (GEMP-400A, pp 203-20)
corrosion by water, 18: 2188
corrosion by water at 260 and 280°C, 18: 22450
corrosion by water and steam at 500 to 950°F, 19: 11682
corrosion by water in ETR G-7 loop, 19: 30669(R) (HW-84573(p.5.1-22))
corrosion by water at 280°C, 19: 37167(R) (HW-84609(p.8.1-7))
corrosion by water at 680°F, effects of heat transfer on, 19: 40196(R) (WCAP-3269-6)
corrosion by water at high temperatures, 19: 39234 (GEAP-4597)
corrosion failure in aqueous iron chloride solutions, stress, 20: 4328 (WCAP-3269-50)
corrosion in reactor, ETR test of, 20: 27425(R) (BNWL-207, pp 5.1-12)
corrosion of, by lithium hydroxide and related solutions at high temperatures, 16: 33433 (WAPD-TM-307)
corrosion of, by steam and hot water, 16: 24128 (WAPD-T-1281)
corrosion of projections on tubes of, 18: 13354(R) (BMI-1657(Del.))
corrosion of stressed, in ferric chloride solutions, 19: 34647
corrosion of tubing of, by steam, 19: 4587 (GEAP-4739)
corrosion of, effects of environmental factors on hydrogen pickup during aqueous, 19: 9625 (WAPD-TM-411)
corrosion properties of, high-temperature, 17: 14744 (WAPD-T-1549)
deuterium absorption in deuterated lithium hydroxide, 18: 27856(R) (HW-79280(p.9.1-4))
development, 17: 14744 (WAPD-T-1549)
diffusion of fission products in, mechanisms of, 19: 39152(R) (BMI-X-10132)
diffusion of fission products in, 20: 2389
diffusion of fission products in irradiated, at 600 to 1200°C, 20: 21232 (BMI-1763)
effects of physical parameters on hydridation and oxidation of, for use as fuel element cladding, 20: 7519 (RCN-41)
embrittlement by steam during dynamic heating, 20: 2257(R) (GEMP-52A, pp 47-52)
evaluation for fuel clad in Connecticut Yankee reactor, 19: 27784 (UNC-5095)
extrusion of thin-walled tubes of, with internal ribs, 18: 10498 (TID-20047)
fabrication and properties of resistance-gathered projections on sheets of, 18: 15664(R) (BMI-1655(Del.))
fabrication and properties of tubes of, with spacing projections, 18: 20450(R) (BMI-1661(Del.))
fabrication into aluminum-lined tubes of, by explosive welding, 20: 37168(R) (BMI-1771)
fabrication into aluminum-lined tubes of, by explosive welding, 20: 37169(R) (BMI-1774)
fabrication of, for CVTR pressure tube, 16: 24973 (CVNA-141)
fabrication of projections on tubes of, 18: 17351(R) (BMI-1659(Del.))
fabrication of projections on sheet and tubing of, 19: 28773 (BMI-X-10096)
fabrication of, clad on zirconium–2.5 niobium pressure tubing, 20: 43862 (TID-23312)
fatigue at 1175°R of cold-worked, mechanisms of, 20: 37235
fatigue limits for, 19: 40196(R) (WCAP-3269-6)
fatigue of cold-worked, mechanisms of, 19: 40195(R) (WCAP-3269-5)
fatigue of fuel element cladding of, biaxial strain, 20: 5134(R) (WCAP-3269-12)
fatigue of thick sections of wrought and weld-metal, notch sensitivity, 19: 30738 (KAPL-3089)
fatigue properties of, effects of superimposed strain and oxide films on, 18: 20521 (KAPL-3016)
fatigue strength in bending, effects of added strains on, 18: 28022
fatigue strength of, effects of mean strain on, 18: 42013 (CONF-446-35)
fatigue strength of, oxide film and additional strain effects on, (E), 19: 20593
fatigue strength of, effects of superimposed strain on bending, 20: 11227
fretting-wear studies in water at 550°F, 20: 29616(R) (BMI-1738)
grain formation in heat-treated cold-worked, 19: 6296 (KAPL-3062)
heat treatment of, formation of large alpha grains induced by, 19: 18429 (KAPL-3066)
hydridation of, effects on mechanical properties, 20: 30902
hydridation of, in water, 20: 11221
hydridation of, in steam, effects of initial oxide layer formation on, 20: 25500
hydride orientation on, dependence on crystallographic texture, 20: 33828
hydride precipitation in, effects of stress on habit planes for, 20: 2355 (WAPD-T-1757(Rev.))
hydride precipitation in stressed and unstressed, habit planes for, 20: 27498 (WAPD-T-1757)
hydrogen absorption in deuterated and undeuterated lithium hydroxide solutions at 275°C, 18: 14407(R) (HW-79766(p.5.1-16))
ignition properties of wastes from machining operations on, 20: 15001 (HW-66930)
joining to chromium–iron–nickel Alloy 600, development of processes for, 19: 13941 (KAPL-3073)
mechanical properties of extruded, at 580°F, 18: 14465 (KAPL-2296)
mechanical properties of tubular, at 500 to 680°F, 19: 40195(R) (WCAP-3269-5)
mechanical properties at 750 to 800°F, 19: 40196(R) (WCAP-3269-6)
mechanical properties of, summary of, 19: 39097 (GEMP-346)
microstructure of cold-worked tubing of, effects of annealing on, 20: 29716 (WAPD-T-1819)
microstructure of, effects of cold-working on, 20: 29716 (WAPD-T-1819)
oxidation by heavy water, 18: 8752(R) (HW-78388(p.9.1-4))
oxidation by lithium hydroxide solutions at 275°C, 18: 32139(R) (HW-81269(p.5.1-23))
oxidation by steam during dynamic heating, 20: 27430(R) (GEMP-400A, pp 203-20)
oxidation by water vapor at 375 and 575°C, kinetics of, 20: 25498
oxidation rates in water-d_2 at 400°C, 17: 37003(R) (HW-78118)
performance as boiling-reactor fuel cladding, 18: 29069
performance as cladding in borated water at high pressures and temperatures, 20: 33791
performance as fuel coatings in PWR, 19: 34632
performance as fuel rod cladding, 20: 5134(R) (WCAP-3269-12)
performance in reactor components, design criteria for, 18: 28023
preferred orientation in, x-ray method for measuring, 20: 9504 (WAPD-TM-472)
properties as cladding and structural material in reactors, 18: 41947
properties as fuel cladding, 18: 30973(R) (HW-76304(p.3.1-19))
properties as fuel cladding, 19: 29651(R) (WCAP-3269-3)
properties for fuel cladding for water-cooled reactors, 20: 35849 (KR-89, pp 82-96)
properties of, mechanical and physical, 19: 45601(R) (WCAP-3750)
properties of, mechanical and physical, 20: 4400 (WCAP-3269-41)
properties of, summary of corrosion, hydridation, and oxidation, 19: 39097 (GEMP-346)
properties, mechanical and physical, (E), 19: 5490(R) (WCAP-3269-2)
radiation effect on mechanical properties at 70 to 600°F, 18: 34233
radiation effects on creep of, 16: 15925(R) (WCAP-4122)
radiation effects on hydridation of purposely defected, 16: 12177 (HW-65465)
radiation effects on mechanical properties of, research program on, 16: 7941 (TID-14763)
radiation effects on, 17: 16734 (CVNA-159)
radiation effects on tubes of, 18: 2354
radiation effects on tensile properties at 343°C, 18: 4761(R) (GEAP-4383)
radiation effects on mechanical properties of, neutron, 18: 14533 (CONF-187-98)
radiation effects on corrosion of, 19: 16018(R) (HW-84281(p.5.26-30))
radiation effects on oxidation by low-oxygen water, neutron, 19: 16016(R) (HW-84281(p.5.1-5))
radiation effects on mechanical properties of, 19: 40195(R) (WCAP-

3269-5)
radiation effects on properties of, summary of, 19: 39097 (GEMP-346)
radiation effects on mechanical properties of, 19: 39234 (GEAP-4597)
radiation effects on tensile properties of, neutron, 19: 40961
radiation effects on hydridation and oxidation of, for use as fuel element cladding, (E), 20: 7519 (RCN-41)
radiation effects on corrosion of, by water, effects of fabrication history on fast-neutron, 20: 23767 (BNWL-88)
radiation effects as fuel claddings of, 20: 28733(R) (GEAP-4919)
radiation effects on fuel element cladding of, in-pile, 20: 33867 (GEAP-4849)
reactions with organic reactor coolants, 20: 33832
reactions with steam, facility for testing, 19: 45601(R) (WCAP-3750)
reactions with steam at high temperature, 20: 33806
reactions with urania at 1900°C, 20: 2257(R) (GEMP-52A, pp 47-52)
reactions with urania in steam, effects of heating rate to 1750°C on, 20: 27409(R) (GEMP-58A)
reactions with urania at 1900 to 2200°C, 20: 27430(R) (GEMP-400A, pp 203-20)
reactions with water at 630 and 650°F, 20: 33827
reactions with water in LOFT experiment, 20: 45112 (IDO-17168)
recrystallization of cold-worked alpha-, primary and secondary, 20: 2330 (KAPL-3091)
recrystallization of as-quenched and beta-quenched, primary and secondary, 20: 2331 (KAPL-3103)
sorption of deuterium in heavy water, 18: 8752(R) (HW-78388(p.9.1-4))
sorptive properties of, for hydrogen, 16: 24128 (WAPD-T-1281)
sorptive properties for deuterium, 18: 7148(R) (HW-78962(p.5.13-23))
specifications for tubing of, for use as fuel jackets, 18: 10448 (HW-66921)
strain fatigue in biaxially stressed, testing procedure for, 20: 23658 (WCAP-3269-42A)
strain fatigue in cold-worked tubular, 20: 23659 (WCAP-3269-42B)
strain fatigue limit of fuel cladding of, biaxial, 20: 12418(R) (WCAP-3739)
strength of, methods for increasing, 19: 40961
strengthening by heat treatment and oxygen addition, 18: 44139 (KAPL-3036)
stress corrosion by aqueous ferric chloride at 68°F, 19: 40196(R) (WCAP-3269-6)
stress-corrosion cracking by boiler water at 500°F and sea water at 550°F, 17: 27749 (KAPL-M-CC-3)
stress corrosion in ferric chloride solutions, 18: 27911
stress relaxation in, by annealing, 18: 37622 (KAPL-M-6155)
stress-strain properties at 580°F under biaxial loading, 18: 14370 (KAPL-M-JOS-2)
temperature distributions in fuel element end cap of, 19: 21674
temperature distributions in, as end caps for annular fuel elements, 19: 29586
tensile properties of tubing of, with oriented hydrides, 17: 4932 (TID-17372)
tensile properties of, effects of hydrogen content and hydride orientation on, 18: 12639 (GEAP-4089(Vol.II)(Paper 14))
testing as cladding for plutonia–urania fuel, 20: 28767 (WCAP-3385-53)
testing of fuel claddings of, economics of nondestructive, 20: 14032
testing of fuel cladding of, eddy current, 20: 14033
testing of tubes of, ultrasonic, 16: 31955 (HW-72802)
thermal expansion of, x-ray method for measuring, 20: 9504 (WAPD-TM-472)
thermal expansion of, effects of hydride phase on, 20: 31745
use in coolant loops of organic-cooled reactors, 20: 33800
use in N.S. *Savannah* fuel element containers, evaluation of, 18: 1286 (ORNL-3476)
weld joint design for tubes of, end closure, 20: 5865 (WCAP-3269-37)
welding duplex tubing of aluminum alloy 1100 and, process development for explosive, 20: 7493(R) (BMI-1748(Del.))
welding of aluminum, process development for explosive, 20: 23582(R) (BMI-1765)
welding of, to aluminum, process development for explosive, 20: 19177(R) (BMI-1757)
welding to aluminum, explosive, 20: 35834(R) (BMI-1767)
welds in, effects of welding process on distortion in, 20: 25566 (KAPL-3120)
Nb–Zircaloy-4–Zr, fabrication of tubular, methods for, 19: 47998(R) (SRO-118)
UO_2–Zircaloy-4–ZrO_2, dissolution of fused, 20: 43067(R) (IDO-14679, pp 6-46)

ZIRCEX PROCESS

(Separation of U from U–Zr fuel elements by hydrochlorination to UCl_4 and $ZrCl_4$, and subsequent $ZrCl_4$ distillation.)
development for TRIGA reactor fuel, 16: 3066 (ORNL-3065)
development of, 16: 32883(R) (ORNL-3314(p.1-39))
dissolution in, 18: 13969
thermodynamics, 19: 19742 (CEA-R-2592)

ZIRCONATES

see also Barium Zirconates
see also Calcium Zirconates
see also Cerium Zirconates
see also Chlorozirconates
see also Europium Zirconates
see also Fluozirconates
see also Lanthanum Zirconates
see also Lead Zirconates
see also Lithium Zirconates
see also Neodymium Zirconates
see also Potassium Oxalatozirconates
see also Potassium Silicozirconates
see also Potassium Zirconates
see also Sodium Oxalatozirconates
see also Sodium Zirconates
see also Strontium Zirconates
see also Yttrium Zirconates
dielectric dispersion of, 18: 42162(R) (TID-20963)
melting points of alkali metal, 17: 29170(R) (ASD-TDR-63-233)
preparation of alkaline-earth, 16: 15126(R) (NP-11584)
properties for magnetohydrodynamic cell insulators, 17: 31012

Zirconia

see Zirconium Oxides

ZIRCONIUM

ablation during re-entry, device for testing, (E), 19: 47117(R) (SC-DC-65-1698)
abrasion of, friction, wear, and work-hardening during, 18: 18363
abundance in solar atmosphere, 16: 29599 (AFOSR-3024)
abundance in solar system, (T), 19: 6433
abundance in sun, (E), 20: 17237
abundances in iron and stone meteorites, 18: 5901
allotropic transformation in, effects of rare earths on, 20: 5891(R) (NYO-2159-1)
alloying characteristics with rare earths, 18: 41924(R) (IITRI-578P19-13)
alloying effects on high-temperature properties of uranium alloys, 16: 2246
alloying effects on properties of niobium, 16: 7897 (WADC-TR-57-344 (Pt.V))
alloying effects on properties of magnesium–thorium alloys, 16: 9246
alloying effects on tantalum and tungsten alloys, 16: 13562(R) (AD-259116)
alloying effects on corrosion of titanium by mercury at 371°C, 16: 12649(R) (ANL-6485)
alloying effects on aluminum–niobium–titanium alloys, 16: 15167 (ARF-2201-15)
alloying effects on aluminum alloy type 7075, 16: 9222
alloying effects on corrosion and rupture behavior of uranium, 16: 9197 (HW-63137)
alloying effects on corrosion of carbon–uranium systems, 16: 9150 (HW-62875)
alloying effects on uranium extrusion, 16: 13546 (HW-62347)
alloying effects on strain-aging in niobium alloys, 16: 21063
alloying effects on aluminum–niobium oxidation by air, 16: 24174 (TID-16032)
alloying effects on oxidation of $NbAl_3$ at 760°C, 16: 27590(R) (DRI-2043)
alloying effects on internal friction in niobium, 16: 33500
alloying effects on mechanical properties of niobium and tungsten, 16: 3443 (ASD-TR-61-3)
alloying effects on aluminum–niobium alloy oxidation, 17: 4902(R) (DRI-2061)
alloying effects on chromium-nickel steel, 17: 11210
alloying effects on iron–nickel–tungsten alloys, 17: 14825(R) (LAR-12)
alloying effects on iron–nickel–tungsten alloys, 17: 14826(R) (LAR-14)
alloying effects on iron–nickel–tungsten alloys, 17: 14827(R) (LAR-17)
alloying effects on ultimate tensile strength of thorium–uranium alloy, 17: 14740 (TID-11295(2nd Ed.))
alloying effects on titanium, 17: 16580(P)
alloying effects on iron self-diffusion, 17: 22177
alloying effects on mechanical properties of vanadium, 17: 25771 (ASD-TDR-62-667)
alloying effects on negative thermal expansion of delta plutonium, 17: 29340
alloying effects on magnesium, 17: 29349
alloying effects on molybdenum–tantalum–tungsten alloys, 17: 29312(R) (ASD-TDR-62-594(Pt.II))
alloying effects on formation of macrostructure of aluminum alloys, 17: 32591
alloying effects on mechanical properties of magnesium–manganese–thorium alloys, 17: 32595
alloying effects on properties and structure of magnesium–thorium alloys,

17: 32596
alloying effects on corrosion resistance of niobium to steam at 540°C, 17: 36221 (BMI-1636)
alloying effects on hardness of chromium, 17: 37548
alloying effects on uranium, effects of quenching temperature on, 17: 39627
alloying effects on austenitic steel, 17: 41437(T,R) (EURAEC-598)
alloying effects on machinability of plutonium–uranium alloy, 17: 40422(R) (ANL-6784)
alloying effects on niobium–tantalum–vanadium alloys, 18: 5732(R) (IITRI-B6007-5)
alloying effects on magnetic, mechanical, and oxidation properties of aluminum–iron alloys, 18: 7226
alloying effects on niobium corrosion by lithium, 18: 14409 (ORNL-3551)
alloying effects on oxidation of niobium at 500 and 1000°, 18: 14413(T) (FTD-TT-63-1020)
alloying effects on fissium–plutonium–uranium alloys, 18: 15563
alloying effects on tensile properties of titanium base alloys at room temperature, 18: 18380
alloying effects on iron–nickel alloys, 18: 24161
alloying effects on niobium oxidation, 18: 25936
alloying effects on electric conductivity, hardness, and structure of niobium, 18: 25999
alloying effects on oxidation of plutonium–uranium alloys, 18: 26893(R) (ANL-6868(p.11-108))
alloying effects on Magnox alloys for use as canning material, 18: 27999
alloying effects on carbon steel corrosion, 18: 30140
alloying effects on high-temperature properties of niobium–tantalum base alloys, 19: 37151(P)
alloying effects on high-temperature properties of niobium–tantalum base alloys, 19: 37152(P)
alpha attenuation by, energy-range relations in, 19: 46324(R) (AGN-8132)
alpha elastic scattering at 24.7 Mev, relative cross sections for, 18: 34902
alpha reactions at 24 Mev, isomer production in, (E), 20: 46717
alpha scattering at 25 Mev by, differential cross sections for elastic (E), 19: 1234 (PAN-347)
analysis, 17: 6020
analysis after neutron irradiation, systematic, 16: 16784
analysis by neutron activation, 17: 33819
analysis for alloying constituents and impurities, polarographic, 16: 18820
analysis for boron by direct absorptiometric method, 17: 5965 (PG-Report-362)
analysis for boron, spectrophotometric, 17: 21641
analysis for boron using curcumin, 17: 25118 (PG-Report-251)
analysis for boron using curcumin, 17: 27265
analysis for cadmium, copper, lead, and zinc, oscillopolarographic, 18: 6759
analysis for calcium in reactor grade, spectrographic, 17: 33793 (PG-Report-441)
analysis for carbon and nitrogen, activation, 16: 12986
analysis for carbon dioxide, carbon monoxide, hydrogen, and nitrogen by hot-vacuum extraction, 17: 14147 (PG-Report-412)
analysis for carbon and hydrogen simultaneously, method for, 18: 1540
analysis for carbon, hydrogen, and oxygen, 19: 15406
analysis for cobalt, spectrographic, 17: 2907 (WAL-TR-823.5/1)
analysis for hafnium, activation, 16: 18832
analysis for hafnium, differential spectrophotometric, 17: 12221
analysis for hafnium, activation, 17: 27289
analysis for hafnium using cyclohexanone, method for, 18: 1552
analysis for hafnium by tape method, quantitative spectrographic, 18: 3699
analysis for hafnium, activation, 18: 5219
analysis for hafnium, activation, 20: 16335(R) (NBS-TN-276)
analysis for hafnium, 20: 29114
analysis for hafnium, 20: 29115
analysis for hydrogen by equilibrium gas pressure functions, 16: 8675 (KAPL-M-AHA-2)
analysis for hydrogen using dosivac, 18: 34060(T,R) (EURAEC-1062)
analysis for hydrogen, equipment for, 18: 33511
analysis for hydrogen, analyzer for, 19: 32059(R) (IDO-14655)
analysis for impurities, methods of spectrochemical, 16: 22038
analysis for impurities by activation, 19: 24418
analysis for impurities, mass spectrometric, 20: 235 (Y-KG-28)
analysis for iron, spectrographic, 17: 2907 (WAL-TR-823.5/1)
analysis for iron, 17: 5946 (AERE-AM-91)
analysis for light rare earths, direct spectrochemical, 18: 37076 (IA-925)
analysis for molybdenum and tin using 8-quinolinol, spectrophotometric, 16: 16314
analysis for niobium, oscillographic, 19: 32092
analysis for nitrogen and oxygen by d-c carbon-arc, gas chromatographic technique, 19: 9069
analysis for nuclear impurities, 16: 28885
analysis for oxygen by sulfur monochloride method, 16: 14631(T) (UCRL-Trans-801(L))
analysis for oxygen by emission spectrography in argon atmosphere, 16: 26904(T) (AEC-tr-5276)
analysis for oxygen, vacuum fusion, 16: 26911
analysis for oxygen, fast-neutron activation, 16: 26914
analysis for oxygen, neutron activation, 16: 28887
analysis for oxygen, activation, 20: 16331 (GA-6568)
analysis for oxygen by helium-3 activation, 20: 36741
analysis for rare earths, spectrographic, 20: 2520(R) (IA-920)
analysis for rhenium by anion exchange, 19: 13220
analysis for sulfur, luminescent method for, 18: 33513
analysis for surface oxygen by neutron activation methods, 19: 24410
analysis for thorium using *N*-benzoyl-*N*-phenylhydroxylamine, gravimetric, 19: 46194
analysis for tin, polarographic, 18: 13673
analysis for titanium, oscillographic, 19: 32092
analysis for trace impurities, mass spectrometric, 19: 26226 (CEA-R-2721)
analysis for vanadium, spectrographic, 17: 2907 (WAL-TR-823.5/1)
analysis for 8 elements by neutron activation, 16: 23633 (TID-7629 (p.239-44))
analysis of, for boron, 17: 5970 (PG-Report-391)
analysis of, for tungsten by solvent extraction using 8-quinolinol, 17: 19952
analysis of standards for hafnium, 16: 8676 (KAPL-M-FW-4)
analysis of very pure, for impurities by radioactivation, 17: 4480
analysis of zone-refined, for impurities, activation, 17: 39004
analysis of, use of activation methods for, 18: 29577
analytical use with Eriochrome cyanine R for spectrophotometric determination of fluorides, 18: 27302
annealing of cold-worked, at temperatures from 300 to 800°C, 16: 3422 (HW-69679)
annealing of deformed, dilatometric and thermal effects during, 19: 2830
annealing of neutron radiation effects on electric conductivity of, 16: 27700(T) (AEC-tr-5263)
annealing, cold-working, and precipitation phenomena in, electron microscope studies on, 18: 22482 (EURAEC-999)
anodic oxide film capacitance on, effects of proton space charge on, 19: 13365
anodic treatment of, process for, 17: 12625(P)
argon-ion reactions on, secondary from, 17: 16836
Auger spectrum, 17: 16810
availability, costs, and purity of, (E), 19: 31532 (BMI-X-151)
band structure, 16: 27673
behavior in surface waters, fission product, 16: 399(T) (CEA-tr-A-1012)
behavior of hydrided in HTRE-2 burnout tests, 16: 8350 (DC-58-3-37)
behavior of, in reduction of fissium oxide, 16: 28641(R) (ANL-6543)
bibliography, 16: 18022 (BM-IC-8048)
bibliography on preparation, fabrication, and uses of, 18: 34151
bibliography on SNAP fuel materials containing, 18: 33128 (NAA-SR-9525(Vol.I))
bonding at 1050 to 1500°F, effects of surface preparation on self-, 19: 42801(R) (BMI-1721(Del.))
bonding by solid-state pressure, 18: 34034(R) (BMI-1672(Del.))
bonding of, effects of interatomic forces and surface contaminants on solid-state pressure, 19: 30642(R) (BMI-1707(Del.))
bonding of, factors affecting solid-state pressure, 19: 18420(R) (BMI-1694(Del.))
bonding of, gas-pressure, 18: 17351(R) (BMI-1659(Del.))
bonding to aluminum, extrusion, 19: 26782 (AECL-2243)
bonding to copper and stainless steel by extrusion, 18: 27937
bonding to ferrous metals, 18: 25962(P)
bonding to magnesium, 18: 30107 (AERE-R-4594)
bonding to stainless steel by hot coextrusion in iron jacket, 18: 41997(P)
bonding to uranium, diffusion in, 17: 25745(R) (NYO-9329)
bonding to zirconium and other materials, brazing alloy, 16: 12173(P)
bonding to zirconium by gas pressure, 18: 20450(R) (BMI-1661(Del.))
bonding to zirconium by solid-state pressure, effects of hydride interphase on, 19: 22865(R) (BMI-1711(Del.))
bonding to zirconium, solid-state pressure, 19: 32676(R) (BMI-1717(Del.))
bonding to zirconium, effects of interatomic forces on pressure, 19: 39091(R) (BMI-1723(Del.))
book: *Critical Review of the Analytical Methods of the Titanium, Vanadium, and Chromium Transition Element Groups*, 18: 3702
book: *New Treatise on Inorganic Chemistry*, Vol. IX, 19: 4162
book: *Rare Metal Extraction by Chemical Engineering Techniques*, 18: 13952
book: *Special Metallurgy*. Vol. 3. *Zirconium and Its Alloys*, 17: 32512
braze cladding of, on steel, technique for vacuum-pressure, 18: 7177
brazing to uranium, 17: 40153(R) (AD-290727)
bremsstrahlung reactions (γ,p) at 24 Mev, direct photoeffect and evaporation contributions in, 17: 38209

brittleness of, effects of hydrogen on, 19: 44716
bromine-80 isomer separation on, 19: 36562
burning, inhibition by halogenated hydrocarbons, 17: 25213
burning of scraps of, tests on, 17: 18436
burning propagation in, 17: 1359(R) (ANL-6569)
burning temperatures in air, 17: 25211
burning velocities in air, 17: 25212
carbon diffusion in beta, 19: 32742
carbon monoxide photodesorption from, efficiency and mechanism of, 19: 7408
carbon monoxide photoinduced desorption from, 19: 5974
carburization of, identification of products from, 18: 201 (JEN-116-DMe/I-11)
casting in expendable molds, 18: 39854 (BM-RI-6509)
catalytic action on phosphoric acid ester decomposition, 17: 33955
catalytic effects on dephosphorylation of phosphoric acid esters, 17: 23071
charged particle reactions with, cross sections for, 17: 34886 (UCRL-10783)
chemical behavior, electrodialysis and extraction studies, 16: 8815(R) (TID-14694)
chemical behavior in acid and aqueous solutions, 17: 6097
chemical properties of, in aqueous solutions, 18: 35508 (UJV-1066/64)
chemical properties, 19: 5860
chemistry, analytical, 16: 8701
chemistry of aqueous solutions of, bibliography on, 18: 23472
chemistry of, in aqueous zirconyl chloride, 17: 14247
chemistry of, in industry, 17: 15989
chemistry of, review of structural aspects of, 19: 4153
chlorination of, corrosion and reaction rates in processing by, 18: 39386
cladding thickness on reactor fuel elements, use of x ray for determination of, 18: 6939
coating with aluminum for hydrogen barrier, 17: 36298 (NAA-SR-Memo-8060(Rev.))
coating with chemical conversion coatings, 16: 27576(P)
coating with steel, 18: 41481(P)
combustion and explosion of droplets of, by flash heating, 20: 12826 (SC-RR-65-569)
combustion in argon–oxygen mixtures, 19: 38583(R) (SC-DC-65-1480)
combustion in oxygen, explosive effects of nitrogen on, (E), 19: 32050
combustion in oxygen, luminous energy of, 19: 42887
combustion of falling droplets of, in air and argon–oxygen, 19: 2275 (SC-DC-64-1559)
combustion of falling drops of, ignited by flash heating, 20: 45672
combustion of, in pyrotechnic mixture with inorganic oxidizer, 19: 42518
combustion of, powders for extinguishing, 20: 46007(P)
combustion of, research summary on, 19: 13671(R) (WASH-1052)
compatibility of coatings of, with plutonium, thorium, and uranium, 17: 8843
compatibility with thorium uranium beryllides, borides, and carbides at 1090°C, 17: 40423(R) (BMI-1639(Del.))
compatibility with iridium at high temperatures, 18: 14493
compatibility with uranium nitrides at 600 to 700°C, 18: 32037(R) (BMI-X-10092)
compatibility with beryllium–thorium–uranium alloy, 18: 34033(R) (BMI-1669(Del.))
compatibility with uranium and uranium carbides, 18: 40827 (EUR-1830.e(Pt.II))
compatibility with uranium nitride, 19: 2717(R) (BMI-X-10100)
compatibility with urania, 20: 11224
compatibility with uranium at 500 to 900°C, 20: 11316
compatibility with water in reactor environment, 20: 14996
compatibility with uranium phosphides at high temperatures, 20: 23640(R) (ANL-7176, pp 45-72)
compatibility with plutonium carbides at 1200 to 1400°C, 20: 29820
conference on hydriding and irradiation effects, Buffalo, New York, Oct. 10–14, 1965, 20: 27420
content and distribution in acid igneous rocks of Africa, 18: 37358
content in alkali igneous rocks, 16: 31970
content in chondrites, 19: 4350
content in granites and zircons, 16: 25629
content in meteorites, tektites, and terrestrial materials, 18: 32339
content in meteorites, role in nucleosynthetic theories, (E/T), 19: 9857
content in minerals and rocks, ratio to hafnium, 16: 25631
content in ratio with hafnium in zircon from Southern California batholith, 18: 39483
content in ratio with hafnium in chondrites, 19: 4350
content in zircons from granitoids of Dnieper area, USSR, 20: 7264
content in zirconyl phosphates, ratio to phosphorus, 17: 27351
contents in meteorites, 19: 37428(R) (N64-32896)
corrosion, 16: 12836
corrosion, analysis of film, 17: 15466(R) (SRO-77)
corrosion and oxidation of annealed and etched, by air and water, 20: 4319 (EURAEC-1457)
corrosion by acid, alkaline, and neutral solutions, effects of halide ions on pitting, 16: 17986
corrosion by acid solutions, 17: 8747
corrosion by acids and chloride salts in chemical plants, 16: 20983
corrosion by alkaline solutions, effects of cathodic polarization on, 18: 30137
corrosion by aluminum–silicon and water of coatings of, on uranium, 19: 40949 (ISC-640)
corrosion by anodization and steam dielectric-loss spectra of films formed in, 18: 41964
corrosion by aqueous chlorides, 19: 29651(R) (WCAP-3269-3)
corrosion by aqueous solutions at high temperatures, electrochemistry of, 19: 30650(R) (ORNL-3789(p.126-38))
corrosion by aqueous hydrofluoric and sulfuric acid solutions, electrochemical, 18: 2181(R) (ORNL-3488(p.91-5))
corrosion by biphenyl, 20: 25491(T) (AECL-2330, pp 179-95)
corrosion by boiling cesium in loop, 18: 18279 (AGN-8041(Del.))
corrosion by boiling cesium, 19: 13913(R) (AFML-TR-64-327)
corrosion by carbon dioxide at 700°C, 16: 4583(P)
corrosion by carbon dioxide at 450°C, 17: 27730(R) (HW-77052)
corrosion by carbon monoxide at 600°C, 18: 7141(R) (HW-77954(p.5.14-15))
corrosion by carbon dioxide at 800 to 1300°F, 18: 12576 (GEAP-4089 (Vol.I)(Paper 3))
corrosion by carbon dioxide at 500 to 700°C and 60 atm, 18: 37630 (A/CONF.28/P/63)
corrosion by carbon dioxide, 19: 11682
corrosion by carbon dioxide and carbon monoxide at 850°C, 19: 28759
corrosion by cesium at 1600 to 2500°F, 16: 16684 (TID-7626(Pt.I) (p.109-10))
corrosion by cesium at high temperatures, design of capsules for testing, 17: 3426(R) (NP-12189)
corrosion by cesium at 1600°F, role of oxygen in, 18: 16447
corrosion by cesium at 1600, 1800, and 2500°F, 20: 5846
corrosion by chloride solutions and water, structure of films formed in, 18: 4205
corrosion by cupric and ferric chloride solutions at 35°C, effects of purity and surface treatment, 16: 15143 (BM-RI-5945)
corrosion by deuterated lithium hydroxide, 18: 27856(R) (HW-79280 (p.9.1-4))
corrosion by deuterated and undeuterated lithium hydroxide solutions at 275°C, 18: 14407(R) (HW-79766(p.5.1-16))
corrosion by gas–oil, hydrogenated terphenyl, and monoisopropylbiphenyl at 330 to 400°C, 20: 25492(T) (AECL-2330, pp 196-217)
corrosion by heavy-water steam at 400°C, 17: 27730(R) (HW-77052)
corrosion by high-pressure flowing steam at 300, 400, and 500°C, 17: 34346(R) (GEAP-4211)
corrosion by high-temperature aqueous solutions, effects of copper sulfate on, 18: 22446(R) (ORNL-3591(p.77-83))
corrosion by hydrochloric acid at 150 to 250°C, effects of impurities on and reactor kinetics, 16: 13533
corrosion by hydrochloric acid, effects of solution heat treatment on, 17: 22118
corrosion by hydrochloric acid, tracer studies of effects of ammonium fluorides, copper chlorides, and iron chlorides on, 20: 29649
corrosion by hydrochloric acid in benzene, ethanol, and ethyl ether, tracer studies of, 20: 35855
corrosion by impure Santowax, 17: 23891 (NAA-SR-7755)
corrosion by liquid sodium, 17: 36873 (LADC-5783)
corrosion by liquid lithium, effects of oxygen on, 18: 14409 (ORNL-3551)
corrosion by liquid potassium chloride–sodium chloride at 700, 800, and 900°C, 18: 24089
corrosion by lithium, effects of oxygen, 16: 22552
corrosion by lithium at 1500 to 1900°F, 17: 6570 (ORNL-2674)
corrosion by lithium, effects of carbon, nitrogen, or oxygen on, 18: 27914
corrosion by lithium at 1500 to 1600°F, 19: 36980 (PWAC-355)
corrosion by molten mixture of potassium and sodium chlorides, 20: 5855 (JPRS-32341, pp 24-31)
corrosion by nitrate–nitrite fused salt mixture at 400 to 600°C, 17: 25724 (TID-18773)
corrosion by nitric and phosphoric acids, 16: 33441
corrosion by oxygen and water vapor at high temperatures, kinetics of, 17: 495 (HW-73511)
corrosion by oxygen, mechanism of, 17: 25722 (GEAP-3999)
corrosion by oxygen and steam at 500°C, 17: 32520
corrosion by oxygenated sodium at 540°C, effects of polarizing current on, 19: 44616(R) (ANL-7000, pp 122-37)
corrosion by perchlorate solutions, pitting, 20: 31687
corrosion by polyphenyls at 330 to 400°C, 16: 22547
corrosion by potassium at high temperature, 16: 16684 (TID-7626(Pt.I) (p.69-86))
corrosion by potassium, effects of oxygen on, 18: 27914

corrosion by potassium hydroxide and potassium sulfate at 50 to 90°C, effects of electrode potential on, 20: 16979
corrosion by reactor coolant, 16: 491(T) (CEA-tr-A-979)
corrosion by sodium in Sodium Reactor Experiment, 16: 1191 (NAA-SR-5363)
corrosion by sodium (liquid), 18: 2187
corrosion by sodium at high temperatures, 18: 44926(R) (ANL-6923(p.46-78))
corrosion by sodium, effects of hydrogen on, 19: 23991(R) (ANL-7003)
corrosion by sodium at 540°C, 19: 29468(R) (ANL-7017)
corrosion by sodium vapor, 19: 40113(R) (ANL-7071)
corrosion by sodium at 540°C, 19: 40112(R) (ANL-7046(p.36-66))
corrosion by steam at 500°C, hydrogen uptake, 16: 485 (AERE-R-3768)
corrosion by steam at 425°C and oxygen at 700°C, 16: 9141(R) (NMI-2101)
corrosion by steam to 550°C, 16: 32084(T,R) (EURAEC-227)
corrosion by steam and water, 17: 1882
corrosion by steam, inhibition using boric acid, 17: 20428(P)
corrosion by steam at 400°C, alloying effects of chromium, iron, niobium, and tin on, 17: 37495(T) (TRG-Inf-Ser-100)
corrosion by steam, effects of additives on, 18: 7134 (AERE-R-4458)
corrosion by steam, additive effects of hydrogen and nitrogen on, 18: 10476(T) (JPRS-22697(p.8-26))
corrosion by steam at 400°C, 18: 24150(T,R) (EURAEC-538)
corrosion by steam, effects of additives on, 18: 26824(R) (ANL-6885)
corrosion by steam and water, 18: 37635 (A/CONF.28/P/445)
corrosion by steam and water at high temperatures, 18: 37632 (A/CONF.28/P/341)
corrosion by steam at 500°C, hydrogen uptake in, 19: 22901
corrosion by steam, effects of boric acid on, 19: 32701(P)
corrosion by steam at 500°C, effects of surface contamination on, 20: 11227
corrosion by sulfuric acid, 16: 33440
corrosion by sulfuric acid solutions, mechanisms of high-temperature, 20: 23602(R) (ORNL-3913, pp 53-73)
corrosion by superheated steam at 540 and 650°C, effects of copper, iron, nickel, and oxygen on, 19: 22899
corrosion by terphenyls, 16: 22551
corrosion by uranyl sulfate solution at 280°C, in-pile, 17: 27750 (ORNL-3099)
corrosion by water at 360°C, effects of annealing atmosphere, cold-work, temperature, and time on, 16: 4492 (HW-69681)
corrosion by water and steam, bibliography, 16: 4504 (VDIT-7.1)
corrosion by water at 85°C, 16: 12063
corrosion by water at 680°F, 16: 16674(R) (ARF-2198-24)
corrosion by water, effects of cathodic polarization, 16: 22154
corrosion by water at high temperatures and pressures, effects of anions, 16: 22557
corrosion by water at 260 and 280°C, 18: 22450
corrosion by water or water vapor in radiation environment, 19: 7870
corrosion cracking by iodine at 350°C, stress-, 20: 5914(R) (GEAP-3771-17)
corrosion cracking in alcohol–acid solution, effects of water on stress, 20: 14988
corrosion, effects of metal clorides in oxide film, 16: 5715(R) (NMI-2098)
corrosion, effects of failure of oxide film and incorporation of foreign ions, 16: 10534(R) (NMI-2102)
corrosion films on, development of stripping method for, 18: 44931(R) (ANL-6936(p.39-72))
corrosion in PRTR, 18: 9646(R) (HW-78388(p.11.1-15))
corrosion in water-cooled reactors, 18: 11373
corrosion mechanisms of, 19: 22870(R) (HW-83601)
corrosion of, by gases at high temperature, bibliographic review of, 17: 20422
corrosion of coatings of, 17: 39555
corrosion of crystals of, by pure water at 680°F, 17: 499(R) (KAPL-2000-19(p.III.1-III.9))
corrosion of crystals of, by water at 680°F, 17: 27748 (KAPL-2257)
corrosion of crystals of, by neutral water at 680°F, 17: 20415 (TID-16895)
corrosion of, effects of gases on, 17: 6020
corrosion of, effects of hydrogen on, 17: 6585
corrosion of high-purity, in demineralized water and superheated steam, effects of iron on, 19: 4628
corrosion of single crystals of, by water at 680°F, 20: 41423
corrosion of stressed, in ferric chloride solutions, 19: 34647
corrosion of, book, 18: 22451
corrosion of, conference papers on, Buffalo, New York, Oct. 10 to 14, 1965, 20: 25495
corrosion of, electrochemical, 18: 14404(R) (EURAEC-95)
corrosion of, measurement by coulostatic galvanostatic single shot method, 18: 12540(R) (EURAEC-493)
corrosion of, research programs on aqueous, 19: 4627
corrosion of, review, 19: 7868
corrosion of, review of oxidation and hydriding kinetics and radiation effects in, 19: 16011 (AERE-R-4820)
corrosion of, review of aqueous, 19: 16013 (CEA-R-2600)
corrosion of, spectrophotometric measurements of oxide films formed in, 19: 13921
corrosion pitting in halide solutions, mechanism of electrochemical, 16: 19291
corrosion product radioactivity in Hanford reactors, effects of deionized water on, 19: 684(R) (HW-81746(p.3.30-2))
corrosion protection of uranium by flame-sprayed deposits, 19: 13922
corrosion resistance of, effects of chromium and tin on, 18: 41969(P)
corrosion resistance and neutron absorption properties of, effects of palladium on, 18: 41970(P)
corrosion resistance of, effects of various added elements on, 18: 41972(P)
corrosion resistance for use in chemical processing industry, 19: 26770
corrosion resistance of, process for improving, 19: 36989(P)
corrosion resistance of, effects of additional metals and cold working on, 19: 36990(P)
corrosion resistance to mercury at 900°F, 20: 2264
corrosion studies of, technical progress review, 17: 11129
corrosion studies, 18: 14396
corrosion testing and resistance, 17: 36231
corrosion-resistant film production on, in aqueous chlorides and sea water, 18: 20481
corrosion-resistant films produced on, in water and aqueous chloride solutions, 19: 22906
creep at high temperature, 18: 26002
creep at 660-1425°C under tensile stress, 19: 47074
creep behavior and dislocation mobility in alpha-, (E/T), 20: 32696
creep-rupture properties, 18: 3190(R) (SRO-95)
creep testing, 18: 15537(R) (SRO-99)
creep under constant load in vacuum, 16: 6739
crystal dislocations in, anisotropy effects on, 16: 33604
crystal elastic moduli and phase transformations in, 18: 28009
crystal orientation in, x-ray diffraction measurements of preferred, 16: 10522 (DP-607)
crystal structure of, 16: 30717(R) (ANL-6516)
crystal structure of, at high pressures, 17: 18834
crystal structure of alpha, 17: 32580
crystal structure and phase studies, 17: 41333(R) (ANL-6677)
crystal structure and phase studies, 18: 25968(R) (ANL-6868(p.267-86))
crystal structure of alpha, effects of rare earth additions on, 18: 34053(R) (TID-20862)
crystal structure of, basal slip kink bands in, 18: 34193
crystal structure and thermal expansion in welded zone, 19: 16115
crystal structure lattice strain in welded, recovery of, 19: 16116
crystal structure of, effects of dissolution of oxygen on, 19: 15510
crystal structure of, effects of annealing on, 20: 4413
crystal structure patterns of, computer program for correcting x-ray diffraction, 20: 9505 (WAPD-TM-521)
crystal structure of, etching dislocations in, 20: 25607
crystal structure of, determination by polarized-light microscopy, 20: 37266
crystallization properties, 20: 4304(R) (ORNL-3870, pp 171-83)
crystallization with thionalid, tracer study of, 16: 12961 (USNRDL-TR-551)
crystallography, interplanar angles, 17: 2095
de Haas-van Alphen effect in crystals of, pulsed-magnetic-field study of, 17: 34457
decomposition by sintering with limestone, 16: 4181
decontamination of, method and solution for, 20: 41214(P)
deformation and delayed failure hydrogen embrittlement, 17: 1049(R) (SRO-73)
deformation and ductility, 17: 15466(R) (SRO-77)
deformation and flow of polycrystalline, effects of pressure on, 19: 37048 (WVT-6431)
deformation and hydrogen embrittlement studies, 16: 17299(R) (SRO-66)
deformation and recovery of, electric conductivity study of, 20: 43959
deformation by strains due to twinning at 77°K, 19: 44725
deformation in creep and tension, contractile strain ratio analysis in plastic, 16: 30807(R) (TID-16574)
deformation modes of polycrystalline, 19: 16204
deformation of crystals of, role of twinning in plastic, 17: 23968(R) (TID-18669)
deformation of, role of twinning in plastic, 16: 30804(R) (TID-15640)
deformation recovery in, activation energies of, 19: 11722(R) (EURAEC-1099)
deformation, stored energy increase and release after, 16: 25821
dehydridation of powders of, 16: 12653(R) (EURAEC-130)
deposition by electrolytic methods, 20: 35870
deposition from chloride solutions, cathodic processes in, 18: 1668

deposition from chloride–fluoride melts, cathodic processes in, 18: 1669
deposition from fused salts, electrolytic, 20: 9448
deposition from fused salt mixtures, electro-, 20: 11260
deposition from fused fluoride bath, 19: 11711
deposition from molten salt solutions at high temperature, electrolytic, 16: 5358(T)
deposition from molten fluorides, 19: 16034
deposition of, by electrophoresis, 16: 30369 (TID-11153)
deposition of coatings of, on ceramic substrates without oxidation, 16: 18007(P)
deposition of coatings of, on molybdenum, niobium, and tantalum, 17: 22147
deposition of coatings of, on molybdenum, stainless steel, steel, and uranium, effects of iodine circulation rate on, 17: 39555
deposition of coatings of, on molybdenum and stainless steel, vapor, 17: 32507
deposition of coatings of, on thorium, use of thorium–zirconium alloy foil for bonding, 16: 512(P)
deposition of, from chloride–fluoride melts, electrolytic, 17: 21700
deposition on graphite and annealing to carbide form, 19: 7918
deposition on metal, method for, 19: 37011
deposition on other metals by electroplating methods, 19: 42827
deposition on plutonium–zirconium alloys, 17: 7547(R) (HW-74761 (p.3.1-39))
deposition on uranium by diffusion from molten magnesium bath, 19: 40949 (ISC-640)
deposition with nickel, niobium, tantalum, and titanium, electrolytic, 18: 26057
deposition, electrolytic, 16: 5658(T) (P) (CEA-tr-X-290)
detection in presence of thorium, ring oven technique for, 19: 30088(T) (JPRS-30087(p.45-9))
determination, 17: 4633
determination as molybdate, amperometric, 18: 39137
determination as pyrophosphate using phosphorus-32 and counting, 20: 258
determination as reduced molybdosulfatozirconic acid, spectrophotometric, 17: 33804
determination as trace in standard rocks G-1 and W-1, spectrographic, 16: 20831
determination as trace impurity in uranium, 18: 29591
determination as trace impurity in plutonium–thorium–uranium and thorium–uranium alloys, 19: 17798
determination by amperometric titration using cupferron, 17: 15861(R) (ORNL-3397(p.117-21))
determination by amperometric titration using *N*-benzoylphenylhydroxylamine, 18: 13695
determination by activation and separation of niobium-97, 19: 26265
determination by bremsstrahlung-activation gamma spectra, 20: 22960
determination by colorimetry using Xylenol Orange after liquid-liquid extraction by tri-n-octylamine, 16: 12974
determination by complexometric methods using pyrocatechol violet, 19: 323
determination by complex formation with substituted acetic acids, 19: 19802
determination by complexometric methods using EDTA, 19: 46219
determination by charged-particle reactions at 2 Mev, 20: 43097
determination by direct complexometric titration with EDTA using Gallein indicator, 18: 41336
determination by iodometric titration using arsenate, 17: 35645
determination by isotope dilution, substoichiometric, 18: 21997
determination by neutron activation using niobium-97, 19: 2255
determination by neutron activation analysis, 20: 33163(T) (AEC-tr-6639, pp 22-7)
determination by neutron activation, 20: 33163(T) (AEC-tr-6639, pp 22-7)
determination by precipitation with *α*-methoxybenzyl acetic acid, 18: 23415(T) (JPRS-24552(p.60-1))
determination by periodate method, micro-, 18: 23420
determination by potentiometric titration using EDTA, equipment for, 20: 5502
determination by radiometric titration, 16: 3331(T) (AEC-tr-4497 (p.215-27))
determination by spectrochemical methods, voltage-fluctuation patterns in, 19: 40416
determination by thermal-neutron activation methods, sensitivity for, 19: 9071
determination by titration using EDTA, 20: 3893
determination, chromatographic and photometric, 17: 6020
determination in and volatilization from tungsten, semiquantitative spectrographic, 16: 4131 (BM-RI-5903)
determination in aluminum, copper, and magnesium alloys, complexometric, 17: 15921
determination in alloys and systems with hafnium and its oxide, activation, 17: 40750
determination in alloys and quartz by indirect polarography, 18: 8305
determination in aqueous or ethanol-water media using potassium dihydrogen phosphate, high-frequency titrimetric, 18: 13657
determination in aluminum–iron alloy, absorptiometric, 18: 17728 (PG-Report-546)
determination in alloys and ores using *p*-iodoamygdalic acid, gravimetric, 18: 17749
determination in aqueous solutions, polarographic, 18: 31379
determination in aluminum and magnesium alloys using Arsenazo III, spectrophotometric, 18: 31413
determination in aluminum and magnesium alloys, photometric, 18: 33512
determination in alloys using vacuum cup electrode, spectrographic, 19: 22103 (TIM-904)
determination in aqueous solutions, design of oxyacetylene burner for measuring sensitivity of spectrophotometric, 20: 29083(R) (UCRL-14767)
determination in beryllium–magnesium alloys by spectral analysis, 16: 22037
determination in boron oxide–silica glass by chelometric titration, 18: 17748
determination in borides, carbides, and nitrides, methods for, 19: 24403 (NP-14952)
determination in clay, acetic acid leachates, sand, and silt, spectrochemical, 16: 4379
determination in copper mixtures, complexometric, 16: 26944
determination in carbide mixtures containing uranium, x-ray fluorescence spectrographic, 18: 1499 (CONF-285-3)
determination in cast iron, photometric, 18: 37105
determination in copper–zirconium alloys by colorimetric methods, 19: 15389
determination in copper by activation, 19: 40422
determination in dissolver solutions, spectrochemical, 16: 5266 (DP-648)
determination in diabase W-1 and granite G-1, spectrographic, 16: 17895
determination in diabase and granite by spark source mass spectrography, 19: 11406
determination in dust samples by microchemical methods and autoradiography, 20: 14472
determination in europium oxide, spectrographic, 17: 2931
determination in fluorides by titration with EDTA, use of vanadyl ion as back-titrant in, 17: 5995
determination in fissium–uranium alloys, fluorescent x-ray spectrometric, 17: 27255
determination in fuel for Molten Salt Reactor Experiment, methods for, 18: 13632(R) (ORNL-3537(p.47-57))
determination in fission product solutions, method for, 20: 40803 (KFK-387)
determination in granite, x-ray fluorescence, 18: 6769
determination in granite, spectrochemical, 18: 17755
determination in glass samples, activation, 20: 14439(R) (GA-5556)
determination in heat-resisting alloys by x-ray fluorescence, 16: 28877
determination in hafnium by x-ray fluorescence methods, 19: 5785
determination in hafnium, activation, 19: 5824
determination in hafnium by activation methods, 19: 42440
determination in iron and nickel base alloys, spectrographic, 16: 11539
determination in iron and stone meteorites, activation, 16: 17896
determination in ignited uranium/zirconium residues, 18: 13640 (PG-Report-515)
determination in industrial solutions, quantometric and spectrographic, 18: 19910
determination in iron and steel using arsenazo III, photometric, 18: 27343
determination in iron and steel using Arsenazo III in nitric acid, photometric, 19: 17812
determination in irradiated fuel effluents, methods for, 20: 22862 (CEA-R-2553)
determination in igneous and metamorphic apatites, spectrographic, 20: 26787
determination in lanthanum oxide, spectrographic, 20: 22895
determination in magnesium alloys using morin, photocolorimetric, 16: 149
determination in minerals and ores, x-ray fluorescence, 16: 152
determination in magnesium–zirconium alloys, x-ray fluorescence, 16: 5283
determination in molybdenum and tungsten by solvent extraction using cupferron, 17: 6012
determination in meteorites, rocks, and sediments, neutron activation, 17: 31986 (TID-19179)
determination in molten salt reactor fuel by automatic, amperometric titration using cupferron, 17: 38930
determination in magnesium alloy, porcelains, and zircon sand by EDTA titration, 18: 1556
determination in molten fluoride systems by voltammetry, 18: 13630(R) (ORNL-3537(p.23-30))

determination in molybdenum, tungsten, and their alloys, classical methods for, 18: 19921
determination in molybdenum alloys, plasma arc technique for spectrochemical, 18: 25268 (ML-TDR-64-36)
determination in mass spectrometer at 10^{-9} gram, 18: 39057 (CONF-520-1)
determination in marine animals and plants and sea water, fluorimetric, 18: 43406
determination in meteorites and minerals, activation, 19: 4078
determination in metals and alloys by mass spectrography using isotope dilution, 19: 15405
determination in molybdenum and molybdenum alloys by ion exchange, 20: 3896
determination in mixtures by x-ray fluorescence using promethium-147/aluminum and tritium/zirconium sources, 20: 3883 (ORNL-IIC-5, pp 154-81)
determination in mixtures of actinides and fission products by paper chromatography, 20: 5509
determination in molybdenum, niobium, and tantalum alloys by ion exchange, 20: 7039
determination in magnesia, by neutron activation, 20: 35386 (AERE-R-5108)
determination in magnesium alloys, quantometric, 20: 43112
determination in niobium by radioactivation analysis, 16: 23633 (TID-7629(p.239-44))
determination in niobium and its alloys, 16: 25294
determination in niobium and niobium pentoxide, 16: 30343
determination in natural materials, 17: 4474
determination in nickel steel and electro-etch residues, activation, 17: 5984
determination in niobium alloys, evaluation method for, 18: 1520
determination in natural materials, activation, 18: 8267 (CONF-151-4)
determination in niobium, photometric, 18: 37102
determination in niobium or niobium oxide by d-c arc excitation, photometric, 19: 26268
determination in niobium or niobium oxide by fusion and d-c arc excitation, photometric, 19: 26269
determination in natural waters, tracer studies of ion adsorption on glass and plastic surfaces in, 19: 30097
determination in niobium carbide–zirconium carbide, method for, 19: 46941 (NP-15514(Vol.3))
determination in niobium–zirconium alloys by spectrography of solutions on cored graphite, 20: 14446 (N64-25607)
determination in ores, x-ray fluorescence, 16: 9967
determination in other metals using catechol violet, colorimetric, 19: 19780
determination in organic solutions by photometric methods, 19: 43972
determination in presence of titanium using quercetin, chromatographic-fluorimetric, 16: 8697
determination in presence of hafnium, titrimetric, 17: 6002
determination in presence of titanium, gravimetric, 17: 19967
determination in presence of hafnium by catalytic activity, 17: 33837
determination in presence of titanium and zirconium using sodium salt of 2,3-dihydroxynaphthalene-6-sulfonic acid, 17: 40743
determination in presence of niobium and yttrium by x-ray spectrum method, 18: 5226
determination in PRTR primary coolant, 18: 19425 (HW-78080)
determination in presence of thorium, spectrophotometric, 18: 17761
determination in polyphenyls, x-ray-spectrographic, 18: 19844 (ISPRA-455)
determination in presence of thorium by precipitation with iodophenylformic acid, 18: 23416(T) (JPRS-24593(p.10-12))
determination in presence of iron by complex formation with dihydroxycoumarin, gravimetric, 18: 31395
determination in presence of uranium, x-ray-fluorescence spectrographic, 18: 35449 (LADC-5830)
determination in presence of uranium by x-ray fluorescence spectrometry, 18: 39077
determination in presence of thorium and titanium using xylenol orange, complexometric, 18: 39125
determination in plutonium by amine extraction and spectrography, 19: 4070
determination in presence of iron and zirconium using arsenate method, 19: 19818
determination in powdered samples by spectrochemical methods, 19: 22120
determination in presence of aluminum and titanium, 19: 30130
determination in presence of thorium, circular furnace separation technique for use in, 19: 36280
determination in process feed solutions by extraction chromatography, 20: 16333 (KR-81)
determination in presence of thorium and uranium using Arsenazo-III, 20: 20614
determination in presence of thorium using ring furnace technique, 20: 22911
determination in powder samples by spectrographic methods, semi-quantitative, 20: 43104
determination in refined uranium materials, x-ray spectrometric, 16: 23621 (TID-7629(p.69-80))
determination in refractory samples, gravimetric, 17: 35657
determination in ratio with hafnium in zircon, direct-reading emission spectrometric, 18: 39129
determination in reactor coolants, polarographic, 19: 11003
determination in refractory materials, titrimetric, 19: 11019
determination in ores and rocks, method for gamma activation, 19: 28277
determination in rare earths by precipitation by 2,5-dihydroxy-1,4-benzoquinone, 20: 26771
determination in sulfate solutions using electromigration, 16: 154
determination in solutions of fission products, development of radio-electrochromatographic method for, 16: 3347(T) (AEC-tr-4497(p.382-8))
determination in steel, photometric, 17: 35653
determination in sulfate solutions of fluoride salts, spectrophotometric, 18: 3298(R) (ORNL-2221(Pts.1-5)(Del.))
determination in solutions in presence of iron and nickel, spectrographic, 18: 31409
determination in solids by spark source mass spectrometry, quantitative, 19: 13247
determination in silicate rocks by ion exchange and spectrophotometry, 19: 17805
determination in sea water by neutron activation methods, 19: 22574
determination in steel containing tungsten, spectrophotometric, 19: 26264
determination in solutions, effects of aluminum, calcium, iron, magnesium, and titanium on polarographic, 19: 34122
determination in solutions using 8-quinolinol, spectrophotometric, 20: 3895
determination in submicrogram amounts, concentration-dependent distribution methods for, 20: 12778 (UJV-1434/65)
determination in silicates, activation, 20: 26782
determination in seawater, activation, 20: 40834
determination in seawater, spectrophotometric, 20: 43088(R) (TID-23295, Sect.5)
determination in tungsten carbide–zirconium boride systems, gravimetric, 16: 1724
determination in thorium-zirconium alloys, spectrophotometric, 16: 25284
determination in titanium and titanium alloys, spectrographic, 17: 2907 (WAL-TR-823.5/1)
determination in tantalum, photometric, 17: 6022
determination in tantalum, 18: 19920
determination in tungsten, spectrophotometric, 18: 25281
determination in tantalum by anion exchange in hydrofluoric–nitric acid mixtures, 18: 35455
determination in tantalum by activation, 19: 24416
determination in tantalum carbide–zirconium carbide, method for, 19: 46941 (NP-15514(Vol.3))
determination in titanium carbide–zirconium carbide, method for, 19: 46941 (NP-15514(Vol.3))
determination in tungsten, spectrophotometric, 19: 314
determination in uranium by x-ray spectrometry, 16: 23655
determination in uranium base alloys, photometric, 16: 26928
determination in uranium–zirconium alloys, volumetric, 16: 14624 (PG-Report-265)
determination in uranium, volumetric, 17: 7606(R) (ORNL-1515)
determination in uranium compounds by x-ray-emission spectroscopy, 17: 14135 (AERE-R-4210)
determination in uranyl nitrate, rapid x-ray fluorescence, 17: 35630(R) (NBL-195)
determination in uranium using TBP, photometric, 18: 1542
determination in uranium using 8-quinolinol, spectrophotometric, 18: 1545
determination in uranium, methods for, 18: 9991
determination in uranium alloys, photometric, 18: 19845 (JAERI-1053)
determination in uranium and its compounds and alloys, methods for, 19: 19823
determination in uranium tetrafluoride, spectrographic, 20: 14473
determination in uranium dioxide, x-ray spectrographic, 20: 18558 (AECL-2526)
determination in uranium compounds after separation by solvent extraction using *N*-benzoylphenylhydroxylamine, spectrographic, 20: 24976 (GAT-524)
determination in vanadium, chemico-spectrographic, 18: 13708
determination in water, silver-spark spectrographic, 17: 1381 (IDO-14591)
determination in waste calcine, 19: 32059(R) (IDO-14655)
determination in water, automated fluorescence, 19: 40403 (BNWL-SA-166)
determination in yttrium oxide–zirconium oxide mixtures by precipitation using cupferron, 18: 25277

determination in zircon using EDTA, 17: 7977
determination in zirconyl solutions by amperometric titration, 18: 6768
determination in zirconium diboride, 18: 19882
determination in zirconium alloys, electrographic, 20: 267
determination in zirconium metal and powders, method for, 20: 1729 (AD-619244)
determination in zirconium minerals, x-ray spectrographic, 20: 27147
determination of, by potentiometric-acidimetric methods, 17: 23288
determination of, bibliography on, 18: 1566
determination of, colorimetric, 18: 1569
determination of, design of quantometer for x-ray, 17: 40751
determination of, in fluoride mixtures, 16: 34073(R) (ORNL-1294)
determination of, in low concentrations, fluorescence, 16: 14378(R) (NYO-2302)
determination of, in uranium–zirconium alloys, 17: 15892
determination of, in presence of alkali metals, chemical spectrographic, 17: 15923
determination of, in zirconyl chloride, amperometric, conductometric, and potentiometric, 17: 23283
determination of, in uranium using Xylenol Orange, 17: 38944
determination of microgram traces in alloys by x-ray fluorescence, 17: 21644
determination of milligram levels of, gravimetric, 17: 27298
determination of, method for, 17: 28801 (IDO-14316(Suppl.4))
determination of, nuclear and radiochemical properties for sensitive and selective, 18: 5240
determination of, optimum pH and reagent specificity for colorimetric, 17: 7964(T) (CEA-tr-R-1620)
determination of, radiometric, 17: 5952 (IA-772)
determination of, review of, 18: 1567
determination of radioactive, in marine organisms, 20: 33215
determination of soluble and insoluble forms of, in magnesium alloys, 16: 12977
determination of traces, colorimetric, 16: 12962(T) (TT-1003)
determination of trace amounts of, in tungsten, 18: 9964 (ASD-TDR-63-358)
determination of traces of, in solutions, spectrochemical, 19: 11031
determination of trace amounts of, by reactor neutron activation methods, 20: 26760
determination of, using thiosalicylic acid, gravimetric, 17: 21639
determination of, x-ray spectrometric, 18: 1589
determination of, paper chromatographic methods for, 18: 29600
determination of, complexometric, 18: 33503
determination of, colorimetric, 18: 37104
determination of, submicrogram radiochromatographic, 19: 313
determination of, use of methaphosphol for, 19: 15403
determination of, preparation of 2-(1,8-dihydroxy-3,6-disulfo-2-naphthylazo)-phenoxyacetic acid for, 19: 17809
determination of, review on methods for, 19: 22108
determination of, reagents for (E), 19: 40441
determination of, using mandelic acid, gravimetric, 20: 35413
determination of, using Arsenazo III, photometric, 20: 36778
determination, photometric, 16: 23653
determination simultaneously with hafnium, thorium, and titanium in ores, spectrographic, 18: 19912
determination simultaneously with sulfur in organic compounds, amperometric, 18: 33514
determination simultaneously with titanium, colorimetric, 19: 4087
determination using diammonium-5,5′-indigo disulfonate, 16: 16322
determination using phenyl-phosphonic acid, gravimetric, 16: 23660
determination using semixylenol orange indicator, 16: 28879
determination using 3-ruthenozide,3,5,7,2′-tetrahydroxyflavone, fluorimetric, 16: 31578
determination using purpurogallin, spectrophotometric, 17: 2923
determination using chlorphosphonazo III, photometric, 17: 6016
determination using arsenazo III, 17: 14192
determination using pyrocatechin violet, colorimetric, 17: 14195
determination using Methylthymol Blue and Xylenol Orange, 17: 19960
determination using 3,5,7-trihydroxyflavone, spectrophotometric, 17: 25133
determination using *N*,*N*′-di-(2-hydroxy-5-sulfophenyl)-C-cyanformazan, photometric, 17: 25157
determination using EDTA, polarographic, 17: 33824
determination using mandelic acid, volumetric, 18: 177
determination using 3′,4′-dihydroxybenzotropolone, 18: 9996
determination using Arsenazo III, spectrophotometric, 18: 13638 (ORNL-3558(p.112-16))
determination using xylenol orange, spectrophotometric, 18: 17750
determination using aromatic carboxylic acids, gravimetric, 18: 19871
determination using flavonol-2′-sulfonic acid, spectrophotometric, 18: 19884
determination using bromanilic acid, spectrometric, 18: 33498
determination using gallein, 18: 37099
determination using β-naphthol-6,8-disulfonic acid, gravimetric, 18: 41323
determination using nuclear fast red, spectrophotometric, 19: 10988
determination using 4,4′-bis[(2″-carboxy-4″, 5″, 6″-trihydroxyphenyl) azo]-2,2′-stilbenedisulfonic acid, complexometric, 19: 30138
determination using 7,8,3′4′-tetrahydroxyflavone, spectrophotometric, 19: 43955
determination using mandelic acid, 19: 46224
determination using *N*-benzoylphenylhydroxylamine, spectrophotometric, 20: 18586
deuterium absorption in deuterated lithium hydroxide, 18: 27856(R) (HW-79280(p.9.1-4))
deuteron elastic scattering at 11.8 Mev, angular distributions, 16: 3637
deuteron elastic scattering at 11.8 Mev, optical model analysis of, 17: 38192
deuteron elastic scattering at 26 Mev, angular distributions from, 18: 28634
deuteron elastic scattering at 15 Mev, strong absorption model analysis of, 18: 42708
deuteron elastic scattering at 26 Mev, optical model analysis of, (E/T), 20: 3053
deuteron inelastic scattering at 13.6 Mev, angular distributions from, 18: 40633
deuteron reactions (d,α) at 15 Mev, cross sections and energy distributions for, 16: 11020
deuteron reactions (d,p) at 13.6 Mev, proton spectra from, 16: 26356
deuteron reactions at 11.8 Mev, optical model parameters for, 18: 1051
deuteron reactions (d,n) at 11.8 Mev, total cross sections for, (E), 19: 35438
deuteron reactions (d,n) with, cross sections and mechanism of, (E), 20: 38159
deuteron reactions at 11.8 Mev, energy spectra from, 20: 40065(R) (BMwF-FB-K-66-01)
deuteron scattering at 11.8 Mev, 17: 31539
deuteron scattering at 11.8 Mev, optical potential ambiguities in, 17: 34944
deuteron scattering at 26.5 Mev, total cross sections for, (E), 19: 5164
development and properties as cladding, review, 16: 16661
development as reactor material, 18: 44075
development for use in plutonium recycle program, summary for 1961, 16: 14376(R) (HW-70000)
diffusion and dissolution of oxygen in, mechanism of, 20: 23615
diffusion and precipitation of hydrogen in, 18: 2220(R) (EURAEC-748)
diffusion and solubility of hydrogen in, effects of alloying additions on, 19: 13349
diffusion coefficient measurements in, for niobium-95 and zirconium-95 at 900 to 1750°C, 18: 4172(R) (ORNL-3470(p.67-74))
diffusion coefficients at 650 and 750°C, self-, 19: 26810(R) (BMI-X-10118)
diffusion from in-pile-destroyed fuel elements, 18: 22530(R) (ORNL-3591(p.175-81))
diffusion from irradiated uranium, effects of burnup and irradiation level on, 16: 25841 (HW-72321)
diffusion from irradiated cerium–cobalt–plutonium alloy to sodium at 550°C, 20: 5848
diffusion from sodium at high temperatures, factors affecting, 20: 40357 (NAA-SR-11766)
diffusion in, 16: 7890 (NP-11196(p.34-41))
diffusion in alpha, 18: 14458 (EIR-49)
diffusion in aluminum, 19: 45471 (AECL-2309)
diffusion in anomalous bcc, mechanism of, 19: 2811
diffusion in bcc phases of, 19: 45471 (AECL-2309)
diffusion in beta-zirconium, temperature dependence of, 18: 41933 (TID-11295(3rd Ed.))
diffusion in body-centered cubic, model for, 17: 41447
diffusion in gamma cerium, electro-, 19: 34722
diffusion in gamma-cerium, gamma-uranium, and epsilon-plutonium, electro-, 20: 23734
diffusion in hydrides of, self-, 20: 8316(R) (NAA-SR-11450, Sect.7)
diffusion in hydrochloric acid solutions, coefficients of self-, 19: 397
diffusion in magnesium at 623°C, electron-probe microanalysis of, 19: 14016
diffusion in molybdenum, niobium, tantalum, and tungsten at 1700 and 1800°C, 17: 1918 (ASD-TDR-62-432)
diffusion in niobium, 16: 2194(R) (NP-11060)
diffusion in niobium–zirconium alloys, tracer studies of, 17: 30988(T) (FTD-TT-63-258)
diffusion in pyrographite-coated uranium carbide–zirconium carbide particles, 19: 30734 (EUR-1819.e(p.91-104))
diffusion in pyrolytic carbon, 18: 37676 (A/CONF.28/P/573)
diffusion in stabilized, coefficients for self-, 19: 40961
diffusion in thorium and uranium dioxides, 19: 47070
diffusion in titanium, 17: 33859 (ARF-2208-16)

diffusion in uranium dioxide single crystals, 19: 5904
diffusion in uranium, effects of carbon on, 19: 18494
diffusion in uranium, 20: 11316
diffusion in zirconium hydrides, 19: 12865(R) (NAA-SR-10501)
diffusion in zirconium hydrides, 19: 27735(R) (NAA-SR-10850)
diffusion in zirconium hydrides, self-, 20: 9379(R) (NAA-SR-11650, Sect.4)
diffusion in zirconium hydride, 20: 35841(R) (NAA-SR-11900)
diffusion in zirconium hydrides, self-, 20: 46966(R) (NAA-SR-12010)
diffusion in, coefficients for tellurium and zirconium, 19: 26810(R) (BMI-X-10118)
diffusion in, parameters for self-, 20: 2356(T) (AERE-Trans-1030)
diffusion into magnesium, 18: 30107 (AERE-R-4594)
diffusion into niobium carbide at 1760°C, 19: 40412 (TIM-924)
diffusion kinetics of oxygen in alpha-phase, 19: 16094
diffusion kinetics of silver in alpha- and beta-, tracer studies of, 20: 43974
diffusion of boron and carbon in, conditions for, 18: 20540
diffusion of boron and carbon in, 18: 36001
diffusion of boron and carbon in surface of, 20: 11228
diffusion of carbon in, 20: 23631
diffusion of carbon in beta-, tracer studies of, 20: 27509
diffusion of carbon, hydrogen, nitrogen, and oxygen in beta-, thermodynamics of, 20: 27509
diffusion of chromium in, grain-boundary and lattice, 18: 39882 (AEET/CD/22)
diffusion of fission products in, at 800, 1000, and 1150°C, 18: 32136(R) (BMI-X-10093)
diffusion of fission products in, 19: 28850
diffusion of fission products in, mechanisms of, 19: 39152(R) (BMI-X-10132)
diffusion of fission products in irradiated, at 600 to 1200°C, 20: 21232 (BMI-1763)
diffusion of helium in, effects of crystal structure on, 19: 14049
diffusion of helium in coatings of, 17: 14845(R) (TID-15434)
diffusion of helium in irradiated, 20: 11227
diffusion of hydrogen in clad and unclad, 16: 11142(R) (DC-56-5-157)
diffusion of hydrogen in films on, at 200 to 700°C, 16: 21035 (NAA-SR-6267)
diffusion of hydrogen in, effects of surface films on, 17: 12708
diffusion of hydrogen in beta-, at 760 to 1010°C, coefficients for, 17: 27844
diffusion of hydrogen in oxide films on, polarographic measurements of, 18: 12641 (GEAP-4089(Vol.II)(Paper 21))
diffusion of hydrogen in, protective effects of surface oxide films against, 18: 22439 (EURAEC-1000)
diffusion of iron in, temperature dependence of, 18: 20561
diffusion of iron in, 20: 5846
diffusion of niobium-95 and zirconium-95 in, temperature dependence, 18: 27967 (ORNL-3617)
diffusion of niobium-95 and zirconium-95 in, 18: 44153 (ORNL-P-425)
diffusion of niobium-95 and zirconium-95 in crystals of, at 900 to 1750°C, 17: 29360
diffusion of nitrogen in, relation to internal friction, 17: 6724
diffusion of oxygen in alpha, determination by microhardness measurements, 16: 15202 (WAPD-TM-306)
diffusion of oxygen in, 17: 11129
diffusion of oxygen in metal and oxidized layers on, 18: 8759
diffusion of oxygen in, coefficient and mechanism of, 20: 11268 (EIR-82)
diffusion of oxygen in zirconium oxides on, nuclear reaction study of, 20: 29817
diffusion of rare gases in, 16: 5736
diffusion of stabilized, mechanism of, 18: 34153
diffusion of tritium at 149 to 240°C in, autoradiographic technique for study of, 16: 30832
diffusion of tritium in, for use as beta source, 17: 18111(T) (AEC-tr-5707)
diffusion of uranium in, alloying effects of molybdenum on, 17: 18821
diffusion of uranium in, temperature dependence of, 20: 11290
diffusion of zirconium-95 in bcc crystals of, 16: 29378 (ORNL-3339)
diffusion of, in beta-phase of Zircaloy-2, 17: 18820
diffusion penetration by plutonium-uranium alloys, 16: 28555 (TID-7623 (p.105-21))
diffusion processes in, review of solute and self-, 20: 29737
diffusion, colloid formation, and electric charge in dilute solutions, tracer studies of, 19: 2285
disintegration of drops by explosion upon re-entry into atmosphere, 18: 33130(R) (SC-DC-64-1061)
dislocation arrangement in deformed, effect of nitrogen and oxygen on, 16: 33420
dislocation arrangements in cold-rolled, 18: 12718 (AE-130)
dislocation behavior of polycrystalline, 20: 43892(R) (IITRI-578-P27-20)
dislocation interaction and movement in annealed foils of, electron microscopic investigation of, 16: 27645
dislocations in deformed, electron microscopic studies of, 17: 20482
dislocations in, etching method for, 20: 37227
dispersion strengthening of, effects of lanthanum, thorium, and yttrium oxides on, 18: 4260 (TID-18430)
dissociation energy of gaseous and heat of vaporization of solid, correlation of, 17: 6095
dissolution, 16: 16464
dissolution and ion exchange behavior in ammonium carbonate solutions, 17: 39035
dissolution by acids, 16: 33431(R) (TID-16833)
dissolution by Citriflex process, chemistry of, 20: 11272 (NP-15661)
dissolution by hydrofluoric acid, flowsheets, 16: 20535(R) (IDO-14583)
dissolution by hydrofluoric acid solutions, 18: 37120
dissolution by hydrofluoric acid, effects of sulfuric acid on, 19: 46957(R) (ORNL-3832, pp 100-6)
dissolution in aqueous hydrofluoric–nitric acids and hydrofluoric–sulfuric acids, equation for, 19: 930(R) (ORNL-3679(p.84-7))
dissolution in bismuth (liquid), development for LMFRE, 16: 9672 (TID-14879)
dissolution in Citriflex Process, 18: 27618(R) (ORNL-TM-833)
dissolution in halide salt–metal systems at 547 to 556°C, 17: 36860(R) (ANL-6648)
dissolution in hydrochloric acid–methanol systems, 16: 7553
dissolution in hydrochloric acid–methanol systems, electrolytic, 16: 13126 (IDO-14573)
dissolution in hydrofluoric acid–nitrogen oxide systems, 17: 2461(R) (BNL-731(p.18-46))
dissolution in hydrofluoric acid, effects of oxygen on, 17: 37245
dissolution in hydrochloric–hydrofluoric acid mixtures and hydrofluoric acid, 18: 4266
dissolution in hydrofluoric–sulfuric acid mixtures, kinetics of, 19: 36341 (ORNL-P-862)
dissolution in hydrofluoric–sulfuric acid system, 20: 4055
dissolution in nitric acid solutions, electrolytic, 17: 32192(R) (DP-839)
dissolution in potassium chloride–sodium chloride mixture, 18: 31517
dissolution in stainless steel vessel without corrosion, 18: 35639 (DP-872)
dissolution of coatings of, on uranium-dioxide fuels, 17: 35951(P)
dissolution of oxygen in, effects of temperature on, 19: 15510
dissolution of, development of Citriflex Process for, 18: 13970
dissolution reaction in hydrofluoric acid–nitric acid solutions, rate constants of, 19: 34178
dissolution studies, 18: 8454
dissolution using hydrofluoric acid, 18: 13962
distribution between lead and zinc, 17: 1359(R) (ANL-6569)
distribution between nitric acid and 10% trilaurylamine solutions, 17: 12364 (NP-12394)
distribution coefficients in alcoholic mineral acid solutions and Dowex-1, 16: 1862(T) (AEC-tr-4875)
distribution coefficient in hydrochloric acid and ion exchange resin, 16: 7503
distribution in irradiated uranium(IV) oxides, (E), 19: 30835
distribution in tissue following inhalation, tracer study, 16: 6287
distribution of, in neutron-irradiated plutonium dioxide suspensions, 20: 41009 (AERE-R-3268)
ductility of coatings of, 17: 39555
ductility of, effects of hydrogen on, 17: 7609(R) (SRO-75)
ductility of, effects of prestraining at liquid-nitrogen temperature on, 17: 23966(R) (TID-18637)
ductility of hydrided, effects of grain size and temperature on, 20: 27488(R) (IITRI-578P27-17)
ductility of polycrystalline alpha-, during tensile deformation, 20: 4374(R) (IITRI-578-P27-12)
ductility of tubular, effects of hydride platelet orientations on, 18: 45031(R) (SRO-106)
ductility of tubular, effects of hydride platelet orientation on, 18: 45032(R) (SRO-107)
ductility of, combined grain size and temperature effects on, 20: 15042(R) (IITRI-578-P27-14)
ductility of, effects of hydride platelet size on, 20: 27437
economic and technological review of, 18: 24076
effects in reactor loss-of-coolant accidents, 20: 3334
effects of additions of, on extrusion and forging of molybdenum alloys, 17: 6589 (ASD-TDR-62-670)
effects of additions of, on extrusion and forging of molybdenum–tungsten alloys, 17: 6589 (ASD-TDR-62-670)
effects of, on strength of pyrographite, 17: 22151(R) (AD-281769)
effects of alloy additions of, on mechanical properties of niobium, 20: 11302
effects of alloying additions of, on oxidation rates of niobium, tantalum, and tungsten, 20: 11227

effects of contact with, on corrosion of Magnox alloys, 19: 11694
effects of corrosion resistance of beryllium to carbon dioxide, 19: 36991(P)
effects of, on determination of thorium in tissues, 20: 45588
effects on alpha-beta transition in hafnium, 19: 6331
effects on aluminum–copper–iron–tin–titanium–vanadium alloys, 18: 35944(R) (WAL-TR-401/303-4)
effects on austenitic grain size in iron and steel, 17: 32627
effects on austenitic grain size and ductility of low-alloy steel, 20: 27481(R) (EURAEC-1419 and App.)
effects on beta phase stability in plutonium, 16: 19352 (HW-SA-2560)
effects on carbon steel corrosion by mercury, 19: 20493
effects on coatability of niobium, 20: 43827 (GTR-19)
effects on colorimetric determination of uranyl ions using Schiff base, 19: 24421
effects on corrosion of carbon steel by mercury, 17: 36233
effects on corrosion resistance and mechanical properties of beryllium, 18: 16448(P)
effects on corrosion of sintered aluminum–iron–nickel compacts by water and steam, 19: 4607(P)
effects on corrosion of beryllium by hot carbon dioxide, 19: 11680
effects on corrosion, stability, and strength of niobium, 20: 43905 (ORNL-3212)
effects on corrosion of container materials by liquid bismuth alloys, 18: 4193 (BNL-811)
effects on coulometric titration of uranium(VI) in aqueous solutions of sodium fluoride, 19: 15357
effects on creep and tensile properties of aluminum-titanium alloys, 16: 25820
effects on creep of Inconel X, (E), 20: 10384(T,R) (EURFNR-3F)
effects on creep of magnesium, 20: 11313
effects on crystal structure of alpha-iron, 20: 13317
effects on crystal structure and properties of thoria-tungsten cermets, 20: 37185
effects on determination of plutonium using Arsenazo III and its analogs, 20: 45614
effects on ductility of steel, 17: 14862(T) (EURAEC-515)
effects on ductility of iodide chromium, 18: 32189
effects on ductility of electron-beam-melted molybdenum, 20: 29783
effects on efficiency of porous tungsten ionizers, 20: 21570 (N-65-29785)
effects on electric and mechanical properties of aluminum, 20: 19241
effects on fabrication and properties of niobium–vanadium alloys, 18: 27858(R) (IITRI-B6007-6)
effects on field emission microscopy, 18: 14063
effects on forging of magnesium, 19: 7886(P)
effects on fracture mechanisms in beryllium single crystals, 20: 23714
effects on grain size of tungsten, 20: 39400 (NASA-TN-D-3531)
effects on heterometric determination of vanadium, 19: 36289
effects on heterometric determination of vanadium using 5,7-diiodo-8-hydroxyquinoline, 20: 257
effects on high-temperature properties of eutectic alloys, 20: 17108
effects on hot shortness of type 347 stainless steel, 17: 32628
effects on hot-working properties of electron-beam-melted molybdenum, 20: 23720
effects on hydrolysis of adenosine-2-phosphate and carboxylase, catalytic, 20: 16420
effects on Inconel X aging, 19: 24098(T,R) (ORNL-tr-538)
effects on isothermal transformation of gamma phase of uranium-base alloys, 19: 7910 (UCRL-7824)
effects on magnetic susceptibility of vanadium oxide, 16: 15126(R) (NP-11584)
effects on mechanical properties of molybdenum–tungsten alloys, 16: 33368(R) (ASD-TDR-62-508)
effects on mechanical properties of thorium–uranium alloys, 18: 18304
effects on mechanical properties of magnesium-manganese-thorium alloys, 18: 32156(T) (JPRS-25069(p.1-31))
effects on mechanical properties of titanium, 19: 11682
effects on mechanical properties of niobium, 19: 11734
effects on mechanical properties of niobium alloys prepared by electron-beam melting, 19: 30768
effects on mechanical properties of aluminum–copper–iron–tin–titanium–vanadium alloys, 19: 46985 (AD-613651)
effects on mechanical properties and microstructure of cobalt and nickel alloys, 20: 27550
effects on mechanical and thermodynamic properties of niobium nitrides, 20: 37274
effects on microstructure of tungsten–thoria dispersion-hardened alloys, 20: 31781
effects on molybdenum crystallization, 20: 35930
effects on niobium, additive, 20: 4299(R) (ORNL-2711)
effects on oxidation resistance of silicon carbide at high temperatures, 19: 36993(P)
effects on phase transformations in steel, 18: 24152(T,R) (EURAEC-1001)
effects on phases in uranium shot, electron microprobe studies of, 18: 32051 (NLCO-915)
effects on plasticity of nickel, 20: 46213
effects on plutonium purification by ion exchange in nitric acid, 18: 13965
effects on polarographic determination of uranium in minerals, 18: 1572
effects on polarographic reduction of nitrate ions, 19: 28238
effects on preparation of uranium carbide by carbothermic reduction of oxide, 20: 33841 (NAA-SR-10624)
effects on properties of hafnium–tantalum–tungsten alloys, 18: 22427(R) (WANL-PR(Q)-002)
effects on properties of beryllium–calcium alloys at high temperatures, 18: 35951(P)
effects on properties of magnesium for use as fuel element can, 19: 20610(P)
effects on properties of molybdenum, 19: 37138
effects on properties of tantalum, 19: 41067
effects on properties of boron steel, 20: 39426
effects on properties of tungsten powder, 20: 43889 (NASA-TN-D-3610)
effects on quantitative separation of niobium and tantalum, 19: 24437
effects on radiation resistance and mechanical properties of plutonium or uranium carbides, 18: 44230(P)
effects on radiation damage to niobium, 18: 24196 (PWAC-278)
effects on recrystallization of annealed aluminum, dispersion, 20: 23695
effects on reduction of europium oxide in vacuum, 20: 23591
effects on resistance of silicate glass to alkali solutions, 18: 32201
effects on sintering of zirconium boride, 19: 26794
effects on spectrophotometric determination of uranium, 16: 30342
effects on spectrophotometric determination of aluminum, 19: 13226
effects on spectrophotometric determination of thorium, 19: 24408
effects on spectrofluorimetric determination of scandium, 20: 14476
effects on strength of thorium at high temperatures, 19: 20560 (ORNL-3777)
effects on structure and tensile properties of molybdenum and molybdenum carbides, 18: 27978
effects on superconductivity of niobium–tin alloys, 18: 44679
effects on superconducting transition temperature of vanadium silicide, 19: 39196
effects on tantalum–tungsten alloys, 18: 34059(R) (WANL-PR(Q)-003)
effects on tensile properties of niobium–tungsten alloys, 18: 34197
effects on tensile properties of magnesium, 19: 11682
effects on tensile properties of niobium alloys, 20: 37245
effects on thermal expansion of niobium, 18: 22516
effects on thermal properties of zirconia, 18: 593 (ARL-63-170)
effects on thorium dioxide–uranium dioxide fuel particle solubility in fluoride–nitric acid solutions, 20: 18819 (AAEC/E-143)
effects on titanium corrosion by mercury, 19: 44616(R) (ANL-7000, pp 122-37)
effects on x-ray-fluorescence determination of hafnium, 19: 5785
elastic module of single crystal alpha, adiabatic, 16: 4575
elastic moduli of crystals of, effects of temperature on, 17: 41333(R) (ANL-6677)
elastic moduli of, effects of temperature on, 19: 11682
elastic properties of monocrystalline, to 1200°K, 18: 25967(R) (ANL-6868(p.231-3))
elastic properties at 4 to 1200°K, 18: 25968(R) (ANL-6868(p.267-86))
elastic properties at room temperature effects of prestrain at 77°K on, 19: 44728
electric arcs between electrodes of, infrared spectra of, 17: 4793
electric conductivity at low temperatures, 16: 3495
electric conductivity at low temperatures, 16: 12118(T) (AEC-tr-5035)
electric conductivity of, temperature effects on, 17: 6814(T) (UCRL-Trans-887(L))
electric conductivity and recrystallization temperature of fused-zone, effects of trace impurities on, 18: 18365
electric conductivity and Hall effect of evaporated films of, effects of chemisorption of nitrogen on, 18: 29668
electric conductivity of plastically deformed, annealing of, (E), 19: 14008
electric conductivity of films of, effects of sorption of carbon monoxide on, 17: 18840
electric conductivity of anodic oxide films on, 20: 23654 (ORNL-TM-1435)
electric conductivity at −196°C, 20: 33864 (EURAEC-1615)
electric conductivity of wires of, effects of high vacuum anneal on, 16: 4572
electric mobility in bismuth (liquid) at 500°C, 17: 4946
electric mobility in liquid bismuth alloys, 18: 546 (IP-488)
electric properties of, in gold–zirconium oxide–zirconium sandwiches, 16: 33497
electrochemical behavior in fused lithium chloride–potassium chloride

melt, polarographic and potentiometric studies of, 18: 17778(R) (NYO-10707)
electrochemical behavior of powders of, 16: 15226
electrochemical behavior in lithium chloride–potassium chloride eutectic, 20: 7111
electrochemical potential and hydrogen overvoltage, 17: 34403 (GEAP-4192)
electrochemical properties, 17: 10512(R) (ORNL-3320(p.83-97))
electrochemical properties of, paper electrophoretic studies of, 18: 41418
electrochemical properties in molten chloride eutectic, 20: 5543
electrodeposition and electroforming of, process for, 18: 14439
electromigration in, Soret effect, 19: 42459(R) (RPI-1044-7)
electron binding energies of, measurements for, 17: 18924
electron energy loss spectra, 16: 12273
electron paramagnetic resonance of, in glass, 17: 8089
electron reactions with, K x-ray emission in, (E), 19: 16377
electron reactions at 2.5 to 4.0 Mev, bremsstrahlung spectra from, (E), 20: 6432
electron scattering at 0.8 and 1.5 Mev, energy-loss spectra, 16: 8136
electron secondary emission coefficient, 16: 12276
electronegativity, 18: 13797
electronic specific heat, (T), 19: 6332
electroplating of sintered, in aqueous electrolytes, 18: 44117
embrittlement by hydrogen, 17: 35154(R) (SRO-92)
embrittlement by hydrogen during slow-bend tests, 20: 14993
embrittlement of alpha-, review of effect of hydrogen on, 20: 37187
emissivity, 17: 31009
emissivity during re-entry ablation, 20: 9091(R) (SC-DC-65-1893)
energy level transitions in, Coster-Kronig, (T), 20: 15238 (CONF-233 (Vol.3), pp 398-418)
energy level widths for, K, (T), 20: 15239 (CONF-233(Vol.3), pp 419-39)
equilibrium potentials in equimolar mixtures of sodium and potassium chlorides, 16: 5360(T)
etching and pickling of, methods and solutions for, 20: 39351(P)
etching in hydrofluoric acid–glycerine–nitric acid solutions, electrolytic, 18: 12540(R) (EURAEC-493)
evaporation and condensation of, design of electron beam device for, 18: 43753
explosibility of powders of, 19: 36698 (BM-RI-6516)
explosion of wires of, in nitrogen, x-ray analysis of nitride aerosol composition and size produced by, 18: 41381
extrusion, 16: 30758
extrusion by hydrostatic methods, 19: 18436
extrusion by hydrostatic methods, 19: 44651
extrusion of, effects on structure, 17: 6654(R) (EURAEC-394)
fabrication and production in Japan, 16: 5662
fabrication and properties as refractory material, 16: 19404
fabrication and properties review, 16: 29328
fabrication and properties of vessels of, for steel casting, 17: 36319
fabrication and properties for process equipment in aerospace, cryogenics, and nuclear engineering, 17: 39556
fabrication and properties for use as superconductors, 18: 34179
fabrication and properties, 18: 37681(R) (EURAEC-1082)
fabrication and quality control of, comparison with titanium, 18: 27930
fabrication by electroforming, 19: 42827
fabrication by extrusion and drawing, 16: 27614
fabrication of bars and tubes of, 19: 32712(P)
fabrication of molybdenum- and stainless-steel-clad, 16: 10473 (DC-57-3-164)
fabrication of rods or tubes of, method for, 19: 22954(P)
fabrication of tubes of, 18: 6493(R) (SRO-96)
fabrication of tubes of, by rotary swaging, 18: 41993(P)
fabrication of tubes of, by hot drawing, 20: 41432
fabrication, ore processing, properties, and uses of, 18: 35950
fatigue, effects of applied stress and hydrogen absorption, 16: 15168(R) (ARF-2230-6)
fatigue, effects of applied stress and hydrogen sorption on static, 16: 25746(R) (ARF-2230-9)
fatigue of, effects of hydrogen and stress on, 17: 526(R) (ARF-2230-12)
fatigue of, effects of hydrogenation on susceptibility to delayed-static, 18: 18406
fatigue properties, 19: 9281(R) (IS-900(Sect.E))
Fermi surface of, 18: 34185
formation and combustion of single droplets of, use of flash heating for, 18: 19927 (CONF-322-9)
fractionation between meteorites and terrestrial rocks, 17: 1637
fracture at 78, 197, and 373°K, mechanisms of, 20: 37231
fracture of, effects of hydrogen and zirconium hydride precipitates on, 19: 23082
fracture of, effects of hydride precipitates on, 20: 27438
fracture of, effects of hydrogen on, 19: 44716
fracture properties of, 20: 31667
frequency dependence of oxidized electrodes of, in oxidation-reduction media, 17: 27397
friction properties of, *in vacuo*, relation of lattice parameter to, 20: 19206 (N-65-17331)
fusion in ultravacuum, design of device for zone, 17: 29344
galvanomagnetic properties at 4.2°K, 18: 44150(R) (ORNL-3670 (p.44-53))
galvanomagnetic properties at 4.2°K, 20: 3920(R) (ORNL-3870, pp 27-37)
gamma attenuation by, effects of hydridation on, 16: 6074 (DC-57-7-51)
gamma coherent scattering at 0.662 and 1.332 Mev, cross sections for, (E/T), 20: 6323
gamma elastic scattering at 662 kev, cross sections for, (E), 19: 35498
gamma heating in, calculations for, (E/T), 20: 6517 (CONF-651101-41)
gamma pair production cross sections for, 17: 7116 (NP-12330(p.186-92))
gamma reactions at 1.119 Mev, absolute cross section for pair production in, 17: 25972
gamma reactions at 1–2 Mev, electron pair cross section Z-dependence from, 17: 28275
gamma scattering by, spectra of nonresonant, (E), 19: 39265(R) (IA-1021)
gamma spectra from 14-Mev neutron activation of, determination by, 19: 26241
gamma spectra in, at 0.2 to 6 Mev, 20: 30722 (KAPL-M-6497)
gamma transition strength functions in, 17: 21062
geochemistry and mineralogy of, in Cherry Mountains (Urals), USSR, book, 19: 20190
grain boundary and intergranular cracking under stress, effects of purity, 16: 5716 (NP-10972)
grain growth in cones at 1000°C, effects of time and wall thickness on, 19: 25024
grain growth in high-temperature phase, 18: 34139
grain size of, effects of zone-fusion purification on, 19: 16095
grinding of, operational techniques and recommendations for, 17: 16613
growth of large single crystals of, using electron-beam furnace, 18: 44052(R) (ORNL-3670(p.147-59))
growth of single crystals of, by electron-beam techniques, 18: 4252(R) (ORNL-3470(p.55-62))
growth of single crystals of, methods for, 19: 23996(R) (ORNL-3650(p.1-110))
growth of single crystals of, using electron-beam heating, 19: 39137
handling hazards and safety procedures for powders of, 16: 25670
handling of, recommendations for safe, 18: 8542 (AHSB(S)R-59)
handling of, safety in, 17: 10863 (RSPP-20(Issue 1))
handling particles of, safety in, 20: 45788(R) (ORNL-3945, pp 27-47)
hardness, 18: 35938(R) (NMI-2129)
hardness of coatings of, 17: 39555
hardness of oxidized, variation profile of, 20: 33898
hardness of, effects of zone-fusion purification on, 19: 16095
hardness testing, sticking to diamonds in, 16: 12163
hazards of handling, 16: 7767 (DC-59-9-223)
heat transfer during consumable-electrode arc casting of, 18: 22207(R) (USBM-U-1109(p.16-18))
helium and hydrogen ion attenuation at 0.1 to 500 Mev, tables for, 20: 41619 (CEA-R-3042)
hydridation, (E), 19: 35622
hydridation, effects on corrosion, 16: 13530 (AERE-R-3881)
hydridation, in-reactor, 18: 37633 (A/CONF.28/P/342)
hydridation in reactors at high temperature, 18: 37668 (A/CONF.28/P/158)
hydridation kinetics, 16: 5654 (APEX-307)
hydridation method, 16: 6089 (APEX-305)
hydridation method for large solid shapes of, 17: 29274(P)
hydridation of, effects of carbon dioxide on, 17: 27730(R) (HW-77052)
hydridation of, effects of carbon dioxide on, 18: 7145(R) (HW-77954 (p.5.31-2))
hydridation of, factors affecting, 18: 2192
hydridation of 50- to 60-lb shapes, 16: 13541 (APEX-546)
hydridation of, at 800°C, effects of oxygen on, 20: 2267
hydridation of, bibliography on, 18: 18285 (DP-803(Del.))
hydridation of, delayed failure from, 18: 6493(R) (SRO-96)
hydridation of, delayed failure from, 18: 6493(R) (SRO-96)
hydridation of, effects of hafnium on, 19: 26776
hydridation of, kinetics, 20: 2222 (EURAEC-1390)
hydridation of, testing equipment and techniques for, 18: 37681(R) (EURAEC-1082)
hydridation of, testing equipment and techniques for, 18: 2236(T,R) (EURAEC-607)
hydridation of, testing equipment and techniques for, 18: 16469(R) (EURAEC-821)
hydridation of, testing equipment and techniques for, 18: 24131(R) (EURAEC-921)
hydride distribution in matrix of, 19: 44676(R) (ANL-7000, pp 176-82)
hydride nucleation and growth in, 20: 2253 (AECL-2297)

hydride orientation in single-crystal tensile specimens of, effects of stress on, 20: 37269
hydride platelet orientation in, effects of stress on, 20: 27437
hydride precipitation in, research program on, 18: 2220(R) (EURAEC-748)
hydride precipitation in, mechanism of, 19: 11722(R) (EURAEC-1099)
hydride precipitation in alpha-, habit planes for, 20: 2355 (WAPD-T-1757(Rev.))
hydride precipitation in large grains of alpha, habit planes for, 20: 27498 (WAPD-T-1757)
hydriding mechanism of, 18: 44037(R) (HW-82651(p.5.1-33))
hydriding procedures for massive, 17: 6649 (DC-61-7-26)
hydrogen absorption in deuterated and undeuterated lithium hydroxide solutions at 275°C, 18: 14407(R) (HW-79766(p.5.1-16))
hydrogen distribution in oxidized, tritium autoradiographic studies of, 19: 13910 (AECL-2085)
hydrogen overvoltage measurement in, 17: 27728(R) (GEAP-4076)
hydrogen overvoltage at, in sulfuric acid, 18: 12642 (GEAP-4089(Vol.II) (Paper 22))
hydrogen transport in, alloying effects of niobium and yttrium on heat of, 18: 5800
hydrolysis, 16: 6391(T) (CEA-tr-R-1431)
ignition in oxygen, spontaneous, 16: 4173
ignition of, flame propagation velocities and temperatures of, 17: 4227(R) (ANL-6635(p.55-9))
ignition studies, 17: 1359(R) (ANL-6569)
ignition temperatures, 17: 40421(R) (ANL-6766)
in-pile corrosion, 17: 6565(R) (EURAEC-413)
inflammability of powdered, at 180 to 1100°C, 18: 44211
internal friction in cold-worked, 16: 29397
internal friction and Young's modulus of cold-worked, 19: 2827
internal friction of, effects of irradiation and plastic deformation on, 19: 11814
ion exchange by silica gel and zirconium phosphate, 18: 13971
ion exchange in chloride media, 16: 30411
ion exchange in concentrated hydrochloric and perchloric acids, distribution coefficients for, 18: 17759
ion exchange on Radgendorf clay, 16: 21865
ion reactions with foils of, sticking factors of rare gas, 19: 34610
ionization by electron and positron impact, 18: 34431
joining to stainless steel tubes, method for, 19: 37018(P)
machining of, effects of friction, surface finish, and tool erosion on electrochemical, 17: 34386
machining of, optimum conditions for turning, 19: 30696 (RDB(C)TM-278)
machining procedures for, 20: 43864 (Y-1550)
magnetic impurity states in, localized, 19: 28840
magnetic susceptibilities of, temperature dependence of, 20: 17069
magnetic susceptibility of, (T), 19: 6332
mechanical and physical properties of, 20: 23649 (NAA-SR-Memo-6532)
mechanical anisotropy of sheets, 16: 19385
mechanical properties, effects of hydrogen, 16: 7875(R) (ARF-2230-3)
mechanical properties at high temperatures, 16: 19339 (BM-RI-5987)
mechanical properties, temperature dependences, 17: 8868(T)
mechanical properties of sponge-source, 18: 1834(R) (IS-700(Sect.E))
mechanical properties of electroclad and electroformed, 18: 14439
mechanical properties, 18: 25894(R) (NMI-2128)
mechanical properties, effects of rare earths on, 18: 34053(R) (TID-20862)
mechanical properties of, effects of hydridation on, 19: 11722(R) (EURAEC-1099)
mechanical properties of, effects of hydrogen and oxygen on, 19: 16172
mechanical properties of, combined effects of hydrogen and oxygen on, 19: 44676(R) (ANL-7000, pp 176-82)
mechanical properties of, effects of hydrogen, 17: 24687(R) (SRO-82)
mechanical properties of, at 250 to 350°C, effects of oxygen on, 20: 4416
mechanical properties of, combined effects of hydrogen and oxygen on, 20: 11227
mechanical properties at room temperature, effects of prestrain at 77°K on, 20: 13246 (CONF-651017-13)
mechanical properties of annealed, rolled-plate at room temperature, effects of prestrain at 77°K on, 20: 37228
melting effects on work hardening properties of, electron beam and inert gas arc, 17: 16712
melting, evaluation of pyrolytic graphite as crucible material for, 16: 15181 (HW-72998)
melting in simulated reentry tests, 19: 39118(R) (SC-DC-65-1520)
melting of, performance of induction furnace for cold-mold, 20: 2352(R) (USBM-RC-1205, pp 9-10)
meson (μ^-) capture by, x-ray spectra from, 17: 26578
metallography of twinning in, 20: 20365
metallurgy, 18: 12661
metallurgy and uses, 16: 12153
metallurgy and uses of, developments in, 18: 28011
metallurgy of, book on, 20: 46147(T) (NASA-TT-F-359)
movement in ground water at Savannah River Plant, 17: 4700
neutron absorption cross sections at 24 kev, (E), 19: 45230
neutron absorption and inelastic scattering by, gamma spectra from, 20: 13966 (UNC-5140)
neutron absorption cross section in pitchblende, thermal, 20: 37994
neutron absorption cross sections of, uncertainties in, 20: 45192 (CONF-660303, pp 88-90)
neutron activation products of, analysis of gamma spectra of fast, 19: 32058(R) (GA-5978)
neutron age in, moments calculations of, 16: 22977
neutron attenuation in hydrided, 16: 6076 (XDC-57-1-32)
neutron attenuation, effects of hydridation on, 16: 6074 (DC-57-7-51)
neutron capture cross sections, 16: 26509
neutron capture cross sections for, 18: 4598
neutron capture cross sections, 18: 12294
neutron capture cross sections, energy dependence of, 18: 15562
neutron coherent scattering amplitude and cross sections for, 18: 7679 (CONF-346-6)
neutron cross sections, 16: 7012 (DC-59-7-171)
neutron cross sections, library of 40-group BPG and spectral "B" codes, 16: 12422 (BAW-158)
neutron cross sections, 16: 33579 (GA-2911)
neutron cross sections for, nine and sixteen group, 17: 22789 (GEMP-173)
neutron cross sections of natural, data compilation of, 18: 6153 (AHSB(S)-R-62)
neutron cross sections of, shell effects on thermal, (E), 19: 47618
neutron elastic scattering at $\theta = 0°$, 16: 4741(R) (TID-14157)
neutron elastic scattering by, threshold effects in, 17: 31514
neutron elastic scattering by, threshold effects and Wigner cusp phenomenon in, 18: 997
neutron elastic scattering at 0.3 to 1.5 Mev, differential cross sections for, 18: 6221
neutron elastic scattering at 0.275 to 0.85 Mev, nonlocal optical model analysis of, 18: 6241
neutron elastic scattering at 0.65 Mev, angular distributions for, 18: 17089
neutron elastic scattering at 3.25 Mev, polarization in, 18: 19103
neutron elastic scattering at 0.5 to 0.8 Mev, cross sections for, 18: 26568
neutron elastic scattering at 5.0 Mev, angular distribution, 18: 26668
neutron elastic scattering at 400 kev, cross section for, 18: 38074(T) (AEC-tr-6398(p.64-9))
neutron elastic scattering at 0.3 to 1.5 Mev, differential cross sections for (E), 19: 3381
neutron elastic scattering by, differential cross section for, (E), 19: 5238
neutron elastic scattering at 0.3 to 1.5 Mev, angular distributions from, (E), 19: 19095 (WASH-1053)
neutron elastic scattering at 0.3 to 1.5 Mev, cross sections for fast, (E), 19: 31215(R) (ANL-7010(p.1-19))
neutron elastic scattering at 0.8 Mev, angular distributions from, (T), 19: 37884
neutron elastic scattering at 1 Mev, differential cross sections for, (E/T), 20: 9981 (WASH-1064)
neutron elastic scattering at 0.8 Mev, cross sections for, (T), 20: 15770
neutron elastic scattering at 0.68 to 1.25 Mev, (E/T), 20: 19805(R) (ANL-7110, pp 1-28)
neutron elastic scattering at 5 Mev, angular distributions from, (E),
neutron inelastic scattering cross sections, 17: 15385(R) (ANL-6683) 20: 46794
neutron four-group cross sections, 20: 12485
neutron inelastic scattering at 0.3 to 1.5 Mev, cross section for excitation of 0.92-Mev level from, 18: 6221
neutron inelastic scattering at 4.0 to 6.5 Mev, energy spectra, 18: 26668
neutron inelastic scattering by, gamma yields from, (E), 19: 35406(T) (ANL-Trans-177)
neutron inelastic scattering at 5.8 and 7.5 Mev, gamma spectra from thermal, (E), 20: 22069
neutron microscopic cross sections for, 17: 41866 (NAA-SR-Memo-8904)
neutron polarization in, measurement as function of scattering angle, 17: 7065
neutron radiative capture cross sections at 30 and 65 kev, 18: 34274(R) (NIRS-2(p.3-15))
neutron reactions, yttrium-90 isomer production in fast, 16: 3705
neutron reactions at 3.7 Mev, cross-section measurements, 16: 8224
neutron reactions at 0.1 to 100 Mev, total cross sections for, 16: 11021
neutron reactions at 3 to 15 Mev, removal cross sections, 16: 29739
neutron reactions (n,p) with, optical model analysis of, 18: 21165 (CONF-490-1)
neutron reactions with, gamma radiation from, 18: 30735(R) (TID-20657)
neutron reactions (n,γ) with, polarization from, (E), 19: 23726
neutron reactions (n,2n) with, fission-averaged cross sections, 19: 29319
neutron reactions (n,γ) at 1 ev to 50 kev, cross sections for, (E), 20: 3032

neutron reactions in, short-lived activities from, (E), 20: 16336(R) (NYO-10175)
neutron resonance absorption integrals for, 16: 26511
neutron resonance integral for, 17: 22566 (TID-18590)
neutron resonance absorption cross sections for, computer program for calculating, 18: 24589 (KAPL-M-6131)
neutron resonance absorption integrals for, (E), 20: 15691 (CEA-R-2840)
neutron resonances, 16: 14046
neutron scattering at 0.4 to 24 Mev, optical model for, 16: 3872(R) (ORNL-3193(p.237-50))
neutron scattering, optical model parameter calculations, 16: 8169 (TID-14569)
neutron scattering angular distribution, 16: 12419 (ANL-5567(Rev.))
neutron scattering resonance cross sections for, fast, 16: 24387
neutron scattering, fast, 16: 26505 (TID-13546)
neutron scattering cross section and resonance parameters for, fast, 17: 28437 (KAPL-2000-20)
neutron scattering at 3.4 Mev by, polarization effects in, 17: 31432
neutron scattering cross sections at 0.3 to 1.5 Mev, 17: 35079(R) (ANL-6749)
neutron scattering at 1 Mev, nonlocal model analysis of, 17: 41873 (WASH-1044)
neutron scattering by, cross sections for, 17: 41873 (WASH-1044)
neutron scattering at 0.275 and 0.85 Mev, optical model analysis of, 18: 7676 (CONF-340-3)
neutron scattering at 0.4 to 1.2 Mev, cross sections for, 18: 9331
neutron scattering at 2.5 Mev, cross sections for inelastic, 18: 14851
neutron scattering by, optical model analysis of, 18: 24625 (WASH-1046)
neutron scattering by, gamma production cross section for, 18: 28579 (TID-20689)
neutron scattering at 3.4 Mev, polarization in, 18: 42613
neutron scattering at 0.275 to 0.850 Mev, 18: 42623(R) (ANL-6879 (p.21-34))
neutron scattering at 3 to 650 kev, cross sections, phase shifts, and strength functions for, (E), 19: 10319
neutron scattering at 2 to 14 Mev by, elastic cross sections for, 19: 5148
neutron scattering by, (E), 19: 14765(R) (ANL-6977)
neutron scattering by, average compound-nucleus cross sections for, (E/T), 19: 17011
neutron scattering by, angular distribution in, 19: 31252
neutron scattering at 14 Mev, cross sections for elastic and inelastic, (E), 20: 34687
neutron slowing down in, use of Monte Carlo method for, 18: 24996(R) (NAA-SR-8888(Sect.VI))
neutron total cross section, thermal, 16: 3718
neutron total cross section of, fast, 17: 20982 (HW-SA-2875)
neutron total cross sections at 0.3 to 2.7 Mev, resonance structure in, 18: 13066
neutron total cross section at 0.002 to 0.1 ev, (E), 19: 33672
neutron total cross sections at high energies, fluctuations in, 20: 38173
neutron transmission resonances at 1 to 3.5 kev, 16: 2319
neutron transmission resonances below 5 kev, 16: 28054
neutron transport properties at 0.3 to 2.7 Mev, 17: 787(T) (AEC-tr-5413)
nitridation, 18: 5729 (ASD-TDR-63-744)
nitridation at 1400 to 1700°C, formation of alpha-solid solutions in, 19: 19877
nuclear moment of inertia, determination of, 17: 38206
nucleation of burning droplets of, effects of supercooling on spearpoint formation during, 20: 31664
occurrence in stone meteorites, determination by neutron activation, 17: 13270
optical properties of small particles of, (T), 20: 5879 (D-910092-6)
organic chemistry of, 17: 18094
oxidation and oxygen sorption at 500 to 3830°R under re-entry conditions, 19: 30653(R) (TID-21723)
oxidation and reduction in halide salt baths, 17: 36860(R) (ANL-6648)
oxidation at high temperatures, dissolution of oxygen in the metallic lattice during, 16: 27650
oxidation at high temperatures, kinetics of, 17: 29286
oxidation at 20 to 400°C, 16: 27684
oxidation at 300 to 900°C, 16: 12119(T) (CEA-tr-A-1039)
oxidation at 400 and 500°C, 16: 17983
oxidation at 400 to 600°C, kinetics of, 18: 20479
oxidation at 400 to 850°C, mechanism of, 19: 933
oxidation at 400 to 600°C and 1 to 760 torr, kinetics and mechanism of, 19: 18409 (COO-1000-1)
oxidation at 700°C, electrochemical model for, 20: 5858
oxidation at 800 and 850°C, kinetics, 17: 8031
oxidation at 800 to 850°C, slow, 18: 14414
oxidation at 800°C, 16: 10466
oxidation at 840 to 1100°C, film growth and oxygen solution processes in, 19: 22902
oxidation at 850 and 950°C, breakaway phenomena in, 19: 18412
oxidation at 850°C, kinetics of, 18: 32091
oxidation by air at 650 to 850°C, mechanism of, 17: 23370
oxidation by argon–oxygen atmosphere below 265°C, 18: 12540(R) (EURAEC-493)
oxidation by carbon dioxide at 650 to 850°C and 15 to 760 mm Hg, 16: 161(T) (CEA-tr-X-399)
oxidation by carbon dioxide, carbon monoxide, and oxygen at temperatures up to 830°C, 17: 23369
oxidation by carbon monoxide at 600°C, 18: 8752(R) (HW-78388(p.9.1-4))
oxidation by carbon dioxide and monoxide at 600 to 850°C, 18: 12584
oxidation by carbon dioxide at 400 to 750°C, additive effects on, 18: 16439 (CEA-2393)
oxidation by carbon dioxide at 350 and 450°C and steam at 425°C, 18: 32139(R) (HW-81269(p.5.1-23))
oxidation by carbon dioxide at high temperatures, 19: 22898
oxidation by carbon dioxide at 600 to 850°C and above 1000°C, 19: 22904
oxidation by carbon oxides and oxygen, 19: 35615(R) (NP-15037)
oxidation by carbon dioxide at 600 to 700°C, effects of copper alloying additions on, 20: 23616
oxidation by dry oxygen at 600 to 850°C, kinetics of, 20: 25503
oxidation by liquid sodium at 400 to 635°C, 16: 10453 (NAA-SR-6674)
oxidation by liquid sodium and oxygen, mechanisms of, 19: 9125
oxidation by lithium hydroxide solutions at 275°C, 18: 32139(R) (HW-81269(p.5.1-23))
oxidation by oxygen at 700°C, 17: 41333(R) (ANL-6677)
oxidation by oxygen and water vapor at 600 to 800°C, properties of, 18: 10489
oxidation by oxygen at 700°C, 18: 25920(R) (ANL-6868(p.338-54))
oxidation by oxygen at 700 to 2000°F, effects of rare earth additions on, 18: 34053(R) (TID-20862)
oxidation by oxygen at 400 to 600°C, kinetics and mechanisms of, 20: 11227
oxidation by oxygen or water vapor at 300 to 360°C, kinetics of, 20: 24995
oxidation by steam at 500°C, effects of surface contamination on, 20: 21268
oxidation by sulfuric acid at 174 to 284°C, anodic film growth in, 20: 25501
oxidation by steam, oxide films from, 19: 2763 (AECL-1999)
oxidation by steam at 500°C and 1000 psi, inhibiting effects of boric acid on, 19: 20492
oxidation by triple carbonate salt, 17: 23957(R) (NMI-7247)
oxidation by water vapor at 1 and 8 torr, 20: 19197
oxidation by water vapor at 375 and 575°C, kinetics of, 20: 25498
oxidation, crack formation in oxide film, 16: 5715(R) (NMI-2098)
oxidation, effects of electrolyte on anodic, 16: 31607
oxidation films on, effects of environment and surface preparation on structure of, 20: 19188(R) (GEAP-5001)
oxidation in acid and base solutions, kinetics of anodic, 17: 32528
oxidation in carbon dioxide and carbon monoxide at 500 to 900°C, 19: 24942
oxidation in dry oxygen, effects of germanium, niobium, and tin, 16: 7528(T) (CEA-tr-X-428)
oxidation in dry oxygen at 600 to 850°C, 16: 22161
oxidation in nitrate solutions, electrolytic, 16: 7522 (IDO-14571)
oxidation in nitric acid, electrolytic, 16: 17759 (DP-647)
oxidation in oxygen atmospheres at 700°C, 17: 12609 (ANL-FGF-402)
oxidation in oxygen and water vapor at 600 to 850°C, 19: 22870(R) (HW-83601)
oxidation in pure oxygen, fission fragment recoil effects on, 16: 10465
oxidation in reactor, electric conductivity study of, 19: 7846 (AECL-2066)
oxidation in simulated reentry tests, 19: 39118(R) (SC-DC-65-1520)
oxidation in thiocyanic acid at 25°C, 20: 14995
oxidation inhibition by boric acid, 16: 17984
oxidation kinetics and thermochemistry, 16: 4495 (NP-11056(p.3-15))
oxidation kinetics at 600 to 850°C, 16: 27648
oxidation kinetics of alpha-phase, at 850°C, 18: 18321
oxidation kinetics of beta-phase, at 950°C in oxygen, 19: 13919
oxidation kinetics and oxide film breakaway of 600 to 850°C, 20: 25497
oxidation kinetics, 20: 29644
oxidation mechanism, 16: 22156
oxidation of, at 800 to 850°C, surface evolution in, 18: 4264
oxidation of coated, 18: 2163(R) (IS-700(Sect.M))
oxidation of, effects of modifications of surface films on, 17: 16591(R) (NMI-1254(p.44-65))
oxidation of, factors affecting, 18: 2192
oxidation of, in dry air, effects of surface conditions on, 16: 29345(T,R) (EURAEC-228)
oxidation of, infrared-spectra studies of, 17: 41381
oxidation of oriented thin layers of, in air and oxygen, 19: 39120
oxidation of poly and single crystals of, at 307 to 815°C, 17: 39613

oxidation of, relations of, with oxide scale formation, 16: 30717(R) (ANL-6516)
oxidation of sheets of, deformation in, 18: 34081
oxidation of, structure of anodic films formed during, 17: 29285
oxidation of, surface temperature during, 17: 30943
oxidation of thin oriented films of, 18: 27870
oxidation of thin films of, kinetics of, 17: 27754
oxidation of, at 550 to 1300°C, kinetics and mechanism of film growth in, 20: 25502
oxidation of, beta spectroscopic and tracer studies of oxygen and metal transport in, 19: 34645
oxidation of, crystal structure of films formed in, 20: 778
oxidation of, current efficiency and formation field at constant current in anodic, 18: 10486
oxidation of, current decrease under potentiostatic operation conditions in anodic, 18: 12585
oxidation of, electrochemical studies of kinetics of film formation in, 19: 28758
oxidation of, electron microscopy of thin films formed in, 19: 46958
oxidation of, film formation kinetics at constant voltage in anodic, 18: 10487
oxidation of, kinetics of, 20: 29648
oxidation of, layer growth in, 18: 14592(R) (PR-P-60)
oxidation of, plasticity of oxide films formed during, 18: 27882 (GEAP-4473)
oxidation of, refractive index and thickness of films formed in anodic, 19: 20489
oxidation of, structure of films formed in, 19: 26816(R) (EURAEC-1334)
oxidation of, to form metal–metal oxide electrode, 19: 22936
oxidation processes at 600 to 850°C, 18: 8759
oxidation properties of, for use in sodium coolant system, 19: 22981 (LA-DC-7050)
oxidation rate of single-crystal, effects of crystallographic orientation on, 20: 4304(R) (ORNL-3870, pp 171-83)
oxidation rates in water-d_2 at 400°C, 17: 37003(R) (HW-78118)
oxidation reaction mechanisms, 19: 44617(R) (ANL-7000, pp 213-26)
oxidation resistance of, in carbon dioxide at 600 and 700°C, 20: 5860
oxidation, relationship of oxidation of anion-deficient zirconia to, 19: 13274 (GEAP-4544)
oxidation, tracer studies of mechanism of, 19: 9098 (UCRL-7631-T)
oxide film breakdown and growth on, in steam, 18: 12589
oxide film formation at 850°C on, oxygen gradient in, 18: 18324
oxide film formation on, hot hardness tests of plasticity of, 19: 25009
oxide film structure on, 19: 44622(R) (EURAEC-1433)
oxide films on foils of, refractive index of anodized, 18: 44052(R) (ORNL-3670(p.147-59))
oxide films on surface of electrodes of, valency changes in, 17: 25203
oxygen diffusion in, determination of coefficient of, 17: 20005
oxygen distribution between liquid potassium and alpha-, at 815°C, 18: 43360(R) (ORNL-3670(p.112-15))
partition coefficients and reciprocal ionic radii, 17: 27562 (INSJ-54)
passivation, 18: 2183(T,R) (EURAEC-285)
passivation by oxide film, electrochemical studies of, 18: 10485
passivation in hydrochloric and sulfuric acids, 16: 12064
performance as cladding for thorium-bearing reactor fuel elements, (E), 19: 31551(R) (SRO-115)
performance as fuel element cladding in large PWR, 20: 12418(R) (WCAP-3739)
performance as reflector in fast rocket reactors, 19: 29769
performance of coatings of, on Pebble Bed Reactor fuel, 16: 9663 (NYO-9064)
phase studies, 17: 11204(T,R) (EURAEC-444)
phase studies of, effects of rare earth additions on, 17: 25782(R) (TID-18791)
phase studies to 1200°C, 16: 98(T) (AEC-tr-4801)
phase transformations, latent heats of allotropic, 16: 30848
phase transformation studies using electric conductivity measurements, 17: 8869(T)
phase transformations in, dislocations during alpha–beta, 17: 29342
phase transformation in, whisker growth from, 18: 8830
phase transformations in, 18: 18307
phase transformations in, relation of c/a ratio and elastic moduli temperature dependence with, 19: 44676(R) (ANL-7000, pp 176-82)
phase transformations, effect of pressure and irradiation on solid-solid, (E), 20: 40306
phase transformation kinetics in, 19: 41033
phase transformations in, martensite, 17: 11239
phase transitions in, effects of rare-earth and yttrium contents on, 16: 33499
photoelectric properties of anodized, 18: 14722(R) (TID-20233)
photoelectric properties of electrodes of, 16: 13705(R) (TID-14943)
photoelectric properties of anodized electrodes of, 18: 14722(R) (TID-20233)
photogalvanic effects of anodized, 18: 569
photogalvanic effects of anodized electrodes of, 18: 569
photon reactions with, proton angular distributions and yields at >8 Mev, 17: 28265
photon transition strength functions in, resonances in, 18: 38192
photoprotons from, angular distribution of, 18: 32817
photovoltaic effects in anodized electrodes of, 16: 10457(R) (TID-14977)
photovoltaic properties of coatings of, on anodized zirconium electrodes, (E), 19: 36768 (TID-21971)
photovoltaic properties of anodized electrodes of, (E), 19: 36768 (TID-21971)
physical properties and uses of, review on, 17: 32503
plastic deformation, role of deformation twinning in, 16: 29384(R) (TID-14983)
plastic deformation, 16: 33989(R) (SRO-72)
plastic deformation of, evaluation of role of twinning in, 17: 4305(R) (SRO-74)
plastic deformation of, mechanisms in, 17: 7609(R) (SRO-75)
plastic deformation of, role of deformation twinning in, 17: 17546(R) (SRO-80)
plastic deformation of, kink bands in, 17: 23966(R) (TID-18637)
plastic deformation of, role of twinning in, 17: 23967(R) (TID-18638)
plastic deformation of, role of twinning in, 17: 28533(R) (SRO-83)
plastic deformation of, role of twinning in, 17: 31733(R) (SRO-84)
plastic deformation of, role of deformation twinning in, 17: 39542(R) (TID-19465)
plastic deformation of hydrided, 17: 41333(R) (ANL-6677)
plastic deformation of, role of twinning in, 18: 10540(R) (TID-20024)
plastic deformation of, role of twinning in, 18: 12638 (GEAP-4089 (Vol.II)(Paper 12))
plastic deformation of hydrided, 18: 25968(R) (ANL-6868(p.267-86))
plastic deformation of, effects of twinning on, 18: 30178(R) (TID-20735)
plastic deformation of, role of twinning in, 18: 37685(R) (TID-20999)
plastic deformation, 18: 39835
plastic deformation of, role of twinning in, 18: 42022(R) (TID-21138)
plastic deformation of foils of, analysis by electron microscopy, 20: 37248
plastic flow of, determination by hardness, 20: 37230
polarization capacity, effects of oxide film formation on, 16: 10039
polarization in aluminum chloride–diethyl ether solution for plating, 19: 25010
polarization in aqueous sulfate solutions, electrochemistry of passivating oxide film formed in, 18: 34063
polarization of, in chloride and chloride–fluoride melts, 17: 30558
polarographic behavior in alcoholic and aqueous solutions, 19: 34122
polishing of, electrolytic process for, 20: 19186(P)
polishing, utilization of "plug" technique in, electrolytic, 16: 10440
positron lifetime in, 16: 3626
potentiometric behavior in potassium sulfate, 16: 27591(R) (EURAEC-284)
precipitation by atrolactic acid and hexahydromandelic acid, 19: 46224
precipitation by gettering action in recrystallized, electron microscopic observations, 19: 9655 (EURAEC-1260)
precipitation by iron hydroxides, 16: 27509
precipitation of zirconium hydride in, crystallography and morphology of, 17: 18788
precipitation of zirconium hydride in alpha crystals of, habit planes for, 16: 13628
precipitation using trichlorobenzenearsonic acid, 19: 9137
precipitation using α-methoxyphenylacetic acid, 19: 2235
precipitation using dimethylbenzenearsonic acid, 19: 9136
precipitation with cerium–cadmium intermetallic compounds from liquid cadmium, 18: 34192
preferred orientation and recrystallization, bibliography on, 16: 3433 (VDIT-46)
preparation and grain size distribution of powdered, by reduction of tetrachloride fused salts, 19: 22950
preparation as radiation target substrate for tritium, 18: 27815(R) (ORNL-TM-718)
preparation by electron-beam refining, 16: 16674(R) (ARF-2198-24)
preparation by electrolysis, 17: 32514(P)
preparation by electrolysis of salts reacted with urea, 20: 23596(P)
preparation by fusion electrolysis, 18: 22435(P)
preparation by fusion electrolysis, device for introducing gases in salt melt for, 19: 22956(P)
preparation by reduction of halide by magnesium, 18: 31544(P)
preparation by vacuum reduction of oxide, 19: 5889
preparation from chloride-fluoride fused-salt melt, electrolytic, 18: 8457
preparation of, by oxide reduction, thermodynamics of, 17: 14269
preparation of, by reduction using magnesium or sodium, 17: 16615
preparation of, by reduction of tetrachloride, 17: 40826(P)
preparation of crystals of, by electron beam melting, 18: 27871(T)
preparation of crystals of, by zone melting at 2320 to 3800°K, 17: 32590

preparation of, design of apparatus and method for, 17: 20408(P)
preparation of, design of apparatus and method for, 17: 20409(P)
preparation of ductile, by calcium reduction and iodide refining of oxide, 16: 22538
preparation of ductile, 19: 11689(P)
preparation of ductile, by reduction of its chloride, development of method for, 19: 26790
preparation of films of, and examination by electron microscope, 16: 10525(R) (EURAEC-21)
preparation of highly dispersed, by irradiation of hydroxide, 16: 32161
preparation of large crystals of, by phase transformation method, 19: 20527
preparation of powders of, 20: 2222 (EURAEC-1390)
preparation of pure, by electrolysis, 17: 29275(P)
preparation of, separation of metal from reaction products in, 17: 20410(P)
preparation of single crystals of, 20: 4304(R) (ORNL-3870, pp 171-83)
preparation of thin films of, 18: 27870
preparation of, by direct iodination of carbide, 19: 46969
preparation, properties and uses of, chemical process monograph on, 19: 18407
preparation, properties, and uses of, review on, 20: 35901
producers in Europe, index, 16: 15119 (EURAEC-32)
production and fabrication for use in reactors, industrial problems created by, 18: 14389
production and properties of, 17: 16707
production and uses, 18: 25898
production and uses in nuclear reactors, 19: 39108
production and uses of, 1965 survey on, 20: 33773
production by alkali fusion of zircons, 16: 28860
production by electrolysis, 18: 37609 (A/CONF.28/P/350)
production by electrolytic reduction of potassium fluozirconate, 19: 11294
production by electrolysis, technique for, 20: 5604(P)
production by fusion electrolysis, 18: 25913(P)
production by fusion electrolysis, 20: 25214(P)
production by igneous electrolysis of zirconium oxide, 18: 27873
production by magnesium reduction of tetrachloride, 18: 27878(P)
production by reduction of chloride, apparatus for, 18: 12569(P)
production by salt electrolysis, 19: 28752(P)
production from tetrachloride by magnesium and sodium reduction, 16: 12087 (BM-RI-5933)
production from zircon, dissolution of alkali fusion cakes in, 20: 9065
production in Euratom countries, installations for, 19: 29470 (EUR-2271.f)
production in U. S., 18: 25908
production of, by electrolysis of fused salts, 17: 14238
production of ductile, by vacuum reduction, 18: 14390
production of nuclear-grade sponge, flowsheet for, 20: 45684
production of pressed products without annealing, 18: 24110
production of sponges of, 20: 21305
production of very pure, process for, 19: 2743(P)
production, economics, and uses of, 1964, 20: 9383
properties, 17: 33610
properties and reactor uses, review, 16: 3490
properties and reactions at elevated temperatures, 16: 4527 (DMIC-160)
properties and uses of, mechanical and physical, 17: 16715
properties and uses of, review of, 19: 36966
properties as cladding for corrosion protection of uranium, 20: 7522
properties as corrosion inhibitor for titanium in mercury at 538°C, 17: 41333(R) (ANL-6677)
properties as fuel element cladding, 18: 15563
properties as fuel cladding for heavy water–gas reactors, French research on, 19: 23034
properties as reactor material, 16: 18050
properties as reactor material, review on, 18: 42067
properties as reactor fuel material, 20: 18182
properties as threshold detector, 18: 17278 (KAPL-M-6101)
properties as x-ray filter, 16: 20086
properties as x-ray filter in radiodiagnosis and radiotherapy, 19: 268
properties at 4.2 to 1130°K, structural and thermal, 20: 21391
properties, data manual, 16: 27632 (TRG-Report-108)
properties for coating metals, 20: 43880
properties for magnetohydrodynamic cell electrodes, 17: 31012
properties for nuclear and space applications, 20: 7503
properties for use as reactor material, 16: 4994
properties for use in chemical process equipment, 17: 425
properties for use as canning and structural material for reactors, 17: 35111
properties for use in reactors, 19: 2760
properties for use as reactor material, 19: 13907
properties for use as oxidation-resistant coating for uranium, 19: 13925
properties for use as fuel-element cladding, 19: 22884
properties for use as reactor material, 19: 26830
properties for use as fuel cladding material in reactors, 19: 39206
properties for use in water-cooled reactors, 19: 42813
properties of debris of, particle size distributions in, 20: 9091(R) (SC-DC-65-1893)
properties of electron beam melted, 16: 19280
properties of, for formation of transition metal pseudosilicides, 17: 18668(R) (AFOSR-2647)
properties of, for use in silicate technology, 18: 7250
properties of hydrided, mechanical and thermal, 16: 10609 (DC-56-3-115)
properties of oxidized, electric and mechanical, 18: 25920(R) (ANL-6868 (p.338-54))
properties of welded sheaths, sheets, and tubes of, corrosion, mechanical, and physical, 18: 7172
properties of zone-refined, 19: 41030
properties of, effects of alloying additives on, 19: 7867 (GEAP-4504)
properties of, effects of sodium coolant on, 20: 46995
properties of, review on, 18: 34180
protective effects of, against corrosion of carbon steel by acids and bases, 19: 22903
proton nonelastic scattering cross sections at 10 Mev, 17: 13581
proton reactions (p,n) with, isobaric states from, 18: 14590(R) (NIRL/R/60)
proton reactions (p,n) at 18.5 Mev, angular distributions of quasielastic, 18: 40587
proton reactions (p,xn) at 400 Mev, effects of target thickness on, 19: 37835(R) (TID-22024)
proton reactions (p,n) at 30 and 50 Mev, isobaric-state excitation in, (E/T), 20: 6361
proton reactions (p,n) at 30 to 50 Mev, distributions from, 20: 15729(R) (RHEL/R-112, pp 37-66)
proton reactions at 0.1 to 0.5 Mev, characteristic x-ray yields from, 16: 33633
proton reactions (p,n) with, time-of-flight neutron spectrum from, 17: 20994 (UCRL-7233)
proton reactions with, niobium isotopes from, 17: 18149
purification by cold-mold-induction and electron-beam melting, effects of additives on, 18: 2174(R) (USBM-U-1082)
purification by controlled addition of other metals, 18: 14384(R) (USBM-U-1091)
purification by electrolysis, 16: 20969(P)
purification by electron-beam melting, 17: 34330(R) (USBM-U-1057)
purification by iodide refining, transfer of nonmetallics during, 18: 10459(T) (JPRS-22697(p.1-7))
purification by iodide refining method in molybdenum-glass vessel with molybdenum electrodes and tungsten filaments, 19: 36558
purification by iodide method and zone refining, 20: 9079
purification by Van Arkel process, optimum conditions for, 16: 32035 (JEN-102-DMe/I-9)
purification by Van Arkel method, 17: 4890
purification by veritical zone fusion under ultravacuum, 17: 34338
purification by zone melting, 18: 8456
purification by zone refining, 18: 44052(R) (ORNL-3670(p.147-59))
purification by zone refining, 19: 36969
purification by zone fusion method, 19: 41030
purification by zone fusion, 20: 4413
purification of, by solid state electrolysis and zone refining, 17: 12603
purification of, by fusion in electron beam furnace, 17: 18685
purification of crystals of, by van Arkel process, 19: 22848 (ORNL-TM-1047(p.53-7))
purification of scrap chips by pickling, 16: 17749(P)
purification of, by displacement of beta phase zone, 20: 35843
purification of, radiochemical method for, 20: 8838 (UCRL-14258)
purification using amine and organophosphorus solvents, 18: 37266 (A/CONF.28/P/456)
purity and recrystallization, 16: 3495
purity and recrystallization, 16: 12118(T) (AEC-tr-5035)
radiation damage, 16: 21086 (AECL-1484)
radiation damage to, effects of anisotropic neutron scattering on, 16: 32153 (TID-11164)
radiation effects on hydrided, 16: 9625 (DC-57-12-710)
radiation effects on electric conductivity, 16: 578(T) (SCL-T-371)
radiation effects on mechanical properties, fast neutron, 16: 572 (REIC-20)
radiation effects on corrosion by chemicals, 16: 17976(R) (EURAEC-94)
radiation effects on electric conductivity of, annealing neutron, 16: 22706
radiation effects on relaxation of elastic stresses in, neutron, 16: 27699(T) (AEC-tr-5257)
radiation effects of fission fragments and neutrons on oxidation of, 16: 31369
radiation effects on mechanical properties of, neutron, 17: 465
radiation effects on corrosion by water, 17: 2018
radiation effects on mechanical properties, 17: 11129

radiation effects on K absorption spectrum, neutron, 17: 14319
radiation effects on oxidation of, 17: 16584(R) (EURAEC-550)
radiation effects on plastic deformation of, 17: 32684
radiation effects on corrosion of, 17: 39485(R) (EURAEC-738)
radiation effects on corrosion of, by oxygen and water vapor, 17: 39482(R) (EURAEC-616)
radiation effects on attenuation decrement in, 17: 41504
radiation effects on electric conductivity of corrosion films on, 18: 7210(R) (HW-77954(p.5.27-9))
solutions, 18: 10470(R) (EURAEC-812)
radiation effects on low-temperature chlorination of, gamma, 18: 12138
radiation effects on electrochemical properties of, in potassium sulfate (BM-RI-6382)
radiation effects on dislocation arrangements in, neutron, 18: 12718 (AE-130)
radiation effects on electrochemical properties of, 18: 14406(R) (EURAEC-852)
radiation effects on crystal lattice of, review on, 18: 14565
radiation effects on, 18: 15568
radiation effects on mechanical properties, 18: 16525 (NP-13657)
radiation effects on mechanical properties of, 18: 16526 (NP-13663)
radiation effects on corrosion of, by oxygen and water vapor, 18: 22524 (EURAEC-874)
radiation effects on, in-pile, 18: 27952(R) (EURAEC-926)
radiation effects on oxidation of, by dry argon–nitrogen–oxygen, argon–oxygen, and oxygen systems at 20°C, 18: 37639(R) (EURAEC-1130)
radiation effects on corrosion by hydrofluoric acid, neutron, 19: 46957(R) (ORNL-3832, pp 100-6)
radiation effects on corrosion of oxide films on, gamma and neutron, 19: 47099
radiation effects on in-pile corrosion of, by aqueous solutions, 20: 5852(R) (EURAEC-1522)
radiation effects on dimensional changes in reactor fuel tubes of, exposed in HWCTR, 20: 25615 (DP-1019)
radiation effects on oxide films on, effects of vacuum annealing on fast-neutron, 20: 27600
radiation effects on phase transformations in, under high pressure, 20: 33968
radiation effects testing in MTR, 16: 10608 (DC-57-11-718)
radiation heating deposition rates in, cross sections for, 17: 36347(R) (NARF-62-18P)
radioinduced corrosion of, 20: 17158(R) (ORNL-3900, pp 82-149)
radioinduced corrosion by oxygen, 20: 23602(R) (ORNL-3913, pp 53-73)
radioinduced creep in neutron-irradiated, transient, 17: 34505
radioinduced growth of, 17: 470
radioinduced production of helium and hydrogen in, neutron, 19: 26901
radioinduced relaxation of elastic stresses in, 17: 455
radioinduced relaxation of stresses in, 18: 42120(T) (AEC-tr-6474)
reaction with xylenol orange, 16: 18918
reactions in chloride slagging of fissium–plutonium–uranium alloys, 20: 5594(R) (ANL-6925, pp 21-106)
reactions in gaseous mixtures, combustion, 20: 29641(R) (SC-DC-65-1691)
reactions in molten beryllium fluoride–lithium fluoride–zirconium fluoride, 19: 9096 (ORNL-P-403)
reactions in plasma jet streams, 19: 30653(R) (TID-21723)
reactions in skull reclamation processes, 20: 5594(R) (ANL-6925, pp 21-106)
reactions of, with water at high temperatures, 16: 30718 (ANL-6548)
reactions of, with phenylfluorone, 17: 18084
reactions with air, nitrogen, and oxygen, effects of pressure and temperature on, 19: 11722(R) (EURAEC-1099)
reactions with alkyl-phosphoric acids to form polymers, 17: 21664 (AERE-R-4281)
reactions with alumina, magnesia, and silica to 500°C, 19: 22997 (TRG-Report-842)
reactions with benzenearsonic acid and its derivatives in acid media, precipitation, 17: 12198
reactions with beryllium, copper, stainless steel, and niobium alloys to 760°C *in vacuo*, 19: 44606 (PWAC-483)
reactions with beryllium to 500°C in carbon dioxide and *in vacuo*, 19: 22997 (TRG-Report-842)
reactions with carbon dioxide at 550 to 750°C, 16: 3410
reactions with carbon dioxide to 500°C, 19: 22997 (TRG-Report-842)
reactions with carbon dioxide at 590 to 730°C at low pressures, 20: 21279
reactions with carbon monoxide and carbon dioxide at 850°C, kinetics of, 20: 31669
reactions with complexing agents, stoichiometry of, 19: 38667
reactions with crucibles of refractory compounds with boron, carbon, and nitrogen at 400 to 1500°C, 19: 37112
reactions with cupferron in sulfuric acid, 16: 30428
reactions with fluoride ions in water, 18: 2189
reactions with graphite–bismuth–uranium systems at 500 to 1100°C, 16: 13585 (TID-14950)
reactions with graphite above 2000°C, kinetics of, 20: 35523
reactions with hydrogen, review, 16: 5301 (HW-66537)
reactions with hydrogen peroxide in alkaline solutions, properties of product in, 18: 25379
reactions with hydrogen in irradiated uranium dioxide fuel elements, 20: 2468
reactions with hydrogen, thermochemical and structural aspects of, 20: 27436
reactions with iodine at 350°C, 19: 8615(R) (GEAP-3771-14)
reactions with iodine at 350 to 455°C, 19: 42804(R) (GEAP-3771-16)
reactions with ions, mechanisms and secondary ion emission coefficients, 16: 1036(T) (AEC-tr-4695)
reactions with liquid sodium at high temperatures, 20: 38499 (ANL-7120, pp 839-47)
reactions with magnesium to 450°C, 19: 22997 (TRG-Report-842)
reactions with Magnox alloy to 400°C, 19: 22997 (TRG-Report-842)
reactions with metals to 700°C in different atmospheres, 19: 22997 (TRG-Report-842)
reactions with molten salts, 17: 179
reactions with nitrosyl fluoride, formation of complex in, 16: 30357 (BNL-6231)
reactions with nitrogen in air by flash-heating, 18: 41393
reactions with nitrogen at 750 to 1000°C, kinetics of, 20: 27439
reactions with oxygen at 840 to 1100°C, diffusion kinetics for, 20: 31669
reactions with phosphorus vapor at 500 to 1100°C, 18: 8332(R) (TID-19990(Paper 5))
reactions with phosphorus at 500 to 1000°C, 20: 29642
reactions with polyacrolein, effects of pH and temperature on precipitate formation in, 18: 23542
reactions with rare earth borides, 18: 25319 (COO-1140-103)
reactions with sodium hydroxide and sodium carbonate, 16: 120 (p.78-82))
reactions with sodium at high temperatures, 19: 39090(R) (ANL-7046
reactions with sodium, high-temperature, 20: 15033(R) (ANL-7152, pp 87-96)
reactions with sodium at high temperatures, 20: 20925(R) (ANL-7055, pp 177-212)
reactions with sodium at 1700 to 2350°C, 20: 31440(R) (ANL-7175, pp 159-83)
reactions with steam, reactor safety studies of, 18: 33678(R) (ANL-6875)
reactions with steam in reactor core meltdown, 19: 29651(R) (WCAP-3269-3)
reactions with steam at high temperatures, kinetics of, 19: 32447(R) (ANL-7020(p.179-97))
reactions with steam in loss-of-coolant reactor accident, calculations, 20: 582 (CONF-650407, pp 938-69)
reactions with steam at high temperatures, 20: 6552(R) (ANL-6925, pp 187-233)
reactions with sulfur, 20: 3863(R) (IS-1200(Sect. C))
reactions with sulfur dioxide, 20: 33270
reactions with uranium di- and monocarbides and nitride at 1000°C, 16: 30829
reactions with uranium monocarbide at 700 to 1000°C, 17: 14740 (TID-11295(2nd Ed.))
reactions with uranium dioxide at 2200°C, 19: 44599(R) (GEMP-50A)
reactions with uranium to 900°C *in vacuo*, 19: 22997 (TRG-Report-842)
reactions with uranium carbides, thermodynamic calculation of, 20: 9432
reactions with uranium nitride at 600 to 700°C, 20: 19187 (BMI-1760)
reactions with volatile fission products, fixation in, 19: 25781(P)
reactions with water, exploding wire study, 17: 9107
reactions with water at high temperatures, 17: 17447
reactions with water, energy release from, 18: 245
reactions with water using laser-beam heating, 18: 15426(R) (ANL-6810)
reactions with water using laser-beam heating, 18: 19456(R) (ANL-6840)
reactions with water at high temperatures, research summary on, 19: 13671(R) (WASH-1052)
reactions with water in reactors, analysis of, 19: 35619
reactions with water at high temperatures, 19: 40195(R) (WCAP-3269-5)
reactions with water at high temperatures during core meltdown, (E/T), 19: 47960(T) (ORNL-tr-694)
reactions with water during reactor accidents, 20: 16019(T) (BMI-X-10154)
reactions with water during reactor coolant-loss accidents, 20: 20925(R) (ANL-7055, pp 177-212)
reactor criticality effects, 18: 30963
reactor criticality effects per atom, (E), 19: 42077 (ANL-7014)
recovery and recrystallization, effects of cold working and composition, 16: 3455 (HW-69678)
recovery kinetics at 150 and 200°C, 19: 26816(R) (EURAEC-1334)

recrystallization behavior of, effect of rare-earth additions on, 17: 25823
recrystallization of deformed, mechanisms of, 20: 33864 (EURAEC-1615)
recrystallization of wires of, effects of high vacuum anneal on, 16: 4572
reduction in molten fluorides, current-voltage curve for, 18: 1635
reduction of hydrogen peroxide and oxygen on electrodes of, 16: 1742
reduction of oxygen on film-covered, production of hydrogen peroxide in, 17: 10623
refinement by melting, oxygen removal, and treatment in electron bombardment furnace, 18: 7168
refining by melting in high static vacuum, zone, 19: 2771
refining powders of, electrolytic, 17: 8270(P)
rolling and recrystallization textures, 16: 6700
scavenging effects on carbon, nitrogen, and oxygen in chromium, 18: 12692
separation by anion exchange in acetic acid–nitric acid medium, 18: 16131
separation by anion exchange in mixed aqueous and non-aqueous systems, 19: 2243
separation by electrodialysis using ion exchange membranes, 18: 31653 (COO-770-12)
separation by ion exchange chromatography, 16: 31577
separation by reversed-phase column chromatography, 17: 1401
separation by reversed-phase chromatography, use of tri-caprylylmonoethyl ammonium chloride and trioctylamine in, 18: 43395
separation by solvent extraction with TBP, 16: 18995
separation by solvent extraction using nitric acid–tributyl phosphate solution, 16: 33074
separation by solvent extraction using dodecylbenzenesulfonic acid, 16: 3075
separation by solvent extraction using *N*-benzoylphenylhydroxylamine, 16: 12989
separation by solvent extraction using bis(di-*n*-hexylphosphinyl)methane, 17: 35937 (IS-284)
separation by solvent extraction using butyl phosphates, 18: 16157(P)
separation by solvent extraction using TBP-Amsco, effects of keto-oximes and nitrites on, 19: 13532(R) (ORNL-TM-1020)
separation by solvent extraction using TBP-Amsco, effects of oximes on, 19: 13532(R) (ORNL-TM-1020)
separation by solvent extraction using long chain amines, 20: 1761
separation for Indian zircon, pilot plant process for, 19: 34266 (AEET-201)
separation from acid solution by solvent extraction with tri-*n*-octyl phosphine oxide-cyclohexane systems, 16: 22275
separation from aluminum by ion exchange, 16: 30436
separation from aluminum, titanium, and vanadium by solvent extraction using thenoyltrifluoroacetone-xylene, 18: 1808
separation from alkaline solutions by hydrated titanium oxide, 19: 5985 (AERE-R-4516)
separation from aluminum and titanium by ion exchange, 19: 30130
separation from aqueous solutions by solvent extraction using Amsco-TBP, suppression of, by oximinoketones and oxalic acid, 17: 3070(R) (ORNL-TM-265)
separation from aqueous nitric acid solutions by solvent extraction using triisooctylamine–xylene, 18: 31663(T) (UCRL-Trans-1078)
separation from aqueous solutions in fluorozirconate ion by ion flotation methods, 19: 22413
separation from beryllium by ion-exchange chromatography, 17: 21793
separation from berkelium by solvent extraction, 19: 22112
separation from bismuth, lead, and titanium by cation exchange, 19: 534
separation from cadmium by coprecipitation with cadmium–cerium alloy, 16: 16464
separation from cations in zircon, chromatographic, 17: 7977
separation from carrier-free niobium-95 by solvent extraction using *N*-benzoyl-*N*-phenylhydroxylamine, 18: 43412
separation from cerium, cesium, and uranyl ions by electrodialysis, 16: 19004(P)
separation from cesium and molybdenum by precipitation from nitric acid solutions, 19: 38778(P)
separation from cesium by ion exchange on zinc ferrocyanide, 20: 7198
separation from cerium, ruthenium, and uranium by ion exchange using 8-quisolinol, 20: 36754
separation from chloride solutions by solvent extraction using amines, 17: 17949(R) (ORNL-TM-449)
separation from chromium, iron, molybdenum, and tin by solvent extraction using ethyl acetate, 18: 1808
separation from cobalt, manganese, nickel, and zinc using ammonium cinnamate, 16: 28900
separation from dissolver solutions, 16: 1854(R) (IDO-14553)
separation from ferrous ions by precipitation using 4-phenyldaphnetin, 18: 41579
separation from fission product mixtures, ion exchange, 17: 244
separation from fission products by solvent extraction using TBP and TOPO, 17: 243
separation from fission products by solvent extraction using D2EHPA, 18: 16147
separation from fission products in air samples by paper chromatography, 19: 317
separation from fission product solutions by ion exchange, 20: 29357
separation from fluorine and uranium, 18: 12276(P)
separation from fuel elements, 17: 39212(P)
separation from fused salts, electrolytic, 18: 10201
separation from hafnium, 16: 3474(R) (USBM-U-863)
separation from hafnium, 16: 4164(T) (FTD-TT-61-75)
separation from hafnium by complexing with bromoamygdalic acid, 16: 5411
separation from hafnium by ion exchange, 16: 10104
separation from hafnium by solvent extraction, 16: 13163(P)
separation from hafnium, lanthanum, thorium, and uranium, using tri-*n*-octylamine-cellulose anion exchanger, 16: 4231
separation from hafnium by quaternary ammonium anion-exchange resin, 16: 18834
separation from hafnium, 16: 17967(R) (USBM-U-887)
separation from hafnium by fractional crystallization and selective leaching, 16: 19374(R) (USBM-U-921)
separation from hafnium by solvent extraction from hydrochloric acid and nitric acid solutions, 16: 20545
separation from hafnium in sulfuric acid solution by anion exchange, 16: 23792(T) (AEC-tr-5099)
separation from hafnium and iron by ion exchange, 16: 25278(T) (SCL-T-423)
separation from hafnium by complexing with β-diketones, 16: 30439
separation from hafnium by solvent extraction using amyl acetate, butyl acetate, and isoamyl alcohol, 16: 7621
separation from hafnium by solvent extraction, 17: 1575(P)
separation from hafnium, 17: 1578(P)
separation from hafnium by solvent extraction, 17: 6020
separation from hafnium, electrolytic, 17: 8262
separation from hafnium by solvent extraction using TBP, 17: 12375
separation from hafnium, chromatographic, 17: 14384
separation from hafnium, methods for, 17: 27401
separation from hafnium by cation exchange, solvent effects in, 17: 35636
separation from hafnium by organic extraction, 18: 3906(P)
separation from hafnium by solvent extraction, 18: 3906(P)
separation from hafnium by electrolysis, 18: 8457
separation from hafnium by ion exchange, 18: 10203
separation from hafnium and other materials by ion exchange, 18: 16155(P)
separation from hafnium by paper chromatography, 18: 17945
separation from hafnium by solvent extraction, 18: 17963(P)
separation from hafnium by precipitation, 18: 17965(P)
separation from hafnium by countercurrent extraction, 18: 23739(P)
separation from hafnium, spectrographic control analysis in, 18: 27621
separation from hafnium by partition of their thiocyanates, 18: 29808
separation from hafnium, chromatographic, 19: 9046(R) (IS-900(Sect. C))
separation from hafnium by electron-beam melting, 19: 4582 (BM-RI-6560)
separation from hafnium using thiocyanic acid, determination of factors for, 19: 18079
separation from hafnium by reversed-phase chromatography, 19: 19752 (IS-T-2)
separation from hafnium, 19: 39108
separation from hafnium by reversed-phase chromatography, 20: 240
separation from hafnium, chromatographic, 20: 3863(R) (IS-1200(Sect. C))
separation from hafnium by ion exchange, 20: 14657(P)
separation from hafnium by liquid-liquid partition of their thiocyanates, 20: 18828
separation from hafnium by liquid-liquid extraction, review of chemistry in, 20: 25200
separation from hafnium by solvent extraction using fatty acids in benzene, 20: 26815
separation from hafnium by ion exchange using anionites, 20: 29352
separation from hydrochloric acid solutions by ion exchange, 16: 30420
separation from hydrochloric acid and sulfate solutions using amines and organophosphorus, 16: 11788(R) (ORNL-TM-107)
separation from hydrochloric, nitric, and sulfuric acid solutions by solvent extraction using *N*-benzoylphenylhydroxylamine, 17: 27305
separation from hydrochloric acid solutions by solvent extraction using 2-ethylhexanol, 19: 36252
separation from hydrochloric acid solutions by solvent extraction using *N*-benzoyl-*N*-phenylhydroxylamine, 19: 43972
separation from hydrochloric acid solutions by solvent extraction using tetrabutyl pyrophosphate and tetrabutyl hypophosphate, tracer studies of, 19: 46451
separation from hydrochloric acid solutions by solvent extraction using quaternary ammonium chlorides, 20: 20816
separation from irradiated fuels, 19: 20084(P)

separation from lanthanides and other metals by paper chromatography using alcohols, 16: 27140
separation from low grade ores, reductive chlorination process for, 20: 4072(P)
separation from metallic mixture by ion exchange chromatography, 17: 5991
separation from metal solutions by anion exchange in ammonium and hydrogen chlorides and fluorides, 18: 17941
separation from metals by precipitation using triethanolamine, 18: 33503
separation from metals by ion exchange on pyrocatechol-*O,O*-diacetic acid, 18: 33508
separation from mercury, 19: 15332(R) (BNL-841(p.52-62))
separation from molybdenum by carrier precipitation, 17: 2242 (TID-16949)
separation from neptunium by solvent extraction using 4-methyl-2-pentanone, 20: 31319 (ISO-SA-10)
separation from niobium and uranium using TBP, 16: 1649(R) (ORNL-TM-1)
separation from niobium by solvent extraction, 16: 17766
separation from niobium by solvent extraction using acetylacetone, 16: 29042
separation from nitrate solutions using alkyl amines, 17: 3873
separation from niobium by solvent extraction using selenious acid, 17: 6022
separation from niobium by TTA in benzene, chromatographic, 17: 20113
separation from nitric-perchloric acid mixtures using TBP, 17: 25370
separation from niobium by paper chromatography, 17: 37157
separation from niobium using phenylacetylhydroxamic acid, gravimetric, 17: 38933
separation from nitrate solutions by solvent extraction using N,N-dialkylamides, 18: 1799(R) (ORNL-3496)
separation from nitric acid by solvent extraction using TBP, 18: 1825
separation from nitric acid by solvent extraction, effects of chlorine and fluorine on, 18: 1828
separation from niobium by thin-layer chromatography, 18: 17949
separation from niobium and protactinium by solvent extraction using benzoylphenylhydroxylamine, 18: 23728
separation from niobium and neptunium by ion exchange, 18: 25294
separation from niobium using salicylhydroxamic acid, radiochemical, 19: 2224
separation from nitric or sulfuric acid solutions, ion exchange selectivity scales for, 19: 9257
separation from nitric acid solutions, solvent extraction using mesityl oxide, 19: 36547
separation from niobium by solvent extraction using benzoyltrifluoroacetone or trifluoroacetylacetone, 20: 18833
separation from niobium by solvent extraction using 8-hydroxyquinaldoxime and caproic acid, 20: 18849
separation from niobium by solvent extraction using *N*-benzoylphenylhydroxylamine, 20: 18586
separation from nitric acid–perchloric acid solutions by solvent extraction using TTA, 20: 25004
separation from niobium by ion exchange, 20: 27044
separation from nitrate solutions by solvent extraction using tributyl phosphate, effects of sulfate ions on, 20: 27048
separation from niobium by solvent extraction using dioctyl ester of methylenediphosphonic acid, 20: 33421
separation from nitric acid solutions by solvent extraction using di- and monoisopentyl esters of methylphosphonic acid, 20: 41051
separation from ores as sodium zirconate, 16: 14763(P)
separation from ores, evaluation of methods for, 17: 220
separation from organophosphorus solvents using acid solutions, 19: 13532(R) (ORNL-TM-1020)
separation from other fission products by sorption on silica gel, 18: 16144
separation from other metal ions by paper chromatography using inorganic solvents, 18: 39388
separation from other metal ions on silica columns treated with dinonyl naphthalenesulfonic acid, 19: 15691
separation from other metals by ion exchange, 19: 15692
separation from other fission products by solvent extraction, 19: 18075
separation from other metals by reversed-phase chromatography, 19: 30331
separation from other elements by electrophoresis in glycolic acid, 19: 40671
separation from other fission products by solvent extraction using benzene–oxine solutions, 19: 46440
separation from other elements by ion exchange, 20: 7197
separation from other elements by precipitation with bismuth phosphate carrier, 20: 7204
separation from other elements by electrophoresis and chromatography, 20: 9070
separation from other inorganic ions by paper chromatography, 20: 12939
separation from other fission products and uranium by chromatography on ion-exchange paper, 20: 35440
separation from other fission products by ion exchange, 20: 35587 (IEA-101)
separation from other elements by ion exchange using triisooctylamine, 20: 43439
separation from oxalic acid solution by solvent extraction using triisooctylamine, effects of uranium on, 19: 22409
separation from perchloric acid solutions using acetophenone, 19: 552
separation from perchloric acid solutions by ion exchange materials, 20: 20823
separation from plutonium and uranium in halide salt–metal systems, 17: 36860(R) (ANL-6648)
separation from plutonium by ion exchange, 20: 35585 (EURAEC-1639)
separation from potassium fluoride solutions by solvent extraction using trioctylamine, effects of acid on, 17: 14403
separation from potassium fluozirconates by solvent extraction using tributyl phosphate, 18: 363
separation from protactinium, chromatographic, 16: 16396
separation from protactinium using arsenazo III and isoamyl alcohol, radiometric, 17: 27306
separation from protactinium by solvent extraction, 19: 30337
separation from protactinium by solvent extraction using quaternary ammonium chlorides, 20: 20816
separation from protactinium by solvent extraction using isoamyl alcohol, 20: 36940
separation from Purex solution by solvent extraction using D2EHPA, 17: 39186(R) (ORNL-3452(p.189-94))
separation from Purex 1WW by solvent extraction using organophosphorus reagents, 19: 13532(R) (ORNL-TM-1020)
separation from rare earths by ion exchange in isopropyl alcohol, 18: 20104
separation from rare earths, thorium, and uranium, chromatographic, 19: 7300
separation from rare earths by ion exchange chromatography, 20: 18827
separation from rhenium by anion exchange chromatography, 19: 24433
separation from scandium by iodate precipitation, 16: 17695
separation from scandium sulfate by solvent extraction using sulfuric acid, 19: 30196
separation from seawater by sorption on ferric hydroxide ion exchange material, 20: 22923
separation from silicate ores, 16: 5427(P)
separation from silicate ores, 16: 5428(P)
separation from silica in zircon, 16: 18998(P)
separation from solutions of uranium–zirconium alloy fuels by barium fluozirconate precipitation, 17: 18200
separation from solutions of uranium(IV) by formate precipitation, 17: 25379(P)
separation from solutions by solvent extraction using hydroxamic acid, 17: 39185(R) (ORNL-3452(p.168-88))
separation from soil, radiochemical methods for, 18: 22185
separation from solutions by solvent extraction, review of methods for, 19: 13543
separation from solutions of irradiated uranium-235 by precipitation and solvent extraction, 19: 36217(R) (IDO-14656)
separation from solutions formed by dissolution of molybdenum–uranium fuel alloys, 20: 4070(P)
separation from strontium by ion exchange, 19: 22443(P)
separation from strontium by rapid solvent extraction using bis(2-ethylhexyl) phosphate, 20: 33191
separation from sulfuric acid solutions by solvent extraction using liquid anion exchange resin, 16: 30317
separation from sulfuric acid solutions by solvent extraction using *N*-benzoyl-*N*-phenylhydroxylaminates, 18: 5237
separation from sulfuric acid solution by solvent extraction, evaluation of organic solvents for, 20: 4061
separation from sulfuric acid solutions by solvent extraction using long-chain amines, 20: 25204
separation from tantalum by solvent extraction of fluorotantalate using chloroform, 17: 12216
separation from thorium nitrate solutions, 17: 40389
separation from thorium and uranium by paper chromatography, 18: 33505
separation from thorium and titanium by reverse-phase paper chromatography, 19: 7294
separation from thorium by selective adsorption on silica gel, 20: 29344
separation from titanium using benzoylphenylhydroxylamine, direct weight gravimetric, 17: 38940
separation from tributyl phosphate, 17: 40954(P)
separation from tungsten, 19: 26264
separation from uranium, photolytic, 16: 7620
separation from uranium by oxidation-reduction in fused salts, 16: 10100 (IS-286)
separation from uranium, 16: 3091(P)

separation from uranium alloy, 16: 19001(P)
separation from uranium fuel solutions by precipitation with sodium formate, 16: 23782 (IDO-14582)
separation from uranium by ion exchange, 16: 30436
separation from uranium by chlorination and fluorination, 17: 15385(R) (ANL-6683)
separation from uranium process solution, tracer studies of effects of temperature and residence times on, 17: 32191 (DP-818)
separation from uranium by chlorination-fluorination, effects of moist hydrochloric acid on, 17: 37001(R) (ANL-6780)
separation from uranium, method for, 17: 40949(P)
separation from uranium by solvent extraction using 8-quinolinol, 18: 1545
separation from uranium by solvent extraction, efficiency of tannin, oxalic acid, tiron, pyrogallol and Arsenazo I as masking reagents in, 18: 13923
separation from uranium and other elements using bromomandelic acid, 18: 25283
separation from uranium by solvent extraction using *n*-butanol, 18: 27623
separation from urine, chromatographic, 19: 519 (TID-7696(p.53-63))
separation from uranium–zirconium alloys by hydrochlorination and volatilization of chloride, 19: 11292
separation from uranium by solvent extraction using 2-butanone, 19: 13548
separation from uranium by complex formation with phthalocyanine, 19: 34279
separation from uranium and plutonium by solvent extraction, 19: 32286
separation from uranium in spent fuel elements, 19: 42609(P)
separation from uranium by partition chromatography on silica-gel column, 20: 9073
separation from uranium by reversed-phase partition chromatography, 20: 10784
separation from uranium by combined ion exchange–solvent extraction using nitric acid–tetrahydrofuran solutions, 20: 20811
separation from uranium by extraction using triisooctylamine, 20: 20598
separation from uranium in aqueous ammonium fluoride solution by precipitation as peroxide, 20: 25218(P)
separation from uranium by fluidized-bed fluoride volatility process, 20: 31321
separation from waste solutions, development of methods for, 16: 1855(R) (IDO-14560)
separation from waste water, methods for, 19: 40276
separation from waste solutions by flotation methods, 20: 10447
separation from water by foaming, 20: 36934
separation from waste solutions by solvent extraction using bis(2-ethylhexyl) phosphate, 20: 45796(R) (ORNL-3945, pp 195-8)
separation from zirconium silicates concentrates, 16: 7606
separation from zircon containing hafnium by liquid-liquid extraction using TBP, 16: 29035 (JEN-99-DQ/I-30)
separation in trace amounts from uranyl nitrate solutions by solvent extraction, tracer studies of, 19: 13540
separation of americium, curium, europium, and promethium from, by paper electrophoresis, 20: 43451
separation of fission product, radiochemical, 16: 24564
separation of, from hafnium by anion exchange, 17: 4633
separation of, from hafnium by extraction as substituted ammonium chlorometallate, 17: 14397
separation of, from zirconium oxide ores, 17: 16533
separation of, from boron, method for, 17: 17999
separation of, from complex fluoride salts in acid solution, 17: 30559
separation of, from bauxite by direct electrolysis and precipitation, economics of, 17: 32065
separation of nitrogen and oxygen from interstitial positions in, 19: 36564(P)
separation of rare earths from, by solvent extraction using butyric acid, 20: 45612
separation of scandium from, by ion exchange chromatography, 19: 533
separation of silver from, by cation exchange chromatography, 20: 40847
separation of, solvent-extraction, 17: 35655
separation of thorium from, by precipitation using fluoboric acid, 18: 5425
separation of thorium from, by ion exchange, 20: 45615
separation of uranium from, 16: 11808(P)
separation of uranium from, by nitrosyl fluoride volatilization, 18: 6882 (BNL-7572)
separation of uranium from, by solvent extraction, 18: 37301(P)
separation of uranium from, using chloride volatility method, 18: 41560 (CEA-R-2508)
separation of, from other fission products by fractional electrolytic dissolution, 20: 35589 (NP-16170)
separation of, from thorium in sulfuric acid solutions by ion exchange, 20: 43147
separation of, from zinc, in hydrochloric acid solutions by ion-exchange chromatography, 20: 45809
separation using solvent extraction with tri-*n*-octyl phosphine oxide, 17: 12347
separation with fluoride from solutions containing hydrofluoric acid, uranium, and zirconium by precipitation, 18: 33690(P)
shear stress in, effects of hydrogen on critical resolved, 19: 44676(R) (ANL-7000, pp 176-82)
shear stress of, effects of hydrogen and oxygen on critical resolved, 20: 5851
slow-bend testing of hydrided, yield-drop in, 20: 857
soaps of, preparation and properties of, 20: 35931
solubility in alpha-iron at 600 to 900°C, 20: 13317
solubility in aluminum, 20: 46200
solubility in beryllium, 17: 20474
solubility in beryllium, 18: 18305
solubility in bismuth (liquid) at 270 to 500°C, 16: 13137
solubility in bismuth at 300 to 700°C, 16: 24216
solubility in chromium, 18: 7249
solubility in copper, 16: 25794
solubility in copper, solid, 17: 11240
solubility in ferrite of low-carbon steels at room temperature, 20: 23723
solubility in fluoride solutions of ethylene glycol and triethanolamine, 17: 30582(R) (IDO-14611)
solubility in fluoboric and hydrofluoric acids, 19: 30106
solubility in hydrofluoric acid, electrochemistry of, 18: 10073
solubility in hydrofluoric, nitric, and sulfuric acids, 19: 5905
solubility in liquid magnesium–zinc alloys, 17: 1359(R) (ANL-6569)
solubility in liquid zinc, 20: 22966 (ANL-7083)
solubility in lithium (liquid) at 482 to 1010°C, 16: 6718 (NEPA-1465)
solubility in lithium–magnesium alloys, 17: 31000
solubility in lithium at 1370°C, 20: 33863 (CNLM-6335)
solubility in magnesium, maximum solid, 16: 19395
solubility in magnesium–zinc solutions at 482 to 758°C, 17: 14116(R) (ANL-6596(p.29-118))
solubility in magnesium–zinc alloys, 20: 31314(R) (ANL-7175, pp 1-41)
solubility in mercury, 17: 31798(R) (BNL-782(p.60-91))
solubility in molten potassium, 20: 2237
solubility in rubidium at 1000 to 2000°F, 17: 16634 (AGN-8063)
solubility in sodium at 1470 to 2507°F, equilibrium, 16: 30365(R) (NRL-5844)
solubility in zinc (liquid), 16: 544
solubility in zinc, 16: 28555 (TID-7623(p.105-21))
solubility of hydrogen in, effects of oxygen on, 19: 13350
solubility of, in copper, 17: 16706
solvent extraction by organo-phosphorus compounds, 16: 140
solvent extraction using triisooctylamine, 16: 13148
solvent extraction with triisooctylamine, 16: 25482(T) (AEC-tr-5197)
solvent extraction from nitric acid solutions by organic phosphates, 16: 27144
solvent extraction using acetylacetone, 16: 29042
solvent extraction from nitric acid solutions, effects of fluoride ion on, 16: 30504
solvent extraction from strong hydrochloric acid, 16: 31687
solvent extraction by 5,7-dinitro-8-quinolinol in cyclohexanone, 16: 14827
solvent extraction by 5,7-dinitro-8-quinolinol in cyclohexanone, pH dependence, 16: 14828
solvent extraction by triisooctylamine from nitric acid solutions, 17: 8259
solvent extraction using TBP, mathematical analysis of, 17: 16165
solvent extraction from hydrochloric and nitric acid solutions by TBP, 17: 25365
solvent extraction from nitric solutions using TBP, mathematical analysis of, 17: 25369
solvent extraction from nitric solutions using tributyl phosphate, 17: 25368
solvent extraction from nitric acid solutions by tertiary amines, 19: 38761(T) (CEA-tr-A-1809)
solvent extraction by tributyl phosphate and di-2-amyl 2-butylphosphonate in short-residence contactors, 19: 40645 (CONF-650918-1)
solvent extraction by Alamine 336–dibutyl cellosolve in contactor, 19: 44108 (AERE-R-4440(Pt.3))
solvent extraction from nitric acid solutions, effects of solvent degradation on, 19: 46430 (ORNL-P-1601)
solvent partition in butyl ether–nitric acid, butyl ether–calcium nitrate, and nitric acid–TBP, 18: 13956
solvent properties for hydrogen at 400 to 520°C, 16: 16752
solvent properties of alpha-, for chromium at 360 to 400°C, 17: 27728 (GEAP-4076)
solvent properties in D2EHPA–hydrochloric acid, 18: 16147
solvent properties for hydrogen at room temperature, 18: 41916 (AD-604409)
solvent properties for hydrogen, as a function of temperature,

19: 24982(R) (EURAEC-1270)
solvent properties of liquid, for carbon at 2700 to 4000°K, 19: 44701(R) (TID-22144)
solvent properties for oxygen, 20: 11268 (EIR-82)
solvent properties for hydrogen, effects of dissolved oxygen on, 20: 31667
solvent properties for hydrogen, effects of alloying additions on, 20: 31667
sorption by cationite ion exchanger from nitric acid solutions of oxychloride, kinetics of, 18: 31675
sorption by nickel-based alloys, tracer studies of, 20: 35912
sorption by peat, 16: 25078
sorption by platinum, gold, silver, stainless steel, glass, and polyvinyl chloride, tracer study of, 17: 35693 (NP-12983)
sorption by silica gel from nitric acid solutions, mechanism of, 18: 35509 (UJV-1079/64)
sorption by uranyl phosphate at 30 to 1020°C, 19: 24442
sorption from aqueous solutions by pyroclastic rocks, 17: 35940 (UJV-951/63)
sorption from hydrochloric acid solutions by zirconium phosphates, 16: 16390
sorption from hydrochloric acid solutions by zirconium phosphates, 16: 32958(T) (KFK-tr-112)
sorption from nitric acid in presence of Arsenazo I, EDTA, and oxalic acid by silica gel, 18: 35536
sorption from nitric acid by silica gel, mechanism of, 18: 35469
sorption from nitric acid by ion exchange paper, 19: 24435
sorption from TBP solutions by silica gel, 19: 15683
sorption of air and oxygen by evaporated films of, 16: 31724
sorption of deuterium, hydrogen, and tritium by, 16: 5388
sorption of hydrogen by, comparison of reaction kinetics of hafnium, 16: 21064
sorption of trace amounts of, on benzenearsonic acid from nitric acid solutions, 20: 23007
sorption on silica gel from nitric acid solution, 19: 30329
sorption, molecular state in, 16: 27042(T) (CEA-tr-R-1597)
sorptive properties for gases, effects of temperature, 16: 31725
sorptive properties for fluorine, 18: 14403 (CI-221)
sorptive properties for bromide ions, tracer studies of, 19: 36562
sorptive properties of films of, for krypton and xenon, relation of surface area to, 17: 39589
sorptive properties for oxygen in liquid potassium at 815°C, 20: 2367
sorptive properties for hydrogen from hydrochloric acid, 20: 11227
sorptive properties of evaporated films of, for krypton and xenon, 20: 21387
sorptive properties of evaporated films of, for carbon monoxide at 0°C, 20: 21388
spark patterns produced by grinding of, 18: 19493(T) (SC-T-64-47)
specific heat, (T), 20: 17084
specific heat at 25 to 1845°C, 18: 2401(R) (IS-700(Sect.P))
specific heat at 25 to 1845°C, 18: 42016 (NP-14281(p.47-54))
spectra of oxide films on, effects of refractive index on infrared, 18: 25925
spectra of, effects of impurities on M-emission band of, 18: 39197
spectra of, effects of electronic structure on x-ray emission, 20: 12846
spectra of, isotopic shifts in, 18: 20002
spectra of, Ohlin structure near limit of continuous x-ray, (E), 19: 44940
spectra of, use of fuel-rich premixed oxyacetylene flame for emission, 18: 25278
spectra of, x-ray fluorescence, 18: 12022
spectral emissivity at high temperatures, 17: 41363 (WADD-TR-60-646 (Pt.II))
sputtering at 50 to 600 ev by rare gas ions, 17: 8931(R) (NP-12389)
sputtering by argon ions, full-plane threshold energies for, 17: 37743
sputtering by hydrogen ions, yields from, 18: 8926
sputtering by noble-gas ions at 100 to 600 ev, yields from, 16: 22753
stain recovery in prestrained, anelastic, 18: 42022(R) (TID-21138)
strengthening by powdered lanthanum, thorium, and yttrium oxide dispersions, 19: 44676(R) (ANL-7000, pp 176-82)
stresses in, x-ray diffraction analysis of, 17: 23872(R) (TID-18626)
structural properties and uses in reactors, survey, 16: 16036
structure of alpha-, effects of preferred orientation on creep, deformation, and fracture in, 20: 2339 (ORNL-P-1753)
structure of crystals of, theoretical investigation of energy band, 16: 2921 (AD-257435)
structure of radiation targets of, x-ray diffraction analysis of, 20: 25605
structure of, angular values between crystallographic planes in, 20: 5898 (WAPD-TM-519)
structure transitions at high pressures in crystals of, hcp to bcc, 17: 27871
superconducting behavior of pressure-induced polymorphs of, 18: 13016
superconducting critical fields and temperatures for, 17: 41592
superconducting properties of, effects of high pressures on, 18: 24560
superconducting transition temperature of, isotope effects on, (E), 19: 23569
superconducting transition temperature, (E), 20: 30316
superconductivity of high-pressure form of, 20: 37985
superconductivity of, 20: 40047
surface-hardening of, by nitridation and oxidation, 18: 4191(P)
surface layer removal by vibratory polishing, 20: 7504
surface properties of, studies by field-emission microscopy, 17: 6634 (AFOSR-2273)
surface properties of beta-phase annealed, effects of oxygen on, 20: 43933
surface tension at melting point, 17: 39612
surface tension of, measurement by electron bombardment heating, 17: 37538
surface tension of, measurement by pendant drop method, 19: 47065
synthesis in halo red giant star HD 122563, spectral analysis of, 19: 28982
technology developments, 16: 19996(R) (SRO-67)
temperature distribution in infinite slab of, computer studies, 17: 3353 (ANL-6319(Rev.))
tensile properties of, effects of interstitial oxygen on, 18: 30226
tensile properties, 19: 11682
tensile properties of hydrided alpha-, 20: 5905
tensile properties of polycrystalline alpha-, 20: 13245 (CONF-651017-7)
tensile properties of hydrided, effects of grain size on, 20: 23708
tensile properties of, of hydrogen on, 20: 27553
tensile properties at 1100 to 1300°C, effects of vacuum on, 20: 46198
testing in re-entry conditions, ablation and oxidation, 20: 9091(R) (SC-DC-65-1893)
testing of, nondestructive, 18: 9636 (ANL-6632)
texture, simple sheer of crystals of, 16: 10580
thermal capacity, 18: 18307
thermal capacity of, from 1.1 to 4.5°K, 17: 22191
thermal capacity of hexagonal, effects of niobium on low-temperature, 20: 3920(R) (ORNL-3870, pp 27-37)
thermal conductivity of superconducting thermal switches of, at 0.3 to 2°K, (E), 19: 23584
thermal conductivity of, black body radiation in, 19: 32763
thermal cycling effects on dimensions and structure, 17: 471
thermal cycling, effects on crystal structure and dimensional stability, 17: 14729 (CRGM-1106)
thermal cycling, microstructural changes during, 16: 21059
thermal cycling of, plastic strain induced by, 18: 39905 (NP-14268)
thermal diffusion in high-temperature phase of, 17: 34441
thermal diffusion of oxygen in β-, method for measuring, 20: 29769
thermal expansion at 800 to 1450°C, 18: 32198
thermal expansion to 1450°C, 18: 34190
thermal expansion to 2000°C, 19: 4678(T)
thermal expansion of alpha crystals of, at room temperature to 860°C, 17: 12658 (ANL-6591)
thermal expansion of alpha crystals of, 17: 41333(R) (ANL-6677)
thermal expansion of alpha-phase, 20: 43956
thermal properties at high temperatures, 16: 4551 (WADD-TR-60-904)
thermal shock tests of, with hydrogen pickup, 18: 7931(R) (PRDC-TR-74)
thermal stress fatigue behavior, 17: 14740 (TID-11295(2nd Ed.))
thermal stresses in, fatigue behavior from, 16: 33467 (ATL-A-127)
thermionic properties, 20: 29801
thermodynamic functions at high temperatures, 17: 40816
thermodynamic properties at zero pressure and 293 to 3000°K, 16: 19354 (LAMS-2640)
thermodynamic properties, 16: 25406
thermodynamic properties, 20: 10816(T) (NASA-TT-F-285)
thermodynamic properties at high temperatures and pressures, 20: 19217 (NP-15933)
thermodynamics in potassium chloride (liquid), oxygen equilibrium potential diagram for, 16: 20426
thermoelectric emission and work function of, in cesium vapor, (E), 19: 6447
toxic properties of, review of, 18: 13423
transformation of, effects of rare earths on allotropic, 20: 5891(R) (NYO-2159-1)
tritium release from foils of, at high temperatures, 19: 26718 (ORNL-3802)
twinning in alpha crystals of, determination of $\{11\bar{2}1\}$, 17: 32632
twinning in, analysis of zig-zag, 17: 18783
twinning in, mechanism of $11\bar{2}1$, 17: 31003
uptake by Sargassum, 18: 37382
use as cathode for electric arc operation in reactive gases, 19: 36360
use as cover for reactor fuel plates, 16: 28476(P)
use as gettering material for hydrogen and oxygen in heat transfer medium in sheathed fuel elements, 20: 10357(P)
use as tracer, survey, 16: 1359
use for electroless and electrolytic coating of bearings and dies, review

of, 19: 4604
use in brazing alloys for niobium, 17: 36257
use in coolant-flow rotameters for water-cooled reactors, 16: 27393(P)
use in oxygen gettering in liquid sodium, 18: 1245 (LADC-5936)
use of tritium-excited, as source in x-ray fluorescence analysis, 20: 3883 (ORNL-IIC-5, pp 154-81)
uses in industry, survey, 17: 1822(T) (JPRS-15907)
uses of granular or powdered, in fuel element end cap cavity to reduce pressure, 18: 42988(P)
uses, review, 16: 3402
vacancy formation energy and concentration in, determination from thermal capacity measurements, 20: 32729(T)
vapor pressure, 20: 331
vapor pressure at 2000°K, 17: 40388
vaporization, 19: 4100 (AD-450678)
vaporization from zirconium carbide hot cathodes, measurement of rate of, 20: 33163(T) (AEC-tr-6639, pp 22-7)
viscosity of liquid, to 2400°K, 20: 5899(T) (JPRS-32341, pp 1-7)
volatilization from fluidized beds of uranium carbide–zirconium carbide at high temperatures, 18: 8326 (LAMS-2994)
wear and corrosion testing of oxidized, as journal bearing material, 20: 43823 (AECL-2566)
welding, 17: 14797
welding by friction, 17: 1908
welding by solid-state methods, 19: 22937
welding by Tig method, 16: 19320
welding by tungsten inert gas process, effects of hydrogen, nitrogen, and oxygen, 17: 34382
welding, industrial procedure for, 16: 6701
welding of, electron-beam, 18: 4220
welding of, evaluation of electron-beam, 16: 31763
welding of, electron beam process for, 19: 24973(P)
welding sheaths, sheets, and tubes of, techniques for, 18: 7172
welding, ultrasonic, 16: 4515 (NP-11054)
work hardening and recovery in, studies of mechanism of, 19: 7901 (EURAEC-1261)
work hardening and recovery, 19: 37106
x-ray emission by, excited by electrons, protons, and primary x rays, 18: 36093
x-ray yields from, L-shell, 18: 40573
xenon-133 ranges and retention at 1–150 kev, energy and flux dependence of, 17: 28002
yield point of polycrystalline alpha-phase, mechanisms affecting, 20: 37229
yield point of, effects of hydrogen on, 19: 41010(R) (IITRI-578P27-10)
yield point phenomena in polycrystalline, studies of, 19: 18450(R) (COO-578-P27-4)
yield points in high-purity, effects of grain diameter on, 19: 32727(R) (COO-578-P27-7)
yield properties of polycrystalline, 20: 43892(R) (IITRI-578-P27-20)
yields from radiolysis of zirconium phthalocyanine, 20: 36886
Young's modulus of, as function of temperature, 18: 39970
zone refining of, redistribution of iron and oxygen during, 20: 37177
zone refining of, method for induction zone, 18: 14398

ZIRCONIUM ACETATES
preparation and uses, 19: 38647
preparation of anhydrous, 18: 6837(P)

ZIRCONIUM ALCOHOLATES
hydrolysis, with secondary and tertiary alkoxide groups, 16: 5323
isopropoxide and tetra-tert butoxide, pyrolysis and synthesis, 16: 24147 (ASD-TDR-62-90)
isopropoxide and t-butoxide, preparation and properties, 17: 27727 (ASD-TDR-63-322)
isopropoxide, infrared spectra, 17: 27727 (ASD-TDR-63-322)
isopropoxide, thermal decomposition in air, argon, helium, and nitrogen, 17: 27727 (ASD-TDR-63-322)
tert-butyl and isopropyl, infrared spectra of, 18: 1720

ZIRCONIUM ALLOY COUPLES
Fe/Nb–Zr/stainless steel, diffusion in bimetallic tubing of, with iron diffusion barrier, inter-, 20: 11215(R) (NASA-CR-54718)
Fe/Nb–Zr/stainless steel/V, diffusion in bimetallic tubing of, with iron and vanadium diffusion barriers, inter-, 20: 11215(R) (NASA-CR-54718)
Mo/Ni/Nb–Zr/stainless steel, diffusion in bimetallic tubing of, with molybdenum and nickel diffusion barriers, inter-, 20: 11215(R) (NASA-CR-54718)
Nb–Zr/stainless steel, diffusion in, 17: 34413 (TID-19109)
Nb–Zr/stainless steel, diffusion in bimetallic tubing of, inter-, 20: 11215(R) (NASA-CR-54718)

ZIRCONIUM ALLOYS
see also Zircaloy-2
see also Zircaloy-3
see also Zircaloy-4
allotropic transformation temperature of binary, effects of alloying element on, 18: 42095
analysis, 17: 6020
analysis for calcium in reactor grade, spectrographic, 17: 33793 (PG-Report-441)
analysis for carbon, hydrogen, and oxygen, 19: 15406
analysis for cobalt, spectrographic, 17: 2907 (WAL-TR-823.5/1)
analysis for hafnium, 20: 29114
analysis for hafnium, 20: 29115
analysis for hydrogen by high-vacuum inductive heating, 18: 12542(R) (GEAP-4484)
analysis for hydrogen, equipment for, 18: 33511
analysis for hydrogen by isotopic equilibration, 19: 17771 (CRDC-1212)
analysis for iron, spectrographic, 17: 2907 (WAL-TR-823.5/1)
analysis for iron, 17: 5946 (AERE-AM-91)
analysis for niobium and zirconium, gravimetric, 18: 35478
analysis for niobium and tantalum, photometric method for, 19: 40442
analysis for oxygen by emission spectrography in argon atmosphere, 16: 26904(T) (AEC-tr-5276)
analysis for oxygen, activation, 18: 19886
analysis for rare earths, gravimetric, 18: 19839 (BM-RI-6430)
analysis for tin, volumetric, 18: 1550
analysis for tin, polarographic, 18: 13673
analysis for vanadium, spectrographic, 17: 2907 (WAL-TR-823.5/1)
analysis of, for boron, 17: 5970 (PG-Report-391)
analysis of, for niobium, photometric, 17: 21658
analysis of surface for nitrogen, 17: 7971
analysis of, collection of methods for, 18: 12542(R) (GEAP-4484)
annealing of cold-worked, at 300 to 800°C, 16: 3422 (HW-69679)
anodic treatment of, process for, 17: 12625(P)
bonding to aluminum, method for diffusionless, 20: 46179(P)
bonding to Inconel, stainless steel, and steel by extrusions, 18: 27937
bonding to zirconium and other materials, brazing alloy, 16: 12173(P)
book: *Special Metallurgy*. Vol. 3. *Zirconium and Its Alloys*, 17: 32512
brazing into corrosion-resistant structures, brazing alloy for, 18: 34114(P)
brazing of, alloys for, 18: 5765(P)
casting of, segregation of tin during, 19: 32696(R) (EURAEC-783)
chemical properties and structure of pyrophorous, 17: 4935(T) (AEC-tr-5545)
chemical properties of pyrophorous, 17: 4935(T) (AEC-tr-5545)
coating with aluminum for hydrogen barrier, 17: 36298 (NAA-SR-Memo-8060(Rev.))
coating with chemical conversion coatings, 16: 27576(P)
conference on development of, Castlewood, Pleasanton, California, Nov. 12 to 14, 1962, 18: 12541 (GEAP-4089(Vols. I and II))
conference on hydriding and irradiation effects, Buffalo, New York, Oct. 10–14, 1965, 20: 27420
constitution of quenched, theory of metastable, 18: 18404
corrosion by acids, carbon dioxide, and liquid metals, alloying effects of molybdenum on, 17: 34352
corrosion by calcium-gettered sodium at 650°C, 19: 14765(R) (ANL-6977)
corrosion by carbon dioxide at 700°C, 16: 5021 (GNEC-176(Del.))
corrosion by carbon dioxide at 700°C, 16: 4583(P)
corrosion by carbon dioxide and water, 16: 32083(T) (CEA-tr-A-1148)
corrosion by carbon dioxide, 17: 40341(R) (GNEC-141(Del.))
corrosion by carbon dioxide at 800 to 1300°F, 18: 12576 (GEAP-4089 (Vol.I)(Paper 3))
corrosion by carbon dioxide at 500 to 700°C and 60 atm, 18: 37630 (A/CONF.28/P/63)
corrosion by chemical cleaning, evaluation of, 19: 36984
corrosion by flowing steam at 650°C, 17: 37001(R) (ANL-6780)
corrosion by gas–oil, hydrogenated terphenyl, and monoisopropylbiphenyl at 330 to 400°C, 20: 25492(T) (AECL-2330, pp 196-217)
corrosion by high-temperature steam, inhibiting effects of boric acid on, 18: 41973(P)
corrosion by impure Santowax, 17: 23891 (NAA-SR-7755)
corrosion by lithium at 1500 to 1900°F, 17: 6570 (ORNL-2674)
corrosion by oxygen and hydrogen chloride at 650 and 750°C, 16: 5656(R) (NMI-2099)
corrosion by oxygen and steam at 500°C, 17: 32520
corrosion by steam to 1200°F, evaluation program, 16: 479(R) (NMI-2097)
corrosion by steam at 500°C, hydrogen uptake, 16: 485 (AERE-R-3768)
corrosion by steam, sorption of hydrogen during, 16: 5674
corrosion by steam, absorption of hydrogen during, 16: 11274
corrosion by steam and water, 16: 20973(R) (ARF-2198-18)
corrosion by steam at 750°F and water at 680°F, 16: 24117(R) (ARF-2198-28)
corrosion by steam, 16: 29338 (GEAP-3462)
corrosion by steam and water, 17: 1882
corrosion by steam, 17: 14740 (TID-11295(2nd Ed.))
corrosion by steam, inhibition using boric acid, 17: 20428(P)
corrosion by steam, 17: 23865(R) (GEAP-4139)
corrosion by steam and water, effects of metal additions on,

17: 23889(R) (ARF-B198-39)
corrosion by steam at 300, 400, and 500°C, 17: 32484(R) (GEAP-4284)
corrosion by steam and water, alloying effects on, 17: 37495(T) (TRG-Inf-Ser-100)
corrosion by steam at 650°C, 17: 40422(R) (ANL-6784)
corrosion by steam at 300, 400, and 500°C, 18: 545(R) (GEAP-4368)
corrosion by steam at temperatures up to 500°C, test facility for, 18: 4196 (GEAP-4393)
corrosion by steam, statistical techniques used in study of, 18: 8750 (GEAP-4453)
corrosion by steam at 300, 400, and 500°C, 18: 12542(R) (GEAP-4484)
corrosion by steam at 540 and 650°C, 18: 25919(R) (ANL-6868(p.190-200))
corrosion by steam and water at high temperatures, 18: 37632 (A/CONF.28/P/341)
corrosion by steam, effects of boric acid on, 19: 37701(P)
corrosion by superheated steam at 540°C, 16: 4505
corrosion by superheated steam at 540°C and 600 psi, 16: 12649(R) (ANL-6485)
corrosion by superheated steam, 17: 41333(R) (ANL-6677)
corrosion by superheated steam, program for evaluation of, 18: 12579 (GEAP-4089(Vol.I)(Paper 8))
corrosion by superheated steam, 18: 21698(R) (ANL-6860)
corrosion by superheated steam, 19: 40977(P)
corrosion by terphenyls, chlorine evolution in, 19: 20469 (EUR-2279.e)
corrosion by terphenyls, research on, 20: 39344 (EUR-2997.e)
corrosion by uranyl sulfate solutions at 235 and 250°C, in-pile loop experiments on, 17: 34348 (ORNL-3131)
corrosion by water and steam, bibliography, 16: 4504 (VDIT-7.1)
corrosion by water at 680°F, 16: 15166 (ARF-2198-21)
corrosion by water at 680°F, 16: 16674(R) (ARF-2198-24)
corrosion by water, 18: 2189
corrosion by water at high temperatures, effects of composition on, 18: 8762
corrosion by water at high temperatures, effects of fluorides on, 18: 10469 (CONF-187-52)
corrosion by water vapor at 300 to 500°C, 19: 2760
corrosion by water during neutron irradiation, 19: 32693 (AECL-2257)
corrosion, effects of impurities and oxide film behavior, 16: 20954(R) (NMI-2104)
corrosion, fundamental study, 16: 20955(R) (NMI-2105)
corrosion in HWCTR, 19: 38262 (DP-964)
corrosion in reactors, 19: 20488
corrosion, mechanism, 16: 15122(R) (NMI-2103)
corrosion mechanisms, 19: 7867 (GEAP-4504)
corrosion of, by gases at high temperature, bibliographic review of, 17: 20422
corrosion of, by high-temperature steam, cracking of oxide films formed in, 17: 16590(R) (NMI-1254(p.3-43))
corrosion of, by high-temperature steam, mechanisms of, 17: 16589(R) (NMI-1254)
corrosion of, by superheated steam, 16: 31197(R) (ANL-6597)
corrosion of, effects of using iodide, sponge, and electrolytic zirconium on, 17: 39659
corrosion of, in high-temperature water cooled reactors, 17: 6567 (HW-SA-2745)
corrosion of, theory of in-pile, 17: 36230 (TID-17974)
corrosion of, conference on, New York, N. Y., Nov. 20, 1963, 19: 13931
corrosion of, conference papers on, Buffalo, New York, Oct. 10 to 14, 1965, 20: 25495
corrosion of, development in in-pile, 20: 7501(R) (TID-22426)
corrosion of, effects of hydrogen uptake on, 20: 7520
corrosion of, effects of oxide films on, 20: 21282
corrosion, oxygen dissolution in, 17: 14740 (TID-11295(2nd Ed.))
corrosion, relation of hydrogen pickup to oxide layer structure in, 16: 20979 (HW-71958-RD)
corrosion resistance and strength in water at 680°F and steam at 750 to 900°F, 18: 12577 (GEAP-4089(Vol.I)(Paper 6))
corrosion resistance in superheated steam, 18: 12578 (GEAP-4089(Vol.I) (Paper 7))
corrosion resistance and neutron absorption properties of, effects of palladium on, 18: 41970(P)
corrosion resistance of, process for improving, 19: 36989(P)
corrosion resistance of, methods for improving, 20: 25507(P)
corrosion studies, 16: 10435(R) (NMI-2100)
corrosion studies on, technical progress review on, 18: 18307
creep in, estimates of grain boundary diffusion, 20: 23709
creep properties, alloying effects of metals, 16: 16772(P)
crystal growth by recrystallization, methods for, 18: 4223
dehydridation, 16: 12653(R) (EURAEC-130)
development, 16: 7890 (NP-11196(p.34-41))
development, 17: 405(R) (ARF-2198-31)
development and evaluation of binary, for fuel assembly brazing, 20: 41425(R) (IITRI-578-P29-2)
development as fuel element cladding material for steam-cooled reactors, 17: 27728(R) (GEAP-4076)
development for in-core reactor uses, 18: 2162(R) (IITRI-B198-46)
development for service in steam, 16: 29338 (GEAP-3462)
development for steam-service fuel element cladding, 17: 14731(R) (GEAP-3979)
development for use as fuel cladding in superheated steam, 18: 12579 (GEAP-4089(Vol.I)(Paper 8))
development for use in nuclear reactors, 20: 9560(P)
development of corrosion-resistant, 16: 19333 (ARF-2198-13)
development of corrosion-resistant, 19: 931 (TID-21221(p.87-109))
development of corrosion-resistant, 19: 7867 (GEAP-4504)
development of, for use in superheated steam, 16: 30717(R) (ANL-6516)
development of, for use in reactors, 16: 30169(R) (ORNL-3313(p.133-78))
development of, for pressurized-water reactors, review of, 17: 18686
development of high-strength corrosion-resistant, 18: 22434(P)
development of high-strength and -temperature, survey on, 20: 33773
development of ternary, for use in 680°F water and steam, 17: 34347(R) (IITRI-B198-43)
development with improved corrosion resistance to steam, 18: 41933 (TID-11295(3rd Ed.))
diffusion of hydrogen in, tracer studies, 16: 7890 (NP-11196(p.34-41))
diffusion processes in, review of solute and self-, 20: 29737
dissolution, 17: 16167(P)
distribution of hydrogen in, during hydrogenation and oxidation, 20: 5851
ductility of Zircaloy tubing, effects of hydride clusters on, 19: 8703(R) (DPST-64-83-10)
economics of, as power reactor fuel cladding, 19: 17264 (AD-422953)
electric potentials across corroding oxides on, measurement of, 20: 5851
etching and pickling of, methods and solutions for, 20: 39351(P)
evaluation for use in superheated steam, 18: 18284 (CONF-187-36)
explosibility of powders of, 19: 36698 (BM-RI-6516)
fabrication, 17: 23865(R) (GEAP-4139)
fabrication, 17: 41333(R) (ANL-6677)
fabrication, 18: 21698(R) (ANL-6860)
fabrication and production in Japan, 16: 5662
fabrication and properties as refractory material, 16: 19404
fabrication and properties, 17: 32484(R) (GEAP-4284)
fabrication and properties for process equipment in aerospace, cryogenics, and nuclear engineering, 17: 39556
fabrication and properties, 18: 545(R) (GEAP-4368)
fabrication and properties, 18: 12542(R) (GEAP-4484)
fabrication and properties for use as superconductors, 18: 34179
fabrication by explosive forming, 19: 22864(R) (BMI-1704)
fabrication for fuel cladding, 19: 42175
fabrication for use in reactors, 19: 37008
fabrication of bars and tubes of, 19: 32712(P)
fabrication of chevron-can and guide-tube components from, by explosive methods, 19: 22865(R) (BMI-1711(Del.))
fabrication of chevron-can and guide-tube components from, by explosive forming, 19: 32676(R) (BMI-1717(Del.))
fabrication of fuel sheath tubes of, economics and specifications for, 18: 39837
fabrication of rods of, 20: 7546(P)
fabrication of, cost reduction in, 18: 12565
fabrication, performance, and properties, as fuel cladding material, 18: 32033 (A/CONF.28/P/255)
failure of, effects of directional hydride precipitation on delayed, 16: 33989(R) (SRO-72)
fatigue, effects of applied stress and hydrogen absorption, 16: 15168(R) (ARF-2230-6)
friction between graphite and, coefficient of, 17: 25774 (NAA-SR-Memo-8336)
handling of, recommendations for safe, 18: 8542 (AHSB(S)R-59)
handling of, safety in, 17: 10863 (RSPP-20(Issue 1))
heat-treatment process for improving corrosion resistance of, 18: 10465(P)
hydridation at 400 and 500°C, 18: 545(R) (GEAP-4368)
hydridation at 400 and 500°C, 18: 12542(R) (GEAP-4484)
hydridation in aqueous thorium oxide and thorium–uranium oxide slurries, 16: 17566(R) (ORNL-3262(p.110))
hydridation in terphenyls, 19: 18417
hydridation method for large solid shapes of, 17: 29274(P)
hydridation of cold-worked and heat-treated, at 280 to 500°C, 20: 9439 (AECL-2511)
hydridation of, during exposure to aqueous thoria and thoria–urania slurries, 17: 26792 (TID-7641(p.353-66))
hydridation of, effects on properties, 17: 32484(R) (GEAP-4284)
hydridation of, effects of oxide films on, 20: 21282
hydridation of, effects of carbon tetrachloride at 400°C on, 20: 39360 (TRG-Report-1255)
hydridation of, in light water reactors, 20: 7521

hydridation of, platelet orientation in, 19: 24089(R) (SRO-114)
hydride platelet formation in tubular, orientation of, 19: 14825(R) (DPST-64-83-9)
hydriding by organic liquids, 18: 38264 (A/CONF.28/P/15)
hydrogen overvoltage and pickup, 17: 34403 (GEAP-4192)
ignition properties of wastes from machining operations on, 20: 15001 (HW-66930)
joining of Zircaloy sheaths of fuel elements to stainless steel-clad thermocouples, 18: 575 (CEA-2290)
joining of Zircaloy to stainless steel by tandem extrusion, 19: 2734
joining to stainless steel by tandem extrusion, 19: 13970
joining to stainless steel tubes, method for, 19: 37018(P)
magnetic moments in dilute iron-group, localized, 19: 38043
magnetization of sonideal type-II superconducting wires of, Procopiu-effect analog in longitudinal, (E), 20: 24277
mechanical properties, 16: 9190(R) (BMI-1549(Del.))
mechanical properties, effects of stress and thermal cycles, 16: 14375(R) (BMI-1557(Del.))
mechanical properties, 17: 14727(R) (BMI-1600(Del.))
mechanical properties, 17: 23865(R) (GEAP-4139)
mechanical properties of, effects of hydridation on, 20: 7521
mechanical properties of, effects of hydrogen on, 20: 11221
mechanical properties of alpha-phase, effects of preferred orientation on, 20: 37226
metallurgy and uses, 16: 12153
oxidation, 17: 6564(R) (DRI-2056)
oxidation by carbon dioxide at 650 to 850°C and 15 to 760 mm Hg, 16: 161(T) (CEA-tr-X-399)
oxidation by liquid sodium at 400 to 635°C, 16: 10453 (NAA-SR-6674)
oxidation by steam at 500°C and 1000 psi, inhibiting effects of boric acid on, 19: 20492
oxidation by terphenyls, 19: 18417
oxidation in electrolytes, oxide film breakdown during, 19: 13912 (AECL-2144)
oxidation mechanism, 16: 22156
oxidation of binary, in oxygen atmosphere at 700°C, 17: 12609 (ANL-FGF-402)
oxidation of, infrared-spectra studies of, 17: 41381
oxidation of, mechanism of breakaway, 20: 25496
performance in organic-cooled reactors, (E), 19: 40218
phase boundaries in binary, effects of solute metallic valence and size on, 20: 35924
phase stabilization, effects of solute valence on, 16: 10584
phase studies of quenched, electron theory in, 19: 26836
phase transformations in, metastable polymorphic, 20: 7619
phase transformations, 18: 18307
pickling of, equations for extrapolation to technological scale, 18: 25902
polishing, utilization of "plug" technique in electrolytic, 16: 10440
preferred orientation and recrystallization, bibliography on, 16: 3433 (VDIT-46)
preparation for use in nuclear reactors, 20: 9561(P)
preparation from oxides by fusion electrolysis, 17: 25719(P)
preparation of alpha-active eutectoid, research program for, 18: 12634 (GEAP-4089(Vol.I)(Paper 5))
preparation of, methods used in metallographic, 20: 4341 (NAA-SR-Memo-10927)
preparation, properties, and uses of, review on, 20: 35901
producers in Europe, index, 16: 15119 (EURAEC-32)
production in electric arc furnace, fabrication of consumable electrodes for, 18: 8741(P)
production of corrosion-resistant, method for, 20: 37194(P)
properties, 17: 11129
properties and reactor uses, review, 16: 3490
properties and structure, 17: 39619
properties and uses of, review of, 19: 36966
properties as bearing material in steam and water, 17: 3427(R) (NP-12233)
properties as cladding and structural materials in reactors, 18: 32072
properties as cladding and structural material in reactors, 18: 41947
properties as cladding for corrosion protection of uranium, 20: 7522
properties as fuel cladding material for reactors, 18: 8840
properties as fuel element cladding in steam and water environments, 18: 34076 (TID-8540(p.213-330))
properties as reactor material, review on, 18: 42067
properties as water-reactor fuel cladding, corrosion-resistance and mechanical strength, 18: 37610 (A/CONF.28/P/419)
properties at 300, 400, and 500°C, mechanical and tensile, 17: 34346(R) (GEAP-4211)
properties, data manual, 16: 27632 (TRG-Report-108)
properties for use as reactor material, 16: 4994
properties for use in chemical process equipment, 17: 425
properties for use in light-water-cooled reactors, 18: 10566
properties for use as pressure tube material in water- cooled power reactors, 18: 12632 (GEAP-4089(Vol.I)(Paper 2))
properties for use in water-cooled reactors, 18: 37668 (A/CONF.28/P/158)
properties for use as fuel cladding for water-cooled power reactors, 18: 37692
properties for use in reactors, 19: 2760
properties for use as fuel-element cladding, 19: 22884
properties for use as reactor material, 19: 26830
properties for use as fuel cladding material in reactors, 19: 39206
properties for use in water-cooled reactors, 19: 42813
properties in superheated steam, 18: 2193
properties of Ozhennite, for fuel cladding for water-cooled reactors, 20: 35849 (KR-89, pp 82-86)
properties of, internal friction measurement for determining, 20: 13321
properties of, research on fundamental, 19: 23163(R) (ORNL-3650(p.111-86))
properties of, review on, 18: 34180
radiation effects on mechanical properties, 16: 33519 (ORNL-TM-337)
radiation effects on properties, review, 16: 33546
radiation effects on mechanical properties of, neutron, 17: 465
radiation effects on mechanical properties of, critical factors in interpretation of, 17: 41515
radiation effects on mechanical properties, 18: 16525 (NP-13657)
radiation effects on corrosion of, by water and steam at 260 to 340°C, 18: 22152
radiation effects on corrosion and hydridation of fuel-cladding, 18: 37633 (A/CONF.28/P/342)
radiation effects on corrosion of, 19: 34745(R) (HW-84384(p.8.1-5))
radiation effects on, evaluation for fast-reactor uses, (E/T), 19: 35634
radioinduced zirconium hydride formation in Zircaloy clad of fuel elements, 17: 36353 (WAPD-TM-351)
reactions with beryllium to 500°C *in vacuo*, 19: 22997 (TRG-Report-842)
reactions with organic reactor coolants, 20: 33832
reactions with sintered aluminum to 550°C *in vacuo*, 19: 22997 (TRG-Report-842)
separation from uranium, 17: 1359(R) (ANL-6569)
soldering to stainless steel, method for, 17: 20444(P)
sorptive properties for hydrogen, 16: 32126(T,R) (EURAEC-328)
specific heats of, relations of, with solute valence, 16: 30170(R) (ORNL-3313(p.179-208))
strength of, effects of carbide or oxide dispersants on, 19: 11682
stress orientation of hydride platelets in tubing of, 17: 41424(R) (DPST-63-74-8)
structural properties and uses in reactors, survey, 16: 16036
structure of pyrophosphorus, 17: 4935(T) (AEC-tr-5545)
superconductivity in, 19: 44678(R) (ANL-7000, pp 186-200)
surface-hardening of, by nitridation and oxidation, 18: 4191(P)
testing of extruded Zircaloy, critical-angle ultrasonic, 19: 7875 (HW-80505)
thermal properties of, 18: 18307
thickness of tube walls of, beta transmission measurements of, 20: 33476
transformation kinetics, 18: 44052(R) (ORNL-3670(p.147-59))
ultrasonic Lamb wave propagation in, 17: 11304 (HW-75499)
ultrasonic response of notches in tubing of, 18: 18347 (HW-77464)
use as cover for reactor fuel plates, 16: 28476(P)
use for electroless and electrolytic coating of bearings and dies, review of, 19: 4604
use in coolant loops of organic-cooled reactors, 20: 33800
uses in industry, survey, 17: 1822(T) (JPRS-15907)
welding, 17: 14797
welding, industrial procedure for, 16: 6701
welding of Zircaloy sheet to hafnium plates, explosive, 19: 46961 (BMI-X-10139)
welding to plutonium-containing fuel elements for reactors use, method for arc, 18: 44120
welding Zircaloy spacing ribs to Zircaloy housing tubes, 19: 11668(R) (DP-945)
Ag–Ti–Zr, tensile properties at room temperature, 18: 18380
Ag–Zr, density of electronic states in, 18: 4247(R) (ORNL-3470(p.20-6))
Ag–Zr, thermal capacity at 1.2 to 4.5°K, 17: 30966 (CONF-22-15)
Al–Be–Mo–Zr, corrosion resistance and mechanical properties, 16: 30891(P)
Al–Be–Mo–Zr, development of high-strength corrosion-resistant, 18: 22434(P)
Al–Cr–Co–Mo–Ni–Ti–V–Zr, surface treatments for IN-100, coating and mechanical, 20: 29706 (NASA-TM-X-53448)
Al–Cr–Cu–Fe–Mo–Sn–Ti–V–Zr, fabrication and properties, 18: 22424(R) (WAL-TR-401/303-2)
Al–Cr–Cu–Fe–Sn–Ti–V–Zr, fabrication and properties, 18: 22424(R) (WAL-TR-401/303-2)
Al–Cr–Fe–Mo–Nb–Zr, machining characteristics, 17: 14778(R) (ASD-TR-7-532a(IX))
Al–Cr–Fe–Nb–Zr, properties, 17: 1997(P)
Al–Cr–Zr, crystallization of intermetallic compounds in, effects of

casting temperature on, 20: 27554
Al–Cr–Zr, oxidation and mechanical properties, 17: 32621
Al–Cu–Fe–Sn–Ti–V–Zr, deformation and heat treatment effects on mechanical properties of, 20: 2309 (AD-615024)
Al–Cu–Fe–Sn–Ti–V–Zr, fabrication and properties of, effects of carbon additions on, 18: 22424(R) (WAL-TR-401/303-2)
Al–Cu–Nb–Zr, creep properties of, 17: 586(P)
Al–Fe–Zr, oxidation and mechanical properties, 17: 32621
Al–Hf–Nb–Ti–Zr, fabrication and tensile properties at 70 and 1600°F, 18: 12538(R) (ARF-B201-27)
Al–Hg–Zr, corrosive effects on titanium of mercury-based, 19: 44616(R) (ANL-7000, pp 122-37)
Al–La–Zr, crystal structure, 20: 2399
Al–Mg–Zr, creep rates, 20: 11313
Al–Mg–Zr, phase studies on intermetallic compounds in extruded and heat-treated, 18: 35985 (BM-RI-6498)
Al–Mo–Sn–Ti–V–Zr, beta transus temperature of, 19: 20462(R) (NRL-6258)
Al–Mo–Sn–Ti–V–Zr, corrosion by sodium chloride, effects of stress on, 20: 33858(R) (AD-634094)
Al–Mo–Sn–Ti–Zr, mechanical properties of, effects of heat treatments on, 19: 41052
Al–Mo–Sn–Zr, carburization by uranium carbide, 18: 10537 (NAA-SR-Memo-9015)
Al–Mo–Sn–Zr, compatibility of 3Z1 with uranium carbide fuels in sodium, 18: 35957 (NAA-SR-7502)
Al–Mo–Sn–Zr, corrosion by terphenyls, 16: 22551
Al–Mo–Sn–Zr, corrosion by sodium, 18: 25937
Al–Mo–Sn–Zr, effects of hydrogenation on delayed failure susceptibility of, 18: 18406
Al–Mo–Sn–Zr, fabrication and welding of alloy 3Z1, 16: 5685 (NAA-SR-6431)
Al–Mo–Sn–Zr, fatigue due to hydrogen embrittlement, 17: 526(R) (ARF-2230-12)
Al–Mo–Sn–Zr, fatigue, effects of applied stress and hydrogen sorption on static, 16: 25746(R) (ARF-2230-9)
Al–Mo–Sn–Zr, properties as claddings for uranium carbide fuels, 17: 16650 (NAA-SR-7696)
Al–Mo–Sn–Zr, thermal conductivity of 3Z1, 18: 12650 (NAA-SR-Memo-9334)
Al–Mo–Ti–Zr, beta transus temperature of, 19: 20462(R) (NRL-6258)
Al–Mo–Ti–Zr, corrosion by sodium chloride, effects of stress on, 20: 33858(R) (AD-634094)
Al–Mo–Zr, properties of, alloying effects of beryllium on, 16: 30891(P)
Al–Mo–Zr, welding of, in various atmospheres, 17: 509 (CW-R&DL-29)
Al–Nb–Ta–Ti–Zr, corrosion by mercury, 18: 10492
Al–Nb–Ti–W–V–Zr, properties for use to 1200°F, 20: 4393 (PWAC-472)
Al–Nb–Ti–Zr, fabrication and mechanical properties at 70 to 1650°F, 18: 12538(R) (ARF-B201-27)
Al–Nb–Ti–Zr, oxidation resistance at 1000°C, alloying effects, 16: 9248(P)
Al–Nb–Ti–Zr, oxidation by air at 1000°F, 18: 12538(R) (ARF-B201-27)
Al–Nb–Zr, corrosion by steam and water, 16: 29346
Al–Nb–Zr, hardness, 17: 27779(R) (DRI-2102)
Al–Nb–Zr, oxidation resistance at 1000°C, 16: 9248(P)
Al–Nb–Zr, phase isotherms at 1100 and 1300°C, 17: 39529(R) (DRI-2117)
Al–Nb–Zr, phase studies, 17: 6729
Al–Nb–Zr, preparation, 17: 6652(R) (DRI-2057)
Al–Ni–Sn–Zr, corrosion by steam at 400°C, 19: 32696(R) (EURAEC-783)
Al–Ni–Sn–Zr, fabrication and properties, 19: 36965(T,R) (EURAEC-618)
Al–Ni–Ti–Zr, corrosion by steam at 400°C, 19: 32696(R) (EURAEC-783)
Al–Ni–Ti–Zr, fabrication and properties, 19: 36965(T,R) (EURAEC-618)
Al–Ni–Zr, corrosion by steam at 400°C, 19: 32696(R) (EURAEC-783)
Al–Ni–Zr, fabrication and properties, 19: 36965(T,R) (EURAEC-618)
Al–Ni–Zr, oxidation and mechanical properties, 17: 32621
Al–Ni–Zr, thermal expansion of, to 1100°C, 19: 24982(R) (EURAEC-1270)
Al–Pu–Zr, phase studies and properties of, bibliographic study of, 16: 32115 (KFK-105)
Al–Sn–Ti–U–V–Zr, mechanical properties, 19: 37074
Al–Sn–Ti–V–Zr, formability characteristics and mechanical properties of, 20: 2308 (AD-614637)
Al–Sn–Ti–V–Zr, mechanical properties of, effects of uranium on, 19: 37074
Al–Sn–Ti–Zr, annealing, 17: 3367 (AD-275092)
Al–Sn–Ti–Zr, corrosion by mercury at 700°F, 16: 16683 (TID-7626(Pt.I) (p.107-8))
Al–Sn–Ti–Zr, corrosion by mercury, 18: 10492
Al–Sn–Ti–Zr, creep properties of, effects of sheet processing variables on, 16: 21009(R) (AD-264815)
Al–Sn–Ti–Zr, creep properties of, effects of composition on, 20: 11335
Al–Sn–Ti–Zr, fabrication and mechanical properties, 17: 12666(R) (NA57H-527-17)
Al–Sn–Ti–Zr, mechanical properties of sheet, 16: 2143(R) (AD-256168)
Al–Sn–Ti–Zr, mechanical properties of weldments, 17: 14886
Al–Sn–Ti–Zr, mechanical properties of diffusion-bonded plates of, 19: 20462(R) (NRL-6258)
Al–Sn–Ti–Zr, phase studies, 20: 13273
Al–Sn–Ti–Zr, production and properties of sheet, 16: 16706(R) (AD-264434)
Al–Sn–Ti–Zr, production of sheet, feasibility of commercial, 17: 22087(R) (AD-285409)
Al–Sn–Ti–Zr, properties of rolled sheet, 16: 19294 (AD-267448)
Al–Sn–Ti–Zr, properties, 17: 3367 (AD-275092)
Al–Sn–Ti–Zr, rolling, 17: 3367 (AD-275092)
Al–Sn–Ti–Zr, rolling, component distribution in ingots, 16: 2142(R) (AD-256167)
Al–Sn–V–Zr, corrosion by steam at 400°C, 19: 32696(R) (EURAEC-783)
Al–Sn–V–Zr, fabrication and properties, 19: 36965(T,R) (EURAEC-618)
Al–Sn–Zr, properties of, 17: 39658
Al–Ti–V–Zr, beta transus temperature of, 19: 20462(R) (NRL-6258)
Al–Ti–V–Zr, corrosion by steam at 400°C, 19: 32696(R) (EURAEC-783)
Al–Ti–V–Zr, fabrication and properties, 19: 36965(T,R) (EURAEC-618)
Al–Ti–V–Zr, welding characteristics, 16: 4510 (DMIC-Memo-140)
Al–Ti–W–V–Zr, properties for use to 1200°C, 20: 4393 (PWAC-472)
Al–Ti–Zr, annealing, 17: 3367 (AD-275092)
Al–Ti–Zr, corrosion by mercury at 700°F, 16: 16683 (TID-7626(Pt.I) (p.107-8))
Al–Ti–Zr, corrosion of nitrided, by mercury to 538°C, effects of inhibitors on, 17: 41333(R) (ANL-6677)
Al–Ti–Zr, corrosion by mercury, 18: 10492
Al–Ti–Zr, creep properties of, effects of sheet processing variables on, 16: 21009(R) (AD-264815)
Al–Ti–Zr, effect of zirconium on lattice parameters of epsilon phase of, 19: 41053
Al–Ti–Zr, fabrication and mechanical properties, 17: 12666(R) (NA57H-527-17)
Al–Ti–Zr, manufacture and properties of sheets, 16: 12027 (NP-11373)
Al–Ti–Zr, mechanical and metallurgical properties, 16: 4547 (WADC-TR-59-595(Pt.II))
Al–Ti–Zr, mechanical properties of sheet, 16: 2143(R) (AD-256168)
Al–Ti–Zr, mechanical properties of, effects of cooling rate on, 16: 21016(R) (AD-266140)
Al–Ti–Zr, mechanical properties of weldments, 17: 14886
Al–Ti–Zr, mechanical properties of diffusion-bonded plates of, 19: 20462(R) (NRL-6258)
Al–Ti–Zr, phase studies and lattice parameters, 16: 22574 (AD-269425)
Al–Ti–Zr, phase studies and properties of, 20: 11332
Al–Ti–Zr, phase studies and properties of, 20: 11333
Al–Ti–Zr, phase studies and properties of, 20: 11334
Al–Ti–Zr, production and properties of sheet, 16: 16706(R) (AD-264434)
Al–Ti–Zr, production of sheet, feasibility of commercial, 17: 22087(R) (AD-285409)
Al–Ti–Zr, properties of rolled sheet, 16: 19294 (AD-267448)
Al–Ti–Zr, properties, 17: 3367 (AD-275092)
Al–Ti–Zr, properties at –400 to 100°F, 19: 26803(R) (AD-611165)
Al–Ti–Zr, rolling, 17: 3367 (AD-275092)
Al–Ti–Zr, rolling, component distribution in ingots, 16: 2142(R) (AD-256167)
Al–Ti–Zr, tensile and thermal properties of, 17: 29358
Al–Ti–Zr, tensile properties of, effects of niobium and tantalum on, 16: 25813
Al–U–Zr, hardness and rollability of, 17: 12697
Al–U–Zr, phase studies of UAl_3–$ZrAl_3$ system in, 16: 4568
Al–U–Zr, preparation and properties as reactor fuel, 19: 32688(P)
Al–V–Zr, corrosion by steam at 400°C, 19: 32696(R) (EURAEC-783)
Al–V–Zr, fabrication and properties, 19: 36965(T,R) (EURAEC-618)
Al–V–Zr, phase studies on intermetallic compounds in, 20: 17075
Al–V–Zr, thermal expansion between 100 and 1100°C, 19: 24982(R) (EURAEC-1270)
Al–Zn–Zr, phase studies, 19: 14059
Al–Zr, analysis for uranium, fluorometric, 18: 25283
Al–Zr, atomic number effects correction in electron probe microanalysis of, 17: 27268
Al–Zr, bibliography on, 17: 23878 (VDIT-74)
Al–Zr, crystal structure, 16: 18048
Al–Zr, crystal structure of intermetallic compound ZrAl in, 16: 21051
Al–Zr, crystal structures of intermetallic compounds $ZrAl_3$ and Zr_2Al_3 in, 16: 12124
Al–Zr, crystal structure of Zr_2Al, 18: 18389
Al–Zr, crystallization of, effects of zirconium additions on, 20: 17072
Al–Zr, crystallization of intermetallic compounds in, effects of casting temperature on, 20: 27554
Al–Zr, deposition from fused salts, electrolytic, 20: 9448

Al–Zr, diffusion and equilibrium in, 18: 37705
Al–Zr, diffusion in, inter-, 20: 5851
Al–Zr, enthalpy, free enthalpy, and entropy of formation of intermetallic compounds Al_3Zr, Al_4Zr_5, and Al_2Zr_3 in, 16: 4581
Al–Zr, fabrication and production of stoichiometric, 19: 42831
Al–Zr, interdiffusion and growth layers in, 19: 978
Al–Zr, oxidation of, distribution of aluminum in oxide film in, 20: 25504
Al–Zr, phase studies, 17: 6729
Al–Zr, phase studies of, atomic size effects in, 19: 23111
Al–Zr, phase studies, 20: 35924
Al–Zr, processing of irradiated, in aqueous solutions, 16: 30495(R) (IDO-14589)
Al–Zr, properties at 800 and 1000°C, 17: 39657
Al–Zr, properties for use as fuel element jacket, 18: 44232(P)
Al–Zr, properties of, electric and mechanical, 20: 19241
Al–Zr, properties of intermetallic compound, 20: 37260
Al–Zr, test casting in dies and molds, 17: 32591
Au–Zr, structure of, 17: 578
Ba–Zr, resistance to scaling at elevated temperatures, 19: 32770(P)
Be–Ca–Zr, development of corrosion-resistant, 17: 37473(P)
Be–Cu–Zr, crystal structure of intermetallic compounds in, 20: 23726
Be–Gd–Zr, high-temperature oxidation resistance of intermetallic compounds in, 18: 27912
Be–Hf–Zr, high-temperature oxidation resistance of intermetallic compounds in, 18: 27912
Be–Mg–Mn–Zr, fabrication and properties, 19: 36970(P)
Be–Nb–Zr, properties to 2750°F, 17: 532 (GEMP-105)
Be–Nb–Zr, properties for brazing niobium, 18: 5758
Be–Ti–Zr, brazing alloy for alumina-to-niobium alloy seals, 19: 40980 (LA-3302)
Be–Ti–Zr, brazing of graphite to, 17: 32547
Be–Ti–Zr, brazing on aluminum, beryllium, uranium oxides, and graphite, 18: 32122
Be–Ti–Zr, properties as brazing alloy, 17: 4912(R) (ORNL-TM-413)
Be–Ti–Zr, properties for brazing on niobium, 18: 5758
Be–Ti–Zr, tensile properties at room temperature, 18: 18380
Be–Ti–Zr, use of, as brazing alloy for refractory metals and alloys, 16: 19328(P)
Be–U–Zr, corrosion by potassium–sodium alloy (liquid), 17: 34329(R) (TID-14146)
Be–U–Zr, fabrication and properties of UBe_{13}–$ZrBe_{13}$, 17: 34329(R) (TID-14146)
Be–U–Zr, high-temperature oxidation resistance of intermetallic compounds in, 18: 27912
Be–U–Zr, properties of intermetallic compounds in, 16: 10517 (DC-60-4-80)
Be–U–Zr, properties, 17: 14740 (TID-11295(2nd Ed.))
Be–Zr, brazing of, specification for, 16: 521 (HW-69715)
Be–Zr, coating developments for, 17: 532 (GEMP-105)
Be–Zr, compatibility with chromium at 2200 and 2500°F, 17: 532 (GEMP-105)
Be–Zr, corrosion of, by argon saturated with water at 1200 to 1600°F, 16: 30723(R) (TID-16478)
Be–Zr, corrosion resistance to carbon dioxide and mechanical properties, 18: 16448(P)
Be–Zr, corrosion by boric acid–potassium hydroxide solutions, 18: 30133 (WCAP-3737)
Be–Zr, corrosion by hot carbon dioxide, 19: 11680
Be–Zr, corrosion resistance to carbon dioxide, 19: 36991(P)
Be–Zr, corrosion by borated water at 600°F, 20: 5846
Be–Zr, development of, for high-temperature uses, 17: 16637(R) (BBC-115)
Be–Zr, development of, for high-temperature reactor uses, 17: 18670(R) (BBC-108)
Be–Zr, development of high-temperature, 17: 20451(R) (BBC-117)
Be–Zr, evaporation rate of $ZrBe_{13}$, 17: 36293(R) (DRI-2079)
Be–Zr, fabrication by splat cooling, 18: 24067(R) (NMI-2127)
Be–Zr, fabrication and properties of splatcooled SLIS, 18: 35938(R) (NMI-2129)
Be–Zr, fabrication and properties of splatcooled SLIS, 19: 34654(R) (NMI-1263)
Be–Zr, high-temperature oxidation resistance of intermetallic compounds in, 18: 27912
Be–Zr, intermetallic compounds in, properties of, for use in aerospace technology, 20: 29770
Be–Zr, machining of, applicability of electric-discharge, 16: 33446 (DC-60-3-173)
Be–Zr, mechanical properties of intermetallic compounds in, effects of composition and structure on, 17: 541 (WADD-TR-60-184(Pt.III))
Be–Zr, mechanical properties of splatcooled, 18: 25894(R) (NMI-2128)
Be–Zr, mechanical properties at 70 to 2500°F, effects of aluminum, nickel, and silicon additions on, 18: 27946(R) (BBC-120)
Be–Zr, mechanical and physical properties of intermetallic compounds in, 19: 7942
Be–Zr, oxidation kinetics at 700 to 1500°C, 16: 12051 (NAA-SR-6493)
Be–Zr, oxidation mechanisms, 16: 9156(R) (TID-14955)
Be–Zr, oxidation of intermetallic compounds in, at 1200 to 1800°F, 16: 30724(R) (TID-16479)
Be–Zr, oxidation stoichiometric, at 1200 to 1800°F, kinetic studies, 16: 27562(R) (TID-16019)
Be–Zr, oxidation of intermetallic compounds $ZrBe_{13}$ and Zr_2Be_{17} in, at 1200 to 2000°F, 16: 24123 (TID-16030)
Be–Zr, oxidation products at 2500°F, 16: 18044 (WADD-TR-60-889)
Be–Zr, oxidation resistance and vapor pressure measurements, 16: 5720(R) (NP-11178)
Be–Zr, oxidation of, at 1200 to 1800°F, 17: 530(R) (DRI-2042)
Be–Zr, oxidation, 17: 6643(R) (BBC-112)
Be–Zr, oxidation, 17: 6653(R) (DRI-2071)
Be–Zr, oxidation of intermetallic compounds in, at high temperatures, 17: 14725(R) (BBC-114)
Be–Zr, oxidation of intermetallic compounds $ZrBe_{13}$ and Zr_2Be_{17} in, at 1200 to 1800°F, 17: 15947(R) (DRI-2088)
Be–Zr, oxidation resistance of, at 1100 to 1700°F, 17: 20450(R) (BBC-116)
Be–Zr, oxidation of aluminum-containing $ZrBe_{13}$ and Zr_2Be_{17} at 650 to 1000°C, 17: 27781(R) (DRI-2105)
Be–Zr, oxidation resistance of $ZrBe_{13}$ and Zr_2Be_{17} at 70 to 2500°F, alloying effects of aluminum, nickel, niobium, and tantalum on, 17: 29313(R) (BBC-118)
Be–Zr, oxidation of $ZrBe_{13}$ and Zr_2Be_{17} at 550 to 1100°C, effects of aluminum additions on, 18: 7136(R) (DRI-2128)
Be–Zr, oxidation by dry and moist air at 1200 to 2700°F, effects of aluminum, nickel, niobium, silicon, and tantalum additions on, 18: 27946(R) (BBC-120)
Be–Zr, oxidation resistance of intermetallic compounds in, at 1000 to 2000°F, 19: 7943
Be–Zr, oxidation and vaporization of $ZrBe_{13}$ and Zr_2Be_{17} at 1533 to 1728°K, 19: 7459
Be–Zr, oxidation of intermetallic compounds $ZrBe_{13}$ and Zr_2Be_{17} in, 19: 11680
Be–Zr, oxidation resistance of, effects of aluminum, nickel, silicon, and tantalum additions on, 20: 5844
Be–Zr, performance as thermionic emitters, 18: 30479(R) (DRI-2137)
Be–Zr, phase studies and thermodynamics of intermetallic compounds in, 19: 41078
Be–Zr, preparation and properties of braze, 19: 26819 (NMI-4787)
Be–Zr, properties of, below 1000°C, 16: 2235
Be–Zr, properties of intermetallic compounds in, 16: 10517 (DC-60-4-80)
Be–Zr, properties of intermetallic compound Zr_2Be_{17} in, effects of fabrication techniques and processing variables on, 16: 25748 (ASD-TDR-62-476)
Be–Zr, properties for high-temperature applications, 17: 543 (WADD-TR-60-889(Pt.II))
Be–Zr, properties to 2750°F, 17: 532 (GEMP-105)
Be–Zr, properties, 17: 11082(R) (BBC-113)
Be–Zr, properties, 17: 14740 (TID-11295(2nd Ed.))
Be–Zr, properties of ZrB_{13} and Zr_2Be_{17} to 2700°F, alloying effects of aluminum, nickel, and titanium on, 17: 34397(R) (BBC-119)
Be–Zr, properties of, effects of aluminum on, 18: 18305
Be–Zr, properties at 1000 to 2100°F, effects of atmosphere and impurities on, 20: 43886(R) (BBC-111)
Be–Zr, stoichiometry and temperature effects on pest degradation in compounds in, 18: 42055
Be–Zr, thermal conductivities of, at 300 to 1000°C, 16: 19393
Be–Zr, thermionic properties, 20: 29801
Be–Zr, use as brazing alloys for refractory metals, 18: 7956(R) (GA-3992(Pt.I))
Be–Zr, wetting behavior of liquid, on solid beryllium, effects of atmosphere and temperature on, 17: 27795 (ORNL-3438)
Be–Zr, wetting behavior of liquid, on solid beryllium, 17: 33323(R) (ORNL-3445(p.199-217))
Be–Zr, wetting behavior on solid beryllium, 18: 28035
Bi–Mo–Zr, corrosion resistance and mechanical properties, 17: 37535
Bi–U–Zr, phase diagram, liquidus curves in, 16: 2251
Bi–Zr, analysis of, source of, variables in, 17: 2464(R) (BNL-731(p.59-94))
Bi–Zr, electric mobility of zirconium in liquid, 18: 546 (IP-488)
Bi–Zr, phase studies and structure, 17: 39653
Bi–Zr, phase studies, 19: 9604(R) (IS-900(Sect.M))
Bi–Zr, preparation and properties, 18: 2163(R) (IS-700(Sect.M))
Bi–Zr, preparation and phase studies on, 20: 13252 (IS-1269)
Bi–Zr, superconductivity, 20: 44554
Ca–Nb–Zr, corrosion by superheated steam, 19: 40977(P)
Ca–Nb–Zr, preparation of corrosion-resistant, 19: 4612(P)
Ca–Zr, oxidation by carbon dioxide up to 600°C, 18: 30192
Cd–Zr, crystal structure of intermetallic compounds in, 20: 11328

Cd–Zr, density of electronic states in, 18: 4247(R) (ORNL-3470(p.20-6))
Cd–Zr, thermal capacity at 1.2 to 4.5°K, 17: 30966 (CONF-22-15)
Ce–fissium–U–Zr, reactions with calcium chloride–magnesium chloride at 1200°C, 19: 17176(R) (ANL-6965(p.1-41))
Ce–Mg–Zn–Zr, ultrasonic wave attenuation and delay in, 19: 32761
Ce–Mg–Zr, mechanical properties at 100 to 300°C, 17: 1920 (BM-RI-6078)
Ce–Mg–Zr, ultrasonic wave attenuation and delay in, 19: 32761
Ce–Nb–Zr, preparation for use in nuclear reactors, 20: 9560(P)
Ce–Th–Zr, properties and structure of, 18: 37670 (A/CONF.28/P/337)
Ce–Zr, electronic state of cerium in, 18: 12693
Co–Fe–Zr, crystal and magnetic properties of, 16: 18039 (TID-14769)
Co–Fe–Zr, electronic specific heats at 1.5 to 4°K, 19: 30743(R) (NYO-3454-1)
Co–Fe–Zr, magnetic and structural properties at 4 to 650°K, 17: 25708(R) (TID-18766)
Co–Fe–Zr, magnetic properties and structure of intermetallic compounds, 17: 36312
Co–Fe–Zr, Mössbauer effect of iron-57 in Laves phases in, 16: 10565
Co–Fe–Zr, thermal capacity for $ZrCo_2$–$ZrFe_2$ phases in, 20: 27494(R) (NYO-3454-6)
Co–Ni–Ti–Zr, mechanical and thermophysical properties of Nivco, at 80 to 1600°C, 18: 41928(R) (NASA-CR-54089)
Co–Ni–Ti–Zr, properties of Nivco in space electric power systems, 20: 4379 (NASA-CR-54091)
Co–Ta–Zr, phase studies, 18: 25970(R) (ANL-6868(p.303-25))
Co–Ti–Zr, magnetic susceptibilities of $TiCo_2$–$ZrCo_2$ in, at 4.2 to 300°K, 20: 27494(R) (NYO-3454-6)
Co–Ti–Zr, tensile properties at room temperature, 18: 18380
Co–V–Zr, atomic arrangements in C14 Laves phase in, 17: 29364
Co–Zr, cobalt ion EPR in intermetallic compounds of, 20: 15963
Co–Zr, crystal structure of Zr_6Co_{23}, 20: 31727
Co–Zr, crystal structure of intermetallic compounds, 20: 41412(R) (IS-1500(Sect. M))
Co–Zr, elastic properties of Laves-phase intermetallic compound, 20: 41412(R) (IS-1500(Sect. M))
Co–Zr, magnetic and structural properties, 16: 18039 (TID-14769)
Co–Zr, oxidation kinetics at 500 to 900°C, 20: 5854(R) (JPRS-32341, pp 8-16)
Co–Zr, phase diagrams of, intermediate phases in, 18: 27976
Co–Zr, phase diagrams at 25 to 950°C, 20: 9516
Co–Zr, phase studies, 17: 4447 (IS-500(Sect.M))
Co–Zr, phase studies, 17: 14740 (TID-11295(2nd Ed.))
Co–Zr, phase studies, 18: 2163(R) (IS-700(Sect.M))
Co–Zr, phase studies, 19: 9604(R) (IS-900(Sect.M))
Co–Zr, phase studies, 20: 14533
Co–Zr, reactions with hydrogen, thermochemical and structural aspects of, 20: 27436
Co–Zr, superconductivity of, 18: 9274
Cr–Cu–Fe–Nb–Zr, fabrication for steam-service, 17: 18713 (GEAP-4115)
Cr–Cu–Nb–Zr, corrosion by high-pressure flowing steam at 300, 400, and 500°C, 17: 34346(R) (GEAP-4211)
Cr–Cu–Nb–Zr, properties for steam-service fuel element cladding, optimization studies, 17: 14731(R) (GEAP-3979)
Cr–Cu–Zr, corrosion by high-pressure flowing steam at 300, 400, and 500°C, 17: 34346(R) (GEAP-4211)
Cr–Fe–Nb–Zr, corrosion by air, carbon dioxide, and water, 17: 504
Cr–Fe–Ni–Sn–Zr, properties for use as fuel element cladding, 19: 20497(P)
Cr–Fe–Sn–Zr, corrosion by steam at temperatures to 1150°F, 20: 9427 (WAPD-TM-546)
Cr–Fe–Zr, corrosion by steam at 750°F, 17: 6561(R) (ARF-2198-34)
Cr–Fe–Zr, corrosion of, oxygen gradients in, 17: 6579
Cr–Fe–Zr, corrosion by steam, 17: 34347(R) (IITRI-B198-43)
Cr–Fe–Zr, corrosion by water at 400°C, 17: 39656
Cr–Fe–Zr, corrosion by steam, 18: 41933 (TID-11295(3rd Ed.))
Cr–Fe–Zr, corrosion by steam, effect of selected fabrication variables on, 19: 26767(R) (GEAP-4821)
Cr–Fe–Zr, corrosion by steam at temperatures to 1150°F, 20: 9427 (WAPD-TM-546)
Cr–Fe–Zr, corrosion by steam at 300 to 500°C, effects of nitrogen impurity content on, 20: 14980(R) (GEAP-5065)
Cr–Fe–Zr, corrosion by steam at 500°C, effects of metallurgical processing variables on, 20: 14980(R) (GEAP-5065)
Cr–Fe–Zr, corrosion by steam, effects of fabrication process and nitride content on, 20: 29660(R) (GEAP-4960)
Cr–Fe–Zr, corrosion by steam at 300, 400, and 500°C, 20: 31677(R) (GEAP-4840)
Cr–Fe–Zr, corrosion of zirconium-base, by steam at 300 to 500°C, 20: 39356(R) (GEAP-5134)
Cr–Fe–Zr, fabrication for steam service, 17: 28713 (GEAP-4115)
Cr–Fe–Zr, hot hardness tests on plasticity of oxide film formation on, 19: 25009
Cr–Fe–Zr, microstructure of, effects of heat treatments on, 20: 29660(R) (GEAP-4960)
Cr–Fe–Zr, oxidation by steam at 750 and 900°F, hydrogen absorption from, 18: 2162(R) (IITRI-B198-46)
Cr–Fe–Zr, phase studies, 17: 16545
Cr–Fe–Zr, properties for use as water reactor fuel cladding, 19: 7867 (GEAP-4504)
Cr–Fe–Zr, properties of, for use as fuel cladding material, 20: 31677(R) (GEAP-4840)
Cr–Fe–Zr, properties of zirconium base, for fuel cladding, 20: 39356(R) (GEAP-5134)
Cr–Fe–Zr, structure of Laves phase in, 17: 23872(R) (TID-18626)
Cr–Fe–Zr, tensile properties at 70 and 750°F, 18: 2162(R) (IITRI-B198-46)
Cr–Mo–Nb–Ti–Zr, mechanical and oxidation properties of, at high temperatures, 16: 27691(P)
Cr–Mo–Zr, corrosion by pressurized water and workability of, 18: 20461
Cr–Mo–Zr, heat treatment effects on mechanical properties and microstructure of, 18: 20461
Cr–Mo–Zr, oxidation and mechanical properties, 17: 32621
Cr–Nb–Sn–U–Zr, corrosion, 17: 39640
Cr–Nb–Ti–Zr, corrosion by steam at 540°C, 17: 36221 (BMI-1636)
Cr–Nb–V–Zr, development and properties for reactor cladding, 18: 7266
Cr–Nb–Zr, corrosion of, by steam and water, 16: 29346
Cr–Nb–Zr, corrosion by steam at 1000°F, 17: 493(R) (BMI-X-10003)
Cr–Nb–Zr, corrosion by high-pressure flowing steam at 300, 400, and 500°C, 17: 34346(R) (GEAP-4211)
Cr–Nb–Zr, corrosion by potassium at 1500 to 1800°F, 18: 5728 (ASD-TDR-63-270(Pt.II))
Cr–Nb–Zr, corrosion films on, composition of, 18: 12580 (GEAP-4089 (Vol.II)(Paper 19))
Cr–Nb–Zr, corrosion by potassium vapor at 1500 to 1800°F, 18: 18282 (BNL-844)
Cr–Nb–Zr, corrosion mechanisms of, 18: 39840 (GEAP-4521)
Cr–Nb–Zr, corrosion by water at 360°C and steam at 400°C, mechanism of, 19: 30681
Cr–Nb–Zr, corrosion by steam at 400 and 450°C, 19: 30668(R) (EURAEC-1274)
Cr–Nb–Zr, oxidation by steam at 750 and 900°F, 18: 2162(R) (IITRI-B198-46)
Cr–Nb–Zr, phase diagram, intermetallic compounds in, 20: 23684
Cr–Nb–Zr, phase studies, 17: 11108(T,R) (EURAEC-307)
Cr–Nb–Zr, phase studies, 17: 14749(T,R) (EURAEC-408)
Cr–Nb–Zr, phase studies, 18: 28036
Cr–Nb–Zr, phase studies, 16: 32084(T,R) (EURAEC-227)
Cr–Nb–Zr, tensile properties of, effects of composition and heat treatment on, 16: 29380 (TID-6155)
Cr–Ni–Zr, corrosion of, oxygen gradients in, 17: 6579
Cr–Ni–Zr, corrosion by water at 400°C, 17: 39656
Cr–Ni–Zr, corrosion by steam, 18: 41933 (TID-11295(3rd Ed.))
Cr–Ni–Zr, oxidation by superheated steam at 540°C, 18: 15663(R) (ANL-6808)
Cr–Sn–Zr, analysis of corrosion films on, for zirconium-to-chromium and -to-tin ratios, 17: 27728(R) (GEAP-4076)
Cr–Sn–Zr, corrosion by air and water at 500°C, 17: 39655
Cr–Sn–Zr, corrosion by water at 400°C, 17: 39656
Cr–Sn–Zr, corrosion by steam and water, 17: 39659
Cr–Sn–Zr, corrosion films on, composition of, 18: 12580 (GEAP-4089 (Vol.II)(Paper 19))
Cr–Sn–Zr, corrosion by water at 360°C and steam at 400°C, mechanism of, 19: 30681
Cr–Sn–Zr, corrosion by steam at temperatures to 1150°F, 20: 9427 (WAPD-TM-546)
Cr–Sn–Zr, oxidation of, causes of second transition point in, 16: 7857
Cr–Sn–Zr, phase diagrams, 17: 39654
Cr–Sn–Zr, properties as cladding for fuel elements, 20: 25614(P)
Cr–Sn–Zr, tensile properties of, effects of composition and heat treatment on, 16: 29380 (TID-6155)
Cr–Ti–Zr, phase studies, 19: 44714
Cr–Ti–Zr, tensile properties at room temperature, 18: 18380
Cr–V–Zr, fabrication of, cracking in, 17: 41427(R) (IITRI-B231-9)
Cr–V–Zr, forgeability and tensile strength, 17: 25771 (ASD-TDR-62-667)
Cr–Zr, corrosion by water at 680°F, 17: 6561(R) (ARF-2198-34)
Cr–Zr, corrosion by steam at 750°F, 17: 6561(R) (ARF-2198-34)
Cr–Zr, corrosion by high-pressure flowing steam at 300, 400, and 500°C, 17: 34346(R) (GEAP-4211)
Cr–Zr, corrosion by steam and water, 17: 39659
Cr–Zr, corrosion by steam, 18: 41933 (TID-11295(3rd Ed.))
Cr–Zr, corrosion by steam at 400°C, mechanism of, 19: 30681
Cr–Zr, electrochemical potential, 17: 34403 (GEAP-4192)
Cr–Zr, free energies of formation of Laves phases in, 16: 13636

Cr–Zr, oxidation by steam at 900°F, 18: 2162(R) (IITRI-B198-46)
Cr–Zr, phase studies, 16: 32084(T,R) (EURAEC-227)
Cr–Zr, phase studies, 17: 14749(T,R) (EURAEC-408)
Cr–Zr, phase studies, 18: 2158(R) (EURAEC-176)
Cr–Zr, phase studies of intermetallic compounds in, 19: 9713(T)
Cr–Zr, phase studies, 19: 44714
Cr–Zr, reactions with hydrogen, thermochemical and structural aspects of, 20: 27436
Cr–Zr, strength, 17: 6561(R) (ARF-2198-34)
Cr–Zr, structural study, 17: 11108(T,R) (EURAEC-307)
Cr–Zr, uptake of hydrogen during steam and water corrosion of, 17: 32519
Cs–Zr, phase studies, 20: 35924
Cu–Fe–Zr, corrosion by steam at 540 to 650°C, 17: 35079(R) (ANL-6749)
Cu–Fe–Zr, corrosion by superheated steam, 17: 41333(R) (ANL-6677)
Cu–Fe–Zr, corrosion by oxygenated sodium at 540 and 650°C, 18: 19456(R) (ANL-6840)
Cu–Fe–Zr, corrosion by steam, effects of additives on, 18: 26824(R) (ANL-6885)
Cu–Fe–Zr, corrosion by steam, 18: 41933 (TID-11295(3rd Ed.))
Cu–Fe–Zr, corrosion by superheated steam, 19: 14765(R) (ANL-6977)
Cu–Fe–Zr, corrosion by liquid metals, measurement of, 19: 17177(R) (ANL-6965(p. 42-83))
Cu–Fe–Zr, corrosion by superheated steam at 540 and 650°C, 19: 22899
Cu–Fe–Zr, corrosion by steam at 540°C, effects of pressure on, 19: 44616(R) (ANL-7000, pp 122-37)
Cu–Mn–Zr, analysis for bonding and inclusions in, by x-ray emission in electron microscopy, 20: 20593
Cu–Mo–Zr, analysis for boron by direct absorptiometric method, 17: 5965 (PG-Report-362)
Cu–Mo–Zr, corrosion by steam at 280 to 500°C and 15 to 800 lb/in.², 17: 12619
Cu–Mo–Zr, corrosion resistance and mechanical properties of, effects of bismuth and niobium on, 17: 37535
Cu–Mo–Zr, corrosion by superheated steam at 500°C, hydrogen uptake from, 17: 41368(T,R) (EURAEC-784)
Cu–Mo–Zr, corrosion by superheated steam at 500°C, hydrogen uptake from, 18: 14386(T,R) (EURAEC-822)
Cu–Mo–Zr, corrosion and hydridation by steam and water, 18: 30134(T,R) (EURAEC-955)
Cu–Mo–Zr, corrosion by steam, effects of heat treatments on copper-base and zirconium-base, 20: 39347 (NP-16239)
Cu–Mo–Zr, effects of transformation reactions on properties of, 17: 14835 (NP-12520)
Cu–Mo–Zr, mechanical properties of, effects of hydrogen content on, 18: 14386(T,R) (EURAEC-822)
Cu–Mo–Zr, oxidation by carbon dioxide up to 600°C, 18: 30192
Cu–Mo–Zr, oxidation by steam, oxide films from, 19: 2763 (AECL-1999)
Cu–Mo–Zr, oxidation resistance of, in carbon dioxide at 600 and 700°C, 20: 5860
Cu–Mo–Zr, properties of compositions being used in reactors, 17: 23995
Cu–Mo–Zr, reactions with carbon dioxide to 500°C, 19: 22997 (TRG-Report-842)
Cu–Mo–Zr, reactions with beryllium to 600°C *in vacuo*, 19: 22997 (TRG-Report-842)
Cu–Mo–Zr, reactions with Magnox alloy to 500°C in carbon dioxide–carbon monoxide, 19: 22997 (TRG-Report-842)
Cu–Nb–Sn–Zr, corrosion by steam at 400 and 450°C, 19: 30668(R) (EURAEC-1274)
Cu–Nb–Zr, abrasion between cylinders and flats of, in water at 550°F, 20: 7490(R) (BMI-1745, Sect.A)
Cu–Nb–Zr, alloy element distribution in bulk metal and oxide film on, 20: 5851
Cu–Nb–Zr, corrosion by air, carbon dioxide, and water, 17: 504
Cu–Nb–Zr, corrosion by high-pressure flowing steam at 300, 400, and 500°C, 17: 34346(R) (GEAP-4211)
Cu–Nb–Zr, corrosion by superheated steam at 500°C, hydrogen uptake from, 17: 41368(T,R) (EURAEC-784)
Cu–Nb–Zr, corrosion by superheated steam at 500°C, hydrogen uptake from, 18: 14386(T,R) (EURAEC-822)
Cu–Nb–Zr, corrosion and hydridation by steam and water, 18: 30134(T,R) (EURAEC-955)
Cu–Nb–Zr, corrosion and hydridation by steam and water, effects on tensile properties, 19: 4616(R) (EURAEC-1161)
Cu–Nb–Zr, corrosion films on, microprobe studies of, 19: 9621 (DP-906)
Cu–Nb–Zr, corrosion by steam at 400 and 450°C, 19: 30668(R) (EURAEC-1274)
Cu–Nb–Zr, corrosion and hydrogen absorption characteristics of, effects of heat treatment on, 20: 25488 (WAPD-TM-500)
Cu–Nb–Zr, effects of hydrogen content on delayed failure of, 17: 14810(R) (ARF-B6005-2)
Cu–Nb–Zr, failure of, factors affecting delayed, 17: 38551(R) (SRO-93)
Cu–Nb–Zr, fatigue of hydrided, effects of heat treatment on, 17: 34404(R) (IITRI-B6005-8)
Cu–Nb–Zr, hot hardness tests on plasticity of oxide film formation on, 19: 25009
Cu–Nb–Zr, hydride precipitates in, effects of heat treatment on strain-induced orientation of, 18: 18341 (AECL-1888)
Cu–Nb–Zr, hydrogen distribution in oxidized, tritium autoradiographic studies of, 19: 13910 (AECL-2085)
Cu–Nb–Zr, hydrogen embrittlement, 18: 5776(R) (IITRI-B6005-11)
Cu–Nb–Zr, hydrogenation of, delayed failure from, 17: 28533(R) (SRO-83)
Cu–Nb–Zr, hydrogenation of, delayed failure from, 17: 42352(R) (SRO-94)
Cu–Nb–Zr, hydrogenation of, delayed failure from, 18: 3190(R) (SRO-95)
Cu–Nb–Zr, mechanical properties of hydrided, effects of fabrication, specimen geometry, and temperature, 17: 22155(R) (ARF-B6005-5)
Cu–Nb–Zr, mechanical properties of, effects of hydrogen content on, 18: 14386(T,R) (EURAEC-822)
Cu–Nb–Zr, radiation effects on tensile properties of, fast-neutron, 20: 2414 (AECL-2272)
Cu–Nb–Zr, radiation effects on tensile properties of, neutron, 20: 9590
Cu–Nb–Zr, stress-rupture of, effects of hydrogen embrittlement on, 17: 31733(R) (SRO-84)
Cu–Nb–Zr, testing for power reactor pressure tubes, 18: 37666 (A/CONF.28/P/22)
Cu–Sn–Zr, development of corrosion resistant, 17: 34357(P)
Cu–Sn–Zr, preparation and properties of corrosion-resistant, 18: 8746(P)
Cu–Ti–Zr, tensile properties at room temperature, 18: 18380
Cu–W–Zr, corrosion of, by carbon dioxide at high temperatures, 16: 4583(P)
Cu–W–Zr, corrosion by steam at 280 to 500°C and 15 to 800 lb/in.², 17: 12619
Cu–W–Zr, plasticity of, effects of annealing in oxygen on, 20: 23677
Cu–W–Zr, production, 20: 9406(P)
Cu–W–Zr, radiation effects on oxidation of, 17: 12621
Cu–Zr, age hardening and conductivity of, affect of oxidation inhibitors and purity on, 17: 11225
Cu–Zr, analysis for zirconium, colorimetric, 19: 15389
Cu–Zr, analysis of, for zirconium, complexometric, 16: 26944
Cu–Zr, compatibility with beryllium at 500 to 650°C in vacuum, 20: 8925
Cu–Zr, conductivity, mechanical properties, and precipitation in, 20: 2334 (NP-15530)
Cu–Zr, corrosion of, at high temperatures, effects of iron impurity on, 16: 15235(P)
Cu–Zr, corrosion by steam at 280 to 500°C and 15 to 800 lb/in.², 17: 12619
Cu–Zr, corrosion by high-pressure flowing steam at 300, 400, and 500°C, 17: 34346(R) (GEAP-4211)
Cu–Zr, corrosion by steam at 540°C, 17: 35079(R) (ANL-6749)
Cu–Zr, corrosion by steam, 18: 2191
Cu–Zr, corrosion by superheated steam at 540 and 650°C, 19: 22899
Cu–Zr, corrosion by steam at 500°C, hydrogen uptake in, 19: 22901
Cu–Zr, corrosion by steam at 540°C, 19: 44616(R) (ANL-7000, pp 122-37)
Cu–Zr, crystal structure and occurrence of intermetallic compound Zr_2Cu in, 19: 9720
Cu–Zr, development of age- and dispersion-hardened copper-base, 20: 29782
Cu–Zr, diffusion in, intermetallic compound formation from, 19: 37131
Cu–Zr, effects of arsenic on electric conductivity of, 17: 4938
Cu–Zr, electric conductivity of type 304 stainless steel-clad wires of, at 80 to 1600°F, 18: 41928(R) (NASA-CR-54089)
Cu–Zr, electrochemical potential and hydrogen overvoltage, 17: 34403 (GEAP-4192)
Cu–Zr, electronic structure of intermetallic compound Zr_2Cu, 19: 16177
Cu–Zr, embrittlement effects of hydrogen on, 18: 34169
Cu–Zr, hydrogen overvoltage measurements in, 17: 27728(R) (GEAP-4076)
Cu–Zr, hydrogen overvoltage at Zr_2Cu in sulfuric acid, 18: 12642 (GEAP-4089(Vol.II)(Paper 22))
Cu–Zr, oxidation by oxygen at 700°C, 17: 41333(R) (ANL-6677)
Cu–Zr, oxidation by superheated steam at 540°C, 18: 15663(R) (ANL-6808)
Cu–Zr, oxidation by carbon dioxide up to 600°C, 18: 30192
Cu–Zr, oxidation in carbon dioxide and carbon monoxide at 500 to 900°C, 19: 24942
Cu–Zr, oxidation at 500 to 900°C, 19: 40976
Cu–Zr, oxidation and oxide film breakaway at 600 to 850°C, 20: 25497
Cu–Zr, oxidation by carbon dioxide at 800°C, 20: 16977
Cu–Zr, oxidation by water vapor at 375 and 575°C, kinetics of, 20: 25498
Cu–Zr, oxidation of, distribution of copper in oxide film in, 20: 25504
Cu–Zr, oxidation of, mechanism of breakaway, 20: 25496
Cu–Zr, oxidation resistance of, in carbon dioxide at 600 and 700°C, 20: 5860
Cu–Zr, oxidation by carbon monoxide at high temperatures, mechanisms of,

20: 37183
Cu–Zr, oxide film growth and breakdown on, 18: 2191
Cu–Zr, oxide film breakdown and growth on steam-exposed, 18: 12589
Cu–Zr, phase studies, 18: 14396
Cu–Zr, phase studies on, 18: 14500
Cu–Zr, phase studies, 20: 35924
Cu–Zr, properties as magnet material, 20: 41097
Cu–Zr, reactions with hydrogen, thermochemical and structural aspects of, 20: 27436
Cu–Zr, resistance to scaling at elevated temperatures, 19: 32770(P)
Cu–Zr, solid solubility of zirconium in copper in, 17: 11240
Cu–Zr, surface preparation of metallographic specimens of, by chemical and electrolytic polishing, 16: 2015 (ORNL-3139)
Cr–Zr, properties of, at high temperatures, 16: 30779 (BMI-1277)
Dy–Zr, magnetic properties of, 17: 32651
Dy–Zr, metallurgical properties and phase studies on, 20: 5891(R) (NYO-2159-1)
Dy–Zr, oxidation by air at 500°C and water at 93 and 177°C, 17: 34330(R) (USBM-U-1057)
Dy–Zr, phase studies, 16: 17967(R) (USBM-U-887)
Dy–Zr, phase studies, 20: 35924
Dy–Zr, physical properties, (E), 19: 16188
Dy–Zr, preparation and properties, 16: 2128
Dy–Zr, surface tension of liquid, 17: 4943
Er–Zr, magnetic properties of, 17: 32651
Er–Zr, metallurgical properties and phase studies on, 20: 5891(R) (NYO-2159-1)
Er–Zr, oxidation by air at 400°C and water at 93 and 177°C, 17: 34330(R) (USBM-U-1057)
Er–Zr, phase studies, 20: 35924
Er–Zr, physical properties, (E), 19: 16188
Er–Zr, preparation and properties, 16: 2128
Er–Zr, surface tension of liquid, 17: 4943
Er–Zr, tensile properties, 16: 1693
Fe–Mo–Zr, oxidation and mechanical properties, 17: 32621
Fe–Mo–Zr, oxidation by steam at 900°F, 18: 2162(R) (IITRI-B198-46)
Fe–Mo–Zr, phase studies, 17: 22209
Fe–Nb–Sn–Zr, corrosion by steam at 400 and 450°C, 19: 30668(R) (EURAEC-1274)
Fe–Nb–Zr, corrosion of, by steam and water, 16: 29346
Fe–Nb–Zr, corrosion by steam at 400 and 450°C, 19: 30668(R) (EURAEC-1274)
Fe–Nb–Zr, oxidation by steam at 750°F, 18: 2162(R) (IITRI-B198-46)
Fe–Ni–W–Zr, oxidation in air at 2000°F, 17: 14724(R) (ARF-2158-15)
Fe–Ni–Zr, corrosion of, by deoxygenated steam, 17: 19720 (ANL-6698)
Fe–Ni–Zr, corrosion by steam at 540°C, 17: 35079(R) (ANL-6749)
Fe–Ni–Zr, corrosion by superheated steam, 17: 41333(R) (ANL-6677)
Fe–Ni–Zr, corrosion by oxygenated sodium at 540 and 650°C, 18: 19456(R) (ANL-6840)
Fe–Ni–Zr, corrosion by steam, 18: 41933 (TID-11295(3rd Ed.))
Fe–Ni–Zr, corrosion by superheated steam, 19: 14765(R) (ANL-6977)
Fe–Ni–Zr, corrosion by liquid metals, measurement of, 19: 17177(R) (ANL-6965(p.42-83))
Fe–Ni–Zr, corrosion by steam at 540°C, effects of alloy microstructure on, 19: 44616(R) (ANL-7000, pp 122-37)
Fe–Ni–Zr, corrosion by steam at 540°C, effects of pressure on, 19: 44616(R) (ANL-7000, pp 122-37)
Fe–Ni–Zr, oxidation by superheated steam at 540°C, 18: 15663(R) (ANL-6808)
Fe–Re–Zr, phase studies, 17: 22209
Fe–Sn–Zr, corrosion by steam at temperatures to 1150°F, 20: 9427 (WAPD-TM-546)
Fe–Sn–Zr, properties as cladding for fuel elements, 20: 25614(P)
Fe–Sn–Zr, radiation effects on mechanical properties of, fast neutron, 16: 572 (REIC-20)
Fe–Sn–Zr, structures in, 17: 6527 (TID-7625(p.30-41))
Fe–Ti–Zr, electronic specific heats at 1.5 to 4°K, 19: 30743(R) (NYO-3454-1)
Fe–Ti–Zr, magnetic and structural properties of, 16: 18039 (TID-14769)
Fe–Ti–Zr, magnetic and structural properties at 4 to 650°K, 17: 25708(R) (TID-18766)
Fe–Ti–Zr, magnetic properties and structure of intermetallic compounds, 17: 36312
Fe–Ti–Zr, Mössbauer effect of iron-57 in Laves phases in, 16: 10565
Fe–Ti–Zr, phase studies and electronic specific heats of $TiFe_2$–$ZrFe_2$, 18: 8862
Fe–Ti–Zr, tensile properties at room temperature, 18: 18380
Fe–Ti–Zr, thermal capacity for $TiFe_2$–$ZrFe_2$ phases in, 20: 27494(R) (NYO-3454-6)
Fe–U–Zr, hyperfine field in, 17: 18815
Fe–U–Zr, phase studies at 800°C, 20: 33924
Fe–V–Zr, corrosion by steam at 750°F, 17: 6561(R) (ARF-2198-34)
Fe–V–Zr, corrosion by steam, 17: 34347(R) (IITRI-B198-43)
Fe–V–Zr, melting points, 18: 44497(R) (MND-2812-2)
Fe–V–Zr, oxidation by steam at 750°F, hydrogen absorption from, 18: 2162(R) (IITRI-B198-46)
Fe–V–Zr, tensile properties at 70 and 750°F, 18: 2162(R) (IITRI-B198-46)
Fe–Y–Zr, magnetic and structural properties of Laves phases in, 19: 30743(R) (NYO-3454-1)
Fe–Y–Zr, magnetic properties and structure of Laves phases in, 20: 27494(R) (NYO-3454-6)
Fe–Y–Zr, thermal capacity of YFe_2–$ZrFe_2$ Laves phases in, 20: 27494(R) (NYO-3454-6)
Fe–Zr, anisotropic hfs interactions of, 18: 26038
Fe–Zr, corrosion of, by superheated steam at 540°C, 16: 4505
Fe–Zr, corrosion of, by water at high temperatures, 16: 3415
Fe–Zr, corrosion of, by water at high temperatures in reactors, 16: 2141
Fe–Zr, corrosion by steam and water, 17: 39659
Fe–Zr, corrosion by carbon dioxide, 18: 27907
Fe–Zr, corrosion by steam at 500°C, hydrogen uptake in, 19: 22901
Fe–Zr, corrosion by superheated steam at 540 and 650°C, 19: 22899
Fe–Zr, crystal structure of Zr_2Fe, 20: 31727
Fe–Zr, electrochemical potential, 17: 34403 (GEAP-4192)
Fe–Zr, embrittlement effects of hydrogen on, 18: 34169
Fe–Zr, enthalpy, free enthalpy, and entropy of formation of intermetallic compound Fe_2Zr in, 16: 4581
Fe–Zr, hyperfine structure of iron-57 spectra in Fe_2Zr, 17: 13236
Fe–Zr, iron-57 NMR in intermetallic compounds of, anisotropic hyperfine interactions in, (E), 20: 24652
Fe–Zr, isomer shift of iron-57 in $ZrFe_2$ at 300 and 800°K, 19: 44678(R) (ANL-7000, pp 186-200)
Fe–Zr, location of intermetallic particles in, 16: 4270 (AERE-R-3845)
Fe–Zr, magnetic and structural properties of, 16: 18039 (TID-14769)
Fe–Zr, magnetic properties of Laves-phase structures in, 16: 16833
Fe–Zr, Mössbauer effect of iron-57 in Laves phases in, 16: 10565
Fe–Zr, Mössbauer effect measurements of hyperfine interactions in Laves phase in, 19: 4683
Fe–Zr, oxidation by steam at 900°F, 18: 2162(R) (IITRI-B198-46)
Fe–Zr, oxidation by water vapor at 375 and 575°C, kinetics of, 20: 25498
Fe–Zr, phase diagram, 16: 19388
Fe–Zr, phase studies, 17: 16544
Fe–Zr, phase studies on, 17: 34425
Fe–Zr, phase studies, 18: 2279
Fe–Zr, phase studies, 18: 14396
Fe–Zr, phase studies, 20: 35924
Fe–Zr, phase transformations in, 16: 25829
Fe–Zr, reactions with hydrogen, thermochemical and structural aspects of, 20: 27436
Fe–Zr, resistance to scaling at elevated temperatures, 19: 32770(P)
Fe–Zr, solubility of nitrogen in, 19: 41065
Fe–Zr, structure, 17: 22177
Fe–Zr, transformation kinetics, 18: 44052(R) (ORNL-3670(p.147-59))
Fe–Zr, uptake of hydrogen during steam and water corrosion of, 17: 32519
Fe–Zr, zirconium-91 NMR in $ZrFe_2$, 18: 39941
fissium–U–Zr, ductility of, effects of aluminum, silicon, titanium, and yttrium additions on, 19: 47004 (NMI-4997, pp 45-54)
fissium–Pu–U–Zr, phase studies on, 20: 5876 (ANL-6974)
fissium–U–Zr, radioinduced swelling in, effects of postirradiation annealing temperature on, 19: 44587(R) (ANL-7000, pp 3-63)
fissium–U–Zr, thermal conductivity of, effects of burnup on, 19: 40112(R) (ANL-7046(p.36-66))
Ga–Ge–Zr, phase studies, 17: 6729
Ga–Ge–Zr, phase studies, 19: 14059
Ga–Nb–Zr, phase studies, 17: 6729
Ga–Zr, phase studies, 16: 30170(R) (ORNL-3313(p.179-208))
Ga–Zr, phase studies of, 17: 582
Gd–Zr, metallurgical properties and phase studies on, 20: 5891(R) (NYO-2159-1)
Gd–Zr, oxidation by air at 450°C and water at 93 and 177°C, 17: 34330(R) (USBM-U-1057)
Gd–Zr, phase studies, 16: 17967(R) (USBM-U-887)
Gd–Zr, phase studies, 20: 35924
Gd–Zr, physical properties, (E), 19: 16188
Gd–Zr, reactor criticality effects of septa of, 17: 24637 (WAPD-BT-28(p.21-6))
Ge–Sn–Zr, corrosion of, in 680°F water, 17: 16582 (ARF-B198-36)
Ge–Sn–Zr, corrosion by water at 680°F, 17: 30905(R) (ARF-B198-42)
Ge–Sn–Zr, oxidation by water at 680°F, 18: 2162(R) (IITRI-B198-46)
Ge–Zn–Zr, phase studies, 19: 14059
Hf–Fe–Zr, Mössbauer effect of iron-57 in Laves phases in, 16: 10565
Hf–Nb–Ti–W–Zr, properties for elevated-temperature service, 19: 6241 (BM-RI-6558)
Hf–Nb–W–Zr, properties for elevated-temperature service, 19: 6241 (BM-RI-6558)

Hf–Os–Zr, phase studies, 18: 25970(R) (ANL-6868(p.303-25))
Hf–Re–Zr, phase studies, 18: 25970(R) (ANL-6868(p.303-25))
Hf–Ta–Zr, fabrication and properties of high-temperature, 20: 27472 (BM-RI-6777)
Hf–Ti–Zr, tensile properties at room temperature, 18: 18380
Hf–Zr, activation analysis for zirconium, 17: 40750
Hf–Zr, analysis for hafnium, x-ray fluorescence spectrometric, 19: 2227
Hf–Zr, corrosion and mechanical properties, 17: 12620
Hf–Zr, corrosion resistance and mechanical properties of, in steam-water systems, 17: 22117
Hf–Zr, corrosion by steam at 316 and 400°C, 17: 27728(R) (GEAP-4076)
Hf–Zr, crystal structure and phase studies, 18: 25968(R) (ANL-6868 (p.267-86))
Hf–Zr, ductility and thermal expansion, 20: 43964
Hf–Zr, elastic properties at 4 to 600°K, 18: 25968(R) (ANL-6868 (p.267-86))
Hf–Zr, electrolytic polishing, 20: 19186(P)
Hf–Zr, electronic and thermal properties, 18: 4247(R) (ORNL-3470 (p.20-6))
Hf–Zr, electronic properties, 18: 44150(R) (ORNL-3670(p.44-53))
Hf–Zr, hydridation at 500 to 900°C at hydrogen pressures of less than 1 atm, 19: 26776
Hf–Zr, hydridation, 19: 26777
Hf–Zr, phase diagram, 20: 31744
Hf–Zr, phase studies, 20: 35924
Hf–Zr, separation of thorium from, by precipitation using pyromellitic, trimellitic, and trimesic acids, 19: 24470
Hf–Zr, thermal expansion of, 17: 14882
Hg–Ni–Zr, corrosive effects on titanium of mercury-based, 19: 44616(R) (ANL-7000, pp 122-37)
Hg–Zr, phase studies, 19: 36949(R) (BNL-900(p.121-97))
Ho–Mo–Zr, magnetic properties of, 17: 32651
Ho–Zr, fracture at 78, 197, and 373°K, mechanisms of, 20: 37231
Ho–Zr, magnetic properties of, 17: 32651
Ho–Zr, metallurgical properties and phase studies on, 20: 5891(R) (NYO-2159-1)
Ho–Zr, phase studies, 20: 35924
Ho–Zr, preparation and properties, 16: 2128
Ho–Zr, surface tension of liquid, 17: 4943
In–Ti–Zr, tensile properties at room temperature, 18: 18380
In–Zr, crystallographic parameters, 17: 18822
In–Zr, density of electronic states in, 18: 4247(R) (ORNL-3470(p.20-6))
In–Zr, diffusion and solubility of hydrogen in, 19: 13349
In–Zr, phase studies, 19: 14060
In–Zr, thermal capacity at 1.2 to 4.5°K, 17: 30966 (CONF-22-15)
Ir–Zr, lattice parameters of Zr_2Ir, 19: 44678(R) (ANL-7000, pp 186-200)
Ir–Zr, phase studies by x-ray diffraction, 19: 7964
Ir–Zr, superconductivity of, 18: 9274
K–Zr, phase studies, 20: 35924
Li–Mg–Th–Zr, preparation and properties at high temperatures, 19: 37153(P)
Li–Zr, phase studies, 20: 35924
Lu–Zr, heats of solution at 300 and 1172°K, 18: 4282
Lu–Zr, metallurgical properties and phase studies on, 20: 5891(R) (NYO-2159-1)
Lu–Zr, phase studies, 20: 35924
Mg–Hg–Zr, corrosive effects on titanium of mercury-based, 19: 44616(R) (ANL-7000, pp 122-37)
Mg–Mn–Zr, cavitation and creep properties of, at 20 to 500°C, 16: 16762
Mg–Mn–Zr, design for fuel element canning, 17: 16730(P)
Mg–Mn–Zr, diffusion of plutonium in MAGZAN-II and ZR55, at 420, 460, and 500°C, 20: 5848
Mg–Mn–Zr, ignition in carbon dioxide, effects of air, oxygen, and water vapor on, 19: 7849 (CEA-R-2494)
Mg–Mn–Zr, performance as reactor components, 18: 37667 (A/CONF.28/P/146)
Mg–rare earths–Zn–Zr, crystal structure, 20: 2399
Mg–rare earths–Zr, crystal structure, 20: 2399
Mg–Th–Zn–Zr, corrosion, 19: 6271(T) (JPRS-27451)
Mg–Th–Zn–Zr, mechanical properties of, at high temperatures, 16: 27688(P)
Mg–Th–Zr, age hardening mechanism in, 19: 4685
Mg–Th–Zr, bonding of HK31, surface preparation and epoxy adhesive for, 19: 36995 (BDX-613-68)
Mg–Th–Zr, corrosion, 19: 6271(T) (JPRS-27451)
Mg–Th–Zr, mechanical properties at 205 to 565°C, 19: 4684
Mg–Th–Zr, plastic anisotropy of HK31A sheet, 19: 39149 (AD-425880)
Mg–Zn, reactions of hydrogen with calcium, cerium, lanthanum, thorium, and ytterium in liquid, 18: 35548
Mg–Zn–Zr, bonding of ZK60, surface preparation and epoxy adhesive for, 19: 36995 (BDX-613-68)
Mg–Zn–Zr, casting, 18: 14452(P)
Mg–Zn–Zr, corrosion resistance of, to carbon dioxide and air at 500°C, alloying effects of beryllium and manganese on, 16: 30892(P)
Mg–Zn–Zr, corrosion, 19: 6271(T) (JPRS-27451)
Mg–Zn–Zr, creep properties of, for use as fuel element can, 16: 15236(P)
Mg–Zn–Zr, hot brittleness of, 19: 37092
Mg–Zn–Zr, oxidation by carbon dioxide–carbon monoxide mixtures at 500 to 700°C, 17: 25739
Mg–Zn–Zr, preparation for casting, 18: 22469(P)
Mg–Zn–Zr, structure, 18: 2258
Mg–Zn–Zr, thermal stress in Z.W. 1, 16: 20811(P)
Mg–Zn–Zr, ultrasonic wave attenuation and delay in, 19: 32761
Mg–Zr, analysis for bonding and inclusions in, by x-ray emission in electron microscopy, 20: 20593
Mg–Zr, analysis of, for zirconium, x-ray fluorescence, 16: 5283
Mg–Zr, corrosion resistance of, to carbon dioxide and air at 500°C, alloying effects of beryllium and manganese on, 16: 30892(P)
Mg–Zr, corrosion by humid air at 350°C, 17: 3420 (BLG-124)
Mg–Zr, corrosion by carbon dioxide at 450 to 550°C, 17: 25737
Mg–Zr, creep behavior of, effects of heat treatment on, 16: 552
Mg–Zr, creep behavior and stress rupture of, in carbon dioxide at 400 and 450 and 200°C, 18: 42058
Mg–Zr, crystal structure, 20: 2399
Mg–Zr, development and fabrication of EdF2, for fuel cans, 20: 15018
Mg–Zr, diffusion of plutonium in, at 420 to 500°C, 19: 47066
Mg–Zr, dissolution using sulfuric acid, flowsheet for, 20: 4048(R) (NP-15406)
Mg–Zr, fabrication and mechanical properties, 17: 25751
Mg–Zr, fatigue of, effects of high-frequency vibrations on, 20: 43957
Mg–Zr, fatigue properties at 200 to 500°C, 17: 27847
Mg–Zr, fine-grain structure in co-extruded, 18: 14503
Mg–Zr, fine-grained structure in magnesium extruded, 18: 34182
Mg–Zr, forging, 19: 7886(P)
Mg–Zr, formation of zirconium hydride in, 18: 5797
Mg–Zr, formation of zirconium hydride in homogenized, 19: 2815
Mg–Zr, grain-boundary denuded zones in, 17: 25796
Mg–Zr, grain-boundary cracking and mode of creep failure in, 18: 26032
Mg–Zr, heat resistance, mechanical properties, and recrystallization of, 18: 16496
Mg–Zr, heat treatment of, effects on creep strength, 18: 42054
Mg–Zr, heat-treatment process for, 20: 4456(P)
Mg–Zr, ignition in carbon dioxide, effects of air, oxygen, and water vapor on, 19: 7849 (CEA-R-2494)
Mg–Zr, mechanical properties, 17: 30925
Mg–Zr, metallurgical properties of, methods for improving, 18: 2290(P)
Mg–Zr, nondestructive method for testing cladding of, 20: 14711
Mg–Zr, oxidation by carbon dioxide–carbon monoxide mixtures at 500 to 700°C, 17: 25739
Mg–Zr, oxidation at 400 to 600°C in damp oxygen, 18: 22449
Mg–Zr, performance of Magnox ZA as reactor components, 18: 37667 (A/CONF.28/P/146)
Mg–Zr, phase diagram, liquidus curve of, 20: 812 (BM-RI-6673)
Mg–Zr, phase study of zirconium-rich phases, 16: 21044(T) (AEC-tr-5127)
Mg–Zr, phase studies, 17: 1920 (BM-RI-6078)
Mg–Zr, phase studies on, 18: 32185
Mg–Zr, preparation and properties, 16: 19255
Mg–Zr, preparation of hafnium-free, 17: 36207
Mg–Zr, production for use as fuel element canning, 19: 30662(P)
Mg–Zr, properties of, for use in canning fuel elements, 17: 25793
Mg–Zr, properties of, for use in canning fuel elements, 17: 25794
Mg–Zr, properties as cladding material in gas-cooled graphite-moderated reactors, 18: 15496(T) (AEC-tr-6329)
Mg–Zr, properties for use as fuel element can, effects of manganin on, 19: 20610(P)
Mg–Zr, recrystallization grain growth of, effects of hydration on, 20: 37252
Mg–Zr, thermophysical properties, 18: 10552
Mg–Zr, ultrasonic wave attenuation and delay in, 19: 32761
Mg–Zr, use for natural-uranium cladding, 18: 37645 (A/CONF.28/P/57)
Mn–Ti–Zr, magnetic moments and superconductivity of, 18: 34700
Mn–Ti–Zr, tensile properties at room temperature, 18: 18380
Mo–Nb–Ta–W–Zr, creep tests on NB132M at 3200°F, 20: 5885(R) (NAS-CR-54773)
Mo–Nb–Ti–U–Zr, ductility of uranium-base, effects of aging, forging, and rolling on, 20: 43883 (AD-637777)
Mo–Nb–Ti–U–Zr, mechanical properties for possible structural use, 19: 9651 (AMRA-TR-64-28)
Mo–Nb–Ti–U–Zr, mechanical properties of high-strength uranium-base, 20: 39440(P)
Mo–Nb–Ti–U–Zr, transformation diagram and kinetics of, 17: 25769(R) (AMRA-CR-63-02/1(F))
Mo–Nb–Ti–W–Zr, forging characteristics, 16: 9162 (DMIC-Memo-143)
Mo–Nb–Ti–Zr, analysis using vacuum cup electrode, 19: 22103 (TIM-904)
Mo–Nb–Ti–Zr, coating with aluminum–tin-base alloys for protection

against oxidation, 17: 39465 (SCNC-328(Del.))
Mo–Nb–Ti–Zr, corrosion by lithium at 1600°F, 19: 36980 (PWAC-355)
Mo–Nb–Ti–Zr, creep properties of niobium-modified TZM, 20: 29705(R) (NAS-CR-54973)
Mo–Nb–Ti–Zr, fabrication and properties of cast and extruded, 18: 12536(R) (AD-412904)
Mo–Nb–Ti–Zr, fabrication and properties of extruded and rolled, 18: 22412(R) (AD-422106)
Mo–Nb–U–Zr, alloying effects of chromium and vanadium on aging and stability of, 17: 39644
Mo–Nb–U–Zr, mechanical properties, 17: 39643
Mo–Nb–U–Zr, mechanical properties of gamma-phase uranium-base, 20: 15060 (UCRL-7771)
Mo–Nb–U–Zr, nonmetallic inclusions in, 16: 30874
Mo–Nb–U–Zr, phase structure of, at 800 and 1000°C, 16: 30872
Mo–Nb–U–Zr, phase studies below 800°C, 17: 39633
Mo–Nb–U–Zr, phase transformation in, at 430 to 550°C, 16: 30873
Mo–Nb–V–Zr, bend ductility of B-66, effects of argon atmosphere contamination on, 19: 9592(R) (ASD-8-170(IV))
Mo–Nb–V–Zr, bonding of B-66, method for diffusion, 20: 5867
Mo–Nb–V–Zr, casting and testing of B-66 ingots, 18: 571(R) (AD-297246)
Mo–Nb–V–Zr, coating evaluation for B-66, oxidation-resistant, 19: 36945 (AD-610867)
Mo–Nb–V–Zr, coating of B-66, with chromium–silicon–titanium systems and silicides, 18: 14373(R) (NP-13498)
Mo–Nb–V–Zr, coatings for B-66 foils, development of high-temperature oxidation-resistant, 18: 30118(R) (RTD-TDR-63-4006(Pt.I))
Mo–Nb–V–Zr, coatings on B-66, properties of oxidation-resistant, 19: 26801(R) (AD-607530)
Mo–Nb–V–Zr, compatibility of rocket nozzles of, with hydrogen, 20: 19228
Mo–Nb–V–Zr, composition, crystal structure, and phases of precipitates in, 16: 22582 (ASD-TDR-62-7)
Mo–Nb–V–Zr, contamination of B-66 by rolling in argon atmosphere, 19: 9592(R) (ASD-8-170(IV))
Mo–Nb–V–Zr, corrosion protection by silicide coatings, 19: 11682
Mo–Nb–V–Zr, corrosion by cesium and lithium above 2500°F, 19: 28766
Mo–Nb–V–Zr, corrosion of B-66, by lithium, effects of oxygen on, 20: 4301(R) (ORNL-3870, pp 102-35)
Mo–Nb–V–Zr, corrosion by cesium vapor and liquid lithium at 2500 to 3400°F of B-66, 20: 5851
Mo–Nb–V–Zr, corrosion by refluxing potassium at 1800 to 2400°F, 20: 25485 (NASA-TN-D-3429)
Mo–Nb–V–Zr, creep-rupture properties of B-66, temperature dependence, 18: 44049(R) (ORNL-3670(p.77-111))
Mo–Nb–V–Zr, creep-rupture properties of, 20: 2336 (ORNL-P-1634)
Mo–Nb–V–Zr, ductility transition temperature of B-66, effects of protective coatings and welding on, 20: 27466
Mo–Nb–V–Zr, ductility, strength, and weldability of, 18: 14448
Mo–Nb–V–Zr, evaporation tests of B-66 in high vacuum, 18: 44049(R) (ORNL-3670(p.77-111))
Mo–Nb–V–Zr, evaporation losses of B-66, at 1200 to 1500°C in high vacuum, 19: 37043 (ORNL-P-1394)
Mo–Nb–V–Zr, evaporation losses in high vacuum of B-66, 20: 4301(R) (ORNL-3870, pp 102-35)
Mo–Nb–V–Zr, extrusion, 17: 3445(R) (NP-12225)
Mo–Nb–V–Zr, extrusion of tubing from, optimization studies, 17: 11140(R) (AMC-TR-7-775(VII))
Mo–Nb–V–Zr, extrusion of tubes of, 17: 23895(R) (AD-403514)
Mo–Nb–V–Zr, extrusion of, program outline for, 17: 25749(R) (WANL-PR-(N)-001)
Mo–Nb–V–Zr, extrusion by Dynapak process of B-66, 19: 30686(R) (AD-608945)
Mo–Nb–V–Zr, fabrication of rolled sheets of B-66, 18: 12591(R) (AD-409960)
Mo–Nb–V–Zr, fabrication of B-66, by rolling, 18: 12593(R) (AD-411155)
Mo–Nb–V–Zr, fabrication and mechanical properties of B-66, 18: 18292(R) (N63-20341)
Mo–Nb–V–Zr, fabrication of B-66, by extrusion and forging, 18: 20484(R) (AD-418992)
Mo–Nb–V–Zr, fabrication of B-66, by extrusion, 18: 20487(R) (WANL-PR-(N)-002)
Mo–Nb–V–Zr, fabrication and properties of coated B-66, 18: 24068(R) (NP-13955)
Mo–Nb–V–Zr, fabrication of extruded B-66, 18: 24093(R) (AD-424593)
Mo–Nb–V–Zr, fabrication and properties of B-66 tubing, 18: 27924(R) (WANL-PR-(N)-004)
Mo–Nb–V–Zr, fabrication of B-66, by rolling, 18: 30106(R) (AD-430773)
Mo–Nb–V–Zr, fabrication B-66 into sheets, 18: 30146(R) (AD-414497)
Mo–Nb–V–Zr, fabrication of B-66 tubing, 18: 41933 (TID-11295(3rd Ed.))
Mo–Nb–V–Zr, fabrication by forging and by extrusion, 19: 11711
Mo–Nb–V–Zr, fabrication and properties of B-66 sheet, 19: 20499(R) (AD-606291)
Mo–Nb–V–Zr, fabrication and properties of B-66 foil, 19: 24945 (ASD-TDR-63-829(Pt.I))
Mo–Nb–V–Zr, fabrication and properties of B-66 strip and foil, 19: 24946 (ASD-TDR-63-829(Pt.II))
Mo–Nb–V–Zr, fabrication of tubing of B-66, 20: 16998
Mo–Nb–V–Zr, joining of foils of B-66, for honeycomb panel fabrication, 18: 37661 (ASD-TDR-63-799(Pt.I))
Mo–Nb–V–Zr, mechanical properties of Pfaudler silicide and TRW chromium–silicon–titanium-coated B-66, in air at 70 to 2600°F, 18: 20523(R) (NP-13811)
Mo–Nb–V–Zr, mechanical properties of B-66, 19: 13978 (AMRA-TR-64-16)
Mo–Nb–V–Zr, oxidation and mechanical properties of coated B-66, 17: 39525(R) (AD-416459)
Mo–Nb–V–Zr, oxidation protection of B-66 by chromium–silicon–titanium coatings at 2000 to 2700°C, 18: 30127 (ASD-TDR-62-934(Pt.II))
Mo–Nb–V–Zr, properties of B66 sheet, 18: 573(R) (AD-422116)
Mo–Nb–V–Zr, properties as space reactor fuel cladding, 18: 9713 (CONF-375-3)
Mo–Nb–V–Zr, properties of coated B-66, to 2600°F, 18: 14373(R) (NP-13498)
Mo–Nb–V–Zr, properties of B-66, to 2600°F, 18: 14353(R) (AD-408310)
Mo–Nb–V–Zr, properties of B-66 foils at high temperatures, effects of coatings on mechanical and thermophysical, 18: 34128 (RTD-TDR-63-4068)
Mo–Nb–V–Zr, properties of welds in B-66, 19: 40989
Mo–Nb–V–Zr, reactions with cesium at 3400°F, metallographic specimen preparation of B-66, 19: 46954 (NMI-5025(Pt.I), pp 39-58)
Mo–Nb–V–Zr, reactions with uranium carbide, nitride, and dioxide, metallographic specimen preparation of B-66, 19: 46954 (NMI-5025(Pt.I), pp 39-58)
Mo–Nb–V–Zr, rolling of foils of B-66, 19: 7871(R) (AD-422001)
Mo–Nb–V–Zr, stress-rupture properties of B-66, 19: 40961
Mo–Nb–V–Zr, tensile properties of welded plates of B-66, 20: 4301(R) (ORNL-3870, pp 102-35)
Mo–Nb–V–Zr, tensile properties of B-66, effects of welds on, 20: 29712(R) (WANL-PR-(P)-009)
Mo–Nb–V–Zr, tensile strength of B-66, at 1100 to 1400°C, 17: 30950(R) (NMI-2117)
Mo–Nb–V–Zr, tests of B-66 tubing, nondestructive, 19: 13950 (ORNL-TM-990)
Mo–Nb–V–Zr, thermal properties, 18: 7201 (ASD-TDR-63-597)
Mo–Nb–V–Zr, thermal properties to melting point, 20: 878
Mo–Nb–V–Zr, weld bend tests of B-66, 19: 13955(R) (WANL-PR-(P)-005)
Mo–Nb–V–Zr, weld stability in B-66, 20: 5866
Mo–Nb–V–Zr, weld structural stability in, 18: 22459(R) (NP-13816)
Mo–Nb–V–Zr, weldability of B-66, 17: 39498 (DMIC-Memo-169)
Mo–Nb–V–Zr, weldability of B-66 sheet, 18: 44049(R) (ORNL-3670 (p.77-111))
Mo–Nb–V–Zr, weldability study of B-66, 19: 24957(R) (WANL-PR(P)-006)
Mo–Nb–V–Zr, weldability studies of B-66, 19: 46966(R) (WANL-PR(P)-007)
Mo–Nb–V–Zr, weldability evaluation of, 20: 39366
Mo–Nb–V–Zr, welding of B66, effects of parameters on TIG welds in, 18: 573(R) (AD-422116)
Mo–Nb–V–Zr, welding of B-66, power force programmed ultrasonic, 18: 12594 (AD-427997)
Mo–Nb–V–Zr, welding of B-66, tungsten-arc, 18: 34058(R) (WANL-PR(P)-003)
Mo–Nb–V–Zr, welding of B-66, equipment and procedures for, 19: 9629(R) (AD-608818)
Mo–Nb–V–Zr, welding parameters for B-66, electron-beam, 20: 5867
Mo–Nb–V–Zr, welding properties of B-66, 20: 27466
Mo–Nb–V–Zr, welds in B-66, thermal stability of, 20: 27467
Mo–Nb–W–Zr, composition, crystal structure, and phases of precipitates in, 16: 22582 (ASD-TDR-62-7)
Mo–Nb–W–Zr, creep testing of F-48, at 2200°F, 17: 35251(R) (BMI-1632(Del.))
Mo–Nb–W–Zr, fabrication and structure, 16: 10470 (ASD-TR-7-784(VI))
Mo–Nb–W–Zr, fabrication and properties of rolled sheet, 17: 6597(R) (DMIC-176)
Mo–Nb–W–Zr, fabrication by vacuum rolling, 17: 36270
Mo–Nb–W–Zr, forging characteristics, 16: 9162 (DMIC-Memo-143)
Mo–Nb–W–Zr, friction and wear of, at high temperatures and in vacuum, 16: 5708 (ASD-TR-61-301)
Mo–Nb–W–Zr, hardness of niobium-base, effects of composition on hot-, 20: 31669
Mo–Nb–W–Zr, homogenization kinetics of sintered, 18: 26047
Mo–Nb–W–Zr, mechanical properties, 17: 14727(R) (BMI-1600(Del.))
Mo–Nb–W–Zr, mechanical properties of warm-extruded and rolled, 17: 32567 (BMI-X-249)

Mo–Nb–W–Zr, mechanical and oxidation properties of F-48, 17: 34415 (UCRL-6187(Rev.))
Mo–Nb–W–Zr, mechanical properties, 18: 18307
Mo–Nb–W–Zr, mechanical properties at 1000 to 1600°C, 19: 23043
Mo–Nb–W–Zr, mechanical properties, 19: 28833
Mo–Nb–W–Zr, mechanical properties of niobium-base, effects of composition on, 20: 7599
Mo–Nb–W–Zr, phase studies, 19: 7968
Mo–Nb–W–Zr, properties of coated, at high temperatures, 16: 9189 (ASD-TR-61-66(Pt.II))
Mo–Nb–W–Zr, properties of F-48, as journal bearing material, 17: 25382 (ASD-TR-61-705)
Mo–Nb–W–Zr, shear strength of F-48 fasteners at room temperature and 1600°F, 17: 36281 (AD-295526)
Mo–Nb–W–Zr, tensile properties, 17: 3378(R) (BMI-1583(Del.))
Mo–Nb–W–Zr, tensile properties, 17: 27878
Mo–Nb–W–Zr, tensile strength of F-48, at 1100 to 1500°C, 17: 30950(R) (NMI-2117)
Mo–Nb–W–Zr, welding, 16: 30741 (ASD-TDR-62-292)
Mo–Nb–Zr, corrosion of, by steam and water, 16: 29346
Mo–Nb–Zr, corrosion resistance and mechanical properties, 17: 37535
Mo–Nb–Zr, oxidation by steam at 900°F, 18: 2162(R) (IITRI-B198-46)
Mo–Nb–Zr, oxidation in air, composition of scale formed during, 18: 10477(T) (JPRS-22697(p.27-38))
Mo–Nb–Zr, phase diagram, 18: 8809(T) (JPRS-22593)
Mo–Nb–Zr, phase studies, 18: 625
Mo–Nb–Zr, phase studies on, 18: 16494
Mo–Nb–Zr, phase studies and properties, 18: 26056
Mo–Nb–Zr, phase studies of, isothermal sections at 1200°C in, 20: 41464
Mo–Nb–Zr, phase transformation kinetics, 16: 15166 (ARF-2198-21)
Mo–Ni–Zr, corrosion by pressurized water and workability of, 18: 20461
Mo–Ni–Zr, heat treatment effects on mechanical properties and microstructure of, 18: 20461
Mo–Ni–Zr, oxidation and mechanical properties, 17: 32621
Mo–Sn–Zr, corrosion by steam and water, 17: 39659
Mo–Th–Zr, properties and structure of, 18: 37670 (A/CONF.28/P/337)
Mo–Ti–Zr, analysis for titanium and zirconium by ion exchange, 20: 3896
Mo–Ti–Zr, analysis for alloying elements and impurities, comparison of results from 25 laboratories on TZM, 20: 18567 (MAB-217-M)
Mo–Ti–Zr, analysis using vacuum cup electrode, 19: 22103 (TIM-904)
Mo–Ti–Zr, bend ductility of TZM, effects of argon atmosphere contamination on, 19: 9592(R) (ASD-8-170(IV))
Mo–Ti–Zr, bend-transition temperature in TZM, 19: 24976(R) (AD-612759)
Mo–Ti–Zr, bonding of TZM, method for diffusion, 20: 5867
Mo–Ti–Zr, brazing developments for, 18: 549(R) (NP-13241)
Mo–Ti–Zr, brazing molybdenum to TZM, brazing alloy development for, 20: 5866
Mo–Ti–Zr, brazing of TZM, exothermic, 17: 27760(R) (NP-12901)
Mo–Ti–Zr, brazing techniques for TZM, 19: 30690(R) (ML-TDR-64-270)
Mo–Ti–Zr, brazing tungsten carbide–cobalt cermet to TZM, use of boron–nickel–silicon for, 20: 4307(R) (ORNL-3870, pp 238-42)
Mo–Ti–Zr, brittle-ductile transition temperature and high-temperature strain aging in, 16: 12080(R) (AD-259795)
Mo–Ti–Zr, cavitation damage to TZM, in liquid sodium, 20: 2243
Mo–Ti–Zr, cavitation damage of TZM in liquid sodium to 1500°F, 20: 46154 (NASA-CR-72035)
Mo–Ti–Zr, coating evaluation for TZM, oxidation-resistant, 19: 36945 (AD-610867)
Mo–Ti–Zr, coating of TZM, with platinum and platinum–rhodium alloy, 18: 20445(R) (AD-434441)
Mo–Ti–Zr, coating of TZM, with palladium–platinum alloy and platinum, 18: 34029(R) (AD-601740)
Mo–Ti–Zr, coating of TZM for oxidation protection at high temperatures, 19: 7845(R) (AD-608135)
Mo–Ti–Zr, coating of TZM for oxidation, 19: 36957(R) (NP-15113)
Mo–Ti–Zr, coating with silicides, 19: 40998(P)
Mo–Ti–Zr, coatings for TZM foils, development of high-temperature oxidation-resistant, 18: 30118(R) (RTD-TDR-63-4006(Pt.I))
Mo–Ti–Zr, compatibility of TZM, with niobium–zirconium alloy in flowing zirconium, 20: 2238
Mo–Ti–Zr, compatibility of TZM, with alumina, beryllia, magnesia, and boron nitride, 20: 17022 (N-65-18933)
Mo–Ti–Zr, compatibility of TZM, with niobium–1 zirconium alloy in refluxing potassium at 2000°F, 20: 13192(R) (NASA-CR-54843)
Mo–Ti–Zr, compression properties at room-temperature of TZM, 19: 24976(R) (AD-612759)
Mo–Ti–Zr, contamination by residual gases in vacuum systems, 18: 14355 (CONF-373-7)
Mo–Ti–Zr, contamination of TZM, by residual gases in high vacuum, 18: 39826 (ORNL-3674)
Mo–Ti–Zr, contamination of TZM by rolling in argon atmosphere, 19: 9592(R) (ASD-8-170(IV))
Mo–Ti–Zr, corrosion of platinum- and platinum–rhodium-clad TZM, by air at 2550°F, 18: 20445(R) (AD-434441)
Mo–Ti–Zr, corrosion by potassium at 2000 to 2200°F, 18: 24091
Mo–Ti–Zr, corrosion by potassium vapor, design of test capsule for, 19: 20473(R) (NASA-CR-54629)
Mo–Ti–Zr, corrosion of TZM by boiling potassium, 19: 34640 (CNLM-6246)
Mo–Ti–Zr, corrosion by cesium and lithium above 2500°F, 19: 28766
Mo–Ti–Zr, corrosion by lithium at high temperatures, 20: 2269
Mo–Ti–Zr, corrosion of TZM, by potassium at high temperatures, 20: 2271
Mo–Ti–Zr, corrosion of TZM, by potassium, 20: 4301(R) (ORNL-3870, pp 102-35)
Mo–Ti–Zr, corrosion by cesium vapor and liquid lithium at 2500 to 3400°F of TZM, 20: 5851
Mo–Ti–Zr, corrosion by potassium at 1010°C of TZM, 20: 7518 (PWAC-501)
Mo–Ti–Zr, corrosion of TZM, by sodium at high temperatures, 20: 25474(R) (BNL-954, pp 122-67)
Mo–Ti–Zr, corrosion of TZM, by potassium at 1600°F, 20: 27432(R) (NASA-CR-54892)
Mo–Ti–Zr, corrosion by hydrochloric, phosphoric, and sulfuric acids at high temperatures, 20: 46158
Mo–Ti–Zr, creep and stress-rupture properties of TZM, in hydrogen at 2000 and 2200°C, 18: 7121(R) (GEMP-29A)
Mo–Ti–Zr, creep at 1800 to 2200°F of TZM, 20: 2333(R) (NASA-CR-54457)
Mo–Ti–Zr, creep of TZM at 2000 and 2130°F, long-time, 19: 18459(R) (NASA-CR-54287)
Mo–Ti–Zr, creep properties in ultra-high vacuum of TZM, long-time, 19: 37039(R) (NASA-CR-54393)
Mo–Ti–Zr, creep properties of TZM, 20: 4301(R) (ORNL-3870, pp 102-35)
Mo–Ti–Zr, creep properties of TZM, 20: 29705(R) (NAS-CR-54973)
Mo–Ti–Zr, creep rupture and fatigue evaluation of TZM, 18: 29103(R) (APS-5071-R)
Mo–Ti–Zr, creep tests on TZC and TZM at high temperatures, 20: 21346(R) (NASA-CR-54895)
Mo–Ti–Zr, dislocation structure in, effects of cold working on, 19: 41015 (MIL-TDR-64-282)
Mo–Ti–Zr, elongation tests and fabrication studies of TZM sheet, 19: 13949(R) (NP-14768)
Mo–Ti–Zr, erosion by sodium at 400, 1000, and 1500°F of TZM, 20: 769(R) (NASA-CR-54459)
Mo–Ti–Zr, erosion by mercury vapor at 640°F of TZM, 20: 11214(R) (NASA-CR-54717)
Mo–Ti–Zr, extrusion of, at 2300 to 2700°F, process evaluation for, 16: 12066(R) (ASD-TR-7-785(IV))
Mo–Ti–Zr, extrusion of tubes of TZM, 17: 41333(R) (ANL-6677)
Mo–Ti–Zr, extrusion of TZM into tube shells, 18: 44049(R) (ORNL-3670(p.77-111))
Mo–Ti–Zr, extrusion of TZM at room temperature, hydrostatic, 19: 6277 (ML-TDR-64-205)
Mo–Ti–Zr, extrusion of TZM into T-sections, 19: 7874(R) (ASD-TDR-7-911(V))
Mo–Ti–Zr, extrusion of complex shapes of TZM, using ceramic dies, 19: 9636(R) (NMI-9700-24)
Mo–Ti–Zr, extrusion of thin H-sections of TZM, 19: 13952(R) (RTD-TR-8-112(Vol.IV))
Mo–Ti–Zr, extrusion of thin H-sections of TZM, 19: 18431(R) (RTD-TR-8-112(V))
Mo–Ti–Zr, extrusion by Dynapak process of TZM, 19: 30686(R) (AD-608945)
Mo–Ti–Zr, extrusion of TZM, process for, 20: 5867
Mo–Ti–Zr, fabrication of rolled sheet, 17: 6597(R) (DMIC-176)
Mo–Ti–Zr, fabrication by vacuum rolling, 17: 36270
Mo–Ti–Zr, fabrication of honeycomb structures of, 17: 36271
Mo–Ti–Zr, fabrication and properties of extruded and rolled, 18: 5727(R) (AD-294579)
Mo–Ti–Zr, fabrication and properties of extruded and sintered TZM, 18: 10449(R) (IITRI-B247-12)
Mo–Ti–Zr, fabrication and testing of brazed honeycomb sandwich panels of TZM, 18: 10494 (AD-427700(p.245-80))
Mo–Ti–Zr, fabrication by extrusion, 18: 12601(R) (RTD-TR-8-112)
Mo–Ti–Zr, fabrication and properties of cast and extruded, 18: 12536(R) (AD-412904)
Mo–Ti–Zr, fabrication of TZM, by extrusion, 18: 18329(R) (ASD-TDR-7-945(IV))
Mo–Ti–Zr, fabrication and properties of extruded and rolled, 18: 22412(R) (AD-422106)

Mo–Ti–Zr, fabrication and properties of forged TZM, 18: 22414(R) (ASD-TR-7-756(X))
Mo–Ti–Zr, fabrication, oxidation, and properties of, 18: 35986 (ERR-FW-049A)
Mo–Ti–Zr, fabrication and properties of forged TZM, 19: 6240(R) (ASD-8-170(V))
Mo–Ti–Zr, fabrication of TZM powder compacts, 19: 7874(R) (ASD-TDR-7-911(V))
Mo–Ti–Zr, fabrication of TZM into thin H-sections by extrusion and drawing, process development for, 19: 7878(R) (RTD-TR-8-112(I))
Mo–Ti–Zr, fabrication and properties, 19: 11676
Mo–Ti–Zr, fabrication of honeycombed-sandwich panels from TZM, 20: 7541
Mo–Ti–Zr, fabrication of missile nose tips of TZM by shear spinning, 20: 25508 (AD-631423)
Mo–Ti–Zr, factors affecting vacuum-arc melting of, 18: 24070 (RTD-TDR-63-4089)
Mo–Ti–Zr, fasteners for use to 3000°F, 19: 32702(R) (AD-609653)
Mo–Ti–Zr, fatigue behavior at high temperatures in ultrahigh vacuum, 20: 824(R) (NASA-CR-54458)
Mo–Ti–Zr, fatigue in sodium at 1000 and 1500°F of TZM, high-frequency, 20: 769(R) (NASA-CR-54459)
Mo–Ti–Zr, fatigue properties at 982°C of stress-relieved TZM, notched, 20: 7572(R) (NASA-CR-54775)
Mo–Ti–Zr, fatigue properties of TZM, at high temperatures, 20: 31710(R) (NASA-CR-54983)
Mo–Ti–Zr, fatigue tests on TZC and TZM at high temperatures, 20: 21347(R) (NASA-CR-54916)
Mo–Ti–Zr, fatigue testing of TZM in liquid sodium at 1000 and 1500°F, 20: 46154 (NASA-CR-72035)
Mo–Ti–Zr, forging of, studies of plasticity in, 17: 18721(T) (FTD-TT-62-1789)
Mo–Ti–Zr, forging of TZM at 2400°F, 18: 44097 (ML-TDR-64-228)
Mo–Ti–Zr, hardness and recrystallization of TZM, at high temperatures, 17: 27760(R) (NP-12901)
Mo–Ti–Zr, joining of, by fiber metal resistance brazing, 16: 20988 (ARF-2232-2)
Mo–Ti–Zr, joining of foils of TZM, for honeycomb panel fabrication, 18: 37661 (ASD-TDR-63-799(Pt.I))
Mo–Ti–Zr, machining, 16: 3417(R) (ASD-TR-7-532a(IV))
Mo–Ti–Zr, machining of TZM, 20: 15014
Mo–Ti–Zr, mechanical properties, 16: 3445 (ASD-TR-61-193)
Mo–Ti–Zr, mechanical properties, 16: 33455(R) (NP-12097)
Mo–Ti–Zr, mechanical properties of TZM, effects of high temperatures and potassium on, 19: 2794 (APL-TDR-64-116(Pt.I))
Mo–Ti–Zr, mechanical properties of TZM at room temperature, 19: 6277 (ML-TDR-64-205)
Mo–Ti–Zr, mechanical and wear properties of TZM, 19: 29732(R) (APS-5152-R2)
Mo–Ti–Zr, mechanical properties of TZM, effects of carbon content on, 19: 41002 (APS-5157-R)
Mo–Ti–Zr, mechanical properties of TZM, effects of forging schedule and ingot processing on, 19: 41002 (APS-5157-R)
Mo–Ti–Zr, mechanical properties at 25 to 3500°F, 20: 21322 (AMRA-TR-65-25)
Mo–Ti–Zr, oxidation tests of coated TZM bolts and nuts, 19: 7844(R) (AD-602500)
Mo–Ti–Zr, oxidation by air at 1000°C, effects of pressure on, 19: 16017(R) (HW-84281(p.5.6-25))
Mo–Ti–Zr, oxidation by oxygen, effects of pressure and temperature on, 19: 23124(R) (HW-83298(p.8.1-4))
Mo–Ti–Zr, performance as fuel cladding in fast reactors, 18: 24952(R) (ANL-6880(p.6-48))
Mo–Ti–Zr, performance as coating on fast reactor fuel elements, 18: 26824(R) (ANL-6885)
Mo–Ti–Zr, phase diagrams, 18: 25985 (WADD-TR-60-132(Pt.III))
Mo–Ti–Zr, phase studies, 16: 27627(R) (NMI-9243)
Mo–Ti–Zr, phase studies, 17: 6668(R) (NMI-9246)
Mo–Ti–Zr, phase studies of, isothermal sections at 1200°C in, 20: 41464
Mo–Ti–Zr, physical properties of TZM sheets, 18: 30165(R) (AD-431114)
Mo–Ti–Zr, physical properties of sheets of TZM, 19: 945(R) (AD-600281)
Mo–Ti–Zr, polygonization effects on elastic limit, microhardness, microstructure, and recrystallization of, 17: 36317
Mo–Ti–Zr, polygonization effects on mechanical properties of, 18: 37722
Mo–Ti–Zr, powder metallurgy, 17: 6668(R) (NMI-9246)
Mo–Ti–Zr, preparation by arc-melting, 16: 16724(R) (NMI-9238)
Mo–Ti–Zr, preparation of vacuum-arc-cast, 16: 18016(R) (AD-265129)
Mo–Ti–Zr, preparation of homogeneous, 17: 12588(R) (NMI-9249)
Mo–Ti–Zr, production and properties of sheets of, 20: 29756
Mo–Ti–Zr, properties of TZM sheet, 18: 573(R) (AD-422116)
Mo–Ti–Zr, properties of TZM foils at high temperatures, effects of coatings on mechanical and thermophysical, 18: 34128 (RTD-TDR-63-4068)
Mo–Ti–Zr, properties of TZM rolled sheet, 19: 18447(R) (AD-423981)
Mo–Ti–Zr, properties of TZM as cladding material for SNAP hydride reactors, 19: 39166 (NAA-SR-Memo-11149)
Mo–Ti–Zr, radiation effects on hardness and oxidation of, by water at 50°C, 18: 32043(R) (HW-81269(p.4.1-64))
Mo–Ti–Zr, radiation effects on mechanical properties of, neutron, 19: 11669(R) (GEMP-41A)
Mo–Ti–Zr, radiation effects on mechanical properties of, 19: 18390(R) (GEMP-43A)
Mo–Ti–Zr, radiation effects on electric and mechanical properties of, neutron, 19: 24916(R) (GEMP-334A)
Mo–Ti–Zr, radiation effects on creep-rupture of TZM, fast-neutron, 20: 9378(R) (GEMP-54A)
Mo–Ti–Zr, radiation effects on tensile properties of TZM, neutron, 20: 27571(R) (BNWL-207, pp 4.1-3)
Mo–Ti–Zr, radiation effects on creep-rupture properties of TZM, fast-neutron, 20: 27582(R) (GEMP-400A, pp 63-98)
Mo–Ti–Zr, radiation effects on hot-hardness of, effects of test temperature on fast-neutron, 20: 27582(R) (GEMP-400A, pp 63-98)
Mo–Ti–Zr, reactions with cesium at 3400°F, metallographic specimen preparation of TZM, 19: 46954 (NMI-5025(Pt.I), pp 39-58)
Mo–Ti–Zr, reactions with uranium carbide, nitride, and dioxide, metallographic specimen preparation of TZM, 19: 46954 (NMI-5025 (Pt.I), pp 39-58)
Mo–Ti–Zr, reactions with niobium–1 zirconium alloy at 2000°F in refluxing potassium, TZM, 20: 9423(R) (NASA-CR-54735)
Mo–Ti–Zr, specifications of TZM, for use in corrosion test loop fabrication, 20: 21293 (R-66SD3007)
Mo–Ti–Zr, strain softening by flexing of TZM sheet, 19: 7887(R) (AD-421621)
Mo–Ti–Zr, strength of, effects of carbon additions on, 17: 6672 (NP-12383)
Mo–Ti–Zr, stress-rupture properties at high temperatures, 19: 37146
Mo–Ti–Zr, stress-rupture at 2000°F of TZM, 20: 31669
Mo–Ti–Zr, substructure of cold-rolled TZM, 19: 13948(R) (NP-14675)
Mo–Ti–Zr, tensile properties at room temperature, 18: 18380
Mo–Ti–Zr, tensile properties of TZM at room temperature and 650°C, 18: 35060(R) (ANL-6904)
Mo–Ti–Zr, tensile properties of recrystallized TZM, 19: 13948(R) (NP-14675)
Mo–Ti–Zr, tensile properties of TZM sheet, 19: 20542(R) (AD-606310)
Mo–Ti–Zr, tensile properties at 1200 and 2000°F of TZM, 19: 24976(R) (AD-612759)
Mo–Ti–Zr, tensile properties of TZM, statistical analysis of variations in, 19: 26802(R) (AD-610564)
Mo–Ti–Zr, tensile properties of, effects of disilicide coatings on, 20: 27549
Mo–Ti–Zr, tensile properties of TZM, effects of brittle coatings on, 20: 37276
Mo–Ti–Zr, testing of TZM, for use in liquid-metal turbine blades and nozzles, 20: 2240
Mo–Ti–Zr, thermal properties, 18: 7201 (ASD-TDR-63-597)
Mo–Ti–Zr, thermal properties to melting point, 20: 878
Mo–Ti–Zr, welding of TZM, effects of parameters on T1G welds in, 18: 573(R) (AD-422116)
Mo–Ti–Zr, welding of brazed joints of, electron-beam, 18: 23123
Mo–Ti–Zr, welding of TZM, equipment and procedures for, 19: 9629(R) (AD-608818)
Mo–Ti–Zr, yield strength of TZM, effects of boiling potassium exposure on, 19: 34640 (CNLM-6246)
Mo–U–Zr, isothermal transformations of gamma-phase, effects of zirconium on, 19: 40958
Mo–U–Zr, mechanical properties, 17: 39643
Mo–U–Zr, phase diagrams and properties of, at 1000 to 625°C, 16: 30865
Mo–U–Zr, phase studies and structure of, at 500, 575, and 600°C, 16: 30866
Mo–V–Zr, oxidation by steam at 900°F, 18: 2162(R) (IITRI-B198-46)
Mo–W–Zr, extrusion of, comparison of high-velocity and conventional, 17: 1889 (ASD-TDR-62-506)
Mo–W–Zr, extrusion and properties of, 19: 18419(R) (AD-424207)
Mo–W–Zr, fabrication and properties of extruded and rolled, 18: 5727(R) (AD-294579)
Mo–W–Zr, fabrication and properties of cast and extruded, 18: 12536(R) (AD-412904)
Mo–W–Zr, fabrication and properties of extruded and rolled, 18: 22412(R) (AD-422106)
Mo–W–Zr, phase diagram, 19: 37090
Mo–W–Zr, phase studies and properties of W_2Zr–Mo_2Zr phase in, 19: 6350
Mo–W–Zr, phase studies, 19: 41035
Mo–Zn, impurity behavior at grain boundaries during recrystallization,

17: 560
Mo–Zr, aging kinetics of, at 1300 to 1500°K, 20: 41466
Mo–Zr, annealing of, tracer studies of grain boundary migration in, 20: 19251
Mo–Zr, beta phase stabilization in, 17: 11213
Mo–Zr, corrosion of, by potassium at 1000 to 1800°F, 16: 16679 (TID-7626(Pt.I)(p.63-8))
Mo–Zr, corrosion by steam and water, 17: 39659
Mo–Zr, corrosion by hydrochloric, phosphoric, and sulfuric acids at high temperatures, 20: 46158
Mo–Zr, critical current density of superconducting, in transverse field of 30 kgauss, 18: 6128
Mo–Zr, diffusion in bcc, 19: 23112
Mo–Zr, electronic properties, 18: 44150(R) (ORNL-3670(p.44-53))
Mo–Zr, free energies of formation of Laves phases in, 16: 13636
Mo–Zr, grain boundary structure in, internal friction studies of, 20: 15128
Mo–Zr, hardness of dispersion-hardened, 17: 20480
Mo–Zr, internal friction in deformed crystals of, 18: 26041(T)
Mo–Zr, internal friction of annealed and deformed, 20: 5846
Mo–Zr, internal friction in deformed, 20: 19250
Mo–Zr, mechanical properties, 16: 3445 (ASD-TR-61-193)
Mo–Zr, melting of, effects of composition on electron-beam, 20: 29674
Mo–Zr, on creep properties of, effects of nitriding, 17: 41461
Mo–Zr, oxidation by carbon dioxide up to 600°C, 18: 30192
Mo–Zr, oxidation in carbon dioxide and carbon monoxide at 500 to 900°C, 19: 24942
Mo–Zr, phase studies, 19: 41035
Mo–Zr, phase studies, 20: 35924
Mo–Zr, polygonization effects on elastic limit, microhardness, microstructure, and recrystallization of, 17: 36317
Mo–Zr, polygonization effects on mechanical properties of, 18: 37722
Mo–Zr, properties at low temperatures, 20: 3920(R) (ORNL-3870, pp 27-37)
Mo–Zr, properties at high temperatures, 20: 4418
Mo–Zr, reactions with hydrogen, thermochemical and structural aspects of, 20: 27436
Mo–Zr, reactions with hydrogen and nitrogen, 20: 29632
Mo–Zr, resistance to scaling at elevated temperatures, 19: 32770(P)
Mo–Zr, self-diffusion of molybdenum in, 17: 32593
Mo–Zr, strength of, effects of carbon additions on, 17: 6672 (NP-12383)
Mo–Zr, strength of, effects of boron additions on, 17: 6672 (NP-12383)
Mo–Zr, superconducting transition temperature of, (E), 20: 8021
Mo–Zr, tensile properties at high temperatures, effects of nitriding on, 17: 23989
Mo–Zr, transformation kinetics, 18: 44052(R) (ORNL-3670(p.147-59))
Mo–Zr, use as brazing alloys for refractory metals, 18: 7956(R) (GA-3992(Pt.I))
Na–Zr, phase studies, 20: 35924
Nb–Pu–U–Zr, hardness and phase studies, 16: 4450(R) (BMI-1546(Del.))
Nb–Pu–U–Zr, phase studies, 16: 17966(R) (BMI-1541(Del.))
Nb–Re–Zr, oxidation by oxygen at 1000°C, kinetics and microstructures of, 20: 37193
Nb–Rh–Zr, superconducting transition temperature, 19: 44678(R) (ANL-7000, pp 186-200)
Nb–Sn–V–Zr, corrosion by steam at 400 and 450°C, 19: 30668(R) (EURAEC-1274)
Nb–Sn–Zr, chemical and mechanical properties of, program for studying radiation effects on, 17: 22229(T-R) (EURAEC-560)
Nb–Sn–Zr, corrosion of, by steam to 550°C, 16: 32084(T,R) (EURAEC-227)
Nb–Sn–Zr, corrosion by steam and water, 17: 6581
Nb–Sn–Zr, corrosion by steam and water, 17: 6535(T) (EURAEC-352)
Nb–Sn–Zr, corrosion by water, 17: 22094 (HW-71023)
Nb–Sn–Zr, corrosion and mechanical properties of, 17: 39472(T,R) (EURAEC-668)
Nb–Sn–Zr, corrosion by steam and water, 17: 39659
Nb–Sn–Zr, corrosion by superheated steam at 400°C, 18: 8735(T,R) (EURAEC-782)
Nb–Sn–Zr, corrosion by steam and water, effects of heat treatment on, 18: 12574 (APED-4364)
Nb–Sn–Zr, corrosion films on, composition of, 18: 12580 (GEAP-4089 (Vol.II)(Paper 19))
Nb–Sn–Zr, corrosion by steam at 400°C, hydrogen pickup in, 18: 14545(T,R) (EURAEC-863)
Nb–Sn–Zr, corrosion by steam and water, 18: 14358(R) (EURAEC-135)
Nb–Sn–Zr, corrosion of $ZrNb_3Sn$ by steam and water, 18: 14360(R) (EURAEC-199)
Nb–Sn–Zr, corrosion by water and steam, 18: 30110 (EUR-86.d)
Nb–Sn–Zr, corrosion and hydrogen pickup in steam and water, effects of heat treatment on, 18: 30138
Nb–Sn–Zr, corrosion mechanisms of, 18: 39840 (GEAP-4521)
Nb–Sn–Zr, corrosion by steam at 400 and 450°C, effects of metal additions on, 18: 41938(T,R) (EURAEC-1058)
Nb–Sn–Zr, corrosion and hydrogen pickup in water and steam at 600 to 900°F, 18: 41957 (KAPL-3018)
Nb–Sn–Zr, corrosion resistance of, effects of various additives on, 18: 41972(P)
Nb–Sn–Zr, corrosion by terphenyls, 19: 2759
Nb–Sn–Zr, corrosion by water at 360°C and steam at 400°C, mechanism of, 19: 30681
Nb–Sn–Zr, corrosion by steam at 400 and 450°C, 19: 30668(R) (EURAEC-1274)
Nb–Sn–Zr, corrosion by water in ETR G-7 loop, 19: 30669(R) (HW-84573(p.5.1-22))
Nb–Sn–Zr, corrosion resistance of, effects of additives and cold working on, 19: 36990(P)
Nb–Sn–Zr, corrosion by steam, effects of antimony, chromium, iron, and vanadium additions on, 20: 2255(R) (EURAEC-1323)
Nb–Sn–Zr, corrosion in reactor, ETR test of, 20: 27425(R) (BNWL-207, pp 5.1-12)
Nb–Sn–Zr, corrosion by steam, composition of oxide film formed by, 20: 31669
Nb–Sn–Zr, creep and fatigue properties of $ZrNb_3Sn$, 18: 14359(R) (EURAEC-136)
Nb–Sn–Zr, crystal structure of, effects of hydrogen on, 16: 33487(T,R) (EURAEC-243)
Nb–Sn–Zr, dispersion and solution strengthening effects on, 18: 5794
Nb–Sn–Zr, effects of metal additions on corrosion of Nb_3SnZr by steam, 18: 18319(T,R) (EURAEC-953)
Nb–Sn–Zr, effects of physical parameters and radiation on fuel element cladding of, (E), 20: 7519 (RCN-41)
Nb–Sn–Zr, elongation of, due to thermal cycling, 16: 10526(R) (EURAEC-86)
Nb–Sn–Zr, fabrication of tubing of, 17: 6600(T) (EURAEC-354)
Nb–Sn–Zr, fabrication and mechanical testing, 18: 37612 (A/CONF.28/P/477)
Nb–Sn–Zr, fabrication and properties of, effects of metal additions on, 18: 41938(T,R) (EURAEC-1058)
Nb–Sn–Zr, fatigue properties of $ZrNb_3Sn$, 18: 14360(R) (EURAEC-199)
Nb–Sn –Zr, hardness of zirconium-base, effects of tempering at 400 to 700°C on, 20: 31669
Nb–Sn–Zr, heat treatment and tensile properties of, 17: 22094 (HW-71023)
Nb–Sn–Zr, hydrogen pickup in steam and water, effects of heat treatment on, 18: 12574 (APED-4364)
Nb–Sn–Zr, length variations induced by thermal cycling in $ZrNb_3Sn$ tubes, 18: 14359(R) (EURAEC-136)
Nb–Sn–Zr, mechanical properties, 16: 33487(T,R) (EURAEC-243)
Nb–Sn–Zr, mechanical properties of, at 25 to 850°C, effects of oxygen, 17: 1947 (TID-17174)
Nb–Sn–Zr, mechanical properties of, hydrogen effects on, 17: 6696(T) (EURAEC-353)
Nb–Sn–Zr, mechanical properties and phases of, effects of hydrogen on, 17: 12693
Nb–Sn–Zr, mechanical properties, 18: 8735(T,R) (EURAEC-782)
Nb–Sn–Zr, phase diagrams, 18: 12633 (GEAP-4089(Vol.I)(Paper 4))
Nb–Sn–Zr, phase studies, 17: 6697(T) (EURAEC-358)
Nb–Sn–Zr, phase studies, 18: 14358(R) (EURAEC-135)
Nb–Sn–Zr, phase studies, 18: 14360(R) (EURAEC-199)
Nb–Sn–Zr, preparation, 16: 20980(T,R) (EURAEC-26)
Nb–Sn–Zr, preparation of, 17: 8890(T,R) (EURAEC-494)
Nb–Sn–Zr, properties for reactor applications, 18: 12633 (GEAP-4089 (Vol.I)(Paper 4))
Nb–Sn–Zr, properties of $ZrNb_3Sn$, 18: 14358(R) (EURAEC-135)
Nb–Sn–Zr, properties for use as cladding materials in water, 18: 30110 (EUR-86.d)
Nb–Sn–Zr, radiation effects on, neutron, 17: 8890(T,R) (EURAEC-494)
Nb–Sn–Zr, radiation effects on, 17: 39472(T,R) (EURAEC-668)
Nb–Sn–Zr, radiation effects on properties of $ZrNb_3Sn_1$, neutron, 18: 14545(T,R) (EURAEC-863)
Nb–Sn–Zr, radiation effects on corrosion and mechanical properties of, neutron, 18: 18418(T,R) (EURAEC-971)
Nb–Sn–Zr, radiation effects on corrosion and mechanical properties of, neutron, 18: 32235(T,R) (EURAEC-1068)
Nb–Sn–Zr, radiation effects on corrosion and mechanical properties of, neutron, 18: 37612 (A/CONF.28/P/477)
Nb–Sn–Zr, radiation effects on oxidation by low-oxygen water, neutron, 19: 16016(R) (HW-84281(p.5.1-5))
Nb–Sn–Zr, radiation effects on corrosion and mechanical properties of, neutron, 19: 16208(R) (EURAEC-1249)
Nb–Sn–Zr, radiation effects on corrosion and mechanical properties of, neutron, 20: 11354
Nb–Sn–Zr, radiation effects on corrosion of, by water, effects of fabrication history on fast-neutron, 20: 23767 (BNWL-88)
Nb–Sn–Zr, stability of martensite structure at 400 to 700°C at times to

2000 hr, 19: 14041
Nb–Sn–Zr, stability of martensite structure in zirconium-base, 20: 11227
Nb–Sn–Zr, superconductivity of fused, 20: 15123
Nb–Sn–Zr, tensile properties of, effects of oxygen on, 16: 15184 (KAPL-2000-17)
Nb–Sn–Zr, tensile properties of, effects of composition and heat treatment on, 16: 29380 (TID-6155)
Nb–Sn–Zr, thermal cycling of, changes in length by, 16: 19380(T,R) (EURAEC-201)
Nb–Sn–Zr, treatment for improved corrosion resistance, 17: 36216(P)
Nb–Sn–Zr, welding, 17: 6535(T) (EURAEC-352)
Nb–stainless steel–Zr, compatibility studies, 20: 8447 (PWAC-491)
Nb–Ta–V–Zr, strength at high temperatures, 20: 2407(P)
Nb–Ta–W–Zr, analysis for alloying elemeats and impurities, comparison of results from 25 laboratories on FS-85, 20: 18567 (MAB-217-M)
Nb–Ta–W–Zr, analysis using vacuum cup electrode, 19: 22103 (TIM-904)
Nb–Ta–W–Zr, bonding of FS-85, to Inconel 600 and stainless steels, process development for explosive, 20: 21295(R) (WANL-PR-(EE)-002)
Nb–Ta–W–Zr, bonding to Hastelloy N, Inconel 600, and types 321 and 347 stainless steels of FS-85, explosive, 20: 11243(R) (WANL-PR(EE)-001)
Nb–Ta–W–Zr, coating of FS-85, with chromium–molybdenum–silicon and chromium–silicon–titanium systems, 18: 14353(R) (AD-408310)
Nb–Ta–W–Zr, coating of FS-85, platinum and platinum–rhodium alloy, 18: 20445(R) (AD-434441)
Nb–Ta–W–Zr, coating of FS-85, with palladium–platinum alloy and platinum, 18: 34029(R) (AD-601740)
Nb–Ta–W–Zr, coating of FS-85 for oxidation protection at high temperatures, 19: 7845(R) (AD-608135)
Nb–Ta–W–Zr, coating of FS-85 for oxidation protection, development of diffusion barriers for ductile, 19: 36957(R) (NP-15113)
Nb–Ta–W–Zr, coatings on FS-85, properties of oxidation-resistant, 19: 26801(R) (AD-607530)
Nb–Ta–W–Zr, contamination of FS-85, by residual gases in high vacuum, 18: 39826 (ORNL-3674)
Nb–Ta–W–Zr, corrosion of platinum- and platinum–rhodium-clad FS-85, by air at 2200 and 2550°F, 18: 20445(R) (AD-434441)
Nb–Ta–W–Zr, corrosion of FS-85 by boiling cesium, 19: 13913(R) (AFML-TR-64-327)
Nb–Ta–W–Zr, corrosion of FS-85, by lithium, effects of oxygen on, 20: 4301(R) (ORNL-3870, pp 102-35)
Nb–Ta–W–Zr, corrosion by lithium in niobium–1-zirconium alloy forced-convection loop, 20: 5853 (TIM-898)
Nb–Ta–W–Zr, creep behavior in ultrahigh vacuum at 2000 and 2200°F, 20: 13256 (NASA-TN-D-3222)
Nb–Ta–W–Zr, creep of FS-85, at 2000°F and 4000 psi stress under vacuum conditions, 18: 44142(R) (NASA-CR-54123)
Nb–Ta–W–Zr, creep of FS-85, at 2000 to 2200°F in ultrahigh vacuum, 20: 21344 (N-65-26653)
Nb–Ta–W–Zr, creep properties of FS-85, 20: 4301(R) (ORNL-3870, pp 102-35)
Nb–Ta–W–Zr, creep properties of FS-85, 20: 31669
Nb–Ta–W–Zr, creep test data of FS-85 at 2000°F and 7000 psi, 19: 9662(R) (NASA-CR-54228)
Nb–Ta–W–Zr, creep-rupture of FS-85 at 982 to 1204°C, effects of annealing on, 20: 35895 (ORNL-TM-1456)
Nb–Ta–W–Zr, ductility of FS-85, effects of aging on bend, 20: 4301(R) (ORNL-3870, pp 102-35)
Nb–Ta–W–Zr, ductility transition temperature of FS-85, effects of protective coatings and welding on, 20: 27466
Nb–Ta–W–Zr, evaporation tests of FS-85 in high vacuum, 18: 44049(R) (ORNL-3670(p.77-111))
Nb–Ta–W–Zr, evaporation losses of FS-85, at 1200 to 1500°C in high vacuum, 19: 37043 (ORNL-P-1394)
Nb–Ta–W–Zr, evaporation losses in high vacuum of FS-85, 20: 4301(R) (ORNL-3870, pp 102-35)
Nb–Ta–W–Zr, fabricability, strength, and weldability of, 20: 29763
Nb–Ta–W–Zr, fabrication and properties, 18: 7265
Nb–Ta–W–Zr, fabrication of FS-85, by rolling, 18: 12593(R) (AD-411155)
Nb–Ta–W–Zr, fabrication and mechanical properties of FS-85, 18: 18292(R) (N63-20341)
Nb–Ta–W–Zr, fabrication of FS-85, by forging, 18: 20484(R) (AD-418992)
Nb–Ta–W–Zr, fabrication and properties of forged and rolled FS-85, 18: 24093(R) (AD-424593)
Nb–Ta–W–Zr, fabrication and properties of FS-85 sheet, 18: 30106(R) (AD-430773)
Nb–Ta–W–Zr, fabrication FS-85 into sheets, 18: 30146(R) (AD-414497)
Nb–Ta–W–Zr, fabrication by forging and cold rolling, 19: 11711
Nb–Ta–W–Zr, fabrication and properties of FS-85 sheet, 19: 20499(R) (AD-606291)
Nb–Ta–W–Zr, mechanical properties, 17: 14802(R) (AD-278727)
Nb–Ta–W–Zr, mechanical properties of coated and uncoated FS-85, in air to 2600°F, 17: 36188(R) (AD-289857)
Nb–Ta–W–Zr, mechanical properties of FS-85, 19: 13978 (AMRA-TR-64-16)
Nb–Ta–W–Zr, preparation and specifications for corrosion loop testing, 20: 4380 (NASA-CR-54761)
Nb–Ta–W–Zr, properties as space reactor fuel cladding, 18: 9713 (CONF-375-3)
Nb–Ta–W–Zr, properties of coated FS-85, to 2600°F, 18: 14353(R) (AD-408310)
Nb–Ta–W–Zr, properties of welds in FS-85, 19: 40989
Nb–Ta–W–Zr, properties as hollow turbine vanes, 20: 16963
Nb–Ta–W–Zr, tensile properties of FS-85 at room temperature to 2600°F, 17: 36279(R) (AD-287509)
Nb–Ta–W–Zr, tensile properties of FS-85, effects of welds on, 20: 29712(R) (WANL-PR-(P)-009)
Nb–Ta–W–Zr, thermal properties, 18: 7201 (ASD-TDR-63-597)
Nb–Ta–W–Zr, thermal properties to melting point, 20: 878
Nb–Ta–W–Zr, weld bend tests of FS-85, 19: 13955(R) (WANL-PR-(P)-005)
Nb–Ta–W–Zr, weldability of FS-85, 17: 39498 (DMIC-Memo-169)
Nb–Ta–W–Zr, weldability of FS-85 sheet, 18: 44049(R) (ORNL-3670 (p.77-111))
Nb–Ta–W–Zr, weldability study of FS-85, 19: 24957(R) (WANL-PR(P)-006)
Nb–Ta–W–Zr, weldability studies of FS-85, 19: 46966(R) (WANL-PR(P)-007)
Nb–Ta–W–Zr, weldability of FS-85, effects of oxygen contamination on, 20: 13264(R) (WANL-PR(P)-008)
Nb–Ta–W–Zr, weldability of FS-85, effects of oxygen contamination on, 20: 29712(R) (WANL-PR-(P)-009)
Nb–Ta–W–Zr, weldability evaluation of, 20: 39366
Nb–Ta–W–Zr, welding of FS-85, electron-beam and tungsten-arc, 18: 34058(R) (WANL-PR(P)-003)
Nb–Ta–W–Zr, welding properties of FS-85, 20: 27466
Nb–Ta–Y–Zr, grain size and hardness of, effects of yttrium additions on, 19: 40953 (PWAC-441)
Nb–Ta–Zr, coating evaluation for FS-82, 19: 9607 (ML-TDR-64-70)
Nb–Ta–Zr, corrosion by lithium at 2000 to 3000°F, 18: 14420
Nb–Ta–Zr, forging characteristics, 16: 9162 (DMIC-Memo-143)
Nb–Ta–Zr, nitrogen and oxygen content of, effects of yttrium additions on, 19: 40953 (PWAC-441)
Nb–Ta–Zr, properties for use in thermal protective systems in space vehicles, 18: 32199
Nb–Ta–Zr, radiation effects on fuel rod jackets of, 19: 26876 (ANL-6750)
Nb–Ta–Zr, reactions with uranium monocarbide at 1000 to 2400°C, 18: 8795 (HW-72031)
Nb–Ta–Zr, superconducting critical currents at 4.2°K, 17: 554
Nb–Ta–Zr, superconductivity, 17: 4886(R) (AD-275610)
Nb–Ta–Zr, superconducting critical current density in, effect of microheterogeneity on, 20: 40020
Nb–Ta–Zr, welding, 16: 30741 (ASD-TDR-62-292)
Nb–Th–Zr, corrosion by water at 300 to 500°C, 17: 39651
Nb–Th–Zr, phase studies and structure at 550 to 1100°C, 17: 39650
Nb–Ti–V–Zr, oxidation of siliconized, at 2200°F, 17: 23942(R) (ARF-B6001-3)
Nb–Ti–V–Zr, oxidation life at 2200°F of siliconized, static, 17: 35997(R) (IITRE-B6001-5)
Nb–Ti–V–Zr, phase studies, 18: 549(R) (NP-13241)
Nb–Ti–V–Zr, properties, 19: 26848
Nb–Ti–V–Zr, properties, effects of composition on, 20: 2340 (ORNL-TM-1131)
Nb–Ti–W–V–Zr, properties for elevated-temperature service, 19: 6241 (BM-RI-6558)
Nb–Ti–Zr, annealing, 17: 35078(R) (ANL-6739)
Nb–Ti–Zr, bend tests of coated D-36, 19: 7844(R) (AD-602500)
Nb–Ti–Zr, bonding of D-36, method for diffusion, 20: 5867
Nb–Ti–Zr, brazing of honeycomb structures of, 18: 39874
Nb–Ti–Zr, brazing, equipment and methods for, 18: 27938
Nb–Ti–Zr, coatings for D-36 foils, development of high-temperature oxidation-resistant, 18: 30118(R) (RTD-TDR-63-4006(Pt.I))
Nb–Ti–Zr, corrosion of, by steam and water, 16: 29346
Nb–Ti–Zr, corrosion by steam at 1000°F, 17: 493(R) (BMI-X-10003)
Nb–Ti–Zr, corrosion by potassium at 1500 to 1800°F, 18: 5728 (ASD-TDR-63-270(Pt.II))
Nb–Ti–Zr, corrosion by sodium at 650°C, 18: 15663(R) (ANL-6808)
Nb–Ti–Zr, corrosion by potassium vapor at 1500 to 1800°F, 18: 18282 (BNL-844)
Nb–Ti–Zr, corrosion by sodium at 650°C, 18: 26893(R) (ANL-6868(p.11-108))
Nb–Ti–Zr, ductility transition temperature of D-36, effects of protective coatings and welding on, 20: 27466

Nb–Ti–Zr, fabrication of high-quality tubing of, 17: 16603 (ANL-FGF-409)
Nb–Ti–Zr, fabrication and testing of brazed honeycomb sandwich panels of D-36, 18: 10494 (AD-427700(p.245-80))
Nb–Ti–Zr, fabrication and properties, 18: 26893(R) (ANL-6868(p.11-108))
Nb–Ti–Zr, fabrication and properties of D-36 foil, 19: 24945 (ASD-TDR-63-829(Pt.I))
Nb–Ti–Zr, fabrication and properties of D-36 strip and foil, 19: 24946 (ASD-TDR-63-829(Pt.II))
Nb–Ti–Zr, fabrication of honeycombed-sandwich panels from D-36, 20: 7541
Nb–Ti–Zr, joining of foils of D-36, for honeycomb panel fabrication, 18: 37661 (ASD-TDR-63-799(Pt.I))
Nb–Ti–Zr, microstructure of, effects of annealing temperature on, 19: 44587(R) (ANL-7000, pp 3-63)
Nb–Ti–Zr, oxidation of, at 1000°C, 16: 9248(P)
Nb–Ti–Zr, oxidation of, by air above 700°C, 16: 3408 (NP-11119)
Nb–Ti–Zr, oxidation, 18: 7157
Nb–Ti–Zr, oxidation-resistant coatings on D-36, performance of commercial, 20: 16973 (NASA-TN-D-3275)
Nb–Ti–Zr, phase diagram, 16: 5743
Nb–Ti–Zr, phase studies on, at 570 to 1100°C, 20: 29785
Nb–Ti–Zr, properties, 18: 2163(R) (IS-700(Sect.M))
Nb–Ti–Zr, properties of D-36 foils at high temperatures, effects of coatings on mechanical and thermophysical, 18: 34128 (RTD-TDR-63-4068)
Nb–Ti–Zr, shear strength of fasteners of, at room temperature and 1600°F, 17: 36281 (AD-295526)
Nb–Ti–Zr, superconductivity of, effects of composition on, 20: 29784
Nb–Ti–Zr, superconductivity of, effects of cold working and heat treatments on, 20: 29787
Nb–Ti–Zr, superconductivity of, effects of microstructure on, 20: 29788
Nb–Ti–Zr, thermal properties, 18: 7201 (ASD-TDR-63-597)
Nb–Ti–Zr, thermal properties to melting point, 20: 878
Nb–Ti–Zr, welding of brazed joints of, electron-beam, 18: 32123
Nb–Ti–Zr, welding properties of D-36, 20: 27466
Nb–U–Zr, corrosion of, by sodium at 1600 and 1800°C, 16: 17966(R) (BMI-1541(Del.))
Nb–U–Zr, corrosion mechanisms of, stress, 16: 12056
Nb–U–Zr, corrosion, 17: 39640
Nb–U–Zr, corrosion resistance and dimensional stability of, methods of preparation for, 18: 44093(P)
Nb–U–Zr, fabrication of corrosion-resistant dimensionally-stable, 17: 22148(P)
Nb–U–Zr, fission product release from, in TREAT meltdown, 19: 17174(R) (ANL-6900(p.232-303))
Nb–U–Zr, mechanical properties and phase studies, 17: 39642
Nb–U–Zr, mechanical properties, 17: 41333(R) (ANL-6677)
Nb–U–Zr, mechanical properties of gamma-phase uranium-base, 20: 15060 (UCRL-7771)
Nb–U–Zr, mechanical properties of gamma-phase, effects of dynamic loading on, 20: 27496 (UCRL-14805)
Nb–U–Zr, phase studies and structure, 16: 30862
Nb–U–Zr, phase studies and polythermal diagrams, 16: 30863
Nb–U–Zr, phase studies and structure, 16: 30864
Nb–U–Zr, phase studies, 17: 39632
Nb–U–Zr, phase studies and properties of, 18: 39912 (UCRL-7869)
Nb–U–Zr, properties of metastable γ-phase, 20: 5843
Nb–U–Zr, properties of, at 150 to 350°C, mechanical and physical, 20: 21356 (UCRL-14724)
Nb–U–Zr, radiation effects on, reactor-excursion, 19: 31462(R) (ANL-7028)
Nb–U–Zr, reactions of molybdenum with uranium in, 18: 34174
Nb–U–Zr, reactions with water during Kiwi-TNT transients, 20: 20925(R) (ANL-7055, pp 177-212)
Nb–U–Zr, thermal cycling effects on crystal structure and dimensional stability, 17: 39639
Nb–U–Zr, transformation of gamma phase of, isothermal, 19: 7910 (UCRL-7824)
Nb–V–Zr, corrosion of, by steam and water, 16: 29346
Nb–V–Zr, creep properties of, at 982 and 1204°C, 20: 27545
Nb–V–Zr, creep testing of, summary of slow-bend, 18: 4255(R) (ORNL-3470(p.98-125))
Nb–V–Zr, development and properties of niobium-base Cb-753, 20: 19214 (N-65-22097)
Nb–V–Zr, melting points, 18: 44497(R) (MND-2812-2)
Nb–V–Zr, phase studies, 17: 11108(T,R) (EURAEC-307)
Nb–V–Zr, phase studies, 17: 14749(T,R) (EURAEC-408)
Nb–V–Zr, phase studies, 18: 28036
Nb–V–Zr, preparation and properties, 16: 22577(R) (ARF-2231-4)
Nb–V–Zr, properties of Cb-753, 20: 21411
Nb–V–Zr, radiation effects on phases in, neutron, 18: 39999 (KAPL-2251)
Nb–W–V–Zr, ductility, strength, and weldability of, 18: 14448
Nb–W–V–Zr, mechanical properties of, effects of carbon on, 17: 34419(R) (WADC-TR-57-344(Pt.VII))
Nb–W–V–Zr, properties for elevated-temperature service, 19: 6241 (BM-RI-6558)
Nb–W–Y–Zr, corrosion by refluxing potassium at 1800 to 2400°F, 20: 25485 (NASA-TN-D-3429)
Nb–W–Zr, aging characteristics of Cb-752 and D-43, 18: 44049(R) (ORNL-3670(p.77-111))
Nb–W–Zr, alloying effects of carbon on creep properties, 17: 1998(P)
Nb–W–Zr, bend tests of coated Cb-752 and D-43, 19: 7844(R) (AD-602500)
Nb–W–Zr, bend tests of electron-beam welds in Cb-752, 19: 13954(R) (WANL-PR(P)-004)
Nb–W–Zr, bonding of, controlling factors in diffusion, 19: 24964
Nb–W–Zr, brazing, equipment and methods for, 18: 27938
Nb–W–Zr, casting and testing of Cb-752 and D-43 ingots, 18: 571(R) (AD-297246)
Nb–W–Zr, coating of D-43, with chromium–silicon–titanium systems and silicides, 18: 14373(R) (NP-13498)
Nb–W–Zr, coating of, with oxidation-resistant silicides, fluidized-bed process for, 20: 43881
Nb–W–Zr, coatings on Cb-752, properties of oxidation-resistant, 19: 26801(R) (AD-607530)
Nb–W–Zr, coatings on D-43, performance of Disil, 19: 37034 (N64-27085)
Nb–W–Zr, contamination of Cb-752, by residual gases in high vacuum, 18: 39826 (ORNL-3674)
Nb–W–Zr, corrosion by sodium at 650°C, 18: 15663(R) (ANL-6808)
Nb–W–Zr, corrosion by sodium at 650°C, 18: 26893(R) (ANL-6868 (p.11-108))
Nb–W–Zr, corrosion by boiling sodium, 19: 22890 (BNL-9018)
Nb–W–Zr, corrosion by sodium at 1260°C, 19: 28764
Nb–W–Zr, corrosion by sodium at 1266°C, 19: 36949(R) (BNL-900 (p.121-97))
Nb–W–Zr, corrosion protection by silicide coatings, 19: 11682
Nb–W–Zr, corrosion by flowing lithium, 20: 2238
Nb–W–Zr, corrosion by bismuth and tin, 20: 2275
Nb–W–Zr, corrosion of Cb-752, by lithium, effects of oxygen on, 20: 4301(R) (ORNL-3870, pp 102-35)
Nb–W–Zr, corrosion by refluxing potassium at 1800 to 2400°F, 20: 25485 (NASA-TN-D-3429)
Nb–W–Zr, creep behavior in ultrahigh vacuum at 2000 and 2200°F, 20: 13256 (NASA-TN-D-3222)
Nb–W–Zr, creep of AS-30 at 2000°F, long-time, 19: 18459(R) (NASA-CR-54287)
Nb–W–Zr, creep properties of Cb-752, 20: 4301(R) (ORNL-3870, pp 102-35)
Nb–W–Zr, creep tests on AS-30 at 3200°F, 20: 5885(R) (NAS-CR-54773)
Nb–W–Zr, creep-rupture properties of D-43, temperature dependence, 18: 44049(R) (ORNL-3670(p.77-111))
Nb–W–Zr, creep-rupture properties of, 20: 2336 (ORNL-P-1634)
Nb–W–Zr, ductility and tensile properties of arc-welded D-43, 19: 37034 (N64-27085)
Nb–W–Zr, ductility transition temperature of Cb-752 effects of protective coatings and welding on, 20: 27466
Nb–W–Zr, effect of carbon on phase equilibria of, 19: 32729(R) (DRI-1092-211)
Nb–W–Zr, effects of carbon on phase equilibria in, 19: 22973(R) (DRI-1092-203)
Nb–W–Zr, effects of carbon and oxygen on phase equilibria in, 20: 7558(R) (DRI-1092-221)
Nb–W–Zr, effects of carbon and oxygen additions on phase equilibria in, 20: 7559(R) (DRI-1092-225)
Nb–W–Zr, effects of carbon and oxygen on phase equilibria in niobium-rich region of, 20: 21329(R) (DRI-1092-229)
Nb–W–Zr, erosion by mercury vapor of Cb-752, 20: 11214(R) (NASA-CR-54717)
Nb–W–Zr, evaporation tests of D-43 in high vacuum, 18: 44049(R) (ORNL-3670(p.77-111))
Nb–W–Zr, evaporation losses of D-43, at 1200 to 1500°C in high vacuum, 19: 37043 (ORNL-P-1394)
Nb–W–Zr, extrusion, 17: 3445(R) (NP-12225)
Nb–W–Zr, fabricability, strength, and weldability of, 20: 29763
Nb–W–Zr, fabrication of sheets, 17: 8757(R) (NP-12446)
Nb–W–Zr, fabrication into H sections, 18: 7163(R) (NP-13410)
Nb–W–Zr, fabrication of rolled sheets of D-43 and Cb-752, 18: 12591(R) (AD-409960)
Nb–W–Zr, fabrication of H sections of Cb-752 and D-43, by drawing and extrusion, 18: 12595(R) (AD-429144)
Nb–W–Zr, fabrication and properties of extruded and rolled D-43, 18: 22411(R) (AD-417692)
Nb–W–Zr, fabrication and properties of coated D-43, 18: 24068(R) (NP-13955)

Nb–W–Zr, fabrication and properties of Cb-752 sheet, 18: 34025(R) (AD-428036)
Nb–W–Zr, fabrication and properties of rolled sheets of Cb-752, 19: 882(R) (AD-600403)
Nb–W–Zr, fabrication and properties of rolled Cb-752, 19: 6239(R) (ASD-8-108(VI))
Nb–W–Zr, fabrication and properties of forged Cb-752, 19: 6240(R) (ASD-8-170(V))
Nb–W–Zr, fabrication and properties of Cb-752 foil, 19: 24945 (ASD-TDR-63-829(Pt.I))
Nb–W–Zr, fabrication and properties of Cb-752 strip foil, 19: 24946 (ASD-TDR-63-829(Pt.II))
Nb–W–Zr, fasteners for use to 3000°F, 19: 32702(R) (AD-609653)
Nb–W–Zr, forging characteristics, 16: 9162 (DMIC-Memo-143)
Nb–W–Zr, forging of, method optimization for closed-die, 16: 15152(R) (ASD-TR-7-782(VIII))
Nb–W–Zr, grain size and microhardness of D-43, effects of annealing temperature on, 19: 37034 (N64-27085)
Nb–W–Zr, hardness of annealed and as-cast, 18: 32138(R) (DRI-2166)
Nb–W–Zr, machining, properties, welding, and working of, 18: 14486
Nb–W–Zr, mechanical properties of Pfaudler silicide and TRW chromium–silicon–titanium-coated D-43, in air at 70 to 2600°F, 18: 20523(R) (NP-13811)
Nb–W–Zr, mechanical properties of Cb-752 and D-43, 19: 13978 (AMRA-TR-64-16)
Nb–W–Zr, phase diagram, 17: 3531
Nb–W–Zr, phase diagram, 18: 8809(T) (JPRS-22593)
Nb–W–Zr, phase equilibria of niobium-rich regions, 17: 16641(R) (DRI-2091)
Nb–W–Zr, phase equilibria in, effects of carbon and oxygen on, 20: 35885(R) (DRI-1092-232)
Nb–W–Zr, phase studies, 17: 39529(R) (DRI-2117)
Nb–W–Zr, phase studies, 18: 8792(R) (DRI-2131)
Nb–W–Zr, phase studies on, 18: 16494
Nb–W–Zr, phase studies, 18: 32138(R) (DRI-2166)
Nb–W–Zr, preparation and properties of, 17: 27779(R) (DRI-2102)
Nb–W–Zr, properties of, for alkali metal containment, 16: 24165(R) (NP-11824)
Nb–W–Zr, properties of Cb-752 as structural material for re-entry vehicles, 18: 7203 (D2-35105)
Nb–W–Zr, properties of coated D-43, to 2600°F, 18: 14373(R) (NP-13498)
Nb–W–Zr, properties of X-110, to 2600°F, 18: 14353(R) (AD-408310)
Nb–W–Zr, properties as hollow turbine vanes, 20: 16963
Nb–W–Zr, radiation effects on mechanical properties of Nb-752, neutron, 18: 14537(R) (HW-79766(p.4.1-76))
Nb–W–Zr, radiation effects on hardness of Cb-752, at 50°C, 18: 32043(R) (HW-81269(p.4.1-64))
Nb–W–Zr, radiation effects on ductility of D-43, fast-neutron, 18: 44049(R) (ORNL-3670(p.77-111))
Nb–W–Zr, radiation effects on mechanical properties of Cb-752, neutron, 19: 30820 (BNWL-23)
Nb–W–Zr, radiation effects on tensile properties of Cb-752, neutron, 20: 27571(R) (BNWL-207, pp 4.1-3)
Nb–W–Zr, rolling of foils of Nb-752, 19: 7871(R) (AD-422001)
Nb–W–Zr, stress effects in corrosion of D-43, by potassium, 20: 2270
Nb–W–Zr, stress-corrosion of D-43, in potassium at 2000 to 2200°F, 19: 9622(R) (NASA-CR-54200)
Nb–W–Zr, tensile and creep properties at 2800 to 3400°F, 17: 37506 (BLR-62-26)
Nb–W–Zr, tensile properties of D-43, to 3000°F, 19: 37034 (N64-27085)
Nb–W–Zr, tensile properties of, effects of disilicide coatings on, 20: 27549
Nb–W–Zr, tensile properties of Cb-752, effects of welds on, 20: 29712(R) (WANL-PR-(P)-009)
Nb–W–Zr, tensile properties of, 20: 37245
Nb–W–Zr, thermal properties, 18: 7201 (ASD-TDR-63-597)
Nb–W–Zr, thermal properties to melting point, 20: 878
Nb–W–Zr, thermophysical properties of D-43, 18: 44049(R) (ORNL-3670(p.77-111))
Nb–W–Zr, weld bend tests of Cb-752, 19: 13955(R) (WANL-PR-(P)-005)
Nb–W–Zr, weld structural stability in, 18: 22459(R) (NP-13816)
Nb–W–Zr, weldability of D-43 sheets, 18: 44049(R) (ORNL-3670 (p.77-111))
Nb–W–Zr, weldability study of Cb-752, 19: 24957(R) (WANL-PR(P)-006)
Nb–W–Zr, weldability studies of Cb-752, 19: 46966(R) (WANL-PR(P)-007)
Nb–W–Zr, weldability evaluation of, 20: 39366
Nb–W–Zr, welding of Nb-752 and D-43, electron-beam and tungsten-arc, 18: 22426(R) (WANL-PR(P)-002)
Nb–W–Zr, welding of Cb-752 and D-43, tungsten-arc, 18: 34058(R) (WANL-PR(P)-003)
Nb–W–Zr, welding properties of Cb-752, 20: 27466
Nb–Y–Zr, corrosion by steam at 400-500°C, 20: 2276(P)
Nb–Y–Zr, grain size and hardness of, effects of yttrium additions on, 19: 40953 (PWAC-441)
Nb–Y–Zr, preparation for use in nuclear reactors, 20: 9561(P)
Nb–Zircaloy-4–Zr, fabrication of tubular, methods for, 19: 47998(R) (SRO-118)
Nb–Zn–Zr, mechanical properties, 18: 7292(R) (HW-77954(p.4.1-12))
Nb–Zr, a-c conductivity of superconducting, 17: 41541 (BSD-TDR-63-147)
Nb–Zr, a-c losses in superconducting wires of, 17: 28099
Nb–Zr, a-c resistance of, 17: 20538 (BSD-TDR-63-60)
Nb–Zr, a-c power losses in superconducting, 18: 36426
Nb–Zr, aging characteristics, 16: 15192 (ORNL-3245)
Nb–Zr, aging of, 16: 30167 (ORNL-3313(p.19-64))
Nb–Zr, aging studies of, 20: 5181(R) (ORNL-3029)
Nb–Zr, aging studies on welds of, 20: 5181(R) (ORNL-3029)
Nb–Zr, analysis for niobium, spectrophotometric, 18: 35465
Nb–Zr, analysis for zirconium by spectrography of solutions, 20: 14446 (N64-25607)
Nb–Zr, analysis of electron-beam welds of, 19: 22984(R) (NASA-CR-54167)
Nb–Zr, analysis of, gamma spectra measurements in activation, 19: 38566
Nb–Zr, annealing effects on superconductivity in, 16: 12131
Nb–Zr, annealing, 17: 35078(R) (ANL-6739)
Nb–Zr, annealing specifications for, 20: 35110 (CNLM-5584(Vol.3))
Nb–Zr, anodization measurements of compositional segregation in, 18: 4250(R) (ORNL-3470(p.45-8))
Nb–Zr, anomalous critical currents in superconducting noninductive coils of, (E), 20: 13674
Nb–Zr, attenuation of 5- to 30-Mc elastic waves in superconducting, 17: 11400
Nb–Zr, beta phase stabilization in, 17: 11213
Nb–Zr, bonding of, to Inconel 600 and stainless steels, process development for explosive, 20: 21295(R) (WANL-PR-(EE)-002)
Nb–Zr, bonding to aluminum and beryllium oxides, 18: 41928(R) (NASA-CR-54089)
Nb–Zr, bonding to beryllium, 19: 11711
Nb–Zr, bonding to metallized alumina, brazing alloy for, 19: 40980 (LA-3302)
Nb–Zr, bonding to alumina–yttria, brazing alloy for, 19: 40980 (LA-3302)
Nb–Zr, bonding to types 321 and 347 stainless steels, explosive, 20: 11243(R) (WANL-PR(EE)-001)
Nb–Zr, bonding to aluminum oxide, development and properties of brazes for, 20: 27445 (LA-DC-7159)
Nb–Zr, brazing and welding of, 20: 5181(R) (ORNL-3029)
Nb–Zr, brazing techniques for bonding to graphite, 20: 2294
Nb–Zr, brazing to beryllium using silver, 19: 44606 (PWAC-483)
Nb–Zr, brazing to beryllium using silver alloys, effects of carbon and silicon coatings on, 19: 44606 (PWAC-483)
Nb–Zr, brittle fracture in liquid-metal coolant loop tubing of, 19: 22984(R) (NASA-CR-54167)
Nb–Zr, brittle fracture of hydrided and nonhydrided cold-worked, 20: 27477(R) (BNWL-207, pp 6.7-12)
Nb–Zr, brittleness of, effects of hydrogen on, 19: 18498
Nb–Zr, brittleness and fracture of, effects of hydrogen on, 19: 44716
Nb–Zr, brittleness at –23 to 265°C, 20: 746(R) (BNWL-120, pp 6.1-11)
Nb–Zr, brittleness of, effects of hydrogen on, 20: 11227
Nb–Zr, burst testing of tubular, 19: 24089(R) (SRO-114)
Nb–Zr, calculation of upper critical field of, 17: 20452 (BSD-TDR-63-62)
Nb–Zr, carburization by uranium carbide, 18: 10537 (NAA-SR-Memo-9015)
Nb–Zr, carburization of, for prevention of galling, 19: 44609 (TIM-927)
Nb–Zr, casting methods improvement for preparation of macrohomogeneous ingots of, 18: 4250(R) (ORNL-3470(p.45-8))
Nb–Zr, cavitation damage in mercury and water, 18: 3955 (NP-13319)
Nb–Zr, cavitation damage in mercury and water, 19: 9623 (NP-14632)
Nb–Zr, cavitation damage in bismuth–lead alloy at 500°F, 19: 24938 (NP-15024)
Nb–Zr, cavitation in bismuth–lead alloy at 500 and 1500°F, ultrasonic-induced, 19: 39116 (NP-15263)
Nb–Zr, cavitation damage in bismuth–lead alloy at 500 and 1500°F, 20: 771 (NP-15558)
Nb–Zr, cavitation damage in mercury and water, 20: 16974 (NP-15889)
Nb–Zr, cavitation damage in liquid, at high temperatures, 20: 33835
Nb–Zr, characteristics of superconducting solenoid of, 17: 12539
Nb–Zr, chromatographic analysis for hydrogen, 17: 2909(T,R) (EURAEC-383)
Nb–Zr, coating development for oxidation protection, 18: 25896(R) (PF-63-3)
Nb–Zr, coating of, evaluation of properties before and after, 17: 1887(R) (AD-273746
Nb–Zr, coating of D-14, with chromium and titanium from fused salt

baths, 18: 18294(R) (NP-13758)
Nb–Zr, coating of D-14 for oxidation protection, 18: 34052 (RTD-TDR-63-4063)
Nb–Zr, coating testing for, 17: 36283 (AD-295530)
Nb–Zr, coating with enamel frits, 16: 13570 (CNLM-2989)
Nb–Zr, coating with aluminum–tin-base alloys for protection against oxidation, 17: 39465 (SCNC-328(Del.))
Nb–Zr, coating with chromium or titanium by deposition from fused-salt baths, 18: 29675
Nb–Zr, coating with silicides for oxidation protection, evaluation, 19: 7876(R) (ML-TDR-64-71)
Nb–Zr, coating with nickel, electroless, 20: 5867
Nb–Zr, coating with silicon by fluidized-bed process, 20: 29630
Nb–Zr, coatings for, development of oxidation-protection, 20: 7517 (PWAC-499)
Nb–Zr, compatibility with fissium–plutonium–uranium alloys at 550 to 650°C, 17: 35079(R) (ANL-6749)
Nb–Zr, compatibility with sodium at 650°C, 17: 41333(R) (ANL-6677)
Nb–Zr, compatibility with plutonium carbide–uranium carbide, 18: 8729 (UNC-5074)
Nb–Zr, compatibility with plutonium carbide–uranium carbide systems at 1500°F, 18: 16426(R) (UNC-5068)
Nb–Zr, compatibility with cesium at 1800 and 2500°F, 18: 22444(R) (MSAR-63-126)
Nb–Zr, compatibility with fissium–plutonium–uranium alloys at 550 to 650°C, 18: 26893(R) (ANL-6868(p.11-108))
Nb–Zr, compatibility with uranium carbide fuels in sodium, 18: 35957 (NAA-SR-7502)
Nb–Zr, compatibility with ceramic insulation materials at high temperatures, 19: 7851 (CNLM-5942)
Nb–Zr, compatibility with plutonium carbide–uranium carbide, 19: 24923(R) (UNC-5081)
Nb–Zr, compatibility with alkali metals at high temperatures, 20: 2236
Nb–Zr, compatibility with TZM alloy in flowing lithium, 20: 2238
Nb–Zr, compatibility with uranium dioxide, 20: 5181(R) (ORNL-3029)
Nb–Zr, compatibility with type 316 stainless steel in 650°C, 20: 7518 (PWAC-501)
Nb–Zr, compatibility with lithium, 20: 8447 (PWAC-491)
Nb–Zr, compatibility with plutonium–uranium carbides at 590 and 820°C, 20: 9437
Nb–Zr, compatibility with TZM molybdenum alloy in refluxing potassium at 2000°F, 20: 13192(R) (NASA-CR-54843)
Nb–Zr, contamination in high vacua at 578 to 1202°C, analysis of, 18: 4255(R) (ORNL-3470(p.98-125))
Nb–Zr, contamination by residual gases in vacuum systems, 18: 14355 (CONF-373-7)
Nb–Zr, contamination by residual gases in high vacuum, 18: 39826 (ORNL-3674)
Nb–Zr, content test and phase studies, 16: 10526(R) (EURAEC-86)
Nb–Zr, corrosion and hydridation of, by gases, steam, and water, 16: 22541 (AECL-1513)
Nb–Zr, corrosion and properties study, 16: 12653(R) (EURAEC-130)
Nb–Zr, corrosion of, by cesium at 1600 to 2500°F, 16: 16684 (TID-7626(Pt.I)(p.109-10))
Nb–Zr, corrosion of, by potassium at high temperatures, 16: 16680 (TID-7626(Pt.I)(p.69-86))
Nb–Zr, corrosion of, by liquid rubidium at 1800°F, 16: 14834 (AGN-8034)
Nb–Zr, corrosion of, by potassium at 1450 to 2000°F, 16: 16678 (TID-7626(Pt.I)(p.42-62))
Nb–Zr, corrosion of, by sodium at 1500 to 2400°F, 16: 16677 (TID-7626 (Pt.I)(p.23-34))
Nb–Zr, corrosion of, by sodium at 2200°F, 16: 20042(R) (BNL-696)
Nb–Zr, corrosion of, by steam and water, 16: 29346
Nb–Zr, corrosion of, by steam and water at 750 to 900 and 680°F, 16: 29337(R) (ARF-2198-26)
Nb–Zr, corrosion of, by steam at 400°C and 200 atm, rates of, 16: 20981(T,R) (EURAEC-27)
Nb–Zr, corrosion of, by steam or water at 360, 400, and 480°C, effects of heat treatment on rates of, 16: 20982(T,R) (EURAEC-85)
Nb–Zr, corrosion of, by steam to 550°C, 16: 32084(T,R) (EURAEC-227)
Nb–Zr, corrosion of, by water, 16: 32086
Nb–Zr, corrosion of, by water at 300 and 350°C, 16: 12735(R) (EURAEC-80)
Nb–Zr, corrosion of, by water at high temperatures and pressures, effects of anions on, 16: 22557
Nb–Zr, corrosion of, effects of heat treatment on, 16: 10526(R) (EURAEC-86)
Nb–Zr, corrosion of, effects of heat treatment on, 16: 3406 (GEAP-3729)
Nb–Zr, corrosion, fabrication, and phase studies, 16: 18613(R) (EURAEC-22)
Nb–Zr, corrosion resistance, 16: 10464
Nb–Zr, corrosion resistance of, effects of heat treatment on, 16: 20980(T,R) (EURAEC-26)
Nb–Zr, corrosion by air, carbon dioxide, and water, 17: 504
Nb–Zr, corrosion by cesium at high temperatures, design of capsules for testing, 17: 3426(R) (NP-12189)
Nb–Zr, corrosion by potassium, 17: 4905(R) (NP-12334)
Nb–Zr, corrosion by steam and water, 17: 6581
Nb–Zr, corrosion of, by steam at 500°C and 1 atm. pressure, 17: 8715(T,R) (EURAEC-451)
Nb–Zr, corrosion by liquid sodium, 17: 11935(R) (ANL-6658)
Nb–Zr, corrosion by steam and water at high temperatures, effects of iron additions on, 17: 12618
Nb–Zr, corrosion by steam at 280 to 500°C and 15 to 800 lb/in.², 17: 12619
Nb–Zr, corrosion of, in water at 680°F and steam at 750 and 900°F, 17: 16586 (GEAP-4098)
Nb–Zr, corrosion of, by rubidium at 1000 to 2000°F, 17: 16634 (AGN-8063)
Nb–Zr, corrosion by mercury at high temperatures, 17: 19726 (BNL-759(p.54-77))
Nb–Zr, corrosion by sodium at 1400 to 2400°F, 17: 19726 (BNL-759 (p.54-77))
Nb–Zr, corrosion by uranyl sulfate solution at 280°C, in-pile, 17: 27750 (ORNL-3099)
Nb–Zr, corrosion resistance and tensile properties of welds in, 17: 32496
Nb–Zr, corrosion hydrogen embrittlement of, 17: 32525
Nb–Zr, corrosion by high-pressure flowing steam at 300, 400, and 500°C, 17: 34346(R) (GEAP-4211)
Nb–Zr, corrosion by sodium at 650°C, 17: 36861(R) (ANL-6764)
Nb–Zr, corrosion by flowing sodium at 650°C, 17: 37001(R) (ANL-6780)
Nb–Zr, corrosion by superheated steam at 500°C, hydrogen sorption during, 17: 39470(T,R) (EURAEC-619)
Nb–Zr, corrosion by steam at 500°C, 17: 39468(T,R) (EURAEC-520)
Nb–Zr, corrosion by steam and water, 17: 39659
Nb–Zr, corrosion by superheated steam at 500°C, hydrogen uptake from, 17: 41368(T,R) (EURAEC-784)
Nb–Zr, corrosion by potassium (liquid), 17: 41339 (GE-62FPD365)
Nb–Zr, corrosion by magnesium-mercury alloys and mercury at 315 to 870°C, 18: 4160(R) (BNL-799(p.74-100))
Nb–Zr, corrosion by sodium at 760 to 1315°C, effects of barium, magnesium and oxygen additions on, 18: 4160(R) (BNL-799(p.74-100))
Nb–Zr, corrosion by potassium at 1500 to 1800°F, 18: 5728 (ASD-TDR-63-270(Pt.II))
Nb–Zr, corrosion by mercury at high temperatures, 18: 7152
Nb–Zr, corrosion by superheated steam at 500°C and water at 350°C, hydrogen uptake from, 18: 14386(T,R) (EURAEC-822)
Nb–Zr, corrosion by water at 300°C, 18: 14357(R) (EURAEC-79)
Nb–Zr, corrosion by water vapor at 400°C, 18: 14418
Nb–Zr, corrosion by liquid cesium, role of oxygen in, 18: 16447
Nb–Zr, corrosion by boiling cesium in loop, 18: 18279 (AGN-8041 (Del.))
Nb–Zr, corrosion by potassium vapor at 1500 to 1800°F, 18: 18282 (BNL-844)
Nb–Zr, corrosion by potassium at 2000 to 2200°F, 18: 24091
Nb–Zr, corrosion by sodium at 650°C, 18: 26893(R) (ANL-6868(p.11-108))
Nb–Zr, corrosion by lithium, effects of carbon, nitrogen, or oxygen on, 18: 27914
Nb–Zr, corrosion and hydridation by steam and water, 18: 30134(T,R) (EURAEC-955)
Nb–Zr, corrosion by steam and water, 18: 37612 (A/CONF.28/P/477)
Nb–Zr, corrosion by water, 18: 37633 (A/CONF.28/P/342)
Nb–Zr, corrosion and hydrogen absorption in steam, 18: 39847
Nb–Zr, corrosion by boiling mercury and sodium, 18: 41933 (TID-11295 (3rd Ed.))
Nb–Zr, corrosion by barium vapor, 18: 44499(R) (MND-2812-4)
Nb–Zr, corrosion and hydridation by steam and water, effects on tensile properties, 19: 4616(R) (EURAEC-1161)
Nb–Zr, corrosion by steam, effects of antimony, chromium, copper, germanium, iron, tellurium, and vanadium, 19: 4615(R) (EURAEC-1115)
Nb–Zr, corrosion cracking by boiling mercury, 19: 7863 (BNL-7642)
Nb–Zr, corrosion mass transfer in potassium to types 316 and 321 stainless steel, 19: 9622(R) (NASA-CR-54200)
Nb–Zr, corrosion by boiling cesium, 19: 13913(R) (AFML-TR-64-327)
Nb–Zr, corrosion by two-phase potassium in loop, 19: 13917 (SY-5463-R)
Nb–Zr, corrosion by Santowax OM coolant at 320 to 400°C, out-of-pile and in-pile, 19: 13911 (AECL-2118)
Nb–Zr, corrosion by boiling mercury, effects of magnesium on, 19: 15991(R) (BNL-841(p.63-101))
Nb–Zr, corrosion by boiling potassium in loop test, 19: 20476 (ORNL-3603)
Nb–Zr, corrosion by boiling sodium, 19: 22890 (BNL-9018)
Nb–Zr, corrosion by liquid potassium, 19: 23996(R) (ORNL-3650(p.1-110))

Nb–Zr, corrosion by sodium at 1260°C, 19: 28764
Nb–Zr, corrosion by ultrasonic-induced cavitation in liquid metals, 19: 28767
Nb–Zr, corrosion by steam at 400 and 450°C, effects of alloy additions on, 19: 30668(R) (EURAEC-1274)
Nb–Zr, corrosion by boiling potassium, 19: 34640 (CNLM-6246)
Nb–Zr, corrosion by potassium–sodium alloy at 1250°F in stainless steel loop, carbon and nitrogen mass transfer in, 19: 34640 (CNLM-6246)
Nb–Zr, corrosion by mercury at high temperatures, 19: 36949(R) (BNL-900(p.121-97))
Nb–Zr, corrosion by sodium at high temperatures, 19: 36949(R) (BNL-900(p.121-97))
Nb–Zr, corrosion by bismuth at 748°C, 19: 36949(R) (BNL-900(p.121-97))
Nb–Zr, corrosion by lithium, effects of zirconium content on, 19: 36980 (PWAC-355)
Nb–Zr, corrosion by lithium, effects of oxygen contamination on, 19: 36980 (PWAC-355)
Nb–Zr, corrosion by lithium, effects of heat treatment and oxygen on, 19: 44620 (CNLM-6344)
Nb–Zr, corrosion by potassium–sodium at 1250°F, effects of carbon, nitrogen, and oxygen on, 19: 44626 (TIM-896)
Nb–Zr, corrosion of, review of oxidation and hydriding kinetics and radiation effects in, 19: 16011 (AERE-R-4820)
Nb–Zr, corrosion of welds in, effects of heat treatments on lithium, 19: 36980 (PWAC-355)
Nb–Zr, corrosion resistance of, effects of production method and aging on, 19: 44629
Nb–Zr, corrosion stress cracking in mercury, 19: 28763
Nb–Zr, corrosion by potassium at 2000°F, 20: 768(R) (NASA-CR-54226)
Nb–Zr, corrosion by boiling and condensing alkali metals, 20: 2268
Nb–Zr, corrosion by potassium at high temperatures, 20: 2271
Nb–Zr, corrosion by potassium–sodium system, 20: 2273
Nb–Zr, corrosion by bismuth and tin, 20: 2275
Nb–Zr, corrosion by potassium–sodium alloys, 20: 5181(R) (ORNL-3029)
Nb–Zr, corrosion by lead at 1400°F, 20: 4308(R) (ORNL-3870, pp 243-60)
Nb–Zr, corrosion by potassium–sodium eutectic, 20: 4323(R) (ORNL-3870, pp 308-11)
Nb–Zr, corrosion by lithium at high temperatures, 20: 4299(R) (ORNL-2711)
Nb–Zr, corrosion by potassium, 20: 4301(R) (ORNL-3870, pp 102-35)
Nb–Zr, corrosion by lithium, effects of oxygen on, 20: 4301(R) (ORNL-3870, pp 102-35)
Nb–Zr, corrosion by cesium at 1600, 1800, and 2500°F, 20: 5846
Nb–Zr, corrosion by potassium at 1070°C, 20: 7518 (PWAC-501)
Nb–Zr, corrosion by sodium at 2000°F, 20: 9423(R) (NASA-CR-54735)
Nb–Zr, corrosion by hydrochloric, phosphoric, and sulfuric acids, effects of alloy composition on, 20: 14997
Nb–Zr, corrosion of welded joints of, by water and steam, 20: 19195
Nb–Zr, corrosion by liquid alkali metals, test loops for studying, 20: 21284
Nb–Zr, corrosion by lead at 1400°F, 20: 23603 (ORNL-TM-1437)
Nb–Zr, corrosion by mercury and sodium at high temperatures, 20: 25474(R) (BNL-954, pp 122-67)
Nb–Zr, corrosion by refluxing potassium at 1800 to 2400°F, 20: 25485 (NASA-TN-D-3429)
Nb–Zr, corrosion by mercury at 593 to 703°C, 20: 29646
Nb–Zr, corrosion by cerium–cobalt–plutonium alloy fuels, effects of carbon on, 20: 31679(R) (LA-3524)
Nb–Zr, corrosion by lead at 1400°F, 20: 31683(R) (ORNL-3936, pp 95-121)
Nb–Zr, corrosion resistance of, effect of heat treatment on, 20: 33849
Nb–Zr, corrosion by steam at 400°C and 120 atm, effects of heat treatment on, 20: 33824
Nb–Zr, corrosion by liquid potassium at high temperatures, 20: 41419(R) (GMAD-3643-5)
Nb–Zr, corrosion of zirconium-base, by steam at high temperatures, 20: 41422
Nb–Zr, corrosion by molten plutonium alloys, carbon effects on, 20: 43829(R) (LA-3582)
Nb–Zr, corrosion by lithium at 2000°F, 20: 43837 (TIM-823)
Nb–Zr, crack propagation tests on pressure tubes of, 20: 7501(R) (TID-22426)
Nb–Zr, crack propagation in hydrided zirconium-base, 20: 9490(R) (BNWL-166, pp 6.15-18)
Nb–Zr, creep and tensile properties, 17: 32568 (CONF-53-5)
Nb–Zr, creep and fatigue properties of $ZrNb_2$, 18: 14359(R) (EURAEC-136)
Nb–Zr, creep and rupture properties at 1600 to 2200°F, 19: 37029 (CNLM-4267)
Nb–Zr, creep at 600°C, 19: 31462(R) (ANL-7028)
Nb–Zr, creep properties of, at high temperatures, alloying effects of copper and molybdenum on, 16: 16772(P)
Nb–Zr, creep properties at 2200°F, 18: 37621(R) (IITRI-B6021-3)
Nb–Zr, creep properties, effects of vacuum gases on slow-bend, 18: 44049(R) (ORNL-3670(p.77-111))
Nb–Zr, creep properties, effects of cold working and annealing on, 20: 4301(R) (ORNL-3870, pp 102-35)
Nb–Zr, creep rupture and fatigue evaluation of, 18: 29103(R) (APS-5071-R)
Nb–Zr, creep rupture properties of, effects of annealing on, 19: 7929
Nb–Zr, creep strength of, effects of vacuum on cantilever beam bend tests of, 18: 14456 (CONF-373-10)
Nb–Zr, creep testing of, summary of slow-bend, 18: 4255(R) (ORNL-3470(p.98-125))
Nb–Zr, critical alternating currents in superconducting films of, 18: 9269
Nb–Zr, critical currents in, effects of carbon, oxygen, and size on, 16: 30798 (ORNL-3303)
Nb–Zr, critical currents in external magnetic field and superconducting properties, 17: 545(T) (AEC-tr-5473)
Nb–Zr, critical current in magnets of, 17: 27944 (NP-12908)
Nb–Zr, critical current and magnetization properties of, 17: 34549(R) (ORNL-3480(p.41-5))
Nb–Zr, critical current degradation and flux jumping in solenoids of heat-treated, 17: 36469
Nb–Zr, critical current-field characteristics of short wire samples in superconducting solenoids, 17: 37729
Nb–Zr, critical current-field relation in, 17: 41542 (BSD-TDR-63-148)
Nb–Zr, critical currents in superconducting, effects of heat treatment on, 18: 6127
Nb–Zr, critical current density of superconducting, in transverse field of 30 kgauss, 18: 6128
Nb–Zr, critical current in rolled strip of superconducting, field-dependent anisotropy of, 18: 6130
Nb–Zr, critical current density of superconducting, in a pulsed magnetic field, 18: 18833
Nb–Zr, critical currents in wires and strips of superconducting, anisotropy and proximity effect in, 18: 36525
Nb–Zr, critical currents in ribbons of superconducting, effects of magnetic field direction and annealing on, 18: 36526
Nb–Zr, critical current training in superconducting, (E), 19: 10215
Nb–Zr, critical currents in superconducting, 19: 16797
Nb–Zr, critical current degradation in wide-strip superconductors of, (E), 19: 41639
Nb–Zr, critical currents of superconducting, effect of magnetic-field rise time on, (E), 19: 43238
Nb–Zr, critical currents in, effect of omega transformation on, (E), 19: 47511
Nb–Zr, critical current of disperse superconducting phases in, 20: 9900
Nb–Zr, critical current density in superconducting, magnetic field dependence of, (E), 20: 26031
Nb–Zr, critical current in, effects of annealing and orientation on, (E), 20: 42569
Nb–Zr, critical-current induced transitions in superconducting, 20: 24273
Nb–Zr, crystal structure of, effects of hydrogen on, 16: 33487(T,R) (EURAEC-243)
Nb–Zr, crystal structure of, preparation of oxide replicas for studies of, 20: 27561
Nb–Zr, crystal structure and electric conductivity of, 20: 29766
Nb–Zr, crystallization and recovery of cold-worked, 19: 44698 (PWAC-465)
Nb–Zr, current-carrying capacity in superconducting solenoids, 17: 6209
Nb–Zr, current density reduction in magnets of, 17: 25873
Nb–Zr, current decay propagation in superconducting, persistent, (E), 19: 47507
Nb–Zr, current degradation in superconducting solenoids of, 19: 37735(R) (N64-33921)
Nb–Zr, current density and magnetic field in cold-worked superconductors of, 19: 41637
Nb–Zr, current degradation in superconducting solenoids of, (E), 20: 21920
Nb–Zr, current degradation in superconductors of, low-frequency alternating, (E), 20: 34449
Nb–Zr, current losses in type II superconducting, 20: 28187
Nb–Zr, current losses and magnetic field aberrations from high-field superconducting wires of, in adiabatic demagnetization apparatus, 20: 37970
Nb–Zr, current-carrying capacity of superconducting, temperature and field dependence of, 18: 34681 (BSD-TDR-64-87)
Nb–Zr, degradation of large superconducting magnets of, (E), 19: 25444
Nb–Zr, degradation phenomena in small superconducting coils of, (E), 20: 17629
Nb–Zr, development, properties, and uses of superconducting,

18: 13010
Nb–Zr, development as reactor material, 19: 914
Nb–Zr, development as fuel jacket material for fast reactors, 20: 38465 (ANL-7120, pp 289-300)
Nb–Zr, diffusion of interstitials in, 16: 33500
Nb–Zr, diffusion of components in, tracer studies of, 17: 30988(T) (FTD-TT-63-258)
Nb–Zr, diffusion in type 316 stainless steel, 17: 36200(R) (NP-13033)
Nb–Zr, diffusion and solubility of hydrogen in, 19: 13349
Nb–Zr, diffusion in bcc, 19: 23112
Nb–Zr, dimensional changes during annealing in, temperature gradient effects on, 18: 26028
Nb–Zr, ductility of zirconium-base, effects of high temperatures on, 20: 41422
Nb–Zr, effects of heat treatment and radiation on mechanical properties, 17: 3550
Nb–Zr, effects of hydrogen on delayed failure of, 17: 14810(R) (ARF-B6005-2)
Nb–Zr, effects of aging temperature on hardness, 17: 22160(R) (DRI-2094)
Nb–Zr, effects on environment, heat treatment, and temperature on corrosion of, 17: 32524
Nb–Zr, effects of cold working and heat treatment on properties of, 17: 41636
Nb–Zr, effects of hydrogenation on delayed failure susceptibility of, 18: 18406
Nb–Zr, effects of surface treatments on emittance of, 19: 22984(R) (NASA-CR-54167)
Nb–Zr, effects of lithium and oxygen on tensile properties of, 20: 5181(R) (ORNL-3029)
Nb–Zr, effects of physical parameters and radiation on fuel element cladding of, (E), 20: 7519 (RCN-41)
Nb–Zr, electric and mechanical properties, 18: 24158
Nb–Zr, electric conductivity in fixed and swept magnetic fields, 17: 41546 (CONF-176-7)
Nb–Zr, electric conductivity of nonideal superconducting, a-c, 18: 18836
Nb–Zr, thermal conductivity, 18: 22475 (BATT-4673-T7)
Nb–Zr, electric conductivity, 18: 22475 (BATT-4673-T7)
Nb–Zr, electric current degradation in superconducting solenoids of, (E), 19: 6608
Nb–Zr, electric conductivity at 4 to 273°K, 19: 13992 (ML-TDR-64-234)
Nb–Zr, electric conductivity at 200 to 1446°C, 19: 47015 (TIM-854)
Nb–Zr, electric conductivity to 1500°C, 20: 5851
Nb–Zr, electric properties of contacts to normal metals, 17: 36453 (TID-19310)
Nb–Zr, electric properties of superconducting, 17: 35260(R) (TID-19135)
Nb–Zr, electric properties near breakdown in superconducting, 18: 9264
Nb–Zr, electric power losses at 50 cps in superconducting, 18: 44677
Nb–Zr, electric properties of normal region in superconducting magnet of, 20: 17610
Nb–Zr, electrochemical potential and hydrogen overvoltage, 17: 34403 (GEAP-4192)
Nb–Zr, electron field emission patterns of, 18: 29662
Nb–Zr, electronic properties, 18: 44150(R) (ORNL-3670(p.44-53))
Nb–Zr, embrittlement effects of hydrogen on, 18: 34169
Nb–Zr, embrittlement by contamination during vacuum treatments, 19: 42809
Nb–Zr, emissivity, 17: 6675(R) (PWA-2128)
Nb–Zr, emissivity measurements at 800 to 5000°K, 18: 20566
Nb–Zr, emissivity of coated, in vacuum, 18: 24138(R) (PWA-2206 (Vol.I))
Nb–Zr, emissivity of coated, in vacuum, 18: 24139(R) (PWA-2206 (Vol.II))
Nb–Zr, emissivity of coated, in vacuum, 18: 24140(R) (PWA-2206 (Vol.III))
Nb–Zr, emissivity, effects of surface treatments on, 20: 4301(R) (ORNL-3870, pp 102-35)
Nb–Zr, emissivity to 1500°C, total hemispherical, 20: 5851
Nb–Zr, emissivity of titanate coatings on, 20: 15057(R) (PWA-2750)
Nb–Zr, emissivity of titanate-coated, at high temperatures, 20: 43816(R) (PWA-2877)
Nb–Zr, emittance at 100 to 1200°C, measurement of total hemispherical, 18: 5809
Nb–Zr, emittance properties of iron titanate coatings on, 19: 18465(R) (PWA-2518)
Nb–Zr, energy gap of high-field superconducting, 18: 26481
Nb–Zr, erosion by water of rotating disks of, 19: 44625 (TIM-894)
Nb–Zr, erosion by mercury, water, and bismuth–lead alloy, cavitation, 20: 29640 (NP-16048)
Nb–Zr, evaporation tests in high vacuum, 18: 44049(R) (ORNL-3670 (p.77-111))
Nb–Zr, evaporation losses of FS-85, at 1200 to 1500°C in high vacuum, 19: 37043 (ORNL-P-1394)
Nb–Zr, evaporation losses in high vacuum, 20: 4301(R) (ORNL-3870, pp 102-35)
Nb–Zr, extrusion at high energy rates, 18: 8769 (LADC-5763)
Nb–Zr, extrusion, 19: 20500 (AFML-TR-64-387)
Nb–Zr, extrusion as clad in uranium carbide fuel elements, 19: 24952 (NMI-2523)
Nb–Zr, extrusion by hydrostatic methods, 19: 18436
Nb–Zr, fabrication, melting, welding, and workability of, 16: 16716 (CNLM-2166)
Nb–Zr, fabrication of arc-melted, for production of 43-kgauss superconducting solenoid, 16: 6564
Nb–Zr, fabrication of beta-quenched, 16: 24137
Nb–Zr, fabrication of tubing of, by spinning, 16: 12068 (CNLM-3342)
Nb–Zr, fabrication of, for mercury corrosion loop, 17: 11131 (AGC-0584-04-5)
Nb–Zr, fabrication and properties of cold-rolled, 17: 41333(R) (ANL-6677)
Nb–Zr, fabrication and properties, 18: 2158(R) (EURAEC-176)
Nb–Zr, fabrication of tube shells of, by floturning, 18: 4255(R) (ORNL-3470(p.98-125))
Nb–Zr, fabrication and superconductivity properties of, 18: 4285
Nb–Zr, fabrication and properties, 18: 14357(R) (EURAEC-79)
Nb–Zr, fabrication of tabular, as reactor fuel cladding, 18: 19456(R) (ANL-6840)
Nb–Zr, fabrication effects on superconducting current capacities of, 18: 21098
Nb–Zr, fabrication and properties, 18: 26893(R) (ANL-6868(p.11-108))
Nb–Zr, fabrication into tube shells by flow turning, 18: 44049(R) (ORNL-3670(p.77-111))
Nb–Zr, fabrication, properties, testing, and uses of superconducting of, 19: 16110
Nb–Zr, fabrication into tubing, development of methods for, 19: 24954 (TID-21790)
Nb–Zr, fabrication into superconducting delay lines, (E), 20: 3612 (CONF-651001-6)
Nb–Zr, fabrication of superconductors of, 20: 39372(P)
Nb–Zr, fabrication of Zircaloy-4-clad pressure tubing of, 20: 43862 (TID-23312)
Nb–Zr, fabrication of loops of, for liquid potassium and sodium, 20: 43879
Nb–Zr, fast neutron effects on critical current in, 18: 9265
Nb–Zr, fatigue behavior in potassium at 800°F, 17: 12036(R) (SY-5396-R3)
Nb–Zr, fatigue due to hydrogen embrittlement, 17: 526(R) (ARF-2230-12)
Nb–Zr, fatigue in lithium at 1600°F from cantilever bending, 17: 35223(R) (SY-5396-R5)
Nb–Zr, fatigue in lithium at 1600°F and potassium at 800°F from cantilever bending, 18: 6516 (SY-5396-R6)
Nb–Zr, fatigue in lithium at 1600°F and potassium at 800°F, cantilever-bending, 18: 12624(R) (ASD-TDR-63-270(Pt.IV))
Nb–Zr, fatigue of, effects of applied stress and hydrogen sorption on static, 16: 25746(R) (ARF-2230-9)
Nb–Zr, fatigue of hydrided, effects of heat treatment on, 17: 34404(R) (IITRI-B6005-8)
Nb–Zr, fatigue properties of $ZrNb_3$, 18: 14360(R) (EURAEC-199)
Nb–Zr, feasibility of labeled, for spacecraft shield ablation measurements, 20: 36353
Nb–Zr, filament structure of superconducting, 18: 18846
Nb–Zr, flux annihilation in superconducting, (E/T), 19: 43239
Nb–Zr, flux creep and jump in superconducting, effect of Joule heating on, 20: 21884
Nb–Zr, flux jumping and training in superconducting solenoids of, 18: 26470
Nb–Zr, forging characteristics, 16: 9162 (DMIC-Memo-143)
Nb–Zr, formation of niobium carbide surface films on, activation energies for, 20: 14992
Nb–Zr, fracture of, effects of hydrogen content and temperature on, 19: 26839
Nb–Zr, fracture properties of zirconium-base, effects of hydrogen and temperature on, 20: 31669
Nb–Zr, grain growth of, effects of cold working and annealing on, 19: 20473(R) (NASA-CR-54629)
Nb–Zr, grain growth in liquid-metal coolant loop tubing of, 19: 22984(R) (NASA-CR-54167)
Nb–Zr, Hall coefficient in normal and superconducting, 17: 12668 (NRL-5874)
Nb–Zr, Hall effect measurements on superconducting magnets of, 20: 17600(R) (ORNL-3908, pp 114-48)
Nb–Zr, hardness, 20: 15073
Nb–Zr, hardness of, effects of cooling rate on, 18: 44133 (CRRM-1200)
Nb–Zr, hardness of, effects of cooling rate and niobium content on, 19: 40961

Nb–Zr, heat treatment for improved corrosion resistance, 19: 34635(P)
Nb–Zr, heat treatment effects on texture of, 20: 37198
Nb–Zr, heat-treatment effects on critical current and temperature of superconducting, 18: 44690
Nb–Zr, hemispherical emittance values at 100 to 1200°C, total, 18: 4255(R) (ORNL-3470(p.98-125))
Nb–Zr, hydridation of, metallographical studies of, 17: 39470(T,R) (EURAEC-619)
Nb–Zr, hydridation effects on properties of, 19: 40959
Nb–Zr, hydridation of, kinetics, 20: 2222 (EURAEC-1390)
Nb–Zr, hydride nucleation and growth in, 20: 2253 (AECL-2297)
Nb–Zr, hydrogen distribution in oxidized, tritium autoradiographic studies of, 19: 13910 (AECL-2085)
Nb–Zr, hydrogen embrittlement of, 17: 8715(T,R) (EURAEC-451)
Nb–Zr, hydrogen embrittlement, 18: 5776(R) (IITRI-B6005-11)
Nb–Zr, hydrogen embrittlement of, review of, 20: 37187
Nb–Zr, hydrogen overvoltage measurements in, 17: 27728(R) (GEAP-4076)
Nb–Zr, hydrogen overvoltages at, in sulfuric acid, 18: 12642 (GEAP-4089(Vol.II)(Paper 22))
Nb–Zr, hydrogen uptake by, 20: 7520
Nb–Zr, hydrogenation, 18: 551(T,R) (EURAEC-224)
Nb–Zr, in-pile stress rupture tests, 17: 14740 (TID-11295(2nd Ed.))
Nb–Zr, inductance of superconducting solenoids of, 20: 26032
Nb–Zr, internal friction measurements, 18: 4255(R) (ORNL-3470(p.98-125))
Nb–Zr, internal friction peak in, dislocation-relaxation, 20: 15122
Nb–Zr, internal friction and relaxation processes in, 20: 17106
Nb–Zr, joining to alumina bodies in ceramic-to-metal seals for high temperatures, 17: 34366 (LAMS-2917)
Nb–Zr, longitudinal critical currents in cold-drawn superconducting, 17: 14961
Nb–Zr, magnetic behavior of superconducting wires of, 18: 13019
Nb–Zr, magnetic diffusivity in cylinder of type-II superconducting, (E), 20: 24279
Nb–Zr, magnetic field stabilization inside superconducting tubes of, 18: 11111
Nb–Zr, magnetic field effects on superconductivity of, 18: 15077
Nb–Zr, magnetic flux jumps in superconducting, 18: 34724
Nb–Zr, magnetic field effects on temperature in superconducting, (E), 19: 5105
Nb–Zr, magnetic field penetration in superconducting, radial velocity of, (E), 19: 39702
Nb–Zr, magnetic flux behavior in wires of superconducting, (E), 19: 16795
Nb–Zr, magnetic flux degradation in superconducting coils of, (E), 19: 47512
Nb–Zr, magnetic flux jumping under adiabatic conditions in superconducting wires of, (E), 19: 33164
Nb–Zr, magnetic fluxoid annihilation instability in superconducting, (E/T), 19: 12441
Nb–Zr, magnetic field effects on ultrasonic wave propagation in, 20: 863
Nb–Zr, magnetic flux annihilation and instabilities in inhomogeneous superconducting, (E), 20: 1132
Nb–Zr, magnetic flux jumps in superconducting NbZr in pulsed magnetic fields, (E), 20: 2921
Nb–Zr, magnetic fields on surface of superconducting, in external magnetic field, (E), 20: 2924
Nb–Zr, magnetic field penetration of thick slabs of superconducting type-II, velocity of, (T), 20: 8011
Nb–Zr, magnetic flux jumps in superconducting, sample geometry effects on, (E), 20: 9916
Nb–Zr, magnetic flux motion in thin-walled tubes of hard superconducting, spatial variations of, (T), 20: 9917
Nb–Zr, magnetic fluxoid annihilation instability in superconducting, (E/T), 20: 21927
Nb–Zr, magnetic field strength at surface of superconducting, EPR measurements for, (E), 20: 21898
Nb–Zr, magnetic flux penetration in superconducting, (E), 20: 42132
Nb–Zr, magnetic hysteresis losses from surface of superconducting, 18: 956
Nb–Zr, magnetic hysteresis losses of high-field superconducting, (T), 20: 26044
Nb–Zr, magnetic induction measurements for superconducting, 17: 37717
Nb–Zr, magnetic moment, 18: 13008(R) (ORNL-3564(p.100-25))
Nb–Zr, magnetic properties of superconducting, 16: 15426
Nb–Zr, magnetic properties of superconducting, effects of cold-working and heat treatment on, 16: 15465
Nb–Zr, magnetic properties of superconducting, effects of cold-working and heat treatment on, 16: 15466
Nb–Zr, magnetic properties of superconducting, effects of temperature on critical field of, 16: 15467
Nb–Zr, magnetic susceptibility, 20: 17106
Nb–Zr, magnetization and transport current in wire of, 17: 39749
Nb–Zr, magnetization of superconducting, relation to magnetic field of a solenoid constructed of the alloy, 18: 9277
Nb–Zr, magnetization of superconducting, 18: 9279
Nb–Zr, magnetization of superconducting wires of, 18: 42563
Nb–Zr, magnetization of superconducting, (E/T), 19: 27372
Nb–Zr, magnetization discontinuities in superconducting, (E), 19: 37740
Nb–Zr, magnetization of superconducting, effect of external current on, (E/T), 20: 19735
Nb–Zr, magnetization of high-field superconducting, a-c losses and hysteresis in, (E), 20: 26043
Nb–Zr, magnetization of superconducting, (E), 20: 42133
Nb–Zr, magnetothermal effects in superconductors of, (E), 19: 14433 (CONF-651-44)
Nb–Zr, magnets of superconducting wires of, 18: 6108
Nb–Zr, mass transport by sodium, 18: 15563
Nb–Zr, mass transfer by sodium, 18: 15568
Nb–Zr, mass transfer from type 316 and 321 stainless steel to, in liquid potassium, research program on, 19: 20474(R) (NASA-CR-54281)
Nb–Zr, mass transfer from Type 316 and 321 stainless steels to, in liquid potassium at 1400°F, 19: 40970(R) (NASA-CR-54390)
Nb–Zr, mass transfer of carbon and nitrogen to, from type-316 stainless steel in liquid potassium, 20: 2239
Nb–Zr, maximum critical field of superconductors of, 17: 8959
Nb–Zr, mechanical properties of, to 550°C, 16: 32084(T,R) (EURAEC-227)
Nb–Zr, mechanical properties, 17: 504
Nb–Zr, mechanical properties of, hydrogen effects on, 17: 6696(T) (EURAEC-353)
Nb–Zr, mechanical properties at −300 to 1200°F, 17: 11075(R) (AD-278043)
Nb–Zr, mechanical properties, 17: 11108(T,R) (EURAEC-307)
Nb–Zr, mechanical properties of hydrided, effects of fabrication, specimen geometry, and temperature on, 17: 22155(R) (ARF-B6005-5)
Nb–Zr, mechanical properties of, effects of high-temperature lithium and potassium on, 17: 30939(R) (SY-5396-R4)
Nb–Zr, mechanical properties of LB-2-coated, effects of coating oxidation test on, 17: 36284 (AD-295547)
Nb–Zr, mechanical and superconductivity properties of, 17: 37542(T)
Nb–Zr, mechanical properties of, effects of hydrogen content on, 17: 39470(T,R) (EURAEC-619)
Nb–Zr, mechanical properties of, effects of hydrogen content on, 17: 39468(T,R) (EURAEC-520)
Nb–Zr, mechanical properties of, effects of hydrogen content on, 17: 41368(T,R) (EURAEC-784)
Nb–Zr, mechanical properties, 18: 7292(R) (HW-77954(p.4.1-12))
Nb–Zr, mechanical properties of, effects of heat treatment on, 18: 12637 (GEAP-4089(Vol.I)(Paper 11))
Nb–Zr, mechanical properties of welded, 18: 37680 (A/CONF.28/P/757)
Nb–Zr, mechanical properties at 1100 and 1300°C, 19: 11734
Nb–Zr, mechanical properties and TTT curves, 19: 18517
Nb–Zr, mechanical properties at high temperatures, 19: 44674(R) (ANL-7000, pp 69-83)
Nb–Zr, mechanical properties of, effects of carbon and oxygen on, 19: 44605 (PWAC-464)
Nb–Zr, mechanical properties of effects of aging, oxygen content, and production method on, 19: 44629
Nb–Zr, mechanical properties of, effects of oxygen on, 20: 4297(R) (IS-1200(Sect.M))
Nb–Zr, mechanical properties of, effects of composition on, 20: 11288(T) (AD-622477)
Nb–Zr, mechanical properties of, effects of beta grain size on, 20: 21368
Nb–Zr, mechanical properties of cold-worked zirconium-base, 20: 31669
Nb–Zr, mechanical properties of, effects of oxygen on, 20: 35887 (IS-T-92)
Nb–Zr, mechanical properties of, effects of composition and heat treatments on, 20: 37236
Nb–Zr, mechanical properties of, effects of oxygen on, 20: 41412(R) (IS-1500(Sect. M))
Nb–Zr, metallographic inspection of test samples of, 16: 32126(T,R) (EURAEC-328)
Nb–Zr, metallography, 16: 20042(R) (BNL-696)
Nb–Zr, metallographic techniques for studying corrosion of, 19: 7863 (BNL-7642)
Nb–Zr, metallographic techniques for preparation of, for microscopy, 20: 16959
Nb–Zr, metallurgical aspects of superconducting, 18: 6129
Nb–Zr, metallurgical bonding to Hastelloy X and stainless steel by extrusion, 18: 27937
Nb–Zr, metallurgical properties and phase studies on, 20: 5891(R) (NYO-

2159-1)
Nb–Zr, microstructure and superconductivity of, effects of cold rolling and heat treatment on, 17: 29369
Nb–Zr, microstructure and training of high-field superconductors of, 18: 4286
Nb–Zr, microstructures, 19: 44610 (TIM-943)
Nb–Zr, microstructure of, effects of annealing temperature on, 19: 44587(R) (ANL-7000, pp 3-63)
Nb–Zr, microstructure, effects of tempering on, 20: 13304
Nb–Zr, microstructure of cast, with low oxygen contents, 20: 19245
Nb–Zr, nickel coatings on, thermal cycling effects, 19: 29468(R) (ANL-7017)
Nb–Zr, nitrogen and oxygen content of, effects of yttrium additions on, 19: 40953 (PWAC-441)
Nb–Zr, nondestructive testing of superconducting wires of, methods development for, 18: 4250(R) (ORNL-3470(p.45-8))
Nb–Zr, nuclear spin-lattice relaxation in type II superconductors of, (E), 19: 41611
Nb–Zr, omega transformation in, 17: 12706
Nb–Zr, omega transformation and segregation processes in, 20: 17105
Nb–Zr, oxidation of, at 1000°C, 16: 9248(P)
Nb–Zr, oxidation of, at 400 and 600°C, kinetics of, 16: 4503(R) (TID-14242
Nb–Zr, oxidation of, at 525 to 1090°C, 16: 2254
Nb–Zr, oxidation of, by air above 700°C, 16: 3408 (NP-11119)
Nb–Zr, oxidation of, causes of second transition point in, 16: 7857
Nb–Zr, oxidation of, during forging, development of coatings to prevent, 16: 13570 (CNLM-2989)
Nb–Zr, oxidation of, in air and steam, effects of additives on, 16: 32078 (AERE-R-4134)
Nb–Zr, oxidation characteristics at 400 to 2200°F, 17: 18705
Nb–Zr, oxidation of, protective effects of aluminum-tin, beryllide, and silicon-titanium coatings against, 17: 22109(R) (ASD-TDR-63-160)
Nb–Zr, oxidation of, effects of zirconium on resistance to, 17: 29291
Nb–Zr, oxidation by water at 360°C, 17: 35078(R) (ANL-6739)
Nb–Zr, oxidation by water containing lithium hydroxide, 18: 2192
Nb–Zr, oxidation in air and steam, 18: 7135 (AERE-R-4459)
Nb–Zr, oxidation in air, composition of scale formed during, 18: 10477(T) (JPRS-22697(p.27-38))
Nb–Zr, oxidation at 500 and 1000°, alloying effects of metals on, 18: 14413(T) (FTD-TT-63-1020)
Nb–Zr, oxidation by carbon dioxide up to 600°C, 18: 30192
Nb–Zr, oxidation at 400 to 600°C and 1 to 760 torr, kinetics and mechanism of, 19: 18409 (COO-1000-1)
Nb–Zr, oxidation at low pressures at 1000 to 1600°F, 19: 24931 (CNLM-5351)
Nb–Zr, oxidation by high-pressure, high-velocity helium at 2050°F, 19: 34639(R) (BNWL-79(p.5.1-11))
Nb–Zr, oxidation protection by aluminum–tin coatings with chromium and titanium additions, 20: 7580 (TIM-945)
Nb–Zr, oxidation by oxygen at 400 to 600°C, kinetics and mechanisms of, 20: 11227
Nb–Zr, oxidation rate of, at 1100°C, 20: 23614
Nb–Zr, oxidation of, kinetics, mechanism, and microstructure of internal, 20: 23619
Nb–Zr, oxidation of, mechanism of breakaway, 20: 25496
Nb–Zr, oxidation kinetics and oxide film breakaway at 600 to 850°C, 20: 25497
Nb–Zr, oxidation of, distribution of niobium in oxide film in, 20: 25504
Nb–Zr, oxidation by oxygen at 1000°C, kinetics and microstructures of, 20: 37193
Nb–Zr, oxygen addition mechanism and solubility in, 19: 2820
Nb–Zr, oxygen content of, 19: 22984(R) (NASA-CR-54167)
Nb–Zr, oxygen content in, 20: 8447 (PWAC-491)
Nb–Zr, paramagnetic susceptibility, 16: 10576
Nb–Zr, paramagnetic helical current flow in superconducting, (E), 19: 23576
Nb–Zr, paramagnetism in cold-worked superconducting wires of, 19: 39749
Nb–Zr, parameters for zirconium self-diffusion in, 20: 2356(T) (AERE-Trans-1030)
Nb-Zr, performance in superconducting solenoids, 17: 4781
Nb–Zr, performance of superconducting magnets of, 18: 11100 (LNF-63/67)
Nb–Zr, performance in superconducting coils for inductive energy storage, 18: 15047
Nb–Zr, performance as cladding for uranium carbide fuels, 18: 23817(R) (ANL-6880(p.72-8))
Nb–Zr, performance as fuel cladding in fast reactors, 18: 24952(R) (ANL-6880(p.6-48))
Nb–Zr, performance as cladding for uranium carbide fuels, 18: 24860(R) (UNC-5071)
Nb–Zr, performance as superconducting magnet, 18: 42554
Nb–Zr, performance as space radiator for thermionic reactor, 19: 3728 (PWA-2319)
Nb–Zr, performance as superconducting solenoids, (E), 19: 10189 (RLE-TR-427)
Nb–Zr, performance of superconducting coils of, in magnetic mirror systems, (E), 19: 10449
Nb–Zr, performance in high-field superconducting magnets, (E), 19: 19018 (ORNL-TM-1083)
Nb–Zr, performance of superconducting, for linac resonant cavities, 19: 27012 (MURA-714(p.540-4))
Nb–Zr, performance of superconducting magnets of, 19: 31335(R) (UCRL-12303)
Nb–Zr, performance as reactor pressure tubes, evaluation, (E), 19: 31551(R) (SRO-115)
Nb–Zr, performance in superconducting magnets, 20: 1120(R) (ORNL-3836, pp 90-110)
Nb–Zr, performance of superconducting solenoids of, 20: 4775 (UCRL-16376)
Nb–Zr, performance as cladding for alloy and carbide fuels, (E), 20: 14007(R) (ANL-7122, pp 1-41)
Nb–Zr, phase diagrams of, effects of oxygen on, 16: 16719 (EURAEC-137)
Nb–Zr, phase diagrams, 17: 556
Nb–Zr, phase diagrams, 18: 12633 (GEAP-4089(Vol.I)(Paper 4))
Nb–Zr, phase diagram, 18: 12635 (GEAP-4089(Vol.I)(Paper 9))
Nb–Zr, phase strengthening in, 17: 6555
Nb–Zr, phase studies, 16: 20981(T,R) (EURAEC-27)
Nb–Zr, phase studies, 16: 20982(T,R) (EURAEC-85)
Nb–Zr, phase studies, 16: 21061
Nb–Zr, phase studies, 16: 22616
Nb–Zr, phase studies, 16: 30783 (EURAEC-283)
Nb–Zr, phase studies and properties, 16: 12735(R) (EURAEC-80)
Nb–Zr, phase studies, 17: 537(R) (TID-17006)
Nb–Zr, phase studies, 18: 14396
Nb–Zr, phase studies of, 18: 18383
Nb–Zr, phase studies, 18: 26003
Nb–Zr, phase studies, 19: 11682
Nb–Zr, phase studies, 20: 35924
Nb–Zr, phase studies of, 20: 41443(R) (COO-588-12)
Nb–Zr, phase transformation kinetics, 16: 15166 (ARF-2198-21)
Nb–Zr, phase transformations in, time-temperature curves for, 18: 12636 (GEAP-4089(Vol.I)(Paper 10))
Nb–Zr, phase transformations in, dilatometric observations of, 19: 14019
Nb–Zr, phase transformations in, omega, 19: 16163
Nb–Zr, phase transformation kinetics, 20: 4390(R) (ORNL-3870, pp 65-9)
Nb–Zr, phase transformations in, effects of niobium content on metastable, 20: 7619
Nb–Zr, phase transformation in, start temperature for martensitic, 20: 19230
Nb–Zr, phase transformation in, kinetics of beta-, 20: 23746
Nb–Zr, phase transformations of, factors affecting, 20: 37234
Nb–Zr, physical properties of, 17: 4225(R) (ANL-6635(p.28-50))
Nb–Zr, pickling conditions for, 18: 12587
Nb–Zr, plastic deformation and tensile properties of, effects of temperature on, 16: 3464 (PWAC-359)
Nb–Zr, plastic flow of, determination by hardness, 20: 37230
Nb–Zr, power losses in superconducting solenoids of, 19: 16448(R) (TID-21380(p.85-111))
Nb–Zr, power losses in superconducting, a-c, (E), 19: 35324
Nb–Zr, preparation of powders of, by igneous electrolysis, 17: 16529(T,R) (EURAEC-509)
Nb–Zr, preparation and properties of heat-treated, 17: 32626
Nb–Zr, preparation and properties of thin-film hard superconducting, 18: 28501
Nb–Zr, preparation of powders of, 20: 2222 (EURAEC-1390)
Nb–Zr, pressure testing of tubular, 19: 47998(R) (SRO-118)
Nb–Zr, procurement and quality evaluation of stock of, for corrosion studies, 19: 40952 (ORNL-TM-1179)
Nb–Zr, production by fused salt electrolysis in sodium chloride–sodium fluoniobate–zirconium tetrafluoride, 18: 16431
Nb–Zr, propagation of normal region in superconducting solenoid of, 20: 42100
Nb–Zr, properties of welded, 17: 11242
Nb–Zr, properties as claddings for uranium carbide fuels, 17: 16650 (NAA-SR-7696)
Nb–Zr, properties of superconducting, at 9.250 Mcps, 17: 16722
Nb–Zr, properties of, effects of annealing temperature and time on critical, 17: 20504
Nb–Zr, properties during superconducting transition, 17: 27942 (NIRL/R/32)
Nb–Zr, properties as superconducting magnet, 17: 32712 (LNF-63/26)
Nb–Zr, properties as cladding for fissium–plutonium–uranium fuel

elements, 17: 41333(R) (ANL-6677)
Nb–Zr, properties of superconducting, 17: 41604
Nb–Zr, properties as cladding for reactor fuel elements, 18: 6412(R) (GEAP-3888)
Nb–Zr, properties for use for containment of boiling mercury or sodium, 18: 12627(R) (BNL-823(p.66-93))
Nb–Zr, properties of, 18: 12565
Nb–Zr, properties for superconducting solenoids, 18: 26474
Nb–Zr, properties for use as superconductive wires, 18: 34200
Nb–Zr, properties for use in water-cooled reactors, 18: 37668 (A/CONF.28/P/158)
Nb–Zr, properties for use as fuel cladding for water-cooled power reactors, 18: 37692
Nb–Zr, properties for use as fuel cladding material, 19: 11679
Nb–Zr, properties as pressure tubes in power reactors, 19: 17328
Nb–Zr, properties for liquid metal loops, 19: 40112(R) (ANL-7046 (p.36-66))
Nb–Zr, properties of cold-worked fuel sheathing tubes of, 19: 39150 (AECL-2250(Pt.I))
Nb–Zr, properties for use in water-cooled reactors, 19: 42813
Nb–Zr, properties at low temperatures, 20: 3920(R) (ORNL-3870, pp 27-37)
Nb–Zr, properties of bimetal tubes of type 316 stainless steel and, 20: 11214(R) (NASA-CR-54717)
Nb–Zr, properties for containment of potassium at high temperatures, 20: 18020(R) (ORNL-3900, pp 2-81)
Nb–Zr, properties of TIG-welded, 20: 23731
Nb–Zr, properties of zirconium-base, for fuel cladding for water-cooled reactors, 20: 35849 (KR-89, pp 82-96)
Nb–Zr, properties at high temperatures, compilation to 1957, 20: 43908 (PWAC-237)
Nb–Zr, properties as bore seal material, 20: 46145 (NASA-CR-54093)
Nb–Zr, properties of zirconium-base, for use in water cooled reactors, 20: 46159(P)
Nb–Zr, pulse transmission by coaxial cables of superconducting, (E), 19: 39740
Nb–Zr, purification by electron-beam melting, 20: 5181(R) (ORNL-3029)
Nb–Zr, radiation effects on stress-rupture strength of, tube burst tests of, 16: 6823(R) (ORNL-3213(p.124-33))
Nb–Zr, radiation effects on superconducting, proton, 17: 6756
Nb–Zr, radiation effects on oxidation of, 17: 12621
Nb–Zr, radiation effects, 17: 17447
Nb–Zr, radiation effects on, 17: 18389 (TID-7652(p.808-18))
Nb–Zr, radiation effects on properties of precipitation-hardening, 17: 31054
Nb–Zr, radiation effects on rupture-stress properties of, 17: 31068
Nb–Zr, radiation effects on stress-rupture properties, 17: 34557(R) (ORNL-3480(p.117-42))
Nb–Zr, radiation effects on properties as semiconductor material, 17: 36347(R) (NARF-62-18P)
Nb–Zr, radiation effects on mechanical properties of, neutron, 18: 14537(R) (HW-79766(p.4.1-76))
Nb–Zr, radiation effects on tensile properties of, 18: 26096
Nb–Zr, radiation effects on bend properties of, neutron, 18: 32226 (ORNL-TM-880)
Nb–Zr, radiation effects on hardness of, at 50°C, 18: 32043(R) (HW-81269(p.4.1-64))
Nb–Zr, radiation effects on mechanical properties of hydrided, 18: 42108 (AECL-1986)
Nb–Zr, radiation effects on ductility of, fast-neutron, 18: 44049(R) (ORNL-3670(p.77-111))
Nb–Zr, radiation effects on creep of, 19: 24089(R) (SRO-114)
Nb–Zr, radiation effects on tensile properties of, neutron, 19: 25046(R) (HW-83615)
Nb–Zr, radiation effects, 19: 27735(R) (NAA-SR-10850)
Nb–Zr, radiation effects on fuel rod jackets of, 19: 26876 (ANL-6750)
Nb–Zr, radiation effects on mechanical properties of, neutron, 19: 30820 (BNWL-23)
Nb–Zr, radiation effects on tensile properties of, neutron, 20: 27571(R) (BNWL-207, pp 4.1-3)
Nb–Zr, radiation effects on sorptive properties of, for hydrogen and oxygen, fast-neutron and gamma, 20: 27599
Nb–Zr, radiation effects on impact properties of hydrided, fast-neutron, 20: 27602
Nb–Zr, radiation effects on tensile properties of, fast-neutron, 20: 27604
Nb–Zr, radiation effects on impact properties of, effects of hydrogen on fast-neutron, 20: 31669
Nb–Zr, radiation effects on critical current peak vs magnetic field behavior of superconducting, 20: 44505
Nb–Zr, reactions with uranium monocarbide at 1000 to 2400°C, 18: 8795 (HW-72031)
Nb–Zr, reactions with sodium at 2100 to 2400°C, 19: 39090(R) (ANL-7046(p.78-82))
Nb–Zr, reactions with fissium–plutonium–uranium alloys at 750°C, 19: 44587(R) (ANL-7000, pp 3-63)
Nb–Zr, reactions with metals at 540 to 760°C *in vacuo*, 19: 44606 (PWAC-483)
Nb–Zr, reactions with oxygen at 2000°F, 19: 47016 (TIM-901)
Nb–Zr, reactions with TZM molybdenum alloy at 2000°F in refluxing potassium, 20: 9423(R) (NASA-CR-54735)
Nb–Zr, reactions with sodium, high-temperature, 20: 15033(R) (ANL-7152, pp 87-96)
Nb–Zr, reactions with sodium at high temperatures, 20: 20925(R) (ANL-7055, pp 177-212)
Nb–Zr, reactions with plutonium uranium carbide at 820°C, 20: 27416(R) (UNC-5134(Vol.1))
Nb–Zr, reactions with oxygen at 1000 to 1600°F, mechanisms of, 20: 31669
Nb–Zr, reactions with liquid sodium at high temperatures, 20: 38499 (ANL-7120, pp 839-47)
Nb–Zr, reactions with uranium mononitride at high temperatures, 20: 37168(R) (BMI-1771)
Nb–Zr, reactions with plutonium nitride and uranium nitride at high temperatures, 20: 37169(R) (BMI-1774)
Nb–Zr, reactor creep tests on heat-treated, 20: 7501(R) (TID-22426)
Nb–Zr, relation between structure anisotropy and superconducting anisotropy in, 17: 20493
Nb–Zr, resistance to sodium corrosion, 17: 31798(R) (BNL-782 (p.60-91))
Nb–Zr, resistive states in superconducting, 18: 15065
Nb–Zr, rupture properties of, effects of exposure to potassium at 1400°F on stress-, 20: 13191(R) (NASA-CR-54476)
Nb–Zr, shear strength of fasteners of, at room temperature and 1600°F, 17: 36281 (AD-295526)
Nb–Zr, solubility in sodium (liquid), 17: 14839(R) (NRL-5904)
Nb–Zr, solubility in cesium at 2500°F, 19: 13913(R) (AFML-TR-64-327)
Nb–Zr, solubility in sodium at 800 to 1380°C, 20: 5846
Nb–Zr, solvent properties of, for oxygen at 1000°C, 16: 13611
Nb–Zr, solvent properties for hydrogen, 20: 5849
Nb–Zr, solvent properties for oxygen at 100 to 1200°C, 20: 16980
Nb–Zr, solvent properties of zirconium-base, for hydrogen to 550°C, 20: 27435
Nb–Zr, sorptive properties of, for hydrogen in steam at 500°C and 1 atm. pressure, 17: 8715(T,R) (EURAEC-451)
Nb–Zr, sorptive properties for hydrogen from steam at 500°C, 17: 39468(T,R) (EURAEC-520)
Nb–Zr, sorptive properties for oxygen at 1000°C and 10^{-8} to 10^{-7} torr, 18: 27903 (NASA-SP-41(p.307-12))
Nb–Zr, sorptive properties for nitrogen, 18: 44049(R) (ORNL-3670 (p.77-111))
Nb–Zr, sorptive properties for nitrogen, kinetics of, 20: 4301(R) (ORNL-3870, pp 102-35)
Nb–Zr, sound absorption in superconducting, u-h-f, 17: 39767
Nb–Zr, specifications of, for use in corrosion test loop fabrication, 20: 21293 (R-66SD3007)
Nb–Zr, stability of carbon-strengthened, at 2000°F, 20: 4397 (TIM-955)
Nb–Zr, strength of CS1830 series of, effects of fabrication on short-time, 17: 36290 (CNLM-4408)
Nb–Zr, strength properties, 19: 20474(R) (NASA-CR-54281)
Nb–Zr, strengthening by oxygen addition and quenching, 19: 39223(P)
Nb–Zr, stress rupture of tubular, 16: 30167 (ORNL-3313(p.19-64))
Nb–Zr, stress-rupture in-pile testing, 17: 5040(R) (ORNL-3364(p.125-50))
Nb–Zr, stress-rupture of, effects of hydrogen embrittlement on, 17: 31733(R) (SRO-84)
Nb–Zr, stress-rupture properties at 980 to 1200°C, 18: 4255(R) (ORNL-3470(p.98-125))
Nb–Zr, stress rupture at 550 and 600°C, 19: 29468(R) (ANL-7017)
Nb–Zr, structure of, temperature effects on, 16: 12653(R) (EURAEC-130)
Nb–Zr, structure effects on mechanical and superconducting properties of, (E), 19: 28863
Nb–Zr, structure and superconducting properties of, effects of oxygen on, 20: 42535
Nb–Zr, superconducting, phase equilibria in, 16: 27671
Nb–Zr, superconducting, behavior of, 16: 30170(R) (ORNL-3313(p.179-208))
Nb–Zr, superconducting, magnetic quenching characteristics of, 16: 15396
Nb–Zr, superconducting, transition temperatures of, 16: 6825(R) (ORNL-3213(p.139-40))
Nb–Zr, superconductivity, 16: 16830
Nb–Zr, superconducting, use of, as iron-core-magnet coils, 16: 15430
Nb–Zr, superconducting, use of, as magnet coils for fields over 100 kgauss, 16: 15460
Nb–Zr, superconducting, use of, for 55-kguass magnets, 16: 15427
Nb–Zr, superconducting, use of, in 30-kgauss solenoid, 16: 15431

Nb–Zr, superconducting, use of, to produce 59-kgauss magnet, 16: 15428
Nb–Zr, superconducting critical currents in, 17: 553
Nb–Zr, superconductivity of, effects of magnetic-field orientation on, 17: 5037(R) (ORNL-3364(p.27-56))
Nb–Zr, superconductivity in, 17: 6807 (UCRL-9819)
Nb–Zr, superconductivity of thin wires of, 17: 8858
Nb–Zr, superconductive properties and technical applications of, 17: 16705
Nb–Zr, superconductivity of, pulsed-magnetic-field studies of, 17: 18907 (TID-17310)
Nb–Zr, superconducting properties, 17: 22365
Nb–Zr, superconducting critical currents in coils and wires of, 17: 24062 (UCRL-10402)
Nb–Zr, superconducting transitions in high magnetic fields, 17: 25938
Nb–Zr, superconducting properties for use in high-field magnets, 17: 28074
Nb–Zr, superconducting critical currents at 4.2°K, 17: 28101
Nb–Zr, superconducting critical fields of, 17: 32224
Nb–Zr, superconductivity, 17: 34438
Nb–Zr, superconductivity and uses of Nb_3Zr, 17: 34451
Nb–Zr, superconductor transition to normal state in solenoids of, 17: 37742
Nb–Zr, superconducting critical current dependence on dI/dt in, 17: 37523
Nb–Zr, superconducting-normal transitions in, 18: 952 (ANL-SBC-1)
Nb–Zr, superconducting behavior of films of, prepared using exploding wires, 18: 2753
Nb–Zr, superconductivity of, upper critical fields for, 18: 2776
Nb–Zr, superconductivity of, mechanism for high-field, 18: 4499
Nb–Zr, superconducting transition temperatures in, pressure effects on, 18: 6120
Nb–Zr, superconducting critical current of, dependence on applied transverse magnetic field, 18: 6131
Nb–Zr, superconducting critical current of ultrafine wire of, dependence on wire size, 18: 6132
Nb–Zr, superconducting wire of, intermediate-state resistance of, 18: 6134
Nb–Zr, superconducting solenoids of, flux jumping in, 18: 13017
Nb–Zr, superconducting critical alternating currents in, 18: 13018
Nb–Zr, superconducting magnets of, 18: 24547
Nb–Zr, superconducting magnets of, 18: 34715
Nb–Zr, superconducting behavior of films of, 18: 42574
Nb–Zr, superconducting properties, 18: 44681
Nb–Zr, superconducting properties of, 19: 12453
Nb–Zr, superconducting properties of, (E), 19: 16764 (AROD-3473:2)
Nb–Zr, superconducting transitions in fast-pulsed magnetic fields, (E), 19: 16779
Nb–Zr, superconducting, alternating current characteristics of, 19: 18480
Nb–Zr, superconducting critical fields for, (T), 19: 19025
Nb–Zr, superconducting critical currents of, (E), 19: 19056
Nb–Zr, superconducting properties of, effects of heating to 300°C for 10 hr on, 19: 20609(P)
Nb–Zr, superconductivity, 19: 39695
Nb–Zr, superconducting critical current density in, method for increasing, (E), 20: 1121(T) (AI-Trans-97)
Nb–Zr, superconducting properties of, effects of heat treatments and microstructure on, 20: 2395
Nb–Zr, superconducting-normal transitions in variable fields, mechanisms of, (E), 20: 2902
Nb–Zr, superconducting properties, (E), 20: 4792
Nb–Zr, superconducting solenoids of, mechanism of current degradation in, 20: 8004
Nb–Zr, superconducting point contacts of, macroscopic quantum interference effects in, (E/T), 20: 11911
Nb–Zr, superconductivity of, 20: 13666 (IPP-4/22)
Nb–Zr, superconductivity of, effects of omega-transformation on, (E), 20: 19722 (N-65-17099)
Nb–Zr, superconducting critical currents and fields in flux-pump fed coils of, (E), 20: 21924
Nb–Zr, superconducting properties, 20: 4390(R) (ORNL-3870, pp 65-9)
Nb–Zr, superconductivity disruption in, in magnetic field, 20: 28181
Nb–Zr, superconducting critical currents in wires of, magnetic field dependence of, (E), 20: 28175
Nb–Zr, superconductivity of, effects of cold working and heat treatments on, 20: 29787
Nb–Zr, superconductivity of, effects of microstructure on, 20: 29788
Nb–Zr, superconductivity of, effects of cold working and heat treatments on, 20: 29789
Nb–Zr, superconducting critical current density of wires of, (E), 20: 30267(T)
Nb–Zr, superconducting critical fields of, angular dependence of upper, (E), 20: 30270
Nb–Zr, superconductivity of, in pulsed magnetic fields, effects of aging on, 20: 32312(R) (UCRL-16658, pp 133-43)
Nb–Zr, superconducting properties of, at elevated temperatures, 20: 34417(R) (N-65-34464)
Nb–Zr, superconducting properties in strong d-c magnetic fields, (E), 20: 37950
Nb–Zr, superconductivity for magnets, 20: 40015(R) (ORNL-TM-1598)
Nb–Zr, superconductivity in surface layers of, (E), 20: 40023
Nb–Zr, superconductivity, 20: 40047
Nb–Zr, superconducting critical current density in, effect of structure on, 20: 40021
Nb–Zr, superconducting properties of copper-enclosed, pressure effects on, 20: 44526
Nb–Zr, superconducting critical field measurements for, resistive effects on surface, 20: 44534
Nb–Zr, surface current effects in superconducting, 20: 30280
Nb–Zr, temperature cycling effects on critical currents in wire of, 18: 42553
Nb–Zr, tensile properties, 16: 20981(T,R) (EURAEC-27)
Nb–Zr, tensile properties at 4.2, 77, and 300°K, 17: 5037(R) (ORNL-3364(p.27-56))
Nb–Zr, tensile properties at 4.2 to 300°K, 17: 41477
Nb–Zr, tensile properties at 20 to 950°C, 18: 25966(R) (ANL-6868 (p.120-32))
Nb–Zr, tensile properties of, effects of copper and specimen geometry on, 19: 26805 (AECL-2207)
Nb–Zr, tensile properties of cold-worked, for use as fuel sheathing, 19: 28807 (AECL-2250)
Nb–Zr, tensile properties of, effect of texture on, 19: 30805
Nb–Zr, tensile properties of pressure tubing of, effects of hot working on, 19: 46539(R) (TID-22249)
Nb–Zr, tensile properties, 18: 3038(R) (ANL-6801)
Nb–Zr, tensile properties of zirconium-base, effects of strain rate and temperature on, 20: 9490(R) (BNWL-166, pp 6.15-18)
Nb–Zr, tensile properties of, effects of precipitation hardening on, 20: 23698
Nb–Zr, testing for power reactor pressure tubes, 18: 37666 (A/CONF.28/P/22)
Nb–Zr, testing for use in liquid-metal turbine blades and nozzles, 20: 2240
Nb–Zr, testing magnets of, 17: 24053(R) (ORNL-3432)
Nb–Zr, testing of, method for maintaining high-purity gas environment for, 19: 18408
Nb–Zr, testing superconducting magnets of, 17: 21388(R) (LNF-63/11)
Nb–Zr, testing tubular, 19: 35778(R) (SRO-116)
Nb–Zr, thermal analysis of ω phase of, 19: 47037
Nb–Zr, thermal conductivity of normal and superconducting, at 1.6–12°K, 17: 39598
Nb–Zr, thermal cycling, effects on crystal structure and dimensional stability, 17: 14729 (CRGM-1106)
Nb–Zr, thermal expansion coefficient at 75 to 1890°F, 19: 16057(R) (AGN-8131)
Nb–Zr, thermal expansion of, effects of hydride phase on, 20: 31745
Nb–Zr, thermal phase transitions in superconducting, 18: 42575
Nb–Zr, thermal properties of, at 500 to 5000°F, 17: 16636 (ASD-TDR-62-765)
Nb–Zr, thermal propagation of normal region in wires of, effect of copper plating on velocity of, 17: 37716
Nb–Zr, thermal propagation of normal boundary in superconducting, (E/T), 19: 16766
Nb–Zr, thermal propagation of normal transitions of superconducting, 20: 24273
Nb–Zr, thermodynamic properties, 16: 13636
Nb–Zr, thermodynamic properties of capsules of, 17: 27792 (NP-12933)
Nb–Zr, thermodynamic properties of nitrogen equilibrium solid solutions in, 20: 13263 (ORNL-TM-1355)
Nb–Zr, thermoelectric power at 9.2 to 330°K, effects of zirconium content on, 20: 17067
Nb–Zr, thermophysical properties, 18: 44049(R) (ORNL-3670(p.77-111))
Nb–Zr, training effect in coil of superconducting, (E), 20: 11895
Nb–Zr, transfer of carbon and nitrogen to, from stainless steels in potassium, 20: 2270
Nb–Zr, transformation kinetics in, 18: 4250(R) (ORNL-3470(p.45-8))
Nb–Zr, transformation kinetics, study of, 18: 44147(R) (ORNL-3670 (p.21-2))
Nb–Zr, transformation kinetics in, 19: 41033
Nb–Zr, transformation temperatures of, effects of cooling rates on, 20: 37233
Nb–Zr, transients in superconducting coil of, 17: 22267 (BSD-TDR-62-116)
Nb–Zr, transport current effects on magnetization of superconducting wires of, 17: 34622
Nb–Zr, transport current effects on magnetic properties of superconduct-

ing (E), 19: 3176
Nb–Zr, tube-burst tests on, 20: 5181(R) (ORNL-3029)
Nb–Zr, ultrasonic attenuation in superconducting, in strong magnetic fields, (E), 19: 21188
Nb–Zr, ultrasonic attenuation in superconductors of, temperature dependence of, 19: 25436(R) (RTD-TR-65)
Nb–Zr, ultrasonic attenuation in nonideal superconducting, flux jumping and magnetization effects on, (E), 20: 17606
Nb–Zr, upper critical fields of superconducting, 18: 11109
Nb–Zr, uptake of carbon, nitrogen, and oxygen by, in liquid metal loops, 20: 41419(R) (GMAD-3643-5)
Nb–Zr, use as loop material for forced-convection corrosion of refractory alloys by lithium, 20: 5853 (TIM-898)
Nb–Zr, use as solenoid lens in electron microscope, 19: 15841
Nb–Zr, use for superconducting magnet coils, 20: 5614
Nb–Zr, use in accelerators and storage rings as superconductors, 18: 16602 (BNL-7534(p.417-47))
Nb–Zr, use in condensers for space power plants, 19: 9331 (PWA-2320 (Vol.1))
Nb–Zr, use in heat transfer tube, 20: 14699(P)
Nb–Zr, use in superconducting magnets, 17: 20438
Nb–Zr, use in superconducting solenoids, 17: 23712
Nb–Zr, use in superconducting solenoids, 18: 36520
Nb–Zr, use in superconducting solenoid, 19: 23594(P)
Nb–Zr, use of superconducting, for magnet development, 20: 34418(R) (N-66-16181)
Nb–Zr, welding, 17: 22092(R) (GE63FPD66)
Nb–Zr, welding, aging behavior in, 17: 8769
Nb–Zr, welding of, effects of gases on, 16: 20807 (NP-11694)
Nb–Zr, welding of, in various atmospheres, 17: 509 (CW-R&DL-29)
Nb–Zr, welding of, 17: 6558
Nb–Zr, welding of, nondestructive testing of zones of, 20: 13320
Nb–Zr, welding properties, 18: 4255(R) (ORNL-3470(p.98-125))
Nb–Zr, welding to current contacts, 17: 36267
Nb–Zr, welding to T-111 alloy, 20: 43830(R) (NASA-CR-72029)
Nb–Zr, wetting by sodium, effects of temperature on, 20: 37168(R) (BMI-1771)
Nb–Zr, x-ray diffraction of nonmetallic phases chemically extracted from, 19: 7973
Nb–Zr, 50-c critical currents in superconducting wires of, 17: 34595
Nd–Zr, fracture at 78, 197, and 273°K, mechanisms of, 20: 37231
Nd–Zr, preparation and properties, 16: 2128
Nd–Zr, surface tension of liquid, 17: 4943
Ni–Nb–Zr, hydrogen embrittlement of, review of, 20: 37187
Ni–Sn–Ti–Zr, corrosion by steam at 400°C, 19: 32696(R) (EURAEC-783)
Ni–Sn–Ti–Zr, fabrication by extrusion, 18: 22428(T,R) (EURAEC-838)
Ni–Sn–Ti–Zr, fabrication and properties, 19: 36965(T,R) (EURAEC-618)
Ni–Sn–Zr, corrosion by steam at 400°C, 18: 22428(T,R) (EURAEC-838)
Ni–Sn–Zr, corrosion by steam at 400°C, 19: 32696(R) (EURAEC-783)
Ni–Sn–Zr, fabrication and properties, 19: 36965(T,R) (EURAEC-618)
Ni–Sn–Zr, properties as cladding for fuel elements, 20: 25614(P)
Ni–Sn–Zr, thermal expansion of, to 1100°C, 19: 24982(R) (EURAEC-1270)
Ni–Th–Zr, properties and structure of, 18: 37670 (A/CONF.28/P/337)
Ni–Ti–Zr, fabrication and properties, 19: 36965(T,R) (EURAEC-618)
Ni–Ti–Zr, tensile properties at room temperature, 18: 18380
Ni–Ti–Zr, thermal expansion of, to 1100°C, 19: 24982(R) (EURAEC-1270)
Ni–Zr, analysis for zirconium, electrographic, 20: 267
Ni–Zr, brittleness and fracture of, effects of hydrogen on, 19: 44716
Ni–Zr, corrosion by steam at 540°C, 17: 35079(R) (ANL-6749)
Ni–Zr, corrosion by steam at 400°C, 18: 24150(T,R) (EURAEC-538)
Ni–Zr, corrosion by steam at 400°C, hydrogen sorption during, 18: 34060(T,R) (EURAEC-1062)
Ni–Zr, corrosion films on, microprobe studies of, 19: 9621 (DP-906)
Ni–Zr, corrosion by superheated steam at 540 and 650°C, 19: 22899
Ni–Zr, corrosion by steam of, 19: 24982(R) (EURAEC-1270)
Ni–Zr, corrosion by steam, effects of aluminum, tin, or titanium on, 19: 24982(R) (EURAEC-1270)
Ni–Zr, corrosion by steam at 540°C, 19: 44616(R) (ANL-7000, pp 122-37)
Ni–Zr, crystal growth and structure of, 19: 22863(R) (AD-606809)
Ni–Zr, crystal structure, 16: 10570
Ni–Zr, crystal structure of intermetallic compound $Ni_{10}Zr_7$ in, 16: 30787 (IS-257)
Ni–Zr, crystal structures of intermetallic compounds NiZr and $NiZr_2$ in, 16: 12122
Ni–Zr, crystal structure of Brillouin zones in, effects of electron-atom ratios on, 19: 26836
Ni–Zr, crystal structure of intermetallic compounds, 20: 41412(R) (IS-1500(Sect. M))
Ni–Zr, effects of additives on high-temperature properties of eutectic, 20: 17108
Ni–Zr, electrochemical potential and hydrogen overvoltage, 17: 34403 (GEAP-4192)
Ni–Zr, embrittlement effects of hydrogen on, 18: 34169
Ni–Zr, extrusion of, effects on structure, 17: 6654(R) (EURAEC-394)
Ni–Zr, hardening of, by formation of intermetallic compounds, 19: 24982(R) (EURAEC-1270)
Ni–Zr, hardening of, by addition of aluminum, tin, or titanium, 19: 24982(R) (EURAEC-1270)
Ni–Zr, hydrogen overvoltage measurements in, 17: 27728(R) (GEAP-4076)
Ni–Zr, hydrogen overvoltage at Zr_2Ni in sulfuric acid, 18: 12642 (GEAP-4089(Vol.II)(Paper 22))
Ni–Zr, impact testing of, high-velocity, 20: 33490 (CONF-651026, pp 737-68)
Ni–Zr, magnetic susceptibility of $ZrNi_5$, at 4 to 300°K, 19: 30743(R) (NYO-3454-1)
Ni–Zr, mechanical properties of, 19: 24982(R) (EURAEC-1270)
Ni–Zr, mechanical properties and microstructure of, effects of small additions of selected elements on, 20: 27550
Ni–Zr, oxidation by oxygen at 700°C, 17: 41333(R) (ANL-6677)
Ni–Zr, oxidation kinetics at 500 to 900°C, 20: 5454(T) (JPRS-32341, pp 8-16)
Ni–Zr, oxidation kinetics and oxide film breakaway at 600 to 850°C, 20: 25497
Ni–Zr, phase diagram, 16: 10578
Ni–Zr, phase diagram, 16: 25819
Ni–Zr, phase studies, 17: 11204(T,R) (EURAEC-444)
Ni–Zr, phase studies, 17: 40153(R) (AD-290727)
Ni–Zr, phase studies and properties of extruded, effects of annealing, quenching, and tempering on, 18: 24150(T,R) (EURAEC-538)
Ni–Zr, reactions with hydrogen and structure of intermetallic compounds in, 16: 19356 (NAA-SR-7132)
Ni–Zr, reactions with hydrogen, thermochemical and structural aspects of, 20: 27436
Ni–Zr, resistance to scaling at elevated temperatures, 19: 32770(P)
Ni–Zr, sorptive properties for hydrogen, 19: 24982(R) (EURAEC-1270)
Ni–Zr, tensile properties, 19: 36965(T,R) (EURAEC-618)
Pb–Zr, diffusion and solubility of hydrogen in, 19: 13349
Pb–Zr, phase studies, 16: 30170(R) (ORNL-3313(p.179-208))
Pb–Zr, phase studies and structure, 17: 39653
Pb–Zr, phase studies, 18: 4247(R) (ORNL-3470(p.20-6))
Pd–Zr, corrosion by uranyl sulfate solution at 280°C, in-pile, 17: 27750 (ORNL-3099)
Pd–Zr, crystal structure and electric conductivity of, 20: 29766
Pd–Zr, electric conductivity and Hall constant of, 17: 580
Pd–Zr, magnetic properties at 90 to 1100°K, 20: 7585(T) (ANL-Trans-251)
Pd–Zr, structure of, 17: 578
Pt–Zr, corrosion by uranyl sulfate solution at 280°C, in-pile, 17: 27750 (ORNL-3099)
Pt–Zr, corrosion by hydrochloric–nitric acid mixtures, 19: 28214(R) (ORNL-3739)
Pt–Zr, corrosion by hydrochloric acid, effects of platinum content on, 20: 11227
Pt–Zr, crystal structure of equiatomic intermetallic compound in, 19: 24994
Pt–Zr, phase studies by x-ray diffraction, 19: 7964
Pu–U–Zr, analysis for trace impurities by anion exchange-partition chromatography and spectrography, 20: 26764
Pu–U–Zr, burnup testing of clad, 20: 36391(R) (ANL-7219, pp 1-27)
Pu–U–Zr, burnup testing of, 20: 45106(R) (ANL-7249)
Pu–U–Zr, compatibility with Hastelloy-X, Incoloy-800, and type-304 stainless steels, 20: 2229
Pu–U–Zr, compatibility with type 304 stainless steel to 800°C, 20: 31666
Pu–U–Zr, compressive strength of, 20: 6601(R) (ANL-7115, pp 1-41)
Pu–U–Zr, corrosion by air, 19: 2753
Pu–U–Zr, corrosion in air, 19: 11679
Pu–U–Zr, corrosion by air at room temperature, 19: 44587(R) (ANL-7000, pp 3-63)
Pu–U–Zr, density and structure of, 20: 16060(R) (ANL-7152, pp 1-49)
Pu–U–Zr, development as fast reactor fuel, 20: 38465 (ANL-7120, pp 289-300)
Pu–U–Zr, development for LMFBR fuel, 20: 42651 (WASH-1065)
Pu–U–Zr, heating characteristics in air, 18: 15663(R) (ANL-6808)
Pu–U–Zr, mechanical and thermal properties of, 19: 29468(R) (ANL-7017)
Pu–U–Zr, mechanical properties and phase diagram of, 20: 31666
Pu–U–Zr, melting temperatures of, 20: 38465 (ANL-7120, pp 289-300)
Pu–U–Zr, oxidation by air at 24°C, 18: 15663(R) (ANL-6808)
Pu–U–Zr, performance as zero-power reactor fuel, 18: 24952(R) (ANL-6880(p.6-48))
Pu–U–Zr, performance as FTR fuel, 20: 42676 (BNWL-281)

Pu–U–Zr, phase studies, 19: 40177(R) (ANL-7046(p.1-35))
Pu–U–Zr, phase studies, 20: 6600(R) (ANL-7105, pp 1-35)
Pu–U–Zr, phase studies, 20: 7569(R) (MLM-1283)
Pu–U–Zr, phase studies, 20: 33778
Pu–U–Zr, phase transformations at 550°C, (E), 20: 14007(R) (ANL-7122, pp 1-41)
Pu–U–Zr, preparation and properties, 18: 37601 (A/CONF.28/P/58)
Pu–U–Zr, properties, 19: 4647 (CEA-R-2531)
Pu–U–Zr, properties as fast-breeder fuel, effects of refractory-metal additions on, 19: 14765(R) (ANL-6977)
Pu–U–Zr, properties as fast power-breeder fuels, 20: 2386
Pu–U–Zr, properties for use as fast reactor fuel, 20: 26394(R) (ANL-7193)
Pu–U–Zr, radiation effects on, in-pile testing of, (E), 20: 14007(R) (ANL-7122, pp 1-41)
Pu–U–Zr, reactions with stainless steel at high temperatures, 19: 40177(R) (ANL-7046(p.1-35))
Pu–U–Zr, reactions with Hastelloy, Incoloy, and stainless steel at high temperatures, 20: 3320(R) (ANL-7082, pp 1-28)
Pu–U–Zr, tensile properties, 20: 6600(R) (ANL-7105, pp 1-35)
Pu–U–Zr, thermal conductivities of, 20: 46963(R) (ANL-7132)
Pu–U–Zr, thermal expansion, 20: 5848
Pu–Zr, chemistry and metallurgy of, 17: 17439
Pu–Zr, cladding with zirconium, 17: 7547(R) (HW-74761(p.3.1-39))
Pu–Zr, crystal structure lattice parameters of delta- and epsilon-phase, 18: 27998
Pu–Zr, etchant for delta-phase stabilized, bright field grain structure, 20: 23590
Pu–Zr, etching of delta-phase, bright-field grain structure, 20: 21233 (BNWL-188)
Pu–Zr, fabrication of zirconium-clad, 17: 13678(R) (HW-75914)
Pu–Zr, fabrication of wire, for use in urania fuel element enrichment, 19: 22921(R) (HW-81603(p.6.1-11))
Pu–Zr, mechanical properties and phase studies, 16: 19352 (HW-SA-2560)
Pu–Zr, performance as fuels in thermal power reactors (E), 19: 3587 (AECL-2102)
Pu–Zr, performance as high-exposure (Hx) fuels in MTR, (T), 19: 31605 (HW-84575)
Pu–Zr, phase diagram, 17: 16567
Pu–Zr, phase diagram, 18: 7220(T) (JPRS-22599)
Pu–Zr, phase diagrams of, 18: 16493
Pu–Zr, phase studies, 17: 16566
Pu–Zr, phase studies of plutonium-base, 20: 46143(R) (HW-66081)
Pu–Zr, phase transformation of delta-stabilized, 17: 8733(P)
Pu–Zr, properties as reactor fuel, 17: 8763
Pu–Zr, radiation effects on cold-rolled, 16: 29435 (ANL-6428)
Pu–Zr, radiation effects on, 17: 16572
Pu–Zr, tensile properties of plutonium-base, effects of temperature on, 20: 46144(R) (HW-67765)
Pu–Zr, thermal expansion of delta phase, 16: 4464
Pu–Zr, thermal expansion of delta, 17: 23953 (LADC-5466)
Pu–Zr, thermodynamic properties of, 18: 44224
Pu–Zr, welding to aluminum, stainless steel, and zirconium alloys, 18: 44120
rare earth–Zr, preparation, 17: 8795(P)
rare earth–Zr, preparation and properties, 16: 12111(R) (TID-14779)
rare earth–Zr, recrystallization behavior, 17: 25823
rare earth–Zr, solid solutions of, electronic states of, 20: 21398
Rb–Zr, oxidation of, mechanism of breakaway, 20: 25496
Rb–Zr, phase studies, 20: 35924
Re–Zr, phase diagram, 17: 8727
Re–Zr, phase studies of, 17: 11213
Re–Zr, properties at low temperatures, 20: 3920(R) (ORNL-3870, pp 27-37)
Re–Zr, work function for, 20: 40297
Rh–Ti–Zr, superconductivity, 18: 21112
Rh–Zr, fine structure of, 18: 11132
Rh–Zr, phase studies by x-ray diffraction, 19: 7964
Rh–Zr, specific heat at 0.9 to 12°K, (E), 19: 39218
Rh–Zr, superconductivity of, effects of valence electron concentration on, 17: 34466
Rh–Zr, superconductivity of, 18: 9274
Rh–Zr, superconductivity and phase transitions, 18: 21104
Rh–Zr, superconductivity, 19: 43235
Ru–Zr, lattice parameters of Zr_2Rh, 19: 44678(R) (ANL-7000, pp 186-200)
Ru–Zr, oxidation of, distribution of ruthenium in oxide film in, 20: 25504
Ru–Zr, phase studies, 17: 37557
Ru–Zr, properties at low temperatures, 20: 3920(R) (ORNL-3870, pp 27-37)
Sb–Cr–Zr, oxidation by steam at 900°F, 18: 2162(R) (IITRI-B198-46)
Sb–Fe–Zr, oxidation by steam at 750°F, 18: 2162(R) (IITRI-B198-46)
Sb–Ge–Zr, corrosion of, in 680°F water, 17: 16582 (ARF-B198-36)
Sb–Ge–Zr, corrosion by water at 680°F, 17: 30905(R) (ARF-B198-42)
Sb–Ge–Zr, oxidation by water at 680°F, 18: 2162(R) (IITRI-B198-46)
Sb–Mo–Zr, oxidation by steam at 900°F, 18: 2162(R) (IITRI-B198-46)
Sb–Nb–Sn–Zr, corrosion by steam at 400 and 450°C, 19: 30668(R) (EURAEC-1274)
Sb–Nb–Zr, corrosion of, in 680°F water, 17: 16582 (ARF-B198-36)
Sb–Nb–Zr, corrosion by water at 680°F, 17: 30905(R) (ARF-B198-42)
Sb–Nb–Zr, corrosion by steam at 400 and 450°C, 19: 30668(R) (EURAEC-1274)
Sb–Nb–Zr, oxidation by water at 680°F, 18: 2162(R) (IITRI-B198-46)
Sb–Sn–Zr, phase studies, 19: 44720
Sb–Ti–Zr, tensile properties at room temperature, 18: 18380
Sb–Zr, corrosion by steam and water at 750 to 900 and 680°F, 16: 29337(R) (ARF-2198-26)
Sb–Zr, corrosion by water at 680°F, 17: 6561(R) (ARF-2198-34)
Sb–Zr, density of electronic states in, 18: 4247(R) (ORNL-3470(p.20-6))
Sb–Zr, diffusion and solubility of hydrogen in, 19: 13349
Sb–Zr, strength, 17: 6561(R) (ARF-2198-34)
Sb–Zr, thermal capacity at 1.2 to 4.5°K, 17: 30966 (CONF-22-15)
Sb–Zr, uptake of hydrogen during steam and water corrosion of, 17: 32519
Sc–Zr, electronic properties, 18: 44150(R) (ORNL-3670(p.44-53))
Sc–Zr, phase studies, 17: 27785 (IS-569)
Sc–Zr, phase studies, 18: 18307
Sc–Zr, scandium-45 hyperfine interactions in, 20: 9658 (IS-T-38)
Sc–Zr, superconductivity, 20: 40047
Sc–Zr, superconducting transition temperature and electronic specific heat of, 20: 42121
Sm–Zr, oxidation by air at 500°C, 17: 34330(R) (USBM-U-1057)
Sm–Zr, physical properties, (E), 19: 16188
Sn–Ti–V–Zr, corrosion by steam at 400°C, 18: 22428(T,R) (EURAEC-838)
Sn–Ti–V–Zr, corrosion by steam at 400°C, 19: 32696(R) (EURAEC-783)
Sn–Ti–V–Zr, fabrication by extrusion, 18: 22428(T,R) (EURAEC-838)
Sn–Ti–V–Zr, fabrication and properties, 19: 36965(T,R) (EURAEC-618)
Sn–Ti–Zr, creep and phase studies, 17: 29348
Sn–Ti–Zr, creep properties at 300 to 700°C, 17: 11211
Sn–Ti–Zr, oxidation at high-temperatures, 17: 39495
Sn–Ti–Zr, tensile properties at room temperature, 18: 18380
Sn–U–Zr, analysis of, for copper, absorptiometric, 16: 12955 (PG-Report-269)
Sn–U–Zr, casting, 19: 2787
Sn–U–Zr, corrosion resistance and preparation of, 17: 36239(P)
Sn–U–Zr, corrosion resistance, 18: 44094(P)
Sn–U–Zr, dissolution of, in Zirflex Process, 16: 11503(R) (ORNL-TM-34)
Sn–U–Zr, dissolution in hydrofluoric acid, additive effects of boron on continuous, 17: 30582(R) (IDO-14611)
Sn–U–Zr, dissolution and processing of irradiated, 18: 17930(R) (IDO-14625)
Sn–U–Zr, dissolution in hydrofluoric acid, effects of boron on, 18: 17929(R) (IDO-14616)
Sn–V–Zr, corrosion by steam at 350, 400, and 480°C, 18: 22428(T,R) (EURAEC-838)
Sn–V–Zr, corrosion by steam at 350, 400, and 480°C, 18: 20476(T,R) (EURAEC-916)
Sn–V–Zr, corrosion by steam at 350, 400, and 480°C, hydrogen sorption during, 18: 34060(T,R) (EURAEC-1062)
Sn–V–Zr, corrosion by steam or water, 19: 24982(R) (EURAEC-1270)
Sn–V–Zr, corrosion by steam at 400°C, 19: 32696(R) (EURAEC-783)
Sn–V–Zr, fabrication and tensile properties of extruded, 18: 22428(T,R) (EURAEC-838)
Sn–V–Zr, fabrication and mechanical properties, effects of heat treatments on, 18: 34060(T,R) (EURAEC-1062)
Sn–V–Zr, fabrication and properties, 19: 36965(T,R) (EURAEC-618)
Sn–V–Zr, mechanical properties at 20, 200, 500, and 700°C, 18: 20476(T,R) (EURAEC-916)
Sn–V–Zr, mechanical properties between 20 and 700°C, 19: 24982(R) (EURAEC-1270)
Sn–V–Zr, oxidation of, causes of second transition point in, 16: 7857
Sn–V–Zr, sorptive properties for hydrogen, 19: 24982(R) (EURAEC-1270)
Sn–V–Zr, thermal expansion between 100 and 1100°C, 19: 24982(R) (EURAEC-1270)
Sn–Zr, analysis for boron, colorimetric, 16: 12978
Sn–Zr, analysis for hydrogen by equilibrium gas pressure functions, 16: 8675 (KAPL-M-AHA-2)
Sn–Zr, analysis for hydrogen by resistivity measurements, 16: 12094 (HW-70977)
Sn–Zr, analysis for hydrogen by Hall currents, 16: 22030
Sn–Zr, analysis for molybdenum and tin using 8-quinolinol, spectrophotometric, 16: 16314
Sn–Zr, analysis for nitrogen, design of modified Kjeldahl apparatus for,

16: 8682 (TID-11411)
Sn–Zr, bonding of, by gas-pressure method, 16: 16701
Sn–Zr, bonding of, to firebox steel by extrusion, 16: 9169 (NMI-4771)
Sn–Zr, bonding of, to iron–nickel alloys, 16: 30744 (CVNA-44)
Sn–Zr, bonding of, to stainless steel, effects of surface preparation on, 16: 28642(R) (BMI-1581(Del.))
Sn–Zr, bonding of, to stainless steel by explosive joining, friction bonding, and modified roll forming, 16: 15154(R) (BMI-X-193)
Sn–Zr, bonding of, to stainless steel by indentation, 16: 2149 (OEL-MET-3306)
Sn–Zr, bonding of, to stainless steel by tandem extrusion, 16: 13548 (NMI-7216)
Sn–Zr, bonding of, to stainless steel by various techniques, 16: 32092 (BMI-1594)
Sn–Zr, bonding of, to type 410 stainless steel, 16: 24149(R) (BMI-X-204)
Sn–Zr, brazing, 16: 7889 (NP-11196(p.16-20))
Sn–Zr, brazing to stainless steel type 304, eutectic, 16: 9179
Sn–Zr, brazing Zircaloy end closures, 16: 33477(R) (NMI-7253)
Sn–Zr, coating with boron and cadmium, 16: 7519 (CRCE-1039)
Sn–Zr, corrosion, 16: 25760 (ORNL-3281)
Sn–Zr, corrosion of, by aqueous thoria–uranía slurries, in-pile tests on, 16: 10621 (ORNL-3222)
Sn–Zr, corrosion of, by chloride solutions, 16: 23528(R) (ORNL-3290)
Sn–Zr, corrosion of, by copper and uranyl nitrate solutions, in-pile autoclave, 16: 5670 (ORNL-3171)
Sn–Zr, corrosion of, by decontaminating solution, 16: 24496
Sn–Zr, corrosion of, by flowing water at 340°C, 16: 19285 (HW-66206)
Sn–Zr, corrosion of, by halide solutions and water at high temperatures, 16: 15144 (BMI-1571)
Sn–Zr, corrosion of, by reactor solutions, 16: 17562(R) (ORNL-3262 (p.80-9))
Sn–Zr, corrosion of, by steam, sorption of hydrogen during, 16: 5674
Sn–Zr, corrosion of, by steam at 425°C and oxygen at 700°C, 16: 9141(R) (NMI-2101)
Sn–Zr, corrosion of, by steam and water, 16: 12050 (HW-71771)
Sn–Zr, corrosion of, by steam and water, 16: 12693
Sn–Zr, corrosion of, by steam and water at 750 and 680°F, effects of impurities on, 16: 10463
Sn–Zr, corrosion of, by steam and water at 750 to 900 and 680°F, 16: 29337(R) (ARF-2198-26)
Sn–Zr, corrosion of, by steam and water at high temperatures, 16: 12664 (WAPD-BT-24(p.27-42))
Sn–Zr, corrosion of, by steam or water at 360, 400, and 480°C rates of, 16: 20982(T,R) (EURAEC-85)
Sn–Zr, corrosion of, by steam–water mixtures, 16: 34082(T,R) (EURAEC-40)
Sn–Zr, corrosion of, by steam–water mixtures at 245 to 287°C at flows of 553 g/cm² sec, 16: 7853 (EURAEC-151)
Sn–Zr, corrosion of, by uranyl sulfate, 16: 31311
Sn–Zr, corrosion of, by uranyl sulfate, effects of excess sulfuric acid on radioinduced, 16: 17981 (ORNL-2943)
Sn–Zr, corrosion of, by water at 200 to 260°C, 16: 1183 (AECL-1265 (Paper 7))
Sn–Zr, corrosion of, by water at 680°F, 16: 7889 (NP-11196(p.16-20))
Sn–Zr, corrosion of, by water at 300°C, effects of fluoride ions on, 16: 20977 (CRGM-1082)
Sn–Zr, corrosion of, by water at 360°C, effects of annealing atmosphere, cold-work, temperature, and time on, 16: 4492 (HW-69681)
Sn–Zr, corrosion of, in PRTR, monitoring of, 16: 34112 (HW-73701(Rev.))
Sn–Zr, corrosion of Zircaloy under nucleate boiling conditions in ammoniated and lithiated water, effects of VEE-shaped crevices on, 16: 19287 (KAPL-2203)
Sn–Zr, corrosion of Zircaloy by alkaline solutions at high temperatures, 16: 22560
Sn–Zr, corrosion-product deposition on, in pressurized water reactors, 16: 1183 (AECL-1265(Paper 7))
Sn–Zr, corrosion resistance of, effects of heat treatment on, 16: 23629(R) (DP-735)
Sn–Zr, corrosion resistance of, effects of partial dissolution of oxide film on aqueous, 16: 7858
Sn–Zr, corrosion resistance of, restoration of, by heat treatment in beta-field structure in molten salt bath, 16: 11157 (WAPD-243)
Sn–Zr, corrosion by air, carbon dioxide, and water, 17: 504
Sn–Zr, corrosion by steam and water, 17: 39659
Sn–Zr, corrosion resistance of, effects of chromium on, 18: 41969(P)
Sn–Zr, corrosion and mechanical strength of new composition, 19: 4706(P)
Sn–Zr, creep, 16: 7890 (NP-11196(p.34-41))
Sn–Zr, creep and rupture data for, correlation of, with time-temperature parameter, 16: 9199 (HW-67641)
Sn–Zr, creep at 500°C, 16: 12653(R) (EURAEC-130)
Sn–Zr, creep properties at 550 to 750°F, 16: 4450(R) (BMI-1546(Del.))
Sn–Zr, crystal orientation in, x-ray diffraction measurements of preferred, 16: 10522 (DP-607)
Sn–Zr, crystal structure of, x-ray diffraction studies of preferred orientation in, 16: 33476 (HW-74429(p.67-79))
Sn–Zr, crystal structure of intermetallic compound $ZrSe_2$ in, 19: 44720
Sb–Zr, crystal structure of intermetallic compound $ZrSb_2$ in, 19: 44702
Sn–Zr, decomposition, electrolytic, 16: 1855(R) (IDO-14560)
Sn–Zr, deformation and fracture of, stress-rate test results on, 16: 30167 (ORNL-3313(p.19-64))
Sn–Zr, deformation of, in creep and tension, contractile strain ratio analysis in plastic, 16: 30807(R) (TID-16574)
Sn–Zr, deformation of, role of twinning in plastic, 16: 30804(R) (TID-15640)
Sn–Zr, density of electronic states in, 18: 4247(R) (ORNL-3470(p.20-6))
Sn–Zr, development of, for use in plutonium recycle program, summary for 1961 on, 16: 14376(R) (HW-70000)
Sn–Zr, development of Zircaloy-1, 17: 14744 (WAPD-T-1549)
Sn–Zr, development, 18: 24077(P)
Sn–Zr, diffusion in uranium carbide at 820°C, 16: 6686(R) (NDA-2162-5)
Sn–Zr, diffusion of hydrogen in alpha-delta, mechanism, 16: 21075
Sn–Zr, dissolution, 16: 16464
Sn–Zr, dissolution of, in anhydrous hydrogen fluoride–hydrogen chloride at 400 to 450°C, 16: 25710(P)
Sn–Zr, dissolution of, in molten fluorides, corrosion of Hy Mu-80 and INOR-8 during, 16: 5665 (BMI-X-184)
Sn–Zr, dissolution of, in nitric acid, electrolytic, 16: 266(R) (DP-626)
Sn–Zr, dissolution of, in nitric acid solutions, electrolytic, 16: 18652(R) (DP-706)
Sn–Zr, dissolution of, in titanium dissolver using nitric, hydrofluoric, and fluoboric acid mixture, 16: 8813 (ORNL-TM-22)
Sn–Zr, distribution of hydrogen in, relations with temperature gradients, 16: 32126(T,R) (EURAEC-328)
Sn–Zr, ductility of Zircaloy cladding on swelling fuel, 16: 16723 (NMI-7211)
Sn–Zr, electric conductivity of, effects of hydrogen on, 16: 12094 (HW-70977)
Sn–Zr, elongation of, due to thermal cycling, 16: 10526(R) (EURAEC-86)
Sn–Zr, equipment and properties for electron beam welding of, 17: 34378
Sn–Zr, etching of, parameters for cathodic, in argon atmospheres, 16: 29315 (HW-73450)
Sn–Zr, extrusion of tubular, cold, 16: 19296(R) (ATL-A-112)
Sn–Zr, fabrication and handling of, 16: 32104
Sn–Zr, fabrication of, 16: 30717(R) (ANL-6516)
Sn–Zr, fabrication of, for CVTR thermal baffles, 16: 17975 (CVNA-113)
Sn–Zr, fabrication of, properties of welded versus seamless tubular, 16: 34065(R) (DP-775)
Sn–Zr, fabrication of, ultrasonic tube drawing, 16: 7868 (NYO-10008)
Sn–Zr, fabrication of tubes of, 16: 24634
Sn–Zr, fabrication of consumable electrodes of, 18: 8741(P)
Sn–Zr, fatigue of, effects of applied stress and hydrogen sorption on static, 16: 25746(R) (ARF-2230-9)
Sn–Zr, Hall effect measurements on, effects of hydrogen on, 16: 3456 (HW-70612)
Sn–Zr, heat transfer to, from uranium dioxide, 16: 18023 (CVNA-127)
Sn–Zr, heat transfer to helium and krypton on surface of, thermal accommodation coefficient for, 16: 13589 (WAPD-252)
Sn–Zr, heat treatment of heavy forged sections of, effects of, on corrosion resistance, mechanical properties, and structure, 16: 5739
Sn–Zr, hydridation, 16: 12750(R) (SRO-65)
Sn–Zr, hydridation, 16: 21810(R) (DP-725)
Sn–Zr, hydridation of, by gaseous hydrogen, effects of oxidation rate on, 16: 22588 (HW-67811)
Sn–Zr, hydridation of, by lithium hydroxide at high temperatures, 16: 33433 (WAPD-TM-307)
Sn–Zr, hydridation of, effects of, on corrosion, 16: 13530 (AERE-R-3881)
Sn–Zr, hydridation of, effects of alloy orientation on, 16: 30065(R) (DP-755)
Sn–Zr, hydridation of sheet, 16: 30064(R) (DP-745)
Sn–Zr, hydrogen embrittlement of, delayed failure from, 16: 28542(R) (SRO-68)
Sn–Zr, ignition of, in oxygen, spontaneous, 16: 4173
Sn–Zr, impact properties and notch toughness of, 16: 32119 (ORNL-TM-336)
Sn–Zr, joining of, to stainless steel, 16: 32105
Sn–Zr, joining of, to stainless steel, development of, 16: 4450(R) (BMI-1546(Del.))
Sn–Zr, joining of, to steel in NPR tube-to-nozzle fabrication, 16: 32096 (HW-72086)
Sn–Zr, joining of tubular, to stainless steel, 16: 29313 (DP-723)
Sn–Zr, Lamb wave propagation in, schlieren image of, 17: 31681(R) (HW-76559)
Sn–Zr, mechanical properties, 16: 25760 (ORNL-3281)
Sn–Zr, mechanical properties of, at high temperatures, 16: 19339

(BM-RI-5987)
Sn–Zr, mechanical properties of, effects of hydriding on, 16: 7889 (NP-11196(p.16-20))
Sn–Zr, mechanical properties of foils of, effects of hydrogen content on, 16: 13571 (CW-R&DL-19)
Sn–Zr, mechanical properties of irradiated sheet, 16: 30064(R) (DP-745)
Sn–Zr, mechanical properties of thin, testing of, for fuel plate compartments, 16: 12665 (WAPD-BT-24(p.43-63))
Sn–Zr, mechanical properties of unirradiated, 16: 26467(R) (HW-73100)
Sn–Zr, mechanical properties, 17: 504
Sn–Zr, metallographic inspection of test samples of, 16: 32126(T,R) (EURAEC-328)
Sn–Zr, neutron diffusion and thermalization in hydrided, 16: 26207
Sn–Zr, notch and pit response of Zircaloy to ultrasonic testing, 16: 19987(R) (HW-73314)
Sn–Zr, oxidation behavior of liquid, 16: 19249(R) (NP-11690)
Sn–Zr, oxidation in nitric acid, electrolytic, 16: 17759 (DP-647)
Sn–Zr, oxidation in water at high temperature, effects of hydrogen and oxygen on, 16: 26467(R) (HW-73100)
Sn–Zr, oxidation kinetics and oxide film breakaway at 600 to 850°C, 20: 25497
Sn–Zr, oxidation of, distribution of tin in oxide film in, 20: 25504
Sn–Zr, oxidation of, mechanism of breakaway, 20: 25496
Sn–Zr, oxidation of, at 850°C, mechanisms of breakaway, 20: 29652
Sn–Zr, oxygen effects on hydrogen pickup during autoclaving, 16: 12095 (HW-72266)
Sn–Zr, parameters for zirconium self-diffusion in, 20: 2356(T) (AERE-Trans-1030)
Sn–Zr, performance as reactor material, 18: 44183
Sn–Zr, phase studies, 20: 35924
Sn–Zr, pickling of Zircaloy, fluorine pick-up in, 18: 14403 (CI-221)
Sn–Zr, plastic deformation, 16: 33989(R) (SRO-72)
Sn–Zr, plastic deformation of, at 77°K, twinning in, 16: 28542(R) (SRO-68)
Sn–Zr, plastic deformation of, role of deformation twinning in, 16: 29384(R) (TID-14983)
Sn–Zr, properties of, for use in process tubes for nuclear superheat reactors, 16: 31254 (GEAP-3784)
Sn–Zr, properties of, effects of stress and temperature on physical, 16: 28642(R) (BMI-1581(Del.))
Sn–Zr, properties of hydrided, 16: 34065(R) (DP-775)
Sn–Zr, properties for use in light-water-cooled reactors, 18: 10566
Sn–Zr, radiation damage, 16: 21086 (AECL-1484)
Sn–Zr, radiation effects, 16: 25760 (ORNL-3281)
Sn–Zr, radiation effects on, in reactor creep measurements, 16: 26467(R) (HW-73100)
Sn–Zr, radiation effects on, corrosion of, by aqueous chlorides, 16: 14772 (ORNL-3265)
Sn–Zr, radiation effects on corrosion of, by uranyl sulfate at 280°C, 16: 17982 (ORNL-2962)
Sn–Zr, radiation effects on fuel element cladding, 16: 30075 (HW-70158(Pt.I))
Sn–Zr, radiation effects on mechanical properties of, 16: 7890 (NP-11196(p.34-41))
Sn–Zr, radiation effects on mechanical properties of, 16: 23269(R) (DP-735)
Sn–Zr, radiation effects on mechanical properties of, at 5×10^{17} to 8×10^{20} nvt, 16: 33566
Sn–Zr, radiation effects on mechanical properties of, fast neutron, 16: 572 (REIC-20)
Sn–Zr, radiation effects on mechanical properties of, review, 16: 626
Sn–Zr, radiation effects on reactions of, with water at high temperatures, 16: 11575 (ANL-6250)
Sn–Zr, radiation effects on stress-rupture strength of, tube burst tests of, 16: 6823(R) (ORNL-3213(p.124-33))
Sn–Zr, radiation effects on mechanical properties of welded, neutron, 16: 30898 (CRGM-1093)
Sn–Zr, reactions of, with aluminum and uranium at 1182 to 1580°C, 16: 9198 (HW-64573)
Sn–Zr, reactions of, with aluminum–plutonium alloys, 16: 4487
Sn–Zr, reactions of, with thoria–urania slurries during 2200-hr Low Intensity Reactor Test, 16: 17568(R) (ORNL-3262(p.114-22))
Sn–Zr, reactions of, with uranium dioxide during radioinduced failures of, 16: 33428 (CRGM-1103)
Sn–Zr, reactions of, with water, thermodynamics of, 16: 12843
Sn–Zr, reactions with uranium dioxide at high temperatures, 16: 33375 (NYO-10469)
Sn–Zr, recovery and recrystallization of, effects of cold working and composition on, 16: 3455 (HW-69678)
Sn–Zr, solubility of Zr,Sn in Nb,Sn at 1300 to 1600°C, 18: 4271
Sn–Zr, solvent properties of, for hydrogen at 400 to 520°C, 16: 16752
Sn–Zr, sonic inspection for cracks in tubular, 16: 3238 (R61CAP9(Rev.))
Sn–Zr, sonic testing of tubular, 16: 30093(R) (SRO-71)
Sn–Zr, stress analysis, 16: 23309 (ACNP-62010)
Sn–Zr, structure, 16: 27666
Sn–Zr, surface and sub-surface defect detection in, by ultrasonic techniques, 16: 11927 (HW-70638)
Sn–Zr, tensile properties, 16: 20981(T,R) (EURAEC-27)
Sn–Zr, tensile properties of, effects of composition and heat treatment on, 16: 29380 (TID-6155)
Sn–Zr, tensile properties of hydrided, 16: 31253(R) (DP-765)
Sn–Zr, testing tubes of, ultrasonic, 16: 28542(R) (SRO-68)
Sn–Zr, thermal capacity of, determination of, from thermal diffusivity data, 16: 31828 (TID-16721)
Sn–Zr, thermal capacity at 1.2 to 4.5°K, 17: 30966 (CONF-22-15)
Sn–Zr, thermodynamic properties of zirconium in, 16: 25406
Sn–Zr, tube production from, by cold extrusion, feasibility of, 16: 7860(R) (ATL-A-125)
Sn–Zr, use in reactor coolant assemblies, end shielding, and moderator vessel, 17: 34379
Sn–Zr, use of, in reactor pressure tubes, 16: 18679
Sn–Zr, welding, 16: 7889 (NP-11196(p.16-20))
Sn–Zr, welding of, development of high-frequency resistance process for, 16: 12071 (HW-67679)
Sn–Zr, welding of, evaluation of electron-beam, 16: 31763
Sn–Zr, welding properties, 16: 10486 (TID-14971)
Sn–Zr, welding techniques for Zircaloy of CVTR fuel assembly, 16: 494 (CVNA-93)
stainless steel–Zr, corrosion by steam at 650°C, 19: 44616(R) (ANL-7000, pp 122-37)
Ta–Ti–V–Zr, phase studies, 18: 549(R) (NP-13241)
Ta–Ti–Zr, tensile properties at room temperature, 18: 18380
Ta–V–Zr, coating for oxidation protection, 19: 20459(R) (IITRI-B6019-6)
Ta–W–Zr, availability, properties, and uses of, 20: 29760
Ta–W–Zr, fabrication and mechanical properties of sheet of, 19: 11700 (ML-TDR-64-63)
Ta–W–Zr, fabrication of tantalum-base, process development for, 20: 11260
Ta–W–Zr, mechanical properties and weldability, 17: 34420(R) (WANL-PR-M-004)
Ta–W–Zr, metallography of as-cast, 19: 22972(R) (DRI-1092-202)
Ta–W–Zr, phase diagrams, 16: 29376(R) (NMI-9237)
Ta–W–Zr, phase diagrams, 18: 25985 (WADD-TR-60-132(Pt.III))
Ta–W–Zr, phase equilibria, research program on, 19: 7894(R) (DRI-2197)
Ta–W–Zr, phase studies, 16: 16724(R) (NMI-9238)
Ta–W–Zr, phase studies, 16: 27627(R) (NMI-9243)
Ta–W–Zr, phase studies, 17: 6668(R) (NMI-9246)
Ta–W–Zr, phase studies, 17: 12588(R) (NMI-9249)
Ta–W–Zr, phase studies on, 18: 16503
Ta–W–Zr, phase studies, 19: 11682
Ta–W–Zr, phase studies, 19: 32730(R) (DRI-1092-212)
Ta–W–Zr, phase studies on, 20: 7557(R) (DRI-1092-220)
Ta–W–Zr, phase studies at 1100 and 1600°C, 20: 17012(R) (DRI-1092-226)
Ta–W–Zr, strength, weldability, and heat treatment of, 20: 21405
Ta–W–Zr, tensile properties of, 17: 27733(R) (NMI-2116)
Ta–Zr, corrosion by mercury at high temperatures, 19: 36949(R) (BNL-900(p.121-97))
Ta–Zr, effects of carbon additions on mechanical properties of, 18: 14489
Ta–Zr, fabrication and properties, 16: 514(R) (AD-255012)
Ta–Zr, fabrication and properties at high temperatures, 18: 7178
Ta–Zr, magnetic induction measurements for superconducting, 17: 37717
Ta–Zr, oxidation of, at high temperatures, 16: 3411
Ta–Zr, oxidation kinetics at 500 to 900°C, 20: 5854(T) (JPRS-32341, pp 8-16)
Ta–Zr, parameters for zirconium self-diffusion in, 20: 2356(T) (AERE-Trans-1030)
Ta–Zr, phase diagram, 16: 25823 (IS-320)
Ta–Zr, phase diagram, 16: 29376(R) (NMI-9237)
Ta–Zr, phase diagram, 17: 14740 (TID-11295(2nd Ed.))
Ta–Zr, phase diagram, 17: 34409(R) (NMI-1253)
Ta–Zr, phase diagram, 17: 39616
Ta–Zr, phase studies, 16: 21036(R) (NMI-9235)
Ta–Zr, phase studies, 16: 27627(R) (NMI-9243)
Ta–Zr, properties at high temperatures, 18: 2226(R) (NMI-1258)
Ta–Zr, radiation effects on mechanical properties of, fast neutron, 16: 572 (REIC-20)
Ta–Zr, thermodynamic properties, 16: 13636
Tb–Zr, heat of solution at 300°K, 18: 4282
Tb–Zr, magnetic properties of, 17: 32651
Tb–Zr, metallurgical properties and phase studies on, 20: 5891(R) (NYO-2159-1)
Tb–Zr, phase studies, 20: 35924

Tc–Zr, phase studies on, 17: 11220
Th–Ti–Zr, corrosion and structure of, 17: 39649
Th–Ti–Zr, properties and structure of, 18: 37670 (A/CONF.28/P/337)
Th–Ti–Zr, tensile properties at room temperature, 18: 18380
Th–U–Zr, additive effects of aluminum and beryllium, 18: 29001(R) (HW-79280(p.5.1-25))
Th–U–Zr, brazing of Zircaloy-2 end caps to, evaluation, 17: 31681(R) (HW-76559)
Th–U–Zr, corrosion and mechanical properties at high temperatures, 17: 39648
Th–U–Zr, corrosion of defected Zircaloy-2 clad, by water at 300°C, 19: 14806(R) (HW-81984(p.5.1-55))
Th–U–Zr, corrosion by water at 120 to 260°C, 19: 22889 (ANL-7006)
Th–U–Zr, extrusion for use in fuel elements, 17: 37003(R) (HW-78118)
Th–U–Zr, fabrication and corrosion testing of Zy-2 clad, 18: 29001(R) (HW-79280(p.5.1-25))
Th–U–Zr, fabrication into fuel tubes, 18: 30152 (HW-79843)
Th–U–Zr, fabrication, 18: 8721(R) (HW-78388(p.5.1-22))
Th–U–Zr, fabrication of Zircaloy-2-clad, 19: 14806(R) (HW-81984 (p.5.1-55))
Th–U–Zr, fabrication of Zircaloy-clad, for corrosion testing, 19: 34628(R) (HW-84384(p.5.1-6))
Th–U–Zr, hardness of, effects of uranium content on, 19: 11679
Th–U^{235}–Zr, irradiation testing in ETR-P-7 facility, 18: 29001(R) (HW-79280(p.5.1-25))
Th–U–Zr, irradiation testing and metallurgical properties, 18: 29002(R) (HW-80284(p.5.1-14))
Th–U–Zr, irradiation testing, 18: 44056(R) (ORNL-3670(p.228-50))
Th–U–Zr, mechanical properties and phase studies at high temperatures, 17: 12660 (ATL-A-128)
Th–U–Zr, microstructure, 18: 22485 (MCW-1483)
Th–U–Zr, phase diagrams, effects of cooling rate on omega, 17: 39647
Th–U–Zr, phase studies, 16: 30882
Th–U–Zr, radiation effects on Zircaloy-2-clad, 18: 8721(R) (HW-78388 (p.5.1-22))
Th–U–Zr, radiation effects on Zircaloy-clad, 19: 22869(R) (HW-83298 (p.5.1-38))
Th–U–Zr, radiation effects on Zircaloy-clad, 19: 34628(R) (HW-84384(p.5.1-6))
Th–U–Zr, radiation effects on Zircaloy-clad, 19: 36953(R) (HW-84609 (p.5.1-5))
Th–U–Zr, radiation effects on, 19: 38755(R) (ORNL-3611)
Th–U–Zr, stress-rupture measurements at 800°C and 4 and 5 ksi, 18: 4175(R) (ORNL-3470(p.196-212))
Th–U–Zr, tensile strength of, aging effects on, 20: 31767
Th–Zr, analysis of, for zirconium, spectrophotometric, 16: 25284
Th–Zr, beta-phase transformations in, 18: 37707
Th–Zr, corrosion by water at 120 to 260°C, 19: 22889 (ANL-7006)
Th–Zr, development for high-temperature oxidation protection of tungsten, 17: 14836(R) (NP-12592)
Th–Zr, mechanical properties at 600°C, 17: 14740 (TID-11295(2nd Ed.))
Th–Zr, mechanical properties at high temperatures, 19: 38755(R) (ORNL-3611)
Th–Zr, nitridation, 18: 5729 (ASD-TDR-63-744)
Th–Zr, oxidation at high temperatures and oxide diffusion behavior, 17: 30937(R) (NP-12968)
Th–Zr, oxidation of nitrided, 17: 30937(R) (NP-12968)
Th–Zr, oxidation at high temperatures, surface, 18: 5729 (ASD-TDR-63-744)
Th–Zr, phase studies, 16: 30877
Th–Zr, phase studies, 16: 30879
Th–Zr, phase studies, 20: 35924
Th–Zr, phase transformations in, 18: 37701
Th–Zr, structure of, effects of heat treatment on, 16: 4574
Th–Zr, tensile properties, effects of thoria on, 18: 44056(R) (ORNL-3670(p.228-50))
Th–Zr, use of, in cladding thorium with zirconium, 16: 512(P)
Ti–U–Zr, phase studies of, at 900°C, 16: 30875
Ti–V–Zr, fabrication and properties, 18: 26893(R) (ANL-6868(p.11-108))
Ti–V–Zr, fabrication and properties, 19: 36965(T,R) (EURAEC-618)
Ti–V–Zr, phase studies, 18: 549(R) (NP-13241)
Ti–V–Zr, tensile properties at room temperature, 18: 18380
Ti–V–Zr, thermal expansion between 100 and 1100°C, 19: 24982(R) (EURAEC-1270)
Ti–V–Zr, use as brazing alloy, 19: 30690(R) (ML-TDR-64-270)
Ti–W–Zr, properties of wrought, 17: 6672 (NP-12383)
Ti–W–Zr, tensile properties at room temperature, 18: 18380
Ti–Zr, chemical ordering in, 20: 36355 (ANL-7182)
Ti–Zr, combustibility temperature of, 19: 37093
Ti–Zr, corrosion of, by hydrochloric and nitric acids, 16: 17988
Ti–Zr, corrosion of, by nitric and phosphoric acids, 16: 33441
Ti–Zr, corrosion of, by sulfuric acid, 16: 33440
Ti–Zr, corrosion rates of, in oxygen and water, electrical measurements on growing scale, 16: 2132 (ANL-6434)
Ti–Zr, corrosion in acid solutions, 17: 8747
Ti–Zr, creep activation in, limiting values for, 18: 34152
Ti–Zr, creep of beta, 18: 26011
Ti–Zr, creep properties, 17: 27830
Ti–Zr, creep properties of, effects of pressure and zirconium content on, 19: 11738
Ti–Zr, creep properties of, effects of phase, temperature, and zirconium content on, 19: 11739
Ti–Zr, deposition from fused salts, electrolytic, 20: 9448
Ti–Zr, ductility and thermal expansion, 20: 43964
Ti–Zr, elastic modulus variations and internal friction in iodide-refined, 16: 13629
Ti–Zr, electric conductivity of, effects of temperature on, 20: 41457(R) (ORO-3291-3)
Ti–Zr, electronic properties, 18: 44150(R) (ORNL-3670(p.44-53))
Ti–Zr, hardness, 19: 11682
Ti–Zr, heat of solution at 300°K, 18: 4282
Ti–Zr, hydrogen reaction kinetics with, 17: 27347
Ti–Zr, ignition temperatures, 17: 40421(R) (ANL-6766)
Ti–Zr, inelastic neutron scattering in, 17: 38060(T)
Ti–Zr, lattice structure of, 17: 41873 (WASH-1044)
Ti–Zr, magnetic moments and superconductivity of, 18: 34700
Ti–Zr, mechanical and metallurgical properties, 16: 4547 (WADC-TR-59-595(Pt.II))
Ti–Zr, neutron inelastic scattering by disordered, cold, 16: 33911
Ti–Zr, neutron inelastic scattering in, 18: 24959 (NP-13910)
Ti–Zr, oxidation of, at high temperatures, 16: 3411
Ti–Zr, oxidation behavior at 700 or 900°C, 17: 36235
Ti–Zr, oxidation properties for use in sodium coolant system, 19: 22981 (LA-DC-7050)
Ti–Zr, oxidation by potassium hydroxide at 90°C, 19: 32698
Ti–Zr, oxidation kinetics at 500 to 900°C, 20: 5854(T) (JPRS-32341, pp 8-16)
Ti–Zr, phase diagram for, 20: 41457(R) (ORO-3291-3)
Ti–Zr, phase studies and tensile properties, 16: 21058
Ti–Zr, phase studies, 20: 35924
Ti–Zr, phase studies, 20: 35928
Ti–Zr, reactions of, with hydrogen, 16: 21072
Ti–Zr, sorptive properties for hydrogen, 17: 22206
Ti–Zr, superconductivity of, 18: 15084
Ti–Zr, superconducting transition anomalies in, (E), 19: 10214
Ti–Zr, temperature effects on mechanical properties of, 18: 10553
Ti–Zr, tensile properties at room temperature, 18: 18380
Ti–Zr, thermodynamic properties, 16: 13636
Ti–Zr, use as getter in removing oxygen from argon, 18: 27862 (NASA-SP-41(p.313-16))
Ti–Zr, vibrational frequency distribution of, neutron inelastic scattering studies of, 17: 39713 (BNL-7240)
U–Zr, analysis for aluminum, spectrographic, 18: 35451 (PG-Report-390)
U–Zr, analysis for trace impurities by anion exchange-partition chromatography and spectrography, 20: 26764
U–Zr, analysis of, for hydrogen by equilibrium gas pressure functions, 16: 8675 (KAPL-M-AHA-2)
U–Zr, analysis of, for zirconium, volumetric, 16: 14624 (PG-Report-265)
U–Zr, analysis of, for zirconium, 17: 15892
U–Zr, annealing irradiated, 18: 34234
U–Zr, bibliography on SNAP fuel materials containing, 18: 33128 (NAA-SR-9525(Vol.I))
U–Zr, bonding and fabrication of Zr-clad, by gas-pressure method, 16: 16701
U–Zr, bonding to ferrous metals, 18: 25962(P)
U–Zr, casting of radiator of, 18: 27919(R) (NMI-1131)
U–Zr, casting of, testing of products from, 20: 29803
U–Zr, chlorination of irradiated, in reprocessing, 18: 16153
U–Zr, cladding with Zirconium-2, bonding mechanisms in, 20: 39361 (WAPD-305)
U–Zr, combustion kinetics of, 20: 43612
U–Zr, compatibility with iron, 20: 2229
U–Zr, corrosion of, by water, effects of cathodic polarization on, 16: 22154
U–Zr, corrosion of, effects of carbon on, 16: 9150 (HW-62875)
U–Zr, corrosion of, effects of hydrogen on, 17: 6585
U–Zr, corrosion by alkaline solutions, effects of cathodic polarization on, 18: 30137
U–Zr, corrosion in aqueous solutions, effects of temperature on, 19: 13926
U–Zr, corrosion inhibition by oxide films on, mechanisms of, 20: 21281
U–Zr, criticality studies, 17: 19033 (NAA-SR-Memo-8195)
U–Zr, criticality studies for fabrication, shipping, and storage of, 17: 30754 (NAA-SR-Memo-8195(Rev.))
U–Zr, criticality conditions and handling safety, 16: 13392 (NAA-SR-Memo-6872)

U–Zr, decontamination of fluoride-volatility plant after processing irradiated, 20: 11032 (ORNL-3891)
U–Zr, detection of metastable phases in, 18: 18385
U–Zr, diffusion in, Kirkendall effect as a function of concentration in, 16: 29393(T) (AEC-tr-5324)
U–Zr, diffusion of fission gases from, during temperature changes in reactor, 16: 23255 (AERE-R-3093)
U–Zr, diffusion of hydrogen in delta-phase, theoretical kinetics and stresses of, 16: 25756 (NAA-SR-6264)
U–Zr, diffusion in gamma phase, 17: 32577(T) (AEC-tr-5931)
U–Zr, diffusion of fission gas from hydrided, 20: 5844
U–Zr, disintegration in mixtures of argon and oxygen and argon and nitrogen, droplet study of, 18: 24933 (AFSWC-TDR-63-51)
U–Zr, dissolution of, by anhydrous hydrogen fluoride–hydrogen chloride at 400 to 450°C, 16: 25710(P)
U–Zr, dissolution of, by hydrofluoric acid–hydrogen peroxide systems, 16: 16464
U–Zr, dissolution of, development of continuous hydrofluoric acid process for, 17: 8242 (IDO-14594)
U–Zr, dissolution, 17: 10246(R) (ORNL-TM-403)
U–Zr, dissolution in titanium equipment, 17: 14378 (ORNL-TM-395)
U–Zr, dissolution process expansions, developments, 17: 30582(R) (IDO-14611)
U–Zr, dissolution-fluorination tests in fused salt volatility process, 17: 40930(R) (ORNL-TM-581)
U–Zr, dissolution of, equipment for, 18: 31683(P)
U–Zr, dissolution in hydrofluoric acid-nitric acid solutions, 18: 31658(R) (IDO-14635)
U–Zr, dissolution in hydrofluoric acid solutions, 18: 10181 (IDO-14619)
U–Zr, dissolution of Zircaloy-clad, using hydrofluoric acid, 18: 16152
U–Zr, dissolution in stainless steel vessel without corrosion, 18: 35639 (DP-872)
U–Zr, dissolution in fused salt fluoride volatility process media, 18: 35641(R) (ORNL-TM-785)
U–Zr, dissolution of irradiated, development of methods for, 19: 7274(R) (IDO-14636)
U–Zr, dissolution in dilute hydrofluoric acid, 19: 11292
U–Zr, dissolution and processing of irradiated Zr-alloy-clad, 16: 20534(R) (IDO-14574)
U–Zr, dissolution by ammonium fluoride, 20: 10964
U–Zr, dissolution of zirconium-clad, flowsheets for semi-continuous, 20: 33411 (IDO-14674)
U–Zr, effects on preparation of uranium carbide by carbothermic reduction of oxide, 20: 33841 (NAA-SR-10624)
U–Zr, enrichment of, autoradiographic determination, 17: 18672 (NAA-SR-7752)
U–Zr, fabrication of tubes of, for driver elements of the Heavy Water Components Test Reactor, 17: 25758
U–Zr, fabrication by casting, 18: 27920(R) (NMI-1123)
U–Zr, fabrication by casting, 18: 27921(R) (NMI-1129)
U–Zr, fabrication and mechanical properties, 18: 20449 (BMI-973(Del.))
U–Zr, fabrication and handling of fuel rods of, (E/T), 19: 8619 (NAA-SR-Memo-9945)
U–Zr, fabrication and properties, 19: 15991(R) (BNL-841(p.63-101))
U–Zr, fabrication of Zr-clad, into tubular fuel elements by extrusion, 16: 21001
U–Zr, hydrochlorization for separation of zirconium, 19: 11292
U–Zr, hydrogen thermal migration in, 19: 11680
U–Zr, irradiation testing of reactor fuel tubes of, 20: 2466
U–Zr, mechanical properties of, 17: 39636
U–Zr, mechanical properties and phase studies, 17: 39637
U–Zr, mechanical properties and phase studies, 17: 39625
U–Zr, mechanical properties and phase studies, 17: 39628
U–Zr, mechanical properties, 17: 39635
U–Zr, mechanical properties of gamma-phase uranium-base, 20: 15060 (UCRL-7771)
U–Zr, mechanical properties, 20: 29803
U–Zr, meltdown in TREAT, 17: 1359(R) (ANL-6569)
U–Zr, microstructure characteristics, 16: 25785
U–Zr, microstructure of, effects of aluminum, iron, phosphorus, and silicon on, 18: 22485 (MCW-1483)
U–Zr, microstructure of uranium-rich, effects of heat treatments on, 20: 21372
U–Zr, neutron multiplication factor of, (E), 20: 22392
U–Zr, nuclear reactions of, in EBR-I, 17: 14121(R) (ANL-6596 (p.211-17))
U–Zr, oxidation of, in nitric acid, electrolytic, 16: 17759 (DP-647)
U–Zr, oxidation, 17: 468
U–Zr, phase decomposition and formation in, effects of composition and cooling on, 19: 26837
U–Zr, phase diagram of uranium-rich, 19: 47014 (RT/MET(64)4)
U–Zr, phase studies, 16: 30856
U–Zr, phase studies and properties of 6 wt % zirconium, 16: 12140
U–Zr, phase studies in uranium-rich end, 16: 15165 (ANL-6055)
U–Zr, phase studies, 17: 29255 (ZFK-WF-13)
U–Zr, phase studies, 17: 39623
U–Zr, phase studies, 17: 39624
U–Zr, phase studies on uranium-rich, 20: 21372
U–Zr, phase studies, 20: 31666
U–Zr, phase studies, 20: 35924
U–Zr, phase studies of uranium-base, 20: 39388 (CEA-R-2956)
U–Zr, phase transformations, 18: 14477 (UCRL-7595)
U–Zr, phase transformations in, effects of cooling rate on, 20: 5843
U–Zr, phase transformations in, structural orientation relation in gamma-to-alpha, 20: 23701
U–Zr, phase transformation in, mechanisms for beta-to-alpha, 20: 27519
U–Zr, physical properties of delta and gamma phases, 16: 4579
U–Zr, preparation of uranium-rich, by coreduction, 16: 29331
U–Zr, preparation and use as reactor fuel in foamy state, 17: 41478(P)
U–Zr, processing of, by fluoride volatility, 16: 32884(R) (ORNL-3314 (p.39-57))
U–Zr, processing of, for uranium recovery, 16: 4215 (ANL-6342)
U–Zr, processing of irradiated, in aqueous solutions, 16: 30495(R) (IDO-14589)
U–Zr, processing of irradiated, 17: 10742 (ORNL-TM-447)
U–Zr, processing of irradiated, for uranium recovery, 17: 34049 (DP-826)
U–Zr, processing for recovery of uranium, developments in, 17: 36860(R) (ANL-6648)
U–Zr, processing of, by fluoride volatility method, 17: 39179(R) (ORNL-3452(p.26-50))
U–Zr, processing of irradiated, equipment contamination and decontamination in, 18: 23705 (ORNL-TM-837)
U–Zr, processing in Volatility Pilot Plant, demonstration run for, 18: 6885 (ORNL-TM-752)
U–Zr, processing by fluidized-bed method, 18: 13976
U–Zr, processing by volatilization, 18: 37280 (A/CONF.28/P/771)
U–Zr, processing by fused-salt fluoride volatility method, 18: 39385
U–Zr, processing in ORNL volatility pilot plant, 18: 39387
U–Zr, processing for uranium recovery, 18: 41560 (CEA-R-2508)
U–Zr, processing by fluoride volatility, 19: 15331(R) (BNL-841(p.18-42))
U–Zr, processing high-enrichment, research on, 20: 7192(R) (K-1649)
U–Zr, processing for uranium recovery by fluoride volatility, 20: 24971(R) (BNL-954, pp 50-83)
U–Zr, processing for uranium recovery by solvent extraction, 20: 27036(R) (IDO-14661, pp 1-44)
U–Zr, processing of irradiated, by fluoride volatility, 20: 35584 (BNL-973)
U–Zr, properties for use as fuel element in gas-graphite reactors, 18: 4818
U–Zr, properties of hydrided, at high temperatures, 18: 12621 (ARF-A6003)
U–Zr, properties as fast reactor fuel, 18: 15563
U–Zr, properties as reactor fission rate detector, 18: 17278 (KAPL-M-6101)
U–Zr, properties as reactor fuel, 18: 34130 (TID-8540(p.331-410))
U–Zr, properties as reactor fuel, 18: 42024 (UJV-926/63)
U–Zr, properties as function of temperature, 20: 43983
U–Zr, radiation effects on enriched, 16: 15239 (ANL-6114)
U–Zr, radiation effects on cladding materials for, 16: 28555 (TID-7623 (p.105-21))
U–Zr, radiation effects on swelling of crystalline, 18: 32042(R) (HW-81269(p.3.1-38))
U–Zr, radiation stability, 19: 11792
U–Zr, radiation effects on Zr-alloy-clad, dimensional stability of tubular, at 1280 Mwd/t, 16: 24237 (DP-709)
U–Zr, radiation effects on restrained and vented, clad, 16: 32136 (ANL-6431)
U–Zr, radiation effects on HWCTR driver tubes of, 20: 9572 (DP-994)
U–Zr, radiation effects on dimensional changes in tubular fuel elements of, exposed in HWCTR, 20: 25615 (DP-1019)
U–Zr, radioinduced swelling, 17: 27730(R) (HW-77052)
U–Zr, radioinduced swelling of Zircaloy-2-clad, 18: 7291(R) (HW-77954 (p.3.21-54))
U–Zr, radioinduced swelling, 18: 8866(R) (HW-78388(p.8.1-7))
U–Zr, radioinduced dimensional changes in tubes of, 19: 8633(R) (DP-935)
U–Zr, radioinduced swelling in clad tubular, 19: 46917(R) (DP-975)
U–Zr, re-entry burnup enhancement of hydrided, 18: 9619 (SC-DC-3553(p.295-327))
U–Zr, reactions with fluorine, hydrofluoric acid, and sodium fluoride for preparation of uranium hexafluoride, 17: 8258
U–Zr, reactions with water in TREAT, 18: 44922(R) (ANL-6800 (p.326-402))
U–Zr, reactions with air, nitrogen, and oxygen, disintegration properties of, 20: 14169 (AFWL-TDR-64-75)

U–Zr, reactivity coefficients in PMA-47 unpoisoned slab core, 16: 19988 (KAPL-M-JRT-2)
U–Zr, reactivity coefficient measurements in Plastic Mockup Assembly, 17: 4254 (TID-17292)
U–Zr, self-diffusion coefficients of gamma-phase uranium in, 16: 29416
U–Zr, self-diffusion of uranium in, mechanism, 16: 2223
U–Zr, separation of components, 16: 19001(P)
U–Zr, separation of uranium from, by fluorination, 16: 5418(P)
U–Zr, separation of uranium from, by volatilization processes, improvement in method for, 16: 27114(P)
U–Zr, separation of uranium from, using zinc (liquid), pyrometallurgical, 16: 11796
U–Zr, separation of uranium from spent fuel, evaluation of four processes for, 16: 22268 (IDO-14564)
U–Zr, separation of zirconium from, 16: 1854(R) (IDO-14553)
U–Zr, separation of uranium from, 17: 245(P)
U–Zr, separation from unirradiated fuel elements by fluoride volatility, 17: 10728 (BNL-6148)
U–Zr, separation by chlorination-fluorination reactions, 17: 36861(R) (ANL-6764)
U–Zr, separation of uranium from, using bromomandelic acid, 18: 25283
U–Zr, separation of uranium from irradiated, by molten-salt fluoride-volatility process, 18: 31671
U–Zr, separation of uranium from enriched, development of fluid bed-volatility process for, 18: 1484(R) (ANL-6687(p.86-152))
U–Zr, separation of uranium from irradiated, using fused-salt fluoride volatility processes, 19: 4247(R) (ORNL-3627(p.29-72))
U–Zr, separation of uranium from, by fluid-bed volatility process, 19: 11293
U–Zr, separation of uranium from, using fluoride solution, 19: 32321(P)
U–Zr, separation of uranium from, by fluid-bed fluoride volatility process, 19: 42606
U–Zr, separation of uranium from, by fused salt electrolysis, 19: 46448
U–Zr, solubility in hydrofluoric acid containing nitric acid, 19: 22429
U–Zr, solubility in hydrofluoric acid, 20: 36946
U–Zr, solvent properties for iron, 20: 33924
U–Zr, structure, 16: 27666
U–Zr, structure of, effects of cooling rate from gamma phase on, 18: 34127 (RT/MET(64)-2)
U–Zr, structure of, effects of heat treatment on, 19: 47014 (RT/MET 64)4)
U–Zr, superconducting properties, 20: 4390(R) (ORNL-3870, pp 65-9)
U–Zr, surface tension and viscosity, 17: 4933 (WADD-TR-60-463(Pt.II))
U–Zr, swelling of irradiated, effects of annealing temperature on, 19: 40958
U–Zr, tensile properties of hydrided, at 700 to 1000°F, 20: 23650 (NAA-SR-Memo-6957)
U–Zr, thermal conductivity of hydrided, 18: 39901 (NAA-SR-Memo-3848)
U–Zr, thermal cycling effects on dimensional stability, 16: 9657(R) (NAA-SR-1109)
U–Zr, thermodynamics of uranium separation by Zircex process from, 19: 19742 (CEA-R-2592)
U–Zr, thermodynamic behavior of rods of, during re-entry, (T), 20: 8438(R) (AE-63-0011)
V–Zr, composition and mechanical and physical properties of, 18: 7267
V–Zr, corrosion by steam at 400°C, 18: 24150(T,R) (EURAEC-538)
V–Zr, corrosion by steam of, 19: 24982(R) (EURAEC-1270)
V–Zr, corrosion by steam, 19: 24982(R) (EURAEC-1270)
V–Zr, crystal structure of, electron microscopic studies of, 18: 20476(T,R) (EURAEC-916)
V–Zr, crystal structure of Brillouin zones in, effects of electron-atom ratios on, 19: 26836
V–Zr, electrochemical potential and hydrogen overvoltage, 17: 34403 (GEAP-4192)
V–Zr, extrusion of, effects on structure, 17: 6654(R) (EURAEC-394)
V–Zr, free energies of formation of Laves phases in, 16: 13636
V–Zr, hardening of, by addition of aluminum, tin, or titanium, 19: 24982(R) (EURAEC-1270)
V–Zr, hardening of, by formation of intermetallic compounds, 19: 24982(R) (EURAEC-1270)
V–Zr, hydrogen overvoltage measurements in, 17: 27728(R) (GEAP-4076)
V–Zr, hydrogen overvoltage at ZrV_2 in sulfuric acid, 18: 12642 (GEAP-4089(Vol.II)(Paper 22))
V–Zr, magnetic induction in hard superconducting, (E), 20: 21893
V–Zr, mechanical properties of, 19: 24982(R) (EURAEC-1270)
V–Zr, oxidation by carbon dioxide up to 600°C, 18: 30192
V–Zr, phase studies, 17: 11204(T,R) (EURAEC-444)
V–Zr, phase studies of, 17: 11213
V–Zr, phase studies and properties of extruded, effects of annealing, quenching, and tempering on, 18: 24150(T,R) (EURAEC-538)
V–Zr, reactions with hydrogen, thermochemical and structural aspects of, 20: 27436
V–Zr, tensile properties, 19: 36965(T,R) (EURAEC-618)
V–Zr, uptake of hydrogen during steam and water corrosion of, 17: 32519
W–Zr, burn-off rate of electrodes of, in uranium dioxide melting furnace, 16: 33461(T,R) (EURAEC-323)
W–Zr, crystal structure, 18: 32138(R) (DRI-2166)
W–Zr, extrusion and properties of, 19: 18419(R) (AD-424207)
W–Zr, extrusion and swaging, 20: 15101
W–Zr, free energies of formation of Laves phases in, 16: 13636
W–Zr, oxidation kinetics at 500 to 900°C, 20: 5854(T) (JPRS-32341, pp 8-16)
W–Zr, phase studies, 19: 41035
W–Zr, properties of wrought, 17: 6672 (NP-12383)
W–Zr, properties at high temperatures, 20: 4418
W–Zr, properties for high-temperature uses, 20: 15101
Y–Zr, diffusion and solubility of hydrogen in, 19: 13349
Y–Zr, mechanical properties, 16: 5315 (WADD-TR-61-123)
Y–Zr, metallurgical properties and phase studies on, 20: 5891(R) (NYO-2159-1)
Y–Zr, oxidation at high temperatures, 17: 30937(R) (NP-12968)
Y–Zr, oxidation at high temperatures, surface, 18: 5729 (ASD-TDR-63-744)
Y–Zr, oxidation in dry air at 1200 and 1600°C, 19: 47034
Y–Zr, phase studies, 16: 13634
Y–Zr, phase studies, 20: 35924
Y–Zr, preparation and properties, 16: 2128
Y–Zr, surface tension of liquid, 17: 4943
Zn–Zr, crystal structure of intermetallic compounds in, 20: 11328
Zn–Zr, ferromagnetic resonance in intermetallic compounds of, (E), 20: 15960
Zn–Zr, itinerant electron ferromagnetism in, 18: 20556
Zn–Zr, structure of intermetallic compound $ZrZn_{22}$ in, 16: 5730

ZIRCONIUM ANTIMONATES
ion exchange properties for cations, 16: 20403
sorptive properties for sodium and strontium, 18: 1614(R) (ORNL-3488 (p.65-90))

ZIRCONIUM ARSENATES
ion exchange properties, 16: 11548(T) (CEA-tr-R-1421)
ion exchange properties of, effects of acids and hydrolysis on, 18: 33535
preparation of granular gels, for ion exchange use, 17: 1373(P)

ZIRCONIUM ARSENIDES
crystal structure, 19: 7945

ZIRCONIUM BORIDES
abrasive properties, 20: 15109
analysis for boron, carbon, silicon and zirconium, 18: 19882
analysis for boron, volumetric, 18: 35453 (PG-Report-573)
analysis for boron by pyrohydrolysis, 19: 19761 (NP-14876)
analysis for boron, method for, 19: 46941 (NP-15514(Vol.3))
analysis, methods for, 19: 24403 (NP-14952)
bibliography on preparation and properties of, 17: 10579 (ASD-TDR-62-873)
binding of di-, by chromium, molybdenum, and tungsten, 19: 46907 (AD-456724)
bonding in nuclear magnetic resonance analysis of, 17: 8081
boron-11 quadrupole resonance in, 17: 3511
chemical bonding and electric conductivity of, 20: 16439
coating with molybdenum or tungsten by chloride and oxide processes, evaluation of, 19: 40986
coating with molybdenum or tungsten by chloride and oxide processes, 20: 29631
combustion in fluorine, calorimetry of, 17: 14118(R) (ANL-6596 (p.164-74))
combustion in fluorine, thermodynamic properties for, 17: 36860(R) (ANL-6648)
combustion in fluorine, calorimetry of, 18: 43440(R) (ANL-6800(p.305-25))
compact preparation, 17: 6520(R) (NP-12373)
conversion of ZrB_{12} to ZrB_2, kinetics and mechanisms of, 20: 36810
corrosion by carbon dioxide mixtures at 2250°C, 17: 416(R) (NP-12130)
corrosion by cerium–cobalt–plutonium alloy at 750°C, 16: 22549
corrosion by hydrogen chloride at 2250°C, 19: 46956 (NP-15514 (Vol.1))
corrosion by liquid magnesium–uranium–zinc alloys with fused chlorides, 20: 20802(R) (ANL-7055, pp 21-98)
crystal lattice parameters, 19: 47009 (NP-15514(Vol.2))
crystal structure, 17: 3500(T) (JPRS-16059)
crystal structure at 25, 750, and 1005°C, 17: 34328(R) (NP-12991)
crystal structure, 18: 35939(R) (NP-12991)
crystal structure, 19: 7467
Debye temperature parameters for, 19: 7467
deposition from fused salts, electrolytic, 20: 9448
diffusion of oxygen in alpha, anodic film dissolution and hardness studies, 19: 44673 (AECL-2268)
effects of films of, on thermal radiation properties of molybdenum, 16: 32039(R) (PWA-1863)

effects on oxidation resistance of graphite, 18: 24087 (WADD-TR-61-72(Vol.XXX))
effects on properties of niobium–titanium alloy for high-temperature use, 18: 14454 (BM-RI-6390)
effects on thermoelectric properties of MCC 50, 19: 12129(R) (ASD-TDR-62-896(Pt.II))
elastic properties of polycrystalline, 17: 34328(R) (NP-12991)
electric conductivity of, at high temperatures, 17: 8856
electric conductivity at high temperatures, 18: 28012(T)
electric properties of, effects of non-metallic atoms on, 17: 8854
emissivity at 800 to 5000°K, relation of structure to, 18: 20566
emissivity, measurement of spectral, 17: 16632(R) (AD-274654)
emissivity measurements to 3000°K, equipment for, 18: 20567
enthalpy at 300 to 750°C, 20: 23012
enthalpy of formation of, 20: 31213(R) (ANL-7175, pp 119-58)
erosion by gases at 3000°K, 16: 16726(R) (NP-11311)
evaporation at high temperature and thermodynamic properties, 16: 10567
evaporation rate and vapor pressure at 1100 to 2000°C, 16: 2208(T) (AEC-tr-4865)
extrusion and sintering, viscous flow in, 16: 12076
fabrication and properties of, review of, 18: 585
fabrication and properties of sintered filters of, 18: 18336
fabrication and properties of hot-pressed and sintered, 18: 35939(R) (NP-14192)
fabrication and properties of MHD cell electrodes of, 19: 6495
fabrication and properties of, for use at high temperatures, 20: 29772
fabrication as thermocouple casings by grinding and sintering, 19: 30706
fabrication of compacts of, by vacuum hot-pressing, 17: 22145
fluorination at high temperatures, kinetics of, 18: 27354(R) (ASD-TDR-62-204(Pt.III))
friction between surfaces of, at high temperatures in vacuum, argon, helium, and nitrogen atmospheres, 19: 28826
galvanomagnetic properties, 17: 416(R) (NP-12130)
hardness of, effects of temperature on, 17: 36316
heat capacity, 17: 6520(R) (NP-12373)
heat content at 410 to 1125°K, 18: 19955
heat of formation, 18: 1603 (CONF-117-14)
heat of formation of bivalent, 18: 43493
heat of formation of di-, 19: 32118(R) (ANL-7020(p.165-74))
inflammability of powdered, at 180 to 1100°C, 18: 44211
interactions with gas flow in MHD generators, 20: 41738
melting temperature, evaluation for space technology, 18: 16521
oxidation at high temperatures, 18: 27354(R) (ASD-TDR-62-204(Pt.III))
oxidation at 1200 to 2000°K, kinetics of, 20: 43840
oxidation at 500 to 1000°C, effects of additions of cobalt, iron, or nickel on, 18: 32200
oxidation at 945 to 1256°C, kinetics of, 18: 30139
oxidation by carbon dioxide at 2250°C, 19: 46956 (NP-15514(Vol.1))
oxidation by oxygen to 1850°K, effects of alloying additions, stoichiometry, and water vapor on, 18: 35939(R) (NP-14192)
oxidation kinetics at 945 to 1256°C, 20: 5845
oxidation of, by carbon dioxide at 2250°C, 17: 20405(R) (NP-12710)
oxidation of, in argon–carbon dioxide mixtures at 2250°C, 17: 6520(R) (NP-12373)
oxidation of, kinetics of, 20: 7527
performance as control materials for high-temperature reactors, 18: 22519
performance as seed material for gas coolant in rocket reactors, (E), 19: 24149 (NASA-CR-212)
phase studies, 18: 35939(R) (NP-14192)
plasticity and strength at 20 to 2500°C, 16: 27679
preparation and properties of, 20: 17085
preparation and properties of crucibles of, 16: 9219(T) (CEA-tr-R-1440)
preparation and purification, 19: 46941 (NP-15514(Vol.3))
preparation by carbothermic reduction of boron and zirconium oxides, 18: 19882
preparation by carbon reduction of oxide with boric oxide, 20: 19702
preparation by powder metallurgical techniques, 17: 34328(R) (NP-12991)
preparation by reactions of boron carbide with zirconium oxide, 18: 39832(T)
preparation by slip casting, method for, 20: 37201
preparation in fluidized beds, 20: 9397
preparation of divalent, by reaction between boric acid, carbon, and zircon, 19: 30657
preparation of stoichiometric, 18: 238
preparation of, electrolytic, 18: 37159
preparation, properties, and aerospace applications, 19: 37142
preparation, properties, and uses, 20: 8900
pressing high density, apparatus for hot, 16: 19267
production, 17: 25280(P)
production from zircon, 17: 8732(P)
properties as magnetohydrodynamic electrodes, 18: 7458 (PWA-2125)
properties for aerospace applications, 19: 37143
properties for magnetohydrodynamic cell electrodes, 17: 31012
properties for very high temperature applications, 18: 10539 (RTD-TDR-63-4096(Pt.I))
properties, mechanical and physical, 16: 30853
properties of, for use in silicate technology, 18: 7250
properties of vapor-deposited, 19: 30775
properties, mechanical and physical, 19: 7456
radiation effects on mechanical properties of, 18: 16526 (NP-13663)
radiation sintering of, 17: 20512 (GEAP-3743(Pt.II))
reactions with carbon at 2092 to 2221°K, mass spectrometric study of, 19: 4100 (AD-450678)
reactions with carbon, high-temperature, 19: 28865
reactions with carbon, thermodynamic data for, 19: 46956 (NP-15514 (Vol.1))
reactions with copper and nickel mattes, slags, molten salts, and refractory metals, 20: 14989
reactions with fluorine at high temperatures, kinetics of, 17: 32130
reactions with fluorine at high temperatures, 18: 3793
reactions with graphite, iridium, and rhodium, 19: 18393(R) (ML-TDR-64-173(Pt.II))
reactions with graphite to 2200°C, 19: 38654
reactions with magnesium and zirconium oxides at 1800 to 2000°C, 18: 43463
reactions with molten metals at 400 to 1500°C, 19: 37112
reactions with molybdenum, niobium, tantalum, and tungsten at 900 to 2200°C, 20: 25578(T) (N-65-35787)
sintering conditions, 17: 22142
sintering of, effects of various metals on, 19: 26794
sintering of, effects of cobalt, iron, or nickel additions on, 20: 31668
sintering of, grain growth during, 20: 21273
sintering of, mechanism of shrinkage in, 20: 23630
spectra at high temperatures, emission, 19: 4661 (WADD-TR-60-646 (Pt.IV))
spectra at 1500 to 2500°K, infrared, 18: 22497 (WADD-TR-60-646 (Pt.3, Vol.II))
spectra of, reflection, 17: 6520(R) (NP-12373)
strength of powdered, at 20 to 2800°C, 18: 39984
structure, nuclear quadrupole studies, 16: 27643
thermal expansion at 25 to 2020°C, 19: 47009 (NP-15514(Vol.2))
thermal properties to 5000°F, 16: 18938
thermal properties, 16: 22597 (WADD-TR-60-924)
thermal properties of, at 500 to 5000°F, 17: 16636 (ASD-TDR-62-765)
thermal properties, 19: 7467
thermodynamic properties at 3000°K and in different atmospheres, 16: 25747 (ASD-TDR-62-204(Pt.I))
thermodynamic properties at 300 to 1200°K, 16: 25401
thermodynamic properties of di-, at 5 to 350°K, 17: 28849
thermodynamic properties, 17: 30961 (ASD-TDR-62-204(Pt.II))
thermodynamic properties, 18: 27354(R) (ASD-TDR-62-204(Pt.III))
thermodynamic properties, 19: 7448
thermodynamic properties, 19: 46956 (NP-15514(Vol.1))
thermoelectric properties, 17: 8855
use in dispersion fuel elements as burnable poison, 17: 22929 (TID-7642(p.369-75))
use in MHD duct electrodes, preparation and testing for, (E), 20: 41718
use of, in nuclear rockets, 17: 8710 (TID-16315(Del.))
vapor pressure at high temperatures, 19: 4661 (WADD-TR-60-646(Pt.IV))
vapor pressure at 2267 to 2445°K, 19: 46956 (NP-15514(Vol.1))
vaporization at 2267 to 2445°K, mass spectrometric study of, 19: 4100 (AD-450678)
vaporization near 2400°K, 16: 16726(R) (NP-11311)
vaporization of, mass-spectrometric studies, 17: 416(R) (NP-12130)
wear resistance of electroslag welding cell of, in molten fluxes, 18: 44168
wetting with liquid aluminum or beryllium oxides, sessile drop studies of, 19: 26826
B_4C–$MoSi_2$–ZrB_2, development of composite of, 20: 9391
BeO–ZrB_2, fabrication of hot-pressed blocks of, 20: 4999(R) (ORNL-2599)
BN–$MoSi_2$–ZrB_2, mechanical properties of composites of, 20: 5845
BN–$MoSi_2$–ZrB_2, tensile properties at 70 to 3500°F, 18: 30170 (CONF-553-1)
Co–ZrB_2, oxidation kinetics at 500 to 1000°C, 20: 5845
Cr–ZrB_2, phase studies, evidence for existence of $CrZrB_2$ in, 20: 13276
Fe–ZrB_2, oxidation kinetics at 500 to 1000°C, 20: 5845
$MoSi_2$–ZrB_2, emittance testing of coatings of, 19: 18465(R) (PWA-2518)
$MoSi_2$–ZrB_2, oxidation of, in argon–carbon dioxide mixtures at 2250°C, 17: 6520(R) (NP-12373)
$MoSi_2$–ZrB_2, oxidation and thermodynamic properties at high temperatures, 18: 35939(R) (NP-14192)
MoSi–ZrB, oxidation of, kinetics of, 20: 7527
$MoSi_2$–ZrB_2, preparation and properties of oxidation-resistant, 16: 9223
$MoSi_2$–ZrB_2, preparation and properties of, 19: 37121

$MoSi_2$–ZrB_2, properties of Boride Z, 17: 12692
$MoSi_2$–ZrB_2, tensile properties of pressed and sintered, at 70 to 3650°F, 18: 7217(R) (TID-19877)
$MoSi_2$–ZrB_2, tensile properties at 70 to 3650°F, 19: 7909 (TID-21430)
$MoSi_2$–ZrB_2, tensile properties at 70 to 3650°F, 19: 26823 (TID-21843)
Mo–ZrB_2, sintering of, effects of composition on, 20: 31698
Mo–ZrB_2, stability and strength at 1650 to 2210°C, 19: 26853
Ni–ZrB_2, oxidation kinetics at 500 to 1000°C, 20: 5845
stainless steel–ZrB_2, fabrication of dispersions of, process development for, 20: 19177(R) (BMI-1757)
UO_2–ZrB_2, preparation and properties, 19: 40960
UO_2–ZrB_2, radiation testing of fuel elements of, 20: 17121 (GEAP-4918)
WC–ZrB_2, analysis of, for tungsten and zirconium, 16: 1724
Zircaloy-2–ZrB_2, burnup of boron-10 in, at 400 to 650°F, 17: 23864(R) (BMI-1619(Del.))
Zircaloy-2–ZrB_2, corrosion by water at 600°F, 17: 23864(R) (BMI-1619(Del.))
Zircaloy-2–ZrB_2, radiation effects on, at high boron burnups at 400 to 500°F, 17: 24004 (BMI-1627)
ZrB_2–$ZrSi_2$, crystal structure of ZrB_2–$ZrSi_2$ phase in, 16: 4175

ZIRCONIUM BROMIDES

complexes with bipyridyl and 1,10-phenanthroline, preparation and properties of, 18: 8361
complexes with ethyl and methyl cyanides, uv spectra of, 18: 41415
crystal structure, 16: 30437
crystal structure of trivalent, 18: 39188
decomposition on hitting hot metal foil in vacuum, 17: 159
density and critical parameters of liquid, 17: 18078
heat of formation and thermodynamic properties, 17: 4501
magnetic properties at 80 to 300°K, 16: 20423
preparation of trivalent, from zirconium tetrabromide and zirconium, 17: 14294
reactions with potassium and potassium amide in liquid ammonia, 17: 23342
solubility in carbon tetrachloride, chloroform and 1,2-dichloroethane, 17: 35810
structure of trivalent, 16: 23682
thermodynamic properties, 20: 10816(T) (NASA-TT-F-285)
$HfBr_4$–$ZrBr_4$, phase studies, 16: 18074
$ZrBr_4$–ZrI_4, phase studies, 16: 18074

ZIRCONIUM BRONZE

analysis for zirconium using *p*-iodoamygdalic acid, gravimetric, 18: 17749

ZIRCONIUM CARBIDE HYDRIDES

crystal structure of, from thermal-neutron powder diffraction studies, 20: 17074

ZIRCONIUM CARBIDES

abrasive properties, 20: 15109
analysis for carbon using electron microprobe, 19: 43966
analysis, methods for, 19: 24403 (NP-14952)
atomic vibration amplitudes, 18: 19987
atomic vibrational amplitudes and Debye temperatures at 25 to 1700°C, 19: 47009 (NP-15514(Vol.2))
bibliography on properties, 17: 27809 (UCRL-7284)
bonding and vacancies in, 18: 16483(T) (AEC-tr-6374)
bonding to tantalum, 16: 15151 (APED-3870)
carbon diffusion in, at 1650 to 2000°C, coefficient for, 20: 46216
coating of, effects of, on oxidation resistance of graphite, 20: 29773
coating with molybdenum or tungsten by chloride and oxide processes, evaluation of, 19: 40986
coating with molybdenum or tungsten by chloride and oxide processes, 20: 29631
comminution of, effects of impact strength, microhardness, shear modulus, and thermal expansion on, 18: 44220(T)
compact preparation, 17: 6520(R) (NP-12373)
compatibility with stainless steel, 17: 41364(T,R) (EURAEC-562)
compatibility with stainless steel at 600°C, 18: 32064(T,R) (EURAEC-1064)
compatibility with stainless steel at 600°C, 19: 7853(R) (EURAEC-1173)
compatibility with stainless steel and uranium carbides at high temperatures, 19: 13874(R) (EURAEC-1179)
compressibility of, effect of high pressure on, 20: 9520
conductivities at high temperatures, electric and thermal, 16: 16733 (WADD-TR-60-581(Pt.II))
containment in graphite crucibles at 3800 to 4700°K, 20: 43174 (NASA-CR-608)
corrosion by carbon dioxide mixtures at 2250°C, 17: 416(R) (NP-12130)
corrosion by carbon dioxide and hydrochloric acid at 2250°C, 17: 34328(R) (NP-12991)
corrosion by cerium–cobalt–plutonium alloy at 750°C, 16: 22549
corrosion by fused fluorides and liquid metals, 17: 7606(R) (ORNL-1515)
corrosion by hydrogen chloride at 2250°C, 19: 46956 (NP-15514 (Vol.1))
corrosion by hydrogen fluoride at 2000 to 3100°K, 20: 2261(R) (UCRI-326)
corrosion by manganese–uranium alloy at 1100°C, 17; 7658(R) (LAMS-2815)
corrosion of, by hydrochloric acid, 17: 20405(R) (NP-12710)
creep rate of polycrystalline, at 1960 to 2060°K, 19: 47009 (NP-15514 (Vol.2))
creep testing, 17: 20405(R) (NP-12710)
crystal lattice parameters as function of carbon content, 19: 34684 (N64-27289)
crystal structure, 18: 12627(R) (BNL-823(p.66-93))
crystal structure, 18: 25970(R) (ANL-6868(p.303-25))
crystal structure, 19: 7467
Debye temperature parameters for, 19: 7467
deformation properties and hardness of, at high temperatures, 20: 33920
deposition of coatings of, on uranium dioxide fuel particles, vapor method for, 17: 34388
deposition on metals by electrophoresis at 19 to 20 mv, 20: 17004
determination in niobium carbide–zirconium carbide, method for, 19: 46941 (NP-15514(Vol.3))
development and evaluation of tantalum and tungsten reinforced, 16: 27624 (ASD-TDR-62-314)
diffusion of carbon in, 20: 23631
diffusion of carbon in, at 1700 to 3000°C, 20: 27530
diffusion of xenon in powdered, 19: 23355(R) (BNL-867(p.1-117))
diffusion of xenon from, temperature effects on, 19: 36949(R) (BNL-900 (p.121-97))
diffusion of xenon in, 20: 20177(R) (BNL-929, pp 83-105)
effects of dispersions of, on hardness of niobium–titanium–vanadium alloys, 17: 41428(R) (IITRI-B6007-4)
effects on austenitic grain size in iron and steel, 17: 32627
effects on dispersion strength of niobium–vanadium alloys, 17: 23943(R) (ARF-B6007-2)
effects on graphite microstructure, 20: 2318(R) (GA-5915(Pt.1))
effects on mechanical properties of tungsten, 16: 3478 (WADD-TR-60-37 (Pt.II))
effects on properties of niobium–titanium alloy for high-temperature use, 18: 14454 (BM-RI-6390)
effects on radiation resistance and mechanical properties of plutonium or uranium carbides, 18: 44230(P)
effects on strength of pyrographite at high temperatures, 17: 22152(R) (AD-285518)
elastic constants at 27°C, 16: 16726(R) (NP-11311)
elastic properties of stoichiometric, 20: 39430
elastic properties at 4.2 to 298°K, (E), 20: 43942
electric conductivities and Hall coefficients, 16: 6749
electric conductivity and Hall effect at 77 to 350°C, 16: 16726(R) (NP-11311)
electric conductivity, 17: 6520(R) (NP-12373)
electric conductivity of, at high temperatures, 17: 8856
electric conductivity at high temperatures, 18: 28012(T)
electric conductivity at 1000 to 2500°K, 19: 30771
electric conductivity of, at 1200 to 3500°K, 20: 41729
electric properties of, effects of non-metallic atoms on, 17: 8854
electric properties of, rigid band model for interpreting, 18: 24137 (NP-13944)
electron structure and bond strength of, relation of, 18: 18395
emissivity at 1600 to 3100°K and 0.4 to 4 μ wavelength, 17: 30832
emissivity at 800 to 5000°K, relation of structure to, 18: 20566
enthalpy at 1275 to 2788°K, 19: 23045
entropy of formation at 298°K, 18: 19974
erosion by gases at 3000°K, 16: 16726(R) (NP-11311)
evaporation rate and vapor pressure at 1100 to 2000°C, 16: 2208(T) (AEC-tr-4865)
evaporation rate at 2300 to 2500°K, 19: 7505
fabrication and properties of, review of, 18: 585
fabrication and properties, 18: 10456(T,R) (EURAEC-733)
fabrication and properties, 18: 14292(T,R) (EURAEC-861)
fabrication and properties, 20: 29727
fabrication and thermal properties, 17: 41364(T,R) (EURAEC-562)
fabrication by hot-pressing, 20: 31699
fabrication into thin plates by pressure compacting or powder rolling, 20: 21303
fabrication into thin plates, methods for, 20: 41430
fabrication of spherical particles of, by powder agglomeration method, 20: 793
Fermi level, 19: 47009 (NP-15514(Vol.2))
figure of merit and atomic characteristics, 19: 2284
flexural strengths at room to 1500°C, development of, 17: 18734 (AD-282047)

flow characteristics of, high-temperature, 17: 6554
fluorination at high temperatures, kinetics of, 18: 27354(R) (ASD-TDR-62-204(Pt.III))
formation at 500 to 1100°C, kinetics of, 16: 13585 (TID-14950)
formation of mixed, in diffusion between uranium and zirconium in presence of carbon, 19: 18494
formation of, in reaction of zirconium with graphite above 2000°C, 20: 35523
free energy of formation, 16: 22582 (ASD-TDR-62-7)
hardness of, effects of temperature on, 17: 36316
heat flow between thermionic electrodes of, 17: 27979
heat of formation, 18: 39889 (BM-RI-6518)
heat transfer in fluidized beds to argon and helium, particle-to-gas, 18: 27655 (LA-3061)
heats of formation, 19: 40961
inflammability of powdered, at 180 to 1100°C, 18: 44211
interactions with gas flow in MHD generators, 20: 41738
iodination of, to prepare pure zirconium, 19: 46969
joining to niobium and tantalum, 16: 19323(P)
magnetic susceptibility, 17: 14858(T) (AEC-tr-5651)
mass loss rates of zirconium from fluidized beds of, 18: 8326 (LAMS-2994)
mechanical properties of hot-pressed, 18: 603 (JPL-TR-32-452)
melting point, 17: 11201(T) (AEC-tr-5598)
melting temperature, evaluation for space technology, 18: 16521
oxidation at high temperatures, 18: 27354(R) (ASD-TDR-62-204(Pt.III))
oxidation at 554 to 652°C, kinetics of, 18: 30139
oxidation by carbon dioxide at 2250°C, 19: 46956 (NP-15514(Vol.1))
oxidation kinetics, 16: 22611
oxidation kinetics of, at 450 to 580°C, 17: 23368
oxidation kinetics at 554 to 652°C, 20: 5845
oxidation of, at 1000 to 2000°K, kinetics of, 17: 21665(R) (ASD-TDR-62-203(Pt.II))
oxidation of cast, by air at 450 to 800°C, 20: 41429(R) (USBM-RC-1249)
oxidation of, in argon–carbon dioxide mixtures at 2250°C, 17: 6520(R) (NP-12373)
performance as diffusion barrier between uranium carbides and refractory metals, 18: 35929(R) (GA-4769(Pt.I))
performance as emitter in hypersonic plasma generators, (E), 19: 20905 (SC-RR-65-54)
performance in focus electrodes in cesium-contact ion thrustors, 20: 31383
performance in high-temperature reactors for space propulsion, 16: 28631
performance in high-temperature reactor fuels, 20: 12378
performance of coatings of, on Pebble Bed Reactor fuel, 16: 9663 (NYO-9064)
phase studies, 17: 22168 (WADD-TD-60-143(Pt.IV))
phase studies, 17: 41364(T,R) (EURAEC-562)
phase studies by differential thermal analysis, 20: 9525
phase studies on, electric conductivity and transformations in, 17: 39560
phase transformation above 2000°C, 17: 27835
physical properties, 17: 11215
physicochemical properties to 2400°K for use as cathodes in thermionic space reactors, 16: 14350(R) (GA-3007)
physicochemical properties for use as cathodes for thermionic space reactors, 16: 5078(R) (GA-2670)
plastic deformation at 2016 and 2134°C, 17: 34328(R) (NP-12991)
plastic deformation of crystalline, 18: 14497
plastic deformation, 19: 11682
preparation, 18: 201 (JEN-116-DMe/I-11)
preparation, 18: 12627(R) (BNL-823(p.66-93))
preparation and properties of, for use in industry, 17: 15989
preparation and properties of, 18: 16498
preparation and properties of cast, 20: 41429(R) (USBM-RC-1249)
preparation and purification, 19: 46941 (NP-15514(Vol.3))
preparation as graphite coating, 19: 7918
preparation by reaction of graphite with zirconium oxide, 19: 19866
preparation in fluidized beds, 20: 9397
preparation of high-purity, using cobalt or iron-nickel alloy bath, 19: 42828
preparation of high-purity, auxiliary metal bath for, 20: 27452
preparation of spherical particles of, procedure and apparatus for, 20: 14971(P)
preparation, properties, and aerospace applications, 19: 37142
production and properties of, 18: 7262
production by carbon reduction in electric arc, 16: 13510 (BM-RI-5951)
production by carbothermic reduction of zirconium dioxide, 19: 12865(R) (NAA-SR-10501)
properties, 16: 4542(R) (NP-11160)
properties as thermionic cathodes to 3000°C, 18: 12426
properties for matrix material in particulate uranium carbide fuels, 20: 39353 (BMWF-FBK-66-07)
properties for thermionic power generation, vaporization, 18: 27980
properties, mechanical and physical, 16: 30853
properties of, dispersion velocity dependence on mechanical and thermal, 17: 27873
properties of, for use in silicate technology, 18: 7250
properties of pyrolytic, chemical and physical, 18: 44223
properties of, at 2000°C, for use in thermionic converters, 20: 29729
properties of, effects of temperature on mechanical and physical, 17: 16760
radiation capacity at 1200 to 3500°K, 20: 41729
radiation effects on pellets of, 20: 20177(R) (BNL-929, pp 83-105)
radiation effects on, neutron, 20: 23774(R) (ORNL-3913, pp 75-109)
radiation effects on mechanical and physical properties of, 17: 16760
reactions of liquid, with liquid carbon in zirconium carbide, 20: 43179(R) (NYO-2082-6)
reactions with copper and nickel mattes, slags, molten salts, and refractory metals, 20: 14989
reactions with fluorine at high temperatures, kinetics of, 17: 32130
reactions with fluorine at high temperatures, 18: 3793
reactions with graphite at 1800 to 2200°C, contact, 18: 30208
reactions with hydrogen, 17: 6520(R) (NP-12373)
reactions with hydrogen chloride, 17: 6520(R) (NP-12373)
reactions with hydrogen at high temperatures, thermodynamic properties of, 17: 38428 (ANL-6656)
reactions with iridium and rhodium, 19: 18393(R) (ML-TDR-64-173(Pt.II))
reactions with magnesium and zirconium oxides at 1800 to 2000°C, 18: 43463
reactions with molybdenum at 1000 to 2100°C, 16: 4555(T) (FTD-TT-61-74)
reactions with molten metals at 400 to 1500°C, 19: 37112
reactions with molybdenum, niobium, tantalum, and tungsten at 900 to 2200°C, 20: 25578(T) (N-65-35787)
reactions with zirconium hydride, structure of ZrC-ZrH_2 formed by, 20: 4378 (NAA-SR-Memo-11542)
review, 18: 39899 (LA-2942)
sintering without binder, pressure, 17: 32583
solubility in hydrofluoric, nitric, and sulfuric acids, 19: 5905
spectral emissivity at high temperatures, 17: 41363 (WADD-TR-60-646 (Pt.II))
spectral emittance at 800 to 5000°F, 16: 18939
stability in acids, alkalis, and oxidizers, 16: 2952
stability in acids, alkalis, and oxidizers, 16: 11583(T) (AEC-tr-5040)
stability in gases, 16: 29421
strength characteristics of pyro-, testing of, 17: 18285(R) (AD-281238)
structure of, x-ray diffraction study of polymorphism in, 18: 4268
structure, effects of composition on lattice parameter, 19: 42847 (LA-DC-6629)
superconducting properties, 19: 20572
surface energy of, calculation of approximate, 17: 41475(T)
testing as high-temperature heater for electric resistance furnaces, 20: 15112
thermal conductivity at 530 to 2100°C, 16: 24192
thermal conductivity and diffusivity of, 17: 14853 (WADD-TR-60-581 (Pt.III))
thermal conductivity at 200 to 2000°C, 18: 12672
thermal conductivity and diffusion, 18: 25986 (WADD-TR-60-581(Pt.IV))
thermal conductivity, 19: 11682
thermal conductivity at 450 to 1150°C, 19: 13874(R) (EURAEC-1179)
thermal conductivity at 1000 to 2500°K, 19: 30771
thermal decomposition, 17: 32036 (CONF-40-2)
thermal diffusivity at 1300 to 1650°C, technique for measurement of, 18: 2242
thermal emittance at 1000 to 2500°K, 19: 30771
thermal expansion, 17: 11110(T,R) (EURAEC-387)
thermal expansion at temperatures up to 2000°C, 17: 12688
thermal expansion at –190 to 26°C, 17: 25202
thermal expansion coefficient of hot-pressed, 18: 603 (JPL-TR-32-452)
thermal expansion, 18: 19987
thermal expansion at 25 to 2080°C, 18: 30195
thermal expansion at high temperatures, 18: 32178
thermal expansion at 200 to 1000°C, 19: 13874(R) (EURAEC-1179)
thermal expansion at 25 to 2040°C, 19: 47009 (NP-15514(Vol.2))
thermal expansion of, to 2700°C, 20: 1839
thermal expansion at 30 to 2390°C, 20: 5846
thermal properties to 5000°F, 16: 18938
thermal properties, 16: 22597 (WADD-TR-60-924)
thermal properties at 450 to 1820°C, 16: 25837(R) (AD-270841)
thermal properties of, at 500 to 5000°F, 17: 16636 (ASD-TDR-62-765)
thermal properties, 19: 7467
thermal shock resistance of compacts of, 16: 24176 (WADD-TR-60-749(Pt.II))
thermionic emission, 17: 3368 (AD-275571)
thermionic emission properties in cesium vapor and *in vacuo*, 17: 20609

thermionic emission properties, 17: 20622
thermionic emission in cesium vapor, 17: 27977
thermionic emission properties of, microstructure effects on, 17: 37532
thermionic emission from cesiated surfaces of, (E), 20: 21584
thermionic properties at 1400 to 2100°K, 16: 33504
thermionic properties at 1400 to 2000°K, 17: 25811
thermodynamic properties at 3000°K and in different atmospheres, 16: 25747 (ASD-TDR-62-204(Pt.I))
thermodynamic properties, 17: 3470 (BMI-1601)
thermodynamic properties at 5 to 350°K, 17: 28848
thermodynamic properties, 17: 30961 (ASD-TDR-62-204(Pt.II))
thermodynamic properties, 18: 27354(R) (ASD-TDR-62-204(Pt.III))
thermodynamic properties of, Schottky-Wagner model predictions and observations of, 19: 7453
thermodynamic properties at 0 to 1200°K, 20: 7115
thermodynamic properties, 20: 10816(T) (NASA-TT-F-285)
thermodynamic properties of, at high temperatures, 20: 15052 (NP-15880)
thermodynamic stability of, review of data on, 19: 23064
thermoelectric and ionic emission of, in cesium vapor, (E), 19: 6448
thermoelectric emission of, on metal substrates, 19: 6351
thermoelectric emission in cesium vapor, 20: 29800
thermoelectric properties, temperature dependence, 16: 15230
thermoelectric properties in cesium vapor, 16: 15348
thermoelectric properties, 17: 8855
thermoelectric properties at 1300 to 2400°K, 18: 44505
thermophysical properties at high temperatures, 18: 14469 (TID-7676 (p.101-4))
use of, in nuclear rockets, 17: 8710 (TID-16315(Del.))
vapor pressure, 17: 41363 (WADD-TR-60-646(Pt.II))
vapor pressure at 2200 to 2900°K, 17: 38428 (ANL-6656)
vapor pressure of, 19: 37134
vapor pressure, thermodynamic calculation, 16: 13582 (R61SD010)
wear resistance of electroslag welding cell of, in molten fluxes, 18: 44168
welding to high melting metals by vacuum diffusion, 19: 22931(T) (JPRS-29550)
wetting by liquid cobalt, copper, iron, and nickel, 20: 1837
wetting with liquid aluminum or beryllium oxides, sessile drop studies of, 19: 26826
work function, 16: 12151
work function of tantalum cathodes coated with, 17: 27975
zirconium vaporization from hot cathodes of, measurement of rate of, 20: 33163(T) (AEC-tr-6639, pp 22-7)
C–HfC–ZUC, phase equilibria and uranium carbide stability in, 17: 39588
Cr_3C_2–SiC–ZrC, oxidation tests at 1400°C, 19: 9624 (SCNC-270)
Cr_3C_2–ZrC, oxidation tests at 1400°C, 19: 9624 (SCNC-270)
C–UC–ZrC, preparation as reactor fuel material, 20: 2305(P)
C–W_2C–ZrC, behavior at 3250°K in graphite crucible, 19: 44701(R) (TID-22144)
graphite–ZrC, diffusion of helium in, 19: 13877(R) (GA-5016(Pt.1))
graphite–ZrC, elastic properties of graphite dispersions, 17: 12687
graphite–ZrC, fabrication and properties of hot-pressed, 19: 13875(R) (GA-4022(Pt.1))
graphite–ZrC, fabrication and properties of hot-pressed, 19: 13877(R) (GA-5016(Pt.1))
graphite–ZrC, fabrication of dispersions of, by hot-working, 20: 21306
graphite–ZrC, fabrication and properties of hot-pressed composites of, 20: 31688 (NASA-CR-507)
graphite–ZrC, fabrication and mechanical properties of, 20: 39367
graphite–ZrC, hot-working characteristics of dispersion of, 19: 13876(R) (GA-4930(Pt.1))
graphite–ZrC, physical properties of hot-worked matrix bodies of, 19: 7902(R) (GA-4617(Pt.1))
graphite–ZrC, preferred orientation in hot-worked, 19: 13983(R) (GA-4675)
graphite–ZrC, properties as magnetohydrodynamic electrodes, 18: 7458 (PWA-2125)
graphite–TaC–ZrC, properties as magnetohydrodynamic electrodes, 18: 7458 (PWA-2125)
graphite–ZrC, properties and structure of hot-pressed, 20: 5089(R) (GA-6181)
graphite–ZrC, thermal shock resistance, 16: 24176 (WADD-TR-60-749 (Pt.II))
HfC–NbC–ZrC, phase studies and structure, 18: 2281
HfC–ZrC, crystal structure of solid solutions in, x-ray studies of, 20: 15074
HfC–ZrC, preparation and properties, 18: 10569
HfC–ZrC, preparation and physical properties of solid solutions in, 19: 37091
HfC–ZrC, preparation and properties, 20: 11330
MoC–UC–ZrC, analysis for molybdenum and zirconium by x-ray fluorescence spectrometry, 18: 39077
MoC–UC–ZrC, x-ray-fluorescence spectrographic analysis for molybdenum and zirconium, 18: 35449 (LADC-5830)
$MoSi_2$–SiC–ZrC, oxidation tests at 1400 and 1500°C, 19: 9624 (SCNC-270)
$MoSi_2$–ZrC, oxidation tests at 1400 and 1500°C, 19: 9624 (SCNC-270)
NbC–NbN–ZrC, Hall coefficient for solid solutions of, 19: 47009 (NP-15514(Vol.2))
NbC–SiC–ZrC, oxidation tests at 1400°C, 19: 9624 (SCNC-270)
NbC–TaC–ZrC, melting point, 17: 11201(T) (AEC-tr-5598)
NbC–UC–ZrC, preparation and high-temperature stability, 18: 44231(P)
NbC–ZrC, analysis for niobium in, oxidimetric, 17: 25150
NbC–ZrC, analysis for niobium and zirconium, method for, 19: 46941 (NP-15514(Vol.3))
NbC–ZrC, corrosion by carbon dioxide and hydrochloric acid at 2250°C, 17: 34328(R) (NP-12991)
NbC–ZrC, electric conductivity, 17: 34328(R) (NP-12991)
NbC–ZrC, Hall effect, 17: 6520(R) (NP-12373)
NbC–ZrC, melting point, 17: 11201(T) (AEC-tr-5598)
NbC–ZrC, oxidation tests at 1400°C, 19: 9624 (SCNC-270)
NbC–ZrC, oxidation by carbon dioxide at 2250°C, 19: 46956 (NP-15514(Vol.1))
NbC–ZrC, phase studies, 16: 2210(T) (AEC-tr-4871)
NbC–ZrC, preparation and properties as electrode to 3000°C, 18: 12425
NbC–ZrC, preparation and properties, 20: 11330
NbC–ZrC, reflection spectra of, 17: 6520(R) (NP-12373)
NbC–ZrC, superconducting critical currents of, (E), 19: 27371
PuC–ZrC, melting point, 18: 22484 (HW-SA-3131)
PuC–ZrC, preparation and properties, 18: 30113(R) (HW-76304(p.2.1-43))
PuC–ZrC, properties at high temperatures, 18: 29002(R) (HW-80284 (p.5.1-14))
ReC–UC–ZrC, analysis for rhenium, x-ray absorption edge method for, 18: 43376 (LA-3135)
SiC–TaC–ZrC, oxidation tests at 1400°C, 19: 9624 (SCNC-270)
SiC–TiC–ZrC, oxidation tests at 1400 and 1500°C, 19: 9624 (SCNC-270)
SiC–VC–ZrC, oxidation tests at 1400°C, 19: 9624 (SCNC-270)
SiC–ZrC, oxidation tests at 1400 and 1500°C, 19: 9624 (SCNC-270)
stainless steel–ZrC, compatibility with uranium carbide–zirconium carbide, 18: 24072(T,R) (EURAEC-934)
TaC–WC–ZrC, properties as graphite coatings, 17: 14776(R) (AD-285214)
TaC–ZrC, analysis for tantalum and zirconium, method for, 19: 46941 (NP-15514(Vol.3))
TaC–ZrC, hot-pressing effects on density and grain size of, 18: 14437
TaC–ZrC, melting point, 17: 11201(T) (AEC-tr-5598)
TaC–ZrC, melting point and tensile strength, 17: 37552
TaC–ZrC, oxidation tests at 1400°C, 19: 9624 (SCNC-270)
TaC–ZrC, phase studies, 16: 2210(T) (AEC-tr-4871)
TaC–ZrC, properties, 16: 4542(R) (NP-11160)
TaC–ZrC, properties of sintered, 17: 39617
TaC–ZrC, properties at high temperatures, methods of determining, 20: 4297(R) (IS-1200(Sect.M))
TaC–ZrC, thermal expansion at temperatures up to 2000°C, 17: 12688
TaC–ZrC, thermal expansion at high temperatures, 18: 32178
TaC–ZrC, thermal expansion at 30 to 2300°C, effects of composition and hot-pressing direction on, 20: 5846
TaC–ZrC thermionic emission properties, 17: 20609
TaC–ZrC, thermoemission properties at 1100 to 2500°C, 19: 23075
TaC–ZrC, wetting with liquid aluminum or beryllium oxides, sessile drop studies of, 19: 26826
ThC–UC–ZrC, phase studies, 16: 30887
ThC–ZrC, phase studies and properties, 16: 30886
TiC–ZrC, analysis for titanium and zirconium, method for, 19: 46941 (NP-15514(Vol.3))
TiC–ZrC, oxidation tests at 1400°C, 19: 9624 (SCNC-270)
TiC–ZrC, phase studies, 16: 2210(T) (AEC-tr-4871)
UC–ZrC, aqueous processing of graphite- and silicon dicarbide-coated fuel elements of, 20: 14638 (NP-15753)
UC–ZrC, carbon-stable regions in, 17: 32617
UC–ZrC, cathode vapor loss of, physical and chemical redeposition methods for reduction of, 17: 16774(R) (GA-3642)
UC–ZrC, compatibility with refractory metals, 18: 9713 (CONF-375-3)
UC–ZrC, compatibility with stainless steel–zirconium carbide, 18: 24072(T,R) (EURAEC-934)
UC–ZrC, compatibility of molybdenum, niobium, and tungsten at high temperatures in, 20: 2332 (LA-3307)
UC–ZrC, compatibility with refractory metals at 2000°C, 20: 4335
UC–ZrC, compatibility with molybdenum, niobium, and tungsten at high temperatures, 20: 27490 (LA-DC-6901)
UC–ZrC, compatibility of thermionic diodes of, with refractory metal coatings at 1800 to 2500°C, 20: 29820
UC–ZrC, corrosion and oxidation resistance and compatibility with graphite, 18: 30142

UC–ZrC, deposition of, by electrophoresis, 16: 30369 (TID-11153)
UC–ZrC, development as fuel for thermionic space power plants, 20: 14959(R) (N65-20797)
UC–ZrC, development as fuel for thermionic space power plants, 20: 14960(R) (N65-20798)
UC–ZrC, development as fuel for thermionic space power plants, 20: 14961(R) (N65-20801)
UC–ZrC, development as cathodes for thermionic space reactors, 20: 19207(R) (N-65-21346)
UC–ZrC, diffusion of refractory alloys and metals in, 18: 35929(R) (GA-4769(Pt.I))
UC–ZrC, diffusion of fission products in, 18: 38406 (A/CONF.28/P/122)
UC–ZrC, diffusion in pyrographite-coated particles of, 19: 30734 (EUR-1819.e(p.91-104))
UC–ZrC, diffusion of xenon-133 from low-dose, low-temperature irradiated fuels of, (E), 20: 4471
UC–ZrC, diffusion of iridium, rhenium, and rhenium–tungsten alloy in, 20: 19211(R) (N-65-21350)
UC–ZrC, diffusion of iridium, rhenium, and rhenium–tungsten alloy in, at 1800°C, 20: 19212(R) (N-65-21351)
UC–ZrC, ductility at 1800°C, 20: 5848
UC–ZrC, electric conductivity, 17: 30970 (GEST-2015)
UC–ZrC, electric conductivity and optical emissivity of, 18: 4245 (LAMS-2965)
UC–ZrC, electron emission in, effects of component proportions on thermionic, 16: 294 (GA-1973)
UC–ZrC, electron emission and vaporization, 17: 16516(R) (GA-3866)
UC–ZrC, electron emission and vaporization rates of, in cesium vapor, 17: 25687(R) (GA-4173)
UC–ZrC, emission and vaporization at low pressures, anodic and porosity effects on, 17: 41338(R) (GA-4391)
UC–ZrC, emission and vaporization testing of, in cesium vapor, 20: 19208(R) (N-65-21347)
UC–ZrC, fabrication, 17: 11311(R) (LAMS-2796)
UC–ZrC, fabrication for irradiation studies, 17: 41338(R) (GA-4391)
UC–ZrC, fabrication by arc casting, 18: 8770 (NAA-SR-Memo-8528)
UC–ZrC, fabrication and testing, 18: 14381 (TID-7676(p.163-9))
UC–ZrC, fabrication by isostatic pressing, 18: 14363(R) (GA-4874)
UC–ZrC, fabrication of fuel elements of, 18: 38406 (A/CONF.28/P/122)
UC–ZrC, fabrication and properties as fuel element material, 19: 15991(R) (BNL-841(p.63-101))
UC–ZrC, fabrication into fuel for thermionic space power plants, 20: 14962(R) (N65-20803)
UC–ZrC, fission product release at high temperatures, 20: 14960(R) (N65-20798)
UC–ZrC, fission product release at 1800°C, 20: 14961(R) (N65-20801)
UC–ZrC, fission product release at high temperatures, 20: 14959(R) (N65-20797)
UC–ZrC, graphite coating of procedure for, 17: 33279
UC–ZrC, mass loss rates of uranium and zirconium from fluidized beds of, 18: 8326 (LAMS-2994)
UC–ZrC, neutron absorption and heating in cylinder of, at 2000°C, 16: 19906 (AERE-M-1011)
UC–ZrC, performance as electrodes in thermionic cells, 17: 3589
UC–ZrC, performance as emitters in thermionic cells, 18: 9064(R) (GA-4012)
UC–ZrC, performance of refractory metal coated, as thermionic emitters, 18: 20874
UC–ZrC, performance as in-pile thermionic electrodes, 18: 26259
UC–ZrC, performance and properties as thermionic emitters, 18: 35929(R) (GA-4769(Pt.I))
UC–ZrC, performance as fuels in nuclear-thermionic cells, 18: 37869 (A/CONF.28/P/132)
UC–ZrC, performance as thermionic fuel elements, (E), 19: 10519
UC–ZrC, phase studies and properties, 16: 30886
UC–ZrC, phase studies, 18: 24133 (LADC-6391)
UC–ZrC, physicochemical properties, 16: 24154(R) (GA-3245)
UC–ZrC, physicochemical properties of, to 2400°K, for use as cathodes in thermionic space reactors, 16: 14350(R) (GA-3007)
UC–ZrC, preparation of submicron powders of, 17: 25687(R) (GA-4173)
UC–ZrC, preparation and fabrication, 17: 37496
UC–ZrC, preparation and high-temperature stability, 18: 44231(P)
UC–ZrC, preparation by consumable electrode technique at 5000°K, 20: 9401
UC–ZrC, preparation of high-purity, 20: 25542(P)
UC–ZrC, production of solid-solution, 19: 24918 (LA-3217)
UC–ZrC, production of solid solutions of, methods for, 20: 27489 (LA-DC-6807)
UC–ZrC, properties of, as thermionic emitter, 16: 33579 (GA-2911)
UC–ZrC, properties of, for use in thermionic reactors, 17: 5577 (GA-3523)
UC–ZrC, properties as emitter in thermionic converters, 17: 14934 (GA-3330)
UC–ZrC, properties as nuclear thermionic cell emitters, 17: 27960
UC–ZrC, properties as thermionic cell emitters, 17: 27962
UC–ZrC, properties and hot-pressing of solid solutions of, additive effects of nickel on, 18: 12567
UC–ZrC, properties for thermionic applications, 18: 14468 (TID-7676 (p.99-100))
UC–ZrC properties of tungsten-clad and unclad, for, use in thermionic cells, 18: 14778(R) (GA-4071)
UC–ZrC, properties as thermionic material, 18: 22715
UC–ZrC, properties as thermionic emitters for cesium-vapor cells, 18: 26253(R) (GA-4677)
UC–ZrC, properties as thermionic electron emitters, 18: 30486(TID-7687(p.27-44))
UC–ZrC, properties for cathodes in thermionic space power plants, 20: 15046(R) (N65-15820)
UC–ZrC, radiation effects on carbon-coated particles, 19: 26888
UC–ZrC, radiation effects, 19: 36949(R) (BNL-900(p.121-97))
UC–ZrC, reactions of, with molybdenum, niobium, tantalum, and tungsten at 1200 to 2000°C, 16: 33468 (GA-3124)
UC–ZrC, reactions with molybdenum-tungsten alloys at high temperatures, 17: 41338(R) (GA-4391)
UC–ZrC, release of fission products from fuel inserts of, 17: 33272
UC–ZrC, surface area of, apparatus for measuring, 18: 14363(R) (GA-4874)
UC–ZrC, thermal conductivity and thermal emission, 17: 30970 (GEST-2015)
UC–ZrC, thermal expansion of polycrystalline solid solution of, at 25 to 1000°C, 19: 39200
UC–ZrC, thermionic properties of, at 1400 to 2100°K, 16: 33504
UC–ZrC thermionic emission properties, 17: 20609
UC–ZrC, thermionic emission properties, 17: 20610
UC–ZrC, thermionic emission by, 17: 27976
UC–ZrC, thermionic electrode design of, 17: 31713(P)
UC–ZrC, thermionic emission stability of clad, in cesium vapor, 17: 41338(R) (GA-4391)
UC–ZrC, thermionic constants, 18: 2421
UC–ZrC, thermodynamic properties, 18: 2222 (LADC-5907)
UC–ZrC, thermoelectric properties of, in cesium vapor, 16: 15348
UC–ZrC, thermoelectric properties at 1700 to 2620°K, 17: 11436
UC–ZrC, thermoelectric properties at 1300 to 2000°K, 17: 25813
UC–ZrC, thermoelectric properties, 18: 30490 (TID-7687(p.92-116))
UC–ZrC, thermoelectric emission, 19: 6351
UC–ZrC, thermoelectric emission in cesium vapor, 20: 29800
UC–ZrC, thermophysical properties at high temperatures, 18: 14469 (TID-7676(p.101-4))
UC–ZrC, use as fuel compacts in nuclear-thermionic cells, 18: 7956(R) (GA-3992(Pt.I))
UC–ZrC, use as thermionic emitters for cesium-vapor cells, 20: 13444(P)
UC–ZrC, vacuum emission of thermionic cell cathodes of, 20: 19209(R) (N-65-21348)
UC–ZrC, vaporization of, in thermoelectric cell cathodes, redeposition studies on, 16: 16807(R) (GA-3093)
UC–ZrC, vaporization at high temperatures, effects of cesium vapor on low-pressure, 17: 41338(R) (GA-4391)
UC–ZrC, vaporization and fission product release rates at 1800 to 2000°C, 18: 14363(R) (GA-4874)
UC–ZrC, vaporization testing in cesium vapor, 20: 19210(R) (N-65-21349)
UC–ZrC, vaporization testing of, in cesium vapor, 20: 19211(R) (N-65-21350)
UC–ZrC, vaporization of, effects of cesium vapor pressure and sample density on rate of, 20: 19212(R) (N-65-21351)
VC–ZrC, oxidation tests at 1400°C, 19: 9624 (SCNC-270)
W_2C–ZrC, melting point, 17: 11201(T) (AEC-tr-5598)
ZrC–ZrH, properties, 19: 40959
Zr–ZrC, phase diagram, 20: 19249

ZIRCONIUM CARBONATES
ion exchange properties, 16: 11548(T) (CEA-tr-R-1421)
preparation by precipitation, 16: 188
solubility in ammonium carbonate solutions, 19: 22235

ZIRCONIUM CHLORIDE ADDITION COMPOUNDS
with amides, formation of, 17: 23242

ZIRCONIUM CHLORIDE COMPLEXES
with bipyridyl and 1,10-phenanthroline, preparation and properties of, 18: 8361
with ethyl and methyl cyanides, uv spectra of, 18: 41415
with ethyl cyanoacetate, preparation and spectra of, 18: 23471
with tributyl phosphate, infrared spectral studies of, 18: 43450(T) (FTD-TT-64-471)

ZIRCONIUM CHLORIDES
see also Cesium Zirconium Chlorides
activity coefficients of tetra-, in mixtures with aluminum trichloride, 19: 9097 (ORNL-P-707)

analysis for silicon by silicomolybdic blue method, 17: 38951
band spectrum, 16: 7572
collection of gaseous tetra-, by condensation in hydrochloric acid, 19: 36221(P)
conversion to very pure zirconium metal, 19: 2743(P)
crystal structure of trivalent, 18: 39188
crystal structure, (E), 19: 9109
decomposition on hitting hot metal foil in vacuum, 17: 159
decomposition pressures above sodium chloride and sodium hexachlorozirconate at 300 to 525°K, 18: 13752
density and critical parameters of liquid, 17: 18078
heat of formation and thermodynamic properties, 17: 4501
hydrolysis in fluidized bed, 18: 1484(R) (ANL-6687(p.86-152))
hydrolysis of, fluid-bed, 17: 1359(R) (ANL-6569)
hydrolysis of, in fluid beds, 17: 19720 (ANL-6698)
magnetic properties at 80 to 300°K, 16: 20423
polarography in acetonitrile, tetraethylammonium perchlorate, and tetraalkylammonium halides, 18: 3692
polarography in fused salt systems, 16: 17680
preparation and properties of, for use in industry, 17: 15989
preparation and properties of divalent, 19: 34157
preparation by chlorination of zirconium dioxide, 18: 31536
preparation by sublimation, 17: 4557(P)
preparation of anhydrous trivalent, 18: 27372
preparation of, by chlorination of hafnium zirconium oxide, 17: 39089
preparation of labeled by slowing down of fission fragments in chlorine-containing gases, 17: 16065
preparation of pure trivalent, 18: 17828
preparation of tetra-, by chlorination of zirconium dioxide–carbon mixture, 18: 35582(P)
production, 17: 4555(P)
production from oxide using carbon tetrachloride entrained by carbon dioxide at 700°C, 16: 33071(T,R) (EURAEC-337)
production of pure tetravalent, 16: 7576(P)
properties in ethanol solution, 16: 17691
properties of, chemical and physical, 17: 6097
purification by fused-salt scrubbing, 17: 1828
reactions of trivalent, thermodynamic properties of disproportionation, 18: 8343
reactions of, with potassium chloride in vapor phase, 17: 18079
reactions of, with molybdenum in hydrogen, 17: 21681
reactions with alkali hydroxides to produce zirconia, 20: 38929(P)
reactions with aluminum chlorides at high temperatures, 19: 38755(R) (ORNL-3611)
reactions with hafnium and phosphoryl chlorides, product volatility, 16: 17629(T) (AEC-tr-4456(p.341-2))
reactions with iodides, 16: 30407
reactions with methanol, methoxide complex formation equilibrium in, 19: 11075
reactions with potassium chloride, tracer study of gaseous, 16: 23709 (JINR-P-957)
reactions with ϵ-butyl acetate, mechanisms of, 19: 17888
reactions with thorium chlorides at high temperatures, 19: 38755(R) (ORNL-3611)
reactions with tributyl phosphate, absorption spectra, 17: 30489
reactions with tributyl phosphate, 18: 1683
reactions with zirconium nitrate, 16: 183
reduction by magnesium and sodium, 16: 12087 (BM-RI-5933)
reduction by magnesium to metal, 18: 31544(P)
reduction by sodium or magnesium in fused salts, 19: 22950
reduction for production of zirconium metal, apparatus for, 18: 12569(P)
reduction of, by magnesium or sodium, preparation of zirconium by, 17: 16615
reduction of tetravalent, by alkali metals at low temperature, 16: 11647
reduction of tetra, preparation of zirconium from, 17: 40826(P)
reduction of tetra-, by magnesium in alkali metal halide melt, 18: 27878(P)
reduction to metal, electrolytic, 18: 10201
reduction to metal, development of method for, 19: 26790
separation by reversed-phase partition chromatography using organophosphorus compounds, 18: 25614
sorption and hydrolysis of radioactive waste, 17: 14117(R) (ANL-6596(p.119-63))
spectra at 575°C, Raman, 17: 25267
spectra of, Raman, 19: 32048(R) (NP-15073)
stability in molten mixtures of alkali and alkaline earth metals, 20: 1822(T) (ANL-Trans-233)
structure of trivalent, 16: 23682
structure of vapor, 16: 27027
thermodynamic properties, 16: 4164(T) (FTD-TT-61-75)
thermodynamic properties, 17: 14289
thermodynamic properties of di- and trivalent, 18: 8343
thermodynamic properties, 20: 10816(T) (NASA-TT-F-285)
volatility relative to hafnium chloride at 450°C, 19: 9154
$AlCl_3$–KCl–$ZrCl_4$, phase studies, 16: 8751
$AlCl_3$–$ZrCl_4$, phase diagram, 19: 9097 (ORNL-P-707)
$AlCl_3$–$ZrCl_4$, phase studies, 18: 22011(R) (ORNL-3591(p.38-58))
$AlCl_3$–$ZrCl_4$, phase studies, 19: 30067(R) (ORNL-3789(p.56-98))
$AlCl_3$–$ZrCl_4$, phase studies, 20: 27040(R) (ORNL-3831)
$AlCl_3$–$ZrCl_4$, phase studies at 100 to 450°C, 20: 26868
$FeCl_3$–KCl–$ZrCl_4$, phase studies, 16: 8751
$HfCl_4$–$ZrCl_4$, phase studies, 16: 18074
KCl–NaCl–$ZrCl_4$, stability of zirconium dichloride in, 20: 1822(T) (ANL-Trans-233)
NaCl–$ZrCl_4$, phase studies, 18: 3298(R) (ORNL-2221(Pts.1-5)(Del.))
$NbCl_4$–KCl–$ZrCl_4$, thermodynamic properties and crystallization, 17: 21713
$ThCl_4$–$ZrCl_4$, phase studies, 18: 22011(R) (ORNL-3591(p.38-58))
$ZrCl_4$–ZrI_4, phase studies, 16: 18074

ZIRCONIUM CHROMATES

ion exchange properties, 16: 11548(T) (CEA-tr-R-1421)

ZIRCONIUM CITRATES

effects of, on strontium-89 and -90 distribution in rats, 17: 12107
effects of, on strontium-89 binding by bones in guinea pigs, 17: 12108
effects on elimination of strontium-90 from mice, 18: 35288
effects on radioisotope uptake and excretion in rats, 18: 3460
protective effects against strontium-90 induced bone cancer in mice, 19: 17677

ZIRCONIUM CLADDING

see also Uranium (Zr Clad)

ZIRCONIUM COMPLEXES

catalytic effects on hydrolysis of salicyl phosphate, 16: 28949
cyclopentadienyl halide, preparation and properties, 19: 22214
distribution of iodide ions in, 16: 12801(R) (IA-685)
formation and properties of, in aqueous solutions, 18: 35508 (UJV-1066/64)
formation and properties of, in oxalic acid–sulfuric acid systems, 20: 7039
formation of, 18: 6711
preparation of, 17: 28912
spectra of, absorption, 17: 15927
spectra of oxygen-containing, infrared, 18: 41455
stability constants of, determination of, by metal distribution between aqueous phase and ion exchanger, 20: 16481
stability of simple fluoride, 16: 5318(T) (CEA-tr-R-1401)
with acetylacetone and benzoylacetone, water effects on disproportionation, 16: 5327
with acetylacetone–ethylenediimines, preparation and structure of, 20: 29203
with alizarin S, effects of pH on structure of, 17: 38936
with Alizarin S, separation by solvent extraction using butanol, 18: 25306
with alkylenepolyaminoacetic acid type chelating agents, preparation, 19: 46299(P)
with α-carboxy-β-methyltropolone, composition of, spectrophotometric studies of, 20: 29179
with aminoacetic acid, preparation and molecular structure of, 18: 41459
with aminodiacetic acid, preparation and molecular structure of, 18: 41459
with ammonium carbonate, properties, 19: 22235
with arsenazo III, formation mechanism of, 17: 6007
with arsenazo III, mechanism of formation of, 18: 10006
with arsenazo, composition of, 19: 362
with benzohydroxamic acid, stability constant for, 19: 24438
with β-hydronaphthazarin and naphthazarin, formation constants and spectra of, 18: 25456
with chlorides, nitrates, and oxalates, formation constants for, 16: 30411
with chlorides, nitrates, oxalates, oxyacids, and sulfates, equilibrium and stability constants of, 18: 27414
with chromotropic acid, composition and stability constants of, 18: 5260
with complexones, stability, 16: 11791(T) (AWRE/TRANS/27)
with cupferron, structure, 16: 30428
with cupferron, radiation effects on, 19: 46761 (NYO-2979-34)
with diantipyrinemethane in hydrochloric acid, composition of, 17: 12291
with diantipyrinemethane–thiocyanates, formation and composition of, 18: 10131
with diantipyrylmethane in hydrochloric acid, composition and stability of, 17: 35822
with diethylenetriaminepentaacetic acid, preparation, properties, and structure, 16: 11610
with diethylenetriaminepentaacetic acid, preparation and properties, 18: 17847
with diethylentriaminepentaacetic acid and 1,2-diaminecyclohexanetetraacetic acid, preparation and stability of, 18: 43522
with dimethyl sulfoxide, preparation and thermal properties, 19: 7419
with dimethyl sulfoxide and perchlorate ions, crystal structure, 19: 13339
with DTPA, radionuclide removal from body using, 20: 18438

with EDTA, nitrilotriacetic acid, and Tiron, formation constants of, 18: 6806
with EDTA, stability of, 18: 194
with EDTA-Tiron and HEDTA, molecular weights of, 18: 12129
with EDTA, mandelic, oxalic, and phenylarsonic acids, solvent extraction studies on formation of, 20: 20561 (JAERI-1099)
with EDTA, migration in electrodialysis cell, 19: 20052 (ORNL-TM-1035)
with EDTA, preparation and structure of, 18: 10076
with ethylenediaminetetraacetic acid, preparation and molecular structure of, 18: 41459
with ethylenediaminetetraacetic acid, formation and stability of polynuclear, 20: 23035
with flavonol, use of absorption and excitation spectra to determine dissociation of, 18: 39272
with fluoride and sulfate, stability constants of, 17: 21675
with fluoride, effects of other cations on, 18: 17771 (DP-842)
with germanium and silicon chalcogenides, preparation and crystal structure, 19: 9152
with hinokitiol, stability constants of, 18: 41421
with malonic, oxalic, succinic, and tartaric acids, formation of, 16: 11676
with Methylthymol Blue and Xylenol Orange, 17: 19960
with molybdate, sulfate and tungstate anions, properties of, 17: 35825
with montmorillonite, fixation of phosphoric ions on, 16: 25305 (CEA-1650)
with *N*-hydroxyethylethylenediaminetriacetic acid, formation and stability of polynuclear, 20: 23035
with nitrilodiacetate derivatives of sulfonphthaleins, 16: 32978
with nitrilotriacetic acid, preparation and properties, 18: 17846
with nitrilotriacetic acid, preparation and molecular structure of, 18: 41459
with organophosphorus compounds, vibration spectra of, 18: 3898
with phenylarsonate, solubility, 18: 41386
with phosphoŏrganic compounds in nitric acid, infrared spectra of, 18: 35567
with phthalocyanines, preparation and properties of, 18: 13826
with pyridine-N-oxide-2-carboxylic acid, preparation and properties of, 17: 227 (IA-736)
with pyrogallolsulfonephthalein, instability constants and spectra of, 18: 10126
with selenoylacetones, formation of, 17: 19984
with selenoyltrifluoroacetone, formation and stability, 17: 35830
with semixylenol orange in perchloric acid, spectra of, 16: 28879
with thenoyltrifluoroacetone, crystallographic and optical properties and spectra of, 17: 34059
with thiocyanates, preparations and properties of, 17: 1482
with tri-n-butylphosphine oxide, structure in, 18: 3897
with triacyloxycyclopentadienyl, formation of, 17: 32144
with trichloroacetic acid, preparation and properties of, 18: 17837
with tropolone, preparation, properties, and structure, 20: 5538
with 1,2-cyclohexanediaminetetraacetic acid, formation and stability of polynuclear, 20: 23035
with 1,2-cyclohexylenedinitrilotetraacetic acid, stabilities and thermodynamic properties, 19: 36406
with 2-carboxypyridine N-oxide, properties of, 17: 8065
with 2,4-pentanedione, gas chromatography of fluorinated and normal, 17: 32068
with 2,4-pentanedione and 1,1,1-trifluoro-2,4-pentanedione, rapid ligand exchange in, 18: 222
with 2,5-dihydroxyquinone, polymerization of, 17: 23237
with 2-hydroxy-3-naphthoic acid, conductometric and potentiometric studies on, 18: 22100
with 2,2′-bipyridine-1,1′-dioxide, preparation and properties of, 20: 25067
with 2,4-pentanedione, ligand exchange in solutions of, nuclear magnetic resonance studies of, 19: 22260
with 2,4-pentanedione and 2,4-trifluoropentanedione, NMR spectra of ligand exchange reactions in, 20: 26836
with 2,4-pentanedione, crystal and molecular structure of, stereoisomerism in, 17: 18030
with 3′,4′-dihydroxybenzotropolone, composition and stability of, 18: 9996
with 8-quinolinol, infrared absorption spectrometry, 17: 30489
with 8-quinolinol, infrared spectral studies of, 18: 43450(T) (FTD-TT-64-471)

ZIRCONIUM COMPOUNDS
butoxide, reactions with acetyl chloride, mechanism of, 19: 17888
chemical properties, 19: 5860
dissolution by nitric acid in titanium containers, corrosion inhibitors for, 20: 7215(P)
machining procedures for, 20: 43864 (Y-1550)
organic, preparation and properties of, for use in industry, 17: 15989
preparation and properties of butyl phosphate, 16: 1855(R) (IDO-14560)
preparation and uses, 19: 38647
preparation of organo polymers as ion exchange materials, 17: 1371(P)
spectra of isopropoxide and tetra-*tert*-butoxide, infrared, 19: 7359(R) (ML-TDR-64-124)
uses in industry, survey, 17: 1822(T) (JPRS-15907)

ZIRCONIUM COUPLES
Nb/Zr, interdiffusion in, 18: 42031
Re–W/Zr, thermoelectric potential at 200 to 1800°C, 19: 37031(R) (GEMP-47A, pp 101-6)
stainless steel/Sn/Zr, roll-form bonding of, 16: 17966(R) (BMI-1541 (Del.))

ZIRCONIUM DEUTERIDES
combustion in oxygen, calorimetry of, 17: 14118(R) (ANL-6596 (p.164-74))
crystal structure and phase studies, 17: 41333(R) (ANL-6677)
enthalpy of formation and heat of combustion of di-, 17: 37198
heat of formation, 16: 20299(R) (ANL-6477(p.155-67))
heat of formation, 17: 8005 (TID-15554)
heat of formation, 17: 7655(R) (ANL-6600)
heat of formation, 17: 40421(R) (ANL-6766)
heats of combustion and formation, 16: 12649(R) (ANL-6485)
thermodynamic properties, 16: 25395
thermodynamic properties, 17: 10597 (TID-15795)

ZIRCONIUM ETHOXIDES
spectra of, infrared, 20: 23037

ZIRCONIUM FERROCYANIDES
distribution of iodide ions in, 16: 12801(R) (IA-685)
preparation and composition, 17: 32101

ZIRCONIUM FLUORIDES
see also Lithium Sodium Zirconium Fluorides
see also Potassium Zirconium Fluorides
see also Sodium Zirconium Fluorides
analysis by potentiometric titration using sodium methylate in methanol, 16: 7530
calcination of wastes of, pilot plant study of fluid-bed, 19: 43623 (IDO-14653)
complexes with hydrazine, preparation and stability of, 19: 46236 (NIJS-R-430)
corrosive effects on nickel and stainless steel at 350 to 830°C, 16: 33438
crystal structure, 17: 25060(R) (ORNL-3417(p.3-16))
crystal structure of $Li_4BeF_4ZrF_8$, 19: 2312
crystal structure, 19: 5884
crystal structure of tetravalent, 19: 25015
determination in presence of hafnium fluorides by x-ray diffraction, 20: 43206
effects on freezing point of sodium fluoride, 17: 6088
electrolysis in sodium chloride, anode effect in, 16: 17970
entropies and heat contents at 273 to 1200°K, 16: 15170 (BM-RI-5964)
equilibrium distribution in complex, 18: 6800
fluorine replacement by chlorine in, 16: 26992
formation, 18: 17771 (DP-842)
formation and decomposition in hydrofluoric acid, 17: 1473
heat of sublimation and vapor pressure, 18: 1676
ionization cross sections and partial pressure in systems with sodium fluorides, 18: 31533
polarography in fused salt systems, 16: 17680
preparation and properties, 16: 178
preparation and properties, 16: 17641(T) (AEC-tr-5087)
preparation and properties of, for use in industry, 17: 15989
preparation properties, and structure of divalent, 18: 33544
preparation, crystal structure and paramagnetism, 19: 9150
properties of molten, for use as reactor fuels, 20: 4376 (JUL-268-RG)
properties of, comparison with hafnium fluorides, 20: 43206
purification, 20: 36950
purification by sublimation, 19: 30744(R) (ORNL-3789(p.323-33))
purification by sublimation, 20: 5528 (ORNL-TM-1292)
purification by vacuum volatilization, 18: 22019(R) (ORNL-3591(p.231-40))
reaction with hydrofluoric acid containing hafnium, 17: 1473
spectra of fluorine-19 in, NMR, 20: 40931
stability constants, 16: 30421
stability constants of, 17: 21675
structure of hydrates of, 17: 28856
thermal capacity and thermodynamic properties at 5 to 307°K, 19: 26312
thermal capacity and thermodynamic properties of tetravalent, at 5 to 307°K, 20: 1809 (COO-1149-30)
thermal decomposition of the trihydrate of, in air, 17: 35700 (TID-17478)
thermodynamic properties at 284 to 1226°K, 16: 8739
thermodynamic properties of liquid and solid systems of, 16: 26960 (ORNL-1956)
thermodynamic properties, 20: 10816(T) (NASA-TT-F-285)

vapor pressure of, bell method measurements of, 19: 9151
vapor pressures, 17: 32116
AlF_3–F–KF–ZrF_4, corrosive effects on HyMu 80, INOR-8, and nickel at 600°C, 19: 6267 (BMI-X-316)
AlF_3–HF–KF–ZrF_4, solvent properties for aluminum, 18: 43717 (ORNL-P-391)
AlF_3–KF–UF_4–ZrF_4, corrosive effects on HyMu-80, INOR-8, and L nickel alloys at 600°C, 19: 13871(R) (BMI-1691(Del.))
AlF_3–KF–ZrF_4, corrosive effects on nickel-base alloys, 18: 2178 (BMI-X-260)
AlF_3–KF–ZrF_4, corrosive effects on HyMu 80 and INOR-8 under fluorination and hydrofluorination conditions, 19: 2744 (BMI-X-315)
AlF_3–KF–ZrF_4, corrosive effects on Inor-8, HYMU-8, and nickel under hydrofluorination conditions, 19: 2716(R) (BMI-1681(Del.))
AlF_3–KF–ZrF_4, melting points of, effects of sodium fluoride on, 20: 9045(R) (ORNL-3830, pp 69-96)
AlF_3–KF–ZrF_4, phase diagram of, 18: 35503 (ORNL-3594)
AlF_3–KF–ZrF_4, phase diagrams, 20: 9045(R) (ORNL-3830, pp 69-96)
AlF_3–KF–ZrF_4, phase studies, 18: 22174(R) (ORNL-3591(p.213-16))
AlF_3–KF–ZrF_4, phase studies, 19: 4247(R) (ORNL-3627(p.29-72))
AlF_3–KF–ZrF_4, use for non-aqueous processing of aluminum-containing fuels, 20: 25224(P)
AlF_3–KF–ZrF_4, uses of fused, in fluoride volatility process for separation of uranium from spent fuel elements, 20: 442
Al–KF–ZrF_4, phase studies, 19: 30323(R) (ORNL-3789(p.306-7))
BeF_2–LiF–NaF–ZrF_4, corrosive effects on nickel alloys at 500°C, 17: 29279 (BMI-X-227)
BeF_2–LiF–NaF–ZrF_4, corrosive effects on nickel alloys and Zircaloy-2 at 500°C, 17: 36222 (BMI-X-253)
BeF_2–LiF–ThF_4–UF_4–ZrF_4, neutron sources in unirradiated, inherent, 17: 36875 (ORNL-TM-611)
BeF_2–LiF–ThF_4–UF_4–ZrF_4, phase studies, 16: 17554(R) (ORNL-3262 (p.3-18))
BeF_2–LiF–ThF_4–UF_4–ZrF_4, phase studies, 17: 7562(R) (ORNL-3369)
BeF_2–LiF–ThF_4–UF_4–ZrF_4, phase studies, 17: 26788 (TID-7641 (p.290-9))
BeF_2–LiF–ThF_4–UF_4–ZrF_4, phase studies, 17: 25060(R) (ORNL-3417(p.3-16))
BeF_2–LiF–ThF_4–UF_4–ZrF_4, properties as reactor fuel, 18: 7129(R) (ORNL-3529(p.71-143))
BeF_2–LiF–ThF_4–UF_4–ZrF_4, radiation effects on, 18: 34050(R) (ORNL-3626(p.59-164))
BeF_2–LiF–ThF_4–UF_4–ZrF_4, radiation effects on, x, 19: 2402
BeF_2–LiF–ThF_4–UF_4–ZrF_4, radiolysis of, fluorine production in, 18: 22111(R) (ORNL-3591(p.16-37))
BeF_2–LiF–ThF_4–UF_4–ZrF_4, reactions with graphite under irradiation, 16: 17555(R) (ORNL-3262(p.19-26))
BeF_2–LiF–ThF_4–UF_4–ZrF_4, spectra of irradiated, absorption and reflectance, 20: 14453(R) (ORNL-3889, pp 12-14)
BeF_2–LiF–UF_4–ZrF_4, analysis for chromium by amperometric titration, 18: 19869
BeF_2–LiF–UF_4–ZrF_4, analysis for uranium, polarographic, 20: 14454(R) (ORNL-3889, pp 17-24)
BeF_2–LiF–UF_4–ZrF_4, corrosive effects of MSRE fuel salt on materials, in-pile, 18: 44055(R) (ORNL-3670(p.216-24))
BeF_2–LiF–UF_4–ZrF_4, corrosive effects on type 304 stainless steel, 20: 4308(R) (ORNL-3870, pp 243-60)
BeF_2–LiF–UF_4–ZrF_4, crystallization of, phase separation in, 19: 30149(R) (ORNL-3789(p.3-35))
BeF_2–LiF–UF_4, phase studies, 16: 17554(R) (ORNL-3262(p.3-18))
BeF_2–LiF–UF_4–ZrF_4, preparation for MSRE, 18: 22172(R) (ORNL-3591(p.59-64))
BeF_2–LiF–UF_4–ZrF_4, production of reactor-fuel, 19: 10566(R) (ORNL-3708(p.288-303))
BeF_2–LiF–UF_4–ZrF_4, production for MSRE fuel, 19: 31608(R) (ORNL-3789(p.99-109))
BeF_2–LiF–UF_4–ZrF_4, properties as reactor fuel, 18: 7129(R) (ORNL-3529(p.71-143))
BeF_2–LiF–UF_4–ZrF_4, properties as fuel for MSRE, 18: 22996
BeF_2–LiF–UF_4–ZrF_4, properties as fuel for high-temperature reactors, 19: 36342 (ORNL-P-899)
BeF_2–LiF–UF_4–ZrF_4, radiation effects on, in-pile, 19: 30825(R) (ORNL-3789(p.36-55))
BeF_2–LiF–UF_4–ZrF_4, radiation effects on, electron, 19: 30825(R) (ORNL-3689(p.36-55))
BeF_2–LiF–UF_4–ZrF_4, separation from rare earths by zone melting, 19: 34100(R) (ORNL-3812(p.121-68))
BeF_2–LiF–UF_4–ZrF_4, vapor pressure, 17: 25062(R) (ORNL-3417(p.41-50))
BeF_2–LiF–UF_4–ZrF_4, zone melting of, segregation of phases in, 19: 34144 (ORNL-3658)
BeF_2–LiF–ZrF_4, crystal structure of stoichiometric, 16: 17554(R) (ORNL-3262(p.3-18))
BeF_2–LiF–ZrF_4, crystallographic and phase studies on, 18: 34050(R) (ORNL-3626(p.59-164))
BeF_2–LiF–ZrF_4, electrochemical studies of uranium in molten, at 480 to 620°C, 20: 43099
BeF_2–LiF–ZrF_4, phase diagram and crystal structure, 18: 22010(R) (ORNL-3591(p.3-15))
BeF_2–LiF–ZrF_4, phase diagram, 19: 10564(R) (ORNL-3708(p.214-51))
BeF_2–LiF–ZrF_4, phase studies of, 17: 7562(R) (ORNL-3369)
BeF_2–LiF–ZrF_4, phase studies, 19: 30149(R) (ORNL-3789(p.3-35))
BeF_2–LiF–ZrF_4, phase studies, 19: 34100(R) (ORNL-3812(p.121-68))
BeF_2–LiF–ZrF_4, phase studies, 20: 22856(R) (ORNL-3913, pp 1-51)
BeF_2–LiF–ZrF_4, properties as reactor fuel, 18: 7129(R) (ORNL-3529 (p.71-143))
BeF_2–LiF–ZrF_4, reactions in molten, spectrophotometric studies of redox, 19: 9096 (ORNL-P-403)
BeF_2–LiF–ZrF_4, separation from rare earth fission products, 20: 32804(R) (ORNL-3936, pp 122-71)
BeF_2–LiF–ZrF_4, solubility of beryllia and zirconia in liquid, 20: 22856(R) (ORNL-3913, pp 1-51)
BeF_2–LiF–ZrF_4, vapor pressure of, 20: 8399(R) (ORNL-3872)
BeF_2–NaF–ZrF_4, phase studies, 16: 17554(R) (ORNL-3262(p.3-18))
BeF_2–ZrF_4, phase studies, 17: 28842
CsF–ZrF_4, crystal structure of Cs_3ZrF_4 in, x-ray diffraction studies, 16: 28919 (ORNL-TM-310)
CsF–ZrF_4, phase equilibrium diagram, 19: 17903
CsF–ZrF_4, phase studies, 17: 25060(R) (ORNL-3417(p.3-16))
F–LiF–NaF–ZrF_4, corrosive effects on nickel fluorinator and nickel alloys at 500°C, 19: 18051 (ORNL-3623)
HF–LiF–NaF–ZrF_4, corrosive effects on INOR-8, effects of cathodic protection on, 19: 920 (BMI-X-312)
HF–LiF–NaF–ZrF_4, corrosive effects on INOR-8 at 650°C, effects of inert gas sparge on, 19: 16012 (BMI-X-329)
HF–LiF–NaF–ZrF_4, corrosive effects on INOR-8 hydrofluorinator at 500 to 650°C, 19: 18051 (ORNL-3623)
KF–NaF–ZrF_4, phase diagram of, liquidus surface in, 18: 16008(T) (ORNL-tr-31)
KF–NaF–ZrF_4, phase studies and structure, 18: 27453
KF–NaF–ZrF_4, spectra of, emission technique for study of, 18: 3744
KF–NaF–ZrF_4, viscosity, 16: 26961 (ORNL-2278)
KF–ZrF_4, corrosive effects on construction materials at 600°C, 18: 7985(R) (BMI-1650(Del.))
KF–ZrF_4, phase studies and solubilities of aqueous, at 20°C, 16: 28946
KF–ZrF_4, solvent properties of fused, for aluminum-base fuels, 20: 45824(P)
LiF–KF–ZrF_4, spectra of, emission technique for study of infrared, 18: 3744
LiF–NaF–UF_4–ZrF_4, corrosive effects of, on nickel fluorinator in conjunction with fluorine, 16: 10455 (ORNL-3253)
LiF–NaF–UF_4–ZrF_4, fluorination, determination of half times for uranium removal in, 17: 37292(R) (ORNL-TM-586)
LiF–NaF–UF_4–ZrF_4, viscosity, 16: 26961 (ORNL-2278)
LiF–NaF–ZrF_4, corrosive effects of, on nickel, 16: 4450(R) (BMI-1546 (Del.))
LiF–NaF–ZrF_4, corrosive effects of, on HyMu-80 at 500°C, 16: 4502 (TID-13691)
LiF–NaF–ZrF_4, corrosive effects of, on INOR-8 hydrofluorinator in conjunction with hydrofluoric acid, 16: 10455 (ORNL-3253)
LiF–NaF–ZrF_4, corrosive effects of liquid, on nickel and nickel alloys, 17: 6571 (ORNL-TM-411)
LiF–NaF–ZrF_4, corrosive effects on nickel-base alloys at 650°C, 17: 34345 (BMI-X-247)
LiF–NaF–ZrF_4, corrosive effects of molten, on nickel alloys at 500 to 650°C, 17: 35251(R) (BMI-1632(Del.))
LiF–NaF–ZrF_4, corrosive effects on construction materials under hydrofluorination conditions, 17: 40423(R) (BMI-1639(Del.))
LiF–NaF–ZrF_4, corrosive effects on HyMu 80 and INOR-8 at 500°C in presence of fluorine and hydrofluoric acid, 18: 10468 (BMI-X-269)
LiF–NaF–ZrF_4, corrosive effects on INOR-8 and HyMu-80 at 650°C during hydrofluorination of stainless steel and Zircaloy-2, 18: 30128 (BMI-X-288)
LiF–NaF–ZrF_4, corrosive effects on HyMu-80 and INOR-8 under hydrofluorination conditions, 18: 34034(R) (BMI-1672(Del.))
LiF–NaF–ZrF_4, corrosive effects on INOR-8 at 650°C, 18: 40970(R) (BMI-1674(Del.))
LiF–NaF–ZrF_4, corrosive effects on HyMu 80 and INOR-8 under fluorination and hydrofluorination conditions, 19: 2744 (BMI-X-315)
LiF–NaF–ZrF_4, corrosive effects on Inor-8 under hydrofluorination conditions, 19: 2716(R) (BMI-1681(Del.))
LiF–NaF–ZrF_4, corrosive effects on INOR-8, effects of argon on, 19: 13871(R) (BMI-1691(Del.))
LiF–NaF–ZrF_4, crystallography and phase studies on, 19: 37101
LiF–NaF–ZrF_4, density and surface tension of liquid, 19: 5875
LiF–NaF–ZrF_4, phase diagram, 18: 22010(R) (ORNL-3591(p.3-15))

LiF–NaF–ZrF_4, phase diagram, 18: 39385
LiF–NaF–ZrF, separation of plutonium hexafluoride from, by volatilization, 17: 39179(R) (ORNL-3452(p.26-50))
LiF–NaF–ZrF_4, separation of uranium hexafluoride from, by continuous fluorination, 20: 45790(R) (ORNL-3945, pp 72-8)
LiF–NaF–ZrF_4, solvent properties for reactor fuels, 18: 39385
LiF–NaF–ZrF_4, viscosity, 16: 26961 (ORNL-2278)
LiF–UF_4–ZrF_4, phase studies and solvent properties, 17: 26765(R) (ORNL-3419)
LiF–UF_4–ZrF_4, radioinduced evolution of fluorine from, 17: 26765(R) (ORNL-3419)
LiF–ZrF_4, activity coefficients of zirconium tetrafluoride in, 17: 25062(R) (ORNL-3417(p.41-50))
LiF–ZrF_4, crystallography and phase studies on, 19: 37101
LiF–ZrF_4, phase studies, 19: 38610
NaCl–K_2NbF_7–ZrF_4, production of niobium–zirconium alloys by electrolysis of, 18: 16431
NaF–UF_4–ZrF_4, corrosive effects on Inconel, effects of thermal cycling on, 18: 29147 (NASA-SP-41(p.273-303))
NaF–UF_4–ZrF_4, fluorination and volatilization of, for uranium separation, 16: 13167(P)
NaF–UF_4–ZrF_4, level measurement of fused, by Inconel level indicators, 16: 31823 (ORNL-TM-331)
NaF–UF_4–ZrF_4, phase diagram, 19: 10564(R) (ORNL-3708(p.214-51))
NaF–UF_4–ZrF_4, phase studies, 17: 7606(R) (ORNL-1515)
NaF–UF_4–ZrF_4, phase studies, 18: 3298(R) (ORNL-2221(Pts.1-5)(Del.))
NaF–UF_4–ZrF_4, separation of uranium from, by boron trifluoride treatment, 16: 8809 (NAA-SR-269)
NaF–UF_4–ZrF_4, solvent properties of liquid, for rare earth fluorides, 16: 23595
NaF–UF_4–ZrF_4, thermal capacity at 550 to 850°C, 17: 7606(R) (ORNL-1515)
NaF–UF_4–ZrF_4, vapor pressures, 18: 3298(R) (ORNL-2221(Pts.1-5)(Del.))
NaF–UF_4–ZrF_4, viscosity, 16: 26961 (ORNL-2278)
NaF–ZrF_4, ionization cross sections and partial vapor pressures, 17: 33891
NaF–ZrF_4, phase diagram, 19: 10564(R) (ORNL-3708(p.214-51))
NaF–ZrF_4, solvent properties of, for argon, helium, neon, and xenon, 16: 18877
NaF–ZrF_4, thermodynamic properties, mass spectrometric studies of, 18: 31533
NaF–ZrF_4, vapor pressure, 18: 3298(R) (ORNL-2221(Pts.1-5)(Del.))
NaF–ZrF_4, viscosity of, 16: 26961 (ORNL-2278)
RbF–NaF–UF_4–ZrF_4, viscosity, 16: 26961 (ORNL-2278)
RbF–NaF–UF_4–ZrF_4, viscosity, 16: 26961 (ORNL-2278)
RbF–UF_4–ZrF_4, viscosity, 16: 26961 (ORNL-2278)

ZIRCONIUM GLUTARATES
preparation of stable gels of, 17: 25205

ZIRCONIUM HALIDES
phase studies, 16: 18074
production process for, 20: 33315(P)

ZIRCONIUM HYDRIDES
ablation during re-entry, device for testing, (E), 19: 47117(R) (SC-DC-65-1698)
ablation of, in vehicle reentry, 20: 33884(R) (SC-CR-66-2029)
analysis for hydrogen by density measurement, 16: 5484 (DC-57-1-141)
analysis for hydrogen by combustion method, 19: 22150
bibliography, 16: 12999 (CNLM-2370-2)
bibliography on preparation and properties, 16: 11577 (CEA-BIB-27)
bibliography on SNAP fuel materials containing, 18: 33128 (NAA-SR-9525(Vol.I))
chemical bonds in, properties of, 20: 12847
cladding, 16: 5654 (APEX-307)
cladding, development of methods for moderators, 16: 6089 (APEX-305)
cladding, evaluation of methods for, 16: 6691 (APEX-306)
cladding for use in moderators, methods development, 16: 7861 (DCL-57-7-37)
combustion in oxygen, calorimetry of, 17: 14118(R) (ANL-6596 (p.164-74))
corrosion by biphenyl, 20: 25491(T) (AECL-2330, pp 179-95)
corrosion inhibition by, 17: 7606(R) (ORNL-1515)
crystal lattice dynamics of, axially symmetric model for, 17: 430
crystal lattice parameter changes in, 16: 5322
crystal orientation in single-crystal zirconium, effects of stress on, 20: 37269
crystal structure of, 16: 31253(R) (DP-765)
crystal structure of, 16: 30717(R) (ANL-6516)
crystal structure of delta, 19: 971(T) (JPRS-26808(p.169-82))
crystal structure, 17: 18074
crystal structure, 17: 41333(R) (ANL-6677)
determination in zirconium alloys, chromatographic, 17: 2909(T,R) (EURAEC-383)
development as reactor moderator material, 17: 17445
development as shielding for space reactors, 18: 32955
development of high-hydrogen-content, 17: 3905
development of variable-hydrogen-content, for reactor moderators, 18: 44037(R) (HW-82651(p.5.1-33))
diffusion in Zircaloy-2, electrothermal effects on, 19: 30737(R) (HW-84573(p.6.1-11))
diffusion in, self, 19: 40286(R) (NAA-SR-11200)
diffusion of fission products in, 19: 27735(R) (NAA-SR-10850)
diffusion of fission products in, 19: 40286(R) (NAA-SR-11200)
diffusion of hydrogen in, loss and migration rate production, 16: 7876 (DC-57-5-107)
diffusion of hydrogen in, nuclear magnetic resonance study, 16: 11620
diffusion of hydrogen from, analysis of pulse heating studies of, 19: 7906 (NAA-SR-Memo-9622)
diffusion of zirconium in, self-, 19: 12865(R) (NAA-SR-10501)
diffusion of zirconium in, 19: 27735(R) (NAA-SR-10850)
diffusion of zirconium in, self-, 20: 8316(R) (NAA-SR-11450, Sect.7)
diffusion of zirconium in, self-, 20: 9379(R) (NAA-SR-11650, Sect.4)
diffusion of zirconium in, 20: 35841(R) (NAA-SR-11900)
diffusion of zirconium in, self-, 20: 46966(R) (NAA-SR-12010)
dissociation pressure isochores for, at 300 to 900°C at 0.01 to 10.0 atm., 18: 27961 (NAA-SR-9374)
dissociation pressure of, effects of temperature on, 20: 45691
effects of heat on clad and unclad, 16: 11196 (DC-56-12-37)
effects on average thermal-neutron capture cross sections of media, (T), 20: 37991
effects on ductility of Zircaloy-2, 20: 31669
effects on fracture of zirconium, 19: 23082
effects on mechanical properties of thin-walled Zircaloy tubing, 19: 22970(R) (DPST-65-83-2(p.8-12))
effects on properties of Zircaloy-2 tubing, 20: 35911
effects on sodium-void coefficient of fast reactors, (T), 19: 29693
effects on tensile properties of Zircaloy-2, 18: 14480 (WAPD-275)
effects on tensile properties of Zircaloy-2, 19: 4690
effects on zirconium solid-state bonding, 19: 22865(R) (BMI-1711(Del.))
elastic properties at high temperatures, 16: 7921
emissivity during re-entry ablation, 20: 9091(R) (SC-DC-65-1893)
enthalpy of formation, 17: 37198
explosibility of powders of, 19: 36698 (BM-RI-6516)
fabrication, 16: 10487 (XDCL-58-7-23)
fabrication by powder metallurgy methods, 18: 8822
fabrication, properties, and uses of, 17: 20403 (NAA-SR-Memo-6836)
fission gas mobility in, 19: 12865(R) (NAA-SR-10501)
fission gas mobility studies in, radiochemical aspects of, 19: 25047 (NAA-SR-Memo-10509)
fission gas mobility in, 20: 8316(R) (NAA-SR-11450, Sect.7)
formation and orientation of crystal platelet, in tubing, 19: 14825(R) (DPST-64-83-9)
formation and structure of, electron microscope studies on, 18: 22482 (EURAEC-999)
formation by reduction of zirconium oxide by magnesium in hydrogen, 18: 17816
formation in homogenized magnesium–zirconium alloys, 19: 2815
formation in magnesium–zirconium alloy, 18: 5797
fracture properties of, 20: 31667
gamma and fast neutron heating in moderators of, for cold neutron production, (T), 20: 36152
gamma transmission in slabs of, (E), 19: 14728 (APEX-581)
gases extracted from hot, analyses of, 19: 36227 (AWRE-O-22/65)
growth in zirconium alloys, 20: 2253 (AECL-2297)
hardness at 25 to 225°C, 20: 29697 (AECL-2538)
heat of combustion of di-, 17: 37198
heat of formation, 16: 20299(R) (ANL-6477(p.155-67))
heat of formation, 17: 8005 (TID-15554)
heat of formation, 17: 7655(R) (ANL-6600)
heat of formation, 17: 40421(R) (ANL-6766)
heats of combustion and formation, 16: 12649(R) (ANL-6485)
heats of formation of, 19: 4113
hydrogen binding in, neutron scattering study of, (E), 19: 4740 (GA-5744)
hydrogen bonding in, neutron scattering study, 19: 46232 (BNWL-SA-239)
magnetic properties of ZrH_2, 20: 32699
magnetic properties, 17: 18074
mechanical properties, 16: 12097(R) (LAR-1)
mechanical properties, 16: 12102(R) (LAR-8)
mechanical properties, 16: 12103(R) (LAR-9)
molecular binding of deuterium and hydrogen in, (E/T), 19: 16817(R) (GA-5554)
molecular binding of deuterium and hydrogen in deuterated, (E/T), 19: 16817(R) (GA-5554)
neutron attenuation, 16: 15612 (GA-2544)
neutron attenuation in, at 0.5 to 12 Mev, 18: 28912
neutron attenuation by, fast, 18: 42618

neutron cross sections at 0.1 to 0.9 ev, 18: 36080(R) (RPI-328-8)
neutron diffusion and thermalization in, 16: 26207
neutron diffusion constant measurements in, 18: 37113 (A/CONF.28/P/763)
neutron diffusion constants of, scattering measurements on, 18: 40475 (JÜL-160-NP)
neutron diffusion in, thermal parameters of, (E), 19: 35378(R) (EANDC(E)-57(U))
neutron diffusion in, decay-time constants and spectra for, (E), 20: 11943
neutron elastic scattering at 0.01 to 0.55 ev, analysis of, 18: 13043 (GA-4490(Rev.))
neutron flux distribution in slabs, emergent gamma flux from, 16: 31177 (NARF-62-6T)
neutron flux distribution in slabs of, 17: 3806
neutron inelastic scattering by, cold, 18: 13030(R) (GA-4434)
neutron inelastic scattering by, spectra of, (E), 19: 23600(R) (RPI-328-20(p.35-9))
neutron inelastic scattering by, thermal, (E), 19: 31234(R) (RPI-328-35(p.120-4))
neutron inelastic scattering by, distributions from cold, (E), 19: 45240
neutron inelastic scattering by, thermal, (E/T), 19: 47549(R) (TID-22141, pp 34-49)
neutron inelastic scattering at 0.238 to 0.570 ev, cross sections for fast, (E), 20: 30325(R) (RPI-328-56, pp 113-34)
neutron inelastic scattering by, differential cross section for, (E), 20: 46563(R) (RPI-328-68, pp 145-60)
neutron moderation in lattices of, 18: 38311 (A/CONF.28/P/645)
neutron reactions at 0.025 to 0.4 ev, total cross sections for, (E), 20: 40069(R) (EANDC(E)-66(U))
neutron scattering, studies using spinning sample method, 16: 7158
neutron scattering, cross sections and spectra, 16: 7178
neutron scattering by, (E/T), 19: 16817(R) (GA-5554)
neutron scattering by, at 0.018 to 0.080 ev, (E), 19: 21200 (KFK-264)
neutron scattering by, theory of thermal, 19: 25454 (NAA-SR-10899)
neutron scattering by, differential cross section of thermal, (E/T), 19: 27389 (GA-6295)
neutron scattering at 0.018, 0.032, and 0.064 Mev, frequency distribution in, (E), 19: 35378(R) (EANDC(E)-57(U))
neutron scattering at 0.06 to 10 ev, differential cross section for, 20: 2963
neutron scattering by, differential cross sections for thermal, (E/T), 20: 4801(R) (GA-6634)
neutron scattering by, angular distributions and diffusion constants from thermal, (E), 20: 6271
neutron scattering by, cross sections for slow, (E/T), 20: 19778(R) (GA-6824)
neutron scattering by, differential cross sections and corrections for thermal, (E), 20: 21939(R) (GA-6930)
neutron scattering by, (E), 20: 27344
neutron scattering cross sections for, thermal, (T), 20: 36139 (GA-7055)
neutron scattering at 296 and 750°K, cross sections for thermal, 20: 36140(R) (GA-7091)
neutron spectra in, temperature coefficient of, 16: 24380
neutron spectra in, temperature coefficient of, 16: 24381
neutron spectra in poisoned, temperature-dependent, 17: 39943(R) (GA-4176)
neutron spectra in, pulsed-source measurements of, (E/T), 20: 13737
neutron spectra in, transient properties of, (E/T), 20: 21941 (IAE-977)
neutron spectra in, 20: 36428 (GA-7072)
neutron spectra of, temperature dependence of, 17: 26392(R) (GA-3853)
neutron thermalization in, 17: 19205 (TID-18432)
neutron thermalization in, 17: 20957 (LA-2834)
neutron thermalization in, measured and theoretical spectra for, 17: 24369(R) (GA-3542)
neutron thermalization in, 17: 26030
neutron thermalization in, 17: 32974 (GA-4328)
neutron thermalization in, 17: 37993(R) (GA-4426)
neutron thermalization in, 18: 22848(R) (GA-4659)
neutron thermalization in, measurement of, 18: 26514
neutron thermalization, 18: 38031 (A/CONF.28/P/360)
neutron thermalization in, integral, 19: 41640(R) (GA-6323)
neutron thermalization in, (E/T), 20: 8035 (GA-5798)
neutron thermalization in, pulsed-source measurements of, (E), 20: 13739
neutron thermalization in, integral, (E/T), 20: 19778(R) (GA-6824)
neutron thermalization in, models for, 20: 22377 (GA-6930, App. B)
neutron total cross sections, 16: 5967
neutron total cross sections, 17: 10148
neutron transmission in slabs of, (E), 19: 14728 (APEX-581)
orientation of platelets of, on Zircaloy tubing, 18: 23137(R) (DPST-64-83-3)
orientation on Zircaloy, dependence on crystallographic texture, 20: 33828
performance as reactor moderator, critical parameters and neutron spectra in, 18: 38332 (A/CONF.28/P/878)
phase diagram, 16: 12099(R) (LAR-3)
phase studies, 19: 40959
phase studies, 20: 5844
phase studies, 17: 41333(R) (ANL-6677)
phase studies, 16: 12102(R) (LAR-8)
phase studies, 16: 12103(R) (LAR-9)
phase studies by x-ray diffraction analysis, 16: 12105 (NAA-SR-6880)
physical properties, (E), 19: 31532 (BMI-X-151)
platelet orientation in, 19: 24088(R) (SRO-112)
precipitation in alpha zirconium crystals, habit planes for, 16: 13628
precipitation in zirconium, 18: 2220(R) (EURAEC-748)
precipitation in Zircaloy-2, effects of elastic stresses on orientation of, 19: 44697 (ORNL-TM-1239)
precipitation in Zircaloy-2, effects of preferred orientation and stress on, 20: 4304(R) (ORNL-3870, pp 171-83)
precipitation in Zircaloy-2 crystals, effects of stress on, 20: 15120
precipitation of, in zirconium, crystallography and morphology of, 17: 18788
precipitation of, in Zircaloy-2, effects of strain on directional, 17: 20453 (CRGM-1135)
preparation, 20: 5844
preparation, 20: 26902
preparation, 18: 35247(R) (NAA-SR-9700)
preparation, 20: 35841(R) (NAA-SR-11900)
preparation and properties for use as reactor moderator, 18: 14394
preparation and properties, 18: 18305
preparation and properties as reactor moderator material, 18: 41945
preparation and self-diffusion in, 20: 22520(R) (NAA-SR-11805)
preparation of ternary, 20: 46966(R) (NAA-SR-12010)
preparation of, methods used in metallographic, 20: 4341 (NAA-SR-Memo-10927)
production, 16: 13541 (APEX-546)
production in zirconium alloys, 18: 30134(T,R) (EURAEC-955)
production of crack-free shaped bodies of delta-phase, 16: 9148(P)
production of crack-free shaped bodies of gamma, 17: 29274(P)
production of fully fabricated, 17: 8792(P)
production of large bodies of delta, 16: 4524(P)
production of low-porosity, by sintering, 19: 42505
production of massive sections of, 17: 6595 (DC-61-7-18)
properties, 16: 12101(R) (LAR-7)
properties, 18: 8822
properties as reactor moderator, 16: 5654 (APEX-307)
properties as reactor moderator, review of, 18: 32032 (A/CONF.28/P/254)
properties as reactor moderator, 18: 38467 (A/CONF.28/P/537)
properties as reactor control material, 19: 24083(R) (HW-83298(p.3.1-10))
properties as reactor moderator, 20: 5844
properties evaluation for use in boiling water-superheat reactors, 16: 15910 (NAA-SR-5943)
properties for use as reactor material, 19: 7470
properties for use in SNAP systems, 19: 17341(R) (NAA-SR-10496)
properties for use as space shielding material, 19: 37104
properties, mechanical and thermal, 16: 12100(R) (LAR-4)
proton resonance, line width and displacement, 16: 5741
radiation effects on clad and unclad, 16: 11196 (DC-56-12-37)
radioinduced formation within Zircaloy clad of fuel elements, mechanism of, 17: 36353 (WAPD-TM-351)
reactions in plasma jet streams, 19: 30653(R) (TID-21723)
reactions with carbon and zirconium oxides at 1000 to 1600°C, hydrogen bonding in, 18: 19981
reactions with oxidizing agents, deuterium tracer studies of, 18: 10031 (AD-403803)
reactions with zirconium carbide, structure of ZrC-ZrH_2 formed by, 20: 4378 (NAA-SR-Memo-11542)
structural testing of stamped moderator assembly, 16: 23259 (DC-59-5-182)
structure of nonstoichiometric beta-, statistical model for, 18: 19959
tensile properties, 16: 12098(R) (LAR-2)
testing in re-entry conditions, ablation and oxidation, 20: 9091(R) (SC-DC-65-1893)
thermal conductivity, 18: 39901 (NAA-SR-Memo-3848)
thermal cycling behavior of slotted tube, 16: 7880 (DC-58-11-13)
thermal cycling effects on moderator, 16: 7241 (DC-58-9-151)
thermal expansion coefficient, 16: 9626 (DC-58-1-191)
thermal expansion properties, 16: 12099(R) (LAR-3)
thermal stability of clad, 16: 6089 (APEX-305)
thermodynamic functions of, calculation from dissociation-pressure data, 17: 6108
thermodynamic functions at high temperatures, 17: 40816
thermodynamic properties, 16: 25395
thermodynamic properties, 17: 10597 (TID-15795)

thermodynamic properties of, composition effects on, 19: 4113
use as heat transfer medium in nuclear reactors, 20: 26411(P)
use as reactor coolant and moderator, 20: 28807(P)
use in purification of iron and molybdenum, 20: 27476(R) (BNWL-207, pp 3.14-16)
use in self-moderating fuel element, 19: 19375(P)
Al–UO_2–ZrH, reactivity measurements in lattices of, near-critical, (E), 20: 14082
BeO–ZrH, reactivity effects on plutonium-fueled reactors, 20: 14122(R) (GA-4451)
Fe–$SrTiO_3$–Y_2O_3–ZrH, electric and thermal properties, 17: 29854(R) (MND-2584-4)
LiH–ZrH_4, liquid-solid equilibrium in, 16: 7545
Mg–ZrH_4, production for use as fuel element canning, 19: 30662(P)
UH–ZrH, criticality studies, 17: 26057
UH–ZrH, criticality studies, 17: 26058
UH–ZrH, decomposition by pulse heating, thermodynamics of, 19: 7469
UH–ZrH, hydrogen evolution in pulse heating, 17: 12587 (NAA-SR-7736)
UH–ZrH, properties of reactor fuel of, in KIWI-TNT, (E), 19: 29592
UH–ZrH, properties of, effects of destructive rapid pulse heating on, 19: 41017 (NAA-SR-10482)
UH–ZrH, pulse heating of, 17: 8808 (NAA-SR-7398)
UH–ZrH, radiation effects on, measurement in TREAT, (E), 20: 6678 (NAA-SR-Memo-11374)
UO_2–ZrH_2, fabrication of fuel pellets of, by cold compacting, 18: 35969 (NAA-SR-Memo-9411)
U–ZrH, burnup during atmospheric re-entry of rocket reactors, (E), 19: 17351 (RTD-TDR-63-3054)
U–ZrH, combustion and disintegration of fuel rods of, 18: 4768
U–ZrH, combustion and disintegration of fuel rods of, during atmospheric re-entry, 18: 11478
U–ZrH_x, criticality studies, 18: 38303 (A/CONF.28/P/361)
U–ZrH, fission product release from irradiated SNAP 10A/2 fuel, 18: 34045 (NAA-SR-9673)
U–ZrH, performance as reactor fuel in SNAPTRAN transient tests, 20: 35138
UH–ZrH, mechanical and physical properties of, 20: 23649 (NAA-SR-Memo-6532)
U–ZrH, properties of, 17: 6559
U–$ZrH_{1.7}$, radiation effects on dimensional stability of stainless steel-clad, 19: 43618
U–ZrH_x, re-entry behavior of fuel elements of, (E), 19: 10628
U–ZrH, shielding properties of, gamma and neutron, 20: 36352
U–Zr–ZrH_2, properties as rocket reactor fuel, testing of, 18: 21698(R) (ANL-6860)
ZrC–ZrH, properties, 19: 40959

ZIRCONIUM HYDROXIDES
dehydration, emanation during, 16: 31661
free energy of formation, 17: 26944(R) (BMI-1630(Del.))
ion exchange properties for xenon oxide in iodate and periodate solutions, 20: 40851
irradiation, preparation of metal and oxide by, 16: 32161
precipitation from nitrates, oxychlorides, and sulfates using barium and sodium hydroxides, 16: 13045
reactions with hydrogen peroxide, 16: 2999
solubility in sodium perchlorate solutions, 20: 36789
sorptive properties for yttrium-90 in acid solution, 19: 376
thermodynamic properties at 2000°K, 17: 25685(R) (BMI-1624(Del.))

ZIRCONIUM IODATES
properties of, for preparation of carrier-free actinides, tracer studies on, 20: 45772
sorptive properties for actinides and lanthanides, 20: 43448
structural properties, 17: 14210 (NBS-MON-25(Sect.1))
use in separation of thorium-234 from lanthanides, 20: 40832

ZIRCONIUM IODIDE, BISCYCLOPENTADIENYL-
preparation by reaction of zirconium iodide with magnesium cyclopentadienide, 20: 35493

ZIRCONIUM IODIDES
crystal structure of trivalent, 18: 39188
decomposition on hitting hot metal foil in vacuum, 17: 159
density and critical parameters of liquid, 17: 18078
deposition of zirconium coating on molybdenum and stainless steel from vapor of, 17: 32507
heat of formation and thermodynamic properties, 17: 4501
magnetic properties at 80 to 300°K, 16: 20423
magnetic properties and preparation, 19: 7416
preparation, 16: 30407
preparation and properties of tri-, 19: 7515
reactions with dinitrogen tetroxide, 16: 13022(T) (NP-tr-850)
reduction of tetravalent, using aluminum, germanium, iron, and mercury, 16: 11634
structure of trivalent, 16: 23682
thermal conductivity of, black body radiation in, 19: 32763
thermodynamic properties, 20: 10816(T) (NASA-TT-F-285)
HfI_4–ZrI_4, phase studies, 16: 18074
ZrB_4–ZrI_4, phase studies, 16: 18074
$ZrCl_4$–ZrI_4, phase studies, 16: 18074

ZIRCONIUM IONS
see also Zirconyl Ions
complex formation by, optimum conditions for, 19: 13374
effect on salt filtration properties of cellophane, 20: 35495
effects on cobalt determination in steel, 20: 43145
effects on copper determination, 20: 36726
effects on dephosphorylation on nucleotides and coenzymes, 19: 60
effects on dephosphorylation of nucleotides and sugar phosphates, 19: 19876
effects on dephosphorylation of cocarboxylase, riboflavin-5-phosphate, and pyridoxal phosphate, 20: 20375
effects on hydrolysis of nucleotides, catalytic, 19: 43708
effects on spectrophotometric determination of erbium, holmium, and neodymium, 20: 43100
electric charges of complex, determination by ion exchange, 18: 39285(T) (AEC-tr-6390(p.475-9))
electrochemical properties of, in fused lithium chloride–potassium chloride media, 17: 18012(R) (TID-18440)
electrogeneration and application to coulometric titrations, 18: 8315
enrichment in bioliths, role of humic acid in, 19: 656
hydrolysis, 17: 1446
polymerization in solutions, dialysis, 16: 182
polysaccharide bond disruption by, 19: 419
reactions with aluminum and copper at 30 kev, x-ray diffraction studies of precipitates from, 17: 1964
reactions with derivatives of Arsenazo III, spectrophotometric studies of, 19: 40426
separation by thin-layer ionophoresis, 18: 10185
separation from aqueous solutions by dibutyl phosphate extraction, equilibria in, 17: 37304
sorption by ion exchange resins, 16: 30436
sorption by polymers, 17: 14354
sorption from perchloric acid solutions by cellulose and resin sulfonic acid exchangers, 18: 35473
sorption on ammonium uranyl phosphate, 19: 32294
sorption on manganese hydroxides, 17: 40792

ZIRCONIUM ISOTOPES
abundance in irradiated uranium-235, 19: 36217(R) (IDO-14656)
alpha scattering by, 17: 41530(R) (ANL-6720(p.43-7))
binding energies and E2 transitions, (T), 19: 6661
decay of isomeric, energy and half life for, (E), 19: 10329
deuteron reactions (d,p) and (d,t), 16: 14009
deuteron reactions (d,p) and (d,t) with, for nuclear structure studies, 17: 34956
deuteron reactions (d,p) with, 17: 41530(R) (ANL-6720(p.43-7))
deuteron reactions at 15 Mev, isomeric states from, (E), 20: 15856
distribution and natural carriers of, in sea water, 20: 31422
energy level spacing and strength functions of, 18: 7696(R) (ORNL-TM-761)
energy level spacings and strength function of even-even, 18: 24625 (WASH-1046)
energy levels, interactions, nuclear moments, and transitions in, 17: 24381 (AD-403411)
energy levels of, theory of low-lying vibrational, 17: 5365
energy levels of, isobaric analogue, 19: 14640
energy levels of, structure from isomeric transition in, (T), 20: 19970
gamma reactions on, cross sections for, 19: 12496
helium-3 reactions (He-3,t) at 18 Mev, (E), 20: 42334
isomeric transitions, M_4-type, 16: 22985 (NP-11747)
mass differences, 17: 21014
masses of even-A, 17: 38102
neutron binding energies in, 18: 32881
neutron capture gamma spectra of, thermal, 17: 41873 (WASH-1044)
neutron configurations in, 16: 26319
neutron reactions (n,n′ γ) at 4.1 Mev, cross section and gamma spectrum for, 18: 30736(R) (TID-20658)
neutron separation energies of even-A, 17: 38102
neutron total cross sections, 17: 41873 (WASH-1044)
nuclear masses and binding energies, 16: 1066
nucleon interactions in, effective, (T), 20: 6337
preparation and properties of radioactive, 19: 4227
preparation of thin self-supporting foils of, by rolling, 20: 25520 (AERE-R-5097, Paper 22)
production and properties of neutron-deficient (N = 41 to 45), 18: 42635 (JINR-P-1724)
production in helium ion and proton reactions with niobium at 240 to 880 Mev, cross sections for, 18: 42745
proton elastic scattering at 22.5 Mev by, cross sections for, 17: 24053(R) (ORNL-3432)

proton elastic scattering at 14.5 Mev, cross sections for, 19: 47705
proton elastic scattering at 14.5 Mev, cross sections for, (E/T), 20: 34638
proton reactions at 22 Mev with, pickup mechanism in, 17: 24053(R) (ORNL-3432)
proton reactions at 14.5 Mev, total cross sections for, (E), 20: 42162 (LA-DC-8075)
purification of electromagnetically separated, 20: 37163
retention by reactor coolant sodium, 18: 11383 (NAA-SR-9163)
separation and purification, method for, 16: 18971
separation from other fission products, large-scale, 18: 31649 (A/CONF.28/P/252)
separation in calutrons, 18: 34007(R) (ORNL-TM-890)

ZIRCONIUM ISOTOPES Zr-80
energy levels of, Hartree-Fock calculations for, 20: 34564
nucleon binding energies and single-particle levels for, (T), 19: 43340
properties of, Hartree-Fock calculations of, (T), 20: 24323 (AD-624314)

ZIRCONIUM ISOTOPES Zr-85
half life, 17: 26507

ZIRCONIUM ISOTOPES Zr-86
decay, 18: 30761
decay of, yttrium-86 levels from, (E), 20: 13856
decay scheme, (E), 20: 24358(R) (UCRL-16580, pp 1-93)

ZIRCONIUM ISOTOPES Zr-87
gamma decay, 18: 30761
half life, 17: 26507

ZIRCONIUM ISOTOPES Zr-88
decay scheme, 16: 4741(R) (TID-14157)
energy levels of, properties of collective, (E), 19: 6671
gamma spectra, (E), 19: 16840(R) (IDO-17050)

ZIRCONIUM ISOTOPES Zr-89
beta decay of, second order effects on shape factor of, 17: 41951
beta emission, pseudoscalar interactions in, 16: 23116
core deformability and electric quadrupole moments, 16: 7026
decay, 18: 2846(R) (TID-19709)
decay of, ratio of electron capture to positron emission in, 18: 2886
decay of 78.4-hr and 4.18-min isomers of, 18: 18985
decay scheme, discrepancies in, 16: 2545
decay scheme for, 16: 33856
energy level densities in, effects of spin on, 16: 33853
energy levels from yttrium-89 (p,n) reactions, 4.83- and 5.03-Mev isobaric analog, (E), 19: 21356
energy levels from proton reactions (p,n) with yttrium-89, isobaric analog, (E), 19: 25511
energy levels of, isobaric-spin splitting of single-particle and single-hole, 17: 9572
energy levels of, wave functions for, 18: 28574(R) (ORNL-3630(p.18-30))
energy levels of, parity and spin of, (E), 20: 22010(R) (NYO-72-28)
energy levels of, parity and spin, (E), 20: 26094 (ORNL-P-2117)
formation in decay of niobium-89, 19: 37835(R) (TID-22024)
gamma decay, 18: 30761
gamma spectra, (E), 19: 16840(R) (IDO-17050)
half life, 17: 2243(R) (TID-17083)
isomeric yield ratio from zirconium-90 (γ,n) reactions to 70 Mev, (E), 19: 43299
positron emission, half life, and production of, 18: 5179 (TID-7673 (p.371-87))
production in reactor by neutron reactions (n,α), 17: 24508
separation from irradiated carrier-free yttrium by solvent extraction using cupferron, 20: 20626
separation from yttrium oxides using ion exchange, radiochemical method for, 20: 16353
use as tracer for external localization of brain tumors by positron scanning, 19: 10929(R) (NYO-1242-1)

ZIRCONIUM ISOTOPES Zr-90
alpha elastic and inelastic scattering at 65 Mev, differential cross sections for, (E/T), 20: 38092
alpha elastic scattering at 43 Mev, collective excitations in, (E), 19: 21386
alpha inelastic scattering at 43 Mev, excitation of collective modes in, 17: 38257
alpha inelastic scattering by, (3⁻,4⁻) doublet energy level from, 18: 24661
alpha inelastic scattering at 34.4 Mev, excitation of 2⁺, 5⁻, and 3⁻ states by, (E), 19: 39844
alpha inelastic scattering at 65 Mev, nuclear structure analysis from, (E/T), 20: 13784 (ORNL-TM-1336)
alpha reactions (α,He-3) at 65 Mev, nuclear structure analysis from, (E/T), 20: 13784 (ORNL-TM-1336)
alpha reactions (α,He-3) at 66 Mev, cross sections for (E/T), 20: 30353(R) (ORNL-3940, pp 1-61)
alpha reactions (α,He-3) at 65 Mev, (E/T), 20: 38092
alpha scattering at 34.4 Mev, angular distributions for, (E), 19: 47623
alpha scattering by, 17: 40436(R) (NYO-10063(p.105-15))
alpha scattering cross sections at 30.5 Mev, (E), 19: 36220(R) (MIT-2098-142)
analysis of first excited state (0+), 16: 5980
bremsstrahlung reactions (γ,n) to 70 Mev, isomeric yield ratio in, (E), 19: 43299
decay of 0.83-sec isomer of, 17: 29634
decay of 1.76 Mev 0⁺ level in, search for two-photon, 17: 19242
deuteron elastic scattering at 12 and 14 Mev, differential cross sections for, (E), 19: 45281 (ORNL-3850)
deuteron inelastic scattering at 15 Mev, angular distributions from, 17: 38271
deuteron inelastic scattering by, effect of data normalization on optical model parameters for, (T), 19: 27550
deuteron reactions (d,p) with, at 7.5 Mev, 16: 30930(R) (NYO-2669)
deuteron reactions (d,α) at 15 Mev, mechanisms for, 16: 32422
deuteron reactions (d,p) at 13.6 Mev, angular distributions from, 17: 24414
deuteron reactions (d,p) at 11.8 Mev, distorted-wave predictions for, 17: 26429(R) (ORNL-3425(p.5-8))
deuteron reactions (d,p) at 11.1 Mev, energy-level excitation in, 17: 26635
deuteron reactions (d,p) with, cross sections and energy levels of, 17: 33066
deuteron reactions (d,t) at 20 Mev, angular distributions and energy spectra from, 17: 38177
deuteron reactions (d,p) at 11.8 Mev, distorted waves approximation in, 17: 38182
deuteron reactions (d,p) with, distorted-wave analysis of, 18: 16909 (ANL-6848(p.30-7))
deuteron reactions (d,He-3) at 21.4 Mev, ground-state configuration from, 18: 36644
deuteron reactions (d,p) with, distorted-wave Born approximation for, 18: 38193
deuteron reactions (d,He-3) with, 18: 42625(R) (ANL-6879(p.65-8))
deuteron reactions (d,p) with, angular distributions from, (T), 19: 12596
deuteron reactions (d,p) at 7 to 11 Mev, (E), 19: 14487 (ANL-6878 (p.61-83))
deuteron reactions (d,p), distorted-wave analysis of, (E/T), 19: 16855(R) (ORNL-3714(Vol.I)(p.1-30))
deuteron reactions (d,p) at less than 4 Mev, optical-model parameters, (T), 19: 16855(R) (ORNL-3714(Vol.I)(p.1-30))
deuteron reactions (d,p) at 12 Mev, angular distributions from, (E), 19: 19095 (WASH-1053)
deuteron reactions (d,p) with, spectra from, 19: 21394
deuteron reactions (d,p) with, DWBA and Coulomb stripping approximations for, (E), 19: 41742
deuteron reactions (d,p) at 12 and 14 Mev, differential cross sections for, (E), 19: 45281 (ORNL-3860)
deuteron reactions (d,p) at 3.5 to 5.5 Mev, angular distributions from, (T), 20: 17691 (ORNL-TM-1235)
deuteron reactions (d,p) below 4 Mev, angular distributions and excitation functions for, (E), 20: 26091 (ORNL-P-1203)
deuteron reactions (d,p) at 11 and 13 Mev, angular-momentum effects on angular distribution from, (E), 20: 32512
deuteron reactions (d,He-3) at 21 Mev, angular distributions from, (E), 20: 34530(T) (CONF-660107-46)
deuteron reactions (d,p) at 2.7 to 3.6 Mev, proton angular distributions from, (E), 20: 38096
deuteron reactions at 11.8 Mev, energy spectra from, 20: 40065(R) (BMwF-FB-K-66-01)
deuteron reactions (d,He-3) at 34.4 Mev, spin dependence of angular distributions from, (E/T), 20: 44800
electromagnetic monopole transitions in, partial widths for 2γ, 18: 16999
energy level configurations in, doublets from, 17: 7105 (NP-12330 (p.122-5))
energy level de-excitation in, two-photon, 17: 31077(R) (CU(PNPL)-228)
energy level excitations in, coherent antiproton-neutron, (T), 20: 42279
energy level transitions in, probability for E2, (T), 19: 10311
energy level transitions in, with double photon emission, (E), 20: 10029
energy level widths, (E/T), 20: 30360 (WASH-1068)
energy levels, 16: 14009
energy levels, 18: 36663
energy levels, (E), 19: 43391
energy levels (E/T), 19: 1568(R) (TID-21113)
energy levels, 18: 16951(R) (TID-20311)
energy levels in, double gamma emission from 1.73-Mev, 17: 4049 (AFOSR-2531)
energy levels in, excited by (d,p) and (d,t) reactions, 17: 34956
energy levels in, excitation of isobaric analog, 18: 15287
energy levels of, electric monopole transitions between, 18: 6252
energy levels of, from (p,α), (p,d), and (p,t) reactions, 17: 26566
energy levels of, location of 4⁻, 18: 24661
energy levels of, identification of 4⁻, 18: 24663

energy levels of, shell model, 18: 30795
energy levels of, half life of, 18: 32797
energy levels of, isobaric analog, 18: 36642
energy levels of, shell model of, 19: 23363(R) (NP-14954)
energy levels of, isobaric spin admixture in, (T), 19: 33313
energy levels of, analysis of isobaric analog, (E), 19: 37813(R) (ORNL-3778(p.97-100))
energy levels of, Coulomb excitation in nitrogen-14 inelastic scattering, (E), 19: 39942
energy levels of, existence of low-lying 4-, 20: 3141
energy levels of, fluctuation averaging for widths of 0.1-kev, (E), 20: 8135
energy levels of, double gamma emission from, (E/T), 20: 22010(R) (NYO-72-28)
energy levels of, central and tensor potentials in shell model calculations of, 20: 28360
energy levels of, shell-model potential parameters for low-lying, (T), 20: 38145
energy levels of, isobaric analogue, (T), 20: 44777
energy levels, configuration mixing, and proton-neutron interaction in, (T), 19: 23678
gamma decay in 0^+-0^+ transition, detection of double, 16: 1063
gamma decay of excited, detection of two-photon, 18: 30717(R) (COO-605-6)
gamma emission in 0^+–0^+ transitions in, double, 18: 34752(R) (CU(PNPL)-234)
gamma emission, probability of double, 16: 5981
gamma reaction (γ,p) with angular distribution and cross section of, 18: 38171
gamma reactions (γ,p) with, quadrupole excitation in, 18: 7721
gamma reactions (γ,n) and (γ,2n), cross sections for, (E), 20: 44660 (UCRL-70002)
gamma reactions (γ,n) and (γ,p), mechanism of, (E), 20: 44778
gamma reactions (γ,n) on, nuclear excited states from, 16: 33853
gamma resonance absorption by, energy levels from, 17: 38160
gamma scattering by, resonance, 18: 11175 (ANL-6797(p.275-87))
gamma spectra, 18: 1050
gamma spectra in two-photon E(0) transitions of, 18: 9326
helium-3 elastic scattering at 12 Mev, 18: 38144
helium-3 reactions (He-3,t) at 18 Mev, (E), 20: 42334
helium-4 reactions at 6 to 42 Mev, excitation functions for, (E), 20: 34529(R) (UR-3591-2)
internal conversion probabilities in, reduced M and N E0, (T), 20: 15771
ion reactions with, unexcited compound nuclei from, (T), 20: 26126
mass difference from strontium-88, 17: 17158
meson (π^+) reactions at 220 to 320 Mev/c, double charge exchange in, (E), 20: 42316
metabolism in rats of, after oral administration of mixed uranium fission products, 19: 40322
neutron capture by, gamma spectrum for thermal, 18: 6179(R) (ORNL-3499(Vol.I)(p.42-6))
neutron capture by, s-wave strength functions for, 18: 26544(R) (ORNL-3582(p.82-4))
neutron capture cross sections at 1–30,000 ev, p and s-wave strength functions from resonances in, 17: 26438(R) (ORNL-3425(p.32-5))
neutron cross sections at 20000 ev, 18: 6165 (NP-13359)
neutron inelastic scattering cross sections, 16: 1023 (KAPL-2163)
neutron inelastic scattering by, 17: 36669 (WASH-1042)
neutron inelastic scattering near threshold, (E), 19: 16973
neutron inelastic scattering at 0 to 200 kev, excited states from, (E/T), 20: 34652
neutron radiative capture cross sections, (T), 19: 19106
neutron reactions (n,p) at 14 Mev, cross section ratios to zirconium-91, 92, and 94, 16: 6019
neutron reactions (n,2n), cross sections for, 16: 7072
neutron reactions at 14.6 Mev, mechanisms and shell effects, 16: 12487
neutron reactions (n,p) at 7.0 to 19.8 Mev, cross sections for, 16: 19782
neutron reactions (n,p) at 14.7 Mev, cross sections, 16: 21352 (NP-11667)
neutron reactions (n,α) at 14.8 Mev, cross sections and product half-life for, 17: 2242 (TID-16949)
neutron reactions (n,2a) at 14.8 Mev, cross sections and product half life for, 17: 2242 (TID-16949)
neutron reactions (n,p), cross sections for, 17: 2242 (TID-16949)
neutron reactions (n,2n) with, cross sections for positron production in, 18: 13061
neutron reactions (n,2n) at 14 Mev, isomeric cross-section ratios for, 18: 18966
neutron reactions (n,p) at 3.55 to 6.02 Mev, cross sections for (E), 19: 3383
neutron reactions (n,2n) at 14 Mev, shell effects in, (T), 19: 12536
neutron reactions (n,pn) at 14 Mev, production of yttrium-89 isomers in, (E), 19: 47566 (AERE-R-5009)
neutron reactions (n,γ) at 1 ev to 50 kev, cross sections for, (E), 20: 3032
neutron reactions (n,p) at 3.55 to 15 Mev, cross sections for, (E), 20: 30418
neutron reactions (n,2n) at 3 Mev above threshold, cross section for, (E), 20: 46614
neutron resonance at 180 to 1490 ev, 16: 5994
neutron resonance absorption by, at 0.021 to 10.1 kev, 18: 36080(R) (RPI-328-8)
neutron resonance structure and s-wave strength function for, (E), 19: 35401 (ORNL-P-1346)
neutron resonance absorption at 0 to 60 kev, structure in, (E), 19: 37809(R) (ORNL-3778(p.76-81))
neutron resonances below 10 kev, 18: 24620(R) (ORNL-TM-874)
neutron scattering at 0.25 to 7 Mev, angular distributions, 16: 9653 (KAPL-2000-16)
neutron scattering by, metastable state production cross section for, 17: 22628
neutron scattering at 3 to 650 kev, cross sections, phase shifts, and strength functions for, (E), 19: 10319
neutron scattering by, zirconium-91 neutron single-particle levels from, (T), 20: 32552
neutron strength functions for, 18: 8919(R) (PR-P-59(p.65-78))
neutron strength functions, (T), 19: 25497
neutron strength functions of, calculation of, 20: 38038
neutron total cross sections for, principal resonances in, 17: 26437 (ORNL-3425(p.32))
neutron total cross sections for, resonances in, 17: 33005 (ORNL-TM-636)
neutron total cross section measurements to 20 kev, 18: 28637
neutron total inelastic cross sections, 18: 2963
nitrogen-15 reactions with, two neutron transfer in, 17: 38080 (JINR-P-1273)
nitrogen-15 reactions at 70 to 120 Mev, cross sections for two-neutron transfer in, 18: 6260
nuclear electric monopole transitions, 16: 9463
nuclear properties of, generalized Hartree-Fock calculations for, (T), 20: 40076 (MIT-2098-255)
nuclear structure of, alpha cluster reduced widths for, 18: 34891
nuclear wave functions, (E), 19: 10257(R) (TID-21335(p.33-107))
nucleon binding energies, energy levels, and potentials for, 18: 21358
nucleon capture at 10 to 40 Mev, cross sections and mechanism for direct, (T), 20: 17737
nucleon interaction potentials in, shell model calculation of, 17: 40031
photoabsorption cross sections of, dipole, (T), 19: 27479
photodisintegration, giant resonance effects in, 16: 18534
photon reactions (γ,n) on, threshold of, 17: 17158
production in proton reactions (p,α), (p,d), and (p,t), pick-up contributions in ground-state, 17: 38230
proton elastic and inelastic scattering at 6.8 Mev, 17: 24414
proton elastic scattering at 22.5 Mev, potentials for, 18: 32844
proton elastic scattering by, optical model parameters for distributions and polarizations from, (E/T), 20: 1157 (ORNL-P-1616)
proton elastic scattering at 40 Mev, cross sections for, (E/T), 20: 30353(R) (ORNL-3940, pp 1-61)
proton elastic scattering at 40 Mev, differential cross sections and polarization for, (E), 20: 32510
proton inelastic scattering by, shell-model form factors for, (T), 20: 13867
proton inelastic scattering at 10 to 20 Mev, multiple excitation and shell model description of, 20: 42229
proton reactions (p,d) with, zirconium-89 energy levels from, 18: 28574(R) (ORNL-3630(p.18-30))
proton reactions (p,α) with, distorted-wave analysis of, (T), 19: 14486 (ANL-6878(p.23-60))
proton reactions (p,α) at 20.2 Mev, distributions from, (E), 19: 37823(R) (ORNL-3800(p.1-49))
proton reactions (p,α) at 20.2 to 22.5 Mev, alpha angular distributions and spectra from, (E/T), 19: 47670
proton reactions (p,p), fine structure near isobaric analog resonances in, 20: 4923
proton reactions (p,n) at 30 and 50 kev, excitation of double analog states in, 20: 10031
proton reactions (p,n) at 14.2 Mev, angular distributions, Q values, and spectra from, (E), 20: 13345(R) (NP-15772)
proton reactions (p,n) at 30 to 50 Mev, distributions from, 20: 15729(R) (RHEL/R-112, pp 37-66)
proton reactions (p,d) at 36 Mev, deuteron spectra from, (E/T), 20: 30353(R) (ORNL-3940, pp 1-61)
proton reactions (p,α) at 20.2 Mev, alpha spectra from, (E/T), 20: 30353(R) (ORNL-3940, pp 1-61)
proton reactions (p,n) at 14.2 Mev, Q-values and differential cross sections for, (E/T), 20: 34520 (INSJ-97)
proton reactions (p,γ) in stars, 16: 12308
proton reactions (p,n) at 19.2 Mev, isomeric states from, 16: 32441

proton reactions (p,d) with, isobaric-spin analog states in, 17: 19361
proton reactions (p,d) at 22 Mev, excited energy levels in, 17: 38234
proton reactions (p,n) at 6.9 to 11.2 Mev, cross sections for, 17: 40056
proton reactions (p,α) and (p,d) at 11.2 Mev, cross sections for, 17: 40056
proton scattering at 40.5 Mev, polarization effects in, (E), 19: 37823(R) (ORNL-3800(p.1-49))
proton scattering at 18.8 Mev, shell-model analysis of angular distributions from, (E/T), 20: 13866
proton scattering by, niobium-91 isobaric analog state from, (E), 20: 24441
proton scattering at 12.7 Mev, cross sections for, (E), 20: 26090 (ORNL-3934)
reactions with hydrogen gas at 10 to 50 kev, stopping powers from, 18: 32453
superconducting transition temperature, (E), 20: 30316

ZIRCONIUM ISOTOPES Zr-91

alpha elastic and inelastic scattering at 65 Mev, differential cross sections for, (E/T), 20: 38092
alpha elastic scattering at 43 Mev, collective excitations in, (E), 19: 21386
alpha inelastic scattering at 65 Mev, nuclear structure analysis from, (E/T), 20: 13784 (ORNL-TM-1336)
alpha reactions (α,He-3) at 65 Mev, nuclear structure analysis from, (E/T), 20: 13784 (ORNL-TM-1336)
alpha reactions (α,He-3) at 66 Mev, cross sections for, (E/T), 20: 30353(R) (ORNL-3940, pp 1-61)
alpha reactions (α,He-3) at 65 Mev, (E/T), 20: 38092
alpha scattering at 34.4 Mev, angular distributions for, (E), 19: 47623
core deformability and electric quadrupole moments, 16: 7026
deuteron elastic scattering at 34.4 Mev, angular distributions from, (E/T), 20: 30353(R) (ORNL-3940, pp 1-61)
deuteron reactions (d,p), spins and parities of certain states, 16: 4837
deuteron reactions (d,p) at 13.6 Mev, angular distributions from, 17: 24414
deuteron reactions (d,p) at 11.1 Mev, energy-level excitation in, 17: 26635
deuteron reactions (d,p) with, cross sections and energy levels of, 17: 33066
deuteron reactions (d,t) at 20 Mev, angular distributions and energy spectra from, 17: 38177
deuteron reactions (d,t) at 11.8 Mev, angular distributions from, (E), 19: 21326
energy levels, 16: 14009
energy levels and nuclear potential, 18: 32881
energy levels, determination of neutron, 16: 21495
energy levels in, excited by (d,p) and (d,t) reactions, 17: 34956
energy levels of, (T), 20: 30350 (JINR-P-2682)
energy levels of, spin values for three-particle isomeric, 18: 28614
energy levels of, low-lying positve parity, 18: 36663
energy levels of, neutron transmission measurements for, (E), 19: 12553
energy levels of, single-particle, (T), 20: 22113
energy levels of, neutron single-particle, (T), 20: 32552
energy-level transition probabilities of, E2, (T), 20: 3115
gamma reactions (γ,n) with, cross sections for, (E), 20: 4849(R) (UCRL-14360, pp 1-50)
gamma reactions (γ,n) and (γ,2n), cross sections for, (E), 20: 44660 (UCRL-70002)
helium-3 reactions (He-3,t) at 18 Mev, (E), 20: 42334
neutron capture by, gamma spectra of p- and s-wave resonances in, 17: 34951
neutron capture by, gamma spectrum for thermal, 18: 6179(R) (ORNL-3499(Vol.I)(p.42-6))
neutron capture by, polarization of gamma rays from, (E), 19: 23633 (UJV-1211/64)
neutron capture cross sections at 1–30,000 ev, p and s-wave strength function from resonances in, 17: 26438 (ORNL-3425(p.32-5))
neutron compound inelastic scattering at 3 Mev, angular correlation functions for, 18: 9402
neutron cross sections at 20000 ev, 18: 6165 (NP-13359)
neutron elastic scattering at 1.509 Mev, polarization in, 17: 31410 (TID-19051)
neutron radiative capture cross sections, (T), 19: 19106
neutron reactions (n,p) at 14 Mev, cross section ratio to zirconium-90, 16: 6019
neutron reactions at 14.6 Mev, mechanisms and shell effects, 16: 12487
neutron reactions (n,p), separation energies for, 17: 2242 (TID-16949)
neutron reactions (n,p), cross sections for, 17: 2242 (TID-16949)
neutron reactions (n,p) at 3.55 to 6.02 Mev, cross sections for (E), 19: 3383
neutron reactions (n,γ) at 1 ev to 50 kev, cross sections for, (E), 20: 3032
neutron reactions (n,p) at 4.32 to 6.02 Mev, cross sections for, (E), 20: 30418
neutron resonance at 180 to 1490 ev, 16: 5994
neutron resonance capture in, gamma spectra from, 17: 41527(R) (ANL-6720(p.2-15))
neutron resonance capture, 18: 2804
neutron resonance capture in, approximation calculations of, 18: 7673 (CONF-187-26)
neutron resonance absorption by, at 0.021 to 10.1 kev, 18: 36080(R) (RPI-328-8)
neutron resonances below 10 kev, 18: 24620(R) (ORNL-TM-874)
neutron total cross sections for, principal resonances in, 17: 26437 (ORNL-3425(p.32))
neutron total cross sections for, resonances in, 17: 33005 (ORNL-TM-636)
neutron total cross section measurements to 20 kev, 18: 28637
nuclear energy splittings of spin-orbit doublets in, 16: 33884
nuclear magnetic resonance in iron–zirconium intermetallic compounds, 18: 39941
nucleon binding energy, (T), 20: 22113
nucleon capture at 10 to 40 Mev, cross sections and mechanism for direct, (T), 20: 17737
proton elastic and inelastic scattering at 6.8 Mev, 17: 24414
proton elastic scattering at 22.5 Mev, potentials for, 18: 32844
proton reactions (p,n) at 12.35 Mev, niobium-91 levels in proton emission from, 20: 30480
proton reactions (p,n) at 13 Mev, isobaric analogue states from, (E), 20: 46577 (AD-630032)
proton reactions (p,d) at 22 Mev, excited energy levels in, 17: 38234
proton reactions (p,d) at 22.3 Mev, distorted-wave analysis of, 17: 38233
proton reactions (p,d) with, pick-up contributions in, 17: 38230
proton reactions (p,α) at 11.2 Mev, cross sections for, 17: 40056
proton reactions (p,n) at 30 and 50 Mev with, excitation of isobaric states in, 17: 41926
sorption by humic acids and peat, 16: 11591
spin-orbit splitting in, 17: 21047
wave function of, 18: 32881

ZIRCONIUM ISOTOPES Zr-92

alpha elastic and inelastic scattering at 65 Mev, differential cross sections for, (E/T), 20: 38092
alpha elastic scattering at 43 Mev, collective excitations in, (E), 19: 21386
alpha reactions (α,He-3) and scattering, distributions from, (E), 19: 37823(R) (ORNL-3800(p.1-49))
alpha reactions (α,He-3) at 65 Mev, nuclear structure analysis from, (E/T), 20: 13784 (ORNL-TM-1336)
alpha reactions (α,He-3) at 66 Mev, cross sections for, (E/T), 20: 30353(R) (ORNL-3940, pp 1-61)
alpha reactions (α,He-3) at 65 Mev, (E/T), 20: 38092
alpha scattering at 34.4 Mev, angular distributions for, (E), 19: 47623
alpha scattering at 65 Mev, nuclear structure analysis from, (E/T), 20: 13784 (ORNL-TM-1336)
deuteron (d,p) reaction with, 19: 3267
deuteron inelastic scattering at 15 Mev, angular distributions from, 17: 38271
deuteron inelastic scattering at 15 Mev, single excitations in, (E), 19: 35486
deuteron reactions (d,p) at 10.85 Mev, energy level excitation in, 16: 11019
deuteron reactions (d,α) at 15 Mev, mechanisms for, 16: 32422
deuteron reactions (d,t) at 20 Mev, angular distributions and energy spectra from, 17: 38177
deuteron reactions (d,p) at 12 Mev, angular distributions from, (E), 19: 19095 (WASH-1053)
deuteron reactions (d,t) at 11.8 Mev, angular distributions from, (E), 19: 21326
deuteron reactions (d,α) at 120 Mev, yttrium-90 levels from, (E), 20: 15799
deuteron reactions (d,p) at 11 and 13 Mev, angular-momentum effects on angular distribution from, (E), 20: 32512
energy level at 2.33 Mev, spin of, 18: 18990
energy level strength functions for, 16: 26518
energy level transitions in, M1-M2 mixing ratios as testing of purity of vibrational, (T), 19: 25503
energy levels, 16: 14009
energy levels, 16: 29828 (LADC-5293)
energy levels in, excited by (d,p) and (d,t) reactions, 17: 34956
energy levels of, 17: 39968 (BNL-7234)
energy levels of, shell model for, 17: 2300
energy levels of, shell model analysis of, (T), 19: 37824(R) (ORNL-3800 (p.50-7))
energy levels of, shell-model calculation using realistic interactions for, 20: 30384
gamma emission by, circular polarization in, (E), 19: 23633 (UJV-1211/64)

gamma reactions (γ,n) with, cross sections for, (E), 20: 4849(R) (UCRL-14360, pp 1-50)
gamma reactions (γ,n) and (γ,2n), cross sections for, (E), 20: 44660 (UCRL-70002)
helium-3 reactions (He-3,t) at 18 Mev, (E), 20: 42334
neutron capture by, gamma spectrum for thermal, 18: 6179(R) (ORNL-3499(Vol.I)(p.42-6))
neutron capture by, s-wave strength functions for, 18: 26544(R) (ORNL-3582(p.82-4))
neutron capture cross sections at 1–30,000 ev p and s-wave strength functions from resonances in, 17: 26438(R) (ORNL-3425(p.32-5))
neutron cross sections at 20000 ev, 18: 6165 (NP-13359)
neutron inelastic scattering cross sections, 16: 1023 (KAPL-2163)
neutron radiative capture cross sections, (T), 19: 19106
neutron reactions (n,p) at 14 Mev, cross section ratio to zirconium-90, 16: 6019
neutron reactions at 14.6 Mev, mechanisms and shell effects, 16: 12487
neutron reactions (n,α) at 7.0 to 19.8 Mev, cross sections for, 16: 19782
neutron reactions (n,np) and (n,pγ) at 14 Mev, cross sections for, 17: 2242 (TID-16949)
neutron reactions (n,p) at 14.8 Mev, cross sections and product half life for, 17: 2242 (TID-16949)
neutron reactions (n,α) at 14 Mev, 18: 17057
neutron reactions (n,p) at 3.55 to 6.02 Mev, cross sections for (E), 19: 3383
neutron reactions (n,p) at 6.0 Mev, cross sections for, (E), 20: 30418
neutron resonance absorption by, at 0.021 to 10.1 kev, 18: 36080(R) (RPI-328-8)
neutron resonance structure and s-wave strength function for, (E), 19: 35401 (ORNL-P-1346)
neutron resonance absorption at 0 to 60 kev, structure in, (E), 19: 37809(R) (ORNL-3778(p.76-81))
neutron resonances below 10 kev, 18: 24620(R) (ORNL-TM-874)
neutron scattering at 3 to 650 kev, cross sections, phase shifts, and strength functions for, (E), 19: 10319
neutron scattering by, optical analysis of, (T), 19: 43276 (NAA-SR-Memo-11456)
neutron strength functions, (T), 19: 25497
neutron strength functions of, calculation of, 20: 38038
neutron total cross sections for, principal resonances in, 17: 26437 (ORNL-3425(p.32))
neutron total cross sections for, resonances in, 17: 33005 (ORNL-TM-636)
neutron total cross section measurements to 20 kev, 18: 28637
nitrogen ion reactions at 44 and 52 Mev, Coulomb excitation in, 18: 7718
nitrogen-15 reactions with, two neutron transfer in, 17: 38080 (JINR-P-1273)
nitrogen-15 reactions at 70 to 120 Mev, cross sections for two-neutron transfer in, 18: 6260
nuclear wave functions, (E), 19: 10257(R) (TID-21335(p.33-107))
nucleon interactions in, potentials for, 18: 26638
parity and spin of, from deuteron scattering data, 20: 15850
proton elastic and inelastic scattering at 6.8 Mev, 17: 24414
proton elastic scattering at 22.5 Mev, potentials for, 18: 32844
proton reactions (p,d) and (p,t) with, mechanisms for, 18: 36605
proton reactions (p,α) at 28 Mev, J-dependence of angular distributions from, (E), 20: 32489
proton reactions (p,γ) in stars, 16: 12308
proton reactions (p,t) at 22 Mev, angular distributions and cross sections for, 17: 26566
proton reactions (p,d) at 22 Mev, excited energy levels in, 17: 38234
proton reactions (p,t) with, pick-up contributions in, 17: 38230
proton reactions (p,d) at 22.3 Mev, distorted-wave analysis of, 17: 38233
proton scattering at 12.7 Mev, cross sections for, (E), 20: 26090 (ORNL-3934)
separation from neutron-deficient molybdenum-93m, 20: 43067(R) (IDO-14679, pp 6-46)
superconducting transition temperature, (E), 20: 30316

ZIRCONIUM ISOTOPES Zr-93

abundance in giant stars, 17: 3913
deuteron reactions (d,p) with, spins of states from, (E), 19: 14495 (ANL-6878(p.279-301))
energy levels, 16: 14009
energy levels, 19: 3267
energy levels, determination of neutron, 16: 21495
energy levels of, shell model for, 17: 2300
energy levels of, parity and spin of, (E), 19: 23726
gamma reactions (γ,n) with, cross sections for, (E), 20: 4849(R) (UCRL-14360, pp 1-50)
production in yttrium-93 decay, mass discrepancies from, 16: 26287 (IS-408)

ZIRCONIUM ISOTOPES Zr-94

alpha elastic scattering at 43 Mev, collective excitations in, (E), 19: 21386
deuteron (d,p) reaction with, 19: 3267
deuteron inelastic scattering at 15 Mev, angular distributions from, 17: 38271
deuteron reactions (d,n) and (d,p), mechanism, 16: 7127
deuteron reactions (d,t) at 20 Mev, angular distributions and energy spectra from, 17: 38177
deuteron reactions (d,p) at 12 Mev, angular distributions from, (E), 19: 19095 (WASH-1053)
deuteron reactions (d,t) at 11.8 Mev, angular distributions from, (E), 19: 21326
deuteron reactions (d,n), cross sections for isomer production in, 19: 25476(R) (TID-21525)
deuteron reactions (d,n) at 15 Mev, isomeric yield ratios for, 20: 16508(R) (NYO-2771-13)
deuteron reactions (d,p) at 11 and 13 Mev, angular momentum effects on angular distribution from, (E), 20: 32512
deuteron reactions at 11.8 Mev, energy spectra from, 20: 40065(R) (BMwF-FB-K-66-01)
energy level strength functions for, 16: 26518
energy levels, 16: 14009
energy levels, 20: 28315
energy levels between 0.92 and 4.25 Mev, (E), 20: 46592(R) (ORNL-3973(Vol.1), pp 1-13)
energy levels in, excited by (d,p) and (d,t) reactions, 17: 34956
gamma reactions (γ,n) and (γ,2n), cross sections for, (E), 20: 44660 (UCRL-70002)
helium-3 reactions (He-3,t) at 18 Mev, (E), 20: 42334
neutron capture by, gamma spectrum for thermal, 18: 6179(R) (ORNL-3499(Vol.I)(p.42-6))
neutron capture by, s-wave strength functions for, 18: 26544(R) (ORNL-3582(p.82-4))
neutron capture cross sections at 1–30,000 ev, p and s-wave strength functions from resonances in, 17: 26438(R) (ORNL-3425(p.32-5))
neutron cross sections at 20000 ev, 18: 6165 (NP-13359)
neutron radiative capture cross sections, (T), 19: 19106
neutron reactions (n,p) at 14 Mev, cross section ratio to zirconium-90, 16: 6019
neutron reactions (n,He³) at 14.5 Mev, cross-section upper limits, 16: 8219
neutron reactions at 14.6 Mev, mechanisms and shell effects, 16: 12487
neutron reactions (n,α) at 7.0 to 19.8 Mev, cross sections for, 16: 19782
neutron reactions (n,np) at 14 Mev, cross sections for, 17: 2242 (TID-16949)
neutron reactions (n,p) at 14.8 Mev, cross sections and product half life for, 17: 2242 (TID-16949)
neutron reactions (n,α) at 14.8 Mev, cross sections and product half-life for, 17: 2242 (TID-16949)
neutron reactions (n,p) at 3.55 to 6.02 Mev, cross sections for (E), 19: 3383
neutron reactions (n,γ) at 1 ev to 50 kev, cross sections for, (E), 20: 3032
neutron reactions (n,p) at 6.0 Mev, cross sections for, (E), 20: 30418
neutron resonance absorption by, at 0.021 to 10.1 kev, 18: 36080(R) (RPI-328-8)
neutron resonance structure and s-wave strength function for, (E), 19: 35401 (ORNL-P-1346)
neutron resonance absorption at 0 to 60 kev, structure in, (E), 19: 37809(R) (ORNL-3778(p.76-81))
neutron resonances below 10 kev, 18: 24620(R) (ORNL-TM-874)
neutron scattering at 3 to 650 kev, cross sections, phase shifts, and strength functions for, (E), 19: 10319
neutron separation energy for, 17: 21014
neutron strength functions, (T), 19: 25497
neutron strength functions of, calculation of, 20: 38038
neutron total cross sections for, principal resonances in, 17: 26437 (ORNL-3425(p.32))
neutron total cross sections for, resonances in, 17: 33005 (ORNL-TM-636)
neutron total cross section measurements to 20 kev, 18: 28637
nitrogen ion reactions at 44 and 52 Mev, Coulomb excitation in, 18: 7718
nitrogen-15 reactions with, two neutron transfer in, 17: 38080 (JINR-P-1273)
nitrogen-15 reactions at 70 to 120 Mev, cross sections for two-neutron transfer in, 18: 6260
nuclear wave functions, (E), 19: 10257(R) (TID-21335(p.33-107))
proton elastic scattering at 22.5 Mev, potentials for, 18: 32844
proton inelastic scattering by, angular distributions and analog state spins from, (E), 20: 19917
proton reactions (p,t) with, mechanisms for, 18: 36605
proton reactions (p,n) at 14.2 Mev, angular distributions, Q values, and spectra from, (E), 20: 13345(R) (NP-15772)
proton reactions (p,n) at 14.2 Mev, Q-values and differential cross sections for, (E/T), 20: 34520 (INSJ-97)

proton reactions (p,γ) in stars, 16: 12308
proton reactions (p,d) at 22 Mev, excited energy levels in, 17: 38234
proton reactions (p,t) at 22 Mev, energy spectra from, 17: 38235
proton reactions (p,d) at 22.3 Mev, distorted-wave analysis of, 17: 38233
proton reactions (p,α) at 11.2 Mev, cross sections for, 17: 40056
proton scattering at 12.7 Mev, cross sections for, (E), 20: 26090 (ORNL-3934)
superconducting transition temperature, (E), 20: 30316

ZIRCONIUM ISOTOPES Zr-95
activity of dust-borne, in Osaka, Japan, Nov. 1962–Dec. 1963, 20: 7275
age and content in fall out, determination of, 17: 39271(T) (AEC-tr-6022)
analysis of fallout particles of, for yttrium-88 on grass, 17: 17998
analysis of mixtures with niobium-95, beta and gamma scintillation spectrometric, 18: 39117
behavior in solutions without carrier, 18: 3848
beta activity measurements in France, 20: 41189 (CEA-R-3020)
beta decay, isospin conservation in, 16: 17084
beta decay of, niobium-95 activity for varied fluxes in zirconium-94 (n,γ) reactions, 17: 26510
beta decay of, β-γ circular polarization correlation in permitted transitions in, (E), 19: 47605
beta decay of, β-γ circular polarization correlations in, (E), 20: 30543
beta decay of, circular polarization of gamma radiation following, 18: 21309
body burden in Alaska, 18: 20231 (HW-SA-3048)
chemical behavior in trace quantities, 17: 2960(T) (UCRL-Trans-599(L))
content and motion in, 19: 36661
content in air and rain from 1962 nuclear explosions, 18: 428 (AERE-R-4384)
content in air and rain, up to 1964, 19: 7696 (AERE-R-4687)
content in air from Chinese detonations in 1964, 20: 8980(R) (BNWL-36, pp 3.1-122)
content in air over Indian and Pacific Oceans in 1961–62, 19: 20158 (NP-14712)
content in air samples collected at Richland, Wash., 1962, 1963, and 1964, 19: 2541
content in air, bones, food, soil, and water in Italy, 1962, 18: 18040 (BIO/03/63)
content in airborne particles in Cincinnati, May 1962 to Dec. 1963, 19: 4367
content in Alaskan water supplies, 1963, 19: 18164
content in animals, birds, fish, and plants in region of Cape Thompson, Alaska, 1959 to 1962, 20: 7319 (PNE-480)
content in atmosphere over Atlantic Ocean, 1958, 16: 32719
content in atmosphere and drinking water, Moncloa Station, Spain, 1964, 19: 46597
content in atmosphere, 1962 to 1963, 20: 2049
content in atmosphere, 1962 through mid-1964, 20: 8980(R) (BNWL-36, pp 3.1-122)
content in atmospheric dust and rain water, 1964–65, 20: 16660 (AERE-R-4997)
content in atmosphere after Chinese atmospheric tests, 20: 23344 (AEET-240)
content in atmosphere over Spokane, Washington, after Chinese nuclear explosion in May 1965, 20: 33573
content in atmosphere from underground nuclear explosion, effects of filtering on, 20: 45833 (UCRL-14778)
content in biosphere of, from fallout, 1959 through 1962, 19: 9367 (IAEA-R-1)
content in brown algae in Black Sea, 18: 4979
content in children and stillborn infants, 17: 27013 (TID-18878)
content in deep bottom ocean feeders, sinking rates for, 18: 8526
content in diet and excreta in Japan, 19: 38894
content in drinking waters in England, 16: 20126
content in dust particles in precipitation, Vienna, Austria, Oct. 1962 to Sept. 1963, 19: 13643
content in environment in Japan, 1961–64, 20: 43615
content in fallout in French territory, 18: 33770 (SCPRI(S)-99)
content in fallout in Dallas, Texas, from Dec. 1962 to July 1963, 19: 28540(R) (TID-21892)
content in fallout from Chinese nuclear test, 19: 32429
content in fallout over Moscow, 1962, 19: 34369
content in fallout particles, 20: 2053
content in fallout, 1963, 20: 5652
content in fallout, 1964, 20: 11018
content in fallout in USSR, 1962, 20: 29406 (NP-14719)
content in fallout from Chinese nuclear tests, 20: 29423
content in fallout particles from high-altitude explosions, 20: 31424
content in fallout from Chinese nuclear test of May 14, 1965, 20: 33530
content in fallout and plankton of Mediterranean Sea, 1963, 20: 41146
content in fallout from Chinese nuclear test, May 1965, 20: 41130(R) (COO-1407-10)
content in fallout at Vilnius, Soviet Union, 1962, 20: 16700
content in fallout and precipation near Leningrad, 20: 16704
content in fractionated fallout particles from land surface burst, 20: 31460
content in ground-level air near Moscow, 1960-1962, 19: 13628 (NP-14718)
content in holothuriae, western Mediterranean, 1962, 19: 46611
content in human lungs from fallout inhalation, 19: 11434
content in individual rain showers at Bombay, 20: 5661 (AEET-215)
content in irradiated uranium carbide cladding, 19: 40286(R) (NAA-SR-11200)
content in juniper trees in Georgia, 20: 29410
content in lake sediments and mollusks, 19: 1996
content in large fallout particles in Japan, 20: 31412
content in man, 16: 28736
content in man of, from inhaled irradiated uranium, 19: 10749
content in marine organisms near Columbia River mouth, interspecies differences in, 17: 24866
content in marine environment, 19: 43663
content in marine organisms in northeast Pacific Ocean, 20: 18903 (RLO-1750-3)
content in natural waters, fallout correlations with, 20: 27161
content in nekton and macroplankton in Pacific Ocean off Oregon coast, 18: 1341(R) (TID-19608)
content in nuclear debris over Sweden, 1962 to 1963, 20: 43524
content in organisms and water in Gulf of Mexico, 20: 18200 (NYO-3450-1, pp 109-29)
content in Pacific Ocean surface water near mouth of Columbia River, 20: 18902 (RLO-1725-41)
content in Pacific Ocean sediments near mouth of Columbia River, 20: 18902 (RLO-1725-41)
content in plants and soil, methods for decreasing, 19: 18209
content in plants of Bucharest region, (E), 19: 30413
content in plants before and after Salmon Event, 20: 16743 (VUF-1021)
content in pulp for photographic paper, 20: 29427
content in rabbit tissues after intravenous injection, 19: 27939
content in rain water, Fayetteville, Arkansas, Oct. 1964, 20: 16663 (TID-21470)
content in rain water and air in Great Britain, 1960 to 1961, 16: 394 (AERE-R-3766)
content in rainwater at Ispra during 1963 and 1964, 19: 34373
content in rainwater at Milan following Chinese nuclear explosions, 19: 42643
content in rainwater and snow in Germany, 1961 to 1963, 20: 16766
content in Savannah River water, July through Dec. 1965, 20: 27195(R) (DPST-66-30-1)
content in sedge from Chariot site environment, 19: 25798 (PNE-447)
content in silt in Escaut River, Belgium, control of, 20: 22515(T) (ORNL-tr-965)
content in sintered uranium dioxide pellet, radial distribution of, 20: 4472
content in soil in King, Ontario, Oct. 1958 to July 1961, 16: 13375
content in stratospheric and tropospheric air filter samples collected in 1961 and 1962, 19: 9755 (HASL-153)
content in stratosphere, 19: 20657(R) (DASA-1309)
content in stratospheric and tropospheric samples in Project Star Dust, 1963, 20: 16727(R) (HASL-168)
content in stratospheric and tropospheric samples in Project Star Dust, 1964, 20: 16728(R) (HASL-169)
content in surface layer of atmosphere over Heis Island and Moscow, 20: 16650
content in Swedish food, 1962, 18: 23790 (NP-13828)
content in tissues of fin whale captured off Oregon coast, 19: 6936
content in Tyrrhenian Sea plankton, 19: 30411
content in U. S. soil samples, 1962 and 1963, 19: 629 (TID-7696(p.101-10))
content in vegetation in Italy, 1961, 17: 27591 (EUR-223.i)
content in vegetation in Northern Alaska from fallout, 17: 27053 (HW-SA-3050)
content of, in lung specimens, effects of age on, 17: 40492(R) (TID-18790)
content of, in brown algae of Solway Firth, 20: 3662 (PG-Report-650)
content of, in marine organisms, 19: 10732
content of, in tuna from Western Pacific, 1962, 18: 27703 (UWFL-90)
content on air filters at Hanford, methods of gamma spectrometry for monitoring, 19: 620(R) (HW-81746(p.3.51-5))
contents in air in Hanford Works Area, 19: 13626 (HW-SA-3742)
contents in animals and plants from Chariot site environment, 19: 25796 (PNE-445)
contents in animals, plants, rain water, and soils from Chariot site environment, 19: 25797 (PNE-446)
contents in animals and plants from Chariot site environment, 19: 25799(R) (PNE-448)

decay curves for precursors of, 20: 40357 (NAA-SR-11766)
decay of, correction factors for, 17: 24384 (AERE-R-4237)
decay patterns in rat tissue, 18: 11604
deposition from helium gas flow at high velocities, 18: 12321
deposition in lungs, calculation of radiation dose from, 19: 22017
deposition on aluminum during corrosion, 17: 8741 (DP-788)
deposition on copper, glass, perspex, platinum, and tin, 16: 7872
deposition on tropospheric aerosols, 20: 31459
deposition rates and concentration in Pittsburgh precipitation, 17: 18328 (NSEC-89)
determination by carrier precipitation, 17: 1375 (AERE-AM-90)
determination by coincidence counting, 17: 4845
determination in air samples, 16: 6639 (DASA-1300(Vol.1))
determination in air by scintillation spectroscopy of gamma spectra, 17: 7778
determination in Alaskan vegetation, gamma spectrometric, 19: 9366 (HW-SA-3316)
determination in aerosols, methods and equipment for, 19: 34258 (NP-15102)
determination in atmospheric and precipitation samples, methods for radiochemical, 20: 14430 (AD-620219)
determination in bovine feces, forage, and grain, gamma spectrometric, 19: 32101
determination in cesium-137 sulfate, 16: 23631 (TID-7629(p.209-16))
determination in Chinese cabbage and spinach, 17: 7779
determination in Columbia River, 20: 8980(R) (BNWL-36, pp 3.1-122)
determination in dust samples, spectrometric, 16: 27461
determination in diet and excreta of Japanese, 1962 and 1963, 18: 20232 (JAERI-1057)
determination in dilute waste solutions by computer resolution of gamma spectra, 19: 9063 (ORNL-3744)
determination in decontamination solutions, 19: 32059(R) (IDO-14655)
determination in drinking and rain water, 20: 7021
determination in fission products by solvent extraction and gamma counting, 18: 160 (AERE-AM-97)
determination in food samples by gamma spectroscopy, 19: 15385
determination in fallout particles, gamma spectrometric, 19: 17821
determination in forest moss, gamma spectrometric, 19: 42249
determination in fallout, gamma spectrometric, Korea, 1964, 20: 9149
determination in fallout and air filter samples, 20: 25004
determination in graphite, method for, 19: 26224 (AERE-R-4872)
determination in human lungs, whole-body counting, 17: 5704 (TID-12790)
determination in heavy-water moderator by sequential analysis, 18: 27287 (DP-886)
determination in IRL Reactor pool by gamma spectrometry, 17: 40702 (TID-7655(p.107-18))
determination in irradiated MITR fuel elements by gamma spectroscopy, 20: 10764 (MITNE-64)
determination in liquids, gamma spectrometric, 18: 33485
determination in lung tissues, spectrometric, 19: 44292(R) (NP-15173)
determination in mixed fission products, radiochemical, 16: 2988
determination in man, computer program for processing data from, 16: 27465(R) (NP-11928)
determination in mixtures with niobium-95, radiometric, 19: 19748 (DP-933)
determination in mixtures with niobium-95 during chemical separation, gamma spectrometric, 19: 30073 (CEA-R-2729)
determination in man of, in isotope mixtures, γ spectrometric, 20: 6923
determination in niobium-95 mixtures by resolution of complex decay curves, 17: 29009
determination in newborns, infants, and children, whole-body, 17: 35432
determination in niobium-95–zirconium-95 mixtures, beta and gamma spectrometric, 18: 39117
determination in niobium-95–zirconium-95 samples, gamma-spectrometric, (E), 19: 22684 (AE-174)
determination in Pacific Ocean, 18: 39109
determination in ratio with niobium-95 in rain water, method for, 17: 38952
determination in rain water, 18: 39506
determination in rain water, 19: 38557
determination in reactor cooling water, fission-product monitor based on, 20: 3909
determination in shore sand and sea silt, gamma-spectrometric, 16: 20323 (PG-Report-312)
determination in sediments near mouth of Columbia River, 17: 15530
determination in seaweed and sea water, spectrometric, 17: 32005
determination in simulated high-altitude radionuclide samples, radiometric, 19: 13203(R) (NYO-3276-8)
determination in sea water, methods for, 20: 1749 (USNRDL-TR-912)
determination in spent fuel elements, 20: 29078(R) (AD-633252)
determination in sea water, gamma spectrometric, 20: 41145
determination in seawater, spectrophotometric, 20: 43088(R) (TID-23295, Sect.5)
determination in urine and feces of, gamma spectrometric, 18: 33264
determination in water supplies, 19: 324
determination of bomb-produced, in fallout particles, 19: 641
determination of, in stratosphere, 17: 6271(R) (NYO-10464)
determination of, in soil samples, gamma spectrometric, 17: 18308
determination of inhaled, in man by whole-body gamma spectrometry, 17: 24853
determination of, in plant material, gamma spectrographic, 18: 171 (TID-19618(App.B))
determination of, procedure for radiochemical, 16: 28871 (LA-1721(2nd Ed.)(Rev.))
determination of, radiochemical, 18: 8288(T) (AEC-tr-6049(p.75-99))
determination of, gamma spectrometric, 19: 32545 (CEA-R-2461)
determination relative to niobium-95, radiochemical, 19: 9054 (AERE-R-4814)
determination using lithium-drifted germanium detector, 19: 32594
deuteron reactions (d,p) with, spins of states from, (E), 19: 14495 (ANL-6878(p.279-301))
diffusion from chromium–iron alloy at 1000°C, 17: 23946(R) (BMI-X-10039)
diffusion from irradiated molybdenum–rhenium–tungsten alloy, 19: 44599(R) (GEMP-50A)
diffusion from irradiated uranium oxidized in air, helium, and steam, 16: 9047
diffusion in bcc zirconium at 900 to 1750°C, 16: 29378 (ORNL-3339)
diffusion in beta zirconium, temperature dependence, 18: 27967 (ORNL-3617)
diffusion in beta-zirconium, 18: 44153 (ORNL-P-425)
diffusion in chromium-iron alloy at 800 to 1200°C, 17: 30964(R) (BMI-X-10050)
diffusion in chromium–iron alloy at 400 to 1200°C, 18: 10522(R) (BMI-X-10072)
diffusion in chromium–iron and chromium–iron–nickel alloys at 600 to 1200°C, 18: 22477(R) (BMI-X-10081)
diffusion in irradiated artificial graphite, 18: 632
diffusion in irradiated fuel element cladding alloys and materials at 600 to 1200°C, 20: 21232 (BMI-1763)
diffusion in pyrolytic graphite couples, 17: 35251(R) (BMI-1632(Del.))
diffusion in uranium(IV) oxides, 16: 10602
diffusion in uranium (IV) oxides, 16: 21046(T) (AEC-tr-5171)
diffusion in uranium, 17: 3471(R) (BMI-X-10017)
diffusion in zirconium crystals at 900 to 1750°C, 17: 29360
diffusion in zirconium at 900 to 1750°C, coefficient for, 18: 4172(R) (ORNL-3470(p.67-74))
diffusion in zirconium at 800, 1000, and 1150°C, 18: 32136(R) (BMI-X-10093)
diffusion of gaseous, from lightly irradiated uranium at 1000 to 2200°C, 17: 35076 (AERE-R-4342)
diffusion of, in aluminum during zone fusion, 20: 33897
dispersion from fallout in seawater, 20: 37037
distribution and half life in rats, 16: 27465(R) (NP-11928)
distribution and volatility in air-burst debris, 20: 9184 (USNRDL-TR-933)
distribution from nuclear excavation in basalt, 20: 613
distribution in Columbia River effluent, 19: 46680
distribution in fetal and maternal rabbit tissues, 19: 43883(R) (UCLA-12-565, pp 65-85)
distribution in ground-level aerosols, 19: 13687
distribution in rats and dogs from inhalation, 17: 40510
distribution in rabbit tissues, fetal and maternal, 19: 22019(R) (UCLA-12-541(p.51-91))
distribution in samples of atmospheric precipitation, effects of sample preparation on, 18: 37372(T) (AEC-tr-6446)
distribution in sea water in Swordfish Program, 20: 18576(R) (TID-22660)
distribution in surface waters, 1956 to 1961, 18: 8525(T) (AEC-tr-6049 (p.233-57))
distribution in water and silt of British estuaries, 20: 45224
distribution of inhaled, in tissues of guinea pigs, 18: 35295
effects of large intraperitoneal injections of, on guinea pigs, 17: 100
effects on determination of rhodium-106 and ruthenium-106 using coincidence methods, 20: 43158
effects on plutonium determination in fission product solutions, 20: 10763 (KR-100)
energy level transitions in, branching ratio for, (E), 20: 11134
energy levels, 16: 14009
energy levels, 19: 3267
energy levels, 20: 28315
energy levels, determination of neutron, 16: 21495
energy levels from zirconium-94 (p,p′) reactions, spin of, (E), 20: 19917
energy levels from beta decay of yttrium-95, (E), 20: 44722
fallout in India, 19: 36650 (AEET-208)
fallout of, from Sept. 1961 to Feb. 1962, 17: 29087 (AEET/AM/31)

fractionation in fallout from Chinese and Russian tests, 20: 43528
gamma activity from, use in whole-body monitoring facility calibration, 20: 6694(R) (MIT-952-2)
gamma activity in air, effects of northerly and southerly winds on, 18: 2393
gamma dose constants for, 20: 46617
gamma dose-rate from, 17: 21925 (AWRE-E-6/63)
gamma dose rate from shielded and unshielded, 18: 18621 (ORNL-3576)
gamma spectra, 16: 12265
gamma spectra, (E), 19: 16840(R) (IDO-17050)
gamma spectra, (E), 20: 36170 (JINR-P-2739)
gamma spectra from terrestrial, time variation, 18: 35746
gamma spectra of, least-squares analysis of, 18: 33926
gamma spectra of, analysis of, 19: 11585
gamma spectra of, in stratospheric fallout, 19: 22544
half life of, determination by direct decay, (E), 19: 37847
incorporation in solid cracking catalyst, process for, 20: 38993(P)
measurement in fallout, 20: 25288
metabolism by dairy cows, 19: 33744
metabolism by fresh water algae, fish, and invertebrates, 19: 8740(R) (IAEA-R-37-5)
metabolism by fresh-water plants, 19: 35939
metabolism by plants, 19: 25838 (NP-14903)
metabolism in mice, 18: 15768(R) (LAMS-3034(p.53-8))
metabolism in rats after inhalation, 19: 40314
metabolism in rats of, in transient equilibrium with niobium-95, 20: 6753
occurrence in marine organisms and particulate material, 17: 30255
precipitation of, with titanium dioxide hydrate, 17: 14271
preparation and separation from niobium-95 by ion exchange, 20: 43433
production by thermal neutron fission of uranium-233 and -235, (E), 19: 47584(R) (ORNL-3832, pp 1-28)
production in yttrium-95 decay, mass discrepancies from, 16: 26287 (IS-408)
properties and metabolism in plants and animal, 17: 33610
proton reactions (p,d) at 22.3 Mev, distorted-wave analysis of, 17: 38233
radioactivity and yield from uranium fission, gravimetric method of determining, 18: 27288 (KFK-199)
radioactivity losses in liquid scintillator solutions, effects of trioctylphosphine oxide on, 19: 28237
radioactivity standardization in mixtures with niobium-95, 18: 24042 (AERE-R-4555)
ranges of fission products of, in aluminum, (E), 20: 17721
removal from leafy vegetables, effectiveness of detergents and water for, 18: 5555
retention of inhaled particles of, in guinea pigs, 18: 29534
separation by calcium phosphate–humic acid flocculation, 18: 24982
separation by solvent extraction using butyl phosphate solutions, 18: 6890
separation by solvent extraction using tributyl phosphate, 17: 37294(T) (AEC-tr-6014)
separation from aqueous solutions, use of silica gel for, 20: 1742 (INR-636/XIII/J)
separation from aqueous solution by sorption on diatomaceous earth, 20: 12938
separation from cerium-144, cesium-137, and strontium-90 by paper electrophoresis, 18: 1739
separation from drinking water using natural sorbents, 19: 24424
separation from fission product mixtures by ion exchange, design of semiautomatic device for, 18: 1805
separation from fission products by solvent extraction using D2EHPA, 18: 16147
separation from fission products by amalgam exchange, radiochemical, 18: 16148
separation from fission products by solvent extraction using TBP, (E), 19: 22417
separation from hydroxides by precipitation, effects of freezing on, 16: 11736
separation from hydrochloric acid by solvent extraction using tribenzylamine, 17: 40935
separation from iron-59 and scandium-46 by anion exchange, 19: 26224 (AERE-R-4872)
separation from irradiated uranium oxides using molten sodium chloride, 20: 43454
separation from irradiated copper ore by column leaching, 20: 45570(R) (ORNL-3945, pp 189-94)
separation from low-level waste solutions, ion exchange method for, 20: 47083(R) (ORNL-3945, pp 79-106)
separation from niobium-95 using Vycor glass, 16: 3044
separation from niobium-95 by solvent extraction using acetylacetone, 18: 6889
separation from niobium-95 by ion exchange on tin phosphate, 18: 13922
separation from niobium-95 by ion exchange on pyrocatechol-*O,O*-diacetic acid, 18: 33508
separation from niobium-95 by solvent extraction using benzene solution of fatty acids, 18: 39116
separation from niobium-95 and hafnium-181, chromatographic, 19: 44118 (UCRL-16015)
separation from niobium-95, chromatographic, 17: 25301
separation from niobium by solvent extraction using diisobutylcarbinol, 20: 33419
separation from other short-lived uranium fission products, chromatographic, 18: 39393
separation from radioisotopes in aqueous solutions by foam chromatography using colloidal manganese dioxide, 20: 20628
separation from sea water, method for, 20: 18576(R) (TID-22660)
separation from sea water, ion exchange, 20: 22872(R) (NIRS-4, pp 12-17)
separation from sea water by sorption by metal sulfide-ion exchange resins, 20: 29345
separation from uranium carbide during oxidation reactions, 16: 33071(T,R) (EURAEC-337)
separation from uranium fission products using ring oven method, 19: 11021
separation from waste solutions by flocculation, 16: 21862
separation from waste water by ion exchange on humic acid, 19: 33678
separation from waste solutions by recycle scavenging–precipitation ion exchange process, 20: 10440 (ORNL-3863)
separation from yttrium-90 in food by solvent extraction using di-(2-ethylhexyl) phosphoric acid, 19: 15386
separation of, from nitric acid, efficiency of AMSCO-TBP in, 17: 10739(R) (ORNL-TM-27)
separation of, from other fission products in air and rain water, 17: 20203
separation of, from americium-241, radiochemical, 17: 19954
separation using chromatographic paper treated with tri-*n*-octyl phosphate, 17: 35943
shielding power sources of, 19: 21595 (TID-7698(Pt.I)(p.33-248))
sorption by ammonium phosphotungstate, effects of ammonium and sodium salts on, 17: 34062
sorption by degraded kerosene, effects of nitroparaffins on, 20: 33423
sorption by ion exchange materials from water, 19: 539
sorption by iron trioxide and monodisperse lucite particles, 19: 4124
sorption by PA-2 aluminum alloys and stainless steel, effects of pH on, 20: 25073
sorption by paper filters, effects of pH, 16: 3345(T) (AEC-tr-4497 (p.353-68))
sorption by river silts, 18: 35238 (STI/DOC/10/28(p.9-20))
sorption by slags, 18: 40965
sorption by soils, effects of disodium salt of EDTA on, 20: 35227
sorption by stainless steel in boiling-water reactor, 16: 20303(R) (ANL-6477(p.224-30))
sorption by tin hydroxide, mechanism of, 18: 31394
sorption from aqueous solutions by manganese dioxide, 16: 16389
sorption from sea water on ferric hydroxide resin, 19: 32787(R) (NIRS-3(1-17))
sorption on sediments in river-estuary systems, 20: 39121
sorption on silica gel, effects of phosphoric acid and iron(III) ions on, 19: 28449
sorption reactions of, on minerals, 20: 41178 (AD-635547)
sorption through burns and wounds in rats, 18: 29232
standardization of, method for absolute, 18: 35591 (RCC-R-175)
storage of solutions in polyethylene bottles, 17: 18141
transport in Columbia River, 20: 25290
transport in river-estuary systems, 20: 39121
uptake and distribution in rat tissues, 18: 11604
uptake and distribution in developing roe of Black Sea fish, 19: 25879
uptake by beach organisms, 18: 21762
uptake by brain tumors, 18: 1471
uptake by corn plants, effects of soil temperature, 16: 17431
uptake by deer lungs, 18: 25693
uptake by maize, effects of soil temperature on, 20: 3668
uptake by man following accidental exposure, 20: 9199
uptake by marine mollusks, 20: 40528
uptake by plants in Georgia piedmont, 20: 12985
uptake, distribution, and excretion by animals, 17: 28637
uptake from fallout by human lungs, 19: 3856
yield in epi-cadmium neutron fission of plutonium-239, (E), 19: 27585
yields from neutron fission of plutonium-239, uranium-235, and uranium-238, 16: 1037(T) (AEC-tr-4696)
yields from 14.7-Mev neutron-induced and spontaneous fission of uranium-238, 19: 19135
yields in proton fission of uranium-238 at 7.1, 9.4, and 12.0 Mev, 20: 37995
yields in thermal neutron fission of plutonium-239, 19: 16873
yields in thermal-neutron fission of uranium-233 and -235, (E), 20: 13783 (ORNL-TM-1333)

ZIRCONIUM ISOTOPES Zr-96

decay to niobium-96, energy for, 17: 21014
deuteron reactions (d,n) and (d,p), mechanism, 16: 7127
deuteron reactions (d,t) at 20 Mev, angular distributions and energy spectra from, 17: 38177
deuteron reactions (d,t) at 11.8 Mev, angular distributions from, (E), 19: 21326
deuteron reactions at 11.8 Mev, energy spectra from, 20: 40065(R) (BMwF-FB-K-66-01)
energy levels, 16: 14009
energy levels and nuclear potential, 18: 32881
energy levels in, excited by (d,p) and (d,t) reactions, 17: 34956
energy levels of, Coulomb excitation in nitrogen-14 inelastic scattering, (E), 19: 39942
neutron capture by, gamma spectrum for thermal, 18: 6179(R) (ORNL-3499(Vol.I)(p.42-6))
neutron capture by, s-wave strength functions for, 18: 26544(R) (ORNL-3582(p.82-4))
neutron capture cross sections at 1–30,000 ev, p and s-wave strength functions from resonances in, 17: 26438(R) (ORNL-3425(p.32-5))
neutron cross sections at 20000 ev, 18: 6165 (NP-13359)
neutron radiative capture cross sections, (T), 19: 19106
neutron reactions (n,p), formation of strontium-93 and yttrium-96 from, 16: 12468
neutron reactions (n,γ) at fission energies, 16: 18429
neutron reactions (n,α) at 14.8 Mev, cross sections and product half-life for, 17: 2242 (TID-16949)
neutron reactions (n,p) at 3.55 to 6.02 Mev, cross sections for (E), 19: 3383
neutron resonance at 180 to 1490 ev, 16: 5994
neutron resonance cross sections of, determination of, by boron absorption technique, 16: 28036 (TID-16059)
neutron resonance structure and s-wave strength function for, (E), 19: 35401 (ORNL-P-1346)
neutron resonance absorption at 0 to 60 kev, structure in, (E), 19: 37809(R) (ORNL-3778(p.76-81))
neutron separation energy for, 17: 21014
neutron strength functions, (T), 19: 25497
neutron strength functions of, calculation of, 20: 38038
neutron total cross sections for, principal resonances in, 17: 26437 (ORNL-3425(p.32))
neutron total cross sections for, resonances in, 17: 33005 (ORNL-TM-636)
neutron total cross section measurements to 20 kev, 18: 28637
nuclear structure of, subshell closure in, 18: 40506 (IS-878)
nuclear wave functions, (E), 19: 10257(R) (TID-21335(p.33-107))
proton elastic and inelastic scattering at 6.8 Mev, 17: 24414
proton elastic scattering at 22.5 Mev, potentials for, 18: 32844
proton reactions (p,t) with, mechanisms for, 18: 36605
proton reactions at 1.8 Bev, isobaric yield distributions in, 18: 7761
proton reactions (p,γ) in stars, 16: 12308
proton reactions (p,t) at 22 Mev with, differential cross section for states excited in, 17: 24053(R) (ORNL-3432)
proton reactions (p,d) at 22 Mev, excited energy levels in, 17: 38234
proton reactions (p,t) at 22 Mev, angular distributions from, 17: 38235
proton reactions (p,d) at 22.3 Mev, distorted-wave analysis of, 17: 38233

ZIRCONIUM ISOTOPES Zr-97

activity in fast neutron activation products of zirconium, calculated, 19: 32058(R) (GA-5978)
decay scheme, 17: 9606
determination in heavy-water moderator by sequential analysis, 18: 27287 (DP-886)
determination in mixed fission products, radiochemical, 16: 2988
determination of, in fission products by solvent extraction using 2-thionyltrifluoroacetone, 17: 14162
determination of, procedure for radiochemical, 16: 28871 (LA-1721(2nd Ed.)(Rev.))
distribution and volatility in air-burst debris, 20: 9184 (USNRDL-TR-933)
distribution from nuclear excavation in basalt, 20: 613
energy levels, 16: 14009
gamma dose constants for, 20: 46617
gamma spectra, 17: 34966
half life, (E), 20: 13783 (ORNL-TM-1333)
production in helium ion fission of uranium-235 and -238, cross sections for, 17: 17126 (TID-18165)
ranges from fission of plutonium-239, radiochemical determination of, 20: 34525 (KFK-401)
reactions with chlorine in gas mixtures, 17: 16065
yield in epi-cadmium neutron fission of plutonium-239, (E), 19: 27585
yields from helium ion-induced fission of lead-207 at 41.1 to 26.3 Mev, 20: 37996
yields from spontaneous fission of uranium-238, 17: 33109
yields from 14.7-Mev neutron-induced fission of uranium-238, 19: 19135
yields in neutron fission of uranium at 14.7 Mev, 18: 44835
yields in neutron fission of natural thorium at 14.7 Mev, 18: 44836
yields in proton fission of uranium-238 at 7.1, 9.4, and 12.0 Mev, 20: 37995

ZIRCONIUM ISOTOPES Zr-98

detection and measurement of, mass-spectrometric, 18: 7853(R) (KR-58)

ZIRCONIUM ISOTOPES Zr-99

fission yield of, 17: 22608

ZIRCONIUM LACTATES

toxic effects of, on guinea pigs, hamsters, and rats, 17: 23041

Zirconium Mandelates

see Mandelic Acid, Zirconium Salts

ZIRCONIUM MINERALS

see also Baddeleyites
see also Zirconium Ores
see also Zircons
analysis for hafnium and zirconium by x-ray spectrography, 20: 27147
hafnium and zirconium abundance ratios in, 20: 27147
industrial hygiene in mines, 17: 27603(T) (JPRS-19866)
preparation and properties of synthetic, 17: 6282
processing, evaluation of methods for, 17: 220
separation of hafnium-enriched fractions from, 16: 29319(R) (USBM-U-952)

ZIRCONIUM MOLYBDATES

cation exchange properties, 16: 20356 (JÜL-32-RC)
ion exchange properties for cesium, francium, and rubidium, 17: 20089
ion exchange properties for elements in nitrate media, 18: 1624
ion exchange properties of, 18: 35572
ion exchange properties for calcium, magnesium, and strontium, 19: 13218
physical properties at 600 to 1325°C, 16: 13003(R) (NP-11299)
preparation of granular gels, for ion exchange use, 17: 1373(P)

ZIRCONIUM NITRATES

analysis for silicon by silicomolybdic blue method, 17: 38951
concentration of aqueous solutions without precipitation of zirconium, 16: 20465(P)
concentration of aqueous solutions of, 17: 28793(P)
diffusion of carbon in, carbide film formation in, 20: 15072
hydrolysis, 17: 1446
properties of, chemical and physical, 17: 6097
reactions with sodium hydroxide, precipitation of zirconium hydroxide in, 16: 13045
separation by reversed-phase partition chromatography using organophosphorus compounds, 18: 25614
solubility and thermal stability, 16: 30414

ZIRCONIUM NITRIDES

analysis for nitrogen by reaction with chlorine and measurement of nitrogen released, 19: 17800
analysis for nitrogen, comparison of hot extraction and Kjeldahl methods for, 20: 40820(T) (IS-Trans-37)
analysis, methods for, 19: 24403 (NP-14952)
atomic vibration amplitudes, 18: 19987
atomic vibrational amplitudes at 25 to 1426°C, 19: 47009 (NP-15514 (Vol.2))
corrosion by mercury, effects of dissolved titanium on, 19: 44616(R) (ANL-7000, pp 122-37)
Debye temperatures at 25 to 1426°C, 19: 47009 (NP-15514(Vol.2))
density and degree of disorder in, 18: 1670
effects on austenitic grain size in iron and steel, 17: 32627
effects on crystal growth of zirconium dioxide, 19: 23033
electric properties of, effects of non-metallic atoms on, 17: 8854
electric properties of, rigid band model for interpreting, 18: 24137 (NP-13944)
electron structure and bond strength of, relation of, 18: 18395
electronic structure of crystals of, 17: 27875
emissivity, measurement of spectral, 17: 16632(R) (AD-274654)
emissivity measurements to 3000°K, equipment for, 18: 20567
fabrication and properties of, review of, 18: 585
fabrication of crucibles of, by pressure-sintering, 19: 34657(R) (RFP-518)
figure of merit and atomic characteristics, 19: 2284
formation by reduction of zirconium oxide by magnesium in nitrogen, 18: 17816
free energy of formation at 1550 to 1750°C, 19: 41065
Hall effect, 17: 6520(R) (NP-12373)
hardness of, 16: 7916
hydridation, 20: 35841(R) (NAA-SR-11900)
non-stoichiometry in, evaluation of, 18: 29673
oxidation at high temperatures, 18: 5729 (ASD-TDR-63-744)
oxidation of, in argon–carbon dioxide mixtures at 2250°C, 17: 6520(R) (NP-12373)
performance as seed material for gas coolant in rocket reactors, (E), 19: 24149 (NASA-CR-212)
physical properties, 16: 15209

physical properties in homogeneity region, 16: 22612
physical properties of crystals of, 17: 27875
preparation, 20: 22520(R) (NAA-SR-11805)
preparation, 20: 46966(R) (NAA-SR-12010)
preparation and physical properties of brown, 19: 9147
preparation and properties of, 18: 16498
preparation and properties of dark blue, 18: 29669
preparation and properties of, 19: 18472(T) (JPRS-28739)
preparation and purification, 19: 46941 (NP-15514(Vol.3))
production by fused salt process, 19: 12865(R) (NAA-SR-10501)
production of, by passage of continuous current through zirconia–yttrium oxide systems at 1300°C, 19: 42470
properties as corrosion inhibitor for titanium in mercury at 538°C, 17: 41333(R) (ANL-6677)
properties, mechanical and physical, 16: 30853
properties of, for use in silicate technology, 18: 7250
reactions with copper and nickel mattes, slags, molten salts, and refractory metals, 20: 14989
reactions with magnesium and zirconium oxides at 1800 to 2000°C, 18: 43463
reactions with molten metals at 400 to 1500°C, 19: 37112
reactions with molybdenum, niobium, tantalum, and tungsten at 900 to 2200°C, 20: 25578(T) (N-65-35787)
reactions with plutonium nitride at high temperatures, 19: 14806(R) (HW-81984(p.5.1-55))
review, 18: 39899 (LA-2942)
sintering conditions, 17: 22142
sintering of, electron density in phase lattices and optimal conditions for, 17: 27767
solubility products in liquid iron at 1550 to 1750°C, 19: 41065
spectra of vaporized, 19: 46982(R) (AD-611856)
spectra of, infrared, 18: 22497 (WADD-TR-60-646(Pt.3, Vol.II))
spectra of, reflection, 17: 6520(R) (NP-12373)
structure, 16: 7916
superconducting critical currents of, (E), 19: 27371
superconducting properties, 19: 20572
surface energy of, calculation of approximate, 17: 41475(T)
thermal conductivity, effects of electronic and crystalline structure, 16: 24208
thermal expansion, 18: 19987
thermal expansion at 25 to 1426°C, 19: 47009 (NP-15514(Vol.2))
thermal properties to 5000°F, 16: 18938
thermal properties, 18: 7201 (ASD-TDR-63-597)
thermal properties, 16: 22597 (WADD-TR-60-924)
thermal properties of, at 500 to 5000°F, 17: 16636 (ASD-TDR-62-765)
thermal properties to melting point, 20: 878
thermal stability, 18: 16473 (HW-SA-3370)
thermodynamic properties, 20: 10816(T) (NASA-TT-F-285)
thermoemission properties of, 17: 39799
use of, in nuclear rockets, 17: 8710 (TID-16315(Del.))
vapor composition and pressure at high temperature, 16: 18922
vapor pressure, 16: 9142(R) (NP-11264)
vapor pressure of, 18: 22497 (WADD-TR-60-646(Pt.3, Vol.II))
InN–ZrN, preparation and crystal structure of H-phase in, 19: 39208
Mo–ZrN, stability and strength at 1650 to 2210°C, 19: 26853
NbC–NbN–ZrN, superconducting properties, 20: 17589 (CONF-650922, pp 541-9)
NbN–ZrN, superconductivity of wires of, (E), 20: 2891
PuN–ZrN, phase studies, 19: 9603(R) (HW-81601(p.2.1-35))
PuN–ZrN, phase studies, 19: 22867(R) (HW-81603(p.2.1-23))
PuN–ZrN, phase studies, 19: 36953(R) (HW-84609(p.5.1-5))
PuN–ZrN, preparation, 18: 35932(R) (HW-81600(p.2.1-23))
ThN–ZrN, development for high-temperature oxidation protection of tungsten, 17: 14836(R) (NP-12592)
ThN–ZrN, oxidation at high temperatures, 18: 5729 (ASD-TDR-63-744)
UN–ZrN, preparation and properties, 18: 32035(R) (BMI-X-10073)

ZIRCONIUM ORES

see also Zirconium Minerals

analysis for rare earths, photometric, 18: 13697
analysis for uranium, spectrographic, 17: 6013
concentration, 17: 25452
processing by reductive chlorination, 20: 4072(P)
reduction to phosphorus-free zirconium oxides, process for, 17: 12308(P)
separation of hafnium and zirconium from oxide, 17: 16533
separation of zirconium from silicate, 16: 5427(P)
separation of zirconium oxide from, 18: 3909(P)
separation of zirconium from silicate, 16: 5428(P)
separation of zirconium from, as sodium zirconate, 16: 14763(P)

ZIRCONIUM OXALATE COMPLEXES

stability, 17: 14279
with ammonium and potassium, preparation and properties, 18: 1690
with potassium salts, preparation and properties, 18: 1690

ZIRCONIUM OXALATES

equilibrium and stability constants of, 18: 27414
precipitation of zirconium hydroxyquinoline from, 16: 183
precipitation of zirconium quinolinolate from, 16: 183
solubility in aqueous solutions, 19: 5911
with hafnium and zirconium, equilibrium and stability constants of, 18: 27414

ZIRCONIUM OXIDES

age determinations by lead-alpha method, 17: 1651
age estimation of, by thorium-230–uranium method, 20: 29441
agglomeration of vaporized, 18: 36837(R) (IITRI-C6007-12)
analysis for antimony, iron, nickel, and zinc, 17: 144
analysis for distribution of alloying elements in, using electron microprobe, 17: 27746(R) (DPST-63-71-1)
analysis for hafnium, spectrographic, 16: 7512
analysis for hafnium, complexometric, 16: 26941
analysis for hafnia traces, spectrochemical, 18: 157 (AEET/ANAL/27)
analysis for hafnium, activation, 18: 39136
analysis for hafnium by neutron activation using semiconductor detector in, 19: 34129
analysis for hafnium, x-ray-fluorescence, 20: 14496
analysis for impurities by hollow-cathode discharge, 16: 26902(T) (AEC-tr-5262)
analysis for impurities, chemical, emission-spectrographic, and mass-spectrographic, 19: 9079
analysis for impurities, spectrochemical, 19: 30070 (AD-611006)
analysis for oxygen by sulfur monochloride method, 16: 14631(T) (UCRL-Trans-801(L))
analysis for oxygen by activation using helium-3 ions, detection limits and sensitivity of, 20: 20565 (ORNL-P-1216)
analysis for sulfur, luminescent method for, 18: 33513
analysis for zirconium, use of fluorescent x-ray instrument for, 19: 13221
bibliography on SNAP fuel materials containing, 18: 33128 (NAA-SR-9525(Vol.I))
bonding and chemical reactions with fluophosphoric acid, mechanism of, 20: 29145 (NP-16047)
bonding of coatings of, to steel, nondestructive ultrasonic testing of, 16: 389(R) (ARF-6043-20)
bonding of, with tantalum at 2248°K, method for, 17: 23930
breakdown of films of, during oxidation of zirconium alloys, 19: 13912 (AECL-2144)
chemical bonding in, mechanism of, 18: 39151 (AD-437101)
chemical bonds in, properties of, 20: 12848
chlorination, 18: 35582(P)
chlorination at 1000 to 1200°C, equilibrium constant for, 16: 1653(T) (AEC-tr-4868)
chlorination by carbon tetrachloride entrained by carbon dioxide at 700°C, 16: 33071(T,R) (EURAEC-337)
chlorination in fluidized bed, 16: 7576(P)
chlorination of, for preparation of zirconium chloride, kinetics of, 18: 31536
chlorination of, uses of electrothermal fluidized-bed processing in, 19: 11135
coating of, by plasma-arc spraying, 17: 32545
coating of, effects of, on oxidation resistance of graphite, 20: 29773
coating with molybdenum or tungsten by chloride and oxide processes, evaluation of, 19: 40986
coating with molybdenum or tungsten by chloride and oxide processes, 20: 29631
comminution of, effects of impact strength, microhardness, shear modulus, and thermal expansion on, 18: 44220(T)
compatibility with graphite in argon and vacuum environments at 800 and 900°C, 17: 25685(R) (BMI-1624(Del.))
compatibility with graphite, 17: 26944(R) (BMI-1630(Del.))
compatibility with cesium vapor at 1800°C, 20: 31669
complexes with dialkyl phosphoric acids, preparation and properties, 18: 25429
content in zircon from Kyoto Prefecture, Japan, 19: 36296
corrosion by barium vapor at 800 to 1000°C, 18: 44498(R) (MND-2812-3)
corrosion by biphenyl, 20: 25491(T) (AECL-2330, pp 179-95)
corrosion by cerium–cobalt–plutonium alloy at 750°C, 16: 22549
corrosion by plasma jets, 19: 9627
corrosion by potassium-seeded gases, 19: 11695
corrosion of, by hydrochloric acid, 17: 20405(R) (NP-12710)
corrosion of Zircoa 1027, by potassium at 1600°F, 20: 27432(R) (NASA-CR-54892)
crystal field properties of, effects of chromium and vanadium on, 19: 33518 (TID-21946)
crystal field properties of, effects of chromium and vanadium on, 20: 36854
crystal growth of, after melting and spraying on cold metal, effects of aluminum and silicon oxides and zirconium nitride on, 19: 23033
crystal growth of, by sintering, 20: 25536
crystal growth using induction plasma torch, stabilized, 16: 5661

crystal lattice constants of tetragonal, at 1150 to 1700°C, 18: 32130 (ARL-64-63)
crystal phase transformations in, twinning in, 18: 27442
crystal structure of tetragonal, 17: 4504
crystal structure of, electric conductivity studies of defect, 18: 12640 (GEAP-4089(Vol.II)(Paper 20))
crystal structure and stabilization mechanism, 18: 18409
crystal structure, 18: 27870
crystal structure, 18: 29607 (UCRL-7370)
crystal structure of films of, on Zircaloy-2, 19: 973
crystal structure of, interaction energy between vacancies in, 19: 9687
crystal structure of, defects in, 19: 9689
crystal structure polymorphic conversion of, effects of heat on, 19: 19925
crystal structure of, effects of crystallite size effect on occurrence of metastable tetragonal, 19: 23048
crystal structure of, in thin films on zirconium, 19: 46958
crystal structure of, erroneous published literature on, 17: 8838
crystal structure of films of, on zirconium surfaces, 20: 778
crystal vibration amplitudes for, mean, 18: 22051
crystallographic transformations at temperatures up to 1750°C, 19: 6142 (ARL-64-82)
decomposition effects on calcium zirconate at 1350 to 1600°C, 16: 31615
defect structure and electric conductivity of tetragonal, 20: 845
defect structure from electric conductivity measurements, 17: 12689
deformation on zirconium, mechanisms of anodic film, 20: 43949
deposition of coatings of, on graphite crucibles for thorium and uranium casting, 17: 12599
deposition of coatings of, on ceramic fuel elements by plasma-jet spraying, 16: 19297(R) (ATL-A-114)
deposition of coatings of, on graphite, 16: 24147 (ASD-TDR-62-90)
deposition of coatings of, on graphite by wash-coating or flame-spraying, 16: 495 (NAA-SR-5833)
deposition of coatings of, on graphite by vaporization of isopropoxides, 17: 27727 (ASD-TDR-63-322)
deposition on actinide oxides, 19: 22958(P)
deposition on copper, stainless steel, and steel by flame-spraying, 16: 4455
deposition on dies for Dynapak extrusion process, 19: 30686(R) (AD-608945)
deposition on graphite by decomposition of alkoxides, 19: 6253 (ML-TDR-64-269)
deposition on graphite by alkoxide decomposition, 20: 36851
deposition on steel of chromium plating containing dispersions of, electrolytic, 20: 21286 (AD-621920)
deterioration of calcia-stabilized, by thermal cycling, 17: 6667 (NASA-TN-D-1595)
determination by electron probe method, correction of atomic number effects in, 17: 27268
determination of, gravimetric, 18: 1570
development and properties of heat shield foams of, 16: 29350 (ASD-TR-61-706(Vol.II))
diffusion and solubility of hydrogen in, 19: 13349
diffusion of fission products in, 18: 14522
diffusion of hydrogen in, 18: 22439 (EURAEC-1000)
diffusion of hydrogen in, 18: 37681(R) (EURAEC-1082)
diffusion of hydrogen in films of, kinetics of, 20: 13201
diffusion of iodine and rare gases in, 18: 16424(R) (GEMP-270A)
diffusion of oxygen in, 16: 22156
diffusion of oxygen in, 17: 25722 (GEAP-3999)
diffusion of oxygen in, electric conductivity studies of, 18: 27354(R) (ASD-TDR-62-204(Pt.III))
diffusion of oxygen in, 19: 18393(R) (ML-TDR-64-173(Pt.II))
diffusion of oxygen in, at 1400°C, 20: 8919
diffusion of oxygen in poly- and single-crystal calcia-stabilized, 20: 23688
diffusion of oxygen in layers of, on zirconium metal, 20: 29817
diffusion of titanium in, 19: 9688
dissolution by acids, 16: 33431(R) (TID-16833)
dissolution by hydrogen fluoride in molten salt, 16: 10102(R) (ORNL-TM-65)
dissolution by hydrofluorination in fused-salt fluorides, 18: 39385
dissolution in fuel sample with calcium and uranium oxides, 20: 43069(R) (IDO-14679, pp 51-9)
dissolution in hydrofluoric acid, 16: 17617(R) (ORNL-TM-122)
dissolution of films of, effects of, on aqueous corrosion resistance of tin–zirconium alloys, 16: 7858
dissolution of hydrated, by nitric acid, 18: 31658(R) (IDO-14635)
dissolution studies, 18: 8454
distribution of iodide ions in, 16: 12801(R) (IA-685)
dust mixtures of, with silicon dioxide, effects on lungs in rats of, 16: 27499
effects as diluent on fission density of dispersion fuels at high burnup, 20: 27565 (AAEC/TM-306)
effects of additives of, on modulus of rupture of beryllia, 19: 44599(R) (GEMP-50A)
effects of films of, on thermal radiation properties of molybdenum, 16: 32039(R) (PWA-1863)
effects on austenitic grain size in iron and steel, 17: 32627
effects on corrosion resistance of copper–zirconium alloys, 20: 37183
effects on creep properties of uranium dioxide, 19: 14022
effects on creep, recrystallization, and sintering of beryllium oxide, 18: 7187
effects on crystal structure of beryllium oxide, 16: 5689 (ORNL-TM-94)
effects on electrochemical properties of lithium silicate glass, 17: 32095
effects on electrochemical properties of glass, 17: 32098
effects on fritting of beryllium oxide, 18: 22500(T) (UCRL-Trans-1042(L))
effects on grain boundary hardening in sintered beryllium oxide, 20: 846
effects on grain size of tungsten, 20: 39400 (NASA-TN-D-3531)
effects on linear thermal expansion of hafnia, 19: 18394 (ML-TDR-64-294)
effects on mechanical properties of sintered and extruded tungsten, 20: 21374
effects on mechanical and thermal properties of aluminum oxide ceramics, 17: 41469
effects on oxidation of uranium dioxide, 17: 12233(T) (JPRS-17403)
effects on oxidation of copper at 800°C, 20: 23686
effects on properties of beryllium oxides, 16: 2732 (GA-2262)
effects on properties and structure of uranium dioxide, 20: 34825
effects on properties of tungsten powder, 20: 43899 (NASA-TN-D-3610)
effects on properties of niobium–titanium alloy for high-temperature use, 18: 14454 (BM-RI-6390)
effects on radioinduced polymerization of solid 3,3-*bis*-chloromethyloxetane, 18: 33651
effects on thermal conductivity of uranium dioxides, 19: 18448 (AECL-2169)
effects on thermodynamic properties of solid solutions in uranium(IV) oxide–yttrium oxide systems, 20: 23713
effects on thermoelectric properties of molybdenum, tantalum, and tungsten at 1500°C, 18: 622
effects on uranium dioxide oxidation, 18: 3765
effects on uranium oxide sintering properties, 17: 12637
elastic properties at high temperatures, 16: 7921
elastic properties of hot-pressed, at 25 to 1000°C, 19: 9686
elastic properties of calcia-stabilized effects of temperature on, 20: 39438
elastic properties of yttria-stabilized, effects of temperature on, 20: 39438
electric conductivity, 17: 6656 (HW-75501)
electric conductivity of stabilized, at 550 to 1200°C, 17: 16683
electric conductivity of, effects of thermionic emission on measurement of, 19: 11752
electric conductivity of calcia-stabilized crystalline, effects of composition and temperature on, 19: 11132
electric conductivity at 1200 to 1750°C, (E), 19: 26856
electric conductivity of films of, on Zircaloy-2, effects of gas atmosphere on, 17: 36225 (HW-76562(Rev.))
electric conductivity of films of, at 180 to 300°C, 20: 7589
electric conductivity at 1100 to 1500°C and 1 to 10^{-4} atm, 20: 8919
electric conductivity of, effects of temperature on, 20: 12850
electric conductivity of anodic films of, on zirconium, 20: 23654 (ORNL-TM-1435)
electric conductivity of flame-sprayed coatings of, 20: 43927
electric conductivity at high pressures and temperatures, 19: 9696
electric properties, 16: 9184(R) (AD-260194)
electric properties of oxygen deficient, 16: 24141(R) (AD-270235)
electric properties, 17: 18736(R) (AD-283667)
electric properties, 18: 44130 (ARL-64-122)
electric properties of calcium-stabilized, effects of defect structure on, 19: 37137
electric properties of films of, sandwiched between gold and zirconium, 16: 33497
electrochemistry of passivating films of, formed on metal by polarization, 18: 34063
electrolysis in sodium fluoride–zirconium fluoride, production of zirconium by igneous, 18: 27873
electron transport number in yttria-stabilized, 18: 18377
electronic conductivity of calcium oxide-stabilized, 20: 23692
electrotransport in, color variation during, (E), 19: 38604
emanation of inhomogeneously labeled, apparatus for, 18: 5694
emissivity and reflectivity at 2100 to 3700°K, 20: 17021 (N-65-18607)
emissivity at 800 to 5000°K, relation of structure to, 18: 20566
emissivity of coatings of, at 200 to 1450°F, total, 16: 30802(R) (PWA-1966)
emissivity of coatings of, to 2200°F, 16: 30800(R) (PWA-1877)
energy levels of molecular zirconium monoxide, ground-state, (E),

19: 24517
extrusion, analysis of plasticizer and vehicle requirements for ultrasonic, 16: 12072 (NYO-10006)
fabrication and properties of spray-dried and hot-pressed, 19: 13898(R) (RFP-490)
fabrication by slip casting from ethanolic suspension, 18: 4218
fabrication of compacts of, 16: 24138
fabrication of crucibles of, by slip casting from ethanolic suspension, 18: 4218
fabrication of hard dense, hot-pressing method and apparatus for, 20: 13230(P)
fabrication of large dense bodies of, 19: 28795(P)
fabrication of nonstabilized, by hot-pressing, 19: 18433
fabrication of spherical particles of, by powder agglomeration method, 20: 793
fission fragment recoil in, expansion induced by, 19: 18547
fission gas release from irradiated, 17: 15532(R) (BMI-1607(Del.))
fluorescence and phosphorescence of, 18: 23661(T) (UCRL-Trans-1048(L))
formation and properties of, on zirconium single crystals in water, 20: 41423
formation and structure of cubic, 16: 18056
formation of corrosion-resistant films of, in aqueous chlorides and sea water, 18: 20481
formation of cubic, 16: 29403
formation of films of, effects of electrolyte on anodic, 16: 31607
formation of, free energy of, 18: 14401 (BNL-7553)
formation on air-oxidized zirconium, factors affecting, 19: 30653(R) (TID-21723)
formation on zirconium in water and aqueous chloride solution, 19: 22906
formation on zirconium at 300 to 900°C, 16: 12119(T) (CEA-tr-A-1039)
fracture of films of, on zirconium alloys, 20: 25496
fracture of films of, on zirconium alloys, 20: 25497
friction testing to 2000°F, 16: 3475 (WADC-TR-59-603(Pt.II))
fusion of powdered, in plasma flames, 19: 7882
hardness, 20: 27505
hardness of doped and pure, at 20 to 725°C, 17: 32484(R) (GEAP-4284)
hardness of, effects of metal additions on hot, 20: 5846
heat of formation of bivalent, 18: 43493
heat of fusion of ZrO_2, 16: 12192
hydrofluorination of, 16: 32884(R) (ORNL-3314(p.39-57))
hydrofluorination in fluidized bed, kinetics of, 19: 40529
hydrogen pickup in layer structure of corrosion product, 16: 20979 (HW-71958-RD)
interactions with gas flow in MHD generators, 20: 41738
ion exchange properties for elements in nitrate media, 18: 1624
isoelectric point of synthetic, 20: 35902
life of crucibles of, effects of calcium oxide and titanium on, 17: 34341
luminescent properties of titanium-activated, 20: 17056
machining characteristics, 17: 34358(R) (ASD-TDR-63-581)
machining studies on pressed, sintered, and arc-cast, 16: 30742(R) (ASD-TR-7-532a(VII))
machining studies on coatings of, 16: 30742(R) (ASD-TR-7-532a(VII))
mechanical properties, 17: 3460(R) (AD-273802)
mechanical properties of calcium-stabilized, effects of temperature at 1600 to 2000°F on, 17: 41455
mechanical properties, effects of iron, aluminum, titanium silicon and phosphorus oxides on, 18: 2261
mechanical properties of films of, at 300 to 900°C on zirconium, 16: 12119(T) (CEA-tr-A-1039)
melting by induction, 19: 11683
melting of, method for electron beam, 19: 6289
metallography of microspheres of, 19: 13889(R) (MLM-1208)
microstructure and sintering of, effects of titanium on, 19: 9688
microstructure of thin films of, from oxidized zirconium, 20: 31755
neutron diffraction properties of, 20: 26396(R) (IDO-17140)
neutron resonance absorption integral of, (E), 20: 14008(R) (ANL-7122, pp 42-69)
oxidation at 450 to 900°C, effects of yttrium additions on, 20: 11227
oxidation of anion-deficient, mechanism, 19: 13274 (GEAP-4544)
oxidation of oxygen-deficient, at 450 to 900°C, kinetics of, 20: 29648
oxidation of, color variations during, 19: 38604
oxygen diffusion in, determination of coefficient of, 17: 20005
oxygen sorbed on, mechanisms for hydrogen reactions with, 20: 20705
performance as magnetohydrodynamic thermal insulation, 18: 12859 (NP-13516)
performance as melting-point temperature sensors up to 6000°F, (E), 19: 30489 (SC-DC-65-1237)
performance as seed material for gas coolant in rocket reactors, (E), 19: 24149 (NASA-CR-212)
performance of dies of, for extrusion of thin H-sections of TZM alloy, 19: 18431(R) (RTD-TR-8-112(V))
permeability of films of, to potassium nitrate, 19: 15492
permeability to oxygen at 1100 to 2050°C, 20: 31731
phase analysis of, method for quantitative, 17: 31008
phase diagrams, 17: 6579
phase inversion and thermal expansion, 16: 19338 (BM-RI-5982)
phase inversion of, 17: 15973
phase stabilization by oxide additions, 17: 32653
phase studies, 17: 21389(R) (MLM-1145)
phase studies of, bibliography on, 16: 33480 (UCRL-6262(Pt.2))
phase transformation, effects of pressure and temperature on monoclinic-tetragonal, 17: 4519
phase transformation of single crystals of, monoclinic-tetragonal, 18: 12033 (ATN-64(9236)-3)
phase transformations at 25 to 1300°C in, monoclinic-tetragonal, 19: 9726
phase transformation of, mechanism of monoclinic-tetragonal, 19: 28810 (BM-RI-6619)
phase transformations in, at 1100 to 2750°C, 19: 34696
phase transformation in, on heating in vacuum and in air, 19: 39190
phase transformation hysteresis, 17: 16667
phase transformations at 1155°C, x-ray analysis of time dependence of, 17: 16750
phase transformation at high temperatures, 17: 27876
phase transformations in, diffusionless, 17: 39559
phase transformations of, effects of magnesium and yttrium oxides on, 20: 3953
phase transformations in submicron, 20: 31736
phase transformations, effects of pressure and irradiation on solid-solid, (E), 20: 40306
phase transformations during cooling, kinetics of polymorphous, 18: 36000
phase transitions in submicron particles of, 19: 14014
phases at high temperatures and pressures, 19: 9696
photoelectric effect at −150 to 25°C, temperature dependence of, 20: 28667
physical properties at 600 to 1325°C, 16: 13003(R) (NP-11299)
physical properties of flame-sprayed coatings of, 16: 2219
physical properties, 17: 3460(R) (AD-273802)
physical properties of, bibliography on, 20: 43911 (UCRL-6262(Pt.1))
plasticity of, effects of doping agents on, 18: 27882 (GEAP-4473)
polarography in fused salt systems, 16: 17680
polarography in lithium and lithium sodium metaphosphates at 750 and 730°C, 18: 1516
polymorphic conversion of, effects of heat on, 18: 5786
preparation and properties of, for use in industry, 17: 15989
preparation and properties of microspheres of, 19: 6254 (MLM-1205)
preparation and properties of foams of, for aerospace uses, 19: 37141
preparation and stability of black nonstoichiometric, 20: 11248
preparation and uses, 19: 38647
preparation by vapor-phase oxidation of chloride, 19: 5923(P)
preparation, composition, and structure of crystalline hydrous, 18: 6808
preparation for use in reactors for gamma absorption, 18: 8825
preparation from zirconyl nitrate solutions, process for, 19: 36434(P)
preparation of crystalline, 16: 17582(R) (ORNL-3262(p.187-94))
preparation of crystals of, by zone melting at 2320 to 3800°K, 17: 32590
preparation of crystalline, from zirconium tetrachloride or its hydrolysis products, 20: 38929(P)
preparation of, from Indian zircon, 17: 14250
preparation of granular gels, for ion exchange use, 17: 1373(P)
preparation of granular, directly from ore, 18: 3909(P)
preparation of highly dispersed, by irradiation of hydroxide, 16: 32161
preparation of high-purity, 20: 41486
preparation of hydrogen-containing, relation to metal oxide bronzes, 17: 32088
preparation of lanthanide niobate-stabilized, method for, 20: 46153(P)
preparation of, method for, 17: 40831(P)
preparation of microspheres of, 20: 43182 (ORNL-TM-1508)
preparation of microspheres of, sol-gel process for, 20: 45794(R) (ORNL-3945, pp 157-75)
preparation of porous low-thermal-conductivity ceramic of, 18: 41955(P)
preparation of purified finely divided, from acidic solutions, 17: 30935(P)
preparation of sols of, with actinide oxides, 19: 2355(P)
preparation of spherical particles of, procedure and apparatus for, 20: 14971(P)
preparation of stabilized, method for, 18: 44068
preparation of tetragonal, at high pressure, 18: 3779
preparation of thin films of, 20: 16946 (ORNL-TM-1161, pp 80-4)
preparation of titanium-activated, 20: 17056
preparation of ultra-high-purity, by decomposition of alkoxides, 19: 6253 (ML-TDR-64-269)
preparation of ultra-high-purity submicron powders, 19: 36382
preparation procedures, ceramographic, 19: 46937 (NMI-6025(Pt.I), pp 1-25)
preparation, properties, and uses of high-temperature, 17: 18678(T)

(AEC-tr-5711)
preparation, properties, and uses, 18: 5740
preparation, properties, and structure of light-weight refractory, 18: 44206
preparation, properties, and aerospace applications, 19: 37142
pressing high density, apparatus for hot, 16: 19267
pressure effects on monoclinic-tetragonal transition of, 17: 8837
processing of, by chlorination, 20: 7188 (EUR-2088.f)
processing waste sludge of, by electrolytic dissolution, 17: 4295(R) (DP-740)
production from chlorides in fluidized beds, 16: 27579(P)
production of high bulk density, 16: 30318(P)
production of hypostoichiometric dioxide, methods for, 20: 37181(P)
production of phosphorus-free, process for, 17: 12308(P)
production of phosphorus-free, from zircon ore, 18: 1705(P)
production of sols of, methods for, 20: 9048(R) (ORNL-3830, pp 174-92)
production of thin coatings of, by flame spraying, 17: 8761
production of zirconium from, by electrolysis in fused salts, 17: 14238
properties and sinterability at high temperatures, effects of aluminum, calcium, magnesium, and titanium oxides on, 18: 34155
properties and uses of, review of, 18: 6834
properties as coating for extrusion liners for use at 1900 to 3600°F, 18: 18329(R) (ASD-TDR-7-945(IV))
properties as fuel particle coating, 18: 39949
properties as nuclear thermionic device material, 18: 24367 (GEST-2022)
properties at high temperatures, effects of calcia or magnesia on, 20: 5851
properties for magnetohydrodynamic cell insulators, 17: 31012
properties for use as ion exchanges for water purification in Parr Shoals Power Reactor, 16: 14612 (CVNA-135)
properties for use in vacuum electrothermics, 19: 11733
properties for use as insulator-seal combination in thermionic cells, 17: 1916(R) (ARF-2215-6)
properties in in-pile thermionic cells, 19: 44685 (CONF-650908-5)
properties of, additive effects of calcium and magnesium oxides on mechanical and thermal, 17: 41469
properties of crystalline, energy-band and ligand-field calculations of, 18: 24296(R) (AD-417517)
properties of, dispersion velocity dependence on mechanical and thermal, 17: 27873
properties of fibers of, 17: 1825
properties of fibers of, as filler for plastics, 18: 21709(R) (MLM-1179)
properties of films of, at 120 to 800°C, optical and structural, 17: 8846(T)
properties of flame-sprayed coatings of, for use in space technology, 18: 16521
properties of heat shield foams of, mechanical and thermal, 16: 29365 (ASD-TR-61-706(Vol.I))
properties of mixtures of different size powders of, mechanical and physical, 18: 28004
properties of refractory-based bricks of, effects of impurities on, 17: 34452
properties of reinforced coatings of, 16: 7920
properties of, bibliography on, 16: 33480 (UCRL-6262(Pt.2))
properties of, literature review of structural and physical, 19: 11720 (ARL-64-205)
properties, x-ray diffraction studies of heat treatment effects, 16: 15171 (DC-61-3-71)
properties, mechanical and thermal, 16: 7922
protective effects of coatings of, on graphite, against thorium alloys, 17: 40393
radiation effects on uranium-doped, 16: 6817(R) (ORNL-3213(p.57-80))
radiation effects on catalytic action in thermal dissociation of ethanol, 17: 4569 (NP-12250)
radiation effects on, fission-fragment, 18: 2352
radiation effects on, 18: 2353
radiation effects on electric conductivity of, 18: 7210(R) (HW-77954 (p.5.27-9))
radiation effects on thermal control coatings of, in nuclear spacecraft, 18: 20603
radiation effects on electric conductivity of films of, gamma, (E), 19: 20621
radiation effects on curvature of poly and single crystals of, fission-fragment, 17: 23864(R) (BMI-1619(Del.))
radiation effects on films of, applied to glass, 16: 21108
radiation effects on electric conductivity of, 20: 2460
radiation effects on optical properties of films of, fast neutrons, 20: 4304(R) (ORNL-3870, pp 171-83)
radiation effects on structure of, neutron, 20: 17148
radiation effects on films of, on zirconium, effects of vacuum annealing on fast-neutron, 20: 27600
radiation effects on, as insulator for nuclear thermionic converters, 20: 27614
radiation effects on phase transformations in, under high pressure, 20: 33968
radioinduced graft polymerization of styrene, vinylphosphonic acid dichloranhydride, and vinylpyridine on, 20: 43311
radioinduced phase transformations in, effects of uranium doping, 16: 25861
radioinduced phase transformations in, neutron and fission fragment, 18: 8885
radioinduced phase changes in films of, effects of heat treatment on recovery of, 17: 39570
radioinduced stresses in, from fission fragment bombardment, 17: 27888 (BMI-1635)
radioinduced swelling of, fission fragment, 20: 11227
reaction with molten potassium fluoborate, 18: 13786
reactions in fused fluoride fuels, 18: 1660
reactions of crucibles of, with titanium, reduction of, 17: 34341
reactions of crucibles of, with nickel-base alloys at high temperatures in vacuum, 16: 6756
reactions with ammonia, phase formation during, 16: 16350
reactions with ammonia at high temperatures, 18: 43451(T) (SC-T-64-1607)
reactions with barium carbonates and barium oxides, 20: 13282
reactions with beryllium to 600°C *in vacuo*, 19: 22997 (TRG-Report-842)
reactions with boron carbide, preparation of zirconium diboride by, 18: 39832(T)
reactions with calcium zirconates at 1350 to 1500°C, 16: 10574
reactions with calcium hydrides at 1000 to 1600°C, hydrogen bonding in, 18: 19981
reactions with carbon and zirconium hydrides at 1000 to 1600°C, hydrogen bonding in, 18: 19981
reactions with cesium vapor at high temperatures, 19: 9628
reactions with chromium, 19: 9122
reactions with copper and nickel mattes, slags, molten salts, and refractory metals, 20: 14989
reactions with gaseous uranium trioxide, effects of substrate symmetry in, 20: 20649 (AEET-CD-24)
reactions with graphite, torsion effusion study of, 18: 35553
reactions with graphite to prepare carbide, 19: 19866
reactions with graphite, torsion effusion study of, 20: 7107
reactions with lanthanum and neodymium oxides in solid state, 20: 36840
reactions with liquid bismuth, 18: 24815(R) (MLM-1184)
reactions with Magnox alloy to 500°C, 19: 22997 (TRG-Report-842)
reactions with metal borides, carbides, and nitrides at 1800 to 2000°C, 18: 43463
reactions with molybdenum, niobium, and tungsten at 1600 to 2100°C, 16: 4555(T) (FTD-TT-61-74)
reactions with molten AMS 5350 steel and Inconel 713C, 20: 16984
reactions with potassium hydroxide (liquid) and sodium hydroxide, 16: 179
reactions with rubidium carbonates or silicates at 870 to 950°C, 20: 12851
reactions with silicon oxides, Gibb's free energy of, 20: 5537
reactions with tungsten carbide at 1300 to 1400°C, preparation of alloys by, 18: 39833(T)
reactions with tungsten at high temperatures, 18: 41373(R) (TID-20951)
reactions with urania, effects of temperature of, 20: 20365
reduction by aluminum, carbon, or silicon in electron bombardment furnace, vacuum, 19: 5889
reduction by calcium carbide or calcium cyanamide, 17: 32059
reduction by magnesium in argon, hydrogen, and nitrogen, formation of hydrides and nitrides by, 18: 17816
reduction of, carbothermic, 19: 12865(R) (NAA-SR-10501)
reduction of, thermodynamics of, 17: 14269
reduction to metal, electrolytic, 18: 10201
reduction to metal by magnesium in hydrogen or nitrogen atmospheres, 20: 7100
reduction to metal by cerium, lanthanum, neodymium, or praseodymium, 20: 7529
reduction, carbothermic, 19: 18393(R) (ML-TDR-64-173(Pt.II))
reflectance of monoclinic, as function of purity, 20: 41486
refractive index of anodic films of, on zirconium foil, 18: 44052(R) (ORNL-3670(p.147-59))
refractive indices of anodized films *in situ* and stripped, 20: 4304(R) (ORNL-3870, pp 171-83)
semiconductivity at 1000°C, 19: 9689
separation from oxides as function of SO_3–ZrO_2 ratio, 17: 32077
sintering and stabilization, 18: 2262
sintering of, mechanism of first stage in, 18: 4217(T) (AEC-tr-6159)
sintering properties, 17: 7662(R) (MLM-1139)
solubilities in molten alkali metal fluorides at 1000 to 1200°C, 17: 8016(T) (AEC-tr-5601)

solubility in borax at 760 to 900°C, 20: 3951
solubility in fused fluorides, 20: 22856(R) (ORNL-3913, pp 1-51)
solubility in hydrochloric acid, 16: 30417
solubility in hydrofluoric, nitric, and sulfuric acids, 19: 5905
solubility in lithium fluoride–beryllium fluoride system, 18: 22011(R) (ORNL-3591(p.38-58))
solubility in lithium fluoride–uranium(IV) fluoride–zirconium fluoride systems, 17: 26765(R) (ORNL-3419)
sonic inspection of bond to Inconel, 16: 19150(R) (WADD-TR-61-91 (Pt.II))
sorption from dilute aqueous solutions of hydrochloric and nitric acids and sodium chloride, 18: 6819
sorptive properties for tributyl phosphates, 17: 1564(R) (IDO-14593)
sorptive properties for hydrogen, 17: 4500(T) (AEC-tr-5529)
sorptive properties for electrolytes, effects of previous hydrogen adsorption on, 17: 4500(T) (AEC-tr-5529)
sorptive properties for radioisotopes in water, 17: 10710
sorptive properties for dibutyl phosphate from organic solutions, 17: 23241
sorptive properties for TBP degradation products, 18: 5415(R) (IDO-14599)
sorptive properties for dibutyl phosphate, 18: 12256(R) (IDO-14621)
sorptive properties for molecular oxygen at 400 to 900°C, mechanism of, 18: 37698
sorptive properties for atomic oxygen at 400 to 900°C, mechanism of, 18: 37699
sorptive properties of hydrous, for dibutyl phosphate from aqueous solutions, 19: 26463 (IDO-14630)
sorptive properties for oxygen, 19: 40961
sorptive properties for hydrogen, 19: 40484
sorptive properties for chloride and potassium ions, effects of pH on, 20: 14651
sorptive properties of hydrous, for molybdenum-99 and technetium-99m in nitric acid solution, 20: 20566 (ORNL-TM-1468)
specific heat at 500 to 1300°C, measurement of mean, 18: 13779
spectra at 4 to 10.5 ev, absorption, 16: 538
spectra in low frequency region, infrared, 18: 23549
spectra of, amplitudes in vibrational, 17: 35721
spectra of corrosion films of, dielectric-loss, 18: 41964
spectra of cubic and monoclinic, infrared absorption, 18: 43442 (ASD-TDR-63-789)
spectra of cubic and monoclinic, infrared, 19: 9121
spectra of films of, on zirconium, effects of refractive index on infrared, 18: 25925
spectra of, infrared, 17: 41381
spectra of molecular, vibrational probabilities for α and γ systems in, 17: 12285(T)
spectra of, absorption, 19: 26327
spectra of, at 1300°K, infrared emission, 20: 1823
spectra of, impurity ion effects on reflectance, 18: 14722(R) (TID-20233)
spectra of, Raman, 19: 19849 (WAPD-T-1760)
spectra, rotational constants for α(C÷X) band system, 16: 24303
spectral emittance at 800 to 5000°F, 16: 18939
spraying of plasma, 17: 6556
stability at high temperatures, 17: 9073
stability in dry hydrogen at 1100 to 2000°C, 20: 14986
stability in gases, 16: 29421
stability in thermal cycling between 1600 and 2100°F, effects of impurities on, 19: 20585
stabilization by calcium oxide, effects of aluminum, iron, silicon, and titanium oxides on, 20: 867
stabilization, effects of impurities and titanium dioxide, 16: 101(T) (NP-tr-799)
stabilization of, effects of iron group oxides on, 18: 4272
strength and structure of, effects of porosity on, 17: 1972
stresses in films of, measurements of, 17: 16685
structure, effects of foreign oxides, 16: 16736(T) (UCRL-Trans-791(L))
structure of corrosion films of, on Zircaloy-2 and zirconium, 20: 19188(R) (GEAP-5001)
structure of films of, formed on zirconium, 19: 44622(R) (EURAEC-1433)
structure of monoclinic, from room temperature to 1095°C, 20: 2314 (ARL-65-140)
structure of, effects of oxide additions on, 19: 26359
structure of, from matrix-isolated vapor spectra, 19: 4661 (WADD-TR-60-646(Pt.IV))
structure, theoretical investigation of energy bands, 16: 2921 (AD-257435)
surface layer removal by vibratory polishing, 20: 7504
tensile strength for machining, effects of PVA binders on, 20: 11277 (RFP-659)
testing for use in shaft seals for potassium space power systems, 20: 2242
thermal conductivity and expansion, 16: 22585 (DC-61-6-4)
thermal conductivity at 200 to 1500°F, 18: 6537(R) (ORNL-TM-603)
thermal conductivity of foams of, for use above 3000°F, 18: 16520
thermal conductivity at high temperatures, 18: 39895 (GEMP-296)
thermal conductivity of powdered, 19: 17174(R) (ANL-6900(p.232-303))
thermal conductivity of partially reduced, 19: 18448 (AECL-2169)
thermal conductivity and total emissivity of coatings of, 19: 23076
thermal conductivity at high temperatures, (E), 19: 39215
thermal conductivity of, transient temperature method for measuring, 19: 40732(R) (CEND-3336-237)
thermal conductivity of powders of, 17: 27368
thermal conductivity of stabilized, to 2200°C, 20: 820 (GE-TM-64-10-4)
thermal conductivity of powders of, at 100 to 850°C, 20: 12854
thermal conductivity of powders of, at 100 to 850°C, (T), 20: 12855
thermal conductivity of powders of, in air at 200 to 1500°F, 20: 23552 (ORNL-3510)
thermal conductivity of powders of, under compressive stress, 20: 45056
thermal energy storage in, in solar-thermionic power supplies, 17: 9113
thermal expansion and structural transformation in solid solutions with MgO, CaO, and CeO_2 at temperatures of 20 to 1800°C, 16: 98(T) (AEC-tr-4801)
thermal expansion of yttrium oxide-stabilized, at 200 to 2200°C, 18: 16500
thermal expansion of axes of tetragonal, at 1150 to 1700°C, 18: 32130 (ARL-64-63)
thermal properties to 5000°F, 16: 18938
thermal properties of, effects of additives on, 18: 593 (ARL-63-170)
thermal properties of resin-impregnated foams of, 18: 10519 (AD-427700 (p.311-37))
thermal properties, 17: 3460(R) (AD-273802)
thermal properties of, at 500 to 5000°F, 17: 16636 (ASD-TDR-62-765)
thermal shock resistance, mechanism of effects of titanium additions on, 18: 42015 (NASA-TN-D-2464)
thermal shock resistance of, effects of grain growth, on, 20: 33901
thermal stability of mixtures of different size powders of, 18: 28004
thermal stabilization using calcium and magnesium oxides, effects of iron oxide on, 16: 24203
thermodynamic properties, 17: 30961 (ASD-TDR-62-204(Pt.II))
thermodynamic properties, 18: 35939(R) (NP-14192)
thermodynamic properties of large products of, 18: 24111
thermodynamic properties of, tables of, 17: 40777(R) (RAD-SR-63-183)
thermodynamic properties, 20: 10816(T) (NASA-TT-F-285)
thermodynamic properties of gaseous, liquid, and solid, at 2180 to 6000°K, 20: 19202 (AD-629571)
thickness and refractive index of films of, on anodized zirconium, 19: 20489
thickness of films of, on zirconium, spectrophotometric measurements of, 19: 13921
use as a diathermanous substance in thermal reactors, 19: 42065(P)
use as charge component in refractory materials for glass furnaces, 16: 32131
use as container material in continuous electrowinning of plutonium, 19: 18397 (RL-SEP-30)
use as corrosion inhibitor in high-temperature gas-cooled reactors, 20: 14021(P)
use as electrodes in MHD generators, (E), 20: 39723
use as radiography contrast medium, pathological effects from, 17: 26972
use as support base for oxide catalyst for oxidation of internal combustion engine exhaust gases, 20: 343(P)
use in development of in-pile method for measuring thermal conductance of fuel elements, 19: 44684 (CEND-3336-241)
use in metal-ceramic structural composite materials, 19: 9609(R) (ML-TDR-64-83)
use in MHD duct walls, preparation and testing for, (E), 20: 41718
use of electrodes of, in magnetohydrodynamic power generators, 17: 9073
use of, in nuclear rockets, 17: 8710 (TID-16315(Del.))
valency changes in films of, on electrodes, 17: 25203
vapor pressure, 17: 3378(R) (BMI-1583(Del.))
vapor pressure at high temperatures, 19: 4661 (WADD-TR-60-646(Pt.IV))
vapor pressure of, expression for, 19: 42801(R) (BMI-1721(Del.))
vaporization at 2300 to 2500°C, spectra of, 17: 11191(R) (NP-12483)
vaporization in magnetohydrodynamic generators, 17: 36334
vaporization in magnetohydrodynamic cells, 18: 4756 (ASD-TDR-63-4019)
vaporization of, species produced by, 20: 43901(R) (NBS-D-154)
vaporization of, to 2300°C, 20: 13265(T) (AD-623208)
vaporization of, thermodynamics of, 20: 36841
vaporization rate in air, 16: 25403
wear characteristics, 16: 30518
wear properties of plasma-arc-deposited coatings of, 20: 21319 (AD-621064)
xenon-133 release from, 18: 8712 (BMI-1651)
xenon-133 diffusion in, thermal release study of fission-recoil, 18: 18373
actinide oxides–ZrO_2, preparation of sols of, 20: 39442(P)

Ag_2O–ZrO_2, crystal structure and phase studies, 17: 37503(R) (AD-290693)

Al_2O_3–$AlPO_4$–ZrO_2–$Zr_3(PO_4)_4$, preparation of foam for insulating materials, 20: 39375(P)

Al_2O_3–CaO–MgO–ZrO_2, phase studies on, 18: 16490

Al_2O_3–CaO–ZrO_2, phase studies on, 18: 10059

Al_2O_3–CaO–ZrO_2, phase studies, 18: 14491

Al_2O_3–Cr_2O_3–MgO–SiO_2–TiO_2–ZrO_2, phase diagrams, 20: 8932

Al_2O_3–Gd_2O_3–ZrO_2, fabrication and properties as reactor poison, 18: 42912(R) (ACNP-64585)

Al_2O_3–Gd_2O_3–ZrO_2, properties as reactor poison, 18: 42913(R) (ACNP-64586)

Al_2O_3–MgO–ZrO_2, melting diagram, 18: 30188

Al_2O_3–MgO–ZrO_2, phase studies, 20: 7621

Al_2O_3–ZrO_2, fabrication of, method for, 20: 29695(P)

Al_2O_3–ZrO_2, preparation for use as abrasive, 19: 32690(P)

Al_2O_3–ZrO_2, preparation of, for use at temperatures to 1750°C, 20: 2382

Al_2O_3–ZrO_2, thermal shock resistance, 16: 24176 (WADD-TR-60-749(Pt.II))

Al–Zircaloy-2–ZrO_2, phase studies, 20: 39380 (AECL-2570)

BaO–SiO_2–ZrO_2, phase studies, 20: 38899

BeO–MgO–ZrO_2, heat storage for solar-thermionic power supplies in, 17: 9113

BeO–MgO–ZrO_2, melting temperatures, 17: 14740 (TID-11295(2nd Ed.))

BeO–MgO–ZrO_2, phase studies, 17: 27833

BeO–MgO–ZrO_2, properties of molten, for fuel matrix for homogeneous thermal nuclear reactors, 20: 31726

BeO–TiO_2–ZrO_2, heat storage for solar-thermionic power supplies in, 17: 9113

BeO–ZrO_2, phase studies, 17: 27833

BeO–ZrO_2, properties of irradiated and unirradiated, 17: 25688(R) (GEMP-177A)

BeO–ZrO_2, radiation effects on mechanical and physical properties, 16: 4586(R) (GEMP-6A)

Bi_2O_3–ZrO_2, phase studies, 19: 9719

B_2O_3–ZrO_2, phase equilibria in, 16: 32106(R) (AD-271937)

B_2O_3–ZrO_2, preparation and sorptive properties for hydrogen, 19: 40484

CaO–CeO_2–ZrO_2, electric conductivity and structure of, at 500 to 1000°C, 20: 14536

CaO–La_2O_3–ZrO_2, phase studies, 18: 20538

CaO–MgO–SiO_2–ZrO_2, properties of, for use as refractory material, 16: 21067

CaO–MgO–ZrO_2, phase studies, 17: 32653

CaO–Sm_2O_3–UO_2–ZrO_2, corrosion and surface properties of, 20: 16089(R) (WAPD-MRP-114)

CaO–TiO_2–ZrO_2, phase studies, 16: 3485

CaO–TiO_2–ZrO_2, structure of compound $CaZrTi_2O_7$ in, 18: 39956(T)

CaO–UO_2–Y_2O_3–ZrO_2, phase studies of, after heating in air at 1400 to 1800°C, 20: 43900(R) (NBS-D-150)

CaO–UO_2–ZrO_2, corrosion by steam at 625°C, 16: 33511(R) (CEND-162)

CaO–UO_2–ZrO_2, corrosion of stainless steel clad, by liquid sodium and water, 18: 14532(R) (CEND-190)

CaO–UO_2–ZrO_2, corrosion by lithium hydroxide at 680°F and steam at 750°F, 18: 45034(R) (WAPD-MRP-109)

CaO–UO_2–ZrO_2, corrosion by ammonium hydroxide, lithium hydroxide, steam, and water at high temperatures, hydrogen sorption from, 19: 12785(R) (WAPD-MRP-110)

CaO–UO_2–ZrO_2, corrosion of sintered, by ammoniated water, 19: 24093(R) (WAPD-MRP-111)

CaO–UO_2–ZrO_2, corrosion of sintered, by aqueous ammonia and deionized water at 630 to 680°C, 19: 31556(R) (WAPD-MRP-112)

CaO–UO_2–ZrO_2, corrosion and surface properties of, 20: 16089(R) (WAPD-MRP-114)

CaO–UO_2–ZrO_2, crystal structure and properties of, 19: 30777

CaO–UO_2–ZrO_2, densities and thermal properties, 19: 39091(R) (BMI-1723(Del.))

CaO–UO_2–ZrO_2, development of, for fuels, 17: 1815 (ANL-6314)

CaO–UO_2–ZrO_2, enthalpy and thermal conductivity at 100 to 2000°C, 19: 46912(R) (BMI-1727(Del.))

CaO–UO_2–ZrO_2, fabrication and properties as reactor fuel, 18: 7932(R) (WAPD-MRP-106)

CaO–UO_2–ZrO_2, fabrication of uranium-235-enriched, autoradiographic detection of alpha-active contamination and isotopic heterogeneity in, 18: 8774 (WAPD-BT-29(p.45-57))

CaO–UO_2–ZrO_2, fabrication by cold pressing and sintering, 18: 14532(R) (CEND-190)

CaO–UO_2–ZrO_2, fabrication and properties as reactor fuel, 18: 21643(R) (WAPD-MRP-107)

CaO–UO_2–ZrO_2, fabrication and properties as reactor fuel, 18: 29060(R) (WAPD-MRP-108)

CaO–UO_2–ZrO_2, fabrication and properties as reactor fuel, 18: 45034(R) (WAPD-MRP-109)

CaO–UO_2–ZrO_2, fabrication and properties as reactor fuel, 19: 12785(R) (WAPD-MRP-110)

CaO–UO_2–ZrO_2, phase relationships and properties, 16: 11191(R) (CEND-147)

CaO–UO_2–ZrO_2, phase studies, 16: 32110(R) (CEND-123)

CaO–UO_2–ZrO_2, phase studies at high temperatures, 16: 33511(R) (CEND-162)

CaO–UO_2–ZrO_2, phase studies, 19: 24093(R) (WAPD-MRP-111)

CaO–UO_2–ZrO_2, physical and thermal properties of, at high temperatures, 20: 33862 (BMI-1775)

CaO–UO_2–ZrO_2, preparation and properties of, for ceramic nuclear fuels, 20: 21302

CaO–UO_2–ZrO_2, properties of, as reactor fuel, 16: 24625

CaO–UO_2–ZrO_2, properties of, evaluation of, for use in spiked cores, 16: 12731 (CEND-150(Pt.V))

CaO–UO_2–ZrO_2, properties of sintered, 16: 2672 (CEND-87)

CaO–UO_2–ZrO_2, properties of single-phase face-centered cubic structures in, 17: 36339 (CEND-158)

CaO–UO_2–ZrO_2, properties for PBF fuel, 19: 35847(R) (IDO-17084)

CaO–UO_2–ZrO_2, properties of, in-pile, 20: 15138 (WAPD-392)

CaO–UO_2–ZrO_2, radiation effects on, at high burnup, 16: 28642(R) (BMI-1581(Del.))

CaO–UO_2–ZrO_2, radiation effects on uranium-235-enriched, stainless steel-clad, at high burnup, 20: 35834(R) (BMI-1767)

CaO–UO_2–ZrO_2, thermal conductivity and expansion, 16: 33511(R) (CEND-162)

CaO–UO_2–ZrO_2, thermal conductivity measurements of, preparation of samples for, 18: 40970(R) (BMI-1674(Del.))

CaO–UO_2–ZrO_2, thermal conductivity at high temperatures, 19: 42801(R) (BMI-1721(Del.))

CaO–Y_2O_3–ZrO_2, ionic conductivity of cubic solid solutions in, 18: 16014

CaO–ZrO_2, corrosion by potassium-seeded gases, 19: 11695

CaO–ZrO_2, crystal structure and phase studies, 17: 37503(R) (AD-290693)

CaO–ZrO_2, diffusion of oxygen in, at high temperatures, 18: 30105(R) (AD-429028)

CaO–ZrO_2, diffusion at 1700 to 2150°C in, cationic self-, 20: 31732

CaO–ZrO_2, disorder-order in fluorite-type cubic solid solutions of, relations with ionic conductivity changes, 17: 30980(R) (NP-12969(Paper III))

CaO–ZrO_2, electric and ionic conductivities, 19: 34194

CaO–ZrO_2, electric conductivity of, relations with anion vacancy concentrations and temperature, 17: 30979(R) (NP-12969(Paper II))

CaO–ZrO_2, electric conductivity and x-ray diffraction studies on fluorite phase in, 17: 37756

CaO–ZrO_2, electric conductivity at 800 to 2000°C, 18: 7225

CaO–ZrO_2, electric conductivity in, 19: 13311

CaO–ZrO_2, electric conductivity at 350 to 1250°C of stabilized cubic, 19: 36338(R) (NP–15160)

CaO–ZrO_2, electric properties, 17: 18736(R) (AD-283667)

CaO–ZrO_2, electronic conduction in, 18: 27869(T) (SC-T-64-910)

CaO–ZrO_2, fusion by high-frequency induction heating, 17: 41450

CaO–ZrO_2, grain growth of $Ca_{0.16}Zr_{0.84}O_{1.84}$, 17: 32135

CaO–ZrO_2, internal friction, 20: 3945

CaO–ZrO_2, performance as electrolyte in electrochemical cells, (E), 19: 13205 (SAN-8002(p.276-85))

CaO–ZrO_2, phase equilibria in, sub-solidus, 18: 20578

CaO–ZrO_2, phase studies, 17: 30979(R) (NP-12969(Paper II))

CaO–ZrO_2, phase studies, 17: 32653

CaO–ZrO_2, preparation, properties, and aerospace applications, 19: 37142

CaO–ZrO_2, preparation of dense and homogeneous samples by melting techniques, 20: 798

CaO–ZrO_2, stability of solid solutions in, 16: 15219

CaO–ZrO_2, structure and properties, 16: 5363(T)

CaO–ZrO_2, structure and electric conductivity of, effects of iron and nickel oxides on, 19: 32736(T) (NP-tr-1236(p.66-73))

CaO–ZrO_2, thermal conductivity in MHD jets, 19: 16195

CaO–ZrO_2, thermal shock resistance of, effects of physical properties on, 20: 33900

CaO–ZrO_2, use in measurement of ionic conductivities and oxygen activities in oxides, 18: 27869(T) (SC-T-64-910)

CaO–ZrO_2, uses as electrolyte in oxygen concentration cells, 19: 46297

$CaZrO_3$–ZrO_2, electric conductivity, 18: 42039

CdO–ZrO_2, crystal structure and phase studies, 17: 37503(R) (AD-290693)

CeO_2–ZrO_2, crystal structure and properties at 1700 to 1750°C, 18: 556

CeO_2–ZrO_2, crystal structure, differential thermal analysis, and thermal expansion of, 18: 23503

Ce_2O_3–ZrO_2, effects of oxygen partial pressures on chemical reactions and transformation in, 20: 25074

CeO_2–ZrO_2, formation and properties of solid solutions of, 17: 34453

Cs_2O_3–ZrO_2, phase studies, 16: 27642(T) (FTD-TT-62-505)

CeO_3–ZrO_3, phase studies, 17: 32653
Ce_2O_3–ZrO_2, phase studies, 19: 42464
Ce_2O_3–ZrO_2, phase studies of, in oxidizing, inert, and reducing atmospheres, 20: 26845
CeO_3–ZrO_3, phase transformations in, fluorite, 19: 358(T) (ORNL-tr-201)
CeO_3–ZrO_3, preparation and properties of, 18: 6822
Cr_2O_3–MgO–ZrO_2, phase studies of, use of chemical analysis in, 20: 35527
Cr_2O_3–ZrO_3, characterization of hot-pressed, 17: 27728(R) (GEAP-4076)
Cr_2O_3–ZrO_2, formation of refractories of, 19: 40997(P)
Cr_2O_3–ZrO_2, phase studies of, at 1500°C, 16: 22573(R) (AD-266459)
Cr–ZrO_2, thermal shock resistance of, 20: 33901
CuO–Cu_2O–ZrO_2, phase studies, 20: 43978
CuO–ZrO_3, characterization of hot-pressed, 17: 27728(R) (GEAP-4076)
CuO–ZrO_3, crystal structure and phase studies, 17: 37503(R) (AD-290693)
Dy_2O_3–ZrO_3, crystal structure of, evolution of, 16: 2224
Dy_2O_3–ZrO_3, crystal structure, differential thermal analysis, and thermal expansion of, 18: 23503
Eu_2O_3–ZrO_2, phase studies, 20: 36815
Fe_3O_4–ZrO_2, characterization of hot-pressed, 17: 27728(R) (GEAP-4076)
Ga_2O_3–ZrO_3, crystal structure and phase studies, 17: 37503(R) (AD-290693)
Gd_2O_3–UO_3–ZrO_3, fabrication and reaction properties, 18: 11396(R) (ACNP-64003)
Gd_2O_3–UO_3–ZrO_3, fabrication and properties as reactor poison, 18: 28958(R) (ACNP-64023)
Gd_2O_3–UO_3–ZrO_3, fabrication and properties as reactor poison, 18: 42912(R) (ACNP-64585)
Gd_2O_3–ZrO_3, crystal structure of, evolution of, 16: 2224
Gd_2O_3–ZrO_3, fabrication and properties as reactor poison, 18: 42912(R) (ACNP-64585)
Gd_2O_3–ZrO_2, phase studies, 19: 42464
Gd_2O_3–ZrO_3, phase transformations in, fluorite, 19: 358(T) (ORNL-tr-201)
Gd_2O_3–ZrO_2, properties as reactor poison, 18: 11396(R) (ACNP-64003)
Ge_2O_3–ZrO_3, ordered states in non-stoichiometric phases of, appearance of, 16: 19383
GeO_2–ZrO_2, phase transformations in, fluorite, 19: 358(T) (ORNL-tr-201)
graphite–ZrO_3, protective effects against oxidation of uranium dioxide compacts coated with, 17: 37477 (BMI-1647)
HfO_2–Ta_2O_5–ZrO_3, thermal expansion to 4000°F, 18: 30105(R) (AD-429028)
HfO_2–Y_2O_3–ZrO_3, thermal expansion to 4000°F, 18: 30105(R) (AD-429028)
HfO_2–ZrO_3, activation analysis for zirconium, 17: 40750
HfO_2–ZrO_2, phase transformations in, fluorite, 19: 358(T) (ORNL-tr-201)
HfO_2–ZrO_3, thermal expansion to 4000°F, 18: 30105(R) (AD-429028)
HfO_2–ZrO_2, thermal expansion of solid solutions of, at 900 to 2500°C, 19: 47045
KBF_4–ZrO_2, melting temperatures, 18: 22080
La_2O_3–UO_2–ZrO_2, phase studies of, after heating in air at 1400 to 1800°C, 20: 43900(R) (NBS-D-150)
La_2O_3–ZrO_3, crystal structure and properties at 1700 to 1750°C, 18: 556
La_2O_3–ZrO_3, crystal structure, differential thermal analysis, and thermal expansion of, 18: 23503
La_2O_3–ZrO_2, electric conductivity, 19: 37094
La_2O_3–ZrO_3, electric conductivity of, at 1200 to 1650°C, 17: 20006
La_2O_3–ZrO_2, formation and properties of solid solutions of, 17: 34453
La_2O_3–ZrO_3, phase studies, 16: 27642(T) (FTD-TT-62-505)
La_2O_3–ZrO_2, phase studies, 19: 42464
La_2O_3–ZrO_3, phase transformations in, fluorite, 19: 358(T) (ORNL-tr-201)
La_2O_3–ZrO_3, preparation and properties of, 18: 6822
Li_2O–SiO_2–ZrO_2, phase studies, 19: 41038
$LuO_{1.5}$–ZrO_2, electric conductivity of, 20: 19243
Lu_2O_3–ZrO_2, phase studies, 19: 42464
MgO–Y_2O_3–ZrO_2, phase studies of, on annealing and cooling, 20: 3953
MgO–ZrO_3, analysis, chemical, 16: 23599 (ARL-180)
MgO–ZrO_3, corrosion by barium vapor at 800 to 1000°C, 18: 44498(R) (MND-2812-3)
MgO–ZrO_2, grain boundary precipitation in, 20: 31738
MgO–ZrO_3, heat storage for solar-thermionic power supplies in, 17: 9113
MgO–ZrO_3, phase boundaries of cubic solid solutions of, 17: 15974
MgO–ZrO_3, phase boundaries of cubic solid solutions at 1400 to 2285°C, 17: 15975
MgO–ZrO_3, phase studies, 17: 27833
MgO–ZrO_2, phase studies, 17: 32653
MgO–ZrO_2, phase studies, 19: 34708
MgO–ZrO_2, preparation, properties, and aerospace applications, 19: 37142
MgO–ZrO_3, radiation effects, 17: 13678(R) (HW-75914)
MgO–ZrO_3, stability of solid solutions in, 16: 15219
MgO–ZrO_2, stability of solid solutions in, 19: 34701
Mo–ZrO_2, stability and strength at 1650 to 2210°C, 19: 26853
Mo–ZrO_2, structure of dispersion-hardened, effects of sintering process on, 20: 17109
Nb_2O_5–ZrO_2, crystal structure of compounds $ZrO_2 \cdot 5Nb_2O_5$ and $ZrO_2 \cdot 7Nb_2O_5$ in, 20: 13281
Nb_2O_5–ZrO_2, phase studies, 19: 26846
Nb_2O_5–ZrO_2, phase studies, 20: 15079
Nd_2O_3–ZrO_3, crystal structure, differential thermal analysis, and thermal expansion of, 18: 23503
Nd_2O_3–ZrO_3, phase studies, 16: 27642(T) (FTD-TT-62-505)
Nd_2O_3–ZrO_2, phase studies, 19: 41037
Nd_2O_3–ZrO_2, phase studies, 19: 42464
Nd_2O_3–ZrO_2, phase studies, 20: 13283
Nd_2O_3–ZrO_3, phase transformations in, fluorite, 19: 358(T) (ORNL-tr-201)
NiO–ZrO_3, characterization of hot-pressed, 17: 27728(R) (GEAP-4076)
paraffin–UO_2–ZrO_2, neutron asymptotic spectra in, (E), 19: 25457 (RPI-328-28)
paraffin–UO_2–ZrO_2, neutron asymptotic and steady-state spectra in, (E), 19: 29561
paraffin–UO_2–ZrO_2, neutron spectra in, asymptotic and steady-state, (E), 19: 39768 (RPI-328-21)
paraffin–ZrO_2, neutron spectra in, 20: 4806(R) (RPI-328-40, pp 1-42)
PbO–TiO_2–ZrO_3, phase studies, 17: 4963
PbO–TiO_2–ZrO_3, separation of titanium and zirconium from, by cation exchange, 19: 534
Pd–Ag–ZrO_2, preparation and properties of zirconia-base cermets of, 20: 37209
PrO–ZrO_2, phase studies, 20: 13279
PuO_2–UO_2–ZrO_2, fabrication of pellets of, 20: 33945(R) (NUMEC-3505-14)
PuO_2–UO_2–ZrO_2, preparation and thermophysical properties, 20: 15054(R) (NUMEC-3505-11)
PuO_2–UO_2–ZrO_2, properties for use in thermal reactors, 20: 4382(R) (NUMEC-3505-8)
PuO_2–UO_2–ZrO_2, properties as reactor fuel, 20: 33945(R) (NUMEC-3505-14)
PuO_3–ZrO_3, compact powder welding to aluminum, stainless steel, and zirconium alloys, 18: 44120
PuO_3–ZrO_3, corrosion resistance to hot water in reactors, 18: 22526 (HW-SA-3128)
PuO_3–ZrO_2, fabrication and testing, 17: 7547(R) (HW-74761(p.3.1-39))
PuO_3–ZrO_3, fabrication by sintering and spheroidization, 17: 33412(R) (MLM-1146)
PuO_3–ZrO_2, irradiation testing, 18: 29001(R) (HW-79280(p.5.1-25))
PuO_3–ZrO_3, pellet welding to aluminum, stainless steel, and zirconium alloys, 18: 44120
PuO_3–ZrO_2, phase diagram, 17: 14740 (TID-11295(2nd Ed.))
PuO_3–ZrO_3, phase diagram, 17: 27836
PuO_3–ZrO_3, phase studies, 16: 12093 (HW-69305)
PuO_3–ZrO_3, phase studies, 16: 14376(R) (HW-70000)
PuO_3–ZrO_3, phase studies and properties of, bibliographic study of, 16: 32115 (KFK-105)
PuO_3–ZrO_3, phase studies, 17: 21389(R) (MLM-1145)
PuO_2–ZrO_2, phase studies, 20: 46144(R) (HW-67765)
PuO_3–ZrO_3, preparation and properties of pellets of, 18: 24815(R) (MLM-1184)
PuO_3–ZrO_3, preparation and properties of spherical particles of, 18: 26008
PuO_3–ZrO_3, preparation and properties of microspheres of, 19: 6254 (MLM-1205)
PuO_3–ZrO_3, radiation effects, 17: 13678(R) (HW-75914)
PuO_3–ZrO_3, radiation effects on, 17: 23866(R) (HW-76300)
PuO_3–ZrO_3, radiation effects, 17: 36198(R) (HW-76301(Paper 3))
PuO_3–ZrO_3, radiation effects on, 18: 2339
PuO_3–ZrO_3, radiation effects on, 18: 12724(R) (HW-76303(p.4.1-43))
PuO_3–ZrO_3, radiation effects on, in ETR, 18: 22526 (HW-SA-3128)
PuO_3–ZrO_3, structure of microspherical, 17: 41350(R) (MLM-1162)
rare earth oxide–ZrO_3, ordered states in non-stoichiometric phases of, appearance of, 16: 19383
Re–W–ZrO_3, preparation and properties, 19: 883(R) (AD-600764)
Sc_2O_3–ZrO_2, electric conductivity, 19: 37094
$ScO_{1.5}$–ZrO_2, electric conductivity of, 20: 19243
Sc_2O_3–ZrO_3, phase studies, 18: 10113
Sc_2O_3–ZrO_3, phase studies, 19: 11753
Sc_2O_3–ZrO_2, phase studies, 19: 42464
Sc_2O_3–ZrO_3, phase transformations in, fluorite, 19: 358(T) (ORNL-tr-201)
Sc_2O_3–ZrO_2, preparation of sols of, 20: 8959(P)
SiO_2–Na_2O–ZrO_2, phase studies, 20: 13284
SiO_3–V_2O_5–ZrO_3, zircon formation in, 18: 42085
SiO_3–ZrO_3, ceramic properties, 16: 24210
SiO_3–ZrO_3, ion exchange properties of, in nitrate melts, 17: 27500
SiO_3–ZrO_3, phase transformations in, fluorite, 19: 358(T) (ORNL-tr-201)
SiO_2–ZrO_2, preparation, properties, and aerospace applications, 19: 37142

SiO_2–ZrO_2, use of phosphate-bonded, as mold for casting molybdenum–uranium alloys, 19: 32674 (AD-610003)
Sm_2O_3–ZrO_2, electric conductivity, 19: 37094
Sm_2O_3–ZrO_2, phase studies, 19: 42464
Sm_2O_3–ZrO_2, phase transformations in, fluorite, 19: 358(T) (ORNL-tr-201)
SnO_2–ZrO_2, crystal structure and phase studies, 17: 37503(R) (AD-290693)
SnO_2–ZrO_2, phase transformations in, fluorite, 19: 358(T) (ORNL-tr-201)
SrO-TiO_2-ZrO_2, phase studies, 17: 1994
SrO–ZrO_2, equilibrium diagram of, 19: 11131
SrO–ZrO_2, phase studies on, 20: 23670
$SrTiO_3$–TiO_2–ZrO_2, phase studies on solid solutions of, at 1300°C, 20: 23671
ThO_2–UO_2–ZrO_2, phase studies on, 20: 2361(T) (WAPD-Trans-21)
ThO_2–ZrO_2, phase studies, 16: 27642(T) (FTD-TT-62-505)
ThO_2–ZrO_2, phase studies, 16: 30888
ThO_2–ZrO_2, phase transformations in, fluorite, 19: 358(T) (ORNL-tr-201)
TiO_2–VO–ZrO_2, phase diagram at 1500°C, 16: 29403
TiO_2–ZrO_2, heat storage for solar-thermionic power supplies in, 17: 9113
TiO_2–ZrO_2, phase transformations in, fluorite, 19: 358(T) (ORNL-tr-201)
Ti–ZrO_2, structure after firing at 1200 to 2000°C, 17: 30530
Ti–ZrO_2, tensile properties of, effects of heat treatments on, 19: 9690
Ti–ZrO_2, thermal shock resistance of, effects of physical properties on, 20: 33900
Ti–ZrO_2, thermal shock resistance of, role of grain boundary in, 20: 33901
Ti–ZrO_2, use in container for molten titanium, 19: 36974(P)
Ti_2O–ZrO_2, crystal structure and phase studies, 17: 37503(R) (AD-290693)
UO_2–UO_3–Y_2O_3–ZrO_2, phase equilibria in air at high temperatures, 20: 43901(R) (NBS-D-154)
UO_2–Y_2O_3–ZrO_2, phase studies of, after heating in air at 1400 to 1800°C, 20: 43900(R) (NBS-D-150)
UO_2–Y_2O_3–ZrO_2, preparation and properties as internal conversion fuel material, 18: 24065(R) (GEMP-34A)
UO_2–Y_2O_3–ZrO_2, preparation of solid solution powders of, for use as reactor fuel, 19: 39094 (CONF-117(p.11-19))
UO_2–Y_2O_3–ZrO_2, preparation procedures, ceramographic, 19: 46937 (NMI-5025(Pt.I), pp 1-25)
UO_2–Zircaloy-4–ZrO_2, dissolution of fused, 20: 43067(R) (IDO-14679, pp 6-46)
UO_2–ZnO, phase studies of, at 1200°C and 6×10^4 atm, 16: 4450(R) (BMI-1546(Del.))
UO_2–ZrO_2, bibliography on SNAP fuel materials containing, 18: 33128 (NAA-SR-9525(Vol.I))
UO_2–ZrO_2, burnup effects on stability of, 17: 22966(R) (BMI-1614(Del.))
UO_2–ZrO_2, coating of, with pyrolytic carbon, 17: 10063 (WAPD-272)
UO_2–ZrO_2, corrosion and reaction rates in chloride volatility processing of, 18: 39386
UO_2–ZrO_2, corrosion of sintered, by ammoniated water, 19: 24093(R) (WAPD-MRP-111)
UO_2–ZrO_2, corrosion by steam and water, 19: 25044(R) (CEND-2936-222)
UO_2–ZrO_2, corrosion of sintered, by aqueous ammonia and deionized water at 630 to 680°C, 19: 31556(R) (WAPD-MRP-112)
UO_2–ZrO_2, crystal structure, 17: 1836
UO_2–ZrO_2, crystal structure and phase studies at 1000 to 1800°C, 18: 15664(R) (BMI-1655(Del.))
UO_2–ZrO_2, crystal structure of calcia-stabilized, 19: 46913(R) (BMI-1733(Del.))
UO_2–ZrO_2, differential thermal analysis, 16: 23652
UO_2–ZrO_2, diffusion of xenon-133 from irradiated plates of, 17: 39678 (WAPD-TM-313)
UO_2–ZrO_2, diffusion at 2000 to 2400°C, 19: 22979 (IDO-17006)
UO_2–ZrO_2, diffusion across boundaries in fuel elements of, 20: 46210
UO_2–ZrO_2, dissolution of Zircaloy-clad irradiated, 18: 17930(R) (IDO-14625)
UO_2–ZrO_2, dissolution in boric acid-hydrofluoric acid-nitric acid-oxalic acid solutions, 18: 31658(R) (IDO-14635)
UO_2–ZrO_2, dissolution by hydrofluorination in fused-salt fluorides, 18: 39385
UO_2–ZrO_2, dissolution in hydrofluoric acid solutions, 19: 11292
UO_2–ZrO_2, electric conductivity at high temperatures, 17: 555
UO_2–ZrO_2, electric conductivity and thermal properties, 18: 17351(R) (BMI-1659(Del.))
UO_2–ZrO_2, energy release of irradiated, 17: 18866 (WAPD-TM-350)
UO_2–ZrO_2, enthalpy as a function of temperature of, 19: 32676(R) (BMI-1717(Del.))
UO_2–ZrO_2, enthalpy and thermal conductivity at 100 to 2000°C, 19: 46912(R) (BMI-1727(Del.))
UO_2–ZrO_2, fabrication and radiation stability of, effects of impurities on, 16: 6698 (WAPD-251)
UO_2–ZrO_2, fabrication, 17: 3378(R) (BMI-1583(Del.))
UO_2–ZrO_2, fabrication, 17: 3379(R) (BMI-1596(Del.))
UO_2–ZrO_2, fabrication, 17: 13876(R) (BMI-1603(Del.))
UO_2–ZrO_2, fabrication and phase relationships, 17: 14727(R) (BMI-1600(Del.))
UO_2–ZrO_2, fabrication, 17: 15532(R) (BMI-1607(Del.))
UO_2–ZrO_2, fabrication and properties as fuel element material, 17: 36931(R) (WAPD-MRP-93)
UO_2–ZrO_2, fabrication and properties as fuel element material, 17: 36932(R) (WAPD-MRP-104)
UO_2–ZrO_2, fabrication of enriched fuel wafers of, 18: 9654 (WAPD-BT-29(p.29-43))
UO_2–ZrO_2, fabrication of uranium-235-enriched, autoradiographic detection of alpha-active contamination and isotopic heterogeneity in, 18: 8774 (WAPD-BT-29(p.45-57))
UO_2–ZrO_2, fabrication into pellets for irradiation, 18: 20450(R) (BMI-1661(Del.))
UO_2–ZrO_2, fabrication and properties as reactor fuel, 18: 45034(R) (WAPD-MRP-109)
UO_2–ZrO_2, fabrication for thermal conductivity testing, 19: 2716(R) (BMI-1681(Del.))
UO_2–ZrO_2, fabrication and properties as reactor fuel, 19: 12785(R) (WAPD-MRP-110)
UO_2–ZrO_2, fabrication of fuel wafers for Shippingport PWR, 19: 14846 (WAPD-BT-31(p.19-25))
UO_2–ZrO_2, fabrication by pressing and sintering, 19: 13871(R) (BMI-1691(Del.))
UO_2–ZrO_2, fabrication and properties, 20: 17005
UO_2–ZrO_2, fission gas release from, in PWR, 16: 6223(R) (WAPD-MRP-94)
UO_2–ZrO_2, fission gas release from irradiated, 19: 25044(R) (CEND-2936-222)
UO_2–ZrO_2, fission-product distribution in irradiated, 20: 29616(R) (BMI-1738)
UO_2–ZrO_2, hardness of compacts of, at temperatures up to 1500°C, 17: 40423(R) (BMI-1639(Del.))
UO_2–ZrO_2, in-pile thermal conductivity of, 18: 3149
UO_2–ZrO_2, irradiation temperatures, 18: 7985(R) (BMI-1650(Del.))
UO_2–ZrO_2, melting point, 19: 22989(R) (ORNL-3776(p.37-40))
UO_2–ZrO_2, melting point, 19: 31478(R) (ORNL-3789(p.251-62))
UO_2–ZrO_2, of, coating with pyrolytic carbon, 16: 24626
UO_2–ZrO_2, partial pressures of, 19: 39091(R) (BMI-1723(Del.))
UO_2–ZrO_2, phase diagrams, 20: 22856(R) (ORNL-3931, pp 1-51)
UO_2–ZrO_2, phase equilibria in air at high temperatures, 20: 43901(R) (NBS-D-154)
UO_2–ZrO_2, phase studies, 16: 27642(T) (FTD-TT-62-505)
UO_2–ZrO_2, phase studies, 16: 4564
UO_2–ZrO_2, phase studies, 16: 30889
UO_2–ZrO_2, phase studies at 1200 to 2350°C, 16: 25765 (WAPD-253)
UO_2–ZrO_2, phase studies, 17: 3379(R) (BMI-1596(Del.))
UO_2–ZrO_2, phase studies, 19: 30651(R) (ORNL-3789(p.239-47))
UO_2–ZrO_2, physical and thermal properties of, at high temperatures, 20: 33862 (BMI-1775)
UO_2–ZrO_2, physical properties and thermal diffusivity of, 19: 30642(R) (BMI-1707(Del.))
UO_2–ZrO_2, preparation of sols of, 19: 2355(P)
UO_2–ZrO_2, preparation of sols of, 19: 11138(P)
UO_2–ZrO_2, preparation of sols of, 19: 34205(P)
UO_2–ZrO_2, preparation of colloidal particle of, 19: 36429(P)
UO_2–ZrO_2, preparation and thermodynamic stability of fibrous fuels of, 20: 23071(R) (AGN-8169)
UO_2–ZrO_2, production porosity control for PWR Core 2, 18: 29059 (WAPD-BT-30(p.81-7))
UO_2–ZrO_2, properties, 17: 3379(R) (BMI-1596(Del.))
UO_2–ZrO_2, properties, 17: 14740 (TID-11295(2nd Ed.))
UO_2–ZrO_2, properties of compacted pellets of, 18: 41919 (BMI-1689)
UO_2–ZrO_2, properties of pressed-sintered, 19: 18421(R) (BMI-1697(Del.))
UO_2–ZrO_2, properties of pressed-sintered, 19: 18420(R) (BMI-1694(Del.))
UO_2–ZrO_2, properties of, effects of calcia additions on in-pile, 20: 15138 (WAPD-292)
UO_2–ZrO_2, radiation effects, 16: 24616
UO_2–ZrO_2, radiation effects, 17: 3378(R) (BMI-1583(Del.))
UO_2–ZrO_2, radiation effects, 17: 6752 (WAPD-264)
UO_2–ZrO_2, radiation effects on phase changes in, 17: 6753 (WAPD-T-1402)
UO_2–ZrO_2, radiation effects on, at high burnup, 17: 11270 (WAPD-T-1455)
UO_2–ZrO_2, radiation effects on calcia-stabilized, at high burnups, 18: 2157(R) (BMI-1644(Del.))
UO_2–ZrO_2, radiation effects on, 18: 20450(R) (BMI-1661(Del.))
UO_2–ZrO_2, radiation effects on, relations with reactor safety, 18: 44268
UO_2–ZrO_2, radiation effects on calcia-stabilized, at high burnup, 19: 2716(R) (BMI-1681(Del.))

UO_3–ZrO_2, radiation effects on thermal conductivity of nickel-clad, 19: 11679
UO_3–ZrO_2, radiation effects on Hastelloy-X-clad, at high temperatures, 19: 18420(R) (BMI-1694(Del.))
UO_3–ZrO_2, radiation effects on calcia-stabilized, 19: 18421(R) (BMI-1697(Del.))
UO_3–ZrO_2, radiation effects on Hastelloy-X-clad, at high temperatures, 19: 18421(R) (BMI-1697(Del.))
UO_3–ZrO_2, radiation effects on calcia-stabilized, at high burnups, 19: 18420(R) (BMI-1694(Del.))
UO_2–ZrO_2, radiation effects on calcia-stabilized, at high burnup, 19: 22864(R) (BMI-1704)
UO_2–ZrO_2, radiation effects at high burnup, 19: 22865(R) (BMI-1711 (Del.))
UO_2–ZrO_2, radiation effects on Hastelloy X-clad, 19: 22865(R) (BMI-1711(Del.))
UO_2–ZrO_2, radiation effects on microstructure, 19: 25044(R) (CEND-2936-222)
UO_2–ZrO_2, radiation effects on coated particulate in loop tests, 19: 31556(R) (WAPD-MRP-112)
UO_2–ZrO_2, radiation effects on calcia-stabilized, at high burnups, 19: 30642(R) (BMI-1707(Del.))
UO_2–ZrO_2, radiation effects on calcia-stabilized, at high burnups, 19: 39091(R) (BMI-1723(Del.))
UO_2–ZrO_2, radiation effects on clad, 19: 39091(R) (BMI-1723(Del.))
UO_2–ZrO_2, radiation effects on stainless steel clad calcia-stabilized, 19: 42801(R) (BMI-1721(Del.))
UO_2–ZrO_2, radiation effects on fibrous fissiochemical fuels of, 19: 46324(R) (AGN-8132)
UO_2–ZrO_2, radiation effects on stability of, 19: 46912(R) (BMI-1727 (Del.))
UO_2–ZrO_2, radiation effects on calcia-stabilized, at high burnups, 19: 46913(R) (BMI-1733(Del.))
UO_2–ZrO_2, radiation effects on calcia-stabilized at high burnup, 19: 46912(R) (BMI-1727(Del.))
UO_3–ZrO_2, radiation effects on fibrous fissiochemical fuels of, 19: 46324(R) (AGN-8132)
UO_2–ZrO_2, radiation stability of, 20: 7627(R) (BMI-1745, Sect. U)
UO_2–ZrO_2, radiation effects on plates of, in-pile, 20: 16089(R) (WAPD-MRP-114)
UO_2–ZrO_2, radiation effects on densification and homogenization of, neutron, 20: 21432 (WAPD-301)
UO_2–ZrO_2, radiation effects on, effects of density, fissioning rate, and temperature on thermal-neutron, 20: 23778 (WAPD-TM-455)
UO_2–ZrO_2, radiation effects on clad boron carbide-poisoned, 20: 33942 (IDO-17157)
UO_2–ZrO_2, radiation effects on calcia-stabilized clad, 20: 37168(R) (BMI-1771)
UO_2–ZrO_2, radiation effects on calcia-stabilized clad, 20: 37169(R) (BMI-1774)
UO_2–ZrO_2, radiation effects on stability of, at high temperatures, 20: 46221 (BMI-1782)
UO_2–ZrO_2, radioinduced homogenization of two-phase mixtures of, 20: 13330
UO_2–ZrO_2, radiolysis in fissiochemical loop, 19: 46324(R) (AGN-8132)
UO_3–ZrO_2, reactions in fuel elements of, 19: 2841
UO_3–ZrO_2, reactivity worth of transverse gaps in, 18: 3094 (CONF-187-12)
UO_2–ZrO_2, sintering of, boron and iron volatilization by, 20: 33847 (WAPD-TM-582)
UO_2–ZrO_2, solubility in hydrofluoric acid, 19: 22429
UO_3–ZrO_2, temperature measurements during irradiation tests, 17: 35251(R) (BMI-1632(Del.))
UO_2–ZrO_2, testing as reactor fuels, 20: 29616(R) (BMI-1738)
UO_3–ZrO_2, thermal conductivity and expansion of, at 20 to 1000°C, 18: 2157(R) (BMI-1644(Del.))
UO_3–ZrO_2, thermal conductivity, 18: 13354(R) (BMI-1657(Del.))
UO_3–ZrO_2, thermal conductivity at 100 to 1000°C, 18: 15664(R) (BMI-1655(Del.))
UO_3–ZrO_2, thermal conductivity at high fission depletion, effective in-pile, 18: 26073 (WAPD-246)
UO_3–ZrO_2, thermal conductivity at 0 to 2600°C, calculations of, 18: 44140 (KAPL-M-6184)
UO_2–ZrO_2, thermal conductivity, 19: 22864(R) (BMI-1704)
UO_2–ZrO_2, thermal conductivity to 2200°C, 19: 25044(R) (CEND-2936-222)
UO_2–ZrO_2, thermal conductivity at high temperatures, 19: 42801(R) (BMI-1721(Del.))
UO_2–ZrO_2, thermal conductivity of aluminum-clad plates of, 20: 43811(R) (BNWL-269, pp 1.1-28)
UO_3–ZrO_2, thermal cycling stability, 18: 7985(R) (BMI-1650(Del.))
UO_2–ZrO_2, thermal properties, 19: 22865(R) (BMI-1711(Del.))
UO_2–ZrO_2, thermal stability, 19: 25044(R) (CEND-2936-222)
UO_x–ZrO_2, vaporization of, species produced by, 20: 43901(R) (NBS-D-154)
UO_3–ZrO_2, wet techniques in fabrication of, 17: 13685 (WAPD-BT-27(p.21-36))
V–ZrO_2, thermal shock resistance of, 20: 33901
W–ZrO_2, development of ductile sheet, 17: 3437(R) (AD-277459)
W–ZrO_2, ductility at low temperatures, 18: 28028
W–ZrO_2, extrusion of, elongation and microstructure from, 20: 27510
W–ZrO_2, fabrication, 20: 29689
W–ZrO_2, mechanical properties of, above 2500°F, 16: 3478 (WADD-TR-60-37(Pt.II))
Yb_2O_3–ZrO_2, crystal structure, differential thermal analysis, and thermal expansion of, 18: 23503
Yb_2O_3–ZrO_2, electric conductivity, 19: 37094
Yb_2O_3–ZrO_2, phase studies, 19: 42464
Yb_2O_3–ZrO_2, phase transformations in, fluorite, 19: 358(T) (ORNL-tr-201)
$YCrO_3$–ZrO_2, ceramic properties, 17: 14801(R) (AD-278452)
YO_3–ZrO_2, analysis for zirconium by precipitation using cupferron, 18: 25277
Y_2O_3–ZrO_2, crystal structure, evolution, 16: 2224
Y_2O_3–ZrO_2, crystal structure and properties at 1700 to 1750°C, 18: 556
Y_2O_3–ZrO_2, electric and ionic conductivities, 19: 34194
Y_2O_3–ZrO_2, electric conductivity at 1000 to 2400°K, 19: 25005
Y_2O_3–ZrO_2, electric conductivity, 19: 37094
Y_2O_3–ZrO_2, electric conductivity at 850 to 1300°C, 19: 42470
Y_2O_3–ZrO_2, electric current passage through, at 1300°C, zirconium nitride production in, 19: 42470
Y_2O_3–ZrO_2, formation and properties of solid solutions of, 17: 34453
Y_2O_3–ZrO_2, phase equilibria in air at high temperatures, 20: 43901(R) (NBS-D-154)
Y_2O_3–ZrO_2, phase studies, 17: 25792
Y_2O_3–ZrO_2, phase studies, 17: 32653
Y_2O_3–ZrO_2, phase studies and structure, 16: 28945
Y_2O_3–ZrO_2, phase studies of, after heating in air at 1400 to 1800°C, 20: 43900(R) (NBS-D-150)
Y_2O_3–ZrO_2, phase transformations in, fluorite, 19: 358(T) (ORNL-tr-201)
Y_2O_3–ZrO_2, preparation and properties of, 18: 6822
Y_2O_3–ZrO_2, preparation of dense and homogeneous samples by melting techniques, 20: 798
Y_2O_3–ZrO_2, preparation of sols of, 20: 8958(P)
Y_2O_3–ZrO_2, properties of, x-ray diffraction studies of heat treatment effects on, 16: 15171 (DC-61-3-71)
Y_2O_3–ZrO_2, vacancies in stabilized cubic, Mössbauer study, 19: 36338(R) (NP–15160)
Y_2O_3–ZrO_2, x-ray fluorescence analysis for yttrium, 18: 39135
Zr–ZrO_2, anion vacancy concentration and diffusion coefficients in, at 386°C, 19: 28832
Zr–ZrO_2, phase studies, 16: 4571
Zr–ZrO_2, phase studies, 16: 15204(T) (AEC-tr-5060)
Zr–ZrO_2, thermal conductivity at 24°C, 18: 23817(R) (ANL-6880 (p.72-8))
Zr–ZrO_2, thermal shock resistance of, 20: 33901

ZIRCONIUM OXYACETATES
preparation and properties, 17: 21710

Zirconium Oxychlorides
see Zirconyl Chlorides

Zirconium Oxyfluorides
see Zirconyl Fluorides

ZIRCONIUM OXYNITRIDES
preparation and structure, 17: 18020
preparation, properties, and structure, 20: 10856

Zirconium Oxysulfides
see Zirconyl Sulfides

ZIRCONIUM PERCHLORATES
complexes with pyridine-1-oxide, spectra of bonding in, 18: 17856
reactions with dimethyl sulfoxide, 19: 7419

ZIRCONIUM PEROXIDES
formation, 16: 2999
precipitation from sulfate solutions, 17: 1483

ZIRCONIUM PHOSPHATE SILICATES
sorptive properties for cesium and strontium in gel form, 20: 38994(R) (AE-232)

ZIRCONIUM PHOSPHATES
see also Calcium Zirconium Phosphates
see also Strontium Zirconium Phosphates
cation exchange properties, 16: 20356 (JÜL-32-RC)
effects on elimination of radioisotopes by mice and rats, 20: 38733
effects on ion-exchange resins, tracer studies of, 19: 18073
effects on thallium-204 sorption by gastrointestinal tract, 19: 36117
ion exchange capacity, effect of thermal treatments, 16: 7617(T) (CEA-tr-X-336)
ion exchange properties for hydrogen and sodium, kinetics, 16: 13050
ion exchange properties for elements in nitrate media, 18: 1624

ion exchange properties of crystalline and gelatinous, 18: 10077
ion exchange properties for cesium, potassium, and rubidium, 18: 13757
ion exchange properties for cesium and hydrogen, 18: 13758
ion exchange properties of, effects of acids and hydrolysis on, 18: 33535
ion exchange properties of, 18: 35572
ion exchange properties for cesium and strontium in acidic effluents, 18: 37281 (A/CONF.28/P/772)
ion exchange properties at 18 to 300°C, 18: 43720
ion exchange properties for thorium-228, 19: 34120
ion exchange properties, 16: 16347
ion exchange properties in electrophoretic separation of inorganic ions, 17: 4467
ion exchange properties at high temperatures, 17: 15865
ion exchange properties of, effects of drying temperature on, 17: 28903
ion exchange properties of, in nitrate melts, 17: 27500
ion exchange properties of, effects of heat treatments on, 20: 10957
ion exchange properties for cesium, potassium, rubidium, and sodium, 20: 22863 (CEA-R-2835)
ion exchange properties for xenon oxide in iodate and periodate solutions, 20: 40851
ionic conductivity, 16: 25349
phosphorus-32-labeled colloids of, preparation and use in treatment of chronic leukemia and lymphomas, 18: 8255
precipitation and/or uptake of uranyl ion by, in hydrochloric acid, 18: 33600
preparation and formula determination, 19: 32293
preparation and properties of crystalline and gelatinous, 18: 10077
preparation and properties of, for use as ion exchanger, 20: 22863 (CEA-R-2835)
preparation of granular gels, for ion exchange use, 17: 1373(P)
preparation of granular, for cation exchange use, 20: 3968(P)
preparation of, method of, 17: 12307(P)
properties and stoichiometry as ion exchange material, 20: 18841
properties as cation exchanger, 19: 30334
properties as ion exchange for separation of americium, berkelium, californium, and curium, 20: 29340
properties for separation of iodic acid and xenon oxide, 20: 41054
properties for use as ion exchanges for water purification in Parr Shoals
properties for use as ion exchange material, 19: 32293
Power Reactor, 16: 14612 (CVNA-135)
properties for use as ion exchanger, 20: 16568
properties for use as ion exchanger, 20: 16582
properties of gels of, for use as ion exchangers, 19: 9256
properties of reinforced zirconium oxide bonded, 16: 7920
separation from other fission products by ion exchange, 20: 3871 (EUR-2497.e)
sorptive properties for yttrium and zirconium, 16: 16390
sorptive properties of high-temperature desiccated, for cesium, 16: 17337
sorptive properties, for chromatography of inorganic ions, 16: 23650
sorptive properties for yttrium and zirconium, 16: 32958(T) (KFK-tr-112)
sorptive properties for radioisotopes in water, 17: 10710
sorptive properties for cesium-137, 17: 16139 (AERE-R-4245)
sorptive properties for plutonium, 17: 39178(R) (ORNL-3452(p.1-25))
sorptive properties for thorium, titanium, uranium, and zirconium, 18: 13971
sorptive properties for plutonium in fission product and uranium mixtures, 18: 17950
sorptive properties for lead and uranium, temperature effects on, 18: 17951
sorptive properties for cesium from acid waste solutions, 19: 7613 (BLG-267)
sorptive properties of gels of, for metal ions, effects of dehydration on, 19: 7622
sorptive properties for inorganic ions, (E), 19: 30309
sorptive properties for protactinium, 20: 9044(R) (ORNL-3830, pp 30-68)
sorptive properties for cesium and strontium in gel form, 20: 38994(R) (AE-232)
sorptive properties of, for metals in nitric acid solutions, 20: 45795(R) (ORNL-3945, pp 176-88)
use for enrichment of heavy water, 18: 22405(P)
use in impregnated papers for chromatographic separations of valency states, 17: 1402
Al_2O_3–$AlPO_4$–ZrO_2–$Zr_3(PO_4)_4$, preparation of foam for insulating materials, 20: 39375(P)

ZIRCONIUM PHOSPHIDES
crystal structure, 19: 7945
preparation and high-temperature properties, 16: 12110(R) (TID-14770)
properties, 19: 2802 (NYO-2541-1)
structural transformation at high temperatures, 18: 234
vaporization, 18: 8800(R) (TID-19990(Paper 3))
vaporization behavior, 18: 3430 (TID-19737)

ZIRCONIUM PHTHALOCYANINES
reactions in, Szilard-Chalmers, 20: 26921 (BNL-10208)

Zirconium Potassium Fluorides
see Potassium Zirconium Fluorides

ZIRCONIUM PYROPHOSPHATES
ion exchange properties for iron, plutonium, uranium, and fission products from solutions, 19: 4258(T) (AEC-tr-6227/2(p.73-86))
sorptive properties for scandium and thorium, 18: 17953
structure, 16: 5321

ZIRCONIUM SALICYLATES
preparation of, effects of pH and salicylic acid concentration on, 19: 7379

ZIRCONIUM SALTS
see also Benzenearsonic Acid, Zirconium Salts
see also Mandelic Acid, Zirconium Salts

ZIRCONIUM SELENIDES
crystal structure of $ZrSe_3$, x-ray studies on, 16: 18036 (NP-11457)
structure of trivalent, 19: 25038

ZIRCONIUM SELENITES
precipitation of, and thermal properties, 18: 8388
thermal decomposition, 18: 10056

ZIRCONIUM SILICATES
see also Sodium Zirconium Silicates
see also Zircons
analysis for hafnium and zirconium by EDTA titration, 18: 1556
decomposition of, using potassium fluosilicate, 20: 29201
distribution of thorium and uranium in, 17: 20197(R) (TID-18456)
emissivity, 17: 6675(R) (PWA-2128)
emissivity of flame-sprayed, on stainless steel at 300 to 1000°F, 16: 14358(R) (PWA-2043)
endurance of coating, 17: 6675(R) (PWA-2128)
fabrication and properties of spray-dried and hot-pressed, 19: 13898(R) (RFP-490)
preparation of alkali-metal, 17: 30564(P)
properties as magnetohydrodynamic insulation, 18: 7458 (PWA-2125)
properties for use as insulator-seal combination in thermionic cells, 17: 1916(R) (ARF-2215-6)
properties of flame-sprayed coatings of, for use in space technology, 18: 16521
radiation effects on, 17: 25080(R) (ORNL-3417(p.217-18))
reactions with calcium oxide at 1300°C for 50 hr, 1200°C for 70 hr, or 1100°C for 120 hr, 19: 46267
reactions with molten AMS 5350 steel and Inconel 713C, 20: 16984
separation of zirconium from, 16: 5427(P)
separation of zirconium from, 16: 5428(P)
thermal properties to 5000°F, 16: 18938
thermal properties, 16: 22597 (WADD-TR-60-924)
thermal properties of, at 500 to 5000°F, 17: 16636 (ASD-TDR-62-765)

ZIRCONIUM SILICIDES
coating of, effects of, on oxidation resistance of graphite, 20: 29773
crystal structure of Zr_5Si_3, 20: 11337
electron structure and physical properties of crystals of, 17: 27875
fabrication and properties of, review of, 18: 585
heats of formation, 16: 20394
magnetic susceptibility, 18: 20541
properties of, for use in silicate technology, 18: 7250
thermionic emissions at 1200 to 1900°K, 17: 25812
ZrB_2–$ZrSi_2$, crystal structure of ZrB_2–$ZrSi_2$ phase in, 16: 4175

Zirconium Sodium Fluorides
see Sodium Zirconium Fluorides

Zirconium Sodium Silicates
see Sodium Zirconium Silicates

ZIRCONIUM SULFATES
analysis for silicon by silicomolybdic blue method, 17: 38951
composition and stability, ion exchange analysis, 16: 11681
entropies and heat contents at 273 to 1200°K, 16: 15170 (BM-RI-5964)
hydrolysis, 17: 1446
hydrolysis in sulfuric acid and in water, 18: 31520
preparation, 20: 9065
preparation and properties of, for use in industry, 17: 15989
preparation of basic, 19: 5922(P)
preparation of basic, 19: 30208(P)
reactions with barium and sodium hydroxides, precipitation of zirconium hydroxide in, 16: 13045
refractive indices of solutions, 18: 31520
spectra of hydrates of, effects of mass-radius and hydrogen bonding on infrared, 20: 7057

ZIRCONIUM SULFIDES
see also Barium Zirconium Sulfides
see also Calcium Zirconium Sulfides
see also Strontium Zirconium Sulfides
crystal structure of, 17: 40783
ion exchange properties, 16: 11548(T) (CEA-tr-R-1421)
properties of, magnetic and thermodynamic, 17: 40783

thermal expansion, 20: 23005
thermodynamic properties, 20: 10816(T) (NASA-TT-F-285)

ZIRCONIUM SYSTEMS
fabrication of refractory composites of, method for, 19: 28794
Al–B–C–Cr–Mo–Ni–Ta–W–Zr, corrosion and properties of TAZ-8A, 20: 46166 (NASA-TN-D-3597)
Al–B–Nb–Ti–Zr, fabrication and mechanical properties at 70 to 1650°F, 18: 12538(R) (ARF-B201-27)
Al–B–Zr, phase studies, 19: 44719
Al–C–Cu–H–N–Sn–Ti–V–Zr, mechanical properties of, 19: 46985 (AD-613651)
Al–C–Mo–Ni–Si–U–Zr, preparation and fabrication as refractory fuel material, 18: 34071(P)
Al–C–Ti–Zr, properties for use to 1200°F, 20: 4393 (PWAC-472)
Al–Fe–Mg–Ni–Si–Ti–Zr, coating with aluminum–nickel layers by chemical deposition, 19: 39143(P)
Al–Si–Zr, crystallographic parameters, 17: 18822
Al–Si–Zr, crystallographic parameters, 17: 18822
Al–Si–Zr, phase diagram at 1200°C, 17: 22196
Al–Si–Zr, phase studies, 17: 6729
Al–Si–Zr, phase studies, 17: 18733 (AD-278041L)
Al–Si–Zr, phase studies, 19: 14060
Al–Si–Zr, structure of phases in, 18: 18388
B–Co–Zr, crystal structure, 20: 20685
B–Co–Zr, crystal structure of stoichiometric, 20: 39416
B–Co–Zr, phase studies, 20: 14533
B–Cr–Zr, development for use in rocket nozzle coatings, 17: 13846(R) (NP-12541)
B–Cr–Zr, phase studies, 16: 33496
B–Cu–Zr, crystal structure, 20: 14532
B–C–Zr, crystal structure and phase studies on, 18: 12703
Be–B–Zr, crystal structure of $ZrBe_3$–ZrB_2, 16: 4175
Be–Si–Zr, crystal structure of $ZrBe_3$–$ZrSi_2$, 16: 4175
Be–Si–Zr, properties for high-temperature applications, 17: 543 (WADD-TR-60-889(Pt.II))
B–Fe–Zr, crystal structure, 20: 14532
B–Fe–Zr, phase diagram for, 20: 46199
B–Fe–Zr, phase studies, 16: 33496
B–Mo–Nb–Ti–Zr, mechanical and thermal properties of niobium-base, 20: 43940
B–Nb–Zr, neutron radiation effects on, 17: 465
B–Ni–Zr, crystal structure, 20: 20685
B–Ni–Zr, crystal structure of stoichiometric, 20: 39416
B–Ni–Zr, phase studies, 16: 33496
B–Si–Zr, crystal structure of compound range ZrB_2–$ZrSi_2$ in, 16: 4175
B–Sn–Zr, properties of, as reactor control material, 16: 32120 (TID-16597)
B–U–Zr, analysis for boron by spectrography, 19: 24417
B–U–Zr, expansion coefficients and structure of, 17: 12695
B–U–Zr, neutron multiplication factor of, (E), 20: 22392
B–U–Zr, phase studies, 17: 18733 (AD-278041L)
B–W–Zr, fabrication and mechanical properties of, 19: 46940(R) (NP-15444)
B–W–Zr, phase studies at 1400°C, 16: 6732
B–Zr, neutron radiation effects on, 17: 465
B–Zr, phase studies, 18: 35939(R) (NP-14192)
B–Zr, preparation, properties, and uses of, review on, 16: 27640(T) (FTD-TT-62-430)
B–Zr, production of, by sintering at 470 to 1150°C, 17: 32497
B–Zr, properties of, as reactor control material, 16: 32120 (TID-16597)
C–Ce–Zr, phase studies, 19: 16130
C–Co–Ti–W–Zr, development and tensile properties of cobalt-base, 20: 21237 (N-65-29395)
C–Co–Zr, phase studies, 20: 17086
C–Cr–Co–Re–Ti–W–Zr, development and tensile and stress-rupture properties of cobalt-base, 20: 21237 (N-65-29395)
C–Cr–Co–Ti–W–Zr, development and tensile and stress-rupture properties of cobalt-base, 20: 21237 (N-65-29395)
C–Cr–Co–Ti–W–Zr, properties for aerospace uses at high temperatures, 18: 42035
C–Cr–Zr, phase studies, 19: 23067
C–Cr–Zr, phase studies, 20: 31669
C–Ge–Zr, crystal structure and phase studies on, 18: 10561
C–Hf–Mo–N–Re–Ta–W–Zr, creep properties at 2400°F, 19: 18401(R) (WANL-PR(Q)-005)
C–Hf–Mo–N–Re–Ta–W–Zr, development of dispersion-strengthened tantalum-base, 20: 21240(R) (WANL-PR-(Q)-006)
C–Hf–Mo–N–Re–Ta–W–Zr, effects of heat treatment on hardness of, 19: 18401(R) (WANL-PR(Q)-005)
C–Hf–Mo–N–Ta–W–Zr, effects of heat treatment on hardness of, 19: 18401(R) (WANL-PR(Q)-005)
C–H–Zr, formation of ternary compounds in, 18: 39821 (IS-875)
C–H–Zr, preparation of stoichiometric, 19: 12865(R) (NAA-SR-10501)
C–In–Zr, superconductivity of Zr_2InC, 20: 6228
C–Mo–Nb–Ta–Ti–W–Zr, creep properties at 1800 to 2200°F of Cb132M, 20: 2333(R) (NASA-CR-54457)
C–Mo–Nb–Ta–W–Zr, erosion by sodium at 400, 1000, and 1500°F of Cb-132M, 20: 769(R) (NASA-CR-54459)
C–Mo–Nb–Ta–W–Zr, extrusion parameters for Cb-132M, 20: 21263(R) (NASA-CR-54911)
C–Mo–Nb–Ta–W–Zr, preparation and specifications for corrosion loop testing, 20: 4380 (NASA-CR-54761)
C–Mo–Nb–Ta–Zr, thermal-mechanical processing of a precipitation-hardenable, dispersion-hardened, 20: 21250
C–Mo–Nb–Ti–Zr, bend and tensile ductility properties of, 20: 21410
C–Mo–Nb–Ti–Zr, corrosion of PWC-533 by boiling potassium, 19: 34640 (CNLM-6246)
C–Mo–Nb–Ti–Zr, extrusion, heat treatment, and rolling of, 19: 32720(R) (AD-609815)
C–Mo–Nb–Ti–Zr, mechanical and metallurgical properties, 19: 32720(R) (AD-609815)
C–Mo–Nb–Ti–Zr, preparation and properties of castings of, 19: 32720(R) (AD-609815)
C–Mo–Nb–Ti–Zr, yield strength of PWC-533, effects of boiling potassium exposure on, 19: 34640 (CNLM-6246)
C–Mo–Nb–W–Zr, corrosion by potassium at 2000 to 2200°F, 18: 24091
C–Mo–Nb–W–Zr, evaluation of protective coatings for, 20: 29651
C–Mo–Nb–W–Zr, thermal properties, 18: 7201 (ASD-TDR-63-597)
C–Mo–Nb–W–Zr, thermal properties to melting point, 20: 878
C–Mo–Nb–Zr, heat treatment of, 20: 14972(P)
C–Mo–Ti–Zr, crack formation in Mo-3 alloy ingots, effects of molybdenum capping on, 20: 37219
C–Mo–Ti–Zr, creep properties in ultra-high vacuum of TZC, long-time, 19: 37039(R) (NASA-CR-54393)
C–Mo–Ti–Zr, creep properties at 1800 to 2200°F of TZC, 20: 2333(R) (NASA-CR-54457)
C–Mo–Ti–Zr, creep properties of TZC, 20: 29705(R) (NAS-CR-54973)
C–Mo–Ti–Zr, creep testing, fabrication, and properties of, 20: 9501 (UCRL-14437)
C–Mo–Ti–Zr, dispersed phase studies in Mo-TZC, 18: 20512 (ASD-TDR-62-7(Pt.II))
C–Mo–Ti–Zr, dispersion-hardening characteristics in, 18: 27979
C–Mo–Ti–Zr, extrusion of, cast and wrought, evaluation of, 16: 3418(R) (ASD-TR-7-785)
C–Mo–Ti–Zr, extrusion of molybdenum-TZC, 19: 20500 (AFML-TR-64-387)
C–Mo–Ti–Zr, extrusion parameters for TZC, 20: 21263 (NASA-CR-54911)
C–Mo–Ti–Zr, extrusion, heat treatment, and rolling of, 19: 32720(R) (AD-609815)
C–Mo–Ti–Zr, fabrication and properties of arc-cast, 18: 32107 (NP-14128)
C–Mo–Ti–Zr, fabrication and properties of TZC, 20: 43830(R) (NASA-CR-72029)
C–Mo–Ti–Zr, fatigue properties at 1093°C of annealed TZC, notched, 20: 7572(R) (NASA-CR-54775)
C–Mo–Ti–Zr, fatigue properties of TZC, at high temperatures, 20: 31710(R) (NASA-CR-54983)
C–Mo–Ti–Zr, mechanical and metallurgical properties, 19: 32720(R) (AD-609815)
C–Mo–Ti–Zr, mechanical properties at high temperatures, 19: 44674(R) (ANL-7000, pp 69-83)
C–Mo–Ti–Zr, microstructure and tensile properties of, effects of composition, heat treatment, and processing on, 20: 5846
C–Mo–Ti–Zr, preparation and properties of castings of, 19: 32720(R) (AD-609815)
C–Mo–Ti–Zr, preparation and specifications for corrosion loop testing, 20: 4380 (NASA-CR-54761)
C–Mo–Ti–Zr, properties at high temperatures, 20: 29756
C–Mo–Ti–Zr, radiation effects on mechanical and thermal properties of, 18: 41921(R) (GEMP-37A)
C–Mo–Ti–Zr, reduction of gross ingot defects in vacuum arc-melted, 19: 7885
C–Mo–Ti–Zr, stress-rupture properties of TZC, at high temperatures and strain rates, 20: 11265 (AD-626375)
C–Mo–U–Zr, preparation and properties, 19: 36949(R) (BNL-900(p.121-97))
C–Mo–W–Zr, extrusion, heat treatment, and rolling of, 19: 32720(R) (AD-609815)
C–Mo–W–Zr, mechanical properties and preparation, 17: 22150(R) (AD-281728)
C–Mo–W–Zr, mechanical and metallurgical properties, 19: 32720(R) (AD-609815)
C–Mo–W–Zr, preparation and properties of castings of, 19: 32720(R) (AD-609815)
C–Mo–W–Zr, thermal properties, 18: 7201 (ASD-TDR-63-597)

C–Mo–W–Zr, thermal properties to melting point, 20: 878
C–Mo–Zr, fabrication and properties of arc-cast, 18: 32107 (NP-14128)
C–Mo–Zr, phase studies of, 17: 23991
C–Mo–Zr, phase studies, 19: 23066
C–Mo–Zr, phase studies, 20: 31669
C–Nb–O–W–Y–Zr, design for improved fabricability and strength at high temperatures, 20: 25610(P)
C–Nb–Ta–V–Zr, preparation and properties of dispersion strengthened, 17: 16514(R) (ARF-B6007-1)
C–Nb–Ta–Zr, heat treatment of, 20: 14972(P)
C–Nb–Ti–V–Zr, evaluation of properties of, 19: 15995 (IITRI-B231-11)
C–Nb–Ti–V–Zr, mechanical properties, 17: 14809(R) (ARF-B231-8)
C–Nb–Ti–V–Zr, mechanical properties, 17: 41427(R) (IITRI-B231-9)
C–Nb–Ti–V–Zr, mechanical properties and oxidation rate, 19: 32754
C–Nb–Ti–Zr, heat treatment of, 20: 14972(P)
C–Nb–V–Zr, fabrication, 17: 41427(R) (IITRI-B231-9)
C–Nb–V–Zr, hardening by annealing, 17: 41428(R) (IITRI-B6007-4)
C–Nb–V–Zr, heat treatment of, 20: 14972(P)
C–Nb–V–Zr, mechanical properties, 17: 14809(R) (ARF-B231-8)
C–Nb–V–Zr, preparation and properties of dispersion strengthened, 17: 16514(R) (ARF-B6007-1)
C–Nb–W–Y–Zr, corrosion by potassium at 2000 to 2200°F, 18: 24091
C–Nb–W–Y–Zr, corrosion by potassium at 2000°F of AS-55, 20: 768(R) (NASA-CR-54226)
C–Nb–W–Y–Zr, microstructure of AS-55 sheet, 19: 13955(R) (WANL-PR-(P)-005)
C–Nb–W–Y–Zr, properties of AS-55 for containment of alkali metals, 17: 41339 (GE-62FPD365)
C–Nb–W–Y–Zr, tensile properties of D-43Y, effects of welds on, 20: 29712(R) (WANL-PR-(P)-009)
C–Nb–W–Y–Zr, weldability study of AS-55, 19: 24957(R) (WANL-PR(P)-006)
C–Nb–W–Y–Zr, weldability of D-43Y, 20: 13264(R) (WANL-PR(P)-008)
C–Nb–W–Zr, aging and recrystallization of D-43, 20: 4301(R) (ORNL-3870, pp 102-35)
C–Nb–W–Zr, aging characteristics of D-43, 19: 13996 (ORNL-P-1051)
C–Nb–W–Zr, bonding of D-43, method for diffusion, 20: 5867
C–Nb–W–Zr, brazing, equipment and methods for, 18: 27938
C–Nb–W–Zr, coatings on D-43, properties of oxidation-resistant, 19: 26801(R) (AD-607530)
C–Nb–W–Zr, contamination of D-43 by residual gases in high vacuum, 18: 39826 (ORNL-3674)
C–Nb–W–Zr, corrosion by potassium at 2000°F of D-43, 20: 768(R) (NASA-CR-54226)
C–Nb–W–Zr, corrosion of D-43, by potassium, 20: 4301(R) (ORNL-3870, pp 102-35)
C–Nb–W–Zr, corrosion of D-43, by lithium, effects of oxygen on, 20: 4301(R) (ORNL-3870, pp 102-35)
C–Nb–W–Zr, corrosion of D-43, by refluxing potassium at 2000°F, stress, 20: 9424(R) (NASA-CR-54844)
C–Nb–W–Zr, corrosion of D-43, by potassium at 2450°F, stress-, 20: 13191(R) (NASA-CR-54476)
C–Nb–W–Zr, corrosion of D-43, by sodium at high temperatures, 20: 25474(R) (BNL-954, pp 122-67)
C–Nb–W–Zr, creep behavior in ultrahigh vacuum at 2000 and 2200°F, 20: 13256 (NASA-TN-D-3222)
C–Nb–W–Zr, creep properties of D-43, 19: 20474(R) (NASA-CR-54281)
C–Nb–W–Zr, ductility of welds in D-43, effects of aging on bend, 20: 4301(R) (ORNL-3870, pp 102-35)
C–Nb–W–Zr, electric conductivity to 1500°C of D-43, 20: 5851
C–Nb–W–Zr, electric conductivity of D-43, at 80 to 400°K, 20: 23749
C–Nb–W–Zr, emissivity to 1500°C of D-43, total hemispherical, 20: 5851
C–Nb–W–Zr, evaluation of protective coatings for, 20: 29651
C–Nb–W–Zr, evaporation losses in high vacuum of D-43, 20: 4301(R) (ORNL-3870, pp 102-35)
C–Nb–W–Zr, extrusion of tubing from, optimization studies, 17: 11140(R) (AMC-TR-7-775(VII))
C–Nb–W–Zr, extrusion of tubes of, 17: 23895(R) (AD-403514)
C–Nb–W–Zr, fabricability, strength, and weldability of, 20: 29763
C–Nb–W–Zr, fabrication into H sections, 18: 7163(R) (NP-13410)
C–Nb–W–Zr, fabrication and properties of sheet, 18: 10497 (RTD-TDR-63-4236)
C–Nb–W–Zr, fabrication by double electrode process, 18: 12562(R) (X63-12299)
C–Nb–W–Zr, fabrication and properties of D-43 strip and foil, 19: 24946 (ASD-TDR-63-829(Pt.II))
C–Nb–W–Zr, fabrication and properties at –325 to 3000°F, 19: 39224(P)
C–Nb–W–Zr, fabrication and mechanical properties of, 19: 46940(R) (NP-15444)
C–Nb–W–Zr, heat treatment of, 20: 14972(P)
C–Nb–W–Zr, mechanical properties of D-43, effects of protective coatings and welding on, 20: 5866
C–Nb–W–Zr, microstructure of D-43, effects of aging on, 20: 17023 (ORNL-TM-1161, pp 208-24)
C–Nb–W–Zr, oxidation and mechanical properties of coated X-110, 17: 39525(R) (AD-416459)
C–Nb–W–Zr, oxidation protection of D-43 by chromium–silicon–titanium coatings at 2000 to 2700°C, 18: 30127 (ASD-TDR-62-934(Pt.II))
C–Nb–W–Zr, preparation and specifications for corrosion loop testing, 20: 4380 (NASA-CR-54761)
C–Nb–W–Zr, properties as space reactor fuel cladding, 18: 9713 (CONF-375-3)
C–Nb–W–Zr, properties of welds in D-43, 19: 40989
C–Nb–W–Zr, properties as hollow turbine vanes, 20: 16963
C–Nb–W–Zr, properties at very high temperatures, 20: 21412
C–Nb–W–Zr, properties of D-43 as bore seal material, 20: 46145 (NASA-CR-54093)
C–Nb–W–Zr, radiation effects on bend properties of D-43, neutron, 18: 32226 (ORNL-TM-880)
C–Nb–W–Zr, rolling of foils of D-43, 19: 7871(R) (AD-422001)
C–Nb–W–Zr, specifications of D-43, for use in corrosion test loop fabrication, 20: 21293 (R-66SD3007)
C–Nb–W–Zr, stress corrosion of D-43 by refluxing potassium, research program on, 19: 20474(R) (NASA-CR-54281)
C–Nb–W–Zr, stress corrosion of D-43 by boiling potassium, research program on, 19: 40970(R) (NASA-CR-54390)
C–Nb–W–Zr, stress-rupture properties of D-43, 19: 40961
C–Nb–W–Zr, tensile properties of welded plates of D-43, 20: 4301(R) (ORNL-3870, pp 102-35)
C–Nb–W–Zr, tensile properties of D-43, 20: 15068
C–Nb–W–Zr, tensile properties of D-43, effects of welds on, 20: 29712(R) (WANL-PR-(P)-009)
C–Nb–W–Zr, tensile properties of D-43, effects of brittle coatings on, 20: 37276
C–Nb–W–Zr, tensile strength of X-110, at 1100 to 1500°C, 17: 30950(R) (NMI-2117)
C–Nb–W–Zr, thermal conductivity of D-43, at 30 to 120°C, 20: 4301(R) (ORNL-3870, pp 102-35)
C–Nb–W–Zr, thermal expansion of D-43, at 80 to 400°K, 20: 23749
C–Nb–W–Zr, thermal properties, 18: 7201 (ASD-TDR-63-597)
C–Nb–W–Zr, weld bend tests of D-43, 19: 13955(R) (WANL-PR-(P)-005)
C–Nb–W–Zr, weld stability in D-43, 20: 5866
C–Nb–W–Zr, weldability study of D-43, 19: 24957(R) (WANL-PR(P)-006)
C–Nb–W–Zr, weldability studies of D-43, 19: 46966(R) (WANL-PR(P)-007)
C–Nb–W–Zr, welding parameters for D-43, electron-beam, 20: 5867
C–Nb–W–Zr, welds in D-43, thermal stability of, 20: 27467
C–Nb–Zr, corrosion of PWC-11 by boiling potassium, 19: 34640 (CNLM-6246)
C–Nb–Zr, corrosion by lithium in niobium–1-zirconium alloy forced-convection loop, 20: 5853 (TIM-898)
C–Nb–Zr, corrosion by potassium at 1070°C, 20: 7518 (PWAC-501)
C–Nb–Zr, development of, with high-temperature strength, 19: 44605 (PWAC-464)
C–Nb–Zr, phase diagrams, 20: 13272
C–Nb–Zr, phase diagrams, 20: 39434
C–Nb–Zr, phase studies on, 18: 34211
C–Nb–Zr, phase studies at 1092 and 1538°C, 20: 4392 (PWAC-461)
C–Nb–Zr, thermal properties to melting point, 20: 878
C–Nb–Zr, x-ray diffraction of nonmetallic phases chemically extracted from, 19: 7973
C–Nb–Zr, yield strength of PWC-11, effects of boiling potassium exposure on, 19: 34640 (CNLM-6246)
C–Ni–Nb–Ti–Zr, creep properties in ultra-high vacuum of AS-30, long-time, 19: 37039(R) (NASA-CR-54393)
C–Ni–Zr, phase studies of nickel-rich, 20: 826 (NP-15535)
Co–O–Zr, phase studies, 16: 547
C–O–Zr, phase studies, 20: 37264
C–Pb–Zr, crystal structure of Zr_3PbC compound in, 18: 36014
C–Pu–U–Zr, fabrication, properties, and structure of, 20: 46156
Cr–HBF_4–HF–HNO_3–Zr, solvent properties for uranium–zirconium alloy, 17: 10246(R) (ORNL-TM-403)
Cr–HBF_4–HNO_3–Zr, corrosive effects of, on pre- and de-filmed titanium, 17: 35618(R) (ORNL-TM-545)
Cr–O–Zr, phase studies at 1200, 1500, and 1700°C, 19: 16149
Cr–O–Zr, phase studies, 20: 11227
Cr–Si–U–Zr, fatigue tests on compression and tension of, 18: 36021
Cr–Te–Zr, corrosion of, in 680°F water, 17: 16582 (ARF-B198-36)
Cr–Te–Zr, corrosion by water at 680°F, 17: 30905(R) (ARF-B198-42)
Cr–Te–Zr, corrosion and mechanical properties, 17: 34347(R) (IITRI-B198-43)
Cr–Te–Zr, oxidation by steam at 750 and 900°F and water at 680°F, hydrogen absorption from, 18: 2162(R) (IITRI-B198-46)
Cr–Te–Zr, tensile properties at 68 and 680°F, 17: 30905(R) (ARF-

B198-42)
Cr–Te–Zr, tensile properties at 70 and 680°F, 18: 2162(R) (IITRI-B198-46)
C–Ru–Zr, structure of filled Ti_2Ni type compounds in, 19: 37107
C–Sn–Zr, crystal structure and phase studies, 18: 12706
C–Ta–V–Zr, coating for oxidation protection, 19: 20459(R) (IITRI-B6019-6)
C–Ta–W–Zr, yield strength at 2400 to 3000°F, 20: 25612(P)
C–Ta–Zr, phase studies, 20: 37270
C–Ta–Zr, thermionic emission properties of, 17: 37532
C–Th–U–Zr, mechanical properties and phase studies at high temperatures, 17: 12660 (ATL-A-128)
C–Th–Zr, crystal structure of, 17: 39645
C–Th–Zr, phase studies at 1100 to 1550°C, 17: 34448
C–Th–Zr, structure, 18: 621
C–Ti–W–Zr, fabrication by double electrode process, 18: 12562(R) (X63-12299)
C–Ti–Zr, tensile properties at room temperature, 18: 18380
C–Tl–Zr, crystal structure of Zr_2TlC compound in, 18: 36014
Cu–P–Zr, oxidation by carbon dioxide up to 600°C, 18: 30192
C–U–Zr, diffusion phenomena in sintered pyrographite-coated, 18: 14520
C–U–Zr, fabrication by high-intensity arc process, 17: 36208
C–U–Zr, fabrication and physical properties, 20: 9400
C–U–Zr, fabrication, properties, and structure of, 20: 46156
C–U–Zr, phase diagram, 18: 44116
C–U–Zr, phase studies, 18: 25269(R) (NLCO-905)
C–U–Zr, phase transformations in, thermodynamics of, 17: 22205
C–U–Zr, phase transformations in, thermodynamics of, 18: 44161(T) (AERE-Trans-1009)
C–U–Zr, properties as thermionic converter, 20: 9400
C–U–Zr, radiation effects on coated fuel particles of, fast-neutron and fission fragment, 20: 9596
C–U–Zr, reactions with niobium, tantalum, and tungsten, 20: 9400
C–U–Zr, vapor pressures to 10,000°R, 20: 8884 (NASA-CR-353)
C–U–Zr, vaporization characteristics at 9,000 and 10,000°R of liquid, calculations, 20: 45626 (NASA-CR-591)
C–W–Zr, fabrication and mechanical properties of, 19: 46940(R) (NP-15444)
C–W–Zr, mechanical properties and preparation, 17: 22150(R) (AD-281728)
C–W–Zr, phase diagrams, 19: 23063
C–W–Zr, phase studies at 1500°C, 19: 37119
C–W–Zr, phase studies, 20: 31669
C–W–Zr, strength at 1650°C and ductility at low temperatures, 20: 25613(P)
C–Zn–Zr, structure of filled Ti_2Ni type compounds in, 19: 37107
C–Zr, fabrication of hypereutectic composites of, with high thermal shock resistance, 20: 29727
C–Zr, phase studies, 16: 24798(R) (WADD-TR-60-143(Pt.III))
C–Zr, phase studies at 3125 to 3150°K, 17: 28828(R) (TID-18951)
C–Zr, phase studies, 19: 30772
C–Zr, preparation, properties, and uses of, review on, 16: 27640(T) (FTD-TT-62-430)
C–Zr, preparation and properties of alloys of, 20: 41471
C–Zr, thermodynamic properties of defect compounds of, models for, (T), 20: 26818 (LA-3481)
D–Zr, deuterium solubility in, 18: 4277
D–Zr, phase studies, 17: 32580
D–Zr, preparation for neutron-generator targets, 18: 18860
Fe–O–Ti–Zr, fabrication and properties of sintered, deformable, 20: 17003
Fe–Te–Zr, oxidation by steam at 750°F, 18: 2162(R) (IITRI-B198-46)
graphite–Zr, properties for aerospace applications, 19: 37144
graphite–Zr, properties of, effects of graphite source material on, 20: 33876(R) (N-66-17087)
HfC–Zr, solidus at 1760°C, 19: 44612(R) (USBM-RC-1199)
Hf–H–Zr, decomposition pressure hysteresis in, 18: 44204
Hf–H–Zr, phase diagrams, 20: 31667
Hf–H–Zr, phase studies, 19: 26776
Hf–H–Zr, phase studies, 19: 26777
Hf–N–Re–Ta–W–Zr, hardness at room temperature, 19: 18401(R) (WANL-PR(Q)-005)
H–Nb–Zr, phase studies, 20: 11225
H–Ni–Zr, crystal structure of compound $NiZrH_3$ in, 16: 10570
HNO_3–Zr, corrosive effects of, on titanium, inhibition by chromium(VI)–hydrofluoric acid solutions of, 16: 16464
H_2O–Zr, fission neutron ages to indium resonance in, 18: 28555
H_2O–Zr, fission-neutron age-to-indium resonance in, 18: 44708 (NAA-SR-Memo-9965)
H_2O–Zr, gamma heating in, calculations for, (E/T), 20: 6517 (CONF-651101-41)
H_2O–Zr, neutron age in, moments calculations of, 16: 22977
H_2O–Zr, neutron age-to-indium resonance in, fission, 18: 40476 (NAA-SR-9503)
H_2O–Zr, neutron age and higher moments in, 19: 10675(R) (NAA-SR-9999)
H_2O–Zr, neutron ages in, 20: 10272(R) (NAA-SR-9339)
H_2O–Zr, reaction thermodynamics, 16: 12843
H_2O–Zr, reactivity calculations for uranium-235-containing, 16: 28421 (WAPD-BT-25(p.87-94))
H–O–Zr, tensile properties, 19: 16172
H–Ti–Zr, phase studies, 17: 12264
H–U–Zr, corrosion and reaction rates in chloride volatility processing of, 18: 39386
H–U–Zr, preparation and properties for use as reactor moderator, 18: 14394
H–U–Zr, thermal migration of hydrogen in, 18: 7228
H–Zr, calculations of integral and partial thermodynamic functions for, 17: 10607 (UCRL-10189)
H–Zr, enthalpy data for, 17: 20023
H–Zr, metallographic structure, 16: 10547(T) (APEX-614)
H–Zr, origin and propagation of microcracks in crystals of, 17: 18790
H–Zr, phase diagram for, at high hydrogen content, composition-pressure isotherms in, at 500 to 850°C, 16: 16754
H–Zr, phase diagrams, 17: 6649 (DC-61-7-26)
H–Zr, phase structure of, effects of hydrogen content and heat treatment on gamma, 16: 27670
H–Zr, phase studies, 16: 21072
H–Zr, phase studies of, 17: 4939
H–Zr, phase studies, 17: 8864
H–Zr, phase studies, 18: 2236(T,R) (EURAEC-607)
H–Zr, phase studies and thermal properties, 18: 13776
H–Zr, phase studies, 18: 27961 (NAA-SR-9374)
H–Zr, phase studies, 20: 7520
H–Zr, phase studies of, by x-ray diffraction, 20: 45688
H–Zr, precipitation in, electron microscope studies of, 16: 33421
H–Zr, precipitation strengthening in crystals of, containing oxygen as impurity, 19: 6311
H–Zr, preparation of crack-free specimens of, 17: 4940
H–Zr, preparation of, for transmission electron microscopy, hydrogen concentration in electrothinning procedures for, 20: 31691
H–Zr, properties, 16: 12104(R) (LAR-10)
H–Zr, properties, 16: 13572 (DC-56-9-130)
H–Zr, properties of solid solutions of, 18: 41916 (AD-604409)
H–Zr, thermal migration of hydrogen in, 18: 7228
H–Zr, thermal stability, 17: 11817
H–Zr, thermodynamic properties of solid solutions of, models for, (T), 20: 26818 (LA-3481)
H–Zr, thermophysical properties of, 17: 4940
Li–O–Zr, equilibrium distribution of oxygen in, at 500 to 800°C, 18: 4253(R) (ORNL-3470(p.63-6))
MoC–Ta–Zr, preparation and properties of dispersion-hardened, 20: 39441(P)
Mo–Nb–N–Zr, heat treatment of, 20: 14972(P)
Mo–Nb–O–Zr, heat treatment of, 20: 14972(P)
Mo–N–Re–Ta–W–Zr, effects of heat treatment on hardness of, 19: 18401(R) (WANL-PR(Q)-005)
Mo–O–Ti–Zr, phase studies, 16: 25826
Mo–Te–Zr, oxidation by steam at 900°F, 18: 2162(R) (IITRI-B198-46)
Nb–N–Ta–Zr, heat treatment of, 20: 14972(P)
Nb–N–Ti–Zr, heat treatment of, 20: 14972(P)
Nb–N–V–Zr, heat treatment of, 20: 14972(P)
Nb–N–W–Zr, heat treatment of, 20: 14972(P)
Nb–N–Zr, equilibrium solid solutions at 1200 to 1800°C in, 20: 2337 (ORNL-P-1677)
Nb–O–Ta–Zr, heat treatment of, 20: 14972(P)
Nb–O–Ti–Zr, heat treatment of, 20: 14972(P)
Nb–O–Ti–Zr, phase diagram at 1500°C, 16: 13635
Nb–O–V–Zr, heat treatment of, 20: 14972(P)
Nb–O–W–Zr, heat treatment of, 20: 14972(P)
Nb–O–Zr, phase studies, 18: 2163(R) (IS-700(Sect.M))
Nb–O–Zr, phase studies on, 18: 34211
Nb–O–Zr, phase studies, 20: 4297(R) (IS-1200(Sect.M))
Nb–O–Zr, phase studies, 20: 16980
Nb–Te–Zr, corrosion of, in 680°F water, 17: 16582 (ARF-B198-36)
Nb–Te–Zr, corrosion by water at 680°F, 17: 30905(R) (ARF-B198-42)
Nb–Te–Zr, corrosion and mechanical properties, 17: 34347(R) (IITRI-B198-43)
Nb–Te–Zr, oxidation by steam at 750 and 900°F and water at 680°F, hydrogen absorption from, 18: 2162(R) (IITRI-B198-46)
Nb–Te–Zr, tensile properties at 68 and 680°F, 17: 30905(R) (ARF-B198-42)
Nb–Te–Zr, tensile properties at 70 and 680°F, 18: 2162(R) (IITRI-B198-46)
Ni–O–Zr, phase studies, 16: 547
N–Re–Ta–W–Zr, creep properties at 2400°F, 19: 18401(R) (WANL-

PR(Q)-005)
N–Ru–Zr, structure of filled Ti_2Ni type compounds in, 19: 37107
N–Ta–W–Zr, effects of heat treatment on hardness of, 19: 18401(R) (WANL-PR(Q)-005)
N–Ti–Zr, tensile properties at room temperature, 18: 18380
N–Zn–Zr, structure of filled Ti_2Ni type compounds in, 19: 37107
Nb–N–Zr, properties of equilibrium solid solutions in, mechanical and thermodynamic, 19: 13991 (ML-TDR-64-134)
Nb–O–Zr, phase studies, 19: 9604(R) (IS-900(Sect.M))
N–Zr, preparation, properties, and uses of, review on, 16: 27640(T) (FTD-TT-62-430)
N–Zr, superconductivity, 17: 41604
O–K–Zr, equilibrium distribution of oxygen in, at 500 to 800°C, 18: 4253(R) (ORNL-3470(p.63-6))
O–K–Zr, phase studies, 19: 41031
O–Na–Zr, equilibrium distribution of oxygen in, at 500 to 800°C, 18: 4253(R) (ORNL-3470(p.63-6))
O–Ru–Zr, structure of filled Ti_2Ni type compounds in, 19: 37107
O–Si–Ti–W–Zr, development of, for protection of tungsten against oxidation at high temperatures, 17: 14837(R) (NP-12595)
O–Si–Ti–W–Zr, development for high-temperature oxidation protection of tungsten, 18: 565(R) (NP-13243)
O–Si–Ti–W–Zr, development for high-temperature oxidation protection of tungsten, 18: 24086(R) (NP-13898)
O–Si–Ti–W–Zr, oxidation resistance of, testing as tungsten coating, 17: 6519(R) (NP-12293)
O–Ta–Ti–Zr, phase studies, 18: 26053
O–Ta–Ti–Zr, phase studies at 1500°C, 20: 5846
O–Ti–Zr, oxygen long-range ordering in, 17: 37801
O–Ti–Zr, phase studies, 17: 36287 (ARL-63-104)
O–Ti–Zr, tensile properties at room temperature, 18: 18380
O–Zr, crystal structure of, ligand field theory of, 17: 27817
O–Zr, crystal structure of, ligand field theory of, 18: 14487
O–Zr, electric conductivity of, at room temperature to 2030°K, 16: 4570
O–Zr, electron energy bands in crystals of, 18: 33543
O–Zr, hardness of solid solutions in, 20: 27505
O–Zr, hydrogen solubility in, 18: 4276
O–Zr, mechanical properties, 18: 30226
O–Zr, oxidation of, at 800°C, 16: 10466
O–Zr, thermodynamic properties of oxygen in, 16: 25384
O–Zr, thermodynamic properties of, 17: 6111
paraffin–U–Zr, neutron spectra in, 19: 23596(R) (RPI-328-20(p.1-8))
PuO_2–Zr, fabrication of, 17: 19575 (HW-75007(Paper 22))
PuO_2–Zr, preparation, 17: 31681(R) (HW-76559)
Sb–Te–Zr, corrosion of, in 680°F water, 17: 16582 (ARF-B198-36)
Sb–Te–Zr, corrosion by water at 680°F, 17: 30905(R) (ARF-B198-42)
Sb–Te–Zr, oxidation by water at 680°F, 18: 2162(R) (IITRI-B198-46)
Si–Ti–W–Zr, properties as protective coatings for tungsten at high temperatures, 19: 13888 (ML-TDR-64-227)
Si–Ti–Zr, tensile properties at room temperature, 18: 18380
Si–U–Zr, phase studies of uranium-rich, 16: 2257
Si–Zr, atomic number effects correction in electron probe microanalysis of, 17: 27268
Si–Zr, combustibility temperature of, 19: 37093
Si–Zr, combustion diagram of, 18: 39935
Si–Zr, phase studies, 19: 14060
Si–Zr, preparation, 16: 20980(T,R) (EURAEC-26)
Si–Zr, preparation, properties, and uses of, review on, 16: 27640(T) (FTD-TT-62-430)
S–Zr, stability and thermodynamics of, 18: 26065
Ta–ThO_2–W–Zr, development of oxidation-resistant, 20: 19193
Ta–WC–Zr, preparation and properties of dispersion-hardened, 20: 39441(P)
Te–Sn–Zr, corrosion of, in 680°F water, 17: 16582 (ARF-B198-36)
Te–Sn–Zr, corrosion by water at 680°F, 17: 30905(R) (ARF-B198-42)
Te–Sn–Zr, oxidation by water at 680°F, 18: 2162(R) (IITRI-B198-46)
Te–V–Zr, oxidation by steam at 900°F, 18: 2162(R) (IITRI-B198-46)
Te–Zr, oxidation mechanism, 17: 1883
ThO_2–W–Zr, crystal structure and properties of tungsten-base, 20: 37185
T–Zr, contamination from activity decrease and diffusion of, 19: 28595
T–Zr, efficiency as x-ray spectroscopy source, 20: 2136
T–Zr, fabrication as radiation target, 18: 27813(R) (ORNL-TM-428)
T–Zr, fabrication and uses of targets of, 20: 16916
T–Zr, use as exciting source for x-ray spectra, 18: 28252
T–Zr, use as source in x-ray fluorescence measurement of tin coating thickness, 19: 28742
U–H_2O–Zr, critical bucklings and extrapolation distances for uranium-235, (T), 19: 40159 (WAPD-T-1774)
U–H_2O–Zr, critical bucklings and extrapolation distances for uranium-235, (T), 19: 40159 (WAPD-T-1774)
U–H_2O–Zr, criticality of water-reflected uranium-235, (E/T), 19: 29524
U^{235}–H_2O–Zr, reactivity of, effects of water gaps and uranium-238 on, 17: 41734 (WAPD-T-1483(Rev.))
U–H_2O–Zr, reactivity effect of water-gap spacing and uranium-238 on enriched, 20: 26434
UO_2–H_2O–Zr, neutron parameters for lattice of, 18: 9580 (WAPD-T-1632)
UP–Zr, compatibility, 20: 15032(R) (ANL-7152, pp 50-72)
U–Zr–ZrH_2, properties as rocket reactor fuel, testing of, 18: 21698(R) (ANL-6860)
U-235–H_2O–Zr, critical bucklings and extrapolation distance for, (T), 19: 40159 (WAPD-T-1774)
Zr–ZrC, phase diagram, 20: 19249
Zr–ZrO_2, anion vacancy concentration and diffusion coefficients in, at 386°C, 19: 28832
Zr–ZrO_2, phase studies, 16: 4571
Zr–ZrO_2, phase studies, 16: 15204(T) (AEC-tr-5060)
Zr–ZrO_2, thermal conductivity at 24°C, 18: 23817(R) (ANL-6880 (p.72-8))
Zr–ZrO_2, thermal shock resistance of, 20: 33901

ZIRCONIUM THIOCYANATES

complexes with diantipyrinemethane, formation of, 18: 10131
properties in perchloric acid media, 19: 552
separation from hafnium thiocyanate by solvent extraction using 4-methyl-2-pentanone, 20: 18828
solvent extraction in three phase system using diantipyrilmethan e, 18: 13950
solvent partition between hydrochloric acid and alcohols, esters, ethers, and ketones, 18: 1553
spectra of complexes, infrared, 16: 18872
with ammonium, cesium, potassium, pyridine, and rubidium, properties, 17: 1482

ZIRCONIUM TITANATES

see also Lead Zirconium Titanates
performance as coating in beryllium emissivity tests, 20: 43816(R) (PWA-2877)
reaction with metal oxides at high temperatures, 16: 5352
temperature effects on transducers of, 19: 39270(R) (TID-21894)

ZIRCONIUM TUNGSTATES

cation exchange properties, 16: 20356 (JÜL-32-RC)
ion exchange properties for elements in nitrate media, 18: 1624
ion exchange properties of, effects of acids and hydrolysis on, 18: 33535
ion exchange properties of, 18: 35572
preparation of granular gels, for ion exchange use, 17: 1373(P)
sorptive properties of gels of, for metal ions, effects of dehydration on, 19: 7622

ZIRCONS

see also Zirconium Silicates
age estimation from fission product tracks, (E), 19: 4382
age estimation of, by uranium–lead method, Ontario, Canada, 20: 18929
age estimation of, errors in uranium–lead method of, 19: 38849
age estimation of, radioactivity-uranium content discordance in, 17: 25458
age estimation of, lead diffusion model for discordance in radioactivity-uranium content ratio, 17: 25459
age estimations of, using lead-uranium method, 20: 18924(R) (NYO-1669-11)
age estimation studies, 16: 16577 (TID-14861(Vols.I&II))
age estimation using uranium–lead isotope systems, 17: 30742
age of northeastern Minnesota, estimations of, 20: 4169
age of, in Japanese granites, 20: 43556
age of, La Sal Mountain, Utah, (E), 19: 20178
ages in granodiorite, discordant isotopic, 17: 8422
alpha activity and thorium concentration in, in Conway granite, 18: 20222
analysis for elements and impurities in, 19: 36296
analysis for europium, gadolinium, and niobium, radiospectroscopic, 18: 6756
analysis for hafnium and zirconium using paper chromatography, 17: 7977
analysis for hafnium and hafnium-zirconium ratio, direct-reading emission spectrometric, 18: 39129
analysis for hafnium, activation, 20: 24993
analysis for hafnium, lead, thorium, uranium, and yttrium, x-ray fluorescence, 20: 35666
analysis for lead, thorium, and uranium, x-ray fluorescence, 16: 26923
analysis for lead and uranium, 19: 22567(R) (NYO-1669-10)
analysis for thorium dioxide in Taiwan, by gamma scintillation spectrometry, 18: 21977
analysis for uranium, polarographic, 18: 1572
analysis for uranium, parameters influencing, 20: 43565
analysis for zirconium using *p*-iodoamygdalic acid, gravimetric, 18: 17749
analysis of natural, for impurities, 17: 4716
analysis of, spectroscopic, 19: 43954
conversion into concentrated aqueous zirconium nitrate solutions, 16: 20465(P)
conversion into metal by alkali fusion, 16: 28860
conversion to phosphorus-free zirconia, 18: 1705(P)

defects in, natural annealing of, 18: 35711
emanation by, effects of temperature on, 16: 31981
fission product tracks in, formation and stability of, (E), 19: 20674
formation in silicon oxide–zirconium oxide systems, 18: 42085
gadolinium ion paramagnetic resonance in, 18: 19945
geochemistry of, in Lueshe carbonatite deposit in Congo Republic, 19: 18137 (EUR-2110.e)
growth and doping of single-crystal, 20: 16960
hafnium and zirconium contents, 16: 25629
hafnium content and hafnium–zirconium ratio in, from Southern California batholith, 18: 39483
hardness of crystalline, micro-, 18: 19953
heat of formation, 16: 22613
helium formation in metamict, mechanism of, 16: 33291
history of, lead-207 to uranium-235 ratio for thermal, 17: 23529
lead–thorium and lead–uranium isotopic variations in Arizona, 19: 660
lead-207/-206 ratio in, 20: 41176
lead/uranium ratios in Panamint Range, 18: 33793
niobium EPR in, 18: 9021(T)
origin of, in metasomatic modified basic rocks, 17: 20206
pleochroic halos produced in biotite-cordierite by, reversal, 19: 38846(T) (ORNL-tr-698)
preparation and properties, 19: 42463
preparation, properties, and structure of light-weight refractory, 18: 44206
processing of, pilot plant for, 19: 34266 (AEET-201)
production and uses of, 1965 survey on, 20: 33773
properties and uses of, review of, 18: 6834
properties of fibers of, 17: 1825
radiation damage in, alpha, 20: 17147
radiation effects, 17: 5041(R) (ORNL-3364(p.151-200))
radiation effects on magnetic resonance of, 17: 35792
radiation effects on, neutron, 19: 30828(R) (ORNL-3789(p.230-8))
radioinduced color centers, 16: 13770
ratio of hafnium and zirconium in, from Kazakhstan igneous region, 18: 1894
ratio of hafnium oxide to zirconium oxide in, from Vishnevye and Ilmenskie Mountains, 17: 16275
reactions with alkali carbonates and alkaline earth metals, 16: 33017
reactions with boric acid and carbon, preparation of zirconium diboride by, 19: 30657
separation from liquids in hydrocyclones, 16: 1727 (AAEC/E-65)
separation of silica and zirconium from, 16: 18998(P)
separation of zirconium from, 20: 9065
sorptive properties for strontium, ruthenium, cesium, and cerium, 18: 37288 (A/CONF.28/P/813)
spectra of color centers in metamict, infrared, 16: 33291
spectra of, nature of linear luminescence, 17: 2967
stability of, at 1180 to 1366°C, 20: 5537
tensile strength for machining, effects of PVA binders on, 20: 11277 (RFP-659)
thermal conductivity of, for use above 3000°F, 18: 16520
thermal conductivity and total emissivity of coatings of, 19: 23076
thermonuclear activities in, 17: 4716
thorium and uranium distributions in accessory, from granitic rocks, 19: 32445
uranium-234, uranium-235, and uranium-238 contents and ratios in, 19: 38849

ZIRCONYL CHLORIDES
analysis of, for zirconium, amperometric, conductometric, and potentiometric, 17: 23283
chemical behavior in aqueous solutions, 17: 6097
chemical behavior in aqueous solutions, 17: 35839
chemistry of zirconium in aqueous solutions of, 17: 14247
polymerization in acid solutions, light-scattering study of, 16: 32976
preparation and uses, 19: 38647
preparation of hydrate of, 20: 9065
purification by zone melting, 18: 544 (CEA-2310)
radiation effects on decomposition of octahydrate of, gamma, 18: 12138 (BM-RI-6382)
reactions of, with dicarboxylic acids, precipitate formations in, 17: 20014
reactions with alkali metal ferrocyanides in acid solutions, 16: 18913
reactions with ammonium carbonates, 18: 5304
reactions with iminodiacetic acid, 19: 5910
reactions with neutral salts, effects on pH of dialyzed, 17: 35718
reactions with oxalates or oxalic acid, 17: 28836(T) (SCL-T-486)
reactions with sodium hydroxide, precipitation of zirconium hydroxide in, 16: 13045
reactions with sulfates and sulfuric acid, 16: 5334
titration with potassium ferrocyanide, amperometric, 18: 6768
$CaCl_2$–H_2O–$ZrOCl_2$, solubility in hydrochloric acid at 25°C, 18: 1682
catechol–H_2O–$ZrOCl_2$, chelate formation in adiabatic compressibility and ultrasonic studies of, 20: 45666

ZIRCONYL FLUORIDES
crystal structure, 17: 25060(R) (ORNL-3417(p.3-16))
hydrolysis products, composition, 16: 25326(T) (AEC-tr-5117)
preparation and properties, 16: 178
preparation and properties, 16: 17641(T) (AEC-tr-5087)
preparation and properties, 16: 17554(R) (ORNL-3262(p.3-18))
preparation and properties, 16: 18869

ZIRCONYL IONS
behavior in solutions, 16: 18914
determination using 5,5'-thiodisalicylic acid, gravimetric, 19: 19812
radioprotective effects in mice, 18: 13567
toxicity of, in mouse, determination by LD_{50} on thirtieth day of, 17: 17719

ZIRCONYL NITRATES
behavior in aqueous solutions and organic solvents, 16: 2935
calcination in sulfur at 150°C, 17: 19697 (DP-713)
catalytic effects on hydrolysis of salicyl phosphate, 16: 28949
chemical behavior in aqueous solutions, 17: 6097
conversion to zirconium oxides, process for, 19: 36434(P)
production of anhydrous, from tetraiodide–nitrogen oxide reactions, 16: 13022(T) (NP-tr-850)

ZIRCONYL OXALATES
preparation and properties, 17: 1467
properties for use as ion exchanger for alkali cations, 20: 18840
sorptive properties for strontium, 16: 26935

ZIRCONYL PERCHLORATES
complex formation reactions with dimethyl sulfoxide, 19: 13339
crystal structure of dihydrate of, x-ray diffraction studies of, 17: 35762
spectra of, infrared, 18: 22028
thermal properties of hydrates of, 19: 22189

ZIRCONYL PHOSPHATES
crystal structure, 16: 10020
electric conductivity and composition of, 18: 27465
electrochemical properties for di- and monovalent ions, 18: 5269
electrochemical properties, 18: 27460
ion exchange equilibria on, tracer study, 16: 10021
ion exchange properties for di- and monovalent ions, 18: 5269
ion exchange properties of granulated, 20: 41055
ion exchange reactions with metallic ions, temperature effects on, 17: 23345
labeling of colloidal, with phosphorus-32, 19: 7599
performance as ion exchange material for potassium isotopes, 19: 15976
preparation of granulated, by freezing, 20: 41055
preparation of phosphorus-32 labeled, method for, 19: 2421
properties as ion exchanger for potassium isotope separation in fused potassium nitrate, 19: 39074
radiation effects on properties of, infrared absorption at 40–1000°C, 17: 27351

ZIRCONYL SULFATES
formation of peroxy complexes of, 17: 1483
preparation and uses, 19: 38647

ZIRCONYL SULFIDES
structure of tetragonal, 16: 23676

ZIRFLEX PROCESS
(NH_4F Process)
construction materials for, corrosion behavior of, 17: 17451
corrosion in, 18: 8454
corrosion of construction materials in, 17: 3428 (ORNL-TM-417)
corrosion of construction materials in, 17: 19724 (BNL-759(p.39-46))
corrosion studies in, 16: 1649(R) (ORNL-TM-1)
corrosive effects of solutions from, on candidate alloys for centrifuge, 19: 20481 (ORNL-3787)
decladding of irradiated Zircaloy-2-clad uranium dioxide, 16: 8814 (ORNL-TM-111)
decladding of Zircaloy-2-clad uranium fuel specimens in, 17: 23434 (ORNL-3404)
decontamination of equipment used in, 19: 4046(R) (ORNL-3627 (p.247-8))
development, 19: 4246(R) (ORNL-3627(p.1-28))
development, 19: 22870(R) (HW-83601)
development, 20: 4048(R) (NP-15406)
development for TRIGA fuel, 16: 4227(R) (ORNL-TM-33)
development for TRIGA reactor fuel, 16: 3066 (ORNL-3065)
development of, 16: 32883(R) (ORNL-3314(p.1-39))
development of continuous modified, 16: 14817(R) (ORNL-TM-112)
development of dissolution step, 17: 10743(R) (ORNL-TM-457)
dissolution in, 18: 13969
dissolution of tin–uranium–zirconium fuels, 16: 11503(R) (ORNL-TM-34)
dissolution rates in, effects of modifications, 16: 1858(R) (ORNL-TM-32)
dissolver solution analysis for plutonium and uranium by multiple-filament mass-spectrometry, 16: 17607
dissolver vessel materials for, evaluation of, 16: 33064 (BNL-752)

efficiency, hot cell demonstration, 16: 27123 (ORNL-TM-187)
equipment contamination and decontamination in, 18: 23705 (ORNL-TM-837)
evaluation of, in hot cells, 17: 39178(R) (ORNL-3452(p.1-25))
head-end techniques for stainless steel, zirconium, and graphite fuel elements, 16: 29051 (ORNL-TM-131)
hot cell demonstration with PWR blanket rods, 16: 20537(R) (ORNL-TM-177)
modification for continuous dissolution, 16: 10102(R) (ORNL-TM-65)
operation of, hot-cell demonstration of, 17: 26189
performance, hot cell demonstration, 16: 11789 (ORNL-TM-130)
preparation of solvent extraction feeds from zirconium-base fuels in modified, 18: 17932 (ORNL-3465)
simulation of, use of analog computer for, 16: 31673 (HW-71054)
waste processing for, strontium and rare earth recovery in, 20: 40476(R) (BNWL-267)

ZOE REACTOR
development and uses of, 18: 38572 (A/CONF.28/P/33)
environs monitoring, 1961 and 1962, 18: 20209 (CEA-2397)
fuel elements for, 18: 15496(T) (AEC-tr-6329)
use in CEA research program, 18: 15618

Zone Melting
see High Temperature Separation Processes

Zorita Reactor (Spain)
see Power Reactors

ZPR-II Reactor
see Zero Power Reactor (Mark II)

ZPR-III Reactor
see Critical Assemblies

ZPR-IV
see Critical Assemblies

ZPR-VI
see Critical Assemblies

ZPT Reactor
see Initial Engine Test

Zyglo
see Dyes

ZYMOSAN
effects on mouse RES, Riley virus effects on plasma enzyme levels following, 20: 45252
effects on protective effects of Properdin against radiation mortality in rats, 19: 7182
effects on radioinduced changes in properdin system in dogs, 20: 31013
effects on radiosensitivity of mice, 20: 26712
protection against effects of radiation sickness on alveolar macrophages and phagocytosis in mice and rats using, 20: 35341
use to inhibit mouse RES, levels of Riley virus in blood following, 20: 45253

DEPOSITORIES OF USAEC REPORTS

In Countries Other than the U.S.

ARGENTINA
Buenos Aires, Comisión Nacional de Energía Atómica
AUSTRALIA
Canberra, Australian National Library
Sutherland, New South Wales, Australian Atomic Energy Commission
AUSTRIA
Vienna, Zentral Bibliothek der Physikalischen Institute der Universität
BELGIUM
Mol-Donk, Centre d'Etude de l'Energie Nucleaire
BOLIVIA
La Paz, Comisión Nacional de Energiá Nuclear
BRAZIL
Rio de Janeiro, Instituto Brasileiro de Bibliografia e Documentacao
São Paulo, Instituto de Energia Atomica, Cidade Universitaria São Paulo
BURMA
Rangoon, Union of Burma Applied Research Institute, Atomic Energy Center Library
CANADA
Hamilton, McMaster University
Ottawa, National Research Council Library
Vancouver, University of British Columbia
CHILE
Santiago, Departamento de Fisica, Universidad de Chile
CHINA
Hsinchu, Taiwan, Free China, National Tsing Hua University
COLOMBIA
Bogota, Instituto De Asuntos Nucleares
COSTA RICA
San Pedro, University of Costa Rica Library
DENMARK
Risö, Danish Atomic Energy Commission
ECUADOR
Quito, Escuela Politécnica Nacional
EL SALVADOR
San Salvador, Universidad de El Salvador, Biblioteca de Energia Nuclear
FINLAND
Helsinki, Teknillisen Korkeakoulun Kirjasto
FRANCE
Gif-sur-Yvette, Centre d'Etudes Nucléaires de Saclay
Paris, Académie des Sciences
GERMANY
Berlin, Hahn-Meitner-Institut für Kernforschung Berlin
Frankfurt/Main, Gmelin-Institut
Munich, Technische Hochschule, Bibliothek
GHANA
Accra, University College of Ghana
GREECE
Athens, Nuclear Research Center "Democritus"
GUATEMALA
Guatemala, Comisión Nacional de Energía Nuclear
INDIA
Bombay, Department of Atomic Energy
INDONESIA
Djogjakarta, Java, Science Faculty Gadjah Mada University
IRAN
Tehran, Tehran University Nuclear Centre
IRAQ
Baghdad, Iraqi Atomic Energy Commission
IRELAND
Dublin, University College
ISRAEL
Rehovoth, Israel Atomic Energy Commission
ITALY
Rome, Centro di Studi Nucleari della Casaccia
Rome, Comitato Nazionale per l'Energia Nucleare
JAPAN
Tokyo, National Diet Library
KOREA
Seoul, Office of Atomic Energy
LEBANON
Beirut, Lebanese National Council for Scientific Research
LUXEMBOURG
Luxembourg, Ministry of Transport and Electricity
MALAYSIA
Kuala Lumpur, University of Malaysia
MEXICO
Mexico, D.F., Comisión Nacional de Energía Nuclear
NETHERLANDS
The Hague, Reactor Centrum Nederland
NEW ZEALAND
Lower Hutt, Institute of Nuclear Sciences
NIGERIA
Ibadan, University of Ibadan
NORWAY
Lilleström, Institutt för Atomenergi
PAKISTAN
Islamabad, Pakistan Institute of Nuclear Science and Technology
PERU
Lima, Junta de Control de Energia Atomica
PHILIPPINE REPUBLIC
Manila, Philippine Atomic Energy Commission
POLAND
Warsaw, Biura Pelnomocnika Rzadu do Spraw Wykorzystania Energii Jadrowej
PORTUGAL
Sacavem, Junta de Energía Nuclear
REPUBLIC OF SOUTH AFRICA
Pretoria, Atomic Energy Board Library
REPUBLIC OF THE CONGO
Leopoldville, Université Lovanium
SPAIN
Madrid, Junta de Energía Nuclear, Biblioteca Documentación y Publicaciones, Ciudad Universitaria
SWEDEN
Nyköping, Aktiebolaget Atomenergi
SWITZERLAND
Zürich, Eidgenössische Technische Hochschule, Bibliothek
THAILAND
Bangkok, Office of the Thai Atomic Energy Commission, Department of Science
TURKEY
Ankara, Turkish Atomic Energy Commission, Atomic Energy Library
UNITED ARAB REPUBLIC
Cairo, Atomic Energy Commission
UNITED KINGDOM
Birmingham, Central Library
Boston Spa, National Lending Library for Science and Technology
Kingston upon Hull, Central Library
Liverpool, Central Library
London, Central Library, Acton
London, National Reference Library
London, Science Museum Library, South Kensington
Manchester, Central Library
Newcastle upon Tyne, Central Library
Nottingham, Central Library
Sheffield, Central Library
URUGUAY
Montevideo, Comision Nacional de Energia Atomica
VENEZUELA
Caracas, Instituto Venezolano de Investigaciones Científicas
VIET-NAM
Saigon, Atomic Energy Office
YUGOSLAVIA
Belgrade, Federal Commission for Nuclear Energy

In International Agencies

AUSTRIA
Vienna, International Atomic Energy Agency
BELGIUM
Brussels, La Bibliotheque EURATOM
FRANCE
Paris, European Nuclear Energy Agency, O.E.C.D.
ITALY
Ispra, EURATOM Research Center
SWITZERLAND
Geneva, United Nations Library

UNITED STATES
GOVERNMENT PRINTING OFFICE
DIVISION OF PUBLIC DOCUMENTS
WASHINGTON, D.C. 20402

OFFICIAL BUSINESS

POSTAGE AND FEES PAID
U.S. GOVERNMENT PRINTING OFFICE

TECHNICAL PROGRESS REVIEWS

The Division of Technical Information, U. S. Atomic Energy Commission, also publishes the Technical Progress Reviews, a series of four quarterly journals on nuclear technology. These journals, compiled by specialists and recognized authorities, summarize, evaluate, and reference the progress of development in four important fields.

Isotopes and Radiation Technology P. S. Baker, A. F. Rupp, and associates, Oak Ridge National Laboratory. Reviews AEC-sponsored projects and related significant worldwide developments in radioisotopes and radiation technology.

Nuclear Safety Wm. B. Cottrell, W. H. Jordan, J. P. Blakely, and associates, Nuclear Safety Information Center, Oak Ridge National Laboratory. Covers topics relevant to the analysis and control of hazards associated with nuclear reactors and with operations involving fissionable materials and the products of nuclear fission.

Power Reactor Technology Argonne National Laboratory. Reviews research, development, design practices, and operating experiences associated with power reactors, including aerospace applications.

Reactor Materials E. M. Simons and associates, Battelle Memorial Institute. Covers the properties, behavior, and fabrication processes of materials used in nuclear reactors and associated equipment.

Availability

SUBSCRIPTION RATE: The Technical Progress Reviews may be purchased from the Superintendent of Documents, U. S. Government Printing Office, Washington, D. C. 20402. *Nuclear Safety* at $3.00 per year for each subscription or $1.00 per issue; each of the other journals at $2.50 per year or $0.70 per issue.

POSTAGE: Postpaid within the United States, Canada, Mexico, and all Central and South American countries except Argentina, Brazil, Guyana, French Guiana, Surinam, and British Honduras. For these Central and South American countries and all other countries, add $0.75 for each annual subscription or $0.20 for a single issue.

REMITTANCE: Payment should be by check, money order, or document coupons and MUST accompany order. Remittances from foreign countries should be made by international money order or draft on an American bank payable to the Superintendent of Documents or by UNESCO book coupons.